PRE- AND POST-KATANGAN GRANITOIDS OF THE GREATER LUFILIAN ARC – GEOLOGY, GEOCHEMISTRY, GEOCHRONOLOGY AND METALLOGENIC SIGNIFICANCE

Volume 1, Text

By Alberto Lobo-Guerrero Sanz

Supervisor: Professor Laurence J. Robb

A thesis submitted to the Faculty of Science
University of the Witwatersrand, Johannesburg
For the Degree of Doctor of Philosophy

Johannesburg, March 12, 2005

PRE- AND POST-KATANGAN GRANITOIDS OF THE GREATER LUFILIAN ARC – GEOLOGY, GEOCHEMISTRY, GEOCHRONOLOGY AND METALLOGENIC SIGNIFICANCE

By Alberto Lobo-Guerrero Sanz

Supervisor: Professor Laurence J. Robb

A thesis submitted to the Faculty of Science
University of the Witwatersrand, Johannesburg
For the Degree of Doctor of Philosophy

Johannesburg, March 12, 2005

A single watch is enough to tell time. If you have access to more than one watch, you can't decide which time is right.

"... You must learn to live with the rules of the geology game, however frustrating: (1) collect bits of data, however incomplete, that bear on a problem, (2) evaluate them, and (3) come to a conclusion, however imperfect. Then (4) be ready to accept and analyze pertinent new data, and (5) repeat."

John E. Warme, Professor in Applied Stratigraphy
Colorado School of Mines, Golden Colorado, 1992 Prospectus.

Aknowledgements

I thank my father for his unconditional support, for guiding me into the world of geology and mineral deposits, and for encouraging me to continue advancing my education.

I thank Andrea, my wife, for accepting to delay our wedding one year (the first year of this Ph.D. research). I also thank her support, understanding and patience during the long days and nights, Christmasses and holidays that were spent developing ideas and editing multiple drafts.

ABSTRACT

This document reports observations, findings and conclusions of the research project entitled “Pre- and Post-Katangan Granitoids of the Greater Lufilian Arc - Geology, Geochemistry, Geochronology and Metallogenic Significance”. The project, structured and supervised by Professor Laurence Robb, was designed to study granitoids that comprise the Greater Lufilian Arc. Its main aims were to define the various granitoids, and study their role in Katangan orogenesis and mineralization. Main fieldwork was concentrated in northwestern Zambia and northern Namibia.

The Greater Lufilian Arc is a curvilinear belt of Neoproterozoic Katangan sediments that was deformed during the Pan African orogeny in Zambia and the Democratic Republic of Congo, and the westward extension of similar rock sequences into Botswana, Angola and Namibia. The mobile belt of the Greater Lufilian Arc also comprises a dominantly Paleoproterozoic basement of deformed granitoids, and a diverse suite of Pan-African granitoids that intrude the Katangan sequences.

A total of 1500 samples were collected in the field; 351 plutonic rocks were analysed. 157 chemical analysis were compiled from various well-documented sources, to reach a total of 508 samples analysed in the database. 38 new zircon U-Pb SHRIMP II and laser ablation ICP-MS ages were produced.

The majority of intrusive rocks from the Greater Lufilian Arc that were analysed (60%) had midalkaline characte. 33% were subalkaline and 7% were alkaline. Mafic rocks are closely associated to felsic rocks in most domains of the Arc. Two thirds of the gabbroids were midalkaline, 1/6 alkaline and 1/6 subalkaline. The average rock type distribution for the entire Lufilian Arc closely resembles that of the Hook Granite Batholith in Zambia.

A frequent field observation is the persistent clustering of small bodies of red-altered granitoids, gabbroids, massive magnetite-hematite and quartz pods that are linked to ages around 550 and 750 Ma. The four-rock association is related to iron oxide-copper-gold (IOCG) mineralization, and seems to be a characteristic of continental extension anorogenic environments.

Another recurrent feature observed in most outcrops of the study area is the presence of two or more contrasting types of plutonic rocks, including mafic, ultramafic and alkaline plugs and dikes. The multiplicity of rock types in a small area seems to be a characteristic of continental extension anorogenic environments. Quartz pods, hydrothermally-emplaced iron oxide bodies and round-pebble hydrothermal breccias are features that occur often in and around IOCG systems throughout the Greater Lufilian Arc.

The main granitoid periods of emplacement present in the study area of the Arc are listed on Table 1. Several more restricted events occurred at 1700, 1600, 880 and 460 Ma.

Table 1 Main Granitoid Terranes in the Greater Lufilian Arc

Age (Ma)	Rock types	Location	Environment of Emplacement	Notes
550 ±50	Granite, alkali granite, quartzmonzonite, syenite, gabbroids	Otjiwarongo, central Namibia, Kaokoland, Damaran intrusives (Namibia), Hook Granite, NW Zambia (Zambia)	Continental epeirogenic uplift	The period may be broken into 3 discrete events.
750 ±50	Granite, alkali granite, syenite and gabbroids with felsic and mafic volcanics	Copperbelt, Kalengwa-Kasempa, NW Zambia (Zambia); Khorixas Inlier and Summas Mountains (Namibia)	Rift-related and continental epeirogenic uplilft.	Intrude Roan and Nguba Lithologies; overlain by Kundelungu and equivalent sediments.
1100 ±50	Granitoids and felsic to mafic volcanics	South of the Copperbelt, West of Lusaka (Zambia); around Omitiomire, Kaokoland and the Witvlei area (Namibia)	Continental rift-related environments	Surrounds Kapvaal Craton from Namaqualand to Irumide Belt in Zambia
1900 ±100	Foliated alkali granie, quartzmonzonite and granite	Copperbelt basement, Mkushi-Serenje, NW Zambia, Domes region (Zambia); Kaokoland, central Namibia, Kamanjab Batholith, Grootfontein Inlier (Namibia)	Not well defined; probably formed in an anorogenic continental extension environment	Period can be broken into 4 discrete events

The Zambian Lufilian Arc and Damara region of Namibia behaved as independent entities from 2200 to 2000 Ma. They also behaved significantly different from 1400 to 850 Ma. Geological history of the two main portions of the Greater Lufilian Arc is consistent from *circa* 800 Ma to the present, and especially during the last 600 million years.

Most areas studied in the Arc show polycyclic geological histories. Repeated anorogenic intrusive events are a common denominator. Prolonged crustal histories have resulted in superimposition of events.

Granitoid rock suites with closely matching chemistry and macroscopic features have been found to form two or three times in the same region, with up to a thousand million years of age difference. These features preclude lithological or detailed geochemical correlation of plutonic rocks.

At least ten clusters of ring complexes were identified in the Arc. Clustering of multiple anorogenic ring complex intrusions can form batholithic size bodies. Clusters are made by amalgamation of multiple ring complexes of varying chemical composition and size. Most of their rocks are midalkaline. Volcanic and plutonic rocks of roughly the same composition occur together. Total duration of ring complex cluster cycles averages 110 Ma, and their plan view geometry is roughly that of an isosceles triangle.

Information currently available on geophysics, geochronology, rock distribution and geochemistry from the Hook Granite Batholith (Zambia) fit quite well with an intracontinental, anorogenic, ring complex cluster origin. The Nchanga Granite (Zambia) has all the characteristics of an anorogenic granite ring complex, and might have contributed to the origin of copper in its environs. Several sources of evidence indicate that the Kamanjab Batholith (Namibia) is an anorogenic cluster of ring complexes. Volcanic and plutonic rocks of similar composition make the batholith. Geological history for the Khorixas Inlier and the Kamanjab Batholith are significantly different.

Complete Wilson cycles were not identified in the study areas of the Greater Lufilian Arc. The dominant magmatic process, as evidenced by the volume of extruded rock, is anorogenic continental epeirogenic uplift, closely-followed in time by a rift-related granitoid emplacement. Coalescing and overprinting aulacogens seem to be the main geological event in the Arc.

Incipient migmatitization and alteration of Paleoproterozoic rocks modified their chemistry to a point where their environment of emplacement cannot be identified by traditional geochemical means.

The anomalous thorium content in some granitoids of the Greater Lufilian Arc induced and maintained long-lived, large convective cells of hydrothermal fluid flow.

E-W-trending regional fracture systems, that run parallel to the elongation of the Arc, play an important role in the emplacement of magmatism and IOCG mineralization. Those structures are generally parallel to the main Lufilian Arc trend, and could have been normal syn-rift faults reactivated multiple times during geological history.

At least eight discrete periods of mineralization were identified in the Greater Lufilian Arc. There is a wide-spread series of midalkaline intrusions emplaced around 750 Ma that produces a variety of mineral deposits. Another event took place around 540±40 Ma. Five less well defined events occurred at ~1970, ~1930, ~1866, 1097-1059 and ~460 Ma. The dominant deposit type is iron oxide-copper-gold mineralization, but other types of mineral deposits are present in the Arc. At least two distinct events of disseminated copper mineralization associated to midalkaline granitoid intrusives were identified in the Kamanjab Batholith; the first took place around 1975 Ma and the second around 1928 Ma.

The main IOCG events that have been identified in the Greater Lufilian Arc took place during eight time periods. The rocks of many IOCG deposits and prospects in the Arc are pristine. There is no significant deformaton involved. Hydrothermal brecciation and other mineralization features are un-deformed.

Three discrete time periods show IOCG mineralization in close temporal spatial association with sedimentary-hosted copper deposits. The first took place around Witvlei (Namibia) from 1108 to 1059 Ma. The second and third ocurred in the basement to the Zambian Copperbelt from 882 to 725 Ma and from 607 to 500 Ma. This idea may generate a new concept for the origin of sedimentary-hosted copper and cobalt deposits.

SHORT TABLE OF CONTENTS

Abstract, v
Short Table of Contents, vii
Detailed Table of Contents, viii
Aknowledgements, iii
Conclusions, 395

1. Introduction, 1
2. Methodology, 4
3. Generalized Geology of the Greater Lufilian Arc, 21
4. Description of Rocks from the Different Domains, 23
    - Zambian domains, 24
        - Hook Granite Batholith, Zambia, 24
        - West Lusaka/Kafue Flats domain, 61
        - Kalengwa-Kasempa Area, Zambia, 70
    - Northwestern Zambia domain, 83
        - Kalene Hill area, 84
        - Introduction to the geology of the Domes Region, NW Zambia, 96
        - Kabompo Dome, 97
        - Mwombezhi Dome, 104
        - Solwezi Dome, 115
        - Conclusions on entire NW Zambia region, 118
    - Zambian Copperbelt, 121
        - Nchanga Granite, 127
        - Nchanga mine area, 137
        - Muliashi Porphyry, 140
        - Deep borehole, Konkola mine, 144
        - Chambishi granite, 148
        - Mufulira granite, 152
        - Samba deposit, 155
        - Conclusions, 158
    - Namibian Domains, 163
        - Kamanjab Batholith, 163
        - Khorixas Inlier, 211
            - Oas farm, 213
            - Lofdal farm, 237
        - Other Small Outcrops in Namibia and Bostwana, 252
            - Mesopotamie, 252
            - Summas Mountains, 260
            - Ugab River outcrops, 262
            - Okwa River Outcrops, Botswana, 264
            - Grootfontein Inlier, 265
            - Environs of Otjiwarongo, 266
            - Review of observations, 277
        - Witvlei, Namibia, 281
5. Thorium Content of Granitoids in the Greater Lufilian Arc, 303
6. Geochronology, 308
    - New radiometric ages, 308
    - Geochronological database and interpretation, 308
    - New Re-Os ages from copper mineralization, Zambian Copperbelt, 312
7. Some Aspects of Anorogenic Intrusive Rocks, 316
    - Comparison of batholithic granitoid bodies with anorogenic ring complex clusters, 317
    - Comparison of Lufilian small basic intrusions with examples from the literature, 334
8. Iron Oxide-Copper-Gold Mineralization in the Greater Lufilian Arc, 337
    - Some notes on iron oxide-copper-gold deposits, 337
    - Iron oxide-copper-gold systems in the Greater Lufilian Arc, 346
    - Some known IOCG-like deposits and prospects, 362
    - Relationship between IOCG and sedimentary-hosted Cu mineralization, 391
    - Sedimentary-hosted Au mineralization in the Greater Lufilian Arc, 391
    - Peculiarities of Zambian and Namibian IOCG systems, 391
    - Conclusions, 392
9. Conclusions, 395
10. References, 405

Appendices

DETAILED TABLE OF CONTENTS

ABSTRACT, v

SHORT TABLE OF CONTENTS, vii

DETAILED TABLE OF CONTENTS, viii

AKNOWLEDGEMENTS, iii

CONCLUSIONS, 395

1. INTRODUCTION, 1
1.1 The Lufilian Arc, 1
1.2 The Project, 1
1.3 Aims of the Project, 1
1.4 Study Areas, 1
1.5 Project Outline, 3
1.5.1 Phase 1, 3
1.5.2 Phase 2, 3
1.5.3 Phase 3, 3
1.5.4 Phase 4, 3
1.5.5 Current Status of Project, 3

2. METHODOLOGY, 4
2.1 Field Sampling, 4
2.1.1 Definition of Granitoid, 4
2.1.2 Sampling Procedure, 4
2.1.3 Referencing Geological Stations, Recording Information and Sample Labeling, 4
2.1.4 Other Field Activities, 5
2.1.5 Field Equipment Used, 5
2.1.6 Bibliographical Research, 5
2.1.7 Office and Laboratory Work, 5
2.2 Petrologic Nomenclature, 7
2.2.1 Total Alkali Diagram, 7
2.2.2 R1/R2 Cationic Classification, 8
2.2.3 Granitoid Classification, 9
2.2.4 Debon & LeFort Cationic Classification Diagrams, 10
2.2.4.1 Q-P DiagraM, 10
2.2.4.2 A-B Diagram, 10
2.2.4.3 QBF Diagram, 10
2.2.4.4 K-B Diagram, 10
2.2.4.5 Mg*-B Diagram, 10
2.3 Geochemistry, 12
2.3.1 Major Oxide Chemistry, 12
2.3.2 Trace Element and Rare Earth Chemistry, 12
2.3.3 Presentation of Chemical Data, 12
2.3.4 Geochemical Threshold Values, 12
2.4 Tectonic Discrimination of Samples, 14
2.4.1 Granitoids, 14
2.4.1.1 Comprehensive method of Barbarin, 1999, 14
2.4.1.2 Major oxide method of Maniar & Piccoli, 1989, 14
2.4.1.3 Definition of anorogenic granitoids, method of Whalen et al, 1987, 15
2.4.1.4 Trace element method of Pearce et al, 1984, 17
2.4.1.5 Discrimination of granitoids from collisional environments, method of Harris at al, 1986, 17
2.4.1.6 Discussion, 17
2.4.1.7 A Novel Approach, 17
2.4.2 Mafic Rocks, 18
2.4.3 Conventions to Tabulate Rock Type and Methods to Evaluate Environment of Emplacement for Samples Studied, 18

3 GENERALIZED GEOLOGY OF THE GREATER LUFILIAN ARC, 21

4 DESCRIPTION OF ROCKS FROM THE DIFFERENT DOMAINS, 23

4.1 ZAMBIAN DOMAINS, 24

4.1.1 HOOK GRANITE BATHOLITH, ZAMBIA, 24

4.1.1.1 Introduction, 24
4.1.1.2 Geochemistry, 25
4.1.1.3 Geological Units, 36
4.1.1.4 Comparison of Hook Granitoids with Ring Complexes, 45
4.1.1.4.1 Airborne Geophysical Image and Definition of Ring Complexes, 45
4.1.1.4.2 Comparison of Hook Granitoids with rocks from Namibian Mesozoic Ring Complexes, 49
4.1.1.5 E-W Transect Across the Kafue Park, Zambia, 55
4.1.1.6 Geochronology and Geological History, 57
4.1.1.7 Environment of Emplacement, 59
4.1.1.8 Conclusions, 59
4.1.1.9 Recommendations, 59

4.1.2 WEST LUSAKA/KAFUE FLATS DOMAIN, ZAMBIA, 61

4.1.2.1 Introduction, 61
4.1.2.2 Geochemistry, 61
4.1.2.3 Lusaka Granite, 66
4.1.2.4 Description of main rock types, 66
4.1.2.4.1 Four rock association, 66
4.1.2.4.2 Granitoids, 67
4.1.2.4.3 Gabbroids, 67
4.1.2.4.4 Iron oxide bodies, 68
4.1.2.5 Thorium content in Kafue Flats area, 68
4.1.2.6 Geochronology, 68
4.1.2.7 Conclusions, 68

4.1.3 KALENGWA-KASEMPA AREA, ZAMBIA, 70

4.1.3.1 Introduction, 70
4.1.3.2 Sampling, 71
4.1.3.3 Geochemistry, 71
4.1.3.4 Analysis of independent samples by elements, 79
4.1.3.5 Analysis by source area, 80
4.1.3.6 Kalengwa Area, 80
4.1.3.6.1 Samples, 80
4.1.3.6.2 Geochronology, 81
4.1.3.6.3 Environment of emplacement, 81
4.1.3.7 Kasempa Area, 81
4.1.3.7.1 Borehole MB-34, 81
4.1.3.7.2 Mufwashi and Chitampa Boreholes, 81
4.1.3.7.3 Geochronology, 82

4.1.4 NORTHWESTERN ZAMBIA DOMAIN, 83

4.1.4.1 Introduction, 83
4.1.4.2 Kalene Hill Area, 84
4.1.4.2.1 Geochemistry, 84
4.1.4.2.2 Description of the various groups, 84
4.1.4.2.2.1 Group 1, 84
4.1.4.2.2.2 Group 2, 84
4.1.4.2.2.3 Group 3, 94
4.1.4.2.2.4 Group 4, 94
4.1.4.2.3 Analysis of independent samples by elements, 94
4.1.4.2.4 Geochronology, 94
4.1.4.2.5 Environment of emplacement, 95
4.1.4.2.6 Conclusions, 95

4.1.4.3 Introduction to the geology of the Domes Region, NW Zambia, 96
4.1.4.4 Kabompo Dome, 97
4.1.4.4.1 Introduction, 97
4.1.4.4.2 Description of samples collected in the field, 97
4.1.4.4.2.1 Samples L-028 and L-029, 97
4.1.4.4.2.2 Sample L-030, 98
4.1.4.4.2.3 Samples L-047 and L-048, 100
4.1.4.4.3 Conclusions, 103
4.1.4.5 Mwombezhi Dome, 104
4.1.4.5.1 Introduction, 104
4.1.4.5.2 Lumwana copper mineralization, 104
4.1.4.5.3 Mafic volcanics from Shilenda, 106
4.1.4.5.4 Chitungulu sodalite syenite, 107
4.1.4.5.4.1 Introduction, 107
4.1.4.5.4.2 Sampling, 107
4.1.4.5.4.3 Description of the rocks, 107
4.1.4.5.4.4 Weathering, jointing and problematic structures for mining, 107
4.1.4.5.4.5 Geochemistry, 110
4.1.4.5.4.6 Environment of emplacement, 113
4.1.4.5.4.7 Geochronology, 114
4.1.4.5.4.8 Conclusions, 114
4.1.4.6 Solwezi Dome, 115
4.1.4.6.1 Introduction, 115
4.1.4.6.2 Sampling, 115
4.1.4.6.3 Samples from the Solwezi Dome, 115
4.1.4.6.4 Geochronology, 116
4.1.4.6.5 Samples from East of Solwezi, 118
4.1.4.6.6 Conclusions, 118
4.1.4.7 Conclusions on the entire NW Zambia Region, 118

4.1.5 ZAMBIAN COPPERBELT, 121
4.1.5.1 Introduction, 121
4.1.5.2 Nchanga Granite, 127
4.1.5.2.1 Introduction, 127
4.1.5.2.2 Sampling, 127
4.1.5.2.3 Main rock types, 128
4.1.5.2.4 Samples P-28 and P-29, 128
4.1.5.2.5 Samples from Chiwempala Hill, 130
4.1.5.2.6 Gray's quarry, 131
4.1.5.2.7 Various dikes, 132
4.1.5.2.8 Geochemistry, 132
4.1.5.2.9 Anorogenic character of the Nchanga Granite, 135
4.1.5.2.10 Conclusions, 136
4.1.5.3 Nchanga mine area, 137
4.1.5.3.1 Introduction, 137
4.1.5.3.2 Comparison of gabbroid rocks,138
4.1.5.3.3 Nchanga lamprophyre dike, 138
4.1.5.3.4 Samples with special character, 139
4.1.5.3.5 Geochronology, 139
4.1.5.3.6 Conclusions, 139
4.1.5.4 Muliashi Porphyry, 140
4.1.5.4.1 Introduction, 140
4.1.5.4.2 Sampling and composition of samples, 140
4.1.5.4.3 Description of samples, 141
4.1.5.4.4 Geochronology, 141
4.1.5.4.5 Discussion on the Muliashi Porphyry and its correlatives, 141
4.1.5.5 Deep borehole, Konkola mine, 144
4.1.5.6 Chambishi Granite, 148
4.1.5.6.1 Introduction, 148
4.1.5.6.2 Geochemistry, 148
4.1.5.6.3 Chambishi gabbroid rocks, 150
4.1.5.6.4 Geochronology, 151
4.1.5.6.5 Environment of emplacement, 151
4.1.5.6.6 Conclusion, 151

4.1.5.7 Mufulira Granite, 152
4.1.5.7.1 Introduction, 152
4.1.5.7.2 Sample description and geochemistry, 152
4.1.5.7.3 Geochronology, 153
4.1.5.7.4 Discussion, 153
4.1.5.8 Samba Deposit, 155
4.1.5.8.1 Introduction, 155
4.1.5.8.2 Sampling and geochemistry, 155
4.1.5.8.3 Geochronology, 157
4.1.5.8.4 Discussion, 157
4.1.5.9 Conclusions on granitoids from the Zambian Copperbelt, 158
4.1.5.9.1 General conclusions, 158
4.1.5.9.2 Tectonic environment of emplacement, 158
4.1.5.9.3 Mineralization, 158
4.1.5.9.4 Lithologic correlation, 159
4.1.5.9.5 Stratigraphic relations, 159

4.2 NAMIBIAN DOMAINS, 163

4.2.1 KAMANJAB BATHOLITH, 163
4.2.1.1 Introduction, 163
4.2.1.2 Geochemistry, 164
4.2.1.3 Main Rock Suites, 173
4.2.1.3.1 Examples of rock suites, 173
4.2.1.3.1.1 Suite B, 173
4.2.1.3.1.2 Suite E, 173
4.2.1.3.1.3 Suite G, 174
4.2.1.3.1.4 Suite H, 174
4.2.1.3.1.5 Suite J, 177
4.2.1.3.1.6 Suite K, 177
4.2.1.3.1.7 Suite M, 177
4.2.1.4 Sample grouping, 179
4.2.1.4.1 Quartzmonzonites, 179
4.2.1.4.2 Alkali granites, 181
4.2.1.4.3 Granites, 182
4.2.1.4.4 Syenites, 183
4.2.1.4.5 Gabbroid rocks, 183
4.2.1.4.6 Rocks that could not be classified into above groups, 184
4.2.1.5 Volcanic rocks, 184
4.2.1.6 Environment of emplacement, 200
4.2.1.7 Evidence of magma mixing-magma mingling, 200
4.2.1.8 Granitoids sampled by Tom Clifford, 201
4.2.1.9 Geochronology, 201
4.2.1.10 Some copper-mineralized systems in the Kamanjab Batholith, 206
4.2.1.11 Discussion, 208
4.2.1.12 Gelbingen farm, 209

4.2.2 KHORIXAS INLIER, 211
4.2.2.1 Introduction, 211
4.2.2.2 OAS FARM, 213
4.2.2.2.1 Introduction, 213
4.2.2.2.2 4-km long N-S transect across Oas Syenite, 213
4.2.2.2.3 Geochemistry, 219
4.2.2.2.4 Zinc enrichment, 229
4.2.2.2.5 Quartzite from Oas farm that might host mineralization,235
4.2.2.2.6 Geochronology, 235
4.2.2.2.7 Environment of emplacement, 236
4.2.2.2.8 Conclusions, 236

4.2.2.3 LOFDAL FARM, 237
4.2.2.3.1 Introduction, 237
4.2.2.3.2 Geochemistry, 237
4.2.2.3.3 Description of outcrops from the Lofdal farm, 238
4.2.2.3.3.1 Dissolution of silicates in granitoids, 238
4.2.2.3.3.2 Carbonatite dikes and iron oxide-copper-gold mineralization, 241
4.2.2.3.3.3 Cross section through series of ultramafic dikes, 244
4.2.2.3.3.4 Magnetite-cemented, polymictic hydrothermal breccia that makes diatreme, 245
4.2.2.3.3.5 Abandoned Lofdal mine, 247
4.2.2.3.3.6 Carbonatite dikes, 248
4.2.2.3.3.6.1 Introduction, 248
4.2.2.3.3.6.2 Geochemistry, 248
4.2.2.3.3.6.3 Economic mineralization in carbonatite dikes, 248
4.2.2.3.3.6.4 High-heat production properties in some of the dikes, 249
4.2.2.3.4 Environment of emplacement, 250
4.2.2.3.5 Geochronology, 251
4.2.2.3.6 Conclusions, 251

4.2.3 OTHER SMALL OUTCROPS IN NAMIBIA AND BOTSWANA, 252
4.2.3.1 Introduction, 252
4.2.3.2 Mesopotamie, 252
4.2.3.2.1 Introduction, 252
4.2.3.2.2 Sampling and geochemisty, 252
4.2.3.2.3 Environment of emplacement, 252
4.2.3.2.4 Geochronology, 259
4.2.3.2.5 Economic geology, 259
4.2.3.3 Summas Mountains, 260
4.2.3.3.1 Sampling and geochemistry, 260
4.2.3.3.2 Geochronology, 261
4.2.3.4 Ugab River outcrops, 262
4.2.3.4.1 Sampling and geochemistry, 262
4.2.3.4.2 Geochronology, 263
4.2.3.5 Okwa River Outcrops, Botswana, 264
4.2.3.6 Grootfontein Inlier, 265
4.2.3.6.1 Sampling and geochemistry, 265
4.2.3.6.2 Geochronology, 265
4.2.3.7 Environs of Otjiwarongo, Namibia, 266
4.2.3.7.1 Introduction, 266
4.2.3.7.2 Field description of main outrcrops, 266
4.2.3.7.3 Pegmatitic rocks, 270
4.2.3.7.4 Geochemistry, 273
4.2.3.7.5 Otjiwarongo Batholith, 274
4.2.3.7.6 Environment of emplacement, 274
4.2.3.7.7 Geochronology, 274
4.2.3.7.8 Discussion, 274
4.2.3.8 Review of observations from Mesopotamie, Summas Mountains, Ugab River, Okwa River, Grootfontein Inlier and Otjiwarongo outcrops, 277

4.2.4 WITVLEI, NAMIBIA, 281
4.2.4.1 Introduccion, 281
4.2.4.2 Field observations, 281
4.2.4.3 Description of the OP-1 borehole, Okatjepuiko Project, 284
4.2.4.4 Geochemistry, 284
4.2.4.5 Environment of emplacement, 291
4.2.4.6 Geochronology, 291
4.2.4.7 Other events of the same age in the region, 292
4.2.4.8 Evidence of iron oxide-copper-gold mineralization and definition of a mineralized belt, 292
4.2.4.9 Conclusions, 293

5 THORIUM CONTENT OF GRANITOIDS IN THE GREATER LUFILIAN ARC, 303

5.1 Introduction, 303
5.2 High Thorium samples, 303
5.3 Values for high-heat generating granitoids, 305

6 GEOCHRONOLOGY, 308

6.1 Introduction, 308
6.2 New radiometric ages, 308
6.3 Geochronological Database and Interpretation, 308
6.3.1 Event diagrams, 309
6.3.2 Compilation of event diagrams, 309
6.4 New Re-Os Ages from Copper Mineralization, Zambian Copperbelt, 312
6.4.1 Basic data, 312
6.4.2 Discussion, 312
6.4.3 Conclusions, 314

7 SOME ASPECTS OF ANOROGENIC INTRUSIVE ROCKS, 316

7.1 Intoduction, 316
7.2 Comparison of batholithic granitoid bodies with anorogenic ring complex clusters, 317
7.2.1 Introduction, 317
7.2.2 Nuba Mountains, Sudan, 318
7.2.3 Central Nigeria ring complexes, 319
7.2.4 Kanye-Gaborone ring complexes, Botswana, 323
7.2.5 Comparison of the three ring complex clusters, 324
7.2.6 Model for the origin of batholithic-size granitoid bodies in anorogenic environments, 326
7.2.7 Ring complex clusters in the Greater Lufilian Arc, 329
7.2.8 Conclusions, 333
7.3 Comparison of Lufilian small basic intrusions with examples from the literature, 334

8 IRON OXIDE-COPPER-GOLD MINERALIZATION IN THE GREATER LUFILIAN ARC, 337

8.1 Introduction, 337
8.2 Some notes on iron oxide-copper-gold deposits, 337
8.3 Iron oxide-copper-gold systems in the Greater Lufilian Arc, 346
8.3.1 Relationship between granitoids and iron oxides, 346
8.3.2 Iron oxide bodies, 349
8.3.3 Breccias, 351
8.3.4 Structural control, 353
8.3.4.1 Rock fracturing to control IOCG mineralization, 353
8.3.4.2 E-W Structures, 354
8.3.4.3 Planar features of iron oxide bodies, 354
8.3.5 Particular hydrothermal alteration features, 357
8.3.5.1 Tourmaline alteration, 357
8.3.5.2 Quartz pods, 357
8.3.5.2.1 Description of QP, 357
8.3.5.2.2 Four rock association, 359
8.3.5.2.3 Particles enclosed in QP, 359
8.3.5.2.4 Studies that can be done on QP, 360
8.3.5.2.5 Practical applications of QP, 360
8.3.5.2.6 Hypothesis about the origin of QP, 360

8.4 Some known IOCG-like deposits and prospects, 362
8.4.1 Namibian deposits and prospects, 362
8.4.1.1 Okatjepuiko Prospect, Witvlei, 362
8.4.1.2 Kombat mine, Otavi Mountains, 363
8.4.1.3 Otjikoto gold deposit, 366
8.4.1.4 Mesopotamie farm, 366
8.4.1.4.1 Copper Valley mineralization on the NW portion of Mesopotamie 504, 367
8.4.1.4.2 Kruger's deposit on the NW portion of Mesopotamie 504, 368
8.4.1.4.3 Mineralization on the NE portion of Mesopotamie 504, 369
8.4.2 Zambian deposits and prospects, 370
8.4.2.1 Evidence of IOCG mineralization under the Copperbelt, 370

8.4.2.2 Dunrobin gold mine, 370
8.4.2.3 Nampundwe pyrite mine, 374
8.4.2.4 Kasempa Region Prospects, 374
8.4.2.5 IOCG prospects and mines around the Hook Granite Batholith, 375
8.4.2.6 Kalengwa copper-silver mine, 377
8.4.3 Other Lufulian Arc IOCG prospects and deposits, 379
8.4.3.1 Quartzite-hosted deposits, Gelbingen farm, Namibia, 379
8.4.3.2 Deposits associated to alkaline rocks and carbonatites, 383
8.4.3.3 IOCG Mineralization in the Democratic Republic of Congo, 388
8.4.3.4 Active exploration in projects in the Greater Lufilian Arc, 390

8.5 Relationship between IOCG and sedimentary-hosted Cu mineralization, 391
8.6 Sedimentary-hosted Au mineralization in the Greater Lufilian Arc, 391
8.7 Peculiarities of Zambian and Namibian IOCG systems, 391
8.8 Conclusions, 392

9 CONCLUSIONS, 395

9.1 Main Granitoid Terranes in the Greater Lufilian Arc, 395
9.2 Polycyclic Geological History, 395
9.3 Rock Types, 395
9.3.1 Mafic, Ultramafic and Alkaline Rocks, 398
9.3.2 Rock Associations in Anorogenic Environments, 398
9.3.3 Quartz Pods, 399
9.3.4 Iron Oxide Bodies, 399
9.3.5 Round-Pebble Hydrothermal Breccias, 399
9.4 Ring Complex Clusters, 399
9.5 Tectonic Environment of Emplacement, 399
9.6 High Thorium, 400
9.7 Correlation of Granitoids, 400
9.8 Main Findings in Specific Domains, 400
9.8.1 Hook Granite Batholith, Zambia, 400
9.8.2 Nchanga Granite, Zambia, 400
9.8.3 Kamanjab Batholith, Namibia, 400
9.8.5 New Temporal Constrain to Katangan Sedimentation, 401
9.8.6 Khorixas Inlier-Kamanjab Batholith, 401
9.8.7 Long-Lived Fractures, 401
9.9 Metallogeny, 401
9.9.1 Metallogenic Epochs, 401
9.9.2 Iron Oxide-Copper-Gold Mineralization, 404
9.9.3 Association of Sedimentary-Hosted Copper Mineralization with IOCG Mineralization, 404

10 REFERENCES, 404-428

10 APPENDICES (Paging in the Appendices volume is independent from the rest of the text)

A Sample Maps, 127
B TAS Diagram for Suites of the Kamanjab Batholith, Namibia, 165
C Geochemistry Database, 1
D Geographic Coordinates of Samples Collected and Geological Stations, 25
E Geochronology Database, 41
F Geochronological Event Diagrams, 67
G Tectonic Environent of Emplacement for Samples, 95
H Partial Transcription of Field Notes, 183
I Other Information, 222
J Raw Data for New Geochronology, 237
K Geochronological Correlation Diagrams, 257

LIST OF FIGURES

1.1 Definition of the study area area and tectonic framework of Southern Africa, 2
2.1 TAS diagram modified by Middlemost, 1994, 1997, 7
2.2 Comparison of the total alkali versus silica diagrams proposed by Middlemost, 1994 and by Wilson, 1989, 8
2.3 R1/R2 diagram of De La Roche et al, 1980, 9
2.4 The Q-P diagram, 11
2.5 The A-B diagram, 11
2.6 The QBF diagram, 11
2.7 The K*-B diagram, 11
2.8 The Mg*-B diagram, 11
3.1 Schematic structural map of Gondwana, 21
4.1 General map of the Hook Granite Batholith, 24
4.2 Correlation diagrams between silica and the major oxides for samples from the Hook Granite Batholith, Zambia, 26
4.3 Enlargement of TAS diagram for Hook Granite Batholith, 28
4.4 TAS diagram for Hook Granite Batholith, 29
4.5 Enlargement of R1/R2 diagram for Hook Granite Batholith, 30
4.6 R1/R2 diagram for Hook Granite Batholith, 31
4.7 Type I, Logarithmic major oxide plot, Hook Granite Batholith, 32
4.8 Type II, Logarithmic major oxide plot, Hook Granite Batholith, 33
4.9 Type III, Logarithmic major oxide plot, Hook Granite Batholith, 33
4.10 Type IV, Logarithmic major oxide plot, Hook Granite Batholith, 33
4.11 Type VII, Logarithmic major oxide plot, Hook Granite Batholith, 34
4.12 Type IX, Logarithmic major oxide plot, Hook Granite Batholith, 34
4.13 Type X, Logarithmic major oxide plot, Hook Granite Batholith, 35
4.14 Type XI, Logarithmic major oxide plot, Hook Granite Batholith, 35
4.15 Compilation of geology for the Hook Granite Batholith, 38
4.16 Structural interpretation of Zambian geology based on aeromagnetic data, 46
4.17 Sanabozi processed airborne geophysical image, Hook Granite Batholith, Namibia overlain by samples collected, 47
4.18 Anorogenic ring structures that can be identified in the Sanabozi geophysical image, Hook Granite Batholith, Zambia, 48
4.20 Logarithmic major oxide plot to compare Namibian granitoid ring complexes with samples from the Hook Granite Batholith, 52
4.21 R1/R2 diagram for Hook Granite Batholith compared to other anorogenic ring complexes, 53
4.21A TAS diagram comparing Hook Granite Batholith with anorogenic ring complexes, 54
4.22 TAS diagram for samples collected along the E-W transect, Hook Granite Batholith, 56
4.23 Hypothetical granitoid ring complex cluster and transect across it, 57
4.24 Schematic representation of the various events that gave rise to the current geology of the Hook Granite Batholith, 58
4.1.2.1 TAS diagram West Lusaka-Kafue Flats, Zambia, 63
4.1.2.2 R1R2 diagram, West Lusaka-Kafue Flats, Zambia, 64
4.1.2.3 Geological map of the Lusaka Granite, 66
4.1.2.4 Photographs of slabs from red-altered granitoids in the Kafue Flats area, Zambia, 67
4.1.3.1 Geological interpretation of airborne magnetic image for northwestern Zambia, 70
4.1.3.2 TAS diagram Kalengwa-Kasempa Area, Zambia, 73
4.1.3.3 R1R2 diagram, Kalengwa-Kasempa Area, Zambia, 74
4.1.3.4 Q-B diagram, Kalengwa-Kasempa Area, Zambia, 75
4.1.3.5 Q-P diagram, Kalengwa-Kasempa Area, Zambia, 76
4.1.3.6 K-B diagram, Kalengwa-Kasempa Area, Zambia, 77
4.1.3.7 Mg-Fe-B diagram, Kalengwa-Kasempa Area, Zambia, 78
4.1.3.8 Photos of red-altered, subvolcanic porphyritic granitoids that were dated; borehole MB-34, Chitampa, Kasempa area, Zambia, 82

4.1.4.1 TAS diagram NW Zambia, 86
4.1.4.2 R1R2 diagram, NW Zambia, 87
4.1.4.3 Q-B diagram, NW Zambia, 88
4.1.4.4 Q-P diagram, NW Zambia, 89
4.1.4.5 K-B diagram, NW Zambia, 90
4.1.4.6 Mg-Fe-B diagram, NW Zambia, 92
4.1.4.7 Generalized geological map of the domes region in Zambia, 96
4.1.4.8 General aspect of the outcrop where samples L-029 and L-030 were collected, 98
4.1.4.9 Main aspects of the outcrop where sample L-030 was collected, 98
4.1.4.10 Detail of the foliation and mineral banding of the rock that intersect at around 5-8 degrees, 99
4.1.4.11 Simplified regional geology and interpreted stratigraphic relations of the southern site of the the Kabompo Dome, 102
4.1.4.12 Geological map with location of sample L-047, Kabompo Dome, Zambia, 101
4.1.4.13 Photographs of slabs, samples L-047* and L-048, 100
4.1.4.14 Cross section of the Malundwe Cu deposit at Lumwana, Zambia, 104
4.1.4.15 Photographs of hand samples and slabs from the Shilenda mafic volcanics, 106
4.1.4.16 Rough map of sodalite syenite quarry, NW Zambia, 108
4.1.4.17 Photographs of slabbed syenites from the Chitungulu sodalite syenite quarry, Zambia, 109
4.1.4.18 TAS diagram sodalite syenite quarry, NW Zambia, 111
4.1.4.19 R1R2 diagram, sodalite syenite quarry, NW Zambia, 112
4.1.4.20 Major oxide logarithmic plot for samples from the Chitungulu sodalite syenite quarry, 114
4.1.4.21 intrusive relationships between the different facies of sodalite syenites observed at the quarry, 109
4.1.4.22 Geological map and cross sections to locate boreholes from the environs of the Kansanshi deposit, Solwesi, Zambia, 117
4.1.4.23 Photographs of slabs from the samples that make L-063, 118
4.1.5.1 TAS diagram Basement to the Copperbelt, Zambia, 122
4.1.5.2 R1R2 diagram, Basement to the Copperbelt, Zambia, 123
4.1.5.3 A-B diagram, Basement to the Copperbelt, Zambia, 124
4.1.5.4 K-B diagram, Basement to the Copperbelt, Zambia, 125
4.1.5.5 Mg-Fe-B diagram, Basement to the Copperbelt, Zambia, 126
4.1.5.6 W-E geological cross section of underground exposure of the Nchanga Granite, 127
4.1.5.7 Geological cross sections through the Nchanga Granite, 130
4.1.5.8 Geological map of the Nchanga Granite, 131
4.1.5.9 Photograph of Nchanga Granite inselberg at the Chiwempala Hill, Zambia, 129
4.1.5.10 Logarithmic scale plot of major oxides to compare Nchanga Granite with Nigerian and Namibian granitoid ring complexes, 133
4.1.5.11 Logarithmic scale plot of minor elements and rare earths to compare Nchanga Granite with Nigerian and Namibian granitoid ring complexes, 134
4.1.5.12 Second logarithmic scale plot of minor elements and rare earths to compare Nchanga Granite with Nigerian and Namibian granitoid ring complexes, 134
4.1.5.13 WSW-ENE Schematic geological cross section throgh the Nchanga Granite along the Nchanga mine, Zambia, 138
4.1.5.14 Main features of the Muliashi Porphyry as observed on outcrops, 142
4.1.5.15 Photographs of slabs from the Muliashi Porphyry, basement to the Copperbelt, Zambia, 143
4.1.5.16 Surface geological map of the Konkola Dome and Nchanga Area, Zambia, 145
4.1.5.17 Stratigraphic column of exploratory Konkola Deep Borehole, Zambia, 146
4.1.5.18 Geological map of the Chambishi-Nkana basin, Zambia, 149
4.1.5.19 Stratigraphy of drillhole into Chambishi gabbros and ganophyres, 150
4.1.5.20 Underground cross section of the Mufulira orebody in relation to the basement highs, 152
4.1.5.21 Geological map of the Mufulira mine environs, Zambia, 153

4.1.5.22 Cross section of the basement of the Mufulira mine area, 154
4.1.5.23 Generalized geological map of the Samba copper deposit in the basement to the Copperbelt, Zambia, 156
4.1.5.24 Eastern borehole-controlled geological cross section, Samba copper deposit, Zambia, 156
4.1.5.25 Western borehole-controlled geological cross section, Samba copper deposit, Zambia, 156
4.1.5.26 Main stratigraphic relationships between rock units in the main Copperbelt area, Zambia, 159
4.2.1.1 Entire TAS diagram Kamanjab Batholith, Namibia, 167
4.2.1.2 Enlargement of main portion, TAS diagram Kamanjab Batholith, Namibia, 168
4.2.1.3 Entire R1R2 diagram Kamanjab Batholith, Namibia, 169
4.2.1.4 Enlargement of main portion, R1R2 diagram Kamanjab Batholith, Namibia, 170
4.2.1.5 Correlation diagrams between silica and the major oxides for samples from the Kamanjab Batholith, Namibia, 174
4.2.1.6 Generalized location of dated samples and geochemical suites in the Kamanjab Batholith, Namibia,175
4.2.1.7 Logarithmic scale plot of major oxides for Quartzmonzonite Group, Kamanjab Batholith, Namibia, 185
4.2.1.8 Logarithmic scale plot of major oxides for Alkali Granite Group, Kamanjab Batholith, Namibia, 186
4.2.1.9 Logarithmic scale plot of major oxides for Granite Group, Kamanjab Batholith, Namibia, 187
4.2.1.10 Logarithmic scale plot of major oxides for Syenite Group, Kamanjab Batholith, Namibia, 188
4.2.1.11 Logarithmic scale plot of major oxides for Gabbroid Group, Kamanjab Batholith, Namibia, 189
4.2.1.12 Logarithmic scale plot of major oxides for Unclassified Group, Kamanjab Batholith, Namibia, 190
4.2.1.13 Logarithmic scale plot of trace elements and rare earths for Quartzmonzonite Group, Kamanjab Batholith, Namibia, 190
4.2.1.14 Logarithmic scale plot of trace elements and rare earths for Alkali Granite Group, Kamanjab Batholith, Namibia, 191
4.2.1.15 Logarithmic scale plot of trace elements and rare earths for Granite Group, Kamanjab Batholith, Namibia, 192
4.2.1.16 Logarithmic scale plot of trace elements and rare earths for Syenite Group, Kamanjab Batholith, Namibia, 193
4.2.1.17 Logarithmic scale plot of trace elements and rare earths for Gabbroid Group, Kamanjab Batholith, Namibia, 194
4.2.1.18 Logarithmic scale plot of trace elements and rare earths for Unclassified Group, Kamanjab Batholith, Namibia, 195
4.2.1.19 Photos of samples from Kamanjab Suite G, 178
4.2.1.20 Photos of samples from Kamanjab Batholith Suite J, 178
4.2.1.21 Photos of rocks with “fuzzy” texture, Kamanjab Batholith, 177
4.2.2.1 Reconaissance map of a syenite ring complex cluster in the Oas farm, Namibia - Main portion of the N-S transect across the Oas Mountains, 215
4.2.2.2 TAS diagram Khorixas Inlier, Namibia, 220
4.2.2.3 Enlargement of main portion, TAS diagram Khorixas Inlier, Namibia, 221
4.2.2.4 R1R2 diagram, Khorixas Inlier, Namibia, 222
4.2.2.5 Enlargement of main portion, R1R2 diagram, Khorixas Inlier, Namibia, 223
4.2.2.6 Q-P diagram, Khorixas Inlier, Namibia, 224
4.2.2.7 Enlargement of main portion, Q-P diagram, Khorixas Inlier, Namibia, 225
4.2.2.8 Mg-Fe-B diagram, Khorixas Inlier, Namibia, 226
4.2.2.9 QBF diagram, Khorixas Inlier, Namibia, 227
4.2.2.10 Logarithmic major oxide plot for the Syenites A and Syenites B groups in the Oas farm, Loftal farm and Ojtiwarongo environs, Namibia, 232

4.2.2.11 Logarithmic trace element plot for the Syenites A and Syenites B groups in the Oas farm, Loftal farm and Ojtiwarongo environs, Namibia, 232
4.2.2.12 Field relationships of mineralized quartzites at the Oas farm, Namibia, 235
4.2.2.13 Generalized map of the Lofdal farm showing geological stations, 239
4.2.2.14 Map of geological stations and sampling, Lofdal farm, Namibia, 240
4.2.2.15 Cross section through mafic and ultramafic dikes, Lofdal farm, Namibia, 244
4.2.2.16 Photograph of a slabbed carbonatite dike from the Lofdal farm, Namibia, 241
4.2.2.17 Photograph of a carbonatite dike with subparallel internal zoning and magnetite, 242
4.2.2.18 Close-up view of a magnetite-rich massive carbonatite body, Lofdal farm, Namibia, 243
4.2.2.19 Photograph of two subparallel carbonatite dikes, 243
4.2.2.20 Sample map, carbonatite diatreme at Lofdal farm, Namibia, 246
4.2.2.21 Large fans of elongated amphibole crystals in an ultramafic dike, Lofdal farm, Namibia, 247
4.2.2.22 Major oxide logarithmic plot of carbonatite samples, Lofdal farm, Namibia, 249
4.2.3.1 TAS diagram of the Ugab River-Summas Mountains-Okwa River-Grootfontein Inlier, Namibia and Botswana, 254
4.2.3.2 R1R2 diagram of the Ugab River-Summas Mountains-Okwa River-Grootfontein Inlier, Namibia and Botswana, 255
4.2.3.3 Sample map of the Mesopotamie farm, Namibia, 257
4.2.3.4 Map of geological stations and sampling, Mesopotamie farm, Namibia, 258
4.2.3.5 TAS diagram Otjiwarongo-Grootfontein Inlier, Namibia, 267
4.2.3.6 R1R2 diagram, Otjiwarongo-Grootfontein Inlier, Namibia, 268
4.2.3.7 Enlargement of main portion, R1R2 diagram, Otjiwarongo-Grootfontein Inlier, Namibia, 269
4.2.3.8 Photograph of granitoid inselbergs on the road Okahandja-Otjiwarongo, Namibia, 266
4.2.3.9 Photographs of slabs from samples L807 and L-811, 272
4.2.3.10 Photographs of granitic pegmatites from the Otjiwarongo Batholith, 272
4.2.4.1 TAS diagram Okatjepuiko, Witvlei, Namibia, 289
4.2.4.2 R1R2 diagram, Okatjepuiko, Witvlei, Namibia, 286
4.2.4.3 QBF diagram, Okatjepuiko, Witvlei, Namibia, 287
4.2.4.4 Map of geological stations and sampling at the Okatjepuiko site, Witvlei, Namibia, 289
4.2.4.5 Logarithmic major oxide plot, granitoid samples, Okatjepuiko prospect, Witvlei, Namibia, 290
4.2.4.6 Logarithmic trace element plot, granitoid samples, Okatjepuiko prospect, Witvlei, Namibia, 290
4.2.4.7 Photo 1. Trap rock breccias from 18.2-22.0 m; borehole OP-1, Okatjepuiko, Witvlei, Namibia.
4.2.4.8 Photo 2. Enlargement with detail at 19.77 m; borehole OP-1, Okatjepuiko
4.2.4.9 Photo 3. Volcanic rocks with vacuoles and dense veinlet network, borehole OP-1
4.2.4.10 Photo 4. Close-up of Fig 4.2.4.8. Details of pink zeolites (?) and very thin white veinlets; borehole OP-1
4.2.4.11 Photo 5. Beginning of hydrothermal brecciation, 33-34 m; borehole OP-1
4.2.4.12 Photo 6. Close-up of photo 5, centered on letter M; borehole OP-1
4.2.4.13 Photo 7. Breccia with abundant chlorite that fills open spaces and veinlets, after 34m; borehole OP-1
4.2.4.14 Photo 8. 4 core fragments, marked with different alteration types; borehole OP-1
4.2.4.15 Photo 9. Beginning of the pink granitoid 54-57 m; borehole OP-1
4.2.4.16 Photo 10. Close-up of photo 9, on the pink granitoid; borehole OP-1
4.2.4.17 Photo 11. Breccia with angular fragments of volcanic rock (68, 69 and 70 m); borehole OP-1
4.2.4.18 Photo 12. Intrusive rock in the middle line of core, surrounded by dark volcanic trap rocks; borehole OP-1
4.2.4.19 Photo 13. Core showing angular fragments of pink granitoid within dark gray trap rock, 73-75m; borehole OP-1
4.2.4.20 Photo 14. Core fragments from 79-82 m; borehole OP-1

4.2.4.21 Slabs of strongly hematitized polymictic hydrothermal breccias from Samples L-644 and L-645
6.4.1 Re-Os ages calculated by Joaquín Ruiz and collaborators at the University of Arizona, 313
6.4.2 Event diagram for three copper mineralizing periods in the Greater Lufilian Arc, 315
7.1 Schematic cross section of the Wonji Fault Belt: an example of a tectomagmataic belt in a continental rift, 316
7.2 Alkaline intrusions of the SW Nuba Mountains, 319
7.3 Event diagram for intrusions from the SW Nuba mountains, Sudan, 318
7.4 Sketch map of cluster of anorogenic ring complexes in central Nigeria, 321
7.5 Event diagram graph for ring complexes in Central Nigeria, 322
7.6 Botsalano ring complex and other possible ring intrusions in the Gaborone-Kanye igneous terrane, Botswana and South Africa, 323
7.7 Event diagram for Gaborone anorogenic ring complex cluster, Botswana/South Africa, 324
7.8 Scheme of what might have taken place to produce one of the granitoid ring complex clusters identified in the Greater Lufilian Arc, 272
7.9 Comparison of event diagrams from three anorogenic ring complex clusters, 325
7.10 Comparison of the outlines of various ring complex clusters, 328
7.11 Event diagram of Anorogenic Complex Cluster periods in the Greater Lufilian Arc, 330
7.12 Comparison of event diagrams from various anorogenic ring complex clusters from the Greater Lufilian Arc, 331
7.13 Sketch map of basalt, trachyte and phonolite plugs of the Filiya area in eastern Nigeria, 334
8.1 Cartoon to illustrate the development process of an iron oxide-copper-gold system, 337
8.2 Generalized geological map of the Salobo Deposit, Carajás, Brazil, 338
8.3 Simplified geochemical log of borehole ALM-FD09, from the Alemão deposit, Carajás, Brazil, 340
8.4 Examples of hydrothermal alteration zonation in IOCG deposits formed in volcanic and plutonic host rocks, 341
8.5 Examples of hydrothermal alteration zonation in IOCG deposits formed in sedimentary sequences, 341
8.6 Geological Map of the Kamanjab Batholith, Namibia, 344
8.7 Iron oxide-coper-gold prospects and deposits, Greater Lufilian Arc, 345
8.8 Quartz bodies, gabbros, felsic granitoids and iron oxide bodies that outcrop together east of Solwesi, Zambia, 347
8.9 Quartz body and metamorphosed gabbros that outcrop together to the norteast of Mwinilunga, Zambia, 347
8.10 Young gabbroic bodies that intersect all rock types to the northeast of Solwesi, Zambia, 348
8.11 Quartz bodies, gabbros and felsic granitoids bodies that outcrop together east of Solwesi, Zambia, 348
8.12 Hill of massive magnetite that outcrops west of Lusaka, Zambia, 348
8.13 Magnetite “disease” in a felsic granitoid that is very light pink when fresh, 350
8.14 Hematite “disease” that overprints a polymictic hydrothermal breccia, 350
8.15 Progressive “red-rock” hydrothermal alteration in round-pebble hydrothermal breccia, 351
8.16 Typical features of polymictic, round-pebble hydrothermal breccia, 352
8.17 Aspect of poly-brecciated polymictic round-pebble hydrothermal breccia, 352
8.18 Typical angular stockwork mineralization in a foliated granitoid host rock, 353
8.19 Typical irregular stockwork mineralization in a felsic non-foliated granitoid, 353
8.20 Schematic geological section across the southeast margin of Kasumbalesa Hill, Zambia, 355
8.21 Stratiform body of magnetite in the Kasempa area of Zambia, 356
8.22 Cross section of stratiform body of magnetite at the Kantonga IOCG deposit, Zambia, 356

8.23 Quartz pod outcrops observed in the Greater Lufilian Arc, Zambia and Namibia, 358
8.24 Types of quartz pod outcrops observed during field work, Greater Lufilian Arc Granitoid Project, 357
8.25 Sedimentary bedding and/or foliation that bends around quartz pods, 359
8.26 Various features of iron oxides in quartz pods of the Lufilian Arc, 361
8.27 Schematic diagram to show process of quartz pod formation, 360
8.29 Geological map of the Witvlei site, and location of the Okatjepuiko IOCG prospect, 362
8.30 Typical mineralization at the Kombat Cu mine, Namibia, 365
8.31 Diagram taken from Deane (1995) to reinterpret origin of the Kombat mine, Namibia, 364
8.32 Underground map that shows core of iron oxide bordered by copper mineralization at the Kombat Mine, Namibia, 365
8.33 Simplified geological map of the Otjikoto gold deposit, Namibia, 366
8.34 Mineralized quartz pod with magnetite and chalcopyrite, 367
8.35 Mineralized samples from the Copper Vallei mine, Mesopotamie farm, Khorixas Inlier, Namibia, 368
8.36 Mineralized quartz-magnetite-sulfide veins at the Dunrobin gold mine, Zambia, 371
8.37 Progressive hydrothermal alteration around mineralized quartz-magnetite-sulfide veinlets at the Dunrobin gold mine, Zambia, 372
8.38 Concentric iron oxide banding around mineralized veinlets at the Dunrobin gold mine, Zambia, 373
8.39 Explanation diagram for Fig 8.37, 371
8.40 Geological map around the Lusaka West area, Zambia, 374
8.41 Geological Map NW of Mumbwa, Hook Granite Batholith Province, Zambia, 375
8.42 Generalized geology of the Kitumba prospect, Kafue Flats, Zambia, 377
8.43 Cross section and map of the Kalengwa mine open pit, Zambia, 378
8.44 Angular hydrothermal breccias and the subvolcanic, porphyritic, rhyolitic intrusive that is responsible for their formation, 379
8.45 Another aspect of hydrothermal breccias cemented by massive magnetite from the Gelbingen farm, Namibia, 380
8.46 Sulfide-bearing hydrothermal breccia-vein cemented by magnetite that intrudes quartzites, 380
8.47 Three close-up aspects of the mineralized breccias from the Gelbingen farm, Namibia, 381
8.48 Another aspect of sulfide-bearing hydrothermal breccia cemented by magnetite that intrudes quartzites, 381
8.49 Network of Sulfide-bearing magnetite veins that form a stockwork in Pan African felsic granitoids, 382
8.50 Aspects of hydrothermal breccias associated to a diatreme body 450 m by 150 m in outcrop, 383
8.51 Another aspect of hydrothermal breccias cemented by massive magnetite, 384
8.52 Sulfide-bearing magnetite-hematite veins associated to ultramafic dikes, 385
8.54 Slab of magnetite-cemented angular polymictic hydrothermal breccia, 385
8.55 Another aspect of round-pebble hydrothermal breccias cemented by magnetite, 386
8.56 Dense packing in round-pebble hydrothermal breccias associated to IOCG systems in the Lufilian Arc, 386
8.57 Angular fragments in a magnetite-cemented hydrothermal breccia from an IOCG mineralized body, 388
8.58 IOCG Mineralized Fracture System, northern Namibia, 387
8.59 General gravimetric map overlain by selected samples and metal values, Tevrede property, northwestern Kamanjab batholith, Namibia, 390
9.1 Distribution of rock types and comparative composition of rock alkalinity in the Greater Lufilian Arc, 397
9.2 Composition of the samples collected in the Greater Lufilian Arc, 398

LIST OF TABLES

2.1 Laboratories where chemical analysis were carried out, 6
2.2 Threshold or notch values used in the Greater Lufilian Arc granitoid project for various elements and oxides, 13
2.3 Synthetic table showing the relationships between main granitic petrogenetic types, their origins, and the geodynamic environment, 15
2.4 Principal mineralogical, petrographical and chemical features of the main types of granitoids, 15
2.5 Review of the main methodologies to study the tectonic environment of emplacement of granitoid rocks, 16
2.6 Acronyms used to shorten rock names (after the use of Debon & LeFort, 1983), 19
2.7 Acronyms for environment of emplacement terms, diagrams of Maniar & Piccoli, 1989, 19
2.8 Acronyms for environment of emplacement terms of mafic rocks, 19
2.9 Acronyms for environment of emplacement terms, diagrams of Harris et al, 1986, 20
4.1 Geological Domains sampled during the Greater Lufilian Arc Granitoid Project, 25
4.1.1 Statistics of rock types in the suite of samples from the Hook Granite Batholith, 36
4.2 Groups of samples from the Hook Granite Batholith, based on major oxide chemistry and logarithmic plots, 27
4.3 High Zn samples from the Hook Granite Batholith, Zambia, 27
4.4 Correlation of mapped units for the Hook Granite Batholith, from published 1:100,000 geological sheets, 37
4.5 Hook Granite Batholith rock types and environment of emplacement, 39
4.6 Chemical analyses of Namibian Mesozoic anorogenic complexes, 50
4.7 Rock groups from Namibian Mesozoic anorogenic granitoid complexes, 50
4.8 Comparative chemical analysis from granite anorogenic ring complexes Hook Granite Batholith samples, 51
4.9 Analysis of samples along E-W transect across the Hook Granite Batholith, Zambia, 55
4.10 Samples collected along the E-W transect through the Kafue Park, Hook Granite Batholith, 55
4.11 List of samples sorted by rock type based on maps/field observations, Hook Granite Batholith, Zambia, 41
4.12 Samples from the E-W transect through the Kafue Park, Hook Granite Batholith, and correspondence with ring complexes from Fig SUCH and geological map units, 56
4.13 Hook Granite samples that show similarities with granitoid samples from Nigerian, Namibian and Corsican anorogenic ring complexes, 50
4.14 Radiometric ages for the Hook Granite Batholith published by Hanson et al, 1993, 57
4.1.2.1 Chemical Analysis of samples from the West Lusaka-Kafue Flats Area, Zambia, 62
4.1.2.2 Rock types from the West Lusaka-Kafue Flats area, Zambia, 62
4.1.2.3 Basic geochemistry and environment of emplacement for samples from the West Lusaka-Kafue Flats, Zambia, 65
4.1.2.4 Statistics of rock types in samples from West Lusaka and Kafue Flats, Zambia, 65
4.1.2.5 Analysis of gossanous massive iron oxide bodies, West Lusaka-Kafue Flats area, Zambia, 68
4.1.2.6 Samples with high Th values from the Kafue Flats, Zambia, 69
4.1.3.1 Chemical Analysis of samples from the Kalengwa-Kasempa Area, Zambia, 72
4.1.3.2 Rock type statistics, samples from Kalengwa and Kasempa region, Zambia, 71
4.1.3.3 Suites of samples from Kalengwa/Kasempa and projection on various geochemical diagrams, 79
4.1.3.4 Rock name, basic geochemistry and environment of emplacement for samples from the Kalengwa and Kasempa region, Zambia, 79
4.1.3.5 Chemical Analisis, Kasempa Area, Zambia, 82
4.1.4.1 Rock type statistics, from Northwestern Zambia, 83
4.1.4.2 Partial rock type statistics, from Northwestern Zambia, 83
4.1.4.3 Chemical Analysis of samples from the Kalene Hill Area, NW Zambia, 85

4.1.4.4 Rock type statistics, from Kalene Hill samples, NW Zambia, 84
4.1.4.5 Samples from Kalene Hill sorted by groups and geochemistry, 93
4.1.4.6 Kalene Hill groups of samples and their projection on various geochemical diagrams, 93
4.1.4.7 Rock name, basic geochemistry and environment of emplacement for samples from the Kabompo Dome, NW Zambia, 97
4.1.4.8 Resources and Reserves at the Lumwana District, Zambia, 105
4.1.4.9 Chemical Analysis of the sodalite syenite quarry, Zambia, 110
4.1.4.10 Chemical character of samples from the Sodalite Syenite Quarry, Zambia, 113
4.1.4.11 Tectonic environment of emplacement for sodalite syenite quarry, Zambia, 113
4.1.4.12 Chemical Analysis of samples from the Solwesi Dome, Zambia, 115
4.1.4.13 Rock name, basic geochemistry and environment of emplacement for samples from the Solwesi Dome, NW Zambia, 116
4.1.5.1 Statistics of rock types, basement to the Copperbelt, Zambia, 121
4.1.5.2 Statistics of rock types, Nchanga Granite, Zambia, 128
4.1.5.3 Rock name, basic geochemistry and environment of emplacement for samples from the Nchanga Granite, Zambia, 128
4.1.5.4 Exchange in values for Na and K in chemical analysis of sample X-34, 132
4.1.5.5 Chemical analysis of samples from the Nchanga Granite and others in the basement to the Zambian Copperbelt, 132
4.1.5.6 Comparison of chemical data from anorogenic ring complexes and the Nchanga Granite, 135
4.1.5.7 Borehole samples collected in the environs of the Nchanga open pit mine, Zambia, 112
4.1.5.8 Rock name and main geochemical parameters of samples from the Nchanga mine, 112
4.1.5.9 Chemical analysis from the Nchanga Mine environs, 112
4.1.5.10 New SHRIMP U-Pb ages from the Copperbelt area, Zambia, 139
4.1.5.11 Chemical analysis of samples from the Muliashi Porphyry, Basement to the Copperbelt, Zambia, 140
4.1.5.12 Chemical characteristics and environment of emplacement for Muliashi Porphyry samples, Zambia, 141
4.1.5.13 Statistics of rock types, Muliashi Porphyry, Zambia, 140
4.1.5.14 Chemical Analysis of samples from the deep borehole, Konkola mine, Zambia, 144
4.1.5.15 Data from borehole samples, Konkola Deep borehole, Zambia, 144
4.1.5.16 Simplified log of exploratory Konkola Deep Borehole, Zambia, 146
4.1.5.17 Geological history interpreted from the Konkola deep borehole, Zambia, 147
4.1.5.18 Chemical analysis of samples from the Chambishi copper mine environs, Zambia, 148
4.1.5.19 Statistics of rock types, Chambishi granite, Zambia, 148
4.1.5.20 Chemical character and environment of emplacement for samples in the Chambishi mine environs, Zambia, 150
4.1.5.21 Chemical analysis of samples from the basement to the Mufulira copper mine, Zambia, 152
4.1.5.22 Main details of analysed samples from the Samba copper deposit, basement to the Copperbelt, Zambia, 157
4.1.5.23 Regional correlation of dated Paleoproterozoic granitoids in the Greater Lufilian Arc, 160
4.1.5.24 Original data, additional samples from the literature on Copperbelt granitoids, Zambia, 161
4.1.5.25 Chemical characteristics and environment of emplacement for samples in the Basement to the Copperbelt, Zambia, 162
4.2.1.1 Chemical Analysis, Kamanjab Batholith Area, Namibia, 165
4.2.1.2 Statistics of rock types, Kamanjab Batholith, Namibia, 173
4.2.1.3 Brief description of analysed samples, Kamanjab Batholith, Namibia, 171
4.2.1.4 Kamanjab Batholith rock suites that are made by two or more rock types, 176
4.2.1.5 Chemical Analysis of the Group of Quartzmonzonites, Kamanjab Batholith, 180
4.2.1.6 Chemical Analysis of the Group of Alkali Granites, Kamanjab Batholith, 181
4.2.1.7 Chemical Analysis of the Group of Granites, Kamanjab Batholith, 182

4.2.1.8 Chemical Analysis of the Group of Syenites, Kamanjab Batholith, 183
4.2.1.9 Chemical Analysis of the Group of Gabbroids, Kamanjab Batholith, 183
4.2.1.10 Chemical Analysis of the Group of unclassified samples, Kamanjab Batholith, 184
4.2.1.11 Comparison of volcanic and plutonic rock types in the Kamanjab Batholith, 184
4.2.1.12 Groups of samples from the Kamanjab Batholith based on chemical similarity, 198
4.2.1.13 Kamanjab rock suites with samples of non-anorogenic or subductional character, 200
4.2.1.14 Chemical Analysis, Samples analysed by Clifford, 1969; Kamanjab Batholith, Namibia, 201
4.2.1.15 Granitoid samples from the Kamanjab Batholith that were dated, 202
4.2.1.16 Hypothetical correlation of the dated samples, Kamanjab Batholith and Grootfontein inlier, Namibia, 203
4.2.1.17 Tentative correlation of the various rock units in the Suites from the Kamanjab Batholith. Namibia, 204
4.2.1.18 Location of samples and geological stations on the Kamanjab Batholith, Namibia, 205
4.2.1.19 Rock suites that show mineralization or hydrothermal alteration; Kamanjab Batholith, sorted by rock suite letter, 207
4.2.1.20 Compilation of data from mineralized suites, Kamanjab Batholith, 208
4.2.1.21 Regional correlation of Paleoproterozoic Granitoids in the Greater Lufilian Arc, 210
4.2.2.1 Statistics of rock types, Khorixas Inlier, Namibia, 211
4.2.2.2 Comparison of samples from the Khorixas Inlier and nearby Summas Mountains, Namibia, 212
4.2.2.3 Chemical Analysis of Samples from the Oas Farm, Namibia, 213
4.2.2.4 Main features of small syenitoid circular bodies found at the Oas farm, Namibia, 217
4.2.2.5 High heat producing rocks in the Oas farm, Namibia; estimated at 750Ma, 214
4.2.2.6 Statistics of rock types, Oas farm, Namibia, 219
4.2.2.7 Sample grouping, Oas farm, Namibia, 228
4.2.2.8 Correlation matrix of samples from the Oas ring complexes using the isocon diagram and visual comparison, 229
4.2.2.9 Comparison of sample groups from various Namibian regions, 233
4.2.2.10 Groups of samples from various Namibian regions, 230
4.2.2.11 Samples form the Oas farm ring complex cluster that were dated, 235
4.2.2.12 Statistics of rock types, Lofdal farm, Namibia, 237
4.2.2.13 Chemical Analysis of Samples from the Lofdal Farm, Namibia, 238
4.2.2.14 Main features of cross section across mafic, ultramafic and carbonatitic dikes, Lofdal farm, Namibia, 245
4.2.2.15 High heat producing rocks in the Lofdal farm, Namibia; estimated at 750Ma, 249
4.2.2.16 Chemistry of carbonatites and dikes, Lofdal farm, Namibia, 250
4.2.3.1 Chemical analysis of samples from the Mesopotamie farm, Namibia, 253
4.2.3.2 Chemical analysis of samples from the Summas Mountains, Namibia, 260
4.2.3.3 Rock types and environment of emplacement for the Summas Mountains, Namibia, 260
4.2.3.4 Chemical Analysis, Ugab River, Namibia, 262
4.2.3.5 Rock types and environment of emplacement for the Ugab River, Namibia, 262
4.2.3.6 Chemical Analysis, Okwa River, Botswana, 264
4.2.3.7 Rock types and environment of emplacement for the Okwa River area, Botswana, 264
4.2.3.8 Chemical Analysis, Grootfontein Inlier, Namibia, 265
4.2.3.9 Rock types and environment of emplacement for the Grootfontein Inlier, Namibia, 265
4.2.3.10 Chemical Analysis, Otjiwarongo environs, Namibia, 271
4.2.3.11 Chemical Analysis, Otjiwarongo pegmatites, Namibia, 270
4.2.3.12 Main details of samples from pegmatitic granitoids, Otjiwarongo batholith, Namibia, 272
4.2.3.13 Statistics of rock types, Otjiwarongo environs, Namibia, 273
4.2.3.14 Rocks from different regions that display very simiar major oxide and trace element chemistry, 273
4.2.3.15 Tentative correlation table for samples from the environs of Otjiwarongo, Namibia, 274
4.2.3.16 Rock types and environment of emplacement for the environs of Otjiwarongo, Namibia, 275

4.2.3.17 Rock types and environment of emplacement for several Namibian domains, 276
4.2.3.18 Groups of rocks from the Ugab-Okwa Domain compared with others in Namibia, 279
4.2.4.1 Description of OP-1 Borehole, Okatjepuiko, Project, Namibia, 283
4.2.4.2 Samples collected from borehole OP-1, Okatjepuiko, Namibia, 284
4.2.4.3 Chemical Analysis, Okatjepuiko, Witvlei, Namibia, 284
4.2.4.4 Statistics of rock types, Okatjepuiko environs, Witvlei, Namibia, 288
4.2.4.5 Comparison of samples from the Okatjepuiko area, Namibia, 288
4.2.4.6 Chemistry of granitoids from the Okatjepuiko Prospect, Namibia, 290
5.1 High Thorium Values from Greater Lufilian Arc Granitoids, 303
5.2 Samples with similar chemical signature as Th-rich samples from the Kafue Flats, Zambia, 305
5.3 Heat production values for various high-heat producing granitoids, 306
5.4 High heat production capacity of Greater Lufilian Arc intrusive rocks calculated at the time of emplacement, 307
6.1 New radiometric ages, Greater Lufilian Arc - sorted by age, 310
6.2 New radiometric ages, Greater Lufilian Arc - sorted by sample number, 311
6.3 Events of magmatism identified in the Greater Lufilian Arc based on the new radiometric ages obtained, 308
6.4 Events associated with three main copper mineralizing periods in the Greater Lufilian Arc, 315
7.1 Radiometric (Rb-Sr) ages from ring complexes, SW Nuba Mountains, Sudan, 318
7.2 Radiometric (Rb-Sr) ages from Nigerian ring complexes, 322
7.3 Chemistry of biotite granites from Nigerian anorogenic ring complexes, 323
7.4 Geochronological data available for Gaborone anorogenic ring complex cluster, Botswana and South Africa, 324
7.5 Compilation of ages from various ring complex clusters in the Greater Lufilian Arc, 330
7.6 Compilation of Anorogenic Complex Cluster Periods in the Greater Lufilian Arc, 329
7.7 Geochronological data from various ring complex clusters leveled to a common age, for comparison, 332
8.1 Data for some iron oxide-copper-gold deposits, 343
8.2 Details of selected IOCG deposits and prospects, Greater Lufilian Arc, Africa, 342
8.3 Discrete periods of iron oxide-copper-gold mineralization that took place in the Greater Lufilian Arc, 393
9.1 Rock type statistics of all samples analysed from the Greater Lufilian Arc, 396
9.2 Number of samples from each rock type for domains of the Greater Lufilian Arc, 396
9.3 Percentages of each rock type for domains of the Greater Lufilian Arc, 397
9.4 Main metallogenic events observed - Greater Lufilian Arc, 402
9.5 Simplified classification of metallogenic events in the Greater Lufilian Arc, 403
9.6 Periods of iron oxide-copper-gold mineralization in the Greater Lufilian Arc, 404

APPENDICES (all page numbers in Appendices volume)

Abbreviated Table of Contents for the Appendices

A	Sample Maps, 120
B	TAS Diagram for Suites of the Kamanjab Batholith, Namibia, 160
C	Geochemistry Database, 1
D	Geographic Coordinates of Samples Collected and Geological Stations, 25
E	Geochronology Database, 41
F	Geochronological Event Diagrams, 67
G	Tectonic Environent of Emplacement for Samples, 95
H	Partial Transcription of Field Notes, 183
I	Other Information, 222
J	Raw Data for New Geochronology, 237
K	Geochronological Correlation Diagrams, 257

A SAMPLE MAPS

M1 Key for Zambian Sample Maps, 121
M2 Sample map, Hook Granite Batholith, Zambia over 1:1'000,000 geological map, 122
M3 Sample map, Hook Granite Batholith, Zambia over 1:100,000 geological sheets, 123
M4 Enlarged sample map, Hook Granite Batholith, Zambia over 1:100,000 geological sheets,
M5 Enlargement of sample, Hook Granite Batholith, northern portion, 124
M6 Enlargement of sample, Hook Granite Batholith, southern portion, 125
M7 Sample map of the Kafue Flats area, Zambia, 126
M8 Sample map, Kalengwa mine environs, Zambia, 127
M9 Sample map, Kasempa environs, Zambia, 128
M10 Sample map, Kalene Hill and Kabompo Dome, NW Zambia, 129
M11 Sample map of Kalene Hill and environs, NW Zambia, 130
M12 Sample map, Domes Area, Zambia, 131
M13 Sample map, Kabompo and Mwombezhi Domes, Zambia, 132
M14 Sample map SE of Mwinilunga, 133
M15 Sample map, Solwesi Dome environs, Zambia, 13
M16 Sample map of the Nchanga Granite, Zambia, 135
M17 Sample map of the Chambishi-Mufulira Area, Zambia, 136
M18 Sample map of the Serenje area, Zambia, 137
M19 Key for Namibian Sample Maps, 138
M20 Sample map of the Khorixas inlier and the Mesopotamie farm, Namibia, 139
M21 Sample map of the Oas and Lofdal farms, Khorixas Inlier, Namibia, 140
M22 Sample map of the Summas Mountains and Ugab River, Namibia, 141
M23 Sample map, Otjiwarongo environs, Namibia, 142
M24 Close-up of sample map, Otjiwarongo environs, Namibia, 143
M25 Sample map, Otavi Mountains, Namibia, 144
M26 Sample map, Witvlei environs, Namibia, 145
M27 Key for Kamanjab Batholith sample maps, Namibia, 146
M28 K-14 portion of sample map, Kamanjab Batholith, Namibia, 148
M29 K-15 portion of sample map, Kamanjab Batholith, Namibia, 149
M30 K-16 portion of sample map, Kamanjab Batholith, Namibia, 150
M31 K-17 portion of sample map, Kamanjab Batholith, Namibia, 151
M32 K-18 portion of sample map, Kamanjab Batholith, Namibia, 152
M33 K-19 portion of sample map, Kamanjab Batholith, Namibia, 153
M34 K-20 portion of sample map, Kamanjab Batholith, Namibia, 154
M35 K-21 portion of sample map, Kamanjab Batholith, Namibia, 155
M36 K-22 portion of sample map, Kamanjab Batholith, Namibia, 156
M37 K-23 portion of sample map, Kamanjab Batholith, Namibia, 157
M38 K-24 portion of sample map, Kamanjab Batholith, Namibia, 158

M39 K-25 portion of sample map, Kamanjab Batholith, Namibia, 159

B TAS DIAGRAM FOR SUITES OF THE KAMANJAB BATHOLITH, NAMIBIA

F1 Suite A, 160
F2 Suite B, 160
F3 Suite C, 161
F4 Suite D, 161
F5 Suite E, 162
F6 Suite F, 162
F7 Suite G, 163
F8 Suite H, 163
F9 Suite I, 164
F10 Suite J, 164
F11 Suite K, 165
F12 Suite L, 165
F13 Suite M, 166
F14 Suite N, 166
F15 Suite P, 167
F16 Suite Q, 167

C GEOCHEMISTRY

A1 Chemical analysis of samples from the Greater Lufilian Arc sorted by region, 1
A2 West Lusaka-Kafue Flats, Zambia, 1
A3 Hook Granite Batholith, Zambia, 2
A4 Serenje, Zambia, 3
A5 Kalengwa-Kasempa Area, Zambia, 4
A6 Northwestern Zambia Region Zambia, 5
A7 Kalene Hill, Archean rocks, Paleoproterozoic Group 2, Paleoproterozoic Group 3, Paleoproterozoic Group 4, Other samples, 5
A7.1 Kabompo Dome, 5
A7.2 Solwesi Dome, 6
A7.3 Mwombezhi Dome, 6
A7.4 Sodalite Syenite Quarry, 6
A7.5 Shilenda, 6
A8 Basement to the Copperbelt, Zambia, 6
A8.1 Muliashi Porphyry, 6
A8.2 Chambishi mine area, 7
A8.3 Samba copper prospect, 7
A8.4 Nchanga Granite, 7
A8.5 Nchanga mine, 7
A8.6 Mufulira Granite, 7
A8.7 Other, 7
A9 Kamanjab Batholith, 8
A10 Felsic volcanics, Namibia; Ugab River, Namibia; Okwa River, Botswana; Summas Mountains, Namibia, 10
A11 Oas farm, Namibia, 11
A12 Lofdal farm, Namibia; Mesopotamie farm, Namibia; other alkaline and gabbroic rocks, Khorixas, Namibia, 12
A13 Otjiwarongo environs, Namibia; Grootfontein Inlier, Otavi Mountains, Namibia; Okatjepuiko, Witvlei, Namibia, 13
A14 Spitskoppe complexes, Namibia; Erongo complex, Namibia; Brandberg complex, Namibia; Nigerian ring complexes, 14
A15 Chemical analysis from the Greater Lufilian Arc sorted by number, 15

D GEOGRAPHIC COORDINATES OF SAMPLES COLLECTED

A16 Zambian samples located on UTM zone 35, 24
A17 Zambian samples located using latitude and longitude (WGS84), 29
A18 Namibian samples that are located in UTM zone 33 (Schwartzeck), 30
A19 Namibian samples that are located in UTM zone 34, (Schwartzeck), 34
A20 Namibian samples that are located using latitude and longitude coordinates (Schwartzeck), 35

E GEOCHRONOLOGY

A21 Compilation of radiometric ages, Greater Lufilian Arc – sorted by chronological order, 38
A22 Compilation of radiometric ages, Greater Lufilian Arc – sorted by region and sites, 46

ZAMBIA

A22.1 Hook Granite Batholith, Zambia, 46
A22.2 Northwestern Zambia, Domes Area, 46
A22.3 Solwesi Dome Area, Zambia, 46
A22.4 Western Lusaka-Kafue Flats Area, Zambia, 46
A22.5 Kalengwa-Kasempa Area, Zambia, 47
A22.6 Mkushi-Serenje Area, Zambia, 47
A22.7 Copperbelt region, Zambia, 47
A22.8 Mufulira Area, Zambia, 48
A22.9 Nchanga Area, Zambia, 48
A22.10 All Basement to the Copperbelt, Zambia (Compilation of Groups), 48
A22.11 Choma-Kalomo Batholith, Zambia, 48
A22.12 Irumde Belt, Zambia, 49
A22.113 Luangwa Valley, Zambia, 49
A22.14 Other Zambia, 50

NAMIBIA

A22.15 True Kamanjab Batholith, Namibia, 50
A22.16 Khorixas Inlier, Namibia, 50
A22.17 All Kamanjab Area, Namibia, 51
A22.18 Witvlei Area and possible correlatives in the region, 51
A22.19 Central Namibia, 53
A22.20 Northernmost Namibia, 53
A22.21 Southernmost Namibia, 53
A22.22 Kaokoveld, Namibia, 53
A22.23 Rehoboth Inlier, Namibia, 54
A22.24 Namibrand-Sasriem Area, Namibia, 54
A22.25 Namaqua Metamorphic Complex, Namibia, 54
A22.26 “Kibaran” rocks of Namibia, 55
A22.27 Other Namibia, 55
A22.28 Other countries relevant to Lufilian Arc project, 55
A22.29 All Zambia (compilation of all Zambian ages), 56
A22.30 All Namibia (compilation of all ages from the country), 60

F EVENT DIAGRAMS

ZAMBIA

A23 Hook Granite Batholith, Zambia, 63
A24 NW Zambia, 64
A25 West Lusaka-Kafue Flats Area, Zambia, 65
A26 Environs of the Nchanga Mine, Zambia, 66
A27 Basement to the main Copperbelt, Zambia, 67
A28 Environs of the Mufulira Area, Zambia, 68
A29 All basement to the Copperbelt, Zambia, 69

A30 Luangwa Valley, Zambia, 70
A31 Mkushi-Serenje Area, Zambia, 71
A32 Choma-Kalomo Batholith, Zambia, 72
A33 Irumide Belt, Zambia, 73
A34 Other Zambian reported ages, 74
A35 All Zambian radiometric ages, 75

NAMIBIA

A36 Kaokoland Area, Namibia, 76
A37 Entire Kamanjab region, Namibia, 77
A38 Khorixas Inlier, Namibia, 78
A39 True Kamanjab Batholith, Namibia, 79
A40 Comparative event diagram for Khorixas Inlier and Kamanjab Batholith, Namibia, 80
A41 Central Namibian Area, 81
A42 Namaqua Metamorphic Complex, Namibia, 82
A43 Witvlei Area and correlatives in the Greater Lufilian Arc, 83
A44 So-called “Kibaran-Age” rocks, Namibia, 84
A45 Southernmost portion of Namibia, 85
A46 Namibrand-Sasriem Area, Namibia, 86
A47 Rehoboth Inlier, Namibia, 87
A48 All Namibian radiometric ages, 88
A49 Radiometric ages of other countries that are related to the Greater Lufilian Arc., 89

G TECTONIC ENVIRONMENT OF EMPLACEMENT

A50 Tectonic environment of emplacement for samples from the Greater Lufilian Arc, 90
A51 Results of determination for environment of emplacement of granitoids based on methodology of Maniar & Piccoli, 1989, 96
A52 Results of determination for anorogenic character of granitoids based on the Whalen et al, 1987 plots, 102
A53 Results of determination for environment of emplacement of granitoids based on methodology of Pearce et al, 1984, 107
A54 Discrimination of granitoids following procedure of Harris et al, 1986, 112
A55 Results of determination for environment of emplacement of granitoids based on methodology of Batchelor & Bowden, 1985, 116
A56 Tectonic environment of mafic rocks, Greater Lufilian Arc project, 117

H PARTIAL TRANSCRIPTION OF FIELD NOTES

ZAMBIA

A57 Field notes taken along E-W transect of the Hook Granite Batholith, 168
A58 Abbreviated description of samples collected in the Hook Granite Batholith by Pepper, 2001, 170
A59 Comments from published Zambian geological survey reports and maps on iron oxide bodies, quartz pods, associated granitoids and round-pebble hydrothermal breccias, 172
A60 Sample description and field relationships in the West Lusaka-Kafue Flats Area, Zambia, 173
A60.1 Quartz pods, 173
A60.2 Granitoids, 173
A60.3 Gabbroids, 174
A60.4 Iron oxide bodies, 175
A60.5 Contact metamorphic rocks, 175
A61 Descriptions of samples from the Kalengwa Area, Zambia by Pepper, 2001, 176
A62 Descriptions of samples collected in the field, Kalene Hill Area, NW Zambia, 178
A63 Field descriptions of samples L-032 to L-034, Kabompo dome, NW Zambia, 1798
A64 Petrography of the Chitungulu sodalite syenites, Mwombezhi Dome, NW Zambia, 180

NAMIBIA

A64 Field notes for a few suites of Cu-mineralized rocks in the Kamanjab Batholith, Namibia, 182
A65.1 Suite G, 182
A65.2 Suite H, 182
A65.3 Suite M, 183
A65.4 Suite N, 184
A66 Field notes on the N-S transect through the Oas Farm, Namibia, 185
A67 Field notes from the Lofdal farm, Namibia, 194
A67.1 Cross section through series of ultramafic dikes, Lofdal farm, Namibia, 197
A67.2 Magnetite-cemented, polymictic hydrothermal breccia that makes a diatreme, 198
A68 Partial field notes collected at the Mesopotamie farm, Namibia, 200
A69 Field notes, Ugab River, Namibia, 201
A70 Field notes, Okwa River, Botswana, 204
A71 Field notes Grootfontein Inlier, Namibia, 205
A72 Field notes from Okatjepuiko, Witvlei, Namibia, 206

I OTHER

A73 Persons interviewed for preparation of fieldwork, during fieldwork, and when processing information, 208
A74 Rock names of samples from the Greater Lufilian Arc Granitoid project, 209
A75 Experiment to test quality of chemical laboratory, 214
A76 Heat production capacity of intrusive rocks from the Greater Lufilian Arc at the time of their emplacement, 216

J RAW DATA FOR NEW GEOCHRONOLOGY

A77.1 Raw data obtained for SHRIMP II U-Pb dating at the Australian National University, Canberra, 221
A77.2 Raw data and processing for zircon dating using U-Pb laser-ablation ICP-MS technique, 225
A78 **CONCORDIA DIAGRAMS**
A78.1 Sample L-030, 227
A78.2 Sample L-047, 227
A78.3 Sample L-075, 228
A78.4 Sample L-158, 228
A78.5 Sample L-160, 229
A78.6 Sample L-207, 229
A78.7 Sample L-213 Concordia diagram for high U zircons + rims, 230
A78.8 Sample L-213 Concordia diagram for cores and rims, 230
A78.9 Sample L-638 Concordia diagram for all zircons including xenocrysts, 231
A78.10 Sample L-638 Concordia diagram for main cluster of zircons, 231
A78.11 Sample L-688 Concordia diagram for all zircons, 232
A78.12 Sample L-688 Histogram of all 12 ages in main cluster, 232
A78.13 Sample L-693, 233
A78.14 Sample L-868, 233
A78.15 Sample L-855 Concordia diagram for all zircons, 234
A78.16 Sample L-855 Concordia diagram for main cluster of ages, 234
A78.17 Sample L-943 Concordia diagram for all zircons, 235
A78.18 Sample L-943 Concordia diagram for main cluster of zircons, 235
A78.19 Sample L-969, 236
A78.20 Sample L-993, 236
A78.21 Sample L-1013 first, 237
A78.22 Sample L-1013 second, 237
A78.23 Sample L-1043 concordia diagram for older group of zircons, 238
A78.24 Sample L-1043 concordia diagram for younger group of zircons, 238

A78.25 Sample L-1043 concordia diagram for all zircons 2, 239
A78.26 Sample L-1043 concordia diagram for all zircons 1, 239

K GEOCHRONOLOGICAL CORRELATION DIAGRAMS

A79 Correlation of dated events, Zambian locations, 240
A80 Correlation of dated events, Namibian locations, 241
A81 Correlation of dated events, Greater Lufilian Arc, 242
A82 Correlation of dated events, Greater Lufilian Arc, first portion (3000 to 1400 Ma), 243
A83 Correlation of dated events, Greater Lufilian Arc, second portion (1400 to 0 Ma), 244

1. INTRODUCTION

This document reports observations, findings and conclusios of the research project entitled “Geochemistry, Geochronology and Metallogeny of Pre-Katangan and Post-Katangan Granitoids in the Greater Lufilian Arc, Zambia and Namibia”. It is presented to the School of Geosciences of the Science Faculty of the University of the Witwatersrand, and constitutes the thesis for the Ph.D. degree in Geology at that institution.

1.1 The Lufilian Arc

The Lufilian Arc of South-Central Africa is defined as the curvilinear belt of Neoproterozoic Katangan sediments that was deformed during the Pan African orogeny in Zambia and the Democratic Republic of the Congo. Those two countries contain the vast stratiform Katanga copper-cobalt ores, as well as the epigenetic polymetallic (Pb, Zn, Cu-Au, and U) ores of the region. The Katangan sequences were deposited over a lengthy period of Neoproterozoic time that extended from around 880 Ma (Lower Roan) to less than 590 Ma (Upper Kundelungu). That interval coincides with the Cryogenian Period, or so-called “Snowball Earth”. The Lufilian Arc also comprises a dominantly Paleoproterozoic basement of deformed granitoids, and a diverse suite of Pan-African granitoids that intrude the Katangan sequences.

Although the Lufilian Arc *per se*, occurs essentially in Zambia and the Democratic Republic of Congo, it is evident that tectonized correlatives of the tectonostratigraphic Katangan entitity extend westwards, beneath Karoo and Kalahari cover in Botswana, into Angola and northern Namibia. The western extension of this arc has only been sporadically studied. At the time of starting this project, there was an urgent need to address that deficit, especially since it is clear that mineralization also extends into Angola and Namibia. The Greater Lufilian Arc covers that large area, as shown on Fig 1.1.

1.2 The Project

This project was structured by Professor Laurence Robb of the University of the Witwatersrand in late 2001. It was designed to study the pre- and post-Katangan granitoids that comprise the Greater Lufilian Arc. Its main purpose was to provide insights into the metallogenic characteristics and potential of the whole belt. Three South African-based mining companies were interested in the project and joined to fund and support it. These were Anglo American Corporation, AngloVaal and BHPBilliton. Granitoids were selected for study because they represent rock types that could potentially provide a great deal of information about the orogenic processes involved in the formation of the Greater Lufilian Arc. They were also likely to be implicated in many of the ore forming processes in the belt. Given that three mining companies were involved in funding this collaborative research project, a study of granitoid evolution and metallogeny was considered to be the best way to avoid compromising any of the individual corporate strategic initiatives that might otherwise have arisen in a project aimed at studying specific exploration targets or deposits.

1.3 Aims of the Project

The main aims of the study of granitoids in the Greater Lufilian Arc were:

1. To evaluate geological relationships of intrusives relative to the Katangan, emplacement style and depths of intrusion.
2. To study the role of granitoids in Katangan orogenesis and mineralization.
3. To define the geochemistry of the granitoids in order to identify their tectonic setting and metallogenic affinities.
4. To study the age of the principal events and evolution of the belt.
5. To improve geological understanding of late granite intrusions in the arc.
6. To assess whether the iron oxide-copper-gold mineral deposit model pertains to the region.
7. To improve the metallogenic models for the belt in order to assist in exploration of known areas, and areas covered by Karoo and Kalahari sediments in eastern Angola, northeast Namibia and Botswana.

1.4 Study Areas

The project was constrained to areas with reasonably good surface exposure, that allowed for adequate representative sampling and definite geological control. Main fieldwork was concentrated in two broad regions: NW Zambia and northern Namibia (Fig 1.1).

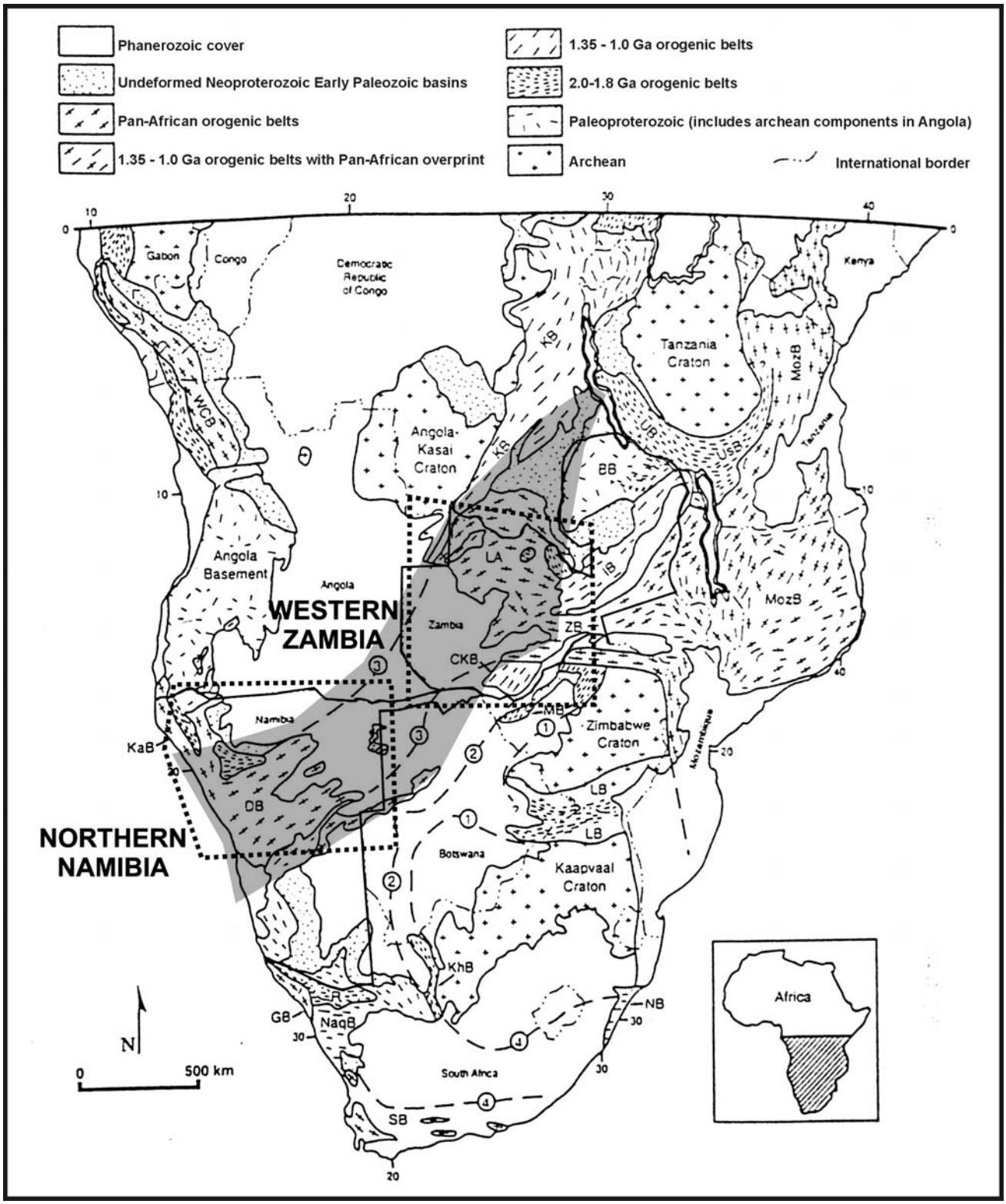

Fig 1.1 Definition of the study area area and tectonic framework of southern Africa. *The Greater Lufilian Arc covers the northern part of Namibia and western part of Zambia, as indicated in gray. Fieldwork was carried out in the two boxed areas. Zambia lies just in the center of the map; Namibia on the lower left. Borders of the two countries were enhanced for reference. Note that the Greater Lufilian Arc, limited by the covers significant portions of the Democratic Republic of Congo, Angola, Botswana, Zambia and Namibia. LA = Lufilian Arc, DB = Damara Belt, KaB = Kaoko Belt, ZB = Zambezi Belt, IB = Irumide Belt, BB = Bangweulu Block, CKB = Choma-Kalomo Block. Figure slightly modified from (Hanson, 2000).*

1.5 Project Outline

The project was subdivided into three discrete phases. Each of them defined by a specific task, budget and delivery date. They each were followed by a report summarizing the results to the funding parties. The following three phases defined the project's objectives and deliverables up to June, 2003:

1.5.1 Phase 1 – April to November 2002. Geological Characteristics of Pre- and Post-Katangan Granitoids.

The main objective of this phase was to collect a representative suite of samples from both study areas and provide definitive geological controls for the samples. Fieldwork began after carrying out a preliminary literature survey and review of information. Much of the phase was dedicated to field work. Specific objectives of the phase included:

- To collect samples representing the compositional variety in each of the major pre- and post-Katangan granitoid bodies in the two study areas.
- To establish geological relationships of the granitoids to the Katangan sequence and its correlatives.
- To collate information relating to the known mineral deposits in and adjacent to these granitoid bodies.

1.5.2 Phase 2 – December 2002 to May 2003. Petrographic and Geochemical Characterization of Pre- and Post-Katangan Granitoids.

The main objective of this phase was the petrographic and geochemical characterization of the sample suite collected in Phase 1. It was a laboratory-based phase that entailed slabbing of all granitoids, and preparation of thin and polished/thin sections of a representative collection of the sample suite. A subset of the samples was analysed for major oxides, trace elements and rare earth elements at various laboratories. Specific objectives included:

- To obtain major and trace element analysis by XRF techniques.
- To evaluate the rare earth content of some samples using various techniques.
- To process and interpret petrographic and geochemical information from the samples.

1.5.3 Phase 3 – June to September 2003. High Precision U-Pb Zircon Geochronology of Pre- and Post-Katangan Granitoids.

The main objective was to provide accurate and precise age dates for each major granitoid unit identified during the previous two stages. Zircons separated from select samples were sent to two geochronological laboratories in Australia and Canada.

1.5.4 Phase 4 – October 2003 to January 2005. Ellaboration of the Ph.D. thesis.

The main objective was to compile, process and interpret all the information obtained during the previous three phases. It was an office-based phase where most of the diagrams were drawn, many references were reviewed, and the thesis was structured. Special attention was given to compilation of geochronological information from the Greater Lufilian Arc and to interpretation of the tectonic environment of emplacement of the various rocks analysed. Several presentations were made at international and South African geological conferences to ventilate some of the ideas and interact with other researchers, especially in the field of iron oxide-copper-gold mineralization (Lobo-Guerrero, 2004a; Lobo-Guerrero, 2003; Lobo-Guerrero, 2004b; Lobo-Guerrero, 2004c; Lobo-Guerrero, 2004d; Lobo-Guerrero, 2004e; Lobo-Guerrero S., 2003).

1.5.5 Current status of project

A total of 1500 samples were collected in the field; 351 were analysed. 157 chemical analysis were compiled from various well-documented sources, to reach a total of 508 samples analysed in the database. 38 new zircon U-Pb ages were produced: 10 of them by laser-ablation ICP-MS techniques at the Memorial University of Newfoundland, Canada, by Marc Poujol and his research group; and 28 by SHRIMP II at the National University of Australia (ANU) by Richard Armstrong and his research group.

Major sampling domains of the Lufilian Arc Granitoid Project will be grouped and described in the following pages. Main findings on geochemistry, petrology and geochronology of the rocks sampled will be exposed for the third time. Future work to be carried out in specific projects and on-going work will also be described.

2 METHODOLOGY

2.1 FIELD SAMPLING

2.1.1 Definition of Granitoid

The term “granitoid” was loosely used during field sampling, to include all felsic to intermediate plutonic rocks. That field classification included all syenites and foid-bearing rocks, as well as diorites and carbonatites. Ocassionally such “granitoids” were intimately associated with small gabbroic bodies. This was noted very early in the project, in northwestern Zambia. Once that the granitoid-gabbroid association was established, mafic rocks that occurred with the “granitoids” were also sampled. Some areas had very little to no rock outcrop, so any *in situ* gabbroid or granitoid exposed on the surface was sampled. Gabbros from regional Mesozoic dike swarms (Karoo) were not sampled.

2.1.2 Sampling Procedure

Most of the samples were taken from the surface. The freshest samples were collected and only the best of that group were selected for chemical analysis and dating. Samples were generally only collected along the main roads. At most, they come from a few hundred meters away from the main road network. For these reasons, samples collected have a bias: they come from the best outcrops available along the main roads in each of the regions. Rocks that did not outcrop well were selected out of the project. A very small number of foot transects was done at special sites. Core from many localities was also observed and sampled, especially in areas with no outcrop.

Transects were made across the intrusive bodies of the Greater Lufilian Arc, with representative sampling of the main outcrops along roads or near them. Information on granitoids was primarily based on published maps and literature. Interviews with key persons, mainly geologists from various geological surveys, mining companies, universities and consulting firms, helped to define which particular regions deserved more attention. Most interviews were recorded on tape and later transcribed. A list of the persons interviewed is presented in the Appendix.

Pre-Katangan and Post-Katangan granitoid rocks were selected for sampling based on their location, representativity, foliation, deformation and composition. Sampling was carried out in areas that had little recent geological work. For example, geochemistry and geochronology of granitoid rocks in some parts of Namibia has been studied in detail during the last ten years (Becker & Brandenburg, 1997; Becker, Diedrichs, Hansen, & Weber, 2000; Becker & Schreiber, 2002; McDermott, Harris, & Hawkesworth, 2000; McDermott & Hawkesworth, 1990; Seth, 1999; Seth, Armstrong, Brandt, Villa, & Kramers, 2003; Seth et al., 1998; Seth, Okrusch, Wilde, & Hoffmann, 2000). Those areas were not considered for sampling. In contrast, most of the Zambian granitic rocks do not have any recent studies, apart from general 1:200,000, and 1:100,000 scale mapping of the Mwinilunga area (Key & De Waele, 2003; Key & Banda, 2000; Key et al., 2002; Key et al., 2000; Key et al., 2001), and work done on the Irumide and Kibaran belts by (De Waele, Fitzsimons, & Nemchin, 2004; De Waele & Tembo, 2000; De Waele, Tembo, & Wingate, 2001; De Waele, Wingate, & Mapani, 2002).

On most occassions, sampling routes were first traversed one way in order to locate all possible outcrops with GPS waypoints; the most favorable outcrops were sampled on the way back. The general approach for sampling was to collect fresh, representative specimens of all the different facies of intrusive rocks within a given area. For example, if a well-exposed outcrop had a granite gneiss intruded by a medium-grained tonalite and a series of uniform gabbroids, homogeneous samples of all three rocks were selected. Choice fell on the least altered, with the minimium of veins and xenoliths. In principle, all samples for chemical analysis and dating were chosen to be approximately 1½ to 2½ kilograms in weight. Ideally, every specimen had fresh, trimmed surfaces on all faces.

2.1.3 Referencing Geological Stations, Recording Information and Sample Labeling

All sampling stations were located on a map and their GPS coodinates were recorded. Depending on the region, published 1:100,000 geological maps had latitude and longitude, or UTM based coordinates. The same coordinates, projection systems and datums of the maps were used for GPS location of stations. Coordinates and reference systems for all sample collection sites, and most geological observation stations have been listed on Tables A16 to A20 in the Appendix. The table is broken down into groups, to account for the various coordinate systems and datums used. Sample locations have been plotted on the maps that come with this document.

When possible, the following observations were recorded on each outcrop: station number, sample number, GPS coordinates, macroscopic field description, structural relations, contacts, foliation, alteration and mineralization. Other information recorded on the field notebook was type of outcrop, its environs and general physiography. The sample, if any, was then placed in a heavy plastic bag along with a cardboard tag labeled on both sides with a waterproof marker. The plastic bag was also labeled on both sides. Its upper portion was cut with a knife and then tied with a square knot to keep the specimen from getting out. Batches of samples were temporarily stored in warehouses and mining company facilities until the moment of driving them to Johannesburg.

2.1.4 Other Field Activities

Although sampling for granitoid rocks was the main objective of the project, several other aspects of the geology were observed. Namely, structural features, mineralization produced by some of the granitoid rocks, and hydrothermal alteration around granitoid bodies. Apart from granitoids and gabbroids, other rocks sampled include: volcanic rocks, iron oxide bodies, quartz pods[1], mafic and ultramafic dikes, carbonatites, and mineralized zones associated (or potentially associated) with granitoids.

2.1.5 Field Equipment Used

The main equipment used for fieldwork was: 10X magnifying glass, HCl bottle, steel scratcher, field magnet, GPS, 4 megapixel high-resolution digital camera, Brunton compass, large sledge hammer, 1 kilogram steel hammer with modified long handle, steel chissel, portable computer and field notebook. A steel pan was also carried along for sampling gravity concentrates. Four wheel drive vehicles were used for all fieldwork. Most field mapping and sampling activities were based on moving tent camps. Small hotels were used to sleep at the main towns and cities. Ninety percent of the fieldwork was done singlehandedly.

2.1.6 Bibliographical Research

Before going to the field, basic cartographic and bibliographic research on granitoids, structural geology and mineral deposits of the Lufilian Arc was carried out. This research was done at the various libaries of the University of the Witwatersrand, the Geological Survey Organization in Lusaka, the Zambian Chamber of Mines in Kalulushi, the Geological Survey of Namibia in Windhoek, and the Geological Survey of South Africa in Pretoria. Some published papers and internal reports from the funding mining companies were also reviewed. Most of the bibliographical research on Zambia was carried out at libraries of the University of the Witwatersrand, the main Johannesburg Public Library, and the library of BHPBilliton in Johannesburg.

2.1.7 Office and Laboratory Work

Once back in Johannesburg, preparation of samples began. First of all, field notes and drawings were reviewed and updated. Lists of sample coordinates were assembled and preliminary sample databases were put together. These included field name of rock, site, coordinates, type of sample collected, and research to be done on each particular sample. Granitoid samples were prepared first, and other samples of mineralized material, iron oxides, volcanic and sedimentary rocks were saved for later evaluation.

After assembling the databases, rock specimens were prepared in the following manner: They were organized by sample number, later they were slabbed using a 40 cm diameter circular diamond blade. The largest possible slabs were kept as counter-samples. Weathered or otherwise altered portions of the samples were sawed off. All of the slabbed surfaces were photographed wet or dry, to obtain the maximum contrast. Representative slabs of all samples were labeled and stored for future reference. Thin and thin-polished petrographical sections were made of selected samples. The remainder of the rocks were carefully crushed and then ground to a medium sand size for zircon-picking. Standard dense media separation, as well as magnetic separation procedures were used at the EGRI-HAL[2] laboratories to concentrate zircons and other minerals of interest. Mineral separates were kept for further reference.

If grinding for zircon-picking was not to be carried out, crushed samples were quartered, and a representative portion was finely ground. Samples were labeled and sent to the chemical laboratory of the School of Geosciences for XRF chemical analysis of major oxides and some trace elements as indicated on Table 2.1.

---

[1]The informal term “quartz pod” will be used to indicate massive quartz bodies that occur throughout the work area as round outcrops of milky to sugary quartz in circular to sub-circular outcrops that range from a few meters in diameter to one kilometer in diameter (See Chapter SUCH).

[2] EGRI-HAL stands for Economic Geology Research Institute-Hugh Alsopp Laboratory of the School of Geosciences, University of the Witwatersrand.

Part of the trace elements and rare earths were analysed by ICPOES at the Chemistry Department of the University of the Witwatersrand and others were analysed by ICPMS at the University of Capetown. Table 2.1 indicates which elements were analysed where and what their detection limits were. All samples, countersamples, slabs and thin sections were filed and stored. They are currently kept at the Department of Geosciences.

All results for iron oxides were given as total iron oxides, expressed in Fe2O3. Several of the samples from the literature had both FeO and Fe2O3 and were kept as such in the geochemical database. Nevertheless, for comparison purposes, total iron oxide expressed as Fe2O3 was used.

Table 2.1 Laboratories where chemical analysis were carried out, with threshold values and detection limits where available.

Element /Cation	Laboratory	Type of Analysis	Detection Limit	Notch
SiO2	SGWits	XRF		50.00
TiO2	SGWits	XRF		1.00
TiO2	SGWits	XRF	0.10%	1.00
Al2O3	SGWits	XRF		15.50
Fe2O3	SGWits	XRF		6.00
MnO	SGWits	XRF		0.150
MgO	SGWits	XRF		2.00
CaO	SGWits	XRF		5.00
Na2O	SGWits	XRF		4.90
K2O	SGWits	XRF		5.50
P2O5	SGWits	XRF		0.30
LOI	SGWits	Difference		2.00
Total	SGWits			
Rb	SGWits	XRF	3	200
Rb	UCT	ICPMS		200
Sr	SGWits	XRF	3	400
Sr	UCT	ICPMS		400
Y	SGWits	XRF	3	60
Y	UCT	ICPMS		60
Zr	SGWits	XRF	8	360
Zr	UCT	ICPMS		360
Nb	SGWits	XRF	3	40
Nb	UCT	ICPMS		40
Co	SGWits	XRF	6	30
Ni	SGWits	XRF	6	16
Cu	SGWits	XRF	6	25
Zn	SGWits	XRF	6	85
Ga	SGWits	XRF	9	26
V	SGWits	XRF	12	100
Cr	SGWits	XRF	12	100
Ba	SGWits	XRF	20	1300
U	SGWits	XRF	6	20

Element	Laboratory	Type of Analysis	Detection Limit	Notch
U	UCT			20
Th	SGWits	XRF	15	37
Th	UCT	ICPMS		37
Sc	SGWits	XRF	10	20
Pb	UCT	ICPMS		20
Sm	SCWits	ICPOES		50
Sm	UCT	ICPMS		50
Nd	SCWits	ICPOES		50
Pr	UCT	ICPMS		15
Ce	SGWits	XRF	12	175
Ce	UCT	ICPMS		175
La	SGWits	XRF	12	95
La	UCT	ICPMS		95
Cs	UCT	ICPMS		3
Hf	SCWits	ICPOES		10
Hf	UCT	ICPMS		10
Ta	SCWits	ICPOES		120
Ta	UCT	ICPMS		120
Eu	SCWits	ICPOES		4
Eu	UCT	ICPMS		4
Gd	SCWits	ICPOES		30
Gd	UCT	ICPMS		30
Tb	SCWits	ICPOES		5
Tb	UCT	ICPMS		5
Dy	UCT	ICPMS		20
Ho	UCT	ICPMS		3
Er	UCT	ICPMS		9
Tm	UCT	ICPMS		35.5
Yb	SCWits	ICPOES		7.5
Yb	UCT	ICPMS		7.5
Lu	SCWits	ICPOES		1.6
Lu	UCT	ICPMS		1.6

NOTES
SGWits = Laboratory of the School of Geosciences, University of the Witwatersrand
SCWits = School of Chemistry, University of the Witwatersrand
UCT =University of Capetown
No analysis were performed for H2O+ and H2O-, SO2, F, Cl, CO2.
Analysis for Mo, Sn, W, Ge, Be, Li, As and Se were not carried out during the project. Samples with such analysis were obtained from external sources.

2.2 PETROLOGIC NOMENCLATURE

Samples were first classified macroscopically in the field using the bare eye and a 10X hand lens. In general, that preliminary classification included main color, grain size, foliation, freshness, basic colors of principal rock constituents, degree of observable hydrothermal alteration and mineralization constituents. Typical descriptions were “fine-grained, pink plagioclase porphyry”, “medium-grained gray granitoid with blue quartz ‘eyes’”, “dark brown, very fine-grained gabbro with disseminated cubic vugs after probable sulfides”, and “well-foliated coarse-grained red porphyritic granitoid with pink plagioclase phenocrysts (2.5 cm average long dimension) and biotite in the foliation planes”.

Two different procedures were used to give proper petrologic names to samples collected for the project, based on their major oxide chemical analysis. These will be discussed below.

2.2.1 Total Alkali Diagram

The modified version of the IUGS Total Alkali versus Silica diagram presented by (Middlemost, 1994b) is a comprehensive and widely accepted standard for plutonic rock nomenclature. It builds upon the total alkali versus silica (TAS) diagram to name volcanic rocks suggested by the IUGS Subcommission for Igneous Rock Nomenclature (LeMaitre et al., 2002 and several other earlier versions). The diagram is made by plotting SiO_2 weight percentages on the abcissa versus the sum of Na_2O and K_2O on the ordinate (Fig 2.1).

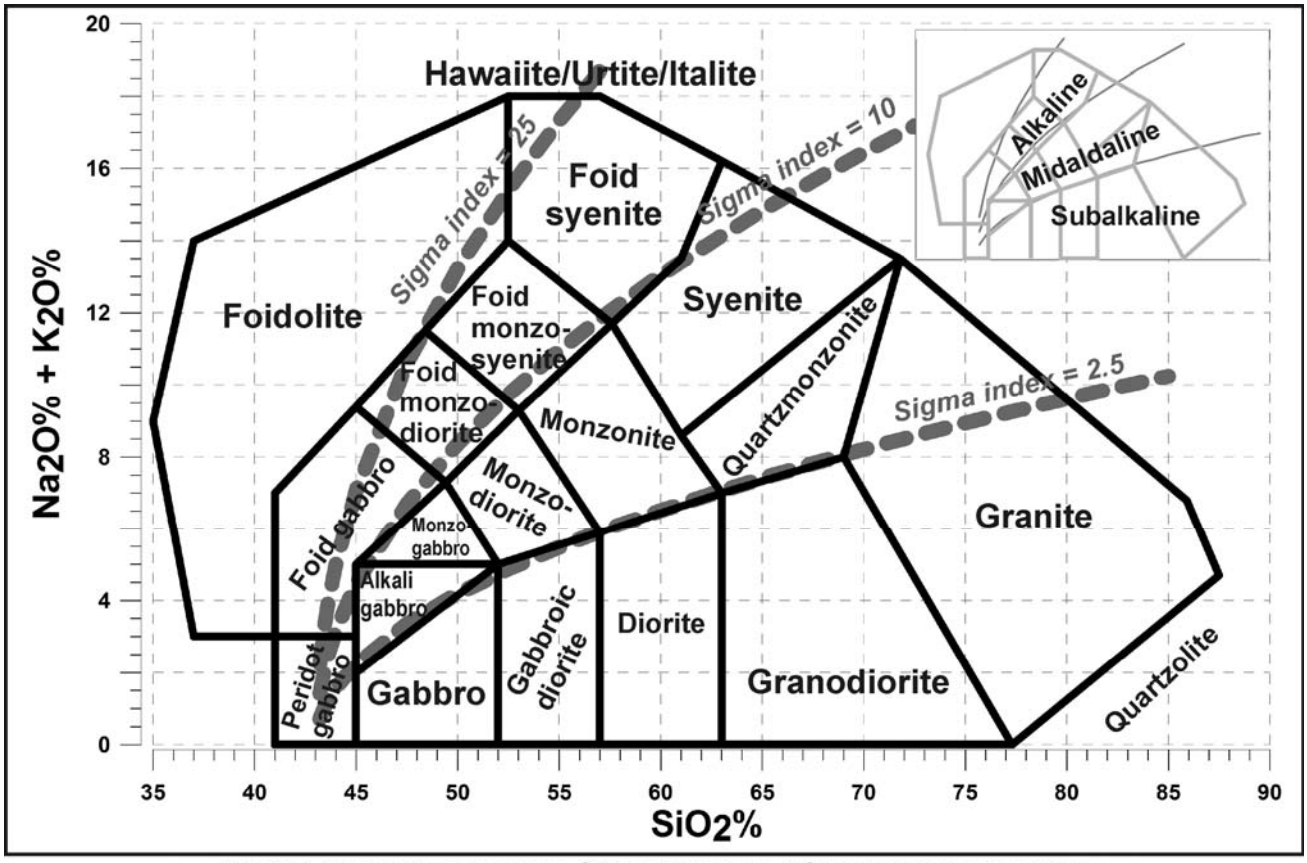

Fig 2.1 Total Alkali versus Silica Diagram, After Middlemost, 1994.
Includes the sigma index to separate alkaline, midalkaline and subalkaline rocks (See inset).

Middlemost, 1997 suggests that three sigma isopleths should be used to separate the subalkaline, midalkaline and alkaline magmatic lineages. The sigma index was devised by Rittmann, 1957, and is equal to:

$$\Sigma \text{ index} = (Na_2O + K_2O)^2/(SiO_2 - 43)$$

Equation 1

“Rocks of the subalkaline suite have sigma values less than 2.5; sigma values between 2.5 and 10 define the midalkaline suite; whereas sigma values in the range 10 to 25 separate the alkaline suite.” (Middlemost,

1997). He further adds that igneous rocks with sigma values that are greater than 25 or negative "should be regarded as special rocks with chemical compositions that set them apart from the normal igneous rocks" (Middlemost, 1997, p. 46). Both the modified TAS diagram for plutonic rocks and the sigma isopleths just described will be used throughout this document. All plutonic rock names, as well as the alkalinity suites are shown on Fig 2.1.

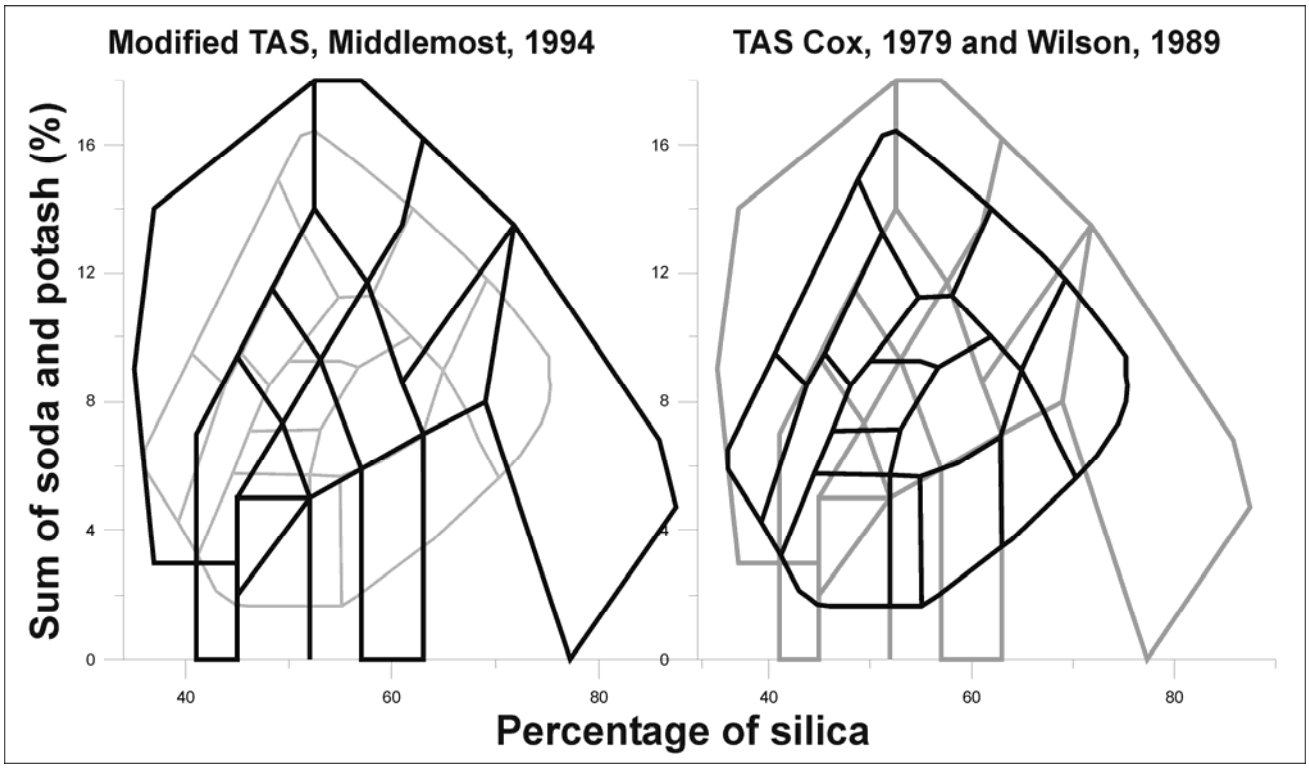

Fig 2.2 Comparison of the total alkali versus silica diagrams proposed by Middlemost, 1994 and by Wilson, 1989. *Both diagrams were plotted at the same scale, to compare the various fields of each method. Note that the fields of granites, syenites and foid syenites in Middlemost's diagram than in Wilson's diagram. Many fresh samples from the Greater Lufilian Arc plotted outside of the Wilson diagram.*

The TAS diagram described by Cox, Bell, & Pankhurst, 1979 and later modified by Wilson, 1989 to include plutonic rocks is not very practical and will not be used here. Its rock names are significantly different from the Middlemost TAS diagram, as shown on Fig 2.2.

2.2.2 R1/R2 Cationic Classification

Classification of plutonic rocks only based on total content of potash, soda and silica is an oversimplification. Other classification procedures use various relations of most major oxides that define intrusive rocks. Perhaps the most used multioxide methodology to classify igneous rocks was devised by the French research group let by Henry De la Roche (De la Roche, Leterrier, Gandclaude, & Marchal, 1980). Common spreadsheet applications and drafting software, make it very simple to apply De la Roche's method for batch plotting of geochemical analysis. The method separates igneous rocks into at least 28 groups using eight cations (SiO_2, Na_2O, K_2O, FeO_3, TiO_2, CaO, MgO and Al_2O_3) to classify the rocks. Parameters R1 and R2 are calculated from millicationic values and plotted against each other. Values for R1 and R2 are calculated as follows:

$$R_1 = 4Si - 11 (Na + K) - 2 (Fe + Ti) \qquad R_2 = 6 Ca + 2 Mg + Al$$

Equations 2

The R1/R2 nomenclature devised by De la Roche and co-workers is the most descriptive of the chemical-based rock nomenclatures available. The facts that it derives from a range multiple cations and that it spans all types of intrusive rocks, makes it a robust system to classify igneous rocks from the Greater Lufilian Arc Granitoid Project. Fig 2.3 illustrates the limits between various rock types and the names used.

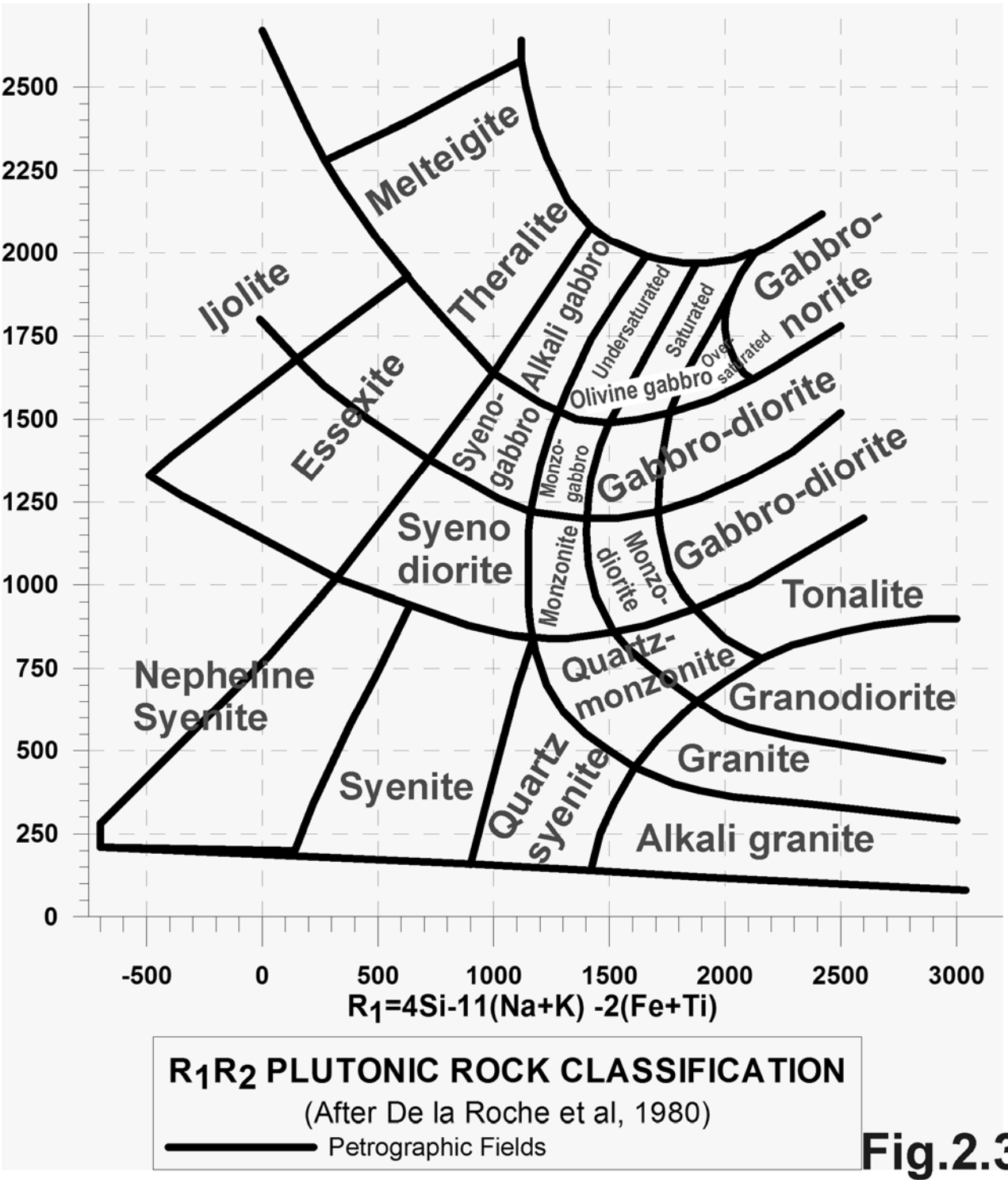

Fig.2.3

2.2.3 Granitoid Classification

Characterization of the different types of granitoids was one of the main tasks of this research project. The granite family, composed by granodiorite, quartz monzonite, monzonite and true granite (sensu modified TAS diagram of Middlemost, 1994b) conforms a very significant portion of the rocks sampled for the Lufilian project. The same group of rocks includes the fields of alkali granite, granite, granodiorite, tonalite, quartz monzonite and monzonite, according to the R1/R2 diagram of De la Roche et al., 1980. Different names for the same rock speciments turn out, because each procedure is based on a contrasting relation of major oxide values.

The systematics of methods proposed by (De la Roche et al., 1980) and by Middlemost, 1994b and Middlemost, 1997 were considered to be more representative of the various rock types and were selected for

nomenclature and discussions of various petrological aspects in this report. All samples with chemical analysis were evaluated with the TAS and R1/R2 methodologies. Table A74 in the Appendix presents results of the nomenclature.

The triangular modal diagrams devised by the IUGS Subcommission on nomenclature of igneous rocks (LeMaitre et al., 2002) offer yet another solution to the complex issue of naming rocks. They were not used for this project due to the amount of samples and the lack of precision of those methods for comparative purposes.

2.2.4 Debon & LeFort Cationic Classification Diagrams

Several of the diagrams presented by Debon & Le Fort, 1988 are useful for rock discrimination and geochemical evaluation. The authors devised ways to standardise description of some geochemical parameters including: quartz content, alumina index, color index, alkali ratio, relationship of quartz-dark minerals-alkalies, sodium versus potassium content, and magnesium versus iron content. The main cationic parameters are calculated in terms of millications and help to produce specially designed plots. The way to calculate these parameters in described clearly in Debon & Le Fort, 1988 and Debon & LeFort, 1983. The main equations for each parameter are listed below. Q is an empiric estimate of the rock's quartz/(quartz + feldspars + muscovite) proportions in volume percentages. P is the alkali ratio. The A parameter is the classical alumina index. B is directly proportional to the weight content of dark minerals in common granitic rocks. F is proportional to the weight content of feldspars + muscovite.

$$Q = Si/3-(K+Na+2Ca/3)$$
$$P = K-(Na+Ca)$$
$$A = Al-(K+Na+2\,Ca)$$
$$B = Fe+Mg+Ti$$
$$F = 555-(Q+B)$$
$$K^* = K/(Na+K)$$
$$Mg^* = Mg/(Fe+Mg)$$

Equations 3

The diagrams devised by Debon & LeFort will be used extensively through the project to compare suites of samples, evaluate their hydrothermal alteration, and define geochemical trends.

1. The Q-P diagram (Fig 2.4), originally designed to name the common plutonic rocks, is useful to evaluate rock associations, geochemical trends, and some types of hydrothermal alteration. The twelve "standard" plutonic rock types, as defined by Debon & LeFort, 1983 are plotted in the middle of the fields.

2. The A-B diagram (Fig 2.5) separates peraluminous minerals and rocks from metaluminous minerals and rocks. It also helps to identify some of the characteristic rock-forming minerals. The plot is sensible to subtle hydrothermal alteration.

3. The QBF diagram (Fig 2.6) is useful to help define geochemical trends of igneous rocks, and aids in distinction of different magmatic associations.

4. The K*-B diagram (Fig 2.7) is useful to help establish sodic, sodic-potassic or potassic character of rocks, as well as to classify their color index into leucocratic, subleucocratic and mesocratic. This plot is sensible to subtle hydrothermal alteration. It also helps to define geochemical trends of igneous rocks.

5. The Mg*-B diagram (Fig 2.8) has a central line made by joining the average values for granite, adamellite, granodiorite, tonalite quartz diorite and gabbro, as defined by Debon & LeFort, 1983. The diagram helps to distinguish between common, magnesian and ferriferous associations. It is sensible to some hydrothermal alterations related to iron oxide-copper gold systems.

The various diagrams defined by Debon & LeFort, 1983 were used extensively during the Greater Lufilian Arc Granitoid Project. Results from the A-B, K*-B and Mg*-B diagrams helped to produce detailed rock names. The basic rock type name was nevertheless given by the TAS diagram modified by Middlemost, 1994b.

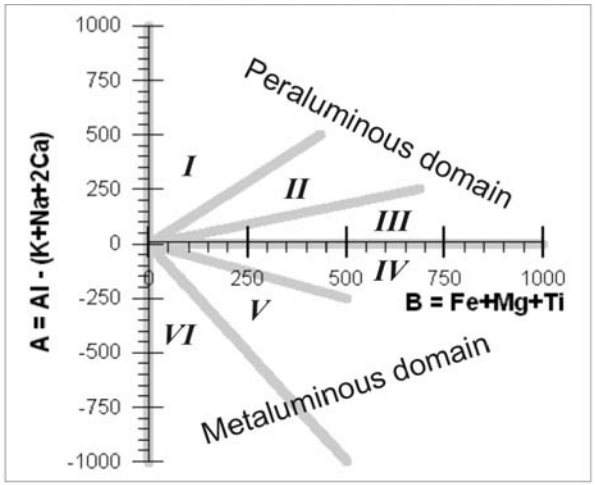

Fig 2.5 AB Diagram

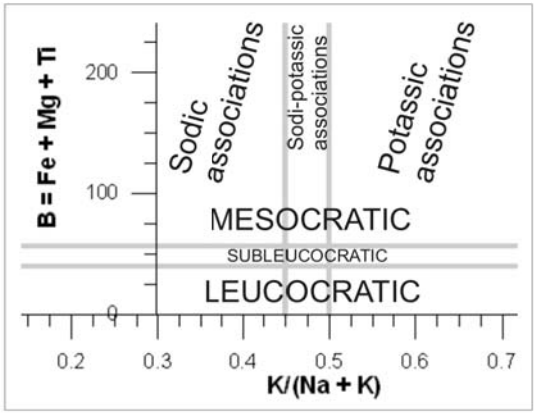

Fig 2.7 KB Diagram

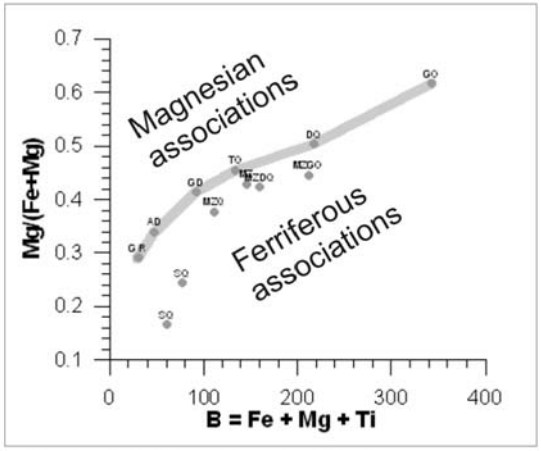

Fig 2.8 MgB Diagram

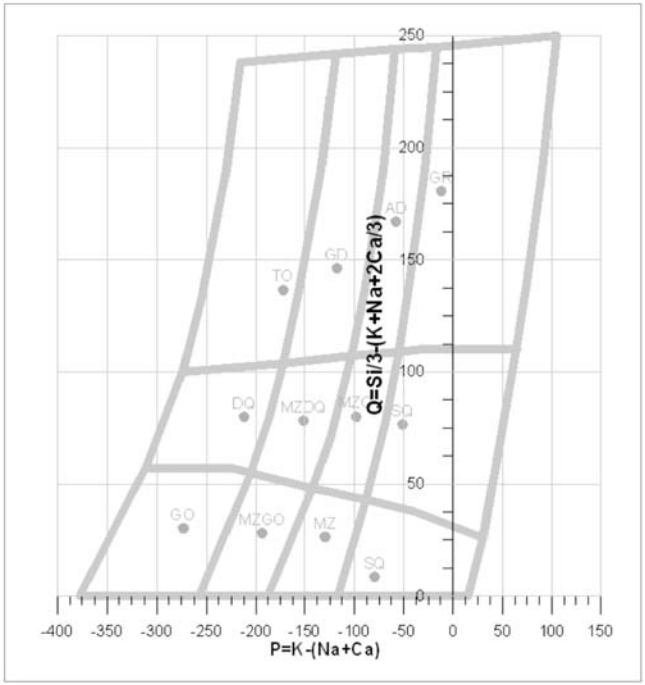

Fig 2.4 QP Diagram

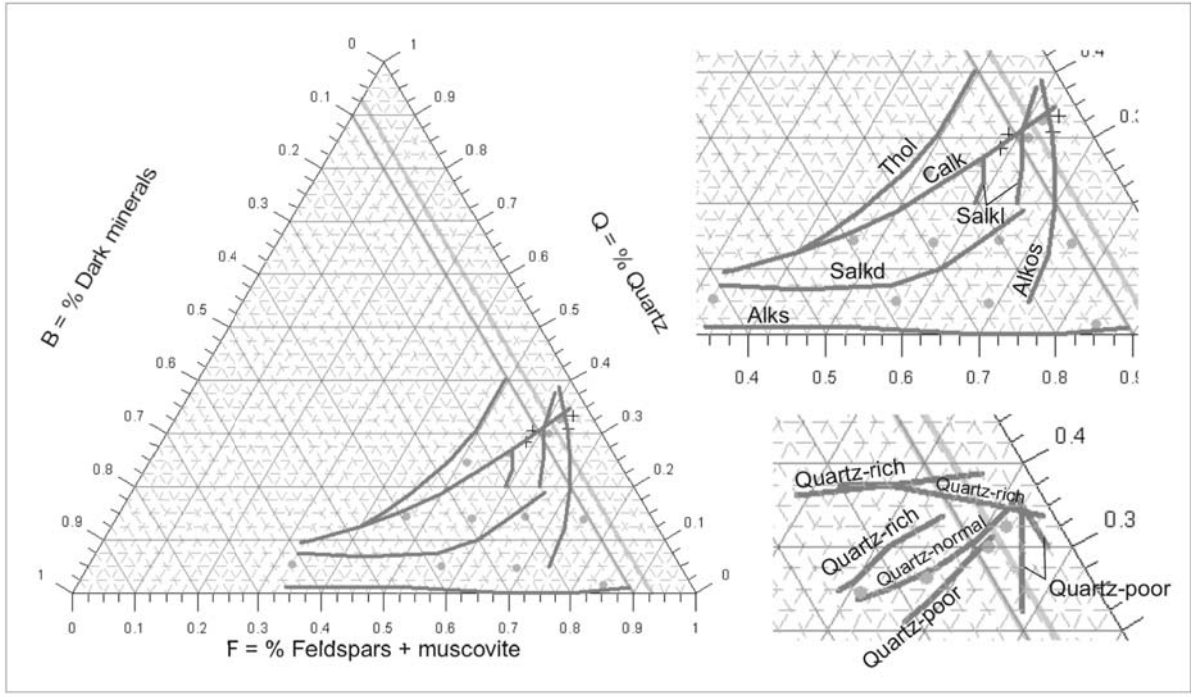

Fig 2.6 QBF Diagram

Figs 2.4 to 2.8 Diagrams of Debon & LeFort, 1988

2.3 GEOCHEMISTRY

2.3.1 Major Oxide Chemistry

The major oxide geochemistry of samples from the Lufilian Arc region will be described using the modified TAS diagram of Middlemost, 1994a; and Middlemost, 1997 and the R1/R2 classification of plutonic rocks by De la Roche et al., 1980. Since most of the rocks sampled fall within the granite field, the 2.5 sigma isopleth was used to separate subalkaline from midalkaline rocks in the modified TAS diagram. It was also used to break the field of granites into alkali granites from granites on the same diagram. Each suite of analysed rock samples was evaluated statistically in terms of their alkalinity using the modified TAS diagram and the sigma isopleths.

All individual samples from the Greater Lufilian Arc granitoid project were first given the R1-R2 basic rock name. Later the methods of Debon & Le Fort, 1988 and Debon & LeFort, 1983 were used to establish their aluminosity, color, sodic-potassic and ferriferous-magnesian parameters. Results of this classification are listed in each of the chapters that describe the sampling domains.

Suites of rocks were studied using the logarithmic diagram of their major oxides. That diagram was found useful to compare the entire major oxide chemistry of samples. It helps to visually evaluate the similarity or dissimilarity of groups of rocks, and will be extensively used throughout this document.

2.3.2 Trace Element and Rare Earth Chemistry

Trace element geochemistry of samples is included in the main geochemical databases (Tables A15 and A1 to A14). In many cases, trace elements and rare earths were used to define geochemical signatures in groups of rocks. Those signatures helped to search for samples with similar chemistry within the database. Logarithmic plots of trace elements and rare earths proved to be very useful in visual comparison of rock suites.

Normalized logarithmic geochemical plots or “spider-diagrams” were not found practical to compare the vast range of rock types and large number of samples from the Greater Lufilian Arc. The wide variety of elements used and normalizing standards selected for plots in numerous publications, made it extremely difficult to use a standardized procedure.

Normalized logarithmic trace element plots were certainly used in the evaluation of several domains and sub-domains. Nevertheless, results obtained from those analyses were meaningless. Now that the geographical, geochemical and geochronological aspects of the domains and sub-domains have been identified, more detailed evaluation of the geochemical database compiled can be done. That escapes the scope of this project.

Trace element and rare earth data have proved to be key in the definition of environment of emplacement. They will be used in a new project to compare samples from the Greater Lufilian Arc with a database of almost 4000 geochemical analysis from granitoids in well-identified geotectonic environments. Neural web geostatistical analysis and specially designed software will be applied, as described under Novel Approach section below.

2.3.3 Presentation of Chemical Data

Chemical analyses were compiled into a main database that is listed on Table A15 in the Appendix. The database was then broken into main sampling domains, and a few domains were further subdivided, as shown on Tables A1 to A14. The entire range of chemical analyses is included in the list of Tables A1 to A15. Geochemical tables in the main text of the document have been reduced and simplified.

2.3.4 Geochemical Threshold Values

To assist in visual evaluation of the geochemical data, threshold or notch values were defined for each of the elements. Threshold values were based on information from the entire database, and in general terms epresent the upper ten percent of the data. Elements that were only analysed in a small group of samples do not have a defined threshold. The values chosen were arbitrary, and were used for interpretation purposes only. Two notch values were used for silica: a lower limit of 50% and an upper limit of 76%. All values above the notches were highlighted in yellow on the geochemical tables. That type of labeling helped to rapidly identify patterns and geochemical signatures in the database.

The first line of most geochemical tables includes the notch values for easy reference. Table 2.2 lists the notch values used. Any values highlighted were considered anomalous. They are considered to be higher than average or relatively enriched. For example, any sample with a loss on ignition over 2% was considered anomalous. Likewise, samples with barium cotent over 1300 ppm or thorium above 37 ppm.

Table 2.2 Threshold or notch values used in the Greater Lufilian Arc granitoid project for various elements and oxides

Sample	Notch
SiO2	50.00
TiO2	1.00
Al2O3	15.50
Fe2O3	6.00
MnO	0.15
MgO	2.00
CaO	5.00
Na2O	4.90
K2O	5.50
P2O5	0.30
LOI	2.00

Sample	Notch
Rb	200
Sr	400
Y	60
Zr	360
Nb	40
Co	30
Ni	16
Cu	25
Zn	85
Ga	26
V	100
Cr	100

Sample	Notch
Ba	1300
U	20
Th	37
Sc	20
Pb	20
Sm	50
Nd	50
Pr	15
Ce	175
La	95
Cs	3
Hf	10

Sample	Notch
Ta	120
As	100
Eu	4
Gd	30
Tb	5
Dy	20
Ho	3
Er	9
Tm	35.5
Yb	7.5
Lu	1.6

2.4 TECTONIC DISCRIMINATION OF SAMPLES

By far, the most difficult task of the Lufilian Arc granitoid project was to define the environment of emplacement of the various rock samples. Established methods for that purpose failed to produce meaningful results for the majority of the samples collected. A completely different approach to the problem was finally tried and it produced significant results. The next two sections describe the procedures followed to study the environment of emplacement in granitoids and mafic rocks.

2.4.1 Granitoids

2.4.1.1 Comprehensive Method of Barbarin, 1999

After reviewing more than twelve different classification schemes to define the environment of emplacement for granitoid rocks, the procedure devised by Barbarin, 1990 and Barbarin, 1999 was found to be the most comprehensive and universal method of evaluation. Tables 2.3, 2.4 and 2.5 show the basic environments and the main parameters of the granitoids produced by each.

Table 2.3 Synthetic table showing the relationships between main granitic petrogenetic types, their origins, and the geodynamic environment. (After Barbarin, 1999)

<table>
<tr><th colspan="2">GRANITOID TYPES</th><th>ORIGIN</th><th>GEODYNAMIC ENVIRONMENT</th></tr>
<tr><td>Muscovite-bearing Peraluminous Granitoids</td><td>MPG</td><td rowspan="2">CRUSTAL ORIGIN
Peraluminous Granitoids</td><td rowspan="2">CONTINENTAL COLLISION</td></tr>
<tr><td>Cordierite-bearing Peraluminous Granitoids</td><td>CPG</td></tr>
<tr><td>K-rich Calc-alkaline Granitoids
(High K - Low Ca)</td><td>LCG</td><td rowspan="2">MIXED ORIGIN
(Crust + Mantle)
Metaluminous and Calc-Alkaline Granitoids</td><td>TRANSITIONAL REGIMES</td></tr>
<tr><td>Amphioble-bearing Calc-alkaline Granitoids
(Low K - High Ca)</td><td>ACG</td><td rowspan="2">SUBDUCTION</td></tr>
<tr><td>Arc Tholeiitic Granitoids</td><td>ATG</td><td rowspan="3">MANTLE ORIGIN

Tholeiitic, Alkaline and Peralkaline Granitoids</td></tr>
<tr><td>Mid-Ocean Ridge Tholeiitic Granitoids</td><td>RTG</td><td rowspan="2">OCEANIC SPREADING OR CONTINENTAL DOMING AND RIFTING</td></tr>
<tr><td>Peralkaline and Alkaline Granitoids</td><td>PAG</td></tr>
</table>

Four main methods to determine environment of emplacement were followed: the major oxide system of Maniar & Piccoli, 1989; the definition of anorogenic granitoids by Whalen, Currie, & Chappell, 1987; the trace element method of Pearce, 1996 and Pearce, Harris, & Tindle, 1984; and the discrimination of granitoids from collisional environments, Method of Harris, Pearce, & Tindle, 1986. The methods and main results will be briefly discussed in the next paragraphs. Various other methods were tried, but did not produce practical results (among them, Sylvester, 1989 and Batchelor & Bowden, 1985).

Barbarin's method was used to solve incoherences from results of other methods. Nevertheless, many samples from the collection produce incongruent results. It is expected that application of the various physical, chemical and mineralogical parameters presented by Barbarin will in time provide more precise environments of emplacement for the granitoids collected in the Lufilian Arc.

2.4.1.2 Major Oxide Method of Maniar & Piccoli, 1989

Maniar & Piccoli, 1989 developed a simple and straightforward procedure to classify the environment of emplacement of granitoid rocks based on major oxide chemical analysis. This enabled most of the rock samples from the Lufilian Arc to be evaluated. After careful processing of all samples that fit the classification scheme, results were color-coded and are listed on Table A51.

Table 2.4 Principal mineralogical, petrographical and chemical features of the main types of granitoids.

(After Barbarin, 1999) [M.E.=microgranular enclaves. O= absent; X=rare or low; XX=common or medium; XXX=abundant or high.]

MINERALS	**MPG**	**CPG**	**KCG**	**ACG**	**RTG**	**PAG**
Biotite	X	XXX	XXX	XX	X	XX
Muscovite	XXX	X	X	O	O	X
Cordierite	O	XX	O	O	O	O
Sill.-And.	O	X	O	O	O	O
Amphibole	O	O	X	XXX	XXX	Alk.amph.
Pyroxene	O	O	O	XX	XXX	Alk.pyr.
Apatite	XXX	XXX	XX	XX	XX	XX
Zircon	X	XX	XXX	XXX	XXX	XXX
Monazite	X	X	O	O	O	O
Garnet	XX	X	O	O	O	X
Tourmaline	XXX	XX	O	O	O	O
Allanite	O	X	XX	XX	X	XX
Titanite	O	O	XX	XXX	X	X
Ilmenite	X	X	X	X	X	XX
Magnetite	O	O	X	XX	XX	XX
Plag An%	0-20	15-40	15-30	20-50	20-50	0-10
PETROGRAPHY						
Petrographic Types	Leucogranites (granites)	(Leucogranites) Granites Granodiorites (Qz diorites)	(Leucogranites) Granites Granodiorites Qz diorites	(Granites) Granodiorites Tonalites Gabbros	Plagiogranites Trondjemites Tonalites Gabbros	Alk. Granites Alk. Syenites Syenites Granites (Gabbros) (Anorthosites)
Associated Rocks						
Metamorphic	O	Migmatites Anatexites	O	O	O	O
Volcanic	O	O	Acid lavas ("Tuffs")	Andesites & dacites	Olivine-bearing Tholeiites	Alkaline lavas
Mafic	O	Qz diorites (Vaugnerites)	Qz diorites Gabbros (Appinites)	Gabbros (in large amounts)	Gabbros (in large amounts)	Gabbros (in large amounts)
Enclaves						
Xenoliths	X	O-X	X	X	X	X
Restites	X	XXX	X	O	O	O
Felsic M.E.	X	O-X	X	X	X	X
Mafic M.E.	O	X	XX	XXX	XXX	X
Differentiation Processes	fractional crystallization	fractional crystallization or restite unmixing	Fractional crystallization and magma mixing	strong fractional crystallization and magma mixing	extreme fractional crystallization	extreme fractional crystallization and subsolidus interactions
CHEMISTRY						
Alumina Index	A≥CNK		CNK>A>NK			A≤NK
A/KCN (molar)	≥1		<1			alkaline
Al2O3	XXX	XXX	XX	XX	XX	X
CaO	X	X	XX	XXX	XX	X
Na2O	XX	XX	XX	XX	XXX	XXX
K2O	XX	XXX	XXX	XX	X	XXX
FeOt+MgO+MnO	X	XX	XX	XXX	XX	XX
Fe3+/(FeOt + MgO)	X	X	XX	XXX	XXX	XX
87Sr/86Sr	0.706 to 0.760	>0.708	0.706 to 0.712	0.706 to 0.708	≤0.704	0.704 to 0.712
End	-4 to -17	-6 to -9	-4 to –9		-	-
delta 18O permil	+10 to +14	+10 to +13	+5 to +10		-	-
delta 34 S permil	-12 to +2		+5 to +20		-	-

2.4.1.3 Definition of Anorogenic Granitoids, Method of Whalen et al, 1987

Whalen et al., 1987 devised a series of geochemical diagrams to discriminate samples that formed in anorogenic environments. The diagrams use Ga/Al, various major element ratios and Y, Ce, Nb and Zr. Many of the diagrams use the most commonly analysed elements, and that allowed a large number of the samples to be processed in numerous diagrams. A bit of interpretation from results was required. A single “anorogenic” signature was not accepted, but only repetitive results from the various diagrams. Similarly, single “non-anorogenic” results were not considered valid. Table A52 lists results of the various plots; the last column of the table indicates interpreted results coming from more than one of the plots.

Table 2.5 Review of the main methodologies to study the tectonic environment of emplacement for granitoid rocks (after Barbarin, 1999)

PARAMETERS	AUTHORS	ORIGIN											
		CRUSTAL		MIXED				MANTLE					
FIRST CHEMICAL NOMENCLATURES	SHAND (1927 & 1943)	PERALUMINOUS rocks		METALUMINOUS rocks						PERALKALINE rocks			
	LACROIX (1933)	Roches CALCO-ALC. HYPERALUMINEUSES		Roches CALCO-ALCALINES						Roches ALCALINES			
PETROGRAPHY	CAPDEVILLA & FLOOR (1970) CAPDEVILLA ET AL (1973)	Granites MESOCRUSTAUX		Granites MIXTES		Granites BASICRUSTAUX							
	ORSINI (1976 & 1979)			A.M. SUB-ALC. ALUMINEAUX		A.M. SUB-ALC. HYPOALUM.	A.M. CALCO-ALC.						
	YANG CHAOQUN (1982)	MM-TYPE		CR-TYPE		MS-TYPE						MD-TYPE	
	TISCHENDORF & PALCHEN (1985)	**Si**	**Ss**	**Si**		**Ikk**	**Iok**	**Imt**				**Ima**	
ENCLAVES	DIDIER & LAMEYRE (1969) DIDIER ET AL.(1982)	C-TYPE (Crustal) ("Leucogranites")		M-TYPE (Mixed or Mantle) ("Monzogranites & Granodiorites")									
MINERALOGY	LAMEYRE (1980) LAMEYRE & BOWEN (1982)	"LEUCOGRANITES" (Crustal fusion)		CALC-ALKALINE Series (High K, Medium K or Low K)				THOLEIITIC Series				(PER) ALKALINE Series	
MAFIC MINERALS	ROSSI& CHEVREMONT (1987)	A.M. ALUMINOPOTASSIQUE (s.s. oucomposites)				A.M. MONZONITIQUE		A.M. CALCOALCALINE	A.M. THOLEITIQUE			A.M. (PER) ALCALINE	
BIOTITE COMPOSITION	NACHIT et al. (1985)	Lignees ALUMINO-POTASSIQUES				Lignees CALCOALCALINES et SUBALCALINES						Lignees ALCALINES et	
ZIRCON MORPHOLOGY	PUPIN (1980 & 1985)	TYPE 1	TYPE 2	TYPE 3		TYPE 4 AND 5		TYPE 7				TYPE 6	
OPAQUE OXIDES	ISHIHARA (1977) CZAMANSKE et al. (1981)	**ILMENITE- Series**					**MAGNETITE - Series**						
GEOCHEMISTRY (Major Elements)	CHAPPELL & WHITE (1974 &1983) COLLINS et al. (1982), WHALEN et al. (1987)		**S-TYPE**			**(I - TYPE)***		**M - TYPE**				**(A - TYPE)**	
	LA ROCHE (1986) LA ROCHE et al. (1980)	**AK-L M.A.**	**AK-G M.A.**			**SA M.A.**	**CA M.A.**	**TH M.A.**				**A-PA M.A.**	
	DEBON & LE FORT (1983 & 1988)	ALUMINOUS M.A.		ALUMINO-CAFEMIC and CAFEMIC M.A. (Subalkaline, calc-alkaline, tholeiitic, and (per)alkaline)									
	MANIAR & PICCOLI (1989)	CCG				POG	CAG	IAG	OP	RRG	CEUG		
GEOCHEMISTRY (Trace Elements)	TAUSON & KOZLOV (1973)	PLUMASITIC LEUCOGR.	ULTRA-MM GRANITES	PALINGENIC GRANIES (Normal and Subalkalines)				PLAGIO-GRANITES				AGPAITIC LEUCOGRANITES	
	PEARCE et al. (1984)	**COLG** - Collision Granites (Syntectonic) (Post-tectonic)					**VAG** Volcanic Arc Granites		**ORG**			**WPG** Within Plate Granites	
ASSOCIATED MINERALIZATION	XU KEQUIN et al. (1982)	TRANSFORMATION -TYPE (Contiental crust)		SYNTEXIS - TYPE (Transitional crust)				MANTLE-DERIVED - TYPE					
TECTONIC ENVIRONMENT	PITCHER (1983 & 1987)	HERCYNOTYPE		CALEDONIAN - TYPE			ANDINO TYPE	W.PACIFIC TYPE				NIGERIA - TYPE	
SUGG. SYNTHETIC CLASSIFICATION		**MPG**	**CPG**			**KCG**	**ACG**	**ATG**	**RTG**			**PAG**	

2.4.1.4 Trace Element Method of Pearce et al, 1984

The experience using tectonic discrimination diagrams devised by Pearce, 1996 and Pearce et al., 1984 for granitoid rocks of the Greater Lufilian Arc was unsatisfactory. “Anorogenic” results from the Whalen et al., 1987 plots were not validated by the procedures of Pearce et al., 1984. In most cases, samples could be plotted on two different diagrams (Nb vs Y and Rb vs Y+Nb), but results were not coherent. When more than two diagrams were used, coherent results seldom came out. In fact, many times the so-called Pearce plots contradict themselves.

Table A53 in the Appendix lists the results of all four diagrams. Coherent results are marked in the last column and a blank space was left when no conclusive results that could be used were obtained from the plots. When two or three of the four diagrams produced a similar environment of emplacement, that was indicated by a code like W2/4, W3/4 or O3/4.

Once all the information was processed, and since most of the results were not completely compatible, the database was sorted to extract as much information from it as possible. Similar results were grouped in order to establish “Pearce-plot rock families”. After testing the method in several sites, no significant results were achieved. The meaning of the “rock families” was not validated by other field observations. A similar procedure was tried by grouping similar results from the (Whalen et al., 1987) plots. Results were sorted and grouped into “Whalen-plot rock families”. These were not significant either.

A very thorough review of the Rb vs (Y+Nb) discrimination diagram of Pearce et al, 1984 was published by Forster, Tischendorf, & Trumbull, 1997. It shows that many granitoids defy the classification schemes devised by Pearce et al., 1984. Geodynamic environment of formation of many granitoid types does not fit well. In fact, incorrect environments are interpreted in many cases. Many ambiguities and mis-classifications arise when the sample suites come from complex polyphyase orogeny that mixes source rocks from different tectonic provenance. Continental arcs and collisional settings that can be closely associated in space and time with extensional regimes are especially prone to misinterpretation using the Pearce et al., 1984 diagrams. In addition to that, differentiation can produce compositional trends that cross field boundaries, especially the “Volcanic Arc Grantiod” and “Within-Plate Granitoid” field boundary.

2.4.1.5 Discrimination of Granitoids from Collisional Environments, Method of Harris et al, 1986

Harris et al., 1986 developed a systematic procedure to evaluate the granitoids from collisional environments. Such environments of emplacement could not be identified using the discrimination procedures of Pearce et al., 1984 and Pearce, 1996. A problem of the Harris’ methodology is that it requires tantalum and halfnium, two elements not commonly analysed for all samples. Basic data and results from the three main plots are listed on Table A54 in the Appendix. No true collisional granitoids were positively identified. Nevertheless, several within-plate and volcanic-arc granitoids were identified.

2.4.1.6 Discussion

Table A50 in the Appendix compiles results from six different methods used to evaluate the environment of emplacement of the various rocks. Coherent results from colums 2, 3 and 4 were marked in red. Incoherent results were marked in light yellow. Additional color coding is indicated at the end of the table. The overall interpretation of results from tectonic environment of emplacement for the granitoids of the Lufilian Arc Granitoid Project was not conclusive for a large proportion of the samples.

Most of the methods to evaluate tectonic environment of emplacement for granitoids were developed for large batches of samples from the same location. Samples from the Greater Lufilian Arc come from many different sites. Few specimens of similar rocks were collected and analyzed at each site, and in most cases only a single one. That makes interpretation of tectonic discrimination diagrams more difficult. For all the procedures of tectonic discrimination, samples were initially treated as single entities and not in cluster form.

2.4.1.7 A Novel Approach

Forster et al, 1997 compiled a substantial database of published geochemical information from suites of granitoids from all over the world that have reasonably well established environments of formation. The database includes some major oxides, trace elements and rare earths. At the time of writing, the author is collaborating with Juan Pablo Lacassie, from the University of Johannesburg, to use Forster’s updated database with neural web geostatistical analysis and specially designed software to compare the chemistry of problematic samples from the present Greater Lufilian Arc study. Lacassie has been using the methods for sedimentary provenance analysis (Lacassie, Roser, Ruiz del Solar, & Herve, 2004). Preliminary results of this approach to evaluate samples from

the Greater Lufilian Arc have been very encouraging, but will not be included in this document. That approach demands a lot of computer processing power, but has proved to be the best way to evaluate the environment of emplacement for granitoid igneous rocks.

A complete re-evaluation of the environment for each of the granitoids analysed will be carried out and presented in a publication after the Ph.D. thesis.

2.4.2 Mafic Rocks

As indicated in previous chapters, many of the sampling sites had only gabbroic rock outcrops, and in most locations mafic and felsic intrusive rocks were intimately associated. Although very few of the mafic rocks collected for the Lufilian Arc Granitoid Project were basalts, they were all analysed following methods devised to discriminate tectonic environment of emplacement for mafic volcanic rocks. Precisely the same approach was made by Kampunzu, Tembo, Matheis, Kapenda, & Huntsman-Mapila, 2000 and Tembo, 1995 to study Katangan mafic igneous rocks of the Democratic Republic of Congo and Zambia. In general terms, the following procedure was followed:

All mafic and ultramafic rocks from the suite of samples collected during fieldwork in the Greater Lufilian Arc were separated based on their major oxide chemistry. Carbonatitic rocks were taken out of the group before further studies. Mafic samples were selected based on the R1-R2 and modified TAS diagrams. Later the systematics of Winchester & Floyd, 1977 was applied to name the various rocks. Most of the samples were certainly not basalts. Some of them turned out to be ultramafic and lamprophyric; but that was discovered later in the process.

Once that was done, discrimination diagrams to evaluate environment of emplacement of mafic volcanic rocks devised by Meschede, 1986; Pearce & Cann, 1973; Wood, 1980; and Shervais, 1982 were used. Each of the procedures was completed independently from the others, in order to compare results. Interpretations from all results are listed on Table A53 in the Appendix. No single sample plots the same on all four of the tectonic discrimination diagrams devised by (Pearce & Cann, 1973).

According to Pearce & Cann, 1973 only rocks with CaO+MgO values between 12 and 20 should be evaluated in their classification. The procedures that follow include a wider range of rocks. On Table A56, samples that fall out of that range were highlighted in pink; these are 33, and account for 37.1% of the samples identified as “mafic rocks”. The process of tectonic discrimination was nevertheless followed for all of the samples, and results are presented on Table A56 in the Appendix. They are also included on tables in each of the chapters from the domains.

2.4.3 Conventions to Tabulate Rock Type and Methods to Evaluate Environment of Emplacement for Samples Studied

All chapters that describe rock domains in this document contain review tables such as that of Table 2.5. Complete tables are included in Appendix G. The first column contains the sample number. The second, the rock name as respectively indicated by the TAS diagrams of Middlemost and the IUGS for plutonic or volcanic rocks. The third column shows the rock type classification of Debon & LeFort. Table 2.6 lists acronyms used to shorten the detailed rock names, after using the various diagrams defined by Debon & LeFort, 1983.

Table 2.5 Review of sample main characteristics and potential environment of emplacement obtained by traditional methods

1	2	3	4	5	6	7	8	9	10
			Methods to Evaluate Environment of Emplacement						
Sample	Rock Name	Debon & LeFort Rock Type Classification	Maniar & Piccoli	Whalen	Pierce	Mafic	Rb/10HfTa	Rb/30HfTa	Nb-Ta
L-012A	quartzmonzonite	metaiv mesoKMg	IAG+CAG	A	O-W1-1				
L-079	Granite	metaiv mesoNaKFe			O-W1-1				
L-353	quartzmonzonite	metav mesoNaKFe		A	W				
L-354	Granodiorite	peraiii mesoNaKFe		A	W				

Table 2.6 Acronyms used to shorten rock names (after the use of Debon & LeFort, 1983)

Convention	Meaning	Debon-LeFort Diagram
pera	peraluminous field	
meta	metaluminous field	
i,ii,iii	locations in the peraluminous field	
iv,v,vi	locations in the metaluminous field	A-B Diagram (Fig 2.5)
leuco	leucocratic field	
subleuco	subleucocratic field	
meso	mesocratic field	
Na	sodic field	
Na-K	sodic-potassic field	
P	Potassic	K*-B Diagram (Fig 2.7)
Mg	Magnesian	
Fe	Ferriferous	Mg*-B Diagram (Fig 2.8)

Columns 4 to 10 of Table 2.5 present the environments of emplacement identified for each rock sample, according to seven different methods described in the previous pages. The fourth column shows results of the major oxide method devised by Maniar & Piccoli, 1989. Table 2.7 lists the acronyms used for environment of emplacement terms deduced after using the various diagrams defined by Maniar & Piccoli, 1989.

Table 2.7 Acronyms for environment of emplacement term, diagrams of Maniar & Piccoli, 1989

Acronym	Meaning
POG	Post-Orogenic Granitoid
IAG+CAG	Island Arc Granitoid + Continental Arc Granitoid
CEUG	Continental Epeirogenic Uplift Granitoid
RRG	Rift-Related Granitoid
OP	Oceanic Plagiogranite
CCG	Continental Collision Granitoid
CCG-IAG-CAG	Imposible to define between these three types
CEUG-RRG	CEUG near the margin with RRG
RRG-CEUG	RRG near the margin with CEUG

The fifth column presents results of the method to identify anorogenic granitoids by Whalen et al, 1987.

Column 6 of Table 2.5 presents results of the Pearce et al, 1984 trace element method to identify environment of emplacement for granitoids.

Column 7 presents results of the various methods to discriminate the tectonic environment of emplacement for the mafic rocks (Meschede, 1986; Pearce & Cann, 1973; Wood, 1980; and Shervais, 1982). Table 2.8 lists the acronyms used for the environment of emplacement of mafic rocks.

Table 2.8 Acronyms for environment of emplacement terms of mafic rocks

Acronym	Meaning
Mor	Mid-Ocean Ridge Basalt
Emor	E-Type Mid-Ocean Ridge Basalt
Wpab	Within-Plate Alkaline Basalt
Vab	Volcanic Arc Basalt
Wpt	Within-Plate Tholeiite
?	Unknown Environment
-	Or
+	And

Columns 8 to 10 show results of the procedure defined by Harris et al, 1986 for granitoids from collisional environments. Table 2.9 lists acronyms used by the authors for the environment of emplacement of such granitoids.

Table 2.9 Acronyms for environment of emplacement terms, diagrams of Harris et al, 1986

Acronym	Meaning
WP	Within-Plate Granitoids
VA	Volkanic Arc Granitoids
II	Type II Collisional Granitoids
VA-	Plots in Volcanic Arc Field but might be Collisional Granitoid
WP-	Plots in Within-Plate Field but might be Collisional Granitoid
OF	Oceanic Floor Granitoid

3 GENERALIZED GEOLOGY OF THE LUFILIAN ARC

The Greater Lufilian Arc is one of many Pan African orogenic belts. These mobile belts are an important component of the African geology and developed extensively throughout the continent. They formed during a series of orogenic cycles over a period of 500 million years (approximately 950 to 450 Ma), to produce the African sector of the Gondwana supercontinent (Fig 1.1). Diverse orogenic styles in the belts range from major continental collision (Mozambique Belt) through the closure of small oceanic tracts (Damara Belt) to major accretionary belts of island arcs and microcontinents (Nubian Shield) (Foster et al., 2001). Orogenic evolution was very diverse through space and time during Pan African times. That makes correlation of stratigraphic sequences, intrusive, metamorphic and tectonic events between the different terranes complex and, in some cases, irrelevant (Foster et al., 2001).

The Lufilian Arc of southern Africa is composed by a Meso- to Neo-Proterozoic rift basin that ceased to exist after closure of the basin during the Pan-African orogeny at approximately 500 Ma (Kampunzu & Cailteaux, 1999). It is made by the extension of the Pan African Katanga fold belt westward into the Damara fold belt (Figs 1.1 and 3.1). Superficial cover of Mesozoic rocks conformed by Karoo deposits and Kalahari sand masks the central portion in NE Namibia, Botswana, Angola and SW Zambia (Fig 1.1). A geological reconstruction map of Gondwana terrains is shown on Fig 3.1. Note the Lufilian Arc emplaced between the Congo Craton and the Kapvaal Craton in the southwestern part of Africa. As shown, similar belts border cratons throughout most of Africa, in parts of eastern South America and India. Note the location of the Carajás province in Brazil, where major IOCG deposits are known to exist (Table 8.1).

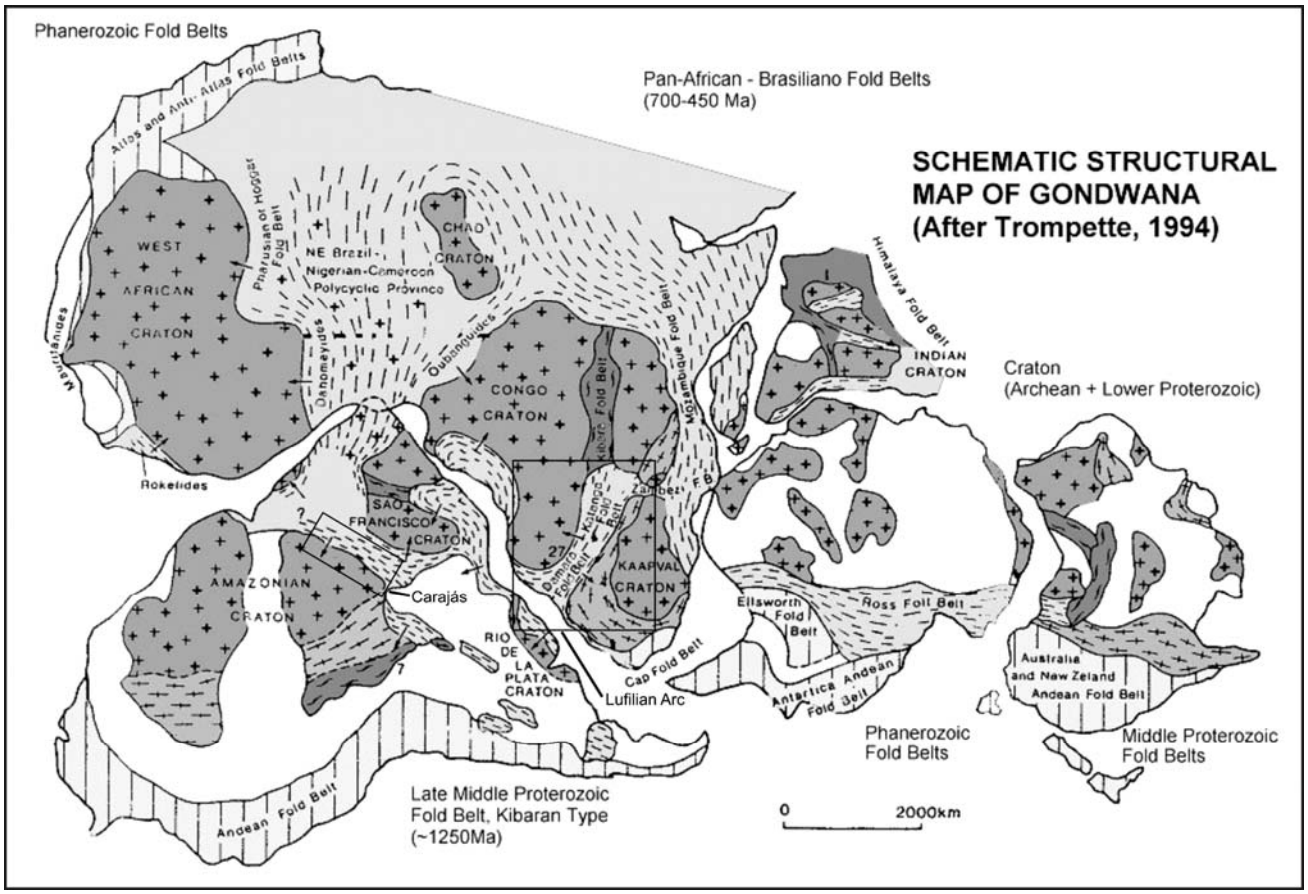

Fig 3.1 Schematic structural map of Gondwana. *This map shows location of the Greater Lufilian Arc roughly in the middle, indicated with a rectangle. It is made by the extension of the Katanga fold belt into the Damara fold belt, and lies between the Congo and Kaapval cratons. Like other Pan-African fold belts, the Greater Lufilian Arc was formed during the amalgamation of continental terranes to conform Gondwana. The prolific mineral province of Carajás in Brazil, off the eastern border of the Guaporé Craton, is indicated by a smaller rectangle. Note similarities among both locations. They lie in between Archean cratons and were formed during collisions. Also note the extense portions of Africa and South America that have similar tectonic features. IOCG mineralization is prospective in most of that area. Figure slightly modified from Trompette, 1994.*

The Damara sequence of rocks (Namibia) and the Katangan sedimentary sequence (Democratic Republic of Congo and Zambia) were deposited during the opening of an ocean (Miller, 1983; Martin & Eder, 1983; Hoffmann, 1990; and Porada, 1989). Katangan rocks host the Copperbelt world-class copper and Co deposits (Mendelsohn, 1961; Unrug, 1988; Kampunzu & Cailteaux, 1999; Miller, 1994; Sweeney & Binda, 1994; and Singer, 1995).

Rocks of the Damara Orogen cover half of northern Namibia. They are made by a thin N-S coastal branch and a thick NE-trending branch. The second one has been divided into a number of contrasting tectonostratigraphic zones (Miller, 1983a; Miller, 1994; Miller, 2002). “The structure and tectonothermal history of the northeast arm of the orogen have been explained in terms of a plate-tectonic model based on the presence of paired metamorphic belts; extensive calc-alkali granite intrusions; an assymetric structure; an intensely thrusted southern margin; and basic and ultrabasic igneous rocks occurring in association with a high-pressure, schistose flycsh.” (Foster et al, 2001, p. B-16).

The Lufilian Arc *sensu stricto* (basically the Pan-African Katangan belt in Zambia and the D.R. Congo) has been intensively studied since the beginning of the twentieth century when mining in the Central African Copperbelt began. The Katangan Supergroup basically consists of a series of basal continental and shallow marine siliciclastics and carbonates; these are overlain by marine shales, dolomites and sandstones; in turn they are overlain by black shales and carbonates. Abundant volcanic material is intercalated with most of the units.

Crustal attenuation and rifting of the MesoProterozoic Rodinia Supercontinent lead to continental break-up and to the formation of an ocean basin. Pre-rift midalkaline granitoid magmatism, syn-rift continental sedimentation, rift-related bimodal tholeiitic volcanism, and granite emplacement took place during 890 to 850 Ma. The early rift basins were filled by continental clastics; later by shallow marine clastics and platform carbonates; and tholeiitic basalts within a succession of oceanic siliciclastics and carbonate rocks. Thick diamictites with interbeds of banded iron formation and impure sandstones were intercalated by rift-related oceanic volcanic rocks.

A short-lived subduction of part of the oceanic basin began by 640 Ma (Tembo & Porada, 2002) before the closure of the Katanga-Damara basin. It was followed by continental collision around 550 Ma, widespread, NE-trending thrusting, emplacement of anorogenic granitoids, and continental-scale shearing.

The considerable thrusting and shearing that took place during continental collision makes stratigraphic correlation of the Katanga Supergroup difficult. The importance of halokinesis in the evolution of the region is very significant and is just beginning to be understood. Significant revisions to the stratigraphy are being made (Cailteaux, 1995; Master et al, 2003).

Midalkaline magmatism took place during the rifting phase. Bimodal midalkaline magmatism and vulcanism occurred during the opening of the Katanga-Damara basin. Widespread midalkaline magmatism occurred after closure of the basin; subalkaline magmatism, during a short-lived subduction-related event; and later anorogenic midalkaline magmatism, during epeirogenic uplift and post orogenic collapse that took place after closure of the basin. Igneous massifs like the Lusaka pluton, Hook Granite Batholith, Kamanjab Batholith, Khorixas Inlier and Otjiwarongo Batholith are examples of granitoid bodies formed by those processes (Figs 4.1 and 4.2). Rocks in the massifs have a wide petrographic variability; they range from alkali granites through quartmonzonites, granites, syenites, diorites and granodiorites into carbonatites. Some of those granitoids are high-heat producers, with elevated Th, K and/or U content (Phillips, 1958a; Phillips, 1958b and Griffiths, 1978). Abundant small gabbroic intrusions accompanied midalkaline magmatism throughout.

4 DESCRIPTION OF ROCKS FROM THE DIFFERENT DOMAINS

Samples collected for the Greater Lufilian Arc Granitoid Project were grouped for preliminary evaluation into geographical domains with apparently similar geological characteristics. The domains were established as a means to present the information in this Ph.D. thesis. These are listed on Table 4.1. The maps of Figs M1 and M19 (presented in the Appendices Volume) show their general location. A few of the domains sampled will not be described in this document. These are marked by an asterisk on Table 4.1. Samples from those domains were incompletely analysed, or did not contain granitoids. The next chapter will describe main characteristics of rocks from each domain, following the same arbitrary order of Table 4.1.

Table 4.1 Geographical-Geological Domains sampled during the Greater Lufilian Arc Granitoid Project. These domains were established for descriptive purposes. They are geographical entities as shown on Figs M1 and M19. (Domains marked with an asterisk did not contain granitoids, or their samples have not been fully studied at the time of writing this document.)

ZAMBIAN DOMAINS	NAMIBIAN DOMAINS
Hook Granite Batholith	Kamanjab Batholith
West Lusaka-Kafue Flats	Khorixas Inlier
Kalengwa-Kasempa Area	Oas farm
NW Zambia	Lofdal farm
Kalene Hill Area	Mesopotamie farm
Kabompo Dome	Several outcrops south of Khorixas Inlier
Mwombezhi Dome	Ugab River Area
Solwezi Dome	Summas Mountains
Sodalite Nepheline Syenite Quarry	Grootfontein Inlier
Main Zambian Copperbelt Area	Otjiwarongo Environs
Nchanga Mine Area	Okwa River, Botswana
Nchanga Granite	**Other domains sampled but not included in this document**
Muliashi Porphyry	
Deep Borehole, Konkola Mine	*Okatjepuiko, Witvlei
Chambishi Granite	*Gelbingen Farm
Mufulira Granite	*Sesfontein Area
Samba Copper Prospect	*Otavi Mountains
Other domains sampled but not included	*Tshoosha/Kalkfontein, Botswana
*Serenje Area	
*Mkushi Area	
*Bwana Mkubwa Area	

4.1 ZAMBIAN DOMAINS

4.1.1 HOOK GRANITE BATHOLITH, ZAMBIA

4.1.1.1 Introduction

The Hook Granite Batholith is located in western Zambia, as indicated on the map of Fig M1, in the Appendix. Its name is derived from a rectangular turn that the Kafue River makes through the granitic massif. Part of the turn is controlled by a N-S fracture zone on its way south and southeast into the Zambezi River (Fig 4.1). It fulfills the definition of batholith because it is “a type of area, where individual plutons are so numerous as to overlap or intersect one another” (Hall, 187, p. 93).

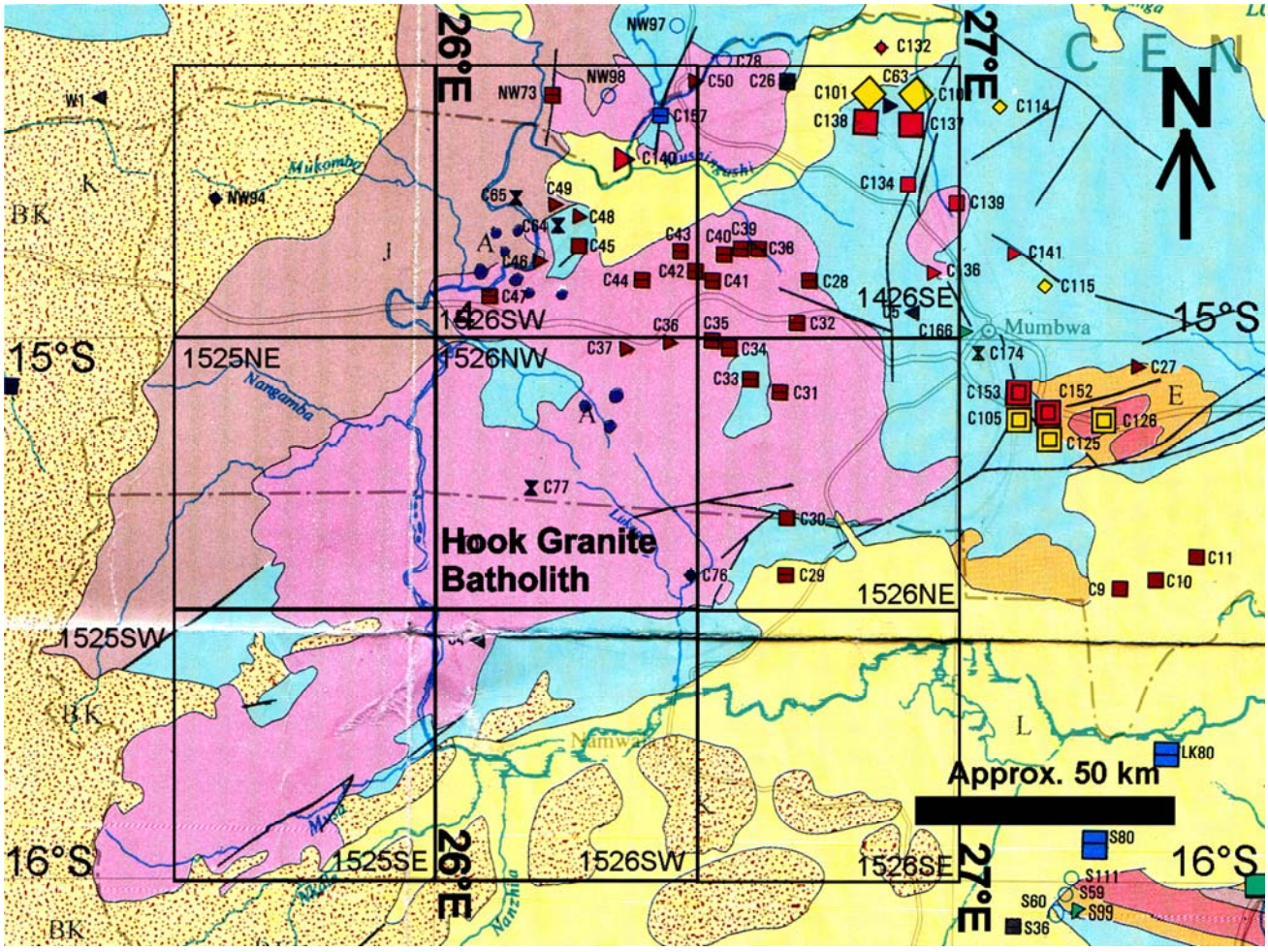

Fig 4.1 General map of the Hook Granite Batholith. *Note the angular turns that the Kafue river does around the batholith. Also note the road that crosses the batholith from east to west from Mumbwa. A sampling transect was done along that road. The roughly triangular shape of the batholith will be discussed on chapter 7. Pink indicates granitoid rocks of the Hook Granite; brown, Mesozoic Karoo rocks; light green, Katangan sediments; orange, meta-sediments; yellow, alluvial and cover; dotted orange, Kalahari sand. The black squares indicate 1:100,000 geological map sheets published by the Zambian Geological Survey. Small dots with symbols indiate various mineral deposits and occurrences. Yellow shapes are gold deposits; red, copper deposits; brown, iron; gray, uranium; purple bowties are kimberlites; blue, evaporites; green, industrial minerals. Specific deposits will not be discussed here. Notice that the SW portion of the batholith, west of the Kafue River, does not have any mineral occurrences. Geology is very similar, but it is less well studied. Taken from 1:2,000,000 geological and mineral occurrence map of Zambia, 1994.*

Surprisingly little is known about this important Zambian batholith. The published 1:100,000 geological maps are less than reconaissance grade, but constitute a formidable amount of work, given the lack of outcrop, access and infrastructure (Phillips, 1958; Simpson, 1962; Cikin, 1971; Cikin, 1972; Page, 1974; Abel, 1976; and Griffiths, 1978). The geological map sheets published by the various authors are shown by large black squares on Fig. 4.1. Reports accompany the maps included in the figure. They deal mainly with petrography of the various mappable units, and contain general descriptions of mineral deposits, hydrothermal alteration

features, structures, and stratigraphic units that cover and were intruded by the batholith. Geological compilation work and geochronology of the batholith was published by Hanson et al, 1993. Attempts to evaluate geochemistry of the Hook Granite have been carried out by Pepper, 2000 and Goagoseb, 2004. In addition to the previously listed documents, reports about mineralization on and around the batholith have been published by Hitzman, 2001; Nisbet, Cooke, Richards, & Williams, 2000; and Nisbet, 2004b. Fig 4.1 shows the main known mineral deposits and occurrences. Structural geology of the intrusive body is not well described or mapped in the publicly-available geological literature. Many of the features observed during field work for this Ph.D. project have never been described in the literature.

This account will first describe the chemistry of samples collected in the batholith; next comes a discussion on problems faced with mapped geological units; that will be followed by evidence of circular complexes in the Hook Granite; and an E-W sampling transect through the batholith; the rest of the chapter will be completed by comments on geochronology, geological history and environment of emplacement of the Hook granitoids.

4.1.1.2 Geochemistry

One-hundred-and-four samples were collected from the main Hook Granite Batholith in an effort to produce a representative spread. Nineteen samples were collected in the field. Forty-four samples were selected from the collection of the Zambian Geological Survey in Lusaka, and located as best as possible according to the author's descriptions and field notes, with help of 1:50,000 and 1:100,000 topographic maps. Major oxide chemical analysis of thirty-three samples X-43 to X-74 were taken directly from Griffiths, 1978, and located according to the author's description and field notes. Finally, eight, reasonably well studied and located samples were recovered (Pepper, 2000).

Most of the samples cluster from 69 to 77% silica. In general terms, geochemistry of the batholith shows the following trends (Fig 4.2): There is a negative correlation of silica with titanium dioxide, alumina, total iron oxide, magnesia, lime and P_2O_5; a positive correlation was observed between silica and potash. Manganese oxide and soda do not correlate. The trends are wide and quite complex, as shown. As will be explained in a later portion of this chapter, each of the trends is made of numerous linear trends that come from different types of granitic rocks from ring complexes, and are unrelated to each other.

Fig 4.3 is a close-up of a modified TAS diagram showing the wide variety of granitoid rocks that occur in the main batholith. Fig 4.4 shows the entire suite of samples on the modified TAS diagram. Fig 4.5 illustrates the same samples on the R1/R2 diagram. The statistics of Table 4.1.1 were obtained from the TAS diagram of samples from the batholith. Only samples that plotted inside the diagram were considered.

Table 4.1.1 Statistics of rock types in the suite of samples from the Hook Granite Batholith
The fifth column (Granitoids) is the sum of underlined rock types.

Group	Rock type	number	%	Granitoids	Groups
Midalkaline Rocks	alkali granite	26	29.21	71.60	71.91
	Quartzmonzonite	20	22.47		
	Syenite	7	7.87		
	Monzonite	5	5.62		
	Monzodiorite	3	3.37		
	Monzogabbro	1	1.12		
	alkali gabbro	2	2.25		
Subalkaline Rocks	Granite	16	17.98	28.40	28.09
	Granodiorite	7	7.87		
	Gabbro-diorite	1	1.12		
	Gabbro	1	1.12		
Total		89	100.00	100.00	100.00

65% of the granitoids fall within the midalkaline field, while 26% of them fall in the subalkaline field. All midalkaline rocks make 72% of the samples, 28% of them are subalkaline. None are alkaline. This is significant, especially when 22.5% of the rocks are quartzmonzonites. The R1/R2 plot for the Hook Granite (Fig 4.5) shows a large range of rock types. Fig 4.6 presents the entire R1/R2 diagram with all the samples that were studied for the batholith.

Many of the samples from X-46 to P-40ii are enriched in K_2O (Table A3). Many of the samples from L-181 to L-345 to L-465 are enriched in Fe_2O_3. Most of the Hook Granite samples have very high contents of Nd, Pr. Ce and La are also high.

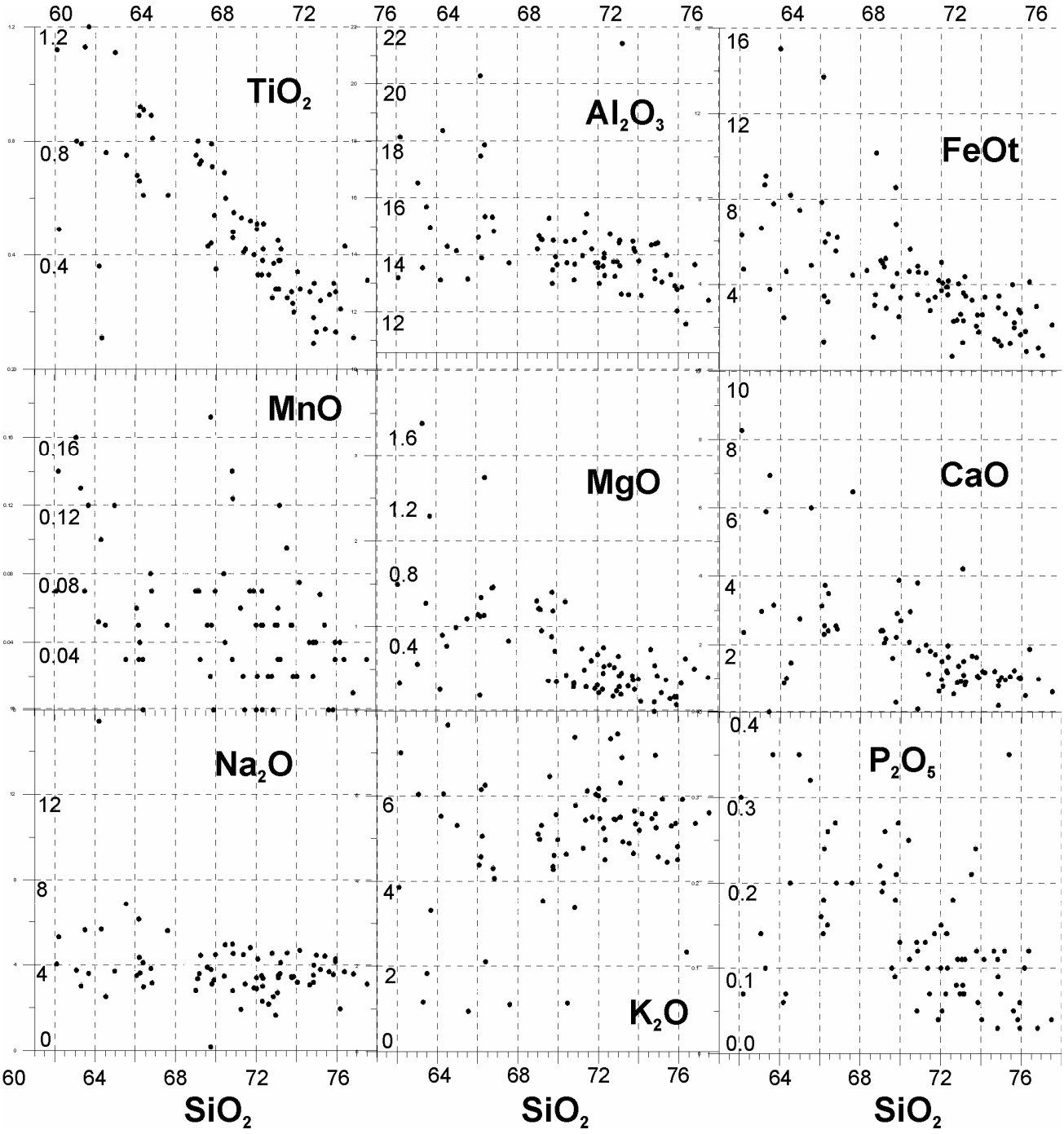

Fig 4.2 Correlation diagrams between silica and the major oxides for samples from the Hook Granite Batholith, Zambia*. All values are in percentage.*

Samples P-57 and P-50 are anomalously enriched in many LREE, Nb and K_2O. P-39 to P-41 have high contents of Rb, Y, Nb, Ga and Co. These are all features of anorogenic granites.

All samples from the Hook Granite were compared with each other using the logarithmic plot of major oxides. Thirteen discrete groups were identified, and they are listed on Table 4.2. 27 samples could not be allocated to any of the groups. Main features of each of the groups is also included on the table. Rock groups that show

similarities with groups of rocks from the Kamanjab Batholith[1] in Namibia are indicated with an asterisk (See Table 4.2). The geochemical diagrams of Figs 4.3 and 4.5 show that the groups behave as independent chemical entities. Logarithmic major oxide plots of the various groups are shown on Figs 4.7 to 4.14.

Part of the samples from the batholith are enriched in copper. Ring complexes[2] with high Cu are underlined of Fig 4.18 (A, E, O, K and P). Chemistry of all the samples is shown on Table A3 in the Appendix.

Table 4.2 Groups of samples from the Hook Granite Batholith, based on major oxide chemistry and logarithmic plots*. *= group that was also in the Kamanjab Batholith. Table 4.5 presents further details on the rock groups. Sub-chapter 4.1.1.3 describes geological units.*

Group	# samples	Characteristics	Rock Type
I*	13	high Fe,Mg,Mn low Si,K	syenite, quartzmonzonite, granodiorite, syenite, tonalite
II*	9	high Mg,P,Mn low Si	gabbroids
III*	6	Order = K,Na,Fe,Ca,Mg,Ti	granite, alkali granite
IV*	6	Order = K,Na,Fe,Ca,Ti,Mg	granite, alkali granite, quartz syenite
VII	9	high K, order = K,Fe,Na,Ca,Mg	granite, granodiorite
VIII			
IX	4	Order = K,Fe,Na,Ca,Ti,Mg	quartz syenite, granite, quartzmonzonite
X	10	Order = K,Fe,Na,Ca,Ti,Mg	granite, quartzmonzonite
XI	8	Order = K,Fe,Ca,Na,Ti,Mg	alkali granite, granite
XII			
XIII			

Another group of samples from the Hook Granite was found to have high Zn values. These are listed on Table 4.3. A few ring complexes[2] contain them. Three of the complexes with high Zn values have gabbroic ring dikes: K, AC and AL. Only a few of the samples from Table 4.3 come from the center of the ring complexes, these are: L-433, L-437.

Table 4.3 High Zn samples from the Hook Granite Batholith, Zambia
For location of ring complexes, see Fig 4.18.

Sample	Ring complex	Rock type (sensu TAS)	Rock type (sensu Dela Roche, 1980)	General rock type	Position within ring dike
L-181	?	Gabbro	Saturated olivine gabbro	Gabbroid	
L-347	K	Gabbro	Gabbro	Gabbroid	Nucleus
L-403	O	Quartzmonzonite	Quartz monzonite	Granitoid	Rim
L-406	O	Gabbro	Alkali gabbro	Gabbroid	Rim
L-410	E	Granodiorite	Granite	Granitoid	Rim
L-433	Q	Monzodiorite	Syeno gabbro	Gabbroid	Nucleus
L-437	P	Monzonite	Syeno diorite	Syenitoid	Nucleus
L-440	AC	Monzogabbro	Gabbro-diorite	Gabbroid	Rim
L-441	K	Quartzmonzonite	Quartz monzonite	Granitoid	Rim
L-444	AQ	Monzodiorite	Gabbro-diorite	Gabbroid	
L-459	?	Diorite	Tonalite	Granitoid	
L-463	AL	Gabbro	Gabbro-diorite	Gabbroid	Rim
L-464	AL	Out of plot, foid	Foid-rich rock	Foid-rich syenitoid	Rim
L-465	AL	Out of plot, foid	Foid-rich rock	Foid-rich syenitoid	Rim

[1] The Kamanjab Batholith of Namibia is discussed in section 4.2.1 of this document.
[2] Relationship of the Hook Granite Batholith with anorogenic ring complexes will be explained in sub-chapters 4.1.1.4 and 4.1.1.5. Fig 4.18 shows the main ring complexes that have been identified in the batholith.

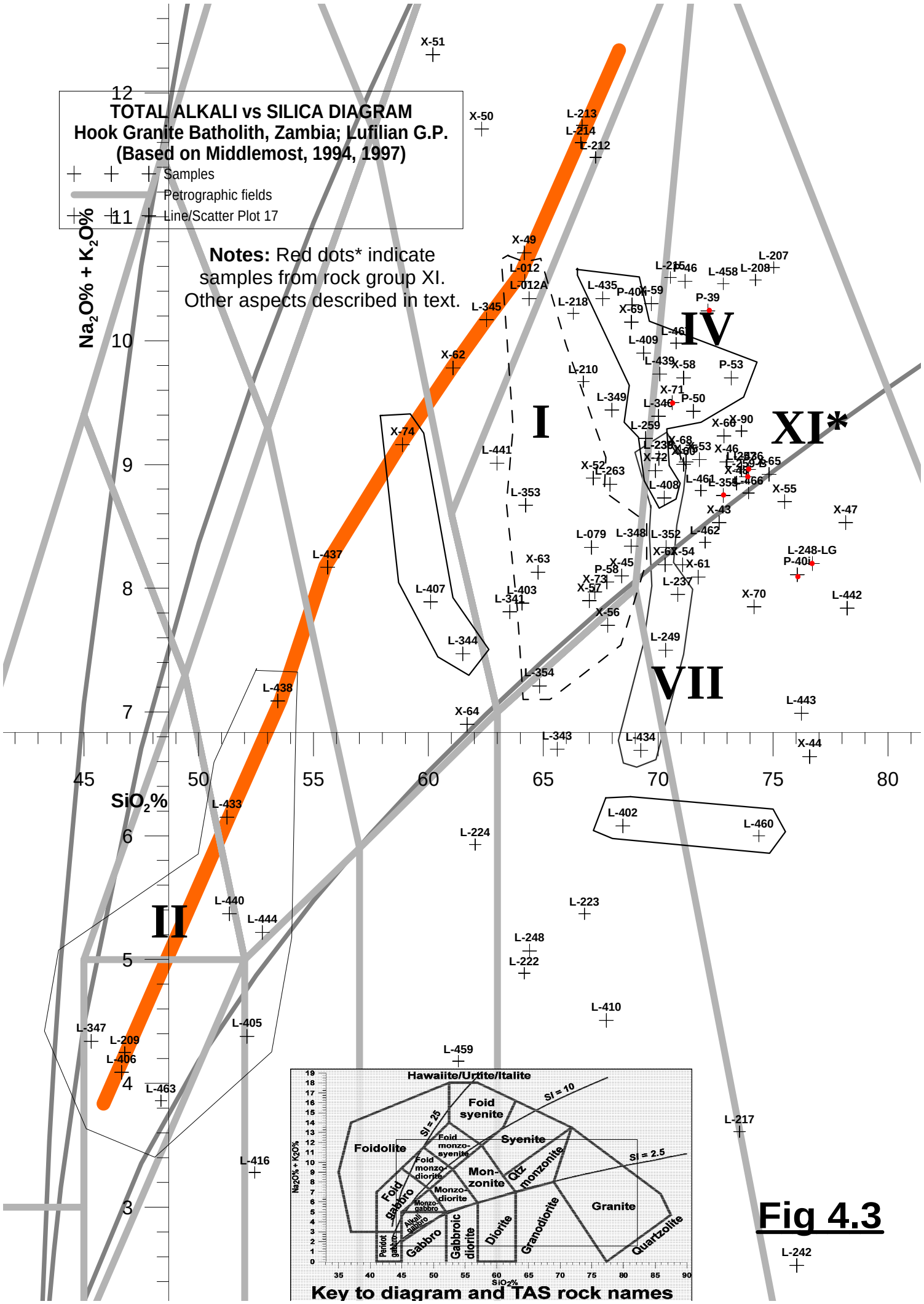
TOTAL ALKALI vs SILICA DIAGRAM
Hook Granite Batholith, Zambia; Lufilian G.P.
(Based on Middlemost, 1994, 1997)
Samples
Petrographic fields
Line/Scatter Plot 17
Notes: Red dots* indicate samples from rock group XI. Other aspects described in text.
Na2O% + K2O%
SiO2%
I
II
IV
VII
XI*
Hawaiite/Urtite/Italite
Foid syenite
Syenite
Foidolite
Foid monzo-syenite
Foid monzo-diorite
Mon-zonite
Qtz monzonite
Monzo-diorite
Foid gabbro
Monzo-gabbro
Alkali gabbro
Peridot gabbro
Gabbro
Gabbroic diorite
Diorite
Granodiorite
Granite
Quartzolite
SI = 10
SI = 25
SI = 2.5
Key to diagram and TAS rock names

Fig 4.3

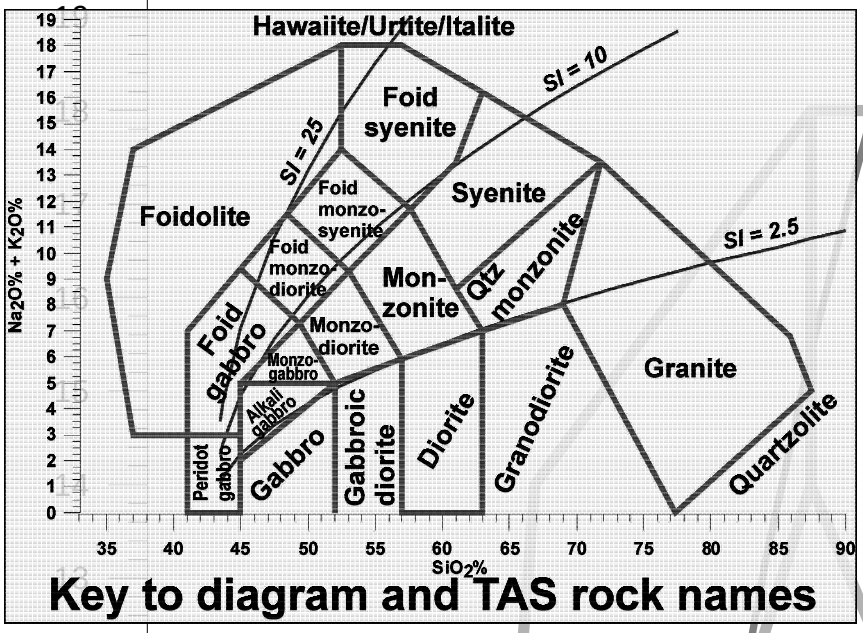

Key to diagram and TAS rock names

Note: The central cluster of samples on the granite and quartzmonzonite fields is better shown on Fig 4.3.

TOTAL ALKALI vs SILICA DIAGRAM
Hook Granite Batholith, Zambia; Lufilian G.P.
(Based on Middlemost, 1994, 1997)

Samples

Petrographic fields

Fig 4.4

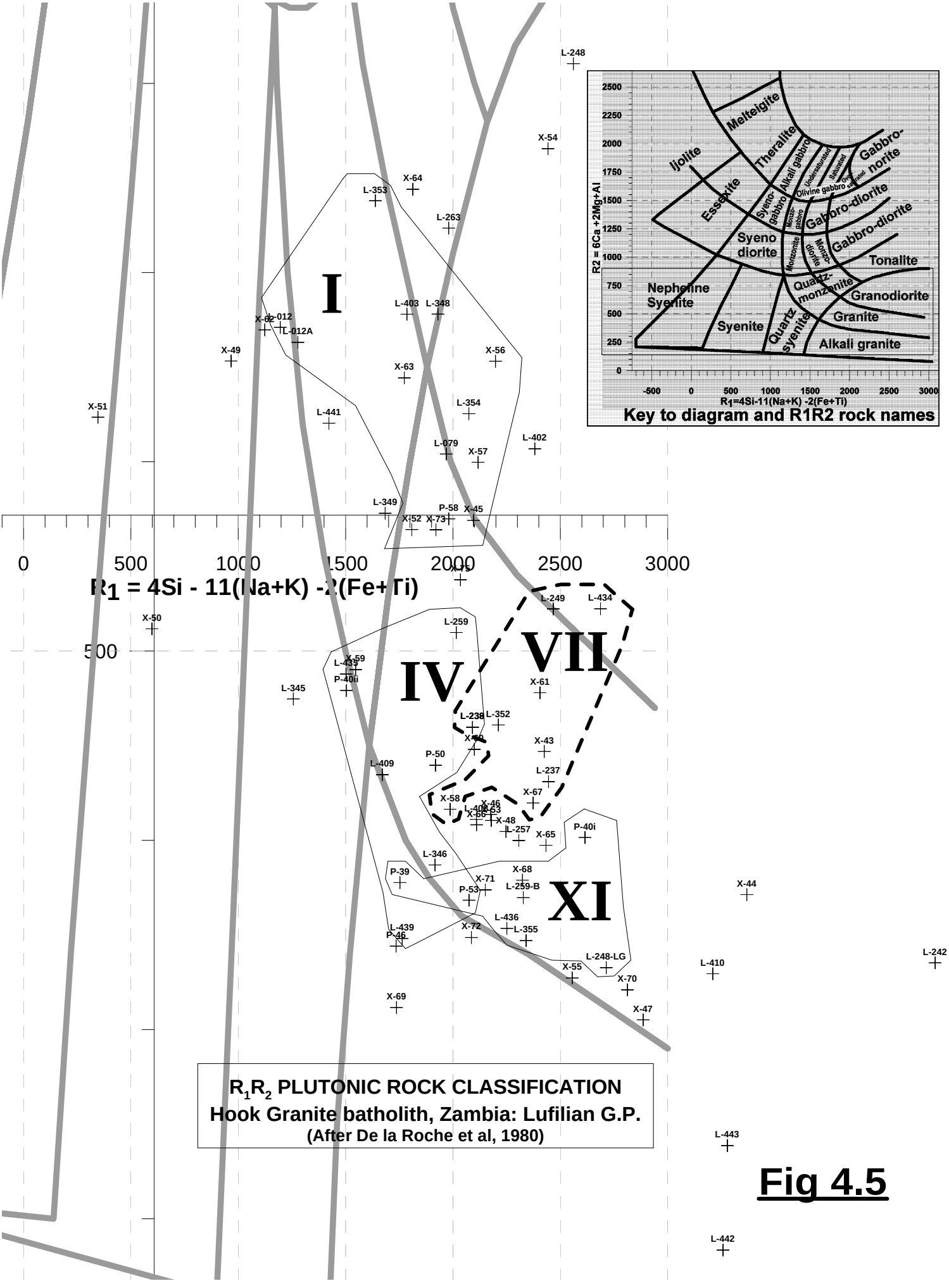

R_1R_2 PLUTONIC ROCK CLASSIFICATION
Hook Granite batholith, Zambia: Lufilian G.P.
(After De la Roche et al, 1980)

Fig 4.5

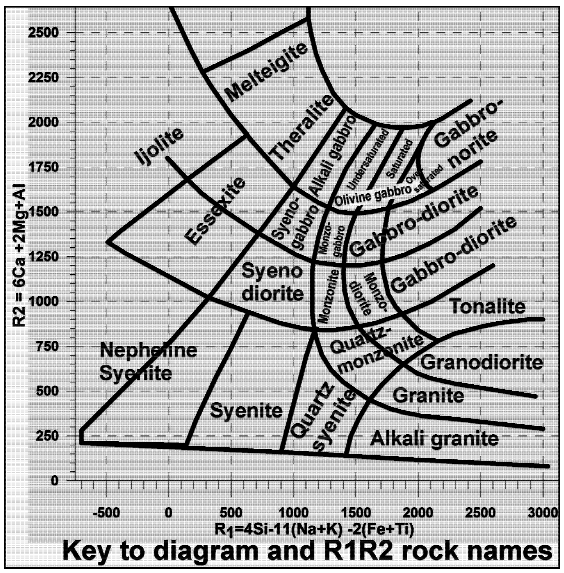

R_1R_2 PLUTONIC ROCK CLASSIFICATION
Hook Granite batholith, Zambia: Lufilian G.P.
(After De la Roche et al, 1980)

Petrographic fields

Samples

Note: The central cluster of samples on the granite and quartzmonzonite fields is better shown on Fig 4.5.

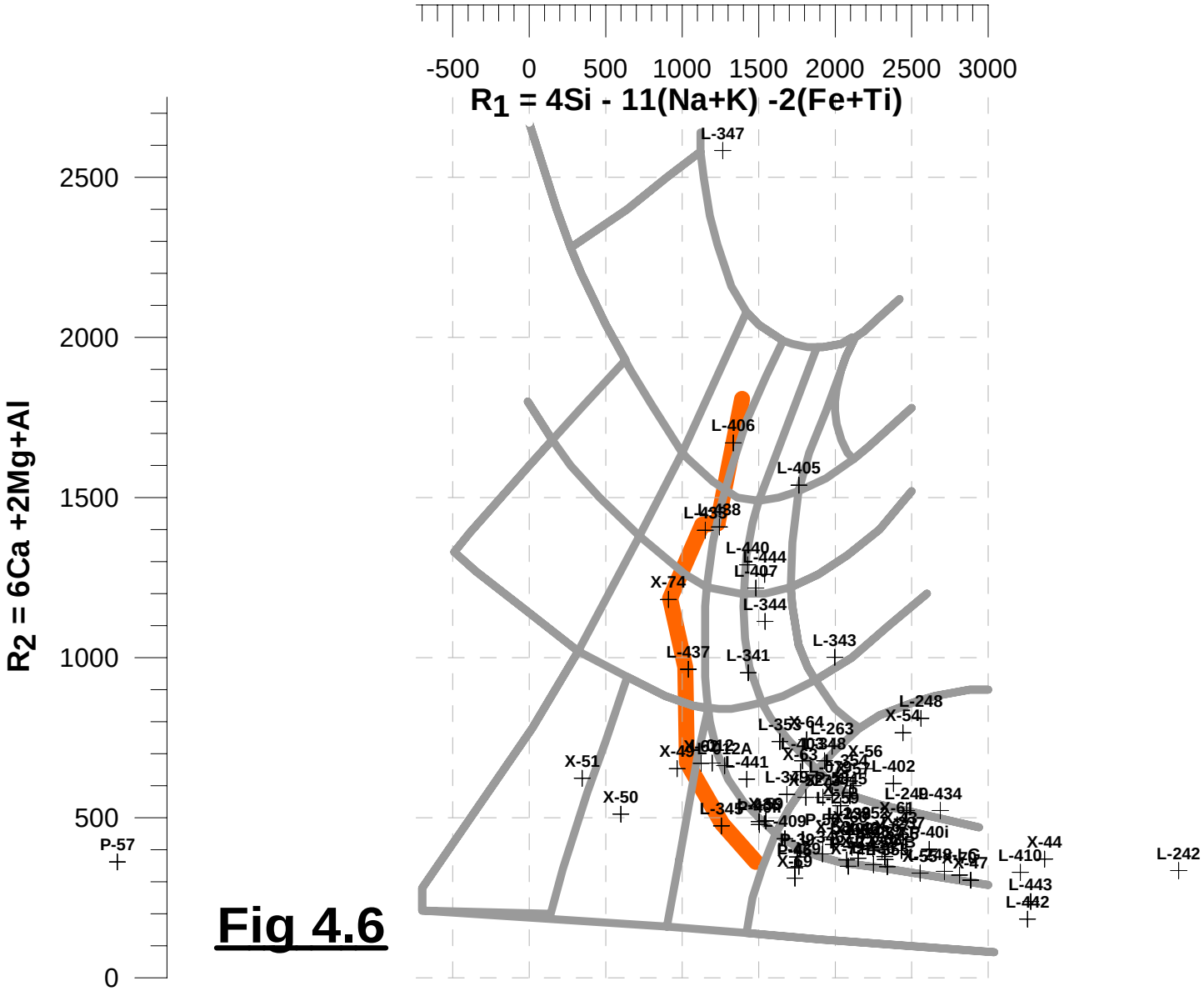

Fig 4.6

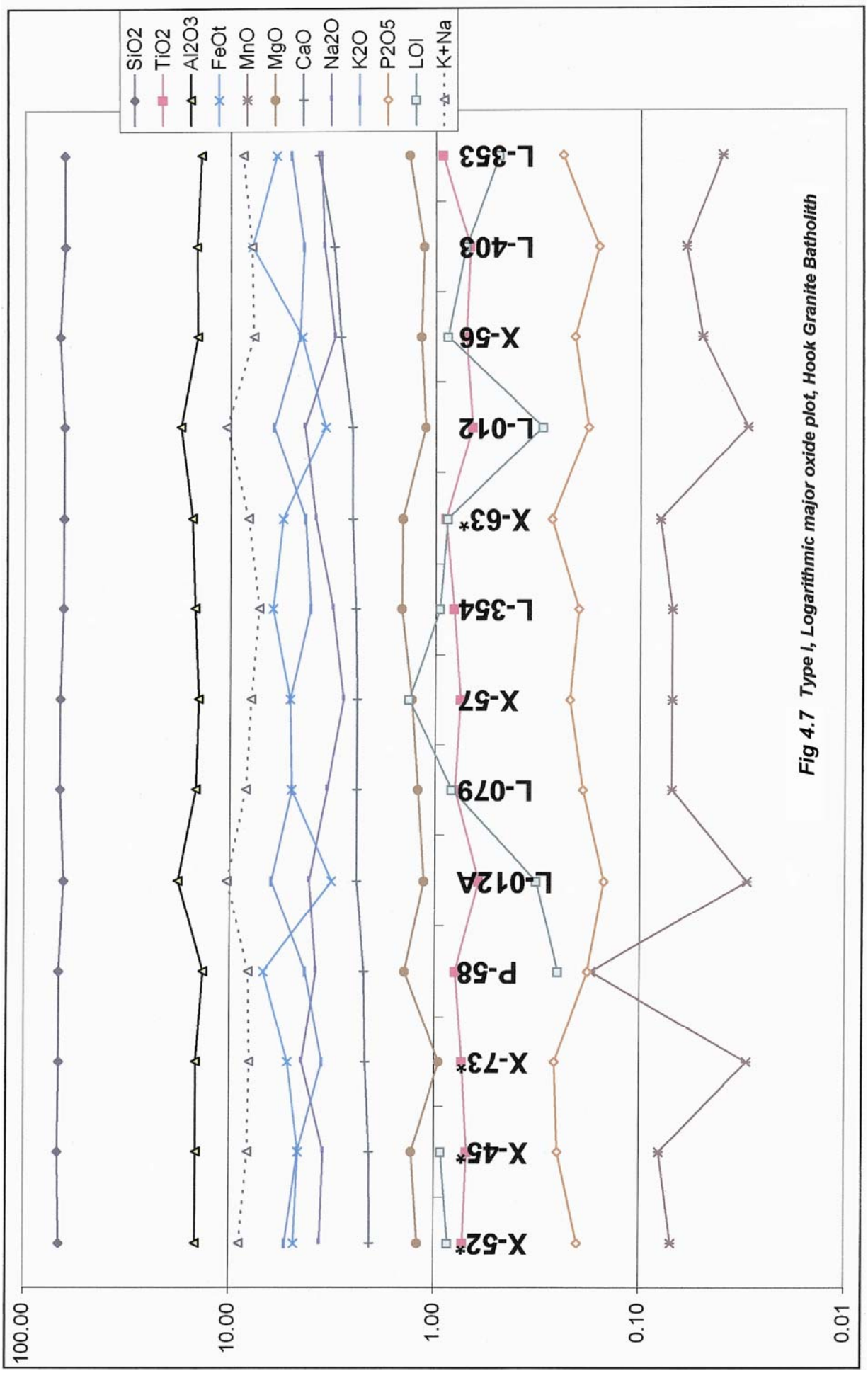

Fig 4.7 Type I, Logarithmic major oxide plot, Hook Granite Batholith

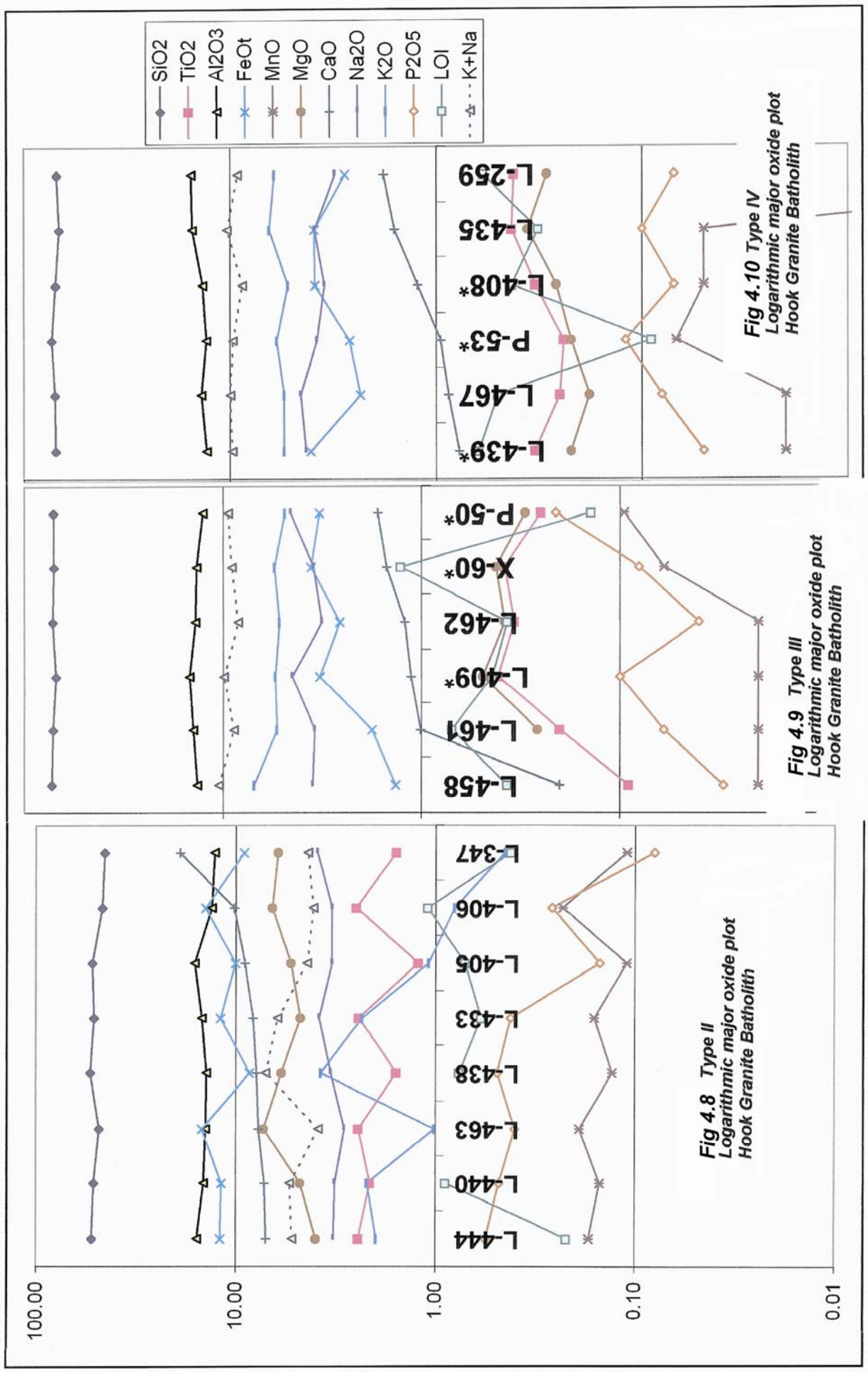

Fig 4.8 Type II
Logarithmic major oxide plot
Hook Granite Batholith

Fig 4.9 Type III
Logarithmic major oxide plot
Hook Granite Batholith

Fig 4.10 Type IV
Logarithmic major oxide plot
Hook Granite Batholith

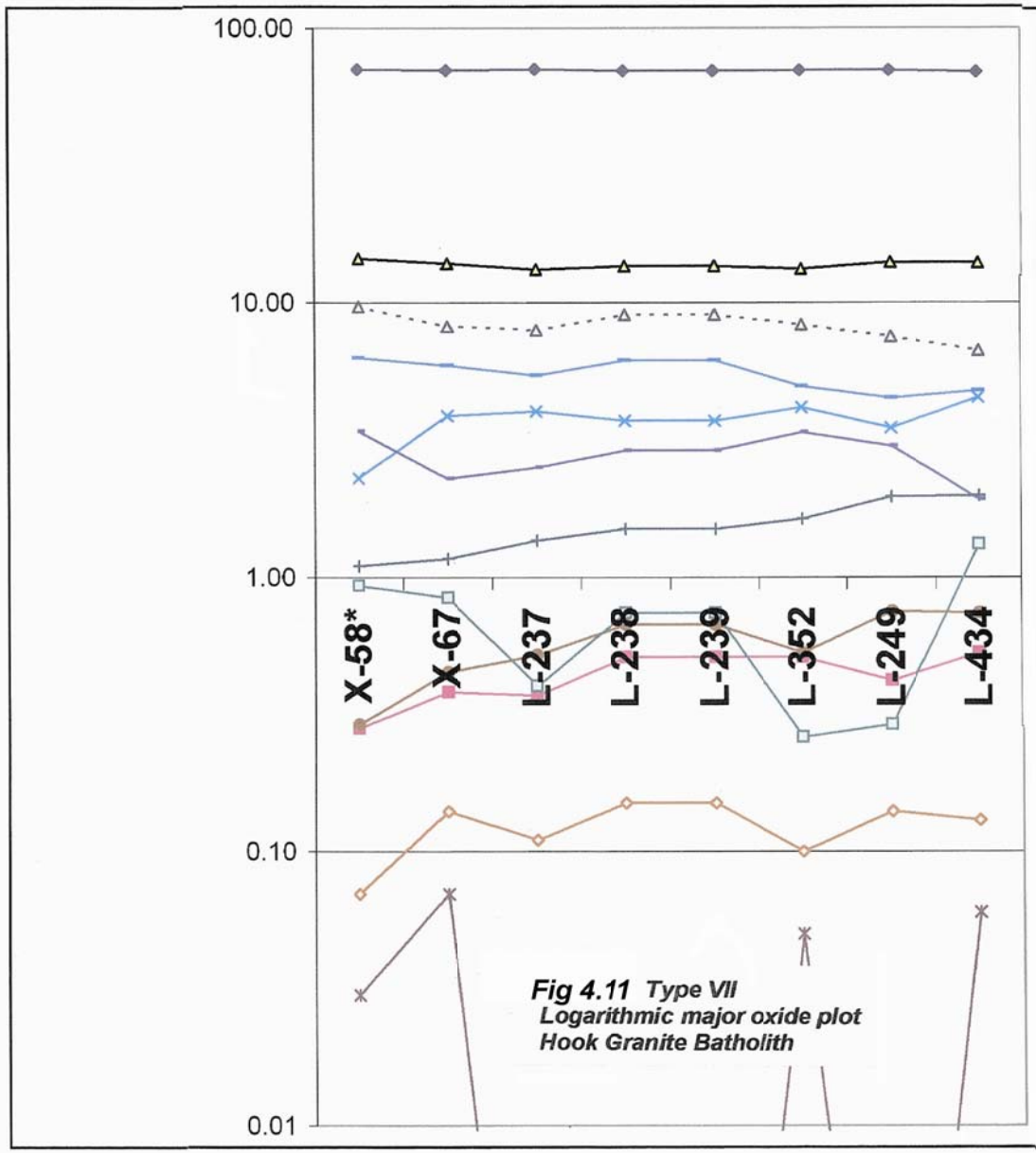

Fig 4.11 Type VII
Logarithmic major oxide plot
Hook Granite Batholith

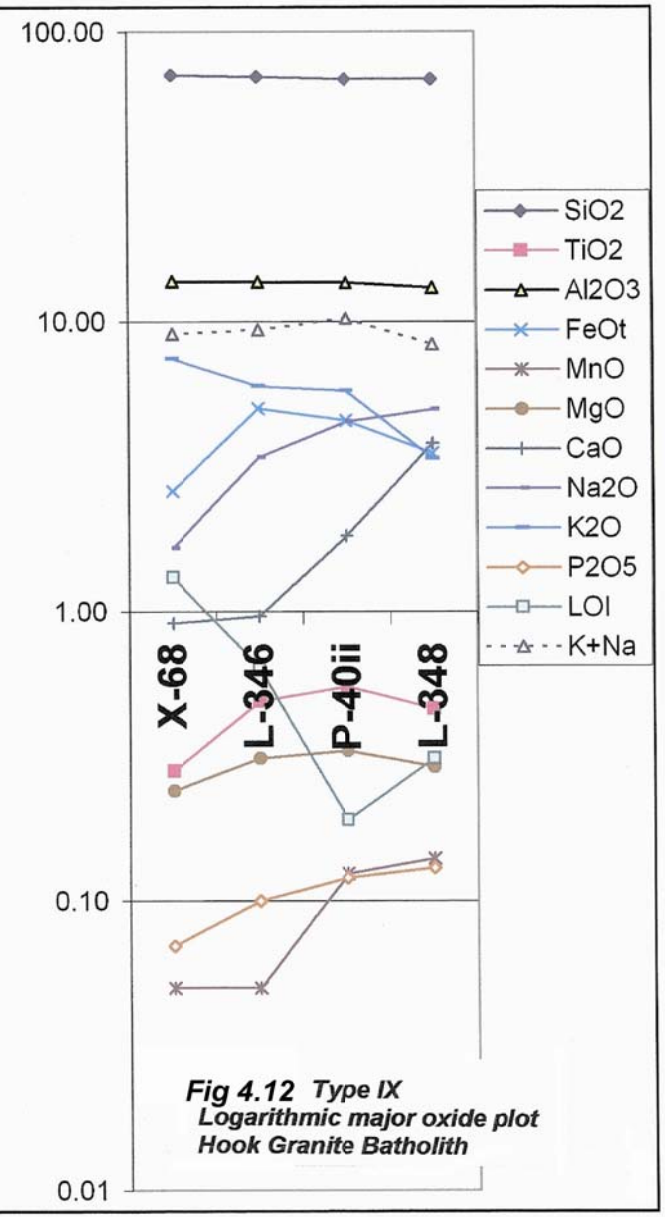

Fig 4.12 Type IX
Logarithmic major oxide plot
Hook Granite Batholith

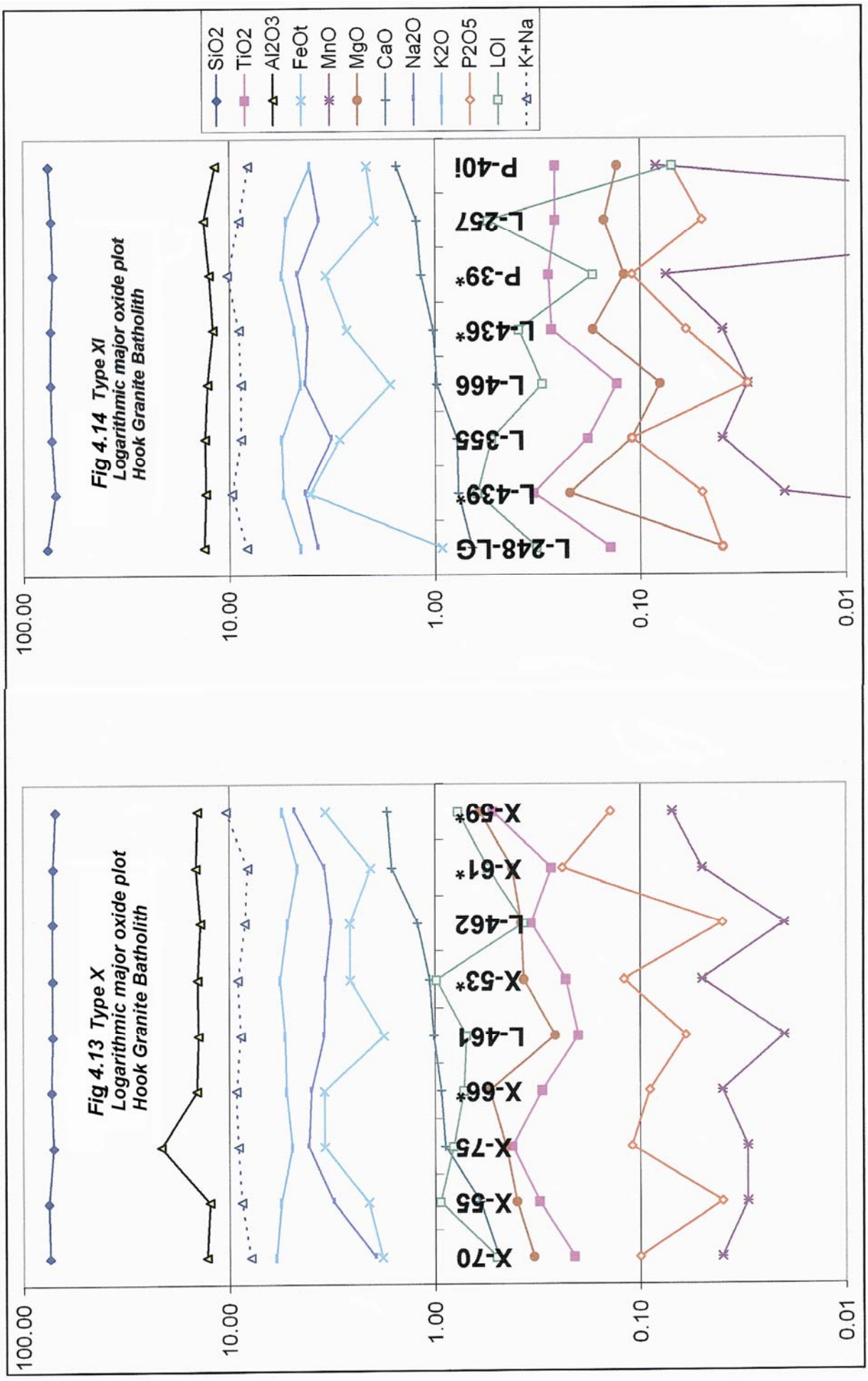
Fig 4.13 Type X
Logarithmic major oxide plot
Hook Granite Batholith
100.00
10.00
1.00
0.10
0.01
X-70
X-55
X-75
X-66*
L-461
X-53*
L-462
X-61*
X-59*
Fig 4.14 Type XI
Logarithmic major oxide plot
Hook Granite Batholith
L-248-LG
L-439*
L-355
L-466
L-436*
P-39*
L-257
P-401
SiO2
TiO2
Al2O3
FeOt
MnO
MgO
CaO
Na2O
K2O
P2O5
LOI
K+Na

4.1.1.3 Geological Units

Geological units from each of the eight published 1:100,000, half-degree by half-degree geological map sheets were correlated on Table 4.4. They were correlated from one map to the next to produce a series of discrete map units. Several units cannot correlate well, due to varying lithologies and mapping strategies of the various authors. In fact, many of the contacts between lithologic units run along map borders. Some roads that can now be used to traverse through the Hook Granite Batholith were not available at the time of mapping. For that reason, many of the outcrops opened during the construction of the roads have not been included in the original mapping. This produced many new mappable units. Examples of such outcrops lie along the E-W road from Mumbwa to eastern Zambia, across the Kafue National Park. Twelve samples were analysed from the most relevant outcrops along the road, and geology along that transect does not coincide with the 1:100,000 geological map sheets (for example on Sheet 1426SE).

For lack of a better system, the mapping units from each map sheet were correlated with those used by Hanson et al, 1993. Results of that process are shown on the map of Fig 4.15 and on Table 4.4. As seen on Table 4.11, there is a wide variability in the chemistry of the samples. This may be due to improper selection of the mapping units, to a large variability in the mapping units, or both. Careful evaluation indicated that in some cases, units Nos. 8 and 1 (from Table 4.4) could be grouped. In others, units 9 and 1 could be grouped. Unit 12 could be grouped with unit 2, unit 9 with 3, and unit 13 with 1.

After finding out that mapping units were not coherent with the geochemistry and field observations, a new approach to group all available samples by chemistry was tried out. All samples from the Hook Granite Batholith with chemical analysis were grouped using major oxide values and logarithmic plots. This is explained on Table 4.5. And later, rocks with similar chemistry were mapped as “units”. The main faults and some lithological contacts were kept as limits between map units, and new polygonal limits were produced between contrasting map units. This exercise had not been completed, when the concept of a ring complex cluster for the batholith was devised.

The scope of this project did not include remapping of the Hook Granite Batholith, but in the opinion of the author, mapped units are not adequate and a major re-mapping effort is needed.

Table 4.4 Correlation of Mapped Units for the Hook Granite Batholith, From Published 1:100,000 Geological Sheets

DESCRIPTION/MAP SHEET	1526NW	1526NE	1426SW	1426SE	1426NW	1525SE/1526SW	1527NW	HANSON PAPER	Ages	No.
	F,B,E,A	D (Porphiroblastic biotite adamellite),A		B	O	D3		Deformed Megacrystic gt	H-2	1
Coarse-grained adamellite, cg porphyroblastic gt-gneiss	F Cg adamellite		N K-rich gt and adamellite	D	N	E3,G,G1,D,A1		Post-Tectonic Megacrystic gt	H-4	2
Grey quatz feldspar porph	A Mcg foliated gt, gt-gneiss		H		H			Heterogeneous gt/Microcrogt Assemblage		3
						D2		Granodiorite and tonalite		4
Sheared leocogt, leucoc gt	H Sheared leucogt	C Mg gt and gt-gneiss, F		A	Q	A,A1		Fine- to M-Grained gt	H-1	5
Syenites and bostonites and carbonatites		H	Q	H Syenite			Syenitic + hybrid complexes	Syenite		6
Migmatitic gneisses						M1 ,M		Migmatite		7
Ca-enriched porphyroblast gt	B adamellite gneiss	A Cg adamellite gneiss				D3				8
Older Qz porph	A Mcg foliated gt, gt-gneiss	C Mg gt and gt-gneiss	O Gneissic gt and cg porph	B	O	D3				9
Basic rocks, dolerites, gabbro	L Dolerites	G Gabbro, oliv gbb, dolerit	F Metagabbro	J Gabbro	F	C	Gabbro			10
Iron oxides		f,M Qz-Mag-hematite	U Hematite	S Fe-silica replacement bodies	U					11
Rapakivi gt			N K-rich gt +adamellite	D Rapakivi gt	N	G				12
Aegirine-augite gts			M Aegirine-augite gt	B Cg porphyrob gt-gneiss	M	D1				13
Qz-tourmaline and Qz veins	K Qz +_ tour veins		V	L Qz veins	V					14
Late leucocratic gt	C Unfoliated pink leucogt					E3 Pale pink leucocratic gt				15
Qz-feldspar porph	J Pk Qz felds porphs								H-3	16
Pink Qz-feldspar porph					J					17
Younger porphs + FeOx + bxs				C Porphyritic K gt						18
Coarse amphibole-Qz monz					D1 Pink, green spotted cg amphibole Qzmonzonite					19
Granodiorites and tonalites						D Grey porphyroblastic g				20
Later biotite Qz monzonite						E Grey to pink fm-g homogeneous biotite g				21
Post-tectonic tourmaline gr						F Unfoliated mc-g post-tectonic tourmaline g				22
Qz feldspar porph		J Qz felds porph							H-5	23
Katanga		P1 Up Kund pelitic schist		Q Shales, slates, schists						24
Quaternary			Y Quaternary	W Alluvium	Y	R				25
Katanga biotite schists	D Biotite schist	N Biotite schist		R		L2 Biotite schist				26
Kundelungu pelitic schists	E Pelitic schist			R		L				27
								E on 1426SE		28
								F on 1426SE		29
								L on 1426SW		30
								E1 on 1525SE		31
								P on 1426SW		32
								S on 1426SW		33

RADIOMETRIC AGES FROM HANSON ET AL, 1993

SAMPLE No.	AGE	ROCK TYPE
H-1	559±18Ma	Deformed, fine- to medium-grained granite
H-2	566±5Ma	Deformed megacrystic granite
H-3	538±1.5Ma	Rhyolite dike within Katangan pendant
H-4	533±3Ma	Post-tectonic megacrystic granite
H-5	551±19Ma	Rhyolite intrusion in Mwembeshi dislocation

COORDINATES OF DATED SAMPLES

UTME	UTMN
479400	8325500
484600	8322500
421100	8317700
435000	8326900
469500	8303700

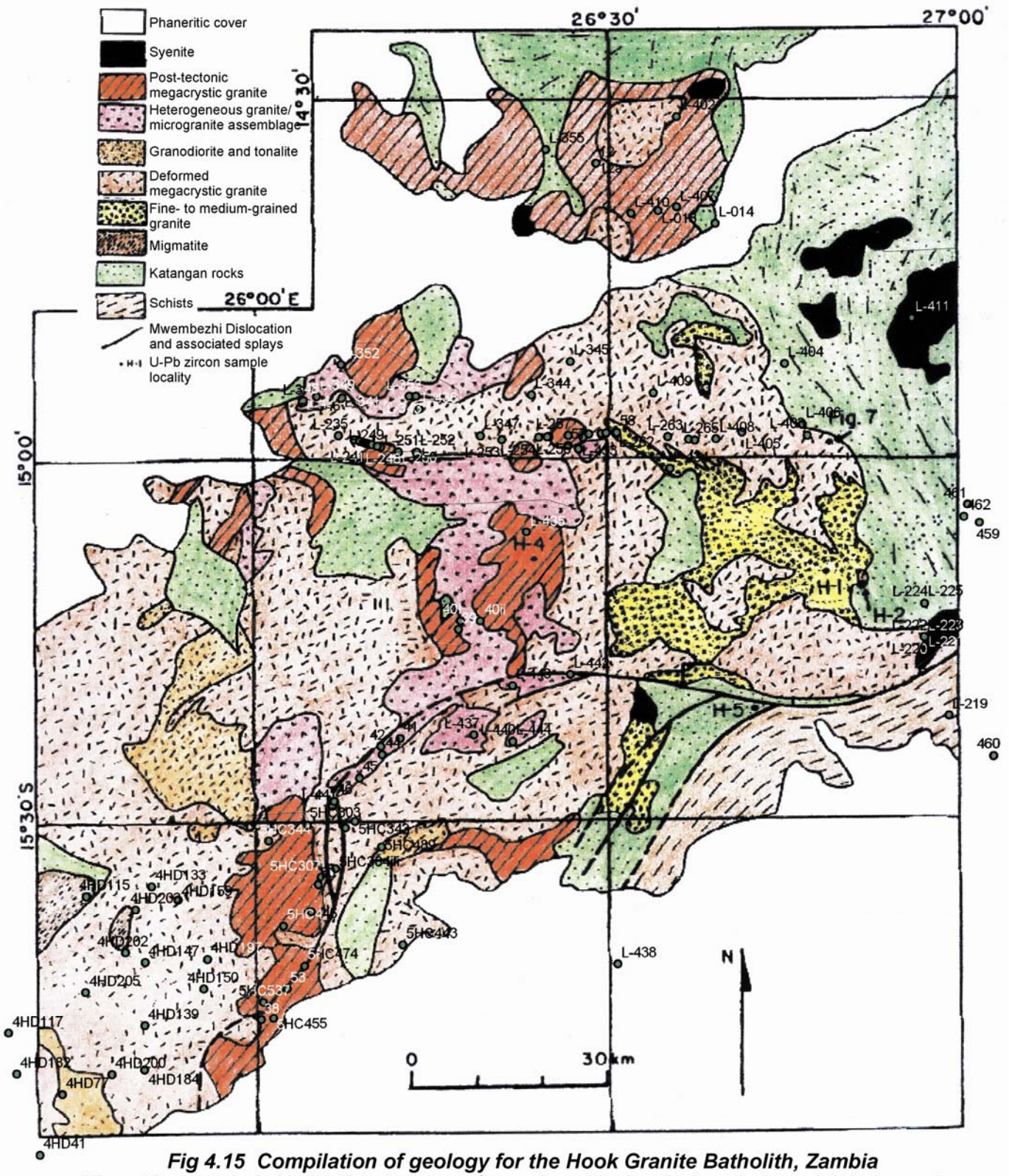

Fig 4.15 Compilation of geology for the Hook Granite Batholith, Zambia
(From Hanson et al, 1993.) Note location of samples with chemical analysis and dated samples. Several rock units end in the border of the map sheets.

Table 4.5 Hook Granite Batholith rock types and environment of emplacement
(see acronym description on section 2.4.3.)

Sample	Rock Name	Debon & LeFort	Maniar & Piccoli	Whalen	Pierce	Mafic	Rb/10HfTa	Rb/30HfTa	Nb-Ta
Type I									
L-012	quartz syenite		IAG+CAG	A			VA-	III	INW-INV
L-012A	quartzmonzonite	metaiv mesoKMg	IAG+CAG	A	O-W1-1				
L-079	granite	metaiv mesoNaKFe			O-W1-1				
L-353	quartzmonzonite	metav mesoNaKFe		A	W				
L-354	granodiorite	peraiii mesoNaKFe		A	W				
L-403	quartzmonzonite	metaiv mesoNaKFe	CEUG	A	W				
P-58	granite	metaiv mesoNaFe					VA-	III	INV-INW
X-45*	granite	metaiv mesoNaKFe							
X-52*	granite	metaiv mesoNaKFe							
X-56	granodiorite	metaiv mesoNaKFe	IAG+CAG						
X-57	granodiorite	metaiv mesoKFe							
X-63*	quartzmonzonite	metaiv mesoNaFe							
X-73*	granite	metaiv mesoNaFe							
Type VII									
L-237	granite	peraiii mesoKFe	CEUG	A	O-W1-1				
L-238	granodiorite	metaiv mesoKFe	CEUG-RRG	A	O3/4				OUTU
L-239	granite	metaiv mesoKFe		A	O-W1-1				
L-249	granite	peraiii mesoNaKFe		A	O3/4				OUTU
L-352	granite	metaiv mesoNaKFe	CEUG	A	O-W1-1				
L-434	granodiorite	peraii mesoKFe	RRG-CEUG	A					
X-58*	granite	peraiii subleucoKFe							
X-67	granite	peraii mesoKFe							
Type IV									
L-259	granite	metaiv, peraiii subleucoKFe		A	W				
L-408*	granite	metaiv mesoNaKFe	CEUG	A	W				
L-435	quartz syenite	metaiv mesoKFe	CEUG	A	O-W1-1				
L-439	alkali granite	metaiv mesoNaKFe	RRG	A	W				
L-467	alkali granite	metav leucoNaFe	RRG-CEUG	A					
P-53*	granite	metav subleucoKFe	CEUG				VA-	II	INV-INW
Type IX									
L-346	granite	metaiv mesoKFe	RRG-CEUG	A	O-W1-1				
L-348	granodiorite	metav mesoNaFe		A	V1/2				
P-40ii	quartz syenite	metav mesoNaKFe	CEUG				VA-	III	INW-INV
X-68	granite	peraii subleucoKFe							
Type X									
L-461	granite	peraii leucoKFe	POG	?N					
L-462	granite	peraiii subleucoKFe	POG	N					
X-53*	granite	peraiii subleucoKFe							
X-55	granite	peraiii subleucoKFe							
X-59*	quartzmonzonite	metav mesoNaFe							
X-61*	granite	peraii subleucoNaKFe	CCG-IAG-CAG						
X-66*	granite	peraiii mesoNaKFe	IAG+CAG						
X-70	granite	perai leucoKFe	CCG						
X-75	granite	perai mesoNaFe							
Type XI									
L-248-LG	granite	perai leucoNaFe	POG	A	O-W1-1				
L-257	granite	metaiv subleucoNaKFe	POG	A	O-W 2-2		WP	WP	OUTU
L-355	granite	peraiii subleucoKFe	CEUG	A	O-W1-1				
L-436*	granite	metav subleucoNaFe	RRG	A	O-W1-1				
L-439*	alkali granite	metaiv mesoNaKFe	RRG	A	W				
L-466	granite	metav leucoNaFe		A					
P-39*	alkali granite	metav subleucoNaFe	CEUG				VA-	VA-	INW-INV
P-40i	granite	metav leucoNaFe					VA-	VA	INV
Type III									
L-409*	granite	metaiv mesoNaFe	CEUG-RRG	A	O-W1-1				
L-458	alkali granite	metaiv leucoKFe		A	O-W1-1				
L-461	granite	peraii leucoKFe	POG	?N					
L-462	granite	peraiii subleucoKFe	POG	N					
P-50*	granite	metav subleucoNaFe	CEUG				VA-	III	OUTD-INW
X-60*	granite	metaiv mesoKFe							

(Continued on the next page)

Table 4.5 Hook Granite Batholith rock types and environment of emplacement

(continues from previous page)

Sample	Rock Name	Debon & LeFort	Maniar & Piccoli	Whalen	Pierce	Mafic	Rb/10HfTa	Rb/30HfTa	Nb-Ta
Type II									
L-347	melteigite	metav mesoNaMg		A	V	vab			
L-405	sat olivine gabbro	metaiv mesoNaFe	IAG+CAG	N	V	Emor			
L-406	alkali gabbro	metav mesoNaFe		A	V	Emor			
L-433	syeno gabbro	metav mesoNaFe		A	O-W1-1	wpt			
L-438	monzogabbro	metav mesoNaMg	IAG+CAG	A	O-W1-1	Wpab			
L-440	gabbro-diorite	metaiv mesoNaFe		A	O-W1-1	Wpab			
L-444	gabbro-diorite	metaiv mesoNaFe	RRG	N?	V1/2	Emor			
L-463	gabbro-diorite	metaiv mesoNaFe		A	V	wpt			
Type Unclassified									
L-241		origin		A	O-W 2-2		VA-	III	INW-INV
L-242	granodiorite	peraii mesoKFe		A	V				
L-248	granodiorite	peraiii mesoNaFe		A	W				
L-259-B*	granite	metaiv subleucoKFe	RRG	A	W				
L-263	quartzmonzonite	metav subleucoKMg	IAG+CAG	A	O-W 2-2				OUTU
L-341	monzonite	metavi mesoNaFe	OP	A	V1/2				
L-343	gabbro-diorite	metav mesoNaFe		A	S1/2				
L-344	monzonite	metav mesoNaFe		A	V1/2				
L-345	quartz syenite	metaiv mesoKFe	CEUG-RRG	A	O-W1-1				
L-349	quartzmonzonite	metav subleucoNaFe		A	W				
L-402	granodiorite	metaiv mesoNaFe	CEUG-RRG	A	W				
L-407	gabbro-diorite	metav mesoNaFe		A	W	wpt+vab			
L-410	granite	peraii mesoKFe	CEUG	A					
L-411	carbonatite	metavi mesoKMg							
L-437	syeno diorite	metav mesoNaFe	CEUG	A	O-W1-1	wpab+wpt			
L-441*	quartzmonzonite	metaiv mesoNaKFe	RRG	A	W				
L-442	alkali granite	peraiii subleucoKFe	RRG	A	O-W1-1				
L-443		peraiii mesoKFe	CEUG	A	O-W1-1				
L-459	tonalite	metaiv mesoNaFe		A					
L-460	granite	metaiv mesoNaFe		A					
L-464	foid out of plot	metaiv mesoKFe	CEUG		V				
L-465	foid out of plot	peraiii mesoKFe	CEUG	A	V				
P-46*	alkali granite	metav mesoKFe	CEUG				VA-	VA-	INW-INV
P-50	granite	metav subleucoNaFe	CEUG				VA-	III	OUTD-INW
P-57*	nepheline syenite	metavi subleucoNaFe					VA-	VA-	INW-INV
X-43	granite	peraii subleucoKMg	CCG-IAG-CAG						
X-44	granite	perai mesoKMg							
X-46	granite	peraiii leucoNaMg	IAG+CAG						
X-47	granite	peraiii leucoKMg							
X-48	granite	metaiv leucoNaMg	IAG+CAG						
X-49	syenite	peraii leucoNaFe			O-W1-1				
X-51	nepheline syenite	metav mesoNaKFe			O3/4				
X-54	granodiorite	metav subleucoKMg							
X-62	quartz syenite	metaiv mesoKFe							
X-64	tonalite	metaiv mesoNaFe	IAG+CAG						
X-65	granite	peraiii leucoNaKMg							
X-69	alkali granite	peraii mesoKFe							
X-71	granite	peraii subleucoKFe							
X-72	alkali granite	peraiii mesoKFe							
X-74	syeno-diorite	metavi mesoNaMg							

Table 4.11 List of Sample Sorted by Rock Type Based on Maps/Field Observations

HOOK GRANITE BATHOLITH, ZAMBIA

21-Jun-04

Sample	SiO2	TiO2	Al2O3	Fe2O3	FeO	MnO	MgO	CaO	Na2O	K2O	P2O5	LOI	Total	Rb	Sr	Y	Zr	Nb	Co	Ni	Cu	Zn	Ga	V	Cr	Ba	U	Th	Sc	Pb	Sm	Nd	Pr	Ce	La	Cs	Hf	Ta	As	Se	Eu	Gd	Tb	Dy	Ho	Er	Tm	Yb	Lu
1	**Deformed megacrystic gt**																																																
4HD139	64.17	0.89	20.28	0.26	1.06	0.05	0.19	2.30	6.14	4.57	0.14	0.49	100.54																																				
4HD147	62.31	0.11	18.36	1.53	3.07	0.10	0.90	1.00	5.67	6.04	0.07	0.98	100.14																																				
4HD150	60.19	0.49	18.14	0.84	3.86	0.14	0.33	2.35	5.31	7.00	0.07	1.55	100.27																																				
4HC343	72.65	0.27	14.34	0.34	1.10	0.04	0.73	1.21	3.07	5.46	0.12	0.55	99.88																																				
4HC344	76.59	0.32	12.60	0.28	2.08	0.04	0.82	0.78	0.87	5.77	0.04	0.49	100.68																																				
L-220																																																	
L-221																																																	
L-222	64.17	0.57	13.11	13.72	0.00	0.00	0.80	0.08	0.15	4.74	0.12	2.46	99.94	304.0	122.0	69.0	275.0	30.0	<6	7	<6	22	29	79	18	499	7.00	20.0	11					220	121														
L-223	66.79	0.57	14.12	10.16	0.00	0.00	0.79	0.08	0.17	5.20	0.10	2.49	100.48	312.0	122.0	77.0	270.0	28.0	<6	<6	<6	27	28	68	18	468	8.00	21.0	<10		2.2	0.6	20.21	250	2			166.0												0.99
L-264																																																	
L-403	64.07	0.68	14.61	7.86	0.00	0.06	1.14	3.13	3.50	4.38	0.16	0.71	100.30	119.0	277.0	83.0	762.0	25.0	9	9	196	89	25	19	19	1054	8.00	17.0	15					141	80														
L-405	52.10	1.22	16.06	10.02	0.00	0.11	5.30	8.98	3.30	1.08	0.15	0.71	99.03	23.0	882.0	24.0	121.0	14.0	37	72	30	53	17	220	35	226	<6	<15	26					78	37														
2	**Post-tectonic megacrystic gt**																																																
38																																																	
5HC537	71.21	0.42	21.42	2.00	1.44	0.03	0.45	0.89	4.10	4.92	0.11	0.81	107.80																																				
L-012	64.19	0.66	17.47	3.45	0.00	0.03	1.12	2.55	4.34	6.14	0.18	0.30	100.43	131.2	516.0	33.1	189.1	29.2	7	9	7	42	20	46	36	1042	4.27	50.4	<10	3.8	15.4	112.1	31.5	293	163	1.08	4.73	1.57	293		2.69	9.76	1.21	6.81	1.22	3.22	0.47	3.14	0.48
L-012A	64.38	0.61	17.86	3.18	0.00	0.03	1.13	2.40	4.10	6.24	0.15	0.32	100.40	143.0	536.0	36.0	360.0	32.0	9	10	9	28	21	33	36	940	<6	49.0	<10					312	216														
L-241	0.00	0.00	0.00	0.00	0.00	0.00	0.00	0.00	0.00	0.00	0.00	0.00	0.00	156.4	229.1	54.7	173.6	24.1	0	0	0	0		0	0	594	0.00	0.0	0	2.4	9.2	45.2	10.98	0	0	1.91	5.17	1.86	0	0	1.64	9.31	1.44	9.41	1.92	5.84	0.87	5.96	0.89
L-243	L-244	L-245		L-246	L-247																																												
L-248	64.40	0.91	15.35	6.34	0.00	0.00	2.74	3.49	2.97	2.10	0.26	0.53	99.08	126.0	300.0	54.0	205.0	42.0	15	15	13	28	25	109	39	271	6.00	<15	21					77	42														
L-248-LG	76.71	0.14	13.26	0.92	0.00	0.00	0.04	0.66	3.71	4.49	0.04	0.32	100.29	121.0	314.0	48.0	206.0	20.0	9	7	8	16	19	35	25	745	<6	27.0	<10					139	68														
L-249	70.32	0.42	14.04	3.50	0.00	0.00	0.75	1.96	3.00	4.50	0.14	0.29	98.93	123.0	309.0	49.0	211.0	23.0	8	7	8	16	19	45	21	716	<6	20.0	<10		0.7	0.7	4.800	124	0			46.24				1.313						0.35	0.69
L-407	60.09	1.12	13.19	6.31	0.00	0.07	1.49	8.27	4.03	3.86	0.30	0.61	99.34	92.0	396.0	79.0	532.0	28.0	13	8	43	40	19	71	29	689	7.00	26.0	14					188	96														
L-435	67.58	0.43	15.29	3.91	0.00	0.05	0.36	1.59	3.89	6.45	0.10	0.32	99.97	142.0	271.0	34.0	389.0	11.0	8	<6	29	34	21	15	13	1227	<6	<15	<10					86	43														
3	**Grey Qz-felds porph**																																																
L-341	63.54	0.75	13.15	4.88	0.00	0.03	1.09	5.99	6.86	0.95	0.32	1.14	98.70	19.0	703.0	76.0	329.0	29.0	11	9	31	21	21	45	20	72	<6	20.0	11					174	89														
L-343	65.60	0.61	13.71	4.43	0.00	0.05	0.83	6.46	5.59	1.11	0.20	0.17	98.76	20.0	616.0	180.0	408.0	40.0	11	7	12	24	19	44	16	187	<6	35.0	12					162	103														
L-346	70.01	0.49	13.71	5.02	0.00	0.05	0.31	0.96	3.40	5.99	0.10	0.64	100.68	195.0	168.0	69.0	469.0	27.0	12	<6	80	77	20	14	<12	774	11.00	24.0	<10					190	98														
L-347	45.32	1.57	12.74	9.07	0.00	0.11	6.14	18.97	3.89	0.45	0.08	0.42	98.76	11.0	497.0	14.0	77.0	6.0	26	21	197	147	22	127	131	48	9.00	29.0	<10					111	57														
L-348	68.82	0.46	13.11	3.52	0.00	0.14	0.29	3.80	4.97	3.37	0.13	0.31	98.92	38.0	762.0	56.0	329.0	19.0	7	<6	13	20	19	43	17	439	<6	40.0	<10					130	61														
L-352	70.34	0.51	13.27	4.15	0.00	0.05	0.53	1.63	3.37	4.96	0.10	0.26	99.17	178.0	166.0	35.0	357.0	20.0	10	11	17	30	19	16	21	861	<6	19.0	<10					212	123														
L-355	72.83	0.18	13.16	2.91	0.00	0.04	0.11	0.78	3.18	5.57	0.11	0.53	99.40	263.0	46.0	46.0	126.0	19.0	<6	7	20	21	18	79	38	135	8.00	21.0	<10					80	37														
4	**Granodiorite and Tonalite**																																																
4HD108	68.41	0.69	14.46	0.29	4.31	0.08	1.29	2.07	3.47	4.63	0.25	0.92	100.87																																				
4HD122	61.68	1.20	14.96	0.77	7.01	0.12	2.29	3.15	3.60	3.30	0.35	1.28	99.71																																				
4HD159	67.17	0.72	14.55	0.48	4.33	0.07	1.20	2.05	3.59	5.30	0.20	0.85	100.51																																				
4HD184	71.06	0.45	14.42	0.03	1.25	0.05	0.65	4.21	2.70	5.49	0.11	0.57	100.99																																				
4HD197	67.80	0.71	14.50	0.90	3.60	0.05	1.18	2.90	3.10	4.60	0.21	0.87	100.42																																				
4HD77	64.77	0.89	15.33	0.73	4.82	0.08	1.45	2.54	3.83	4.30	0.27	0.87	99.88																																				
5HC489	58.87	0.46	14.09	2.03	2.44	0.07	2.10	7.49	6.09	3.07	0.17	0.00	96.88																																				
5	**Sheared leucogranite**																																																
58	67.76	0.79	13.46	6.83	0.00	0.17	1.40	2.21	3.78	4.27	0.18	0.25	100.85	210.0	189.0	66.0	223.0	30.0	77	4	21	72	26	45	12	680	4.00	24.0	8	12.0	10.3	50.5	13.10	107	53	5.00	6.00	2.10	1	30	2.10	9.90	1.50	8.50	1.70	4.70	33.4	3.90	0.60
5HC384ii	70.96	0.28	13.75	1.02	1.58	0.05	0.24	0.91	1.65	7.44	0.07	1.31	99.26																																				
5HC443	68.83	0.48	14.51	4.05	0.79	0.03	0.33	0.10	2.79	7.36	0.05	0.00	99.32																																				
5HC474	69.88	0.40	13.71	1.80	2.37	0.07	0.27	0.62	2.92	6.03	0.04	0.55	98.66																																				
L-262																																																	
L-408	70.26	0.33	13.59	3.87	0.00	0.05	0.26	1.23	3.49	5.24	0.07	0.43	98.82	241.0	95.0	104.0	348.0	33.0	7	6	15	34	23	<12	13	483	12.00	32.0	<10					241	121														
L-409	69.36	0.41	14.76	3.25	0.00	0.02	0.49	1.13	4.47	5.43	0.10	0.44	99.86	206.0	151.0	43.0	313.0	32.0	6	<6	10	16	19	25	12	677	13.00	53.0	<10					120	60														
L-442	78.22	0.33	8.81	3.27	0.00	0.03	0.00	0.10	0.23	7.61	0.06	0.34	99.00	227.0	44.0	99.0	349.0	18.0	<6	<6	16	16	12	27	<12	618	<6	44.0	<10					288	149														
L-443	76.23	0.44	9.57	5.13	0.00	0.03	0.10	0.43	0.20	6.79	0.05	0.40	99.37	201.0	24.0	64.0	391.0	48.0	8	7	12	14	14	28	<12	499	<6	100.0	<10					49	25														

6	**Syenite**																																																
Sample	SiO2	TiO2	Al2O3	Fe2O3	FeO	MnO	MgO	CaO	Na2O	K2O	P2O5	LOI	Total	Rb	Sr	Y	Zr	Nb	Co	Ni	Cu	Zn	Ga	V	Cr	Ba	U	Th	Sc	Pb	Sm	Nd	Pr	Ce	La	Cs	Hf	Ta	As	Se	Eu	Gd	Tb	Dy	Ho	Er	Tm	Yb	Lu
L-212	67.27	0.40	15.94	2.89	0.00	0.00	0.15	0.81	4.44	7.04	0.03	0.71	99.69	149.0	117.0	51.0	336.0	49.0	8	<6	32	17	22	<12	<12	503	8.00	79.0	<10					250	130														
L-213	66.68	0.36	17.40	3.03	0.00	0.00	0.08	0.23	6.87	4.87	0.03	0.60	100.17	73.0	193.0	27.0	596.0	39.0	8	6	18	22	25	22	<12	762	12.00	163.0	<10		4.4	42.1	69.13	137	20		16.48	39.14			0.663							0.7	0.8
L-214	66.63	0.39	17.62	1.54	0.00	0.03	0.00	0.24	7.68	3.92	0.06	0.63	98.74	65.0	167.0	24.0	662.0	77.0	<6	12	20	15	25	19	81	657	7.00	104.0	<10					181	89														
L-215	70.53	0.23	16.82	0.65	0.00	0.00	0.00	0.15	10.32	0.19	0.03	0.36	99.30	7.0	72.0	15.0	443.0	23.0	6	7	6	9	27	<12	<12	71	<6	193.0	<10					18	<12														
L-217	73.54	0.39	10.80	3.98	0.00	0.09	3.40	1.35	0.64	2.97	0.15	2.41	99.72	124.0	48.0	10.0	128.0	10.0	86	17	8	43	13	67	502	805	<6	<15	11		6.8	28.2	53.20	89	30			58.60											0.8
L-218	66.30	0.52	15.92	4.64	0.00	0.00	0.49	2.01	4.79	5.43	0.11	0.21	100.42	202.0	344.0	46.0	601.0	53.0	8	<6	6	30	22	15	16	793	8.00	99.0	<10		16.7	74.6	264.5	342	135		7.513	65.38			1.450							2.1	1.1
L-260	L-395																																																
L-411	8.09	0.09	0.85	0.57	0.00	0.02	4.72	43.80	0.04	0.35	0.16	41.87	100.56	6.0	87.0	4.0	17.0	3.0	<6	<6	<6	16	<9	<12	<12	23	<6	<15	45					12	<12														
L-460	74.38	0.43	11.58	4.11	0.00	0.03	0.62	1.86	3.67	2.33	0.12	0.34	99.47	68.0	482.0	13.0	632.0	7.0	8	9	19	63	18	22	14	596	<6	20.0	<10					197	102														
L-466	73.93	0.13	12.78	1.65	0.00	0.03	0.08	0.98	4.27	4.50	0.03	0.30	98.68	351.0	83.0	31.0	75.0	39.0	<6	<6	15	21	24	<12	14	225	<6	23.0	<10					57	27														
L-467	70.78	0.25	13.75	2.33	0.00	0.02	0.18	0.87	4.53	5.45	0.08	0.50	98.74	145.0	1046.0	29.0	208.0	18.0	7	10	12	30	22	16	<12	2676	<6	67.0	<10					224	130														
7	**K felds migmatite**																																																
4HD 115	72.98	0.13	14.41	0.10	1.05	0.04	0.42	1.03	4.45	4.57	0.07	0.79	100.04																																				
4HD 117	78.16	0.15	11.55	0.00	0.86	0.02	0.70	0.41	2.45	6.08	0.40	0.18	100.96																																				
4HD 190	75.50	0.31	12.40	1.50	0.60	0.03	0.40	0.60	3.10	5.60	0.04	0.94	101.02																																				
4HD200	67.00	0.75	14.20	1.10	4.00	0.07	1.30	2.40	2.80	5.10	0.22	1.34	100.28																																				
4HD202	71.10	0.28	14.50	1.20	1.10	0.03	0.29	1.10	3.40	6.30	0.07	0.93	100.30																																				
4HD 203	69.70	0.52	14.20	1.00	2.40	0.07	0.60	1.70	4.80	5.50	0.14	0.77	101.40																																				
8	**Ca-enriched porphyroblast gt**																																																
39	72.16	0.28	12.57	3.40	0.00	0.08	0.12	1.17	4.67	5.57	0.11	0.17	100.13	404.0	43.0	109.0	309.0	59.0	56	4	<3	12	29	<4	5	182	19.00	71.0	4	11.0	21.4	114.1	33.00	290	145	2.00	10.00	2.50	<1	12	0.80	19.40	3.10	18.30	3.60	9.20	34.4	7.30	1.10
40i	76.05	0.26	11.74	2.15	0.00	0.08	0.13	1.54	4.06	4.05	0.07	0.07	100.13	150.0	92.0	48.0	335.0	27.0	61	12	<3	26	26	<4	9	309	6.00	20.0	2	8.0	9.3	45.6	11.90	98	51	1.00	11.00	1.30	2	8	1.50	8.80	1.40	8.30	1.70	5.00	35.3	5.00	0.80
9	**Older qz porph**																																																
57	62.19	0.36	13.11	2.44	0.00	0.05	0.26	0.86	15.42	5.52	0.06	0.21	100.27	225.0	45.0	375.0	404.0	48.0	63	21	<3	1	24	<4	<4	286	10.00	51.0	6	5.0	79.0	499.4	133.60	735	579	2.00	11.00	2.60	<1	5	7.60	80.50	10.00	55.60	11.10	28.9	35.9	21.4	3.30
L-235																																																	
L-236																																																	
L-237	70.85	0.37	13.24	4.02	0.00	0.00	0.52	1.36	2.51	5.44	0.11	0.40	98.83	151.0	276.0	74.0	194.0	24.0	8	6	25	16	18	28	<12	815	<6	26.0	<10					273	148														
L-238	70.04	0.46	14.22	4.47	0.00	0.00	0.70	2.13	3.09	4.42	0.17	0.45	100.16	110.0	399.0	59.0	238.0	26.0	8	<6	28	19	19	37	27	647	<6	27.0	12		15.0	50.8	105.6	130	44			67.75			1.313							3.4	1.28
L-239	70.02	0.51	13.56	3.71	0.00	0.00	0.67	1.50	2.89	6.16	0.15	0.74	99.92	156.0	260.0	58.0	240.0	27.0	7	<6	9	18	18	33	15	747	6.00	24.0	<10					130	67														
L-240																																																	
L-254																																																	
L-257	73.62	0.26	13.30	1.97	0.00	0.00	0.15	1.23	3.67	5.29	0.05	0.55	100.10	214.0	117.0	53.0	208.0	25.0	6	<6	<6	13	22	<12	14	321	16.00	74.0	<10		113.8	43.0	114.8	192	66		5.363	26.34			0.663							4.0	1.18
L-258																																																	
L-259	69.45	0.42	15.44	2.77	0.00	0.00	0.29	1.80	3.10	6.11	0.07	0.59	100.05	174.0	199.0	72.0	402.0	47.0	7	<6	<6	21	20	13	26	911	7.00	21.0	11					113	58														
L-259-B	73.83	0.30	12.91	2.80	0.00	0.00	0.17	1.01	3.55	5.35	0.04	0.44	100.42	204.0	118.0	214.0	292.0	39.0	<6	<6	12	28	20	<12	15	617	10.00	29.0	<10					277	209														
L-345	62.53	0.76	14.29	8.20	0.00	0.05	0.77	1.46	2.52	7.65	0.20	0.40	98.83	210.0	366.0	61.0	494.0	18.0	7	11	19	27	23	67	24	1440	6.00	<15	<10					174	94														
10	**Gabbro**																																																
L-219																																																	
L-406	46.64	2.48	13.15	14.14	0.00	0.23	6.55	10.17	3.29	0.80	0.26	1.09	98.80	11.0	282.0	38.0	180.0	17.0	43	73	80	104	18	374	106	118	<6	<15	37					29	18														
L-416	52.44	0.65	15.34	8.63	0.00	0.15	7.28	12.42	2.55	0.73	0.07	0.20	100.46	6.0	126.0	17.0	41.0	5.0	34	72	94	84	17	195	217	43	6.00	<15	42					<12	<12														
L-433	51.23	2.42	14.76	11.92	0.00	0.16	4.74	8.16	3.82	2.33	0.42	0.59	100.55	71.0	396.0	44.0	261.0	22.0	28	11	45	99	20	275	62	384	7.00	<15	27					96	52														
L-434	69.24	0.53	13.96	4.52	0.00	0.06	0.74	1.98	1.92	4.77	0.13	1.32	99.17	149.0	247.0	8.0	411.0	7.0	8	9	25	35	16	19	18	869	<6	<15	30					18	<12														
L-437	55.61	1.95	14.33	9.89	0.00	0.14	2.79	5.09	3.77	4.40	0.52	0.58	99.07	113.0	395.0	52.0	404.0	32.0	21	8	121	132	22	144	21	736	<6	<15	18					111	56														
L-438	53.44	1.57	14.02	8.54	0.00	0.13	5.89	7.86	3.34	3.75	0.49	0.76	99.79	171.0	402.0	43.0	390.0	31.0	27	77	43	71	19	163	250	592	7.00	22.0	22					99	55														
L-440	51.34	2.12	14.48	11.82	0.00	0.15	4.77	7.19	3.18	2.19	0.48	0.89	98.61	74.0	395.0	39.0	348.0	19.0	32	29	27	99	21	244	101	373	<6	<15	29					56	29														
L-444	52.77	2.43	15.66	11.98	0.00	0.17	3.98	7.06	3.24	1.98	0.56	0.22	100.05	43.0	404.0	41.0	170.0	21.0	33	14	27	108	21	245	54	396	6.00	<15	33					67	36														
L-463	48.36	2.43	14.19	14.79	0.00	0.19	7.26	7.68	2.85	1.01	0.40	-0.53	98.63	25.0	255.0	38.0	193.0	15.0	39	11	16	153	21	133	94	285	<6	<15	30					30	18														
L-464	5.46	0.07	0.00	77.5	0.00	0.08	0.50	6.09	0.10	0.52	0.06	3.16	93.53	14.0	13.0	16.0	17.0	3.0	25	185	184	122	<9	34	<12	142	29.00	<15	37					<12	<12														
11	**Iron oxides**																																																
Sample	SiO2	TiO2	Al2O3	Fe2O3	FeO	MnO	MgO	CaO	Na2O	K2O	P2O5	LOI	Total	Rb	Sr	Y	Zr	Nb	Co	Ni	Cu	Zn	Ga	V	Cr	Ba	U	Th	Sc	Pb	Sm	Nd	Pr	Ce	La	Cs	Hf	Ta	As	Se	Eu	Gd	Tb	Dy	Ho	Er	Tm	Yb	Lu
L-465	14.01	0.58	2.56	64.7	0.00	0.03	0.70	0.17	0.06	0.43	0.12	12.85	96.25	25.0	76.0	9.0	129.0	17.0	13	85	143	102	11	127	<12	694	24.00	<15	36					<12	<12														

12	Rapakivi gt																																																
50	71.53	0.25	12.60	3.26	0.00	0.10	0.30	1.66	4.55	4.88	0.21	0.14	99.34	376.0	66.0	163.0	312.0	107.0	40	16	<3	30	27	<4	4	314	62.00	256.0	3	23.0	54.3	334.8	100.20	899	505	4.00	9.00	3.20	1	8	1.20	39.60	6.00	32.20	6.20	16.3	5.70	11.40	1.60
5HC303	74.82	0.11	13.65	0.38	0.65	0.01	0.50	0.98	3.57	5.35	0.03	0.58	100.63																																				
5HC307	72.86	0.30	14.37	0.79	2.66	0.04	0.54	0.93	3.98	5.25	0.09	0.72	102.53																																				
5HC317	70.30	0.38	13.88	0.60	3.27	0.07	0.45	1.17	2.29	5.90	0.14	0.84	99.29																																				
5HC445	74.17	0.21	12.86	0.00	1.80	0.04	0.33	0.49	1.94	5.91	0.10	0.50	98.35																																				
13	Aegirine-augite gt																																																
L-344	61.49	1.13	15.69	3.77	0.00	0.07	1.27	6.94	5.64	1.83	0.40	0.98	99.21	47.0	555.0	126.0	485.0	41.0	10	<6	13	25	27	44	22	577	6.00	24.0	15					209	107														
L-349	67.98	0.35	13.65	3.38	0.00	0.07	0.35	2.69	4.47	4.97	0.13	0.82	98.86	108.0	423.0	55.0	230.0	32.0	7	11	24	16	19	21	16	590	<6	23.0	<10					106	50														
L-353	64.23	0.92	13.89	5.97	0.00	0.04	1.34	3.73	3.62	5.05	0.24	0.49	99.52	120.0	400.0	152.0	404.0	20.0	10	<6	67	24	21	36	19	606	6.00	20.0	12					141	73														
L-436	73.93	0.27	12.03	2.68	0.00	0.04	0.17	1.02	4.15	4.81	0.06	0.39	99.55	235.0	74.0	45.0	303.0	31.0	<6	<6	10	21	21	<12	<12	195	26.00	99.0	<10					223	114														
14	Qz-Tourmaline and Qz veins																																																
L-013	L-014																																																
16	Qz feldspar porph																																																
L-439	70.07	0.33	12.99	4.06	0.00	0.02	0.22	0.77	4.27	5.46	0.05	0.62	98.86	243.0	66.0	90.0	572.0	46.0	<6	3	21	16	25	<12	<12	163	19.00	90.0	<10					237	124														
18	Younger porphyritic K granite																																																
L-410	67.74	0.44	12.99	8.55	0.00	0.02	0.88	0.29	0.17	4.34	0.09	3.18	98.69	233.0	16.0	25.0	177.0	33.0	9	9	489	218	17	51	14	187	7.00	32.0	<10					147	80														
20	Grey porphyroblastic gt																																																
5HC485	67.24	0.73	14.52	2.90	2.30	0.03	0.95	2.17	4.44	3.53	0.26	0.00	99.07																																				
21	Grey to pink fm-g homogeneous biotite g																																																
4HD133	73.41	0.14	13.97	0.16	1.08	0.05	0.37	1.05	4.41	4.44	0.35	0.59	100.02																																				
4HD182	71.79	0.23	14.21	0.31	2.26	0.05	0.37	1.06	3.40	5.64	0.12	0.98	100.42																																				
4HD205	71.10	0.38	13.60	1.10	2.50	0.06	0.42	1.50	3.50	5.50	0.08	1.27	101.01																																				
4HD41	71.74	0.27	14.47	0.32	1.73	0.05	0.42	1.62	3.44	4.65	0.24	0.55	99.50																																				
53	73.18	0.24	13.04	2.62	0.00	0.07	0.22	0.95	3.78	5.92	0.12	0.09	100.14	421.0	59.0	54.0	179.0	48.0	71	19	<3	<1	24	<4	24	209	21.00	43.0	2	11.0	5.6	25.7	8.00	78	44	6.00	6.00	2.50	6	6	0.80	6.00	1.10	6.70	1.50	4.70	31.8	4.80	0.80
5HC455	70.61	0.33	14.72	1.41	0.86	0.02	0.55	0.54	2.17	7.33	0.18	0.73	99.45																																				
28																																																	
L-265																																																	
L-354	64.83	0.81	14.83	6.19	0.00	0.07	1.46	2.45	3.15	4.06	0.20	0.95	99.00	138.0	207.0	77.0	435.0	25.0	11	17	115	78	20	71	22	977	<6	22.0	12					156	82														
29																																																	
L-404																																																	
30																																																	
L-253																																																	
31	Fine-to medium-grained biotite quartz monzonite																																																
4HD48	61.07	0.80	16.53	1.03	5.61	0.16	0.56	2.97	3.75	6.03	0.14	0.84	99.49																																				
32	Post-tectonic qz porph																																																
L-224	62.03	0.58	13.42	15.02	0.00	0.00	0.62	0.07	0.24	5.69	0.11	2.33	100.13	261.0	103.0	35.0	301.0	28.0	9	8	<6	21	24	76	16	1065	8.00	19.0	<10					120	65														
L-225																																																	
33	Post-tectonic adamellite																																																
Sample	SiO2	TiO2	Al2O3	Fe2O3	FeO	MnO	MgO	CaO	Na2O	K2O	P2O5	LOI	Total	Rb	Sr	Y	Zr	Nb	Co	Ni	Cu	Zn	Ga	V	Cr	Ba	U	Th	Sc	Pb	Sm	Nd	Pr	Ce	La	Cs	Hf	Ta	As	Se	Eu	Gd	Tb	Dy	Ho	Er	Tm	Yb	Lu
L-255	L-256																																																

3-9	**Grey Qz-felds porph**																																																
41	42	44	45																																														
46	71.17	0.38	12.62	4.35	0.00	0.12	0.20	0.81	3.59	6.89	0.07	0.16	100.20	398.0	65.0	89.0	257.0	53.0	48	4	<3	45	27	<4	9	387	10.00	46.0	1	11.0	16.9	93.1	25.70	217	110	3.00	11.00	2.80	26	28	1.40	15.50	2.40	14.00	2.80	7.90	4.90	7.40	1.10
40i	76.05	0.26	11.74	2.15	0.00	0.08	0.13	1.54	4.06	4.05	0.07	0.07	100.13	150.0	92.0	48.0	335.0	27.0	61	12	<3	26	26	<4	9	309	6.00	20.0	2	8.0	9.3	45.6	11.90	98	51	1.00	11.00	1.30	2	8	1.50	8.80	1.40	8.30	1.70	5.00	35.3	5.00	0.80
40ii	68.86	0.55	13.67	4.56	0.00	0.12	0.33	1.82	4.52	5.77	0.12	0.19	100.32	195.0	110.0	77.0	391.0	52.0	53	14	<3	53	27	11	19	503	<2	15.0	5	10.0	15.9	78.8	20.00	157	71	1.00	11.00	3.30	<1	22	2.00	14.40	2.40	14.20	2.80	7.50	34.9	6.40	1.00
L-441	62.98	1.11	14.13	7.49	0.00	0.12	0.99	2.75	3.71	5.30	0.35	0.46	99.39	180.0	226.0	74.0	414.0	46.0	10	<6	13	88	24	28	<12	893	6.00	19.0	12					187	98														
9-1	**Older qz porphyry**																																																
L-250	L-251	L-252		L-261																																													
L-079	67.09	0.80	14.65	4.99	0.00	0.07	1.21	2.40	3.35	4.98	0.19	0.83	100.56	165.0	216.0	40.0	332.0	24.0	14	12	41	45	0	68	40	1291	0.00	0.0	0					0	0														
L-139	75.60	0.09	11.88	1.50	0.00	0.03	0.62	0.14	1.61	7.87	0.01	0.79	100.14	399.0	17.0	40.0	75.0	41.0	10	7	55	34	23	14	47	769	<6	26.0	<10					42	12														
L-175	74.72	0.41	12.60	2.96	0.00	0.00	0.41	1.08	2.71	4.60	0.09	0.32	99.90	221.0	63.0	45.0	229.0	29.0	9	7	31	31	15	28	17	541	<6	25.0	<10		5.9	30.1	47.8	153	19			41.58			0.263							1.30	0.84
L-181	49.82	1.08	15.86	11.33	0.00	0.16	6.30	11.28	2.94	0.24	0.06	0.86	99.94	7.0	157.0	29.0	62.0	8.0	34	30	57	94	16	293	35	<22	<6	<15	35					<12	<12														
L-195	61.25	0.38	15.84	8.67	0.00	0.09	0.04	2.35	5.66	5.03	0.09	0.51	99.91	89.0	130.0	115.0	1054	80.0	<6	<6	10	71	40	13	<12	2151	8.00	<15	<10		15.8	44.1	74.25	118	25			145.1			3.888	1.463						7.50	2.20
L-199													10.3	786.7	42.2	533.6	46.6								399	8.85	38.7		5.6	20.0	137.1	35.6	288	95	0.67	10.8	2.65			5.38	12.6	1.58	9.10	1.61	4.24	0.59	3.76	0.53
L-207	75.03	0.07	13.63	0.68	0.00	0.00	0.00	0.11	4.32	6.27	0.01	0.26	100.39	123.0	182.0	12.0	432.0	6.0	8	6	10	13	0	<12	13	557	0.00	0.0	0				4.575	0	2		19.10				0.225	0.625							0.44
L-208	74.23	0.05	13.85	0.87	0.00	0.03	0.00	0.12	4.36	6.13	0.05	0.24	99.93	137.0	178.0	12.0	431.0	33.0	<6	<6	14	10	25	<12	238	517	9.00	132.0	<10					35	20														
L-209	46.78	1.81	16.06	9.69	0.00	0.05	7.51	11.46	2.34	1.91	0.57	0.60	98.79	53.0	1592.0	27.0	111.0	17.0	36	42	29	52	19	243	50	1437	<6	<15	27					113	61														
L-210	66.74	0.43	17.99	3.52	0.00	0.00	0.29	0.69	9.58	0.09	0.14	0.39	99.87	4.0	275.0	30.0	474.0	36.0	6	7	143	13	22	28	<12	83	7.00	74.0	<10					372	223														
L-211	L-229	L-230	L-231																																														
L-242	76.03	0.29	10.81	5.91	0.00	0.01	2.03	0.21	0.57	1.96	0.11	1.21	99.14	42.0	228.0	33.0	256.0	11.0	14	18	8	12	38	87	309	617	7.00	<15	29					148	112														
L-259	69.45	0.42	15.44	2.77	0.00	0.00	0.29	1.80	3.10	6.11	0.07	0.59	100.05	174.0	199.0	72.0	402.0	47.0	7	<6	<6	21	20	13	26	911	7.00	21.0	11					113	58														
L-259-B	73.83	0.30	12.91	2.80	0.00	0.00	0.17	1.01	3.55	5.35	0.04	0.44	100.42	204.0	118.0	214.0	292.0	39.0	<6	<6	12	28	20	<12	15	617	10.00	29.0	<10					277	209														
L-263	67.90	0.54	13.93	2.49	0.00	0.00	0.71	3.88	3.29	5.55	0.27	0.54	99.13	83.0	640.0	51.0	244.0	26.0	7	<6	23	15	20	34	16	920	<6	19.0	10		118.9	46.7	91.5	118	32			29.10			1.813							2.86	1.06
L-402	68.46	0.60	13.71	5.64	0.00	0.04	0.43	2.96	4.94	1.14	0.11	0.82	98.85	70.0	286.0	178.0	602.0	44.0	7	10	12	29	22	25	20	272	6.00	21.0	12					178	107														
L-458	72.83	0.09	13.43	1.35	0.00	0.02	0.00	0.20	3.52	6.94	0.03	0.37	98.78	277.0	30.0	72.0	45.0	13.0	<6	<6	9	11	18	<12	13	129	8.00	<15	<10					38	42														
L-459	61.30	0.79	13.54	9.09	0.00	0.13	3.38	5.88	3.02	1.16	0.10	0.63	99.02	87.0	204.0	22.0	81.0	8.0	26	40	111	107	19	181	57	287	<6	<15	23					54	30														
L-461	71.85	0.20	14.11	1.77	0.00	0.02	0.26	1.01	3.45	5.34	0.06	0.70	98.77	178.0	241.0	14.0	65.0	10.0	<6	<6	30	36	18	<12	13	1222	<6	15.0	<10					43	21														
L-462	72.04	0.34	13.78	2.58	0.00	0.02	0.38	1.21	3.18	5.19	0.04	0.37	99.13	114.0	630.0	5.0	95.0	11.0	<6	<6	11	32	17	25	<12	3607	<6	16.0	<10					61	25														

4.1.1.4 Comparison of Hook Granitoids with Ring Complexes

Some portions of the Hook Granite Batholith may have formed by the amalgamation of granitoid anorogenic ring complexes. Several supporting facts to this hypothesis will be presented in the next pages.

4.1.1.4.1 Airborne Geophysical Image and Definition of Ring Complexes

The aeromagnetic interpretation of Zambian geology published by Nisbet et al., 2000, and shown on Fig 4.16, illustrates many circular features. The Hook Granite lies roughly in the center of the figure. These circular features probably are annular complexes that make the batholith. Part of the original geophysical image is shown on Fig 4.17. The image is basically a digital blend of airborne magnetometry and radiometry with other electromagnetic information. It is based on the Sanabozi TMI geophysical database used by Equinox Limited for mineral exploration in Zambia. White represents high magnetic values. A pseudo-topography of magnetic values has been illuminated from the NW to enhance perception of relief.

Fig 18 is a transparent overlay on Fig 4.17. It shows an interpretation of the geology around the Hook Granite Batholith, based on the geophysical image just described and other information published by (Nisbet et al., 2000 and Nisbet, 2004b). The various ring complexes are labeled in the figure for easy reference.

The majority of the rock samples obtained come from ring dikes. Several granitoids were collected from a granite ring dike of complex A: L-436, L-348, L-349, L-343 and they contain high Cu. L-352 was collected from further inside the same ring complex. Other samples that seem to come from potential ring dikes are: L-404, L-403, and L-406 (complex O, high Cu); L-263, L-408 (M); L-258 and L-359 (L); L-441 and L-257 (K high Cu); L-435 (P high Cu); P-40ii (Q); P-39 and other (R); P-42 (AA); L-440 (AC); L-442 (AF); L-254 and L-257 (J); L-410 (E?); X-74 (AD); and L-216 (AN). L-406 is a gabbro, and it probably comes from a gabbroic ring dike. See Table 4.12.

A few of the rock specimens come from intrusions along major structures. Samples P-46, X-59, X-50 and X-66 probably were emplaced along one of the main N-S-trending fracture zones that are well defined on the geophysical image (Figs 4.17 and 4.18). L-348 also seems to have been collected on granitoids extruded along that fracture zone. P-044, P-045, X-44 were collected along or very near another important N-S fracture. The granitoids could have been emplaced at an earlier time and were later exposed by displacement of the faults.

Differential erosion generates a sampling bias in granitoids from the Hook Granite. Rocks that stand out topographically tend to be sampled; valley-forming granitoids remain unsampled. Fig 4.16 shows that very few of the rock specimens collected come from the nucleus of ring complexes. These are: L-352 (A high Cu); L-264, L-265 (M); L-347 (K high Cu); L-433 (Q); P-40i (R); L-262, P-58, L-261, L-260, L-259 (L); L-255 and L-256 (J); L-014 (C); L253, P-57 (K high Cu); L-437 (P high Cu); L-433, L-40ii (AQ); L-013, L-407 (E with high Cu).

The granitoids that lie in between ring complexes probably came from older ring complexes. Most of the Th-rich rocks are of that type (See section 4.1.1.2 on geochemisty). They probably formed in an earlier generation of intrusions, and later were overprinted by newer granitoid ring complexes.

An interesting group of well-located samples is P-39, L-40i, P-40ii. These come from the rims of ring complexes Q and R.

Many structures present on the geophysical image of Fig 4.17 (and mapped on Fig 4.18) do not correspond with those mapped on the published geological sheets. Most N-S structures and WSW-ENE structures are evident on the geophysical image and were not described or mapped in the published geology. The ring structures are not even hinted. There is not enough outcrop to map structure or geology adequately at 1:100,000 scale.

A lensoid N-S fault structure that is present on the map by Hanson et al, 1993 (and on the Zambian Geological Survey maps) shows up well on the geophysical image (westernmost portion of Figs 4.17 and 4.18). A few samples (P-50, P-46 and others) were collected from the middle of the fault duplex. That fault is the same very long N-S fracture that is evident on the geophysical image, connects the Hook Granite to the Kasempa area to the north (Figs 4.18 and 4.16), and seems to be the site of emplacement of massive iron oxide bodies and iron oxide-copper-gold mineralization.

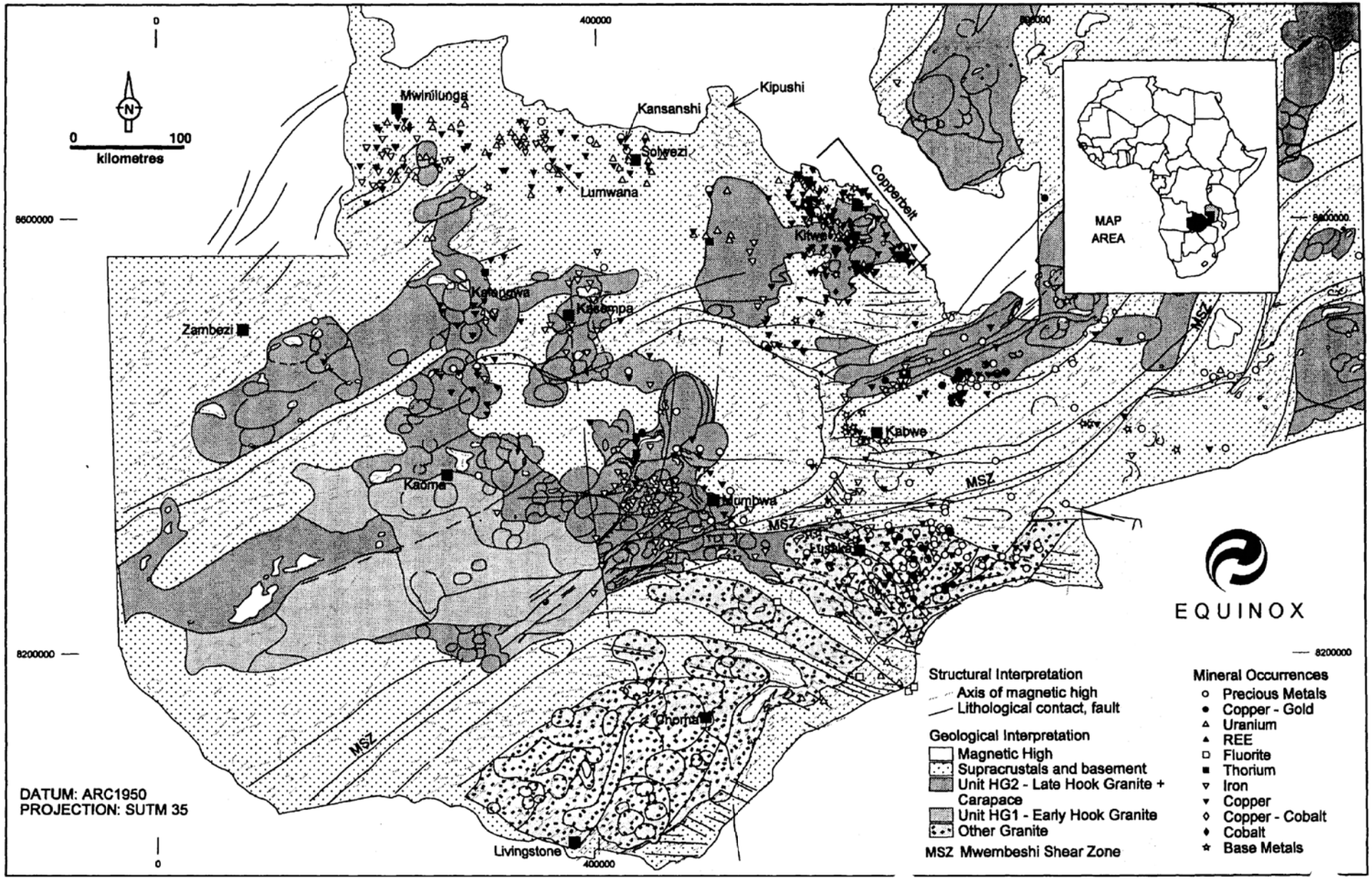

Fig 4.16 Structural interpretation of Zambian geology based on aeromagnetic data. Note the abundant annular structures and numerous WSW-ENE lineaments. Also note N-S lineaments. From Nisbet et al, 2000.

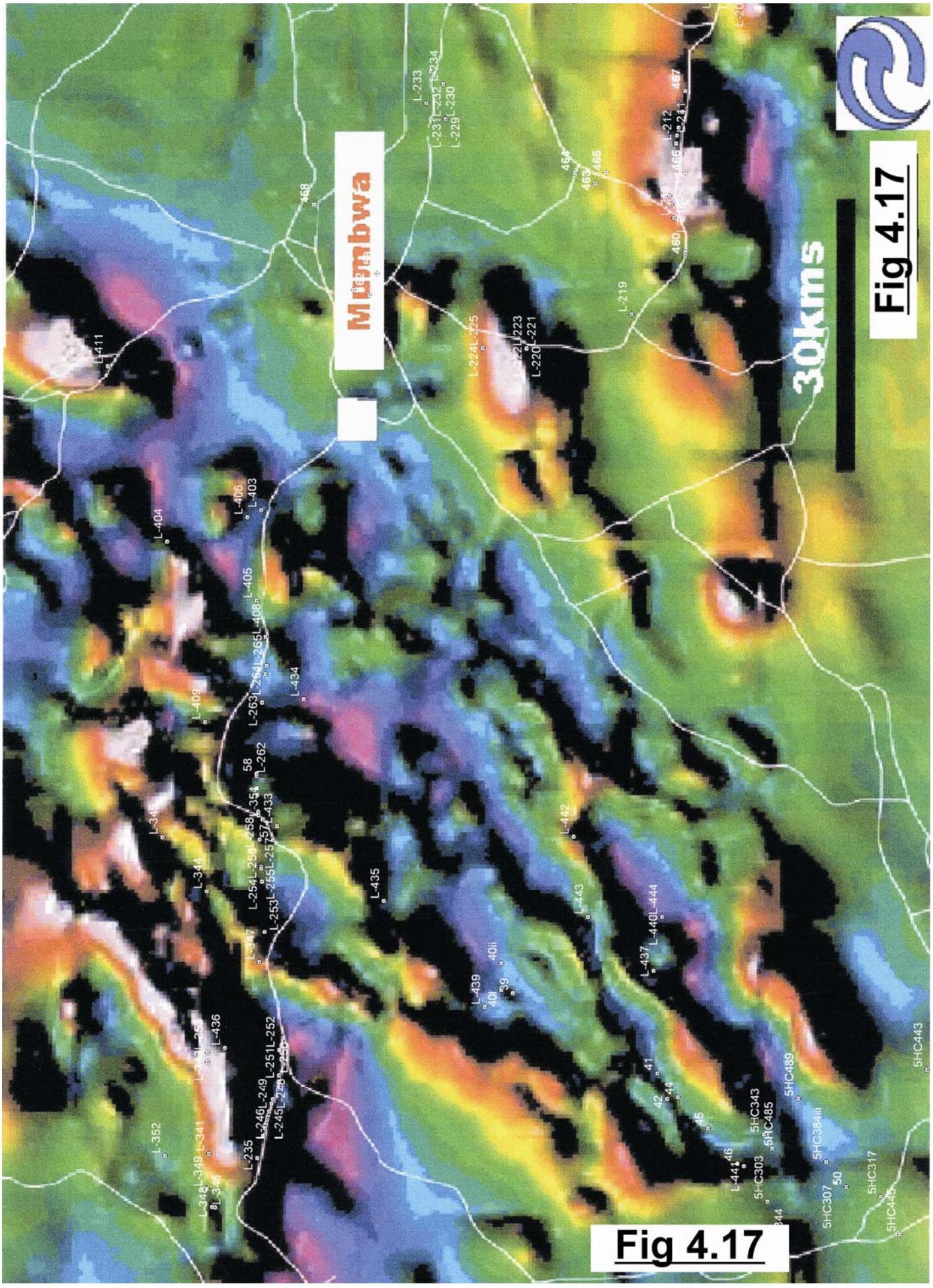
Mumbwa
30kms
Fig 4.17
Fig 4.17

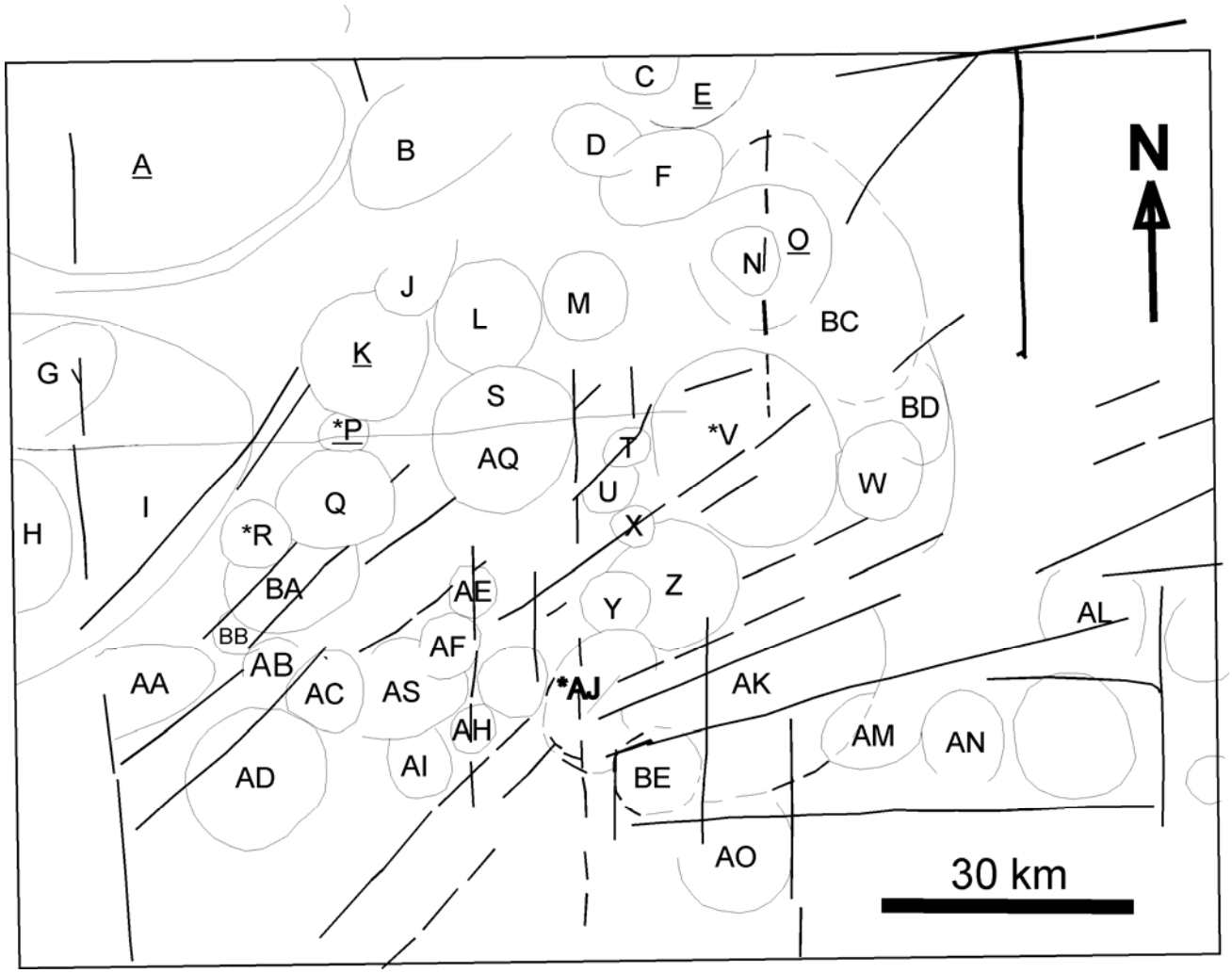

Fig 4.18. Anorogenic ring structures that can be identified in the Sanabozi geophysical image, Hook Granite Batholith, Zambia. *Thick lines are fractures. Thin lines are geophysical ring lineaments. The letters serve to designate the various ring structures. Based on interpretation of Fig 4.17 with input from Fig 4.16 and Nisbet, 2004a and Nisbet, 2004b. The letter of complexes with high copper content are underlined. Stars indicate ring complexes dated by Hanson et al, 1993.*

The south-western half of the Hook Granite (the part that lies west of the Kafue River) seems to have been down-faulted along the same N-S structure, and is now less-well exposed. That same fault controls the N-S deflection of the Kafue River across the Hook Granite Batholith. Maybe the textural change shown by the geophysical image is due to different data sources or a different scale of coverage of geophysical information.

Some of the mapped syenite bodies that lie to the northeast and east of the main Hook Granite Batholith (Fig 4.1) seem to be isolated from it. They intrude Katangan metasediments, have been called “outliers” or “satellites” of the batholith, and could be younger or older than the main batholith.

Samples **L-207** and **L-213**, from some of the satellite bodies, were dated during this project. Their ages are very similar to ages published by Hanson et al, 1993 for the Hook Granite. That implies that the satellite bodies are isolated ring complexes, apophysis of ring complexes that did not outcrop, or portions of the main batholith that are partially covered by fluvial deposits. The image of Nisbet presents an explanation for such intrusive bodies (Fig 4.17). **L-213** sampled a syenitoid that produced one of the strongest magnetic anomalies in the environs of the Hook Granite. It will be discussed in detail below.

The geology mapped by the Zambian Geological Survey and published on reports (Phillips, 1958; Simpson, 1962; Cikin, 1971; Cikin, 1972; Page, 1974; Abel, 1976; and Griffiths, 1978) does not bear any resemblance with the geophysical interpretation published by Nisbet, 2004a and Nisbet, 2004b. Field observations along the E-W transect do not relate to the published geological map sheets either. The same can be said of some of the structures mapped. The map published by Hanson et al, 1993 is just a compilation of older 1:100,000 geological map sheets. It does not relate to field observations or to the geophysical interpretations.

When syenites and quartz syenites from the Hook Granite are plotted on the published maps, these seem to be spread out in no particular location. Some of them are even related to the granite bodies. Gabbroic bodies are also widely distributed throughout. These are common features in anorogenic ring complexes.

4.1.1.4.2 Comparison of Hook granitoids with rocks from Namibian Mesozoic ring complexes

A review of literature on Mesozoic Namibian anorogenic complexes showed that the Erongo and Brandberg complexes, two of the countrie's larger ring complexes are exclusively made of granites. Fig 4.19 shows their location on a simplified geological map. Brandberg measures 25 x 30 km. If several bodies of that size were to overprint each other, a batholithic-size body of granite would result. This would happen if the granitic bodies would occur with the density of the Sudanese Nuba Mountains (See chapter 7). Two smaller Namibian anorogenic granitic complexes are Klein Spitskoppe and Gross Spitzkoppe. Chemical analyses from the four Namibian complexes are listed on Table 4.6. Neoproterozoic granitic ring complexes from northern Mali studied by Liegeois & Black, 1987 have equivalent compositions and dimensions.

Simple evaluation was carried out to define the general chemistry of the four mentioned Namibian granitic complexes. This was later compared with granitoids from the Hook Granite Batholith. Based on the R1/R2 diagram of De la Roche et al, 1980, samples from the Namibian anorogenic complexes may be grouped into five sets (A to E), as indicated on Table 4.7 and presented on Fig 4.5. Major oxide chemistry is very similar between samples X-97, X-98, X-99, X-100 and X-101 (Groups A, D and E); and between samples X-92, X-93, X-94, X-95 and X-96 (Groups B and C). These make two sets of comparable rocks.

Several particular geochemical features were observed in the chemical analysis from Namibian Mesozoic anorogenic granite ring complexes (Table 4.2). Among others, the samples contain high potash, Rb, Y, Nb, and Zr, and low Sr. When those signatures were compared with all samples from the Hook Granite, 10 samples produce a good match. These are listed on Table 4.8.

A particular minor element signature is common in rocks from the Nigerian ring complexes, Namibian granite anorogenic complexes and those of the Hook Granite Batholith. All three groups have high values for Rb, Y, Nb, Th, Pb, Ce, La, and low values for Sr and Zr (Table 4.8).

If anomalous enrichment in Rb, Y, Nb, Th and Pb (all of them at the same time) is assumed to be the chemical signature of some anorogenic granitoid ring complexes, then rocks with that signature from any province could have been formed as anorogenic granite ring complexes. A search for rocks with similar chemical signature in the entire Greater Lufilian Arc sample database shows that only a few suites of rocks have similar signatures.

There is no match for the major oxide chemistry from Nigerian granitoid complexes with the Hook Granite. Namibian rocks correlate much better. Certain samples from the Hook Granite display very similar chemistry to the Mesozoic Namibian granitoid ring complexes, as shown on Table 4.8 and Fig 4.20.

Samples considered to come from anorogenic ring complexes are L-259B, L-408, L-409, L-436, L-439, L-441, P-39, P-46, P-53, P-57, and P-58 (Table 4.8). Others considered to be of the same origin due to major oxide similarities were X-43, X-45, X-52, X-58, X-59, X-60, X-61, X-63, X-66 and X-73. Unfortunately the last group of samples was not analysed for trace elements or rare earths. Fig 4.20 illustrates the similarity of their major oxide composition. There is a remarkable correlation between the samples, and they all probably originated as anorogenic ring complexes.

On the modified TAS diagram, several groups of samples from the Hook Granite Batholith display similarities with rocks from suites of anorogenic ring complexes (Fig 4.21) The TAS diagram includes rocks from complexes such as Pan-African and Evisa granitoids of Nigeria, and others of Corsica. Nchanga Granite samples were also plotted for comparison. Part of the samples with similarities to the ring complexes are directly associated with the rock groups identified for the Hook Granite. The Nchanga Granite also displays close association with some Nigerian ARC rocks. Results are listed on Table 4.13.

Furthermore, a midalkaline linear trend of rocks has been observed on the TAS diagram for the Hook Granite Batholith (Fig. 4.21). The trend seems to be a special feature of a portion of the Hook Granite batholith, but its relevance is not yet well understood. Samples that make the trend have been listed on Table 4.13.

Table 4.6 Chemical analyses of Namibian Mesozoic anorogenic complexes
From Harris & le Roex, 2002, pgs. 10 and 26. Numbers refer to Lufilian Arc database.

#	Sample	SiO2	TiO2	Al2O3	FeOt	MnO	MgO	CaO	Na2O	K2O	P2O5	LOI	Total
	Notch	50.00	1.00	15.50	6.00	0.15	2.00	5.00	4.90	5.50	0.30	2.00	
Spitzkoppe Complexes													
X-92	CH9308	76.99	0.10	11.73	2.06	0.02	0.08	0.74	3.03	5.23	0.02	0.52	100.52
X-93	CH9309	76.04	0.04	12.83	1.57	0.02	0.04	0.62	3.89	4.93	0.01	0.46	100.45
X-94	CH9310	75.67	0.04	12.94	1.71	0.02	0.05	0.65	4.05	4.84	0.02	0.45	100.44
X-95	SMER11	69.75	0.51	12.55	5.77	0.08	0.11	2.30	2.55	6.29	0.09	1.38	101.38
Erongo Complex													
X-96	ERG	76.26	0.07	13.30	1.43	0.03	0.06	0.43	3.08	5.07	0.26	-	99.99
Brandberg Complex													
X-97	CH9301	74.98	0.16	10.39	5.06	0.07	0.06	0.16	4.43	4.69	0.00	0.66	100.66
X-98	CH9302	71.34	0.48	13.14	4.71	0.11	0.23	0.91	3.45	5.53	0.11	0.98	100.99
X-99	CH9306	71.05	0.45	13.09	4.38	0.11	0.30	1.46	3.46	5.60	0.10	0.49	100.49
X-100	CH9307	70.25	0.50	13.51	4.37	0.11	0.38	1.52	3.58	5.66	0.11	0.28	100.27
X-101	CH9401	69.97	0.55	13.70	4.65	0.11	0.30	1.88	3.59	5.15	0.11	0.56	100.57

#	Sample	Rb	Sr	Y	Zr	Nb	Ni	Cu	Zn	V	Cr	Ba	Sc	Ce	La	Na+K
	Notch	200	400	60	360	40	16	25	85	100	100	1300	20	175	95	
Spitzkoppe Complexes																
X-92	CH9308	473	14	157	196	141	3	3	44	2	7	75	2	148	84	8.3
X-93	CH9309	604	2	208	112	88	2	3	58	6	2	9	1	63	26	8.8
X-94	CH9310	620	1	214	128	83	4	4	45	2	7	2	-	54	21	8.9
X-95	SMER11	243	81	68	474	24	-	-	-	-	-	1051	10	162	77	8.8
Erongo Complex																
X-96	ERG	637	25	155	60	26	10	2	38			76	6			8.2
Brandberg Complex																
X-97	CH9301	1241	18	438	537	95						14		459	207	9.1
X-98	CH9302	211	111	66	483	56						856		134	64	9
X-99	CH9306	210	112	110	455	53						807		163	85	9.1
X-100	CH9307	209	111	78	505	61						808		144	66	9.2
X-101	CH9401	188	132	73	472	51								112	54	8.7

Table 4.7 Rock groups from Namibian Mesozoic anorogenic granitoid complexes and comparison with samples from the Hook Granite Batholith, Zambia
Based on R1/R2 diagram and chemical data from Table 4.5. See plots on Fig 4.21.

Site/Group	A	B	C	D	E
Spitskoppe	X-95	X-93, X-94	X-92		
Erongo			X-96		
Brandberg	X-99, X-100, X-101			X-98	X-97
Hook Granite Batholith	P-40ii, P-50, L-408	L-139	L-458	P-39, P-46, L-259B, L-436	L-442, L-443

Table 4.13 Hook Granite samples that show similarities with granitoid samples from Nigerian, Namibian and Corsican anorogenic ring complexes. *Underlined samples are members of the Hook Granite Batholith rock group indicated on third column. All data was obtained from TAS diagram of Fig 4.21.*

Anorogenic ring complexes	Sample numbers from Hook Granite Batholith	Hook Granite Batholith Rock Group
Young Nigerian, Namibian and Corsican ARC	X-46, L-257, L-436, L-355, L-259B, X-43, L-46, X-66, L-442, X-90, X-65, X-55, L-248-LG, P-40i	**XII**
Namibian Mesozoic ARC	L-238, L-239, X-72, L-408, X-68, X-75, X-60	
PanAfrican Nigerian black and white granitoids	L-343, L-354, L-341, L-403, X-63, L-079, X-52, L-263, L-348, X-45, P-58, X-73, X-57, X-56	**I**

Hook Granite midalkaline linear trend	L-213, L-212, L-214, X-49, L-012, L-012A, L-345, X-62, X-74, L-437, L-402, L-438, L-433, L-209

Nchanga Granite rocks that are similar to Nigerian ARC	L-151, L-154, L-153, L-162, X-43, X-36; also to a minor extent: P-29, X-35 and X-37

Table 4.8

Comparative chemical analysis from granite anorogenic ring complexes Hook Granite Batholith samples. (Boxes in yellow are anomalous values)
(complete trace element analysis on Table A3 in Appendix)

Anorogenic Granite Complexes, Nigeria

Sample	SiO2	TiO2	Al2O3	Fe2O3	FeO	MnO	MgO	CaO	Na2O	K2O	P2O5	LOI	Total	Rb	Sr	Y	Zr	Nb	Co	Ni	Cu	Zn	Ga	V	Cr	Ba	U	Th	Sc	Pb	Sm	Nd	Pr	Ce	La	Cs	Hf	Ta	As	Se	Eu	Gd	Tb	Dy	Ho	Er	Tm	Yb	Lu
AMN24	72.60	0.29	14.1	0.90	1.73	0.07	0.43	1.01	3.36	5.74	0.07	0.47	100.74	185	100	63	246	57				61		9		362		27		22				144	59		6													
B34	76.00	0.10	11.7	0.37	0.89	0.02	0.09	0.83	3.78	5.77	0.04	0.24	99.87	574	4	115	141	158				60		12		39		40		74				114	64		5													
DR11	76.70	0.14	13.4	0.00	1.16	0.03	0.05	0.33	4.41	3.58	0.02	0.34	100.12	966	0	87	81	119				103		4		0		61		47				149	88		9													
DW1	78.03	0.06	12.1	0.33	0.89	0.01	0.09	0.52	4.59	3.56	0.01	0.42	100.65	389	22	356	207	205				77		0		71		42		16				275	169		10													
FG5	77.44	0.08	12.0	0.37	0.87	0.02	0.07	0.49	3.89	4.45	0.01	0.34	100.02	347	3	189	161	148				42		0		43		39		27				117	64		8													
JON147	73.20	0.18	14.2	0.67	1.19	0.02	0.08	0.73	3.45	5.32	0.03	0.98	100.03	296	38	227	330	118				126		0		264		41		38				251	218		8													
KD12	76.50	0.10	12.8	0.35	0.84	0.02	0.07	0.46	4.17	4.39	0.01	0.34	100.08	283	4	144	147	96				48		0		4		36		41				62	27		6													
MD333	75.40	0.10	13.3	0.01	0.96	0.02	0.04	0.34	4.26	4.53	0.01	0.20	99.20	620	0	139	129	78			9	68		0		0		66		70				79	28		9													
NG208	75.70	0.20	13.2	1.48	0.01	0.03	0.09	0.44	3.41	5.10	0.01	0.66	100.31	318	29	75	186	80				70		2		151		63		57				156	83		7													
PAN112	73.90	0.15	14.9	0.43	0.80	0.02	0.67	0.43	3.98	5.17	0.02	0.61	101.06	192	28	117	234	88						0		80		25		22				195	189		7													
RN75	75.90	0.11	12.9	0.33	1.05	0.05	0.02	0.24	3.91	4.31	0.01	0.88	99.66	979	15	696	399	214			120	376		0		109		111		56				296	234		28													
T15A	74.30	0.08	11.7	0.33	0.89	0.02	0.01	0.26	3.88	4.59	0.01	0.64	96.75	502	1	86	166	132			7	61		3		0		69		37				153	166		7													

Mesozoic Anorogenic Granite Complexes, Namibia

Sample	SiO2	TiO2	Al2O3	Fe2O3	FeO	MnO	MgO	CaO	Na2O	K2O	P2O5	LOI	Total	Rb	Sr	Y	Zr	Nb	Co	Ni	Cu	Zn	Ga	V	Cr	Ba	U	Th	Sc	Pb	Sm	Nd	Pr	Ce	La	Cs	Hf	Ta	As	Se	Eu	Gd	Tb	Dy	Ho	Er	Tm	Yb	Lu
X-100	70.25	0.5	13.5	4.37		0.11	0.38	1.52	3.58	5.66	0.11	0.28		209	111	78	505	61								808								144	66															
X-101	69.97	0.55	13.7	4.65		0.11	0.3	1.88	3.59	5.15	0.11	0.56		188	132	73	472	51																112	54															
X-92	76.99	0.1	11.7	2.06		0.02	0.08	0.74	3.03	5.23	0.02	0.52		473	14	157	196	141		3	3	44		2	7	75			2					148	84															
X-93	76.04	0.04	12.8	1.57		0.02	0.04	0.62	3.89	4.93	0.01	0.46		604	2	208	112	88		2	3	58		6	2	9			1					63	26															
X-94	75.67	0.04	12.9	1.71		0.02	0.05	0.65	4.05	4.84	0.02	0.45		620	1	214	128	83		4	4	45		2	7	2			-					54	21															
X-95	69.75	0.51	12.6	5.77		0.08	0.11	2.3	2.55	6.29	0.09	1.38		243	81	68	474	24		-	-	-		-	-	1051			10					162	77															
X-96	76.26	0.07	13.3	1.43		0.03	0.06	0.43	3.08	5.07	0.26	-		637	25	155	60	26		10	2	38				76			6																					
X-97	74.98	0.16	10.4	5.06		0.07	0.06	0.16	4.43	4.69	0	0.66		1241	18	438	537	95								14								459	207															
X-98	71.34	0.48	13.1	4.71		0.11	0.23	0.91	3.45	5.53	0.11	0.98		211	111	66	483	56								856								134	64															
X-99	71.05	0.45	13.1	4.38		0.11	0.3	1.46	3.46	5.6	0.1	0.49		210	112	110	455	53								807								163	85															

Samples from Hook Granite that are similar to ring complex granites

Sample	SiO2	TiO2	Al2O3	Fe2O3	FeO	MnO	MgO	CaO	Na2O	K2O	P2O5	LOI	Total	Rb	Sr	Y	Zr	Nb	Co	Ni	Cu	Zn	Ga	V	Cr	Ba	U	Th	Sc	Pb	Sm	Nd	Pr	Ce	La	Cs	Hf	Ta	As	Se	Eu	Gd	Tb	Dy	Ho	Er	Tm	Yb	Lu
L-259-B	73.83	0.30	12.9	2.80		0.00	0.17	1.01	3.55	5.35	0.04	0.44	100.42	204	118	214	292	39	<6	<6	12	28	20	<12	15	617	10	29	<10					277	209															
L-408	70.26	0.33	13.6	3.87		0.05	0.26	1.23	3.49	5.24	0.07	0.43	98.82	241	95	104	348	33	7	6	15	34	23	<12	13	483	12	32	<10					241	121															
L-409	69.36	0.41	14.8	3.25		0.02	0.49	1.13	4.47	5.43	0.10	0.44	99.86	206	151	43	313	32	6	<6	10	16	19	25	12	677	13	53	<10					120	60															
L-436	73.93	0.27	12.0	2.68		0.04	0.17	1.02	4.15	4.81	0.06	0.39	99.55	235	74	45	303	31	<6	<6	10	21	21	<12	<12	195	26	99	<10					223	114															
L-439	70.07	0.33	13.0	4.06		0.02	0.22	0.77	4.27	5.46	0.05	0.62	98.86	243	66	90	572	46	<6	3	21	16	25	<12	<12	163	19	90	<10					237	124	9.73														
L-441	62.98	1.11	14.1	7.49		0.12	0.99	2.75	3.71	5.30	0.35	0.46	99.39	180	226	74	414	46	10	<6	13	88	24	28	<12	893	6	19	12					187	98															
P-39	72.16	0.28	12.6	3.40		0.08	0.12	1.17	4.67	5.57	0.11	0.17	100.13	404	43	109	309	59	56	4	<3	12	29	<4	5	182	19	71	4	11	21	114	33	290	145	2	10	3	<1	12	1	19	3	18	4	9	34	7	1
P-46	71.17	0.38	12.6	4.35		0.12	0.20	0.81	3.59	6.89	0.07	0.16	100.20	398	65	89	257	53	48	4	<3	45	27	<4	9	387	10	46	1	11	17	93	26	217	110	3	11	3	26	28	1	16	2	14	3	8	5	7	1
P-50	71.53	0.25	12.6	3.26		0.10	0.30	1.66	4.55	4.88	0.21	0.14	99.34	376	66	163	312	107	40	16	<3	30	27	<4	4	314	62	256	3	23	54	335	100	899	505	4	9	3	1	8	1	40	6	32	6	16	6	11	2
P-53	73.18	0.24	13.0	2.62		0.07	0.22	0.95	3.78	5.92	0.12	0.09	100.14	421	59	54	179	48	71	19	<3	<1	24	<4	24	209	21	43	2	11	6	26	8	78	44	6	6	3	6	6	1	6	1	7	2	5	32	5	1
P-57	62.19	0.36	13.1	2.44		0.05	0.26	0.86	15.42	5.52	0.06	0.21	100.27	225	45	375	404	48	63	21	<3	1	24	<4	<4	286	10	51	6	5	79	499	134	735	579	2	11	3	<1	5	8	81	10	56	11	29	36	21	3
P-58	67.76	0.79	13.5	6.83		0.17	1.40	2.21	3.78	4.27	0.18	0.25	100.85	210	189	66	223	30	77	4	21	72	26	45	12	680	4	24	8	12	10	51	13	107	53	5	6	2	1	30	2	10	2	9	2	5	33	4	1
X-45	68.41	0.69	14.5	4.60		0.08	1.29	2.07	3.47	4.63	0.25																																							
X-52	67.17	0.72	14.6	4.81		0.07	1.20	2.05	3.59	5.30	0.20																																							
X-53	71.79	0.23	14.2	2.57		0.05	0.37	1.06	3.40	5.64	0.12																																							
X-58	71.10	0.28	14.5	2.30		0.03	0.29	1.10	3.40	6.30	0.07																																							
X-59	69.70	0.52	14.2	3.40		0.07	0.60	1.70	4.80	5.50	0.14																																							
X-60	71.10	0.38	13.6	3.60		0.06	0.42	1.50	3.50	5.50	0.08																																							
X-61	71.74	0.27	14.5	2.05		0.05	0.42	1.62	3.44	4.65	0.24																																							
X-63	64.77	0.89	15.3	5.55		0.08	1.45	2.54	3.83	4.30	0.27																																							
X-66	72.86	0.30	14.4	3.45		0.04	0.54	0.93	3.98	5.25	0.09																																							
X-73	67.24	0.73	14.5	5.20		0.03	0.95	2.17	4.44	3.53	0.26																																							

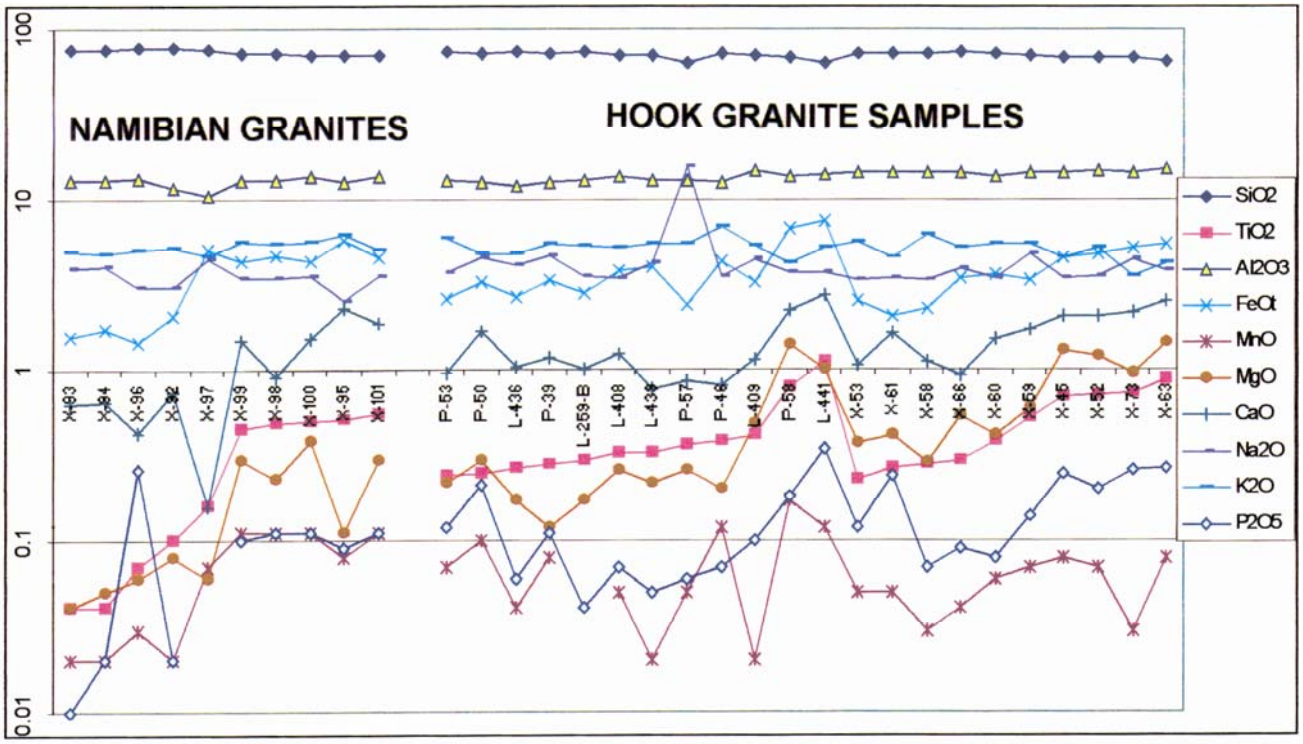

Fig 4.20 Logarithmic major oxide plot to compare Namibian granitoid ring complexes with samples from the Hook Granite Batholith. FeOt represents total iron oxides. Samples on the left come from the Nigerian complexes; the other are from the Hook Granite. The ten samples from the right lack trace element analysis.

In conclusion, the chemistry of granitoids from the Mesozoic anorogenic complexes from Namibia is quite similar in trace element and major oxide geochemistry to some samples from the Hook Granite. These are shown on Table 4.8.

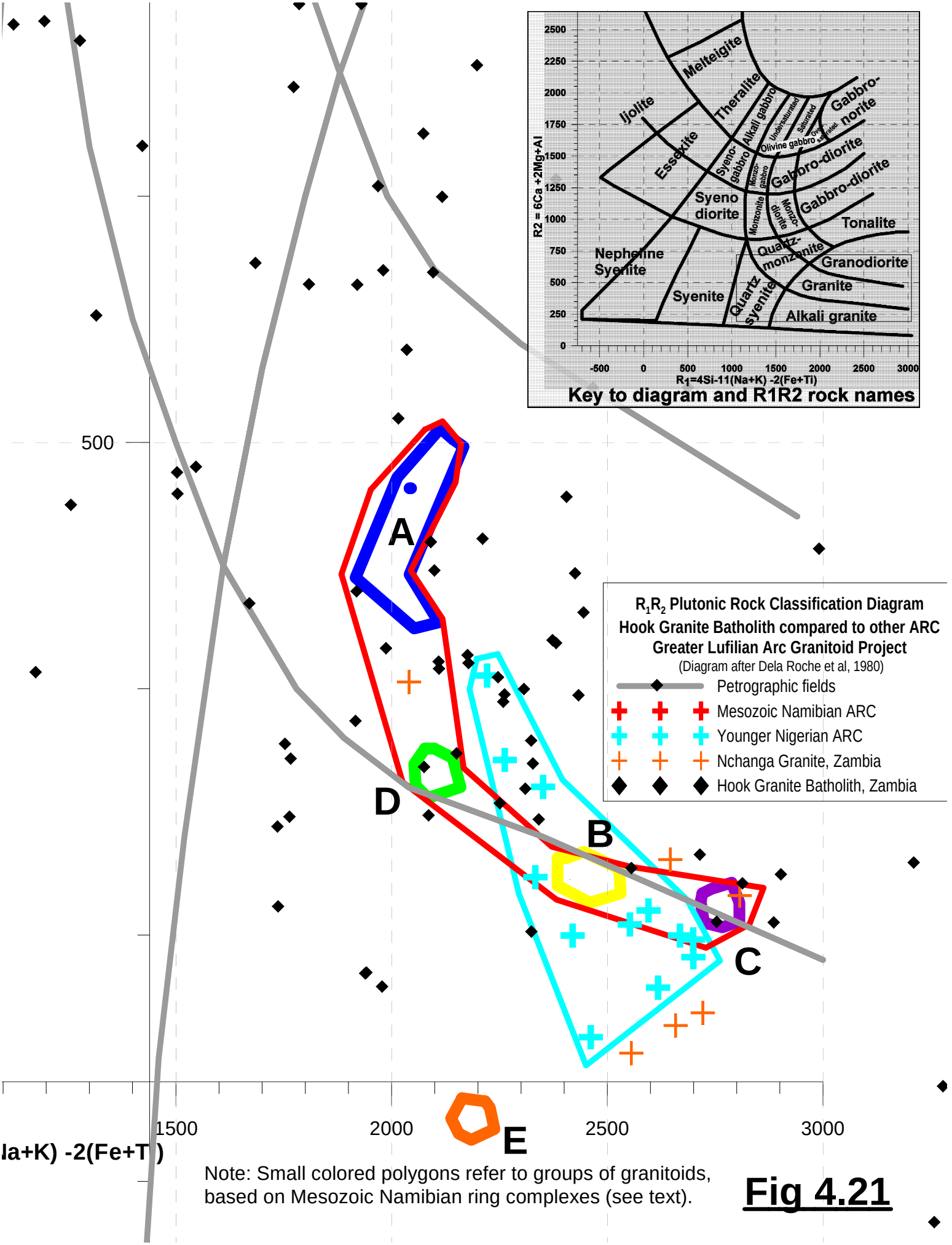

Note: Small colored polygons refer to groups of granitoids, based on Mesozoic Namibian ring complexes (see text).

Fig 4.21

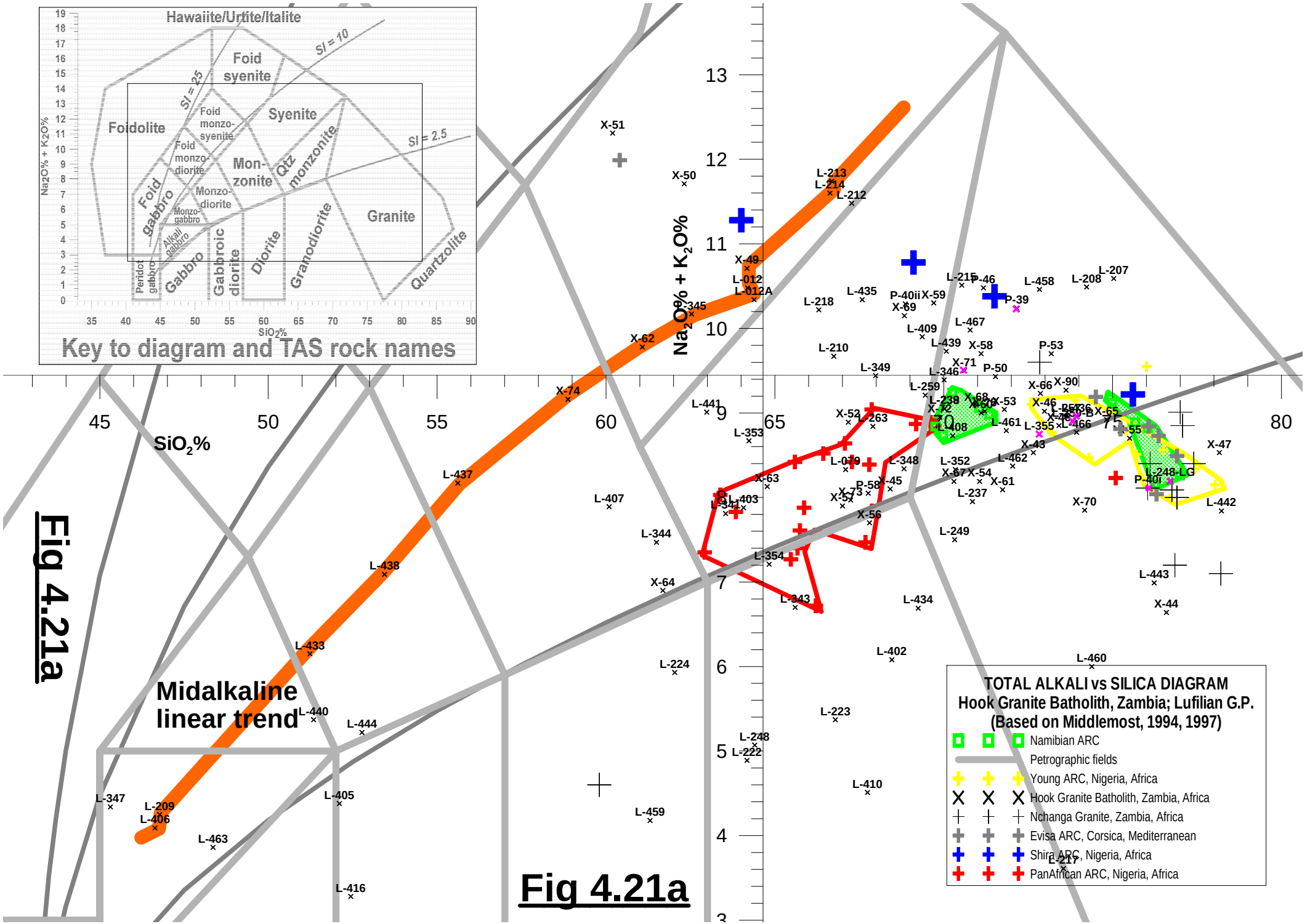

Fig 4.21a

Fig 4.21a

4.1.1.5 E-W transect across the Kafue Park, Zambia

A well-paved road runs E-W across the Hook Granite Batholith in the Kafue National Park (Figs 4.1 and M2 to M5, in Appendix). Since most of the rest of the batholith lacks good infrastructure, detailed sampling was carried out along that main road. Outcrop is sparse along the transect, rarely of good quality. In most cases, relationships between the various types of rocks identified was not clear. A total of 57 outcrops were visited along the 90 kilometer transect; each outcrop was located using a GPS. Only representative outcrops were fully described and sampled. Thirty samples were collected, twelve of them were analysed and they are listed on Table 4.9. Differences based on grain size, main constituents and foliation helped to name and group them in the field. At least five different generations of granitoids were identified along the transect. Part of the rocks contain more xenoliths than others. Hydrothermal brecciation, minor mineralization and tourmalinization were observed in a few places. A summary of main field observations along the transect is included in Appendix A57.

Table 4.9 Analysis of samples along E-W transect across the Hook Granite Batholith, Zambia
(X= samples collected in the field; P = samples by Pepper, 1999; Z = from Zambian Geological Survey. (complete elemental on Table A3, in the Appendix)

Sample	#	SiO2	TiO2	Al2O3	Fe2O3	MnO	MgO	CaO	Na2O	K2O	P2O5	Rb	Sr	Y	Zr	Nb	Co	Ni	Cu	Zn	Ga	V	Cr	Ba	U	Th
L-237 X	VII	71.99	0.38	13.45	4.08	0	0.53	1.38	2.55	5.53	0.11	151	276	74	194	24	8	6	25	16	18	28	<12	815	<6	26
L-238 X	VII	70.25	0.46	14.26	4.48	0	0.7	2.14	3.1	4.43	0.17	110	399	59	238	26	8	<6	28	19	19	37	27	647	<6	27
L-239 X		70.61	0.51	13.67	3.74	0	0.68	1.51	2.91	6.21	0.15	156	260	58	240	27	7	<6	9	18	18	33	15	747	6	24
L-241 X		0	0	0	0		0	0	0	0	0	156	229	55	174	24	0	0	0	0		0	0	594	0	0
L-242 X		77.64	0.3	11.04	6.03	0.01	2.07	0.21	0.58	2	0.11	42	228	33	256	11	14	18	8	12	38	87	309	617	7	<15
L-248 X		65.34	0.92	15.57	6.43	0	2.78	3.54	3.01	2.13	0.26	126	300	54	205	42	15	15	13	28	25	109	39	271	6	<15
L-248-lg X	XI	76.73	0.14	13.26	0.92	0	0.04	0.66	3.71	4.49	0.04	121	314	48	206	20	9	7	8	16	19	35	25	745	<6	27
L-249 X	VII	71.3	0.43	14.24	3.55	0	0.76	1.99	3.04	4.56	0.14	123	309	49	211	23	8	7	8	16	19	45	21	716	<6	20
L-257 X		73.96	0.26	13.36	1.98	0	0.15	1.24	3.69	5.31	0.05	214	117	53	208	25	6	<6	<6	13	22	<12	14	321	16	74
L-259 X	XI	69.83	0.42	15.53	2.79	0	0.29	1.81	3.12	6.14	0.07	174	199	72	402	47	7	<6	<6	21	20	13	26	911	7	21
L-259-b X		73.86	0.3	12.92	2.8	0	0.17	1.01	3.55	5.35	0.04	204	118	214	292	39	<6	<6	12	28	20	<12	15	617	10	29
L-263 X	C	68.89	0.55	14.13	2.53	0	0.72	3.94	3.34	5.63	0.27	83	640	51	244	26	7	<6	23	15	20	34	16	920	<6	19
L-354 Z		66.12	0.83	15.12	6.31	0.07	1.49	2.5	3.21	4.14	0.2	138	207	77	435	25	11	17	115	78	20	71	22	977	<6	22
L-403 Z		64.33	0.68	14.67	7.89	0.06	1.14	3.14	3.51	4.4	0.16	119	277	83	762	25	9	9	196	89	25	19	19	1054	8	17
L-405 Z	II	52.99	1.24	16.33	10.19	0.11	5.39	9.13	3.36	1.1	0.15	23	882	24	121	14	37	72	30	53	17	220	35	226	<6	<15
L-406 Z	II	47.73	2.54	13.46	14.47	0.24	6.7		3.37	0.82	0.27	11	282	38	180	17	43	73	80		18	374	106	118	<6	<15
L-408 Z	IV	71.41	0.34	13.81	3.93	0.05	0.26	1.25	3.55	5.33	0.07	241	95	104	348	33	7	6	15	34	23	<12	13	483	12	32
P-58 P	I1	67.19	0.78	13.35	6.77	0.17	1.39	2.19	3.75	4.23	0.18	210	189	66	223	30	77	4	21	72	26	45	12	680	4	24

If the transect is considered to be representative of the main batholith, it consists of granites and minor granodiorite that correspond to the map units listed on Table 4.4. From the TAS diagram of Fig 4.22, one might conclude that there are six distinct rock types in the batholith. After processing data of the transect, geology observed in the outcrops was not coherent with the map units indicated on Table 4.4. Map units did not make any geological sense. Table 4.10 shows the ways in which samples from the transect can be grouped.

Table 4.10 Samples collected along the E-W transect through the Kafue Park, Hook Granite Batholith
(Underlined samples were anaysed.) Map units are correlated on Table 4.12.

Map Unit (Table 4.5)	Map sheet	Sample Numbers
O	1426SW +1426SE	L-235, L-236, L-237, L-238, L-239, L-240, L-250, L-251, L-252, L-254, P-57, L-257, L-258, L-259, L-354, L-261, L-263
N	1426SW	L-241, L-245, L-246, L-244, L-248, L-249, L-247
L	1426SW	L-253, L-255, L-256
H	1426SW	L-260
A	1426SW	L-262, P-58
B	1426SE	L-405, L-403
Unidentified	1426SE	L-406, L-408

The E-W transect along the Kafue National Park intersected complexes J (4), K (2), L (8), M (4), and O (2) (See Table 4.12). In all cases except for ring complex K, both rim and nucleus were sampled (Fig 4.17 and Table 4.12). Some portions of the ring complexes contain anomalous copper, and part of them are also enriched in zinc, as shown. Outcrops are scattered around and they lack continuity to enable proper geological mapping to be done. In the field, it is virtually impossible to establish that one is looking at ring complexes, because the various relations of rocks exposed do not provide clues.

Fig 4.23 illustrates a hypothetical case of a ring complex cluster. Something similar might have been the case of the Hook Granite Batholith. The hypothetical transect across the series of ring complexes produces a lithological variation that is difficult to interpret without having the map of the ring complexes. Several such detailed traverses may help in understanding the geology and interpreting the geological history of the rock massif.

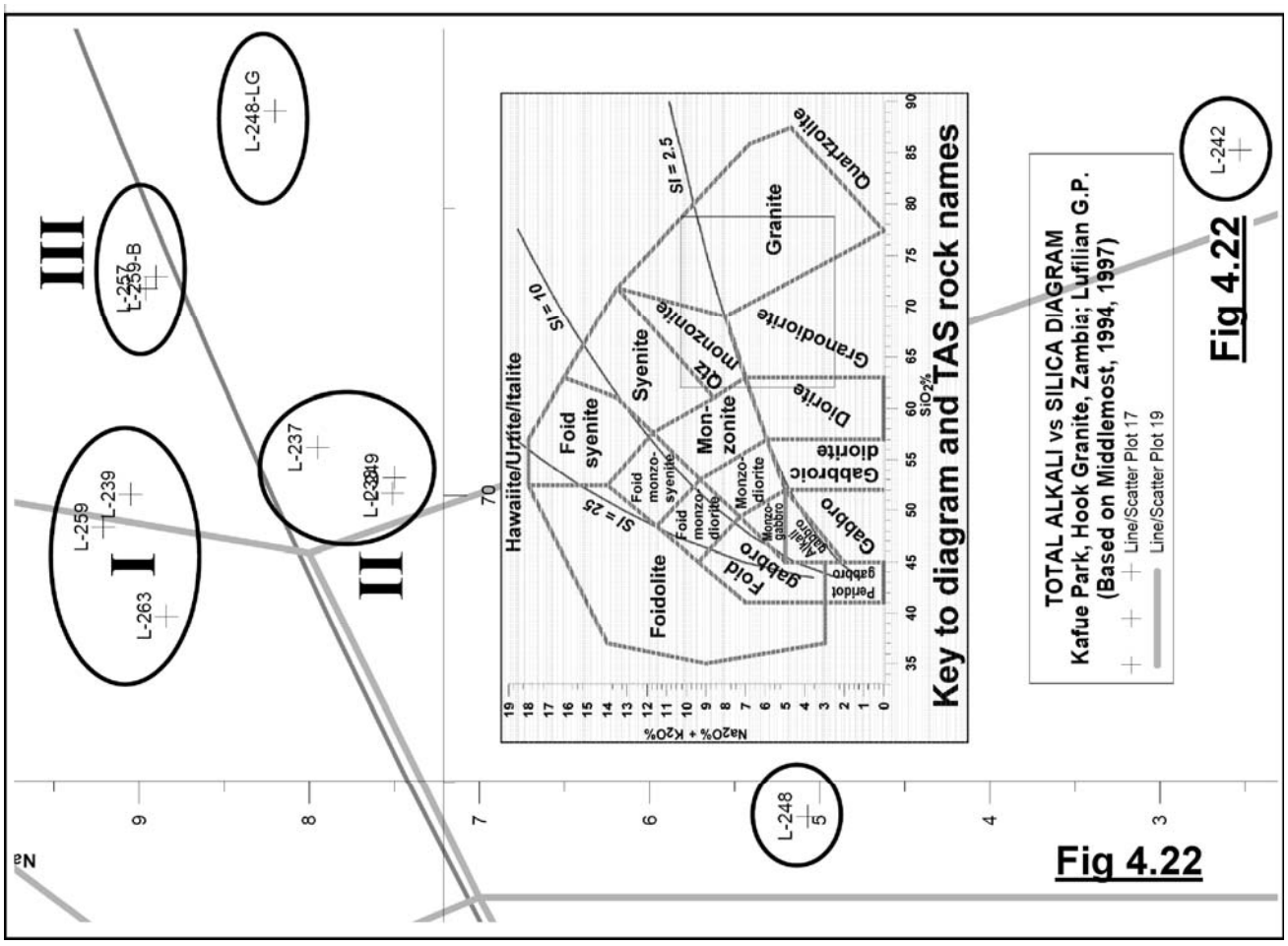

Fig 4.22 Total alkali versus silica diagram for samples collected along the E-W transect through the Kafue Park, Hook Granite Batholith, Zambia. *See more details in text.*

4.1.1.6 Geochronology and Geological History

Hanson et al, 1993 compiled the geology of the Hook Granite Batholith and dated what they considered were the main geological events of the batholith. Table 4.13 lists their ages and Fig 4.15 illustrates the position of samples dated. UTM coordinates of the samles have been included on Table 4.4. Other ages available for the Hook Granite and its environs are listed on Table A22.1 in the Appendix. These ages were plotted on the event diagram of Fig A23 (Appendix). Based on that diagram, the time span for emplacement of the Hook Granite Batholith is 40 million years (from 570 to 530 Ma). See also Table 4.13 with correlation of the various geological map sheets and their geological units.

Table 4.14 Radiometric ages for the Hook Granite Batholith published by Hanson et al, 1993. *All information was extracted from the original publication. Coordinates of the samples are listed on Table 4.4. Ring complex location is shown on Fig 4.18.*

Sample	Age (Ma)	Rock type	Ring complexes dated
H-1	559±18	Deformed, fine- to medium-grained granite	V
H-2	566±5	Deformed megacrystic granite	V
H-3	538±1.5	Rhyolite dike within Katangan pendant	R
H-4	533±3	Post-tectonic megacrystic granite	P?
H-5	551±19	Rhyolite intrusion in Mwembezhi Dislocation	AJ

Hanson and co-workers define six different intrusive events for the batholith. There might be younger ones, since they did not date any of the syenitic bodies, which seem to have come later, according to recent field observations. Intrusives dated around 750 Ma might have been precursors to the main Hook Granite event.

Table 4.12 Samples from the E-W transect through the Kafue Park, Hook Granite Batholith, *and correspondence with ring complexes from Fig 4.18 and geological map units of Table 4.4*
(X= samples collected in the field; P= samples by Pepper, 1999; Z=from Zambian Geological Survey. Underlined samples have chemical analysis. The last two columns indicate high Cu or Zn values.)

Samples	Source	Chemical rock type	New unit (Table 4.5)	Map unit (Table 4.5)	Map sheet	Ring complex (Fig 4.6)	Position	Rock type (sensu TAS)	Cu	Zn
L-254	X		9	O	1426SW	**J**	nucleus	Granite		
L-255	X			L	1426SW		rim	Granite		
L-256	X			L	1426SW		nucleus	Granite		
L-257	X	XI	9	O	1426SW		rim	Granite		
L-253	X			L	1426SW	**K**	nucleus	Quartz pod		
P-57	P	unclassified	9	O	1426SW		nucleus	Granite	X	
L-258	X		9	O	1426SW	**L**	nucleus	Granite		
L-259	X	XI	9	O	1426SW		nucleus	Granite		
L-259B	X	Unclassified	9	O	1426SW		nucleus	Granite		
L-260	X		3	H	1426SW		nucleus	lt bn granite		
L-261	X		9	O	1426SW		nucleus	Granitoid+cp	X	
L-262	X				1426SE		nucleus	granitoid+cp+py	X	
L-354	Z	I	9	O	1426SW		rim	Granodiorite	X	
L-433	Z	II			1426SW		rim	Syenogabbro	X	X
L-263	X	Unclassified	9	O	1426SW	**M**	rim	foliated granitoid		
L-264	X		1	B	1426SE		nucleus	foliated granitoid		
L-265	X			?	1426SE		nucleus	bn granitoid		
L-408	Z	IV		?	1426SE		rim	Granite		
L-403	Z	VII	1	B	1426SE	**O**	rim	Quartzmonzonite	X	X
L-406	Z	II		?	1426SE		rim	alkali gabbro	X	X
P-58	Z	II			1426SE		nucleus	Granite		
L-235	X		9	O	1426SW	Unidentified		granitoid		
L-236	X		9	O	1426SW	Unidentified		Hornfels		
L-237	X	VII	9	O	1426SW	Unidentified		Granite	X	
L-238	X	VII	9	O	1426SW	Unidentified		Granodiorite		
L-239	X	VII	9	O	1426SW	Unidentified		granite		
L-240	X		9	O	1426SW	Unidentified		granitoid		
L-241	X	Unclassified	2	N	1426SW	Unidentified		Foidolite		
L-244	X		2	N	1426SW	Unidentified		pink granitoid		
L-245	X		2	N	1426SW	Unidentified		pink granitoid		
L-246	X		2	N	1426SW	Unidentified		gray granitoid		
L-247	X		2	N	1426SW	Unidentified		foliated granitoid		
L-248	X	Unclassified	2	N	1426SW	Unidentified		Granodiorite		
L-248LG	X	XI			1426SW	Unidentified		granitoid		
L-249	X	VII	2	N	1426SW	Unidentified		Granite		
L-250	X		9	O	1426SW	Unidentified		granitoid		
L-251	X		9	O	1426SW	Unidentified		granitoid		
L-252	X		9	O	1426SW	Unidentified		granitoid		
L-405	Z	II	1	B	1426SE	Unidentified		s. oliv. Gabbro	X	

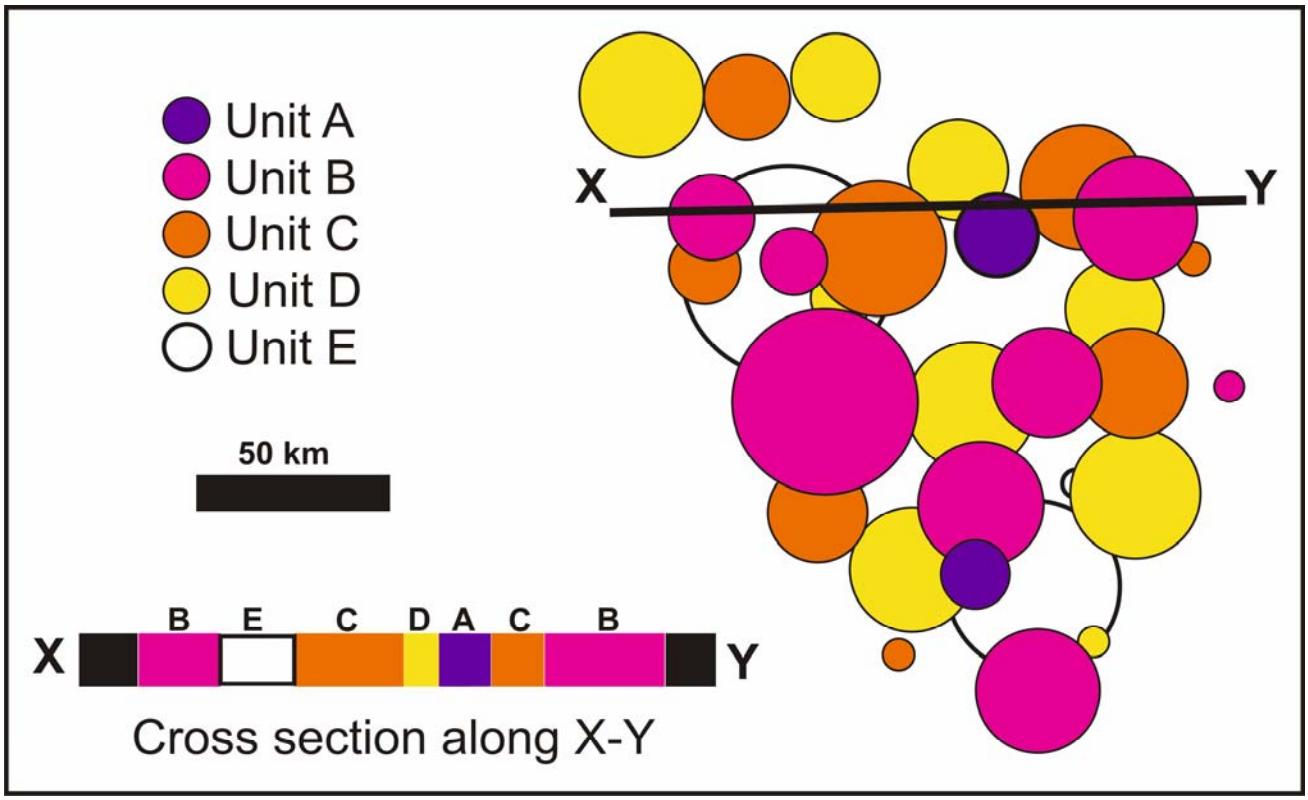

Fig 4.23 Hypothetical granitoid ring complex cluster and transect across it. *Notice that if a series of five different generations of granitoid ring complex structures intrude and intersect each other, a complex assembly of igneous lithologies can form. Each of the separate intrusive events (A to E) was made of a few ring complexes widely spread in the area. In the hypothetical case, each generation of ring complexes has a uniform lithology. A chance orientation for a geological transect along X-Y results in the geology shown. Interpretation of that geology based on the single transect is quite complex, especially if the outcrop density is not good. Compare with Fig 4.18.*

Hanson et al, 1993 dated samples that come from various granite ring complexes. Ring Complex V had samples **H-1** inside and **H-2** on the rim; both could be dating the same event. **H-5** is located on the rim of ring AJ; no samples from this project were collected there. **H-5** was said to be a rhyolite intrusion into the Mwembezhi Dislocation; that sample dates at least one of the intrusive events that took place along that major structure. **H-3** comes from the same site as **L-40i** and both lie on the rim of ring R. according to Hanson et al, 1993, **H-3** comes from a rhyolite dike within a Katangan pendant. **H-4** could come from the rim of not very well defined complex P.

A tentative geological history for the Hook Granite Batholith may be established out of interpreting its geophysical image with the radiometric ages published by Hanson et al, 1993. Four distinct events of faulting can be established, and using cross-cutting relationships of the various ring complexes, the sequence of events illustrated on Fig 4.24 turns out. Note that available rock dating does not include a large portion of the plutons on Fig 4.24. If ring complexes AO and AQ were dated geochronologically, the geological history of the batholith would be much better constrained. These two seem to be the oldest and youngest ring complexes, based on data available. The basement to the oldest granite complexes is also made by granitoids; these rocks are probably the oldest in the batholith and have not been given names.Timing of the structural evolution could also be defined precisely by dating ring complexes that are younger and older than the faults.

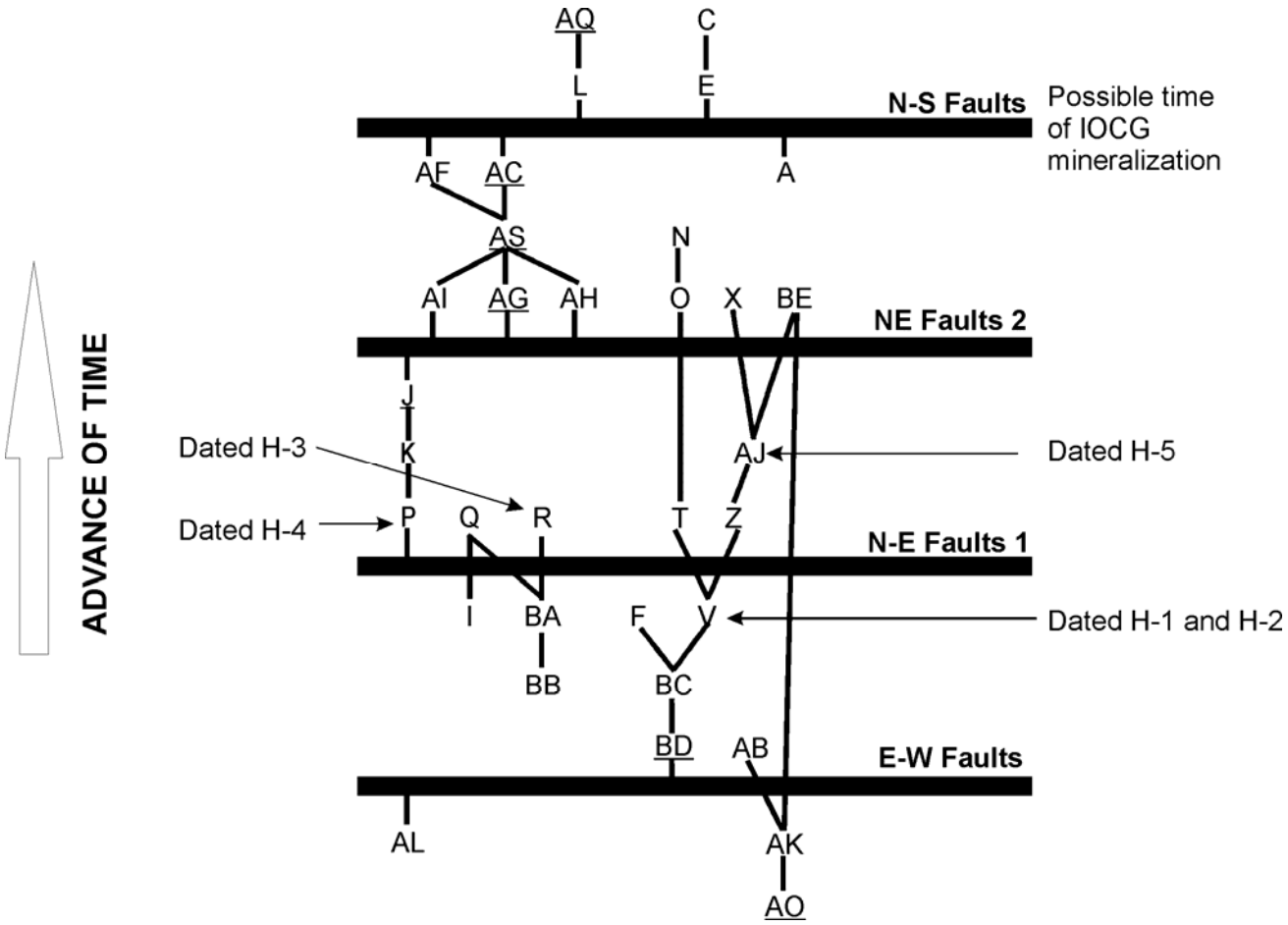

Fig 4.24 Schematic representation of the various events that gave rise to the current geology of the Hook Granite Batholith. *Each letter represents the emplacement of a single granitoid ring complex. Time advances upward. The diagram is based on cross-cutting relationships observed in interpreted geophysical images (Fig 4.18). Four distinct generations of faulting are recognized, and they help to establish the order of emplacement. Only events joined by black lines have direct sequential order. For example, V is older than T, that is older than O. Nevertheless, the temporal relationship between V, F, BA and I has not established. Underlined ring complexes could be dated to refine geological history of the Hook Granite Batholith.*

As previously discussed, IOCG mineralization took place along various N-S faults. The age of those events in uncertain, but probably younger than 532 Ma.

If the batholith was made by amalgamation of anorogenic granitoid ring complexes, geochronological studies of Hanson et al, 1993 are not representative of the entire Hook Granite; especially for the pre-tectonism granitoid phases. The geological model on which they based their observations and geochronological deductions was partially wrong. There might be significant changes in the picture if more ring complexes were dated. Case studies from other similar size, ring complex clusters, such as those in the Nuba mountains of Sudan and in central Nigeria show that the main intrusive event is pre-dated and post-dated by various other anorogenic intrusions (Section 7.2).

The model here presented for the Hook Granite could be refined by dating rocks of ring complexes AQ, AC, AS, AG, U, BD, and AO. These are underlined on Fig 4.23. The new information would produce a much better constrained geological history of the batholith. Dating complexes AF, AC, A, L and E would provide a good geochronological grasp on the timing of the N-S faults, and could help to constrain the age of at least one of the IOCG mineralizing events.

4.1.1.7 Environment of Emplacement

At least the samples listed on Table 4.8 formed in intra-plate anorogenic rift environments, by comparison with samples from anorogenic ring complexes in Sudan, Namibia and Nigeria. All other samples that come from some of the ring complexes mapped on Fig 4.18 probably have a similar origin. The last phases of rift magmatism in the batholith seem to have taken place in close temporal association with tectonism. Table 4.5 shows that granitoids in groups IV, VII and IX formed as continental epeirogenic uplift granitoids, in an anorogenic environment. Part of the samples indicate a post orogenic environment of emplacement. Associated gabbroid rocks formed in continental extensional environments. The environment of emplacement of all samples from the batholith will be refined using the automated process of comparison described in section 2.4.

4.1.1.8 Conclusions

We can conclude that information currently available on geophysics, geochronology, rock distribution and geochemistry from the Hook Granite Batholith fit quite well with an intracontinental, anorogenic, ring complex cluster origin. A series of ring complexes roughly centered on the same place for a period of at least forty million years could very well have produced a body of the size of the current Hook Granite. More than fifty individual ring complexes have been identified.

The Hook Granite Batholith is mainly made of midalkaline granitoids. Alkali granites, quartzmonzonites and granites make up 70% of all samples. Rock composition varies widely from one ring complex to the next, and also within individual ring complexes. The suite of 104 samples collected from the batholith has been grouped into eight main types, but 40% of them do not classify into those groups.

A 90 kilometer E-W transect across the batholith sampled five different ring complexes and proved that published geological maps do not represent the reality.

Many features of iron oxide-copper-gold mineralization were identified in the batholith. Some of them include massive iron oxide bodies, red-altered intrusives, round-pebble hydrothermal brecciation, gold, copper, zinc and silver occurrences and some old mines. Several of the samples analysed carry copper enrichment. Zinc values are high in a few granites and syenites, as well as in most of the gabbroids analysed. Zinc-rich samples come from at least nine different ring complexes.

4.1.1.9 Recommendations

There is so little outcrop in the Hook Granite area, that field mapping on its own is not enough to understand the geology. Airborne geophysics should be used to guide and help interpret the field observations. Good geological maps of the Hook Granite Batholith could be made by going back to the original field maps and using the outlines of the outcrops. If only mapped real data is re-interpreted with the airborne geophysics, a reasonable geological map may be produced. All of the samples collected by Zambian Geological Survey geologists should be precisely located on topographical maps, using the original field notebooks. Many of these samples have already been analysed during the Lufilian Arc granitoid project. Such samples can be used to re-map the entire area.

All samples collected during the mapping of the Hook Granite could be precisely located with a few days of office work at the Zambian Geological Survey. Once their precise location is known, well-selected samples could be dated to complete the process. Wherever new roads or ways of access are available, additional sampling and mapping could be carried out to complete those portions of the maps. The entire project could be completed in two month’s time by the Zambian Geological Survey, and should not be expensive to execute.

4.1.2 WEST LUSAKA AND KAFUE FLATS REGION, ZAMBIA

4.1.2.1 Introduction

This portion of Zambia is known to have various copper occurrences associated to iron oxide bodies that outcrop as prominent hills (See Fig 8.12). The Nampundwe pyrite mine[1] is located in the West Lusaka region, while the Dunrobin and Matala gold mines, the Lewis-Marie copper mines, and the Kitumba and Kantonga copper deposits, occur to the north of the Kafue Flats area. Shimyoka, another mineralized domain where various mineral deposits have been sought for in the last decade, lies just south of the Kafue Flats area. As illustrated on Figs 8.40 and M7, Cu, Zn, Au and Fe occurrences are known throughout this zone.

4.1.2.2 Geochemistry

Twenty nine chemical analyses of samples conform the database of Table 4.1.2.1. The Zambian Geological Survey provided **L-416** and **L-458** to **L-467**, analysis for **X-90** (labeled "Lusaka Granite") comes from Simpson, Drysdall, & Lambert, 1963, p. 25; the remainding seventeen samples were collected during field work by the author. The rocks analysed can be grouped into six discrete types, as shown on Figs 4.1.2.1 and 4.1.2.2. These are listed on Table 4.1.2.2.

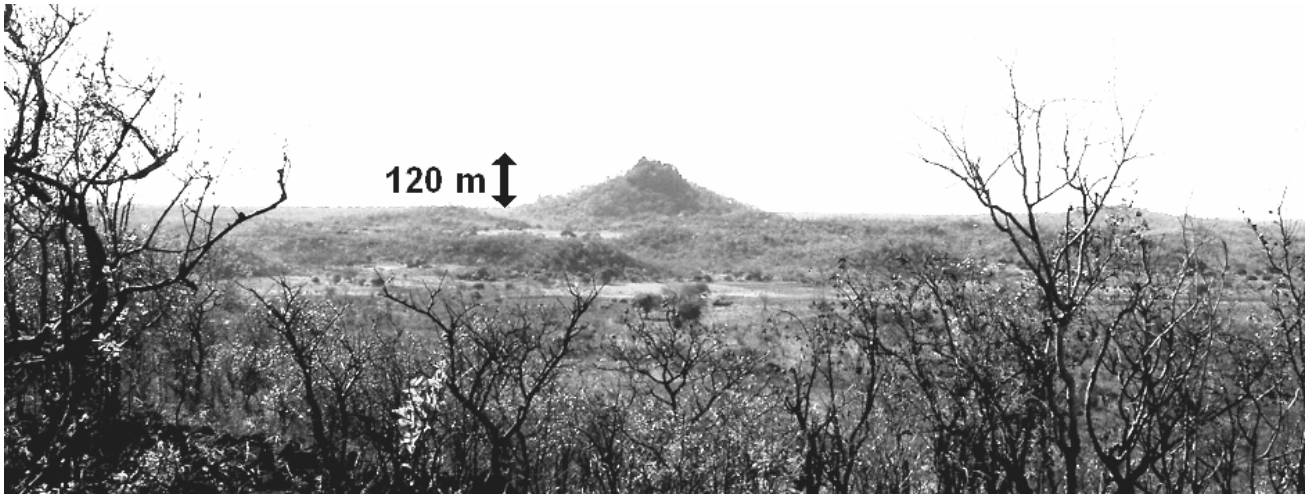

Fig 8.12 (brought in from Chapter 12) Hill of massive magnetite that outcrops west of Lusaka, Zambia*. As shown here, massive iron oxide bodies in this part of the Lufilian Arc produce these interesting geomorphological features. They stand out up to 120 meters above the average flat plateau. In the foreground, rolling hills are syenitic intrusive bodies. Small gabbroic bodies are also found in the environs. Abundant hydrothermal breccias with sulfide mineralization occur here too.*

The West Lusaka and Kafue Flats region has very abundant small gabbroic bodies (group D); nevertheless, these were not sampled as often, and few of the ones collected were analysed. Group F is made of single sample **L-217**; it contains abnormally high Cr, anomalous Mg, Pr, Co and Ni, and very low Na and Al. At the time of collection the rock was thought to be a red syenite, but its chemistry indicates granodioritic composition. Group G is made of hydrothermally altered granites that plot as granodiorite-diorite on the TAS diagram (Fig 4.1.2.1). Samples **L-222**, **L-223** and **L-224** contain anomalous iron oxide, high loss on ignition, abnormally high Rb and Ce and low Mn, Ca and Na. In addition, two samples of massive iron oxide were collected (**L-464** and **L-465**).

The pattern of multiple compositional fields re-occurs here, and is fully recognized. Four contrasting rock types that occur together. Granites B probably are the host rock, and alkali granites A, syenites C and gabbros D were intruded into them, giving rise to the large iron oxide bodies and sulfidation in the region. Quartz pods are also quite common in some parts, especially around **L-175**.

[1] The Nampundwe pyrite mine was previously called King Edward mine.

Table 4.1.2.1 Chemical Analysis of samples from the West Lusaka-Kafue Flats Area, Zambia
(Complete elemental analysis on Table A2, Appendix)

Sample	SiO2	TiO2	Al2O3	FeOt	MnO	MgO	CaO	Na2O	K2O	P2O5	LOI	Total
Notch	50.00	1.00	15.50	6.00	0.15	2.00	5.00	4.90	5.50	0.30	2.00	
Notch	50.00	1.00	15.50	6.00	0.15	2.00	5.00	4.90	5.50	0.30	2.00	
L-175	74.72	0.41	12.60	2.96	0.00	0.41	1.08	2.71	4.60	0.09	0.32	99.90
L-181	49.82	1.08	15.86	11.33	0.16	6.30	11.28	2.94	0.24	0.06	0.86	99.94
L-195	61.25	0.38	15.84	8.67	0.09	0.04	2.35	5.66	5.03	0.09	0.51	99.91
L-207	75.03	0.07	13.63	0.68	0.00	0.00	0.11	4.32	6.27	0.01	0.26	100.39
L-208	74.23	0.05	13.85	0.87	0.03	0.00	0.12	4.36	6.13	0.05	0.24	99.93
L-209	46.78	1.81	16.06	11.33	0.05	7.51	11.46	2.34	1.91	0.57	0.60	98.79
L-210	66.74	0.43	17.99	3.52	0.00	0.29	0.69	9.58	0.09	0.14	0.39	99.87
L-212	67.27	0.40	15.94	2.89	0.00	0.15	0.81	4.44	7.04	0.03	0.71	99.69
L-213	66.68	0.36	17.40	3.03	0.00	0.08	0.23	6.87	4.87	0.03	0.60	100.17
L-214	66.63	0.39	17.62	1.54	0.03	0.00	0.24	7.68	3.92	0.06	0.63	98.74
L-215	70.53	0.23	16.82	0.65	0.00	0.00	0.15	10.32	0.19	0.03	0.36	99.30
L-217	73.54	0.39	10.80	3.98	0.09	3.40	1.35	0.64	2.97	0.15	2.41	99.72
L-218	66.30	0.52	15.92	4.64	0.00	0.49	2.01	4.79	5.43	0.11	0.21	100.42
L-222	64.17	0.57	13.11	13.72	0.00	0.80	0.08	0.15	4.74	0.12	2.46	99.94
L-223	66.79	0.57	14.12	10.16	0.00	0.79	0.08	0.17	5.20	0.10	2.49	100.48
L-224	62.03	0.58	13.42	15.02	0.00	0.62	0.07	0.24	5.69	0.11	2.33	100.13
L-416	52.44	0.65	15.34	8.63	0.15	7.28	12.42	2.55	0.73	0.07	0.20	100.46
L-458	72.83	0.09	13.43	1.35	0.02	0.00	0.20	3.52	6.94	0.03	0.37	98.78
L-459	61.30	0.79	13.54	9.09	0.13	3.38	5.88	3.02	1.16	0.10	0.63	99.02
L-460	74.38	0.43	11.58	4.11	0.03	0.62	1.86	3.67	2.33	0.12	0.34	99.47
L-461	71.85	0.20	14.11	1.77	0.02	0.26	1.01	3.45	5.34	0.06	0.70	98.77
L-462	72.04	0.34	13.78	2.58	0.02	0.38	1.21	3.18	5.19	0.04	0.37	99.13
L-463	48.36	2.43	14.19	14.79	0.19	7.26	7.68	2.85	1.01	0.40	-0.53	98.63
L-464	5.46	0.07	0.00	77.49	0.08	0.50	6.09	0.10	0.52	0.06	3.16	93.53
L-465	14.01	0.58	2.56	64.74	0.03	0.70	0.17	0.06	0.43	0.12	12.85	96.25
L-466	73.93	0.13	12.78	1.65	0.03	0.08	0.98	4.27	4.50	0.03	0.30	98.68
L-467	70.78	0.25	13.75	2.33	0.02	0.18	0.87	4.53	5.45	0.08	0.50	98.74
X-90	73.62	0.31	12.90	2.21	0.05	0.42	1.13	3.37	5.90	0.10	0.44	100.45

Sample	Rb	Sr	Y	Zr	Nb	Co	Ni	Cu	Zn	Ga	V	Cr	Ba	U	Th	Sc	Sm	Nd	Pr	Ce	La	Hf	Ta	Eu	Gd	Yb	Lu
Notch	200	400	60	360	40	30	16	25	85	26	100	100	1300	20	37	20	50	50	15	175	95	10	120	4.0	30	7.5	1.6
L-175	221	63	45	229	29	9	7	31	31	15	28	17	541	<6	25	<10	6	30	48	153	19		42	0.3		1.3	0.8
L-181	7	157	29	62	8	34	30	57	94	16	293	35	<22	<6	<15	35				<12	<12						
L-195	89	130	115	1054	80	<6	<6	10	71	40	13	<12	2151	8	<15	<10	16	44	74	118	25		145	3.9	1.5	7.5	2.2
L-199	10	787	42	534	47								399	9	39		20	137	36	288	95	11	3	5.4	13	3.8	0.5
L-207	123	182	12	432	6	8	6	10	13	0	<12	13	557	0	0	0			5	0	2	19		0.2	0.6		0.4
L-208	137	178	12	431	33	<6	<6	14	10	25	<12	238	517	9	132	<10				35	20						
L-209	53	1592	27	111	17	36	42	29	52	19	243	50	1437	<6	<15	27				113	61						
L-210	4	275	30	474	36	6	7	143	13	22	28	<12	83	7	74	<10				372	223						
L-212	149	117	51	336	49	8	<6	32	17	22	<12	<12	503	8	79	<10				250	130						
L-213	73	193	27	596	39	8	6	18	22	25	22	<12	762	12	163	<10	4	42	69	137	20	16	39	0.7		0.7	0.8
L-214	65	167	24	662	77	<6	12	20	15	25	19	81	657	7	104	<10				181	89						
L-215	7	72	15	443	23	6	7	6	9	27	<12	<12	71	<6	193	<10				18	<12						
L-217	124	48	10	128	10	86	17	8	43	13	67	502	805	<6	<15	11	7	28	53	89	30		59				0.8
L-218	202	344	46	601	53	8	<6	6	30	22	15	16	793	8	99	<10	17	75	265	342	135	8	65	1.5		2.1	1.1
L-222	304	122	69	275	30	<6	7	<6	22	29	79	18	499	7	20	11				220	121						
L-223	312	122	77	270	28	<6	<6	<6	27	28	68	18	468	8	21	<10	2	1	20	250	2		166				1.0
L-224	261	103	35	301	28	9	8	<6	21	24	76	16	1065	8	19	<10				120	65						
L-416	6	126	17	41	5	34	72	94	84	17	195	217	43	6	<15	42				<12	<12						
L-458	277	30	72	45	13	<6	<6	9	11	18	<12	13	129	8	<15	<10				38	42						
L-459	87	204	22	81	8	26	40	111	107	19	181	57	287	<6	<15	23				54	30						
L-460	68	482	13	632	7	8	9	19	63	18	22	14	596	<6	20	<10				197	102						
L-461	178	241	14	65	10	<6	<6	30	36	18	<12	13	1222	<6	15	<10				43	21						
L-462	114	630	5	95	11	<6	<6	11	32	17	25	<12	3607	<6	16	<10				61	25						
L-463	25	255	38	193	15	39	11	16	153	21	133	94	285	<6	<15	30				30	18						
L-464	14	13	16	17	3	25	185	184	122	<9	34	<12	142	29	<15	37				<12	<12						
L-465	25	76	9	129	17	13	85	143	102	11	127	<12	694	24	<15	36				<12	<12						
L-466	351	83	31	75	39	<6	<6	15	21	24	<12	14	225	<6	23	<10				57	27						
L-467	145	1046	29	208	18	7	10	12	30	22	16	<12	2676	<6	67	<10				224	130						

Table 4.1.2.2 Rock types from the West Lusaka-Kafue Flats area, Zambia

Rock type	**Group**	**Samples**
alkali granites	**A**	L-207*, L-208, L-458, L-467
Granites	**B**	L-175, L-460, L-461, L-462, L-460, X-90
syenites and quartz syenites	**C**	L-195, L-210, L-212, L-213*, L-214, L-215, L-218
Gabbros	**D**	L-181, L-209, L-416, L-436, L-463, X-11
Tonalite	**E**	L-459
Anomalous granodiorite	**F**	L-217
Hydrothermally altered granite	**G**	L-222, L-223, L-224

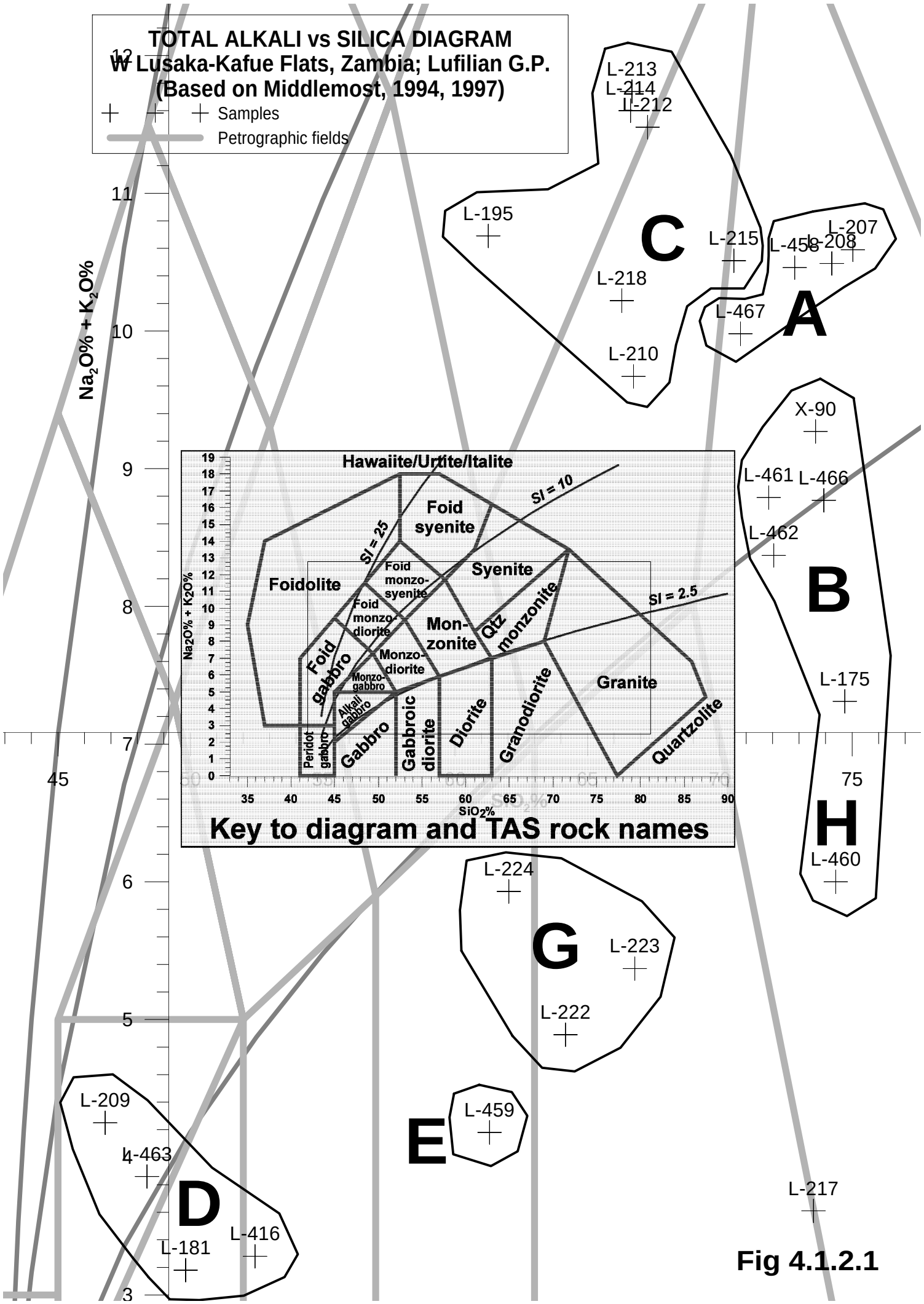
TOTAL ALKALI vs SILICA DIAGRAM
W Lusaka-Kafue Flats, Zambia; Lufilian G.P.
(Based on Middlemost, 1994, 1997)
Samples
Petrographic fields
Na2O% + K2O%
SiO2%
L-213
L-214
L-212
L-195
C
L-215
L-458
L-207
L-208
L-218
L-467
A
L-210
X-90
L-461
L-466
L-462
B
L-175
H
L-460
L-224
G
L-223
L-222
L-209
L-463
D
L-416
L-181
E
L-459
L-217
Hawaiite/Urtite/Italite
Sl = 10
Sl = 25
Sl = 2.5
Foid syenite
Foidolite
Foid monzo-syenite
Syenite
Foid monzo-diorite
Mon-zonite
Qtz monzonite
Foid gabbro
Monzo-diorite
Monzo-gabbro
Alkali gabbro
Peridot gabbro
Gabbro
Gabbroic diorite
Diorite
Granodiorite
Granite
Quartzolite
Key to diagram and TAS rock names

Fig 4.1.2.1

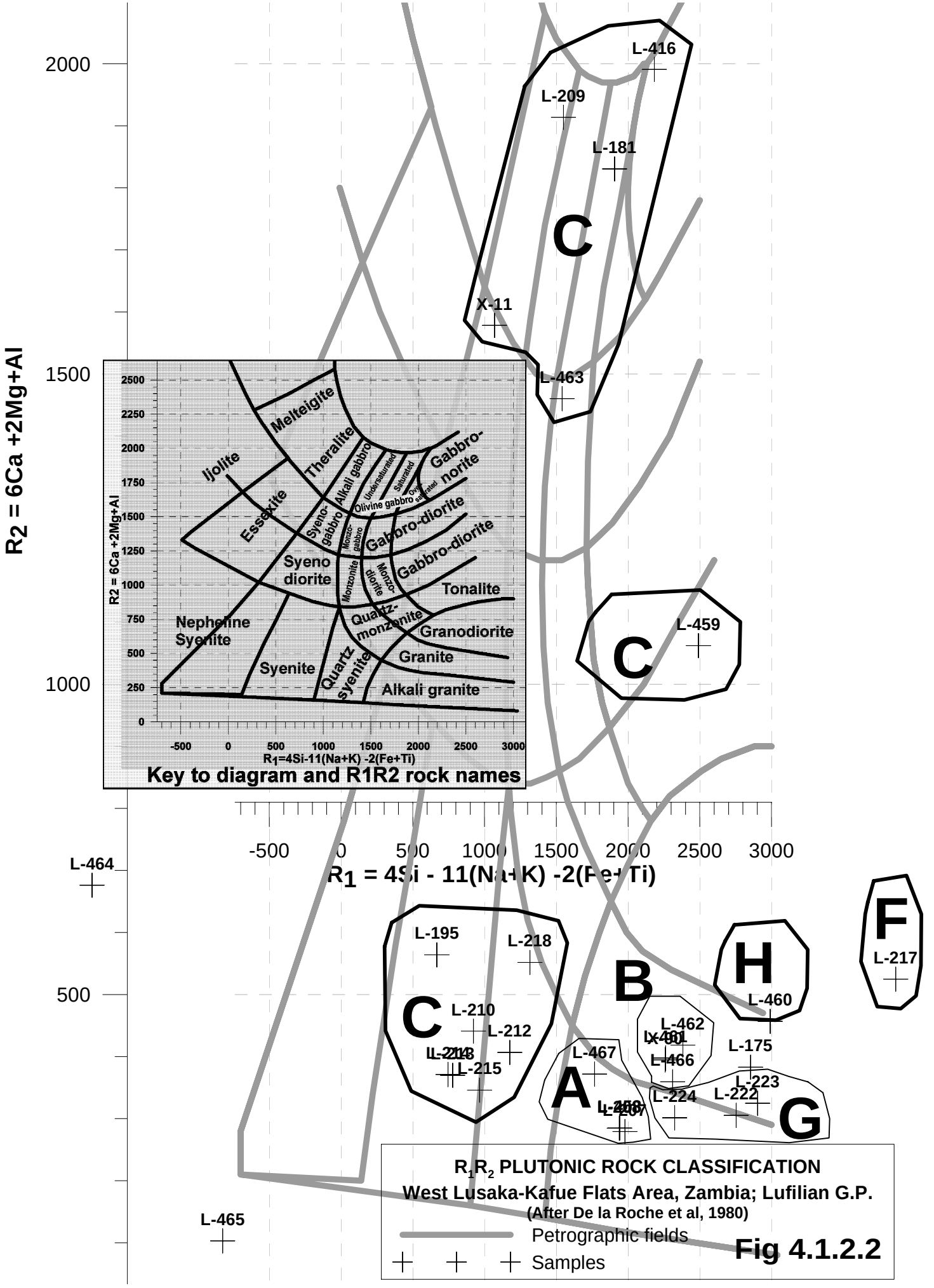
R2 = 6Ca +2Mg+Al
2000
1500
1000
500
L-416
L-209
L-181
C
X-11
L-463
L-459
C
L-464
L-465
-500
0
500
1000
1500
2000
2500
3000
R1 = 4Si - 11(Na+K) -2(Fe+Ti)
Melteigite
Ijolite
Theralite
Alkali gabbro
Olivine gabbro
Gabbro-norite
Essexite
Syeno-gabbro
Gabbro-diorite
Syeno diorite
Monzonite
Monzo-diorite
Tonalite
Nepheline Syenite
Quartz-monzonite
Granodiorite
Syenite
Quartz syenite
Granite
Alkali granite
Key to diagram and R1R2 rock names
L-195
L-218
C
L-210
L-212
L-214
L-215
B
H
L-460
L-462
L-461
L-466
L-175
L-467
A
L-223
L-222
L-224
G
F
L-217
R1R2 PLUTONIC ROCK CLASSIFICATION
West Lusaka-Kafue Flats Area, Zambia; Lufilian G.P.
(After De la Roche et al, 1980)
Petrographic fields
Samples

Fig 4.1.2.2

Table 4.1.2.3 Basic geochemistry and environment of emplacement for samples from the West Lusaka-Kafue Flats, Zambia (See acronym description on section 2.4.3.)

Sample	Rock Name	Debon & LeFort	Maniar & Piccoli	Whalen	Pearce	Mafic	Rb/10HfTa	Rb/30HfTa	Nb-Ta
L-175	Granite	Peraii subleucoKFe	POG	A	O3/4				OUTU
L-181	Saturated olivine gabbro	Metav mesoNaFe	IAG+CAG	N	V	emor			
L-195	Syenite	Metav mesoNaFe	CEUG	A	O-W 2-2				OUTU
L-199	Syenite				O 2/4		WP	WP	INW
L-207*	alkali granite	Metav leucoNaKFe		?					
L-208	alkali granite	Metaiv leucoNaKFe		A					
L-209	alkali gabbro	Metav mesoNaFe		N		emor			
L-210	Syenite	Peraiii mesoNaFe	OP	A	V1/2				
L-212	quartz syenite	Metaiv subleucoKFe	CEUG	A	O-W1-1				
L-213*	Syenite	Peraiii subleucoKFe	CEUG	A	O3/4		WP	WP	OUTU
L-214	Syenite	Peraiii leucoNaFe		A	W				
L-215	Syenite	Metav leucoNaFe		A	V				
L-217	Granodiorite	Peraii subleucoKMg		N?	O2/3				OUTU
L-218	quartz syenite	Metaiv mesoNaFe	CEUG	A	O3/4		WP	WP	OUTU
L-222	alkali granite	Peraii subleucoKFe	CEUG	A	O-W1-1				
L-223	Granite	Peraii mesoKFe	CEUG	A	O2/3				OUTU
L-224	alkali granite	Peraii mesoKFe	CEUG	A	O-W1-1	wpab			
L-416	Gabbro norite	Metav mesoNaMg							
L-458	alkali granite	Metaiv leucoKFe		A	O-W1-1				
L-459	Tonalite	Metaiv metaNaFe		A					
L-460	Granite	Metaiv mesoNaFe		A					
L-461	Granite	Peraii leucoKFe	POG	?N					
L-462	Granite	Peraiii subleucoKFe	POG	N					
L-463	Gabbro-diorite	Metaiv mesoNaFe		A	V	wpt			
L-464	mass. iron oxide	Metaiv mesoKFe	CEUG		V				
L-465	mass. iron oxide	Peraiii mesoKFe	CEUG	A	V				
L-466	Granite	Metaiv leucoNaFe		A					
L-467	alkali granite	Metaiv leucoNaFe	RRG-CEUG	A					
X-11		Metav subleucoKFe							
X-90	Granite	Metaiv subleucoKFe							

65% of the granitoids from the West Lusaka/Kafue Flats region fall within the midalkaline field, while 35% of them fall in the subalkaline field (Table 4.1.2.4). All midalkaline rocks make 60% of the samples, 40% of them are subalkaline.

Table 4.1.2.4 Statistics of rock types in samples from West Lusaka and Kafue Flats, Zambia
The fifth column (granitoids) is the sum of underlined rock types.

Group	Rock type	number	%	Granitoids	Groups
Midalkaline Rocks	Alkali granite	7	25.93	65.00	59.26
	Quartzmonzonite	2	7.41		
	Syenite	4	14.81		
	Monzogabbro	1	3.70		
	Alkali gabbro	2	7.41		
Subalkaline Rocks	Granite	4	14.81	35.00	40.74
	Granodiorite	3	11.11		
	Diorite	2	7.41		
	Gabbro-diorite	1	3.70		
	Gabbro	1	3.70		
Total		27	100.00	100.00	100.00

We will now proceed to describe the Lusaka Granite, continue describing the main rock types in the West Lusaka and Kafue Flats region, and discuss the high thorium content of Kafue Flats rocks.

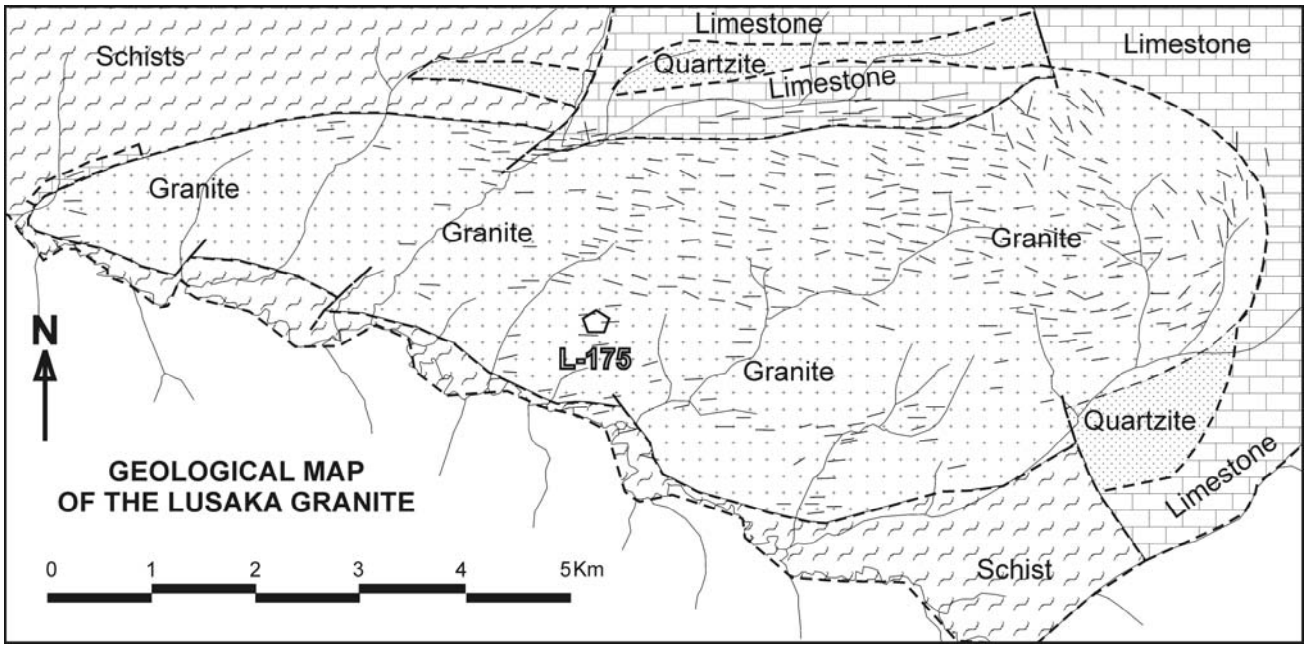

Fig 4.1.2.3 Geological map of the Lusaka Granite. *Taken from Thieme, 1968. Note location of sample* ***L-175****.*

4.1.2.3 Lusaka Granite

The Lusaka Granite is an elongated stock that intrudes into slightly folded and metamorphosed Katanga limestones, and siliciclastics. It has a drop-like shape, as shown on Fig 4.1.2.3. **L-175** comes from an outcrop of the Lusaka Granite, a coarse-grained, foliated, pink peraluminous subleucocratic potassic ferriferous granite with abundant coarse biotite, and quartz porphyroblasts in ellipsoids. The main foliation at the sampling site was 120/37°S, with lineations along the intersection with 125/37°N. Outcrops are generally flat, and follow horizontal planes of foliation. Many quartz pods occur around **L-175**. The pluton is considered to have formed at approximately 820 Ma. Thieme, 1968 states that **X-90** is a representative sample from the Lusaka Granite and it is a metaluminous subleucocratic potassic ferriferous granite. Tables 4.1.2.1 and 4.1.2.3 shows that it differers from **L-175**, which was the most representative rock in the outcrops visited.

As discussed by Thieme, 1968 #38, the center of the granite is unfoliated, and it grades into strongly gneissose rocks towards the eastern and western boundaries (Fig 4.1.2.3). Foliation is parallel to the boundaries. “The internal structures of the pluton suggest a combination of internal intrusive forces and external regional deformation during the waning phases of the Lufilian orogeny.” Additional references on the Lusaka Granite are: DeSwardt & Simpson, 1972; Drysdall & Garrard, 1964; Snelling, Johnson, & Drysdall, 1972.

The environment of emplacement of **L-175** and **X-90** is not easy to interpret based on the two chemical analyses available. Whalen plots indicate anorogenic origin, and the Maniar & Picolli method indicates a post orogenic origin. A working hypothesis for the Lusaka Granite is that is formed as a single anorogenic granite ring complex; it was later deformed.

4.1.2.4 Description of Main Rock Types

4.1.2.4.1 Four Rock Association

Small bodies of red-altered granitoids, gabbros, iron oxide bodies and quartz pods occur together in the West Lusaka-Kafue Flats area. These four rock features are associated with iron oxide-copper-gold mineralization throughout the Greater Lufilian Arc. In this case, the four-rock association is hosted by Katangan carbonates of the Lusaka Formation (marked light blue on Fig 8.40). Hydrothermal brecciation and coarse-grain sodic alteration (scapolitization) in the carbonates are commonly observed around the four-rock association. Both syenites and alkali granites are closely related to gabbroids. At times, the features of mineralization and alteration resemble skarn.

Descriptions of all the granitoids, gabbroids, iron oxide bodies and quartz pods collected during fieldwork in the West Lusaka/Kafue Flats area are included in Appendix 60. They have been grouped by rock type for

description purposes, but these rocks generally occur in close association in the field. Discussions on their field relations, geochemistry, environment of emplacement and other geological data are were also included there.

4.1.2.4.2 Granitoids

Samples **L-207*** and **L-213*** are good representatives of the red-altered granitoids and were dated. Both of them contain miarolitic cavities; these are evidence of boiling that took place during rock formation. Degassification from magma, or boiling, is a very important clue for mineralization; in other parts of the same magma chamber, rocks might have experienced violent hydrothermal explosions. This observation is relevant for mineral exploration.

L-207*, a red, metaluminous leucocratic sodic-potasssic ferriferous alkali granite from West Lusaka, comes from a series of granitoids that are intimately associated with small gabbroic bodies (See photograph on Fig 4.1.2.4). **L-213*** is a red, peraluminous subleucocratic potassic ferriferous syenite with small miarolitic cavities and disseminated specular hematite (Fig 4.1.2.4). This sample has evidence of intense hydrothermal alteration, probably due to its high thorium content and heat production capacity. Chapter 5 comments about thorium-related heat production capacity in greater detail. The rock also contains anomalous Pr, Zr, Na_2O and Al_2O_3. Both **L-207*** and **L-213*** were dated; their geochronology is discussed on subchapter 4.1.2.6.

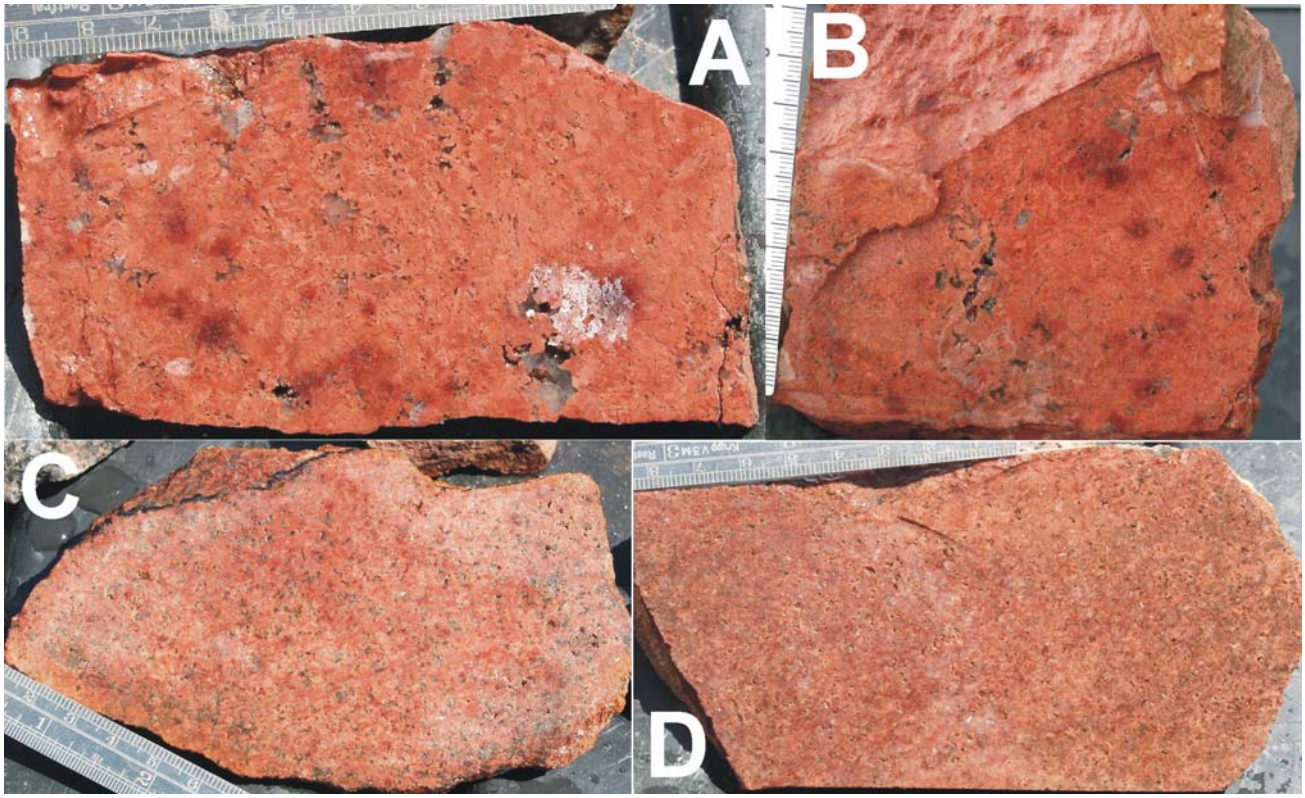

***Fig 4.1.2.4 Photographs of slabs from red-altered granitoids in the Kafue Flats area, Zambia**. A comes from sample **L-207**; B, from **L-208**; C, from **L-213**; D from **L-215**. Notice the abundant, large miarolitic cavities in A and B. Part of them have been filled by quartz, others are empty. C and D display abundant, but smaller miarolitic cavities. Most of the cavities in C and D are empty. Samples of A and C were dated. See more details in the text. All scales in millimeters.*

Part of the granitoids in the Kafue Flats display disseminations of specular hematite and others are intersected by abundant specularite veinlets. The majority of the granitoids are anorogenic, and formed in a continental epeirogenic uplift environment, as shown on Table 4.1.2.3. Most granitoids from the suite are enriched in the light rare elements.

4.1.2.4.3 Gabbroids

Many gabbros outcrop in the West Lusaka/Kafue Flats region. Only a few of these abundant gabbroid rock outcrops were analysed. They contain significant metal mineralization and may be source for copper, zinc and

other economic metallic enrichment in the region. Some occur as small isolated bodies that intersect any type of rock, as dikes or sills with various granitoids, or as gabbro only ring complexes. The Appendix includes descriptions of the main samples observed and studied.

4.1.2.4.4 Iron Oxide Bodies

Massive bodies of magnetite and/or hematite are hosted by Katangan limestones and dolostones. Sometimes the entire soil is made of only magnetite sand and gravel. Part of the iron oxide bodies contain sulfides and/or gossans after various sulfides. They may contain metals besides Fe, including Cu, Mn and others (See Table 4.1.2.1). Although gold and silver were not analysed, they could be present in economic concentrations.

Many of the iron oxide bodies overprint breccioid textures. It is common to see hydrothermal breccias flooded by coarse, metallic hematite or magnetite. There generally is a relict igneous texture in some of the iron oxide bodies. This may be due to progressive overprinting and replacement of the silicates by iron oxides.

L-464 and **L-465**, two samples from massive iron oxide bodies associated to a gabbroic ring complex in the Kafue Flats area were analysed (Table 4.1.2.1). Fig M7 shows their location. The rocks are extremely vuggy; before being leached, their vugs contained copper, nickel and zinc sulfides, among other metals. That elemental enrichment is an evidence of IOCG-type mineralization.

Table 4.1.2.5
Analysis of gossanous massive iron oxide bodies, West Lusaka-Kafue Flats area, Zambia

Sample	SiO2	TiO2	Al2O3	Fe2O3	MnO	MgO	CaO	Na2O	K2O	P2O5	LOI	Total
Notch	50.00	1.00	15.50	6.00	0.15	2.00	5.00	4.90	5.50	0.30	2.00	
L-464	5.46	0.07	0.00	77.49	0.08	0.50	6.09	0.10	0.52	0.06	3.16	93.53
L-465	14.01	0.58	2.56	64.74	0.03	0.70	0.17	0.06	0.43	0.12	12.85	96.25

Sample	Rb	Sr	Y	Zr	Nb	Co	Ni	Cu	Zn	Ga	V	Cr	Ba	U	Th	Sc	Ce
Notch	200	400	60	360	40	30	16	25	85	26	100	100	1300	20	37	20	175
L-464	14	13	16	17	3	25	185	184	122	<9	34	<12	142	29	<15	37	<12
L-465	25	76	9	129	17	13	85	143	102	11	127	<12	694	24	<15	36	<12

4.1.2.5 Thorium content in Kafue Flats Area

Some syenites and quartz syenites from the Kafue Flats area contain extremely high values of thorium. These are listed on Table 4.1.2.1. That Th enrichment is more than ten times the average value for most granitoids in Zambia and Namibia; such values are among the highest in samples collected during the Greater Lufilian Arc granitoid project. Abundance of Th in an igneous rock enables it to act as a long-lived heat engine. This can generate and focus hydrothermal fluid flow for a long time. It possibly is a key ingredient for the occurrence of iron oxide-copper-gold mineralization. Chapter 5 contains more information on high thorium content of granitoids in the Greater Lufilian Arc. Sample **L-257** from the Hook Granite, and several others listed on Table 5.1, also contain anomalous thorium and are related to granitoids in the Kafue Flats.

Samples **L-212** and **L-218** contain much more potassium than normal, and their soda content is far lower than the rest of the high-Th samples listed on Table 4.1.2.6.

4.1.2.6 Geochronology

Zircon concentrates from sample **L-207*** gave a zircon U-Pb SHRIMP II age of 538.2±3.3 Ma. Sample **L-213*** gave a SHRIMP II age of 550±25 Ma; several xenocrystic zircons were dated at 1872±14 Ma (Table A22.4). Both of the young ages could represent the same intrusive event, given the error overlap. The large error in age for **L-213*** could be due to intense hydrothermal alteration due to the rock's extraordinary Th content.

4.1.2.7 Conclusions

The granitoids and gabbroids from the West Lusaka – Kafue Flats region formed in an anorogenic uplift environment. There is a close association of gabbroids with red-altered granitoids, bodies of massive iron oxide and quartz pods. Gabbroids of various ages and origins intersect the rest of the rock types in the region. High thorium content in many of the granitoids induced and maintained a long-lived flow of hydrothermal fluids

in the region. Several large iron oxide-copper-gold prospects are known in the area, and there is very good potential to find new, large, economic, iron oxide-copper gold mineralization in the region.

Table 4.1.2.6 Samples with high Th values from the Kafue Flats, Zambia

Samples contain high values in alumina, soda, Zr, Nb, Ce, La and low values for lime. Note the extraordinary heat capacity of these rocks at the time of emplacement. Any value of heat capacity above 4 is anomalous.

Sample	Rock Name	SiO2	Al2O3	Fe2O3	CaO	Na2O	K2O	LOI	Total	Y	Zr	Nb	Cu	Ga
L-199	Syenite									42	534	47		
L-210	Syenite	66.74	17.99	3.52	0.70	9.58	0.10	0.39	99.87	30	474	36	143	22
L-212	Quartz syenite	67.27	15.94	2.89	0.80	4.44	7.00	0.71	99.69	51	336	49	32	22
L-213*	Syenite	66.68	17.4	3.03	0.20	6.87	4.90	0.60	100.2	27	596	39	18	25
L-214	Syenite	66.63	17.62	1.54	0.20	7.68	3.90	0.63	98.74	24	662	77	20	25
L-215	Syenite	70.53	16.82	0.65	0.20	10.3	0.20	0.36	99.30	15	443	23	6	27
L-218	Quartz syenite	66.30	15.92	4.64	2.00	4.79	5.40	0.21	100.4	46	601	53	6	22

Sample	Zn	U	Th	Sm	Nd	Pr	Ce	La	Cs	Hf	Eu	Gd	Yb	Lu	Heat Capacity
L-199		9	39	20	137	36	288	95	1	11	5	13	4	1	2.924
L-210	13	7	74				372	223							5.325
L-212	17	8	79				250	130							6.56
L-213*	22	12	163	4	42	69	137	20		17	1		1	1	12.211
L-214	15	7	104				181	89							7.873
L-215	9	<6	193				18	<12							13.449
L-218	30	8	99	17	75	265	342	135		8	1		2	1	7.743

4.1.3 KALENGWA-KASEMPA AREA, ZAMBIA

4.1.3.1 Introduction

The Kalengwa and Kasempa areas lie in the Northwestern Province of Zambia (Figs M1, M8 and M9). They occur in the same geographical area, their geology is comparable, and have similar general characteristics; for these reasons, they have been grouped together for discussion. The area may be reached by road from the Copperbelt, through Solwesi into Kasempa. Access from Mumbwa in the south is possible, but the roads are in bad shape. It lies halfway between the Hook Granite batholith and the border with the Democratic Republic of Congo.

The region is underlain by Katangan siliciclastics and carbonates. These in turn are covered by Mesozoic sediments and recent sands. The Katangan sediments were intruded by various midalkaline granitoids and gabbroids. These have been grouped by some researchers into anorogenic ring complexes. There are very few outcrops in the Kasempa and Kalengwa areas. Outcrops of granitoids are especially scarce.

The geophysical image of Fig 4.1.3.1 shows that the Kalengwa-Kasempa area is made up of several large ring structures. Kalengwa has at least four ring structures with a diameter of 15 km and one with 25 km diameter. It is centered in another ring structure with diameter of 55 km; several smaller rings structures are also evident. The Kasempa area is made by of such structures with diameters around 20 km, some with diameter of 10-15 km, and one with 50 km diameter; several smaller ring structures are also present. Some very large magnetic anomalies like at Chitampa and Kametete are evident in geophysical images of this region (Nisbet, Cooke, Richards, & Williams, 2000; Nisbet, 2004a and Nisbet, 2004b). See also Fig. 4.16.

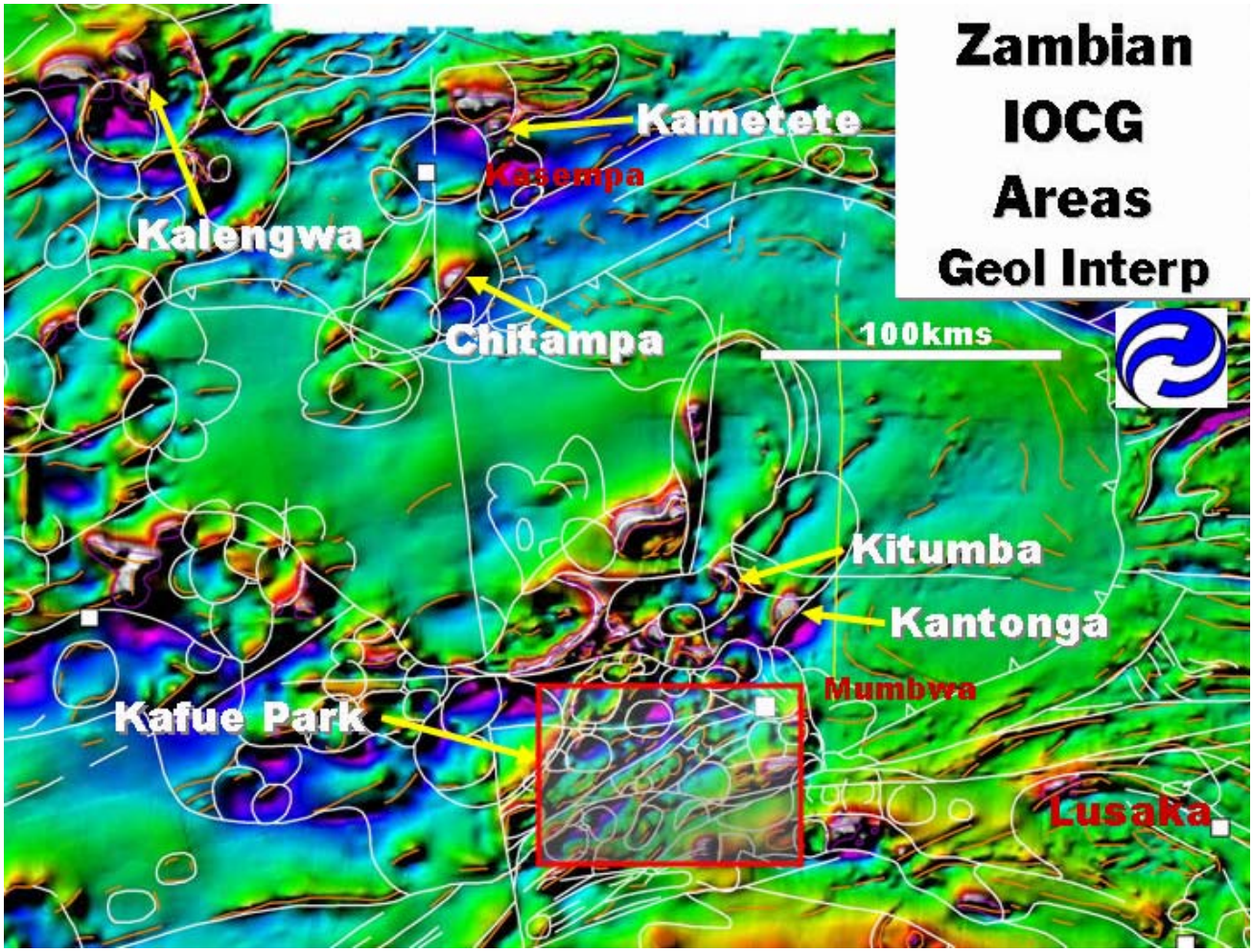

Fig 4.1.3.1 Geological interpretation of airborne magnetic image for northwestern Zambia. *Note the abundant circular features that are represented in many parts of the figure. Also note the N-S-trending structures that extend for hundreds of kilometers. The Kalengwa and Kasempa areas are dominated by large annular structures that are considered to be anorogenic ring complexes. Same color coding as explained for Fig 4.17, which is located in the red rectagle. Extracted from Nisbet, 2004b.*

The Kalengwa mine is considered by many to be one of the major exponents of iron oxide-copper-gold deposits in Zambia. It was one of the most profitable copper deposits in the country, and paid for its own infrastructure in a remote location, separated from the rest of the main Copperbelt. Few reports on the deposit are publicly available today. Hydrothermal brecciation, as well as gabbroid rocks seem to have played important roles in the formation of the original deposit. Most of the mined copper minerals were enriched by supergene concentration; copper oxides and few sulfides were found near the surface. There is more information about the Kalengwa mine in section 8.4.2.6.

The Kasempa area has been explored for its copper and gold potential since the early twentieth century by various mining companies. Numerous prospects and mineral occurrences are known from the district. Many boreholes drilled in the region are kept at the Kalulushi coreshed. Both the Kalengwa and Kasempa areas have significant potential for iron oxide-copper-gold mineralization.

4.1.3.2 Sampling

Although the road from Kasempa to Mumbwa was traversed during fieldwork for this project, there is very little outcrop and no samples were collected. All samples were obtained from indirect sources. A total of 27 chemical analysis were collected (Table 4.1.3.1); 18 were chemical analysis from previous reports, and 9 were physical samples from boreholes and outcrops visited by other researchers. More details on the samples will be given for each section.

4.1.3.3 Geochemistry

Samples from the Kalengwa-Kasempa region fall within the midalkaline and alkaline fields as shown on Fig 4.1.3.2. Midalkaline and alkaline rocks dominate as seen on Table 4.1.3.2. This is probably related to the ring complex composition. 82% of the granitoids from the Kalengwa-Kasempa region fall within the midalkaline field while the rest are subalkaline. All midalkaline rocks make 64% of the samples, 29% are alkaline and 7%, subalkaline.

Table 4.1.3.2 Rock type statistics, samples from Kalengwa and Kasempa region, Zambia
The fifth column (granitoids) is the sum of underlined rock types.

Group	Rock type	number	%	Granitoids	Groups
Midalkaline Rocks	alkali granite	2	7.14	81.82	64.29
	quartzmonzonite	3	10.71		
	syenite	2	7.14		
	monzonite	2	7.14		
	monzodiorite	3	10.71		
	monzogabbro	3	10.71		
	alkali gabbro	3	10.71		
Subalkaline Rocks	granite	1	3.57	18.18	7.14
	granodiorite	1	3.57		
Alkaline Rocks	foid monzo-diorite	1	3.57		28.57
	foid gabbro	7	25.00		
Total		28	100.00	100.00	100.00

Geochemistry from Kalengwa and Kasempa will be discussed jointly.

The TAS diagram (Fig 4.1.3.2) shows a wide spread distribution of rock chemistry that spans the entire midalkaline field in at least five discrete clusters (Table 4.1.3.2). Most rocks from the Kalengwa area fall in the mid-alkaline field except for **L-322**, **L-321** and the foid-bearing rocks of the Kasempa area. Most rocks display evidence of hydrothermal alteration, especially **L-321**.

The different geochemical diagrams (Figs 4.1.3.2 to 4.1.3.7) helped to establish seven main geochemical suites of contrasting rock types in the Kalengwa-Kasempa area (See Table 4.1.3.3). This variety of rock types is a feature observed in several other mineralized areas of the Greater Lufilian Arc. Rocks that fall in the general gabbroid field have extremely different chemistries. Some of them are intrusive and others effusive rocks. These observations are common in anorogenic mafic, midalkaline and alkaline ring complexes.

Table 4.1.3.1 Chemical Analysis of samples from the Kalengwa-Kasempa Area, Zambia
(Complete elemental analysis on Table A5, Appendix)

Sample	SiO2	TiO2	Al2O3	Fe2O3	MnO	MgO	CaO	Na2O	K2O	P2O5	LOI	Total	Rb	Sr	Y	Zr	Nb	Co	Ni
Notch	50.00	1.00	15.50	6.00	0.15	2.00	5.00	4.90	5.50	0.30	2.00		200	400	60	360	40	30	16
L-139	75.60	0.09	11.88	1.50	0.03	0.62	0.14	1.61	7.87	0.01	0.79	100.14	399	17	40	75	41	10	7
L-313	54.29	1.67	13.47	10.37	0.06	5.07	4.92	4.55	0.80	0.67	4.40	100.27	21	164	89	445	40	14	12
L-314	43.72	7.81	12.73	11.28	0.08	6.68	7.01	3.38	0.36	0.64	6.73	100.42	14	77	56	25	36	20	19
L-318	47.28	3.04	15.31	7.93	0.04	6.86	13.85	4.18	0.56	0.38	0.96	100.39	9	154	37	163	27	23	53
L-321	71.94	0.71	9.67	11.04	0.03	3.43	0.30	0.68	0.05	0.12	2.40	100.37	6	81	59	242	18	96	18
L-322	70.45	0.74	13.65	5.38	0.02	0.48	0.08	0.13	7.57	0.08	1.74	100.32	168	30	37	264	30	12	7
L-323	67.04	0.81	14.15	7.57	0.02	0.52	0.19	0.17	8.21	0.17	1.61	100.46	173	29	37	302	35	26	9
L-324	62.05	0.97	14.50	7.90	0.06	1.43	1.71	3.85	6.29	0.29	1.25	100.30	112	230	57	362	35	20	16
L-325	60.42	1.15	16.98	11.07	0.02	0.91	0.06	0.08	6.75	0.29	2.82	100.55	227	37	346	372	31	28	13
P-13	65.76	0.82	14.67	5.87	0.10	1.00	2.40	5.77	3.89	0.24	0.21	100.52	90	301	45	157	30	70	11
P-17	64.11	0.97	14.29	7.35	0.08	0.80	2.43	3.95	5.62	0.26	0.18	99.86	107	372	54	327	32	84	16
P-25	51.44	2.40	20.38	8.73	0.71	3.91	5.28	6.42	1.71	0.38	0.12	100.72	55	348	24	107	14	33	6
P-26	76.20	0.13	11.58	0.93	0.05	<.1	0.25	10.51	0.03	0.03	0.08	99.71	7	15	170	705	243	39	4
X-76	55.35	1.48	14.63	10.86	0.10	4.43	2.43	0.91	7.34	0.50	1.65	99.69	209	199	56	591	28	13	11
X-77	61.50	1.10	15.15	7.30	0.11	1.58	2.81	4.39	5.07	0.34	1.21	100.59	182	313	48	339	34	15	<9
X-78	51.81	3.13	15.06	11.46	0.06	7.53	1.00	3.02	4.48	0.33	2.67	100.54	137	109	32	290	46	25	102
X-79	48.31	4.07	11.38	9.92	0.21	9.92	5.90	2.58	1.14	0.57	6.34	100.34	18	234	32	358	44	47	70
X-80	45.03	3.27	13.53	16.29	0.09	6.04	5.05	5.14	3.32	0.53	2.13	100.41	97	112	48	325	55	24	81
X-81	46.37	3.96	13.46	15.27	0.05	6.20	4.88	4.91	2.96	0.54	1.92	100.52	103	94	55	302	48	17	88
X-82	48.60	1.56	13.71	18.47	0.08	2.02	5.07	7.38	1.05	0.81	1.52	100.26	32	122	61	567	84	<9	10
X-83	46.07	2.56	14.20	17.60	0.15	5.97	5.84	3.60	3.20	0.32	0.85	100.37	88	105	27	177	32	17	44
X-84	46.07	3.95	12.30	12.67	0.06	3.44	8.56	5.49	0.87	0.91	6.14	100.47	27	106	59	444	89	11	11
X-85	47.35	2.56	14.08	13.25	0.14	7.29	8.22	4.21	0.61	0.32	2.54	100.58	21	287	26	173	37	36	69
X-86	45.88	3.96	12.72	16.75	0.25	5.61	7.19	3.78	1.46	0.31	2.23	100.14	37	319	33	201	40	14	36
X-87	46.09	2.86	13.80	14.33	0.23	6.98	7.07	4.90	0.32	0.41	3.05	100.06	13	344	31	208	42	18	50
X-88	45.24	2.00	14.37	11.55	0.11	10.97	4.11	2.72	5.24	0.20	3.85	100.37	147	69	25	131	21	35	201
X-89	46.20	3.57	8.68	14.36	0.18	11.42	6.07	4.30	2.70	0.67	1.85	100.01	56	337	36	223	53	37	30

Sample	Cu	Zn	Ga	V	Cr	Ba	U	Th	Sc	Sm	Nd	Pr	Ce	La	Cs	Hf	Ta	As	Se	Eu	Gd	Tb	Dy	Ho	Er	Tm	Yb	Lu
Notch	25	85	26	100	100	1300	20	37	20	50	50	15	175	95	3	10	120	100		4.0	30	5.0	20	3	9	36	7.5	1.6
L-139	55	34	23	14	47	769	<6	26	<10				42	12														
L-313	42	39	23	102	21	104	7	<15	36				139	75														
L-314	28	49	18	438	50	60	<6	<15	55				27	16														
L-318	9	22	19	258	99	20	<6	<15	30				68	33														
L-321	16	30	15	157	95	65	<6	<15	12				102	61														
L-322	13	35	21	49	33	498	<6	27	<10				171	74														
L-323	17	28	20	58	32	525	<6	30	<10				153	71														
L-324	62	121	21	96	27	1004	13	48	11				190	74														
L-325	55	48	26	114	<12	508	6	27	<10				1460	819														
P-13	<3	4	23	55	22	787	10	56	7	10	59	17	153	80	<1	9	3	1	35	2.1	9.5	1.3	8	2	5	35	4.6	0.8
P-17	63	23	24	103	11	782	11	48	10	12	64	17	136	47	1	8	2	3	88	2.4	11.7	1.5	9	2	5	36	5.0	0.8
P-25	40	13	24	98	90	120	<2	2	20	4	15	3	22	9	1	2	1	12	107	1.7	4.5	0.7	4	1	2	34	2.1	0.3
P-26	<3	<1	68	<4	24	22	6	76	1	7	15	3	24	8	<1	31	5	1	7	0.7	11.8	3.3	28	7	21	36	23.0	3.4
X-76	295	50		139	<9	1379																						
X-77	7	47		92	11	1189																						
X-78	20	100		415	117	118																						
X-79	35	146		458	74	75																						
X-80	12	23		327	142	141																						
X-81	7	22		324	135	148																						
X-82	777	47		58	<9	233																						
X-83	102	44		325	79	384																						
X-84	26	59		138	<9	152																						
X-85	11	182		318	36	127																						
X-86	124	167		522	<9	303																						
X-87	9	134		315	23	119																						
X-88	<2	168		326	515	112																						
X-89	7	228		474	9	155																						

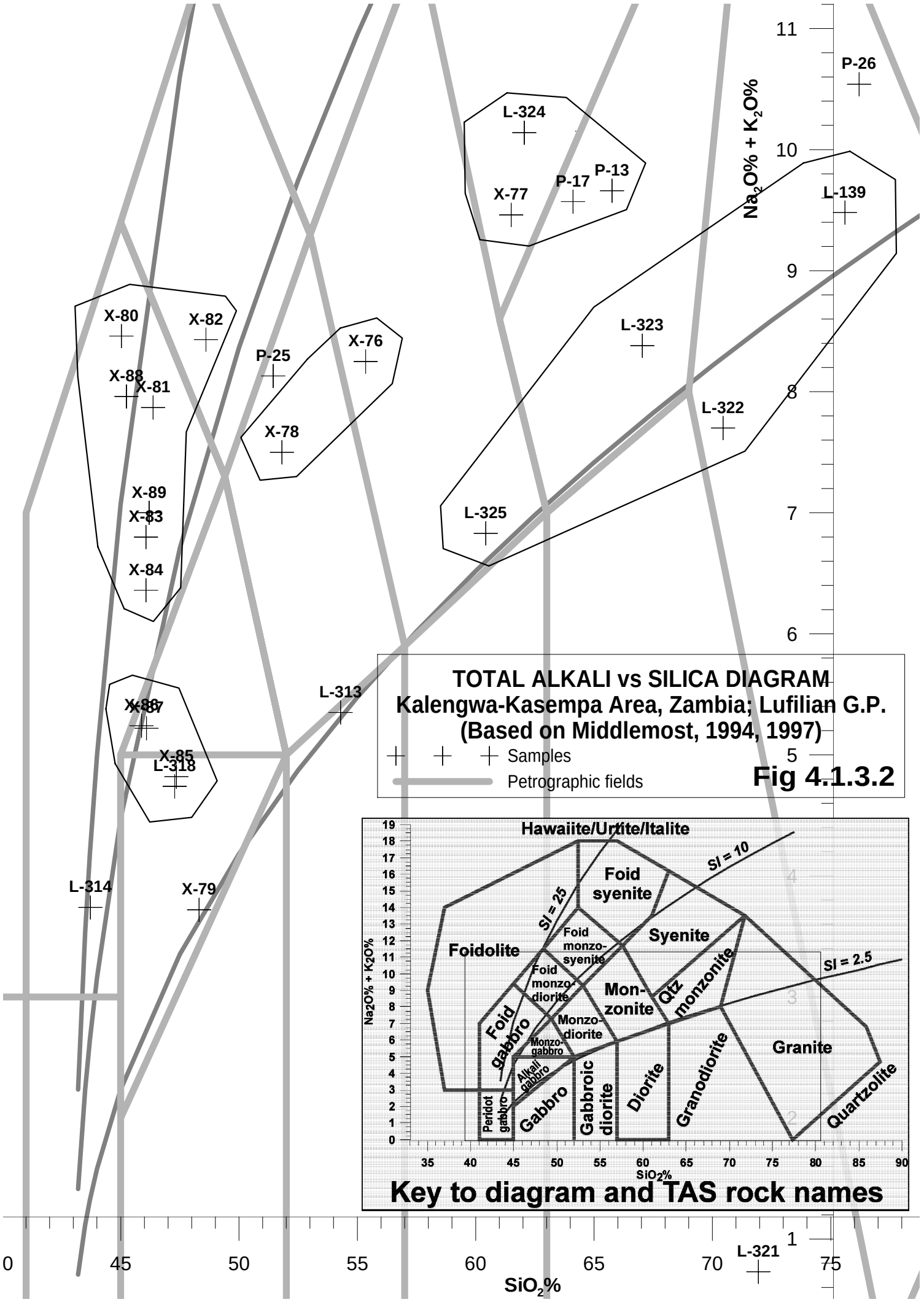

TOTAL ALKALI vs SILICA DIAGRAM
Kalengwa-Kasempa Area, Zambia; Lufilian G.P.
(Based on Middlemost, 1994, 1997)

Samples

Petrographic fields

Fig 4.1.3.2

Key to diagram and TAS rock names

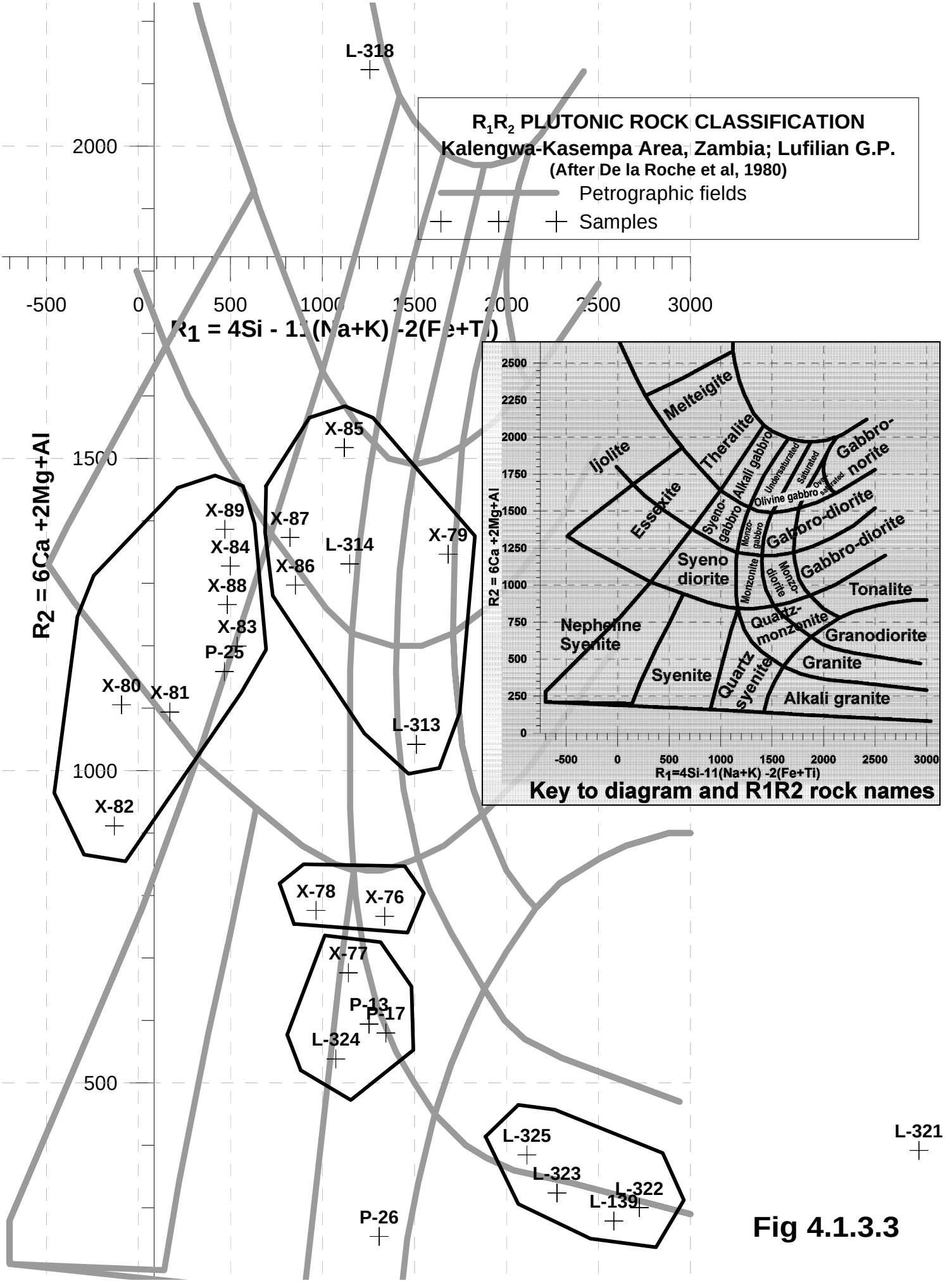
R1R2 PLUTONIC ROCK CLASSIFICATION
Kalengwa-Kasempa Area, Zambia; Lufilian G.P.
(After De la Roche et al, 1980)
Petrographic fields
Samples
R1 = 4Si - 11(Na+K) -2(Fe+Ti)
R2 = 6Ca +2Mg+Al
L-318
X-85
X-89
X-87
X-84
L-314
X-79
X-86
X-88
X-83
P-25
X-80
X-81
L-313
X-82
X-78
X-76
X-77
P-13
P-17
L-324
L-325
L-323
L-322
L-139
L-321
P-26
Melteigite
Ijolite
Theralite
Alkali gabbro
Olivine gabbro
Gabbro-norite
Essexite
Syeno-gabbro
Monzo-gabbro
Gabbro-diorite
Syeno diorite
Monzonite
Monzo-diorite
Tonalite
Nepheline Syenite
Quartz-monzonite
Granodiorite
Syenite
Quartz syenite
Granite
Alkali granite
Key to diagram and R1R2 rock names

Fig 4.1.3.3

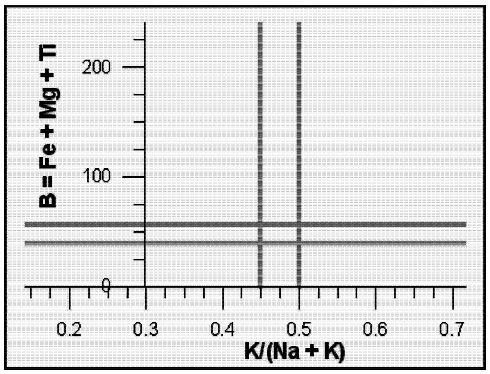

K-B Diagram (After Debon & LeFort, 1994)
Kalengwa-Kasempa Area, Zambia;
Lufilian Arc Granitoid Project

Fig 4.1.3.4

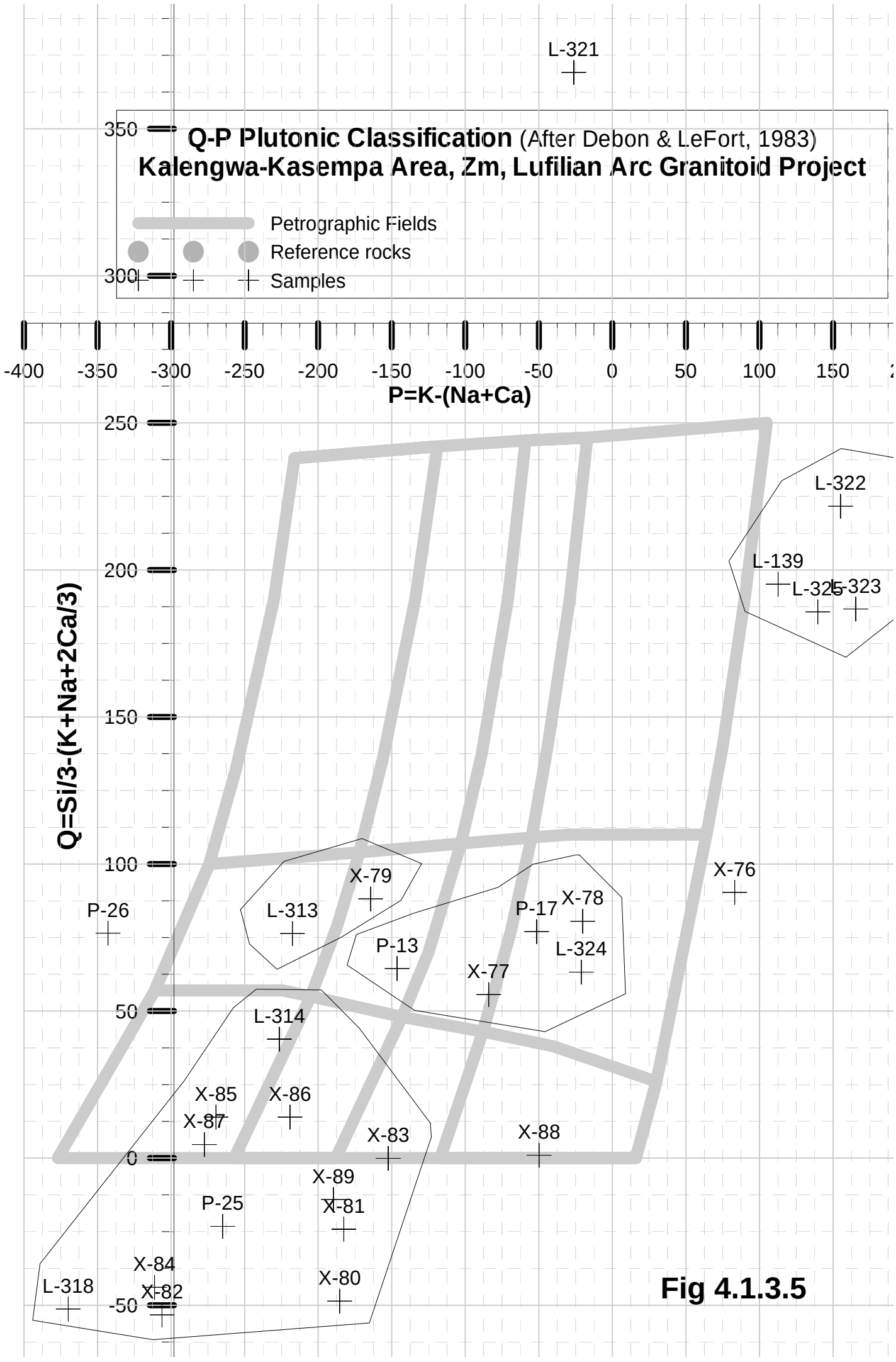
Q-P Plutonic Classification (After Debon & LeFort, 1983)
Kalengwa-Kasempa Area, Zm, Lufilian Arc Granitoid Project
Petrographic Fields
Reference rocks
Samples
P=K-(Na+Ca)
Q=Si/3-(K+Na+2Ca/3)
350
300
250
200
150
100
50
0
-50
-400
-350
-300
-250
-200
-150
-100
-50
0
50
100
150
L-321
L-322
L-139
L-325
L-323
X-79
L-313
P-26
X-76
X-78
P-17
L-324
P-13
X-77
L-314
X-85
X-86
X-87
X-83
X-88
X-89
X-81
P-25
X-84
X-80
L-318
X-82

Fig 4.1.3.5

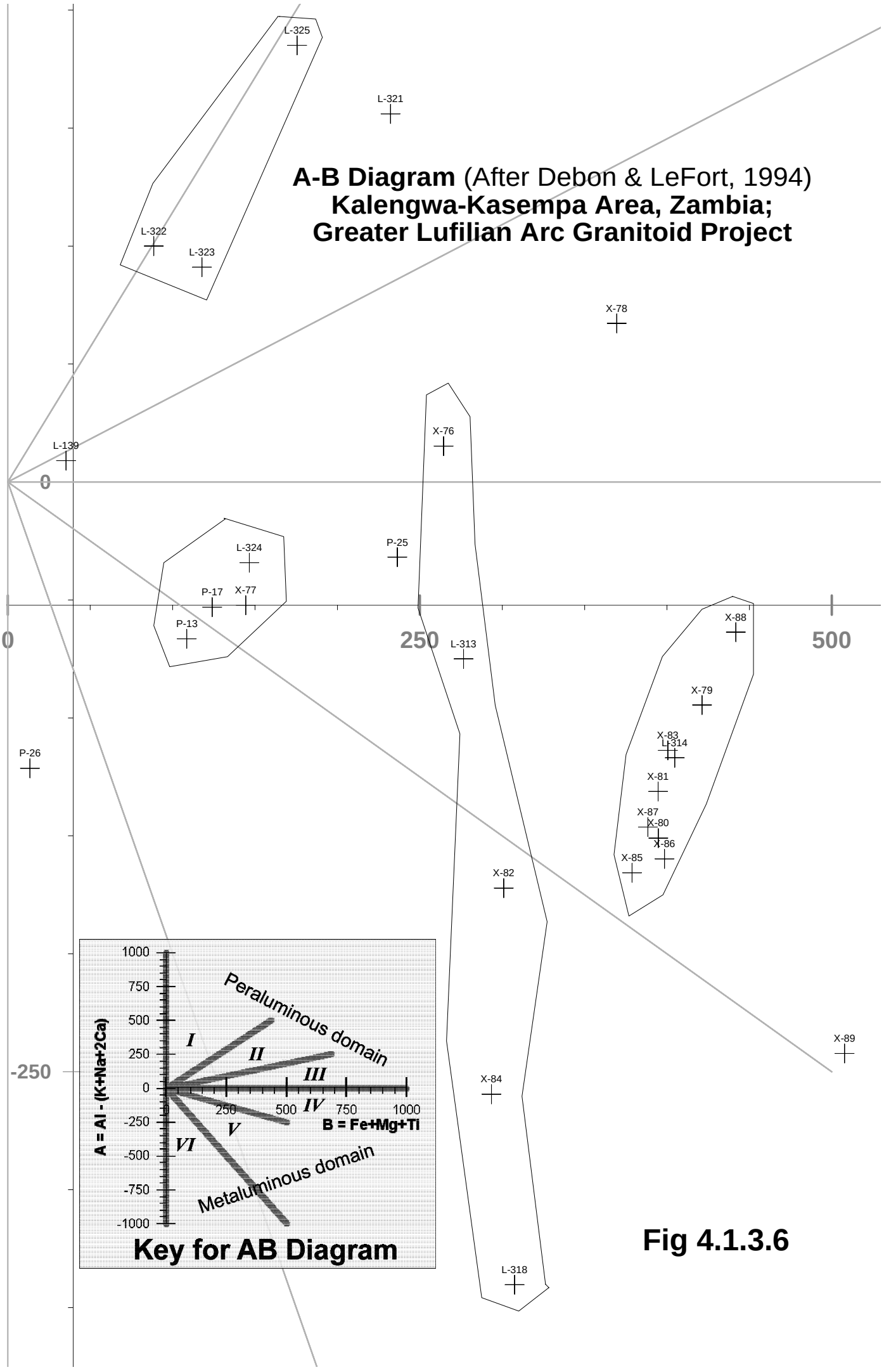
A-B Diagram (After Debon & LeFort, 1994)
Kalengwa-Kasempa Area, Zambia;
Greater Lufilian Arc Granitoid Project
L-325
L-321
L-322
L-323
X-78
X-76
L-139
0
L-324
P-25
P-17
X-77
P-13
0
250
500
L-313
X-88
X-79
X-83
L-314
X-81
X-87
X-80
X-86
X-85
P-26
X-82
X-89
X-84
-250
L-318
1000
750
500
250
0
-250
-500
-750
-1000
A = Al - (K+Na+2Ca)
B = Fe+Mg+Ti
Peraluminous domain
Metaluminous domain
I
II
III
IV
V
VI
Key for AB Diagram

Fig 4.1.3.6

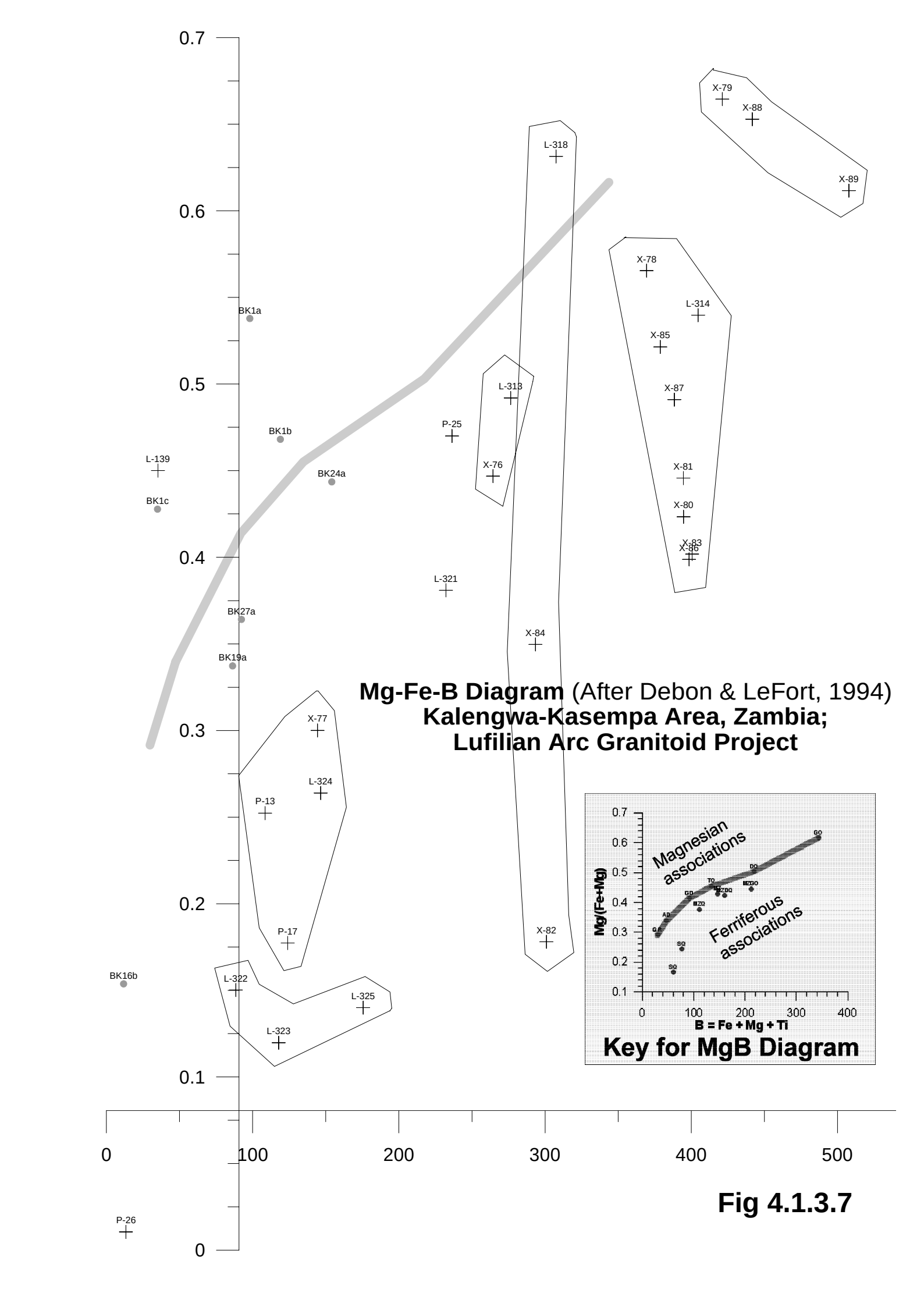
0.7
0.6
0.5
0.4
0.3
0.2
0.1
0
0
100
200
300
400
500
X-79
X-88
X-89
L-318
X-78
L-314
X-85
X-87
L-313
P-25
X-76
X-81
X-80
X-83
X-86
L-321
X-84
X-82
BK1a
BK1b
L-139
BK24a
BK1c
BK27a
BK19a
X-77
L-324
P-13
P-17
BK16b
L-322
L-325
L-323
P-26
Mg-Fe-B Diagram (After Debon & LeFort, 1994)
Kalengwa-Kasempa Area, Zambia;
Lufilian Arc Granitoid Project
Mg/(Fe+Mg)
B = Fe + Mg + Ti
Magnesian associations
Ferriferous associations
Key for MgB Diagram

Fig 4.1.3.7

As shown on Table 4.1.3.3, samples from the Kalengwa/Kasempa area can be grouped into six main suites and others made by single samples. The diagrams proposed by Debon & Le Fort, 1988 and Debon & LeFort, 1983 are very useful for evaluating the trends of the different suites. These are also included on Table 4.1.3.4. A few samples that are significantly different were placed on their own suites (6 to 8). These do not fall on any of the other trends. Suite 1 produced well-defined trends of differentiation. **L-314** from Kalengwa seems to follow the same pattern and was grouped with that suite.

Table 4.1.3.3
Suites of samples from Kalengwa/Kasempa and projection on various geochemical diagrams

Suite	Lithology	AB	MgB	KB	QB	QP	TAS	R1-R2	Samples
1	Foid gabbroids or essexites	Trend	Trend	Trend	Cluster	Cluster		Cluster	X-80, X-81, X-82, X-83, X-84, X-85, L-314
2	Granite	Cluster	Trend	Trend	Trend		spread	Cluster	L-139, L-322, L-323, L-325
3	Quartz syenite	Cluster	Cluster	Trend		Trend	Cluster	Cluster	P-13, P-17, X-77 and L-324
4	Gabbroid	Trend	Trend	Cluster	Trend	Trend		Cluster	L-313, X-79
5	Non-foid gabbroids	Trend	Long trend	Cluster	Trend		Cluster	Cluster	X-86, X-87
6	Gabbroid		Trend	Separate	Trend	Distant	Cluster	Distant	X-79, X-88, X-89
6	Lamprophyre	Na	Na	Na	Na	Na	na	Na	L-318
7	Altered granodiorite	Na	Na	Na	Na	Na	Na	Na	L-321
8	Quartz syenite	Na	Na	Na	Na	Na	Na	Na	P-26
9	Quartz monzonite-syenite	near	near	near	near	near	Near		X-76, X-78

Table 4.1.3.4 Rock name, basic geochemistry and environment of emplacement for samples from the Kalengwa and Kasempa region, Zambia (See acronym description on section 2.4.3.)

Sample	Rock Name	Debon & LeFort	Maniar & Piccoli	Whalen	Pearce	Mafic	Rb/10HfTa	Rb/30HfTa	Nb-Ta
L-139	Granite	peraiii leucoKMg		A					
L-313	Monzodiorite	metaiv mesoNaFe							
L-314	Syeno gabbro	metaiv mesoNaFe							
L-318	Theralite	metav mesoNaMg							
L-321	Granodiorite (altered)	peraii mesoNaFe	OP	A	V1/2				
L-322	Alkali granite	peraii mesoKFe	RRG	A	O-W1-1				
L-323	Alkali granite	peraii mesoKFe	RRG	A	O-W1-1				
L-324	quartz syenite	metaiv mesoKFe	RRG-CEUG	A	W				
L-325	Granite	peraii mesoKFe	RRG	A	W				
P-13	quartz syenite	metav mesoNaFe					VA-	WP	INW
P-17	quartz syenite	metaiv mesoNaKFe					VA-	WP	INW
P-25	Essexite	metaiv mesoNaFe	IAG+CAG			Wpab	VA-	III-WP	INV
P-26	quartz syenite	metavi leucoNaFe					OF	WP	OUTD
X-76	quartz syenite	peraiii mesoKFe	RRG		O-W1-1	Wpab			
X-77	Quartzmonzonite	metaiv mesoNaFe	RRG		O-W1-1	Wpab			
X-78	Syenite	peraiii mesoNaKFe		A		Wpab			
X-79	gabbro-diorite	metaiv mesoNaFe		A	V1/2	Wpab			
X-80	nepheline syenite	metaiv mesoNaFe	RRG	A	W	Wpab			
X-81	Essexite	metaiv mesoNaFe	RRG	A	W	Wpab			
X-82	nepheline syenite	metav mesoNaFe	RRG	A	V1/2	Wpab			
X-83	syeno diorite	metaiv mesoNaFe	RRG	N		Wpab			
X-84	essexite	Metav mesoNaFe		A	V1/2	Wpab			
X-85	syeno gabbro	metaiv mesoNaFe		N	V1/2	Wpab			
X-86	syeno diorite	metaiv mesoNaFe	RRG	N	V1/2	Wpab			
X-87	syeno gabbro	metaiv mesoNaFe		N	V1/2	Wpab			
X-88	essexite	metaiv mesoKFe		N		Wpab			
X-89	essexite	metaiv mesoNaFe		N	W	Wpab			

4.1.3.4 Analysis of Independent Samples by Elements

L-321 seems to have been subject to Na_2O, Al_2O_3 and K_2O depletion, and MgO, Co, Ni, V and Fe_2O_3 enrichment by hydrothermal alteration. **L-322** to **L-325** come from a similar region and they all show evidence

of potassic alteration. Conversely, potassium is very low in **L-313**, **L-314**, **L-318**, **L-321** and **P-26**. Note the significant enrichment in copper shown by some rocks of this suite (**L-313**, **L-324**, **L-325**, **P-17** and **P-25**). Cobalt is high in **L- 321** and in **P-13**, **P-17**, **P-25** and **P-26**. Vanadium is high in **L-311**, **L-313**, **L-314**, **L-318**, **L-321**, **L-325**, **and P-17**.

P-26, an altered quartz syenite is extremely enriched in Na, contains high Th and is enriched in multiple metals: Y, Zr, Nb, Co. Before being altered and mineralized, the rock might have been like **P-13** or **P-17** (See original description by Pepper, 2000 in Appendix A61). **P-26** is also enriched in Hf and in the heavy rare earths Dy, Ho, Er, Tm, Yb and Lu. Samples **P-13** and **P-17** are enriched in Nd and Pr.

The suites of quartz syenites and granites all are high-heat producers. Although **L-139** is not very enriched in Th, maybe other granitoids from the MB-34 borehole might be; the rest of the elements for that sample have an incipient Th-associated signature.

P-25, **L-311**, **L-313**, **L-314** and **L-318** are enriched in Sc. Potash is highly enriched in **L-322**, **L-323**, **L-324** and **L-325**. This is evident in Table 4.1.3.1. **L-325** is very enriched in Ce and La and probably also in the other LREE. **L-324**, **P-13** and **P-17** are very similar in many ways.

X-86 and **X-87** is similar to **L-318** in the TAS diagram; that is not true in the R1/R2 diagram. The last sample probaby has been hydrothermally altered. **X-76** seems to be similar to **L-324**; that is true in both R1/R2 and in the TAS diagrams (Figs 4.1.3.2 and 4.1.3.3). **X-76**, **X-77**, **X-78**, **L-324**, **P-13** and **P-17** seem to have very similar chemistry on the R1R2 diagram, but they separate into two discrete clusters on the TAS diagram. **X-76**, and **X-78** behave independently from the rest, especially on the Debon & Le Fort diagrams (Figs 4.1.3.4 to 4.1.3.7).

4.1.3.5 Analysis by Source Area

L-321, **L-322**, **L-323** and **L-324** come from the “meta-gabbro”, or “albite-chlorite rock” that is associated to the Kalengwa deposit (See Fig 8.43). Their chemistry is very different: **L-321** is a peraluminous mesocratic sodic ferriferous altered granodiorite; **L-322** and **L-323** are peraluminous mesocratic potassic ferriferous alkali granites; and **L-324** is a metaluminous mesocratic potassic ferriferous quartz syenite. The four samples seem to have been part of the same body of rock; their varying chemistry is probably due to differential hydrothermal alteration and/or original chemical disparity. The rocks formed in a rift-related environment, as shown on Table 4.1.3.4.

L-322 and **L-323** are probaby the least altered rocks from which **L-321**, **L-324** and **L-325** could have been hydrothermally altered. The original rock may have had a completely different composition altogether.

X-80, **X-81**, **X-82**, **X-83**, **X-84** and **X-88** are all similar and form a cluster of foid gabbros or essexites. **P-25** is similar to this group. **X-79**, **X-85**, **X-86** and **X-87** are non-foid gabbroids. **X-76**, **X-77** and **X-78** are syenitoids. Thus, the suite of samples from boreholes in the Kasempa area has at least three contrasting chemistries. See Table 4.1.3.3. Note that the KB and MgB diagrams (Figs 4.1.3.6 and 4.1.3.7) group all these rocks in a particular trend.

Rock samples **L-318**, **L-319**, **L-320** and **P-13** go together in the Kalengwa Ndenda granitoid area. This proves that the Ndenda region has at least those two types of contrasting rocks. These are metaluminous mesocratic sodic ferriferous quartz syenite (**P-13**) and metaluminous mesocratic sodic magnesic theralite (**L-318**)

Samples **P-14**, **P-16**, **P-17** and **L-313** come from the same region. They also have contrasting chemistry. **L-313** is a monzodiorite, while **P-17** is a metaluminous mesocratic sodic-potassic ferriferous quartz syenite. Samples **X-87** and **X-86** are similar to **X-88** in the R1/R2 and TAS diagrams. They are syeno-diorite and syeno-gabbro, and probably contain high Th values. **L-324**, **P-13**, **P-17** and **P-26** are all high heat producing granitoids.

Mafic and ultramafic lithologies were observed in boreholes CHIT-8, K-1 and RKN 719 and RKN 801. Studies of those boreholes will not be included in this document.

4.1.3.6 Kalengwa

4.1.3.6.1 Samples

Chemistry of intrusive rocks collected around the Kalengwa deposit is very important for exploration and to gain insight on its possible environment of formation. A total of thirteen samples from the Kalengwa area were

obtained from various sources. Samples **L-312** to **L-326** were collected in the field by Mr. Jon Woodhead, exploration geologist at the Kitwe office of AngloAmerican Corporation (Woodhead, J., personal communication, 2002). **Samples P-13**, **P-17**, **P-25** and **P-26** were collected and processed by (Pepper, 2000). An abstract of Pepper's descriptions and observations on the samples is included in Appendix A61.

4.1.3.6.2 Geochronology

There is no published radiometric age on rocks from the Kalengwa area. The age of intrusive rocks has to be younger than the siliciclastic and carbonate sequences that host them. The age of the sedimentary rocks is not known either, and only loose lithostratigraphic correlations have been attempted (Berbeleac et al., 1979; Evans, 2004 (estimated); Janneker, 2002 and Williams, 1997). If the hypothesis of common origin for the Kasempa and Kalengwa intrusive rocks is true, then the anorogenic complexes that formed at Kalengwa around 750 Ma.

4.1.3.6.3 Environment of Emplacement

All the granitoids from the Kalengwa area formed in anorogenic environments, and possibly as rift-related granitoids as shown on Table 4.1.3.4. All of the gabbroid rocks formed as within-plate alkali basalts. This information, added to the numerous large ring structures from the map produced by (Nisbet et al., 2000) makes a strong case in favor of midalkaline anorogenic ring complexes that intruded Katangan sediments are the most probable environment of emplacement.

4.1.3.7 KASEMPA AREA

A total of fifteen samples from the Kasempa area were studied for this project. All came from boreholes. One came from borehole MB-34 and fourteen from various boreholes drilled by Billiton in the Kasempa area.

4.1.3.7.1 Borehole MB-34

The MB-34 borehole was located in the Chitampa area of Kasempa, as indicated on Fig M9. It was drilled to a depth of 1484 feet[2] in the middle of one of the largest magnetic anomalies of the region, and was completed on June 19, 1958. The hole was logged at 1:500 scale at the Kalulushi coreshed. Fifty-four samples for studies of mineralization, hydrothermal alteration and brecciation were collected.

The borehole has iron oxide-copper-gold mineralization, polymictic, multi-stage, round-pebble hydrothermal breccias and various types of hydrothermal alteration including red-rock alteration, massive magnetite and "hematite-disease" alteration. Parts of this is discussed and illustrated on the chapter about iron oxide-copper-gold mineralization. Results of the research on round-pebble hydrothermal breccias, hydrothermal alteration and mineralization will not be included here.

Relatively unaltered granitoids were sought for chemical analysis, and only **L-139** was analysed from a depth of 1305.3 feet. It is one of several subvolcanic porphyritic, peraluminous leucocratic potassic magnesic granites responsible for mineralization at the Chitampa site. Sample **L-142** was dated; it comes from the same suite of subvolcanic porphyritic intrusives as **L-139**. Zircons from six of the mineralizing granitoids were separated.

4.1.3.7.2 Mufwashi and Chitampa Boreholes

Six boreholes were drilled at the Chitampa and Mufwashi areas of Kasempa by Billiton (Fig M9). The boreholes were sunk to test iron oxide-copper-gold mineralization hosted by Katangan carbonates and siliciclastics, and to help define local stratigraphy. A significant part of the boreholes intersected previously unidentified diamictites. They were sampled during an un-finished M.Sc. project at the University of the Witwatersrand (Janneker, 2002 and Janneker, D., personal communication, 2003). Fourteen samples of intrusive rocks were analysed from boreholes CH5, MUF1, MUF2, MUF3, MUF3 and MUF4. They were added to the geochemical database of this project (A5). Coordinates of the boreholes are listed in Appendix A16.

Samples **X-76** to **X-89** come from various mafic and syenitic dikes that are intimately associated with the mineralization (Janneker, D., personal communication, 2003).

---

[2] The original borehole was measured and recovered in feet. 1484 feet are approximately equal to 453 meters.

Table 4.1.3.5 Chemical Analisis, Kasempa Area, Zambia
(complete elemental analysis on Table A5, Appendix)

Sample	Original #	SiO2	TiO2	Al2O3	Fe2O3	MnO	MgO	CaO	Na2O	K2O	P2O5	LOI	Total	Rb	Sr	Y	Zr	Nb	Co	Ni	Cu	Zn	Ga	V	Cr	Ba
X-76	CH5/01	55.35	1.48	14.63	10.86	0.10	4.43	2.43	0.91	7.34	0.50	1.65	99.69	209	199	56	591	28.0	13	11	295	50		139	<9	1379
X-77	CH5/05	61.50	1.10	15.15	7.30	0.11	1.58	2.81	4.39	5.07	0.34	1.21	100.59	182	313	48	339	34.0	15	<9	7	47		92	11	1189
X-78	MUF1/15	51.81	3.13	15.06	11.46	0.06	7.53	1.00	3.02	4.48	0.33	2.67	100.54	137	109	32	290	46.0	25	102	20	100		415	117	118
X-79	MUF2/04	48.31	4.07	11.38	9.92	0.21	9.92	5.90	2.58	1.14	0.57	6.34	100.34	18	234	32	358	44.0	47	70	35	146		458	74	75
X-80	MUF3/02	45.03	3.27	13.53	16.29	0.09	6.04	5.05	5.14	3.32	0.53	2.13	100.41	97	112	48	325	55.0	24	81	12	23		327	142	141
X-81	MUF3/03	46.37	3.96	13.46	15.27	0.05	6.20	4.88	4.91	2.96	0.54	1.92	100.52	103	94	55	302	48.0	17	88	7	22		324	135	148
X-82	MUF3/09	48.60	1.56	13.71	18.47	0.08	2.02	5.07	7.38	1.05	0.81	1.52	100.26	32	122	61	567	84.0	<9	10	777	47		58	<9	233
X-83	MUF3/11	46.07	2.56	14.20	17.60	0.15	5.97	5.84	3.60	3.20	0.32	0.85	100.37	88	105	27	177	32.0	17	44	102	44		325	79	384
X-84	MUF3/13	46.07	3.95	12.30	12.67	0.06	3.44	8.56	5.49	0.87	0.91	6.14	100.47	27	106	59	444	89.0	11	11	26	59		138	<9	152
X-85	MUF4/01	47.35	2.56	14.08	13.25	0.14	7.29	8.22	4.21	0.61	0.32	2.54	100.58	21	287	26	173	37.0	36	69	11	182		318	36	127
X-86	MUF4/02	45.88	3.96	12.72	16.75	0.25	5.61	7.19	3.78	1.46	0.31	2.23	100.14	37	319	33	201	40.0	14	36	124	167		522	<9	303
X-87	MUF4/03	46.09	2.86	13.80	14.33	0.23	6.98	7.07	4.90	0.32	0.41	3.05	100.06	13	344	31	208	42.0	18	50	9	134		315	23	119
X-88	MUF4/09	45.24	2.00	14.37	11.55	0.11	10.97	4.11	2.72	5.24	0.20	3.85	100.37	147	69	25	131	21.0	35	201	<2	168		326	515	112
X-89	MUF4/17	46.20	3.57	8.68	14.36	0.18	11.42	6.07	4.30	2.70	0.67	1.85	100.01	56	337	36	223	53.0	37	30	7	228		474	9	155
L-139		75.60	0.09	11.88	1.50	0.03	0.62	0.14	1.61	7.87	0.01	0.79	100.14	399	17	40	75	41.0	10	7	55	34	23	14	47	769

4.1.3.7.3 Geochronology

A zircon concentrate of **L-142**, from borehole MB-34 (1373.5 feet) was dated by U-Pb SHRIMP II at approximately 750 Ma[3]. That is at least one of the ages of emplacement for ring complexes in the Kalengwa-Kasempa area, and does not overrule the presence of younger intrusives. Geochronology of the Kalengwa-Kasempa area is still in its early stages. **L-139** comes from the same borehole as **L-142** (MB-34), and is the same type of subvolcanic porphyritic, peraluminous leucocratic potassic magnesic granite (Fig 4.1.3.8). The normal analysis for environment of emplacement did not produce any valid results for **L-139**. Most probably, the granites were emplaced in an anorogenic rift-related or continental epeirogenic uplift environment.

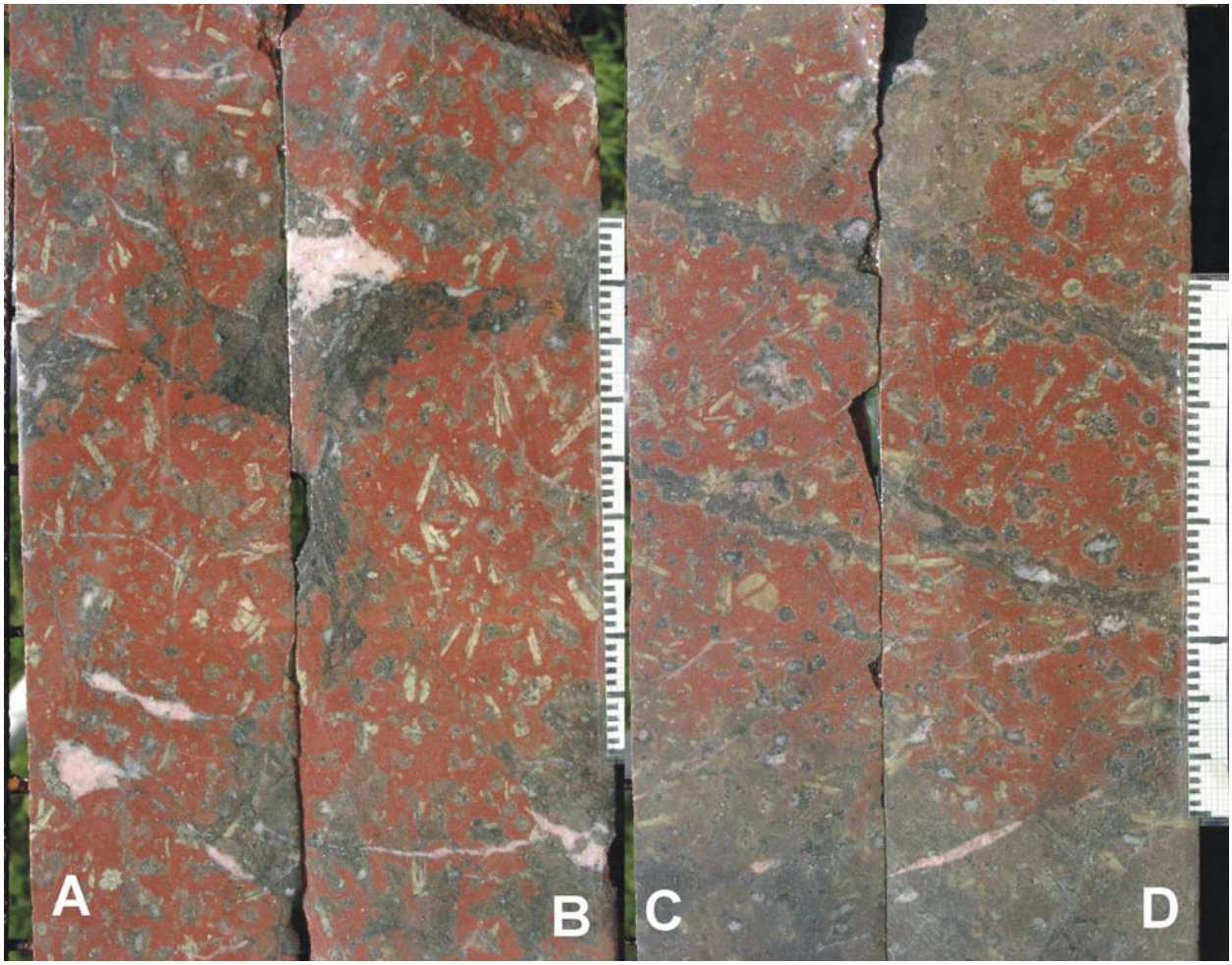

Fig 4.1.3.8 Photos of red-altered, subvolcanic porphyritic granitoids that were dated; borehole MB-34, Chitampa, Kasempa area, Zambia*. A and B come from sample L-129, and C and D from L-127. More details in the text. Gray material is the silicate-sulfide matrix to hydrothermal breccias and stockworks. Mm for scale.*

[3] 750 Ma is a preliminary age. Complete results have not been produced by the ANU.

4.1.4 NORTHWESTERN ZAMBIA DOMAIN

4.1.4.1 Introduction

This portion of northwestern Zambia comprises the environs of Mwinilunga and Kalene Hill as well as the Domes Area and shown on Figs M1, M10 and M12. It has a large areal extent and very little outcrop. It will be subdivided into four areas, as follows: Kalene Hill, Kabompo Dome, Mombwezhi Dome, and Solwezi[1] Dome, as illustrated on Figs M1 and 4.1.4.7. Samples collected from each of these areas are described from west to east in the following pages. A special section about a sodalite syenite quarry is included with the Mwombezhi Dome.

Granitoids from northwestern Zambia are equally spread between midalkaline and subalkaline rocks: 45% of all rocks collected come from midalkaline rocks, 36% from subalkaline rocks and 20% from alkaline rocks (Table 4.1.4.1). This domain has the larger proportion of subalkaline rocks in the Greater Lufilian Arc granitoid project.

Table 4.1.4.1 Rock type statistics, from Northwestern Zambia
The fifth column (granitoids) is the sum of underlined rock types.

Group	Rock type	Number	%	Granitoids	Groups
Midalkaline Rocks	Alkali granite	7	12.50	50.00	44.64
	Quartzmonzonite	8	14.29		
	Syenite	2	3.57		
	Monzonite	1	1.79		
	Monzodiorite	1	1.79		
	Monzogabbro	1	1.79		
	Alkali gabbro	5	8.93		
Subalkaline Rocks	Granite	10	17.86	50.00	35.71
	Granodiorite	8	14.29		
	Diorite	1	1.79		
	Gabbro	1	1.79		
Alkaline Rocks	Foid syenite	8	14.29		19.64
	Foid gabbro	2	3.57		
	Foidolite	1	1.79		
Total		56	100.00	100.00	100.00

If samples from the sodalite syenite quarry are not considered, rocks analysed are still spread out almost equally between midalkaline and subalkaline rocks. Nevetheless, a 6.5% of rocks is still alkaline, as shown on Table 4.1.4.2. A large portion of the samples come from the Kalene Hill area, which contains a significant number of subalkaline or calc-alkaline rocks. This shows that the domain is a mix of several magmatic environments that were active through time.

Table 4.1.4.2 Partial rock type statistics, from Northwestern Zambia
The fifth column (granitoids) is the sum of underlined rock types.

Group	Rock type	number	%	Granitoids	Groups
Midalkaline Rocks	Alkali granite	7	15.22	48.57	52.17
	Quartzmonzonite	8	17.39		
	Syenite	1	2.17		
	Monzonite	1	2.17		
	Monzodiorite	1	2.17		
	Monzogabbro	1	2.17		
	Alkali gabbro	5	10.87		
Subalkaline Rocks	Granite	10	21.74	51.43	41.30
	Granodiorite	8	17.39		
	Gabbro	1	2.17		
Alkaline Rocks	Foid gabbro	2	4.35		6.52
	Foidolite	1	2.17		
Total		46	100.00	100.00	100.00

[1] Solwezi is a Zambian term with several spellings in use. This document uses Solwezi instead of “Solwesi”.

4.1.4.2 Kalene Hill Area, Zambia

This northwestern portion of Zambia borders with the Democratic Republic of Congo to the north and Angola to the west, as indicated on Fig M1. There is very little outcrop in the region. Some of the best outcrops were roadcuts and foundations for bridges over perennial creeks. The rocks from this part of the Lufilian Arc are mainly granites, granodiorites, quartzmonzonites, alkali granites, gabbro and syenite (Figs 4.1.4.2 and 4.1.4.1). Thirty-one samples make the database of Kalene Hill, as shown on Table 4.1.4.3. Six samples from the fieldwork were analysed. 24 rock samples were collected during mapping of 1:100,000 scale geological sheets 1124NW, 1023SE and 1024SW (Key & Banda, 2000). These were kindly supplied by the Zambian Geological Survey in Lusaka (See Map of Fig M11). The original report includes UTM coordinates of all samples. Renumbering of samples from Key & Banda, 2000 is listed on Table 4.4.4.5.

Detailed field descriptions of outcrops and specimens collected are included in Appendix A62.

4.1.4.2.1 Geochemistry

Granitoids from the Kalene Hill area are equally spread between the midalkaline and subalkaline fields. Midalkaline and subalkaline rocks are evenly spread too, as shown on Table 4.1.4.4. In addition to that, midalkaline and subalkaline rocks are each broken into two dominant rock groups.

Table 4.1.4.4 Rock type statistics, from Kalene Hill samples, NW Zambia
The fifth column (granitoids) is the sum of underlined rock types.

Group	Rock type	number	%	Granitoids	Groups
Midalkaline Rocks	Alkali granite	6	20.00	50.00	50.00
	Quartzmonzonite	7	23.50		
	Syenite	1	3.33		
	Monzodiorite	1	3.33		
Subalkaline Rocks	granite	7	23.33	50.00	50.00
	granodiorite	7	23.33		
	gabbro	1	3.33		
Total		30	100.00	100.00	100.00

Table 4.4.4.5 groups the various samples into three map types (fifth column), based on the maps and report of Key & Banda, 2000 and Key et al., 2000 Archean rocks were marked with letter A, and Paleoproterozoic rocks were marked with B. Samples that correspond with uncertain map units have a question mark.

4.1.4.2.2 Description of the Various Groups

As seen on Table 4.4.4.5, rocks from Kalene Hill can be divided at least into four groups, listed below in tentative chronological order. The first group is a suite of Archean rocks made of pink, iron-rich mainly metaluminous granites and alkaline granites (map type A) that was intruded by mafic dikes and syenites. It corresponds with map unit A and covers a particular area in the NW part of the geological map (Fig M11). All rocks in the suite are enriched in Cu and Pr. There is a good correlation of the various oxides against silica.

Group 2 is a suite of Paleoproterozoic leucocratic to mesocratic, sodic to potassic, pink to red granites, alkaline granites and granites that correspond to map unit B and were probably formed in an anorogenic continental epeirogenic uplift environment. More precise definition of the environment will not be made here. These are associated with minor mafic intrusions. Group 2 samples are enriched in Pr and K and have low Ca content. This group of rocks seems to have emplaced itself at approximately 1928 Ma, as indicated by the SHRIMP age of **L-030*** discussed below under the section for the Kabompo Dome. This group plots as a linear trend in the KB, MgB and QBF plots of Debon & LeFort and as a cluster on R1R2 and TAS diagrams as illustrated on Figs 4.1.4.1 to 4.1.4.6 and shown on Table 4.4.4.6. Unaltered members of the group are all subleucocratic to leucocratic. There is a slight correlation when the various oxides are plotted against silica.

Additional samples from the NW Zambia region that fall into this group are **L-030***, **L-060b**, **L-360**, **L-420** and **L-421**. If **L-030*** and **L-060** (samples from the Kabompo and Solwezi Domes, respectively) are included in the group, they are somewhat different from the “average”. This is probably due to hydrothermal alteration.

The group is far from homogeneous (See Fig 4.1.4.5). Detailed geochemistry of samples from Group 2 varies significantly, especially in terms of minor elements. A few samples seem to deviate from the “average” cluster, due to moderate or strong hydrothermal alteration. These include **L-377**, **L-368**, **L-366**, and to a minor extent, **L-375**, **L-360** and **L-380**. **L-366** is enriched in Fe, Ti, P_2O_5 Zn, Zr, Ce, La, Eu, Gd, Nd, Pr, Yb and Lu. **L-368** is

enriched in Mg, Ba, Zr, Ce, La, Mg, Ti and P_2O_5. A subgroup of group 2 may be made. It includes **L-026**, **L-365**, **L-366**, **L-368** and **L-378**. These samples contain high Zn, Fe, Ce, La and Zr in comparison with the rest of the suite; in addition, part of these show low Ca and deviate from the "average" composition.

Table 4.1.4.3 Chemical Analysis of samples from the Kalene Hill Area, NW Zambia
(Complete elemental analysis on Table A7, Appendix)

Sample	SiO2	TiO2	Al2O3	FeOt	MnO	MgO	CaO	Na2O	K2O	P2O5	LOI	Total
Notch	50.00	1.00	15.50	6.00	0.15	2.00	5.00	4.90	5.50	0.30	2.00	
Archean rocks												
L-372	54.14	0.84	17.15	9.33	0.12	3.24	7.00	4.31	2.25	0.28	1.85	100.51
L-373	72.41	0.25	14.10	2.22	0.03	0.41	1.36	3.49	4.20	0.05	0.93	99.45
L-375	69.92	0.45	12.64	4.64	0.07	0.33	1.04	3.27	5.81	0.13	0.77	99.07
L-376	59.71	0.51	17.93	5.54	0.09	1.10	2.05	6.07	4.94	0.12	0.83	98.89
Paleoproterozoic rocks												
L-027	67.24	0.53	15.50	4.74	0.09	1.38	4.31	3.75	1.72	0.19	1.02	100.47
L-023	67.01	0.56	14.95	5.02	0.07	1.83	2.74	3.71	3.60	0.19	0.80	100.48
L-025	70.60	0.40	13.80	3.70	0.05	0.73	1.82	3.19	4.80	0.08	0.96	100.13
L-026	71.92	0.37	13.46	3.29	0.04	0.67	1.98	3.23	4.51	0.08	0.82	100.37
L-362	64.93	0.66	14.31	9.33	0.07	1.39	3.79	3.72	2.15	0.17	1.66	98.65
L-363	65.30	0.64	15.16	2.22	0.09	1.23	3.11	3.95	3.37	0.16	1.49	99.80
L-369	71.39	0.21	13.38	4.64	0.03	0.49	1.80	4.10	3.83	0.04	1.74	98.90
L-370	74.09	0.20	12.02	5.54	0.03	0.26	0.95	4.32	4.07	0.04	0.88	99.44
L-377	69.88	0.26	12.62	3.07	0.04	0.28	1.27	5.06	5.45	0.05	1.01	98.99
L-364	74.42	0.19	11.94	2.26	0.02	0.40	0.26	3.54	5.07	0.04	0.68	98.82
L-365	72.12	0.48	12.08	4.21	0.04	1.25	0.45	2.64	4.87	0.12	1.33	99.59
L-378	73.20	0.22	12.15	3.08	0.04	0.23	0.84	3.95	4.18	0.05	0.84	98.78
L-020	74.44	0.22	12.70	2.48	0.05	0.28	0.58	3.03	5.85	0.02	0.75	100.40
L-379	72.89	0.21	12.77	2.54	0.03	0.45	0.72	6.12	2.92	0.07	0.62	99.34
Other												
L-367	72.13	0.48	11.76	4.45	0.06	1.30	3.17	1.69	2.41	0.13	1.70	99.28
L-023	67.01	0.56	14.95	5.02	0.07	1.83	2.74	3.71	3.60	0.19	0.80	100.48
L-024	48.01	2.10	12.37	18.91	0.28	4.93	8.74	1.70	0.43	0.17	1.16	98.80
L-357	61.26	0.49	17.43	5.33	0.07	1.08	2.85	4.92	3.59	0.22	1.77	99.01
L-358	63.11	0.65	15.74	6.29	0.07	1.04	3.80	4.03	2.31	0.17	1.51	98.72
L-359	66.92	0.41	14.63	4.21	0.06	0.79	2.31	3.91	4.84	0.12	1.07	99.27
L-360	68.89	0.31	14.44	3.71	0.04	0.60	1.23	3.18	6.02	0.07	0.91	99.40
L-361	63.38	0.74	15.35	6.08	0.06	1.57	3.80	4.38	2.06	0.22	1.49	99.13
L-366	67.02	0.66	13.23	5.79	0.09	0.90	1.76	4.05	4.28	0.18	0.92	98.88
L-368	67.04	0.71	14.00	4.96	0.05	1.32	0.98	3.41	4.64	0.17	1.39	98.67
L-371	70.77	0.25	14.56	1.78	0.03	0.40	1.37	4.85	4.06	0.08	1.04	99.19
L-374	70.46	0.20	14.58	2.28	0.04	0.31	1.75	5.02	3.92	0.05	0.77	99.38
L-380	70.37	0.39	13.41	3.59	0.05	0.27	0.92	3.65	5.94	0.09	0.69	99.37

Sample	Rb	Sr	Y	Zr	Nb	Co	Ni	Cu	Zn	Ga	V	Cr	Ba	U	Th	Sc	Sm	Nd	Pr	Ce	La	Hf	Ta	Eu	Gd	Yb	Lu
Notch	200	400	60	360	40	30	16	25	85	26	100	100	1300	20	37	20	50	50	15	175	95	10	120	4.0	30	7.5	1.6
Archean rocks																											
L-372	86	764	11	193	8	20	9	57	116	21	23	18	423	<6	<15	24				135	71						
L-373	114	353	31	147	8	6	7	17	28	14	198	12	1215	<6	17	<10	105	15	35	90	10	3	21	0.2			0.6
L-375	140	197	47	365	30	7	11	26	55	18	22	19	1228	<6	21	<10				296	145						
L-376	74	419	29	280	27	11	<6	18	58	20	67	<12	1036	<6	<15	<10				174	95						
Paleoproterozoic rocks																											
L-027	49	619	21	123	13	7	<6	<6	49	18	68	161	573	<6	<15	12				107	58						
L-023	78	376	24	133	13	10	6	<6	44	16	80	219	1283	<6	<15	12	7	50	77	127	44		61	0.7		1.3	1.1
L-025	91	370	11	108	10	6	8	9	71	17	38	42	1390	<6	<15	<10	4	32	47	85	20		25	0.8		0.6	0.8
L-026	85	384	12	392	14	6	7	8	55	16	38	42	1367	<6	<15	<10				97	41						
L-362	77	452	35	221	9	9	8	17	93	19	79	22	1523	<6	<15	10				113	61						
L-363	119	398	31	202	9	11	6	18	69	20	73	20	1054	<6	<15	<10				82	40						
L-369	78	254	51	135	25	<6	6	119	118	16	53	20	789	<6	<15	<10	114	19	57	86	27		23	0.6	1.4		0.7
L-370	279	61	7	195	6	<6	10	10	32	21	16	<12	264	9	52	<10				145	73						
L-377	255	69	91	174	17	<6	9	167	109	19	12	19	365	8	45	<10				135	71						
L-364	236	34	42	207	10	<6	9	9	23	20	59	23	198	8	44	<10				179	88						
L-365	146	81	75	353	24	8	7	24	38	19	<12	15	881	<6	26	<10				212	114						
L-378	216	69	79	255	19	<6	10	163	98	19	<12	15	371	6	33	<10				267	135						
L-020	226	91	53	228	19	<6	<6	9	64	18	<12	47	553	10	62	<10	11	88	145	286	75		73	3.3		2.7	1.3
L-379	139	54	59	84	27	<6	14	17	15	25	<12	20	133	10	<15	<10				39	18						
Other																											
L-367	59	232	237	162	22	10	<6	7	61	15	29	14	1518	<6	<15	<10				80	42						
L-023	78	376	24	133	13	10	6	<6	44	16	80	219	1283	<6	<15	12	7	50	77	127	44		61	0.7		1.3	1.1
L-024	16	78	51	140	11	57	66	236	149	22	470	79	108	6	<15	43	14	39	39	25	19		391			2.3	2.1
L-357	69	568	67	298	29	10	9	36	70	21	<12	12	1645	<6	<15	<10				111	55						
L-358	80	492	29	233	13	12	10	479	261	22	58	16	950	<6	<15	14	10	28	69	106	32		98	0.2		0.6	1.1
L-359	120	359	28	192	13	8	8	11	54	22	64	26	1134	<6	<15	10				149	76						
L-360	100	369	67	134	15	7	6	9	46	16	40	20	2144	<6	<15	<10				114	57						
L-361	118	544	17	246	8	12	15	20	78	21	36	<12	844	<6	<15	12				162	84						
L-366	142	188	54	448	19	7	<6	13	86	20	21	12	1082	<6	<15	11	10	139	247	347	139		88	6.1	42.5	13.2	2.6
L-368	112	156	18	565	10	10	8	13	61	18	38	15	1652	<6	<15	<10				189	101						
L-371	104	650	59	127	23	<6	10	10	38	18	<12	15	1474	<6	<15	<10				110	52						
L-374	97	473	10	105	6	<6	<6	9	33	17	17	14	1054	<6	<15	<10				49	23						
L-380	177	135	57	365	28	7	10	116	83	18	17	13	1129	<6	18	<10	15	66	188	241	95	1	44	1.5	2.9	2.5	1.1

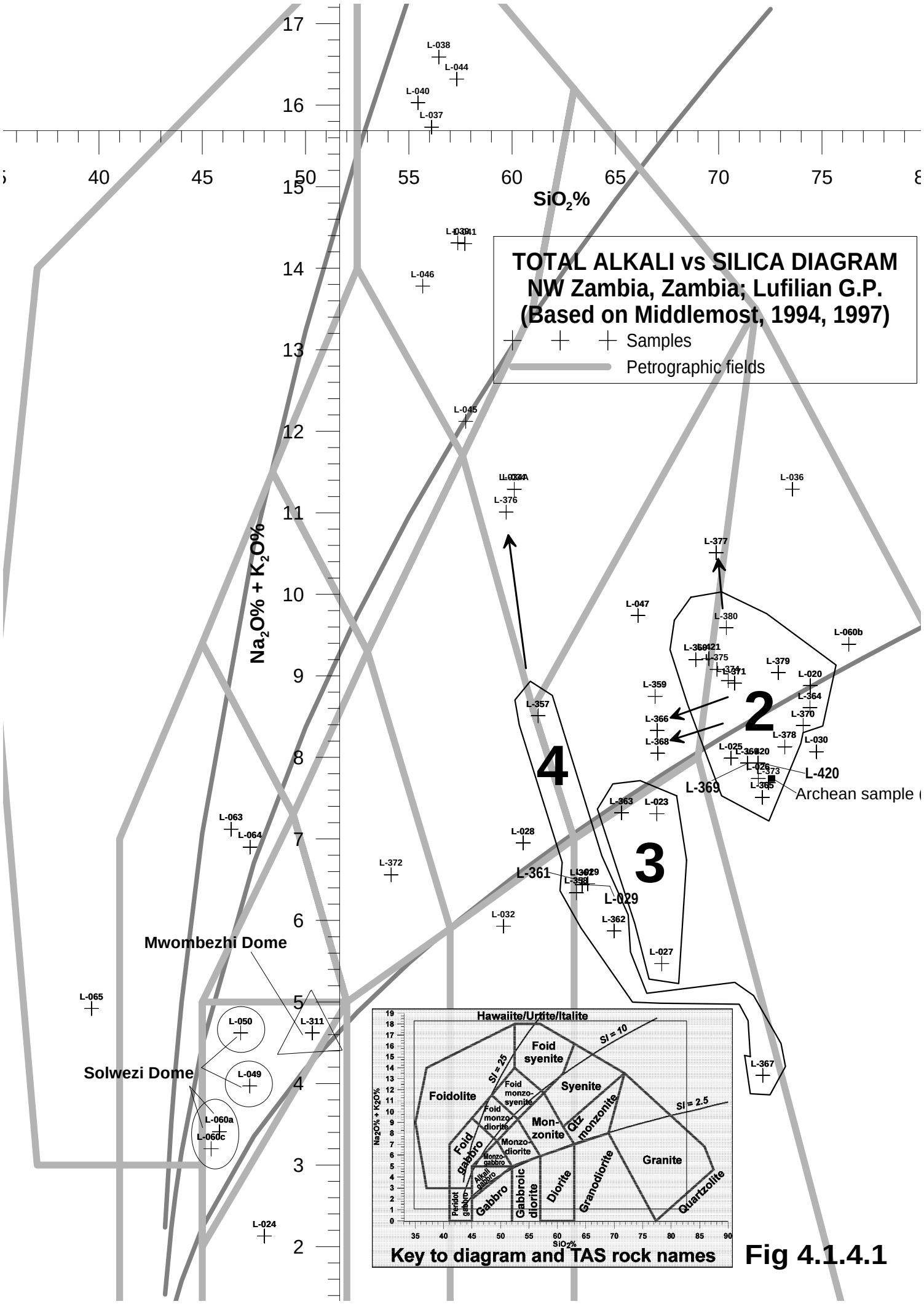
TOTAL ALKALI vs SILICA DIAGRAM
NW Zambia, Zambia; Lufilian G.P.
(Based on Middlemost, 1994, 1997)
Samples
Petrographic fields
SiO2%
Na2O% + K2O%
17
16
15
14
13
12
11
10
9
8
7
6
5
4
3
2
40
45
50
55
60
65
70
75
L-038
L-044
L-040
L-037
L-046
L-045
L-376
L-036
L-377
L-047
L-380
L-060b
L-375
L-379
L-020
L-359
L-364
L-357
L-366
L-370
L-368
L-378
L-030
L-025
L-420
L-369
L-363
L-023
L-028
L-361
L-029
L-362
L-027
L-032
L-372
L-063
L-064
L-065
L-050
L-311
L-049
L-060a
L-060c
L-024
L-367
2
3
4
Mwombezhi Dome
Solwezi Dome
Archean sample
Hawaiite/Ultite/Italite
Foid syenite
Syenite
Foidolite
Foid monzo-syenite
Foid monzo-diorite
Monzo-diorite
Monzo-gabbro
Mon-zonite
Qtz monzonite
Granite
Foid gabbro
Alkali gabbro
Peridot gabbro
Gabbro
Gabbroic diorite
Diorite
Granodiorite
Quartzolite
SI = 10
SI = 2.5
SI = 25
Key to diagram and TAS rock names

Fig 4.1.4.1

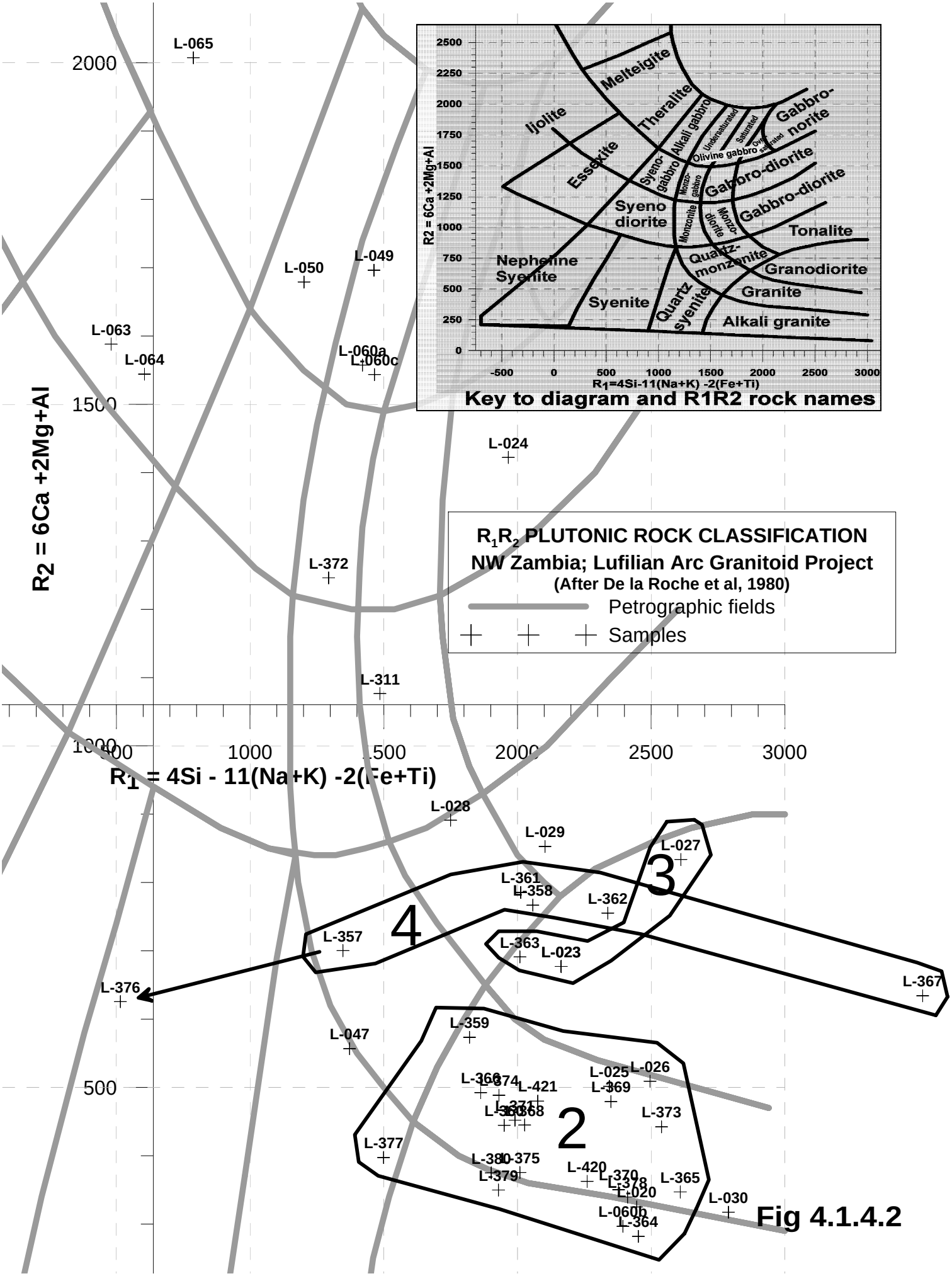
L-065
L-050
L-049
L-063
L-064
L-060a
L-060c
L-024
L-372
L-311
L-028
L-029
L-027
L-361
L-358
L-362
L-357
L-363
L-023
L-376
L-367
L-359
L-047
L-025
L-026
L-369
L-421
L-373
L-377
L-420
L-370
L-365
L-378
L-020
L-030
L-060b
L-364
L-379
2
3
4
2000
1500
1000
500
1000
1500
2000
2500
3000
R2 = 6Ca +2Mg+Al
R1 = 4Si - 11(Na+K) -2(Fe+Ti)
R1R2 PLUTONIC ROCK CLASSIFICATION
NW Zambia; Lufilian Arc Granitoid Project
(After De la Roche et al, 1980)
Petrographic fields
Samples
Melteigite
Ijolite
Theralite
Alkali gabbro
Olivine gabbro
Gabbro-norite
Essexite
Syeno-gabbro
Gabbro-diorite
Syeno diorite
Monzonite
Monzo-diorite
Tonalite
Nepheline Syenite
Quartz-monzonite
Granodiorite
Syenite
Quartz syenite
Granite
Alkali granite
Key to diagram and R1R2 rock names

Fig 4.1.4.2

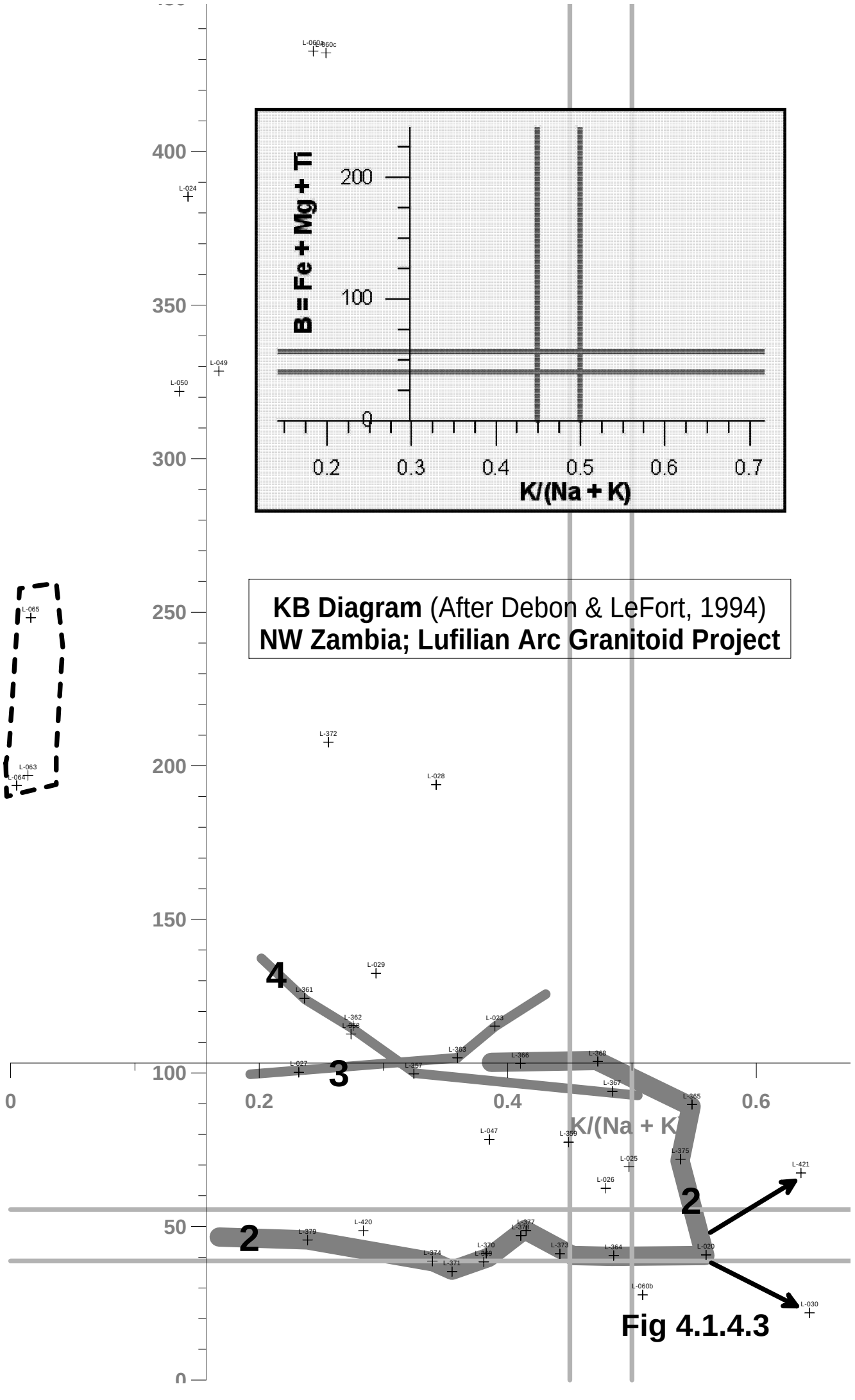
B = Fe + Mg + Ti
200
100
0
0.2
0.3
0.4
0.5
0.6
0.7
K/(Na + K)
KB Diagram (After Debon & LeFort, 1994)
NW Zambia; Lufilian Arc Granitoid Project
400
350
300
250
200
150
100
50
0
0
0.2
0.4
0.6
K/(Na + K)
4
3
2
2
L-060a
L-060c
L-024
L-049
L-050
L-065
L-063
L-064
L-372
L-028
L-029
L-361
L-362
L-023
L-363
L-027
L-357
L-366
L-368
L-367
L-365
L-047
L-359
L-375
L-025
L-026
L-421
L-379
L-420
L-374
L-371
L-370
L-373
L-364
L-020
L-060b
L-030

Fig 4.1.4.3

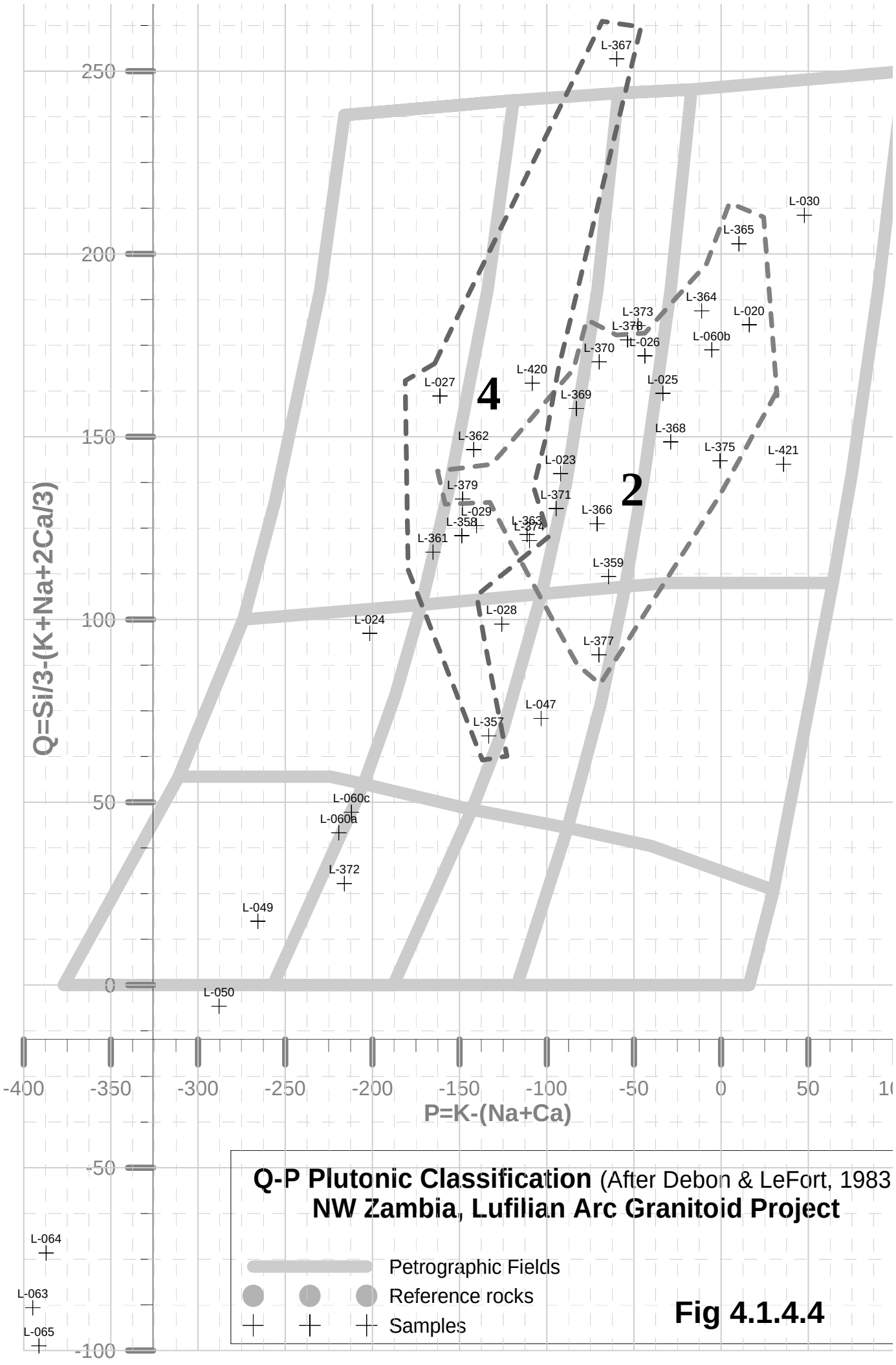
Q=Si/3-(K+Na+2Ca/3)
P=K-(Na+Ca)
250
200
150
100
50
0
-50
-100
-400
-350
-300
-250
-200
-150
-100
-50
0
50
4
2
L-367
L-030
L-365
L-364
L-020
L-373
L-378
L-060b
L-026
L-370
L-420
L-027
L-025
L-369
L-368
L-362
L-375
L-421
L-023
L-379
L-371
L-029
L-366
L-358
L-363
L-374
L-361
L-359
L-028
L-024
L-377
L-047
L-357
L-060c
L-060a
L-372
L-049
L-050
L-064
L-063
L-065
Q-P Plutonic Classification (After Debon & LeFort, 1983
NW Zambia, Lufilian Arc Granitoid Project
Petrographic Fields
Reference rocks
Samples
Fig 4.1.4.4

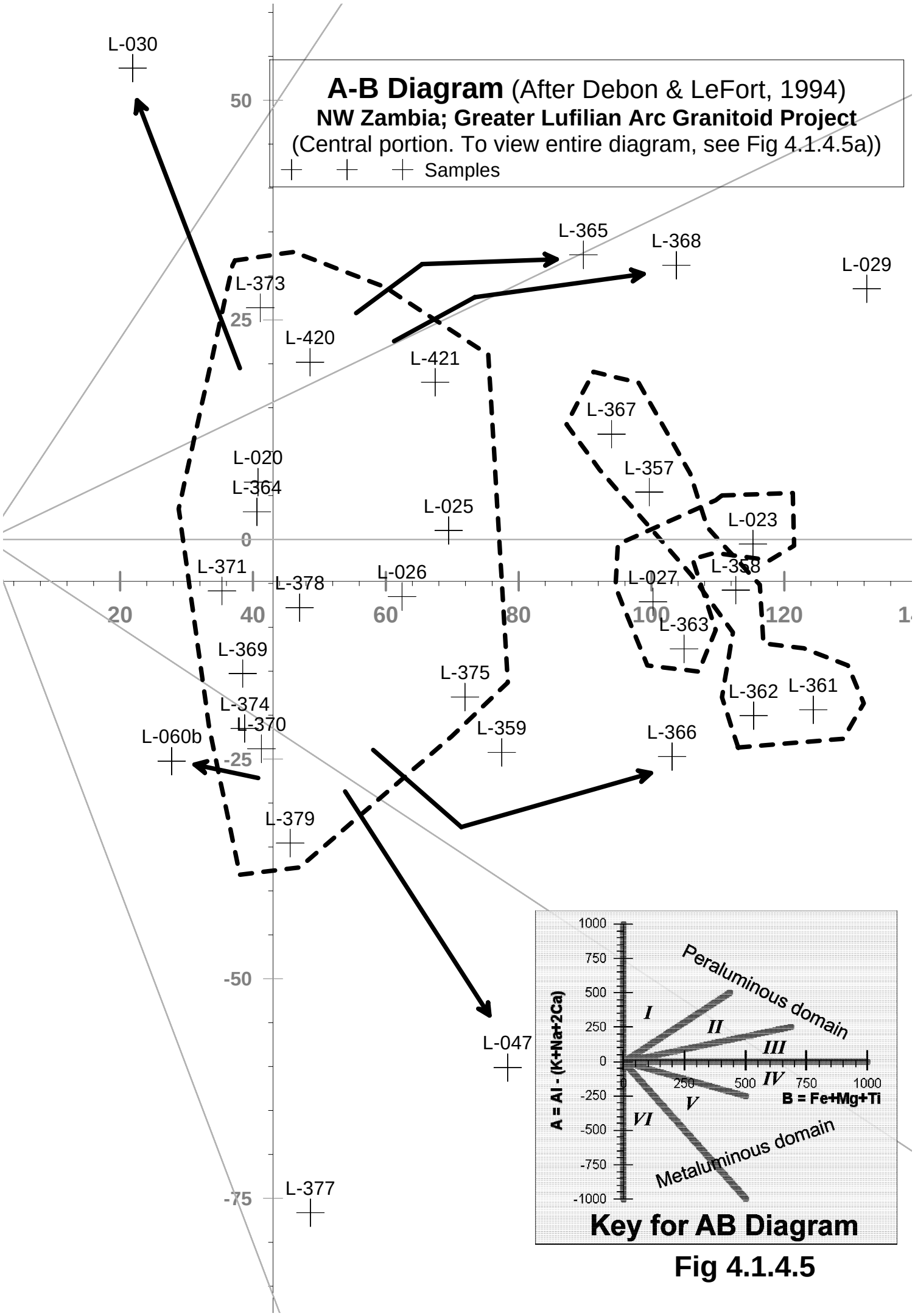
A-B Diagram (After Debon & LeFort, 1994)
NW Zambia; Greater Lufilian Arc Granitoid Project
(Central portion. To view entire diagram, see Fig 4.1.4.5a))
Samples
L-030
L-365
L-368
L-029
L-373
L-420
L-421
L-367
L-020
L-364
L-357
L-025
L-023
L-371
L-378
L-026
L-027
L-358
L-363
L-369
L-375
L-362
L-361
L-374
L-370
L-060b
L-359
L-366
L-379
L-047
L-377
50
25
0
-25
-50
-75
20
40
60
80
100
120
Peraluminous domain
Metaluminous domain
I
II
III
IV
V
VI
A = Al - (K+Na+2Ca)
B = Fe+Mg+Ti
1000
750
500
250
0
-250
-500
-750
-1000
Key for AB Diagram

Fig 4.1.4.5

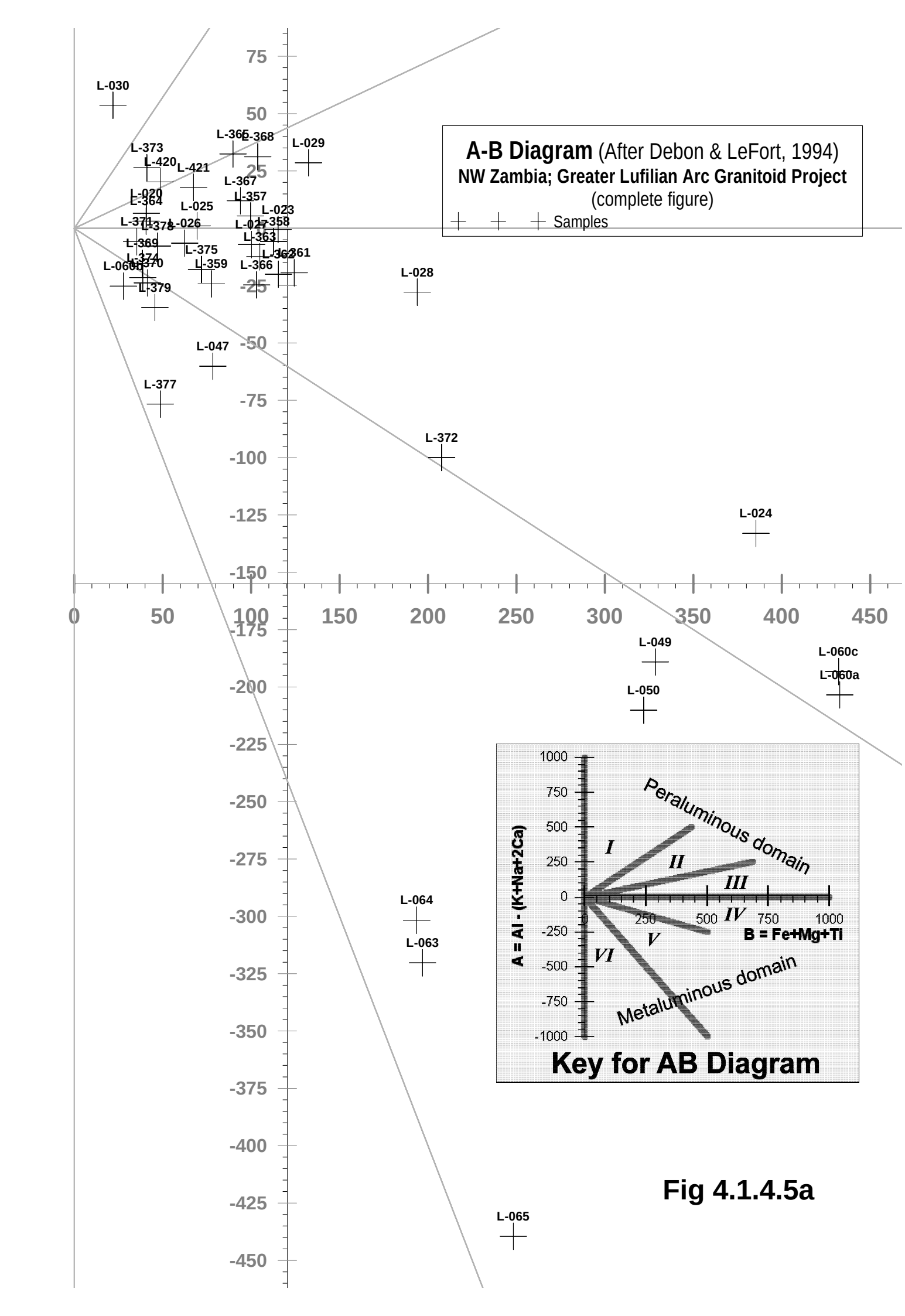
A-B Diagram (After Debon & LeFort, 1994)
NW Zambia; Greater Lufilian Arc Granitoid Project
(complete figure)
Samples
L-030
L-373
L-420
L-421
L-365
L-368
L-029
L-367
L-357
L-020
L-364
L-025
L-023
L-371
L-378
L-026
L-027
L-358
L-369
L-363
L-375
L-362
L-261
L-374
L-370
L-359
L-366
L-060b
L-379
L-028
L-047
L-377
L-372
L-024
L-049
L-060c
L-060a
L-050
L-064
L-063
L-065
75
50
25
-25
-50
-75
-100
-125
-150
-175
-200
-225
-250
-275
-300
-325
-350
-375
-400
-425
-450
0
50
100
150
200
250
300
350
400
450
1000
750
500
250
0
-250
-500
-750
-1000
A = Al - (K+Na+2Ca)
B = Fe+Mg+Ti
Peraluminous domain
Metaluminous domain
I
II
III
IV
V
VI
Key for AB Diagram

Fig 4.1.4.5a

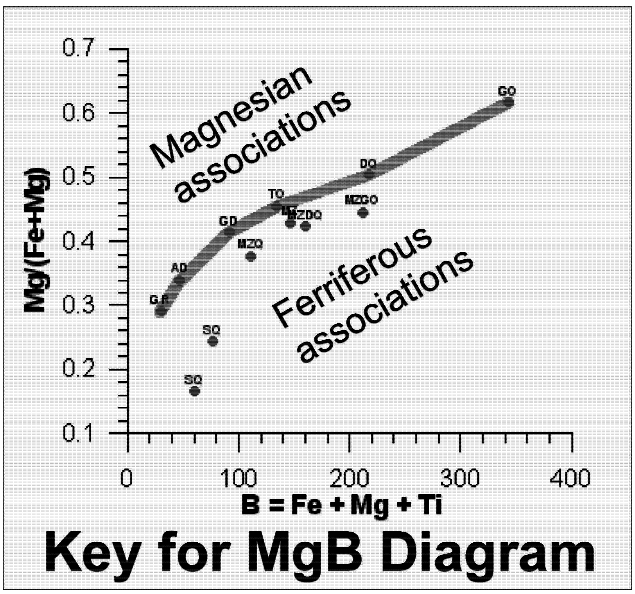

Key for MgB Diagram

Mg-Fe-B Diagram (After Debon & LeFort, 1994)
NW Zambia; Lufilian Arc Granitoid Project

Fig 4.1.4.6

Table 4.4.4.5 Samples from Kalene Hill sorted by groups and geochemistry

(^ = sample with hydrothermal alteration. * = dated sample. High-heat producing rocks are underlined. # = high Cu and Zn content. $ high Cu only. Z = high zinc only. Original sample numbers, from Key & Banda, 2000. See acronym description on section 2.4.3.)

Group 1							
#	**Rock Type**	**Debon & LeFort**	**Orig #**	**Map type**	Maniar & Pic	**Whalen**	**Pearce**
L-372*#	Monzo-gabbro	Metaluminous iv mesocratic Na Fe	3DA100	A	IAG+CAG	A	
L-373*	Granite	Peraluminous ii subleucocratic Na Fe	3DA101	A	POG	N	
L-374	Granite	Metaluminous v subleucocratic Na high Fe	3DA103	?		N	
L-375$	Granite	Metaluminous iv mesocratic K high Fe	3DA106	A	CEUG	A	O-W1-1
L-376	Syenite	Metaluminous iv mesocratic Na Fe	3DA107	A	CEUG	A	O-W1-1
L-380#	Alkali granite	Metaluminous iv mesocratic K high Fe	3DA117	A	CEUG-RRG	A	O3/4
Group 2							
#	**Rock Type**	**Debon & LeFort**	**Orig #**	**Map type**	Maniar & Pic	**Whalen**	**Pearce**
L-020	Alkali granite	Peraluminous iii subleucocratic K high Fe		B	POG	A	O3/4
L-025^	Granite	Peraluminous iii mesocratic Na-K Fe		B		N	O3/4
L-026^	Granite	Metaluminous iv mesocratic Na-K Fe		B	POG	A	
L-360	Granite	Peraluminous iii mesocratic K Fe	3DA045	?	CEUG	A	O-W1-1
L-364	Alkali granite	Peraluminous iii subleucocratic Na-K Fe	3DA060	B		A	
L-365^	Granite	Peraluminous iii mesocratic K Fe	3DA072	B		A	O-W1-1
L-366#	Granite	Metaluminous iv mesocratic Na Fe	3DA073	B	CEUG-RRG	A	O-W 2-2
L-368^	Granite	Peraluminous iii mesocratic Na-K Fe	3DA083	?	RRG-CEUG	A	
L-369#	Granite	Peraluminous iv leucocratic Na Mg	3DA093	B		A	?
L-370	Granite	Peraluminous iv subleucocratic Na Fe	3DA097	B	CEUG	A	
L-371	Granite	Metaluminous iv leucocratic Na Mg	3DA098	?	POG	A	O-W1-1
L-377#	Quartz syenite	Metaluminous v subleucocratic Na Fe	3DA109	B	CEUG	A	O2/3
L-378#	Granite	Metaluminous iv subleucocratic Na Fe	3DA110	B	CEUG-RRG	A	O-W1-1
L-379	Alkali granite	Metaluminous v subleucocratic Na Fe	3DA111	B		A	O-W1-1
Group 3							
#	**Rock Type**	**Debon & LeFort**	**Orig #**	**Map type**	Maniar & Pic	**Whalen**	**Pearce**
L-023	Granodiorite	Metaluminous iv mesocratic Na Fe	L-023	B		N	O3/4
L-027	Granodiorite	Metaluminous iv mesocratic Na Fe	L-027	B	IAG+CAG	N	V
L-363	Granodiorite	Metaluminous iv mesocratic Na Fe	3DA059	B		N	
Group 4							
#	**Rock Type**	**Debon & LeFort**	**Orig #**	**Map type**	Maniar & Pic	**Whalen**	**Pearce**
L-357	Quartz monzonite	Peraluminous iii mesocratic Na Fe	3DA034	?	CEUG	A	W
L-358#	Quartz monzonite	Metaluminous iv mesocratic Na Fe	3DA035	?		A	O3/4
L-359	Granite	Metaluminous iv mesocratic Na Fe	3DA036	?	CEUG	A	
L-361	Quartz monzonite	Metaluminous iv mesocratic Na Fe	3DA056	?		A	
L-362#	Granodiorite	Metaluminous iv mesocratic Na Fe	3DA058	B		A	
L-367	Granodiorite	Peraluminous iii mesocratic Na-K Fe	3DA082	B		A	W
Other Samples							
#	**Rock Type**	**Debon & LeFort**	**Orig #**	**Map type**	Maniar & Pic	**Whalen**	**Pearce**
L-024#	Gabbro-diorite	Metaluminous iv mesocratic Na high Fe	L-024	B	RRG	A	V2/4

Table 4.1.4.6 Kalene Hill groups of samples and their projection on various geochemical diagrams

Group	**# samples**	**AB**	**MgB**	**KB**	**QB**	**QP**	**QBF**	**TAS**	**R1R2**
1	6	Disperse	Disperse		Disperse	Disperse	Disperse	Disperse	Disperse
2	14	Cluster	Trend	Long curvy trend	Disperse	Large cluster	Elongated cluster	Cluster	Cluster
3	3	Trend	Trend	Trend	Disperse	Curve	Curved trend	Curve	Curve
4	6	Trend	Curvy trend	Trend	Disperse	Disperse	Trend	Trend	Curvy trend
X	1	-	-	-	-	-	-	-	-

Group 3 is a widespread series of three Paleoproterozoic, metaluminous, sodic, ferriferous, black and white granodiorites that could have formed in a magmatic arc environment and corresponds to map unit B. It is enriched in Al, Pr, and Cr. There is a good correlation of the various oxides against silica. This group plots as a trend in the K B and MgB plots of Debon LeFort (Figs 4.1.4.5 and 4.1.4.6).

Group 4 is a series of six Paleoproterozoic, mesocratic, sodic, ferriferous, black and white granodiorites and quartzmonzonites that formed in an anorogenic continental epeirogenic uplift environment and corresponds to map unit B. It is enriched in Sr, Pr, Te, and has high loss on ignition. There is a good correlation of the various oxides against silica. This group plots as a linear trend in the Debon & LeFort K vs B and Mg vs B diagrams (Figs 4.1.4.5 and 4.1.4.6). Rock groups 3 and 4 occur in close association. **L-359** seems to be hydrothermally altered, as a variation from group 2 rocks by the intrusion of group 4 rocks (**L-358**).

4.1.4.2.3 Analysis of Independent Samples by Elements

All the samples from the Kalene Hill area that were analyzed for Pr are enriched in that element. There is no valid explanation for that fact yet.

High heat producing granites (due to high Th) are **L-020**, **L-364**, **L-370**, and **L-377**.

Several samples from the Kalene Hill suite are enriched in copper. Three of them are Archean granitoids: **L-372***, **L-375** and **L-380**. The last is highly enriched. This is very important; especially if the copper mineralization is hypogene. Other high Cu samples are: **L-024**, **L-357**, **L-358**, **L-369**, **L-377** and **L-378**. Only one of the high heat producing granitoids (**L-377**) contains anomalous copper. Only two of the Cu-rich rocks are gabbroids (**L-024** and **L-372***); seven are granitoids.

Samples with high zinc include: **L-024**, **L-358**, **L-362**, **L-366**, **L-369**, **L-372***, **L-377** and **L-378**. Of these, only **L-372*** and **L-024** are gabbroids; the rest are granitoids. **L-372*** is the only Archean rock.

Samples **L-369**, **L-372***, **L-377**, **L-378** and **L-380** are all felsic intrusive rocks and contain abundant Cu and Zn (Table 4.1.4.3). This might be significant for Cu and Zn mineralization in the region. Of the group of samples with high Cu and Zn, **L-376**, **L-377** and **L-379** also contain high sodium.

None of the samples studied contain anomalous uranium or niobium.

Cerium and lanthanum are high in: **L-364**, **L-365**, **L-366**, **L-367**, **L-375**, **L-376**, **L-378** and **L-380**.

Cobalt is enriched only in **L-024**.

4.1.4.2.4 Geochronology

Zircon concentrates from two samples from the Kalene Hill area were dated by (Key et al., 2001) using U-Pb SHRIMP II methods. These are **L-372*** and **L-373*** (respectively 3DA100 and 3DA101 in Key's original numbering). **L-372*** is a metaluminous mesocratic sodic ferriferous monzogabbro that intersects the foliated, peraluminous subleucocratic sodic ferriferous granite **L-373***.

The age of emplacement for **L-373*** is 2538±10 Ma. A metamorphic overprint dated 714±66 Ma was identified. **L-372*** produced an age of emplacement of 2535±11 Ma. It had xenocrystic zircons with an age of 2543±5 Ma that correlate well with the age of emplacement for **L-373***. Key et al., 2001 established that rocks from Group 1 were formed in the Archean (See Table A22.2 and event diagram A24 in the Appendix).

L-373* formed in a post-orogenic environment of emplacement. The environment of **L-372*** has not been identified. It could be a continental arc basalt, as indicated by the diagrams of Pearce & Cann, 1976.

Rocks from Group 2 seem to have been emplaced from 1913 to 1952 Ma, as indicated by the SHRIMP age of **L-030***, a sample that correlates well with Group 2, and other similar ages in the environs. Geochronology of **L-030*** will be discussed under the section for the Kabompo Dome.

A tentative order of intrusion for the groups of rocks from the Kalene Hill may be established: Group 1 was intruded by 2. 4 intruded 2. 3 probably also intruded 2. 3 and 4 might be of similar age and there is no evidence for relative age difference among them.

4.1.4.2.5 Environment of Emplacement

As shown on Table 4.1.4.5, most of the Archean rocks formed in a continental epeirogenic uplift environment, except for **L-373** and **L-374** that formed in a post orogenic environment. Proterozoic samples formed in anorogenic, mainly continental epeirogenic environments, except for four; these are **L- 023, L-025**, **L-027** and **L-363**, as shown on Table 4.1.4.5. **L-027** may have formed in an island arc environment, and the environment of the other three samples is uncertain. The new procedure to compare trace and major oxide element chemistry with a database of over 4000 well-located chemical analysis of granitoids using artificial intelligence may help to identify the true environment of emplacement of all the granitoids in the Kalene Hill area.

4.1.4.2.6 Conclusions

Four distinct groups of rocks were identified in the Kalene Hill area. One is Archean and three are Paleoproterozoic.

Archean rocks from Group 1 are enriched in copper.

Paleoproterozoic rocks from Group 2 are widely spread, similar rocks are known in the Mwombezhi and Solwezi domes, and probably also occur in the basement to the Copperbelt. Some of them contain high Th. Some contain high Cu values.

There are several Paleoproterozoic granitoids enriched in copper and zinc.

Minor subductional magmatism may have taken place during the Paleoproterozoic to form part of the rocks present at Kalene Hill.

4.1.4.3 INTRODUCTION TO THE GEOLOGY OF THE DOMES REGION, NW ZAMBIA

From west to east, the Domes region of northwestern Zambia can be subdivided into three main zones: the Kabompo Dome, the Mwombezhi Dome and the Solwezi Dome (Fig M12). Discussion of sampling and results will be presented in that order. Lack of outcrop, and strong overprint by younger orogenies mask Paleoproterozoic structures and geology of the domes region in Zambia.

Very little literature is available on the geology of that part of the country. Paleoproterozoic rocks are exposed in the basement domes; these are covered by younger Mesoproterozoic and Neoproterozoic supracrustal rocks. Neoproterozoic orogenies modified the domes deforming and thrusting their rocks into the arcuate trend that is known today. Domes tend to run parallel to the main structural trend of the Lufilian Arc, as indicated on Fig 4.1.4.7.

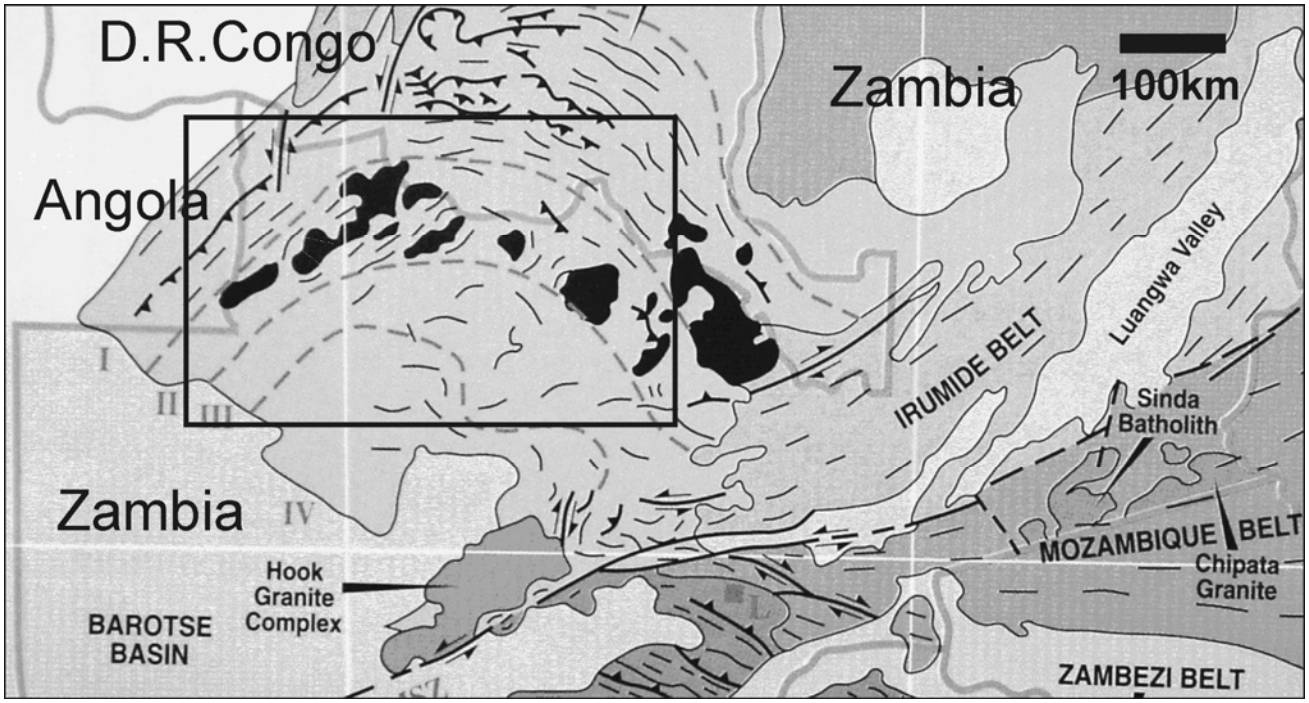

Fig 4.1.4.7 Generalized geological map of the domes region in Zambia. *The black rectangle encloses the main domes. Note the arcuate shape of the domes, and their extension of approximately 500 km along the Lufilian Arc. Rock outcrops are only a very small portion of the domes, most of the land is covered by regolith. Extracted from Porada, 1989.*

In northwestern Zambia, geology is largely obscured by thick soil cover, Karoo rocks, calcrete and Kalahari sand. Outcrops of the domes are only sparsely exposed along river and stream beds.

All the domes are composed of gneisses, migmatites, amphibolites, metagranites and quartz-kyanite-muscovite schists. The oldest rocks are considered to be biotite and hornblende gneisses derived from both sedimentary and igneous protoliths. No detailed subdivision of the gneisses has been attempted, and great portions of the domes appear on geological maps as large, uniform units (Klinck, 1977; Master, 1996 and Mulela & Seifert, 1980 - 1998). Typical paragenesis of the gneisses are:

a) biotite + K-feldspar + quartz + garnet + sulfides
b) biotite + epidote + sphene
c) hornblende + plagioclase + quartz + sphene + scapolite
d) biotite + quartz + epidote

Migmatites are closely associated with the gneisses from which they were derived. The melanosome of the migmatites contains more biotite than the gneisses, while the paleosomes comprise fine-grained gneiss and pegmatitic microcline granite. Massive and foliated granites intrude the gneisses and are considered to be partly responsible for migmatitization. Quartz+kyanite+muscovite±epidote±K-feldspar is the dominant mineral assemblage in the schists, which are mainly found at the basement-cover contact. Kyanite-bearing biotite schist occurs as lenses and bands within the gneisses. Amphibolites interbanded with the gneisses are a minor component of the basement domes; their typical mineral assemblage is: hornblende+plagio-

clase+quartz±biotite±epidote. These rocks are commonly converted to talc-chlorite schists along shear zones (Master, 1996).

Neoproterozoic Katangan metasedimentary rocks contain economic mineralization in the Domes region. The largest mineral deposits are copper mineralization at Lumwana in the Mwombezhi Dome (Benham, Greig, & Vink, 1976; Master, 1996; Equinox Resources, 2003; and Equinox Resources, 2004). Main copper production from the Domes Region historically came from the Kansanshi mine just north of the Solwezi Dome. This is a deposit enriched in copper, gold, uranium and silver (Broughton, Hitzman, & Stephens, 2002; Hitzman, 2001; Master, 1996; O'Brien, 1958; Torrealday, 2000; Torrealday, 2001; and Torrealday et al., 2000). Basement rocks contain minor disseminated and vein copper mineralization. The region has been explored for other minerals, including gold, uranium (Jay, 1960 in Meneghel, 1981a; Meneghel, 1981b; Meneghel, 1981c; Cosi et al., 1989; Cosi et al., 1992; and Master, 1996), rare earths, cobalt, nickel, manganese, iron and diamonds. Deposits at Lumwana and Kansanshi are currently being developed into world-class copper mines.

The following chapters will discuss new geological findings from the Kabompo, Mwombezhi and Solwezi Domes.

4.1.4.4 Kabompo Dome

4.1.4.4.1 Introduction

Rocks of the Kabompo Dome consist of a complex of migmatized gneiss, hornblendite and amphibolite. These rocks are overlain by migmatitized psamites and pelites. Katanga quartzites, and talc-muscovite and kyanite-bearing schists surround the rocks of higher metamorphism. The various gneisses, migmatites and amphibolites are described by Klinck, 1977.

Four samples were collected in the field. Table A7.1 lists their chemical analyses. Table 4.1.4.7 presents their basic geochemistry and results of studies to understand their environment of emplacement. Very few outcrops were found, and the greatest amount of information will be extracted from them. Geology, geochemistry and other aspects of the main rocks observed in the Kabompo Dome will be described in the following pages.

Table 4.1.4.7 Rock name, basic geochemistry and environment of emplacement for samples from the Kabompo Dome, NW Zambia

(Samples with an asterisk were dated. See acronym description on section 2.4.3.)

Sample	Rock Name	Debon & LeFort	Maniar & Piccoli	Whalen	Pearce	Mafic	Rb/10HfTa	Rb/30Hf/Ta	Nb-Ta
L-028	Quartzmonzonite	Metaiv mesoNaMg		N	O3/4				OUTU
L-029	Tonalite	Peraiii mesoNaMg		N					
L-030*	Granite	Perai leucoKFe	POG	A	S2/4 O2/4		VA-	II	INV
L-047*	quartz syenite	Metav mesoNaFe	CEUG	A	W3/4				OUTU

4.1.4.4.2 Description of Samples Collected in the Field

4.1.4.4.2.1 Samples L-028 and L-029

Sample **L-028** was identified in the field as an amphibolite. It is a black and white, metaluminous sodic magnesic quartzmonzonite, that plots near the border with the monzodiorite field. No *in situ* outcrops were found; but 6- to 10-meter diameter boulders of the same material were seen along the river. Several samples of that rock were collected under a bridge located on UTM coordinates 35L 0282993/8698411, 1843m, as shown on Figs M13 and M10. Based on the chemistry, this sample can be assigned to an undefined orogenic environment of emplacement (Table 4.1.4.7). It has high total Fe, Mg, Sr, Ni, Cu and Pr.

L-029 was collected from under a bridge on UTM 35L 0281721/8699392. Very little rock outcrops could be seen for kilometers around. Large boulders of amphibolite-facies, foliated schists or gneisses were sampled on the river bed. They are not *in situ*, but are reasonably well located, according to the geological map sheet. The chemistry of this black, andalusite, peraluminous, mesocratic sodic magnesic tonalite only allows to state that it formed in an orogenic environment (Fig 4.1.4.7). The sample is enriched in alumina, Mg, Sr, Ni and Cu. No analysis for Pr was carried out.

4.1.4.4.2.2 Sample L-030*

By far the best outcrop seen in many tens of kilometers was the box cut to access a bridge along the main paved road from Solwezi to Mwinilunga, on UTM coordinates 35L 0295813/8692365, 1405masl. **L-030*** was collected from a 35 m long outcrop on the southern side of the road, although both sides are well exposed. Figs 4.1.4.8 to 4.1.4.10 illustrate main aspects of the outcrop. All three were drawn at 90° to the main rock foliation.

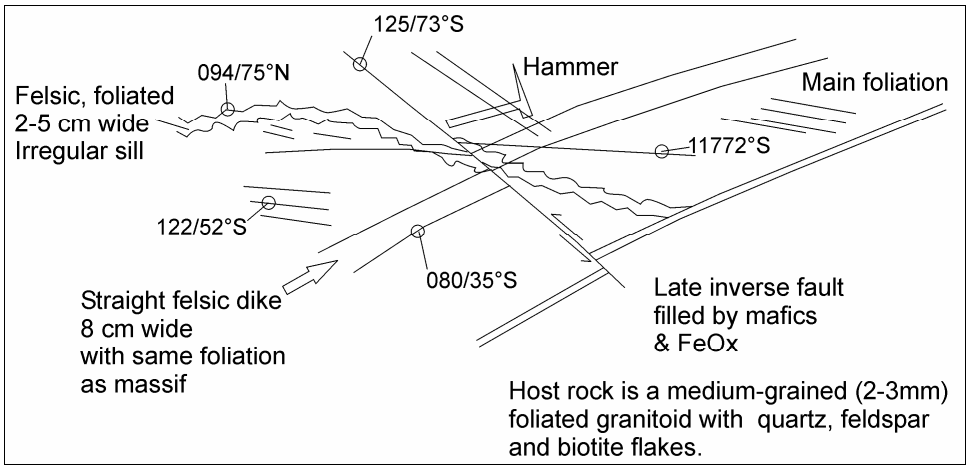

Fig 4.1.4.8 General aspect of the outcrop where samples L-029 and L-030 were collected. *Geological hammer for scale.*

A straight, 8 cm wide dike of felsic gneiss with quartz augen lies along the main foliation. Medium-grained quartz-feldspar and biotite flakes make the darker bands. Several generations of 2.5 cm-wide, irregular felsic sills that intersect the main rock foliation are cut by small displacement thrust faults. Late inverse faults, 5 mm wide, filled by mafic minerals and iron oxides cut all other structures and break the main foliation. Most quartz in the thrust faults and gneisses tends to be brown and smokey. Rock foliation is at an angle to the gneissic light and dark banding. Note the angles of white banding, augen in both light gray mass and in lighter bands (Fig 4.1.4.10). Some of the quartz-rich veins display small refolds, as shown on Fig 4.1.4.9.

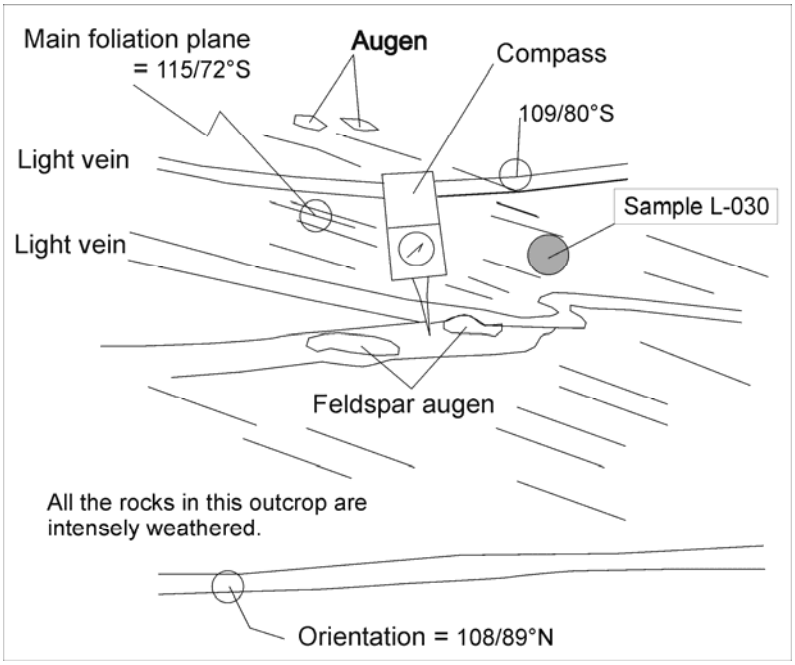

Fig 4.1.4.9. Main aspects of the outcrop where sample L-030 was collected.
More details are included in the text. Brunton geological compass for scale.

L-030* was dated by U-Pb SHRIMP II analysis on zircons and is one of the few samples that has complete rare earth analysis (Fig 21, Appendix). It is a foliated, peraluminous leucocratic potassic ferriferous granite and was formed at 1927.6±7.1 Ma (See Tables 4.1.4.7 and A7.1). Complete geochronological analysis from the sample is not available at the time of writing this document.

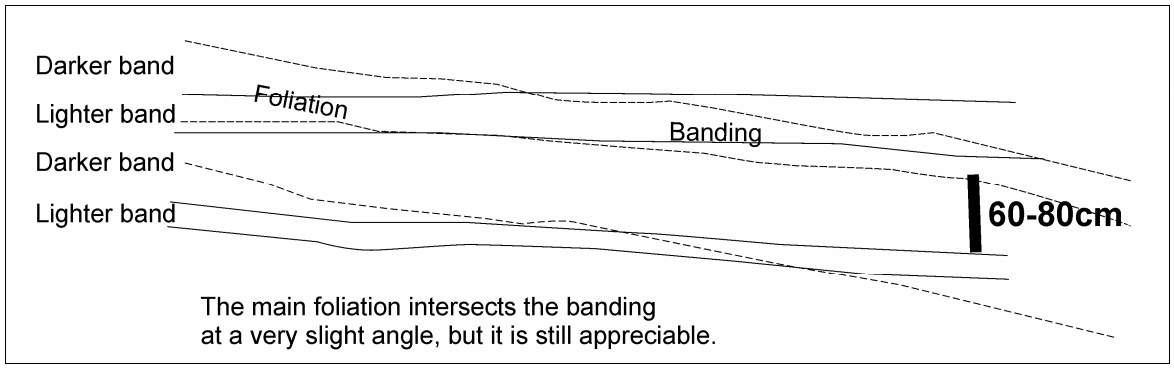

Fig 4.1.4.10 Detail of the foliation and mineral banding of the rock that intersect at around 5-8 degrees.

L-030* was collected as an oriented representative fragment (Fig 4.1.4.9). Its precise location is indicated on the map of Fig M13. It is made by feldspar augen and light refolded bands. This was the freshest possible sample of the rock in the entire outcrop, but it still displays some weathering, and it does not carry apparent magnetite. Main jointing in the outcrop is 095/31°S. Quartz veins are oriented 107/59.5°S with slickensides in "normal" faulting direction (Figs 4.1.4.9 and 4.1.4.8). General foliation on the opposite side of the road was 130/89°W. Another joint that carries a 6 mm quartz vein was oriented 199/55°S. **L-030*** is slightly enriched in uranium and thorium. It is a high-heat producing granitoid, and at the time emplacement it had a 5.0 heat production value as indicated on Chapter 5.

The chemical signature of **L-030*** is very similar to that of **L-364**, **L-370** and **L-020**. That includes K, Rb, Ca, Sr, Ba and most of the other major oxides, minor elements and rare earths. It can be established with a good degree of certainty that Group 2 rocks from the Kalene Hill suite formed in the same environment. They might have been produced during the same geological event. Thus, we can tentatively give Group 2 rocks an approximate age of 1928 Ma. That makes sense, because Key et al., 2001 established SHRIMP II U-Pb zircon ages for feldspar-phyric granitoids at 1934±6 Ma and 1940±2.8 Ma in the Mwinilunga area, just east of the Kalene Hill area. This is also part of the Kabompo Dome.

Detrital zircons from the environs of the Kalumbila deposit were dated by Steven & Armstrong, 2003 and produced ages of 1924 to 1913 Ma and 1952 to 1939 Ma. These ages are all very near in time and could be the evidence of a major event of magmatism in the Kabompo Dome (See Table A22.3 and event diagram of Fig A24).

L-031 was collected from the same outcrop, in a more competent fragment of float of fine-grained foliated gneiss that had very similar macroscopic composition. This sample has not been analysed.

The environment of emplacement for this granite is somewhat difficult to establish, because the various schemes produce conflicting results. It has potassic alteration; for that reason, the Maniar & Piccoli, 1989 tectonic discrimination process state that it formed as a post-orogenic granitoid (Table 4.1.4.7). This is probably wrong, but other tectonic discrimination methodologies don't produce trustworthy results either. The Whalen diagrams clearly show that it is an anorogenic granitoid. Pearce, Harris, & Tindle, 1984 discrimination procedures do not produce any clear results, while the process presented by Harris, Pearce, & Tindle, 1986 indicate that the rock formed in a volcanic arc.

If the anology of **L-030*** with the suite of Group 2 from the Kalene Hill area is extended, then **L-030*** probably formed in a continental epeirogenic uplift.

Field descriptions of samples **L-032** to **L-034** are included in Appendix A63.

4.1.4.4.2.3 Samples L-047* and L-048

Instructions from Peter Mann of the AngloAmerican exploration office in Kitwe served as guide to find obscure outcrops where **L-047*** and **L-048** were collected (Mann, P., personal communication, 2002). There is very little outcrop in the region; no outcrops were seen along the entire route from the main paved road. Both samples come from large boulders that lie semi-buried on the ground, under cover of high grass and abundant shrubs. **L-047*** comes from UTM coordinates 35L 0320870/8660393. **L-048** (Fig 4.1.4.13) was collected exactly 50 m SW of the previous sample. The general location of the sampling sites is shown on the maps of Figs M13, 4.1.4.11 and 4.1.4.12.

L-047* is a metaluminous mesocratic sodic ferriferous quartz syenite; it represents an intrusive event that cuts the "basement" granodiorites in NW Zambia and Katangan siliciclastics and carbonates. Fig 4.1.4.13 shows general macroscopic features of the sample. Complete chemical analysis is presented on Table A7.1. This rock represents a large mapped area (See Fig M13). Studying it is very relevant, because it might have some genetic association with the Kalumbila Co-Ni-Cu deposit, which lies immediately to the south east (Steven & Armstrong, 2003). **L-047*** is highly enriched in almost all the rare earths; Y, Zr, Nb, Nd, Pr, Ce, La, Yb, Eu, Tb and Lu are all very high. In fact the sample has the highest values of such elements in the collection of rocks from NW Zambia. It also has a high Na content and very low Cu, Zn, Co, Ni or Th. The sample lies isolated in all of the geochemical diagrams (Figs 4.1.4.1 to 4.1.4.6). It is a midalkaline rock and is not related to any of the other rocks in the NW Zambia suite.

Fig 4.1.4.13 Slabs of L-047* and L-048. *Note the abundant open spaces in between the crystals. This red-altered rock is associated with small bodies of gabbroids and massive iron oxide as seen on Fig 4.1.4.11. It probably is associated with iron oxide-copper-gold mineralization. Both scales in centimeters and millimeters.*

Both samples have abundant miarolitic cavities, as seen on Fig 4.4.4.13. Quartz fills part of the voids between potassium feldspar and nepheline. Maybe the original rock lacked quartz altogether and that mineral came later after the more alkaline minerals in the rock were formed. This topic was not evaluated in detail. Textures from granitoids that are responsible for iron oxide-copper-gold mineralization in the Kafue Flats and around the Hook Granite batholith have many similar features to those of **L-047***. The fact that a quartz syenite is so enriched in some rare earths and minor elements is very significant. The following rocks have chemical signatures similar to **L-047***: **L-195**, **L-259**, **L-402**, **L-439** and **L-713**.

L-047* was provisionally dated for this project at approximately 730 Ma. Precise U-Pb zircon SHRIMP II data is not available at the time of writing this document. Geological events with similar ages in NW Zambia are listed on Table A22.3 and illustrated on the event diagram of Fig A24. Regional-scale metamorphic events were reported by Cosi et al., 1989; Cosi et al., 1992 and Key et al., 2001 (Events 2, 3 and 4 of Fig A24). Key et al., 2001 report felsic volcanism with a SHRIMP II U-Pb age of 735±5 Ma at Luamata, and a 765±5 Ma basalt effusion at Lwanu in the Mwinilunga area. These events are very near in time and space to the emplacement of **L-047***. Unfortunately, the chemistry of volcanic rocks dated by Key et al., 2001 is not available for comparison and interpretation. They probably are midalkaline rocks.

Fig 4.1.4.12 Geological map with location of sample L-047, Kabompo Dome, Zambia.
From the AngloAmerican exploration office, Kitwe.

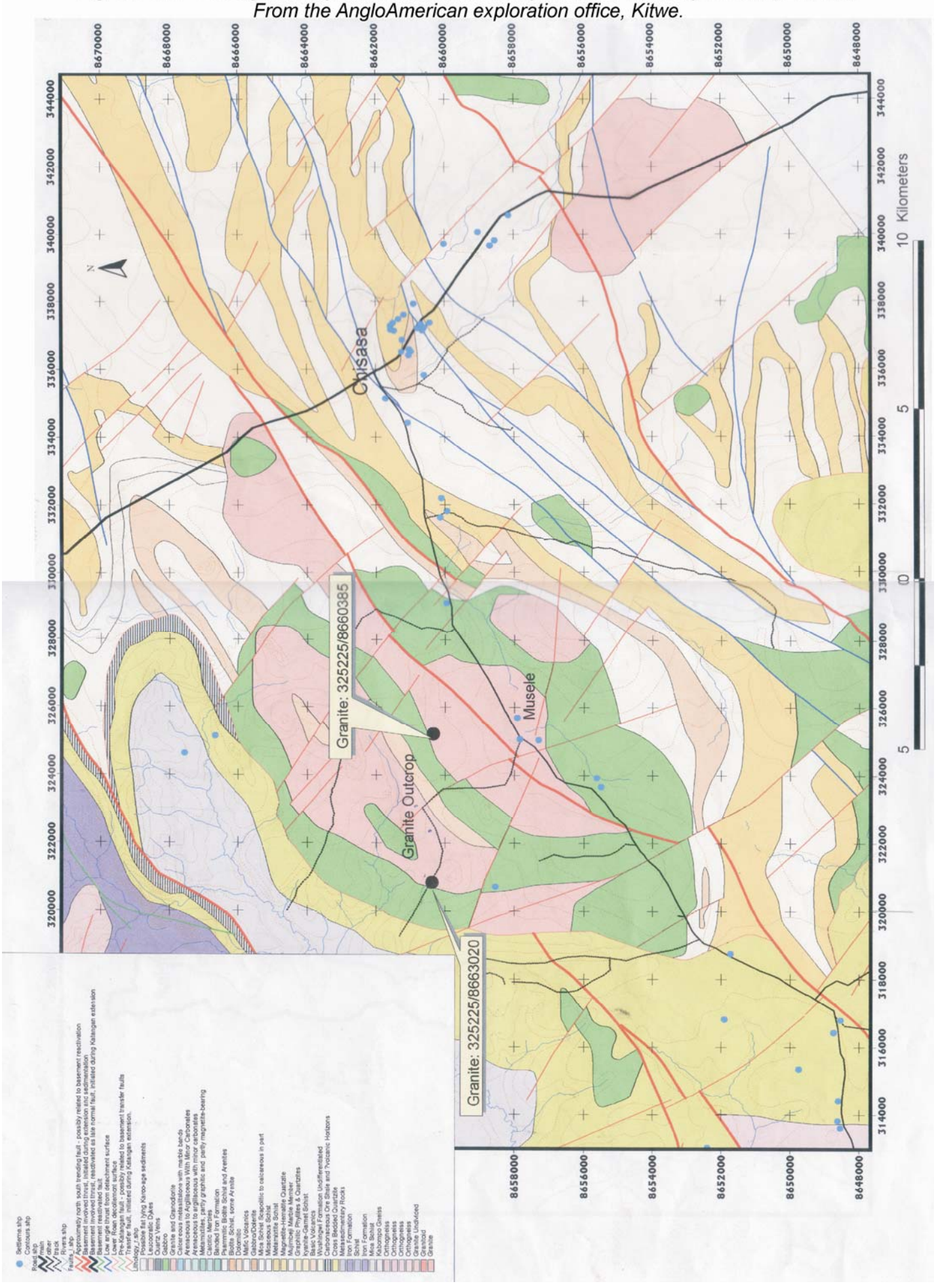

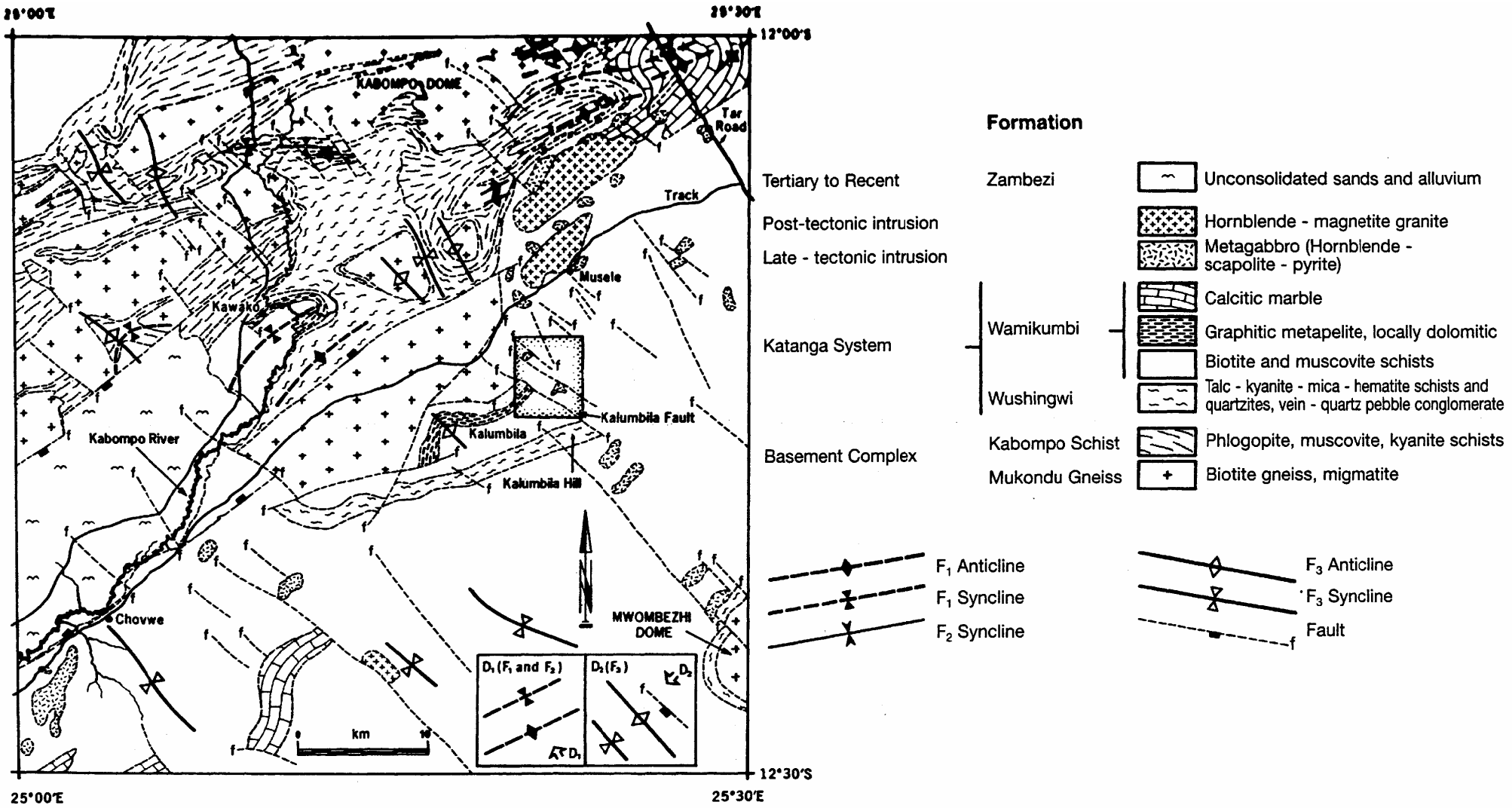

Fig 4.1.4.11 Simplified regional geology and interpreted stratigrapic relations of the southern site of the Kabompo Dome. From Steven, 2003. Note location of granite outcrops and abundant small bodies of gabbroid rocks. The Kalumbila sedimentary-hosted cobalt, copper, nickel deposit is located within the rectangle. Siliciclastic rocks and carbonates fold around the granitoid rocks of the domes. The scale bar is 10 km long.

Sample **L-047*** has been interpreted as a continental-epeirogenic uplift granitoid. It probably formed as a single ring complex. The various granitoid bodies mapped may be faulted portions of a single body (Figs 4.1.4.11 and 4.1.4.12).

The evaluation of sample **L-047*** opens a new concept for exploration in the southeastern portion of the Kabompo Dome. Rocks like **L-047*** were very explosive and produced hydrothermal brecciation. The intrusives intersected Katangan siliciclastics, dark shales and carbonates. There is some minor epigenetic copper mineralization in the environs, gold mineralization, red-altered quartz syenites with abundant miarolitic cavities and explosive brecciation, nearby iron oxide bodies, abundant small gabbroic bodies, strong widespread sodic alteration, and red-rock alteration. All of those features are common in the environs of iron oxide-copper-gold systems (Chapter 8). In addition to that, there is a nearby sedimentary-hosted Co-Ni-Cu deposit.

The south eastern portion of the Kabompo Dome is another location where iron oxide-copper-gold mineralization may be associated to sedimentary-hosted copper mineralization in the Greater Lufilian Arc.

4.1.4.4.3 Conclusions

Foliated, peraluminous, leucocratic to subleucocratic, ferriferous granites and alkali granites were emplaced at least from 1952 to 1913 Ma in the Kabompo Dome. This is probably the evidence of a major anorogenic magmatic event that is present in the Kalene Hill, Kabompo Dome and Solwezi Dome. The granitoids were emplaced in a continental epeirogenic uplift environment.

The south eastern portion of the Kabompo Dome has all the characteristics of being prospective ground to explore for iron oxide-copper-gold mineralization. Red-altered quartz syenites with abundant miarolitic cavities that were emplaced around 730 Ma in a continental epeirogenic uplift environment are intimately associated with small gabbroic bodies and massive iron oxide bodies. They intersect Katangan siliciclastics, organic shales and carbonates. There might be a relationship between iron oxide-copper gold systems and sedimentary-hosted Co-Ni-Cu mineralization in that part of the Kabompo Dome.

4.1.4.5 Mwombezhi Dome

4.1.4.5.1 Introduction

According to Master, 1996 and Mulela & Seifert, 1980 - 1998, the basement of the Mwombezhi Dome comprises the following units:

a) A biotite-rich migmatitic complex, dominated by granites and biotite-hornblende gneisses that are intruded by syenites and microgranite stocks and dikes.

b) Muscovite-phlogopite schists with epidote, biotite, kyanite, quartz and feldspar porphyroblasts produced by shearing of the migmatitic complex. This rock-type represents major shear zones in the basement.

c) Scapolite-garnet metagabbros and hornblendites and amphibolites occur as lenses and bands within the other components of the dome.

d) Katangan meta-sediments that unconformably overlay the crystalline basement of the dome.

Significant subhorizontal shearing of basement and Katangan sediments with later folding of the sheared rocks, produced the complex structural setup of the Mwombezhi Dome. All four rock units were folded into large east-west-trending structures.

Outcrops of the Mwombezhi Dome are uncommon. Nevertheless, 15 granitoid samples were collected from the Chitungulu sodalite syenite that lies just north of the dome, and three from the Shilenda area, south of the dome. Eleven samples of the syenite quarry and one from Shilenda were analysed. This chapter will review general aspects of the Lumwana copper deposit, the Shilenda mafic volcanics, and the sodalite syenite quarry.

4.1.4.5.2 Lumwana Copper Mineralization

The Lumwana copper mineralization is probably the largest completely undeveloped resource of copper in Zambia today. General location of Lumwana is indicated on Fig M13. It occurs within refolded folds and shear zones in the Mwombezhi Dome. The camp is made by several mineralized areas, the most important of which are Malundwe and Chimiwungu. A short visit to the deposit, with assistance of geologists from Equinox and Phelps Dodge is the basis for the following account.

In principle, mineralization at the deposits is hosted in highly deformed metavolcanics. The age of these schists is not known, but may be the extrusive equivalents of the granitoid sampled in **L-030***. And have an age of *circa* 1930 Ma. The age of mineralization has not been well constrained.

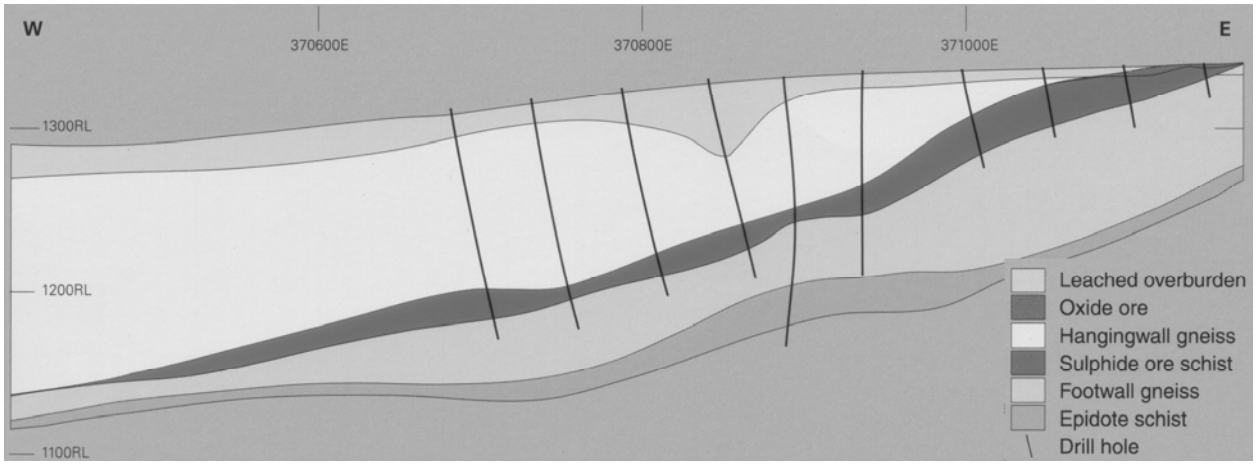

Fig 4.1.4.14 Cross section of the Malundwe Cu deposit at Lumwana, Zambia. *Geology here is greatly simplified. Note the width of mineralization and the depth at which the ore is known. Malundwe is planned to be mined as an open pit; underground operations probably will begin in the last stages of the project. The footwall gneiss is considered to be a meta-granitoid, and the hangingwall schists and gneisses are metavolcanics. Horizontal marks are every 200 m and vertical marks are every 100 m. Image from* Equinox Resources, 2004.

The mineralized body is a 100 m wide sheet that occurs at an approximate depth of 150 m in an area of 1400 m by 4000 m (Fig 4.1.4.14). The body sometimes thins to around 50 m. Mineralization at the Malundwe

deposit is thought to be syn-metamorphic. A shear zone at upper amphibolite facies took place at the same time as mineralization. Publicly available figures on reserves and resources from the Lumwana district are listed on Table 4.1.4.8.

Table 4.1.4.8 Resources and Reserves at the Lumwana District, Zambia
(From Equinox Resources, 2003; and Equinox Resources, 2004)

Lumwana Resource					
Deposit	**Class**	**Tonnage**	**Grade**		
		(Mt)	Cu%	Co (ppm)	Au (g/t)
Malundwe	Measured	47.0	1.14	137	0.05
	Indicated	83.3	0.80	160	0.01
	Inferred	31.4	0.74	115	0.03
	Subtotal	161.7	0.89	144	0.03
Chimiwungo	Measured	82.5	0.76	296	0.02
	Indicated	56.7	0.75	228	0.02
	Inferred	600.4	0.64	48	0.01
	Subtotal	739.6	0.66	89	0.01
	Total	**901.2**	**0.70**	**99**	**0.01**
Lumwana Ore Reserves					
Deposit	**Class**	**Tonnage**	**Grade**		
		(Mt)	Cu%	Co (ppm)	Au (g/t)
Malundwe	Proved	42.6	1.09	140	0.05
	Probable	44.7	0.79	116	0.01
	Total Ore Reserves	87.3	0.94	128	0.03
	Inferred Resource	8.3	0.64	80	0.02
	Total Mineral Resources	95.6	0.91	124	0.03
Chimiwungo	Proved	80.1	0.69	295	0.02
	Probable	37.9	0.68	202	0.02
	Total Ore Reserves	118.0	0.69	265	0.02
	Inferred Resource	134.6	0.60	57	0.01
	Total Mineral Resources	252.6	0.64	154	0.01
Lumwana Combined	Proved	122.7	0.83	241	0.03
	Probable	82.6	0.74	155	0.01
	Total Ore Reserves	205.3	0.79	207	0.02
	Inferred Resource	142.9	0.61	58	0.01
	Total Mineral Resources	**348.3**	**0.72**	**146**	**0.02**

Malundwe contains abundant copper, gold, cobalt and minor uranium mineralization. Co was concentrated in hinge zones during folding, but it source is not yet clear. Uranium was introduced much later during shearing, or along the shear zone (Bouda, Steven, personal communication, 2002). The mining operation will leach uranium from select portions of the deposit. Gold is much lower grade at the Chimiwungu deposit than elsewhere at Lumwana. Fig 4.4.4.14 shows a generalized cross section of Malundwe.

Meta volcanic units at Malundwe underwent extreme shearing and metamorphism. Temperature and pressure of metamorphism are thought to be 650°C and 13kbars; that corresponds to upper amphibolite facies. Very coarse kyanite porphyroblasts were rotated by shearing of the rocks. Quartz-feldspar partial melts in the rock are abundant. Some pegmatitic veins that occur in the deposit might indicate a possible relationship of mineralization with the migmatitization process. There is also abundant red garnet; copper is present in the shearing shadow of the garnets. Extensive red-rock alteration is ubiquitous: pink is iron oxide, white is the gneiss. It is not quite clear when copper mineralization took place. In June, 2002, the source of copper and the age of mineralization were uncertain (Bouda, Steven, personal communication, 2002).

At the Chipata site, granitic gneiss intrudes the Lumwana mineralized rocks (Bouda, Steven, personal communication, 2002).

4.1.4.5.3 Mafic Volcanics from Shilenda

Mafic volcanics with very particular surface textures were sampled around the site of Shilenda, just south of the Mwombezhi Dome, as shown on Figs M12 and M13. Samples **L-311** and **L-319** are green to black lati-andesites with a micro-pillow texture, joined by a white substance that erodes more readily than the surrounding rock, to form a very irregular surface (Figs 4.1.4.15). The white material is a sodium-rich carbonate that is readily disolvable in the surface environment.

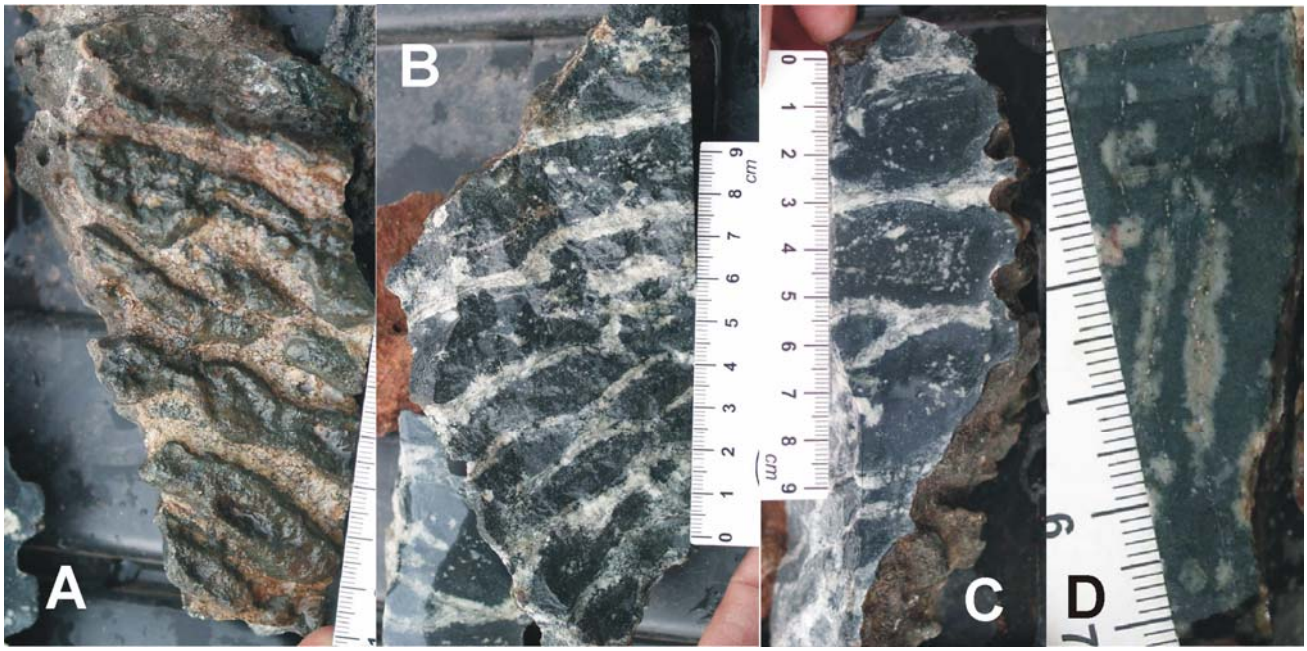

Fig 4.1.4.15 Photographs of hand samples and slabs from the Shilenda mafic volcanics*. A shows the irregular surface that the rocks display on outcrop. B is a fresh cut with the hammer, and C and D are slabbed surfaces. Note that the white substance is less resistant to erosion and weathers negatively. The right side of C shows a perpendicular cross section of the surface, with deep incision along the sodium carbonate white material. C also shows concentric zonation and crystal size distribution of the black lava particles. Coarser crystals tend to be in the middle, while the chilled margins have finer size. All scales are in millimeters. More details in the text.*

The separate fragments in the breccia display concentric mineral zonation, and concentric crystal size distribution. Coarser grains tend to be in the middle. Most of the fragments have a lensoid shape in cross section. That texture may be due to progressive cooling of the semi-molten lava and rapid quenching of the borders, or to some degassing process. The rock has many similarities with hyaloclastites. Chemical analysis of nearby rocks show gabbroic compositions. Klinck, 1977 described these rocks as autobrecciated lavas. Most of the autobreccias carry sulfides including pyrite and chalcopyrite that have primary origin. The rocks have been altered to scapolite, hornblende and epidote.

Sample **L-311** is a metaluminous mesocratic sodic magnesic lati-andesite. The various procedures to evaluate environment of emplacement for mafic volcanic rocks do not coincide in their interpretation of the tectonic environment for the rock. The Ti-Zr-Y diagram of Pearce & Cann, 1973 indicate that it is a calcalkaline basalt. Using the procedure by Meschede, 1986, the sample falls in the field of within-plate tholeiites and volcanic arc basalts.

The precise age of the lavas is not known, but they are probably extrusive correlatives of the abundant Neo-Proterozoic gabbroid bodies that intersect Katangan meta sediments in the area.

4.1.4.5.4 Chitungulu Sodalite Syenite

4.1.4.5.4.1 Introduction

Rocks of this sodalite syenite quarry are important because they intrude into Katangan metasediments and could produce a minimum age for their deposition. The quarry is located NW of Solwezi along the Chitungulu river, northeast of the Mukumbi Lubinga village, and is currently mined for its striking cobalt-blue, speckled dimension stone.

The occurrence of foid-bearing syenites is composed of at least five bodies with ellipsoidal perimeter, each of one to a few hundred meters in diameter that make a ring complex cluster. These are the only mapped such features, but there are probably many more alkaline intrusions of varying composition that intersect Katangan sediments in the region. The bodies of syenite are closely related to many gabbroid intrusions of similar dimensions. A few gold and copper occurrences and abundant bodies of massive iron oxides have been mapped in the environs. The Lumwana deposits lie 18 km south of the sodalite syenites. The quarry site was found by following large boulders of sodalite syenite up the river. There was no clear outcrop on the surface.

The largest body of syenite occurs near a right bend of the Chitungulu river and covers approximately 2.6 square kilometers. The quarry was visited because it is one of the few well mapped intrusions into Katangan rocks, and because of its accessibility. This account will only describe the largest of the three syenite bodies.

4.1.4.5.4.2 Sampling

A reconnaissance geological map of the quarry with all the sampling sites is presented on Fig 4.1.4.16. According to the mine geologist, Mr. Remo Tognaletta from GTM Stones Limited, it is the first geological map ever made of that deposit (Tognaletta, R., personal communication, 2002). Eleven samples were taken from the most representative rock units at the quarry. Two more major oxide analysis of nepheline syenites from the same locality were compiled from the literature[2]. All samples and their chemistry are listed on Table 4.1.4.9.

4.1.4.5.4.3 Description of the rocks

Syenites at the quarry are equigranular, medium- to coarse-grained, and ocassionally become porphyritic with large feldspar crystals. A recently re-edited report of the Zambian Geological Survey states that the proper petrographical name for the sodalite syenite is aegirine ditroite (Mulela & Seifert, 1980 - 1998). Petrography of the sodalite syenites was described in some detail by Mulela & Seifert, 1980 - 1998, and is included in the Appendix. Colors of the rock vary greatly: from white to light blue, gray, pink, brown, red and even into light green, as discussed below.

The main product of the quarry is a light gray, bluish, massive, non-foliated, metaluminous subleucocratic, markedly ferriferous sodalite syenite. The rock has abundant blue specks of sodalite that displays uniform texture and no preferential crystal orientation (Fig 4.1.4.17 B, C and D). Samples **L-037**, **L-043** and **L-044** are typical of the “blue” rock. That type of rock is not easy to find fresh at the quarry, because most of the faces have been weathered along joints. The “blue” rock contains a few white xenoliths made of plagioclase, quartz and disperse magnetite. An unidentified hard, gray sulfide is also present in the sodalite syenite.

All rock types at the deposit carry abundant magnetite, as seen on Fig. 4.1.4.17, and nepheline is a rock-forming mineral. Various facies of foid syenites intrude into each other and grade from one composition to another, in a way not completely well established. They may obey to telescoping plugs of slightly varying composition.

L-045 is a red, finer grained variety of the syenite. **L-046** is a fresh “brown”, coarse-grained syenite. **L-039** is a pink syenite that intrudes the blue and gray syenite bodies. All contacts are net, and none of the rocks is foliated. **L-040** contains a 4-cm wide, massive vein of blue sodalite; that is not commonly found at the quarry. Although **L-041** is a darker variety of syenite, its chemistry is very similar to the other rocks (Table 4.1.4.9).

4.1.4.5.4.4 Weathering, Jointing and Problematic Structures for Mining

Nepheline weathers readily on the surface environment, and produces a white, etched rock with angular vugs. Most of the rock at the quarry is deeply weathered along the main joints. Surface alteration of feldspathoids along the fractures extends for more than fifty meters below the surface. “Brown” and “pink” varieties of

[2] These samples were labeled ZGSI and ZGSII, that stands for Zambian Geological Survey I and II.

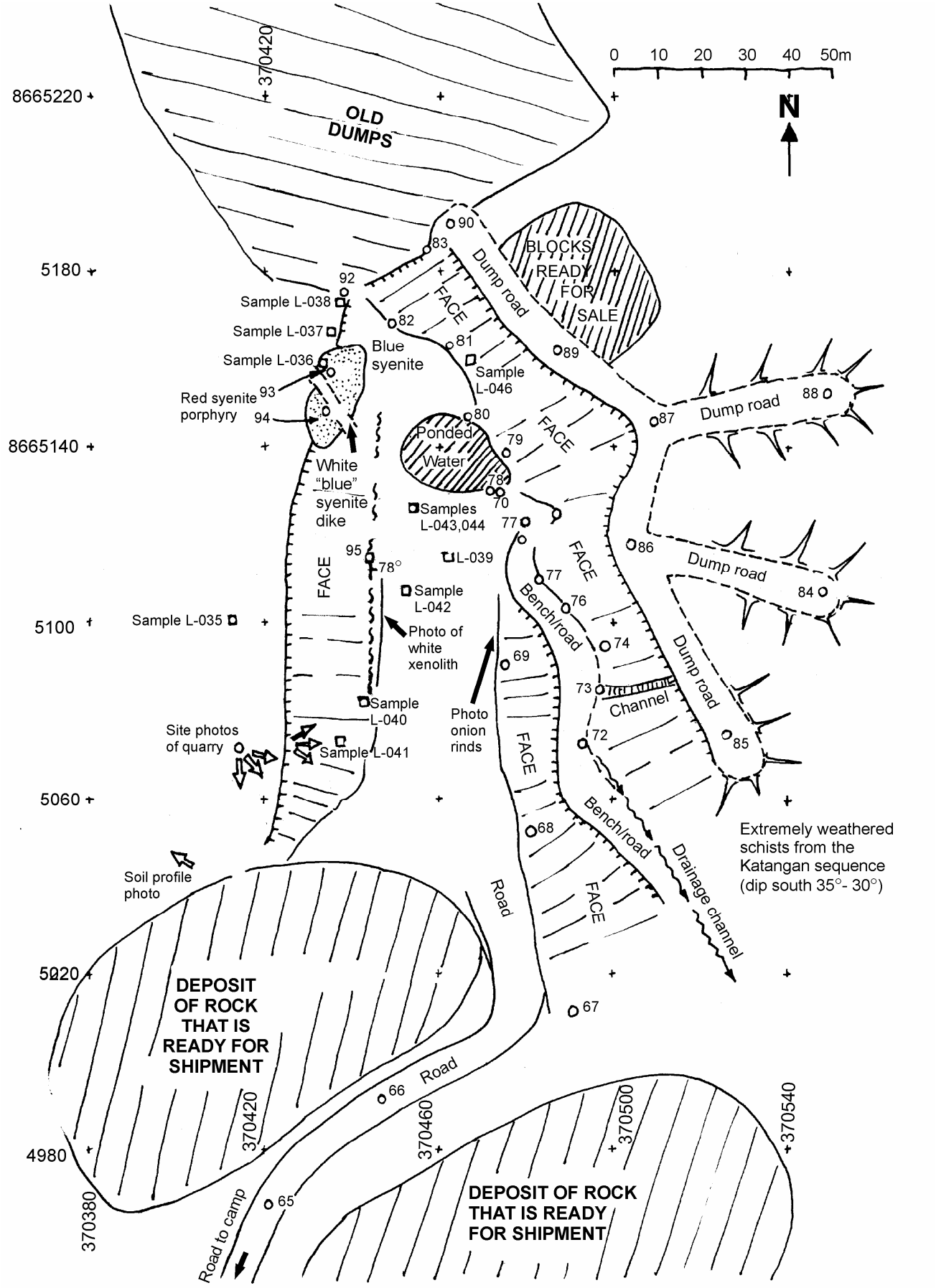

Fig 4.1.4.16 Rough Map of Sodalite Syenite Quarry, NW Zambia
Quarry owned by GTM Stones, Lusaka, Zambia.
by Alberto Lobo-Guerrero S., M.Sc.,Min.Ex., June 15, 2002

syenite in the quarry are difficult to find fresh (Fig 4.1.4.17A and G). The soil produced by weathering of the sodalite nepheline syenites contains a high proportion of magnetite.

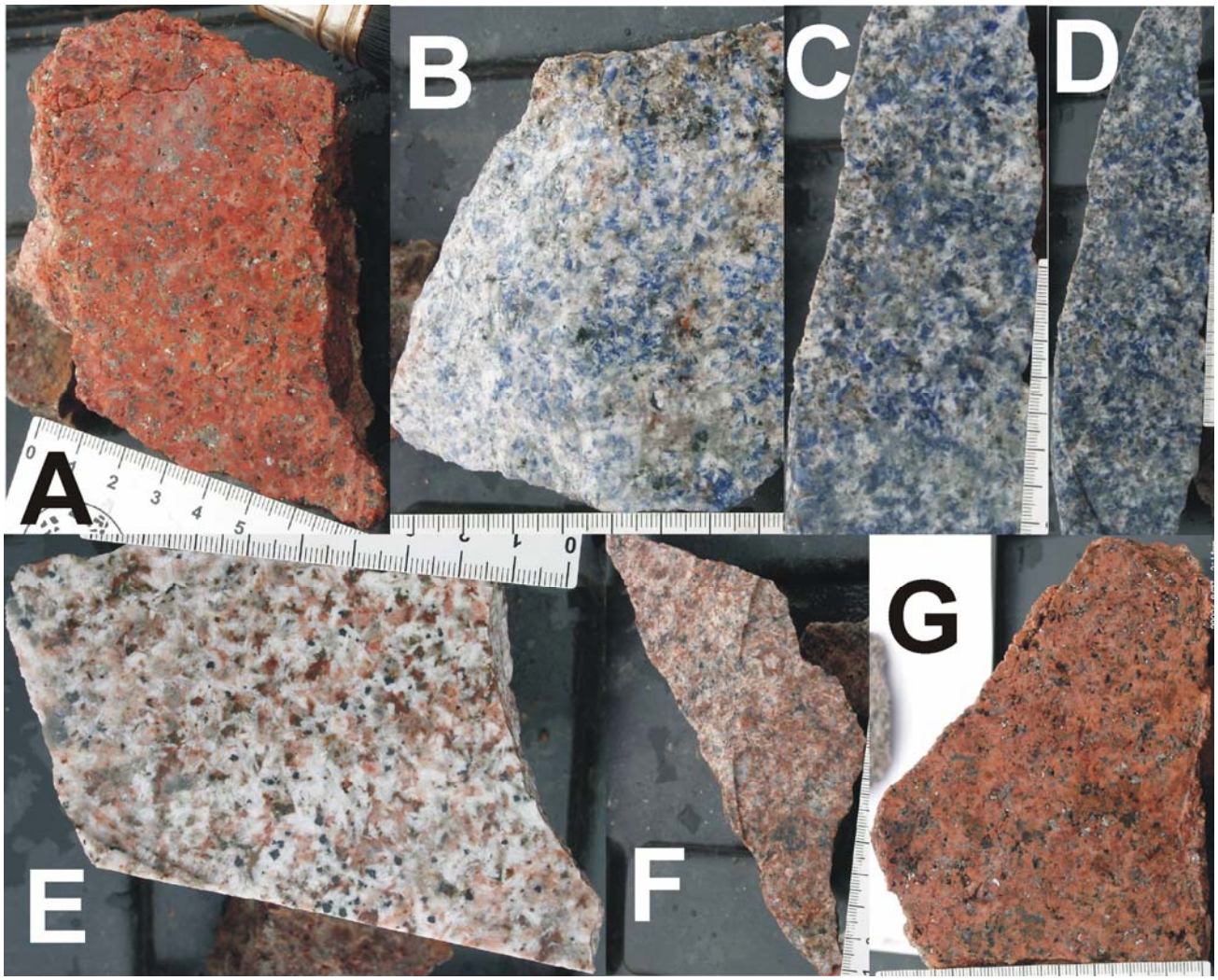

Fig 4.1.4.17 Photographs of slabbed syenites from the Chitungulu sodalite syenite quarry, Zambia. *A is sample L-036; B, L-037; C, L-044; D, L-043; E, L-039; F, L-046; G, L-045. B, C and D are typical "blue" syenites. A and G are "red" syenites and E and F are "brown" syenites. Note the rock texture in E and F. A is more weathered (or hydrothermally altered?) than the other rocks. B displays a white weathering rim towards the left, due to feldspathoid kaolinization. All scales in millimeters. See more descriptions in text.*

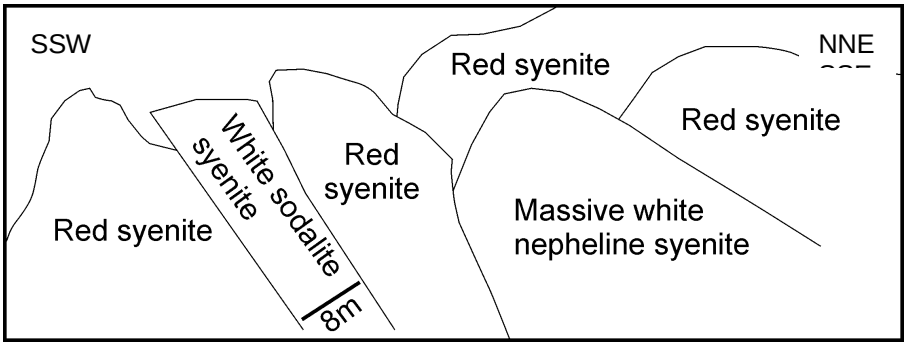

Fig 4.1.4.21 Intrusive relationships between the different facies of sodalite syenites observed at the quarry*. There is no clear order of intrusion, and maybe that can be explained by gradual facial changes of the syenites within a single intrusive event. See more details in the text.*

The red syenite at WPT 092 (**L-036**) (See Figs 4.1.4.21 and 4.1.4.16) is intruded by irregular bodies of light gray to white, finer-grained "blue" sodalite syenite that weathers white. There is an 8m wide dike of sodalite syenite intersecting the red syenite. Contacts between the various units are straight. No xenoliths of the red syenite were found in the blue syenite.

The outcrop of syenite at the quarry shows a massive, sparsely-jointed non-foliated granitoid. Main joint families are 044/89°W, 080/02°W, 060/64°S, and151/88°NE. These are unevenly spaced, approximately every 5 meters. They are open and display weathering and white leaching (See Fig. 4.1.4.17B). The spacious jointing enables blocks of 2-6 meters on side to be cut for dimension stone exploitation.

Black veins, a few centimeters wide are a problem for mining. They extend for at least 200m and are oriented 118/57°S. An important shear zone crosses the quarry on its western side with orientation 000/78°E. Hydrothermal alteration and fracturing occurs in the surrounding rock for at least 1 m, and 3m in some places. No blocks of good quality for dimension stone can be cut near the shear zone.

4.1.4.5.4.5 Geochemistry

Thirteen chemical analysis of rocks from the quarry are listed on Table 4.1.4.9. Chemistry of the samples plots on plutonic rock diagrams as illustrated on Figs 4.1.4.18 and 4.1.4.19. All samples analysed except for two are foid-bearing syenites. Fig 4.2.4.20 illustrates the chemical variation of rocks at the quarry in a logarithmic major oxide diagram.

Table 4.1.4.9 Chemical Analysis of the sodalite syenite quarry, Zambia
(Complete elemental analysis on Table A7.4, Appendix)

Sample	SiO2	TiO2	Al2O3	Fe2O3	FeO	MnO	MgO	CaO	Na2O	K2O	P2O5	LOI	Total	Rb	Sr	Y	Zr	Nb	Co	Ni
Notch	50.00	1.00	15.50	6.00		0.15	2.00	5.00	4.90	5.50	0.30	2.00		200	400	60	360	40	30	16
L-032	59.58	1.09	15.52	7.08	0.00	0.07	3.07	5.01	2.80	3.13	0.54	0.82	98.71	110	566	26	284	23	25	34
L-034	60.10	0.04	23.01	3.98	0.00	0.07	0.11	0.14	6.82	4.47	0.07	1.68	100.49	79	342	27	708	92	<6	12
L-036	73.57	1.10	15.97	1.46	0.00	0.02	0.12	0.10	0.03	0.25	0.09	7.83	100.54	34	51	30	635	38	<6	26
L-037	56.10	0.04	21.65	3.00	0.00	0.12	0.04	1.20	10.22	5.51	0.05	2.53	100.46	92	465	33	792	101	<6	7
L-038	56.45	0.12	21.07	3.77	0.00	0.08	0.00	0.32	12.27	4.32	0.07	2.01	100.48	72	244	29	859	114	<6	7
L-039	57.37	0.05	21.32	3.71	0.00	0.20	0.08	0.75	9.68	4.63	0.06	2.64	100.49	87	355	37	808	120	<6	<6
L-040	55.44	0.04	20.98	5.81	0.00	0.34	0.02	1.29	9.89	6.14	0.06	0.44	100.45	75	283	38	922	135	2	8
L-041	57.71	0.05	20.81	4.02	0.00	0.07	0.00	0.60	8.89	5.41	0.02	2.85	100.45	85	283	33	950	134	<6	<6
L-044	57.32	0.03	21.02	3.15	0.00	0.14	0.00	0.65	12.04	4.28	0.05	1.70	100.38	109	616	107	1758	178	4	8
L-045	57.75	0.10	20.94	6.96	0.00	0.03	0.00	0.14	7.96	4.16	0.06	1.17	99.27	58	367	20	186	98	<6	11
L-046	55.67	0.05	20.92	3.40	0.00	0.19	0.09	1.07	8.51	5.27	0.06	5.21	100.44	82	311	30	670	82	<6	6
ZGSI	58.04	Tr	20.76	4.45		0.20	0.09	0.95	9.22	4.81	Tr	1.99	100.51							
ZGSII	56.31	Tr	19.89	4.28	0.30	0.16	0.26	0.74	8.33	5.75	n.d.	3.56	99.58							

Sample	Cu	Zn	Ga	V	Cr	Ba	U	Th	Sc	Pb	Sm	Nd	Pr	Ce	La	Cs	Hf	Ta	As	Eu	Gd	Tb	Dy	Ho	Er	Tm	Yb	Lu
Notch	25	85	26	100	100	1300	20	37	20	20	50	50	15	175	95	3	10	120	100	4	30	5	20	3	9	36	8	2
L-032	17	58	19	151	78	703	<6	<15	16		8	54	83	109	37			96		1							1	1
L-034	8	18	17	74	87	705	<6	20	11					311	134													
L-036	36	37	28	52	30	196	<6	36	<10					282	240													
L-037	10	171	25	<12	117	423	9	17	<10		108	39	71	139	63			51		0							1	1
L-038	12	108	26	<12	65	318	8	32	<10					261	146													
L-039	12	127	27	<12	68	349	9	30	<10					231	166													
L-040	8	106	25	4	139	261	8	30	<10					278	186													
L-041	6	98	27	<12	<12	347	11	22	<10					183	109													
L-044	10	227	26	11	120	1441	10	31	<10		0		4	196	0			37			1.5	1.2					0.3	0.7
L-045	32	34	27	<12	45	764	7	18	<10	1.9	7.1	58	20	214	158	0.3	2.4	9.7	214	1.2	4.7	0.8	4.5	0.8	2.1	0.3	2.0	0.3
L-046	115	168	24	<12	51	526	<6	29	<10		1	1	7	204	1			44			1	1					0	1

Table 4.1.4.10 lists the rock name, macroscopic field description and general geochemical parameters of the samples, according to Debon & LeFort, 1983 and Debon & LeFort, 1988.

In general terms, rocks from the quarry display homogeneous chemistry. They contain abundant alumina and soda, accompanied by high values of Zr, Nb, Zn, Ga, Ce and La. As shown by the TAS diagram of Fig 4.1.4.18, most samples plot on the nepheline syenite portion. **L-037**, **L-038**, **L-040** and **L-044** are similar to each other both chemically and macroscopically. They are all blue sodalite nepheline syenites. **L-039**, **L-045**, **L-046** and **L-041** are chemically similar to each other, but differ slightly from the group of sodalite-rich syenites. The first three are varieties of pink syenite, while the fourth is a dark, finer-grained rock collected near the north-south-trending shear zone, as indicated on the map of Fig 4.1.4.16. The only rocks with significant copper enrichment are those of the pink variety, especially **L-046** (Fig 4.1.4.17F). This last sample also has a high loss on ignition, but does not deviate significantly from the average syenite at the quarry.

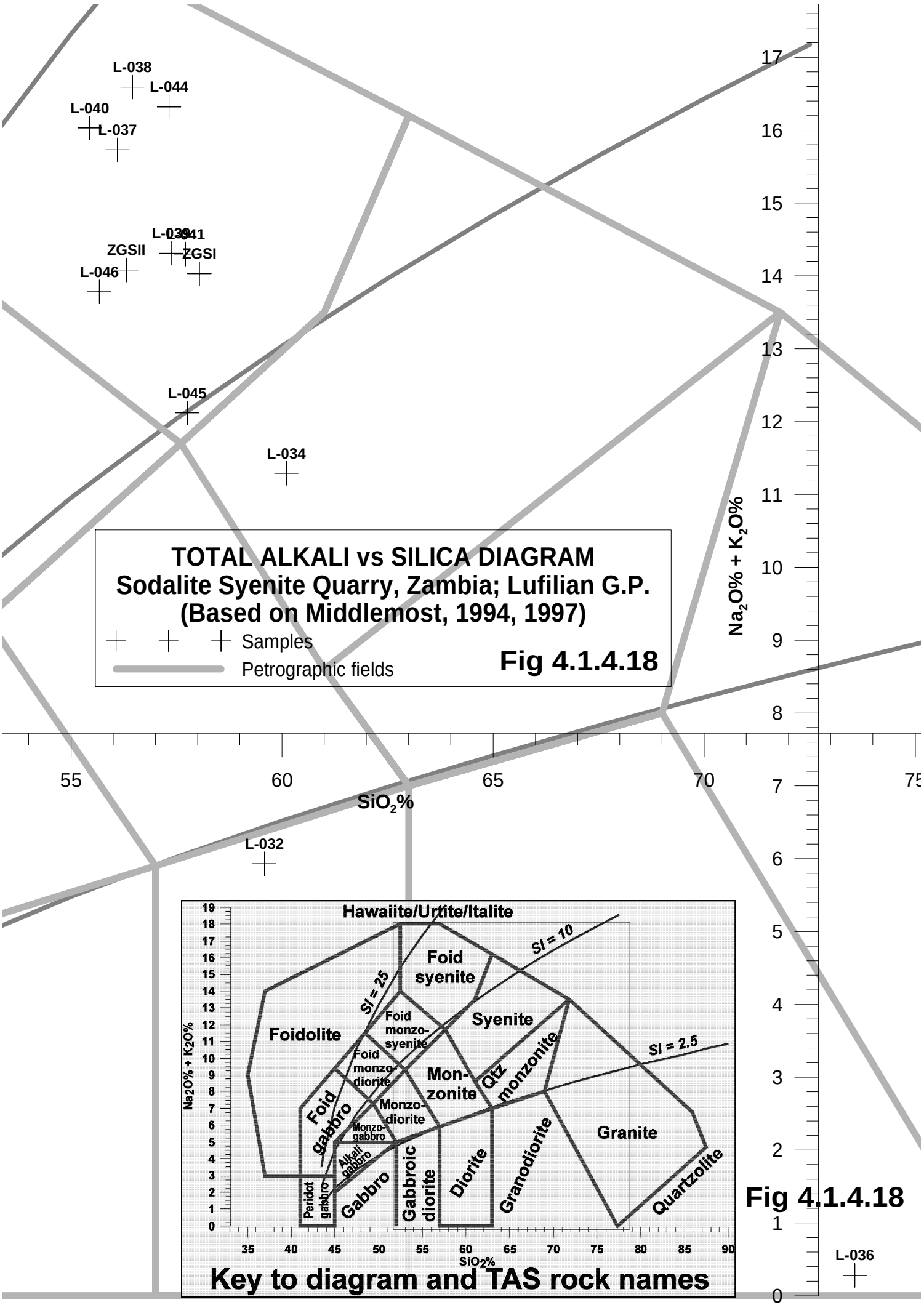
L-038
L-044
L-040
L-037
L-039
L-041
ZGSII
ZGSI
L-046
L-045
L-034
L-032
L-036
TOTAL ALKALI vs SILICA DIAGRAM
Sodalite Syenite Quarry, Zambia; Lufilian G.P.
(Based on Middlemost, 1994, 1997)
Samples
Petrographic fields
Fig 4.1.4.18
$Na_2O\% + K_2O\%$
$SiO_2\%$
55
60
65
70
75
Hawaiite/Urtite/Italite
Sl = 10
Sl = 25
Sl = 2.5
Foid syenite
Foidolite
Foid monzo-syenite
Syenite
Foid monzo-diorite
Mon-zonite
Qtz monzonite
Foid gabbro
Monzo-diorite
Monzo-gabbro
Granite
Alkali gabbro
Peridot gabbro
Gabbro
Gabbroic diorite
Diorite
Granodiorite
Quartzolite
Key to diagram and TAS rock names

Fig 4.1.4.18

R_1R_2 PLUTONIC ROCK CLASSIFICATION
Sodalite Nepheline Syenite, Zambia; Lufilian G.P.
(After De la Roche et al, 1980)
Petrographic fields
Samples

Fig 4.1.4.19

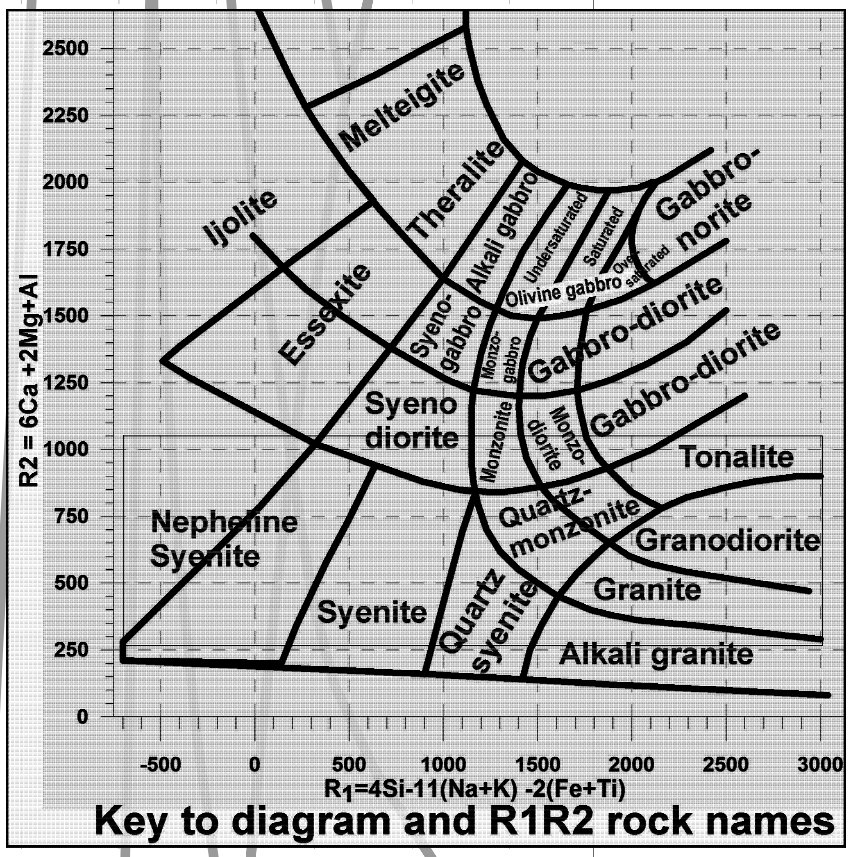

L-032
L-037
L-040
L-046
ZGSI
L-039
L-044
ZGSII
L-041
L-034
L-038
L-045
L-036

1000
500

-500 0 500 1000 1500 2000 2500 3000

R_1 = 4Si - 11(Na+K) -2(Fe+Ti)

Fig 4.1.4.19

Table 4.1.4.10 Chemical character of samples from the Sodalite Syenite Quarry, Zambia
(see acronym description on section 2.4.3.)

Sample	Rock Name	Aluminosity, color, Na/K, Fe/Mg	Macroscopic field description
L-032	Gabbro-diorite	Metaluminous v mesocratic Na low Fe	mafic dike
L-034	Syenite	Peraluminous I subleucocratic Na high Fe	Syenite
L-036	Granodiorite	Peraluminous I leucocratic K high Fe	"red" syenite
L-040	Nepheline syenite	Metaluminous v mesocratic Na high Fe	"blue" syenite with sodalite vein
L-045	Nepheline syenite	Peraluminous ii mesocratic Na High Fe	"pink" syenite
L-037	Nepheline syenite	Metaluminous v subleucocratic Na high Fe	"blue" syenite
L-038	Nepheline syenite	Metaluminous v subleucocratic Na high Fe	"blue" syenite
L-039	Nepheline syenite	Metaluminous v subleucocratic Na high Fe	"pink" syenite
L-041	Nepheline syenite	Metaluminous v subleucocratic Na high Fe	Dark gray fine-grained syenite
L-044	Nepheline syenite	Metaluminous v subleucocratic Na high Fe	"blue" syenite
L-046	Nepheline syenite	Metaluminous v subleucocratic Na high Fe	"brown" syenite
ZGSI	Nepheline syenite	Metaluminous iv subleucocratic Na Mg	"blue" syenite
ZGSII	Nepheline syenite	Metaluminous iv subleucocratic Na Mg	"blue" syenite

Four of the samples collected differ from the main chemistry of nepheline syenite: these are **L-032**, **L-045**, **L-034** and **L-036**. The first is a gabbro-diorite, the second a granodiorite. **L-045**, **L-034** and **L-036** have more silica than normal for nepheline syenitic rocks; they may have been contaminated by Katangan siliciclastics during intrusion. **L-045** and **L-036** also are enriched in copper.

The red granitoid porphyry of **L-036** differs significantly from the suite of rocks; it might be a different type of rock altogether (Fig 4.1.4.17A). It displays abnormally high loss on ignition, is enriched in Ti, has the lowest alumina value of the suite, contains normative quartz, higher Th and U values, and it probably was depleted in Na and K. The sample was collected from a small intrusive body that intersected the blue syenite and was itself intersected by a dike of sodalite syenite (See the map of Fig 4.1.4.16).

Few analysis for rare earths were carried out. Only one representative sample (**L-045**) was analysed for the complete suite of elements, and it displays a slight enrichment in the light rare earths. That seems to be the case in the rest of the rocks, based on the figures for Ce and La.

A gabbroic dike (**L-032**) intrudes the syenites. It carries some unidentified black minerals and is enriched in V, Sr, Ni, Nd and Pr; it also carries abundant magnetite. Although P_2O_5 and Zr contents are high in the suite of rocks from the quarry, no outstanding values of U and Th were recorded, except in **L-036** with 36 ppm Th.

4.1.4.5.4.6 Environment of Emplacement

As illustrated on Table 4.1.4.11, all samples plot on the "anorogenic" portion of the Whalen diagrams, and most plot on the the "within plate" environment of Pearce et al., 1984. The mafic dike of **L-032** formed in a within-plate environment. None of the samples produced coherent results in the procedure devised by Maniar & Piccoli, 1989 to evaluate environment of emplacement. Bodies of nepheline syenite worldwide are known to form in environments of continental crust extension.

Syenites from the Chitungulu quarry probably formed as one in a series of anorogenic ring complexes.

Table 4.1.4.11 Tectonic environment of emplacement for sodalite syenite quarry, Zambia
(See acronym description on section 2.4.3.)

Sample	Whalen	Pearce	Mafic	Harris		
				Rb/10HfTa	Rb/30HfTa	Nb-Ta
L-032	A	O3/4	Wpab			OUTU
L-034	A	V1/2				
L-036	A	W				
L-037	A	O-W 2-2				OUTU
L-038	A	W				
L-039	A	W				
L-040	A	W				
L-041	A	W				
L-044	A	O-W 2-2				OUTU
L-045	A	W3/4		WP	WP	INW
L-046	A	O2/3				OUTU

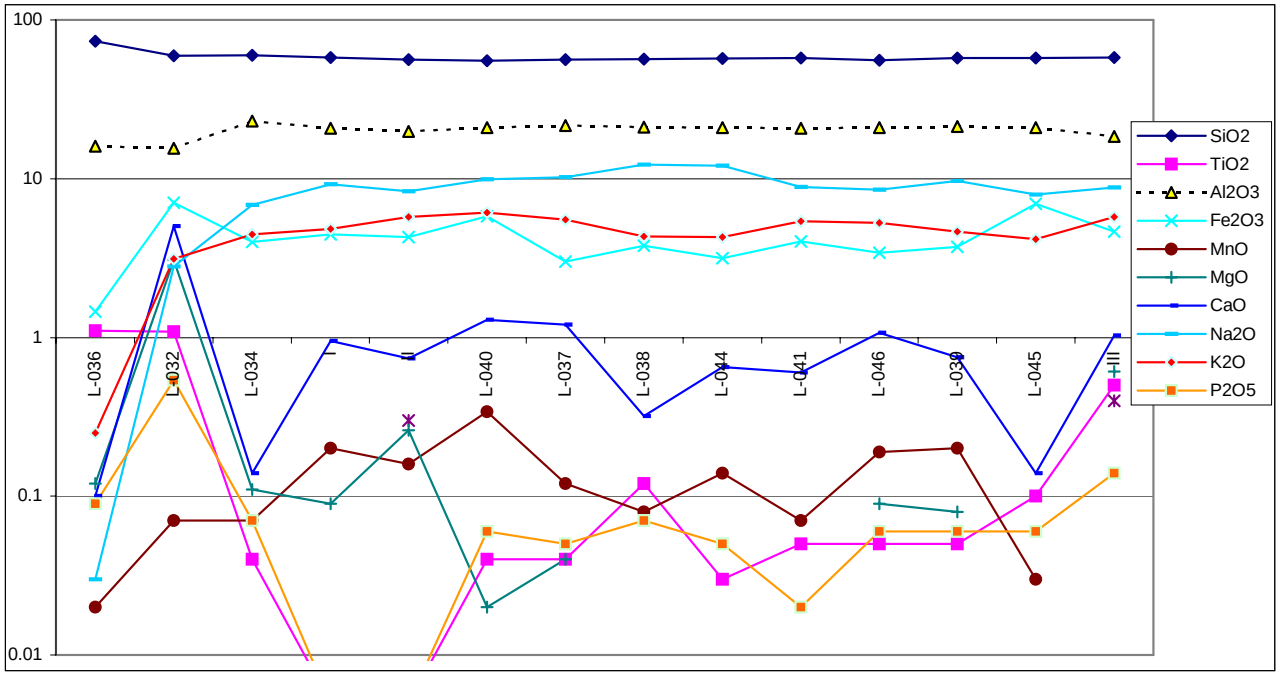

Fig 4.1.4.20 Major oxide logarithmic plot for samples from the Chitungulu sodalite syenite quarry.
Note general similarity betweeen most of the samples, except for L-032 and L-036. More discussion on the geochemistry is included in the text.

4.1.4.5.4.7 Geochronololgy

During the 1980's, Italian geologists from the AGIP SPA Corporation established that the nepheline syenites at the quarry cooled below 350°C at 413±5 Ma, based on K/Ar in biotite (Cosi et al., 1989; Cosi et al., 1992). (See Tables A22.2). The same group dated zircons from the sodalite syenite quarry and produced a U/Pb age of 458 to 427 Ma (Cosi et al., 1989; Cosi et al., 1992). That age may still be reflecting orogenic events and not the original time of emplacement.

A zircon concentrate from sample **L-043** was sent to the ANU for U-Pb SHRIMP II dating and results are not available at the time of editing this document. The new age will be correlated with the other two just described. Cores of zircons are expected to be older than previously thought, approximately around 750 to 780 Ma. It could provide a good time constrain to Katangan sedimentation in that portion of the Greater Lufilian Arc.

4.1.4.5.4.8 Conclusions

The Chitungulu sodalite syenites that occur north of the the Mwombezhi Dome in NW Zambia formed as an anorogenic, alkaline ring complex that intruded siliciclastic Katangan meta-sediments. Several facies of foid-bearing syenites intersect each other. The rock is quarried for its striking cobalt-blue speckled dimension stone. The typical rock is a white, medium- to fine-grained, metaluminous subleucocratic sodic ferriferous sodalite nepheline syenite. Deep joints that enhance weathering of the rock, some minor dikes and shear zones, sometimes render it useless for extraction. A new SHRIMP II age is expected to place further constrains on the time of deposition of the Katangan sequence.

4.1.4.6 Solwezi Dome

4.1.4.6.1 Introduction

Four different rock types can be identified in the Solwezi Dome, and relationships between them are not well exposed. According to Master, 1996, these are:

a) Migmatitic gneiss occurs mainly in the central part of the dome. They are composed by a garnetiferous biotite gneiss in which pegmatitic leucosomes are well developed parallel to the gneissic foliation.
b) A poorly-exposed leucocratic two mica granite covers the northern part of the dome. Its main constituents are sodic plagioclase, perthitic microcline, quartz, biotite and muscovite.
c) A fine-grained gneiss, which is compositionally similar to the migmatitic gneiss, but is fine-grained, and has less well developed gneissic banding.
d) Metabasites occur as lozenge-shaped bodies within mega shear zones that intersect the other rock types.

The lower units of the Solwezi Dome metasedimentary envelope are muscovite-hematite quartzites and schists, while the upper units are dominantly marbles. Metasedimentary rocks outcrop in concentric aureoles around the main body of the dome, as seen on the generalized geological map of Fig M15. Isolated wedges of Katangan metasediments are mapped in the central part of the dome.

4.1.4.6.2 Sampling

Outcrops of the granitoids that make the basement of the Solwezi Dome were very difficult to find in the field. Ten samples collected in and around the dome are listed on Table 4.4.4.12 and shown on Fig M15. They include 3 samples from mafic intrusive rocks that intersect Katangan metasediments in boreholes around the Kansanshi mine, 2 from outcrops of mafic intrusives, and 2 from outcrops of felsic granitoids from the core of the dome itself.

Rock name, basic geochemistry and environment of emplacement of the samples collected are listed in Table 4.1.4.13. Figs 4.1.4.1 to 4.1.4.6 are geochemical diagrams of their properties. As seen on Fig 4.1.4.1, most of the samples are midalkaline.

Table 4.1.4.12 Chemical Analysis of samples from the Solwezi Dome, Zambia
(Complete elemental analysis on Table A7.2, Appendix)

Sample	*SiO2*	*TiO2*	*Al2O3*	*FeOt*	*MnO*	*MgO*	*CaO*	*Na2O*	*K2O*	*P2O5*	*LOI*	*Total*
Notch	50.00	1.00	15.50	6.00	0.15	2.00	5.00	4.90	5.50	0.30	2.00	
L-063	46.39	0.84	12.95	3.10	0.09	5.95	9.71	6.97	0.15	0.12	14.12	100.39
L-064	47.31	0.82	12.99	3.23	0.10	5.76	9.38	6.85	0.05	0.12	13.87	100.48
L-065	39.63	0.57	9.98	4.16	0.11	7.62	13.40	4.80	0.12	0.07	19.80	100.26
L-060a	45.83	4.36	11.86	17.84	0.26	6.24	9.49	2.29	1.12	0.43	0.38	100.11
L-060b	76.30	0.15	11.89	1.79	0.04	0.14	0.53	3.65	5.74	0.04	0.28	100.55
L-060c	45.43	4.31	11.83	17.86	0.28	6.23	9.37	2.11	1.09	0.45	0.42	99.57
L-049	47.30	2.03	15.47	13.49	0.25	5.41	10.51	3.04	0.93	0.22	0.92	99.58
L-050	46.86	2.06	15.40	13.35	0.21	5.20	10.46	3.73	0.89	0.27	0.52	98.95

Sample	*Rb*	*Sr*	*Y*	*Zr*	*Nb*	*Co*	*Ni*	*Cu*	*Zn*	*Ga*	*V*	*Cr*	*Ba*	*U*	*Th*	*Sc*	*Sm*	*Nd*	*Pr*	*Ce*	*La*	*Hf*	*Ta*	*Eu*	*Gd*	*Yb*	*Lu*
Notch	200	400	60	360	40	30	16	25	85	26	100	100	1300	20	37	20	50	50	15	175	95	10	120	4.0	30	7.5	1.6
L-063	4	51	19	192	7	<6	18	7	22	21	86	36	<20	<6	<15	23				25	16						
L-064	4	51	19	175	7	<6	18	8	28	20	92	36	<20	<6	<15	24				16	<12						
L-065	4	125	24	108	8	<6	20	8	29	12	102	45	<20	<6	<15	30	6	2	19	15	10		71			1.0	0.8
L-060a	149	64	19	128	10	31	39	20	105		396	38	477	5	47	0	4	27	9	113	61	4	1	0.6	2.7	2.7	0.4
L-060b	154	64	23	141	13	<6	<6	14	25	22	<12	54	481	<6	<15	35				37	20						
L-060c	24	330	38	165	27	37	39	29	101		387	33	118														
L-049	13	346	30	109	17	34	46	143	119	19	296	85	127	<6	<15	31				23	<12						
L-050	11	321	31	114	16	46	49	91	70	18	321	171	93	<6	<15	34				30	<12						

4.1.4.6.3 Samples from the Solwezi Dome

L-420 and **L-421** come from foliated granitoids in the core of the Solwezi Dome (Fig M13) and were selected from the rock collection of the Zambian Geological Survey in Lusaka. **L-420** is a peraluminous subleucocratic sodic ferriferous biotite granite. **L-421** is a peraluminous mesocratic potassic ferriferous granite. It is enriched in K, Rb, Cu, Ba, Th, Ce, La, P_2O_5 and Ti. Both samples correlate quite well with the chemistry of Group 2 from the Kalene Hill area; both probably formed by the same geological process in the same environment. They might even have a similar age, but that has not been confirmed. **L-420** always plots in the middle of the Group 2 cluster, while **L-421** deviates from the cluster (See Figs 4.1.4.3 to 4.1.4.6). **L-420** has evidence of sodic alteration, while **L-421** has evidence of potassic alteration. Their chemistry indicates a post-orogenic origin in the (Maniar & Piccoli, 1989) process. Nevertheless, if their association with group 2 from the other domes is correct, they probably formed in a continental epeirogenic uplift environment.

Numerous outcrops of gabbro and other basic rocks were observed, especially to the east and northeast of the Solwezi Dome. No physical relationships with the host rocks were established due to poor outcrop. These gabbroids are not as deformed as those in the Solwezi Dome, and are considered to be mainly pod-shaped bodies and not dikes.

Table 4.1.4.13 Rock name, basic geochemistry and environment of emplacement for samples from the Solwezi Dome, NW Zambia (See acronym description on section 2.4.3.)

Sample	Rock Name	Debon & LeFort	Maniar & Piccoli	Whalen	Pearce	Mafic	Rb/10HfTa	Rb/30Hf/Ta	Nb-Ta
Solwezi Dome									
L-049	Saturated olivine gabbro	Metav mesoNaFe				wpab			
L-050	Undersaturated olivine gabbro	Metav mesoNaFe				emor			
L-060a	saturated olivine gabbro	Metaiv mesoNaFe				wpab			
L-060c	saturated olivine gabbro	Metav leucoKFe				wpt			
L-060b	Granite	Metaiv mesoNaFe		A	O				
L-420	Granite	Peraii subleucoNaFe	POG	A					
L-421	Granite	Peraiii mesoKFe	POG	A					
East of Solwezi Dome									
L-063	Essexite	Metav mesoNaMg				?			
L-064	Essexite	Metav mesoNaMg				wpab			
L-065	Theralite	Metav mesoNaMg				arc			OUTU

Samples **L-049** and **L-050** are gabbros from outcrops north of the Kansanshi deposit. **L-049** is a metaluminous sodic ferriferous saturated olivine gabbro, and **L-050** is a metaluminous sodic ferriferous undersaturated olivine gabbro. The environment of emplacement of these rocks has been interpreted as within-plate alkali basalt and e-morb, respectively. They are similar to **L-060a**, **L-060c**, and to a lesser degree, to **L-024**. As is typical in that type of gabbroids, they contain high values for Co, Ni, Cu, Zn and V.

L-060a to **L-060c** were collected from core in boreholes that intersect intrusive rocks cutting mineralized metasediments within and around the Kansanshi deposit (See Figure M13). **L-060a** and **L-060b** were taken from boreholes K-256 from a depth of 158.70m and 166.28m respectively. **L-060c** comes from borehole K-292 at a depth of 109.15m. A geological map from the exploration company that drilled at Kansanshi (Fig 4.1.4.22 A) shows the location of the two boreholes. Cross sections prepared by the same group to illustrate underground geology around the boreholes are shown on Figs 4.1.4.22 B and C.

Very little else may be said about the saturated olivine gabbros **L-060a** and **L-060c** (Fig 4.1.4.22), because they are somewhat weathered. They clearly intrude into Katangan rocks and produce contact metamorphic haloes. They contain anomalous Ti, P2O5, Th, Pb as well as Co, Ni, Cu, Zn and V. Various procedures to evaluate the environment of emplacement indicate that the samples formed in an anorogenic within-plate environment.

No *in situ* granitoids were identified in the environs of the Kansanshi deposit. The only outcropping rocks were the gabbroids just described. **L-060b** is a fine- to medium-grained, metaluminous mesocratic sodic ferriferous biotite alkali granite with foliated texture and coarse plagioclase that makes augen. It is very similar to samples of Group 2 from the Kalene Hill and Mwombezhi Dome areas. If it forms part of that group, it displays slight hydrothermal alteration, as shown on Figs 4.1.4.1 to 4.1.4.6. This rock could be a granite dike or a xenolith transported during intrusion of the gabbroic bodies into Katangan sediments. Relationships in the borehole were not clear in one way or another. The sample displays hydrothermal alteration related to potassic enrichment, Ca and Fe depletion and has high Sc content. The alteration observed would be reasonable in any case. **L-060b** is a high heat producing granite, due to its high Th content. It formed in an un-defined anorogenic environment. This rock may represent the basement to the Katangan rocks in the environs of the Kansanshi mine.

4.1.4.6.4 Geochronology

A zircon concentrate of **L-060a** was dated by U-Pb SHRIMP II at approximately 750 Ma. Definitive geochronological data are not available at the time of editing this document. That age correlates well with SHRIMP II ages published by Barron, Broughton, Armstrong & Hitzman, 2003 for a gabbro located immediately north of the Kansanshi mine. They report an age of 762±8.6 Ma. Another gabbro, from the schist and phyllite unit of the domes region dated by Barron et al., 2003 produced a SHRIMP II age of 745±7.8 Ma, with metamorphic overgrowths in zircons which returned an age of 510±7.8 Ma. Similar age rocks occur throughout NW Zambia, as shown on Tables A22.3 and A22.2, and illustrated on the event diagram of Fig A24.

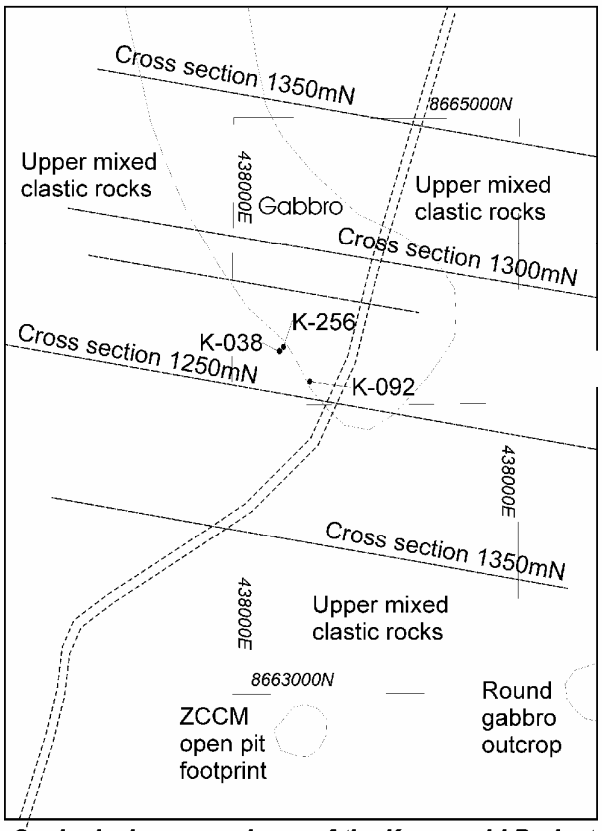

Geological map, environs of the Kansanshi Project showing location of boreholes and cross sections

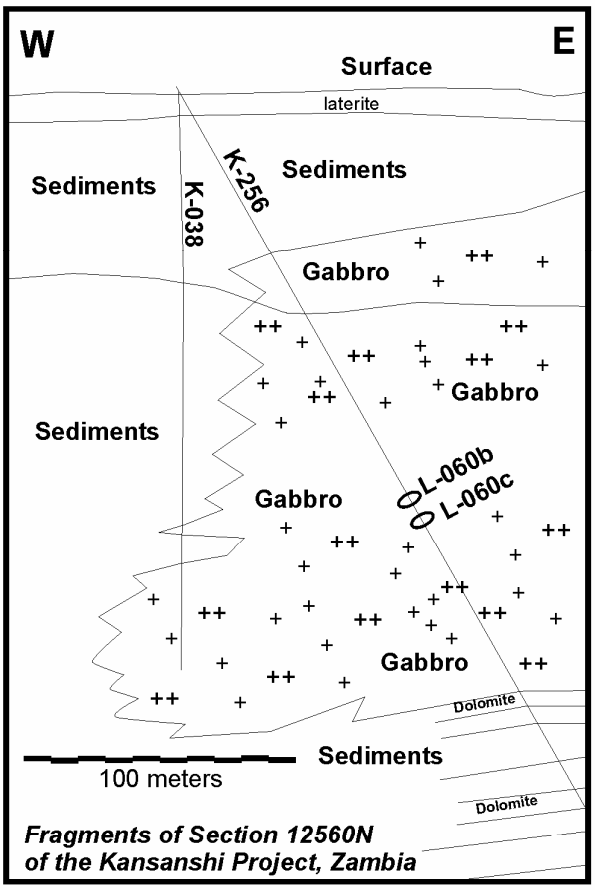

Fragments of Section 12560N of the Kansanshi Project, Zambia

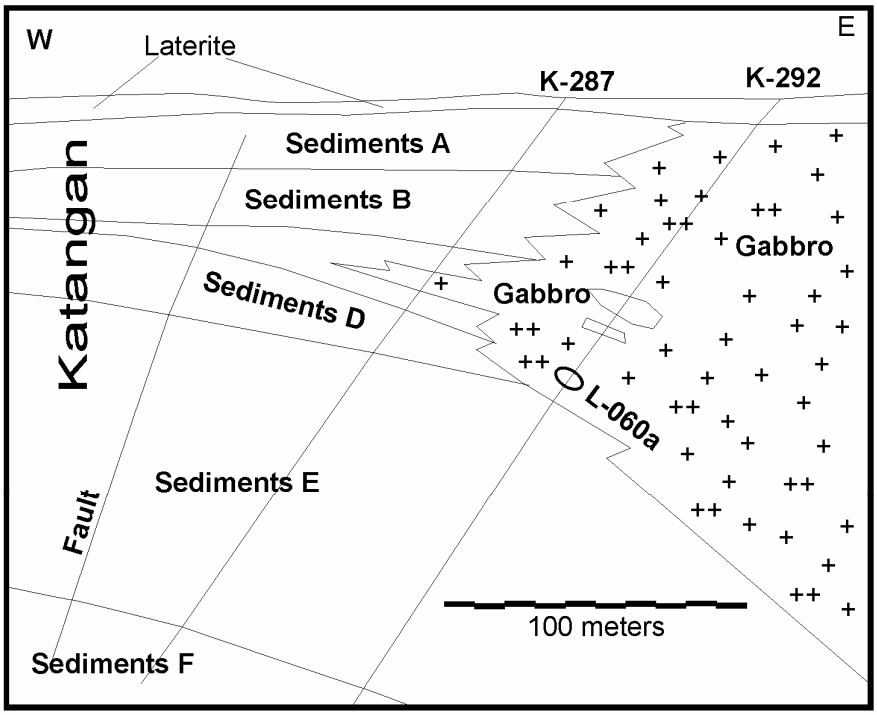

Simplified diagram from Section 12550N, Kansanshi Project, Zambia

Fig 4.1.4.22 Geological map and cross sections to locate boreholes from the environs of the Kansanshi deposit, Solwezi, Zambia. *Sample location is indicated on the cross sections. Basic information obtained from Carruthers, H., personal communication, 2002.*

4.1.4.6.5 Samples from East of Solwezi

Three samples of a pink, fine-grained rock (Fig 4.1.4.23) were collected east of the Solwezi Dome along the main road: **L-063**, **L-064** and **L-065** (Figs M12 and M15). These were exceptionally fresh and produced a bell tinge when hammered. Field observations indicated they were a fine-grained intrusive or well-cemented fine-grained volcanic rock (Fig 4.1.1.23). Their uncommon chemistry (very high CaO, high Mg, Na, Ni, Sc, V, Pr, and extremely low Ba and Rb) was not easy to understand. The loss on ignition for the samples is high: respectively, 14.12%, 13.87%, 19.8%. Such high values may be related to abundant CO_2 related to a high content of calcium and other carbonates.

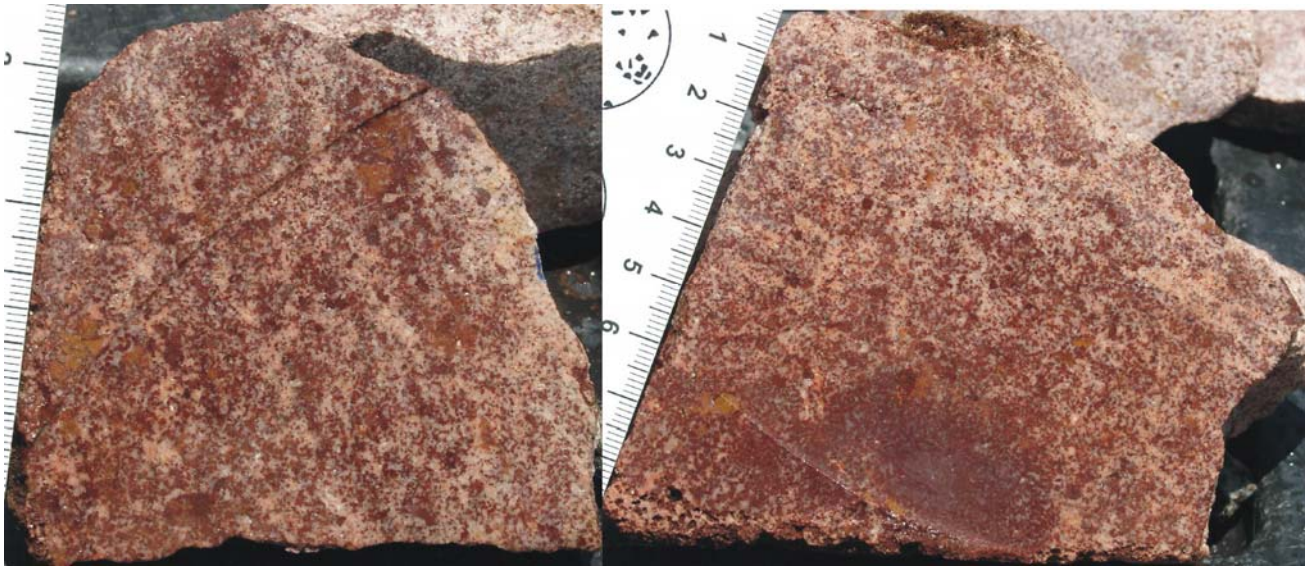

Fig 4.1.4.23 Photographs of slabs from the samples that make L-063. *These rocks are essexites, and were the freshest igneous rocks available in many kilometers. Other notes in text. Scales are in millimeters.*

L-063 and **L-064** are essexites, and **L-065** is a melteigite. They all have metaluminous mesocratic sodic magnesic character. **L-063** and **L-064** are alkaline rocks; L-065 is alkaline. The samples plot as foid gabbros and foidolite on the TAS diagram modified by Middlemost, 1994a. These uncommon rocks probably formed in an anorogenic, rift-related environment.

4.1.4.6.6 Conclusions

The granitoids from the nucleus of the Solwezi Dome are similar to those of group 2 identified in Kalene Hill.

The gabbroids that were studied in the environs of the Solwezi Dome were emplaced at *circa* 750 Ma in an anorogenic within-plate environment into Katangan sediments. Some of them produced large bodies that were able to transport xenoliths from the basement.

Anorogenic alkaline mafic intrusions (essexites and melteigites) were intruded in rift-related environments east of Solwezi.

4.1.4.7 Conclusions on the Entire NW Zambia Region

Foliated, peraluminous, leucocratic to subleucocratic, ferriferous granites and alkali granites were emplaced at least from 1952 to 1913 Ma in Kalene Hill and the Kabompo, Mwombezhi and Solwezi domes. This is probably the evidence of a major anorogenic magmatic event. The granitoids were emplaced in a continental epeirogenic uplift environment. Some of the rocks contain high Th. Some contain high Cu values. This was identified as Group 2 of Kalene Hill.

Archean rocks from Kalene Hill are enriched in copper.

Several Paleoproterozoic granitoids were found to be enriched in copper and zinc.

There is evidence of minor subductional magmatism in Paleoproterozoic rocks of Kalene Hill.

Katangan metasediments were intruded in anorogenic rift-related environments by alkaline and midalkaline rocks at the Chitungulu sodalite syenite quarry and essexites and melteigites east of Solwezi.

The south eastern portion of the Kabompo Dome is prospective for IOCG mineralization. Red-altered quartz syenites with miarolitic cavities were emplaced *circa* 730 Ma in a continental epeirogenic uplift environment. They are intimately associated with small gabbroic bodies and massive iron oxide bodies. There might be a relationship between IOCG systems and sedimentary-hosted Co-Ni-Cu mineralization in that part of Zambia.

Gabbroids that were studied in the environs of the Solwezi Dome were emplaced at *circa* 750 Ma in an anorogenic within-plate environment into Katangan sediments. Some of them produced large bodies that were able to transport xenoliths from the basement.

4.1.5 MAIN ZAMBIAN COPPERBELT

4.1.5.1 Introduction

Sampling in the environs of the Zambian Copperbelt was carried out to establish the chemical composition of the basement granitoids and to find intrusive rocks that cut the Katangan sedimentary sequence. This chapter will cover the results of observations and analysis for rocks from the Nchanga, Chambishi, Mufulira[1], and Muliashi granitoids, rocks that host the Samba deposit and some intrusive rocks that intersect the mineralized sequence at the Nchanga mine.

The project's current database has 51 samples analysed. Table A8 discriminates the chemical analyses into the different areas. Coordinates of all samples are listed on the Appendix A16. Their chemical analyses are presented on Table A8, and they are located on Figs M1, M16 and M17.

Rocks from the region span a large range of lithologies, mainly granitoids, gabbroids and syenitoids (Figs 4.1.5.1 and 4.1.5.2). In general terms, geochemistry for the suite of samples shows that 62% are subalkaline and the rest are midalkaline. Forty percent of the total rocks are midalkaline, 52% are subalkaline and 8% are alkaline. As shown on Table 4.1.5.1, most of the samples are granites, alkali granites, granodiorites and quartzmonzonites. Minor gabbroids and syenitoids constitute a small percentage of the rocks sampled.

Table 4.1.5.1 Statistics of rock types, basement to the Copperbelt, Zambia
The fifth column (granitoids) is the sum of underlined rock types.

Group	Rock type	Number	%	Granitoids	Groups
Midalkaline Rocks	Alkali granite	6	12.00	37.84	40.00
	Quartzmonzonite	5	10.00		
	Syenite	2	4.00		
	Monzonite	1	2.00		
	Monzodiorite	2	4.00		
	Monzogabbro	3	6.00		
	Alkali gabbro	1	2.00		
Subalkaline Rocks	Granite	15	30.00	62.16	52.00
	Granodiorite	8	16.00		
	Diorite	2	4.00		
	Gabbro	1	2.00		
Alkaline Rocks	Foid syenite	1	2.00		8.00
	Foid monzo-diorite	1	2.00		
	Foid gabbro	2	4.00		
Total		50	100.00	100.00	100.00

[1] The local term Mufulira has varied spelling in English. Among these, "Mufulila" and "Mufulida" have also been used in the geological literature. Mufulira was chosen in this document, for being the most widely used term.

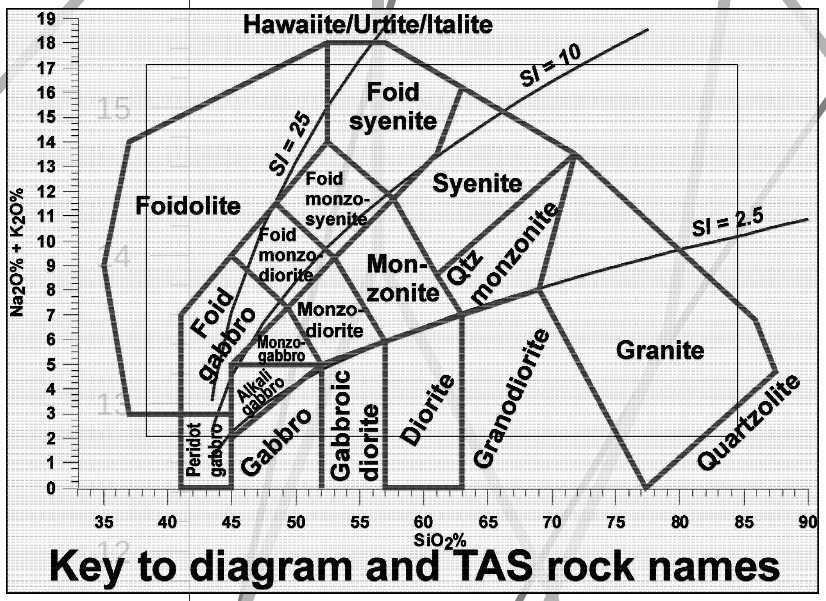

Key to diagram and TAS rock names

$Na_2O\% + K_2O\%$

$SiO_2\%$

L-167 and L-167A

X-40 X-39 P-28 X-09 P-29 L-173 L-172 X-02 X-01 L-151 L-154 L-077 L-166 L-076 L-162 L-153 X-41 L-161 L-160 X-34 X-36 L-150 X-05 L-159 L-168 L-158 X-03 X-35 L-157 X-37 L-155 X-08 L-279 X-42 X-07 L-273 X-06 X-11 L-163 X-14 L-268 L-170 X-38 X-10 X-04 L-269 X-13

TOTAL ALKALI vs SILICA DIAGRAM
Copperbelt Granitoids, Zambia; Lufilian G.P.
(Based on Middlemost, 1994, 1997)

Samples

Petrographic fields

Fig 4.1.5.1

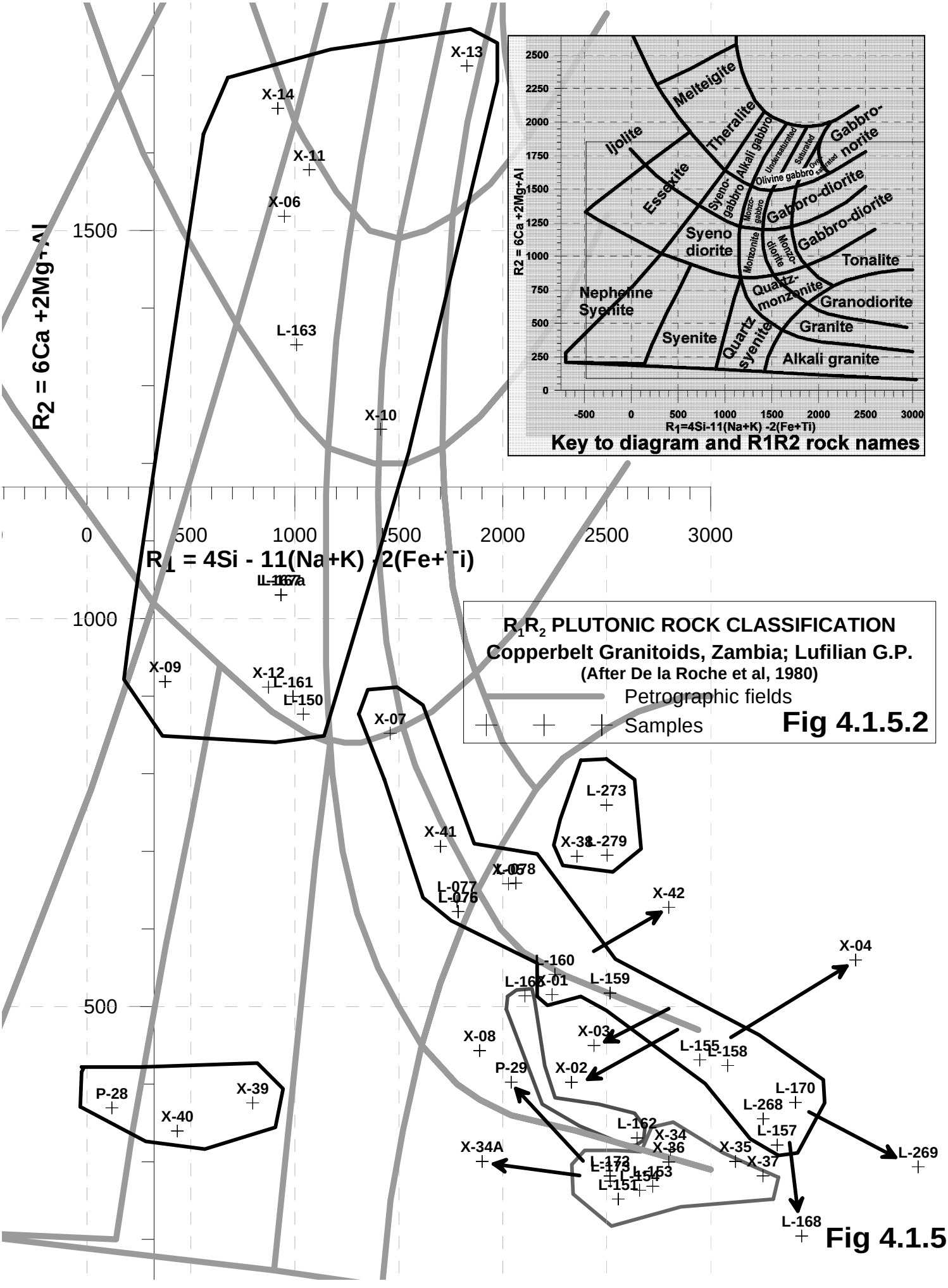
R2 = 6Ca +2Mg+Al
R1 = 4Si - 11(Na+K) -2(Fe+Ti)
0
500
1000
1500
2000
2500
3000
X-13
X-14
X-11
X-06
L-163
X-10
X-09
X-12
L-161
L-150
X-07
L-273
X-41
X-38
L-279
L-077
L-076
X-42
X-04
L-160
L-159
X-03
X-08
L-155
L-158
P-29
X-02
P-28
X-39
X-40
L-170
L-268
L-162
X-34
X-34A
X-36
X-35
L-157
L-269
X-37
L-173
L-153
L-154
L-151
L-168
Melteigite
Ijolite
Theralite
Alkali gabbro
Olivine gabbro
Gabbro-norite
Essexite
Syeno-gabbro
Monzo-gabbro
Gabbro-diorite
Syeno diorite
Monzonite
Monzo-diorite
Tonalite
Nepheline Syenite
Quartz-monzonite
Granodiorite
Syenite
Quartz syenite
Granite
Alkali granite
Key to diagram and R1R2 rock names
R1=4Si-11(Na+K) -2(Fe+Ti)
R2 = 6Ca +2Mg+Al
R1R2 PLUTONIC ROCK CLASSIFICATION
Copperbelt Granitoids, Zambia; Lufilian G.P.
(After De la Roche et al, 1980)
Petrographic fields
Samples
Fig 4.1.5.2

Fig 4.1.5.2

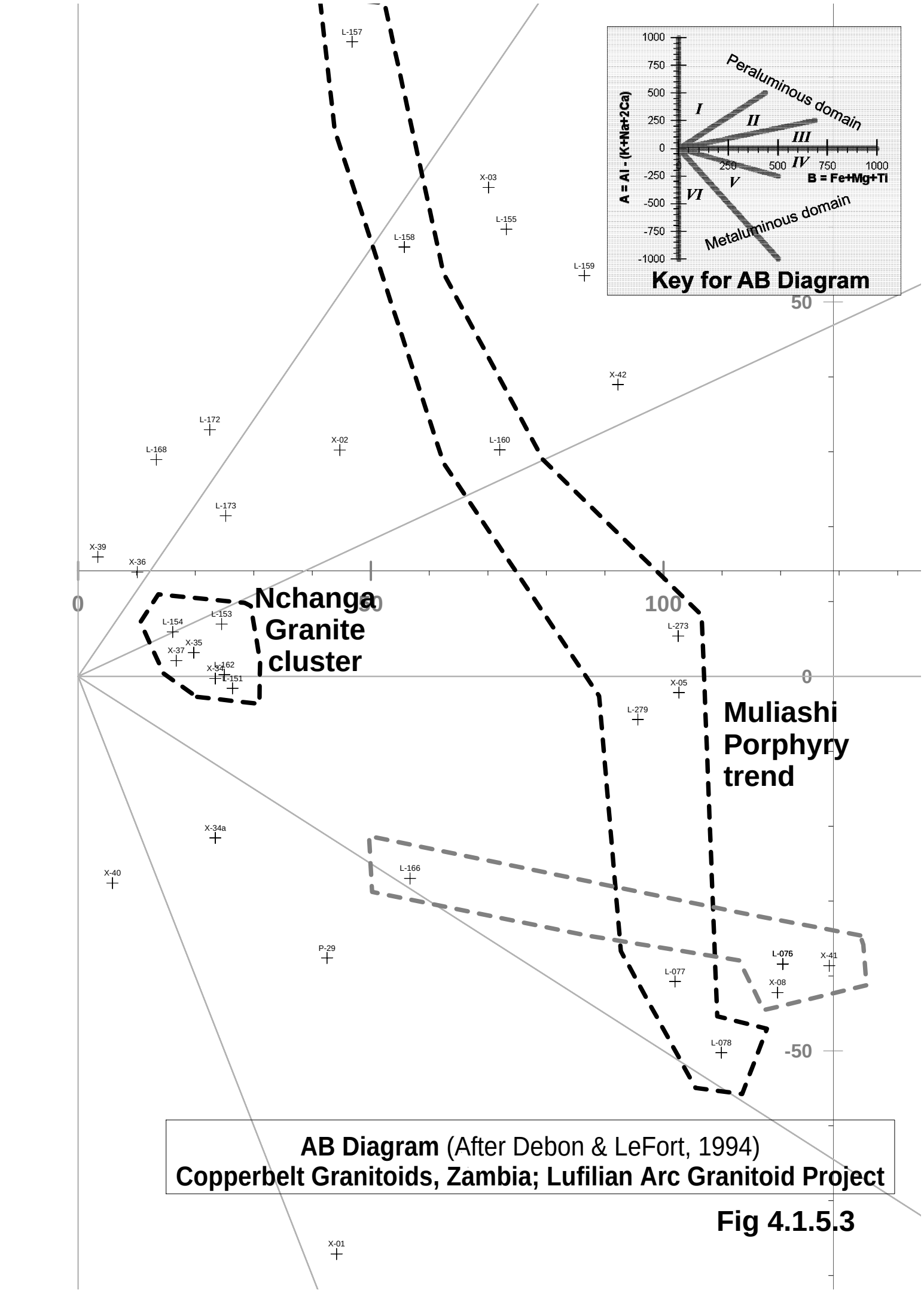

AB Diagram (After Debon & LeFort, 1994)
Copperbelt Granitoids, Zambia; Lufilian Arc Granitoid Project

Fig 4.1.5.3

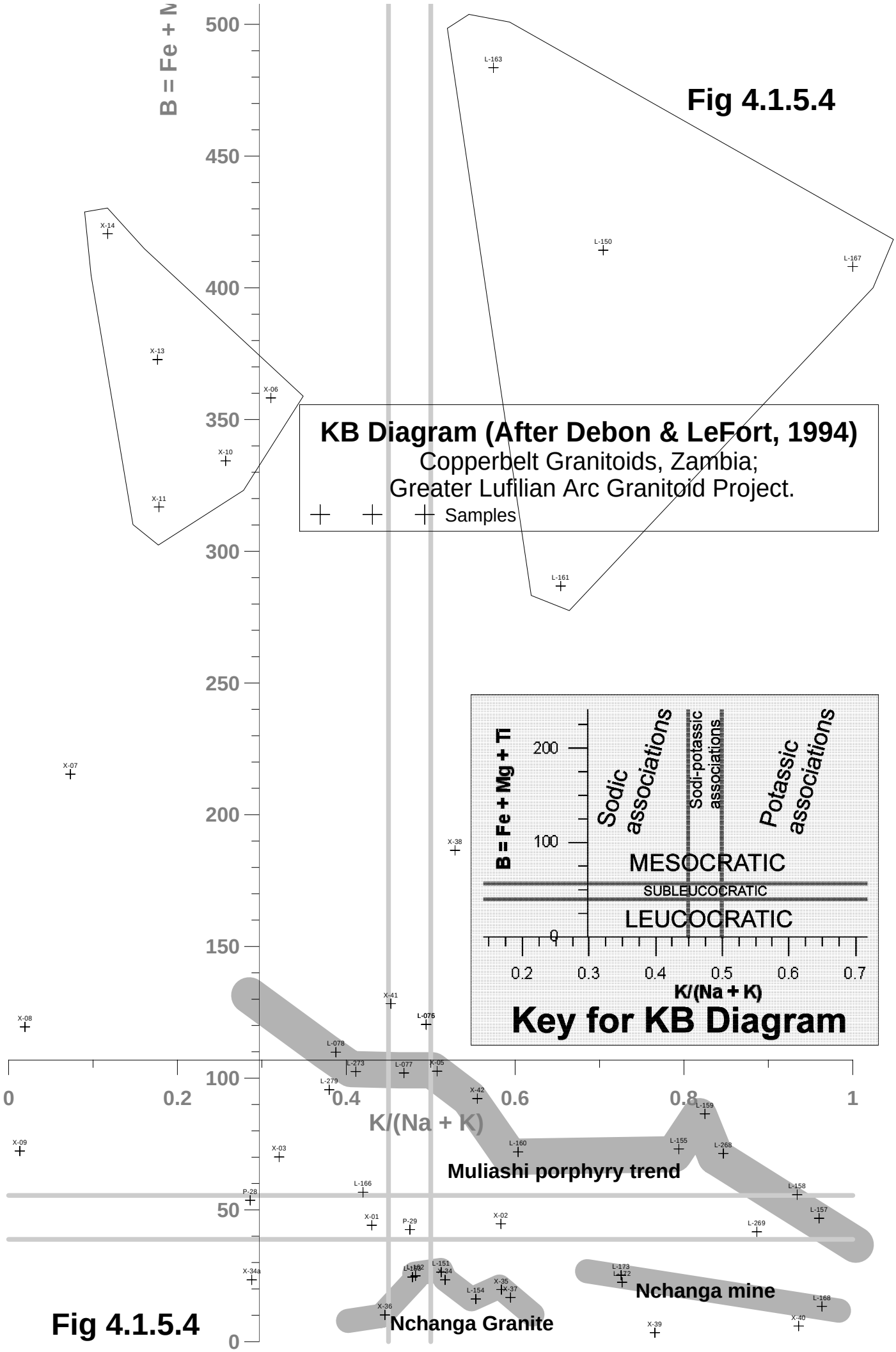
B = Fe + M
500
450
400
350
300
250
200
150
100
50
0
0
0.2
0.4
0.6
0.8
1
K/(Na + K)
Fig 4.1.5.4
KB Diagram (After Debon & LeFort, 1994)
Copperbelt Granitoids, Zambia;
Greater Lufilian Arc Granitoid Project.
Samples
B = Fe + Mg + Ti
200
100
0
Sodic associations
Sodi-potassic associations
Potassic associations
MESOCRATIC
SUBLEUCOCRATIC
LEUCOCRATIC
0.2
0.3
0.4
0.5
0.6
0.7
K/(Na + K)
Key for KB Diagram
Muliashi porphyry trend
Nchanga mine
Nchanga Granite
Fig 4.1.5.4

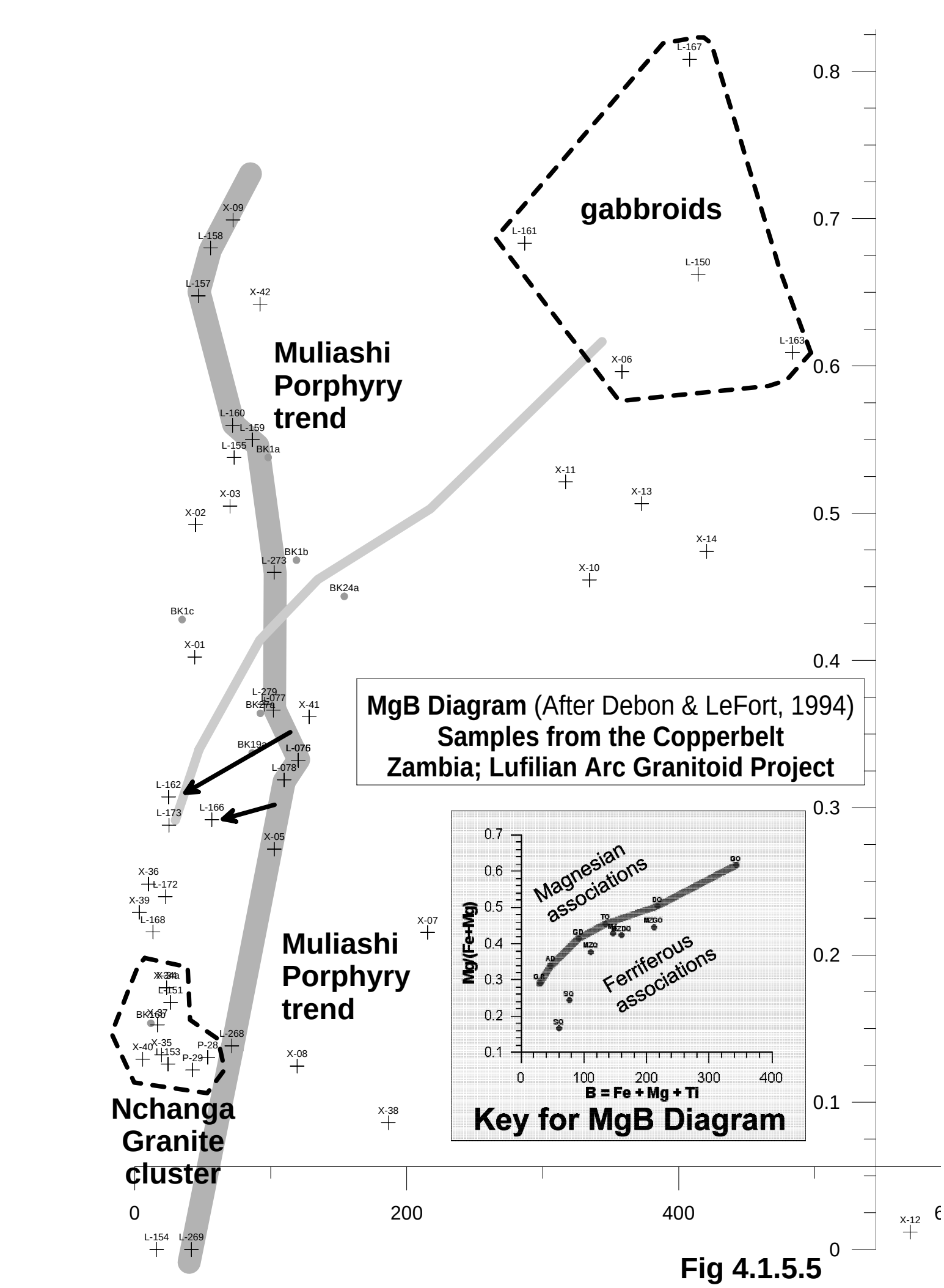
gabbroids
Muliashi Porphyry trend
Muliashi Porphyry trend
Nchanga Granite cluster
MgB Diagram (After Debon & LeFort, 1994)
Samples from the Copperbelt
Zambia; Lufilian Arc Granitoid Project
Magnesian associations
Ferriferous associations
Mg/(Fe+Mg)
B = Fe + Mg + Ti
Key for MgB Diagram
L-167
L-161
L-150
L-163
X-06
X-09
L-158
L-157
X-42
L-160
L-159
L-155
BK1a
X-03
X-02
BK1b
L-273
BK24a
BK1c
X-01
X-11
X-13
X-14
X-10
L-279
L-077
BK-276
X-41
BK19a
L-076
L-078
L-162
L-173
L-166
X-05
X-36
L-172
X-39
L-168
X-07
L-151
BK-167
L-268
X-40
X-35
P-28
L-153
P-29
X-08
X-38
L-154
L-269
X-12
0.8
0.7
0.6
0.5
0.4
0.3
0.2
0.1
0
0
200
400

Fig 4.1.5.5

4.1.5.2 Nchanga Granite

4.1.5.2.1 Introduction

The Nchanga Granite is an isolated, roughly ellipsoidal body of pink to red and gray, medium- to coarse-grained granite body that is exposed to the south of the Nchanga copper mine. That mine is the largest copper deposit in Africa, and a major mine by any standard. A large portion of the Chingola town is built on the Nchanga Granite. Its dimensions are roughly 9.5 x 15 kilometers (Figs M16 and 4.1.5.8).

A comprehensive review of the Nchanga Granite, its geology, structure and relation with mineralization was published by Garlick, 1973. Armstrong, Robb, Master, Kruger, & Mumba, 1999 dated the emplacement of the Nchanga Granite at 877±11Ma. In the past, some authors called the granitoid body "Nchanga Red Granite". This document prefers the name "Nchanga Granite".

Among the new findings are that the Nchanga Granite has all the characteristics of an anorogenic ring complex, and that it might have contributed to the origin of copper in its environs. The Nchanga red granite, or part of it high heat producing granite that probably maintained a long-lived circulation of hydrothermal fluids. Sections 8.4.2.1 and 8.5 of this document discuss iron oxide-copper-gold mineralization that may be associated with the Nchanga Granite.

4.1.5.2.2 Sampling

Some new data can be interpreted from the chemical analyses compiled by Garlick, 1973, and from the evaluation of samples collected and studied for this project. Thirteen samples have been analysed from the Nchanga Granite. Nine were collected in the field; of these, three were analysed. Two reasonably well documented samples with complete chemical analysis from the center of the Nchanga Granite come from Pepper, 2000. Seven major oxide analysis, mainly from Gray's quarry were extracted from Garlick, 1973. Part of them were previously disclosed in other publications of the Northern Rhodesia Geological Survey. A sample from the deep borehole at Konkola that was put in for geotechnical studies of a new deep shaft correlates well with Nchanga Granite rocks and was included here (Table 4.1.5.5).

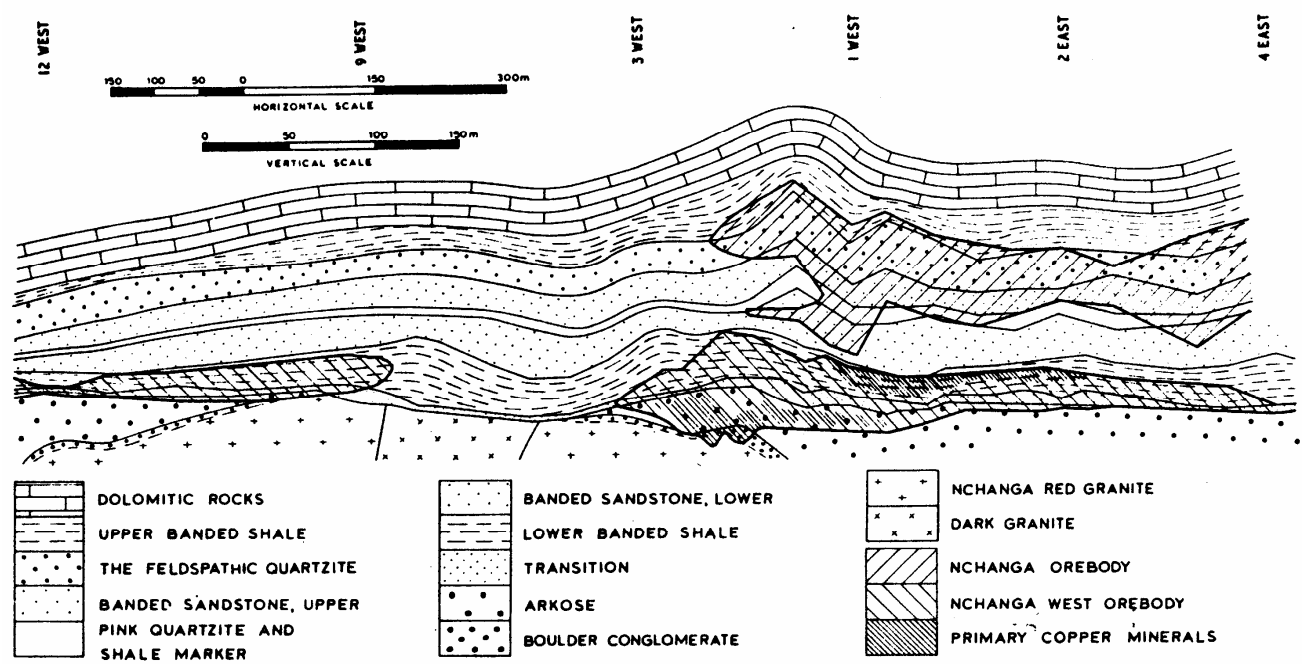

Fig 4.1.5.6 W-E geological cross section of underground exposure of the Nchanga Granite*. Drawn along 970 level at Nchanga Mine. As shown, two different granitoids make the pluton. It formed a positive paleotopography. Copper mineralization extends six meters into the granitoid at the site. It is partly hosted in fractures, and partly disseminated in metamorphosed paleosol where microcline lost its perthitic texture. The unconformable character of Katangan sediments and of mineralization pinching on top of the granitoid is also apparent. Vertical and horizontal scales are not the same, as indicated. Taken directly from Fleischer, Garlick & Haldane, 1976, p. 268.*

4.1.5.2.3 Main Rock Types

Samples analysed for the Nchanga Granite show a wide compositional variety. 73% of the granitoids have subalkaline character, while the rest are midalkaline (Table 4.1.5.2). Three quarters of the total samples are subalkaline rocks, the remaining quarter is made by midalkaline rocks. Two thirds of all the samples are granites *sensu stricto*.

Table 4.1.5.2 Statistics of rock types, Nchanga Granite, Zambia
The fifth column (granitoids) is the sum of underlined rock types.

Group	Rock type	number	%	Granitoids	Groups
Midalkaline Rocks	Alkali granite	1	8.33	27.27	25.00
	Syenite	2	16.67		
Subalkaline Rocks	Granite	8	66.67	72.73	75.00
	Diorite	1	8.33		
Total		12	100.00	100.00	100.00

Table 4.1.5.3 Rock name, basic geochemistry and environment of emplacement for samples from the Nchanga Granite, Zambia (See acronym description on section 2.4.3.)

Sample	Rock type	Debon & LeFort	Maniar & Picc	Whalen	Pearce	Rb/10HfTa	Rb/30HfTa	Nb-Ta	
P-28	Nepheline syenite	Metaluminous iv subleucocratic Na Fe	?			VA-	VA-III	INW-INV	
P-29	Granite	Metaluminous iv subleucocratic Na-K Fé				VA-	III	INW-INV	
L-151	alkali granite	Metaluminous iv leucocratic K Fe	RRG	A	W3/4	WP-	III	OUTU	
L-153	alkali granite	Peraluminous iii leucocratic Na-K Fe	RRG	A	W				
L-154	alkali granite	Peraluminous ii leucocratic K Fe	?	A	O-W 2-2	WP-	WP-III	OUTU	
L-162	Granite	Peraluminous iii leucocratic Na-K Mg	POG	A					
X-34	Alkali granite	Metaluminous iv leucocratic K Fe	Pog-rrg						
X-35	Granite	Peraluminous iii leucocratic K Fe	?						
X-36	alkali granite	Peraluminous i leucocratic Na low Mg	POG						
X-37	Granite	Peraluminous iii leucocratic K Fe	?						
X-38	Granodiorite	Metaluminous iv mesocratic K Fe	RRG						
X-39	Syenite	Peraluminous i leucocratic K low Mg	?						
X-40	Syenite	Metaluminous iv leucocratic K Fe	?						

4.1.5.2.4 Samples P-28 and P-29

According to Pepper, 2000, **P-28** was collected from one of many rounded inselberg outcrops near the side of the Kitwe-Chingola road. The outcrop is located roughly in the middle of the Nchanga Granite (Fig M16). It is a white to slightly pink, very coarse (>2cm crystals), porphyritic, metaluminous subleucocratic sodic ferriferous syenite. It has feldspar phenocrystals of up to 2-3 cm, no obvious mineral orientation and minor chlorite alteration. It also contains clear subhedral to anhedral quartz and chloritized biotite. Macroscopically, Pepper described the rock as made of “60% plagioclase, 30% quartz, 10% biotite, <5% amphiboles”. No petrographical work was done on it. Thin sections and hand samples were not available for re-evaluation.

P-29 was collected by Pepper, 2000 from large inselberg outcrops near the main road (Fig M16). Its external general appearance is similar to that of **P-28**. It is a white to slightly pink, holocrystaline porphyritic, metaluminous subleucocratic sodic to potassic ferriferous granite with minor chlorite alteration of the biotite and no specific crystal orientation. It contains porphyritic plagioclase phenocrystals up to 3 cm. Macroscopically, the rock is made of 55% plagioclase, 35% quartz, 10% biotite, <3% amphiboles. Under the microscope, the rock is a porphyritic granite that cooled slowly. Its biotites are partially chloritized, very small epidote crystals occur inside plagioclase, and there is complex intergrowth of different feldspar compositions. A portion of

the slide studied by Pepper contained abundant zircons. Microscopically the rock is made of 40% quartz, 25% plagioclase, 15% perthite (micro), 10% microcline, <10% epidote, ~5% biotite, <5% amphibole, <5% chlorite, <3-4% allanite, <2% muscovite, <2% sphene, <2% opaques (magnetite?)

Based on the chemical analysis of **P-28** provided by Pepper, 2000, the rock is a nepheline syenite *sensu* De la Roche, Leterrier, Gandclaude, & Marchal, 1980. It plots as a syenite on the TAS diagram modified by Middlemost, 1994. According to the IUGS software to evaluate rock nomenclature and calculate CIPW norms, **P-28** is the plutonic equivalent of a comenditic trachyte. That is "a variety of peralkaline trachyte of TAS field T in which Al_2O_3>1.33 x total iron as (FeO + 4.4)" (LeMaitre et al., 2002). It contains normative albite, orthoclase and quartz; other minerals present in order of abundance are: sodium metasilicate, diopside, acmite, hypersthene, ilmenite, hydroxiapatite, and zircon.

A strong albitization of the core of the Nchanga Granite could produce the high Na_2O value of **P-28**. In any case, the presence of that amount of sodium in a rock is extraordinary.

Samples **P-28** and **P-29** from Nchanga Granite are enriched in all REE, Th and Cu. The chemistry of **P-28** and **P-29** has slightly lower silica, higher total iron oxide, Ca, Na, Ti and Mn than the rest of the rocks from the Nchanga Granite suite. **P-29** falls into the Nchanga Granite general trends in the various geochemical plots, while **P-28** definitely has a contrasting chemistry (Figs 4.1.5.1 to 4.1.5.5). It is interesting to note that the MgB plot of Debon LeFort (Fig 4.1.5.5) shows both **P-28** and **P-29** well within the general trend of the other Nchanga Granite rocks, although enrichment in total iron and magnesium were identified for **P-28**.

After comparing the chemistry of samples **P-28** and **P-29** using the isocon diagram of Grant, 1986, both rocks actually have very similar basic chemistry. Major changes have taken place after hydrothermal albitization, especially with respect to the rare earths. The amount of Na_2O doubled in **P-28**; it was also enriched in total iron, P_2O_5, MnO, MgO, As, Pb, Ni, Rb, Zr, Zn, Y, Th, U, Pr, Sm, Dy, Gd, Eu, Sm, La, Ce and all the other rare earths. There were depletions in CaO, Sr, Sc and Cu. K_2O, Sc, Ba, Cr, Al_2O_3 and SiO_2 remained relatively constant. A relative change in the rock volume during alteration is not apparent, although albitization involves a net volume reduction.

Several questions come to mind. What produced the severe alteration of **P-28**? Why was only that portion of the Nchanga Granite altered? Why were the other samples not altered? **L-162** does not seem to have been altered in the way that the other samples were. Did the alteration take place along the NW-SE fault that is shown on the map of Fig 4.1.5.8?

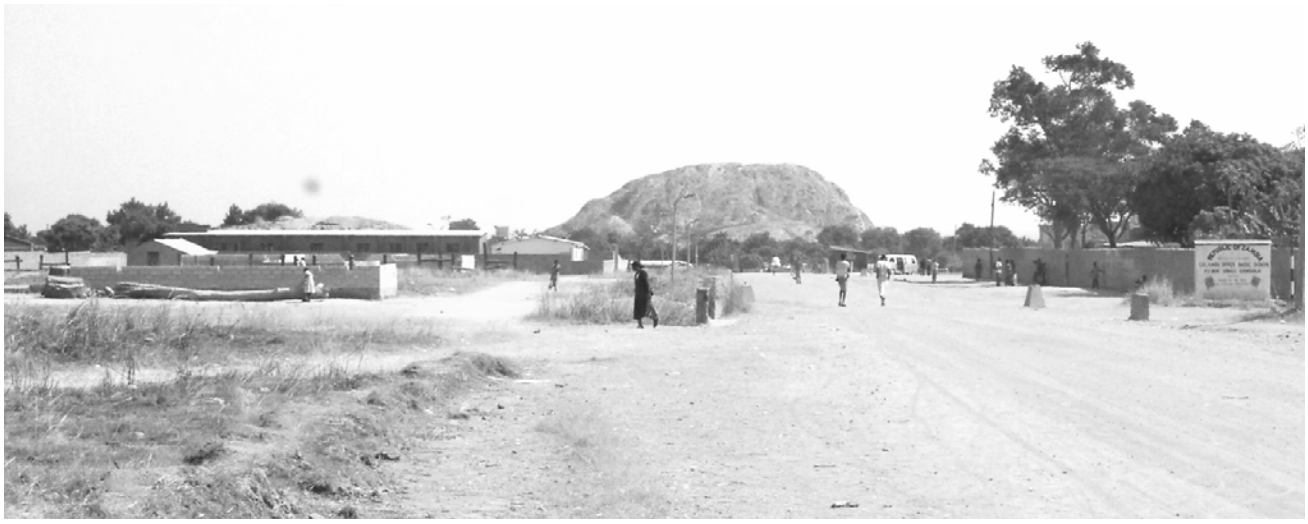

Fig 4.1.5.9 Inselberg and whaleback of Nchanga Granite at the Chiwempala Hill*. This is probably the best outcrop of the pluton. Several samples were collected from there and from the lower outcrops that lie to the left of the main hill. The hill stands out due to silicification along many intersecting shear zones. Several other hills have been used as source for road and railroad ballast.*

4.1.5.2.5 Samples from Chiwempala Hill

One of the best outcrops of the Nchanga Granite is made by a granite inselberg at the Chiwemupala Hill, approximately 5 km south of the Nchanga mine (Fig 4.1.5.8). **L-151** was collected from there. The rock is a metaluminous leucocratic potassic ferriferous alkali granite, and was produced in a rift-related anorogenic environment. The granite massif has been subject to at least three distinct families of shearing in different directions along which quartz veins formed. Almost every linear meter has several quartz veins or small shear zones filled by quartz braiding. The inselberg is probably due to the dense quartz veining and silicification of the massif (Fig 4.1.5.9).

Samples **L-153** and **L-154** come from an outcrop of lower elevation that lies a few hundred meters southeastward from the previously described inselberg (Fig 4.1.5.8). Plagioclase phenocrystals in these outcrops are 4-5 cm in diameter. Layers 1 to 5 meters thick of fine and coarser-grained porphyritic rock are clearly discernible. **L-153** is a slightly-foliated, metaluminous leucocratic sodic to potassic ferriferous alkali granite. **L-154** is a peraluminous leucocratic potassic ferriferous alkali granite. The average plane of foliation is 130/79° N. This rock was produced in a rift-related anorogenic environment (Table 4.1.5.3.).

L-151 and **L-153** have large (up to 3 cm) angular plagioclase porphyroblasts with a pink nucleus and white rim. Coarse (2-5 mm), anhedral blue quartz phenocrysts are another characteristic feature of both samples.

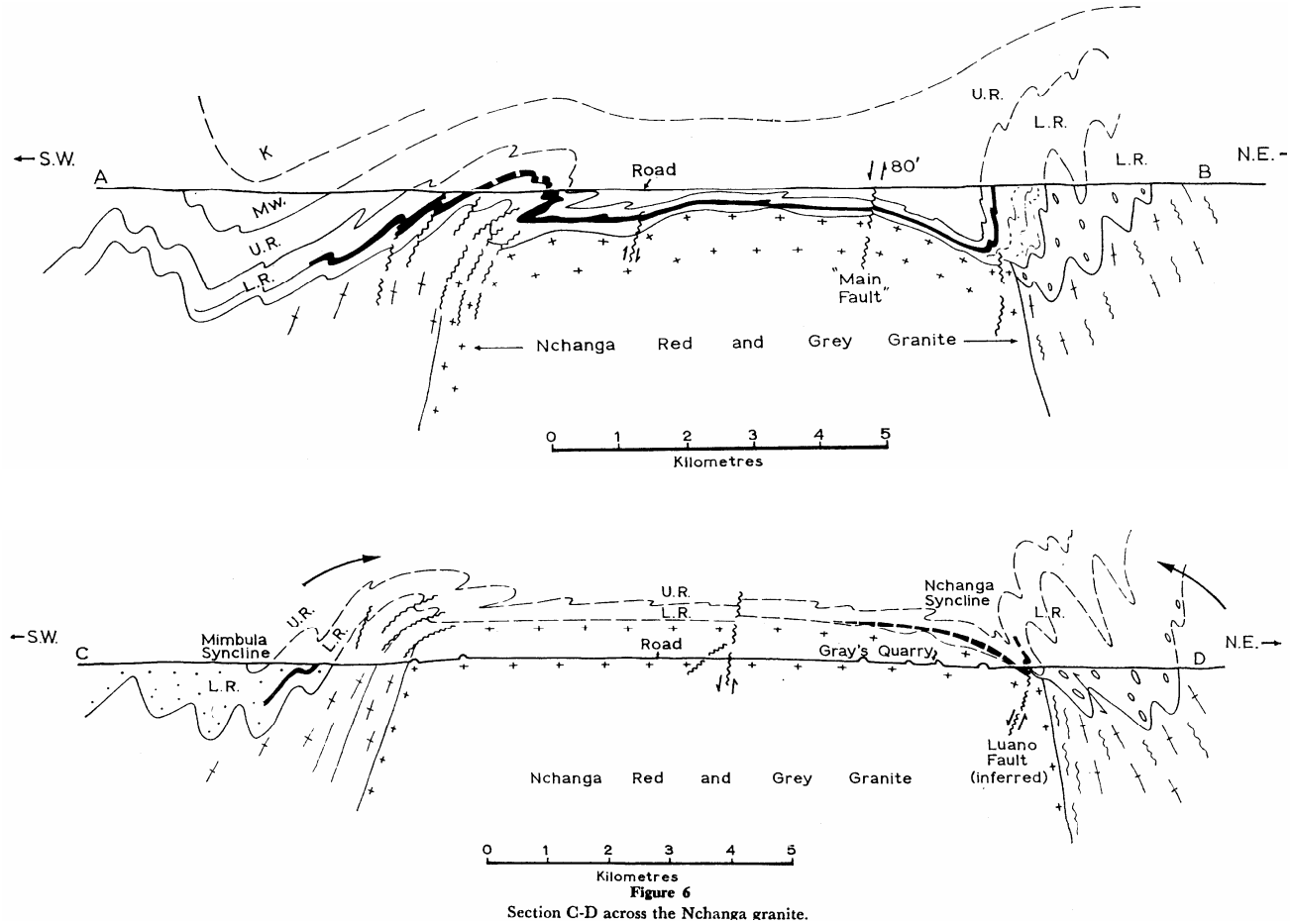

Figure 6
Section C-D across the Nchanga granite.

Fig 4.1.5.7 Geological cross sections through the Nchanga Granite*. Location of the sections is indicated on Fig 4.1.5.8. Section AB, across the Nchanga mine area, shows the main fault where the "lamprophyre" was intruded. Katangan sediments over the Nchanga Granite were not as severely folded as elsewhere. Section CD shows Gray's Quarry and the Chiwempala Hill, the location of the road, and the extension of the fault. Note refolding of Katangan sediments on the borders of the pluton, and that the limits of the pluton are drawn vertically. Section CD shows several inselbergs of the granitoid; one of them is exploited at Gray's Quarry. Taken from Garlick, 1973.*

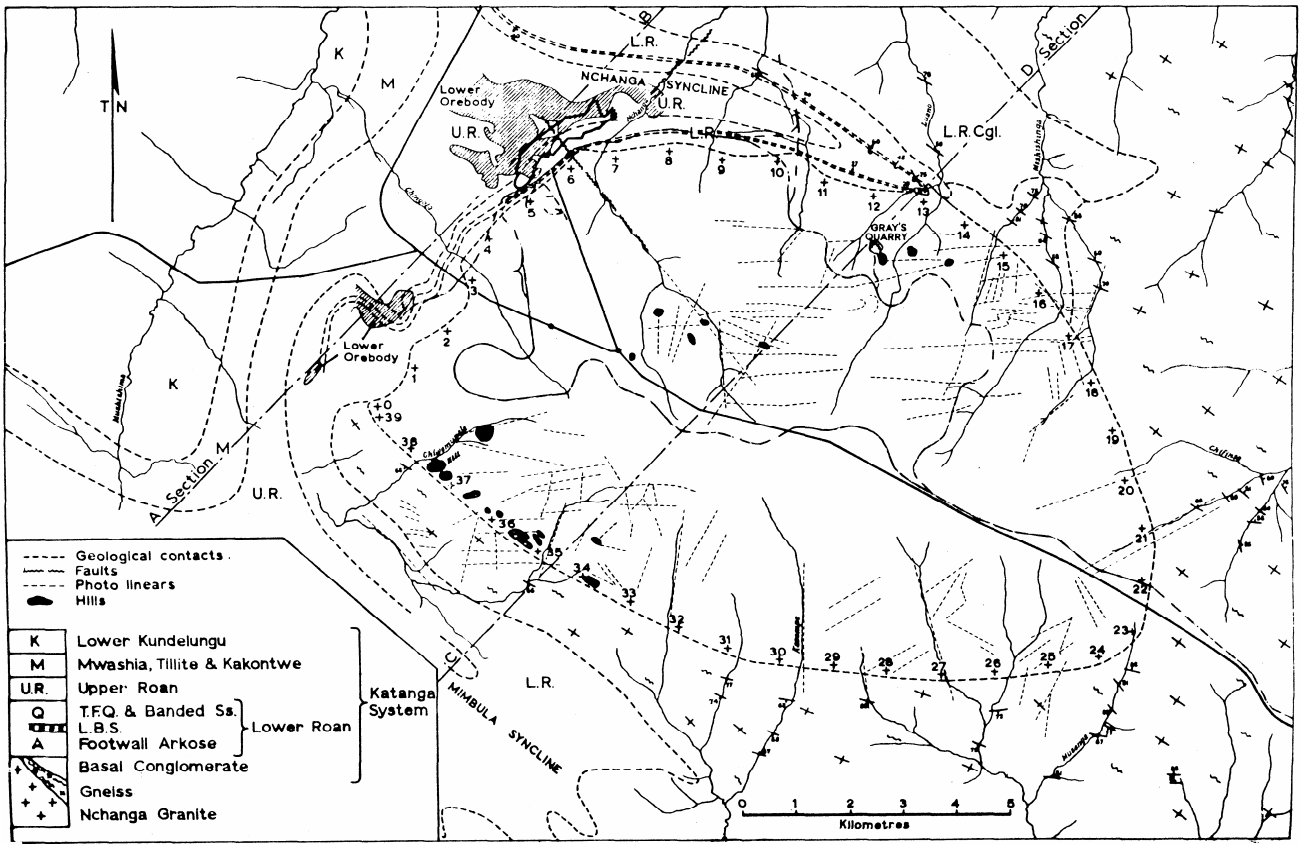

Fig 4.1.5.8 Geological map of the Nchanga Granite*. The numbers around the pluton are stations measured every kilometer for reference in the original description. Note the location of Gray's Quarry around No. 13, and the Chiwempala Hills around No. 37. Parts of the Nchanga mine are found from Nos. 1 to 8. The "lamprophyre" dike described in the text is emplaced along the fault that outcrops at the Nchanga mine in No. 6. As shown, numerous E-W trending fracture zones were identified on air photographs. There is a road that intersects the pluton roughly NW-SE, and several observations were made on outcrops along it. Main inselbergs are indicated by black irregular shapes. Cross sections AB and CD are included on Fig 4.1.5.7. Foliation of the rocks that surround the Nchanga Granite is uniform in NW-SE direction: that corresponds approximately with the surface deformation of the . Figure taken from Garlick, 1973.*

4.1.5.2.6 Gray's Quarry

Gray's quarry is located on the NE part of the pluton, as shown on Figs M16 on the site of 2006. Samples **X-35** and **X-36** that come from the typical red and grey granites at the quarry are very similar. At first glance, the only parameters that seem to vary between them are Ti and P. A closer look shows that both are peraluminous leucocratic potassic ferriferous granites. **X-34**, an alkali granite, has roughly the same chemistry as the previous two samples described. **X-36** is a peraluminous leucocratic sodic low magnesic alkali granite aplite, and shows a minor enrichment in Na with depletions in K, Ca, Ti and Mn compared to the rest of the other rocks at the quarry.

Garlick, 1973 states that the values of Na_2O and K_2O for sample **X-34** were misplaced by previous authors. He exchanged the values to make them fit with the rest of the data. With the information that is now available, the original data presented by Mendelsohn, 1961 and earlier by other authors makes more sense. It is shown on Table 4.1.5.4 as **X-34a**. A higher value for soda is compatible with hydrothermally altered rocks that deviate from the average composition. The change does not modify the TAS diagram (Fig 4.1.5.1), but transforms the sample from a granite into an alkali granite on the R1/R2 diagram (Fig 4.1.5.2). Other geochemical diagrams show that **X-34a** deviates from the main cluster of the Nchanga Granite (Figs 4.1.5.3 to 4.1.5.5). A comparison of the rest of the samples collected in the Nchanga Granite point that the chemical analysis for **X-34** is probably correct. Most of the samples contain K2O values around 5%. See Table 4.1.5.4.

Table 4.1.5.4 Exchange in values for Na and K in chemical analysis of sample X-34.

Sample	SiO2	TiO2	Al2O3	Fe2O3	FeO	MnO	MgO	CaO	Na2O	K2O	P2O5	LOI	Total
X-34	76.75	0.09	11.78	0.82	0.58	0.03	0.16	0.72	3.08	5.01	0.1	0.84	99.96
X-34a	76.75	0.09	11.78	0.82	0.58	0.03	0.16	0.72	5.01	3.08	0.1	0.84	99.96

4.1.5.2.7 Various Dikes

Dikes of varying composition occur on and around the Nchanga Granite. Some of them are syenitic and granodioritic; others granitic. The last three samples of Table 4.1.5.5 show completely different chemistry and are not related to the main Nchanga Granite body. They are not related to each other either. **X-39** (Gray's quarry pegmatite microcline) and **X-40** (Nkana vein adularia) are similar to each other in general composition. They plot as syenites on the R1/R2 and TAS diagrams. **X-39** is a peraluminous leucocratic potassic magnesic syenite, while **X-40** is a metaluminous leucocratic potassic ferriferous syenite. They are both enriched in potash and could be potassic segregations of the general Nchanga Granite body. **X-38**, described by Garlick as a biotite-rich schlieren rock from Gray's quarry, is a bizzare mafic rock of the type called lamprophyre in the Copperbelt. It plots as a metaluminous mesocratic potassic ferriferous granodiorite. These dikes seem to be related to the Nchanga Granite, as late intrusions in the system.

L-168, L-170, **L-171**, **L-172*** and **L-173** are other dikes that will be discussed in the next chapter. **L-172*** and **L-173** are extremely similar in composition to rocks from the Nchanga Granite. But they have to be younger, because they intersect Katangan sediments.

4.1.5.2.8 Geochemistry

Table 4.1.5.5 Chemical analysis of samples from the Nchanga Granite and others in the basement to the Zambian Copperbelt

(complete elemental analyses are on Table A8.4, Appendix)

No.	SiO2	TiO2	Al2O3	FeT	MnO	MgO	CaO	Na2O	K2O	P2O5	LOI	Total	Rb	Sr	Y	Zr	Nb	Co	Ni	Cu	Zn	Ga	V	Cr	Ba	U	Th
X-34	76.75	0.09	11.78	1.40	0.03	0.16	0.72	3.08	5.01	0.10	0.85	99.97															
X-34a	76.75	0.09	11.78	1.40	0.03	0.16	0.72	5.01	3.08	0.10	0.85	99.97															
X-35	76.84	0.08	10.70	1.30	0.04	0.10	0.80	2.30	4.90	0.02	0.84	97.92															
X-36	76.90	0.01	12.30	0.60	0.01	0.10	0.50	3.60	4.40	0.04	0.43	98.89															
X-37	78.20	0.04	10.30	1.10	0.04	0.10	0.70	2.20	4.90	0.01	0.53	98.12															
L-162	76.11	0.19	12.33	1.25	0.00	0.28	0.70	3.48	4.92	0.03	0.59	99.88	119	155	14	96	10	6	<6	7	22	13	17	15	793	<6	<15
L-151	77.00	0.10	11.82	1.67	0.03	0.17	0.11	3.47	5.54	0.02	0.51	100.44	351	32	158	197	91	10	8	42	39	24	<12	42	441	11	65
L-153	77.40	0.07	11.91	1.65	0.03	0.12	0.27	3.51	4.89	0.01	0.51	100.37	438	25	117	106	70	<6	8	58	33	24	<12	60	236	11	44
L-154	77.07	0.07	12.06	1.22	0.00	0.00	0.25	3.07	5.78	0.01	0.50	100.05	478	27	68	122	58	7	<6	17	22	23	<12	<12	255	<6	44
P-28	68.49	0.34	12.40	3.43	0.12	0.26	1.06	8.74	5.32	0.11	0.13	100.27	345	58	617	261	64	34	19	<3	97	24	<4	8	689	13	98
P-29	72.84	0.31	13.07	2.71	0.11	0.19	1.28	4.04	5.56	0.08	0.17	100.19	278	79	89	183	46	38	3	6	58	22	<4	8	724	9	65
X-38	59.80	1.10	10.40	12.6	0.30	0.60	4.30	1.70	2.90	0.08	1.06	94.84															
X-39	66.60	0.01	18.00	0.20	0.02	0.03	0.20	2.40	11.90	0.01	1.13	100.50															
X-40	64.80	0.01	16.70	0.40	0.01	0.03	0.10	0.70	15.50	0.00	0.00	98.25															

The suite of samples from the Nchanga Granite crosses the fields of alkaline to non-alkaline rocks. That happens especially on the TAS diagram (Fig 4.1.5.1). All samples are leucocratic and only two (28 and 29) are subleucocratic.

All samples from the Nchanga Granite that were analysed for Th are strongly enriched in it; to a point that they are all high-heat producing granitoids.

Most of the samples from the Nchanga Granite contain high values of K_2O. They are all leucocratic in character and tend to be ferric according to the MgB Debon LeFort diagram.

L-151, **L-153**, **L-154**, **P-28** and **P-29** all have very similar chemical signature. They contain high values for K_2O, Sc, Ba, Cr, Al_2O_3, SiO_2. Maybe all the samples from the Nchanga area carry that same chemical signature. U

Samples **L-151**, **L-153** and **L-154** (more foliated) display lower Ca values than the first four samples, but correlate well with them in the various plots (Figs 4.1.5.1 to 4.1.5.5 and logarithmic plots of Figs 4.1.5.10 and 4.1.5.11).

As shown on the table above, **L-162** has very similar major oxide chemistry to the rest of the samples from the Nchanga Granite. It falls neatly into the trends of the Nchanga Granite in the various plots (Figs 4.1.5.1 to 4.1.5.5). That body was intersected in the Konkola deep borehole that is described later on in this chapter. It

could constitute an apophysis of the Nchanga Granite body, or another isolated anorogenic plutonic body that formed in a similar environment and intruded into the Muliashi Porphyry. Nevertheless, **L-162** does not show any of the minor element and rare earth enrichment that is evident in other samples from the Nchanga Granite (Table 4.1.5.5).

L-162 correlates very well with **X-36**, the gray granite of Gray's quarry. Maybe these two rocks are isolated representatives of the original composition of the Nchanga Granite that was turned pink by subsequent hydrothermal alteration. Plot MgB of Debon LeFort shows that **L-162** suffered minor alteration. Maybe sample **L-162** has the original, unaltered Nchanga Granite chemistry.

That hydrothermal enrichment probably is not present in apophyses of the Nchanga Granite.

Samples from the Nchanga Granite plot as an elongated cluster on the R1/R2 diagram, as a curved line on the TAS diagram, as a cluster on the BMg diagram, and as a trend on the KB diagram (Figs 4.1.5.1 to 4.1.5.5).

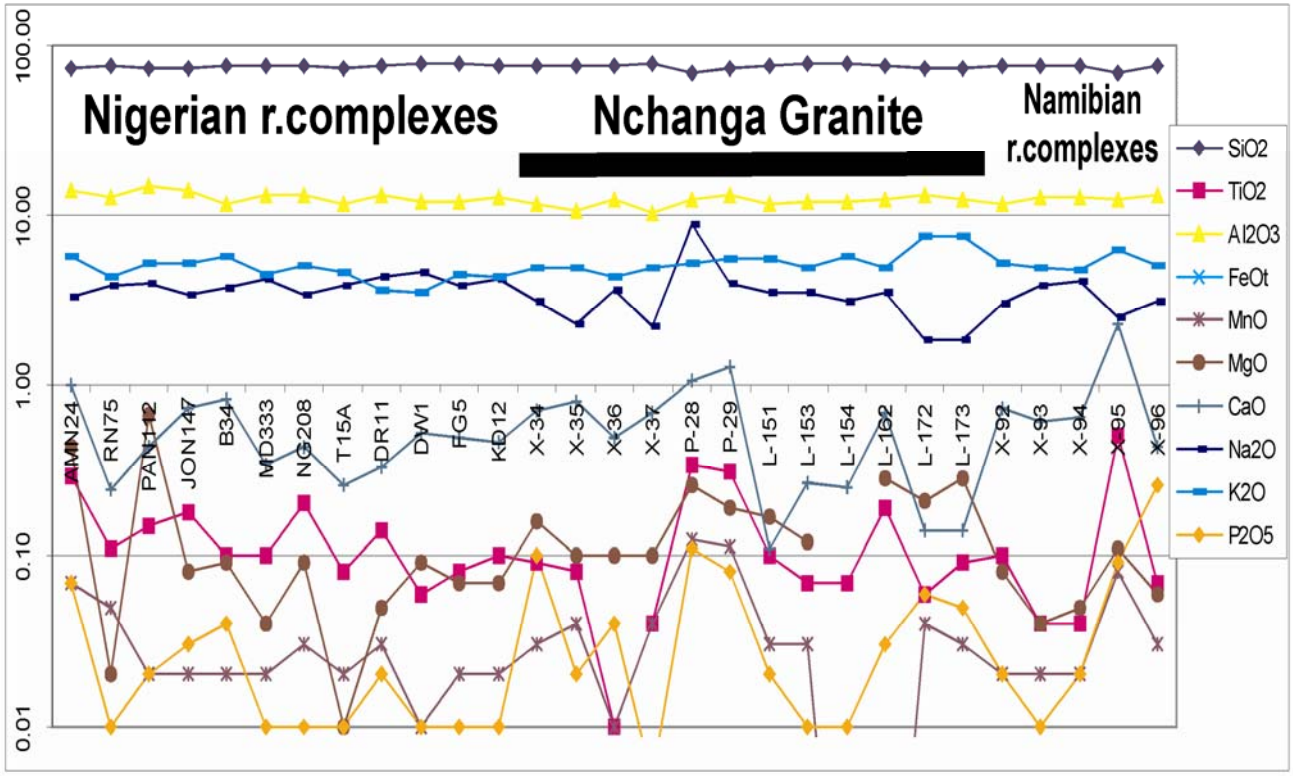

Fig 4.1.5.10 Logarithmic scale plot of major oxides to compare Nchanga Granite with Nigerian and Namibian granitoid ring complexes. *All major oxides behave in roughly the same way. Only Mg, Mn and P_2O_5 are higher in the Nchanga Granite. The first twelve samples, up to KD12 come from Nigerian granitoids; the last five (X-92 to X-96) come from Namibian granitoids. X-34 to L-173 come from the Nchanga Granite. Same numbering scheme and order for Figs 4.1.5.11 and 4.1.5.12. For more details, see Table 4.1.5.6.*

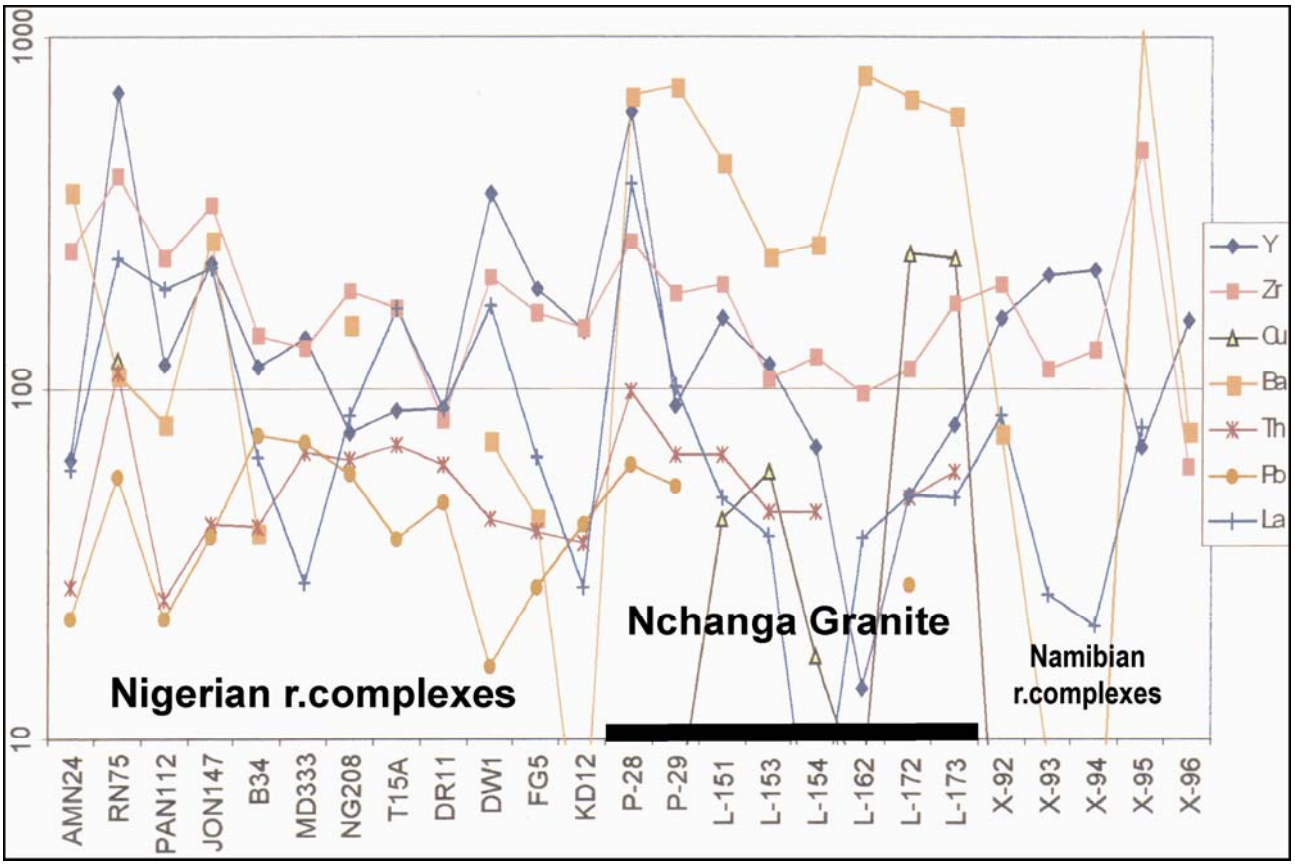

Fig 4.1.5.11 Logarithmic scale plot of minor elements and rare earths to compare Nchanga Granite with Nigerian and Namibian granitoid ring complexes. *Note that the Nchanga Granite has higher Ba and Cu values. The ranges for Zr are equivalent.*

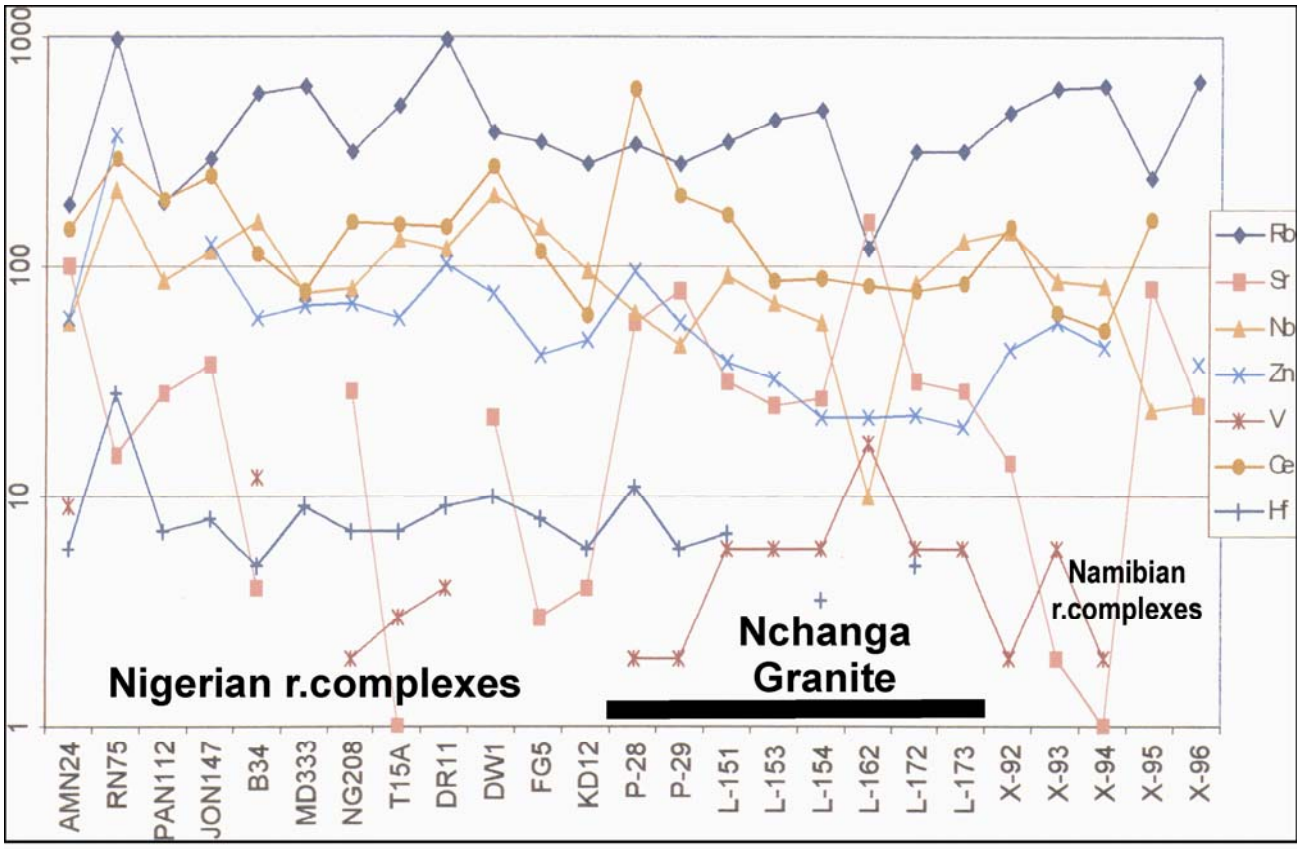

Fig 4.1.5.12 Logarithmic scale plot of minor elements and rare earths to compare Nchanga Granite with Nigerian and Namibian granitoid ring complexes. *Note that Sr and Rb are roughly equal; Zn is lower; Nb and Ce are slightly lower.*

4.1.5.2.9 Anorogenic character of the Nchanga Granite

Many separate observations lead to conclude that the Nchanga Granite is an anorogenic ring complex. The following section will present that evidence.

First of all, the shape of the Nchanga Granite is characteristic of slightly deformed anorogenic ring complexes. The map of Fig 4.1.5.8 was carefully prepared following outcrops along the outline of the Nchanga Granite. Figs 4.1.5.7 show geologically-controlled cross sections through that map. Cross sections drawn by other authors also maintain the same general pattern for the Nchanga Granite (Figs 4.1.5.13): cylindrical geometry with subvertical walls. The pluton acted as a rigid buttress against which the surrounding sediments flowed and folded, as indicated in Fig 4.1.5.7 and 4.1.5.13. The oval shape displayed by the pluton is a feature commonly observed worldwide in granitic anorogenic complexes that have been subject to slight deformation. Numerous examples of similar bodies are found in Bonin, 1986; Nuelle, Day, Sidder, & Seeger, 1992; and Wooley, 2001.

Chemistry of biotite granites from the Nigerian anorogenic ring complexes and from some of the Namibian Mesozoic granitic ring complexes shows significant similarities with samples from the Nchanga Granite (Table 4.1.5.7, Fig 4.1.5.10). High values for Rb, Y, Nb, Th, Pb, Ce and La are all present in analysis from the Nchanga Granite. Equivalent figures occur in samples from Spitskoppe and Erongo Namibian granitoid ring anorogenic complexes. Samples from the Nchanga Granite contain more Ba and Cu (Fig 4.1.5.10A). Zn, Nb and Ce are slightly lower in the Nchanga Granite (Fig 4.1.5.10B). All other values for ranges of the elements publicly available are similar. This is another observation that supports the hypothesis that the Nchanga Granite is an anorogenic ring complex.

L-162 does not have the chemical signature of the rest of the samples from the Nchanga Granite. It does not contain high Rb, Y, Nb, Th, Pb, Ce or La, although the major oxide composition is akin to that of the rest of the samples from the suite. **L-162** might be an apophyses of the main Nchanga Granite that was subject to depletion in some elements. If this hypothesis is true, then the original rock contained low Sr and Ba, while most of the rest of the metals and minor elements were depleted by later processes.

Table 4.1.5.6 Comparison of chemical data from anorogenic ring complexes and the Nchanga Granite
(Complete trace element analysis on Table A8.4)

Sample	SiO2	TiO2	Al2O3	Fe2O3	FeO	FeOt	MnO	MgO	CaO	Na2O	K2O	P2O5	LOI	Total	Rb	Sr	Y	Zr	Nb	Cu	Zn	V	Ba	Th	Pb	Ce	La	Hf
Nigerian granitoid ring complexes																												
AMN24	72.60	0.29	14.07	0.90	1.73	2.63	0.07	0.43	1.01	3.36	5.74	0.07	0.47	100.74	185	100	63	246	57		61	9	362	27	22	144	59	6
RN75	75.90	0.11	12.85	0.33	1.05	1.38	0.05	0.02	0.24	3.91	4.31	0.01	0.88	99.66	979	15	696	399	214	120	376	0	109	111	56	296	234	28
PAN112	73.90	0.15	14.88	0.43	0.80	1.23	0.02	0.67	0.43	3.98	5.17	0.02	0.61	101.06	192	28	117	234	88			0	80	25	22	195	189	7
JON147	73.20	0.18	14.18	0.67	1.19	1.86	0.02	0.08	0.73	3.45	5.32	0.03	0.98	100.03	296	38	227	330	118		126	0	264	41	38	251	218	8
B34	76.00	0.10	11.74	0.37	0.89	1.26	0.02	0.09	0.83	3.78	5.77	0.04	0.24	99.87	574	4	115	141	158		60	12	39	40	74	114	64	5
MD333	75.40	0.10	13.33	0.01	0.96	0.97	0.02	0.04	0.34	4.26	4.53	0.01	0.20	99.20	620	0	139	129	78	9	68	0	0	66	70	79	28	9
NG208	75.70	0.20	13.18	1.48	0.01	1.49	0.03	0.09	0.44	3.41	5.10	0.01	0.66	100.31	318	29	75	186	80		70	2	151	63	57	156	83	7
T15A	74.30	0.08	11.74	0.33	0.89	1.22	0.02	0.01	0.26	3.88	4.59	0.01	0.64	96.75	502	1	86	166	132	7	61	3	0	69	37	153	166	7
DR11	76.70	0.14	13.36	0.00	1.16	1.16	0.03	0.05	0.33	4.41	3.58	0.02	0.34	100.12	966	0	87	81	119		103	4	0	61	47	149	88	9
DW1	78.03	0.06	12.14	0.33	0.89	1.22	0.01	0.09	0.52	4.59	3.56	0.01	0.42	100.65	389	22	356	207	205		77	0	71	42	16	275	169	10
FG5	77.44	0.08	11.99	0.37	0.87	1.24	0.02	0.07	0.49	3.89	4.45	0.01	0.34	100.02	347	3	189	161	148		42	0	43	39	27	117	64	8
KD12	76.50	0.10	12.83	0.35	0.84	1.19	0.02	0.07	0.46	4.17	4.39	0.01	0.34	100.08	283	4	144	147	96		48	0	4	36	41	62	27	6
Nchanga Granite																												
X-34	76.75	0.09	11.78	0.82	0.58	1.40	0.03	0.16	0.72	3.08	5.01	0.10	0.84	99.96														
X-34a	76.75	0.09	11.78	0.82	0.58	1.40	0.03	0.16	0.72	5.01	3.08	0.10	0.84	99.96														
X-35	76.84	0.08	10.7	1.3		1.30	0.04	0.10	0.80	2.30	4.90	0.02	0.69	97.77														
X-36	76.9	0.01	12.3	0.6		0.60	0.01	0.10	0.50	3.60	4.40	0.04	0.35	98.81														
X-37	78.2	0.04	10.3	1.1		1.10	0.04	0.10	0.70	2.20	4.90	0.005	0.44	98.025														
P-28	68.49	0.34	12.40	3.43		3.43	0.12	0.26	1.06	8.74	5.32	0.11	0.13	100.27	345	58	617	261	64	<3	97	<4	689	98.0	61	600	383	11
P-29	72.84	0.31	13.07	2.71		2.71	0.11	0.19	1.28	4.04	5.56	0.08	0.17	100.19	278	79	89	183	46	6	58	<4	724	65.0	53	204	101	6
L-151	77.00	0.10	11.82	1.67		1.67	0.03	0.17	0.11	3.47	5.54	0.02	0.51	100.44	351	32	158	197	91	42	39	<12	441	65.0		167	49	7
L-153	77.40	0.07	11.91	1.65		1.65	0.03	0.12	0.27	3.51	4.89	0.01	0.51	100.37	438	25	117	106	70	58	33	<12	236	44.0		87	38	
L-154	77.07	0.07	12.06	1.22		1.22	0.00	0.00	0.25	3.07	5.78	0.01	0.50	100.05	478	27	68	122	58	17	22	<12	255	44.0		90	4	4
L-162	76.11	0.19	12.33	1.25		1.25	0.00	0.28	0.70	3.48	4.92	0.03	0.59	99.88	119	155	14	96	10	7	22	17	793	<15		82	37	
L-172	74.42	0.06	13.07	1.32		1.32	0.04	0.21	0.14	1.85	7.48	0.06	0.71	99.36	316	32	49	113	85	242	23	<12	668	48.5	27	79	50	5
L-173	74.69	0.09	12.55	1.37		1.37	0.03	0.28	0.14	1.87	7.51	0.05	0.78	99.36	314	29	78	172	128	232	20	<12	598	58.0		85	49	
Spitzkoppe Complexes, Namibia																												
X-92	76.99	0.1	11.73	2.06		2.06	0.02	0.08	0.74	3.03	5.23	0.02	0.52		473	14	157	196	141	3	44	2	75			148	84	
X-93	76.04	0.04	12.83	1.57		1.57	0.02	0.04	0.62	3.89	4.93	0.01	0.46		604	2	208	112	88	3	58	6	9			63	26	
X-94	75.67	0.04	12.94	1.71		1.71	0.02	0.05	0.65	4.05	4.84	0.02	0.45		620	1	214	128	83	4	45	2	2			54	21	
X-95	69.75	0.51	12.55	5.77		5.77	0.08	0.11	2.30	2.55	6.29	0.09	1.38		243	81	68	474	24	-	-	-	1051			162	77	
Erongo Complex, Namibia																												
X-96	76.26	0.07	13.3	1.43		1.43	0.03	0.06	0.43	3.08	5.07	0.26	-		637	25	155	60	26	2	38		76					

The following diagrams illustrate the small range of variation for the major oxides, minor elements and some rare earths. When plotted on a logarithmic scale, values for major oxides and minor elements are comparable. These rocks, as seen, have striking similarities in their chemical character.

There might have been some reactivation of magmatism in the Nchanga Granite at the Nchanga mine after the emplacement of the Katangan sediments, and after copper-cobalt mineralization. The dikes L-168, L-170, L-172, and L-173 seem to be chemically related to the Nchanga Granite as shown on Table A.8. L-172 and L-173 have similar minor element chemistry to the Nchanga Granite chemistry, except that they contain high values of chrome and copper, lower Na_2O and higher K_2O. Sr and Rb are in the same ranges. Zn is lower, and Nb and Ce are slightly lower.

After taking a closer look at the Nchanga Granite, the following questions come to mind:
1) Are there many more Nchanga-like plutons under Katangan rocks in the Zambian Copperbelt?
2) Could the anorogenic ring complex of the Nchanga Granite may be in some way responsible for copper mineralization at the Nchanga mine?
3) Could an iron oxide-copper-gold mineral deposit have formed on the upper portion of the Nchanga Granite before erosion?
4) Could the copper in at least part of the Zambian Copperbelt have been produced by the event of emplacement of the Nchanga Granite and later eroded and re-mobilized to favorable stratigraphic-redox traps in the Katangan sediments?

Figure A26 shows an event diagram of the radiometric ages available from the Nchanga mine area.

4.1.5.2.10 Conclusions

1. The Nchanga Granite has all the characteristics of an anorogenic granite ring complex. It probably formed as a granite plug in an anorogenic ring complex cluster[2] that is not well exposed, and lies in the basement of the Zambian Copperbelt.

2. Chemistry of the Nchanga Granite crosses the fields of midalkaline to subalkaline rocks.

3. The pluton behaves as a coherent cluster in all geochemical diagrams.

4. The pluton, or parts of it, are high heat producing granites that probably maintained a long-lived circulation of hydrothermal fluids.

5. The Nchanga Granite might have contributed to the origin of copper in its environs.

[2] The term anorogenic ring complex cluster will be introduced in chapter 7.

4.1.5.3 Nchanga Mine Area

4.1.5.3.1 Introduction

Several dikes that evidently intersect the mineralized Katangan sedimentary sequence in the environs of the Nchanga mine were sampled in boreholes at the Nchanga mine core warehouse. The boreholes, samples collected and depths are listed on Table 4.1.5.7. Results of the chemical analysis are listed on Table 4.1.5.9. Interpretation of the major oxide chemistry and detailed geochemical parameters are listed on Table 4.1.5.8.

The rocks sampled were not fresh, but weathered and altered. In any case, the best rocks were chosen for zircon picking.

Table 4.1.5.7 Borehole samples collected in the environs of the Nchanga open pit mine, Zambia.
(underlined sample numbers indicate chemical analysis)

Sample	Borehole	depth (m)	Field description	R1R2 nomenclature	Shrimp II age (Ma)
L-167a	NOP-681	52.70	Weathered granitoid	Essexite	
L-168	NOP-681	33.00	Weathered granitoid	alkali granite	
L-169*	NOP-681	105.00	Weathered granitoid	alkali granite	765±3 emplacement age; 1860±10 inherited zircon
L-170	NOP-681	43.55	Weathered granitoid	Granite	
L-171	NOP-836	302.90	Basal polymictic sedimentary breccia	n.a.	
L-172	NOP-589	76.41	Granitoid dike	alkali granite	
L-173	NOP-589	74.28	Granitoid dike	alkali granite	
L-172c*	NOP-589	composite	composite of L-172 and L-173	alkali granite	765±3*[3] emplacement age

Table 4.1.5.8 Rock name and main geochemical parameters of samples from the Nchanga Mine
(See acronym description on section 2.4.3.)

Sample	Rock type	Debon & LeFort geochemical characteristics
L-150	Syeno-diorite dike	Peraluminous iii mesocratic K high Fe
L-167a	Syeno-diorite dike	Peraluminous ii mesocratic K high Fe+Mg
L-168*	Alkali granite	Peraluminous I leucocratic K Fe
L-170	Granite	Peraluminous I mesocratic K Mg
L-172*	Alkali granite	Peraluminous I leucocratic K Fe
L-173	Alkali granite	Peraluminous I leucocratic K Mg

Table 4.1.5.9 Chemical analysis from the Nchanga Mine environs

Sample	SiO2	TiO2	Al2O3	Fe2O3	MnO	MgO	CaO	Na2O	K2O	P2O5	LOI	Total	Rb	Sr	Y	Zr	Nb
Notch	50.00	1.00	15.50	6.00	0.150	2.00	5.00	4.90	5.50	0.30	2.00		200	400	60	360	40
L-150	51.05	2.91	15.47	10.19	0.00	10.09	0.68	1.69	6.12	0.36	1.16	99.72	361	24	45	150	28
L-167	47.14	0.78	19.71	6.10	0.08	12.98	0.00	0.00	8.70	0.08	4.00	99.57	255	64	101	781	147
L-168	79.68	0.15	10.06	0.72	0.02	0.10	0.02	0.19	7.61	0.08	0.59	99.22	132	125	19	258	11
L-170	70.45	0.86	15.35	3.22	0.03	1.50	0.01	0.02	5.02	0.13	3.05	99.64	110	46	42	320	79
L-172	74.42	0.06	13.07	1.32	0.04	0.21	0.14	1.85	7.48	0.06	0.71	99.36	316	32	49	113	85
L-173	74.69	0.09	12.55	1.37	0.03	0.28	0.14	1.87	7.51	0.05	0.78	99.36	314	29	78	172	128

Sample	Co	Ni	Cu	Zn	Ga	V	Cr	Ba	U	Th	Sc	Sm	Nd	Pr	Ce	La	Ta	Eu	Gd	Yb	Lu
Notch	30	16	25	85	26	100	100	1300	20	37	20	50	50	15	175	95	120	4	30	7.5	1.6
L-150	851	191	623	66	24	424	94	349	6	<15	29	13	13	55	18	7	221			0.263	1.250
L-167	266	57	1896	65	28	95	74	615	12	37	12				43	13					
L-168	32	<6	261	10	<9	16	59	1190	<6	<15	<10			10	61	1				0.175	0.48
L-170	131	14	1954	25	29	92	335	766	10	<15	11	6	26	30	44	21	46	0.188	1.963	1.413	0.888
L-173	11	6	232	20	22	<12	453	598	7	58	<10				85	49					

Sample	Co	Ni	Cu	Zn	Ga	V	Cr	Ba	U	Th	Sc	Pb	Sm	Nd	Pr	Ce	La	Cs	Hf	Ta	Eu	Gd	Tb	Dy	Ho	Er	Tm	Yb	Lu
Notch	30	16	25	85	26	100	100	1300	20	37	20	20	50	50	15	175	95	3	10	120	4	30	5	20	3	9	36	8	2
L-172	9	8	242	23	21	<12	618	668	5	48	<10	27	9	41	11	79	50	1	5	3	0	7	1	10	2	7	1	7	1

As seen on Table 4.1.5.9, most of the samples have high potassium values, and all of them contain anomalous copper. That could have been brought recently, as impregnations in microfractures due to migration of copper-saturated fluids. Cobalt values may have been increased in a similar way.

[3] Radiometric age data marked with an asterisk has not been completely determined. These should be considered preliminary data obtained by the U-Pb SHRIMP system on zircons. Most of this work was done at the ANU in Canberra.

L-170, L-172 and L-173 contain high chromium.
L-172 and L-173 have almost identical values for all elements. Their macroscopic features were also similar.
L-167 and L-170 have high values for losses on ignition.
Three samples contain enough thorium to make them high heat producing granites: L-167, L-173 and L-172.

4.1.5.3.2 Comparison of Gabbroid Rocks

L-167a and **L-150** are both syeno-diorites and they seem to be similar to alkaline mafic rocks **L-161** and **L-163** from the Konkola deep borehole described under the Muliashi Porphyry section (4.1.5.4).

Both groups of mafic rocks were emplaced in extensional environments. Thus both the Muliashi Porphyry around Konkola and the Katangan rocks in the environs of the Nchanga mine were intruded by rocks of similar compostion. Maybe the chemical similarities of these rocks are mere coincidence and they were emplaced at different times. Maybe they are all from the same event of mafic dikes. That is not completely well understood yet, and only **L-150** was observed in the field. If the rocks happened to have been emplaced during the same event, then there would be several coincidences between the Nchanga and Konkola areas: the mafic rocks and the Nchanga-like granites.

All four samples (L-150, L-161, L-163, L-167a) have high alumina values
L-150, L-161 and L-163 hive high Co, Ni, V, Ti and contain Na and Ca.
L-167a has high Y, Zr, Nb, Ca, Cu, Th, K. No Ca or Na.
L-150, L-161 and L-167a have high K
L-150 has high Cu
L-161 and L-163 have low Cu
L-150, L-161 high Rb/Sr
L-163 low Rb/Sr high Mn, low K

4.1.5.3.3 Nchanga Lamprophyre Dike

One of the main structures of the Nchanga open pit is the so-called “lamprophyre dike”. It outcrops on the southern wall of the pit, and has been reasonably well documented in the literature (Figs 4.1.5.6, 4.1.5.13, 4.1.5.7, 4.1.5.8). According to the mine geolosits, it normally contains 3-7% Cu, higher grade than most of the orebody. A well-located sample of the dike was collected, its coordinates are listed in the Appendix.

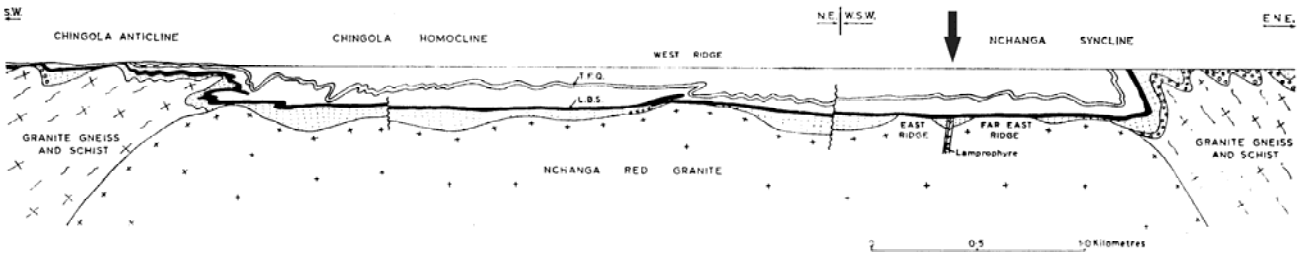

Fig 4.1.5.13 WSW-ENE Schematic geological cross section throgh the Nchanga Granite along the Nchanga mine, Zambia*. Note the folds of Katangan sediments over the Nchanga pluton, the normal faults, and the irregular paleotopography of the granitoid surface. Sedimentary beds were strongly folded around the pluton. The “lamprophyre” dike is illustrated to the right of the image. Taken from Garlick, 1973.*

L-150 is an extremely fresh, highly micaceous, 5-15 m wide, peraluminous potassic ferriferous syenodiorite dike with very slight foliation. It does not show alteration like the surrounding rocks. As observed on the pit face, it was intruded into highly sheared rocks with abundant hydrothermalism, along a pre-existing shear zone. The Katangan sediments that overlie the Nchanga Granite display major drag folds towards the shear zone. This was seen on outcrop and is shown on the various maps and cross sections (Figs 4.1.5.6, 4.1.5.13, 4.1.5.7, 4.1.5.8). Abundant thin hydrothermal quartz veins cut the nearby mineralized Katangan host rocks, but the gabbro is not altered or cut by any significant quartz veins. The contact of **L-150** with the Nchanga Granite is chilled; it has quartz recrystallization and a halo of contact alteration. The dike does not seem to have been subject to shearing or hydrothermal alteration, nor seems to have been subject to major fluid flow. The mafic dike is full of secondary Cu minerals that impregnate both matrix and surfaces.

4.1.5.3.4 Samples with Special Character

L-168, **L-172** and **L-173** are a completely independent group of rocks; different from the Muliashi Porphyry and the Nchanga Granite. They follow a leucocratic trend on the KB diagram, and it is not related to neither of the trends of the Nchanga Granite or the Muliashi Porphyry. It simply runs parallel. The **L-168**, **L-172**, **L-173** trend on the MgB diagram seems to run along the critical or common Mg-Fe line of Debon & LeFort.

4.1.5.3.5 Geochronology

Two intrusive rocks that intersect Katangan sediments under the Nchanga open pit were dated by the SHRIMP II method at approximately 765 Ma. These are **L-169** and **L-172c**. Details of the sampling sites and sample numbers are listed on Table 4.1.5.7. An inherited zircon in **L-169** gave and age of 1860±10Ma. **L-169** is very similar to sample **L-168**.

In principle, the SHRIMP ages of **L-172c** and **L-169** are within error of each other. They define an intrusive event, or at least one of the last intrusive events in the environs of the Nchanga copper mine. The new ages are very significant, because they provide the oldest age of deposition for the Katanga sedimentary sequence at Nchanga. That is a significant bracket for the deposition and mineralization.

If funds become available, the lamprophyre of **L-150** should be dated. It could provide another age constrain for copper mineralization at Nchanga.

Below is a list of the new radiometric SHRIMP zircon U-Pb ages obtained in the northern portion of the Copperbelt. These all plotted in the event diagram of Figs A29 and A27.

Table 4.1.5.10 New SHRIMP U-Pb ages from the Copperbelt area, Zambia

Number	Field description of sample	Age (Ma)
L-172c	Alkali granite dike in a borehole	765±3*[4]
L-169	Alkali granite dike in a borehole	765±3*
L-169	Dike in a borehole, inherited zircon	1860±10
L-075	Rapakivi granite from the Muliashi Porphyry	1865±5.4
L-160	Undeformed light gray granitoid from the Muliashi Porphyry in the Konkola deep borehole	1866±5.4
L-158	Foliated pink granitoid from the Muliashi Porphyry in the Konkola deep borehole	1874±14

4.1.5.3.6 Conclusions

Mafic rocks studied in the Nchanga mine area were emplaced in anorogenic extensional environments.

Alkali granite dikes studied do not seem to be directly related to the Nchanga Granite. They formed in an extensional, anorogenic environment.

New radiometric ages of the felsic, midalkaline dikes (~765 Ma) provide an oldest age of deposition for the Katanga sedimentary sequence at Nchanga. That also provides a significant bracket age for mineralization.

[4] Radiometric age data marked with an asterisk has not been completely determined. These should be considered preliminary data obtained by the U-Pb SHRIMP system on zircons. Most of this work was done at the ANU in Canberra.

4.1.5.4 Muliashi Porphyry

4.1.5.4.1 Introduction

Muliashi Porphyry is the name given to some of the coarse-grained to porphyritic granitoids that make the basement to the Katanga sedimentary rocks throughout most of the Copperbelt area. In some publications this body is refered to as the “gray granite”. The rock is often a pink granite, due to minor natural variations in chemical composition and overprinted potassic alteration. Sometimes the granites vary into gneisses; and they often have sub-spherical 1.5 to 6 cm diameter feldspar porphyroblasts that grew over a previous foliated texture with abundant biotite. Major oxide chemical analysis of these rocks were provided by Mendelsohn, 1961 and are listed on Tables 4.1.5.24 and 4.1.5.11.

This body of granites is widely spread in the basement to the Copperbelt. Similar gray and gray-pink granitoids are observed as basement around Konkola (old Bancroft area), Chambishi, Mufulira, Nkana and around the Roan Antelope mine. Chemistry from the various sites indicates a large similarity between them. This sub-chapter will review the main observations and findings from geochemical studies and geochronology in those rocks.

Table 4.1.5.11 Chemical analysis of samples from the Muliashi Porphyry, Basement to the Copperbelt, Zambia

Sample	SiO2	TiO2	Al2O3	Fe2O3	FeO	MnO	MgO	CaO	Na2O	K2O	P2O5	LOI	Total	Rb	Sr	Y	Zr	Nb	Co	Ni	Cu
Notch	50.00	1.00	15.50	6.00		0.15	2.00	5.00	4.90	5.50	0.30	2.00		200	400	60	360	40	30	16	25
L-075	65.53	0.91	13.91	5.81	0.00	0.07	1.46	2.59	3.43	5.10	0.23	1.14	100.18	162	217	33	50	17	0	0	0
L-076	65.53	0.91	13.91	5.81	0.00	0.07	1.46	2.59	3.43	5.10	0.23	1.14	100.18	182	212	48	361	26	22	16	105
L-077	66.70	0.79	14.45	4.66	0.00	0.06	1.36	2.66	3.78	5.06	0.21	0.77	100.50	174	216	39	290	22	14	11	28
L-078	67.56	0.89	13.59	5.37	0.00	0.07	1.27	3.08	3.93	3.78	0.23	0.81	100.58	143	235	47	343	25	19	13	31
L-157	75.81	0.19	12.48	1.25	0.00	0.00	1.16	0.18	0.19	6.95	0.03	1.39	99.63	225	12	12	107	17	26	8	7
L-158	73.58	0.20	12.85	1.36	0.00	0.00	1.46	0.93	0.33	7.11	0.04	2.00	99.87	233	19	13	109	16	32	7	<6
L-159	68.02	0.64	14.23	2.82	0.00	0.00	1.74	1.42	0.95	6.80	0.16	2.10	98.87	303	47	34	209	28	38	7	<6
L-160	67.96	0.55	14.78	2.29	0.00	0.00	1.47	1.67	2.46	5.69	0.16	2.10	99.14	264	40	49	223	32	39	9	<6
X-01	73.81	0.08	12.29	0.37	1.52	0.04	0.70	2.24	4.21	4.83	0.04	0.66	100.79								
X-02	72.56	0.23	14.28	0.94	0.68	0.02	0.83	0.76	2.88	6.12	0.05	1.96	101.31								
X-03	70.95	0.42	15.07	1.13	1.29	0.03	1.32	0.83	4.23	3.03	0.11	2.60	101.01								
X-04	75.20	0.33	10.10	1.55	1.69	0.04	2.81	2.08	2.02	2.13	0.34	2.36	100.65								
X-05	65.27	0.84	15.18	3.20	1.94	0.08	1.01	2.90	3.00	4.70	0.31	1.39	99.82								

Sample	Zn	Ga	V	Cr	Ba	U	Th	Sc	Pb	Sm	Nd	Pr	Ce	La	Cs	Hf	Ta	Eu	Gd	Tb	Dy	Ho	Er	Tm	Yb	Lu
Notch	85	26	100	100	1300	20	37	20	20	50	50	15	175	95	3	10	120	4	30	5	20	3	9	35.5	7.5	1.6
L-075	0	16	0	0	1339	<6	16	<10	21	9	53	13	160	61	2	1	1	1.9	7.8	1.1	6.7	1.3	3.5	0.5	3.2	0.5
L-076	35	17	82	56	1344	<6	17	10					137	61												
L-077	46	18	59	41	1391	<6	14	<10		11	35	86	119	41			75	1.1							1.2	1.1
L-078	48	17	74	51	964	<6	18	10					131	61												
L-157	14	14	20	15	618	<6	18	<10					43	17												
L-158	13	14	20	14	628	6	26	<10		108	26	63	76	31		2	8	0.5								0.6
L-159	19	17	57	18	919	11	24	10					118	60												
L-160	18	16	47	16	805	<6	15	13		118	42	102	156	49			28	1.1							2.8	1.0

4.1.5.4.2 Sampling and composition of samples

Four samples were collected from an outcrop along the Muliashi river. Five analysis were compiled from the literature. Additional samples from the Konkola deep borehole, the Chambishi area and the Samba copper deposit serve to complete the suite. These will be discussed independently in later chapters.

Table 4.1.5.13 indicates that 62.5% of the samples available from the Muliashi Porphyry are subalkaline while the rest are midalkaline rocks. Most of the samples are granites and granodiorites. This includes rocks from the Samba deposit.

Table 4.1.5.13 Statistics of rock types, Muliashi Porphyry, Zambia
The fifth column (granitoids) is the sum of underlined rock types.

Group	Rock type	Number	%	Granitoids	Groups
Midalkaline Rocks	Alkali granite	2	12.50	37.50	37.50
	Quartzmonzonite	4	25.00		
Subalkaline Rocks	Granite	5	31.25	62.50	62.50
	Granodiorite	5	31.25		
Total		16	100.00	100.00	100.00

Table 4.1.5.12 Chemical characteristics and environment of emplacement for Muliashi Porphyry samples, Zambia (See acronym description on section 2.4.3.)

Sample	Rock type	Debon & LeFort	Maniar & Picc	Whalen	Pearce	Rb/10HfTa	Rb/30HfTa	Nb-Ta
L-075*	Quartzmonzonite	Metaluminous iv mesocratic Na-K Fe	?	N	S2/4 O2/4	VA	II	INV
L-076	Quartzmonzonite	Metaluminous iv mesocratic Na-K Fe	?	A	O-W1-1			
L-077	Quartzmonzonite	Metaluminous iv mesocratic Na-K Fe	?	A	O3/4			OUTU
L-078	Granodiorite	Metaluminous iv mesocratic Na Fe	?	A	O-W1-1			
L-157	Granite	Peraluminous i subleucocratic K Fe	?	A				
L-158*	Granite	Peraluminous ii mesocratic K low Fe Mg		N	O2/3	WP-	II	OUTU
L-159	Granod-granite	Peraluminous i mesocratic K Mg	?	A	O-W1-1			
L-160*	Granite	Peraluminous ii mesocratic K Mg	?	A	O3/4			OUTU
L-161	Syeno-diorite dike	Peraluminous ii mesocratic K high Fe Mg	?	A	O-W1-1	Wpab-wpt		
L-163	Syeno-gabbro dike	Peraluminous i mesocratic K high Fe	?	N		Emor		
X-01	Granite	Metaluminous iv subleucocratic Na Mg	iag-cag					
X-02	Granite	Peraluminous ii subleucocratic K Mg	iag-cag,ccg					
X-03	Granite	Peraluminous ii mesocratic Na Mg	Ccg					
X-04	Altered granodiorite	Peraluminous ii mesocratic Na Mg	?					
X-05	Granodiorite	Metaluminous iv mesocratic K Fe	RRG					

The suite from the Muliashi Porphyry crosses the fields of alkaline to non-alkaline rocks. That happens especially on the TAS diagram

4.1.5.4.3 Description of samples

A well exposed outcrop of the Muliashi Porphyry was studied near the Muliashi river. Fig 4.1.5.14 illustrates main relationships of intrusive rocks at the site. Coordinates of the samples collected are presented in the Appendix A16. Figs 4.1.5.13 are slabbed surfaces of the samples. Large samples were collected at this site and analysed in detail. The results are listed on Table 4.1.5.14. The rocks are metaluminous mesocratic sodic to potassic ferriferous biotite quartzmonzonites. Although the samples were collected from the freshest possible rocks, geochemistry shows that they have been subject to weathering.

There is blue, opalescent quartz and biotite in the slightly-foliated matrix. Many very fine-grained, white to light gray aplite dikes cut the rock. Mafic, preferentially-oriented, spindle shape xenoliths with reaction rims and lesser development of plagioclase orbicles occur throughout. There are many pink potassic feldspar porphyroblasts that enclose mafic minerals and seem to grow over the previously-foliated matrix. Mafic minerals remain as witness of previous texture. **L-075** comes from the freshest rock possible. Plagioclase orbicles are concentrically zoned: the outer rim is white, then light green-gray, later pink, and in the core, white or gray. Outer rims weather more readily. Coloration reflects the varying composition of the feldspar. Such spheres are more resistant to weathering and produce a grape-like surface texture made by spheres of different sizes (Figs 4.1.5.14 and 4.1.5.15). All samples are anorogenic granitoids.

4.1.5.4.4 Geochronology

Zircons from sample **L-075** were dated by SHRIMP II U/Pb methods to obtain an age of 1864.9±5.4 Ma.

4.1.5.4.5 Discussion on the Muliashi Porphyry and its Correlatives

Several of the rocks from the Muliashi Porphyry contain significant copper, even when they are distant from the coppper mines. That might be due to an original hypogene high copper content, to contamination by groundwater, or to a combination of both.

Most of the samples are mesocratic.

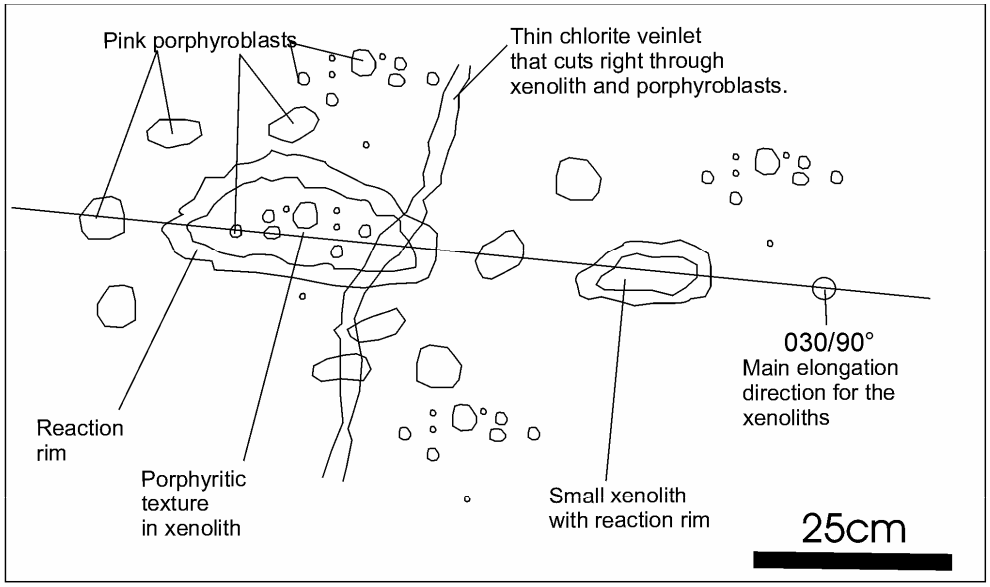

Xenolith with darker, finer-grained reaction rim around it, and corroded, round shape. Its composition is more mafic than that of the porphyry.

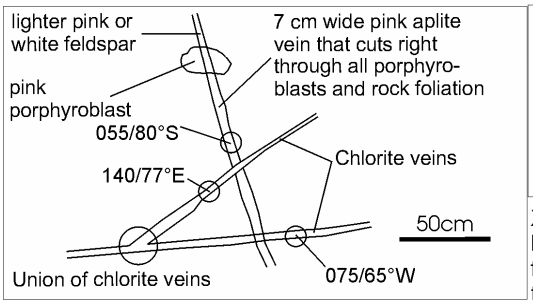

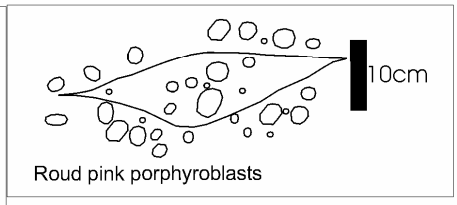

Xenolith with elongated shape and less orbicles than the surrounding rock, in a gray, fine-grained matrix. This is quite common in the Muliashi Porphyry.

Fig 4.1.5.14 Main features of the Muliashi Porphyry as observed on outcrops. Photographs of the same.

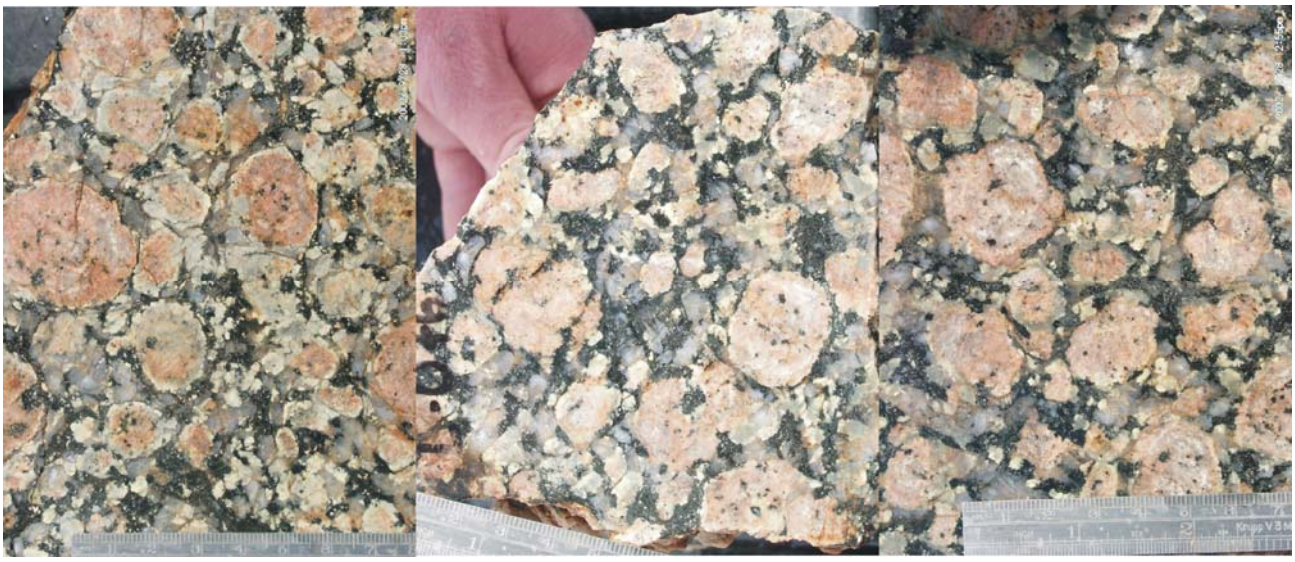

Fig 4.1.5.13 Photographs of slabs from the Muliashi Porphyry, basement to the Copperbelt, Zambia. *Samples L-075 and L-076. Note the overgrowth of spherical potasium feldspar porphyroblasts. There was a previous medium-grained igneous texture that was overprinted by the macrocrysts. Most of the matrix is made of biotite. See description in text. Scales in centimeters and inches.*

The Muliashi Porphyry plots as a distinct trend on the R1R2, TAS, AB, QP, KB, MgB and QB diagrams. On the TAS diagram, the Muliashi Porphyry trend extends well into the field of monzonites (**X-07**) along the limit between granite and granodiorite, as illustrated (Fig 4.1.5.1 and 4.1.5.2). Some samples like **X-04** (Nkana) and **X-09** (Chambishi) seem to be regionally altered versions of the Muliashi Porphyry. Samples from the Mufulira granite (**X-41** and **L-166**) follow the general trend of the Muliashi Porphyry. Three samples **X-38**, **L-273** and **L-279**) seem to be a special variation of the Muliashi Porphyry. Maybe they were produced by a particular type of magma mixing or enrichment in biotite by country-rock assymilation.

L-268 and **L-269** from the Samba copper prospect seem to lie along the Muliashi Porphyry trend on the AB diagram of Debon & LeFort. **L-273** and **L-279** lie on that trend on the MgB diagram. **L-268**, **L-273** and **L-279** (and **L-269**?) lie on the Muliashi Porphyry line on the KB diagram. The QP diagram does not show any reasonable correlation between the two groups of samples. On the QB diagram, **L-273**, **L-279**, **L-268** and **L-269** seem to run along the same general trend as the Muliashi Porphyry. On the R1R2 diagram, **L-268** lies just in the middle of the Muliashi trend. **L-279** and **L-273**, as well as **L-269** are off the main trend. The TAS diagram shows no direct correlation with the Muliashi trend, unless we connect it with the Chambishi samples (**L-155** and Chambishi Gray). In that case, there is a long, winding trend of samples that connects the Muliashi to the Chambishi and then to the Samba samples. On the MgB diagram, the Samba trend continues along the trend of the Muliashi Porphyry. In conclusion, there are clear trends that continue the Muliashi line on the MgB diagram, the KB diagram, the AB diagram, partially on the R1R2 diagram and not at all on the QP diagram. Samples from the Samba deposit plot on the main Muliashi Porphyry trend.

Mafic rocks that intersect the basement to the Copperbelt were emplaced after the Katangan sediments were consolidated, and in some cases after the copper-cobalt mineralization took place. The chemistry of dikes that intersect the Katangan rocks varies widely from midalkaline felsic to gabbroid.

Although the various methods to evaluate environment of emplacement for Muliashi Porphyry granitoids did not produce coherent results, the majority of those samples have an anorogenic origin, according to the method of Whalen et al, 1987 (Table 4.1.5.12). There is no evidence that indicates the plutonic and volcanic rocks in the suite formed in a magmatic arc, as Master et al, 2003 indicate. The information available does not support a subductional origin for the Muliashi Porphyry. Further work will be carried out to define the environment of emplacement of these rocks using artificial intelligence and a large geochemical database, as indicated on section 2.4.1.7.

4.1.5.5 Deep Borehole, Konkola Mine

The deep operations of the Konkola deposit certainly are one of the largest un-developed copper resources of Zambia. Konkola is located on Fig 4.1.5.16, on the eastern limb of the Konkola dome. The deposit is shared with the Democratic Republic of Congo and the Congolese portion is called Musoshi, as shown on Fig 4.1.5.16. Feasibility studies for the project indicate that major capital investment is required and the Zambian government is not prepared to go ahead on it without private capital. Several multinational corporations have evaluated the project.

ZCCM, the Zambian entity that managed most of that nation's copper deposits for the last twenty years, drilled a deep borehole to study geological and geotechnical features of the rocks in order to plan and build a new deep shaft to exploit copper resources around the so-called Konkola Deep area. Significant portions of that borehole were exposed by ZCCM geologists for logging and sampling. The borehole log, as described by ZCCM geologists, is synthesized on Table 4.1.5.16 and Fig 4.1.5.17. L-157 to L-163 were collected from the deep borehole. Table 4.1.5.15 shows main data from the samples, including depth of collection, temporary unit names for interpretation and SHRIMP ages. Chemical analysis from samples are listed on Table 4.1.5.14. Samples collected are described below.

Table 4.1.5.14 Chemical Analysis of samples from the deep borehole, Konkola mine, Zambia
(Complete elemental analysis on Table A8.2, Appendix)

Sample	*SiO2*	*TiO2*	*Al2O3*	*FeOt*	*MnO*	*MgO*	*CaO*	*Na2O*	*K2O*	*P2O5*	*LOI*	*Total*
Notch	50.00	1.00	15.50	6.00	0.15	2.00	5.00	4.90	5.50	0.30	2.00	
L-157	75.81	0.19	12.48	1.25	0.00	1.16	0.18	0.19	6.95	0.03	1.39	99.63
L-158	73.58	0.20	12.85	1.36	0.00	1.46	0.93	0.33	7.11	0.04	2.00	99.87
L-159	68.02	0.64	14.23	2.82	0.00	1.74	1.42	0.95	6.80	0.16	2.10	98.87
L-160	67.96	0.55	14.78	2.29	0.00	1.47	1.67	2.46	5.69	0.16	2.10	99.14
L-162	76.11	0.19	12.33	1.25	0.00	0.28	0.70	3.48	4.92	0.03	0.59	99.88

Sample	*Rb*	*Sr*	*Y*	*Zr*	*Nb*	*Co*	*Ni*	*Cu*	*Zn*	*Ga*	*V*	*Cr*	*Ba*	*U*	*Th*	*Sc*	*Sm*	*Nd*	*Pr*	*Ce*	*La*	*Hf*	*Ta*	*Eu*	*Gd*	*Yb*	*Lu*
Notch	200	400	60	360	40	30	16	25	85	26	100	100	1300	20	37	20	50	50	15	175	95	10	120	4.0	30	7.5	1.6
L-157	225	12	12	107	17	26	8	7	14	14	20	15	618	<6	18	<10				43	17						
L-158	233	19	13	109	16	32	7	<6	13	14	20	14	628	6	26	<10	108	26	63	76	31	2	8	0.5			0.6
L-159	303	47	34	209	28	38	7	<6	19	17	57	18	919	11	24	10				118	60						
L-160	264	40	49	223	32	39	9	<6	18	16	47	16	805	<6	15	13	118	42	102	156	49		28	1.1		2.8	1.0
L-162	119	155	14	96	10	6	<6	7	22	13	17	15	793	<6	<15					82	37						

Table 4.1.5.15 Data from borehole samples, Konkola Deep borehole, Zambia

Sample	Age (Ma)	Depth (m)	Field description	Lithology	Notes	Unit for interpretation
L-157		44.10	Medium gray granitoid	Granite	Similar to L-158, intrudes Unit A	C
L-158	1874±14	45.86	Medium gray granitoid	Granite	Similar to L-157	C
L-159		123.02	Pink coarse-grained foliated granitoid	Granite-granodiorite	Abundant biotite, strong foliation	A
L-160	1866±5.4	127.44	Pink coarse-grained foliated granitoid	Granite	Strong foliation. Overprinted by large, round K feldspar porphyroblasts and abundant biotite. Similar to L-075, L-076 and L-155 (Muliashi Porphyry).	A
L-161		776.62	Foliated fine-grained gabbroid	Syenodiorite	Foliated, fine-grained mass with large white plagioclase augen. Some with rotation; serpentinized.	D
L-162		889.50	Light gray coarse-grained granitoid	Coarse-granied granite	Coarse-grained, unfoliated, with minor biotite, mafics are mainly amphybole.	B
L-163		812.08	Gabbroid	Syeno-gabbro	Very fine-grained, foliated, serpentinized gabbroid.	E

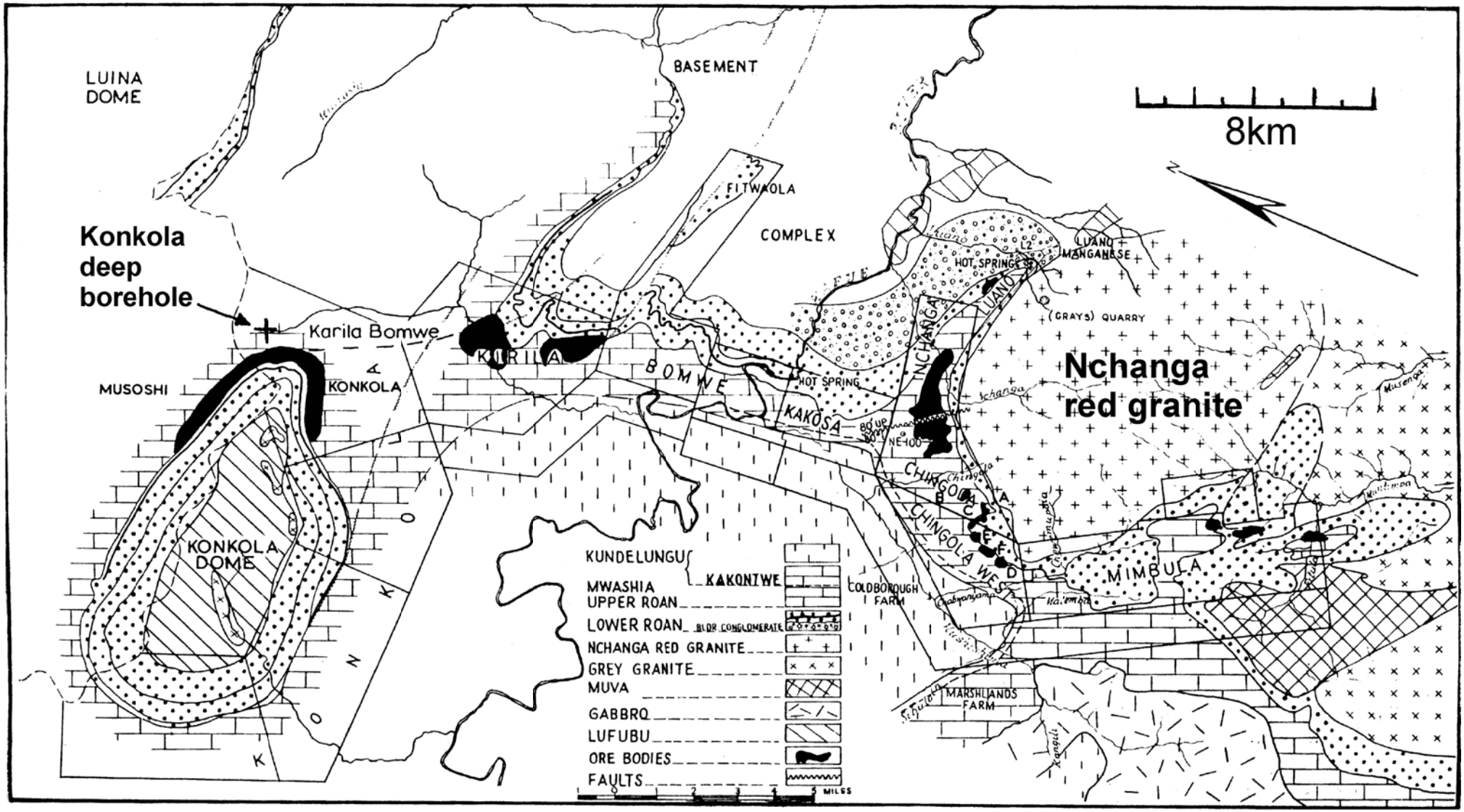

Fig 4.1.5.14 Surface geological map of the Konkola Dome and Nchanga Area, Zambia. *Note the mineralized rocks marked in black. The Konkola deep borehole was designed to exploit the lower portion of the rich Konkola orebody. Approximate location of the borehole is marked on the figure. The limit between the D.R. Congo and Zambia crosses through the Konkola Dome, as shown. The Congolese portion of the deposit is called Musoshi. A large portion of the Nchanga Granite is also drawn on the map. Taken from Fleischer, Garlick & Haldane, 1976.*

Table 4.1.5.16 Simplified log of exploratory Konkola Deep Borehole, Zambia

From	To	Lithology	Thickness	Unit	Samples
0.00	40.30	Conglomerate and conglomeratic sandstone.	40.30		
40.30	65.70	Grey coarse-grained quartz porphyry in a biotite groundmass.	25.40	C	L-157, L-158
65.70	80.70	Dark gray foliated quartz feldspar granitic porphyry.	15.00		
80.70	112.20	Light gray to pink quartz porphyry with pink calcite veinlets and straining in the feldspars.	31.50		
112.20	205.70	Pink to gray porphyroblastic augen gneiss of pink feldspar 5 cm in diameter.	93.50		
205.70	320.80	Pink to gray quartz feldspar foliated gneiss.	115.10	A	L-159, L-160
320.80	506.60	Dark gray porphyritic, foliated quartz feldspar micaceous gneiss.	185.80		
506.60	584.50	Pink to gray biotite porphoroblastic gneiss in dark biotite groundmass.	77.90		
584.50	667.70	Dark gray porphyroblastic biotite-felspar-quartz gneiss.	83.20		
667.70	785.60	Black to dark gray porphyroblastic biotite schist.	117.90	D	L-161
785.60	815.35	Black biotite-rich schist.	29.75	E	L-163
815.35	820.35	Pink to dark gray porphyrytic foliated feldspar-quartz-biotite gneiss	5.00		
820.35	900.00	Gray to pink coarse-grained granite with potassium feldspar	79.65	B	L-162

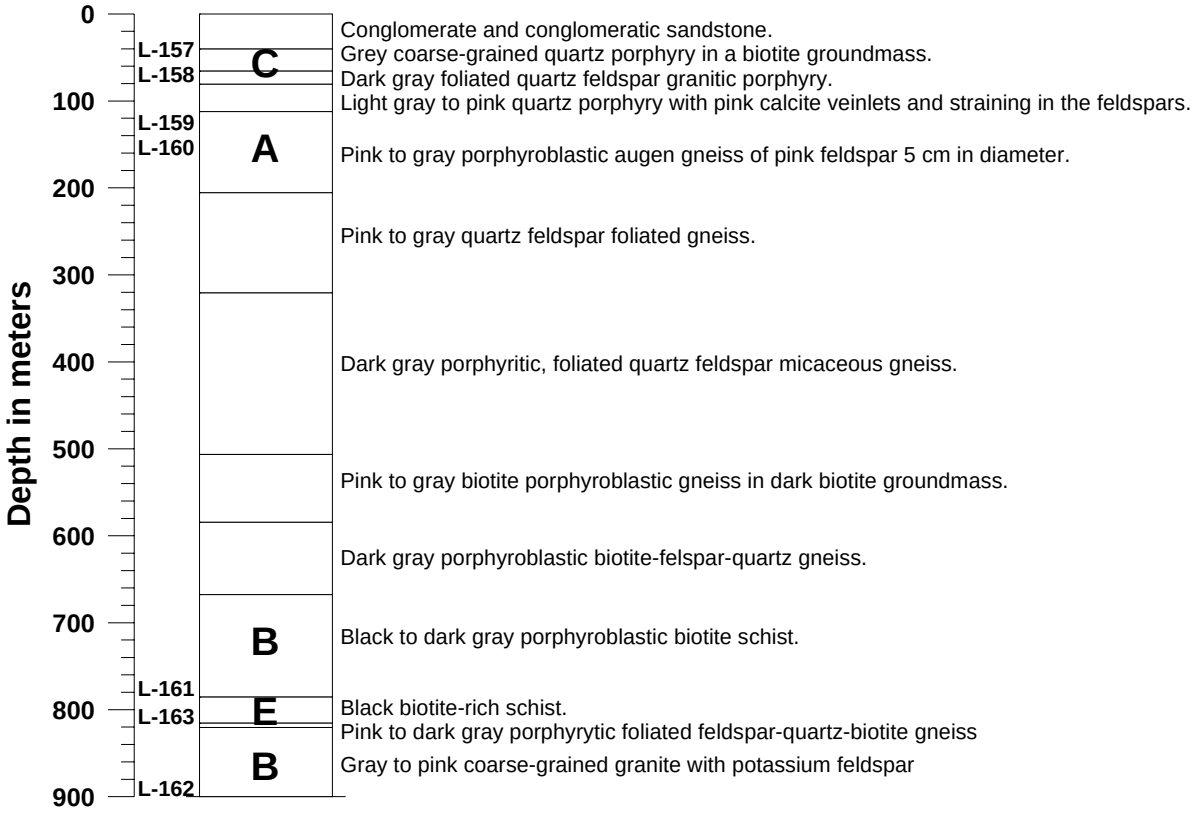

Fig 4.1.5.17 Stratigraphic column of exploratory Konkola Deep Borehole, Zambia

L-157 and **L-158** were collected from a gray porphyritic granite *sensu stricto*, at the depths shown on Table 4.1.5.15 and make Unit C. Both are enriched in K, Rb and Co. Maybe that was due to alteration by fluids related to nearby Cu-Co mineralization.

L-162 sampled a light gray to white granite and makes Unit B. This sample is not enriched in K, Rb and Co. It has remarkably similar major oxide chemistry to the rocks sampled at the inselberg of the Nchanga Granite.

L-159 and **L-160** come from a pink, coarse-grained porphyritic gneissose granite, with abundant quartz veining, fracturing and foliation; they make Unit A. Anomalous K_2O, Rb, Co, Sm and Pr are the same as in samples **L-158**, **L-159** and **L-160**.

L-161 is a syenodiorite porphyry that makes Unit D. Its major oxide composition is remarkably similar to that of **L-150** from the mafic dike at the Nchanga mine. They both probably had a similar origin and could be from the same geological event. **L-161** seems to have formed in an extensive anorogenic within-plate environment and probably **L-150** did too.

L-163 is a peraluminous potassic ferriferous syeno-gabbro dike and makes Unit E. Most samples from that rock type were extremely foliated into a schistose, talcous rock, probably serpentinized. Cobalt, chrome, vanadium and nickel contents are high, as would be expected of a mafic rock. It was probably emplaced in an extensive anorogenic within-plate environment.

Units A and C are chemically distinct. Unit A contains high Ca, Al, Ce, Ba and Sr, while C has low Ca, Al, Ce, Sr and Ba.

Copper is surprisingly low in units B and C. They were assembled before the copper enrichment process took place, and were kept away from it. This amalgamation of both units has very little evidence of quartz veining and deformation.

In principle, relationships observed in the core showed that there were three generations of granitoids. One was more foliated than the other, and a series of mafic intrusives were significantly more deformed and sheared to conform schistose texture of mylonites. The following structural relationships were observed at the hole: C intrudes A. B intrudes A and C. D and E intrude B, A and C. A tentative geological history is listed on Table 4.1.5.17.

Table 4.1.5.17 Geological history interpreted from the Konkola deep borehole, Zambia

Order	Event
1	Pink granitoid of Unit A was intruded.
2	Pink granitoid of Unit A was deformed and its porphyroblasts grew.
3	Pink granitoid was intruded by medium gray granitoid (Unit C).
4	1000 milllion years later, a white, coarse-grained Nchanga Granite-like pluton (Unit B) intruded into the pink (A) and gray (C) granitoids.
5	Gabbroic dikes (Units D and E) intruded the older rocks.
6	Deformation of the entire suite took place; mafic dikes were serpentinized and sheared, granitoid rocks suffered less deformation.

Conclusions

Geochemical and geochronological data from the Konkola deep borehole helped to deduce the geological history in the environs of Konkola. There might be an anorogenic granitoid intrusion similar to the Nchanga Granite in the area.

It might happen that correlation of **L-162** with rocks from the Nchanga Granite is wrong. **L-162** should be dated and further evaluated. The possibility of other Nchanga Granite-like bodies in the basement to the Copperbelt is very relevant and should be investigated.

4.1.5.6 Chambishi Granite

4.1.5.6.1 Introduction

The Chambishi copper mine is located near Kitwe, Zambia, as shown on Figs M17 and 4.1.5.18. It is the northernmost copper mineralization of a series of deposits in the Chambishi-Nkana basin. Katangan siliciclastics and carbonates unconformably overlie basement granitoids. Gabbroids that intrude the Katangan metasediments are an important lithology in the basin. A single sample (**L-155**) was collected from the granite that outcrops as basement on the Chambishi open pit (Fig 4.1.5.18). Seven chemical analysis of various rocks from the environs of the mine were also compiled for this project, labeled with the prefix X, and are listed on Table 4.1.5.18.

Table 4.1.5.18 Chemical analysis of samples from the Chambishi copper mine environs, Zambia
(complete elemental analysis on Table A8.2, Appendix)

Sample	Original #	SiO2	TiO2	Al2O3	Fe2O3	FeO	MnO	MgO	CaO	Na2O	K2O	P2O5	LOI	Total	Na+K
Notch		50.00	1.00	15.50	6.00		0.150	2.00	5.00	4.90	5.50	0.30	2.00		
L-155	L-155	72.00	0.28	12.99	2.57	0.00	0.00	1.51	0.95	1.03	6.03	0.09	1.71	99.17	7.06
X-42	Chambishi Gray	68.64	0.3	13.95	1.14	1.25	0.06	2.29	2.25	2.13	4.04	0.11	3.54	99.7	6.17
X-06	Chambishi amphibolite 51	46.85		15.87	3.33	7.40	0.11	8.61	7.29	3.65	2.50	0.15	3.06	98.82	6.15
X-07	Chambishi transition amphibolitic granophyre 52	58.63		13.08	6.07	6.68	0.15	1.87	4.70	5.50	0.66	0.32	1.66	99.32	6.16
X-08	Chambishi granophyre 53	67.94		12.08	7.23	1.01	0.04	0.60	1.65	6.70	0.20	0.07	1.70	99.22	6.90
X-09	Chambishi granophyre 54	59.26		16.65	1.26	0.43	0.06	2.04	4.59	9.80	0.20	0.65	4.48	99.42	10.00
X-10	Chambishi amphibolite 55	47.87		14.53	4.50	9.05	0.15	6.13	6.12	2.95	1.55	0.37	7.22	100.44	4.50
X-11	Chambishi amphibolite 56	48.19		14.53	4.13	7.18	0.12	6.66	9.00	4.25	1.40	0.17	3.60	99.23	5.65

Sample	Rb	Sr	Y	Zr	Nb	Co	Ni	Cu	Zn	Ga	V	Cr	Ba	U	Th	Sc	Sm	Nd	Pr	Ce	La	Ta	Eu	Yb	Lu
Notch	200	400	60	360	40	30	16	25	85	26	100	100	1300	20	37	20	50	50	15	175	95	120	4	7.5	1.6
L-155	219	62	20	99	13.0	61	12	<6	26	15	44	21	848	<6	<15	<10	109.6	25.34	56.81	69	23	36.41	0.5	0.2	0.713

4.1.5.6.2 Geochemistry

Although eight samples might not be representative, Table 4.1.5.19 shows statistics of their alkalinity discrimination. 80% of the granitoids from the Chambishi mine area fall within the subalkaline field, the rest in the midalkaline field. 62.5% of the samples available from the Chambishi granite are subalkaline, the rest are midalkaline.

Table 4.1.5.19 Statistics of rock types, Chambishi granite, Zambia
The fifth column (granitoids) is the sum of underlined rock types.

Midalkaline Rocks	alkali granite	1	12.50	20.00	37.50
	monzogabbro	1	12.50		
	alkali gabbro	1	12.50		
Subalkaline Rocks	granite	1	12.50	80.00	62.50
	granodiorite	3	37.50		
	gabbro	1	12.50		
Total		8	100.00	100.00	100.00

L-155 was collected on GPS station 0613444/8600564, from the granite basement in the Chambishi open pit as shown on Fig 4.1.5.18. Katangan sedimentary rocks lie unconformably on top of it and are exposed at the pit as well as underground. It is a fresh, foliated, peraluminous mesocratic potassic ferriferous biotite granite with high high K, Co, Sm and Pr.

Garlick, 1973 states that **X-42** is a representative sample of the Chambishi Gray granite. The rock is effectively a peraluminous mesocratic potassic ferriferous granodiorite.

Both L-155 and X-42 fall within the general trends of the Muliashi Porphyry granitoids. L-155 has very similar chemistry to L-158 from the Muliashi Porphyry. They plot together on all the geochemical diagrams. X-42

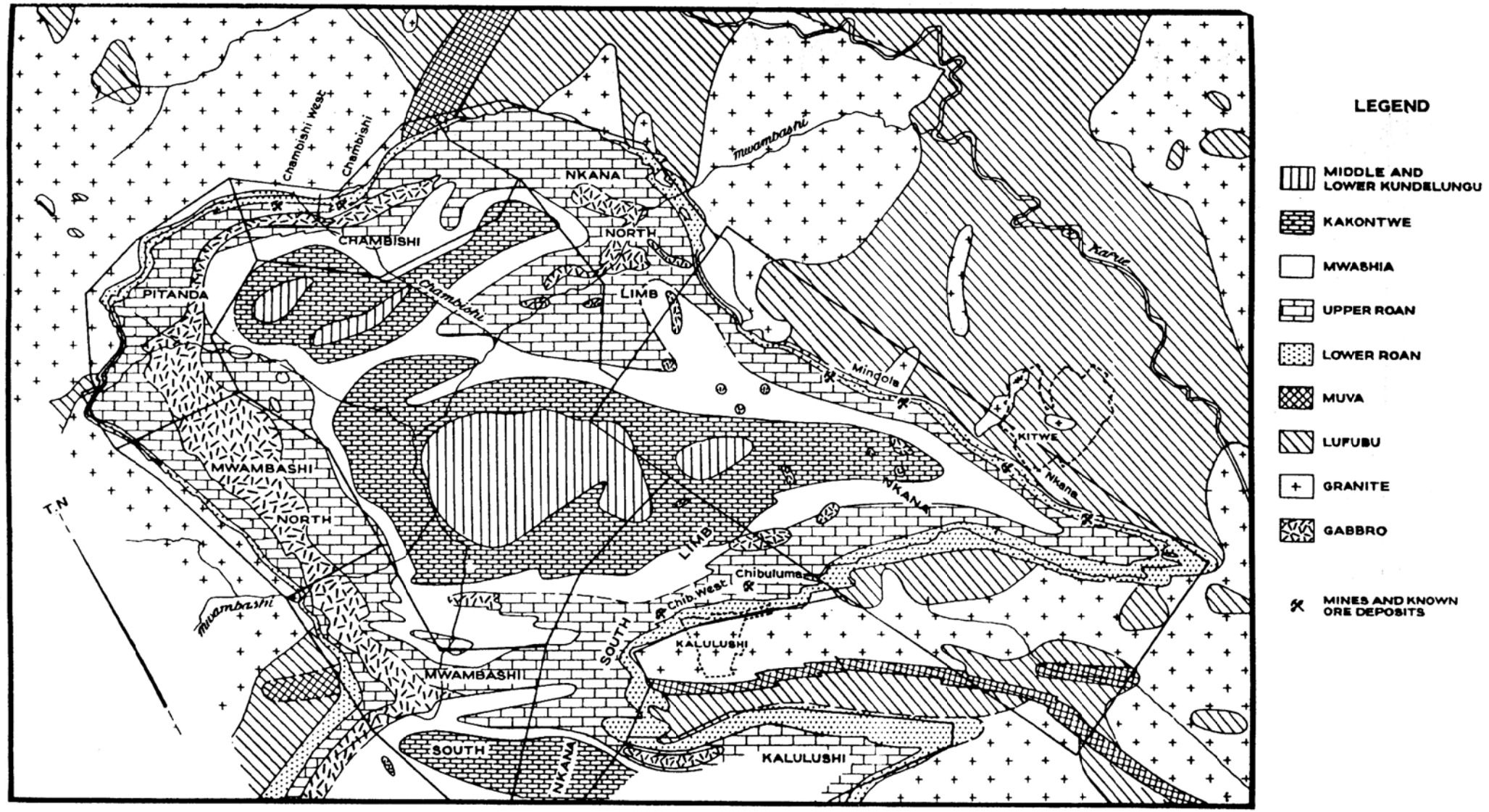

Fig 4.1.5.16 Geological map of the Chambishi-Nkana basin, Zambia. *There is abundant gabbroid outcrops, especially around the Mwabashi and Mwabashi North areas. The same body extends into the environs of the Chambishi mine. Much smaller mafic bodies are present in the Nkana North and Nkana areas. Taken from Mendelsohn, 1961.*

shows a slight deviation from the main trend on the R1/R2 diagram, due to hydrothermal alteration. This is also evident on its high losses on ignition.

Table 4.1.5.20 Chemical character and environment of emplacement for samples in the Chambishi mine environs, Zambia (See acronym description on section 2.4.3.)

Sample	Rock type	Debon & LeFort	Maniar & Piccoli	Whalen	Pearce	Nb-Ta
L-155	Granite	peraluminous ii mesocratic K Fe	?	N	O3/4	OUTU
X-42	Granodiorite	peraluminous ii mesocratic K Fe	?			
X-06	Syenogabbro	metaluminous iv mesocratic Na Fe	?			
X-07	Quartzmonzonite	metaluminous iv mesocratic Na Fe	Rrg-ceug			
X-08	Granite	metaluminous iv mesocratic Na Fe	Rrg-ceug			
X-09	Nepheline syenite	VI mesocratic Na Mg	?			
X-10	Gabbro	metaluminous iv mesocratic Na Fe	?			
X-11	Syenogabbro	metaluminous iv mesocratic Na Fe	?			

4.1.5.6.3 Chambishi Gabbroid Rocks

Mwambashi gabbros are a major outcropping rock type in the environs of the Chambishi mine, as well as around Nkana North and Chibuluma mines. This can be seen on Fig 4.1.5.18. Several samples of these rocks were reported by Mendelsohn, 1961. The samples are listed on Table 4.1.5.18. **X-6**, **X-10**, **X-11** and **X-13** are representative of the gabbroid rocks.

Below is a literal transcription[5] from a report on the Chambishi gabbroids and related "granophyres". It is very important, because it may be evidence of iron oxide-copper-gold mineralization in the environs of the Chambishi deposit. That mineralization seems to be associated to the gabbroids.

> "At 200 to 400 feet above the base of the dolomite a thick, somewhat irregular sill interrupts the sedimentary section. The dark, greenish-grey to almost black, coarsely crystalline rock consists of amphibole enclosing light-colored patches of scapolite pseudomorphs after plagioclase feldspar. Rarely a sub-ophitic texture is apparent. Most of the rock can be called amphibolite. There are a few pegmatitic zones of coarser scapolite and amphibole. Zones of chloritic rock and amphibole, commonly with narrow dolomite veins and a sparse mineralization of pyrite, a little pyrrhotite, and chalcopyrite, represent shear zones. See Appendix 1, Nos. 51-56."[6]
>
> "The deepest drill hole on the property passed through 400 feet of gabbro in the top of this sill, then through about 170 feet of granophyre, then through 25 feet of magnetite-rich rock, 110 feet of gabbro, 50 feet of dolomite, and finally 25 feet of gabbro. These thicknesses are measured perpendicular to the contacts, which generally show 1 foot or more of fine-grained chilled margin."

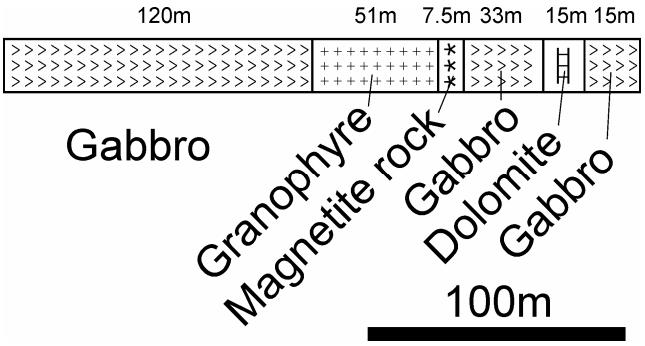

Fig 4.1.5.19 Stratigraphy of drillhole into Chambishi gabbros and granophyres*. The dimensions have been modified to the metric system. Top is to the left. Based on description by Garlick, W.G. in Mendelsohn, 1961, page 287.*

[5] Underlining was added here to stress important information.
[6] Mendelsohn's samples **51** to **56** have been re-numbered in this document with numbers X-06 to X-11, as shown on Table 4.1.5.24.

> "The surface distribution of the meta-gabbro through Chambishi and adjacent grants indicates that it is intruded apparently as a sill into the Upper Roan dolomite. Four drill holes have been collared in gabbro and passed through the contact into underlying dolomite. In the eastern part of Chambishi the meta-gabbro cuts across the bedding of the Upper Roan dolomite and reaches the base of the Mwashia. Detailed pitting in 1930 at a basal contact of the gabbro indicated that it was intruded essentially parallel to the bedding of the Upper Roan dolomite, even where the latter is folded. This observation and the almost complete scapolitization and amphibolitization of the gabbro with evidence of many shear zones indicates that it was probably intruded either before or during the folding. This tentative conclusion is based on observations in decomposed formation in pits and from a few drillholes." From report by Garlick, W.G. in Mendelsohn, 1961, page 287.

The stratigraphy of the borehole described is shown in meters on Fig 4.1.5.19. The granophyre described in the text was sampled as **X-07**, **X-08** and **X-09** (Table 4.1.5.18). Based on their chemistry, we know that they respectively are a quartzmonzonite, a granite and a nepheline syenite. These rocks intrude the Katangan metasediments as sills, along with the gabbroids.

The gabbroids, in turn are samples **X-06**, **X-10** and **X-11**. From their major oxide chemical analysis, we know that they are metaluminous sodic syenogabbros and a gabbro.

According to Garlick, at the base of the granophyre sequence lies 7.5 meters of "magnetite rock". The description is not specific, to be sure if that means a body of massive magnetite, but it probably does.

This implies that the gabbroids, granophyres and "magnetite-rock" were intimately related. All three probably formed in the same series of events, during a short time span. In addition, the gabbroids and granophyres show evidence of hydrothermal alteration. Table 4.1.5.18 indicates that their losses on ignition are high, the granophyres contain anomalous sodium, and two of them, anomalous iron. This may be evidence of hydrothermal albitization and hematitization.

The presence of massive iron oxides, midalkaline intrusions, hydrothermal alteration and nearby related copper mineralization, are all indications of a potential iron oxide-copper-gold environment in the environs of Chambishi.

4.1.5.6.4 Geochronology

Rainaud et al (2004) dated a sample of what she calls "Chambishi Granite" from borehole NN75, drilled in the Chambishi South-East prospect, 13 km NE of drill hole BN53. The sample was collected near the bottom of the hole, "14 meters below the nonconformable contact between the basal Roan Group sediments of the Katanga Supergroup, and an underlying granite". She describes the sample as a medium to coarse-grained, weakly foliated biotite granite. Her age of emplacement for the granite, based on $^{207}Pb/^{206}Pb$ is of 1983±5 Ma.

4.1.5.6.5 Environment of Emplacement

Although the environment of emplacement for samples **L-155** and **X-42** is not clear, they behave as a cluster with the Muliashi Porphyry rocks on most of the geochemical diagrams, and formed roughly at the same time. An undefined anorogenic environment seems to fit best for the Chambishi granite, just as for the Muliashi Porphyry.

X-07 and **X-08** are given a rift-related or continental epeirogenic uplift environment of emplacement by the method of Maniar & Piccoli. The rest of the gabbroids and granophyres have a midalkaline affinity and probably formed in an anorogenic environment as rift granitoids or continental epeirogenic uplift granitoids.

4.1.5.6.6 Conclusion

There are some similarities between the suites of rocks from Chambishi and Muliashi. Both have equivalent granitoids of comparable age, they both also contain midalkaline intermediate to mafic rocks.

A large volume of gabbroid rocks intruded the Katangan metasediments in the environs of Chambishi. Those rocks were acccompanied by the emplacement of granophyres, an iron oxide body and characteristic sodic and hematite alterations. That might be evidence for iron-copper-gold mineralization at or around the Chambishi deposit. This concept has to be further evaluated.

4.1.5.7 Mufulira Granite

4.1.5.7.1 Introduction

The Mufulira deposit is one of Zambia's major historical copper producers. It is located near the border with the D.R.Congo. The district contained sedimentary-hosted copper mineralization that lead to the underground operation of the Mufulira mine. According to Fleischer, Garlick & Haldane, 1976, it contained around fifteen million tonnes of recoverable copper, and once was the world's deepest copper mine. It had an average grade of 3.47% Cu.

Several samples of the Mufulira granite were collected from a large outcrop along a main road, near the Mufulira Zambian Army firing range, as illustrated on Figs M17 and 4.1.5.21. Sample coordinates are presented in Appendix A16. One sample from that site was analysed and its chemistry is presented on Table A8.6.

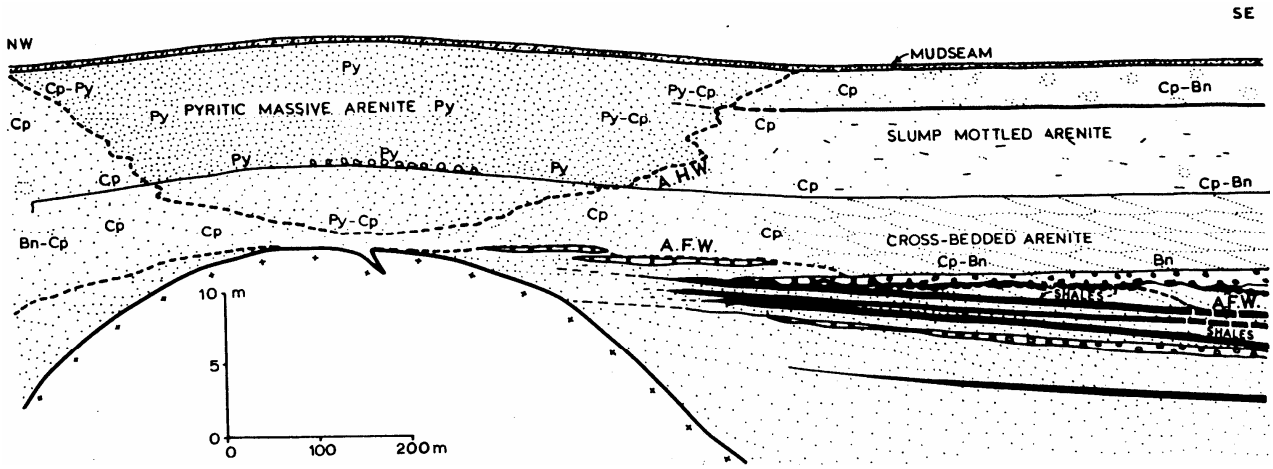

Fig 4.1.5.20 Underground cross section of the Mufulira West orebody in relation to the basement highs. *The granite paleo-hill has a fissure that is filled by chalcopyrite-rich arkose. Note zonation of mineralization: pyrite is abundant as the mineralized layers get near the paleo-hill. Chalcopyrite, chalcopyrite-bornite and then bornite occur as the distance progressively increases from the granite paleo hill. Vertical and horizontal scales are very different, as illustrated. Taken from Fleischer, Garlick & Haldane, 1976, p. 320.*

4.1.5.7.2 Sample description and geochemistry

L-166 is a medium-grained, pink metaluminous mesocratic sodic ferriferous granite with no visible xenoliths. It is intersected by minor aplitic thin white veinlets spaced every 15 cm that are more resistant to weathering. This sample has low cobalt values. Samples **L-160**, **X-01** and **X-02** are very similar to **L-166**; they plot together on most diagrams. Many of the trace element values are comparable. Total iron, K, Rb, Sr, Sm, Nd, Pr, Cu, Zn, Cr and Ba are almost equivalent in the four samples. This suite contains no Cu, some Co, and low Ba. The rock probably formed as a post-orogenic granitoid in an anorogenic environement.

Table 4.1.5.21 Chemical analysis of samples from the basement to the Mufulira copper mine, Zambia

Sample	SiO2	TiO2	Al2O3	Fe2O3	FeO	MnO	MgO	CaO	Na2O	K2O	P2O5	LOI	Total	Na+K
Notch	50.00	1.00	15.50	6.00		0.150	2.00	5.00	4.90	5.50	0.30	2.00		
X-41	64.2	1.05	14.8	2.89	2.68	0.05	1.68	3.11	3.7	4.65	0.31	0.97	100	8.35
L-166	70.84	0.39	13.91	2.93	0.00	0.00	0.61	1.97	4.13	4.54	0.13	0.44	99.89	8.67

Sample	Rb	Sr	Y	Zr	Nb	Co	Ni	Cu	Zn	Ga	V	Cr	Ba	U	Th	Sc	Sm	Nd	Pr	Ce	La	Hf	Ta	Eu	Yb	Lu
Notch	200	400	60	360	40	30	16	25	85	26	100	100	1300	20	37	20	50	50	15	175	95	10	120	4	7.5	2
X-41								1500					1600													
L-166	209	89	31	89	18	6	<6	22	18	15	<12	17	741	<6	15.0	<10	109	34.36	63.5	105	35	3.063	3.313	0.713	0.863	1

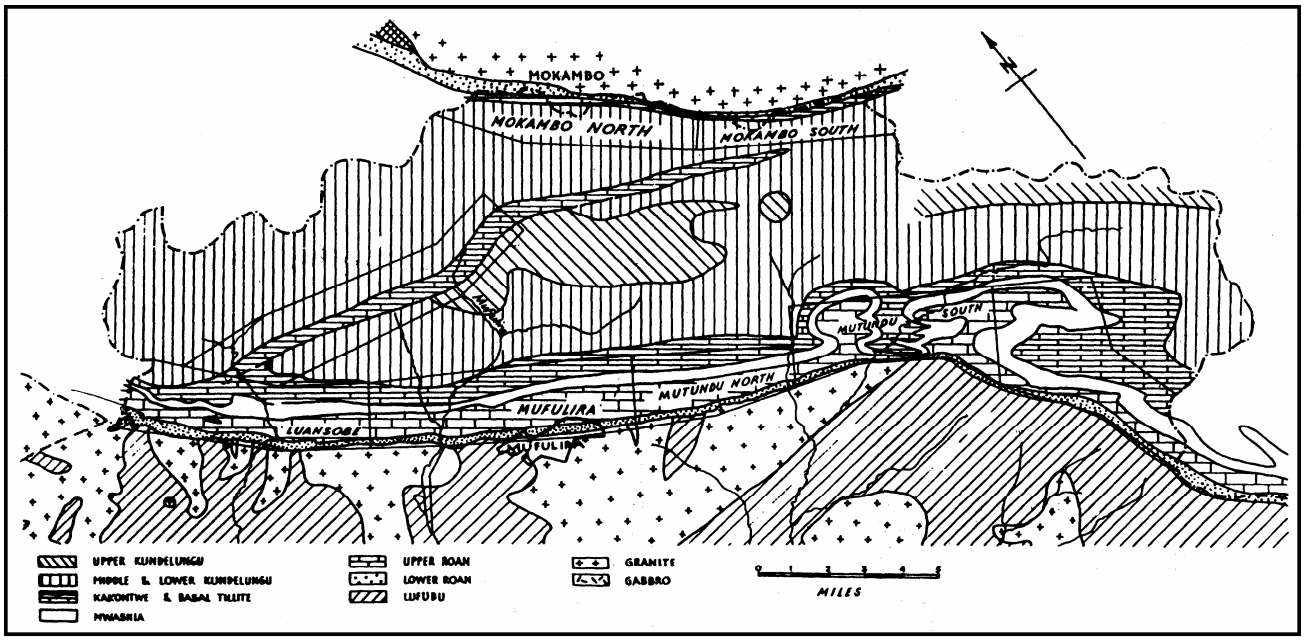

Fig 4.1.5.21 Geological map of the Mufulira mine environs, Zambia. *Note location of the border with D.R.Congo, indicated as a dash-dot line. Taken from Fleischer, Garlick & Haldane, 1976, p. 304.*

A Major oxide chemical analysis from the Mufulira "tonalite" was published by Garlick, 1973. The rock of sample **X-41** is actually a quartzmonzonite with high TiO_2 and P_2O_5. It is the only sample with those characteristics in the basement to the Copperbelt. Samples **L-075**, **L-076** and **L-077** have similar composition, and they plot roughly in the same location on most diagrams. This suite contains high Cu and Ba and low Co, Rb and K. The high values of copper for **X-41** must obey to some type of hypogene copper enrichment, and that is very significant.

Rainaud, et al, 2003 describe two distinct granitoid phases in the environs of the Mufulira mine. They are precisely the two rock types just described.

1. "The western Mufulira Grey Granodiorite, which is the most abundant, is uniformily grey and is characterized by xenoliths of Lufubu schists. This is a typical biotite-granodiorite (also called tonalite by Darnley, 1960), comprising epidote, plagioclase, quartz, biotite (sometimes altered to chlorite), scarce muscovite, magnetite, ilmenite and sphene." (X-41 is a representative sample of that rock.)
2. "The pink granite comprises microcline, quartz, scarce plagioclase, and abundant muscovite (but no biotite or epidote) together with magnetite, rutile and hematite as accesory minerals. This granite lacks xenoliths of Lufubu schists." (L-166 is representative of that phase.)

4.1.5.7.3 Geochronology

Rainaud, et al 2003 dated the pink granite at 1993 ±7.1 Ma. They state that "The ages of the Mufulira Lufubu schists (1968 Ma) and the Mufulira Pink Granite, together with the fact that the Mufulira Grey Granodiorite contains xenoliths of Lufubu schists, indicate that the pink and grey granites are not two phases of the same granite, but are two separate intrusions emplaced at different times."

"The older intrusion is the Mufulira Pink Granite dated at 1994 Ma. This was followed by extrusion of the Lufubu volcanics in the Mufulira region at 1968 Ma, an event that was followed by the intrusions of the Mufulira Grey Granodiorite, which, following model 1 of Cahen et al., 1970c, may be ca. 1945 Ma in age." This makes sense. Similar features are observed in the Muliashi Porphyry, where the same two types of granitoids were sampled.

4.1.5.7.4 Discussion

If **X-41** and **L-166** are representative of the Mufulira area, then that area has precisely the same petrographical and physical features of the Muliashi Porphyry: two different rock types. Both rock types plot together with the Muliashi Porphyry samples on all geochemical diagrams as shown (Figs 4.1.5.1 to 4.1.5.5).

A cross section of the Mufulira deposit was published by Fleischer, Garlick & Haldane, 1976. The basement portion of that section has been modified with the recently understood structural relationships of the basement as shown on Fig 4.1.5.22. The bornite, chalcopyrite and pyrite mineralization in veins of the basement has not been satisfactorily explained. It might be related to the emplacement of the gray granite, as indicated. This should be looked into in greater detail.

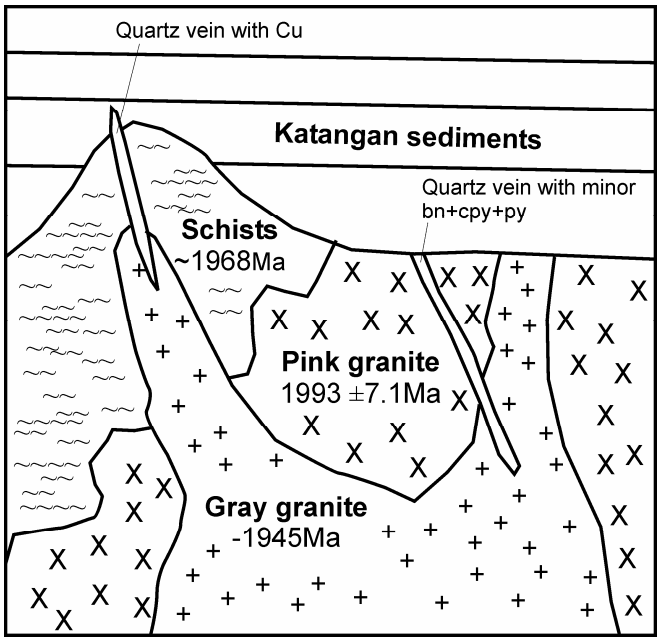

Fig 4.1.5.22 Cross section of the basement of the Mufulira mine area*. It includes all the observations and new geochronology. Copper-bearing quartz veins were exposed on the surface at the time of deposition of the Katangan sediments. Those seem to be related to the emplacement of the gray granite. Modified from the generalized stratigraphic column of Mufulira, by Fleischer, Garlick & Haldane, 1976*.

4.1.5.8 Samba Deposit

4.1.5.8.1 Introduction

The so-called Samba "Cu-Porphyry", hosted in the basement to the Katangan sedimentary sequence to the south west of the main Copperbelt was also evaluated during the Greater Lufilian Arc granitoid project. The following pages will illustrate the results of that evaluation.

On 1978, Wakefield published a paper about a Paleoproterozoic deformed porphyry-type copper deposit in the basement of the Zambian Copperbelt (Wakefield, 1978). That paper has caused a lot of confusion. The Samba deposit has reserves of over 50 Mt of 0.5% Cu, and is the largest concentration of copper mineralization in the pre-Katangan basement of the Copperbelt. According to Master, "The deposit, situated at 27°50'E, 12°43'S, consists of disseminated pyrite, chalcopyrite and bornite in deformed pre-Katangan granodioritic and quartzmonzonitic porphyritic intrusive rocks, with associated quartz-sericite and biotite-quartz-sericite schists." (Master, 1996, p. 8).

Fig 4.1.5.23 shows a generalized geological map of the deposit, and Figs 4.1.5.24 and 4.1.5.25 are two controlled cross sections to illustrate general geometry of the deposit.

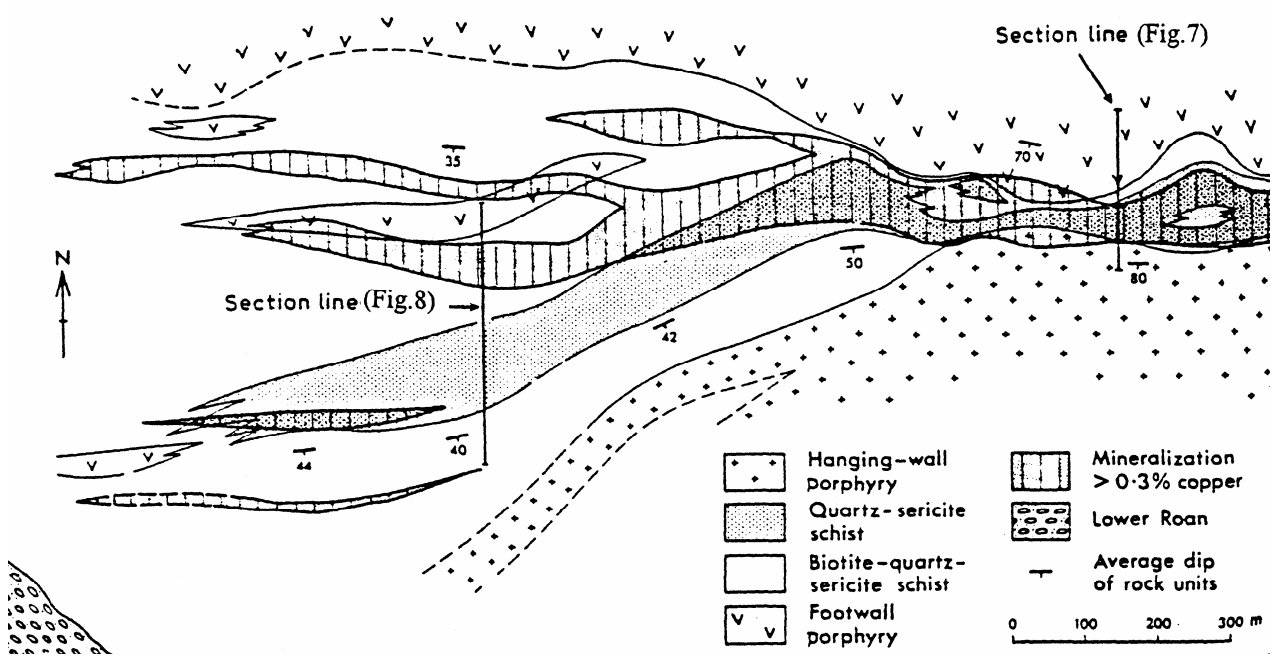

Fig 4.1.5.23 Generalized geological map of the Samba copper deposit in the basement to the Copperbelt, Zambia*. Note the location of cross sections of Figs 4.1.5.24 and 4.1.5.25. From Wakefield, 1978.*

4.1.5.8.2 Sampling and Geochemistry

A representative suite of 18 samples from the deposit was collected from boreholes CT-115, CT-116, CT-124 and CT-130 at the Kalulushi coreshed (samples **L-268** to **L-284**). Boreholes CT-115 are shown on Figs 4.1.5.24. Four samples were analysed for this research project: **L-268**, **L-269**, **L-273** and **L-279**. Their location, field description and rock name are included on Table 4.1.5.22. Chemistry of the samples is listed on Table A8.3, and is plotted on Figs 4.1.5.1 to 4.1.5.5. The rocks analysed were hosting mineralization, and were the most likely samples to have been porphyrytic volcanic rocks.

The samples are rhyolitic and rhyodacitic, fine- to medium-grained, volcaniclastic rocks (Table 4.1.5.22). **L-268** and **L-269** were subject to intense hydrothermal alteration. They produce high losses on ignition due to abundant hydrous minerals. They were subject to silicification and got a significant input of chrome. **L-268** is highly enriched in copper.

Samples **L-268** and **L-170** are strikingly similar on the TAS and R1R2 diagrams (Figs 4.1.5.1 and 4.1.5.2). Maybe both rocks were subject to similar processes. They have high Cr, Cu, Al, their loss on ignition is 3 to 3.6, and they contain low Th and Zn. Nevetheless, their Nb and Cu values are different.

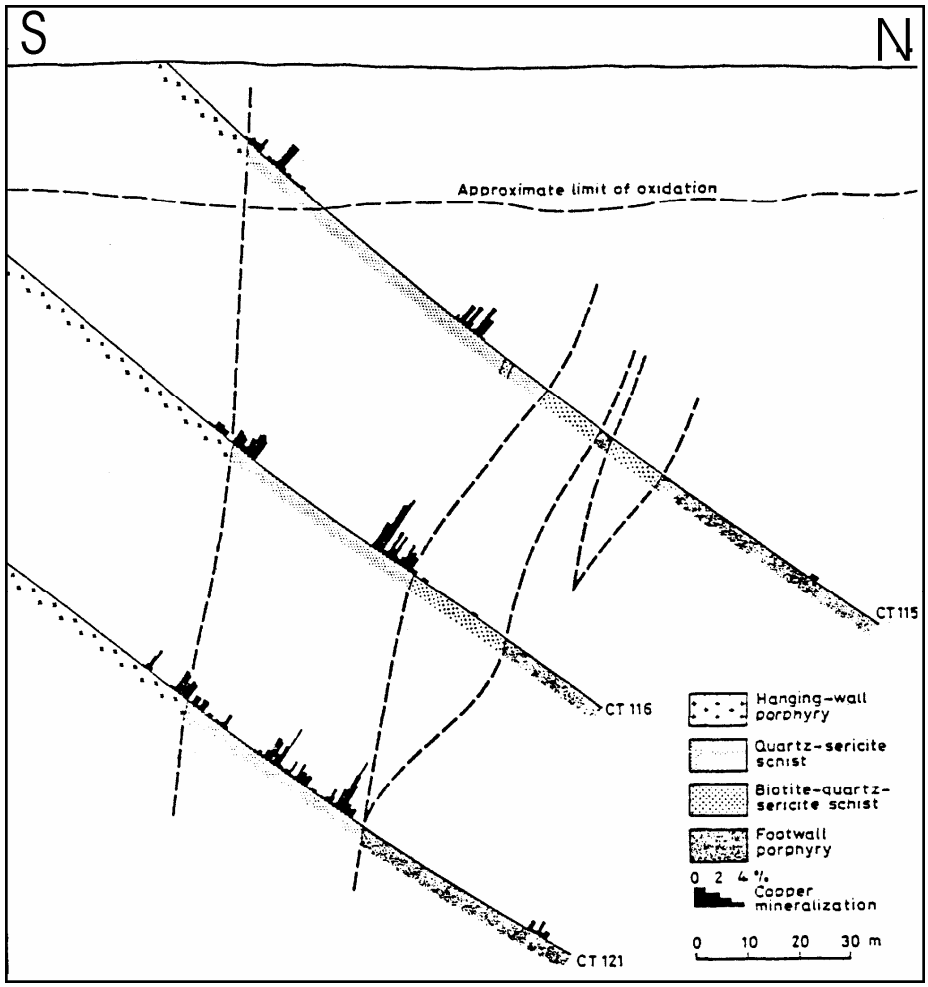

Fig 4.1.5.24 Eastern borehole-controlled geological cross section, Samba copper deposit, Zambia*. It is marked as the section line from Fig 7 on Fig 4.1.5.23. Taken from Wakefield, 1978.*

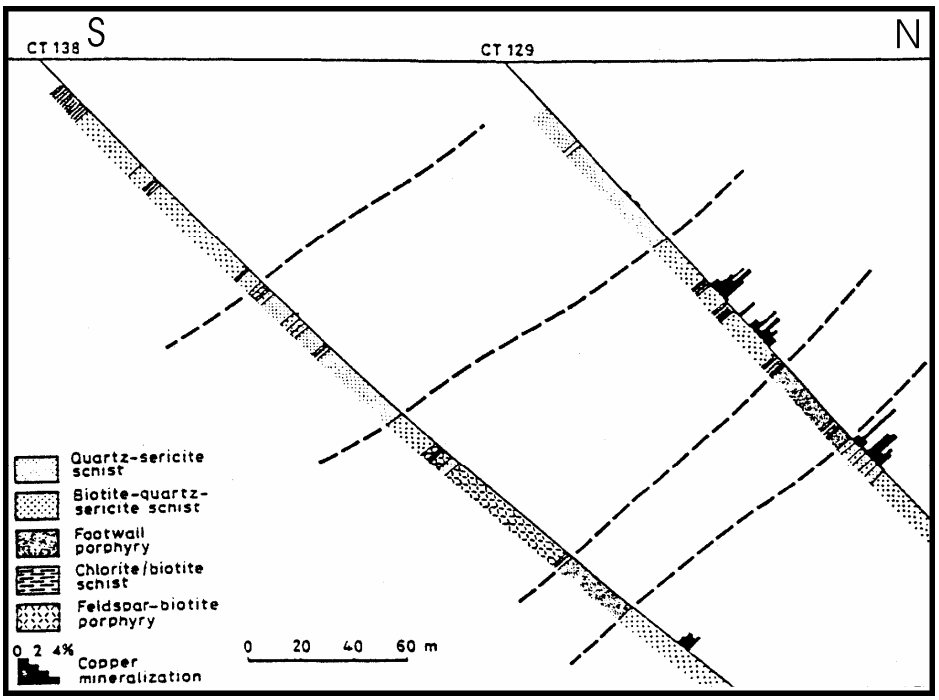

Fig 4.1.5.25 Western borehole-controlled geological cross section, Samba copper deposit, Zambia*. It is marked as section line of Fig 8 on Fig 4.1.5.23. Taken from Wakefield, 1978.*

Table 4.1.5.22 Main details of analysed samples from the Samba copper deposit, basement to the Copperbelt, Zambia

Sample Number	Borehole	Depth (feet)	Field Description	Rock Name
L-269	CT-115	241.1	Fractured schistose rocks that contain disseminated chalcopyrite and pyrite.	Peraluminous subleucocratic potassic ferriferous rhyolite
L-273	CT-115	257.0	Biotite schist with sulfide veinlets.	Peraluminous mesocratic sodic magnesic rhyodacite
L-279	CT-116	195.2	Schists after igneous rock (?)	Metaluminous mesocratic sodic ferriferous rhyodacite
L-268	CT-124	315.5	Schist with stockwork and hematite/goethite oxidation of pyrite	Peraluminous mesocratic potassic ferriferous rhyolite

Samba samples plot along the general trend of the Muliashi Porphyry rocks in most of the Debon & LeFort diagrams (Figs 5.1.5.1 to 5.1.5.5). Deviation from the main trend in some of the diagrams is probably due to hydrothermal alteration associated to the mineralizing processes.

Rainaud, Master, Armstrong, & Robb, 2003 comment that schists from the Samba deposit are part of the Lufubu Schist Group of rocks. This had been previously hinted by Master, 1996, when he stated the likelihood of Samba rocks being "of Paleoproterozoic age", and "related to other Paleoproterozoic granitoids in the Kafue Anticline and surrounding areas (e/g. Mufulira, Mokambo, Luina and Roan Antelope granites)."

4.1.5.8.3 Geochronology

Rainaud et al., 2003 dated schists from the same boreholes and produced a U-Pb SHRIMP age in zircons of 1964±12Ma (Table A22.7). That is the age of the volcanic protolith for the schists. The relevance of that age to mineralization, and the type and origin of the Samba copper concentration are not well understood. Several questions remain: Do the zircons have evidence of a strong metamorphic event? Is that process reflected in their shape and ages? Rainaud was not able to solve these questions (Rainaud, C., personal communication, 2003).

4.1.5.8.4 Discussion

Observation of core from the original boreholes drilled to explore the Samba property did not detect any intrusive porphyritic rocks; only what seemed to be metamorphosed fine- to medium-grained volcanic rocks.

Few aspects of typical porphyry copper mineralization were evident. No significant brecciation or stockworking was seen. Hydrothermal alteration patterns and minerals were not those of a porphyry copper deposit. Mineralization of coarse bornite and chalcopyrite in veins and disseminated fashion was observed in core; but many of the patterns common in copper porphyry systems known from the Central Andes and the North American Cordillera were missing.

The author looked at the core at approximately the same time as Richard Sillitoe did. And, after discussing the issue together in Kitwe, both agreed that the mineralization does not seem to be due to porphyry copper processes or bears resemblance with those mineralized systems (Sillitoe, R., personal communication, 2002).

One of the main problems to consider the Samba "porphyry" a true porphyry copper deposit is the strong deformation of its host rocks. They all are schistose and lack true plutonic character. If mineralized volcanic rocks were the protolith of the schists, induration of parts of the rock by silicification, potassic and phyllic alteration would be expected; that would preclude schistose deformation. No evidence of epidote, nor phyllic, argillic or potassic alteration was seen.

A possible origin of copper mineralization at the Samba prospect could be a high sulfidation copper dissemination in volcanic ash. This probably took place in an anorogenic environment like that of the Muliashi Porphyry-Lufubu Schist group of rocks. Ash was subject to deformation and metamorphism that reconcentrated iron and copper sulfides, to become what is now the Samba prospect.

Samba "porphyry" is a misnomer and should be changed definitely for "Samba copper deposit" to avoid further confusion.

4.1.5.9 Conclusions on Granitoids in the Copperbelt

General Conclusions

1. The Nchanga Granite has all the characteristics of an anorogenic granite ring complex. Chemistry of its rocks cross the fields of midalkaline to subalkaline rocks. The pluton behaves as a coherent cluster in all geochemical diagrams. The pluton, or parts of it, is made of high heat producing granites that probably maintained a long-lived circulation of hydrothermal fluids. The Nchanga Granite might have contributed to the origin of copper in its environs.

2. Mafic rocks and midalkaline granitic dikes were studied in the Nchanga mine area. Both were emplaced in anorogenic extensional environments. The granitic dikes were dated at ~765 Ma. They provide an oldest age of deposition for the Katanga sedimentary sequence at Nchanga, and might provide a significant bracket age for mineralization.

3. Mafic rocks that intersect the basement to the Copperbelt were emplaced after the Katangan sediments were consolidated, and in some cases, after the copper-cobalt mineralization took place. The chemistry of dikes that intersect the Katangan rocks varies widely from midalkaline felsic to gabbroid.

4. The Muliashi Porphyry plots as a distinct trend on all geochemical diagrams evaluated. A few of the samples studied display variations by hydrothermal alteration or metamorphism. Samples from the Chambishi and Mufulira environs, as well as from the Samba copper deposit, plot on the Muliashi Porphyry trend.

5. Geochemical and geochronological data from the Konkola deep borehole helped to deduce part of the geological history in the environs of that mine. There might be an anorogenic granitoid intrusion similar to the Nchanga Granite in the area.

6. A large portion of the rocks in the basement to the Copperbelt are enriched in K_2O, Rb and Pr. Select groups of samples are enriched in Nb and Cu.

Tectonic Environment of Emplacement

7. The procedure of (Maniar & Piccoli, 1989) cannot identify environment of emplacement for 70% of the granitoids in the basement to the Copperbelt. Few samples produce meaningful results, as indicated on Table 4.1.5.25. This is probably due to particular modifications of the rocks at regional scale that make them unrecognizeable by the Maniar & Piccoli procedures.

8. Intense sodic alteration and hematitization were observed in the basement to the Copperbelt. Maybe other unidentified processes of regional metamorphism have occurred, that modify the basic chemistry of rocks. One alteration process could be a net enrichment in potassium that is evident in the abundant biotite and alkali feldspar overgrowth.

9. The regional metamorphic process mentioned in the previous conclusion seems to have taken place before the emplacement of the Nchanga Granite, because the method of Maniar & Piccoli, 1989 produced results for several samples from the Nchanga Granite and young intrusives that cut Katangan sediments at Chambishi. Results of the methods to evaluate granitoid environment of emplacement were not clear for rocks older than the Nchanga Granite.

10. Although the various methods to evaluate environment of emplacement for Muliashi Porphyry granitoids did not produce coherent results, the majority of those samples have an anorogenic origin, according to the method of Whalen et al, 1987 (Table 4.1.5.12). There is no evidence that indicates the plutonic and volcanic rocks in the suite formed in a magmatic arc, as Master et al, 2003 indicate. The information available does not support a subductional origin for the Muliashi Porphyry. Further work will be carried out to define the environment of emplacement of these rocks using artificial intelligence and a large geochemical database, as indicated on section 2.4.1.7.

Mineralization

11. A large volume of gabbroid rocks intruded the Katangan metasediments in the environs of Chambishi. Those rocks were acccompanied by the emplacement of granophyres, an iron oxide body and characteristic sodic and hematite alterations. That might be evidence for iron-copper-gold mineralization at or around the Chambishi deposit. The concept has to be studied further.

12. Rocks from the Muliashi Porphyry contain significant copper that might have a hypogene origin.

13. Mineralization of the Samba copper deposit does not seem to be due to porphyry copper processes or bears resemblance with those mineralized systems.

Lithologic Correlation

14. Rocks with “identical” chemistry may form from the same protolith, in similar environments that are very separated in time. This occurs with samples from the suites of Muliashi Porphyry and Mufulira. They both have pink and gray granitoids with similar compositions, but the ages of the rocks are completely different.

Stratigraphic Relations

15. The stratigraphic model that Robb, Master and Rainaud have been using for the basement to the Zambian Copperbelt during the past few years can be slightly modified with the new information from this research project. Fig 4.1.5.26 illustrates most of the relevant intrusive and stratigraphic relations. It shows the new radiometric ages obtained for this project.

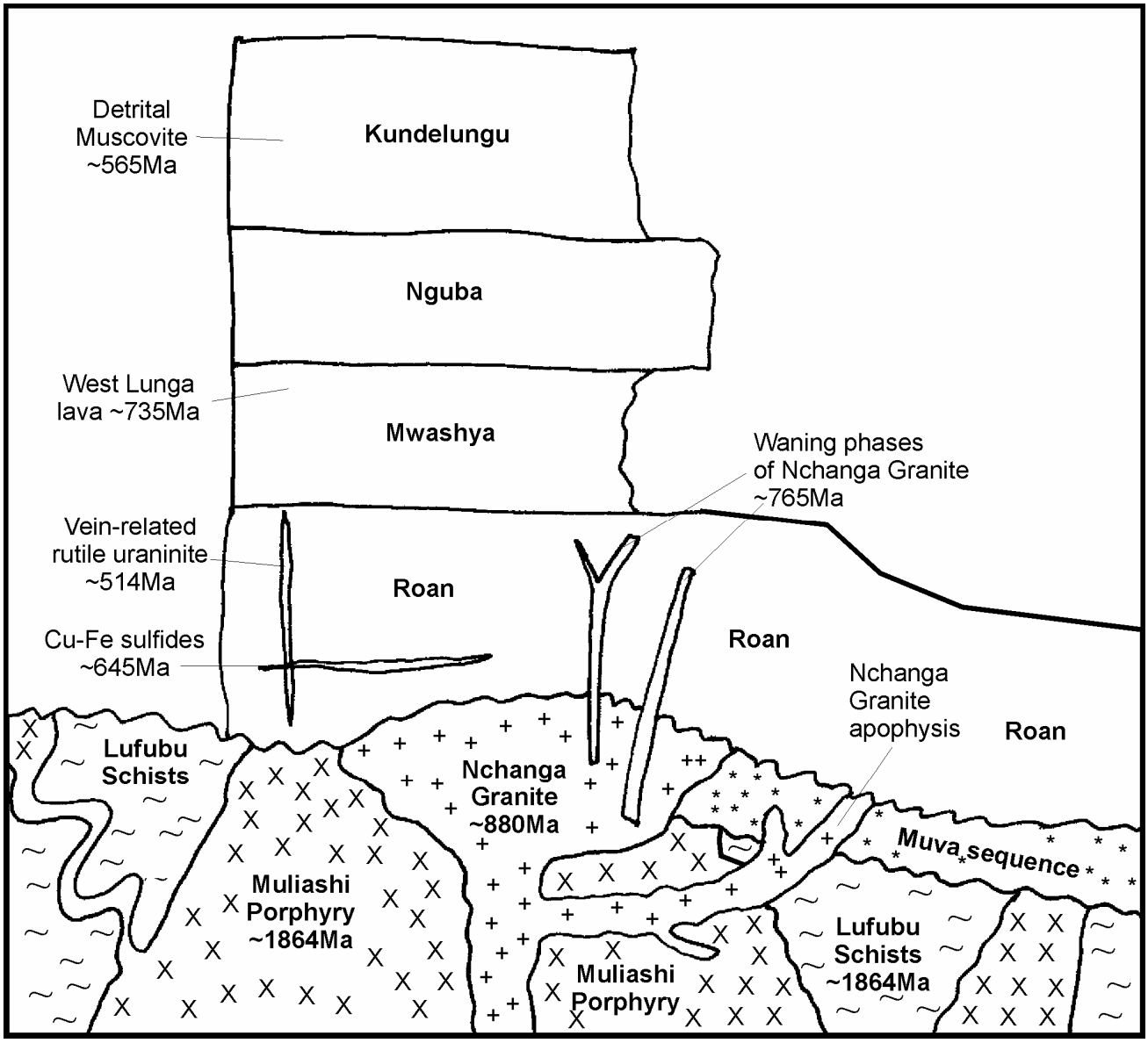

***Fig 4.1.5.26 Main stratigraphic relationships between rock units in the main Copperbelt area, Zambia**. Figure modified after model of the Economic Geology Research Institute [Robb, L., personal communication, 2003].*

Table 4.1.5.23 Regional correlation of dated Paleoproterozoic granitoids in the Greater Lufilian Arc

Event	Kalene Hill, Zm	Grootfontein, Nm	Kamanjab, Nm	Mufulira, Zm	Konkola, Zm	Muliashi, Zm	NW Zambia	Fe/Mg
9					L-158 gray gt 1874;14			
8	1872;14		L-944 granite 1856;24 L-993		L-160 pink gt 1866;5.4	L-075 1865;5.4 X-1, X-2 quartzmonzonite	granite 1864	
6	1945	L-1045 quartzmonzonite	L-868 quartzmonzonite 1937;14 L-945 L-855 granite 1939;19	X-41 gray quartzmonzonite ~1945			L-030 granite 1927	ferriferous
5			L-864 granodiorite			Samba 1964;12		magnesic
4			L-969 syenite 1976;42			L-155 Chambishi granite 1983;5		
3		L-1043 granite 1997;39		L-166 pink granite 1993;7.1			1994	
2			L-968 granite					

Table 4.1.5.24 Original data, additional samples from the literature on Copperbelt granitoids, Zambia

Samples from Garlick, 1973

#	Sample	SiO2	TiO2	Al2O3	Fe2O3	FeO	MnO	MgO	CaO	Na2O	K2O	P2O5	CO2	S	H2O+	H2O-	Cu	F	BaO	Total	
X-34	Nchanga Red Granite	76.75	0.09	11.78	0.82	0.58		0.03	0.16	0.72	3.08	5.01	0.10	0.05	0.01	0.79	nil		tr.	nil	99.97
X-35	Gray's Quarry Red	76.84	0.08	10.70	1.30		1.30	0.04	0.10	0.80	2.30	4.90	0.02	0.05	0.15	0.45	0.19			0.01	97.93
X-36	Gray's Quarry Aplite	76.90	0.01	12.30	0.60		0.60	0.01	0.10	0.50	3.60	4.40	0.04	0.07	0.08	0.25	0.03			0.01	98.90
X-37	Gray's Quarry Grey	78.20	0.04	10.30	1.10		1.10	0.04	0.10	0.70	2.20	4.90	0.01	0.03	0.09	0.32	0.09			0.01	98.13
X-38	Gray's Quarry Schlieren	59.80	1.10	10.40	12.6		0.30	0.30	0.60	4.30	1.70	2.90	0.08	0.03	0.07	0.92	0.04			0.01	94.85
X-39	Gray's Quarry pegmatite microcline	66.60	0.01	18.00	0.20		0.20	0.02	0.03	0.20	2.40	11.90	0.01	0.09	0.18	0.71	0.15			0.01	100.51
X-40	Nkana vein adularia	64.80	0.01	16.70	0.40		0.40	0.01	0.03	0.10	0.70	15.50			tr.					0.49	98.74
X-42	Chambishi Grey	68.64	0.30	13.95	1.14	1.25		0.06	2.29	2.25	2.13	4.04	0.11	1.77	tr.	1.68	0.09			0.03	99.73
X-41	Mufulira Tonalite	64.19	1.05	14.80	2.89	2.68		0.05	1.68	3.11	3.70	4.65	0.31	0.08	0.18	0.85	0.04	0.15	0.16		100.57

Samples from Mendelsohn, 1961

#	Sample	SiO2	TiO2	Al2O3	Fe2O3	FeO	MnO	MgO	CaO	Na2O	K2O	P2O5	CO2	S	H2O+	H2O-	H2OT	Cu	F	BaO	Cl	ZrO2	equiv	FeS2	total
X-01	Roan Antelope Gray Granite 1	73.81	0.08	12.29	0.37	1.52	0.04	0.70	2.24	4.21	4.83	0.04			0.33										100.5
X-42	Chambishi Gray Granite 2	68.64	0.30	13.95	1.14	1.25	0.06	2.29	2.25	2.13	4.04	0.11	1.77	tr	1.68	0.09				0.03					99.73
X-02	Mokambo adamellite 3	72.56	0.23	14.28	0.94	0.68	0.02	0.83	0.76	2.88	6.12	0.05			0.93	0.05				0.06		0			100.4
X-03	Mwekera gray granite 4	70.95	0.42	15.07	1.13	1.29	0.03	1.32	0.83	4.23	3.03	0.11	tr	tr	1.21	0.09				0.05					99.76
X-04	Ndola gray granite 5	75.20	0.33	10.10	1.55	1.69	0.04	2.81	2.08	2.02	2.13	0.34	0.07	0.02	0.91	0.20				0.08	0.05	nil			99.62
X-41	Mufulira tonalite 7	64.19	1.05	14.80	2.87	2.68	0.05	1.68	3.11	3.70	4.65	0.31	0.08	0.18	0.85	0.04		0.15	0.16				0.2		100.4
X-05	Bancroft Muliashi Porphyry 8	65.27	0.84	15.18	3.20	1.94	0.08	1.01	2.90	3.00	4.70	0.31	0.05	tr	1.32	0.02				nil	tr				99.82
X-34a	Nchanga red granite 9	76.75	0.09	11.78	0.82	0.58	0.03	0.16	0.72	5.01	3.08	0.10	0.05	0.01	0.79	nil			tr.	nil	tr				99.97
X-12	Chiringoli phosphatic schist 48	30.05	0.37	8.60	39.65	4.48	0.05	0.27	6.82			5.78	nil				4	nil			0.35				100.5
X-13	Lufubu river norite SW of Chibuluma 49	49.41	2.67	12.71	2.18	10.07	0.14	6.93	10.46	2.46	0.80	0.46	0.06	tr	0.85	0.12				0.03	0.4		0.1		99.65
X-14	Lufwanyama valley scapolitized gabbro 50	46.76	3.30	10.31	5.81	9.10	0.14	7.25	10.24	4.26	0.86	0.38	nil	0.22	1.04	0.17				nil	1.4		0.3		100.9
X-06	Chambishi amphibolite 51	46.85		15.87	3.33	7.40	0.11	8.61	7.29	3.65	2.50	0.15			1.43	0.10								0.2	97.46
X-07	Chambishi transition amphybolitic granophyre 52	58.63		13.08	6.07	6.68	0.15	1.87	4.70	5.50	0.66	0.32			0.75	0.08								0.8	99.32
X-08	Chambishi granophyre 53	67.94		12.08	7.23	1.01	0.04	0.60	1.65	6.70	0.20	0.07	0.88		0.24	0.17								0.1	98.86
X-09	Chambishi granophyre 54	59.26		16.65	1.26	0.43	0.06	2.04	4.59	9.80	0.20	0.65	2.46		0.69	0.32								0.2	98.56
X-10	Chambishi amphibolite 55	47.87		14.53	4.50	9.05	0.15	6.13	6.12	2.95	1.55	0.37			3.35	0.26								0.2	97.03
X-11	Chambishi amphibolite 56	48.19		14.53	4.13	7.18	0.12	6.66	9.00	4.25	1.40	0.17			1.73	0.07								0.3	97.71

Table 4.1.5.25 Sample discrimination by location, chemical character and environment of emplacement, Copperbelt region, Zambia.

Muliashi Porphyry

Sample	Rock type	Debon & LeFort	Maniar & Picc	Whalen	Pierce	Rb/10HfTa	Rb/30HfTa	Nb-Ta
L-075*	Quartzmonzonite	IV meso Na-K Fe	?	N	S2/4 O2/4	VA	II	INV
L-076	Quartzmonzonite	IV meso Na-K Fe	?	A	O-W1-1			
L-077	Quartzmonzonite	IV meso Na-K Fe	?	A	O3/4			OUTU
L-078	Granodiorite	IV meso Na Fe	?	A	O-W1-1			
L-157	Granite	I subleuco K Fe	?	A				
L-158*	Granite	II meso K low Fe Mg		N	O2/3	WP-	II	OUTU
L-159	Granod-granite	II meso K Mg	?	A	O-W1-1			
L-160	Granite	II meso K Mg	?	A	O3/4			OUTU
L-161	Syeno-diorite dike	II meso K high Fe Mg	?	A	O-W1-1	wpab-wpt		
L-163	Syeno-gabbro dke	III meso K high Fe	?	N		emor		
X-01	Granite	V subleuco Na Mg	lag-cag					
X-02	Granite	II subleuco K Mg	lag-cag,ccg					
X-03	Granite	II meso Na Mg	Ccg					
X-04	Altered granodior.	III meso Na Mg	?					
X-05	Granodiorite	IV meso K Fe	RRG					

Nchanga Granite

Sample	Rock type	Debon & LeFort	M & P	Whalen	Pierce	Rb/10	Rb/30	Nb-Ta
P-28	Nepheline syenite	VI subleuco Na Fe	?			VA-	VA-III	INW-INV
P-29	Granite	VI subleuco Na-K Fe				VA-	III	INW-INV
L-151	alkali granite	IV leuco K Fe	RRG	A	W3/4	WP-	III	OUTU
L-153	alkali granite	III leuco Na-K Fe	RRG	A	W			
L-154	alkali granite	II leuco K Fe	?	A	O-W 2-2	WP-	WP-III	OUTU
L-162	Granite	III leuco Na-K Mg	POG	A				
X-34	Alkali granite	IV leuco K Fe	Pog-rrg					
X-35	Granite	III leuco K Fe	?					
X-36	alkali granite	I leuco Na low Mg	POG					
X-37	Granite	III leuco K Fe	?					
X-38	Granodiorite	V meso K Fe	RRG					
X-39	Syenite	I leuco K low Mg	?					
X-40	Syenite	VI leuco K Fe	?					

Nchanga Mine Area

Sample	Rock type	Debon & LeFort	M & P	Whalen	Pierce	Mafic	Rb/10	Rb/30	Nb-Ta
L-150	syeno-diorite dike	III meso K high Fe	?	A	O3/4	emor			OUTU
L-167a	syeno-diorite dike	II meso K high Fe+Mg		A	W	wpab			
L-168*	alkali granite	I leuco K Fe	?	A?	O2/3				
L-170	Granite	I meso K Mg	?	A	O-W 2-2				OUTU
L-172*	alkali granite	I leuco K Fe	?	A	O-W 2-2		VA-	III-II	INW
L-173	alkali granite	I leuco K Mg	?	A	W				

Chambishi Granite

Sample	Rock type	Debon & LeFort	M&P	Whalen	Pearce	Rb/10HfTa	Rb/30HfTa	Nb-Ta
L-155	Granite	peraluminous ii mesocratic K Fe	?	N	O3/4			OUTU
X-42	Granodiorite	peraluminous ii mesocratic K Fe	?					
X-06	Syenogabbro	metaluminous iv mesocratic Na Fe	?					
X-07	Quartzmonzonite	metaluminous iv mesocratic Na Fe	Rrg-ceug					
X-08	Granite	metaluminous iv mesocratic Na Fe	Rrg-ceug					
X-09	Nepheline syenite	VI mesocratic Na Mg	?					
X-10	Sat. olivine gabbro	metaluminous iv mesocratic Na Fe	?					
X-11	Syenogabbro	metaluminous iv mesocratic Na Fe	?					

Mufulira Granite

Sample	Rock type	Debon & LeFort	M&P	Whalen	Pearce	Rb/10HfTa	Rb/30HfTa	Nb-Ta
L-166	Granite	metaluminous iv mesocratic Na Fe	POG	N	V2/4 O2/4	VA-	III	OUTU
X-41	Quartzmonzonite	metaluminous iv mesocratic Na-K Fe	?					

Samba Copper Prospect

Sample	Rock type	Debon & LeFort	M&P	Whalen	Pearce	Rb/10HfTa	Rb/30HfTa	Nb-Ta
L-268	Granite	peraluminous iii mesocratic K Fe						
L-269	Granite	Peraluminous i subleucocratic K Fe						
L-273	Granodiorite	peraluminous iii mesocratic Na Mg						
L-279	Granodiorite	metaluminous iv mesocratic Na Fe						

* Zircons from this sample were dated by U/Pb SHRIMP.

4.2 NAMIBIAN DOMAINS

4.2.1 KAMANJAB BATHOLITH, NAMIBIA

4.2.1.1 Introduction

The Kamanjab Batholith is one of the most significant geological features on northern Namibia. Surprisingly, very little was known about its geology until 2003. Only generalized maps and a few isolated reports were available; little or no comprehensive literature on this large unit of igneous rocks could be found. Age constraints were not very tight. The mineral potential of the region was considered to be significant. For these reasons, the batholith constitutes one of the main foci for sampling in this project.

The Kamanjab Batholith may be reached by a 300 km paved road from Windhoek, capital of Namibia. It lies roughly south-west of the Etosha Natural National Park. A few farms in the region have airstrips for small aircraft. Most of the secondary roads are unpaved, but are in general good shape. The area has electrical power lines supplied by the main Namibian grid. A few farm homesteads are connected with the main Namibian telephone grid, and some farmers have microwave and radio communications. The nearest well-equipped hospital is in Otwijarongo. The nearest gas stations are located in Outjo and Khorixas, approximately 100 km from the main batholith. Some farms sell diesel fuel and gasoline in small quantities at a surcharge.

Rainfall is very low in the semi-desert climate of the Kamanjab region. All the drainage system is ephemeral; no rivers or creeks are perennial. There is a rapid decrease in rainfall towards the western portion of the Kamanjab Batholith, where the Etendeka Plateau and the Namib desert begin. As discussed by Frets, 1969, “the year can be divided into a dry winter period with moderate temperature and a hot summer period with occasional rainfall. The proper rainy season occurs from November/December to April. Years with a normal rainfall alaternate, however, with drought years.” Each farm has several water wells that constitute the main source of water. Most of the pumping is done using small wind-driven pumps and engines. A few private, small dams gather water during the rainy seasons. Vegetation is scarce, short and thorny. A portion of the land, especially towards the northeastern part of the batholith, is covered by extensive game farms and bad quality pastures for cattle. Small numbers of various types of antelopes, zebra, wildebeast, giraffe, desert elephant and rhinoceros are seen occasionally. Desert lizards, small mammals and snakes are commonly found in the rocky outcrops and inselbergs. Main economic activities of the region are game viewing and extensive goat and sheep raising. A great portion of the land is barren; no industrial crops are grown; most foods are brought from outside.

The Kamanjab Batholith has been given several names in the literature. Some of these are: Franzfontein Granite, Fransfontein Granite Suite, Huab Gneiss, Kamanjab Granitic Complex and Kamanjab Inlier. The term Kamanjab Batholith is proposed here to name the plutonic body and its associated volcaniclastic material.

The best map available of the entire batholith was a 1:200,000 compilation by Ajagbe, 2001, based on the 1:1’000,000 scale geological map of Namibia. Some portions of the batholith were available at 1:100,000 scale (Frets, 1969; Porada, 1974; and Anonymous, 1997). Geological sheet *2014 Fransfontein* that covers the southern part of the Kamanjab Batholith was available at 1:250,000 scale in preliminary form at the Geological Survey of Namibia. Geological reports on the area were published by Clifford, Rooke, & Allsopp, 1962b; Clifford, Nicolaysen, & Burger, 1962a; Siedner, 1968; Clifford, Rooke, & Allsopp, 1969; Frets, 1969; Guj, 1970; Porada, 1974; Burger & Coetze, 1975; Burger, Clifford, & Miller, 1976; Tegtmeyer & Kroner, 1985; Steven, 2000; Steven, 2001a; Steven, 2001b; and Steven & Armstrong, 2002.

Various types of mineralization have been identified throughout the Kamanjab Batholith. The literature available indicates significant copper, gold and fluorite occurrences and mines. A review of mineral resources of the Kamanjab Batholith region was compiled by Ajagbe, 2001. Namibian copper mineralization was reviewed by Schneider & Seeger, 1992 and gold mineralization was reviewed by Burnett, 1999; both reports include some information about deposits and prospects in the batholith. Several company reports have been issued during the past few years on the merits of the iron oxide-copper-gold Tevrede property, located in the northwestern portion of the batholith (Anonymous, 2003; Boulder Mining, 2002; Boulder Mining, 2002-2004; Boulder Mining, 2003a; Boulder Mining, 2003b; Boulder Mining, 2004a; and Boulder Mining, 2004b).

Reconnaissance field sampling was done along the main public roads that transect the batholith. Very few volcanic rocks were sampled. 170 samples were collected in the field; 97 of those were analysed. Nineteen additional chemical analyses of samples were compiled from the literature, for a total database of 116 samples. Table 4.2.1.1 lists their chemical analysis. All samples collected in the Kamanjab Batholith are

located on the series of maps of Figs M27 to M39. A guide to find waypoints and samples is presented on Table 4.2.1.18. Maps have been consecutively numbered with the prefix “K-“. For example, L-958 is located on the southeastern corner of map sheet K-18. That is codified as K-18 SE. Sample L-942 is located on the western central portion of the same map. It has been codified as K-18 WC. For easy reference, a key map for all the larger scale maps has been included (Fig M27). Table 4.2.1.3 lists general characteristics of all samples collected in the Kamanjab Batholith.

The following pages will describe main findings in the Kamanjab Batholith.

4.2.1.2 Geochemistry

The Kamanjab Batholith is made by a series of three major rock types with five or six subordinate types that make dikes and smaller plutonic bodies. At first sight it seems to have a rather homogeneous chemistry, because almost 60% of the rocks cluster around the quartzmonzonite-alkali granite lithologies on the TAS diagram (Figs 4.2.1.1 and 4.2.1.2). Nevertheless, after careful inspection, several clear distinctions between rock types are apparent.

73% of the granitoids from the Kamanjab Batholith fall within the midalkaline field, while 27% of them fall in the subalkaline field (Table 4.2.1.2). 69% of all rocks sampled are in the midalkaline field, 27% are subalkaline and 5% are alkaline. By far the most abundant rocks in the batholith are quartzmonzonites; more that a third of all samples collected come from that group. The dominance of midalkaline rocks stresses the fact that the batholith formed in an anorogenic environment.

Table No. 4.2.1.1 CHEMICAL ANALYSIS OF SAMPLES IN THE KAMANJAB INLIER, NAMIBIA; GREATER LUFILIAN ARC

Sample	SiO2	TiO2	Al2O3	Fe2O3	FeO	MnO	MgO	CaO	Na2O	K2O	P2O5	LOI	Total	Rb	Sr	Y	Zr	Nb	Co	Ni	Cu	Zn	Ga	V	Cr	Ba	U	Th	Sc	Pb	Sm	Nd	Pr	Ce	La	Cs	Hf	Ta	Eu	Gd	Tb	Dy	Ho	Er	Tm	Yb	Lu	Li	Be	Ge	Mo	Na+K
Notch	50.00	1.0	15.5	6.00		0.15	2.00	5.00	4.90	5.5	0.3	2.00		200	400	60	360	40	30	16	25	85	26	100	100	1300	20	37	20	20	50	50	15	175	95	3	10	120	4	30	5	20	3	9	35.5	7.5	1.6					
L-832	73.67	0.32	12.24	1.83	0.00	0.04	0.14	0.46	4.39	5.23	0.11	0.63	99.06	154	297	38	307	15.0	8	10	19	70	17	46	<12	1468	<6	19.0	<10					121	58																	9.62
L-834	59.92	0.47	16.55	4.88	0.00	0.05	0.10	1.72	0.29	14.1	0.12	1.28	99.44	283	70	49	274	20.0	7	<6	14	19	9	26	<12	1842	7.0	25.0	<10		12.06	41.53	111.4	192	54		2.88	77.3	0.70							2.45	1.28					14.4
L-835	65.67	0.65	15.35	3.98	0.00	0.08	0.87	2.29	4.41	4.48	0.19	1.44	99.41	135	203	38	342	15.0	<6	<6	7	68	17	40	<12	1318	<6	15.0	10					127	60																	8.89
L-836	67.42	0.74	14.82	4.07	0.00	0.10	0.86	2.21	4.08	4.77	0.20	0.79	100.06	159	266	40	343	17.0	6	<6	19	69	0	45	<12	1272	0.0	0.0	0					0	0																	8.85
L-838	67.61	0.61	14.50	3.84	0.00	0.09	0.82	2.37	3.62	4.48	0.18	0.50	98.62	208	69	22	93	15.6	<6	8	10	30	15	12	<12	552	4.0	21.2	<10					130	55																	8.10
L-839	76.62	0.29	11.26	1.41	0.00	0.04	0.23	0.35	3.05	5.28	0.07	0.47	99.07	218	67	27	163	17.0	<6	9	19	35	13	12	<12	565	<6	16.0	<10					102	44																	8.33
L-840	70.88	0.42	13.61	2.64	0.00	0.07	0.48	1.29	3.97	4.93	0.13	0.75	99.17	176	247	37	237	15.0	<6	8	20	47	16	20	<12	1054	<6	18.0	<10					127	62																	8.90
L-842	65.32	0.68	14.27	4.45	0.00	0.10	1.13	2.64	4.17	3.50	0.19	2.76	99.21	141	316	38	361	16.0	10	11	37	83	16	49	13	1668	<6	16.0	12		11.19	33.40	82.63	135	41		1.48	62.9	1.013							1.64	1.08					7.67
L-843	75.42	0.33	12.58	1.52	0.00	0.03	0.25	0.31	3.01	4.39	0.10	1.13	99.07	163	61	41	199	20.0	<6	<6	6	25	14	16	177	907	<6	21.0	<10		113.0	35.20	74.00	126	32		3.95	10.0	0.65							2.04	0.88					7.40
L-844	68.18	0.63	14.42	3.75	0.00	0.08	0.82	2.22	3.87	4.35	0.20	1.02	99.54	137	259	39	345	16.0	6	7	20	62	17	42	<12	1378	6.0	16.0	<10					129	63																	8.22
L-846	67.61	0.60	14.35	3.72	0.00	0.08	0.89	1.97	4.09	4.59	0.18	0.78	98.86	134	246	44	306	16.0	6	10	18	56	15	39	<12	1240	<6	19.0	<10		11.76	41.76	86.50	133	45			50.4	1.00							1.913	1.09					8.68
L-849	73.54	0.33	12.99	1.74	0.00	0.02	0.20	0.14	3.78	5.57	0.04	0.55	98.90	189	43	24	243	27.0	<6	7	<6	22	18	17	217	451	<6	16.0	<10		107.3	30.33	47.85	152	20		1.013	33.7	0.26							0.24	0.38					9.35
L-855	76.63	0.15	11.87	1.14	0.00	0.02	0.05	0.25	4.70	4.06	0.02	0.25	99.14	88	39	10	71	10.0	<6	10	9	11	15	<12	<12	328	<6	<15	<10					39	16																	8.76
L-857	73.33	0.32	13.00	1.84	0.00	0.04	0.43	1.21	4.01	4.21	0.11	1.00	99.50	155	211	17	141	14.0	<6	9	26	28	15	22	<12	1081	<6	<15	<10					80	38																	8.22
L-863	64.77	0.71	14.71	5.42	0.00	0.08	1.57	3.06	3.37	3.86	0.24	1.14	98.93	155	288	33	228	19.0	14	15	23	72	18	100	122	1004	<6	17.0	11					89	44																	7.23
L-864	66.28	0.74	14.57	5.01	0.00	0.09	1.56	2.96	3.05	4.14	0.33	1.62	100.35	97	249	23	39	11.9	10	16	28	58	16	91	273	1039	3.1	13.4	10	17.4	6.19	37.8	9.86	78	45	0.83	1.38	0.8	1.27	5.35	0.73	4.38	0.86	2.38	0.34	2.22	0.32					7.19
L-864	0.00	0.00	0.00	0.00	0.00	0.00	0.00	0.00	0.00	0.00	0.00	0.00	0.00	0	0	0	0	0.0	0	0	0	0	<9				<6	<15	<10					23	<12																	0.00
L-865	66.29	0.76	14.63	4.88	0.00	0.08	1.51	2.53	3.09	4.38	0.27	1.26	99.68	179	240	34	241	19.0	10	20	21	68	17	84	226	1100	<6	16.0	10					129	67																	7.47
L-868	66.57	0.77	14.29	4.73	0.00	0.10	1.11	2.09	3.56	4.38	0.29	1.15	99.04	112	186	32	22	15.3	10	13	14	:	19	68	114	1100	<6	<15	10	14.6	8.72	52.03	13.28	154	79	1.07	0.84	0.6	1.83	7.21	0.99	6.12	1.18	3.36	0.47	3.09	0.45					7.94
L-874	96.83	0.09	0.64	0.69	0.00	0.01	0.00	0.02	0.02	0.31	0.03	0.08	98.72	11	8	5	29	4.0	<6	13	8	6	17	<12	538	30	6.0	17.0	11					144	73																	0.33
L-874a	67.47	0.89	13.68	4.67	0.00	0.10	1.05	1.71	3.48	4.99	0.27	1.09	99.40	155	181	57	348	24.0	12	14	19	69		63	17	1380																										8.47
L-875	66.20	0.78	14.38	5.11	0.00	0.12	1.18	2.90	3.74	4.25	0.30	1.32	100.28	138	222	46	329	23.0	7	13	14	68	18	71	181	1294	<6	<15	10		12.16	42.90	111.4	157	54			76.6	1.59							1.96	1.23					7.99
L-877	66.24	0.93	13.94	5.04	0.00	0.09	1.14	2.08	3.48	4.74	0.41	1.24	99.33	140	224	54	377	23.0	9	16	22	75	19	62	17	1371	<6	17.0	10					169	87																	8.22
L-878	67.83	0.67	13.61	4.34	0.00	0.09	0.95	1.67	3.73	4.58	0.23	1.08	98.78	152	176	57	329	19.0	9	12	34	71	19	46	16	1143	<6	17.0	<10		12.29	39.36	92.38	150	41			56.1	1.150							2.56	1.213					8.31
L-895	55.24	0.90	18.42	6.32	0.00	0.11	3.12	4.54	4.23	4.61	0.50	1.93	99.92	164	840	22	172	7.0	18	43	164	69	18	134	91	1382	<6	<15	14		8.250	23.24	53.84	74	22			98.6	0.33							0.36	0.91					8.84
L-898	69.20	0.58	12.94	5.11	0.00	0.08	0.60	1.62	4.21	5.14	0.15	0.09	99.72	112	193	33	215	15.0	<6	7	17	46		27	189	1049																										9.35
L-899	71.98	0.41	12.65	2.41	0.00	0.06	0.72	1.79	4.23	3.72	0.11	0.69	98.77	112	193	33	210	18.0	<6	7	17	46	17	26	182	1049	<6	16.0	<10					119	56																	7.95
L-900	67.40	0.67	14.52	4.30	0.00	0.08	1.12	2.21	4.83	4.01	0.21	0.90	100.25	101	244	40	361	16.0	8	8	17	43	17	48	<12	1239	<6	16.0	11					127	61																	8.84
L-902	77.60	0.17	12.00	0.96	0.00	0.02	0.08	0.11	4.16	4.81	0.10	0.34	100.35	160	35	18	95	22.0	<6	7	33	15	15	13	<12	131	<6	25.0	<10					85	39																	8.97
L-903	79.24	0.19	10.48	1.02	0.00	0.02	0.12	0.14	2.98	4.99	0.04	0.32	99.54	262	21	23	103	16.0	<6	8	10	15	13	<12	<12	132	<6	25.0	<10					80	38																	7.97
L-904	76.77	0.24	11.40	1.61	0.00	0.05	0.16	0.10	3.59	4.81	0.05	0.45	99.23	242	44	30	149	18.0	<6	8	15	37	15	<12	14	233	<6	21.0	<10		107.0	29.65	49.94	99	23			7.2	0.28							1.30	0.90					8.40
L-905	77.13	0.29	11.44	1.46	0.00	0.03	0.23	0.54	5.65	1.54	0.06	0.51	98.88	75	80	40	160	19.0	<6	9	17	23	13	13	<12	672	<6	22.0	<10					116	55																	7.19
L-906	76.57	0.27	12.23	1.45	0.00	0.03	0.07	0.32	3.00	5.97	0.03	0.42	100.36	254	43	51	164	21.0	<6	7	37	14	13	<12	269	219	<6	19.0	<10					122	62																	8.97
L-907	71.26	0.43	13.59	2.43	0.00	0.06	0.51	1.34	3.85	5.07	0.11	0.52	99.17	175	181	41	248	16.0	<6	8	11	44	15	24	<12	1136	<6	16.0	<10					135	69																	8.92
L-908	66.78	0.41	16.95	1.82	0.00	0.08	0.28	0.22	9.57	2.63	0.03	0.34	99.11	96	28	10	66	15.5	<6	8	12	53	26	<12	<12	125	<6	15.0	<10	9.7	2.50	17.12	5.04	82	40	1.49	2.03	1.1	0.29	1.92	0.28	1.78	0.37	1.19	0.20	1.64	0.29					12.2
L-909	71.39	0.41	13.73	1.94	0.00	0.07	0.35	0.72	4.37	4.96	0.08	0.91	98.93	153	134	46	285	18.0	<6	8	25	56	17	15	<12	1346	<6	18.0	<10					163	82																	9.33
L-910	70.84	0.59	13.17	3.28	0.00	0.04	0.51	0.53	4.21	4.24	0.20	1.11	98.72	129	126	44	360	17.0	<6	8	12	47	16	26	<12	1115	<6	<15	<10					152	76																	8.45
L-911	72.60	0.37	14.49	2.24	0.00	0.03	0.81	0.22	0.16	5.19	0.11	2.40	98.62	170	16	45	344	27.0	<6	10	33	48	19	17	139	398	<6	19.0	<10					145	75																	5.35
L-912	73.33	0.37	13.50	1.75	0.00	0.02	0.70	0.22	2.05	5.30	0.08	1.55	98.87	139	29	38	273	20.0	<6	7	9	34	17	15	<12	787	<6	16.0	<10					148	47																	7.35
L-917	71.65	0.73	12.99	3.87	0.00	0.08	1.25	0.71	3.95	4.48	0.20	0.63	100.54	113	116	16	39	15.2	6	12	17	50	15	46	15	967	<6	<15	<10	13.4	5.26	30.24	7.86	85	42	1.40	1.36	0.9	1.04	4.56	0.63	3.72	0.68	1.87	0.27	1.86	0.27					8.43
L-919	87.60	0.31	4.60	3.09	0.00	0.03	0.08	0.09	0.12	2.09	0.04	0.79	98.84	79	9	11	99	8.0	6	15	13	14	<9	27	32	297	<6	<15	<10					55	26																	2.21
L-920	36.93	0.23	6.77	1.19	0.00	0.03	0.22	0.29	2.90	2.72	0.06	49.0	100.35	124	81	20	208	15.0	<6	<6	16	29	14	17	134	1088	<6	<15	<10		113.1	35.71	61.91	99	29			18.9	0.66							0.20	0.70					5.62
L-922	68.49	0.77	14.39	4.18	0.00	0.07	0.89	1.69	3.76	4.88	0.23	0.98	100.33	143	206	56	426	27.0	8	9	15	58	18	56	244	1598	<6	16.0	10		22.13	52.85	122.3	159	56			61.6	1.73	4.29						2.49	1.13					8.64
L-923	70.32	0.62	13.18	3.95	0.00	0.06	0.59	0.92	4.03	4.67	0.17	1.02	99.53	162	156	56	425	21.0	6	12	11	55	18	37	<12	1168	<6	21.0	<10					159	89																	8.70
L-924	71.99	0.63	12.33	2.83	0.00	0.05	0.57	1.46	3.58	3.97	0.13	1.69	99.23	82	63	46	359	22.0	8	9	14	26	15	38	<12	1811	<6	19.0	<10					158	79																	7.55
L-938	70.06	0.58	13.36	3.13	0.00	0.05	0.58	1.70	4.16	4.11	0.19	0.90	98.82	76	244	38	294	19.0	6	7	11	44	16	40	266	1785	<6	<15	<10	23.8	117.0	49.23	83.50	96	37	1.37	3.22	38.5	1.43	3.22	0.53	3.70	0.77	2.40	0.39	1.213	0.89					8.27
L-939	68.27	0.56	15.25	3.83	0.00	0.08	0.63	1.89	3.55	5.28	0.14	0.74	100.22	132	422	22	166	11.0	15	16	29	68	16	89	23	1059	<6	<15	11		8.325	30.34	57.99	77	28			77.5								0.58	0.93					8.83
L-940	62.87	0.57	14.38	5.03	0.00	0.09	1.98	6.05	4.02	3.40	0.20	0.69	99.28	133	422	23	173	12.0	14	13	22	64	18	94	17	1043	<6	<15	11		9.050	25.39	64.13	90	31			79.8	0.43							0.64	0.98					7.42
L-943	74.31	0.15	13.23	1.77	0.00	0.04	0.03	0.75	3.70	5.72	0.11	0.29	100.10	137	123	4	65	7.2	<6	9	19	17	14	13	15	350	<6	28.0	<10	18.5	0.91	6.77	2.16	42	20	2.27	3.29	0.5	0.15	0.72	0.10	0.64	0.14	0.46	0.09	0.83	0.17					9.42
L-945	67.85	0.52	15.01	3.25	0.00	0.07	0.55	1.40	4.19	5.08	0.11	0.92	98.95	169	235	45	386	18.0	9	8	20	64	18	2	13	1409	<6	19.0	<10		12.43	41.88	115.1	178	53			61.2	0.85	1.66						2.46	1.13					9.27
L-946	67.96	0.48	14.78	2.89	0.00	0.06	0.59	1.58	4.39	5.01	0.12	0.73	98.59	165	232	38	250	19.0	6	8	8	45	16	30	185	1451	<6	<15	<10					175	88																	9.40
L-948	70.39	0.65	13.17	3.48	0.00	0.11	0.62	1.58	4.48	4.47	0.13	0.41	99.49	160	174	63	368	21.0	7	8	10	73	17	22	<12	1424	<6	15.0	<10					175	92																	8.95
L-951	66.61	0.52	15.75	3.69	0.00	0.02	0.04	0.50	11.34	0.33	0.12	0.19	99.11	4	30	50	261	24.0	<6	10	6	9	16	39	137	<20	<6	22.0	<10		10.83	28.36	109.6	166	14			48.5	0.71	3.14						1.89	1.09					11.67
L-952	67.68	0.59	15.55	4.09	0.00	0.02	0.15	0.73	10.86	0.35	0.15	0.22	100.39	6	38	36	308	23.0	<6	9	6	10	16	31	173	52	<6	<15	<10					38	27																	11.21
L-955	67.86	0.41	16.46	3.50	0.00	0.05	0.11	0.33	10.16	0.19	0.23	0.82	100.12	4	37	40	340	17.0	<6	13	333	142	21	36	<12	30	<6	<15	16		13.25	62.33	671.3	965	405			42.8	0.40							1.79	1.03					10.4
L-956	61.48	2.00	9.60	15.05	0.00	0.04	0.23	2.72	7.38	0.01	0.92	0.23	99.66	5	36	63	321	14.0	9	11	7	17	17	91	<12	51	<6	<15	24			41.30	97.50	116	63			297								3.05	2.13					7.39
L-957	75.71	0.31	11.71	1.52	0.00	0.04	0.21	1.09	2.90	4.90	0.05	0.66	99.10	126	135	32	207	20.0	<6	7	<6	36	14	<12	228	571	<6	26.0	<10		112.1	34.19	59.59	156	79		3.20	7.2	0.28							0.34	0.68					7.80
L-958	47.73	1.22	15.13	13.06	0.00	0.23	7.23	8.03	3.57	0.36	0.22	2.21	98.99	5	188	34	105	5.0	63	122	59	119	19	296	107	297	<6	<15	37					15	<12																	3.93
L-963	88.82	0.21	4.22	2.07	0.00	0.03	0.19	0.14	1.00	1.77	0.06	0.66	99.17	63	17	18	133	8.0	8	11	20	15	<9	25	12	308	<6	<15	<10					64	31																	2.77
L-965	67.45	0.59	13.65	6.24	0.00	0.03	0.32	0.69	4.10	5.73	0.19	0.42	99.41	156	43	88	358	29.0	<6	11	8	24	17	33	12	741	7.00	30.0	<10					125	56																	9.83

Table No. 4.2.1.1 CHEMICAL ANALYSIS OF SAMPLES IN THE KAMANJAB INLIER, NAMIBIA; GREATER LUFILIAN ARC (Cont.)

Sample	SiO2	TiO2	Al2O3	Fe2O3	FeO	MnO	MgO	CaO	Na2O	K2O	P2O5	LOI	Total	Rb	Sr	Y	Zr	Nb	Co	Ni	Cu	Zn	Ga	V	Cr	Ba	U	Th	Sc	Pb	Sm	Nd	Pr	Ce	La	Cs	Hf	Ta	Eu	Gd	Tb	Dy	Ho	Er	Tm	Yb	Lu	Li	Be	Ge	Mo	Na+K
Notch	50.00	*1.0*	*15.5*	*6.00*		*0.15*	*2.00*	*5.00*	*4.90*	*5.5*	*0.3*	2.00		200	*400*	*60*	*360*	*40*	*30*	*16*	*25*	*85*	*26*	*100*	*100*	1300	*20*	*37*	*20*	*20*	*50*	*50*	*15*	*175*	*95*	*3*	*10*	*120*	*4*	*30*	*5*	*20*	*3*	*9*	*35.5*	*7.5*	*1.6*					
L-966	68.15	0.60	12.90	6.30	0.00	0.02	0.16	0.43	4.46	5.68	0.19	0.27	99.16	144	39	74	108	17.1	<6	9	6	19	16	42	193	708	5.82	27.2	<10	17.8	6.29	34.8	9.84	103	45	0.41	3.12	1.2	0.89	7.00	1.36	10.3	2.34	7.51	1.13	7.93	1.21					10.14
L-967	70.72	0.48	12.92	3.64	0.00	0.07	0.46	1.11	3.78	5.05	0.12	0.63	98.98	269	119	83	395	22.0	8	9	13	60	17	31	<12	883	8.00	36.0	<10					259	130																	8.83
L-967a	0.00	0.00	0.00	0.00	0.00	0.00	0.00	0.00	0.00	0.00	0.00	0.00	0.00	0	0	0	0	0.0	0	0	0	0	15	0	0	0	<6	20.0	<10					153	119																	0.00
L-968	72.13	0.34	13.69	2.21	0.00	0.03	0.17	0.89	3.99	4.79	0.05	0.51	98.80	136	145	37	225	15.0	7	9	20	86	15	16	<12	1370	<6	23.0	<10		110.0	16.73	28.51	110	11		2.86	26.2								0.49	0.76					8.78
L-969	59.46	0.49	19.16	4.28	0.00	0.05	0.68	0.38	0.55	14.31	0.08	0.84	100.28	393	66	59	293	24.0	6	<6	47	53	22	61	<12	2451	6.00	29.0	<10		10.51	36.03	92.38	159	37		7.20	60.2	0.66							3.05	1.29					14.9
L-971	64.34	0.54	17.73	1.51	0.00	0.09	0.14	0.68	4.58	8.51	0.11	0.69	98.92	148	66	47	358	22.0	<6	9	10	14	13	34	<12	2236	<6	<15	<10					137	81																	13.1
L-973	71.06	0.42	12.34	2.89	0.00	0.04	0.12	1.90	0.51	9.97	0.09	0.97	100.31	266	42	47	249	19.0	6	<6	141	70	9	28	12	1800	<6	18.0	<10		9.588	33.88	96.50	128	42		5.85	36.5	0.50							3.23	1.138					10.5
L-975	72.48	0.35	13.19	2.05	0.00	0.06	0.27	0.82	3.81	5.40	0.10	0.56	99.09	164	149	34	215	16.0	7	9	45	47	14	19	<12	1327	<6	21.0	<10					137	68																	9.21
L-976	72.48	0.37	13.10	1.84	0.00	0.04	0.29	0.71	4.00	5.29	0.06	0.50	98.68	195	113	55	203	21.0	<6	10	8	29		18	209	1114					115.8	48.35	91.75		71		3.23	13.4	1.03	2.21						2.93	1.08					9.29
L-977	74.68	0.27	11.99	1.72	0.00	0.04	0.24	0.55	3.86	5.21	0.04	0.45	99.05	121	81	27	197	13.0	<6	8	<6	39	15	12	<12	766	<6	16.0	<10					110	57																	9.07
L-978	76.43	0.22	11.10	2.76	0.00	0.10	0.04	0.28	4.16	5.19	0.05	0.18	100.51	139	58	15	133	16.9	<6	10	37	73	20	14	20	264	3.59	19.1	<10	21.3	2.08	13.4	4.14	50	25	0.75	5.11	1.0	0.29	1.79	0.29	2.06	0.48	1.79	0.33	2.76	0.49					9.35
L-979	66.06	0.48	15.03	3.97	0.00	0.09	1.33	3.18	4.23	3.67	0.14	0.79	98.97	108	435	35	143	15.0	10	10	76	88	16	68	242	1077	<6	<15	11					92	44																	7.90
L-980	67.03	0.53	15.05	4.32	0.00	0.09	1.37	3.20	4.47	3.48	0.18	0.77	100.49	115	424	32	157	17.0	10	15	28	62	17	72	200	1140	<6	<15	<10					104	52																	7.95
L-982	66.31	0.56	15.11	3.80	0.00	0.09	1.18	3.09	4.72	3.57	0.19	0.80	99.42	99	495	25	176	12.0	11	10	11	56	17	54	<12	1245	<6	<15	<10		8.588	26.96	66.38	74	30			53.8	0.36							0.55	0.83					8.29
L-983	72.59	0.29	13.57	1.83	0.00	0.04	0.07	0.90	4.08	4.95	0.04	0.51	98.87	197	156	28	181	17.0	<6	6	7	32	15	13	<12	963	<6	19.0	<10					90	39																	9.03
L-985	72.90	0.46	12.76	2.61	0.00	0.05	0.29	1.39	3.72	4.25	0.06	0.63	99.12	123	219	5	51	6.1	<6	7	9	46	14	25	173	1580	1.49	17.1	<10	25.6	3.41	33.2	9.78	103	61	2.13	1.48	0.2	1.09	2.00	0.20	0.97	0.17	0.46	0.07	0.54	0.10					7.97
L-987a	45.74	2.33	16.73	14.31	0.00	0.17	4.10	10.53	2.62	1.59	0.46	1.99	100.57	22	598	11	18	1.9	41	8	75	109	17	429	<12	397	<6	<15	36	7.7	2.50	10.86	2.08	<12	<12	0.29	0.51	0.0	1.03	2.95	0.39	2.37	0.46	1.20	0.15	0.92	0.13					4.21
L-987b	40.92	2.62	19.28	13.71	0.00	0.19	4.13	12.81	2.45	0.79	1.19	2.06	100.15	35	646	19	31	4.0	28	<6	37	72	17	307	<12	284	<6	<15	32			7.100	29.40	16	5			284									1.34					3.24
L-990	53.79	0.31	13.92	7.16	0.00	0.15	8.22	7.59	5.52	0.32	0.10	2.29	99.37	10	267	12	84	10.0	38	178	73	69	13	75	584	187	<6	<15	20					39	22																	5.84
L-991	48.45	0.96	11.97	11.52	0.00	0.19	11.57	9.20	3.07	0.46	0.12	1.70	99.21	7	217	20	53	9.0	64	251	83	93	12	255	870	188	<6	<15	35					19	12																	3.53
L-992	50.94	0.49	19.38	7.11	0.00	0.15	5.16	9.79	3.16	1.87	0.09	2.25	100.39	67	659	10	28	3.4	27	53	35	53	16	144	100	460	0.24	0.9	26	4.4	1.92	9.78	2.25	19	9	0.49	0.75	0.13	0.79	2.03	0.30	1.93	0.39	1.11	0.16	1.04	0.15					5.03
L-993	71.34	0.39	13.57	2.03	0.00	0.05	0.39	1.42	3.97	5.33	0.07	0.81	99.37	115	224	27	75	11.5	<6	6	8	34	15	24	160	1595	<6	17.0	<10	22.5	7.25	47.18	12.68	139	69	0.45	2.38	0.59	1.21	5.76	0.82	5.12	1.00	2.86	0.42	2.84	0.41					9.30
L-994	70.70	0.40	13.83	2.09	0.00	0.05	0.43	1.46	3.95	5.07	0.09	0.73	98.80	110	226	37	208	19.0	6	7	10	33	15	32	195	1763	<6	<15	<10					142	70																	9.02
L-995	39.21	3.69	11.13	22.15	0.00	0.26	7.20	10.83	1.60	0.53	1.13	1.13	98.86	14	449	21	27	4.0	59	<6	54	128	19	491	<12	457	<6	<15	45					<12	<12																	2.13
L-996	69.95	0.44	14.71	2.86	0.00	0.06	0.50	1.75	4.30	4.78	0.11	0.95	100.41	121	274	24	78	13.9	6	9	67	71	16	30	<12	1498	2.82	14.9	<10	23.0	6.17	39.6	10.8	113	49	0.69	2.30	0.83	1.22	4.96	0.74	4.69	0.93	2.78	0.42	2.93	0.42					9.08
L-997	69.62	0.34	15.29	1.59	0.00	0.04	0.27	0.51	5.88	5.33	0.05	0.73	99.65	135	65	57	241	22.0	8	9	8	24	16	19	<12	542	<6	33.0	<10		111.4	28.71	57.06	156	21		4.19	11.06								2.45	0.95					11.21
L-998	64.78	0.73	15.67	4.59	0.00	0.11	1.41	2.78	4.52	4.03	0.24	1.33	100.19	103	300	34	347	15.0	6	9	29	96	18	53	13	2134	<6	<15	10		10.00	32.01	78.50	106	38			63.0	0.94								1.04	1.03					8.55
L-999	67.68	0.49	14.73	3.02	0.00	0.07	0.74	1.83	4.31	4.65	0.13	1.19	98.84	140	252	37	288	20.0	<6	9	10	58	17	33	205	1537	<6	16.0	<10		9.700	36.04	91.88	144	44		1.53	39.2	0.83							1.49	0.89					8.96
L-1000	67.91	0.47	15.37	2.32	0.00	0.06	0.52	1.06	4.28	5.11	0.10	1.68	98.88	192	112	37	251	18.0	<6	10	62	58	17	35	<12	1206	<6	20.0	<10		11.55	90.10	152.3	134	80			82.0	3.48								2.58	1.20					9.39
L-1002	77.59	0.26	11.61	1.64	0.00	0.05	0.10	0.32	3.59	4.97	0.03	0.33	100.49	180	40	25	134	22.0	<6	8	6	14	14	10	<12	180	<6	28.0	<10		104.0	18.61	52.50	87	26		3.35	5.4								1.60	0.93					8.56
L-1003	68.00	0.50	15.07	2.73	0.00	0.05	0.58	1.60	4.64	5.26	0.12	0.69	99.24	145	242	40	289	16.0	<6	8	12	47	17	32	<12	1796	<6	15.0	<10		8.450	28.94	79.13	133	26		2.58	31.7	0.78							1.71	0.95					9.90
L-1005	71.20	0.48	12.46	3.35	0.00	0.06	0.56	1.47	3.93	4.47	0.18	0.76	98.92	171	218	46	298	18.0	7	9	15	50	17	26	16	1194	<6	18.0	<10					132	64																	8.40
L-1007	64.26	0.56	15.15	5.20	0.00	0.10	1.92	3.56	4.03	3.92	0.20	0.55	99.45	169	234	45	318	16.0	7	10	22	61	17	38	<12	1413	<6	22.0	<10					160	78																	7.95
L-1009	66.67	0.69	15.06	4.31	0.00	0.09	1.05	2.81	4.12	4.42	0.26	0.88	100.36	129	347	38	354	15.0	7	7	18	71	17	53	<12	1757	<6	16.0	10					115	55																	8.54
L-1010	63.36	0.80	15.40	5.08	0.00	0.11	1.26	3.27	4.15	4.24	0.34	1.17	99.18	138	385	37	372	15.0	9	10	21	74	18	53	<12	1944	<6	<15	12					110	55																	8.39
L-1011	66.33	0.64	14.74	3.94	0.00	0.09	0.94	2.72	4.53	4.43	0.19	0.82	99.37	152	302	38	308	20.0	7	9	21	73	17	50	126	1322	<6	17.0	10					129	66																	8.96
L-1012	64.77	0.68	15.28	4.30	0.00	0.20	0.95	3.01	5.41	3.94	0.20	0.97	99.71	132	337	42	332	22.0	8	10	9	331	17	53	105	1550	<6	17.0	<10					139	74																	9.35
L-1013	67.41	0.61	14.33	4.04	0.00	0.08	0.94	2.09	4.00	4.72	0.21	0.95	99.38	171	240	39	331	16.0	6	10	26	67	17	47	<12	1290	<6	19.0	<10		108.4	40.58	79.25	131	35			48.2	0.64							1.74	0.98					8.72
C-1	74.03	0.27	12.73	1.15	1.51	0.05	0.31	0.48	3.67	5.09	0.05	0.71	100.05	100	50	70	500	30.0	<10	<10	n.d		25	<3	10	1200				25.0					95			<100										<3	<3	<30	<3	8.76
C-2	69.71	0.68	14.17	1.69	1.57	0.04	0.84	0.82	4.10	5.30	0.27	0.67	99.86	70	110	45	550	30.0					25	35	25	2100				8.0					90														35				9.40
C-3	68.63	0.67	15.43	1.74	1.03	0.10	0.51	1.99	4.50	4.42	0.18	0.50	99.70	90	350	140	700	40.0					25	35	11	2500				25.0					130														30				8.92
C-4	73.63	0.33	14.16	1.13	0.24	0.02	0.00	0.50	3.14	6.35	0.07	0.44	100.01	200	80	20	380	20.0					20	9	13	1200				40.0					95														11				9.49
C-5	75.35	0.27	13.18	1.08	0.22	0.02	0.00	0.62	3.15	5.50	0.05	0.36	99.80	110	100	35	280	10.0					20	5	15	1400				30.0					65														12				8.65
C-6	66.09	0.69	14.60	3.06	1.72	0.08	1.81	2.54	3.25	4.71	0.28	1.11	99.94	150	480	25	280	<10					20	85	18	1900				14.0					75														25				7.96
C-7	69.29	0.47	14.55	1.81	1.48	0.06	1.19	2.83	3.33	4.40	0.17	0.46	100.04	230	650	25	320	10.0					19	70	35	1700				16.0					70														13				7.73
C-8	73.88	0.33	13.85	0.87	0.24	0.03	0.18	0.26	4.05	5.93	0.09	0.39	100.10	130	40	55	450	15.0					20	7	11	400				20.0					65														4				9.98
C-9	73.30	0.32	13.20	2.93	0.48	0.01	0.00	0.24	3.46	5.67	0.07	0.34	100.02	130	50	80	650	30.0					30	<3	14	1200				12.0					85														9				9.13
C-10	68.63	0.49	15.01	1.62	1.44	0.07	1.22	2.74	4.41	3.60	0.20	0.57	100.00	65	720	25	230	<10					20	55	30	1900				18.0					70														20				8.01
C-11	78.84	0.29	10.79	0.95	0.27	0.03	0.09	0.60	2.94	5.20	0.06	0.22	100.28	120	65	55	180	18.0					15	5	25	560				20.0					100														<3				8.14
C-13 (w	75.89	0.41	12.46	1.07	0.13	n.d.	0.05	0.25	3.60	5.71	0.04	0.50	100.11	100	40	65	650	40.0	<10	<10	n.d.		25	<3	10	1000				30.0					90			<100										<3	<3	<30	<3	9.31
C-14	48.69	1.26	13.27	4.86	8.71	0.18	6.15	10.49	2.41	1.05	0.22	0.50	97.79																																									3.46

Felsic volcanics, Namibia

Notch	50.00	*1.0*	*15.5*	*6.00*		*0.15*	*2.00*	*5.00*	*4.90*	*5.5*	*0.3*	2.00		200	*400*	*60*	*360*	*40*	*30*	*16*	*25*	*85*	*26*	*100*	*100*	1300	*20*	*37*	*20*	*20*	*50*	*50*	*15*	*175*	*95*	*3*	*10*	*120*	*4*	*30*	*5*	*20*	*3*	*9*	*35.5*	*7.5*	*1.6*					
Notch	50.00	*1.0*	*15.5*	*6.00*		*0.15*	*2.00*	*5.00*	*4.90*	*5.5*	*0.3*	2.00		200	*400*	*60*	*360*	*40*	*30*	*16*	*25*	*85*	*26*	*100*	*100*	1300	*20*	*37*	*20*	*20*	*50*	*50*	*15*	*175*	*95*	*3*	*10*	*120*	*4*	*30*	*5*	*20*	*3*	*9*	*35.5*	*7.5*	*1.6*					
X-16	75.93	0.26	12.08	2.96	0.32	0.01	0.36	0.48	7.93	0.13	0.07	0.42	100.95																																									8.06
X-17	72.07	0.33	13.36	3.76	0.25	0.02	1.33	1.01	7.95	0.30	0.04	0.49	100.91																																									8.25
X-18	69.24		12.00					0.55	3.83	5.36		0.00	90.98																																										9.19
X-19	72.02	0.32	13.78	2.24	1.02	0.02	0.20	0.39	4.07	5.18	0.03	0.65	99.92																																									9.25
X-20	76.01	0.23	12.05	0.80	0.91	0.03	0.20	1.02	3.09	5.02	0.01	1.14	100.51																																									8.11

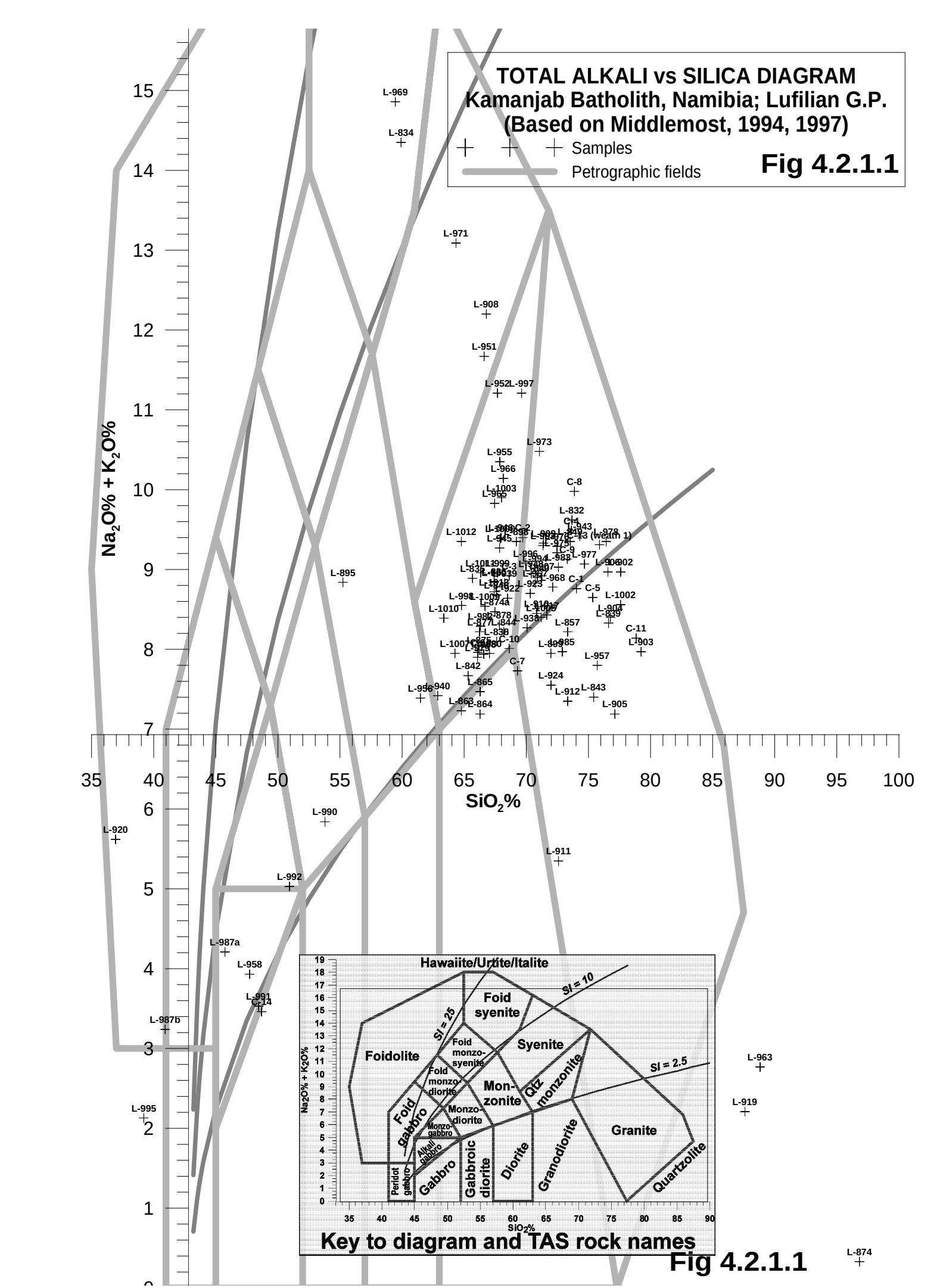
TOTAL ALKALI vs SILICA DIAGRAM
Kamanjab Batholith, Namibia; Lufilian G.P.
(Based on Middlemost, 1994, 1997)
Samples
Petrographic fields
Fig 4.2.1.1
Na2O% + K2O%
SiO2%
Hawaiite/Urtite/Italite
Foid syenite
Syenite
Foidolite
Foid monzo-syenite
Foid monzo-diorite
Mon-zonite
Qtz monzonite
Monzo-diorite
Monzo-gabbro
Foid gabbro
Alkali gabbro
Peridot gabbro
Gabbro
Gabbroic diorite
Diorite
Granodiorite
Granite
Quartzolite
SI = 10
SI = 25
SI = 2.5
Key to diagram and TAS rock names
Fig 4.2.1.1

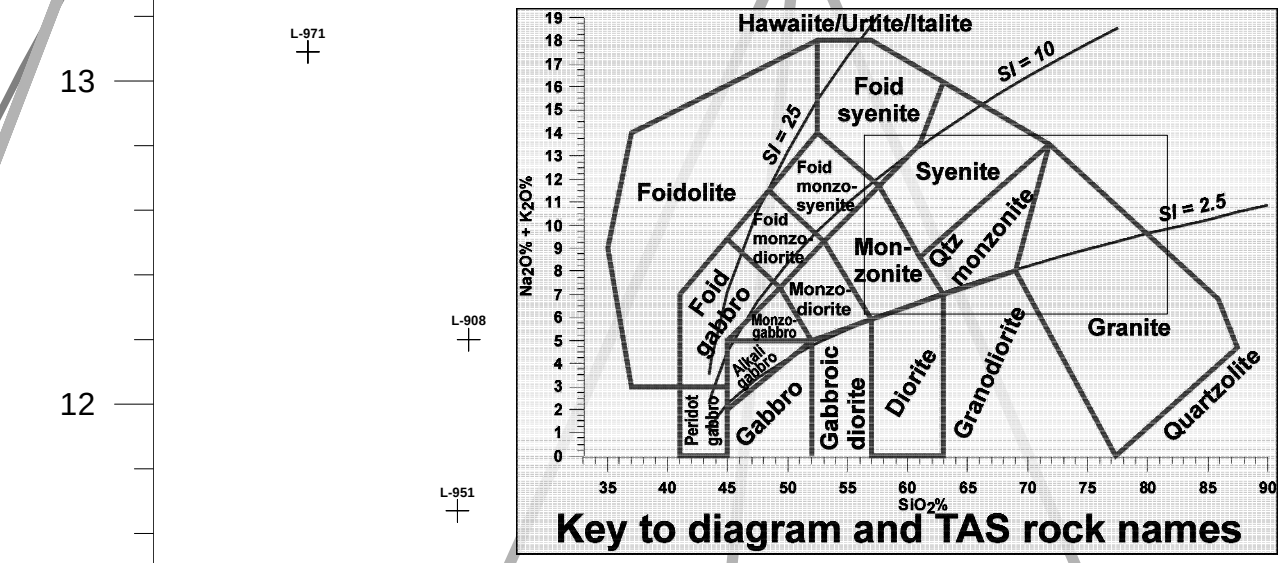

TOTAL ALKALI vs SILICA DIAGRAM
Kamanjab Batholith, Namibia; Lufilian G.P.
(Based on Middlemost, 1994, 1997)

Samples

Petrographic fields

Fig 4.2.1.2

$Na_2O\% + K_2O\%$

$SiO_2\%$

Fig 4.2.1.2

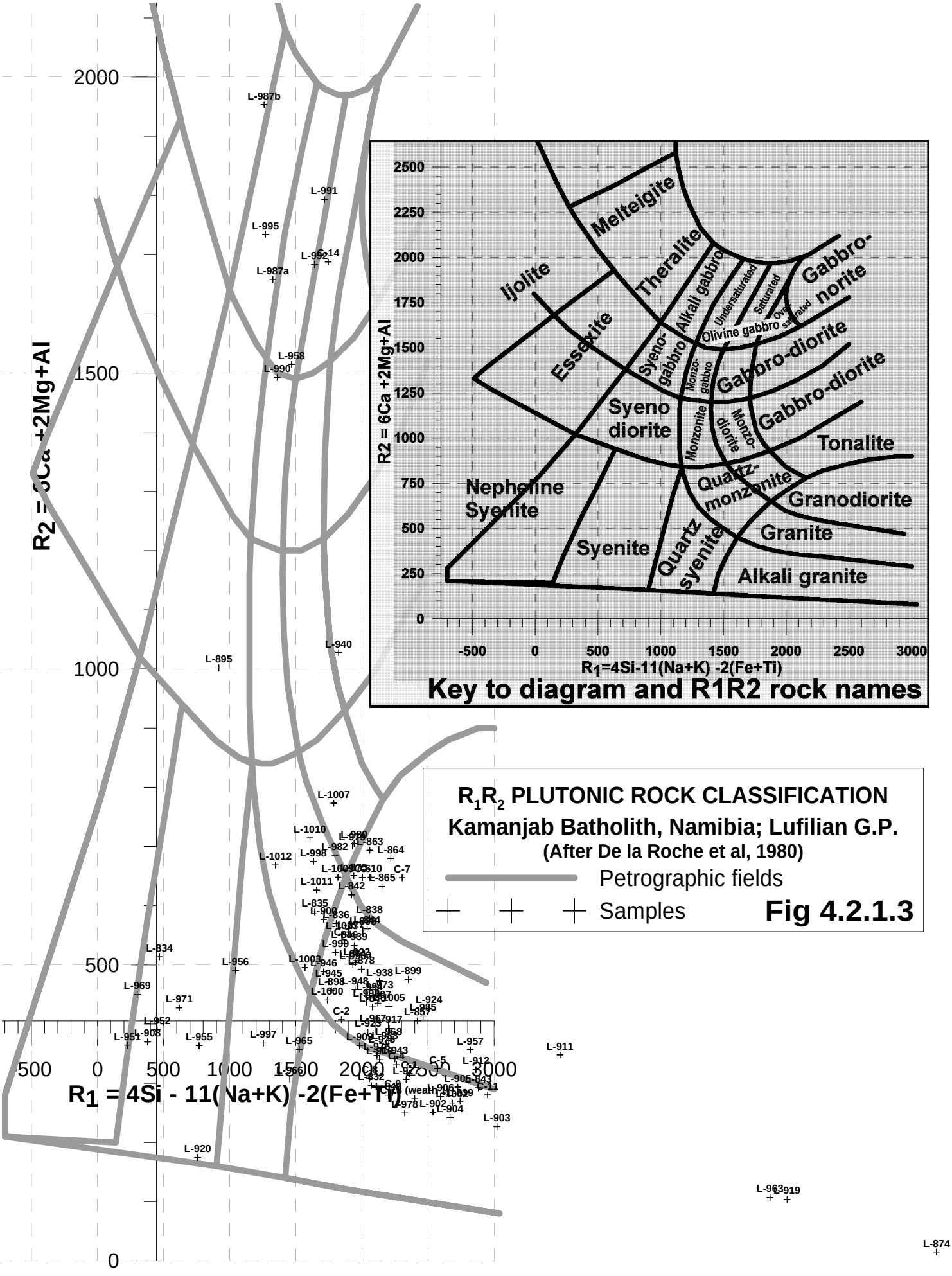
R2 = 6Ca +2Mg+Al
R1 = 4Si - 11(Na+K) -2(Fe+Ti)
2000
1500
1000
500
0
-500
0
500
1000
1500
2000
2500
3000
L-987b
L-991
L-995
L-992
L-987a
L-958
L-990
L-940
L-895
L-1007
L-1010
L-1012
L-998
L-1011
L-835
L-834
L-956
L-969
L-971
L-952
L-951
L-903
L-955
L-997
L-965
L-920
L-911
L-957
L-912
L-904
L-902
L-978
L-963
L-919
L-874
R2 = 6Ca +2Mg+Al
R1=4Si-11(Na+K) -2(Fe+Ti)
Melteigite
Ijolite
Theralite
Alkali gabbro
Undersaturated
Saturated
Gabbro-norite
Olivine gabbro
Essexite
Syeno-gabbro
Monzo-gabbro
Gabbro-diorite
Syeno diorite
Monzonite
Monzo-diorite
Tonalite
Nepheline Syenite
Quartz-monzonite
Granodiorite
Syenite
Quartz syenite
Granite
Alkali granite
Key to diagram and R1R2 rock names
R1R2 PLUTONIC ROCK CLASSIFICATION
Kamanjab Batholith, Namibia; Lufilian G.P.
(After De la Roche et al, 1980)
Petrographic fields
Samples
Fig 4.2.1.3

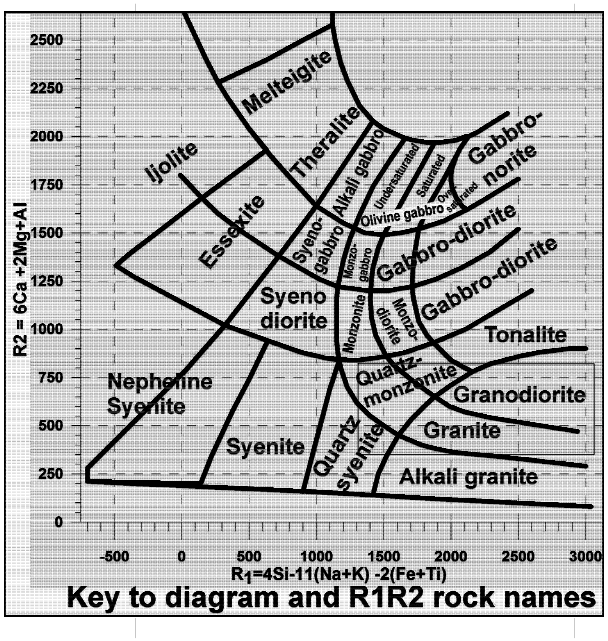

R_1R_2 PLUTONIC ROCK CLASSIFICATION

Kamanjab Batholith, Namibia; Lufilian G.P.

(After De la Roche et al, 1980)

Petrographic fields

Samples

Fig 4.2.1.4

Fig 4.2.1.4

Table 4.2.1.3 Brief description of analysed samples, Kamanjab Batholith, Namibia

sample	Brief Description	blue qz	xenoliths	myarolites	foliated	volcanic	sulfides
L-832	foliated m-g gtd near mapped shear zone. General foliation 051/86NW				x		
L-834	f-g subvolcanic rk light pink to light gray; w/ myarolites, small porphyries. ridge that cuts road. Hard rk. More resistant to weathering than surrounding granitic rocks.			x		x	
L-835	foliated, gneissose intrusive. Small o.c. Maybe basement gneiss or sheared granite. Foliation 100/71S.				x		
L-836	foliated porphyritic rk. Seems to be vulcaniclastic deposit. Forms ridges as if a dike or tabular sedimentary unit. W/ very thin epidote veinlets. Foliation is not apparent in handsample. 170/71 = gral foliation.				x	x	
L-838	m-g, non-foliated gtd						
L-839	Large outcrop of gtd. Very hard to find fresh sample. Series of hills by road.						
L-840	Gtd. Hard to find fresh. Cut by quartz vein						
L-842	Bk, glassy, porphyritic lava(?). Not very dense. Chalcedony (?) fills vacuoles. Maybe conforms a suvbolcanic dike. No time to complete the minimum outcrop size.					x	
L-843	foliated, porphyritic gtd w/ white porphyroclasts; looks like a deformed subvolcanic rk. W/ blue qtz porphyries. Bk matrix. Nearby qtz veins seem to have carried sulfides.	x				x	
L-844	Textural variation of L-843, with bk matrix., cut by qtz veins w/ sulfides.	x					
L-846	gtds w/ qtz veining, abundant qtz some w/ vugs						
L-849	gtd hard to find fresh						
L-850	fg, gray, homogeneous granite, w/ occasional xenoliths of dk green amphybolite. Fresh rock. O.c. by road		x				
L-855	only rock from that part of the world. Could not carry out any more detailed work.						
L-857	oc of gtd by road.						
L-863	Foliated gtd in large outcrop. Fresh sample (diorite?)				x		
L-864	Foliated gtd, ready to slab. W/ epidote veinlets and sheared, pink, coarse porphyroblasts; main foliation 035 suvbertical. Large outcrop				x		
L-864							
L-865	End of very large oc of fol gtd. Continues from L-864. Compound for a large sample. Dateable				x		
L-868	Coarse gtd w/ blue qurtz, zoned plagioclase, auhedral, rectangular; some rounded. Abundant qz veins cut rk. Good for dating.	x					
L-874							
L-874-	low lying gtd from Kamdescha farm						
L-875	low lying gtd from Kamdescha farm, very fresh						
L-877	large o/c of gtd by main road. Many small hills						
L-878	gtd by main road. Freshest possible						
L-895	Subvolcanic porphyritic rk. From Gelbingen farm					x	
L-898	C-g porphyritic, foliated gtd. Very large outcrop on both sides of road. Main fol= 065/73S				x		
L-899	vf-g metavolcanic rk, fresh, w/ chlorite, main foliation 045/90, there are two minor foliations.				x	x	
L-900	C-g, foliated gtd, low lying oc just by road. Main foliation=040/74W				x		
L-902	Long hill outcrop that extends for kilometers perpendicular to road. (probably foliated vertically, at right angle to road)						
L-903	M-g gtd. Large outcrop on both sides of road. But by numerous 5cm qtz veins, probable quartzite xenoliths		x				
L-904	M-g gtd hill by road						
L-905	M-g gtd						
L-906	very fresh m-g gtd, cuts both sides of road. Good for dating.						
L-907	vc-g porphyritic gtd. Large outcrop on both sides of road. Hard to find completely fresh. Intense chloritization.						
L-908	M-g gtd medium gray color. Large outcrop on both sides of road						
L-909	volcanic rk, foliated into a schistose rk; very good outcrop. As fresh as could be found.				x	x	
L-910	volcanic k, foliated to look like schists. Maybe chemistry compares to some of intrusives. Many outcrops.				x	x	
L-911	Schistose rk of probable volcanic origin. Representative sample for geochem and comparison. These rocks do not form high hills				x	x	
L-912	Representative sample of slightly metamorphosed volcanic rks; schistose, outcrop both sides of road				x	x	
L-917	Foliated porphyritic gtd; gneissose texture, abundant micas give it schistosity. Fol=070/79S				x		
L-919	Orthoquartzitic quartzite. This rock cuts through ridge made of volcanic rocks.						
L-920	dike of fine-med g gtd underformed and cuts foliated schistose volc. Rks. It probably also cuts fold intrusive rks of hill. Very fresh large sample. Very low-lying outcrop. Approximate strike of dike=060.						
L-922	Foliated granitoid that makes hill				x		

sample	Brief Description	bl qz	xenol	myar	foliat	volc	sulfs
L-923	M-g gtd from large hill						
L-924	Foliated gtd				x		
L-938	Whaleback of fold gtd q/ qtz veins. Vein in sample runs 050 strike.				x		
L-939	C-g gray gtd w/ abundant xenoliths that show preferential flow orientation. Very good outcrop.		x				
L-940	Enclaves of bk amphybolitic material in L-939		x				
L-943	dikes of f-g gtd that cut c-g gtd w/ foliation (L-945 and 939)						
L-945	Fol c-g porphyritic gtd. (same as L-945 and 939) large enclaves are overprinted by large K-spar porphyroblasts.Good description.				x		
L-946	small isolated o/c of same rock L-945. Extremely fresh				x		
L-948	intruded c-g fol gtd				x		
L-951	small o/c of slightly foliated gtd that is extremely fresh. Maybe freshness is due to albitization				x		
L-952	Two facies of banding in the c-g porphyritc gtd. This one is white						
L-955	fine-grained (volcanic-looking) slightly-foliated, very felsi rk. High Cu,Na,Zn,Al				x	x	
L-956	Coarse-grained foliated granitoid, high Fe,Ti,Na,Al,P2O5. Good descriptions				x		
L-957	very fine-grained, silicic, glassy, pink rk w/ some rare coarse crystals. Subvolcanic (?) metamorphosed volcanic rk? Very fresh for chemical analysis.					x	
L-958	Gabbroic rk that is slightly foliated				x		
L-963	Bx w/ abundant angular vugs. Assay and slab. Whole rock chem analysis						x
L-965	Several samples of bxs w/ abundant angular vugs that might have carried sulfides. Slab & study. May be relect gossan. Might indicate sulfide types.high Zr.						
L-966	Foliated, pink intrusive. Not as coarse as "normal" granitoid. Fresh. High Zr.				x		
L-967	Pink, coarse-grained intrusive, to make sure it's the same, as fresh as could be found. Big outcrop.						
L-967a							
L-968	"Country rock" porphyry that is hydrothermally altered (Clay alteration).						
L-969	Porphyry w/ gossanous vugs after disseminated sulfides, mainly py.						x
L-971	porphyry w/ gossanous vugs after disseminated sulfides						x
L-973	Porphyritic rk of the L-969 type w/ vugs, gossanous w/ diss bornite (?) + blue, cubic, translucent mineral (flourite?) + purple translucent mineral	x					x
L-975	M-g gtd w/ minor diss sulfides						x
L-976	Fresh M-g gtd						
L-977	fg gtd (volcanic?), small, low-lying outcrop					x	
L-978	C-g gtd w/ blue qtz phenocrystals. Very fresh rk. 2 o/c by road	x					
L-979	C-g gtd in large o/c by road. No visible blue qtz						
L-980	c-g gtd in large o/c by road, more mafic than L-979, slightly foliated				x		
L-982	C-g, slightly foliated gtd in very large o/c by road				x		
L-983	C-g gtd w/ slight foliation				x		
L-985	M-g gtd that makes large hill; fresh						
L-987a	Fresh dioritic (?) porphyry w/ diss py. Looks like porphyry copper rk type. Unweathered and sulfides are fresh. Probably subvolcanic rk. More mafic than other seen today.					x	x
L-987b	Pink, f-g porphyritic rk w/ diss sulfides						x
L-990	Coarse gabbro w/ white band (plag?) (vein?) high Cu						x
L-991	Coarse gabbro w/ white band (plag?) (vein?) high Cu						x
L-992	Intermediate to mafic med-to-coarse gtd rk w/o sulfides.						
L-993	Pink, fine-grained, porphyritic rk w/ blue qtz porphyroblasts and diss sulfides ncluding cpy. Large for dating + geochem	x					x
L-994	Pink, fine-grained, porphyritic rk w/ blue qtz porphyroblasts and diss sulfides including cpy. Fresh	x					x
L-995	Gabbro (or mafic rk) w/ diss py + cpy; high Ti,Fe,Ca,Cu						x
L-996	M-g gtd not very good outcrop. High Cu						x
L-997	pink rk						.
L-998	brown rk						
L-999	strongly foliated gtd w/ megacrysts of hexagonal form (apatite or zircon?) Neither seems reasonable from cheman				x		
L-1000	Med-g gtd, fresh on both sides of road high Cu						x
L-1002	Intensely-fractured and qtz-veined massif of med-g, pink gtd. Possibly hydrothermally altered. Freshest possible						
L-1003	Slightly foliated coarse-grained volcanic rk (?) from basement (?)				x	x	
L-1005	Coarse-g, fol, porphyritic gtd intruded by pink aplitic dikes						
L-1007	Foliated, pink, porphyritic gtd.				x		
L-1009	Foliated, med-g gtd				x		
L-1010	Foliated, med-g gtd				x		
L-1011	Very fresh, coarse-g, foliated, porphyritic gtd w/ bk matrix				x		
L-1012	Very fresh, coarse-g, foliated, porphyritic gtd w/ bk matrix				x		
L-1013	Coarse-g gtd						

Table 4.2.1.2 Statistics of rock types, Kamanjab Batholith, Namibia
The fifth column (granitoids) is the sum of underlined rock types.

Group	Rock type	Number	%	Granitoids	Groups
Midalkaline Rocks	Alkali granite	26	24.07	73.40	68.52
	Quartzmonzonite	38	35.19		
	Syenite	3	2.78		
	Monzonite	2	1.85		
	Monzodiorite	1	0.93		
	Monzogabbro	1	0.93		
	Alkali gabbro	3	2.78		
Subalkaline Rocks	Granite	22	20.37	26.60	26.85
	Granodiorite	3	2.78		
	Quartzolite	3	2.78		
	Garbo	1	0.93		
Alkaline Rocks	Foid syenite	2	1.85		4.63
	Foidolite	2	1.85		
	Peridot gabbro	1	0.93		
Total		108	99.07	100.00	100.00

In general terms, geochemistry of the Kamanjab Batholith shows the following trends (Fig 4.2.1.5): There is a negative correlation of silica with titanium dioxide, alumina, total iron oxide, manganese oxide, magnesia, lime, soda and P_2O_5; a positive correlation was observed between silica and potash. The correlation trends are very narrow and rather simple, as illustrated. There is a general uniformity in the chemical variation of the rocks. Most of the samples cluster from 63 to 78% silica.

The diagrams of Si vs total iron, Si vs Al and modified TAS show two very distinct groups of granitoids (See Fig 4.2.1.5). Samples in each of the two separate groups from the two diagrams are the same. After various studies, it became clear that the two groups have clear geochemical and physical distinctions. This will be discussed again in greater detail on section 4.2.1.6.

Characteristic barium (and La?) enrichment is widespread throughout the batholith. Samples L-987 to L-992 all show enrichment in Mn, Mg, Ca, Cu and Sc. That suite seems to have formed in a non-anorogenic environment related to crustal contamination. Some groups of samples have high Pr values.

4.2.1.3 Main Rock Suites

At least two contrasting rock types were identified in most of the regions visited throughout the Kamanjab Batholith. These contrasting rocks outcrop together in close spatial association. Each suite of samples was collected to obtain the representative rock types from a given, relatively small area.

Table 4.2.1.4 reviews main aspects of each of the suites. In this case, rock names are based on the modified TAS diagram, and they have been plotted on Figs F1 to F16 in the Appendix. The suites are well spread across the Kamanjab Batholith, as shown on Fig 4.1.2.6. Six suites are described below for greater clarity; more detailed descriptions of the rock suites are included in Appendix A64. Rock subgroups that make the suites are normally different from those of other suites. No two suites were identical.

Although several rock types may be represented in a suite, that does not mean the entire universe of rock types is present. There are many conditions that bias sampling. For these reasons, the number of rock types in each of the suites of Table 4.2.1.4 should be considered to be an absolute minimum of the true conditions.

Macroscopically visible sulfides were found to be present in a few of the suites. Copper primary sulfides and secondary minerals were also detected in select locations. This will be further described in section 4.2.1.10.

4.2.1.3.1 Examples of Rock Suites

Suite B (Fig F2) has at least six distinct rock types: **L-843** and **L-839** make two different groups of granites; **L-840** is an alkali granite; **L-1011** and **L-1012**, **L-838** and **L-842,** and **L-1010** make three contrasting groups of quartzmonzonites.

Suite E (Fig F5) is made by three distinct rock types: **L-908** in the syenite field; **L-904**, **L-905**, **L-906, L-911** and **L-912** in at least three parts of the granite field, **L-907**, **L-909** and **L-910** in the alkali granite field.

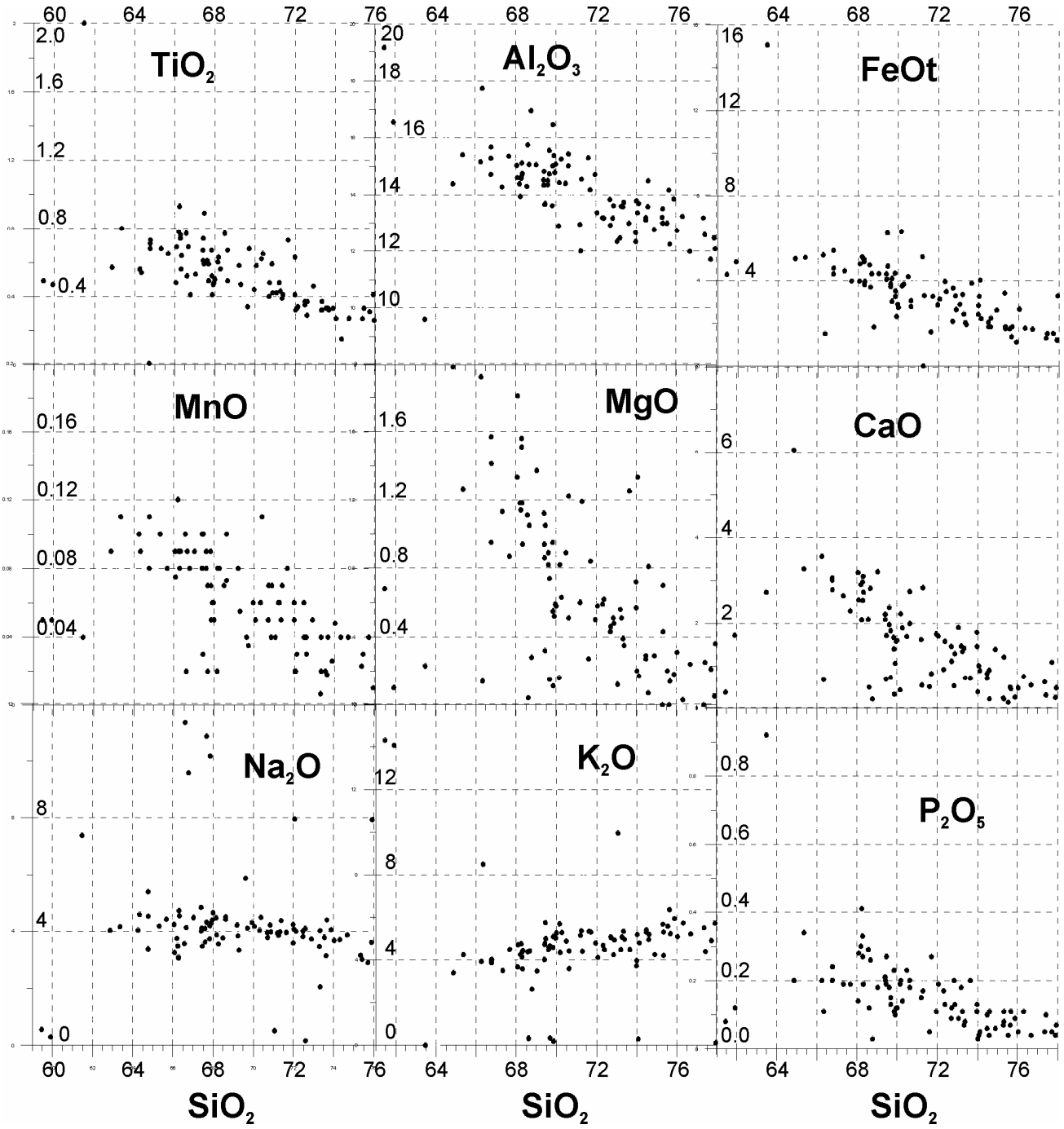

Fig 4.2.1.5 Correlation diagrams between silica and the major oxides for samples from the Kamanjab Batholith, Namibia. *All values are in percentage.*

Suite G (Fig F7) has **L-940** in the monzonite-quartzmonzonite limit; **L-939**, **L-945**, **L-946** and **L-948** in the quartzmonzonite-alkali granite field, and **L-943*** in the alkali granite. **L-939** is a medium-grained granite. **L-940** is one the very abundant mafic xenoliths contained by **L-939**. **L-945** is a foliated, coarse-grained granitoid that acts as host to all the other rocks in the suite. **L-943*** is one of many dikes that intersect **L-945**, **L-939** and **L-948**. All the chemistries are roughly similar, but on closer examination, they can be discriminated. The two main rock types have a non-anorogenic signature. Figs 4.2.1.19 are typical textures of the four types of rocks. Note that all of them show the "fuzzy" texture, especially Fig 4.2.1.19C. **L-943*** that was dated is shown too.

In **Suite H** (Fig F8), **L-958** is an alkali grabbro; **L-956** is a monzonite; **L-957** is a granite, **L-951** and **L-952** span the syenite and quartzmonzonite fields; and **L-955** is a quartzmonzonite. The environs of this suite contain abundant mineralized hydrothermal breccias hosted in quartzites and mainly conformed by quartzites. Samples of the breccias contain sulfides. None of the samples has been assayed to date. Figs 4.2.1.20 are typical textures of three of the suite's main rock types.

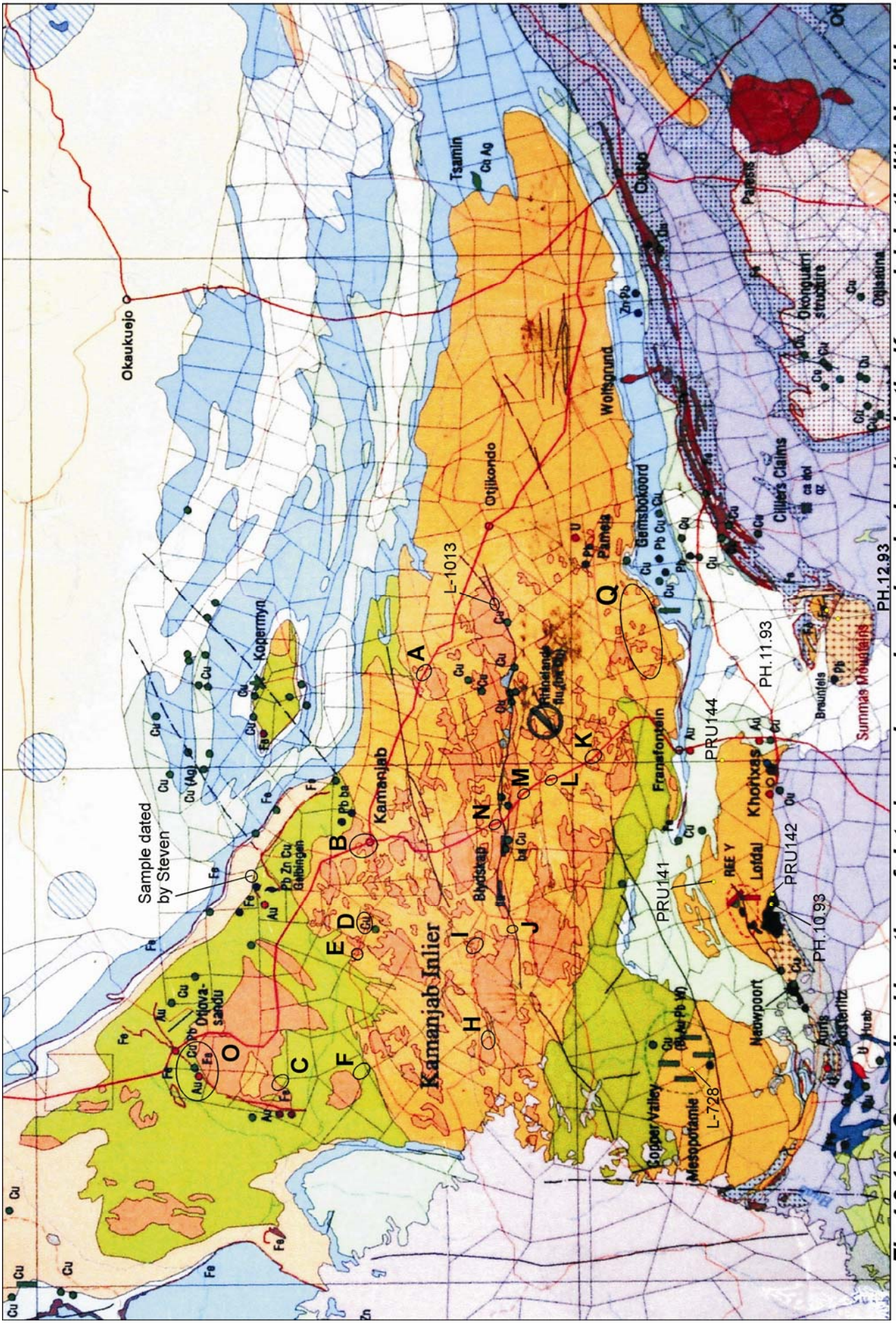

Fig 4.2.1.6 Generalized location of dated samples and geochemical suites in the Kamanjab batholith, Namibia.

Table 4.2.1.4 Kamanjab Batholith rock suites that are made by two or more rock types

(Underlined suites are mineralized. Dated samples are marked with an asterisk.
Photographed samples are in italics. Bold samples were not analysed.)

	Sample number	Samples Analysed	Rock Types (sensu TAS) (#, quality, types)	Environment of emplacement	Map	Notes	Rock Groups TAS diagram
A	4	**L-832, L-834, L-835**	3 Very good. Quartzmonzonite, alkali granite, nepheline syenite	Anorogenic	K-17 CE		1, 8, 10
B	10	*L-838, L-839*, L-840, L-842, L-843, L-1010, L-1011, L-1012	6 Good Granite and Quartzmonzonite	Non-Anorogenic (L-838)	K-16 C		3, 5, 6, 8, 9, 10, 14
C	9	L-863, L-864, L-865, L-868*, *L-874*, L-874-, L-875, ***L-867A, L-871, L-873***	4 Very good. 2 quartzmonzonites, granodiorite and altered granite	Non Anorogenic, subduction? (L-864, L-868)	K-14 SW	Contains Au and Fe mineralization, near major N-S fault	8, 11, P, Q
D	6	L-898, L-899, *L-900, L-902,* L-903	3 Good. Quartzmonzonite, granite	Anorogenic Rift-related	K-16 WC	Disseminated Cu mineralization	5, 10, 12
E	10	*L-904*, L-905, L-906, *L-907*, L-908, L-909, L-910, L-911, L-912	6 Very good. Syenite, granite, alkali granite	Anorogenic	K-16 WC		2, 9, 10, 12, 13, 14
F	4	*L-919*, L-920, *L-922*	3 Very good. Quartzmonzonite, gabbro and altered granite	Anorogenic	K-15 NW		3, 5, Q
G	9	*L-939, L-940, L-943*, L-945*, L-946, *L-948*	4: 2 quartzmonzonite, 2 alkali granite	Non Anorogenic (L-940)	K-18 WC		5, 7, 9, 10
H	10	L-951, L-952, *L-955, L-956,* L-957, *L-958,* ***L-954***	4 Very good. Granite, gabbro, monzonite	Non-Anorogenic (L-958?)	K-18 SC	Disseminated Cu mineralization	3, 7, 10, G
I	7	*L-963*, L-965, L-966, L-967, *L-967a*	4 Good. Quartzmonzonite, alkaline granite, altered granitoid, monzonite	Anorogenic	K-19 WC		5, 9, P, Q
J	6	*L-968, L-969*, L-971, L-973*, L-975, L-976	4 Very good. Nepheline syenite, syenite, alkali granite	Anorogenic	K-19 SW	Disseminated Cu mineralization	1, 2, 4, 9
K	6	*L-977a, L-978*, L-979, *L-980, L-982*	3 Very good. Quartzmonozonite, alkali granite	Non-Anorogenic, Subduction (L-979, L-980, L-982)	K-21 NW	One of the rock types was not analysed.	8, 10
L	4	*L-983*, L-985, ***L-984, L-986***	3 Not clear. Granite, alkali granite		K-20 CW	One of the rock types was not analysed.	9
M	13	L-987, *L-987a, L-990, L-991*, L-992, L-993*, L-994, L-995, *L-996, L-997*, L-998	6 very good. Alkali granite, quartzmonzonite, various gabbroids, quartz syenite	Non-Anorogenic, Subduction (L-991)	K-20 CW	Disseminated Cu mineralization. Seems to have a large fractionation sequence.	3, 6, 9, G
N	6	L-998, L-999, *L-1000*, L-1001, *L-1002*, *L-1003*	2 good, quartzmonzonite, granite	Anorogenic	K-24 C	Disseminated Cu mineralization around a major E-W fracture zone.	5, 10
O	1	*L-855** (See sample plotted on the TAS diagram for Suite A)	3 granite	Anorogenic	K-14 WC	Host to IOCG mineralization at Tevrede, NW Kamanjab, Namibia	5, 8, 10
P	5	C-2, C-3, C-4, C-5, C-6	3 Simple. Quartzmonzonite, alkali granite	Anorogenic	K-24		5, 8, 10
Q	11	C-1, C-2, C-3, C-4, C-5, C-6, C-7, C-8, C-9, C-10, C-12	4 Simple. Quartzmonzonite, alkali granite	Non-Anorogenic, maybe subductional. (C-10)	K-24	Zircons from suite dated collectively by Clifford, 1969.	5, 8, 10, 15

Suite J (Fig F10) is made by at least four distinct rock types. **L-969** is a nepheline syenite; **L-971** is a syenite; **L-973** is a granite of group D; and **L-968**, **L-975** and **L-976** are granites of group K. The copper anomaly shown by the granitoids is marked by significant potassic enrichment (Table 4.2.1.1). That alteration was what originally called attention to the samples. Note the high Rb to Sr ratios in the suite of rocks. L-971 has miarolitic cavities. Also note the fuzzy texture in L-968 and L-969. As shown on the location map, this suite occurs along a major E-W trending fault zone (Fig 4.2.1.6).

Suite K is composed of three contrasting rock types. Fig F11 shows two of them, a quartzmonzonite (**L-979**, **L-980** and **L-982**), and an alkali granite (**L-977** and **L-978**).

Suite M (Fig F13) is special, because it has a wide range of rock types that make at least six contrasting groups of rocks. **L-993**, **L-994** and **L-996** are alkali granites; **L-997** and **L-998** are two distinct types of quartzmonzonites; **L-990** is a monzodiorite; **L-992** is a monzogabbro; **L-987a** and **L-991** are alkali gabbros; **L-987b** is a foid gabbro; and **L-995** is a peridot gabbro. Significant disseminated copper mineralization is associated to the suite. Varied types of mineralization occur along the fracture zone, including iron oxide-copper gold systems.

L-993 is a dioritic rock with xenoliths. **L-995** contains high Ti, Fe, Ca and Cu. **L-997** intrudes **L-998. L-996** also contains high Cu. **L-997** has abundant miarolitic cavities.

Table 4.2.1.4 shows that most of the different suites have granites or alkali granites in common. Whenever intrusive relationships were observed, these rocks were the oldest, make the local basement, and were intruded by quartzmonzonites, syenites, other granitoids and/or gabbroids (See also Table 4.2.1.17). In the process, the older granites were sometimes heavily altered. The samples that plot as quartzolites are intensely silicified granites from that group. **L-874** from Suite C is an example of that type of rock with silica alteration.

Fig 4.2.1.21 shows a few of these rocks. Although the images are in sharp focus, the crystalline texture of the granitoids is not distinct. That is a common feature observed in the majority of rocks throughout the Kamanjab Batholith. Most of the mineral constituents have been “soldered” together by hydrothermal or metamorphic processes.

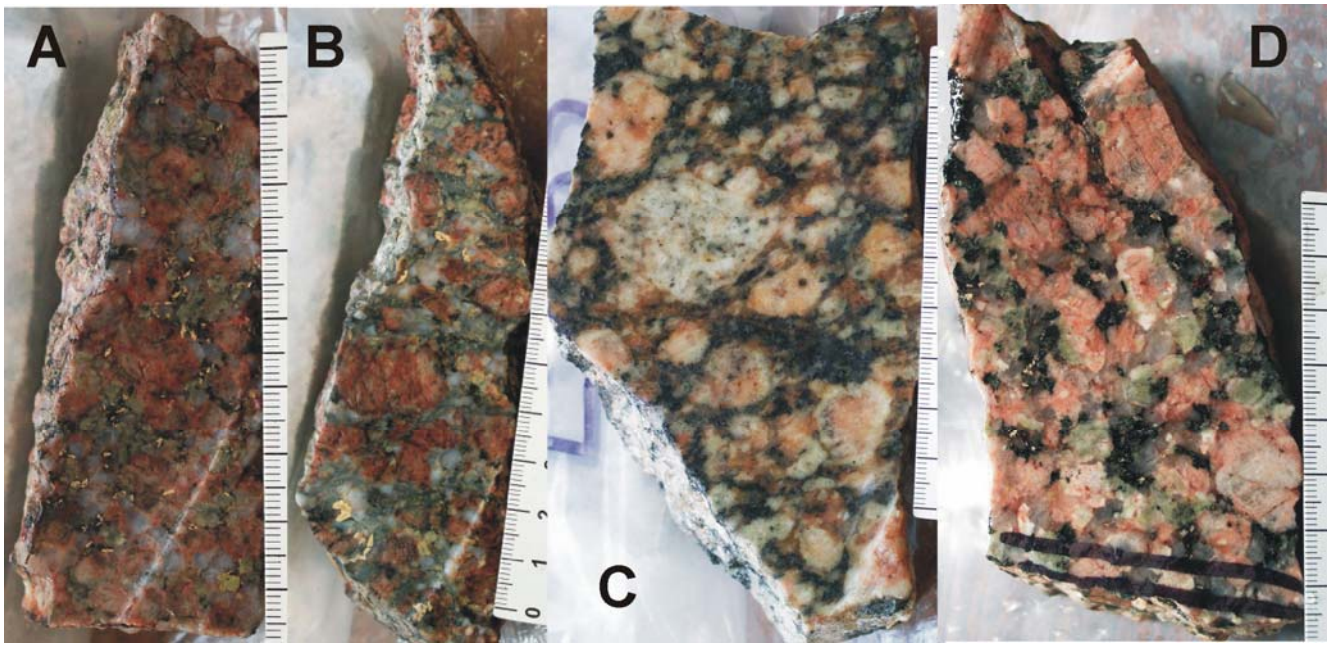

Fig 4.2.1.21 Photos of rocks with “fuzzy” texture, Kamanjab Batholith. *A, L-923; B, L-853; C, L-1006a; D, 1007b (quartmonzonite). These samples show gradational contacts between crystals and coarse blue quartz phenocrystals. Both features seem to have formed by incipient migmatitization. More details in the text. Scale in millimeters.*

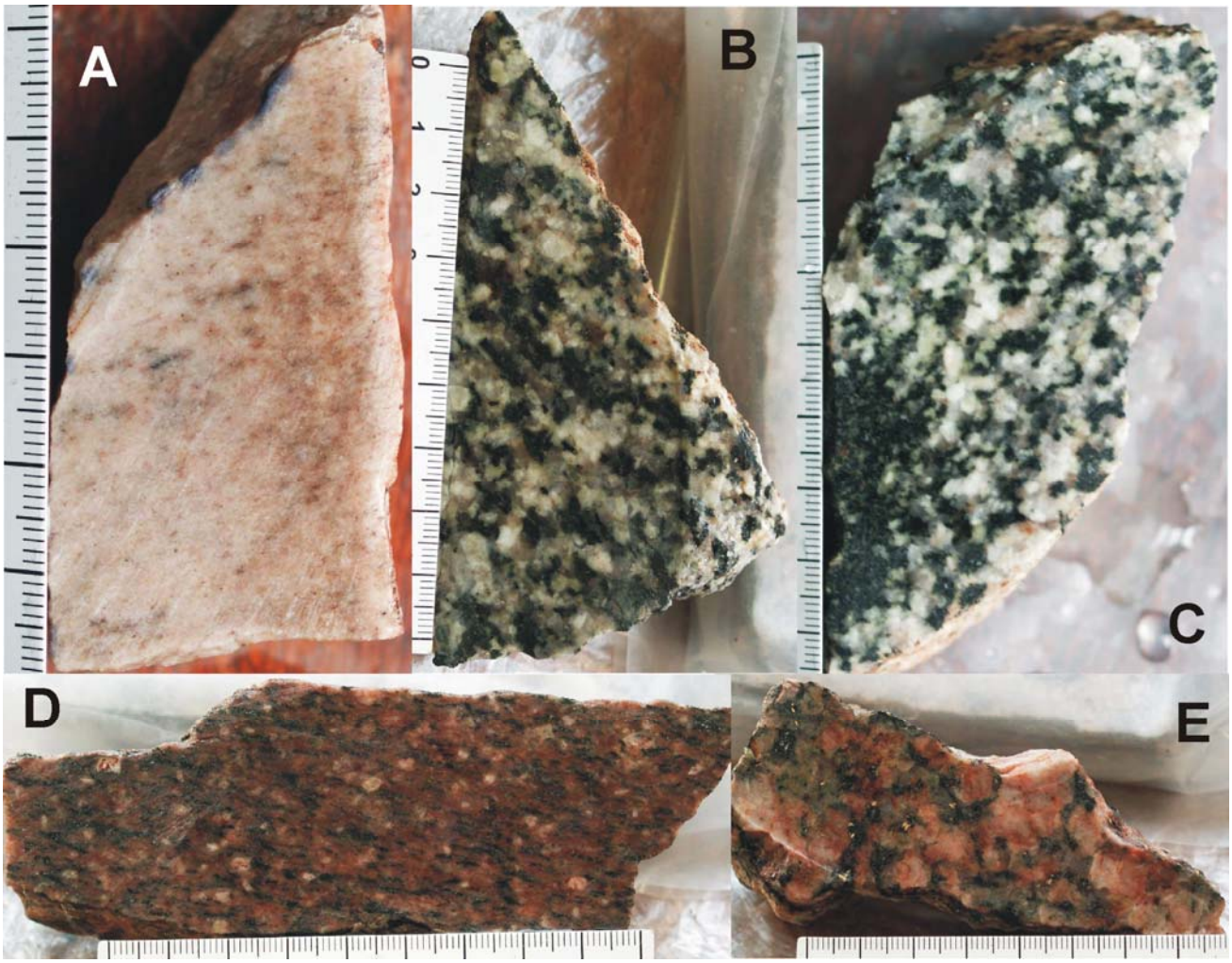

Fig 4.2.1.19 Photos of samples from Kamanjab Suite G*. A, L-939a; B, L-940; C, L-943b; D, L-945; and E, L-948.*

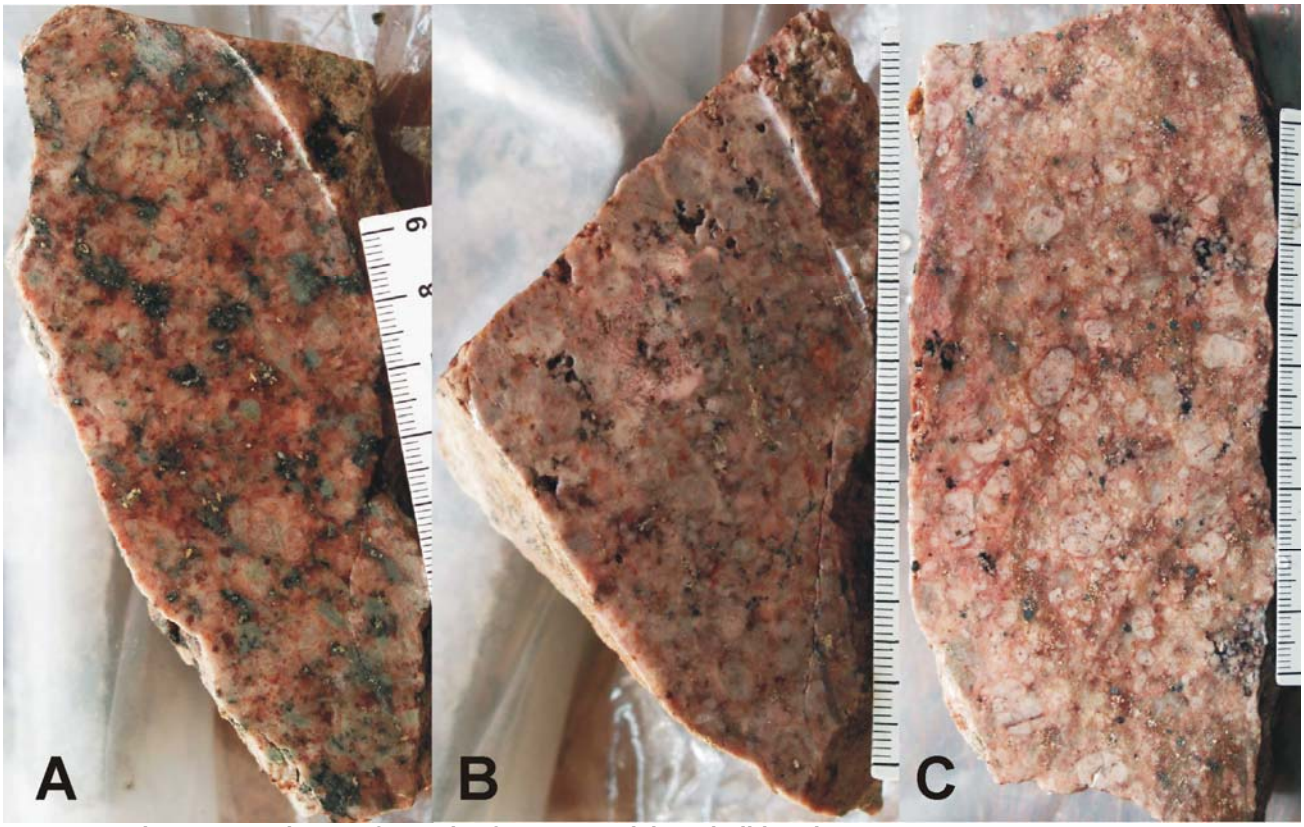

Fig 4.2.1.20 Photos of samples from Kamanjab Batholith Suite J*. A, L-968; B, L-971; C, L-973.*

4.2.1.4 Sample Grouping

The samples from the Kamanjab Batholith were geochemically subdivided using logarithmic major oxide plots into five main rock groups and a few unclassified samples, as indicated on Table 4.2.1.12. The main groups are: 1) Quartzmonzonites, 2) Alkali granites, 3) Granites, 4) Syenites, and 5) Gabbroid rocks. Chemical analyses of the samples sorted by groups are listed on Tables 4.2.1.5 to 4.2.1.10, and they have been plotted as major oxide logarithmic diagrams on Figs 4.2.1.7 to 4.2.1.12. Trace elements and some rare earths were plotted on Figs 4.2.1.13 to 4.2.1.18. Geochemical characteristics of the various groups are described below.

4.2.1.4.1 The **Group of Quartzmonzonites** is made of samples that are mainly quartzmonzonites *sensu* the R1/R2 diagram of De la Roche, 1982. More than 95% of the samples that make the group are metaluminous and mesocratic. The majority is sodic and all are ferriferous. A typical rock of that group is a metaluminous iv mesocratic sodic ferriferous quartzmonzonite. Granodiorites and granites are also included with quartzmonzonites. Surprisingly, the group has the largest number of non-anorogenic samples, as shown by the procedure of Whalen et al, 1987 (Table 4.2.1.12). Three of the samples (**L-979**, **L-980** and **L-982**) plot as granitoids of island arc or continental arc environment in the diagrams of Maniar & Piccoli, 1985. Samples from the Group of Quartzmonzonites are preety homogeneous, as shown on the close match of the logarithmic major oxide diagrams (Fig 4.2.1.7), and on the R1R2 and TAS diagrams (Figs 4.2.1.2 and 4.2.1.4). In comparison with the rest of the granitoids in the Kamanjab Batholith, they contain relatively high values of total iron, MgO, P_2O_5, MnO (around 0.1%), and TiO_2; SiO2 and K_2O values are low. The variation in CaO is minimal, and values for K_2O, Na_2O and total iron are all very similar to each other (Fig 4.2.1.7). Barium is normally high, and most of the samples analysed contain anomalous Pr. The general order of abundance for the major oxides below Fe, Na and K is: Ca, Mg, Ti, P, Mn.

Trace element logarithmic plots also show similar chemistry among the group of quartzmonzonites. Most elements except for chrome have elemental values that oscillate in less than an order of magnitude. The general order of abundance for trace elements is the following: Ba, Sr, Zr, Rb, Zn, V, Y, Cu, Ga, Th, Nb, Sc, Ni, Co, U.

Samples from the quartzmonzonite group produce a dense cluster in most of the geochemical variation diagrams. They constitute a discrete and probably related family of rocks.

Table 4.2.1.5 Chemical Analysis of the Group of Quartzmonzonites, Kamanjab Batholith

Sample	SiO2	TiO2	Al2O3	FeOt	MnO	MgO	CaO	Na2O	K2O	P2O5	LOI	Total	Rb	Sr	Y	Zr	Nb	Co	Ni	Cu
C-10	68.63	0.49	15.01	3.06	0.07	1.22	2.74	4.41	3.60	0.20	0.57	100.00	65	720	25	230	<10			
C-6	66.09	0.69	14.60	4.78	0.08	1.81	2.54	3.25	4.71	0.28	1.11	99.94	150	480	25	280	<10			
C-7	69.29	0.47	14.55	3.29	0.06	1.19	2.83	3.33	4.40	0.17	0.46	100.04	230	650	25	320	10			
L-1007	64.26	0.56	15.15	5.20	0.10	1.92	3.56	4.03	3.92	0.20	0.55	99.45	169	234	45	318	16	7	10	22
L-1009	66.67	0.69	15.06	4.31	0.09	1.05	2.81	4.12	4.42	0.26	0.88	100.36	129	347	38	354	15	7	7	18
L-1010	63.36	0.80	15.40	5.08	0.11	1.26	3.27	4.15	4.24	0.34	1.17	99.18	138	385	37	372	15	9	10	21
L-1011	66.33	0.64	14.74	3.94	0.09	0.94	2.72	4.53	4.43	0.19	0.82	99.37	152	302	38	308	20	7	9	21
L-1012	64.77	0.68	15.28	4.30	0.20	0.95	3.01	5.41	3.94	0.20	0.97	99.71	132	337	42	332	22	8	10	9
L-1013	67.41	0.61	14.33	4.04	0.08	0.94	2.09	4.00	4.72	0.21	0.95	99.38	171	240	39	331	16	6	10	26
L-832	73.67	0.32	12.24	1.83	0.04	0.14	0.46	4.39	5.23	0.11	0.63	99.06	154	297	38	307	15	8	10	19
L-835	65.67	0.65	15.35	3.98	0.08	0.87	2.29	4.41	4.48	0.19	1.44	99.41	135	203	38	342	15	<6	<6	7
L-836	67.42	0.74	14.82	4.07	0.10	0.86	2.21	4.08	4.77	0.20	0.79	100.06	159	266	40	343	17	6	<6	19
L-838	67.61	0.61	14.50	3.84	0.09	0.82	2.37	3.62	4.48	0.18	0.50	98.62	208	69	22	93	16	<6	8	10
L-842	65.32	0.68	14.27	4.45	0.10	1.13	2.64	4.17	3.50	0.19	2.76	99.21	141	316	38	361	16	10	11	37
L-844	68.18	0.63	14.42	3.75	0.08	0.82	2.22	3.87	4.35	0.20	1.02	99.54	137	259	39	345	16	6	7	20
L-846	67.61	0.60	14.35	3.72	0.08	0.89	1.97	4.09	4.59	0.18	0.78	98.86	134	246	44	306	16	6	10	18
L-863	64.77	0.71	14.71	5.42	0.08	1.57	3.06	3.37	3.86	0.24	1.14	98.93	155	288	33	228	19	14	15	23
L-864	66.28	0.74	14.57	5.01	0.09	1.56	2.96	3.05	4.14	0.33	1.62	100.35	97	249	23	39	12	10	16	28
L-865	66.29	0.76	14.63	4.88	0.08	1.51	2.53	3.09	4.38	0.27	1.26	99.68	179	240	34	241	19	10	20	21
L-868	66.57	0.77	14.29	4.73	0.10	1.11	2.09	3.56	4.38	0.29	1.15	99.04	112	186	32	22	15	10	13	14
L-875	66.20	0.78	14.38	5.11	0.12	1.18	2.90	3.74	4.25	0.30	1.32	100.28	138	222	46	329	23	7	13	14
L-877	66.24	0.93	13.94	5.04	0.09	1.14	2.08	3.48	4.74	0.41	1.24	99.33	140	224	54	377	23	9	16	22
L-878	67.83	0.67	13.61	4.34	0.09	0.95	1.67	3.73	4.58	0.23	1.08	98.78	152	176	57	329	19	9	12	34
L-900	67.40	0.67	14.52	4.30	0.08	1.12	2.21	4.83	4.01	0.21	0.90	100.25	101	244	40	361	16	8	8	17
L-940	62.87	0.57	14.38	5.03	0.09	1.98	6.05	4.02	3.40	0.20	0.69	99.28	133	422	23	173	12	14	13	22
L-979	66.06	0.48	15.03	3.97	0.09	1.33	3.18	4.23	3.67	0.14	0.79	98.97	108	435	35	143	15	10	10	76
L-980	67.03	0.53	15.05	4.32	0.09	1.37	3.20	4.47	3.48	0.18	0.77	100.49	115	424	32	157	17	10	15	28
L-982	66.31	0.56	15.11	3.80	0.09	1.18	3.09	4.72	3.57	0.19	0.80	99.42	99	495	25	176	12	11	10	11
L-998	64.78	0.73	15.67	4.59	0.11	1.41	2.78	4.52	4.03	0.24	1.33	100.19	103	300	34	347	15	6	9	29

Sample	Zn	Ga	V	Cr	Ba	U	Th	Sc	Pb	Sm	Nd	Pr	Ce	La	Cs	Hf	Ta	Eu	Gd	Tb	Dy	Ho	Er	Tm	Yb	Lu
C-10		20	55	30	1900				18					70												
C-6		20	85	18	1900				14					75												
C-7		19	70	35	1700				16					70												
L-1007	61	17	38	<12	1413	<6	22	<10					160	78												
L-1009	71	17	53	<12	1757	<6	16	10					115	55												
L-1010	74	18	53	<12	1944	<6	<15	12					110	55												
L-1011	73	17	50	126	1322	<6	17	10					129	66												
L-1012	331	17	53	105	1550	<6	17	<10					139	74												
L-1013	67	17	47	<12	1290	<6	19	<10		108	41	79	131	35			48	0.6							1.7	1.0
L-832	70	17	46	<12	1468	<6	19	<10					121	58												
L-835	68	17	40	<12	1318	<6	15	10					127	60												
L-836	69	0	45	<12	1272	0	0	0					0	0												
L-838	30	15	12	<12	552	4	21	<10					130	55												
L-842	83	16	49	13	1668	<6	16	12		11	33	83	135	41		1.5	63	1.0							1.6	1.1
L-844	62	17	42	<12	1378	6	16	<10					129	63												
L-846	56	15	39	<12	1240	<6	19	<10		12	42	87	133	45			50	1.0							1.9	1.1
L-863	72	18	100	122	1004	<6	17	11					89	44												
L-864	58	16	91	273	1039	3	13	10	17	6	38	10	78	45	0.8	1.4	1	1.3	5.3	0.7	4.4	0.9	2.4	0.3	2.2	0.3
L-865	68	17	84	226	1100	<6	16	10					129	67												
L-868	.	19	68	114	1100	<6	<15	10	15	9	52	13	154	79	1.1	0.8	1	1.8	7.2	1.0	6.1	1.2	3.4	0.5	3.1	0.4
L-875	68	18	71	181	1294	<6	<15	10		12	43	111	157	54			77	1.6							2.0	1.2
L-877	75	19	62	17	1371	<6	17	10					169	87												
L-878	71	19	46	16	1143	<6	17	<10		12	39	92	150	41			56	1.2							2.6	1.2
L-900	43	17	48	<12	1239	<6	16	11					127	61												
L-940	64	18	94	17	1043	<6	<15	11		9	25	64	90	31			80	0.4							0.6	1.0
L-979	88	16	68	242	1077	<6	<15	11					92	44												
L-980	62	17	72	200	1140	<6	<15	<10					104	52												
L-982	56	17	54	<12	1245	<6	<15	<10		9	27	66	74	30			54	0.4							0.6	0.8
L-998	96	18	53	13	2134	<6	<15	10		10	32	79	106	38			63	0.9							1.0	1.0

4.2.1.4.2 The **Group of Alkali Granites** is less well constrained. It mainly has leucocratic to subleucocratic ferriferous granitoids. It is composed by alkali granites and granites of varying character, as shown on Table 4.2.1.6 and Fig 4.2.1.8. The name of the group was derived from the majority of the samples. One of the main features of these rocks is that potash is more abundant than soda, and soda is more abundant than total iron; all three are clearly separated from each other on the logarithmic major oxide plot. MnO and P_2O_5 values tend to be low, and silica high. The general order of abundance for major oxides is: K, Na, Fe, Ca, Ti, Mg, P, Mn. Trace element correlation is not very close, although most elements have a small range of variation, as shown on Fig 4.2.1.14.

Table 4.2.1.6 Chemical Analysis of the Group of Alkali Granites, Kamanjab Batholith

Sample	SiO2	TiO2	Al2O3	FeOt	MnO	MgO	CaO	Na2O	K2O	P2O5	LOI	Total	Rb	Sr	Y	Zr	Nb	Co	Ni	Cu
C-11	78.84	0.29	10.79	1.22	0.03	0.09	0.60	2.94	5.20	0.06	0.22	100.28	120	65	55	180	18			
C-13 (w	75.89	0.41	12.46	1.20	n.d.	0.05	0.25	3.60	5.71	0.04	0.50	100.11	100	40	65	650	40	<10	<10	n.d.
C-4	73.63	0.33	14.16	1.37	0.02	0.00	0.50	3.14	6.35	0.07	0.44	100.01	200	80	20	380	20			
C-5	75.35	0.27	13.18	1.30	0.02	0.00	0.62	3.15	5.50	0.05	0.36	99.80	110	100	35	280	10			
C-8	73.88	0.33	13.85	1.11	0.03	0.18	0.26	4.05	5.93	0.09	0.39	100.10	130	40	55	450	15			
C-9	73.30	0.32	13.20	3.41	0.01	0.00	0.24	3.46	5.67	0.07	0.34	100.02	130	50	80	650	30			
L-1002	77.59	0.26	11.61	1.64	0.05	0.10	0.32	3.59	4.97	0.03	0.33	100.49	180	40	25	134	22	<6	8	6
L-839	76.62	0.29	11.26	1.41	0.04	0.23	0.35	3.05	5.28	0.07	0.47	99.07	218	67	27	163	17	<6	9	19
L-843	75.42	0.33	12.58	1.52	0.03	0.25	0.31	3.01	4.39	0.10	1.13	99.07	163	61	41	199	20	<6	<6	6
L-849	73.54	0.33	12.99	1.74	0.02	0.20	0.14	3.78	5.57	0.04	0.55	98.90	189	43	24	243	27	<6	7	<6
L-855	76.63	0.15	11.87	1.14	0.02	0.05	0.25	4.70	4.06	0.02	0.25	99.14	88	39	10	71	10	<6	10	9
L-902	77.60	0.17	12.00	0.96	0.02	0.08	0.11	4.16	4.81	0.10	0.34	100.35	160	35	18	95	22	<6	7	33
L-903	79.24	0.19	10.48	1.02	0.02	0.12	0.14	2.98	4.99	0.04	0.32	99.54	262	21	23	103	16	<6	8	10
L-904	76.77	0.24	11.40	1.61	0.05	0.16	0.10	3.59	4.81	0.05	0.45	99.23	242	44	30	149	18	<6	8	15
L-905	77.13	0.29	11.44	1.46	0.03	0.23	0.54	5.65	1.54	0.06	0.51	98.88	75	80	40	160	19	<6	9	17
L-906	76.57	0.27	12.23	1.45	0.03	0.07	0.32	3.00	5.97	0.03	0.42	100.36	254	43	51	164	21	<6	7	37
L-909	71.39	0.41	13.73	1.94	0.07	0.35	0.72	4.37	4.96	0.08	0.91	98.93	153	134	46	285	18	<6	8	25
L-912	73.33	0.37	13.50	1.75	0.02	0.70	0.22	2.05	5.30	0.08	1.55	98.87	139	29	38	273	20	<6	7	9
L-917	71.65	0.73	12.99	3.87	0.08	1.25	0.71	3.95	4.48	0.20	0.63	100.54	113	116	16	39	15	6	12	17
L-943	74.31	0.15	13.23	1.77	0.04	0.03	0.75	3.70	5.72	0.11	0.29	100.10	137	123	4	65	7	<6	9	19
L-957	75.71	0.31	11.71	1.52	0.04	0.21	1.09	2.90	4.90	0.05	0.66	99.10	126	135	32	207	20	<6	7	<6
L-968	72.13	0.34	13.69	2.21	0.03	0.17	0.89	3.99	4.79	0.05	0.51	98.80	136	145	37	225	15	7	9	20
L-973	71.06	0.42	12.34	2.89	0.04	0.12	1.90	0.51	9.97	0.09	0.97	100.31	266	42	47	249	19	6	<6	141
L-975	72.48	0.35	13.19	2.05	0.06	0.27	0.82	3.81	5.40	0.10	0.56	99.09	164	149	34	215	16	7	9	45
L-976	72.48	0.37	13.10	1.84	0.04	0.29	0.71	4.00	5.29	0.06	0.50	98.68	195	113	55	203	21	<6	10	8
L-977	74.68	0.27	11.99	1.72	0.04	0.24	0.55	3.86	5.21	0.04	0.45	99.05	121	81	27	197	13	<6	8	<6
L-978	76.43	0.22	11.10	2.76	0.10	0.04	0.28	4.16	5.19	0.05	0.18	100.51	139	58	15	133	17	<6	10	37
L-983	72.59	0.29	13.57	1.83	0.04	0.07	0.90	4.08	4.95	0.04	0.51	98.87	197	156	28	181	17	<6	6	7
L-985	72.90	0.46	12.76	2.61	0.05	0.29	1.39	3.72	4.25	0.06	0.63	99.12	123	219	5	51	6	<6	7	9
L-997	69.62	0.34	15.29	1.59	0.04	0.27	0.51	5.88	5.33	0.05	0.73	99.65	135	65	57	241	22	8	9	8
X-18	69.24		12.00	0.00			0.55	3.83	5.36		0.00	90.98								
X-19	72.02	0.32	13.78	3.26	0.02	0.20	0.39	4.07	5.18	0.03	0.65	99.92								
X-20	76.01	0.23	12.05	1.71	0.03	0.20	1.02	3.09	5.02	0.01	1.14	100.51								

Sample	Zn	Ga	V	Cr	Ba	U	Th	Sc	Pb	Sm	Nd	Pr	Ce	La	Cs	Hf	Ta	Eu	Gd	Tb	Dy	Ho	Er	Tm	Yb	Lu
C-11		15	5	25	560				20					100												
C-13 (w		25	<3	10	1000				30					90			<100									
C-4		20	9	13	1200				40					95												
C-5		20	5	15	1400				30					65												
C-8		20	7	11	400				20					65												
C-9		30	<3	14	1200				12					85												
L-1002	14	14	10	<12	180	<6	28	<10		104	19	53	87	26		3.4	5								1.6	0.9
L-839	35	13	12	<12	565	<6	16	<10					102	44												
L-843	25	14	16	177	907	<6	21	<10		113	35	74	126	32		4.0	10	0.7							2.0	0.9
L-849	22	18	17	217	451	<6	16	<10		107	30	48	152	20		1.0	34	0.3							0.2	0.4
L-855	11	15	<12	<12	328	<6	<15	<10					39	16												
L-902	15	15	13	<12	131	<6	25	<10					85	39												
L-903	15	13	<12	<12	132	<6	25	<10					80	38												
L-904	37	15	<12	14	233	<6	21	<10		107	30	50	99	23			7	0.3							1.3	0.9
L-905	23	13	13	<12	672	<6	22	<10					116	55												
L-906	14	13	<12	269	219	<6	19	<10					122	62												
L-909	56	17	15	<12	1346	<6	18	<10					163	82												
L-912	34	17	15	<12	787	<6	16	<10					148	47												
L-917	50	15	46	15	967	<6	<15	<10	13	5	30	8	85	42	1.4	1.4	1	1.0	4.6	0.6	3.7	0.7	1.9	0.3	1.9	0.3
L-943	17	14	13	15	350	<6	28	<10	19	1	7	2	42	20	2.3	3.3	1	0.1	0.7	0.1	0.6	0.1	0.5	0.1	0.8	0.2
L-957	36	14	<12	228	571	<6	26	<10		112	34	60	156	79		3.2	7	0.3							0.3	0.7
L-968	86	15	16	<12	1370	<6	23	<10		110	17	29	110	11		3	26								0.5	0.8
L-973	70	9	28	12	1800	<6	18	<10		10	34	97	128	42		6	37	0.5							3.2	1.1
L-975	47	14	19	<12	1327	<6	21	<10					137	68												
L-976	29		18	209	1114					116	48	92		71		3.2	13	1.0	2.2						2.9	1.1
L-977	39	15	12	<12	766	<6	16	<10					110	57												
L-978	73	20	14	20	264	4	19	<10	21	2	13	4	50	25	0.8	5.1	1	0.3	1.8	0.3	2.1	0.5	1.8	0.3	2.8	0.5
L-983	32	15	13	<12	963	<6	19	<10					90	39												
L-985	46	14	25	173	1580	1	17	<10	26	3	33	10	103	61	2.1	1.5	0	1.1	2.0	0.2	1.0	0.2	0.5	0.1	0.5	0.1
L-997	24	16	19	<12	542	<6	33	<10		111	29	57	156	21		4.2	11								2.5	1.0

4.2.1.4.3 The **Group of Granites** is very homogeneous. It is almost exclusively made of granites *sensu stricto*. Ranges of variation for most of the major oxides are small as shown on Table 4.2.1.7 and Fig 4.2.1.9. In general terms, the order of abundance of the oxides is: K_2O, Na_2O, FeOt, CaO, MgO, TiO_2, P_2O_5 and MnO. P_2O_5 is normally higher than 1 and MnO is lower than 1. In general, total iron values are higher than for the group of alkali granites, MgO and TiO_2 values are much higher, and lime has a small range of variation. Ba and Pr values tend to be high. Trace element values are quite uniform for the group of granites, except for chrome, as shown on Fig 4.2.1.15.

Table 4.2.1.7 Chemical Analysis of the Group of Granites, Kamanjab Batholith

Sample	SiO2	TiO2	Al2O3	FeOt	MnO	MgO	CaO	Na2O	K2O	P2O5	LOI	Total	Rb	Sr	Y	Zr	Nb	Co	Ni	Cu
C-2	69.71	0.68	14.17	3.26	0.04	0.84	0.82	4.10	5.30	0.27	0.67	99.86	70	110	45	550	30			
C-3	68.63	0.67	15.43	2.77	0.10	0.51	1.99	4.50	4.42	0.18	0.50	99.70	90	350	140	700	40			
L-1000	67.91	0.47	15.37	2.32	0.06	0.52	1.06	4.28	5.11	0.10	1.68	98.88	192	112	37	251	18	<6	10	62
L-1003	68.00	0.50	15.07	2.73	0.05	0.58	1.60	4.64	5.26	0.12	0.69	99.24	145	242	40	289	16	<6	8	12
L-1005	71.20	0.48	12.46	3.35	0.06	0.56	1.47	3.93	4.47	0.18	0.76	98.92	171	218	46	298	18	7	9	15
L-840	70.88	0.42	13.61	2.64	0.07	0.48	1.29	3.97	4.93	0.13	0.75	99.17	176	247	37	237	15	<6	8	20
L-857	73.33	0.32	13.00	1.84	0.04	0.43	1.21	4.01	4.21	0.11	1.00	99.50	155	211	17	141	14	<6	9	26
L-898	69.20	0.58	12.94	5.11	0.08	0.60	1.62	4.21	5.14	0.15	0.09	99.72	112	193	33	215	15	<6	7	17
L-907	71.26	0.43	13.59	2.43	0.06	0.51	1.34	3.85	5.07	0.11	0.52	99.17	175	181	41	248	16	<6	8	11
L-910	70.84	0.59	13.17	3.28	0.04	0.51	0.53	4.21	4.24	0.20	1.11	98.72	129	126	44	360	17	<6	8	12
L-922	68.49	0.77	14.39	4.18	0.07	0.89	1.69	3.76	4.88	0.23	0.98	100.33	143	206	56	426	27	8	9	15
L-923	70.32	0.62	13.18	3.95	0.06	0.59	0.92	4.03	4.67	0.17	1.02	99.53	162	156	56	425	21	6	12	11
L-924	71.99	0.63	12.33	2.83	0.05	0.57	1.46	3.58	3.97	0.13	1.69	99.23	82	63	46	359	22	8	9	14
L-938	70.06	0.58	13.36	3.13	0.05	0.58	1.70	4.16	4.11	0.19	0.90	98.82	76	244	38	294	19	6	7	11
L-939	68.27	0.56	15.25	3.83	0.08	0.63	1.89	3.55	5.28	0.14	0.74	100.22	132	422	22	166	11	15	16	29
L-945	67.85	0.52	15.01	3.25	0.07	0.55	1.40	4.19	5.08	0.11	0.92	98.95	169	235	45	386	18	9	8	20
L-946	67.96	0.48	14.78	2.89	0.06	0.59	1.58	4.39	5.01	0.12	0.73	98.59	165	232	38	250	19	6	8	8
L-948	70.39	0.65	13.17	3.48	0.11	0.62	1.58	4.48	4.47	0.13	0.41	99.49	160	174	63	368	21	7	8	10
L-967	70.72	0.48	12.92	3.64	0.07	0.46	1.11	3.78	5.05	0.12	0.63	98.98	269	119	83	395	22	8	9	13
L-993	71.34	0.39	13.57	2.03	0.05	0.39	1.42	3.97	5.33	0.07	0.81	99.37	115	224	27	75	11	<6	6	8
L-994	70.70	0.40	13.83	2.09	0.05	0.43	1.46	3.95	5.07	0.09	0.73	98.80	110	226	37	208	19	6	7	10
L-999	67.68	0.49	14.73	3.02	0.07	0.74	1.83	4.31	4.65	0.13	1.19	98.84	140	252	37	288	20	<6	9	10

Sample	Zn	Ga	V	Cr	Ba	U	Th	Sc	Pb	Sm	Nd	Pr	Ce	La	Cs	Hf	Ta	Eu	Gd	Tb	Dy	Ho	Er	Tm	Yb	Lu
C-2		25	35	25	2100				8					90												
C-3		25	35	11	2500				25					130												
L-1000	58	17	35	<12	1206	<6	20	<10		12	90	152	134	80			82	3.5							2.6	1.2
L-1003	47	17	32	<12	1796	<6	15	<10		8	29	79	133	26		2.6	32	0.8							1.7	1.0
L-1005	50	17	26	16	1194	<6	18	<10					132	64												
L-840	47	16	20	<12	1054	<6	18	<10					127	62												
L-857	28	15	22	<12	1081	<6	<15	<10					80	38												
L-898	46		27	189	1049																					
L-907	44	15	24	<12	1136	<6	16	<10					135	69												
L-910	47	16	26	<12	1115	<6	<15	<10					152	76												
L-922	58	18	56	244	1598	<6	16	10		22	53	122	159	56			62	1.7	4.3						2.5	1.1
L-923	55	18	37	<12	1168	<6	21	<10					159	89												
L-924	26	15	38	<12	1811	<6	19	<10					158	79												
L-938	44	16	40	266	1785	<6	<15	<10	24	117	49	84	96	37	1.4	3.2	38	1.4	3.2	0.5	3.7	0.8	2.4	0.4	1.2	0.9
L-939	68	16	89	23	1059	<6	<15	11		8	30	58	77	28			78								0.6	0.9
L-945	64	18	2	13	1409	<6	19	<10		12	42	115	178	53			61	0.9	1.7						2.5	1.1
L-946	45	16	30	185	1451	<6	<15	<10					175	88												
L-948	73	17	22	<12	1424	<6	15	<10					175	92												
L-967	60	17	31	<12	883	8	36	<10					259	130												
L-993	34	15	24	160	1595	<6	17	<10	23	7	47	13	139	69	0.5	2.4	1	1.2	5.8	0.8	5.1	1.0	2.9	0.4	2.8	0.4
L-994	33	15	32	195	1763	<6	<15	<10					142	70												
L-999	58	17	33	205	1537	<6	16	<10		10	36	92	144	44		1.5	39	0.8							1.5	0.9

4.2.1.4.4 The **Group of Syenites** is far from homogeneous. Nepheline syenites, syenites and quartz syenites have been joined together. In broad terms, these rocks have low K and Mg, and high Na. The general order of abundance of the major oxides, is Na, Fe, Ca, Ti, K. Table 4.2.1.8 lists the chemical analysis of members of this group. Their major oxides are plotted on Fig 4.2.1.10 and their trace elements are plotted on Fig 4.2.1.16.

Table 4.2.1.8 Chemical Analysis of the Group of Syenites, Kamanjab Batholith

Sample	SiO2	TiO2	Al2O3	FeOt	MnO	MgO	CaO	Na2O	K2O	P2O5	LOI	Total	Rb	Sr	Y	Zr	Nb	Co	Ni	Cu
X-16	75.93	0.26	12.08	3.28	0.01	0.36	0.48	7.93	0.13	0.07	0.42	100.95								
X-17	72.07	0.33	13.36	4.01	0.02	1.33	1.01	7.95	0.30	0.04	0.49	100.91								
L-955	67.86	0.41	16.46	3.50	0.05	0.11	0.33	10.16	0.19	0.23	0.82	100.12	4	37	40	340	17	<6	13	333
L-951	66.61	0.52	15.75	3.69	0.02	0.04	0.50	11.34	0.33	0.12	0.19	99.11	4	30	50	261	24	<6	10	6
L-952	67.68	0.59	15.55	4.09	0.02	0.15	0.73	10.86	0.35	0.15	0.22	100.39	6	38	36	308	23	<6	9	6
L-908	66.78	0.41	16.95	1.82	0.08	0.28	0.22	9.57	2.63	0.03	0.34	99.11	96	28	10	66	16	<6	8	12
L-920	36.93	0.23	6.77	1.19	0.03	0.22	0.29	2.90	2.72	0.06	49.01	100.35	124	81	20	208	15	<6	<6	16
L-971	64.34	0.54	17.73	1.51	0.09	0.14	0.68	4.58	8.51	0.11	0.69	98.92	148	66	47	358	22	<6	9	10
L-969	59.46	0.49	19.16	4.28	0.05	0.68	0.38	0.55	14.31	0.08	0.84	100.28	393	66	59	293	24	6	<6	47
L-834	59.92	0.47	16.55	4.88	0.05	0.10	1.72	0.29	14.06	0.12	1.28	99.44	283	70	49	274	20	7	<6	14
L-956	61.48	2.00	9.60	15.05	0.04	0.23	2.72	7.38	0.01	0.92	0.23	99.66	5	36	63	321	14	9	11	7
L-997	69.62	0.34	15.29	1.59	0.04	0.27	0.51	5.88	5.33	0.05	0.73	99.65	135	65	57	241	22	8	9	8
L-965	67.45	0.59	13.65	6.24	0.03	0.32	0.69	4.10	5.73	0.19	0.42	99.41	156	43	88	358	29	<6	11	8
L-966	68.15	0.60	12.90	6.30	0.02	0.16	0.43	4.46	5.68	0.19	0.27	99.16	144	39	74	108	17	<6	9	6
L-863	64.77	0.71	14.71	5.42	0.08	1.57	3.06	3.37	3.86	0.24	1.14	98.93	155	288	33	228	19	14	15	23

Sample	Zn	Ga	V	Cr	Ba	U	Th	Sc	Pb	Sm	Nd	Pr	Ce	La	Cs	Hf	Ta	Eu	Gd	Tb	Dy	Ho	Er	Tm	Yb	Lu
L-834	19	9	26	<12	1842	7	25	<10		12	42	111	192	54		2.9	77	0.7							2.5	1.3
L-863	72	18	100	122	1004	<6	17	11					89	44												
L-908	53	26	<12	<12	125	<6	15	<10	10	2	17	5	82	40	1.5	2.0	1	0.3	1.9	0.3	1.8	0.4	1.2	0.2	1.6	0.3
L-920	29	14	17	134	1088	<6	<15	<10		113	36	62	99	29			19	0.7							0.2	0.7
L-951	9	16	39	137	<20	<6	22	<10		11	28	110	166	14			49	0.7	3.1						1.9	1.1
L-952	10	16	31	173	52	<6	<15	<10					38	27												
L-955	142	21	36	<12	30	<6	<15	16		13	62	671	965	405			43	0.4							1.8	1.0
L-956	17	17	91	<12	51	<6	<15	24			41	98	116	63			297								3.1	2.1
L-965	24	17	33	12	741	7	30	<10					125	56												
L-966	19	16	42	193	708	6	27	<10	18	6	35	10	103	45	0.4	3.1	1	0.9	7.0	1.4	10	2.3	7.5	1.1	7.9	1.2
L-969	53	22	61	<12	2451	6	29	<10		11	36	92	159	37		7.2	60	0.7							3.1	1.3
L-971	14	13	34	<12	2236	<6	<15	<10					137	81												
L-997	24	16	19	<12	542	<6	33	<10		111	29	57	156	21		4	11								2.5	1.0

4.2.1.4.5 All **Gabbroid Rocks** have been grouped together for convenience. This group of samples has the lowest values for silica, at times total iron exceeds alumina, and lime is normally around 10%. Special characteristics for the group include: high Mg, Mn and P. None of the major oxides is below 0.1 percent. The order of the oxide abundance varies widely as shown on Fig 4.2.1.11 and on Table 4.2.1.9. Surprisingly, trace elements are very uniform, except for chrome and niobium, as illustrated on Fig 4.2.1.17.

Table 4.2.1.9 Chemical Analysis of the Group of Gabbroids, Kamanjab Batholith

Sample	SiO2	TiO2	Al2O3	FeOt	MnO	MgO	CaO	Na2O	K2O	P2O5	LOI	Total	Rb	Sr	Y	Zr	Nb	Co	Ni	Cu
C-14	48.69	1.26	13.27	13.57	0.18	6.15	10.49	2.41	1.05	0.22	0.50	97.79								
L-895	55.24	0.90	18.42	6.32	0.11	3.12	4.54	4.23	4.61	0.50	1.93	99.92	164	840	22	172	7	18	43	164
L-958	47.73	1.22	15.13	13.06	0.23	7.23	8.03	3.57	0.36	0.22	2.21	98.99	5	188	34	105	5	63	122	59
L-987a	45.74	2.33	16.73	14.31	0.17	4.10	10.53	2.62	1.59	0.46	1.99	100.57	22	598	11	18	2	41	8	75
L-987b	40.92	2.62	19.28	13.71	0.19	4.13	12.81	2.45	0.79	1.19	2.06	100.15	35	646	19	31	4	28	<6	37
L-990	53.79	0.31	13.92	7.16	0.15	8.22	7.59	5.52	0.32	0.10	2.29	99.37	10	267	12	84	10	38	178	73
L-991	48.45	0.96	11.97	11.52	0.19	11.57	9.20	3.07	0.46	0.12	1.70	99.21	7	217	20	53	9	64	251	83
L-992	50.94	0.49	19.38	7.11	0.15	5.16	9.79	3.16	1.87	0.09	2.25	100.39	67	659	10	28	3	27	53	35
L-995	39.21	3.69	11.13	22.15	0.26	7.20	10.83	1.60	0.53	1.13	1.13	98.86	14	449	21	27	4	59	<6	54

Sample	Zn	Ga	V	Cr	Ba	U	Th	Sc	Pb	Sm	Nd	Pr	Ce	La	Cs	Hf	Ta	Eu	Gd	Tb	Dy	Ho	Er	Tm	Yb	Lu
L-895	69	18	134	91	1382	<6	<15	14		8	23	54	74	22			99	0.3							0.4	0.9
L-958	119	19	296	107	297	<6	<15	37					15	<12												
L-987a	109	17	429	<12	397	<6	<15	36	8	3	11	2	<12	<12	0.3	0.5	0	1.0	2.9	0.4	2.4	0.5	1.2	0.2	0.9	0.1
L-987b	72	17	307	<12	284	<6	<15	32			7	29	16	5			284									1.3
L-990	69	13	75	584	187	<6	<15	20					39	22												
L-991	93	12	255	870	188	<6	<15	35					19	12												
L-992	53	16	144	100	460	0	1	26	4	2	10	2	19	9	0.5	0.7	0	0.8	2.0	0.3	1.9	0.4	1.1	0.2	1.0	0.2
L-995	128	19	491	<12	457	<6	<15	45					<12	<12												

A few rocks could not be classified into the above groups, and they were left as undefined. Some of them have been subject to hydrothermal alteration.

Table 4.2.1.10 Chemical Analysis of the Group of unclassified samples, Kamanjab Batholith

Sample	SiO2	TiO2	Al2O3	FeOt	MnO	MgO	CaO	Na2O	K2O	P2O5	LOI	Total	Rb	Sr	Y	Zr	Nb	Co	Ni	Cu
C-1	74.03	0.27	12.73	2.66	0.05	0.31	0.48	3.67	5.09	0.05	0.71	100.05	100	50	70	500	30	<10	<10	n.d
L-874	96.83	0.09	0.64	0.69	0.01	0.00	0.02	0.02	0.31	0.03	0.08	98.72	11	8	5	29	4	<6	13	8
L-874a	67.47	0.89	13.68	4.67	0.10	1.05	1.71	3.48	4.99	0.27	1.09	99.40	155	181	57	348	24	12	14	19
L-899	71.98	0.41	12.65	2.41	0.06	0.72	1.79	4.23	3.72	0.11	0.69	98.77	112	193	33	210	18	<6	7	17
L-911	72.60	0.37	14.49	2.24	0.03	0.81	0.22	0.16	5.19	0.11	2.40	98.62	170	16	45	344	27	<6	10	33
L-919	87.60	0.31	4.60	3.09	0.03	0.08	0.09	0.12	2.09	0.04	0.79	98.84	79	9	11	99	8	6	15	13
L-963	88.82	0.21	4.22	2.07	0.03	0.19	0.14	1.00	1.77	0.06	0.66	99.17	63	17	18	133	8	8	11	20
L-996	69.95	0.44	14.71	2.86	0.06	0.50	1.75	4.30	4.78	0.11	0.95	100.41	121	274	24	78	14	6	9	67

Sample	Zn	Ga	V	Cr	Ba	U	Th	Sc	Pb	Sm	Nd	Pr	Ce	La	Cs	Hf	Ta	Eu	Gd	Tb	Dy	Ho	Er	Tm	Yb	Lu
C-1		25	<3	10	1200				25					95			<100									
L-874	6	17	<12	538	30	6	17	11					144	73												
L-874a	69		63	17	1380																					
L-899	46	17	26	182	1049	<6	16	<10					119	56												
L-911	48	19	17	139	398	<6	19	<10					145	75												
L-919	14	<9	27	32	297	<6	<15	<10					55	26												
L-963	15	<9	25	12	308	<6	<15	<10					64	31												
L-996	71	16	30	<12	1498	3	15	<10	23	6	40	11	113	49	0.7	2.3	1	1.2	5.0	0.7	4.7	0.9	2.8	0.4	2.9	0.4

Three of the five main rock groups can be easily distinguished on the TAS and R1R2 diagrams. These are the group of gabbroids, that of syenites and the unclassified samples. Alkali granites, granites and quartzmonzonites cluster closely in both diagrams and are difficult to separate. The diagrams of Si vs total iron, and Si vs Al can be used to separate quartzmonzonites from granites and alkali granites (See Fig 4.2.1.5). Close inspection of the TAS diagram can also achieve that discrimination (Fig 4.2.1.2). Discrimination between the alkali granite and granite groups was only possible using the logarithmic major oxide diagrams.

4.2.1.5 Volcanic Rocks

Volcanic and volcaniclastic rocks that have almost the same compositions as their plutonic counterparts, coexist in the Kamanjab Batholith. This is due to the intermediate level of erosion in the plutonic/volcanic systems. Volcanic rocks correlate well with their plutonic equivalents. For example, **X-16** and **X-17** analysed by Frets, 1969, are the volcanic equivalent of nepheline syenites. Trachytic rock **L-834** is very similar to its plutonic counterpart **L-969**. Rhyolitic rock **L-836** has very similar chemistry to its granitic counterpart **L-1013**; their major oxide and trace element chemistry is almost identical. Something equivalent takes place between **L-842** and **L-1011**. **L-842** is a rhyolite with vacuoles and black matrix that carries significant copper; **L-1011** is a quartzmonzonite. **X-18**, **X-19** and **X-20** correlate well with the group of alkali granites. Table 4.2.1.11 presents examples of this feature, and their chemical similarity can be viewed on Figs 4.2.1.7 to .2.1.11.

Table 4.2.1.11 Comparison of volcanic and plutonic rock types in the Kamanjab Batholith
(See Figs 4.2.1.7 to 4.2.1.11)

Volcanic Rocks		**Plutonic Rocks**	
Sample	**Rock type**	**Sample**	**Rock type**
X-16, X-17	Alkali rhyolite, rhyolite	No precise match	Nepheline syenite
L-834	Trachyte	L-969	Nepheline syenite
L-836	Rhyolite	L-1013	Granite
L-909	Alkali rhyolite	L-976	Alkali granite
L-842	Rhyolite with black matrix	L-1011	quartzmonzonite
L-977, X-18	Alkali rhyolite	L-839, L-976	Alkali granite
L-1003	Quartz latite	L-946, L-948	Granite
X-18	Alkali rhyolite	L-977	Alkali granite
X-20	Rhyolite	L-957	Granite

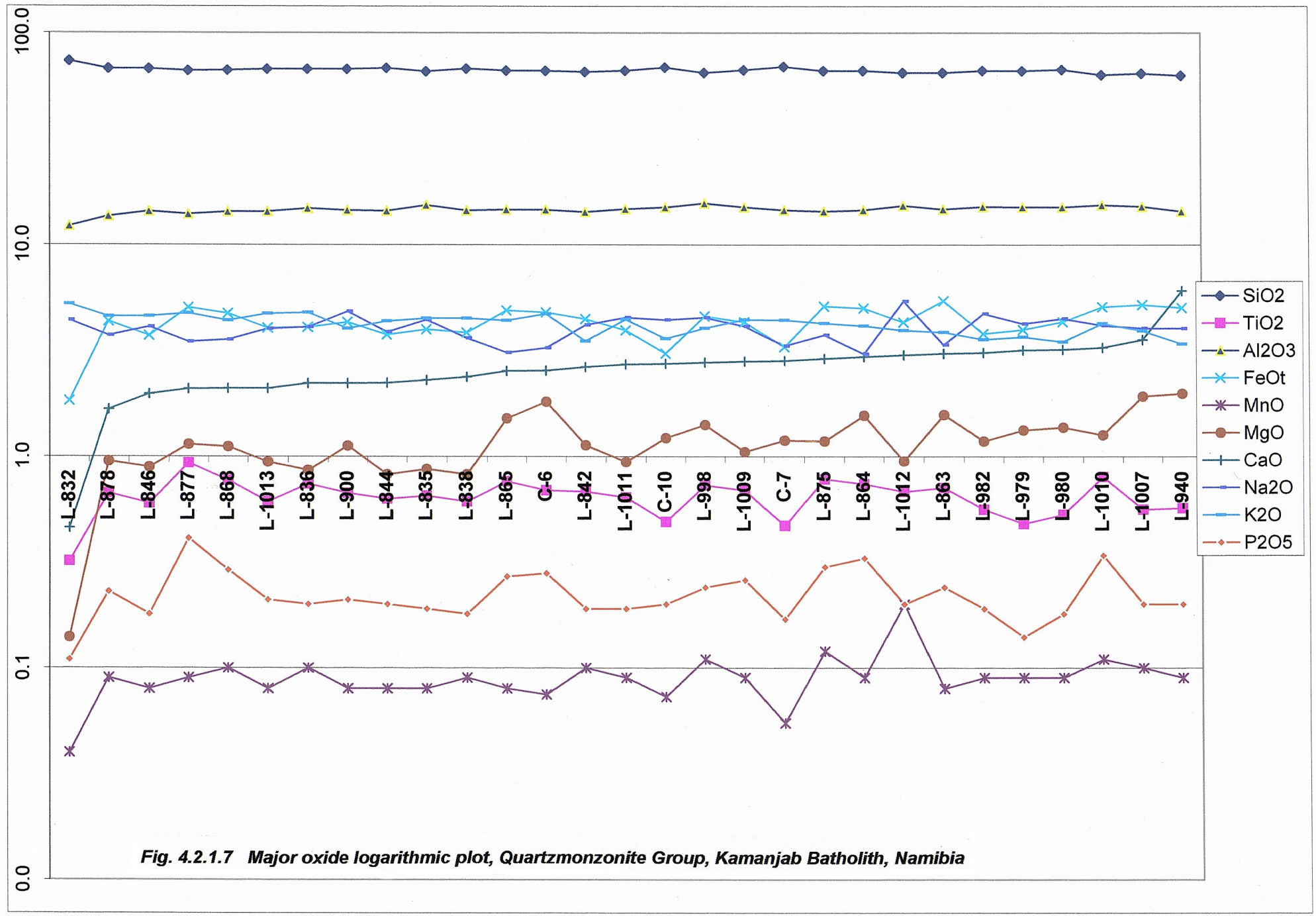

Fig. 4.2.1.7 Major oxide logarithmic plot, Quartzmonzonite Group, Kamanjab Batholith, Namibia

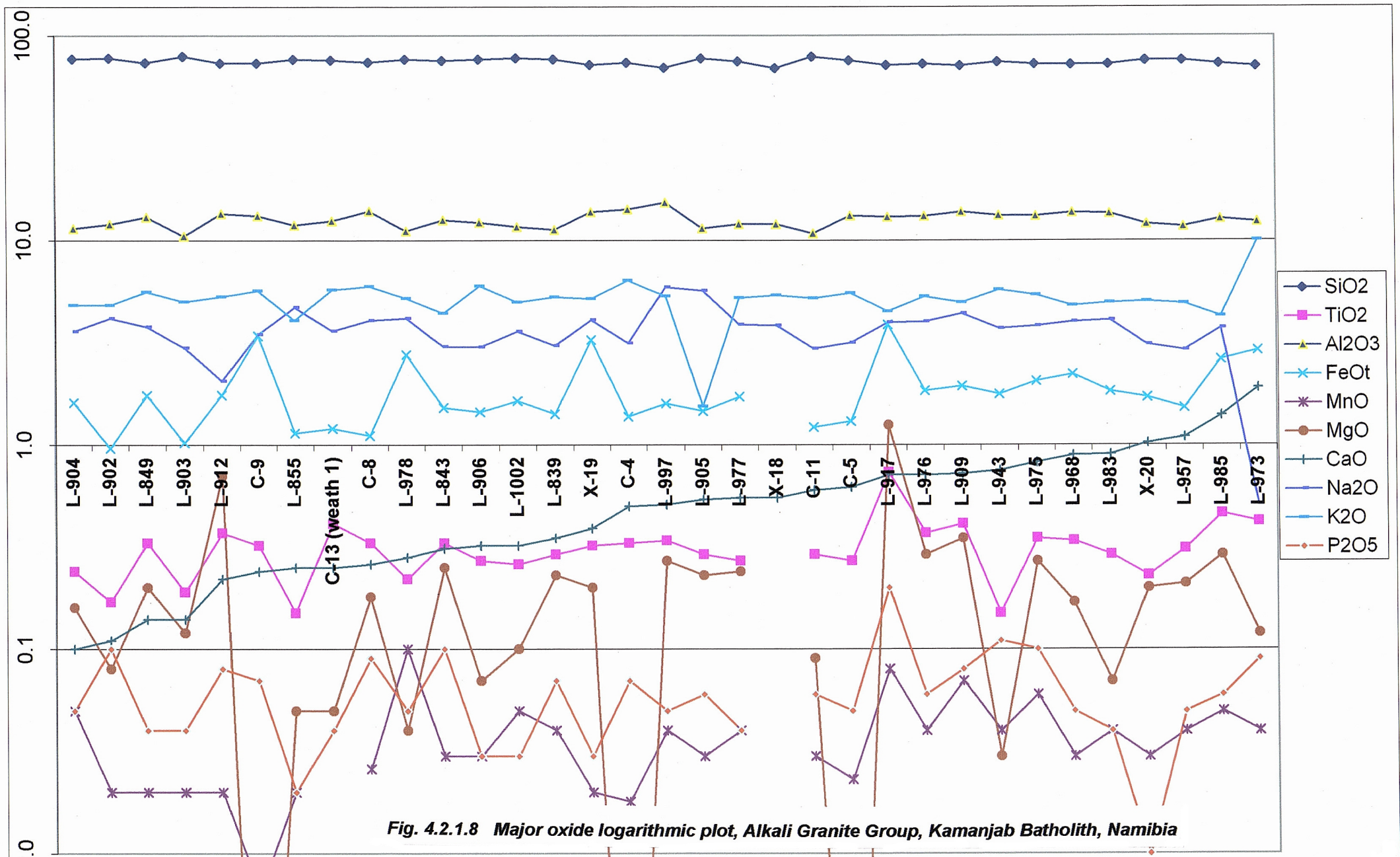

Fig. 4.2.1.8 Major oxide logarithmic plot, Alkali Granite Group, Kamanjab Batholith, Namibia

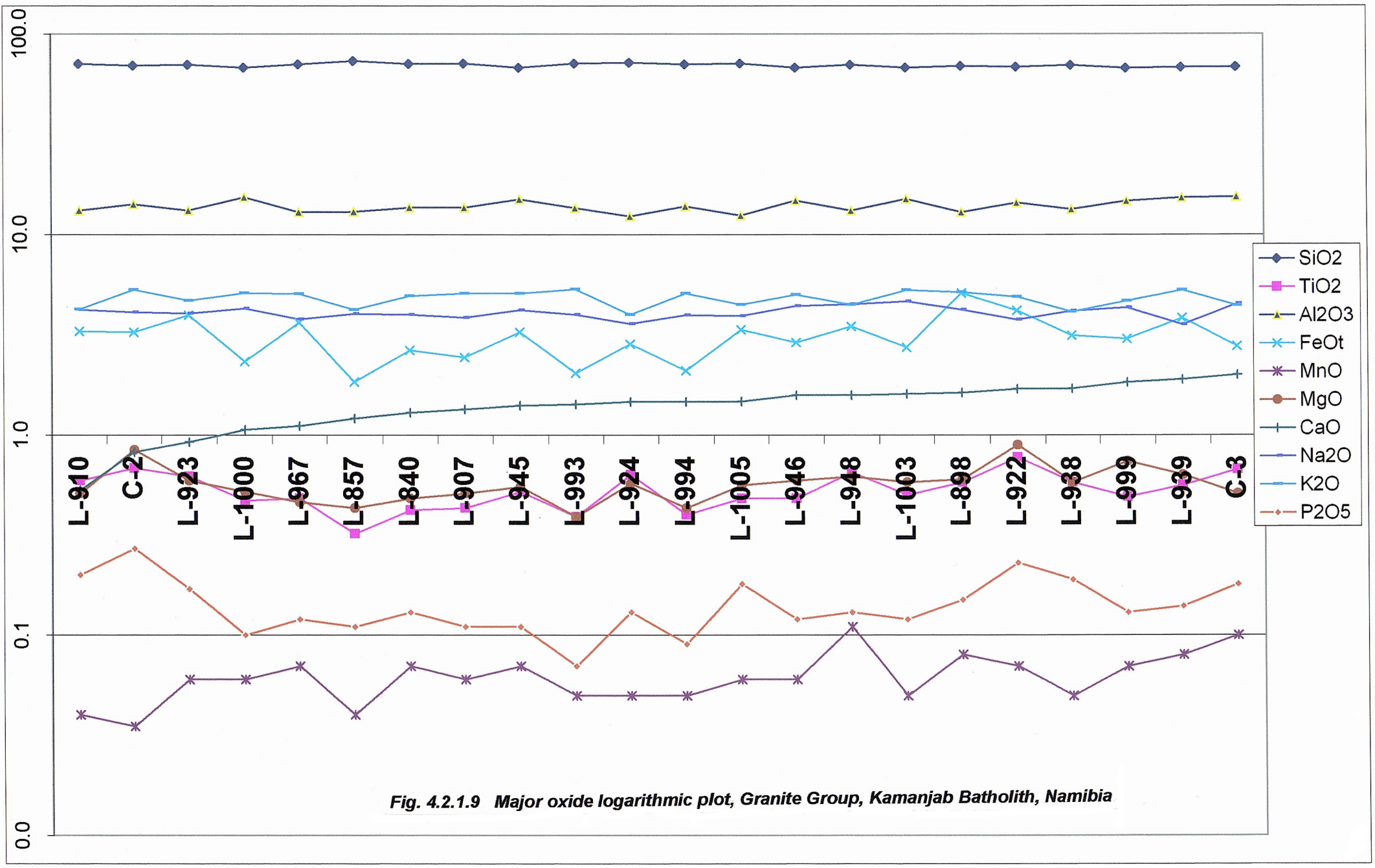

Fig. 4.2.1.9 Major oxide logarithmic plot, Granite Group, Kamanjab Batholith, Namibia

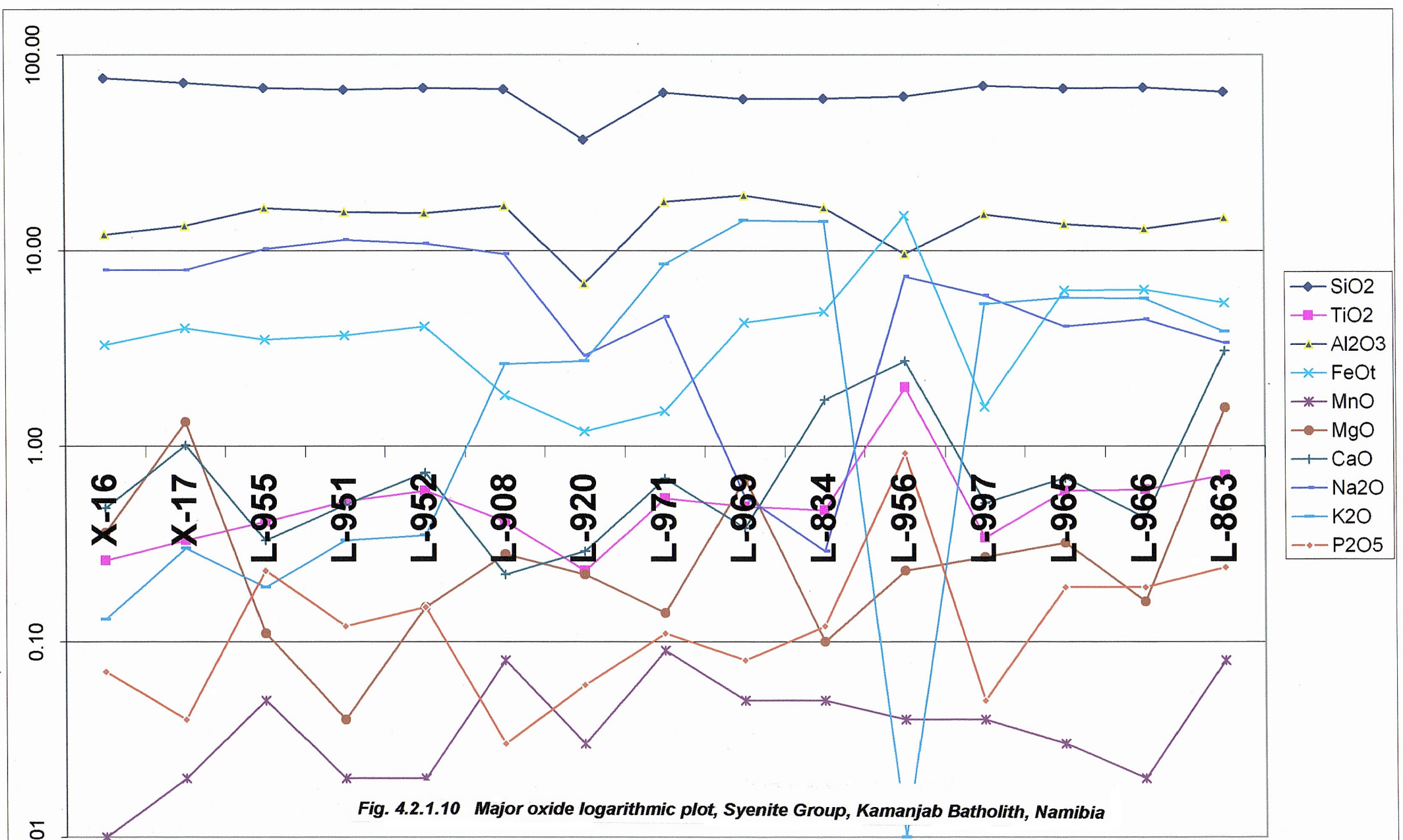

Fig. 4.2.1.10 Major oxide logarithmic plot, Syenite Group, Kamanjab Batholith, Namibia

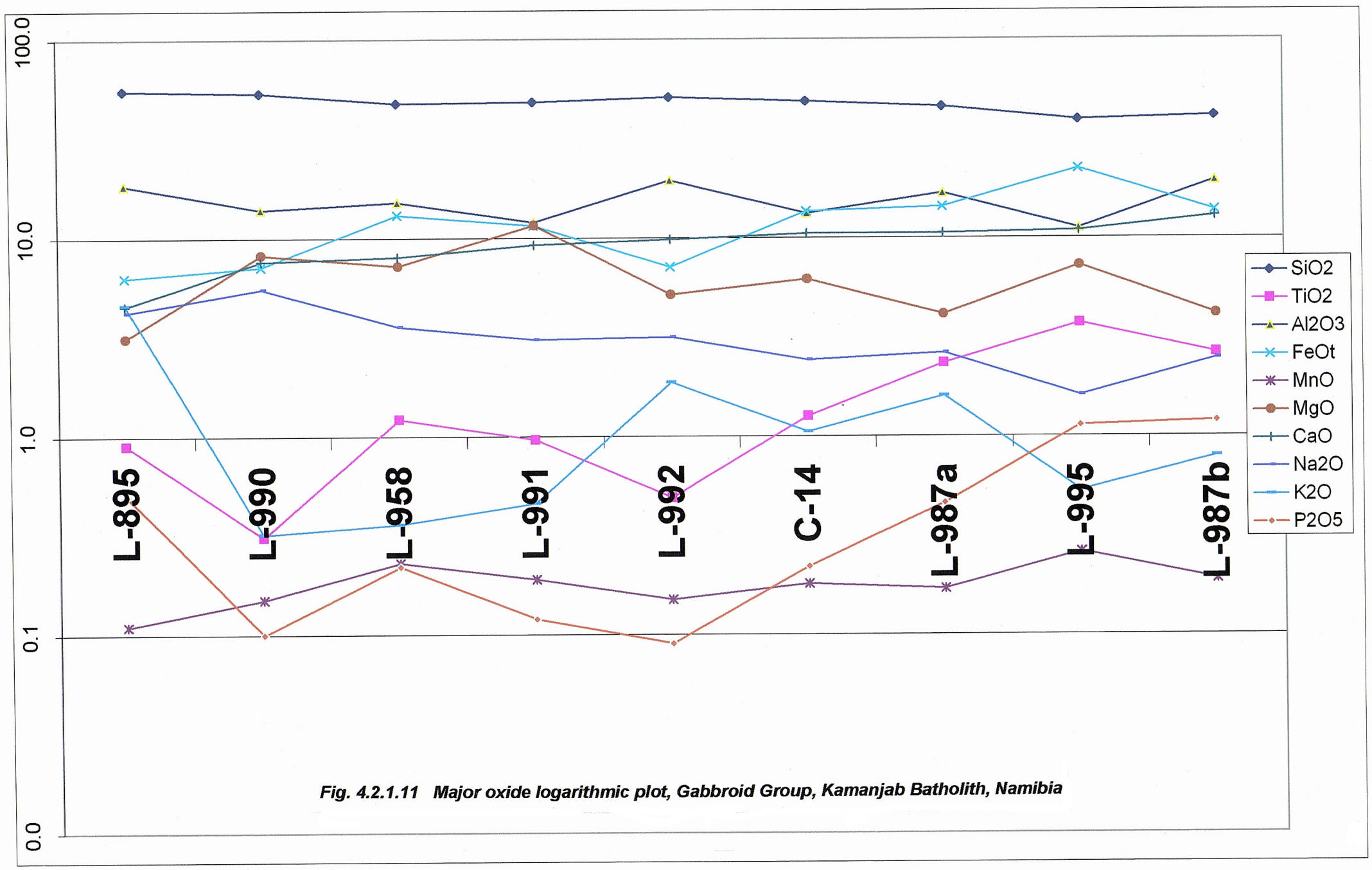

Fig. 4.2.1.11 Major oxide logarithmic plot, Gabbroid Group, Kamanjab Batholith, Namibia

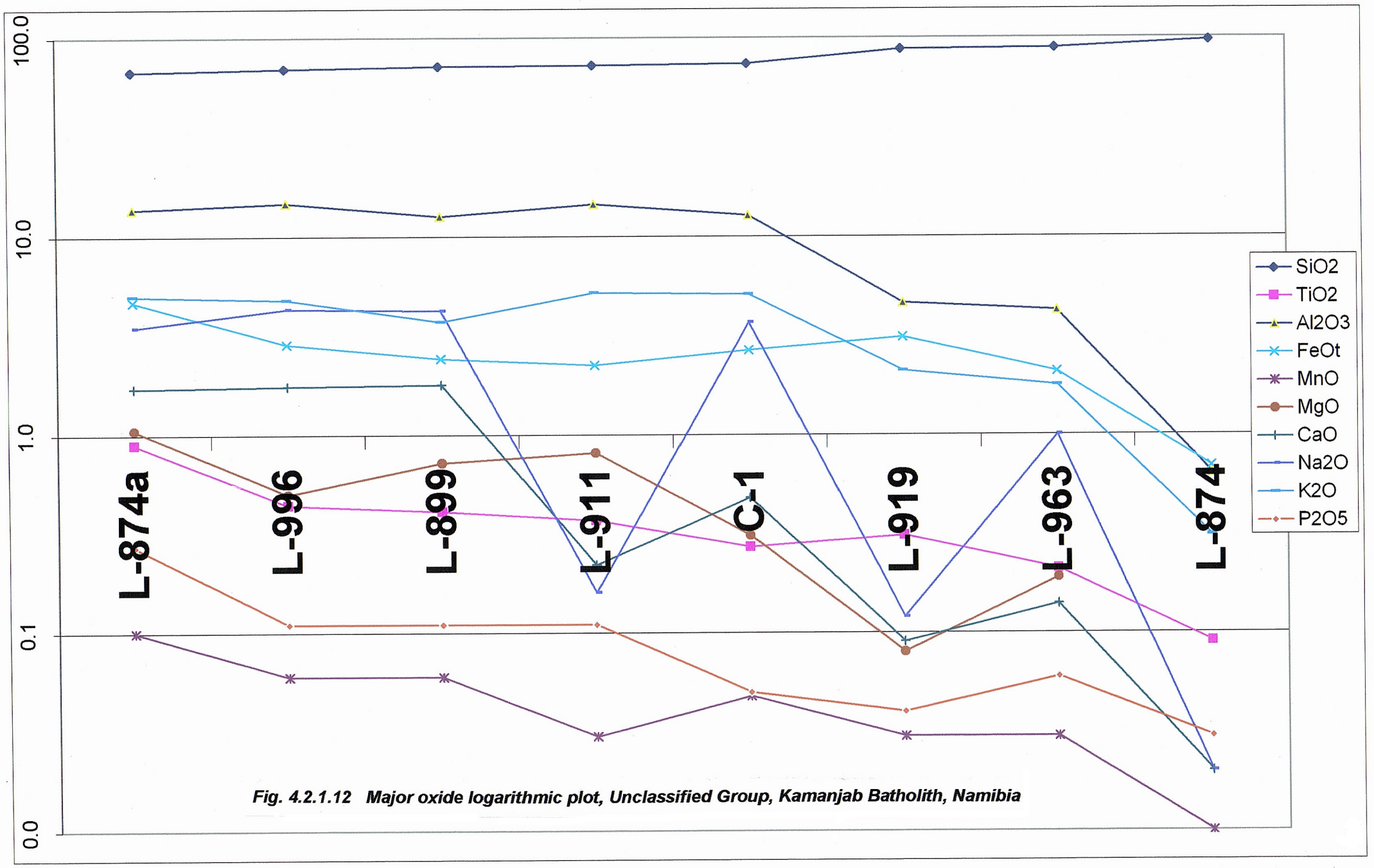

Fig. 4.2.1.12 Major oxide logarithmic plot, Unclassified Group, Kamanjab Batholith, Namibia

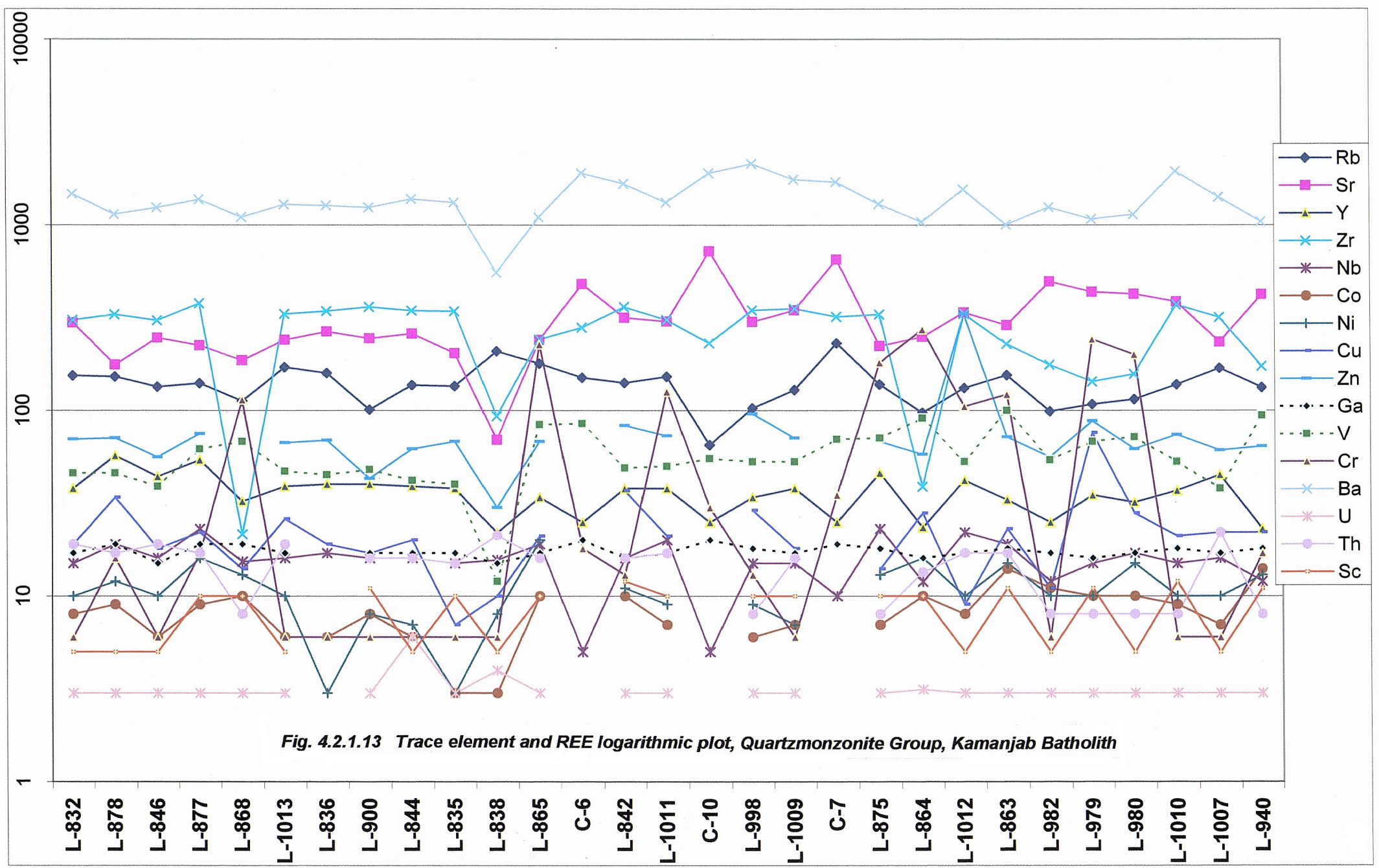

Fig. 4.2.1.13 Trace element and REE logarithmic plot, Quartzmonzonite Group, Kamanjab Batholith

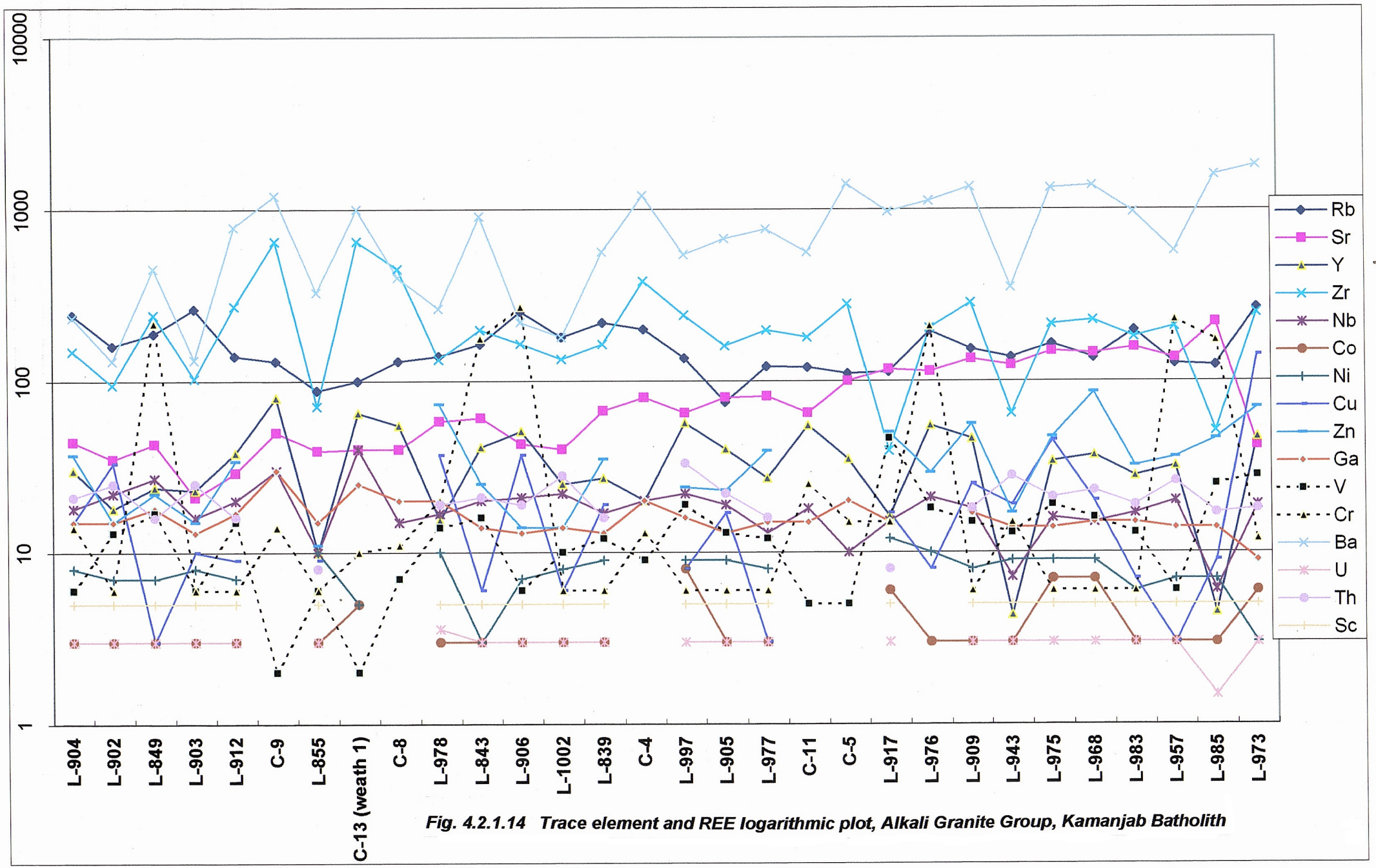

Fig. 4.2.1.14 Trace element and REE logarithmic plot, Alkali Granite Group, Kamanjab Batholith

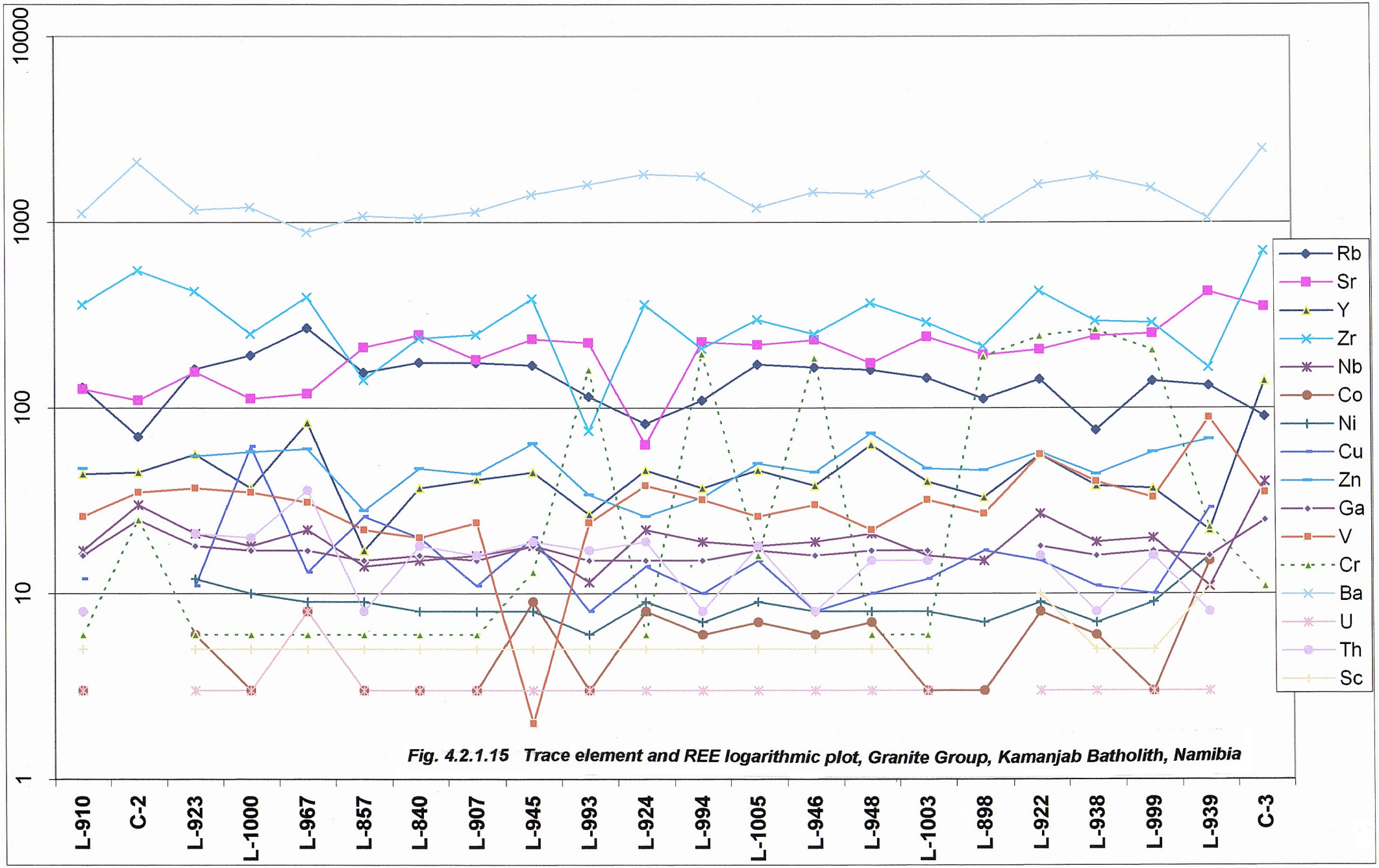

Fig. 4.2.1.15 Trace element and REE logarithmic plot, Granite Group, Kamanjab Batholith, Namibia

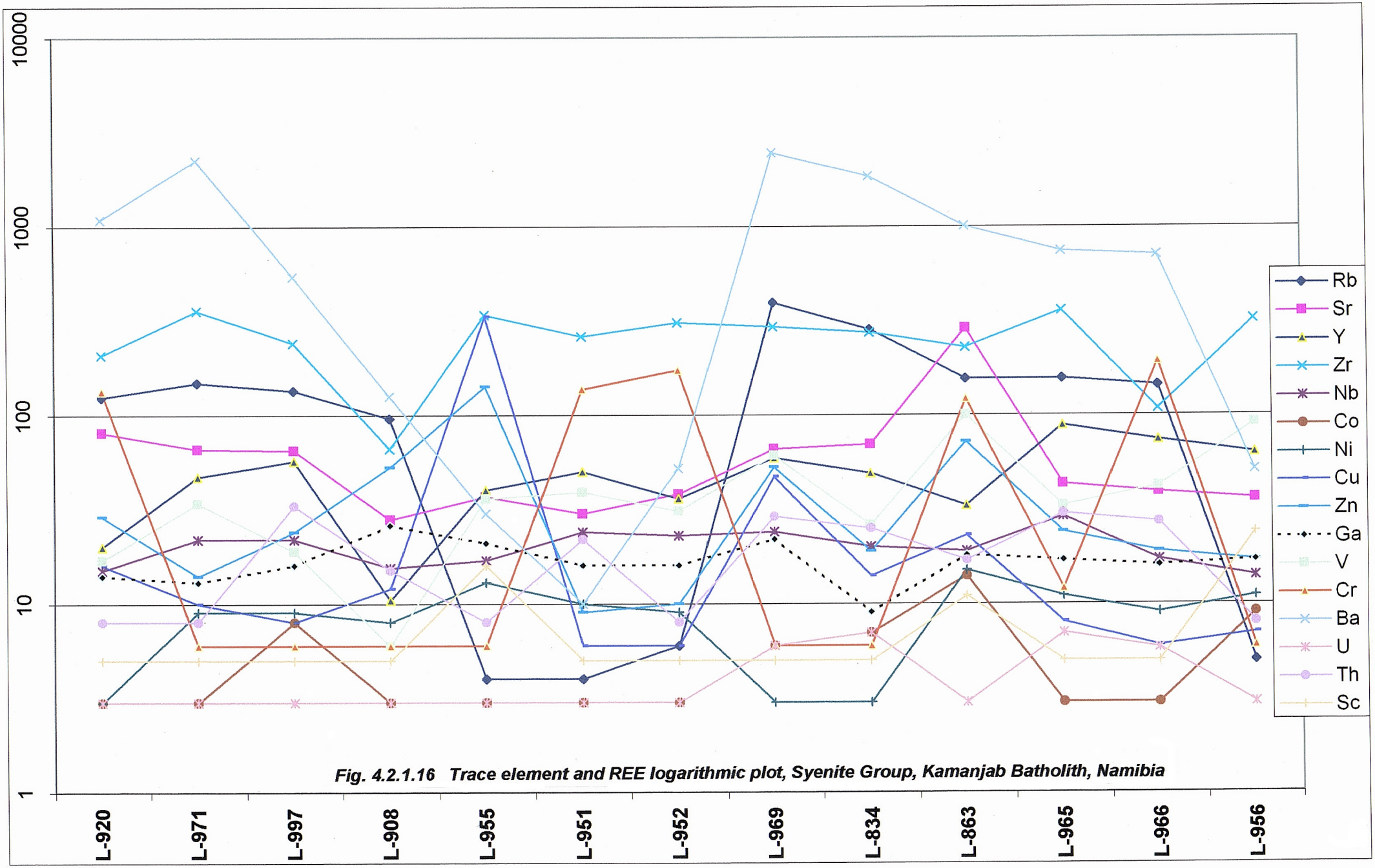

Fig. 4.2.1.16 Trace element and REE logarithmic plot, Syenite Group, Kamanjab Batholith, Namibia

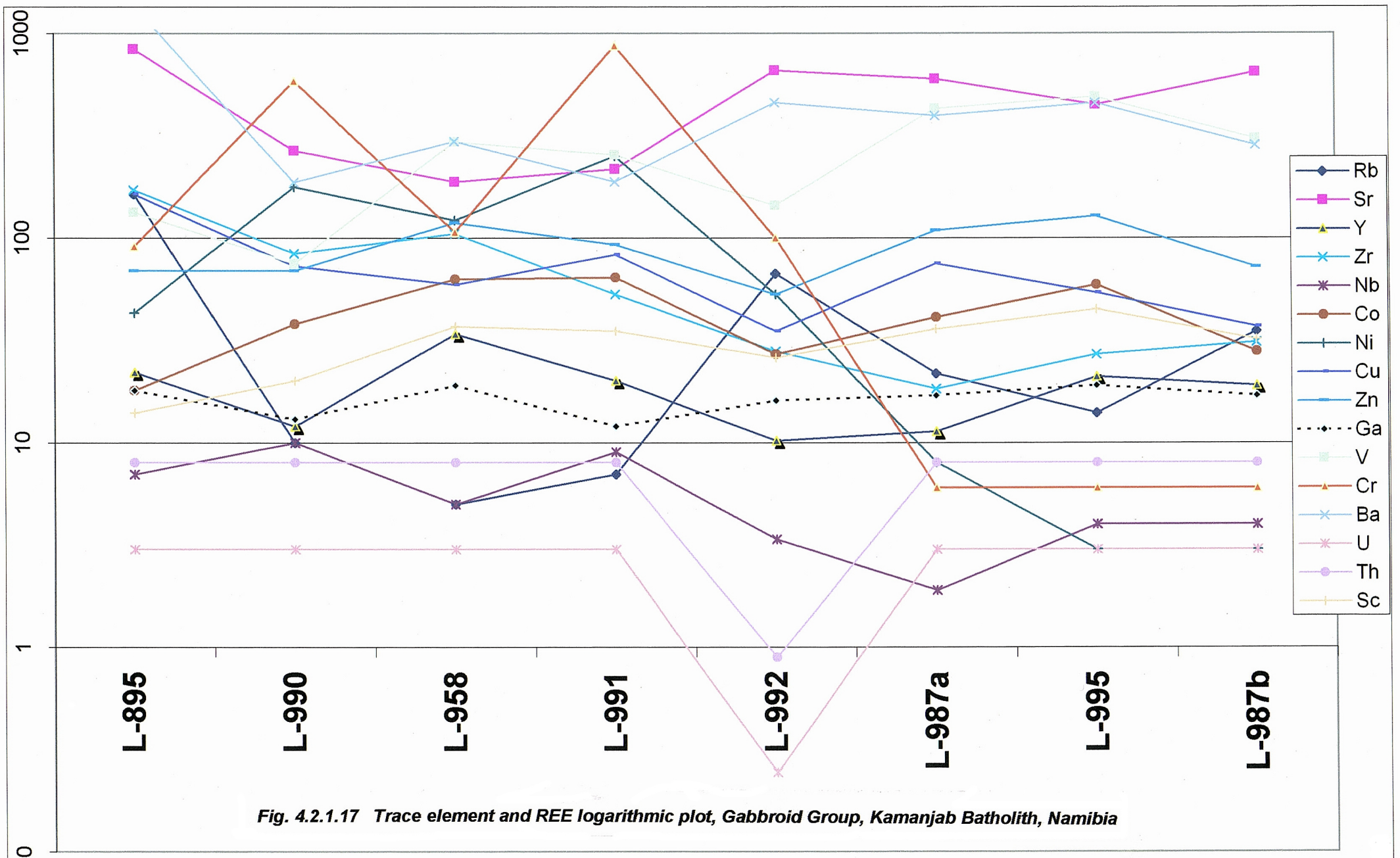

Fig. 4.2.1.17 Trace element and REE logarithmic plot, Gabbroid Group, Kamanjab Batholith, Namibia

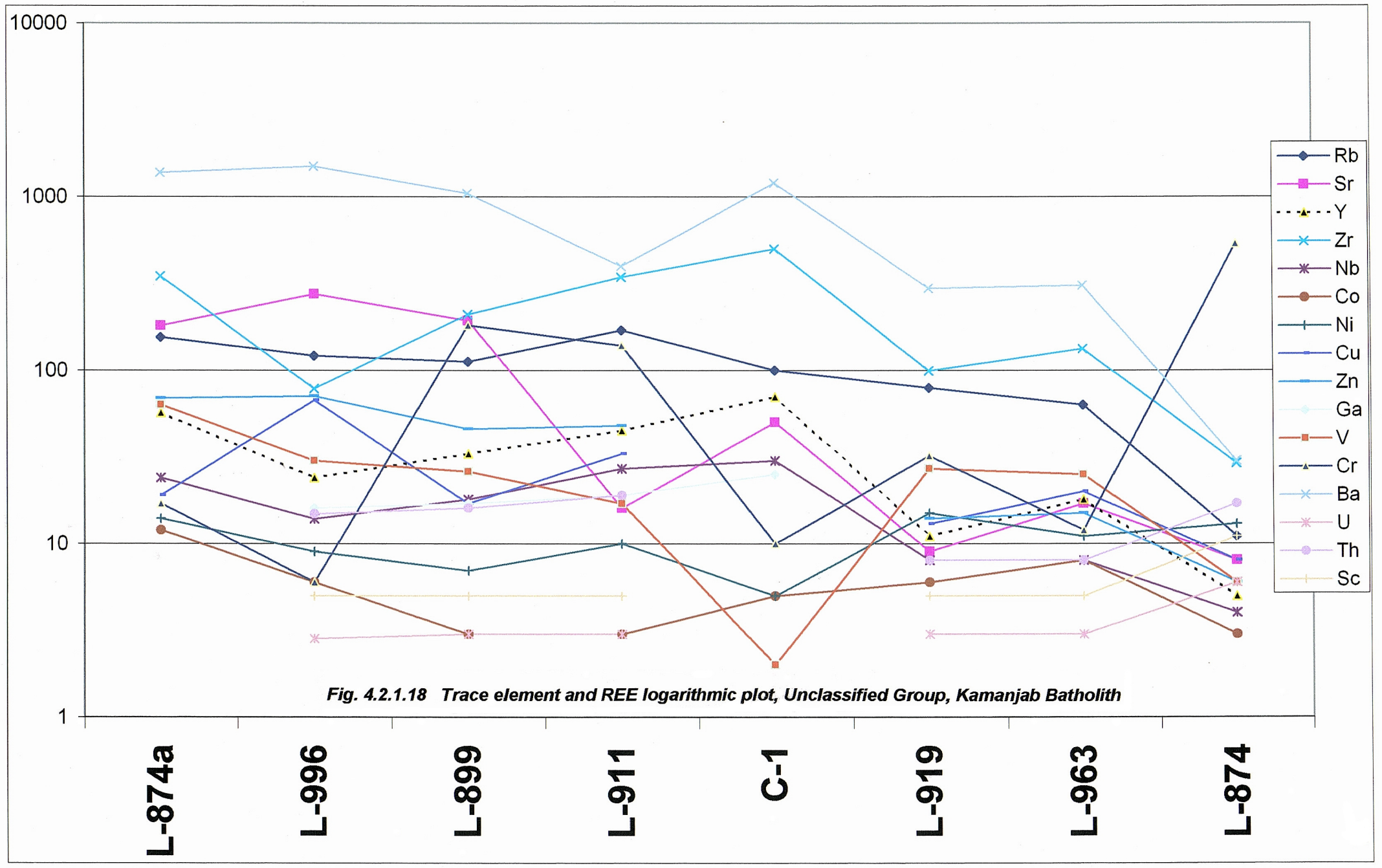

Fig. 4.2.1.18 Trace element and REE logarithmic plot, Unclassified Group, Kamanjab Batholith

Table 4.2.1.12 Groups of samples from the Kamanjab Batholith based on chemical similarity
(see acronym description on section 2.4.3.)

Group of Quartzmonzonites									
Sample	Rock Name	Debon & LeFort	Maniar & Piccoli	Whalen	Pierce	Mafic	Rb/10HfTa	Rb/30HfTa	Nb-Ta
L-832	alkali granite	metav leuco Na Fe	POG	A					
L-835	quartzmonzonite	metaiv meso Na Fe		A					
L-836	granite	metaiv meso Na Fe		A?					
L-838	granite	metaiv meso Na Fe		N					
L-842	granite	metaiv meso Na Fe		A	O3/4		WP	WP	OUTU
L-844	granite	metaiv meso Na Fe		A					
L-846	granite	metaiv meso Na Fe		A	O2/3				OUTU
L-863	granite	metaiv meso Na Fe		A					
L-864	granodiorite	metaiv meso Na-K Fe		N	S2/4 O2/4		VA-	II	INV
L-865	granodiorite	peraiii meso Na-K		A					
L-868	granite	metaiv meso Na Fe		N	S2/4 O2/4		VA-	II	INV
L-875	granodiorite	metaiv meso Na Fe		A?	O3/4				OUTU
L-877	granite	metaiv meso Na-K Fe	RRG	A	O-W1-1				
L-878	granite	metaiv meso Na Fe		A	O3/4				OUTU
L-900	quartzmonzonite	metaiv meso Na Fe		A					
L-940	gabbro-diorite	metav meso Na Fe		N	O3/4				OUTU
L-979	quartzmonzonite	metaiv meso Na Fe	IAG-CAG	N					
L-980	quartzmonzonite	metaiv meso Na Fe	IAG-CAG	N					
L-982	quartzmonzonite	metaiv meso Na Fe	IAG-CAG	N					OUTU
L-998	quartzmonzonite	metaiv meso Na Fe		A	O3/4				OUTU
L-1007	quartzmonzonite	metaiv meso Na Fe		A					
L-1009	quartzmonzonite	metaiv meso Na Fe		A					
L-1010	quartzmonzonite	metaiv meso Na Fe		A					
L-1011	quartzmonzonite	metav meso Na Fe		A	O-W1-1				
L-1012	Quartzmonzonite	metav meso Na Fe		A	O-W1-1				
L-1013	Granite	metaiv meso Na Fe		A	O3/4				OUTU
C-6	Granodiorite	metaiv meso Na-K Fe							
C-7	Granodiorite	metaiv meso Na-K Mg							
C-10	Granodiorite	metaiv meso Na Mg	IAG-CAG						
Group of Alkali Granites									
Sample	Rock Name	Debon & LeFort	Maniar & Piccoli	Whalen	Pierce	Mafic	Rb/10HfTa	Rb/30HfTa	Nb-Ta
L-839	alkali granite	metaiv leuco K Fe		A					
L-843	alkali granite	perai leuco Na-K		A	O-W 2-2		WP-	WP	OUTU
L-849	alkali granite	peraiii leuco Na-K Fe	RRG-CEUG	A	O3/4		WP	WP	OUTU
L-855	granite	metav leuco Na Fe	RRG-CEUG	A					
L-902	alkali granite	metaiv leuco Na Fe	RRG-CEUG	A					
L-903	alkali granite	metaiv leuco K Fe		A					
L-904	alkali granite	peraiii leuco Na-K Fe	RRG-CEUG	A					OUTU
L-905	alkali granite	metaiv leuco Na Fe	POG	N?	O-W1-1				
L-906	alkali granite	peraiii leuco K Fe	POG	A	O-W1-1				
L-909	alkali granite	metaiv leuco Na Fe	POG	A	O-W1-1				OUTU
L-912	granite	perai subleu K Mg		A	O-W1-1				
L-917	granite	peraiii meso Na Fe		A	S2/4 O2/4		VA-	II	INV
L-943	granite	metaiv leuco K Fe	CEUG-RRG	A	S2/4 O2/4		VA-	VA	INV
L-957	granite	metaiv leuco K Fe	POG	A	O3/4		WP-	WP	OUTU
L-968	granite	peraiii leuco Na Fe	CEUG-RRG	A	O3/4		WP	WP	OUTU
L-973	granite	metav subleu K Fe		A	O3/4		WP	WP	OUTU
L-975	granite	metaiv leuco Na-K Fe	POG	A					
L-976	alkali granite	metaiv leuco Na-K Fe	POG	A	O-W 2-2		WP-	WP	OUTU
L-977	alkali granite	metav leuco Na-K Fe	POG	A					
L-978	alkali granite	metav leuco Na-K Fe	RRG	A	S2/4 O2/4		VA-	VA	INV
L-983	granite	metaiv leuco Na Fe	CEUG-RRG	A					
L-985	Granite	metaiv subleu Na Fe	POG	N	S2/3		VA-	VA	OUTD-INV
L-997	Quartz syenite	metav leuco Na Fe	CEUG	A	O-W 2-2		WP-	WP	OUTU
L-1002	Alkali granite	metaiv leuco Na-K Fe	RRG	A			VA-	III	OUTU
C-4	Alkali granite	peraii leuco K Fe							
C-5	Granite	peraii leuco K Fe							
C-8	Alkali granite	peraiii leuco Na-K Fe	POG						
C-9	Alkali granite	peraii subleu K Fe	RRG						
C-11	Alkali granite	metav leuco K Fe							
C-13	Alkali granite	metaiv leuco K Fe	RRG						
X-18	Alkali granite	metavi leuco Na-K							
X-19	Alkali granite	peraiii subleu Na-K Fe	CEUG						
X-20	Granite	metaiv leuco K Fe	POG						

Group of Granites									
Sample	Rock Name	Debon & LeFort	Maniar & Piccoli	Whalen	Pierce	Mafic	Rb/10HfTa	Rb/30HfTa	Nb-Ta
L-840	Granite	metaiv subleu Na Fe	POG	A					
L-857	Alkali granite	metaiv leuco Na Mg	POG	N					
L-898	Granite	metaiv meso Na Fe	RRG-CEUG	A					
L-907	Granite	metaiv subleu Na-K Fe	POG	A					
L-910	Alkali granite	peraiii meso Na Fe	RRG-CEUG	A	O-W1-1				
L-922	Granite	metaiv meso Na-K Fe		A	O3/4				OUTU
L-923	granite	metaiv meso Na Fe	RRG-CEUG	A	O-W1-1				
L-924	granite	metaiv meso Na Fe		A	O-W1-1				
L-938	granite	metaiv meso Na Fe		A	O3/4		WP	WP	OUTU
L-939	granite	peraiii meso Na-K Fe	CEUG-RRG	N?	O3/4				OUTU
L-945	granite	peraiii meso Na Fe	CEUG	A	O3/4				OUTU
L-946	granite	metaiv meso Na Fe		A	O-W1-1				
L-948	granite	metav meso Na Fe		A	O-W1-1				
L-967	granite	metaiv meso Na-K Fe	RRG-CEUG	A	O-W1-1				
L-993	granite	metaiv subleu Na-K Fe	POG	N?	S2/4 O2/4		VA-	VA	INV
L-994	granite	metaiv subleu Na-K Fe	POG	A	O-W1-1				
L-999	granite	metaiv meso Na Fe		A	O3/4		WP-	WP	OUTU
L-1000	granite	peraiii subleu Na Fe		A	O3/4				OUTU
L-1003	quartzmonzonite	metaiv subleu Na Fe	POG	A	O3/4		WP	WP	OUTU
L-1005	granite	metaiv meso Na Fe	RRG	A	O-W1-1				
C-2	granite	peraiii meso Na-K Fe	RRG						
C-3	granite	metaiv meso Na Fe							
Group of Syenites									
Sample	Rock Name	Debon & LeFort	Maniar & Piccoli	Whalen	Pierce	Mafic	Rb/10HfTa	Rb/30HfTa	Nb-Ta
L-920	syenite	metav leuco Na Fe	CEUG	A	O3/4	wpab			OUTU
L-969	nepheline syenite	peraii meso K Fe	CEUG	A	O3/4		WP	WP	OUTU
L-951	nepheline syenite	metav subleu Na Fe	OP	A	V2/4				OUTU
L-971	nepheline syenite	metaiv leuco K Fe	CEUG	A	O-W1-1				
L-952	nepheline syenite	metav meso Na Fe	OP	A	V1/2				
L-834	syenite	metav meso K Fe	CEUG	A	O3/4		WP	WP	OUTU
L-956	syenite	metav meso Na Fe	OP	A					OUTU
L-908	syenite	metav leuco Na Fe	CEUG	A	S2/4 O2/4		VA-	III	INV
L-955	nepheline syenite	metaiv subleu Na Fe	OP	A	V3/4				OUTU
L-965	quartz syenite	metaiv meso Na-K Fe	CEUG	A	W				
L-966	quartz syenite	metaiv meso Na-K Fe	CEUG-RRG	A			VA-	III	INV
L-997	quartz syenite	metav leuco Na Fe	CEUG	A	O-W 2-2		WP-	WP	OUTU
Group of Gabbroids									
Sample	Rock Name	Debon & LeFort	Maniar & Piccoli	Whalen	Pierce	Mafic	Rb/10HfTa	Rb/30HfTa	Nb-Ta
L-895	syeno-diorite	metaiv meso Na Mg		N?	O3/4	wpt+vab-cab			OUTU
L-958	und-sat oliv gabbro	metaiv meso Na Fe		NZn?	V	arc			
L-987a	alkali granite	metav meso Na Fe		NZn?		emor	VA-	VA	OUTD
L-987b	theralite	metav meso Na Fe		N	V2/3	morb-iat-cab			OUTU
L-990	monzo-gabbro	metav meso Na Mg		N		wpab			
L-991	und-sat oliv gabbro	metaiv meso Na Fe		N	V	arc			
L-992	und-sat oliv gabbro	metaiv meso Na Mg	IAG-CAG	N	S2/4 O2/4	emor	VA-	VA	INV
L-995	alkali gabbro	metaiv meso Na Fe	RRG	A	V	morb-wpt			
C-14	ov sat oliv gabbro	metav meso Na Fe							
Group of samples that are not classified									
Sample	Rock Name	Debon & LeFort	Maniar & Piccoli	Whalen	Pierce	Mafic	Rb/10HfTa	Rb/30HfTa	Nb-Ta
L-874	out of plot high Si	peraiii leuco K Fe	RRG	A	V				
L-874a	granite	metaiv meso Na-K Fe			O-W1-1				
L-899	granite	metav subleu Na Mg		A					
L-911	granite quartzolite	perai subleu K Mg		A	O-W1-1				
L-919	out of plot high Si	peraii subleu K Fe	RRG						
L-963	out of plot high Si	peraiii leuco K Fe	RRG						
L-996	granite	Metaiv subleu Na Fe		N?	S2/4 O2/4		VA-	III	INV
C-1	alkali granite	Peraiii subleu Na-K Fe	POG						
X-16	alkali granite	Metav subleu Na Fe	RRG						
X-17	granite	Metaiv meso Na Fe							

4.2.1.6 Environment of Emplacement

As stated on section 2.4 of this document, the methods to define granitoid environment of emplacement based on geochemical data do not work well for Paleoproterozoic rocks. Nevertheless, the tests showed that several samples from the Kamanjab Batholith have a non-anorogenic character. A few samples seem to have been emplaced in a subductional environment. Table 4.2.1.13, extracted from Tables 4.2.1.12 and 4.2.1.4, shows details of the suites that contain such rocks, and Fig 4.2.1.6 shows their location. The spatial distribution of the suites is large; they practically cover all the batholith. This probably reflects a period of time when mantle rocks mixed with crustal rocks, producing a particular type of magmatism and vulcanism. This was not necessarily subduction magmatism. Not all rocks emplaced during that time have the mixed chemical signature. The areal extent of plutons with mixed-chemistry does not seem to be very large; that probably is due to the fact that crust and mantle mixing ocurred only during short periods of time in isolated places. The volume of rock formed was not as large as that of typical anorogenic magmatism.

Table 4.2.1.13 Kamanjab rock suites with samples of non-anorogenic or subductional character.
(Non-anorogenic samples have a #. Bold samples show subductional environment of emplacement. Dated samples marked with an asterisk. Underlined suites are mineralized.)

	Samples Analysed	Rock Types (sensu TAS) (#, quality, types)	Environment of emplacement	Map	Notes
B	L-838#, L-839, L-840, L-842, L-843, L-1010, L-1011, L-1012	2 Simple. Granite# and Quartzmonzonite	Non-Anorogenic (L-838)	K-16 C	
C	L-863, **L-864#**, L-865, **L-868#****, L-874, L-874-, L-875	3 Very good. Quartzmonzonite, **granodiorite#** and **altered granite#**	Non Anorogenic, subduction? (L-864, L-868)	K-14 SW	Contains Au and Fe mineralization, near major N-S fault
G	L-939, L-940, L-943*, L-945, L-946, L-948	4: 2 quartzmonzonite, 2 alkali granite	Non Anorogenic (L-940)	K-18 WC	
H	L-951, L-952, L-955, L-956, L-957, **L-958#**	4 Very good. Granite, **gabbro#**, monzonite	Non-Anorogenic (L-958?)	K-18 SC	Disseminated Cu mineralization
K	L-977a, L-978, **L-979#, L-980#, L-982#**	2 Very good. **Quartzmonzonite#**, alkali granite	Non-Anorogenic, Subduction (L-979, L-980, L-982)	K-21 NW	
M	**L-987#**, L-987a, L-990, L-991#**, L-992**, **L-993#***, L-994, L-995, L-996, L-997, L-998	6 very good. Alkali granite, quartzmonzonite, various **gabbroids#**, **granite#,** quartz syenite	Non-Anorogenic, Subduction (L-987?, L-987A, L-990, L-991, L-992, L-993?)	K-20 CW	Disseminated Cu mineralization. Seems to have a large fractionation sequence.
Q	C-1, C-2, C-3, C-4, C-5, C-6, C-7, C-8, C-9, **C-10**, C-12	2 (or 3) Simple. Quartzmonzonite, alkali granite, **granodiorite**	Non-Anorogenic, maybe subductional. (C-10)	K-24	Zircons from suite dated collectively by Clifford, 1969.

If the number of samples analysed represents the entire batholith, then 15% of the rocks in the batholith have a non-anorogenic origin, and 8% indicate mixed origin. This observation has to take into account that 7 out of 9 gabbroid rocks turned out to be non-anorogenic, and the procedure of Whalen et al, 1987 was not designed for mafic rocks.

The environment of emplacement for all samples of the Greater Lufilian Arc is currently being reviewed using geostatistical artificial intelligence cluster techniques. Preliminary results shown on Table 4.2.1.12 may be due to crustal contamination and not to true subduction processes.

4.2.1.7 Evidence of Magma Mixing-Magma Mingling

There are many indications of magma mixing in the Kamanjab Batholith. These include rapakivi and antirapakivi textures, abundant mafic inclusions and hybrid inclusions, diffuse nature of crystal contacts, ovoidal alkali feldspar pseudophenocrysts in some rocks, and spongy cellular plagioclase.

The presence of two or more contrasting rock types implies that there were many pulses of magma with different compositions that were emplaced in a small area. Suites that display evidence of five or six contrasting rock types must have had a lot of mixing and interaction of the magmas. One of the important aspects of magma mixing and mingling is that these processes destabilize the ionic balance of incoming magma and may act as precipitation agent for various new minerals and metal-bearing sulfides.

4.2.1.8 Granitoids sampled by Tom Clifford

Clifford and his co-workers carried out pioneering work on the chemistry and geochronology of the Kamanjab Batholith (Clifford et al., 1962a; Clifford et al., 1962b; and Clifford et al., 1969). Table 4.2.1.14 shows chemical analysis of the samples he collected. This was the only publicly available geochemical information on the batholith before 1992. Preliminary plots of their chemistry indicated a large heterogeinity. Ten of Clifford's samples were studied as Suite Q (Fig F16). **C-1**, **C-4**, **C-5**, **C-8** and **C-9** make a cluster that spans from alkali granite to granite; **C-2** and **C-3**, and **C-6** make two clusters of quartzmonzonites; while **C-7** and **C-10** make a cluster in the triple point of quartzmonzonite, granodiorite and granite.

Clifford et al., 1962a identified that mafic rocks (**C-14**) intersected the granitoids and were fossilized by the Otavi sedimentary rocks. They also identified some red granitoids[1] (**C-13**) that, according to them were subject to sub-aereal "weathering" before deposition of the Otavi siliciclastic and carbonate sequences. Clifford and his research group evaluated the rest of the granitoids as a single entity. Nevertheless, these rocks of varying composition formed at different times, as discussed in the following sections.

Table 4.2.1.14 Chemical Analysis, Samples analysed by Clifford et al., 1969; Kamanjab Batholith, Namibia
(Complete analysis is on Tables 4.2.1.1 and A9)

Sample	SiO2	TiO2	Al2O3	Fe2O3	FeO	MnO	MgO	CaO	Na2O	K2O	P2O5	LOI	Total	Rb	Sr	Y	Zr	Nb	Ga	V	Cr	Ba	Pb	La	Ta	Li	Be
C-1	74.03	0.27	12.73	1.15	1.51	0.05	0.31	0.48	3.67	5.09	0.05	0.71	100.05	100	50	70	500	30	25	<3	10	1200	25.0	95	<100	<3	<3
C-2	69.71	0.68	14.17	1.69	1.57	0.04	0.84	0.82	4.10	5.30	0.27	0.67	99.86	70	110	45	550	30	25	35	25	2100	8.0	90		35	
C-3	68.63	0.67	15.43	1.74	1.03	0.10	0.51	1.99	4.50	4.42	0.18	0.50	99.70	90	350	##	700	40	25	35	11	2500	25.0	130		30	
C-4	73.63	0.33	14.16	1.13	0.24	0.02	0.00	0.50	3.14	6.35	0.07	0.44	100.01	200	80	20	380	20	20	9	13	1200	40.0	95		11	
C-5	75.35	0.27	13.18	1.08	0.22	0.02	0.00	0.62	3.15	5.50	0.05	0.36	99.80	110	100	35	280	10	20	5	15	1400	30.0	65		12	
C-6	66.09	0.69	14.60	3.06	1.72	0.08	1.81	2.54	3.25	4.71	0.28	1.11	99.94	150	480	25	280	<10	20	85	18	1900	14.0	75		25	
C-7	69.29	0.47	14.55	1.81	1.48	0.06	1.19	2.83	3.33	4.40	0.17	0.46	100.04	230	650	25	320	10	19	70	35	1700	16.0	70		13	
C-8	73.88	0.33	13.85	0.87	0.24	0.03	0.18	0.26	4.05	5.93	0.09	0.39	100.10	130	40	55	450	15	20	7	11	400	20.0	65		4	
C-9	73.30	0.32	13.20	2.93	0.48	0.01	0.00	0.24	3.46	5.67	0.07	0.34	100.02	130	50	80	650	30	30	<3	14	1200	12.0	85		9	
C-10	68.63	0.49	15.01	1.62	1.44	0.07	1.22	2.74	4.41	3.60	0.20	0.57	100.00	65	720	25	230	<10	20	55	30	1900	18.0	70		20	
C-11	78.84	0.29	10.79	0.95	0.27	0.03	0.09	0.60	2.94	5.20	0.06	0.22	100.28	120	65	55	180	18	15	5	25	560	20.0	100		<3	
C-13	75.89	0.41	12.46	1.07	0.13	n.d.	0.05	0.25	3.60	5.71	0.04	0.50	100.11	100	40	65	650	40	25	<3	10	1000	30.0	90	<100	<3	<3
C-14	48.69	1.26	13.27	4.86	8.71	0.18	6.15	10.49	2.41	1.05	0.22	0.50	97.79														

The granitoids sampled and analysed by Clifford et al., 1969 have been included in the database of the Greater Lufilian Arc granitoid project. Such samples were located as best as possible, with the help of the author, using 1:50,000 scale topographical maps that were not available at the time of original sampling (Clifford, T., personal communication, 2003). The samples have been numbered with the same digits and a "C" prefix for identification.

The chemistry of the samples helped to assign them to various rock groups of the Kamanjab Batholith. **C-6**, **C-7** and **C-10** were assigned to the group of alkali granites; **C-4**, **C-5**, **C-8**, **C-9** and **C-11** to the group of granites; **C-14** is listed with the gabbroids; while **C-2** and **C-3** were assigned to the group of quartzmonzonites. **C-1** has some similarities with the group of alkali granites.

4.2.1.9 Geochronology

New radiometric ages for samples from the Kamanjab Batholith were produced during this project, and are listed on Table 4.2.1.15. Rocks from several suites spread out across the batholith were selected, to obtain the greatest representativity, and date some of the main mineralizing events. Table A22.17 presents all trustworthy geochronological data from the Kamanjab area, and Table A22.15 lists only the ages that come from the main portion of the batholith. Geochronology proved to be definitive for the interpretation of the Kamanjab Batholith, its history and metallogenic events.

The "younger" granitoids from some suites were tested on purpose, to see if there was a significant magmatic event overprinted on the Paleoproterozoic granitoids. Ages of 750 Ma were expected, but none were found. The "old" intrusions of the suites still remain to be tested. Rocks older than 2000 Ma are expected to occur. Xenocrystic ages of ~2600 Ma and ~2500 Ma were found in **L-855** and **L-969** (Table 4.2.1.15). That might be the age of the granite basement of the Kamanjab Batholith. Until recently, such ages were unthinkable for the batholith. Zircons from several of the perceived-to-be old samples, were picked and are ready for dating. The order of priority for the rest of the samples to date is: **L-968**, **L-864**, **L-985**, **L-1045** and **L-945**, as indicated on

[1] The reddened rocks identified by Clifford may be hematite-altered granitoids produced by hydrothermal alteration.

Table 4.2.1.15. The chemistry of the other "old" granitoids listed on that table (i.e. **L-864** and **L-945**) is completely different. See the Tables 4.2.1.12 and 4.2.1.16.

Events 13 and 14 from Table A22.15, correlate reasonably well with each other. They represent an important moment of magmatism. Samples **L-1043** and **L-1045** correlate well with rocks from the Kamanjab Batholith both geochemically and geochronologically. In fact, **L-1043** and **L-855** have similar chemistry, age of emplacement and xenocrystic zircon ages.

Table 4.2.1.15 Granitoid samples from the Kamanjab Batholith that were dated.
(Zircon concentrates from all samples were dated for this project by laser ablation ICPMS at the Memorial University of Newfoundland, Canada, except for C-1. Precise locations of the rest of the dated samples from the batholith could not be obtained.)

Name of site	Suite	Sample	Description	Age (Ma)	Error (Ma)	Priority
Kamdescha farm	C	L-868	Quartzmonzonite. Young intrusive. Related to sulfidation and maybe to IOCG mineralization	1937	14	Dated
Kamdescha farm	C	L-864	Granodiorite. Old granitoid. Hosts L-868 and is the local basement.			2
Tevrede farm	P	L-855	Granite. Sample collected at the Tevrede property. Could be one of the intrusives associated with IOCG mineralization.	1937	19	Dated
Tevrede farm	P	L-855	Inherited zircons	~2500		Dated
N of Kamanjab town	Q	L-985	Granite. Average composition of the granitoids from the Kamanjab Batholith. Easily accessible.			3
Mineralized area 2	J	L-969	Foid syenite. Associated to disseminated copper mineralization in the Kamanjab Batholith. Has strong potassic alteration.	1976	42	Dated
Mineralized area 2	J	L-968	Granite. Hosts L-969 and shows minor mineralization.			1
Mineralized area 3	M	L-993	Granite. Associated to copper dissemination in the Kamanjab Batholith. Has potassic alteration.	1866	13	Dated
Intrusive along E-W fault		L-1013	Quartzmonzonite. Could be one of the young intrusives. Emplaced along a main E-W fracture.	1878	15	Dated
End of road W of Kamanjab Batholith	G	L-943	Granite. Is one of many young granioitd dikes that intersect L-945, L-939 and L-948.	1877	39	Dated
End of road W of Kamanjab Batholith	G	L-945	Quartzmonzonite. Old, foliated, coarse-grained granitoid that acts as host to all other rocks in the suite.			5
Franzfontein granite, Franzfontein	Q	C-1	Alkali granite. Studied and analysed by Clifford et al, 1962; Clifford et al, 1969; and Burger et al, 1976. Located in the southern portion of the Kamanjab Batholith	1730	30	Dated
Otavi Mountains, basement		L-1043	Granite. The youngest granitoid in the region. Intrudes into L-1045.	1939	64	Dated
Otavi Mountains, basement		L-1043	Inherited zircons	2544	78	Dated
Otavi Mountains, basement		L-1045	Quartzmonzonite. Old granitoid in the region. Part of the Grootfontein Inlier. Very little is known about the basement in this part of Namibia.			4

At least two ages for copper mineralization exist at the Kamanjab Batholith: the mineralizing granitoid of Suite J is dated at 1976±42Ma and that of suite M, at 1866±13Ma. These are separated by 110 Ma. The copper event from copper mineralization of suite J may be correlated with the 1987±4Ma age for Khoabendus granitoids of Hoffman & Kroner published by Seth et al., 1998 (Table A22.15, and Fig A39).

The age of the Cu-mineralization event of suite M, dated at 1866±13Ma is within error of the quartz-eye rhyolite dated at 1862±6Ma by Steven & Armstrong, 2002 at the Gelbingen farm, in the NE portion of the Kamanjab Batholith. The age of mineralization at the Gelbingen farm could be the same, although the subvolcanic rhyolitic intrusive that seems to be producing mineralization at Gelbingen has not been dated.

The age of the mineralizing intrusion at Suite J is also very near to the time of emplacement for **L-1013**. This might be very relevant, since **L-1013** was emplaced along a major E-W fracture (Fig 4.2.1.6).

The granitoid that hosts copper mineralization of the suite J has an unknown age. Sample **L-968** should be dated with the highest priority. Of all the samples collected, it has potential to become the oldest known granitoid of the Kamanjab Batholith.

The anorogenic magmatism of **L-864** must be dated. That rock may be representing an event of subductional-related magmatism and should be studied. The sample does not seem to correlate with any of the other ones on the geochemical database. It could be younger or older than **L-969**; but definitely older than ~1957Ma.

Inherited zircons from the Kamanjab region indicate ages of *circa* 2500 Ma and 2125 Ma for the basement to the batholith. It is possible that some of the undated rocks from the batholith are that old.

All ages from the Kamanjab region have been put together on the event diagram of Fig A37 (Table A22.17). It shows a continuum of emplacement events from 1980 to 1560 Ma. A closer look helps to identify three discrete shorter events: 1991 to 1923, ~1900 to 1776, and 1755 to 1632 Ma. These lasted 68, 124 and 123 Ma, respectively. The last of the three lapses occurs mainly in the Khorixas Inlier. Information available is not enough to define if the first and second events are separate or form the same series of magmatism.

There is no record of magmatic events from 800 to 740 Ma in the main Kamanjab Batholith. Events Nos. 4 to 15 on Fig A37 are all from the Khorixas Inlier and environs. That indicates that geological history of the main Kamanjab Batholith and the Khorixas Inlier was different after circa 1600 Ma (Fig A40).

Table 4.2.1.16 shows a hypothetical correlation of rocks based on rock types and new geochronological data for the Kamanjab Batholith. The age of **L-945** is probably ~1937Ma and it seems to correlate with **L-868**, **L-855** and **L-1045**.

Table 4.2.1.16 Hypothetical correlation of the dated samples, Kamanjab Batholith and Grootfontein inlier, Namibia. (Base data from Table 4.2.1.15. Lithological correlation based on the same chemical groups, as indicated on Tables 4.2.1.12 and 4.2.1.5 to 4.2.1.7).

Suite/Unit	**C**	**J**	**G**	**M**	**P**	**Q**	
Region	Kamanjab	Kamanjab	Kamanjab	Kamanjab	Kamanajab	Kamanjab	Grootfontein
Alkali Granite						**C-1** alkali granite, 1739;30	
Alkali Granite			**L-944** young granite 1856;24 Ma	**L-993*** granite 1866;13 Cu			**L-1043** young granite ~1887;39 Ma
Quartzmonzonite	**L-868*** young quartzmonzonite 1937;14 Ma IOCG		**L-945** old quartzmonzonite		**L-855** granite 1939;19		**L-1045** Old quartzmonzonite ~1900?
Granodiorite	**L-864** old granodiorite						
Alkali Rocks		**L-969*** young foid syenite 1976;42					
Granites		**L-968** old granite 2600Ma?			~2500 Ma		

The event diagram for the Kamanjab Batholith (Fig A39) looks very much like that of the anorogenic granitic complex clusters. Chapter 7 defines the main characteristics of anorogenic ring complex clusters, in terms of time distribution of intrusions and length of magmatic events. Section 7.2.7 shows similarities of the Kamanjab Batholith with other ring complex clusters in the Greater Lufilian Arc.

Zircon concentrates from several samples were dated by Clifford et al., 1969 and Burger et al, 1976 (Nos. 3, 4, 7 and 11 on Table A22.15 and Fig A39). If the hypotheses presented above[2] are true, then Burger et al, 1976 grouped rocks of three different ages and compositions to yield zircons for U-Pb dating. It is commonly understood today that the methods used for dating of large amounts of zircons in a single batch are not precise. As shown on the event diagrams of Figs A39 and A37, ages 3 and 4 of Clifford et al., 1969 are too young by more than a hundred and twenty million years.

[2] This refers to the hypotheses of 1) extensive quartzmonzonite extrusion in the Kamanjab Batholith around 1937 Ma, 2) alkaline granites being intruded at around 1856 Ma, and 3) granites being the basement of such intrusions.

Table 4.2.1.17 Tentative correlation of the various rock units in the Suites from the Kamanjab Batholith. Namibia

(Asterisks mark mineralized suites and mineralizing granitoids. # indicates samples with non-anorogenic environment of emplacement. Ag=alkali granite, Alk=alkaline, Gb=gabbro, Gd=granodiorite, Gt=granite, Qm=quartzmonzonite. This table is an enlargement of Table 4.2.1.16.) The term “non-anorogenic” is used here to describe environments of granitoid emplacement that do not fit the anorogenic paramaters in discrimination methodologies commonly used today. The origin of such rocks is not clear at the time of writing. Nevertheless, such rocks probably did not form in subductional environments.

Events	A	B	C*	D*	E	F	G*	H*	I	J*	K	L	M*	N*	O*	P	Q	Gelbingen *	Grootfontein
Anorogenic magmatism																	Ag C-1 1739; 30		
Anorogenic magmatism																		1862±6 Ma L-849 Alk Gt*	
Anorogenic magmatism				Gt*	Alk Gt		Alk Gt L-934 1856;24*		Ag	Ag	Ag	Ag	Ag L-993 1866;13*				Ag		Gt L-1043 ~1887;39
Non-anorogenic magmatism 2	Qm	Am, Gt L-838#	Am L-868#	Qm		Qm	Qm L-945		Qm		Qm subduc-tion L-979#, L-980#, L-982#		Qm	Qm	Gt L-855 1939; 19		Qm		Qm L-1045 ~1900
Non-anorogenic magmatism 1			Gd L-864#				Gt, L-939, L-949, gb, L-940#	Gb L-958#					Gabbroids, L-991#				Gd C-10#		
Anorogenic magmatism										Syenite L-969* 1876;42									
Anorogenic magmatism	Gt		Gt			Gt		Gt	Gt	Gt L-968		Gt		Gt					
										Gt ~2600						Gt ~2500			~2600

Table 4.2.1.18 Location of samples and geological stations on the Kamanjab Batholith, Namibia

(Map number indicates maps of Figs M28 to M35. Samples and stations are listed in alphabetical order.)

map	place	sample
K-24	SW	C-1
K-21	NC	C-10
K-24	CW	C-10
K-21	SE	C-12
K-24	SC	C-12
K-21	SE	C-2
K-24	SC	C-2
K-21	SE	C-3
K-24	SC	C-3
K-21	SE	C-4
K-24	SC	C-4
K-21	SE	C-5
K-24	SC	C-5
K-24	SC	C-6
K-24	CW	C-7
K-21	CN	C-8
K-24	CW	C-8
K-21	CW	C-9
K-24	SW	C-9
K-23	WC	CW
K-19	SE	L-1000
K-20	NW	L-1000
K-23	SW	L-1000
K-25	C	L-1000
K-19	SE	L-1001
K-25	C	L-1001
K-19	CE	L-1002
K-25	C	L-1002
K-19	CE	L-1003
K-19	CE	L-1004
K-25	NW	L-1004
K-19	CW	L-1005
K-19	CW	L-1006
K-23	SW	L-1006
K-19	CN	L-1007
K-16	SC	L-1008
K-19	NE	L-1008
K-23	WC	L-1008
K-25	NW	L-1008
K-16	SC	L-1009
K-23	WC	L-1009
K-16	SC	L-1010
K-16	C	L-1011
K-16	SC	L-1012
K-23	WC	L-1012
K-22	WC	L-1013
K-23	SE	L-1013
K-24	CN	L-1013
K-24	SC	L-784
K-14	CW	L-803
K-14	CW	L-804
K-22	CN	L-830
K-24	NC	L-830
K-22	NW	L-831
K-24	NC	L-831
K-17	CE	L-832
K-17	CE	L-833
K-23	CE	L-833
K-17	CE	L-834
K-17	C	L-835
K-23	CE	L-835
K-17	NC	L-836
K-23	CE	L-836
K-16	C	L-837
K-16	CE	L-837
K-16	C	L-838
K-16	C	L-838
K-16	C	L-839
K-16	C	L-839
K-23	WC	L-839
K-16	C	L-843
K-16	C	L-844
K-16	NC	L-845
K-23	NW	L-845
K-16	NC	L-846
K-23	NW	L-846
K-14	SE	L-847
K-23	NW	L-847
K-14	SE	L-848
K-23	NW	L-848
K-14	SC	L-849
K-14	SE	L-849
K-23	NW	L-849
K-14	SC	L-850
K-14	SC	L-851
K-14	SC	L-852
K-23	NW	L-852
K-14	NW	L-855
K-14	C	L-857
K-14	CW	L-862
K-14	SW	L-863
K-14	SW	L-864
K-14	SW	L-865
K-14	SW	L-866
K-14	SW	L-867
K-14	SW	L-868
K-14	SW	L-869
K-14	SW	L-869
K-14	SW	L-870
K-14	SW	L-871
K-14	SW	L-872
K-14	SW	L-873
K-14	SW	L-874
K-14	SW	L-875
K-14	SC	L-876
K-14	SC	L-877
K-14	SC	L-878
K-16	WC	L-898
K-16	WC	L-899
K-16	WC	L-900
K-16	WC	L-901
K-23	WC	L-901
K-16	WC	L-902
K-16	WC	L-903
K-23	WC	L-903
K-16	WC	L-904
K-16	WC	L-905
K-16	WC	L-906
K-16	WC	L-907
K-15	NE	L-908
K-16	WC	L-908
K-15	NE	L-909
K-15	NE	L-910
K-15	NE	L-911
K-15	C	L-912
K-15	C	L-913
K-15	C	L-914
K-15	C	L-915
K-15	C	L-916
K-15	C	L-917
K-15	C	L-918
K-15	NW	L-919
K-15	NW	L-920
K-15	NE	L-923
K-15	NE	L-924
K-15	NW	L-937
K-18	NW	L-938
K-18	WC	L-939
K-18	WC	L-940
K-18	WC	L-941
K-18	WC	L-942
K-18	WC	L-943
K-18	WC	L-944
K-18	WC	L-945
K-18	SC	L-948
K-18	SC	L-949
K-18	SC	L-950
K-18	SC	L-952
K-18	SC	L-953
K-18	SC	L-954
K-18	SC	L-955
K-18	SC	L-956
K-18	SE	L-957
K-18	SE	L-958
K-18	SE	L-959
K-19	WC	L-960
K-23	SW	L-960
K-19	WC	L-962
K-19	WC	L-963
K-23	SW	L-963
K-19	WC	L-964
K-23	SW	L-964
K-19	WC	L-965
K-19	WC	L-966
K-19	WC	L-967
K-23	SW	L-967
K-19	SW	L-971
K-19	SW	L-972
K-23	SW	L-972
K-19	SW	L-973
K-23	SW	L-973
K-19	SW	L-974
K-23	SW	L-974
K-19	SW	L-975
K-23	SW	L-975
K-19	SW	L-976
K-23	SW	L-976
K-19	CW	L-977
K-21	NW	L-977
K-23	SW	L-977
K-21	NW	L-978
K-24	WC	L-978
K-20	SC	L-979
K-21	NW	L-979
K-24	WC	L-979
K-20	SC	L-980
K-21	NW	L-980
K-24	WC	L-980
K-20	SC	L-981
K-21	NW	L-981
K-24	WC	L-981
K-20	SC	L-982
K-21	NW	L-982
K-24	WC	L-982
K-20	CW	L-983
K-24	WC	L-983
K-20	CW	L-984
K-20	CW	L-985
K-25	SE	L-985
K-20	CW	L-986
K-25	SE	L-986
K-20	CW	L-987
K-25	SE	L-987
K-20	CW	L-988
K-25	SE	L-988
K-20	CW	L-989
K-25	SE	L-989
K-20	CW	L-990
K-25	SE	L-990
K-20	CW	L-991
K-25	SE	L-991
K-20	CW	L-992
K-25	SE	L-992
K-20	CW	L-993
K-25	SE	L-993
K-20	CW	L-994
K-25	SE	L-994
K-20	CW	L-995
K-25	SE	L-995
K-20	CW	L-996
K-25	SE	L-996
K-20	NW	L-997
K-25	SE	L-997
K-20	NW	L-998
K-25	SE	L-998
K-19	SE	L-999
K-20	NW	L-999
K-23	SW	L-999
K-25	C	L-999
K-25	NW	S102
K-16	NC	S11
K-21	SW	S122
K-24	SW	S122
K-20	NW	S141
K-23	SW	S141
K-25	NW	S151
K-14	SC	S17
K-23	NW	S17
K-17	C	S2
K-14	SW	S21
K-14	SW	S24
K-14	SW	S27
K-14	SW	S31
K-14	SW	S32
K-14	SW	S36
K-14	SW	S38
K-14	SW	S41
K-14	SW	S42
K-23	WC	S425
K-14	SW	S43
K-14	SC	S59
K-22	CE	S59
K-16	WC	S62A
K-16	WC	S63
K-16	WC	S67
K-23	WC	S68
K-23	WC	S70
K-15	CE	S74
K-15	NE	S78
K-15	NE	s79
K-15	NE	S79
K-15	NE	S80
K-15	NE	S80
K-15	NE	S81
K-15	NE	S82
K-15	NE	S85
K-15	NE	S87
K-15	NE	S87
K-15	EC	S88
K-15	EC	S89
K-18	NC	S89
K-15	EC	S90
K-15	EC	S91
K-18	WC	S91
K-18	NC	S95
K-21	SW	S95
K-24	SW	S95
K-20	NW	S98
K-23	SW	S98
K-19	EC	S99
K-20	NW	S99
K-23	SW	S99
K-25	C	S99
K-16	CW	W100
K-23	WC	W100
K-16	CW	W101
K-23	WC	W101
K-16	WC	W102
K-23	WC	W102
K-16	WC	W103
K-23	WC	W103
K-23	WC	W104
K-16	WC	W105
K-16	WC	W106
K-16	WC	W107
K-16	WC	W108
K-15	WC	W109
K-16	WC	W109
K-15	WC	W110
K-23	WC	W110
K-15	WC	W111
K-23	WC	W111
K-23	WC	W112
K-15	CE	W113
K-15	CE	W114
K-18	NC	W114
K-15	EC	W115
K-18	NC	W115
K-15	EC	W116
K-18	NC	W116
K-18	NC	W117
K-18	WC	W118
K-18	WC	W119
K-18	WC	W120
K-18	WC	W121
K-18	WC	W122
K-18	WC	W123
K-18	WC	W124
K-18	WC	W125
K-24	WC	W362
K-21	NW	W364
K-24	WC	W364
K-20	SC	W366
K-21	NW	W366
K-24	WC	W366
K-20	SC	W367
K-21	NW	W367
K-24	WC	W367
K-20	SC	W368
K-20	SC	W368
K-24	WC	W368
K-20	SC	W369
K-21	NW	W369
K-21	NW	W370
K-20	SC	W371
K-21	NW	W371
K-24	WC	W371
K-20	SC	W372
K-24	WC	W372
K-24	WC	W373
K-20	CW	W374
K-20	SC	W374
K-24	WC	W374
K-20	CW	W375
K-24	WC	W375
K-20	CW	W376
K-24	WC	W376
K-20	CW	W377
K-24	WC	W377
K-20	CW	W379
K-20	CW	W380
K-25	SE	W381
K-20	CW	W382
K-20	CW	W384
K-25	SE	W384
K-20	NW	W385
K-20	NW	W386
K-20	NW	W387
K-20	NW	W388
K-20	NW	W389
K-20	NW	W390
K-20	NW	W391
K-23	SW	W391
K-23	SW	W391
K-25	C	W391
K-19	EC	W392
K-20	NW	W392
K-25	C	W392
K-19	EC	W393
K-25	C	W393
K-19	EC	W394
K-23	SW	W394
K-25	C	W394
K-25	C	W395
K-19	EC	W396
K-20	CW	W396
K-25	C	W396
K-19	EC	W397
K-23	SW	W397
K-25	C	W397
K-25	C	W398
K-19	EC	W-398
K-19	EC	W399
K-23	SW	W399
K-25	C	W399
K-19	EC	W400
K-23	SW	W401
K-25	C	W401
K-19	EC	W402
K-23	SW	W402
K-25	C	W402
K-23	SW	W403
K-25	C	W403
K-23	SW	W404
K-25	C	W404
K-19	EC	W405
K-23	SW	W405
K-25	NW	W405
K-19	EC	W406
K-23	SW	W406
K-25	NW	W406
K-19	EC	W407
K-25	NW	W407
K-19	EC	W408
K-23	SW	W408
K-25	NW	W408
K-19	EC	W409
K-23	SW	W409
K-25	NW	W409
K-19	EC	W410
K-23	SW	W410
K-25	NW	W410
K-19	EC	W411
K-23	SW	W411
K-25	NW	W411
K-23	WC	W412
K-25	NW	W412
K-16	CE	W413
K-23	WC	W413
K-16	CE	W414
K-23	WC	W414
K-16	CE	W415
K-16	CE	W417
K-16	CE	W418
K-23	WC	W418
K-23	WC	W419
K-16	CE	W420
K-23	WC	W420
K-16	CE	W421
K-23	WC	W422
K-16	CE	W423
K-23	WC	W423
K-16	CE	W424
K-16	CE	W425
K-16	NC	W427
K-16	NC	W430
K-16	NC	W431
K-23	NW	W431
K-16	NC	W432
K-23	NW	W432
K-16	NC	W433
K-23	NW	W433
K-16	NC	W434
K-23	NW	W434
K-14	SC	W435
K-14	SC	W436
K-14	SC	W437
K-23	NW	W437
K-14	SC	W438
K-14	SC	W439
K-23	NW	W439
K-23	NW	W440
K-14	SC	W442
K-14	SC	W443
K-14	SC	W445
K-14	SW	W446
K-14	SW	W447
K-24	WC	W463
K-16	CW	W503
K-16	CW	W504
K-16	CW	W505
K-14	SC	W510
K-14	C	W511
K-14	C	W513
K-14	C	W514
K-14	C	W515
K-14	NC	W517
K-14	NC	W519
K-14	NC	W521
K-14	NC	W523
K-14	NC	W525
K-14	NC	W527
K-14	NC	W529
K-14	NC	W530
K-14	NC	W531
K-14	NC	W532
K-14	C	W534
K-23	NW	W536
K-23	NW	W543
K-23	NW	W569
K-23	NW	W569
K-24	EC	W57
K-23	NW	W571
K-23	NW	W578
K-23	NW	W578
K-22	SE	W58
K-24	NE	W58
K-24	NC	W59
K-15	NE	W598
K-15	NE	W599
K-22	CE	W60
K-24	NC	W60
K-15	EC	W600
K-22	CE	W61
K-24	NC	W61
K-22	CE	W62
K-24	NC	W62
K-24	NC	W63
K-22	CN	W64
K-24	NC	W64
K-22	NW	W65
K-24	NC	W65
K-24	NC	W65
K-22	NW	W66
K-22	NW	W67
K-23	CE	W67
K-24	NC	W67
K-22	NW	W68
K-23	CE	W68
K-24	NC	W68
K-22	NW	W69
K-23	CE	W69
K-24	NC	W69
K-17	SE	W70
K-23	CE	W70
K-24	NC	W70
K-17	EC	W71
K-23	CE	W71
K-17	EC	W72
K-23	CE	W72
K-17	EC	W73
K-23	CE	W73
K-17	EC	W74
K-17	EC	W75
K-23	CE	W75
K-17	C	W76
K-23	CE	W76
K-17	C	W77
K-23	CE	W77
K-17	C	W78
K-23	CE	W78
K-17	C	W79
K-23	CE	W79
K-17	C	W80
K-23	CE	W80
K-17	C	W81
K-23	C	W81
K-23	CE	W81
K-17	C	W82
K-23	C	W82
K-17	C	W83
K-23	C	W83
K-17	NW	W84
K-23	C	W84
K-17	NW	W85
K-23	C	W85
K-16	EC	W86
K-17	NW	W86
K-23	C	W86
K-16	EC	W87
K-23	C	W87
K-16	CE	W88
K-23	C	W88
K-16	CE	W89
K-23	C	W89
K-16	CE	W90
K-23	C	W90
K-16	C	W91
K-23	WC	W92
K-16	C	W94
K-16	C	W95
K-23	WC	W95
K-16	C	W96
K-23	WC	W96
K-16	C	W97
K-23	WC	W97
K-16	CW	W98
K-23	WC	W98
K-16	CW	W99
K-23	WC	W99

4.2.1.10 Some Copper-Mineralized Systems in the Kamanjab Batholith

Suites D, H, J, M and N contain varied disseminated copper mineralization (See Table 4.2.1.4). Such suites have macroscopic similarity with those of typical porphyry copper deposits, but a closer look shows that the granitoid rocks are midalkaline and alkaline. In addition to that, hydrothermal alterations observed were not those associated with typical porphyry copper mineralization. Suites C and O seem to contain iron oxide-copper-gold mineralization. The Gelbingen farm also has IOCG mineralization, but only a very small outcrop of subvolcanic porphyritic intrusives was found. Some of these mineralized areas were sought for, because they occur along major east-west-trending faults that show abundant mineralization all along. The locations were easy to sample, for being along main public roads and displaying clear evidence of hydrothermal alteration and mineralization. Reasons for emplacement of the mineralized suites that do not occur along mapped major fractures are not well understood. Suites D, J, N and O are entirely related to anorogenic magmatism, while C, H and M may have had a partial subductional component (Table 4.2.1.4).

None of the mineralized sites was described in detail. Field notes of the sites are included in the Appendix**.** Maybe the presence of differing magmas was the trigger for mineralization to occur. Mixing of magmas and/or mingling of contrasting lithologies could have produced the precipitation of some sulfides.

Porphyritic intrusive rocks of the suites H, J and M had abundant chalcopyrite and pyrite dissemination. Such features may be diagnostic of significant hydrothermal mineralization in the environs. The three suites contain contrasting rock types that occur in close association (Table 4.2.1.4).

The copper mineralization of Suite M (samples **L-987** to **L-996**) may have been produced by the interaction of the contrasting gabbroids and granitoids. Both groups of rocks carry anomalous copper in the form of visible chalcopyrite; as may be expected, mafic rocks have higher values. Total iron content in the mafic rocks is high, probably due to sulfide mineralization. Mafic rocks also show high losses on ignition, and anomalous values of Mn, Ca, Mg, V, Cr and Ni. Thus, gabbroic rocks could be a source of metals for suite M. Another interesting feature is that felsic rocks carry somewhat high K values, don't carry as much Cu and are enriched in chromium. The entire suite has low Rb to Sr ratios.

L-1000, a sample from Suite N, contains anomalous Cu and is located along the main fracture that bisects the Kamanjab massif from east to west. Many copper occurrences and associated iron oxide bodies are known to occur along that east-west-trending fracture zone (Fig 4.2.1.6).

Common aspects of the mineralized suites from Tables 4.2.1.4 and 4.2.1.19 have been grouped in Table 4.2.1.20. Many useful deductions for exploration of mineral deposits in the Kamanjab Batholith can be made from Table 4.2.1.19. Mineralization tends to occur either along major fault systems or along the margins of anorogenic plutons. The majority of the sulfide disseminations observed in the batholith occur near or along major fault systems. Nepheline syenites with disseminated sulfides were emplaced along major fault systems.

The type of intrusive rocks present in a suite seems to play a role in mineralization. Apart from the observations already presented on multiple types of rocks that make Suites A to Q, some rock types show particular involvement in the mineralizing processes. Quartzmonzonites are directly involved in four mineralized suites. Nepheline syenites carry disseminated sulfides in four suites. These two rock types, and their volcanic counterpart, seem to be the most important mineralizing agents in the Kamanjab Batholith.

A few of the mineralized suites share common features. Suites U, V and W are all IOCG-like, and occur near redox contrasts on the margins of anorogenic plutons. Suites I and X contain disseminated sulfides associated to fault zones and hosted by quartzites. In general, quartzite-hosted mineralization is located near or along major fault systems, and displays significant brecciation, quartz veining and gossanous vugs.

Table 4.2.1.19
Rock suites that show mineralization or hydrothermal alteration in the Kamanjab Batholith, Namibia
Sorted by Rock Suite Letter

(Dated samples are marked with an asterisk. Photographed samples are in italics. Bold samples were not analysed. Key: abund.=abundant, diss=dissemination, gtd=granitoid, hydroth.=hydrothermal, mag=magnetite, mnzn=mineralization, qz=quartz, rk=rock, sulfs=sulfides, w/=with)

	Sample Number	Samples Analysed	Rock Types (sensu TAS) (evidence of mineralization)	Map	Mineralization Type	Notes
C	9	L-863, L-864, L-865, L-868*, *L-874*, L-874-, L-875, ***L-867A, L-871, L-873***	Quartzmonzonites, granodiorite and altered granite. Silicification in some samples.	K-14 SW	IOCG	Contains Au and Fe mineralization, near major N-S fault epidote, qz, angular vugs, sulfs
D	6	L-898, L-899, *L-900, L-902,* L-903	Quartzmonzonite, granite, volcanics. Some quartz veins and minor chloritization.	K-16 WC	Not known.	Disseminated Cu mineralization. No macroscopic evidence. Near Cu prospect..
F	4	*L-919*, L-920, *L-922*	Quartzmonzonite, gabbro and altered granite, volcanics and quartzites.	K-15 NW	Not known. Minor evidence	Qz vein w/ specularite cube, wide qz veins
H	10	L-951, L-952, *L-955, L-956,* L-957, *L-958,* ***L-954***	Granite, gabbro, monzonite, nepheline syenite with disseminated sulfides	K-18 SC	Nepheline syenite with Cu diss.	Disseminated Cu mineralization, angular vugs.
I	7	*L-963*, L-965, L-966, L-967, *L-967a* several non-analysed	Quartzites, quartzmonzonite, alkaline granite, altered granitoid, monzonite. Abundant mineralized breccias.	K-19 WC	Unidentified hydrothermal mineralization	Abund. Brecciation, sulfidation in quartzites. May be related to NW-SE regional fault zone.
J	6	*L-968, L-969*, L-971, L-973*, L-975, L-976	Nepheline syenite, syenite + granite with diss Cu, alkali granite. Abundant hydroth. alteration and sulfidation.	K-19 SW	Nepheline syenite + other rks w/ Cu diss.	Diss. Cu mineralization, hydroth. alteration including K. Along E-W regional fault zone.
M	13	L-987, *L-987a, L-990, L-991*, L-992, L-993*, L-994, L-995, *L-996, L-997*, L-998	Alkali granite, quartzmonzonite, various gabbroids, quartz syenite. Most contain disseminated sulfides and show hydrothermal alteration.	K-20 CW	Gabbroids and granitoids with disseminated copper.	Disseminated Cu mnzn. Large fractionation sequence. May be related to branch of E-W regional fault zone.
N	6	L-998, L-999, *L-1000*, *L-1001*, *L-1002*, *L-1003, L-1004*	Quartzmonzonite, granite Vugs in schistose rks; miarolites. Large amount of mineralization, quartz veining, quartz pods (?)	K-25 C	Unidentified hydrothermal mineralization	Disseminated Cu mineralization around a major E-W fracture zone.
O	1	*L-855** (See sample plotted on the TAS diagram for Suite A)	Granite	K-14 WC	IOCG	Host to IOCG mineralization at Tevrede, NW Kamanjab, Namibia
R	1	*L-836*	Foliated porphyritic metaluminous mesocratic sodic ferriferous rhyolite	K-17 NC	Just alteration, type unknown.	With epidote veinlets. Near border of pluton.
S		L-846	Granitoids with quartz veining and abundant quartz float in the environs. Part of the quartz has vugs.	K-16 NC	Unidentified hydrothermal mineralization	Vugs in quartz veins and quartz float.
T	3	**L-852, *L-853*, L-854**	Medium-grained granitoid with quartz and epidote veins.	K-14 SC	Unidentified hydrothermal mineralization	qz veins w/ sulfs + possible hydroth mnzn. On border of pluton.
U	2	***L-858*, L-859**	Mag-rich, 2-3 cm wide veins cut fine-grained gtd. Quartz pods.	K-14 SW	IOCG?	Qz with large angular vugs. Outside of a pluton, hosted in meta-sediments.
V	3	**L-914, L-915, L-916**	Redox contrast in contact aphibolite/quartzite has diss sulfs. Some coarse magnetite.	K-15 C	Possible IOCG or other large dissemination in rock contact.	Wide quartz veins with gossans and sulfides. Very large gossanous vugs. Near border of pluton.
W	13	**L-925 to L-937** No chemical analysis	Redox contrast with black shales. Abundant “vuggy silicates”. Very abundant mineralization.	K-15 WC	IOCG or other unidentified.	Qz float w/ mag + sulfs, gossanous vugs. Border of plutons, redox contrast.
X	2	L-959, *L-960* No chemical analysis	Quartzites with disseminated sulfides, dense fracture networks and abundant quartz veinlets, granitoids	K-18 SE K-19	Unidentified hydrothermal mineralization	Densely-fractured, gossanous gtd. May be related to NW-SE regional fault zone.

The presence of miarolitic cavities in various granitoids is another feature that appears in five suites; it seems to be key in processes that lead to dissemination of sulfides but not to IOCG mineralization.

Various types of gossanous vugs and quartz veining occur in a lot of the suites. Quartz pods tend to occur in the environs of IOCG-type mineralization.

In general terms, the presence of granitoids (granodiorites, nepheline syenites and other granitoids) produces mineralization in multiple environments, along major faults and on the margins of plutonic bodies.

Table 4.2.1.20 Compilation of data from various mineralized rock suites in the Kamanjab Batholith, Namibia

Name\Rock Suite	C	D	F	H	I	J	M	N	O	R	S	T	U	V	W	X	Y	G	Gelbingen
IOCG	X								X				X	X	X				X
Disseminated sulfides		X		X	X	X	X	X		X	X	X				X	X		
Near or along major fault systems	X			X	X	X	X	X								X	X		X
On margin of anorogenic plutons		X								X		X	X	X	X				X
Quartzmonzonite association	X				X			X									X		
Other granitoid association		X				X	X		X		X	X				X			X
Nepheline syenite association				X	X	X	X												
Quartzite-hosted					X											X			X
Mafic rock association							X												
Redox contrast or contrasting lithology association													X	X	X				?
Brecciation					X											X			X
Quartz veining	X		X		X			X			X	X	X	X	X	X	X		X
Magnetite association			X										X	X	X				X
Gossanous vugs	X	X		X	X	X					X		X	X	X	X	X		X
Miarolitic cavities						X	X	X				X					X		
Epidote	X									X		X							
Potassic alteration						X	X											X	
Black shale association															X				

Mafic rocks were not sampled or described in as great detail as the granitoids. They are under-represented. For that reason, deductions on the relevance of mafic rocks to mineralization derived from Tables 4.2.1.19 and 4.2.1.20 may be wrong.

Most of the suites that show mineralization or hydrothermal alteration are not well understood at the time of writing this report.

4.2.1.11 Discussion

The present study of the Kamanjab Batholith was only of a reconnaissance nature. Although the number of samples is large, variation in rock types is too great for it to be representative. No detail work was carried out in any of the locations visited. The quality of outcrops and their interconectivity did not allow for many structural relationships between rock types to be established.

Nevertheless, based on some of the radiometric ages and on general observations, a table that correlates the various granitoid units in all rock suites has been devised. It makes geological sense at the locations visited. Table 4.2.1.17 is based on lithologic and geochemical data, as well as on the partial geochronological information available.

In the few cases where radiometric ages are available, quartzmonzonites seem to be a discrete event of intrusion in an anorogenic environment. Many of the suites of Table 4.2.1.4 contain that rock unit. Quartzmonzonites seem to have produced mineralization.

A widespread characteristic of the Kamanjab Batholith is that most sites have suites of two or more contrasting rock types. No two suites are identical, and there is a large variety of rock types that make them.

Ten geochemical transects were drawn in different directions across the Kamanjab Batholith, but results were not meaningful. Even though all of the representative types of rock from each site were sampled, in most areas the lithology changed very often and no correlations could be established. The reason for that great rock variability may be that the batholith is made of multiple granitic ring complex intrusions, each with slightly varying chemistry. Radiometric, magnetometric and gravimetric images from the Kamanjab Batholith were not available at adequate resolution to detect circular structures, but they are to be expected.

There is no direct proof of the presence of ring complexes at the Kamanjab Batholith. Nevertheless, several sources of evidence point to the batholith as a cluster of ring complexes. Among others, these are: 1) the lack of continuity in the rock types along traverses, 2) the presence of multiple rocks types in at least fifteen discrete sites, 3) General anorogenic character of most of the rocks, 4) three quarters of the rocks in the suite are midalkaline, 4) the size and shape of the batholith, as well as its event diagram has similarities with other ring complex clusters, as indicated on section 7.3.

Rocks from the Kamanjab batholith and the Khorixas inlier seem to have had a similar geological history up to 1600 Ma. After that, both massifs underwent significantly different geological events. They seem to have had a common geological history once more for the past 550 Ma.

A common feature observed throughout the Kamanjab Batholith is the “out-of-focus” texture. More than 70% of the samples from the masif display gradational contacts between crystals. The contacts between grains may have been softened by incipient metamorphism or hydrothermal alteration. The original net crystal boundaries have been recrystallized and rocks lost their pristine intrusive textures. The texture is generally associated with coarse blue quartz phenocrystals with gradational margins. These features may be an indication of incipient migmatitization that was experienced by the entire batholith. Further work on this issue is needed.

4.2.1.12 Gelbingen Farm, Outlier of Kamanjab Batholith, Namibia

This farm is located to the northeast of the Kamanjab Batholith, as shown on Fig 4.2.1.6. A single, very small outcrop of subvolcanic coarse-grained, porphyritic intrusion with rhyolite composition was observed at the farm. The intrusion seems to be associated with gold, iron and sulfide mineralization hosted by brittle quartzites. Hydrothermal brecciation, massive iron oxide bodies and many gossans after various sulfides were sampled and described. Their interpretation will not be part of this document.

L-985 is a porphyritic subvolcanic intrusive that occurs in the Gelbingen Farm. The rhyolitic rock contains well zoned plagioclase phenocrystals and no quartz is visible to the bare eye (Fig 8.45). Petrographic analysis of **L-985** shows strong hydrothermal alteration. Most of the plagioclases are altered to clays and sericite. This type of rock is considered to have generated iron oxide-copper-gold mineralization at the Gelbingen farm. It was emplaced in an anorogenic environment at around 1862±6Ma, by correspondence with rhyolitic volcanic rocks dated by Steven, 2002 at the farm. Several descriptions of mineralization and types of breccias from the Gelbingen Farm are included in section 8.4.3.1.

Table 4.2.1.21 Regional correlation of Paleoproterozoic granitoids in the Greater Lufilian Arc.

Event	Kalene Hill, Zm	Kamdescha, Nm	Tevrede, Nm	Grootfontein, Nm	Kamanajab, Nm	Mufulira, Zm	Konkola, Zm	Muliashi, Zm	NW Zambia	Fe/Mg
9							L-158 gray gt 1874;14			
8	1872;14			L-1043 granite 1997;39	L-934 granite 1856;24		L-160 pink gt 1866;5.4	L-075 1865;5.4 X-1, X-2 quartzmonzonite	granite 1864	
6	1945	L-868 quartzmonzonite 1937;14	L-855 granite 1939;19	L-1045 quartzmonzonite	L-868 quartzmonzonite 1937;14	X-41 gray quartzmonzonite ~1945			L-030 granite 1927	ferriferous
5		L-864 granodiorite						Samba 1964;12		magnesic
4					L-969 syenite 1976;42			L-155 Chambishi granite 1983;5		
3						L-166 pink granite 1993;7.1			1994	
2		granite	Granite		L-968 granite					

4.2.2 KHORIXAS INLIER

4.2.2.1 Introduction

The Khorixas Inlier is an isolated, fault-bounded body of rocks that is located to the west of the Khorixas town in Damaraland, Namibia, as shown on Fig M20. Climate is very dry and vegetation is mainly grasses and short thorny bush. The inlier is mainly composed of granitoid rocks and was sampled during the Greater Lufilian Arc grantiod project. Description of the Khorixas Inlier will be broken in two parts: one on the Oas Farm and the other on the Lofdal farm. Observations and sampling of the Mesopotamie farm was also included under the Khorixas Inlier heading, although it does not form part of the inlier strictly speaking, but makes another fault-bound entity.

The Khorixas Inlier is heavily inclined toward midalkaline and alkaline rocks. 71% of the granitoids from that domain fall within the midalkaline field while 29% of them fall in the subalkaline field (Table 4.2.2.1). All midalkaline rocks make 60.5% of the samples. 26% are sulbalkaline and 14% are alkaline rocks. Carbonatites in this area play an important role. They have been kept apart from the other rocks in the evaluation of alkalinity, and make 17% of the samples studied.

Table 4.2.2.1 Statistics of rock types, Khorixas Inlier, Namibia
The fifth column (granitoids) is the sum of underlined rock types.

Group	Rock type	number	%	Granitoids	Groups
Midalkaline Rocks	alkali granite	10	23.26	70.97	60.47
	Quartzmonzonite	1	2.33		
	Syenite	9	20.93		
	Monzonite	2	4.65		
	Monzogabbro	1	2.33		
	alkali gabbro	3	6.98		
Subalkaline Rocks	Granite	8	18.60	29.03	25.58
	Granodiorite	1	2.33		
	gabbro-diorite	1	2.33		
	Gabbro	1	2.33		
Alkaline Rocks	foid monzosyenite	4	9.30		13.95
	foid gabbro	1	2.33		
	peridot gabbro	1	2.33		
Total		43	97.67	100.00	100.00
	Carbonatite	9			
Total		52			

Table 4.2.2.2 lists all samples collected in the Mesopotamie, Oas and Lofdal farms, along with their main geochemical parameters and studies for environment of emplacement. Samples from the Summas Mountains were included there too, for comparision purposes, and will be discussed independently in the following chapter.

A regional model on the nature of granitoids and their metallogenic significance at Mesopotamie, Lofdal and Oas farms in Namibia was put together during the Greater Lufilian Arc granitoid project. Fig 8.6 shows the location of the study area. Most of the mineralization at those sites is controlled by major E-W trending fault systems. In fact, most of the mineralization observed in or around the Kamanjab Batholith seems to be controlled by subparallel regional E-W-trending major fractures. The term E-W structures is used here somewhat loosely. Most of the structures that fall under that denomination are actually N68°E; they follow the general trend of the Lufilian Arc. Rifting and later collision fronts had roughly the same relative orientation.

Table 4.2.2.2 Comparison of samples from the Khorixas Inlier and nearby Summas Mountains, Namibia

(Samples with asterisk were dated. See acronym description on section 2.4.3.)

Mesopotamie Farm, Namibia									
Sample	Rock Name	Debon & LeFort	Maniar & Piccoli	Whalen	Pearce	Mafic	Rb/10HfTa	Rb/30HfTa	Nb-Ta
L-759*	Granite	peralum i leuco KFe		A					
L-772	alkali granite	metalum v leuco KFe		A					
L-773	Granite	peralum i leuco NaFe		A	W				
L-783	Granite	peralum ii meso Na-KFe		A	O-W1-1		WP	WP	OUTU
L-784	Granite	metalum iv meso Na-KFe	RRG-CEUG	A	O3/4				
Oas Farm, Namibia									
Sample	Rock Name	Debon & LeFort	Maniar & Piccoli	Whalen	Pearce	Mafic	Rb/10HfTa	Rb/30HfTa	Nb-Ta
L-668*	Syenite	metalum iv meso NaFe	RRG	A	O-W 2-2	wpab	WP-	WP	INW
L-669	Syenite	metalum iv meso NaFe	CEUG	A	W		WP-	WP	INW
L-670	nepheline syenite	metalum iv meso NaFe	RRG	A	O-W 2-2	?			OUTU-NEA
L-675	Syenite	peralum i subleuco NaFe	CEUG	A	W3/4	wpab			OUTU
L-676	Syenite	metalum iv meso NaFe	RRG-CEUG	A	W	wpab			
L-691	Monzonite	metalum iv meso NaFe	RRG-CEUG	A	W	wpt			
L-693*	alkali granite	metalum iv meso NaFe	RRG	A	W3/4		WP-	WP	INW
L-694	nepheline syenite	metalum v meso NaFe	RRG	A	W	wpab			
L-695	nepheline syenite	metalum iv meso NaFe	RRG-CEUG	A	O-W 1-1	wpab			
L-697	Syenite	metalum v meso NaFe	RRG-CEUG	A	W3/4	wpab	WP-	WP	OUTU-NEA
L-698	alkali granite	metalum v meso NaFe	RRG-CEUG	A	O-W 2-2				OUTU
L-699	Syenite	metalum iv meso NaFe	CEUG	A	W				
L-708	Pyroxenite	metalum v meso NaFe	IAG-CAG	A	W?	wpab			
L-712	alkali granite	peralum iii leuco NaFe	POG	A	V				
L-713	quartz syenite	metalum v leuco NaFe		A	O-W 2-2		WP	W	OUTU
L-714	Granite	metalum v leuco NaMg	OP	A	V				
L-714a	alkali granite	peralum ii leuco NaFe		A	V				
L-715	Granite	metalum iv meso Na-KFe	RRG-CEUG	A	O3/4				OUTU
L-716*	Granite	metalum iv subleuco NaFe	CEUG-RRG	A	S2/4O2/4		VA-	VA	INV
L-1019	alkali granite	metalum v subleuco NaFe	RRG	A	V2/4		WP-	WP	INW
L-1020	Granite	metalum v meso NaFe		A	W				
Lofdal Farm, Namibia									
Sample	Rock Name	Debon & LeFort	Maniar & Piccoli	Whalen	Pearce	Mafic	Rb/10HfTa	Rb/30HfTa	Nb-Ta
L-722	Carbonatite	metalum vi meso KFe		A					OUTU
L-728*	Granite	metalum vi subleuco NaFe	OP	A	?		WP-	WP	INW
L-729	Granite	metalum iv subleuco Na-KFe	POG	A	O-W 1-1				
L-740	nepheline syenite	peralum ii meso NaFe	CEUG	A	O3/4	?			OUTU
L-741	nepheline syenite	metalum iv meso KFe	CEUG	A	O-W 2-2	wpab			OUTU
L-742	granite	metalum iv meso NaMg		A	O2/3				OUTU
L-754	diorite	metalum iv meso KFe	RRG	N		arc			
L-1021	Granite	metalum iv subleuco NaFe	RRG	A	W				
L-1022	nepheline syenite	peralum iii meso Na-KFe		A	O2/3	?			OUTU
L-1023	sat. olivine gabbro	metalum v meso NaFe	IAG+CAG	?NZn	V	emor			
L-1024a	Carbonatite	metalum vi meso KMg		A					
L-1024c	Carbonatite	metalum vi meso KMg		A					
L-1025	undersat. oliv. gab.	metalum v meso NaFe		A		arc	WP	WP	OUTD-INV
L-1027	nepheline syenite	metalum v meso KFe		A	W-O 2-2	?			OUTU
L-1032	Undersat. oliv. gab.	metalum iv meso NaFe		N	V2/4	emor	WP	WP	OUTU
Summas Mountains, Namibia (Volcanic Rocks)									
Sample	Rock Name	Debon & LeFort	Maniar & Piccoli	Whalen	Pearce	Mafic	Rb/10HfTa	Rb/30HfTa	Nb-Ta
L-789	Syenite	metalum iv meso NaFe	RRG-CEUG	A	O-W 2-2				OUTU
L-791	Alkali rhyolite	peralum ii leuco KFe	RRG-CEUG	A	W3/4		WP-	WP	INW
L-791a	Alkali rhyolite	peralum iii meso Na-KFe			W				

4.2.2.2 OAS FARM, NAMIBIA

4.2.2.2.1 Introduction

The Oas farm is located in the eastern portion of the Khorixas Inlier that lies south of the Kamanjab batholith, in Damaraland, northern Namibia. The farm may be reached along dirt roads from the town of Khorixas. General location is shown on Fig M20.

The suite of chemical analyses from the Oas farm is made by a total of 29 samples. They may be subdivided geographically into 19 from the N-S transect, 2 from mineralized quartzites, 2 that come from outcrops along the route of access, and 6 more samples with major oxide chemistry that were compiled from a report by (Frets, 1969). The Sample database is listed on Table 4.2.2.3. Petrographically they may be grouped into three sets: granitoids that make the host rocks (or "basement"), some syenitic rocks, and a few gabbroic rocks.

Table 4.2.2.3 Chemical Analysis of Samples from the Oas Farm, Namibia
(complete elemental analysis on Table A12, Appendix)

Sample	SiO2	TiO2	Al2O3	Fe2O3	MnO	MgO	CaO	Na2O	K2O	P2O5	LOI	Rb	Sr	Y	Zr	Nb	Co	Ni	Cu	Zn	Ga	V	Cr	Ba	U	Th	Sc	Pb	Sm	Nd	Pr	Ce	La	Hf	Ta	Eu
Notch	50.00	1.00	15.50	6.00	0.15	2.00	5.00	4.90	5.50	0.30	2.00	200	400	60	360	40	30	16	25	85	26	100	100	1300	20	37	20	20	50	50	15	175	95	10	120	4
L-668	62.61	0.89	17.32	4.83	0.14	0.72	1.80	6.42	4.79	0.36	0.59	121	474	69	710	193	7	7	6	127	26	14	139	2037	7	22	<10		14	101	182	235	110	4	23	1
L-669	64.34	0.61	16.76	4.66	0.12	0.36	1.46	6.43	4.80	0.23	0.74	115	350	73	378	204	<6	9	7	146	28	<12	124	1647	9	31	<10	22	18	102	28	267	137	8	12	4
L-670	57.01	1.45	15.14	11.08	0.21	1.42	2.33	6.69	3.35	0.53	1.32	173	1219	73	1843	458	<6	9	9	85	42	<12	18	767	17	46	<10		3	27	72	219	42		74	0
L-675	60.71	0.10	21.99	3.59	0.09	0.13	0.94	4.92	6.41	0.03	1.61	125	384	123	1520	345	7	9	23	167	30	20	17	1321	10	78	11			140	592	844	440		238	3
L-676	59.35	0.87	18.13	5.92	0.17	1.24	2.05	5.20	5.55	0.24	1.84	226	634	58	553	139	7	7	11	177	26	19	31	1591	<6	19	<10					180	85			
L-691	50.24	3.31	12.95	14.15	0.21	4.13	6.53	2.95	2.82	0.55	1.51	151	589	52	368	62	39	32	190	166	19	357	66	617	<6	<15	33					110	61			
L-693*	71.37	0.48	11.65	6.47	0.14	0.19	0.77	4.62	4.46	0.09	0.31	86	98	31	132	105	6	7	14	128	33	<12	60	241	2	9	<10	5	13	114	35	357	216	3	5	1
L-694	59.18	1.09	17.07	5.91	0.17	1.01	2.48	6.84	4.89	0.36	0.54	106	633	39	333	93	7	<6	10	107	23	27	<12	1995	<6	<15	<10					166	87			
L-695	46.29	3.29	13.34	13.54	0.48	3.19	4.92	4.10	3.51	0.68	6.78	197	399	53	329	54	27	22	89	120	19	353	28	639	<6	<15	26					64	30			
L-697	59.94	0.86	16.90	5.28	0.17	0.99	2.06	6.58	4.59	0.32	1.54	169	491	151	1363	432	8	9	5	129	26	<12	117	1444	15	51	<10			127	480	582	291	2	108	5
L-698	71.68	0.46	11.40	5.84	0.10	0.10	0.85	4.91	4.10	0.10	0.40	77	45	50	329	124	<6	7	7	104	35	<12	207	157	<6	<15	<10		16	67	228	372	143		92	0
L-699	63.41	0.28	17.28	5.27	0.20	0.34	0.93	7.40	4.73	0.12	0.56	98	114	75	1246	307	<6	10	7	147	34	<12	126	458	15	50	<10					470	310			
L-708	47.15	0.47	8.72	11.27	0.53	13.12	14.2	1.46	1.77	0.04	1.79	86	578	146	469	126	16	26	13	279	17	68	14	2096	<6	<15	23					258	97			
L-712	79.11	0.04	12.04	0.83	0.04	0.11	0.40	5.47	1.95	0.01	0.54	33	159	12	17	7	<6	10	8	35	18	<12	47	662	<6	<15	<10		107		13	41	7	2		0
L-713	71.32	0.16	14.36	2.37	0.05	0.08	0.32	5.76	5.66	0.02	0.41	117	94	30	277	71	<6	8	9	53	25	19	49	909	<6	<15	<10		121	80	295	436	188	1	25	1
L-714a	77.55	0.05	13.19	0.73	0.03	0.17	0.85	6.33	0.76	0.02	0.67	16	338	9	250	9	<6	9	8	40	23	<12	50	538	<6	16	<10		106		3	83		3		0
L-714b	74.47	0.12	14.63	0.94	0.04	0.12	0.59	8.15	0.94	0.05	0.41	16	152	25	237	50	<6	8	<6	17	0	12	160	606	0	0	0					0	0			
L-715	72.13	0.48	13.02	3.49	0.09	0.48	1.12	3.88	4.88	0.12	0.50	118	147	58	348	25	8	11	12	67	18	28	47	1230	<6	19	<10		76	39	88	154	44		39	1
L-716*	73.88	0.30	12.54	2.79	0.04	0.41	0.98	4.49	3.98	0.04	0.68	69	164	38	332	16	8	11	12	51	16	19	57	1389	7	24	<10	9	7	42	11	134	66	7	1	1
L-1016	77.33	0.10	1.04	2.18	0.47	2.02	6.71	0.50	0.09	0.13	8.00	6	124	8	15	4	<6	<6	56	14	<9	<12	351	33	<6	<15	12					24	<12			
L-1016a	79.38	0.10	0.80	2.49	0.45	1.96	5.74	0.55	0.13	0.04	7.50	5	140	6	37	4	<6	7	28	27	<9	13	15	57	<6	<15	10					23	<12			
L-1019	72.23	0.41	13.17	3.00	0.11	0.24	0.79	6.18	3.79	0.08	0.41	50	101	31	290	47	<6	10	9	62	17	<12	253	1351	2	17	<10	29	8	47	12	110	60	7	2	2
L-1020	70.82	0.58	12.68	4.01	0.10	0.76	1.57	5.17	3.14	0.09	0.31	70	173	52	445	22	<6	8	64	85	17	19	<12	1364	<6	19	<10					180	95			

Sample	SiO2	TiO2	Al2O3	Fe2O3	FeO	MnO	MgO	CaO	Na2O	K2O	P2O5	LOI
X-21	60.78	0.87	16.97	1.13	4.10	0.16	0.99	1.94	5.65	5.27	0.22	1.78
X-22	64.42	1.12	14.69	4.34	1.80	0.07	1.37	1.17	3.71	5.64	0.25	1.78
X-23	63.81	0.59	14.21	3.67	1.10	0.15	1.48	2.27	4.37	6.00	0.09	3.13
X-24	51.29	0.40	19.06	5.95	1.05	0.42	0.82	4.79	6.75	5.19	0.30	3.38
X-25	47.49	2.22	14.47	3.74	8.09	0.05	6.73	11.57	1.24	0.77	0.30	2.80
X-26	48.82	1.03	12.21	3.62	6.54	0.15	13.68	9.63	1.77	1.10	0.59	1.16

4.2.2.2.2 4-km Long N-S Transect Across Oas Syenite

Very little is written about the geology of the Oas Syenite, its chemistry, environment of emplacement, mineralization and associated hydrothermal alteration. The main references on the geology of this part of Namibia are Frets, 1969; Hoffmann, Hawkings, Isachsen, & Bowring, 1996; and Miller & Burger, 1983. Reports by Schneider & Seeger, 1999 and Burnett, 1999 describe some copper and gold occurrences in the Khorixas Inlier.

A 4 km long N-S geological transect was carried out along a road, across the Oas Syenite, ro produce a reconnaissance geological map (Fig 4.2.2.1). The road where the transect was done may be reached from Khorixas as indicated below: A gravel road leads southwest from Khorixas, as shown on 1:50,000 scale topographic sheet 2014BD. The Bella Vista farm intersection is crossed westward. After passing on to map sheet 2014BC, in the Bloemhoef 484 farm, there is a NNW gravel road. That road should be followed northward up to the farmhouse of the Oas 486 farm. From there, a rough mountain road continues north. That is the site of the N-S transect.

A reconnaissance geological map of exposures along the road was produced (Fig 4.2.2.1). Nine midalkaline ring complexes that make a cluster were identified along the transect. Field notes on the transect, slightly

edited with results from geochemical and geochronological data, are included in Appendix A66. The location of all geological and sampling stations is also included in the Appendices A18 and A19. Most stations are shown on the maps of Fig 4.2.2.1.

These syenitic bodies were emplaced along with explosive brecciation events. Massive magnetite and hematite were observed in many sites; iron oxide hydrothermal alteration ("red-rock" and "brown-rock" types), quartz pods, widespread sulfidation, and abundant gossans were sampled and mapped in the area. The type of mineralization displays many characteristics of iron oxide-copper-gold systems.

Type and amount of mineralization are still to be defined. Zinc, rare earths, possibly gold, copper and other metals are expected to occur in economic amounts. Part of the syenitoids could act as potential zinc source for various styles of mineralization in the Katangan rocks.

Mapping and sampling along the transect will probably help solve issues about hydrothermal fluids, processes and different events that produced mineralization. Table 4.2.2.4 the main features of the nine syenitoid circular complexes that were discovered at the Oas farm. That includes estimated size of the bodies, composition, heat production capacity, associated structures and dikes, as well as age of emplacement. The map of Fig 4.2.2.1 presents the main geological observations of the area. At least four of the circular bodies are made by high-heat producing syenitoids. Several of the complexes seem to have produced iron oxide-copper-gold mineralization.

The syenites of the Oas farm contain significant potential for iron oxide-copper-gold mineralization. More detailed geological maps, maps of alteration and studies of the associated mineralization were prepared and will be published elsewhere.

Most of the samples from the Oas syenite suite, including mafic and felsic rocks, are endowed with anomalous zinc (See Table 4.2.2.3). None are truly enriched in copper. This does not include any of the mineralized samples; those were not analysed for the Greater Lufilian Arc granitoid project. Assays for gold, copper, zinc and other metals will not be included in this document.

Extensive bodies of massive quartz occur throughout the Oas farm (see section 8.3.5.2). These seem to be associated with a widespread event of silicification, and with quartzites.

At the time of emplacement, part of the Oas syenitoids were high-heat producing rocks. Four of the samples are especially enriched in thorium and they are listed on Table 4.2.2.5. The heat generating capacity of these rocks established and maintained long-lived, large hydrothermal fluid circuits. That probably was a determining factor in the mineralizing capacity of the magmatic systems.

Table 4.2.2.5 High heat producing rocks in the Oas farm, Namibia; estimated at 750Ma.

Sample	Uranium (ppm)	Thorium (ppm)	Potassium (%)	Heat producing value (muW-m3)	U/Th
L-670	17	46	3.35	4.166	0.370
L-675	10	78	6.41	6.603	0.128
L-697	15	51	4.59	4.628	0.294
L-699	15	50	4.73	4.579	0.300

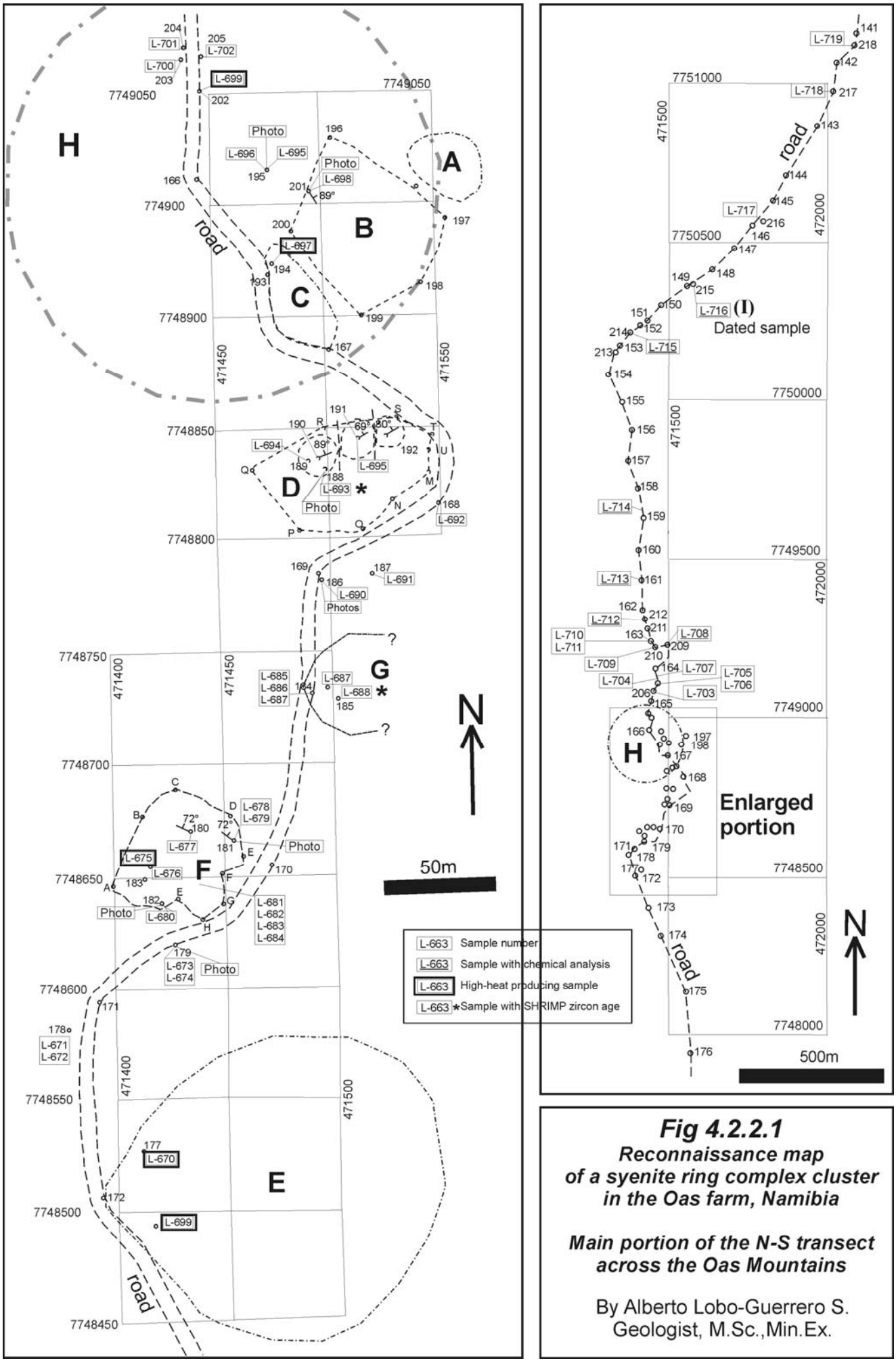

Fig 4.2.2.1

Reconnaissance map of a syenite ring complex cluster in the Oas farm, Namibia

Main portion of the N-S transect across the Oas Mountains

By Alberto Lobo-Guerrero S.
Geologist, M.Sc.,Min.Ex.

Table 4.2.2.4 Main features of small syenitoid circular bodies found at the Oas farm, Namibia (See location map, Fig 4.2.2.1)
(Dated samples are marked with an asterisk. An "H" was added to the humber of high heat producing rocks.)

Body	Geological stations	Number of samples	Analysed samples	Perimeter	Shape	Area	Composition	Dikes	Heat production capacity	Age	Additional Notes
A	0	0	0	Assumed	Oval	estimated 30 x 35 m diameter	Syenitoid	None observed	Unknown	Estimated	Observed but not mapped nor samples collected.
B	7	1	1 (L-698)	Mapped	Circular	75 m diameter	syenite but not analysed	several generations of mafic dikes	Unknown	Estimated	Explosive brecciation. Many quartz veins surround hill. Breccia vein/dike with hematite and angular fragments.
C	3	1	1 (L-697H)	Not well constrained	Uncertain	Minimum 25 x 50 m	Syenite	Not observed	High	Estimated	Syenite cut by network of magnetite-rich veinlets.
D	14	3	3 (L-693*, L-694, L-695)	Mapped	Oval	80 x 50 m	Nepheline syenite	Several L-795 alkali granite + nepheline syenite	Low	Dike L-693* is ~765;4.5 Ma	Three independent hills. Photos.
E	3	2	3 (L-668*, L-669, L-670H)	1/3 way around	Circular estimated	150 m diameter estimated	Syenite + nepheline syenite	Not observed	High	L-668* is 762;12 Ma	Intensely fractured and recemented.
F	14	10 (L-678)	2 (L-675H, L-676)	Mapped	Roughly circular	60 m diameter	Syenite	Not observed	Very high	Estimated	Abundant IOCG evidence. Massive magnetite bodies + vugs + sulfides. Abundant magnetite-filled veins and stockworks. L-678 has xenolith of pink granitoid. Photos.
G	3	5 (L-685 to L-688*)	1 (L-688*)	Not mapped	?	More than 10 m; true size is uncertain	Syenite	None observed	Low	L-688* is 762;4.5 Ma	Not identified as ring complex during field work. Composition similar to body E. With braided quartz veins + hematite + sulfides; diss. sulfides.
H	1	5	1 (L-699H)	Not mapped	Roughly circular	200 m diameter estimated	Syenite	Yes	High	?	Intersected by many quartz veins with magnetite +sulfides. Very altered and weathered, with abundant gossans. Strong red-rock alteration.
I	2	1	1 (L-716*)	Not mapped	?	Unknown	Gneissic granite	Yes	Low	L-716* is 745; Ma	Not identified as a circular body in the field. Large red rock alteration.
Basement	8 (L-691, L-712, L-713, L-715, L-1019, L-1020)				Granite, alkali granite			Yes	Low	?	Not well studied.

4.2.2.2.3 Geochemistry

A significant portion of the rocks from the Oas farm is made of granites and alkali granites. The rest are syenites, nepheline syenites and gabbroids (Figs 4.2.2.2). 85% of the granitoids from the Oas farm fall within the midalkaline field, while 15% of them fall in the subalkaline field (Table 4.2.2.6). All midalkaline rocks make 74% of the samples. 18.5% are sulbalkaline and 7.5% are alkaline rocks. Rocks from this farm exemplify the problem of plutonic rock nomenclature. A suite of rocks that petrographically is considered to be syenitic, plots as granodioritic and dioritic in the modified TAS diagram (Fig 4.2.2.3). The R1/Rs2diagram (Fig 4.2.2.5) shows them to be syenites and nepheline syenites.

Table 4.2.2.6 Statistics of rock types, Oas farm, Namibia

The fifth column (granitoids) is the sum of underlined rock types.

Group	Rock type	Number	%	Granitoids	Groups
Midalkaline Rocks	alkali granite	7	25.93	85.00	74.07
	Quartzmonzonite	1	3.70		
	Syenite	9	33.33		
	Monzodiorite	1	3.70		
	Monzogabbro	1	3.70		
	Alkali gabbro	1	3.70		
Subalkaline Rocks	Granite	3	11.11	15.00	18.52
	Gabbro	2	7.41		
Alkaline Rocks	Foid monzosyenite	1	3.70		7.41
	Foid gabbro	1	3.70		
Total		27	100.00	100.00	100.00

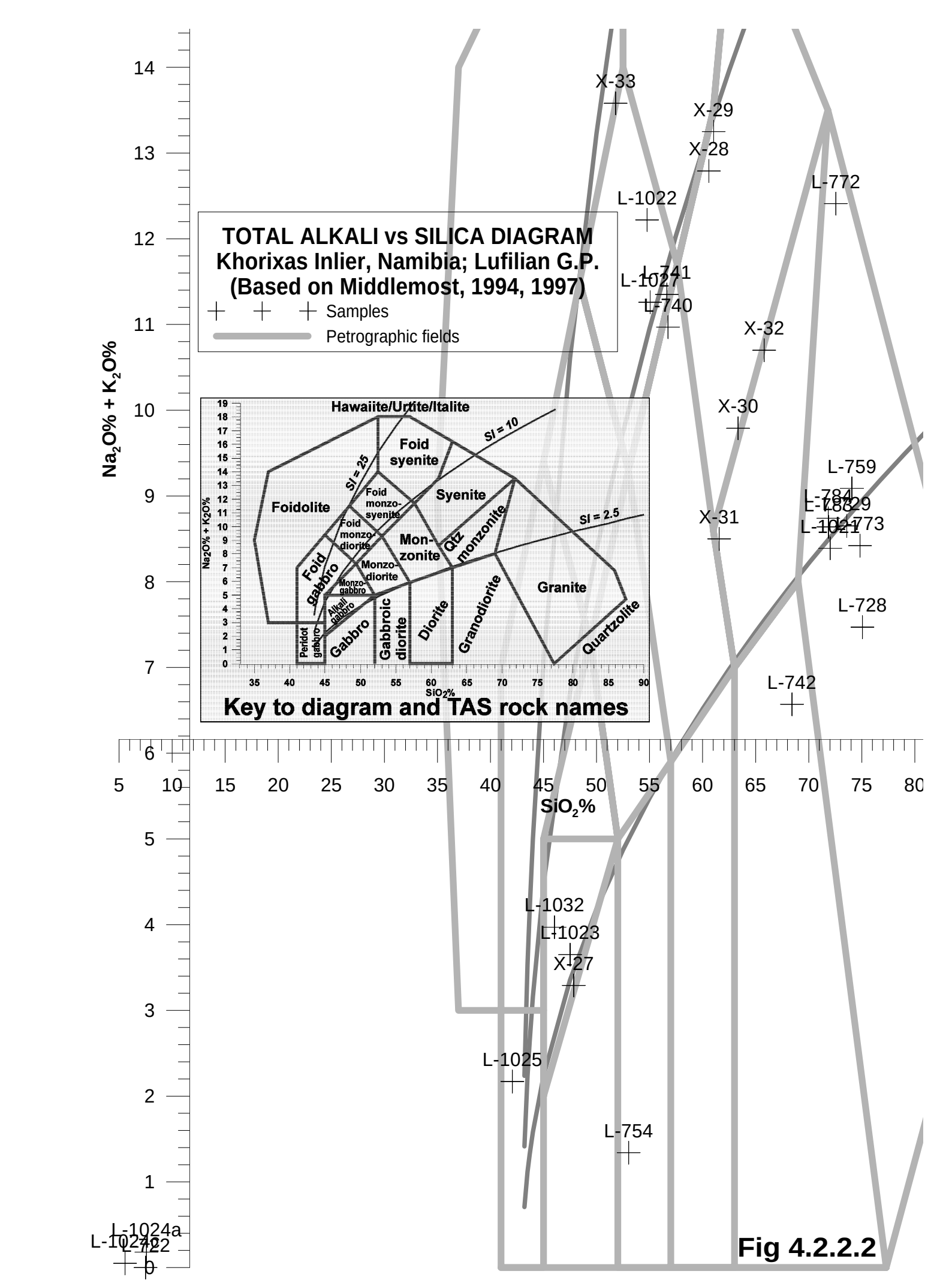
TOTAL ALKALI vs SILICA DIAGRAM
Khorixas Inlier, Namibia; Lufilian G.P.
(Based on Middlemost, 1994, 1997)
Samples
Petrographic fields
Na2O% + K2O%
SiO2%
Hawaiite/Urtite/Italite
Foid syenite
Foidolite
Foid monzo-syenite
Syenite
Foid monzo-diorite
Mon-zonite
Qtz monzonite
Monzo-diorite
Monzo-gabbro
Foid gabbro
Alkali gabbro
Peridot gabbro
Gabbro
Gabbroic diorite
Diorite
Granodiorite
Granite
Quartzolite
SI = 10
SI = 25
SI = 2.5
Key to diagram and TAS rock names
X-33
X-29
X-28
L-772
L-1022
L-741
L-1027
L-740
X-32
X-30
L-759
L-784
L-1029
L-773
X-31
L-1021
L-728
L-742
L-1032
L-1023
X-27
L-1025
L-754
L-1024a
L-1024b
L-722

Fig 4.2.2.2

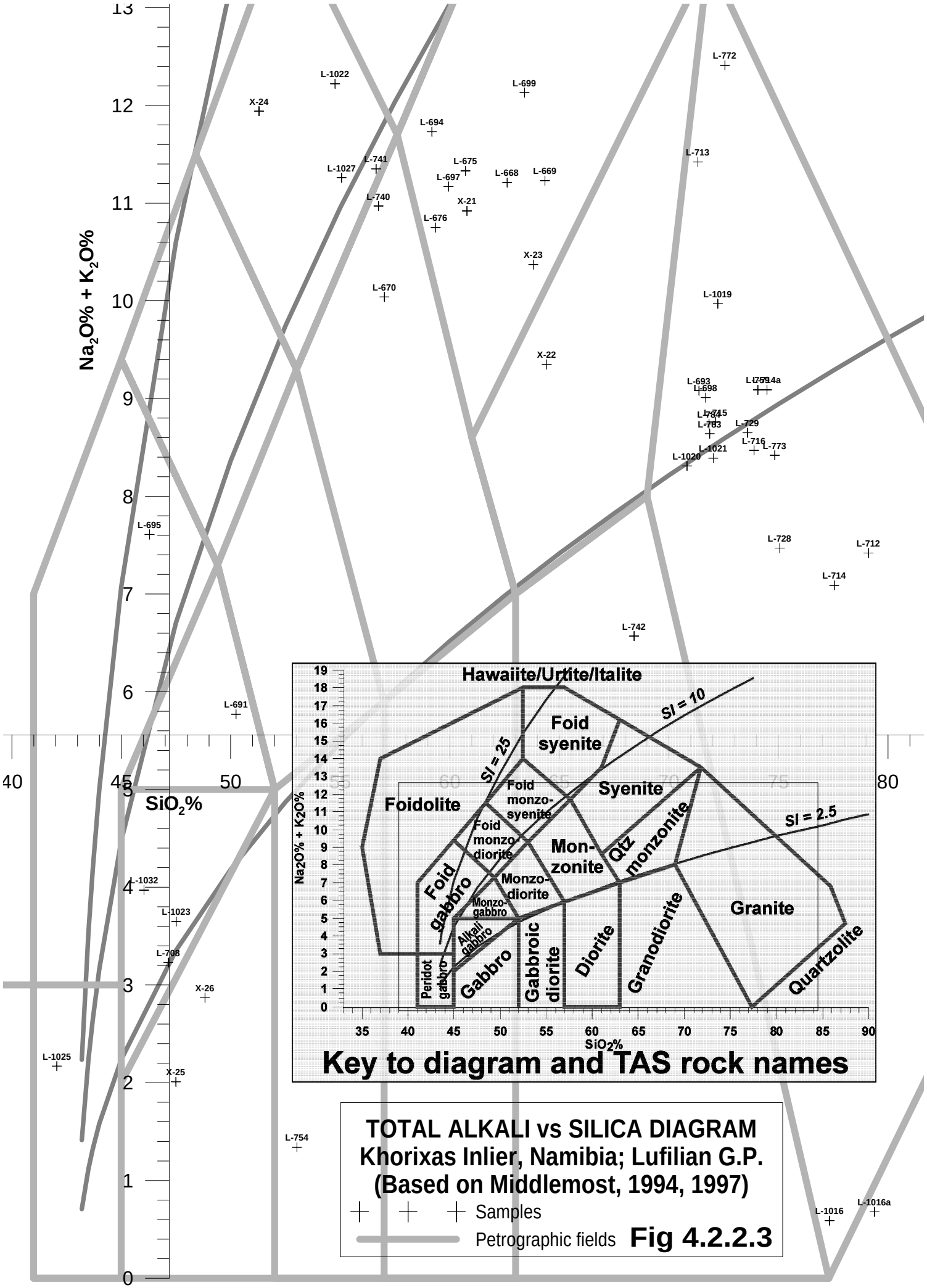

TOTAL ALKALI vs SILICA DIAGRAM
Khorixas Inlier, Namibia; Lufilian G.P.
(Based on Middlemost, 1994, 1997)

Samples

Petrographic fields

Fig 4.2.2.3

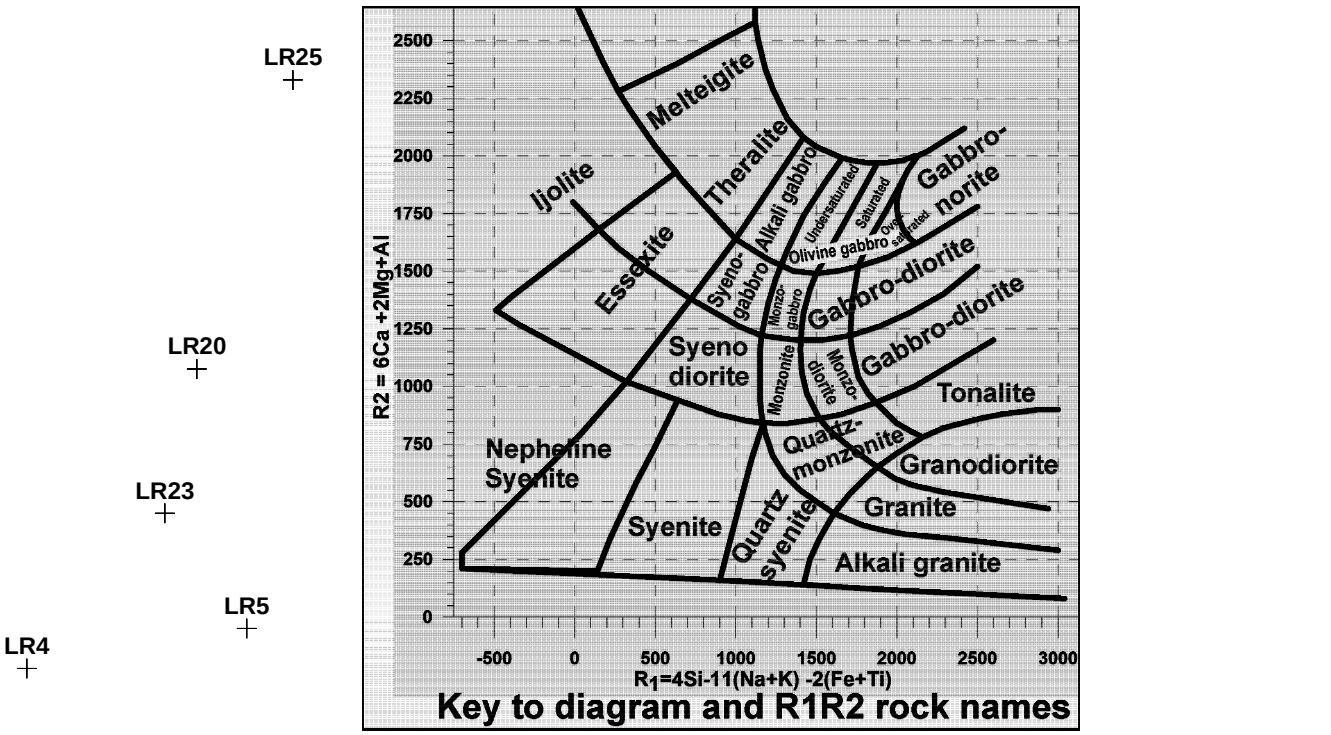
Melteigite
Theralite
Ijolite
Essexite
Alkali gabbro
Olivine gabbro
Gabbro-norite
Syeno-gabbro
Monzo-gabbro
Gabbro-diorite
Syeno diorite
Monzonite
Monzo-diorite
Tonalite
Quartz-monzonite
Granodiorite
Nepheline Syenite
Syenite
Quartz syenite
Granite
Alkali granite
R2 = 6Ca +2Mg+Al
R1=4Si-11(Na+K) -2(Fe+Ti)
Key to diagram and R1R2 rock names

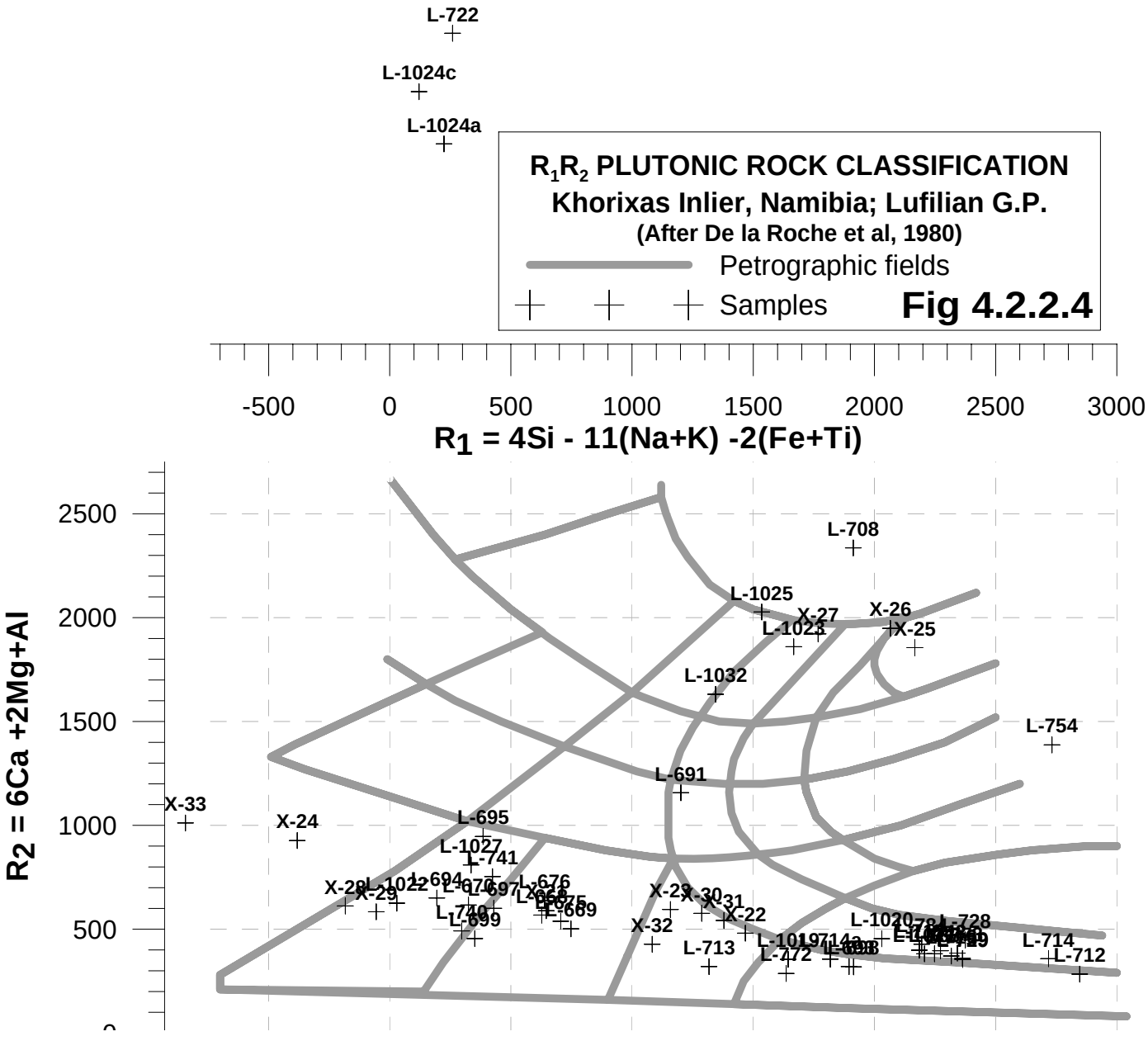
R1R2 PLUTONIC ROCK CLASSIFICATION
Khorixas Inlier, Namibia; Lufilian G.P.
(After De la Roche et al, 1980)
Petrographic fields
Samples
Fig 4.2.2.4
R1 = 4Si - 11(Na+K) -2(Fe+Ti)
R2 = 6Ca +2Mg+Al

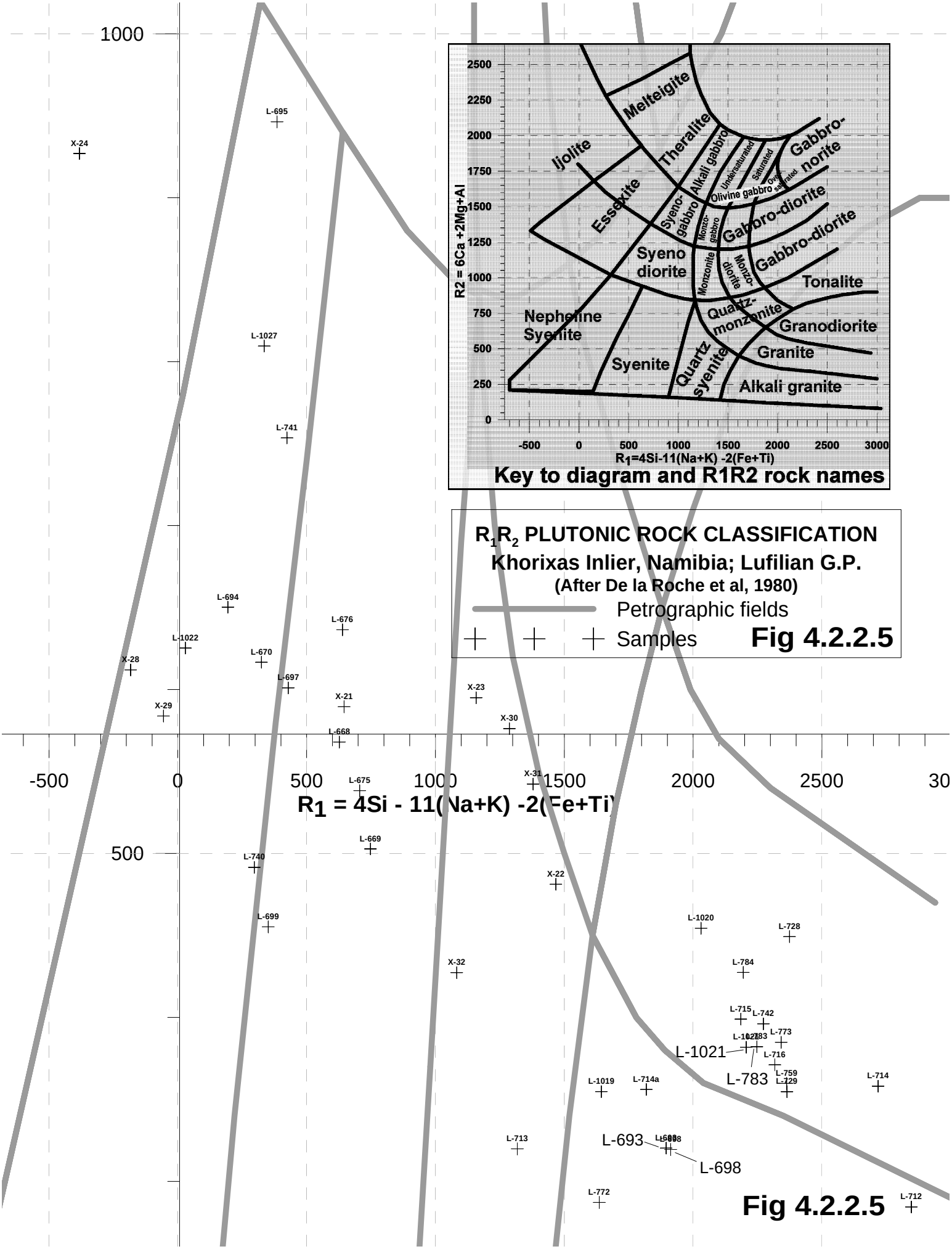
Melteigite
Theralite
Ijolite
Essexite
Alkali gabbro
Gabbro-norite
Olivine gabbro
Syeno-gabbro
Monzo-gabbro
Gabbro-diorite
Syeno diorite
Monzonite
Monzo-diorite
Tonalite
Quartz-monzonite
Granodiorite
Nepheline Syenite
Syenite
Quartz syenite
Granite
Alkali granite
Undersaturated
Saturated
Oversaturated
R2 = 6Ca +2Mg+Al
R1=4Si-11(Na+K) -2(Fe+Ti)
Key to diagram and R1R2 rock names
R1R2 PLUTONIC ROCK CLASSIFICATION
Khorixas Inlier, Namibia; Lufilian G.P.
(After De la Roche et al, 1980)
Petrographic fields
Samples
Fig 4.2.2.5
R1 = 4Si - 11(Na+K) -2(Fe+Ti)
L-1021
L-783
L-693
L-698
Fig 4.2.2.5

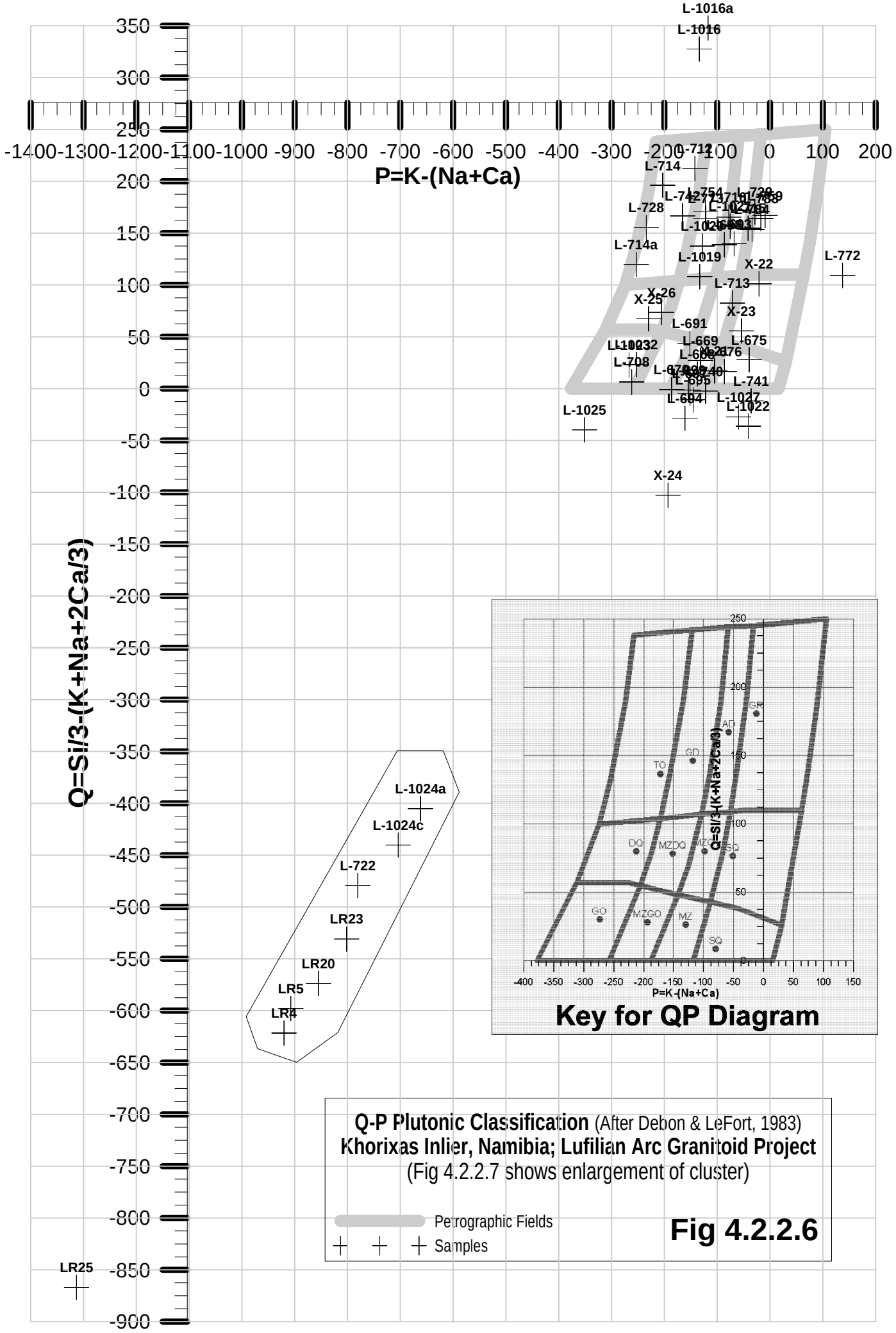
P=K-(Na+Ca)
Q=Si/3-(K+Na+2Ca/3)
-1400 -1300 -1200 -1100 -1000 -900 -800 -700 -600 -500 -400 -300 -200 -100 0 100 200
350 300 250 200 150 100 50 0 -50 -100 -150 -200 -250 -300 -350 -400 -450 -500 -550 -600 -650 -700 -750 -800 -850 -900
L-1016a
L-1016
L-712
L-714
L-754
L-728
L-714a
L-1019
L-772
X-22
L-713
X-26
X-25
X-23
L-691
L-669
L-675
L-708
L-741
L-1027
L-1025
L-1022
X-24
L-1024a
L-1024c
L-722
LR23
LR20
LR5
LR4
LR25
Key for QP Diagram
GR
AD
GD
TO
DQ
MZDQ
MZ
SQ
GO
MZGO
P=K-(Na+Ca)
Q-P Plutonic Classification (After Debon & LeFort, 1983)
Khorixas Inlier, Namibia; Lufilian Arc Granitoid Project
(Fig 4.2.2.7 shows enlargement of cluster)
Petrographic Fields
Samples
Fig 4.2.2.6

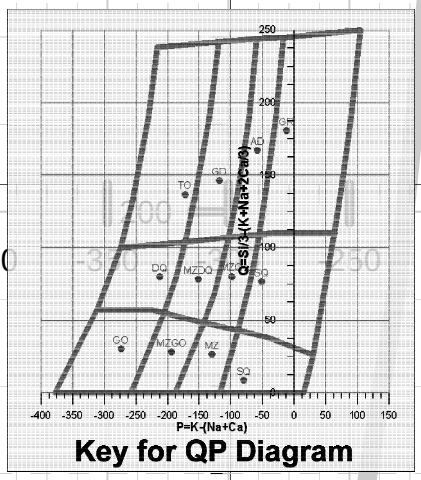

L-712
L-714
L-742
L-754
L-773
L-729
L-759
L-783
L-716
L-1021
L-728
L-715
L-784
L-1020
L-698
L-693
L-714a
L-1019
L-772
X-22
L-713
X-26
X-25
X-23
L-691
L-669
L-675
L-1023
L-1032
X-21
L-676
L-668
L-708
L-670
L-699
L-740
L-697
L-695
L-741
L-694
L-1027
L-1022
L-1025

Q-P Plutonic Classification (After Debon & LeFort, 1983)
Khorixas Inlier, Namibia; Lufilian Arc Granitoid Project

Petrographic Fields
Samples

Fig 4.2.2.7

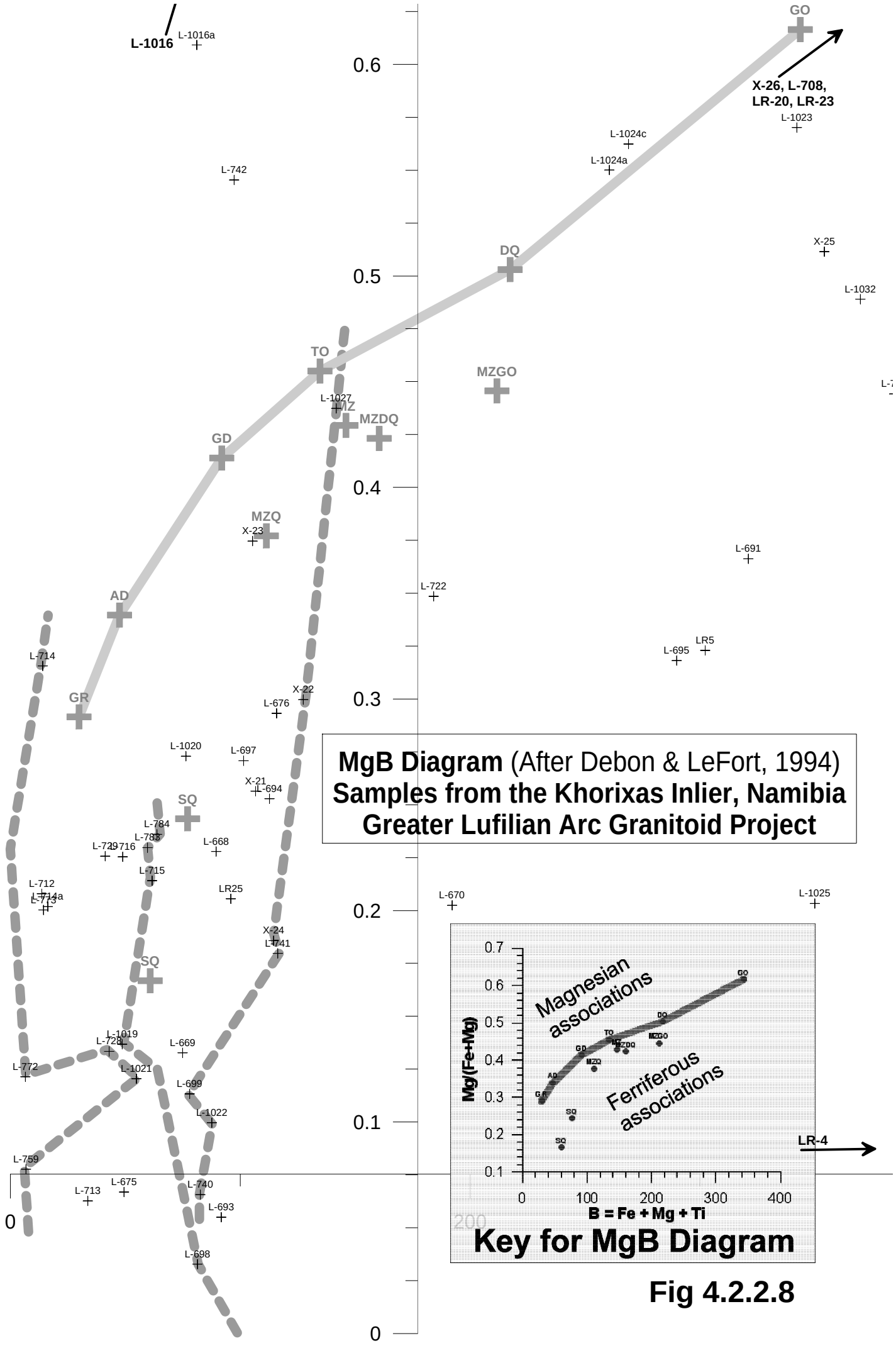
GO
X-26, L-708,
LR-20, LR-23
DQ
TO
MZGO
MZ
MZDQ
GD
MZQ
AD
GR
SQ
SQ
SQ
L-1016
L-1016a
L-1023
L-1024c
L-1024a
L-742
X-25
L-1032
L-691
L-722
LR5
L-695
L-714
X-22
L-676
L-1020
L-697
X-21
L-694
L-784
L-783
L-729
L-716
L-668
L-715
L-712
L-714a
L-713
LR25
L-670
L-1025
X-24
L-741
L-1019
L-728
L-669
L-772
L-1021
L-699
L-1022
L-759
L-675
L-713
L-740
L-693
L-698
0.6
0.5
0.4
0.3
0.2
0.1
0
0
200
LR-4
MgB Diagram (After Debon & LeFort, 1994)
Samples from the Khorixas Inlier, Namibia
Greater Lufilian Arc Granitoid Project
Mg/(Fe+Mg)
B = Fe + Mg + Ti
Magnesian associations
Ferriferous associations
Key for MgB Diagram

Fig 4.2.2.8

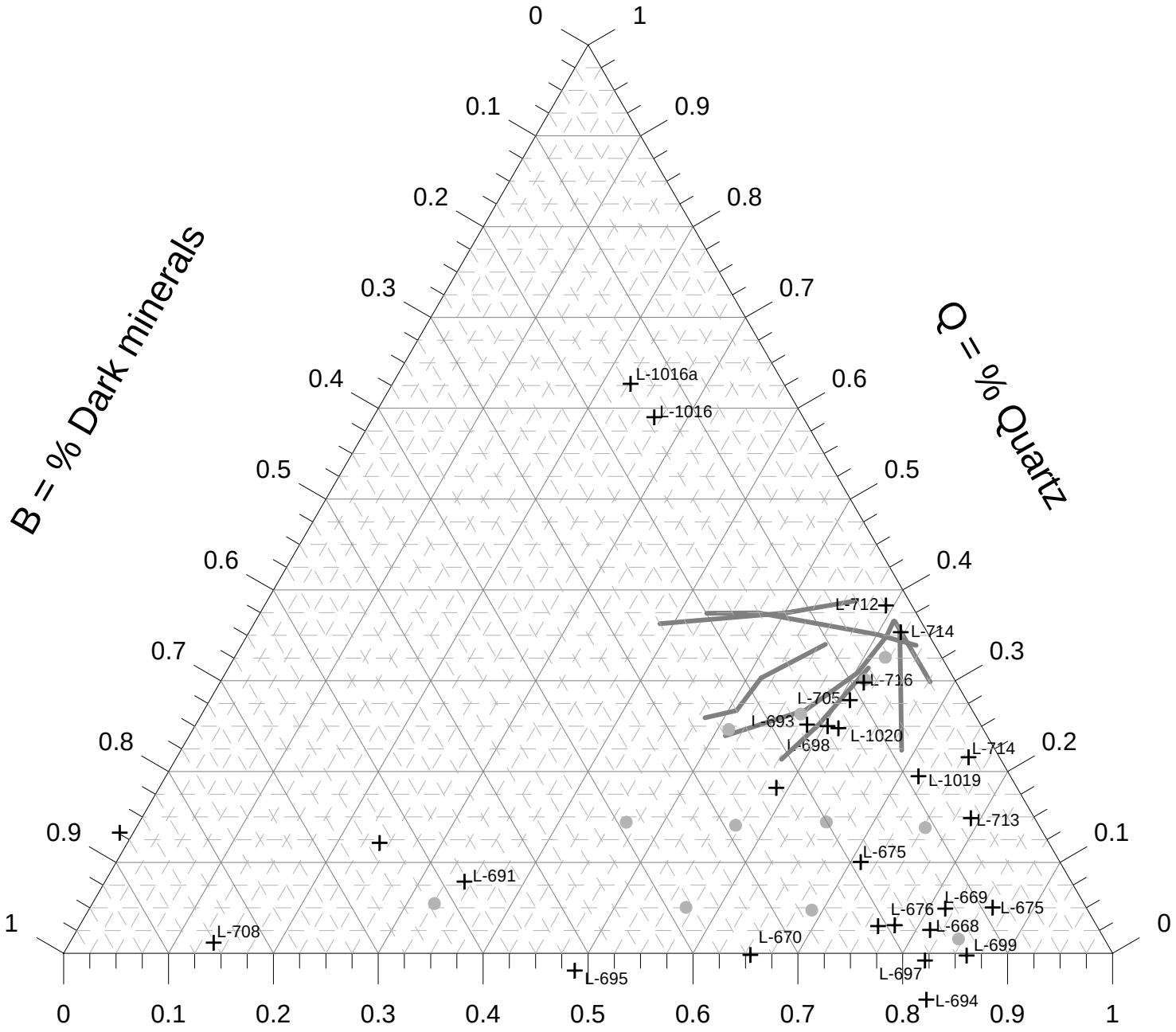

QBF ternary diagram (after Debon & LeFort, 1994)
Samples from the Oas Farm, Khorixas Inlier, Namibia
Greater Lufilian Arc Granitoid Project

Reference samples (Debon & LeFort)

Samples

Fig 4.2.2.9

The samples from the Oas Farm that were analysed could be separated into four rock groups: 1) basement rocks, 2) massive intrusions of midalkaline and alkaline character, 3) dikes that intersect the second group, and 4) younger granitoids. These are listed on Table 4.2.2.7, along with their main geochemical characteristics and studies on environment of emplacement.

Table 4.2.2.7 Sample grouping, Oas farm, Namibia
(*dated samples. See acronym description on section 2.4.3.)

Basement									
Sample	Rock Name	Debon & LeFort	Maniar & Piccoli	Whalen	Pearce	Mafic	Rb/10HfTa	Rb/30HfTa	Nb-Ta
L-712	alkali granite	peralum iii leuco NaFe	POG	A	V				
L-713	quartz syenite	metalum v leuco NaFe		A	O-W 2-2		WP	W	OUTU
L-714	Granite	metalum v leuco NaMg	OP	A	V				
L-714a	alkali granite	peralum ii leuco NaFe		A	V				
L-715	Granite	metalum iv meso Na-Kfe	RRG-CEUG	A	O3/4				OUTU
L-716*	Granite	metalum iv subleuco NaFe	CEUG-RRG	A	S2/4O2/4		VA-	VA	INV
L-1019	alkali granite	metalum v subleuco NaFe	RRG	A	V2/4		WP-	WP	INW
L-1020	Granite	metalum v meso NaFe		A	W				
Massive Intrusives									
Sample	Rock Name	Debon & LeFort	Maniar & Piccoli	Whalen	Pearce	Mafic	Rb/10HfTa	Rb/30HfTa	Nb-Ta
L-668*	Syenite	metalum iv meso NaFe	RRG	A	O-W 2-2	wpab	WP-	WP	INW
L-669	Syenite	metalum iv meso NaFe	CEUG	A	W		WP-	WP	INW
L-670	Nepheline syenite	metalum iv meso NaFe	RRG	A	O-W 2-2	?			OUTU-NEA
L-675	Syenite	peralum i subleuco NaFe	CEUG	A	W3/4	wpab			OUTU
L-676	Syenite	metalum iv meso NaFe	RRG-CEUG	A	W	wpab			
L-694	Nepheline syenite	metalum v meso NaFe	RRG	A	W	wpab			
L-695	Nepheline syenite	metalum iv meso NaFe	RRG-CEUG	A	O-W 1-1	wpab			
L-697	Syenite	metalum v meso NaFe	RRG-CEUG	A	W3/4	wpab	WP-	WP	OUTU-NEA
L-699	Syenite	metalum iv meso NaFe	CEUG	A	W				
X-21	Syenite								
X-22	Quartz syenite								
X-23	Quartz syenite								
Dikes									
Sample	Rock Name	Debon & LeFort	Maniar & Piccoli	Whalen	Pearce	Mafic	Rb/10HfTa	Rb/30HfTa	Nb-Ta
L-691	Monzonite	metalum iv meso NaFe	RRG-CEUG	A	W	wpt			
L-693*	alkali granite	metalum iv meso NaFe	RRG	A	W3/4		WP-	WP	INW
L-698	alkali granite	metalum v meso NaFe	RRG-CEUG	A	O-W 2-2				OUTU
L-708	Pyroxenite	metalum v meso NaFe	IAG-CAG	A	W?	wpab			
X-24	Nepheline syenite								
X-25	Gabbro								
X-26	Saturated olivine gabbro								
Quartzites									
Sample	Rock Name	Debon & LeFort	Maniar & Piccoli	Whalen	Pearce	Mafic	Rb/10HfTa	Rb/30HfTa	Nb-Ta
L-1016	Quartzite								
L-1016a	Quartzite								

Most samples that come from the Oas farm N-S transect are enriched in Nd, Pr, Ce, La, Nb, Zr, Sm, Nd, Pr and Y. They are also high in Na, Mn and Zn. These make up a suite of rocks that are very similar to each other, and may have been emplaced at approximately the same time.

Samples of syenite and nepheline syenite from the main cluster of ring complexesFig 4.2.2.1) show some additional similarities. Results from a simplified isocon diagram comparison of each of these samples with all the rest are shown on the matrix of Table 4.2.2.8. The following conclusions were reached: the main group of samples is **L-668**, **L-669**, **L-694**, **L-697** and **L-699**. Samples **L-670**, **L675** and **L-676** are similar to each other.

Samples **L-676**, **L-691**, **L-693***, **L-695** and **L-698** are different from the main batch. **L-698** and **L-693*** are very similar to each other, and different from other rocks in the suite. They are also very similar to **L-713**, **L-715** and **L-716***. In other plots, they are similar to **L-1020** and **L-1019**. **L-716*** was dated and turned out to be younger than the syenite ring complexes.

Table 4.2.2.8 Correlation matrix of samples from the Oas ring complexes using the isocon diagram (Grant, 1986) and visual comparison.

(Conventions: B = bad, C = some change or variation, **G** = good, **VG** = very good, ~ = reasonable.)

	L-669	L-670	L-675	L-676	L-691	L-693*	L-694	L-695	L-697	L-698	L-699
L-668	**G**	C	C	~	C	B	**G**	C	**G**	C	**G**
L-669		~	~	C	C	B	**G**	C	~	~	**VG**
L-670			~	B	B	B	B	C	B	B	~
L-675				~	B	B	~	B	B	B	~
L-676					C	B	~	~	~	B	B
L-691						B	B	C	B	B	B
L-693*							C	B	B	**G**	B
L-694								~	**VG**	B	G
L-695									B	B	C
L-697										B	**G**
L-698											C

L-712, **L-713**, **L-714** and **L-714a** are all leucocratic. **L-668**, **L-669**, **L-670**, **L-675**, **L-694** and **L-697** make a straight line on the R1R2 diagram (Fig 4.2.2.5). The same samples plot as a trend on the QBF diagram of Debon & LeFort (Fig 4.2.2.9). Samples **L-668**, **L-669**, **L-670**, **L-675**, **L-676**, **L-694**, **L-695**, **L-697**, **L-699**, **L-708**; all are in the ALKS suite of rocks on the QBF diagram (Fig 4.2.2.9). On the same diagram, **L-693***, **L-698**, **L-714**, **L-715**, **L-716*** and **L-1020** plot on one of the "quartz-poor" aluminous types.

L-694 and **L-697** have very similar chemistry. **L-669** and **L-699** are also very similar to each other. **L-693*** and **L-698** are very different from the rest of the rocks in the suite; they are extremely similar to each other.

L-1019 seems to have significant hydrothermal alteration.

On the R1/R2 diagram, **L-716*** forms a dense cluster of granites with **L-715** (Oas farm), **L-728**, **L-729**, **L-742**, **L-1021** (Lofdal farm), **L-759**, **L-773**, **L-783** and **L-784** (Mesopotamie farm). See Fig 4.2.2.5. The minor element chemistry is uniform too. These samples probably come from several suites of rocks, that formed at different times. All of these granites seem to have formed in anorogenic environments, according to the Whalen plots; the ones that produce coherent results from the Pearce diagrams are within-plate granites, and the ones that produce coherent results from the Maniar & Piccoli procedure were formed in rift-related environments. They all formed in a similar environment, from the same protolith, but at different times.

Table 4.2.2.9 compiles most of the groups of rocks with similar chemical features from the different sampling domains in Namibia, except for the Kamanjab Batholith. There are many similarities between the various domains. Logarithmic major oxide and trace element diagrams of the groups of Syenites A and B have been plotted on Figs 4.2.2.10 and 4.2.2.11 to show their chemical similarity.

4.2.2.2.4 Zinc Enrichment

All syenites and gabbros from various Namibian regions are enriched in zinc, as shown on Table 4.2.2.9. Part of the alkali granites and granites are also zinc-enriched. A large portion of the rocks mentioned come from the Oas farm (See Table 4.2.2.3).

Table 4.2.2.10 Groups of samples from various Namibian regions. (Grouping according to Table 4.2.2.9) (complete elemental analysis on Table A15, Appendix)

Sample	SiO2	TiO2	Al2O3	Fe2O3	FeO	MnO	MgO	CaO	Na2O	K2O	P2O5	LOI	Total	Rb	Sr	Y	Zr	Nb	Co	Ni	Cu	Zn	Ga	V	Cr	Ba	U	Th	Sc	Nd	Pr	Ce	La
Notch	50	1	15.5	6		0.15	2	5	4.9	5.5	0.3	2		200	400	60	360	40	30	16	25	85	26	100	100	1300	20	37	20	50	15	175	95
Basement granites																																	
Sample	SiO2	TiO2	Al2O3	Fe2O3	FeO	MnO	MgO	CaO	Na2O	K2O	P2O5	LOI	Total	Rb	Sr	Y	Zr	Nb	Co	Ni	Cu	Zn	Ga	V	Cr	Ba	U	Th	Sc	Nd	Pr	Ce	La
L-715	72.1	0.48	13.02	3.49	0	0.09	0.48	1.12	3.88	4.88	0.12	0.5	100.2	118	147	58	348	25	8	11	12	67	18	28	47	1230	<6	19	<10	39	88	154	44
L-716*	73.9	0.3	12.54	2.79	0	0.04	0.41	0.98	4.49	3.98	0.04	0.68	100.1	69	164	38	332	16	8	11	12	51	16	19	57	1389	7	24	<10	42	11	134	66
L-729	73.6	0.31	12.64	2.31	0	0.05	0.34	0.84	3.69	4.96	0.03	1.7	100.5	113	82	46	281	24	<6	6	6	60		<12	58	957							
L-759	74.1	0.03	14.47	0.47	0	0.04	0.02	0.7	3.55	5.54	0.06	0.94	99.9	109	124	20	16	7	<6	<6	<6	12	13	<12	185	649	<6	<15	<10			12	<12
L-773	74.8	0.06	14.98	0.87	0	0.02	0.11	0.8	5.35	3.07	0.04	0.41	100.5	76	71	103	64	14	<6	10	8	43	20	<12	47	176	<6	<15	<10			25	<12
L-783	71.9	0.45	13.96	3.32	0	0.08	0.5	0.78	3.49	5.15	0.18	0.71	100.5	223	85	54	273	22	<6	6	9	49	17	25	239	859	<6	27	<10			161	75
L-784	71.8	0.39	13.23	3.59	0	0.06	0.56	1.31	3.67	5.07	0.09	0.7	100.5	193	105	58	312	23	<6	7	7	59	17	23	63	1049	7	26	<10	37	99	155	51
L-1021	72	0.43	12.86	3.47	0	0.05	0.24	1.1	4.37	4.02	0.07	0.53	99.2	83	92	84	464	33	<6	8	5	29	17	<12	250	1355	<6	18	<10			143	61
L-712	79.1	0.04	12.04	0.83	0	0.04	0.11	0.4	5.47	1.95	0.01	0.54	100.5	33	159	12	17	7	<6	10	8	35	18	<12	47	662	<6	<15	<10		13	41	7
L-714	77.6	0.05	13.19	0.73	0	0.03	0.17	0.85	6.33	0.76	0.02	0.67	100.4	16	338	9	250	9	<6	9	8	40	23	<12	50	538	<6	16	<10		3	83	
L-728	75.1	0.16	10.35	2.83	0	0.14	0.22	2.2	6.61	0.86	0.06	2.04	100.5	23	140	58	212	33	<6	10	15	45	18	14	67	581	5	21	15	82	20	171	73
L-742	68.4	0.18	10	3.45	0	0.2	2.09	0.9	5.4	1.17	0.03	8.44	100.3	59	181	41	310	26	11	13	32	227	19	18	44	802	<6	21	<10	33	52	79	44
L-1020	70.8	0.58	12.68	4.01	0	0.1	0.76	1.57	5.17	3.14	0.09	0.31	99.2	70	173	52	445	22	<6	8	64	85	17	19	<12	1364	<6	19	<10			180	95
Quartzites																																	
L-1016	77.3	0.1	1.04	2.18	0	0.47	2.02	6.71	0.5	0.09	0.13	8	98.6	6	124	8	15	4	<6	<6	56	14	<9	<12	351	33	<6	<15	12			24	<12
L-1016a	79.4	0.1	0.8	2.49	0	0.45	1.96	5.74	0.55	0.13	0.04	7.5	99.1	5	140	6	37	4	<6	7	28	27	<9	13	15	57	<6	<15	10			23	<12
Syenite A																																	
Sample	SiO2	TiO2	Al2O3	Fe2O3	FeO	MnO	MgO	CaO	Na2O	K2O	P2O5	LOI	Total	Rb	Sr	Y	Zr	Nb	Co	Ni	Cu	Zn	Ga	V	Cr	Ba	U	Th	Sc	Nd	Pr	Ce	La
L-668	62.6	0.89	17.32	4.83	0	0.14	0.72	1.8	6.42	4.79	0.36	0.59	100.5	121	474	69	710	193	7	7	6	127	26	14	139	2037	7	22	<10	101	182	235	110
L-669	64.3	0.61	16.76	4.66	0	0.12	0.36	1.46	6.43	4.8	0.23	0.74	100.5	115	350	73	378	204	<6	9	7	146	28	<12	124	1647	9	31	<10	102	28	267	137
L-670	57	1.45	15.14	11.08	0	0.21	1.42	2.33	6.69	3.35	0.53	1.32	100.5	173	1219	73	1843	458	<6	9	9	85	42	<12	18	767	17	46	<10	27	72	219	42
L-675	60.7	0.1	21.99	3.59	0	0.09	0.13	0.94	4.92	6.41	0.03	1.61	100.5	125	384	123	1520	345	7	9	23	167	30	20	17	1321	10	78	11	140	592	844	440
L-676	59.4	0.87	18.13	5.92	0	0.17	1.24	2.05	5.2	5.55	0.24	1.84	100.6	226	634	58	553	139	7	7	11	177	26	19	31	1591	<6	19	<10			180	85
L-694	59.2	1.09	17.07	5.91	0	0.17	1.01	2.48	6.84	4.89	0.36	0.54	99.5	106	633	39	333	93	7	<6	10	107	23	27	<12	1995	<6	<15	<10			166	87
L-697	59.9	0.86	16.9	5.28	0	0.17	0.99	2.06	6.58	4.59	0.32	1.54	99.2	169	491	151	1363	432	8	9	5	129	26	<12	117	1444	15	51	<10	127	480	582	291
L-699	63.4	0.28	17.28	5.27	0	0.2	0.34	0.93	7.4	4.73	0.12	0.56	100.5	98	114	75	1246	307	<6	10	7	147	34	<12	126	458	15	50	<10			470	310
L-1022	54.8	0.44	20.41	5.9	0	0.2	0.33	1.95	4.97	7.25	0.13	2.78	99.1	189	616	24	767	249	7	<6	11	171	36	14	<12	629	8	<15	<10	28	48	61	19
LL14	57	1	17	9	0	0	1	3	6	5	0	1	99.5	280	355	161	2052	364	4		5	133		4	0	1161	22	83	5				
X-21	60.8	0.87	16.97	1.13	4.1	0.16	0.99	1.94	5.65	5.27	0.22	1.78	99.9																				
Syenite B																																	
L-695	46.3	3.29	13.34	13.54	0	0.48	3.19	4.92	4.1	3.51	0.68	6.78	100.1	197	399	53	329	54	27	22	89	120	19	353	28	639	<6	<15	26			64	30
L-741	56.6	0.47	19.54	7.23	0	0.44	0.8	3.09	4.14	7.21	0.11	0.91	100.6	169	548	49	640	337	<6	<6	14	164	34	14	18	1955	19	<15	<10	52	211	248	131
L-1027	55.1	0.81	15.77	5.91	0	0.27	2.32	3.6	4.38	6.88	0.23	3.58	98.8	177	429	37	621	220	14	42	25	134	24	45	174	1043	<6	<15	<10	58	136	239	72
LL10	56.5	1.24	17.84	6.85	0	0.19	1.96	3.78	5.74	4.86	0.74	0.74	99.7	135	965	36	340	99	11	3	0	78		44	0	1366	9	25	1				
LL15	62	1	16	6	0	0	1	4	6	5	0	4	99.7	118	328	31	305	47	10	9	0	73		125	22	1308	3	26	15				
X-24	51.3	0.4	19.06	5.95	1.05	0.42	0.82	4.79	6.75	5.19	0.3	3.38	99.4																				
Alkali granites																																	
Sample	SiO2	TiO2	Al2O3	Fe2O3	FeO	MnO	MgO	CaO	Na2O	K2O	P2O5	LOI	Total	Rb	Sr	Y	Zr	Nb	Co	Ni	Cu	Zn	Ga	V	Cr	Ba	U	Th	Sc	Nd	Pr	Ce	La
L-693	71.4	0.48	11.65	6.47	0	0.14	0.19	0.77	4.62	4.46	0.09	0.31	100.6	86	98	31	132	105	6	7	14	128	33	<12	60	241	2	9	<10	114	35	357	216
L-698	71.7	0.46	11.4	5.84	0	0.1	0.1	0.85	4.91	4.1	0.1	0.4	99.9	77	45	50	329	124	<6	7	7	104	35	<12	207	157	<6	<15	<10	67	228	372	143
L-713	71.3	0.16	14.36	2.37	0	0.05	0.08	0.32	5.76	5.66	0.02	0.41	100.5	117	94	30	277	71	<6	8	9	53	25	19	49	909	<6	<15	<10	80	295	436	188
L-714	74.5	0.12	14.63	0.94	0	0.04	0.12	0.59	8.15	0.94	0.05	0.41	100.5	16	152	25	237	50	<6	8	<6	17	0	12	160	606	0	0	0			0	0
L-772	72.6	0.03	14.29	0.43	0	0.03	0.03	0.05	2.34	10.1	0.02	0.67	100.5	201	100	7	<8	4	<6	<6	8	28	13	<12	44	579	<6	<15	<10			21	<12
L-1019	72.2	0.41	13.17	3	0	0.11	0.24	0.79	6.18	3.79	0.08	0.41	100.4	50	101	31	290	47	<6	10	9	62	17	<12	253	1351	2	17	<10	47	12	110	60
LL3b	70.3	0.04	16.91	0.47	0	0.01	0.24	0.37	2.44	9.09	0.09	1.2	100.0	348	252	9	5	4	2	1	0	7		7	1	495	1	0	5				
Gabbroids																																	
Sample	SiO2	TiO2	Al2O3	Fe2O3	FeO	MnO	MgO	CaO	Na2O	K2O	P2O5	LOI	Total	Rb	Sr	Y	Zr	Nb	Co	Ni	Cu	Zn	Ga	V	Cr	Ba	U	Th	Sc	Nd	Pr	Ce	La
L-691	50.2	3.31	12.95	14.15	0	0.21	4.13	6.53	2.95	2.82	0.55	1.51	99.4	151	589	52	368	62	39	32	190	166	19	357	66	617	<6	<15	33			110	61
L-708	47.2	0.47	8.72	11.27	0	0.53	13.1	14.2	1.46	1.77	0.04	1.79	100.5	86	578	146	469	126	16	26	13	279	17	68	14	2096	<6	<15	23			258	97
L-1032	46	1.99	15.47	14.07	0	0.33	6.8	9.26	3.22	0.75	0.42	1.94	100.3	10	322	48	132	9	47	45	26	163	15	345	218	299	<6	<15	40	42	61	<12	40
L-1023	47.5	0.82	15.7	11.39	0	0.21	7.63	11	2.78	0.87	0.09	2.31	100.3	19	177	23	45	5	51	86	11	157	19	246	354	223	<6	<15	42			33	20
L-1025	42.1	1.06	1.26	21.42	0	0.77	2.76	17.4	1.61	0.56	3.85	7.4	100.2	30	1546	50	1312	##	42	10	29	207	12	334	106	214	86	20	33	183	47	396	176
X-25	47.5	2.22	14.47	3.74	8.09	0.05	6.73	11.6	1.24	0.77	0.3	2.8	99.5																				
X-26	48.8	1.03	12.21	3.62	6.54	0.15	13.7	9.63	1.77	1.1	0.59	1.16	100.3																				
Carbonatites																																	
L-722	7.5	0.04	0.13	9.55	0	0.68	2.58	43.8	0	0	0.03	36.2	100.5	7	210	260	119	13	23	<6	5	37	<9	194	12	145	6	27	54		16	10	<12
L-1024a	7.58	0.07	0.57	9.33	0	0.79	5.76	37.2	0.03	0.15	0.23	38.8	100.5	6	335	62	9	44	28	21	177	59	<9	23	<12	115	19	20	49	543	179	2058	1583
L-1024c	5.56	0.06	0.2	9.37	0	0.84	6.08	39.5	0.01	0.04	0.23	38.7	100.6	10	325	92	18	31	29	11	116	29	<9	24	<12	99	20	18	49			1786	1383
Other																																	
L-713	71.3	0.16	14.36	2.37	0	0.05	0.08	0.32	5.76	5.66	0.02	0.41	100.5	117	94	30	277	71	<6	8	9	53	25	19	49	909	<6	<15	<10	80	295	436	188
L-754	53	1.59	13.32	16.18	0	0.28	6.53	7.5	0.32	1.02	0.3	0.15	100.2	318	84	40	94	8	50	53	94	252	17	393	178	235	<6	<15	49			25	12
Granite F																																	
Sample	SiO2	TiO2	Al2O3	Fe2O3	FeO	MnO	MgO	CaO	Na2O	K2O	P2O5	LOI	Total	Rb	Sr	Y	Zr	Nb	Co	Ni	Cu	Zn	Ga	V	Cr	Ba	U	Th	Sc	Nd	Pr	Ce	La
L-605	76.6	0.12	12.03	1.16	0	0.01	0.02	0.81	3.42	5.47	0.07	0.41	100.1	198	99	7	89	7	<6	<6	9	19	13	<12	227	772	<6	42	<10			148	102
L-791b	76.4	0.14	12.55	1.25	0	0.02	0	0.51	3.09	5.85	0.03	0.29	100.1	270	74	83	70	65	<6	10	<6	15	22	16	234	332	8	17	<10			224	108
L-793	74.9	0.33	12.39	2.15	0	0.08	0.24	1	3.28	5.24	0.14	0.37	100.1	251	140	81	213	78	<6	7	7	34	19	22	390	435	12	61	<10	51	175	234	98
L-797	75.1	0.21	13.05	1.92	0	0.04	0.08	0.51	3.62	4.63	0.08	0.61	99.9	225	107	23	199	38	<6	6	<6	33	21	17	372	658	6	37	<10			132	76
L-802	73.3	0.23	14.56	1.83	0	0.05	0.29	1.08	3.46	4.55	0.13	0.84	100.4	234	141	32	142	41	<6	6	<6	51	19	22	260	745	<6	15	<10			77	38
L-812	75.6	0.08	12.89	1.27	0	0.03	0.25	1.29	4.03	4.17	0.09	0.71	100.4	141	104	86	215	10	<6	8	9	67	13	<12	34	439	17	30	<10			93	55
L-1043	72.4	0.34	13.62	2.4	0	0.04	0.57	0.57	2.76	5.77	0.1	1.27	99.9	276	85	71	207	17	7	9	51	30	14	28	<12	525	<6	44	<10	42	89	140	35
L-1044	73.4	0.25	12.72	2.04	0	0.04	0.39	0.49	2.79	5.94	0.11	1.1	99.3	293	67	47	166	16	6	9	115	70	12	20	12	415	<6	36	<10			109	44
L-1046	72.8	0.33	12.73	2.4	0	0.03	0.55	0.76	2.61	5.45	0.12	1.39	99.2	283	61	69	193	16	6	9	30	27	13	25	16	473	<6	42	<10			126	53
LL2a	75.7	0.02	14.98	0.67	0	0.01	0.06	0.12	3.62	4.86	0.04	1.36	100.1	181	35	10	19	19	2	1	14	8		11	0	104	2	4	2				

LL3a	75.9	0.03	13.87	0.68	0	0.01	0.05	0.39	2.87	5.93	0.01	1.19	99.8	156	182	13	29	0	2	1	14	4		5	3	659	0	7	1				
X-20	76	0.23	12.05	0.8	0.91	0.03	0.2	1.02	3.09	5.02	0.01	1.14	100.5																			
Granite G																																
Sample	SiO2	TiO2	Al2O3	Fe2O3	FeO	MnO	MgO	CaO	Na2O	K2O	P2O5	LOI	Total	Rb	Sr	Y	Zr	Nb	Co	Ni	Cu	Zn	Ga	V	Cr	Ba	U	Th	Sc	Nd	Pr	Ce	La
L-715	72.1	0.48	13.02	3.49	0	0.09	0.48	1.12	3.88	4.88	0.12	0.5	100.2	118	147	58	348	25	8	11	12	67	18	28	47	1230	<6	19	<10	39	88	154	44
L-810	73.9	0.06	14.05	1.11	0	0.04	0.16	1.04	4	5.44	0.04	0.5	100.3	173	85	7	<8	7	9	10	13	50	14	<12	56	249	<6	<15	<10			24	<12
LL1	73.4	0.09	14.65	0.8	0	0.01	0.27	1	3.34	6.24	0.2	1.26	100.0	150	176	17	42	6	3	3	13	11		6	1	1468	0	5	2				
Granite I																																
L-606	72.6	0.36	12.83	3.51	0	0.06	0.48	1.32	3.22	5.19	0.07	0.73	100.3	185	105	38	202	17	<6	6	7	61	18	20	57	781	<6	38	<10			227	149
L-729	73.6	0.31	12.64	2.31	0	0.05	0.34	0.84	3.69	4.96	0.03	1.7	100.5	113	82	46	281	24	<6	6	6	60		<12	58	957							
L-759	74.1	0.03	14.47	0.47	0	0.04	0.02	0.7	3.55	5.54	0.06	0.94	99.9	109	124	20	16	7	<6	<6	<6	12	13	<12	185	649	<6	<15	<10			12	<12
L-783	71.9	0.45	13.96	3.32	0	0.08	0.5	0.78	3.49	5.15	0.18	0.71	100.5	223	85	54	273	22	<6	6	9	49	17	25	239	859	<6	27	<10			161	75
L-798	72.6	0.26	14.07	2.13	0	0.08	0.26	1.09	3.42	5.17	0.12	0.91	100.2	222	204	26	229	48	<6	<6	<6	40	20	16	285	1117	7	27	<10			211	102
L-799	73.1	0.08	13.93	1.96	0	0.06	0.04	0.95	3.84	4.84	0.13	0.63	99.6	153	168	53	183	14	<6	7	11	19	18	29	326	727	7	<15	<10			102	36
L-809	71.6	0.07	14.95	1.24	0	0.03	0.23	0.87	3.46	7.52	0.06	0.5	100.5	253	92	19	<8	9	<6	7	11	56	16	<12	27	301	<6	<15	<10			29	<12
L-1021	72	0.43	12.86	3.47	0	0.05	0.24	1.1	4.37	4.02	0.07	0.53	99.2	83	92	84	464	33	<6	8	5	29	17	<12	250	1355	<6	18	<10			143	61
LL11	73	0	14	2	0	0	0	1	3	6	0	1	99.9	287	134	34	210	16	2	1	0	30		20	3	880	3	55	5				
LL18	76	0	13	1	0	0	0	1	3	7	0	1	100.1	178	84	8	55	3	0			8		5	4	316	5	4	1				
LL4	74.7	0.1	13.5	1.59	0	0.03	0.1	0.8	3.49	5.74	0.02	0.41	100.1	365	50	32	138	29	1		0	27		1	0	235	4	52	5				

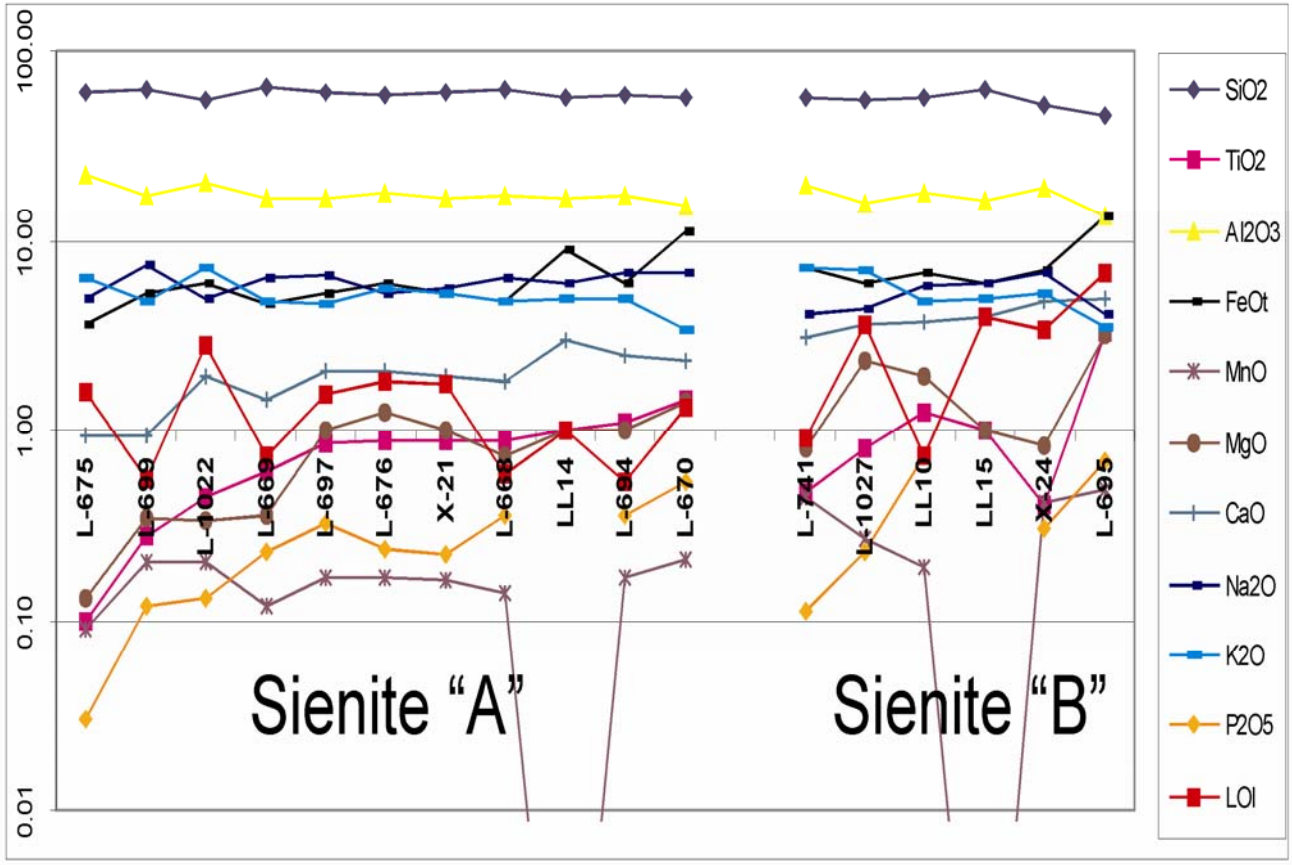

Fig 4.2.2.10 Logarithmic major oxide plot for the Syenites A and Syenites B groups in the Oas farm, Loftal farm and Ojtiwarongo environs, Namibia

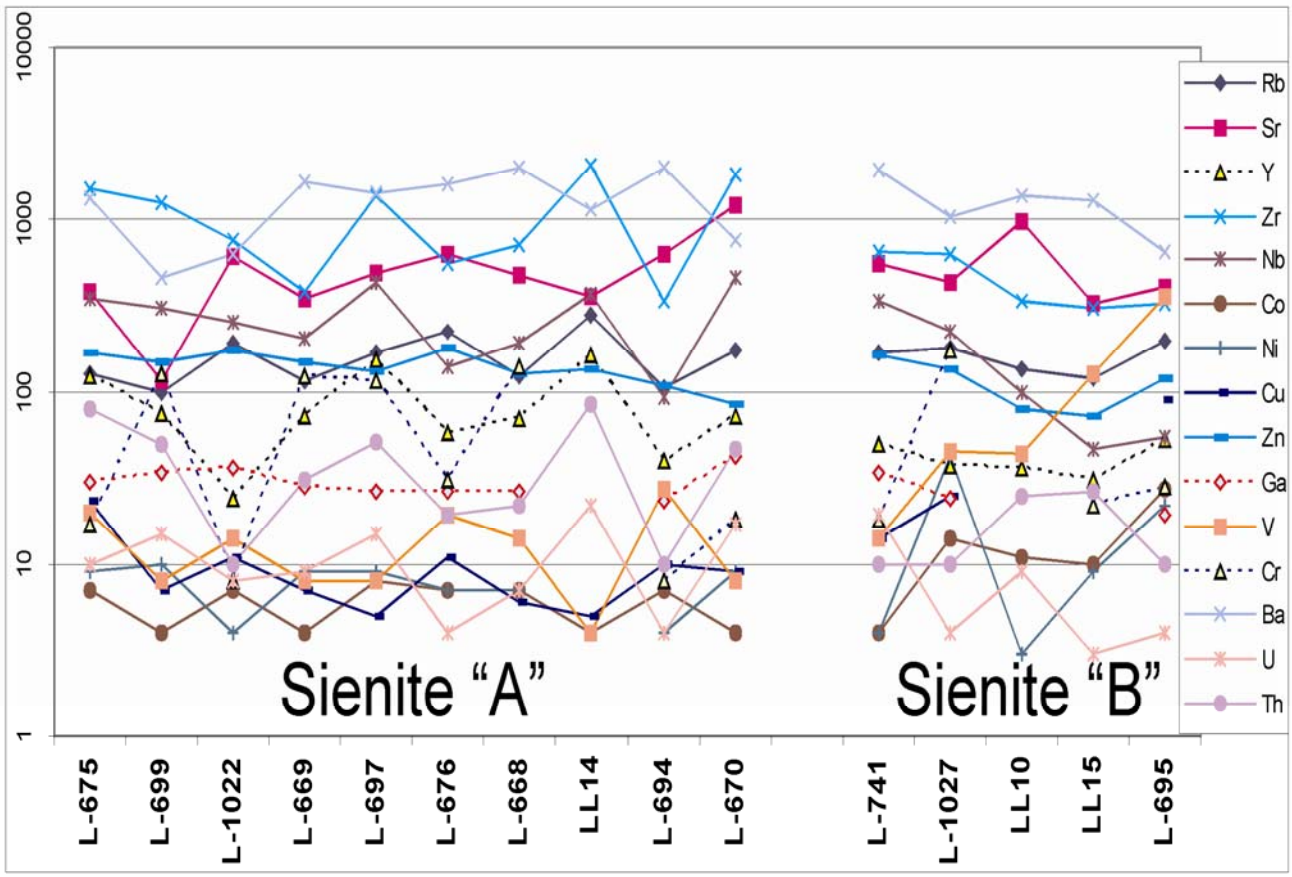

Fig 4.2.2.11 Logarithmic trace element plot for the Syenites A and Syenites B groups in the Oas farm, Loftal farm and Ojtiwarongo environs, Namibia

Table 4.2.2.9 Comparison of sample groups from various Namibian regions (Based mainly on geochemical similarities.)

Group	Oas	Lofdal	Mesopotamie	Summas Mts.	Otjiwarongo	AVMIN	Felsic Volc.	Grootfontein	Okwa River	Ugab River	NW Zambia	Hook Granite	Age	Environment
Syenite A	L-676, L-699, L-675, **L-668***, L-669, L-670, L-695, L-697, X-21	L-1022			LL14								762±12 (L-668)	
Syenite B	L-694, X-24	L-1027, L-741			LL10, LL15									
Alkali Granite	**L-693***, L-698, L-1019, L-713, L-714a		L-772 **B**	L-791a	LL3b, L-1039, L-1039a, L-1039c		X-16, X-18, X-19		L-600A				~750 (L-693*)	Rfit-related anorogenic gtd.
Gabbro	L-708, X-25, X-26, L-691	L-1032,L-1023,L-1025												
Base Granite B	L-1020, L-714, L-712	L-742, **L-728***											~1750(L-728)	
Granite F	X-20			L-791b	LL2a, LL3a, LL17a	L-812		**L-043***, L-1044, L-1046	L-605	L-793, L-802, L-797, **L-796***	L-364, L-370	L-257, L-409	1887±39 (L-1043) ~1700 (L-796)	
Granite G	L-715				LL1	L-810								
Granite I		L-1021, L-729	L-759 L-758* **A**		LL11, LL4, LL18	L-809, L-813, **L-808***, L-815		L-1042	L-606	L-798, L-799			540 (L-745) ~550 (L-808c) (L-758) 750±5Ma relict at 1692±10Ma	Anorogenic undetermined environment
Carbonatite		L-1024a,L-1024c,L-722										L-411		
Quartzite	L-1016,L-1016a													
Syenite C	L-40													
Base Granite A	**L-716***	L-729, L-1021	L-759 , L-773										~745±15 (L-716*)	Rift-Related Anorogenic
Other	L-713	L-754												
		L-729, L-1021	L-783, L-784, L-793 + schists **D**										1692±10Ma (L-758)	Within-plate Rift-Related anorogenic gtds
				L-789	L-1037, L-1038, LJ1									
Quartz pods														

4.2.2.2.5 Quartzite from Oas Farm that might host mineralization.

The chemical analyses of **L-1016** and **L-1016a** show high content of silica, CaO, MgO, Cu and high loss on ignition; extremely low K, Na and other oxides (Table 4.2.2.3). In thin section, the rocks are quartzites with partial carbonate cement and strong hydrothermal overprint. The rock is light gray to white under the surface weathering crust (red-brown to dark gray color). Numerous quartz veins intersect the quartzites and in some areas significant iron oxide mineralization accompanies the quartz. Extensive exposures of the quartzite are covered by hydrothermal breccias and stockworks.

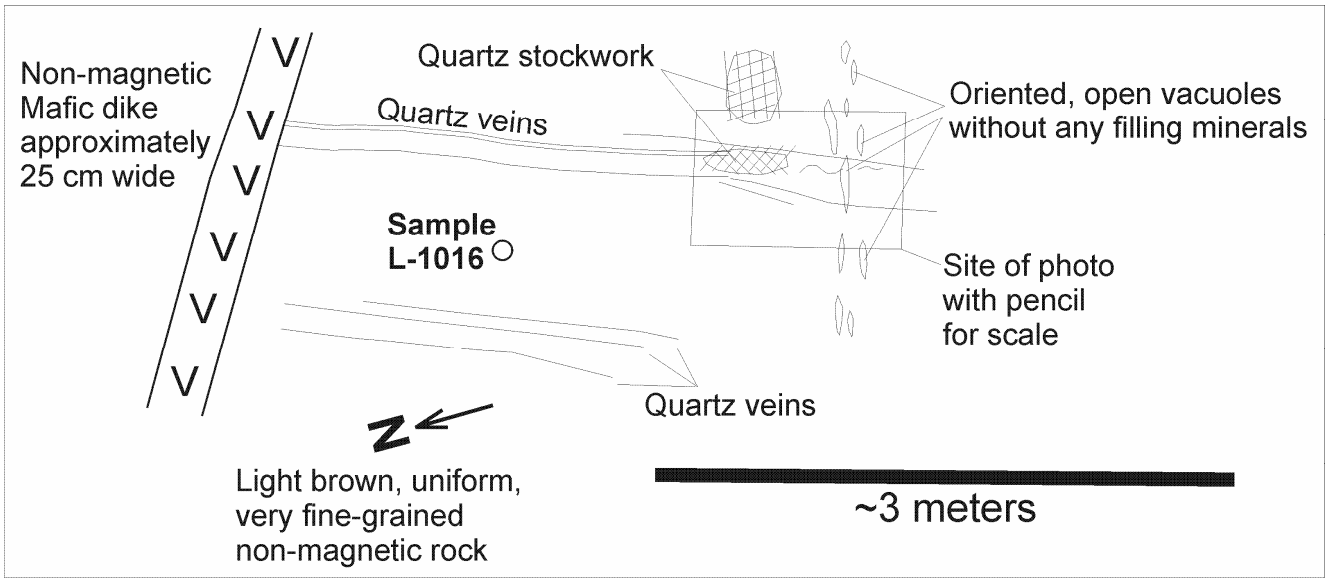

***Fig 4.2.2.12 Field relationships of mineralized quartzites at the Oas farm**, Namibia. Note size of the stockworking, quartz veins that intersect the quartzites and the open vugs. Other descriptions in the text.*

Fig 4.2.2.12 is a sketch of field relationships observed around geological station S170. The rock makes massive outcrops, has a dark gray to brown surface weathering color, rings like a bell when hammered, and displays abundant elongated vugs that are alligned. These look like elongated vacuoles in a lava. Parts of the rock contain lensoid fragments of what seems to be a schistose or slaty material, after clay. Those fragments are seldom longer than five centimeters. The rock's induration makes it behave in a brittle way, and after fracturing, it becomes a good host for mineralization.

4.2.2.2.6 Geochronology

Three new isotopic ages were produced from rocks at the Oas farm during this project. Zircons from samples **L-716***, **L-688*** and **L-693*** were dated by U-Pb SHRIMP II techniques (Table 4.2.2.11).

Table 4.2.2.11 Samples from the Oas farm ring complex cluster that were dated

Sample	Description	Age (Ma)	Notes
L-688*	Slightly-magnetic, brown-colored fine- to medium-grained syenite with little visible quartz	762±12	Structural relationships indicate that the rock is older than **L-689**.
L-693*	Fine-grained, medium gray, metaluminous mesocratic sodic ferriferous, biotite-rich, non-calcareous alkali granite, with strong magnetic content	765±4.5	Structural relationships indicate that the rock is younger than **L-688*.**
L-716*	Gneissic, medium-grained, pink and black layered, metaluminous subleucocratic sodic ferriferous granite with macroscopic potassium feldspar+quartz+biotite and no appreciable magnetite	745±5	Youngest known intrusion at the Oas farm.

The first intrusion of syenites (**L-688***) was closely followed by an intrusion of granite (**L-693***), and approximately 20 Ma later, by the intrusion of alkali granite (**L-693***). There might be at least two different minor younger intrusive events that intersect the other plutonic rocks, but they do not seem to be as relevant for mineralization. A quartz syenite from the Oas farm was dated by Hoffmann et al., 1996 at 756±2 Ma.

The protolith of intrusive rocks at the Oas farm probably are granites with ages of emplacement that oscillate in the range of 2192 to 2124 Ma, as indicated by inherited zircons in samples from the Oas farm dated by Tegtmeyer & Kroner, 1985. Even though none of such rocks have been specifically dated, they could be part of the group of foliated granites and alkaline granites observed at the farm. These might be correlative with the oldest rocks from the Kamanjab batholith.

Two granites in the nearby Lofdal and Mesopotamie farms were dated for the Greater Lufilian Arc project. These are **L-758*** and **L-728***. They produced ages of 750±5 Ma and 1750±5 Ma respectively.

Radiometric ages available for granitoids from the Oas farm in Namibia were plotted on the event diagram of Fig A38, along with other ages known for the Khorixas Inlier, the Summas Mountains and the Mesopotamie farm (Table A22.16). A minimum span of 113 Ma (Fig A38), broken into at least two discrete events of intrusion took place. There was one that is not so precisely constrained, from 853 to 827 Ma, and an almost continuous series of intrusive events from 801 to 740 Ma (Table A22.16). This evidence shows that the Oas farm – consequentially the Khorixas Inlier - had a long-lived series of alkaline events of intrusion that took place in roughly the same place. The events of the Oas farm are akin to those studied for anorogenic alkaline complexes in various provinces worldwide. This is discussed on section 7.2.

4.2.2.2.7 Environment of Emplacement

Table 4.2.2.7 shows the results of studies to devise the environment of emplacement for this important sample. The following is a description of the environments for the various groups of rocks.

The basement granitoids observed at the Oas farm all formed in anorogenic environments. L-713, L-715, L-716, L-1019 and L-1020 have many similarities and formed in a rift-related environment. L-712 seems to have formed as a post orogenic granitoid in an anorogenic environment, and L-714 as an oceanic plagiogranite. These last two samples are considered to be the two oldest rock types in the Oas farm. The syenites and nepheline syenites and alkali granites formed in a continuum of continental epeirogenic uplift to rift related environments. The dikes formed mainly in rift-related environments.

4.2.2.2.8 Conclusions

A basement of Paleoproterozoic gneisses was intruded by a series of zinc-rich midalkaline small anorogenic complexes for a period that lasted from 801 to 740 Ma. Dikes of compositions that vary from alkali granite to ultramafic and hyperalkaline and carbonatitic intruded the whole sequence during the midalkaline magmatism. Several of the intrusive events produced significant hydrothermal brecciation. Massive iron oxide bodies were emplaced along favourable structures. Iron sulfides and possibly sulfides of zinc and copper, along with gold and silver were later deposited on or around the magnetite and hematite bodies. Widespread red-rock and brown-rock hematite alteration and sodic alteration modified the surrounding rocks. Quartz podding and some silicification replaced in suitable redox sites in granitoids. All this took place in a continuum of continental epeirogenic uplift to rift related environments.

At least nine circular midalkaline intrusions were emplaced to make a ring complex cluster at the Oas farm.

The entire domain of the Oas syenites is prospective for iron oxide-copper-gold mineralization, and maybe for various types of zinc mineralization. Economic rare earth deposits and maybe thorium mineral enrichments can probably also be found in association with the midalkaline and alkaline intrusive rocks.

4.2.2.3 LOFDAL FARM, NAMIBIA

4.2.2.3.1 Introduction

The Lofdal farm is located in the eastern portion of the Khorixas Inlier, to the west of the town of the same name in Damaraland, northern Namibia (Fig M20). The farm hosts a wide variety of rock types. As observed on Figs 4.2.2.2 to 4.2.2.5, granites, nepheline syenites, alkali gabbros and carbonatites occur together and produce a complex set of minerals, mineralization, alteration and geology. This is probably a product of overprinting intrusions over a long period of time. Older granites were intruded by alkaline rocks in a rift environment. Major iron oxide bodies, sulfidation and emplacement of breccia pipes are related to the alkaline plutonism. Repetitive explosive hydrothermal events produced particular hydrothermal brecciation and what seems to be economic iron oxide-copper-gold mineralization.

This chapter will cover some aspects of geochemistry, environment of emplacement and geochronology of the Lofdal area. A description of the field sampling will follow, and will close with some comments on carbonatites.

4.2.2.3.2 Geochemistry

Table 4.2.2.1.2 lists 21 representative samples collected at Lofdal. Fifteen samples were analysed for the Greater Lufilian Arc granitoid project, and six chemical analysis come from technical reports. Chemistry of only a small portion of the samples collected is available. Most rocks were slabbed for macroscopic studies; none of the mineralized samples have been assayed to date.

20% of the granitoids from the Lofdal farm fall within the midalkaline field, while 80% of them fall in the subalkaline field (Table 4.2.2.12). All midalkaline rocks make 8% of the samples. 58% are sulbalkaline and 33% are alkaline rocks. This suite of rocks is more enriched in alkaline rocks than most of the others in the Greater Lufilian Arc. Carbonatites are extremely important. They account for almost half of the total samples. The Lofdal farm subdomain is clearly dominated by subalkaline and alkaline rocks.

Table 4.2.2.12 Statistics of rock types, Lofdal farm, Namibia
The fifth column (granitoids) is the sum of underlined rock types.

Group	Rock type	Number	%	Granitoids	Groups
Midalkaline Rocks	Monzonite	1	8.33	20.00	8.33
Subalkaline Rocks	Granite	3	25.00	80.00	58.33
	Granodiorite	1	8.33		
	gabbro-diorite	1	8.33		
	Gabbro	2	16.67		
Alkaline Rocks	foid monzosyenite	3	25.00		33.33
	peridot gabbro	1	8.33		
Total		12	91.67	100.00	100.00
	Carbonatite	9			
Total		**21**			

Foliated granitic rocks are represented by **L-728***, **L-729**, **L-742** and **L-1021** the various intrusions and the mineralization. The nepheline syenite **L-1027** hosts mineralized magnetite-cemented brecia pipes. **L-740**, **L-741**, and **L-1022** come from dikes that intrude granites in different parts of the Lofdal farm. **L-1023**, **L-1025**, and **L-1032** are gabbros with various compositions and magnetite content. Some of them intrude as dikes, others are large bodies that host various other intrusions. **L-754** is an ultramafic lamprophyric rock (See Table 4.2.2.2).

Many of the rocks that were analyzed carry significant amounts of Nd, Pr, Ce, La, Nb, Zr and Y. Some of them are also enriched in Zn. Losses on ignition also tend to be high in a large portion of the samples studied (Table 4.2.2.13).

All syenites and gabbros from the Lofdal and Oas farms display a particular enrichment in zinc, and part of the alkali granites and granites that were intruded by zinc-rich rocks have it too.

Table 4.2.2.13 Chemical Analysis of Samples from the Lofdal Farm, Namibia
(complete elemental analysis are included on Table A12 in the Appendix)

Sample	SiO2	TiO2	Al2O3	Fe2O3	MnO	MgO	CaO	Na2O	K2O	P2O5	LOI	Rb	Sr	Y	Zr	Nb	Co	Ni	Cu	Zn	Ga	V	Cr	Ba	U	Th	Sc	Pb	Sm	Nd	Pr	Ce	La	Hf	Ta	Eu
Notch	50.00	1.00	15.50	6.00	0.15	2.00	5.00	4.90	5.50	0.30	2.00	200	400	60	360	40	30	16	25	85	26	100	100	1300	20	37	20	20	50	50	15	175	95	10	120	4
L-722	7.50	0.04	0.13	9.55	0.68	2.58	43.8	0.00	0.00	0.03	36.2	7	210	260	119	13	23	<6	5	37	<9	194	12	145	6	27	54		17		16	10	<12		229	
L-728*	75.06	0.16	10.35	2.83	0.14	0.22	2.20	6.61	0.86	0.06	2.04	23	140	58	212	33	<6	10	15	45	18	14	67	581	5	21	15	24	17	82	20	171	73	6	3	3
L-729	73.58	0.31	12.64	2.31	0.05	0.34	0.84	3.69	4.96	0.03	1.70	113	82	46	281	24	<6	6	6	60		<12	58	957												
L-740	56.74	0.26	18.91	5.92	0.18	0.21	1.03	6.29	4.68	0.03	6.26	170	442	26	1803	563	<6	11	8	189	42	<12	27	617	27	18	<10		9	22	72	112	36		115	1
L-741	56.63	0.47	19.54	7.23	0.44	0.80	3.09	4.14	7.21	0.11	0.91	169	548	49	640	337	<6	<6	14	164	34	14	18	1955	19	<15	<10		15	52	211	248	131		127	2
L-742	68.41	0.18	10.00	3.45	0.20	2.09	0.90	5.40	1.17	0.03	8.44	59	181	41	310	26	11	13	32	227	19	18	44	802	<6	21	<10		3	33	52	79	44		72	1
L-754	53.02	1.59	13.32	16.18	0.28	6.53	7.50	0.32	1.02	0.30	0.15	318	84	40	94	8	50	53	94	252	17	393	178	235	<6	<15	49					25	12			
L-1021	72.02	0.43	12.86	3.47	0.05	0.24	1.10	4.37	4.02	0.07	0.53	83	92	84	464	33	<6	8	5	29	17	<12	250	1355	<6	18	<10					143	61			
L-1022	54.76	0.44	20.41	5.90	0.20	0.33	1.95	4.97	7.25	0.13	2.78	189	616	24	767	249	7	<6	11	171	36	14	<12	629	8	<15	<10		3	28	48	61	19		94	0
L-1023	47.51	0.82	15.70	11.39	0.21	7.63	11.0	2.78	0.87	0.09	2.31	19	177	23	45	5	51	86	11	157	19	246	354	223	<6	<15	42					33	20			
L-1024a	7.58	0.07	0.57	9.33	0.79	5.76	37.2	0.03	0.15	0.23	38.8	6	335	62	9	44	28	21	177	59	<9	23	<12	115	19	20	49	2	50	543	179	2058	1583	0	n.d.	7
L-1024c	5.56	0.06	0.20	9.37	0.84	6.08	39.5	0.01	0.04	0.23	38.7	10	325	92	18	31	29	11	116	29	<9	24	<12	99	20	18	49					1786	1383			
L-1025	42.06	1.06	1.26	21.42	0.77	2.76	17.4	1.61	0.56	3.85	7.40	30	1546	50	1312	1425	42	10	29	207	12	334	106	214	86	20	33	5	28	183	47	396	176	10	34	8
L-1027	55.06	0.81	15.77	5.91	0.27	2.32	3.60	4.38	6.88	0.23	3.58	177	429	37	621	220	14	42	25	134	24	45	174	1043	<6	<15	<10			58	136	239	72		94	2
L-1032	46.04	1.99	15.47	14.07	0.33	6.80	9.26	3.22	0.75	0.42	1.94	10	322	48	132	9	47	45	26	163	15	345	218	299	<6	<15	40		109	42	61	<12	40	4	23	1

4.2.2.3.3 Description of outcrops from the Lofdal farm

Field notes, corrected with results of geochemistry and geochronology are included in Appendix A67. Coordinates of geological stations and sampling sites are also in Appendix A18. Fig 4.2.2.13 is a topographical map of the sampling sites and geological stations. Fig 4.2.2.14 shows greater detail and coordinates of the sampling area. The small map on the lower left portion of the figure shows relative location of the various study areas. Samples with chemical analysis have been underlined. Dated samples are marked with a star.

4.2.2.3.3.1 Dissolution of silicates in granitoids

Many granitoids in the Lofdal farm display severe dissolution effects. Both quartz and feldspars have been partially dissolved out of the rocks, to produce a "spongy" texture[1]. Sample **L-726** is one of the clearest examples of that feature. Fig 4.2.2.14 shows its location. The sample is a coarse- to fine-grained granitoid with abundant myarolitic cavities filled by brown, druzy hematite. The rock is spongy, has extremely light density, and shows evidence of massive silicate leaching. Part of the vugs were filled by specularite. It is one of many similar rocks in the environs. Carbonatite bodies and dikes, as well as ultramafic dikes, outcrop very few meters away; quartz pods[2] and quartz-feldspar pegmatites with gossanous vugs are also present in the area.

The partial corrosion of the granitoids seems to have taken place in a hyperalkaline environment, related to the emplacement of the carbonatites, under CO_2 saturation. This is a working hypothesis.

Silica etching process described for the Lofdal farm were observed in other locations during the Greater Lufilian Arc granitoid project. Granitoid "corrosion" was observed in the Kafue Flats area of Zambia. The etched granitoids in that case are syenites. Carbonatites have not been reported there, but the host rocks are Katangan carbonates. Quartz pods and small gabbroic bodies are ubiquitous. Abundant massive iron oxide bodies and evidence of iron oxide-copper-gold mineralization was observed in the environs.

[1] Vugginess in calcalkaline volcanics is a feature commonly sought during the exploration of mineral deposits in high sulfidation environments. "Spongy" rock and "vuggy silica" are terms used to describe the textures of sub-volcanic and volcanic rocks that have been etched in highly acid environments produced by the oxidation of pyrite. Feldspars and most of the other rock constituents except for quartz are leached. The corrosion features observed at the Lofdal farm are different.

[2] The quartz pods are described on the chapter on iron oxide-copper-gold mineralization.

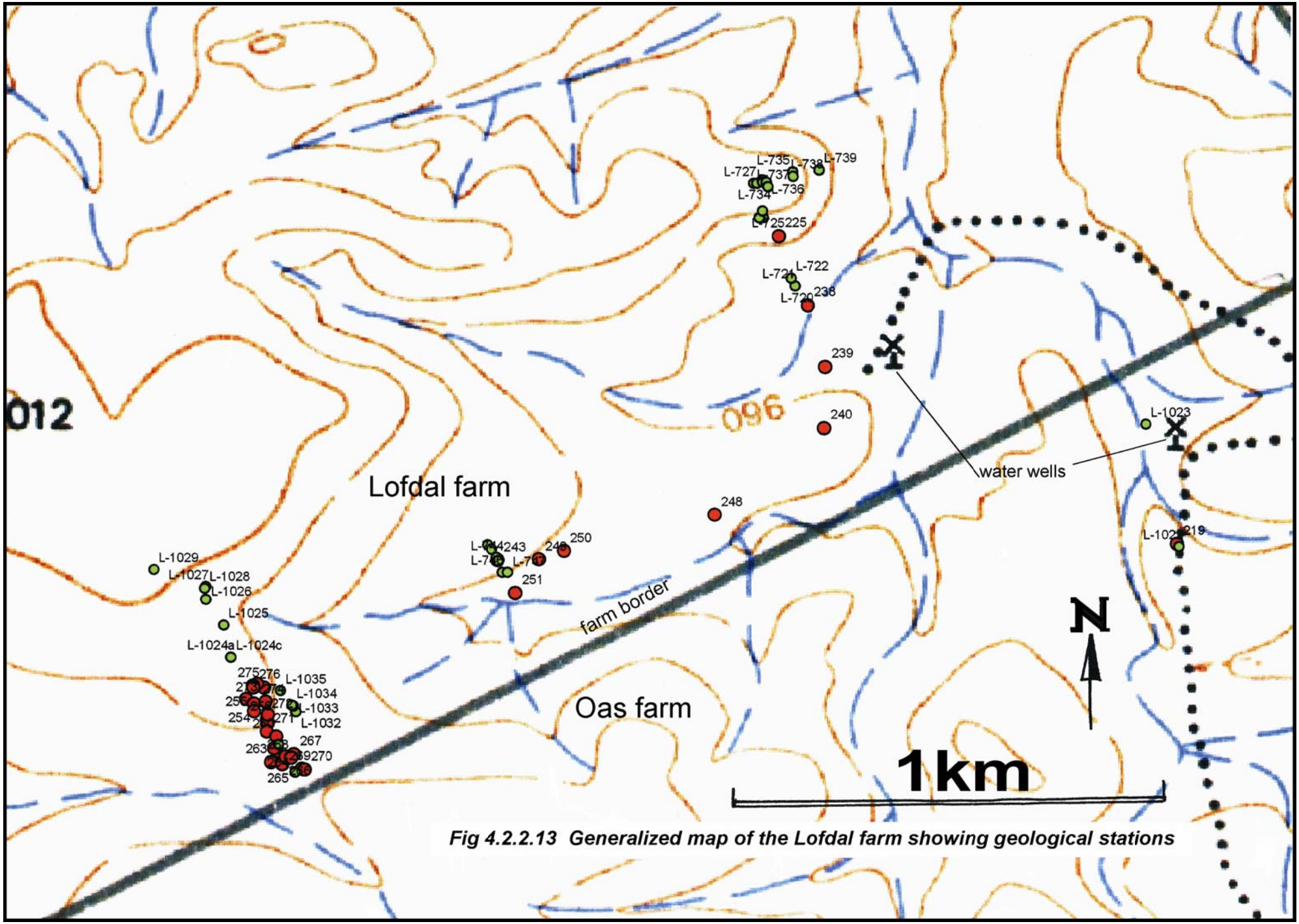

Fig 4.2.2.13 Generalized map of the Lofdal farm showing geological stations

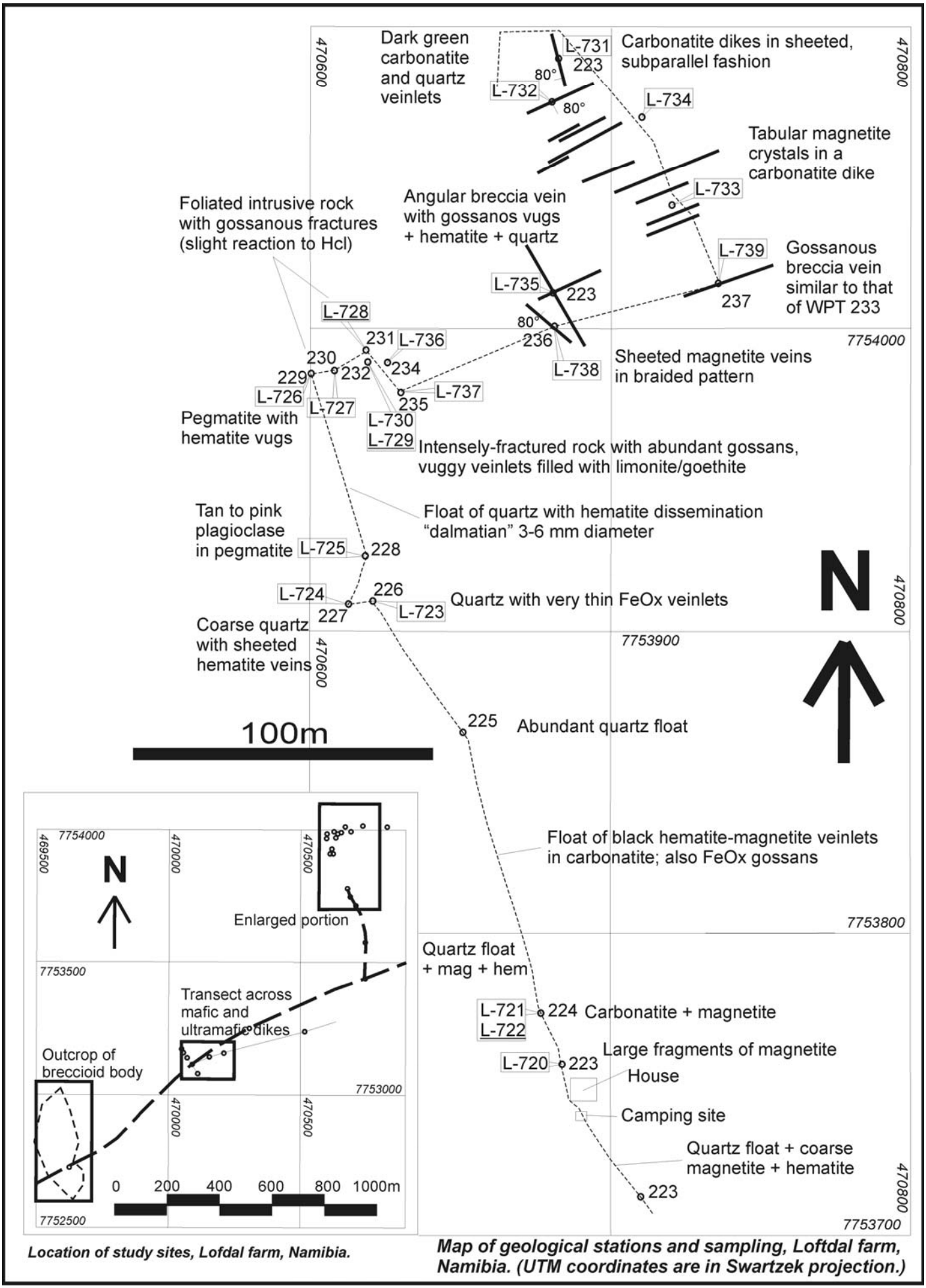

Location of study sites, Lofdal farm, Namibia.

Map of geological stations and sampling, Loftdal farm, Namibia. (UTM coordinates are in Swartzek projection.)

Fig 4.2.2.14

4.2.2.3.3.2 Carbonatite dikes and iron oxide-copper-gold mineralization

Numerous mafic dikes and carbonatites were observed in the easternmost portion of the Lofdal farm (Fig 4.2.2.14). Carbonatites outcropped as both dikes and large bodies. Several of the carbonatites are associated with magnetite and sulfide mineralization. The map of Fig 4.2.2.14 shows the main geological stations and sampling sites. Field descriptions are included in Appendix A67.1.

Several dike swarms were observed and sampled at the Lofdal farm, many of which are carbonatitic in composition. All of them have a NE-SW general strike, and roughly sub-vertical dips. Many of the dikes outcrop for over a hundred meters. Their widths vary widely from a few centimeters to over six meters. Some of such dikes might be responsible for iron oxide-copper-gold mineralization. A carbonatite diatreme was found along strike one of the dikes; and magnetite-sulfide cemented, coarse-grained polymictic breccias make most of the diatreme. These dikes intersect a series of quartz-feldspathic granitic gneisses (**L-742** and other samples). Carbonatite dikes run sub-parallel to other mafic and ultramafic dikes swarms. Some compositions of dikes associated with carbonatites include: gabbro, alkali gabbro, syenite, alkali granite, phonolite, tinguaite and lamprophyres of various types. They extend for dozens of kilometers along strike, as shown on the map by Frets, 1969. These dikes sometimes produce anomalous radiometric signatures due to their high thorium content. According to Niku-Paavola, Siegfried, & Mariano, 2002, thorium content may reach up to 14.4% weight percent.

An example of the type of features observed is described below. Sheeted magnetite veins in braided patterns with abundant sulfides were identified. One of them is represented by sample **L-738**. A fine-grained, foliated, pink granitoid was intersected by braided magnetite + hematite + quartz + sulfide veinlets that vary in width from 1.0 to 0.3 cm. They intersect each other at uniform angles, making a trellis pattern, as shown on Fig 8.58. The vein system is approximately one meter wide. Almost every single one of the veinlets in the vein system contains gossanous vugs with weathered sulfides. Magnetite in some of the veinlets is partially martitized. The surface expression of the vein system is a linear gossan. The vein system extends for at least twenty meters along strike. Many sub-parallel vein systems occur in the region. The average foliation of the host rock is 130/76°N. The same orientation and similar features are often seen around this site. Fig 8.58 show two slabs from the sample, to illustrate the textures of mineralization. The rock is very similar to rocks from around the Hook Granite batholith, Zambia and to mineralized stockworks from the Tevrede iron oxide-copper-gold deposit in Namibia.

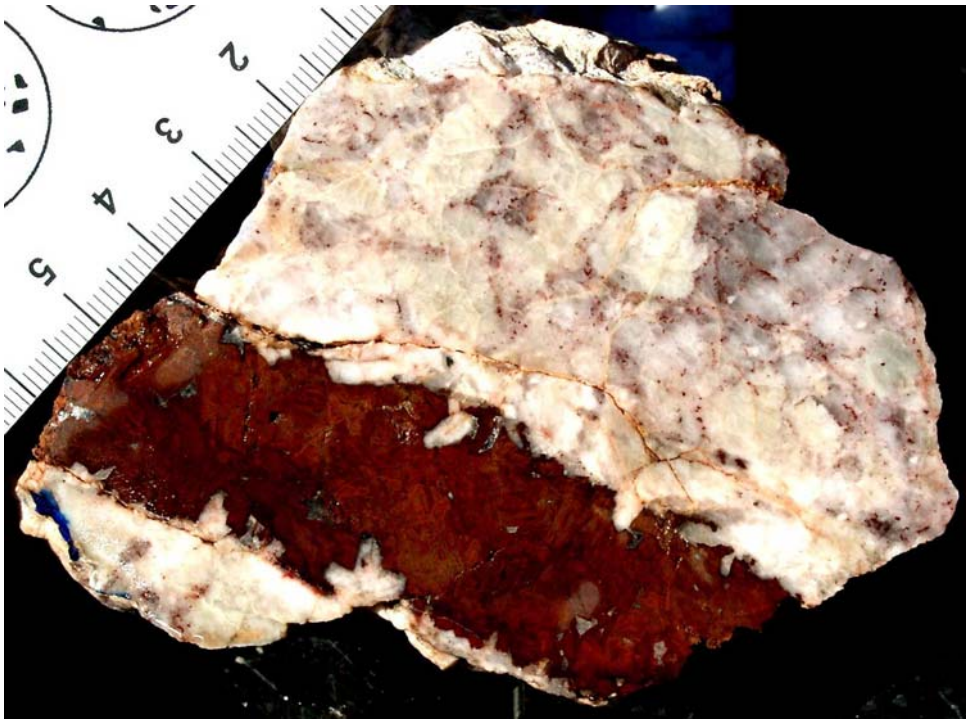

Fig 4.2.2.16 Photograph of a slabbed carbonatite dike from the Lofdal farm, Namibia*. The host is a coarse-grained, foliated alkali granite. Note the irregular borders of the dike, with fragments of the crystals from the host rock extending towards the dike. There are chill margins from the dike into the granitoid. Millimeters for scale.*

Fig 4.2.2.17 Photograph of a carbonatite dike with subparallel internal zoning and magnetite*. This is one of the iron-rich carbonatite dikes from the Lofdal farm, Namibia. There is abundant sulfidation that accomanies some of the massive iron oxides in the dikes and around them. The composition of these dikes is indicated on Table 4.2.2.16. For scale, card is ten centimeters long.*


2002/10/13 11:24am


2002/10/13 9:58am

(Photographs from the previous page)

Fig 4.2.2.18 (upper photo) Close-up view of a magnetite-rich massive carbonatite body, Lofdal farm, Namibia*. Sample* ***L-722*** *came from this same intrusive body. Note the characteristic carbonate surface dissolution features. The white spots are the remains of HCl tests. Some bodies like this contain abundant gossans after sulfidation. They are described on the field notes and located on Fig 4.2.2.14. Chemical analysis of this sample is included on Table 4.2.2.16.*

Fig 4.2.2.19 (lower photo) Photograph of two subparallel carbonatite dikes. *One of them was sampled and makes Fig. 4.2.2.16. The composition of these dikes is indicated on Table 4.2.2.16.*

4.2.2.3.3.3 Cross Section Through Series of Ultramafic Dikes

Many sub-parallel mafic and ultramafic dikes were observed in the Lofdal farm. A series of seven sub-parallel dikes was studied along a 140 m long transect that ran perpedicular to the main strike of the dikes (Fig 4.2.2.15 and Table 4.2.2.14). In other locations, dikes are closer together and very abundant. See field photos taken towards the west on Fig 4.2.2.17 and 4.2.2.19. The location of the typical cross section is indicated on Fig 4.2.2.14. Detailed field descriptions are included in Appendix A67.1 and Table 4.2.2.14.

L-742 is the host rock to the series of dikes studied. Unfortunately, samples **L-743**, **L-744**, **L-745**, **L-746** and **L-747** were not analysed. These were other dikes, including three carbonatites (**L-743**, **L-745** and **L-746**). Dozens of satellite dikes run subparallel to the main ones that were sampled.

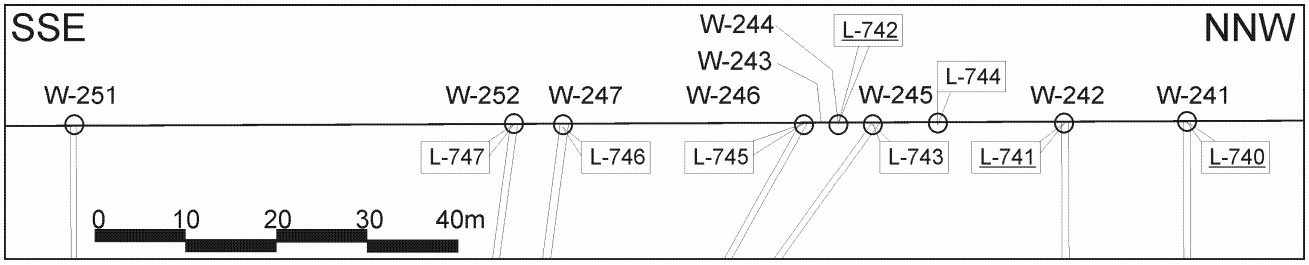

Fig 4.2.2.15 Cross section through mafic and ultramafic dikes, Lofdal farm, Namibia*. This section is located on Fig 4.2.2.14. More description in text.*

Table 4.2.2.14 Main features of cross section across mafic, ultramafic and carbonatitic dikes, Lofdal farm, Namibia
(Underlined samples were analysed)

WPT	Sample	Composition	Additional description	Orientation	Width	Iron oxide	Other
241	L-740	Peraluminous sodic ferriferous trachy phonolite	Very fine-grained, glassy, gray-reddish to dark pink-brown; no reaction to HCl. It has conchoidal fracture and sharp edges.	056°90°	1 m	w/ diss fine magnetite	
242	L-741	Metaluminous potassic ferriferous trachy phonolite	Magnetic, dark gray to black, subvolcanic. With extremely fine-grained matrix, plagioclase porphyries, open vacuoles; does not react to HCl; chloritization. Nepheline blades 2-3mm wide, range to 2cm long.	078°90°			
243		Carbonatite	Black to dark brown with hematitic banding along the foliation, coarse hematite clusters and gossanous texture.	60°/78°S		Very abundant iron oxides	
244	L-742	Metaluminous sodic magnesian biotite granite	Very fine-grained, medium gray, foliated, with slightly magnetic character.				
245	L-743	Carbonatite	Brown, very magnetic, with internal flow banding.	085/52°S	1m	abundant earthy goethite after sulfides	
246	L-745	Carbonatite	Strongly magnetic, very fine-grained, medium gray; internal flow banding; intersects L-742. Alteration halo around dike; sample has 2 “quenched” margins.	095/49°S	4-5 cm	none visible	
247	L-746	Carbonatite	Weathering surfaces show clusters of iron oxide-rich substance that do not weather as much. The surface is brown/yellow and has a very irregular texture like lapiez corrosion in karstic environments.	064/83°S		abundant braided black magnetite bodies that contain sulfides	minimun length = 400m
251		Carbonatite	With abundant iron oxide alteration and red-rock alteration in the host rocks.	Subvertical	25-30 cm		
252	L-747	Quartz vein	With red iron oxide stains, thin red-filled joints, and some black-filled joints.	050/90°	10-15 cm		

4.2.2.3.3.4 Magnetite-Cemented, Polymictic Hydrothermal Breccia that Makes a Diatreme

A magnetite-cemented diatreme was discovered at the Lofdal farm, along one of main farm roads. It is located on a saddle, as shown on Fig 2.2.2.20, near the easternmost corner of the farm (See inset of Fig 4.2.2.14, and 4.2.2.13). The diatreme seems to have been a blow-up of a carbonatite dike. Massive magnetite and coarse sulfides cement the polymictic angular fragments of the diatreme. Fig 4.2.2.20 is a map of the diatreme. Field descriptions of geological stations and sampling sites are included in Appendix A67.2.

The major portion of the diatreme is made by highly magnetic, coarse-grained, polymictic, angular hydrothermal breccias with gossanous surfaces. Many of the clasts display corrosion edges and hydrothermal alteration. The sulfide portion of the matrix was completely leached, to a point that no fresh sulfides are present. Coarse massive, gossanous magnetite was observed lying all around over the diatreme. Typical descriptions and photographs of rocks from the diatreme are included in the chapter on iron oxide-copper-gold mineralization.

Two types of rocks were identified as hosts to the diatreme (Fig 4.2.2.20). The first is a coarse-grained, metaluminous mesocratic potassic ferriferous nepheline syenite, represented by **L-1027**. It has abundant submillimetric circular vugs and contains high K, Zr, Zn and Nb. It produced a 3.58% loss on ignition. The other host rock is a massive, very dark, green to black, foliated, metaluminous mesocratic sodic ferriferous undersaturated olivine gabbro, represented by **L-1032**. The average dip of its foliation is 65°SE. The rock has similar chemistry to **L-754** and **L-1023**.

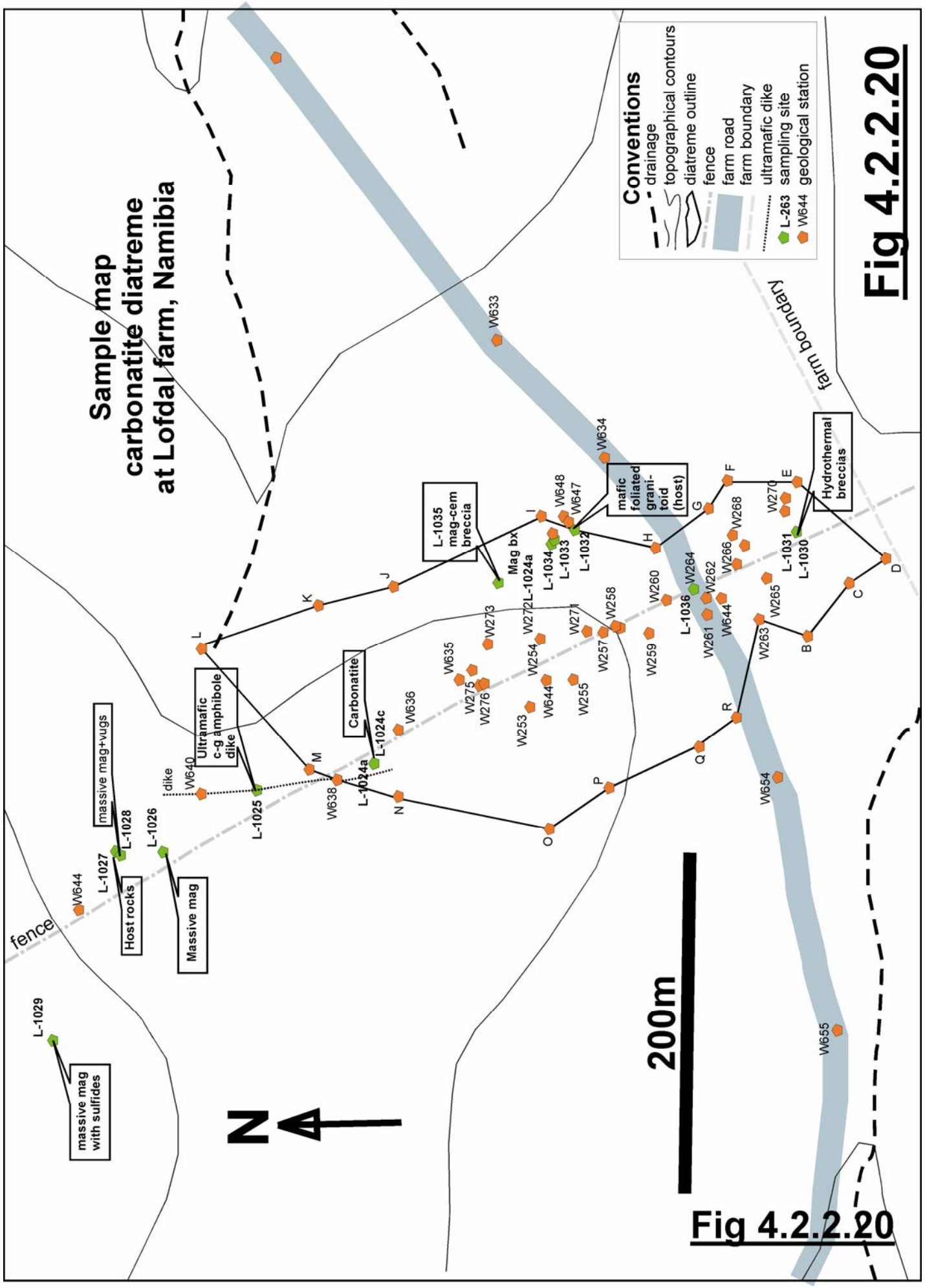
Sample map
carbonatite diatreme
at Lofdal farm, Namibia
Conventions
drainage
topographical contours
diatreme outline
fence
farm road
farm boundary
ultramafic dike
L-263 sampling site
W644 geological station
Fig 4.2.2.20
farm boundary
fence
dike
Ultramafic c-g amphibole dike
Carbonatite
L-1024c
L-1024a
L-1025
L-1026
L-1027
L-1028
massive mag+vugs
Host rocks
Massive mag
L-1029
massive mag with sulfides
L-1035 mag-cem breccia
Mag bx
L-1034
L-1033
L-1032
mafic foliated granitoid (host)
L-1036
L-1031
L-1030
Hydrothermal breccias
W633
W634
W654
W655
W635
W636
W638
W640
W644
W647
W648
W253
W254
W255
W257
W258
W259
W260
W261
W262
W263
W264
W265
W266
W268
W270
W271
W272
W273
W275
W276
A
B
C
D
E
F
G
H
I
J
K
L
M
N
O
P
Q
R
200m
N

Fig 4.2.2.20

A mafic dike with peculiar texture was observed on the northwestern portion of the diatreme, as shown by sample **L-1025** on Fig 4.2.2.20 (waypoints W636, W639, and W640). It is a subvertical, black, magnetic, metaluminous sodic ferriferous undersaturated olivine gabbro dike, with extremely large radial pyroxene crystals. The rock has a decimetric, radial, conic crystal structure. It might indicate paleo-verticality at the time of emplacement. It trends in a general N-S direction. See photo on Fig 4.2.2.21. The sample has anomalous enrichement in U, Ti, P, Zn and V; very high Sr, Sr and Nb; low Al_2O_3, K, Na and Rb. It produced a 7.4% loss on ignition. Its copper content is also significant, and it contains 86.4 ppm uranium. The dike is two meters wide at times, but thins; it was followed for at least two hundred meters. The chemistry of this dike will be discussed along with carbonatitic dikes in the next few pages.

Fig 4.2.2.21 Large fans of elongated amphibole crystals in an ultramafic dike, Lofdal farm, Namibia*. The crystals are sometimes up to thirty centimeters long. Site of sample* ***L-1025****. Analysis of this sample is included on Table 4.2.2.16. Steel scratcher is 15 cm long.*

4.2.2.3.3.5 Abandoned Lofdal Mine

Several samples were collected from the abandoned Lofdal mine at UTM 0466547/7755980, (Fig M21). These are numbered **L-749** to **L-753**. There is very little to see at the mine site. The mine exploited subvertical rare earth-bearing veins and pegmatites striking 075°. That orientation is sub-parallel to most of the dike swarms in the region, as discussed by Frets, 1969. Among the abandoned machinery was a Wilfley table, some crushers, water pumps, storage equipment, as well as drilling and pumping compressors. Many exploration trenches and pits were found and they follow the main strike of the system. Abudant iron oxide and some charcoal lies on the ground around the pits.

4.2.2.3.3.6 Carbonatite Dikes

4.2.2.3.3.6.1 Introduction

Maybe the most relevant types of rocks present at the Lofdal farm are its numerous dikes of mafic, ultramafic and alkaline nature. Among the dikes, carbonatites constitute a very important portion. The dikes have a clear economic relevance, especially because they might contain significant rare earth element or base metal-precious metal accumulations. This sub-chapter will discuss some aspects of carbonatites at the Lofdal farm.

Many carbonatite dikes and intrusive bodies were observed and sampled at the farm. Several of the carbonatites are associated with magnetite and sulfide mineralization. Evident iron oxide-copper-gold mineralization was observed in at least two different sites. Fig 8.58 was taken from a mineralized fracture system conformed by interweaved quartz-magnetite-sulfide veinlets. Abundant gossans that remain after leaching of sulfides including chalcopyrite were sampled from each of the different sites. Copper carbonate and copper sulphate stains were observed in some cases. Free gold is thought to be present in gossans at most of the mineralized sites.

Several dike swarms were observed and sampled at the Lofdal farm, many of which are carbonatitic in composition. All of them have a NE-SW general strike, and roughly sub-vertical dips. Many of the dikes outcrop for over a hundred meters. Their widths vary widely from a few centimeters to over six meters. Some of such dikes might be responsible for iron oxide-copper-gold mineralization. A carbonatite diatreme was found along strike one of the dikes; and magnetite-sulfide cemented, coarse-grained polymictic breccias make most of the diatreme. These dikes intersect a series of quartz-feldspathic granitic gneisses (**L-742** and other samples). Carbonatite dikes run sub-parallel to other mafic and ultramafic dikes swarms. Some compositions of dikes associated with carbonatites include: gabbro, alkali gabbro, syenite, alkali granite, phonolite, tinguaite and lamprophyres of various types. They extend for dozens of kilometers along strike, as shown on the map by Frets, 1969. These dikes sometimes produce anomalous radiometric signatures due to their high thorium content. According to Niku-Paavola, Siegfried, & Mariano, 2002, thorium content may reach up to 14.4% weight percent.

4.2.2.3.3.6.2 Geochemistry

Table 4.2.2.16 presents chemical analysis of three carbonatites collected at the Lofdal farm, along with six samples compiled from reports on carbonatitic dikes in the environs, a single carbonatite from the Hook Granite batholith, and seven other dikes that are associated with carbonatites at the Lofdal farm. They vary widely in major oxide and trace element composition. Fig 4.2.2.22 is a logarithmic plot of the carbonatites for visual comparison. Part of the carbonatites were plotted on Figs 4.2.2.2, 4.2.2.4 and 4.2.2.6 along with the rest of the samples for comparison. Note on 4.2.2.6 that the carbonatites produce a linear trend.

Dike chemistry has a wide range of compositions, as shown on Table 4.2.2.15 and Fig 4.2.2.22. Most of the samples in the suite have high values for Fe2O3 and MnO, and low Na and K. Carbonatites obviously have high values for CaO. The only common trait between carbonatites sampled at Lofdal is that they have high CaO and Y content; the rest of the elements vary widely in a large spectrum of values. Scandium is high, but not in all cases. Many samples from the suite of carbonatites and carbonatite dikes from Lofdal are enriched in Cu. Ce and La are enriched in some but not all rocks.

In the case of samples labeled LR, the total seems to have been recalculated to 100% without CO2 or water content. Maybe the values for major oxides are not readily comparable to those coming from the rest of the Lofdal region. Anyhow, values for CO2, water and other volatiles were not reported for the LR or AM samples.

4.2.2.3.3.6.3 Economic Mineralization in Carbonatite Dikes

From the data available, part of the carbonatite dikes are enriched in the light rare earths, but there is no information on the heavy rare earth content for six samples of carbonatite dikes from Lofdal. Evidence cited by Mariano, 2001 for studies of similar dikes from farms Lofdal 491 and Bergville 490, indicates that their Tb, Eu, and Dy content may be quite high. Based on cathodoluminiscence spectra, he states that the type of xenotime found in carbonatite vein at the Lofdal farm “could be a good source material for Y, Tb, Eu and other mid atomic-number and heavy lanthanides”. Y is anomalously enriched in all the carbonatites sampled, except for **L-411**, as shown on Table 4.2.2.16. Ce and La are enriched in part of them and in some of the mafic dikes sampled.

Mariano, 2001 states that sample **AM1** was collected from a ferruginous carbonatite. No other elemental data is available. Its high Y value derives from xenotime mineralization. Studies done by Mariano on the sample

indicate that it contains “an appreciable quantity of Eu”, but the actual figures are not given. **AM1** contains at least 2% weight xenotime, and other minerals include: monazite, apatite, parisite and thorite. Mariano states that xenotime is probably amenable to effective concentration and separation from other minerals including thorite.

According to Mariano, 2001, “primary crystallization of xenotime in a carbonatite is rarely encountered, making the Lofdal occurrence very unusual. The mineral churchite ($YPO_4 \cdot 2H_2O$) which occurs in the Mount Weld laterite of Australia is a product of supergene weathering. It is fine-grained and inextricably associated with ferric iron oxides and other deleterious mineral components, while the Lofdal xenotime is relatively coarse and should be amenable to concentration.” He states that Eu content in that xenotime should be on the weight percent level. In other current deposits, minerals with that element contain less than 0.05 weight percent Eu.

4.2.2.3.3.6.4 High heat production properties in some of the dikes

Part of the carbonatite and mafic dikes of the Lofdal farm carry high values of thorium, as indicated on Table 4.2.2.15. If the areal concentration of those dikes is high, they may significantly increase the flow of heat, and power large hydrothermal fluid flow cells. Table 4.2.2.15 shows the heat producing value for dikes in the Lofdal farm at the time of emplacement. The heat flow for the entire region due to the presence of these dikes was evidently high, and that does not take into consideration the thermal anomaly produced by doming and rifting. Long-lived flow of hydrothermal fluids were probably an important component of the iron oxide-copper-gold systems observed in the Khorixas Inlier. Thorium-rich dikes may even be bulk-mined for their thorium content in areas of high dike concentration.

Table 4.2.2.15 High heat producing rocks in the Lofdal farm, Namibia; estimated at 750Ma.

Sample	Uranium	Thorium	Potassium	Time	Heat producing value	U/Th
	(PPM)	(PPM)	(%)	(Ba)	(muW-m3)	
L-1024a	19.00	20.0	0.15	0.75	1.973	0.950
L-1024c	20.00	18.0	0.04	0.75	1.849	1.111
L-1025	86.4	19.5	0.56	0.75	4.017	4.423
LR25	24	7730	0.01	0.75	535.017	0.003
LR23	15	130	0.10	0.75	9.450	0.115
LR20	0	36	0.04	0.75	2.494	0.000
LR5	26	2347	0.53	0.75	163.080	0.011
LR4	28	1593	0.04	0.75	110.953	0.018
AM-1	11	1019		0.75	70.777	0.011

Fig 4.2.2.22 Major oxide logarithmic plot of carbonatite samples, Lofdal farm, Namibia

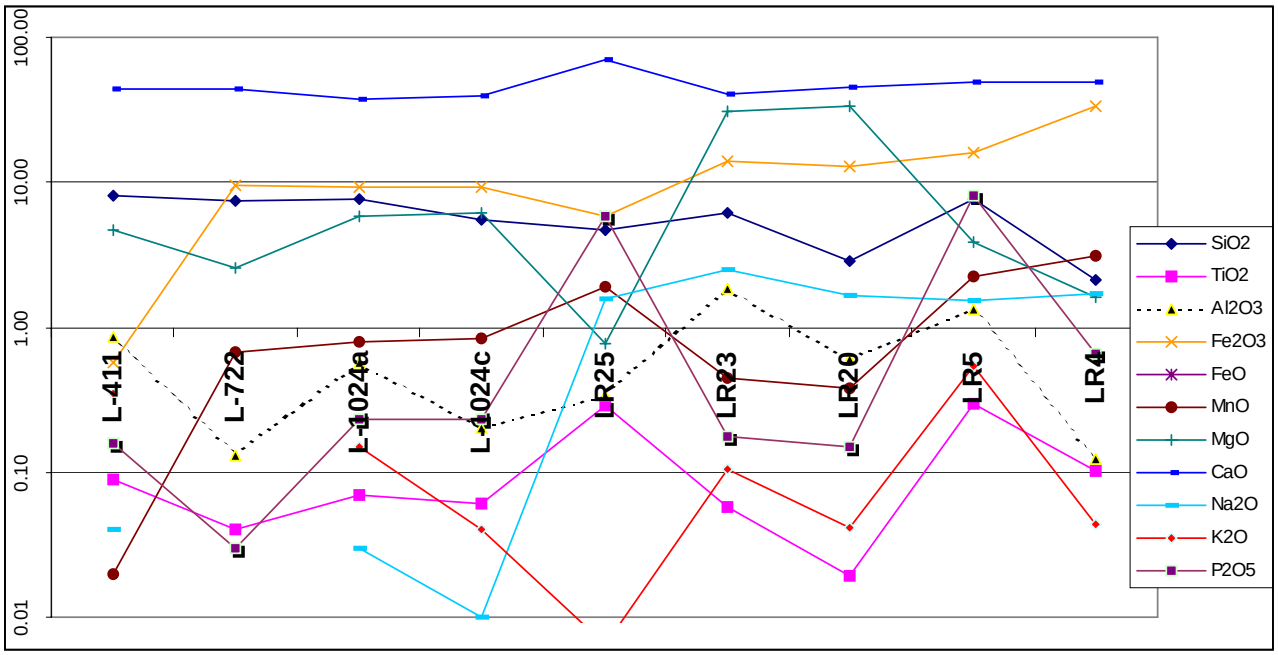

Table 4.2.2.16 Chemistry of carbonatites and dikes, Lofdal farm, Namibia
(Major oxide values are expressed in percentage, values for all other elements are in parts per million.)

Sample	Notch	L-411	L-722	L-1024a	L-1024c	LR25	LR23	LR20	LR5	LR4	AM-1	L-1025	L-740	L-741	L-1023	L-1022	L-1027
SiO2	50.00	8.09	7.50	7.58	5.56	4.673	6.138	2.875	7.666	2.133		42.06	56.74	56.63	47.51	54.76	55.06
TiO2	1.00	0.09	0.04	0.07	0.06	0.29	0.06	0.02	0.30	0.10		1.06	0.26	0.47	0.82	0.44	0.81
Al2O3	15.50	0.85	0.13	0.57	0.20	0.34	1.84	0.60	1.32	0.12		1.26	18.91	19.54	15.70	20.41	15.77
Fe2O3	6.00	0.57	9.55	9.33	9.37	5.85	14.0	12.9	16.1	33.4		21.42	5.92	7.23	11.39	5.90	5.91
MnO	0.150	0.02	0.68	0.79	0.84	1.89	0.45	0.38	2.24	3.12		0.77	0.18	0.44	0.21	0.20	0.27
MgO	2.00	4.72	2.58	5.76	6.08	0.76	30.5	33.1	3.89	1.61		2.76	0.21	0.80	7.63	0.33	2.32
CaO	5.00	43.80	43.77	37.24	39.51	70.8	40.6	45.0	48.8	48.6		17.44	1.03	3.09	10.97	1.95	3.60
Na2O	4.90	0.04	0.00	0.03	0.01	1.58	2.47	1.67	1.51	1.71		1.61	6.29	4.14	2.78	4.97	4.38
K2O	5.50	0.35	0.00	0.15	0.04	0.01	0.10	0.04	0.53	0.04		0.56	4.68	7.21	0.87	7.25	6.88
P2O5	0.30	0.16	0.03	0.23	0.23	5.82	0.18	0.15	8.09	0.66		3.85	0.03	0.11	0.09	0.13	0.23
LOI	2.00	41.87	36.24	38.75	38.66							7.40	6.26	0.91	2.31	2.78	3.58
Total		100.56	100.52	100.50	100.56							100.19	100.51	100.57	100.28	99.12	98.81
Rb	200	6	7	6	10	1	6	0	19	0		30	170	169	19	189	177
Sr	400	87	210	335	325	6765	941	1166	1669	1054	1839	1546	442	548	177	616	429
Y	60	4	260	62	92	12358	2633	152	4033	2761	8630	50	26	49	23	24	37
Zr	360	17	119	9	18	65	327	97	130	44		1312	1803	640	45	767	621
Nb	40	3.0	13.0	44.1	31.0	128	152	22	181	598		1425.4	563.0	337.0	5.0	249.0	220.0
Co	30	<6	23	28	29	167	71	16	90	44		42	<6	<6	51	7	14
Ni	16	<6	<6	21	11	58	53	44	46	21		10	11	<6	86	<6	42
Cu	25	<6	5	177	116	166	41	31	89	0		29	8	14	11	11	25
Zn	85	16	37	59	29	899	53	79	45	99		207	189	164	157	171	134
Ga	26	<9	<9	<9	<9	0	0	0	0	-5		12	42	34	19	36	24
V	100	<12	194	23	24	191	62	115	36	0		334	<12	14	246	14	45
Cr	100	<12	12	<12	<12	50	86	85	114	0		106	27	18	354	<12	174
Ba	1300	23	145	115	99	469	25	32	393	0	114	214	617	1955	223	629	1043
U	20	<6	6.00	19.00	20.00	24	15	0	26	28	11	86.4	27.00	19.00	<6	8.00	<6
Th	37	<15	27.0	20.0	18.0	7730	130	36	2347	1593	1019	19.5	18.0	<15	<15	<15	<15
Sc	20	45	54	49	49	7	19	0	0	0		33	<10	<10	42	<10	<10
Pb	20			2.4		0	71	10	91	438	330	4.8					
Sm	50		17.16	50.29		673	0	0	655	0		27.7	8.750	14.68		2.638	
Nd	50			543.29		1335	0	0	1734	2003	748	183	22.20	51.69		27.54	58.35
Pr	15		15.61	178.89		0	88	0	486	0		47.1	71.88	210.8		47.69	136.1
Ce	175	12	10	2058	1786	3341	0	0	4909	6950	1726	396	112	248	33	61	239
La	95	<12	<12	1583	1383	2342	32	37	3846	5436	1061	176	36	131	20	19	72
Cs	3			0.06		0	0	25	18	3		0.39					
Hf	10			0.11		8	13	0	7	7		10.1					
Ta	120		229.3	n.d.		35	449	42	75	2199		33.6	114.8	127.0		94.38	94.25
As	100			0		0	24	6	49	93	78						
Se				0													
Eu	4			7.27								8.30	0.500	1.813		0.375	1.663
Gd	30			28.38								21.9					
Tb	5			3.20								2.59					
Dy	20			14.82								13.0					
Ho	3			2.54								2.12					
Er	9			6.75								5.37					
Tm	35.5			1.02								0.85					
Yb	7.5		0.263	7.22								7.25	0.138	1.863			1.063
Lu	1.6		0.863	1.10								1.48	0.838	1.100		0.763	0.838
Be						0	0	0	0	0							
Mo						75	5	2	21	74							
Sn						27	0	0	0	12							
Sb						3	0	0	73	0							
W						368	109	14	124	137	183						

Source of samples:
L-411: Hook Granite batholith, Zambia, this document.
L-722, **L-740, L-741**, **L-1022**, **L-1023**, **L-1024a**, **L-1024c**, **L-1025**, **L-1027**: Lofdal farm, Namibia, this document.
LR4, **LR5**, **LR20**, **LR23**, **LR25**: Lofdal and Bergville farms, Namibia, (Niku-Paavola et al., 2002).
AM-1, Lofdal farm, Namibia,
Types of samples:
L-740, **L-741**, **L-1022**, **L-1023**, **L-1025**, **L-1027**: mafic and ultramafic dikes.
AM-1, **L-411**, **L-722**, **L-1024a**, **L-1024c**, **LR4**, **LR5**, **LR20**, **LR23**, **LR25**: carbonatites.

4.2.2.3.4 Environment of Emplacement

All rocks from the Lofdal farm that were analysed display anorogenic character[3]. Several of the methods to evaluate environment of emplacement indicate within-plate origin for them (Table 4.2.2.2). From the evidence available, the basement granites, the undersaturated olivine gabbros that host a carbonatitic diatreme, and

[3] Whalen's analysis for samples **L-1023**, **L –1032** and **L-754** is not valid, because the procedure was designed for granitoid rocks

the numerous carbonatitic, midalkaline, alkaline and ultramafic rocks from Lofdal formed in a continental epeirogenic uplift environment followed by incipient rifting processes. Multiple recycling of continental crust with mantle input has probably taken place during the Proterozoic.

4.2.2.3.5 Geochronology

A single sample was dated from the Lofdal farm during this project. Zircons from sample **L-728** were dated using the U-Pb SHRIMP II method at the ANU, to produce an preliminary age of 1750±5 Ma. Complete geochronological data is not available at the time of writing this document. Fig A38 is an event diagram with all radiometric ages available from the Khorixas Inlier.

L-728 is part of the Base Granite B of Tables 4.2.2.7 ad 4.2.2.9. It was collected in the easternmost portion of the Lofdal farm, from a fine-grained, banded, dark pink to red-brown, fine-grained, metaluminous, subleucocratic sodic ferriferous granite. Similar foliated granites host most of the younger intrusives and part of the mineralization at the Lofdal farm. **L-742**, that hosts the carbonatite dikes at the site of the transect has almost the same chemistry as **L-728**. **L-738** illustrated on Fig 8.58 has the same physical features of **L-728** and is located approximately 70 meters away from it.

4.2.2.3.6 Conclusions

Alkaline and midalkaline rocks predominate in the Lofdal farm. They intruded a series of ~1750 Ma foliated granites. A carbonatite diatreme intruded foliated ultramafic rocks and nepheline syenites. All of these rocks were emplaced in anorogenic continental extensional environments

N70°E-trending dike swarms were present in most of the Lofdal farm. Many dikes of widely varying compositions were found during fieldwork. Some of them are carbonatitic, ultramafic, peralkaline and lamprophyric. It is extremely difficult to identify the various lithologies and their associated minerals in the field.

The effects of severe etching processes in granitoids by carbonatitic corrosion were seen throughout the Lofdal farm.

Zinc enrichement in many syenites, potential IOCG mineralization associated with carbonatites and at least one diatreme, as well as rare earth mineralization associated to alkaline dikes and carbonatites are the economic mineralization observed.

4.2.3 OTHER SMALL OUTCROPS IN NAMIBIA AND BOTSWANA

4.2.3.1 INTRODUCTION

4.2.3.2 MESOPOTAMIE FARM, NAMIBIA

4.2.3.2.1 Introduction

The Mesopotamie 504 farm is located W of the Lofdal farm. It lies outside of the Khorixas Inlier, in a separate, fault-bound block (Fig M20). Various types of granites, including granites with graphic textures occur at the farm and seem to be responsible for copper mineralization in the Copper Vallei deposit. Part of the granites has been metamorphosed into gneisses. Most of the granitoids intrude a series of metapelitic (or metavolcanic?) schistose rocks; in a few cases, the basement was made of gneissose granitoids.

Mineralization observed at the Mesopotamie farm conforms to the models of iron oxide-copper-gold deposits. A geological model, with maps and samples of the mineralized rocks is herein presented. Five representative samples were analyzed and they are listed on Table 4.2.3.1. Chemistry of these rocks was plotted on Figs 4.2.3.1 and 4.2.3.2. As seen, all are granites. Several quartz pods were also mapped in the field. Sampling stations and sites of other geological observations are located on Fig 4.2.3.3.

Table 4.2.3.1 Chemical analysis of samples from the Mesopotamie farm, Namibia
(complete elemental analysis can be found on Table A12, Appendix)

Sample	SiO2	TiO2	Al2O3	Fe2O3	MnO	MgO	CaO	Na2O	K2O	P2O5	LOI	Total	Rb	Sr	Y	Zr	Nb	Co	Ni	Cu	Zn	Ga	V	Cr	Ba	U	Th	Sc	Sm	Nd	Pr	Ce	La	Ta	Eu	Yb
Notch	50.00	1.00	15.50	6.00	0.15	2.00	5.00	4.90	5.50	0.30	2.00		200	400	60	360	40	30	16	25	85	26	100	100	1300	20	37	20	50	50	15	175	95	120	4	8
L-759	74.06	0.03	14.47	0.47	0.04	0.02	0.70	3.55	5.54	0.06	0.94	99.88	109	124	20	16	7	<6	<6	<6	12	13	<12	185	649	<6	<15	<10				12	<12			
L-772	72.55	0.03	14.29	0.43	0.03	0.03	0.05	2.34	10.07	0.02	0.67	100.51	201	100	7	<8	4	<6	<6	8	28	13	<12	44	579	<6	<15	<10				21	<12			
L-773	74.83	0.06	14.98	0.87	0.02	0.11	0.80	5.35	3.07	0.04	0.41	100.54	76	71	103	64	14	<6	10	8	43	20	<12	47	176	<6	<15	<10				25	<12			
L-783	71.86	0.45	13.96	3.32	0.08	0.50	0.78	3.49	5.15	0.18	0.71	100.48	223	85	54	273	22	<6	6	9	49	17	25	239	859	<6	27	<10				161	75			
L-784	71.83	0.39	13.23	3.59	0.06	0.56	1.31	3.67	5.07	0.09	0.70	100.50	193	105	58	312	23	<6	7	7	59	17	23	63	1049	7	26	<10	11	37	99	155	51	42	1	4

There is possible IOCG mineralization at Mesopotamie 504. These mineralizations are associated to major E-W-trending fracture zones (Fig M20) and contain copper sulfides that surround masses of magnetite and/or hematite.

L-783 and L-784 were collected from the basement rocks at Mesopotamie. They host mineralization and are cut by the other intrusives.

4.2.3.2.2 Sampling and Geochemistry

All geological stations from the Mesopotamie farm are located on the map of Fig 4.2.3.4. Field descriptions were updated with geochemical and geochronological information, and are included in Appendix A68.

Samples collected from the Mesopotamie farm can be grouped in four units as follows: **A**, **L-758** and **L-759** from a white granite with graphic texture; **B**, **L-772** from a light gray to white graphic alkali granite vein; **C**, **L-773** from a coarse-grained pegmatitic granitoid; and **D**, **L-779**, **L-783** and **L-784** from an augen granite gneiss that probably makes the regional basement and could be the protolith to the granitods **L-758** and **L-759**. Chemical data shows that **L-783** and **L-784** are almost identical; these are roughly similar to **L-758** and **L-773**. **L-772** is very different in all aspects from the other samples. It is highly enriched in K2O and depleted in CaO. The series of schists observed in various outcrops throughout the farm were probably formed as volcanic rocks at the same time as Unit **D**.

Unit **B** is similar to **L-713** and **L-1019** from the Oas farm. The major oxide chemistry of units **C** and **D** has similarities with samples from the Lofdal farm (**L-728**, **L-729** and **L-1021**) and the Oas farm (**L-715** and **L-716***). Fig 4.2.3.2 shows this on the R1/R2 diagram. Thus the Mesopotamie farm conforms a series of rocks similar to those of the Oas and Lofdal farms. That makes sense, since the three farms line in the Khorixas inlier.

4.2.3.2.3 Environment of Emplacement

All granitoids sampled at the Mesopotamie farm have an anorogenic origin. No significant results were obtained from the various methodologies to evaluate environment of emplacement, except for **L-773** and **L-784**. Both of them fall in the “within-plate” category of Pearce et al, 1984. **L-783** and **L-784** come from the same basic rock unit. **L-772** is an alkali granite and probably was formed as a rift-related granitoid. The origin

TOTAL ALKALI vs SILICA DIAGRAM
Ugab River-Okwa River-Summas Mts.-Grootfontein-Felsic Volcanics, Namibia; Lufilian G.P.
(Based on Middlemost, 1994, 1997)

Samples

Petrographic fields

Fig 4.2.3.1

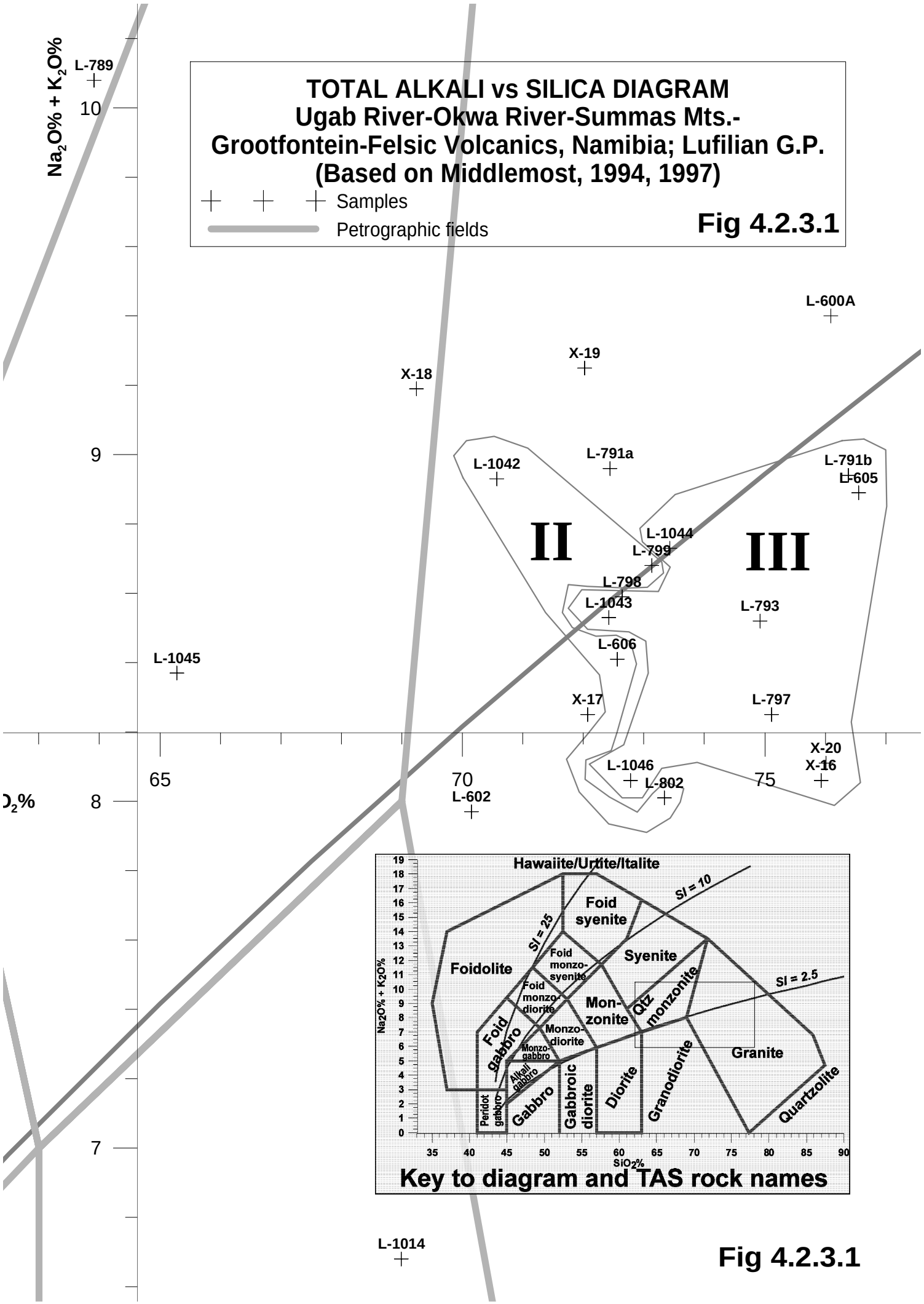

Key to diagram and TAS rock names

Fig 4.2.3.1

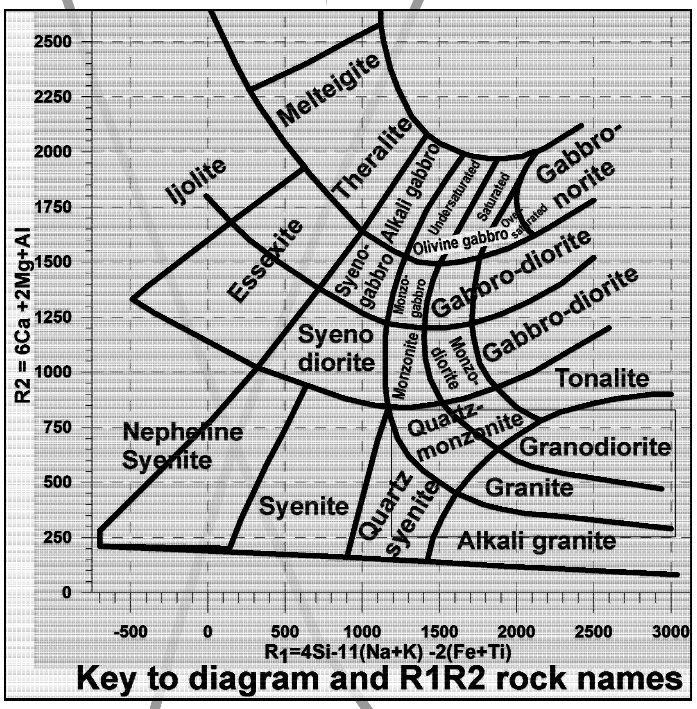

R_1R_2 PLUTONIC ROCK CLASSIFICATION
Ugab River-Okwa River-Summas Mountains-Grootfontein-Felsic Volcanics, Namibia; Lufilian G.P.
(After De la Roche et al, 1980)

Petrographic fields

Samples

Fig 4.2.3.2

L-1045
L-1014
L-602
L-789
X-17
L-606
L-802
L-798
II
L-799
L-1042
L-793
L-1043
L-1046
X-20
III
L-791a
X-19
L-1044
L-605
L-797
X-16
L-791b
X-18
L-600A

500
1000
1500
2000
2500

= 4S - 11(Na+K) -2(Fe+Ti)

Fig 4.2.3.2

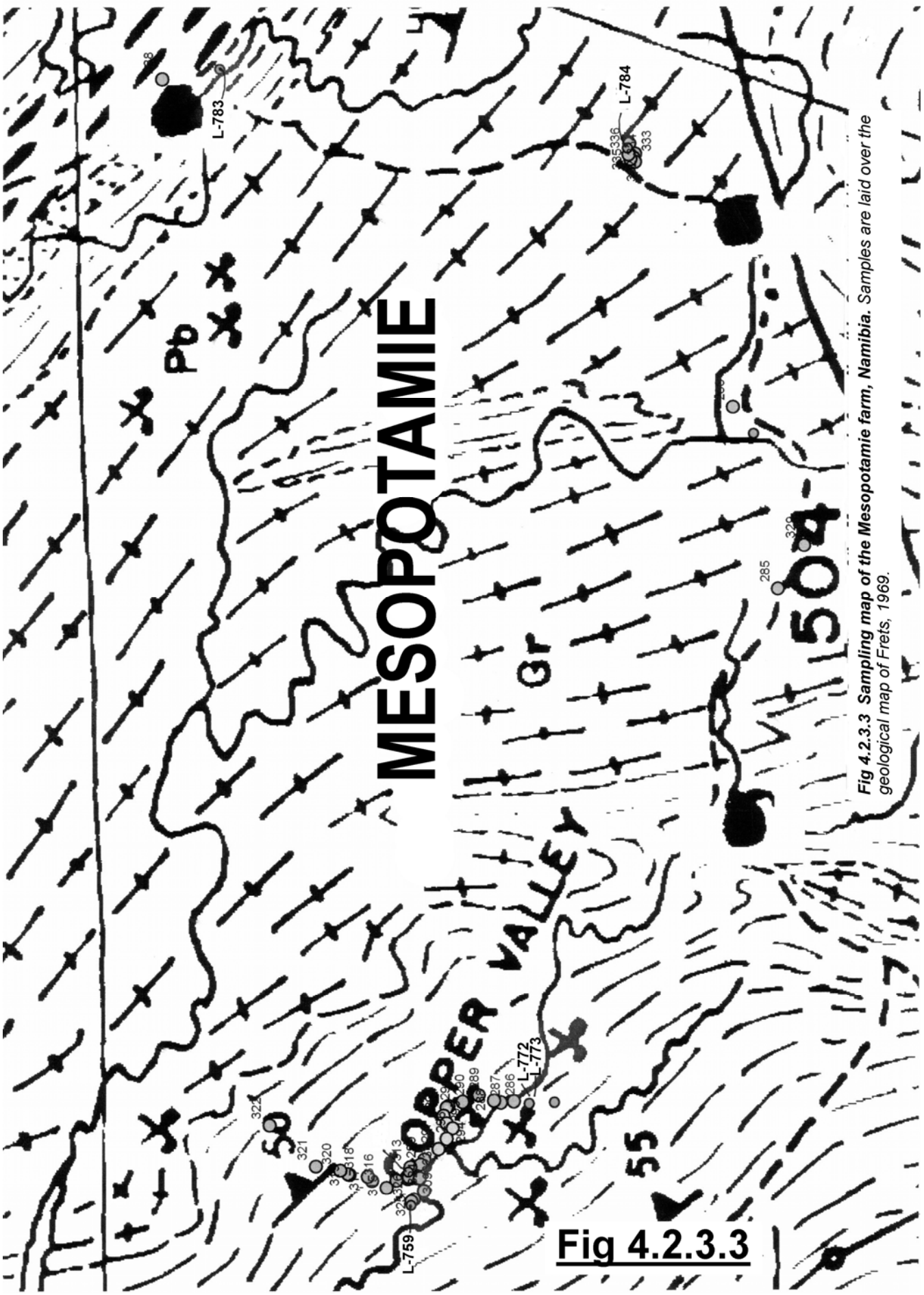

Fig 4.2.3.3 Sampling map of the Mesopotamie farm, Namibia. *Samples are laid over the geological map of Frets, 1969.*

Fig 4.2.3.3

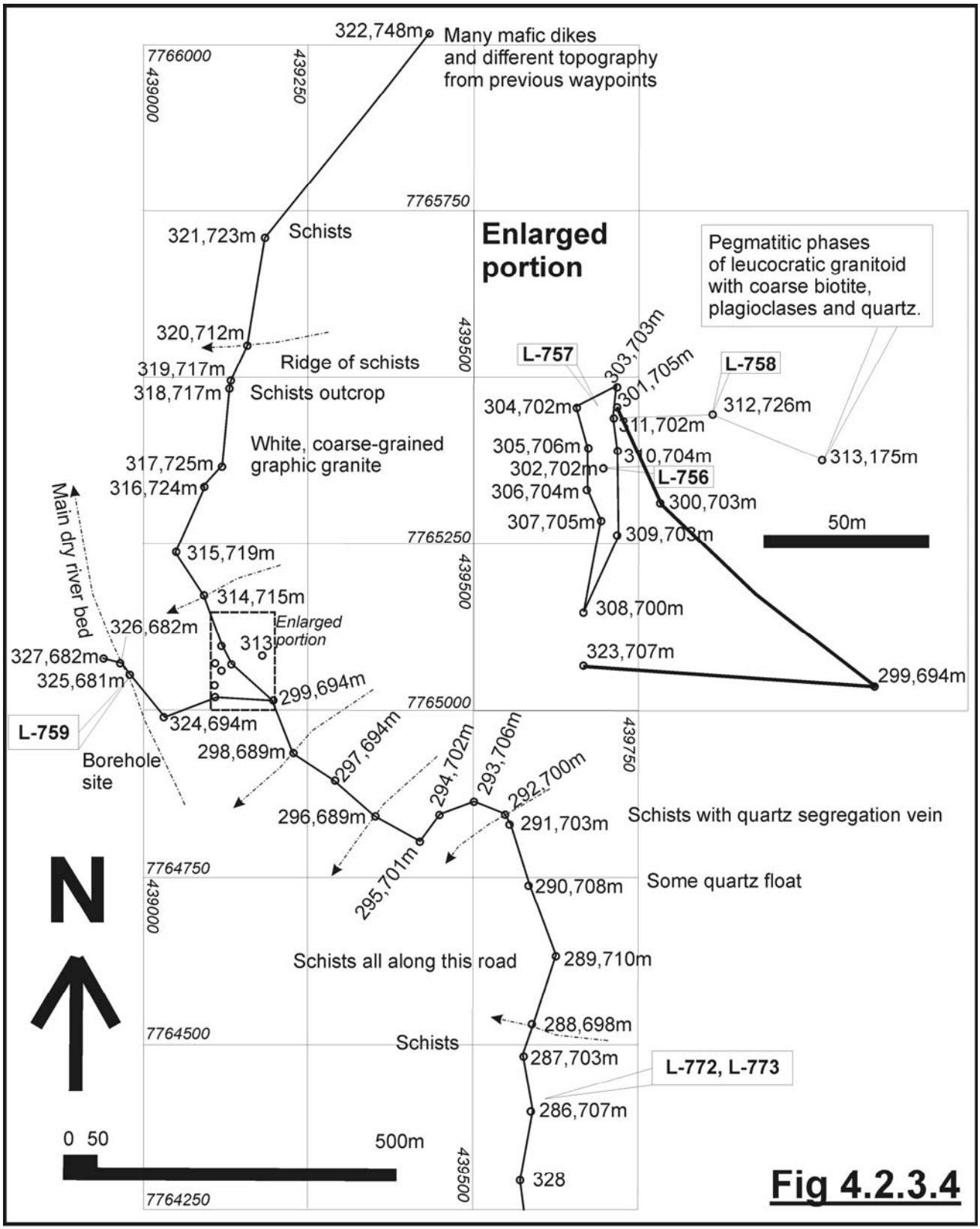

Fig 4.2.3.4 Map of geological stations and sampling, Mesopotamie farm, Namibia

of **L-759** cannot be defined any further. Thus, probable environments of emplacement for the four rock units is as follows: **B**, **C** and **D** formed in rift-related environments; **A** formed in an undetermined anorogenic environment.

4.2.3.2.4 Geochronology

In principle, the only chronological relationships that can be established are that unit **B** intersects unit **C**, that units **A** and **C** intersect unit **D**. Other relationships between **A** and **B**, and **A** and **C** are uncertain.

As indicated on Table A22.16, zircon concentrates from **L-758** were dated to give an age of 750±5 Ma. Inherited zircons in the sample gave an age of 1692±10 Ma. The sample was collected from the NW corner of the farm, as seen on Figs 4.2.3.3. Since **L-758** and **L-759** were taken from the same granitic body (unit **A**), we can assume that age and chemistry of both samples is the same. **L-779**, **L-783** and **L-784** correlate well with samples from other suites macroscopically, microscopically and chemically (high Pr, Th and Rb). They behave as basement for the other intrusive rocks in the Mesopotamie farm. We will thus assign a temporary age of 1690 Ma to these rocks. Their striking similarities allow us to give such an age to those rocks of group **D**. For the time being, groups **B** and **C** have not been dated in any way.

4.2.3.2.5 Economic Geology

There are three distinct mineralized areas at the Mesopotamie 504 farm. All have some characteristics of iron oxide-copper-gold deposits. These will be described in chapter 8. Iron oxide-copper-gold mineralization at the Copper Valley deposit could have been produced by unit **A** or by a later mineralizing event.

4.2.3.3 SUMMAS MOUNTAINS, NAMIBIA

4.2.3.3.1 Sampling and Geochemistry

Some samples were collected in the northern portion of the Summas Mountains, as illustrated on the map of Fig M22. Their chemistry is listed on Table 4.2.3.2 and is plotted on Figs 4.2.3.1 and 4.2.3.2. See location of sampling sites on M22. Chemistry of the dated volcanic rocks is not supplied by them. These rocks were probably emplaced in a rift-related environment. According to Roy Miller, the rocks that make the Mitten Fold and all three of the outcrops are made of the same granitoid rocks, but they are increasingly sheared towards the south, to the point where they seem to be a volcanic rock. All three have similar compositions (Miller, R., personal communications, 2003).

Table 4.2.3.2 Chemical analysis of samples from the Summas Mountains, Namibia
(complete analysis of all elements on Table A12, Appendix)

Sample	SiO2	TiO2	Al2O3	Fe2O3	MnO	MgO	CaO	Na2O	K2O	P2O5	LOI	Total	Na+K
Notch	50.00	1.00	15.50	6.00	0.150	2.00	5.00	4.90	5.50	0.30	2.00		
L-789	63.91	1.38	14.35	7.45	0.07	1.13	1.09	4.87	5.21	0.41	0.55	100.42	10.08
L-791a	72.44	0.40	13.01	3.67	0.06	0.32	0.54	3.80	5.16	0.10	0.61	100.11	8.96
L-791b	76.38	0.14	12.55	1.25	0.02	0.00	0.51	3.09	5.85	0.03	0.29	100.11	8.94

Sample	Rb	Sr	Y	Zr	Nb	Co	Ni	Cu	Zn	Ga	V	Cr	Ba	U	Th	Sc	Sm	Nd	Pr	Ce	La	Hf	Ta	Eu	Yb	Lu
Notch	200	400	60	360	40	30	16	25	85	26	100	100	1300	20	37	20	50	50	15	175	95	10	120	4	7.5	1.6
L-789	125	29	66	715	149	<6	6	10	80	21	32	135	1019	8	15	<10	15	50	136	196	67		128	2.03	3.88	1.58
L-791a	141	25	97	685	130	<6	7	<6	35	17	<12	220	637	6	32	<10	109	23	37	63	18	2	7	0.438	5.688	1.400
L-791b	270	74	83	70	65	<6	10	<6	15	22	16	234	332	8	17	<10				224	108					

Major WNW-ESE-, ENE-WSW-, and N-S–trending structures cut the rocks around the Summas Mountains and were unconformably overlain by Damara sedimentary sequences including base conglomerates and turbiditic sequences.

Several geochemical features of the three volcanic rocks from the Summas Mountains include high Y, Nb and Cr, low Ca, and low metallic content.

Table 4.2.3.3 Rock types and environment of emplacement for the Summas Mountains, Namibia
(See acronym description on section 2.4.3.)

Sample	Rock Name	Debon & LeFort	Maniar & Piccoli	Whalen	Pearce	Rb/10HfTa	Rb/30HfTa	Nb-Ta
L-789	quartz syenite	metalumi iv meso NaFe	RRG-CEUG	A	O-W 2-2			OUTU
L-791a	alkali granite	peralum ii leuco KFe	RRG-CEUG	A	W3/4	WP-	WP	INW
L-791b	alkali granite	peralum iv meso Na-KFe			W			

The following is a direct transcription from the field notebook.

L-786, taken on WPT 342 at 967 m. Slightly foliated, light brown, very glass-rich, translucent volcanic rock. The foliation may be syn-sedimentary bedding. Fresh samples are hard to find. Some vacuoles and porphyritic crystals are still present in the rock. Foliation plane is 100/45° N.

L-787 Vugs with sulfides and gossanous textures in volcanic rocks. Try to identify what the sulfides were using the methods of Blanchard, 1967.

L-788 Another aspect of the volcanics, that are slightly foliated and contain goethite in vugs after sulfides.

WPT 343 at 994 m. **L-789**: Slightly magnetic, subvolcanic metaluminous sodic ferriferous quartz trachyte with white porphyritic plagioclase and open vacuoles.This rock formed in a rift-related environment.

L-792 from WPT 343, Magnetic subvolcanic rock with compressional foliation.

L-790 Fine-grained medium brown to red crystalline rock. Similar to the matrix of L-789 with specks of chalcopyrite and gossanous specks. No crystals or macrocrystals.

WPT 344, 1028 m. **L-791a**: Finely laminated, pink/red fine-grained volcaniclastic, vitreous peraluminous leucocratic potassic ferriferous alkali rhyolitic ash with conchoidal fracture. Lamination = 180/67° W. This tuff formed in a rift-related environment.

L-791b was collected from another fine-grained, laminated, pink peraluminous sodic to potassic ferriferous alkali rhyolite.

WPT 345, 951 m. Some clasts in the river bed contain quartz with magnetite/hematite inclusions.

The volcanic rocks oberved in the Summas Mountains willl be compiled and correlated with other suites of Namibian rocks in the next few pages.

The amount of sulfidation observed in volcanic rocks from the Summas Mountains may be indication of economic mineralization. Rhyolitic magmas carry a lot of volatiles and metals, and they tend to be extremely explosive. Many high sulfidation and low sulfidation epithermal systems with economic gold mineralization are hosted in rhyolitic tuffs. Other metals like tin, silver and molybdenum might be present too. None of the samples from the Summas Mountains was assayed.

4.2.3.3.2 Geochronology

Hoffmann, Hawkings, Isachsen, & Bowring, 1996 dated two volcanic rocks in the Summas Mountains. They were given a U-Pb zircon age of 746±2 and 747±2 Ma (Table A22.16). Their ages are within error of each other. As seen on Fig A38 they form part of magmatic and volcanic activity associated to the emplacement of the Oas ring complex cluster.

4.2.3.4 UGAB RIVER OUTCROPS, NAMIBIA

A well exposed series of granitoids outcrops along two different intersections of the Ugab River with main roads. These are located south of the Khorixas Inlier, as shown on Fig M22. Field observations are included in Appendix A69; a few photographs and diagrams are also included there.

4.2.3.4.1 Sampling and Geochemistry

Geological stations and sampling sites are shown on Fig M22. Only the samples with a box were analysed, and their chemical analysis are listed on Table 4.2.3.4. As seen on Table 4.2.3.4, most samples from the Ugab River contain high values of Rb, Nb, Cr, Sm, Nd, Pr, Ce and La. **L-793** and **L-797** contain high Th values; they are high heat producing granitoids, as shown on Table 5.4.

Additional comments on geochemistry of the Ugab River and other sampling areas in Namibia with similar characteristics will be presented in the review of this chapter.

Rocks with enrichment in Cr and Rb are not very common in nature. Only a handful of samples from the Greater Lufilian Arc geochemical database have similar major oxide values to samples from the Ugab River and are enriched in Cr and Rb. These include: **L-602** from the Okwa River in Botswana, **L-754** from the Lofdal farm, **L-783** from the Mesopotamie farm, **L-791** from the Summas Mountains, **L-906** from the Kamanjab batholith, and **L-1037** from the Otjiwarongo environs. These rocks were found to be related, as indicated on Table 4.2.3.18.

Table 4.2.3.4 Chemical Analysis, Ugab River, Namibia
(complete elemental analysis on Table A12 in the Appendix)

Sample	SiO2	TiO2	Al2O3	Fe2O3	MnO	MgO	CaO	Na2O	K2O	P2O5	LOI	Total	Na+K
Notch	50.00	1.00	15.50	6.00	0.150	2.00	5.00	4.90	5.50	0.30	2.00		
L-793	74.92	0.33	12.39	2.15	0.08	0.24	1.00	3.28	5.24	0.14	0.37	100.14	8.52
L-797	75.11	0.21	13.05	1.92	0.04	0.08	0.51	3.62	4.63	0.08	0.61	99.86	8.25
L-798	72.64	0.26	14.07	2.13	0.08	0.26	1.09	3.42	5.17	0.12	0.91	100.15	8.59
L-799	73.13	0.08	13.93	1.96	0.06	0.04	0.95	3.84	4.84	0.13	0.63	99.59	8.68
L-802	73.34	0.23	14.56	1.83	0.05	0.29	1.08	3.46	4.55	0.13	0.84	100.36	8.01

Sample	Rb	Sr	Y	Zr	Nb	Co	Ni	Cu	Zn	Ga	V	Cr	Ba	U	Th	Sc	Sm	Nd	Pr	Ce	La	Hf	Ta	Eu	Yb	Lu
Notch	200	400	60	360	40	30	16	25	85	26	100	100	1300	20	37	20	50	50	15	175	95	10	120	4	7.5	1.6
L-793	251	140	81	213	78	<6	7	7	34	19	22	390	435	12	61	<10	119	51	175	234	98	1.8	28	0.938	6.6	1.7
L-797	225	107	23	199	38	<6	6	<6	33	21	17	372	658	6	37	<10				132	76					
L-798	222	204	26	229	48	<6	<6	<6	40	20	16	285	1117	7	27	<10				211	102					
L-799	153	168	53	183	14	<6	7	11	19	18	29	326	727	7	<15	<10				102	36					
L-802	234	141	32	142	41	<6	6	<6	51	19	22	260	745	<6	15	<10				77	38					

Although only sample **L-793** was analysed for Pr in the Ugab River suite, its values are significantly higher than the notch. The Pr enrichment is also known to many Namibian samples, including most from the Summas Mountains, Mesopotamie farm, Oas farm, Lofdal farm, Grootfontein, Okajepuiko and Okwa River. In general, Zambian rocks do not display such high Pr values.

Table 4.2.3.5 Rock types and environment of emplacement for the Ugab River, Namibia
(See acronym description on section 2.4.3.)

Sample	*Rock Name*	*Debon & LeFort*	*Maniar & Piccoli*	*Whalen*	*Pearce*	*Rb/10HfTa*	*Rb/30HfTa*	*Nb-Ta*
L-793	Granite	metaiv leuco Na Fe	POG	A	W3/4	WP-	WP	OUTU
L-795*	granite							
L-796*	granite							
L-797	granite	peraii leuco Na-K Fe	RRG-CEUG	A				
L-798	granite	peraii leuco Na-K Fe	POG	A				
L-799	granite	peraii leuco Na-K Fe		A				
L-802	granite	peraii leuco Na-K Fe		N				

The suite of samples from the Okwa River is very similar to that of the Ugab River (See Table 4.2.13). The same anomaly of Th, Cr, Rb and rare earths is present. When suites I and II of Table 4.2.3.18 are plotted on the TAS diagram (Fig 4.2.3.1), they are very close; but when plotted on the R1R2 diagram (Fig 4.2.3.2), they make two separate clusters. **L-606** and **L-798** are extremely similar. They plot almost on top of each other.

These two suites of rocks are very close. Based on geochemical similarities, one can confidently state that the two domains may be linked together as a single entity. It is very improbable that two different suites of rocks, carrying the same major oxide and trace element signatures occur in two different sites and not be related. They probably formed in the same environment and from the same source rocks. That does not mean that they have the same age, but the possibility is large.

Appendix A69 contains a transcription of all observations, geological stations and sampling carried out at the Ugab River outcrops. Notes were updated with chemical analysis and geochronological information. Coordinates of stations and samples are listed on Appendix A18.

Table 4.2.3.18 compiles the suites of igneous rocks from the Ugab River, Okwa River and Summas Mountains with some from Otjiwarongo and Grootfontein to evaluate their chemical similarities and establish possible correlations.

4.2.3.4.2 Geochronology

Zircons from two samples of that Ugab River suite (**L-795*** and **L-796***) were approximately dated by U-Pb zircon SHRIMP II at the ANU (Table A22.16) Final results are not available at the time of editing this document.

L-795*, a gray, coarse, porphyritic granite with abundant biotite and magnetite clusters, gave an age of ~540 Ma; it also contained xenocrystic zircons with ages around 1200 Ma.

L-796*, a pink granite with red quartz clusters, zoned red plagioclase and no magnetite, gave an age of ~750 Ma. That age came as a surprise, for the gray, foliated, porphyritic rock seemed to be older. There might be two generations of gray granites at the Ugab River outcrops.

Additional comments on geochronology of the Ugab River and other sampling areas will be presented in the review of this chapter.

4.2.3.5 OKWA RIVER OUTCROPS, BOTSWANA

One of the few outcrops of pre-Katangan granitoids in Botswana is located along the intersection of the main Trans-Kalahari road with the Okwa River. Sharad Master from the University of the Witwatersrand suggested visiting that outcrop (Master, S., personal communication, 2002). It is a reasonably well-exposed pavement outcrop; topography is almost flat, the river bed has very bad definition, and no river banks are visible.

According to Singletary et al., 1998, the Okwa River outcrops of granite and orthogneiss in the Qwangwadum Valley have given K-Ar ages of approximately 650-500 Ma. “Pb/Pb ages for discordant zircons from the gneiss suggest a crystallization age of approximately 2.07 Ga and WR eNd(t) and T(DM) of -3.5 and 2.65 Ga, respectively”. Their data indicates that reworked Archean crust of Eburnian age is present in northwestern Botswana. They suggest that the Okwa River gneiss represents basement inliers like those of the Damara belt to the southwest in Namibia and the Lufilian Arc to the northeast in Zambia. Geophysical evidence and regional structural trends that are known beneath the Kalahari semi-desert are consistent with that model (Singletary et al., 1998).

Seven samples were collected in the field, and four were analysed. Their chemistry is listed on table 4.2.3.6 plotted on Figs 4.2.3.1 and 4.2.3.2. A transcription of the field notes taken on the outcrops is included in the Appendix, as well as coordinates of all samples collected. Their environment of emplacement and geochemical characteristics are listed on Table 4.2.3.7.

Table 4.2.3.6 Chemical Analysis, Okwa River, Botswana
(complete elemental analysis on Table A12 in the Appendix)

Sample	SiO2	TiO2	Al2O3	Fe2O3	MnO	MgO	CaO	Na2O	K2O	P2O5	LOI	Total	Na+K
Notch	50.00	1.00	15.50	6.00	0.150	2.00	5.00	4.90	5.50	0.30	2.00		
L-600A	76.09	0.13	11.83	1.93	0.04	0.07	0.45	3.85	5.55	0.06	0.40	100.40	9.40
L-602	70.15	0.49	13.13	3.63	0.06	0.83	1.80	3.43	4.54	0.16	0.98	99.20	7.97
L-605	76.55	0.12	12.03	1.16	0.01	0.02	0.81	3.42	5.47	0.07	0.41	100.07	8.89
L-606	72.56	0.36	12.83	3.51	0.06	0.48	1.32	3.22	5.19	0.07	0.73	100.33	8.41

Sample	Rb	Sr	Y	Zr	Nb	Co	Ni	Cu	Zn	Ga	V	Cr	Ba	U	Th	Sc	Pb	Sm	Nd	Pr	Ce	La	Hf	Ta	Eu	Gd	Yb	Lu
Notch	200	400	60	360	40	30	16	25	85	26	100	100	1300	20	37	20	20	50	50	15	175	95	10	120	4	30	8	2
L-600A	160	59	23	137	14	<6	6	14	29	15	<12	68	508	<6	43	<10					141	77						
L-602	214	137	64	305	26	8	7	9	60	18	13	189	716	<6	36	<10		14	62	169	213	86		53	1		4	1
L-605	198	99	7	89	7	<6	<6	9	19	13	<12	227	772	<6	42	<10					148	102						
L-606	185	105	38	202	17	<6	6	7	61	18	20	57	781	<6	38	<10					227	149						

Table 4.2.3.7 Rock types and environment of emplacement for the Okwa River area, Botswana
(See acronym description on section 2.4.3.)

Sample	***Rock Name***	***Debon & LeFort***	***Maniar & Piccoli***	***Whalen***	***Pearce***	***Nb-Ta***
L-600A	alkali granite	metav leuco Na-K Fé	RRG-CEUG	A		
L-602	granite	metaiv meso Na-K Fé		A	O3/4	OUTU
L-605	granite	metav leuco Na Fe		A		
L-606	granite	metaiv meso Na Fe	RRG-CEUG	A		

All rocks collected show high thoroum content. Two of them contain high chromium. Tentative lithologic and geochemical correlations are shown on Table 4.2.3.18.

4.2.3.6 GROOTFONTEIN INLIER, NAMIBIA

4.2.3.6.1 Sampling and Geochemistry

Outcrops of intrusive rocks were found southeast of the Kombat mining area in the Grootfontein inlier, under sediments of the Otavi sequence. These were discovered under instructions from Geologist Arno Guenzel of Ongopolo Corporation (Guenzel, A., personal communication, 2003). General location of the outcrops is shown on Fig M25. Seven samples were collected in the field, and five of them were analysed.

In addition to that, Mr Guenzel kindly supplied a series of granitoid samples from boreholes drilled into the basement of the Grootfontein Inlier. He provided approximate coordinates of the drill sites. A composite of those sampes was analysed. The representative sample, **L-1014**, is a coarse-grained, peraluminous mesocratic sodic magnesic biotite granodiorite. It has a special chemical signature: 1632 PPM Ba, 176 PPM Cr and low Ce, La and Pr. The only samples with similar geochemical features are **L-985**, **L-993**, **L-994, L-999** from the Kamanjab batholith. They are roughly similar in other aspects too, but don't plot near on TAS or R1R2 diagrams.

Chemical analysis of the samples is listed on Table 4.2.3.8, Figs 4.2.3.1 and 4.2.3.2 show their plots on geochemical diagrams. A transcription of the field notes taken on the outcrops is included in the Appendix. Their environment of emplacement and geochemical characteristics are listed on Table 4.2.3.16.

Some Grootfontein samples are enriched in K2O, Th, Rb, Y and Cu.

Table 4.2.3.8 Chemical Analysis, Grootfontein Inlier, Namibia
(complete elemental analysis on Table A13 in the Appendix)

Sample	SiO2	TiO2	Al2O3	Fe2O3	MnO	MgO	CaO	Na2O	K2O	P2O5	LOI	Total	Na+K
Notch	50.00	1.00	15.50	6.00	0.15	2.00	5.00	4.90	5.50	0.30	2.00		
L-1014	68.99	0.40	14.2	3.21	0.05	1.35	2.61	3.04	3.64	0.11	1.80	99.41	6.68
L-1042	70.57	0.26	14.13	2.58	0.06	0.45	0.67	2.79	6.14	0.10	1.35	99.10	8.93
L-1043*	72.42	0.34	13.62	2.40	0.04	0.57	0.57	2.76	5.77	0.10	1.27	99.86	8.53
L-1044	73.43	0.25	12.72	2.04	0.04	0.39	0.49	2.79	5.94	0.11	1.10	99.30	8.73
L-1045	65.28	0.40	17.54	2.82	0.08	0.36	3.60	6.67	1.70	0.11	1.41	99.97	8.37
L-1046	72.78	0.33	12.73	2.40	0.03	0.55	0.76	2.61	5.45	0.12	1.39	99.15	8.06

Sample	Rb	Sr	Y	Zr	Nb	Co	Ni	Cu	Zn	Ga	V	Cr	Ba	U	Th	Sc	Pb	Sm	Nd	Pr	Ce	La	Hf	Ta	Eu	Gd	Yb	Lu
Notch	200	400	60	360	40	30	16	25	85	26	100	100	1300	20	37	20	20	50	50	15	175	95	10	120	4	30	8	2
L-1014	59	321	5	43.2	2.5	9	20	13	43	13	60	173	1632	<6	<15	<10	14	2.27	18.6	4.86	64	34	1.0	n.d.	1.76	1.76	0.4	.007
L-1042	317	68	65	161	17	7	12	20	29	14	16	<12	471	<6	35	<10		110	45	79	106	34	4	27	0	1	4	1
L-1043*	276	85	71	207	17	7	9	51	30	14	28	<12	525	<6	44	<10		109	42	89	140	35	2	37	1		9	2
L-1044	293	67	47	166	16	6	9	115	70	12	20	12	415	<6	36	<10					109	44						
L-1045	90	471	107	246	24	5	7	48	18	20	24	<12	116	<6	57	12		12	15	48	154	16		298	0		2	2
L-1046	283	61	69	193	16	6	9	30	27	13	25	16	473	<6	42	<10					126	53						

Table 4.2.3.16 Rock types and environment of emplacement for the Grootfontein Inlier, Namibia
(See acronym description on section 2.4.3.)

Sample	*Rock Name*	*Debon & LeFort*	*Maniar & Piccoli*	*Whalen*	*Pearce*	*Rb/10HfTa*	*Rb/30HfTa*	*Nb-Ta*
L-1014	granodiorite	peraiii meso Na Mg	IAG_CAG	?N				
L-1042	granite	peraii subleuco K Fe	POG	A		WP-	WP	OUTU
L-1043*	granite	peraii subleuco K Fe	POG	A	O-W 2-2	WP	WP	OUTU
L-1044	granite	peraii leuco K Fe	POG	A	O-W1-1			
L-1045	quartzmonzonite	metav subleuco Na Fe		A	W3/4			OUTU
L-1046	granite	peraii subleuco K Fe	POG	A	O-W1-1			

4.2.3.6.2 Geochronology

Zircons concentrated from a single sample of the Grootfontein Inlier were dated by laser ablation ICPMS at the Memorial University in Newfoundland, Canada. **L-1043***, a fine, felsic, porphyritic, almost un-foliated, peraluminous, subleucocratic potassic ferriferous biotite granite gave a U-Pb age of 1939±64 Ma, with xenocrystic zircons that dated 2544±78 Ma. Geochronological data for this sample was extremely complex to interpret, and further work may end up refining the ages (Table 4.2.1.15). The relevance of this age will be discussed in the next few pages.

4.2.3.7 ENVIRONS OF OTJIWARONGO, NAMIBIA

4.2.3.7.1 Introduction

Very little outcrop of intrusive rocks is to be found in the environs of Otjiwarongo, Namibia (Figs M23 and M24). Most of the rocks are covered by carbonates, Kalahari sand and calcrete. The presence of a significant batholith (approximately as large as the Kamanjab batholith) under cover northeast of the town of Otjiwarongo is a fact known by a few geologists. Geophysicist Branko Corner first detected the body of batholithic dimensions for AngloVaal Namibia (Lombard, A., personal communication, 2003). The Otjikoto gold deposit is thought to have been produced by that plutonic body. This chapter reviews samples from the environs of Otjiwarongo, and describes pegmatitic apophyses of the Otjiwarongo batholith. A single sample from Otjiwarongo pegmatites was dated.

Geologists from AVMIN in Windhoek spent months looking for outcrops of intrusive rocks in that part of the world. They provided locations of their outcrops and complete chemical analysis of 18 such rocks and some petrographical details (Wilton, J, 2003, personal communication). These are labeled with the “LL-“ and “LJ-“ prefix on Table 4.2.3.10. Seven samples were collected and analysed from pegmatitic rocks that were considered by geologists from AVMIN Namibia to be part of the Otjiwarongo batholith (L-808 to L-815) (Lombard, A., 2003, personal communication). Six rock samples collected in the field were added to AVMIN’s samples to compose the Otjiwarongo suite, a database of 31 rock samples (Table 4.2.3.10). Figs 4.2.3.6 and 4.2.3.7 has them plotted on the R1/R2 diagram and Fig 4.2.3.5, on the modified TAS diagram. Rock compositions are again bimodal. Granites dominate, although alkali granite, various quartz syenites and minor granodiorite are also present. See Table 4.2.3.13. LL-9 and L-814 are rocks of complex petrology or probably hydrothermally altered.

4.2.3.7.2 Field Description of Main Outcrops

There are very few outcrops of granitoids exposed in the environs of Otjiwarongo. Some of the reasonable outcrops are out of bounds, because farm owners have locked their properties away from the public. The few outcrops that were visited are described below.

The following is a transcription of sampling field notes around Otjiwarongo, modified with laboratory results. Coordinates of samples are in Appendix D.

L-850 was sampled from a large outcrop along the main road from Okahandja to Otjiwarongo, 10 km before Otjiwarongo. Photo 4.2.3.8 taken towards the SE shows the place where the sample was collected (hill on the left). See also Figs M23 and M24. The rock is a fresh, fine-grained, homogeneous, gray, peraluminous subleucocratic ferriferous biotite micro-granite with occasional xenoliths of dark green amphybolite. The sample does not correlate well with any of the rest of rocks collected in the environs of Otjiwarongo. It probably formed in an anorogenic rift environment.

Fig 4.2.3.8 Photograph of granitoid inselbergs on the road Okahandja-Otjiwarongo, Namibia*. Sample L-850 was collected from the hill on the left of the image. The one on the back was observed but not sampled. This is the typical type of granitoid outcrop in most of Namibia. Very few of them are present in the environs of Otjiwarongo. It is not clear if these granitoids intersect the Damaran siliciclastic and calcareous rocks.*

An elongated whaleback ridge granitoid outcrop located just north of Otjiwarongo was visited with Geologist John Wilton from AngloVaal Mining in Windhoek. This was the best outcrop of granitoids in many thousands of kilometers. Its coordinates are 20°27.169’S/16°39.159’E (See Fig M24). The entire outcrop seems to be a

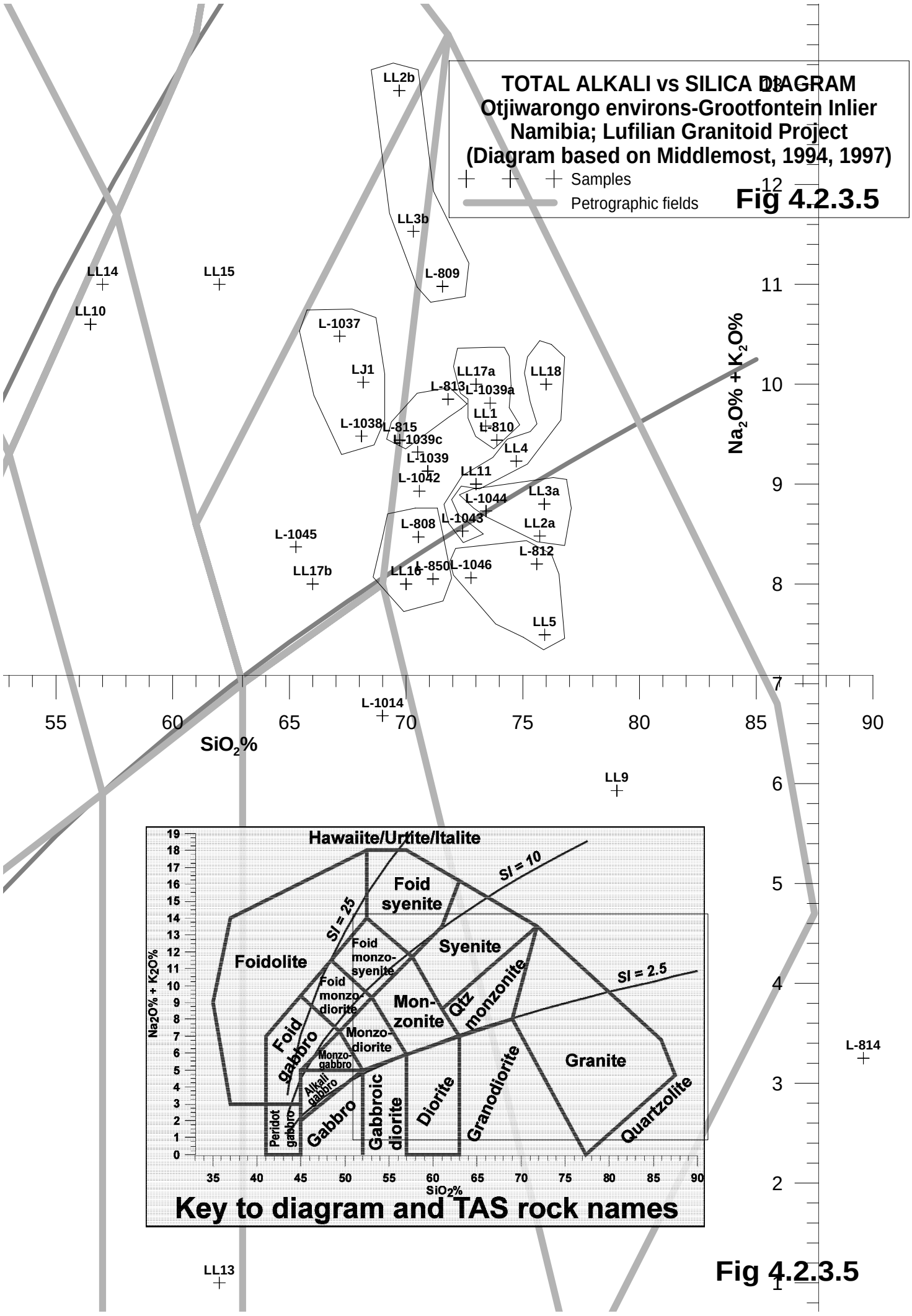
TOTAL ALKALI vs SILICA DIAGRAM
Otjiwarongo environs-Grootfontein Inlier
Namibia; Lufilian Granitoid Project
(Diagram based on Middlemost, 1994, 1997)
Samples
Petrographic fields
Fig 4.2.3.5
LL2b
LL3b
L-809
LL14
LL15
LL10
L-1037
LJ1
LL17a
LL18
L-813
L-1039a
LL1
L-1038
L-815
L-810
L-1039c
LL4
L-1039
L-1042
LL11
L-1044
LL3a
L-808
L-1043
LL2a
L-1045
L-812
LL17b
LL16
L-850
L-1046
LL5
L-1014
LL9
L-814
LL13
$Na_2O\% + K_2O\%$
$SiO_2\%$
Hawaiite/Urtite/Italite
Sl = 10
Sl = 25
Sl = 2.5
Foid syenite
Foidolite
Foid monzo-syenite
Syenite
Foid monzo-diorite
Mon-zonite
Qtz monzonite
Foid gabbro
Monzo-diorite
Monzo-gabbro
Granite
Alkali gabbro
Peridot gabbro
Gabbro
Gabbroic diorite
Diorite
Granodiorite
Quartzolite
Key to diagram and TAS rock names
Fig 4.2.3.5

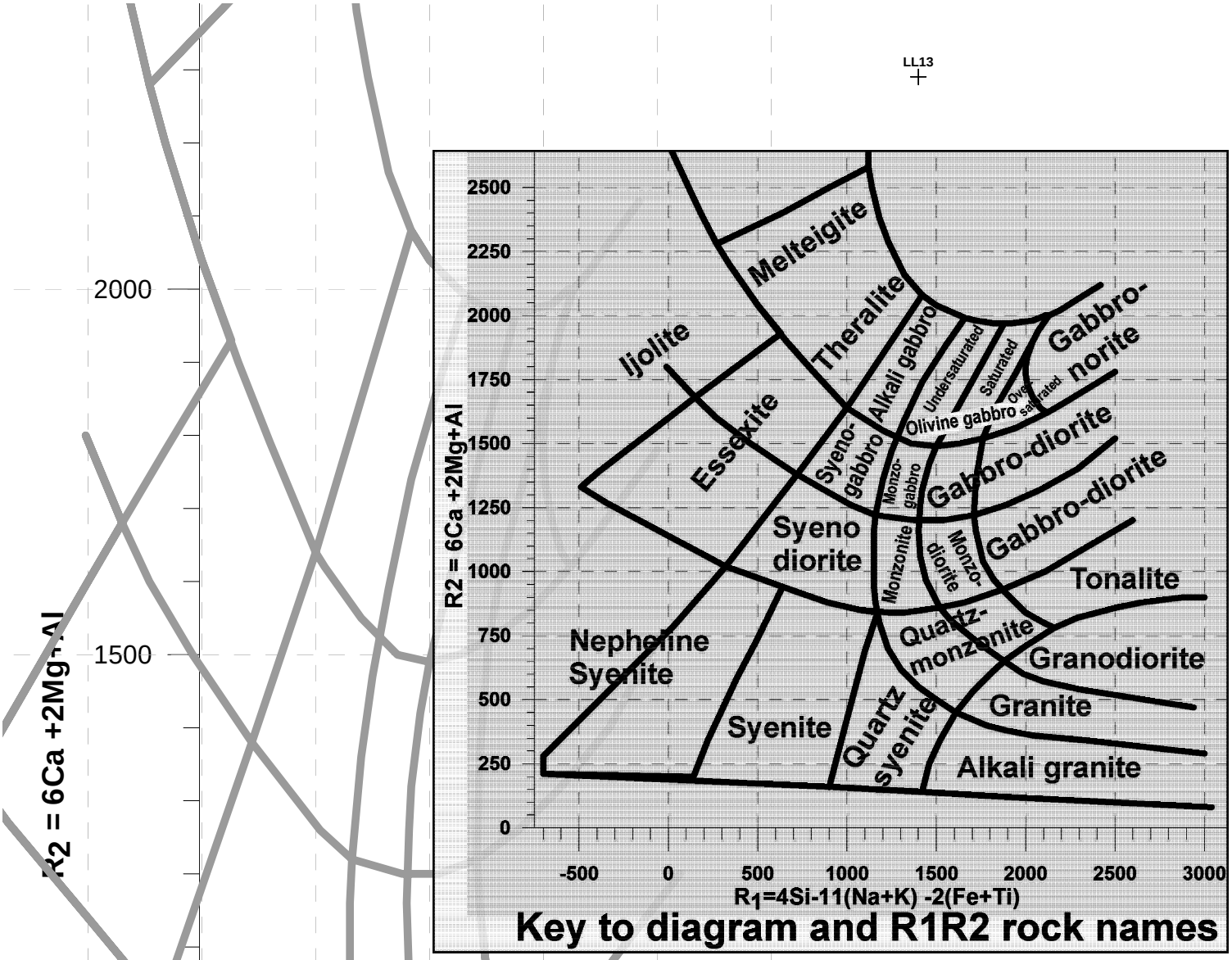

R_1R_2 PLUTONIC ROCK CLASSIFICATION

Otjiwarongo Environs, Namibia; Lufilian G.P.

(After De la Roche et al, 1980)

Petrographic fields

Samples

$R_2 = 6Ca + 2Mg + Al$

$R_1 = 4Si - 11(Na+K) - 2(Fe+Ti)$

LL13 LL10 LL15 L-1045 LL14 LL17b L-1014 LL16 LJ1 L-1037 L-1038 L-1039 L-850 LL5 L-809 LL3b LL1 L-810 LL17a LL11 L-1042 LL18 L-1048 L-1046 L-1039c L-1039 L-1039a L-1044 LL3a LL2a LL2b LL9 L-814

Fig 4.2.3.6

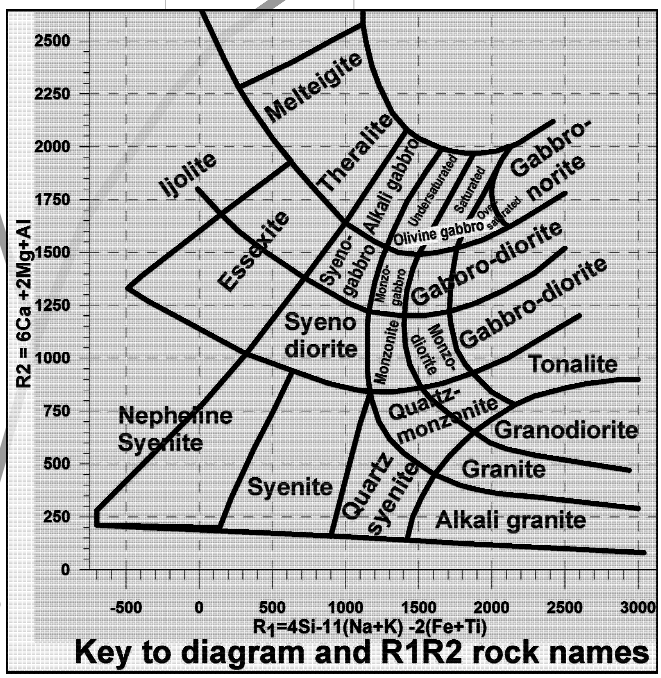

R_1R_2 PLUTONIC ROCK CLASSIFICATION

Otjiwarongo and Grootfontein Environs, Namibia; Lufilian G.P.

(After De la Roche et al, 1980)

Petrographic fields

Samples

Fig 4.2.3.7

Fig 4.2.3.7

thick dike, with are several granitoid facies, probably due to flow banding. The whaleback ridge is elongated along 100°. Part of the large, flat lying outcrop was used as a quarry for road ballast.

The two main rock types observed in the outcrop were sampled. **L-1037** is a medium- to fine-grained foliated, light gray, peraluminous mesocratic potassic magnesic biotite quartzmonzonite. One of the younger granitoids, collected from the northern side of the railroad, **L-1038**, is a peraluminous subleucocratic potassic magnesic biotite granite.

Several samples were collected from different facies of a relatively weathered rock that makes another large granitoid outcrop located approximately 20 km north of Otjiwarongo. It is the only granitoid outcrop mapped in the 1:1,000,000 scale geological map sheet of Namibia (Fig M23) as well as in the 1:250,000 scale geological map sheet of Otjiwarongo. **L-1039** is a pink, medium-grained, peraluminous leucocratic ferriferous alkali granite that weathers into a deep orange color on the surface. The entire outcrop probably has been subject to strong potassic alteration. **L-1039**, **L-1039a** and **L-1039c** are various samples from the site. Samples **LL31**, **LL3b, LL28** were collected from other portions of the same outcrop.

Euhedral magnetite crystals from 1 cm to 5 mm diameter make clusters that are disseminated in some portions of the outcrop. Sample **L-1040** contains them. It was collected for chemical analysis and to compare with magnetite from other sources. The clusters seem to be the product of albitization in the rock.

4.2.3.7.3 Pegmatitic rocks

Geologist Anton Lombard, who worked at the Windhoek exploration office of Anglo Vaal, suggested sampling several pegmatitic granitoids intersected in boreholes drilled by him. In his opinion, those rocks might be the only representatives from the covered Otjiwarongo batholith. That batholith is considered to be the intrusive body responsible for mineralization at the Otjikoto gold deposit.

L-807 to **L-815** come from boreholes NRD-1 and SCH-2 and were drilled on 1999 and 2000 by AVMIN (they are located respectively on stations 5000 and 5001 on Fig M24). The boreholes show domes of strongly-foliated igneous rocks intruded by younger, underformed pegmatitic granitoid bodies (Fig 4.2.3.10). The pegmatitic apophyses lie on top of small intrusive bodies that came from the blind Otjiwarongo batholith. **L-808** to **L-815** have chemical analysis as shown on Table 4.2.3.11. Depth and field description of the samples is listed on Table 4.2.3.12. **L-808** has complete chemical analysis including all rare earths.

Table 4.2.3.11 Chemical Analysis, Otjiwarongo pegmatites, Namibia
(complete elemental analysis on Table A13, Appendix)

Sample	SiO2	TiO2	Al2O3	Fe2O3	MnO	MgO	CaO	Na2O	K2O	P2O5	LOI	Total	Na+K
Notch	50.00	1.00	15.50	6.00	0.150	2.00	5.00	4.90	5.50	0.30	2.00		
L-808*	70.53	0.14	15.35	1.50	0.05	0.42	1.71	4.80	3.67	0.07	2.04	100.28	8.47
L-809	71.56	0.07	14.95	1.24	0.03	0.23	0.87	3.46	7.52	0.06	0.50	100.49	10.98
L-810	73.89	0.06	14.05	1.11	0.04	0.16	1.04	4.00	5.44	0.04	0.50	100.33	9.44
L-812	75.60	0.08	12.89	1.27	0.03	0.25	1.29	4.03	4.17	0.09	0.71	100.41	8.20
L-813	71.80	0.04	15.51	0.86	0.03	0.12	1.40	4.26	5.59	0.08	0.78	100.47	9.85
L-814	89.59	0.02	5.33	0.65	0.02	0.02	0.84	2.94	0.31	0.04	0.63	100.39	3.25
L-815	69.73	0.30	14.51	3.35	0.08	0.84	1.34	3.85	5.59	0.16	0.65	100.40	9.44

Sample	Rb	Sr	Y	Zr	Nb	Co	Ni	Cu	Zn	Ga	V	Cr	Ba	U	Th	Sc	Pb	Sm	Nd	Pr	Ce	La	Cs	Hf	Ta	Gd	Dy	Er	Yb
Notch	200	400	60	360	40	30	16	25	85	26	100	100	1300	20	37	20	20	50	50	15	175	95	3	10	120	30	20	9	8
L-808*	140	89	12	29	14	<6	7	10	71	16	13	39	154	<6	<15	<10	32	2	9	2	26	<12	6	1	1	2	2	1	1
L-809	253	92	19	<8	9	<6	7	11	56	16	<12	27	301	<6	<15	<10					29	<12							
L-810	173	85	7	<8	7	9	10	13	50	14	<12	56	249	<6	<15	<10					24	<12							
L-812	141	104	86	215	10	<6	8	9	67	13	<12	34	439	17	30	<10					93	55							
L-813	173	115	65	77	6	<6	9	13	23	14	<12	42	625	13	21	<10					63	22							
L-814	23	38	5	<8	4	<6	7	10	54	<9	<12	77	50	<6	<15	<10					26	<12							
L-815	214	122	43	268	25	<6	8	10	75	17	12	68	584	42	16	<10					68	29							

A few gabbroid dikes were intersected in the boreholes (**L-807** and **L-811**). These have not been analysed, but are foliated and amphibolitized (See photos in Fig 4.2.3.9). They probably are mid alkaline gabbroids, and were emplaced soon after the pegmatites, in an anorogenic environment.

L-808* is a very coarse-grained, pink, peraluminous leucocratic potassic magnesic graphic granite. **L-808** to **L-815** indicate chemistry of the pegmatitic intrusives intersected in the boreholes.

Table 4.2.3.10 Chemical Analysis, Otjiwarongo environs, Namibia
(complete elemental analysis is on Appendix A13)

Sample	SiO2	TiO2	Al2O3	Fe2O3	MnO	MgO	CaO	Na2O	K2O	P2O5	LOI	Total	Na+K
Notch	50.00	1.00	15.50	6.00	0.150	2.00	5.00	4.90	5.50	0.30	2.00		
L-808	70.53	0.14	15.35	1.50	0.05	0.42	1.71	4.80	3.67	0.07	2.04	100.28	8.47
L-809	71.56	0.07	14.95	1.24	0.03	0.23	0.87	3.46	7.52	0.06	0.50	100.49	10.98
L-810	73.89	0.06	14.05	1.11	0.04	0.16	1.04	4.00	5.44	0.04	0.50	100.33	9.44
L-812	75.60	0.08	12.89	1.27	0.03	0.25	1.29	4.03	4.17	0.09	0.71	100.41	8.20
L-813	71.80	0.04	15.51	0.86	0.03	0.12	1.40	4.26	5.59	0.08	0.78	100.47	9.85
L-814	89.59	0.02	5.33	0.65	0.02	0.02	0.84	2.94	0.31	0.04	0.63	100.39	3.25
L-815	69.73	0.30	14.51	3.35	0.08	0.84	1.34	3.85	5.59	0.16	0.65	100.40	9.44
L-850	71.15	0.38	13.69	2.97	0.05	0.47	1.56	3.09	4.96	0.10	0.48	98.90	8.05
L-1037	67.15	0.44	16.05	2.51	0.02	0.77	1.33	2.99	7.49	0.15	0.46	99.36	10.48
L-1038	68.09	0.44	15.77	2.42	0.02	0.69	1.39	3.03	6.45	0.17	0.40	98.87	9.48
L-1039	70.93	0.25	13.72	2.43	0.01	0.03	0.57	3.62	5.51	0.10	1.71	98.88	9.13
L-1039a	73.60	0.10	13.76	0.98	0.02	0.06	0.47	3.67	6.14	0.03	0.53	99.36	9.81
L-1039c	70.50	0.34	13.95	3.40	0.02	0.00	0.71	3.38	5.94	0.11	2.16	100.51	9.32
LJ1	68.16	0.46	16.02	2.81	0.02	0.89	1.54	2.85	7.17	0.16	0.55	100.07	10.02
LL1	73.41	0.09	14.65	0.80	0.01	0.27	1.00	3.34	6.24	0.20	1.26	100.02	9.58
LL10	56.48	1.24	17.84	6.85	0.19	1.96	3.78	5.74	4.86	0.74	0.74	99.67	10.60
LL11	73.00	0.00	14.00	2.00	0.00	0.00	1.00	3.00	6.00	0.00	1.00	99.86	9.00
LL13	62.00	1.00	11.00	4.00	0.00	3.00	18.00	1.00	0.00	0.00	7.00	100.02	1.00
LL14	57.00	1.00	17.00	9.00	0.00	1.00	3.00	6.00	5.00	0.00	1.00	99.52	11.00
LL15	62.00	1.00	16.00	6.00	0.00	1.00	4.00	6.00	5.00	0.00	4.00	99.73	11.00
LL16	70.00	1.00	14.00	3.00	0.00	1.00	2.00	3.00	5.00	0.00	0.00	99.49	8.00
LL17a	73.00	0.00	14.00	1.00	0.00	0.00	1.00	3.00	7.00	0.00	1.00	99.75	10.00
LL17b	66.00	1.00	16.00	5.00	0.00	1.00	3.00	3.00	5.00	0.00	0.00	99.77	8.00
LL18	76.00	0.00	13.00	1.00	0.00	0.00	1.00	3.00	7.00	0.00	1.00	100.07	10.00
LL2a	75.73	0.02	14.98	0.67	0.01	0.06	0.12	3.62	4.86	0.04	1.36	100.11	8.48
LL2b	69.71	0.00	16.92	0.31	0.01	0.00	0.04	2.54	10.40	0.13	0.60	100.06	12.94
LL3a	75.92	0.03	13.87	0.68	0.01	0.05	0.39	2.87	5.93	0.01	1.19	99.77	8.80
LL3b	70.31	0.04	16.91	0.47	0.01	0.24	0.37	2.44	9.09	0.09	1.20	99.96	11.53
LL4	74.72	0.10	13.50	1.59	0.03	0.10	0.80	3.49	5.74	0.02	0.41	100.08	9.23
LL5	75.94	0.03	14.40	0.33	0.00	0.00	1.44	4.03	3.46	0.03	0.64	99.67	7.49
LL9	79.03	0.02	14.86	0.39	0.00	0.01	0.02	0.30	5.63	0.00	3.19	100.25	5.93

Sample	Rb	Sr	Y	Zr	Nb	Co	Ni	Cu	Zn	Ga	V	Cr	Ba	U	Th	Sc	Pb	Sm	Nd	Pr	Ce	La	Cs	Hf	Ta	Eu	Gd	Dy	Er	Yb
Notch	200	400	60	360	40	30	16	25	85	26	100	100	1300	20	37	20	20	50	50	15	175	95	3	10	120	4	30	20	9	8
L-808	140	89	12	29	14	<6	7	10	71	16	13	39	154	<6	<15	<10	32	2	9	2	26	<12	6	1	1	0	2	2	1	1
L-809	253	92	19	<8	9	<6	7	11	56	16	<12	27	301	<6	<15	<10					29	<12								
L-810	173	85	7	<8	7	9	10	13	50	14	<12	56	249	<6	<15	<10					24	<12								
L-812	141	104	86	215	10	<6	8	9	67	13	<12	34	439	17	30	<10					93	55								
L-813	173	115	65	77	6	<6	9	13	23	14	<12	42	625	13	21	<10					63	22								
L-814	23	38	5	<8	4	<6	7	10	54	<9	<12	77	50	<6	<15	<10					26	<12								
L-815	214	122	43	268	25	<6	8	10	75	17	12	68	584	42	16	<10					68	29								
L-850	254	153	22	241	15	7	7	23	57	17	27	13	919	<6	46	<10		116	43	131	161	67		4.7	34	0.6				0.2
L-1037	204	190	22	149	16	<6	6	8	41	17	15	156	1143	<6	105	<10					288	157								
L-1038	185	178	26	247	18	<6	8	13	39	16	14	162	975	<6	112	<10					316	175								
L-1039	160	562	19	156	20	<6	7	21	11	18	<12	230	793	<6	26	<10					88	46								
L-1039a	168	205	12	38	2	<6	8	6	11	13	12	250	1060	<6	<15	<10	25	3	18	5	55	23	3	1	0	1	3	2	1	1
L-1039c	172	547	24	162	24	<6	7	29	12	18	<12	309	776	<6	32	<10					103	55								
LJ1	196	191	24	259	17	4		30	42		15	0	954	1	95	4														
LL1	150	176	17	42	6	3	3	13	11		6	1	1468	0	5	2														
LL10	135	965	36	340	99	11	3	0	78		44	0	1366	9	25	1														
LL11	287	134	34	210	16	2	1	0	30		20	3	880	3	55	5														
LL13	12	701	42	128	6	9	26	3	58		101	66	448	4	5	10														
LL14	280	355	161	2052	364	4		5	133		4	0	1161	22	83	5														
LL15	118	328	31	305	47	10	9	0	73		125	22	1308	3	26	15														
LL16	230	152	24	320	30	4	2	0	33		39	9	790	3	33	4														
LL17a	202	57	12	29	9	2		5	8		4	6	220	5	3	1														
LL17b	140	208	22	311	16	13	2	2	60		50	7	1167	4	18	9														
LL18	178	84	8	55	3	0			8		5	4	316	5	4	1														
LL2a	181	35	10	19	19	2	1	14	8		11	0	104	2	4	2														
LL2b	356	67	7	4	1	2	1	0	2		0	1	205	0	2	0														
LL3a	156	182	13	29	0	2	1	14	4		5	3	659	0	7	1														
LL3b	348	252	9	5	4	2	1	0	7		7	1	495	1	0	5														
LL4	365	50	32	138	29	1		0	27		1	0	235	4	52	5														
LL5	180	89	47	48	11	1		6	4		0	0	151	5	11	1														
LL9	256	26	9	33	9	2	2	1	3		12	3	285	2	3	2														

Fig 4.2.3.9 Photographs of slabs from samples L807 and L-811*. These slightly deformed mafic dikes with abundant plagioclase amygdules intersect the pegmatites of the Otjiwarongo Batholith. Scale in millimeters.*

Fig 4.2.3.10 Photographs of granitic pegmatites from the Otjiwarongo Batholith. *Note graphic textures, amphibole needles and lack of deformation. A composite of these samples was dated. Depths are marked in blue. Bottom is to the left. For scale, the core slabs are 5.5 cm wide.*

Table 4.2.3.12 Main details of samples from pegmatitic granitoids, Otjiwarongo batholith, Namibia

Sample	Borehole	Depth	Field Notes	Rock Name	Remarks
L-807	NRD1	120.57	Albitization	alkali gabbro?	See photo on Fig 4.2.3.9
L-808*	NRD1	161.79	Pink pegmatitic granites with graphic texture	peral leuco potassic magnesic granite	
L-809	NRD1	162.42	Pink pegmatitic granites with graphic texture	meta leuco potassic ferriferous alkali granite	
L-810	NRD1	161.81	Pink pegmatitic granites with graphic texture	meta leuco sodic to potassic ferriferous granite	The rock was previously cooked and later intruded by pegmatites.
L-811	NRD1	172.28	Schistose amphibolite	alkali gabbro?	Scapolite opens its space in the schists with white plagioclase that floods rock matrix.
L-812	SCH-2	87.51	Mineralized graphitic schist	meta leuco sodic magnesic granite	22 ppb Au, 36 ppm Pb, 76 ppm Cu, 69 ppm Zn
L-813	SCH-2	82.94	Graphitic schist	meta leuco sodic to potassic ferriferous granite	
L-814	SCH-2	158.68	Amphibole albite schist	meta leuco sodic ferriferous, out of plot, high Si	
L-815	SCH-2	195.80	Pegmatitic granite	meta mesocratic sodic to potassic ferriferous granite	

4.2.3.7.4 Geochemistry

76% of the granitoids from the Otjiwarongo region fall within the midalkaline field, while 24% of them fall in the subalkaline field (Fig 4.2.3.5, Table 4.2.3.13). All midalkaline rocks make 71% of the samples, 29% of them are subalkaline and none alkaline. As noted, there is a single quartzolite.

Table 4.2.3.13 Statistics of rock types, Otjiwarongo environs, Namibia
The fifth column (granitoids) is the sum of underlined rock types.

Group	Rock type	number	%	Granitoids	Groups
Midalkaline Rocks	Alkali granite	13	41.94	75.86	70.97
	Quartzmonzonite	5	16.13		
	Syenite	2	6.45		
	Monzonite	2	6.45		
Subalkaline Rocks	Granite	7	22.58	24.14	29.03
	Diorite	1	3.23		
	Quartzolite	1	3.23		
Total		31	100.00	100.00	100.00

Many samples from Otjiwarongo are enriched in K2O, some are enriched in Cr.

Samples **LL13**, **LL12**, **LJ1** were collected near the sampling site for **L-1037**, probably from the same large outcrop. All contain very high Th content. They are extremely high heat producing rocks due to abundant potassium and thorium. The analyses of **LL12** and LL-28 were not available.

LL13 is more mafic, it contains Cu, V, Mg, Ca and Ni. Very high Th, Cr, Rb, K alteration and high alumina. **LJ1** with high Cu. **LL13** low Th.

Several samples were collected and analysed by Anglo Vaal from the same site where **L-1037** and **L-1039** were sampled (Figs M23 and M24). **LL3a** and **LL3b** have high K2O, but somewhat different chemistry. Although **L-1039a** has 29 ppm of Cu, **LL3a** and **LL3b** have much less and very much less Cr. Very low Th compared to medium Th values in **L-1039**. Samples **L-1039** and **L-1039c** contain enough Th and K to be high heat producers (Table 4.2.3.10).

LL2b and **LL3b** are very similar to each other; **LL3a** and **LL2a** are very similar too. Both types of rocks are exposed in two different outcrops that are approximately 10 km away from each other. That means that the same pluton extends further north along the road (Fig M24).

LL1 is similar to **L-1-39a** and **LL3a**, except for the high Cr and Ba.

L-815 is a very high heat producing granite. It contains high U. It has some similarities with **LL16** and **L-1042**, but neither of them contain anomalous U.

L-808, **L-813** and **L-814** do not correlate with any of the other samples.

L-809 correlates with **LL-11** except in Th value

A few samples from completely different regions were found to have equivalent geochemistry. They are listed on Table 4.2.3.9. Their chemical similarity indicates a similar origin and environment of emplacement. That does not mean they have the same age. All the samples listed formed in anorogenic continental extensional environments.

Table 4.2.3.9 Rocks from different regions that display very similar major oxide and trace element chemistry.

Region	Sample numbers
Grootfontein Inlier	L-1043, L-1044, L-1046
Mufulira Granite	L-166
Hook Granite Batholith	L-257, L-409
NW Zambia	L-370, L-364, L-020, L-030
Otjiwarongo environs	LL-4, LL-11, L-16, LJ-1

Samples from the environs of Otjiwarongo could be grouped into seven discrete groups based on their major oxide chemistry. The groups are shown on Figs. 4.2.3.5 and 4.2.3.7. Other geochemical diagrams did not produce significant results, because the groups of samples clustered together and overprinted each other. Table 4.2.3.15 shows the various groups of samples and the locations where they were sampled.

4.2.3.7.5 Otjiwarongo Batholith

The Otjiwarongo batholith may be responsible for mineralization at the Kombat mine. All observations and critical reading of literature available on the mine lead to conclude it formed as a deposit of the iron oxide-copper-gold family. Section 8.4.1.2 describes this in greater detail. Probably other copper deposits in the Kombat region have similar origin. All the occurrences of gold that surround Kombat are hydrothermal and could be attributed to the hidden batholith. It could also produce mineralization of the sediment-hosted gold type (so-called “Carlin ‘type’”) in the Otavi carbonate sequence. Several copper occurrences around Otjiwarongo and copper and gold occurrences NE of the same town seem to be of hydrothermal origin too. In fact, isotopic signatures from the Kombat mine indicate that sulfides have a magmatic input (Pirajno, Kinnaird, Fallick, Boyce, & Petzel, 1993). This is a very significant intrusive body to understand. Knowing more about it might lead to many major new mineral discoveries in Namibia.

The age of the Otjiwarongo Batholith is very significant, because it indicates that large-scale magmatism took place at that time. It is also significant, because the Otjiwarongo Batholith is probably responsible for IOCG mineralization at Kombat and Otjikoto gold deposit in Namibia.

4.2.3.7.6 Environment of Emplacement

All the samples from the environs of Otjiwarongo were emplaced in anorogenic environments, as indicated by the procedure of Whalen et al. Few of the samples produce coherent results from the Pearce and Maniar & Piccoli methods (Table 4.2.3.14). Those that do, indicate continental within-plate rift-related magmatism or continental epeirogenic uplift.

4.2.3.7.7 Geochronology

A zircon concentrate from composite sample **L-808c*** was dated to produce a preliminary SHRIMP U/Pb age of 550 Ma. The radiometric age is dating one of the last magmatic events of the Otjiwarongo batholith, and is the only geochronological constraint on the batholith. That age correlates well with the Zambian Hook Granite batholith, and the Damaran granitoids in Namibia. There are very few radiometric ages from rocks in this part of Namibia.

4.2.3.7.8 Discussion

The evidence obtained from macroscopic description and chemistry of the rocks collected from the environs of Otjiwarongo lead to think that the basement rocks in that part of Namibia are very similar to the rocks in the basement to the Grootfontein Inlier, the Zambian Copperbelt and northwestern Zambia, and probably have the same age. Table 4.2.3.15 groups the various samples from the environs of Otjiwarongo into several groups. Most of the groups are made of samples that come from more than one sampling site. The groups were plotted on Figs 4.2.3.5 and 4.2.3.7.

Table 4.2.3.15 Tentative correlation table for samples from the environs of Otjiwarongo, Namibia
(Letters indicate sites, roman numerals indicate rock types.)

	B	C	A	D	Other
					LL13 anomalous, altered
					LL9, altered granite
					L-1014, granodiorite
					L-814, altered granite, quartzolite
					L-808
		L-1039, L-1039c			
	LL13				
II		LL3a		LL2a	L-1044
III			LL4, LL5, LL11, LL16, L-810, L-812, L-850, L-1046		L-1043, LL18
V	LL17a	L-1039a, LL3b		LL2b	L-809, LL18, L-815, LL36, LL16, L-1042
VI	L-1038, L-1037, LJ1				L-813, L-815

The few samples collected that might come from the Otjiwarongo Batholith were dated at *circa* 550 Ma. This age is probably one of the latest in a series of intrusive events that made the batholith. The pegmatitic character of these rocks made it impossible to define their environment of emplacement precisely. Nevertheless, they formed in an anorogenic environment.

The age of most of the granitoids sampled in the environs of Otjiwarongo is uncertain. Several of them may be part of the basement to the Damara siliciclastic and carbonate rocks that have been exposed on surface due to tectonic uplift. Others may be intersecting such sequences. No relationships were directly observed in the field. Further indications of the geological setting of the granitoids may be possible, if funding for dating the granitoids becomes available.

Table 4.2.3.17 Rock types and environment of emplacement for the environs of Otjiwarongo, Namibia
(See acronym description on section 2.4.3.)

Sample	*Rock Name*	*Debon & LeFort*	*Maniar & Piccoli*	*Whalen*	*Pearce*	*Mafic*	*Rb/10HfTa*	*Rb/30HfTa*	*Nb-Ta*
L-808*	Granite pegmatite	Peraiii leuco K Mg	IAG-CAG	N	S2/4 O2/4		VA-	II	INV
L-809	Alkali granite	Metaiv leuco K Fe	IAG-CAG	A					
L-810	Pegmatitic granite	Metaiv leuco Na-K Fe		A					
L-812	Granite	Metav leuco Na Mg		A					
L-813	Granite	Metaiv leuco Na-K Fe		A					
L-814	Quartzolite, High silica	Metavi leuco Na Fe							
L-815	Pegmatitic granite	Metaiv meso NaK Fe		A	O-W1-1				
L-850	Granite	Peraiii subleuco Na Fe	POG	A	O3/4		WP	WP	OUTU
L-1037	Quartzmonzonite	Peraiii meso K Mg		A					
L-1038	Granite	Peraii subleuco K Mg		A					
L-1039	Alkali granite	Peraii leuco K Fe	CEUG	A					
L-1039a	Alkali granite	Peraiii leuco K Fe		A	S2/4 O2/4		VA-	VA	INV
L-1039c	Alkali granite	Peraiii subleuco K Fe	CEUG	A					
LJ1	Granite	Peraiii meso K Mg		A					
LL1	Granite	Peraii leuco K Mg	IAC+CAG	A					
LL10	Nepheline syenite	Metaiv meso Na Fe		A	W	wpab			
LL11	Granite	Peraii leuco K Fe		A					
LL13	Out of plot, high Ca+Si	Metavi meso Na Mg	OP	A	V	arc			
LL14	Nepheline syenite	Metaiv meso Na Fe	RRG	A	W	wpab			
LL15	Syenite	Metav meso Na Fe		A					
LL16	Granite-granodiorite	Peraiii meso Na Mg		A					
LL17a	Granite	Metav leuco K Fe		A					
LL17b	Granodiorite	Peraiii meso K Fe	RRG	A					
LL18	Granite	Metavi leuco K Fe		A					
LL2a	Alkali granite	Perai leuco Na-K Fe		A					
LL2b	Quartz syenite	Perai leuco K Fe		A					
LL3a	Alkali granite	Perai leuco K Fe		A					
LL3b	Alkali granite	Perai leuco K Mg	CCG	A					
LL4	Granite	Peraiii leuco K Fe	POG	A	O-W1-1				
LL5	Granite	Perai leuco Na Fe		A					
LL9	Granite	Perai leuco K Fe		A					

Table 4.2.3.14 Rock types and environment of emplacement for several Namibian domains

(See acronym description on section 2.4.3.)

Ugab River, Namibia									
Sample	*Rock Name*	*Debon & LeFort*	*Maniar & Piccoli*	*Whalen*	*Pearce*	*Mafic*	*Rb/10HfTa*	*Rb/30HfTa*	*Nb-Ta*
L-793	Granite	metaiv leuco Na Fe	POG	A	W3/4		WP-	WP	OUTU
L-795*	Granite								
L-796*	Granite								
L-797	Granite	peraii leuco Na-K Fe	RRG-CEUG	A					
L-798	Granite	peraii leuco Na-K Fe	POG	A					
L-799	Granite	peraii leuco Na-K Fe		A					
L-802	Granite	peraii leuco Na-K Fe		N					
Otjiwarongo Environs, Namibia									
Sample	*Rock Name*	*Debon & LeFort*	*Maniar & Piccoli*	*Whalen*	*Pearce*	*Mafic*	*Rb/10HfTa*	*Rb/30HfTa*	*Nb-Ta*
L-808*	Granite	Peraiii leuco K Mg	IAG-CAG	N	S2/4 O2/4		VA-	II	INV
L-809	Alkali granite	Metaiv leuco K Fe	IAG-CAG	A					
L-810	Granite	Metaiv leuco Na-K Fe		A					
L-812	Granite	Metav leuco Na Mg		A					
L-813	Granite	Metaiv leuco Na-K Fe		A					
L-814	out of plot, high Si	Metavi leuco Na Fe							
L-815	Granite	Metaiv meso NaK Fe		A	O-W1-1				
L-850	Granite	Peraiii subleuco Na Fe	POG	A	O3/4		WP	WP	OUTU
L-1037	Quartzmonzonite	Peraiii meso K Mg		A					
L-1038	Granite	Peraii subleuco K Mg		A					
L-1039	Alkali granite	Peraii leuco K Fe	CEUG	A					
L-1039a	Alkali granite	Peraiii leuco K Fe		A	S2/4 O2/4		VA-	VA	INV
L-1039c	Alkali granite	Peraiii subleuco K Fe	CEUG	A					
LJ1	Granite	Peraiii meso K Mg		A					
LL1	Granite	Peraii leuco K Mg	IAC+CAG	A					
LL10	Nepheline syenite	Metaiv meso Na Fe		A	W	wpab			
LL11	Granite	Peraii leuco K Fe		A					
LL13	out of plot, high Ca+Si	Metavi meso Na Mg	OP	A	V	arc			
LL14	Nepheline syenite	Metaiv meso Na Fe	RRG	A	W	wpab			
LL15	syenite	Metav meso Na Fe		A					
LL16	Granite-granodiorite	Peraiii meso Na Mg		A					
LL17a	Granite	Metav leuco K Fe		A					
LL17b	Granodiorite	Peraiii meso K Fe	RRG	A					
LL18	Granite	Metavi leuco K Fe		A					
LL2a	Alkali granite	Perai leuco Na-K Fe		A					
LL2b	Quartz syenite	Perai leuco K Fe		A					
LL3a	Alkali granite	Perai leuco K Fe		A					
LL3b	Alkali granite	Perai leuco K Mg	CCG	A					
LL4	Granite	Peraiii leuco K Fe	POG	A	O-W1-1				
LL5	Granite	Perai leuco Na Fe		A					
LL9	Granite	Perai leuco K Fe		A					
Grootfontein Inlier, Otavi Mountains, Namibia									
Sample	*Rock Name*	*Debon & LeFort*	*Maniar & Piccoli*	*Whalen*	*Pearce*	*Mafic*	*Rb/10HfTa*	*Rb/30HfTa*	*Nb-Ta*
L-1014	granodiorite	Peraiii meso Na Mg	IAG_CAG	?N					
L-1042	Granite	Peraii subleuco K Fe	POG	A			WP-	WP	OUTU
L-1043*	Granite	Peraii subleuco K Fe	POG	A	O-W 2-2		WP	WP	OUTU
L-1044	Granite	Peraii leuco K Fe	POG	A	O-W1-1				
L-1045	Quartzmonzonite	Metav subleuco Na Fe		A	W3/4				OUTU
L-1046	Granite	Peraii subleuco K Fe	POG	A	O-W1-1				
Okwa River, Botswana									
L-600A	Alkali granite	Metav leuco Na-K Fe	RRG-CEUG	A					
L-602	Granite	Metaiv meso Na-K Fe		A	O3/4				OUTU
L-605	Granite	Metav leuco Na Fe		A					
L-606	Granite	Metaiv meso Na Fe	RRG-CEUG	A					

Summas Mountains, Namibia								
Sample	*Rock Name*	*Debon & LeFort*	*Maniar & Piccoli*	*Whalen*	*Pearce*	*Rb/10HfTa*	*Rb/30HfTa*	*Nb-Ta*
L-789	Quartz syenite	Metalumi iv meso NaFe	RRG-CEUG	A	O-W 2-2			OUTU
L-791a	Alkali granite	Peralum ii leuco KFe	RRG-CEUG	A	W3/4	WP-	WP	INW
L-791b	Alkali granite	Peralum iv meso Na-KFe			W			

4.2.3.8 REVIEW OF OBSERVATIONS FROM THE OKWA RIVER, UGAB RIVER, GROOTFONTEIN AND SUMMAS MOUNTAINS OUTCROPS

The outcrops of the Okwa River in Botswana, the Ugab River and Grootfontein Inlier in Namibia that have been described in the previous pages are quite remarkable. Especially given the scarcity of outcrops in Botswana.

When geochemical data from the Ugab River, the Summas Mountains, Okwa River, Otjiwarongo[1], Grootfontein and the new Felsic volcanics are plotted on the R1/R2 diagram (Fig 4.2.2.1), several groups of similar rock types can be constructed, as indicated on Table 4.2.3.18. Groups II and III are common to the Okwa River, the Ugab River and the Grootfontein sampling areas. Chemistry, microscopic and macroscopic features of both rock types from each of the sites is remarkably similar, and one of them was present in the Summas Mountains, as shown on Table 4.2.2.10. That cannot be a coincidence. These bodies of rock probably came from the same type of magma. Derived from melting similar rocks. They probably suffered the same geological processes, and may have formed during the same events. Both of the foliated porphyritic granitoids contain mafic elongated lenses of xenolithic material that has been incompletely assymilated by the magma.

In addition, group III has two samples from the other domains, the Summas Mountains and the felsic volcanic rocks from Frets, 1969. Apart from that, when compiling the information another similarity was found between one of the samples from the Summas Mountains, three from the group of felsic volcanics and some from the Otjiwarongo area, here listed as group V. L-789 correlates well with samples from the Otjiwarongo area and conform group VI. Samples X-17 and L-1045 differ significantly from the other groups and are listed on their own, apart as groups VII and VIII.

The detailed chemistry of volcanic rocks from the Summas Mountains (L-791b) matched with granitoids from the Ugab River and the Okwa River sampling sites. The high Cr, Nb and Y signatures are unmistakable. The major oxide chemistry of the suite does not show anything special that can help to identify them positively from other rocks. Potentially all rocks in the suite contain high values of Sm, Nd and Pr, but this was not tested for all the samples. As illustrated on the table below, all rocks from group III contain high thorium values. No rocks from the Ugab River on group III contain anomalous thorium, while those of the Okwa River and Grootfontein do. The geochemical diagrams devised by Debon & LeFort did not produce any significant results.

Since the rocks at the Ugab River were dated, (540 Ma) one could probably extend the same age to rocks from the Okwa River and Grootfontein. The ~750 Ma age from xenocrystic zircons in the granites dated from the Ugab River may be a key to the source of the thorium, the chromium or some of the other “strange” enrichments. L-796, L793 and L-797 are the same type of rock with high Th. Maybe there was some special type of magma mixing that produced the Th enrichment.

All samples from the Grootfontein Inlier (event L-1044) have high copper. Two from Otjiwarongo do so too, and they don’t come from the same suite. None of the other samples contain anomous copper. Maybe copper in these regions is secondary and was brought in after the granitoids were emplaced. This might mean that there is more copper to be found around the Grootfontein Inlier and the Otjiwarongo batholith. Copper might have been introduced along with the thorium.

Probably suites II and III both formed in post orogenic environments. These environments may indicate both orogenic and non-anorogenic in the Whalen et al, 1987 plots.

II and III are better identified on the R1R2 diagram. The TAS diagram mixes them, as shown on Figs 4.2.3.10.

The new age obtained for a sample from the Grootfontein Inlier correlates well with rock type and ages from the Kamanjab Batholith.

[1] The Otjiwarongo domain will be described in the following chapter. Nevertheless, it is treated in this review because of its striking similarities with the Okwa, Ugab and Grootfontein domains.

Table 4.2.3.18 Groups of rocks from the Ugab-Okwa Domain compared with others in Namibia
(Underlined samples have chemical analysis. The # symbol indicates high heat producing granites)

Suite	Okwa River	Ugab River	Grootfontein	Summas Mts.	Otjiwarongo	Felsic Volcanics	NW Zambia
I	**L-602#** A Granite						
II	**L-606#** Medium-grained granite not as foliated as L-605. A ARG-CEUG	**L-798#** (f-medium-grained gray granite without pink felds. May be facies of "pink" granitoid) A POG **L-799** (m-c-g brown, porph granite with yellow quartz, magnetite + transparent to yellow plag) A **L-802** (non-mag f-medium-grained pink granite that grades from previous gray gtd. With small spindle-shaped, biot-rich xenolith and coarse biotite "eyes") N **L-795*** (c-g gray porph gtd + biot + mag clusters) ~540 Ma	**L-1042** c-g, porphyritic, foliated granite; copper; A POG WPG		**LL-2a**, **LL3a**		
III	**L-605#** A c-g, foliated granite. Old	**L-793** (c-g pink biotite granite with abund mag in clusters. Could be c-g facies of pink gtd) **L-797** (medium-grained pink biotite granite with pink felds, rare mag + red qz) **L-796*** (pink gtd + red qz clusters, no mag + zoned red plag), ~1700 Ma; **L-794**, **L-800**	**L-1043*#**f-g, felsic porphyritic granite with little foliation; Cu; A POG WP; 1939±64 Ma **L-1044#** f-g granite; seems to cut through L1042; Cu; A POG **L-1046#** c-g porphyritic grantie; copper; A POG	**L-791b** (pink-rd f-lam, vitreous, f-g alkali rhyolite tuff +conch. Fract.; A WPG; within plate granite	**L850#**, **LL4#**, **LL11#**, **LL5**, **LL-810**, **L-812#**, **LL14#**, **LL16#**	**X-20**? Rhyolite	**L-364**, **L370**
IV	**L-600A#** lt pink, non-fol porph. alkali granite with fine matrix. Cut by pink dike. A ARG-CEUG						
V				**L-791a** (pink-rd f-lam, vitreous, f-g, volcaniclastic alkali rhyolite (ash?) +conch. fract.); A RRG-CEUG	**L-1039** relatively weathered c-g gtd; conforms large whaleback outcrop; Cu **L-1039a** c-g gtd **L-1039c** c-g gtd; Cu **LL17a**, **LL3b**, **LL2b**, **L-809**	**X-16, X-18, X-19**; alkali rhyolites	
VI				**L-789** (~mag subvolcanic quartz trachyte with white porphyritic plagioclase + open vacuoles); A PPG-CEUG	**L-1038#** m-f-g, foliated, lt gy gtd **L-1037#** m-f-g, foliated, lt gy gtd; very high Ht **LJ-1#**; Cu; very high Th		
VII						**X-17**; rhyolite	
VIII			**L-1045#** c-g porphyritic quartzmonzonite, Copper; A		**LL17b**		
IX			**L-1014** N IAC-CAG				

4.2.4 WITVLEI, NAMIBIA

4.2.4.1 Introduction

The Okatjepuiko mineralized site and its associated granitoid rocks were visited by suggestion of Geologist Eckart Freyer, of the AngloAmerican exploration office in Windhoek (Freyer, E., 2002, personal communication). The site is located on Figs M26 and M19. Freyer offered information on a prospect he had recently been exploring, that displayed some special characteristics of iron oxide-copper-gold mineralization. He found ore-grade gold and copper mineralization on surface samples (3.5 gAu/ton and multi percent Cu). The mineralization seems to lie underneath and beside the Witvlei sedimentary-hosted copper deposit. The latter deposit has been said to be very similar to those of the typical Zambian Copperbelt (Anhaeusser & Button, 1973; Borg, 1995; Borg & Maiden, 1986; Maiden, 1996; Maiden, Innes, King, Master, & Pettit, 1984; Maiden, Master, & Borg, 1986; Main, 1978; McManus, 1994; Mendelsohn, 1981; Mendelsohn, 1986; Mendelsohn, 1989; Ruxton & Clemmey, 1986; Steven, 1992; and Steven, 1993). It is readily accessible by road, and has a railroad nearby (Fig M26).

Half a day of looking at the scarce outcrops, mapping and sampling, and a day describing core from two boreholes proved that Freyer was correct in his appreciation: the Okatjepuiko prospect could very well be an iron oxide-copper-gold deposit. Two boreholes drilled at the site were sampled and described at the exploration office of AngloAmerican in Windhoek. Part of the samples collected were analysed; they are listed on Table 4.5.5.4 and plotted on Figs 4.2.4.1 to 4.2.4.3. Although the number of samples is small, some special characteristics emerge; those will be described here.

Parts of the Okatjepuiko area have been explored by mining corporations for the past four decades. Sedimentary-hosted copper mineralization in the environs of the Okatjepuiko farm has been known all along. Fig 8.29 shows a few of the known mineralized sites, in the environs of Witvlei, as shown on the Namibian mineral deposit map. Several authors have described mineralization from Witvlei to be “typical” copperbelt-type deposits. Very little or no reference has been made on previous reports about gold, plutonic rocks associated with mineralization or iron oxide-copper-gold mineralization. Several of the reports make general mention of mafic rocks as a source for primary copper mineralization, but give few details about that issue.

A large amount of additional petrographic, mineralogic, and hydrothermal alteration information has been produced, geochemical and geophysical data from various entities has been processed, but will not be included in this document. Further discussion on Okatjepuiko and its associated iron oxide-copper-gold mineralization is included on section 8.4.1.1 of this document.

4.2.4.2 Field Observations

The Okatjepuiko 154 farm was visited on October 10th, 2002. Clear evidence of hydrothermal mineralization of Cu (and Au?) was observed at the farm. Field descriptions, updated with laboratory results are listed in Appendix A72. The coordinates of all geological stations and sampling sites are also in the Appendix. Geological stations and sampling sites are drawn on Fig 8.2.5.4.

Some of the rocks display round-clast hydrothermal brecciation overprinted by extreme red-brown hematite alteration. Samples **L-644** and **L-645** show those features. The original clastic texture of the rock - a breccia cemented by nepheline syenite - has almost vanished. Both the matrix and clasts of the breccia were replaced by a pervasive brown-red hematite alteration. Fig 4.2.1.21 illustrates these features. The alteration process is gradational.

Another significant geochemical feature of the suite of samples is that felsic rocks associated with mineralization have very little magnetism. They contain secondary, magnetite-rich veinlets; but that is a hydrothermal overprint and not a primary feature.

L-638 was selected for complete chemical analysis. This rock is a pink, medium-grained, metaluminous leucocratic potassic ferriferous alkali granite with magnetite veinlets. It seems to be one of the intrusives responseble for iron oxide-copper-gold mineralization at Okatjepuiko, and formed in a rift-related anorogenic environment. Strong magnetism in the rock is due to the high density of magnetite veinlets. It also offers a clear gravimetric contrast with the neighbouring rocks.

Table 4.2.4.1 Description of OP-1 Borehole, Okatjepuiko Project, Namibia. Depth in meters.

Depth	Description	Samples/Photos
0.62	Brown soil	
3.85	Dark to light green, weathered rock fragments that crumble easily. Medium-grained, weathered, magnetic subvolcanic, porphyritic,pink to pink-white metaluminous subleucocratic sodic ferriferous granite, with black crystals 1-2 mm ø.	**L-816***, 3.21m
4.00	Same as above, with gray tinction.	
6.00	Weathered, broken fragments of gray, red and black "clayey" rocks (lamprophyres?) with tinted surfaces.	
7.02	Weathered, broken fragments of yellow to gray rock, as above, but more consolidated, coarse grained to finer. All rocks from here to the surface are weathered.	
8.90	Dark gray to green, fine-grained, microporphyritic volcanic rock with 0.5 to 1 mm plagioclase phenocrystals and abundant green epidote veinlets.	
8.91	Red granitic vein with chlorite + epidote rims.	
13.00	Moderately magnetic, dar, fine-grained volcanic rock with green veins. There is a pink granitic vein from 12.13 to 12.14m.	
13.13	Dense network of white and light green veinlets with chlorite and epidote in a dark gray trap rock with white and freen 5-10 mm ø amygdules. Abundant hydrothermal alteration.	
15.52	Lighter, very fine-grained intrusive rock with no veins. Halo on contact.	
17.22	Medium density green veining in a dark, fine-grained dark green to black volcanic rock. Contains secondary Cu minerals	
17.77	Densely veined dark trap rock with epidotization in veins and vacuoles.	
18.90	Dark trap rock, with light amygdules ± 10 mm ø. Epidotization in veins and amygdules.	
22.30	Weakly magnetic, dark trap rock with fine green veins in a medium density veining pattern.	Ph 1,2
30.00	Dark gray to black fine-grained trap rock with fine green veining and light patches of hydrothermal alteration. Vacuoles are filled by somewhat epidotized pink and white plagioclase. The rock is cut by shear zones that are filled with serpentine, epidote and chlorite.	Ph 3,4, **C37**, 29.5m
30.01	Dense green veining.	
33.45	Dark rock with very little fine veining	Ph 5
34.35	Intermediate to strongly magnetic dark green trap rock with submillimetric to millimetric pink amygdules.	Ph 6
54.00	Dark trap rock with intermediate veining density; patches of white veins with yellow stains; occasional white amygdules ± 5 mm ø. Weakly magnetic due to disseminated magnetite.	Ph7,8, **L-818**, 29.5m
55.45	Denser dark gray trap rock with larger pink amygdules.	Ph. 9, 10, **L-819**, 53.6m
60.80	Beginning of pink granitic veining. Mixture of medium-grained gray and pink granitoids.	**L-820**, 57.37m; **L-821**, 60.17m
62.44	Medium-grained, dark gray intrusive rock with yellow to green veins and staining. Intense green stain (secondary copper carbonate and sulphate) at 62.44m.	
63.50	Moderately - to weakly-magnetic, fine-grained, dark gray trap rock. With intense surface malachite staining at 63.5m.	
65.00	Medium-grained granitoid with ink banding. Intense green malachite stain at 65.00m.	**L-822**, 63.75m
66.05	Dark gray to black trap rock with light mottled patches of alteration and intense green Cu staining.	**L-823**, 65.5m
66.70	Lighter trap rock with pink mottled patches of alteration.	
67.70	Medium-grained, dark gray intrusive rock with oxidized copper green speckles.	
68.13	Pink, medium-grained granitoid that encloses fragments of the dark gray trap rocks. Cut by millimetric dark gray veins.	Ph 11, 12
68.60	Medium-grained, dark gray intrusives with little macroscopically-detectable hydrothermal alteration.	Ph 11, 12
70.00	Weakly magnetic to non-magnetic, altered, medium-grained, pink granitoids with enclosed angular fragments of the trap rock. Intense yellow to green staining and shearing at 69.45m.	Ph 11, 12
74.80	Intensely altered, green speckled, fine-grained trap rock with gray veins, green copper carbonate and sulphate staining. Some pinkish and "quartzey" inclusions (=albite?). Abundant puyrple very thin veinlets that make stockworks.	Ph 13, **L-824**, 72.45m; **L-825**, 75.19m
76.61	Intensely-fractured, pinkish gray granitoid, with some rounded fragments. Turquoise chalcanthite staining along part of the fracture surfaces.	
77.52	Similar as above, but with more whole, purply/dark pink granitoid rock mixed with gray trap rock.	**L-826**, 77.1m
78.35	Dark gray trap rock with black spotty mineralization; veining is masked by some sort of hydrothermal alteration (sodic?).	
85.00	Moderately to weakly magnetic, medium-grained pink intrusive that encloses very fine-grained dark gray trap rocks. There is grading between medium-grained gray and pink zones. Ocassional green/yellow staining in the trap.	Ph 14, **L-827**, 79.11m; **L-828**, 80.63m
87.27	Dark gray, fine- to medium-grained trap rock. With occasional white quaretz veinlets.	
87.55	Pinkish staining of the medium to dark gray trap rock. (= albitization?)	
92.78	Non-magnetic to slightly magnetic, dark gray trap rocks with slight green staining. Very little disseminated magnetite.	
100.00	Gray trap rocks with pink angular fragments and pink subvolcanci granitoid rock with dark gray included angular fragments. Ocassional yellowish-green stainig of the dark gray trap rocks, thin white veinlets, and also some very thin magnetite veinlets. Purpley-pink medium-grained granitoids with black veins.	

4.2.4.3 Description of the OP-1 borehole, Okatjepuiko Project

Core from two boreholes drilled into the Okatjepuiko deposit were observed and described at the AngloAmerican office in Windhoek. Table 4.2.4.1 contains a rapid lithological log of borehole OP-1. Table 4.2.4.2 lists main information on the samples collected from the borehole. Sample **L-816*** was dated, and that will be discussed in the Geochronology section below. Figures 4.2.4.7 to 4.3.5.20 show photographs of core from the borehole. Table 4.2.4.1 refers to the photographs in order, using numbers 1 to 14.

4.2.4.4 Geochemistry

Chemical analysis from samples collected at the Okatjepuiko prospect show strong sodic alteration, Cu enrichment, and general high Pr values (Table 4.5.5.4). All rocks from this area are also enriched in Ni, Co, Zn, Cr and V. Th and U values are below the limit of detection. Values of Rb, Sr, Y, Zr and Nb are very low.

Table 4.2.4.2 Samples collected from borehole OP-1, Okatjepuiko, Namibia

(The term "trap rock" was used for mafic, fine-grained rocks that could not be better identified macroscopically.)

Sample	Depth (m)	Description
L-816*	3.21	Medium-grained, weathered, magnetic, subvolcanic, porphyritic, pink to pink-white, metaluminous subleucocratic sodic ferriferous granite
L-817	29.50	Dark gray-black, fine-grained intrusive rock with vacuoles filled by epidotized pink and white plagioclase. Cut by shear zones filled with serpentine, epidote and chlorite.
L-818	38.23	Dark gray trap rock with intermediate veining density and occasional white amygdules ±5mm ∅. Weakly magnetic due to disseminated magnetite
L-819	53.60	Denser dark gray trap rock with larger pink plagioclase amygdules
L-820	57.37	Mixture of medium-grained gray and pink granitoids
L-821	60.17	Mixture of medium-grained gray and pink granitoids
L-822	63.75	Medium-grained granitoid with pink banding
L-823	65.50	Dark gray to black trap rock with light mottled amygdules and intense green Cu staining
L-824	72.45	Intensely altered, green speckled, fine-grained trap rock with grey veins, green copper carbonate and sulphate staining. Some pink amygdules that may be filled by albite. Abundant purple very thin veinlets that make stockworks.
L-825	75.19	Light green-gray trap rock with pink amygdules and intense alteration
L-826	77.10	Intensely-fractured pink-gray rock, with some rounded fragments. Chalcanthite staining along part of fracture surfaces.
L-827	79.11	Moderately to weakly magnetic, medium-grained pink intrusive with angular fragments of trap rock
L-828	80.63	Moderately magnetic, medium-grained pink intrusive with fragments of green-stained gray trap rock

Table 4.2.4.3 Chemical Analysis, Okatjepuiko, Witvlei, Namibia

(Total iron oxides were grouped under FeOt. complete elemental analysis is on Table A13, Appendix)

Sample	SiO2	TiO2	Al2O3	FeOt	MnO	MgO	CaO	Na2O	K2O	P2O5	LOI	Total	Na+K
Notch	50.00	1.00	15.50	6.00	0.150	2.00	5.00	4.90	5.50	0.30	2.00		
L-625	74.31	0.32	12.49	2.19	0.04	0.42	0.94	5.72	2.00	0.10	0.70	99.23	7.72
L-626	75.44	0.32	12.53	3.15	0.05	0.57	0.71	5.99	1.04	0.06	0.63	100.49	7.03
L-633	51.27	1.55	16.00	10.81	0.18	6.69	7.17	3.71	1.69	0.26	1.07	100.40	5.40
L-635	62.14	0.98	15.43	6.05	0.12	3.29	3.28	7.37	0.22	0.15	1.00	100.03	7.59
L-637	69.84	0.53	13.33	5.85	0.06	0.58	2.19	5.95	0.76	0.10	1.00	100.19	6.71
L-638	77.05	0.18	11.68	2.36	0.04	0.14	0.62	4.27	3.73	0.02	0.42	100.51	8.00
L-641	50.76	2.24	13.78	12.16	0.24	6.49	7.32	4.30	0.62	0.40	1.90	100.21	4.92
L-645	56.67	1.27	14.07	9.26	0.09	0.42	5.87	8.40	0.16	0.33	3.96	100.50	8.56
L-648	72.50	0.35	12.81	4.25	0.05	0.69	0.64	7.27	1.32	0.06	0.59	100.53	8.59
L-649	73.86	0.30	12.07	4.77	0.06	0.53	0.64	5.74	1.86	0.05	0.56	100.44	7.60
L-816*	74.57	0.30	12.43	3.00	0.06	0.39	1.37	6.02	1.96	0.04	0.44	100.58	7.98

Sample	Rb	Sr	Y	Zr	Nb	Co	Ni	Cu	Zn	Ga	V	Cr	Ba	U	Th	Sc	Pb	Sm	Nd	Pr	Ce	La	Hf	Ta	Eu	Gd	Tb	Dy	Yb	Lu
Notch	200	400	60	360	40	30	16	25	85	26	100	100	1300	20	37	20	20	50	50	15	175	95	10	120	4	30	5	20	8	2
L-625	43	78	49	280	30	<6	15	753	26	15	21	123	493	<6	<15	<10					125	54								
L-626	18	64	50	263	30	<6	13	1078	41	17	21	53	609	<6	<15	<10		11	33	66	112	31		39	1				3	1
L-633	56	239	26	123	13	52	115	499	110	17	279	202	550	<6	<15	31		13	16	36	43	11		224			6		1	1
L-635	9	33	31	241	19	20	64	64	46	20	134	101	58	<6	<15	19		9	24	49	67	21		90	1		3		1	1
L-637	17	165	56	727	29	8	18	128	34	20	26	49	359	<6	<15	10		123	61	134	180	93	3	34	1				4	2
L-638	59	91	35	148	18	<6	9	95	29	15	14	66	751	<6	<15	<10	11	8	41	10	116	53	4	1	1	7	1	7	4	1
L-641	27	195	33	131	15	48	90	704	133	17	262	196	247	<6	<15	34			12	46	28	<12								
L-645	5	67	38	214	17	9	21	6	21	19	113	185	87	<6	<15	26					49	22								
L-648	25	69	21	248	12	6	17	1546	44	13	47	67	1144	<6	<15	<10					89	30								
L-649	37	63	16	193	11	9	19	2238	37	11	50	78	1330	<6	<15	<10					74	19								
L-816*	43	91	52	284	32	<6	13	104	62	17	18	81	386	<6	<15	<10		116	36	72	122	33	1	33	1				3	1

TOTAL ALKALI vs SILICA DIAGRAM
Okatjepuiko, Witvlei, Namibia; Lufilian G.P.
(Based on Middlemost, 1994, 1997)

Samples

Petrographic fields

Fig 4.2.5.1

L-645
L-648
L-816
L-638
L-625
L-649
L-635
L-626
L-637
L-633
L-6415

8
7
6

50 55 60 65 70 75

SiO_2%

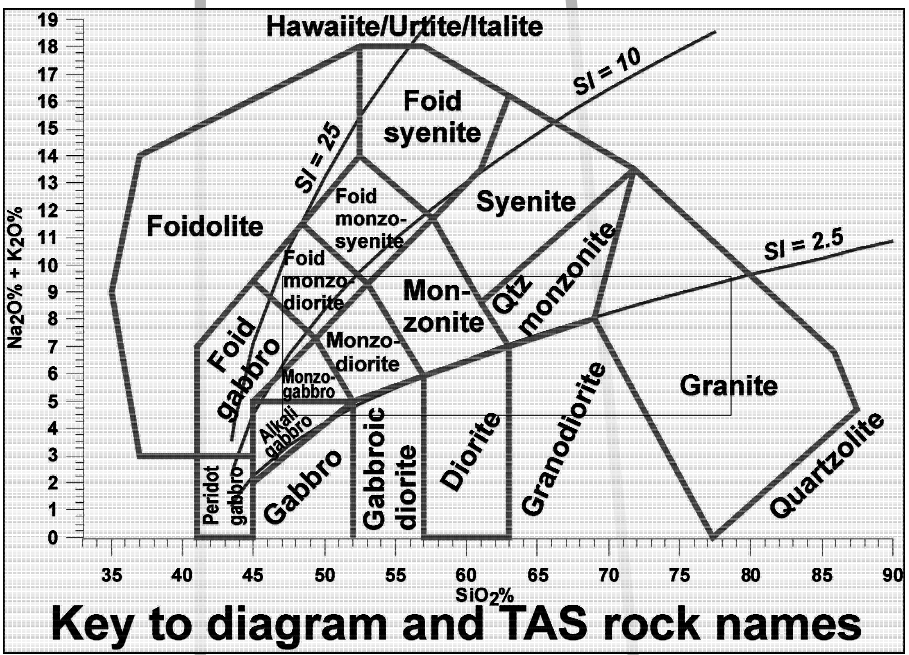

Key to diagram and TAS rock names

Fig 4.2.4.1

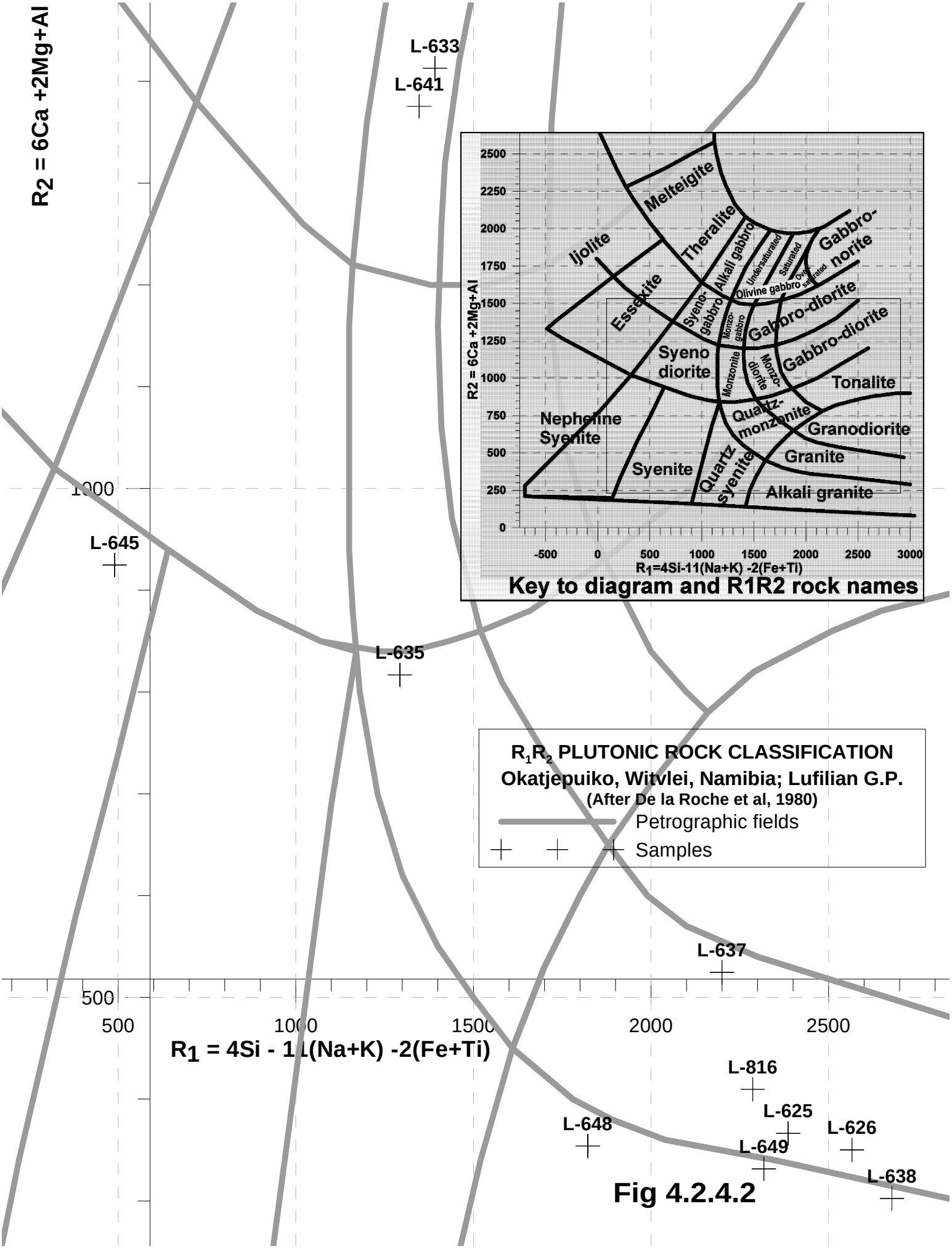
R2 = 6Ca +2Mg+Al
L-633
L-641
L-645
L-635
L-637
L-816
L-625
L-626
L-648
L-649
L-638
1000
500
500
1000
1500
2000
2500
R1 = 4Si - 11(Na+K) -2(Fe+Ti)
Melteigite
Ijolite
Theralite
Alkali gabbro
Olivine gabbro
Gabbro-norite
Essexite
Syeno-gabbro
Monzo-gabbro
Gabbro-diorite
Syeno diorite
Monzonite
Monzo-diorite
Tonalite
Quartz-monzonite
Granodiorite
Nepheline Syenite
Syenite
Quartz syenite
Granite
Alkali granite
Key to diagram and R1R2 rock names
R1=4Si-11(Na+K) -2(Fe+Ti)
R1R2 PLUTONIC ROCK CLASSIFICATION
Okatjepuiko, Witvlei, Namibia; Lufilian G.P.
(After De la Roche et al, 1980)
Petrographic fields
Samples

Fig 4.2.4.2

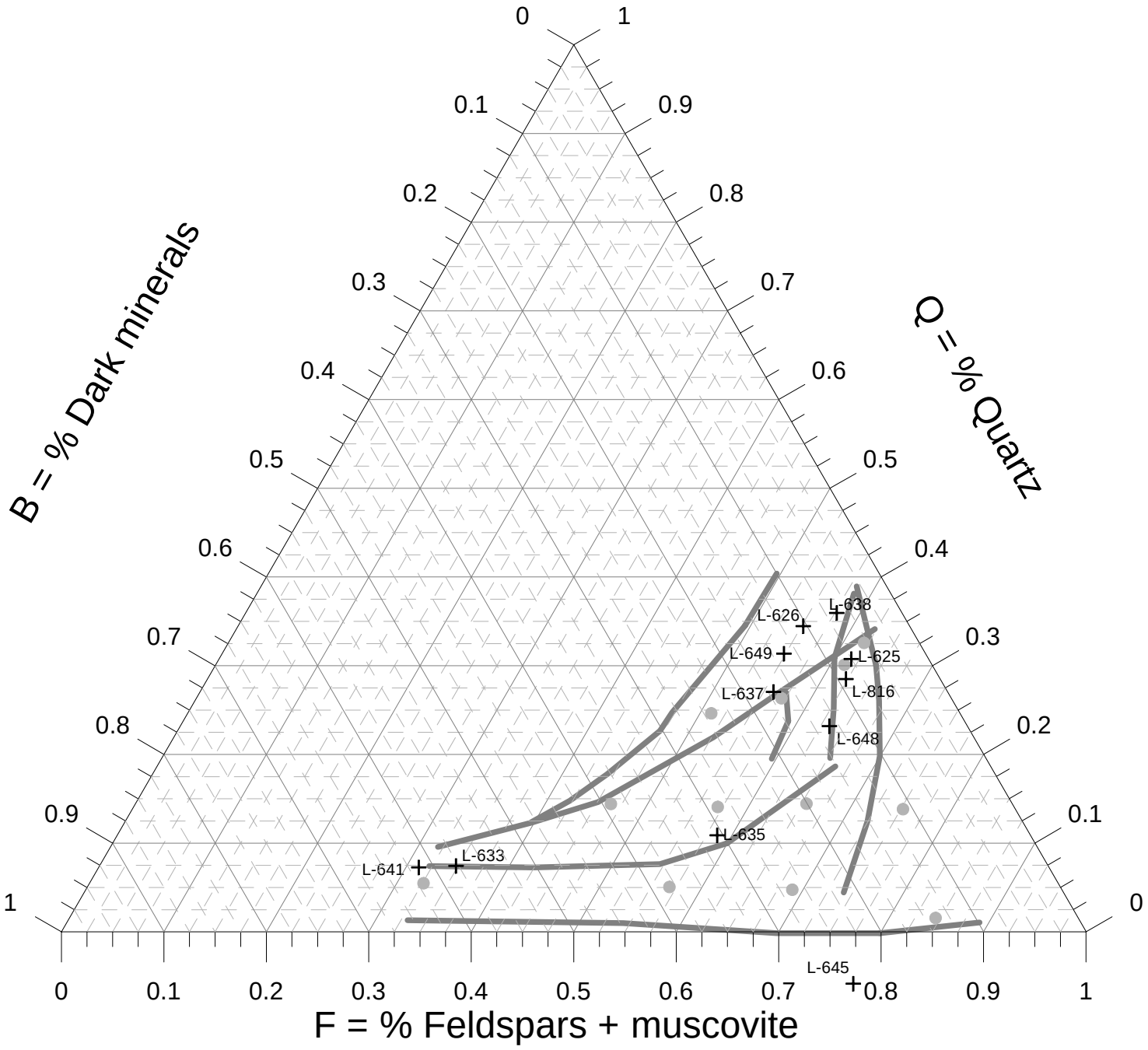

QBF ternary diagram (after Debon & LeFort, 1994)
Samples from the Okatjepuiko Farm, Witvlei, Namibia
Greater Lufilian Arc Granitoid Project

Reference samples (Debon & LeFort)
Samples

Fig 4.2.4.3

Table 4.2.4.4 Statistics of rock types, Okatjepuiko environs, Witvlei, Namibia
Based on the modified TAS diagram of Middlemost, 1994. The fifth column (granitoids) is the sum of underlined rock types.

Group	Rock type	number	%	Granitoids	Groups
Midalkaline Rocks	Alkali granite	1	9.09	33.33	45.45
	Monzonite	2	18.18		
	Monzogabbro	1	9.09		
	Alkali gabbro	1	9.09		
Subalkaline Rocks	Granite	5	45.45	66.67	54.55
	Granodiorite	1	9.09		
Total		11	100.00	100.00	100.00

Although the number of samples analysed is too small to be representative, statistics on their composition may be revealing. Two thirds of the granitoids from the Okatjepuiko deposit fall within the subalkaline field, while one third are midalkaline granitoids (Table 4.2.4.4). Midalkaline and subalkaline rocks are roughly equal in general figures.

Gabbroids have been under-represented in the current sampling; those are more abundant and they seem to play an important role in the iron oxide-copper-gold mineralization style. Only a few of the multiple gabbroid rocks observed were sampled. Mafic rocks make over 70% of material intersected at boreholes OP-1 and OP-2, and no mafic rocks from the boreholes were analysed. Part of those rocks may turn out to be alkaline, including nepheline syenites.

Table 4.2.4.5 Comparison of samples from the Okatjepuiko area, Namibia
(See acronym description on section 2.4.3.)

Sample	Rock Name	Debon & LeFort	Maniar&Piccoli	Whalen	Pearce	Mafic	Rb/10HfTa	Rb/30HfTa	Nb-Ta
L-625	Granite	metaiv subleuco Na Fe	POG	A	V1/2				
L-626	Granite	peraiii meso Na Fe	POG	A					OUTU
L-633	Monzo-gabbro	metaiv meso Na Fe		N?Zn		arc			OUTU
L-635	Quartzmonzonite	metaiv meso Na Fe	OP	A	V2/4	wpab			OUTU
L-637	Granite	metaiv meso Na Fe	OP	A			WP	WP	OUTU
L-638	Alkali granite	metaiv leuco Na Fe	RRG	A	S2/4 O2/4		VA-	VA	INV
L-641	Monzo-gabbro	metaiv meso Na Fe		N?Zn	V	wpab			
L-645	Nepheline syenite	metav meso Na Fe	RRG-CEUG	A	V	wpt			
L-648	Alkali granite	metaiv meso Na Fe		A	V				
L-649	Alkali granite	metaiv meso Na Fe	RRG	N?	V				
L-816*	Granite	metav subleuco Na Fe	POG	A			WP	WP	OUTU

A special feature that stands out on Table 4.2.4.5 is that all rocks display a sodic ferriferous nature. There is a greater proportion of metaluminous mesocratic rocks. Fig 4.2.4.2 shows that the cluster of granites has **L-816*** just in the center. The same is observed on the TAS diagram (Fig 4.2.4.1). Chemistry of these granites has been reasonably documented by six samples, listed on Table 4.2.4.6. Comparison of these samples shows a clear pattern.

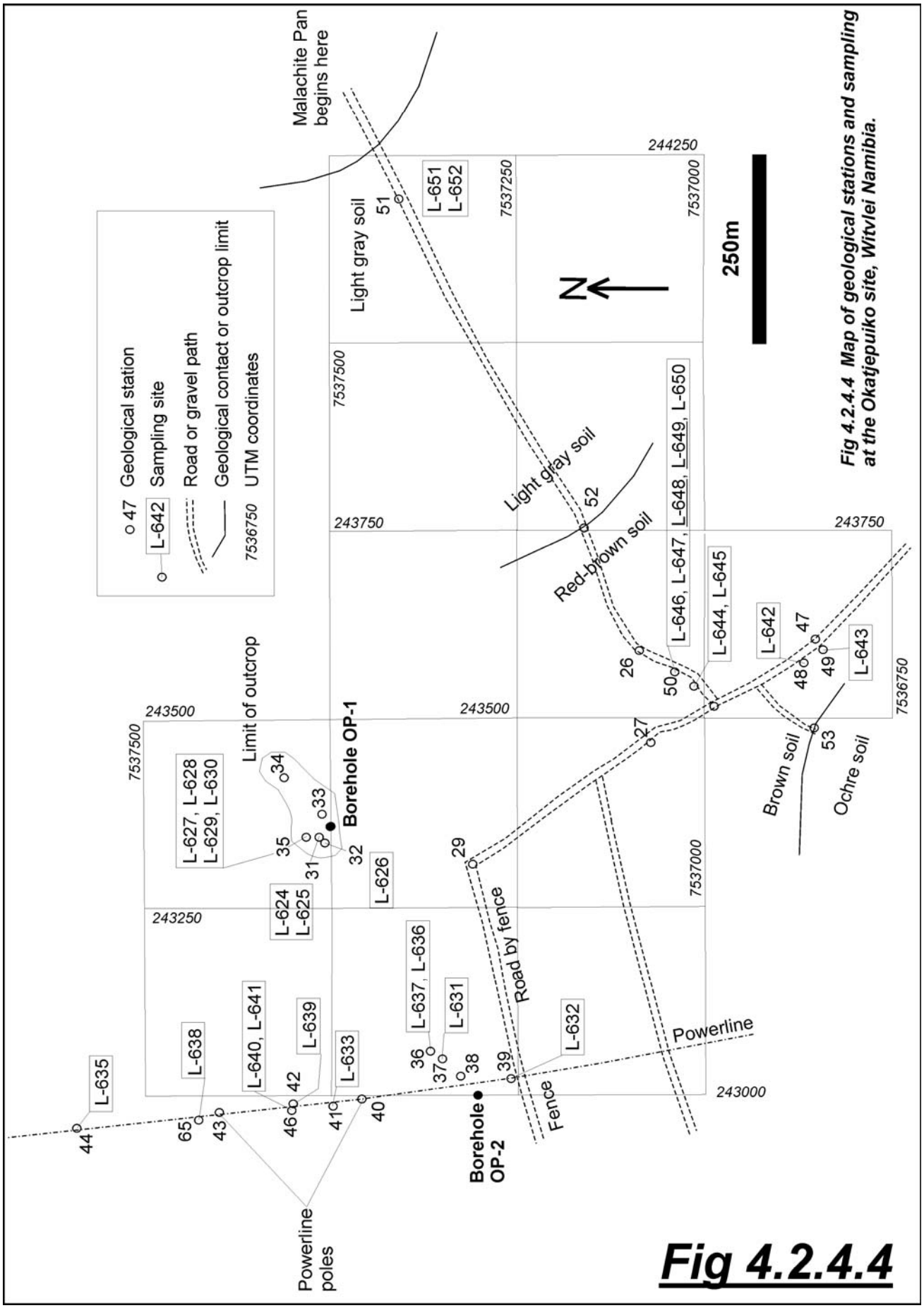

Fig 4.2.4.4 Map of geological stations and sampling at the Okatjepuiko site, Witvlei Namibia.

Fig 4.2.4.4

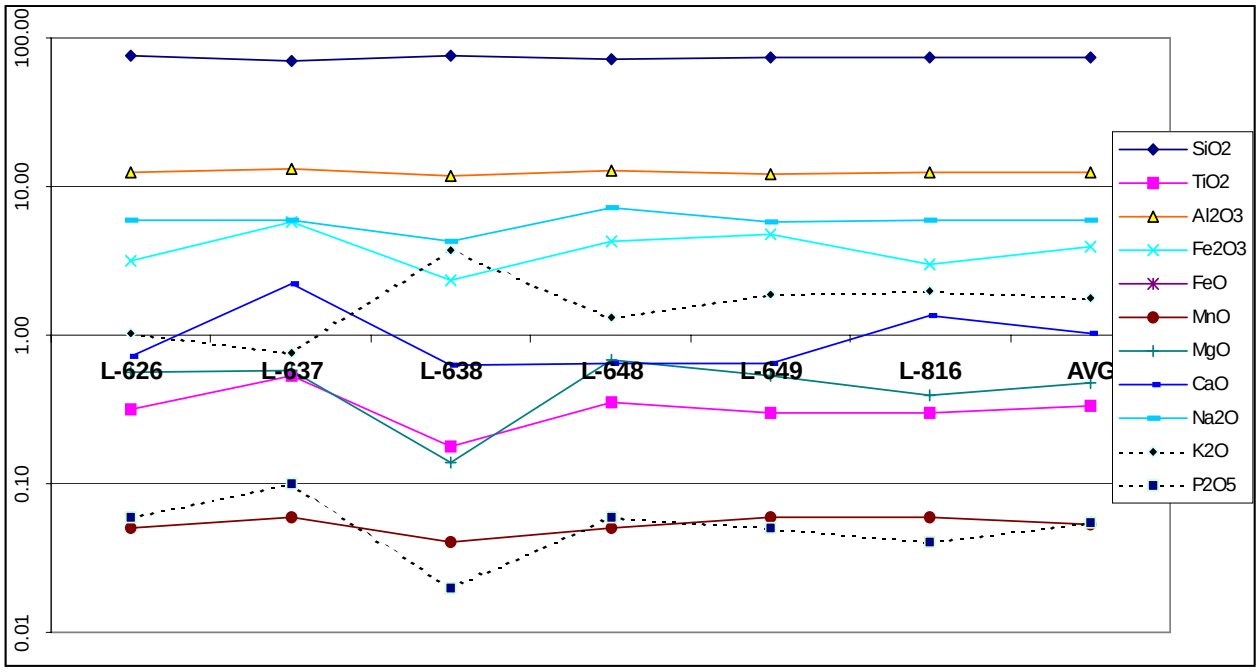

Fig 4.2.4.5 Logarithmic major oxide plot, granitoid samples, Okatjepuiko prospect, Witvlei, Namibia.

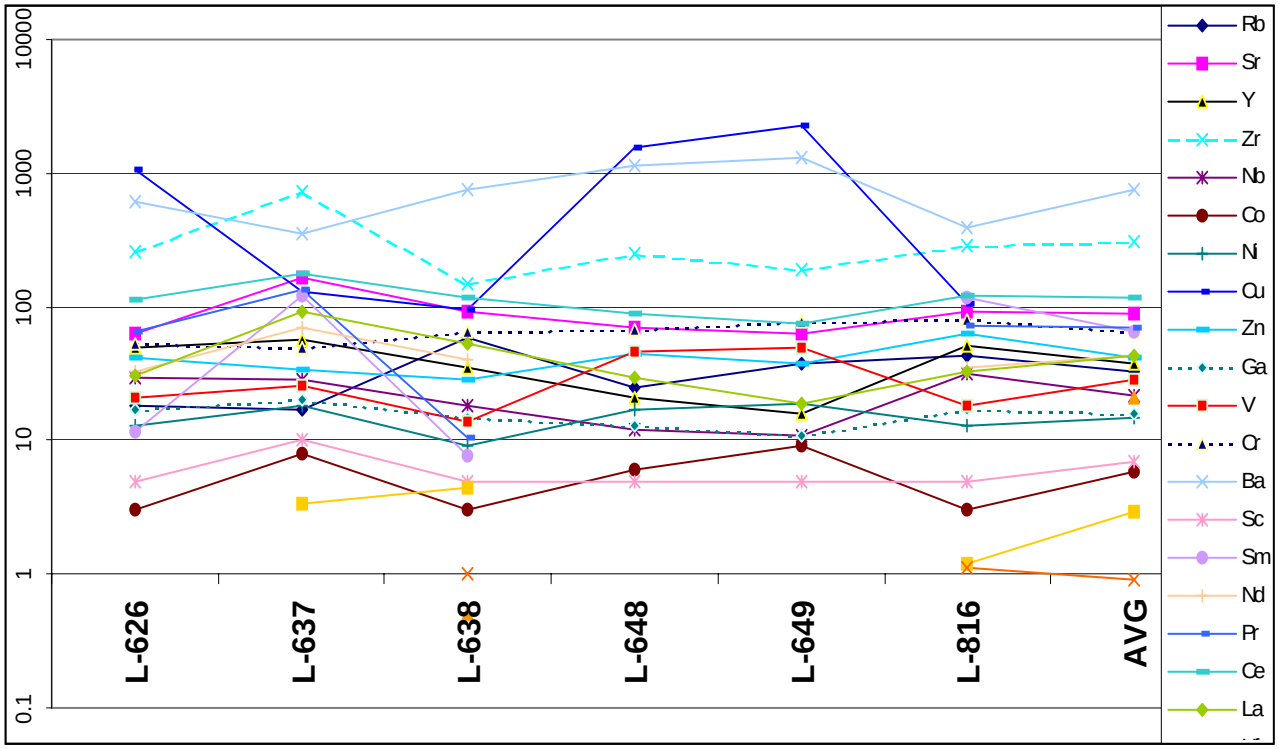

Fig 4.2.4.6 Logarithmic trace element plot, granitoid samples, Okatjepuiko prospect, Witvlei, Namibia.
(Values below the limit of detection were estimated to be half of the limit.)

Table 4.2.4.6 Chemistry of granitoids from the Okatjepuiko Prospect, Namibia
(Extracted from Table 4.5.5.4.)

Sample	SiO2	TiO2	Al2O3	FeOt	MnO	MgO	CaO	Na2O	K2O	P2O5	Rb	Sr	Y	Zr	Nb	Co	Ni	Cu	Zn	Ga	V	Cr	Ba	Sc	Sm	Nd	Pr	Ce	La	Hf	Ta	Eu
L-626	75.44	0.32	12.53	3.15	0.05	0.57	0.71	5.99	1.04	0.06	18	64	50	263	30	<6	13	1078	41	17	21	53	609	<10	11.5	33.3	65.5	112	31			
L-637	69.84	0.53	13.33	5.85	0.06	0.58	2.19	5.95	0.76	0.10	17	165	56	727	29	8	18	128	34	20	26	49	359	10	123	69.8	134.1	180	93	3.313		
L-638	77.05	0.18	11.68	2.36	0.04	0.14	0.62	4.27	3.73	0.02	59	91	35	148	18	<6	9	95	29	15	14	66	751	<10	7.71	40.9	10.4	116	53	4.36	0.51	1.02
L-648	72.50	0.35	12.81	4.25	0.05	0.69	0.64	7.27	1.32	0.06	25	69	21	248	12	6	17	1546	44	13	47	67	1144	<10				89	30			
L-649	73.86	0.30	12.07	4.77	0.06	0.53	0.64	5.74	1.86	0.05	37	63	16	193	11	9	19	2238	37	11	50	78	1330	<10				74	19			
L-816*	74.57	0.30	12.43	3.00	0.06	0.39	1.37	6.02	1.96	0.04	43	91	52	284	32	<6	13	104	62	17	18	81	386	<10	116	35.6	72.1	122	33	1.200		1.1
Average	73.9	0.3	12.5	3.9	0.05	0.48	1.03	5.87	1.78	0.1	33	90	38	311	22	5.8	15		41	16	29	66	763	7	64.2	42.7	70.5	116	43.1	2.96	21	0.9

All the samples from the Okatjepuiko suite, except for **L-645** contain very high copper values, as seen on Tables 4.2.4.3 and 4.2.4.6. **L-645** is a hydrothermal breccia with an intense overprint of hydrothermal red iron oxide alteration Fig. 4.2.2.21. The high copper values are also shown on the logarithmic plot of trace element values for granitoids in the Okatjepuiko suite (Fig 4.2.4.5). An important observation is that copper enrichment is seen both on mafic and felsic igneous rocks.

A portion of the anomalous copper content in rocks from Okatjepuiko may have secondary origin, in the form of copper carbonates, sulfates and phosphates hosted in joints and rock cleavage. Nevertheless, the major proportion of the copper has primary hydrothermal origin. It is hosted in sulfides, iron oxides and silicates that are main rock constituents. Detailed studies to define the location of copper in the samples were not carried out.

The major oxide logarithmic plot for Okatjepuiko granitoids shows that they have very uniform chemistry. One of the main features is the high values for Na_2O. That is probably an indication of hydrothermal sodic alteration. The general order of major oxide concentration is: SiO_2, Al_2O_3, Na_2O, FeOt, K_2O, CaO, MgO, TiO_2, P_2O_5 and MnO. Average values for each of the major oxides is listed on Table 4.2.4.6 and plotted on Fig. 4.2.4.5.

The chemistry of trace elements for the suite of granitoids is also rather uniform. Table 4.2.4.6 lists the values for trace elements and Fig 4.2.4.5 shows their logarithmic plot. As illustrated, the variation for most of the elements occurs in a narrow range, often less than half of an order of magnitude. Copper is the metal with the greatest relative variation. Thorium values are surprisingly low, below the level of precise detection. Uranium is also very low. Cobalt values are relatively low, and certainly far from economic concentration. The general order of abundance of some trace elements is the following: Zr, V, Zn, Nb, Co. That elemental abundance is very characteristic and was not observed in the other sample suites from the Greater Lufilian Arc.

The role of the abundant types of mafic and ultramafic rocks including alkaline gabbros, gabbros and lamprophyres observed in the Okatjepuiko area is not well understood. Those rocks might serve as source for various metals including: Co, Ni, Co, Cr and V. Very few samples of mafic and ultramafic rocks were analysed, and that information is probably not enough to produce relevant results. Further studies on the mafic and alkaline rocks should be carried out.

4.2.4.5 Environment of Emplacement

Results of some processes to evaluate environment of emplacement for the various rock types are listed on Table 4.2.4.5. The procedure developed by Whalen et al, 1989 indicates that all samples analysed were formed in anorogenic environments. Most of the results from other methods produce conflicting results. There must have been a significant mixing of crustal rocks in the formation of the granitoids, because the Harris and Pearce diagrams indicate volcanic arc signatures. Nevertheless, post orogenic environment and rift-related environment seem to be prevalent. The hydrothermal alteration that is evident in most rocks probably changed their chemistry to a point where traditional methods to evaluate granitoid environment of emplacement are useless.

The granitoids from Okatjepuiko were collected in a relatively small area. The chemistry of the rocks is rather uniform as shown in the last few pages. They probably formed in a single tectonic environment; or in a slowly changing environment, such as incipient rifting that took place after post orogenic collapse.

Further studies are currently being done with neural web software to compare geochemistry of several thousand samples with Okatjepuiko rocks. This is expected to help define the tectonic environment of emplacement for the granitoids.

4.2.4.6 Geochronology

A zircon concentrate from a single sample in the Okatjepuiko area was dated at the ANU in Canberra. Sample **L-816*** came from a subvolcanic, porphyritic, metaluminous subleucocratic potassic ferriferous granite in borehole OP-1. A composite of zircons from various parts of the same granitoid was dated using radiometric U-Pb SHRIMP II techniques. It gave an age of 1097.6±5.9 Ma. Xenocrystic zircons in the same sample indicated ages of 1194.6±11 Ma and 1871±6.8 Ma. The sample comes from one of the plutonic bodies responsible for copper and gold mineralization at Okatjepuiko.

The sequence of rocks that holds copper mineralization at the Witvlei sedimentary-hosted copper deposit was dated in the Ghanzi section, Botswana, at 1106 Ma, on a conformable, largely volcanic material [Schwartz et

al, 1996] (See event 72 on Table A22.18 and on the event diagram of Fig A43). Subvolcanic intrusive rocks associated to IOCG mineralization at Witvlei (Okatjepuiko farm) were dated in this project at ~1098 Ma. The question that immediately comes to mind is: Are these two types of mineralization related?

4.2.4.7 Other Events of the Same Age in the Region

Many radiometric ages are available from Southern Africa around 1098 Ma. Table A22.18 a selection of zircon U-Pb geochronological data from that lapse of time. The event diagram of Fig A43 illustrates the density of ages and great temporal continuity of the spread of data available. Data from sample **L-816*** has been highlighted there for comparison.

The last decade has seen a very large amount of geochronological data been produced on the *circa* 1100 Ma volcanic and plutonic belts of Southern Africa, including the southern portion of the Greater Lufilian Arc. It is common knowledge now that the time span of the granitoids and volcanics extends continuously from 1250 Ma to 1000 Ma as listed on Table A22.18 and shown on Fig A43.

The plutonic-magmatic belt extends for several thousands of kilometers along the border of the Kalahari Craton. It is not so well exposed under the Kalahari desert, and that area is precisely in the middle of the Greater Lufilian Arc granitoid project.

Recent work in parts of the Irumide and Kibaran belts of Zambia and the D.R.Congo by DeWaele and co-workers [De Waele, 2004; and De Waele, Fitzsimons, & Nemchin, 2004 (as well as dozens of papers cited in the reference section)] have greatly enhanced the knowledge of the *circa* 1100 Ma age span. The Namibian and northern South Africa counterpart has had abundant work done in recent decades and literally hundreds of geochronological data are available (See references in Table A22.18).

The Ghanzi-Chobe ridge in Botswana is an area that correlates well with the Witvlei granitoid and sedimentary sequence. According to Singletary et al., 1998 bimodal volcanic rocks occur in the north-east-trending Ghanzi-Chobe ridge. They state that “the Ghanzi-Chobe Ridge volcanics occupy a rift superimposed on a pre-existing Kibaran orogenic belt continuous with coeval terranes to the north in Zambia, and to the south in the Namaqua belt of South Africa” (Singletary et al., 1998).

Mafic volcanic rocks have been identified in the *circa* 1100 Ma belts in Namibia. Amygdaloidal basalts, quartzites, conglomerates and acid volcanic rocks in the Rehoboth-Witvlei area were intruded by granites of the Gamsberg Suite and numerous diabase and quartz porphyry sills and dikes (Miller, 1992). Underformed quartz-feldspar porphyries and pyroclastic rocks of *circa* 1100 Ma are found in several locations, including the Nuckopft and Guperas formations (Miller, 1992).

Pfurr, Ahrendt, Hansen, & Weber, 1991 published Rb-Sr ages of 1049±28 Ma for volcano-sedimentary units in the Rostock massifs of the Southern Marginal Zone of the Damara Orogen, Namibia, and maximum U-Pb zircon ages of around 1200 Ma. In general, a period of granitoid emplacement and volcanic activity between 1200-1050 Ma is indicated by the results. That is precisely what Fig A43 shows. Pfurr and co-workers further state that the emplacement of the (*circa* 1100 Ma) igneous rocks is related to collision-induced rifting, complementary to the Kibaran Orogenesis.

Further SHRIMP geochronological data from the Okatjepuiko deposit may help to better define the geological evolution of this prospective area.

4.2.4.8 Evidence of Iron Oxide-Copper-Gold Mineralization and Definition of a Mineralized Belt

The Okatjepuiko mineralization lies in the middle of a rectangular 3 x 6 km magnetic anomaly produced by a cluster of many small magnetic bodies of subvolcanic porphyritic intrusions. The Okatjepuiko prospect lies in the center of the anomalous zone, just in the middle of a small granitic intrusion. Other evidence of a suitable environment for the presence of iron oxide-copper-gold mineralized systems in the environs of Okatjepuiko includes dissemination of copper sulfides in granites and mafic lavas, explosive brecciation, abundant presence of secondary copper minerals and stockworking. Gabbros as well as felsic intrusive rocks outcrop in the area. Subrounded-clast hydrothermal breccias with intense brown-rock and red-rock (iron oxide) alteration also outcrop. Vuggy massive magnetite and hematite fragments occur as float; in fact, a strong magnetic anomaly guided exploration to the site. Among the types of hydrothermal alteration observed are sodic alteration and progressive hematitization that overprints previous textures to a point where they are unrecognizable. All of these ingredients point to an iron oxide-copper-gold mineralization at depth, under the previously identified sedimentary-hosted copper deposit. Gold is not present in the sedimentary-hosted copper deposit; it probably remained underneath in the original hypogene deposit.

Evidence of IOCG mineralization under at least one of the sedimentary-hosted copper deposits of Namibia is very important. The presence of both hydrothermal copper and gold under the Witvlei deposit is relevant to understand the regional metallogeny, and could lead to a completely different source for copper in the Greater Lufilian Arc.

The model of mineralization identified at the Okatjepuiko farm is not restricted to the environs of Witvlei; it can be applied along the NE and SW extensions of a belt made of rocks with similar chemistry and age that occur along more than 600 km across Namibia and Botswana. The entire “Kalahari Copper Belt”, as described by Maiden et al, 1984, could be prospective for IOCG mineralization. The belt has been given different names. This type of mineralization probably extends NW into the well defined Ghanzi-Chobe Belt, of Botswana (Modie, 2000); and SE into the Rehoboth and Helmeringhausen areas of Namibia. Borg, 1995 considers that the belt is an aborted rift basin that underwent tectonic inversion.

4.2.4.8 Conclusions

1. The Okatjepuiko prospect has all the characteristics of an iron oxide-copper-gold deposit.

2. Sodic ferriferous felsic granitoids that are closely associated with fine-grained mafic rocks were emplaced in an anorogenic environment into siliciclastic, carbonate and volcanic sequences and they produced the iron oxide-copper-gold mineralization. The chemistry of the granitoids is reasonably well defined. That of associated mafic and ultramafic rocks is not that well constrained.

3. There are many radiometric ages around 1100 Ma in the environs of the Greater Lufilian Arc. There seems to have been a widespread, temporally and spatially continuous volcanic and plutonic anorogenic belt from 1250 to 1000 Ma.

4. More than 90% of the samples analysed from the Okatjepuiko suite contain highly anomalous copper concentrations. Both mafic and felsic igneous rocks show that enrichment. Although a portion of the copper content is the product of secondary migration into joints and rock cleavage, most of the copper has primary hydrothermal origin. It is hosted by sulfides, iron oxides and silicates that are main rock constituents.

5. The fact that sample **L-816*** (and probably other granitoids like **L-638**) was emplaced at 1097.6±5.9 Ma is very significant. It proves the juxtaposition of an iron oxide-copper-gold mineralization underneath the sedimentary-hosted copper deposit at Witvlei, Namibia. This metallogenic event occurred at 1110 ma. Secondary copper in the sedimentary-hosted deposit probably came from the IOCG deposit that lies underneath. This idea may generate a new concept for the origin of the Copperbelt copper and cobalt deposits.

   That concept is a major breakthrough. It could change the geological model of formation for the well-endowed Zambian Copperbelt, and could help devise new ways to explore for base metal deposits in the Lufilian Arc and elsewhere. Phenomena similar to that of the Witvlei-Okatjepuiko pair might have taken place in many locations, throughout geological time. There is additional evidence of IOCG mineralization related to sediment-hosted copper in other parts of Namibia and Zambia. This topic will be dealt on Chapter 8, section 8.4.1.1.

6. Finding IOCG and related sedimentary-hosted copper mineralization at Witvlei is also significant because it opens an entire new age gap for the exploration of base metal deposits in the Lufilian Arc and in the surrounding environment, including South Africa.

7. All the mineralized rocks from Okatjepuiko are pristine. There is no significant deformation involved. The mafic volcanic rocks show some foliation and shearing, but mineralization seems to have taken place after the deformation. Hydrothermal brecciation and other mineralization features are un-deformed. This may be very useful to study mineralization and alteration processes.

Fig 4.2.4.7. Photo 1. *Trap rock breccias from 18.20 to 22.0 m; from borehole OP-1, Okatjepuiko, Witvlei, Namibia. Notice abundant evidence of shearing. Part of the fractures in the mafic rocks show serpentinite.*

Fig 4.2.4.8. Photo 2. *Enlargement with detail at 19.77 m from borehole OP-1, Okatjepuiko, Witvlei, Namibia. Note copper mineralization associated with hematite that fills part of the veinlets in a stockwork.*

Fig 4.2.4.9. Photo 3. *Volcanic rocks with vacuoles and dense veinlet network. These occur around 26 to 29 m of borehole OP-1, Okatjepuiko prospect, Witvlei Namibia.*

Fig 4.2.4.10. Photo 4. *Close-up of Fig 4.2.4.8. Details of pink zeolites (?) and very thin white veinlets. Part of the veinlets and vacuoles are filled by albite. From borehole OP-1, Okatjepuiko, Witvlei, Namibia.*

Fig 4.2.4.11. Photo 5. *Beginning of hydrothermal brecciation, 33 to 34 m, borehole OP-1, Okatjepuiko, Witvlei, Namibia. Also note significant shearing in the mafic rocks.*

Fig 4.2.4.12. Photo 6. *Close-up of photo 5, centered on letter M. Beginning of hydrothermal brecciation.*

Fig 4.2.4.13. Photo 7. *Breccia with abundant chlorite that fills open spaces and veinlets, after 34m, borehole OP-1, Okatjepuiko prospect, Namibia.*

Fig 4.2.4.14. Photo 8. *4 core fragments, marked with different alteration types. Note overprinting of veining, part of which is albite. The base is to upper left. 47 to 50 m. Borehole OP-1, Okatjepuiko, Witvlei, Namibia.*

Fig 4.2.4.15. Photo 9. *Beginning of the pink granitoid 54-57 m. Note intrusive brecciation. Borehole OP-1, Okatjepuiko.*

Fig 4.2.4.16. Photo 10. *Close-up of photo 9, on the pink granitoid. Borehole OP-1, Okatjepuiko, Witvlei, Namibia.*

Fig 4.2.4.17. Photo 11. *Breccia with angular fragments of volcanic rock (68 m, 69 m and 70 m). From borehole OP-1.*

Fig 4.2.4.18. Photo 12. *Intrusive rock in the middle line of core, surrounded by dark volcanic trap rocks. Upper left is bottom. Borehole OP-1, Okatjepuiko, Witvlei, Namibia.*

Fig 4.2.4.19. Photo 13. *Core showing angular fragments of pink granitoid within dark gray trap rock, from 73- 75m. The third fragment is taped. Borehole OP-1, Okatjepuiko prospect, Witvlei, Namibia.*

Fig 4.2.4.20. Photo 14. *Core fragments from 79-82 m. At 79 m there are thin black, magnetite veinlets in stockwork. Angular fragments of black volcanic rocks and pink granitoid. Borehole OP-1, Okatjepuiko, Witvlei, Namibia.*

Fig 4.2.4.21. Slabs of strongly hematitized polymictic hydrothermal breccias from Samples L-644 and L-645. *The left photograph was taken from a dry slab, while the other two were taken from a wet slab. Wetting enhances the contrast of the particles. The first two come from the same slab of* ***L-644****; the middle photo is a close-up of the first. The third photo comes from* ***L-645****. On the second and third photos, note the angularity and variability of the clasts. The matrix has been almost completely replaced by hematite. The rock as a whole has a deep red-brown color. Abundant albite veining and strong albitization account for the rocks' induration. When hammered it produces a strong bell tinge. This type of rock forms large outcrops in the environs of the Okatjepuiko prospect. Its surface weathers to a deep brown color. In a few cases, the surface is tinted by thin layers of secondary copper carbonates, phosphates and sulphates. That takes place, even when the copper content is very low. For scale, centimeter bars on the left, and millimeters on the middle and right photos.*

5 THORIUM CONTENT OF SOME GRANITOIDS IN THE GREATER LUFILIAN ARC

5.1 Introduction

As discussed on section 4.1.2.5, eight samples from the Kafue Flats area were found to contain extremely high values of thorium. Th enrichment in those rocks is more than ten times the average value for most granitoids in Zambia and Namibia. Abundance of Th in an igneous rock enables it to act as a long-lived heat engine. This can generate and focus hydrothermal fluid flow for a long time; and possibly is a key ingredient for the occurrence of certain types of iron oxide-copper-gold mineralization.

A simple method to determine the Th content of a rock is using a radiometer. Such machines can directly measure radioactivity due to uranium, thorium and potassium. The tools may be taken to the field or flown. Field mapping of radioactivity in rocks could indicate localities with high counts and serve as a guide in the location of various mineral exploration targets.

5.2 High Thorium Samples

Most of the samples collected by Pepper, 2000 (at Kalengwa, the Hook Granite and the Nchanga Granite, Zambia) contain anomalous Th. These are labeled with a P- prefix on Table 5.1. Pepper probably sampled granitoids in sites where significant mineralization was present and known. One conclusion derived from reviewing his work is that thorium enrichment is a key element for mineralization. High thorium values were observed in granitoids from northwestern Zambia, the Nchanga Red Granite, the Hook Granite, as well as in the Ugab River, around Otjiwarongo, Grootfontein and the Okwa River (Table 5.1).

Table 5.1 High Thorium Values from Greater Lufilian Arc Granitoids
(Sample numbers without a prefix are "L-" samples. Those from the Otjiwarongo batholith labeled with a double consonant prefix were collected by AVMIN.)

Region	Samples
Kafue Flats, Zm	208, 210, 212, 213*, 214, 215, 218
Hook Granite Batholith, Zm	012, 012A, 257, 409, 436, 439, P-39, P-50, P-53, P-57
Kalengwa, Zm	324, P-13, P-17, P-26
Kalene Hill/Mwinilunga, Zm	020, 030, 060, 364, 370, 377, 421
Nchanga Granite, Zm	151, 153, 154, 172, 173, P-28, P-29, X-34
Kamanjab Batholith, Nm	850
Ugab River, Nm	793
Oas Farm, Nm	670, 675, 697, 699
Otjiwarongo Batholith, Nm	1037, 1038, LJ1, LL11, LL14, LL4
AVMIN pegmatite, Nm	815
Grootfontein, Nm	1043, 1045, 1046
Okwa River, Botswana	600A, 602, 605, 606
Okatjepuiko, Witvlei, Nm	None

As indicated in earlier chapters of this document, chemical parameters of some syenites and alkali granites from the Oas Farm, the Hook Granite and the Otjiwarongo batholith are very similar to each other. Thorium enrichment in the Nchanga Granite is of a different nature from that of the Kafue Flats. The chemical signature of intrusive rocks there does not match its counterpart of the Hook Granite, Otjiwarongo Batholith and Oas farm.

None of the Namibian Damara granites reported in the literature are known to have Th values as high as those found during this research project (Becker & Brandenburg, 1997; Becker, Diedrichs, Hansen, & Weber, 2000; Haack, Gohn, & Hartmann, 1983; Jung, Mezger, & Hoernes, 1998; McDermott, Harris, & Hawkesworth, 2000; and Seth, Okrusch, Wilde, & Hoffmann, 2000). Very little information was available on geochemistry of Zambian granitic bodies (Griffiths, 1978a; and Griffiths, 1978b)

The mineral form in which the thorium enrichment resides was not studied during the Greater Lufilian Arc granitoid project. It is not clear if the high thorium content is a primary feature or a secondary overprint brought in with hydrothermal alteration. Note for example, the case of P-28 and P-29 from the Nchanga Granite.

After searching for multi-element matches for geochemical parameters of thorium-rich samples from the Kafue Flats, best matches came from NW Zambia, the Hook Granite Batholith, the Oas Farm and Otjiwarongo. Results are listed on Table 5.2. Most of the rocks have a significant enrichment in Al, Na, Zr, Ce, La and some

Table 5.2 Samples with similar chemical signature as Th-rich samples from the Kafue Flats, Zambia.

Anomalous values are highlighted in gray. Notice that samples for the Kafue Flats used as example for matching, contain high values in alumina, soda, Zr, Nb, Ce, La and low values for lime. The last column has values for estimated heat capacity at time of emplacement. (Find complete elemental analysis on Table A15, Appendix.)

Sample	SiO2	Al2O3	Fe2O3	CaO	Na2O	K2O	LOI	Total	Y	Zr	Nb	Cu	Zn	Ga	U	Th	Sm	Nd	Pr	Ce	La	Cs	Hf	Eu	Gd	Yb	Lu	Heat Capacity
COPPERBELT BASEMENT, ZAMBIA																												
P-28	68.49	12.40	3.43	1.06	8.74	5.32	0.13	100.27	617	261	64	<3	97	24	13	98	75	359	90	600	383	5	11	6.4	98	39	5.9	7.989
NW ZAMBIA																												
L-036	73.57	15.97	1.46	0.10	0.03	0.25	7.83	100.54	30	635	38	36	37	28	<6	36				282	240							2.605
L-038	56.45	21.07	3.77	0.32	12.27	4.32	2.01	100.48	29	859	114	12	108	26	8	32				261	146							2.775
L-039	57.37	21.32	3.71	0.75	9.68	4.63	2.64	100.49	37	808	120	12	127	27	9	30				231	166							2.903
L-040	55.44	20.98	5.81	1.29	9.89	6.14	0.44	100.45	38	922	135	8	106	25	8	30				278	186							3.062
L-044	57.32	21.02	3.15	0.65	12.04	4.28	1.70	100.38	107	1758	178	10	227	26	10	31	0.3		4	196	0				1.5	0.3	0.7	2.957
L-046	55.67	20.92	3.40	1.07	8.51	5.27	5.21	100.44	30	670	82	115	168	24	<6	29	0.5	1	7	204	1				0.6	0.3	0.7	2.743
KAFUE FLATS, ZAMBIA																												
L-199									42.2	534	47				9	39	20	137	36	288	95	0.7	11	5.4	13	3.8	0.5	2.924
L-210	66.74	17.99	3.52	0.69	9.58	0.09	0.39	99.87	30	474	36	143	13	22	7	74				372	223							5.325
L-212	67.27	15.94	2.89	0.81	4.44	7.04	0.71	99.69	51	336	49	32	17	22	8	79				250	130							6.56
L-213*	66.68	17.40	3.03	0.23	6.87	4.87	0.60	100.17	27	596	39	18	22	25	12	163	4.4	42	69	137	20		17	0.7		0.7	0.8	12.211
L-214	66.63	17.62	1.54	0.24	7.68	3.92	0.63	98.74	24	662	77	20	15	25	7	104				181	89							7.873
L-215	70.53	16.82	0.65	0.15	10.32	0.19	0.36	99.30	15	443	23	6	9	27	<6	193				18	<12							13.449
L-218	66.30	15.92	4.64	2.01	4.79	5.43	0.21	100.42	46	601	53	6	30	22	8	99	17	75	265	342	135		7.5	1.5		2.1	1.1	7.743
HOOK GRANITE BATHOLITH, ZAMBIA																												
P-57	62.19	13.11	2.44	0.86	15.42	5.52	0.21	100.27	375	404	48	<3	1	24	10	51	79	499	134	735	579	2	11	7.6	81	21	3.3	4.302
L-012	64.19	17.47	3.45	2.55	4.34	6.14	0.30	100.43	33.1	189	29	7	42	20	4	50	15	112	32	293	163	1.1	4.7	2.7	9.8	3.1	0.5	4.365
L-012A	64.38	17.86	3.18	2.40	4.10	6.24	0.32	100.40	36	360	32	9	28	21	<6	49				312	216							4.246
L-325	60.42	16.98	11.07	0.06	0.08	6.75	2.82	100.55	346	372	31	55	48	26	6	27				1460	819							
L-408	70.26	13.59	3.87	1.23	3.49	5.24	0.43	98.82	104	348	33	15	34	23	12	32				241	121							3.203
L-439	70.07	12.99	4.06	0.77	4.27	5.46	0.62	98.86	90	572	46	21	16	25	19	90				237	124							7.437
L-443	76.23	9.57	5.13	0.43	0.20	6.79	0.40	99.37	64	391	48	12	14	14	<6	100				49	25							7.839
OAS FARM, NAMIBIA																												
L-669	64.34	16.76	4.66	1.46	6.43	4.80	0.74	100.51	72.7	378	204	7	146	28	9	31	18	102	28	267	137	0.7	8.2	4	15	6	0.7	2.993
L-670	57.01	15.14	11.08	2.33	6.69	3.35	1.32	100.53	73	1843	458	9	85	42	17	46	3.1	27	72	219	42			0.3		2.1	1	4.078
L-675	60.71	21.99	3.59	0.94	4.92	6.41	1.61	100.52	123	1520	345	23	167	30	10	78		140	592	844	440			3.4	4.2	6.5	2	6.47
L-697	59.94	16.90	5.28	2.06	6.58	4.59	1.54	99.23	151	1363	432	5	129	26	15	51		127	480	582	291		1.7	4.6	16	10	2.1	4.52
L-699	63.41	17.28	5.27	0.93	7.40	4.73	0.56	100.52	75	1246	307	7	147	34	15	50				470	310							4.468
OTJIWARONGO, NAMIBIA																												
LJ1	68.16	16.02	2.81	1.54	2.85	7.17	0.55	100.07	24	259	17	30	42		1	95												7.484
LL10	56.48	17.84	6.85	3.78	5.74	4.86	0.74	99.67	36	340	99	0	78		9	25												2.586
LL14	57.00	17.00	9.00	3.00	6.00	5.00	1.00	99.52	161	2052	364	5	133		22	83												6.982
LL15	62.00	16.00	6.00	4.00	6.00	5.00	4.00	99.73	31	305	47	0	73		3	26												2.502
L-1037	67.15	16.05	2.51	1.33	2.99	7.49	0.46	99.36	22	149	16	8	41	17	<6	105				288	157							8.271
L-1038	68.09	15.77	2.42	1.39	3.03	6.45	0.40	98.87	26	247	18	13	39	16	<6	112				316	175							8.626

are earths; part are also enriched in Y, Zn and Ga. Samples from the Hook Granite Batholith differ from the rest because they have high K and low Na values. Notably, no samples from the Kamanjab Batholith have a chemical signature precisely like that of the Kafue Flats thorium-rich rocks. Another surprising fact was to discover that none of the granitoids from Witvlei, Namibia carry anomalous Th or U.

High thorium samples from the Nchanga Granite did not match the Kafue Flats' chemical signature. Nevertheless, they are highly enriched in thorium. P-28 is the only sample with a signature similar to rocks from the Kafue Flats, but its chemistry is intensely modified. Probably the high values of rare earths were brought to it by hydrothermal processes, at the same time as the sodium alteration took place. This topic has to be studied in greater detail.

5.3 Values for High-Heat Generating Granitoids

Calculations were carried out to define the calorific properties of the rocks from the Greater Lufilian Arc that contain anomalous thorium. Heat generating capacity calculations involve K, Th and U, which are the radiogenic elements that contribute the most, and are listed in order of increasing importance. According to Klominsky, Partington, McNaughton, Ho, & Groves, 1996, high-heat-producing granitoids have the following values today:

$$\mathbf{A = 0.081\ (K_2O) + 0.261\ (U) + 0.072\ (Th)}$$

A is expressed in $\mu W/m^3$, K_2O is in %, U and Th are expressed in PPM.

Equation No. 3A

For comparison, a few A values of known batholiths are listed on Table 5.3.

Table 5.3 Heat production values for various high-heat producing granitoids (in $\mu W/m^3$)

Granitoid	A value	Reference
Cornubian Batholith, Britain	4.0 – 5.7	Webb, Tindle, Barritt, Brown, & Miller, 1985; Lee et al, 1987
Bushveld granites	4.3 – 12.8	McNaughton et al, 1993
Northern Australia	5.7 – 6.3	Solomon & Heinrich, 1992
Young Intrusive Suite, Cullen Batholith, Australia	6.69	Klominsky et al., 1996
Early Intrusive Suite, Cullen Batholith, Australia	5.70	Klominsky et al., 1996
Transitional Intrusive Suite, Cullen Batholith, Australia	5.71	Klominsky et al., 1996

If a value of A≥4 is taken as anomalous for heat producing in granitoids, ninety-nine of the granitoids sampled in the Greater Lufilian Arc are high-heat producers today using equation 3A. This is approximately a fourth of the samples analised and that is very significant.

A table with estimated heat production value of all samples at their approximate age of emplacement is very useful to evaluate which of the regions were high heat producers throughout the geological history. Corrections must be made using the rocks' approximate age of emplacement. The formula to calculate these values comes from Gibson & Jones, 2002.

$$\mathbf{H(\tau) = [0.9929 \times 0.0918 \times M_U \times e^{(0.1551\tau)} + 0.071 \times 0.5726 \times M_U \times e^{(0.98485\tau)} + 0.256 \times M_{Th} \times e^{(0.0498\tau)} + 0.348 \times M_K \times e^{(0.554\tau)}] \times \rho \times 10^{-4}}$$

$H(\tau)$ = heat producing capacity of the rock in $\mu W/m^3$
M_U = uranium content of rock in ppm
M_{Th} = thorium content of rock in ppm
M_K = potassium content of rock in percentage
ρ = density of rock in kg/m^3
τ = age of rock in billions of years

Equation No. 4

The heat producing capacity of all the samples was estimated for the time of their emplacement using Equation No. 4. Precise age of emplacement is unknown for many of the igneous rock units studied in the Greater Lufilian Arc. Nevertheless, an estimate of their age has been made in order to obtain values for the heat production capacity [$\mathbf{H(\tau)}$]. Table A76 in the Appendix lists results of the calculation for all samples from this project. Seventy of the samples collected from the Greater Lufilian Arc turned out to be high heat producers at the time of emplacement using that equation. Samples with the higher values from that table are included on Table 5.4.

Table 5.4 High heat production capacity of Greater Lufilian Arc intrusive rocks.
Calculated at the time of emplacement.

Sample number	U (ppm)	Th (ppm)	K (%)	Time (BA)	Heat producing value	U/Th
West Lusaka, Zambia						
L-207 prox	9.00	132.0	6.27	0.55	10.181	0.068
L-208	9.00	132.0	6.13	0.55	10.163	0.068
L-210	7.00	74.0	0.09	0.55	5.327	0.095
L-212	8.00	79.0	7.04	0.55	6.587	0.101
L-213	12.00	163.0	4.87	0.55	12.232	0.074
L-214	7.00	104.0	3.92	0.55	7.889	0.067
L-215	3.00	193.0	0.19	0.55	13.450	0.016
L-218	8.00	99.0	5.43	0.55	7.764	0.081
Hook Granite, Zambia						
L-012	4.27	50.4	6.14	0.55	4.388	0.085
L-012A	3.00	49.0	6.24	0.55	4.268	0.061
L-257	16.00	74.0	5.29	0.55	6.248	0.216
L-348	3.00	40.0	3.37	0.55	3.280	0.075
L-409	13.00	53.0	5.43	0.55	4.728	0.245
L-436	26.00	99.0	4.81	0.55	8.202	0.263
L-439	19.00	90.0	5.46	0.55	7.462	0.211
L-442	3.00	44.0	7.61	0.55	4.097	0.068
L-443	3.00	100.0	6.79	0.55	7.863	0.030
L-458	8.00	7.5	6.94	0.55	1.632	1.067
L-464	29.00	7.5	0.52	0.55	1.417	3.867
L-465	24.00	7.5	0.43	0.55	1.262	3.200
L-467	3.00	67.0	5.45	0.55	5.412	0.045
P-39	19.00	71.0	5.57	0.55	6.163	0.268
P-46	10.00	46.0	6.89	0.55	4.345	0.217
P-50	62.00	256.0	4.88	0.55	20.096	0.242
P-53	21.00	43.0	5.92	0.55	4.329	0.488
P-57	10.00	51.0	5.52	0.55	4.516	0.196
Kalengwa-Kasempa Area, Zambia						
L-324	13.00	48.0	6.29	0.55	4.492	0.271
L-325	6.00	27.0	6.75	0.55	2.899	0.222
P-13	10.00	56.0	3.89	0.55	4.653	0.179
P-17	11.00	48.0	5.62	0.55	4.350	0.229
P-26	6.00	76.0	0.03	0.55	5.429	0.079
Northwestern Zambia Region, Zambia						
Paleoproterozoic rocks						
L-370	9.00	52.0	4.07	1.89	5.045	0.173
L-377	8.00	45.0	5.45	1.89	4.890	0.178
L-364	8.00	44.0	5.07	1.89	4.719	0.182
L-020	10.00	62.0	5.85	1.89	6.253	0.161
L-379	10.00	7.5	2.92	1.89	1.701	1.333
Other						
L-030	16.00	40.0	5.91	1.89	4.989	0.400
L-060	4.91	46.5	1.12	1.89	3.714	0.106
L-420	13.00	37.0	2.98	1.89	3.876	0.351
L-421	3.00	57.0	6.69	1.89	5.851	0.053
Basement to the Copperbelt, Zambia						
Nchanga Granite						
P-28	13.00	98.0	5.32	0.88	7.989	0.133
P-29	9.00	65.0	5.56	0.88	5.621	0.138
L-151	11.00	65.0	5.54	0.88	5.680	0.169
L-153	11.00	44.0	4.89	0.88	4.129	0.250
L-154	3.00	44.0	5.78	0.88	4.018	0.068
Nchanga Mine						
L-167	12.00	37.0	8.70	0.5	3.977	0.324
L-172	5.31	48.5	7.48	0.5	4.429	0.109
L-173	7.00	58.0	7.51	0.5	5.139	0.121
Kamanjab Inlier, Namibia						
L-834	7.00	25.0	14.06	1.8	5.582	0.280
L-850	3.00	46.0	4.96	1.8	4.560	0.065

Sample number	U (ppm)	Th (ppm)	K (%)	Time (BA)	Heat producing value	U/Th
L-906	3.00	19.0	5.97	1.8	2.951	0.158
L-943	3.00	28.0	5.72	1.8	3.509	0.107
L-965	7.00	30.0	5.73	1.8	3.806	0.233
L-966	5.82	27.2	5.68	1.8	3.551	0.215
L-967	8.00	36.0	5.05	1.8	4.087	0.222
L-969	6.00	29.0	14.31	1.8	5.883	0.207
L-971	3.00	7.5	8.51	1.8	2.803	0.400
L-973	3.00	18.0	9.97	1.8	3.901	0.167
L-997	3.00	33.0	5.33	1.8	3.756	0.091
Ugab River 2, Namibia						
L-793	12.00	61.0	5.24	0.75	5.322	0.197
L-797	6.00	37.0	4.63	0.75	3.396	0.162
L-798	7.00	27.0	5.17	0.75	2.812	0.259
Owka River, Botswana						
L-600A	3.00	43.0	5.55	0.75	3.852	0.070
L-602	3.00	36.0	4.54	0.75	3.225	0.083
L-605	3.00	42.0	5.47	0.75	3.772	0.071
L-606	3.00	38.0	5.19	0.75	3.455	0.079
Oas Farm, Namibia						
L-668	7.00	22.0	4.79	0.75	2.412	0.318
L-669	9.00	31.0	4.80	0.75	3.096	0.290
L-670	17.00	46.0	3.35	0.75	4.166	0.370
L-675	10.00	78.0	6.41	0.75	6.603	0.128
L-676	3.00	19.0	5.55	0.75	2.193	0.158
L-697	15.00	51.0	4.59	0.75	4.628	0.294
L-699	15.00	50.0	4.73	0.75	4.579	0.300
L-713	3.00	7.5	5.66	0.75	1.414	0.400
Lofdal Farm, Namibia						
L-1025	86.4	19.5	0.56	0.75	4.017	4.423
LR25	24	7730	0.01	0.75	535.017	0.003
LR23	15	130	0.10	0.75	9.450	0.115
LR5	26	2347	0.53	0.75	163.080	0.011
LR4	28	1593	0.04	0.75	110.953	0.018
AM-1	11	1019		0.75	70.777	0.011
Otjiwarongo Environs, Namibia						
L-1037	3.00	105.0	7.49	0.55	8.298	0.029
L-1038	3.00	112.0	6.45	0.55	8.649	0.027
L-1039	3.00	26.0	5.51	0.55	2.585	0.115
L-1039c	3.00	32.0	5.94	0.55	3.055	0.094
LJ1	1.00	95.0	7.17	0.55	7.509	0.011
LL11	3.00	55.0	6.00	0.55	4.652	0.055
LL14	22.00	83.0	5.00	0.55	7.005	0.265
LL4	4.00	52.0	5.74	0.55	4.440	0.077
Grootfontein Inlier, Otavi Mountains, Namibia						
L-1042	3.00	35.0	6.14	0.55	3.288	0.086
L-1043	3.00	44.0	5.77	0.55	3.863	0.068
L-1044	3.00	36.0	5.94	0.55	3.331	0.083
L-1045	3.00	57.0	1.70	0.55	4.243	0.053
L-1046	3.00	42.0	5.45	0.55	3.684	0.071
Nigerian Ring Complexes						
RN75		111	4.31	0.15	8.112	0.000
JON147		41	5.32	0.15	3.377	0.000
B34		40	5.77	0.15	3.354	0.000
MD333		66	4.53	0.15	5.024	0.000
NG208		63	5.10	0.15	4.875	0.000
T15A		69	4.59	0.15	5.238	0.000
DR11		61	3.58	0.15	4.582	0.000
DW1		42	3.56	0.15	3.267	0.000
FG5		39	4.45	0.15	3.150	0.000
KD12		36	4.39	0.15	2.937	0.000

6 GEOCHRONOLOGY

6.1 Introduction

One of the main objectives of the project was to define the age of emplacement of key granitoids in the Greater Lufilian Arc. This chapter presents the main findings and results in this respect. The first section presents the new radiometric ages obtained. The second, describes the database of radiometric ages compiled for the project, and several diagrams devised to evaluate geochronological information. The third section discusses a few Re-Os ages that were obtained from sulfides in the Zambian Copperbelt.

In mature, well-studied and mapped regions, a single age does not mean much. On relatively un-studied regions, a single age may represent the only evidence or a major geological event, and should be treated carefully.

6.2 New Radiometric Ages

Twenty seven samples were selected for zircon U-Pb radiometric dating, and 38 new ages were obtained. 10 of them by laser-ablation ICP-MS techniques at the Memorial University of Newfoundland, Canada, by Marc Poujol and his research group; and 28 by SHRIMP II at the Australia National University[1] by Richard Armstrong and his research group.

Table 6.1 compiles all the new ages in chronological order, and Table 6.2 lists them by sample number. Raw data from each of the geochronological laboratories is presented in Appendix A77. The diagrams to interpret radiometric ages are presented in Appendix A78. A few of the tables and diagrams are missing, because they have not been produced by the ANU. As discussed in the introduction, a few of the ages sent to Australia have not been completely processed.

The samples dated have been presented and discussed in each of the relevant sections of this document.

The new radiometric ages helped to define ten discrete events of magmatism. These are listed on Table 6.3.

Table 6.3 Events of magmatism identified in the Greater Lufilian Arc based on the new radiometric ages obtained

Event of magmatism	Time Lapse (Ma)	Period	No. of ages	Associated Mineralization
1	534 - 555	Neoproterozoic	4	IOCG
2	742 - 770	Neoproterozoic	9	IOCG
3	875 - 885	Neoproterozoic	1	IOCG?
4	1091 - 1013	Mesoproterozoic	1	IOCG
5	1682 - 1710	Paleoproterozoic	2	-
6	1745 - 1755	Paleoproterozoic	1	-
7	1850 - 1890	Paleoproterozoic	9	Disseminated Cu
8	1920 - 1951	Paleoproterozoic	4	IOCG
9	1966 - 1986	Paleoproterozoic	1	Disseminated Cu
10	~2500	Archean	2	-

6.3 Geochronological Database and Interpretation

A total of 512 radiometric ages from Namibia and Zambia were compiled, including 38 produced for this project. The majority of those ages come from zircon U-Pb. Tables A21 and A22 present the compilation. Table A21 lists all the ages in chronological order, and Table A22 discriminates the data by country and by regions within the countries. The geochronological database serves as background for the evaluation of the new radiometric ages obtained.

[1] The Australia National University will be refered to as ANU.

6.3.1 Event Diagrams

Data from Table A22 was used to produce a series of event diagrams (Figs A23 to A49) that help to visually understand the temporal and spatial distribution of the dated events. The numbers on the lower portion of the event diagrams refer to numbers on the first columns of the corresponding tables in Appendix A22. The event diagrams have been used throughout this document to discuss aspects of the geology of the Greater Lufilian Arc. They were used to interpret the areas of study for the project.

6.3.2 Compilation of Event Diagrams

In the event diagrams, intrusive events are just as important as the hiatus between them. The main event diagrams from the Greater Lufilian Arc were interpreted in terms of lapses of intrusion and hiatuses. That information was compiled in a series of correlation diagrams. The principal lapses of intrusion were labeled with letters. The correlation diagram for Zambia is Fig A79. The correlation diagram for Namibia is Fig A80. The complete diagram for the Greater Lufilian Arc is Fig A81. It was broken in two for ease of interpretation: Fig A82 is the first portion, from 3000 to 1400 Ma; Fig A83 is the second portion, from 1400 to 0 Ma.

Many observations can be made from the correlation diagrams. A few of the lapses of intrusion occur throughout the Greater Lufilian Arc. Others are more restricted. One of the main observations is that there has been an equal amount of intrusive events through time. That can be deduced from observing the event diagrams for entire countries. Fig A35, the event diagram for all information from Zambia, has continuous events with very short hiatus. Fig A48 has longer hiatus.

The geochronological data available for the Greater Lufilian Arc does not display any periodicity of intrusive events, nor displays a net increase or decrease in intrusive activity.

The following are some observations from the geochronological correlation diagrams.

1. Tectonothermal event C is widespread in the Greater Lufilian Arc.

2. Hiatus of U is widely spread, as well as hiatus R and those of S1 and T, and V.

3. Intrusive events of local extension are: A, B, H, J, M, P, S, Y, Z, AC and AF.

4. In general terms, the geological history of the Mkushi, Mufulira, Copperbelt Basic, All Basement to the Coperbelt, and NW Zambia areas are very similar to each other. Evidence from geochemistry shows that they were emplaced in similar environments, and display equivalent tectonic and magmatic events.

5. The Zambian Lufilian Arc and Damara region of Namibia did not behave in a similar way from 2200 to 2000 Ma. They probably were independent entities. They also behaved significantly different from 1400 to 850 Ma.

6. Events D are important in the Kamanjab environs as well as in the whole of Namibia.

7. Geological history for the Khorixas Inlier and the Kamanjab Batholith are significantly different. They probably were not in the same geographic position all the time. The circa 750 Ma tectonothermal event is not known in the Kamanjab. Older basement is known in the Khorixas Inlier than at the Kamajab. This is discussed in more detail in section 4.2.1.13

8. Events K, M, N and O are not generally present in Namibia. Event N is present in the Kamanjab environs; M is present in Central Namibia.

9. Event L is important at the environs of Nchanga, as well as events E, D', D and C.

Table 6.1 New Radiometric Ages, Greater Lufilian Arc - sorted by age

by Alberto Lobo-Guerrero, Geologist, M.Sc., Min.Ex.
Economic Geology Research Institute, University of the Witwatersrand
Johannesburg, December 22, 2004

Metallogenic Significance	Sample No.	Sampling site/Event site	Rock Type	Age (Ma)	Environment	Source	Event
IOCG, FeOx	L-207	Nampundwe,Zm	Alkali granite	538.2±3.3	CEUG A	ANU	
	L-795	Ugab River, Nm	Granite	540±4	RRG A	ANU	**1**
	L-213	Kafue Flats,Zm	Syenite	550±25	CEUG A	ANU	
Au, IOCG, Sed-hosted Au	L-808c	Otjiwarongo pegmatitic granitoid	Granite pegmatite	550±5	Undefined	ANU	
IOCG?	L-047	Mombwezhi Dome, Zm	Quartz syenite	745.9±3.4	CEUG A	ANU	
	L-716	Oas Farm, Nm (basement)	Granite	745±5	RRG A	ANU	
	L-060	Kansanshi mine, Zm	Saturated olivine gabbro	750±5	WPAB	ANU	
IOCG	L-142	MB-34 intrusives, Kasempa,Zm	Subvolcanic porphyritic granite	750±5	A undefined	ANU	
IOCG	L-758	Mesopotamie Farm,Nm	Graphic granite	750±5	W Within plate	ANU	**2**
	L-688	Oas Farm,Nm (older intrusive)	Syenite	762±12	RRG A	ANU	
	L-169	Nchanga open pit intrusives, Zm	Alkali granite in borehole	765±3	A undefined	ANU	
	L-172c	Nchanga open pit intrusives, Zm	Alkali granite	765±3	A undefined	ANU	
IOCG, FeOx, REE	L-693	Oas Farm, Nm (young intrusive)	Dark subvolcanic alkali granite	765±4.5	RRG A	ANU	
	L-169	Nchanga open pit intrusives, Zm	Inherited zircons in alkali granite	880±5		ANU	3
Cu, Au, IOCG	L-638	Witvlei Gtd,Nm	Alkali granite	1097.6±5.9	RRG A	ANU	4
	L-758	Mesopotamie Farm,Nm	inherited zircons in gtd	1692±10		ANU	**5**
	L-795	Ugab,Nm	inherited zircons in gtd	1700±10		ANU	
	L-728	Lofdal Farm,Nm	Granite	1750±5		ANU	6
	L-169	Nchanga Intrusives, Zm	Inherited zircons in alkali granite	1860±10		ANU	
	L-075	Muliashi Porphyry,Zm	Quartzmonzonite	1864.9±5.4	A undefined	ANU	
	L-166	Konkola Deep Borehole,Zm	Undeformed white granite	1866.4±5.4	N undefined	ANU	
Disseminated Cu	L-993	Mineralized area 3, Kamanjab Batholith	Granite with potassic alteration	1866±13	Undefined	MU	
	L-160	Konkola Deep Borehole,Zm	Granite	1867.9±4.8	A undefined	ANU	**7**
	L-213	Old Kafue Basement,Zm	Inherited zircons in syenite	1872±14		ANU	
	L-158	Konkola Deep Borehole,Zm	Foliated pink granite	1873.7±7.7	N undefined	ANU	
	L-943	End of road W of Kamanjab Batholith	Granite	1877±39	CEUG A	MU	
	L-1013	Along E-W fault, Kamanjab Batholith	Granite along E-W fracture.	1878±15	A undefined	MU	
IOCG?	L-030	Mwinilunga, Western Zambia	Granite	1927.6±7.1	POG, A	ANU	
IOCG, Au, Cu	L-868	Kamdescha f., Kamanjab Batholith	Granite	1937±14	VAG N	MU	**8**
IOCG	L-855	Tevrede f., Kamanjab Batholith	Alkali granite	1937±19	RRG A	MU	
	L-1043	Otavi Mountains, Namibia	Granite	1939±64	POG, A	MU	
Disseminated Cu	L-969	Mineralized area 2, Kamanjab Batholith	Nepheline syenite, K alteration	1976±42	CEUG A	MU	9
	L-855	Tevrede f., Kamanjab Batholith	inherited zircons	~2500		MU	**10**
	L-1043	Otavi Mountains, Namibia	Inherited zircons	2544±78		MU	

ANU = Australia National University, Canberra, Australia. MU = Memorial University in St. John's, Newfoundland, Canada. The last column refers to magmatic events.

Table 6.2 New Radiometric Ages, Greater Lufilian Arc - sorted by sample number

by Alberto Lobo-Guerrero, Geologist, M.Sc., Min.Ex.
Economic Geology Research Institute, University of the Witwatersrand
Johannesburg, December 22, 2004

Metallogenic Significance	Sample No.	Sampling site/Event site	Rock Type	Age (Ma)	Environment	Source
IOCG?	L-030	Mwinilunga, Western Zambia	Granite	1927.6±7.1	POG, A	ANU
IOCG?	L-047	Mombwezhi Dome, Zm	Quartz syenite	745.9±3.4	CEUG A	ANU
	L-060	Kansanshi mine, Zm	Saturated olivine gabbro	750±5	WPAB	ANU
	L-075	Muliashi Porphyry,Zm	Quartzmonzonite	1864.9±5.4	A undefinec	ANU
IOCG	L-142	MB-34 intrusives, Kasempa,Zm	Subvolcanic porphyritic granite	750±5	A undefinec	ANU
	L-158	Konkola Deep Borehole,Zm	Foliated pink granite	1873.7±7.7	N undefinec	ANU
	L-160	Konkola Deep Borehole,Zm	Granite	1867.9±4.8	A undefinec	ANU
	L-166	Konkola Deep Borehole,Zm	Undeformed white granite	1866.4±5.4	N undefinec	ANU
	L-169	Nchanga open pit intrusives, Zm	Alkali granite in borehol	765±3	A undefinec	ANU
	L-169	Nchanga open pit intrusives, Zm	Inherited zircons in alkali granit	880±5		ANU
	L-169	Nchanga Intrusives, Zm	Inherited zircons in alkali granit	1860±10		ANU
	L-172c	Nchanga open pit intrusives, Zm	Alkali granite	765±3	A undefinec	ANU
IOCG, FeOx	L-207	Nampundwe,Zm	Alkali granite	538.2±3.3	CEUG A	ANU
	L-213	Kafue Flats,Zm	Syenite	550±25	CEUG A	ANU
	L-213	Old Kafue Basement,Zm	Inherited zircons in syenite	1872±14		ANU
Cu, Au, IOCG	L-638	Witvlei Gtd,Nm	Alkali granite	1097.6±5.9	RRG A	ANU
	L-688	Oas Farm,Nm (older intrusive	Syenite	762±12	RRG A	ANU
IOCG, FeOx, REE	L-693	Oas Farm, Nm (young intrusive)	Dark subvolcanic alkali granit	765±4.5	RRG A	ANU
	L-716	Oas Farm, Nm (basement)	Granite	745±5	RRG A	ANU
	L-728	Lofdal Farm,Nm	Granite	1750±5	CEUG A	ANU
IOCG	L-758	Mesopotamie Farm,Nm	Graphic granite	750±5	W Within plate	ANU
	L-758	Mesopotamie Farm,Nm	inherited zircons in gtc	1692±10		ANU
	L-795	Ugab River, Nm	Granite	540±4	RRG A	ANU
	L-795	Ugab,Nm	inherited zircons in gtc	1700±10		MU
Au, IOCG, Sed-hosted Au	L-808c	Otjiwarongo pegmatitic granitoi	Granite pegmatite	550±5	Undefinec	ANU
IOCG	L-855	Tevrede f., Kamanjab Batholitl	Alkali granite	1937±19	RRG A	MU
	L-855	Tevrede f., Kamanjab Batholitl	inherited zircons	~2500		MU
IOCG, Au, Cu	L-868	Kamdescha f., Kamanjab Batholitl	Granite	1937±14	VAG N	MU
	L-943	End of road W of Kamanjab Batholitl	Granite	1877±39	CEUG A	MU
Disseminated Cu	L-969	Mineralized area 2, Kamanjab Batholit	Nepheline syenite, K alteratio	1976±42	CEUG A	MU
Disseminated Cu	L-993	Mineralized area 3, Kamanjab Batholit	Granite with potassic alteratio	1866±13	Undefinec	MU
	L-1013	Along E-W fault, Kamanjab Batholitl	Granite along E-W fracture	1878±15	A undefinec	MU
	L-1043	Otavi Mountains, Namibia	Granite	1939±64	POG, A	MU
	L-1043	Otavi Mountains, Namibia	Inherited zircons	2544±78		MU

6.4 NEW Re-Os AGES FROM COPPER MINERALIZATION IN THE ZAMBIAN COPPERBELT

6.4.1 Basic Data

Re/Os ages on sulfides from copper mineralization collected in the Zambian Copperbelt, indicate that there is a significant overlap of mineralization with intrusion ages of granitoids described in this research project. A five-point isochron with analyses from chalcopyrite, carrolite and bornite from the Nkana, Chibuluma and Nchanga deposits, produced an age of 583±24 Ma, and a $^{187}Os/^{188}Os$ initial value of 1.22±0.13 (MSWD=0.67). This was indicated by Barra, Broughton, Ruiz, & Hitzman, 2004 and (Ruiz, J., personal communication, August, 2004). According to the authors from the University of Arizona, the sulfides have Os concentrations that range from 24 to 75 ppt and Re concentrations between 0.6 and 5.8 ppb (Fig 6.4.1). A later version of that age provided by Ruiz (Ruiz, J., personal communication, December, 2004) is 576±41 Ma based on seven points with a $^{187}Os/^{188}Os$ initial value of 1.37±0.32 (MSWD=4.0) (Fig 6.4.1).

This is definitely not a chance issue. A growing amount of evidence points in the direction of a discrete mineralizing event at around 583 Ma. Barra et al., 2004 assume that the mineralizing event is related to the Pan African orogenic events.

A Re-Os molybdenite age of 525.7±3.4 Ma was determined by the same group of researchers for mineralization at the Nkana mine. In this case, the molybdenite gave concentrations of 1789 ppb for Re and 325 for Os. This proves that there were at least two mineralizing events at Nkana.

The other age reported by the working group of the University of Arizona headed by Ruiz is 825±69 Ma for copper mineralization at the Konkola deposit, with a $^{187}Os/^{188}Os$ initial value of 11.4±1.7 (MSWD=1.8) (Ruiz, J., personal communication, December, 2004). An earlier version of that age was 776±150 Ma with a $^{187}Os/^{188}Os$ initial value of 10.8±5.5 (MSWD=1.7) (Ruiz, J., personal communication, August, 2004). These new ages are quite relevant, because they may serve as evidence of an older age for deposition of the Katangan sediments, and as an age of mineralization. The geochronological information is within error of the ages recorded for some dikes sampled under the Nchanga open pit during this research project (**L-172c** and **L-169**). Armstrong, Robb, Master, Kruger, & Mumba, 1999 found that the Nchanga Granite was emplaced at 877±11 Ma. This age overlaps with that of copper mineralization at Konkola. Furthermore, there is Nchanga Granite-like chemistry in granitoids from the Konkola deep borehole.

This indicates that there were at least three discrete mineralizing events in the Zambian Copperbelt. One centered on 825 Ma, a second on 583 Ma, and a third on 525 Ma. Table 6.4 presents dated events associated with three main copper events known in the Greater Lufilian Arc. Fig 6.4.2 illustrates the timing of the three events.

6.4.2 Discussion

One of the questions that comes to mind after analysing the Re-Os ages is “Could the waning anorogenic intrusive events related to the Nchanga Granite have produced copper mineralization at Konkola and Nchanga?”

There might be a probable relationship between the anorogenic intrusion of the Nchanga Granite and copper mineralization at Nchanga and Konkola. Given the evidence, a magmatic-related origin seems reasonable for at least one of the copper-cobalt mineralizing events in the Nchanga and Konkola area.

The presence of Nchanga-like intrusives in the Konkola deep borehole indicates that this possibility is very certain. There might be several high-thorium anorogenic granitic complexes like the Nchanga Granite that lie unidentified underneath the rift-related basin where the Katanga sedimentary sequence was laid. The deposition of the Katangan sequence of sediments must have taken place very soon after the intrusion of the anorogenic Nchanga Granite ring complex (dated at 877±11 Ma by Armstrong et al., 1999). There must have been rapid uplift or tectonic tilting in a rift environment to allow for the volcanic facies of the ring complex to be eroded, the lower Katanga deposits to cover the Nchanga Granite unconformably, and later for intrusive events related to the waning activity of the Nchanga Granite ring complex to intersect the recently deposited and mineralized (?) Kantangan rocks. Currently available resolution of radiometric ages to date mineralization, is not enough to develop a more specific sequence of events. But mineralization took place soon after the anorogenic events of intrusion. Mineralization probably took place around 760 Ma. That age is also within the error of Re/Os data provided by Ruiz and his working group at the University of Arizona, and is one of the ages for IOCG mineralization that comes out from the Lufilian Arc Granitoid project both in Zambia and Namibia.

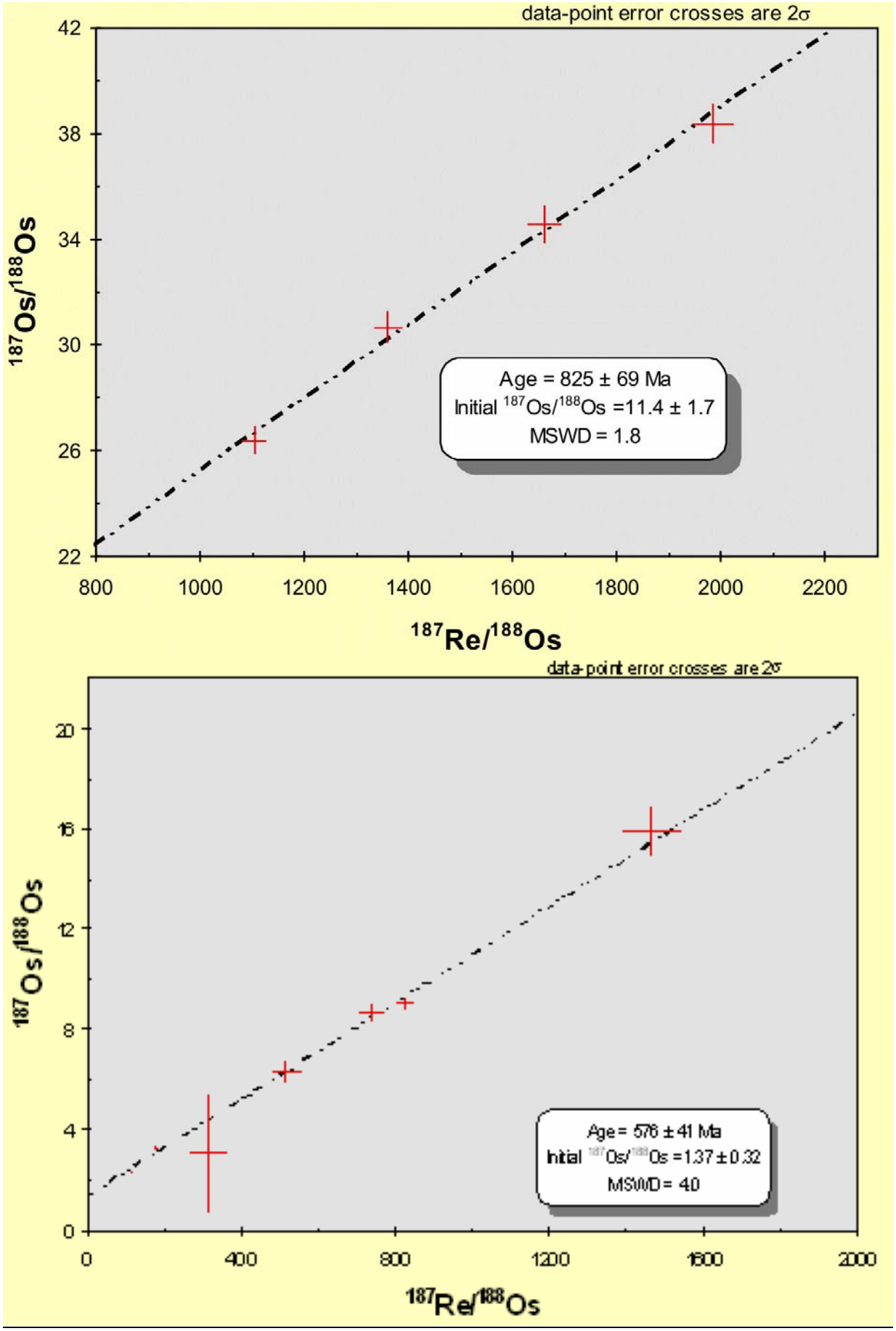

Fig 6.4.1 Re-Os ages calculated by Joaquín Ruiz and collaborators at the University of Arizona. **(Ruiz, J., personal communication, 2004.)**

Two well-represented epochs of anorogenic granitoid intrusion that occur throughout the Greater Lufilian Arc and have been studied in this project are: (1) the sporadic, but widely distributed, small igneous intrusions at 750±50 Ma; and (2) the widespread and voluminous granitoid magmatism at 550±50 Ma (Table 6.4 and Fig 6.4.2). Both of these epochs are related to iron oxide-copper-gold mineralization. If we were able to associate the second period of IOCG mineralization (~550 Ma) to the copper-cobalt mineralizing event recorded by (Barra et al., 2004) for Cu-Co mineralization at several mines in the Copperbelt (583±24 Ma), we have one concordance between IOCG mineralization and so-called sedimentary-hosted Cu-Co mineralization. If we relate the ~750 Ma age of IOCG mineralization with the 825±69 Ma copper mineralization at Konkola, we have another concordance between IOCG mineralization and sedimentary-hosted Cu mineralization.

This could mean that there is some sort of link between IOCG and sedimentary-hosted Cu mineralization in at least three discrete periods of geological time in the Greater Lufilian Arc (the Witvlei area and the Zambian Copperbelt) (Fig 6.4.2). That probably happened more often, but is not yet documented from enough locations to call attention of researchers. This three-legged coincidence might be more relevant than considered at first. It could mean that there is a direct tie between both types of deposits. Maybe the origin of copper in sedimentary-hosted copper deposits has a clear source in magmatic-related IOCG events. Maybe the rapid erosion of the surface expression of mineralized IOCG systems gave rise to the Cu-Co Sedimentary-hosted Cu deposits.

The origin for cobalt in the Copperbelt and in other sedimentary-hosted copper deposits has been a mystery. Epigenetic IOCG mineralization certainly could provide copper, cobalt and other related metals. Zinc enrichment in anorogenic syenites and alkali granites may be the single source, or one of multiple sources, for the large economic zinc mineralization known in the Greater Lufilian Arc.

As seen on Table 6.4 and Fig 6.4.2, the **Copperbelt 1** series of events might have ocurred as follows: after the emplacement of the Nchanga Granite (event 11), large-scale hydrothermal convection of fluids was established and powered by the high-heat producing nature of the Nchanga Granite and other similar bodies like the Konkola Granite. Copper mineralization took place at Konkola and in the Copperbelt (10, 9), then dikes were emplaced into Katangan rocks (8), later came the regional event of intrusion and IOCG mineralization (7). Notice that the error of event 10 allows it to have taken place during an extensive time range. In a similar way, event 7 has a long range of time. Copper and cobalt mineralization could have taken place at any time after the emplacement of the Nchanga Granite and deposition of the Kagangan sediments. The dikes that intersect Copperbelt mineralization under the Nchanga open pit do not carry significant mineralization. They postdate the main event of copper mineralization at the Nchanga mine. There is close temporal association between the time of IOCG mineralization and that of sedimentary copper mineralization.

The **Copperbelt 2** series of events probably occurred as follows: Regional Cu-Co mineralization in the Copperbelt (6), resetting of radiometric watch at Konkola (5), regional IOCG mineralization (4), localized IOCG mineralization (3), copper mineralization at the Nkana mine (2), and mineralization of copper and cobalt in the Congolese Copperbelt. Again, event 6 could have taken place during a long lapse of time.

6.4.3 Conclusions

Secondary copper in sedimentary-hosted deposits probably came from IOCG deposits. This is a new concept for the origin of Copperbelt Cu-Co deposits. At least three discrete time periods show that close temporal spatial association.

Table 6.4 Events associated with three main copper mineralizing periods in the Greater Lufilian Arc.
(Numbers refer to the events of Fig 6.4.2)

#	Event, Site, Type, Source	Age (Ma)	Error	From	To
1	Congolese Cu-Co mineralization (this report)	506.5	6.5	500	513
2	Cu mineralization at Nkana, Zm (Re-Os, Barra et al., 2004)	525.7	3.4	522.3	529.1
3	533Ma IOCG mineralization, Zm (shrimp, this report)	533	4	529	537
4	Greater Lufilian Arc IOCG mineralization (shrimp, this report)	550	50	500	600
5	Resetting age Konkola, Zm (shrimp, L-158, this report)	562	18	544	580
6	Copperbelt Cu-Co mineralization, Zm (Re-Os, Ruiz)	583	24	559	607
7	Greater Lufilian Arc IOCG mineralization (shrimp, this report)	775	50	725	825
8	Nchanga mine intrusives, Zm (shrimp, L-172c, L-169, this report)	765	3	762	768
9	Initial Cu Copperbelt, Zm (Robb, personal communication)	776	20	756	796
10	Konkola Cu mineralization, Zm (Re-Os, Ruiz)	825	69	756	894
11	Nchanga Granite, Zm (shrimp, Armstrong et al., 1999)	877	5	872	882
12	Witvlei IOCG, Nm (shrimp, this report)	1098	5.9	1059	1104
13	Kwebe Mills, Ghanzi, Botswana (Schwartz, 1996)	1106	2	1104	1108

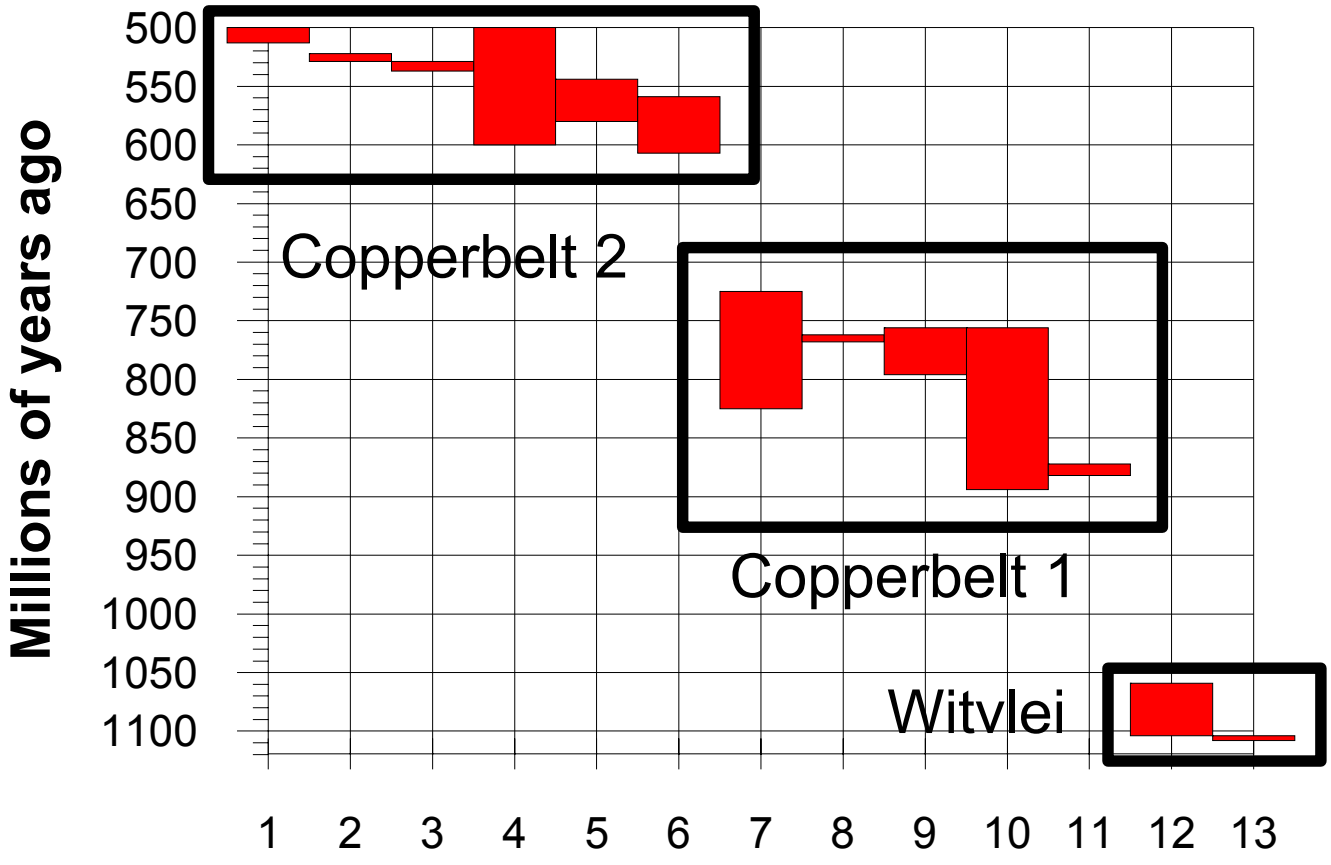

Fig 6.4.2 Event diagram for three copper mineralizing periods in the Greater Lufilian Arc.

7 SOME ASPECTS OF ANOROGENIC INTRUSIVE ROCKS

7.1 INTRODUCTION

Continental rifts are environments where granitoids, gabbroids and alkaline rocks may coexist short distances from one another. Extensional continental rift systems favor the formation of midalkaline felsic magmas. Both plutonic and volcanic rocks are produced from those magmas and may form characteristic ring complexes. Midalkaline mafic magmas also occur in the environs of the felsic magmas. A wide range of gabbroids, syenitoids and ultramafic rocks may form from the mafic magmas. The close association of such diverse rock types enhances magma mixing and there is potential for many types of mineralization.

A model of rift-related intrusions was prepared by Kazmin & Byakov, 2000, and is included on Fig. 7.1. Note the different types of small intrusive bodies that originate from the same mafic magma chamber in the middle of the figure. Chemistry of each intrusive event is unique. Large mafic and felsic chambers may exist at the same time within very short distances, as illustrated. The chamber to the left is one of them. They occur much higher in the crust. With sufficient erosion from the upper layers of syn-rift sediments, the granitoids and mafic intrusive rocks may be exposed on surface. Carbonatites, syenites, gabbroids, alkali granites and granites coexist in this environment. They intrude pre-rift, syn-rift, and post-rift sediments.

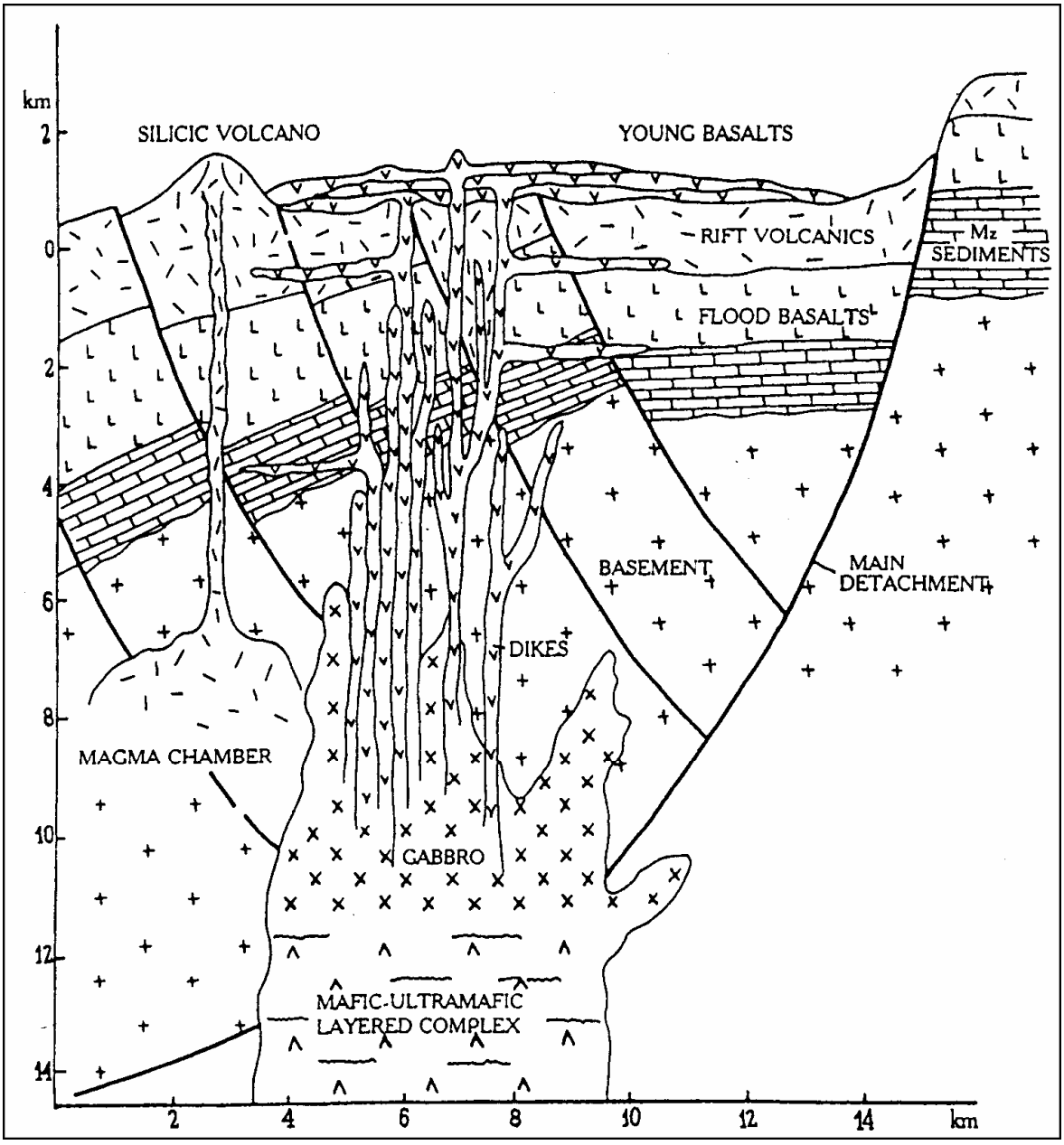

Fig 7.1 Schematic cross section of the Wonji Fault Belt: an example of a tectomagmataic belt in a continental rift. *More details in text.Taken from Kazmin & Byakov, 2000.*

Most of the rifting processes abort before oceanic crust is able to form. The rifting process may repeat itself in time, producing magmas with very similar chemical characteristics.

If more felsic magmatic bodies like the one illustrated on the cross section of Fig. 7.1, occur along successive parallel cross sections, large volumes of granitods may accumulate with time. The ring complexes formed may eventually gain enough areal density to produce the ring complex clusters that are discussed in the next section.

This chapter will begin by comparing granitoid batholithic bodies with three case studies of anorogenic ring complex clusters. It continues defining main characteristics of some ring complex clusters in the Greater Lufilian Arc. Finally, it describes the occurrence of multiple, small gabbroic bodies that are known to occur in anorogenic extensional settings and compares them with similar features observed in the Greater Lufilian Arc.

7.2 COMPARISON OF BATHOLITHIC GRANITOID BODIES WITH ANOROGENIC RING COMPLEX CLUSTERS

7.2.1 Introduction

Similarities have been observed between some of the batholithic intrusive bodies in the Greater Lufilian Arc and clusters of anorogenic ring complexes described in the literature. This chapter presents those observations. Well documented African examples have been used as far as possible.

7.2.2 Nuba Mountains, Sudan

Fig 7.3 shows the emplacement time span for a series of Sudanese rift-related ring complexes (Wooley, 2001). Table 7.1 shows the actual data. This example was taken from a large field of granitoids and alkaline rocks in the SW Nuba Mountains of Sudan, located west of the White Nile River, as shown on Fig 7.2. There were at least three discrete events of intrusion that took place in roughly the same location. These occurred from 531 to 497 Ma, from 275 to 216 Ma, and from 171 to 149 Ma. Taking into account the errors, the first event could have lasted for 38 Ma, the second for 59 Ma and the third for 22 Ma. There is no progressive advance of magmatism in any direction. Masakin Tiwal had two intrusive events separated by 275 Ma (Nos. 6 and 11 on Table 7.1). The old intrusions are separated from the main "batch" of intrusions that occur from near 275-216 Ma.

Table 7.1 Radiometric (Rb-Sr) ages from ring complexes, SW Nuba Mountains, Sudan
chronologically sorted (from compilation of African alkaline rocks and carbonatites by Wooley, 2001. Numbers refer to those listed by Wooley.)

#	Name and Number of Site	Age (Ma)	Error	From	To
1	Jebel Demik 76	160	11	149	171
2	Jebel Lado 87	222	6	216	228
3	Jebel Tabaq 70	228	17	211	245
4	Jebel Talodi 89	229	15	214	244
5	Jebel Kadugli 79	238	12	226	250
6	Masakin Tiwal 85	239	10	229	249
7	Moro-Limon Hills 84	246	2	244	248
8	Jebel Keiga, Umm Dugo 77	248	4	244	252
9	Jebel Tuna, Kafina, Debkaya 81	251	7	244	258
10	Jebel Moro West 83	261	14	247	275
11	Masakin Tiwal 85	514	17	497	531

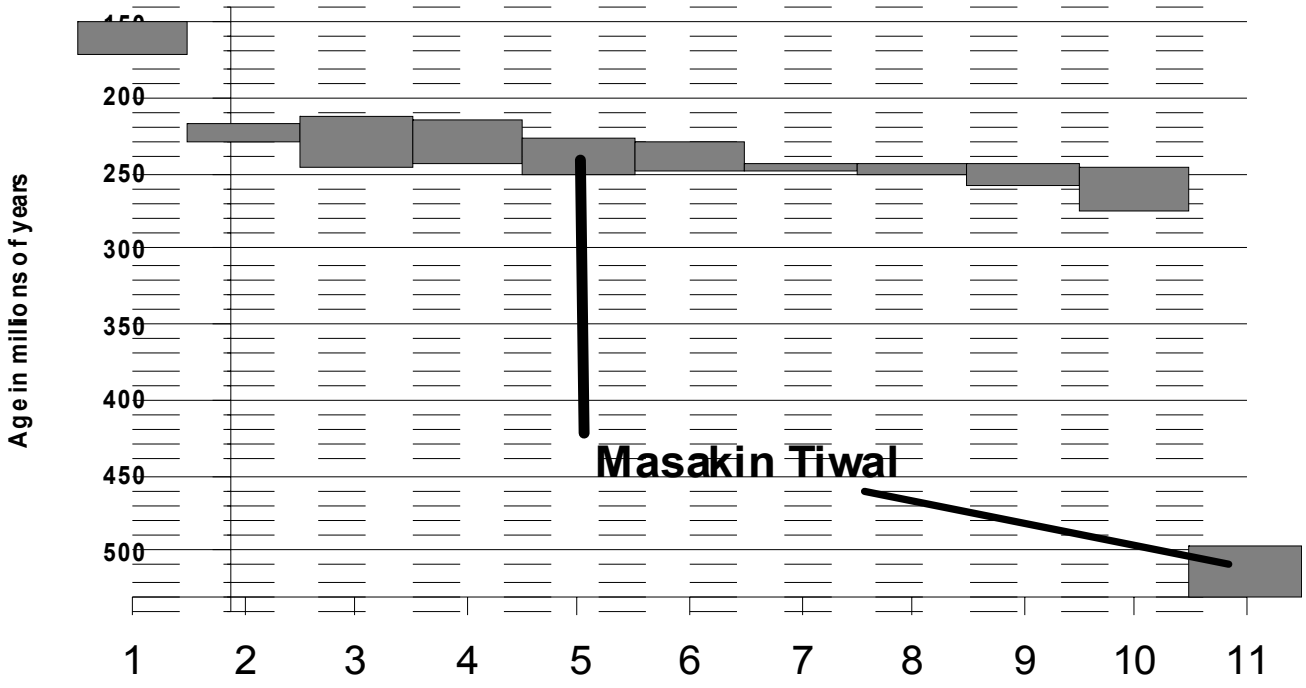

Fig 7.3 Event diagram for intrusions from the SW Nuba Mountains, Sudan. (Number of events from Table 7.1).

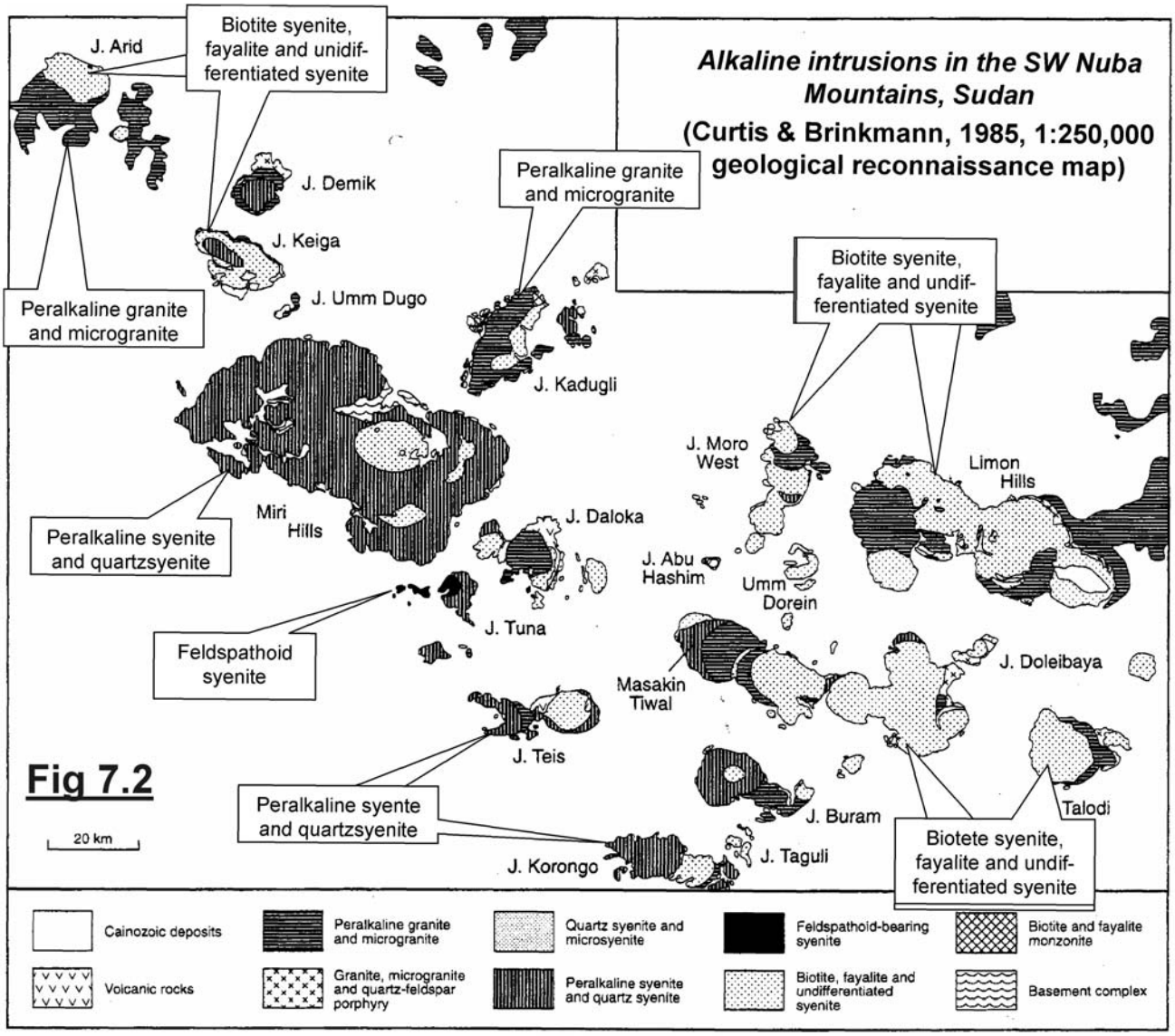

Fig 7.2 Alkaline intrusions of the SW Nuba Mountains, Sudan. Note the varying average composition for each of the complexes. In a few locations, such as the Miri Hills, Masakin Tiwal and the Limon Hills, several ring complexes amalgamated together. (After Curtis & Brinkmann, 1985, in Wooley, 2001 p. 305.)

7.2.3 Central Nigeria ring complexes

Another example of anorogenic ring complexes from Nigeria shows variations on the same topic (Bowden et al., 1987; Kinnaird, Batchelor, Whitley, & MacKenzie, 1985; and Kinnaird & Bowden, 1991). In this case, a cluster of granitic circular complexes was emplaced at the times shown on Table 7.2 and Fig 7.5. The time span is comparable to that of the Sudanese complexes previously described. The information available from Nigerian intrusions shows at least five discrete periods of emplacement, namely: 216-210, 194-180, 175-170, 167-164 and 158-138 Ma. The total time span for the groups of intrusions is 78 million years. If only the main portion is included, the span shortens to 34 Ma. Here, once more, there are some precursor events followed by a main batch of intrusions that were emplaced during a short period of time, and by a waning stage. This example has striking similarities to that from the Nuba Mountains of Sudan. Its dimensions (Fig 7.4) are roughly the same as those of the Kamanjab and Hook batholiths. In addition to that, the Nigerian complexes are mainly composed of biotite granite (Table 7.3). This cluster of complexes was already included in discussions about the Nchanga Granite on section 4.1.5.2.

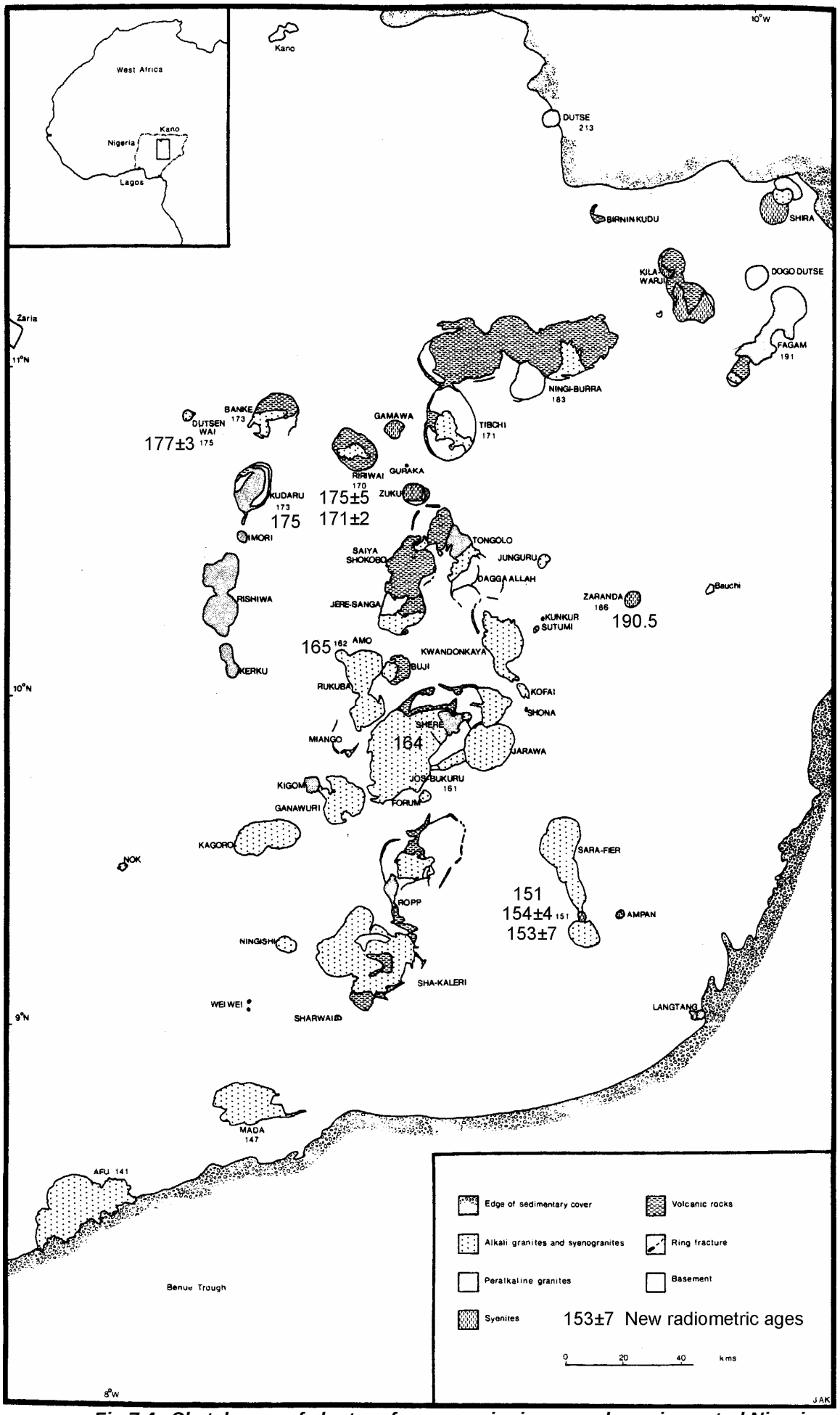

Fig 7.4 Sketch map of cluster of anorogenic ring complexes in central Nigeria (after Kinnaird, 1985; Bowden, 1987 and Wooley, 2001). Ages in Ma.

Table 7.2 Radiometric (Rb-Sr) ages from Nigerian ring complexes

Sorted chronologically from Wooley, 2001; numbers refer to those listed by Wooley. An arbitrary 3 Ma error was added to starred sites (Afu, Mada, Tibchi, Ningi-Burra, Fagam and Dutse) from Bowden et al., 1987.

	Name and number of site	Age (Ma)	Error	From	To
1	Afu*	141	3	138	144
2	Mada*	147	3	144	150
3	Sara-Fier & Pankshin 38	153	7	146	160
4	Sara-Fier & Pankshin 38	154	4	150	158
5	Jos Bukaru & Shere 31	164	4	160	168
6	Jos Bukaru & Shere 31	165	2	163	167
7	Amo & Pukuba 33	165	3	162	168
8	Ririwai 13	171	2	169	173
9	Tibchi*	171	3	168	174
10	Banke 14	173	2	171	175
11	Banke 14	173	3	170	176
12	Dutzenwai 15	173	3	170	176
13	Kundaru 16	173	3	170	176
14	Ririwai 13	175	5	170	180
15	Kundaru 16	175	16	159	191
16	Ririwai 13	176	5	171	181
17	Dutzenwai 15	177	3	174	180
18	Ningi-Burra*	183	3	180	186
19	Zaranda 25	190	15	175	205
20	Fagam*	191	3	188	194
21	Dutse*	213	3	210	216

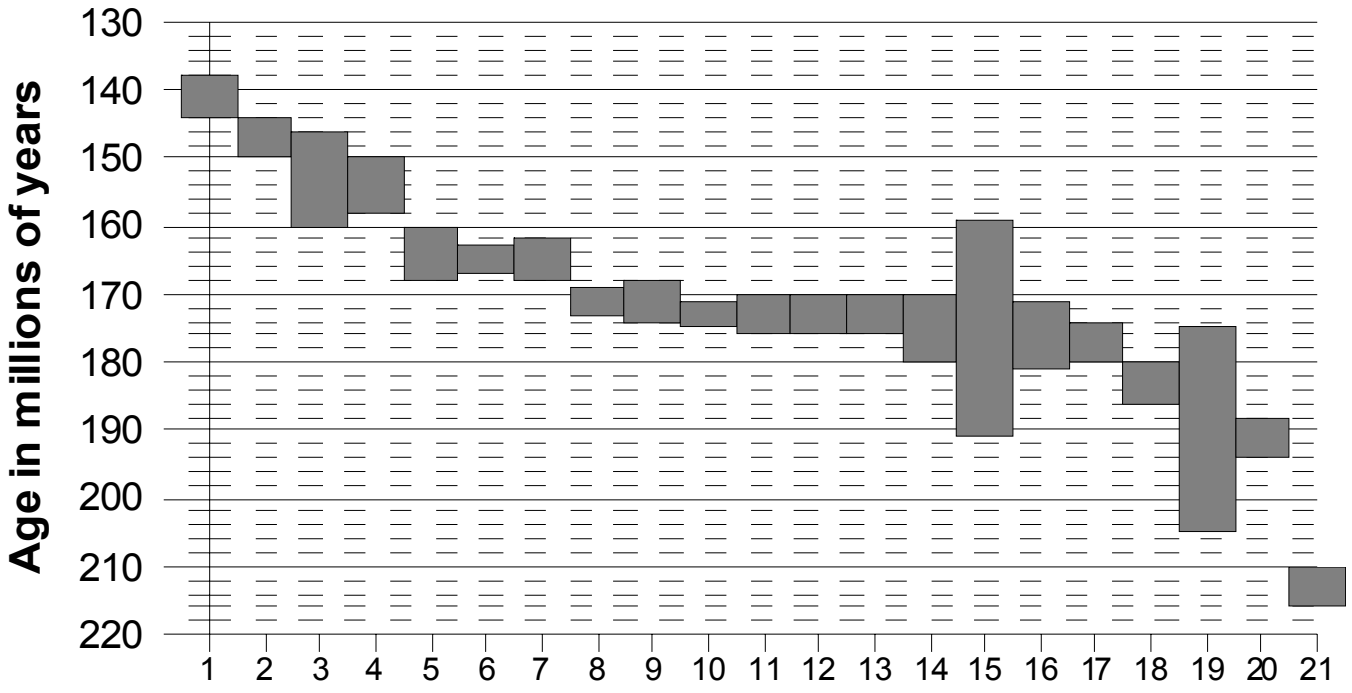

Fig 7.5 Event diagram graph for ring complexes in Central Nigeria. (Number of events from Table 7.2).

Table 7.3 Chemistry of biotite granites from Nigerian anorogenic ring complexes
(from Bowden et al., 1987)

Complex	Sample	SiO2	TiO2	Al2O3	Fe2O3	FeO	FeOt	MnO	MgO	CaO	Na2O	K2O	P2O5	LOI	Total	Rb	Sr	Y	Zr	Nb	Cu	Zn	V	Ba	Th	Pb	Ce	La	Hf	Li	Be	Sn
	Notch	50.00	1.00	15.50	6.00			0.15	2.00	5.00	4.90	5.50	0.30	2.00		200	400	60	360	40	25	85	100	1300			175	95				
Amo	AMN24	72.60	0.29	14.07	0.90	1.73	2.63	0.07	0.43	1.01	3.36	5.74	0.07	0.47	100.74	185	100	63	246	57		61	9	362	27	22	144	59	6	34	5	8
Ririwai	RN75	75.90	0.11	12.85	0.33	1.05	1.38	0.05	0.02	0.24	3.91	4.31	0.01	0.88	99.66	979	15	696	399	214	120	376	0	109	111	56	296	234	28	391	7	40
Pankshin	PAN112	73.90	0.15	14.88	0.43	0.80	1.23	0.02	0.67	0.43	3.98	5.17	0.02	0.61	101.06	192	28	117	234	88			0	80	25	22	195	189	7	25	8	19
Jos Bukuru	JON147	73.20	0.18	14.18	0.67	1.19	1.86	0.02	0.08	0.73	3.45	5.32	0.03	0.98	100.03	296	38	227	330	118		126	0	264	41	38	251	218	8	32	14	39
Banke	B34	76.00	0.10	11.74	0.37	0.89	1.26	0.02	0.09	0.83	3.78	5.77	0.04	0.24	99.87	574	4	115	141	158		60	12	39	40	74	114	64	5	205	9	145
Mada	MD333	75.40	0.10	13.33	0.01	0.96	0.97	0.02	0.04	0.34	4.26	4.53	0.01	0.20	99.20	620	0	139	129	78	9	68	0	0	66	70	79	28	9	158	8	0
Ningi	NG208	75.70	0.20	13.18	1.48	0.01	1.49	0.03	0.09	0.44	3.41	5.10	0.01	0.66	100.31	318	29	75	186	80		70	2	151	63	57	156	83	7	13	16	34
Tib` chi	T15A	74.30	0.08	11.74	0.33	0.89	1.22	0.02	0.01	0.26	3.88	4.59	0.01	0.64	96.75	502	1	86	166	132	7	61	3	0	69	37	153	166	7	122	12	
Dress	DR11	76.70	0.14	13.36	0.00	1.16	1.16	0.03	0.05	0.33	4.41	3.58	0.02	0.34	100.12	966	0	87	81	119		103	4	0	61	47	149	88	9	558	15	76
Dutsen	DW1	78.03	0.06	12.14	0.33	0.89	1.22	0.01	0.09	0.52	4.59	3.56	0.01	0.42	100.65	389	22	356	207	205		77	0	71	42	16	275	169	10	138	10	10
Faban	FG5	77.44	0.08	11.99	0.37	0.87	1.24	0.02	0.07	0.49	3.89	4.45	0.01	0.34	100.02	347	3	189	161	148		42	0	43	39	27	117	64	8	67	13	10
Kudaru	KD12	76.50	0.10	12.83	0.35	0.84	1.19	0.02	0.07	0.46	4.17	4.39	0.01	0.34	100.08	283	4	144	147	96		48	0	4	36	41	62	27	6	56	9	

7.2.4 Kanye-Gaborone ring complexes, Botswana

As shown on Table 7.4 and Fig 7.7, the Gaborone anorogenic ring complex cluster that lies in between Botswana and South Africa formed at least during a period of 20 Ma (Grobler, 1996). If we take into consideration event 12, then the lapse of time increases to approximately 72 Ma. There seems to have been a precursor event (13) 160 million years before. Other U-Pb radiometric ages that are not so well constrained (events 14 to 17) indicate that there might be other moments of intrusion before and after the main known lapse from 2840 to 2768 Ma. These precursor and tailing events are not well studied, and the entire ring complex cluster could very well have formed during a longer time. Only a relatively small portion of the ring complex cluster is exposed, and radiometric ages are available from that eastern portion. The possible extension of the ring complex cluster to the east is estimated by Grobler in some 300 km. Main features of the complex are shown on the map of Fig. 7.6.

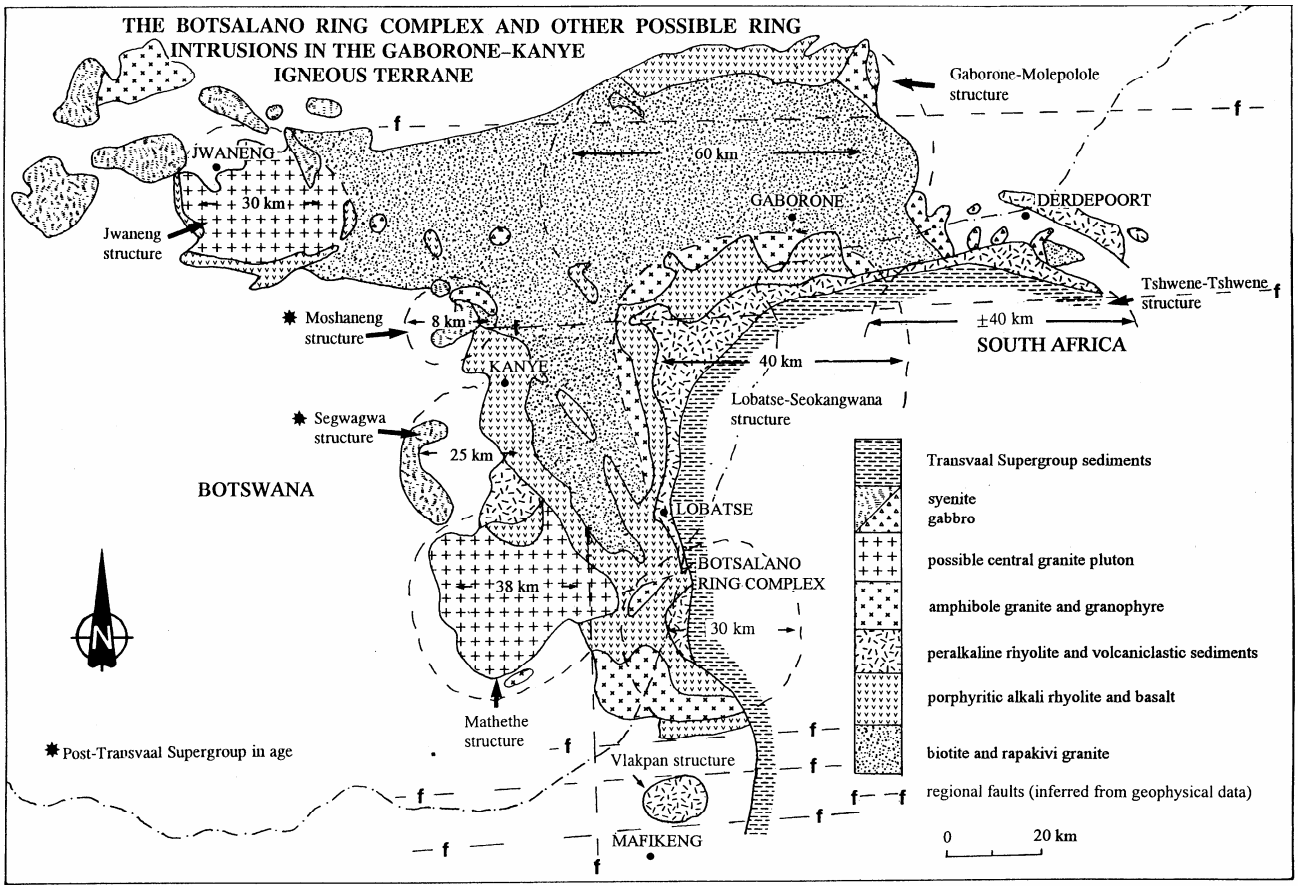

Fig 7.6 The Botsalano ring complex and other possible ring intrusions in the Gaborone-Kanye igneous terrane, Botswana and South Africa (after Grobler, 1996).

Table 7.4 Geochronological data available for Gaborone anorogenic ring complex cluster, Botswana and South Africa. Data from (Grobler, 1996).

#	Site	Age (Ma)	Error	From	To
1	Mmathethe Granite	2775.2	7.4	2767.8	2782.6
2	Lobatse rhyolite**	2780	5	2775	2785
3	Kanye Formation rhyolite	2780	6	2774	2786
4	Plantation porphyry (Lobatse)	2781.1	1.9	2779.2	2783
5	Thamaga rapakivi granite	2782.2	5	2777.2	2787.2
6	Main phase of Kgale granite	2783.1	2	2781.1	2785.1
7	Gaborone Granite granophyre	2783.1	1.2	2781.9	2784.3
8	Kanye Formation rhyolite	2784.7	1.7	2783	2786.4
9	Kanye Fm. rhyolite	2784.8	1.8	2783	2786.6
10	Spherulitic porphyritic	2784.9	1.9	2783	2786.8
11	Rhyolite and granophyre	2785.1	1.1	2784	2786.2
12	Majwana Granite (Kubung)	2830	10	2820	2840
13	Gaborone Granite Derdepoort*	3010	10	3000	3020
14	Plantation porphyry	2630	100	2530	2730
15	Platberg group	2643	100	2543	2743
16	Gaborone Granite Derdepoort	2825	100	2725	2925
17	West Kubung diorite	2932	250	2682	3182

* an error of 10 Ma was added for plotting and comparison.
** an error of 5 Ma was added for plotting and comparison.

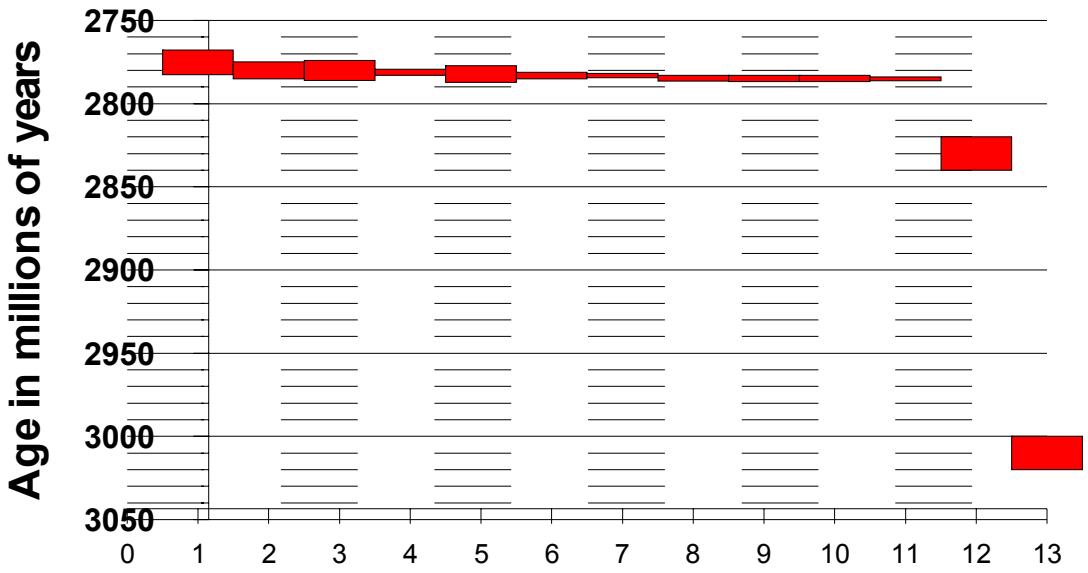

Fig 7.7 Event diagram for Gaborone anorogenic ring complex cluster, Botswana/South Africa. Data comes from Grobler, 1996. (Number of events from Table 7.4).

7.2.5 Comparison of the three ring complex clusters

Finally, a direct comparison of the event diagrams from the three anorogenic ring complex clusters just reviewed helps to understand their similarities better. Fig 7.9 presents event diagrams from the Nuba Mountains, the central Nigerian ring complexes and the Kanye-Gaborone complexes of Botswana. They have been leveled to a common central time point and plotted at the same scale. If one takes into consideration sampling errors, that not all of the ring complexes present in each of the clusters has been dated, and that several different dating techniques have been used, the three diagrams can be said to represent equivalent geological processes. Precursor events more than 200 Ma before the main group of intrusions are present in both the Sudanese and Botswanan clusters.

Volcanic and plutonic rocks of roughly the same composition occur together in all three complex clusters, and in most of the world's ring complexes. The amount of volcanic rocks decreases with successive levels of erosion, to a point where only granitic rocks are left and all volcanic rocks are eroded.

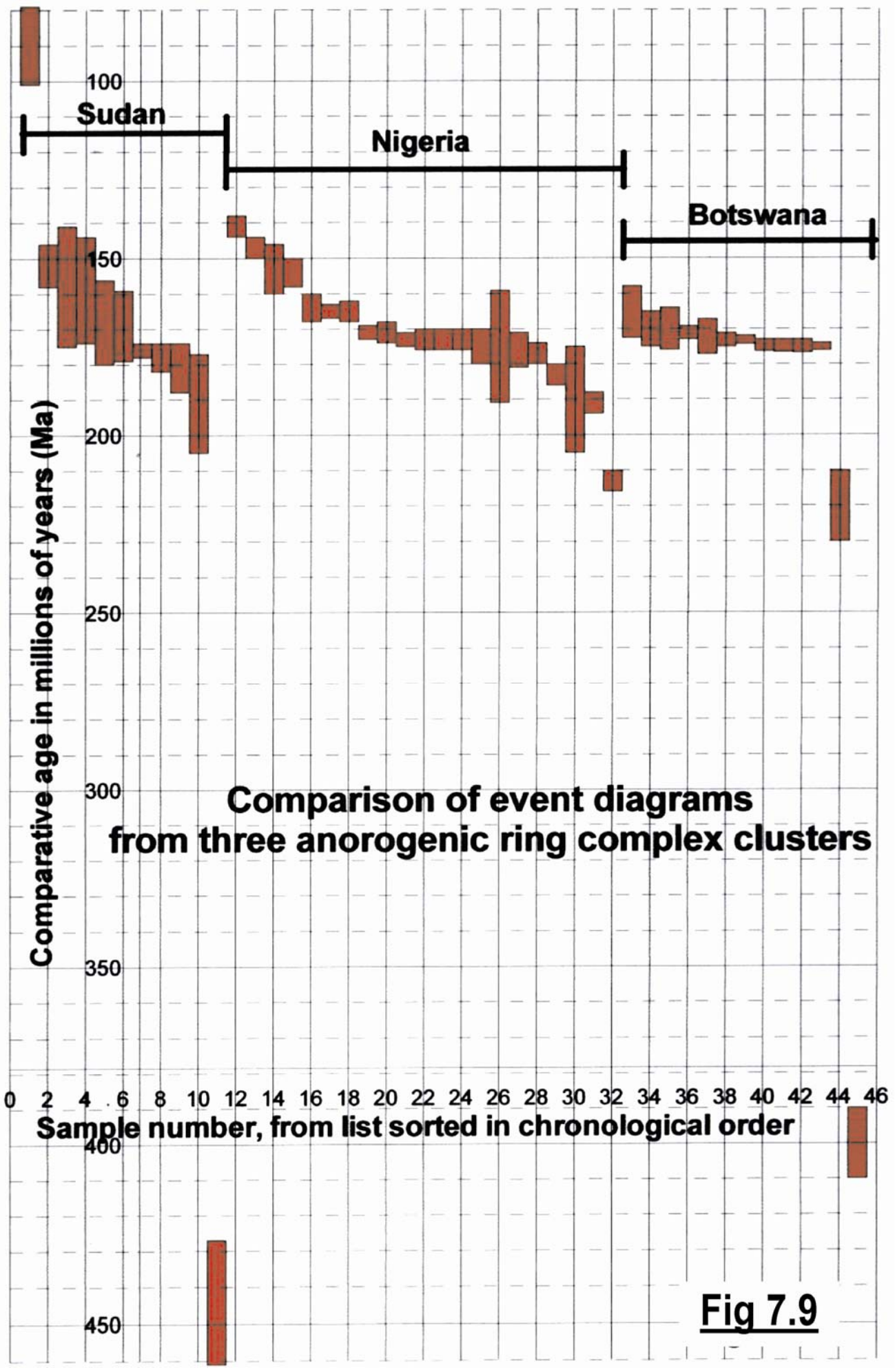
Sudan
Nigeria
Botswana
Comparative age in millions of years (Ma)
100
150
200
250
300
350
400
450
0 2 4 6 8 10 12 14 16 18 20 22 24 26 28 30 32 34 36 38 40 42 44 46
Sample number, from list sorted in chronological order
Comparison of event diagrams
from three anorogenic ring complex clusters

Fig 7.9

Individual anorogenic complexes tend to have circular outcrop, hence the name “circular” or “ring” complex. Clusters of ring complexes tend to have the shape of isosceles triangles in plan view.

This can be considered the model for anorogenic ring complex clusters. Clusters identified in the Greater Lufilian Arc will be compared with it in the next pages.

7.2.6 Model for the origin of batholithic-size granitoid bodies in anorogenic environemnts.

New ideas on the origin of granitic bodies have been proposed by numerous working groups and individuals during the last fifteen years. Some review articles on the subject include Clemens & Mawer, 1992; Glazner, Bartley, Colemena, Gray, & Taylor, 2004; Hutton, 1996; and Vigneresse, 1995. The existence of batholithic size magma chambers is physically impossible. Long-term amalgamation of very small magma chambers, amalgamation of numerous consecutive dikes, and granitic magma transport by fracture propagation seem to be the most energy efficient systems to accumulate large volumes of granitoid rocks and account for the majority of batholiths.

The three, reasonably well-documented, case studies of anorogenic complex clusters described in the previous section form the basis for the genetic model for batholithic-sized anorogenic bodies proposed here.

Many African ring complexes are made of midalkaline granitoids. If such ring complexes intrude very near each other as shown on Fig 7.2, batholitic size bodies may form. Larger magma bodies develop underneath the ring complexes, and once lithified, subsequent erosion can expose them. This process explains the formation of large plutonic bodies like the Hook Granite and the Kamanjab batholith in anorogenic rift-related environments.

The process could also help to explain the large compositional variety of batholiths like the Hook Granite. They did not form during a single event, but by amalgamation of multiple small discrete plutons, each with its own chemistry. Regional heat re-sets the geochronological clocks of some rocks, and continuously metamorphoses older intrusions. This method is proposed as origin for granitoid batholiths in anorogenic environments.

Fig 7.8 shows a cluster of granitic ring complexes (unit E) overprinted by a cluster of quartzmonzonitic ring complexes (D) and later by a third cluster of alkali granite ring complexes (C). Two more generations of ring complexes (B and A) came later. The end result is complex geology, abundant thermal metamorphism and hydrothermal alteration of the older plutons, as well as widespread opportunities for magma mixing processes to occur. Each event of granitic ring complexes produced contemporaneous vulcanism of equivalent composition. Depending on the level of erosion of the ring complex cluster, one will find only volcanic rocks, a mixture of volcanic and plutonic rocks, or only plutonic rocks in ring complexes.

The shapes, and internal and external characeristics of granitic plutons are purely arrival phenomena dictated by local structure, kinematics, and stress states [Clemens & Mawer, 1992, p. 339]. But in the case of large granitoid ring complex clusters, there seems to be an underlying mechanism that leads to the formation of isosceles triangle shapes.

The triangular shapes of the Kamanjab and Hook Granite batholiths, as well as their size, are comparable to those of the three ring complex clusters described in the previous section. Fig 7.10A shows the outlines of the five entities drawn at the same scale, and rotated for simpler comparison.

At first glance, the outlines of the Kamanjab batholith and Hook Granite batholith show many similarities. Their area is approximately the same. Both display a roughly isosceles triangular shape; if one is laid over the other, the silhouette of their perimetral triangles is almost the same size and shape. In the position that the two outlines are laid, both bodies are composed of a principal large, elongated portion and several other smaller portions separated from the main body by a fracture that is parallel to one of the longest sides of the triangle (Fig 7.10B). Both bodies have small satellite intrusions that fall outside of the main triangular outline.

The outlines of the Nuba Mountains and the Central Nigerian ring complex clusters also display several similarities. In both cases, the main portion of the cluster can be circumscribed by an isosceles triangle of roughly the same size and shape. In both cases, there are fractures that run parallel to the longest side of the triangle that separate the ring complexes. Again, both clusters have small satellite intrusions that fall outside of the main triangular outline. The Central Nigerian ring complex cluster a large number of ring complexes that fall outside the main triangle.

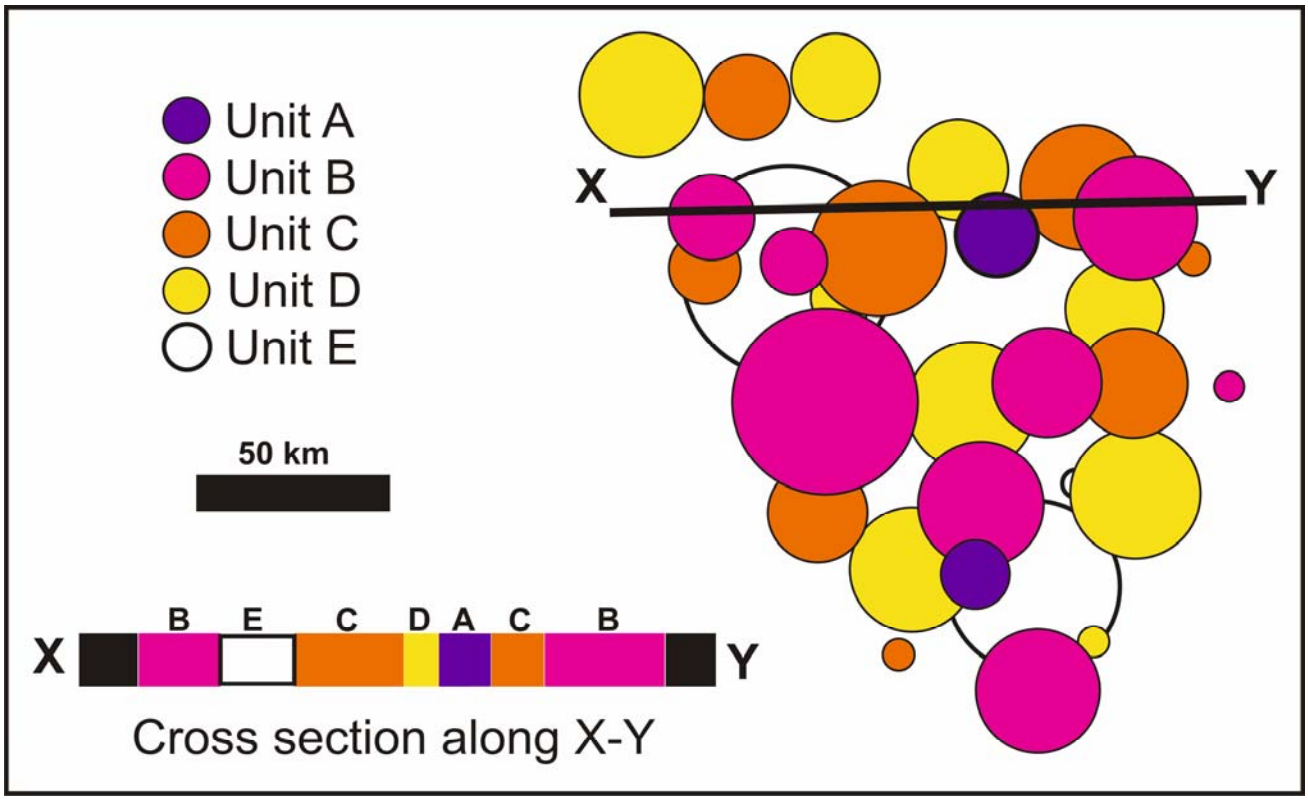

Fig 7.8 Plan view of what might have taken place to produce one of the granitoid ring complex clusters identified in the Greater Lufilian Arc. *Notice that if a series of five different generations of granitoid ring complex structures intrude and intersect each other, a complex assembly of igneous lithologies can form. Each of the separate intrusive events (A to E) was made of a few ring complexes widely spread in the area. In the hypothetical case, each generation of ring complexes has a uniform lithology. A chance orientation for a geological transect along X-Y results in the geology shown. Interpretation of that geology based on the single transect is quite complex, especially if the outcrop density is not good. The geology of the Hook Granite Batholith and the Kamanjab Batholith are very much like this.*

The Kanye-Gaborone ring complex cluster is less well defined than the other clusters, shows the general triangular shape, but it also has three additional ring complexes that significantly modify its overall shape.

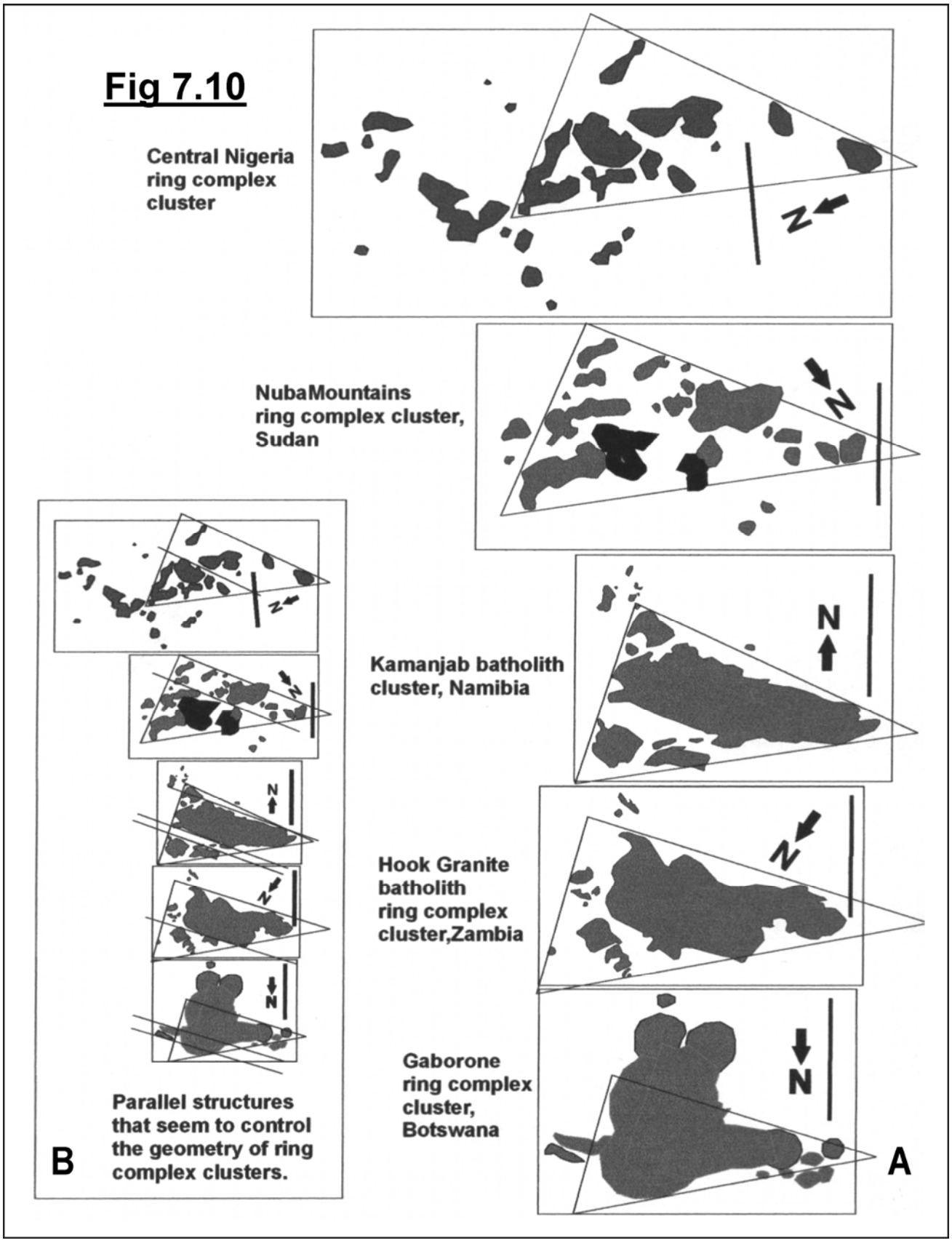

Fig 7.10 Comparison of the outlines of various African ring complex clusters. (All scale bars are 100 km long). Note that most of the ring complex clusters may be circumscribed by an isosceles triangle of similar dimensions. The outlines have been rotated for evaluation. All north arrows kept their original orientation.

7.2.7 Ring Complex Clusters in the Greater Lufilian Arc

The anorogenic granitoid-magmatic events that produce ring complex clusters seem to have a consistent time span of ~110 Ma. This is seen on many locations of the Greater Lufilian Arc, as shown on Table 7.6 below. The Sudanese Nuba Mountains, Nigerian and Gaborone granite ring complex clusters have been included in the table for comparison.

Table 7.6 Compilation of Anorogenic Complex Cluster Periods in the Greater Lufilian Arc

#	Name	Time Lapse	Magmatism	Central Age	Number of Radiometric Ages	Precursor Events	Tailing Events	Areal Extent	Event Diagram (page)	Example or main body
1	Nigeria	~75 Ma	Granite	170	21	1			New	Jos Bukuru
2	Nuba Mts., Sudan	~70, 120Ma	Granite	250	11	1	1		New	Masakin Tiwal
3	Hook Granite	~110 Ma	Granite, alkali granite	500	8	?			138	Hook Granite batholith
4	West Lusaka 2	~120 Ma	Syenite	550	16	?			139	Hook Satellites
5	NW Zambia 2	~100 Ma	Quartz syenite, gabbro	720	7	2			137	Peter Mann's pluton
6	Kafue Flats	~140 Ma	Granite	750	10	yes			139	Lusaka Granite
7	Khorixas 1	~110 Ma	Syenite, nepheline syenite	760	8	no	no		150	Oas Syenite
8	Khorixas 2	~105 Ma	Granite, quartzmonzonite	1800	3	?	2		150	Khorixas Inlier
9	Irumide	~100 Ma		1870	10	2			New	
10	NW Zambia 1	~110 Ma	Granite	1920	7	?			137	L-030
11	Kamanjab	~110 Ma	Granite, quartzmonzonite	1925	8	2	yes		149	Kamanjab batholith
12	Mufulira	~120 Ma	Granite, tonalite	2000	7				141	Mufulira Granite
13	Mkushi-Serenje	~100 Ma	Granite	2050	9	2			New	
14	Kanye-Gaborone, Botswana and South Africa	~72 Ma	Granite-rhyolite	2800	17	1	Maybe	200 x 120 km (may be 300 x 150 km	New	Gaborone and Jwaneng

At least ten of those anorogenic complex cluster periods have been documented in the Greater Lufilian Arc during this project. That represents the regions with enough geochronological data to produce meaningful results, and is definitely an incomplete list. The gaps in the event diagram of Fig 7.11 are time periods with less reliable data and do not necessarily mean that anorogenic ring complex clusters only formed in particular moments (See Fig A81, for example). What should be understood from the diagram is that the process has been taking place on what is now the African plate, at least during the past 2.8 billion years.

If the information from Table 7.5 is considered as totally representative of reality, then three main periods of anorogenic ring complex cluster formation are in evidence in the Greater Lufilian Arc: one from 2100 to 1820 Ma, a second from 815 to 670 Ma, and a third from 610 to 445 Ma. That is just a partial observation.

In addition to that, Fig 7.11 shows that two of the regions have had two completely distinct periods of anorogenic ring complex cluster formation. The events from the NW Zambia region are separated by 1095 Ma, while the events from the Khorixas region are separated by 933 Ma. In both cases, the clusters of ring complexes formed in roughly the same areas. This may be another recurrent feature of the ring complex clusters that probably has not been made evident due to scarce geochronological information.

The two clusters from West Lusaka are not illustrated on Fig 7.11. They trail one after the other, separated by 50 Ma (Fig A25), and Nos. 5 and 6 on Fig 7.12. The end of West Lusaka 1 is the beginning of West Lusaka 2.

Table 7.5 Compilation of ages from various ring complex clusters in the Greater Lufilian Arc

No.	Name	Central Age	Difference	From	To	Lapse
1	Central Nigeria	170	37.5	208	133	75
2	Nuba Mountains, Sudan	250	60	310	190	120
3	Hook Granite	500	55	555	445	110
4	West Lusaka	550	60	610	490	120
5	NW Zambia 2	720	50	770	670	100
6	Kafue Flats	750	70	820	680	140
7	Khorixas1	760	55	815	705	110
8	Khorixas 2	1800	52.5	1853	1748	105
9	Irumide	1870	50	1920	1820	100
10	NW Zambia 1	1920	55	1975	1865	110
11	Kamanjab	1925	55	1980	1870	110
12	Mufulira	2000	60	2060	1940	120
13	Mkushi-Serenje	2050	50	2100	2000	100
14	Gaborone Cluster, Botswana	2800	36	2836	2764	72

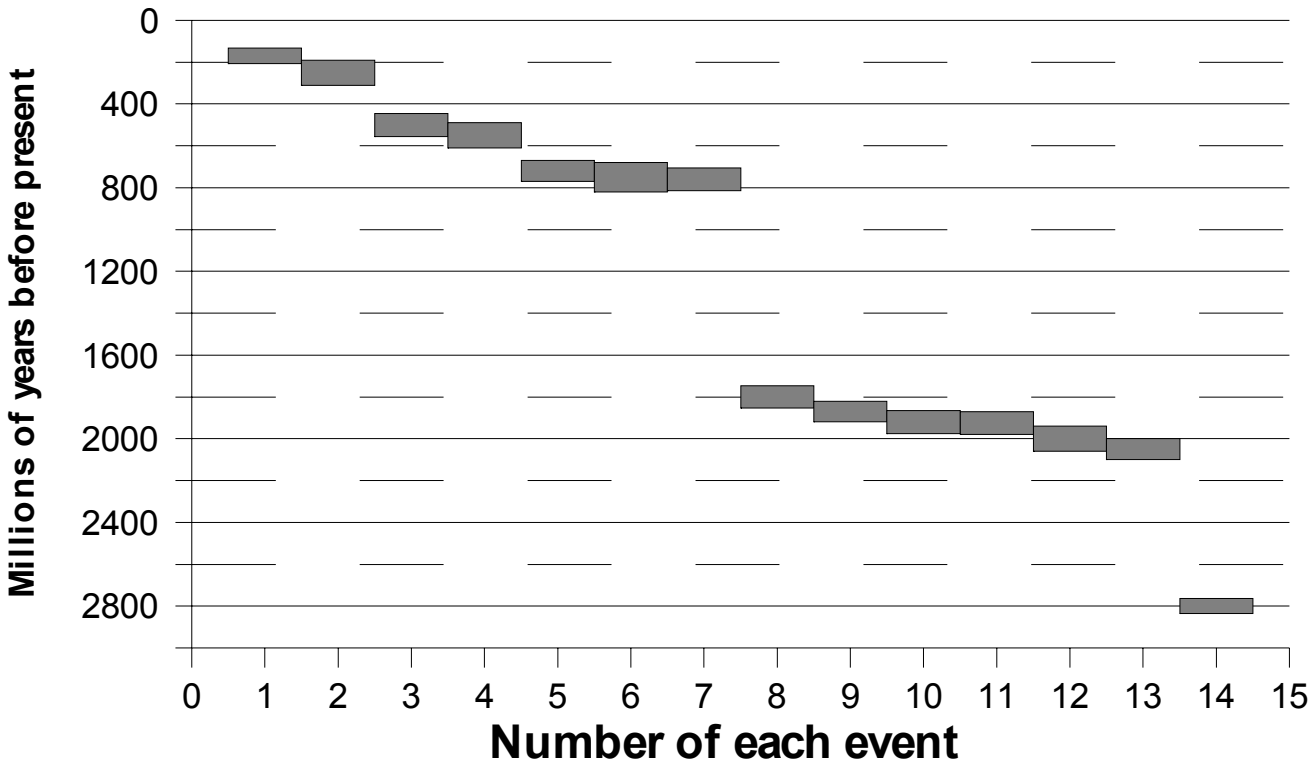

Fig 7.11 Event diagram of Anorogenic Complex Cluster periods in the Greater Lufilian Arc
(With three additions from Botswana, Nigeria and Sudan for comparison) Gaps may be due to incomplete information more than to periods of quiescence. More thorough compilations of geochronological data from the African Plate are necessary to complete the picture.

The event diagrams for some of anorogenic ring complex clusters were leveled to allow for direct comparison of their features. Fig 7.12 includes event diagrams from nine clusters plotted at the same scale, and centered on a uniform arbitrary age datum (230 Ma). Note that there are many similarities. Precursor and trailing intrusions occur in many of the clusters. 110 Ma seems to be the common duration for most of the clusters.

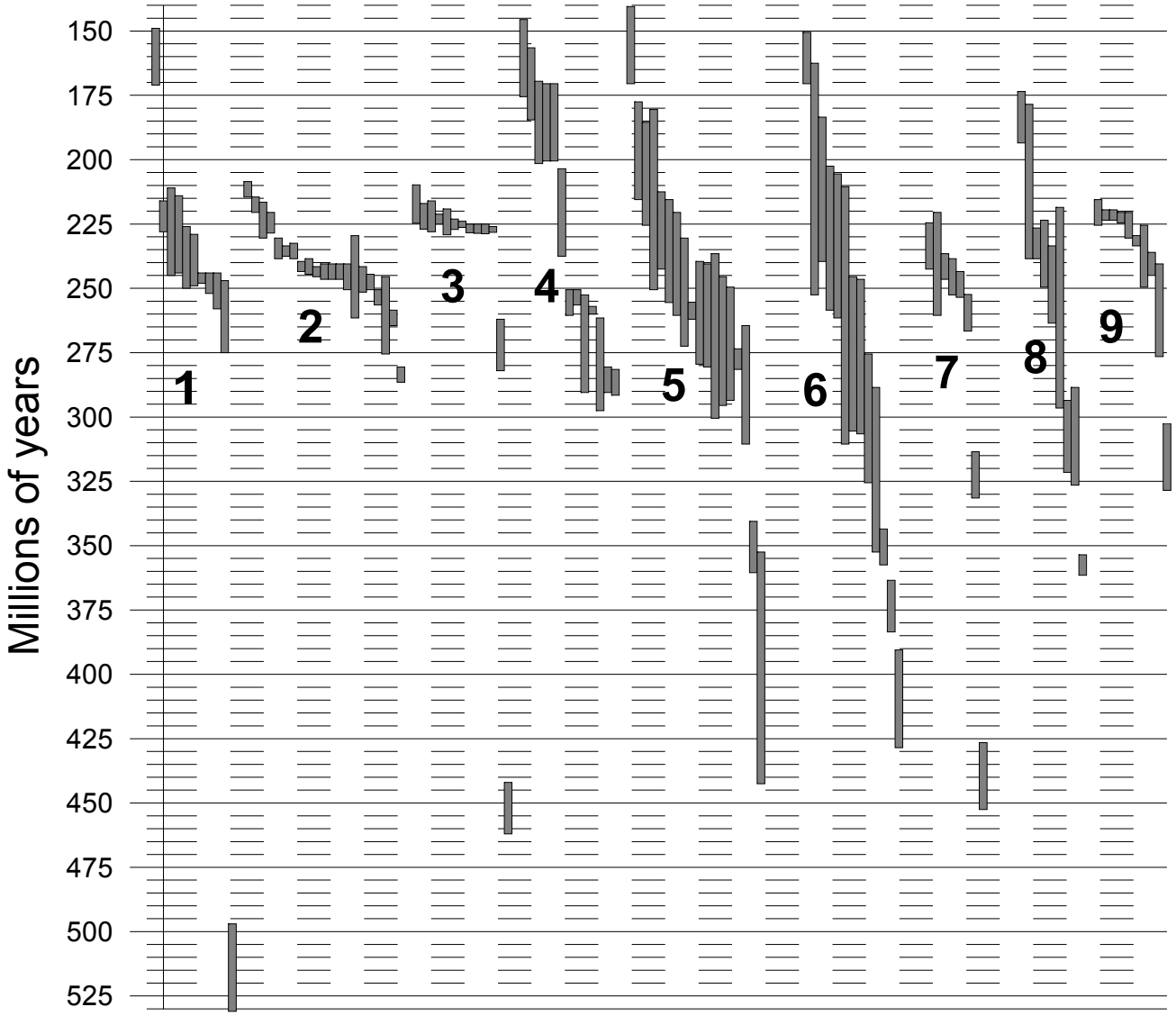

Fig 7.12 Comparison of event diagrams from various anorogenic ring complex clusters from the Greater Lufilian Arc.

Ages of the various complexes have been leveled to allow for comparison. Original data is on Table A22 and modified ages are on Table 7.7. Data from Sudanese, Nigerian and Kanye-Gaborone clusters were also included. Reference numbers of the event plots: **1**, Nuba Mountains, Sudan; **2**, Central Nigeria; **3**, Kanye-Gaborone, Botswana; **4**, Hook Granite batholith, Zambia; **5**, West Lusaka 1, Zambia; **6**, West Lusaka 2, Zambia; **7**, Mufulira, Zambia; **8**, Kamanjab batholith, Namibia; **9**, Khorixas Inlier, Namibia.

Note, for example, that clusters from the Hook Granite, West Lusaka 1, West Lusaka 2, and the Kamanjab batholith show very similar shapes, total length and distribution. Data available for the Mufulira and Khorixas Inlier clusters has some similarities. There are precursor events more than one hundred million years before the main Kanye, West Lusaka 1, West Lusaka 2, and Mufulira clusters.

The ring complex clusters require long-lived mantle plumes that remain relatively still in one place for at least the 110 million years. In several cases, anorogenic complex clusters formed in roughly the same place with 800 million years of difference or more. Examples of this have already been mentioned in the Khorixas inlier and NW Zambia. Another series of such events with a long hiatus is the basement to the Nchanga Granite.

Table 7.7 Range of dates for comparison of event diagrams from various anorogenic ring complex clusters, Greater Lufilian Arc Granitoid Project. *Ages of the various complexes have been leveled to a central value to allow for comparison. Data is plotted on Event diagrams of Fig 7.14.*

No.	From	To
Sudanese R.C.C.		
2	149	171
3	216	228
4	211	245
5	214	244
6	226	250
7	229	249
8	244	248
9	244	252
10	244	258
11	247	275
12	497	531
Kanye RCC (Bots.)		
36	209.8	224.6
37	217	227
38	216	228
39	221.2	225
40	219.2	229.2
41	223.1	227.1
42	223.9	226.3
43	225	228.4
44	225	228.6
45	225	228.8
46	226	228.2
47	262	282
48	442	462

No.	From	To
Nigerian R.C.C.		
14	208.5	214.5
15	214.5	220.5
16	216.5	230.5
17	220.5	228.5
18	230.5	238.5
19	233.5	237.5
20	232.5	238.5
21	239.5	243.5
22	238.5	244.5
23	241.5	245.5
24	240.5	246.5
25	240.5	246.5
26	240.5	246.5
27	240.5	250.5
28	229.5	261.5
29	241.5	251.5
30	244.5	250.5
31	250.5	256.5
32	245.5	275.5
33	258.5	264.5
34	280.5	286.5

No.	From	To
W Lusaka 1 R.C.C.		
64	140.5	170.5
65	177.5	215.5
66	185.5	225.5
67	180.5	250.5
68	212.5	242.5
69	215.5	255.5
70	220.5	260.5
71	230.5	272.5
72	255.4	262
73	239.5	279.5
74	240.5	280.5
75	236.5	300.5
76	245.5	295.5
77	249.5	293.5
78	273.5	281.5
79	264.5	310.5
80	340.5	360.5
81	352.5	442.5

No.	From	To
W Lusaka 2 R.C.C.		
83	55.5	105.5
84	59.5	103.5
85	83.5	91.5
86	74.5	120.5
87	150.5	170.5
88	162.5	252.5
89	183.5	239.5
90	202.5	258.5
91	205.5	261.5
92	210.5	310.5
93	245.5	305.5
94	246.5	306.5
95	275.5	325.5
96	288.5	352.5
97	343.5	357.5
98	363.5	383.5
99	390.5	428.5
100	613.5	637.5
101	617.5	655.5

No.	From	To
Hook Granite R.C.C.		
50	175.5	145.5
51	184.5	156.5
52	201.5	169.5
53	200.5	170.5
54	200.5	170.5
55	237.5	203.5
56	260.5	250.5
57	256.5	250.5
58	290.5	252.5
59	260	257
60	297.5	261.5
61	290.5	280.5
62	291.5	281.5
Mufulira R.C.C.		
103	224.5	242.5
104	220.5	260.5
105	236.5	246.5
106	238.5	252.5
107	243.5	253.5
108	252.4	266.6
109	313.5	331.5
110	426.5	452.5

No.	From	To
Kamanjab R.C.C.		
112	-69.5	-29.5
113	2.5	62.5
114	60.5	80.5
115	173.5	193.5
116	178.5	238.5
117	226.5	238.5
118	223.5	249.5
119	233.5	263.5
120	218.5	296.5
121	293.5	321.5
122	288.5	326.5
123	353.5	361.5
Khorixas 1 R.C.C.		
125	215.5	225.5
126	219.5	223.5
127	219.5	223.5
128	220.5	224.5
129	220.5	230.5
130	229.5	233.5
131	225.5	249.5
132	236	245
133	240.5	276.5
134	302.5	328.5

Very few of the old anorogenic complex clusters remain as discrete entities. Most of them have been broken up. For example, the Khorixas-Ugab-Mesopotamie-Summas domain in Namibia is very fragmented.

7.2.8 Conclusions

Clustering of multiple anorogenic ring complex intrusions can form batholithic size bodies.

Clusters of anorogenic granitoid ring complexes have been produced from Archean times and up to the past 140 Ma in what is now the African Plate; they probably have been forming all through the period in between, including the present. Eastern African examples in the rift valleys indicate that similar processes are still active today. A few normal faults with vertical displacement of over two kilometers expose syenites and granitoids underneath recent trachitic and rhyolitic vulcanism. Many young ring complexes have not been eroded enough to expose their ring shape roots and lie under volcanic fields.

Ring complex clusters have the following characteristics: 1) Multiple ring complexes of varying chemical composition and size that might intersect each other. 2) Volcanic and plutonic rocks of roughly the same composition occur together. 3) Successive magmatic events of varying composition allowed for abundant opportunities of magma mixing and recycling of crustal materials. 4) The plan view geometry of ring complex clusters is roughly that of an isosceles triangle. 5) Less voluminous precursor and waning events of magmatism may occur. 6) The principal chemical composition of the magmas is midalkaline, but may ocassionally vary to alkaline and subalkaline. In extreme cases, it may be peralkaline and can even produce significant carbonatitic rocks. 7) Isolated bodies of mafic and ultramafic rocks often come in the latter stages of the process.

At least ten clusters of ring complexes were identified in the Greater Lufilian Arc. They all display the general characteristics listed above. Their event diagrams show roughly the same parameters that have been identified in African ring complex clusters from the literature. Total duration of ring complex cluster cycles averages 110 Ma.

Several cycles of ring complex clusters have repeatedly occurred in roughly the same location in at least three different localities. These repeated cycles were separated 1095 Ma in NW Zambia, 933 Ma at the Khorixas area, and 50 Ma in West Lusaka.

The relevance of these observations on ring complex clusters are far reaching. They will probably be useful to help understand Proterozoic geology and the formation of contintental crust.

7.3 COMPARISON OF LUFILIAN SMALL BASIC INTRUSIONS WITH EXAMPLES FROM THE LITERATURE

The ubiquitous presence of abundant small gabbroic and midalkaline bodies in portions of the Greater Lufilian Arc was intriguing. These rocks intersect any lithologies, including siliciclastics, carbonates, granitoids and various metamorphic rocks. Parts of Nigeria have rocks with similar characteristics being formed today in rift-related environments. The following pages describe an example that can help understand the origin of the mafic bodies of the Greater Lufilian Arc.

The map from the Filiya area in eastern Nigeria (Fig 7.13) shows hundreds of small bodies of mafic and alkaline rocks that were emplaced into various rock types from 10 to 20 millions years ago. Some of the bodies form plugs or needles that "vary geomorphologically from small mounds several meters high to substantial peaks. Tangale peak, for instance, rises to more than 600 m above low sandstone hills." (Wooley, 2001, p. 247). Many smaller bodies have not been mapped. These numerous bodies of small intrusives were emplaced in an anorogenic environment within a continental plate that is being rifted.

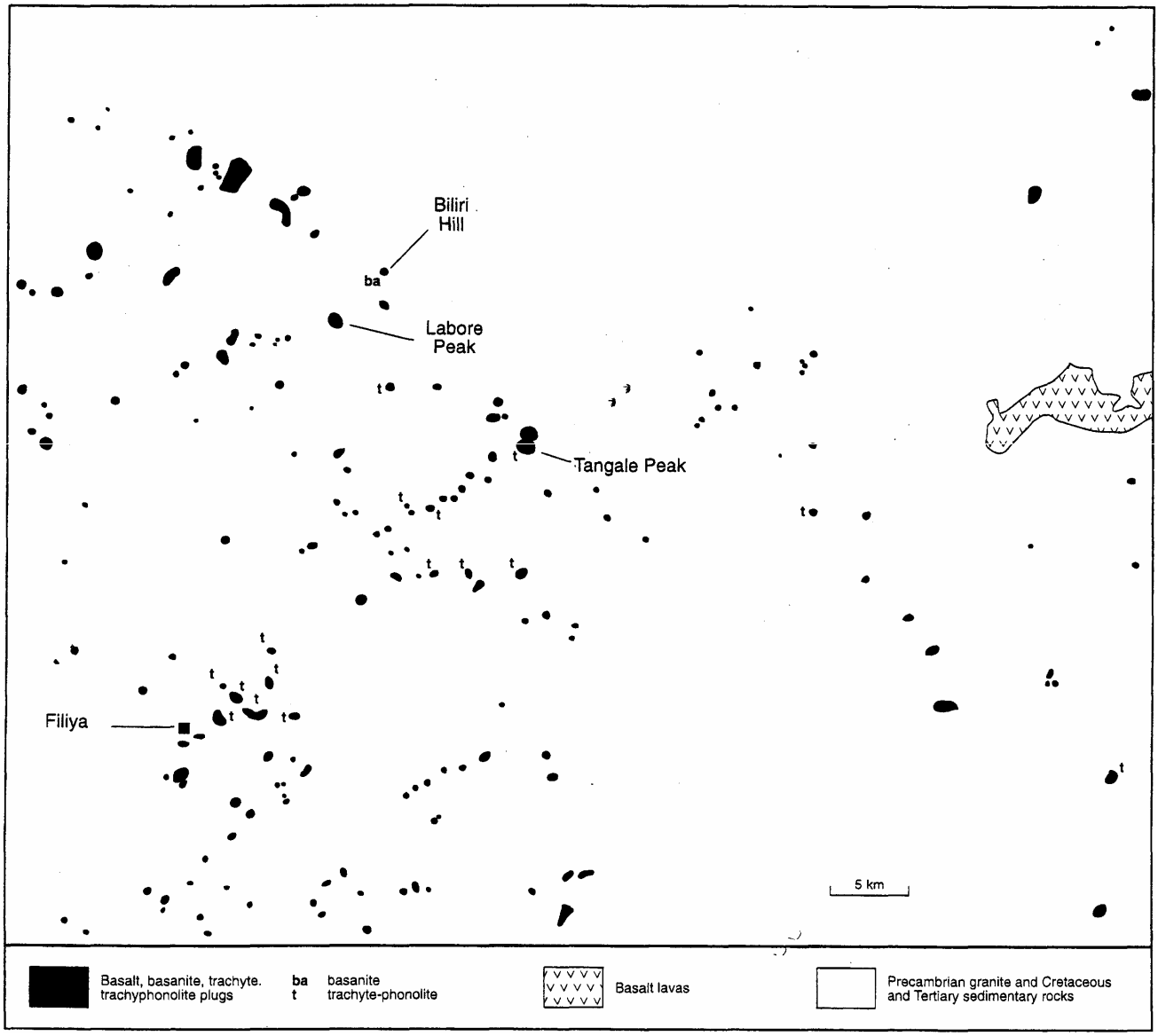

Fig 7.13 Sketch map of basalt, trachyte and phonolite plugs of the Filiya area in eastern Nigeria (after Carter et al, 1963 in Wooley, 2001, p.248) Note that several ENE-WSW linear trends can be identified.

These are typical intrusive features that form in rift environments. Some of the plugs behaved as feeders to volcanoes and others as feeders to dikes and sills. Many of these bodies were emplaced along weak structural zones and may be roughly aligned (Fig 7.13). They take place as the continental crust thins due to

extensional tectonics and the mantle reaches nearer to the surface. Fig 7.1 shows an example of what happens underneath an active rift zone today.

This is very similar to the abundant bodies of mafic rocks and syenites that are known from parts of the Greater Lufilian Arc. The only difference is that the level of erosion in the Lufilian Arc is deeper than that from Nigeria. Regions like West Lusaka and northwest of Solwezi, Zambia, display abundant such small bodies of gabbro, syenite and other alkaline intrusions. In some cases, gabbroic bodies are a few kilometers in diameter, and may even amalgamate into larger ones. Very few Katangan age volcanic rocks associated with the small mafic intrusions remain. For example, see Figs 8.8, and 8.9 to 8.11.

By analogy with the Filiya mafic bodies, the following is an explanation for a large part of the widespread small gabbroic bodies in the Greater Lufilian Arc: They were emplaced as mafic plugs in large, within-plate areas that are being subject to incipient rifting. The mafic plugs could intersect the sedimentary cover of the plate, including marine and continental deposits. A portion of the mafic bodies are eclogite facies oceanic rocks that represent an ophiolitic melange.

8 IRON OXIDE-COPPER-GOLD MINERALIZATION IN THE GREATER LUFILIAN ARC

8.1 INTRODUCTION

Large mineral deposits of the iron oxide-copper-gold family are thought to be present in the Greater Lufilian Arc of western Zambia and northern Namibia. This chapter reviews main features of the deposit type and describes evidence for such deposits in the region, including iron oxide bodies, hydrothermal breccias and alteration features.

As Foster et al, 2001 state, “Pan-African sequences of Africa have tended not to be the first priority for mineral exploration when assessed against the historical perspective of exploration successes and mineral production in Archean, early Proterozoic and Phanerozoic terranes. However, recent advances in understanding of the evolution of Pan-African sequences and a number of recent exploration successes suggest that Pan-African terranes merit more attention than was previously accorded to them.”

8.2 SOME NOTES ON IRON OXIDE-COPPER-GOLD DEPOSITS

Iron oxide-copper-gold (IOCG) mineral deposits comprise a recently-identified type of mineral deposits. IOCGs are known to have formed in Meso- and Neo-Proterozoic rocks of Australia, Canada, Brazil, Scandinavia, the United States, China and Russia. Phanerozoic deposits occur along the Andean chain in Chile and Peru. Brazilian examples of Archean age are also known. The relatively recent international recognition of the deposit family is expected to result in many more mineralized provinces in the ranges of geological time and geographical distribution, including Africa. A brief overview of this deposit family is given below, based on published information and personal observations of some mineralized systems (Oreskes & Einaudi, 1990; Hitzman, Oreskes, & Einaudi, 1992; Barton & Johnson, 1996; Kerrich, Goldfarb, Groves, & Garwin, 2000; Jensen & Barton, 2000; Partington & Williams, 2000; Barton & Johnson, 2000; Haynes, 2000; Hitzman, 2000; Pollard, 2000; Piche & Jebrak, 2003; Sillitoe, 2003; Sillitoe, 2002; Hitzman, 2004a; Barton & Johnson, 2004b; Barton & Johnson, 2004a; and Wall, 2004).

Most of these deposits are located in zones of extensional tectonics, occur mainly along past rift zones or aulacogens and are situated along major structures. Table 8.1 lists a few of the major IOCG deposits with their principal features. Most are related to felsic and mafic intrusive rocks of so-called “anorogenic” type. There is no direct relationship with intrusive rocks in many of the small deposits and in the “distal” portions of mineralized systems. The size of the alteration and mineralization footprint of IOCG systems is very large, typical diameters are in the order of hundreds of kilometers.

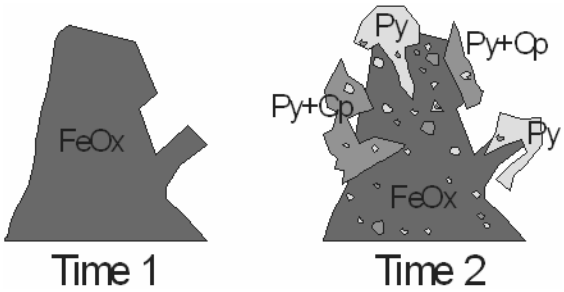

Fig 8.1 Cartoon to illustrate the development process of an iron oxide-copper-gold system. *The emplacement of massive iron oxide bodies takes place first, and later sulfidation nucleates around or within the massive iron oxide. The two processes seem to be independent, and are not necessarily related. Massive iron oxide may have a different origin from the sulfidation process. Three of many alternatives for the origin of massive iron oxide are: 1) the iron oxide may have been deposited as a banded iron formation, 2) hydrothermal emplacement of iron oxide by replacement of granitoids, 3) hydrothermal emplacement of iron oxide by selective replacement of layered rocks. At a smaller scale, other origins include 4) disseminated magetite in a granitoid rock, and 5) massive sodic alteration of a biotite-bearing granitoid that turned biotite into magnetite. The cartoon shows pyrite (light gray) and chalcopyrite (darker gray), but sulfidation may be only pyrite, or may include other copper sulfides like bornite. As shown, sulfidation may occur as large bodies in the contact between massive iron oxide bodies and their host rocks, or disseminations within the iron oxide bodies. In some cases, significant addition of rare earth elements takes place. These processes can take place at many scales. Massive iron oxide bodies can be kilometers in diameter or a few millimeters.*

In general terms, the mineralized deposits contain an iron oxide nucleus (magnetite and/or hematite) that was replaced by pyrite and chalcopyrite. Magnetite might have been demagnetized into martite and/or hematite; and later, part or all of the iron oxides are replaced by sulfides (Fig 8.1). The Salobo deposit, located in the

Carajás province of Brazil is a good example to explain here. Location of Carajás is outlined on Fig 3.1. As observed on the schematic map of alteration and mineralization from its 250 m level (Fig 8.2), note the iron oxides in the center and nucleation of copper content around it. Both iron and potassium alteration increase their intensity towards the middle of the system, which is controlled by a major fracture. Mineralization consists of a sub-vertical lensoid body 6km long and approximately 100m wide. This is hosted in hydrothermal breccias and metagraywackes that have been almost entirely replaced by iron oxides. The deposit is a tabular body, but was clearly emplaced hydrothermally (Goad, Mumin, Duke, Neale, & Mulligan, 2000; Haynes, 2000; Lindenmayer, 1994; Lindenmayer & Fyfe, 1994; Mark, H.S., Williams, Valenta, & Crookes, 2000; Pollard, 2000; Requia & Fontbote, 2000; Requia, Stein, Fontboté, & Chiaradia, 2003; and Souza & Vieira, 2000). The deposit has not been mined due to high metallurgical costs derived from the complex composition of its copper ore.

Light rare earth elements (LREE) and gold are sometimes present in economic quantities in iron oxide-copper-gold deposits. Uranium content might be significant; many other metals like silver, cobalt, and manganese may occur in economic concentrations. Copper mineralization seems to be associated with flow of meteoric fluids and redox reactions on or around the iron oxides as described by (Barton & Johnson, 2000). LREEs may be associated with apatite. Fluorine is another element that may be present in economic quantities. The Brazilian Alemão IOCG deposit, also located in the Carajás Province (Fig 3.1, general location on Fig 3.3) contains significant fluorine. Note that gold, copper, cobalt, thorium, uranium, potassium and fluorine nucleate around and in the iron oxide bodies that are marked with a star. The origin of gold and LREEs is not very clear, and current views on this issue are polemic (Barton & Johnson, 2000; Hitzman, 2004a; Barton & Johnson, 2004b; and Wall, 2004). The causes of hydrothermal alteration, disolution of silicates and transportation of metals are other uncertain issues (Piche & Jebrak, 2003). In some cases, evaporites formed in sabkha, playa or salt lake environments are considered to be an important source of halogens for the highly-alkaline and/or F-rich solutions; basinal brines and/or mixing with sea water may also play a role (Kirkham, 2003; Barton & Johnson, 2000; and Warren, 2000). The origin of elements like cobalt, nickel, zinc and probably also copper and gold in many IOCG systems seem to be associated with mafic (and ultramafic ?) rocks, in a manner not yet completely understood.

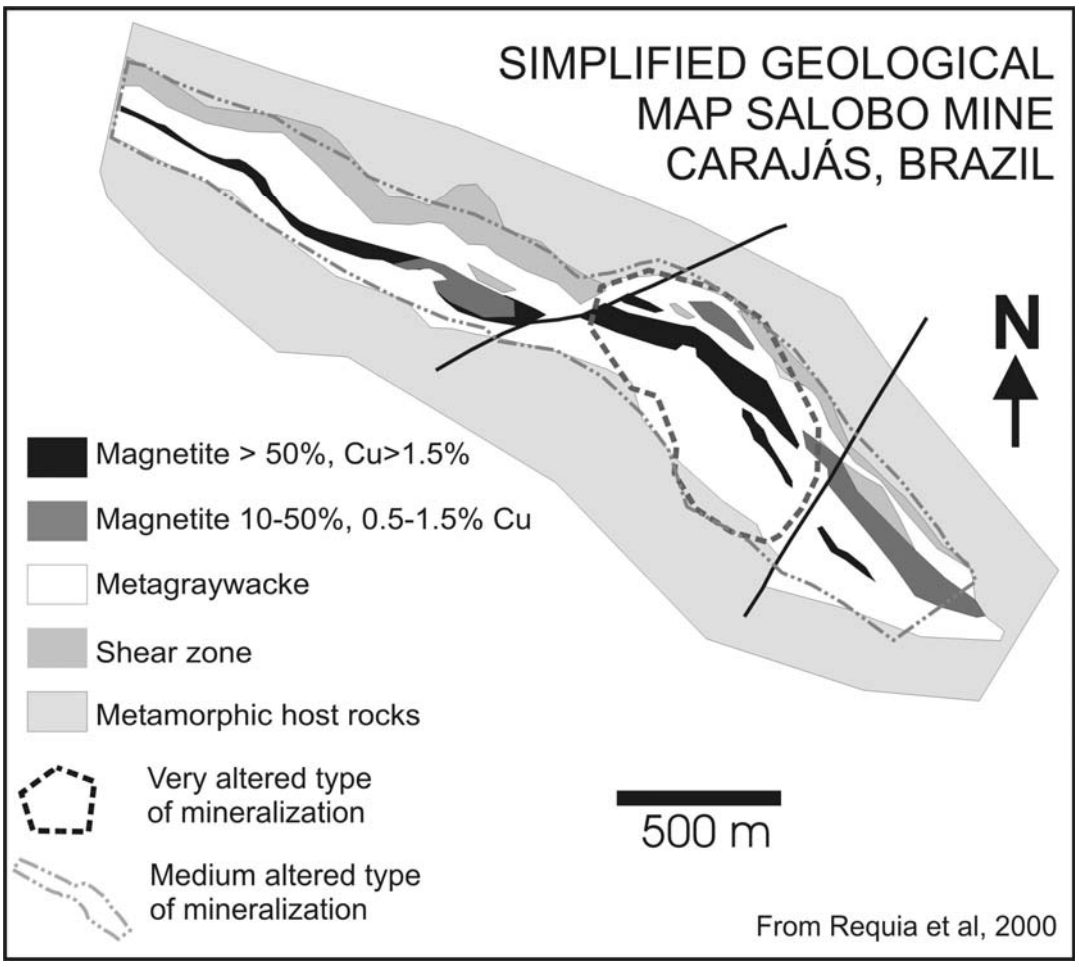

Fig 8.2 Generalized geological map of the Salobo Deposit, Carajás, Brazil. *Note size and distribution of the copper and gold mineralization around iron oxide bodies. Also note the "banana" shape of the orebody in plan view. Other notes in text. The Carajás district is located on Fig 3.1.*

Zoned hydrothermal alteration takes place in almost all mineralized IOCG deposits. Various alteration patterns depend on depth of emplacement and host rock chemistry. In general terms, from shallow to deep levels, these generally are: albitization, scapolitization, potassic alteration, sericitization and silicification (Figs 8.4 and 8.5). Bear in mind that alteration patterns and types vary immensely from deposit to deposit, depending on the composition of intrusives and host rocks. At times large quartz-only rocks occur on the surface above IOCG mineralization. This seems to be produced by leaching of silicates in the center of the systems to allow for the emplacement of iron oxide bodies, and precipitation of the silica farther out.

Massive hematitization and so-called “red-rock” (“brown rock”) alteration are widespread and affect most types of host rocks. Regional sodic alteration marks zones of hydrothermal circulation around the mineralized deposits. Textural replacements of rock constituents are common. There seems to be a particular order of hydrothermal alteration and mineralization in the “typical” IOCG deposits. First comes a strong albitization of the country rock. Then high temperature Fe±K±Ca alteration; this is represented by biotite-garnet-K feldspar-amphibole-clinopyroxene-magnetite. Mineralization and low temperature alteration come last (sulfides± magnetite±hematite–carbonate±sericite/chlorite). The last phase of sulfidation may contain both Cu and Au.

Explosive brecciation occurs in most of the known deposits. An important portion of the largest orebodies shows evidence of multiple explosive fragmentation (Table 8.1). This is quite evident at the Mantoverde mine and its environs in Chile (Astudillo, 2003; Geología, 2003; Zamora & Castillo, 2001; also personal observations), at Candelaria mine in Chile (Sillitoe, 2003; Sillitoe, 2002; Marschik, Leveille, & Martin, 2000; also personal observations), at the Raul-Condestable mine, Peru (Injoque Espinoza, 2002; and personal observations), as well as at the Olympic Dam mine in Australia (Ferris, Schwarz, & Heithersay, 2002; Oreskes & Einaudi, 1990; Reeve, Cross, Smith, & Oreskes, 1990; Reynolds, 2000; and Skirrow, Bastrakov, Davidson, Raymend, & Heithersay, 2002).

Geometry of the mineralized bodies varies substantially; by far the commonest deposits are veins. Some are massive replacements that grade into stockworks, others are breccia pipes or diatremes, others are tabular bodies that run concordant with rock foliation or stratification. Composite deposits comprising veins, breccias, stockworked zones and replacement mantos are common (See Table 8.1).

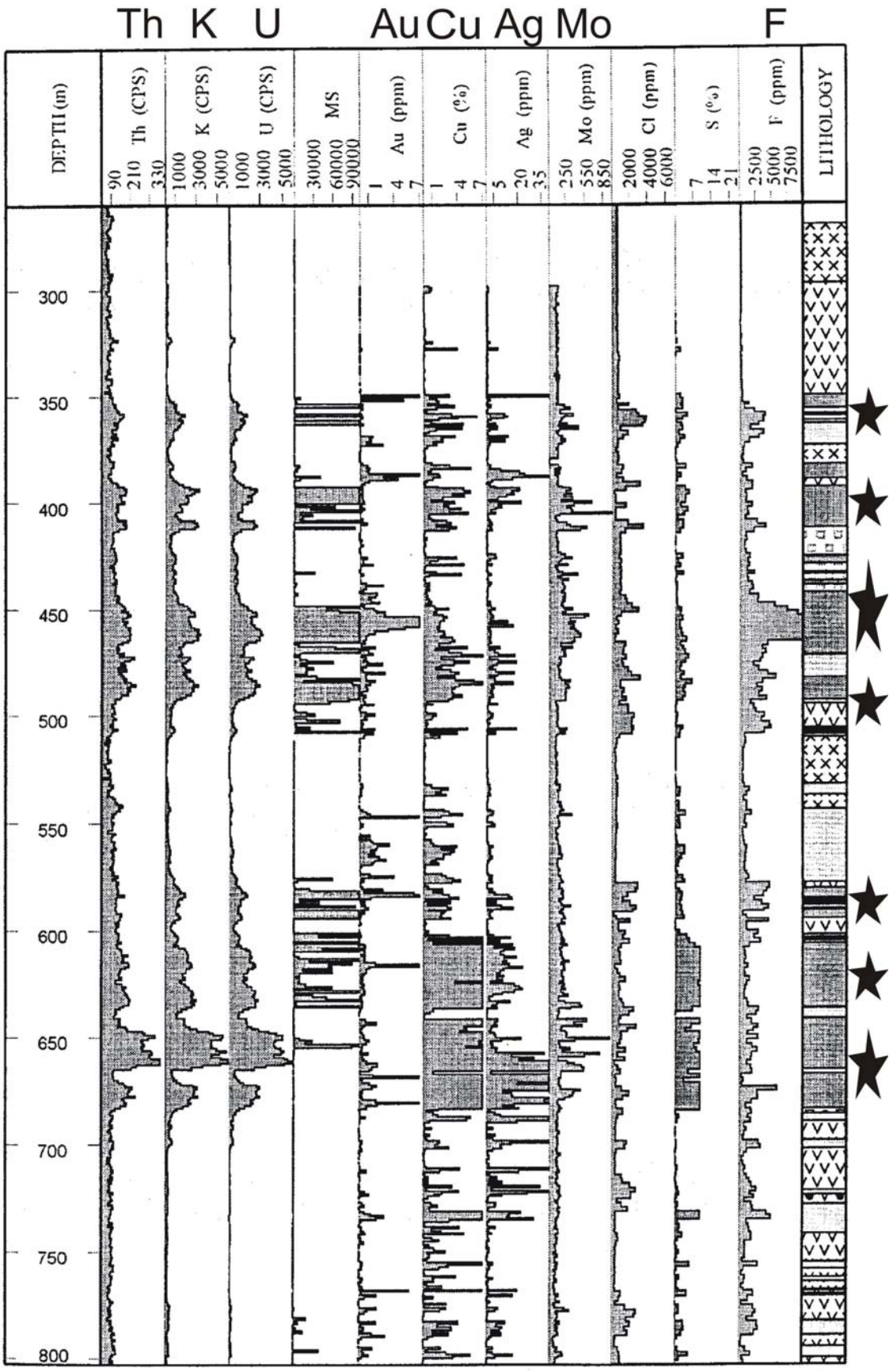

Fig 8.3 Simplified geochemical log of borehole ALM-FD09, from the Alemão deposit, Carajás, Brazil*. Massive iron oxide bodies in this iron oxide-copper-gold deposit are marked with stars on the right of the log. Note that some of the bodies are over fifty meters thick. For scale, tick marks on the left of the log are set every fifty meters. Iron oxides served as site for nucleation of economic mineralization at this site. Note presence of fluorine. Slightly modified from Ronze, Soares, dos Santos, Barreira, & Proterozoic, 2000.*

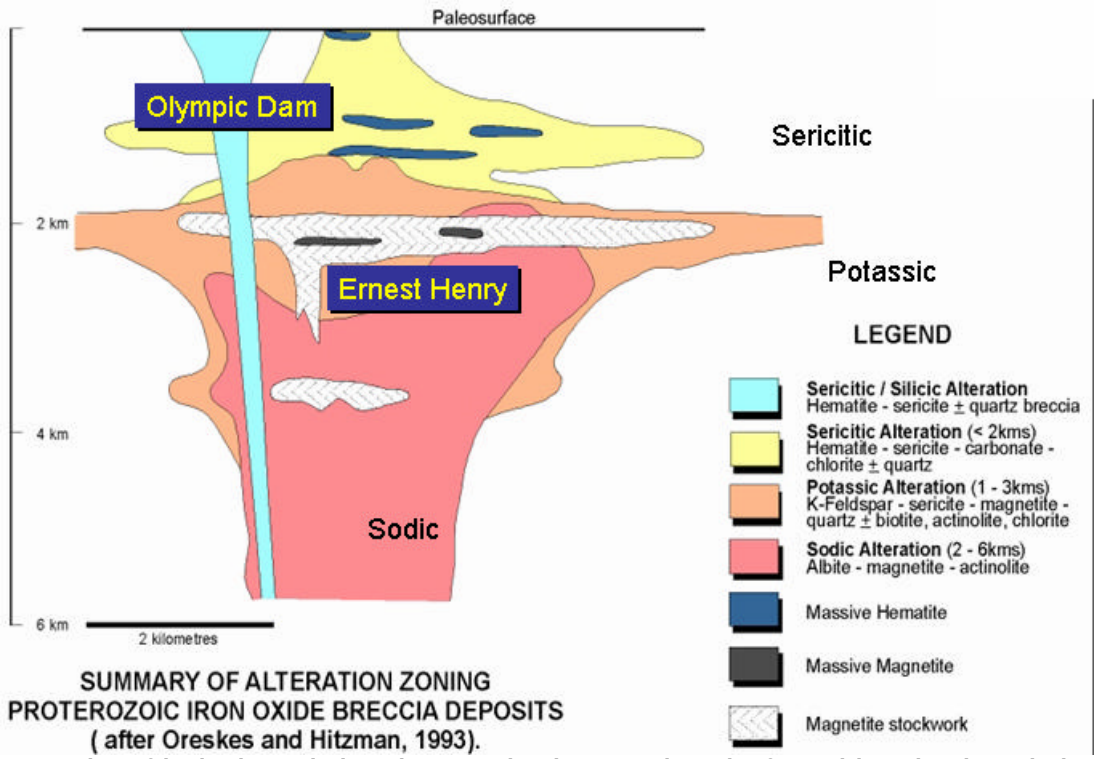

Fig 8.4 Examples of hydrothermal alteration zonation in IOCG deposits formed in volcanic and plutonic host rocks. *Note that most alteration affects large volumes of rock, particularly sodic alteration. Note that the breccia pipe may be cemented by massive magnetite or hematite. Approximate location of Olympic Dam and Ernest Henry deposits is shown for better comprehension. Taken from Nisbet et al., 2004a.*

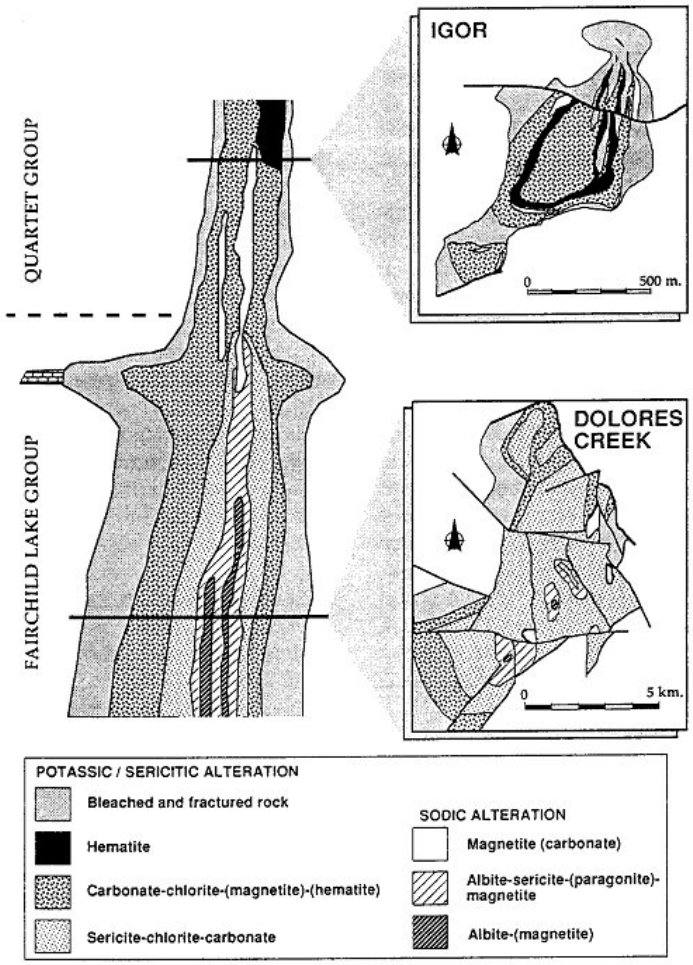

Fig 8.5 Examples of hydrothermal alteration zonation in IOCG deposits formed in sedimentary sequences. *Based on examples from the Wernecke Mountains in the Yukon, Canada. Note that total vertical extension of the diagram is 5 km and its widest portion is also 5 km. Alteration and mineralization are greater in reactive rocks like carbonates. From Hitzman et al., 1992.*

Details of selected IOCG deposits and prospects, Lufilian Arc, Africa

Deposit/ Prospect	Tons x10^6	Cu wt.%	Au g/t	Mineralization Styles	Associated Metals	Associated Rocks
Okatjepuiko, Witvlei, Nm	Undim.	Undim. X n.a.	Undim. X n.a.	Ht bxs in subvolcanic porphyritic intermediate rks. FeOx bodies replacing bxs + fracs. Bn rk altn	Cu,Au	Subvolcanic porphyritic intrusions, gabs + felsic intrusions, subrounded ht bxs
Kombat Mine, Nm	~12	~2.94	X n.a.	Large FeOx bodies serve as nucleus for copper sulfs hosted in ht bxs + stwks. Grades of silver and lead: ~20gAg/t,~2%Pb.	Ag,Pb,Mn,Zn,Ba, As,P,Ni,Co	Otjiwarongo Batholith may be source
Otjikoto Au Deposit, Nm	n.a. ****	n.a.****	n.a.****	FeOx nucleation? Coarse free Au, tourmalinization, sheeted vein systems controlled by E-W structures	PGEs,Cu,B	Otjiwarongo Batholith may be source, hosted by albitized metapelites, siliciclastics + carb
Mesopotamie Farm Area, Nm	n.a.	X n.a.	X n.a.	Massive FeOx bodies along E-W structures + sulfidation around them. Ht bxs.	Au,Cu,LREE	Graphic alkali granites intrude other gtds
Dunrobin Au Mine, Zm	~0.002	n.a.	9.3*	Structurally-controlled; FeOx nucleates sulfidation+Au. Diss + replacements in country rks. Qtz+py veins. Replacement FeOx bodies.	Ag,Bi,Mn,Pb,Sb, As	hosted by folded Katangan carb + gtds
Nampundwe Pyrite Mine, Zm	23 (Cu) 10 (Fe)	0.79	X n.a.	Selective mag replacement in folded sedimentary rocks. Specularite-matrix in polymictic multiphase ht bxs associated to gtds.	16% pyrite. 57% Fe	Small bodies of gab +felsic intrusives, mag-bear diorite; lamprophyres
Kasempa Prospect Area, Zm	n.a.****	X n.a.****	X n.a.****	Selective mag replacement in folded sedimentary rocks. Massive FeOx w/ sulfs. Stwks, round-pebble ht bxs, sheeted mag veins. Various large size prospects.	LREE,Co,Au?	Small bodies of alkaline gabs intrude Katangan lss, masive FeOx hills; lamprophyres
Kalengwa Mine, Zm	0.6 init 1.9 fin	16 init 9.44 fin	n.a.	Tabular replacement in sediments, ht bxs, supergene enrichment to chalcocite body; polymictic hydrothermal bxs; Cu sulfs dissemination	50gAg/t,LREE,U**	gabic rocks, hosted by Katangan siliciclastics. Syenites + granites; lamprophyres
Quartzite-Hosted Deposits, Nm	n.a.	X n.a. **	n.a. **	Sulf-bear ht bx veins cemented by mag, hydroth. Bx bodies. All frac controlled.	LREE,Fe,U,Zn **	Brittle quartzites + carb, small subvolcanic porphyritic bodies, + qtz blobs
Deposits in Alkaline Rocks + Carbonatites, Nm	n.a.	X n.a.	X n.a.	Diatremes, stwks, bx bodies, round-pebble ht bxs, braided veins, masive FeOx bodies, controlled by regional structures.	Fe,LREE,Zr,La, Nb,Zn**	Lamprophyre + carbonatite dikes, syenites, alkaline granites
Tevrede deposit, Kamanjab, Nm	n.a. ****	X n.a. ****	n.a. ****	Ht polymictic bxs cemented by mag and/or hematite; braided vein systems, stwks, frac-controlled mnzn. Massive FeOx bodies	LREE**	alkaline granites, granites
Shimyoka Area, Kafue Flats, Zm	Cubic kms****	0.2 **	X n.a. ****	FeOx bodies w/ diss cp+py, ht bxs, shear zones, stwks. Mnzn related to intrusive bodies.	LREE,P,F,U,Co	Syenites, Katangan carb, qtz bodies, gabs, red-altered gtds
Kantonga prospect, Zm	n.a. ****	X n.a. ****	X n.a.****	Tabular replacement of mag & hem in sedimentary units; large bodies of mag and hem filled polymictic ht bxs; stwks; various Cu sulfs disseminated in FeOx.	Cu,Au,Mn,LREE, phosphates	Syenites and granites that intrude Katangan carbs, syenites and granodiorites
Kitumba prospect, Zm	Cubic kms, n.a.****	X n.a. ****	X n.a. ****	Very large extension of hem-filled polymictic ht bxs & stwks w/ py and cp, bornite, digenite & covellite. Large zones with massive mag.	Cu,Au,Mn,LREE, Phosphates	Syenites, granites, granodiorites and diorites that intrude Katangan carbs and other metaseds
Silver King, Zm	n.a.	X n.a.	n.a.	Sideritic ht bxs, supergene Cu mnzn	Ag,Au,Cu,LREE	Lamprophyre dikes
Sable Antelope, Zm	n.a.	X n.a.	n.a.	Sulf-bear FeOx-filled ht bxs, diatremes, bn-rk altn, network of fissure veins, FeOx bodies	Ag,Ba,Zn,LREE**	Hosted by Katangan massive white or pink dol ls, in flank of anticline
Hippo Mine, Zm	0.016	9.4 ***	2.1	Sulf-bear frac-controlled FeOx, bx + stwk	Fe, F, As, Pb, Zn	Hosted by Katangan silststone. Very little outcrop, all covered
Luiswishi Mine, D.R. Congo	8**	2.5	X n.a.**	Tabular FeOx controlled by fault system. Supergene Cu-Co mnzn. Not true strata-control	1.15%Co,Ni	Hosted by Katangan dol shales, dols, carbonaceous shales
Shituru mine, D.R. Congo	0.085**	2	0.2-0.5**	Fault-controlled, tabular FeOx body underlain by oxidized Cu-Co mnzn. Stwk, shear zone w/ mylonitization, and sed-hosted sulf mnzn w/ organic carbon. Carolite in bk shales, specular hem nucleates sulfs.	1.59 Aug/t in slimes dump, Co(0.05-0.1%),U	Hosted by Katangan bk shales, siltstones and carbs
Kamoya mine, D.R. Congo	1.2**	2.5	<0.01**	Fault-controlled, tabular FeOx body underlain by oxidized Cu-Co mnzn. Stwk, shear zone w/ mylonitization, and sed-hosted sulf mnzn w/ organic carbon. Carolite in bk shales, specular hem nucleates sulfs.	0.58% Co 0.2-0.3% Ni Pd, Zn, La, Ta	Hosted by Katangan ls, dols, sandstones, siltstones and bk shales

CONVENTIONS: *Dunrobin mine produced over 40,000oz of gold by 1935. It produced 13,817oz of gold from 1936 to 1961. ** not well studied. *** Hippo mine produced 2280 tons of ore at an average grade of 27.4% Cu. **** Well studied by mining companies, but information is not publicly available. altn = alteration; bear = bearing; bn = brown; bx = breccia; bxs = breccias; carb = carbonate; cp = chalcopyrite; D.R.Congo = Democratic Republic of Congo; diss = disseminated, dissemination; dol = dolomite, dolostone; FeOx = iron oxide; fin = final; frac = fracture; gab = gabbro; gtd = granitoid; ht = hydrotermal; init = initial; LREE = light rare earth elements; mag = magnetite; n.a. = not available; Nm = Namibia; po = pyrrhotite; py = pyrite; qtz = quartz; rk = rock; stwk = stockwork ;sulf = sulfide; undim. = undimensioned; X n.a. = metal is present but data is not available; Zm = Zambia.

Table 8.2 Details of selected IOCG deposits and prospects, Greater Lufilian Arc, Africa

TABLE 8.1 DATA FOR SOME IRON OXIDE-COPPER-GOLD DEPOSITS

Deposit	T (x10^6)	Cu (%)	Au(g/t)	Ag(g/t)	Mineralization Styles	Associated Metals	Age	References
Raul-Condestable,Peru	>500	0.7	0.5	5	Veins,mantos,disseminations	Co,Mo,Zn,Pb,As,LREE	~115	Injoque, J., personal communication, 2002
Mina Justa,Peru	209	0.86	minor	present	Irregular vein-like replacement body		~155	Rio Tinto, 2003 in Sillitoe, 2003
Marcona,Peru	>1000	50-60%Fe			Replacement mantos + veins	Cu,Ag,Au	150	Injoque, 1989
Candelaria,Chile	470	0.95	0.22	3.19	Bx,skarn	As,Mo,Pb,Zn,LREE	114	Marshik et al, 2000
Mantos Blancos,Chile	500	0.6			Bxs,stwks,veins	Ag		Urrutia, J., personal communication, 2003
Susana,Chile	>100	?			Diatreme bx	Ag		Espinoza et al, 1996
Manto Verde,Chile	~300 >450sulf	0.6	0.53sulf		Bx,fault zones,diatreme	LREE	117	Zamora & Castillo,2001, Personal Communications, Urrutia, J., 2003
Santos,Chile	19	1.7	0.4		Vein,bx	Ag		Marshik & Fontbote, 1996
Punta del Cobre District,Chile	~120	1.5	0.2-0.6	8	Structural zone	Zn,LREE,Mo	~115	Marshik & Fontbote, 2001
Minita Despreciada,Chile	3	16			Veins	Mo,U	114	Espinoza et al, 1996
Cerro Negro,Chile	249 (49)	0.4(0.71)	~0.15		Bx,mantos,stwks,veins			Atna Resources Press Release, 2002
Teresa de Colmo,Chile	70	0.8	trace		Bx pipe			Hooper & Correa, 2000
Salobo,Brazil	789	0.96	0.52	5.5	Vertical,thick,massive FeOx lenses,bx	Co,Mo,Ni,REE,U	2579?	Lindenmayer & Texeira,1999; Requia et al, 2003; Souza & Vieira, 2000, 2004
Alemão,Brazil	170	1.5	0.82		Bx bodies	Mo,U	EprotZc	Barreira et al, 1999
Igarape Bahia,Brazil	23.4		2.9		Bx		EprotZc	Tavaza et al, 1998
Sossego,Brazil	355	1.1	0.28		Hydrothermal veins and bx bodies	Co,Ni	EprotZc	Fanton, 2001; Leveille, 2001
Cristalino,Brazil	~200	1.4	0.25		Stwk	Co,Ni	EprotZc	Huhn et al, 1999
Pojuca,Brazil	58	0.9			Stratiform replacemnt, Fe stone-hosted veins	Au,Co,Ni,Mo,Zn	EprotZc	Winter, 1994
Pahtohavare,Sweden	1.15	2.1	0.9		Bx	Co	EprotZc	Lindblom et al, 1996; Freitsch et al, 1997
Bidjovagge,Norway	3	1.8	0.5		Vein,stwk	REE,U,Te,Co,Ni	EprotZc	Bjorkykke et al,1987; Ettner et al, 1993
Aitik,Sweden	606(+850rs)	0.37	0.2	3	Vein,bx	Mo,U	1.87Ga	Wanhainen et al, 2003
Olympic Dam,Australia	2000	1.6	0.6		Diatreme bx complex	Co,Ag,U,REE	MprotZc	Reeve et al, 1990
Ernest Henry,Australia	166	1.1	0.54		Bx matrix and replacement in shear zone network	Co,Mo,REE	MprotZc	Ryan, 1998
Mount Elliot,Australia	2.47	3.7	2.1		Skarn,bx in brittle faults	Co,Ni	MprotZc	Fortowski & McCraken, 1998
Starra,Australia	7.4	1.88	3.8		Shearzone-controlled Fe stone-hosted	Co	MprotZc	Rotherham et al, 1998
Osborne,Australia	11.2	3.51	1.49		Bx,shearzone-hosted Fe stone	Ag,Co,Mo,Bi,Te,Se,Hg,Sn	MprotZc	Adshead et al, 1998
Greenmount,Australia	3.6	1.5	0.78		Vein,stwk and replacement	Co	MprotZc	Kremarov & Stewart,1988
Eloise,Australia	3.1	5.5	1.4		Vein,bx,stwk in shearzone	Ag,Co,Ni,Zn	MprotZc	Baker, 1998;Gold Gazette, Feb. 1995
Warrego,Australia	5	139kT(2.6)	1.5Moz(2)		Fe stone-hosted in fold limb	Bi	EprotZc	Goulevitch,1975; Wedeking & Cove,1990

Notes: bx = breccia, stwk = stockwork, Fe stone = ironstone, mProtZc = MesoProterozoic, eProtZc = Early Proterozoic, rs = total resources, sulf = sulfide reserves.

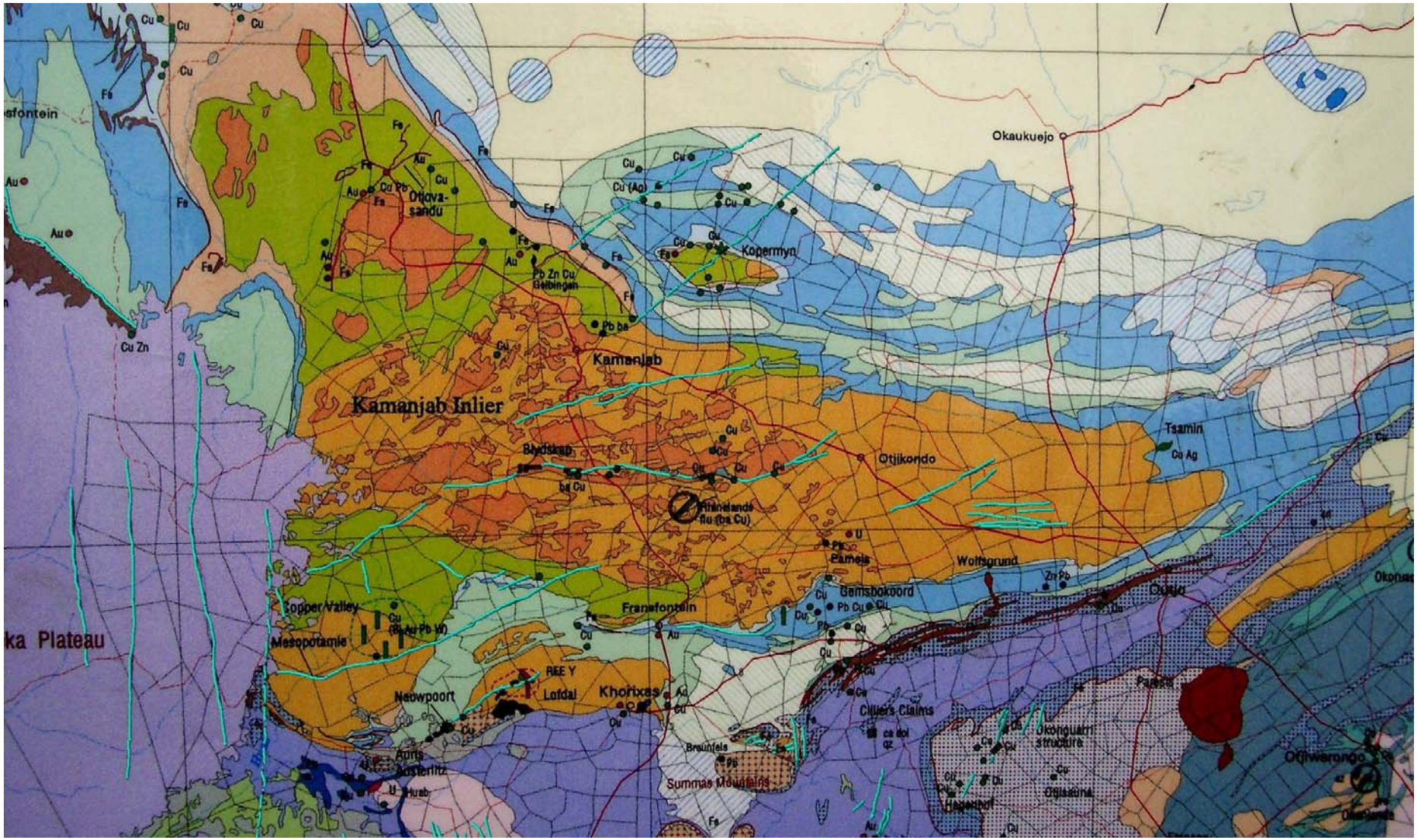

Fig 8.6 Geological Map of the Kamanjab Batholith, Namibia. *Note the fracture zones drawn in light blue. E-W-trending fractures control copper, iron, zinc and gold mineral occurrences. For reference, light blue units are Katangan-age sedimentary rocks including carbonates and siliciclastics. Light orange is composed by meta-sedimentary and metavolcanic rocks. Light green are volcanic rocks. Dark orange is made up of granitoid rocks of the Franzfontein suite. Note the various mineralized sites at the Khorixas Inlier, the Mesopotamie farm, the Gelbingen Farm, Koppermyn and Otjavasandu (Tevrede). There is active drilling at the last site to explore a large Cu and Au mineralized area. Taken from the Mineral Map of Namibia, 1998, 1:1'000,000 scale, published by the Geological Survey of Namibia, Windhoek.*

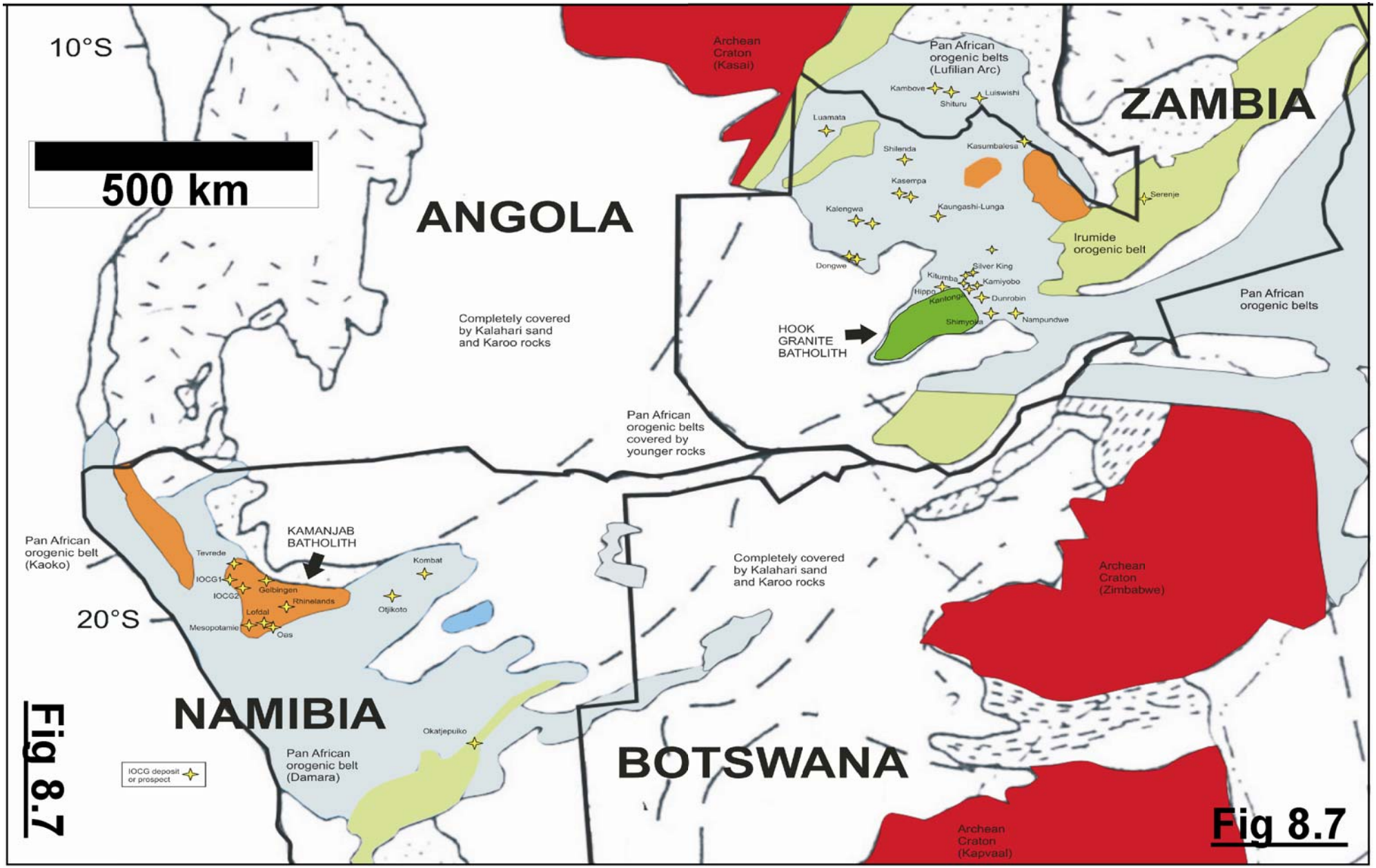

By Alberto Lobo-Guerrero S., January, 2004

Fig 8.7 Iron oxide-copper-gpld prospects and deposits, Greater Lufilian Arc

8.3 IRON OXIDE-COPPER-GOLD SYSTEMS IN THE LUFILIAN ARC

IOCG systems occur on and around the granitoid massifs of the Lufilian Arc (Fig 8.7). Proper environments for development of those systems are widely spread throughout. Massive iron oxide bodies with associated sulfides and other mineralization seem to have formed by replacement and infill of the host rocks. These can be of various types, including true granites, syenites, carbonatites, quartz "pods[1]", albitized schists, volcaniclastic deposits and carbonates.

"Pregnant" granitoids have produced extensive hydrothermal alteration and variable iron oxide mineralization, especially when intruding reactive rocks like carbonates, black shales or carbonatites. Large bodies of hydrothermal iron oxide rocks are found near the intrusive contacts. Many types of mineralization geometries are known, including breccia pipes as well as tabular vertical and horizontal breccioid bodies (Stohl, 1972; Stohl, 1977; Hitzman, 2001; Phillips, 1959; and Phillips, 1958a). Subvolcanic porphyritic intrusives and apophyses of the main massifs account for most of the mineralization. In general terms, the margins of plutons or their distal satellite bodies seem to be better environments for IOCG systems.

The following pages will describe relationships between granitoid and iron oxide bodies, types and features of iron oxide bodies, hydrothermal iron oxide alteration, hydrothermal brecciation in Lufilian Arc IOCG systems, structural control and particular alteration features.

8.3.1 RELATIONSHIP BETWEEN GRANITOIDS AND IRON OXIDES

Evidence of close temporal and spatial relationships between the iron oxide bodies and granitic rocks is widely spread throughout the Lufilian Arc. An association of four types of rocks is common in many parts: iron oxide bodies (of both magnetite and/or hematite), small gabbroic bodies, small outcrops of red-altered felsic or syenitic intrusives and quartz bodies (See Figs 8.8 to 8.11). Some localities show coarse magnetite-bearing intermediate intrusive rocks with weak copper mineralization. This is seen on outcrops near Otjiwarongo, Namibia; it occurs in some rocks of the Hook Granite Massif and in sites around Kasempa and the Kafue Flats region of Zambia. At times, magnetite fills thin veins in the intrusives; these may grade into sheeted veins and/or stockworks. Coarse magnetite is often associated with sulfides.

Magnetite "clusters" up to 1 cm in diameter in granitoids and subvolcanic rocks may produce a black and white "dalmatian rock" texture in some intrusive rocks located NE of Otjiwarongo, Namibia. The origin of this type of texture is not very clear. It might be produced by immiscible iron oxide "droplets" in the magma, by iron oxide nucleation and growth, or as a secondary alteration that overprints previous intrusive textures. The last alternative seems more plausible, because preliminary macroscopic and petrographic studies show that magnetite is emplaced after all of the other minerals of the rock. As a working hypothesis, part or all of the silicates seem to dissolve in order to make space for the iron oxides. This may take place during sodic alteration (albitization) of the rock, where biotite acts as nucleus for the replacement of magnetite.

Throughout the Lufilian Arc, small gabbroic bodies (i.e.: dikes, plugs and sills) seem to be associated with most copper and gold occurrences related to iron oxide bodies, in a manner not yet well understood. The same seems to be true in most western South American IOCG deposits (Injoque, Atkin, Harvey, & Snelling, 1988; Injoque, 2002; Sillitoe, 2003 and personal observations). Figs 8.8 to 8.11 illustrate the type of small mafic bodies that occur. Subvolcanic dacitic porphyritic intrusives in the Andean IOCG systems are called *"ocoitas"*.

[1] A description of the quartz pods is included below in the chapter Particular Alteration Features (6.4.4.2.).

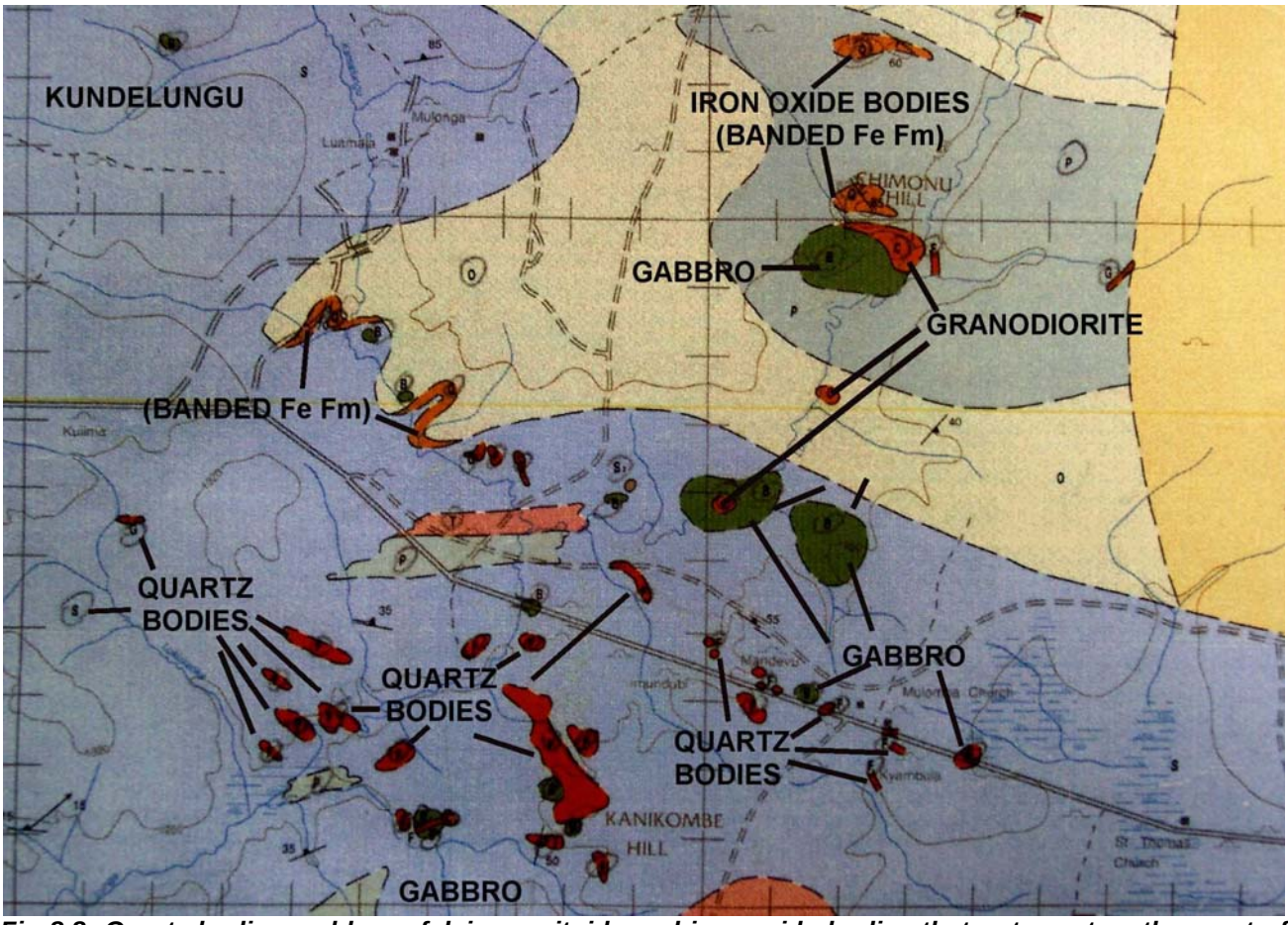

Fig 8.8 Quartz bodies, gabbros, felsic granitoids and iron oxide bodies that outcrop together east of Solwesi, Zambia. *These are all small bodies of rocks that occur together in a rift environment. The double line that cuts across from left to right is the main road from Kitwe to Mwinilunga; Kitwe to the east, Mwinilunga to the west. Host rocks in this case are Katangan carbonates and siliciclastic units. Compare this map with that from Filuya, Nigeria on section 7.3, that shows many small mafic bodies. For scale, tick marks are separated 1 km. Interpreted from public 1:100,000 scale geological map sheet published by the Zambian Geological Survey Organization, Lusaka.*

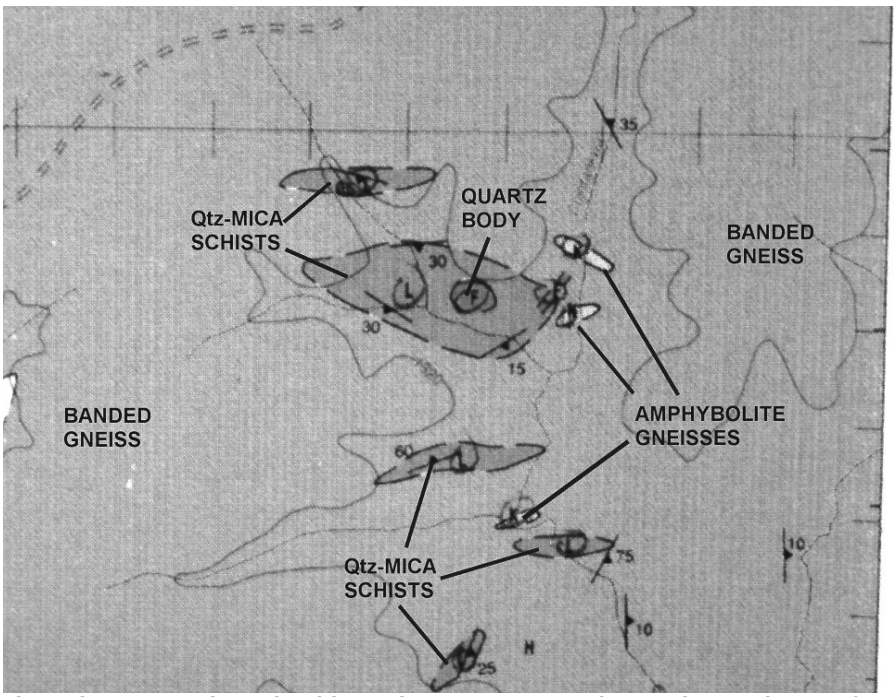

Fig 8.9 Quartz body and metamorphosed gabbros that outcrop together to the northeast of Mwinilunga, Zambia. *Host rocks are gneisses from the domes. Outcrops are outlined in darker color. The double broken line is a tertiary open road. For scale, tick marks are separated 1 km. Interpreted from public 1:100,000 scale geological map sheet published by the Zambian Geological Survey Organization.*

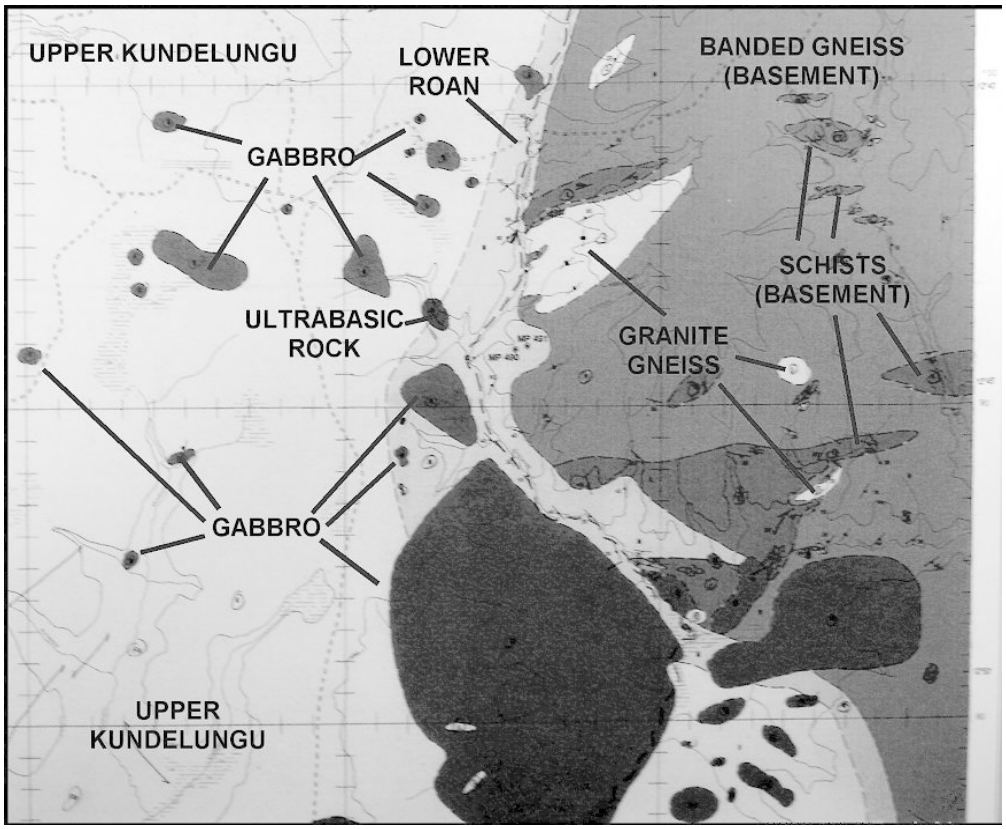

Figs 8.10 and 8.11 Young gabbroic bodies that intersect all rock types to the northeast of Solwesi, Zambia. *Most of the bodies are too small to map at this scale. Many quartz bodies and float of magnetite are also present, but they were not identified by cartographers. Small felsic intrusives also outcrop, but are hard to find due to weathering. For scale, tick marks are separated 1 km. Interpreted from public 1:100,000 scale geological map sheet published by the Zambian Geological Survey Organization. Fig 8.11 is an enlargement of Fig 8.10. Many smaller quartz bodies and felsic intrusives that outcrop are too small to be mapped. Gabbroic rocks are younger than all Katangan units mapped here.*

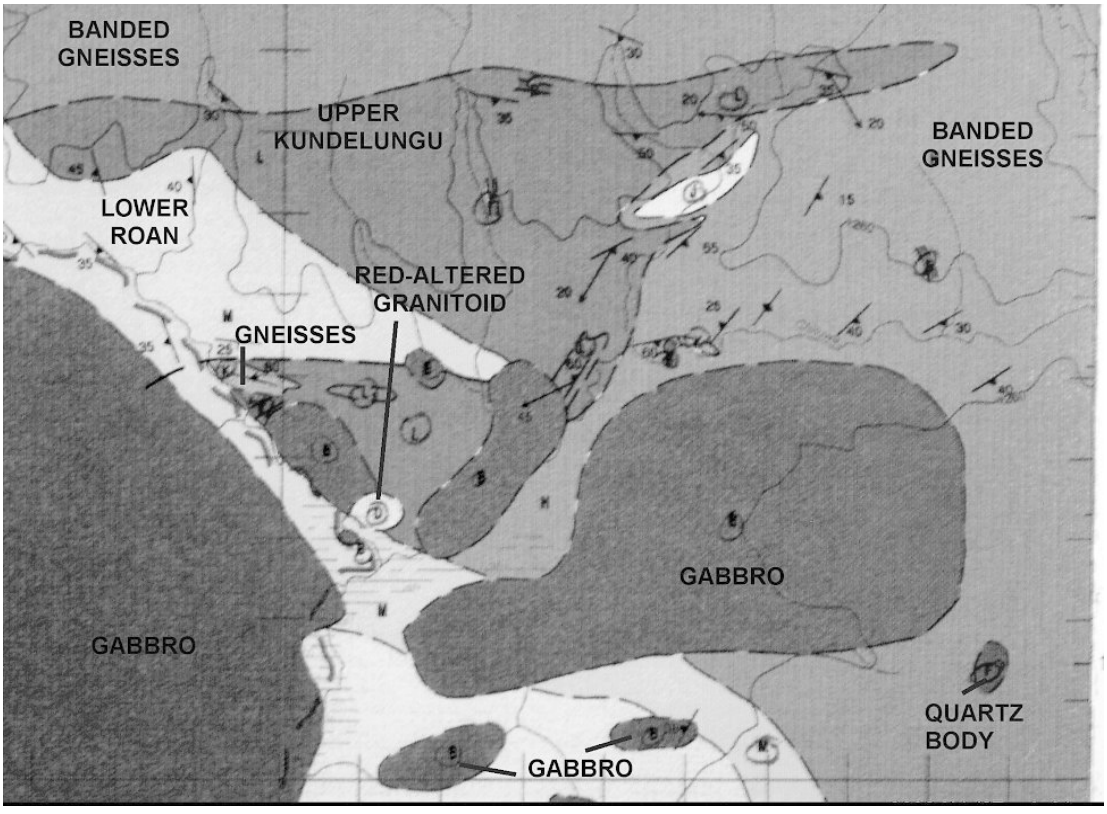

Work on gabbroic rocks from the Lufilian Arc is continuing. As a working hypothesis, gabbros and dioritic rocks are thought to be the source of copper, cobalt and other metals like zinc, nickel, molybdenum and

platinum group metals that are enriched in some IOCG deposits and prospects. Gabbroids may be one of multiple sources. Gabbros predate main mineralization in some of the deposits with reasonable geochronological data. They could have been altered by large hydrothermal IOCG systems driven by more felsic plutons, enriched in sodium and silica and depleted in metals. Barron, Broughton, Armstrong, & Hitzman, 2003 carried out research along the same lines, and Kapenda, Kampunzu, Cabanis, Namegabe, & Tshimanga, 1998; and Kampunzu, Tembo, Matheis, Kapenda, & Huntsman-Mapila, 2000 also evaluate the relevance of small mafic igneous rocks in the Lufilian Arc.

8.3.2 IRON OXIDE BODIES

Iron oxide bodies in the Lufilian Arc occur as cement for hydrothermal breccias and filling for numerous fracture zones (Brandt, 1955; Cikin, 1968; Dawson, 1982; Drakulic, 1984; Drakulic, 1984; Johns, 1982; Moore, 1964; Phillips, 1958; Phillips, 1959; Stohl, 1972; and Stohl, 1977; also personal observations near Lusaka and in the Kafue flats region, Zambia). Nambian geological literature contains very few descriptions of iron oxide bodies, although massive hematite and magnetite bodies have been observed by the author at many locations. Host rocks of iron oxide bodies in the Lufilian Arc generally display sodic and sodic-calcic alteration. Part of the iron oxide bodies carry associated sulfide mineralization, including pyrite and copper minerals like bornite and chalcopyrite (Dawson, 1982; Cikin, 1968; Burnard et al., 1990a; Burnard et al.,1990b; Burnard et al, 1993; and Hitzman, 2001). Some of the known IOCG deposits and prospects in the region contain very particular chemical signatures. These may be marked by abundance of one or more of the following: uranium, LREE minerals, phosphorus, cobalt, barium minerals, silver, platinum group elements, titanium minerals and vanadium, apart from copper and/or gold. Some deposits do not contain any copper. A significant number of the previous elements have affinity to mafic and ultramafic rocks. Two iron oxide samples from the Greater Lufilian Arc were analysed and they are described on the chapter about the West Lusaka-Kafue Flats area, Zambia (4.1.2.4.4).

In locations of western Zambia, large iron oxide bodies display a particular geomorphological expression. They protrude as needles up to a hundred meters above the average elevation of the plateau. An example of this can be seen on Fig 8.12 which depicts a magnetite hill located just to the west of Lusaka and very near to the site of the Nampundwe (or King Edward) pyrite mine. Gabbros and red syenites occur in the environs. Some of these iron oxide bodies carry disseminated sulfides. Similar hills occur near Kasempa, to the NW of Mumbwa and also in the Democratic Republic of Congo. The Namibian counterpart of Zambian iron oxide bodies does not form such structures, probably due to less rainfall.

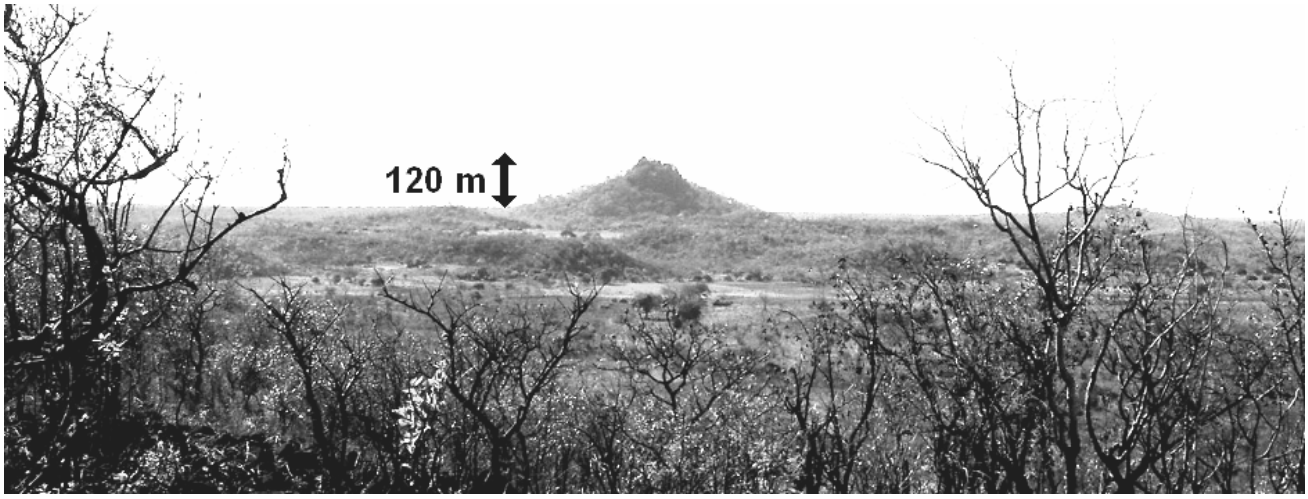

Fig 8.12 Hill of massive magnetite that outcrops west of Lusaka, Zambia*. As shown here, massive iron oxide bodies in this part of the Greater Lufilian Arc produce these interesting geomorphological features. They stand out up to 120 meters above the average flat plateau. In the foreground, rolling hills are syenitic intrusive bodies. Small gabbroic bodies are also found in the environs. Abundant hydrothermal breccias with sulfide mineralization occur here too.*

Iron oxide bodies emplace themselves after the dissolution of the host rock takes place. A gradual change from normal rock into iron oxide has been observed, progressive advance induced by hydrothermal dissolution of silicates and replacement by iron oxide. Probably fluorine-rich solutions play an important role in the process.

Progressive iron oxide alteration overprints textures of granitic rocks, sedimentary rocks and hydrothermal breccias; sometimes to a point where the original rock is unidentifiable. This was observed around many intrusive bodies; there is a gradual change from unaltered rock to similar rock with the “black and white texture” or the “magnetite disease” (Fig 8.13) that progressively becomes a 100% magnetite rock. Red hematite also produces similar alteration features, as shown on Fig 8.14. Fig 8.15 shows some aspects of the progressive alteration. Core fragments were taken from portions of exactly the same host rock, along a borehole, at intervals separated every three meters. As shown, progressive iron oxide overprinting is an example of how iron oxide can make its space in a rock by dissolving its space out. The intrusive body that produced the alteration is located towards the hematite-enrichment. It was a subvolcanic porphyritic rock. In this case, the host rock to alteration is a polymictic, round pebble hydrothermal explosive breccia. These breccias will be discussed further in this chapter. Equivalent gradual change was observed in several granitoids. Another interesting iron oxide mineralization feature is illustrated on Fig 8.37.

Fig 8.13 Magnetite “disease” in a felsic granitoid that is very light pink when fresh*. Progressive magnetite replacement of silicates near mineralized IOCG systems in the Lufilian Arc. This type of hydrothermal alteration grades from very slight to completely pervasive. From borehole MB-34, Kasempa area, Zambia. For scale, ticks are millimeters.*

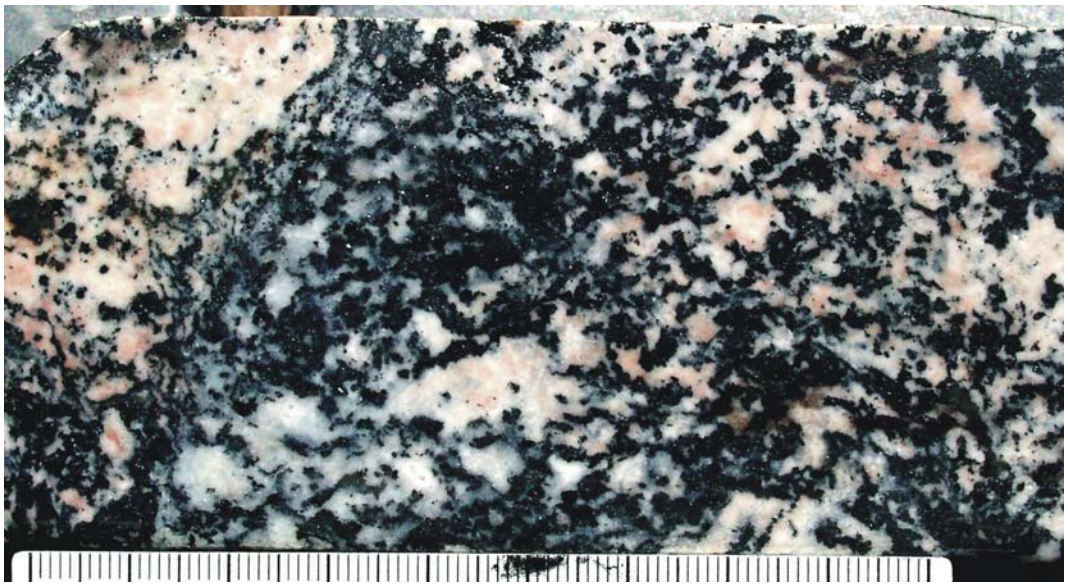

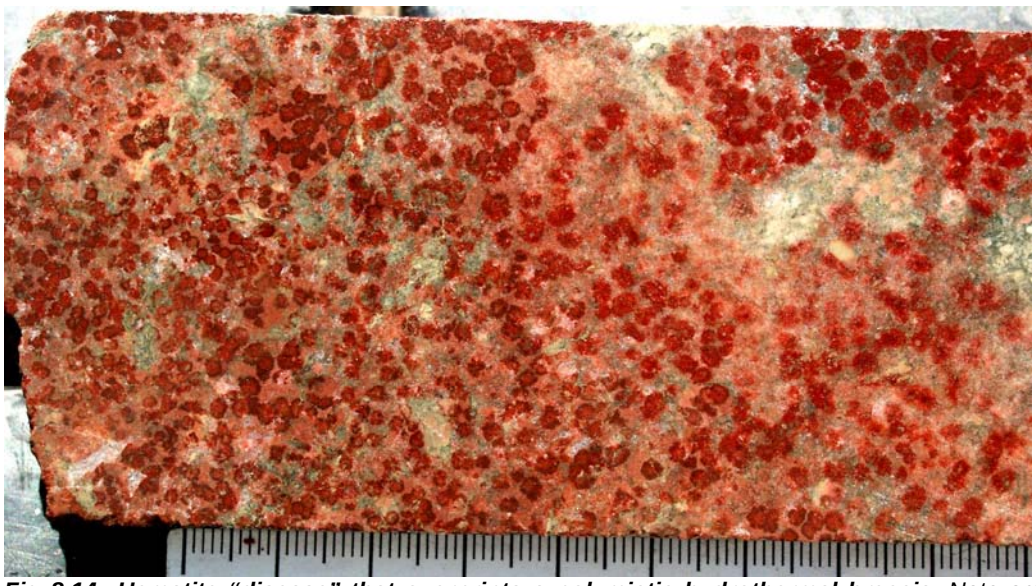

Fig 8.14 Hematite “disease” that overprints a polymictic hydrothermal breccia*. Note small round clusters of red hematite that nucleate and grow until the entire volume of the rock is replaced by minute hematite crystals. Sometimes the previous texture is completely obliterated, and original protolith cannot be recognized. All components of the previous rock have been replaced by a massive, non-selective process. This type of hydrothermal alteration increases towards the IOCG mineralization, and towards the intrusive bodies responsible for the alteration/mineralization. From borehole MB-34, Kasempa area, Zambia. For scale, centimetric/millimetric lines.*

Fig 8.15 Progressive "red-rock" hydrothermal alteration in round-pebble hydrothermal breccia*. The freshest rock[2] in the lower core gradually changes into an entirely deep red rock in the upper one. This is an example of hydrothermal iron oxide alteration. It can take place in almost any type of rock, obliterating previous textures and all features. Sometimes previous quartz fractures seem to be leached away and nothing is left behind except for the massive red mass full of disseminated hematite crystals. A fragment in the lower core has "hematite disease". Note the polymictic character of the breccia and rounding of some clasts. Fragments are altered in very different ways as seen. The large fragment to the left of the second core from the bottom shows concentric hematite alteration advancing inward. Rounding of clasts will be explained in the following item. Core fragments were taken every 3 m to show variation, but a complete alteration continuum occurs in outcrop and core. From borehole MB-34, Kasempa area, Zambia. See details in text. Diameter of core is 5 cm.*

8.3.3 BRECCIAS

Multiphase hydrothermal breccias with strong K-iron alteration (biotite-sericite-magnetite-hematite) and pyrite occur on or around iron oxide bodies in the Greater Lufilian Arc. Sometimes these breccias have a matrix of metallic hematite and/or magnetite, with evidence of explosive hydrothermal activity. Initial Na feldspathization (albitization) is overprinted by biotitization (potassic alteration).

Round-clast breccias cemented by iron oxides are a common feature in some portions of the IOCG systems of the Lufilian Arc. Figs 8.15, 8.16 and 8.17 show polymictic round-pebble hydrothermal breccias that surround subvolcanic porphyrytic intrusions in IOCG systems in northwestern Zambia. Clasts of various intrusive, sedimentary and metamorphic rocks are present. Packing is very dense and almost all clasts are rounded. It seems that corrosion of extremely alkaline or acid hydrothermal solutions etched angular rock fragments, rounding them.

[2] The ¨freshest rock" is slightly altered. Its fragments and matrix contain minute disseminated chlorite and amphiboles. As illustrated, part of the clasts display "hematite disease". The varied chemistry of the clasts reacts in different ways to the types of hydrothermal alteration.

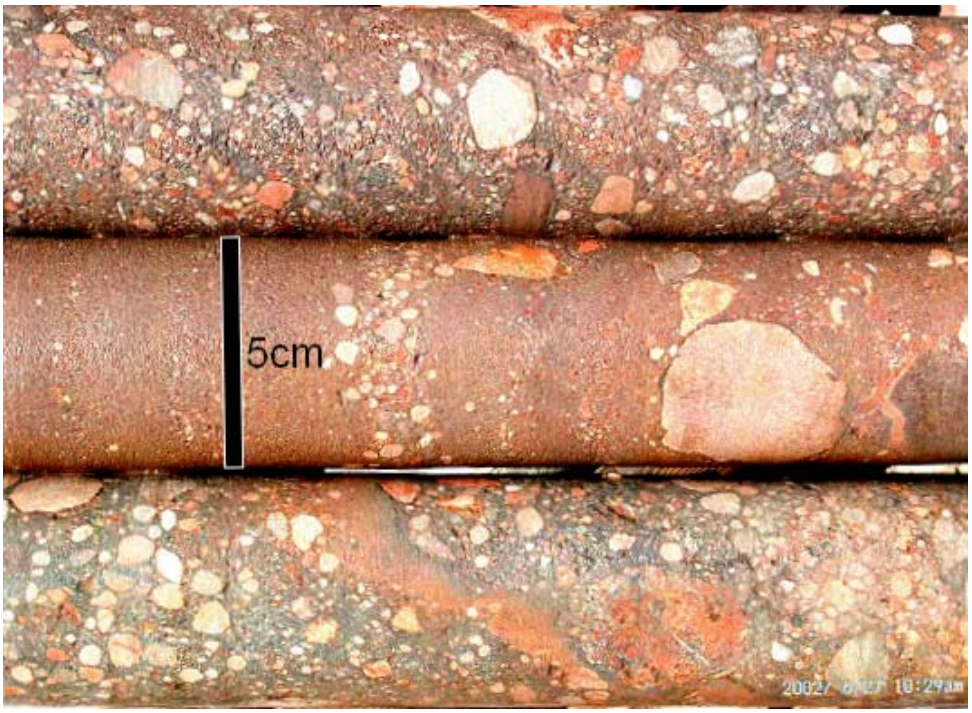

Fig 8.16 Typical features of polymictic, round-pebble hydrothermal breccia. *This type of breccia seems to form by extreme corrosion of hyper-alkaline fluids that move around in IOCG systems. Fragments that were previously angular are corroded. Clasts display severe packing and matrix is mainly smaller, more resistant grains. Note variable grain size and composition. From borehole MB-34, Kasempa area, Zambia. See details in text.*

Fig 8.17 Aspect of poly-brecciated polymictic round-pebble hydrothermal breccia. *The large fragment to the upper left of the photograph is composed of angular pebbles and polymictic fragments, including angular fragments of chalcopyrite and pyrite. It has been rounded itself and makes up a large clast of the new breccia. The round fragments also contain sulfide and magnetite clasts. For scale, millimetric ruler. Note that some fragments are more angular in this portion of core. From borehole MB-34, Kasempa area, Zambia. Read more details in text.*

Round fragments in hydrothermal breccias have been mis-identified in the past as ‘Grand’ and ‘Petit Conglomerats’, as ‘tectonic breccias’ and as ‘sedimentary breccias’ (Johns, 1982; Cailteux, 1995; Stohl, 1972; Pollard, 2000; and Binda, 1995). Part of the angular hydrothermal breccias and stockworks observed at the Kombat mine, Namibia, were mis-interpreted as “collapse breccias”. See chapter on the Kombat mine in the next pages.

8.3.4 STRUCTURAL CONTROL

Structural control of IOCG deposits is held by intrusive-host rock contacts, more reactive stratigraphic units, crustal scale fractures like the Mwembezhi dislocation in Zambia, and local fractures in brittle rocks. We will now review aspects of rock fracturing to control IOCG, and major E-W controlling structures in the Lufilian Arc.

8.3.4.1 ROCK FRACTURING TO CONTROL IOCG MINERALIZATION

Albitization and silicification enhance rock brittleness, they allow rocks to fracture and become good hosts for IOCG mineralization. Quartzites also behave in a brittle manner and produce favorable sites for new minerals. Densely-fractured rocks sometimes host rich mineralization. Figs 8.18 and 8.19 from northern Namibia illustrate that. Fig 8.19 shows a three-dimensional network of irregular fractures that grades into a hydrothermal jigsaw breccia and later into an angular transported breccia. Fractures in the stockwork of Fig 8.18 are formed by three distinct families of joints that are roughly perpendicular to each other. Both stockwork systems account for hundreds to thousands of cubic meters of iron oxide mineralization with sulfides, akin to IOCG mineralization. On both cases, note that mineralization takes place from the fractures into the host rock.

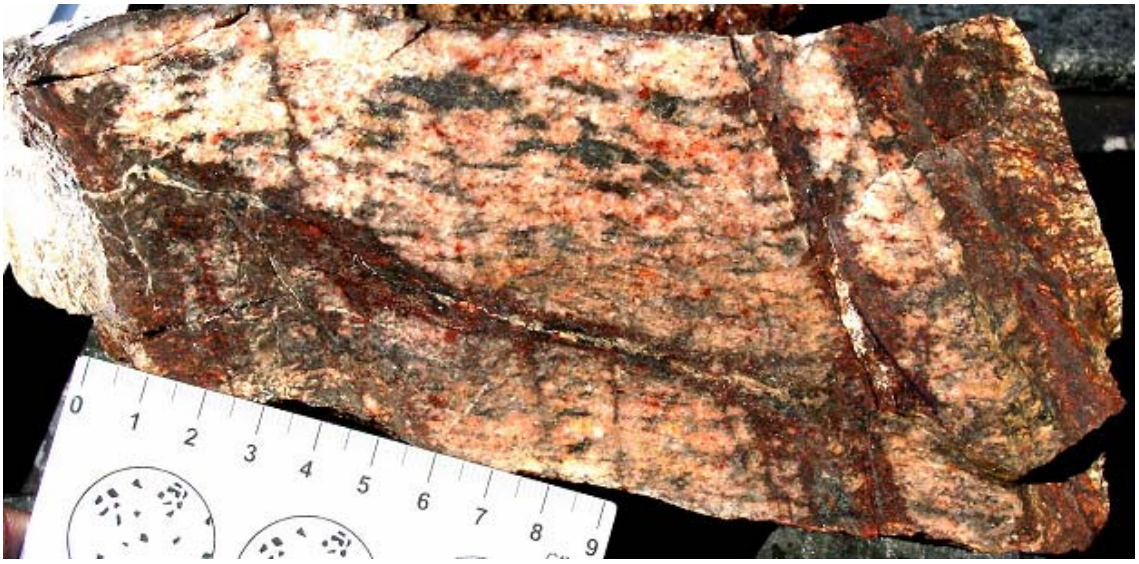

Fig 8.18 Typical angular stockwork mineralization in a foliated granitoid host rock. *This pattern of fracturing is produced by three sub-perpendicular joint families and allows for very large volumes of IOCG mineralization. See text for further details. Scale in centimeters.*

Fig 8.19 Typical irregular stockwork mineralization in a felsic non-foliated granitoid. *This pattern of random fracturing does not seem to follow any rule. IOCG mineralization is hosted by this type of stockwork, and it grades from fresh, undisturbed rock through hydrothermal jigsaw breccias and into breccias with completely displaced clasts. From one of the mineralized areas along the N-S transect, Oas farm, Namibia. Scale in centimeters and millimeters.*

8.3.4.2 E-W STRUCTURES

A regional model on the nature of granitoids and their metallogenic significance at Mesopotamie, Lofdal and Oas farms in Namibia was put together, as shown on Fig 8.6. Most of the mineralization observed in or around the Kamanjab Batholith and the Khorixas Inlier seems to be controlled by subparallel regional E-W-trending major fault systems. The term E-W structures is used here somewhat loosely. Most of the structures that fall under that denomination are actually N68ºE; they follow the general trend of the Lufilian Arc. Rifting and later collision fronts had roughly the same relative orientation.

The major controlling structure of the Luiswishi, Shituru and Kamoya mines in the Democratic Republic of Congo is also an E-W trending fault. Main orientation of the mineralization and planar iron oxide bodies at these sites almost coincides. The Otjikoto gold deposit NW of Otjiwarongo, Namibia is also related to a system of these E-W trending faults.

These E-W structures may be long-lived crustal fractures that remain in place since the onset of rifting. They probably were reactivated through time as varying types of structures, including strike-slip faults and normal faults. Structures that originally were normal faults associated to the rifting events, could have been reactivated into thrusts during basin inversion. Henry, Clendenin, Stanistreet, & Maiden, 1990 discuss some aspects of these features and the origin of main faults in central and northern Namibia.

Most of the fault systems may not be accurately mapped due to lack of outcrop in parts of the Lufilian Arc. Recent mapping in NW Zambia by Key et al., 2002, shows abundant previously un-identified E-W thrust faults. An E-W structure connects the northern part of the Summas Mountains (Fig 8.6) and repeats the lithology. It may be a fracture of similar orientation to the previously described, that acted as thrust fault repeating stratigraphy. Various types of mineralization observed in the Kamajab Batholith are also associated to those E-W structures (Fig 8.6). The southern portion of the Tevrede farm (NW of Kamanjab Batholith, Fig 8.6), site of IOCG deposits under exploration, seems to be controlled by that type of structure. Another one seems to enter the Gelbingen farm and controls mineralization there.

These E-W fractures are quite evident in the published geological maps (Fig 8.6), for they allign copper, iron and gold mineralization (Schneider & Seeger, 1999; Burnett, 1999; Burnett, 2000; and Ajagbe, 2001). A N-S fracture controls gold mineralization to the W of the Kamdescha Farm in Namibia. The main fractures that control the Kombat mine and its satellite deposits in the Otavi Mountains of Namibia also run E-W. This may be a regional feature that is relevant for intrusion and controls the migration of mineralizing fluids (Fig 8.6).

The Mwembezhi Dislocation in Zambia is another major NE-SW structure that controls granitoid intrusion and associated mineralization (Simpson, 1962; Simpson & Stillman, 1963; DeSwardt & Simpson, 1972; Abell, 1976; Griffiths, 1978; Krishnan, 1978; Unrug, 1983; Coward, 1984; Kasolo & Foster, 1991; Hanson, Wardlaw, Wilson, & Mwale, 1993; and Molak, 1995). See country map of Zambia on Figs M1 and 4.3. The Kasempa area, in Zambia, also has important E-W structures that control magmatism and metallogeny. Several other major fractures run parallel to the Mwembezhi Dislocation, including the Mkushi and Serenje faults.

Some of the E-W faults cut across the batholiths, limit them, serve as conduits for the extrusion of granitoid rocks, and control mineralization. They played a very important role in the emplacement of granitic rocks throughout the Lufilian Arc and have not been adequately studied. The Mwembezhi Dislocation, one of Zambia's largest structural features, has not been well mapped, described or understood.

8.3.4.3 PLANAR FEATURES OF IRON OXIDE BODIES

Iron oxide bodies may display layering and/or bedding. Sometimes discrete massive iron oxide bodies are interlayered with plane-structured units that are presumably derived from shales and other types of bedding. At first sight, these planar features may look like banded iron formations; they are produced by selective replacement that conforms thick, extensive, stratabound iron oxide bodies. Some of those bodies have been mis-identified as banded iron formations in the Lufilian Arc.

Nevertheless, they show a close spatial (and temporal?) relationship with hydrothermal magnetite-bearing intrusive bodies, and display relict round-pebble hydrothermal brecciation. The Kasumbalesa body of Zambia is an example of these features (Fig 8.20), as described by Stohl, 1972; Madi-Lugali, 1975; and Bala-Bala & Madi-Lugali, 1979. Surprisingly, none of the Congolese authors knew about the writings of geologists working on the same tabular body in the Zambian side of the border, and viceversa. Dikelike magnetite and/or hematite veins occur as feeders to the tabular conformable iron oxide bodies.

The age of the iron oxide mineralization at Kasumbalesa, in the border between the D.R.Congo and Zambia, is clearly older than the *Grand Conglomerat*, because large fragments of iron oxide with the same features as Kasumbalesa are seen inside the Great Conglomerate that lies on top of the tabular iron oxide layer (Stohl, 1972; Watts, 1991). This is very significant. There might be a relationship between the gabbroic bodies that occur in the lower Roan and the iron oxide bodies, as seen to the east of Solwesi and elsewhere.

Another similar example was found at the Kamoya Cu-Co mine in the Democratic Republic of Congo. Ongoing research at the northern wall of the main pit showed that a tabular iron oxide body indicated to be a banded iron formation had at least three diagonal branches of iron oxide and cuts diagonally across stratification. It is thought to have been emplaced along a fault zone that cuts indurated volcanic ash. In some cases, the iron oxide body carries sulfides. Almost all of the secondary copper mineralization at the deposit lies west of the iron oxide band (below it).

Stohl, 1972 shows that the iron oxide body at Kasumbalesa is intersected by quartz-tourmaline-iron oxide veins (Fig 8.20). In the D.R.Congo an in parts of Zambia, the *Grand Conglomerat* is very magnetic, because it contains the erosional product of magnetite layers. These are similar to some veins seen near the Hippo mine (Cikin, 1968; O'Brien, 1958; and Page, 1974), Zambia and others near the Gelbingen farm in Namibia.

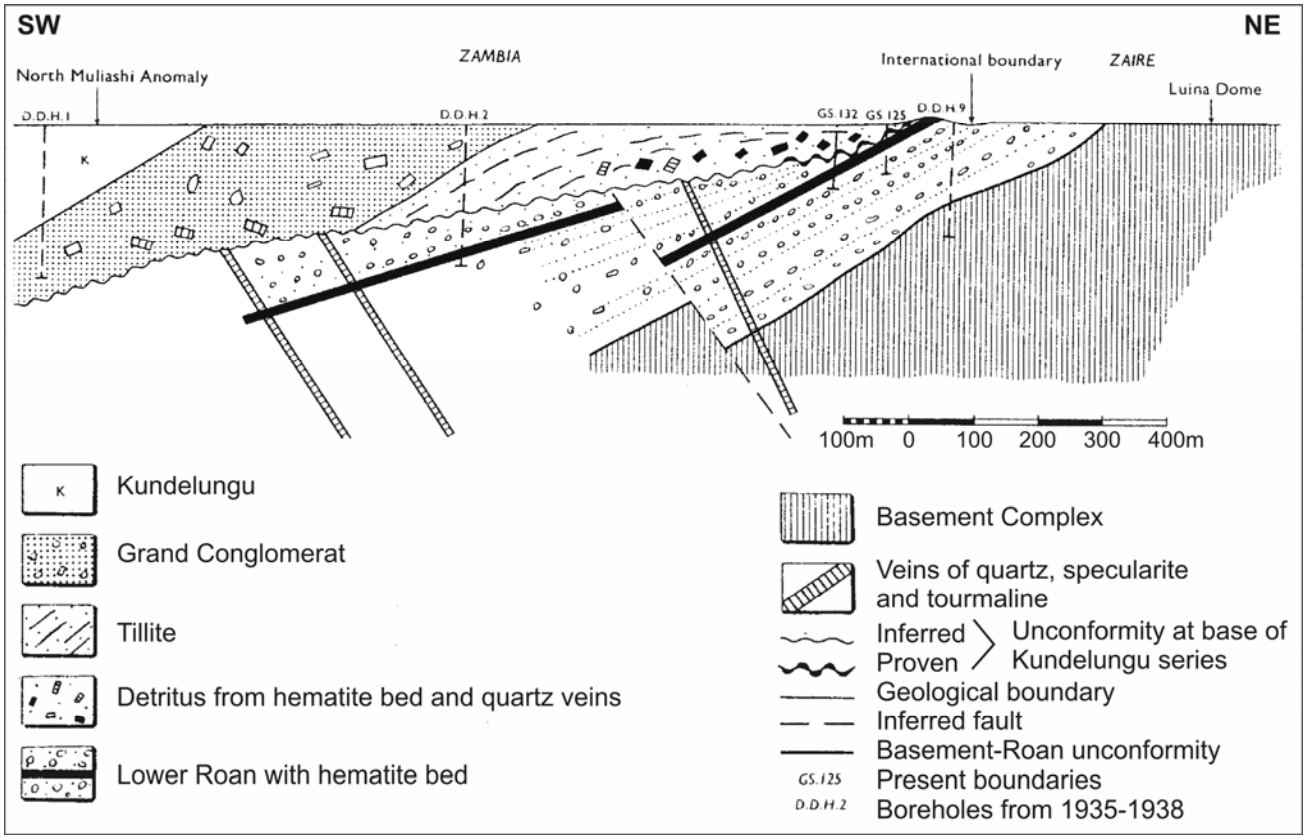

Fig 8.20 Schematic geological section across the southeast margin of Kasumbalesa Hill, Zambia. *Vertical and horizontal scales are equal. From Stohl, 1972. Note the stratiform layer of massive hematite, here interpreted as hydrothermal replacement of iron oxide within favourable beds with a suitable redox setting. Also note the unconformity, and angular fragments of massive iron oxide and vein material.*

A stratiform magnetite-hematite body occurs in the Kasempa area of Zambia. Fig 8.21 presents evidence of this, as shown on aeromagnetic images processed by BHP-Billiton. A doubly plunging syncline is very evident in the maps of that area, as shown on Fig M9.

The Kantonga IOCG prospect also is associated to a tabular iron oxide replacement body (Fig 8.22) The deposit is associated to mafic intrusive rocks, apophyses of the Hook Granite Batholith. Note the lateral extension of the bodies.

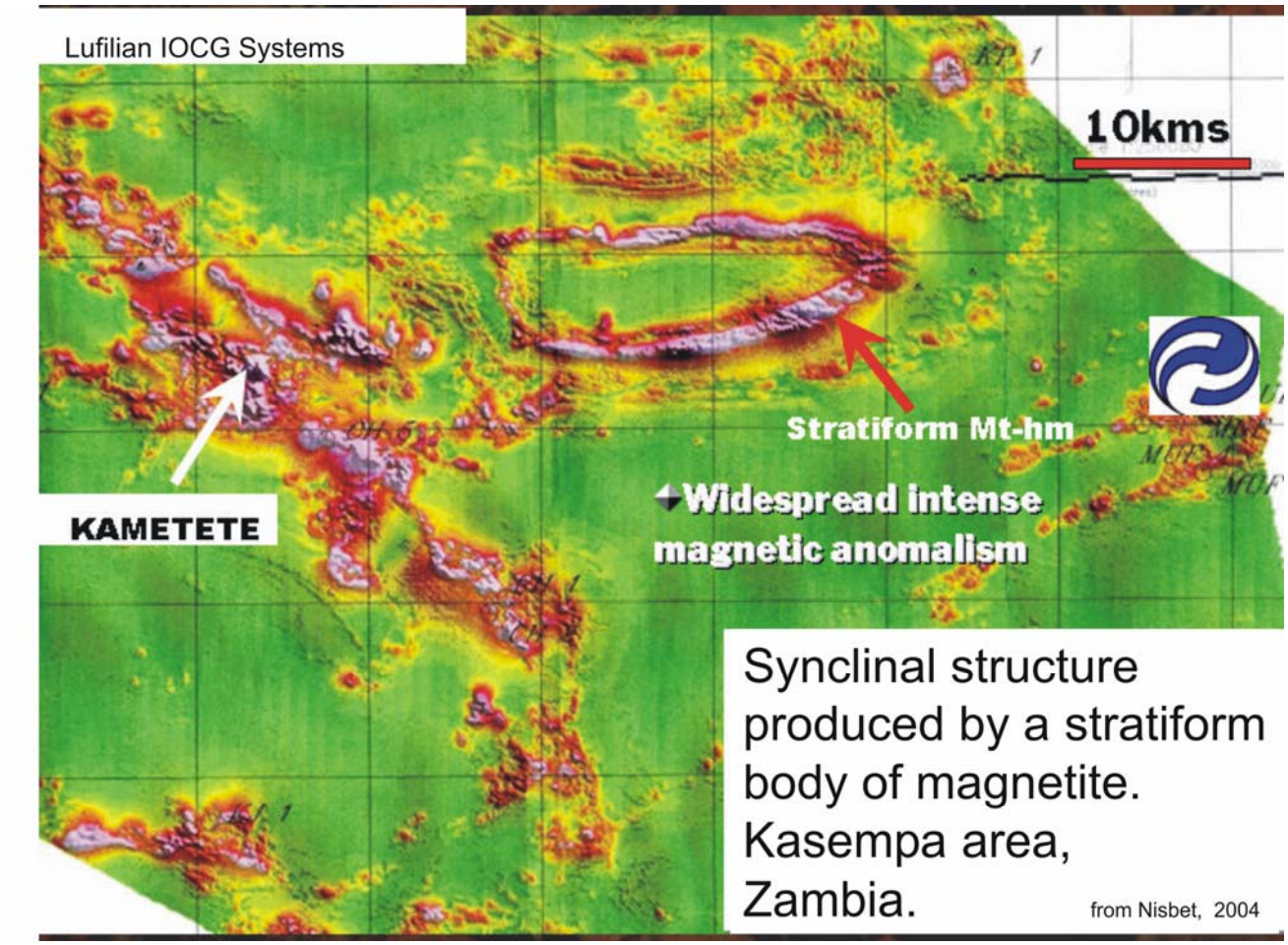

Fig 8.21 Stratiform body of magnetite in the Kasempa area of Zambia. *This type of tabular replacement of iron oxides in sedimentary beds is observed in numerous locations throughout the Greater Lufilian Arc. Taken from Nisbet, 2004b; the image was originally developed by BHPBilliton.*

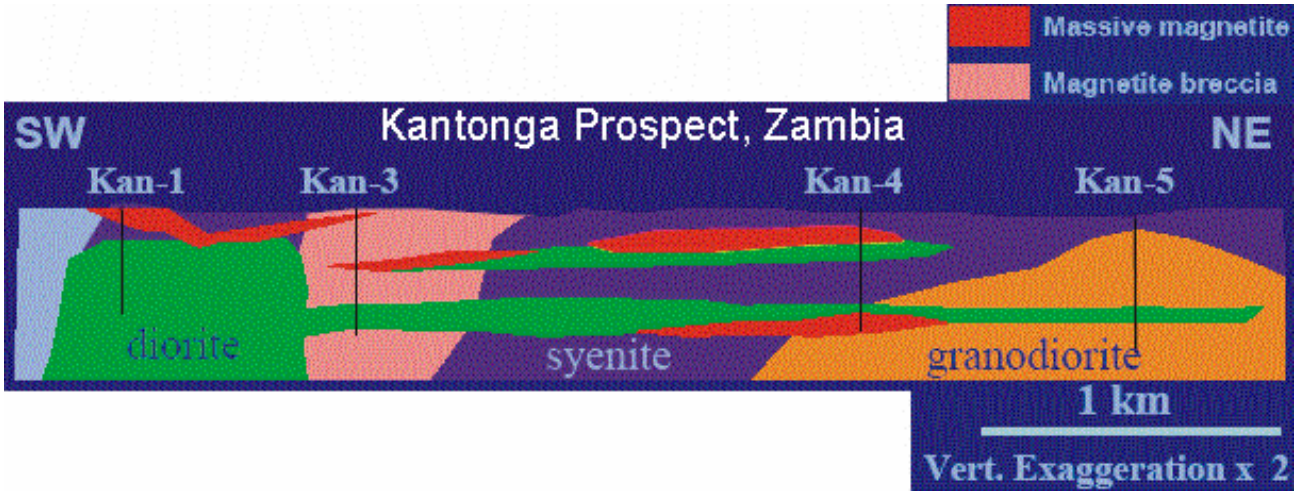

Fig 8.22 Cross section of stratiform body of magnetite at the Kantonga IOCG deposit, Zambia. *Interlayering of discrete, massive iron oxide bodies with mafic sills. Thick, extensive, strata-bound iron oxide bodies were produced by selective replacement. There is a close spatial (and temporal?) relationship with hydrothermal iron oxide-bearing intrusive bodies. Part of the iron oxide bodies display relict round-pebble hydrothermal brecciation. Note the pink diatreme cemented by magnetite. From Hitzman, 2004b.*

8.3.5 PARTICULAR HYDROTHERMAL ALTERATION FEATURES

Particular hydrothermal alteration features observed in the Lufilian Arc will be described below. Alteration from nearby mineralizing systems overprint each other. Sodic alteration is widespread and very important in the iron oxide-copper-gold systems of the Greater Lufilian Arc. Scapolitization and albitization were observed in various types of rocks around the IOCG systems. At times, alteration extends a few hundred kilometers away from the center of the systems. Sodic alteration will not be discussed here.

8.3.5.1 TOURMALINE ALTERATION

A special type of hydrothermal alteration was observed in the western Kamanjab Batholith, and around Otjiwarongo, Namibia (Figs 8.6 and 8.33). Monotonous bands of black tourmaline and quartz, each five to ten mm wide produce the “zebra alteration” pattern. This alteration was seen to occur in silicified quartzites and sometimes in albitized schists and siliciclastic rocks. Portions of the western Hook Granite Batholith also display patterned black tourmaline in red granites and syenites. In this case, the tourmaline occurs as braided and sheeted veins. Yet in other cases, tourmaline was found to be the matrix of hydrothermal breccias. No chemical analysis of these rocks has been carried out to date, but it is expected that copper and maybe gold may be associated with tourmalinization. Significant boron enrichment is another of the “typical” alteration patterns of some IOCG mineralization.

8.3.5.2 QUARTZ “PODS”

Quartz pods are a particular feature that has been identified in most of the Lufilian Arc study region of Zambia and Namibia. The term “quartz pod” (here shortened as QP) is an informal name coined by the author for massive or sugary quartz bodies of varying dimensions. Features are very different from those of vein quartz and pegmatitic quartz bodies; what seems most different is their geometry. The shape of quartz pods appears to be roughly cylindrical, outcrops of undeformed bodies are round to elliptical, and their diameter varies from a few to several hundred meters. Some mapped bodies of quartz exceed four kilometers in diameter. There is geophysical evidence of even larger bodies. Quartz pods occur near intrusive bodies and around iron oxide-copper-gold mineralized systems. Most of the pods are made of white quartz, but color may vary greatly. Examples show change from milky white to dark gray smokey tones and to light pink or yellow tints. These colors are probably due to abundant gas, salt, iron oxide and sulfide micro-inclusions. Both translucent and milky varieties of quartz occur together. Different portions of a single body may be saccaroidal and/or massive. Quartz pods are seldom mapped in published geological maps of Zambia and Namibia. Identifying them in the field and studying their physical-chemical features may aid in the exploration of iron oxide-copper-gold mineralization.

8.3.5.2.1 Description of Quartz Pods

Quartz pods seem to be a particular characteristic of the Lufilian Arc, and may somehow be related to rift environments. They occur in many different types of rocks including limestones, dolostones, granitoids, various schists and gneisses. The author has seen them occur in an extensive region, roughly 2000 km by 300 km; QP are also expected to be found in SE Angola, the Katanga province of the Democratic Republic of Congo, and NW Botswana (See Fig 8.23). The author tried to locate them wherever they weree spotted, sampled them for regional comparison, and whenever time allowed, walked around them with a GPS to study their surface geometry (Fig 8.24) Several dozens of QP were intersected along the roads. Points of intersection were recorded, and constitute a simple measument of the size and abundance of quartz bodies in the Lufilian Arc. That chance sampling is not representative, but it is all available for the time being. A few of the QP were sampled with the hope to find particular chemical or physical features of use in exploration. Preliminary results described here are a by-product of field sampling for a regional project on granitoids in portions of the Greater Lufilian Arc.

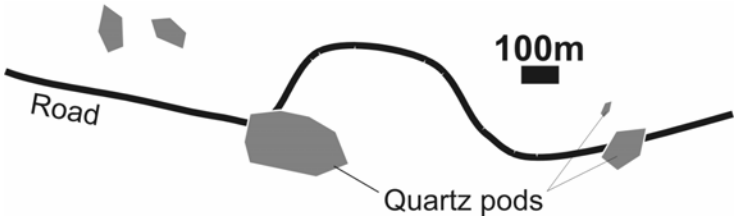

Fig 8.24 Types of quartz pod outcrops observed during field work, Greater Lufilian Arc Granitoid Project. *QP were encountered along the main roads (thick black line) while sampling for granitoid rocks in Zambia and Namibia. A few of the perimeters (gray polygons) were measured by walking with a GPS.*

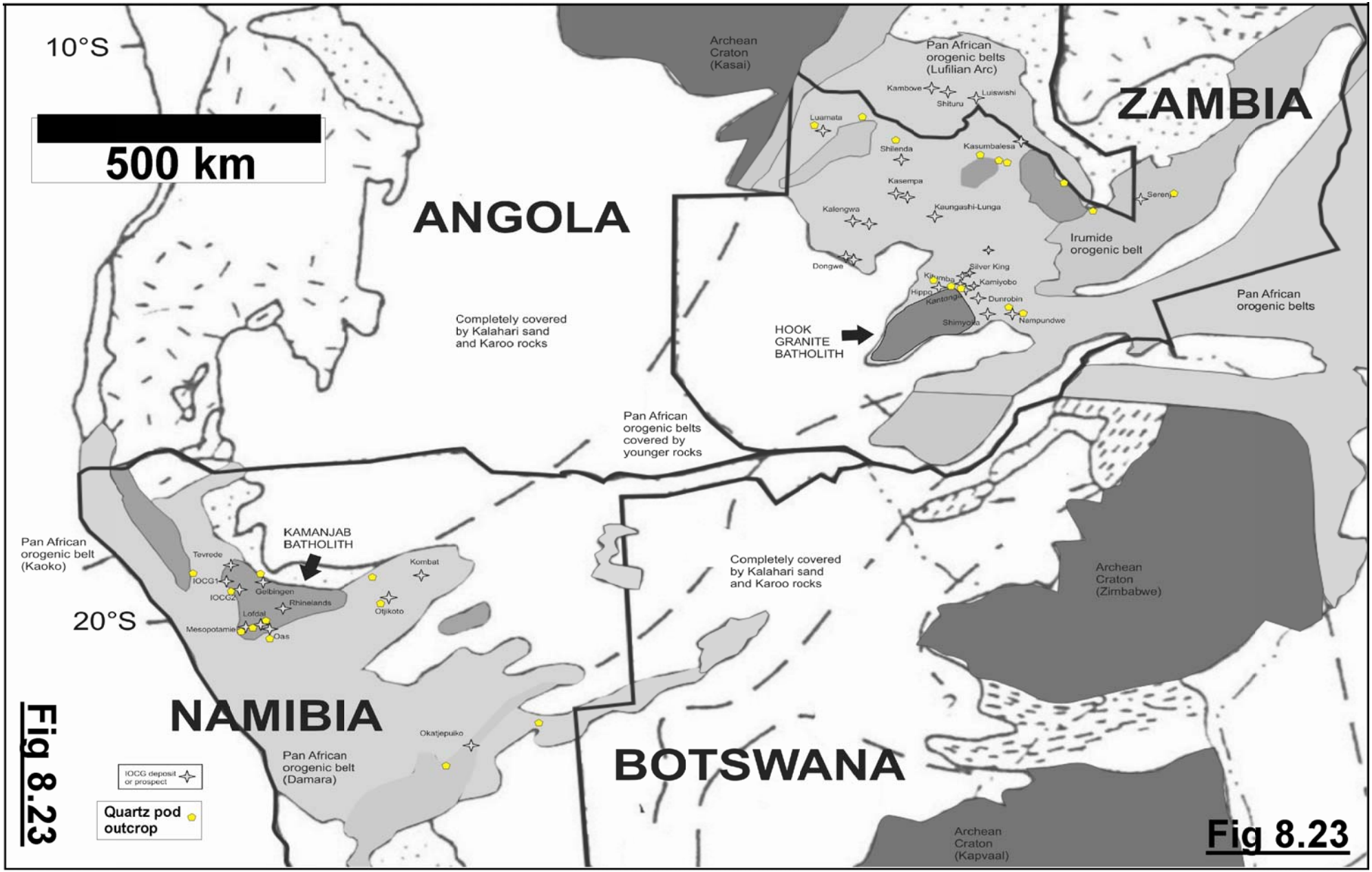

Fig 8.23. Quartz pod outcrops observed in the Greater Lufilian Arc, Zambia and Namibia. *Yellow pentagons represent quartz pods. Note that many quartz pods occur near iron oxide-copper-gold mineralization. By Alberto Lobo-Guerrero S., Jan., 2004.*

In many locations, QP have been found to host IOCG mineralization. At times QP themselves acted as brittle rocks to hold massive magnetite and/or specular hematite mineralization with accompanying sulfides. This is shown on Fig 8.26 D-H.

The Egue farm, located NE of Otjiwarongo, Namibia and in the environs of the Otjikoto gold deposit has a massive quartz body, 500 meters in diameter. After carrying out airborne and field geophysics, the Namibian division of Anglo American drilled in the center of the body searching for metallic mineralization and could not find the bottom of the quartz body. A borehole 325 meters deep was collared in quartz and finished in quartz with minor disseminated pyrite. In this case, the quartz pod seems to be associated with the Otjiwarongo Batholith, a large granitoid entity that lies beneath Kalahari sand, Katangan carbonates and calcrete. The Otjikoto gold deposit, currently being developed by AngloVaal, is located a few kilometers away from the QP; the Kombat copper mine also seems to be related to the Otjiwarongo Batholith. Both mineralizations have recently been classified by the author as iron oxide-copper-gold deposits. There might be more of these deposits under cover.

Sometimes the country rock is deformed upward around QP, as if they had somehow intruded themselves forcefully in a fashion similar to that of diapirs (Fig 8.25). This behavior was observed in outcrops located to the west of the University of Namibia, Windhoek, as shown to the author by Dr. David Robertson from the same university.

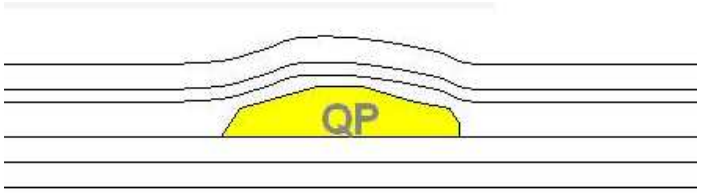

Fig 8.25 Sedimentary bedding and/or foliation that bends around quartz pods. *In some locations, country rocks have been seen to fold around the quartz bodies. The reason for this behavior is unknown. It might be due to differential compaction of the various beds and non-compaction of quartz pods, or dissolution of water-soluble salts in the country rock. The diagram has no particular scale.*

Some published map sheets of Zambia have QP on them. Very few references specifically describe these bodies; maybe they were considered to be simple quartz veins of minor importance. There is very little mention of quartz bodies in Namibian geological literature.

Two Zambian locations display well-exposed QP. One is located west of Kitwe along a road near the Congolese border. Another lies east of Solwesi and is shown on Fig 8.8. Both occur in clusters and have bodies that are more than 500 meters in diameter.

8.3.5.2.2 Four Rock Association

A four-fold rock association is observed in many parts of the Lufilian Arc. This is made up by small bodies of gabbro or diorite, small bodies of red-tinted felsic instrusive rocks, massive iron oxide bodies (magnetite and/or hematite) and quartz bodies. All of these seem to occur in rift environments, and their origin is not yet completely understood (See Fig 8.8). Explaining the ubiquitous presence of these four rock types might provide ideas for the origin of iron oxide-copper-gold mineralization in the Greater Lufilian Arc, and more importantly, may give clues for mineralization elsewhere.

8.3.5.2.3 Particles Enclosed in QP

On some locations, the large quartz bodies contain isolated spherical iron oxide (hematite and/or magnetite) inclusions that vary in size from a 10 cm diameter to 1.5 cm diameter as shown on Fig 8.26D. It seems that the iron “bubbles” occur inside the quartz as if they were immiscible substances or xenocrysts. At times, hematite or magnetite cubes occur in quartz (See Figs 8.26A, B and C). Sometimes xenoliths of any type of country rock are included within the quartz bodies. Shapes of these xenoliths vary widely. Many questions still remain unanswered: Can the FeOx spheres in quartz be a product of immiscible fluids, or incomplete assymilation of previous euhedral iron oxide minerals? What are the relationships with gabbroic bodies, small syenitic bodies and iron oxide bodies?

At times the brittle character of quartz allows it to be host for braided or sub-parallel sheeted veinlet systems filled by hematite and sulfides (Fig 8.26H). Numerous field examples show braided veins, stockworks and various breccias where quartz is both the host rock and the single component of clasts. Figs 8.26

D-H illustrate that well, at the scale of a hand sample. Similar features were observed on samples from Tevrede, a rich copper and gold IOCG prospect in the northwest Kamanjab region, Namibia (www.bouldermining.com).

Fig 8.26G is a slab of massive milky quartz that is host to brecciation and specular hematite mineralization with iron and copper sulfides. This is a fragment from a quartz pod that behaved in a brittle manner and offered a good host for IOCG mineralization.

8.3.5.2.4 Studies that can be Done on the QP

Investigations on the QP might reveal interesting chemical signatures that will probably contribute to the field exploration of IOCG deposits in southern Africa. On-going research on QP includes detailed macroscopic analysis of features, measurement of radioactivity and fluorescence under various wavelengths, cathodoluminiscence studies, detailed determination of specific gravity, chemical analysis, bibliographical review, studies of H and O isotopes, rare earth content, halogen content, fluid inclusion studies to detect salinity and temperature of emplacement, decrepitation studies to evaluate detailed chemical composition of the fluid inclusions, metallic content, study of the contacts with iron oxide inclusions, and study of the braided veins, their contacts with quartz and chemical characteristics.

The three-dimensional geometry of quartz bodies might be studied in a few well-known outcrops using seismic profiling, electrical resistivity profiles, vertical electrical soundings and electrical tomography. Detailed IP profiles may also contribute significantly. Four sites for this have been identified in the Greater Lufilian Arc. They are all easily accessible along main roads.

8.3.5.2.5 Practical Applications of the QP

The fact that QP are related with iron oxide-copper-gold mineralized systems is very significant. Their positive identification as part of IOCG systems might become a major breakthrough in mineral exploration. If as thought, the detailed chemical signature of quartz bodies from mineralized IOCG systems is found to be somewhat anomalous and characteristic, chemical analysis of outcropping quartz bodies and of large areas with quartz float may provide a new exploration tool. Positive field identification of IOCG-related QP could help to select prospective areas for IOCG deposits.

Abundant float of white quartz in a circular area may be detected easily on arid regions. Outcrops of these quartz bodies offer a good color contrast with the country rock; thus black and white air photographs may be an aid to their location. The large outcrop area of some QP can make them identifiable in ASTER images and on other remotely-sensed images. Large QP in part of the Kamanjab Batholith in Namibia are evident on ASTER and hyperspectral airborne images.

8.3.5.2.6 Hypothesis About the Origin of QP

The origin of the QP is not well understood. Many hypotheses for their occurrence come to mind. They may be a type of silicification alteration that is not yet well documented in the literature. The idea of hyper-alkaline fluids dissolving silica in one place and producing the quartz bodies in another place was briefly proposed by Behr, Ahrendt, Porada, Rohrs, & Weber, 1983 while studying chloride-rich inclusions in QP. Sabkha environments near rift systems certainly could produce very saline fluids. But how can the space for the pods come to be? How did silica get in place? The most reasonable working hypothesis based on field observations, is that QP are produced by extremely alkaline fluids rich in HF that dissolve silica in rocks replacing it by iron sulfides (Fig 8.27). Silica migrates further out and precipitates quartz bodies. But again, the question is how can the space for quartz bodies be produced? How could one detect fluorine in fluid inclusions if the way to dissolve silicates involves HF?

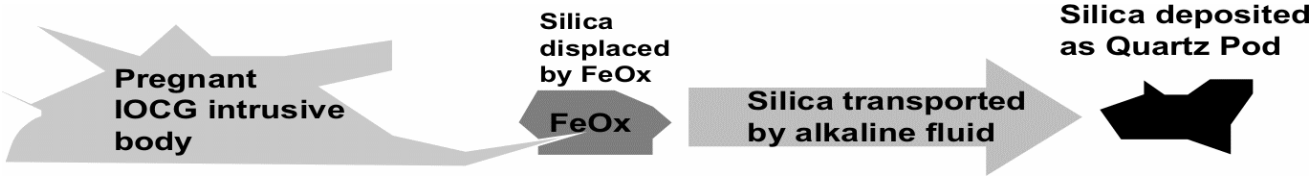

Fig 8.27 Schematic diagram to show process of quartz pod formation. *Space for the emplacement of massive magnetite bodies was dissolved out from the host rocks. Silica from the dissolved minerals migrated outward from the site and later became massive quartz pods in favorable emplacement sites. All the process is carried out by warm hydrothermal fluids. This process may occur at varying scales. The radius of magnetite bodies and quartz pods may be up to a few kilometers long.*

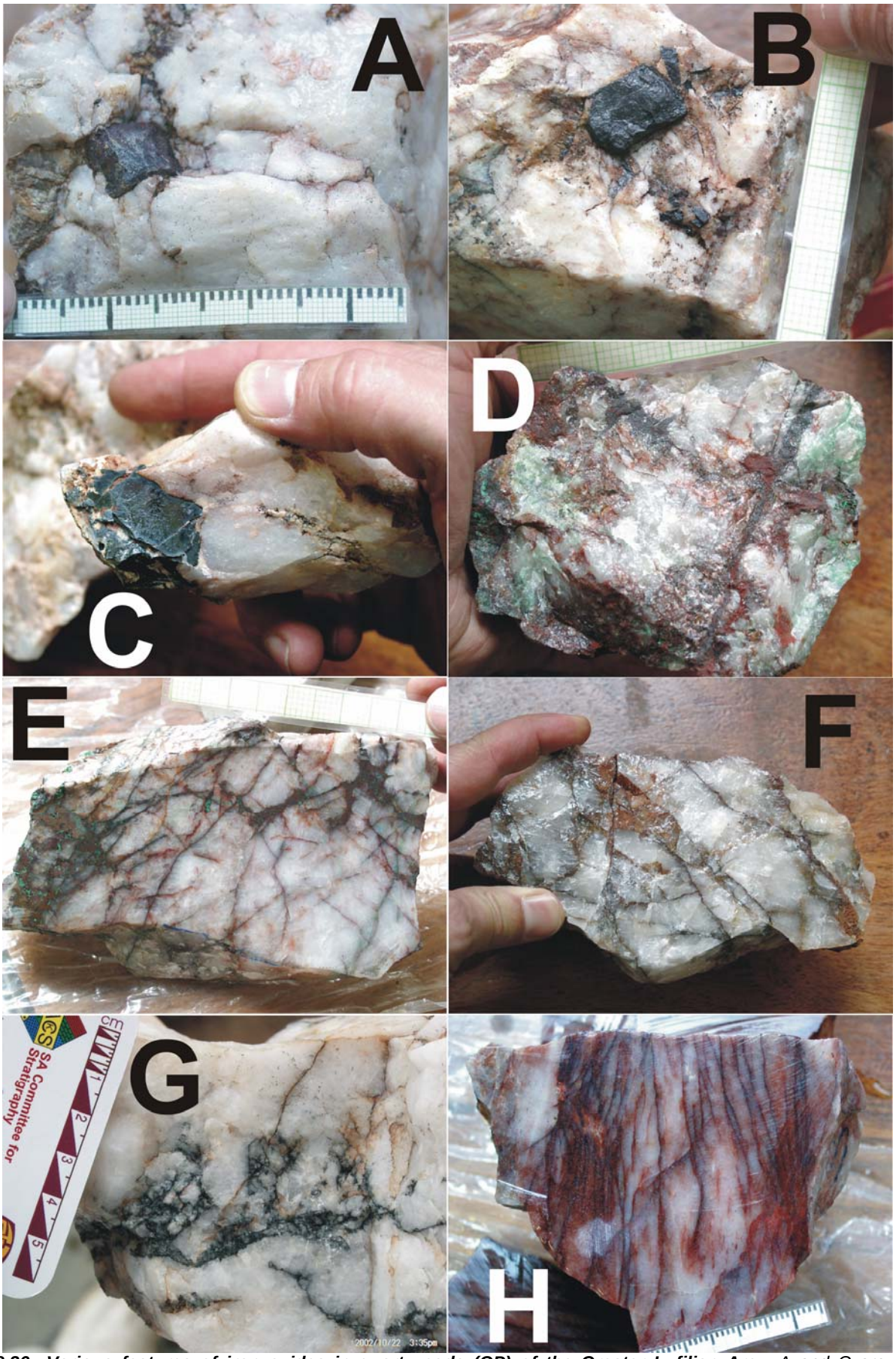

Fig 8.26 Various features of iron oxides in quartz pods (QP) of the Greater Lufilian Arc. *A and C are cubic fragments of magnetite hosted by a QP. B is a sub-rounded fragment of magnetite found inside a QP. D, portion of a sulfide-rich, magnetite-filled stockwork hosted in a QP. E and F are sulfide-rich, magnetite stockworks hosted in QP. Field of view is 15cm. G is a hydrothermal angular clast breccia cemented by magnetite that is hosted in a QP. Clasts are made of quartz fragments. H is a series of closely-packed, subparalled sheeted veinlets hosted in a QP. A and E have scale marks every mm; B and D, every 2mm.*

8.4 SOME KNOWN IOCG-LIKE DEPOSITS AND PROSPECTS

The Greater Lufilian Arc of Zambia and Namibia is a prospective zone for the exploration of economic IOCG mineralization. Below is a description of some operating deposits and prospects that are very akin to IOCG systems. Mines and occurrences in the Democratic Republic of Congo that are considered to be of IOCG origin will be described later. Table 8.2 compiles some of the main IOCG deposits. Fig 8.7 illustrates the location of the main deposits and prospects.

8.4.1 NAMIBIAN DEPOSITS AND PROSPECTS

8.4.1.1 OKATJEPUIKO PROSPECT, WITVLEI, NAMIBIA

An un-dimensioned IOCG deposit exists under the Witvlei sedimentary-hosted copper deposit at the Okatjepuiko farm, Namibia. As seen on Fig 8.29, several authors describe mineralization from Witvlei to be a "typical" copperbelt deposit (Borg & Maiden, 1986; Maiden, Innes et al, 1984; Steven, 1993; Ruxton & Clemmey, 1986; and Anhaeusser & Button, 1973; and Moodie, 2000). Eckhart Freyer of Anglo American exploration in Namibia offered abundant information on the deposit and the region (Freyer, E., personal communications, 2002, 2003). See general location on Fig M26. More details are included on section 4.2.2.6.

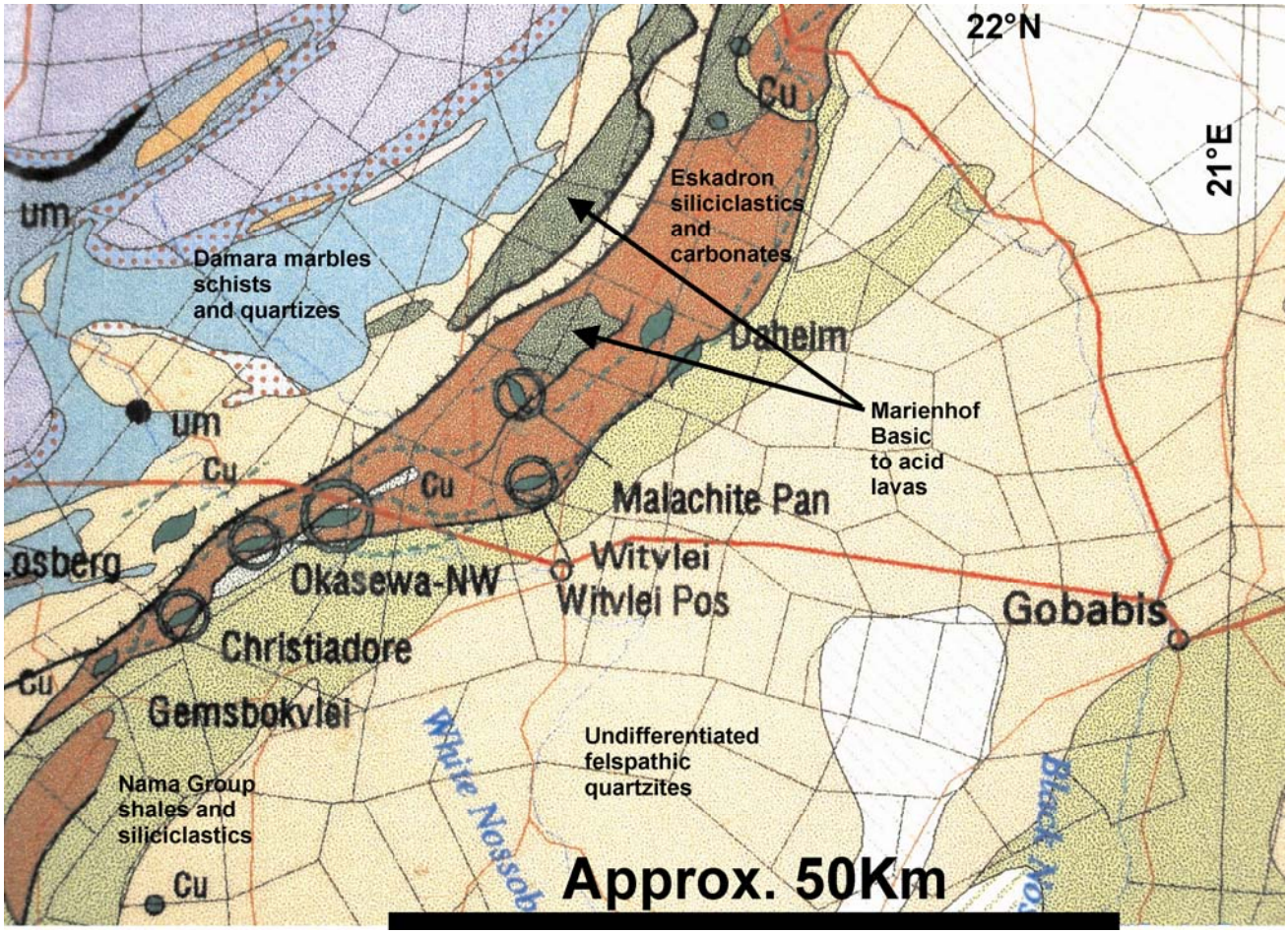

Fig 8.29 Geological map of the Witvlei site, and location of the Okatjepuiko IOCG prospect. *As shown, the main road (in red) from Gobabis to Windhoek cuts across the map. There is also a railroad that runs parallel to that road. Farm boundaries are marked by polygons. Note the "Malachite Pan" and Witvlei Pan that are located around the mineralized area. The belt of dark rocks that runs NE-SW extends under cover into Botswana, and further southwest in Namibia. Note the round and sygmoid symbols that indicate tabular copper mineralization. More details in text and on section 4.2.2.6..*

Rich gold and copper mineralization (3.5 gAu/ton and multi percent Cu) has been found on surface samples (Freyer, E., personal communication, 2003). A subvolcanic porphyritic intrusive rock seems to produce mineralization. Gabbros as well as felsic intrusive rocks outcrop at the Okatjepuiko area. Subrounded-clast hydrothermal breccias with intense brown (iron oxide) alteration also outcrop. Massive magnetite and hematite fragments occur as float. In fact, a strong magnetic anomaly guided exploration to the site. Gold is not present in the sedimentary-hosted copper deposit; it probably remained underneath in the original hypogene deposit. All of these ingredients point to an iron oxide-copper-gold mineralization at depth.

Evidence of IOCG mineralization under at least one of the sedimentary-hosted copper deposits of Namibia is very important. The presence of both hydrothermal copper and gold under the Witvlei deposit is relevant to understand the regional metallogeny, and could lead to a completely different source for copper in the Greater Lufilian Arc.

This type of mineralization probably extends NW into the Ghanzi-Chobe Belt, of Botswana (Moodie, 2000; and Steven, 1993). Other belts of similar age in the region can be prospected for IOCG mineralization.

Another possible case of IOCG under a sedimentary-hosted deposit might exist in Zambia. The Kalumbila, sedimentary-hosted copper (nickel-cobalt) deposit in NW Zambia described by Steven & Armstrong, 2003 is closely associated to small granitoid and gabbroic intrusions, and might be underlain by an IOCG deposit.

8.4.1.2 KOMBAT MINE, OTAVI MOUNTAINS, NAMIBIA

The Otjiwarongo Batholith, intrusive body that measures approximately 200 km by 40 km wide, is thought to exist undercover below carbonates and Mesozoic sands to the NE of Otjiwarongo, Namibia. Geophysical evidence produced by Dr. Branko Corner for Anglo Vaal supports the presence of that hidden batholith (Corner, B., personal communication, 2003). It may be responsible for the known abundant copper and gold mineralization in the region, including the Kombat mine, Uis West, Asis North, and others in the Kombat district. The mine is owned and operated by Ongopolo Corporation, a Namibian-based mining company. It has been active since the 1960's, and is one of the major copper producers in the country. The reserve database has been increased progressively with time to allow for further underground development. Five or six year's worth of reserves are all known, but new ones are found as the mine is exploited.

Ongoing investigations at the Kombat copper mine in the Otavi Mountains of Namibia (See location on Figs M25, M19 and 8.33) show physical features that are akin to the iron oxide-copper-gold (IOCG) deposit type (Table 8.2). Brecciation and stockworks of hydrothermal origin host most of the ore-grade rocks at the mine (Fig 8.30). Primary copper mineralization always occurs near or around large bodies of iron oxides (Innes, 1983; Galloway, 1988; Deane, 1995; Innes, 1986; Songe, 1957; Pirajno & Joubert, 1993; and personal observations). Figs 8.31 and 8.32 illustrate this well. No direct relationship with granitoid rocks has been established to date. Frank Melcher (Melcher, F., personal communication, 2003 and Melcher et al, 2003) state that sulfur isotopes for the Kombat mine are in the 30-24 $d^{34}S$ range, which indicates an igneous input. That had been previously established by (Pirajno, Kinnaird, Fallick, Boyce, & Petzel, 1993).

Field observations and critical reading of literature available on the mine lead to conclude it is a deposit of the IOCG family (a copper-rich end-member). Probably other copper deposits in the Kombat region have similar origin. All the primary occurrences of gold that surround Kombat are hydrothermal and could also be attributed to the hidden batholith (Figs M25 and 8.33). The same igneous body could also produce mineralization of the sediment-hosted gold (so-called "Carlin type") in the Otavi carbonate sequence (described on chapter 6.5.5.).

The several portions of the Kombat mine are controlled by a regional E-W fault as well as the other copper deposits in the region. Copper sulfides nucleate around iron oxide bodies of different shapes and sizes. This is shown on Figs 8.31 and 8.32 and others.

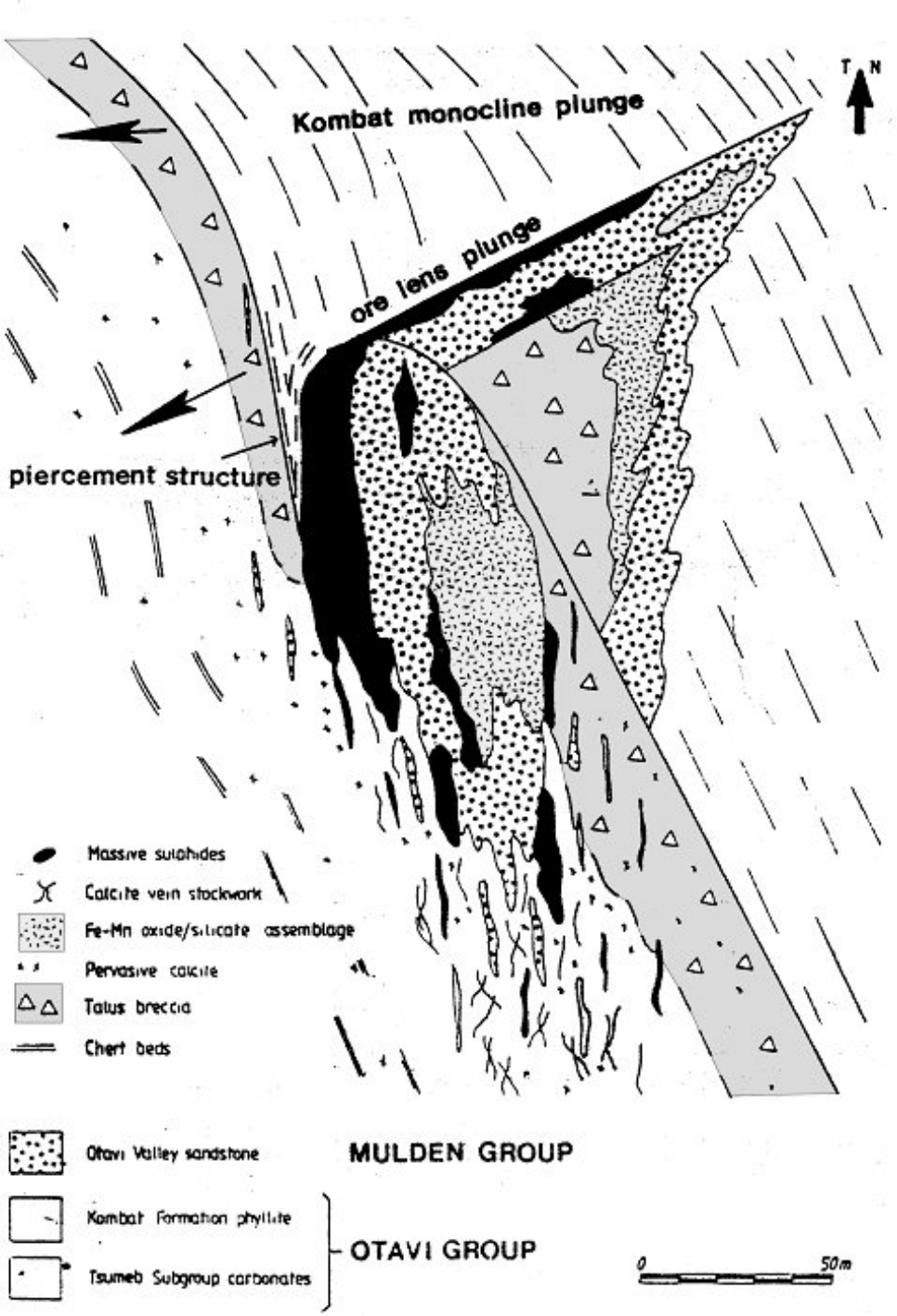

Fig 8.31 Diagram taken from Deane, 1995 to reinterpret origin of the Kombat mine, Namibia. *This three-dimensional picture of a typical ore lens at the mine shows that large iron oxide bodies with minor manganese act as nucleus for pyrite and copper sulfide mineralization. Note the scale for dimensions of the magnetite bodies that are marked with the small dots. The large dots are a fine hydrothermal breccia that is called "Otavi sandstone" at the mine. It seems to be the residual of carbonate disolution by acid fluids. Coarse-grained breccias and stockworks are indicated by the material with triangles. Massive mineralization of copper sulfides is marked in black. The deposit has tectonic overprinting and foliation, that re-mobilized and sheared both host rocks and mineralization.*

Fig 8.30 Typical mineralization at the Kombat Cu mine, Namibia*. This photograph shows the type of stockworking that occurs at the mine. It contains basically bornite, chalcopyrite and pyrite. Large volumes of three-dimensional fracturing like the one depicted account for most of the rich mineralization at the mine. Massive bodies of sulfides are found in parts of the breccia voids. As described in the text, the origin of mineralization seems to be associated to the Otjiwarongo batholith and everything indicates that it is an IOCG deposit.*

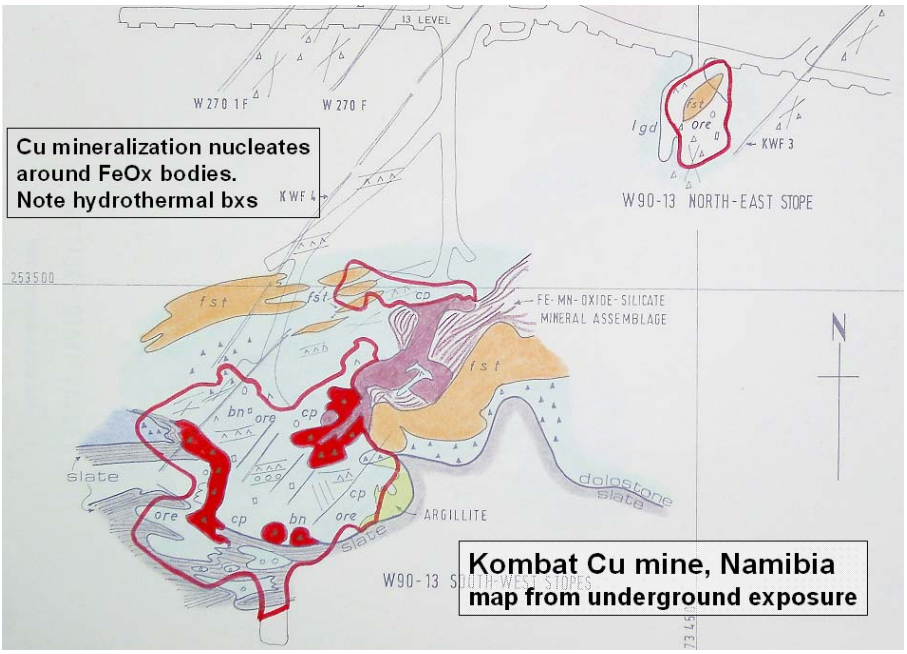

Fig 8.32 Underground map that shows core of iron oxide bordered by copper mineralization at the Kombat Mine, Namibia. *Note that underground exposures show manganese-rich iron oxide bodies – in violet- (sometimes massive, sometimes "banded" and "bedded"), surrounded by hydrothermal breccias. High grade mineralization is marked in red, and the thick red line indicates economic mineralization. Note that all the copper sulfides occur around the iron oxide bodies. This map is one of many cross sections and maps produced by mine geologists that show similar features. Since the purpose of miners is not to map iron oxides, these are seldom depicted in three-dimensions. This diagram was extracted from internal reports reviewed at the mine library.*

8.4.1.3 OTJIKOTO GOLD DEPOSIT, NAMIBIA

Otjikoto is another deposit that seems to be associated to the Otjiwarongo batholith. It occurs in the northern portion of the Lufilian Arc in Namibia. Fig 8.33, a generalized map produced by the AVMIN geological staff based on compilation, field mapping and geophysical interpretation, shows general geology in the environs of Otjikoto. The Kombat mine is also shown there for location and general context. Mineralization at Otjikoto has direct association to magnetic iron oxide bodies and is controlled by E-W fractures, parallel to the main Lufilian Arc elongation. The mineralized sheeted vein system is preferentially hosted within albitized pelitic and siliciclastic rocks in marbles of the Karibib Formation. Just as discussed previously, hydrothermal processes that indurated the host rocks at Otjikoto enabled them to fracture in brittle fashion. According to Wilton, Lombard, & Philpot, 2002, "individual veins range from 1 to 10 cm in width. There is an apparent strong correlation between vein density and grade. Vein mineralogies comprise various proportions of pyrrhotite, magnetite, pyrite, with associated large rounded almandine garnets, amphibole and free gold." Metamorphic foliation overprints mineralization. A significant component of the mineralization at Otjikoto comprises coarse gold. Tourmalinization is one of the observed types of hydrothermal alteration. Other metals of mafic affinity are associated to the deposit. The characteristics described above point to classify the Otjikoto deposits as a gold-rich member of the IOCG family.

A very aggressive drilling campaign was carried out at the deposit during 2003, and pilot mining will soon be advanced. It could soon become a large underground mine. Very little public information on the deposit was made available.

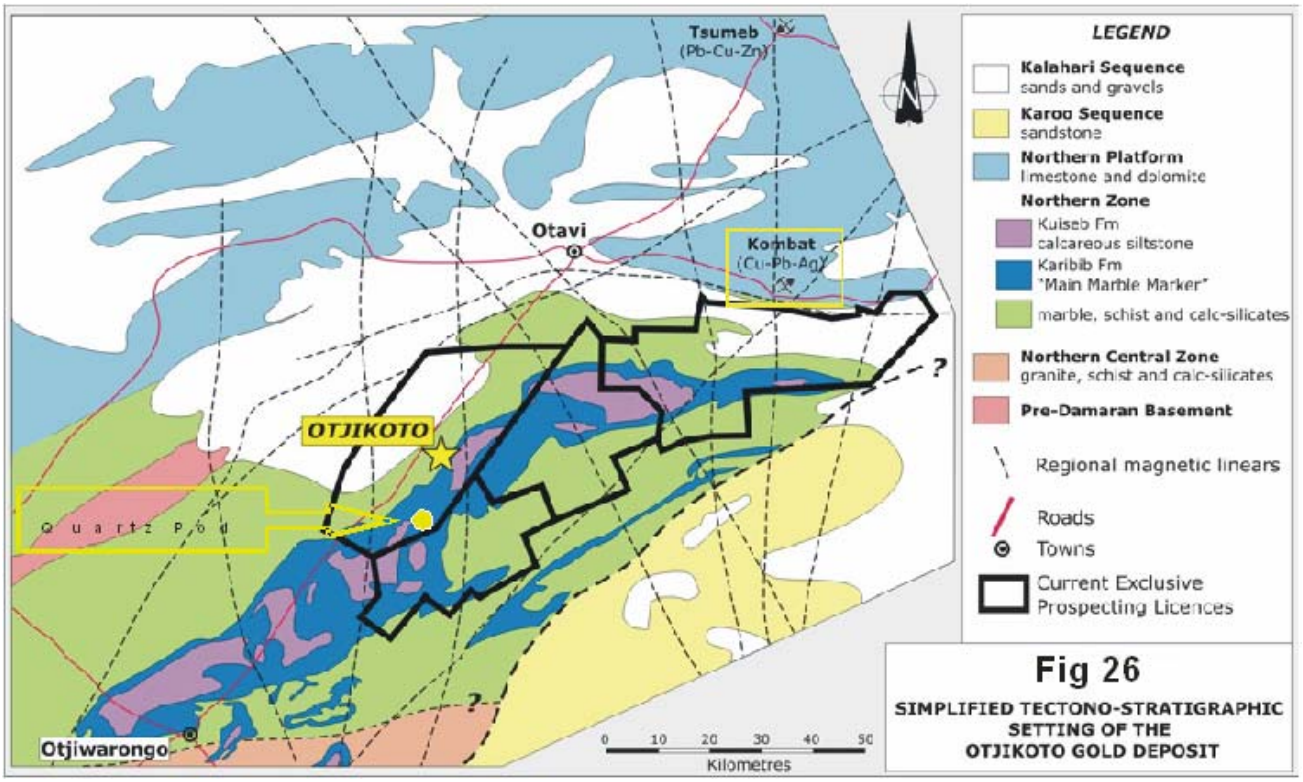

Fig 8.33 Simplified geological map of the Otjikoto gold deposit, Namibia. *This map was produced by the Namibian office of Anglo Vaal and published in Wilton et al., 2002. Dark lines indicate exploration licences; broken lines are magnetic lineaments; most of the rocks are different forms of carbonates, marbles and calcareous siltstones. There are almost no outcrops in the entire area, except in the northern portion of the map, underlain by Otavi limestones. Note location of the Kombat mine and main roads.*

8.4.1.4 MESOPOTAMIE FARM, NAMIBIA

The Mesopotamie farm, located in the southwestern corner of the Kamanjab Batholith in Namibia has significant known copper mineralization of IOCG type (Figs 8.6 and M20 for location). Various granitoids, including graphic texture alkali granites occur at the farm and seem responsible for the copper mineralization of the Copper Vallei deposit. Massive iron oxide bodies emplaced along E-W vein systems and related sulfidation account for the copper mineralization. Gold is thought to occur along with the copper. Hydrothermal breccias were mapped and many quartz "pods" were also identified during reconnaissance work at the farm.

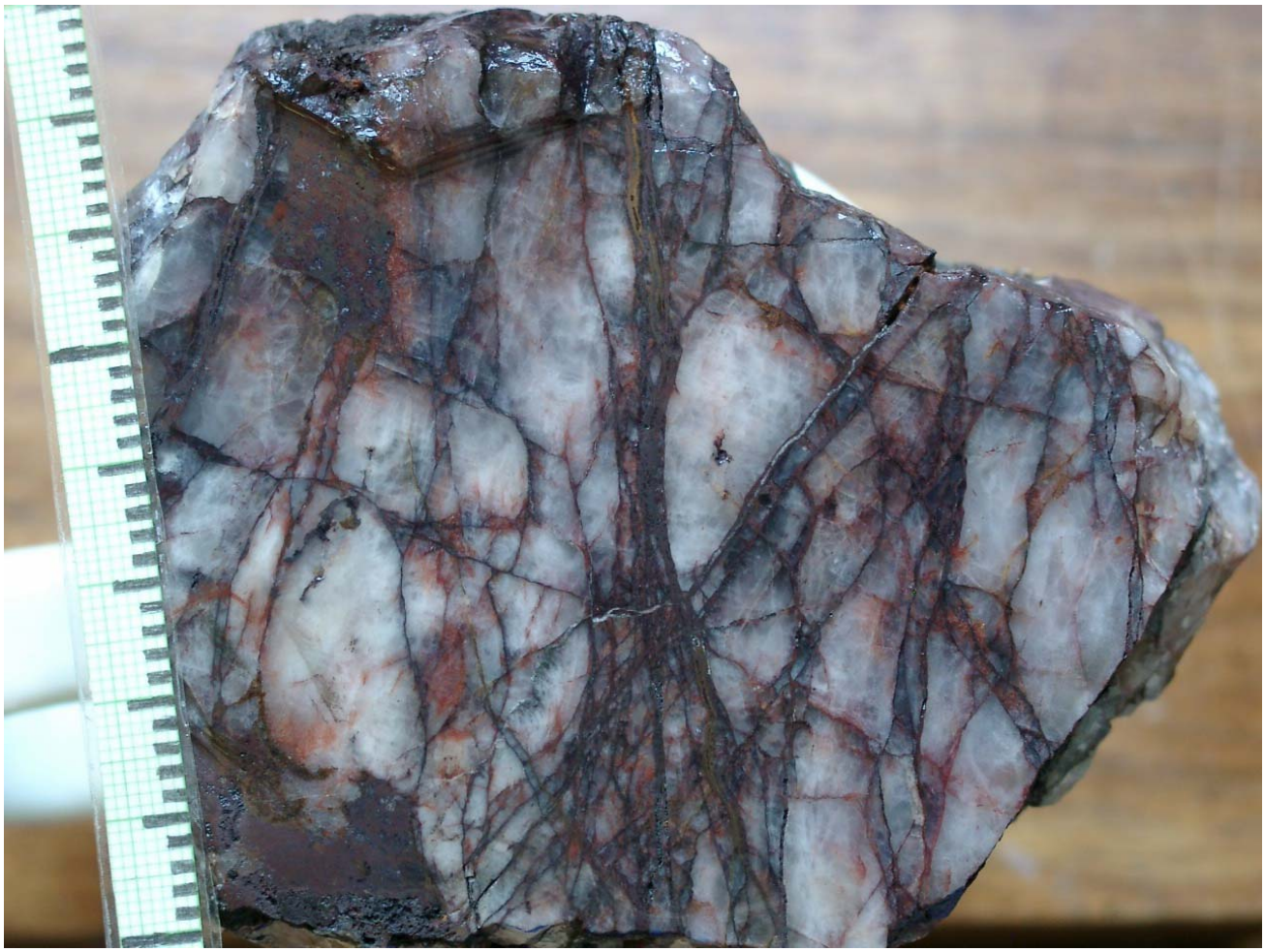

Fig 8.34 Mineralized quartz pod with magnetite and chalcopyrite. *Sample L-756b from the Mesopotamie farm, Namibia. Sulfides were present in the vugs along veinlets and especially in the lower left portion of hematite,*

The chapter on the Mesopotamie farm (4.2.2.4.2) covered most of the geological background of the area. Aspects of iron oxide-copper-gold mineralization at the farm will be discussed here. The old mine located on the northwestern corner of the Lofdal farm farm exploited oxidized copper sulfides by crushing, leaching and precipitating copper on iron scrap. A large proportion of the gold, bismuth and other metals were probably not recovered. The small operation seems to have run bankrupt after finding hard to process sulfide ore in the pits. Dozens of exploration pits were observed; no large, old pits were found. Very small dumps indicate a small total extracted volume of rock. The type of mineralization at this deposit seems to be of iron oxide-copper-gold type.

8.4.1.4.1 Copper Valley mineralization on the NW portion of Mesopotamie 504.

According to the bibliographical compilation carried out by Schneider & Seeger, 1992, the Copper Valley deposit, located on the northwestern corner of the farm Mesopotamie 504, is made by discontinuous quartz lenses with sporadic concentrations of galena, chalcocite and native gold. Such veins appear to be confined to subsidiary faults and shear zones. Host rocks to the mineralization are locally altered to chlorite-sericite schist, talc, brown carbonate and epidote (Songe, 1958 in Schneider & Seeger, 1992, p. 2.3-9).

Six trenches were opened up in a group of Cu-bearing quartz veins prior to 1924. “During the period 1950 to 1952 more than 1000 tons of handcobbed ore grading 20 to 30% copper were produced by open cast mining.” The discontinuous quartz veins, “up to 60 m in length and 1 to 1.5 m in width, carry sporadic concentrations of chalcocite, chalcopyrite and sparse pyrite. They strike mainly parallel to the N-NW trending foliation of the gneiss and schist or transect the structural grain at right angles. Although the ore near surface has been worked out, open-cast mining may be resumed with a very low stripping ratio as the dip of the major quartz body is slightly steeper than that of the slope on which it crops out.” (Schneider & Seeger, 1992, p. 2.3-9).

Many mineralized specimens were collected at the Copper Valley mine site (**L-760** to **L-770**). Some of these include crushed material from an old silo, finely crushed and leached tailings, and grab samples from the

dumps. Gossanous vugs after sulfides with copper carbonates, quartz and hematite are ubiquitous. Abundant fragments of quartz veins with hematite networks and remnants of sulfides were observed. In many cases, hematite blobs are the site for nucleation for chalcopyrite and bornite (Fig 8.35). For example, **L-771** is a fragment from a quartz vein that encloses an angular particle of the schistose host rock; it contains vuggy veins and gossanous boxworks after sulfides.

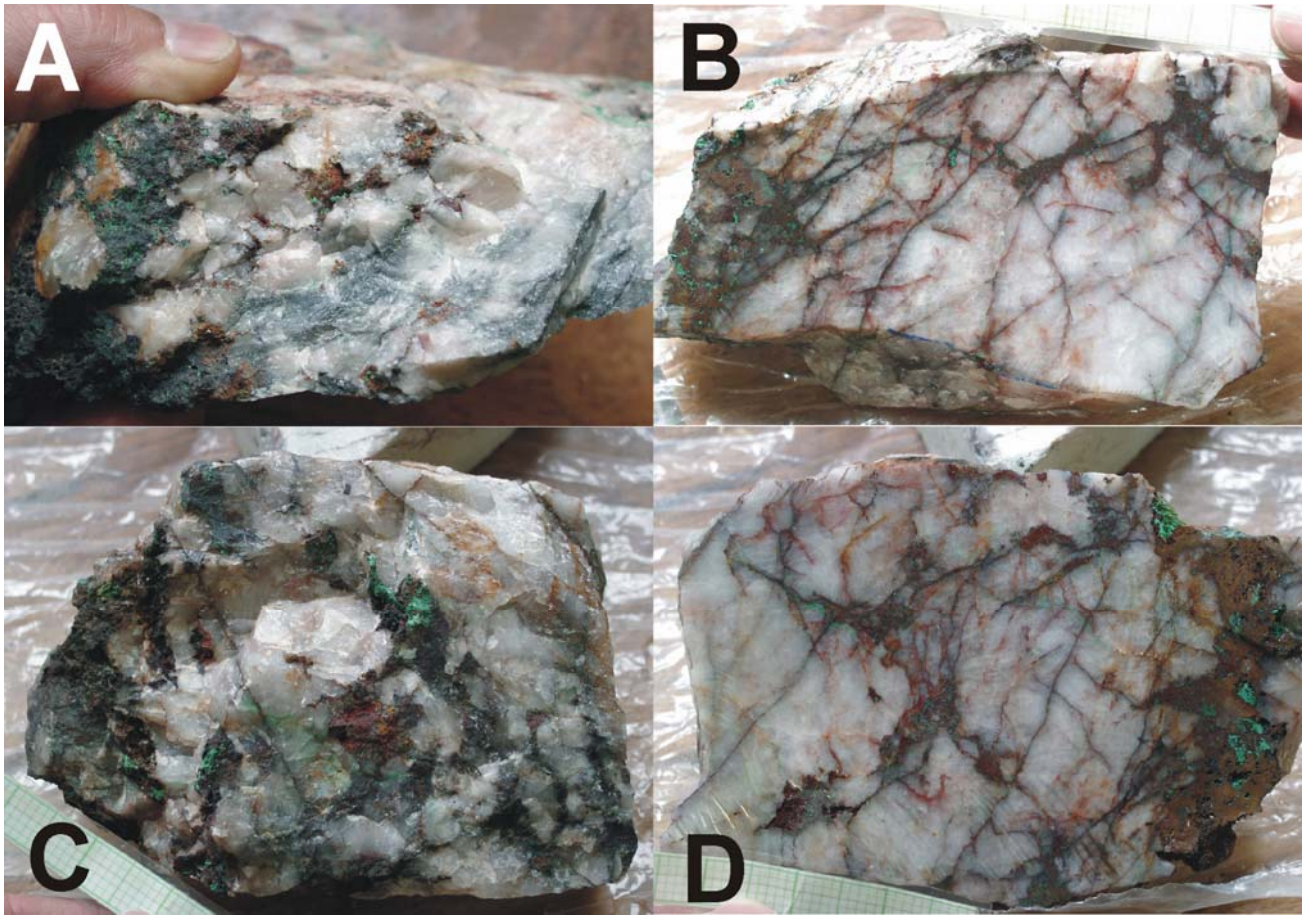

Fig 8.35 Mineralized samples from the Copper Vallei mine, Mesopotamie farm, Khorixas Inlier, Namibia. *Quartz pods with magnetite, chalcopyrite and pyrite. A and C are photographs of exposed surfaces, while B and D are slabs. Note the abundant sulfidation, that normally comes together with magnetite. The dense veining is typical of samples found at the old pits and mine site. A, sample L-766a; B, L-765j; C, L-765c; D, L-765g. Scales in millimeters.*

Some specimens collected from the refuse pile are good examples of the entire mineralized system (**L-774** to **L-778**). These include vuggy quartz veins with dusty chalcocite and Cu carbonates; quartz veins with fine hematite veinlets, iron oxide dust, gossanous vugs and Cu carbonates; and quartz veins with dense hematite stockworks that grade into hydrothermal breccias with vugs after sulfides and intense Cu carbonate stains. Figs 8.34 and 8.35 show aspects of the mineralization.

8.4.1.4.2 Kruger's Deposit on the NW portion of Mesopotamie 504.

"Kruger's deposit lies in augen-gneiss of the Huab Complex on a steep mountain slope close to the Copper Valley prospect near the northwestern boundary of the farm Mesopotamie 504. The copper occurs in a quartz vein that strikes NNE and dips 50 to 55° E. The length of the vein is 45 m and its maximum thickness 2 m near the center of the deposit. A narrow sheet of phyllitic schist adjoins the vein, while the hanging wall is silicified. Mineralization is locally rich where the vein thickens. The copper minerals are mainly malachite, shattuckite, chrysocolla and occasional dioptase, accompanied by hematite, specularite and limonite. Bornite has been noted at only one place." (Schneider & Seeger, 1992, p. 2.3-9).

"An ore sample from one of the copper occurrences on the farm Mesopotamie 504 (probably from Copper Valley) contains a surprising variety of minerals. These include native copper, cuprite, chalcocite, malachite, azurite, chrysocolla, plancheite, a very rare black mineral with a spinel-type structure, a yellowish-green

mineral close to calciovolborthite, native bismuth, bismite, bismutite, beyerite, clinobisvanite, the newly named mineral namibite, galena, scheelite, cuprotungstite, iodagyrite and embolite. The deposit has been opened by trenches over a strike length of 25 m.” (Schneider & Seeger, 1992, p. 2.3-9).

8.4.1.4.3 Mineralization on the NE portion of Mesopotamie 504.

“In the granitic gneiss on the NE part of the farm, sporadic Cu-Pb-Bi-Au-Ag mineralization in lenticular quartz pods occurs in fault zones striking east and dipping steeply north. Handcobbed chalcocite concentrates have been reported to carry 68.5 g/t gold, whereas galena concentrates contained 685 g/t gold. Numerous trenches and pits, one open cast and one 12-m-deep shaft were excavated during previous exploration. Some metallurgical testwork has been carried out.” (Schneider & Seeger, 1992, p. 2.3-9).

Additional Cu-rich mineralization associated with gold is known to occur in the nearby Korechas 381 and Navarre 383 farms. These occurrences were not visited, but might also be related to IOCG. Field notes collected at the Mesopotamie farm are included in the Appendix.

8.4.2 ZAMBIAN DEPOSITS AND PROSPECTS

Zambian deposits like Kalengwa, the Dunrobin mine (gold), Sanje (iron ore), Kansanshi mine (copper, gold) Nampundwe mine (pyrite, copper and minor gold), Kantonga (copper, gold and uranium?) and Kasumbalesa (iron, gold?) on the D.R. Congo border with Zambia and others, also display some characteristics of the IOCG deposits (See Table 8.2). Relation to intrusive rocks at these deposits is not evident. The first three are fracture-controlled and display evidence of strong hydrothermal activity. Intrusive rocks that heated the systems are thought to be nearby and under cover.

7.4.2.1 EVIDENCE OF IOCG MINERALIZATION UNDER THE ZAMBIAN COPPERBELT

Evidence of IOCG mineralization under, or very near sedimentary-hosted copper mineralization has been found in several sites of the Zambian Copperbelt. The chapters on the Nchanga Granite (4.1.5.2), Mufulira (4.1.5.7) and Chambishi (4.1.5.6) already discussed part of these issues. Below are some additional comments on the topic.

Mendelsohn, 1961 and Garlick, 1973 present evidence of iron oxide-copper-gold mineralization in several sites of the basement to the Copperbelt. Portions of the Muliashi porphyry and the Nchanga Granite are probable sources for at least part of the copper in the sedimentary-hosted copper deposits of the Copperbelt. Very little publicly-available research has been carried out in this field. Descriptions of the IOCG prospects are short and lack detail. Nevertheless, several of such occurrences contain primary copper sulfides and gold. Gray's quarry, the Maunga, Nsato and Kafue Areas are some of the zones in the basement to the Copperbelt that contain evidence of iron oxide-copper-gold mineralization. These mineralized areas are associated with magnetite and hematite, most of them carry specularite and tourmaline. They occur in stockworks, veins or shear zones. The association quartz-hematite-tourmaline-chalcopyrite is recurrent in surface occurrences.

At the Nsato area, "a linear magnetic anomaly, which may be associated with a granite contact or a basic dike, was outlined by geophysical surveys. The follow-up work and diamond drilling revealed veins and disseminations of chalcopyrite and bornite in biotite schists and impure schistose quartzites. The copper minerals occur as isolated grains in the matrices and as veins along joints and planes of schistosity. Seams and scattered grains of magnetite and hematite are fairly common. Neither the extent nor the source of the mineralization are known" (Mendelsohn, 1961 , p. 34). The magnetic anomaly could be due to tabular body of magnetite that nucleates sulfidation.

Also, "In several localities, copper minerals have been discovered near granite, pegmatite, and basic intrusives. Minor amounts of malachite, chalcopyrite, and bornite are present along joints, quartz veins, and as disseminations in the country rock. In a few localities the host rock contains scattered grains and veinlets of magnetite and specularite, and has been silicified, feldspathized and seritized." (Mendelsohn, 1961, p. 33).

The Miku and Chondwe areas contain both copper and gold mineralization that is not well documented in the report by Pienaar in (Mendelsohn, 1961).

8.4.2.2 DUNROBIN GOLD MINE, ZAMBIA

Very little information is publicly available from the Dunrobin mine. It was a medium-scale operation that mined only oxide mineralization from open pits and minor underground works. The origin of the deposit is not well understood. From reconnaissance work carried out, IOCG features that were seen include: very important role of iron oxide bodies to nucleate sulfidation and gold; particular hydrothermal alteration features; very clear structural control for mineralization is evident in the pits; there are some copper showings in the environs, strong hydrothermal alteration and brecciation were observed in and around the main mine; free gold was observed in some of the gossans. Mineralization is hosted by carbonates thought to be correlative with Katangan units like the Lusaka Formation.

Typical hydrothermal veins of the Dunrobin mine are shown on Fig 8.36. Note the interbranching and braiding of these quartz veins with massive magnetite and hematite. These iron oxide minerals served as nuclei for pyrite and other sulfides where gold is hosted. Similar features were observed at various scales. The host rock around these veins is almost entirely transformed by brown-rock (hematite) alteration. Note the 35 cm steel mallet for scale.

Fig 8.36 Mineralized quartz-magnetite-sulfide veins at the Dunrobin gold mine, Zambia*. Note steel hammer for scale. Most of the host rock is heavily altered by hematitization. More details in text.*

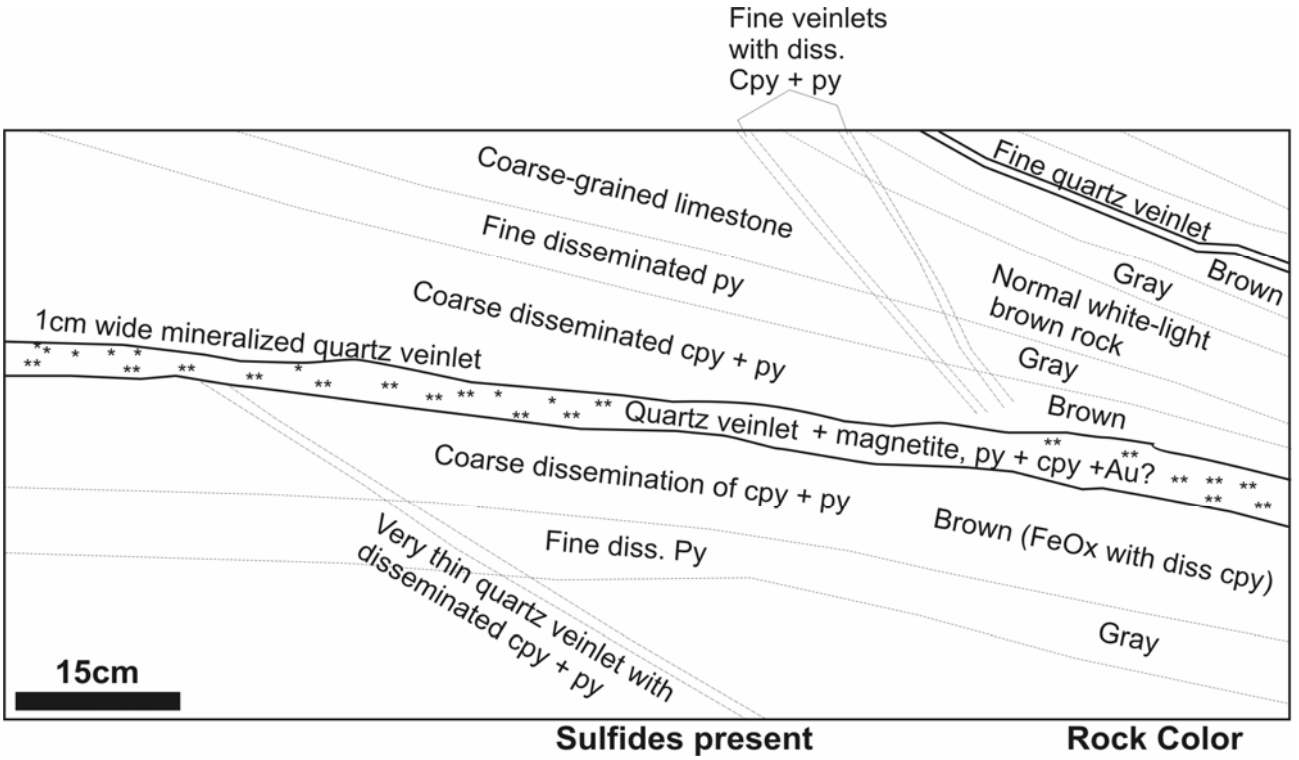

Fig. 8.39 Explanation diagram for Fig 8.37. *Progressive hydrothermal mineralization around quartz-magnetite-sulfide veinlets at the Dunrobin gold mine, Zambia.*

Fig 8.37 Progressive hydrothermal alteration around mineralized quartz-magnetite-sulfide veinlets at the Dunrobin gold mine, Zambia. *Note steel scratcher for scale. Potassic alteration in very thin veinlets, and silicification are overprinted by later gold-bearing quartz-magnetite veinlets. Progressive hematitization of the host rock takes place away from the second generation of veinlets. Most of the host rock is heavily altered by hematitization that gives it a deep brown color. Originally the rock was a felsic granitoid. More details in text.*

Fig 8.38 Concentric iron oxide banding around mineralized veinlets at the Dunrobin gold mine, Zambia*. Host rocks in this case are Katangan carbonates, probably correlatives of the Lusaka Formation. This particular type of alteration and mineralization produces large volumes of brown, gossanous rock. When weathered, coarse free gold can be easily extracted. Parts of the main ore grade material at the mine seem to have been of this type.*

Professor Allan Clark of Queen's University in Kingston Ontario calls the texture here depicted "riglites" (Personal communication, 2004). According to him, the texture is also called "Racoon tail" banding. Riglites are a common feature in some skarn deposits, and have also been described in Mississippi Valley Type Zn-Pb deposits. The same structures have been called "piedra famelicana" in Spanish deposits by Professor Lluis Fontboté from the University of Geneve, Switzerland.

Fig 8.37 illustrates another aspect of gradual host rock hematitization. In this case the rock is granitic; numerous veinlets intersect it conforming a series of phacoids. Note progressive hematite impregnation in the host rock. At times this alteration completely obliterates the original texture and main mineralogy of the host rock. Zones of denser veining are completely brown. The accompanying diagram illustrates various other features of the veinlets and their hydrothermal alteration. A metallic scratcher is used for scale. The sketch of Fig. 8.39 serves to understand the various features of alteration and mineralization on Fig 8.37.

Another interesting aspect of the intense iron oxide alteration that takes place around mineralized veins of the Dunrobin mine is shown on Fig 8.38. Concentric iron oxide alteration that spreads out from contiguous veins replaces the host rock and produces a particular banding in the rock that in a way is similar to Leisegang rings. Extensive volumes of similarly altered rock are found around and within the Dunrobin gold mine. Here too, a progressive disolution of the host rock and replacement first by iron oxides and later by sulfides seems to be the governing rule. Gold comes late, with pyrite and other sulfides that are emplaced on top or within the previously deposited hematite. Note steel ruler with centimeters and inches for scale.

8.4.2.3 NAMPUNDWE PYRITE MINE

The Nampundwe mine, previously called “King Edward Mine” is a pyrite mine currently exploited as a source of sulfur for smelting processes by the private corporation KCM at Nchanga. As observed on Fig 8.40 it is emplaced in Katangan carbonates and siliciclastics of the Lusaka Formation, just west of Lusaka. Very few references discuss the geology of this deposit in detail (Burnard, Vaughan, & Sweeney, 1990a; Burnard, Vaughan, & Sweeney, 1990b; Burnard, Sweeney, Vaughan, Spiro, & Thirlwall, 1993; Phillips, 1958a; Reeve, 1963; Simpson, 1962; Stohl, 1977; and Tembo & Porada, 2002). The deposit has been mis-identified as a sedimentary exhalative mineralization (Burnard et al., 1990a; Burnard et al., 1990b; and Burnard et al., 1993). Its association with large iron oxide bodies of hydrothermal origin is certain (Figs 8.12 and 8.40); part of the deposit is spatially related to the large magnetite hill shown on Fig 8.12; small bodies of gabbro and felsic intrusives occur in its environs; it is basically a pyrite deposit, but contains minor chalcopyrite and gold; many copper and gold occurrences are known around the deposit. A working hypothesis is that the Nampundwe mine is a pyrite-rich end-member of the IOCG clan of deposits. Similar types of mineralization are known in the Marcona area and Raúl-Condestable mine of Peru; both are currently being mined and explored for their iron oxide-copper-gold potential.

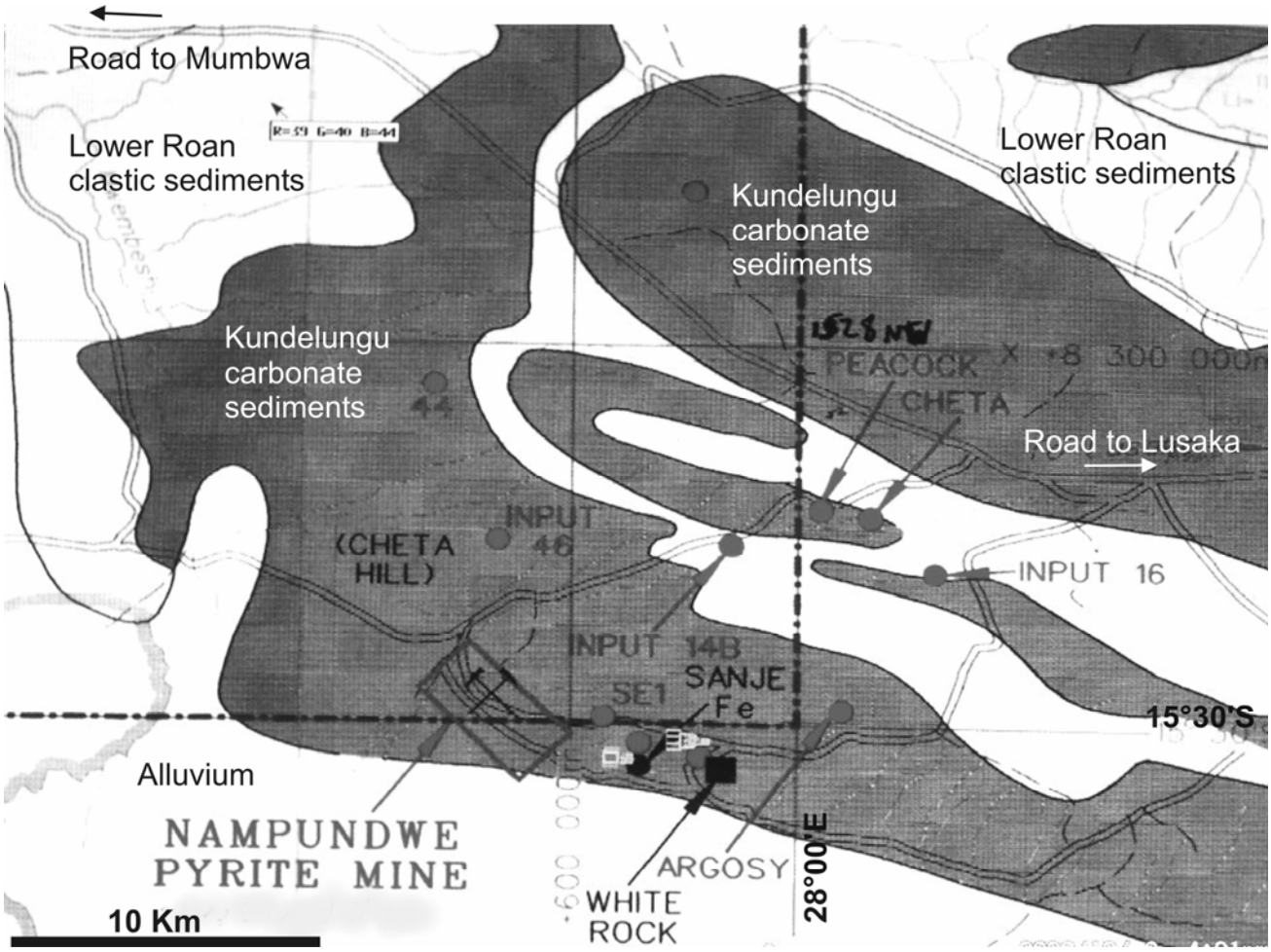

Fig 8.40 Geological map around the Lusaka West area, Zambia. *Note dark dots that indicate iron oxide mineralization and lighter ones that indicate copper and gold mineralization. The Nampundwe pyrite mine is located near the lower third left portion of the map. Most of the rocks shown are carbonates. Note Peacock and Cheta copper prospects, as well as Sanje iron deposit operated by Zambian collieries. Double lines are main roads. Small squares are sampling sites for intrusive rocks, that are not mapped. The photograph of Fig 8.12 was taken in one of the iron oxide hills. More details in text. Compilation geological map from Billiton. Special geophysical tests were carried out at the Input sites.*

8.4.2.4 KASEMPA REGION PROSPECTS, ZAMBIA

The Kasempa region of Zambia has IOCG mineralization associated to small bodies of alkaline gabbros and syenites that intrude Katangan limestones. The chapter on that portion of Zambia describes its main geology. Hydrothermal brecciation and various forms of iron oxide alteration are widespread. Massive bodies of iron

oxide have been identified and sampled. Large magnetic and gravimetric anomalies as well as soil geochemistry Cu, Co, Ag, As and Au anomalies have been identified.

Numerous companies have carried out significant exploration in this part of Zambia, including Roan Selection Trust, Phelps Dodge, Iscor, Billiton and Anglo Vaal. Part of the aeromagnetic anomalies were drilled. The most promising anomaly is the Chitampa prospect, where borehole MB-34 was drilled in the 1970's. Various aspects of brecciation, hydrothermal alteration and mineralization at the borehole will be described in this chapter. The Kasempa area is not definitively explored, and many of the anomalies identified have not been followed up. See the chapter on the Kalengwa-Kasempa area for descriptions on samples from part of the boreholes drilled by Billiton at Kasempa.

The Lufupa prospect of the Kasempa area in Zambia also displays sedimentary-hosted copper mineralization. It is located near IOCG prospects and iron oxide-cemented brecciation and veining. It was drilled by Roan Selection Trust.

8.4.2.5 IOCG PROSPECTS AND MINES AROUND THE HOOK GRANITE BATHOLITH, ZAMBIA

The northwestern portion of the Hook Granite Batholith contains abundant mineralization of various types. As shown on Fig 8.41, zinc, silver, copper, gold and iron deposits occur in a wide area. Mines like the Hippo mine (Cikin, 1968), Blue Jacket, Lou-Lou and others were well known in the early twentieth century. All of them are akin to the iron oxide-copper-gold type. Some are enriched in silver or lead or zinc or copper, but they are all associated to iron oxide bodies and round-pebble hydrothermal brecciation. The region has been called the Mumbwa district by some authors, and the "Great Concession" by others. Two samples of iron oxide bodies were analysed from this area and they are enriched in Zn, Cu, Ce and other minerals (See complete description on section 4.1.2 about the West Lusaka-Kafue Flats area).

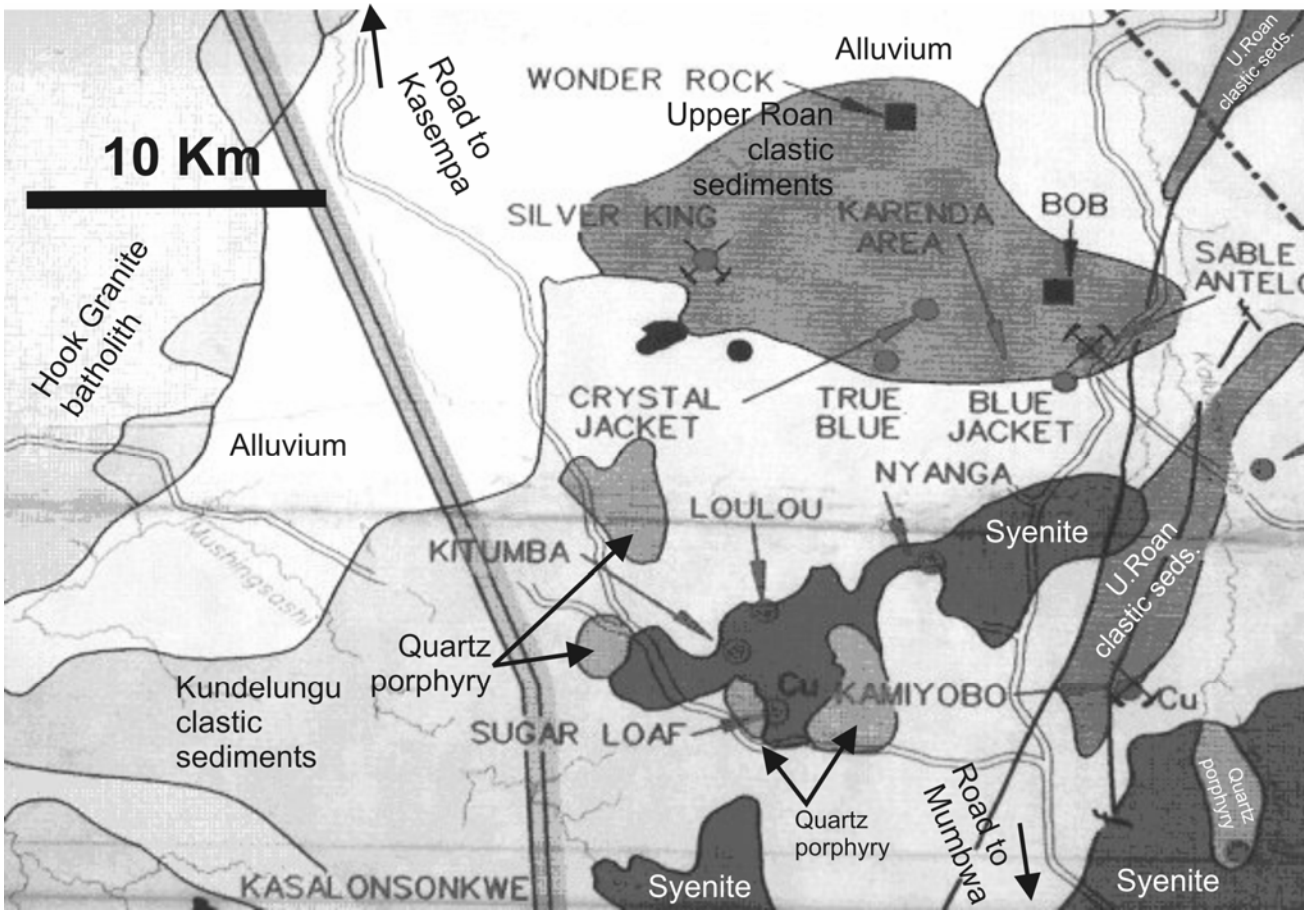

***Fig 8.41 Geological Map NW of Mumbwa, Hook Granite Batholith, Zambia**. Black squares and shapes are massive iron oxide bodies. Gray dots are copper occurrences and mines. Part of them contain silver and gold. Dark gray rocks are syenitic intrusions and light gray ones are granitic intrusions. These granitoid bodies seem to be apophyses of the Hook Granite Batholith (in very light gray, upper left corner), or small ring complexes. The town of Mumbwa lies just in the lower right corner. The thin double line is the main road. The N-S thick light gray line is the eastern limit of the Kafue National Park. More details in text. Compilation map from Billiton.*

Many small IOCG prospects have been explored around the Hook Granite in Zambia during the past ten years. None have been proven large or rich enough to warrant large-scale mining. There are numerous massive iron oxide and copper occurrences in and around the Hook Granite Batholith. Katangan siliciclastics and carbonates that are intruded by various bodies of the batholith account for iron oxide, gold and copper mineralization. Sites like the Luiri Hills, Shimyoka, Kamiyobo, Kitumba, Kantonga, and Lou Lou prospects are just a few of the mines and prospects around Mumbwa and west of Lusaka that contain IOCG mineralization and determine a large prospective province (Fig 8.41). Small copper, silver, zinc and lead mines operated in the area during the century. There is abundant evidence of replacement mineralization in breccias accompany the intrusion of syenites and alkali granites. The following are references that described various types of mineralization in the area: Brandt, 1955; Brandt, 1956; Nisbet, Cooke, Richards, & Williams, 2000; Nisbet, 2004a; Nisbet, 2004b; O'Brien, 1958; Phillips, 1957; Phillips, 1958a; Phillips, 1958b; Phillips, 1959; Sikazwe, 1999; and Simpson, 1962. See also the map of IOCG mineralization in the Greater Lufilian Arc (Fig 8.7) For example, the Shimyoka district contains several cubic kilometers of 0.2% Cu, as defined by Billiton in the late 1990's.

During the 1990's Billiton "undertook a large program of exploration at Kitumba-Kantonga, following up initially on INPUT and Aeromagnetic surveys flown by the United Nations, whose drill results included 100m averaging 0.98% Cu at the Sugarloaf prospect." Significant reconnaissance work was carried out, including rock chip and soil geochemistry, airborne and ground-based geophysics followed by drilling. "They outlined extensive areas of anomalous geochemistry and IOCG style alteration and brecciation of Kundelungu metasediments and Hook Granite syenites, the most interesting areas being the Kitumba and Kantonga Prospects." (Nisbet, 2004b).

"At Kitumba, an 8x3 km sized, Cu-Au anomalous sericite-hematite alteration system was outlined, associated with significant aeromagnetic, IP, and CSAMT anomalism. Hematite-quartz-sericite-apatite-barite-siderite alteration assemblages are described, suggesting the system is a "shallow level' system comparable in size and alteration assemblages to Olympic Dam. Drilling intersected wide, low grade Cu-Au mineralization, a typical intercept being of the order of 125m @ 0.2% Cu." (Nisbet, 2004b). Fig 8.42 shows a simplified geological map of Kitumba, its widespread breccia bodies and hydrothermal alteration. Note comparison of various features with the Olympic Dam and Ernest Henry deposits, at the same scale.

Very large, ridge-producing ring dikes, with an approximate diameter of 40 km, make up the northern portion of the Hook Granite, just north of Kitumba. This is evident on the airborne geophysical image presented by Nisbet, 2004a (Fig 4.5). These are portions of large anorogenic ring complexes.

"At Kantonga, intense aeromagnetic anomalies are associated with several large Cu soil anomalies. Drilling intersected brecciated Kundelungu metasediments and Hook syenites, with extensive albite-garnet-epidote-actinolite-magnetite-Kspar-calcite-apatite alteration. Sulfides were dominantly pyrite, with minor chalcopyrite. The alteration assemblages suggest the Kantonga system was formed at deeper levels to Kitumba, probably more akin to Ernest Henry" (Nisbet, 2004b). Fig 8.22 shows a cross section through the main mineralization at Kantonga. Note the dimensions of alteration, the widespread iron oxide alteration and the tabular bodies of magnetite. Explosive hydrothermal brecciation and round-pebble hydrothermal breccias are a common feature at Kantonga.

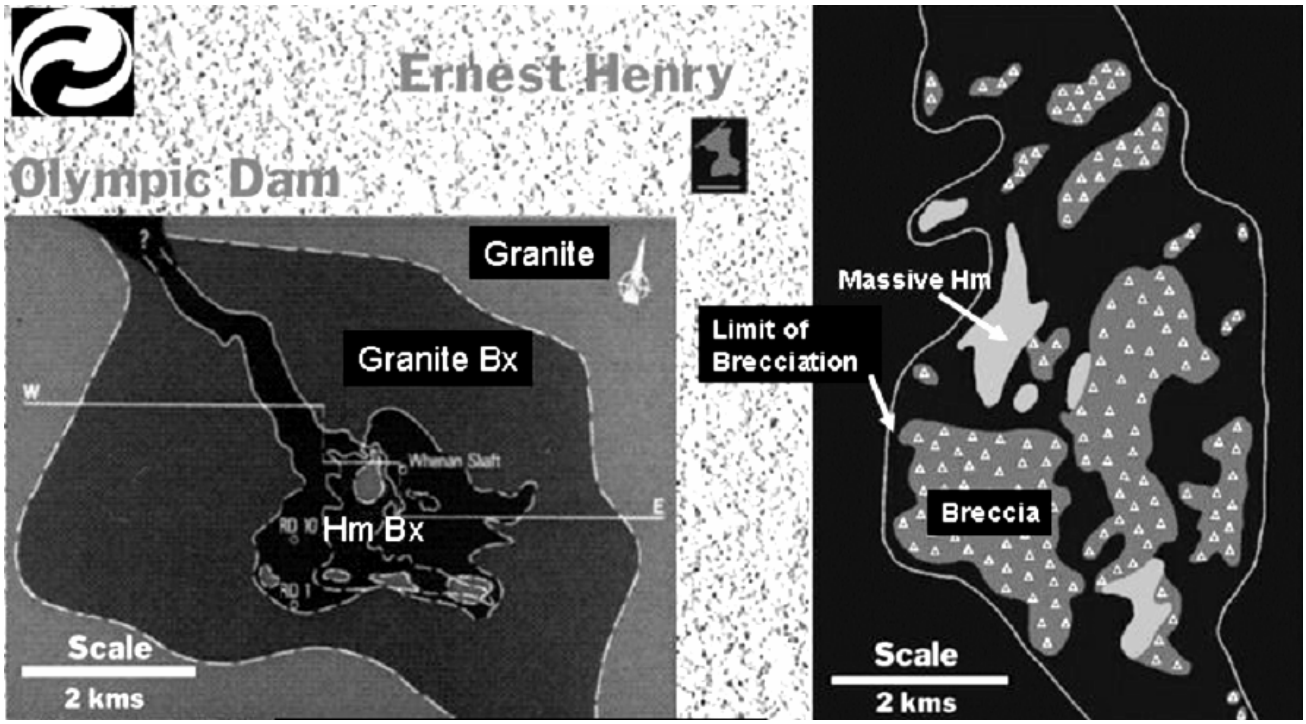

Fig 8.42 Generalized geology of the Kitumba prospect, Kafue Flats, Zambia. *Hydrothermal breccias and massive iron oxide bodies with abundant sulfide mineralization is what makes this large hydrothermal IOCG system. Note that the size of the mineralized brecciation and alteration is approximately the same as that of the Olympic Dam deposit in Australia. Ernest Henry has also been included at the same scale for reference. Figure from Nisbet, 2004b.*

8.4.2.6 KALENGWA COPPER MINE, ZAMBIA

The Kalengwa mine is thought to be one of the major exponents of iron oxide-copper-gold deposits in Zambia. It was one of the most profitable copper deposits in the country, and paid for its own infrastructure in a remote location, separated from the rest of the main Copperbelt (See location on Figs 8.7, M8 and M1). Few reports on the deposit are publicly available today. Initially proven reserves were of 600,000 tons at 16% Cu, according to Ellis & McGregor, 1967. Total production according to Hitzman & Broughton, 2003, was 1.9 million tons of 9.44% Cu, 50 gAg/t. Hydrothermal brecciation, as well as gabbros and monzodiorites seem to have played important roles in the formation of the original deposit. Most of the mined copper minerals came from a massive chalcocite body enriched by supergene concentration; copper oxides and a few sulfides were found near the surface (Fig 8.43). The deposit was completely blind; no part of it outcropped. Discovery of Kalengwa was produced by straightforward geochemical exploration.

The deposit was hosted by Katangan siliciclastic rocks and limestones. It consisted of a tabular body of round-pebble hydrothermal breccias, calcareous conglomerates, sandstones and siltstones replaced by primary copper sulfides (chalcopyrite, bornite and chalcocite) surrounded by a large halo of red-rock and brown-rock (hematite) alteration (Fig 8.43). An association of syenites and granites seems to have produced the mineralization. Ongoing research on samples from the mine includes detailed chemical analysis of various intrusive rocks in its environs. See the chapter on the Kalengwa-Kasempa area for descriptions of part of that research.

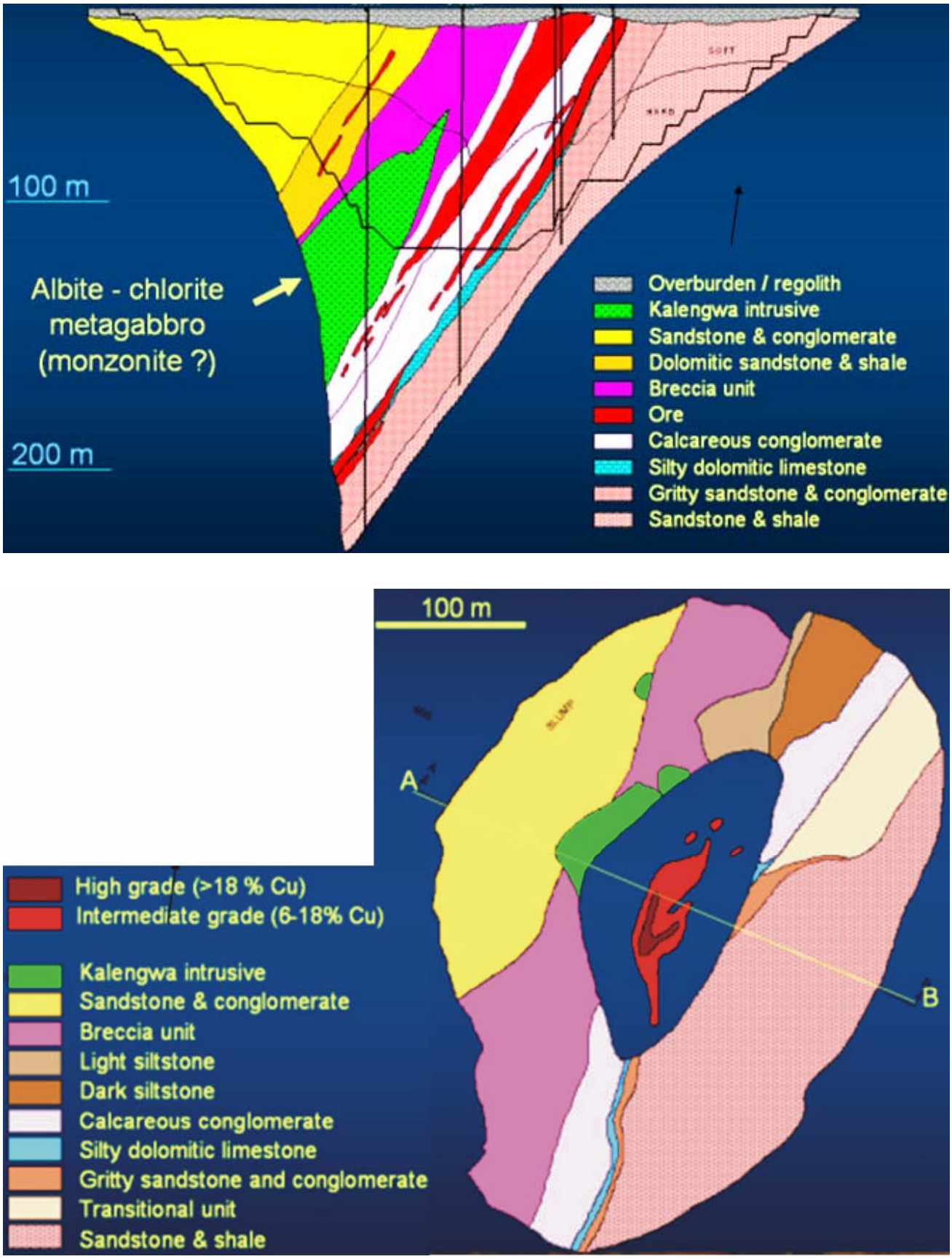

Fig 8.43 Cross section and map of the Kalengwa mine open pit, Zambia. *Note the body of mafic intrusives that is considered to have produced the mineralization. Total production from the mine was 1.9 million tons @ 9.4% Cu with 50g/t Ag. Taken from Nisbet, 2004b; Nisbet, 2004b and Woodhead, J. Personal communication, 2004.*

8.4.3 OTHER LUFILIAN ARC IOCG PROSPECTS AND DEPOSITS

8.4.3.1 QUARTZITE-HOSTED DEPOSITS, GELBINGEN FARM NAMIBIA

Some prospects associated with the large intrusive bodies in the Lufilian Arc, have gold- and copper-rich surface samples. These occur around larger magmatic bodies. Small apophysis of subvolcanic porphyritic intrusive bodies are responsible for gold, iron and sulfide mineralization. In some cases, very small intrusive bodies are the only evidence of magmatism (Fig 8.44). Abundant magnetite- and hematite-filled fractures carry gossans after copper and iron sulfides. All of this is hosted in brittle quartzites. These features were observed at the Gelbingen farm in Namibia.

Figs 8.45 to 8.48 illustrate some of the breccioid mineralization. Part of the region was previously explored for its zinc content; that may be associated to the IOCG environment. Large bodies of quartz - so-called “quartz pods” - are present in extensive areas. No evidence of zinc mineralization was seen during the reconnaissance visit.

Sedimentary-exhalative Zn-Pb deposits have been sought throughout parts of northern Namibia, especially around the Gelbinggen farm, but companies that focused on those exploration targets for decades, overlooked copper-gold hydrothermal mineralization and its high potential. Very small subvolcanic porphyritic intrusive bodies outcrop in few places and seem to be introducing mineralization and alteration. Unmapped, regional E-W structures control both intrusions and mineralization.

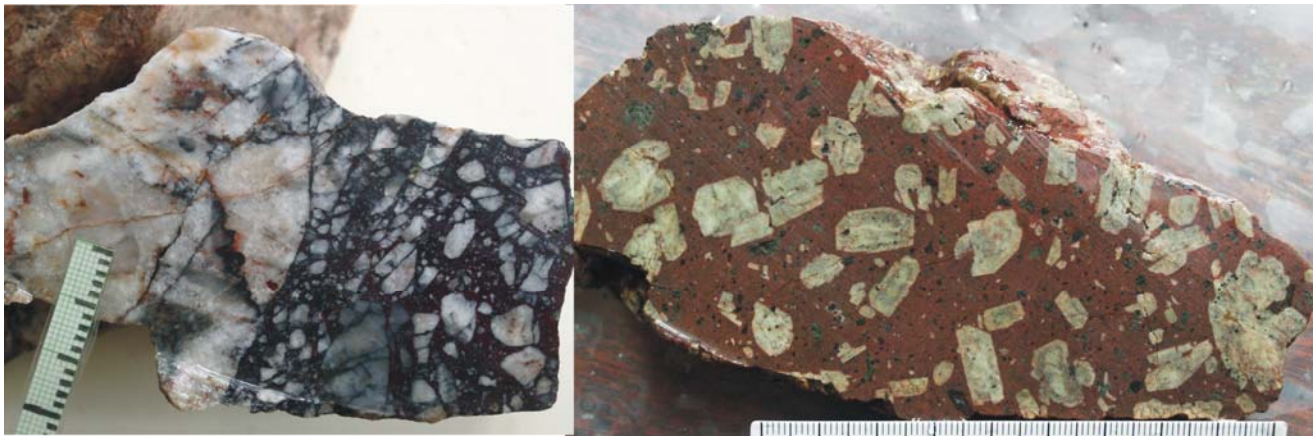

Fig 8.44 Angular hydrothermal breccias and the subvolcanic, porphyritic, rhyolitic intrusive that is responsible for their formation. *Both photographs are at approximately the same scale. Ruler in millimeters. Collected at the Gelbingen farm, Namibia.*

Stockworks of magnetite veins with sulfidation were observed in the environs. The photograph of Fig 8.49 is typical of the alteration and mineralization seen.

Quartzite-hosted IOCG mineralization was also observed on the western border of the Kamanjab Batholith, in association with N-S-trending major fault systems. All characteristics are similar to those just described from the Gelbingen farm on the north-eastern border of the batholith (Fig 8.6).

Fig 8.45 Another aspect of hydrothermal breccias cemented by massive magnetite from the Gelbingen farm, Namibia*. 14 cm marker for scale. Note slight deformation in breccia clasts. Black is magnetite. Part of the vugs were originally filled by sulfides. This particular breccia is associated to large bodies of carbonatitic dikes and diatremes. More details in text.*

Fig 8.46 Sulfide-bearing hydrothermal breccia-vein cemented by magnetite that intrudes quartzites. *. Located in the Gelbingen Farm, to the northeast of the Kamanjab Batholith, Namibia. The brittle behavior of quartzite produced extraordinary rock fracturing and IOCG mineralization in various locations of the Lufilian Arc. This is an example of these breccia bodies. They are associated with small porphyritic subvolcanic intrusives of intermediate composition. (Note smaller breccia veins that extend to the central and lower part of the the photo. They are more enriched in sulfides than the thicker vein above.) See text for more details.*

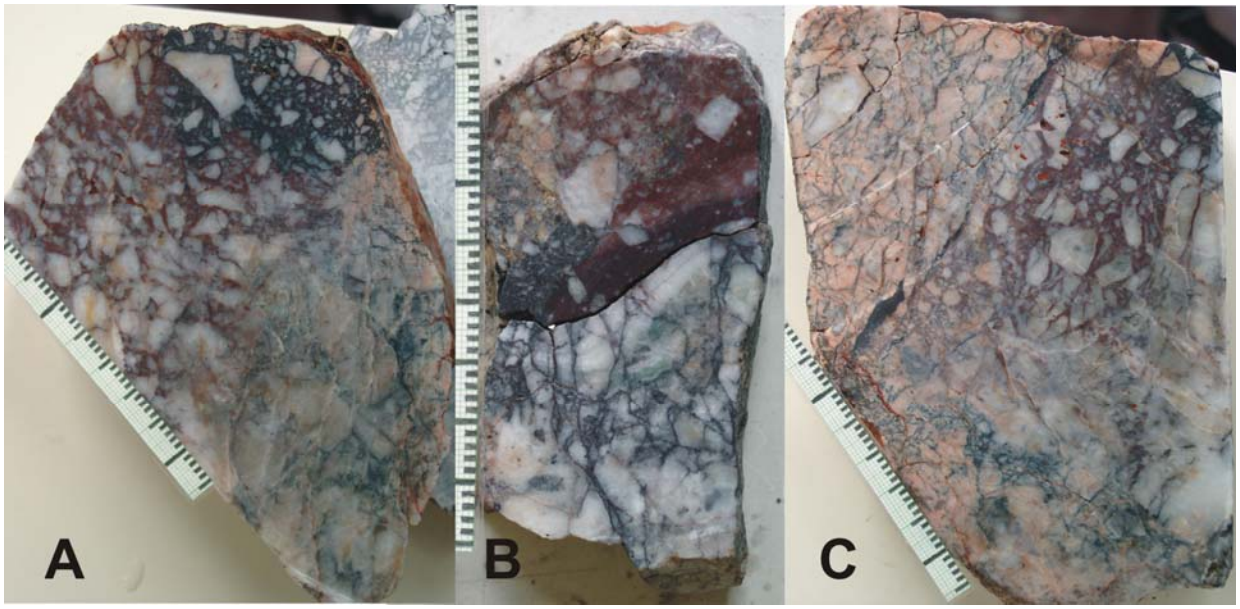

Fig 8.47 Three close-up aspects of the mineralized breccias from the Gelbingen farm, Namibia. *Sample B had strong calcanthite staining on its surface. All scales in millimeters. In this case all clasts are made of quartzite. The matrix is magnetite and sulfide-rich silica. Some outcrops of this breccioid material may reach twenty meters in length. No assays have been carried out at the moment of editing this document.*

Fig 8.48 Another aspect of sulfide-bearing hydrothermal breccia cemented by magnetite that intrudes quartzites. *These were observed in the Gelbingen farm, Namibia. Note type of clasts and clear cut contacts with the white quartzite. Angular fragments are exclusively made of white quartize, and to a lesser extent by milky white quartz. Multigram gold-bearing samples were collected near this site. Again, brittle behavior of the quartzite enhanced the formation of physical traps for IOCG mineralization. The matrix of this breccia contains many small angular fragments in a fractal distribution. Hammer for scale. More details in text.*

Fig 8.49 Network of sulfide-bearing magnetite veins that form a stockwork in Pan African felsic granitoids*. Fifteen-centimeter marker for scale. These stockworks grade into magnetite-cemented dikes, magnetite-rich carbonatite dikes on one direction and into hydrothermal breccias on the other. Granitic rocks have been whitened by albitization; that probably increased their brittleness. Very little iron oxide alteration stems away from this web of veinlets, as seen here. Large volumes of rock display similar features in specific portions of the Gelbingen farm.*

8.4.3.2 DEPOSITS ASSOCIATED TO ALKALINE ROCKS AND CARBONATITES

Highly alkaline rocks including syenites, lamprophyre dikes and carbonatites seem to have been emplaced in rift environments during late Pan African times throughout the Lufilian Arc. Most of these rocks contain anomalous zinc, copper and rare earths. Gold is known to occur in some systems, but is thought to be present in many others. IOCG mineralization is present at the Lofdal and Oas farms in the Khorixas Inlier. Below are examples from some of the prospects associated to such rocks.

NeoProterozoic syenitic and carbonatitic magmas are associated with hydrothermal brecciation, diatremes, massive iron oxide bodies and iron oxide-filled veins in parts of Namibia and Zambia. Figs 8.50 and 8.51 illustrate brecciation and mineralization associated to carbonatites in the Lofdal farm, Khorixas inlier, Namibia. Portions of the iron oxide bodies carry significant vugs and gossans after sulfide mineralization. In some occasions fresh bornite is observed on surface. Fig 8.52 shows a magnetite-pyrite-chalcopyrite vein system from other parts of the Lofdal farm, Khorixas Inlier, Namibia.

Fig 8.53 illustrates typical polymictic hydrothermal breccias cemented by magnetite, that carry abundant vugs and were previously filled by sulfides of various types. This is part of a carbonatitic diatreme from the Lofdal farm, Namibia. Several features of IOCG mineralization were observed in these breccioid bodies. Ongoing work using techniques presented by Ronald Blanchard to study gossans and boxwork wil provide more details on precursor sulfides. Bornite, chalcopyrite and pyrite boxworks have been identified. Note the roundness of clasts due to corrosion, and haloes of alteration that rim the clasts. Most clasts are touching each other; this indicates dense packing and lack of matrix that seems to be characteristic of round-pebble hydrothermal breccias. For scale, the card has marks in centimeters and inches.

Fig 8.50 Aspects of hydrothermal breccias associated to a diatreme body 450 m by 150 m in outcrop, Lofdal farm, Khorixas Inlier, Namibia. *The polymictic breccias are cemented by massive magnetite and abundant coarse sulfides. Note corrosion of the fragments. This type of rock generated positive topography. Similar bodies probably can be detected with airborne magnetometry and gravimetry. Steel hammer included for scale. More details in text.*

Fig 8.51 Polymictic hydrothermal breccia cemented by magnetite that is associated to an extremely explosive IOCG system in the Lofdal farm, Namibia. *Note dense packing of fragments, variable clast size, their rounding and alteration haloes of iron oxide. Note the wide variety of clast types that include gneiss, bedded volcanic rocks, sandstone, various granitoids and schists. The abundant open vugs are a significant feature. Most of these carried sulfides and have been leached. This type of rock is like a sponge: an ideal host for mineralization. Slight rounding of clasts is interpreted to have been produced by hyper-alkaline hydrothermal solutions. Various lithologies were attacked to different degrees. Rock foliation or bedding also produced anisotropic reactions to chemical attack. Abrasion between clasts also must have contributed to rounding. More notes in text. For scale, card with centimeters and inches; the arrow is oriented northward.*

Fig 8.53 shows yet another aspect of hydrothermal breccia pipes associated to carbonatite diatremes in the Loftal farm. A slabbed surface of a polymictic hydrothermal breccia cemented by magnetite shows angular clasts and smaller angular clasts that make up the matrix. Note concentric potassic alteration in the rims of each of the clasts. Clasts of igneous rocks and stratified volcanic and sedimentary rocks can be seen here.

Figs 8.54 and 8.55 are other images of vuggy, polymictic, round-pebble hydrothermal breccias cemented by mangnetite in a breccia pipe that occurs in carbonatite environment. Again, note corrosion of clasts thought to have been produced by extremely alkaline fluids. See the concentric alteration rims on every clast. Also note the dense packing, where clast-to-clast contact is the rule.

Angular clasts are more common in portions of the diatremes. Fig 8.56 illustrates a case of slight clast imbrication. Some clasts display corrosion, the matrix is made of smaller clasts, and the cement is magnetite.

Additional IOCG mineralization of the Lufilian Arc include series of granites, nepheline syenites, alkali gabbros and carbonatites that occur together and produce a complex set of minerals, mineralization and geology. These occur in the Oas farm of the Khorixas inlier, Namibia. They are thought to have been produced by overprinting of intrusions over a long period of time; in a rift environment, alkaline rocks intruded previous granites and mafic rocks. Major iron oxide bodies, sulfidation and emplacement of breccia pipes are related to the alkaline plutonism. Repetitive explosive hydrothermal events produced particular hydrothermal brecciation and what seems to be economic IOCG mineralization. Some systems under evaluation contain significant amounts of rare earths, Zr, La, Nb, as well as Cu, Au and Zn.

Fig 8.53 Slab of magnetite-cemented angular polymictic hydrothermal breccia. *From Sample **L-748**, collected in a carbonatite diatreme of the Lofdal farm, Namibia. This is part of the same breccia body where the previous photograph was taken. Note corrosion of clasts and concentric alteration of their rims. Also note heterogeneity of clast composition, varying clast size and angularity. On the surface this rock is very gossanous, because it carries abundant sulfides. For scale, centimeters. The image has been digitally enhanced to increase contrast between rock types. More details in text.*

Fig 8.52 Sulfide-bearing magnetite-hematite veins associated to ultramafic dikes from the Lofdal farm*. At times they produce stockworks, braided vein, and sheeted vein systems. Copper carbonates are found among the gossans that occur wherever this type of IOCG mineralization outcrops. The host rock in this case is a true granite. Sometimes the country rock is heavily altered by iron oxides. Only slight red-rock alteration spreads out from the veins, as illustrated here. For scale, steel hammer in foreground. More details in text.*

Fig 8.54 Another aspect of heterolithic round-pebble hydrothermal breccias cemented by magnetite. *Taken from a carbonatite diatreme of the Lofdal farm, Namibia. Note dense packing and most grains touching their neighbors. This type of material cannot flow on its own in the current state. It has denser packing than a box full of spheres. Alkaline corrosion is interpreted to have produced clast rounding. The initial proportion of matrix in the breccia must have been much greater, and fragments must have been angular. Some vugs carry sulfides. Clasts have multiple compositions. For scale, card with centimeters and inches; oriented northward.*

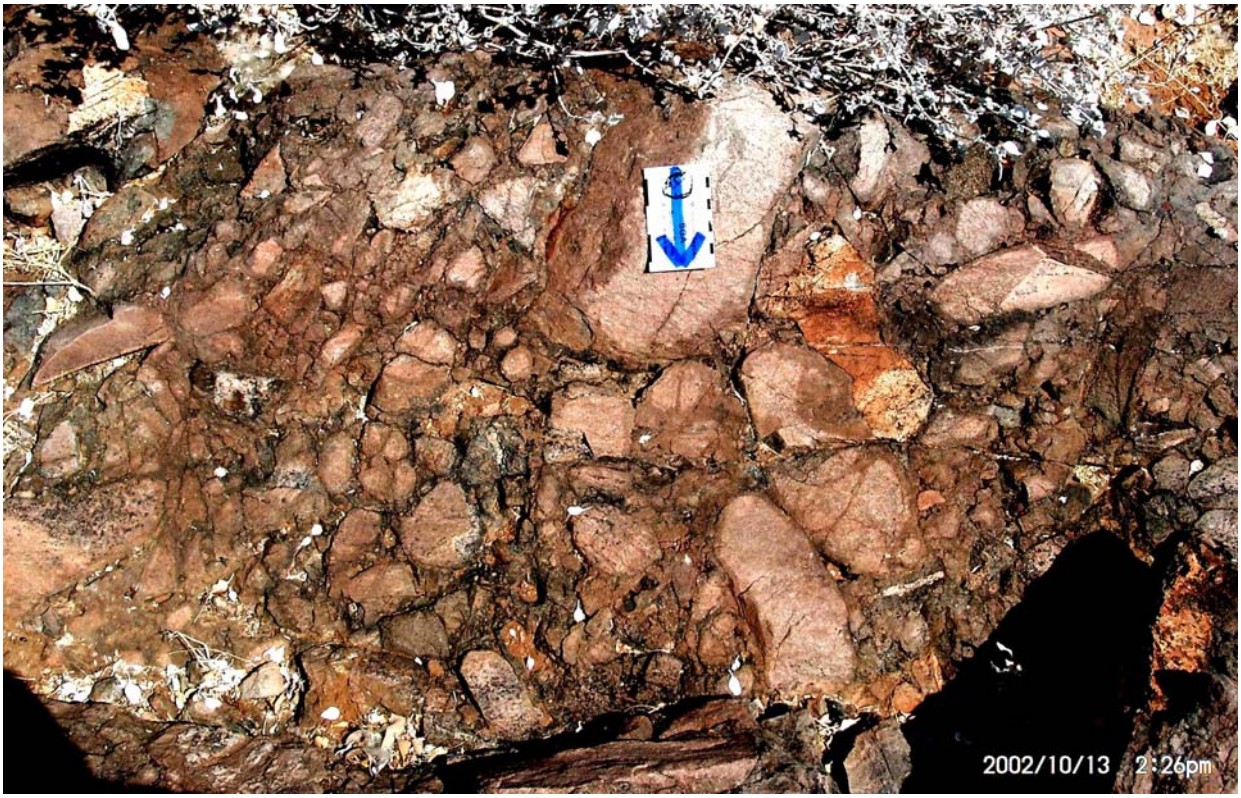

Fig 8.55 Dense packing in heterolithic round-pebble hydrothermal breccias associated to IOCG systems in the Lufilian Arc. *Photo taken from a carbonatite diatreme, Lofdal farm. Note iron oxide impregnation in the rims of the round clasts. Composition is heterogeneous, although not apparent. Note clast size variation. Cement is magnetite. Scale in centimeters and inches; arrow points northward. This type of breccia has been called sedimentary "conglomerate". It is clearly a hydrothermal breccia, associated to a highly explosive hydrothermal system. Its clasts were corroded by abrasion and by chemical attack of magmatic-related (or magmatically-driven) fluids. Abundant vugs were filled by sulfides that are now leached.*

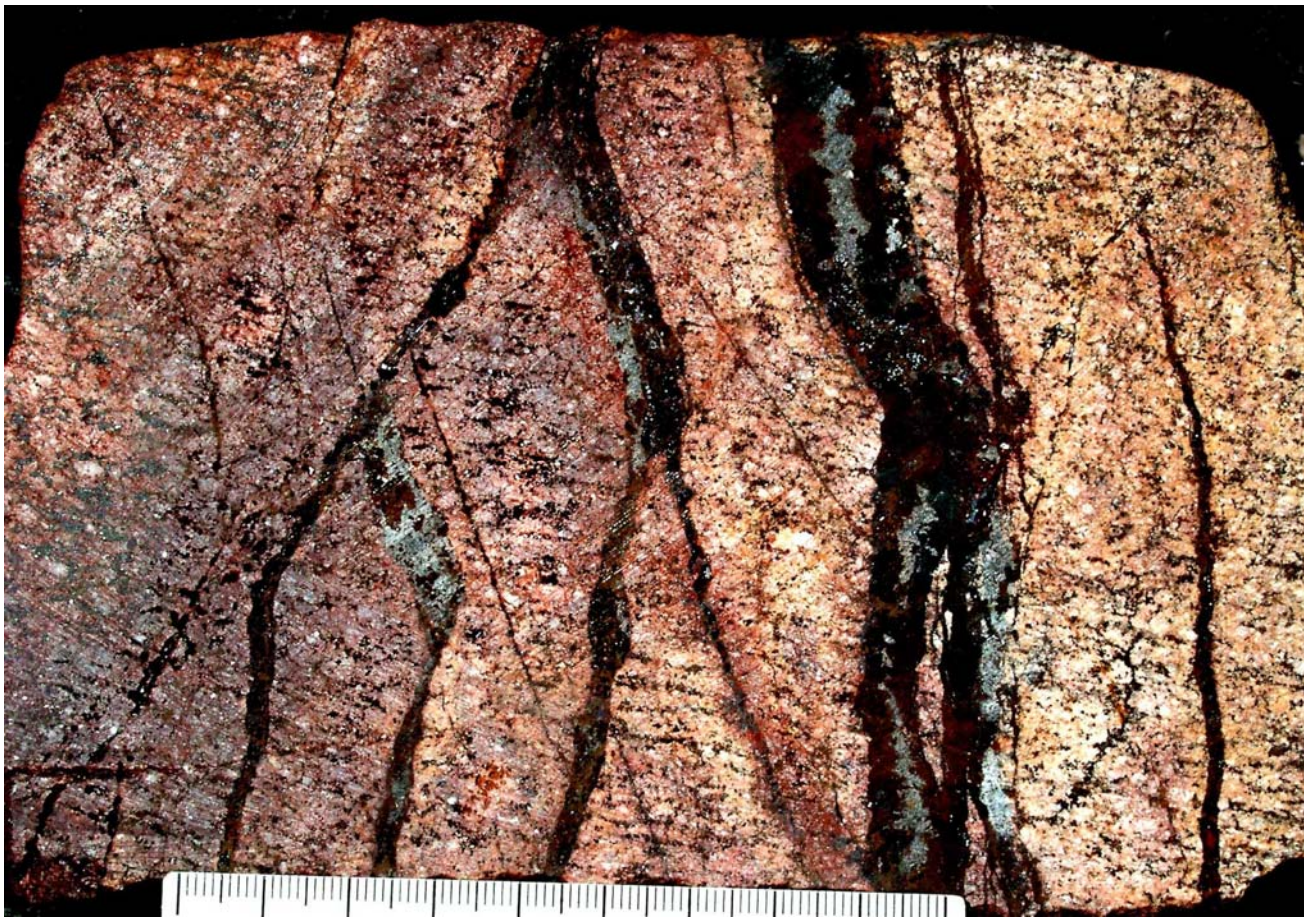

Fig 8.57 IOCG Mineralized Fracture System, that branches from a series of sub-parallel carbonatite dikes in the Lofdal farm, Namibia*. Slab of Sample* ***L-738k****. Note the type of rhomboidal quartz-magnetite veins that intersect an albitized foliated granitoid; the host rock was embrittled by sodic alteration. This type of material forms part of a vein system that is approximately a meter wide and contains abundant vugs after sulfides. The same structures occur at different scales, from hand specimen to 1:5000 and 1:10,000. No samples from the site have been assayed for Au, Cu or other elements. On the bottom, another slab from a nearby rock (****L-738m****) that shows similar features. Left, wet slab; right dry slab. Note magnetite and sulfide dissemination, as well as red hematitization towards the upper part of both slabs.*

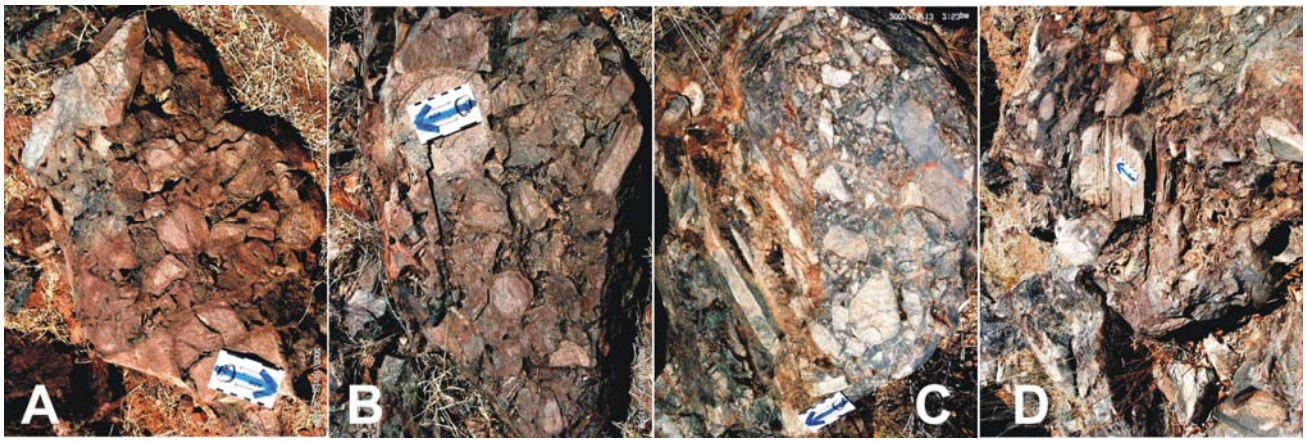

***Fig 8.56 Angular fragments in a polymictic magnetite-cemented hydrothermal breccia from an IOCG mineralized body that is hosted by a carbonatite diatreme from the Lofdal farm, Namibia. A** and **B** show dense round-clast packing and abundant voids in the matrix that were previously filled by coarse sulfides. Note that most large clasts display corrosion and concentric alteration. Note slight imbrication of the fragments on **C**, to produce a shingle breccia towards the upper right. Vugs with pyrite, very gossanous surfaces. Copper sulfides were identified in some of the gossans that fill large vugs between tabular breccia fragments. Angular fragments in the left side of the picture display dense packing and evident transportation. Their strong angularity is evidence of transportation over a short distance. **D** shows a wide variety of clast types, including metasediments with fine bedding. More details in text. In all four photographs, the arrow points north, and the card shows both centimeters and inches.*

Other study areas of the Lofdal and Oas farms contain significant potential for IOCG mineralization. Massive magnetite and hematite was observed in many sites, and abundant gossans after sulfides were sampled and mapped. Carbonatite dikes and intrusive bodies are associated with magnetite and sulfide mineralization. Fig 8.57 was taken from a mineralized fracture system conformed by interweaved quartz-magnetite-sulfide veinlets. Abundant gossans that are relict after sulfides including chalcopyrite were sampled in the environs. The sulfides previously present in gossans and boxwork were positively identified using techniques described by Blanchard, 1968. Free gold is thought to exist in most of the mineralized sites.

8.4.3.3 IOCG MINERALIZATION IN THE DEMOCRATIC REPUBLIC OF CONGO

Although the primary focus of the Greater Lufilian Arc granitoid project was not the Democratic Republic of Congo, several field observations were made, they are relevant to iron oxide-copper-gold mineralization, and will be discussed below.

Tabular iron oxide bodies occur at the Luiswishi, Shituru and Kamoya deposits located in the Katanga province, D.R. Congo. These tabular iron oxide bodies that intersect Katangan sedimentary rocks of the Lower Mwashya have been mis-identified as itabirites. On-going research at those sites indicates a hydrothermal origin for the iron oxide bodies. In all three cases, structurally controlled iron oxide bodies are not concordant with stratification, and branch[3]. These bodies have traditionally been considered to be banded iron formations; the author of this paper believes that they were emplaced under a brittle environment, after the sediments were lithified. This observation is relevant, because it could imply that Luiswishi, Shituru and Kamoya are all iron oxide-copper-gold deposits. Further work on this is currently being carried out. The Likasi mine, in fact the entire discrict including Shituru mine, contains gold in pyrite. The dumps of Shituru contain 2 gAu/ton. According to Doug Jack (Jack, D., personal communication, 2003), tailings of Likasi, that were under evaluation by First Quantum Minerals in July 2003 for their re-treatment, contain 1.59 gAu/ton. The Kamoya deposit contains gold, but average content is less than 0.01 g/Au/ton. In addition to this, the Kakontwe limestones and dolomites at several Congolese sites have been replaced by iron oxide of hydrothermal origin. Historically, gold has not been systematically evaluated or recovered in the copper/cobalt-rich deposits of Katanga.

[3] Massive, tabular hematite bodies that bifurcate or branch were observed and documented in at least three different locations in the D.R.Congo. The bodies also cut across stratigraphic markers. These two features do not occur in banded iron formations, which are deposited as sedimentary beds. The best explanation for the occurrence of the iron oxide tabular bodies just described is that they were hydrothermally emplaced along fractures, in the fashion of veins (See section 8.3.4.3). They definitely are not BIF. The lateral extension of tabular iron oxide bodies in The D.R.C. could be explained if they were emplaced along a regional fracture.

The Kisanga iron oxide prospect that was visited in the D.R. Congo on July 23rd, 2003 is emplaced in Kakontwe limestone and seems to be a hydrothermal breccia with megaclasts imperfectly cemented by goethite. The rock has massive red-rock iron oxide alteration. Many polymictic, angular, clast-supported hydrothermal breccias were found to be cemented by iron oxide. Most of the rocks that outcrop in the quarry contain irregular angular vugs after pyrite. There is iron oxide stain (goethite-limonite) along most joints, but not on the fragments themselves. There is no evidence of copper at the quarry, but gold may certainly be present. Ongoing research on samples from the site will be presented soon.

Preliminary observation of the D.R. Congo mineral occurrence map shows that there are many iron oxide mineralizations spread out in a very large area. 70 of these are mapped in the southern Shaba area. Most are massive bodies with no particular orientation. Four out of five tabular FeOx bodies have NE-SW orientation. These are Kasekelesa, located W of Kolwesi, Kabompo, an un-named occurrence in the headwaters of the Lualaba river near the Zambian border, and an occurrence located north of Kiabana.

There is a clear alignment of “tabular” copper and copper-cobalt deposits that runs NW-SE. It extends from the Etoile mine, Rwashi, Luwishi, Kibolo, Kippo, Kishia 5, Shituru, Likasi, Kambove. Several un-named occurrrences are also present. In total, the aligned and subparallel tabular mineralizations mapped are 12. Three massive iron oxide occurrences are also present along the same alignment, the NW-SE feature follows the regional structural trend and extends for 300 kilometers. The NW part of the lineament cuts across regional stratigraphy. It seems to have been controlled by a deep-tapping thrust fault.

The evidence of hydrothermal mineralization associated with the copper and cobalt deposits in the D.R. Congo that was discussed above, clearly points towards an important input of IOCG systems in the mineralization. No granitoids nor mafic intrusives were observed during a two-week field visit mainly dedicated to stratigraphy of the Katangan rocks. Nevertheless, a large volume of volcanic rocks was observed. Most of the sedimentary Katangan sequence in the region is allochtonous; it was transported northward hundreds of kilometers by thrusts. It is improbable that complete IOCG systems (including intrusive rocks) will be found in the Congo, due to the tectonic disruption. Only distal facies hosted in the upper volcanic and sedimentary sequences will be present. The roots of the systems were left behind to the south. Remobilization of the metals from primary IOCG mineralization and other sources, probably took place during the Lufilian orogeny to produce the copper and copper-cobalt deposits known today.

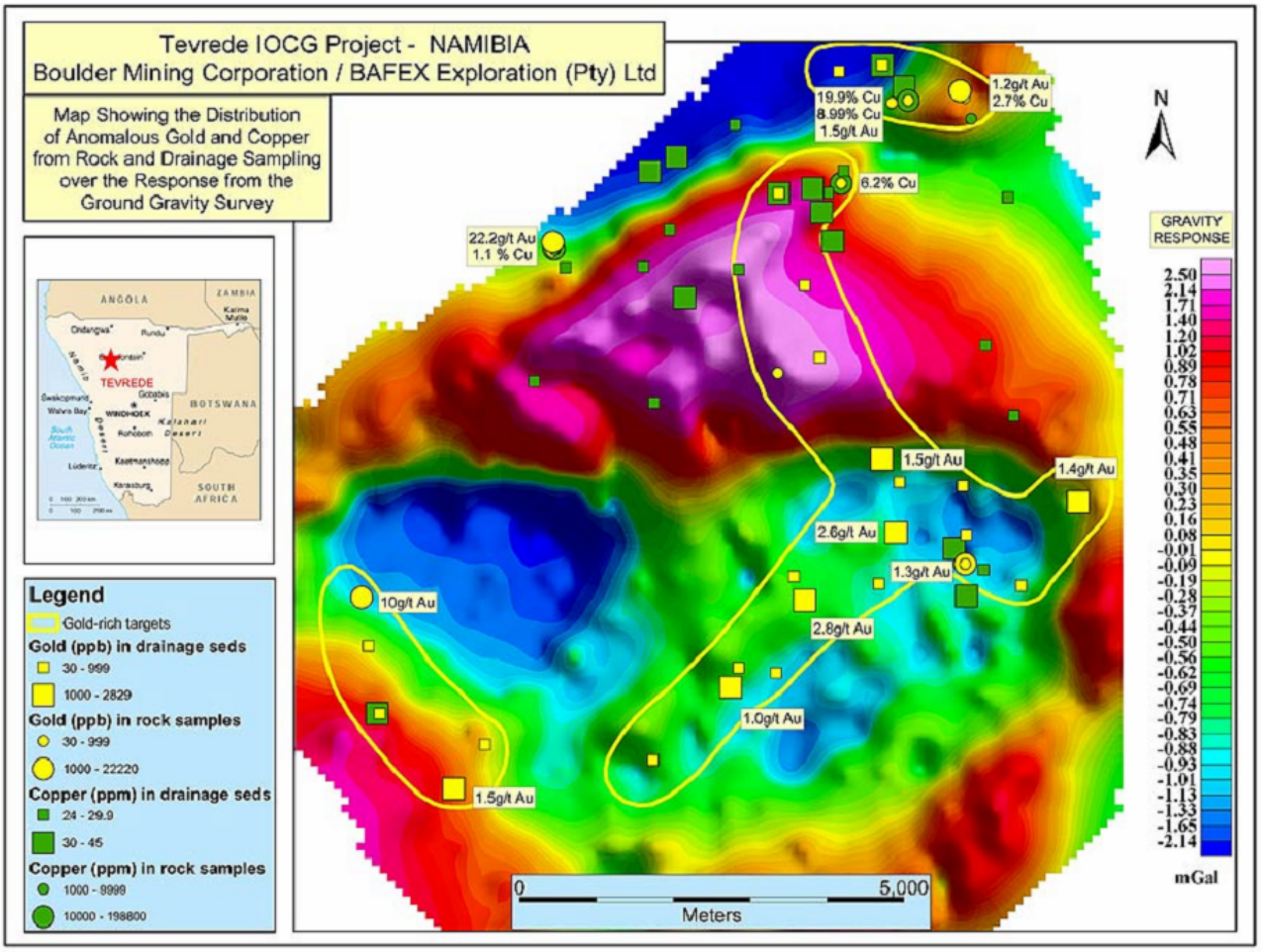

Fig 8.58 General gravimetric map overlain by selected samples and metal values, Tevrede property, northwestern Kamanjab batholith, Namibia. *The image is self explanatory. Note dimensions of the mineralized area, high content of copper and gold in some samples and site of the anomalies. This is part of an ongoing exploration project for IOCG. Drilling was carried out in this and other locations, but results are not yet known. The circular features depicted probably define a ring complex. Image published by the Boulder Mining Corporation of Canada, www.bouldermining.com.*

8.4.3.4 ACTIVE EXPLORATION PROJECTS IN THE LUFILIAN ARC

At the time of writing this document (August, 2004), at least two small mineral exploration companies are actively investing in ground and airborne geophysics, soil and rock sampling and diamond drilling of gold and copper-rich prospects in the northwestern Kamanjab Batholith and around the Hook Granite, the Kalengwa area and the Zambian Serenje area and other sites in eastern Zambia with excellent results.

Fig 8.58 is a gravity map from the Tevrede project of BAFEX Exploration, a junior exploration company that carries out successful activity in the northwestern part of the Kamanjab Batholith, Namibia (Fig 8.6). Preliminary results from soil and rock sampling are plotted on top of the gravimetric map. Note the significant dimensions of the mineralized area. Evidence from publicly available information on the prospect indicate that it is a large and well-endowed IOCG system. Part of the mineralization is hosted in felsic intrusive rocks that have been hydrothermally brecciated and cemented by magnetite. Stockworks and braided magnetite-quartz-sulfide veins were seen in samples at the headquarters of BAFEX in Windhoek (McKenzie, Chris, personal communications, 2002, 2003). If drilling campaigns carried out during the last months of 2003 were successful, there will probably be a new gold and copper mine in this part of Namibia.

8.5 RELATIONSHIP BETWEEN IOCG AND SEDIMENTARY-HOSTED Cu MINERALIZATION

The origin of sedimentary-hosted Cu mineralization may be secondary, derived from primary mineralization in IOCG systems. Several IOCG systems that lie under sedimentary-hosted Cu deposits probably gave origin to their copper mineralization.

"Exotic mineralization" is the term given to some very large copper deposits hosted in Quaternary or Upper Tertiary sedimentary rocks and/or in permeable volcanic rocks in the environs of large Chilean copper deposits (Munchmeyer, 1996; Munchmeyer & Urqueta, 1974; Camus, 2003; and Dold, 2003). Both copper porphyry and iron oxide-copper-gold deposits are known to be the source for source for exotic copper accumulation in nearby porous rocks.

The natural oxidation of pyrite and chalcopyrite in primary copper deposits liberates copper, iron and other metals from the hypogene mineralization. The upward flow of groundwater, produced by strong evaporation regimes in arid regions leaches copper from hypogene copper-rich deposits, leaving insoluble substances like gold behind. Copper-rich fluids are then transported into favourable porous and permeable lithologies with a suitable redox contrast where the metal precipitates. The process just described takes place today, and its rates of copper accumulation have been estimated by Dold, 2003 for several locations in the Atacama desert of Chile.

The same process might have taken place in many locations during the Meso and NeoProterozoic to generate exotic copper accumulations in adequate environments. Presence of organic matter in black shales or carbonates might have provided the redox change required for copper secondary minerals to precipitate. Subsequent metamorphism and tectonism could have transformed the transported copper sulfides, phosphates, sulphates and carbonates that were hosted in the sediments into other mineral forms.

Similar phenomena might have taken place along the Greater Lufilian Arc. The rapid exposure of IOCG deposits formed previous to rifting could have been eroded at great speed during rifting, and their products concentrated in secondary traps within sediments in the rift basins. Exotic copper accumulations could have occurred in favorable porous and permeable lithologies where suitable redox contrasts took place.

8.6 SEDIMENTARY-HOSTED GOLD MINERALIZATION IN THE LUFILIAN ARC

There is potential for hydrothermal sedimentary-hosted gold ("Carlin type") mineralization in the carbonates and dirty limestones that lie on top of the Otjiwarongo Batholith. This region is roughly shown on the map of Figs 8.33 and M25. Other parts of the Lufilian Arc show evidence of this type of gold mineralization. Some of them are areas east of Sesfontein in Namibia (Figs M19 and 8.6); the region where the Lusaka Formation (dolomites, siliciclastics and limestones) is intruded by small granitoid bodies to the west of Lusaka, Zambia (Fig 8.40, see also section 4.1.2); and the environs of Tshoosha (town previously called Kalkfontein) in Botswana, along the Transkalahari road. The Navachab gold mine in Namibia displays many similarities to the sedimentary-hosted gold mineralization at the Pinzon deposit in Nevada, U.S.A.

8.7 PECULIARITIES OF ZAMBIAN AND NAMIBIAN IOCG SYSTEMS

In western Zambia and northern Namibia, the IOCG prospects and evidence of mineralization seem to differ from the published literature on the deposit type. First of all, rocks of most of the mineralized systems have not been subject to high temperatures and strong metamorphic deformation. In general, they tend to be undeformed. Most of the original hydrothermal textures are pristine. High temperature gradients due to nearby plutons seem to be the only major alteration source. Nevertheless, it can be said that the *circa* 550 Ma and 750 Ma events that produced IOCG mineralization were the last major tectonothermal processes, after which there has been relative stability.

Some alteration features that are not commonly described in the literature on IOCG deposits have been identified. Some of these are: quartz "pods", round clast hydrothermal breccias, corrosion of the fragments in some of the magnetite-matrix breccias and progressive hematitization of the country rock to allow for emplacement of iron oxide bodies of any size. The riglite alteration is not associated to IOCG in the literature.

Very few metallic sulfides are visible on the surface in the Lufilian Arc. At times, black chalcocite is mis-identified as black moss or as Mn-iron oxides. This mineral has commonly been overlooked, and seems to be the most common copper sulfide on the surface in Namibian territory.

8.8 CONCLUSIONS

1. Most IOCG mineralization in the Lufilian Arc seems to be related to mafic midalkaline and ultramafic intrusives that occur at the same time as felsic midalkaline intrusives. Relationships between both rock types to produce mineralization are not well understood. In the few well documented cases available, mafic and ultramafic rocks, intruded before the main mineralization, and they might be contributing a significant portion of the metals, including Cu, Zn, Co, Mo, Mn, PGEs and even Au. In others, syenites or alkali granites are the main mineralizing intrusives.

2. In the Lufilian Arc, subvolcanic porphyritic intrusives and apophysis of ring complexes that are separated from the main ring complex clusters account for most of the IOCG mineralization.

3. Iron oxide is a major component in IOCG systems. It occurs as massive magnetite, massive hematite, or disseminated fashions of both. Emplacement of these iron oxides at macroscopic, mesoscopic and microscopic scales is thought to have been produced by gradual replacement of the host rock. The process seems to involve silicate disolution by hyper-alkaline hydrothermally-driven solutions.

4. Sometimes iron oxide bodies display structural control, and they are emplaced along faults, joints and stockworks. At other times, they are emplaced in space dissolved out from silicate (intrusive and siliciclastic) or carbonate rocks. The second process of emplacement is not fully understood at the time of writing this document.

5. Most of the massive iron oxide bodies do not display sulfidation nor any other metallic mineralization. They are considered “barren”. Only a few of the bodies of massive iron oxide became mineralized for reasons not well understood.

6. E-W-trending regional fracture systems that run parallel to the elongation of the Greater Lufilian Arc play an important role in IOCG mineralization. They acted as routes for intrusion, channels for fluids and control for ore deposition. Such structures are generally parallel to the main Lufilian Arc trend, and could have been normal syn-rift faults that reactivated throughout geological history. Some N-S-trending structures are also mineralized and they are sub-perpendicular to the main trend of the Lufilian Arc.

7. Hydrothermal alteration patterns in IOCG systems vary widely. They seem to be dependant on the types of intrusive rocks that produce them and rocks that host them. Sodic alteration of various types is ubiquitous and its role in IOCG processes is not well understood. Evaporites present in the Katanga-Damara sedimentary sequences were probably one of the sources of sodium.

8. Massive, three-dimensional quartz pods are emerging as a type of alteration that is associated to IOCG systems in the Greater Lufilian Arc. They seem to be a special type of silicification. Hyper-alkaline, hydrothermal solutions seem to be involved in the transportation of silica and emplacement of the quartz pods.

9. Round-pebble hydrothermal breccias are another feature that occurs often in and around IOCG systems throughout the Greater Lufilian Arc. They seem to have been produced by hyper-alkaline solutions that corroded previously angular hydrothermal breccia. In some cases, they act as good hosts for sulfide mineralization.

10. Many mineral deposits and prospects found in the Lufilian Arc are being interpreted as IOCG. These include the Dunrobin, Nampundwe and Kalengwa mines in Zambia; Luiswishi, Shituru and Kamoya in the Democratic Republic of Congo; and the Kombat, Copper Vallei, Otjikoto, and Tevrede deposits in Namibia, among others. Many new prospects with IOCG characteristics are emerging. Some large districts like the Kitumba-Kantonga area and the Kasempa-Kalengwa district in Zambia, and the Lofdal-Oas in the Khorixas Inlier of Namibia are promising for the future. The Otjiwarongo Batholith has potential, but involves exploring under cover.

11. An iron oxide-copper-gold deposit seems to lie underneath a sedimentary-hosted “Copperbelt-type” copper deposit at the Okatjepuiko farm, near Witvlei, Namibia. The IOCG mineralization seems to have been the source of copper for the sedimentary-hosted copper deposit. If this can be proven, a new model for copper mineralization in central Africa might emerge.

12. There are several locations where IOCG and sedimentary hosted Cu mineralization seem to be associated. Part of these occur in the Zambian Copperbelt, and may be one of the sources for secondary Cu mineralization in the Copperbelt.

13. The main IOCG events that have been identified took place during seven discrete time periods. From youngest to oldest these are listed on Table 8.3. This is a first attempt to temporally constrain the IOCG mineralization in the Greater Lufilian Arc. The possible IOCG events that took place in the basement to the Zambian Copperbelt (at Chambishi, Mufulira, the main Copperbelt, Konkola and Nchanga) are not very well defined or constrained geochronologically. The tentative age of ~825 Ma is derived from interpretations discussed on section 6.4 of this report. Other possible IOCG mineralization in the basement to the Copperbelt are discussed in this chapter and on section 4.1.5.

Table 8.3 Discrete periods of iron oxide-copper-gold mineralization that took place in the Greater Lufilian Arc.

Period	Main representative mineralization
~460 Ma	Sasare[4], Zambia
~533 Ma	Hook Granite Batholith satellites, Zambia
~550 Ma	Otjiwarongo, Namibia; Kafue Flats, Zambia
~746 Ma	Kalengwa-Kasempa, Zambia; Khorixas, Namibia
~825 Ma	Copperbelt, Zambia (possible, see section 6.4)
~1078 Ma	Witvlei, Omitiomire, Namibia
~1937 Ma	Kamanjab Batholith, Namibia

[4] IOCG mineralization at Sasare is included here for completeness. The source of information about mineralization and geochronology in that part of Zambia cannot be made public.

9 CONCLUSIONS

9.1 Main Granitoid Terranes in the Greater Lufilian Arc

The nature of the granitoid terranes in the study area of the Greater Lufilian Arc can be summarized as follows:

1. Foliated alkali granite, quartzmonzonite and granite were emplaced at 1900±100 Ma. They are present beneath the Katanga Supergroup in the Copperbelt, the Mkushi-Serenje area, NW Zambia, and the Domes region (Zambia); Kaokoland, central Namibia, the Kamanjab Batholith and Grootfontein Inlier (Namibia). The environment of emplacement for these rocks has not been well identified, but tends to be anorogenic. This period may be broken into at least four discrete events.

2. Generally poorly outcropping pre-Katanga granitoid and felsic to mafic volcanics were emplaced at 1100±50 Ma. They are present south of the Copperbelt, and west of Lusaka (Zambia); around Omitiomire, Kaokoland and the Witvlei area (Namibia). These rocks surround the Kapvaal Craton continuously from Namaqualand in South Africa, to the Irumide Belt in Zambia. They were emplaced in anorogenic continental rift–related environments.

3. Sporadic, but widely distributed, small igneous intrusions were emplaced at 750±50 Ma. They comprise granite, alkali granite, syenite and gabbro with felsic and mafic volcanics, as observed in the Copperbelt, Kalengwa-Kasempa and NW Zambia (Zambia); Khorixas Inlier and Summas Mountains (Namibia). These bodies intrude Roan and Nguba Formation lithologies but are generally overlain by (Upper) Kundelungu sediments and their Namibian equivalents. They were emplaced in anorogenic rift-related and continental epeirogenic uplift environments.

4. Widespread and voluminous granitoid magmatism (Pan African) was emplaced at 550±50 Ma. It is well preserved in the environs of Otjiwarongo, central Namibia, Kaokoland, and in west-central Zambia (including the Hook Granite Batholith), but also sporadically detected in NW Zambia. The Otjiwarongo batholith, a covered pluton in Namibia, may be similar to the Hook Granite batholith in size, rock type and age. These rocks were emplaced in continental epeirogenic uplift and rift-related environments. This period may be broken into at least three discrete events.

5. Several, more restricted magmatic events occur during the last 2000 Ma in the Greater Lufilian Arc. Examples of this are the Nchanga Granite in Zambia (880 Ma); magmatism at 1700 Ma in the Khorixas Inlier, Namibia; and at 1600 in the Kamanjab Batholith.

The Zambian Lufilian Arc and Damara region of Namibia behaved in a different way from 2200 to 2000 Ma; they were independent entities. They also behaved significantly different from 1400 to 850 Ma. Geological history of the two main portions of the Greater Lufilian Arc is consistent from *circa* 800 Ma to the present, and especially during the last 600 Ma.

9.2 Polycyclic Geological History

Most areas studied in the Greater Lufilian Arc show polycyclic geological histories. Repeated anorogenic intrusive events are a common denominator. Source rocks for the various melts come from previously-formed intrusive rocks and siliciclastics. Prolonged crustal histories have resulted in superimposition of events. Two Namibian examples illustrate this. In the Otjiwarongo environs, Neoproterozoic granites intruded anorogenic Paleoproterozoic granites, and both were intruded almost in the same location by two large Mesozoic alkaline complexes. At the Oas farm, a Mesozoic mafic feeder pipe cuts through 750 Ma alkaline intrusions that had intruded Paleoproterozoic anorogenic granitoids. Melts and sedimentary rocks have been re-worked in each of the areas; a lot of magma mixing and crustal contamination processes were involved in the formation of the granitoids.

9.3 Rock Types

The majority of the rocks from the Greater Lufilian Arc that were analysed had midalkaline character. Table 9.1 compiles statistics on sample composition and alkalinity that were carried out in all sampling domains. Any rock that plotted outside of the fields of the modified TAS diagram was not included in the statistics.

Table 9.1 Rock type statistics of all samples analysed from the Greater Lufilian Arc

Group	Rock type	number	%	Granitoids	Groups
Midalkaline Rocks	Alkali granite	102	22.13	63.93	59.87
	Quartzmonzonite	83	18.00		
	Syenite	32	6.94		
	Monzonite	17	3.69		
	Monzodiorite	10	2.17		
	Monzogabbro	12	2.60		
	Alkali gabbro	20	4.34		
Subalkaline Rocks	Granite	99	21.48	36.07	32.75
	Granodiorite	33	7.16		
	Diorite	6	1.30		
	Gabbro-diorite	3	0.65		
	Quartzolite	4	0.87		
	Gabbro	6	1.30		
Alkaline Rocks	foid syenite	11	2.39		7.38
	foid monzosyenite	4	0.87		
	foid monzo-diorite	2	0.43		
	foid gabbro	12	2.60		
	Foidolite	3	0.65		
	Peridot gabbro	2	0.43		
Total		461	99.57	100.00	100.00
	Carbonatite	10			
Total including carbonatites		471			

The database of 471 samples was broken into domains as indicated on Table 9.2. Rock type percentages for each domain is listed on Table 9.3.

Table 9.2 Number of samples from each rock type for domains of the Greater Lufilian Arc.

Rock type/ Region	Hook Granite	NW Zambia	Copperbelt	Kamanjab	Khorixas	Okwa,Ugab,Summas,Grootf	Otjiwarongo	Okatjepuiko	KalengwaKasempa	West Lusaka Kafue Flats	total	
alkali granite	26	7	6	26	10	4	13	1	2	7	102	Midaldaline
quartzmonzonite	20	8	5	38	1	1	5		3	2	83	
syenite	7	2	2	3	9	1	2		2	4	32	
monzonite	5	1	1	2	2		2	2	2		17	
monzodiorite	3	1	2	1					3		10	
monzogabbro	1	1	3	1	1			1	3	1	12	
alkali gabbro	2	5	1	3	3			1	3	2	20	
granite	16	10	15	22	8	11	7	5	1	4	99	Subalkaline
granodiorite	7	8	8	3	1	1		1	1	3	33	
diorite		1	2				1			2	6	
gabbro-diorite	1				1					1	3	
quartzolite				3			1				4	
gabbro	1	1	1	1	1					1	6	
foid syenite		8	1	2							11	Alkaline
foid monzosyenite					4						4	
foid monzo-diorite			1						1		2	
foid gabbro		2	2		1				7		12	
foidolite		1		2							3	
peridot gabbro				1	1						2	
carbonatite	1				9						10	
Total	90	56	50	108	43	18	31	11	27	27	461	

Table 9.3 Percentages of each rock type for domains of the Greater Lufilian Arc.

Rock type/ Region	Hook Granite	NW Zambia	Copperbelt	Kamanjab	Khorixas	Okwa,Ugab,Summas,Grootf	Otjiwarongo	Okatjepuiko	KalengwaKasempa	West Lusaka Kafue Flats	Kalene Hill	Nchanga Granite	Muliashi Porphyry	Chambishi	Oas Farm	Lofdal farm	Percentage	
alkali granite	29.2	12.5	12	24.1	23.3	22.2	41.9	9.09	7.14	25.9	20	8.33	12.5	12.5	25.9		22.13	Midaldaline
quartzmonzonite	22.5	14.3	10	35.2	2.33	5.56	16.1		10.7	7.41	23.5		25		3.7		18.00	
syenite	7.87	3.57	4	2.78	20.9	5.56	6.45		7.14	14.8	3.33	16.7			33.3		6.94	
monzonite	5.62	1.79	2	1.85	4.65		6.45	18.2	7.14							8.33	3.69	
monzodiorite	3.37	1.79	4	0.93					10.7		3.33				3.7		2.17	
monzogabbro	1.12	1.79	6	0.93	2.33			9.09	10.7	3.7				12.5	3.7		2.60	
alkali gabbro	2.25	8.93	2	2.78	6.98			9.09	14.3	7.41				12.5	3.7		4.34	
granite	18	17.9	30	20.4	18.6	61.1	22.6	45.5	3.57	14.8	23.3	66.7	31.3	12.5	11.1	25	21.48	Subalkaline
granodiorite	7.87	14.3	16	2.78	2.33	5.56		9.09	3.57	11.1	23.3		31.3	37.5		8.33	7.16	
diorite		1.79	4				3.23			7.41		8.33					1.30	
gabbro-diorite	1.12				2.33					3.7						8.33	0.65	
quartzolite				2.78			3.23										0.87	
gabbro	1.12	1.79	2	0.93	2.33					3.7	3.33			12.5	7.41	16.7	1.30	
foid syenite		14.3	2	1.85													2.39	Alkaline
foid monzosyenite					9.3										3.7	25	0.87	
foid monzo-diorite			2						3.57								0.43	
foid gabbro		3.57	4		2.33				25						3.7		2.60	
foidolite		1.79		1.85													0.65	
peridot gabbro				0.93	2.33											8.33	0.43	

60%, 33%, 7% is the percentage relationship of midalkaline to subalkaline to alkaline rock groups for the entire project (Fig 9.1). 64%, 36% is the percentage relationship of midalkaline to subalkaline granitoids. Carbonatites make 2.1% of the total samples. If the suite of mafic rocks collected are considered representative of reality, then midalkaline gabbroids make 66%; alkaline gabbroids, 18%; and subalkaline gabbroids, 17%.

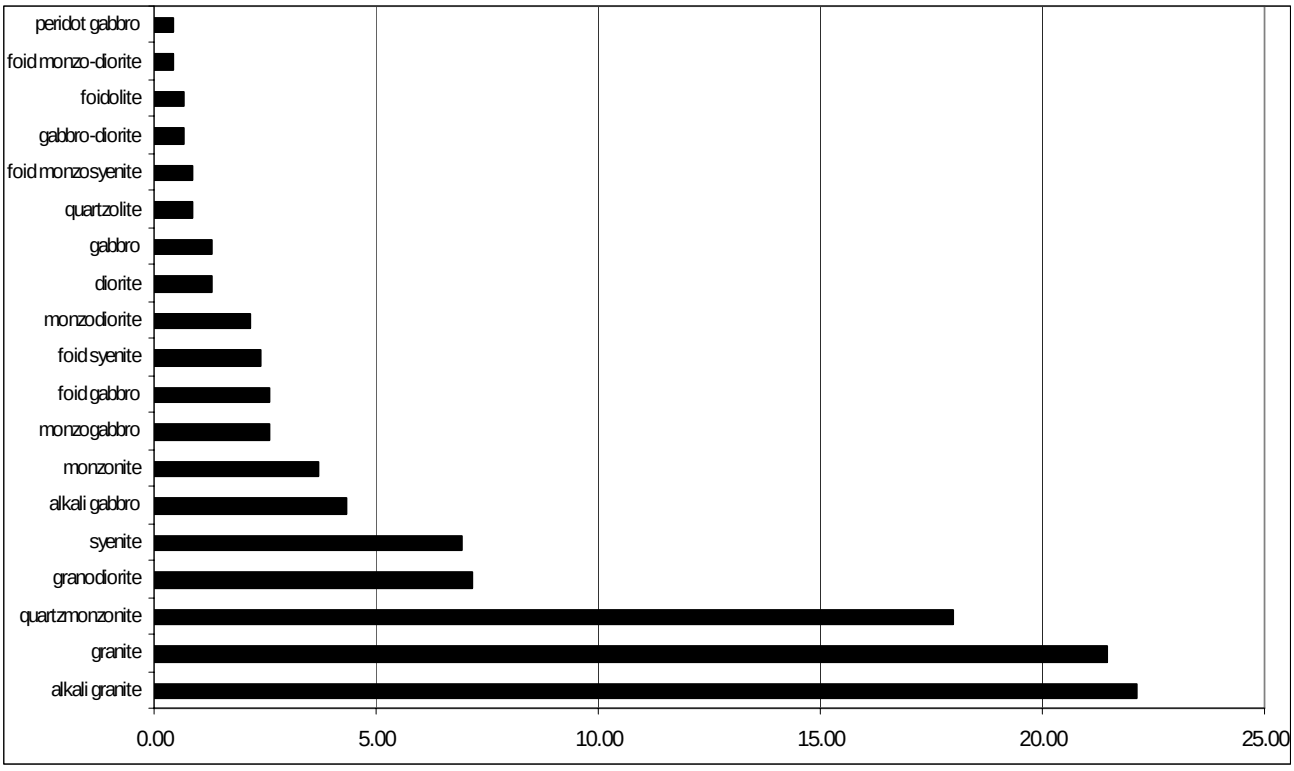

Fig 9.1 Distribution of rock types and comparative composition of rock alkalinity in the Greater Lufilian Arc granitoid project. Based on the names of the modified TAS diagram of Middlemost, 1994a.
Note the absolute domination of alkali granite, granite and quartzmonzonite. Together these rock types account for almost 62% of all samples studied. That is also clear on Fig. 9.2.

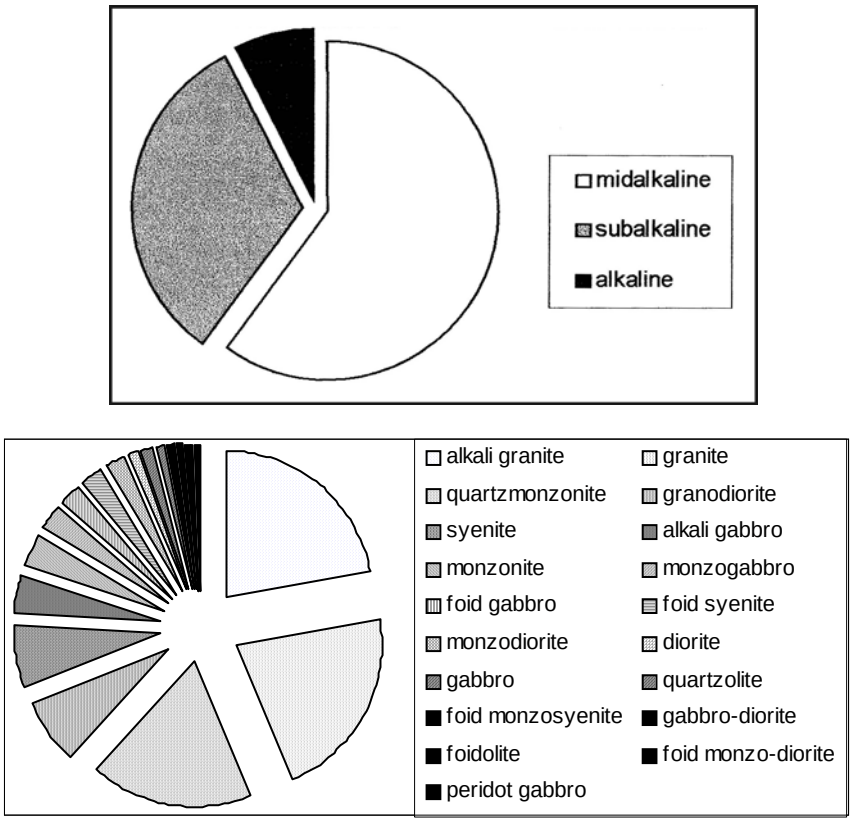

Fig 9.2 Composition of the samples collected in the Greater Lufilian Arc. *The upper pie diagram* ***groups rocks according to*** *their alkalinity, sensu Middlemost, 1994. The lower diagram breaks the samples into their respective rock types.*

Midalkaline rocks predominate, whatever the point of view. That corresponds with the continental extension, anorogenic environment that has ruled formation of plutonic rocks in the Greater Lufilian Arc.

The average rock type distribution for the entire Greater Lufilian Arc closely resembles that of the Hook Granite Batholith, as indicated on Table 9.3.

9.3.1 Mafic, Ultramafic and Alkaline Rocks

Mafic, ultramafic, carbonatitic and alkaline intrusions are well represented, albeit volumetrically minor, in most domains of the Greater Lufilian Arc that were studied. In certain cases, these rocks might be implicated in mineralizing processes (Kalengwa deposit, Lofdal rare earth mineralization and Lofdal carbonatites). These rocks occur in anorogenic epeirogenic uplift and rift-related environments. Mafic rocks are under-represented in the geochemical database, because they were not the primary sampling target.

The widespread small gabbroic bodies in the Greater Lufilian Arc were emplaced as mafic plugs in large, within-plate areas that were being subject to incipient rifting. The mafic plugs could intersect the sedimentary cover of the plate, including marine and continental deposits. A modern day analogue of the same process takes place in the environs of Filiya, Nigeria.

9.3.2 Rock Associations in Anorogenic Environments

A frequent field observation is the persistent clustering of small bodies of red-altered granitoids, gabbroids, massive magnetite-hematite and quartz pods that are linked to ages around 550 and 750 Ma. The four-rock association seems to be a characteristic of continental extension anorogenic environments. It is spatially related to iron oxide-copper-gold mineralization.

A recurrent feature observed in most outcrops of the study area is the presence of two or more contrasting types of plutonic rocks. In some cases gabbroids and granitoids; in others, syenitoids and granitoids; even three or four types of granites and alkali granites. Many of the small areas also contain mafic, ultramafic and alkaline plugs and dikes of varying composition, such as lamprophyres, carbonatite and nepheline syenite.

The multiplicity of rock types in a small area seems to be another characteristic of continental extension anorogenic environments.

9.3.3 Quartz Pods

Quartz pods have been identified throughout most of the Greater Lufilian Arc region. They differ from veins, boudinaged veins and pegmatitic quartz units, particularly in geometry: outcrops of undeformed bodies are typically round to elliptical, and vary from a few to several-hundred meters in diameter. Dimensions of some quartz pods exceed four kilometers in diameter and there is geophysical evidence of even larger ones. They seem to be a special type of silicification. Hyper-alkaline, hydrothermal solutions seem to be involved in the transportation of silica and emplacement of the quartz pods. Quartz pods are emerging as a type of alteration that is associated to IOCG systems in the Greater Lufilian Arc. Improved identification in the field and an increased understanding of their physico-chemical features may aid in the exploration of mineral deposits.

9.3.4 Iron Oxide Bodies

Masive bodies of magnetite and/or hematite at macroscopic, mesoscopic and microscopic scales emplaced themselves by gradual replacement of the host rock. The process seems to involve silicate dissolution by hyper-alkaline hydrothermally-driven solutions.

9.3.5 Round-Pebble Hydrothermal Breccias

Round-pebble hydrothermal breccias occur often in and around IOCG systems throughout the Greater Lufilian Arc. They seem to have been produced by hyper-alkaline solutions that corroded previously angular hydrothermal breccias. In some cases, they act as good hosts for sulfide mineralization.

9.4 Ring Complex Clusters

Clusters of anorogenic granitoid ring complexes have been produced all along from Archean times to the present. Clustering of multiple anorogenic ring complex intrusions can form batholithic size bodies.

At least ten clusters of ring complexes were identified in the Greater Lufilian Arc. Ring complex clusters have the following characteristics: 1) Multiple ring complexes of varying chemical composition and size that might intersect each other. 2) Volcanic and plutonic rocks of roughly the same composition occur together. 3) Successive magmatic events of varying composition allowed for abundant opportunities of magma mixing and recycling of crustal materials. 4) The plan view geometry of un-tectonized ring complex clusters is roughly that of an isosceles triangle. 5) Less voluminous precursor and waning events of magmatism may occur. 6) The principal chemical composition of the magmas is midalkaline, but may ocassionally vary to alkaline and subalkaline. In extreme cases, it may be peralkaline and can even produce carbonatitic rocks. 7) Isolated bodies of mafic and ultramafic rocks often come in the latter stages of the process. 8) Total duration of ring complex cluster cycles averages 110 Ma.

Several cycles of ring complex clusters have repeatedly occurred in roughly the same location in at least three different localities. These repeated cycles were separated 1095 Ma in NW Zambia; 933 Ma at the Khorixas area, Namibia; and 50 Ma in West Lusaka, Zambia.

9.5 Tectonic Environment of Emplacement

The tectonic environment of emplacement for part of the rocks collected is not yet well constrained; active research is currently being carried out to address this issue. Nevertheless, several clear patterns are emerging: 1) The largest portion of granitoids collected are midalkaline rocks that formed in an anorogenic continental epeirogenic uplift environment. 2) Next come those formed in rift environments. 3) Another significant group of rocks formed in a post orogenic granitization environment. 4) Continent-continent collision environments were not positively identified. 5) Subductional magmatism seems to have been very restricted both in terms of time and areal extension. There is evidence of minor such magmatism in Paleoproterozoic rocks of Kalene Hill and in portions of the Kamanjab Batholith. In any given area, two or more of these settings may be superimposed. Anorogenic continental extension is the main geological process of the Arc.

Complete Wilson cycles were not identified in the domains of the Greater Lufilian Arc that were studied. The dominant magmatic process, as evidenced by the volume of extruded rock, is anorogenic continental epeirogenic uplift, closely-followed in time by a rift-related granitoid emplacement. Coalescing and overprinting aulacogens seem to be the main type of geological event in the arc.

The environment of emplacement of Paleoproterozoic rocks that occur throughout the Arc cannot be identified using the established methods for granitoid environment of emplacement. Intense sodic alteration and hematitization were observed in part of these rocks. Another alteration process is a net enrichment in potassium that is evident by the abundant biotite and alkali feldspar overgrowth. Part of the rocks showed diffuse crystal margins and abundant blue quartz phenocrystals. Incipient migmatitization of these rocks may have modified their chemistry to a point where they don't fit traditional procedures to evaluate granitoid environment of emplacement. The alteration processes just mentioned seem to have taken place before ~880 Ma, because the environment of emplacement of younger rocks can be identified.

9.6 High Thorium

High values of thorium were found in part of the granitoids of NW Zambia, Kafue Flats, Hook Granite Batholith (Zambia), Oas farm and Otjiwarongo environs (Namibia). They are high-heat producing rocks. The anomalous thorium content in some granitoids of the Greater Lufilian Arc induced and maintained long-lived, large convective cells of hydrothermal fluid flow.

High-thorium granitoids in all five domains have a particular trace element chemical signature that is not common, and probably were subjected to analogous geological processes at different points in time.

9.7 Correlation of Granitoids

Granitoid rock suites with closely matching chemistry and macroscopic features have been found to form in the same region, two or three times with up to a thousand million years of age difference. Source rocks and environment of emplacement for the anorogenic intrusive events were the same: for that reason, magmatic products turned out equivalent. These features preclude lithological or detailed geochemical correlation.

Rocks from the suites of Muliashi Porphyry and Mufulira, Zambia are an example of this. They both have pink and gray granitoids with similar compositions, but the ages of the rocks are completely different.

Several lithological correlations have been developed for granitoids in various domains of the Greater Lufilian Arc. The rocks cannot be properly correlated until more geochronological information is available.

9.8 Main Findings in Specific Domains

9.8.1 Hook Granite Batholith, Zambia

Information currently available on geophysics, geochronology, rock distribution and geochemistry from the Hook Granite Batholith fit quite well with an intracontinental, anorogenic, ring complex cluster origin. The batholith is mainly composed by midalkaline granitoids. Alkali granites, quartzmonzonites and granites make up 70% of all rocks.

9.8.2 Nchanga Granite, Zambia

The Nchanga Granite has all the characteristics of an anorogenic granite ring complex. Chemistry of its rocks crosses the midalkaline to subalkaline fields. Parts of the pluton are made of high heat producing granites that maintained a long-lived circulation of hydrothermal fluids. The Nchanga Granite might have contributed to the origin of copper in its environs.

9.8.3 Kamanjab Batholith, Namibia

Sixteen suites with more than two contrasting rock types were identified in the Kamanjab Batholith. No two suites are identical, and they are made by a large variety of rock types. This multiplicity of rock types at a given site is one of the characteristics of anorogenic environments in the Greater Lufilian Arc.

There is no direct proof of the presence of ring complexes at the Kamanjab Batholith. Nevertheless, several sources of evidence point to the batholith as a cluster of ring complexes. Among others, these are: 1) the lack of continuity in the rock types along traverses; 2) the presence of multiple rocks types in at least fifteen discrete sites; 3) General anorogenic character of most of the rocks; 4) three quarters of the rocks in the suite are midalkaline; 4) the size and shape of the batholith, as well as its event diagram has similarities with other ring complex clusters.

9.8.5 New Temporal Constrain to Katangan Sedimentation

Granitic dikes emplaced at the Nchanga mine area in anorogenic extensional environments were dated at ~765 Ma. They provide the youngest age of deposition for that portion of the Katanga sedimentary sequence at Nchanga (Roan sediments), and might provide a significant bracket age for mineralization.

9.8.6 Khorixas Inlier-Kamanjab Batholith

Geological history for the Khorixas Inlier and the Kamanjab Batholith are significantly different. They probably were not in the same geographic position all the time. Older basement is known in the Khorixas Inlier than at the Kamajab. The two regions seem to have had a common geological history for the past 550 Ma.

9.8.7 Long-Lived Fractures

E-W-trending regional fracture systems that run parallel to the elongation of the Greater Lufilian Arc play an important role in the emplacement of magmatism and IOCG mineralization. They acted as routes for intrusion, channels for fluids and control for ore deposition. Those structures are generally parallel to the main Lufilian Arc trend, and could have been normal syn-rift faults that have been reactivated throughout geological history. Some N-S-trending structures are also mineralized and they are sub-perpendicular to the main trend of the Lufilian Arc.

9.9 Metallogeny

Various types of mineralization were seen to be associated with intrusive rocks along the Greater Lufilian Arc (Table 9.4). These include rare earth mineralization associated to alkaline dikes and carbonatites in the Khorixas Inlier, sedimentary-hosted gold (so-called “Carlin”-style deposits), several low-sulfidation hydrothermal gold occurrences, low sulfidation hydrothermal copper depostis, epigenetic copper vein deposits, alkaline porphyry molybdenum (-copper?) style mineralization, sedimentary-hosted copper-cobalt deposits, and a wide variety of iron oxide-copper-gold and related deposits and prospects. Several Paleoproterozoic rocks throughout the Greater Lufilian Arc are enriched in copper. Some Mesoproterozoic syenites and alkali granites are enriched in zinc. The significance of the latter observation remains unclear. Paleoproterozoic copper-rich rocks could be the source of metal for later events. Incipient migmatitization of those rocks could have remobilized the copper. Copper is probably being recycled. Very little skarn mineralization was observed in Katangan carbonates, even though they are intruded by multiple plutonic episodes. Possible exceptions occur around the Hook batholith. The Samba deposit is not considered to be a copper porphyry; it is a low sulfidation epithermal copper mineralization hosted in pyroclastic rocks that were sheared during regional metamorphism.

9.9.1 Metallogenic Epochs

At least eight discrete periods of mineralization can be interpreted from Table 9.4 (The same are simplified on Table 9.5). Where possible, radiometric ages have been used to place the various events. Most have been assigned to specific ages by correlation or association. Six deposits could not be placed chronologically and are included at the bottom of the list. There is a wide-spread series of mid-alkaline intrusions emplaced around 750 Ma that produces a variety of mineral deposits. Another such event (separated in at least three different phases: 500-513, 550 and 583 Ma) took place around 540±40 Ma. Five less well defined events took place as indicated on Table 9.5. From old to young, they occurred at ~1970, ~1930, ~1866, 1097-1059 and ~460 Ma (See Tables 9.4 and 9.5). The dominant deposit type is iron oxide-copper-gold mineralization.

The age of sedimentary-hosted copper mineralization in the Copperbelt is currently being re-evaluated using Re-Os dating at the University of Arizona. Three tentative ages for them are 796-756, ~583 and ~550 Ma.

The main events of sedimentary-hosted gold mineralization in Namibia are ~750 Ma in the environs of Sesfontein, ~550 Ma in Eastern Namibia. The age of the Zambian deposits and prospects could not be estimated.

At least two distinct events of disseminated copper mineralization associated to midakaline granitoid intrusives were identified in the Kamanjab Batholith. The first took place around 1975 Ma and the second around 1928 Ma.

Table 9.4 Main Metallogenic Events Observed - Greater Lufilian Arc

Commodities	Mine, Deposit, Prospect, Event	Deposit Type	Age	@	Tectonic Environment
Au	Sasare,Zm	IOCG	460		anorogenic continental rift+
Au,Cu,(Pb?)	Navachab Mine, Nm	structurally-controlled carbonate replacement	~490	E	?
Cu,Au	Kansanshi Mine,Zm	?	500-513	E	extension
Cu,Co,Au,U	Shituru Mine, D.R.Congo	IOCG	500-513#	E	extension
Cu,Co,Ni	Luiswishi Mine, D.R.Congo	IOCG	500-513#	E	extension
Cu,Co,Ni,Au,U,etc.	Kamoya Mine, D.R.Congo	IOCG	500-513#	E	extension
Mo	Marinkas Kwela Deposit, Nm	Mo porphyry	520-560	E	anorogenic continental rift
Cu,Au,Mn,LREE	Kitumba deposit,Zm	IOCG	533	E	anorogenic continental rift
Cu,Au,Mn,LREE	Kantonga deposit, Zm	IOCG	533	E	anorogenic continental rift
Cu,Ag,Au,Fe	Hook Satellites, Zm	IOCG	533	E	anorogenic continental rift+
Au,<Cu	Dunrobin Mine, Zm	Au-rich IOCG	533	E	anorogenic continental rift+
Py,Cu,Au	Nampundwe Mine, Zm	IOCG	538(L-207)	E	anorogenic continental rift+
Cu,Au,As,Pb,Zn	Hippo Mine, Zm	IOCG	538	E	anorogenic continental rift+
Au	Otavi Mts., Nm	Sed-hosted Au	~550	E	anorogenic continental rift
Au	Otjiwarongo, Nm	Sed-hosted Au	~550	E	anorogenic continental rift
Cu,Au	Kombat Mine, Nm	IOCG	~550*	E	anorogenic continental rift
Au	Otjikoto Mine, Nm	IOCG	~550*	E	anorogenic continental rift
Cu,Au	Kafue Flats, Zm	IOCG	550(L-211)	E	anorogenic continental rift
Au	Kamanjab, Nm	Au epithermal	570-677	E	?
Zn,Pb	Kabwe Mine, Zm	?	?	E	?
-	Verangian Glaciation	-	580	E	-
Cu,Co	CuBelt minzn, Nchanga Mine, Zm	Sedimentary-hosted Cu	583	E	-
Cu,Co	CuBelt minzn, Mufulira Mine, Zm	Sedimentary-hosted Cu	583	E	anorogenic continental rift+
Cu,Co	CuBelt minzn, Musoshi Mine, Zm	Sedimentary-hosted Cu	583	E	
Cu,Co	CuBelt minzn, Chambishi Mine, Zm	Sedimentary-hosted Cu	583	E	
-	Marinoan Glaciation	-	630		-
-	Sturtian Glaciation	-	710		-
Cu,Ag,LREE,U,Au?	Kalengwa Mine, Zm	IOCG	745	I	anorogenic continental rift+
Cu,Au,LREE	Kasempa Area, Zm	IOCG	750	I	anorogenic continental rift+
Cu,Au?	Kametete deposit, Zm	IOCG	750	I	anorogenic continental rift+
Au	Sesfontein, Nm	Sed-hosted Au	745-756	I	anorogenic continental rift
Cu,Nb,REE,Au?	Kesya carbonatite, Zm	IOCG	745-756?	I	anorogenic continental rift+
Cu,Co	Copper Valley prospects + mine, Nm	IOCG	745-756	I	anorogenic continental rift+
REE,Zn,Cu?,Au?	Oas farm prospects, Nm	IOCG	745-756	I	anorogenic continental rift+
REE,Cu?,Au?	Lofdal farm prospects, Nm	IOCG	745-756	I	anorogenic continental rift+
Cu,Co,Ni	Luamata deposit, Zm	IOCG	745-756	I	anorogenic continental rift+
Cu,Co	Copperbelt initial Cu minzn, Zm	Sedimentary-hosted Cu	756-796	I	anorogenic continental rift
Cu	Omitiomire deposit, Zm	Sedimentary-hosted Cu	L or younger		anorogenic continental rift
Au,Cu	Kamachopolo, SW Kasempa, Zm	Low sulfid. epithermal	L or younger		anorogenic continental rift
Au	Lunga, Zm	Low sulfid. epithermal	L or younger		anorogenic continental rift
Cu	Mkushi mines and prospects, Zm	Intrusion-related minzn	1059	L	extension
Cu,Au	Witvlei deposit, Nm	IOCG	1097(L-638)	L	anorogenic continental rift+
Cu,Au?,Ag?	Mnzd area 3 Kamanjab Batholith, Nm	Disseminated Cu	1866(L-993)		
Cu,Cu,LREE	Mwinilunga, W Zm	IOCG?	1928(L-030)	U	
Cu,Cu,LREE	Kamdescha f., Kamanjab Batholith,Nm	IOCG, Au, Cu	1937(L-868)	U	
Cu,Cu,LREE	Tevrede f., Kamanjab Bathlith,Nm	IOCG	1937(L-855)	U	
Cu,Mo	Samba Cu prospect, Zm	schist-hosted Cu	1965	V	?
Cu,Au?,Ag?	Mnzd area 2, Kamanjab Batholith,Nm	Disseminated Cu	1876(L-969)		
Co,Ni,Cu	Kalumbila deposit, Zm	Sedimentary-hosted Cu derived from an IOCG	*	I	hydrothermal rift-related brines,can be I,L or even older up to 1800Ma.
Cu	Lumpuna prospect, SW Luanshya,Zm	Cu porphyry	?		Subduction
Cu	Chifumpa, 80km SE Kasempa, Zm	Cu porphyry	?		Subduction
Au,<Cu	Karibarembi, 49km S Kalenwa, Zm	Sed-hosted Au	?		
Au,<Cu	Kililamirombwe, 124km SSE Kasempa,Zm	Sed-hosted Au	?		
Cu	Dongwe, Zm	High+low sulf. epitherm	?		Subduction

+Tectonic environment of emplacement was inferred from geochemistry. *The age is based on a nearby similar age. #Estimated age.

@Magmatic event in geochronological correlation diagrams (Figs A79 to A83).

The age of the six last items of the table is uncertain.

Table 9.5

Simplified Classification of Metallogenic Events in the Greater Lufilian Arc

By Alberto Lobo-Guerrero, M.Sc., Min.Ex., December, 2004
Economic Geology Research Institute, University of the Witwatersrand, Johannesburg

Commodities	Location	Deposit Type	Age	*	Environment
Au	Sasare, Zm	IOCG	460		ACR
Cu,Co,Ni, Au,U,Fe	Kansanshi, Zm + some southern Congolese Fe + Cu-Co deposits	IOCG + Kansanshi veins	500-513	Eo	Extension
Mo	Marinkas Kwela	Mo porphyry	520-560	E	ACR
Cu,Au,Fe, REE,Ag,Zn,Pb	Hook Granite batholith satellite bodies, Zm	IOCG	~533	E1	ACR
Cu,Au	Otjiwarongo, Otavi Mts., Nm; Kafue Flats, Zm	IOCG + Sedimentary-hosted Au + Navachab,Nm	~550	E2	ACR
Cu,Co (U)	Copperbelt and Congolese Cu-Co mineralization hosted in sediments; remobilization and mineralization	Sed-hosted Cu (epigenetic overprint)	~583	E3	Event related to Verangian Glaciation?
Cu,Co,Ni,Au	Kabompo Dome, Zm	IOCG, sed-hosted Co-Ni-Cu	~730	I	CEUG
Cu,Au,REE, Ag,Mn	Kalengwa-Kasempa area,Zm Oas, Lofdal, Mesopotamie, Nm	IOCG	~745-756	I	ACR
Cu,Co	Initial copper mineralization in the Zambian Copperbelt (and Katanga?)	Sed-hosted Cu	756-796	I-J	ACR
Cu,Au	Witvlei, Nm; Mkushi,Zm; Omitiomire,Zm	IOCG + Intrusive related mineralization	1059-1097	L	ACR
Au,As,Bi,Sb	Karibarembi and Kililamirombwe, Zm	Sed-hosted Au	L or younger	L	ACR
Cu,Au?	Kamanjab Batholith, Nm	IOCG, hydrothermal Cu dissemination	1866	U	environment cannot be identified - probably CEUG
Cu,Au?	Kabompo Dome, Mwinilunga, Lumwana, Zm	Schist-hosted Cu	1928	U	?
Cu, Au,Fe,F,REE	Kamanjab Batholith, Nm; Mwinilunga, Zm (?)	IOCG	1930	U	ACR
Cu,Mo	Samba, Zm	Schist-hosted Cu	1965	V	?
Cu,Au,Ag?	Kamanjab Batholith, Nm	Hydrothermal Cu dissemination	1975	V	CEUG

NOTE: ACR = Anorogenic continental rift. CEUG = continental epeirogenic uplift granitization.
* Letters in the fifth column refer to labels for magmatic events in geochronological correlation diagrams (Figs A79 to A83). White and gray coloration serves to separate major metallogenic times.

9.9.2 Iron Oxide-Copper-Gold Mineralization

The iron oxide copper-gold (IOCG) style of mineralization is far broader in terms of both spatial distribution and age of emplacement than previously thought. IOCG deposits have been identified in both Namibia and Zambia. In Namibia, for example, the IOCG deposit Tevrede is currently being explored by junior mining corporations in the northwestern portion of the Kamanjab batholith; in addition, the Kombat copper mine in the Otavi Mountains and Otjikoto, a gold deposit in the environs of Otjiwarongo, seem to be IOCG deposits. Several IOCG-like mineralized areas were identified at the Oas, Lofdal, Mesopotamie and Gelbingen farms as outliers to the Kamanjab Batholith. Zambia also has several known IOCG deposits like the Kalengwa copper-silver mine, the Kitumba and Kantonga copper deposits and others around the Kasempa area. The Nampundwe pyrite mine as well as Dunrobin gold mine also have IOCG characteristics.

Quartzites are good hosts for mineralization. This was observed in several Namibian areas, including the southern part of the Oas farm, the Gelbingen farm and the western portion of the Kamdescha farm, bordering the Kamanjab Batholith. Quartzites fracture in a brittle manner that is ideal for hydrothermal brecciation. Equivalent rocks might host mineralization in Zambia.

The main IOCG events that have been identified in the Greater Lufilian Arc took place during eight time periods. These are listed on Table 9.6. The possible IOCG events that took place in the basement to the Zambian Copperbelt (at Chambishi, Mufulira, the main Copperbelt, Konkola and Nchanga) are not very well defined or constrained geochronologically.

Table 9.6 Periods of iron oxide-copper-gold mineralization in the Greater Lufilian Arc.

Period	Main representative mineralization
~460 Ma	Sasare, Zambia
~533 Ma	Hook Granite Batholith satellites, Zambia
~550 Ma	Otjiwarongo, Namibia; Kafue Flats, Zambia
~746 Ma	Kalengwa-Kasempa, Zambia; Khorixas, Namibia
~825 Ma	Copperbelt, Zambia (possible, see section 6.4)
~1078 Ma	Witvlei, Omitiomire, Namibia
~1937 Ma	Kamanjab Batholith, Namibia

The rocks of many IOCG deposits and prospects in the Greater Lufilian Arc are pristine. There is no significant deformaton involved. Hydrothermal brecciation and other mineralization features are un-deformed. This may be very useful to study mineralization and alteration processes.

9.9.3 Association of Sedimentary Hosted Copper Mineralization with IOCG Mineralization

A significant finding is the juxtaposition of iron-oxide-copper-gold mineralization underneath the sedimentary-hosted copper deposit at Witvlei, Namibia. This metallogenic event occurred at 1110 Ma. Secondary copper in the sedimentary-hosted deposit might have come from the IOCG deposit that lies underneath. This idea may generate a new concept for the origin of the Copperbelt-Katanga copper and cobalt deposits. The concept also opens an entire new age gap for the exploration of base metal mineralization in the Greater Lufilian Arc and the surrounding environment, including South Africa. There is additional evidence of IOCG mineralization related to sediment-hosted copper in other parts of Namibia and Zambia, including the Chambishi area and parts of the basement to the Copperbelt.

At least three discrete time periods show IOCG mineralization in close temporal spatial association with sedimentary-hosted copper deposits. The first took place around Witvlei from 1108 to 1059 Ma. The second and third ocurred in the basement to the Zambian Copperbelt from 882 to 725 Ma and from 607 to 500 Ma.

10 BIBLIOGRAPHY

Abell, R. S. (1976) *The Geology of the Lukomezi River Area - Explanation of Degree Sheet 1526 NW Quarter* (Geological Report 33), Republic of Zambia, Ministry of Mines and Industry, Geological Survey, Lusaka, Zambia.

Adamson, R. G., & Teichmann, R. F. H. (1986) The Matchless Cupreous Pyrite Deposit, South West Africa/ Namibia, In C. R. Anhaeusser & S. Maske (Eds.), *Mineral Deposits of Southern Africa*, Geological Society of South Africa, Johannesburg, South Africa, 1755-1760.

Agar, R. A. (1981) Copper Mineralization and Magmatic Hydrothermal Brines in the Rio Pisco Section of the Peruvian Coastal Batholith, *Economic Geology*, 76(3): 677-693.

Ahrendt, H., Behr, H. J., Clauer, N., Porada, H., & Weber, K. (1983) K-Ar Age Determinations From the Northern Damara Branch and Their Implications for the Structural and Metamorphic Evolution of the Damara Orogen, South West Africa/Namibia, *Special Publications of the Geological Society of South Africa*, 11: 299-306.

Ajagbe, S. D. (2001) Kamanjab Sheet 1914, *Mineral Resources of Namibia, Economic Geology 1:250,000 Map Series - Summary of Mineral Deposits and Occurrences*, 90, Namibian Geological Survey, Windhoek, Namibia.

Alderton, D. H. M. (1998) The Genesis of Tellurium-Rich Epithermal Precious-Metal Deposits; Examples from Western Romania, In Anonymous (Ed.), *Geological Society of America, 1998 Annual Meeting*, Boulder, CO, United States: Geological Society of America (GSA), 30(7): 301.

Ameglio, L., Page, P., & Jacob, R. E. (2000) 3D-Geometry of the Mon Repos Granodiorite (Goas Dioritic Suite, Damara Belt, Namibia) Inferred from Gravity Data, In A. F. M. Kisters & R. J. Thomas (Eds.), *Geocongress 2000; A New Millennium on Ancient Crust; 27th Earth Science Congress of the Geological Society of South Africa*, Pergamon, Oxford, United Kingdom.

Ameglio, L., Wackerly, R., Jacob, R. E., & Hutchins, D. (2000) Geophysical Imaging of the Goas Dioritic Complex in the Damara Belt (Karibib, Namibia), In A. F. M. Kisters & R. J. Thomas (Eds.), *Geocongress 2000; A New Millennium on Ancient Crust; 27th Earth Science Congress of the Geological Society of South Africa*, Pergamon, Oxford, United Kingdom.

Ammerman, P. J. G. (1994) *Resource Base and Investment Potential of the Zambian Copper Mining Industry,* Unpublished B.Sc., Princeton University, Princeton, N.J., United States.

Anderson, J. L. (1983) Proterozoic Anorogenic Granite Plutonism of North America, Geological Society of America, 161: 133-153.

Andrews, S. C. P. (1986) Gold-Bearing Fluvial and Associated Tidal Marine Sediments of Proterozoic Age in the Mporokoso Basin, Northern Zambia, *Sedimentary Geology*, 48(3-4): 193-222.

Andrews, S. C. P. (1989) The Mid-Proterozoic Mporokoso Basin, Northern Zambia; Sequence Stratigraphy, Tectonic Setting and Potential for Gold and Uranium Mineralization, *Precambrian Research*, 44(1): 1-17.

Andrews, S. C. P., & Mulumba, B. P. (1987) Empirical Guides to Gold Enrichment in Proterozoic Quartz-Pebble Conglomerates in Northern Zambia, *Journal of African Earth Sciences, 6*(4), 595-601.

Andrews, S. C. P., Sliwa, A. S., & Unrug, R. (1984) Primary Gold Occurrences in Zambia and Their Geological Controls, In R. P. Foster (Ed.), *Gold '82; the Geology, Geochemistry and Genesis of Gold Deposits*, A.A. Balkema, Rotterdam, Netherlands, 493-505.

Andrews, S. C. P., & Unrug, R. (1984) Gold in the Sedimentary Cover of the Bangweulu Block, Northern Zambia, In R. P. Foster (Ed.), *Gold '82; the Geology, Geochemistry and Genesis of Gold Deposits*, A.A. Balkema, Rotterdam, Netherlands, 221-237.

Anhaeusser, C. R., & Button, A. (1973) A Petrographic and Mineragraphic Study of the Copper-Bearing Formations in the Witvlei Area, South West Africa, *Transactions of the Geological Society of South Africa*, 76: 279-299.

Anhaeusser, C. R., & Button, A. (1976) A Review of Southern African Stratiform Ore Deposits, Their Position in Time and Space, In K. H. Wolf (Ed.), *Handbook of Strata-Bound and Stratiform Ore Deposits* (Vol. 5, Regional Studies and Specific Deposits), Elsevier Publ. Co., New York, 257-319

Annels, A. E. (1979) Mufulira Greywackes and Their Associated Sulphides, *Institution of Mining and Metallurgy, Transactions, Section B: Applied Earth Science*, 88: B15-B23.

Annels, A. E. (1980) The Genetic Relevance of Recent Studies at Mufulira Mine, Zambia, *Annales de la Societe Geologique de Belgique,* 102(2): 431-449.

Annels, A. E. (1984) The Geotectonic Environment of Zambian Copper Cobalt Mineralization, *Journal of the Geological Society of London*, 141: 279-289.

Annels, A. E. (1986) Ore Genesis in the Zambia Copperbelt, with Particular Reference to the Northern Sector of the Chambishi Basin, *GAC, MAC, CGU; 1986 Joint Annual Meeting; Program with Abstracts*, Geological Association of Canada, Waterloo, ON, Canada, 11: 41.

Annels, A. E., & Simmonds, J. R. (1984) Cobalt in the Zambian Copperbelt, In S. N. Punukollu & S. C. P. Andrews (Eds.), *Proterozoic; Evolution, Mineralization, and Orogenesis*, Elsevier, Amsterdam, The Netherlands, 25(1-3): 75-98.

Annels, A. E., Vaughan, D. J., & Craig, J. R. (1983) Conditions of Ore Mineral Formation in Certain Zambian Copperbelt Deposits with Special Reference to the Role of Cobalt, *Mineralium Deposita*, 18(1): 71-88.

Anonymous (1986) The Geology & Mineral Resources of Zambia and Neighbouring Countries, *AGID News*, 47: 12-18.

Anonymous (2003) Boulder Mining Corp. (BDR-V) New Coverage, *Hard Rock Analyst Journal*, 3(9): 1-4.

Armstrong, R. A., Master, S., Robb, L. J., & Lobo-Guerrero, A. (2004) Geochronology of the Nchanga Granite, and Constraints on the Maximum Age of the Katanga Supergroup, Zambian Copperbelt, *Journal of African Earth Sciences*, in press.

Armstrong, R. A., Robb, L. J., Master, S., Kruger, F. J., & Mumba, P. A. C. C. (1999) New U-Pb Age Constraints on the Katangan Sequence, Central African Copperbelt, In H. E. Frimmel (Ed.), *11th International Conference of the Geological Society of Africa; Earth Resources for Africa*, Pergamon, London, 28(4a): 6-7

Astudillo, C. (2003, October, 2003) Distribución y Caracterización de Carbonatos en Mantoverde, Provincia de Chañaral, Tercera Región, Chile, *CD Actas del X Congreso Geológico Chileno*, Sociedad Geológica de Chilel, Concepción, Chile.

Bailey, D. K. (1957) Carbonatites in the Rufunsa Valley, Central Province, *Records of the Geological Survey of Northern Rhodesia, 1957*, 35-42.

Bailey, D. K. (1959) *Carbonatites and Intrusive Limestone in the Central and Southern Provinces of Northern Rhodesia,* Unpublished Ph.D., University of Dublin, Trinity College, Dublin.

Baker, A. J. M., & Brooks, R. R. (1988) Botanical Exploration for Minerals in the Humid Tropics, *Journal of Biogeography*, 15(1): 221-229.

Bala-Bala, S., & Madi-Lugali, L. (1979) A Propos de la Position Stratigraphique et de L'Origine du Minerai de Fer de Kasumbalesa, *Ann. Fac. Sc. Lubumbashi*, 2: 103-111.

Banda, A. (1994) Technical Report on the Allied Copper Deposit, *Zambian Journal of Applied Earth Sciences*, 8(1): 99-104.

Barbarin, B. (1990) Granitoids: Main Petrogenetic Classifications in Relation to Origin and Tectonic Setting, *Geological Journal*, 25: 227-238.

Barbarin, B. (1999) A Review of the Relationships Between Granitoid Types, Their Origins and Their Geodynamic Environments, *Lithos,* 46: 605-626.

Barr, J. M., & Reid, D. L. (1993) Hydrothermal Alteration at the Haib Porphyry Copper Deposit, Namibia: Stable Isotope and Fluid Inclusion Patterns, *Communications of the Geological Survey of Namibia*, 8(1992/1993): 23-34.

Barra, F., Broughton, D., Ruiz, J., & Hitzman, M. (2004) *Multi-Stage Mineralization in the Zambian Copperbelt Based on Re-Os Isotope Constraints*, Geological Society of America, 2004 Denver Annual Meeting.

Barron, J. W., Broughton, D. W., Armstrong, F. A., & Hitzman, M. W. (2003, July 14 to 24) Petrology, Geochemistry and Age of Gabbroic Bodies in the Solwezi Area, Northwestern Zambia, *3rd. IGCP 450 Conference on Proterozoic Sediment-Hosted Base Metal Deposits of Western Gondwana,* Lubumbashi, Katanga, D.R.Congo.

Barton, M. D., & Johnson, D. A. (1996) Evaporitic-Source Model for Igneous-Related Fe Oxide-(REE-Cu-Au-U) Mineralization, *Geology,* 24(3): 259-262.

Barton, M. D., & Johnson, D. A. (2000) Alternative Brine Sources for Fe-Oxide(-Cu-Au) Systems: Implications for Hydrothermal Alteration and Metals, In T. Porter (Ed.), *Hydrothermal Iron Oxide Copper-Gold & Related Deposits: A Global Perspective*, Australian Mineral Foundation, Adelaide, Australia, 43-60.

Barton, M. D., & Johnson, D. A. (2004a) Footprints of Fe-Oxide(-Cu-Au) Systems, *SEG 2004 - Predictive Mineral Discovery Under Cover - CD*, Society of Economic Geologists, Perth, Western Australia.

Barton, M. D., & Johnson, D. A. (2004b) *Footprints of Fe-Oxide(-Cu-Au) Systems* [Power Point presentation during SEG 2004 Predictive Mineral Discovery Under Cover], Society of Economic Geologists, Perth, Western Australia.

Batchelor, R. A., & Bowden, P. (1985) Petrogenetic Interpretation of Granitoid Rock Series Using Multicationic Parameters, *Chemical Geology*, 48: 43-55.

Beaudry, C., & Schafer, R. (Eds.). (2004) *Exploration for Iron Oxide-Hosted Copper-Gold Deposits - Short Course*, Prospectors and Developers Association of Canada, Toronto, Canada.

Becker, T., & Brandenburg, A. (1997) The Evolution of the Alberta Complex, Naub Diorite and Elim Formation Within the Rehoboth Basement Inlier, Namibia: Geochemical Constraints, *Communications of the Geological Survey of Namibia*, 12: 29-39.

Becker, T., Diedrichs, B., Hansen, B., T., & Weber, K. (2000) Weener Igneous Complex: Geochemistry and Implications for the Evaluation of the Palaeoproterozoic Rehoboth Basement Inlier; Namibia, *Communications of the Geological Survey of Namibia,* 12: 41-52.

Becker, T., & Schreiber, U. (2002) *Guidebook to Excursion: Mesoproterozoic Belts of Namibia, 28 July to 4 August, 2002*, Technical Meeting IGCP Projects 418/440, Windhoek, Namibia.

Behr, H., Ahrendt, H., Porada, H., Rohrs, J., & Weber, K. (1983a) Upper Proterozoic Playa and Sabkha Deposits in the Damara Orogen, SWA/Namibia, *Special Publication of the Geological Society of South Africa*, 11: 1-20.

Behr, H. J., Ahrendt, H., Martin, H., Porada, H., Roehrs, J., & Weber, K. (1983b) Sedimentology and Mineralogy of Upper Proterozoic Playa-Lake Deposits in the Damara Orogen, In H. Martin & F. W. Eder (Eds.), *Intracontinental Fold Belts; Case Studies in the Variscan Belt of Europe and the Damara Belt in Namibia*, Springer-Verlag, Berlin, Germany, 577-610.

Behr, H. J., Ahrendt, H., Porada, H., & Weber, K. (1983) The Sole Dolomite at the Base of the Naukluft Nappe Complex, *Special Publications of the Geological Society of South Africa*, 11: 185-197.

Behr, H. J., & Schmidt, M. A. (1987) The Role of Sedimentary and Tectonic Brines in the Damara Orogen, Namibia, In J. S. Hanor, Y. K. Kharaka, & L. S. Land (Eds.), *Geochemistry of Waters in Deep Sedimentary Basins; Selected Contributions from the Penrose Conference*, Pergamon, Oxford, 2(5-6): 535-542.

Benham, D. G., Greig, D. D., & Vink, B. W. (1976) Copper Occurrences of the Mombezhi Ddome Area, Northwestern Zambia, *Economic Geology*, 71: 433-442.

Berbeleac, I., Micu, C., Kusko, M., Balasa, E., Asztalos, S. T., & Costache, C. (1979) Relationships of the Katanga System, Post-Tectonic Magmatism and the Tectonics of the Kasempa Area, Northwestern Province of Zambia, *Rev. Roum. Geol. Geophis. et Geogr., Boucarest, Geologie*, 23(1): 53-61.

Berhorst, V., Porada, H., & Wolf, J. (1990) Tectonic structures in northern parts of the Khomas Trough, Damara Belt, interpreted in terms of collision tectonics in a forearc, In Anonymous (Ed.), *15th Colloquium of African Geology*, Centre International pour la Formation et les Echanges Geologiques (CIFEG), Paris, France, 20: 247.

Bernasconi, A. (1986) The Marinkas Kwela Alkali Intrusive - A Porphyry Molybdenum System of Cambrian Age in Southern South West Africa/Namibia, In C. R. Anhaeusser & S. Maske (Eds.), *Mineral Deposits of Southern Africa*, Geological Society of South Africa, Johannesburg, South Africa, 2: 1587-1591.

Berube, D., & Jebrak. (1999) High Precision Boundary Fractal Analysis for Shape Characterization, *Computers & Geosciences*, 1059-1071.

Binda, P. L. (1984) *Detrital Copper Sulfides in Stratiform Deposits*, Society of Economic Paleontologists and Mineralogists; First Annual Midyear Meeting, Tulsa, OK, United States.

Binda, P. L. (1987) *Depositional Environment and Copper Mineralization of the Footwall Rocks at Muliashi South, Zambian Copperbelt*, Colloquium on African Geology - Current Research in African Earth Sciences, Rotterdam, Netherlands.

Binda, P. L. (1988) *Evidence for Land-Derived Metals in the Stratiform Deposits of the Zambian Copperbelt*, IAS International Symposium on Sedimentology Related to Mineral Deposits, Beijing, China.

Binda, P. L. (1994a) *Cenozoic Analogies for the Katangan Copper Deposits of Zambia*, Centenaire des Premieres Etudes sur la Geologie Shabienne (Zaire), "Gisements Stratiformes de Cuivre et Mineralisations Associees", Brussels, Belgium.

Binda, P. L. (1994b) Stratigraphy of Zambian Copperbelt Orebodies, In A. B. Kampunzu & R. T. Lubala (Eds.), Neoproterozoic Belts of Zambia, Zaire and Namibia*, Special Issue of the Journal of African Earth Sciences*, 19(4): 251-264.

Binda, P. L. (1995) Reflections on Metallogenic Models for Sediment-Hosted Stratiform Copper Deposits, In M. Wendorff & L. Tack (Eds.), *Late Proterozoic Belts in Central and Southwestern Africa; IGCP Project 302*, Koninklijk Museum voor Midden - Afrika, Tervuren, Belgium, 101: 77-86.

Binda, P. L., & Porada, H. (1995) Observations on the Katangan Breccias of Zambia, In M. Wendorff & L. Tack (Eds.), *Late Proterozoic Belts in Central and Southwestern Africa; IGCP Project 302*, Koninklijk Museum voor Midden - Afrika, Tervuren, Belgium, 101: 49-62.

Blanchard, R. (1969) Interpretation of Leached Outcrops, *Nevada Bureau of Mines Bulletin,* Mackay School of Mines, University of Nevada, Reno, 66: 196.

Bloomfield, K. (1981) The Pan-African Event in Malawi and Eastern Zambia, In D. R. Hunter (Ed.), *Precambrian of the Southern Hemisphere*, Elsevier, Amsterdam, 743-754.

Bonin, B. (1986) *Ring Complex Granites and Anorogenic Magmatism*. Paris: Bureau de Recherches Geologiques et Minieres - North Oxford Academic, 189.

Borg, G. (1995) Metallogenesis of Neoproterozoic Basins in Namibia and Botswana, *Communications of the Geological Survey of Namibia*, 10: 109-119.

Borg, G. (2000) Regional Controls on Sediment-Hosted Pb-Zn (Ba-Cu) Occurrences Within the Pan African Orogenic Belts of Namibia, *Communications of the Geological Survey of Namibia*, 12: 211-220.

Borg, G., Graf, N., & Maiden, K. J. (1987) The Klein Aub Fault Zone - A Wrench Fault System in Middle Proterozoic Metasediments in Central SWA/Namibia, *Communications of the Geological Survey of Namibia*, 3: 91-98.

Borg, G., & Maiden, K. (1986) Stratabound Copper-Silver-Gold Mineralization of Late Proterozoic Age Along the Margin of the Kalahari Craton in SWA/Namibia and Botswana, *Canadian Mineralogist*, 24: 178.

Boric, R., Holmgren, C., Wilson, N. S. F., & Zentili, M. (2002) The Geology of the El Soldado Manto Type Cu (Ag) Deposit, Central Chile, In T. M. Porter (Ed.), *Hydrothermal Iron Oxide Copper-Gold & Related Deposits: A Global Perspective*, PGC Publishing, Adelaide, Australia, 2: 163-184.

Boulder Mining, C. (2002) Boulder Acquires Outstanding Iron Oxide-Copper-Gold (IOCG) Project in Namibia, *press release, April 2, http//www.bouldermining.com*, 2.

Boulder Mining, C. (2002-2004) Various internet press releases on the Tevrede property in NW Namibia, *http://www.bouldermining.com*.

Boulder Mining, C. (2003a) Impressive Gold Copper Results from Tevrede Point to Strong Iron Oxide Copper-Gold Targets, *press release, January 20, http//www.bouldermining.com*, 4.

Boulder Mining, C. (2003b) Tevrede Property - Namibia: An Outstanding Iron Oxide-Copper-Gold Project, *press release, September 3, http//www.bouldermining.com/tevrede.project.htm*, 3.

Boulder Mining, C. (2004a) Exploration Program Commences on Tevrede Copper-Gold Project, p*ress release, March 22, http://www.bouldermining.com*, 2.

Boulder Mining, C. (2004b) Reconnaissance Drilling Confirms Gold Discovery, *press release, January 23, http//www.bouldermining.com*, 4.

Bowden, P., Batchelor, R. A., Chappell, B. W., Didier, J., & Lameyre, J. (1984) Petrological, Geochemical and Source Criteria for the Classification of Granitic Rocks: A Discussion, *Physics of the Earth and Planetary Interiors*, 35: 1-11.

Bowden, P., Black, R., Martin, R. F., Ike, E. C., Kinnaird, J. A., & Batchelor, R. A. (1987) Niger-Nigerian Alkaline Ring Complexes: A Classic Example of African Phanerozoic Anorogenic Mid-Plate Magmatism, In J. G. Fitton & B. G. J. Upton (Eds.), *Alkaline Igneous Rocks*, Blackwell Scientific Publications - The Geological Society, Oxford.

Bowden, P., Herd, D., & Kinnaird, J. A. (1995) The Significance of Uranium and Thorium Concentrations in Pegmatitic Leucogranites (Alaskites), Rossing Mine, Swakopmund, Namibia, *Communications of the Geological Survey of Namibia*, 10: 43-49.

Bowden, P., Tack, L., Williams, I. S., & Deblond, A. (1999) Transpression and Transtensional Granite Magmatism in the Central Damaran (Pan-African) Orogenic Belt, Western Namibia, In H. E. Frimmel (Ed.), *11th International Conference of the Geological Society of Africa; Earth Resources for Africa*, Pergamon, London, 28(4a): 13-14.

Bowen, R., & Gunatilaka, A. (1976) The Zambian Copperbelt, *Science Progress*, 63(249): 87-109.

Brandt, R. (1985) Preliminary Report on the Stratigraphy of the Damara Sequence and the Geology and Geochemistry of the Damaran Granites in an Area Between Walvis Bay and Karibib, *Communications of the Geological Survey of South West Africa/Namibia* 1: 31-43.

Brandt, R. (1987) Evolution of the Pan-African Granitic Rocks of the Damara Orogen, Namibia, In G. Matheis & H. Schandelmeier (Eds.), *Current Research in African Earth Sciences,* 14: 121-125.

Brandt, R. T. (1954) Mumbwa District - Notes on the Geology and Mineralization in the Mumbwa District, *Records of the Geological Survey of Northern Rhodesia, 1954*, 11-14.

Brandt, R. T. (1955a) The Geology and Mineral Resources of the Big Concession - Mumbwa District, *Bulletin, 2*, 56.

Brandt, R. T. (1955b) Geology and Mineralization in the "Big Concession", *Northern Rhodesia Records of the Geological Survey for the Year Ending December 31, 1953*, 10-11.

Brandt, R. T. (1955c) Mumbwa District - Geology and Mineralization of the "Big Concession", *Records of the Geological Survey of Northern Rhodesia* (For the Year ending 31st December, 1953), 10-11.

Brandt, R. T. (1956a) Examination of Dumps at the Sable Antelope Mine, Mumbwa District, *Northern Rhodesia Records of the Geological Survey for Year Ending 31st December 1954*, 14-15.

Brandt, R. T. (1956b) The Kamiyobo Copper Prospect, Mumbwa District, *Northern Rhodesia Records of the Geological Survey for Year Ending 31st December 1954*, 12-15.

Branquet, Y., Cheilletz, A., Laumonier, B., & Giuliani, G. (1999) Fluidization During Tectonics; The Hydrothermal Breccias in Colombian Emerald Deposits, In Anonymous (Ed.), *European Union of Geosciences Conference Abstracts; EUG 10*, Cambridge Publications, Cambridge, United Kingdom, 4(1): 618).

Broderick, T. J. (1981) The Zambezi Metamorphic Belt in Zimbabwe, In D. R. Hunter (Ed.), *Precambrian of the Southern Hemisphere*, 739-743.

Broughton, D. W., Hitzman, M. W., & Stephens, A. J. (2002) Exploration History and Geology of the Kansanshi Cu (-Au) Deposit, Zambia, *Special Publication 9*, Society of Economic Geologists, 141-153.

Brown, A. C. (1981) The Timing of Mineralization in Stratiform Copper Deposits, In K. H. Wolf (Ed.), *Regional Studies and Specific Deposits*, Elsevier Sci. Publ. Co., Amsterdam, 9: 1-23.

Brown, A. C. (1992) Sediment-Hosted Stratiform Copper Deposits, *Geoscience Canada*, 19(3): 125-141.

Brown, A. G. (1966) The Geology of the Monze Area - Explanation of Degree Sheet 1627, NW Quarter, *Report of the Geological Survey* 17, Geological Survey of Zambia, Lusaka, Zambia.

Brynard, H. J., & Andreoli, M. A. G. (1988) An Overview of the Regional, Geological and Structural Setting of the Uraniferous Granites in the Damara Orogen, Namibia, In J. Moore (Ed.), *Recognition of Uranium Provinces; Proceedings of a Technical Committee Meeting*, International Atomic Energy Agency, Vienna, Austria, 195-212.

Bryner, L. (1968) Proposed Terminology for Hydrothermal Breccias and Conglomerates, *Economic Geology*, 63(6): 692.

Buehn, B., Doerr, W., & Brauns, C. M. (1999) Petrology and Age of the Otjisazu Carbonatite Complex, Namibia; Implications for the Pre- and Syn-Orogenic Damaran Evolution, In H. E. Frimmel (Ed.), *11th International Conference of the Geological Society of Africa; Earth Resources for Africa*, Pergamon, London, 28(4a):14-15.

Buehn, B., Rankin, A. H., Schneider, J., & Dulski, P. (2002) The Nature of Orthomagmatic, Carbonatitic Fluids Precipitating REE, Sr-Rich Fluorite; Fluid-Inclusion Evidence From the Okorusu Fluorite Deposit, Namibia, *Chemical Geology*, 186(1-2): 75-98.

Buehn, B., & Stanistreet, I. G. (1991a) Interaction of Basin Evolution and Glacial Events in Late Proterozoic Manganese Deposits at Otjosondu, Damara Belt, Namibia, In Anonymous (Ed.), *Sixth Meeting of the European Union of Geosciences*, Blackwell Scientific Publications, Oxford, 3(1): 409.

Buehn, B., & Stanistreet, I. G. (1991b) A Sedimentary and Genetic Model for the Late Proterozoic Otjosondu Manganese Deposits, Damara Belt, Namibia, Controlled by Basin Evolution and Glaciation, In P. G. Eriksson (Ed.), *Precambrian Sedimentary Basins of Southern Africa,* Blackwell Scientific Publications, Oxford,3(3): 4.

Buehn, B., & Stanistreet, I. G. (1993) A Correlation of Structural Patterns and Lithostratigraphy at Otjosondu with the Damara Sequence of the Southern Central Zone, Namibia, *Communications of the Geological Survey of Namibia*, 8: 15-21.

Buehn, B., Stanistreet, I. G., & Charlesworth, E. G. (1991a) Multiple Deformation Patterns in the Otjosondu Manganese Mining Area, Eastern Damara Belt, Namibia, *Communications of the Geological Survey of Namibia*, 7: 15-19.

Buehn, B., Stanistreet, I. G., & Okrusch, M. (1991b) *Genesis of Late Proterozoic Sedimentary Manganese Deposits at Otjosondu, Damara Mobile Belt, East Central Namibia*, *Economic Geology Research Unit Information Circular* 234, University of the Witwatersrand, Johannesburg, South Africa.

Buehn, B., Stanistreet, I. G., & Okrusch, M. (1992a) Late Proterozoic Manganese and Iron Formations at Otjosondu/ Namibia in the Light of Source, Transport and Depositional Regime, In Anonymous (Ed.), *29th International Geological Congress; Abstracts*, (29: 212).

Buehn, B., Stanistreet, I. G., & Okrusch, M. (1992b) Late Proterozoic Outer Shelf Manganese and Iron Deposits at Otjosondu (Namibia) Related to the Damaran Oceanic Opening, *Economic Geology*, 87(5): 1393-1411.
Buehn, B., Stanistreet, I. G., & Okrusch, M. (1993) Preservation of Sedimentary Features in Late Proterozoic Manganese and Iron Formation (Namibia) Through Upper Amphibolite Facies Metamorphism; Protoliths, Paleoenvironments and Ore Genesis, In S. Ishihara, T. Urabe, & H. Ohmoto (Eds.), *Mineral Resources Symposia; Volume C, Selected Papers from the Symposia I-3-47, II-16-5, II-16-10, and II-16-12; Ferro-Manganese Deposits, Anoxic Sediments and Massive Sulfide Deposits* (Vol. Special Issue 17), Tokyo, Japan: Shigen Chishitsu Gakkai - Society of Resource Geologists of Japan, 12-26.
Buerger, A. J., & Coertze, F. J. (1975) Age Determinations - April 1972 to March 1974, *Annuary of the Geological Survey of South Africa,* 10: 135-141.
Buhn, B., Stanistreet, I. G., & Charlesworth, E. G. (1993) Fold Shape Variation Controlling Interference Mechanisms and Patterns During Oblique Fold Superpositions in the Damara Orogen, Eastern Namibia, *Annales Tectonicae,* 7(2): 113-128.
Bulambo, M., De Waele, B., Kampunzu, A. B., & Tembo, F. (2004, 2-7 June, 2004) Shrimp U-Pb Geochronology of the Choma-Kalomo Block (Zambia) and Geological Implications, *20th Colloquium of African Geology*, Orleans, France.
Burger, A. J., Clifford, T. N., & Miller, R. M. (1976) Zircon U-Pb Ages of the Franzfontein Granitic Suite, Northern South West Africa, *Precambrian Research*, 3: 415-431.
Burger, A. J., & Coertze, F. J. (1975) Age Determinations - April 1972 to March 1974, *Annuary of the Geological Survey of South Africa,* 11: 135-141.
Burger, A. J., & Coertze, F. J. (1978) Summary of Age Determinations Carried Out During the Period April 1974 to March 1975, *Annuary of the Geological Survey of South Africa*, 11: 317-321.
Burke, K. (1992) *Continental Rifts and Mineral Resources*, Geological Society of America, 1992 Annual Meeting, Boulder, CO, United States.
Burnard, P., Vaughan, D. J., & Sweeney, M. A. (1990a) *Contrasting Styles of Copper Mineralization in Zambia; the Nampundwe Deposit and the Copperbelt*, Etudes Recentes sur la Geologie de l'Afrique; 15 (Super e) Colloque de Geologie Africaine; Resumes Detailles, Paris, France.
Burnard, P., Vaughan, D. J., & Sweeney, M. A. (1990b) *A Geochemical, Geological and Isotopic Investigation of the Nampundwe Deposit, Zambia; Evidence for Central African Volcanogenic/ Exhalative Ores?*, In Anonymous (Ed.), *15th Colloquium of African Geology*, Centre International pour la Formation et les Echanges Geologiques (CIFEG), Paris, France, 20.
Burnard, P. G., Sweeney, M. A., Vaughan, D. J., Spiro, B., & Thirlwall, M. F. (1993) Sulfur and Lead Isotope Constraints on the Genesis of a Southern Zambian Massive Sulfide Deposit, *Economic Geology*, 88(2): 418-436.
Burnett, R. J. (1999) Gold, In G. I. C. Schneider (Ed.), *Mineral Deposits of Namibia CD edition*, Geological Survey of Namibia, Windhoek, 37 p.
Cahen, L., Snelling, N. J., Delhal, J., & Vail, J. R. (1984) *The Geochronology and Evolution of Africa*, Clarendon Press, Oxford.
Cailteux, J. (1991) La Tectonique Intra-Katanguienne Dans La Region Nor-Ouest De L'Arc Lufilien (Shaba, Rep. du Zaire), *Annales de la Societe Geologique de Belgique*, 113(2): 199-215.
Cailteux, J. (1994) Lithostratigraphy of the Neoproterozoic Shaba-Type (Zaire) Roan Supergroup and Metallogenesis of Associated Stratiform Mineralization, In A. B. Kampunzu & R. T. Lubala (Eds.), Neoproterozoic Belts of Zambia, Zaire and Namibia, Special Issue, *Journal of African Earth Sciences*, 19(4): 279-301.
Cailteux, J., Binda, P. L., Katekesha, W. M., Kampunzu, A. B., Intiomale, M. M., Kapenda, D., Kaunda, C., Ngongo, K., Tshiauka, T., & Wendorff, M. (1994) Lithostratigraphical Correlation of the Neoproterozoic Roan Supergroup from Shaba (Zaire) and Zambia, in the Central African Copper-Cobalt Metallogenic Province, In A. B. Kampunzu & R. T. Lubala (Eds.), Neoproterozoic Belts of Zambia, Zaire and Namibia, Special Issue, *Journal of African Earth Sciences*, 19(4): 265-278.
Cailteux, J. L. H., Binda, P. L., Kampunzu, H. A. B., Katekesha, W. M., Kaunda, C., & Wendorff, M. (1995) Results of Lithostratigraphic Correlation of the Late Proterozoic Roan Supergroup Between Zambia and Zaire, Central African Copperbelt,
In M. Wendorff & L. Tack (Eds.), *Late Proterozoic Belts in Central and Southwestern Africa; IGCP Project 302*, Koninklijk Museum voor Midden - Afrika, Tervuren, Belgium, 101: 21-27.
Cailteux, J. L. H., & Kampunzu, H. A. B. (1995) The Katangan Tectonic Breccias in the Shaba Province (Zaire) and their Genetic Significance, In M. Wendorff & L. Tack (Eds.), *Late Proterozoic Belts in Central and Southwestern Africa; IGCP Project 302*, Koninklijk Museum voor Midden - Afrika, Tervuren, Belgium, 101: 63-76.
Cairney, T. (1958) *The Geology of the Leopards Hill Area - Explanation of the Degree Sheet 1528 SE Quarter* (21), Geological Survey of Zambia, Lusaka.
Cairney, T. (1967) *The Geology of the Leopards Hill Area - Explanation of Degree Sheet 1528, SE Quarter* (Geological Report 21), Zambian Geological Survey, Lusaka.
Calles, M. R., Miranda, G. M. A., & Garza, R. A. P. (1988) The Matoma and Condesa Ag-Pb-Zn Chimneys, Two Magmatic-Hydrothermal Breccias of El Potosi Mine, Santa Eulalia, Chihuahua, Mexico, In K. F. Clark, P. C. Goodell, & J. M. Hoffer (Eds.), *Stratigraphy, Tectonics and Resources of Parts of Sierra Madre Occidental Province, Mexico*, El Paso Geological Society, El Paso, Texas, United States, 1988: 269-282.
Camus, F. (2003) *Geología de los Sistemas Porfiríticos en los Andes de Chile*, Servicio Nacional de Geología y Minería, Santiago, Chile.
Carlon, C. J. (2000) Iron Oxide Systems and Base Metal Mineralization in Northern Sweden, In T. M. Porter (Ed.), *Hydrothermal Iron Oxide Copper-Gold & Related Deposits: A Global Perspective*, PGC Publishing, Adelaide, Australia, 1: 283-296.
Carten, R. B. (1986) Sodium-Calcium Metasomatism: Chemical, Temporal, and Spatial Relationships at the Yerington, Nevada, Porphyry Copper Deposit, *Economic Geology*, 81: 1495-1519.
Carvajal, C. R., & Palacios, C. (1999) A Newly Described post Early Cretaceous Epithermal Deposit, Central Chile, In Anonymous (Ed.), *Geological Society of America, 1999 Annual Meeting*, Geological Society of America, 31(7): 405-406.
Chabu, M. (1989) *Carbonate Hosted Zinc-Lead-Copper Deposits of Kakontwe Basin of Zaire and Zambia (Central Africa)*, 28th International Geological Congress.
Chamberlain, I. C. L. (1982) Nickel Prospecting in Zambia with Reference to Four Locations, *Geochemistry in Zambia*; Report of the AGID Geochemical Workshop, Lusaka.
Chapman, D. S. (1983) Thermal Regime of the Luanshya Mine, Republic of Zambia, *Geoexploration*, 21(4): 265-281.
Charlet, J. M., & Makabu, G. (2000) La Prospection des Gisements Caches d'Uranium et Metaux Associes par les Techniques Gaz, le Cas du Katanga, *Bulletin des Siences de l'Academie Royale des Sciences d'Outre-Mer*, 46(3): 319-338.
Chetty, D., & Frimmel, H. E. (2000) The Role of Evaporites in the Genesis of Base Metal Sulphide Mineralisation in the Northern Platform of the Pan-African Damara Belt, Namibia; Geochemical and Fluid Inclusion Evidence from Carbonate Wall Rock Alteration, *Mineralium Deposita*, 35(4): 364-376.
Cikin, M. (1968) A Preliminary Report on the Geology and Ore Reserves of the Hippo Mine, Kafue National Park, *Economic Report 19*, Zambian Geological Survey Department, Lusaka, Zambia.
Cikin, M. (1972) Geology of the North-Eastern Margin of the Hook Granite Massif, Central Province, *Records of the Geological Survey of Zambia*, 12: 43-54.

Cikin, M., & Drysdall, A. R. (1971) The Geology of the Big Concession - Explanation of Degree Sheet 1426, SE Quarter - With a Section on Economic Geology, *Report of the Geological Survey* No. 27, Ministry of Mines and Mining Development, Geological Survey, Lusaka, Zambia, 72 p.

Clague, S., & Ogilvie, P. (2002) Joumbira Zinc Project, Otjiwarongo, Namibia, *11th IAGOD Quadrennial Symposium and Geocongress CD*, Windhoek, Namibia.

Clark, J. P., & Browne, P. R. L. (1998) Surface Alteration Between Orakeikorako and Te Kopia Thermal Areas, In S. F. Simmons, O. E. Morgan, & M. G. Dunstall (Eds.), *Proceedings of the 20th New Zealand Geothermal Workshop 1998*, University of Auckland Geothermal Institute, Centre for Continuing Education, Auckland, New Zealand, 20: 271-276.

Clarke, D. B. (1992) *Granitoid Rocks*, Chapman and Hall, London.

Clemens, J. D., & Mawer, C. K. (1992) Granitic Magma Transport by Fracture Propagation, *Tectonophysics*, 204: 339-360.

Clemmey, H. (1977) The Genetic Significance of Mineralized Pre-Roan Weathering Horizons on the Zambian Copperbelt, In A. M. Evans (Ed.), *Mineralization Associated with Acid Magmatism and Other Aspects of Ore Geology*, Institution of Mining and Metallurgy, London, 86: B162.

Clifford, T. N., Nicolaysen, L. O., & Burger, A. J. (1962) Petrology and Age of the Pre-Otavi Basement Granite at Franzfontein, Northern South-West Africa, *Journal of Petrology, 3:* 244-279.

Clifford, T. N., Rooke, J. M., & Allsopp, H. L. (1962) Petrochemistry and Age of the Franzfontein Granitic Rocks of Northern South-West Africa, *Geochimica et Cosmochimica Acta, 33*: 973-986.

Collins, W. J., Beams, S. D., White, A. J. R., & Chappell, B. W. (1982) Nature and Origin of A-type Granites with Particular Reference to Southeastern Australia, *Contributions to Mineralogy and Petrology, 80*: 189-200.

Collinston, W. P., & Schoch, A. E. (2000) Mid-Proterozoic Tectonic Evolution Along the Orange River on the Border Between South Africa and Namibia, *Communications of the Geological Survey of Namibia, 12*: 53-62.

Cooke, R. (1965) *Preliminary Report on the Ondundu Gold and Copper Occurrences Otjohorongo Reserve, Namibia*, Geological Survey of Namibia, Windhoek, Namibia.

Cooper, A. F. (1988) Geology of Dicker Willem, A Subvolcanic Carbonatite Complex in South-West Namibia, *Communications of the Geological Survey of Namibia, 4*: 3-12.

Corner, B. (1983) *An Interpretation of the Aeromagnetic Data Covering Portion of the Damara Orogenic Belt, With Special Reference to the Occurrence of Uraniferous Granite*, unpublished report.

Corner, B. (2000) Crustal Framework of Namibia Derived from Magnetic and Gravity Data, *Communications of the Geological Survey of Namibia, 12*: 13-19.

Corner, B. (2002) Ring Structures in Southern Africa, *Geocongress 2002 - CD*, Geological Society of South Africa-Geological Society of South Namibia, Windhoek, Namibia.

Corner, B. (2003) Geophysical Mapping of Major Structures of Southern Africa and an Assessment of Kimberlite Correlation, *International Kimberlite Conference - CD*, Vancouver, Canada.

Corner, B., Cartwright, J., & Swart, R. (2002) Volcanic Passive Margin of Namibia: A Potential Fields Perspective, *Geological Society of America, Special Paper 362:* 203-220.

Corriveau, L., & P., G. M. (1991) Coexisting K-Rich Alkaline and Shoshonitic Magmatism of Arc Affinities in the Proterozoic: A Reassessment of Syenitic Stocks in the Southwestern Grenville Province, *Contributions to Mineralogy and Petrology, 113*: 262-279.

Cosi, M., De, B. A., Gosso, G., Hunziker, J., Martinotti, G., Moratto, S., Robert, J. P., & Ruhlman, F. (1989) *Preliminary Report on Age Work Performed on Rocks and Minerals of the North-Western Prospecting Licences of AGIP in Zambia* (unpublished), Lusaka.

Cosi, M., De, B. A., Gosso, G., Hunziker, J., Martinotti, G., Moratto, S., Robert, J. P., & Ruhlman, F. (1992) Late Proterozoic Thrust Tectonics, High-Pressure Metamorphism and Uranium Mineralization in the Domes area, Lufilian Arc, Northwestern Zambia, In G. Gaal & K. J. Schulz (Eds.), *Precambrian Metallogeny Related to Plate Tectonics*, 58(1-4): 215-240.

Coward M. P., & Daly, M. C. (1984) Crustal Lineaments and Shear Zones in Africa: Their Relationship to Plate Movements, *Precambrian Research, 24:* 27-45.

Cox, K. G., Bell, J. D., & Pankhurst, R. J. (1979) *The Interpretation of Igneous Rocks,* Allen and Unwin, London.

Cox, R. A., Rivers, T., Mapani, B., Tembo, F., & De Waele, B. (2002) New U-Pb Data for the Irumide Belt: LAM-ICP-MS Results for the Luangwa Terrane, *11th IAGOD Quadrennial Symposium and Geocongress CD*, Windhoek, Namibia.

Creaser, R. A., Price, R. C., & Wormald, R. J. (1991) A-Type Granites Revisited: Assessment of a Residual-Source Model, *Geology, 19*: 163-166.

Croaker, M., Selley, D., & Mwale, G. (2004) Neoproterozoic Sediment-Hosted Cu-Co Mineralization at the Nkana-Mindola Deposit, Zambia, *SEG 2004 - Predictive Mineral Discovery Under Cover - CD*, Society of Economic Geologists, Perth, Western Australia.

Cutten, H., Fernandez-Alonso, M., De Waele, E. B., & Tack, L. (2004, 2-7 June, 2004) *Age Constraints for Basin Evolution and Sedimentation in the "Northeastern Kibaran Belt"*, 20th Colloquium of African Geology, Orleans, France.

Daliran, F. (2002) Kiruna-Type Iron Oxide-Apatite Ores and "Apatitites" of the BAFQ District, Iran, With an Emphasis on the REE Geochemistry of Their Apatites, In T. M. Porter (Ed.), *Hydrothermal Iron Oxide Copper-Gold & Related Deposits: A Global Perspective*, PGC Publishing, Adelaide, Australia, 2: 303-320.

Daly, M. C. (1986a) Crustal Shear Zones and Thrust Belts: Their Geometry and Continuity in Central Africa, *Philosophical Transactions of the Royal Society of London*, A 317: 111-128.

Daly, M. C. (1986b) The Intra-Cratonic Irumide Belt of Zambia and its Bearing on Collision Orogeny During the Proterozoic of Africa, Collision Tectonics, *Geological Society Special Publication*, 19: 321-328.

Daly, M. C., & 1986. (1986) *The Tectonic and Thermal Evolution of the Irumide Belt, Zambia,* Unpublished Ph.D., University of Leeds, Leeds.

Daly, M. C., Chakraborty, S. K., Kasolo, P., Musiwa, M., Mumba, P., Naidu, B., Namateba, C., Ngambi, O., & Coward, M. P. (1984) The Lufilian Arc and Irumide Belt of Zambia: Results of a Geotraverse Across Their Intersection, *Journal of African Earth Sciences, 2*(4): 311-318.

Davidson, G., J., Davis, B., K., & Garner, A. (2002) Structural and Geochemical Constraints on the Emplacement of the Monakoff Oxide Cu-Au (-Co-U-REE-Ag-Zn-Pb) Deposit, Mt. Isa Inlier, Australia, In T. M. Porter (Ed.), *Hydrothermal Iron Oxide Copper-Gold & Related Deposits: A Global Perspective*, PGC Publishing, Adelaide, Australia, 2: 49-75.

Dawson, A. L. (1982a) The Inyati Copper Prospect, Northwestern Province, Zambia, In D. C. Turner (Ed.), *Geochemistry in Zambia; Report of the AGID Geochemical Workshop*, Association of Geoscientists for International Development, 9: 54-64.

Dawson, A. L. (1982b) The Kalengwa Copper Deposit, Northwestern Province, Zambia, In D. C. Turner (Ed.), *Geochemistry in Zambia; Report of the AGID Geochemical Workshop*, Association of Geoscientists for International Development, 9: 65-76.

de Carvalho, H., & Alves, P. (1993) *The Precambrian of SW Angola and NW Namibia; General Remarks, Correlation Analysis, Economic Geology*, Vol. 4, Instituto de Investigacao Cientifica Tropical, Lisbon, Portugal.

de Carvalho, H., Pereira, C. J., Silva, Z. C. G., & Vialette, Y. (1985) The Kibaran Cycle in South West Angola, In P. Bowden, J. A. Kinnaird, & H. F. D. Van (Eds.), *13th Colloquium of African Geology; Abstracts*, Centre International pour la Formation et les Echanges Geologiques (CIFEG), Paris, France, 3: 52-53.

de Castro, F., Tallarico, F., & Araujo, J. (2004) The IOCG Deposits of the Carajas Mineral District, In C. Beaudry (Ed.), *Exploration for Iron Oxide-Hosted Copper-Gold Deposits - Short Course*, Prospectors and Developers Association of Canada, Toronto, pp. 2

de Kock, G. S. (1987) The Tectonostratigraphy and Basin Development of a Portion of the Damara Orogen Southeast of Karibib, S. W. A, In Anonymous (Ed.), *Abstracts of the Annual Congress of the Tectonics Division of the Geological Society of South Africa*, Pretoria, South Africa, 21: 104.

de Kock, G. S. (1991) Tectonostratigraphy and Basin Evolution of the Damara Orogen Southeast of Karibib, Namibia, In P. G. Eriksson (Ed.), *Precambrian Sedimentary Basins of Southern Africa*, Blackwell Scientific Publications, Oxford, 3: 7-8.

de Kock, G. S. (1992) Forearc Basin Evolution in the Pan-African Damara Belt, Central Namibia; the Hureb Formation of the Khomas Zone, *Precambrian Research, 57*(3-4): 169-194.

de Kock, G. S., Eglington, B., Armstrong, R. A., Harmer, R. E., & Walraven, F. (2000) U-Pb and Pb-Pb Ages of the Naauwpoort Rhyolite, Kawakeup Leptite and Okongava Diorite: Implications for the Onset of Rifting and of Orogenesis in the Damara Belt, Namibia, *Communications of the Geological Survey of Namibia, 12*: 81-88.

De la Roche, H., Leterrier, J., Gandclaude, P., & Marchal, M. (1980) A Classification of Volcanic and Plutonic Rocks Using R1R2-Diagram and Major-Element Analyses - Its Relationships with Current Nomenclature, *Chemical Geology*, 29: 183-210.

De Swardt, A. M. J. (1962) Structural Relationships in the Northern Rhodesian Copperbelt: An Alternative Explanation, *Occasional Paper, Northern Rhodesia Geological Survey*, Lusaka, 30:15-28.

De Waele, B. (1998) Geology and Stratigraphy of the Mupamadzi River Area and Correlation with the Adjoining Areas Within the Irumide Belt, *Zambian Journal of Applied Earth Sciences*, 11(1): 34-48.

De Waele, B. (2004) A U-Pb Shrimp Geochronological Database for the Irumide Belt of Zambia: From Paleoproterozoic Sedimentation to Late Mesoproterozoic Magmatism, *32nd International Geological Congress - Memoirs*, Florence, Italy.

De Waele, B., & Fitzsimons, I. C. W. (2004) The Age and Detrital Fingerprint of the Muva Supergroup of Zambia: Molassic Deposition to the Southwest of the Ubendian Belt, *Geoscience Africa 2004 - CD*, Geological Society of South Africa, Johannesburg, South Africa.

De Waele, B., Fitzsimons, I. C. W., & Nemchin, A. A. (2004, 2-7 June, 2004) *Paleoproterozoic to Mesoproterozoic Deposition, Magmatism and Metamorphism at the Southeastern Margin of the Congo Craton: The Geological History of the Irumide Belt*, 20th Colloquium of African Geology, Orleans, France.

De Waele, B., Fitzsimons, I. C. W., & Wingate, M. T. D. (2003a) *The Tectonothermal History of the Irumide Belt of Zambia, Regional Significance of New Geochronological Constraints*, The Assembly and Breakup of Rodinia, South China Field Symposium, Hangzou, China.

De Waele, B., & Mapani, B. (2002) Geology and Correlation of the Central Irumide Belt, *Journal of African Earth Sciences*, 35: 385-397.

De Waele, B., Nemchin, A. A., & Kampunzu, A. B. (2003) *The Bangweulu Block of Northern Zambia: Where is the Pre-Ubendian Crust?*, The Assembly and Breakup of Rodinia - South China Field Symposium, Hangzou, China.

De Waele, B., & Tembo, F. (1999) *A Review of Geochronological Data on the Irumide Orogeny, Zambia*, International Conference IGCP 418 Evolution of the Kibaran Belt, Kitwe, Zambia.

De Waele, B., & Tembo, F. (2000) *Geochemical and Petrological Characteristics of Granitic Rocks in the Serenje Area, Central Irumide Belt, Zambia*, Geocongress 2000: 27th Earth Science Congress of the Geological Society of South Africa, Capetown, South Africa.

De Waele, B., Tembo, F., & Key, R. (2000) Towards a Better Understanding of the Mesoproterozoic Irumide Belt of Zambia: Report on a Geotraverse Across the Belt - Report of the Third Annual Field Meeting of IGCP 418 - The Kibaran of Southwestern Africa, *Episodes*, 23(2): 126-130.

De Waele, B., Tembo, F., & Wingate, M. T. D. (2001a) *Characterization of Syn- and Post-Collisional Granite Magmatism, and Metavolcanics in the Irumide Belt, Zambia*, Abstract volume, 4th Annual Field Meeting IGCP 418, Durban, South Africa.

De Waele, B., Tembo, F., & Wingate, M. T. D. (2001b) *A Review of the Geochronology of the Irumide Belt, Zambia*, 4th International Archean Symposium, Perth, Western Australia.

De Waele, B., Wingate, M. T. D., Fitzsimons, I. C. W., & Mapani, B. S. E. (2003) Untying the Kibaran Knot: A Reassessment of Mesoproterozoic Correlations in Southern Africa Based on SHRIMP U-Pb Data from the Irumide Belt, *Geology*, 31(6): 509-512.

De Waele, B., Wingate, M. T. D., & Mapani, B. S. E. (2002) Geochronological Constraints on Granitoid Magmatism and Deformation in the SW Irumide Belt, Zambia, *11th IAGOD Quadrennial Symposium and Geocongress CD*, Windhoek, Namibia.

Deane, J., G. (1995) The Structural Evolution of the Kombat Deposits, Otavi Mountainland, Namibia, *Communications of the Geological Survey of Namibia*, 10: 99-107.

Debon, F., & Le Fort, P. (1988) A Cationic Classification of Common Plutonic Rocks and Their Magmatic Associations: Principles, Method, Applications, *Bulletin Mineralogique*, 111: 493-510.

Debon, F., & LeFort, P. (1983) A Chemical-Mineralogical Classification of Common Plutonic Rocks and Associations, *Transactions of the Royal Society of Edinburgh: Earth Sciences*, 73: 135-149.

deKlerk, S. L. (2001) Gold Deposits in the SADC Region, *Mineral Resources Survey Programme - Southern African Development Community - Mining Sector Coordinating Unit*, 4: 107.

DeSwardt, A. M. J., Garrard, P., & Simpson, J. G. (1965) Major Zones of Transcurrent Dislocation and Superposition of Orogenic Belts in Part of Central Africa, *Geological Society of America Bulletin*, 76: 89-102.

DeSwardt, A. M. J., & Simpson, J. G. (1972) A Structural Interpretation for Part of Zambia, *Records of the Geological Survey of Zambia,* 12: 31-35.

Dingeldey, D. P., Durr, S. B., Charlesworth, E. G., Franz, L., Okrusch, M., & Stanistreet, I. G. (1994) A Geotraverse Through the Northern Coastal Branch of the Damaran Orogen West of Sesfontein, Namibia, In A. B. Kampunzu & R. T. Lubala (Eds.), Neoproterozoic Belts of Zambia, Zaire and Namibia, *Journal of African Earth Sciences*, Special Issue 19; 4: 315-329.

Dold, B. (2003) Enrichment Processes in Oxidizing Sulfide Mine Tailings: Lessons for Supergene Ore Formation, *SGA News,* 16(1):10-15.

Dombrowski, A. Hoernes, S., & Okrusch, M. (1996) Scapolitization in the Kuiseb Formation of the Damara Orogen: Geochemical and Stable Isotope Evidence for Fluid Infiltration Along Deep Crustal Shear Zones, *Communications of the Geological Survey of Namibia*, 11: 21-29.

Dow, R. J., & Hitzman, M. W. (2002) Geology of the Arizaro and Lindero Prospects, Salta Province, Northwest Argentina: Mid-Miocene Hydrothermal Fe-Ox Copper-Gold Mineralization, In T. M. Porter (Ed.), *Hydrothermal Iron Oxide Copper-Gold & Related Deposits: A Global Perspective*, PGC Publishing, Adelaide, Australia, 2: 153-161

Downing, K. N. (1983) The Stratigraphy and Palaeoenvironment of the Damara Sequence in the Okahandka Lineament Area, In R. G. Miller (Ed.), *Evolution of the Damara Orogen of South West Africa-Namibia,* Geological Society of South Africa, Johannesburg, South Africa, 11: 37-41.

Downing, K. N., & Coward, M. P. (1981) The Okahandja Lineament and its Significance for Damaran Tectonics in Namibia, *Band 70, Heft 3,(un-identified German journal)*, 972-1000.
Drakulic, D. (1984a) Hydrothermal Iron Ore Deposits Genetically Associated with Consolidation of Basic Magma in the North West Zambia (Chisaca Area Between Solwesi and Mwinilunga), Tezisy; *27-y Mezhdonarodnyy Geologicheskiy Kongress - Abstracts; 27th International Geological Congress*.
Drakulic, D. (1984b) Some New Aspects of the Cu-Deposits Genesis in the Copperbelt; Zambia, *Tezisy; 27-y Mezhdunarodnyy Geologicheskiy Kongress--Abstracts; 27th International Geological Congress*.
Drysdall, A. R., & Garrard, P. (1964) Significance of the Radiometric Ages of the Nchanga and Lusaka Granites, Northern Rhodesia, *Geological Magazine*, 101(2): 161-168.
Drysdall, A. R., & Stillman, C. J. (1966) Scapolite From the Katanga Carbonate Rocks of the Lusaka District, *Records of the Geological Survey of Zambia*, 10: 20-24.
Duerr, S. B., Dingeldey, D. P., & Prave, A. R. (1997) Tale of Three Cratons; Tectonostratigraphic Anatomy of the Damara Orogen in Northwestern Namibia and the Assembly of Gondwana; Discussion and Reply, *Geology*, 25(12): 1149-1151.
Dunai, T., Stoessel, G. F. U., & Ziegler, U. R. F. (1989) Note: A Sr Isotope Study of the Eureka Carbonatite, Damaraland, Namibia, *Communications of the Geological Survey of Namibia*, 5: 89-90.
Duncan, A. R., Newton, S. R., van den Berg, C., & Reid, D. L. (1989) Geochemistry and Petrology of Dolerite Sills in the Huab River Valley, Damaraland, North-Western Namibia, *Communications of the Geological Survey of Namibia*, 5: 5-17.
Eby, G. N. (1990) The A-Type Granitoids: A Review of Their Occurrence and Chemical Characteristics and Speculations on Their Pterogenesis, *Lithos*, 26: 115-134.
Eby, G. N. (1992) Chemical Subdivision of the A-Type Granitoids: Petrogenetic and Tectonic Implications, *Geology*, 20: 641-644.
Eglington, B. M., & Armstrong, R. A. Geochronological and Isotopic Constraints on the Mesoproterozoic Namaqua-Natal Belt: Evidence from Deep Borehole Intersections in South Africa, *Precambrian Research*, 125: 179-189.
Ellis, M. W., & McGregor, J. A. (1967) The Kalengwa Copper Deposit in North-Western Zambia, *Economic Geology*, 62: 781-797.
Equinox Resources, L. (2003) *Quarterly Report to Shareholders for the Three Months Ended 31 December 2003* , Perth, Australia.
Equinox Resources, L. (2004) *Equinox Resources Limited Annual Report 2003*, Perth, Australia.
Eriksson, K. A., & Chuck, R. G. (1985) Aulacogens; Sedimentological and Tectonic Evolution and Associated Mineralization, In K. H. Wolf (Ed.), *General Studies*, Elsevier Sci. Publ., Amsterdam, Netherlands, pp. 461-529.
Eugster, H. P. (1986) *Geochemical Environments of Sediment-Hosted Ore Deposits*, GAC, MAC, CGU 1986 Joint Annual Meeting, Waterloo, ON, Canada.
Evans, M. J. (2004 -estimated) *Mineral Exploration at Chitampa, Kasempa Area, Zambia* (internal Power Point promotional presentation 18 p.), Johannesburg: Metorex Corporation.
Evers, T. J. J. M., & Bowen, M. P. (1989) Lithogeochemistry as a Tool for Extending Mineral Resources; the Brandberg West Sn-W Deposit, Damaraland, South West Africa/ Namibia, In G. L. Coetzee (Ed.), *Exploration Geochemistry in Southern Africa; Compilation of Papers, Partly Based on Symposium on Exploration Geochemistry*, Elsevier, Amsterdam, 34(1): 47-62.
Fanton, J., Lancaster, O. J., Almeida, A. J., Leveille, R. A., & Vieira, S. (2001) Discovery and Geology of the Sossego Copper-Gold Deposit, Carajás District, Pará State, Brazil, *ProExplo '2001 - CD*, Instituto de Ingenieros de Minas del Perú, Lima, Peru.
Fernandez-Alonso, M., Tahon, A., & Tack, L. (2002) *The "Northeastern Kibaran Belt" (NKB) Reconsidered: Evidence from a GIS-Compilation Presented as a 1:500,000-Scale Geological Map*, Technical Meeting IGCP Projects 418/440, Windhoek, Namibia.
Ferré, E.C., Caby, R., Peucat, J. J., Capdevila, R., Monié, P. (1998) Pan-African, Post-Collisional, Ferro-Potassic Granite and Quartz-Monzonite Plutons of Eastern Nigeria, *Lithos*, 45: 255-279.
Ferris, G. M., Schwarz, M. P., & Heithersay, P. (2002) The Geological Framework, Distribution and Controls of Fe-Oxide Cu-Au Mineralization in the Gawler Craton, South Australia - Part I - Geological and Tectonic Framework, In T. M. Porter (Ed.), *Hydrothermal Iron Oxide Copper-Gold & Related Deposits: A Global Perspective*, PGC Publishing, Adelaide, Australia, 2: 9-31.
Fershtater, G. B., & Rapoport, M. S. (2000) Granite Magmatism and Related Ore Mineralization in the Urals, Russia, In A. Kremenetsky, B. Lehman, & R. Seltmann (Eds.), *Ore-Bearing Granites of Russia and Adjacent Countries*, Institute of Mineralogy, Geochemistry and Crystal Chemsitry of Rare Elements, Moscow, 97-111.
Fitton, J. G., & Upton, B. G. J. (1987) *Alkaline Igneous Rocks*, Vol. 30, Blackwell Scientific Publications - The Geological Society, Oxford.
Fitzsimons, I. C. W., & De Waele, B. (2004, 27-28 May, 2004) *Precambrian Crustal Lineaments in Africa: Using Precise U-Pb Geochronology to Test Correlations Across Shear Zones*, Continental Tectonics, Geological Society of London, London.
Flavianu, L. S. (2004) *Petrographic and Geochemical Investigacion of Possible Iron Oxide-Cu-Au Related Mineralization at Oas Farm in the Neoproterozoic Rocks of the Khorixas Inlier, Northern Namibia,* Unpublished honours thesis, University of the Witwatersrand, Johannesburg.
Fleischer, V. D. (1984) Discovery, Geology and Genesis of Copper-Cobalt Mineralisation at Chambishi Southeast Prospect, Zambia, In S. N. Punukollu & S. C. P. Andrews (Eds.), *Proterozoic: Evolution, Mineralization, and Orogenesis*, 25(1-3): 119-133.
Fleischer, V. D., Garlick, W. G., & Haldane, R. (1976) Geology of the Zambian Copperbelt, In K. H. Wolf (Ed.), *Handbook of Strata-Bound and Stratiform Ore Deposits*, Elsevier, 1: 223-352.
Foley, S., & Peccerillo, A. (1992) Potassic and Ultrapotassic Magmas and Their Origin, *Lithos* (Special Issue on Potasic and Ultrapotassic Magmas and their Origin, edited by Peccerillo, A.), 181-185.
Forster, H.-J., Tischendorf, G., & Trumbull, R. B. (1997) An Evaluation of the Rb vs. (Y+Nb) Discrimination Diagram to Infer Tectonic Setting of Silicic Igneous rocks, *Lithos*, 40: 261-293.
Foster, R. P., Leahy, K., Hunns, D. A., Pelham, S. R., S.R., L., & Harrison, A. E. (2001) *Pan-African Teranes: Realizing the Metal Potential*, Second Annual Astralian African Mining Conference, Perth, Australia.
Fourie, P. J. (2000) The Vergenoeg Fayalite Iron Oxide Fluorite Deposit, South Africa: Some New Aspects, In T. M. Porter (Ed.), *Hydrothermal Iron Oxide Copper-Gold & Related Deposits: A Global Perspective*, PGC Publishing, Adelaide, Australia, 1: 309-320).
Francois, A. (1995) Le Contact Entre le Socle Kibarien et la Couverture Katanguienne dans la Region de Kolwezi (Shaba, Zaire), *Bulletin de la Societe Belge de Geologie = Bulletin van de Belgische Vereniging voor Geologie*, 104(3-4): 283-289.
Fraser, T. M. (1994) Hydrothermal Breccias and Associated Alteration of the Mount Polley Copper-Gold Deposit, In B. Grant & J. M. Newell (Eds.), *Geological Fieldwork 1993; a Summary of Field Activities and Current Research*, Province of British Columbia, Ministry of Energy, Mines and Petroleum Resources, Victoria, British Columbia, Canada, pp. 259-267.
Freeman, P. V. (1983a) History of Mining and Exploration in Zambia, *Exploration and Mining in Zambia - Proterozoic 83 Souvenir*, Geological Society of Zambia, Lusaka, 4 p.
Freeman, P. V. (1983b) Mining in Zambia Today, *Exploration and Mining in Zambia - Proterozoic 83 Souvenir*, Geological Society of Zambia, Lusaka, 3 p.
Freeman, P. V. (1988) *Descriptions of Some Mineral Deposits Discovered or Re-Investigated in the Post World War II Period* (Internal un-published company report), ZCCM Limited, Lusaka, Zambia.
Frets, D. C. (1969) Geology and Structure of the Huab-Welwitschia Area - South West Africa, *Chamber of Mines Precambrian Research Unit, Capetown, South Africa,* Bulletin 5: 235.

Friehauf, K. C., Smith, R. C., & Volkert, R. A. (2002) Comparison of the Geology of Proterozoic Iron Oxide Deposits in the Adirondack and Mid-Atlantic Belt of Pennsylvania, New Jersey and New York, In T. M. Porter (Ed.), *Hydrothermal Iron Oxide Copper-Gold & Related Deposits: A Global Perspective*, PGC Publishing, Adelaide, Australia, 2: 247-252.

Frimmel, H. E. (2000) The Pan-African Gariep Belt in Southwestern Namibia and Western South Africa, *Communications of the Geological Survey of Namibia*, 12: 197-209.

Frimmel, H. E., Deane, J. G., & Chadwick, P. J. (1997) Pan-African Tectonism and the Genesis of Base Metal Sulfide Deposits in the Northern Foreland of the Damara Orogen, Namibia, In D. F. Sangster (Ed.), *Carbonate-Hosted Lead-Zinc Deposits*, Society of Economic Geologists, Special Publication 4: 204-217.

Frimmel, H. E., & Frank, W. (1998) Neoproterozoic Tectono-Thermal Evolution of the Gariep Belt and its Basement, Namibia and South Africa, *Precambrian Research*, 90(1-2): 1-28.

Frimmel, H. E., Zartman, R. E., & Spath, A. (2001) The Richtersveld Igneous Complex, South Africa: U-Pb Zircon and Geochemical Evidence for the Beginning of Neoproterozoic Continental Breakup, *Journal of Geology*, 109: 493-508.

Frindt, S., & Haapala, I. (2002) *The Cretaceous Gross Spitzkoppe Granite Stock in Namibia, a Highly Evolved A-Type Granite with Structures and Textures Demonstrating Magma Flow, Undercooling and Vapor Saturation During Crystallization*,11th IAGOD Quadrennial Symposium and Geocongress CD, Windhoek, Namibia.

Frindt, S., Poutiainen, M., & Haapala, I. (2002) *Greisen Mineralization Associated with the Evolved Gross Spitzkoppe Topaz-Bearing Granite Stock, Western Namibia*,11th IAGOD Quadrennial Symposium and Geocongress CD, Windhoek, Namibia.

Gair, H. S. (1957) The Plateau Series and the So-Called Luapula Porphyries in the Northern Province, *Records of the Geological Survey of Northern Rhodesia, 1957*, 50-58.

Galloway, C. (1988) *The Geology of the Kombat Mine and Environs* (Consulting Report), Windhoek: Tsumeb Corporation Limited.

Garlick, W. G. (1961) Chambishi-Nkana Basin, In F. Mendelsohn (Ed.), *The Geology of the Northern Rhodesian Copperbelt*, Macdonald, London, 281-342.

Garlick, W. G. (1973) The Nchanga Granite, In L. A. Lister (Ed.), *Symposium on Granites, Gneisses and Related Rocks*, Special Publication 3, Geological Society of South Africa, Johannesburg, 455-474.

Garlick, W. G. (1981) Sabkhas, Slumping, and Compaction at Mufulira, Zambia, *Economic Geology*, 76(7): 1817-1847.

Garlick, W. G. (1982) Erosion of the Folded Copper-Rich Arenite Filling of a Rolled-up Algal Mat, Mufulira, Zambia, *Economic Geology, 77*(8): 1934-1939.

Garlick, W. G. (1986) *Genetic Interpretation From Ore Relations to Algal Reefs in Zambia and Zaire*, GAC, MAC, CGU 1986 Joint Annual Meeting, Waterloo, ON, Canada.

Garlick, W. G. (1989a) Genetic Interpretation From Ore Relations to Algal Reefs in Zambia and Zaire, In R. W. Boyle, A. C. Brown, C. W. Jefferson, E. C. Jowett, & R. V. Kirkham (Eds.), *Sediment-Hosted Stratiform Copper Deposits*, Geological Association of Canada, Toronto, 36: 471-498.

Garlick, W. G. (1989b) Mineralization Controls and Source of Metals in the Lufilian Fold Belt, Shaba (Zaire), Zambia, and Angola; A Discussion, *Economic Geology*, 84(4): 966-969.

Garnett, D. L., & Rea, W. J. (1985) Geochemical Prospecting in the Area Around the Otjihase Copper Deposit, Namibia; A Case History, In G. R. Davis (Ed.), *Prospecting in Areas of Desert Terrain*, Inst. Min. and Metall., London, 191-208.

Geología, Ddepartamento de (2003) *Geología del Distrito Mantoverde - División Mantoverde* (unpublished report), Anglo American Chile.

Germs, G. J. B. (1983) Implications of a Sedimentary Facies and Depositional Environmental Analysis of the Nama Group in South West Africa-Namibia, In R. G. Miller (Ed.), *Evolution of the Damara Orogen of South West Africa-Namibia*, Publication 11, Geological Society of South Africa, Johannesburg, 11: 89-114.

Germs, G. J. B. (1995) The Neoproterozoic of Southwestern Africa, With Emphasis on Platform Stratigraphy and Paleontology, In A. H. Knoll & M. Walter (Eds.), *Neoproterozoic Stratigraphy and Earth History*, 73(1-4): 137-151.

Gibson, R. L., & Jones, M. Q. W. (2002) Late Archean to Palaeoproterozoic Geotherms in the Kaapvaal Craton, South Afirca: Constraints on the Thermal Evolution of the Witwatersrand Basin, *Basin Research*, 14: 169-181.

Glazner, A. F., Bartley, J. M., Colemena, D. S., Gray, W., & Taylor, R. Z. (2004) Are Plutons Assembled Over Millions of Years by Amalgamation from Small Magma Chambers?, *GSA Today*, 14(4/5): 4-11.

Goad, R., El, Mumin, H., Duke, N. A., Neale, K. L., & Mulligan, D. L. (2000) Geology of the Proterozoic Iron Oxide-Hosted, Nico Cobalt-Gold-Bismuth, and Sue-Dianne Copper-Silver Deposits, Southern Great Bear Magmatic Zone, Northwest Territories, Canada, In T. M. Porter (Ed.), *Hydrothermal Iron Oxide Copper-Gold & Related Deposits: A Global Perspective*, PGM Publishers, Adelaide, Australia, 1: 249-267.

Goagoseb, E. E. (2004) *The Geological, Mineralogical and Chemical Characteristics of the Neoproterozoic Hook Granite Batholith in Zambia,* Unpublished honours thesis, University of the Witwatersrand, Johannesburg, South Africa.

Goscombe, B., Armstrong, R., & Barton, J. M. (1998) Tectonometamorphic Evolution of the Chewore Inliers: Partial Re-Equilibration of High-Grade Basement During the Pan-African Orogeny, *Journal of Petrology*, 39(7): 1347-1384.

Goscombe, B., Armstrong, R., & Barton, J. M. (2000) Geology of teh Chewore Inliers, Zimbabwe: Constraining the Mesoproterozoic to Paleozoic Evolution of the Zambezi Belt, *Journal of African Earth Sciences*, 30(3): 589-627.

Grainger, C. J., Groves, D. I., & Costa, C. H. C. (2002) The Epigenetic Sediment-Hosted Serra Pelada Au-PGE Deposit and Its Potential Genetic Association with Fe Oxide Cu-Au Mineralization within the Carajas Mineral Province, Amazon Craton, Brazil, In T. M. Porter (Ed.), *Hydrothermal Iron Oxide Copper-Gold & Related Deposits: A Global Perspective*, PGC Publishing, Adelaide, Australia, 2: 227-245.

Grant, J. A. (1986) The Isocon Diagram - A Simple Solution to Gresens' Equation for Metasomatic Alteration, *Economic Geology*, 81: 1976-1982.

Greenberg, J. K. (1990) Anorogenic Granite Associations as Products of Progressive Continental Evolution, In C. f. Gower, T. Rivers, & B. Ryan (Eds.), *Mid-Proterozoic Laurentia-Baltica*, Special Paper 38, Geological Association of Canada, Ottawa, 447-457.

Greig, D. D. (1972) *Geology of the Malundwe Copper Deposit, NW Zambia* , Lusaka, Zambia: Internal company report.

Griffiths, C. M. (1978a) *Geology of the Ngoma, Namwana and Mala Areas*, *Report* 77, Republic of Zambia, Ministry of Mines and Mineral Development, Geological Survey Department, Lusaka.

Griffiths, J. (1978b) *The Itezhi-Tezhi Uranium Anomaly*, *Technical Report* 86, Zambian Geological Survey, Lusaka.

Grobler, D. F. (1996) *The Geology, Geochemistry and Geochronology of the Gaborone Granite Suite and Kanye Formation North of Mafikeng, South Africa,* Unpublished Ph.D., University of the Witwatersrand, Johannesburg, South Africa.

Guernsey, T. D. (1941) *A Prospector's Guide to Mineral Occurrences in Northern Rhodesia*, The British South Africa Company, Salisbury, Rhodesia.

Guilbert, J. M. (2001) *Linkages Among Hydrothermal Ore Deposit Types*, ProExplo '2001 CD, Lima, Peru.

Guilloux, L. (1982) *Etude Chimique des Series Porteuses de Quelques Grands Gisements du Type Kupferschiefer*, Vol. 43, Foundation Scientifique de la Geologie et de ses Applications, Nancy, France.

Guj, P. (1970) The Relationships Between the "Fransfontein Granite" and the Huab and Khoabendus Formations Northwest of Fransfontein, South West Africa, *Annals of the Geological Survey of South Africa*, 8: 49-51.

Guney, M. (1980) Thermal Heat Balance in Mindola Mine, Zambian Copperbelt, *Institution of Mining and Metallurgy, Transactions, Section A: Mining Industry*, 89: A165-A173.
Gunthorpe, R. J., & Buerger, A. D. (1986) Geology and Economic Evaluation of the Otjisazu Alkaline Igneous Complex, Central South West Africa/ Namibia, In C. R. Anhaeusser & S. Maske (Eds.), *Mineral Deposits of Southern Africa*, Geological Society of South Africa, Johannesburg, South Africa, 2255-2260.
Gupta, A. K., & Yagi, K. (1980) *Petrology and Genesis of Leucite-Bearing Rocks*, Springer-Verlag, Berlin.
Haack, U., & Gohn, E. (1988) Rb-Sr Data on Some Pegmatites in the Damara Orogen (Namibia), *Communications of the Geological Survey of South West Africa/Namibia*, 4: 13-17.
Haack, U., Gohn, E., & Hartmann, O. (1983) Radiogenic Heat Generation in Damaran Rocks, In R. Miller (Ed.), *Evolution of the Damara Orogen of South West Africa/Namibia*, Special Publication No. 11, Geological Society of South Africa, Johanensburg, pp. 225-231
Haeussinger, H., Okrusch, M., & Scheepers, D. (1993) Geochemistry of Premetamorphic Hydrothermal Alteration of Metasedimentary Rocks Associated with the Gorob Massive Sulfide Prospect, Damara Orogen, Namibia, *Economic Geology*, 88(1): 72-90.
Hall, A. (1987) *Igneous Petrology,* Longman Scientific & Technical, Essex, England, 573p.
Hambleton, J. B. B., Toens, P. D., & Levin, M. (1984) Time-Bound Characteristics and Tectonic Control of Southern Africa's Uranium Deposits, In N. A. Bogdanov (Ed.), *Special Session of the International "Lithosphere" Programme*, International Geological Congress, 9(1): 352.
Hancock, M. C. (1977) *The Kalulushi East Copper Deposit*, International Conference on the Utilization of Mineral Resources in Developing Countries, Lusaka, Zambia.
Hanson, G. N. (1978) The Application of Trace Elements to the Petrogenesis of Igneous Rocks of Granitic Composition, *Earth and Planetary Science Letters*, 38: 26-43.
Hanson, R. E. (2000) *Proterozoic Tectonic Evolution of Southern Africa*, 31st, Internacional Geological Congress CD, Rio de Janeiro.
Hanson, R. E., Wardlaw, M. S., Wilson, T. J., & Mwale, G. (1993) U-Pb Zircon Ages from the Hook Granite Massif and Mwembeshi Dislocation: Constraints on Pan-African Deformation, Plutonism, and Transcurrent Shearing in Central Zambia, *Precambrian Research*, 63: 189-209.
Hanson, R. E., Wilson, T. J., Brueckner, H. K., Onstott, T. C., Wardlaw, M. S., Johns, C. C., & Hardcastle, K. C. (1988) Reconnaissance Geochronology, Tectonothermal Evolution, and Regional Significance of the Middle Proterozoic Choma-Kalomo Block, Southern Zambia, *Precambrian Research*, 42: 39-61.
Hanson, R. E., Wilson, T. J., & Wardlaw, M. S. (1988) Deformed Batholiths in the Pan-African Zambezi Belt, Zambia - Age and Implications for Regional Proterozoic Tectonics, *Geology*, 16: 1134-1037.
Harmer, R. E. (2000) Mineralization of the Phalaborwa Complex and the Carbonatite Connection in Iron Oxide-Cu-Au-U-REE Deposits, In T. M. Porter (Ed.), *Hydrothermal Iron Oxide Copper-Gold & Related Deposits: A Global Perspective*, PGC Publishing, Adelaide, Australia, 1: 331-340.
Harris, C., & le Roex, A. (2002) *Mesozoic Damaraland Anorogenic Complexes, Namibia, Field Excursion A1*, 11th IAGOD Quadrennial Symposium and Geocongress CD, Windhoek, Namibia.
Harris, N. B. W., Pearce, J. A., & Tindle, A. G. (1986) Geochemical Characteristics of Collision-Zone Magmatism, In M. P. Coward & A. C. Ries (Eds.), *Collision Tectonics*, Geological Society, Special Publication No. 19, London, 67-81.
Hawkes, N., Clark, A. H., & Moody, T. C. (2002) Marcona and Pampa de Pongo: Giant Mesozoic Fe-(Cu, Au) Deposits in the Peruvian Coastal Belt, In T. M. Porter (Ed.), *Hydrothermal Iron Oxide Copper-Gold & Related Deposits: A Global Perspective*, PGC Publishing,Adelaide, Australia, 2: 115-130.
Hawkesworth, C. J., Gendhill, A. R., Roddick, J. C., Miller, R. M., & Kroner, A. (1983) Rb-Sr and 40Ar/39Ar Studies Bearing on Models for the Thermal Evolution of the Damara Belt, Namibia, *Special Publications of the Geological Society of South Africa*, 11: 323-338.
Haynes, D. W. (2000) Iron Oxide Copper (-Gold) Deposits: Their Position in the Ore Deposit Spectrum and Modes of Origin, In T. Porter (Ed.), *Hydrothermal Iron Oxide Copper-Gold & Related Deposits: A Global Perspective*, Australian Mineral Foundation, Adelaide, Australia, 1: 71-90.
Hays, J. (1957) The Zhima River Catchment Area, Kalomo - Sheet 1726, NE Quarter, *Records of the Geological Survey of Northern Rhodesia for 1956*, Lusaka, 19-23.
Heath, D. C. (1960) *Geological Report Ondundu Copper Mine*, Windhoek, Namibia: Geological Survey of Namibia.
Hegenberger, W. (1982) *The Regional Geology of Northeast South West Africa/Namibia* (open file report RG 6), Geological Survey of Namibia, Windhoek.
Heins, R., Hering, C., Liebetrau, V., Behr, H. J., & Porada, H. (1990) The Lithology of Some Metamorphic Playa Lake Deposits in the Duruchaus Formation (Upper Proterozoic), Damara Orogen, Namibia, In Anonymous (Ed.), *15th Colloquium of African Geology*, Centre International pour la Formation et les Echanges Geologiques (CIFEG), Paris, France, 20: 90.
Henry, G., Clendenin, C. W., Stanistreet, I. G., & Maiden, K. J. (1990) Multiple Detachment Model for the Early Rifting Stage of the Late Proterozoic Damara Orogen in Namibia, *Geology*, 18(1): 67-71.
Henry, G., Maiden, K. J., & Stanistreet, I. G. (1986) Tectonic and Sedimentological Development of an Ensialic Rift; the Central Rift Zone of the Damara Orogen, South West Africa/ Namibia, In Anonymous (Ed.), *Sediments Down-Under; 12th International Sedimentological Congress*, Bureau of Mineral Resources, Geology and Geophysics, Canberra, Australia, 138p.
Herrington, R., Smith, M., Maslennikov, V., Belogub, E., & Armstrong, R. (2002) A Short Review of Paleozoic Hydrothermal Magnetite Iron-Oxide Deposits of the South and Central Urals and Their Geological Setting, In T. M. Porter (Ed.), *Hydrothermal Iron Oxide Copper-Gold & Related Deposits: A Global Perspective*, PGC Publishing, Adelaide, Australia, 2: 343-353.
Hitchon, B. (1957) Notes on a Reconnaissance of the Zimba-Kalomo Area, *Records of the Geological Survey of Northern Rhodesia, 1957*, Lusaka, 23-25.
Hitzman, M. W. (1994) Source Basins for Sediment-Hosted Stratiform Cu Deposits; Implications for the Structure of the Zambian Copperbelt, *Journal of African Earth Sciences*, 30(4): 855-863.
Hitzman, M. W. (1998) *Petrographic Studies of "Ore Shale" from the Zambian Copperbelt Implications for Models of Ore Formation*, Geological Society of America, 1998 Annual Meeting, Boulder, CO, United States.
Hitzman, M. (2000a) Iron Oxide-Cu-Au Deposits: What, Where, When, and Why, In T. Porter (Ed.), *Hydrothermal Iron Oxide Copper-Gold & Related Deposits: A Global Perspective*, Australian Mineral Foundation, Adelaide, Australia, 1: 9-25.
Hitzman, M. W. (2000b) Source Basins for Sediment-Hosted Stratiform Cu Deposits: Implications for the Structure of the Zambian Copperbelt, *Journal of African Earth Sciences*, 30(4): 855-863.
Hitzman, M. W. (2001) *Fe Oxide-Cu-Au Systems in the Lufilian Orogen of Southern Africa*, Geological Society of America, 2001 Annual Meeting, Boulder, CO, United States.
Hitzman, M. W. (2004a) *Exploration for Iron Oxide-Hosted Copper-Gold Deposits* [Power Point presentation], In C. Beaudry (Ed.), *Exploration for Iron Oxide-Hosted Copper-Gold Deposits - Short Course*, Prospectors and Developers Association of Canada, Toronto.
Hitzman, M. W. (2004b) IOCG Deposits - Introduction, Geology and Tectonic Settings, In C. Beaudry (Ed.), *Exploration for Iron Oxide-Hosted Copper-Gold Deposits - Short Course*, Prospectors and Developers Association of Canada, Toronto, pp. 2.

Hitzman, M., & Broughton, D. (2003) *Mineralization in and Adjacent to the African Copperbelt*, Mineralogy and Geochemistry of Base Metal Deposits in Southern Africa - Implications for Exploration and Beneficiation, Rand Afrikaans University, Johannesburg.
Hitzman, M. W., Oreskes, N., & Einaudi, M. T. (1992) Geological Characteristics and Tectonic Setting of Proterozoic Iron Oxide (Cu-U-Au-REE) Deposits, *Precambrian Research*, 58: 241-287.
Hoal, B. G. (1989) The Geological History of the Awasib Mountain Terrain and its Relationship to the Sinclair Sequence and Namaqualand Metamorphic Complex, *Communications of the Geological Survey of Namibia*, 5: 41-51.
Hoal, B. G. (1990) The Geology and Geochemistry of the Proterozoic Awasib Mountain Terrain, Southern Namibia, *Special Publication of the Geological Survey of Namibia*, V. 11, Windhoek, Namibia.
Hoal, B. G., & Hearman, L. M. (1995) The Sinclair Sequence: U-Pb Age Constraints from the Awasib Mountain Area, *Communications of the Geological Survey of Namibia*, 10: 883-991.
Hoffmann, K. (1990) *Sedimentary Depositional History of the Damara Belt Related to Continental Breakup, Passive to Active Margin Transition and Foreland Basin Development*, Geocongress 90, Capetown, South Africa.
Hoffmann, K. H. (1983) Lithostratigraphy and Facies of the Swakop Group of the Southern Damara Belt, SWA-Namibia, In R. G. Miller (Ed.), *Evolution of the Damara Orogen of South West Africa-Namibia*, Geological Society of South Africa, Johannesburg, 11: 43-63.
Hoffmann, P. F., Hawkings, D. P., Isachsen, C. E., & Bowring, S. A. (1996) Precise U-Pb Zircon Ages for Early Damaran Magmatism in the Summas Mountains and Welwitschia Inlier, Northern Damara Belt, Namibia, *Communications of the Geological Survey of Namibia*, 11: 47-52.
Hoffmann, P. F., Kaufman, A., J., Halverson, G. P., & Schrag, D. P. (1998) A Neoproterozoic Snowball Earth, *Science*, 281: 1342-1346.
Hoffmann, P. F., Swart, R., Freyer, E. E., & Guowei, H. (1994) *Damara Orogen of Northwest Namibia - Geological Excursion Guide*, Proterozoic Crustal and Metallogenic Evolution, Geological Society of Namibia, Windhoek, Namibia.
Holcombe, C. J. (1985) Paleoflow Modeling for Sedimentary Orebodies, *Economic Geology*, 80(1): 172-179.
Hollaway, J. (1987) Gold Mining Opportunities in Sub-Saharan Africa, *Mining Magazine (London)*, 157(2): 133-137.
Hopper, D., & Correa, A. (2000) The Panulcillo and Teresa de Colmo Copper Deposits: Two Contrasting Examples of Fe-Ox Cu-Au Mineralization from the Coastal Cordillera of Chile, In T. M. Porter (Ed.), *Hydrothermal Iron Oxide Copper-Gold & Related Deposits: A Global Perspective*, PGC Publishing, Adelaide, Australia, 1: 177-189.
Horstmann, U., Ahrendt, H., Clauer, N., & Porada, H. (1985) Relationships Between Molasse Deposition and Orogeny as Deduced from K/ Ar-Age Determinations in the Pan-African Damara Sequence, SWA/ Namibia, In P. Bowden, J. A. Kinnaird, & H. F. D. Van (Eds.), *13th Colloquium of African Geology; Abstracts*, Centre International pour la Formation et les Echanges Geologiques (CIFEG), Paris, France, 3: 84-85.
Hunt, J. P. (2004) Iron Oxide-Copper-Gold-Type Alteration and Mineralization: Bushveld Complex, Rooiberg District, *SEG 2004 - Predictive Mineral Discovery Under Cover CD*, Perth, Australia.
Hunter, D. R. (1986) Intracontinental Fold Belts; Case Studies in the Variscan Belt of Europe and the Damara Belt in Namibia; Book Review, *Lithos*, 19(2): 166-168.
Hutchins, D. G., & Lynam, A. P. (1985) The Proceedings of a Seminar on the Mineral Exploration of the Kalahari (October, 1983), *Bulletin - Geological Survey Department, Republic of Botswana*, 29: 364.
Hutton, D. H. W. (1996) The 'Space Problem' in the Emplacement of Granite, *Episodes*, 19(4): 114-119.
Injoque Espinoza, J. (2002) Fe Oxide-Cu-Au Deposits in Peru An Integrated View, In T. M. Porter (Ed.), *Hydrothermal Iron Oxide Copper-Gold & Related Deposits: A Global Perspective*, PGC Publishing, Adelaide, Australia, 2: 97-113.
Injoque, J. (2002) Información Reciente Sobre Yacimientos FeOx-Cu-Au (series of personal communications).
Injoque, J., Atkin, B., Harvey, P., & Snelling, N. (1988) Mineralogía y Geocronología del Skarn Geotermal de Hierro de Marcona, *Boletín de la Sociedad Geológica del Perú*, 78: 65-80.
Innes, J. (1983) *Notes on an Underground Visit - Asis West - 12-10-82* (Un-published internal report), Tsumeb, Namibia: Tsumeb Corporation Limited.
Innes, J., & Chaplin, R. C. (1986) Ore Bodies of the Kombat Mine, South West Africa/Namibia, In C. R. Anhaeusser & S. Maske (Eds.), *Mineral Deposits of Southern Africa*, Geological Society of South Africa, Johannesburg, South Africa, 1: 1789-1805.
Irvine, T. N., & Baragar, W. R. A. (1971) A Guide to the Chemical Classification of the Common Volcanic Rocks, *Canadian Journal of Earth Sciences*, 8: 523-548.
Jackson, M. P. A., Warin, O. N., Woad, G. M., & Hudee, M. R. (2003) Neoproterozoic Allochthonous Salt Tectonics During the Lufilian Orogeny in the Katangan Copperbelt, Central Africa, *GSA Bulletin*, 115(3): 314-330.
Jackson, N. J., Drysdall, A. R., & Stoeser, D. B. (1985) Alkali Granite-Related Nb-Zr-REE-U-Th Mineralization in the Arabian Shield, *High Heat Production (HHP) Granites, Hydrothermal Circulation and Ore Genesis*, The Institution of Mining and Metallurgy, St. Austell, Cornwall, England, pp. 479-487.
Jacob, R. E., Moore, J. M., & Armstrong, R. A. (2000) Zircon and Titanite Age Determinations from Igneous Rocks in the Karibib District, Namibia: Implications for Navachab Veins-Style Gold Mineralization, *Communications fo the Geological Survey of Namibia*, 12: 157-166.
Jacobs, J., Fanning, C. M., & Bauer, W. (2002) *Timing of Grenville-Age vs. Pan-African Medium- to High-Grade Metamorphism in Western Dronning Maud Land (East Antarctica) and Significance for Correlations in Rodinia and Gondwana*, Technical Meeting IGCP Projects 418/440, Windhoek, Namibia.
Jacobsen, J. B. E., & McCarthy, T. S. (1976a) The Copper-Bearing Breccia Pipes of the Messina District, South Africa, *Mineralium Deposita*, 11: 33-45.
Jacobsen, J. B. E., & McCarthy, T. S. (1976b) An Unusual Hydrothermal Copper Deposit at Messina, South Africa, *Economic Geology*, 71: 117-130.
Janneker, D. (2002) *Various Drafts, Geochemical Data, Stratigraphic Columns and Maps of the Un-Finished M.Sc. Project on Stratigraphy and Iron Oxide-Copper-Gold Mineralization in the Kasempa Area, Zambia*, School of Geosciences, University of the Witwatersrand, Johannesburg, South Africa.
Jasper, M. J. U., Charlesworth, E. G., & Stanistreet, I. G. (1994a) Effects of Oceanic Closure and Continental Collision Along the Southern Coastal Branch (Gariep Belt) of the Late Proterozoic/ Early Palaeozoic Damara Orogen, Southern Namibia, *Economic Geology Research Unit Information Circular* 282, University of the Witwatersrand, Johannesburg, South Africa.
Jasper, M. J. U., Stanistreet, I. G., & Charlesworth, E. G. (1993) Preliminary Results of a Study of the Structural and Sedimentological Evolution of the Late Proterozoic/ Early Paleozoic Gariep Belt, Southern Namibia, *Communications of the Geological Survey of Namibia*, 8: 99-118.
Jasper, M. J. U., Stanistreet, I. G., & Charlesworth, E. G. (1994b) Recognition of Inversion Tectonics Within the Pan African Gariep Belt (Damara Orogen) in Southern Namibia, *Economic Geology Research Unit Information Circular* 285, University of the Witwatersrand, Johannesburg, South Africa.
Jebrak, M. (1992) Les Textures Intra-Filoniennes, Marqueurs des Conditions Hydrauliques et Tectoniques, *Chronique de la Recherche Miniere*, 506: 25-35.

Jebrak, M. (1997) Hydrothermal Breccias in Vein-Type Ore Deposits; A Review of Mechanisms, Morphology and Size Distribution, *Ore Geology Reviews*, 12(3): 111-134.
Jebrak, M. (2002) *Magmatic-Hydrothermal Breccias in Proterozoic Cu-Au-Fe-Oxide Deposits: Processes and Exploration Significance*, Geocongress 2002 CD, Windhoek, Namibia.
Jensen, E. P., & Barton, M. D. (2000) Gold Deposits Related to Alkaline Magmatism, In S. G. a. B. Hagemann, P.E. (Ed.), *Gold in 2000,* Reviews 13, Society of Economic Geology.
John, T. (2001) *Subduction and Continental Collision in the Lufilian Arc-Zambesi Belt Orogen: A Petrological, Geochemical and Geochronological Study of Eclogites and Whiteschists (Zambia), Unpublished manuscript.*
Johns, C. C. (1982) *The Kahare Ironstone (A Preliminary Investigation)* (92), Zambian Geological Survey Department, Lusaka, Zambia.
Johns, C. C. (1985) Geological Investigations in the Kalahari Region of Zambia, *Seminar on the Mineral Exploration of the Kalahari*, Lobatsi, Botswana.
Johnson, M. L., Wentzell, C. Y., & Elen, S. (1997) Multicolored Bismuth-Bearing Tourmaline from Lundazi, Zambia, *Gems and Gemmology*, 33(3): 204-211.
Johnson, S. P., & Oliver, G. J. H. (2000) Mesoproterozoic Oceanic Subduction, Island Arc Formation and the Initiation of Back-Arc Spreading in the Kibaran Belt of Central , Southern Africa: Evidence from the Ophiolite Terrane, Chewore Inliers, Northern Zimbabwe, *Precambrian Research*, 103: 125-146.
Johnson, S. P., Oliver, G. J. H., Tembo, F., De Waele, B., & Rivers, T. (2004) Mesoproterozoic Supra-Subduction Magmatism and Accretionary Tectonics in the Southern Irumide Belt, Central Southern Africa, *Geocience Africa 2004 CD*, Johannesburg, South Africa.
Johnson, S. P., & T., R. (2004) A Review of the Mesoproterozoic to Early Paleozoic Magmatic and Tectonothermal History of Central Southern Africa: Implications for Rodinia and Gondwana Reconstructions, *Geoscience Africa 2004* CD, Johannesburg, South Africa.
Jowett, E. C., & Cathles, L. M., III. (1988) *Evolution of Ideas About the Genesis of Stratiform Cu-Ag Deposits*, Geological Society of America Centennial Celebration, Boulder, CO, United States.
Jung, S., Hoernes, S., & Mezger, K. (2000) Geochronology and Petrogenesis of Pan-African, Syn-Tectonic, S-Type and Post-Tectonic A-Type Granite (Namibia): Products of Melting of Crustal Sources, Fractional Crystallization and Wall Rock Entrainment, *Lithos*, 50: 259-187.
Jung, S., Hoffer, E., Masberg, P., & Hoernes, S. (1995) Geochemistry of Granitic In-Situ Low-Melt Fractions - An Example From the Central Damara Orogen, *Communications of the Geological Survey of Nambia*, 10: 21-31.
Jung, S., & Mezger, K. (2001) Geochronology in Migmatites; a Sm-Nd, U-Pb and Rb-Sr Study From the Proterozoic Damara Belt (Namibia); Implications for Polyphase Development of Migmatites in High-Grade Terranes, *Journal of Metamorphic Geology*, 19(1): 77-97.
Jung, S., Mezger, K., & Hoernes, S. (1998) Petrology and Geochemistry of Syn- to Post-Collisional Metaluminous A-Type Granites - A Major and Trace Element and Nd-Sr-Pb-O Isotope Study from the Proterozoic Damara Belt, Namibia, *Lithos*, 45: 147-175.
Kabengele, M., Mashala, T., & Loris, N. B. T. (2003, July 14 to 24) Geochemistry of the Lower Mwashya Pyroclastic Rocks in the Likasi-Kambove Area (D.R. Congo), *3rd. IGCP-450 Conference and Guide Book of the Field Workshop*, Lubumbashi, Katanga, D.R. Congo.
Kamona, A. F. (1994) Mineralization Types in the Mozambique Belt of Eastern Zambia, *First meeting of IGCP 348, International Field Workshop (Mozambique and Related Belts), Zambia and Malawi*.
Kamona, A. F., Leveque, J., Friedrich, G., & Haack, U. (1999) Lead Isotopes of the Carbonate-Hosted Kabwe, Tsumeb, and Kipushi Pb-Zn-Cu Sulphide Deposits in Relation to Pan African Orogenesis in the Damaran-Lufilian Fold Belt of Central Africa, *Mineralium Deposita*, 34(3): 273-283.
Kamona, F., & Friedrich, G. (1994) Die Blei-Zink-Lagerstaette Kabwe in Zentral Sambia, *Erzmetall*, 47(1): 34-44.
Kamona, F., Friedrich, G., Sweeney, M. A., & Fallick, A. E. (1991) Stable Isotopes of the Kabwe Lead-Zinc Deposit, In M. Pagel & J. L. Leroy (Eds.), *Source, Transport and Deposition of Metals*, A. A. Balkema, Rotterdam, Netherlands, 313-316.
Kamona, F., & Friedrich, G. H. (1989) Mineralogy and Geochemistry of the Kabwe Pb-Zn Deposit, Zambia, *Referate der Vortraege und Poster, 67, Jahrestagung der Deutschen Mineralogischen Gesellschaft*, E. Schweizerbart'sche Verlagsbuchhandlung, Stuttgart, Germany: 1: 91.
Kamona, F., Friedrich, G. H., & Sweeney, M. A. (1990) *The Kabwe Pb-Zn Deposit in Central Zambia,* In Anonymous (Ed.), *15th Colloquium of African Geology*, Centre International pour la Formation et les Echanges Geologiques (CIFEG), Paris, France, 20.
Kampunzu, A. B., & Cailteaux, J. (1999) Tectonic Evolution of the Lufilian Arc (Central African Copperbelt) During Neoproterozoic Pan African Orogenesis, *Gondwana Research*, 2: 401-421.
Kampunzu, A. B., & Lubala, R. T. (Eds.) (1991) *Magmatism in Extensional Structural Settings - The Phanerozoic African Plate*, Springer-Verlag, Berlin, Germany.
Kampunzu, A. B., & Lubala, R. T. (1994) *Neoproterozoic Belts of Zambia, Zaire and Namibia, Journal of African Earth Sciences*, Special Issue 19: 4.
Kampunzu, A. B., Tembo, F., Matheis, G., Kapenda, D., & Huntsman-Mapila, P. (2000) Geochemistry and Tectonic Setting of Mafic Igneous Units in the Neoproterozoic Katangan Basin, Central Africa: Implications for Rodinia Break-Up, *Gondwana Research,* 3(2): 125-153.
Kapenda, D., Kampunzu, A. B., Cabanis, B., Namegabe, M., & Tshimanga, K. (1998) Petrology and Geochemistry of Post-Kinematic Mafic Rocks from the Paleoproterozoic Ubendian Belt, NE Katanga (Democratic Republic of Congo), *Geol. Rundsch.*, 87: 345-362.
Kasch, K. W. (1983) The Structural Geology, Metamorphic Petrology and Tectonothermal Evolution of the Southern Damara Belt Around Omitara; S.W.A. Namibia, *Bulletin of the Chamber of Mines Precambrian Research Uni*t, v. 27, University of Cape Town, Department of Geology, Cape Town, South Africa.
Kasolo, P. C., & Foster, R. P. (1991) Fluid-Channeling and Gold Mineralization Within the Late Proterozoic Mwembeshi Shear Zone, Zambia, *Brazil Gold '91.*
Katz, E. F. (1981) A Tour of African Countries, *Lapidary Journal*, 34(11): 2320.
Kazmin, V. G., & Byakov, A. F. (2000) Magmatism and Crustal Accretion in Continental Rifts, *Journal of African Earth Sciences*, 30(3): 555-568.
Keller, P. (1984) Tsumeb, *Lapis (Muenchen)*, 9(7-8): 13-63.
Keller, P. (1991) The Occurrence of Li-Fe-Mn Phosphate Minerals in Granitic Pegmatites of Namibia, *Communications of the Geological Survey of Namibia*, 7: 21-34.
Keller, P., Roda, R. E., Pesquera, P. A., & Fontan, F. (1999) Chemistry, Paragenesis and Significance of Tourmaline in Pegmatites of the Southern Tin Belt, Central Namibia, *Chemical Geology*, 158(3-4): 203-225.
Kerr, I. D. (1998) *Mineralogy, Chemistry and Hydrothermal Evolution of the Pea Ridge Fe-oxide-REE Deposit, Missouri, USA*, un-published report.

Kerr, S. B. (1997) Geology of the Mercur Gold Mine, Oquirrh Mountains, Utah, In D. A. John & G. H. Ballantyne (Eds.), *Geology and Ore Deposits of the Oquirrh and Wasatch Mountains, Utah*, Special Publication of the Society of Economic Geologists, 29: 241-253.

Kerrich, R., Goldfarb, R., Groves, D., & Garwin, S. (2000) The Geodynamics of World-Class Gold Deposits: Characteristics, Space-Time Distribution, and Origins, In S. G. a. B. Hagemann, P.E. (Ed.), *Gold in 2000*, Reviews in Economic Geology, Society of Economic Geologists, 13: 501-551.

Key, R., & De Waele, B. (2003) *A Multi-Element Baseline Geochemical Database from the Western Extension of the Central Africa Copper Belt in NW Zambia*, 6th International Symposium on Environmental Geochemistry, University of Edinburgh, Edinburgh, Scotland.

Key, R. M., & Banda, J. (2000) *Geology of the Kalene Hill Area - Explanation of Those Parts of Quarter Degree Sheets 1124NW, 1023SE and 1024SW That Lie in Zambia* (Geological Report 107), Geological Survey Organization, Republic of Zambia, Lusaka, Zambia

Key, R. M., Liyungu, A. K., Njambu, F. M., Somwe, V., Banda, J., Mosley, P. N., & Armstrong, R. A. (2002) The Western Arm of the Lufilian Arc in NW Zambia and Its Potential for Copper Mineralization, *Journal of African Earth Sciences*, In Press, v. 31.

Key, R. M., Liyungu, A. K., Njamu, F. M., Banda, J., Mosley, P. N., & Somwe, V. (2000) *The Geology and Stream Sediment Geochemistry of the Mwinilunga Sheet - Explanation of That Part of 1:250,000 Sheet SC-35-13 That Lies in Zambia*, Geological Survey Department, Republic of Zambia, Lusaka, Zambia.

Key, R. M., Liyungu, A. K., Njamu, F. M., Somwe, V., Banda, J., Mosley, P. N., & Armstrong, R. A. (2001) The Western Arm of the Lufilian Arc in NW Zambia and its Potential for Copper Mineralization, *Journal of African Earth Sciences*, 33(3-4): 503-528.

Kihn, C. M. (1977) *Prospecting in Zambia*, Papers Presented at the International Conference on the Utilization of Mineral Resources in Developing Countries, Lusaka, Zambia.

King, C. H. M. (1991) Relationship Between Chaotic Debris Flow Breccia Deposits and Some Pb-Zn Occurrences Within the Tsumeb Carbonate Sequence in the Otavi Mountainland, Namibia, In P. G. Eriksson (Ed.), *Precambrian Sedimentary Basins of Southern Africa*, Blackwell Scientific Publications, Oxford, 3(3): 17.

Kinnaird, J. A., Batchelor, R. A., Whitley, J. E., & MacKenzie, A. B. (1985) Geochemistry, Mineralization and Hydrothermal Alteration of the Nigerian High Heat Producing Granites, *High Heat Production (HHP) Granites, Hydrothermal Circulation and Ore Genesis*, The Institution of Mining and Metallurgy, St. Austell, Cornwall, England, pp. 169-195.

Kinnaird, J. A., Bowden, P., & Oliver, G. J. H. (1992) Magmatism, Uranium Mineralisation and Hydrothermal Activity; Granitic Examples from the Damaran Orogen of Namibia, In P. E. Brown & B. W. Chappell (Eds.), *The Second Hutton Symposium on the Origin of Granites and Related Rocks; Proceedings*, Geological Society of America, 272: 493.

Kinnaird, J. S., & Bowden, P. (1991) Magmatism and Mineralization Associated with Phanerozoic Anorogenic Plutonic Complexes of the African Plate, In A. B. Kampunzu & R. T. Lubala (Eds.), *Magmatism in Extensional Structural Settings*, Springer-Verlag, Berlin, 410-485.

Kirkham, R. (2003, July 14 to 24) Sediment-Hosted Copper Deposits and Occurrences of the World, unpublished MS-Power Point presentation, *Proterozoic Sediment-Hosted Base Metal Deposits of Western Gondwana, 3rd IGCP-450 Conference and Guide Book of the Field Workshop*, Lubumbashi, Katanga, D.R. Congo.

Kirkham, R. V. (1986) *Distribution of Sediment-Hosted Stratiform Copper Deposits; an Introduction*, GAC, MAC, CGU 1986 Joint Annual Meeting, *Program with Abstracts,* Waterloo, ON, Canada.

Kirkham, R. V. (1990) *Models for Sediment-Hosted Stratiform Copper Deposits*, 8th IAGOD Symposium in Conjunction with International Conference on Mineral Deposit Modeling, Stuttgart, Germany.

Kirkham, R. V. (1995) Sediment-Hosted Stratiform Copper Deposits; An Overview, In W. R. Smyth (Ed.), *Exploration in British Columbia 1995; Part A, Overview of Exploration Activity and Part B, Geological Descriptions of Properties*, British Columbia Ministry of Mines and Petroleum Resources, Victoria, BC, Canada, 1995: 147.

Kitchon, B. (1958) Notes on a Reconnaissance of the Zimba-Kalomo Area, *Records of the Geological Survey of Northern Rhodesia, 1956*: 23-25.

Klemd, R., Maiden, K., Okrusch, M., & Richter, P. (1987) Die metamorphe Kupferlagerstaette Matchless (SWA/ Namibia) und ihr Nebengestein, In Anonymous (Ed.), *Referate der Vortraege und Poster; 65. Jahrestagung der Deutschen Mineralogischen Gesellschaft*, E. Schweizerbart'sche Verlagsbuchhandlung, Stuttgart, Germany, 65(1): 90.

Klemd, R., Maiden, K. J., Okrusch, M., & Richter, P. (1989) Geochemistry of the Matchless Metamorphosed Massive Sulfide Deposit, South West Africa/ Namibia; Wall-Rock Alteration During Submarine Ore-forming Processes, *Economic Geology*, 84(3): 603-617.

Klinck, B. A. (1977) *The Geology of the Kabompo Dome Area - Explanation of Degree Sheet 1224, NE Quarter* (44), Geological Survey of Zambia, Lusaka, Zambia.

Klominsky, J., Partington, G. A., McNaughton, N. J., Ho, S. E., & Groves, D. I. (1996) Radiothermal Granites of the Cullen Batholith and Associated Mineralization (Australia), *Czech Geological Survey Bulletin*, V. 5, Prague, Czhechoslovakia.

Knight, J., Joy, S., Lowe, J., Cameron, J., Merrillees, J., Nag, S., Shah, N., Dua, G., & Jhala, K. (2002) The Khetri Copper Belt, Rajasthan: Iron Oxide Copper-Gold terrane in the Proterozoic of NW India, In T. M. Porter (Ed.), *Hydrothermal Iron Oxide Copper-Gold & Related Deposits: A Global Perspective*, PGC Publishing, Adelaide, Australia, 2: 321-341.

Kossinowski, M. H. F. (1982) MESONRM, A Fortran Program for the Improved Version of Mesonorm Calculation, *Computers & Geosciences*, 8(1): 11-20.

Krishnan, R. (1978) *The Nature and Distribution of Gold Mineralization in the Pre-Katanga Rocks of Zambia*, unpublished internal report, Geological Survey of Zambia, Lusaka, Zambia.

Kroener, A. (1984) Dome Structures and Basement Reactivation in the Pan-African Damara Belt of Namibia, In A. Kroener & R. Greiling (Eds.), *Precambrian Tectonics Illustrated*, E. Schweizerbart'sche Verlagsbuchhandl, (Naegele u. Obermiller), Stuttgart, Germany, 191-206.

Kukla, C., Kramm, U., Kukla, P. A., & Okrush, M. (1991) U-Pb Monazite Data Relating to Metamorphism and Granite Intrusion in the Northwestern Khomas Trough, Damara Orogen, Central Namibia, *Communications of the Geological Survey of Namibia*, 7: 49-54.

Kukla, P. A. (1992) *Tectonics and Sedimentation of a Late Proterozoic Damaran Convergent Continental Margin, Khomas Hochland, Central Namibia*, un-published internal report, Ministry of Mines and Energy, Geological Survey of Namibia, Windhoek, Namibia.

Kukla, P. A., Charlesworth, E. G., Stanistreet, I. G., & Opitz, C. (1989) Downward-Facing Structures in the Khomas Trough of the Damara Orogen, Namibia, *Communications of the Geological Survey of South West Africa/Namibia*, 5: 53-57.

Kukla, P. A., & Stanistreet, I. G. (1990a) Tectonic Setting of the Late Proterozoic Khomas Hochland Accretionary Prism of the Damara Orogen, Central Namibia, *Economic Geology Research Unit Information Circular*, University of the Witwatersrand, Johannesburg, South Africa.

Kukla, P. A., & Stanistreet, I. G. (1990b) Tectonics and Sedimentation of a Late Proterozoic (Damaran) Accretionary Prism, Central Namibia, In Anonymous (Ed.), *15th Colloquium of African Geology*, Centre International pour la Formation et les Echanges Geologiques (CIFEG), Paris, France, 20: 267.

Kukla, P. A., & Stanistreet, I. G. (1991) Record of the Damaran Khomas Hochland Accretionary Prism in Central Namibia; Refutation of an "Ensialic" Origin of a Late Proterozoic Orogenic Belt, *Geology*, 19(5): 473-476.
Kukla, P. A., & Stanistreet, I. G. (1993) Sedimentation and Tectonics of the Khomas Hochland Accretionary Prism, Along a Late Proterozoic Active Continental Margin, Damara Sequence, Central Namibia, In L. E. Frostick & R. J. Steel (Eds.), *Tectonic Controls and Signatures in Sedimentary Successions*, Blackwell, Oxford, 20: 481-497.
Lacassie, J. P., Roser, B., Ruiz del Solar, J., & Herve, F. (2004) Discovering Geochemical Patterns Using Self-Organizing Neural Networks: A New Perspective for Sedimentary Provenance Analysis, *Sedimentary Geology*, 165: 175-191.
Larson Rhodes, A., & Oreskes, N. (1999) Oxygen Isotope Composition of Magnetite Deposits at El Laco, Chile: Evidence of Formation from Isotopically Heavy Fluids, *Special Publication 7*, Society of Economic Geologists, 333-351.
Larson Rhodes, A., Oreskes, N., & Sheets, S. (1999) Geology and Rare Earth Element Geochemistry of Magnetite Deposits at El Laco, Chile, *Special Publication 7*, Society of Economic Geologists, 299-332.
Laznicka, P. (2002) Wernecke Mountains (Yukon) Breccias and Scattered Ore Occurences: What Contribution to FeOx-Cu-Au-U Metallogeny?, In T. M. Porter (Ed.), *Hydrothermal Iron Oxide Copper-Gold & Related Deposits: A Global Perspective*, PGC Publishing, Adelaide, Australia, 2: 253-271.
Leach, D. L. (1988) Hydrothermal Breccias in Mississippi Valley-Type Deposits, *Geological Society of America; 1988 Centennial Celebration*, Geological Society of America, 20(7): 140.
Legg, C. (1976) *The Geology and Mineralisation of the Mkushi Copper Deposits*, Geological Survey of Zambia, Lusaka, Zambia.
Legg, C. A., & Namateba, C. (1982) Regional Zoning of Tin-Tantalum-Niobium Pegmatites in Masuku Area, Southern Province, Zambia, In A. M. Evans (Ed.), *Metallization Associated with Acid Magmatism*, John Wiley & Sons, Chichester, U.K., 181-190.
LeMaitre, R. W. e., Streckeisen, A., Zanettin, B., LeBas, M. J., Bonin, B., Bateman, P., Bellieni, G., Dudek, A., Efremova, S., Keller, J., Lameyre, J., Sabine, P. A., Schimd, R., Sorensen, H., & Woolley, A. R. (2002) *Igneous Rocks - A Classification and Glossary of Terms*, 2nd. ed., Cambridge University Press, London.
Leveille, R. A., & Marshik, R. (2001) Iron Oxide Copper-Gold Deposits in South America, *ProExplo '2001 CD*, Lima, Peru.
Liegeois, J. P., & Black, R. (1987) Alkaline Magmatism Subsequent to Collision in the Pan-African Belt of the Adrar del Iforas (Mali), In J. G. Fitton & B. G. J. Upton (Eds.), *Alkaline Igneous Rocks*, Blackwell Scientific Publications, Oxford, 381-402.
Lindenmayer, Z. (1994) Nota Preliminar Sobre as Intrusoes Granitoides do Deposito de Cobre do Salobo, Carajás, *Acta Geológica Leopoldensia*, 40: 153-177.
Lindenmayer, Z. G., & Fyfe, W. S. (1994) The Salobo Cu (Au, Ag,Mo) Deposit, Serra dos Carajás, Brazil, *7o. Congreso Geológico Chileno - CD*, Universidad de Concepción, Concepcion, Chile.
Lobo-Guerrero. (2004a) *Iron Oxide-Copper-Gold Mineralization in the Lufilian Arc of Zambia and Namibia* [Poster presentation at the Geoscience Africa Geological Congress, August, 2004], Geological Society of South Africa, Johannesburg.
Lobo-Guerrero, A. (2003a) *Interim Report: Description of the Various Sampling Sites - Lufilian Arc Granitoid Project, Namibia and Zambia*, Economic Geology Research Institute, School of Geosciences, University of the Witwatersrand, Johannesburg.
Lobo-Guerrero, A. (2003b, October, 2003) Meso- and Neo-Proterozoic Granitoid-Related Iron Oxide-Copper-Gold Mineralization in the Lufilian Arc of Zambia and Namibia, *X Congreso Geológico Chileno - CD*, Universidad de Concepción, Concepción, Chile.
Lobo-Guerrero, A. (2004b) Granitoid-Related Iron-Oxide-Copper-Gold Minerlization, Greater Lufilian Arc, Zambia and Namibia, *SEG 2004 - Predictive Mineral Discovery Under Cover*, Society of Economic Geologists, Perth, Western Australia.
Lobo-Guerrero, A. (2004c) Iron Oxide-Copper-Gold, Granitoid-Related Mineralization in the Lufilian Arc, Zambia and Namibia, *Geoscience Africa - CD*, Geological Society of South Africa, Johannesburg, South Africa.
Lobo-Guerrero, A. (2004d) Quartz Pods - An Exploration Guide to Iron Oxide-Copper-Gold Mineralization?, *Geoscience Africa - CD*, Geological Society of South Africa, Johannesburg, South Africa.
Lobo-Guerrero, A. (2004e) Quartz Pods: An Exploration Guide to Iron-Oxide-Copper-Gold Mineralization?, *SEG 2004 - Predictive Mineral Discovery Under Cover*, Society of Economic Geologists, Perth, Western Australia.
Lobo-Guerrero S., A. (2003) Meso- and Neo-Proterozoic Granitoid-Related Iron Oxide-Copper-Gold Mineralization in the Lufilian Arc of Western Zambia and Northern Namibia, *GeoForum 2003 - CD*, Geological Society of South Africa, Johannesburg, South Africa.
Loiselle, M. C., & Wones, D. R. (1979) Characteristics and Origin of Anorogenic Granites, *1979 Annual Meeting,* Geological Society of America.
Lombaard, A. F., Guenzel, A., Innes, J., & Krueger, T. L. (1986) The Tsumeb Lead-Copper-Zinc-Silver Deposit, South West Africa/ Namibia, , In C. R. Anhaeusser & S. Maske (Eds.), *Mineral Deposits of Southern Africa*, Geological Society of South Africa, Johannesburg, South Africa, 1761-1787.
Lorilleux, G., Jebrak, M., Cuney, M., & Baudemont, D. (2002) Polyphase Hydrothermal Breccias Associated with Unconformity-Related Uranium Mineralization (Canada); From Fractal Analysis to Structural Significance, *Journal of Structural Geology, 24*(2), 323-338.
Lur, Y. A. M. (1978) Alteration of Ores During Epigenesis and Metamorphism in the Copper Deposits of the Red Bed Associations, *International Geology Review, 20*(6): 627-636.
Lustwerk, R. L., & Rose, A. W. (1983) *Source and Segregation of Transition Metals During Diagenetic Formation of the Redstone Stratiform Copper Deposit, Mackenzie Mts., N.W.T., Canada*, The Geological Society of America, 96th Annual Meeting, Boulder, CO, United States.
Machado, N., Lindenmayer, Z., Kroch, T. E., & Lindenmayer, D. (1991) U-Pb Geochronology of Archean Magmatism and Basement Reactivation in the Carajás Area, Amazon Shield, Brazil, *Precambrian Research*, 49: 329-354.
MacKenzie, C. (2002) Personal Communication About Sampling on Mineral Licences Held by BAFEX, *October 6, Windhoek, Namibia*.
Madi-Lugali, L. (1975) Observations sur le Conglomerat de Base du Systeme du Katanga Dans la Region de Kasumbalesa-M'Baya (Shaba Sud-Oriental), *Annales de la Faculte de Sciences - Geologie et Geographie*, 1: 69-84.
Maiden, K. (1996) Kalahari Copper Belt, Namibia and Botswana, photocopies from uncertain source, 159-164.
Maiden, K. J., Innes, A. H., King, M. J., Master, S., & Pettit, I. (1984) Regional Controls on the Localization of Stratabound Copper Deposits: Proterozoic Examples from Southern Africa and South Australia, *Precambrian Research*, 25: 99-118.
Maiden, K. J., Master, S., & Borg, G. (1986) Rift-Related Stratabound Copper-Precious Metal Deposits in Southern Africa, In Anonymous (Ed.), *Sediments Down-Under; 12th International Sedimentological Congress*, Bureau of Mineral Resources, Geology and Geophysics, Canberra, Australia, 197 p.
Main, J., V. (1978) *Witvlei Prospect, Prospecting Grant M46/3/149 - Report Summarizing Exploration Results for the Period October 1976 to December 1978*, Windhoek, Namibia: Anglo American Prospecting Services (Pty) Ltd., South West Africa.
Maksaev, V. (2001) *Reseña Metalogénica de Chile y de los Procesos que Determinan la Metalogénesis Andina* (unpublished report), Santiago, Chile.
Maksaev, V., & Zentilli, M. (2002) Chilean Strata-Bound Cu-(Ag) Deposits: An Overview, In T. M. Porter (Ed.), *Hydrothermal Iron Oxide Copper-Gold & Related Deposits: A Global Perspective*, PGC Publishing, Adelaide, Australia, 2: 185-105.
Maloof, A. C., & Hoffman, P. F. (1999) Superposed Folding at the Junction of the Inland and Coastal Belts, Damaran Orogen, NW Namibia, In Anonymous (Ed.), *Geological Society of America, 1999 Annual Meeting*, Boulder, CO, United States: Geological Society of America, 31(7): 179.

Mambwe, S. H., & Mwape, F. N. (1991) *Rare Earth Occurrences and Potential of Zambia*, International Conference on Rare Earth Minerals and Minerals for Electronic Uses, Hat Yai, Thailand.
Mambwe, S. H., & Sikatali, C. (1994) *Mineralisation and Potential of the Gemstone Industry of Zambia*, Industrial Minerals in Developing Countries (no further references available on this report).
Maniar, P. D., & Piccoli, P. M. (1989) Tectonic Discrimination of Granitoids, *Geological Society of America Bulletin*, 101: 635-643.
Mapani, B. E. S., & Moore, T. A. (1989-1995) *Geology of the Serenje Area - Explanation of Degree Sheet 1330, NW Quarter* (Geological Report 51), Geological Survey Department, Republic of Zambia, Lusaka, Zambia.
Mapani, B. S., Rivers, T., Tembo, F., De Waele, B., & Katongo, C. (2004) *Terrane Subdivision of the Irumide Orogen in Zambia: A Testable Tectonic Hypothesis*, 20th Colloquium of African Geology, Orleans, France.
Mapani, B. S. E., & Samama, J. (1999) *Mineralisation and Geologic Evolution of Neoproterozoic Kabwe Zn-Pb Mine; A Review*, 11th international Conference of the Geological Society of Africa; Earth Resources for Africa, London.
Mariano, A. N. (2001) *Xenotime-Bearing Carbonatite Veins from Lofdal, Damaraland, Namibia*, Carlisle, Maryland, USA, unpublished geological consulting report.
Marjonen, R. K. (1970 - 2000) *Geology of the Mufulira-Kitwe Area - Explanation of Degree Sheet 1228, Part of NW Quarter and SW Quarter* (60), Geological Survey Department, Republic of Zambia, Lusaka, Zambia.
Mark, G., H.S., O. N., Williams, P. J., Valenta, R. K., & Crookes, R. A. (2000) The Evolution of the Ernest Henry Fe-Oxide-(Cu-Au) Hydrothermal System, In T. M. Porter (Ed.), *Hydrothermal Iron Oxide Copper-Gold & Related Deposits: A Global Perspective*, PGC Publishing, Adelaide, Australia, 1: 123-136.
Marschik, R., Leveille, R. A., & Martin, W. (2000) La Candelaria and the Punta del Cobre District, Chile: Early Cretaceous Iron-Oxide Cu-Au(-Zn-Ag) Mineralization, In T. M. Porter (Ed.), *Hydrothermal Iron Oxide Copper-Gold & Related Deposits: A Global Perspective*, PGC Publishing, Adelaide, Australia, 1: 163-175.
Marsh, J. S., Erlank, A. J., & Duncan, A. R. (1991) Preliminary Geochemical Data for Dolerite Dikes and Sills of the Southern Part of the Etendeka Igneous Province, *Communications of the Geological Survey of Namibia, 7*: 71-73.
Martin, H. (1983) Alternative Geodynamic Models for the Damara Orogeny; A Critical Discussion, In H. Martin & F. W. Eder (Eds.), *Intracontinental Fold Belts; Case Studies in the Variscan Belt of Europe and the Damara Belt in Namibia*, Springer-Verlag, Berlin, 913-945.
Martin, H., & Behr, H. J. (1983) Generalized Comparison of the Variscan with the Damara Orogen, In H. Martin & F. W. Eder (Eds.), *Intracontinental Fold Belts; Case Studies in the Variscan Belt of Europe and the Damara Belt in Namibia*, Springer-Verlag, Berlin, 1-6.
Martin, H., & Eder, F. W. (1983) *Intracontinental Fold Belts; Case Studies in the Variscan Belt of Europe and the Damara Belt in Namibia*, Springer-Verlag, Berlin.
Martin, H., Porada, H., & Walliser, O. H. (1985) Mixtite Deposits of the Damara Sequence, Namibia, Problems of Interpretation, In M. Deynoux (Ed.), *Glacial Record*, 51(1-4): 159-196.
Mason, R. (1981) The Damara Mobile Belt in South West Africa/Namibia, In D. R. Hunter (Ed.), *Precambrian of the Southern Hemisphere*, Elsevier, Amsterdam, 754-802.
Master, S. (1995) *Bibliography of the Geology and Mineral Resources of the Central African Copperbelt and Katangan Sequence in Zambia, Zaire, Angola and Zimbabwe (1877-1995)*, *Economic Geology Research Unit Information Circular 291*, University of the Witwatersrand, Johannesburg, South Africa.
Master, S. (1996a) *Excursion Guidebook; Palaeoproterozoic of Zambia and Zimbabwe*, *Economic Geology Research Unit Information Circular 302*, University of the Witwatersrand, Johannesburg, South Africa.
Master, S. (1996b) The Palaeoproterozoic Magondi Mobile Belt, NW Zimbabwe, In S. Master (Ed.), *Excursion Guidebook; Palaeoproterozoic of Zambia and Zimbabwe, Economic Geology Research Unit Information Circular*, University of the Witwatersrand, Johannesburg, South Africa, 302: 21-61.
Master, S. (1998) *A Review of the World-Class Katangan Metallogenic Province and the Central African Copperbelt; Tectonic Setting, Fluid Evolution, Metal Sources, and Timing of Mineralization*, Recueil des Resumes; Carrefour des Sciences de la Terre, Waterloo, ON, Canada.
Master, S. (2003a) *Introduction to Stratabound Sediment-Hosted Cu Deposits* [Power Point presentation], School of Geosciences, University of the Witwatersrand, Johannesburg, South Africa.
Master, S. (2003b) *Ore Genesis Models for Stratabound Sediment-Hosted Copper Deposits* [Power Point presentation], School of Geosciences, University of the Witwatersrand, Johannesburg, South Africa.
Master, S. (2003c) *Tectonic Setting of Sedimentary Basins* [Power Point presentation], School of Geosciences, University of the Witwatersrand, Johannesburg, South Africa.
Master, S., Rainaud, C., Armstrong, R. A., Phillips, D., & Robb, L. J. (2003) Provenance Ages of the Neoproterozoic Katanga Supergroup (Central African Copperbelt), Based on Shrimp U-Pb and Laser 40 Ar/39Ar Dating of Detrital Zircons and Muscovites, with Implications for Basin Evolution, *Economic Geology Research Institute, Information Circular, 376*: 23.
Master, S., Rainaud, C. L., Armstrong, R. A., Phillips, D., & Robb, L. J. (2002) *Contributions to the Geology and Mineralization of the Central African Copperbelt: II. Neoproterozoic Deposition of the Katanga Supergroup with Implications for Regional and Global Correlations*, 11th IAGOD Quadrennial Symposium and Geocongress CD, Windhoek, Namibia.
Matheson, G. D., & Newman, D. (1966) Geology and Structure of the Lusaka Area, *Records of the Geological Survey of Zambia*, 10: 10-19.
Matton, G., & Jebrak, M. (2004 (submitted)) Resolving the Richat Enigma: Doming and Hydrothermal Karstification Above and Alkaline Complex, *Geology*, 15.
Maynard, J. B. (1991) Copper: Product of Diagenesis in Rifted Basins, In E. R. Force, J. J. Eidel, & J. B. Maynard (Eds.), *Sedimentary and Diagenetic Mineral Deposits; A Basin Analysis Approach to Exploration*, Socorro, NM, United States, Special Publication 5, Society of Economic Geologists, 199-207.
McCarthy, T. S., & Jacobsen, J. B. E. (1976) The Mineralizing Fluids at the Artonvilla Copper Deposit: An Example of a Silica-Deficient, Alkaline Hydrothermal System, *Economic Geology*, 71: 131-138.
McCourt, S., Armstrong, R., & Bisnath, A. (2002) *U-Pb Zircon Ages from the Tugela Terrane Natal Belt, South Africa: Constraints on Accretion Tectonics Associated with the Assembly of Rodinia*, Technical Meeting IGCP Projects 418/440, Windhoek, Namibia.
McDermott, F., Harris, N. B. W., & Hawkesworth, C. J. (1985) Geochemical Variations in Damara Granitoids; A Guide to Orogenic Evolution, In P. Bowden, J. A. Kinnaird, & H. F. D. Van (Eds.), *13th Colloquium of African Geology; Abstracts*, Centre International pour la Formation et les Echanges Geologiques (CIFEG), Paris, France, 3: 118-119.
McDermott, F., Harris, N. B. W., & Hawkesworth, C. J. (2000) Geochemical Constraints on the Petrogenesis of Pan-African A-Type Granites in the Damara Belt, Namibia, *Communications of the Geological Survey of Namibia, 12*: 139-148.
McDermott, F., & Hawkesworth, C. J. (1990) Intracrustal Recycling and Upper-Crustal Evolution; A Case Study From the Pan-African Damara Mobile Belt, Central Namibia, In B. K. Nelson & P. Vidal (Eds.), *Development of Continental Crust Through Geological Time,* Elsevier, Amsterdam, 83(3-4): 263-280.

McGowan, R., Roberts, S., Foster, R. P., Boyce, A. J., & Coller, D. (2002) *The Nchanga Deposits: Implications for the Origin of Zambian Copperbelt Mineralisation*, 11th IAGOD Quadrennial Symposium and Geocongress CD, Windhoek, Namibia.
McGowan, R. R., Roberts, S., Foster, R. P., Boyce, A. J., & Coller, D. (2003) Origin of the Copper-Cobalt Deposits of the Zambian Copperbelt: An Epigenetic View from Nchanga, *Geology*, 31(6): 497-500.
McManus, M. N. C. (1994) *Southern Damara Belt and Nama Foreland Basin - Excursion 2*, Conference on Proterozoic Crustal & Metallogenic Evolution, Windhoek, Namibia.
Mendelsohn, F. (Ed.). (1961) *The Geology of the Northern Rhodesian Copperbelt*, Macdonald, London.
Mendelsohn, F. (1981) Precambrian Geology of Zaire and Zambia, In D. R. Hunter (Ed.), *Precambrian of the Southern Hemisphere*, Elsevier, Amsterdam, 721-739.
Mendelsohn, F. (1986) *Southern Angola - Preliminary Exploration Assessment* (M165), Johannesburg, South Africa: consulting report for Gold Fields of South Africa.
Mendelsohn, F. (1989) Central-Southern African Ore Shale Deposits, *Special Paper of the Geological Association of Canada*, 36: 453-470.
Meneghel, L. (1982) *Trial Geochemical Prospecting Over the Kimberlite Pipes of the Kundelungu Plateau, Shaba Province, Zaire*, Geochemistry in Zambia, AGID Geochemical Workshop, Lusaka, Zambia.
Meneghel, L. (1977) *The Occurrence of Uranium in the Katanga System of North-Western Zambia*, Bulletin of the Geological Survey of Zambia, vol. 89, Lusaka, Zambia.
Meneghel, L. (1981a) *Methodology and History of Discovery of Uranium Mineralization in North-Western Province of Zambia*, Uranium Exploration Case Histories/ Advisory Group Meeting on Case Histories of Uranium Exploration, Vienna, Austria.
Meneghel, L. (1981b) A Model of the Processes Forming Sedimentary-Hosted Uranium Deposits, *Economic Geology*, 76(3): 727-732.
Meneghel, L. (1981c) The Occurrence of Uranium in the Katanga System of Northwestern Zambia, *Economic Geology*, 76(1): 56-68.
Meschede, M. (1986) A Method of Discriminating Between Different Types of Mid-Ocean Ridge Basalts and Continental Tholeiites with the Nb-Zr-Y Diagram, *Chemical Geology*, 56: 207-218.
Meyer, C. (1988) Ore Deposits as Guides to Geologic History of the Earth, *Annual Review of Earth and Planetary Sciences, 16*: 147-171.
Microsearch II. (2001) *Petrographic Description of Thin Sections (from the Kalengwa Area, Zambia)*, Ambase Exploration Namibia (Pty) Ltd. (unpublished internal report).
Middlemost, E. (1994a) Naming Materials in the Magma/Igneous Rock System, *Earth Science Reviews*, 37: 215-224.
Middlemost, E. (1994b) Towards a Comprehensive Classification of Igneous Rocks and Magmas, *Earth Science Reviews*, 31: 207-218.
Middlemost, E. (1997) *Magmas, Rocks and Planetary Development - A Survey of Magma/Igneous Rock Systems*, Longman, London.
Miller, R. (1983a) Evolution of the Damara Orogen of South West Africa/Namibia, In Miller, R. (ed.) *The Pan African Damara Orogen of South West Africa/Namibia*, Special Publication 11, Geological Society of South Africa, Johannesburg.
Miller, R. (1983b) (ed.) *The Pan African Damara Orogen of South West Africa/Namibia*, Special Publication 11, Geological Society of South Africa, Johannesburg.
Miller, R. (1994) *Excursion Through the Damara Orogen*, Conference on Proterozoic Crustal and Metallogenic Evolution, Windhoek, Namibia.
Miller, R. M. (1983c) Economic Implication of Plate Tectonic Models of the Damara Orogen, *Special Publications of the Geological Society of South Africa, 11*: 385-395.
Miller, R. M. (1983d) A Possible Model for the Damara Orogen in the Light of Recent Data, In N. Rast & F. N. Delany (Eds.), *Geodynamics of Orogenic Belts*, American Geophysical Union, Washington, D.C., 10: 31-34.
Miller, R. M. (1983e) Tectonic Implications of the Contrasting Geochemistry of Damaran Mafic Volcanic Rocks, South West Africa-Namibia, In R. G. Miller (Ed.), *Evolution of the Damara Orogen of South West Africa-Namibia*, Special Publication 11, Geological Society of South Africa, Johannesburg, 115-138.
Miller, R. M. (1991) The Framework of the Damara Orogen, Namibia, In P. G. Eriksson (Ed.), *Precambrian Sedimentary Basins of Southern Africa*, Blackwell Scientific Publications, Oxford, 3(3): 22-23.
Miller, R. M. (1992) Stratigraphy, *Mineral Resources of Namibia* Windhoek, Geological Survey of Namibia, Windoek, Namibia, 1.2-1 to 22).
Miller, R. M. (2000) The Agate Mountain Carbonatite Complex, Cape Fria NW Namibia, *Communications of the Geological Survey of Namibia, 12*: 325-336.
Miller, R. M. (2002) *Excursion Through the Neoproterozoic Damara Orogen*, 11th Quadriennial IAGOD Symposium and Geocongress 2002, Windhoek, Namibia.
Miller, R. M., Barnes, S. J., & Balkwill, G. (1983a) Possible Active Margin Deposits Within the Southern Damara Orogen - The Kuiseb Formation Between Okahandja and Windhoek, In R. G. Miller (Ed.), *Evolution of the Damara Orogen of South West Africa-Namibia*, Special Publication No. 11, Geological Society of South Africa, Johannesburg, 73-88.
Miller, R. M., & Burger, A. J. (1983a) U-Pb Zircon Age of the Early Damaran Naauwpoort Formation, In R. G. Miller (Ed.), *Evolution of the Damara Orogen of South West Africa-Namibia*, Special Publication 11, Geological Society of South Africa, Johannesburg, 267-272.
Miller, R. M., & Burger, A. J. (1983b) U-Pb Zircon Ages of Members of the Salem Granitic Suite Along the Northern Edge of the Central Damaran Granite Belt, In R. G. Miller (Ed.), *Evolution of the Damara Orogen of South West Africa-Namibia*, Special Publication 11, Geological Society of South Africa, Johannesburg, 273-280.
Miller, R. M., Freyer, E. E., & Halbich, W. (1983b) A Turbidite Succesion Equivalent to the Entire Swakop Group, In R. G. Miller (Ed.), *Evolution of the Damara Orogen of South West Africa-Namibia*, Special Publication 11, Geological Society of South Africa, Johannesburg, 67-71.
Milner, S. C., & Ewart, A. (1989) The Geology of the Goboboseb Mountain Volcanics and their Relationship to the Messum Complex, Namibia, *Communications of the Geological Survey of Namibia, 5*: 31-40.
Milner, S. C., Le, R. A., & Watkins, R. T. (1993) Rb-Sr Age Determinations of Rocks From the Okenyenya Igneous Complex, Northwestern Namibia, *Geological Magazine, 130*(3): 335-343.
Minnitt, R. C. A. (1986) Porphyry Copper-Molybdenum Mineralization at Haib River, South West Africa/Namibia, In C. R. Anhaeusser & S. Maske (Eds.), *Mineral Deposits of Southern Africa*, Geological Society of South Africa, Johannesburg, South Africa, 2: 1567-1585.
Mitchell, A. H. G., & Garson, M. S. (1981) *Mineral Deposits and Global Tectonic Settings*, Academic Press, London.
Miyashiro, A. (1978) Nature of Alkalic Volcanic Rock Series, *Contributions to Mineralogy and Petrology, 66*: 91-104.
Moodie, B. N. (2000) Geology and Mineralization in the Meso- to Neoproterozoic Ghanzi-Chobe Belt of Northwest Botswana, *Journal of African Earth Sciences, 30*(3): 467-474.
Molak, B. (1995) Some Structural and Petrological Aspects of the Cu (Co) Mineralization in the Copperbelt and Northwestern Provinces of Zambia, In M. Wendorff & L. Tack (Eds.), *Late Proterozoic Belts in Central and Southwestern Africa; IGCP Project 302*, Koninklijk Museum voor Midden - Afrika, Tervuren, Belgium, 101: 95-102.

Moles, N., Parnell, J., & Ruffell, A. (1992) *Prediction of Sediment-Hosted Ores Using Sequence Stratigraphy in Basin Analysis*, Mineral Deposit Modelling in Relation to Crustal Reservoirs of the Ore-Forming Elements, British Geological Survey, Keyworth, United Kingdom.

Money, N. J. (1972) An Outline of the Geology of Western Zambia, *Records of the Geological Survey of Zambia, 12*: 103-123.

Moore, J. M., Jacob, R. E., Harris, C., & Armstrong, R. A. (1999) The Navachab Gold Deposit, Namibia; a Mesothermal Sheeted-Vein/ Skarn System Related to the Pan-African Damaran Orogen, In H. E. Frimmel (Ed.), *11th international Conference of the Geological Society of Africa; Earth Resources for Africa,* Pergamon, London, 28 (4a): 50-51.

Moore, T. A. (1964) *The Geology of the Chisamba Area - Explanation of Degree Sheet 1428, SW Quarter*, Geological Report 5, Northern Rhodesia Geological Survey, Lusaka.

Mouillac, J. L., Valois, J. P., & Walgenwitz, F. (1986) The Goanikontes Uranium Occurrence in South West Africa/Namibia, In C. R. Anhaeusser & S. Maske (Eds.), *Mineral Deposits of Southern Africa*, Geological Society of South Africa, Johannesburg, South Africa, 1:1833-1843.

Mountford, B. R. (1982) The Chipirinyuma Massive Sulphide Deposit, Eastern Province, Zambia, *Geochemistry in Zambia*, Report of the AGID Geochemical Workshop, Lusaka, Zambia.

Mpande, M. M., & Royle, A. G. (1982) Spatial Variation in the Orebodies of the Zambian Copperbelt, *Proceedings; Twelfth Congress of the Council of Mining and Metallurgical Institutions,* Marshalltown, South Africa.

Mulela, D., & Seifert, A. V. (1980 - 1998) Geology of the Mwombezhi Dome and Jiwundu Swamp Areas - Explanation of Degree Sheet 1225 NE Quarter and 1125, part of SE Quarter, *Geological Report 83,* Geological Survey Department, Lusaka, Zambia.

Munchmeyer, C. (1996) Exotic Deposits-Products of Lateral Migration of Supergene Solutions from Porphyry Copper Deposits, In F. Camus, R. Sillitoe, & R. Petersen (Eds.), *Andean Copper Deposits: New Discoveries, Mineralization, Styles and Metallogeny,* Society of Economic Geologists, Special Publication, 5: 43-58.

Munchmeyer, C., & Urqueta, I. (1974) Geología del Yacimiento Exótica, *Coloquio Sobre Fenómenos de Alteración y Metamorfismo en Rocas Volcánicas e Intrusivas,* Universidad de Chile, Departamento de Geología, Santiago, Chile.

Mustard, R., Blenkinsop, T., McKeagney, C., Huddleston, H., C., & Partington, G. (2004) New Perspectives on IOCG Deposits, MT Isa Eastern Succession, Northwest Queensland, *SEG 2004 - Predictive Mineral Discovery Under Cover - CD*, Society of Economic Geologists, Perth, Western Australia.

Mwamba, K., & Sikazwe, O. N. (2002) The Kabulanshishi Copper Sulphide Deposit, Cchongwe District, Lusaka Province, Zambia: A Field Investigation, *11th IAGOD Quadrennial Symposium and Geocongress CD*, Windhoek, Namibia.

Namateba, C. (1986) Irumide; the Kibaran Belt of Zambia, *Newsletters-Bulletin - UNESCO, 5*: 163-172.

Naslund, H. R., Henriquez, F., Nystrom, J. O., Vivallo, W., & Dobbs, F. M. (2002) Magmatic Iron Ores and Associated Mineralization: Examples from the Chilean High Andes and Coastal Cordillera, In T. M. Porter (Ed.), *Hydrothermal Iron Oxide Copper-Gold & Related Deposits: A Global Perspective*, PGC Publishing, Adelaide, Australia, 2: 207-226.

Newton, A. R. (1957) Some New Katanga Sequences and Their PossibleSignificance in Relation to the System as a Whole, *Records of the Geological Survey of Northern Rhodesia, 1957*, 42-50.

Newton, A. R. (1958) Preliminary Notes on the Quartz-Biotite-Schist Series of the Monze Area, Sheet 1627 NE Quarter - Gwembe District, *Records of the Geological Survey of Northern Rhodesia, 1958*, 18-19.

Newton, A. R. (1961) An Unusual Gabbroic Intrusion from Northern Rhodesia, *Geological Magazine*, 98(5): 417-422.

Newton, A. R. (1968) Some New Katanga Sequences and Their Possible Significance in Relation to the System as a Whole, *Records of the Geological Survey of Northern Rhodesia, 1956*: 42-50.

Nex, P., & Kinnaird, N. A. (1995) Granites and Their Mineralization in the Swakop River Area Around Gonikontes, Namibia, *Communications of the Geological Survey, Namibia*, 10: 51-56.

Niku-Paavola, V., Siegfried, P., & Mariano, A. N. (2002) *Yttrium and HREE-Rich Carbonatite Veins of Lofdal, Damaraland, Namibia*, 11th Quadriennial IAGOD Symposium and Geocongress, Windhoek, Namibia.

Nisbet, B., Cooke, J., Richards, M., & Williams, C. (2000) Exploration for Iron Oxide Copper Gold Deposits in Zambia and Sweden: Comparison with the Australian Experience, In T. M. Porter (Ed.), *Hydrothermal Iron Oxide Copper-Gold & Related Deposits: A Global Perspective*, PGC Publishing, Adelaide, Australia, 1: 297-308.

Nisbet, B. W. (2004a) IOCG Mineralization in the Kiruna Region, Norbotten, Northern Sweden, In C. Beaudry (Ed.), *Exploration for Iron Oxide-Hosted Copper-Gold Deposits - Short Course*, Prospectors and Developers Association of Canada, Toronto, pp. 6

Nisbet, B. W. (2004c) *IOCG Mineralization in Zambia* [MS-Power Point presentation] In C. Beaudry (Ed.), *Exploration for Iron Oxide-Hosted Copper-Gold Deposits - Short Course*, Prospectors and Developers Association of Canada, Toronto, 52 p.

Nisbet, B. W. (2004b) IOCG Mineralization in Zambia, In C. Beaudry (Ed.), *Exploration for Iron Oxide-Hosted Copper-Gold Deposits - Short Course*, Prospectors and Developers Association of Canada, Toronto, pp. 6

Nortemann, M. F. J., Mucke, A., Weber, K., & Meinert, L. D. (2000) Mineralogy of the Navachab Skarn Deposit, Namibia: An Unusual Au-Bearing Skarn in High-Grade Metamorphic Rocks, *Communications of the Geological Survey of Namibia, 12*: 149-156.

Notebaart, C. W. (1978) Cupriferous Micas from the Chingola Area, Zambian Copperbelt, *Institution of Mining and Metallurgy, Transactions, Section B: Applied Earth Science*, 87 May: 74-78.

Nuelle, L. M., Day, W. C., Sidder, G. B., & Seeger, C. M. (1992) Geology and Mineral Paragenesis of the Pea Ridge Iron Ore Mine, Washington County, Missouri - Origin of the Rare-Earth-Element- and Gold-Bearing Breccia Pipes, *United States Geological Survey Bulletin*, 1989-A-C, A1-A11.

Nyambe, I. A. (1999a) Heavy Mineral Concentrations in the Mesoproterozoic Mbala Formation of the Mporokoso Group, Makasa Hill area, Northern Zambia; Implications for Precious Metal Exploration, *11th International Conference of the Geological Society of Africa; Earth Resources for Africa,* London.

Nyambe, I. A. (1999b) Mineral Resources of Zambia; Implications on Exploration, Exploitation and Geourban Growth, *11th International Conference of the Geological Society of Africa; Earth Resources for Africa,* London.

Obolenskiy, A. A., Rodionov, S. M., Ariunbileg, S., Dejidmaa, G., E.G., D, Dorjgotov. D., O., G., Hwan Hwang, D., Sun, F., Gotovsuren, A., S.N., L., Li, X., Nokleberg, W. J., & Ogasawara, M. (2003) *Mineral Deposit Models for Northeast Asia*, United States Geological Survey, Menlo Park, California, (http://minerals.usgs.gov/west/projects/minres.html).

O'Brien, P. L. A. (1954) Economic Geology - Some Mineral Ocurrences of the Eastern Province, *Records of the Geological Survey of Northern Rhodesia* (For the Year ending 31st december, 1953), Lusaka, Northern Rhodesia.

O'Brien, P. L. A. (1955) Some Mineral Occurrences of the Eastern Province, *Records of the Geological Survey of Northern Rhodesia* (for the Year ending 31st December, 1953), Lusaka, Northern Rhodesia, 13-16.

O'Brien, P. L. A. (1958) Copper deposits and Their Environment in Northern Rhodesia, *Northern Rhodesia Geological Survey Occasional Paper*, 24: 133-146.

Ojala, V. J., Eilu, P., Groves, D. I., O'Brien, H. E., & Peltonen, P. (2004) *Metasomatized Mantle: Implications for Metallogeny of the Fennoscandian Shield*, *SEG 2004 - Predictive Mineral Discovery Under Cover - CD*, Society of Economic Geologists, Perth, Western Australia.

Okitaudji, L. R. (1994) L'Evolution des Modeles Genetiques des Gisements de Cuivre-Cobalt Dans l'Arc Cuprifere du Shaba et de la Zambie; Discussion, In J. M. Charlet (Ed.), *Centenaire des Premieres Etudes Sur la Geologie Shabienne (Zaire), "Gisements Stratiformes de Cuivre et Mineralisations Associees"*, Academie Royale des Sciences d'Outre-Mer, Brussels, Belgium, 101-121.

Okitaudji, L. R. (2000) Les Bacteries Fossiles du Proterozoique Superieur (1000-600 m.a.) et Leur Role Dans la Concentration du Cuivre et du Cobalt des Gisements de l'Arc Cuprifere du Shaba (Republique Democratique du Congo), *Bulletin de l'Academie et de la Societe Lorraine des Sciences*, 39(1-4): 23-32.

Okitaudji, L. R., & Unilu, B. P. (1990) La Metallogenese du Cuivre et du Cobalt en Afrique Centrale (Shaba, Zaire, Zambie), In Anonymous (Ed.), *15th Colloquium of African Geology*, Centre International pour la Formation et les Echanges Geologiques (CIFEG), Paris, France, 20: 267.

Okrusch, M., Buehn, B., Hoernes, S., Katz, L. K., & Woermann, E. (1992) High-Grade Metamorphism and its Petrological Implications of Sedimentary Manganese Deposits at Otjosondu, Damara Belt, Namibia, In Anonymous (Ed.), *29th International Geological Congress; Abstracts*, International Union of Geological Sciences, 29: 213.

Oliver, G. J. H. (1994) Mid-Crustal Detachment and Domes in the Central Zone of the Damaran Orogen, Namibia, In A. B. Kampunzu & R. T. Lubala (Eds.), *Neoproterozoic Belts of Zambia, Zaire and Namibia Namibia, Journal of African Earth Sciences*, Special Issue, 19(4): 331-344.

Oliver, G. J. H. (1995) The Central Zone of the Damara Orogen, Namibia, as a Deep Metamorphic Core Complex, *Communications of the Geological Survey of Namibia*, 10: 33-41.

Oliver, G. J. H., Johnson, S. P., Williams, I. S., & Herd, D. A. (1998) Relict 1.4 Ga Oceanic Crust in the Zambezi Valley, Northern Zimbabwe: Evidence for Mesoproterozoic Supercontinental Fragmentation, *Geology*, 26(6): 571-573.

Oliver, G. J. H., & Kinnaird, J. A. (1996) The Rossing-SJ Dome, Central Zone, Damara Belt, Namibia: An Example of Mid-Crustal Extensional Ramping, *Communications of the Geological Survey of Namibia*, 11: 53-64.

Oreskes, N., & Einaudi, M. T. (1990) Origin of Rare Earth Element-Enriched Hematite Breccias at the Olympic Dam Cu-U-Au-Ag Deposit, Roxby Downs, South Australia, *Economic Geology*, 85(1): 1-28.

Osterman, C. (1999) *The Geology and Genesis of the Orebodies of the Kombat Mine, Namibia,* Unpublished Ph.D., Colorado School of Mines, Golden, Colorado.

Oyarzun, R., Oyarzun, J., Menard, J. J., & Lillo, J. (2003) The Cretaceous Iron Belt of Northern Chile: Role of Oceanic Plates, A Superplume Event and a Major Shear Zone, *Minerliium Deposita*, 38: 640-646.

Page, T. C. (1974) *The Geology of the Lubungu and Lungu Areas - Explanation of Degree Sheet 1426 NW and SW Quarters* (Geological Report 39), Geological Survey, Lusaka, Zambia.

Pandey, B. K., Chabria, T., & Gupta, J. N. (1995) Geochronological Characterisation of the Proterozoic Terrains of Peninsular India; Relevance to the First Order Target Selection for Uranium Exploration, *Exploration and Research for Atomic Minerals*, 8: 187-213.

Park, C. F. (1961) A Magnetite "Flow" in Northern Chile, *Economic Geology*, 56: 431-441.

Parker, A. J. (1990) Gawler Craton and Stuart Shelf - Regional Geology and Mineralization, In E. E. Hughes (Ed.), *Geology of the Mineral Deposits of Australia and Papua New Guinea,* The Australian Institute of Mining and Metallurgy, Melbourne, Australia, 2: 999-1008.

Partington, G. A., & Williams, P. J. (2000) Proterozoic Lode Gold and (Iron)-Copper-Gold Deposits: A Comparison of Australian and Global Examples, In S. G. Hagemann & P. E. Brown (Eds.), *Gold in 2000*, Reviews in Economic Geology, Society of Economic Geologists, 13: 69-101.

Pearce, J. (1996) Sources and Settings of Granitic Rocks, *Episodes*, 19(4): 120-125.

Pearce, J. A., & Cann, J. R. (1973) Tectonic Setting of Basic Volcanic Rocks Determined Using Trace Element Analysis, *Earth and Planetary Science Letters*, 19: 290-300.

Pearce, J. A., Harris, N. B. W., & Tindle, A., G. (1984) Trace Element Discrimination Diagrams for the Tectonic Interpretation of Granitic Rocks, *Journal of Petrology*, 25(4): 956-983.

Peccerillo, A., & Taylor, S. R. (1976) Geochemistry of Eocene Calc-Alkaline Volcanic Rocks From the Kastamonu Area, Northern Turkey, *Contributions to Mineralogy and Petrology*, 58: 63-81.

Pepper, L. (2000) *Zambian Regional Granitoid Study: A Petrological and Geochemical Investigation,* Unpublished MGeol Independent Research Project, University of Southampton, Southampton, England.

Perkin, D. J. (1983) Proterozoic Stratabound Uranium Deposits; A Proposed New Class, *Sixth Australian Geological Convention; Lithosphere Dynamics and Evolution of Continental Crust,* Sydney, N.S.W., Australia.

Pfurr, N., Ahrendt, B. T., Hansen, B. T., & Weber, K. (1991) U-Pb and Rb-Sr Isotopic Study of Granitic Genisses and Associated Metavolcanic Rocks from the Rostock Massifs, Southern Margin of the Damara Orogen: Implications for Lithostratigraphy of this Crustal Segment, *Communications of the Geological Survey of Namibia*, 7: 35-48.

Pfurr, N., Ahrendt, H., & Weber, K. (1990) U/ Pb and Rb/ Sr Isotopic Study of Red Granitic Gneisses and Associated Metavolcanics in the Area of the Rostock Massifs, Southern Margin Zone of the Damara Orogen, Namibia and Their Implications for the Lithostratigraphy of This Crustal Segment, In Anonymous (Ed.), *15th Colloquium of African Geology*, Centre International pour la Formation et les Echanges Geologiques (CIFEG), Paris, France, 20: 185.

Phillips, K. (1955) The Nambala Iron Deposits, Mumbwa District, *Northern Rhodesia Records of the Geological Survey for the Year Ending December 31, 1953*, 17-20.

Phillips, K. (1957a) Further Information Concerning the Nature and Origin of the Nambala-Sonkwe Iron Deposits, *Records of the Geological Survey Organization of Northern Rhodesia for the Year Ending 31st December 1955,* 10-12.

Phillips, K. (1957b) Progress in Fieldwork - Luiri Hilll sheet 1527NW, *Northern Rhodesia Records for the Year Ending December 1955*, 3-4.

Phillips, K. (1958a) A Regional Outline of Certain Metalliferous zones and Their Bearing Upon Some Problems of Granitization in Northern Rhodesia, *Ocassional Paper of the Department of Geological Survey*, 23: 15.

Phillips, K. A. (1954) Preliminary Notes on the Geology of the South-East Part of the Mumbwa District, *Records of the Geological Survey, Northern Rhodesia* (For the Year ending 31st December, 1952), 14-16.

Phillips, K. A. (1958b) *The Geology and Metalliferous Deposits of the Luiri Hill Area (Mumbwa District) - Explanation of Degree Sheet 1527, NW Quarter* (Report No. 4, 67 p.), Northern Rhodesia Department of Geological Survey, Lusaka, 67.

Phillips, K. A. (1958c) A Summary of the Geology of the Luiri Hill Area, Sheet 1527, NW Quarter - Mumbwa District, *Records of the Geological Survey of Northern Rhodesia, 1956*, 8-15.

Phillips, K. A. (1959) Some Interpretations Arising from a Remapping of the Katanga Systems Southeast of Mumbwa, Northern Rhodesia, XX Congreso Geológico Internacional, Ciudad de México, México.

Piche, M., & Jebrak, M. (2003) Normative Minerals and Alteration Indices Developed for Mineral Exploration, *Journal of Geochemical Exploration*.

Pirajno, F. (1986) Sn-W Metallogeny in the Damara Province, Namibia, In C. D. Branch (Ed.), *Proceedings of the Eighth Australian Geological Convention; Earth Resources in Time and Space,* Geological Society of Australia, Sydney, N.S.W., Australia, 15: 157-158.

Pirajno, F., & Jacob, R. E. (1987) Sn-W Metallogeny in the Damara Orogen, South West Africa/ Namibia, *Transactions of the Geological Society of South Africa*, 90(3): 239-255.

Pirajno, F., & Jacob, R. E. (1988) Gold Mineralisation in the Intracontinental Branch of the Damara Orogen, Namibia, In A. D. T. Goode, E. L. Smyth, W. D. Birch, & L. I. Bosma (Eds.), *Bicentennial Gold 88; Extended Abstracts; Poster Programme,* Geological Society of Australia, Sydney, N.S.W., Australia, 23(1-2): 168-171.

Pirajno, F., & Jacob, R. E. (1991) Gold Mineralisation in the Intracontinental Branch of the Damara Orogen, Namibia; A Preliminary Survey, *Journal of African Earth Sciences*, 13(3-4): 305-311.

Pirajno, F., Jacob, R. E., & Petzel, V. F. W. (1991) Distal Skarn-Type Gold Mineralization in the Central Zone of the Damara Orogen, Namibia, In E. A. Ladeira (Ed.), *Brazil Gold '91; The Economics, Geology, Geochemistry and Genesis of Gold Deposits; Proceedings,* A. A. Balkema, Rotterdam, Netherlands, 95-100.

Pirajno, F., Kinnaird, J. A., Fallick, A. E., Boyce, A. J., & Petzel, V. W. F. (1993) A Preliminary Regional Sulphur Isotope Study of Selected Samples from Mineralized Deposits of the Damara Orogen, Namibia, *Communications of the Geological Survey of Namibia, 8*: 81-97.

Pirajno, F., Petzel, V. F. W., & Jacob, R. E. (1987) Geology and Ateration-Mineralization of the Brandberg West Sn-W Deposit, Damara Orogen, South West Africa/ Namibia, *Transactions of the Geological Society of South Africa*, 90(3): 256-269.

Pirajno, F., & Schlogl, H. U. (1987) The Alteration-Mineralization of the Krantzberg Tungsten Deposit, South West Africa/ Namibia, *Transactions of the Geological Society of South Africa*, 90(4): 499-508.

Piranjo, F., & Joubert, B. D. (1993) An Overview of Carbonate-Hosted Mineral Deposits in the Otavi Mountain Land, Namibia: Implicaitons of Ore Genesis, *Journal of African Earth Sciences*, 16(3): 165-172.

Pitcher, W. S. (1979) The Nature, Ascent and Emplacement of Granitic Magmas, *Journal of the Geological Society, London*, 136: 627-662.

Pitcher, W. S. (1982) Granite Type and Tectonic Environment, In K. J. Hsu (Ed.), *Mountain Building Processes,* Academic Press, London, 19-40.

Plant, J. A., O'Brien, C., Tarney, J., & Hurdley, J. (1985) Geochemical Criteria for the Recognition of High Heat Production Granites, *High Heat Production (HHP) Granites, Hydrothermal Circulation and Ore Genesis*, The Institution of Mining and Metallurgy, St. Austell, Cornwall, England, 263-285.

Pollard, P. J. (2000) Evidence of a Magmatic Fluid and Metal Source for Fe-Oxide Cu-Au Mineralization, In T. M. Porter (Ed.), *Hydrothermal Iron Oxide Copper-Gold & Related Deposits: A Global Perspective*, PGC Publishing, Adelaide, Australia, 1: 27-41.

Pollington, N. (2004) *Sulfide Mineral Chemistry at Konkola North, Zambia*, *SEG 2004 - Predictive Mineral Discovery Under Cover - CD*, Society of Economic Geologists, Perth, Western Australia.

Porada, H. (1986) Stratigraphy and Facies in the Upper Proterozoic Damara Orogen, Namibia, Based on a Geodynamic Model, *Precambrian Geology*, 3: 37-56.

Porada, H. (1989) Pan-African Rifting and Orogenesis in Southern Equatorial Africa and Eastern Brazil, *Precambrian Research*, 44: 103-136.

Porada, H., Ahrendt, H., Behr, H. J., & Weber, K. (1983) The Joint of the Coastal and Intracontinental Branches of the Damara Orogen, Namibia, South West Africa, In H. Martin & F. W. Eder (Eds.), *Intracontinental Fold Belts; Case Studies in the Variscan Belt of Europe and the Damara Belt in Namibia*, Springer-Verlag, Berlin, 901-912.

Porada, H., & Behr, H. J. (1988) Setting and Sedimentary Facies of Late Proterozoic Alkali Lake (Playa) Deposits in the Southern Damara Belt of Namibia, In M. J. Jackson (Ed.), *Aspects of Proterozoic Sedimentary Geology*, 58(2-4): 171-194.

Porada, H., & Wittig, R. (1983a) Turbidites and Their Significance for the Geosynclinal Evolution of the Damara Orogen, South West Africa-Namibia, In R. G. Miller (Ed.), *Evolution of the Damara Orogen of South West Africa-Namibia,* Geological Society of South Africa, Johannesburg, South Africa, 11: 21-36.

Porada, H., & Wittig, R. (1983b) Turbidites in the Damara Orogen, In H. Martin & F. W. Eder (Eds.), *Intracontinental Fold Belts; Case Studies in the Variscan Belt of Europe and the Damara Belt in Namibia*, Springer-Verlag, Berlin, 543-576.

Porada, H. R. (1974) The Khoabendus Formation in the Area Northwest of Kamanjab and in the Southeastern Kaokoveld, South West Africa, *South West Africa Series of the Geological Survey of South Africa*, 4: 23.

Porter, T. M. (2002) Iron Oxide Alteration/Mineralizing Systems and Copper-Gold & Related Mineralization, In T. M. Porter (Ed.), *Hydrothermal Iron Oxide Copper-Gold & Related Deposits: A Global Perspective*, PGC Publishing, Adelaide, Australia, 2: 3-6.

Poulsen, K. H. (1996) Carlin-Type Gold Deposits and Their Potential Occurrence in the Canadian Cordillera, *Cordillera and Pacific Margin*, Geological Survey of Canada, Ottawa, ON, Canada, 1-9.

Prave, A. R. (1994) The Maieberg-Mulden Foreland Basin; New Insights on the Neoproterozoic Damara Orogen of Namibia, In Anonymous (Ed.), *Geological Society of America, 1994 Annual Meeting,* Boulder, Colorado, Geological Society of America*,* 26(7): 406-407.

Prave, A. R. (1996) Tale of Three Cratons; Tectonostratigraphic Anatomy of the Damara Orogen in Northwestern Namibia and the Assembly of Gondwana, *Geology*, 24(12): 1115-1118.

Premoli, C. (1999) Mineral Resources of the Lufilian Arc; A Modern Database, *11th International Conference of the Geological Society of Africa; Earth Resources for Africa*, London.

Pretorius, D. A. (1985) The Kalahari Foreland, Its Marginal Troughs and Overthrust Belts, and The Regional Structure of Botswana, In D. G. Hutchins & A. P. Lynam (Eds.), *The Proceedings of a Seminar on the Mineral Exploration of the Kalahari; October, 1983,*: Republic of Botswana, Geological Survey Department, Lobatsi, Botswana, 29: 294-319.

Preussinger, H. (1990) Host-Rock Geology of the Metamorphosed Massive Sulfide Deposits at Gorob in the Pan-African Damara Orogen, Namibia, *Journal of African Earth Sciences*, 10(4): 717-732.

Punukollu, S. N. (1983) Future of Mineral Exploration and Mining in Zambia, *Exploration and Mining in Zambia - Proterozoic 83 Souvenir*, Geological Society of Zambia, Lusaka, Zambia, 7.

Pupin, J. P. (1980) Zircon and Granite Petrology, *Contributions to Mineralogy and Petrology*, 73: 207-220.

Purves, W. D. (1973) Engineering Implications of Granite Weathering, In L. A. Lister (Ed.), *Symposium on Granites, Gneisses and Related Rocks*, Geological Society of South Africa, Johannesburg, Special Publication 3: 163-166.

Rainaud, C., Master, S., Armstrong, R. A., & Robb, L. J. (2003a) A Cryptic Mesoarchean Terrane in the Basement to the Central African Copperbelt, *Journal of the Geological Society, London*, 160: 11-14.

Rainaud, C., Master, S., Armstrong, R. A., & Robb, L. J. (2003b) *Geochronology and Nature of the Paleoproterozoic Basement in the Central African Copperbelt (Zambia and the Democratic Republic of Congo), with Regional Implications,* draft for publication, presented at short course on sedimentary-hosted copper deposits held in Kitwe, Zambia, 2003, 86-102.

Rainaud, C. L., Armstrong, R. A., Master, S., Robb, L. J., & Mumba, P. A. C. C. (2002a) Contributions to the Geology and Mineralization of the Central African Copperbelt: I. Nature and Geochronology of the Pre-Katangan Basement, *11th IAGOD Quadrennial Symposium and Geocongress CD*, Windhoek, Namibia.

Rainaud, C. L., Master, S., Armstrong, R. A., Phillips, D., & Robb, L. J. (2002b) Contributions to the Geology and Mineralization of the Central African Copperbelt: IV. Monazite U-Pb Dating and 40Ar-39Ar Thermochronology of Metamorphic Events During the Lufilian Orogeny, *11th IAGOD Quadrennial Symposium and Geocongress CD*, Windhoek, Namibia.

Ray, G. E., & Dich, L. A. (2002) The Productora Prospect in North-Central Chile: An Example of and Intrusion-Related, Candelaria Type Fe-Cu-Au Hydrothermal System, In T. M. Porter (Ed.), *Hydrothermal Iron Oxide Copper-Gold & Related Deposits: A Global Perspective*, PGC Publishing, Adelaide, Australia, 2: 131-151.

Reardon, N. C. (1992) *Magmatic-Hydrothermal Systems and Associated Magnetite-Apatite-Actinolite Deposits, Echo Bay, Northwest Territories*, leaflet handed during the 2003 PDAC Convention, Prospectors and Developers Association of Canada, Toronto.

Reeve, J. S., Cross, K. C., Smith, R. N., & Oreskes, N. (1990) Olympic Dam Copper-Uranium-Gold-Silver Deposit, In E. E. Hughes (Ed.), *Geology of the Mineral Deposits of Australia and Papua New Guinea,* The Australian Institute of Mining and Metallurgy, Melbourne, Australia, 2: 1009-1035.

Reeve, W. H. (1954) Mpika District - A Preliminary Reconnaissance of the Nsalu and Chiromo Hills, *Records of the Geological Survey of Northern Rhodesia* (For the Year ending 31st December, 1953), Lusaka, Northern Rhodesia.

Reeve, W. H. (1963) The Geology and Mineral Resources of Northern Rhodesia, *Bulletin of the Geological Survey of Northern Rhodesia, 3*: 213.

Reid, D. L., Mallin, S., & Allsopp, H. L. (1988) Rb-Sr Ages of Granites in the Rehoboth-Nauchas Area, South West Africa/Namibia, *Communications of the Geological Survey of Namibia*, 4: 19-27.

Requia, K., & Fontbote, L. (2000) The Salobo Iron Oxide Copper-Gold Deposit, Carajás, Northern Brazil, In T. M. Porter (Ed.), *Hydrothermal Iron Oxide Copper-Gold & Related Deposits: A Global Perspective*, PGC Publishing, Adelaide, Australia, 1: 225-236.

Requia, K., Stein, H., Fontboté, L., & Chiaradia, M. (2003) Re-Os and Pb-Pb Geochronology of the Archean Salobo Iron Oxide Copper-Gold Deposit, Carajás Mineral Province, Northern Brazil, *Mineralium Deposita*, 38: 727-738.

Reuning, E. (1937) The Goldfields of Ondundu, South West Africa, *Geologische Rundschau - English translation of a report in German,* 28: 18.

Reynolds, L. J. (2000) Geology of the Olympic Dam Cu-U-Au-Ag-REE Deposit, In T. M. Porter (Ed.), *Hydrothermal Iron Oxide Copper-Gold & Related Deposits: A Global Perspective*, PGC Publishing, Adelaide, Australia, 1: 93-104.

Richards, J. P., Ronacher, E., & Johnston, M. (1998) New Mineralization Styles at the Porgera Gold Deposit, Papua New Guinea, In Anonymous (Ed.), *Geological Society of America, 1998 Annual Meeting*, Boulder, CO, Geological Society of America, 30(7): 302.

Richards, T. E. (1986) Geological Characteristics of Rare-Metal Pegmatites of the Uis Type in the Damara Orogen, South West Africa/ Namibia, In C. R. Anhaeusser & S. Maske (Eds.), *Mineral Deposits of Southern Africa*, Geological Society of South Africa, Johannesburg, South Africa, 1845-1862.

Rickwood, P. C. (1989) Boundary Lines Within Petrologic Diagrams Which Use Oxide of Major and Minor Elements, *Lithos, 22*, 247-263.

Rittmann, A. (1957) On the Serial Character of Igneous Rocks, *The Egyptian Journal of Geology, 1*(1): 23-48.

Rivers, T., & Johnson, S. (2002) *Construction of the Southern Africa Craton: Relationships Between the Mesoproterozoic Irumide, Kibaran and Natal-Namaqua Orogens*, Technical Meeting IGCP Projects 418/440, Windhoek, Namibia.

Robb, L. (2004) *Introduction to Ore-Forming Processes*, Blackwell, Oxford.

Robb, L. J., Master, S., Greyling, L. N., Yao, Y., & Rainaud, C. L. (2002) Contributions to the Geology and Mineralization of the Central African Copperbelt: V. Speculations Regarding the 'Snowball Earth' and Redox Controls on Stratiform Cu-Co and Pb-Zn Mineralization, *11th IAGOD Quadrennial Symposium and Geocongress CD*, Windhoek, Namibia.

Rogers, J. J. W., & Greenberg, J. K. (1981) Trace Elements in Continental-Margin Magmatism: Part III Alkali Granites and Their Relationship to Cratonization: Summary, *Geological Society of America Bulletin, 92*(1): 6-9.

Rogers, J. J. W., & Greenberg, J. K. (1990) Late-Orogenic, Post-Orogenic, and Anorogenic Granites: Distinction by Major Element and Trace-Element Chemistry, and Possible Origins, *Journal of Geology, 98*: 291-309.

Rollinson, H. R. (1994) *Using Geochemical Data: Evaluation, Presentation, Interpretation*, Longman Scientific & Technical, London.

Ronze, P. C., Soares, A. D. V., dos Santos, M. G., Barreira, C. F., & Proterozoic. (2000) Alemao Copper-Gold (U-REE) Deposit, Carajás, Brazil, In T. M. Porter (Ed.), *Hydrothermal Iron Oxide Copper-Gold & Related Deposits: A Global Perspective*, PGC Publishing, Adelaide, Australia, 1: 191-202.

Rose, A. W., & Bianchi, G. C. (1985) Adsorption of Cu, Ag, and Other Metals on Fe-oxides as a Control on Elemental Composition of Stratiform and Redbed Copper Deposits, *The Geological Society of America, 98th Annual Meeting*, Boulder, Colorado, United States of America.

Rose, A. W., Herrick, D. C., & Deines, P. (1985) An Oxygen Sulfur Isotope Study of Skarn-Type Magnetite Deposits of the Cornwall Type, Southeastern Pennsylvania, *Economic Geology*, 80: 418-443.

Ruxton, P. A. (1986) Sedimentology, Isotopic Signature and Ore Genesis of the Klein Aub Copper Mine, South West Africa/Namibia, In C. R. Anhaeusser & S. Maske (Eds.), *Mineral Deposits of Southern Africa*, Geological Society of South Africa, Johannesburg, South Africa, 1: 1725-1738.

Ruxton, P. A., & Clemmey, H. (1986) Late Proterozoic Stratabound Red Bed-Copper Deposits of the Witvlei Area, South West Africa/Namibia, In C. R. Anhaeusser & S. Maske (Eds.), *Mineral Deposits of Southern Africa*, Geological Society of South Africa, Johannesburg, South Africa, 1: 1739-1754.

Saviaro, K., Phil, L., & Agar, R. (1980) *Uranium Channel Anomalies from the 1973-76 Airborne Geophysical Survey of Zambia*, Volume 89, Geological Survey of Zambia, Lusaka, Zambia.

Sawkins, F. J. (1990) *Metal Deposits in Relation to Plate Tectonics*, 2nd ed., Springer-Verlag, Berlin.

Schandelmeier, H., Burhani, M., de, V. G. P., & Cooray, P. G. (1977) The Geology of the North Eastern Region of Zambia with Special Reference to the Kawimbe-Nsokolo-Mambwe Area, *International Conference on the Utilization of Mineral Resources in Developing Countries*, Lusaka, Zambia.

Schneider, G. I. C., & Seeger, K. G. (1999) Copper, In G. I. C. Schneider (Ed.), *Mineral Deposits of Namibia, CD edition*, Geological Survey of Namibia, Windhoe, Namibia, 172 p.

Schwarzer, R. R., & Rogers, J. J. W. (1974) A Worldwide Comparison of Alkali Olivine Basalts and Their Differentiation Trends, *Earth and Planetary Science Letters*, 23: 286-296.

Searle, D. L. (1972) The Stratigraphy of the Plateau Series of the Senga Hill Area, *Records of the Geological Survey of Zambia*, 12: 55-62.

Seeger, C. M. (2000) Southeast Missouri Iron Metallogenic Province: Characteristics and General Chemistry, In T. M. Porter (Ed.), *Hydrothermal Iron Oxide Copper-Gold & Related Deposits: A Global Perspective*, PGC Publishing, Adelaide, Australia, 1: 237-248.

Seifert, N. (1986) Geochronologische Untersuchungen an Basement-Gesteinen am Suedrand des Damara-Orogens (Namibia), *Schweizerische Mineralogische und Petrographische Mitteilungen, 66*(3): 483-484.
Seltmann, R., Koroteeev, V., Fershtater, G., & Smirnov, V. (2000) The Eroded Uralian Paleozoic Ocean to Continent Transition Zone: Granitoids and Related Ore Deposits, *International Field Conference in the Urals, Russia; IGCP Project 373 "Correlation, Anatomy and Magmatic-Hydrothermal Evolution of Ore-Bearing Felsic Igneous Systems in Eurasia",* 18-30 July, 2000, Yekaterinburg, Russia.
Seth, B. (1999) *Crustal Evolution of the Kaoko Belt, NW Namibia - Geochemical and Geochronological Study of Archean to Mesoproterozoic Basement Gneisses and Pan-African Migmatites and Granitoids,* Unpublished Ph.D., Julius-Maxilimians-Universitat, Wurzburg, Germany.
Seth, B., Armstrong, R. A., Brandt, S., Villa, I. M., & Kramers, J. D. (2003) Mesoproterozoic U-Pb and Pb-Pb Ages of Granulites in NW Namibia: Reconstructing a Complete Orogenic Cycle, *Precambrian Research*, 126: 147-168.
Seth, B., Kroner, A., Mezger, K., Nemchin, A. A., Pidgeon, R. T., & Okrusch, M. (1998) Archean to Neoproterozoic Magmatic Events in the Kaoko Belt of NW Namibia and Their Geodynamic Sygnificance, *Precambrian Research*, 92: 341-363.
Seth, B., Okrusch, M., Wilde, M., & Hoffmann, K. H. (2000) The Voetspoor Intrusion, Southern Kaoko Zone, Namibia: Mineralogical, Geochemical and Isotopic Constraints for the Origin of a Syenitic Magma, *Communications of the Geological Survey of Namibia*, 12: 125-137.
Shervais, J. W. (1982) Ti-V Plots and the Petrogenesis of Modern Ophiolitic Lavas, *Earth and Planetary Science Letters,* 59: 101-118.
Sidder, G. B., Day, W. C., Nuelle, L. M., Seeger, C. M., & Kisvarsanyi, E. B. (1993) Mineralogic and Fluid-Inclusion Studies of the Pea Ridge Iron-Rare-Earth-Element Deposit, Southeast Missouri, In R. W. Scott, P. S. Detra, & B. R. Berger (Eds.), Advances Related to United States and International Mineral Resources: Developing Frameworks and Exploration Strategies, *United States Geological Survey Bulletin* 2039: 201-216.
Siedner, G. (1968) Distribution of Alkali Metals and Thallium in Some South-West African Granites, *Geochimica et Cosmochimica Acta,* 32: 1303-1315.
Sikaswe, O. N., Koller, F., Abart, R., & Kamona, A. F. (2002) Geology and Geochemistry of the Marie Copper Sulphide Deposit, Mumbwa District, Central Zambia, *11th IAGOD Quadrennial Symposium and Geocongress CD*, Windhoek, Namibia.
Sikatali, C., & Njamu, M. (1992) A Uranium Orientation Survey in Sikaneka Area, Southern Zambia, *Journal of African Earth Sciences,* 14(2): 275-282.
Sikazwe, O. N. (1999) The Lewis-Marie Copper Deposits, Central Zambia: Geology, Structure and Mineralisation, *11th International Conference of the Geological Society of Africa; Earth Resources for Africa*, London.
Sikazwe, O. N., & Simukanga, S. (1996) A Bibliography of Undergraduate Theses in the School of Mines (1982-1986), *Zambian Journal of Applied Earth Sciences*, 10(1): 62-75.
Sikka, D., & Nehru, C. E. (1997) Review of Precambrian Porphyry Cu+ or -Mo+ or -Au Deposits with Special Reference to Malanjkhand Porphyry Copper Deposit, Madhya Pradesh, India, *Journal of the Geological Society of India*, 49(3): 239-288.
Sikombe, W. B. (1982) *Lochinvar Gypsum Mine, Zambia: A Case Study in Production of an Industrial Mineral*, Regional Workshop: Strategies for Small-Scale Mining and Mineral Industries.
Sillitoe, R. (2003) Iron Oxide-Copper-Gold Deposits: an Andean View, *Mineralium Deposita*, 38: 787-812.
Sillitoe, R. H. (1996) Granites and Metal Deposits, *Episodes*, 19(4): 126-133.
Sillitoe, R. H. (2002) *Iron Oxide-Copper-Gold Deposits - An Andean View*, *11th IAGOD Quadrennial Symposium and Geocongress CD*, Windhoek, Namibia.
Simmonds, J. (1998) The Central African Copperbelt: Tectonic Overview, Metallogeny and Analysis of Current Research, *The Assembly and Breakup of Rodinia: Proceedings of a Workshop*, Sydney, N.S.W., Australia.
Simpson, J. G. (1962) *The Geology of the Mwembeshi River Area - Explanation of Degree Sheet 1527, NE Quarter* (Geological Report 11), Northern Rhodesia Geological Survey, Lusaka.
Simpson, J. G., Drysdall, A. R., & Lambert, H. H. J. (1963) *The Geology and Groundwater Resources of the Lusaka Area* (Geological Report 16), Northern Rhodesia Geological Survey, Lusaka.
Simpson, J. G., & Stillman, C. J. (1963) Metamorphism and Reaction Phenomena in Gabbros of the Mwembeshi and Lusaka Areas, *Records of the Geological Survey of Northern Rhodesia*, 9: 10-14.
Singer, D. A. (1995) World-Class Base and Precious Metal Deposits - A Quantitative Analysis, *Economic Geology*, 90, 88-104.
Singletary, S., Martin, M., Hanson, R., Bowring, S., Key, R., Majaule, T., Mapeao, R., Ramokate, L., & Direng, B. (1998) Distribution of Proterozoic Orogenic Provinces Beneath the Kalahari Desert in Botswana, In Anonymous (Ed.), *Geological Society of America, 1998 Annual Meeting,* Geological Society of America, Boulder, Colorado, 30(7): 98.
Skirrow, R. G. (2000) Gold-Copper-Bismuth Deposits of the Tennant Creek District, Australia: A Reappraisal of Diverse High-Grade Systems, In T. M. Porter (Ed.), *Hydrothermal Iron Oxide Copper-Gold & Related Deposits: A Global Perspective*, PGC Publishing, Adelaide, Australia, 1: 149-160.
Skirrow, R. G., Bastrakov, E., Davidson, G., Raymend, O. L., & Heithersay, P. (2002) The Geological Framework, Distribution and Controls of Fe-Oxide Cu-Au Mineralization in the Gawler Craton, South Australia - Part I - Alteration and Mineralization, In T. M. Porter (Ed.), *Hydrothermal Iron Oxide Copper-Gold & Related Deposits: A Global Perspective*, PGC Publishing, Adelaide, Australia, 2: 33-47.
Skripchenko, N. S. (1986) Zoning and Concentration of Mineralization in Sandstone- and Shale-Hosted Copper Deposits, *International Geology Review*, 28(11): 1313-1326.
Sleigh, D. W. W. (2002) The Selwyn Line Tabular Iron-Copper-Gold System, Mount Isa Inlier, NW Queensland, Asutralia, In T. M. Porter (Ed.), *Hydrothermal Iron Oxide Copper-Gold & Related Deposits: A Global Perspective*, PGC Publishing, Adelaide, Australia, 2: 77-93.
Sliwa, A. S., & Nguluwe, C. A. (1984) Geological Setting of Zambian Emerald Deposits, In S. N. Punukollu & S. C. P. Andrews (Eds.), *Proterozoic: Evolution, Mineralization, and Orogenesis*, Elsevier, Amsterdam, 25(1-3): 213-228.
Smirnov, V. I. (1977) *Ore Deposits of the USSR*., Vol. 1, Pitman Publishing, London.
Smith, A. G. (1966a) Basal Relations of the Katanga System in the Kafue Area, *Records of the Geological Survey of Zambia*, 10: 5-9.
Smith, A. G. (1966b) *The Geology of the Kapiri Mposhi Area Explanation of Degree Sheet 1328, SE Quarter* (Report of the Geological Survey 18), Zambia Geological Survey, Lusaka.
Smith, A. G. (1966c) Local Influences on the Development of Dambos in Zambia, *Records of the Geological Survey of Zambia*, 10, 30-34.
Smith, A. G. (1972) Lufilian Shearing and Metamorphism Near Kafue, *Records of the Geological Survey of Zambia*, 10: 1-4.
Smith, A. G., Simpson, J. G., Phillips, K. A., Newton, A. R., & Drysdall, A. R. (1960) Precambrian Stratigraphy of Part of the Central Province, *Records of the Northern Rhodesia Geological Survey, 1959*, 20-25.
Smith, C. G. (2001) Always the Bridesmaid, Never the Bride: Cobalt Geology and Results, *Institution of Mining and Metallurgy, Transactions, Section B: Applied Earth Science*, 110: 75-80.
Smith, C. G., & Gunn, A. G. (2000) Always the Bridesmaid, Never the Bride: Cobalt Geology and Resources, In Anonymous (Ed.), *Annual Commodity Meeting on Cobalt; Abstracts*, Institution of Mining and Metallurgy and Institution of Mining Engineers, Doncaster, United Kingdom, 3: 35).

Smith, E. I. (1983) Geochemistry and Evolution of the Early Proterozoic, Post-Penokean Rhyolites, Granites, and Related Rocks of South-Central Winsconsin, U.S.A., *Geological Society of America Bulletin*, 160; 113-128.
Smith, M., & Chengyu, W. (2000) The Geology of the Bayan Obo Fe-REE-Nb Deposit: A Review, In T. M. Porter (Ed.), *Hydrothermal Iron Oxide Copper-Gold & Related Deposits: A Global Perspective*, PGC Publishing, Adelaide, Australia, 1: 271-281.
Smith, R. J. (2002) Geophysics of Iron Oxide Copper-Gold Deposits, In T. M. Porter (Ed.), *Hydrothermal Iron Oxide Copper-Gold & Related Deposits: A Global Perspective*, PGC Publishing, Adelaide, Australia, 2: 357-367.
Smithies, R. H., & Marsh, J. S. (1996) Alkaline Rocks in the Kuboos-Bremen Igneous Province, Southern Namibia: the Grootpenseiland and Marinkas Kwela Complexes, *Communications of the Geological Survey of Namibia*, 11: 12-20.
Snelling, M. J., Hamilton, E. I., Drysdall, A. R., & Stillman, C. J. (1964) A Review of Age Determinations from Northern Rhodesia, *Economic Geology*, 59(6): 961-981.
Snelling, N. J., Johnson, R. L., & Drysdall, A. R. (1972) The Geochronology of Zambia, *Records of the Geological Survey of Zambia*, 12: 19-30.
Snowball, G. J. (1960) A Bibliography of Northern Rhodesia Geology, *Records of the Northern Rhodesia Geological Survey, 1959*, 35-75.
Songe, G. (1976) *Exploration in the Environs of Tsumeb, South West Africa* (Internal consulting report to the Tsumeb Corporation Limited), University of Stellenbosch, Stellenbosch, South Africa.
Songe, P. G. (1957) *Revision of the Geology fo the Otavi Mountainland, South West Africa* (Internal consulting report), Tsumeb Corporation Limited, Tsumeb, Namibia.
Sorensen, H. (1974) *The Alkaline Rocks*, John Wiley & Sons, London.
Souza, L. H., & Vieira, E. A. P. (2000) Salobo 3 Alpha Deposit: Geology and Mineralization, In T. M. Porter (Ed.), *Hydrothermal Iron Oxide Copper-Gold & Related Deposits: A Global Perspective*, PGC Publishing, Adelaide, Australia, 1: 213-224.
Stanistreet, I. G., & Charlesworth, E. G. (2001) Damaran Basement-Cored Fold Nappes Incorporating Pre-Collisional Basins, Kaoko Belt, Namibia, and Controls on Mesozoic Supercontinental Break-Up, *South African Journal of Geology*, 104(1): 1-12.
Stanistreet, I. G., Kukla, P. A., & Henry, G. (1991a) Basinal Responses to the Opening and Closing of the Late Proterozoic Khomas Sea, and Adamastor Ocean to Form the Damara Orogen, Namibia, In Anonymous (Ed.), *IAS 12th Regional Meeting; Abstracts for Papers and Posters*, International Association of Sedimentologists, 12: 54.
Stanistreet, I. G., Kukla, P. A., & Henry, G. (1991b) Sedimentary Basinal Responses to a Late Precambrian Wilson Cycle; the Damara Orogen and Nama Foreland, Namibia, In P. G. Eriksson (Ed.), *Precambrian Sedimentary Basins of Southern Africa*, Blackwell Scientific Publications, Oxford, 3(3): 27-28.
Starkey, R. J., & Frost, B. R. (1983) Factors Controlling Copper Transport and Deposition Under Oxidizing Conditions, *The Geological Society of America, 96th Annual Meeting*, Boulder, CO, United States.
Staude, J. M. (2001) Geology, Geochemistry, and Formation of Au-(Cu) Mineralization and Advanced Argillic Alteration in the Mulatos District, Sonora, Mexico, *Special Publication* 8, Society of Economic Geologists, 199-218.
Steven, N. (1992) Note: The Potential for Stratabound Copper (-Siilver-Platinum) Mineralization in the Rehoboth-Dordabis-Witvlei Area, Central Namibia: A New Approach, *Communications of the Geological Survey of Namibia*, 8(1992-1993): 151-154.
Steven, N. (2001a) *Field Visit to the ~1800 Ma-Old Khoabendus Group, Northwestern Namibia* (internal report for Rio Algom), Rockwater Consulting cc., Capetown, South Africa.
Steven, N. (2001b) *Summary of Previous Exploration Work in the Khoabendus Group, Kamanjab Area, Northwestern Namibia* (internal report for Rio Algom), Rockwater Consulting cc., Capetown, South Africa.
Steven, N., & Armstrong, R. (2002) The Potential for Clastic-Hosted Zinc Deposits in the Upper Khoabendus Group Near Kamanjab, N.W. Namibia, *11th IAGOD Quadrennial Symposium and Geocongress CD*, Windhoek, Namibia.
Steven, N., & Armstrong, R. (2003) A Metamorphosed Proterozoic Carbonaceous Shale-Hosted Co-Ni-Cu Deposit at Kalumbila, Kabompo Dome: The Copperbelt Ore Shale in Northwestern Zambia, *Economic Geology*, 98: 893-909.
Steven, N. M. (1991) Turbidite-Hosted Gold Mineralization at the Sandamap Noord Prospect, Central Namibia, In E. A. Ladeira (Ed.), *Brazil Gold '91; The Economics, Geology, Geochemistry and Genesis of Gold Deposits; Proceedings,* A. A. Balkema, Rotterdam, Netherlands.
Steven, N. M. (1993a) The Potential for Stratabound Copper (-Silver-Platinum) Mineralisation in the Rehoboth-Dordabis-Witvlei Area, Central Namibia; A New Approach, *Communications of the Geological Survey of Namibia. Department of Economic Affairs, 8*: 151-154.
Steven, N. M. (1993b) *A Study of Epigenetic Mineralization in the Central Zone of the Damara Orogen, Namibia, With Special Reference to Gold, Tungsten, Tin and Rare Earth Elements*, Vol. 16, Sociedad Nacional de Mineria y Petroleo, Lima, Peru.
Steven, N. M. (1993c) Tourmalinite Mineralisation in Central Namibia; Evidence for an Epigenetic Origin, In Anonymous (Ed.), *Geological Association of Canada-Mineralogical Association of Canada; Annual Meeting; Program with Abstracts*, Waterloo, ON, Canada, 1993: 100.
Steven, N. M. (2000a) Exploration for Volcanogenic Massive Sulphide (VMS) Deposits in the Khoabendus Group, Near Kamanjab, Northwestern Namibia: The Wrong Tectonic Setting and an Alternative Exploration Model, *Economic Geology Research Unit Information* Circular, Economic Geology Research Unit, University of the Witwatersrand, Johannesburg, South Africa, 341: 15.
Steven, N. M. (2000b) A Shaba-Type Cu-Co(-Ni) Deposit at Luamata, West of the Kabompo Dome, Northwestern Zambia, *Exploration and Mining Geology*, 9(3-4): 277-287.
Steven, N. M., Armstrong, R. A., & Moore, J. M. (1993) New Rb-Sr data from the Central Zone of the Damara Orogen, Namibia, *Communications of the Geological Survey of Namibia*, 8: 5-14.
Steven, N. M., Badenhorst, F. P., & Petzel, V. F. W. (1994) A Review of Gold Occurrences in the Northern and Central Zones of the Damara Orogen and the Underlying Mid-Proterozoic Basement, Central Namibia, *Communications of the Geological Survey, Namibia*, 9: 63-77.
Steven, N. M., & Hartnady, C. J. H. (1993) Early Palaeozoic Gold Metallogeny in the Damara Orogen, Central Namibia, In Anonymous (Ed.), *Geological Association of Canada-Mineralogical Association of Canada; Annual Meeting; Program with Abstracts,* Geological Association of Canada, Waterloo, ON, Canada,1993: 100.
Steven, N. M., & Moore, J. M. (1994) Pan-African Tungsten Skarn Mineralization at the Otjua Prospect, Central Namibia, *Economic Geology*, 89(7): 1431-1453.
Steven, N. M., & Moore, J. M. (1995) Tourmalinite Mineralization in the Late Proterozoic Kuiseb Formation of the Damara Orogen, Central Namibia; Evidence for a Replacement Origin, *Economic Geology*, 90(5): 1098-1117.
Stillman, C. J. (1965) *The Geology of the Musofu River and Mkushi Areas - Explanation of Degree Sheet 1329, Part of NW Quarter and SW Quarter* (Geological Report 12), Zambian Geological Survey, Lusaka, Zambia.
Stillman, C. J., & De Swardt, A. M. J. (1965) The Response to Lufilian Folding of the Basement Complex Around the Northern Edge of the Mpande Dome, Northern Rhodesia, *The Journal of Geology*, 73(1): 131-141.
Stohl, J. (1972) The Kundelungu-Lower Roan Uncomformity at Kasumbalesa, Near Chililabombwe, *Records of the Geological Survey of Zambia*, 12: 95-101.
Stohl, J. (1977) The Geology of the Iron Deposits West of Lusaka, Zambia, *Geologicke Prace*, 67: 247-285.

Stowe, C. W., Hartnady, C. J. H., & Joubert, P. (1984) Proterozoic Tectonic Provinces of Southern Africa, In S. N. Punukollu & S. C. P. Andrews (Eds.), *Proterozoic; Evolution, Mineralization, and Orogenesis,* Elsevier, Amsterdam, 25(1-3): 229-231.
Strickland, C. D., & Martyn, J. E. (2002) The Guelb Moghrein Fe-Oxide Copper-Gold-Cobalt Deposit and Associated Mineral Occurrences, Mauritania: A Geological Introduction, In T. M. Porter (Ed.), *Hydrothermal Iron Oxide Copper-Gold & Related Deposits: A Global Perspective*, PGC Publishing, Adelaide, Australia, 2: 275-291.
Stuart-Smith, P. G., Needham, R. S., Page, R. W., & Wyborn, L. A. I. (1993) Geology and Mineral Deposits of the Cullen Mineral Field, Northern Territory, *Bulletin of the Australian Geological Survey Organization*, 229: 155.
Swart, R. (1986) A Note on an Occurrence of Scapolite in the Northern Zone of the Damara Orogen, *Communications of the Geological Survey of Namibia*, 2: 61-62.
Sweeney, M., & Tembo, F. (1987) Amphibolites of the Zambian Copperbelt: A Preliminary Study, In G. Matheis & H. Schandelmeier (Eds.), *Current Research in African Earth Sciences*, 14: 401-404.
Sweeney, M., Turner, P., & Vaughan, D. J. (1986) Stable Isotope and Geochemical Studies in the Role of Early Diagenesis in Ore Formation, Konkola Basin, Zambian Copper Belt, *Economic Geology*, 81(8): 1838-1852.
Sweeney, M. A. (1990a) *The Occurrence and Possible Mode of Formation of Willemite Deposits in Zambia*, Etudes Recentes Sur la Geologie de l'Afrique; 15 (Super e) Colloque de Geologie Africaine, Paris, France.
Sweeney, M. A. (1990b) *The Occurrence and Possible Mode of Formation of Willemite Deposits in Zambia,* In Anonymous (Ed.), *15th Colloquium of African Geology*, Centre International pour la Formation et les Echanges Geologiques (CIFEG), Paris, France, 20.
Sweeney, M. A., & Binda, P. L. (1986) The Role of Diagenesis in the Formation of the Konkola Cu-Co Orebody of the Zambian Copperbelt, *1986 Joint Annual Meeting of GAC, MAC and CGU*, Waterloo, ON, Canada.
Sweeney, M. A., & Binda, P. L. (1989a) Mineralization Controls and Source of Metals in the Lufilian Fold Belt, Shaba (Zaire), Zambia, and Angola: A Discussion, *Economic Geology*, 84(4): 963-964.
Sweeney, M. A., & Binda, P. L. (1989b) The Role of Diagenesis in the Formation of the Konkola Cu-Co Orebody of the Zambian Copperbelt, In R. W. Boyle, A. C. Brown, C. W. Jefferson, E. C. Jowett, & R. V. Kirkham (Eds.), *Sediment-Hosted Stratiform Copper Deposits*, Geological Association of Canada, Toronto, ON, Canada, 36: 499-518.
Sweeney, M. A., & Binda, P. L. (1994) Some Constraints on the Formation of the Zambian Copperbelt Deposits, In A. B. Kampunzu & R. T. Lubala (Eds.), Neoproterozoic Belts of Zambia, Zaire and Namibia*, Special Issue of the Journal of African Earth Sciences*, 19(4): 303-313.
Sweeney, M. A., Binda, P. L., & Vaughan, D. J. (1991a) Genesis of the Ores of the Zambian Copperbelt, *Ore Geology Reviews*, 6(1): 51-76.
Sweeney, M. A., Burnard, P., Vaughan, D. J., & Kamona, F. (1990) *A Zonation in Central African Metallogenesis: Implications for Base Metal Mineralization in Central Zambia*, Etudes Recentes sur la Geologie de l'Afrique; 15 (super e) Colloque de Geologie Africaine, Paris, France.
Sweeney, M. A., Pattrick, R. A. D., Vaughan, D. J., & Turner, P. (1991b) The Nature and Genesis of the Willemite Deposits of Zambia, In M. Pagel & J. L. Leroy (Eds.), *Source, Transport and Deposition of Metals*, A. A. Balkema, Rotterdam, 139-142.
Sweeney, M. A., Vaughan, D. J., & Binda, P. (1991c) The Geochemistry of the Basement Complex of the Zambian Copperbelt: Implications for Mineralisation, In M. Pagel & J. L. Leroy (Eds.), *Source, Transport and Deposition of Metals*, A. A. Balkema, Rotterdam, 359-362.
Sylvester, P. J. (1989) Post-Collisional Alkaline Granites, *Journal of Geology*, 97: 261-280.
Tack, L., Fernandez-Alonso, M., Tahon, A., & Wingate, M. (2002) Meso- and Neoproterozoic Emplacement Ages of Magmatic Rocks in Burundi: New Constraints for the Geodynamic Evolution of the "Northeastern Kibaran Belt" (NKB), *Technical Meeting IGCP Projects 418/440*, Windhoek, Namibia.
Tack, L., Pedrosa-Soares, C., Deblond, A., & Fernandez-Alonso, M. (2002) The Aracuai (Brasiliano)- West Congo (Pan African) Orogenic System: Considerations on the Breakup History of the Pre-Existing Rodinia Supercontinent, *Technical Meeting IGCP Projects 418/440*, Windhoek, Namibia.
Tarney, J., & Jones, C. E. (1994) Trace Element Geochemistry of Orogenic Igneous Rocks and Crustal Growth Models, *Journal of the Geological Society, London*, 151: 855-868.
Tassinari, C. C. G., Munizaga, F., & Ramirez, R. (1993) Edad y Geoquímica Isotópica Rb-Sr del Yacimiento de Cobre Mantos Blancos: Relación Temporal con el Magmatismo Jurásico, *Revista Geológica de Chile*, 20(2): 193-205.
Tauson, L. V., & Kozlov, V. D. (1972) *Distribution Functions and Ratios of Trace-Element Concentrations as Estimators of the Ore-Bearing Potential of Granites*, *Geochemical Exploration 1972 - Proceedings of the IV International Geochemical Exploration Symposium*, 17-20 April, London.
Tavaza, E., & Gouveia de Oliveira, C. (2000) The Igarapé Bahía Au-Cu-(REE-U) Deposit, Carajás Mineral Province, Northern Brazil, In T. M. Porter (Ed.), *Hydrothermal Iron Oxide Copper-Gold & Related Deposits: A Global Perspective*, PGC Publishing, Adelaide, Australia, 1: 203-212.
Tavener-Smith, R. (1961) *The Geology of the Mapanza Mission Area Explanation of Degree Sheet 1626 NE Quarter* (Report of the Geologial Survey 10), Northern Rhodesia Geological Survey, Lusaka, Northern Rhodesia.
Taverner-Smith. (1958) A Prelimininary Account of the Geology of the Area Around Mapanza Mission, Sheet 1626 NE Quarter - Choma and Namwala Districts, *Records of the Geological Survey of Northern Rhodesia, 1958*: 16-18.
Tegtmeyer, A., & Kroner, A. (1985) U-Pb Zircon Ages for Granitoid Gneisses in Northern Namibia and Their Significance for Proterozoic Crustal Evolution of Southwestern Africa, *Precambrian Research, 28*: 311-326.
Tembo, F. (1995) Preliminary Results on the Petrology and Geochemistry of Metabasites from the Copperbelt and Eastern Domes Region, Zambia, In M. Wendorff & L. Tack (Eds.), *Late Proterozoic Belts in Central and Southwestern Africa; IGCP Project 302*, Koninklijk Museum voor Midden - Afrika, Tervuren, Belgium, 101: 103-110.
Tembo, F., & De Waele, B. (2001) Extensional and Compressional Magmatism in the Mesoproterozoic Irumide Belt of Zambia: A Record of Rifting, Continental Rupture and Collision, *Gondwana Annual Asia Conference*, Tokyo, Japan.
Tembo, F., De Waele, B., John, T., & Katongo, C. (2000a) Geochemical Characteristics of Metabasites from the Chongwe Area, Southern Irumide Belt, Zambia, *Geocongress 2000: 27th Earth Science Congress of the Geological Society of South Africa*, Capetown, South Africa.
Tembo, F., De Waele, B., & Nkemba, S. (2002) Syn- to Post-Orogenic Granitoid Magmatism in the Irumide Belt of Zambia: Geochemical Evidence, *Africa Geosciences Review*, 9(1): 1-17.
Tembo, F., Namateba, C., & Master, S. (1996) Palaeoproterozoic Geology of the Domes area, Northwestern Zambia, In S. Master (Ed.), *Excursion Guidebook; Palaeoproterozoic of Zambia and Zimbabwe*, *Economic Geology Research Unit Information Circular,* University of the Witwatersrand, Johannesburg, South Africa, 301: 1-11.
Tembo, F., & Porada, H. (2002) Geotectonic Evolution and Base Metal Mineralization in the Neoproterozoic Katanga Orogen of Central Africa - A Review, *11th IAGOD Quadrennial Symposium and Geocongress CD*, Windhoek, Namibia.
Tembo, F., Rivers, T., De Waele, B., Mapani, B., & Katongo, C. (2000b) *Terrane Mapping of the Irumide Orogen in Eastern Zambia: Reconnaissance Geochemistry of the Meta-Igneous Rocks*, IGCP 840 Meeting, Kitwe, Zambia.

Tembo, W. (1994) The Mineralogy and Geochemistry of Cobalt Minerals at the Kirilabomwe South Orebody, Konkola, *Zambian Journal of Applied Earth Sciences*, 8(1): 107.
Thieme, J. G. (1968) Structure and Petrography of the Lusaka Granite, *Records of the Geological Survey of Zambia*, 11, 69-75.
Thompson, T. B. (1993) Hydrothermal Breccias, In C. L. Williams (Ed.), *Handout for the Symposium on North Eastern Nevada Breccia Bodies,* Geological Society of Nevada, Reno, NV, United States, 19: 4.
Thomson, G., & Sweeney, M. A. (1995) Palaeomagnetic Results from the Zambia Copperbelt, In M. Wendorff & L. Tack (Eds.), *Late Proterozoic Belts in Central and Southwestern Africa; IGCP Project 302*, Koninklijk Museum voor Midden - Afrika, Tervuren, Belgium, 101: 111-120.
Thomson, G., Sweeney, M. A., & Banda, T. (1990) *Palaeomagnetic Results from Ore Bodies in Central Zambia,* In Anonymous (Ed.), *15th Colloquium of African Geology*, Centre International pour la Formation et les Echanges Geologiques (CIFEG), Paris, France, 20.
Timm, J. (2001) *Subduction and Continental Collision in the Lufilian Arc-Zambezi Belt Orogen: A Petrological, Geochemical, and Geochronological Study of Eclogites and Whiteschists (Zambia),* Unpublished Ph.D., Christian-Albrechts-Universitat, Kiel.
Torrealday, H. I. (2000) *Mineralization and Alteration of the Kansanshi Copper Deposit, Zambia,* Unpublished Master's, Colorado School of Mines, Golden, Colorado, United States.
Torrealday, H. I. (2001) Mineralization and Ateration of the Kansanshi Copper Deposit, Zambia - Student Research Grant Abstracts, In R. L. Nielsen (Ed.), *SEG Newsletter*, Society of Economic Geologists, 44: 13-14.
Torrealday, H. I., Hitzman, M., Stein, H. J., Markley, R. J., Armstrong, R., & Broughton, D. (2000) Re-Os and U-Pb Dating of the Vein-Hosted Mineralizations at the Kansanshi Copper Deposit, Northern Zambia, *Economic Geology*, 95(5): 1165-1170.
Trompete, R. (1994) *Geology of Western Gondwana (2000-500 Ma) - Pan-African-Brasiliano Aggregation of South America and Africa* (Carozzi, Albert V., Trans.), A.A. Balkema, Rotterdam.
Tshiauka, T., Katekesha, W. M., Cailteux, J., Intiomale, M. M., Kampunzu, A. B., Kapenda, D., Chabu, M., Ngongo, K., Mutombo, K., & Nkanika, W. R. (1995) Lithostratigraphy of the Neoproterozoic Katangan Sedimentary Sequences in the Musoshi Copper District (SE Shaba, Zaire) and Incidences on Copper and Cobalt Economic Geology in Central Africa, In M. Wendorff & L. Tack (Eds.), *Late Proterozoic Belts in Central and Southwestern Africa; IGCP Project 302*, Koninklijk Museum voor Midden - Afrika, Tervuren, Belgium, 101: 29-48.
Turner, D. C. (1988) Volcanic Carbonatites of the Kaluwe Complex, Zambia, *Journal of the Geological Society, London*, 145: 95-106.
Turner, D. C., Andersen, L. S., Punukollu, S. N., Sliwa, A., & Tembo, F. (1989) Igneous Phosphate Resources in Zambia, In A. J. G. Notholt, R. P. Sheldon, & D. F. Davidson (Eds.), *Phosphate Deposits of the World*, Cambridge University Press, Cambridge, U.K., Volume 2, Phosphate Rock Resources, 247-257.
Tuttle, O. F., & Gittins, J. (1966) *Carbonatites*, Wiley, New York.
Uhlig, S. (1987) Lithology and Geochemistry of the Upper Proterozoic Duruchaus Formation (Namibia) and Related Copper Mineralizations, In Anonymous (Ed.), *Abstracts; Proterozoic Geochemistry - IGCP Conference*, Lund, Sweden, 85-86.
Uhlig, S. (1989) Importance of Regional Metamorphism to the Formation of Stratabound Copper Mineralisations; An Example of the Late Proterozoic Duruchaus Formation in Namibia, *Cuadernos do Laboratorio Xeoloxico de Laxe*, 14: 177-200.
Unrug, R. (1983) The Lufilian Arc: A Microplate in the Pan-African Collision Zone of the Congo and the Kalahari Cratons, *Precambrian Research*, 21: 181-196.
Unrug, R. (1986) Landsat-Based Structural Map of the Lufilian Arc and the Kundelungu Aulacogen, Shaba (Zaire), Zambia, and Angola, and the Tectonic Position of Cu, Co, U, Au, Zn, Pb, and Fe Mineralization, *1986 Joint Annual Meeting of GAC, MAC and CGU*, Waterloo, ON, Canada.
Unrug, R. (1988) Mineralization Controls and Source of Metals in the Lufilian Fold Belt, Shaba (Zaire), Zambia, and Angola, *Economic Geology*, 83(6): 1247-1258.
Unrug, R. (1989a) Landsat-Based Structural Map of the Lufilian Fold Belt and the Kundelungu Aulacogen, Shaba (Zaire), Zambia, and Angola, and the Regional Position of Cu, Co, U, Au, Zn, and Pb Mineralization, In R. W. Boyle, A. C. Brown, C. W. Jefferson, E. C. Jowett, & R. V. Kirkham (Eds.), *Sediment-Hosted Stratiform Copper Deposits*, Geological Association of Canada, Toronto, 36: 519-524.
Unrug, R. (1989b) Mineralization Controls and Source of Metals in the Lufilian Fold Belt, Shaba (Zaire), Zambia, and Angola: A Reply, *Economic Geology*, 84(4): 969-970.
Unrug, R. (1990) Post-Kibaran Rifting to Katangan Transpression; Late Proterozoic Evolution of the Kalahari and Congo Cratons Margins, Southern Africa, In Anonymous (Ed.), *Geological Society of America, 1990 Annual Meeting*, Boulder, Colorado, United States, Geological Society of America, 22(7): 264.
Vail, J. R., Snelling, N. J., & D.C., R. (1968) Pre-Katangan Geochronology of Zambia and Adjacent Parts of Central Africa, *Canadian Journal of Earth Sciences*, 5: 621-628.
Van Zijl, J. S. V., & DeBeer, J. H. (1983) Electrical Structure of the Damara Orogen and Its Tectonic Significance, *Special Publications of the Geological Society of South Africa*, 11: 369-379.
Verwoerd, W. J. (1967) *The Carbonatites of South Africa and South West Africa*, Vol. Handbook No. 6, Geological Survey of South Africa, Pretoria, South Africa.
Verwoerd, W. J. (1993) Update on Carbonatites of South Africa and Namibia, In W. J. Verwoerd (Ed.), *Special Issue on Carbonatites*, Bureau for Scientific Publications at the Foundation for Education, Science and Technology, Pretoria, South Afrca, 96(3): 75-95.
Vielreicher, N. M., Groves, D. I., & Vielreicher, R. M. (2000) The Phalaborwa (Palabora) Deposit and its Potential Connection to Iron-Oxide Copper-Gold Deposits of Olympic Dam Type, In T. M. Porter (Ed.), *Hydrothermal Iron Oxide Copper-Gold & Related Deposits: A Global Perspective*, PGC Publishing, Adelaide, Australia, 1: 321-329.
Vigneresse, J. L. (1995) Crustal Regime of Deformation and Ascent of Granitic Magma, *Tectonophysics*, 249: 187-202.
Vila, T., Lindsay, N., & Zamora, R. (1996) Geology of the Manto Verde Copper Deposit, Northern Chile: A Specularite-Rich, Hydrothermal-Tectonic Breccia Related to the Atacama Fault Zone, In F. Camus, R. M. Sillitoe, R. Petersen, & P. Sheahan (Eds.), *Andean Copper Deposits, New Discoveries, Mineralization, Styles and Metallogeny*, Society of Economic Geologists, Special Publication 5: 157-170.
Viljoen, R. P., Minnitt, R. C. A., & Viljoen, M. J. (1986) Porphyry Copper-Molybdenum Mineralization at the Lorelei, South West Africa/Namibia, In C. R. Anhaeusser & S. Maske (Eds.), *Mineral Deposits of Southern Africa*, Geological Society of South Africa, Johannesburg, South Africa, 2: 1559-1565.
Viljoen, W. G. (2002) *Copper-Gold Mineralization in the Onguati Area, Karibib District, Southern Central Zone, Namibia*, *11th IAGOD Quadrennial Symposium and Geocongress CD*, Windhoek, Namibia.
Voevodin, V. N., Voevodina, S. A., Krutov, N. K., & Makeev, N. P. (1979) Hydrothermal Breccias in Diatremes in the Tungsten Deposits of the Far East, *Soviet Geology and Geophysics*, 20(9): 18-24.
Wakefield, J. (1978) Samba: A Deformed Porphyry-Type Copper Deposit in the Basement of the Zambian Copperbelt, *Institution of Mining and Metallurgy, Transactions, Section B: Applied Earth Science*, 87 May: 43-52.

Wall, V. J., Clemens, J. D., & Clarke, D. B. (1987) Models for Granitoid Evolution and Source Compositions, *Journal of Geology*, 95: 731-749.
Wanhainen, C., Broman, C., & Martinsson, O. (2003) The Aitik Cu-Au-Ag-Deposit in Northern Sweden: A Product of High Salinity Fluids, *Mineralium Deposita*, 38: 715-726.
Warren, J. K. (2000) Evaporites, Brines and Bae Metals: Low Temperature Ore Emplacement Controlled by Evaporite Diagenesis, *Australian Journal of Earth Sciences*, 47: 179-208.
Watkins, R. T., & LeRoex, A. P. (1991) Petrology and Structure of Syenite Intrusions of the Okenyenya Igneous Complex, *Communications of the Geological Survey of Namibia*, 7: 55-70.
Watts, Griffits & McOuat, (1991) *Assessment of Mineral Exploration Opportunities in Zambia*, consulting report presented to the Government of the Republic of Zambia, Toronto, Canada.
Watts, J. T., Tooms, J. S., & Webb, J. S. (1963) Geochemical Dispersion of Niobium From Pyrochlore-Bearing Carbonatites in Northern Rhodesia, *Bulletin of the Institution of Mining and Metallurgy*, August 1963, 681 (Transactions 72 (1962-1963, II): 729-792.
Webb, P. C., Tindle, A. G., Barritt, S. D., Brown, G. C., & Miller, J. F. (1985) Radiothermal Granites of the United Kingdom: Comparison of Fractionation Patterns and Variation of Heat Production for Selected Granites, *High Heat Production (HHP) Granites, Hydrothermal Circulation and Ore Genesis*, The Institution of Mining and Metallurgy, St. Austell, Cornwall, England, 409-424.
Weber, K., Ahrendt, H., & Hunziker, J. C. (1983) Geodynamic Aspects of Structural and Radiiometric Investigations on the Northern and Southern Margins of the Damara Orogen, South West Africa/Namibia, *Special Publications of the Geological Society of South Africa*, 11: 307-319.
Whalen, J. B., Currie, K., L., & Chappell, B. W. (1987) A-Type Granites: Geochemical Characteristics, Discrimination and Petrogenesis, *Contributions to Mineralogy and Petrology*, 95: 407-419.
Williams, P. J. (1997) *Observations on Cu-Au Exploration in the Kasempa and Mumbwa Project Areas* (Technical Report No. 15/97 prepared for Billiton Exploration and Development - Africa Region), James Cook University, Sydney, Australia.
Williams, P. J., Dkong, G., Ryan, C. G., Pollard, P. J., Rotherman, J. F., Mernagh, T. P., & Chapman, L. H. (2001) Geochemistry of Hypersaline Fluid Inclusions from the Starra (Fe Oxide)-Au-Cu Deposit, cloncurry District, Queensland, *Economic Geology*, 96: 875-883.
Williams, P. J., & Skirrow, R. g. (2000) Overview of Iron Oxide-Copper-Gold Deposits in the Curnomona Province and Cloncurry District (Easern Mount Isa Block), Australia, In T. M. Porter (Ed.), *Hydrothermal Iron Oxide Copper-Gold & Related Deposits: A Global Perspective*, PGC Publishing, Adelaide, Australia, 1: 105-122.
Williams-Jones, I. E. (1984) *The Petrology of the Basalts of the Dordabis Formation, in the Vicinity of Dordabis in Central SWA/Namibia,* Unpublished M.Sc., Rhodes University, Grahamstown, South Africa.
Wilson, M. (1989) *Igneous Petrogenesis - A Global Tectonic Approach*, Unwin Hyman, London.
Wilson, T. J., Hanson, R. E., & Wardlaw, M. S. (1993) Late Proterozoic Evolution of the Zambezi Belt, Zambia: Implications for Regional Pan-African Tectonics and Shear Displacements in Gondwana, *Gondwana Eight*, 69-82.
Wilton, J., Lombard, P. J. A., & Philpot, H. G. (2002) *Discovery of the Otjikoto Gold Deposit, Namibia*, *11th IAGOD Quadrennial Symposium and Geocongress CD*, Windhoek, Namibia.
Winchester, J. A., & Floyd, P. A. (1977) Geochemical Discrimination of Different Magma Series and Their Differentiation Products Using Immobile Elements, *Chemical Geology*, 20: 325-343.
Windley, B. F. (1993) Uniformitarianism Today: Plate Tectonics is the Key to the Past, *Journal of the Geological Society, London*, 150: 7-19.
Wolf, J., Berhorst, V., & Porada, H. (1990) Development of Tectono-Metamorphic Layering in Metagraywackes of the Kuiseb Formation (Upper Swakop Group) in Northern Parts of the Khomas Trough, Damara Belt, Namibia, In Anonymous (Ed.), *15th Colloquium of African Geology*, Centre International pour la Formation et les Echanges Geologiques (CIFEG), Paris, France, 20: 293.
Wood, D. A. (1980) The Application of a Th-Hf-Ta Diagram to Problems of Tectonomagmatic Classification and to Establishing the Nature of Crustal Contamination of Basaltic Lavas of the British Tertiary Volcanic Province, *Earth and Planetary Science Letters*, 50: 11-30.
Wooley, A. R. (2001) *Alkaline Rocks and Carbonatites of the World - Part 3: Africa*, The Geological Society, London.
Wright, J. B. (1969) A simple Alkalinity Ratio and its Application to Questions of Non-Orogenic Granite Genesis, *Geological Magazine,* 106(4): 370-384.
Wyborn, L. (1999) *Metallogeny of Australian Proterozoic Granites*. Perth, Western Australia: Centre for Teaching and Research in Strategic Mineral Deposits - Australian Geological Survey Organization.
Wyman, B., Cooke, D. R., & Large, R. R. (1997) Cambrian Granite-Related Copper-Gold Mineralisation in the Southern Mt. Read Volcanics, A Possible Submarine Porphyry Copper System in Western Tasmania, Australia, In Anonymous (Ed.), *Geological Society of America, 1997 Annual Meeting,* Boulder, Colorado, United States, Geological Society of America, 29(6): 63.
Yardley, B. W. D., Banks, D. A., & Barnicoat, A. C. (2000) The Chemistry of Crustal Brines: Tracking Their Origins, In T. M. Porter (Ed.), *Hydrothermal Iron Oxide Copper-Gold & Related Deposits: A Global Perspective*, PGC Publishing, Adelaide, Australia, 1: 61-70.
Zamora, R., & Castillo, B. (2001) *Mineralización de Fe-Cu-Au en el Distrito Mantoverde, Cordillera de la Costa, III Región de Atacama, Chile*, ProExplo '2001, Instituto de Ingenieros de Minas del Perú, Lima, Perú.
Zen, E.-A., & White, A. (1989) FROGS (Friends of Granite) Report Winter 1989 - Commentaries on the Significance of Cordierite and Muscovite in Peraluminous Felsic Magmas, *EOS*, 70(7): 109-111.
Ziegler, U. R. F., & Stoessel, G. F. U. (1989) K-Ar, Rb-Sr and Geochemical Investigations int he Mooirivier Complex, South Western Windhoek District and North-Western Maltahohe District, Namibia, *Communications of the Geological Survey of Namibia*, 5: 69-75.
Ziegler, U. R. F., & Stoessel, G. F. U. (1990) Isotope Geology and Geochemistry of the Rehoboth Basement Inlier, Namibia/ S.W. Africa; A Multimethod Case History, *Bulletin der Vereinigung Schweizerisches Petroleum -Geologen und -Ingenieur*, 56(130): 13-33.
Ziegler, U. R. F., & Stoessel, G. F. U. (1991) New Constraints on the Age of the Weener Intrusive Suite, the Gamsberg Granite and the Crustal Evolution of the Rehoboth Basement Inlier, Namibia, *Communications of the Geological Survey of Namibia*, 7: 75-78.
Ziegler, U. R. F., & Stoessel, G. F. U. (1993) *Age Determinations in the Rehoboth Basement Inlier, Namibia*, Geological Survey of Namibia, Windhoek, Namibia, Special Publication, Volume 14.

Contact information of the author

Last Name: **Lobo-Guerrero Sanz**

Name: **Alberto**

e-mail addresses: **ageo@iname.com**

ageo@logemin.com

Paper mail address: **Calle 127A No. 53A-28, office 309**
Bogota, Colombia

Home address: **Calle 109 No. 13-98**
Bogota, Colombia

Business telephone: **+57-1-6435364**

Home telephone: **+57-1-6586040**

PRE- AND POST-KATANGAN GRANITOIDS OF THE GREATER LUFILIAN ARC – GEOLOGY, GEOCHEMISTRY, GEOCHRONOLOGY AND METALLOGENIC SIGNIFICANCE

Volume 2, Appendices

By Alberto Lobo-Guerrero Sanz

Supervisor: Professor Laurence J. Robb

A thesis submitted to the Faculty of Science
University of the Witwatersrand, Johannesburg
For the Degree of Doctor of Philosophy

Johannesburg, March 12, 2005

ABSTRACT

This document reports observations, findings and conclusions of the research project entitled “Pre- and Post-Katangan Granitoids of the Greater Lufilian Arc - Geology, Geochemistry, Geochronology and Metallogenic Significance”. The project, structured and supervised by Professor Laurence Robb, was designed to study granitoids that comprise the Greater Lufilian Arc. Its main aims were to define the various granitoids, and study their role in Katangan orogenesis and mineralization. Main fieldwork was concentrated in northwestern Zambia and northern Namibia.

The Greater Lufilian Arc is a curvilinear belt of Neoproterozoic Katangan sediments that was deformed during the Pan African orogeny in Zambia and the Democratic Republic of Congo, and the westward extension of similar rock sequences into Botswana, Angola and Namibia. The mobile belt of the Greater Lufilian Arc also comprises a dominantly Paleoproterozoic basement of deformed granitoids, and a diverse suite of Pan-African granitoids that intrude the Katangan sequences.

A total of 1500 samples were collected in the field; 351 plutonic rocks were analysed. 157 chemical analysis were compiled from various well-documented sources, to reach a total of 508 samples analysed in the database. 38 new zircon U-Pb SHRIMP II and laser ablation ICP-MS ages were produced.

The majority of intrusive rocks from the Greater Lufilian Arc that were analysed (60%) had midalkaline characte. 33% were subalkaline and 7% were alkaline. Mafic rocks are closely associated to felsic rocks in most domains of the Arc. Two thirds of the gabbroids were midalkaline, 1/6 alkaline and 1/6 subalkaline. The average rock type distribution for the entire Lufilian Arc closely resembles that of the Hook Granite Batholith in Zambia.

A frequent field observation is the persistent clustering of small bodies of red-altered granitoids, gabbroids, massive magnetite-hematite and quartz pods that are linked to ages around 550 and 750 Ma. The four-rock association is related to iron oxide-copper-gold (IOCG) mineralization, and seems to be a characteristic of continental extension anorogenic environments.

Another recurrent feature observed in most outcrops of the study area is the presence of two or more contrasting types of plutonic rocks, including mafic, ultramafic and alkaline plugs and dikes. The multiplicity of rock types in a small area seems to be a characteristic of continental extension anorogenic environments. Quartz pods, hydrothermally-emplaced iron oxide bodies and round-pebble hydrothermal breccias are features that occur often in and around IOCG systems throughout the Greater Lufilian Arc.

The main granitoid periods of emplacement present in the study area of the Arc are listed on Table 1. Several more restricted events occurred at 1700, 1600, 880 and 460 Ma.

Table 1 Main Granitoid Terranes in the Greater Lufilian Arc

Age (Ma)	Rock types	Location	Environment of Emplacement	Notes
550 ±50	Granite, alkali granite, quartzmonzonite, syenite, gabbroids	Otjiwarongo, central Namibia, Kaokoland, Damaran intrusives (Namibia), Hook Granite, NW Zambia (Zambia)	Continental epeirogenic uplift	The period may be broken into 3 discrete events.
750 ±50	Granite, alkali granite, syenite and gabbroids with felsic and mafic volcanics	Copperbelt, Kalengwa-Kasempa, NW Zambia (Zambia); Khorixas Inlier and Summas Mountains (Namibia)	Rift-related and continental epeirogenic uplilft.	Intrude Roan and Nguba Lithologies; overlain by Kundelungu and equivalent sediments.
1100 ±50	Granitoids and felsic to mafic volcanics	South of the Copperbelt, West of Lusaka (Zambia); around Omitiomire, Kaokoland and the Witvlei area (Namibia)	Continental rift-related environments	Surrounds Kapvaal Craton from Namaqualand to Irumide Belt in Zambia
1900 ±100	Foliated alkali granie, quartzmonzonite and granite	Copperbelt basement, Mkushi-Serenje, NW Zambia, Domes region (Zambia); Kaokoland, central Namibia, Kamanjab Batholith, Grootfontein Inlier (Namibia)	Not well defined; probably formed in an anorogenic continental extension environment	Period can be broken into 4 discrete events

The Zambian Lufilian Arc and Damara region of Namibia behaved as independent entities from 2200 to 2000 Ma. They also behaved significantly different from 1400 to 850 Ma. Geological history of the two main portions of the Greater Lufilian Arc is consistent from *circa* 800 Ma to the present, and especially during the last 600 million years.

Most areas studied in the Arc show polycyclic geological histories. Repeated anorogenic intrusive events are a common denominator. Prolonged crustal histories have resulted in superimposition of events.

Granitoid rock suites with closely matching chemistry and macroscopic features have been found to form two or three times in the same region, with up to a thousand million years of age difference. These features preclude lithological or detailed geochemical correlation of plutonic rocks.

At least ten clusters of ring complexes were identified in the Arc. Clustering of multiple anorogenic ring complex intrusions can form batholithic size bodies. Clusters are made by amalgamation of multiple ring complexes of varying chemical composition and size. Most of their rocks are midalkaline. Volcanic and plutonic rocks of roughly the same composition occur together. Total duration of ring complex cluster cycles averages 110 Ma, and their plan view geometry is roughly that of an isosceles triangle.

Information currently available on geophysics, geochronology, rock distribution and geochemistry from the Hook Granite Batholith (Zambia) fit quite well with an intracontinental, anorogenic, ring complex cluster origin. The Nchanga Granite (Zambia) has all the characteristics of an anorogenic granite ring complex, and might have contributed to the origin of copper in its environs. Several sources of evidence indicate that the Kamanjab Batholith (Namibia) is an anorogenic cluster of ring complexes. Volcanic and plutonic rocks of similar composition make the batholith. Geological history for the Khorixas Inlier and the Kamanjab Batholith are significantly different.

Complete Wilson cycles were not identified in the study areas of the Greater Lufilian Arc. The dominant magmatic process, as evidenced by the volume of extruded rock, is anorogenic continental epeirogenic uplift, closely-followed in time by a rift-related granitoid emplacement. Coalescing and overprinting aulacogens seem to be the main geological event in the Arc.

Incipient migmatitization and alteration of Paleoproterozoic rocks modified their chemistry to a point where their environment of emplacement cannot be identified by traditional geochemical means.

The anomalous thorium content in some granitoids of the Greater Lufilian Arc induced and maintained long-lived, large convective cells of hydrothermal fluid flow.

E-W-trending regional fracture systems, that run parallel to the elongation of the Arc, play an important role in the emplacement of magmatism and IOCG mineralization. Those structures are generally parallel to the main Lufilian Arc trend, and could have been normal syn-rift faults reactivated multiple times during geological history.

At least eight discrete periods of mineralization were identified in the Greater Lufilian Arc. There is a wide-spread series of midalkaline intrusions emplaced around 750 Ma that produces a variety of mineral deposits. Another event took place around 540±40 Ma. Five less well defined events occurred at ~1970, ~1930, ~1866, 1097-1059 and ~460 Ma. The dominant deposit type is iron oxide-copper-gold mineralization, but other types of mineral deposits are present in the Arc. At least two distinct events of disseminated copper mineralization associated to midalkaline granitoid intrusives were identified in the Kamanjab Batholith; the first took place around 1975 Ma and the second around 1928 Ma.

The main IOCG events that have been identified in the Greater Lufilian Arc took place during eight time periods. The rocks of many IOCG deposits and prospects in the Arc are pristine. There is no significant deformaton involved. Hydrothermal brecciation and other mineralization features are un-deformed.

Three discrete time periods show IOCG mineralization in close temporal spatial association with sedimentary-hosted copper deposits. The first took place around Witvlei (Namibia) from 1108 to 1059 Ma. The second and third ocurred in the basement to the Zambian Copperbelt from 882 to 725 Ma and from 607 to 500 Ma. This idea may generate a new concept for the origin of sedimentary-hosted copper and cobalt deposits.

ABBREVIATED TABLE OF CONTENTS

Abstract
Short Table of Contents
Detailed Table of Contents
Aknowledgements

1. Introduction, 1
2. Methodology, 4
3. Generalized Geology of the Greater Lufilian Arc, 21
4. Description of Rocks from the Different Domains, 23
    - Zambian domains, 24
        - Hook Granite Batholith, Zambia, 24
        - West Lusaka/Kafue Flats domain, 46
        - Kalengwa-Kasempa Area, Zambia, 53
    - Northwestern Zambia domain, 60
        - Kalene Hill area, 61
        - Introduction to the geology of the Domes Region, NW Zambia, 72
        - Kabompo Dome, 73
        - Mwombezhi Dome, 80
        - Solwezi Dome, 91
        - Conclusions on entire NW Zambia region, 94
    - Zambian Copperbelt, 96
        - Nchanga Granite, 102
        - Nchanga mine area, 112
        - Muliashi Porphyry, 115
        - Deep borehole, Konkola mine, 120
        - Chambishi granite, 124
        - Mufulira granite, 129
        - Samba deposit, 132
        - Conclusions, 136
    - Namibian Domains, 142
        - Kamanjab Batholith, 142
        - Khorixas Inlier, 182
            - Oas farm, 184
            - Lofdal farm, 207
        - Other Small Outcrops in Namibia and Bostwana, 223
            - Mesopotamie, 223
            - Summas Mountains, 228
            - Ugab River outcrops, 230
            - Okwa River Outcrops, Botswana, 232
            - Grootfontein Inlier, 234
            - Review of observations, 235
        - Environs of Otjiwarongo, Namibia, 237
        - Witvlei, Namibia, 245
5. Thorium Content of Granitoids in the Greater Lufilian Arc, 253
6. Geochronology, 257
    - New radiometric ages, 257
    - Geochronological database and interpretation, 257
    - New Re-Os ages from copper mineralization, Zambian Copperbelt, 262
7. Some Aspects of Anorogenic Intrusive Rocks, 265
    - Comparison of batholithic granitoid bodies with anorogenic ring complex clusters, 266
    - Comparison of Lufilian small basic intrusions with examples from the literature, 279
8. Iron Oxide-Copper-Gold Mineralization in the Greater Lufilian Arc, 281
    - Some notes on iron oxide-copper-gold deposits, 281
    - Iron oxide-copper-gold systems in the Greater Lufilian Arc, 289
    - Some known IOCG-like deposits and prospects, 305
    - Relationship between IOCG and sedimentary-hosted Cu mineralization, 334
    - Sedimentary-hosted Au mineralization in the Greater Lufilian Arc, 334
    - Peculiarities of Zambian and Namibian IOCG systems, 335
    - Conclusions, 335
9. Conclusions, 337
10. References, 347

Appendices

9 CONCLUSIONS

9.1 Main Granitoid Terranes in the Greater Lufilian Arc

The nature of the granitoid terranes in the study area of the Greater Lufilian Arc can be summarized as follows:

1. Foliated alkali granite, quartzmonzonite and granite were emplaced at 1900±100 Ma. They are present beneath the Katanga Supergroup in the Copperbelt, the Mkushi-Serenje area, NW Zambia, and the Domes region (Zambia); Kaokoland, central Namibia, the Kamanjab Batholith and Grootfontein Inlier (Namibia). The environment of emplacement for these rocks has not been well identified, but tends to be anorogenic. This period may be broken into at least four discrete events.

2. Generally poorly outcropping pre-Katanga granitoid and felsic to mafic volcanics were emplaced at 1100±50 Ma. They are present south of the Copperbelt, and west of Lusaka (Zambia); around Omitiomire, Kaokoland and the Witvlei area (Namibia). These rocks surround the Kapvaal Craton continuously from Namaqualand in South Africa, to the Irumide Belt in Zambia. They were emplaced in anorogenic continental rift–related environments.

3. Sporadic, but widely distributed, small igneous intrusions were emplaced at 750±50 Ma. They comprise granite, alkali granite, syenite and gabbro with felsic and mafic volcanics, as observed in the Copperbelt, Kalengwa-Kasempa and NW Zambia (Zambia); Khorixas Inlier and Summas Mountains (Namibia). These bodies intrude Roan and Nguba Formation lithologies but are generally overlain by (Upper) Kundelungu sediments and their Namibian equivalents. They were emplaced in anorogenic rift-related and continental epeirogenic uplift environments.

4. Widespread and voluminous granitoid magmatism (Pan African) was emplaced at 550±50 Ma. It is well preserved in the environs of Otjiwarongo, central Namibia, Kaokoland, and in west-central Zambia (including the Hook Granite Batholith), but also sporadically detected in NW Zambia. The Otjiwarongo batholith, a covered pluton in Namibia, may be similar to the Hook Granite batholith in size, rock type and age. These rocks were emplaced in continental epeirogenic uplift and rift-related environments. This period may be broken into at least three discrete events.

5. Several, more restricted magmatic events occur during the last 2000 Ma in the Greater Lufilian Arc. Examples of this are the Nchanga Granite in Zambia (880 Ma); magmatism at 1700 Ma in the Khorixas Inlier, Namibia; and at 1600 in the Kamanjab Batholith.

The Zambian Lufilian Arc and Damara region of Namibia behaved in a different way from 2200 to 2000 Ma; they were independent entities. They also behaved significantly different from 1400 to 850 Ma. Geological history of the two main portions of the Greater Lufilian Arc is consistent from *circa* 800 Ma to the present, and especially during the last 600 Ma.

9.2 Polycyclic Geological History

Most areas studied in the Greater Lufilian Arc show polycyclic geological histories. Repeated anorogenic intrusive events are a common denominator. Source rocks for the various melts come from previously-formed intrusive rocks and siliciclastics. Prolonged crustal histories have resulted in superimposition of events. Two Namibian examples illustrate this. In the Otjiwarongo environs, Neoproterozoic granites intruded anorogenic Paleoproterozoic granites, and both were intruded almost in the same location by two large Mesozoic alkaline complexes. At the Oas farm, a Mesozoic mafic feeder pipe cuts through 750 Ma alkaline intrusions that had intruded Paleoproterozoic anorogenic granitoids. Melts and sedimentary rocks have been re-worked in each of the areas; a lot of magma mixing and crustal contamination processes were involved in the formation of the granitoids.

9.3 Rock Types

The majority of the rocks from the Greater Lufilian Arc that were analysed had midalkaline character. Table 9.1 compiles statistics on sample composition and alkalinity that were carried out in all sampling domains. Any rock that plotted outside of the fields of the modified TAS diagram was not included in the statistics.

Table 9.1 Rock type statistics of all samples analysed from the Greater Lufilian Arc

Group	Rock type	number	%	Granitoids	Groups
Midalkaline Rocks	Alkali granite	102	22.13	63.93	59.87
	Quartzmonzonite	83	18.00		
	Syenite	32	6.94		
	Monzonite	17	3.69		
	Monzodiorite	10	2.17		
	Monzogabbro	12	2.60		
	Alkali gabbro	20	4.34		
Subalkaline Rocks	Granite	99	21.48	36.07	32.75
	Granodiorite	33	7.16		
	Diorite	6	1.30		
	Gabbro-diorite	3	0.65		
	Quartzolite	4	0.87		
	Gabbro	6	1.30		
Alkaline Rocks	foid syenite	11	2.39		7.38
	foid monzosyenite	4	0.87		
	foid monzo-diorite	2	0.43		
	foid gabbro	12	2.60		
	Foidolite	3	0.65		
	Peridot gabbro	2	0.43		
Total		461	99.57	100.00	100.00
	Carbonatite	10			
Total including carbonatites		471			

The database of 471 samples was broken into domains as indicated on Table 9.2. Rock type percentages for each domain is listed on Table 9.3.

Table 9.2 Number of samples from each rock type for domains of the Greater Lufilian Arc.

Rock type/ Region	Hook Granite	NW Zambia	Copperbelt	Kamanjab	Khorixas	Okwa,Ugab,Summas,Grootf	Otjiwarongo	Okatjepuiko	KalengwaKasempa	West Lusaka Kafue Flats	total	
alkali granite	26	7	6	26	10	4	13	1	2	7	102	Midaldaline
quartzmonzonite	20	8	5	38	1	1	5		3	2	83	
syenite	7	2	2	3	9	1	2		2	4	32	
monzonite	5	1	1	2	2		2	2	2		17	
monzodiorite	3	1	2	1					3		10	
monzogabbro	1	1	3	1	1			1	3	1	12	
alkali gabbro	2	5	1	3	3			1	3	2	20	
granite	16	10	15	22	8	11	7	5	1	4	99	Subalkaline
granodiorite	7	8	8	3	1	1		1	1	3	33	
diorite		1	2				1			2	6	
gabbro-diorite	1				1					1	3	
quartzolite				3			1				4	
gabbro	1	1	1	1	1					1	6	
foid syenite		8	1	2							11	Alkaline
foid monzosyenite					4						4	
foid monzo-diorite			1						1		2	
foid gabbro		2	2		1				7		12	
foidolite		1		2							3	
peridot gabbro				1	1						2	
carbonatite	1				9						10	
Total	90	56	50	108	43	18	31	11	27	27	461	

Table 9.3 Percentages of each rock type for domains of the Greater Lufilian Arc.

Rock type/ Region	Hook Granite	NW Zambia	Copperbelt	Kamanjab	Khorixas	Okwa,Ugab,Summas,Grootf	Otjiwarongo	Okatjepuiko	KalengwaKasempa	West Lusaka Kafue Flats	Kalene Hill	Nchanga Granite	Muliashi Porphyry	Chambishi	Oas Farm	Lofdal farm	Percentage	
alkali granite	29.2	12.5	12	24.1	23.3	22.2	41.9	9.09	7.14	25.9	20	8.33	12.5	12.5	25.9		22.13	Midaldaline
quartzmonzonite	22.5	14.3	10	35.2	2.33	5.56	16.1		10.7	7.41	23.5		25		3.7		18.00	
syenite	7.87	3.57	4	2.78	20.9	5.56	6.45		7.14	14.8	3.33	16.7			33.3		6.94	
monzonite	5.62	1.79	2	1.85	4.65		6.45	18.2	7.14							8.33	3.69	
monzodiorite	3.37	1.79	4	0.93					10.7		3.33				3.7		2.17	
monzogabbro	1.12	1.79	6	0.93	2.33			9.09	10.7	3.7				12.5	3.7		2.60	
alkali gabbro	2.25	8.93	2	2.78	6.98			9.09	14.3	7.41				12.5	3.7		4.34	
granite	18	17.9	30	20.4	18.6	61.1	22.6	45.5	3.57	14.8	23.3	66.7	31.3	12.5	11.1	25	21.48	Subalkaline
granodiorite	7.87	14.3	16	2.78	2.33	5.56		9.09	3.57	11.1	23.3		31.3	37.5		8.33	7.16	
diorite		1.79	4				3.23			7.41		8.33					1.30	
gabbro-diorite	1.12				2.33					3.7						8.33	0.65	
quartzolite				2.78			3.23										0.87	
gabbro	1.12	1.79	2	0.93	2.33					3.7	3.33			12.5	7.41	16.7	1.30	
foid syenite		14.3	2	1.85													2.39	Alkaline
foid monzosyenite					9.3										3.7	25	0.87	
foid monzo-diorite			2						3.57								0.43	
foid gabbro		3.57	4		2.33				25						3.7		2.60	
foidolite		1.79		1.85													0.65	
peridot gabbro				0.93	2.33											8.33	0.43	

60%, 33%, 7% is the percentage relationship of midalkaline to subalkaline to alkaline rock groups for the entire project (Fig 9.1). 64%, 36% is the percentage relationship of midalkaline to subalkaline granitoids. Carbonatites make 2.1% of the total samples. If the suite of mafic rocks collected are considered representative of reality, then midalkaline gabbroids make 66%; alkaline gabbroids, 18%; and subalkaline gabbroids, 17%.

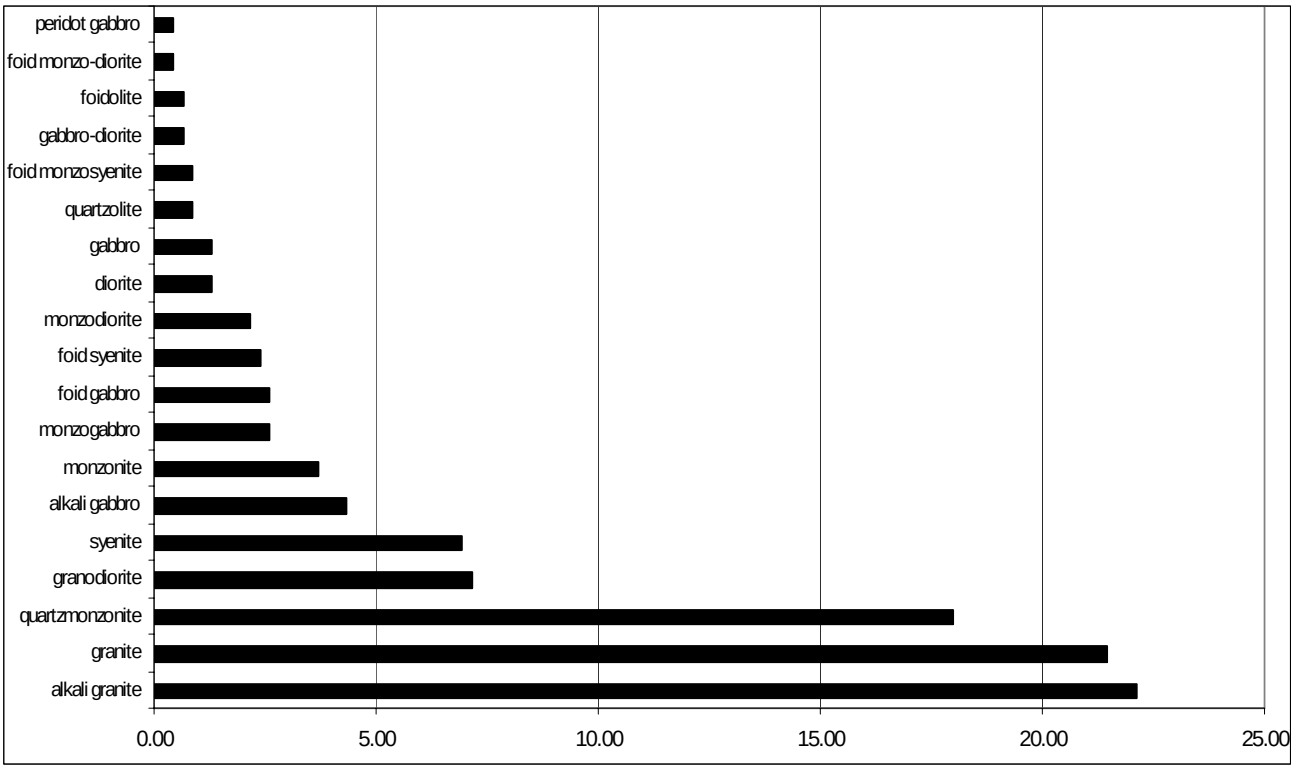

Fig 9.1 Distribution of rock types and comparative composition of rock alkalinity in the Greater Lufilian Arc granitoid project. Based on the names of the modified TAS diagram of Middlemost, 1994a.
Note the absolute domination of alkali granite, granite and quartzmonzonite. Together these rock types account for almost 62% of all samples studied. That is also clear on Fig. 9.2.

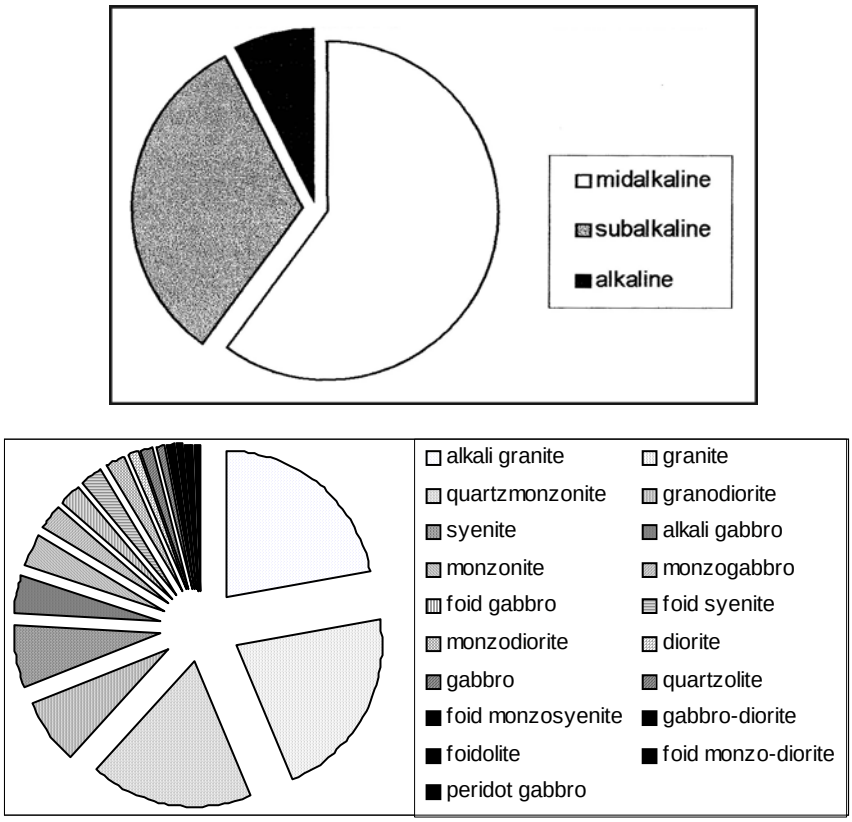

Fig 9.2 Composition of the samples collected in the Greater Lufilian Arc. *The upper pie diagram* ***groups rocks according to*** *their alkalinity, sensu Middlemost, 1994. The lower diagram breaks the samples into their respective rock types.*

Midalkaline rocks predominate, whatever the point of view. That corresponds with the continental extension, anorogenic environment that has ruled formation of plutonic rocks in the Greater Lufilian Arc.

The average rock type distribution for the entire Greater Lufilian Arc closely resembles that of the Hook Granite Batholith, as indicated on Table 9.3.

9.3.1 Mafic, Ultramafic and Alkaline Rocks

Mafic, ultramafic, carbonatitic and alkaline intrusions are well represented, albeit volumetrically minor, in most domains of the Greater Lufilian Arc that were studied. In certain cases, these rocks might be implicated in mineralizing processes (Kalengwa deposit, Lofdal rare earth mineralization and Lofdal carbonatites). These rocks occur in anorogenic epeirogenic uplift and rift-related environments. Mafic rocks are under-represented in the geochemical database, because they were not the primary sampling target.

The widespread small gabbroic bodies in the Greater Lufilian Arc were emplaced as mafic plugs in large, within-plate areas that were being subject to incipient rifting. The mafic plugs could intersect the sedimentary cover of the plate, including marine and continental deposits. A modern day analogue of the same process takes place in the environs of Filiya, Nigeria.

9.3.2 Rock Associations in Anorogenic Environments

A frequent field observation is the persistent clustering of small bodies of red-altered granitoids, gabbroids, massive magnetite-hematite and quartz pods that are linked to ages around 550 and 750 Ma. The four-rock association seems to be a characteristic of continental extension anorogenic environments. It is spatially related to iron oxide-copper-gold mineralization.

A recurrent feature observed in most outcrops of the study area is the presence of two or more contrasting types of plutonic rocks. In some cases gabbroids and granitoids; in others, syenitoids and granitoids; even three or four types of granites and alkali granites. Many of the small areas also contain mafic, ultramafic and alkaline plugs and dikes of varying composition, such as lamprophyres, carbonatite and nepheline syenite.

The multiplicity of rock types in a small area seems to be another characteristic of continental extension anorogenic environments.

9.3.3 Quartz Pods

Quartz pods have been identified throughout most of the Greater Lufilian Arc region. They differ from veins, boudinaged veins and pegmatitic quartz units, particularly in geometry: outcrops of undeformed bodies are typically round to elliptical, and vary from a few to several-hundred meters in diameter. Dimensions of some quartz pods exceed four kilometers in diameter and there is geophysical evidence of even larger ones. They seem to be a special type of silicification. Hyper-alkaline, hydrothermal solutions seem to be involved in the transportation of silica and emplacement of the quartz pods. Quartz pods are emerging as a type of alteration that is associated to IOCG systems in the Greater Lufilian Arc. Improved identification in the field and an increased understanding of their physico-chemical features may aid in the exploration of mineral deposits.

9.3.4 Iron Oxide Bodies

Masive bodies of magnetite and/or hematite at macroscopic, mesoscopic and microscopic scales emplaced themselves by gradual replacement of the host rock. The process seems to involve silicate dissolution by hyper-alkaline hydrothermally-driven solutions.

9.3.5 Round-Pebble Hydrothermal Breccias

Round-pebble hydrothermal breccias occur often in and around IOCG systems throughout the Greater Lufilian Arc. They seem to have been produced by hyper-alkaline solutions that corroded previously angular hydrothermal breccias. In some cases, they act as good hosts for sulfide mineralization.

9.4 Ring Complex Clusters

Clusters of anorogenic granitoid ring complexes have been produced all along from Archean times to the present. Clustering of multiple anorogenic ring complex intrusions can form batholithic size bodies.

At least ten clusters of ring complexes were identified in the Greater Lufilian Arc. Ring complex clusters have the following characteristics: 1) Multiple ring complexes of varying chemical composition and size that might intersect each other. 2) Volcanic and plutonic rocks of roughly the same composition occur together. 3) Successive magmatic events of varying composition allowed for abundant opportunities of magma mixing and recycling of crustal materials. 4) The plan view geometry of un-tectonized ring complex clusters is roughly that of an isosceles triangle. 5) Less voluminous precursor and waning events of magmatism may occur. 6) The principal chemical composition of the magmas is midalkaline, but may ocassionally vary to alkaline and subalkaline. In extreme cases, it may be peralkaline and can even produce carbonatitic rocks. 7) Isolated bodies of mafic and ultramafic rocks often come in the latter stages of the process. 8) Total duration of ring complex cluster cycles averages 110 Ma.

Several cycles of ring complex clusters have repeatedly occurred in roughly the same location in at least three different localities. These repeated cycles were separated 1095 Ma in NW Zambia; 933 Ma at the Khorixas area, Namibia; and 50 Ma in West Lusaka, Zambia.

9.5 Tectonic Environment of Emplacement

The tectonic environment of emplacement for part of the rocks collected is not yet well constrained; active research is currently being carried out to address this issue. Nevertheless, several clear patterns are emerging: 1) The largest portion of granitoids collected are midalkaline rocks that formed in an anorogenic continental epeirogenic uplift environment. 2) Next come those formed in rift environments. 3) Another significant group of rocks formed in a post orogenic granitization environment. 4) Continent-continent collision environments were not positively identified. 5) Subductional magmatism seems to have been very restricted both in terms of time and areal extension. There is evidence of minor such magmatism in Paleoproterozoic rocks of Kalene Hill and in portions of the Kamanjab Batholith. In any given area, two or more of these settings may be superimposed. Anorogenic continental extension is the main geological process of the Arc.

Complete Wilson cycles were not identified in the domains of the Greater Lufilian Arc that were studied. The dominant magmatic process, as evidenced by the volume of extruded rock, is anorogenic continental epeirogenic uplift, closely-followed in time by a rift-related granitoid emplacement. Coalescing and overprinting aulacogens seem to be the main type of geological event in the arc.

The environment of emplacement of Paleoproterozoic rocks that occur throughout the Arc cannot be identified using the established methods for granitoid environment of emplacement. Intense sodic alteration and hematitization were observed in part of these rocks. Another alteration process is a net enrichment in potassium that is evident by the abundant biotite and alkali feldspar overgrowth. Part of the rocks showed diffuse crystal margins and abundant blue quartz phenocrystals. Incipient migmatitization of these rocks may have modified their chemistry to a point where they don't fit traditional procedures to evaluate granitoid environment of emplacement. The alteration processes just mentioned seem to have taken place before ~880 Ma, because the environment of emplacement of younger rocks can be identified.

9.6 High Thorium

High values of thorium were found in part of the granitoids of NW Zambia, Kafue Flats, Hook Granite Batholith (Zambia), Oas farm and Otjiwarongo environs (Namibia). They are high-heat producing rocks. The anomalous thorium content in some granitoids of the Greater Lufilian Arc induced and maintained long-lived, large convective cells of hydrothermal fluid flow.

High-thorium granitoids in all five domains have a particular trace element chemical signature that is not common, and probably were subjected to analogous geological processes at different points in time.

9.7 Correlation of Granitoids

Granitoid rock suites with closely matching chemistry and macroscopic features have been found to form in the same region, two or three times with up to a thousand million years of age difference. Source rocks and environment of emplacement for the anorogenic intrusive events were the same: for that reason, magmatic products turned out equivalent. These features preclude lithological or detailed geochemical correlation.

Rocks from the suites of Muliashi Porphyry and Mufulira, Zambia are an example of this. They both have pink and gray granitoids with similar compositions, but the ages of the rocks are completely different.

Several lithological correlations have been developed for granitoids in various domains of the Greater Lufilian Arc. The rocks cannot be properly correlated until more geochronological information is available.

9.8 Main Findings in Specific Domains

9.8.1 Hook Granite Batholith, Zambia

Information currently available on geophysics, geochronology, rock distribution and geochemistry from the Hook Granite Batholith fit quite well with an intracontinental, anorogenic, ring complex cluster origin. The batholith is mainly composed by midalkaline granitoids. Alkali granites, quartzmonzonites and granites make up 70% of all rocks.

9.8.2 Nchanga Granite, Zambia

The Nchanga Granite has all the characteristics of an anorogenic granite ring complex. Chemistry of its rocks crosses the midalkaline to subalkaline fields. Parts of the pluton are made of high heat producing granites that maintained a long-lived circulation of hydrothermal fluids. The Nchanga Granite might have contributed to the origin of copper in its environs.

9.8.3 Kamanjab Batholith, Namibia

Sixteen suites with more than two contrasting rock types were identified in the Kamanjab Batholith. No two suites are identical, and they are made by a large variety of rock types. This multiplicity of rock types at a given site is one of the characteristics of anorogenic environments in the Greater Lufilian Arc.

There is no direct proof of the presence of ring complexes at the Kamanjab Batholith. Nevertheless, several sources of evidence point to the batholith as a cluster of ring complexes. Among others, these are: 1) the lack of continuity in the rock types along traverses; 2) the presence of multiple rocks types in at least fifteen discrete sites; 3) General anorogenic character of most of the rocks; 4) three quarters of the rocks in the suite are midalkaline; 4) the size and shape of the batholith, as well as its event diagram has similarities with other ring complex clusters.

9.8.5 New Temporal Constrain to Katangan Sedimentation

Granitic dikes emplaced at the Nchanga mine area in anorogenic extensional environments were dated at ~765 Ma. They provide the youngest age of deposition for that portion of the Katanga sedimentary sequence at Nchanga (Roan sediments), and might provide a significant bracket age for mineralization.

9.8.6 Khorixas Inlier-Kamanjab Batholith

Geological history for the Khorixas Inlier and the Kamanjab Batholith are significantly different. They probably were not in the same geographic position all the time. Older basement is known in the Khorixas Inlier than at the Kamajab. The two regions seem to have had a common geological history for the past 550 Ma.

9.8.7 Long-Lived Fractures

E-W-trending regional fracture systems that run parallel to the elongation of the Greater Lufilian Arc play an important role in the emplacement of magmatism and IOCG mineralization. They acted as routes for intrusion, channels for fluids and control for ore deposition. Those structures are generally parallel to the main Lufilian Arc trend, and could have been normal syn-rift faults that have been reactivated throughout geological history. Some N-S-trending structures are also mineralized and they are sub-perpendicular to the main trend of the Lufilian Arc.

9.9 Metallogeny

Various types of mineralization were seen to be associated with intrusive rocks along the Greater Lufilian Arc (Table 9.4). These include rare earth mineralization associated to alkaline dikes and carbonatites in the Khorixas Inlier, sedimentary-hosted gold (so-called “Carlin”-style deposits), several low-sulfidation hydrothermal gold occurrences, low sulfidation hydrothermal copper depostis, epigenetic copper vein deposits, alkaline porphyry molybdenum (-copper?) style mineralization, sedimentary-hosted copper-cobalt deposits, and a wide variety of iron oxide-copper-gold and related deposits and prospects. Several Paleoproterozoic rocks throughout the Greater Lufilian Arc are enriched in copper. Some Mesoproterozoic syenites and alkali granites are enriched in zinc. The significance of the latter observation remains unclear. Paleoproterozoic copper-rich rocks could be the source of metal for later events. Incipient migmatitization of those rocks could have remobilized the copper. Copper is probably being recycled. Very little skarn mineralization was observed in Katangan carbonates, even though they are intruded by multiple plutonic episodes. Possible exceptions occur around the Hook batholith. The Samba deposit is not considered to be a copper porphyry; it is a low sulfidation epithermal copper mineralization hosted in pyroclastic rocks that were sheared during regional metamorphism.

9.9.1 Metallogenic Epochs

At least eight discrete periods of mineralization can be interpreted from Table 9.4 (The same are simplified on Table 9.5). Where possible, radiometric ages have been used to place the various events. Most have been assigned to specific ages by correlation or association. Six deposits could not be placed chronologically and are included at the bottom of the list. There is a wide-spread series of mid-alkaline intrusions emplaced around 750 Ma that produces a variety of mineral deposits. Another such event (separated in at least three different phases: 500-513, 550 and 583 Ma) took place around 540±40 Ma. Five less well defined events took place as indicated on Table 9.5. From old to young, they occurred at ~1970, ~1930, ~1866, 1097-1059 and ~460 Ma (See Tables 9.4 and 9.5). The dominant deposit type is iron oxide-copper-gold mineralization.

The age of sedimentary-hosted copper mineralization in the Copperbelt is currently being re-evaluated using Re-Os dating at the University of Arizona. Three tentative ages for them are 796-756, ~583 and ~550 Ma.

The main events of sedimentary-hosted gold mineralization in Namibia are ~750 Ma in the environs of Sesfontein, ~550 Ma in Eastern Namibia. The age of the Zambian deposits and prospects could not be estimated.

At least two distinct events of disseminated copper mineralization associated to midakaline granitoid intrusives were identified in the Kamanjab Batholith. The first took place around 1975 Ma and the second around 1928 Ma.

Table 9.4 Main Metallogenic Events Observed - Greater Lufilian Arc

Commodities	Mine, Deposit, Prospect, Event	Deposit Type	Age	@	Tectonic Environment
Au	Sasare,Zm	IOCG	460		anorogenic continental rift+
Au,Cu,(Pb?)	Navachab Mine, Nm	structurally-controlled carbonate replacement	~490	E	?
Cu,Au	Kansanshi Mine,Zm	?	500-513	E	extension
Cu,Co,Au,U	Shituru Mine, D.R.Congo	IOCG	500-513#	E	extension
Cu,Co,Ni	Luiswishi Mine, D.R.Congo	IOCG	500-513#	E	extension
Cu,Co,Ni,Au,U,etc.	Kamoya Mine, D.R.Congo	IOCG	500-513#	E	extension
Mo	Marinkas Kwela Deposit, Nm	Mo porphyry	520-560	E	anorogenic continental rift
Cu,Au,Mn,LREE	Kitumba deposit,Zm	IOCG	533	E	anorogenic continental rift
Cu,Au,Mn,LREE	Kantonga deposit, Zm	IOCG	533	E	anorogenic continental rift
Cu,Ag,Au,Fe	Hook Satellites, Zm	IOCG	533	E	anorogenic continental rift+
Au,<Cu	Dunrobin Mine, Zm	Au-rich IOCG	533	E	anorogenic continental rift+
Py,Cu,Au	Nampundwe Mine, Zm	IOCG	538(L-207)	E	anorogenic continental rift+
Cu,Au,As,Pb,Zn	Hippo Mine, Zm	IOCG	538	E	anorogenic continental rift+
Au	Otavi Mts., Nm	Sed-hosted Au	~550	E	anorogenic continental rift
Au	Otjiwarongo, Nm	Sed-hosted Au	~550	E	anorogenic continental rift
Cu,Au	Kombat Mine, Nm	IOCG	~550*	E	anorogenic continental rift
Au	Otjikoto Mine, Nm	IOCG	~550*	E	anorogenic continental rift
Cu,Au	Kafue Flats, Zm	IOCG	550(L-211)	E	anorogenic continental rift
Au	Kamanjab, Nm	Au epithermal	570-677	E	?
Zn,Pb	Kabwe Mine, Zm	?	?	E	?
-	Verangian Glaciation	-	580	E	-
Cu,Co	CuBelt minzn, Nchanga Mine, Zm	Sedimentary-hosted Cu	583	E	-
Cu,Co	CuBelt minzn, Mufulira Mine, Zm	Sedimentary-hosted Cu	583	E	anorogenic continental rift+
Cu,Co	CuBelt minzn, Musoshi Mine, Zm	Sedimentary-hosted Cu	583	E	
Cu,Co	CuBelt minzn, Chambishi Mine, Zm	Sedimentary-hosted Cu	583	E	
-	Marinoan Glaciation	-	630		-
-	Sturtian Glaciation	-	710		-
Cu,Ag,LREE,U,Au?	Kalengwa Mine, Zm	IOCG	745	I	anorogenic continental rift+
Cu,Au,LREE	Kasempa Area, Zm	IOCG	750	I	anorogenic continental rift+
Cu,Au?	Kametete deposit, Zm	IOCG	750	I	anorogenic continental rift+
Au	Sesfontein, Nm	Sed-hosted Au	745-756	I	anorogenic continental rift
Cu,Nb,REE,Au?	Kesya carbonatite, Zm	IOCG	745-756?	I	anorogenic continental rift+
Cu,Co	Copper Valley prospects + mine, Nm	IOCG	745-756	I	anorogenic continental rift+
REE,Zn,Cu?,Au?	Oas farm prospects, Nm	IOCG	745-756	I	anorogenic continental rift+
REE,Cu?,Au?	Lofdal farm prospects, Nm	IOCG	745-756	I	anorogenic continental rift+
Cu,Co,Ni	Luamata deposit, Zm	IOCG	745-756	I	anorogenic continental rift+
Cu,Co	Copperbelt initial Cu minzn, Zm	Sedimentary-hosted Cu	756-796	I	anorogenic continental rift
Cu	Omitiomire deposit, Zm	Sedimentary-hosted Cu	L or younger		anorogenic continental rift
Au,Cu	Kamachopolo, SW Kasempa, Zm	Low sulfid. epithermal	L or younger		anorogenic continental rift
Au	Lunga, Zm	Low sulfid. epithermal	L or younger		anorogenic continental rift
Cu	Mkushi mines and prospects, Zm	Intrusion-related minzn	1059	L	extension
Cu,Au	Witvlei deposit, Nm	IOCG	1097(L-638)	L	anorogenic continental rift+
Cu,Au?,Ag?	Mnzd area 3 Kamanjab Batholith, Nm	Disseminated Cu	1866(L-993)		
Cu,Cu,LREE	Mwinilunga, W Zm	IOCG?	1928(L-030)	U	
Cu,Cu,LREE	Kamdescha f., Kamanjab Batholith,Nm	IOCG, Au, Cu	1937(L-868)	U	
Cu,Cu,LREE	Tevrede f., Kamanjab Bathlith,Nm	IOCG	1937(L-855)	U	
Cu,Mo	Samba Cu prospect, Zm	schist-hosted Cu	1965	V	?
Cu,Au?,Ag?	Mnzd area 2, Kamanjab Batholith,Nm	Disseminated Cu	1876(L-969)		
Co,Ni,Cu	Kalumbila deposit, Zm	Sedimentary-hosted Cu derived from an IOCG	*	I	hydrothermal rift-related brines,can be I,L or even older up to 1800Ma.
Cu	Lumpuna prospect, SW Luanshya,Zm	Cu porphyry	?		Subduction
Cu	Chifumpa, 80km SE Kasempa, Zm	Cu porphyry	?		Subduction
Au,<Cu	Karibarembi, 49km S Kalenwa, Zm	Sed-hosted Au	?		
Au,<Cu	Kililamirombwe, 124km SSE Kasempa,Zm	Sed-hosted Au	?		
Cu	Dongwe, Zm	High+low sulf. epitherm	?		Subduction

+Tectonic environment of emplacement was inferred from geochemistry. *The age is based on a nearby similar age. #Estimated age.

@Magmatic event in geochronological correlation diagrams (Figs A79 to A83).

The age of the six last items of the table is uncertain.

Table 9.5

Simplified Classification of Metallogenic Events in the Greater Lufilian Arc

By Alberto Lobo-Guerrero, M.Sc., Min.Ex., December, 2004
Economic Geology Research Institute, University of the Witwatersrand, Johannesburg

Commodities	Location	Deposit Type	Age	*	Environment
Au	Sasare, Zm	IOCG	460		ACR
Cu,Co,Ni, Au,U,Fe	Kansanshi, Zm + some southern Congolese Fe + Cu-Co deposits	IOCG + Kansanshi veins	500-513	Eo	Extension
Mo	Marinkas Kwela	Mo porphyry	520-560	E	ACR
Cu,Au,Fe, REE,Ag,Zn,Pb	Hook Granite batholith satellite bodies, Zm	IOCG	~533	E1	ACR
Cu,Au	Otjiwarongo, Otavi Mts., Nm; Kafue Flats, Zm	IOCG + Sedimentary-hosted Au + Navachab,Nm	~550	E2	ACR
Cu,Co (U)	Copperbelt and Congolese Cu-Co mineralization hosted in sediments; remobilization and mineralization	Sed-hosted Cu (epigenetic overprint)	~583	E3	Event related to Verangian Glaciation?
Cu,Co,Ni,Au	Kabompo Dome, Zm	IOCG, sed-hosted Co-Ni-Cu	~730	I	CEUG
Cu,Au,REE, Ag,Mn	Kalengwa-Kasempa area,Zm Oas, Lofdal, Mesopotamie, Nm	IOCG	~745-756	I	ACR
Cu,Co	Initial copper mineralization in the Zambian Copperbelt (and Katanga?)	Sed-hosted Cu	756-796	I-J	ACR
Cu,Au	Witvlei, Nm; Mkushi,Zm; Omitiomire,Zm	IOCG + Intrusive related mineralization	1059-1097	L	ACR
Au,As,Bi,Sb	Karibarembi and Kililamirombwe, Zm	Sed-hosted Au	L or younger	L	ACR
Cu,Au?	Kamanjab Batholith, Nm	IOCG, hydrothermal Cu dissemination	1866	U	environment cannot be identified - probably CEUG
Cu,Au?	Kabompo Dome, Mwinilunga, Lumwana, Zm	Schist-hosted Cu	1928	U	?
Cu, Au,Fe,F,REE	Kamanjab Batholith, Nm; Mwinilunga, Zm (?)	IOCG	1930	U	ACR
Cu,Mo	Samba, Zm	Schist-hosted Cu	1965	V	?
Cu,Au,Ag?	Kamanjab Batholith, Nm	Hydrothermal Cu dissemination	1975	V	CEUG

NOTE: ACR = Anorogenic continental rift. CEUG = continental epeirogenic uplift granitization.
* Letters in the fifth column refer to labels for magmatic events in geochronological correlation diagrams (Figs A79 to A83). White and gray coloration serves to separate major metallogenic times.

9.9.2 Iron Oxide-Copper-Gold Mineralization

The iron oxide copper-gold (IOCG) style of mineralization is far broader in terms of both spatial distribution and age of emplacement than previously thought. IOCG deposits have been identified in both Namibia and Zambia. In Namibia, for example, the IOCG deposit Tevrede is currently being explored by junior mining corporations in the northwestern portion of the Kamanjab batholith; in addition, the Kombat copper mine in the Otavi Mountains and Otjikoto, a gold deposit in the environs of Otjiwarongo, seem to be IOCG deposits. Several IOCG-like mineralized areas were identified at the Oas, Lofdal, Mesopotamie and Gelbingen farms as outliers to the Kamanjab Batholith. Zambia also has several known IOCG deposits like the Kalengwa copper-silver mine, the Kitumba and Kantonga copper deposits and others around the Kasempa area. The Nampundwe pyrite mine as well as Dunrobin gold mine also have IOCG characteristics.

Quartzites are good hosts for mineralization. This was observed in several Namibian areas, including the southern part of the Oas farm, the Gelbingen farm and the western portion of the Kamdescha farm, bordering the Kamanjab Batholith. Quartzites fracture in a brittle manner that is ideal for hydrothermal brecciation. Equivalent rocks might host mineralization in Zambia.

The main IOCG events that have been identified in the Greater Lufilian Arc took place during eight time periods. These are listed on Table 9.6. The possible IOCG events that took place in the basement to the Zambian Copperbelt (at Chambishi, Mufulira, the main Copperbelt, Konkola and Nchanga) are not very well defined or constrained geochronologically.

Table 9.6 Periods of iron oxide-copper-gold mineralization in the Greater Lufilian Arc.

Period	Main representative mineralization
~460 Ma	Sasare, Zambia
~533 Ma	Hook Granite Batholith satellites, Zambia
~550 Ma	Otjiwarongo, Namibia; Kafue Flats, Zambia
~746 Ma	Kalengwa-Kasempa, Zambia; Khorixas, Namibia
~825 Ma	Copperbelt, Zambia (possible, see section 6.4)
~1078 Ma	Witvlei, Omitiomire, Namibia
~1937 Ma	Kamanjab Batholith, Namibia

The rocks of many IOCG deposits and prospects in the Greater Lufilian Arc are pristine. There is no significant deformaton involved. Hydrothermal brecciation and other mineralization features are un-deformed. This may be very useful to study mineralization and alteration processes.

9.9.3 Association of Sedimentary Hosted Copper Mineralization with IOCG Mineralization

A significant finding is the juxtaposition of iron-oxide-copper-gold mineralization underneath the sedimentary-hosted copper deposit at Witvlei, Namibia. This metallogenic event occurred at 1110 Ma. Secondary copper in the sedimentary-hosted deposit might have come from the IOCG deposit that lies underneath. This idea may generate a new concept for the origin of the Copperbelt-Katanga copper and cobalt deposits. The concept also opens an entire new age gap for the exploration of base metal mineralization in the Greater Lufilian Arc and the surrounding environment, including South Africa. There is additional evidence of IOCG mineralization related to sediment-hosted copper in other parts of Namibia and Zambia, including the Chambishi area and parts of the basement to the Copperbelt.

At least three discrete time periods show IOCG mineralization in close temporal spatial association with sedimentary-hosted copper deposits. The first took place around Witvlei from 1108 to 1059 Ma. The second and third ocurred in the basement to the Zambian Copperbelt from 882 to 725 Ma and from 607 to 500 Ma.

APPENDICES VOLUME

Abbreviated Table of Contents

A Sample Maps, 127
B TAS Diagram for Suites of the Kamanjab Batholith, Namibia, 165
C Geochemistry Database, 1
D Geographic Coordinates of Samples Collected and Geological Stations, 25
E Geochronology Database, 41
F Geochronological Event Diagrams, 67
G Tectonic Environent of Emplacement for Samples, 95
H Partial Transcription of Field Notes, 183
I Other Information, 222
J Raw Data for New Geochronology, 237
K Geochronological Correlation Diagrams, 257

APPENDICES VOLUME

Complete Table of Contents

APPENDIX A SAMPLE MAPS, 127

M1 Key for Zambian Sample Maps, 128
M2 Sample map, Hook Granite Batholith, Zambia over 1:1'000,000 geological map, 129
M3 Sample map, Hook Granite Batholith, Zambia over 1:100,000 geological sheets, 130
M4 Enlarged sample map, Hook Granite Batholith, Zambia over 1:100,000 geological sheets, (See Fig 4.15)
M5 Enlargement of sample, Hook Granite Batholith, northern portion, 131
M6 Enlargement of sample, Hook Granite Batholith, southern portion, 132
M7 Sample map of the Kafue Flats area, Zambia, 133
M8 Sample map, Kalengwa mine environs, Zambia, 134
M9 Sample map, Kasempa environs, Zambia, 135
M10 Sample map, Kalene Hill and Kabompo Dome, NW Zambia, 136
M11 Sample map of Kalene Hill and environs, NW Zambia, 137
M12 Sample map, Domes Area, Zambia, 138
M13 Sample map, Kabompo and Mwombezhi Domes, Zambia, 139
M14 Sample map SE of Mwinilunga, 140
M15 Sample map, Solwesi Dome environs, Zambia, 141
M16 Sample map of the Nchanga Granite, Zambia, 142
M17 Sample map of the Chambishi-Mufulira Area, Zambia, 143
M18 Sample map of the Serenje area, Zambia, 144
M19 Key for Namibian Sample Maps, 145
M20 Sample map of the Khorixas inlier and the Mesopotamie farm, Namibia, 146
M21 Sample map of the Oas and Lofdal farms, Khorixas Inlier, Namibia, 147
M22 Sample map of the Summas Mountains and Ugab River, Namibia, 148
M23 Sample map, Otjiwarongo environs, Namibia, 149
M24 Close-up of sample map, Otjiwarongo environs, Namibia, 150
M25 Sample map, Otavi Mountains, Namibia, 151
M26 Sample map, Witvlei environs, Namibia, 152
M27 Key for Kamanjab Batholith sample maps, Namibia, 153
M28 K-14 portion of sample map, Kamanjab Batholith, Namibia, 154
M29 K-15 portion of sample map, Kamanjab Batholith, Namibia, 155
M30 K-16 portion of sample map, Kamanjab Batholith, Namibia, 156
M31 K-17 portion of sample map, Kamanjab Batholith, Namibia, 157
M32 K-18 portion of sample map, Kamanjab Batholith, Namibia, 158
M33 K-19 portion of sample map, Kamanjab Batholith, Namibia, 159
M34 K-20 portion of sample map, Kamanjab Batholith, Namibia, 160
M35 K-21 portion of sample map, Kamanjab Batholith, Namibia, 161
M36 K-22 portion of sample map, Kamanjab Batholith, Namibia, 162
M37 K-23 portion of sample map, Kamanjab Batholith, Namibia, 163
M38 K-24 portion of sample map, Kamanjab Batholith, Namibia, 164
M39 K-25 portion of sample map, Kamanjab Batholith, Namibia, 165

APPENDIX B
TAS DIAGRAM FOR SUITES OF THE KAMANJAB BATHOLITH, NAMIBIA, 165

F1 Suite A, 166
F2 Suite B, 167
F3 Suite C, 168
F4 Suite D, 169
F5 Suite E, 170
F6 Suite F, 171
F7 Suite G, 172

F8 Suite H, 173
F9 Suite I, 174
F10 Suite J, 175
F11 Suite K, 176
F12 Suite L, 177
F13 Suite M, 178
F14 Suite N, 179
F15 Suite P, 180
F16 Suite Q, 181

APPENDIX C GEOCHEMISTRY DATABASE, 1

A1 Chemical analysis of samples from the Greater Lufilian Arc sorted by region, 2
A2 West Lusaka-Kafue Flats, Zambia, 2
A3 Hook Granite Batholith, Zambia, 3
A4 Serenje, Zambia, 4
A5 Kalengwa-Kasempa Area, Zambia, 5
A6 Northwestern Zambia Region Zambia, 6
A7 Kalene Hill, Archean rocks, Paleoproterozoic Group 2, Paleoproterozoic Group 3, Paleoproterozoic Group 4, Other samples, 6
A7.1 Kabompo Dome, 6
A7.2 Solwesi Dome, 7
A7.3 Mwombezhi Dome, 7
A7.4 Sodalite Syenite Quarry, 7
A7.5 Shilenda, 7
A8 Basement to the Copperbelt, Zambia, 7
A8.1 Muliashi Porphyry, 7
A8.2 Chambishi mine area, 8
A8.3 Samba copper prospect, 8
A8.4 Nchanga Granite, 8
A8.5 Nchanga mine, 8
A8.6 Mufulira Granite, 8
A8.7 Other, 8
A9 Kamanjab Batholith, 9
A10 Felsic volcanics, Namibia; Ugab River, Namibia; Okwa River, Botswana; Summas Mountains, Namibia, 11
A11 Oas farm, Namibia, 12
A12 Lofdal farm, Namibia; Mesopotamie farm, Namibia; other alkaline and gabbroic rocks, Khorixas, Namibia, 13
A13 Otjiwarongo environs, Namibia; Grootfontein Inlier, Otavi Mountains, Namibia; Okatjepuiko, Witvlei, Namibia, 14
A14 Spitskoppe complexes, Namibia; Erongo complex, Namibia; Brandberg complex, Namibia; Nigerian ring complexes, 15
A15 Chemical analysis from the Greater Lufilian Arc sorted by number, 16

APPENDIX D GEOGRAPHIC COORDINATES OF SAMPLES COLLECTED, 25

A16 Zambian samples located on UTM zone 35, 26
A17 Zambian samples located using latitude and longitude (WGS84), 31
Zambian samples that are located in UTM zone 36, 31
A18 Namibian samples that are located in UTM zone 33 (Schwartzeck), 32
A19 Namibian samples that are located in UTM zone 34, (Schwartzeck), 36
A20 Namibian samples that are located using latitude and longitude coordinates (Schwartzeck), 37

APPENDIX E GEOCHRONOLOGY, 41
A21 Compilation of radiometric ages, Greater Lufilian Arc – sorted by chronological order, 42
A22 Compilation of radiometric ages, Greater Lufilian Arc – sorted by region and sites, 50
ZAMBIA, 50
A22.1 Hook Granite Batholith, Zambia, 50
A22.2 Northwestern Zambia, Domes Area, 50
A22.3 Solwesi Dome Area, Zambia, 50
A22.4 Western Lusaka-Kafue Flats Area, Zambia, 50
A22.5 Kalengwa-Kasempa Area, Zambia, 51
A22.6 Mkushi-Serenje Area, Zambia, 51
A22.7 Copperbelt region, Zambia, 51
A22.8 Mufulira Area, Zambia, 52
A22.9 Nchanga Area, Zambia, 52
A22.10 All Basement to the Copperbelt, Zambia (Compilation of Groups), 52
A22.11 Choma-Kalomo Batholith, Zambia, 52
A22.12 Irumide Belt, Zambia, 53
A22.13 Luangwa Valley, Zambia, 53
A22.14 Other Zambia, 54
NAMIBIA, 54
A22.15 True Kamanjab Batholith, Namibia, 54
A22.16 Khorixas Inlier, Namibia, 54
A22.17 All Kamanjab Area, Namibia, 55
A22.18 Witvlei Area and possible correlatives in the region, 55
A22.19 Central Namibia, 57
A22.20 Northernmost Namibia, 57
A22.21 Southernmost Namibia, 57
A22.22 Kaokoveld, Namibia, 57
A22.23 Rehoboth Inlier, Namibia, 58
A22.24 Namibrand-Sasriem Area, Namibia, 58
A22.25 Namaqua Metamorphic Complex, Namibia, 58
A22.26 “Kibaran” rocks of Namibia, 59
A22.27 Other Namibia, 59
OTHER, 59
A22.28 Other countries relevant to Lufilian Arc project, 59
A22.29 All Zambia (compilation of all Zambian ages), 60
A22.30 All Namibia (compilation of all ages from the country), 64

APPENDIX F EVENT DIAGRAMS, 67
ZAMBIA, 68
A23 Hook Granite Batholith, Zambia, 68
A24 NW Zambia, 69
A25 West Lusaka-Kafue Flats Area, Zambia, 70
A26 Environs of the Nchanga Mine, Zambia, 71
A27 Basement to the main Copperbelt, Zambia, 72
A28 Environs of the Mufulira Area, Zambia, 73
A29 All basement to the Copperbelt, Zambia, 74
A30 Luangwa Valley, Zambia, 75
A31 Mkushi-Serenje Area, Zambia, 76
A32 Choma-Kalomo Batholith, Zambia, 77
A33 Irumide Belt, Zambia, 78
A34 Other Zambian reported ages, 79
A35 All Zambian radiometric ages, 80

APPENDIX F (cont.)

NAMIBIA, 81

A36 Kaokoland Area, Namibia, 81
A37 Entire Kamanjab region, Namibia, 82
A38 Khorixas Inlier, Namibia, 83
A39 True Kamanjab Batholith, Namibia, 84
A40 Comparative event diagram for Khorixas Inlier and Kamanjab Batholith, Namibia, 85
A41 Central Namibian Area, 86
A42 Namaqua Metamorphic Complex, Namibia, 87
A43 Witvlei Area and correlatives in the Greater Lufilian Arc, 88
A44 So-called “Kibaran-Age” rocks, Namibia, 89
A45 Southernmost portion of Namibia, 90
A46 Namibrand-Sasriem Area, Namibia, 91
A47 Rehoboth Inlier, Namibia, 92
A48 All Namibian radiometric ages, 93
A49 Radiometric ages of other countries that are related to the Greater Lufilian Arc, 94

APPENDIX G TECTONIC ENVIRONMENT OF EMPLACEMENT, 95

A50 Tectonic environment of emplacement for samples from the Greater Lufilian Arc, 96
A51 Results of determination for environment of emplacement of granitoids based on methodology of Maniar & Piccoli, 1989, 102
A52 Results of determination for anorogenic character of granitoids based on the Whalen et al, 1987 plots, 108
A53 Results of determination for environment of emplacement of granitoids based on methodology of Pearce et al, 1984, 113
A54 Discrimination of granitoids following procedure of Harris et al, 1986, 118
A55 Results of determination for environment of emplacement of granitoids based on methodology of Batchelor & Bowden, 1985, 122
A56 Tectonic environment of mafic rocks, Greater Lufilian Arc project, 123

APPENDIX H PARTIAL TRANSCRIPTION OF FIELD NOTES, 183

ZAMBIA, 184

A57 Field notes taken along E-W transect of the Hook Granite Batholith, 184
A58 Abbreviated description of samples collected in the Hook Granite Batholith by Pepper, 2001, 186
A59 Comments from published Zambian geological survey reports and maps on iron oxide bodies, quartz pods, associated granitoids and round-pebble hydrothermal breccias, 188
A60 Sample description and field relationships in the West Lusaka-Kafue Flats Area, Zambia, 189
A60.1 Quartz pods, 189
A60.2 Granitoids, 189
A60.3 Gabbroids, 190
A60.4 Iron oxide bodies, 191
A60.5 Contact metamorphic rocks, 191
A61 Descriptions of samples from the Kalengwa Area, Zambia by Pepper, 2001, 192
A62 Descriptions of samples collected in the field, Kalene Hill Area, NW Zambia, 193
A63 Field descriptions of samples L-032 to L-034, Kabompo dome, NW Zambia, 194
A64 Petrography of the Chitungulu sodalite syenites, Mwombezhi Dome, NW Zambia, 195

APPENDIX H (cont.)

NAMIBIA, 196

A65 Field notes for a few suites of Cu-mineralized rocks in the Kamanjab Batholith, Namibia, 196
A65.1 Suite G, 196
A65.2 Suite H, 196
A65.3 Suite M, 197
A65.4 Suite N, 198
A66 Field notes on the N-S transect through the Oas Farm, Namibia, 199
A67 Field notes from the Lofdal farm, Namibia, 207
A67.1 Cross section through series of ultramafic dikes, Lofdal farm, Namibia, 210
A67.2 Magnetite-cemented, polymictic hydrothermal breccia that makes a diatreme, 211
A68 Partial field notes collected at the Mesopotamie farm, Namibia, 213
A69 Field notes, Ugab River, Namibia, 214
A70 Field notes, Okwa River, Botswana, 217
A71 Field notes Grootfontein Inlier, Namibia, 218
A72 Field notes from Okatjepuiko, Witvlei, Namibia, 219

APPENDIX I OTHER INFORMATION, 223

A73 Persons interviewed for preparation of fieldwork, during fieldwork, and when processing information, 223
A74 Rock names of samples from the Greater Lufilian Arc Granitoid project, 224
A75 Experiment to test quality of chemical laboratory, 229
A76 Heat production capacity of intrusive rocks from the Greater Lufilian Arc at the time of their emplacement, 231

APPENDIX J RAW DATA FOR NEW GEOCHRONOLOGY, 237

A77.1 Raw data obtained for SHRIMP II U-Pb dating at the Australian National University, Canberra, 238
L-030, 238
L-075, 238
L-158, 238
L-160, 239
L-207, 239
L-213, 240
L-638, 240
L-688, 241
A77.2 Raw data and processing for zircon dating using U-Pb laser-ablation ICP-MS technique, 242
L-855, 242
L-868, 242
L-943, 242
L-969, 242
L-993, 243
L-1013, 243
L-1043, 243
A78 **CONCORDIA DIAGRAMS, 244**
A78.1 Sample L-030, 244
A78.2 Sample L-047, 244
A78.3 Sample L-075, 245
A78.4 Sample L-158, 245
A78.5 Sample L-160, 246
A78.6 Sample L-207, 246
A78.7 Sample L-213 Concordia diagram for high U zircons + rims, 247
A78.8 Sample L-213 Concordia diagram for cores and rims, 247
A78.9 Sample L-638 Concordia diagram for all zircons including xenocrysts, 248

APPENDIX J (cont.)

A78.10 Sample L-638 Concordia diagram for main cluster of zircons, 248
A78.11 Sample L-688 Concordia diagram for all zircons, 249
A78.12 Sample L-688 Histogram of all 12 ages in main cluster, 249
A78.13 Sample L-693, 250
A78.14 Sample L-868, 250
A78.15 Sample L-855 Concordia diagram for all zircons, 251
A78.16 Sample L-855 Concordia diagram for main cluster of ages, 251
A78.17 Sample L-943 Concordia diagram for all zircons, 252
A78.18 Sample L-943 Concordia diagram for main cluster of zircons, 252
A78.19 Sample L-969, 253
A78.20 Sample L-993, 253
A78.21 Sample L-1013 first, 254
A78.22 Sample L-1013 second, 254
A78.23 Sample L-1043 concordia diagram for older group of zircons, 255
A78.24 Sample L-1043 concordia diagram for younger group of zircons, 255
A78.25 Sample L-1043 concordia diagram for all zircons 2, 256
A78.26 Sample L-1043 concordia diagram for all zircons 1, 256

APPENDIX K GEOCHRONOLOGICAL CORRELATION DIAGRAMS, 257

A79 Correlation of dated events, Zambian locations, 258
A80 Correlation of dated events, Namibian locations, 259
A81 Correlation of dated events, Greater Lufilian Arc, 260
A82 Correlation of dated events, Greater Lufilian Arc, first portion (3000 to 1400 Ma), 261
A83 Correlation of dated events, Greater Lufilian Arc, second portion (1400 to 0 Ma), 262

APPENDIX C
GEOCHEMISTRY

A1	Chemical analysis of samples from the Greater Lufilian Arc sorted by region, 2
A2	West Lusaka-Kafue Flats, Zambia, 2
A3	Hook Granite Batholith, Zambia, 3
A4	Serenje, Zambia, 4
A5	Kalengwa-Kasempa Area, Zambia, 5
A6	Northwestern Zambia Region Zambia, 6
A7	Kalene Hill, Archean rocks, Paleoproterozoic Group 2, Paleoproterozoic Group 3, Paleoproterozoic Group 4, Other samples, 6
A7.1	Kabompo Dome, 6
A7.2	Solwesi Dome, 7
A7.3	Mwombezhi Dome, 7
A7.4	Sodalite Syenite Quarry, 7
A7.5	Shilenda, 7
A8	Basement to the Copperbelt, Zambia, 7
A8.1	Muliashi Porphyry, 7
A8.2	Chambishi mine area, 8
A8.3	Samba copper prospect, 8
A8.4	Nchanga Granite, 8
A8.5	Nchanga mine, 8
A8.6	Mufulira Granite, 8
A8.7	Other, 8
A9	Kamanjab Batholith, 9
A10	Felsic volcanics, Namibia; Ugab River, Namibia; Okwa River, Botswana; Summas Mountains, Namibia, 11
A11	Oas farm, Namibia, 12
A12	Lofdal farm, Namibia; Mesopotamie farm, Namibia; other alkaline and gabbroic rocks, Khorixas, Namibia, 13
A13	Otjiwarongo environs, Namibia; Grootfontein Inlier, Otavi Mountains, Namibia; Okatjepuiko, Witvlei, Namibia, 14
A14	Spitskoppe complexes, Namibia; Erongo complex, Namibia; Brandberg complex, Namibia; Nigerian ring complexes, 15
A15	Chemical analysis from the Greater Lufilian Arc sorted by number, 16

Table No. A1 A2 CHEMICAL ANALYSIS OF SAMPLES FROM THE GREATER LUFILIAN ARC SORTED BY REGION

West Lusaka-Kafue Flats, Zambia

Sample	SiO2	TiO2	Al2O3	Fe2O3	FeO	MnO	MgO	CaO	Na2O	K2O	P2O5	LOI	Total	Rb	Sr	Y	Zr	Nb	Co	Ni	Cu	Zn	Ga	V	Cr	Ba	U	Th	Sc	Pb	Sm	Nd	Pr	Ce	La	Cs	Hf	Ta	As	Se	Eu	Gd	Tb	Dy	Ho	Er	Tm	Yb	Lu	Li	Be	Ge	Mo	Na+K	Sn
Notch	50.00	*1.00*	*15.50*	*6.00*		*0.150*	*2.00*	*5.00*	*4.90*	*5.50*	*0.30*	2.00		200	*400*	*60*	*360*	*40*	*30*	*16*	*25*	*85*	*26*	*100*	*100*	1300	*20.0*	*37*	*20*	*20*	*50*	*50*	*15*	*175*	*95*	*3*	*10*	*120*	*##*		*4*	*30*	*5*	*20*	*3*	*9*	*35.5*	*7.5*	*1.6*						
L-175	74.72	0.41	12.60	2.96	0.00	0.00	0.41	1.08	2.71	4.60	0.09	0.32	99.90	221	63	45	229	29.0	9	7	31	31	15	28	17	541	<6	25.0	<10		5.913	30.08	47.8	153	19			41.58			0.263							1.300	0.838					7.31	
L-181	49.82	1.08	15.86	11.33	0.00	0.16	6.30	11.28	2.94	0.24	0.06	0.86	99.94	7	157	29	62	8.0	34	30	57	94	16	293	35	<22	<6	<15	35					<12	<12																			3.18	
L-195	61.25	0.38	15.84	8.67	0.00	0.09	0.04	2.35	5.66	5.03	0.09	0.51	99.91	89	130	##	1054	80.0	<6	<6	10	71	40	13	<12	2151	8.0	<15	<10		15.84	44.14	74.3	118	25			145.1			3.888	1.463						7.500	2.200					10.69	
L-199														10	787	42	534	46.6								399	8.8	38.7		5.6	20.0	137	35.6	288	95	0.67	10.8	2.65			5.38	12.6	1.58	9.10	1.61	4.24	0.59	3.76	0.53					0.00	
L-207	75.03	0.07	13.63	0.68	0.00	0.00	0.00	0.11	4.32	6.27	0.01	0.26	100.39	123	182	12	432	6.0	8	6	10	13	0	<12	13	557	0.0	0.0	0				4.58	0	2		19.10			0.225	0.63							0.438				10.59	
L-208	74.23	0.05	13.85	0.87	0.00	0.03	0.00	0.12	4.36	6.13	0.05	0.24	99.93	137	178	12	431	33.0	<6	<6	14	10	25	<12	238	517	9.0	132.0	<10					35	20																	10.49	
L-209	46.78	1.81	16.06	9.69	0.00	0.05	7.51	11.46	2.34	1.91	0.57	0.60	98.79	53	1592	27	111	17.0	36	42	29	52	19	243	50	1437	<6	<15	27					113	61																	4.25	
L-210	66.74	0.43	17.99	3.52	0.00	0.00	0.29	0.69	9.58	0.09	0.14	0.39	99.87	4	275	30	474	36.0	6	7	143	13	22	28	<12	83	7.0	74.0	<10					372	223																	9.67	
L-212	67.27	0.40	15.94	2.89	0.00	0.00	0.15	0.81	4.44	7.04	0.03	0.71	99.69	149	117	51	336	49.0	8	<6	32	17	22	<12	<12	503	8.0	79.0	<10					250	130																	11.48	
L-213	66.68	0.36	17.40	3.03	0.00	0.00	0.08	0.23	6.87	4.87	0.03	0.60	100.17	73	193	27	596	39.0	8	6	18	22	25	22	<12	762	12.0	163.0	<10		4.43	42.11	69.13	137	20		16.48	39.14			0.663							0.738	0.813					11.74	
L-214	66.63	0.39	17.62	1.54	0.00	0.03	0.00	0.24	7.68	3.92	0.06	0.63	98.74	65	167	24	662	77.0	<6	12	20	15	25	19	81	657	7.0	104.0	<10					181	89																	11.60	
L-215	70.53	0.23	16.82	0.65	0.00	0.00	0.00	0.15	10.32	0.19	0.03	0.36	99.30	7	72	15	443	23.0	6	7	6	9	27	<12	<12	71	<6	193.0	<10					18	<12																	10.51	
L-217	73.54	0.39	10.80	3.98	0.00	0.09	3.40	1.35	0.64	2.97	0.15	2.41	99.72	124	48	10	128	10.0	86	17	8	43	13	67	502	805	<6	<15	11		6.750	28.16	53.20	89	30			58.60											0.763				3.61	
L-218	66.30	0.52	15.92	4.64	0.00	0.00	0.49	2.01	4.79	5.43	0.11	0.21	100.42	202	344	46	601	53.0	8	<6	6	30	22	15	16	793	8.0	99.0	<10		16.74	74.63	265	342	135		7.513	65.38			1.450							2.063	1.063					10.22	
L-222	64.17	0.57	13.11	13.72	0.00	0.00	0.80	0.08	0.15	4.74	0.12	2.46	99.94	304	122	69	275	30.0	<6	7	<6	22	29	79	18	499	7.0	20.0	11					220	121																	4.89	
L-223	66.79	0.57	14.12	10.16	0.00	0.00	0.79	0.08	0.17	5.20	0.10	2.49	100.48	312	122	77	270	28.0	<6	<6	<6	27	28	68	18	468	8.0	21.0	<10		2.188	0.575	20.21	250	2			166.0											0.988				5.37	
L-224	62.03	0.58	13.42	15.02	0.00	0.00	0.62	0.07	0.24	5.69	0.11	2.33	100.13	261	103	35	301	28.0	9	8	<6	21	24	76	16	1065	8.0	19.0	<10					120	65																	5.93	
L-416	52.44	0.65	15.34	8.63	0.00	0.15	7.28	12.42	2.55	0.73	0.07	0.20	100.46	6	126	17	41	5.0	34	72	94	84	17	195	217	43	6.0	<15	42					<12	<12																	3.28	
L-458	72.83	0.09	13.43	1.35	0.00	0.02	0.00	0.20	3.52	6.94	0.03	0.37	98.78	277	30	72	45	13.0	<6	<6	9	11	18	<12	13	129	8.0	<15	<10					38	42																	10.46	
L-459	61.30	0.79	13.54	9.09	0.00	0.13	3.38	5.88	3.02	1.16	0.10	0.63	99.02	87	204	22	81	8.0	26	40	111	##	19	181	57	287	<6	<15	23					54	30																	4.18	
L-460	74.38	0.43	11.58	4.11	0.00	0.03	0.62	1.86	3.67	2.33	0.12	0.34	99.47	68	482	13	632	7.0	8	9	19	63	18	22	14	596	<6	20.0	<10					197	102																	6.00	
L-461	71.85	0.20	14.11	1.77	0.00	0.02	0.26	1.01	3.45	5.34	0.06	0.70	98.77	178	241	14	65	10.0	<6	<6	30	36	18	<12	13	1222	<6	15.0	<10					43	21																	8.79	
L-462	72.04	0.34	13.78	2.58	0.00	0.02	0.38	1.21	3.18	5.19	0.04	0.37	99.13	114	630	5	95	11.0	<6	<6	11	32	17	25	<12	3607	<6	16.0	<10					61	25																	8.37	
L-463	48.36	2.43	14.19	14.79	0.00	0.19	7.26	7.68	2.85	1.01	0.40	-0.53	98.63	25	255	38	193	15.0	39	11	16	##	21	133	94	285	<6	<15	30					30	18																	3.86	
L-464	5.46	0.07	0.00	77.49	0.00	0.08	0.50	6.09	0.10	0.52	0.06	3.16	93.53	14	13	16	17	3.0	25	185	184	##	<9	34	<12	142	29.0	<15	37					<12	<12																	0.62	
L-465	14.01	0.58	2.56	64.74	0.00	0.03	0.70	0.17	0.06	0.43	0.12	12.85	96.25	25	76	9	129	17.0	13	85	143	##	11	127	<12	694	24.0	<15	36					<12	<12																	0.49	
L-466	73.93	0.13	12.78	1.65	0.00	0.03	0.08	0.98	4.27	4.50	0.03	0.30	98.68	351	83	31	75	39.0	<6	<6	15	21	24	<12	14	225	<6	23.0	<10					57	27																	8.77	
L-467	70.78	0.25	13.75	2.33	0.00	0.02	0.18	0.87	4.53	5.45	0.08	0.50	98.74	145	1046	29	208	18.0	7	10	12	30	22	16	<12	2676	<6	67.0	<10					224	130																	9.98	
X-90	73.62	0.31	12.90	0.54	1.67	0.05	0.42	1.13	3.37	5.90	0.10	0.44	100.45				370																																					9.27	

Table No. A3 CHEMICAL ANALYSIS OF SAMPLES FROM THE GREATER LUFILIAN ARC SORTED BY REGION

Hook Granite, Zambia

Sample	SiO2	TiO2	Al2O3	Fe2O3	FeO	MnO	MgO	CaO	Na2O	K2O	P2O5	LOI	Total	Rb	Sr	Y	Zr	Nb	Co	Ni	Cu	Zn	Ga	V	Cr	Ba	U	Th	Sc	Pb	Sm	Nd	Pr	Ce	La	Cs	Hf	Ta	As	Se	Eu	Gd	Tb	Dy	Ho	Er	Tm	Yb	Lu	Li	Be	Ge	Mo	Na+K	Sn
Notch	50.00	*1.00*	*15.50*	*6.00*		*0.150*	*2.00*	*5.00*	*4.90*	*5.50*	*0.30*	2.00		200	*400*	*60*	*360*	*40*	*30*	*16*	*25*	*85*	*26*	*100*	*100*	1300	*20*	*37*	*20*	*20*	*50*	*50*	*15*	*175*	*95*	*3*	*10*	*120*	*##*		*4*	*30*	*5*	*20*	*3*	*9*	*35.5*	*7.5*	*1.6*						
L-012	64.19	0.66	17.47	3.45	0.00	0.03	1.12	2.55	4.34	6.14	0.18	0.30	100.43	131	516	33	189	29.2	7	9	7	42	20	46	36	1042	4.3	50.4	<10	3.8	15.4	112	31.5	293	163	1.08	4.73	1.57	293		2.69	9.76	1.21	6.81	1.22	3.22	0.47	3.14	0.48					10.48	
L-012A	64.38	0.61	17.86	3.18	0.00	0.03	1.13	2.40	4.10	6.24	0.15	0.32	100.40	143	536	36	360	32.0	9	10	9	28	21	33	36	940	<6	49.0	<10					312	216																		10.34	
L-079	67.09	0.80	14.65	4.99	0.00	0.07	1.21	2.40	3.35	4.98	0.19	0.83	100.56	165	216	40	332	24.0	14	12	41	45	0	68	40	1291	0.0	0.0	0					0	0																		8.33	
L-237	70.85	0.37	13.24	4.02	0.00	0.00	0.52	1.36	2.51	5.44	0.11	0.40	98.83	151	276	74	194	24.0	8	6	25	16	18	28	<12	815	<6	26.0	<10					273	148																		7.95	
L-238	70.02	0.51	13.56	3.71	0.00	0.00	0.67	1.50	2.89	6.16	0.15	0.74	99.92	156	260	58	240	27.0	7	<6	9	18	18	33	15	747	6.0	24.0	<10					130	67																		9.05	
L-239	70.02	0.51	13.56	3.71	0.00	0.00	0.67	1.50	2.89	6.16	0.15	0.74	99.92	156	260	58	240	27.0	7	<6	9	18	18	33	15	747	6.0	24.0	<10					130	67																		9.05	
L-241	0.00	0.00	0.00	0.00	0.00	0.00	0.00	0.00	0.00	0.00	0.00	0.00	0.00	156	229	55	174	24.1	0	0	0	0	0	0	0	594	0.0	0.0	0	2.4	9.21	45.22	10.98	0	0	1.91	5.17	1.86	0	0	1.64	9.31	1.44	9.41	1.92	5.84	0.87	5.96	0.89					0.00	
L-242	76.03	0.29	10.81	5.91	0.00	0.01	2.03	0.21	0.57	1.96	0.11	1.21	99.14	42	228	33	256	11.0	14	18	8	12	38	87	309	617	7.0	<15	29					148	112																		2.53	
L-248	64.40	0.91	15.35	6.34	0.00	0.00	2.74	3.49	2.97	2.10	0.26	0.53	99.08	126	300	54	205	42.0	15	15	13	28	25	109	39	271	6.0	<15	21					77	42																		5.07	
L-248-L	76.71	0.14	13.26	0.92	0.00	0.00	0.04	0.66	3.71	4.49	0.04	0.32	100.29	121	314	48	206	20.0	9	7	8	16	19	35	25	745	<6	27.0	<10					139	68																		8.20	
L-249	70.32	0.42	14.04	3.50	0.00	0.00	0.75	1.96	3.00	4.50	0.14	0.29	98.93	123	309	49	211	23.0	8	7	8	16	19	45	21	716	<6	20.0	<10		0.700	0.725	4.800	124	0			46.24				1.313						0.350	0.688					7.50	
L-257	73.62	0.26	13.30	1.97	0.00	0.00	0.15	1.23	3.67	5.29	0.05	0.55	100.10	214	117	53	208	25.0	6	<6	<6	13	22	<12	14	321	16.0	74.0	<10		113.8	42.95	114.8	192	66		5.36	26.34			0.663							4.013	1.18					8.96	
L-259	69.45	0.42	15.44	2.77	0.00	0.00	0.29	1.80	3.10	6.11	0.07	0.59	100.05	174	199	72	402	47.0	7	<6	<6	21	20	13	26	911	7.0	21.0	11					113	58																		9.21	
L-259-B	73.83	0.30	12.91	2.80	0.00	0.00	0.17	1.01	3.55	5.35	0.04	0.44	100.42	204	118	##	292	39.0	<6	<6	12	28	20	<12	15	617	10.0	29.0	<10					277	209																		8.90	
L-263	67.90	0.54	13.93	2.49	0.00	0.00	0.71	3.88	3.29	5.55	0.27	0.54	99.13	83	640	51	244	26.0	7	<6	23	15	20	34	16	920	<6	19.0	10		118.9	46.66	91.5	118	32			29.10			1.813							2.863	1.063					8.84	
L-341	63.54	0.75	13.15	4.88	0.00	0.03	1.09	5.99	6.86	0.95	0.32	1.14	98.70	19	703	76	329	29.0	11	9	31	21	21	45	20	72	<6	20.0	11					174	89																		7.81	
L-343	65.60	0.61	13.71	4.43	0.00	0.05	0.83	6.46	5.59	1.11	0.20	0.17	98.76	20	616	##	408	40.0	11	7	12	24	19	44	16	187	<6	35.0	12					162	103																		6.70	
L-344	61.49	1.13	15.69	3.77	0.00	0.07	1.27	6.94	5.64	1.83	0.40	0.98	99.21	47	555	##	485	41.0	10	<6	13	25	27	44	22	577	6.0	24.0	15					209	107																		7.47	
L-345	62.53	0.76	14.29	8.20	0.00	0.05	0.77	1.46	2.52	7.65	0.20	0.40	98.83	210	366	61	494	18.0	7	11	19	27	23	67	24	1440	6.0	<15	<10					174	94																		10.17	
L-346	70.01	0.49	13.71	5.02	0.00	0.05	0.31	0.96	3.40	5.99	0.10	0.64	100.68	195	168	69	469	27.0	12	<6	80	77	20	14	<12	774	11.0	24.0	<10					190	98																		9.39	
L-347	45.32	1.57	12.74	9.07	0.00	0.11	6.14	18.97	3.89	0.45	0.08	0.42	98.76	11	497	14	77	6.0	26	21	197	##	22	127	131	48	9.0	29.0	<10					111	57																		4.34	
L-348	68.82	0.46	13.11	3.52	0.00	0.14	0.29	3.80	4.97	3.37	0.13	0.31	98.92	38	762	56	329	19.0	7	<6	13	20	19	43	17	439	<6	40.0	<10					130	61																		8.34	
L-349	67.98	0.35	13.65	3.38	0.00	0.07	0.35	2.69	4.47	4.97	0.13	0.82	98.86	108	423	55	230	32.0	7	11	24	16	19	21	16	590	<6	23.0	<10					106	50																		9.44	
L-352	70.34	0.51	13.27	4.15	0.00	0.05	0.53	1.63	3.37	4.96	0.10	0.26	99.17	178	166	35	357	20.0	10	11	17	30	19	16	21	861	<6	19.0	<10					212	123																		8.33	
L-353	64.23	0.92	13.89	5.97	0.00	0.04	1.34	3.73	3.62	5.05	0.24	0.49	99.52	120	400	##	404	20.0	10	<6	67	24	21	36	19	606	6.0	20.0	12					141	73																		8.67	
L-354	64.83	0.81	14.83	6.19	0.00	0.07	1.46	2.45	3.15	4.06	0.20	0.95	99.00	138	207	77	435	25.0	11	17	115	78	20	71	22	977	<6	22.0	12					156	82																		7.21	
L-355	72.83	0.18	13.16	2.91	0.00	0.04	0.11	0.78	3.18	5.57	0.11	0.53	99.40	263	46	46	126	19.0	<6	7	20	21	18	79	38	135	8.0	21.0	<10					80	37																		8.75	
L-402	68.46	0.60	13.71	5.64	0.00	0.04	0.43	2.96	4.94	1.14	0.11	0.82	98.85	70	286	##	602	44.0	7	10	12	29	22	25	20	272	6.0	21.0	12					178	107																		6.08	
L-403	64.07	0.68	14.61	7.86	0.00	0.06	1.14	3.13	3.50	4.38	0.16	0.71	100.30	119	277	83	762	25.0	9	9	196	89	25	19	19	1054	8.0	17.0	15					141	80																		7.88	
L-405	52.10	1.22	16.06	10.02	0.00	0.11	5.30	8.98	3.30	1.08	0.15	0.71	99.03	23	882	24	121	14.0	37	72	30	53	17	220	35	226	<6	<15	26					78	37																		4.38	
L-406	46.64	2.48	13.15	14.14	0.00	0.23	6.55	10.17	3.29	0.80	0.26	1.09	98.80	11	282	38	180	17.0	43	73	80	##	18	374	106	118	<6	<15	37					29	18																		4.09	
L-407	60.09	1.12	13.19	6.31	0.00	0.07	1.49	8.27	4.03	3.86	0.30	0.61	99.34	92	396	79	532	28.0	13	8	43	40	19	71	29	689	7.0	26.0	14					188	96																		7.89	
L-408	70.26	0.33	13.59	3.87	0.00	0.05	0.26	1.23	3.49	5.24	0.07	0.43	98.82	241	95	##	348	33.0	7	6	15	34	23	<12	13	483	12.0	32.0	<10					241	121																		8.73	
L-409	69.36	0.41	14.76	3.25	0.00	0.02	0.49	1.13	4.47	5.43	0.10	0.44	99.86	206	151	43	313	32.0	6	<6	10	16	19	25	12	677	13.0	53.0	<10					120	60																		9.90	
L-410	67.74	0.44	12.99	8.55	0.00	0.02	0.88	0.29	0.17	4.34	0.09	3.18	98.69	233	16	25	177	33.0	9	9	489	##	17	51	14	187	7.0	32.0	<10					147	80																		4.51	
L-411	8.09	0.09	0.85	0.57	0.00	0.02	4.72	43.80	0.04	0.35	0.16	41.87	100.56	6	87	4	17	3.0	<6	<6	<6	16	<9	<12	<12	23	<6	<15	45					12	<12																		0.39	
L-433	51.23	2.42	14.76	11.92	0.00	0.16	4.74	8.16	3.82	2.33	0.42	0.59	100.55	71	396	44	261	22.0	28	11	45	99	20	275	62	384	7.0	<15	27					96	52																		6.15	
L-434	69.24	0.53	13.96	4.52	0.00	0.06	0.74	1.98	1.92	4.77	0.13	1.32	99.17	149	247	8	411	7.0	8	9	25	35	16	19	18	869	<6	<15	30					18	<12																		6.69	
L-435	67.58	0.43	15.29	3.91	0.00	0.05	0.36	1.59	3.89	6.45	0.10	0.32	99.97	142	271	34	389	11.0	8	<6	29	34	21	15	13	1227	<6	<15	<10					86	43																		10.34	
L-436	73.93	0.27	12.03	2.68	0.00	0.04	0.17	1.02	4.15	4.81	0.06	0.39	99.55	235	74	45	303	31.0	<6	<6	10	21	21	<12	<12	195	26.0	99.0	<10					223	114																		8.96	
L-437	55.61	1.95	14.33	9.89	0.00	0.14	2.79	5.09	3.77	4.40	0.52	0.58	99.07	113	395	52	404	32.0	21	8	121	##	22	144	21	736	<6	<15	18					111	56																		8.17	
L-438	53.44	1.57	14.02	8.54	0.00	0.13	5.89	7.86	3.34	3.75	0.49	0.76	99.79	171	402	43	390	31.0	27	77	43	71	19	163	250	592	7.0	22.0	22					99	55																		7.09	
L-439	70.07	0.33	12.99	4.06	0.00	0.02	0.22	0.77	4.27	5.46	0.05	0.62	98.86	243	66	90	572	46.0	<6	3	21	16	25	<12	<12	163	19.0	90.0	<10					237	124																		9.73	
L-440	51.34	2.12	14.48	11.82	0.00	0.15	4.77	7.19	3.18	2.19	0.48	0.89	98.61	74	395	39	348	19.0	32	29	27	99	21	244	101	373	<6	<15	29					56	29																		5.37	
L-441	62.98	1.11	14.13	7.49	0.00	0.12	0.99	2.75	3.71	5.30	0.35	0.46	99.39	180	226	74	414	46.0	10	<6	13	88	24	28	<12	893	6.0	19.0	12					187	98																		9.01	
L-442	78.22	0.33	8.81	3.27	0.00	0.03	0.00	0.10	0.23	7.61	0.06	0.34	99.00	227	44	99	349	18.0	<6	<6	16	16	12	27	<12	618	<6	44.0	<10					288	149																		7.84	
L-443	76.23	0.44	9.57	5.13	0.00	0.03	0.10	0.43	0.20	6.79	0.05	0.40	99.37	201	24	64	391	48.0	8	7	12	14	14	28	<12	499	<6	100.0	<10					49	25																		6.99	
L-444	52.77	2.43	15.66	11.98	0.00	0.17	3.98	7.06	3.24	1.98	0.56	0.22	100.05	43	404	41	170	21.0	33	14	27	##	21	245	54	396	6.0	<15	33					67	36																		5.22	
X-43	72.65	0.27	14.34	0.34	1.10	0.04	0.73	1.21	3.07	5.46	0.12	0.55	99.88																																										8.53	
X-44	76.59	0.32	12.60	0.28	2.08	0.04	0.82	0.78	0.87	5.77	0.04	0.49	100.68																																										6.64	
X-45	68.41	0.69	14.46	0.29	4.31	0.08	1.29	2.07	3.47	4.63	0.25	0.92	100.87																																										8.10	
X-46	72.98	0.13	14.41	0.10	1.05	0.04	0.42	1.03	4.45	4.57	0.07	0.79	100.04																																										9.02	
X-47	78.16	0.15	11.55	0.00	0.86	0.02	0.70	0.41	2.45	6.08	0.40	0.18	100.96																																										8.53	
X-48	73.41	0.14	13.97	0.16	1.08	0.05	0.37	1.05	4.41	4.44	0.35	0.59	100.02																																										8.85	

Table No. A3 CHEMICAL ANALYSIS OF SAMPLES FROM THE GREATER LUFILIAN ARC SORTED BY REGION

Hook Granite, Zambia (cont.)

Sample	SiO2	TiO2	Al2O3	Fe2O3	FeO	MnO	MgO	CaO	Na2O	K2O	P2O5	LOI	Total	Rb	Sr	Y	Zr	Nb	Co	Ni	Cu	Zn	Ga	V	Cr	Ba	U	Th	Sc	Pb	Sm	Nd	Pr	Ce	La	Cs	Hf	Ta	As	Se	Eu	Gd	Tb	Dy	Ho	Er	Tm	Yb	Lu	Li	Be	Ge	Mo	Na+K	Sn
Notch	50.00	*1.00*	*15.50*	*6.00*		*0.150*	*2.00*	*5.00*	*4.90*	*5.50*	*0.30*	2.00		200	*400*	*60*	*360*	*40*	*30*	*16*	*25*	*85*	*26*	*100*	*100*	1300	*20*	*37*	*20*	*20*	*50*	*50*	*15*	*175*	*95*	*3*	*10*	*120*	*##*		*4*	*30*	*5*	*20*	*3*	*9*	*35.5*	*7.5*	*1.6*					
X-49	64.17	0.89	20.28	0.26	1.06	0.05	0.19	2.30	6.14	4.57	0.14	0.49	100.54																																												10.71
X-50	62.31	0.11	18.36	1.53	3.07	0.10	0.90	1.00	5.67	6.04	0.07	0.98	100.14																																												11.71
X-51	60.19	0.49	18.14	0.84	3.86	0.14	0.33	2.35	5.31	7.00	0.07	1.55	100.27																																												12.31
X-52	67.17	0.72	14.55	0.48	4.33	0.07	1.20	2.05	3.59	5.30	0.20	0.85	100.51																																												8.89
X-53	71.79	0.23	14.21	0.31	2.26	0.05	0.37	1.06	3.40	5.64	0.12	0.98	100.42																																												9.04
X-54	71.06	0.45	14.42	0.03	1.25	0.05	0.65	4.21	2.70	5.49	0.11	0.57	100.99																																												8.19
X-55	75.50	0.31	12.40	1.50	0.60	0.03	0.40	0.60	3.10	5.60	0.04	0.94	101.02																																												8.70
X-56	67.80	0.71	14.50	0.90	3.60	0.05	1.18	2.90	3.10	4.60	0.21	0.87	100.42																																												7.70
X-57	67.00	0.75	14.20	1.10	4.00	0.07	1.30	2.40	2.80	5.10	0.22	1.34	100.28																																												7.90
X-58	71.10	0.28	14.50	1.20	1.10	0.03	0.29	1.10	3.40	6.30	0.07	0.93	100.30																																												9.70
X-59	69.70	0.52	14.20	1.00	2.40	0.07	0.60	1.70	4.80	5.50	0.14	0.77	101.40																																												10.30
X-60	71.10	0.38	13.60	1.10	2.50	0.06	0.42	1.50	3.50	5.50	0.08	1.27	101.01																																												9.00
X-61	71.74	0.27	14.47	0.32	1.73	0.05	0.42	1.62	3.44	4.65	0.24	0.55	99.50																																												8.09
X-62	61.07	0.80	16.53	1.03	5.61	0.16	0.56	2.97	3.75	6.03	0.14	0.84	99.49																																												9.78
X-63	64.77	0.89	15.33	0.73	4.82	0.08	1.45	2.54	3.83	4.30	0.27	0.87	99.88																																												8.13
X-64	61.68	1.20	14.96	0.77	7.01	0.12	2.29	3.15	3.60	3.30	0.35	1.28	99.71																																												6.90
X-65	74.82	0.11	13.65	0.38	0.65	0.01	0.50	0.98	3.57	5.35	0.03	0.58	100.63																																												8.92
X-66	72.86	0.30	14.37	0.79	2.66	0.04	0.54	0.93	3.98	5.25	0.09	0.72	102.53																																												9.23
X-67	70.30	0.38	13.88	0.60	3.27	0.07	0.45	1.17	2.29	5.90	0.14	0.84	99.29																																												8.19
X-68	70.96	0.28	13.75	1.02	1.58	0.05	0.24	0.91	1.65	7.44	0.07	1.31	99.26																																												9.09
X-69	68.83	0.48	14.51	4.05	0.79	0.03	0.33	0.10	2.79	7.36	0.05	0.00	99.32																																												10.15
X-70	74.17	0.21	12.86	0.00	1.80	0.04	0.33	0.49	1.94	5.91	0.10	0.50	98.35																																												7.85
X-71	70.61	0.33	14.72	1.41	0.86	0.02	0.55	0.54	2.17	7.33	0.18	0.73	99.45																																												9.50
X-72	69.88	0.40	13.71	1.80	2.37	0.07	0.27	0.62	2.92	6.03	0.04	0.55	98.66																																												8.95
X-73	67.24	0.73	14.52	2.90	2.30	0.03	0.95	2.17	4.44	3.53	0.26	0.00	99.07																																												7.97
X-74	58.87	0.46	14.09	2.03	2.44	0.07	2.10	7.49	6.09	3.07	0.17	0.00	96.88																																												9.16
X-75	71.21	0.42	21.42	2.00	1.44	0.03	0.45	0.89	4.10	4.92	0.11	0.81	107.80																																												9.02
P-39	72.16	0.28	12.57	3.40	0.00	0.08	0.12	1.17	4.67	5.57	0.11	0.17	100.13	404	43	##	309	59.0	56	4	<3	12	29	<4	5	182	19.0	71.0	4	11.0	21.40	#####	33.00	290	145	2.00	10.00	2.50	<1	12	0.80	19.40	3.10	18.30	3.60	9.20	34.4	7.30	1.10					10.24
P-46	71.17	0.38	12.62	4.35	0.00	0.12	0.20	0.81	3.59	6.89	0.07	0.16	100.20	398	65	89	257	53.0	48	4	<3	45	27	<4	9	387	10.0	46.0	1	11.0	16.90	93.10	25.70	217	110	3.00	11.00	2.80	26	28	1.40	15.50	2.40	14.00	2.80	7.90	4.90	7.40	1.10					10.48
P-50	71.53	0.25	12.60	3.26	0.00	0.10	0.30	1.66	4.55	4.88	0.21	0.14	99.34	376	66	##	312	107.0	40	16	<3	30	27	<4	4	314	62.0	256.0	3	23.0	54.30	334.8	100.2	899	505	4.00	9.00	3.20	1	8	1.20	39.6	6.00	32.2	6.20	16.30	5.70	11.40	1.60					9.43
P-53	73.18	0.24	13.04	2.62	0.00	0.07	0.22	0.95	3.78	5.92	0.12	0.09	100.14	421	59	54	179	48.0	71	19	<3	<1	24	<4	24	209	21.0	43.0	2	11.0	5.60	25.70	8.00	78	44	6.00	6.00	2.50	6	6	0.80	6.00	1.10	6.70	1.50	4.70	31.80	4.80	0.80					9.70
P-57	62.19	0.36	13.11	2.44	0.00	0.05	0.26	0.86	15.42	5.52	0.06	0.21	100.27	225	45	##	404	48.0	63	21	<3	1	24	<4	<4	286	10.0	51.0	6	5.0	79.00	499.4	133.6	735	579	2.00	11.00	2.60	<1	5	7.60	80.5	10.00	55.6	11.10	28.9	35.9	21.40	3.30					20.94
P-58	67.76	0.79	13.46	6.83	0.00	0.17	1.40	2.21	3.78	4.27	0.18	0.25	100.85	210	189	66	223	30.0	77	4	21	72	26	45	12	680	4.0	24.0	8	12.0	10.30	50.50	13.10	107	53	5.00	6.00	2.10	1	30	2.10	9.90	1.50	8.50	1.70	4.70	33.4	3.90	0.60					8.05
P-40i	76.05	0.26	11.74	2.15	0.00	0.08	0.13	1.54	4.06	4.05	0.07	0.07	100.13	150	92	48	335	27.0	61	12	<3	26	26	<4	9	309	6.0	20.0	2	8.0	9.30	45.60	11.90	98	51	1.00	11.00	1.30	2	8	1.50	8.80	1.40	8.30	1.70	5.00	35.3	5.00	0.80					8.11
P-40ii	68.86	0.55	13.67	4.56	0.00	0.12	0.33	1.82	4.52	5.77	0.12	0.19	100.32	195	110	77	391	52.0	53	14	<3	53	27	11	19	503	<2	15.0	5	10.0	15.90	78.80	20.00	157	71	1.00	11.00	3.30	<1	22	2.00	14.40	2.40	14.20	2.80	7.50	34.9	6.40	1.00					10.29

Table No. A4 Serenje, Zambia

Sample	SiO2	TiO2	Al2O3	Fe2O3	FeO	MnO	MgO	CaO	Na2O	K2O	P2O5	LOI	Total	Rb	Sr	Y	Zr	Nb	Co	Ni	Cu	Zn	Ga	V	Cr	Ba	U	Th	Sc	Pb	Sm	Nd	Pr	Ce	La	Cs	Hf	Ta	As	Se	Eu	Gd	Tb	Dy	Ho	Er	Tm	Yb	Lu	Li	Be	Ge	Mo	Na+K	Sn
Notch	50.00	*1.00*	*15.50*	*6.00*		*0.150*	*2.00*	*5.00*	*4.90*	*5.50*	*0.30*	2.00		200	*400*	*60*	*360*	*40*	*30*	*16*	*25*	*85*	*26*	*100*	*100*	1300	*20*	*37*	*20*	*20*	*50*	*50*	*15*	*175*	*95*	*3*	*10*	*120*	*##*		*4*	*30*	*5*	*20*	*3*	*9*	*35.5*	*7.5*	*1.6*					
P-32	73.45	0.26	12.59	1.67	0.00	0.06	0.10	0.94	4.34	6.61	0.08	0.14	100.10	334	72	23	57	12.0	58	10	<3	14	17	<4	20	862	<2	7.0	3	48.0	3.60	15.80	4.30	36	18	3.00	4.00	0.90	<1	4	1.30	3.80	0.60	3.50	0.60	1.40	36.4	1.00	0.10					10.95
P-33	68.30	0.54	14.41	3.20	0.00	0.10	0.73	1.53	5.65	6.09	0.19	0.20	100.74	230	222	81	157	19.0	52	6	<3	45	21	31	13	2028	<2	16.0	7	21.0	16.60	78.50	19.40	121	57	2.00	4.00	2.40	<1	13	2.90	16.70	2.30	12.80	2.60	7.00	33.10	5.60	0.80					11.74
P-35	74.32	0.25	13.99	1.48	0.00	0.07	0.33	1.12	6.19	2.54	0.07	0.18	100.36	83	188	2	99	6.0	41	2	<3	35	19	11	21	558	2.00	8.0	1	20.0	1.60	9.40	2.70	26	15	1.00	3.00	0.40	<1	5	0.50	1.20	0.10	0.60	0.10	0.20	33.4	0.20	0.00					8.73
X-15	67.63	0.59	14.37	2.02	1.66	0.07	1.15	1.90	4.59	5.21	0.26	0.86	100.31				592																																												9.80

Table No. A5 CHEMICAL ANALYSIS OF SAMPLES FROM THE GREATER LUFILIAN ARC SORTED BY REGION

Kalengwa-Kasempa Area, Zambia

Sample	SiO2	TiO2	Al2O3	Fe2O3	FeO	MnO	MgO	CaO	Na2O	K2O	P2O5	LOI	Total	Rb	Sr	Y	Zr	Nb	Co	Ni	Cu	Zn	Ga	V	Cr	Ba	U	Th	Sc	Pb	Sm	Nd	Pr	Ce	La	Cs	Hf	Ta	As	Se	Eu	Gd	Tb	Dy	Ho	Er	Tm	Yb	Lu	Li	Be	Ge	Mo	Na+K	Sn
Notch	50.00	*1.00*	*15.50*	*6.00*		*0.150*	*2.00*	*5.00*	*4.90*	*5.50*	*0.30*	2.00		200	*400*	*60*	*360*	*40*	*30*	*16*	*25*	*85*	*26*	*100*	*100*	1300	*20*	*37*	*20*	*20*	*50*	*50*	*15*	*175*	*95*	*3*	*10*	*120*	*##*		*4*	*30*	*5*	*20*	*3*	*9*	*35.5*	*7.5*	*1.6*						
L-139	75.60	0.09	11.88	1.50	0.00	0.03	0.62	0.14	1.61	7.87	0.01	0.79	100.14	399	17	40	75	41.0	10	7	55	34	23	14	47	769	<6	26.0	<10					42	12																					9.48
L-313	54.29	1.67	13.47	10.37	0.00	0.06	5.07	4.92	4.55	0.80	0.67	4.40	100.27	21	164	89	445	40.0	14	12	42	39	23	102	21	104	7.0	<15	36					139	75																					5.35
L-314	43.72	7.81	12.73	11.28	0.00	0.08	6.68	7.01	3.38	0.36	0.64	6.73	100.42	14	77	56	25	36.0	20	19	28	49	18	438	50	60	<6	<15	55					27	16																					3.74
L-318	47.28	3.04	15.31	7.93	0.00	0.04	6.86	13.85	4.18	0.56	0.38	0.96	100.39	9	154	37	163	27.0	23	53	9	22	19	258	99	20	<6	<15	30					68	33																					4.74
L-321	71.94	0.71	9.67	11.04	0.00	0.03	3.43	0.30	0.68	0.05	0.12	2.40	100.37	6	81	59	242	18.0	96	18	16	30	15	157	95	65	<6	<15	12					102	61																					0.73
L-322	70.45	0.74	13.65	5.38	0.00	0.02	0.48	0.08	0.13	7.57	0.08	1.74	100.32	168	30	37	264	30.0	12	7	13	35	21	49	33	498	<6	27.0	<10					171	74																					7.70
L-323	67.04	0.81	14.15	7.57	0.00	0.02	0.52	0.19	0.17	8.21	0.17	1.61	100.46	173	29	37	302	35.0	26	9	17	28	20	58	32	525	<6	30.0	<10					153	71																					8.38
L-324	62.05	0.97	14.50	7.90	0.00	0.06	1.43	1.71	3.85	6.29	0.29	1.25	100.30	112	230	57	362	35.0	20	16	62	##	21	96	27	1004	13.0	48.0	11					190	74																					10.14
L-325	60.42	1.15	16.98	11.07	0.00	0.02	0.91	0.06	0.08	6.75	0.29	2.82	100.55	227	37	##	372	31.0	28	13	55	48	26	114	<12	508	6.0	27.0	<10					1460	819																					6.83
P-13	65.76	0.82	14.67	5.87	0.00	0.10	1.00	2.40	5.77	3.89	0.24	0.21	100.52	90	301	45	157	30.0	70	11	<3	4	23	55	22	787	10.0	56.0	7	4.0	9.90	58.80	16.50	153	80	<1	9.00	2.70	1	35	2.10	9.50	1.30	8.00	1.70	4.50	34.9	4.60	0.80					9.66
P-17	64.11	0.97	14.29	7.35	0.00	0.08	0.80	2.43	3.95	5.62	0.26	0.18	99.86	107	372	54	327	32.0	84	16	63	23	24	103	11	782	11.0	48.0	10	5.0	11.90	64.10	17.30	136	47	1.00	8.00	2.40	3	88	2.40	11.70	1.50	9.00	1.80	5.10	35.7	5.00	0.80					9.57
P-25	51.44	2.40	20.38	8.73	0.00	0.71	3.91	5.28	6.42	1.71	0.38	0.12	100.72	55	348	24	107	14.0	33	6	40	13	24	98	90	120	<2	2.0	20	4.0	4.00	15.10	3.20	22	9	1.00	2.00	1.30	12	107	1.70	4.50	0.70	4.20	0.90	2.30	33.6	2.10	0.30					8.13
P-26	76.20	0.13	11.58	0.93	0.00	0.05	<.1	0.25	10.51	0.03	0.03	0.08	99.71	7	15	##	705	243.0	39	4	<3	<1	68	<4	24	22	6.0	76.0	1	5.0	6.90	15.00	3.20	24	8	<1	31.00	4.80	1	7	0.70	11.80	3.30	27.5	6.70	21.30	35.7	23.00	3.40					10.54
X-76	55.35	1.48	14.63	10.86	0.00	0.10	4.43	2.43	0.91	7.34	0.50	1.65	99.69	209	199	56	591	28.0	13	11	295	50		139	<9	1379																																8.25
X-77	61.50	1.10	15.15	7.30	0.00	0.11	1.58	2.81	4.39	5.07	0.34	1.21	100.59	182	313	48	339	34.0	15	<9	7	47		92	11	1189																																9.46
X-78	51.81	3.13	15.06	11.46	0.00	0.06	7.53	1.00	3.02	4.48	0.33	2.67	100.54	137	109	32	290	46.0	25	102	20	##		415	117	118																																7.50
X-79	48.31	4.07	11.38	9.92	0.00	0.21	9.92	5.90	2.58	1.14	0.57	6.34	100.34	18	234	32	358	44.0	47	70	35	##		458	74	75																																3.72
X-80	45.03	3.27	13.53	16.29	0.00	0.09	6.04	5.05	5.14	3.32	0.53	2.13	100.41	97	112	48	325	55.0	24	81	12	23		327	142	141																																8.46
X-81	46.37	3.96	13.46	15.27	0.00	0.05	6.20	4.88	4.91	2.96	0.54	1.92	100.52	103	94	55	302	48.0	17	88	7	22		324	135	148																																7.87
X-82	48.60	1.56	13.71	18.47	0.00	0.08	2.02	5.07	7.38	1.05	0.81	1.52	100.26	32	122	61	567	84.0	<9	10	777	47		58	<9	233																																8.43
X-83	46.07	2.56	14.20	17.60	0.00	0.15	5.97	5.84	3.60	3.20	0.32	0.85	100.37	88	105	27	177	32.0	17	44	102	44		325	79	384																																6.80
X-84	46.07	3.95	12.30	12.67	0.00	0.06	3.44	8.56	5.49	0.87	0.91	6.14	100.47	27	106	59	444	89.0	11	11	26	59		138	<9	152																																6.36
X-85	47.35	2.56	14.08	13.25	0.00	0.14	7.29	8.22	4.21	0.61	0.32	2.54	100.58	21	287	26	173	37.0	36	69	11	##		318	36	127																																4.82
X-86	45.88	3.96	12.72	16.75	0.00	0.25	5.61	7.19	3.78	1.46	0.31	2.23	100.14	37	319	33	201	40.0	14	36	124	##		522	<9	303																																5.24
X-87	46.09	2.86	13.80	14.33	0.00	0.23	6.98	7.07	4.90	0.32	0.41	3.05	100.06	13	344	31	208	42.0	18	50	9	##		315	23	119																																5.22
X-88	45.24	2.00	14.37	11.55	0.00	0.11	10.97	4.11	2.72	5.24	0.20	3.85	100.37	147	69	25	131	21.0	35	201	<2	##		326	515	112																																7.96
X-89	46.20	3.57	8.68	14.36	0.00	0.18	11.42	6.07	4.30	2.70	0.67	1.85	100.01	56	337	36	223	53.0	37	30	7	##		474	9	155																																7.00

Table No. A6 CHEMICAL ANALYSIS OF SAMPLES FROM THE GREATER LUFILIAN ARC SORTED BY REGION

Northwestern Zambia Region, Zambia

Table No. A7 Kalene Hill

Archean rocks

Sample	SiO2	TiO2	Al2O3	Fe2O3	FeO	MnO	MgO	CaO	Na2O	K2O	P2O5	LOI	Total	Rb	Sr	Y	Zr	Nb	Co	Ni	Cu	Zn	Ga	V	Cr	Ba	U	Th	Sc	Pb	Sm	Nd	Pr	Ce	La	Cs	Hf	Ta	As	Se	Eu	Gd	Tb	Dy	Ho	Er	Tm	Yb	Lu	Li	Be	Ge	Mo	Na+K	Sn
Notch	50.00	*1.00*	*15.50*	*6.00*		*0.150*	*2.00*	*5.00*	*4.90*	*5.50*	*0.30*	2.00		200	*400*	*60*	*360*	*40*	*30*	*16*	*25*	*85*	*26*	*100*	*100*	1300	*20*	*37*	*20*	*20*	*50*	*50*	*15*	*175*	*95*	*3*	*10*	*120*	*##*		*4*	*30*	*5*	*20*	*3*	*9*	*35.5*	*7.5*	*1.6*					
L-372	54.14	0.84	17.15	9.33	0.00	0.12	3.24	7.00	4.31	2.25	0.28	1.85	100.51	86	764	11	193	8.0	20	9	57	##	21	23	18	423	<6	<15	24					135	71																				6.56
L-373	72.41	0.25	14.10	2.22	0.00	0.03	0.41	1.36	3.49	4.20	0.05	0.93	99.45	114	353	31	147	8.0	6	7	17	28	14	198	12	1215	<6	17.0	<10		105.3	14.70	34.69	90	10		3.05	21.31			0.200								0.600					7.69
L-374	70.46	0.20	14.58	2.28	0.00	0.04	0.31	1.75	5.02	3.92	0.05	0.77	99.38	97	473	10	105	6.0	<6	<6	9	33	17	17	14	1054	<6	<15	<10					49	23																		8.94
L-375	69.92	0.45	12.64	4.64	0.00	0.07	0.33	1.04	3.27	5.81	0.13	0.77	99.07	140	197	47	365	30.0	7	11	26	55	18	22	19	1228	<6	21.0	<10					296	145																		9.08
L-376	59.71	0.51	17.93	5.54	0.00	0.09	1.10	2.05	6.07	4.94	0.12	0.83	98.89	74	419	29	280	27.0	11	<6	18	58	20	67	<12	1036	<6	<15	<10					174	95																		11.01
L-380	70.37	0.39	13.41	3.59	0.00	0.05	0.27	0.92	3.65	5.94	0.09	0.69	99.37	177	135	57	365	28.0	7	10	116	83	18	17	13	1129	<6	18.0	<10		14.90	65.63	187.9	241	95		0.69	44.41			1.500	2.85							2.488	1.13				9.59

Paleoproterozoic Group 2

Sample	SiO2	TiO2	Al2O3	Fe2O3	FeO	MnO	MgO	CaO	Na2O	K2O	P2O5	LOI	Total	Rb	Sr	Y	Zr	Nb	Co	Ni	Cu	Zn	Ga	V	Cr	Ba	U	Th	Sc	Pb	Sm	Nd	Pr	Ce	La	Cs	Hf	Ta	As	Se	Eu	Gd	Tb	Dy	Ho	Er	Tm	Yb	Lu	Li	Be	Ge	Mo	Na+K	Sn
Notch	50.00	*1.00*	*15.50*	*6.00*		*0.150*	*2.00*	*5.00*	*4.90*	*5.50*	*0.30*	2.00		200	*400*	*60*	*360*	*40*	*30*	*16*	*25*	*85*	*26*	*100*	*100*	1300	*20*	*37*	*20*	*20*	*50*	*50*	*15*	*175*	*95*	*3*	*10*	*120*	*##*		*4*	*30*	*5*	*20*	*3*	*9*	*35.5*	*7.5*	*1.6*					
L-020	74.44	0.22	12.70	2.48	0.00	0.05	0.28	0.58	3.03	5.85	0.02	0.75	100.40	226	91	53	228	19.0	<6	<6	9	64	18	<12	47	553	10.0	62.0	<10		11.13	88.15	144.8	286	75			73.2			3.33								2.68	1.28				8.88
L-025	70.60	0.40	13.80	3.70	0.00	0.05	0.73	1.82	3.19	4.80	0.08	0.96	100.13	91	370	11	108	10.0	6	8	9	71	17	38	42	1390	<6	<15	<10		4.163	31.91	47.41	85	20			24.6			0.750		0.900						0.563	0.83				7.99
L-026	71.92	0.37	13.46	3.29	0.00	0.04	0.67	1.98	3.23	4.51	0.08	0.82	100.37	85	384	12	392	14.0	6	7	8	55	16	38	42	1367	<6	<15	<10					97	41																		7.74
L-360	68.89	0.31	14.44	3.71	0.00	0.04	0.60	1.23	3.18	6.02	0.07	0.91	99.40	100	369	67	134	15.0	7	6	9	46	16	40	20	2144	<6	<15	<10					114	57																		9.20
L-364	74.42	0.19	11.94	2.26	0.00	0.02	0.40	0.26	3.54	5.07	0.04	0.68	98.82	236	34	42	207	10.0	<6	9	9	23	20	59	23	198	8.0	44.0	<10					179	88																		8.61
L-365	72.12	0.48	12.08	4.21	0.00	0.04	1.25	0.45	2.64	4.87	0.12	1.33	99.59	146	81	75	353	24.0	8	7	24	38	19	<12	15	881	<6	26.0	<10					212	114																		7.51
L-366	67.02	0.66	13.23	5.79	0.00	0.09	0.90	1.76	4.05	4.28	0.18	0.92	98.88	142	188	54	448	19.0	7	<6	13	86	20	21	12	1082	<6	<15	11		10.44	139.3	247.0	347	139			88.13			6.08	42.5							13.2	2.600				8.33
L-368	67.04	0.71	14.00	4.96	0.00	0.05	1.32	0.98	3.41	4.64	0.17	1.39	98.67	112	156	18	565	10.0	10	8	13	61	18	38	15	1652	<6	<15	<10					189	101																		8.05
L-369	71.39	0.21	13.38	1.89	0.00	0.03	0.49	1.80	4.10	3.83	0.04	1.74	98.90	78	254	51	135	25.0	<6	6	119	##	16	53	20	789	<6	<15	<10		114.3	19.38	57.14	86	27			23.1			0.600	1.363								0.688				7.93
L-370	74.09	0.20	12.02	2.58	0.00	0.03	0.26	0.95	4.32	4.07	0.04	0.88	99.44	279	61	7	195	6.0	<6	10	10	32	21	16	<12	264	9.0	52.0	<10					145	73																		8.39
L-371	70.77	0.25	14.56	1.78	0.00	0.03	0.40	1.37	4.85	4.06	0.08	1.04	99.19	104	650	59	127	23.0	<6	10	10	38	18	<12	15	1474	<6	<15	<10					110	52																		8.91
L-377	69.88	0.26	12.62	3.07	0.00	0.04	0.28	1.27	5.06	5.45	0.05	1.01	98.99	255	69	91	174	17.0	<6	9	167	##	19	12	19	365	8.0	45.0	<10					135	71																		10.51
L-378	73.20	0.22	12.15	3.08	0.00	0.04	0.23	0.84	3.95	4.18	0.05	0.84	98.78	216	69	79	255	19.0	<6	10	163	98	19	<12	15	371	6.0	33.0	<10					267	135																		8.13
L-379	72.89	0.21	12.77	2.54	0.00	0.03	0.45	0.72	6.12	2.92	0.07	0.62	99.34	139	54	59	84	27.0	<6	14	17	15	25	<12	20	133	10.0	<15	<10					39	18																		9.04

Paleoproterozoic Group 3

Sample	SiO2	TiO2	Al2O3	Fe2O3	FeO	MnO	MgO	CaO	Na2O	K2O	P2O5	LOI	Total	Rb	Sr	Y	Zr	Nb	Co	Ni	Cu	Zn	Ga	V	Cr	Ba	U	Th	Sc	Pb	Sm	Nd	Pr	Ce	La	Cs	Hf	Ta	As	Se	Eu	Gd	Tb	Dy	Ho	Er	Tm	Yb	Lu	Li	Be	Ge	Mo	Na+K	Sn
Notch	50.00	*1.00*	*15.50*	*6.00*		*0.150*	*2.00*	*5.00*	*4.90*	*5.50*	*0.30*	2.00		200	*400*	*60*	*360*	*40*	*30*	*16*	*25*	*85*	*26*	*100*	*100*	1300	*20*	*37*	*20*	*20*	*50*	*50*	*15*	*175*	*95*	*3*	*10*	*120*	*##*		*4*	*30*	*5*	*20*	*3*	*9*	*35.5*	*7.5*	*1.6*					
L-023	67.01	0.56	14.95	5.02	0.00	0.07	1.83	2.74	3.71	3.60	0.19	0.80	100.48	78	376	24	133	13.0	10	6	<6	44	16	80	219	1283	<6	<15	12		6.93	49.95	76.63	127	44			61.23			0.738		1.43						1.300	1.13				7.31
L-027	67.24	0.53	15.50	4.74	0.00	0.09	1.38	4.31	3.75	1.72	0.19	1.02	100.47	49	619	21	123	13.0	7	<6	<6	49	18	68	161	573	<6	<15	12					107	58																		5.47
L-363	65.30	0.64	15.16	5.30	0.00	0.09	1.23	3.11	3.95	3.37	0.16	1.49	99.80	119	398	31	202	9.0	11	6	18	69	20	73	20	1054	<6	<15	<10					82	40																		7.32

Paleoproterozoic Group 4

Sample	SiO2	TiO2	Al2O3	Fe2O3	FeO	MnO	MgO	CaO	Na2O	K2O	P2O5	LOI	Total	Rb	Sr	Y	Zr	Nb	Co	Ni	Cu	Zn	Ga	V	Cr	Ba	U	Th	Sc	Pb	Sm	Nd	Pr	Ce	La	Cs	Hf	Ta	As	Se	Eu	Gd	Tb	Dy	Ho	Er	Tm	Yb	Lu	Li	Be	Ge	Mo	Na+K	Sn
Notch	50.00	*1.00*	*15.50*	*6.00*		*0.150*	*2.00*	*5.00*	*4.90*	*5.50*	*0.30*	2.00		200	*400*	*60*	*360*	*40*	*30*	*16*	*25*	*85*	*26*	*100*	*100*	1300	*20*	*37*	*20*	*20*	*50*	*50*	*15*	*175*	*95*	*3*	*10*	*120*	*##*		*4*	*30*	*5*	*20*	*3*	*9*	*35.5*	*7.5*	*1.6*					
L-357	61.26	0.49	17.43	5.33	0.00	0.07	1.08	2.85	4.92	3.59	0.22	1.77	99.01	69	568	67	298	29.0	10	9	36	70	21	<12	12	1645	<6	<15	<10					111	55																		8.51
L-358	63.11	0.65	15.74	6.29	0.00	0.07	1.04	3.80	4.03	2.31	0.17	1.51	98.72	80	492	29	233	13.0	12	10	479	##	22	58	16	950	<6	<15	14		9.988	28.21	68.8	106	32			98.13			0.188								0.563	1.063				6.34
L-359	66.92	0.41	14.63	4.21	0.00	0.06	0.79	2.31	3.91	4.84	0.12	1.07	99.27	120	359	28	192	13.0	8	8	11	54	22	64	26	1134	<6	<15	10					149	76																		8.75
L-361	63.38	0.74	15.35	6.08	0.00	0.06	1.57	3.80	4.38	2.06	0.22	1.49	99.13	118	544	17	246	8.0	12	15	20	78	21	36	<12	844	<6	<15	12					162	84																		6.44
L-362	64.93	0.66	14.31	5.80	0.00	0.07	1.39	3.79	3.72	2.15	0.17	1.66	98.65	77	452	35	221	9.0	9	8	17	93	19	79	22	1523	<6	<15	10					113	61																		5.87
L-367	72.13	0.48	11.76	4.45	0.00	0.06	1.30	3.17	1.69	2.41	0.13	1.70	99.28	59	232	##	162	22.0	10	<6	7	61	15	29	14	1518	<6	<15	<10					80	42																		4.10

Other Samples

Sample	SiO2	TiO2	Al2O3	Fe2O3	FeO	MnO	MgO	CaO	Na2O	K2O	P2O5	LOI	Total	Rb	Sr	Y	Zr	Nb	Co	Ni	Cu	Zn	Ga	V	Cr	Ba	U	Th	Sc	Pb	Sm	Nd	Pr	Ce	La	Cs	Hf	Ta	As	Se	Eu	Gd	Tb	Dy	Ho	Er	Tm	Yb	Lu	Li	Be	Ge	Mo	Na+K	Sn
L-024	48.01	2.10	12.37	18.91	0.00	0.28	4.93	8.74	1.70	0.43	0.17	1.16	98.80	16	78	51	140	11.0	57	66	236	##	22	470	79	108	6.00	<15	43		13.59	38.8	39.5	25	19			391.4					3.100						2.250	2.088				2.13

Table No. A7.1 Kabompo Dome

Sample	SiO2	TiO2	Al2O3	Fe2O3	FeO	MnO	MgO	CaO	Na2O	K2O	P2O5	LOI	Total	Rb	Sr	Y	Zr	Nb	Co	Ni	Cu	Zn	Ga	V	Cr	Ba	U	Th	Sc	Pb	Sm	Nd	Pr	Ce	La	Cs	Hf	Ta	As	Se	Eu	Gd	Tb	Dy	Ho	Er	Tm	Yb	Lu	Li	Be	Ge	Mo	Na+K	Sn
Notch	50.00	*1.00*	*15.50*	*6.00*		*0.150*	*2.00*	*5.00*	*4.90*	*5.50*	*0.30*	2.00		200	*400*	*60*	*360*	*40*	*30*	*16*	*25*	*85*	*26*	*100*	*100*	1300	*20*	*37*	*20*	*20*	*50*	*50*	*15*	*175*	*95*	*3*	*10*	*120*	*##*		*4*	*30*	*5*	*20*	*3*	*9*	*35.5*	*7.5*	*1.6*					
L-028	60.53	0.60	14.99	6.80	0.00	0.09	4.08	3.69	3.88	3.07	0.26	1.58	99.57	124	581	20	155	16.0	26	52	79	45	16	79	89	532	<6	17.0	17		5.88	43.06	63.88	109	32			95.3					2.93						0.650	1.03				6.95
L-029	63.66	0.66	17.38	5.28	0.00	0.05	2.34	3.70	3.95	2.50	0.26	0.70	100.48	88	542	12	147	11.0	20	23	26	49	18	87	51	574	<6	<15	11					89	45																		6.45
L-030	74.74	0.10	13.50	1.47	0.00	0.04	0.09	0.45	2.16	5.91	0.00	1.92	100.38	262	67	15	128	16.2	<6	7	22	34	16	13	15	391	16.0	40.0	<10	35.7	2.87	14.89	4.15	76	26	2.70	4.00	1.24	0	0	0.39	2.41	0.41	2.81	0.59	1.87	0.30	2.17	0.34				8.07
L-047	66.09	0.46	14.68	5.40	0.00	0.08	0.20	2.42	4.99	4.75	0.08	0.54	99.70	110	83	##	634	105.0	<6	<6	<6	47	22	12	<12	1015	6.0	<15	10			127.3	186.3	308	164			68.50			6.438	29.4	7.750						19.71	3.538				9.74

Table No. CHEMICAL ANALYSIS OF SAMPLES FROM THE GREATER LUFILIAN ARC SORTED BY REGION
Northwestern Zambia Region, Zambia (cont.)

Table No. A7.2 Solwesi Dome

Sample	SiO2	TiO2	Al2O3	Fe2O3	FeO	MnO	MgO	CaO	Na2O	K2O	P2O5	LOI	Total	Rb	Sr	Y	Zr	Nb	Co	Ni	Cu	Zn	Ga	V	Cr	Ba	U	Th	Sc	Pb	Sm	Nd	Pr	Ce	La	Cs	Hf	Ta	As	Se	Eu	Gd	Tb	Dy	Ho	Er	Tm	Yb	Lu	Li	Be	Ge	Mo	Na+K	Sn
Notch	50.00	*1.00*	*15.50*	*6.00*		*0.150*	*2.00*	*5.00*	*4.90*	*5.50*	*0.30*	2.00		200	*400*	*60*	*360*	*40*	*30*	*16*	*25*	*85*	*26*	*100*	*100*	1300	*20*	*37*	*20*	*20*	*50*	*50*	*15*	*175*	*95*	*3*	*10*	*120*	*##*		*4*	*30*	*5*	*20*	*3*	*9*	*35.5*	*7.5*	*1.6*					
L-049	47.30	2.03	15.47	13.49	0.00	0.25	5.41	10.51	3.04	0.93	0.22	0.92	99.58	13	346	30	109	17.0	34	46	143	##	19	296	85	127	<6	<15	31					23	<12																						3.97
L-050	46.86	2.06	15.40	13.35	0.00	0.21	5.20	10.46	3.73	0.89	0.27	0.52	98.95	11	321	31	114	16.0	46	49	91	70	18	321	171	93	<6	<15	34					30	<12																						4.62
L-060a	45.83	4.36	11.86	17.84	0.00	0.26	6.24	9.49	2.29	1.12	0.43	0.38	100.11	149	64	19	128	9.5	31	39	20	##		396	38	477	4.9	46.5	0	20.4	3.67	27.0	9.06	113	61	0.87	4.08	1.16			0.57	2.65	0.44	3.02	0.66	2.15	0.36	2.73	0.42					3.41
L-060b	76.30	0.15	11.89	1.79	0.00	0.04	0.14	0.53	3.65	5.74	0.04	0.28	100.55	154	64	23	141	13.0	<6	<6	14	25	22	<12	54	481	<6	<15	35					37	20																						9.39
L-060c	45.43	4.31	11.83	17.86	0.00	0.28	6.23	9.37	2.11	1.09	0.45	0.42	99.57	24	330	38	165	27.0	37	39	29	##		387	33	118																															3.20
L-420	71.91	0.31	13.61	2.62	0.00	0.02	0.48	0.67	4.95	2.98	0.06	1.08	98.69	187	93	38	178	28.0	8	10	31	26	18	20	20	532	13.0	37.0	<10					165	103																						7.93
L-421	69.53	0.52	14.84	3.30	0.00	0.03	0.79	1.40	2.52	6.69	0.24	0.74	100.60	278	240	17	303	18.0	7	<6	34	24	18	42	19	1428	<6	57.0	<10					229	101																						9.21
East of Solwesi Dome																																																								
L-063	46.39	0.84	12.95	3.10	0.00	0.09	5.95	9.71	6.97	0.15	0.12	14.12	100.39	4	51	19	192	7.0	<6	18	7	22	21	86	36	<20	<6	<15	23					25	16																						7.12
L-064	47.31	0.82	12.99	3.23	0.00	0.10	5.76	9.38	6.85	0.05	0.12	13.87	100.48	4	51	19	175	7.0	<6	18	8	28	20	92	36	<20	<6	<15	24					16	<12																						6.90
L-065	39.63	0.57	9.98	4.16	0.00	0.11	7.62	13.40	4.80	0.12	0.07	19.80	100.26	4	125	24	108	8.0	<6	20	8	29	12	102	45	<20	<6	<15	30		5.65	1.725	18.83	15	10			71.00																			0.988	0.763			4.92

Table No. A7.3 Mwombezhi Dome

Sodalite Syenite Quarry

Sample	SiO2	TiO2	Al2O3	Fe2O3	FeO	MnO	MgO	CaO	Na2O	K2O	P2O5	LOI	Total	Rb	Sr	Y	Zr	Nb	Co	Ni	Cu	Zn	Ga	V	Cr	Ba	U	Th	Sc	Pb	Sm	Nd	Pr	Ce	La	Cs	Hf	Ta	As	Se	Eu	Gd	Tb	Dy	Ho	Er	Tm	Yb	Lu	Li	Be	Ge	Mo	Na+K	Sn
Notch	50.00	*1.00*	*15.50*	*6.00*		*0.150*	*2.00*	*5.00*	*4.90*	*5.50*	*0.30*	2.0		200	*400*	*60*	*360*	*40*	*30*	*16*	*25*	*85*	*26*	*100*	*100*	1300	*20*	*37*	*20*	*20*	*50*	*50*	*15*	*175*	*95*	*3*	*10*	*120*	*##*		*4*	*30*	*5*	*20*	*3*	*9*	*35.5*	*7.5*	*1.6*					
L-032	59.58	1.09	15.52	7.08	0.00	0.07	3.07	5.01	2.80	3.13	0.54	0.82	98.71	110	566	26	284	23.0	25	34	17	58	19	151	78	703	<6	<15	16		7.98	54.33	82.8	109	37			96.13			0.713								1.050	1.063			5.93
L-034	60.10	0.04	23.01	3.98	0.00	0.07	0.11	0.14	6.82	4.47	0.07	1.68	100.49	79	342	27	708	92.0	<6	12	8	18	17	74	87	705	<6	20.0	11					311	134																						11.29
L-034A	60.10	0.04	23.01	3.98	0.00	0.07	0.11	0.14	6.82	4.47	0.07	1.68	100.49	79	342	27	708	92.0	<6	12	8	18	17	74	87	705	<6	20.0	11					311	134																						11.29
L-036	73.57	1.10	15.97	1.46	0.00	0.02	0.12	0.10	4.47	6.82	0.09	7.83	100.54	34	51	30	635	38.0	<6	26	36	37	28	52	30	196	<6	36.0	<10					282	240																						11.29
L-037	56.10	0.04	21.65	3.00	0.00	0.12	0.04	1.20	10.22	5.51	0.05	2.53	100.46	92	465	33	792	101.0	<6	7	10	##	25	<12	117	423	9.0	17.0	<10		108.3	38.65	70.88	139	63			50.70			0.413								0.688	0.68			15.73
L-038	56.45	0.12	21.07	3.77	0.00	0.08	0.00	0.32	12.27	4.32	0.07	2.01	100.48	72	244	29	859	114.0	<6	7	12	##	26	<12	65	318	8.0	32.0	<10					261	146																						16.59
L-039	57.37	0.05	21.32	3.71	0.00	0.20	0.08	0.75	9.68	4.63	0.06	2.64	100.49	87	355	37	808	120.0	<6	<6	12	##	27	<12	68	349	9.0	30.0	<10					231	166																						14.31
L-040	55.44	0.04	20.98	5.81	0.00	0.34	0.02	1.29	9.89	6.14	0.06	0.44	100.45	75	283	38	922	135.0	2	8	8	##	25	4	139	261	8.0	30.0	<10					278	186																						16.03
L-041	57.71	0.05	20.81	4.02	0.00	0.07	0.00	0.60	8.89	5.41	0.02	2.85	100.45	85	283	33	950	134.0	<6	<6	6	98	27	<12	<12	347	11.0	22.0	<10					183	109																						14.30
L-044	57.32	0.03	21.02	3.15	0.00	0.14	0.00	0.65	12.04	4.28	0.05	1.70	100.38	109	616	##	1758	178.0	4	8	10	##	26	11	120	1441	10.0	31.0	<10		0.263		4.488	196	0			37.10				1.48	1.150						0.288	0.713			16.32
L-045	57.75	0.10	20.94	6.96	0.00	0.03	0.00	0.14	7.96	4.16	0.06	1.17	99.27	58	367	20	186	97.6	<6	11	32	34	27	<12	45	764	7.2	17.8	<10	1.9	7.13	57.9	20.0	214	158	0.29	2.38	9.70	214		1.22	4.71	0.77	4.50	0.77	2.09	0.31	2.01	0.27					12.12
L-046	55.67	0.05	20.92	3.40	0.00	0.19	0.09	1.07	8.51	5.27	0.06	5.21	100.44	82	311	30	670	82.0	<6	6	115	##	24	<12	51	526	<6	29.0	<10		0.53	0.550	6.700	204	1			44.38				0.64	1.400						0.250	0.688			13.78
ZGSI	58.04	Tr	20.76	4.45		0.20	0.09	0.95	9.22	4.81	Tr	1.99	100.51																																												
ZGSII	56.31	Tr	19.89	4.28	0.30	0.16	0.26	0.74	8.33	5.75	n.d.	3.56	99.58																																											
Shilenda																																																							
L-311	50.33	3.00	14.97	10.04	0.00	0.00	5.02	4.99	3.78	0.84	1.25	5.18	99.40	26	76	59	326	36.0	15	<6	19	39	19	121	16	88	8.00	<15	40					76	44																						4.62

Table No. A8 Granitoids in the Copperbelt, Zambia

Table No. A8.1 Muliashi Porphyry

Sample	SiO2	TiO2	Al2O3	Fe2O3	FeO	MnO	MgO	CaO	Na2O	K2O	P2O5	LOI	Total	Rb	Sr	Y	Zr	Nb	Co	Ni	Cu	Zn	Ga	V	Cr	Ba	U	Th	Sc	Pb	Sm	Nd	Pr	Ce	La	Cs	Hf	Ta	As	Se	Eu	Gd	Tb	Dy	Ho	Er	Tm	Yb	Lu	Li	Be	Ge	Mo	Na+K	Sn
Notch	50.00	*1.00*	*15.50*	*6.00*		*0.150*	*2.00*	*5.00*	*4.90*	*5.50*	*0.30*	2.00		200	*400*	*60*	*360*	*40*	*30*	*16*	*25*	*85*	*26*	*100*	*100*	1300	*20*	*37*	*20*	*20*	*50*	*50*	*15*	*175*	*95*	*3*	*10*	*120*	*##*		*4*	*30*	*5*	*20*	*3*	*9*	*35.5*	*7.5*	*1.6*					
L-075	65.53	0.91	13.91	5.81	0.00	0.07	1.46	2.59	3.43	5.10	0.23	1.14	100.18	162	217	33	50	16.8	0	0	0	0	16	0	0	1339	<6	16.0	<10	21.1	9.40	53.11	13.45	160	61	2.48	1.38	0.81	0	0	1.89	7.80	1.11	6.66	1.26	3.52	0.49	3.17	0.45					8.53
L-076	65.53	0.91	13.91	5.81	0.00	0.07	1.46	2.59	3.43	5.10	0.23	1.14	100.18	182	212	48	361	26.0	22	16	105	35	17	82	56	1344	<6	17.0	10					137	61																						8.53
L-077	66.70	0.79	14.45	4.66	0.00	0.06	1.36	2.66	3.78	5.06	0.21	0.77	100.50	174	216	39	290	22.0	14	11	28	46	18	59	41	1391	<6	14.0	<10		11.11	35.10	86.3	119	41			75.13			1.088								1.213	1.088			8.84
L-078	67.56	0.89	13.59	5.37	0.00	0.07	1.27	3.08	3.93	3.78	0.23	0.81	100.58	143	235	47	343	25.0	19	13	31	48	17	74	51	964	<6	18.0	10					131	61																						7.71
L-157	75.81	0.19	12.48	1.25	0.00	0.00	1.16	0.18	0.19	6.95	0.03	1.39	99.63	225	12	12	107	17.0	26	8	7	14	14	20	15	618	<6	18.0	<10					43	17																						7.14
L-158	73.58	0.20	12.85	1.36	0.00	0.00	1.46	0.93	0.33	7.11	0.04	2.00	99.87	233	19	13	109	16.0	32	7	<6	13	14	20	14	628	6.00	26.0	<10		107.9	26.04	63.13	76	31		2.100	8.23			0.450								0.588					7.44
L-159	68.02	0.64	14.23	2.82	0.00	0.00	1.74	1.42	0.95	6.80	0.16	2.10	98.87	303	47	34	209	28.0	38	7	<6	19	17	57	18	919	11.00	24.0	10					118	60																						7.75
L-160	67.96	0.55	14.78	2.29	0.00	0.00	1.47	1.67	2.46	5.69	0.16	2.10	99.14	264	40	49	223	32.0	39	9	<6	18	16	47	16	805	<6	15.0	13		117.8	42.35	102.1	156	49			27.91			1.13								2.788	0.988			8.15
L-163	43.65	1.23	15.61	14.61	0.00	0.30	11.50	4.45	1.80	3.69	0.14	2.97	99.95	149	179	25	85	9.0	172	410	<6	##	15	228	292	478	<6	<15	22					16	<12																						5.49
L-161	51.48	1.05	20.52	6.92	0.00	0.10	7.54	1.15	2.18	6.26	0.37	1.89	99.47	225	54	40	319	29.0	93	26	<6	##	24	102	18	1829	<6	30.0	17					128	64																						8.44
X-01	73.81	0.08	12.29	0.37	1.52	0.04	0.70	2.24	4.21	4.83	0.04	0.66	100.79																																											
X-02	72.56	0.23	14.28	0.94	0.68	0.02	0.83	0.76	2.88	6.12	0.05	1.96	101.31																																										
X-03	70.95	0.42	15.07	1.13	1.29	0.03	1.32	0.83	4.23	3.03	0.11	2.60	101.01																																										
X-04	75.20	0.33	10.10	1.55	1.69	0.04	2.81	2.08	2.02	2.13	0.34	2.36	100.65																																										
X-05	65.27	0.84	15.18	3.20	1.94	0.08	1.01	2.90	3.00	4.70	0.31	1.39	99.82																																										

Table No. CHEMICAL ANALYSIS OF SAMPLES FROM THE GREATER LUFILIAN ARC SORTED BY REGION
Basement to the Copperbelt, Zambia (cont.)

Table No. A8.2 Chambishi Mine Area

Sample	SiO2	TiO2	Al2O3	Fe2O3	FeO	MnO	MgO	CaO	Na2O	K2O	P2O5	LOI	Total	Rb	Sr	Y	Zr	Nb	Co	Ni	Cu	Zn	Ga	V	Cr	Ba	U	Th	Sc	Pb	Sm	Nd	Pr	Ce	La	Cs	Hf	Ta	As	Se	Eu	Gd	Tb	Dy	Ho	Er	Tm	Yb	Lu	Li	Be	Ge	Mo	Na+K	Sn
Notch	50.00	*1.00*	*15.50*	*6.00*		*0.150*	*2.00*	*5.00*	*4.90*	*5.50*	*0.30*	2.00		200	*400*	*60*	*360*	*40*	*30*	*16*	*25*	*85*	*26*	*100*	*100*	1300	*20*	*37*	*20*	*20*	*50*	*50*	*15*	*175*	*95*	*3*	*10*	*120*	*##*		*4*	*30*	*5*	*20*	*3*	*9*	*35.5*	*7.5*	*1.6*					
L-155	72.00	0.28	12.99	2.57	0.00	0.00	1.51	0.95	1.03	6.03	0.09	1.71	99.17	219	62	20	99	13.0	61	12	<6	26	15	44	21	848	<6	<15	<10		109.6	25.34	56.81	69	23			36.41			0.53							0.23	0.713					7.06
X-42	68.6	0.3	14	1.14	1.25	0.06	2.29	2.25	2.13	4.04	0.11	3.54	99.7																																										6.17
X-06	46.85		15.87	3.33	7.40	0.11	8.61	7.29	3.65	2.50	0.15	3.06	98.82																																										6.15
X-07	58.63		13.08	6.07	6.68	0.15	1.87	4.70	5.50	0.66	0.32	1.66	99.32																																										6.16
X-08	67.94		12.08	7.23	1.01	0.04	0.60	1.65	6.70	0.20	0.07	1.70	99.22																																										6.90
X-09	59.26		16.65	1.26	0.43	0.06	2.04	4.59	9.80	0.20	0.65	4.48	99.42																																										10.00
X-10	47.87		14.53	4.50	9.05	0.15	6.13	6.12	2.95	1.55	0.37	7.22	100.44																																										4.50
X-11	48.19		14.53	4.13	7.18	0.12	6.66	9.00	4.25	1.40	0.17	3.60	99.23																																										5.65

Table No. A8.3 Samba copper prospect

Sample	SiO2	TiO2	Al2O3	Fe2O3	FeO	MnO	MgO	CaO	Na2O	K2O	P2O5	LOI	Total	Rb	Sr	Y	Zr	Nb	Co	Ni	Cu	Zn	Ga	V	Cr	Ba	U	Th	Sc	Pb	Sm	Nd	Pr	Ce	La	Cs	Hf	Ta	As	Se	Eu	Gd	Tb	Dy	Ho	Er	Tm	Yb	Lu	Li	Be	Ge	Mo	Na+K	Sn
Notch	50.00	*1.00*	*15.50*	*6.00*		*0.150*	*2.00*	*5.00*	*4.90*	*5.50*	*0.30*	2.00		200	*400*	*60*	*360*	*40*	*30*	*16*	*25*	*85*	*26*	*100*	*100*	1300	*20*	*37*	*20*	*20*	*50*	*50*	*15*	*175*	*95*	*3*	*10*	*120*	*##*		*4*	*30*	*5*	*20*	*3*	*9*	*35.5*	*7.5*	*1.6*					
L-268	69.51	0.69	16.52	4.32	0.00	0.01	0.35	0.13	0.54	4.53	0.17	3.62	100.39	178	37	48	275	22.00	10	10	942	14	19	72	187	1116	<6	19.00	13.00					151	81																						5.07
L-269	75.84	0.31	13.87	3.02	0.00	0.00	0.00	0.20	0.31	3.67	0.21	3.03	100.46	94	20	16	179	19.00	<6	8	6	11	15	27	185	291	<6	<15	<10					83	41																						3.98
L-273	65.92	0.52	14.92	4.14	0.00	0.12	1.78	3.54	2.94	3.12	0.18	2.98	100.16	128	110	31	173	14.00	18	9	49	38	16	77	206	966	<6	<15	15.00					101	56																						6.06
L-279	67.94	0.63	14.39	4.41	0.00	0.08	1.31	3.25	3.31	3.08	0.22	1.29	99.91	123	204	39	285	19.00	7	13	6	51	16	64	302	810	6.00	20	<10		10.43	33.43	80.8	140	39			69.3			0.900							1.60	1.08					6.39

Table No. A8.4 Nchanga Granite

Sample	SiO2	TiO2	Al2O3	Fe2O3	FeO	MnO	MgO	CaO	Na2O	K2O	P2O5	LOI	Total	Rb	Sr	Y	Zr	Nb	Co	Ni	Cu	Zn	Ga	V	Cr	Ba	U	Th	Sc	Pb	Sm	Nd	Pr	Ce	La	Cs	Hf	Ta	As	Se	Eu	Gd	Tb	Dy	Ho	Er	Tm	Yb	Lu	Li	Be	Ge	Mo	Na+K	Sn
Notch	50.00	*1.00*	*15.50*	*6.00*		*0.150*	*2.00*	*5.00*	*4.90*	*5.50*	*0.30*	2.00		200	*400*	*60*	*360*	*40*	*30*	*16*	*25*	*85*	*26*	*100*	*100*	1300	*20*	*37*	*20*	*20*	*50*	*50*	*15*	*175*	*95*	*3*	*10*	*120*	*##*		*4*	*30*	*5*	*20*	*3*	*9*	*35.5*	*7.5*	*1.6*					
X-34	76.8	0.09	11.8	0.82	0.58	0.03	0.16	0.72	3.08	5.01	0.1	0.84	99.96																																										8.09
X-34a	76.8	0.09	11.8	0.82	0.58	0.03	0.16	0.72	5.01	3.08	0.1	0.84	99.96																																										8.09
X-35	76.8	0.08	10.7	1.3		0.04	0.1	0.8	2.3	4.9	0.02	0.69	97.77																																										7.20
X-36	76.9	0.01	12.3	0.6		0.01	0.1	0.5	3.6	4.4	0.04	0.35	98.81																																										8.00
X-37	78.2	0.04	10.3	1.1		0.04	0.1	0.7	2.2	4.9	0.01	0.44	98.03																																										7.10
X-38	59.8	1.1	10.4	12.6		0.3	0.6	4.3	1.7	2.9	0.08	0.99	94.77																																										4.60
X-39	66.6	0.01	18	0.2		0.02	0.03	0.2	2.4	11.9	0.01	0.95	100.3																																										14.30
X-40	64.8	0.01	16.7	0.4		0.01	0.03	0.1	0.7	15.5	0	0	98.25																																										16.20
P-28	68.49	0.34	12.40	3.43	0.00	0.12	0.26	1.06	8.74	5.32	0.11	0.13	100.27	345	58	##	261	64.0	34	19	<3	97	24	<4	8	689	13.0	98.0	5	61.0	75.30	#####	89.80	600	383	5.00	11.00	2.90	4	7	6.40	97.8	16.20	98.2	20.3	53.3	40.9	38.70	5.90					14.06
P-29	72.84	0.31	13.07	2.71	0.00	0.11	0.19	1.28	4.04	5.56	0.08	0.17	100.19	278	79	89	183	46.0	38	3	6	58	22	<4	8	724	9.0	65.0	6	53.0	16.20	82.60	23.20	204	101	3.00	6.00	2.20	2	7	1.70	14.80	2.40	14.40	2.90	8.10	36.9	8.20	1.40					9.60
L-151	77.00	0.10	11.82	1.67	0.00	0.03	0.17	0.11	3.47	5.54	0.02	0.51	100.44	351	32	##	197	91.0	10	8	42	39	24	<12	42	441	11.0	65.0	<10		113.8	48.59	96.88	167	49		6.94	13.56			0.538							10.61	2.200					9.01
L-153	77.40	0.07	11.91	1.65	0.00	0.03	0.12	0.27	3.51	4.89	0.01	0.51	100.37	438	25	##	106	70.0	<6	8	58	33	24	<12	60	236	11.0	44.0	<10					87	38																						8.40
L-154	77.07	0.07	12.06	1.22	0.00	0.00	0.00	0.25	3.07	5.78	0.01	0.50	100.05	478	27	68	122	58.0	7	<6	17	22	23	<12	<12	255	<6	44.0	<10		105.1	2.513	22.06	90	4		3.59	9.98										2.363	0.888					8.85
L-162	76.11	0.19	12.33	1.25	0.00	0.00	0.28	0.70	3.48	4.92	0.03	0.59	99.88	119	155	14	96	10.0	6	<6	7	22	13	17	15	793	<6	<15	<10					82	37																						8.40

Table No. A8.5 Nchanga Mine

Sample	SiO2	TiO2	Al2O3	Fe2O3	FeO	MnO	MgO	CaO	Na2O	K2O	P2O5	LOI	Total	Rb	Sr	Y	Zr	Nb	Co	Ni	Cu	Zn	Ga	V	Cr	Ba	U	Th	Sc	Pb	Sm	Nd	Pr	Ce	La	Cs	Hf	Ta	As	Se	Eu	Gd	Tb	Dy	Ho	Er	Tm	Yb	Lu	Li	Be	Ge	Mo	Na+K	Sn
Notch	50.00	*1.00*	*15.50*	*6.00*		*0.150*	*2.00*	*5.00*	*4.90*	*5.50*	*0.30*	2.00		200	*400*	*60*	*360*	*40*	*30*	*16*	*25*	*85*	*26*	*100*	*100*	1300	*20*	*37*	*20*	*20*	*50*	*50*	*15*	*175*	*95*	*3*	*10*	*120*	*##*		*4*	*30*	*5*	*20*	*3*	*9*	*35.5*	*7.5*	*1.6*					
L-150	51.05	2.91	15.47	10.19	0.00	0.00	10.09	0.68	1.69	6.12	0.36	1.16	99.72	361	24	45	150	28.0	851	191	623	66	24	424	94	349	6.0	<15	29		12.9	13.43	54.96	18	7			220.8										0.263	1.250					7.81
L-167a	47.14	0.78	19.71	6.10	0.00	0.08	12.98	0.00	0.00	8.70	0.08	4.00	99.57	255	64	##	781	147.0	266	57	1896	65	28	95	74	615	12.0	37.0	12					43	13																						8.70
L-168	79.68	0.15	10.06	0.72	0.00	0.02	0.10	0.02	0.19	7.61	0.08	0.59	99.22	132	125	19	258	11.0	32	<6	261	10	<9	16	59	1190	<6	<15	<10				9.900	61	1														0.175	0.48					7.80
L-170	70.45	0.86	15.35	3.22	0.00	0.03	1.50	0.01	0.02	5.02	0.13	3.05	99.64	110	46	42	320	79.0	131	14	1954	25	29	92	335	766	10.0	<15	11		6.038	25.63	30.29	44	21			46.49			0.188	1.963						1.413	0.888					5.04
L-172	74.42	0.06	13.07	1.32	0.00	0.04	0.21	0.14	1.85	7.48	0.06	0.71	99.36	316	32	49	113	85.0	9	8	242	23	21	<12	618	668	5.3	48.5	<10	27.3	8.66	41.2	11.3	79	50	1.13	4.97	3.20			0.41	7.22	1.32	9.90	2.23	7.30	1.12	7.27	1.00					9.33
L-173	74.69	0.09	12.55	1.37	0.00	0.03	0.28	0.14	1.87	7.51	0.05	0.78	99.36	314	29	78	172	128.0	11	6	232	20	22	<12	453	598	7.0	58.0	<10					85	49																						9.38

Table No. A8.6 Mufulira Granite

Sample	SiO2	TiO2	Al2O3	Fe2O3	FeO	MnO	MgO	CaO	Na2O	K2O	P2O5	LOI	Total	Rb	Sr	Y	Zr	Nb	Co	Ni	Cu	Zn	Ga	V	Cr	Ba	U	Th	Sc	Pb	Sm	Nd	Pr	Ce	La	Cs	Hf	Ta	As	Se	Eu	Gd	Tb	Dy	Ho	Er	Tm	Yb	Lu	Li	Be	Ge	Mo	Na+K	Sn
X-41	64.2	1.05	14.8	2.89	2.68	0.05	1.68	3.11	3.7	4.65	0.31	0.97	100.1																																											8.35
L-166	70.84	0.39	13.91	2.93	0.00	0.00	0.61	1.97	4.13	4.54	0.13	0.44	99.89	209	89	31	89	18.0	6	<6	22	18	15	<12	17	741	<6	15.0	<10		109.0	34.36	63.50	105	35		3.06	3.313			0.713							0.863	0.68					8.67

Other

Sample	SiO2	TiO2	Al2O3	Fe2O3	FeO	MnO	MgO	CaO	Na2O	K2O	P2O5	LOI	Total	Rb	Sr	Y	Zr	Nb	Co	Ni	Cu	Zn	Ga	V	Cr	Ba	U	Th	Sc	Pb	Sm	Nd	Pr	Ce	La	Cs	Hf	Ta	As	Se	Eu	Gd	Tb	Dy	Ho	Er	Tm	Yb	Lu	Li	Be	Ge	Mo	Na+K	Sn
Notch	50.00	*1.00*	*15.50*	*6.00*		*0.150*	*2.00*	*5.00*	*4.90*	*5.50*	*0.30*	2.00		200	*400*	*60*	*360*	*40*	*30*	*16*	*25*	*85*	*26*	*100*	*100*	1300	*20*	*37*	*20*	*20*	*50*	*50*	*15*	*175*	*95*	*3*	*10*	*120*	*##*		*4*	*30*	*5*	*20*	*3*	*9*	*35.5*	*7.5*	*1.6*					
X-12	30.05	0.37	8.60	39.65	4.48	0.05	0.27	6.82			5.78	0.35	96.42																																												0.00
X-13	49.41	2.67	12.71	2.18	10.07	0.14	6.93	10.46	2.46	0.80	0.46	2.38	100.67																																												3.26
X-14	46.76	3.30	10.31	5.81	9.10	0.14	7.25	10.24	4.26	0.86	0.38	4.05	102.46																																												5.12

Table No. A9 CHEMICAL ANALYSIS OF SAMPLES FROM THE GREATER LUFILIAN ARC SORTED BY REGION

Kamanjab Inlier, Namibia

Sample	SiO2	TiO2	Al2O3	Fe2O3	FeO	MnO	MgO	CaO	Na2O	K2O	P2O5	LOI	Total	Rb	Sr	Y	Zr	Nb	Co	Ni	Cu	Zn	Ga	V	Cr	Ba	U	Th	Sc	Pb	Sm	Nd	Pr	Ce	La	Cs	Hf	Ta	As	Se	Eu	Gd	Tb	Dy	Ho	Er	Tm	Yb	Lu	Li	Be	Ge	Mo	Na+K	Sn
Notch	50.00	1.00	15.50	6.00		0.150	2.00	5.00	4.90	5.50	0.30	2.00		200	400	60	360	40	30	16	25	85	26	100	100	1300	20	37	20	20	50	50	15	175	95	3	10	120	##		4	30	5	20	3	9	35.5	7.5	1.6						
L-832	73.67	0.32	12.24	1.83	0.00	0.04	0.14	0.46	4.39	5.23	0.11	0.63	99.06	154	297	38	307	15.0	8	10	19	70	17	46	<12	1468	<6	19.0	<10					121	58																					9.62
L-834	59.92	0.47	16.55	4.88	0.00	0.05	0.10	1.72	0.29	14.06	0.12	1.28	99.44	283	70	49	274	20.0	7	<6	14	19	9	26	<12	1842	7.0	25.0	<10		12.06	41.53	111.4	192	54		2.88	77.3			0.700							2.450	1.28						14.35
L-835	65.67	0.65	15.35	3.98	0.00	0.08	0.87	2.29	4.41	4.48	0.19	1.44	99.41	135	203	38	342	15.0	<6	<6	7	68	17	40	<12	1318	<6	15.0	10					127	60																					8.89
L-836	67.42	0.74	14.82	4.07	0.00	0.10	0.86	2.21	4.08	4.77	0.20	0.79	100.06	159	266	40	343	17.0	6	<6	19	69	0	45	<12	1272	0.0	0.0	0					0	0																					8.85
L-838	67.61	0.61	14.50	3.84	0.00	0.09	0.82	2.37	3.62	4.48	0.18	0.50	98.62	208	69	22	93	15.6	<6	8	10	30	15	12	<12	552	4.0	21.2	<10					130	55																					8.10
L-839	76.62	0.29	11.26	1.41	0.00	0.04	0.23	0.35	3.05	5.28	0.07	0.47	99.07	218	67	27	163	17.0	<6	9	19	35	13	12	<12	565	<6	16.0	<10					102	44																					8.33
L-840	70.88	0.42	13.61	2.64	0.00	0.07	0.48	1.29	3.97	4.93	0.13	0.75	99.17	176	247	37	237	15.0	<6	8	20	47	16	20	<12	1054	<6	18.0	<10					127	62																					8.90
L-842	65.32	0.68	14.27	4.45	0.00	0.10	1.13	2.64	4.17	3.50	0.19	2.76	99.21	141	316	38	361	16.0	10	11	37	83	16	49	13	1668	<6	16.0	12		11.19	33.40	82.63	135	41		1.48	62.88			1.013							1.638	1.08						7.67
L-843	75.42	0.33	12.58	1.52	0.00	0.03	0.25	0.31	3.01	4.39	0.10	1.13	99.07	163	61	41	199	20.0	<6	<6	6	25	14	16	177	907	<6	21.0	<10		113.0	35.20	74.00	126	32		3.95	9.950			0.650							2.038	0.88						7.40
L-844	68.18	0.63	14.42	3.75	0.00	0.08	0.82	2.22	3.87	4.35	0.20	1.02	99.54	137	259	39	345	16.0	6	7	20	62	17	42	<12	1378	6.0	16.0	<10					129	63																					8.22
L-846	67.61	0.60	14.35	3.72	0.00	0.08	0.89	1.97	4.09	4.59	0.18	0.78	98.86	134	246	44	306	16.0	6	10	18	56	15	39	<12	1240	<6	19.0	<10		11.76	41.76	86.50	133	45			50.38			1.000							1.913	1.088						8.68
L-849	73.54	0.33	12.99	1.74	0.00	0.02	0.20	0.14	3.78	5.57	0.04	0.55	98.90	189	43	24	243	27.0	<6	7	<6	22	18	17	217	451	<6	16.0	<10		107.3	30.33	47.9	152	20		1.013	33.66			0.263							0.238	0.38						9.35
L-855	76.63	0.15	11.87	1.14	0.00	0.02	0.05	0.25	4.70	4.06	0.02	0.25	99.14	88	39	10	71	10.0	<6	10	9	11	15	<12	<12	328	<6	<15	<10					39	16																					8.76
L-857	73.33	0.32	13.00	1.84	0.00	0.04	0.43	1.21	4.01	4.21	0.11	1.00	99.50	155	211	17	141	14.0	<6	9	26	28	15	22	<12	1081	<6	<15	<10					80	38																					8.22
L-863	64.77	0.71	14.71	5.42	0.00	0.08	1.57	3.06	3.37	3.86	0.24	1.14	98.93	155	288	33	228	19.0	14	15	23	72	18	100	122	1004	<6	17.0	11					89	44																					7.23
L-864	66.28	0.74	14.57	5.01	0.00	0.09	1.56	2.96	3.05	4.14	0.33	1.62	100.35	97	249	23	39	11.9	10	16	28	58	16	91	273	1039	3.1	13.4	10	17.4	6.19	37.8	9.86	78	45	0.83	1.38	0.83			1.27	5.35	0.73	4.38	0.86	2.38	0.34	2.22	0.32						7.19
L-864	0.00	0.00	0.00	0.00	0.00	0.00	0.00	0.00	0.00	0.00	0.00	0.00	0.00	0	0	0	0	0.0	0	0	0	0	<9				<6	<15	<10					23	<12																					0.00
L-865	66.29	0.76	14.63	4.88	0.00	0.08	1.51	2.53	3.09	4.38	0.27	1.26	99.68	179	240	34	241	19.0	10	20	21	68	17	84	226	1100	<6	16.0	10					129	67																					7.47
L-868	66.57	0.77	14.29	4.73	0.00	0.10	1.11	2.09	3.56	4.38	0.29	1.15	99.04	112	186	32	22	15.3	10	13	14	.	19	68	114	1100	<6	<15	10	14.6	8.72	52.03	13.28	154	79	1.07	0.84	0.55	0	0	1.83	7.21	0.99	6.12	1.18	3.36	0.47	3.09	0.45						7.94
L-874	96.83	0.09	0.64	0.69	0.00	0.01	0.00	0.02	0.02	0.31	0.03	0.08	98.72	11	8	5	29	4.0	<6	13	8	6	17	<12	538	30	6.0	17.0	11					144	73																					0.33
L-874a	67.47	0.89	13.68	4.67	0.00	0.10	1.05	1.71	3.48	4.99	0.27	1.09	99.40	155	181	57	348	24.0	12	14	19	69		63	17	1380																														8.47
L-875	66.20	0.78	14.38	5.11	0.00	0.12	1.18	2.90	3.74	4.25	0.30	1.32	100.28	138	222	46	329	23.0	7	13	14	68	18	71	181	1294	<6	<15	10		12.16	42.90	111.4	157	54			76.63			1.588							1.963	1.23						7.99
L-877	66.24	0.93	13.94	5.04	0.00	0.09	1.14	2.08	3.48	4.74	0.41	1.24	99.33	140	224	54	377	23.0	9	16	22	75	19	62	17	1371	<6	17.0	10					169	87																					8.22
L-878	67.83	0.67	13.61	4.34	0.00	0.09	0.95	1.67	3.73	4.58	0.23	1.08	98.78	152	176	57	329	19.0	9	12	34	71	19	46	16	1143	<6	17.0	<10		12.29	39.36	92.38	150	41			56.10			1.150							2.563	1.213						8.31
L-895	55.24	0.90	18.42	6.32	0.00	0.11	3.12	4.54	4.23	4.61	0.50	1.93	99.92	164	840	22	172	7.0	18	43	164	69	18	134	91	1382	<6	<15	14		8.250	23.24	53.84	74	22			98.63			0.33							0.363	0.913						8.84
L-898	69.20	0.58	12.94	5.11	0.00	0.08	0.60	1.62	4.21	5.14	0.15	0.09	99.72	112	193	33	215	15.0	<6	7	17	46		27	189	1049																														9.35
L-899	71.98	0.41	12.65	2.41	0.00	0.06	0.72	1.79	4.23	3.72	0.11	0.69	98.77	112	193	33	210	18.0	<6	7	17	46	17	26	182	1049	<6	16.0	<10					119	56																					7.95
L-900	67.40	0.67	14.52	4.30	0.00	0.08	1.12	2.21	4.83	4.01	0.21	0.90	100.25	101	244	40	361	16.0	8	8	17	43	17	48	<12	1239	<6	16.0	11					127	61																					8.84
L-902	77.60	0.17	12.00	0.96	0.00	0.02	0.08	0.11	4.16	4.81	0.10	0.34	100.35	160	35	18	95	22.0	<6	7	33	15	15	13	<12	131	<6	25.0	<10					85	39																					8.97
L-903	79.24	0.19	10.48	1.02	0.00	0.02	0.12	0.14	2.98	4.99	0.04	0.32	99.54	262	21	23	103	16.0	<6	8	10	15	13	<12	<12	132	<6	25.0	<10					80	38																					7.97
L-904	76.77	0.24	11.40	1.61	0.00	0.05	0.16	0.10	3.59	4.81	0.05	0.45	99.23	242	44	30	149	18.0	<6	8	15	37	15	<12	14	233	<6	21.0	<10		107.0	29.65	49.94	99	23			7.188			0.28							1.300	0.900						8.40
L-905	77.13	0.29	11.44	1.46	0.00	0.03	0.23	0.54	5.65	1.54	0.06	0.51	98.88	75	80	40	160	19.0	<6	9	17	23	13	13	<12	672	<6	22.0	<10					116	55																					7.19
L-906	76.57	0.27	12.23	1.45	0.00	0.03	0.07	0.32	3.00	5.97	0.03	0.42	100.36	254	43	51	164	21.0	<6	7	37	14	13	<12	269	219	<6	19.0	<10					122	62																					8.97
L-907	71.26	0.43	13.59	2.43	0.00	0.06	0.51	1.34	3.85	5.07	0.11	0.52	99.17	175	181	41	248	16.0	<6	8	11	44	15	24	<12	1136	<6	16.0	<10					135	69																					8.92
L-908	66.78	0.41	16.95	1.82	0.00	0.08	0.28	0.22	9.57	2.63	0.03	0.34	99.11	96	28	10	66	15.5	<6	8	12	53	26	<12	<12	125	<6	15.0	<10	9.7	2.50	17.12	5.04	82	40	1.49	2.03	1.06	0	0	0.29	1.92	0.28	1.78	0.37	1.19	0.20	1.64	0.29						12.20
L-909	71.39	0.41	13.73	1.94	0.00	0.07	0.35	0.72	4.37	4.96	0.08	0.91	98.93	153	134	46	285	18.0	<6	8	25	56	17	15	<12	1346	<6	18.0	<10					163	82																					9.33
L-910	70.84	0.59	13.17	3.28	0.00	0.04	0.51	0.53	4.21	4.24	0.20	1.11	98.72	129	126	44	360	17.0	<6	8	12	47	16	26	<12	1115	<6	<15	<10					152	76																					8.45
L-911	72.60	0.37	14.49	2.24	0.00	0.03	0.81	0.22	0.16	5.19	0.11	2.40	98.62	170	16	45	344	27.0	<6	10	33	48	19	17	139	398	<6	19.0	<10					145	75																					5.35
L-912	73.33	0.37	13.50	1.75	0.00	0.02	0.70	0.22	2.05	5.30	0.08	1.55	98.87	139	29	38	273	20.0	<6	7	9	34	17	15	<12	787	<6	16.0	<10					148	47																					7.35
L-917	71.65	0.73	12.99	3.87	0.00	0.08	1.25	0.71	3.95	4.48	0.20	0.63	100.54	113	116	16	39	15.2	6	12	17	50	15	46	15	967	<6	<15	<10	13.4	5.26	30.24	7.86	85	42	1.40	1.36	0.92	0	0	1.04	4.56	0.63	3.72	0.68	1.87	0.27	1.86	0.27						8.43
L-919	87.60	0.31	4.60	3.09	0.00	0.03	0.08	0.09	0.12	2.09	0.04	0.79	98.84	79	9	11	99	8.0	6	15	13	14	<9	27	32	297	<6	<15	<10					55	26																					2.21
L-920	36.93	0.23	6.77	1.19	0.00	0.03	0.22	0.29	2.90	2.72	0.06	49.01	100.35	124	81	20	208	15.0	<6	<6	16	29	14	17	134	1088	<6	<15	<10		113.1	35.71	61.91	99	29			18.89			0.663							0.200	0.700						5.62
L-922	68.49	0.77	14.39	4.18	0.00	0.07	0.89	1.69	3.76	4.88	0.23	0.98	100.33	143	206	56	426	27.0	8	9	15	58	18	56	244	1598	<6	16.0	10		22.13	52.85	122.3	159	56			61.63			1.73	4.29						2.488	1.13						8.64
L-923	70.32	0.62	13.18	3.95	0.00	0.06	0.59	0.92	4.03	4.67	0.17	1.02	99.53	162	156	56	425	21.0	6	12	11	55	18	37	<12	1168	<6	21.0	<10					159	89																					8.70
L-924	71.99	0.63	12.33	2.83	0.00	0.05	0.57	1.46	3.58	3.97	0.13	1.69	99.23	82	63	46	359	22.0	8	9	14	26	15	38	<12	1811	<6	19.0	<10					158	79																					7.55
L-938	70.06	0.58	13.36	3.13	0.00	0.05	0.58	1.70	4.16	4.11	0.19	0.90	98.82	76	244	38	294	19.0	6	7	11	44	16	40	266	1785	<6	<15	<10	23.8	117.0	49.23	83.50	96	37	1.37	3.22	38.46			1.43	3.22	0.53	3.70	0.77	2.40	0.39	1.213	0.888						8.27
L-939	68.27	0.56	15.25	3.83	0.00	0.08	0.63	1.89	3.55	5.28	0.14	0.74	100.22	132	422	22	166	11.0	15	16	29	68	16	89	23	1059	<6	<15	11		8.33	30.34	57.99	77	28			77.50										0.58	0.93						8.83
L-940	62.87	0.57	14.38	5.03	0.00	0.09	1.98	6.05	4.02	3.40	0.20	0.69	99.28	133	422	23	173	12.0	14	13	22	64	18	94	17	1043	<6	<15	11		9.050	25.39	64.13	90	31			79.8			0.43							0.638	0.98						7.42
L-943	74.31	0.15	13.23	1.77	0.00	0.04	0.03	0.75	3.70	5.72	0.11	0.29	100.10	137	123	4	65	7.2	<6	9	19	17	14	13	15	350	<6	28.0	<10	18.5	0.91	6.77	2.16	42	20	2.27	3.29	0.51	0	0	0.15	0.72	0.10	0.64	0.14	0.46	0.09	0.83	0.17						9.42
L-945	67.85	0.52	15.01	3.25	0.00	0.07	0.55	1.40	4.19	5.08	0.11	0.92	98.95	169	235	45	386	18.0	9	8	20	64	18	2	13	1409	<6	19.0	<10		12.43	41.88	115.1	178	53			61.16			0.850	1.663						2.463	1.13						9.27
L-946	67.96	0.48	14.78	2.89	0.00	0.06	0.59	1.58	4.39	5.01	0.12	0.73	98.59	165	232	38	250	19.0	6	8	8	45	16	30	185	1451	<6	<15	<10					175	88																					9.40
L-948	70.39	0.65	13.17	3.48	0.00	0.11	0.62	1.58	4.48	4.47	0.13	0.41	99.49	160	174	63	368	21.0	7	8	10	73	17	22	<12	1424	<6	15.0	<10					175	92																					8.95
L-951	66.61	0.52	15.75	3.69	0.00	0.02	0.04	0.50	11.34	0.33	0.12	0.19	99.11	4	30	50	261	24.0	<6	10	6	9	16	39	137	<20	<6	22.0	<10		10.83	28.36	109.6	166	14			48.54			0.713	3.138						1.888	1.088						11.67
L-952	67.68	0.59	15.55	4.09	0.00	0.02	0.15	0.73	10.86	0.35	0.15	0.22	100.39	6	38	36	308	23.0	<6	9	6	10	16	31	173	52	<6	<15	<10					38	27																					11.21

Table No. A9 CHEMICAL ANALYSIS OF SAMPLES FROM THE GREATER LUFILIAN ARC SORTED BY REGION

Kamanjab Inlier, Namibia (cont.)

Sample	SiO2	TiO2	Al2O3	Fe2O3	FeO	MnO	MgO	CaO	Na2O	K2O	P2O5	LOI	Total	Rb	Sr	Y	Zr	Nb	Co	Ni	Cu	Zn	Ga	V	Cr	Ba	U	Th	Sc	Pb	Sm	Nd	Pr	Ce	La	Cs	Hf	Ta	As	Se	Eu	Gd	Tb	Dy	Ho	Er	Tm	Yb	Lu	Li	Be	Ge	Mo	Na+K	Sn
Notch	50.00	1.00	15.50	6.00		0.150	2.00	5.00	4.90	5.50	0.30	2.00		200	400	60	360	40	30	16	25	85	26	100	100	1300	20	37	20	20	50	50	15	175	95	3	10	120	##		4	30	5	20	3	9	35.5	7.5	1.6						
L-955	67.86	0.41	16.46	3.50	0.00	0.05	0.11	0.33	10.16	0.19	0.23	0.82	100.12	4	37	40	340	17.0	<6	13	333	##	21	36	<12	30	<6	<15	16		13.3	62.33	671.3	965	405			42.79			0.400							1.788	1.03						10.35
L-956	61.48	2.00	9.60	15.05	0.00	0.04	0.23	2.72	7.38	0.01	0.92	0.23	99.66	5	36	63	321	14.0	9	11	7	17	17	91	<12	51	<6	<15	24			41.30	97.50	116	63			297.1										3.050	2.13						7.39
L-957	75.71	0.31	11.71	1.52	0.00	0.04	0.21	1.09	2.90	4.90	0.05	0.66	99.10	126	135	32	207	20.0	<6	7	<6	36	14	<12	228	571	<6	26.0	<10		112.1	34.19	59.59	156	79		3.20	7.188			0.28							0.338	0.68						7.80
L-958	47.73	1.22	15.13	13.06	0.00	0.23	7.23	8.03	3.57	0.36	0.22	2.21	98.99	5	188	34	105	5.0	63	122	59	##	19	296	107	297	<6	<15	37					15	<12																				3.93
L-963	88.82	0.21	4.22	2.07	0.00	0.03	0.19	0.14	1.00	1.77	0.06	0.66	99.17	63	17	18	133	8.0	8	11	20	15	<9	25	12	308	<6	<15	<10					64	31																		2.77
L-965	67.45	0.59	13.65	6.24	0.00	0.03	0.32	0.69	4.10	5.73	0.19	0.42	99.41	156	43	88	358	29.0	<6	11	8	24	17	33	12	741	7.00	30.0	<10					125	56																		9.83
L-966	68.15	0.60	12.90	6.30	0.00	0.02	0.16	0.43	4.46	5.68	0.19	0.27	99.16	144	39	74	108	17.1	<6	9	6	19	16	42	193	708	5.82	27.2	<10	17.8	6.29	34.8	9.84	103	45	0.41	3.12	1.20			0.89	7.00	1.36	10.3	2.34	7.51	1.13	7.93	1.21						10.14
L-967	70.72	0.48	12.92	3.64	0.00	0.07	0.46	1.11	3.78	5.05	0.12	0.63	98.98	269	119	83	395	22.0	8	9	13	60	17	31	<12	883	8.00	36.0	<10					259	130																		8.83
L-967a	0.00	0.00	0.00	0.00	0.00	0.00	0.00	0.00	0.00	0.00	0.00	0.00	0.00	0	0	0	0	0.0	0	0	0	0	15	0	0	0	<6	20.0	<10					153	119																		0.00
L-968	72.13	0.34	13.69	2.21	0.00	0.03	0.17	0.89	3.99	4.79	0.05	0.51	98.80	136	145	37	225	15.0	7	9	20	86	15	16	<12	1370	<6	23.0	<10		110.0	16.73	28.51	110	11		2.86	26.16										0.488	0.763						8.78
L-969	59.46	0.49	19.16	4.28	0.00	0.05	0.68	0.38	0.55	14.31	0.08	0.84	100.28	393	66	59	293	24.0	6	<6	47	53	22	61	<12	2451	6.00	29.0	<10		10.51	36.03	92.38	159	37		7.20	60.24			0.663							3.050	1.288						14.86
L-971	64.34	0.54	17.73	1.51	0.00	0.09	0.14	0.68	4.58	8.51	0.11	0.69	98.92	148	66	47	358	22.0	<6	9	10	14	13	34	<12	2236	<6	<15	<10					137	81																		13.09
L-973	71.06	0.42	12.34	2.89	0.00	0.04	0.12	1.90	0.51	9.97	0.09	0.97	100.31	266	42	47	249	19.0	6	<6	141	70	9	28	12	1800	<6	18.0	<10		9.588	33.88	96.50	128	42		5.85	36.50			0.500							3.23	1.138						10.48
L-975	72.48	0.35	13.19	2.05	0.00	0.06	0.27	0.82	3.81	5.40	0.10	0.56	99.09	164	149	34	215	16.0	7	9	45	47	14	19	<12	1327	<6	21.0	<10					137	68																		9.21
L-976	72.48	0.37	13.10	1.84	0.00	0.04	0.29	0.71	4.00	5.29	0.06	0.50	98.68	195	113	55	203	21.0	<6	10	8	29		18	209	1114					115.8	48.35	91.8		71		3.23	13.38			1.03	2.213						2.93	1.08						9.29
L-977	74.68	0.27	11.99	1.72	0.00	0.04	0.24	0.55	3.86	5.21	0.04	0.45	99.05	121	81	27	197	13.0	<6	8	<6	39	15	12	<12	766	<6	16.0	<10					110	57																		9.07
L-978	76.43	0.22	11.10	2.76	0.00	0.10	0.04	0.28	4.16	5.19	0.05	0.18	100.51	139	58	15	133	16.9	<6	10	37	73	20	14	20	264	3.59	19.1	<10	21.3	2.08	13.4	4.14	50	25	0.75	5.11	1.02			0.29	1.79	0.29	2.06	0.48	1.79	0.33	2.76	0.49						9.35
L-979	66.06	0.48	15.03	3.97	0.00	0.09	1.33	3.18	4.23	3.67	0.14	0.79	98.97	108	435	35	143	15.0	10	10	76	88	16	68	242	1077	<6	<15	11					92	44																		7.90
L-980	67.03	0.53	15.05	4.32	0.00	0.09	1.37	3.20	4.47	3.48	0.18	0.77	100.49	115	424	32	157	17.0	10	15	28	62	17	72	200	1140	<6	<15	<10					104	52																		7.95
L-982	66.31	0.56	15.11	3.80	0.00	0.09	1.18	3.09	4.72	3.57	0.19	0.80	99.42	99	495	25	176	12.0	11	10	11	56	17	54	<12	1245	<6	<15	<10		8.588	26.96	66.38	74	30			53.76			0.363							0.550	0.83						8.29
L-983	72.59	0.29	13.57	1.83	0.00	0.04	0.07	0.90	4.08	4.95	0.04	0.51	98.87	197	156	28	181	17.0	<6	6	7	32	15	13	<12	963	<6	19.0	<10					90	39																		9.03
L-985	72.90	0.46	12.76	2.61	0.00	0.05	0.29	1.39	3.72	4.25	0.06	0.63	99.12	123	219	5	51	6.1	<6	7	9	46	14	25	173	1580	1.49	17.1	<10	25.6	3.41	33.2	9.78	103	61	2.13	1.48	0.19			1.09	2.00	0.20	0.97	0.17	0.46	0.07	0.54	0.10						7.97
L-987a	45.74	2.33	16.73	14.31	0.00	0.17	4.10	10.53	2.62	1.59	0.46	1.99	100.57	22	598	11	18	1.9	41	8	75	##	17	429	<12	397	<6	<15	36	7.7	2.50	10.86	2.08	<12	<12	0.29	0.51	0.03	0	0	1.03	2.95	0.39	2.37	0.46	1.20	0.15	0.92	0.13						4.21
L-987b	40.92	2.62	19.28	13.71	0.00	0.19	4.13	12.81	2.45	0.79	1.19	2.06	100.15	35	646	19	31	4.0	28	<6	37	72	17	307	<12	284	<6	<15	32			7.100	29.40	16	5			284.3								1.338						3.24
L-990	53.79	0.31	13.92	7.16	0.00	0.15	8.22	7.59	5.52	0.32	0.10	2.29	99.37	10	267	12	84	10.0	38	178	73	69	13	75	584	187	<6	<15	20					39	22																		5.84
L-991	48.45	0.96	11.97	11.52	0.00	0.19	11.57	9.20	3.07	0.46	0.12	1.70	99.21	7	217	20	53	9.0	64	251	83	93	12	255	870	188	<6	<15	35					19	12																		3.53
L-992	50.94	0.49	19.38	7.11	0.00	0.15	5.16	9.79	3.16	1.87	0.09	2.25	100.39	67	659	10	28	3.4	27	53	35	53	16	144	100	460	0.24	0.9	26	4.4	1.92	9.78	2.25	19	9	0.49	0.75	0.13			0.79	2.03	0.30	1.93	0.39	1.11	0.16	1.04	0.15						5.03
L-993	71.34	0.39	13.57	2.03	0.00	0.05	0.39	1.42	3.97	5.33	0.07	0.81	99.37	115	224	27	75	11.5	<6	6	8	34	15	24	160	1595	<6	17.0	<10	22.5	7.25	47.18	12.68	139	69	0.45	2.38	0.59	0	0	1.21	5.76	0.82	5.12	1.00	2.86	0.42	2.84	0.41						9.30
L-994	70.70	0.40	13.83	2.09	0.00	0.05	0.43	1.46	3.95	5.07	0.09	0.73	98.80	110	226	37	208	19.0	6	7	10	33	15	32	195	1763	<6	<15	<10					142	70																		9.02
L-995	39.21	3.69	11.13	22.15	0.00	0.26	7.20	10.83	1.60	0.53	1.13	1.13	98.86	14	449	21	27	4.0	59	<6	54	##	19	491	<12	457	<6	<15	45					<12	<12																		2.13
L-996	69.95	0.44	14.71	2.86	0.00	0.06	0.50	1.75	4.30	4.78	0.11	0.95	100.41	121	274	24	78	13.9	6	9	67	71	16	30	<12	1498	2.82	14.9	<10	23.0	6.17	39.6	10.8	113	49	0.69	2.30	0.83			1.22	4.96	0.74	4.69	0.93	2.78	0.42	2.93	0.42						9.08
L-997	69.62	0.34	15.29	1.59	0.00	0.04	0.27	0.51	5.88	5.33	0.05	0.73	99.65	135	65	57	241	22.0	8	9	8	24	16	19	<12	542	<6	33.0	<10		111.4	28.71	57.06	156	21		4.188	11.06										2.450	0.950						11.21
L-998	64.78	0.73	15.67	4.59	0.00	0.11	1.41	2.78	4.52	4.03	0.24	1.33	100.19	103	300	34	347	15.0	6	9	29	96	18	53	13	2134	<6	<15	10		10.00	32.01	78.50	106	38			63.00			0.938							1.038	1.03						8.55
L-999	67.68	0.49	14.73	3.02	0.00	0.07	0.74	1.83	4.31	4.65	0.13	1.19	98.84	140	252	37	288	20.0	<6	9	10	58	17	33	205	1537	<6	16.0	<10		9.700	36.04	91.88	144	44		1.53	39.16			0.83							1.488	0.888						8.96
L-1000	67.91	0.47	15.37	2.32	0.00	0.06	0.52	1.06	4.28	5.11	0.10	1.68	98.88	192	112	37	251	18.0	<6	10	62	58	17	35	<12	1206	<6	20.0	<10		11.6	90.10	152.3	134	80			82			3.48							2.58	1.200						9.39
L-1002	77.59	0.26	11.61	1.64	0.00	0.05	0.10	0.32	3.59	4.97	0.03	0.33	100.49	180	40	25	134	22.0	<6	8	6	14	14	10	<12	180	<6	28.0	<10		104.0	18.61	52.50	87	26		3.35	5.388										1.600	0.93						8.56
L-1003	68.00	0.50	15.07	2.73	0.00	0.05	0.58	1.60	4.64	5.26	0.12	0.69	99.24	145	242	40	289	16.0	<6	8	12	47	17	32	<12	1796	<6	15.0	<10		8.450	28.94	79.13	133	26		2.58	31.71			0.78							1.713	0.950						9.90
L-1005	71.20	0.48	12.46	3.35	0.00	0.06	0.56	1.47	3.93	4.47	0.18	0.76	98.92	171	218	46	298	18.0	7	9	15	50	17	26	16	1194	<6	18.0	<10					132	64																		8.40
L-1007	64.26	0.56	15.15	5.20	0.00	0.10	1.92	3.56	4.03	3.92	0.20	0.55	99.45	169	234	45	318	16.0	7	10	22	61	17	38	<12	1413	<6	22.0	<10					160	78																		7.95
L-1009	66.67	0.69	15.06	4.31	0.00	0.09	1.05	2.81	4.12	4.42	0.26	0.88	100.36	129	347	38	354	15.0	7	7	18	71	17	53	<12	1757	<6	16.0	10					115	55																		8.54
L-1010	63.36	0.80	15.40	5.08	0.00	0.11	1.26	3.27	4.15	4.24	0.34	1.17	99.18	138	385	37	372	15.0	9	10	21	74	18	53	<12	1944	<6	<15	12					110	55																		8.39
L-1011	66.33	0.64	14.74	3.94	0.00	0.09	0.94	2.72	4.53	4.43	0.19	0.82	99.37	152	302	38	308	20.0	7	9	21	73	17	50	126	1322	<6	17.0	10					129	66																		8.96
L-1012	64.77	0.68	15.28	4.30	0.00	0.20	0.95	3.01	5.41	3.94	0.20	0.97	99.71	132	337	42	332	22.0	8	10	9	##	17	53	105	1550	<6	17.0	<10					139	74																		9.35
L-1013	67.41	0.61	14.33	4.04	0.00	0.08	0.94	2.09	4.00	4.72	0.21	0.95	99.38	171	240	39	331	16.0	6	10	26	67	17	47	<12	1290	<6	19.0	<10		108.4	40.58	79.3	131	35			48.23			0.638							1.738	0.98						8.72
C-1	74.03	0.27	12.73	1.15	1.51	0.05	0.31	0.48	3.67	5.09	0.05	0.71	100.05	100	50	70	500	30.0	<10	<10	n.d		25	<3	10	1200				25.0				95			<100								<3	<3	<30	<3				8.76
C-2	69.71	0.68	14.17	1.69	1.57	0.04	0.84	0.82	4.10	5.30	0.27	0.67	99.86	70	110	45	550	30.0					25	35	25	2100				8.0				90												35						9.40
C-3	68.63	0.67	15.43	1.74	1.03	0.10	0.51	1.99	4.50	4.42	0.18	0.50	99.70	90	350	##	700	40.0					25	35	11	2500				25.0				130												30						8.92
C-4	73.63	0.33	14.16	1.13	0.24	0.02	0.00	0.50	3.14	6.35	0.07	0.44	100.01	200	80	20	380	20.0					20	9	13	1200				40.0				95												11						9.49
C-5	75.35	0.27	13.18	1.08	0.22	0.02	0.00	0.62	3.15	5.50	0.05	0.36	99.80	110	100	35	280	10.0					20	5	15	1400				30.0				65												12						8.65
C-6	66.09	0.69	14.60	3.06	1.72	0.08	1.81	2.54	3.25	4.71	0.28	1.11	99.94	150	480	25	280	<10					20	85	18	1900				14.0				75												25						7.96
C-7	69.29	0.47	14.55	1.81	1.48	0.06	1.19	2.83	3.33	4.40	0.17	0.46	100.04	230	650	25	320	10.0					19	70	35	1700				16.0				70												13						7.73
C-8	73.88	0.33	13.85	0.87	0.24	0.03	0.18	0.26	4.05	5.93	0.09	0.39	100.10	130	40	55	450	15.0					20	7	11	400				20.0				65												4						9.98
C-9	73.30	0.32	13.20	2.93	0.48	0.01	0.00	0.24	3.46	5.67	0.07	0.34	100.02	130	50	80	650	30.0					30	<3	14	1200				12.0				85												9						9.13
C-10	68.63	0.49	15.01	1.62	1.44	0.07	1.22	2.74	4.41	3.60	0.20	0.57	100.00	65	720	25	230	<10					20	55	30	1900				18.0				70												20						8.01
C-11	78.84	0.29	10.79	0.95	0.27	0.03	0.09	0.60	2.94	5.20	0.06	0.22	100.28	120	65	55	180	18.0					15	5	25	560				20.0				100												<3						8.14
C-13 (w	75.89	0.41	12.46	1.07	0.13	n.d.	0.05	0.25	3.60	5.71	0.04	0.50	100.11	100	40	65	650	40.0	<10	<10	n.d.		25	<3	10	1000				30.0				90			<100								<3	<3	<30	<3				9.31
C-14	48.69	1.26	13.27	4.86	8.71	0.18	6.15	10.49	2.41	1.05	0.22	0.50	97.79																																									3.46

Felsic volcanics, Namibia

Sample	SiO2	TiO2	Al2O3	Fe2O3	FeO	MnO	MgO	CaO	Na2O	K2O	P2O5	LOI	Total	Rb	Sr	Y	Zr	Nb	Co	Ni	Cu	Zn	Ga	V	Cr	Ba	U	Th	Sc	Pb	Sm	Nd	Pr	Ce	La	Cs	Hf	Ta	As	Se	Eu	Gd	Tb	Dy	Ho	Er	Tm	Yb	Lu	Li	Be	Ge	Mo	Na+K	Sn
Notch	50.00	*1.00*	*15.50*	*6.00*		*0.150*	*2.00*	*5.00*	*4.90*	*5.50*	*0.30*	2.00		200	*400*	*60*	*360*	*40*	*30*	*16*	*25*	*85*	*26*	*100*	*100*	1300	*20*	*37*	*20*	*20*	*50*	*50*	*15*	*175*	*95*	*3*	*10*	*120*	*##*		*4*	*30*	*5*	*20*	*3*	*9*	*35.5*	*7.5*	*1.6*					
X-16	75.93	0.26	12.08	2.96	0.32	0.01	0.36	0.48	7.93	0.13	0.07	0.42	100.95																																														8.06
X-17	72.07	0.33	13.36	3.76	0.25	0.02	1.33	1.01	7.95	0.30	0.04	0.49	100.91																																														8.25
X-18	69.24		12.00					0.55	3.83	5.36		0.00	90.98																																														9.19
X-19	72.02	0.32	13.78	2.24	1.02	0.02	0.20	0.39	4.07	5.18	0.03	0.65	99.92																																														9.25
X-20	76.01	0.23	12.05	0.80	0.91	0.03	0.20	1.02	3.09	5.02	0.01	1.14	100.51																																														8.11

Ugab River, Namibia

Sample	SiO2	TiO2	Al2O3	Fe2O3	FeO	MnO	MgO	CaO	Na2O	K2O	P2O5	LOI	Total	Rb	Sr	Y	Zr	Nb	Co	Ni	Cu	Zn	Ga	V	Cr	Ba	U	Th	Sc	Pb	Sm	Nd	Pr	Ce	La	Cs	Hf	Ta	As	Se	Eu	Gd	Tb	Dy	Ho	Er	Tm	Yb	Lu	Li	Be	Ge	Mo	Na+K	Sn
Notch	50.00	*1.00*	*15.50*	*6.00*		*0.150*	*2.00*	*5.00*	*4.90*	*5.50*	*0.30*	2.00		200	*400*	*60*	*360*	*40*	*30*	*16*	*25*	*85*	*26*	*100*	*100*	1300	*20*	*37*	*20*	*20*	*50*	*50*	*15*	*175*	*95*	*3*	*10*	*120*	*##*		*4*	*30*	*5*	*20*	*3*	*9*	*35.5*	*7.5*	*1.6*					
L-793	74.92	0.33	12.39	2.15	0.00	0.08	0.24	1.00	3.28	5.24	0.14	0.37	100.14	251	140	81	213	78.0	<6	7	7	34	19	22	390	435	12.00	61.0	<10		119.3	50.99	175.4	234	98		1.800	28.5			0.938							6.63	1.700					8.52
L-797	75.11	0.21	13.05	1.92	0.00	0.04	0.08	0.51	3.62	4.63	0.08	0.61	99.86	225	107	23	199	38.0	<6	6	<6	33	21	17	372	658	6.00	37.0	<10					132	76																					8.25
L-798	72.64	0.26	14.07	2.13	0.00	0.08	0.26	1.09	3.42	5.17	0.12	0.91	100.15	222	204	26	229	48.0	<6	<6	<6	40	20	16	285	1117	7.00	27.0	<10					211	102																					8.59
L-799	73.13	0.08	13.93	1.96	0.00	0.06	0.04	0.95	3.84	4.84	0.13	0.63	99.59	153	168	53	183	14.0	<6	7	11	19	18	29	326	727	7.00	<15	<10					102	36																					8.68
L-802	73.34	0.23	14.56	1.83	0.00	0.05	0.29	1.08	3.46	4.55	0.13	0.84	100.36	234	141	32	142	41.0	<6	6	<6	51	19	22	260	745	<6	15.0	<10					77	38																					8.01

Owka River, Botswana

Sample	SiO2	TiO2	Al2O3	Fe2O3	FeO	MnO	MgO	CaO	Na2O	K2O	P2O5	LOI	Total	Rb	Sr	Y	Zr	Nb	Co	Ni	Cu	Zn	Ga	V	Cr	Ba	U	Th	Sc	Pb	Sm	Nd	Pr	Ce	La	Cs	Hf	Ta	As	Se	Eu	Gd	Tb	Dy	Ho	Er	Tm	Yb	Lu	Li	Be	Ge	Mo	Na+K	Sn
Notch	50.00	*1.00*	*15.50*	*6.00*		*0.150*	*2.00*	*5.00*	*4.90*	*5.50*	*0.30*	2.00		200	*400*	*60*	*360*	*40*	*30*	*16*	*25*	*85*	*26*	*100*	*100*	1300	*20*	*37*	*20*	*20*	*50*	*50*	*15*	*175*	*95*	*3*	*10*	*120*	*##*		*4*	*30*	*5*	*20*	*3*	*9*	*35.5*	*7.5*	*1.6*					
L-600A	76.09	0.13	11.83	1.93	0.00	0.04	0.07	0.45	3.85	5.55	0.06	0.40	100.40	160	59	23	137	14.0	<6	6	14	29	15	<12	68	508	<6	43.0	<10					141	77																					9.40
L-602	70.15	0.49	13.13	3.63	0.00	0.06	0.83	1.80	3.43	4.54	0.16	0.98	99.20	214	137	64	305	26.0	8	7	9	60	18	13	189	716	<6	36.0	<10		14.31	62.39	169.4	213	86			53.19			0.813							4.213	1.338					7.97
L-605	76.55	0.12	12.03	1.16	0.00	0.01	0.02	0.81	3.42	5.47	0.07	0.41	100.07	198	99	7	89	7.0	<6	<6	9	19	13	<12	227	772	<6	42.0	<10					148	102																					8.89
L-606	72.56	0.36	12.83	3.51	0.00	0.06	0.48	1.32	3.22	5.19	0.07	0.73	100.33	185	105	38	202	17.0	<6	6	7	61	18	20	57	781	<6	38.0	<10					227	149																					8.41

Summas Mountains, Namibia, (Volcanic Rocks)

Sample	SiO2	TiO2	Al2O3	Fe2O3	FeO	MnO	MgO	CaO	Na2O	K2O	P2O5	LOI	Total	Rb	Sr	Y	Zr	Nb	Co	Ni	Cu	Zn	Ga	V	Cr	Ba	U	Th	Sc	Pb	Sm	Nd	Pr	Ce	La	Cs	Hf	Ta	As	Se	Eu	Gd	Tb	Dy	Ho	Er	Tm	Yb	Lu	Li	Be	Ge	Mo	Na+K	Sn
Notch	50.00	*1.00*	*15.50*	*6.00*		*0.150*	*2.00*	*5.00*	*4.90*	*5.50*	*0.30*	2.00		200	*400*	*60*	*360*	*40*	*30*	*16*	*25*	*85*	*26*	*100*	*100*	1300	*20*	*37*	*20*	*20*	*50*	*50*	*15*	*175*	*95*	*3*	*10*	*120*	*##*		*4*	*30*	*5*	*20*	*3*	*9*	*35.5*	*7.5*	*1.6*					
L-789	63.91	1.38	14.35	7.45	0.00	0.07	1.13	1.09	4.87	5.21	0.41	0.55	100.42	125	29	66	715	149.0	<6	6	10	80	21	32	135	1019	8.00	15.0	<10		15.46	50.01	136.3	196	67			127.6			2.03							3.88	1.58					10.08
L-791a	72.44	0.40	13.01	3.67	0.00	0.06	0.32	0.54	3.80	5.16	0.10	0.61	100.11	141	25	97	685	130.0	<6	7	<6	35	17	<12	220	637	6.00	32.0	<10		109	22.50	36.51	63	18		2.04	7.288			0.438							5.688	1.400					8.96
L-791b	76.38	0.14	12.55	1.25	0.00	0.02	0.00	0.51	3.09	5.85	0.03	0.29	100.11	270	74	83	70	65.0	<6	10	<6	15	22	16	234	332	8.00	17.0	<10					224	108																					8.94

Table No. A11 CHEMICAL ANALYSIS OF SAMPLES FROM THE GREATER LUFILIAN ARC SORTED BY REGION

Oas Farm, Namibia

Sample	SiO2	TiO2	Al2O3	Fe2O3	FeO	MnO	MgO	CaO	Na2O	K2O	P2O5	LOI	Total	Rb	Sr	Y	Zr	Nb	Co	Ni	Cu	Zn	Ga	V	Cr	Ba	U	Th	Sc	Pb	Sm	Nd	Pr	Ce	La	Cs	Hf	Ta	As	Se	Eu	Gd	Tb	Dy	Ho	Er	Tm	Yb	Lu	Li	Be	Ge	Mo	Na+K	Sn
Notch	50.00	*1.00*	*15.50*	*6.00*		*0.150*	*2.00*	*5.00*	*4.90*	*5.50*	*0.30*	2.00		200	*400*	*60*	*360*	*40*	*30*	*16*	*25*	*85*	*26*	*100*	*100*	1300	*20*	*37*	*20*	*20*	*50*	*50*	*15*	*175*	*95*	*3*	*10*	*120*	##		*4*	*30*	*5*	*20*	*3*	*9*	*35.5*	*7.5*	*1.6*						
L-668	62.61	0.89	17.32	4.83	0.00	0.14	0.72	1.80	6.42	4.79	0.36	0.59	100.47	121	474	69	710	193.0	7	7	6	##	26	14	139	2037	7.0	22.0	<10		13.58	101.4	182.0	235	110		4.45	23.33			0.850	3.85						2.38	1.03						11.21
L-669	64.34	0.61	16.76	4.66	0.00	0.12	0.36	1.46	6.43	4.80	0.23	0.74	100.51	115	350	73	378	204.4	<6	9	7	##	28	<12	124	1647	9.0	31.0	<10	21.7	17.80	102.1	28.00	267	137	0.70	8.24	12.29	0	0	3.96	14.64	2.26	14.05	2.62	7.39	1.00	5.97	0.73						11.23
L-670	57.01	1.45	15.14	11.08	0.00	0.21	1.42	2.33	6.69	3.35	0.53	1.32	100.53	173	1219	73	1843	458.0	<6	9	9	85	42	<12	18	767	17.0	46.0	<10		3.13	27.46	72.13	219	42			74.00			0.288							2.088	0.988						10.04
L-675	60.71	0.10	21.99	3.59	0.00	0.09	0.13	0.94	4.92	6.41	0.03	1.61	100.52	125	384	##	1520	345.0	7	9	23	##	30	20	17	1321	10.0	78.0	11			140.0	591.5	844	440			238.0			3.438	4.23						6.513	1.98						11.33
L-676	59.35	0.87	18.13	5.92	0.00	0.17	1.24	2.05	5.20	5.55	0.24	1.84	100.56	226	634	58	553	139.0	7	7	11	##	26	19	31	1591	<6	19.0	<10					180	85																							10.75
L-691	50.24	3.31	12.95	14.15	0.00	0.21	4.13	6.53	2.95	2.82	0.55	1.51	99.35	151	589	52	368	62.0	39	32	190	##	19	357	66	617	<6	<15	33					110	61																							5.77
L-693	71.37	0.48	11.65	6.47	0.00	0.14	0.19	0.77	4.62	4.46	0.09	0.31	100.55	86	98	31	132	105.3	6	7	14	##	33	<12	60	241	2.3	8.6	<10	4.8	13.2	114	35.3	357	216	0.23	2.81	4.94			0.94	7.69	0.92	5.26	0.97	2.65	0.43	3.26	0.54						9.08
L-694	59.18	1.09	17.07	5.91	0.00	0.17	1.01	2.48	6.84	4.89	0.36	0.54	99.54	106	633	39	333	93.0	7	<6	10	##	23	27	<12	1995	<6	<15	<10					166	87																							11.73
L-695	46.29	3.29	13.34	13.54	0.00	0.48	3.19	4.92	4.10	3.51	0.68	6.78	100.12	197	399	53	329	54.0	27	22	89	##	19	353	28	639	<6	<15	26					64	30																							7.61
L-697	59.94	0.86	16.90	5.28	0.00	0.17	0.99	2.06	6.58	4.59	0.32	1.54	99.23	169	491	##	1363	432.0	8	9	5	##	26	<12	117	1444	15.0	51.0	<10			127.3	480.3	582	291		1.713	107.9			4.550	15.49						10.2	2.08						11.17
L-698	71.68	0.46	11.40	5.84	0.00	0.10	0.10	0.85	4.91	4.10	0.10	0.40	99.94	77	45	50	329	124.0	<6	7	7	##	35	<12	207	157	<6	<15	<10		16.00	66.88	227.6	372	143			92.13			0.250							2.03	1.338						9.01
L-699	63.41	0.28	17.28	5.27	0.00	0.20	0.34	0.93	7.40	4.73	0.12	0.56	100.52	98	114	75	1246	307.0	<6	10	7	##	34	<12	126	458	15.0	50.0	<10					470	310																							12.13
L-708	47.15	0.47	8.72	11.27	0.00	0.53	13.12	14.15	1.46	1.77	0.04	1.79	100.47	86	578	##	469	126.0	16	26	13	##	17	68	14	2096	<6	<15	23					258	97																							3.23
L-712	79.11	0.04	12.04	0.83	0.00	0.04	0.11	0.40	5.47	1.95	0.01	0.54	100.54	33	159	12	17	7.0	<6	10	8	35	18	<12	47	662	<6	<15	<10		107		13.44	41	7		1.700				0.213								0.638						7.42
L-713	71.32	0.16	14.36	2.37	0.00	0.05	0.08	0.32	5.76	5.66	0.02	0.41	100.51	117	94	30	277	71.0	<6	8	9	53	25	19	49	909	<6	<15	<10		120.8	80.38	294.6	436	188		0.96	24.54			0.763							1.200	0.88						11.42
L-714	77.55	0.05	13.19	0.73	0.00	0.03	0.17	0.85	6.33	0.76	0.02	0.67	100.35	16	338	9	250	9.0	<6	9	8	40	23	<12	50	538	<6	16.0	<10		106.0		2.950	83			3.213				0.188								0.488						7.09
L-714a	74.47	0.12	14.63	0.94	0.00	0.04	0.12	0.59	8.15	0.94	0.05	0.41	100.46	16	152	25	237	50.0	<6	8	<6	17	0	12	160	606	0.0	0.0	0					0	0																							9.09
L-715	72.13	0.48	13.02	3.49	0.00	0.09	0.48	1.12	3.88	4.88	0.12	0.50	100.19	118	147	58	348	25.0	8	11	12	67	18	28	47	1230	<6	19.0	<10		75.8	38.91	87.88	154	44			38.90			1.13							3.588	1.363						8.76
L-716	73.88	0.30	12.54	2.79	0.00	0.04	0.41	0.98	4.49	3.98	0.04	0.68	100.13	69	164	38	332	15.9	8	11	12	51	16	19	57	1389	7.0	24.0	<10	9.2	7.00	41.87	11.18	134	66	0.83	6.58	0.73	0	0	1.48	5.96	0.90	6.07	1.28	4.03	0.63	4.55	0.70						8.47
L-1016	77.33	0.10	1.04	2.18	0.00	0.47	2.02	6.71	0.50	0.09	0.13	8.00	98.57	6	124	8	15	4.0	<6	<6	56	14	<9	<12	351	33	<6	<15	12					24	<12																							0.59
L-1016a	79.38	0.10	0.80	2.49	0.00	0.45	1.96	5.74	0.55	0.13	0.04	7.50	99.14	5	140	6	37	4.0	<6	7	28	27	<9	13	15	57	<6	<15	10					23	<12																							0.68
L-1019	72.23	0.41	13.17	3.00	0.00	0.11	0.24	0.79	6.18	3.79	0.08	0.41	100.41	50	101	31	290	46.9	<6	10	9	62	17	<12	253	1351	1.8	17.0	<10	29.0	7.79	47.2	12.5	110	60	0.15	7.31	2.12			2.05	6.81	0.95	5.85	1.15	3.36	0.49	3.38	0.50						9.97
L-1020	70.82	0.58	12.68	4.01	0.00	0.10	0.76	1.57	5.17	3.14	0.09	0.31	99.23	70	173	52	445	22.0	<6	8	64	85	17	19	<12	1364	<6	19.0	<10					180	95																							8.31
X-21	60.78	0.87	16.97	1.13	4.10	0.16	0.99	1.94	5.65	5.27	0.22	1.78	99.86																																																		10.92
X-22	64.42	1.12	14.69	4.34	1.80	0.07	1.37	1.17	3.71	5.64	0.25	1.78	100.36																																																		9.35
X-23	63.81	0.59	14.21	3.67	1.10	0.15	1.48	2.27	4.37	6.00	0.09	3.13	100.87																																																		10.37
X-24	51.29	0.40	19.06	5.95	1.05	0.42	0.82	4.79	6.75	5.19	0.30	3.38	99.40																																																		11.94
X-25	47.49	2.22	14.47	3.74	8.09	0.05	6.73	11.57	1.24	0.77	0.30	2.80	99.47																																																		2.01
X-26	48.82	1.03	12.21	3.62	6.54	0.15	13.68	9.63	1.77	1.10	0.59	1.16	100.30																																																		2.87

Table No. A12 CHEMICAL ANALYSIS OF SAMPLES FROM THE GREATER LUFILIAN ARC SORTED BY REGION

Lofdal Farm, Namibia

Sample	SiO2	TiO2	Al2O3	Fe2O3	FeO	MnO	MgO	CaO	Na2O	K2O	P2O5	LOI	Total	Rb	Sr	Y	Zr	Nb	Co	Ni	Cu	Zn	Ga	V	Cr	Ba	U	Th	Sc	Pb	Sm	Nd	Pr	Ce	La	Cs	Hf	Ta	As	Se	Eu	Gd	Tb	Dy	Ho	Er	Tm	Yb	Lu	Li	Be	Ge	Mo	Na+K	Sn
Notch	50.00	1.00	15.50	6.00		0.150	2.00	5.00	4.90	5.50	0.30	2.00		200	400	60	360	40	30	16	25	85	26	100	100	1300	20	37	20	20	50	50	15	175	95	3	10	120	##		4	30	5	20	3	9	35.5	7.5	1.6							
L-722	7.50	0.04	0.13	9.55	0.00	0.68	2.58	43.77	0.00	0.00	0.03	36.2	100.52	7	210	##	119	13.0	23	<6	5	37	<9	194	12	145	6.00	27.0	54		17.16		15.61	10	<12			229.3											0.263	0.863					0.00	
L-728	75.06	0.16	10.35	2.83	0.00	0.14	0.22	2.20	6.61	0.86	0.06	2.04	100.53	23	140	58	212	33.0	<6	10	15	45	18	14	67	581	4.64	20.9	15	24.2	17.2	82.2	20.2	171	73	0.33	6.35	2.52			3.25	14.4	2.01	12.1	2.23	6.18	0.99	6.52	1.07					7.47	
L-729	73.58	0.31	12.64	2.31	0.00	0.05	0.34	0.84	3.69	4.96	0.03	1.70	100.45	113	82	46	281	24.0	<6	6	6	60		<12	58	957																										8.65	
L-740	56.74	0.26	18.91	5.92	0.00	0.18	0.21	1.03	6.29	4.68	0.03	6.26	100.51	170	442	26	1803	563.0	<6	11	8	##	42	<12	27	617	27.0	18.0	<10		8.750	22.20	71.88	112	36			114.8			0.500							0.138	0.838					10.97	
L-741	56.63	0.47	19.54	7.23	0.00	0.44	0.80	3.09	4.14	7.21	0.11	0.91	100.57	169	548	49	640	337.0	<6	<6	14	##	34	14	18	1955	19.00	<15	<10		14.68	51.69	210.8	248	131			127.0			1.813							1.863	1.100					11.35	
L-742	68.41	0.18	10.00	3.45	0.00	0.20	2.09	0.90	5.40	1.17	0.03	8.44	100.27	59	181	41	310	26.0	11	13	32	##	19	18	44	802	<6	21.0	<10		2.538	32.53	52.30	79	44			71.88			0.588							1.350	0.600					6.57	
L-754	53.02	1.59	13.32	16.18	0.00	0.28	6.53	7.50	0.32	1.02	0.30	0.15	100.21	318	84	40	94	8.0	50	53	94	##	17	393	178	235	<6	<15	49					25	12																			1.34	
L-1021	72.02	0.43	12.86	3.47	0.00	0.05	0.24	1.10	4.37	4.02	0.07	0.53	99.16	83	92	84	464	33.0	<6	8	5	29	17	<12	250	1355	<6	18.0	<10					143	61																8.39	
L-1022	54.76	0.44	20.41	5.90	0.00	0.20	0.33	1.95	4.97	7.25	0.13	2.78	99.12	189	616	24	767	249.0	7	<6	11	##	36	14	<12	629	8.00	<15	<10		2.638	27.54	47.69	61	19			94.38			0.38								0.763					12.22	
L-1023	47.51	0.82	15.70	11.39	0.00	0.21	7.63	10.97	2.78	0.87	0.09	2.31	100.28	19	177	23	45	5.0	51	86	11	##	19	246	354	223	<6	<15	42					33	20																			3.65	
L-1024a	7.58	0.07	0.57	9.33	0.00	0.79	5.76	37.24	0.03	0.15	0.23	38.8	100.50	6	335	62	9	44.1	28	21	177	59	<9	23	<12	115	19.00	20.0	49	2.4	50.29	543.3	178.9	2058	1583	0.06	0.11	n.d.	0	0	7.27	28.4	3.20	14.82	2.54	6.75	1.02	7.22	1.10					0.18	
L-1024c	5.56	0.06	0.20	9.37	0.00	0.84	6.08	39.51	0.01	0.04	0.23	38.7	100.56	10	325	92	18	31.0	29	11	116	29	<9	24	<12	99	20.0	18.0	49					1786	1383																0.05	
L-1025	42.06	1.06	1.26	21.42	0.00	0.77	2.76	17.44	1.61	0.56	3.85	7.40	100.19	30	1546	50	1312	1425	42	10	29	##	12	334	106	214	86.4	19.5	33	4.8	27.7	183	47.1	396	176	0.39	10.1	33.6			8.30	21.9	2.59	13.0	2.12	5.37	0.85	7.25	1.48					2.17	
L-1027	55.06	0.81	15.77	5.91	0.00	0.27	2.32	3.60	4.38	6.88	0.23	3.58	98.81	177	429	37	621	220.0	14	42	25	##	24	45	174	1043	<6	<15	<10			58.35	136.1	239	72			94.3			1.663							1.063	0.838					11.26	
L-1032	46.04	1.99	15.47	14.07	0.00	0.33	6.80	9.26	3.22	0.75	0.42	1.94	100.29	10	322	48	132	9.0	47	45	26	##	15	345	218	299	<6	<15	40		109.3	42.20	61.28	<12	40		3.53	22.53			0.600							3.588	1.138					3.97	
LR25	4.673	0.29	0.34	5.85		1.89	0.76	70.8	1.58	0.01	5.82			1	6765	65	128	167	58	166	##	0	191	50	469	24	7730	7	0	673	1335	0	3341	2342	0	8	35	0											0	75	1.59	27
LR23	6.138	0.06	1.84	14.0		0.45	30.5	40.6	2.47	0.10	0.18			6	941	2633	327	152	71	53	41	53	0	62	86	25	15	130	19	71	0	0	88	0	32	0	13	449	24											0	5	2.57	0
LR20	2.875	0.02	0.60	12.9		0.38	33.1	45.0	1.67	0.04	0.15			0	1166	##	97	22	16	44	31	79	0	115	85	32	0	36	0	10	0	0	0	0	37	25	0	42	6											0	2	1.71	0
LR5	7.666	0.30	1.32	16.1		2.24	3.89	48.8	1.51	0.53	8.09			19	1669	4033	130	181	90	46	89	45	0	36	114	393	26	2347	0	91	655	1734	486	4909	3846	18	7	75	49											0	21	2.05	0
LR4	2.133	0.10	0.12	33.4		3.12	1.61	48.6	1.71	0.04	0.66			0	1054	2761	44	598	44	21	0	99	-5	0	0	0	28	1593	0	438	0	2003	0	6950	5436	3	7	2199	93											0	74	1.75	12
AM-1															1839	8630										114	11	1019		330		748		1726	1061				78													0.00	

Mesopotamie Farm, Copper Vallei Mine, Namibia

Sample	SiO2	TiO2	Al2O3	Fe2O3	FeO	MnO	MgO	CaO	Na2O	K2O	P2O5	LOI	Total	Rb	Sr	Y	Zr	Nb	Co	Ni	Cu	Zn	Ga	V	Cr	Ba	U	Th	Sc	Pb	Sm	Nd	Pr	Ce	La	Cs	Hf	Ta	As	Se	Eu	Gd	Tb	Dy	Ho	Er	Tm	Yb	Lu	Li	Be	Ge	Mo	Na+K	Sn
Notch	50.00	1.00	15.50	6.00		0.150	2.00	5.00	4.90	5.50	0.30	2.00		200	400	60	360	40	30	16	25	85	26	100	100	1300	20	37	20	20	50	50	15	175	95	3	10	120	##		4	30	5	20	3	9	35.5	7.5	1.6							
L-759	74.06	0.03	14.47	0.47	0.00	0.04	0.02	0.70	3.55	5.54	0.06	0.94	99.88	109	124	20	16	7.0	<6	<6	<6	12	13	<12	185	649	<6	<15	<10					12	<12																9.09	
L-772	72.55	0.03	14.29	0.43	0.00	0.03	0.03	0.05	2.34	10.07	0.02	0.67	100.51	201	100	7	<8	4.0	<6	<6	8	28	13	<12	44	579	<6	<15	<10					21	<12																12.41	
L-773	74.83	0.06	14.98	0.87	0.00	0.02	0.11	0.80	5.35	3.07	0.04	0.41	100.54	76	71	##	64	14.0	<6	10	8	43	20	<12	47	176	<6	<15	<10					25	<12																8.42	
L-783	71.86	0.45	13.96	3.32	0.00	0.08	0.50	0.78	3.49	5.15	0.18	0.71	100.48	223	85	54	273	22.0	<6	6	9	49	17	25	239	859	<6	27.0	<10					161	75																8.64	
L-784	71.83	0.39	13.23	3.59	0.00	0.06	0.56	1.31	3.67	5.07	0.09	0.70	100.50	193	105	58	312	23.0	<6	7	7	59	17	23	63	1049	7.00	26.0	<10		11.3	37.06	98.50	155	51		1.513	41.66			0.78							3.938	1.400					8.74	

Other alkaline and gabbroic rocks to compare with (used by Frets)

Sample	SiO2	TiO2	Al2O3	Fe2O3	FeO	MnO	MgO	CaO	Na2O	K2O	P2O5	LOI	Total	Rb	Sr	Y	Zr	Nb	Co	Ni	Cu	Zn	Ga	V	Cr	Ba	U	Th	Sc	Pb	Sm	Nd	Pr	Ce	La	Cs	Hf	Ta	As	Se	Eu	Gd	Tb	Dy	Ho	Er	Tm	Yb	Lu	Li	Be	Ge	Mo	Na+K	Sn
Notch	50.00	1.00	15.50	6.00		0.150	2.00	5.00	4.90	5.50	0.30	2.00		200	400	60	360	40	30	16	25	85	26	100	100	1300	20	37	20	20	50	50	15	175	95	3	10	120	##		4	30	5	20	3	9	35.5	7.5	1.6							
X-27	47.85	1.47	16.84	2.70	8.50	0.19	6.66	11.79	2.54	0.75	0.27	0.46	100.02																																													3.29	
X-28	60.59	0.58	14.99	2.44	2.30	1.13	0.91	2.55	8.98	3.81	tr	1.00	99.28																																													12.79	
X-29	61.03		18.63	3.66			1.04	1.56	7.68	5.57		0.41	99.58																																													13.25	
X-30	63.34	0.57	16.00	4.17	1.69	0.11	0.35	2.29	3.93	5.86	0.17	2.04	100.52																																													9.79	
X-31	61.56	0.82	15.25	4.29	3.89	0.25	1.28	1.68	4.10	4.40	0.16	1.24	98.92																																													8.50	
X-32	65.80	0.60	15.40	3.84	0.28	0.06	0.11	1.12	5.60	5.10	0.38	1.05	99.34																																													10.70	
X-33	51.80	0.32	18.20	2.24	2.09	0.17	2.56	4.93	8.22	5.36	0.50	3.69	100.08																																													13.58	

Table No. A13 CHEMICAL ANALYSIS OF SAMPLES FROM THE GREATER LUFILIAN ARC SORTED BY REGION

Otjiwarongo Environs, Namibia

Sample	SiO2	TiO2	Al2O3	Fe2O3	FeO	MnO	MgO	CaO	Na2O	K2O	P2O5	LOI	Total	Rb	Sr	Y	Zr	Nb	Co	Ni	Cu	Zn	Ga	V	Cr	Ba	U	Th	Sc	Pb	Sm	Nd	Pr	Ce	La	Cs	Hf	Ta	As	Se	Eu	Gd	Tb	Dy	Ho	Er	Tm	Yb	Lu	Li	Be	Ge	Mo	Na+K	Sn
Notch	50.00	*1.00*	*15.50*	*6.00*		*0.150*	*2.00*	*5.00*	*4.90*	*5.50*	*0.30*	2.00		200	*400*	*60*	*360*	*40*	*30*	*16*	*25*	*85*	*26*	*100*	*100*	1300	*20*	*37*	*20*	*20*	*50*	*50*	*15*	*175*	*95*	*3*	*10*	*120*	##		*4*	*30*	*5*	*20*	*3*	*9*	*35.5*	*7.5*	*1.6*						
L-808	70.53	0.14	15.35	1.50	0.00	0.05	0.42	1.71	4.80	3.67	0.07	2.04	100.28	140	89	12	29	13.9	<6	7	10	71	16	13	39	154	<6	<15	<10	32.4	2.03	9.16	2.46	26	<12	5.99	1.17	1.22	0	0	0.50	1.81	0.31	2.11	0.42	1.29	0.21	1.48	0.22					8.47
L-809	71.56	0.07	14.95	1.24	0.00	0.03	0.23	0.87	3.46	7.52	0.06	0.50	100.49	253	92	19	<8	9.0	<6	7	11	56	16	<12	27	301	<6	<15	<10					29	<12																				10.98
L-810	73.89	0.06	14.05	1.11	0.00	0.04	0.16	1.04	4.00	5.44	0.04	0.50	100.33	173	85	7	<8	7.0	9	10	13	50	14	<12	56	249	<6	<15	<10					24	<12																				9.44
L-812	75.60	0.08	12.89	1.27	0.00	0.03	0.25	1.29	4.03	4.17	0.09	0.71	100.41	141	104	86	215	10.0	<6	8	9	67	13	<12	34	439	17.00	30.0	<10					93	55																				8.20
L-813	71.80	0.04	15.51	0.86	0.00	0.03	0.12	1.40	4.26	5.59	0.08	0.78	100.47	173	115	65	77	6.0	<6	9	13	23	14	<12	42	625	13.00	21.0	<10					63	22																				9.85
L-814	89.59	0.02	5.33	0.65	0.00	0.02	0.02	0.84	2.94	0.31	0.04	0.63	100.39	23	38	5	<8	4.0	<6	7	10	54	<9	<12	77	50	<6	<15	<10					26	<12																				3.25
L-815	69.73	0.30	14.51	3.35	0.00	0.08	0.84	1.34	3.85	5.59	0.16	0.65	100.40	214	122	43	268	25.0	<6	8	10	75	17	12	68	584	42.0	16.0	<10					68	29																				9.44
L-850	71.15	0.38	13.69	2.97	0.00	0.05	0.47	1.56	3.09	4.96	0.10	0.48	98.90	264	153	22	241	15.0	7	7	23	57	17	27	13	919	<6	46.0	<10		116.9	48.33	131.0	171	67		4.76	34.13			0.588							0.18	0.73					8.05
L-1037	67.15	0.44	16.05	2.51	0.00	0.02	0.77	1.33	2.99	7.49	0.15	0.46	99.36	204	190	22	149	16.0	<6	6	8	41	17	15	156	1143	<6	105.0	<10					288	157																				10.48
L-1038	68.09	0.44	15.77	2.42	0.00	0.02	0.69	1.39	3.03	6.45	0.17	0.40	98.87	185	178	26	247	18.0	<6	8	13	39	16	14	162	975	<6	112.0	<10					316	175																				9.48
L-1039	70.93	0.25	13.72	2.43	0.00	0.01	0.03	0.57	3.62	5.51	0.10	1.71	98.88	160	562	19	156	20.0	<6	7	21	11	18	<12	230	793	<6	26.0	<10					88	46																				9.13
L-1039a	73.60	0.10	13.76	0.98	0.00	0.02	0.06	0.47	3.67	6.14	0.03	0.53	99.36	168	205	12	38	2.1	<6	8	6	11	13	12	250	1060	<6	<15	<10	24.9	3.17	17.63	4.60	55	23	2.53	1.29	0.08	0	0	1.07	2.98	0.39	2.17	0.40	1.09	0.15	0.98	0.15					9.81
L-1039c	70.50	0.34	13.95	3.40	0.00	0.02	0.00	0.71	3.38	5.94	0.11	2.16	100.51	172	547	24	162	24.0	<6	7	29	12	18	<12	309	776	<6	32.0	<10					103	55																				9.32
LJ1	68.16	0.46	16.02	2.81	0.00	0.02	0.89	1.54	2.85	7.17	0.16	0.55	100.07	196	191	24	259	17.0	4		30	42		15	0	954	1.00	95.0	4																												10.02
LL1	73.41	0.09	14.65	0.80	0.00	0.01	0.27	1.00	3.34	6.24	0.20	1.26	100.02	150	176	17	42	6.0	3	3	13	11		6	1	1468	0.00	5.0	2																																9.58
LL10	56.48	1.24	17.84	6.85	0.00	0.19	1.96	3.78	5.74	4.86	0.74	0.74	99.67	135	965	36	340	99.0	11	3	0	78		44	0	1366	9.00	25.0	1																																10.60
LL11	73.00	0.00	14.00	2.00	0.00	0.00	0.00	1.00	3.00	6.00	0.00	1.00	99.86	287	134	34	210	16.0	2	1	0	30		20	3	880	3.00	55.0	5																																9.00
LL13	62.00	1.00	11.00	4.00	0.00	0.00	3.00	18.00	1.00	0.00	0.00	7.00	100.02	12	701	42	128	6.0	9	26	3	58		101	66	448	4.00	5.0	10																																1.00
LL14	57.00	1.00	17.00	9.00	0.00	0.00	1.00	3.00	6.00	5.00	0.00	1.00	99.52	280	355	##	2052	364.0	4		5	##		4	0	1161	22.0	83.0	5																																11.00
LL15	62.00	1.00	16.00	6.00	0.00	0.00	1.00	4.00	6.00	5.00	0.00	4.00	99.73	118	328	31	305	47.0	10	9	0	73		125	22	1308	3.00	26.0	15																																11.00
LL16	70.00	1.00	14.00	3.00	0.00	0.00	1.00	2.00	3.00	5.00	0.00	0.00	99.49	230	152	24	320	30.0	4	2	0	33		39	9	790	3.00	33.0	4																																8.00
LL17a	73.00	0.00	14.00	1.00	0.00	0.00	0.00	1.00	3.00	7.00	0.00	1.00	99.75	202	57	12	29	9.0	2		5	8		4	6	220	5.00	3.0	1																																10.00
LL17b	66.00	1.00	16.00	5.00	0.00	0.00	1.00	3.00	3.00	5.00	0.00	0.00	99.77	140	208	22	311	16.0	13	2	2	60		50	7	1167	4.00	18.0	9																																8.00
LL18	76.00	0.00	13.00	1.00	0.00	0.00	0.00	1.00	3.00	7.00	0.00	1.00	100.07	178	84	8	55	3.0	0			8		5	4	316	5.00	4.0	1																																10.00
LL2a	75.73	0.02	14.98	0.67	0.00	0.01	0.06	0.12	3.62	4.86	0.04	1.36	100.11	181	35	10	19	19.0	2	1	14	8		11	0	104	2.00	4.0	2																																8.48
LL2b	69.71	0.00	16.92	0.31	0.00	0.01	0.00	0.04	2.54	10.40	0.13	0.60	100.06	356	67	7	4	1.0	2	1	0	2		0	1	205	0.00	2.0	0																																12.94
LL3a	75.92	0.03	13.87	0.68	0.00	0.01	0.05	0.39	2.87	5.93	0.01	1.19	99.77	156	182	13	29	0.0	2	1	14	4		5	3	659	0.00	7.0	1																																8.80
LL3b	70.31	0.04	16.91	0.47	0.00	0.01	0.24	0.37	2.44	9.09	0.09	1.20	99.96	348	252	9	5	4.0	2	1	0	7		7	1	495	1.00	0.0	5																																11.53
LL4	74.72	0.10	13.50	1.59	0.00	0.03	0.10	0.80	3.49	5.74	0.02	0.41	100.08	365	50	32	138	29.0	1		0	27		1	0	235	4.00	52.0	5																																9.23
LL5	75.94	0.03	14.40	0.33	0.00	0.00	0.00	1.44	4.03	3.46	0.03	0.64	99.67	180	89	47	48	11.0	1		6	4		0	0	151	5.00	11.0	1																																7.49
LL9	79.03	0.02	14.86	0.39	0.00	0.00	0.01	0.02	0.30	5.63	0.00	3.19	100.25	256	26	9	33	9.0	2	2	1	3		12	3	285	2.00	3.0	2																																5.93

Grootfontein Inlier, Otavi Mountains, Namibia

Sample	SiO2	TiO2	Al2O3	Fe2O3	FeO	MnO	MgO	CaO	Na2O	K2O	P2O5	LOI	Total	Rb	Sr	Y	Zr	Nb	Co	Ni	Cu	Zn	Ga	V	Cr	Ba	U	Th	Sc	Pb	Sm	Nd	Pr	Ce	La	Cs	Hf	Ta	As	Se	Eu	Gd	Tb	Dy	Ho	Er	Tm	Yb	Lu	Li	Be	Ge	Mo	Na+K	Sn
Notch	50.00	*1.00*	*15.50*	*6.00*		*0.150*	*2.00*	*5.00*	*4.90*	*5.50*	*0.30*	2.00		200	*400*	*60*	*360*	*40*	*30*	*16*	*25*	*85*	*26*	*100*	*100*	1300	*20*	*37*	*20*	*20*	*50*	*50*	*15*	*175*	*95*	*3*	*10*	*120*	##		*4*	*30*	*5*	*20*	*3*	*9*	*35.5*	*7.5*	*1.6*						
L-1014	68.99	0.41	14.20	3.21	0.00	0.05	1.35	2.61	3.04	3.64	0.11	1.80	99.41	58.9	321	5	43.2	2.55	9.0	20.0	13.00	43	13	60	173	1632	<6	<15	<10	14.1	2.27	18.16	4.86	64	34.0	0.24	1.00	n.d.	0.0	0.0	1.27	1.76	0.20	1.08	0.20	0.51	0.07	0.44	0.07					6.68
L-1042	70.57	0.26	14.13	2.58	0.00	0.06	0.45	0.67	2.79	6.14	0.10	1.35	99.10	317	68	65	161	17.0	7	12	20	29	14	16	<12	471	<6	35.0	<10		109.9	44.76	78.50	106	34		3.63	26.99			0.413	0.78						3.88	1.213					8.93
L-1043	72.42	0.34	13.62	2.40	0.00	0.04	0.57	0.57	2.76	5.77	0.10	1.27	99.86	276	85	71	207	17.0	7	9	51	30	14	28	<12	525	<6	44.0	<10		109.1	41.74	89.3	140	35		1.713	36.96			0.750							8.700	1.850					8.53
L-1044	73.43	0.25	12.72	2.04	0.00	0.04	0.39	0.49	2.79	5.94	0.11	1.10	99.30	293	67	47	166	16.0	6	9	115	70	12	20	12	415	<6	36.0	<10					109	44																				8.73
L-1045	65.28	0.40	17.54	2.82	0.00	0.08	0.36	3.60	6.67	1.70	0.11	1.41	99.97	90	471	##	246	24.0	5	7	48	18	20	24	<12	116	<6	57.0	12		12.20	14.56	48.3	154	16			297.8			0.188							2.238	1.68					8.37
L-1046	72.78	0.33	12.73	2.40	0.00	0.03	0.55	0.76	2.61	5.45	0.12	1.39	99.15	283	61	69	193	16.0	6	9	30	27	13	25	16	473	<6	42.0	<10					126	53																				8.06

Okatjepuiko, Witvlei, Namibia

Sample	SiO2	TiO2	Al2O3	Fe2O3	FeO	MnO	MgO	CaO	Na2O	K2O	P2O5	LOI	Total	Rb	Sr	Y	Zr	Nb	Co	Ni	Cu	Zn	Ga	V	Cr	Ba	U	Th	Sc	Pb	Sm	Nd	Pr	Ce	La	Cs	Hf	Ta	As	Se	Eu	Gd	Tb	Dy	Ho	Er	Tm	Yb	Lu	Li	Be	Ge	Mo	Na+K	Sn
Notch	50.00	*1.00*	*15.50*	*6.00*		*0.150*	*2.00*	*5.00*	*4.90*	*5.50*	*0.30*	2.00		200	*400*	*60*	*360*	*40*	*30*	*16*	*25*	*85*	*26*	*100*	*100*	1300	*20*	*37*	*20*	*20*	*50*	*50*	*15*	*175*	*95*	*3*	*10*	*120*	##		*4*	*30*	*5*	*20*	*3*	*9*	*35.5*	*7.5*	*1.6*						
L-625	74.31	0.32	12.49	2.19	0.00	0.04	0.42	0.94	5.72	2.00	0.10	0.70	99.23	43	78	49	280	30.0	<6	15	753	26	15	21	123	493	<6	<15	<10					125	54																				7.72
L-626	75.44	0.32	12.53	3.15	0.00	0.05	0.57	0.71	5.99	1.04	0.06	0.63	100.49	18	64	50	263	30.0	<6	13	1078	41	17	21	53	609	<6	<15	<10			10.56	33.25	65.50	112	31			38.58			1.038							3.050	1.238					7.03
L-633	51.27	1.55	16.00	10.81	0.00	0.18	6.69	7.17	3.71	1.69	0.26	1.07	100.40	56	239	26	123	13.0	52	115	499	##	17	279	202	550	<6	<15	31			12.91	15.65	35.9	43	11			224.0					5.638					0.563	1.23					5.40
L-635	62.14	0.98	15.43	6.05	0.00	0.12	3.29	3.28	7.37	0.22	0.15	1.00	100.03	9	33	31	241	19.0	20	64	64	46	20	134	101	58	<6	<15	19			9.03	23.53	48.81	67	21			90.3			0.650		2.688					0.900	1.08					7.59
L-637	69.84	0.53	13.33	5.85	0.00	0.06	0.58	2.19	5.95	0.76	0.10	1.00	100.19	17	165	56	727	29.0	8	18	128	34	20	26	49	359	<6	<15	10			123	60.93	134.1	180	93		3.313	34.34			0.588							4.300	1.53					6.71
L-638	77.05	0.18	11.68	2.36	0.00	0.04	0.14	0.62	4.27	3.73	0.02	0.42	100.51	59	91	35	148	17.5	<6	9	95	29	15	14	66	751	<6	<15	<10	10.8	7.71	40.96	10.40	116	53	0.41	4.36	0.51	0	0	1.02	7.02	1.09	6.94	1.36	3.85	0.54	3.56	0.51					8.00
L-641	50.76	2.24	13.78	12.16	0.00	0.24	6.49	7.32	4.30	0.62	0.40	1.90	100.21	27	195	33	131	15.0	48	90	704	##	17	262	196	247	<6	<15	34				12.08	46.00	28	<12																				4.92
L-645	56.67	1.27	14.07	9.26	0.00	0.09	0.42	5.87	8.40	0.16	0.33	3.96	100.50	5	67	38	214	17.0	9	21	6	21	19	113	185	87	<6	<15	26					49	22																				8.56
L-648	72.50	0.35	12.81	4.25	0.00	0.05	0.69	0.64	7.27	1.32	0.06	0.59	100.53	25	69	21	248	12.0	6	17	1546	44	13	47	67	1144	<6	<15	<10					89	30																				8.59
L-649	73.86	0.30	12.07	4.77	0.00	0.06	0.53	0.64	5.74	1.86	0.05	0.56	100.44	37	63	16	193	11.0	9	19	2238	37	11	50	78	1330	<6	<15	<10					74	19																				7.60
L-816	74.57	0.30	12.43	3.00	0.00	0.06	0.39	1.37	6.02	1.96	0.04	0.44	100.58	43	91	52	284	32.0	<6	13	104	62	17	18	81	386	<6	<15	<10		115.9	35.64	72.13	122	33		1.200	32.86			1.13							2.68	1.18					7.98

Table No. A14 CHEMICAL ANALYSIS OF SAMPLES FROM THE GREATER LUFILIAN ARC SORTED BY REGION

Spitzkoppe Complexes, Namibia

Sample	SiO2	TiO2	Al2O3	Fe2O3	FeO	MnO	MgO	CaO	Na2O	K2O	P2O5	LOI	Total	Rb	Sr	Y	Zr	Nb	Co	Ni	Cu	Zn	Ga	V	Cr	Ba	U	Th	Sc	Pb	Sm	Nd	Pr	Ce	La	Cs	Hf	Ta	As	Se	Eu	Gd	Tb	Dy	Ho	Er	Tm	Yb	Lu	Li	Be	Ge	Mo	Na+K	Sn
Notch	50.00	*1.00*	*15.50*	*6.00*		*0.150*	*2.00*	*5.00*	*4.90*	*5.50*	*0.30*	2.00		200	*400*	*60*	*360*	*40*	*30*	*16*	*25*	*85*	*26*	*100*	*100*	1300	*20*	*37*	*20*	*20*	*50*	*50*	*15*	*175*	*95*	*3*	*10*	*120*	*##*		*4*	*30*	*5*	*20*	*3*	*9*	*35.5*	*7.5*	*1.6*							
X-92	77	0.1	11.7	2.06		0.02	0.08	0.74	3.03	5.23	0.02	0.52		473	14	##	196	141		3	3	44		2	7	75			2					148	84																					8.26	
X-93	76	0.04	12.8	1.57		0.02	0.04	0.62	3.89	4.93	0.01	0.46		604	2	##	112	88		2	3	58		6	2	9			1					63	26																					8.82	
X-94	75.7	0.04	12.9	1.71		0.02	0.05	0.65	4.05	4.84	0.02	0.45		620	1	##	128	83		4	4	45		2	7	2		-						54	21																					8.89	
X-95	69.8	0.51	12.6	5.77		0.08	0.11	2.3	2.55	6.29	0.09	1.38		243	81	68	474	24	-	-	-		-	-	1051			10					162	77																					8.84	

Erongo Complex, Namibia

Sample	SiO2	TiO2	Al2O3	Fe2O3	FeO	MnO	MgO	CaO	Na2O	K2O	P2O5	LOI	Total	Rb	Sr	Y	Zr	Nb	Co	Ni	Cu	Zn	Ga	V	Cr	Ba	U	Th	Sc	Pb	Sm	Nd	Pr	Ce	La	Cs	Hf	Ta	As	Se	Eu	Gd	Tb	Dy	Ho	Er	Tm	Yb	Lu	Li	Be	Ge	Mo	Na+K	Sn
X-96	76.3	0.07	13.3	1.43		0.03	0.06	0.43	3.08	5.07	0.26	-		637	25	##	60	26		10	2	38				76			6																									8.15	

Brandberg Complex, Namibia

Sample	SiO2	TiO2	Al2O3	Fe2O3	FeO	MnO	MgO	CaO	Na2O	K2O	P2O5	LOI	Total	Rb	Sr	Y	Zr	Nb	Co	Ni	Cu	Zn	Ga	V	Cr	Ba	U	Th	Sc	Pb	Sm	Nd	Pr	Ce	La	Cs	Hf	Ta	As	Se	Eu	Gd	Tb	Dy	Ho	Er	Tm	Yb	Lu	Li	Be	Ge	Mo	Na+K	Sn
Notch	50.00	*1.00*	*15.50*	*6.00*		*0.150*	*2.00*	*5.00*	*4.90*	*5.50*	*0.30*	2.00		200	*400*	*60*	*360*	*40*	*30*	*16*	*25*	*85*	*26*	*100*	*100*	1300	*20*	*37*	*20*	*20*	*50*	*50*	*15*	*175*	*95*	*3*	*10*	*120*	*##*		*4*	*30*	*5*	*20*	*3*	*9*	*35.5*	*7.5*	*1.6*							
X-97	75	0.16	10.4	5.06		0.07	0.06	0.16	4.43	4.69	0	0.66		1241	18	##	537	95								14								459	207																					9.12	
X-98	71.3	0.48	13.1	4.71		0.11	0.23	0.91	3.45	5.53	0.11	0.98		211	111	66	483	56								856								134	64																					8.98	
X-99	71.1	0.45	13.1	4.38		0.11	0.3	1.46	3.46	5.6	0.1	0.49		210	112	##	455	53								807								163	85																					9.06	
X-100	70.3	0.5	13.5	4.37		0.11	0.38	1.52	3.58	5.66	0.11	0.28		209	111	78	505	61								808								144	66																					9.24	
X-101	70	0.55	13.7	4.65		0.11	0.3	1.88	3.59	5.15	0.11	0.56		188	132	73	472	51																112	54																					8.74	

Nigerian Ring Complexes

Sample	SiO2	TiO2	Al2O3	Fe2O3	FeO	MnO	MgO	CaO	Na2O	K2O	P2O5	LOI	Total	Rb	Sr	Y	Zr	Nb	Co	Ni	Cu	Zn	Ga	V	Cr	Ba	U	Th	Sc	Pb	Sm	Nd	Pr	Ce	La	Cs	Hf	Ta	As	Se	Eu	Gd	Tb	Dy	Ho	Er	Tm	Yb	Lu	Li	Be	Ge	Mo	Na+K	Sn
Notch	50.00	*1.00*	*15.50*	*6.00*		*0.150*	*2.00*	*5.00*	*4.90*	*5.50*	*0.30*	2.00		200	*400*	*60*	*360*	*40*	*30*	*16*	*25*	*85*	*26*	*100*	*100*	1300	*20*	*37*	*20*	*20*	*50*	*50*	*15*	*175*	*95*	*3*	*10*	*120*	*##*		*4*	*30*	*5*	*20*	*3*	*9*	*35.5*	*7.5*	*1.6*							
AMN24	72.60	0.29	14.07	0.90	1.73	0.07	0.43	1.01	3.36	5.74	0.07	0.47	100.74	185	100	63	246	57				61		9		362		27		22				144	59		6														34	5		9.10	8
RN75	75.90	0.11	12.85	0.33	1.05	0.05	0.02	0.24	3.91	4.31	0.01	0.88	99.66	979	15	##	399	214			120	##		0		109		111		56				296	234		28														391	7		8.22	40
PAN112	73.90	0.15	14.88	0.43	0.80	0.02	0.67	0.43	3.98	5.17	0.02	0.61	101.06	192	28	##	234	88						0		80		25		22				195	189		7														25	8		9.15	19
JON147	73.20	0.18	14.18	0.67	1.19	0.02	0.08	0.73	3.45	5.32	0.03	0.98	100.03	296	38	##	330	118				##		0		264		41		38				251	218		8														32	14		8.77	39
B34	76.00	0.10	11.74	0.37	0.89	0.02	0.09	0.83	3.78	5.77	0.04	0.24	99.87	574	4	##	141	158				60		12		39		40		74				114	64		5														205	9		9.55	##
MD333	75.40	0.10	13.33	0.01	0.96	0.02	0.04	0.34	4.26	4.53	0.01	0.20	99.20	620	0	##	129	78			9	68		0		0		66		70				79	28		9														158	8		8.79	0
NG208	75.70	0.20	13.18	1.48	0.01	0.03	0.09	0.44	3.41	5.10	0.01	0.66	100.31	318	29	75	186	80				70		2		151		63		57				156	83		7														13	16		8.51	34
T15A	74.30	0.08	11.74	0.33	0.89	0.02	0.01	0.26	3.88	4.59	0.01	0.64	96.75	502	1	86	166	132			7	61		3		0		69		37				153	166		7														122	12		8.47	
DR11	76.70	0.14	13.36	0.00	1.16	0.03	0.05	0.33	4.41	3.58	0.02	0.34	100.12	966	0	87	81	119				##		4		0		61		47				149	88		9														558	15		7.99	76
DW1	78.03	0.06	12.14	0.33	0.89	0.01	0.09	0.52	4.59	3.56	0.01	0.42	100.65	389	22	##	207	205				77		0		71		42		16				275	169		10														138	10		8.15	10
FG5	77.44	0.08	11.99	0.37	0.87	0.02	0.07	0.49	3.89	4.45	0.01	0.34	100.02	347	3	##	161	148				42		0		43		39		27				117	64		8														67	13		8.34	10
KD12	76.50	0.10	12.83	0.35	0.84	0.02	0.07	0.46	4.17	4.39	0.01	0.34	100.08	283	4	##	147	96				48		0		4		36		41				62	27		6														56	9		8.56	

Table No. A15 CHEMICAL ANALYSIS OF SAMPLES FROM THE GREATER LUFILIAN ARC SORTED BY NUMBER

Sample	SiO2	TiO2	Al2O3	Fe2O3	FeO	MnO	MgO	CaO	Na2O	K2O	P2O5	LOI	Total	Rb	Sr	Y	Zr	Nb	Co	Ni	Cu	Zn	Ga	V	Cr	Ba	U	Th	Sc	Pb	Sm	Nd	Pr	Ce	La	Cs	Hf	Ta	As	Se	Eu	Gd	Tb	Dy	Ho	Er	Tm	Yb	Lu	Li	Be	Ge	Mo	Na+K	Sn
Notch	50.00	1.00	15.50	6.00		0.150	2.00	5.00	4.90	5.50	0.30	2.00		200	400	60	360	40	30	16	25	85	26	100	100	1300	20	37	20	20	50	50	15	175	95	3	10	120	100		4	30	5	20	3	9	35.5	7.5	1.6						
AM-1															1839	8630										114	11	1019		330		748		1726	1061				78																	0.00
C-1	74.03	0.27	12.73	1.15	1.51	0.05	0.31	0.48	3.67	5.09	0.05	0.71	100.05	100	50	70	500	30.0	<10	<10	n.d		25	<3	10	1200				25.0					95				<100										<3	<3	<3(	<3	8.76
C-10	68.63	0.49	15.01	1.62	1.44	0.07	1.22	2.74	4.41	3.60	0.20	0.57	100.00	65	720	25	230	<10					20	55	30	1900				18.0					70														20				8.01
C-11	78.84	0.29	10.79	0.95	0.27	0.03	0.09	0.60	2.94	5.20	0.06	0.22	100.28	120	65	55	180	18.0					15	5	25	560				20.0					100														<3				8.14
C-13 (we	75.89	0.41	12.46	1.07	0.13	n.d.	0.05	0.25	3.60	5.71	0.04	0.50	100.11	100	40	65	650	40.0	<10	<10	n.d.		25	<3	10	1000				30.0					90				<100										<3	<3	<3(	<3	9.31
C-14	48.69	1.26	13.27	4.86	8.71	0.18	6.15	10.49	2.41	1.05	0.22	0.50	97.79																																											3.46
C-2	69.71	0.68	14.17	1.69	1.57	0.04	0.84	0.82	4.10	5.30	0.27	0.67	99.86	70	110	45	550	30.0					25	35	25	2100				8.0					90														35				9.40
C-3	68.63	0.67	15.43	1.74	1.03	0.10	0.51	1.99	4.50	4.42	0.18	0.50	99.70	90	350	140	700	40.0					25	35	11	2500				25.0					130														30				8.92
C-4	73.63	0.33	14.16	1.13	0.24	0.02	0.00	0.50	3.14	6.35	0.07	0.44	100.01	200	80	20	380	20.0					20	9	13	1200				40.0					95														11				9.49
C-5	75.35	0.27	13.18	1.08	0.22	0.02	0.00	0.62	3.15	5.50	0.05	0.36	99.80	110	100	35	280	10.0					20	5	15	1400				30.0					65														12				8.65
C-6	66.09	0.69	14.60	3.06	1.72	0.08	1.81	2.54	3.25	4.71	0.28	1.11	99.94	150	480	25	280	<10					20	85	18	1900				14.0					75														25				7.96
C-7	69.29	0.47	14.55	1.81	1.48	0.06	1.19	2.83	3.33	4.40	0.17	0.46	100.04	230	650	25	320	10.0					19	70	35	1700				16.0					70														13				7.73
C-8	73.88	0.33	13.85	0.87	0.24	0.03	0.18	0.26	4.05	5.93	0.09	0.39	100.10	130	40	55	450	15.0					20	7	11	400				20.0					65														4				9.98
C-9	73.30	0.32	13.20	2.93	0.48	0.01	0.00	0.24	3.46	5.67	0.07	0.34	100.02	130	50	80	650	30.0					30	<3	14	1200				12.0					85														9				9.13
L-012	64.19	0.66	17.47	3.45	0.00	0.03	1.12	2.55	4.34	6.14	0.18	0.30	100.43	131	516	33	189	29.2	7	9	7	42	20	46	36	1042	4.27	50.4	<10	3.8	15.4	112	31.5	293	163	1.08	4.73	1.57	293	2.69	9.76	1.21	6.81	1.22	3.22	0.47	3.14	0.48					10.48
L-012A	64.38	0.61	17.86	3.18	0.00	0.03	1.13	2.40	4.10	6.24	0.15	0.32	100.40	143	536	36	360	32.0	9	10	9	28	21	33	36	940	<6	49.0	<10					312	216																			10.34
L-020	74.44	0.22	12.70	2.48	0.00	0.05	0.28	0.58	3.03	5.85	0.02	0.75	100.40	226	91	53	228	19.0	<6	<6	9	64	18	<12	47	553	10.00	62.0	<10		11.13	88.15	144.8	286	75			73.15		3.33						2.68	1.275					8.88
L-023	67.01	0.56	14.95	5.02	0.00	0.07	1.83	2.74	3.71	3.60	0.19	0.80	100.48	78	376	24	133	13.0	10	6	<6	44	16	80	219	1283	<6	<15	12	6.925	49.95	76.63	127	44			61.23		0.738		1.43				1.300	1.125					7.31
L-024	48.01	2.10	12.37	18.91	0.00	0.28	4.93	8.74	1.70	0.43	0.17	1.16	98.80	16	78	51	140	11.0	57	66	236	149	22	470	79	108	6.00	<15	43	13.59	38.8	39.45	25	19			391.38				3.100				2.250	2.088					2.13
L-025	70.60	0.40	13.80	3.70	0.00	0.05	0.73	1.82	3.19	4.80	0.08	0.96	100.13	91	370	11	108	10.0	6	8	9	71	17	38	42	1390	<6	<15	<10	4.163	31.91	47.41	85	20			24.55		0.750		0.900				0.563	0.825					7.99
L-026	71.92	0.37	13.46	3.29	0.00	0.04	0.67	1.98	3.23	4.51	0.08	0.82	100.37	85	384	12	392	14.0	6	7	8	55	16	38	42	1367	<6	<15	<10					97	41																			7.74
L-027	67.24	0.53	15.50	4.74	0.00	0.09	1.38	4.31	3.75	1.72	0.19	1.02	100.47	49	619	21	123	13.0	7	<6	<6	49	18	68	161	573	<6	<15	12					107	58																			5.47
L-028	60.53	0.60	14.99	6.80	0.00	0.09	4.08	3.69	3.88	3.07	0.26	1.58	99.57	124	581	20	155	16.0	26	52	79	45	16	79	89	532	<6	17.0	17	5.875	43.06	63.88	109	32			95.25				2.93				0.650	1.025					6.95
L-029	63.66	0.66	17.38	5.28	0.00	0.05	2.34	3.70	3.95	2.50	0.26	0.70	100.48	88	542	12	147	11.0	20	23	26	49	18	87	51	574	<6	<15	11					89	45																			6.45
L-030	74.74	0.10	13.50	1.47	0.00	0.04	0.09	0.45	2.16	5.91	0.00	1.92	100.38	262	67	15	128	16.2	<6	7	22	34	16	13	15	391	16.00	40.0	<10	35.7	2.87	14.89	4.15	76	26	2.70	4.00	1.24	0	0	0.39	2.41	0.41	2.81	0.59	1.87	0.30	2.17	0.34					8.07
L-032	59.58	1.09	15.52	7.08	0.00	0.07	3.07	5.01	2.80	3.13	0.54	0.82	98.71	110	566	26	284	23.0	25	34	17	58	19	151	78	703	<6	<15	16	7.975	54.33	82.75	109	37			96.13		0.713						1.050	1.063					5.93
L-034	60.10	0.04	23.01	3.98	0.00	0.07	0.11	0.14	6.82	4.47	0.07	1.68	100.49	79	342	27	708	92.0	<6	12	8	18	17	74	87	705	<6	20.0	11					311	134																			11.29
L-036	73.57	1.10	15.97	1.46	0.00	0.02	0.12	0.10	0.03	0.25	0.09	7.83	100.54	34	51	30	635	38.0	<6	26	36	37	28	52	30	196	<6	36.0	<10					282	240																			0.28
L-037	56.10	0.04	21.65	3.00	0.00	0.12	0.04	1.20	10.22	5.51	0.05	2.53	100.46	92	465	33	792	101.0	<6	7	10	171	25	<12	117	423	9.00	17.0	<10		108.3	38.65	70.88	139	63			50.70		0.413						0.688	0.675					15.73
L-038	56.45	0.12	21.07	3.77	0.00	0.08	0.00	0.32	12.27	4.32	0.07	2.01	100.48	72	244	29	859	114.0	<6	7	12	108	26	<12	65	318	8.00	32.0	<10					261	146																			16.59
L-039	57.37	0.05	21.32	3.71	0.00	0.20	0.08	0.75	9.68	4.63	0.06	2.64	100.49	87	355	37	808	120.0	<6	<6	12	127	27	<12	68	349	9.00	30.0	<10					231	166																			14.31
L-040	55.44	0.04	20.98	5.81	0.00	0.34	0.02	1.29	9.89	6.14	0.06	0.44	100.45	75	283	38	922	135.0	2	8	8	106	25	4	139	261	8.00	30.0	<10					278	186																			16.03
L-041	57.71	0.05	20.81	4.02	0.00	0.07	0.00	0.60	8.89	5.41	0.02	2.85	100.45	85	283	33	950	134.0	<6	<6	6	98	27	<12	<12	347	11.00	22.0	<10					183	109																			14.30
L-044	57.32	0.03	21.02	3.15	0.00	0.14	0.00	0.65	12.04	4.28	0.05	1.70	100.38	109	616	107	1758	178.0	4	8	10	227	26	11	120	1441	10.00	31.0	<10		0.263		4.488	196	0			37.10			1.48	1.150				0.288	0.713					16.32
L-045	57.75	0.10	20.94	6.96	0.00	0.03	0.00	0.14	7.96	4.16	0.06	1.17	99.27	58	367	20	186	97.6	<6	11	32	34	27	<12	45	764	7.24	17.8	<10	1.9	7.13	57.9	20.0	214	158	0.29	2.38	9.70	214	1.22	4.71	0.77	4.50	0.77	2.09	0.31	2.01	0.27					12.12
L-046	55.67	0.05	20.92	3.40	0.00	0.19	0.09	1.07	8.51	5.27	0.06	5.21	100.44	82	311	30	670	82.0	<6	6	115	168	24	<12	51	526	<6	29.0	<10		0.525	0.550	6.700	204	1			44.38			0.638	1.400				0.250	0.688					13.78
L-047	66.09	0.46	14.68	5.40	0.00	0.08	0.20	2.42	4.99	4.75	0.08	0.54	99.70	110	83	458	634	105.0	<6	<6	<6	47	22	12	<12	1015	6.00	<15	10			127.3	186.3	308	164			68.50		6.438	29.43	7.750				19.71	3.538					9.74
L-049	47.30	2.03	15.47	13.49	0.00	0.25	5.41	10.51	3.04	0.93	0.22	0.92	99.58	13	346	30	109	17.0	34	46	143	119	19	296	85	127	<6	<15	31					23	<12																			3.97
L-050	46.86	2.06	15.40	13.35	0.00	0.21	5.20	10.46	3.73	0.89	0.27	0.52	98.95	11	321	31	114	16.0	46	49	91	70	18	321	171	93	<6	<15	34					30	<12																			4.62
L-060a	45.83	4.36	11.86	17.84	0.00	0.26	6.24	9.49	2.29	1.12	0.43	0.38	100.11	149	64	19	128	9.5	31	39	20	105		396	38	477	4.91	46.5	0	20.4	3.67	27.0	9.06	113	61	0.87	4.08	1.16		0.57	2.65	0.44	3.02	0.66	2.15	0.36	2.73	0.42					3.41
L-060b	76.30	0.15	11.89	1.79	0.00	0.04	0.14	0.53	3.65	5.74	0.04	0.28	100.55	154	64	23	141	13.0	<6	<6	14	25	22	<12	54	481	<6	<15	35					37	20																			9.39
L-060c	45.43	4.31	11.83	17.86	0.00	0.28	6.23	9.37	2.11	1.09	0.45	0.42	99.57	24	330	38	165	27.0	37	39	29	101		387	33	118																														3.20
L-063	46.39	0.84	12.95	3.10	0.00	0.09	5.95	9.71	6.97	0.15	0.12	14.12	100.39	4	51	19	192	7.0	<6	18	7	22	21	86	36	<20	<6	<15	23					25	16																			7.12
L-064	47.31	0.82	12.99	3.23	0.00	0.10	5.76	9.38	6.85	0.05	0.12	13.87	100.48	4	51	19	175	7.0	<6	18	8	28	20	92	36	<20	<6	<15	24					16	<12																			6.90
L-065	39.63	0.57	9.98	4.16	0.00	0.11	7.62	13.40	4.80	0.12	0.07	19.80	100.26	4	125	24	108	8.0	<6	20	8	29	12	102	45	<20	<6	<15	30		5.65	1.725	18.83	15	10			71.00								0.988	0.763					4.92
L-075	65.53	0.91	13.91	5.81	0.00	0.07	1.46	2.59	3.43	5.10	0.23	1.14	100.18	162	217	33	50	16.8	0	0	0	0	16	0	0	1339	<6	16.0	<10	21.1	9.40	53.11	13.45	160	61	2.48	1.38	0.81	0	0	1.89	7.80	1.11	6.66	1.26	3.52	0.49	3.17	0.45					8.53
L-076	65.53	0.91	13.91	5.81	0.00	0.07	1.46	2.59	3.43	5.10	0.23	1.14	100.18	182	212	48	361	26.0	22	16	105	35	17	82	56	1344	<6	17.0	10					137	61																			8.53
L-077	66.70	0.79	14.45	4.66	0.00	0.06	1.36	2.66	3.78	5.06	0.21	0.77	100.50	174	216	39	290	22.0	14	11	28	46	18	59	41	1391	<6	14.0	<10		11.11	35.10	86.25	119	41			75.13		1.088						1.213	1.088					8.84
L-078	67.56	0.89	13.59	5.37	0.00	0.07	1.27	3.08	3.93	3.78	0.23	0.81	100.58	143	235	47	343	25.0	19	13	31	48	17	74	51	964	<6	18.0	10					131	61																			7.71
L-079	67.09	0.80	14.65	4.99	0.00	0.07	1.21	2.40	3.35	4.98	0.19	0.83	100.56	165	216	40	332	24.0	14	12	41	45	0	68	40	1291	0.00	0.0	0					0	0																			8.33
L-139	75.60	0.09	11.88	1.50	0.00	0.03	0.62	0.14	1.61	7.87	0.01	0.79	100.14	399	17	40	75	41.0	10	7	55	34	23	14	47	769	<6	26.0	<10					42	12																			9.48
L-150	51.05	2.91	15.47	10.19	0.00	0.00	10.09	0.68	1.69	6.12	0.36	1.16	99.72	361	24	45	150	28.0	851	191	623	66	24	424	94	349	6.00	<15	29		12.85	13.43	54.96	18	7			220.8								0.263	1.250					7.81
L-151	77.00	0.10	11.82	1.67	0.00	0.03	0.17	0.11	3.47	5.54	0.02	0.51	100.44	351	32	158	197	91.0	10	8	42	39	24	<12	42	441	11.00	65.0	<10		113.8	48.59	96.88	167	49		6.938	13.56		0.538						10.61	2.200					9.01
L-153	77.40	0.07	11.91	1.65	0.00	0.03	0.12	0.27	3.51	4.89	0.01	0.51	100.37	438	25	117	106	70.0	<6	8	58	33	24	<12	60	236	11.00	44.0	<10					87	38																			8.40
L-154	77.07	0.07	12.06	1.22	0.00	0.00	0.00	0.25	3.07	5.78	0.01	0.50	100.05	478	27	68	122	58.0	7	<6	17	22	23	<12	<12	255	<6	44.0	<10		105.1	2.513	22.06	90	4		3.588	9.975								2.363	0.888					8.85

Table No. A15 CHEMICAL ANALYSIS OF SAMPLES FROM THE GREATER LUFILIAN ARC SORTED BY NUMBER

Sample	SiO2	TiO2	Al2O3	Fe2O3	FeO	MnO	MgO	CaO	Na2O	K2O	P2O5	LOI	Total	Rb	Sr	Y	Zr	Nb	Co	Ni	Cu	Zn	Ga	V	Cr	Ba	U	Th	Sc	Pb	Sm	Nd	Pr	Ce	La	Cs	Hf	Ta	As	Se	Eu	Gd	Tb	Dy	Ho	Er	Tm	Yb	Lu	Li	Be	Ge	Mo	Na+K	Sn
Notch	*50.00*	*1.00*	*15.50*	*6.00*		*0.150*	*2.00*	*5.00*	*4.90*	*5.50*	*0.30*	*2.00*		*200*	*400*	*60*	*360*	*40*	*30*	*16*	*25*	*85*	*26*	*100*	*100*	*1300*	*20*	*37*	*20*	*20*	*50*	*50*	*15*	*175*	*95*	*3*	*10*	*120*	*100*		*4*	*30*	*5*	*20*	*3*	*9*	*35.5*	*7.5*	*1.6*					
L-155	72.00	0.28	12.99	2.57	0.00	0.00	1.51	0.95	1.03	6.03	0.09	1.71	99.17	219	62	20	99	13.0	61	12	<6	26	15	44	21	848	<6	<15	<10		109.6	25.34	56.81	69	23			36.41			0.53							0.23	0.713					7.06
L-157	75.81	0.19	12.48	1.25	0.00	0.00	1.16	0.18	0.19	6.95	0.03	1.39	99.63	225	12	12	107	17.0	26	8	7	14	14	20	15	618	<6	18.0	<10					43	17																			7.14
L-158	73.58	0.20	12.85	1.36	0.00	0.00	1.46	0.93	0.33	7.11	0.04	2.00	99.87	233	19	13	109	16.0	32	7	<6	13	14	20	14	628	6.00	26.0	<10		107.9	26.04	63.13	76	31		2.100	8.225			0.450								0.588					7.44
L-159	68.02	0.64	14.23	2.82	0.00	0.00	1.74	1.42	0.95	6.80	0.16	2.10	98.87	303	47	34	209	28.0	38	7	<6	19	17	57	18	919	11.00	24.0	10					118	60																			7.75
L-160	67.96	0.55	14.78	2.29	0.00	0.00	1.47	1.67	2.46	5.69	0.16	2.10	99.14	264	40	49	223	32.0	39	9	<6	18	16	47	16	805	<6	15.0	13		117.8	42.35	102.1	156	49			27.91			1.13							2.788	0.988					8.15
L-161	51.48	1.05	20.52	6.92	0.00	0.10	7.54	1.15	2.18	6.26	0.37	1.89	99.47	225	54	40	319	29.0	93	26	<6	160	24	102	18	1829	<6	30.0	17					128	64																			8.44
L-162	76.11	0.19	12.33	1.25	0.00	0.00	0.28	0.70	3.48	4.92	0.03	0.59	99.88	119	155	14	96	10.0	6	<6	7	22	13	17	15	793	<6	<15	<10					82	37																			8.40
L-163	43.65	1.23	15.61	14.61	0.00	0.30	11.50	4.45	1.80	3.69	0.14	2.97	99.95	149	179	25	85	9.0	172	410	<6	240	15	228	292	478	<6	<15	22					16	<12																			5.49
L-166	70.84	0.39	13.91	2.93	0.00	0.00	0.61	1.97	4.13	4.54	0.13	0.44	99.89	209	89	31	89	18.0	6	<6	22	18	15	<12	17	741	<6	15.0	<10		109.0	34.36	63.50	105	35		3.063	3.313			0.713							0.863	0.675					8.67
L-167	47.14	0.78	19.71	6.10	0.00	0.08	12.98	0.00	0.00	8.70	0.08	4.00	99.57	255	64	101	781	147.0	266	57	1896	65	28	95	74	615	12.00	37.0	12					43	13																			8.70
L-167a	47.14	0.78	19.71	6.10	0.00	0.08	12.98	0.00	0.00	8.70	0.08	4.00	99.57	255	64	101	781	147.0	266	57	1896	65	28	95	74	615	12.0	37.0	12					43	13																			8.70
L-168	79.68	0.15	10.06	0.72	0.00	0.02	0.10	0.02	0.19	7.61	0.08	0.59	99.22	132	125	19	258	11.0	32	<6	261	10	<9	16	59	1190	<6	<15	<10				9.900	61	1													0.175	0.475					7.80
L-170	70.45	0.86	15.35	3.22	0.00	0.03	1.50	0.01	0.02	5.02	0.13	3.05	99.64	110	46	42	320	79.0	131	14	1954	25	29	92	335	766	10.00	<15	11		6.038	25.63	30.29	44	21			46.49			0.188	1.963						1.413	0.888					5.04
L-172	74.42	0.06	13.07	1.32	0.00	0.04	0.21	0.14	1.85	7.48	0.06	0.71	99.36	316	32	49	113	85.0	9	8	242	23	21	<12	618	668	5.31	48.5	<10	27.3	8.66	41.2	11.3	79	50	1.13	4.97	3.20			0.41	7.22	1.32	9.90	2.23	7.30	1.12	7.27	1.00					9.33
L-173	74.69	0.09	12.55	1.37	0.00	0.03	0.28	0.14	1.87	7.51	0.05	0.78	99.36	314	29	78	172	128.0	11	6	232	20	22	<12	453	598	7.00	58.0	<10					85	49																			9.38
L-175	74.72	0.41	12.60	2.96	0.00	0.00	0.41	1.08	2.71	4.60	0.09	0.32	99.90	221	63	45	229	29.0	9	7	31	31	15	28	17	541	<6	25.0	<10		5.913	30.08	47.8	153	19			41.58			0.263							1.300	0.838					7.31
L-181	49.82	1.08	15.86	11.33	0.00	0.16	6.30	11.28	2.94	0.24	0.06	0.86	99.94	7	157	29	62	8.0	34	30	57	94	16	293	35	<22	<6	<15	35					<12	<12																			3.18
L-195	61.25	0.38	15.84	8.67	0.00	0.09	0.04	2.35	5.66	5.03	0.09	0.51	99.91	89	130	115	1054	80.0	<6	<6	10	71	40	13	<12	2151	8.00	<15	<10		15.84	44.14	74.25	118	25			145.1			3.888	1.463						7.500	2.200					10.69
L-199														10	787	42	534	46.6							399	8.85	38.7		5.6	20.0	137	35.6	288	95	0.67	10.8	2.65			5.38	12.6	1.58	9.10	1.61	4.24	0.59	3.76	0.53					0.00
L-207	75.03	0.07	13.63	0.68	0.00	0.00	0.00	0.11	4.32	6.27	0.01	0.26	100.39	123	182	12	432	6.0	8	6	10	13	0	<12	13	557	0.00	0.0	0				4.575	0	2		19.10			0.225	0.63						0.438					10.59
L-208	74.23	0.05	13.85	0.87	0.00	0.03	0.00	0.12	4.36	6.13	0.05	0.24	99.93	137	178	12	431	33.0	<6	<6	14	10	25	<12	238	517	9.00	132.0	<10					35	20																			10.49
L-209	46.78	1.81	16.06	9.69	0.00	0.05	7.51	11.46	2.34	1.91	0.57	0.60	98.79	53	1592	27	111	17.0	36	42	29	52	19	243	50	1437	<6	<15	27					113	61																			4.25
L-210	66.74	0.43	17.99	3.52	0.00	0.00	0.29	0.69	9.58	0.09	0.14	0.39	99.87	4	275	30	474	36.0	6	7	143	13	22	28	<12	83	7.00	74.0	<10					372	223																			9.67
L-212	67.27	0.40	15.94	2.89	0.00	0.00	0.15	0.81	4.44	7.04	0.03	0.71	99.69	149	117	51	336	49.0	8	<6	32	17	22	<12	<12	503	8.00	79.0	<10					250	130																			11.48
L-213	66.68	0.36	17.40	3.03	0.00	0.00	0.08	0.23	6.87	4.87	0.03	0.60	100.17	73	193	27	596	39.0	8	6	18	22	25	22	<12	762	12.00	163.0	<10		4.425	42.11	69.13	137	20		16.48	39.14			0.663							0.738	0.813					11.74
L-214	66.63	0.39	17.62	1.54	0.00	0.03	0.00	0.24	7.68	3.92	0.06	0.63	98.74	65	167	24	662	77.0	<6	12	20	15	25	19	81	657	7.00	104.0	<10					181	89																			11.60
L-215	70.53	0.23	16.82	0.65	0.00	0.00	0.00	0.15	10.32	0.19	0.03	0.36	99.30	7	72	15	443	23.0	6	7	6	9	27	<12	<12	71	<6	193.0	<10					18	<12																			10.51
L-217	73.54	0.39	10.80	3.98	0.00	0.09	3.40	1.35	0.64	2.97	0.15	2.41	99.72	124	48	10	128	10.0	86	17	8	43	13	67	502	805	<6	<15	11		6.750	28.16	53.20	89	30			58.60											0.763					3.61
L-218	66.30	0.52	15.92	4.64	0.00	0.00	0.49	2.01	4.79	5.43	0.11	0.21	100.42	202	344	46	601	53.0	8	<6	6	30	22	15	16	793	8.00	99.0	<10		16.74	74.63	264.5	342	135		7.513	65.38			1.450							2.063	1.063					10.22
L-222	64.17	0.57	13.11	13.72	0.00	0.00	0.80	0.08	0.15	4.74	0.12	2.46	99.94	304	122	69	275	30.0	<6	7	<6	22	29	79	18	499	7.00	20.0	11					220	121																			4.89
L-223	66.79	0.57	14.12	10.16	0.00	0.00	0.79	0.08	0.17	5.20	0.10	2.49	100.48	312	122	77	270	28.0	<6	<6	<6	27	28	68	18	468	8.00	21.0	<10		2.188	0.575	20.21	250	2			166.0											0.988					5.37
L-224	62.03	0.58	13.42	15.02	0.00	0.00	0.62	0.07	0.24	5.69	0.11	2.33	100.13	261	103	35	301	28.0	9	8	<6	21	24	76	16	1065	8.00	19.0	<10					120	65																			5.93
L-237	70.85	0.37	13.24	4.02	0.00	0.00	0.52	1.36	2.51	5.44	0.11	0.40	98.83	151	276	74	194	24.0	8	6	25	16	18	28	<12	815	<6	26.0	<10					273	148																			7.95
L-238	70.02	0.51	13.56	3.71	0.00	0.00	0.67	1.50	2.89	6.16	0.15	0.74	99.92	156	260	58	240	27.0	7	<6	9	18	18	33	15	747	6.00	24.0	<10					130	67																			9.05
L-239	70.02	0.51	13.56	3.71	0.00	0.00	0.67	1.50	2.89	6.16	0.15	0.74	99.92	156	260	58	240	27.0	7	<6	9	18	18	33	15	747	6.00	24.0	<10					130	67																			9.05
L-241	0.00	0.00	0.00	0.00	0.00	0.00	0.00	0.00	0.00	0.00	0.00	0.00	0.00	156	229	55	174	24.1	0	0	0	0		0	0	594	0.00	0.0	0	2.4	9.21	45.22	10.98	0	0	1.91	5.17	1.86	0	0	1.64	9.31	1.44	9.41	1.92	5.84	0.87	5.96	0.89					0.00
L-242	76.03	0.29	10.81	5.91	0.00	0.01	2.03	0.21	0.57	1.96	0.11	1.21	99.14	42	228	33	256	11.0	14	18	8	12	38	87	309	617	7.00	<15	29					148	112																			2.53
L-248	64.40	0.91	15.35	6.34	0.00	0.00	2.74	3.49	2.97	2.10	0.26	0.53	99.08	126	300	54	205	42.0	15	15	13	28	25	109	39	271	6.00	<15	21					77	42																			5.07
L-248-LC	76.71	0.14	13.26	0.92	0.00	0.00	0.04	0.66	3.71	4.49	0.04	0.32	100.29	121	314	48	206	20.0	9	7	8	16	19	35	25	745	<6	27.0	<10					139	68																			8.20
L-249	70.32	0.42	14.04	3.50	0.00	0.00	0.75	1.96	3.00	4.50	0.14	0.29	98.93	123	309	49	211	23.0	8	7	8	16	19	45	21	716	<6	20.0	<10		0.700	0.725	4.800	124	0			46.24				1.313						0.350	0.688					7.50
L-257	73.62	0.26	13.30	1.97	0.00	0.00	0.15	1.23	3.67	5.29	0.05	0.55	100.10	214	117	53	208	25.0	6	<6	<6	13	22	<12	14	321	16.00	74.0	<10		113.8	42.95	114.8	192	66		5.363	26.34			0.663							4.013	1.175					8.96
L-259	69.45	0.42	15.44	2.77	0.00	0.00	0.29	1.80	3.10	6.11	0.07	0.59	100.05	174	199	72	402	47.0	7	<6	<6	21	20	13	26	911	7.00	21.0	11					113	58																			9.21
L-259-B	73.83	0.30	12.91	2.80	0.00	0.00	0.17	1.01	3.55	5.35	0.04	0.44	100.42	204	118	214	292	39.0	<6	<6	12	28	20	<12	15	617	10.00	29.0	<10					277	209																			8.90
L-263	67.90	0.54	13.93	2.49	0.00	0.00	0.71	3.88	3.29	5.55	0.27	0.54	99.13	83	640	51	244	26.0	7	<6	23	15	20	34	16	920	<6	19.0	10		118.9	46.66	91.5	118	32			29.10			1.813							2.863	1.063					8.84
L-268	69.51	0.69	16.52	4.32	0.00	0.01	0.35	0.13	0.54	4.53	0.17	3.62	100.39	178	37	48	275	22.00	10	10	942	14	19	72	187	1116	<6	19.00	13.00					151	81																			5.07
L-269	75.84	0.31	13.87	3.02	0.00	0.00	0.00	0.20	0.31	3.67	0.21	3.03	100.46	94	20	16	179	19.00	<6	8	6	11	15	27	185	291	<6	<15	<10					83	41																			3.98
L-273	65.92	0.52	14.92	4.14	0.00	0.12	1.78	3.54	2.94	3.12	0.18	2.98	100.16	128	110	31	173	14.00	18	9	49	38	16	77	206	966	<6	<15	15.00					101	56																			6.06
L-279	67.94	0.63	14.39	4.41	0.00	0.08	1.31	3.25	3.31	3.08	0.22	1.29	99.91	123	204	39	285	19.00	7	13	6	51	16	64	302	810	6.00	20	<10		10.43	33.43	80.75	140	39			69.25			0.900							1.60	1.075					6.39
L-311	50.33	3.00	14.97	10.04	0.00	0.00	5.02	4.99	3.78	0.84	1.25	5.18	99.40	26	76	59	326	36.0	15	<6	19	39	19	121	16	88	8.00	<15	40					76	44																			4.62
L-313	54.29	1.67	13.47	10.37	0.00	0.06	5.07	4.92	4.55	0.80	0.67	4.40	100.27	21	164	89	445	40.0	14	12	42	39	23	102	21	104	7.00	<15	36					139	75																			5.35
L-314	43.72	7.81	12.73	11.28	0.00	0.08	6.68	7.01	3.38	0.36	0.64	6.73	100.42	14	77	56	25	36.0	20	19	28	49	18	438	50	60	<6	<15	55					27	16																			3.74
L-318	47.28	3.04	15.31	7.93	0.00	0.04	6.86	13.85	4.18	0.56	0.38	0.96	100.39	9	154	37	163	27.0	23	53	9	22	19	258	99	20	<6	<15	30					68	33																			4.74
L-321	71.94	0.71	9.67	11.04	0.00	0.03	3.43	0.30	0.68	0.05	0.12	2.40	100.37	6	81	59	242	18.0	96	18	16	30	15	157	95	65	<6	<15	12					102	61																			0.73
L-322	70.45	0.74	13.65	5.38	0.00	0.02	0.48	0.08	0.13	7.57	0.08	1.74	100.32	168	30	37	264	30.0	12	7	13	35	21	49	33	498	<6	27.0	<10					171	74																			7.70
L-323	67.04	0.81	14.15	7.57	0.00	0.02	0.52	0.19	0.17	8.21	0.17	1.61	100.46	173	29	37	302	35.0	26	9	17	28	20	58	32	525	<6	30.0	<10					153	71																			8.38
L-324	62.05	0.97	14.50	7.90	0.00	0.06	1.43	1.71	3.85	6.29	0.29	1.25	100.30	112	230	57	362	35.0	20	16	62	121	21	96	27	1004	13.00	48.0	11					190	74																			10.14

Table No. A15 CHEMICAL ANALYSIS OF SAMPLES FROM THE GREATER LUFILIAN ARC SORTED BY NUMBER

Sample	SiO2	TiO2	Al2O3	Fe2O3	FeO	MnO	MgO	CaO	Na2O	K2O	P2O5	LOI	Total	Rb	Sr	Y	Zr	Nb	Co	Ni	Cu	Zn	Ga	V	Cr	Ba	U	Th	Sc	Pb	Sm	Nd	Pr	Ce	La	Cs	Hf	Ta	As	Se	Eu	Gd	Tb	Dy	Ho	Er	Tm	Yb	Lu	Li	Be	Ge	Mo	Na+K	Sn
Notch	50.00	1.00	15.50	6.00		0.150	2.00	5.00	4.90	5.50	0.30	2.00		200	400	60	360	40	30	16	25	85	26	100	100	1300	20	37	20	20	50	50	15	175	95	3	10	120	100		4	30	5	20	3	9	35.5	7.5	1.6						
L-325	60.42	1.15	16.98	11.07	0.00	0.02	0.91	0.06	0.08	6.75	0.29	2.82	100.55	227	37	346	372	31.0	28	13	55	48	26	114	<12	508	6.00	27.0	<10					1460	819																					6.83
L-341	63.54	0.75	13.15	4.88	0.00	0.03	1.09	5.99	6.86	0.95	0.32	1.14	98.70	19	703	76	329	29.0	11	9	31	21	21	45	20	72	<6	20.0	11					174	89																					7.81
L-343	65.60	0.61	13.71	4.43	0.00	0.05	0.83	6.46	5.59	1.11	0.20	0.17	98.76	20	616	180	408	40.0	11	7	12	24	19	44	16	187	<6	35.0	12					162	103																					6.70
L-344	61.49	1.13	15.69	3.77	0.00	0.07	1.27	6.94	5.64	1.83	0.40	0.98	99.21	47	555	126	485	41.0	10	<6	13	25	27	44	22	577	6.00	24.0	15					209	107																					7.47
L-345	62.53	0.76	14.29	8.20	0.00	0.05	0.77	1.46	2.52	7.65	0.20	0.40	98.83	210	366	61	494	18.0	7	11	19	27	23	67	24	1440	6.00	<15	<10					174	94																					10.17
L-346	70.01	0.49	13.71	5.02	0.00	0.05	0.31	0.96	3.40	5.99	0.10	0.64	100.68	195	168	69	469	27.0	12	<6	80	77	20	14	<12	774	11.00	24.0	<10					190	98																					9.39
L-347	45.32	1.57	12.74	9.07	0.00	0.11	6.14	18.97	3.89	0.45	0.08	0.42	98.76	11	497	14	77	6.0	26	21	197	147	22	127	131	48	9.00	29.0	<10					111	57																					4.34
L-348	68.82	0.46	13.11	3.52	0.00	0.14	0.29	3.80	4.97	3.37	0.13	0.31	98.92	38	762	56	329	19.0	7	<6	13	20	19	43	17	439	<6	40.0	<10					130	61																					8.34
L-349	67.98	0.35	13.65	3.38	0.00	0.07	0.35	2.69	4.47	4.97	0.13	0.82	98.86	108	423	55	230	32.0	7	11	24	16	19	21	16	590	<6	23.0	<10					106	50																					9.44
L-352	70.34	0.51	13.27	4.15	0.00	0.05	0.53	1.63	3.37	4.96	0.10	0.26	99.17	178	166	35	357	20.0	10	11	17	30	19	16	21	861	<6	19.0	<10					212	123																					8.33
L-353	64.23	0.92	13.89	5.97	0.00	0.04	1.34	3.73	3.62	5.05	0.24	0.49	99.52	120	400	152	404	20.0	10	<6	67	24	21	36	19	606	6.00	20.0	12					141	73																					8.67
L-354	64.83	0.81	14.83	6.19	0.00	0.07	1.46	2.45	3.15	4.06	0.20	0.95	99.00	138	207	77	435	25.0	11	17	115	78	20	71	22	977	<6	22.0	12					156	82																					7.21
L-355	72.83	0.18	13.16	2.91	0.00	0.04	0.11	0.78	3.18	5.57	0.11	0.53	99.40	263	46	46	126	19.0	<6	7	20	21	18	79	38	135	8.00	21.0	<10					80	37																					8.75
L-357	61.26	0.49	17.43	5.33	0.00	0.07	1.08	2.85	4.92	3.59	0.22	1.77	99.01	69	568	67	298	29.0	10	9	36	70	21	<12	12	1645	<6	<15	<10					111	55																					8.51
L-358	63.11	0.65	15.74	6.29	0.00	0.07	1.04	3.80	4.03	2.31	0.17	1.51	98.72	80	492	29	233	13.0	12	10	479	261	22	58	16	950	<6	<15	14	9.988	28.21	68.75		106	32			98.13		0.188								0.563	1.063				6.34
L-359	66.92	0.41	14.63	4.21	0.00	0.06	0.79	2.31	3.91	4.84	0.12	1.07	99.27	120	359	28	192	13.0	8	8	11	54	22	64	26	1134	<6	<15	10					149	76																					8.75
L-360	68.89	0.31	14.44	3.71	0.00	0.04	0.60	1.23	3.18	6.02	0.07	0.91	99.40	100	369	67	134	15.0	7	6	9	46	16	40	20	2144	<6	<15	<10					114	57																					9.20
L-361	63.38	0.74	15.35	6.08	0.00	0.06	1.57	3.80	4.38	2.06	0.22	1.49	99.13	118	544	17	246	8.0	12	15	20	78	21	36	<12	844	<6	<15	12					162	84																					6.44
L-362	64.93	0.66	14.31	5.80	0.00	0.07	1.39	3.79	3.72	2.15	0.17	1.66	98.65	77	452	35	221	9.0	9	8	17	93	19	79	22	1523	<6	<15	10					113	61																					5.87
L-363	65.30	0.64	15.16	5.30	0.00	0.09	1.23	3.11	3.95	3.37	0.16	1.49	99.80	119	398	31	202	9.0	11	6	18	69	20	73	20	1054	<6	<15	<10					82	40																					7.32
L-364	74.42	0.19	11.94	2.26	0.00	0.02	0.40	0.26	3.54	5.07	0.04	0.68	98.82	236	34	42	207	10.0	<6	9	9	23	20	59	23	198	8.00	44.0	<10					179	88																					8.61
L-365	72.12	0.48	12.08	4.21	0.00	0.04	1.25	0.45	2.64	4.87	0.12	1.33	99.59	146	81	75	353	24.0	8	7	24	38	19	<12	15	881	<6	26.0	<10					212	114																					7.51
L-366	67.02	0.66	13.23	5.79	0.00	0.09	0.90	1.76	4.05	4.28	0.18	0.92	98.88	142	188	54	448	19.0	7	<6	13	86	20	21	12	1082	<6	<15	11	10.44	139.3	247.0		347	139			88.13		6.08	42.50							13.2	2.600				8.33
L-367	72.13	0.48	11.76	4.45	0.00	0.06	1.30	3.17	1.69	2.41	0.13	1.70	99.28	59	232	237	162	22.0	10	<6	7	61	15	29	14	1518	<6	<15	<10					80	42																					4.10
L-368	67.04	0.71	14.00	4.96	0.00	0.05	1.32	0.98	3.41	4.64	0.17	1.39	98.67	112	156	18	565	10.0	10	8	13	61	18	38	15	1652	<6	<15	<10					189	101																					8.05
L-369	71.39	0.21	13.38	1.89	0.00	0.03	0.49	1.80	4.10	3.83	0.04	1.74	98.90	78	254	51	135	25.0	<6	6	119	118	16	53	20	789	<6	<15	<10	114.3	19.38	57.14		86	27			23.1		0.600	1.363							0.688					7.93
L-370	74.09	0.20	12.02	2.58	0.00	0.03	0.26	0.95	4.32	4.07	0.04	0.88	99.44	279	61	7	195	6.0	<6	10	10	32	21	16	<12	264	9.00	52.0	<10					145	73																					8.39
L-371	70.77	0.25	14.56	1.78	0.00	0.03	0.40	1.37	4.85	4.06	0.08	1.04	99.19	104	650	59	127	23.0	<6	10	10	38	18	<12	15	1474	<6	<15	<10					110	52																					8.91
L-372	54.14	0.84	17.15	9.33	0.00	0.12	3.24	7.00	4.31	2.25	0.28	1.85	100.51	86	764	11	193	8.0	20	9	57	116	21	23	18	423	<6	<15	24					135	71																					6.56
L-373	72.41	0.25	14.10	2.22	0.00	0.03	0.41	1.36	3.49	4.20	0.05	0.93	99.45	114	353	31	147	8.0	6	7	17	28	14	198	12	1215	<6	17.0	<10	105.3	14.70	34.69		90	10		3.050	21.31		0.200								0.600					7.69
L-374	70.46	0.20	14.58	2.28	0.00	0.04	0.31	1.75	5.02	3.92	0.05	0.77	99.38	97	473	10	105	6.0	<6	<6	9	33	17	17	14	1054	<6	<15	<10					49	23																					8.94
L-375	69.92	0.45	12.64	4.64	0.00	0.07	0.33	1.04	3.27	5.81	0.13	0.77	99.07	140	197	47	365	30.0	7	11	26	55	18	22	19	1228	<6	21.0	<10					296	145																					9.08
L-376	59.71	0.51	17.93	5.54	0.00	0.09	1.10	2.05	6.07	4.94	0.12	0.83	98.89	74	419	29	280	27.0	11	<6	18	58	20	67	<12	1036	<6	<15	<10					174	95																					11.01
L-377	69.88	0.26	12.62	3.07	0.00	0.04	0.28	1.27	5.06	5.45	0.05	1.01	98.99	255	69	91	174	17.0	<6	9	167	109	19	12	19	365	8.00	45.0	<10					135	71																					10.51
L-378	73.20	0.22	12.15	3.08	0.00	0.04	0.23	0.84	3.95	4.18	0.05	0.84	98.78	216	69	79	255	19.0	<6	10	163	98	19	<12	15	371	6.00	33.0	<10					267	135																					8.13
L-379	72.89	0.21	12.77	2.54	0.00	0.03	0.45	0.72	6.12	2.92	0.07	0.62	99.34	139	54	59	84	27.0	<6	14	17	15	25	<12	20	133	10.00	<15	<10					39	18																					9.04
L-380	70.37	0.39	13.41	3.59	0.00	0.05	0.27	0.92	3.65	5.94	0.09	0.69	99.37	177	135	57	365	28.0	7	10	116	83	18	17	13	1129	<6	18.0	<10	14.90	65.63	187.9		241	95		0.688	44.41		1.500	2.850							2.488	1.125				9.59
L-402	68.46	0.60	13.71	5.64	0.00	0.04	0.43	2.96	4.94	1.14	0.11	0.82	98.85	70	286	178	602	44.0	7	10	12	29	22	25	20	272	6.00	21.0	12					178	107																					6.08
L-403	64.07	0.68	14.61	7.86	0.00	0.06	1.14	3.13	3.50	4.38	0.16	0.71	100.30	119	277	83	762	25.0	9	9	196	89	25	19	19	1054	8.00	17.0	15					141	80																					7.88
L-405	52.10	1.22	16.06	10.02	0.00	0.11	5.30	8.98	3.30	1.08	0.15	0.71	99.03	23	882	24	121	14.0	37	72	30	53	17	220	35	226	<6	<15	26					78	37																					4.38
L-406	46.64	2.48	13.15	14.14	0.00	0.23	6.55	10.17	3.29	0.80	0.26	1.09	98.80	11	282	38	180	17.0	43	73	80	104	18	374	106	118	<6	<15	37					29	18																					4.09
L-407	60.09	1.12	13.19	6.31	0.00	0.07	1.49	8.27	4.03	3.86	0.30	0.61	99.34	92	396	79	532	28.0	13	8	43	40	19	71	29	689	7.00	26.0	14					188	96																					7.89
L-408	70.26	0.33	13.59	3.87	0.00	0.05	0.26	1.23	3.49	5.24	0.07	0.43	98.82	241	95	104	348	33.0	7	6	15	34	23	<12	13	483	12.00	32.0	<10					241	121																					8.73
L-409	69.36	0.41	14.76	3.25	0.00	0.02	0.49	1.13	4.47	5.43	0.10	0.44	99.86	206	151	43	313	32.0	6	<6	10	16	19	25	12	677	13.00	53.0	<10					120	60																					9.90
L-410	67.74	0.44	12.99	8.55	0.00	0.02	0.88	0.29	0.17	4.34	0.09	3.18	98.69	233	16	25	177	33.0	9	9	489	218	17	51	14	187	7.00	32.0	<10					147	80																					4.51
L-411	8.09	0.09	0.85	0.57	0.00	0.02	4.72	43.80	0.04	0.35	0.16	41.87	100.56	6	87	4	17	3.0	<6	<6	<6	16	<9	<12	<12	23	<6	<15	45					12	<12																					0.39
L-416	52.44	0.65	15.34	8.63	0.00	0.15	7.28	12.42	2.55	0.73	0.07	0.20	100.46	6	126	17	41	5.0	34	72	94	84	17	195	217	43	6.00	<15	42					<12	<12																					3.28
L-420	71.91	0.31	13.61	2.62	0.00	0.02	0.48	0.67	4.95	2.98	0.06	1.08	98.69	187	93	38	178	28.0	8	10	31	26	18	20	20	532	13.00	37.0	<10					165	103																					7.93
L-421	69.53	0.52	14.84	3.30	0.00	0.03	0.79	1.40	2.52	6.69	0.24	0.74	100.60	278	240	17	303	18.0	7	<6	34	24	18	42	19	1428	<6	57.0	<10					229	101																					9.21
L-433	51.23	2.42	14.76	11.92	0.00	0.16	4.74	8.16	3.82	2.33	0.42	0.59	100.55	71	396	44	261	22.0	28	11	45	99	20	275	62	384	7.00	<15	27					96	52																					6.15
L-434	69.24	0.53	13.96	4.52	0.00	0.06	0.74	1.98	1.92	4.77	0.13	1.32	99.17	149	247	8	411	7.0	8	9	25	35	16	19	18	869	<6	<15	30					18	<12																					6.69
L-435	67.58	0.43	15.29	3.91	0.00	0.05	0.36	1.59	3.89	6.45	0.10	0.32	99.97	142	271	34	389	11.0	8	<6	29	34	21	15	13	1227	<6	<15	<10					86	43																					10.34
L-436	73.93	0.27	12.03	2.68	0.00	0.04	0.17	1.02	4.15	4.81	0.06	0.39	99.55	235	74	45	303	31.0	<6	<6	10	21	21	<12	<12	195	26.00	99.0	<10					223	114																					8.96
L-437	55.61	1.95	14.33	9.89	0.00	0.14	2.79	5.09	3.77	4.40	0.52	0.58	99.07	113	395	52	404	32.0	21	8	121	132	22	144	21	736	<6	<15	18					111	56																					8.17
L-438	53.44	1.57	14.02	8.54	0.00	0.13	5.89	7.86	3.34	3.75	0.49	0.76	99.79	171	402	43	390	31.0	27	77	43	71	19	163	250	592	7.00	22.0	22					99	55																					7.09

Table No. A15 CHEMICAL ANALYSIS OF SAMPLES FROM THE GREATER LUFILIAN ARC SORTED BY NUMBER

Sample	SiO2	TiO2	Al2O3	Fe2O3	FeO	MnO	MgO	CaO	Na2O	K2O	P2O5	LOI	Total	Rb	Sr	Y	Zr	Nb	Co	Ni	Cu	Zn	Ga	V	Cr	Ba	U	Th	Sc	Pb	Sm	Nd	Pr	Ce	La	Cs	Hf	Ta	As	Se	Eu	Gd	Tb	Dy	Ho	Er	Tm	Yb	Lu	Li	Be	Ge	Mo	Na+K	Sn
Notch	50.00	1.00	15.50	6.00		0.150	2.00	5.00	4.90	5.50	0.30	2.00		200	400	60	360	40	30	16	25	85	26	100	100	1300	20	37	20	20	50	50	15	175	95	3	10	120	100		4	30	5	20	3	9	35.5	7.5	1.6						
L-439	70.07	0.33	12.99	4.06	0.00	0.02	0.22	0.77	4.27	5.46	0.05	0.62	98.86	243	66	90	572	46.0	<6	3	21	16	25	<12	<12	163	19.00	90.0	<10					237	124																						9.73
L-440	51.34	2.12	14.48	11.82	0.00	0.15	4.77	7.19	3.18	2.19	0.48	0.89	98.61	74	395	39	348	19.0	32	29	27	99	21	244	101	373	<6	<15	29					56	29																						5.37
L-441	62.98	1.11	14.13	7.49	0.00	0.12	0.99	2.75	3.71	5.30	0.35	0.46	99.39	180	226	74	414	46.0	10	<6	13	88	24	28	<12	893	6.00	19.0	12					187	98																						9.01
L-442	78.22	0.33	8.81	3.27	0.00	0.03	0.00	0.10	0.23	7.61	0.06	0.34	99.00	227	44	99	349	18.0	<6	<6	16	16	12	27	<12	618	<6	44.0	<10					288	149																						7.84
L-443	76.23	0.44	9.57	5.13	0.00	0.03	0.10	0.43	0.20	6.79	0.05	0.40	99.37	201	24	64	391	48.0	8	7	12	14	14	28	<12	499	<6	100.0	<10					49	25																						6.99
L-444	52.77	2.43	15.66	11.98	0.00	0.17	3.98	7.06	3.24	1.98	0.56	0.22	100.05	43	404	41	170	21.0	33	14	27	108	21	245	54	396	6.00	<15	33					67	36																						5.22
L-458	72.83	0.09	13.43	1.35	0.00	0.02	0.00	0.20	3.52	6.94	0.03	0.37	98.78	277	30	72	45	13.0	<6	<6	9	11	18	<12	13	129	8.00	<15	<10					38	42																						10.46
L-459	61.30	0.79	13.54	9.09	0.00	0.13	3.38	5.88	3.02	1.16	0.10	0.63	99.02	87	204	22	81	8.0	26	40	111	107	19	181	57	287	<6	<15	23					54	30																						4.18
L-460	74.38	0.43	11.58	4.11	0.00	0.03	0.62	1.86	3.67	2.33	0.12	0.34	99.47	68	482	13	632	7.0	8	9	19	63	18	22	14	596	<6	20.0	<10					197	102																						6.00
L-461	71.85	0.20	14.11	1.77	0.00	0.02	0.26	1.01	3.45	5.34	0.06	0.70	98.77	178	241	14	65	10.0	<6	<6	30	36	18	<12	13	1222	<6	15.0	<10					43	21																						8.79
L-462	72.04	0.34	13.78	2.58	0.00	0.02	0.38	1.21	3.18	5.19	0.04	0.37	99.13	114	630	5	95	11.0	<6	<6	11	32	17	25	<12	3607	<6	16.0	<10					61	25																						8.37
L-463	48.36	2.43	14.19	14.79	0.00	0.19	7.26	7.68	2.85	1.01	0.40	-0.53	98.63	25	255	38	193	15.0	39	11	16	153	21	133	94	285	<6	<15	30					30	18																						3.86
L-464	5.46	0.07	0.00	77.49	0.00	0.08	0.50	6.09	0.10	0.52	0.06	3.16	93.53	14	13	16	17	3.0	25	185	184	122	<9	34	<12	142	29.00	<15	37					<12	<12																						0.62
L-465	14.01	0.58	2.56	64.74	0.00	0.03	0.70	0.17	0.06	0.43	0.12	12.85	96.25	25	76	9	129	17.0	13	85	143	102	11	127	<12	694	24.00	<15	36					<12	<12																						0.49
L-466	73.93	0.13	12.78	1.65	0.00	0.03	0.08	0.98	4.27	4.50	0.03	0.30	98.68	351	83	31	75	39.0	<6	<6	15	21	24	<12	14	225	<6	23.0	<10					57	27																						8.77
L-467	70.78	0.25	13.75	2.33	0.00	0.02	0.18	0.87	4.53	5.45	0.08	0.50	98.74	145	1046	29	208	18.0	7	10	12	30	22	16	<12	2676	<6	67.0	<10					224	130																						9.98
L-600A	76.09	0.13	11.83	1.93	0.00	0.04	0.07	0.45	3.85	5.55	0.06	0.40	100.40	160	59	23	137	14.0	<6	6	14	29	15	<12	68	508	<6	43.0	<10					141	77																						9.40
L-602	70.15	0.49	13.13	3.63	0.00	0.06	0.83	1.80	3.43	4.54	0.16	0.98	99.20	214	137	64	305	26.0	8	7	9	60	18	13	189	716	<6	36.0	<10		14.31	62.39	169.4	213	86			53.19		0.813										4.213	1.338					7.97
L-605	76.55	0.12	12.03	1.16	0.00	0.01	0.02	0.81	3.42	5.47	0.07	0.41	100.07	198	99	7	89	7.0	<6	<6	9	19	13	<12	227	772	<6	42.0	<10					148	102																						8.89
L-606	72.56	0.36	12.83	3.51	0.00	0.06	0.48	1.32	3.22	5.19	0.07	0.73	100.33	185	105	38	202	17.0	<6	6	7	61	18	20	57	781	<6	38.0	<10					227	149																						8.41
L-625	74.31	0.32	12.49	2.19	0.00	0.04	0.42	0.94	5.72	2.00	0.10	0.70	99.23	43	78	49	280	30.0	<6	15	753	26	15	21	123	493	<6	<15	<10					125	54																						7.72
L-626	75.44	0.32	12.53	3.15	0.00	0.05	0.57	0.71	5.99	1.04	0.06	0.63	100.49	18	64	50	263	30.0	<6	13	1078	41	17	21	53	609	<6	<15	<10		10.56	33.25	65.50	112	31			38.58		1.038										3.050	1.238					7.03
L-633	51.27	1.55	16.00	10.81	0.00	0.18	6.69	7.17	3.71	1.69	0.26	1.07	100.40	56	239	26	123	13.0	52	115	499	110	17	279	202	550	<6	<15	31		12.91	15.65	35.85	43	11			224.0			5.638								0.563	1.225					5.40
L-635	62.14	0.98	15.43	6.05	0.00	0.12	3.29	3.28	7.37	0.22	0.15	1.00	100.03	9	33	31	241	19.0	20	64	64	46	20	134	101	58	<6	<15	19		9.025	23.53	48.81	67	21			90.25		0.650		2.688								0.900	1.075					7.59
L-637	69.84	0.53	13.33	5.85	0.00	0.06	0.58	2.19	5.95	0.76	0.10	1.00	100.19	17	165	56	727	29.0	8	18	128	34	20	26	49	359	<6	<15	10		122.5	60.93	134.1	180	93		3.313	34.34		0.588										4.300	1.525					6.71
L-638	77.05	0.18	11.68	2.36	0.00	0.04	0.14	0.62	4.27	3.73	0.02	0.42	100.51	59	91	35	148	17.5	<6	9	95	29	15	14	66	751	<6	<15	<10	10.8	7.71	40.96	10.40	116	53	0.41	4.36	0.51	0	0	1.02	7.02	1.09	6.94	1.36	3.85	0.54	3.56	0.51					8.00
L-641	50.76	2.24	13.78	12.16	0.00	0.24	6.49	7.32	4.30	0.62	0.40	1.90	100.21	27	195	33	131	15.0	48	90	704	133	17	262	196	247	<6	<15	34			12.08	46.00	28	<12																						4.92
L-645	56.67	1.27	14.07	9.26	0.00	0.09	0.42	5.87	8.40	0.16	0.33	3.96	100.50	5	67	38	214	17.0	9	21	6	21	19	113	185	87	<6	<15	26					49	22																						8.56
L-648	72.50	0.35	12.81	4.25	0.00	0.05	0.69	0.64	7.27	1.32	0.06	0.59	100.53	25	69	21	248	12.0	6	17	1546	44	13	47	67	1144	<6	<15	<10					89	30																						8.59
L-649	73.86	0.30	12.07	4.77	0.00	0.06	0.53	0.64	5.74	1.86	0.05	0.56	100.44	37	63	16	193	11.0	9	19	2238	37	11	50	78	1330	<6	<15	<10					74	19																						7.60
L-668	62.61	0.89	17.32	4.83	0.00	0.14	0.72	1.80	6.42	4.79	0.36	0.59	100.47	121	474	69	710	193.0	7	7	6	127	26	14	139	2037	7.00	22.0	<10		13.58	101.4	182.0	235	110		4.450	23.33		0.850	3.850									2.38	1.025					11.21
L-669	64.34	0.61	16.76	4.66	0.00	0.12	0.36	1.46	6.43	4.80	0.23	0.74	100.51	115	350	73	378	204.4	<6	9	7	146	28	<12	124	1647	9.00	31.0	<10	21.7	17.80	102.06	28.00	267	137	0.70	8.24	12.29	0	0	3.96	14.64	2.26	14.05	2.62	7.39	1.00	5.97	0.73					11.23
L-670	57.01	1.45	15.14	11.08	0.00	0.21	1.42	2.33	6.69	3.35	0.53	1.32	100.53	173	1219	73	1843	458.0	<6	9	9	85	42	<12	18	767	17.00	46.0	<10		3.125	27.46	72.13	219	42			74.00		0.288										2.088	0.988					10.04
L-675	60.71	0.10	21.99	3.59	0.00	0.09	0.13	0.94	4.92	6.41	0.03	1.61	100.52	125	384	123	1520	345.0	7	9	23	167	30	20	17	1321	10.00	78.0	11			140.0	591.5	844	440			238.0		3.438	4.23									6.513	1.975					11.33
L-676	59.35	0.87	18.13	5.92	0.00	0.17	1.24	2.05	5.20	5.55	0.24	1.84	100.56	226	634	58	553	139.0	7	7	11	177	26	19	31	1591	<6	19.0	<10					180	85																						10.75
L-691	50.24	3.31	12.95	14.15	0.00	0.21	4.13	6.53	2.95	2.82	0.55	1.51	99.35	151	589	52	368	62.0	39	32	190	166	19	357	66	617	<6	<15	33					110	61																						5.77
L-693	71.37	0.48	11.65	6.47	0.00	0.14	0.19	0.77	4.62	4.46	0.09	0.31	100.55	86	98	31	132	105.3	6	7	14	128	33	<12	60	241	2.29	8.6	<10	4.8	13.2	114	35.3	357	216	0.23	2.81	4.94		0.94	7.69	0.92	5.26	0.97	2.65	0.43	3.26	0.54					9.08
L-694	59.18	1.09	17.07	5.91	0.00	0.17	1.01	2.48	6.84	4.89	0.36	0.54	99.54	106	633	39	333	93.0	7	<6	10	107	23	27	<12	1995	<6	<15	<10					166	87																						11.73
L-695	46.29	3.29	13.34	13.54	0.00	0.48	3.19	4.92	4.10	3.51	0.68	6.78	100.12	197	399	53	329	54.0	27	22	89	120	19	353	28	639	<6	<15	26					64	30																						7.61
L-697	59.94	0.86	16.90	5.28	0.00	0.17	0.99	2.06	6.58	4.59	0.32	1.54	99.23	169	491	151	1363	432.0	8	9	5	129	26	<12	117	1444	15.00	51.0	<10			127.3	480.3	582	291		1.713	107.9		4.550	15.49									10.2	2.075					11.17
L-698	71.68	0.46	11.40	5.84	0.00	0.10	0.10	0.85	4.91	4.10	0.10	0.40	99.94	77	45	50	329	124.0	<6	7	7	104	35	<12	207	157	<6	<15	<10		16.00	66.88	227.6	372	143			92.13		0.250										2.03	1.338					9.01
L-699	63.41	0.28	17.28	5.27	0.00	0.20	0.34	0.93	7.40	4.73	0.12	0.56	100.52	98	114	75	1246	307.0	<6	10	7	147	34	<12	126	458	15.00	50.0	<10					470	310																						12.13
L-708	47.15	0.47	8.72	11.27	0.00	0.53	13.12	14.15	1.46	1.77	0.04	1.79	100.47	86	578	146	469	126.0	16	26	13	279	17	68	14	2096	<6	<15	23					258	97																						3.23
L-712	79.11	0.04	12.04	0.83	0.00	0.04	0.11	0.40	5.47	1.95	0.01	0.54	100.54	33	159	12	17	7.0	<6	10	8	35	18	<12	47	662	<6	<15	<10		106.5		13.44	41	7		1.700			0.213									0.638						7.42
L-713	71.32	0.16	14.36	2.37	0.00	0.05	0.08	0.32	5.76	5.66	0.02	0.41	100.51	117	94	30	277	71.0	<6	8	9	53	25	19	49	909	<6	<15	<10		120.8	80.38	294.6	436	188		0.963	24.54		0.763									1.200	0.875					11.42
L-714	77.55	0.05	13.19	0.73	0.00	0.03	0.17	0.85	6.33	0.76	0.02	0.67	100.35	16	338	9	250	9.0	<6	9	8	40	23	<12	50	538	<6	16.0	<10		106.0		2.950	83			3.213			0.188										0.488					7.09
L-714a	74.47	0.12	14.63	0.94	0.00	0.04	0.12	0.59	8.15	0.94	0.05	0.41	100.46	16	152	25	237	50.0	<6	8	<6	17	0	12	160	606	0.00	0.0	0					0	0																						9.09
L-715	72.13	0.48	13.02	3.49	0.00	0.09	0.48	1.12	3.88	4.88	0.12	0.50	100.19	118	147	58	348	25.0	8	11	12	67	18	28	47	1230	<6	19.0	<10		75.75	38.91	87.88	154	44			38.90		1.13										3.588	1.363					8.76
L-716	73.88	0.30	12.54	2.79	0.00	0.04	0.41	0.98	4.49	3.98	0.04	0.68	100.13	69	164	38	332	15.9	8	11	12	51	16	19	57	1389	7.00	24.0	<10	9.2	7.00	41.87	11.18	134	66	0.83	6.58	0.73	0	0	1.48	5.96	0.90	6.07	1.28	4.03	0.63	4.55	0.70					8.47
L-722	7.50	0.04	0.13	9.55	0.00	0.68	2.58	43.77	0.00	0.00	0.03	36.24	100.52	7	210	260	119	13.0	23	<6	5	37	<9	194	12	145	6.00	27.0	54		17.16		15.61	10	<12			229.3											0.263	0.863					0.00
L-728	75.06	0.16	10.35	2.83	0.00	0.14	0.22	2.20	6.61	0.86	0.06	2.04	100.53	23	140	58	212	33.0	<6	10	15	45	18	14	67	581	4.64	20.9	15	24.2	17.2	82.2	20.2	171	73	0.33	6.35	2.52		3.25	14.4	2.01	12.1	2.23	6.18	0.99	6.52	1.07					7.47
L-729	73.58	0.31	12.64	2.31	0.00	0.05	0.34	0.84	3.69	4.96	0.03	1.70	100.45	113	82	46	281	24.0	<6	6	6	60		<12	58	957																																8.65
L-740	56.74	0.26	18.91	5.92	0.00	0.18	0.21	1.03	6.29	4.68	0.03	6.26	100.51	170	442	26	1803	563.0	<6	11	8	189	42	<12	27	617	27.00	18.0	<10		8.750	22.20	71.88	112	36			114.8		0.500										0.138	0.838					10.97
L-741	56.63	0.47	19.54	7.23	0.00	0.44	0.80	3.09	4.14	7.21	0.11	0.91	100.57	169	548	49	640	337.0	<6	<6	14	164	34	14	18	1955	19.00	<15	<10		14.68	51.69	210.8	248	131			127.0		1.813										1.863	1.100					11.35
L-742	68.41	0.18	10.00	3.45	0.00	0.20	2.09	0.90	5.40	1.17	0.03	8.44	100.27	59	181	41	310	26.0	11	13	32	227	19	18	44	802	<6	21.0	<10		2.538	32.53	52.30	79	44			71.88		0.588										1.350	0.600					6.57

Table No. A15 CHEMICAL ANALYSIS OF SAMPLES FROM THE GREATER LUFILIAN ARC SORTED BY NUMBER

Sample	SiO2	TiO2	Al2O3	Fe2O3	FeO	MnO	MgO	CaO	Na2O	K2O	P2O5	LOI	Total	Rb	Sr	Y	Zr	Nb	Co	Ni	Cu	Zn	Ga	V	Cr	Ba	U	Th	Sc	Pb	Sm	Nd	Pr	Ce	La	Cs	Hf	Ta	As	Se	Eu	Gd	Tb	Dy	Ho	Er	Tm	Yb	Lu	Li	Be	Ge	Mo	Na+K	Sn
Notch	50.00	1.00	15.50	6.00		0.150	2.00	5.00	4.90	5.50	0.30	2.00		200	400	60	360	40	30	16	25	85	26	100	100	1300	20	37	20	20	50	50	15	175	95	3	10	120	100		4	30	5	20	3	9	35.5	7.5	1.6						
L-754	53.02	1.59	13.32	16.18	0.00	0.28	6.53	7.50	0.32	1.02	0.30	0.15	100.21	318	84	40	94	8.0	50	53	94	252	17	393	178	235	<6	<15	49					25	12																						1.34
L-759	74.06	0.03	14.47	0.47	0.00	0.04	0.02	0.70	3.55	5.54	0.06	0.94	99.88	109	124	20	16	7.0	<6	<6	<6	12	13	<12	185	649	<6	<15	<10					12	<12																						9.09
L-772	72.55	0.03	14.29	0.43	0.00	0.03	0.03	0.05	2.34	10.07	0.02	0.67	100.51	201	100	7	<8	4.0	<6	<6	8	28	13	<12	44	579	<6	<15	<10					21	<12																						12.41
L-773	74.83	0.06	14.98	0.87	0.00	0.02	0.11	0.80	5.35	3.07	0.04	0.41	100.54	76	71	103	64	14.0	<6	10	8	43	20	<12	47	176	<6	<15	<10					25	<12																						8.42
L-783	71.86	0.45	13.96	3.32	0.00	0.08	0.50	0.78	3.49	5.15	0.18	0.71	100.48	223	85	54	273	22.0	<6	6	9	49	17	25	239	859	<6	27.0	<10					161	75																						8.64
L-784	71.83	0.39	13.23	3.59	0.00	0.06	0.56	1.31	3.67	5.07	0.09	0.70	100.50	193	105	58	312	23.0	<6	7	7	59	17	23	63	1049	7.00	26.0	<10		11.25	37.06	98.50	155	51		1.513	41.66			0.78							3.938	1.400					8.74
L-789	63.91	1.38	14.35	7.45	0.00	0.07	1.13	1.09	4.87	5.21	0.41	0.55	100.42	125	29	66	715	149.0	<6	6	10	80	21	32	135	1019	8.00	15.0	<10		15.46	50.01	136.3	196	67			127.6			2.03							3.88	1.575					10.08
L-791a	72.44	0.40	13.01	3.67	0.00	0.06	0.32	0.54	3.80	5.16	0.10	0.61	100.11	141	25	97	685	130.0	<6	7	<6	35	17	<12	220	637	6.00	32.0	<10		108.5	22.50	36.51	63	18		2.038	7.288			0.438							5.688	1.400					8.96
L-791b	76.38	0.14	12.55	1.25	0.00	0.02	0.00	0.51	3.09	5.85	0.03	0.29	100.11	270	74	83	70	65.0	<6	10	<6	15	22	16	234	332	8.00	17.0	<10					224	108																						8.94
L-793	74.92	0.33	12.39	2.15	0.00	0.08	0.24	1.00	3.28	5.24	0.14	0.37	100.14	251	140	81	213	78.0	<6	7	7	34	19	22	390	435	12.00	61.0	<10		119.3	50.99	175.4	234	98		1.800	28.45			0.938							6.63	1.700					8.52
L-797	75.11	0.21	13.05	1.92	0.00	0.04	0.08	0.51	3.62	4.63	0.08	0.61	99.86	225	107	23	199	38.0	<6	6	<6	33	21	17	372	658	6.00	37.0	<10					132	76																						8.25
L-798	72.64	0.26	14.07	2.13	0.00	0.08	0.26	1.09	3.42	5.17	0.12	0.91	100.15	222	204	26	229	48.0	<6	<6	<6	40	20	16	285	1117	7.00	27.0	<10					211	102																						8.59
L-799	73.13	0.08	13.93	1.96	0.00	0.06	0.04	0.95	3.84	4.84	0.13	0.63	99.59	153	168	53	183	14.0	<6	7	11	19	18	29	326	727	7.00	<15	<10					102	36																						8.68
L-802	73.34	0.23	14.56	1.83	0.00	0.05	0.29	1.08	3.46	4.55	0.13	0.84	100.36	234	141	32	142	41.0	<6	6	<6	51	19	22	260	745	<6	15.0	<10					77	38																						8.01
L-808	70.53	0.14	15.35	1.50	0.00	0.05	0.42	1.71	4.80	3.67	0.07	2.04	100.28	140	89	12	29	13.9	<6	7	10	71	16	13	39	154	<6	<15	<10	32.4	2.03	9.16	2.46	26	<12	5.99	1.17	1.22	0	0	0.50	1.81	0.31	2.11	0.42	1.29	0.21	1.48	0.22					8.47
L-809	71.56	0.07	14.95	1.24	0.00	0.03	0.23	0.87	3.46	7.52	0.06	0.50	100.49	253	92	19	<8	9.0	<6	7	11	56	16	<12	27	301	<6	<15	<10					29	<12																						10.98
L-810	73.89	0.06	14.05	1.11	0.00	0.04	0.16	1.04	4.00	5.44	0.04	0.50	100.33	173	85	7	<8	7.0	9	10	13	50	14	<12	56	249	<6	<15	<10					24	<12																						9.44
L-812	75.60	0.08	12.89	1.27	0.00	0.03	0.25	1.29	4.03	4.17	0.09	0.71	100.41	141	104	86	215	10.0	<6	8	9	67	13	<12	34	439	17.00	30.0	<10					93	55																						8.20
L-813	71.80	0.04	15.51	0.86	0.00	0.03	0.12	1.40	4.26	5.59	0.08	0.78	100.47	173	115	65	77	6.0	<6	9	13	23	14	<12	42	625	13.00	21.0	<10					63	22																						9.85
L-814	89.59	0.02	5.33	0.65	0.00	0.02	0.02	0.84	2.94	0.31	0.04	0.63	100.39	23	38	5	<8	4.0	<6	7	10	54	<9	<12	77	50	<6	<15	<10					26	<12																						3.25
L-815	69.73	0.30	14.51	3.35	0.00	0.08	0.84	1.34	3.85	5.59	0.16	0.65	100.40	214	122	43	268	25.0	<6	8	10	75	17	12	68	584	42.00	16.0	<10					68	29																						9.44
L-816	74.57	0.30	12.43	3.00	0.00	0.06	0.39	1.37	6.02	1.96	0.04	0.44	100.58	43	91	52	284	32.0	<6	13	104	62	17	18	81	386	<6	<15	<10		115.9	35.64	72.13	122	33		1.200	32.86			1.13							2.68	1.175					7.98
L-832	73.67	0.32	12.24	1.83	0.00	0.04	0.14	0.46	4.39	5.23	0.11	0.63	99.06	154	297	38	307	15.0	8	10	19	70	17	46	<12	1468	<6	19.0	<10					121	58																						9.62
L-834	59.92	0.47	16.55	4.88	0.00	0.05	0.10	1.72	0.29	14.06	0.12	1.28	99.44	283	70	49	274	20.0	7	<6	14	19	9	26	<12	1842	7.00	25.0	<10		12.06	41.53	111.4	192	54		2.875	77.25			0.700							2.450	1.275					14.35
L-835	65.67	0.65	15.35	3.98	0.00	0.08	0.87	2.29	4.41	4.48	0.19	1.44	99.41	135	203	38	342	15.0	<6	<6	7	68	17	40	<12	1318	<6	15.0	10					127	60																						8.89
L-836	67.42	0.74	14.82	4.07	0.00	0.10	0.86	2.21	4.08	4.77	0.20	0.79	100.06	159	266	40	343	17.0	6	<6	19	69	0	45	<12	1272	0.00	0.0	0					0	0																						8.85
L-838	67.61	0.61	14.50	3.84	0.00	0.09	0.82	2.37	3.62	4.48	0.18	0.50	98.62	208	69	22	93	15.6	<6	8	10	30	15	12	<12	552	3.98	21.2	<10					130	55																						8.10
L-839	76.62	0.29	11.26	1.41	0.00	0.04	0.23	0.35	3.05	5.28	0.07	0.47	99.07	218	67	27	163	17.0	<6	9	19	35	13	12	<12	565	<6	16.0	<10					102	44																						8.33
L-840	70.88	0.42	13.61	2.64	0.00	0.07	0.48	1.29	3.97	4.93	0.13	0.75	99.17	176	247	37	237	15.0	<6	8	20	47	16	20	<12	1054	<6	18.0	<10					127	62																						8.90
L-842	65.32	0.68	14.27	4.45	0.00	0.10	1.13	2.64	4.17	3.50	0.19	2.76	99.21	141	316	38	361	16.0	10	11	37	83	16	49	13	1668	<6	16.0	12		11.19	33.40	82.63	135	41		1.475	62.88			1.013							1.638	1.075					7.67
L-843	75.42	0.33	12.58	1.52	0.00	0.03	0.25	0.31	3.01	4.39	0.10	1.13	99.07	163	61	41	199	20.0	<6	<6	6	25	14	16	177	907	<6	21.0	<10		113.0	35.20	74.00	126	32		3.950	9.950			0.650							2.038	0.875					7.40
L-844	68.18	0.63	14.42	3.75	0.00	0.08	0.82	2.22	3.87	4.35	0.20	1.02	99.54	137	259	39	345	16.0	6	7	20	62	17	42	<12	1378	6.00	16.0	<10					129	63																						8.22
L-846	67.61	0.60	14.35	3.72	0.00	0.08	0.89	1.97	4.09	4.59	0.18	0.78	98.86	134	246	44	306	16.0	6	10	18	56	15	39	<12	1240	<6	19.0	<10		11.76	41.76	86.50	133	45			50.38			1.000							1.913	1.088					8.68
L-849	73.54	0.33	12.99	1.74	0.00	0.02	0.20	0.14	3.78	5.57	0.04	0.55	98.90	189	43	24	243	27.0	<6	7	<6	22	18	17	217	451	<6	16.0	<10		107.3	30.33	47.85	152	20		1.013	33.66			0.263							0.238	0.375					9.35
L-850	71.15	0.38	13.69	2.97	0.00	0.05	0.47	1.56	3.09	4.96	0.10	0.48	98.90	264	153	22	241	15.0	7	7	23	57	17	27	13	919	<6	46.0	<10		116.9	48.33	131.0	171	67		4.763	34.13			0.588							0.18	0.725					8.05
L-855	76.63	0.15	11.87	1.14	0.00	0.02	0.05	0.25	4.70	4.06	0.02	0.25	99.14	88	39	10	71	10.0	<6	10	9	11	15	<12	<12	328	<6	<15	<10					39	16																						8.76
L-857	73.33	0.32	13.00	1.84	0.00	0.04	0.43	1.21	4.01	4.21	0.11	1.00	99.50	155	211	17	141	14.0	<6	9	26	28	15	22	<12	1081	<6	<15	<10					80	38																						8.22
L-863	64.77	0.71	14.71	5.42	0.00	0.08	1.57	3.06	3.37	3.86	0.24	1.14	98.93	155	288	33	228	19.0	14	15	23	72	18	100	122	1004	<6	17.0	11					89	44																						7.23
L-864	66.28	0.74	14.57	5.01	0.00	0.09	1.56	2.96	3.05	4.14	0.33	1.62	100.35	97	249	23	39	11.9	10	16	28	58	16	91	273	1039	3.14	13.4	10	17.4	6.19	37.8	9.86	78	45	0.83	1.38	0.83			1.27	5.35	0.73	4.38	0.86	2.38	0.34	2.22	0.32					7.19
L-864	0.00	0.00	0.00	0.00	0.00	0.00	0.00	0.00	0.00	0.00	0.00	0.00	0.00	0	0	0	0	0.0	0	0	0	0	<9				<6	<15	<10					23	<12																						0.00
L-865	66.29	0.76	14.63	4.88	0.00	0.08	1.51	2.53	3.09	4.38	0.27	1.26	99.68	179	240	34	241	19.0	10	20	21	68	17	84	226	1100	<6	16.0	10					129	67																						7.47
L-868	66.57	0.77	14.29	4.73	0.00	0.10	1.11	2.09	3.56	4.38	0.29	1.15	99.04	112	186	32	22	15.3	10	13	14	.	19	68	114	1100	<6	<15	10	14.6	8.72	52.03	13.28	154	79	1.07	0.84	0.55	0	0	1.83	7.21	0.99	6.12	1.18	3.36	0.47	3.09	0.45					7.94
L-874	96.83	0.09	0.64	0.69	0.00	0.01	0.00	0.02	0.02	0.31	0.03	0.08	98.72	11	8	5	29	4.0	<6	13	8	6	17	<12	538	30	6.00	17.0	11					144	73																						0.33
L-874a	67.47	0.89	13.68	4.67	0.00	0.10	1.05	1.71	3.48	4.99	0.27	1.09	99.40	155	181	57	348	24.0	12	14	19	69		63	17	1380																																8.47
L-875	66.20	0.78	14.38	5.11	0.00	0.12	1.18	2.90	3.74	4.25	0.30	1.32	100.28	138	222	46	329	23.0	7	13	14	68	18	71	181	1294	<6	<15	10		12.16	42.90	111.4	157	54			76.63			1.588							1.963	1.225					7.99
L-877	66.24	0.93	13.94	5.04	0.00	0.09	1.14	2.08	3.48	4.74	0.41	1.24	99.33	140	224	54	377	23.0	9	16	22	75	19	62	17	1371	<6	17.0	10					169	87																						8.22
L-878	67.83	0.67	13.61	4.34	0.00	0.09	0.95	1.67	3.73	4.58	0.23	1.08	98.78	152	176	57	329	19.0	9	12	34	71	19	46	16	1143	<6	17.0	<10		12.29	39.36	92.38	150	41			56.10			1.150							2.563	1.213					8.31
L-895	55.24	0.90	18.42	6.32	0.00	0.11	3.12	4.54	4.23	4.61	0.50	1.93	99.92	164	840	22	172	7.0	18	43	164	69	18	134	91	1382	<6	<15	14		8.250	23.24	53.84	74	22			98.63			0.33							0.363	0.913					8.84
L-898	69.20	0.58	12.94	5.11	0.00	0.08	0.60	1.62	4.21	5.14	0.15	0.09	99.72	112	193	33	215	15.0	<6	7	17	46		27	189	1049																																9.35
L-899	71.98	0.41	12.65	2.41	0.00	0.06	0.72	1.79	4.23	3.72	0.11	0.69	98.77	112	193	33	210	18.0	<6	7	17	46	17	26	182	1049	<6	16.0	<10					119	56																						7.95
L-900	67.40	0.67	14.52	4.30	0.00	0.08	1.12	2.21	4.83	4.01	0.21	0.90	100.25	101	244	40	361	16.0	8	8	17	43	17	48	<12	1239	<6	16.0	11					127	61																						8.84
L-902	77.60	0.17	12.00	0.96	0.00	0.02	0.08	0.11	4.16	4.81	0.10	0.34	100.35	160	35	18	95	22.0	<6	7	33	15	15	13	<12	131	<6	25.0	<10					85	39																						8.97
L-903	79.24	0.19	10.48	1.02	0.00	0.02	0.12	0.14	2.98	4.99	0.04	0.32	99.54	262	21	23	103	16.0	<6	8	10	15	13	<12	<12	132	<6	25.0	<10					80	38																						7.97
L-904	76.77	0.24	11.40	1.61	0.00	0.05	0.16	0.10	3.59	4.81	0.05	0.45	99.23	242	44	30	149	18.0	<6	8	15	37	15	<12	14	233	<6	21.0	<10		107.0	29.65	49.94	99	23			7.188			0.28							1.300	0.900					8.40
L-905	77.13	0.29	11.44	1.46	0.00	0.03	0.23	0.54	5.65	1.54	0.06	0.51	98.88	75	80	40	160	19.0	<6	9	17	23	13	13	<12	672	<6	22.0	<10					116	55																						7.19

Table No. A15 CHEMICAL ANALYSIS OF SAMPLES FROM THE GREATER LUFILIAN ARC SORTED BY NUMBER

Sample	SiO2	TiO2	Al2O3	Fe2O3	FeO	MnO	MgO	CaO	Na2O	K2O	P2O5	LOI	Total	Rb	Sr	Y	Zr	Nb	Co	Ni	Cu	Zn	Ga	V	Cr	Ba	U	Th	Sc	Pb	Sm	Nd	Pr	Ce	La	Cs	Hf	Ta	As	Se	Eu	Gd	Tb	Dy	Ho	Er	Tm	Yb	Lu	Li	Be	Ge	Mo	Na+K	Sn
Notch	50.00	1.00	15.50	6.00		0.150	2.00	5.00	4.90	5.50	0.30	2.00		200	400	60	360	40	30	16	25	85	26	100	100	1300	20	37	20	20	50	50	15	175	95	3	10	120	100		4	30	5	20	3	9	35.5	7.5	1.6						
L-906	76.57	0.27	12.23	1.45	0.00	0.03	0.07	0.32	3.00	5.97	0.03	0.42	100.36	254	43	51	164	21.0	<6	7	37	14	13	<12	269	219	<6	19.0	<10					122	62																						8.97
L-907	71.26	0.43	13.59	2.43	0.00	0.06	0.51	1.34	3.85	5.07	0.11	0.52	99.17	175	181	41	248	16.0	<6	8	11	44	15	24	<12	1136	<6	16.0	<10					135	69																						8.92
L-908	66.78	0.41	16.95	1.82	0.00	0.08	0.28	0.22	9.57	2.63	0.03	0.34	99.11	96	28	10	66	15.5	<6	8	12	53	26	<12	<12	125	<6	15.0	<10	9.7	2.50	17.12	5.04	82	40	1.49	2.03	1.06	0	0	0.29	1.92	0.28	1.78	0.37	1.19	0.20	1.64	0.29						12.20
L-909	71.39	0.41	13.73	1.94	0.00	0.07	0.35	0.72	4.37	4.96	0.08	0.91	98.93	153	134	46	285	18.0	<6	8	25	56	17	15	<12	1346	<6	18.0	<10					163	82																						9.33
L-910	70.84	0.59	13.17	3.28	0.00	0.04	0.51	0.53	4.21	4.24	0.20	1.11	98.72	129	126	44	360	17.0	<6	8	12	47	16	26	<12	1115	<6	<15	<10					152	76																						8.45
L-911	72.60	0.37	14.49	2.24	0.00	0.03	0.81	0.22	0.16	5.19	0.11	2.40	98.62	170	16	45	344	27.0	<6	10	33	48	19	17	139	398	<6	19.0	<10					145	75																						5.35
L-912	73.33	0.37	13.50	1.75	0.00	0.02	0.70	0.22	2.05	5.30	0.08	1.55	98.87	139	29	38	273	20.0	<6	7	9	34	17	15	<12	787	<6	16.0	<10					148	47																						7.35
L-917	71.65	0.73	12.99	3.87	0.00	0.08	1.25	0.71	3.95	4.48	0.20	0.63	100.54	113	116	16	39	15.2	6	12	17	50	15	46	15	967	<6	<15	<10	13.4	5.26	30.24	7.86	85	42	1.40	1.36	0.92	0	0	1.04	4.56	0.63	3.72	0.68	1.87	0.27	1.86	0.27						8.43
L-919	87.60	0.31	4.60	3.09	0.00	0.03	0.08	0.09	0.12	2.09	0.04	0.79	98.84	79	9	11	99	8.0	6	15	13	14	<9	27	32	297	<6	<15	<10					55	26																						2.21
L-920	36.93	0.23	6.77	1.19	0.00	0.03	0.22	0.29	2.90	2.72	0.06	49.01	100.35	124	81	20	208	15.0	<6	<6	16	29	14	17	134	1088	<6	<15	<10		113.1	35.71	61.91	99	29			18.89			0.663							0.200	0.700						5.62
L-922	68.49	0.77	14.39	4.18	0.00	0.07	0.89	1.69	3.76	4.88	0.23	0.98	100.33	143	206	56	426	27.0	8	9	15	58	18	56	244	1598	<6	16.0	10		22.13	52.85	122.3	159	56			61.63			1.73	4.288						2.488	1.125						8.64
L-923	70.32	0.62	13.18	3.95	0.00	0.06	0.59	0.92	4.03	4.67	0.17	1.02	99.53	162	156	56	425	21.0	6	12	11	55	18	37	<12	1168	<6	21.0	<10					159	89																						8.70
L-924	71.99	0.63	12.33	2.83	0.00	0.05	0.57	1.46	3.58	3.97	0.13	1.69	99.23	82	63	46	359	22.0	8	9	14	26	15	38	<12	1811	<6	19.0	<10					158	79																						7.55
L-938	70.06	0.58	13.36	3.13	0.00	0.05	0.58	1.70	4.16	4.11	0.19	0.90	98.82	76	244	38	294	19.0	6	7	11	44	16	40	266	1785	<6	<15	<10	23.8	117.0	49.23	83.50	96	37	1.37	3.22	38.46			1.43	3.22	0.53	3.70	0.77	2.40	0.39	1.213	0.888						8.27
L-939	68.27	0.56	15.25	3.83	0.00	0.08	0.63	1.89	3.55	5.28	0.14	0.74	100.22	132	422	22	166	11.0	15	16	29	68	16	89	23	1059	<6	<15	11		8.325	30.34	57.99	77	28			77.50										0.58	0.925						8.83
L-940	62.87	0.57	14.38	5.03	0.00	0.09	1.98	6.05	4.02	3.40	0.20	0.69	99.28	133	422	23	173	12.0	14	13	22	64	18	94	17	1043	<6	<15	11		9.050	25.39	64.13	90	31			79.75			0.43							0.638	0.975						7.42
L-943	74.31	0.15	13.23	1.77	0.00	0.04	0.03	0.75	3.70	5.72	0.11	0.29	100.10	137	123	4	65	7.2	<6	9	19	17	14	13	15	350	<6	28.0	<10	18.5	0.91	6.77	2.16	42	20	2.27	3.29	0.51	0	0	0.15	0.72	0.10	0.64	0.14	0.46	0.09	0.83	0.17						9.42
L-945	67.85	0.52	15.01	3.25	0.00	0.07	0.55	1.40	4.19	5.08	0.11	0.92	98.95	169	235	45	386	18.0	9	8	20	64	18	2	13	1409	<6	19.0	<10		12.43	41.88	115.1	178	53			61.16			0.850	1.663						2.463	1.125						9.27
L-946	67.96	0.48	14.78	2.89	0.00	0.06	0.59	1.58	4.39	5.01	0.12	0.73	98.59	165	232	38	250	19.0	6	8	8	45	16	30	185	1451	<6	<15	<10					175	88																						9.40
L-948	70.39	0.65	13.17	3.48	0.00	0.11	0.62	1.58	4.48	4.47	0.13	0.41	99.49	160	174	63	368	21.0	7	8	10	73	17	22	<12	1424	<6	15.0	<10					175	92																						8.95
L-951	66.61	0.52	15.75	3.69	0.00	0.02	0.04	0.50	11.34	0.33	0.12	0.19	99.11	4	30	50	261	24.0	<6	10	6	9	16	39	137	<20	<6	22.0	<10		10.83	28.36	109.6	166	14			48.54			0.713	3.138						1.888	1.088						11.67
L-952	67.68	0.59	15.55	4.09	0.00	0.02	0.15	0.73	10.86	0.35	0.15	0.22	100.39	6	38	36	308	23.0	<6	9	6	10	16	31	173	52	<6	<15	<10					38	27																						11.21
L-955	67.86	0.41	16.46	3.50	0.00	0.05	0.11	0.33	10.16	0.19	0.23	0.82	100.12	4	37	40	340	17.0	<6	13	333	142	21	36	<12	30	<6	<15	16		13.25	62.33	671.3	965	405			42.79			0.400							1.788	1.025						10.35
L-956	61.48	2.00	9.60	15.05	0.00	0.04	0.23	2.72	7.38	0.01	0.92	0.23	99.66	5	36	63	321	14.0	9	11	7	17	17	91	<12	51	<6	<15	24			41.30	97.50	116	63			297.1										3.050	2.125						7.39
L-957	75.71	0.31	11.71	1.52	0.00	0.04	0.21	1.09	2.90	4.90	0.05	0.66	99.10	126	135	32	207	20.0	<6	7	<6	36	14	<12	228	571	<6	26.0	<10		112.1	34.19	59.59	156	79		3.200	7.188			0.28							0.338	0.675						7.80
L-958	47.73	1.22	15.13	13.06	0.00	0.23	7.23	8.03	3.57	0.36	0.22	2.21	98.99	5	188	34	105	5.0	63	122	59	119	19	296	107	297	<6	<15	37					15	<12																						3.93
L-963	88.82	0.21	4.22	2.07	0.00	0.03	0.19	0.14	1.00	1.77	0.06	0.66	99.17	63	17	18	133	8.0	8	11	20	15	<9	25	12	308	<6	<15	<10					64	31																						2.77
L-965	67.45	0.59	13.65	6.24	0.00	0.03	0.32	0.69	4.10	5.73	0.19	0.42	99.41	156	43	88	358	29.0	<6	11	8	24	17	33	12	741	7.00	30.0	<10					125	56																						9.83
L-966	68.15	0.60	12.90	6.30	0.00	0.02	0.16	0.43	4.46	5.68	0.19	0.27	99.16	144	39	74	108	17.1	<6	9	6	19	16	42	193	708	5.82	27.2	<10	17.8	6.29	34.8	9.84	103	45	0.41	3.12	1.20			0.89	7.00	1.36	10.3	2.34	7.51	1.13	7.93	1.21						10.14
L-967	70.72	0.48	12.92	3.64	0.00	0.07	0.46	1.11	3.78	5.05	0.12	0.63	98.98	269	119	83	395	22.0	8	9	13	60	17	31	<12	883	8.00	36.0	<10					259	130																						8.83
L-967a	0.00	0.00	0.00	0.00	0.00	0.00	0.00	0.00	0.00	0.00	0.00	0.00	0.00	0	0	0	0	0.0	0	0	0	0	15	0	0	0	<6	20.0	<10					153	119																						0.00
L-968	72.13	0.34	13.69	2.21	0.00	0.03	0.17	0.89	3.99	4.79	0.05	0.51	98.80	136	145	37	225	15.0	7	9	20	86	15	16	<12	1370	<6	23.0	<10		110.0	16.73	28.51	110	11		2.863	26.16										0.488	0.763						8.78
L-969	59.46	0.49	19.16	4.28	0.00	0.05	0.68	0.38	0.55	14.31	0.08	0.84	100.28	393	66	59	293	24.0	6	<6	47	53	22	61	<12	2451	6.00	29.0	<10		10.51	36.03	92.38	159	37		7.200	60.24			0.663							3.050	1.288						14.86
L-971	64.34	0.54	17.73	1.51	0.00	0.09	0.14	0.68	4.58	8.51	0.11	0.69	98.92	148	66	47	358	22.0	<6	9	10	14	13	34	<12	2236	<6	<15	<10					137	81																						13.09
L-973	71.06	0.42	12.34	2.89	0.00	0.04	0.12	1.90	0.51	9.97	0.09	0.97	100.31	266	42	47	249	19.0	6	<6	141	70	9	28	12	1800	<6	18.0	<10		9.588	33.88	96.50	128	42		5.850	36.50			0.500							3.23	1.138						10.48
L-975	72.48	0.35	13.19	2.05	0.00	0.06	0.27	0.82	3.81	5.40	0.10	0.56	99.09	164	149	34	215	16.0	7	9	45	47	14	19	<12	1327	<6	21.0	<10					137	68																						9.21
L-976	72.48	0.37	13.10	1.84	0.00	0.04	0.29	0.71	4.00	5.29	0.06	0.50	98.68	195	113	55	203	21.0	<6	10	8	29		18	209	1114					115.8	48.35	91.75		71		3.225	13.38			1.03	2.213						2.93	1.075						9.29
L-977	74.68	0.27	11.99	1.72	0.00	0.04	0.24	0.55	3.86	5.21	0.04	0.45	99.05	121	81	27	197	13.0	<6	8	<6	39	15	12	<12	766	<6	16.0	<10					110	57																						9.07
L-978	76.43	0.22	11.10	2.76	0.00	0.10	0.04	0.28	4.16	5.19	0.05	0.18	100.51	139	58	15	133	16.9	<6	10	37	73	20	14	20	264	3.59	19.1	<10	21.3	2.08	13.4	4.14	50	25	0.75	5.11	1.02			0.29	1.79	0.29	2.06	0.48	1.79	0.33	2.76	0.49						9.35
L-979	66.06	0.48	15.03	3.97	0.00	0.09	1.33	3.18	4.23	3.67	0.14	0.79	98.97	108	435	35	143	15.0	10	10	76	88	16	68	242	1077	<6	<15	11					92	44																						7.90
L-980	67.03	0.53	15.05	4.32	0.00	0.09	1.37	3.20	4.47	3.48	0.18	0.77	100.49	115	424	32	157	17.0	10	15	28	62	17	72	200	1140	<6	<15	<10					104	52																						7.95
L-982	66.31	0.56	15.11	3.80	0.00	0.09	1.18	3.09	4.72	3.57	0.19	0.80	99.42	99	495	25	176	12.0	11	10	11	56	17	54	<12	1245	<6	<15	<10		8.588	26.96	66.38	74	30			53.76			0.363							0.550	0.825						8.29
L-983	72.59	0.29	13.57	1.83	0.00	0.04	0.07	0.90	4.08	4.95	0.04	0.51	98.87	197	156	28	181	17.0	<6	6	7	32	15	13	<12	963	<6	19.0	<10					90	39																						9.03
L-985	72.90	0.46	12.76	2.61	0.00	0.05	0.29	1.39	3.72	4.25	0.06	0.63	99.12	123	219	5	51	6.1	<6	7	9	46	14	25	173	1580	1.49	17.1	<10	25.6	3.41	33.2	9.78	103	61	2.13	1.48	0.19			1.09	2.00	0.20	0.97	0.17	0.46	0.07	0.54	0.10						7.97
L-987a	45.74	2.33	16.73	14.31	0.00	0.17	4.10	10.53	2.62	1.59	0.46	1.99	100.57	22	598	11	18	1.9	41	8	75	109	17	429	<12	397	<6	<15	36	7.7	2.50	10.86	2.08	<12	<12	0.29	0.51	0.03	0	0	1.03	2.95	0.39	2.37	0.46	1.20	0.15	0.92	0.13						4.21
L-987b	40.92	2.62	19.28	13.71	0.00	0.19	4.13	12.81	2.45	0.79	1.19	2.06	100.15	35	646	19	31	4.0	28	<6	37	72	17	307	<12	284	<6	<15	32			7.100	29.40	16	5			284.3											1.338						3.24
L-990	53.79	0.31	13.92	7.16	0.00	0.15	8.22	7.59	5.52	0.32	0.10	2.29	99.37	10	267	12	84	10.0	38	178	73	69	13	75	584	187	<6	<15	20					39	22																						5.84
L-991	48.45	0.96	11.97	11.52	0.00	0.19	11.57	9.20	3.07	0.46	0.12	1.70	99.21	7	217	20	53	9.0	64	251	83	93	12	255	870	188	<6	<15	35					19	12																						3.53
L-992	50.94	0.49	19.38	7.11	0.00	0.15	5.16	9.79	3.16	1.87	0.09	2.25	100.39	67	659	10	28	3.4	27	53	35	53	16	144	100	460	0.24	0.9	26	4.4	1.92	9.78	2.25	19	9	0.49	0.75	0.13			0.79	2.03	0.30	1.93	0.39	1.11	0.16	1.04	0.15						5.03
L-993	71.34	0.39	13.57	2.03	0.00	0.05	0.39	1.42	3.97	5.33	0.07	0.81	99.37	115	224	27	75	11.5	<6	6	8	34	15	24	160	1595	<6	17.0	<10	22.5	7.25	47.18	12.68	139	69	0.45	2.38	0.59	0	0	1.21	5.76	0.82	5.12	1.00	2.86	0.42	2.84	0.41						9.30
L-994	70.70	0.40	13.83	2.09	0.00	0.05	0.43	1.46	3.95	5.07	0.09	0.73	98.80	110	226	37	208	19.0	6	7	10	33	15	32	195	1763	<6	<15	<10					142	70																						9.02
L-995	39.21	3.69	11.13	22.15	0.00	0.26	7.20	10.83	1.60	0.53	1.13	1.13	98.86	14	449	21	27	4.0	59	<6	54	128	19	491	<12	457	<6	<15	45					<12	<12																						2.13
L-996	69.95	0.44	14.71	2.86	0.00	0.06	0.50	1.75	4.30	4.78	0.11	0.95	100.41	121	274	24	78	13.9	6	9	67	71	16	30	<12	1498	2.82	14.9	<10	23.0	6.17	39.6	10.8	113	49	0.69	2.30	0.83			1.22	4.96	0.74	4.69	0.93	2.78	0.42	2.93	0.42						9.08
L-997	69.62	0.34	15.29	1.59	0.00	0.04	0.27	0.51	5.88	5.33	0.05	0.73	99.65	135	65	57	241	22.0	8	9	8	24	16	19	<12	542	<6	33.0	<10		111.4	28.71	57.06	156	21		4.188	11.06										2.450	0.950						11.21
L-998	64.78	0.73	15.67	4.59	0.00	0.11	1.41	2.78	4.52	4.03	0.24	1.33	100.19	103	300	34	347	15.0	6	9	29	96	18	53	13	2134	<6	<15	10		10.00	32.01	78.50	106	38			63.00			0.938							1.038	1.025						8.55

Table No. A15 CHEMICAL ANALYSIS OF SAMPLES FROM THE GREATER LUFILIAN ARC SORTED BY NUMBER

Sample	SiO2	TiO2	Al2O3	Fe2O3	FeO	MnO	MgO	CaO	Na2O	K2O	P2O5	LOI	Total	Rb	Sr	Y	Zr	Nb	Co	Ni	Cu	Zn	Ga	V	Cr	Ba	U	Th	Sc	Pb	Sm	Nd	Pr	Ce	La	Cs	Hf	Ta	As	Se	Eu	Gd	Tb	Dy	Ho	Er	Tm	Yb	Lu	Li	Be	Ge	Mo	Na+K	Sn
Notch	*50.00*	*1.00*	*15.50*	*6.00*		*0.150*	*2.00*	*5.00*	*4.90*	*5.50*	*0.30*	*2.00*		*200*	*400*	*60*	*360*	*40*	*30*	*16*	*25*	*85*	*26*	*100*	*100*	*1300*	*20*	*37*	*20*	*20*	*50*	*50*	*15*	*175*	*95*	*3*	*10*	*120*	*100*		*4*	*30*	*5*	*20*	*3*	*9*	*35.5*	*7.5*	*1.6*						
L-999	67.68	0.49	14.73	3.02	0.00	0.07	0.74	1.83	4.31	4.65	0.13	1.19	98.84	140	252	37	288	20.0	<6	9	10	58	17	33	205	1537	<6	16.0	<10		9.700	36.04	91.88	144	44		1.525	39.16			0.83							1.488	0.888						8.96
L-1000	67.91	0.47	15.37	2.32	0.00	0.06	0.52	1.06	4.28	5.11	0.10	1.68	98.88	192	112	37	251	18.0	<6	10	62	58	17	35	<12	1206	<6	20.0	<10		11.55	90.10	152.3	134	80			81.95			3.48							2.58	1.200						9.39
L-1002	77.59	0.26	11.61	1.64	0.00	0.05	0.10	0.32	3.59	4.97	0.03	0.33	100.49	180	40	25	134	22.0	<6	8	6	14	14	10	<12	180	<6	28.0	<10		104.0	18.61	52.50	87	26		3.350	5.388										1.600	0.925						8.56
L-1003	68.00	0.50	15.07	2.73	0.00	0.05	0.58	1.60	4.64	5.26	0.12	0.69	99.24	145	242	40	289	16.0	<6	8	12	47	17	32	<12	1796	<6	15.0	<10		8.450	28.94	79.13	133	26		2.575	31.71			0.78							1.713	0.950						9.90
L-1005	71.20	0.48	12.46	3.35	0.00	0.06	0.56	1.47	3.93	4.47	0.18	0.76	98.92	171	218	46	298	18.0	7	9	15	50	17	26	16	1194	<6	18.0	<10					132	64																		8.40
L-1007	64.26	0.56	15.15	5.20	0.00	0.10	1.92	3.56	4.03	3.92	0.20	0.55	99.45	169	234	45	318	16.0	7	10	22	61	17	38	<12	1413	<6	22.0	<10					160	78																		7.95
L-1009	66.67	0.69	15.06	4.31	0.00	0.09	1.05	2.81	4.12	4.42	0.26	0.88	100.36	129	347	38	354	15.0	7	7	18	71	17	53	<12	1757	<6	16.0	10					115	55																		8.54
L-1010	63.36	0.80	15.40	5.08	0.00	0.11	1.26	3.27	4.15	4.24	0.34	1.17	99.18	138	385	37	372	15.0	9	10	21	74	18	53	<12	1944	<6	<15	12					110	55																		8.39
L-1011	66.33	0.64	14.74	3.94	0.00	0.09	0.94	2.72	4.53	4.43	0.19	0.82	99.37	152	302	38	308	20.0	7	9	21	73	17	50	126	1322	<6	17.0	10					129	66																		8.96
L-1012	64.77	0.68	15.28	4.30	0.00	0.20	0.95	3.01	5.41	3.94	0.20	0.97	99.71	132	337	42	332	22.0	8	10	9	331	17	53	105	1550	<6	17.0	<10					139	74																		9.35
L-1013	67.41	0.61	14.33	4.04	0.00	0.08	0.94	2.09	4.00	4.72	0.21	0.95	99.38	171	240	39	331	16.0	6	10	26	67	17	47	<12	1290	<6	19.0	<10		108.4	40.58	79.25	131	35			48.23			0.638							1.738	0.975						8.72
L-1014	68.99	0.41	14.20	3.21	0.00	0.05	1.35	2.61	3.04	3.64	0.11	1.80	99.41	59	321	5	43	2.55	9.0	20.0	13.0	43	13	60.0	173	1632	<6	<15	<10	14.1	2.27	18.16	4.86	64.0	34.0	0.24	1.00	n.d.	0.0	0.0	1.27	1.76	0.20	1.08	0.20	0.51	0.07	0.44	0.07						6.68
L-1016	77.33	0.10	1.04	2.18	0.00	0.47	2.02	6.71	0.50	0.09	0.13	8.00	98.57	6	124	8	15	4.0	<6	<6	56	14	<9	<12	351	33	<6	<15	12					24	<12																		0.59
L-1016a	79.38	0.10	0.80	2.49	0.00	0.45	1.96	5.74	0.55	0.13	0.04	7.50	99.14	5	140	6	37	4.0	<6	7	28	27	<9	13	15	57	<6	<15	10					23	<12																		0.68
L-1019	72.23	0.41	13.17	3.00	0.00	0.11	0.24	0.79	6.18	3.79	0.08	0.41	100.41	50	101	31	290	46.9	<6	10	9	62	17	<12	253	1351	1.82	17.0	<10	29.0	7.79	47.2	12.5	110	60	0.15	7.31	2.12			2.05	6.81	0.95	5.85	1.15	3.36	0.49	3.38	0.50						9.97
L-1020	70.82	0.58	12.68	4.01	0.00	0.10	0.76	1.57	5.17	3.14	0.09	0.31	99.23	70	173	52	445	22.0	<6	8	64	85	17	19	<12	1364	<6	19.0	<10					180	95																		8.31
L-1021	72.02	0.43	12.86	3.47	0.00	0.05	0.24	1.10	4.37	4.02	0.07	0.53	99.16	83	92	84	464	33.0	<6	8	5	29	17	<12	250	1355	<6	18.0	<10					143	61																		8.39
L-1022	54.76	0.44	20.41	5.90	0.00	0.20	0.33	1.95	4.97	7.25	0.13	2.78	99.12	189	616	24	767	249.0	7	<6	11	171	36	14	<12	629	8.00	<15	<10		2.638	27.54	47.69	61	19			94.38			0.38								0.763						12.22
L-1023	47.51	0.82	15.70	11.39	0.00	0.21	7.63	10.97	2.78	0.87	0.09	2.31	100.28	19	177	23	45	5.0	51	86	11	157	19	246	354	223	<6	<15	42					33	20																		3.65
L-1024a	7.58	0.07	0.57	9.33	0.00	0.79	5.76	37.24	0.03	0.15	0.23	38.75	100.50	6	335	62	9	44.1	28	21	177	59	<9	23	<12	115	19.00	20.0	49	2.4	50.29	543.29	178.89	2058	1583	0.06	0.11	n.d.	0	0	7.27	28.38	3.20	14.82	2.54	6.75	1.02	7.22	1.10						0.18
L-1024c	5.56	0.06	0.20	9.37	0.00	0.84	6.08	39.51	0.01	0.04	0.23	38.66	100.56	10	325	92	18	31.0	29	11	116	29	<9	24	<12	99	20.00	18.0	49					1786	1383																		0.05
L-1025	42.06	1.06	1.26	21.42	0.00	0.77	2.76	17.44	1.61	0.56	3.85	7.40	100.19	30	1546	50	1312	1425.4	42	10	29	207	12	334	106	214	86.4	19.5	33	4.8	27.7	183	47.1	396	176	0.39	10.1	33.6			8.30	21.9	2.59	13.0	2.12	5.37	0.85	7.25	1.48						2.17
L-1027	55.06	0.81	15.77	5.91	0.00	0.27	2.32	3.60	4.38	6.88	0.23	3.58	98.81	177	429	37	621	220.0	14	42	25	134	24	45	174	1043	<6	<15	<10			58.35	136.1	239	72			94.25			1.663							1.063	0.838						11.26
L-1032	46.04	1.99	15.47	14.07	0.00	0.33	6.80	9.26	3.22	0.75	0.42	1.94	100.29	10	322	48	132	9.0	47	45	26	163	15	345	218	299	<6	<15	40		109.3	42.20	61.28	<12	40		3.525	22.53			0.600							3.588	1.138						3.97
L-1037	67.15	0.44	16.05	2.51	0.00	0.02	0.77	1.33	2.99	7.49	0.15	0.46	99.36	204	190	22	149	16.0	<6	6	8	41	17	15	156	1143	<6	105.0	<10					288	157																		10.48
L-1038	68.09	0.44	15.77	2.42	0.00	0.02	0.69	1.39	3.03	6.45	0.17	0.40	98.87	185	178	26	247	18.0	<6	8	13	39	16	14	162	975	<6	112.0	<10					316	175																		9.48
L-1039	70.93	0.25	13.72	2.43	0.00	0.01	0.03	0.57	3.62	5.51	0.10	1.71	98.88	160	562	19	156	20.0	<6	7	21	11	18	<12	230	793	<6	26.0	<10					88	46																		9.13
L-1039a	73.60	0.10	13.76	0.98	0.00	0.02	0.06	0.47	3.67	6.14	0.03	0.53	99.36	168	205	12	38	2.1	<6	8	6	11	13	12	250	1060	<6	<15	<10	24.9	3.17	17.63	4.60	55	23	2.53	1.29	0.08	0	0	1.07	2.98	0.39	2.17	0.40	1.09	0.15	0.98	0.15						9.81
L-1039c	70.50	0.34	13.95	3.40	0.00	0.02	0.00	0.71	3.38	5.94	0.11	2.16	100.51	172	547	24	162	24.0	<6	7	29	12	18	<12	309	776	<6	32.0	<10					103	55																		9.32
L-1042	70.57	0.26	14.13	2.58	0.00	0.06	0.45	0.67	2.79	6.14	0.10	1.35	99.10	317	68	65	161	17.0	7	12	20	29	14	16	<12	471	<6	35.0	<10		109.9	44.76	78.50	106	34		3.625	26.99			0.413	0.78						3.88	1.213						8.93
L-1043	72.42	0.34	13.62	2.40	0.00	0.04	0.57	0.57	2.76	5.77	0.10	1.27	99.86	276	85	71	207	17.0	7	9	51	30	14	28	<12	525	<6	44.0	<10		109.1	41.74	89.25	140	35		1.713	36.96			0.750							8.700	1.850						8.53
L-1044	73.43	0.25	12.72	2.04	0.00	0.04	0.39	0.49	2.79	5.94	0.11	1.10	99.30	293	67	47	166	16.0	6	9	115	70	12	20	12	415	<6	36.0	<10					109	44																		8.73
L-1045	65.28	0.40	17.54	2.82	0.00	0.08	0.36	3.60	6.67	1.70	0.11	1.41	99.97	90	471	107	246	24.0	5	7	48	18	20	24	<12	116	<6	57.0	12		12.20	14.56	48.25	154	16			297.8			0.188							2.238	1.675						8.37
L-1046	72.78	0.33	12.73	2.40	0.00	0.03	0.55	0.76	2.61	5.45	0.12	1.39	99.15	283	61	69	193	16.0	6	9	30	27	13	25	16	473	<6	42.0	<10					126	53																		8.06
LJ1	68.16	0.46	16.02	2.81	0.00	0.02	0.89	1.54	2.85	7.17	0.16	0.55	100.07	196	191	24	259	17.0	4		30	42		15	0	954	1.00	95.0	4																									10.02
LL1	73.41	0.09	14.65	0.80	0.00	0.01	0.27	1.00	3.34	6.24	0.20	1.26	100.02	150	176	17	42	6.0	3	3	13	11		6	1	1468	0.00	5.0	2																									9.58
LL10	56.48	1.24	17.84	6.85	0.00	0.19	1.96	3.78	5.74	4.86	0.74	0.74	99.67	135	965	36	340	99.0	11	3	0	78		44	0	1366	9.00	25.0	1																									10.60
LL11	73.00	0.00	14.00	2.00	0.00	0.00	0.00	1.00	3.00	6.00	0.00	1.00	99.86	287	134	34	210	16.0	2	1	0	30		20	3	880	3.00	55.0	5																									9.00
LL13	62.00	1.00	11.00	4.00	0.00	0.00	3.00	18.00	1.00	0.00	0.00	7.00	100.02	12	701	42	128	6.0	9	26	3	58		101	66	448	4.00	5.0	10																									1.00
LL14	57.00	1.00	17.00	9.00	0.00	0.00	1.00	3.00	6.00	5.00	0.00	1.00	99.52	280	355	161	2052	364.0	4		5	133		4	0	1161	22.00	83.0	5																									11.00
LL15	62.00	1.00	16.00	6.00	0.00	0.00	1.00	4.00	6.00	5.00	0.00	4.00	99.73	118	328	31	305	47.0	10	9	0	73		125	22	1308	3.00	26.0	15																									11.00
LL16	70.00	1.00	14.00	3.00	0.00	0.00	1.00	2.00	3.00	5.00	0.00	0.00	99.49	230	152	24	320	30.0	4	2	0	33		39	9	790	3.00	33.0	4																									8.00
LL17a	73.00	0.00	14.00	1.00	0.00	0.00	0.00	1.00	3.00	7.00	0.00	1.00	99.75	202	57	12	29	9.0	2		5	8		4	6	220	5.00	3.0	1																									10.00
LL17b	66.00	1.00	16.00	5.00	0.00	0.00	1.00	3.00	3.00	5.00	0.00	0.00	99.77	140	208	22	311	16.0	13	2	2	60		50	7	1167	4.00	18.0	9																									8.00
LL18	76.00	0.00	13.00	1.00	0.00	0.00	0.00	1.00	3.00	7.00	0.00	1.00	100.07	178	84	8	55	3.0	0			8		5	4	316	5.00	4.0	1																									10.00
LL2a	75.73	0.02	14.98	0.67	0.00	0.01	0.06	0.12	3.62	4.86	0.04	1.36	100.11	181	35	10	19	19.0	2	1	14	8		11	0	104	2.00	4.0	2																									8.48
LL2b	69.71	0.00	16.92	0.31	0.00	0.01	0.00	0.04	2.54	10.40	0.13	0.60	100.06	356	67	7	4	1.0	2	1	0	2		0	1	205	0.00	2.0	0																									12.94
LL3a	75.92	0.03	13.87	0.68	0.00	0.01	0.05	0.39	2.87	5.93	0.01	1.19	99.77	156	182	13	29	0.0	2	1	14	4		5	3	659	0.00	7.0	1																									8.80
LL3b	70.31	0.04	16.91	0.47	0.00	0.01	0.24	0.37	2.44	9.09	0.09	1.20	99.96	348	252	9	5	4.0	2	1	0	7		7	1	495	1.00	0.0	5																									11.53
LL4	74.72	0.10	13.50	1.59	0.00	0.03	0.10	0.80	3.49	5.74	0.02	0.41	100.08	365	50	32	138	29.0	1		0	27		1	0	235	4.00	52.0	5																									9.23
LL5	75.94	0.03	14.40	0.33	0.00	0.00	0.00	1.44	4.03	3.46	0.03	0.64	99.67	180	89	47	48	11.0	1		6	4		0	0	151	5.00	11.0	1																									7.49
LL9	79.03	0.02	14.86	0.39	0.00	0.00	0.01	0.02	0.30	5.63	0.00	3.19	100.25	256	26	9	33	9.0	2	2	1	3		12	3	285	2.00	3.0	2																									5.93
LR20	2.875	0.02	0.60	12.9		0.38	33.1	45.0	1.67	0.04	0.15			0	1166	152	97	22	16	44	31	79	0	115	85	32	0	36	0	10	0	0	0	0	37	25	0	42	6											0	2	1.71	0
LR23	6.138	0.06	1.84	14.0		0.45	30.5	40.6	2.47	0.10	0.18			6	941	2633	327	152	71	53	41	53	0	62	86	25	15	130	19	71	0	0	88	0	32	0	13	449	24											0	5	2.57	0
LR25	4.673	0.29	0.34	5.85		1.89	0.76	70.8	1.58	0.01	5.82			1	6765	12358	65	128	167	58	166	899	0	191	50	469	24	7730	7	0	673	1335	0	3341	2342	0	8	35	0											0	75	1.59	27

Table No. A15 CHEMICAL ANALYSIS OF SAMPLES FROM THE GREATER LUFILIAN ARC SORTED BY NUMBER

Sample	SiO2	TiO2	Al2O3	Fe2O3	FeO	MnO	MgO	CaO	Na2O	K2O	P2O5	LOI	Total	Rb	Sr	Y	Zr	Nb	Co	Ni	Cu	Zn	Ga	V	Cr	Ba	U	Th	Sc	Pb	Sm	Nd	Pr	Ce	La	Cs	Hf	Ta	As	Se	Eu	Gd	Tb	Dy	Ho	Er	Tm	Yb	Lu	Li	Be	Ge	Mo	Na+K	Sn
Notch	50.00	1.00	15.50	6.00		0.150	2.00	5.00	4.90	5.50	0.30	2.00		200	400	60	360	40	30	16	25	85	26	100	100	1300	20	37	20	20	50	50	15	175	95	3	10	120	100		4	30	5	20	3	9	35.5	7.5	1.6						
LR4	2.133	0.10	0.12	33.4		3.12	1.61	48.6	1.71	0.04	0.66			0	1054	2761	44	598	44	21	0	99	-5	0	0	0	28	1593	0	438	0	2003	0	6950	5436	3	7	2199	93												0			1.75	12
LR5	7.666	0.30	1.32	16.1		2.24	3.89	48.8	1.51	0.53	8.09			19	1669	4033	130	181	90	46	89	45	0	36	114	393	26	2347	0	91	655	1734	486	4909	3846	18	7	75	49												0			2.05	0
P-13	65.76	0.82	14.67	5.87	0.00	0.10	1.00	2.40	5.77	3.89	0.24	0.21	100.52	90	301	45	157	30.0	70	11	<3	4	23	55	22	787	10.00	56.0	7	4.0	9.90	58.80	16.50	153	80	<1	9.00	2.70	1	35	2.10	9.50	1.30	8.00	1.70	4.50	34.90	4.60	0.80					9.66	
P-17	64.11	0.97	14.29	7.35	0.00	0.08	0.80	2.43	3.95	5.62	0.26	0.18	99.86	107	372	54	327	32.0	84	16	63	23	24	103	11	782	11.00	48.0	10	5.0	11.90	64.10	17.30	136	47	1.00	8.00	2.40	3	88	2.40	11.70	1.50	9.00	1.80	5.10	35.70	5.00	0.80					9.57	
P-25	51.44	2.40	20.38	8.73	0.00	0.71	3.91	5.28	6.42	1.71	0.38	0.12	100.72	55	348	24	107	14.0	33	6	40	13	24	98	90	120	<2	2.0	20	4.0	4.00	15.10	3.20	22	9	1.00	2.00	1.30	12	107	1.70	4.50	0.70	4.20	0.90	2.30	33.60	2.10	0.30					8.13	
P-26	76.20	0.13	11.58	0.93	0.00	0.05	<.1	0.25	10.51	0.03	0.03	0.08	99.71	7	15	170	705	243.0	39	4	<3	<1	68	<4	24	22	6.00	76.0	1	5.0	6.90	15.00	3.20	24	8	<1	31.00	4.80	1	7	0.70	11.80	3.30	27.50	6.70	21.30	35.70	23.00	3.40					10.54	
P-28	68.49	0.34	12.40	3.43	0.00	0.12	0.26	1.06	8.74	5.32	0.11	0.13	100.27	345	58	617	261	64.0	34	19	<3	97	24	<4	8	689	13.00	98.0	5	61.0	75.30	359.30	89.80	600	383	5.00	11.00	2.90	4	7	6.40	97.80	16.20	98.20	20.30	53.30	40.90	38.70	5.90					14.06	
P-29	72.84	0.31	13.07	2.71	0.00	0.11	0.19	1.28	4.04	5.56	0.08	0.17	100.19	278	79	89	183	46.0	38	3	6	58	22	<4	8	724	9.00	65.0	6	53.0	16.20	82.60	23.20	204	101	3.00	6.00	2.20	2	7	1.70	14.80	2.40	14.40	2.90	8.10	36.90	8.20	1.40					9.60	
P-32	73.45	0.26	12.59	1.67	0.00	0.06	0.10	0.94	4.34	6.61	0.08	0.14	100.10	334	72	23	57	12.0	58	10	<3	14	17	<4	20	862	<2	7.0	3	48.0	3.60	15.80	4.30	36	18	3.00	4.00	0.90	<1	4	1.30	3.80	0.60	3.50	0.60	1.40	36.40	1.00	0.10					10.95	
P-33	68.30	0.54	14.41	3.20	0.00	0.10	0.73	1.53	5.65	6.09	0.19	0.20	100.74	230	222	81	157	19.0	52	6	<3	45	21	31	13	2028	<2	16.0	7	21.0	16.60	78.50	19.40	121	57	2.00	4.00	2.40	<1	13	2.90	16.70	2.30	12.80	2.60	7.00	33.10	5.60	0.80					11.74	
P-35	74.32	0.25	13.99	1.48	0.00	0.07	0.33	1.12	6.19	2.54	0.07	0.18	100.36	83	188	2	99	6.0	41	2	<3	35	19	11	21	558	2.00	8.0	1	20.0	1.60	9.40	2.70	26	15	1.00	3.00	0.40	<1	5	0.50	1.20	0.10	0.60	0.10	0.20	33.40	0.20	0.00					8.73	
P-39	72.16	0.28	12.57	3.40	0.00	0.08	0.12	1.17	4.67	5.57	0.11	0.17	100.13	404	43	109	309	59.0	56	4	<3	12	29	<4	5	182	19.00	71.0	4	11.0	21.40	114.10	33.00	290	145	2.00	10.00	2.50	<1	12	0.80	19.40	3.10	18.30	3.60	9.20	34.40	7.30	1.10					10.24	
P-40i	76.05	0.26	11.74	2.15	0.00	0.08	0.13	1.54	4.06	4.05	0.07	0.07	100.13	150	92	48	335	27.0	61	12	<3	26	26	<4	9	309	6.00	20.0	2	8.0	9.30	45.60	11.90	98	51	1.00	11.00	1.30	2	8	1.50	8.80	1.40	8.30	1.70	5.00	35.30	5.00	0.80					8.11	
P-40ii	68.86	0.55	13.67	4.56	0.00	0.12	0.33	1.82	4.52	5.77	0.12	0.19	100.32	195	110	77	391	52.0	53	14	<3	53	27	11	19	503	<2	15.0	5	10.0	15.90	78.80	20.00	157	71	1.00	11.00	3.30	<1	22	2.00	14.40	2.40	14.20	2.80	7.50	34.90	6.40	1.00					10.29	
P-46	71.17	0.38	12.62	4.35	0.00	0.12	0.20	0.81	3.59	6.89	0.07	0.16	100.20	398	65	89	257	53.0	48	4	<3	45	27	<4	9	387	10.00	46.0	1	11.0	16.90	93.10	25.70	217	110	3.00	11.00	2.80	26	28	1.40	15.50	2.40	14.00	2.80	7.90	4.90	7.40	1.10					10.48	
P-50	71.53	0.25	12.60	3.26	0.00	0.10	0.30	1.66	4.55	4.88	0.21	0.14	99.34	376	66	163	312	107.0	40	16	<3	30	27	<4	4	314	62.00	256.0	3	23.0	54.30	334.80	100.20	899	505	4.00	9.00	3.20	1	8	1.20	39.60	6.00	32.20	6.20	16.30	5.70	11.40	1.60					9.43	
P-53	73.18	0.24	13.04	2.62	0.00	0.07	0.22	0.95	3.78	5.92	0.12	0.09	100.14	421	59	54	179	48.0	71	19	<3	<1	24	<4	24	209	21.00	43.0	2	11.0	5.60	25.70	8.00	78	44	6.00	6.00	2.50	6	6	0.80	6.00	1.10	6.70	1.50	4.70	31.80	4.80	0.80					9.70	
P-57	62.19	0.36	13.11	2.44	0.00	0.05	0.26	0.86	15.42	5.52	0.06	0.21	100.27	225	45	375	404	48.0	63	21	<3	1	24	<4	<4	286	10.00	51.0	6	5.0	79.00	499.40	133.60	735	579	2.00	11.00	2.60	<1	5	7.60	80.50	10.00	55.60	11.10	28.90	35.90	21.40	3.30					20.94	
P-58	67.76	0.79	13.46	6.83	0.00	0.17	1.40	2.21	3.78	4.27	0.18	0.25	100.85	210	189	66	223	30.0	77	4	21	72	26	45	12	680	4.00	24.0	8	12.0	10.30	50.50	13.10	107	53	5.00	6.00	2.10	1	30	2.10	9.90	1.50	8.50	1.70	4.70	33.40	3.90	0.60					8.05	
X-01	73.81	0.08	12.29	0.37	1.52	0.04	0.70	2.24	4.21	4.83	0.04	0.66	100.79																																											9.04	
X-02	72.56	0.23	14.28	0.94	0.68	0.02	0.83	0.76	2.88	6.12	0.05	1.96	101.31																																										9.00	
X-03	70.95	0.42	15.07	1.13	1.29	0.03	1.32	0.83	4.23	3.03	0.11	2.60	101.01																																										7.26	
X-04	75.20	0.33	10.10	1.55	1.69	0.04	2.81	2.08	2.02	2.13	0.34	2.36	100.65																																										4.15	
X-05	65.27	0.84	15.18	3.20	1.94	0.08	1.01	2.90	3.00	4.70	0.31	1.39	99.82																																										7.70	
X-06	46.85		15.87	3.33	7.40	0.11	8.61	7.29	3.65	2.50	0.15	3.06	98.82																																										6.15	
X-07	58.63		13.08	6.07	6.68	0.15	1.87	4.70	5.50	0.66	0.32	1.66	99.32																																										6.16	
X-08	67.94		12.08	7.23	1.01	0.04	0.60	1.65	6.70	0.20	0.07	1.70	99.22																																										6.90	
X-09	59.26		16.65	1.26	0.43	0.06	2.04	4.59	9.80	0.20	0.65	4.48	99.42																																										10.00	
X-10	47.87		14.53	4.50	9.05	0.15	6.13	6.12	2.95	1.55	0.37	7.22	100.44																																										4.50	
X-11	48.19		14.53	4.13	7.18	0.12	6.66	9.00	4.25	1.40	0.17	3.60	99.23																																										5.65	
X-12	30.05	0.37	8.60	39.65	4.48	0.05	0.27	6.82			5.78	0.35	96.42																																										0.00	
X-13	49.41	2.67	12.71	2.18	10.07	0.14	6.93	10.46	2.46	0.80	0.46	2.38	100.67																																										3.26	
X-14	46.76	3.30	10.31	5.81	9.10	0.14	7.25	10.24	4.26	0.86	0.38	4.05	102.46																																										5.12	
X-15	67.63	0.59	14.37	2.02	1.66	0.07	1.15	1.90	4.59	5.21	0.26	0.86	100.31				592																																									9.80	
X-16	75.93	0.26	12.08	2.96	0.32	0.01	0.36	0.48	7.93	0.13	0.07	0.42	100.95																																										8.06	
X-17	72.07	0.33	13.36	3.76	0.25	0.02	1.33	1.01	7.95	0.30	0.04	0.49	100.91																																										8.25	
X-18	69.24		12.00					0.55	3.83	5.36		0.00	90.98																																											9.19	
X-19	72.02	0.32	13.78	2.24	1.02	0.02	0.20	0.39	4.07	5.18	0.03	0.65	99.92																																										9.25	
X-20	76.01	0.23	12.05	0.80	0.91	0.03	0.20	1.02	3.09	5.02	0.01	1.14	100.51																																										8.11	
X-21	60.78	0.87	16.97	1.13	4.10	0.16	0.99	1.94	5.65	5.27	0.22	1.78	99.86																																										10.92	
X-22	64.42	1.12	14.69	4.34	1.80	0.07	1.37	1.17	3.71	5.64	0.25	1.78	100.36																																										9.35	
X-23	63.81	0.59	14.21	3.67	1.10	0.15	1.48	2.27	4.37	6.00	0.09	3.13	100.87																																										10.37	
X-24	51.29	0.40	19.06	5.95	1.05	0.42	0.82	4.79	6.75	5.19	0.30	3.38	99.40																																										11.94	
X-25	47.49	2.22	14.47	3.74	8.09	0.05	6.73	11.57	1.24	0.77	0.30	2.80	99.47																																										2.01	
X-26	48.82	1.03	12.21	3.62	6.54	0.15	13.68	9.63	1.77	1.10	0.59	1.16	100.30																																										2.87	
X-27	47.85	1.47	16.84	2.70	8.50	0.19	6.66	11.79	2.54	0.75	0.27	0.46	100.02																																										3.29	
X-28	60.59	0.58	14.99	2.44	2.30	1.13	0.91	2.55	8.98	3.81	tr	1.00	99.28																																										12.79	
X-29	61.03		18.63	3.66			1.04	1.56	7.68	5.57		0.41	99.58																																											13.25	
X-30	63.34	0.57	16.00	4.17	1.69	0.11	0.35	2.29	3.93	5.86	0.17	2.04	100.52																																										9.79	
X-31	61.56	0.82	15.25	4.29	3.89	0.25	1.28	1.68	4.10	4.40	0.16	1.24	98.92																																										8.50	
X-32	65.80	0.60	15.40	3.84	0.28	0.06	0.11	1.12	5.60	5.10	0.38	1.05	99.34																																										10.70	
X-33	51.80	0.32	18.20	2.24	2.09	0.17	2.56	4.93	8.22	5.36	0.50	3.69	100.08																																										13.58	
X-34	76.75	0.09	11.78	0.82	0.58	0.03	0.16	0.72	3.08	5.01	0.1	0.84	99.96																																										8.09	
X-34a	76.75	0.09	11.78	0.82	0.58	0.03	0.16	0.72	5.01	3.08	0.1	0.84	99.96																																										8.09	
X-35	76.84	0.08	10.7	1.3		0.04	0.1	0.8	2.3	4.9	0.02	0.69	97.77																																										7.20	

Table No. A15 CHEMICAL ANALYSIS OF SAMPLES FROM THE GREATER LUFILIAN ARC SORTED BY NUMBER

Sample	*SiO2*	*TiO2*	*Al2O3*	*Fe2O3*	*FeO*	*MnO*	*MgO*	*CaO*	*Na2O*	*K2O*	*P2O5*	*LOI*	*Total*
Notch	*50.00*	*1.00*	*15.50*	*6.00*		*0.150*	*2.00*	*5.00*	*4.90*	*5.50*	*0.30*	*2.00*	
X-36	76.9	0.01	12.3	0.6		0.01	0.1	0.5	3.6	4.4	0.04	0.35	98.81
X-37	78.2	0.04	10.3	1.1		0.04	0.1	0.7	2.2	4.9	0.01	0.44	98.025
X-38	59.8	1.1	10.4	12.6		0.3	0.6	4.3	1.7	2.9	0.08	0.99	94.77
X-39	66.6	0.01	18	0.2		0.02	0.03	0.2	2.4	11.9	0.01	0.95	100.32
X-40	64.8	0.01	16.7	0.4		0.01	0.03	0.1	0.7	15.5	0	0	98.25
X-41	64.19	1.05	14.8	2.89	2.68	0.05	1.68	3.11	3.7	4.65	0.31	0.97	100.08
X-42	68.64	0.3	13.95	1.14	1.25	0.06	2.29	2.25	2.13	4.04	0.11	3.54	99.7
X-43	72.65	0.27	14.34	0.34	1.10	0.04	0.73	1.21	3.07	5.46	0.12	0.55	99.88
X-44	76.59	0.32	12.60	0.28	2.08	0.04	0.82	0.78	0.87	5.77	0.04	0.49	100.68
X-45	68.41	0.69	14.46	0.29	4.31	0.08	1.29	2.07	3.47	4.63	0.25	0.92	100.87
X-46	72.98	0.13	14.41	0.10	1.05	0.04	0.42	1.03	4.45	4.57	0.07	0.79	100.04
X-47	78.16	0.15	11.55	0.00	0.86	0.02	0.70	0.41	2.45	6.08	0.40	0.18	100.96
X-48	73.41	0.14	13.97	0.16	1.08	0.05	0.37	1.05	4.41	4.44	0.35	0.59	100.02
X-49	64.17	0.89	20.28	0.26	1.06	0.05	0.19	2.30	6.14	4.57	0.14	0.49	100.54
X-50	62.31	0.11	18.36	1.53	3.07	0.10	0.90	1.00	5.67	6.04	0.07	0.98	100.14
X-51	60.19	0.49	18.14	0.84	3.86	0.14	0.33	2.35	5.31	7.00	0.07	1.55	100.27
X-52	67.17	0.72	14.55	0.48	4.33	0.07	1.20	2.05	3.59	5.30	0.20	0.85	100.51
X-53	71.79	0.23	14.21	0.31	2.26	0.05	0.37	1.06	3.40	5.64	0.12	0.98	100.42
X-54	71.06	0.45	14.42	0.03	1.25	0.05	0.65	4.21	2.70	5.49	0.11	0.57	100.99
X-55	75.50	0.31	12.40	1.50	0.60	0.03	0.40	0.60	3.10	5.60	0.04	0.94	101.02
X-56	67.80	0.71	14.50	0.90	3.60	0.05	1.18	2.90	3.10	4.60	0.21	0.87	100.42
X-57	67.00	0.75	14.20	1.10	4.00	0.07	1.30	2.40	2.80	5.10	0.22	1.34	100.28
X-58	71.10	0.28	14.50	1.20	1.10	0.03	0.29	1.10	3.40	6.30	0.07	0.93	100.30
X-59	69.70	0.52	14.20	1.00	2.40	0.07	0.60	1.70	4.80	5.50	0.14	0.77	101.40
X-60	71.10	0.38	13.60	1.10	2.50	0.06	0.42	1.50	3.50	5.50	0.08	1.27	101.01
X-61	71.74	0.27	14.47	0.32	1.73	0.05	0.42	1.62	3.44	4.65	0.24	0.55	99.50
X-62	61.07	0.80	16.53	1.03	5.61	0.16	0.56	2.97	3.75	6.03	0.14	0.84	99.49
X-63	64.77	0.89	15.33	0.73	4.82	0.08	1.45	2.54	3.83	4.30	0.27	0.87	99.88
X-64	61.68	1.20	14.96	0.77	7.01	0.12	2.29	3.15	3.60	3.30	0.35	1.28	99.71
X-65	74.82	0.11	13.65	0.38	0.65	0.01	0.50	0.98	3.57	5.35	0.03	0.58	100.63
X-66	72.86	0.30	14.37	0.79	2.66	0.04	0.54	0.93	3.98	5.25	0.09	0.72	102.53
X-67	70.30	0.38	13.88	0.60	3.27	0.07	0.45	1.17	2.29	5.90	0.14	0.84	99.29
X-68	70.96	0.28	13.75	1.02	1.58	0.05	0.24	0.91	1.65	7.44	0.07	1.31	99.26
X-69	68.83	0.48	14.51	4.05	0.79	0.03	0.33	0.10	2.79	7.36	0.05	0.00	99.32
X-70	74.17	0.21	12.86	0.00	1.80	0.04	0.33	0.49	1.94	5.91	0.10	0.50	98.35
X-71	70.61	0.33	14.72	1.41	0.86	0.02	0.55	0.54	2.17	7.33	0.18	0.73	99.45
X-72	69.88	0.40	13.71	1.80	2.37	0.07	0.27	0.62	2.92	6.03	0.04	0.55	98.66
X-73	67.24	0.73	14.52	2.90	2.30	0.03	0.95	2.17	4.44	3.53	0.26	0.00	99.07
X-74	58.87	0.46	14.09	2.03	2.44	0.07	2.10	7.49	6.09	3.07	0.17	0.00	96.88
X-75	71.21	0.42	21.42	2.00	1.44	0.03	0.45	0.89	4.10	4.92	0.11	0.81	107.80
X-76	55.35	1.48	14.63	10.86	0.00	0.10	4.43	2.43	0.91	7.34	0.50	1.65	99.69
X-77	61.50	1.10	15.15	7.30	0.00	0.11	1.58	2.81	4.39	5.07	0.34	1.21	100.59
X-78	51.81	3.13	15.06	11.46	0.00	0.06	7.53	1.00	3.02	4.48	0.33	2.67	100.54
X-79	48.31	4.07	11.38	9.92	0.00	0.21	9.92	5.90	2.58	1.14	0.57	6.34	100.34
X-80	45.03	3.27	13.53	16.29	0.00	0.09	6.04	5.05	5.14	3.32	0.53	2.13	100.41
X-81	46.37	3.96	13.46	15.27	0.00	0.05	6.20	4.88	4.91	2.96	0.54	1.92	100.52
X-82	48.60	1.56	13.71	18.47	0.00	0.08	2.02	5.07	7.38	1.05	0.81	1.52	100.26
X-83	46.07	2.56	14.20	17.60	0.00	0.15	5.97	5.84	3.60	3.20	0.32	0.85	100.37
X-84	46.07	3.95	12.30	12.67	0.00	0.06	3.44	8.56	5.49	0.87	0.91	6.14	100.47
X-85	47.35	2.56	14.08	13.25	0.00	0.14	7.29	8.22	4.21	0.61	0.32	2.54	100.58
X-86	45.88	3.96	12.72	16.75	0.00	0.25	5.61	7.19	3.78	1.46	0.31	2.23	100.14
X-87	46.09	2.86	13.80	14.33	0.00	0.23	6.98	7.07	4.90	0.32	0.41	3.05	100.06
X-88	45.24	2.00	14.37	11.55	0.00	0.11	10.97	4.11	2.72	5.24	0.20	3.85	100.37
X-89	46.20	3.57	8.68	14.36	0.00	0.18	11.42	6.07	4.30	2.70	0.67	1.85	100.01
X-90	73.62	0.31	12.90	0.54	1.67	0.05	0.42	1.13	3.37	5.90	0.10	0.44	100.45
ZGSI	58.04	Tr	20.76	4.45		0.20	0.09	0.95	9.22	4.81	Tr	1.99	100.51
ZGSII	56.31	Tr	19.89	4.28	0.30	0.16	0.26	0.74	8.33	5.75	n.d.	3.56	99.58

Sample	*Rb*	*Sr*	*Y*	*Zr*	*Nb*	*Co*	*Ni*	*Cu*	*Zn*	*Ga*	*V*	*Cr*	*Ba*	*U*	*Th*	*Sc*	*Pb*	*Sm*	*Nd*	*Pr*	*Ce*	*La*	*Cs*	*Hf*	*Ta*	*As*	*Se*	*Eu*	*Gd*	*Tb*	*Dy*	*Ho*	*Er*	*Tm*	*Yb*	*Lu*	*Li*	*Be*	*Ge*	*Mo*	*Na+K*	*Sn*
Notch	*200*	*400*	*60*	*360*	*40*	*30*	*16*	*25*	*85*	*26*	*100*	*100*	*1300*	*20*	*37*	*20*	*20*	*50*	*50*	*15*	*175*	*95*	*3*	*10*	*120*	*100*		*4*	*30*	*5*	*20*	*3*	*9*	*35.5*	*7.5*	*1.6*						
X-36																																									8.00	
X-37																																									7.10	
X-38																																									4.60	
X-39																																									14.30	
X-40																																									16.20	
X-41																																									8.35	
X-42																																									6.17	
X-43																																									8.53	
X-44																																									6.64	
X-45																																									8.10	
X-46																																									9.02	
X-47																																									8.53	
X-48																																									8.85	
X-49																																									10.71	
X-50																																									11.71	
X-51																																									12.31	
X-52																																									8.89	
X-53																																									9.04	
X-54																																									8.19	
X-55																																									8.70	
X-56																																									7.70	
X-57																																									7.90	
X-58																																									9.70	
X-59																																									10.30	
X-60																																									9.00	
X-61																																									8.09	
X-62																																									9.78	
X-63																																									8.13	
X-64																																									6.90	
X-65																																									8.92	
X-66																																									9.23	
X-67																																									8.19	
X-68																																									9.09	
X-69																																									10.15	
X-70																																									7.85	
X-71																																									9.50	
X-72																																									8.95	
X-73																																									7.97	
X-74																																									9.16	
X-75																																									9.02	
X-76	209	199	56	591	28.0	13	11	295	50		139	<9	1379																												8.25	
X-77	182	313	48	339	34.0	15	<9	7	47		92	11	1189																												9.46	
X-78	137	109	32	290	46.0	25	102	20	100		415	117	118																												7.50	
X-79	18	234	32	358	44.0	47	70	35	146		458	74	75																												3.72	
X-80	97	112	48	325	55.0	24	81	12	23		327	142	141																												8.46	
X-81	103	94	55	302	48.0	17	88	7	22		324	135	148																												7.87	
X-82	32	122	61	567	84.0	<9	10	777	47		58	<9	233																												8.43	
X-83	88	105	27	177	32.0	17	44	102	44		325	79	384																												6.80	
X-84	27	106	59	444	89.0	11	11	26	59		138	<9	152																												6.36	
X-85	21	287	26	173	37.0	36	69	11	182		318	36	127																												4.82	
X-86	37	319	33	201	40.0	14	36	124	167		522	<9	303																												5.24	
X-87	13	344	31	208	42.0	18	50	9	134		315	23	119																												5.22	
X-88	147	69	25	131	21.0	35	201	<2	168		326	515	112																												7.96	
X-89	56	337	36	223	53.0	37	30	7	228		474	9	155																												7.00	
X-90				370																																					9.27	
ZGSI																																										
ZGSII																																										
																																									0.00	

APPENDIX D
GEOGRAPHIC COORDINATES OF SAMPLES COLLECTED

A16	Zambian samples located on UTM zone 35, 26
A17	Zambian samples located using latitude and longitude (WGS84), 31 Zambian samples that are located in UTM zone 36, 31
A18	Namibian samples that are located in UTM zone 33 (Schwartzeck), 32
A19	Namibian samples that are located in UTM zone 34, (Schwartzeck), 36
A20	Namibian samples that are located using latitude and longitude coordinates (Schwartzeck), 37

Table A16 Zambian samples that are located in UTM zone 35

ID	UTMEAST	UTMNORTH	UTMZONE	ROCK	LOCATION	SAMPLE	PAGE	ANALYSIS
5	731700	8457266	35L	Mkushi Mine Granites	Site of Patrick Mumba's work	L-005	12	5a
6	731700	8457266	35L	Mkushi Mine Granites	Site of Patrick Mumba's work	L-006	12	
7	731700	8457266	35L	Mkushi Mine Granites	Site of Patrick Mumba's work	L-007	12	
8	731700	8457266	35L	Mkushi Mine Granites	Site of Patrick Mumba's work	L-008	12	
9	600660	8609383	35L	Nchanga Granite	na	L-009	15	
10	438010	8662976	35L	Cu minzn, Kansanshi Mine	na	L-010	16	
11	438010	8662976	35L	Cu minzn, Kansanshi Mine	na	L-011	16	
13	454177	8379381	35L	Mineralized Quartz Veins	na	L-013	17	
14	462917	8377465	35L	Several Hydrothermal veins	na	L-014	18	
20	185354	8761659	35L	Granitoid	Kalene Hill	L-020	22	x
21	185354	8761659	35L	Granitoid	Kalene Hill	L-021	22	
22	188112	8765321	35L	Granitoid	Kalene Hill	L-022	23	
23	188112	8765321	35L	Granitoid	Kalene Hill	L-023	23	
24	191378	8764946	35L	Gabbro	Kalene Hill	L-024	23	x
25	192873	8762357	35L	Granitoid	Kalene Hill	L-025	23	x
26	192873	8762357	35L	Granitoid	Kalene Hill	L-026	23	x
27	192873	8762357	35L	Granitoid	Kalene Hill	L-027	23	x
28	282993	8698411	35L	Non-foliated amphybolite	Mwinilunga	L-028	23	x
29	281721	8699392	35L	Amphybolite	Mwinilunga	L-029	26	x
30	295813	8692365	35L	Gneiss	Mwinilunga	L-030	26	x
31	295813	8692365	35L	Gneiss	Mwinilunga	L-031	26	
32	309413	8685473	35L	Gneiss	Mwembezhi	L-032	27	x
33	318288	8680411	35L	Soil (after granitoid)	Mwembezhi	L-033	27	
34	318288	8680411	35L	Termite Mound (after granitoid)	Mwembezhi	L-034	27	
35	370413	8665100	35L	Magnetite sand	Solwesi, Nepheline syenite quarr	L-035	31	
36	370433	8665159	35L	Red syenite	Solwesi, Nepheline syenite quarr	L-036	33	x
37	370435	8665166	35L	Blue syenite	Solwesi, Nepheline syenite quarr	L-037	34	2
38	370437	8665173	35L	Blue syenite	Solwesi, Nepheline syenite quarr	L-038	34	x
39	370462	8665115	35L	Pink Granitoid that cuts the blue syenite	Solwesi, Nepheline syenite quarr	L-039	34	x
40	370443	8665082	35L	Massive blue nepheline sodalite	Solwesi, Nepheline syenite quarr	L-040	34	x
41	370437	8665073	35L	Massive non-foliated blue rock	Solwesi, Nepheline syenite quarr	L-041	35	x
42	370452	8665107	35L	Black, crystalline, massive mineral that fills	Solwesi, Nepheline syenite quarr	L-042	35	
43	370454	8665126	35L	Fresh "blue" syenite	Solwesi, Nepheline syenite quarr	L-043	35	
44	370454	8665126	35L	Fresh "blue" syenite	Solwesi, Nepheline syenite quarr	L-044	35	x
45	370479	8665123	35L	Finer-grained variety of pink syenite	Solwesi, Nepheline syenite quarr	L-045	35	x
46	370467	8665160	35L	Fresh "brown", coarse-grained syenite	Solwesi, Nepheline syenite quarr	L-046	35	x
47	320870	8660393	35L	Granitoid	Site suggested by Peter Mann	L-047	36	x
48	320900	8660423	35L	Granitoid	Site suggested by Peter Mann	L-048	36	
49	437651	8665739	35L	Gabbro	Solwesi	L-049	37	x
50	437683	8665710	35L	Gabbro	Solwesi	L-050	37	x
51	438010	8662976	35L	Cu minzn	Kansanshi Open Pit	L-051	38	
52	438010	8662976	35L	Cu minzn, vein	Kansanshi Open Pit	L-052	38	
53	438010	8662976	35L	Cu minzn, vein	Kansanshi Open Pit	L-053	38	
54	438010	8662976	35L	Cu minzn, vein	Kansanshi Open Pit	L-054	38	
55	438010	8662976	35L	Secondary Cu minzn	Kansanshi Open Pit	L-055	38	
56	438010	8662976	35L	Secondary Cu minzn	Kansanshi Open Pit	L-056	38	
57	438010	8662976	35L	Secondary Cu minzn	Kansanshi Open Pit	L-057	38	
58	438010	8662976	35L	Secondary Cu minzn	Kansanshi Open Pit	L-058	38	
59	438270	8664080	35L	Granitoid, Diorite	K-292 borehole, Kansanshi Mine	L-059	38	x
60	438180	8664200	35L	Granitoid, Diorite	K-256 borehole, Kansanshi Mine	L-060	38	2
61	438180	8664200	35L	Granitoid, Diorite	K-256 borehole, Kansanshi Mine	L-061	38	
62	482227	8643322	35L	Massive Qtz	Solwesi	L-062	39	
63	477452	8645003	35L	Granitoid w/ FeOx altn?	na	L-063	39	x
64	477452	8645003	35L	Granitoid, fresh	na	L-064	39	x
65	477452	8645003	35L	Granitoid, pink, fresh	na	L-065	39	x
68	496214	8639513	35L	f-g Granitoid	na	L-068	40	
69	496887	8639716	35L	Qtz blobs	Solwesi	L-069	40	
70	496887	8639716	35L	Qtz blobs	Solwesi	L-070	40	
71	496887	8639716	35L	Qtz blobs	Solwesi	L-071	40	
72	496887	8639716	35L	Qtz blobs	Solwesi	L-072	40	
75	602900	8632253	35L	Granitoid	Muliashi Porphyry	L-075	44	
76	602900	8632253	35L	Granitoid	Muliashi Porphyry	L-076	45	x
77	602900	8632253	35L	Granitoid	Muliashi Porphyry	L-077		x
78	602900	8632253	35L	Granitoid	Muliashi Porphyry	L-078		x
79	458795	8465379	35L	Polymictic bx	K-1 borehole, Kaungashi, Lunga A	L-079	45	x
80	458795	8465379	35L	Stkwk in syenite (magnetic?)	K-1 borehole, Kaungashi, Lunga A	L-080	45	
81	458795	8465379	35L	Granitoid	K-1 borehole, Kaungashi, Lunga A	L-081	45	
82	458795	8465379	35L	Stkwk in syenite w/ magnetite	K-1 borehole, Kaungashi, Lunga A	L-082	45	
83	458795	8465379	35L	Granitoid	K-1 borehole, Kaungashi, Lunga A	L-083	45	
84	458795	8465379	35L	Granitoid	K-1 borehole, Kaungashi, Lunga A	L-084	45	
85	458795	8465379	35L	Serpentinitized shear zone (?)	K-1 borehole, Kaungashi, Lunga A	L-085	45	
86	458795	8465379	35L	Stkwk w/ red calc matrix ~ jigsaw bx in granit	K-1 borehole, Kaungashi, Lunga A	L-086	45	
87	458795	8465379	35L	Granitoid, f-g w/ foliation & red veins	K-1 borehole, Kaungashi, Lunga A	L-087	45	
88	458795	8465379	35L	Granitoid, f-g, dk green	K-1 borehole, Kaungashi, Lunga A	L-088	45	
89	458795	8465379	35L	Polymictic bx	K-1 borehole, Kaungashi, Lunga A	L-089	45	
90	458795	8465379	35L	Gray Syenite	K-1 borehole, Kaungashi, Lunga A	L-090	45	
91			35L	Granitoid	KW-22 borehole, with Avmin	L-091	45	
95			35L	Breccia	MB-34 borehole	L-095	66	
147	593617	8616605	35L	Basal Conglomerate	Nchanga Mine	L-147	68	
148	594696	8617011	35L	Massive Cu minzn along "lamprophyre"	Nchanga Mine	L-148	68	
149	594696	8617011	35L	Sheared sediments with Cu mnzn along "lam	Nchanga Mine	L-149	68	
150	594696	8617011	35L	Gabbro from "Lamprophyre"	Nchanga Mine	L-150	68	x
151	591327	8609982	35L	Granitoid	Nchanga Granite	L-151	69	x
152	591820	8609722	35L	Granitoid	Nchanga Granite	L-152	70	
153	591792	8609693	35L	Granitoid	Nchanga Granite	L-153	70	x
154	591781	8609668	35L	Granitoid	Nchanga Granite	L-154	70	x
155	613444	8600564	35L	Granitoid	Chambishi Open Pit	L-155	71	x
163			35L	Gabbro, very foliated?	VS-3B borehole, Konkola Deep Sh	L-163	72	x
164	636861	8611323	35L	Granitoid	Mufulira Granite	L-164	72	

ID	UTMEAST	UTMNORTH	UTMZONE	ROCK	LOCATION	SAMPLE	PAGE	ANALYSIS
165	636883	8611342	35L	Granitoid	Mufulira Granite	L-165	72	
166	636891	8611330	35L	Granitoid	Mufulira Granite	L-166	72	x
167	626463	8602164	35L	Schist	Lufubu Schist under bridge	L-167	72	x
168			35L	Granitoid	NOP-681 borehole, Nchanga Mine	L-168	73	x
170			35L	Granitoid	NOP-681 borehole, Nchanga Mine	L-170	73	x
171			35L	Nchanga Bx	NOP-836 borehole, Nchanga Mine	L-171	73	
173			35L	Granitoid	NOP-589 borehole, Nchanga Mine	L-173	73	x
174	621165	8309439	35L	Qtz blob	West Lusaka	L-174	73	
175	622333	8310267	35L	Foliated Granitoid	West Lusaka	L-175	73	x
176	622623	8310157	35L	Qtz, massive, sugary	West Lusaka	L-176	74	
177	622623	8310157	35L	Qtz, massive, pink	West Lusaka	L-177	74	
178	622623	8310157	35L	Qtz w/ hem blog	West Lusaka	L-178	74	
181	600818	8284839	35L	Mafic Intrusive with garnet	West Lusaka	L-181	74	
182	600750	8284708	35L	Mafic Intrusive with garnet	West Lusaka	L-182	74	
183	603222	8285377	35L	Magnetite-hematite Bx	West Lusaka	L-183	75	
184	603222	8285377	35L	Magnetite Bx	West Lusaka	L-184	75	
185	603222	8285377	35L	Hematite jigsaw bx	West Lusaka	L-185	75	
186	603222	8285377	35L	Hematite jigsaw bx	West Lusaka	L-186	75	
187	603222	8285377	35L	Hematite angular bx	West Lusaka	L-187	75	
195	602827	8285288	35L	Syenite	West Lusaka	L-195	75	
196	602834	8285513	35L	Granitoid ?	West Lusaka	L-196	75	
197	602834	8285513	35L	Granitoid (contact metamorph.)	West Lusaka	L-197	75	
198	536409	8292271	35L	Gabbro	West Lusaka	L-198	76	
199	536409	8292271	35L	Syenite	West Lusaka	L-199	76	
200	535941	8292080	35L	Gabbro w/ epidote	West Lusaka	L-200	76	
201	535941	8292080	35L	Gabbro w/ epidote	West Lusaka	L-201	76	
202	535941	8292080	35L	Sandstone w/ hematite	West Lusaka	L-202	76	
203	535941	8292080	35L	Gabbro	West Lusaka	L-203	76	
204	533464	8288234	35L	Magnetite + hematite (skarn?)	Mamba Coilliery Magnetite mine	L-204	76	
205	533464	8288234	35L	Skarn tremolite-actinolite (sulfides?)	Mamba Coilliery Magnetite mine	L-205	76	
206	533464	8288234	35L	Skarn rocks	Mamba Coilliery Magnetite mine	L-206	76	
207	520902	8295961	35L	f-g Syenite w/ epidote?	na	L-207	77	
208	520902	8295961	35L	c-g Syenite w/ epidote?	na	L-208	77	
209	520902	8295961	35L	m-g Gabbro w/ epidote?	na	L-209	77	
210	519179	8296368	35L	f-g Syenite, pink	na	L-210	77	
211	518327	8296538	35L	porph. Syenite	na	L-211	77	
212	517461	8296629	35L	Syenite	na	L-212	77	
213	511614	8297405	35L	Syenite	na	L-213	77	
214	511614	8297405	35L	Syenite + hematite diss	na	L-214	77	
215	511614	8297405	35L	Syenite	na	L-215	77	
216	510646	8297211	35L	Bn Syenite	na	L-216	77	
217	510646	8297211	35L	f-g Syenite, red	na	L-217	77	
218	509106	8296883	35L	f-g Syenite, pink w/ bk needles	na	L-218	78	
219	498596	8301830	35L	2 Gabbro samples	na	L-219	78	
220	494828	8314088	35L	Syenite + hematite + qtz	na	L-220	78	
221	494828	8314088	35L	Syenite + hematite + qtz	na	L-221	78	
222	494828	8314088	35L	Syenite + hematite + qtz	na	L-222	78	
223	494828	8314088	35L	Syenite + hematite + qtz	na	L-223	78	
224	494875	8319257	35L	Granitoid, coarse + hematite	na	L-224	78	
225	494875	8319257	35L	Granitoid, coarse + hematite	na	L-225	78	
226	520190	8323570	35L	Concentric banding	Dun Robin Mine	L-226	79	
227	520190	8323570	35L	Concentric banding	Dun Robin Mine	L-227	79	
228	520190	8323570	35L	Concentric banding	Dun Robin Mine	L-228	79	
229	520190	8323570	35L	Free Au in Gossan	Dun Robin Mine	L-229	79	
230	520190	8323570	35L	Free Au in Gossan	Dun Robin Mine	L-230	79	
231	520190	8323570	35L	Concentric banding	Dun Robin Mine	L-231	79	
232	520190	8323570	35L	Stkwk + Au	Dun Robin Mine	L-232	79	
233	522000	8325777	35L	Metaconglomerate	Dun Robin Mine	L-233	79	
234	524120	8323852	35L	Qtz blob	Matala Mine ?	L-234	80	
235	405295	8345145	35L	Granitoid	Kafue Park	L-235	81	
236	407722	8344484	35L	Granitoid	Kafue Park	L-236	81	
237	408553	8344258	35L	Granitoid	Kafue Park	L-237	81	
238	409136	8344100	35L	Granitoid, coarse, with sulfides	Kafue Park	L-238	81	
239	409510	8343996	35L	Granitoid, coarse	Kafue Park	L-239	81	
240	409748	8343937	35L	Granitoid, coarse	Kafue Park	L-240	81	
241	410062	8343846	35L	Granitoid w/ diss sulfides	Kafue Park	L-241	81	
242	410387	8343757	35L	Bx, angular, of bk & red material	Kafue Park	L-242	81	
243	410387	8343757	35L	Bx, angular, of bk & red material	Kafue Park	L-243	81	
244	410337	8343780	35L	Granitoid	Kafue Park	L-244	81	
245	410436	8343754	35L	Granitoid, pink, 2 samples	Kafue Park	L-245	81	
246	410436	8343754	35L	Granitoid, gray, c-g	Kafue Park	L-246	81	
247	411817	8343369	35L	Granitoid, m-g, foliated	Kafue Park	L-247	81	
248	411300	8343517	35L	Granitoid, m-g, foliated	Kafue Park	L-248	82	
249	411300	8343517	35L	Granitoid, m-g, foliated	Kafue Park	L-249	82	
250	414509	8342637	35L	Granitoid, m-g, foliated	Kafue Park	L-250	82	
251	414509	8342637	35L	Granitoid, m-g, foliated	Kafue Park	L-251	82	
252	417308	8342625	35L	Granitoid, m-g, foliated	Kafue Park	L-252	82	
253	430325	8344423	35L	Quartz blobs, pink-purple	Kafue Park	L-253	82	
254	435923	8344774	35L	Granitoid, f-m-g, gray	Kafue Park	L-254	82	
255	437504	8344870	35L	Granitoid, m-g, bn, w/ sulfides	Kafue Park	L-255	82	
256	437300	8344864	35L	Granitoid, good outcrop	Kafue Park	L-256	82	
257	440501	8345047	35L	Granitoid, pink, f-m-g, purple mnzn	Kafue Park	L-257	83	
258	443166	8345205	35L	Granitoid, lt gray m-f-g w/ sulfides	Kafue Park	L-258	83	
259	443600	8345232	35L	Granitoid, bn, m-g	Kafue Park	L-259	83	
260	445480	8345341	35L	Granitoid, lt bn w/ sulfides	Kafue Park	L-260	83	
261	446235	8345377	35L	Granitoid, gray-pink, mf-g, w/ diss cpy	Kafue Park	L-261	83	
262	447650	8345462	35L	Granitoid, foliated w/ sulfides ?	Kafue Park	L-262	83	
263	455666	8344828	35L	Granitoid, gray, foliated, w/ porphyroblasts	Kafue Park	L-263	83	
264	458846	8344455	35L	Granitoid, extremely foliated	Kafue Park	L-264	83	
265	459827	8344327	35L	Granitoid, bn, f-g	Kafue Park	L-265	83	
266	658649	8591610	35L	Qtz blob	Eyes NE of Kitwe	L-266	95	

ID	UTMEAST	UTMNORTH	UTMZONE	ROCK	LOCATION	SAMPLE	PAGE	ANALYSIS
267	659696	8589920	35L	Qtz pegmatite + muscovite	Eyes NE of Kitwe	L-267	95	
268			35L	Stkwk + hematite in schist	CT-124 borehole, Samba	L-268	96	
278	306500	8507500	35L	Schist after porphyritic igneous rock? W/ qtz \	CT-116 borehole, Samba	L-278	96	
285	309650	8507300	35L	Granitoid, coarse + hematite, cpy, py	RKN-719 borehole	L-285	97	
294	309655	8507190	35L	Bk hematite filling veins in stkwk	RKN-801 borehole	L-294	97	
311	362655	8628407	35L	Banded gabbro	Shilenda, Jon Woodhead, Zamang	L-311		
312	362655	8628407	35L	Gabbro w/ py mnzn	Shilenda, Jon Woodhead, Zamang	L-312	0	
313	298404	8505075	35L	Syenite w/ fine specularite diss	Jikambo Old pits, Jon Woodhead,	L-313	0	
314	285600	8528650	35L	F-g granitoid rock	Kalengwa North, Jon Woodhead, Z	L-314	0	
315	287600	8528700	35L	vitrophyre w/ patchy hematitization	Kalengwa North, Jon Woodhead, Z	L-315	0	
316	297000	8521000	35L	Granitoid	Kalengwa Ndenda, Jon Woodhead	L-316	0	
317	297000	8521000	35L	Granitoid	Kalengwa Ndenda, Jon Woodhead	L-317	0	
318	297000	8521000	35L	Granitoid	Kalengwa Ndenda, Jon Woodhead	L-318	0	
319	297000	8521000	35L	Granitoid	Kalengwa Ndenda, Jon Woodhead	L-319	0	
320	297000	8521000	35L	Granitoid	Kalengwa Ndenda, Jon Woodhead	L-320	0	
321	283300	8511500	35L	ferro-gabbro/diorite?	Kalengwa Mine, Jon Woodhead, Z	L-321	0	
322	283300	8511500	35L	ferro-gabbro/diorite?	Kalengwa Mine, Jon Woodhead, Z	L-322	0	
323	283300	8511500	35L	ferro-gabbro/diorite?	Kalengwa Mine, Jon Woodhead, Z	L-323	0	
324	283300	8511500	35L	ferro-gabbro/diorite?	Kalengwa Mine, Jon Woodhead, Z	L-324	0	
325	299386	8507419	35L	quartzmonzonite (altered)	Jikambo RKN-719 samples, Jon W	L-325	0	
326	299386	8507419	35L	quartzmonzonite (altered)	Jikambo RKN-719 samples, Jon W	L-326	0	
327			35L	4DC-1 Granitoid porphyry (Rept. 111, Lumwa	Geological Survey, Lusaka	L-327	0	
328			35L	4DC-1 Granitoid porphyry	Geological Survey, Lusaka	L-328	0	
329			35L	4DC-1 Granitoid porphyry	Geological Survey, Lusaka	L-329	0	
330			35L	4DC-8 Foliated granite. (dated 1940Ma)	Geological Survey, Lusaka	L-330	0	
331			35L	4DC-9 Foliated granite	Geological Survey, Lusaka	L-331	0	
			35L	4DC-10 Schist (after altered granite)	Geological Survey, Lusaka	L-332	0	
333			35L	4DC-11 Porphyroblastic schist	Geological Survey, Lusaka	L-333	0	
334			35L	4DC-16 Granitoid (coarse gneiss)	Geological Survey, Lusaka	L-334	0	
335			35L	4DC-55 Porphyritic gneiss	Geological Survey, Lusaka	L-335	0	
336			35L	4DC-100 Gabbro	Geological Survey, Lusaka	L-336	0	
337			35L	4DC-232 Gabbro, foliated, porphyroblastic	Geological Survey, Lusaka	L-337	0	
338			35L	4DC-274 Porphyritic granitoid	Geological Survey, Lusaka	L-338	0	
339			35L	4DC-29 Fine grained intrusive breccia	Geological Survey, Lusaka	L-339	0	
340			35L	4DC-6 Granitoid	Geological Survey, Lusaka	L-340	0	
341	405750	8350800	35L	5GC-164 Felsic granitoid. Aegirine augite gne	Geological Survey, Lusaka	L-341	0	
342			35L	5GC-180 Coarse gneiss after granitoid. Pyrox	Geological Survey, Lusaka	L-342	0	
343	416000	8351000	35L	5GC-Granitoid, foliated. Pyroxene scapolite g	Geological Survey, Lusaka	L-343	0	
344	434800	8351200	35L	5GC-236, Coarse granitoid. Aegirine augite g	Geological Survey, Lusaka	L-344	0	
345	440750	8356400	35L	5GC-240 Pink syenite ?	Geological Survey, Lusaka	L-345	0	
346	399750	8350000	35L	5GC-250 Coarse granitoid. Qtz felds porphyr	Geological Survey, Lusaka	L-346	0	
347	427000	8345000	35L	5GC-251 Foliated granitoid. Qtz felds porphy	Geological Survey, Lusaka	L-347	0	
348	399800	8350400	35L	5GC-258 Foliated granitoid. Pyroxene scapo	Geological Survey, Lusaka	L-348	0	
349	401800	8351000	35L	5GC-259 Foliated granitoid. Pyroxene scapo	Geological Survey, Lusaka	L-349	0	
350			35L	5GC-265 F-m g granitoid. Monzonite + qtz di	Geological Survey, Lusaka	L-350	0	
351			35L	5GC-267 Pink-red granitoid	Geological Survey, Lusaka	L-351	0	
352	405500	8355900	35L	5GC-283 Quartz feldespathic porphyry	Geological Survey, Lusaka	L-352	0	
353	417000	8351000	35L	5GC-284 Granitoid w/ py	Geological Survey, Lusaka	L-353	0	
354	442750	8344700	35L	5GC-330 Coarse granitoid (Quartz feldspathi	Geological Survey, Lusaka	L-354	0	
355	437000	8389000	35L	5GC-402 Coarse granitoid (Quartz feldspathi	Geological Survey, Lusaka	L-355	0	
356			35L	5GC-53 Medium grained granitoid	Geological Survey, Lusaka	L-356	0	
357	202615	8771063	35L	3DA-34 Med. Granitoid (Rept 107, Kalene Hil	Geological Survey, Lusaka	L-357	0	
358	202615	8771063	35L	3DA-35 Foliated granitoid	Geological Survey, Lusaka	L-358	0	
359	202615	8771063	35L	3DA-36 Foliated granitoid	Geological Survey, Lusaka	L-359	0	
360	198992	8767035	35L	3DA-45 Med granitoid	Geological Survey, Lusaka	L-360	0	
361	202131	8775612	35L	3DA-56 Med granitoid. Massive med-grained	Geological Survey, Lusaka	L-361	0	
362	203141	8776017	35L	3DA-58 med granitoid. Gray granite	Geological Survey, Lusaka	L-362	0	
363	203846	8776213	35L	3DA-59 Med granitoid	Geological Survey, Lusaka	L-363	0	
364	194000	8769500	35L	3DA-60 Med granitoid. Chloritized scales of b	Geological Survey, Lusaka	L-364	0	
365	190353	8757416	35L	3DA-72 Med granitoid	Geological Survey, Lusaka	L-365	0	
366	184965	8762141	35L	3DA-73 Med granitoid. Coarse biot leukogran	Geological Survey, Lusaka	L-366	0	
367	191505	8761399	35L	3DA-82 Foliated granitoid	Geological Survey, Lusaka	L-367	0	
368	182724	8766986	35L	3DA-83 Granitoid porphyry	Geological Survey, Lusaka	L-368	0	
369	195407	8762331	35L	3DA-93 Granitoid. Massive granite	Geological Survey, Lusaka	L-369	0	
370	179530	8790750	35L	3DA-97 Granitoid. Masive porph. Granite	Geological Survey, Lusaka	L-370	0	
371	175705	8791238	35L	3DA-98 Granitoid	Geological Survey, Lusaka	L-371	0	
372	180757	8787339	35L	3DA-100 Med grained gabbro	Geological Survey, Lusaka	L-372	0	
373	180757	8787339	35L	3DA-101 Granitoid	Geological Survey, Lusaka	L-373	0	
374	187816	8791635	35L	3DA-103 Granitoid	Geological Survey, Lusaka	L-374	0	
375	182396	8783618	35L	3DA-106 Foliated Granitoid	Geological Survey, Lusaka	L-375	0	
376	180961	8782807	35L	3DA-107 Foliated Granitoid	Geological Survey, Lusaka	L-376	0	
377	191903	8770914	35L	3DA-109 Fine grained granitoid	Geological Survey, Lusaka	L-377	0	
378	190430	8770699	35L	3DA-110 Coarse granitoid	Geological Survey, Lusaka	L-378	0	
379	191290	8769017	35L	3DA-111 Fine grained gabbro. Massive porp	Geological Survey, Lusaka	L-379	0	
380	179813	8777986	35L	3DA-117 Foliated granitoid	Geological Survey, Lusaka	L-380	0	
381			35L	5GB-42 Porphyritic granitoid (Rept 31)	Geological Survey, Lusaka	L-381	0	
382			35L	5GB-Hematite stkwk in granitoid	Geological Survey, Lusaka	L-382	0	
383			35L	5GB-44 Fine grained rock w/ Fe Ox	Geological Survey, Lusaka	L-383	0	
384			35L	5GB-45 Massive hematite	Geological Survey, Lusaka	L-384	0	
385			35L	5GB-46 Hematite-altered granitoid	Geological Survey, Lusaka	L-385	0	
386			35L	5GB-48 Fine grained volcanic rock	Geological Survey, Lusaka	L-386	0	
387			35L	5GB-49 Fine grained volcanic rock	Geological Survey, Lusaka	L-387	0	
388			35L	5GB-50 Very fine-grained granitoid	Geological Survey, Lusaka	L-388	0	
389			35L	5GB-51 Red rock-altered granitoid	Geological Survey, Lusaka	L-389	0	
390			35L	5GB-52 Massive hematite	Geological Survey, Lusaka	L-390	0	
391			35L	5GB-96 Red rock-altered granitoid. Syenite,	Geological Survey, Lusaka	L-391	0	
392			35L	5GB-97 Red rock-altered granitoid. Syenite,	Geological Survey, Lusaka	L-392	0	
393			35L	5GB-101 Red rock-altered granitoid	Geological Survey, Lusaka	L-393	0	
394			35L	5GB-103 Volcanic porphyry w/ red rock altn.	Geological Survey, Lusaka	L-394	0	
395			35L	5GB-163 Hematitized wall rock. Tourmaline	Geological Survey, Lusaka	L-395	0	
396			35L	5GB-166 Granitoid	Geological Survey, Lusaka	L-396	0	

ID	UTMEAST	UTMNORTH	UTMZONE	ROCK	LOCATION	SAMPLE	PAGE	ANALYSIS
397			35L	N-90 Granitoid. Gneiss (rept 60)	Geological Survey, Lusaka	L-397	0	
398			35L	N-127 Gabbro	Geological Survey, Lusaka	L-398	0	
399			35L	N-235 Foliated granitoid	Geological Survey, Lusaka	L-399	0	
400			35L	N-265 Volcanic rock (pre-Karroo) Foliated gra	Geological Survey, Lusaka	L-400	0	
401			35L	N-218 Foliated granitoid	Geological Survey, Lusaka	L-401	0	
402	457000	8394000	35L	5GD-36 Foliated granitoid (rept 27)	Geological Survey, Lusaka	L-402	0	
403	477000	8345000	35L	5GD-43 Porphyritic granitoid	Geological Survey, Lusaka	L-403	0	
404	473500	8356000	35L	5GD-56 Granitoid	Geological Survey, Lusaka	L-404	0	
405	467000	8345500	35L	5GD-77 Gabbro	Geological Survey, Lusaka	L-405	0	
406	476200	8346600	35L	5GD-82 Gabbro	Geological Survey, Lusaka	L-406	0	
407	457000	8380000	35L	5GD-153 Rapakivi granitoid	Geological Survey, Lusaka	L-407	0	
408	463000	8344500	35L	5GD-147 Red granitoid	Geological Survey, Lusaka	L-408	0	
409	453500	8351500	35L	5GD-167 Red granitoid	Geological Survey, Lusaka	L-409	0	
410	450000	8379000	35L	5GD-184 Porphyritic granitoid (volc. Rk?)	Geological Survey, Lusaka	L-410	0	
411	493000	8363000	35L	5GD-229 White coarse-g granitoid (marble?)	Geological Survey, Lusaka	L-411	0	
412			35L	5GD-356 Granitoid	Geological Survey, Lusaka	L-412	0	
413			35L	3DC-130 Vuggy hematite (rept 110 Mwinilung	Geological Survey, Lusaka	L-413	0	
414			35L	7ED-6 Coarse gneiss after granitoid (rept 20)	Geological Survey, Lusaka	L-414	0	
415			35L	3DB-174 Massive hematite (rept 108)	Geological Survey, Lusaka	L-415	0	
416	671000	8244000	35L	7HD-230 Gabbro (repy 21)	Geological Survey, Lusaka	L-416	0	
417	671000	8244000	35L	7HD-250 Foliated granitoid	Geological Survey, Lusaka	L-417	0	
418			35L	5EA-4 Gneiss (foliated granitoid) (repy 36)	Geological Survey, Lusaka	L-418	0	
419			35L	5EA-6 Granitoid	Geological Survey, Lusaka	L-419	0	
422			35L	5EA-162 Foliated granitoid	Geological Survey, Lusaka	L-422	0	
423	755000	8458000	35L	8FC-16 Granitoid (rept 12)	Geological Survey, Lusaka	L-423	0	
424	755000	8458000	35L	8FC-17 Granitoid	Geological Survey, Lusaka	L-424	0	
425	755000	8458000	35L	8FC-18 White granitoid	Geological Survey, Lusaka	L-425	0	
426	747000	8476500	35L	8FC-50 Massive quartz + hematite	Geological Survey, Lusaka	L-426	0	
427			35L	8FC-59 Foliated granitoid	Geological Survey, Lusaka	L-427	0	
428			35L	8FC-81 Foliated granitoid	Geological Survey, Lusaka	L-428	0	
429	762000	8497000	35L	8FC-233 Mafic xenolith in granitoid (non-foliat	Geological Survey, Lusaka	L-429	0	
430			35L	8FC-423 Fine grained foliated granitoid	Geological Survey, Lusaka	L-430	0	
431	763200	8482500	35L	8FC-450 Foliated granitoid	Geological Survey, Lusaka	L-431	0	
432	765200	8452200	35L	8FC-460 Foliated granitoid	Geological Survey, Lusaka	L-432	0	
433	442000	8343000	35L	5HA-3 Gabbro (rept 33)	Geological Survey, Lusaka	L-433	0	
434	456000	8340000	35L	5HA-4 Gabbro	Geological Survey, Lusaka	L-434	0	
435	433700	8330500	35L	5HA-6 Undeformed (?) coarse granitoid	Geological Survey, Lusaka	L-435	0	
436	417500	8349000	35L	5HA-13 Pink med-g granitoid	Geological Survey, Lusaka	L-436	0	
437	426100	8299000	35L	5HA-17 Fine grained gabbro. Dike	Geological Survey, Lusaka	L-437	0	
438	448000	8264000	35L	5HA-20 Gabbro. Dike	Geological Survey, Lusaka	L-438	0	
439	422000	8318700	35L	5HA-21 Orange porphyritic granitoid. Dike	Geological Survey, Lusaka	L-439	0	
440	432000	8298000	35L	5HA-24 Gabbro. Dike	Geological Survey, Lusaka	L-440	0	
441	404500	8288300	35L	5HA-42 Med-g granitoid	Geological Survey, Lusaka	L-441	0	
442	440800	8308400	35L	5HA-69 Pink granitoid	Geological Survey, Lusaka	L-442	0	
443	432000	8306700	35L	5HA-70 Pink foliated granitoid	Geological Survey, Lusaka	L-443		
444	432000	8298000	35L	5HA-86 Fine dark gabbro	Geological Survey, Lusaka	L-444		
445	676000	8529000	35L	7FB-146 Granitoid (rept 20)	Geological Survey, Lusaka	L-445	89	
446	669500	8522000	35L	7FB-153 Foliated granitoid	Geological Survey, Lusaka	L-446		
447	669500	8522000	35L	7FB-154 Foliated granitoid	Geological Survey, Lusaka	L-447		
448	666000	8522000	35L	7FB-155 Foliated granitoid	Geological Survey, Lusaka	L-448		
449	680000	8529000	35L	7FB-165 Foliated granitoid	Geological Survey, Lusaka	L-449		
450	685000	8525000	35L	7FB-172 Foliated granitoid	Geological Survey, Lusaka	L-450		
451	684000	8527000	35L	7FB-173 Felsic, white granitoid	Geological Survey, Lusaka	L-451		
452			35L	7FB-176 Foliated granitoid	Geological Survey, Lusaka	L-452		
453	666000	8522000	35L	7FB-176 Schist, clay altered	Geological Survey, Lusaka	L-453		
454	676000	8530000	35L	7FB-178 Granitoid	Geological Survey, Lusaka	L-454		
455	676000	8529000	35L	7FB-181 Granitoid	Geological Survey, Lusaka	L-455		
456	666000	8522000	35L	7FB-188 Gneiss	Geological Survey, Lusaka	L-456		
457	672000	8537000	35L	7FB-189 (175) Granitoid	Geological Survey, Lusaka	L-457		
468			35L	7GB-78 Granitoid w/ hematite/magnetite	Geological Survey, Lusaka	L-468		
469			35L	7GB-189 Granitoid	Geological Survey, Lusaka	L-469		
470			35L	5GB-102	Geological Survey, Lusaka	L-470		
			35L	Gabbro, coarse grained	West Lusaka	L-180A	74	
	525465	8325280	35L	Quartz blobs	na	L-233A	80	
	600660	8609383	35L	Nchanga Granite	na	L-9A	15	
	376000	8248000	35L	Calcium-enriched porphyritic granite	Hook Granite	4HD184		
	406500	8285000	35L	Calcium-enriched porphyritic granite	Hook Granite	5HC485		
	412000	8282000	35L	Calcium-enriched porphyritic granite	Hook Granite	5HC489		
	367000	8274500	35L	Migmatitic gneisses and granites	Hook Granite	4HD115		
	355300	8253700	35L	Migmatitic gneisses and granites	Hook Granite	4HD117		
	353000	8237500	35L	Migmatitic gneisses and granites	Hook Granite	4HD190		
	373000	8266000	35L	Migmatitic gneisses and granites	Hook Granite	4HD202		
	374500	8272500	35L	Migmatitic gneisses and granites	Hook Granite	4HD203		
	376000	8254850	35L	Coarse amphibole-quartz monzonite	Hook Granite	4HD139		
	376000	8264500	35L	Coarse amphibole-quartz monzonite	Hook Granite	4HD147		
	385000	8260500	35L	Coarse amphibole-quartz monzonite	Hook Granite	4HD150		
	345500	8243000	35L	Granodiorites and tonalites	Hook Granite	4HD108		
	349000	8237700	35L	Granodiorites and tonalites	Hook Granite	4HD122		
	371000	8247300	35L	Granodiorites and tonalites	Hook Granite	4HD200		
	363500	8244300	35L	Granodiorites and tonalites	Hook Granite	4HD77		
	381000	8274000	35L	Porphyroblastic biotite granite	Hook Granite	4HD159		
	385500	8265000	35L	Porphyroblastic biotite granite	Hook Granite	4HD197		
	408000	8286000	35L	Porphyroblastic biotite granite	Hook Granite	5HC343		
	394700	8283100	35L	Porphyroblastic biotite granite	Hook Granite	5HC344		
	405000	8278700	35L	Porphyritic alkali procataclasite	Hook Granite	5HC384iii		
	415300	8267000	35L	Porphyritic alkali procataclasite	Hook Granite	5HC443		
	400200	8264000	35L	Porphyritic alkali procataclasite	Hook Granite	5HC474		
	377000	8276000	35L	fine to medium-grained biotite granite	Hook Granite	4HD133		
	356500	8247400	35L	fine to medium-grained biotite granite	Hook Granite	4HD182		
	367000	8260000	35L	fine to medium-grained biotite granite	Hook Granite	4HD205		
	360100	8235000	35L	fine to medium-grained biotite granite	Hook Granite	4HD41		

ID	UTMEAST	UTMNORTH	UTMZONE	ROCK	LOCATION	SAMPLE	PAGE	ANALYSIS
	341500	8252500	35L	Biotite quartz monzonite	Hook Granite	4HD48		
	394000	8258500	35L	Leukocratic granite	Hook Granite	5HC537		
	395500	8256000	35L	Tourmaline granite	Hook Granite	5HC455		
	400600	8285500	35L	Post-Tectonic granite	Hook Granite	5HC303		
	402700	8277500	35L	Post-Tectonic granite	Hook Granite	5HC307		
	401200	8272250	35L	Post-Tectonic granite	Hook Granite	5HC317		
	397000	8270000	35L	Post-Tectonic granite	Hook Granite	5HC445		
13	296925	8520339	35L	granitoid	Kalengwa Area Zambia	13		
14	298382	8503683	35L	granitoid	Kalengwa Area Zambia	14		
16	298276	8503764	35L	granitoid	Kalengwa Area Zambia	16		
17	299599	8503979	35L	granitoid	Kalengwa Area Zambia	17		
22	264690	8487350	35L	granitoid	Kalengwa Area Zambia	22		
24	283550	8551745	35L	granitoid	Kalengwa Area Zambia	24		
25	282635	8549632	35L	granitoid	Kalengwa Area Zambia	25		
26	299047	8529075	35L	granitoid	Kalengwa Area Zambia	26		
28	594794	8612062	35L	granitoid	Chingola, Zm	28		
29	600795	8609306	35L	granitoid	Chingola, Zm	29		
38	393638	8255771	35L	granitoid	Kafue Park, Hook Granite, Zm	38		
39	423570	8315373	35L	granitoid	Kafue Park, Hook Granite, Zm	39		
41	414825	8298503	35L	granitoid	Kafue Park, Hook Granite, Zm	41		
42	411907	8297321	35L	granitoid	Kafue Park, Hook Granite, Zm	42		
44	412093	8296082	35L	granitoid	Kafue Park, Hook Granite, Zm	44		
45	408665	8292534	35L	granitoid	Kafue Park, Hook Granite, Zm	45		
46	404790	8289083	35L	granitoid	Kafue Park, Hook Granite, Zm	46		
50	402228	8276327	35L	Post-Tectonic granite	Kafue Park, Hook Granite, Zm	50		
53	397596	8260510	35L	Tourmaline granite	Kafue Park, Hook Granite, Zm	53		
57	440441	8343507	35L	granitoid	Kafue Park, Hook Granite, Zm	57		
58	447852	8345457	35L	granitoid	Kafue Park, Hook Granite, Zm	58		
	423932	8316746	35L	granitoid	Kafue Park, Hook Granite, Zm	40I		Y
	426932	8316746	35L	granitoid	Kafue Park, Hook Granite, Zm	40ii		Y
2001	398200	8529500	35L	u	CH-5 Kasempa area, Dale Janneke	CH-5		Y
2002	448480	8530400	35L	u	MUF-1 Kasempa area, Dale Janne	MUF-1		Y
2003	449400	8530400	35L	u	MUF-2 Kasempa area, Dale Janne	MUF-2		Y
2004	448650	8527650	35L	u	MUF-3 Kasempa area, Dale Janne	MUF-3		Y
2005	447750	8530090	35L	u	MUF-4 Kasempa area, Dale Janne	MUF-4		Y
2006	599700	8614500	35L	granitoid	Gray's Quarry, Nchanga Granite	Gray's Quarry		y
2007	649000	8606000	35L	granitoid	Mufulira	Mufulira G		y
2008	614000	8601000	35L	granitoid	Chambishi	Chambishi G		y
2009	594400	8611200	35L	granitoid	Nchanga Red granite	Nchanga Red G		y
6010	358646	8476200	35L	Subvolcanic porphyritic granitoid	Chit-8 Borehole, Chitampa, Kasem	CHIT-8, AVMIN		y
6011	387800	8481200	35L	Subvolcanic porphyritic granitoid	MB-34 Borehole, Chitampa, Kasen	MB-34		y

Table A17 Zambian samples that are located using latitude and longitude coordinates (WGS84)

SAMPLE	E	S	ROCK	LOCATION	PAGE	ANALYSIS
8A	28.633250000	-13.715260000	Muva Quartzite	Big sampl	12	
12	26.485972222	-14.590916667	Hook Granite 1	na	16	
12a	26.486155556	-14.591208333	Hook Granite 2	na	17	
420	26.466666667	-12.250000000	5EA-11 Granitoid	Geologica	0	
421	26.483333333	-12.266666667	5EA-17 Granitoid	Geologica	0	
458	27.100000000	-15.025000000	A-1208 Pink granitoid (rept)	Geologica	90	
459	27.030000000	-15.091666667	A-1247 Gabbro. Mineralized and al	Geologica		
460	27.050000000	-15.416666667	A-1260 Foliated granitoid (minera	Geologica		
461	27.013333333	-15.066666667	A-1267 Fine-grained granitoid	Geologica		
462	27.008333333	-15.083333333	A-1268 Fine grained granitoid	Geologica		
463	27.121666667	-15.321666667	A-1351 Gabbro	Geologica		
464	27.133333333	-15.300000000	A-1353 Massive hematite	Geologica		
465	27.133333333	-15.333333333	A-1360 Porous massive hematite	Geologica		
466	27.133333333	-15.416666667	A-1364 Med-g granitoid	Geologica		
467	27.216666667	-15.416666667	A-1365 Med-g granitoid	Geologica		

Zambian samples that are located in UTM zone 36

ID	UTMEAST	UTMNORTH	UTMZONE	ROCK	LOCATION	SAMPLE	PAGE	ANALYSIS
32	189947	8531605	36L	granitoid	Serenje, Zm	32	u	y
33	187103	8541206	36L	granitoid	Serenje, Zm	33	u	y
34	185730	8554091	36L	granitoid	Serenje, Zm	34	u	y
35	180902	8553214	36L	granitoid	Serenje, Zm	35	u	y

Table A18 Namibian samples that are located in UTM zone 33 (Schwartzeck)

ID	UTMEAST	UTMNORTH	UTMZONE	SAMPLE	PAGE	DATE	ROCK	LOCATION	ELEVATION
492	539840	7809922	na	L-830	5	22403	na		
493	534537	7811450	na	L-831	5	22403	na		
506	472892	7827884	na	L-840	7	22503	na		
170	470574	7745499	33K	L-1015	45	30803	Mafic gtd from dike	Way to Oas Farm	na
170	470574	7745499	33K	L-1016	45	30803	Glassy vfg rk w/ sub// vugs (lava?) + qz	way to Oas Farm	889
170	470574	7745499	33K	L-1016a	45	30803	Volc rk w/o vacuoles	Way to Oas Farm	na
170	470574	7745499	33K	L-1017	45	30803	mnzd	u	na
171	470780	7746140	33K	L-1018	47	30803	mag from sand in dry ck	na	na
	471546	7747493	na	L-1019	47	30803	Fol fg gtd	Way to Oas Farm	na
	471562	7747737	na	L-1020	47	30803	Mafic fol gtd	Oas Farm house	na
	471474	7753169	na	L-1022	47	30803	Porphyritic subvolcanic rk, dike	way to Loftdal farm	na
626	471408	7753443	na	L-1023	49	30803	Fresh mafic fol gtd	way to Loftdal farm	na
637	469519	7752923	na	L-1024a		30803	Carbonatite for dating	Lofdal	na
637	469519	7752923	na	L-1024c		30803	Carbonatite for dating	Lofdal	na
639	469504	7752995	33K	L-1025	49	30803	Mafic rk w/ radial macroxts, magnetic	Lofdal bx	na
641	469468	7753052	33K	L-1026	49	30803	Massive magnetite	Lofdal bx	na
643	469468	7753081	33K	L-1027	49	30803	Massive mag w/ goss vugs after sulfs	Lofdal bx	na
642	469465	7753077	33K	L-1028	49	30803	Cg gtd w/ circular vugs	Lofdal bx	na
645	469360	7753119	33K	L-1029	49	30803	Gossanous mag	Lofdal bx	na
646	469653	7752666	33K	L-1030	49	30803	Large bx	Lofdal bx	na
646	469653	7752666	33K	L-1031	49	30803	Smal bx	Lofdal bx	na
649	469654	7752801	33K	L-1032	51	30803	Mafic fol gtd	Lofdal bx	na
650	469649	7752814	33K	L-1033	51	30803	Mag jigsaw bx	Lofdal bx	na
652	469646	7752816	33K	L-1034	51	30803	Mag bx w/ igneous clasts	Lofdal bx	na
653	469623	7752848	33K	L-1035	51	30803	Ang bx	Lofdal bx	na
221	466169	7754051	33K	L-1036		30803	Big sample of mag bx	Lofdal bx	na
220	469619	7752727	33K	L-1036		30803	Big sample of mag bx	Lofdal bx	na
689	685140	7751116	33K	L-1039a	57	31003	Weathered gtd	Otjiwarongo	na
689	685140	7751116	33K	L-1039c	57	31003	Weathered gtd	Otjiwarongo	na
689	685140	7751116	33K	L-1040	57	31003	FeOx	Otjiwarongo	na
617	798316	7820893	na	L-1041		30703	X Carbonate bx, base of Otavi sequence	Otavi	na
618	798318	7820909	na	L-1042		30703	Y Cg porph fol gtd	Otavi	na
618	798318	7820909	na	L-1043		30703	Z Fg felsic porph rk w/ little foliation	Otavi	na
618	798318	7820909	na	L-1044		30703	XX Fresh gtd	Otavi	na
619	798172	7821133	na	L-1045		30703	Yb Fresh gtd	Otavi	na
619	798172	7821133	na	L-1046		30703	XXb Fresh gtd	Otavi	na
164	471364	7740547	33K	L-1047	45	30803	stwk in bn rk	entrance to Oas Farm	807
			na	L-1048			FeOx bx	Borehole AV-12-160, Kombat	na
			na	L-1049			Bx	Kombat mine	na
			na	L-1050			Bx	Kombat mine	na
			na	L-1051			Bx	Kombat mine	na
			na	L-1052			Bx	Kombat mine	na
			na	L-1053			Bx	Kombat mine	na
			na	L-1054			Bx	Kombat mine	na
			na	L-1055			Bx	Kombat mine	na
	466547	7755980	na	L-551			na	na	na
26	243590	7536839	34K	L-618	9	100802	quartz veins	Klein Windhoek	na
26	243590	7536839	34K	L-619	9	100802	quartz veins	Klein Windhoek	na
31	243338	7537266	34K	L-624	10	100802	M-f-g Gtd	Okatjepuiko	na
26	243590	7536839	34K	L-624a	9	100802	quartz veins	Klein Windhoek	na
31	243338	7537266	34K	L-625	10	100802	na	Okatjepuiko	na
32	243335	7537261	34K	L-626	10	100802	M-f-g intrusive w/ FeOx veins	Okatjepuiko	na
35	243343	7537284	34K	L-627	10	100802	F-g chloritized gtd w/ bk hem	Okatjepuiko	na
35	243343	7537284	34K	L-628	10	100802	F-g chloritized gtd w/ bk hem	Okatjepuiko	na
35	243343	7537284	34K	L-629	10	100802	F-g chloritized gtd w/ bk hem	Okatjepuiko	na
35	243343	7537284	34K	L-630	10	100802	F-g chloritized gtd w/ bk hem	Okatjepuiko	na
37	243050	7537104	34K	L-631	10	100802	Red jasper bx	Okatjepuiko	na
39	243021	7537009	34K	L-632	11	100802	Dk bn vf-g volc rk w/ white plag phenxt	Okatjepuiko	na
41	242991	7537254	34K	L-633	11	100802	F-m-g gtd w/ chlorite veinlets, monzogab	Okatjepuiko	na
43	242977	7537404	34K	L-634	11	100802	Bk-dk gn volc rk (basalt?) subvolc?	Okatjepuiko	na
44	242959	7537593	34K	L-635	11	100802	Med gray porh vold rk	Okatjepuiko	na
36	243060	7537117	34K	L-636	10	100802	Dk volc rk w/ pk veinlets	Okatjepuiko	na
36	243060	7537117	34K	L-637	10	100802	Lt vold rk w/ plag & slight fol (flow ban	Okatjepuiko	na
42	242988	7537303	34K	L-639	11	100802	na	Okatjepuiko	na
46	242979	7537303	34K	L-640		100802	F-g pk gtd w/ bk volc rk xenoliths	Okatjepuiko	na
46	242979	7537303	34K	L-641		100802	F-g dk gn-dk gray vold rk (xenolith? Monz	Okatjepuiko	na
48	243578	7536616	34K	L-642		100802	F-g bk volc rk Fol. W/ mass FEOx altn	Okatjepuiko	na
49	243591	7536591	34K	L-643		100802	Gtd w/ FeOx veinlets	Okatjepuiko	na
50	243566	7536780	34K	L-646		100802	Bn-rk altn that masks text w/ vug white q	Okatjepuiko	na
50	243566	7536780	34K	L-647		100802	Rd-rk altn w/ cc veinlets n stwk	Okatjepuiko	na
50	243566	7536780	34K	L-648		100802	Bn-rk altn w/ Cu stains + goss	Okatjepuiko	na
50	243566	7536780	34K	L-649		100802	Unid f-g rk w/ silicif + FeOx altn Cu sta	Okatjepuiko	na
50	243566	7536780	34K	L-650		100802	Bx of bn-rk altd rk w/ cc veins	Okatjepuiko	na
51	244142	7537156	34K	L-651		100802	Metallic hem	Okatjepuiko	na
51	244142	7537156	34K	L-652		100802	F-g dk volc rk; pervasive FeOx altn	Okatjepuiko	na
653	349377	7890241	33K	L-653	17	101002	Goss schist (Au?)	NW of Sesfontein	na
654	349377	7890241	33K	L-654	17	101002	Goss schist (Au?)	NW of Sesfontein	na
655	348478	7890333	33K	L-655	17	101002	qz from qz blob	NW of Sesfontein	na
656	348478	7890333	33K	L-656	17	101002	Dirty ls cut by qz bxwk w/ sulfs	NW of Sesfontein	na
657	348478	7890333	33K	L-657	17	101002	Dirty ls cut by series of qz veinlets	NW of Sesfontein	na
658	348478	7890333	33K	L-658	17	101002	De-calcified explosive calcarous bx	NW of Sesfontein	na
659	348478	7890333	33K	L-659	17	101002	De-calcified ls w/ FeOx after sulfs	NW of Sesfontein	na
660	347477	7890212	33K	L-660	18	101002	Ls w/ weathered sulfs + qz veinlets	NW of Sesfontein	na
661	347477	7890212	33K	L-661	18	101002	Qz blob w/ sulfide veinlet intersection	NW of Sesfontein	na
662	340091	7893346	33K	L-662	18	101002	Bx w/ pink qz frags cemented by qz	NW of Sesfontein	na
663	340091	7893346	33K	L-663	18	101002	Calc olig bx; concentric bk bands	NW of Sesfontein	na
664	342717	7892842	33K	L-664	19	101002	Arkosic ss. Epupa Complex	NW of Sesfontein	na
665	342717	7892842	33K	L-665	19	101002	Pk qz w/ bk hem xtal	NW of Sesfontein	na
666	471473	7748315	33K	L-666	21	101102	Pan concentrate from loose sand	Oas Farm	na

ID	UTMEAST	UTMNORTH	UTMZONE	SAMPLE	PAGE	DATE	ROCK	LOCATION	ELEVATION
667	471473	7748315	33K	L-667	21	101102	Mag concentrate fro loose sand	Oas Farm	na
668	471439	7748404	33K	L-668	21	101102	M-g gtd cut by qz+mag veinlets	Oas Farm	na
669	471439	7748404	33K	L-669	21	101102	Ang hyd. Bx of pk gtd w/ mag+qz	Oas Farm	na
670	471411	7748527	33K	L-670	21	101102	M-g gray-pk gtd +mag+sulfs?	Oas Farm	na
671	471378	7748582	33K	L-671	21	101102	F-g bn gtd +qz+sulfs vts +mag	Oas Farm	na
672	471378	7748582	33K	L-672	21	101102	Vein qz w/ vthin rd FeOx fracs +sulfs	Oas Farm	na
673	471427	7748620	33K	L-673	22	101102	Massive mag from qz+mag+sulfs vein	Oas Farm	na
674	471427	7748620	33K	L-674	22	101102	M-fg pk gtd cut by qz-mag stwk	Oas Farm	na
675	471427	7748620	33K	L-675	22	101102	M-g gtd w/ abund mag clusters +mag vein	Oas Farm	na
676	471408	7748649	33K	L-676	22	101102	Massive mag veinlet +sulfs?, martitized	Oas Farm	na
677	471435	7748670	33K	L-677	22	101102	Qz vein w/ bladed bk hem+sulfs?	Oas Farm	na
678	471455	7748666	33K	L-678	22	101102	M-g pk gtd	Oas Farm	na
679	471435	7748670	33K	L-679	22	101102	Pk gtd w/ bk mag clustes, veined	Oas Farm	na
680	471425	7748638	33K	L-680	23	101102	Gtd w/ abund vfg mag	Oas Farm	na
681	471435	7748655	33K	L-681	23	101102	Massive bx mag vein w/ ang rk frags	Oas Farm	na
682	471435	7748655	33K	L-682	23	101102	F-mg gy-pk gtd w/ mag veinlet	Oas Farm	na
683	471435	7748655	33K	L-683	23	101102	Mg pk-bn gtd cut by //bk mag veinlets	Oas Farm	na
684	471435	7748655	33K	L-684	23	101102	Massive bx mag + sulfs?	Oas Farm	na
685	471491	7748732	33K	L-685	24	101102	Braided network of qz +hem+sulfs? Veins	Oas Farm	na
686	471491	7748732	33K	L-686	24	101102	Braided qz veins w/ hem+sulfs? Au?	Oas Farm	na
687	471491	7748732	33K	L-687	24	101102	Qz vein w/ hem clusters + sulfs?	Oas Farm	na
688	471503	7748729	33K	L-688	24	101102	F-mg bn gtd w/ little qz, magnetic	Oas Farm	na
689	471503	7748729	33K	L-689	24	101102	Qz bx vein w/ bk massive hem layer	Oas Farm	na
690	471496	7748781	33K	L-690	24	101102	Mg gtd w/ mafic min clusters +mag	Oas Farm	na
691	471519	7748783	33K	L-691	25	101102	Vfg bk-dk gn rk, non-mag, dense, dike? Mo	Oas Farm	na
692	471549	7748814	33K	L-692	25	101102	Vfg bk rk w/ abund 0.5mm cubic vugs	Oas Farm	na
693	471497	7748831	33K	L-693	25	101102	Fg gtd, high mag, high qz	Oas Farm	na
694	471491	7748835	33K	L-694	25	101102	Mg gy gtd, ~mag low Qz	Oas Farm	na
695	471513	7748845	33K	L-695	25	101102	Vfg bk rk -mag cut by qz+hem veins	Oas Farm	na
696	471476	7748965	33K	L-696	25	101102	Mfg gtd cut by qz+hem veinlets	Oas Farm	na
194	471477	7748923	33K	L-697		101202	Mg bn-pk gtd cut by mag veins	Oas Farm	na
201	471494	7748955	33K	L-698		101202	Fg bn-gy gtd w/ diss py	Oas Farm	na
202	471446	7749001	33K	L-699		101202	Mg bn gtd w/ mafic min clusters	Oas Farm	na
203	471438	7749017	33K	L-700		101202	Vuggy, gossanous qz vein. Sulfs?	Oas Farm	na
204	471439	7749022	33K	L-701		101202	Bk intrusive w/ fine acicular needles	Oas Farm	na
205	471442	7749018	33K	L-702		101202	Qz druzes + goss vugs in qz veins	Oas Farm	na
206	471454	7749083	33K	L-703		101202	Qz druzes + goss vugs in qz veins	Oas Farm	na
207	471465	7749111	33K	L-704		101202	Sheeted qz+hem veinlets	Oas Farm	na
	471465	7749111	na	L-705			Vfg bn intrusive w/ braided qz-hem veins	Oas Farm	na
	471465	7749111	na	L-706			Vein of vfg intrusive w/ vugs + goss sulf	Oas Farm	na
208	471464	7749143	33K	L-707		101202	Mg pk gtd cut by ntwk of qz veins	Oas Farm	na
209	471495	7749231	33K	L-708		101202	F-mg dk gn-bk intrusive, -mag, chloritize	Oas Farm	na
210	471456	7749236	33K	L-709		101202	Fg pk intrusive cut by braided qz+chlorit	Oas Farm	na
211	471435	7749288	33K	L-709a		101202	na	Oas Farm	na
163	471443	7749248	33K	L-710		101202	Fg dk gn-gy intrusive cut by qz+hem+sulfs	Oas Farm	na
163	471443	7749248	33K	L-711		101202	Fg fol gtd cut by veins +Au?+sulfs?	Oas Farm	na
212	471428	7749313	33K	L-712		101202	F-mg gold intrusive cut by qz veins	Oas Farm	na
161	471417	7749439	33K	L-713		101203	F-mg gtd w/ smoky qz +sulfs?	Oas Farm	1011
159	471419	7749631	33K	L-714		101202	Mg pk gtd w/ braided qz+sulfs? Veins	Oas Farm	na
214	471383	7750213	33K	L-715		101202	Pk gneiss > mag	Oas Farm	na
215	471571	7750360	33K	L-716		101202	Pk gneiss -mag	Oas Farm	na
216	471782	7750569	33K	L-717		101202	Milky qz w/ bk joints	Oas Farm	na
217	472021	7750981	33K	L-718		101202	Milky white qz in part s/ sugary texture	Oas Farm	na
218	472085	7751127	33K	L-719		101202	Vfg pk intrusive w/ no mag	Lofdal Farm, Field	na
223	470685	7753757	33K	L-720		101202	Mass mag w/ carb vein + vugs	Lofdal Farm, Field	na
223	470685	7753757	33K	L-721		101202	Vuggy white qz w/ hem blob	Lofdal Farm, Field	na
224	470677	7753774	33K	L-722		101202	F-mg gn carbonatite w/ xenolithic frags	Lofdal Farm, Field	na
226	470621	7753910	33K	L-723		101202	Mikly white qz w/ abund bk joints	Lofdal Farm, Field	na
227	470613	7753909	33K	L-724		101202	M<ilky white qz w/ braided mag veinlets s	Lofdal Farm, Field	na
228	470619	7753925	33K	L-725		101202	V coarse plag xtal w/ qz inclusions	Lofdal Farm, Field	na
229	470601	7753986	33K	L-726		101202	C-g gtd w/ dissol cavities +bk hem	Lofdal Farm, Field	na
230	470608	7753986	33K	L-727		101202	F-g pk gtd w/ qz-hem veins +sulfs+Au?	Lofdal Farm, Field	na
231	470619	7753994	33K	L-728		101202	Fg dk pk intrusive cut by vf qz veins	Lofdal Farm, Field	na
232	470620	7753989	33K	L-729		101202	F-mg pk intrusive w/ qz veins + gossan	Lofdal Farm, Field	na
232	470620	7753989	33K	L-730		101202	F-mg intrusive w/ qz+hem+sulf ntwk Bx?	Lofdal Farm, Field	na
232	470620	7753989	33K	L-730a		101202	na	Lofdal Farm, Field	na
232	470620	7753989	33K	L-731		101202	Orange-Bn carbonatite dike, non-mag	Lofdal Farm, Field	na
232	470620	7753989	33K	L-732		101202	Fol ck gy carbonatite dike w/ wz lens	Lofdal Farm, Field	na
232	470620	7753989	33K	L-733		101202	Large tabular mag blades in carbonatite	Lofdal Farm, Field	na
232	470620	7753989	33K	L-734		101202	White qz w/ corroded frags of martite + c	Lofdal Farm, Field	na
233	470681	7754012	33K	L-735		101202	Mg pk gtd "chewed" by carbonatite	Lofdal Farm, Field	na
234	470627	7753989	33K	L-736		101202	Fol m-fg gtd cut by qz-mag-sulf veins	Lofdal Farm, Field	na
235	470630	7753979	33K	L-737		101202	Qz intersected by banded mag veinlets	Lofdal Farm, Field	na
236	470682	7754002	33K	L-738		101202	Fg ph gtd w/ braided mag-hem-qz veins	Lofdal Farm, Field	na
237	470736	7754016	33K	L-739		101202	Extremely vuggy cg intrusive +mag=qz vein	Lofdal Farm, Field	na
241	470051	7753177	33K	L-740		101202	Vfg dk -bn rk w/ fine diss mag	Lofdal Farm, Field	na
242	470059	7753166	33K	L-741		101202	Porph dk gy-bk rk w/ vfg matrix, mag. Vac	Lofdal Farm, Field	na
244	470069	7753143	33K	L-742		101202	Vfg med gy intrusve, slightly magnetic	Lofdal Farm, Field	na
245	470069	7753148	33K	L-743		101202	Bn carbonatite, > mag, flow bands, sulf?	Lofdal Farm, Field	na
245	470069	7753148	33K	L-744		101202	M-cg pk gtd w/ qz veinlets -mag	Lofdal Farm, Field	na
246	470072	7753141	33K	L-745		101202	Vfg med gy intrusive > mag, internal flow	Lofdal Farm, Field	na
247	470081	7753115	33K	L-746		101202	Carbonatite w/ braided mag veins	Lofdal Farm, Field	na
252	470091	7753115	33K	L-747		101202	Qz w/ rd stain + thin rd-filled joints	Lofdal Farm, Field	na
220	469619	7752727	33K	L-748		101202	Ang bx w/ vuggy surfaces + mag (Au?)	Lofdal Farm, Field	na
	466547	7755980	na	L-749			Qz w/ minor lt gn micas in batches	Lofdal Farm, Field	na
	466547	7755980	na	L-750			Mnzd samples	Lofdal Farm, Field	na
	466547	7755980	na	L-751			Mnzd samples	Lofdal Farm, Field	na
	466547	7755980	na	L-752			Mnzd samples	Lofdal Farm, Field	na
	466547	7755980	na	L-753			Mnzd samples	Lofdal Farm, Field	na
278	466549	7755506	33K	L-754		101302	Mnzd samples	Lofdal Farm, Field	na
279	466552	7755496	33K	L-755		101302	Bk material w/ f vugs, braided qz veins	Lofdal Farm, Field	na

ID	UTMEAST	UTMNORTH	UTMZONE	SAMPLE	PAGE	DATE	ROCK	LOCATION	ELEVATION
279	466552	7755496	33K	L-756		101302	Qz + hem cut by braided bk hem veinelst,	Mesopotamie Farm	na
279	466552	7755496	33K	L-757		101302	Qz from Qz blob	Mesopotamie Farm	na
312	439148	7765096	33K	L-758		101302	White, gossanous, graphic granite	Mesopotamie Farm	na
327	438940	7765078	33K	L-759		101302	Pegmatitic intrusive w/ graphic texture	Mesopotamie Farm	na
328	439572	7764296	33K	L-760		101302	Crushed ore grade material, Cu Valley min	Mesopotamie Farm	na
328	439572	7764296	33K	L-761		101302	Finely crushed material, Cu Valley mine	Mesopotamie Farm	na
328	439572	7764296	33K	L-762		101302	Finely crushed material, Cu Valley mine	Mesopotamie Farm	na
328	439572	7764296	33K	L-763		101302	Mnzd rk w/ gossan + hem Cu	Mesopotamie Farm	na
328	439572	7764296	33K	L-764		101302	Qz vein w/ hem ntwk +sulfs	Mesopotamie Farm	na
328	439572	7764296	33K	L-765		101302	Milky white qz q/ ntwk of bk hem + sulfs	Mesopotamie Farm	na
328	439572	7764296	33K	L-766		101302	Qz q/ FeOx veinelts, hem blobs + sulfs	Mesopotamie Farm	na
328	439572	7764296	33K	L-767		101302	Bx w/ qz, ang hem, martite, Cu carbs	Mesopotamie Farm	na
328	439572	7764296	33K	L-768		101302	Qz-bk hem -Cu carbs, vugs after sulfs	Mesopotamie Farm	na
328	439572	7764296	33K	L-769		101302	Qz=hem vein w/ abund vugs after sulfs	Mesopotamie Farm	na
328	439572	7764296	33K	L-770		101302	Qz vein w/ FeOx ntwk, hem blobs +vugs	Mesopotamie Farm	na
328	439572	7764296	33K	L-771		101302	Qz vein w/ rk frags and bxwk after sulfs	Mesopotamie Farm	na
	439579	7764129	na	L-772			Lt gy-white graphic granite	Mesopotamie Farm	703
	439579	7764129	na	L-773			Pegmatitic intrusive w/ graphic texture	Mesopotamie Farm	na
328	439572	7764296	33K	L-774		101302	Vuggy qz vein w/ dusty chalcocite + Cu ca	Mesopotamie Farm	na
328	439572	7764296	33K	L-775		101302	Qz vein w/ chacocite + Cu carbs	Mesopotamie Farm	na
328	439572	7764296	33K	L-776		101302	Qz w/ fine hem veinlets, goss vugs, Cu ca	Mesopotamie Farm	na
328	439572	7764296	33K	L-777		101302	Qz + stwk of hem veinlets, grades to bx	Mesopotamie Farm	na
328	439572	7764296	33K	L-778		101302	Gossans of different types	Mesopotamie Farm	na
284	443718	7762833	33K	L-779		101302	Intensely fractured fol gtd	Mesopotamie Farm	na
330	445478	7763678	33K	L-780		101402	Mass white qz from blob	Mesopotamie Farm	na
330	445478	7763678	33K	L-781		101402	Mass qz w/ vthin hem veinlets	Mesopotamie Farm	na
337	445963	7766384	33K	L-782		101402	Mass qz vein, no FeOx, vugs after sulfs	Mesopotamie Farm	na
337	445963	7766384	33K	L-783		101402	Gneiss	Mesopotamie Farm	na
339	543938	7762661	33K	L-784		101502	Coarse augen gneiss	Volcanics	na
340	536655	7734183	33K	L-785		101502	Calcareous turbidite	Volcanics	na
342	531468	7735504	33K	L-786		101602	Lt bn slightly foliated volc rk	Volcanics	na
342	531468	7735504	33K	L-787		101602	Volc rk w/ vugs - gossanous texture	Volcanics	na
342	531468	7735504	33K	L-788		101602	slightly fol volc rk w/ vugs -gossanous	Volcanics	na
343	531284	7735131	33K	L-789		101602	Slightly mag, porph. Subvolc. Intrusive	Sumas Mountains	na
343	531284	7735131	33K	L-790		101602	Fg bn-rd crystalline rk, cpy specks	Sumas Mountains	na
344	531251	7735039	33K	L-791		101602	Fg laminated pk volc rk (ash?)	Sumas Mountains	na
343	531284	7735131	33K	L-792		101602	Magnetic foliated subvolcanic rk	Sumas Mountains	na
355	495836	7693248	33K	L-793		101602	Cg pk granitoid + mag inclusions	Ugab River	na
356	495856	7693220	33K	L-794		101602	Pk gtd w/ slight foliation	Ugab River	na
358	496026	7693138	33K	L-795		101602	Porphyritic gy intrusive w/ mafic cluster	Ugab River	na
360	496058	7693188	33K	L-796		101602	Pk gtd w/ red qz clustes - mag	Ugab River	na
353	489966	7699063	33K	L-797		101602	Mg pk gtd w/ red qz + pk felds	Ugab River	na
352	488901	7700138	33K	L-798		101602	F-mg gy ftd	Ugab River	na
351	485783	7702912	33K	L-799		101602	Bn porphyritic rk w. yellow qz, <mag	Ugab River	na
351	485783	7702912	33K	L-800		101602	Mg gy gtd	Ugab River	na
349	483857	7707373	33K	L-801		101602	Gy gtd w/ dark red, soft macroxts	Ugab River	na
348	483650	7710515	33K	L-802		101602	F-mg pk gtd - mag	Ugab River	na
454	427928	7855082	33K	L-803		101702	Qz w/ abund dk gy-bk thin fractures	Kaokoveld	na
456	428321	7854990	33K	L-804		101702	White volc rk (orthoquaretzitic ss) w/ qz	Kaokoveld	na
458	714650	7500288	33K	L-805		101702	Ang hydroth bx w/ stwk +hem+goethite	Kaokoveld	na
458	714650	7500288	33K	L-806		101702	Explosive rhyolitic volc bx w. gossanous	Kaokoveld	na
			na	L-807			albitized rock	Borehole NRD-1, AVMIN	na
			na	L-808			pegmatitic intrusive	Borehole NRD-1, AVMIN	na
			na	L-809			albitized rock	Borehole NRD-1, AVMIN	na
			na	L-810			albitized country rock	Borehole NRD-1, AVMIN	na
			na	L-811			pegmatitic intrusive	Borehole NRD-1, AVMIN	na
			na	L-812			intrusive rocks	Borehole SCH-2, AVMIN	na
			na	L-813			Granite	Borehole SCH-2, AVMIN	na
			na	L-814			intrusive rocks	Borehole SCH-2, AVMIN	na
			na	L-815			Granite	Borehole SCH-2, AVMIN	na
			na	L-816			Weathered green intrusive	Borehole OP-2, Okatjepuiko	na
			na	L-817			Weakly magnetic dark green intrusive w/ f	Borehole OP-2, Okatjepuiko	na
			na	L-818			Dark intrusive w/ pink inclusions	Borehole OP-2, Okatjepuiko	na
			na	L-819			Pink intrusive in hydrothermal bx	Borehole OP-2, Okatjepuiko	na
			na	L-820			Pink granitic intrusive	Borehole OP-2, Okatjepuiko	na
			na	L-821			Pink granitic intrusive w/ veining	Borehole OP-2, Okatjepuiko	na
			na	L-822			Mg dk intrusive, mod magnetic with pk ban	Borehole OP-2, Okatjepuiko	na
			na	L-823			Dark intrusive w/ intense green staining	Borehole OP-2, Okatjepuiko	na
			na	L-824			Green speckled rk w/ grey veins and stain	Borehole OP-2, Okatjepuiko	na
			na	L-825			Pinkish gray intrusive rk very ractured,	Borehole OP-2, Okatjepuiko	na
			na	L-826			Bx of pink and dk gray rocks w/ Cu staini	Borehole OP-2, Okatjepuiko	na
			na	L-827			Pink intrusive as matrix to hydroth bx.	Borehole OP-2, Okatjepuiko	na
			na	L-828			Pink intrusive as matrix to hydroth bx.	Borehole OP-2, Okatjepuiko	na
			na	L-829			na	Borehole OP-2, Okatjepuiko	na
	539840	7809922	na	L-830	5		Coarse gtd, round porphyritic plag	Outcho-Kamanjab road	na
	534537	7811450	na	L-831	5		Coarse pk gtd, round plag porph	road side, Amolinda Farm?	na
	472861	7827894	na	L-840	7		Gtd	na	na
	472892	7827884	na	L-841	7		Qz from body or vein	gps perimeter	na
	676453	7730297	na	L-850	5		Fg gray homogeneous gtd	10 Km before Otjiwarongo	na
	462665	7752725	na	L-851	5		Qz w/ bk veins + dk gray color, veins	Loftdal Farm	na
	436172	7864144	na	L-855	11		Gtd	Tevrede property	na
	444509	7859376	na	L-856	11		Gtd	N Kamanjab	na
	442898	7856938	na	L-857	11		Gtd	N Kamanjab	na
552	474970	7852874	na	L-879	15	22703	Bx	Gelbingen farm	na
552	474970	7852874	na	L-879b	15	22703	Several samples Bx, Qz, etc	Gelbingen farm	na
552	474970	7852874	na	L-880	17	22703	Lgt gn stains in Qz and Porph fol rk	Gelbingen farm	na
555	475302	7852837	na	L-881	17	22703	Schist	Gelbingen farm	na
559	475297	7852715	na	L-882	17	22703	Bx mnzd	Gelbingen farm	na
555	475302	7852837	na	L-883	17	22703	Qz + toumaline	Gelbingen farm	na
556	475344	7852747	na	L-883	17	22703	Bx	Gelbingen farm	na
555	475302	7852837	na	L-884	17	22703	Bx	Gelbingen farm	na

ID	UTMEAST	UTMNORTH	UTMZONE	SAMPLE	PAGE	DATE	ROCK	LOCATION	ELEVATION
555	475302	7852837	na	L-885	17	22703	Bx	Gelbingen farm	na
555	475302	7852837	na	L-886	17	22703	Mnzd FeOx bx	Gelbingen farm	na
559	475297	7852715	na	L-887	17	22703	Qz-FeOx	Gelbingen farm	na
555	475302	7852837	na	L-888	19	22703	Zebra rk qz tourmaline	Gelbingen farm	na
574	478444	7851242	na	L-890	21	22703	FeOx, mnzd	Gelbingen farm	na
579	475998	7851002	na	L-891	21	22703	FeOx + vugs after sulfides	Gelbingen farm	na
580	475800	7851143	na	L-892	21	22703	Bx, mnzd	Gelbingen farm	na
580	475800	7851143	na	L-893	21	22703	FeOx	Gelbingen farm	na
580	475800	7851143	na	L-894	21	22703	FeOx, vuggy vein	Gelbingen farm	na
585	473644	7852581	na	L-895	21	22703	Subvolcanic porphyry	Gelbingen farm	na
585	473644	7852581	na	L-896	21	22703	Mnzd	Gelbingen farm	na
585	473644	7852581	na	L-897	21	22703	Bx FeOx	Gelbingen farm	na
594			na	L-902			Granitoid	na	na
5637	502010	7767010	33K	c-1			Granitoid	Clifford's Kamanjab samples	na
5638	526000	7768000	33K	c-2			Granitoid	Clifford's Kamanjab samples	na
5638	531650	7772120	33K	c-3			Granitoid	Clifford's Kamanjab samples	na
5639	531650	7772120	33K	c-4			Granitoid	Clifford's Kamanjab samples	na
5639	531650	7772120	33K	c-5			Granitoid	Clifford's Kamanjab samples	na
5640	533010	7769980	33K	c-6			Granitoid	Clifford's Kamanjab samples	na
5640	526150	7789450	33K	c-7			Granitoid	Clifford's Kamanjab samples	na
5641	515800	7780950	33K	c-8			Granitoid	Clifford's Kamanjab samples	na
5641	511850	7773570	33K	c-9			Granitoid	Clifford's Kamanjab samples	na
5642	520650	7788000	33K	c-10			Granitoid	Clifford's Kamanjab samples	na
5642	527000	7769980	33K	c-12			Granitoid	Clifford's Kamanjab samples	na

Table A19 Namibian samples that are located in UTM zone 34 (Schwartzeck)

ID	UTMEAST	UTMNORTH	UTMZONE	SAMPLE	LOCATION	PAGE
13	575044	7521992	34K	L-600	Okwa River, Botswana	na
14	575038	7521989	34K	L-601	Okwa River, Botswana	na
15	575054	7522050	34K	L-602	Okwa River, Botswana	na
16	575118	7522210	34K	L-603	Okwa River, Botswana	na
17	575141	7522225	34K	L-604	Okwa River, Botswana	na
18	575255	7522389	34K	L-605	Okwa River, Botswana	na
19	575253	7522388	34K	L-606	Okwa River, Botswana	na
20	485728	7551409	34K	L-607	Kalkfontein, Botswana	na
26	243590	7536839	34K	L-618	Klein Windhoek	9
26	243590	7536839	34K	L-619	Klein Windhoek	9
26	243590	7536839	34K	L-624a	Klein Windhoek	9
26	243590	7536839	34K	L-618	Okatjepuiko	10
26	243590	7536839	34K	L-619	Okatjepuiko	10
26	243590	7536839	34K	L-624	Okatjepuiko	10
31	243338	7537266	34K	L-624	Okatjepuiko	10
31	243338	7537266	34K	L-625	Okatjepuiko	10
31	243338	7537266	34K	L-624a	Okatjepuiko	10
32	243335	7537261	34K	L-626	Okatjepuiko	10
35	243343	7537284	34K	L-627	Okatjepuiko	10
35	243343	7537284	34K	L-628	Okatjepuiko	10
35	243343	7537284	34K	L-629	Okatjepuiko	10
35	243343	7537284	34K	L-630	Okatjepuiko	10
36	243060	7537117	34K	L-636	Okatjepuiko	10
36	243060	7537117	34K	L-637	Okatjepuiko	10
37	243050	7537104	34K	L-631	Okatjepuiko	11
39	243021	7537009	34K	L-632	Okatjepuiko	11
41	242991	7537254	34K	L-633	Okatjepuiko	11
42	242988	7537303	34K	L-639	Okatjepuiko	11
43	242977	7537404	34K	L-634	Okatjepuiko	11
44	242959	7537593	34K	L-635	Okatjepuiko	11
45	242969	7537428	34K	L-638	Okatjepuiko	11
46	242979	7537303	34K	L-640	Okatjepuiko	12
46	242979	7537303	34K	L-641	Okatjepuiko	12
48	243578	7536616	34K	L-642	Okatjepuiko	12
49	243591	7536591	34K	L-643	Okatjepuiko	12
50	243566	7536780	34K	L-646	Okatjepuiko	13
50	243566	7536780	34K	L-647	Okatjepuiko	13
50	243566	7536780	34K	L-648	Okatjepuiko	13
50	243566	7536780	34K	L-649	Okatjepuiko	13
50	243566	7536780	34K	L-650	Okatjepuiko	13
51	244142	7537156	34K	L-652	Okatjepuiko	14
51	244142	7537156	34K	L-651	Okatjepuiko	14
607	485728	7551409	34K	L-607	Kalkfontein, Botswana	5
608	485946	7551851	34K	L-608	Kalkfontein, Botswana	5
609	485946	7551851	34K	L-609	Kalkfontein, Botswana	5
610	485946	7551851	34K	L-610	Kalkfontein, Botswana	5
611	485946	7551851	34K	L-611	Kalkfontein, Botswana	5
612	485946	7551851	34K	L-612	Kalkfontein, Botswana	5
613	485946	7551851	34K	L-613	Kalkfontein, Botswana	6
614	485946	7551851	34K	L-614	Kalkfontein, Botswana	6
615	485946	7551851	34K	L-615	Kalkfontein, Botswana	6
616	485946	7551851	34K	L-616	Kalkfontein, Botswana	6
617	485946	7551851	34K	L-617	Kalkfontein, Botswana	6
625	243338	7537266	34K	L-625	Okatjepuiko	10

Table A20 Namibian samples that are located using latitude and longitude coordinates (Schwartzeck)

ID	E	S	ROCK	LOCATION	SAMPLE	PAGE	ANALYSIS
832	15.191350000	-19.723933333	Foliated mg gtd	Near mapp	L-832	7	x
833	15.185883333	-19.722033333	Coarse gtd	na	L-833	7	
834	15.166016667	-19.709000000	Lt p fg subvolcanic rk w/ miarolites	na	L-834	7	x
835	15.091300000	-19.685350000	Foliated gneissose intrusive?	na	L-835	7	x
836	14.091300000	-19.615266667	Foliated porphiritic rk, vulcaniclasti	ridge, ta	L-836	7	x
836	15.091300000	-19.615266667	Foliated porphiritic rk, vulcaniclasti	ridge, ta	L-836	7	x
837	14.836000000	-19.624800000	Coarse porphyritic gtd, slight foliati	NW of Kamanjab	L-837	7	
838	14.825300000	-19.625300000	Mg non-fol gtd	na	L-838	7	x
839	14.796016667	-19.627800000	Gtd	na	L-839	7	x
842	14.742350000	-19.645000000	Bk glassy porph lava ? chalced in vacu	na	L-842	7	x
843	14.837583333	-19.610150000	Fol gtd w/ porphyrob, w/ blue qtz porp	N of Kamanjab	L-843	7	x
844	14.837583333	-19.610150000	Fol gtd w/ porphyrob, w/ blue qtz porp	N of Kamanjab	L-844	9	x
845	14.827766667	-19.573033333	Porph rk w/ pk plag porph	N Kamanjab	L-845	9	
846	14.814083333	-19.533166667	Gtd	N Kamanjab	L-846	9	x
847	14.680133333	-19.464900000	orthoquartzite	N Kamanjab	L-847	9	
848	14.670033333	-19.456466667	metavolcanic rk w/ qz clasts	N Kamanjab	L-848	9	x
849	14.644000000		gtd	N Kamanjab	L-849	9	x
852	14.581483333	-19.435166667	Mg intrusive w/ qz veins, epidote vein	N Kamanjab	L-852	9	
853	14.558050000	-19.443633333	Gtd	N Kamanjab	L-853	9	
854	14.558050000	-19.443633333	associated qz veins + sulfides+ hydrot	N Kamanjab	L-854	9	
858	14.388033333	-19.467383333	Dk gray cg intrusive rk	na	L-858	11	
859	14.388033333	-19.467383333	magnetite-rich veins that cut fg intru	na	L-859	11	
860	14.387050000	-19.463400000	Gneiss	na	L-860	11	
861	14.385350000	-19.448483333	Magnetite concentrate from dry river b	dry river	L-861	11	
862	14.408050000	-19.374150000	Slightly foliated gtd	na	L-862	11	
863	14.421983333	-19.481850000	Foliated gtd (diorite?)	na	L-863	11	x
864	14.387850000	-19.464983333	Foliated gtd w/ epidote veins, sheared	na	L-864	11	x
865	14.387133333	-19.462283333	Foliated gtd w/ epidote veins, sheared	na	L-865	13	x
866	14.384150000	-19.450300000	Qz vein, non-minzd	na	L-866	13	
867	14.387133333	-19.442150000	Vcg fol porph gtd w/ blue qz	na	L-867	13	
868	14.387133333	-19.442150000	Mg porph gtd	na	L-868	13	x
869	14.393116667	-19.435783333	Cg gtd, fol. Rapakiwi	na	L-869	13	
870	14.396850000	-19.433983333	Cg gtd, fol. Rapakiwi	na	L-870	13	
871	14.409083333	-19.429833333	Fg felsic gtd, volc?	na	L-871	13	
872	14.413033333	-19.428000000	Gossanous qz w/ sulfs, cubic hematite	Kamdescha	L-872	13	
873	14.415550000	-19.426966667	Vfg intrusive rk, felsic, silicic, vit	Kamdescha	L-873	13	
874	14.440883333	-19.424783333	Gtd	Kamdescha	L-874	13	x
875	14.447083333	-19.424816667	Fresh gtd	na	L-875	15	x
876	14.504700000	-19.443933333	Fol gtd, augen gneiss	na	L-876	15	
877	14.526283333	-19.445050000	Gtd	na	L-877	15	x
878	14.548266667	-19.444000000	Gtd	na	L-878	15	x
898	14.722516667	-19.623383333	Foliated porhp gtd	Gelbingen	L-898	23	x
899	14.702400000	-19.611066667	Fine grained volcanic rk	Gelbingen	L-899	23	x
900	14.686883333	-19.609283333	Fine grained granitoid	Gelbingen	L-900	23	x
901	14.666900000	-19.623266667	Weathered granitoid	Berg Vall	L-901	23	
903	14.670666667	-19.605033333	Gtd	na	L-903	23	x
904	14.654500000	-19.594000000	Gtd	na	L-904	23	x
905	14.651700000	-19.593966667	Gtd	na	L-905	23	x
906	14.648116667	-19.594100000	Fresh, dateable gtd	na	L-906	23	x
907	14.640383333	-19.595166667	Coarse gd porphyritic gtd	na	L-907	23	x
908	14.631700000	-19.593016667	Gray mg gtd	na	L-908	23	x
909	14.606600000	-19.576666667	Foliated fg volcanic rk	na	L-909	23	x
910	14.575750000	-19.580000000	Fine grained volcanic rk	na	L-910	23	x
911	14.550233333	-19.553250000	Fresh volc rk; schist	na	L-911	23	x
912	14.542650000	-19.605000000	Fine grained, schistose volcanic rk	na	L-912	23	x
913	14.496266667	-19.603616667	Quartzite to compare with Muva	na	L-913	23	
914	14.460050000	-19.611483333	Mnzd, euhedral hematite + vugs	na	L-914	25	
915	14.460050000	-19.611483333	Mnzd, quartzite + goss vugs, magnetite	na	L-915	25	
916	14.460050000	-19.611483333	Mnzd, vugs after sulfides	na	L-916	25	
917	14.453316667	-19.612716667	Foliated porph. gtd	na	L-917	25	x
918	14.443400000	-19.615500000	Fg gtd w/ qz veins	na	L-918	25	
919	14.430016667	-19.602400000	Volcanic rk that makes ridge	na	L-919	25	x
920	14.408316667	-19.585583333	Fresh gtd in undeformed dike	na	L-620	25	x
921	14.408316667	-19.585583333	Qz vein + FeOx cube	na	L-921	25	
922	14.408316667	-19.585583333	Fol gtd	na	L-922	25	x
923	14.398466667	-19.568716667	Gtd	na	L-923	25	x
924	14.402583333	-19.551383333	Fol gtd	na	L-924	27	x
925	14.363150000	-19.606516667	Mnzd, very porous w/ cubic vugs	na	L-925	27	
926	14.363150000	-19.606516667	Mnzd, very porous w/ cubic vugs	na	L-926	27	
927	14.363150000	-19.606516667	Mnzd, very porous w/ cubic vugs	na	L-927	27	
928	14.363150000	-19.606516667	Mnzd, very porous w/ cubic vugs	na	L-928	27	
929	14.363600000	-19.606916667	Mnzd + FeOx, strange gossans	na	L-929	27	
930	14.363600000	-19.606916667	Mnzd + FeOx, strange gossans, bxwk	na	L-930	27	
931	14.364866667	-19.607316667	FeOx, vuggy rks	na	L-931	27	
932	14.364866667	-19.607316667	FeOx, vuggy rks, w/ vuggy hematite	na	L-932	27	
933	14.365333333	-19.607316667	Bx w/ FeOx+sulfides + qz	na	L-933	27	
934	14.365333333	-19.607316667	Vuggy FeOx + Qz	na	L-934	27	
935	14.365333333	-19.607316667	Massive FeOx + qz + opal	na	L-935	27	
936	14.365333333	-19.607316667	Several samples of vuggy FeOx	na	L-936	27	
937	14.369483333	-19.614333333	Hematitized schist, FeOx	na	L-937	29	
938	14.319616667	-19.682166667	Fol gtd + Qz	na	L-938	29	x
939	14.312500000	-19.715833333	Cg gtd	na	L-939	29	x
940	14.312500000	-19.715833333	Mafic gtd as enclave in L-939	na	L-940	29	x
941	14.294800000	-19.738716667	Fol gtd	na	L-941	29	
942	14.284366667	-19.758216667	Fol gtd	na	L-942	29	
943	14.284366667	-19.758216667	Fg gtd in dikes	na	L-943	29	x
944	14.284366667	-19.758216667	white pegmatitic veins	na	L-944	29	
945	14.318100000	-19.772033333	Fol gtd	na	L-945	29	x
946	14.337533333	-19.761683333	Fresh fol gtd	na	L-946	29	x
947	14.396566667	-19.797750000	Cg underformed (?) gtd	na	L-947	29	
948	14.396566667	-19.797750000	Fol gtd intruded by L-947	na	L-948	29	x

ID	E	S	ROCK	LOCATION	SAMPLE	PAGE	ANALYSIS
949	14.426816667	-19.811833333	Bk fg volc rk w/ angular large vugs	na	L-949	29	
950	14.426816667	-19.811833333	Bk fg volc rk	na	L-950	29	
951	14.452350000	-19.815750000	Fresh fol gtd	na	L-951	29	x
952	14.452350000	-19.815750000	White bands in cg porph gtd	na	L-952	29	x
953	14.452350000	-19.815750000	Pink band in cg porph gtd	na	L-953	29	
954	14.452350000	-19.815750000	Dk gn, fol fg gtd	na	L-954	29	
955	14.452350000	-19.815750000	Felsic fg fol gtd	na	L-955	29	x
956	14.474850000	-19.814250000	Cg fol gtd	na	L-956	31	x
957	14.499483333	-19.809816667	Fresh subvolcanic rk?	na	L-957	31	x
958	14.515950000	-19.808083333	Gabbroic rk, fol, in dikes	na	L-958	31	x
959	14.567183333	-19.808383333	Cg porph fol porph gtd	na	L-959	31	
960	14.615150000	-19.800200000	Mnzd, sheeted veins & stwk	na	L-960	31	
961	14.629550000	-19.807933333	Mnzd bx	na	L-961	33	
962	14.629550000	-19.807933333	Mnzd bx w/ abundant vugs	na	L-962	35	
963	14.629550000	-19.807933333	Mnzd bx	na	L-963	35	x
964	14.629550000	-19.807933333	Mnzd bx	na	L-964	35	
965	14.629550000	-19.807933333	Mnzd bx	na	L-965	35	x
966	14.650350000	-19.820133333	Fresh pk fol gtd	na	L-966	31	x
967	14.667250000	-19.823100000	Pk fol gtd	na	L-967	33	x
968	14.682316667	-19.880983333	Hydrothermally altered gtd	na	L-968	33	x
969	14.682316667	-19.880983333	Mnzd gtd, porph w/ goss vugs after dis	na	L-969	33	x
970	14.682316667	-19.880983333	Mnzd gtd, porph w/ goss vugs after sul	na	L-970	33	
971	14.682316667	-19.880983333	Mnzd gtd, porph w/ goss vugs after sul	na	L-971	33	x
972	14.682316667	-19.880983333	Mnzd gtd, porph w/ goss vugs after sul	na	L-972	33	
973	14.681483333	-19.882600000	Mnzd gtd, porph w/ diss bornite (?) fl	na	L-973	33	x
974	14.683183333	-19.878966667	Fg pk gtd	na	L-974	33	
975	14.683183333	-19.878966667	Mg gtd w/ minor diss sulfs	na	L-975	33	x
976	14.681416667	-19.888900000	Fresh mg gtd	na	L-976	33	x
977	14.705066667	-19.830666667	na	na	L-977a	33	
	15.042000000	-20.072650000	na L-977a		L-977a	33	
978	15.037900000	-20.064833333	Fresch cg gtd w/ blue qz	na	L-978	35	x
979	15.029633333	-20.057400000	Cg gtd w/o blue qz	na	L-979	35	x
980	15.024666667	-20.052900000	Mcg gtd	na	L-980	35	x
981	15.009800000	-20.040483333	Fol cg gtd w/ blue qz	na	L-981	35	
982	15.003166667	-20.034800000	Fol cg gtd	na	L-982	35	x
983	14.983450000	-19.994650000	Fol cg gtd	na	L-983	35	x
984	14.980333333	-19.989333333	Less fol cg gtd w/ blue qz	na	L-984	35	
985	14.966766667	-19.968283333	Fresh fold gtd	na	L-985	35	x
986	14.963183333	-19.955716667	Fresh gtd	na	L-986	35	
	14.961750000	-19.936016667	L-987a Subvolcanic Diorite (?)	na	L-987a	35	
	14.961750000	-19.936016667	L-987b Subvolcanic Diorite (?)	na	L-987b	35	
988	14.961616667	-19.937533333	Cg gabbro w/ diss py	na	L-988	37	
989	14.961616667	-19.937533333	Mg gabbro w/ diss py	na	L-989	37	
990	14.961616667	-19.937533333	Cg gabbro w/ white plag vein	na	L-990	37	x
991	14.961616667	-19.937533333	Cg gabbro	na	L-991	37	x
992	14.961650000	-19.938366667	Intermediate gtd w/o sulfides	na	L-992	37	x
993	14.961800000	-19.935083333	Fresh pk fg porph w/ blue qtz + diss c	na	L-993	37	x
994	14.961800000	-19.935083333	Fresh gtd (asL-993) w/ visible cpy	na	L-994	37	x
995	14.961800000	-19.935083333	Gabbro w/ diss py + cpy	na	L-995	37	x
996	14.958716667	-19.926483333	Mg gtd	na	L-996	37	x
997	14.951850000	-19.916000000	Pk gtd	na	L-997	37	x
998	14.951850000	-19.916000000	Bn gtd	na	L-998	37	x
999	14.926183333	-19.891950000	Fol, very porphyritic gtd, w/ hexagona	na	L-999	37	x
1000	14.904783333	-19.873633333	Fresh gtd	na	L-1000	37	x
1001	14.898333333	-19.869066667	Qz w/ schistose dark rk + abdnt vugs	na	L-1001	39	
1002	14.880883333	-19.838566667	Hydrothermally altered gtd ?	na	L-1002	39	x
1003	14.862250000	-19.816933333	Fol cg volcanic rk	na	L-1003	39	x
1004	14.855816667	-19.801350000	Fg subvolcanic rk	na	L-1004	39	
1005	14.724400000	-19.810616667	Fol cg porph gtd	na	L-1005	39	x
1006	14.717000000	-19.805066667	Fol porph gtd	na	L-1006	39	
1007	14.775883333	-19.777466667	Pk fol porph gtd	na	L-1007	39	x
1008	14.830700000	-19.735116667	Fol fg gtd (volc?)	Kamanjabb-	L-1008	39	
1009	14.840600000	-19.692250000	Fol gtd	na	L-1009	39	x
1010	14.856000000	-19.676383333	Fol gtd	na	L-1010	39	x
1011	14.856666667	-19.655250000	Fresh fol porph gtd	na	L-1011	39	x
1012	14.856666667	-19.655250000	Fresh fol porph gtd	na	L-1012	39	x
1013	15.306083333	-19.854616667	Gtd	way to Le	L-1013	43	x
1014	18.250000000	-19.533333333	Mafic gtd	Grootfont	L-1014	47	x
1037	16.652650000	-20.452816667	Fol gtd	Otjiwaron	L-1037	57	x
1038	16.652650000	-20.452816667	Fol gtd	Otjiwaron	L-1038	57	x
5000	16.879850000	-20.270190000	pegmatites from Otjiwarongo Batholith	Borehole NRD-1, AVI	5000		X
5001	16.892070000	-20.222700000	pegmatites from Otjiwarongo Batholith	Borehole SCH-2, AVI	5001		X
5003	16.799267000	-20.367317000	Alkali granite	Wagner 14	LL1		y
5004	16.810383000	-20.270733000	Monzo granite	Jagerhof 11	LL2a		y
5005	16.810383000	-20.270733000	Alkali granite pegmatite	Jagerhoff 11	LL2b		y
5006	16.774167000	-20.330350000	Syenogranite	Drukwerk 13	LL3a		y
5007	16.774167000	-20.330350000	Alkali granite pegmatite	Drukwerk 13	LL3b		y
5008	16.699567000	-20.528233000	Syenogranite	Pinnacles 310	LL4		y
5009	16.712333000	-20.543567000	Syenogranite	Pinnacles 310	LL5		y
5010	17.067399000	-20.139827000	Alkali granite	Houmoed 95	LL9		y
5011	16.579000000	-19.942500000	Biotite syenite	Langelee/Meyerton	LL10		y
5012	16.647000000	-20.453000000	Syenogranite	Otjiwarongo	LJ1		y
5013	16.702650000	-20.532090000	Granodiorite	Pinnacles 310	LL11		y
5014	16.647380000	-20.453130000	NA	Otjiwarongo	LL12		y
5015	16.642537000	-20.456522000	Wollastonite granulite	Otjiwarongo	LL13		y
5016	16.203540000	-20.710140000	Olivine Syenite	Niederungsfelde	LL14		y
5017	16.220260000	-20.813090000	Higly altered olivine syenite	Neu Lehmputz	LL15		y
5018	16.129560000	-20.975030000	Quartz Syenite	Georg-Ferdinanhohe	LL16		y
5019	16.162370000	-21.764060000	Quartz Syenite	Otjakatjongo	LL17a		y
5020	16.162370000	-21.764060000	Quartz Syenite	Otjakatjongo	LL17b		y
5021	16.633540000	-21.916240000	Granodiorite	Ozombanda	LL18		y
5022	16.743352000	-20.459556000	Granitoid	Doornlaagte 299	LL21		na
5023	16.798257000	-20.369058000	Granitoid	Wagner 14	N19		na
5024	16.775259000	-20.377979000	Granitoid	Wagner 14	LL26b		na

ID	E	S	ROCK	LOCATION	SAMPLE	PAGE	ANALYSIS
5025	16.825615000	-20.335396300	Granitoid	Wagner 14	N26		na
5026	16.825798000	-20.353341000	Granitoid	Wagner 14	LL27		na
5027	16.781246000	-20.332666000	Granitoid	Wagner 14	LL28		na
5028	16.815101000	-20.396347000	Granitoid	Wagner 14	LL30		na
5029	16.738760000	-20.471835000	Granitoid	Doornlaagte 299	LL2Oa		na
5030	16.738760000	-20.471835000	Granitoid	Doornlaagte 299	LL2Oc		na

APPENDIX E
GEOCHRONOLOGY

A21	Compilation of radiometric ages, Greater Lufilian Arc – sorted by chronological order, 42
A22	Compilation of radiometric ages, Greater Lufilian Arc – sorted by region and sites, 50
ZAMBIA	
A22.1	Hook Granite Batholith, Zambia, 50
A22.2	Northwestern Zambia, Domes Area, 50
A22.3	Solwesi Dome Area, Zambia, 50
A22.4	Western Lusaka-Kafue Flats Area, Zambia, 50
A22.5	Kalengwa-Kasempa Area, Zambia, 51
A22.6	Mkushi-Serenje Area, Zambia, 51
A22.7	Copperbelt region, Zambia, 51
A22.8	Mufulira Area, Zambia, 52
A22.9	Nchanga Area, Zambia, 52
A22.10	All Basement to the Copperbelt, Zambia (Compilation of Groups), 52
A22.11	Choma-Kalomo Batholith, Zambia, 52
A22.12	Irumide Belt, Zambia, 53
A22.113	Luangwa Valley, Zambia, 53
A22.14	Other Zambia, 54
NAMIBIA	
A22.15	True Kamanjab Batholith, Namibia, 54
A22.16	Khorixas Inlier, Namibia, 54
A22.17	All Kamanjab Area, Namibia, 55
A22.18	Witvlei Area and possible correlatives in the region, 55
A22.19	Central Namibia, 57
A22.20	Northernmost Namibia, 57
A22.21	Southernmost Namibia, 57
A22.22	Kaokoveld, Namibia, 57
A22.23	Rehoboth Inlier, Namibia, 58
A22.24	Namibrand-Sasriem Area, Namibia, 58
A22.25	Namaqua Metamorphic Complex, Namibia, 58
A22.26	“Kibaran” rocks of Namibia, 59
A22.27	Other Namibia, 59
OTHER	
A22.28	Other countries relevant to Lufilian Arc project, 59
A22.29	All Zambia (compilation of all Zambian ages), 60
A22.30	All Namibia (compilation of all ages from the country), 64

Table A21
COMPILATION OF RADIOMETRIC AGES, GREATER LUFILIAN ARC
SORTED BY CHRONOLOGICAL ORDER, January 19, 2005

Compiled by Alberto Lobo-Guerrero, Geologist, M.Sc.,Min.Ex.
Economic Geology Research Institute, University of the Witwatersrand, Johannesburg, South Africa

Note: Samples highlighted in light gray are from Zambia; those in dark gray come from other countries.

sample	Site/Event	Rock type	age	error	max	min	material	type	1/8
	Nkana mine,Zm	Botryoidal pitchblende vein	235	35	270	200	Pitchblend	U-Pb	Snelling et al, 1972
	Luanshya mine,Zm	Pitchblende in vein	365	40	405	325	Pitchblend	U-Pb	Snelling et al, 1972
	Sinda Granite,Zm	Gtd	380	10	390	370	Biotite	Rb-Sr	Snelling et al, 1972
L-030	Kabompo Dome, Zm	diorite-granodiorite gneiss	419	250	669	169	zircon	Pb/U shrimp	This report
	Leopard's Hill area,Zm	Biotite-garnet schist	435	15	450	420	Muscovite	K-Ar	Snelling et al, 1972
	Hook Granite,Zm	Pegmatite	440	15	455	425	Muscovite	K-Ar	Snelling et al, 1972
	Khan-Swakop River, Nm	Schist, cooling age of biotite (350degC)	448		448	448	Biotite	Rb-Sr	Hawkesworth et al, 1983
	Hook Granite,Zm	Biotite granite gneiss	450	14	464	436	biotite	K-Ar	Snelling et al, 1972
	Nkana mine,Zm	Metasediment with uraninite	452	24	476	428	Uraninite	U-Pb	Snelling et al, 1972
	Nkana mine,Zm	Schistose granulite	455	20	475	435	Biotite	Rb-Sr	Snelling et al, 1972
	Lusandwa Syenite,Zm	Syenite	455	5	460	450	Biotite	Rb-Sr	Snelling et al, 1972
	Hook Granite,Zm	Porphyroblastic gneiss	458	122	580	336	Biotite	K-Ar	Snelling et al, 1972
	Rossing Mine, Nm	Uraniferous alaskite, late alaskite	458	8	466	450	w.r.	Rb-Sr	Steven et al, 1993
	Lylands Quarry, Ndola,Zm	Galena	460		460	460	Galena	Pb	Snelling et al, 1972
	Chapalapata, Sasare,Zm	Granite	460		460	460	Biotite	Rb-Sr	Snelling et al, 1972
	Hook Granite,Zm	Biotite-hornblende granite	465	16	481	449	Biotite	K-Ar	Snelling et al, 1972
	Hook Granite,Zm	Biotite-hornblende granite	465	15	480	450	Hornblend	K-Ar	Snelling et al, 1972
	Khan-Swakop River, Nm	Schist, cooling age of biotite (350degC)	465	5	470	460	Biotite	Rb-Sr	Hawkesworth et al, 1983
	Sandamap Mine, Central Zone,Nm	Stanniferous pegmatite	468	14	482	454	w.r.	Rb-Sr	Steven et al, 1993
	Minga Migmatite, Great East Rd,Zm	Migmatite	470		470	470	Biotite	Rb-Sr	Snelling et al, 1972
	Sandamap Noord, Central Zone,Nm	Pegmatite	473	23	496	450	w.r.	Sr/Sr	Steven et al, 1993
	Mpande Dome,Zm	Microgranite	476	19	495	457	Muscovite	K-Ar	Snelling et al, 1972
	Otjozondjou, Nm	Diorite	478	4	482	474	Hornblend	Ar/Ar	Hawkesworth et al, 1983
	Bukanda near Luapula River,Zm	Galena	480		480	480	Galena	Pb	Snelling et al, 1972
	Stinkbank, Central Zone, Nm	Uraniferous leucogranite, scheelite skarn	484	25	509	459	w.r.	Rb-Sr	Steven et al, 1993
	Leopard's Hill area,Zm	Schist	485	20	505	465	Biotite	K-Ar	Snelling et al, 1972
	Nkana mine,Zm	Uraninite in sediment	485	16	501	469	Uraninite	U-Pb	Snelling et al, 1972
	Lundazi,Zm	Mica-beryl pegmatite	485		485	485	Betafite	U-Pb	Snelling et al, 1972
	Huab Complex,Nm	Gtd (Tectonic event age)	488		537	437	zircon	U-Pb	Tegtmeyer & Kroner, 1985
	Gray's Quarry, Nchanga, Zm	Red granite	490	20	510	470	Biotite	K-Ar	Snelling et al, 1972
	Gray's Quarry, Nchanga, Zm	Red granite	490	15	505	475	Biotite	Rb-Sr	Snelling et al, 1972
	Navachab Mine, Cental Zone, Nm	Biotite in skarn	490		490	490	Bt	Rb-Sr	Steven et al, 1993
	Kohero Tin mine, Central Zone, Nm	Stanniferous pegmatite	492	11	503	481	w.r.	Rb-Sr	Steven et al, 1993
	Kafue Rhyolites,Zm	Sheared tuff	495	35	530	460	w.r.	Rb-Sr	Snelling et al, 1972
	Serenje area,Zm	Biotite gneiss	495	20	515	475	Biotite	K-Ar	Snelling et al, 1972
	Nkana mine, Mindola,Zm	Schistose granulite	495	20	515	475	Biotite	K-Ar	Snelling et al, 1972
	Uis Mine, Central Zone, Nm	Stanniferous pegmatite	496	30	526	466	w.r.	Rb-Sr	Steven et al, 1993
	Hook Granite,Zm	Granite	500	17	517	483	Granite	Rb-Sr	Snelling et al, 1972
	Chinyunyu zone,Zm	Sheared granite	500	20	520	480	Biotite	K-Ar	Snelling et al, 1972
	Kansanshi Mine, Zm	Carbonate-molybdenite-monazite veins	502.4	1.7	504	501	Molybden	Re-Os	Torrealday et al, 2003
	Kansanshi Mine, Zm	Carbonate-molybdenite-monazite veins	503	15	518	488	Brannerite	U-Pb	Darnley, 1961
	Kipushi Mine, D.R.Congo	Syn- to post-tectonic metamorphic veins	504.5		496	513	Rutile	U-Pb	Richards, 1988
	Mufulira West mine, Zm	Basement granite	505	20	525	485	Biotite	K-Ar	Snelling et al, 1972
	Chinyunyu zone,Zm	Sheared granite	505	20	525	485	Biotite	K-Ar	Snelling et al, 1972
	Ohere, Central Zone, Nm	Leucogranite	506	135	641	371	w.r.	Sr/Sr	Steven et al, 1993
	Lusaka Granite,Zm	Granite	507	15	522	492	Biotite	Rb-Sr	Snelling et al, 1972
	Goniakontes alaskite, Nm	Alaskite, post-tectonic doming intrusion	508	2	510	506	uraninite,	U-Pb	Briqueau et al, 1980
	Gamigab Prospect, Central Zone, Nm	Cassiterite veins	510		510	510	Muscovite	Rb-Sr	Steven et al, 1993
	Rossing Mine, Nm	Uraniferous alaskite, early alaskite	510		510	510	w.r.	Rb-Sr	Steven et al, 1993
	Khan formation, Goniakonites, Nm	Syn-metamorphic growth	510	3	513	507	monazite	U-Pb	Briqueau et al, 1980
	Kansanshi mine, Zm	Minzd qz vein	511	11	522	500	zircon	U-Pb	Torrealday et al, 2000
	Sandamap Noord, Central Zone,Nm	Leucogranite phacolith	512	19	531	493	w.r.	Sr/Sr	Steven et al, 1993
	Salem Granite, Goas, Nm	Granite, syn-metamorphic intrusion	512	40	552	472	zircon	U-Pb	Allsopp at al, 1983
	Kansanshi Mine, Zm	Cpy-rich veins	512.4	1.2	514	511	Molybden	Re-Os	Torrealday et al, 2003
	Leopard's Hill area,Zm	Katangan mica quartzite	515	20	535	495	Biotite	K-Ar	Snelling et al, 1972
	Luanshya mine, Zm	Lufubu Schist	515	100	615	415	Actinolite	K-Ar	Snelling et al, 1972
	Mufulira West mine, Zm	Basement granite	515	25	540	490	Biotite	Rb-Sr	Snelling et al, 1972
	Rubicon mine, Cental Zone, Nm	Petalite in pegmatite	515	36	551	479	Amb, Kfel	Rb-Sr	Steven et al, 1993
	Kansanshi mine,Zm	Vein	520	20	540	500	Brannerite	U-Pb	Snelling et al, 1972
	Leopard's Hill area,Zm	Sheared gneiss	520	20	540	500	Biotite	K-Ar	Snelling et al, 1972
	Nkana mine,Zm	Uraninite	520	20	540	500	Uraninite	U-Pb	Snelling et al, 1972
Mo Porp	Marinkas Kwela, Nm	Syenite,gt,cb	520		550	490	zircon	U-Pb	Bernasconi, 1986
	Luanshya mine, Zm	Lufubu Schist	530	30	560	500	Biotite	K-Ar	Snelling et al, 1972
	Lusaka Granite,Zm	Granite	531	21	552	510	Biotite	K-Ar	Snelling et al, 1972
H-4	Hook Granite, Zm	Post-Tectonic megacrystic granite	533	3	536	530	zircon	U-Pb	Hanson et al, 1993
	Goniakontes, red granite, Nm	Granite, syn-metamorphic anatexis	534	7	541	527	zircon, m	U-Pb	Briueu et al, 1980
	Hook Granite, Zm	tectonic activity	535		540	530	zircon	U-Pb	Hanson et al, 1993
	Nkana mine,Zm	Uraninite in Lower Roan	535	21	556	514	Uraninite	U-Pb	Snelling et al, 1972
H-3	Hook Granite, Zm	Rhyolite dike within Katangan	538	1.5	540	537	zircon	U-Pb	Hanson et al, 1993

RADIOMETRIC AGES IN CHRONOLOGICAL ORDER, GREATER LUFILIAN ARC (cont.) 2/8

sample	Site/Event	Rock type	age	error	max	min	material	type	reference
L-207	Nampundwe,Zm	Gtd	538.2	3.3	542	535	zircon	U-Pb	This report
	Lusaka Area, Zm	metasediments?	539	20	559	519	w.r.	Rb-Sr	Barr et al, 1978
	Lusaka Granite,Zm	Granite	540	20	560	520	Biotite	K-Ar	Snelling et al, 1972
L-795	Ugab River, Nm	Gtd	540	4	544	536	zircon		This report
	Salem Granite, Ohere Oos, Nm	Granite	542	11	553	531	w.r.	Sr/Sr	Steven et al, 1993
	Kipushi Mine, D.R.Congo	Breccia Pipe	546	18	564	528	Zircon	U-Pb	Walraven & Chabu, 1994
	Kafue Rhyolites,Zm	Rhyolitic tuff	548	32	580	516	w.r.	Rb-Sr	Snelling et al, 1972
L-213	Kafue Flats,Zm	Syenite	550	25	575	525	zircon	U-Pb	This report
	Sachenga mica claims,Zm	Pegmatite	550	20	570	530	Muscovite	K-Ar	Snelling et al, 1972
	Mivula Syenite,N Province,Zm	Syenite	550	20	570	530	Biotite	K-Ar	Snelling et al, 1972
	Gariep Complex Intrusives,Nm		550		600	500			Miller, 1999
H-5	Hook Granite, Zm	Rhyolite intrusion in Mwembezhi dislocation	551	19	570	532	zircon	U-Pb	Hanson et al, 1993
	Lusaka Granite,Zm	Granite	551	22	573	529	Biotite	K-Ar	Snelling et al, 1972
BK-19	Kaoko belt, Hoanib River, NW Nm	Coarse-g monzogranite	551.9	1.5	553	550	zircon	U-Pb	Seth et al, 1998
	Damara syn to post-tectonic intrusives,Nm	Granites	555		650	460			Miller, 1999
	Lusaka Area, Zm	metasediments?	557	4	561	553	w.r.	K-Ar	Barr et al, 1978
	Kamanjab Batholith,Nm	Gtd	558	20	578	538	zircon	U-Pb	Clifford et al, 1969
H-1	Hook Granite, Zm	Deformed f-mg granite	559	18	577	541	zircon	U-Pb	Hanson et al, 1993
	Kamfinsa Quarry,Zm	Pegmatite	560	20	580	540	Biotite	K-Ar	Snelling et al, 1972
	Kafue Rhyolites,Zm	Porphyritic Rhyolite	562	40	602	522	w.r.	Rb-Sr	Snelling et al, 1972
L-158	Konkola Deep Borehole,Zm, resetting age	Foliated pink gtd	562	18	580	544	zircon em	Pb/U shrimp	This report
BK-43	Kaoko belt, Hoanib River, NW Nm	Cg late tectonic granite (migmatite)	563.8	1.5	565	562	zircon	Pb/Pb	Seth et al, 1998
	Hook Granite, Zm	Syntectonic granitic plutonism	565		570	560	zircon	U-Pb	Hanson et al 1993
	Migmatitic biotite gneiss,Zm	Migmatitic biotite gneiss,Zm	565	24	589	541	Biotite	K-Ar	Snelling et al, 1972
BK-43	Kaoko belt, Hoanib River, NW Nm	Cg late tectonic granite (migmatite)	565	13	578	552	zircon	Pb/Pb	Seth et al, 1998
H-2	Hook Granite, Zm	Deformed megacrystic granite	566	5	571	561	zircon	U-Pb	Hanson et al, 1993
	Lusaka Granite,Zm	Granite	567	23	590	544	Biotite	K-Ar	Snelling et al, 1972
	Migmatitic biotite gneiss,Zm	Migmatitic biotite gneiss,Zm	567	24	591	543	Biotite	K-Ar	Snelling et al, 1972
BK-24	Kaoko belt, Hoanib River, NW Nm	Foliated cg granodioritic gneiss	567.2	1.5	569	566	zircon	U-Pb	Seth et al, 1998
BK-17	Kaoko belt, Hoanib River, NW Nm	Metamorphic age in granitic gneiss	578	57	635	521	zircon	U-Pb	Seth et al, 1998
BK-426	Kaoko belt, Hoanib River, NW Nm	Granodioritic augen gneiss	580	3	583	577	zircon	U-Pb	Seth et al, 1998
	Nchanga,Zm	Nchanga red granite	583	90	673	493	w.r.	Rb-Sr	Snelling et al, 1972
BK-43	Kaoko belt, Hoanib River, NW Nm	Xenocrystic zircon in migmatite	584.3	1.6	586	583	zircon	Pb/Pb	Seth et al, 1998
BK-19	Kaoko belt, Hoanib River, NW Nm	Xenocrystic zircon in cg monzogranite	588.1	1.4	590	587	zircon	U-Pb	Seth et al, 1998
	Luangwa River, border Mozambique, Zm	Lower intercept, deformed orthogneiss	590	50	640	540	zircon	LAM ICPMS	Cox et al, 2002
KES232	Namibrand-Sesriem area	Hebron 136 Neuhof felsic volcanics	594	10	604	584	zircon	U-Pb	Burger & Walraven, 1978
KES232	Namibrand-Sesriem area	Hebron 136 Neuhof felsic volcanics	594	10	604	584	zircon	U-Pb	Burger & Walraven, 1978
BK-426	Kaoko belt, Hoanib River, NW Nm	Xenocrystic zircon in augen gneiss	620	42	662	578	zircon	U-Pb	Seth et al, 1998
BK-43	Kaoko belt, Hoanib River, NW Nm	Xenocrystic zircon in migmatite	625	9	634	616	zircon	U-Pb	Seth et al, 1998
	Lusaka Series,Zm	Vein in Lusaka series	630		630	630	Galena	Pb	Snelling et al, 1972
BK-426	Kaoko belt, Hoanib River, NW Nm	Xenocrystic zircon in augen gneiss	630	8	638	622	zircon	U-Pb	Seth et al, 1998
	Serenje area,Zm	Kalonga metasiltite	645	25	670	620	Muscovite	K-Ar	Snelling et al, 1972
BK-27	Kaoko belt, Hoanib River, NW Nm	Coarse-grain augen gneiss	656	8	664	648	zircon	U-Pb	Seth et al, 1998
	Mpande Dome,Zm	Microgranite	677	45	722	632	K-feldspa	Rb-Sr	Snelling et al, 1972
	Nkombwa Carbonatite,Zm	Fenite	680	25	705	655	Phlogopit	K-Ar	Snelling et al, 1972
	Lusaka Granite,Zm	Granite	681	28	709	653	K-feldspa	Rb-Sr	Snelling et al, 1972
	Mafingi Group Phyllite,Zm	Phyllite	690	20	710	670	w.r.	K-Ar	Snelling et al, 1972
	Old Millberg Claims,Zm	Galena	695		695	695	Galena	Pb	Snelling et al, 1972
	Lusaka Granite,Zm	Granite	700	28	728	672	K-feldspa	Rb-Sr	Snelling et al, 1972
	Rosh Pinah Formation,Nm		700		700	700			Hoffman, 1989
	Lusaka Granite,Zm	Granite	703	28	731	675	w.r.	Rb-Sr	Snelling et al, 1972
	Kabompo Dome, Zm	Met event (amphibolite facies)	708	7	715	701		K/Ar	Cosi et al, 1992
BK-426	Kaoko belt, Hoanib River, NW Nm	Xenocrystic zircon in augen gneiss	710	80	790	630	zircon	U-Pb	Seth et al, 1998
	Galena veins near Kabwe,Zm	Galena	712		712	712	Galena	Pb	Snelling et al, 1972
3DA-101	Kasai Shield, Zm	Met event	714	66	780	648	zircon	U-Pb	Key et al, 2001
	Mpande Dome,Zm	Microgranite	730	50	780	680	w.r.	Rb-Sr	Snelling et al, 1972
3DA-51	Kasai Shield, Zm	Met event	734	63	797	671	zircon	U-Pb	Key et al, 2001
	Chiwanda,Zm	Galena	734		734	734	Galena	Pb	Snelling et al, 1972
	Luamata, NWZm	Felsic volcanic	735	5	740	730	zircon	U-Pb	Key et al, 2001
	Oas Farm,Nm	Syenite	736		869	595	zircon	U-Pb	Tegtmeyer & Kroner, 1985
	Kabompo Dome, Zm	Met event (high pressure)	744	8	752	736		Rb/Sr	AGIP, 1985
	Lusaka Granite,Zm	Granite	745	70	815	675	w.r.	Rb-Sr	Snelling et al, 1972
	Lusaka Granite,Zm	Granite	745	30	775	715	w.r.	Rb-Sr	Snelling et al, 1972
L-716	Oas Farm, Nm (basement)	Host gtd	745	5	750	740	zircon	U-Pb	This report
L-047	Mombwezhi Dome, Zm	Quartzmonzonite	745.9	3.4	749	743	zircon	U-Pb	This report
	Lusaka Granite,Zm	Granite	746	30	776	716	K-feldspa	Rb-Sr	Snelling et al, 1972
PH.11.9	Summas Mountains,Nm	Rhyolitic lava flow	746	2	748	744	zircon	U-Pb	Hoffman et al, 1996
PH.12.9	Summas Mountains	Ash-flow tuff	746	2	744	748	zircon	U-Pb	Hoffman et al, 1996
PH.11.9	Lower Ugab rhyolite lava	Rhyolite lava	747	2	745	749	zircon	U-Pb	Hoffman et al, 1996
L-060	Kansanshi mine, Zm	Diorite	750	5	755	745	zircon	U-Pb	This report
L-142	MB-34 intrusives, Kasempa,Zm	Subvolcanic porphyritic intrusive	750	5	755	745	zircon	U-Pb	This report
L-758	Mesopotamie Farm,Nm	Graphic granite	750	5	755	745	zircon	U-Pb	This report
	Serenje area,Zm	Pegmatite	755	30	785	725	Muscovite	K-Ar	Snelling et al, 1972
PH.10.9	Oas Farm,Nm	Quartz syenite	756	2	758	754	zircon	U-Pb	Hoffman et al, 1996
L-688	Oas Farm,Nm (older intrusive)	Syenite intrusion	762	12	774	750	zircon	U-Pb	This report
	Lwanu basalt, Mwinilunga, NW Zm	Basalt	765	5	770	760	zircon	U-Pb	Key et al, 2001
L-172c	Nchanga open pit intrusives, Zm	Lamprophyre in borehole	765	3	768	762	zircon	U-Pb	This report
L-169	Nchanga open pit intrusives, Zm	Lamprophyre in borehole	765	3	768	762	zircon	U-Pb	This report
L-693	Oas Farm, Nm (young intrusive)	Dark subvolcanic intrusive (alkali gtd)	765	4.5	770	761	zircon	U-Pb	This report
	Lusaka Granite,Zm	Granite	770	25	795	745	w.r.	K-Ar	Snelling et al, 1972
	Mafingi Group Phyllite,Zm	Phyllite	770	25	795	745	w.r.	K-Ar	Snelling et al, 1972

RADIOMETRIC AGES IN CHRONOLOGICAL ORDER, GREATER LUFILIAN ARC (cont.) 3/8

sample	Site/Event	Rock type	age	error	max	min	material	type	reference
	Damara volcanics,Nm	Alkaline ignimbrites	780		840	720			Miller, 1999
	Oas Farm, Nm	Gtd	783	18	801	765	zircon	U-Pb	Burger & Kroner in Tegtmeyer,1985
	Lusaka Granite,Zm	Granite	790	32	822	758	w.r.	Rb-Sr	Barr et al, 1978
	Ngoma Gneiss, W Lusaka, Zm	Gneiss	820	7	827	813	zircon	U-Pb	Wilson,1993 in De Waele et al,2001a
	Luanshya mine, Zm	Pegmatite in lower Roan	840	40	880	800	Microcline	Rb-Sr	Snelling et al, 1972
PRU142	Oas Farm, Nm	Gtd	840	13	853	827	zircon	U-Pb	Kroner in Tegtmeyer,1985
	Lusaka Granite, W Lusaka, Zm	Granite	843	10	853	833			Cahen,1984 in De Waele & T,1999
	Lusaka Granite,Zm	Granite	846	68	914	778	zircon	U-Pb	Barr et al, 1978
	Isoka District, Zm	Porphyroblastic biotite gneiss	870	36	906	834	Biotite	K-Ar	Snelling et al, 1972
	Kibaran orogeny, D.R.Congo	pegmatites that cut Roan	870	42	912	828	K-feldspa	Rb-Sr	Caen et al, 1984
	Nchanga Red Granite,Zm	Gtd	877	5	882	872	zircon	U-Pb	Armstrong et al, 2004 (in prep)
	Kafue Rhyolites, W Lusaka, Zm	Rhyolite	879	19	898	860	zircon	U-Pb	Wardlaw in De Waele et al,2001a
	Nchanga open pit intrusives, Zm	inherited zircons	880	5	885	875	zircon	U-Pb	This report
	Serenje area,Zm	Kalonga metasiltstone	885	36	921	849	Muscovite	K-Ar	Snelling et al, 1972
	Isoka District, Zm	Porphyroblastic biotite gneiss	890	36	926	854	Biotite	K-Ar	Snelling et al, 1972
	Northeast of Chinsali,Zm	Biotite gneiss	905	36	941	869	Biotite	K-Ar	Snelling et al, 1972
	Richtersveld Intrusive Complex,Nm		920		920	920			Miller, 1999
	Rufunsa Area, Eastern Zm	Granite	927		927	927	zircon	U-Pb	Barr et al, 1978
RehBI	Gamsberg, Uitdraai granite	Ghoab Oos 381	930	70	1000	860	zircon	U-Pb	Hugo & Schalk, 1974
RehBI	Gamsberg, Uitdraai granite	Ghoab Oos 381	930	70	1000	860	zircon	U-Pb	Hugo & Schalk, 1974
RehBI	Gamsberg, Uitdraai granite	Ghoab Oos 381	932	50	982	882	zircon	U-Pb	Burger & Coertze, 1975
RehBI	Gamsberg, Uitdraai granite	Uitdraai Oos 296	932	50	982	882	zircon	U-Pb	Hugo & Schalk, 1974
RehBI	Gamsberg, Uitdraai granite	Ghoab Oos 381	932	50	982	882	zircon	U-Pb	Burger & Coertze, 1975
RehBI	Gamsberg, Uitdraai granite	Uitdraai Oos 296	932	50	982	882	zircon	U-Pb	Hugo & Schalk, 1974
	G4 gtd Irumide B.,Zm	Coarse biotite granite	943	5	948	938	zircon	shrimp U-Pb	De Waele et al, 2003c
	Rufunsa Area, Eastern Zm	Granite and porphyry	945	30	975	915	zircon	U-Pb	Barr et al, 1978
RehBI	Gamsberg S	Oorwinning 134	948	20	968	928	zircon	U-Pb	Burger & Coertze, 1975
KES5	Namibrand-Sesriem area	Oorwinning 134 granite	948	20	968	928	zircon	U-Pb	Burger & Coertze, 1975
RehBI	Gamsberg S	Oorwinning 134	948	20	968	928	zircon	U-Pb	Burger & Coertze, 1975
KES5	Namibrand-Sesriem area	Oorwinning 134 granite	948	20	968	928	zircon	U-Pb	Burger & Coertze, 1975
	Rufunsa Area, Eastern Zm	Porphyry	955		955	955	zircon	U-Pb	Barr et al, 1978
	near Kariba Dam, Zm	Amphibolite	960	30	990	930	Bt-w.r.	Rb-Sr	Snelling et al, 1972
	Chinsali, Irumide B., Zm	Kaunga Granite	970	5	975	965	zircon	U-Pb	Daly, 1986 in De Waele & Mapani, 2002
RehBI	Gamsberg S	Oorwinning 134	976	20	996	956	zircon	U-Pb	Burger & Coertze, 1978
KES13	Namibrand-Sesriem area	Oorwinning 134 porphyry	976	20	996	956	zircon	U-Pb	Burger & Coertze, 1975
RehBI	Gamsberg S	Oorwinning 134	976	20	996	956	zircon	U-Pb	Burger & Coertze, 1978
KES13	Namibrand-Sesriem area	Oorwinning 134 porphyry	976	20	996	956	zircon	U-Pb	Burger & Coertze, 1975
	Chinsali, N Irumide B.,Zm	Mutangoshi (or grey) biotite granite	1009	12	1021	997	zircon	shrimp U-Pb	De Waele & Mapani, 2002
RehBI	Gamsberg, Kobos granite	Nauzerus 1	1010	70	1080	940	zircon	U-Pb	Hugo & Schalk, 1974
RehBI	Gamsberg, Kobos granite	Nauzerus 1	1010	70	1080	940	zircon	U-Pb	Hugo & Schalk, 1974
	Namaqua, Nm	Luderitz Tschaukaib granite	1012	10	1022	1002	zircon	U-Pb	Burger, 1976
	Namaqua, Nm	Luderitz Tschaukaib granite	1012	10	1022	1002	zircon	U-Pb	Burger, 1976
	Serenje area, Zm	Sasa, leucocratic biotite porphyritic granite	1018	6	1024	1012	zircon	shrimp U-Pb	De Waele et al,2001a
	Namaqua, Nm	Luderitz Tschaukaib granite	1018	10	1028	1008	zircon	U-Pb	Burger, 1976
	Namaqua, Nm	Luderitz Tschaukaib granite	1018	10	1028	1008	zircon	U-Pb	Burger, 1976
	Mutangoshi granite, N Irumide B.,Zm	Mesocratic, fine-grained granite	1021	3	1024	1018	zircon	shrimp U-Pb	De Waele & Mapani, 2002
	Serenje area, Zm	Porphyritic granite	1022	12	1034	1010	zircon	shrimp U-Pb	De Waele et al,2001a
	Namaqua, Nm	Luderitz Glockenberg granite	1022	10	1032	1012	zircon	U-Pb	Burger, 1976
	Namaqua, Nm	Luderitz Glockenberg granite	1022	10	1032	1012	zircon	U-Pb	Burger, 1976
	Serenje area, Zm	Porphyritic granite	1024	13	1037	1011	zircon	shrimp U-Pb	De Waele et al,2001a
	Serenje area, Zm	Porphyritic granite	1025	10	1035	1015	zircon	shrimp U-Pb	De Waele et al,2001a
	G4 gtd. W Irumide B.,Zm	Anorogenic porph biot granite gneiss	1027	13	1040	1014	zircon	shrimp U-Pb	De Waele et al, 2003c
BK-27	Kaoko belt, Hoanib River, NW Nm	Xenocrystic zircon in augen gneiss	1032	130	1162	902	zircon	U-Pb	Seth et al, 1998
	Serenje area, Zm	Porphyritic granite	1033	15	1048	1018	zircon	shrimp U-Pb	De Waele et al, 2002b
	G4 gtd Irumide B.,Zm	Coarse biotite granite	1036	13	1049	1023	Nd isotop	shrimp U-Pb	De Waele et al, 2003b
	G4 gtd Irumide B.,Zm	Coarse biotite granite	1037	16	1053	1021	Nd isotop	shrimp U-Pb	De Waele et al, 2003b
	Serenje area, Zm	Porphyritic granite	1038	10	1048	1028	zircon	shrimp U-Pb	De Waele et al,2001a; De Waele & M, 2002
	G4 gtd Irumide B.,Zm	Coarse biotite granite	1042	47	1042	948	zircon	shrimp U-Pb	De Waele et al, 2003c
	Luangwa River, border Mozambique, Zm	Metamorphism, deformed orthogneiss	1043	19	1062	1024	zircon	LAM ICPMS	Cox et al, 2002
	Phoenix mica claims,Zm	Pegmatite	1045	30	1075	1015	Muscovite	Rb-Sr	Snelling et al, 1972
	Phoenix mica claims,Zm	Pegmatite	1050	40	1090	1010	Muscovite	Rb-Sr	Snelling et al, 1972
BK-426	Kaoko belt, Hoanib River, NW Nm	Xenocrystic zircon in augen gneiss	1052	4	1056	1048	zircon	U-Pb	Seth et al, 1998
	Namaqua, Nm	Townlands tonalitic augengneiss	1052	10	1062	1042	zircon	U-Pb	Burger, 1976
	Namaqua, Nm	Townlands tonalitic augengneiss	1052	10	1062	1042	zircon	U-Pb	Burger, 1976
	Mutangoshi granite, N Irumide B.,Zm	Coarse-grained felsic granite	1053	7	1060	1046	zircon	shrimp U-Pb	De Waele & Mapani, 2002
	G4 gtd. W Irumide B.,Zm	Anorogenic porph biot granite gneiss	1055	13	1068	1042	zircon	shrimp U-Pb	De Waele et al, 2003c
	G4 gtd Irumide B.,Zm	Coarse biotite granite	1055	13	1068	1042	zircon	shrimp U-Pb	De Waele et al, 2003c

RADIOMETRIC AGES IN CHRONOLOGICAL ORDER, GREATER LUFILIAN ARC (cont.) 4/8

sample	Site/Event	Rock type	age	error	max	min	material	type	reference
	Mtuga aplites, Mkushi,Zm	emplacement of aplite	1059	26	1085	1033	zircon	U-Pb	Rainaud, et al, 2004
RehBl	Gamsberg, Kobos granite	Kanaus S 336	1064	20	1084	1044	zircon	U-Pb	Burger & Coertze, 1975
RehBl	Gamsberg, Kobos granite	Kanaus S 336	1064	20	1084	1044	zircon	U-Pb	Burger & Coertze, 1975
	Chipata Area, Eastern Zm	Granitic orthogneiss	1071	8	1079	1063	zircon	Pb/Pb	Haslam et al, 1986
RehBl	Gamsberg, Gamsberg granite	Gamsberg 23	1077	26	1202	1010	zircon	U-Pb	Nagel, 2000
RehBl	Gamsberg, Gamsberg granite	Gamsberg 23	1077	26	1202	1010	zircon	U-Pb	Nagel, 2000
RehBl	Gamsberg, Gamsberg granite	Hohenheim 24	1078	30	1108	1048	zircon	U-Pb	Burger & Coertze, 1975
RehBl	Gamsberg, Gamsberg granite	Hohenheim 24	1078	30	1108	1048	zircon	U-Pb	Burger & Coertze, 1975
RehBl	Gamsberg, Gamsberg granite	Gamsberg 23	1079	30	1142	1038	zircon	U-Pb	Nagel, 2000
RehBl	Gamsberg, Gamsberg granite	Gamsberg 23	1079	30	1142	1038	zircon	U-Pb	Nagel, 2000
RehBl	Gamsberg, Gamsberg granite	Hohenheim 24	1080	70	1150	1010	zircon	U-Pb	Hugo & Schalk, 1974
	Namaqua, Nm	Hottentots Bay Namaqua augengneiss	1080	10	1090	1070	zircon	U-Pb	Burger, 1976
	Namaqua, Nm	Hottentots Bay Namaqua augengneiss	1080	10	1090	1070	zircon	U-Pb	Burger, 1976
RehBl	Gamsberg, Gamsberg granite	Hohenheim 24	1080	70	1150	1010	zircon	U-Pb	Hugo & Schalk, 1974
	Namaqua, Nm	Grasplatz quartz monzonitic gneiss	1082	10	1092	1072	zircon	U-Pb	Burger, 1976
	Namaqua, Nm	Grasplatz quartz monzonitic gneiss	1082	10	1092	1072	zircon	U-Pb	Burger, 1976
RehBl	Nauzerus G, Kartatsaus F	Uitdraai Oos 296	1083	30	1113	1053	zircon	U-Pb	Burger & Coertze, 1975
RehBl	Nauzerus G, Kartatsaus F	Uitdraai Oos 296	1083	30	1113	1053	zircon	U-Pb	Burger & Coertze, 1975
RehBl	Gamsberg, Rostock granite	Greilingshof 107	1084	8	1092	1076	zircon	U-Pb	Pfurr et al, 1990
RehBl	Gamsberg, Rostock granite	Greilingshof 107	1084	8	1092	1076	zircon	U-Pb	Pfurr et al, 1990
	Namaqua, Nm	Luderitz Glockenberg granite	1086	10	1096	1076	zircon	U-Pb	Burger, 1976
	Namaqua, Nm	Luderitz Glockenberg granite	1086	10	1096	1076	zircon	U-Pb	Burger, 1976
	Mkushi Gneiss, Zm	Granitic gneiss (zircon rims)	1088	159	1247	929	zircon	shrimp U-Pb	Robb in De Waele et al,2001a
RehBl	Gamsberg, Gamsberg granite	Abendruhe 411	1089	30	1119	1059	zircon	U-Pb	Burger & Coertze, 1975
RehBl	Gamsberg, Gamsberg granite	Abendruhe 411	1089	30	1119	1059	zircon	U-Pb	Burger & Coertze, 1975
RehBl	Nauzerus G, Kartatsaus F	Kaartatsaus 293	1090	30	1120	1060	zircon	U-Pb	Burger & Coertze, 1975
RehBl	Nauzerus G, Kartatsaus F	Kaartatsaus 293	1090	70	1160	1020	zircon	U-Pb	Hugo & Schalk, 1974
RehBl	Nauzerus G, Kartatsaus F	Kaartatsaus 293	1090	70	1160	1020	zircon	U-Pb	Hugo & Schalk, 1974
RehBl	Nauzerus G, Kartatsaus F	Kaartatsaus 293	1090	30	1120	1060	zircon	U-Pb	Burger & Coertze, 1975
RehBl	Nauzerus G, Kartatsaus F	Kaartatsaus 293	1090	70	1160	1020	zircon	U-Pb	Hugo & Schalk, 1974
RehBl	Nauzerus G, Kartatsaus F	Kaartatsaus 293	1090	70	1160	1020	zircon	U-Pb	Hugo & Schalk, 1974
RehBl	Oorlogsende F	Epukiro area	1094	30	1112	1074	zircon	U-Pb	Hegenberger & Burger, 1985
RehBl	Oorlogsende F	Epukiro area	1094	30	1112	1074	zircon	U-Pb	Hegenberger & Burger, 1985
	Mpande Dome (south), Southern Zm	Fine-grained granite	1095	12	1107	1083	zircon	U-Pb	De Waele et al, 2000a
RehBl	Gamsberg, Gamsberg granite	Gamsberg 23	1095	30	1216	1074	zircon	U-Pb	Nagel, 2000
RehBl	Gamsberg, Gamsberg granite	Gamsberg 23	1095	30	1216	1074	zircon	U-Pb	Nagel, 2000
RehBl	Gamsberg, Rostock granite	Greilingshof 107	1097	24	1121	1073	zircon	U-Pb	Pfurr et al, 1990
RehBl	Gamsberg, Rostock granite	Greilingshof 107	1097	24	1121	1073	zircon	U-Pb	Pfurr et al, 1990
RehBl	Gamsberg, Rostock granite	Greilingshof 107	1099	16	1115	1083	zircon	U-Pb	Pfurr et al, 1990
RehBl	Gamsberg, Rostock granite	Greilingshof 107	1099	16	1115	1083	zircon	U-Pb	Pfurr et al, 1990
	Lusaka Granite,Zm	Granite	1100	70	1170	1030	Plagioclas	Rb-Sr	Snelling et al, 1972
RehBl	Gamsberg, Rostock granite	Rostock S 414	1102	7	1109	1095	zircon	U-Pb	Pfurr et al, 1990
RehBl	Gamsberg, Rostock granite	Rostock S 414	1102	7	1109	1095	zircon	U-Pb	Pfurr et al, 1990
RehBl	Gamsberg, Koichas granite	Kangas 371	1104	20	1124	1084	zircon	U-Pb	Burger & Coertze, 1975
RehBl	Gamsberg, Koichas granite	Kangas 371	1104	20	1124	1084	zircon	U-Pb	Burger & Coertze, 1975
	Mpande Gneiss, Southern Zm	Granitic orthogneiss	1106	19	1125	1087	zircon	U-Pb	Hanson et al, 1988, 1994
RehBl	Gamsberg, Biesespoort granite	Biesiepoort 275	1110	30	1140	1080	zircon	U-Pb	Burger & Coertze, 1978
RehBl	Gamsberg, Gamsberg granite	Nauzerus 1	1110	30	1140	1080	zircon	U-Pb	Burger & Coertze, 1975
RehBl	Gamsberg, Biesespoort granite	Biesiepoort 275	1110	30	1140	1080	zircon	U-Pb	Burger & Coertze, 1978
RehBl	Gamsberg, Gamsberg granite	Nauzerus 1	1110	30	1140	1080	zircon	U-Pb	Burger & Coertze, 1975
	Namaqua, Nm	Hottentots Bay Namaqua augengneiss	1114	10	1124	1104	zircon	U-Pb	Burger, 1976
	Namaqua, Nm	Hottentots Bay Namaqua augengneiss	1114	10	1124	1104	zircon	U-Pb	Burger, 1976
	Namaqua, Nm	Jannelspan F. Garub station, Aus biot schist	1116	10	1126	1106	zircon	U-Pb	Burger, 1976
	Namaqua, Nm	Jannelspan F. Garub station, Aus biot schist	1116	10	1126	1106	zircon	U-Pb	Burger, 1976
	Mafingi Hills,Zm	Granite gneiss	1120	30	1150	1090	Plagioclas	Rb-Sr	Snelling et al, 1972
RehBl	Oorlogsende F	Epukiro area	1127	30	1157	1097	zircon	U-Pb	Burger & Walraven, 1980
RehBl	Oorlogsende F	Epukiro area	1127	30	1157	1097	zircon	U-Pb	Burger & Walraven, 1980
RehBl	Nauzerus G, Nuckopf F	Lekkerwater 144	1130	75	1205	1055	zircon	U-Pb	Ziegler & Stoessel, 1993
RehBl	Nauzerus G, Nuckopf F	Lekkerwater 144	1130	75	1205	1055	zircon	U-Pb	Ziegler & Stoessel, 1993
	Namaqua, Nm	Luderitz felsic volcanics	1131	10	1141	1121	zircon	U-Pb	Burger, 1976
	Namaqua, Nm	Luderitz felsic volcanics	1131	10	1141	1121	zircon	U-Pb	Burger, 1976
RehBl	Gamsberg, Gamsberg granite	Gamsberg 23	1132	26	1158	1106	zircon	U-Pb	Ziegler & Stoessel, 1993
RehBl	Nauzerus G, Nuckopf F	Kunineib 378	1132	75	1207	1057	zircon	U-Pb	Hilken, 1977
	Namaqua, Nm	Luderitz felsic volcanics	1132	10	1142	1122	zircon	U-Pb	Burger, 1976
	Namaqua, Nm	Luderitz felsic volcanics	1132	10	1142	1122	zircon	U-Pb	Burger, 1976
RehBl	Gamsberg, Gamsberg granite	Gamsberg 23	1132	26	1158	1106	zircon	U-Pb	Ziegler & Stoessel, 1993
RehBl	Nauzerus G, Nuckopf F	Kunineib 378	1132	75	1207	1057	zircon	U-Pb	Hilken, 1977
RehBl	Oorlogsende F	Epukiro area	1144	30	1174	1114	zircon	U-Pb	Burger & Walraven, 1979
RehBl	Oorlogsende F	Epukiro area	1144	30	1174	1114	zircon	U-Pb	Burger & Walraven, 1979
	Mafingi Hills,Zm	Lamprophyre	1145	60	1205	1085	riebeckite	K-Ar	Snelling et al, 1972
RehBl	Gamsberg, Ganeib granite	Danigas 289	1150	30	1180	1120	zircon	U-Pb	Burger & Coertze, 1975
RehBl	Gamsberg, Ganeib granite	Danigas 289	1150	30	1180	1120	zircon	U-Pb	Burger & Coertze, 1975
KES7	Namibrand-Sesriem area	Sesriem 134 Eesaam F	1170	30	1200	1140	zircon	U-Pb	Burger & Coertze, 1975
KES7	Namibrand-Sesriem area	Sesriem 134 Eesaam F	1170	30	1200	1140	zircon	U-Pb	Burger & Coertze, 1975
CK4	Choma-Kalomo Batholith, Zm	Medium-grained two mica granite	1174	27	1201	1147	zircon	shrimp U-Pb	Bulambo et al, 2004
CK12	Choma-Kalomo Batholith, Zm	Gneiss containing mica-rich restites	1177	70	1247	1107	zircon	shrimp U-Pb	Bulambo et al, 2004
RehBl	Gamsberg, Kobos granite	Nauchas 14	1178	20	1198	1158	zircon	U-Pb	Burger & Coertze, 1975
	Namaqua, Nm	Luderitz Glockenberg granite	1178	10	1188	1168	zircon	U-Pb	Burger, 1976

RADIOMETRIC AGES IN CHRONOLOGICAL ORDER, GREATER LUFILIAN ARC (cont.) 5/8

sample	Site/Event	Rock type	age	error	max	min	material	type	reference
	Namaqua, Nm	Luderitz Glockenberg granite	1178	10	1188	1168	zircon	U-Pb	Burger, 1976
RehBl	Gamsberg, Kobos granite	Nauchas 14	1178	20	1198	1158	zircon	U-Pb	Burger & Coertze, 1975
CK25	Choma-Kalomo Batholith, Zm	Foliated, med-coarse-g biotite granite	1181	9	1190	1172	zircon	shrimp U-Pb	Bulambo et al, 2004
	Namaqua, Nm	Luderitz felsic volcanics	1184	10	1194	1174	zircon	U-Pb	Burger, 1976
	Namaqua, Nm	Luderitz felsic volcanics	1184	10	1194	1174	zircon	U-Pb	Burger, 1976
RehBl	Gamsberg, Gamsberg granite	Corona 223	1186	30	1240	1147	zircon	U-Pb	Nagel, 2000
RehBl	Gamsberg, Gamsberg granite	Corona 223	1186	30	1240	1147	zircon	U-Pb	Nagel, 2000
CK10	Choma-Kalomo Batholith, Zm	Foliated med-coarse-g biotite granite	1188	11	1199	1177	zircon	shrimp U-Pb	Bulambo et al, 2004
L-638	Okatjepuiko,Nm xenocrystic	Granitoid	1194	11	1205	1183	zircon	Pb/U shrimp	This report
RehBl	Gamsberg, Rostock granite	Rostock S 414	1194	26	1220	1168	zircon	U-Pb	Pfurr et al, 1990
	Namaqua, Nm	Luderitz Glockenberg granite	1194	10	1204	1184	zircon	U-Pb	Burger, 1976
	Namaqua, Nm	Luderitz Glockenberg granite	1194	10	1204	1184	zircon	U-Pb	Burger, 1976
RehBl	Gamsberg, Rostock granite	Rostock S 414	1194	26	1220	1168	zircon	U-Pb	Pfurr et al, 1990
	Basement, Kabompo Dome,Zm	Gtd	1200	50	1250	1150	zircon	U-Pb	AGIP, 1985
	Lusaka Granite,Zm	Granite	1200	96	1296	1104	Plagioclas	Rb-Sr	Snelling et al, 1972
RehBl	Gamsberg, Rostock granite	Rostock N 393	1207	15	1222	1192	zircon	U-Pb	Pfurr et al, 1990
RehBl	Gamsberg, Rostock granite	Rostock N 393	1207	15	1222	1192	zircon	U-Pb	Pfurr et al, 1990
RehBl	porphyry dike	Marienhof 577	1210	7	1217	1203	zircon	U-Pb	Ziegler & Stoessel, 1993
RehBl	Gamsberg S	Morgenroth 17	1210	8	1218	1202	zircon	U-Pb	Ziegler & Stoessel, 1993
RehBl	porphyry dike	Marienhof 577	1210	7	1217	1203	zircon	U-Pb	Ziegler & Stoessel, 1993
RehBl	Gamsberg S	Morgenroth 17	1210	8	1218	1202	zircon	U-Pb	Ziegler & Stoessel, 1993
RehBl	Nauzerus G, Nuckopf F	Areb North 202	1221	35	1257	1192	zircon	U-Pb	Schalk, 1970
RehBl	Nauzerus G, Nuckopf F	Areb North 202	1221	35	1257	1192	zircon	U-Pb	Schalk, 1970
RehBl	Nauzerus G, Kartatsaus F	Spitskop F	1232	30	1262	1202	zircon	U-Pb	Burger & Coertze, 1978
RehBl	Nauzerus G, Kartatsaus F	Spitskop F	1232	30	1262	1202	zircon	U-Pb	Burger & Coertze, 1978
	Namaqua, Nm	Luderitz granite	1233	10	1243	1223	zircon	U-Pb	Burger, 1976
	Namaqua, Nm	Luderitz granite	1233	10	1243	1223	zircon	U-Pb	Burger, 1976
	Namaqua, Nm	Luderitz granite	1264	10	1274	1254	zircon	U-Pb	Burger, 1976
	Namaqua, Nm	Luderitz granite	1264	10	1274	1254	zircon	U-Pb	Burger, 1976
	Aunis Gneiss, Awasib Mtns,Nm	Tonalite gneiss	1271	62	1333	1209			Hoal, 1990
KES231	Namibrand-Sesriem area	Hebron 136 Neuhof felsic volcanics	1294	25	1319	1269	zircon	U-Pb	Burger & Walraven, 1978
KES231	Namibrand-Sesriem area	Hebron 136 Neuhof felsic volcanics	1294	25	1319	1269	zircon	U-Pb	Burger & Walraven, 1978
KES9	Namibrand-Sesriem area	Draaihook 119 Nubib granite	1302	20	1322	1282	zircon	U-Pb	Burger & Coertze, 1975
KES9	Namibrand-Sesriem area	Draaihook 119 Nubib granite	1302	20	1322	1282	zircon	U-Pb	Burger & Coertze, 1975
	Lusaka Granite,Zm	Granite	1305	65	1370	1240	Plagioclas	Rb-Sr	Snelling et al, 1972
RehBl	Oorlogsende F	Epukiro area	1313	30	1343	1283	zircon	U-Pb	Burger & Walraven, 1980
RehBl	Oorlogsende F	Epukiro area	1313	30	1343	1283	zircon	U-Pb	Burger & Walraven, 1980
	Orue gneisses, S Angola	Gneiss	1334	21	1355	1313	zircon	U-Pb	Bassot et al, 1981
	Mivula Hill, Central Irumide B., Zm	Syenite	1341	16	1357	1325	w.r.	Rb-Sr	Tembo in De Waele et al, 2000a
KES6	Namibrand-Sesriem area	Sesriem 134 Nubib granite	1350	40	1390	1310	zircon	U-Pb	Burger & Coertze, 1975
KES6	Namibrand-Sesriem area	Sesriem 134 Nubib granite	1350	40	1390	1310	zircon	U-Pb	Burger & Coertze, 1975
	Siasikobole granite, Choma-Kalomo,Zm	Granite	1352	14	1366	1338	zircon	U-Pb	Hanson et al, 1998b
CK13	Choma-Kalomo Batholith, Zm	Augen (ortho) gneiss	1368	10	1378	1358	zircon	shrimp U-Pb	Bulambo et al, 2004
	Lusenga Syenite,Zm	Syenite	1390	200	1590	1190	w.r.	Rb-Sr	Snelling et al, 1972
	Chewore Ophiolite, Zm	Plagiogranite sheet in ophiolite	1393	22	1415	1371	zircon	shrimp U-Pb	Johnson & Oliver, 2000; Oliver, et al, 1998
	Magmatic event in Irumide B., Zm	Large syntectonic granite bodies	1407	39	1446	1368	w.r.	Rb-Sr	Daly, 1986; De Waele et al, 2000a
	Ufipa Gneiss near Mbala,Zm	Gneiss	1425	50	1475	1375	Biotite	K-Ar	Snelling et al, 1972
	Alberta Basic Complex,Rehoboth,Nm	Layered gabbroic rocks	1442	32	1474	1410			Reid et al, 1988
	Khairab Basalt, Awasib Mtns,Nm	Mafic high-alumina metavolcanic rocks	1460		1460	1460			Hoal, 1990
BK-17	Kaoko belt, Hoanib River, NW Nm	Foliated red granitic gneiss	1507	16	1523	1491	zircon	U-Pb	Seth et al, 1998
	Rehoboth Area, Nm	Granitic and basic rocks	1545		1670	1420			Miller, and Shalk, 1988
	Kamfinsa Quarry,Zm	Pegmatite	1550	50	1600	1500	Biotite	K-Ar	Snelling et al, 1972
	G2 gtd. Lubu Gt, W Irumide B.Zm	Granite gneiss	1551	33	1584	1518	zircon	shrimp U-Pb	De Waele et al, 2003c
3DA-57	Kasai Shield, NW Zm	Aphyric med-g gtd	1561	10	1571	1551	zircon	U-Pb	Key et al, 2001
	Kamanjab Batholith,Nm	tectonic activity	1580	20	1600	1560	zircon	U-Pb	Burger et al, 1976
	Lumi gneissic granite,Zm	Granite	1590	50	1640	1540	Biotite	K-Ar	Snelling et al, 1972
	G2 Mutangoshi/Musalango gn, N Irumide B.Zm	Anorogenic porph biot granite gneiss	1610	26	1636	1584	zircon	shrimp U-Pb	De Waele et al, 2003c
	Mkushi area,Zm	Aplite cutting Mkushi Gneiss	1625	50	1675	1575	w.r.	Rb-Sr	Snelling et al, 1972
	G2 Lukamfwa Hill gtd.W Irumide B.,Zm	Anorogenic porph biot granite gneiss	1627	12	1639	1615	zircon	shrimp U-Pb	De Waele et al, 2003c
	Luanshya mine, Zm	Pegmatite in Lufubu	1635	180	1815	1455	K-feldspa	Rb-Sr	Snelling et al, 1972
	G2 Lukamfwa Hill gtd.W Irumide B.,Zm	Anorogenic porph biot granite gneiss	1639	14	1653	1625	zircon	shrimp U-Pb	De Waele et al, 2003c
	Swartmodder Granite,Rehoboth,Nm	Leucocratic granite	1639	25	1664	1614			Reid et al, 1988 and Shalk, 1988
	Serenje area, Irumide B.,Zm	Granite gneiss	1647	10	1657	1637	zircon	shrimp U-Pb	De Waele & Mapani, 2002
	G2 Lukamfwa Hill gtd.W Irumide B.,Zm	Anorogenic porph biot granite gneiss	1650	4	1654	1646	zircon	shrimp U-Pb	De Waele et al, 2003c
KES230	Namibrand-Sesriem area	Sesriem 137 Eensam qtz porphyry	1656	40	1696	1616	zircon	U-Pb	Burger & Walraven, 1978
KES230	Namibrand-Sesriem area	Sesriem 137 Eensam qtz porphyry	1656	40	1696	1616	zircon	U-Pb	Burger & Walraven, 1978
	Serenje area, Irumide B.,Zm	Granite gneiss	1661	8	1669	1653	zircon	shrimp U-Pb	De Waele & Mapani, 2002
	Franzfontein Granite, Nm	Granite	1662	30	1692	1632	zircon	U-Pb	Burger et al, 1976
	G2 Lukamfwa Hill gtd.W Irumide B.,Zm	Anorogenic porph biot granite gneiss	1664	4	1668	1660	zircon	shrimp U-Pb	De Waele et al, 2003c
L-758	Mesopotamie Farm,Nm	inherited zircons in gtd	1692	10	1702	1682	zircon	U-Pb	This report
L-796	Ugab,Nm	inherited zircons in gtd	1700	10	1710	1690	zircon	U-Pb	This report
	Naub Diorite, Rehoboth Area,Nm	hornblende-biotite gneiss	1725	52	1777	1673			Reid et al, 1988
	Kate granite, Tanzania	Granite	1725	70	1795	1655	K-feldspa	Rb-Sr	Snelling et al, 1972

RADIOMETRIC AGES IN CHRONOLOGICAL ORDER, GREATER LUFILIAN ARC (cont.) 6/8

sample	Site/Event	Rock type	age	error	max	min	material	type	reference
	Namaqua, Nm	Luderitz augen gneiss	1742	10	1752	1732	zircon	U-Pb	Burger, 1976
	Namaqua, Nm	Luderitz augen gneiss	1742	10	1752	1732	zircon	U-Pb	Burger, 1976
PRU141	Huab Complex,Nm	Granitic gneiss	1749		1827	1679	zircon	U-Pb	Tegtmeyer & Kroner, 1985
	Roan Antelope mine,Zm	Granite	1750	50	1800	1700	K-feldspa	K-Ar	Snelling et al, 1972
L-728	Lofdal Farm,Nm	Foliated Gtd	1750	5	1755	1745	zircon	U-Pb	This report
	Haib porphyry Cu deposit,Nm	Metamorphism	1750	20	1770	1730		Rb-Sr	Minnit, 1986; Barr & Reid, 1993
	Namaqua, Nm	Luderitz augen gneiss	1752	10	1762	1742	zircon	U-Pb	Burger, 1976
	Namaqua, Nm	Luderitz augen gneiss	1752	10	1762	1742	zircon	U-Pb	Burger, 1976
	Namaqua, Nm	Luderitz hbl-gneiss	1755	10	1765	1745	zircon	U-Pb	Burger, 1976
	Namaqua, Nm	Luderitz hbl-gneiss	1755	10	1765	1745	zircon	U-Pb	Burger, 1976
RehBI	Nauzerus G, Nuckopf F	Auchas 347	1770	35	1805	1735	zircon	U-Pb	Burger & Coertze, 1978
RehBI	Nauzerus G, Nuckopf F	Auchas 347	1770	35	1805	1735	zircon	U-Pb	Burger & Coertze, 1978
RehBI	Gamsberg, Kobos granite	Kwakwas 251	1775	10	1785	1765	zircon	U-Pb	Nagel, 2000
RehBI	Gamsberg, Kobos granite	Kwakwas 251	1775	10	1785	1765	zircon	U-Pb	Nagel, 2000
	Plateau Series,Zm	Pegmatite cutting Plateau Series	1785	70	1855	1715	K-feldspa	K-Ar	Snelling et al, 1972
	Epupa Complex,Nm	Augen gneiss	1795		1828	1766	zircon	U-Pb	Tegtmeyer & Kroner, 1985
	Elim Formation, Rehoboth Area,Nm	Quartzites, siliciclastics and volcanics	1795		1860	1730			Miller, 1999
PRU144	Huab Complex,Nm	Gtd	1811		1850	1776	zircon	U-Pb	Tegtmeyer & Kroner, 1985
	Khoabendus Group,Nm	Felsic metavolcanics	1813		1860	1765	zircon	U-Pb	Burger & Coertze, 1973
	Franzfontein Granite, Nm	Granite	1838	30	1868	1808	zircon	U-Pb	Burger et al, 1976
	Kalumbila, NW Zm	sediments	1845		1860	1830	zircon	U-Pb	Steven & Armstrong, 2000
	Manshya River Group, Irumide B., Zm	Rhyolitic tuff	1856	4	1860	1852	zircon	shrimp U-Pb	De Waele et al, 2003c
	Etoile mine, D.R.Congo	Roan Group tuff (xenocrystic zircons)	1858	24	1882	1834	zircon	U-Pb	Rainaud, et al, 2004
L-169	Nchanga Intrusives, Zm	Lamprophyre in borehole (inherited zircons)	1860	10	1870	1850	zircon	U-Pb	This report
	Mansa, Irumide B., Zm	Undeformed biot. Gt into Luapula volcs.	1860	13	1873	1847	zircon	shrimp U-Pb	De Waele et al, 2003c
	Mansa, Irumide B., Zm	Undeformed biot. Gt into Luapula volcs.	1862	8	1870	1854	zircon	shrimp U-Pb	De Waele et al, 2003c
	Mansa, Irumide B., Zm	Luapula acid volcanics	1862	19	1881	1843	zircon	shrimp U-Pb	De Waele et al, 2003c
	Gelbingen Farm, Nm	Quartz eye rhyolite	1862	6	1868	1856	zircon	U-Pb	Steven & Armstrong, 2002
L-075	Muliashi Porphyry,Zm	Rapakivi granite	1865	5.4	1870	1860	zircon	U-Pb	This report
	Mansa, Irumide B., Zm	Undeformed biot. Gt into Luapula volcs.	1866	9	1875	1857	zircon	shrimp U-Pb	De Waele et al, 2004a
L-993	Kamanjab Batholith,Nm	Granite	1866	13	1853	1879	zircon	U-Pb	This report
L-160	Konkola Deep Borehole,Zm	Undeformed white gtd	1866	5.4	1872	1861	zircon	U-Pb	This report
L-160	Konkola Deep Borehole,Zm	Gray gtd	1868	4.8	1873	1863	zircon	shrimp concordia age	This report
	Mansa, Irumide B., Zm	Luapula acid volcanics	1868	7	1875	1861	zircon	shrimp U-Pb	De Waele et al, 2003c
L-638	Okatjepuiko,Nm xenocrystic	Granitoid	1871	6.8	1878	1864	zircon	Pb/Pb shrimp	This report
	Weener Quartz Diorite,Rehoboth,Nm	Medium-grained quartzdiorite	1871	143	2014	1728			Seifert, 1986
L-213	Old Kafue Basement,Zm	Inherited zircons in syenite	1872	14	1886	1858	zircon	U-Pb	This report
	Kinsenda Lufubu Schist, Luina Dome, D.R.Congo	metatrachyandesite	1874	8.3	1882	1865	zircon	U-Pb	Rainaud et al, 2004
L-158	Konkola Deep Borehole,Zm	Foliated pink gtd	1874	14	1888	1860	zircon	U-Pb	This report
L-1013	Kamanjab Batholith,Nm	Quartzmonzonite	1878	15	1863	1893	zircon	U-Pb	This report
	Manshya River Group, Irumide B., Zm	Rhyolitic tuff	1879	13	1892	1866	zircon	shrimp U-Pb	De Waele et al, 2003c
	Muva sequence, SW Chinsali, Zm	Conformable metarhyolite	1880	12	1892	1868	zircon	shrimp U-Pb	De Waele & Mapani, 2002
	Kamanjab inlier, Nm	bimodal vulc + intrusion	1880	80	1960	1800	zircon	U-Pb	Burger et al, 1976
	Kalumbila, NW Zm	sediments	1887		1896	1878	zircon	U-Pb	Steven & Armstrong, 2000
L-943	Kamanjab Batholith,Nm	Granite	1887	39	1848	1926	zircon	U-Pb	This report
	Lorelei porphyry Cu-Mo,Nm	Granodiorite	1900	50	1950	1850		inferred	Viljoen, Minnit,Viljoen, 1986
	Haib porphyry Cu deposit,Nm	Gtd	1900	5	1905	1895	zircon	U-Pb	Reid, personal communication, 2003
	Kalumbila, NW Zm	sediments	1919		1924	1913	zircon	U-Pb	Steven & Armstrong, 2000
	Ababis Inlier, Nm	Basement gneisses	1925		2255	1645	zircon	U-Pb	Jacob et al, 1978
L-030	Mwinilunga, NW Zm	Foliated Gtd	1928	7.1	1935	1921	zircon	U-Pb	This report
	Kabompo Dome, Zm	Feldspar-phyric gtd	1934	6	1940	1928	zircon	U-Pb	Key et al, 2001
	Luwalizi Granite, NE Irumide B., Zm	Weakly deformed granite	1937	10	1947	1927	zircon	shrimp U-Pb	De Waele et al, 2003c
L-868	Kamanjab Batholith,Nm	Quartzmonzonite	1937	14	1923	1951	zircon	U-Pb	This report
L-855	Kamanjab Batholith,Nm	Granite	1937	19	1918	1956	zircon	U-Pb	This report
L-1045	Grootfontein Inlier, Nm	Quartzmonzonite	1939	64	1875	2003	zircon	U-Pb	This report
	Kabompo Dome, Zm	Feldspar-phyric gtd	1940	2.8	1943	1937	zircon	U-Pb	Key et al, 2001
	Luwalizi Granite, NE Irumide B., Zm	Weakly deformed granite	1942	6	1948	1936	zircon	shrimp U-Pb	De Waele et al, 2003c
	Tumas Dome, Nm	Basement gneisses	1945	18	1963	1927	zircon	U-Pb	Jacob et al, 1978, Burger & Jacob, unpub. data in Kroner et al, 1991
	Kalumbila, NW Zm	sediments	1946		1952	1939	zircon	U-Pb	Steven & Armstrong, 2000
	Namaqua, Nm	Luderitz Kunguib granodiorite	1952	10	1962	1942	zircon	U-Pb	Burger, 1976
	Namaqua, Nm	Luderitz Kunguib granodiorite	1952	10	1962	1942	zircon	U-Pb	Burger, 1976
	Kaoko Belt, 45 km NW Sesfontein,Nm	partly sheared monzogranite	1961	0.6	1962	1960	zircon	U-Pb	Hoffman & Kroner, unpub in Seth, 1998
BK-439	Kaoko belt, NW Nm	Cg monzogranitic augen gneiss	1961	4	1965	1957	zircon	U-Pb	Seth et al, 1998
	Damaran metased, Navachab mine, Nm	Detrital zircons in Damaran metaseds	1962	10	1972	1952	zircon	U-Pb	Jacob et al, 2003
	Samba Cu prospect,Zm	felsic metavolcanic schist	1964	12	1976	1952	zircon	U-Pb	Rainaud et al, 2004
	Mufulira Lufubu schist,Zm	blastoporphyritic metavolcanic	1968	9	1977	1959	zircon	U-Pb	Rainaud et al, 2004

RADIOMETRIC AGES IN CHRONOLOGICAL ORDER, GREATER LUFILIAN ARC (cont.) 7/8

sample	Site/Event	Rock type	age	error	max	min	material	type	reference
BK-10	Kaoko belt, Hoanib River, NW Nm	Foliated syenogranitic orthogneiss	1971	7	1978	1964	zircon	U-Pb	Seth et al, 1998
	Mufulira mine,Zm	Mufulira granite	1975	20	1995	1955	Zircon	U-Pb	Snelling et al, 1972
	Mulungushi bridge, Kabwe,Zm	Augen gneiss	1976	5	1981	1971	zircon	U-Pb	Rainaud, et al, 2004
L-969	Kamanjab Batholith,Nm	Foid syenite	1976	42	1934	2018	zircon	U-Pb	This report
	Kaoko Belt, 30 km NW Sesfontein,Nm	partly sheared monzogranite	1978	0.6	1978	1977	zircon	U-Pb	Hoffman & Kroner, unpub in Seth, 1998
	Namaqua, Nm	Luderitz Kunguib granodiorite	1978	10	1988	1968	zircon	U-Pb	Burger, 1976
	Namaqua, Nm	Luderitz Kunguib granodiorite	1978	10	1988	1968	zircon	U-Pb	Burger, 1976
	Chambishi basin Lufubu Schist,Zm	Meta-andesite	1980	7	1987	1973	zircon	U-Pb	Rainaud et al, 2004
	Chambishi granite,Zm	Coarse-grained undeformed monzogranite	1983	5	1988	1978	zircon	U-Pb	Rainaud et al, 2004
BK-5	Kaoko belt, NW Nm	Dioritic orthogneiss	1985	23	2008	1962	zircon	U-Pb	Seth et al, 1998
	Khoabendus Formation,Nm	Flow-banded rhyolite	1987	4	1991	1983	zircon	Pb/Pb ev	Hoffman & Kroner, unpub in Seth, 1998
	Mufulira Pink Granite,Zm	Granite	1994	7.1	2001	1987	zircon	U-Pb	Rainaud et al, 2004
	Kalumbila, NW Zm	sediments	1994		2001	1987	zircon	U-Pb	Steven & Armstrong, 2000
	Mtuga aplites, Mkushi,Zm	Inherited zircons	1998	18	2016	1980	zircon	U-Pb	Rainaud, et al, 2004
	Orange River Group,Nm		2000		2000	2000			Miller, 1999
	Mtuga aplites, Mkushi,Zm	Inherited zircons	2009	4	2013	2005	zircon	U-Pb	Rainaud, et al, 2004
BK-10	Kaoko belt, Hoanib River, NW Nm	Xenocrystic zircon in syenogranitic orthogneiss	2033		2033	2033	zircon	U-Pb	Seth et al, 1998
	Mkushi Gneiss, SE Irumide B.,Zm	Variably deformed biotite granite and highly deformed mylonitic granitoids	2036	7	2043	2029	zircon	shrimp U-Pb	De Waele et al, 2003c
	Mkushi Gneiss, Zm	Granitic gneiss	2036	22	2058	2014	zircon	shrimp U-Pb	Robb in De Waele et al,2001a
	Mkushi Gneiss, Zm	Variably deformed biotite granite and highly deformed mylonitic granitoids	2037	12	2049	2025	zircon	shrimp U-Pb	De Waele et al, 2003c
	Mkushi Gneiss, Zm	Gtd	2049	6	2055	2043	zircon	U-Pb	Rainaud et al, 2004
	Kamono school, Luangwa Terrane, Zm	Foliated granitoid	2050	10	2060	2040	zircon	LAM ICPMS	Cox et al, 2002
	Mkushi Gneiss, Zm	Variably deformed biotite granite and highly deformed mylonitic granitoids	2052	13	2065	2039	zircon	shrimp U-Pb	De Waele et al, 2003c
	Mufulira Lufubu schist,Zm	blastoporphyritic metavolcanic (inherited zircons)	2057	9	2066	2048	zircon	U-Pb	Rainaud et al, 2004
3DA-150	Kasai Shield, Zm	Porphyritic gtd	2058	7	2065	2051	zircon	U-Pb	Key et al, 2001
	Mtuga aplites, Mkushi,Zm	Inherited zircons	2064	15	2079	2049	zircon	U-Pb	Rainaud, et al, 2004
	Mtuga aplites, Mkushi,Zm	Inherited zircons	2072	9	2081	2063	zircon	U-Pb	Rainaud, et al, 2004
	Mansa, Irumide B., Zm	Luapula acid volcanics (Model age)	2095	9	2104	2086	Nd isotop	Tchur	De Waele et al, 2003b
	Kunene Complex,Nm	Anorthosites	2100		2100	2100			Miller, 1999
	Mansa, Irumide B., Zm	Undeformed biot. Gt (Model age)	2116	11	2127	2105	Nd isotop	Tchur	De Waele et al, 2003b
PRU142	Oas Farm,Nm	Syenite, inherited zircons	2124		2192	2070	zircon	U-Pb	Tegtmeyer & Kroner, 1985
	Mansa, Irumide B., Zm	Luapula acid volcanics (Model age)	2135	14	2149	2121	Nd isotop	Tchur	De Waele et al, 2003b
	Mansa, Irumide B., Zm	Undeformed biot. Gt (Model age)	2159	14	2173	2145	Nd isotop	Tchur	De Waele et al, 2003b
	Samba Cu prospect,Zm	Inherited zircon	2160	25	2185	2135	zircon	U-Pb	Rainaud et al, 2004
	Kasai Shield, Zm	Porphyritic gtd	2169	5	2174	2164	zircon	U-Pb	This report
	Kalumbila, NW Zm	sediments	2170		2189	2151	zircon	U-Pb	Steven & Armstrong, 2000
	Mufulira Lufubu schist,Zm	blastoporphyritic metavolcanic (inherited zircons)	2174	13	2187	2161	zircon	U-Pb	Rainaud et al, 2004
BK-5	Kaoko belt, NW Nm	Xenocrystic zircon in dioritic orthogneiss	2281	0.9	2282	2280	zircon	U-Pb	Seth et al, 1998
BK-5	Kaoko belt, NW Nm	Xenocrystic zircon in dioritic orthogneiss	2287	10	2297	2277	zircon	U-Pb	Seth et al, 1998
	G2 Lukamfwa Hill gtd.W Irumide B.,Zm	Anor porph biot granite gn (Model age)	2310	55	2365	2255	Nd isotop	Tchur	De Waele et al, 2003b
	Samba Cu prospect,Zm	Inherited zircon	2336	9	2345	2327	zircon	U-Pb	Rainaud et al, 2004
	Mpika, Irumide B.,Zm	Intermediate+mafic volcs (Model age)	2338	109	2447	2229	Nd isotop	Tchur	De Waele et al, 2003b
	Damaran metased, Navachab mine, Nm	Detrital zircons in Damaran metaseds	2360	5	2365	2355	zircon	U-Pb	Jacob et al, 2003
	Luwalizi Granite, NE Irumide B., Zm	Weakly deformed gt (Model age)	2372	23	2395	2349	Nd isotop	Tchur	De Waele et al, 2003b
	Mkushi Gneiss, SE Irumide B.,Zm	Biotite granite (Model age)	2400	17	2417	2383	Nd isotop	Tchur	De Waele et al, 2003b
	Luwalizi Granite, NE Irumide B., Zm	Weakly deformed gt (Model age)	2400	17	2417	2383	Nd isotop	Tchur	De Waele et al, 2003b
	Samba Cu prospect,Zm	Inherited zircon	2423	13	2436	2410	zircon	U-Pb	Rainaud et al, 2004
	Damaran metased, Navachab mine, Nm	Detrital zircons in Damaran metaseds	2428	9	2437	2419	zircon	U-Pb	Jacob et al, 2003
L-855	Kamanjab Batholith,Nm	inherited zircons in gtd	2500	19	2481	2519	zircon	U-Pb	This report
	Manshya River Group, Irumide B., Zm	Rhyolitic tuff (Model age)	2532	109	2641	2423	Nd isotop	Tchur	De Waele et al, 2003b
3DA-100	Kasai Shield, Jimbe Bridge,Zm	Granulite	2535	11	2546	2524	zircon	U-Pb	Key et al, 2001
3DA-101	Kasai Shield, NW Zm	Foliated gtd	2538	10	2548	2528	zircon	U-Pb	Key et al, 2001
3DA-100	Kasai Shield, Jimbe Bridge,Zm	Granulite	2543	5	2548	2538	zircon	U-Pb	Key et al, 2001
L-1045	Grootfontein Inlier, Nm	inherited zircons in gtd	2549	78	2471	2627	zircon	U-Pb	This report
BK-29	Kaoko belt, NW Nm	Coarse-grained quartz-monzonitic augen gneiss	2584	0.6	2585	2584	zircon	U-Pb	Seth et al, 1998
BK-1	Kaoko belt, NW Nm	Grey, coarse-grained monzonitic augen gneiss	2585	1.2	2587	2584	zircon	U-Pb	Seth et al, 1998
BK-5	Kaoko belt, NW Nm	Xenocrystic zircon in dioritic orthogneiss	2600		2600	2600	zircon	U-Pb	Seth et al, 1998
BK-5	Kaoko belt, NW Nm	Xenocrystic zircon in dioritic orthogneiss	2605	11	2616	2594	zircon	U-Pb	Seth et al, 1998
BK-446	Kaoko belt, NW Nm	Quartz-monzodioritic gneiss	2616	5	2621	2611	zircon	U-Pb	Seth et al, 1998
BK-3	Kaoko belt, NW Nm	Fol Quartz-monzodioritic orthogneiss	2645	6	2651	2639	zircon	U-Pb	Seth et al, 1998
	Mtuga aplites, Mkushi,Zm	Inherited zircons	2688	8	2696	2680	zircon	U-Pb	Rainaud, et al, 2004
	Changwena Hill, Ndabala, SW Serenje,Zm	Quartzite, oldest detrital age	2720	20	2740	2700	monazite,	U-Pb	Snelling et al, 1964
	Irumi Hill, Irumide B.,Zm	Irumi quartzite, oldest detrital age	2720	24	2744	2696	monazite,	U-Pb	Snelling et al, 1964; Vail et al, 1968
	Changwena River, Irumi Hill,Zm	Monazite	2720	20	2740	2700	Monazite	U-Pb	Snelling et al, 1972
	Changwena River, Irumi Hill,Zm	Monazite	2720	20	2740	2700	Monazite	U-Pb	Snelling et al, 1972
	Mtuga aplites, Mkushi,Zm	Inherited zircons	2730	7	2737	2723	zircon	U-Pb	Rainaud, et al, 2004

RADIOMETRIC AGES IN CHRONOLOGICAL ORDER, GREATER LUFILIAN ARC (cont.) 8/8

sample	Site/Event	Rock type	age	error	max	min	material	type	reference
	Kapiri Mposhi, Zm	Granite	2738	4	2742	2734	zircon	shrimp U-Pb	De Waele et al, 2003c
	Etoile mine, D.R.Congo	Roan Group tuff (xenocrystic zircons)	2802	36	2838	2766	zircon	U-Pb	Rainaud, et al, 2004
	G4 gtd Irumide B.,Zm	Coarse biotite granite (Model age)	2808	35	2843	2773	Nd isotop	Tchur	De Waele et al, 2003b
	Luangwa River, border Mozambique, Zm	Strongly-deformed granodiorite-diorite orthogneiss	2808	14	2822	2794	zircon	LAM ICPMS	Cox et al, 2002
	Etoile mine, D.R.Congo	Roan Group tuff (xenocrystic zircons)	2831	16	2847	2815	zircon	U-Pb	Rainaud, et al, 2004
	Damaran metased, Navachab mine, Nm	Detrital zircons in Damaran metaseds	2870	6	2876	2864	zircon	U-Pb	Jacob et al, 2003
	Damaran metased, Navachab mine, Nm	Detrital zircons in Damaran metaseds	2872	4	2876	2868	zircon	U-Pb	Jacob et al, 2003
	Mpika, Irumide B.,Zm	Intermediate+mafic volcs (Model age)	2909	31	2940	2878	Nd isotop	Tchur	De Waele et al, 2003b
	G4 gtd Irumide B.,Zm	Coarse biotite granite (Model age)	2948	18	2966	2930	Nd isotop	Tchur	De Waele et al, 2003b
	Manshya River Group, Irumide B., Zm	Rhyolitic tuff (Model age)	2961	152	3113	2809	Nd isotop	Tchur	De Waele et al, 2003b
	G2 Lukamfwa Hill gtd.W Irumide B.,Zm	Anor porph biot granite gn (Model age)	3199	229	3428	2970	Nd isotop	Tchur	De Waele et al, 2003b
	Manshya River Group, Irumide B., Zm	Rhyolitic tuff (Model age)	3238	55	3293	3183	Nd isotop	Tchur	De Waele et al, 2003b

Table A22
COMPILATION OF RADIOMETRIC AGES, LUFILIAN ARC (ZAMBIA & NAMIBIA)

SORTED BY REGION AND SITES. January 19, 2005

Compiled by Alberto Lobo-Guerrero, Geologist, M.Sc.,Min.Ex.,

Economic Geology Research Institute, University of the Witwatersrand, Johannesburg, South Africa

1/

HOOK GRANITE BATHOLITH, ZAMBIA

	sample	Site/Event	Rock type	age	error	max	min	material	type	reference
1		Hook Granite,Zm	Pegmatite	440	15	455	425	Muscovite	K-Ar	Snelling et al, 1972
2		Hook Granite,Zm	Biotite granite gneiss	450	14	464	436	biotite	K-Ar	Snelling et al, 1972
3		Hook Granite,Zm	Porphyroblastic gneiss	458	122	580	336	Biotite	K-Ar	Snelling et al, 1972
4		Hook Granite,Zm	Biotite-hornblende granite	465	16	481	449	Biotite	K-Ar	Snelling et al, 1972
5		Hook Granite,Zm	Biotite-hornblende granite	465	15	480	450	Hornblend	K-Ar	Snelling et al, 1972
6		Hook Granite,Zm	Granite	500	17	517	483	Granite	Rb-Sr	Snelling et al, 1972
7	H-4	Hook Granite, Zm	Post-Tectonic megacrystic granite	533	3	536	530	zircon	U-Pb	Hanson et al, 1993
8		Hook Granite, Zm	tectonic activity	535		540	530	zircon	U-Pb	Hanson et al, 1993
9	H-3	Hook Granite, Zm	Rhyolite dike within Katangan	538	1.5	540	537	zircon	U-Pb	Hanson et al, 1993
10	H-5	Hook Granite, Zm	Rhyolite intrusion in Mwembezhi dislocation	551	19	570	532	zircon	U-Pb	Hanson et al, 1993
11	H-1	Hook Granite, Zm	Deformed f-mg granite	559	18	577	541	zircon	U-Pb	Hanson et al, 1993
12		Hook Granite, Zm	Syntectonic granitic plutonism	565		570	560	zircon	U-Pb	Hanson et al 1993
13	H-2	Hook Granite, Zm	Deformed megacrystic granite	566	5	571	561	zircon	U-Pb	Hanson et al, 1993

NORTHWESTERN ZAMBIA, DOMES AREA

	sample	Site/Event	Rock type	age	error	max	min	material	type	reference
1	L-030	Kabompo Dome, Zm	diorite-granodiorite gneiss	419	250	669	169	zircon	Pb/U shrimp	This report
2		Kabompo Dome, Zm	Met event (amphibolite facies)	708	7	715	701		K/Ar	Cosi et al, 1992
3	3DA-101	Kasai Shield, Zm	Met event	714	66	780	648	zircon	U-Pb	Key et al, 2001
4	3DA-51	Kasai Shield, Zm	Met event	734	63	797	671	zircon	U-Pb	Key et al, 2001
5		Luamata, NWZm	Felsic volcanic	735	5	740	730	zircon	U-Pb	Key et al, 2001
6		Kabompo Dome, Zm	Met event (high pressure)	744	8	752	736		Rb/Sr	AGIP, 1985
7	L-047	Mombwezhi Dome, Zm	Quartzmonzonite	745.9	3.4	749	743	zircon	U-Pb	This report
8		Lwanu basalt, Mwinilunga, NW Zm	Basalt	765	5	770	760	zircon	U-Pb	Key et al, 2001
9		Basement, Kabompo Dome,Zm	Gtd	1200	50	1250	1150	zircon	U-Pb	AGIP, 1985
10	3DA-57	Kasai Shield, NW Zm	Aphyric med-g gtd	1561	10	1571	1551	zircon	U-Pb	Key et al, 2001
11		Kalumbila, NW Zm	sediments	1845		1860	1830	zircon	U-Pb	Steven & Armstrong, 2000
12		Kalumbila, NW Zm	sediments	1887		1896	1878	zircon	U-Pb	Steven & Armstrong, 2000
13		Kalumbila, NW Zm	sediments	1919		1924	1913	zircon	U-Pb	Steven & Armstrong, 2000
14	L-030	Mwinilunga, NW Zm	Foliated Gtd	1928	7.1	1935	1921	zircon	U-Pb	This report
15		Kabompo Dome, Zm	Feldspar-phyric gtd	1934	6	1940	1928	zircon	U-Pb	Key et al, 2001
16		Kabompo Dome, Zm	Feldspar-phyric gtd	1940	2.8	1943	1937	zircon	U-Pb	Key et al, 2001
17		Kalumbila, NW Zm	sediments	1946		1952	1939	zircon	U-Pb	Steven & Armstrong, 2000
18		Kalumbila, NW Zm	sediments	1994		2001	1987	zircon	U-Pb	Steven & Armstrong, 2000
19	3DA-150	Kasai Shield, Zm	Porphyritic gtd	2058	7	2065	2051	zircon	U-Pb	Key et al, 2001
20		Kasai Shield, Zm	Porphyritic gtd	2169	5	2174	2164	zircon	U-Pb	This report
21		Kalumbila, NW Zm	sediments	2170		2189	2151	zircon	U-Pb	Steven & Armstrong, 2000
22	3DA-100	Kasai Shield, Jimbe Bridge,Zm	Granulite	2535	11	2546	2524	zircon	U-Pb	Key et al, 2001
23	3DA-101	Kasai Shield, NW Zm	Foliated gtd	2538	10	2548	2528	zircon	U-Pb	Key et al, 2001
24	3DA-100	Kasai Shield, Jimbe Bridge,Zm	Granulite	2543	5	2548	2538	zircon	U-Pb	Key et al, 2001

SOLWESI DOME AREA, ZAMBIA

	sample	Site/Event	Rock type	age	error	max	min	material	type	reference
1		Kansanshi Mine, Zm	Carbonate-molybdenite-monazite veins	502.4	1.7	504	501	Molybden	Re-Os	Torrealday et al, 2003
2		Kansanshi Mine, Zm	Carbonate-molybdenite-monazite veins	503	15	518	488	Brannerite	U-Pb	Darnley, 1961
3		Kansanshi mine, Zm	Minzd qz vein	511	11	522	500	zircon	U-Pb	Torrealday et al, 2000
4		Kansanshi Mine, Zm	Cpy-rich veins	512.4	1.2	514	511	Molybden	Re-Os	Torrealday et al, 2003
5		Kansanshi mine,Zm	Vein	520	20	540	500	Brannerite	U-Pb	Snelling et al, 1972
6	L-060	Kansanshi mine, Zm	Diorite	750	5	755	745	zircon	U-Pb	This report

WESTERN LUSAKA, KAFUE FLATS AREA, ZAMBIA

	sample	Site/Event	Rock type	age	error	max	min	material	type	reference
1		Leopard's Hill area,Zm	Biotite-garnet schist	435	15	450	420	Muscovite	K-Ar	Snelling et al, 1972
2		Mpande Dome,Zm	Microgranite	476	19	495	457	Muscovite	K-Ar	Snelling et al, 1972
3		Leopard's Hill area,Zm	Schist	485	20	505	465	Biotite	K-Ar	Snelling et al, 1972
4		Kafue Rhyolites,Zm	Sheared tuff	495	35	530	460	w.r.	Rb-Sr	Snelling et al, 1972
5		Lusaka Granite,Zm	Granite	507	15	522	492	Biotite	Rb-Sr	Snelling et al, 1972
6		Leopard's Hill area,Zm	Katangan mica quartzite	515	20	535	495	Biotite	K-Ar	Snelling et al, 1972
7		Leopard's Hill area,Zm	Sheared gneiss	520	20	540	500	Biotite	K-Ar	Snelling et al, 1972
8		Lusaka Granite,Zm	Granite	531	21	552	510	Biotite	K-Ar	Snelling et al, 1972
9	L-207	Nampundwe,Zm	Gtd	538.2	3.3	542	535	zircon	U-Pb	This report
10		Lusaka Area, Zm	metasediments?	539	20	559	519	w.r.	Rb-Sr	Barr et al, 1978
11		Lusaka Granite,Zm	Granite	540	20	560	520	Biotite	K-Ar	Snelling et al, 1972
12		Kafue Rhyolites,Zm	Rhyolitic tuff	548	32	580	516	w.r.	Rb-Sr	Snelling et al, 1972
13	L-213	Kafue Flats,Zm	Syenite	550	25	575	525	zircon	U-Pb	This report
14		Lusaka Granite,Zm	Granite	551	22	573	529	Biotite	K-Ar	Snelling et al, 1972
15		Lusaka Area, Zm	metasediments?	557	4	561	553	w.r.	K-Ar	Barr et al, 1978
16		Kafue Rhyolites,Zm	Porphyritic Rhyolite	562	40	602	522	w.r.	Rb-Sr	Snelling et al, 1972
17		Lusaka Granite,Zm	Granite	567	23	590	544	Biotite	K-Ar	Snelling et al, 1972
18		Lusaka Series,Zm	Vein in Lusaka series	630		630	630	Galena	Pb	Snelling et al, 1972
19		Mpande Dome,Zm	Microgranite	677	45	722	632	K-feldspa	Rb-Sr	Snelling et al, 1972
20		Lusaka Granite,Zm	Granite	681	28	709	653	K-feldspa	Rb-Sr	Snelling et al, 1972
21		Lusaka Granite,Zm	Granite	700	28	728	672	K-feldspa	Rb-Sr	Snelling et al, 1972
22		Lusaka Granite,Zm	Granite	703	28	731	675	w.r.	Rb-Sr	Snelling et al, 1972
23		Mpande Dome,Zm	Microgranite	730	50	780	680	w.r.	Rb-Sr	Snelling et al, 1972
24		Lusaka Granite,Zm	Granite	745	70	815	675	w.r.	Rb-Sr	Snelling et al, 1972
25		Lusaka Granite,Zm	Granite	745	30	775	715	w.r.	Rb-Sr	Snelling et al, 1972
26		Lusaka Granite,Zm	Granite	746	30	776	716	K-feldspa	Rb-Sr	Snelling et al, 1972
27		Lusaka Granite,Zm	Granite	770	25	795	745	w.r.	K-Ar	Snelling et al, 1972
28		Lusaka Granite,Zm	Granite	790	32	822	758	w.r.	Rb-Sr	Barr et al, 1978
29		Ngoma Gneiss, W Lusaka, Zm	Gneiss	820	7	827	813	zircon	U-Pb	Wilson,1993 in De Waele et al,2001a

WESTERN LUSAKA, KAFUE FLATS AREA, ZAMBIA (cont.)

	sample	Site/Event	Rock type	age	error	max	min	material	type	reference
30		Lusaka Granite, W Lusaka, Zm	Granite	843	10	853	833			Cahen,1984 in De Waele & T,1999
31		Lusaka Granite,Zm	Granite	846	68	914	778	zircon	U-Pb	Barr et al, 1978
32		Kafue Rhyolites, W Lusaka, Zm	Rhyolite	879	19	898	860	zircon	U-Pb	Wardlaw in De Waele et al,2001a
33		Mpande Dome (south), Southern Zm	Fine-grained granite	1095	12	1107	1083	zircon	U-Pb	De Waele et al, 2000a
34		Lusaka Granite,Zm	Granite	1100	70	1170	1030	Plagioclas	Rb-Sr	Snelling et al, 1972
35		Mpande Gneiss, Southern Zm	Granitic orthogneiss	1106	19	1125	1087	zircon	U-Pb	Hanson et al, 1988, 1994
36		Lusaka Granite,Zm	Granite	1200	96	1296	1104	Plagioclas	Rb-Sr	Snelling et al, 1972
37		Lusaka Granite,Zm	Granite	1305	65	1370	1240	Plagioclas	Rb-Sr	Snelling et al, 1972
38	L-213	Old Kafue Basement,Zm	Inherited zircons in syenite	1872	14	1886	1858	zircon	U-Pb	This report

KALENGWA-KASEMPA AREA, ZAMBIA

	sample	Site/Event	Rock type	age	error	max	min	material	type	reference
1	L-142	MB-34 intrusives, Kasempa,Zm	Subvolcanic porphyritic intrusive	750	5	755	745	zircon	U-Pb	This report

MKUSHI-SERENJE AREA, ZAMBIA

	sample	Site/Event	Rock type	age	error	max	min	material	type	reference
1		Serenje area,Zm	Biotite gneiss	495	20	515	475	Biotite	K-Ar	Snelling et al, 1972
2		Serenje area,Zm	Kalonga metasiltite	645	25	670	620	Muscovite	K-Ar	Snelling et al, 1972
3		Serenje area,Zm	Pegmatite	755	30	785	725	Muscovite	K-Ar	Snelling et al, 1972
4		Serenje area,Zm	Kalonga metasiltstone	885	36	921	849	Muscovite	K-Ar	Snelling et al, 1972
5		Serenje area, Zm	Sasa, leucocratic biotite porphyritic granite	1018	6	1024	1012	zircon	shrimp U-Pb	De Waele et al,2001a
6		Serenje area, Zm	Porphyritic granite	1022	12	1034	1010	zircon	shrimp U-Pb	De Waele et al,2001a
7		Serenje area, Zm	Porphyritic granite	1024	13	1037	1011	zircon	shrimp U-Pb	De Waele et al,2001a
8		Serenje area, Zm	Porphyritic granite	1025	10	1035	1015	zircon	shrimp U-Pb	De Waele et al,2001a
9		Serenje area, Zm	Porphyritic granite	1033	15	1048	1018	zircon	shrimp U-Pb	De Waele et al, 2002b
10		Serenje area, Zm	Porphyritic granite	1038	10	1048	1028	zircon	shrimp U-Pb	De Waele et al,2001a; De Waele & M, 2002
11		Mtuga aplites, Mkushi,Zm	emplacement of aplite	1059	26	1085	1033	zircon	U-Pb	Rainaud, et al, 2004
12		Mkushi Gneiss, Zm	Granitic gneiss (zircon rims)	1088	159	1247	929	zircon	shrimp U-Pb	Robb in De Waele et al,2001a
13		Mkushi area,Zm	Aplite cutting Mkushi Gneiss	1625	50	1675	1575	w.r.	Rb-Sr	Snelling et al, 1972
14		Serenje area, Irumide B.,Zm	Granite gneiss	1647	10	1657	1637	zircon	shrimp U-Pb	De Waele & Mapani, 2002
15		Serenje area, Irumide B.,Zm	Granite gneiss	1661	8	1669	1653	zircon	shrimp U-Pb	De Waele & Mapani, 2002
16		Mtuga aplites, Mkushi,Zm	Inherited zircons	1998	18	2016	1980	zircon	U-Pb	Rainaud, et al, 2004
17		Mtuga aplites, Mkushi,Zm	Inherited zircons	2009	4	2013	2005	zircon	U-Pb	Rainaud, et al, 2004
18		Mkushi Gneiss, SE Irumide B.,Zm	Variably deformed biotite granite and highly deformed mylonitic granitoids	2036	7	2043	2029	zircon	shrimp U-Pb	De Waele et al, 2003c
19		Mkushi Gneiss, Zm	Granitic gneiss	2036	22	2058	2014	zircon	shrimp U-Pb	Robb in De Waele et al,2001a
20		Mkushi Gneiss, Zm	Variably deformed biotite granite and highly deformed mylonitic granitoids	2037	12	2049	2025	zircon	shrimp U-Pb	De Waele et al, 2003c
21		Mkushi Gneiss, Zm	Gtd	2049	6	2055	2043	zircon	U-Pb	Rainaud et al, 2004
22		Mkushi Gneiss, Zm	Variably deformed biotite granite and highly deformed mylonitic granitoids	2052	13	2065	2039	zircon	shrimp U-Pb	De Waele et al, 2003c
23		Mtuga aplites, Mkushi,Zm	Inherited zircons	2064	15	2079	2049	zircon	U-Pb	Rainaud, et al, 2004
24		Mtuga aplites, Mkushi,Zm	Inherited zircons	2072	9	2081	2063	zircon	U-Pb	Rainaud, et al, 2004
25		Mpika, Irumide B.,Zm	Intermediate+mafic volcs (Model age)	2338	109	2447	2229	Nd isotop	Tchur	De Waele et al, 2003b
26		Mkushi Gneiss, SE Irumide B.,Zm	Biotite granite (Model age)	2400	17	2417	2383	Nd isotop	Tchur	De Waele et al, 2003b
27		Mtuga aplites, Mkushi,Zm	Inherited zircons	2688	8	2696	2680	zircon	U-Pb	Rainaud, et al, 2004
28		Changwena Hill, Ndabala, SW Serenje,Zm	Quartzite, oldest detrital age	2720	20	2740	2700	monazite,	U-Pb	Snelling et al, 1964
29		Mtuga aplites, Mkushi,Zm	Inherited zircons	2730	7	2737	2723	zircon	U-Pb	Rainaud, et al, 2004
30		Mpika, Irumide B.,Zm	Intermediate+mafic volcs (Model age)	2909	31	2940	2878	Nd isotop	Tchur	De Waele et al, 2003b

COPPERBELT REGION, ZAMBIA

	sample	Site/Event	Rock type	age	error	max	min	material	type	reference
1		Nkana mine,Zm	Botryoidal pitchblende vein	235	35	270	200	Pitchblen	U-Pb	Snelling et al, 1972
2		Luanshya mine,Zm	Pitchblende in vein	365	40	405	325	Pitchblen	U-Pb	Snelling et al, 1972
3		Nkana mine,Zm	Metasediment with uraninite	452	24	476	428	Uraninite	U-Pb	Snelling et al, 1972
4		Nkana mine,Zm	Schistose granulite	455	20	475	435	Biotite	Rb-Sr	Snelling et al, 1972
5		Lylands Quarry, Ndola,Zm	Galena	460		460	460	Galena	Pb	Snelling et al, 1972
6		Nkana mine,Zm	Uraninite in sediment	485	16	501	469	Uraninite	U-Pb	Snelling et al, 1972
7		Nkana mine, Mindola,Zm	Schistose granulite	495	20	515	475	Biotite	K-Ar	Snelling et al, 1972
8		Luanshya mine, Zm	Lufubu Schist	515	100	615	415	Actinolite	K-Ar	Snelling et al, 1972
9		Nkana mine,Zm	Uraninite	520	20	540	500	Uraninite	U-Pb	Snelling et al, 1972
10		Luanshya mine, Zm	Lufubu Schist	530	30	560	500	Biotite	K-Ar	Snelling et al, 1972
11		Nkana mine,Zm	Uraninite in Lower Roan	535	21	556	514	Uraninite	U-Pb	Snelling et al, 1972
12	L-158	Konkola Deep Borehole,Zm, resetting age	Foliated pink gtd	562	18	580	544	zircon em	Pb/U shrimp	This report
13		Luanshya mine, Zm	Pegmatite in lower Roan	840	40	880	800	Microcline	Rb-Sr	Snelling et al, 1972
14		Luanshya mine, Zm	Pegmatite in Lufubu	1635	180	1815	1455	K-feldspa	Rb-Sr	Snelling et al, 1972
15		Roan Antelope mine,Zm	Granite	1750	50	1800	1700	K-feldspa	K-Ar	Snelling et al, 1972
16	L-075	Muliashi Porphyry,Zm	Rapakivi granite	1865	5.4	1870	1860	zircon	U-Pb	This report
17	L-160	Konkola Deep Borehole,Zm	Undeformed white gtd	1866	5.4	1872	1861	zircon	U-Pb	This report
18	L-160	Konkola Deep Borehole,Zm	Gray gtd	1868	4.8	1873	1863	zircon	shrimp concordi a age	This report
19	L-158	Konkola Deep Borehole,Zm	Foliated pink gtd	1874	14	1888	1860	zircon	U-Pb	This report
20		Samba Cu prospect,Zm	felsic metavolcanic schist	1964	12	1976	1952	zircon	U-Pb	Rainaud et al, 2004
21		Samba Cu prospect,Zm	Inherited zircon	2160	25	2185	2135	zircon	U-Pb	Rainaud et al, 2004
22		Samba Cu prospect,Zm	Inherited zircon	2336	9	2345	2327	zircon	U-Pb	Rainaud et al, 2004
23		Samba Cu prospect,Zm	Inherited zircon	2423	13	2436	2410	zircon	U-Pb	Rainaud et al, 2004

MUFULIRA AREA, ZAMBIA

	sample	Site/Event	Rock type	age	error	max	min	material	type	reference
1		Mufulira West mine, Zm	Basement granite	505	20	525	485	Biotite	K-Ar	Snelling et al, 1972
2		Mufulira West mine, Zm	Basement granite	515	25	540	490	Biotite	Rb-Sr	Snelling et al, 1972
3		Mufulira Lufubu schist,Zm	blastoporphyritic metavolcanic	1968	9	1977	1959	zircon	U-Pb	Rainaud et al, 2004
4		Mufulira mine,Zm	Mufulira granite	1975	20	1995	1955	Zircon	U-Pb	Snelling et al, 1972
5		Mulungushi bridge, Kabwe,Zm	Augen gneiss	1976	5	1981	1971	zircon	U-Pb	Rainaud, et al, 2004
6		Chambishi basin Lufubu Schist,Zm	Meta-andesite	1980	7	1987	1973	zircon	U-Pb	Rainaud et al, 2004
7		Chambishi granite,Zm	Coarse-grained undeformed monzogranite	1983	5	1988	1978	zircon	U-Pb	Rainaud et al, 2004
8		Mufulira Pink Granite,Zm	Granite	1994	7.1	2001	1987	zircon	U-Pb	Rainaud et al, 2004
9		Mufulira Lufubu schist,Zm	blastoporphyritic metavolcanic (inherited zircons)	2057	9	2066	2048	zircon	U-Pb	Rainaud et al, 2004
10		Mufulira Lufubu schist,Zm	blastoporphyritic metavolcanic (inherited zircons)	2174	13	2187	2161	zircon	U-Pb	Rainaud et al, 2004

NCHANGA AREA, ZAMBIA

	sample	Site/Event	Rock type	age	error	max	min	material	type	reference
1		Gray's Quarry, Nchanga, Zm	Red granite	490	20	510	470	Biotite	K-Ar	Snelling et al, 1972
2		Gray's Quarry, Nchanga, Zm	Red granite	490	15	505	475	Biotite	Rb-Sr	Snelling et al, 1972
3		Nchanga,Zm	Nchanga red granite	583	90	673	493	w.r.	Rb-Sr	Snelling et al, 1972
4	L-172c	Nchanga open pit intrusives, Zm	Lamprophyre in borehole	765	3	768	762	zircon	U-Pb	This report
5	L-169	Nchanga open pit intrusives, Zm	Lamprophyre in borehole	765	3	768	762	zircon	U-Pb	This report
6		Nchanga Red Granite,Zm	Gtd	877	5	882	872	zircon	U-Pb	Armstrong et al, 2004 (in prep)
7		Nchanga open pit intrusives, Zm	inherited zircons	880	5	885	875	zircon	U-Pb	This report
8	L-169	Nchanga Intrusives, Zm	Lamprophyre in borehole (inherited zircons)	1860	10	1870	1850	zircon	U-Pb	This report

ALL BASEMENT TO THE COPPERBELT REGION, ZAMBIA (COMPILATION OF GROUPS)

1										
2		Nkana mine,Zm	Botryoidal pitchblende vein	235	35	270	200	Pitchblend	U-Pb	Snelling et al, 1972
3		Luanshya mine,Zm	Pitchblende in vein	365	40	405	325	Pitchblend	U-Pb	Snelling et al, 1972
4		Nkana mine,Zm	Metasediment with uraninite	452	24	476	428	Uraninite	U-Pb	Snelling et al, 1972
5		Nkana mine,Zm	Schistose granulite	455	20	475	435	Biotite	Rb-Sr	Snelling et al, 1972
6		Lylands Quarry, Ndola,Zm	Galena	460		460	460	Galena	Pb	Snelling et al, 1972
7		Nkana mine,Zm	Uraninite in sediment	485	16	501	469	Uraninite	U-Pb	Snelling et al, 1972
8		Gray's Quarry, Nchanga, Zm	Red granite	490	20	510	470	Biotite	K-Ar	Snelling et al, 1972
9		Gray's Quarry, Nchanga, Zm	Red granite	490	15	505	475	Biotite	Rb-Sr	Snelling et al, 1972
10		Nkana mine, Mindola,Zm	Schistose granulite	495	20	515	475	Biotite	K-Ar	Snelling et al, 1972
11		Mufulira West mine, Zm	Basement granite	505	20	525	485	Biotite	K-Ar	Snelling et al, 1972
12		Luanshya mine, Zm	Lufubu Schist	515	100	615	415	Actinolite	K-Ar	Snelling et al, 1972
13		Mufulira West mine, Zm	Basement granite	515	25	540	490	Biotite	Rb-Sr	Snelling et al, 1972
14		Nkana mine,Zm	Uraninite	520	20	540	500	Uraninite	U-Pb	Snelling et al, 1972
15		Luanshya mine, Zm	Lufubu Schist	530	30	560	500	Biotite	K-Ar	Snelling et al, 1972
16		Nkana mine,Zm	Uraninite in Lower Roan	535	21	556	514	Uraninite	U-Pb	Snelling et al, 1972
17	L-158	Konkola Deep Borehole,Zm, resetting age	Foliated pink gtd	562	18	580	544	zircon em	shrimp	This report
18		Nchanga,Zm	Nchanga red granite	583	90	673	493	w.r.	Rb-Sr	Snelling et al, 1972
19	L-172c	Nchanga open pit intrusives, Zm	Lamprophyre in borehole	765	3	768	762	zircon	U-Pb	This report
20	L-169	Nchanga open pit intrusives, Zm	Lamprophyre in borehole	765	3	768	762	zircon	U-Pb	This report
21		Luanshya mine, Zm	Pegmatite in lower Roan	840	40	880	800	Microcline	Rb-Sr	Snelling et al, 1972
22		Nchanga Red Granite,Zm	Gtd	877	5	882	872	zircon	U-Pb	Armstrong et al, 2004 (in prep)
23		Nchanga open pit intrusives, Zm	inherited zircons	880	5	885	875	zircon	U-Pb	This report
24		Luanshya mine, Zm	Pegmatite in Lufubu	1635	180	1815	1455	K-feldspa	Rb-Sr	Snelling et al, 1972
25		Roan Antelope mine,Zm	Granite	1750	50	1800	1700	K-feldspa	K-Ar	Snelling et al, 1972
26	L-169	Nchanga Intrusives, Zm	Lamprophyre in borehole (inherited zircons)	1860	10	1870	1850	zircon	U-Pb	This report
27	L-075	Muliashi Porphyry,Zm	Rapakivi granite	1865	5.4	1870	1860	zircon	U-Pb	This report
28	L-160	Konkola Deep Borehole,Zm	Undeformed white gtd	1866	5.4	1872	1861	zircon	U-Pb	This report
29	L-160	Konkola Deep Borehole,Zm	Gray gtd	1868	4.8	1873	1863	zircon	shrimp concordia age	This report
30	L-158	Konkola Deep Borehole,Zm	Foliated pink gtd	1874	14	1888	1860	zircon	U-Pb	This report
31		Samba Cu prospect,Zm	felsic metavolcanic schist	1964	12	1976	1952	zircon	U-Pb	Rainaud et al, 2004
32		Mufulira Lufubu schist,Zm	blastoporphyritic metavolcanic	1968	9	1977	1959	zircon	U-Pb	Rainaud et al, 2004
33		Mufulira mine,Zm	Mufulira granite	1975	20	1995	1955	Zircon	U-Pb	Snelling et al, 1972
34		Mulungushi bridge, Kabwe,Zm	Augen gneiss	1976	5	1981	1971	zircon	U-Pb	Rainaud, et al, 2004
35		Chambishi basin Lufubu Schist,Zm	Meta-andesite	1980	7	1987	1973	zircon	U-Pb	Rainaud et al, 2004
36		Chambishi granite,Zm	Coarse-grained undeformed monzogranite	1983	5	1988	1978	zircon	U-Pb	Rainaud et al, 2004
37		Mufulira Pink Granite,Zm	Granite	1994	7.1	2001	1987	zircon	U-Pb	Rainaud et al, 2004
38		Mufulira Lufubu schist,Zm	blastoporphyritic metavolcanic (inherited zircons)	2057	9	2066	2048	zircon	U-Pb	Rainaud et al, 2004
39		Samba Cu prospect,Zm	Inherited zircon	2160	25	2185	2135	zircon	U-Pb	Rainaud et al, 2004
40		Mufulira Lufubu schist,Zm	blastoporphyritic metavolcanic (inherited zircons)	2174	13	2187	2161	zircon	U-Pb	Rainaud et al, 2004
41		Samba Cu prospect,Zm	Inherited zircon	2336	9	2345	2327	zircon	U-Pb	Rainaud et al, 2004
42		Samba Cu prospect,Zm	Inherited zircon	2423	13	2436	2410	zircon	U-Pb	Rainaud et al, 2004

CHOMA-KALOMO BATHOLITH, ZAMBIA

	sample	Site/Event	Rock type	age	error	max	min	material	type	reference
1	CK4	Choma-Kalomo Batholith, Zm	Medium-grained two mica granite	1174	27	1201	1147	zircon	shrimp U-Pb	Bulambo et al, 2004
2	CK12	Choma-Kalomo Batholith, Zm	Gneiss containing mica-rich restites	1177	70	1247	1107	zircon	shrimp U-Pb	Bulambo et al, 2004
3	CK25	Choma-Kalomo Batholith, Zm	Foliated, med-coarse-g biotite granite	1181	9	1190	1172	zircon	shrimp U-Pb	Bulambo et al, 2004
4	CK10	Choma-Kalomo Batholith, Zm	Foliated med-coarse-g biotite granite	1188	11	1199	1177	zircon	shrimp U-Pb	Bulambo et al, 2004
5		Siasikobole granite, Choma-Kalomo,Zm	Granite	1352	14	1366	1338	zircon	U-Pb	Hanson et al, 1998b
6	CK13	Choma-Kalomo Batholith, Zm	Augen (ortho) gneiss	1368	10	1378	1358	zircon	shrimp U-Pb	Bulambo et al, 2004

IRUMIDE BELT, ZAMBIA

	sample	Site/Event	Rock type	age	error	max	min	material	type	reference
1		G4 gtd Irumide B.,Zm	Coarse biotite granite	943	5	948	938	zircon	shrimp U-Pb	De Waele et al, 2003c
2		Chinsali, Irumide B., Zm	Kaunga Granite	970	5	975	965	zircon	U-Pb	Daly, 1986 in De Waele & Mapani, 2002
3		Chinsali, N Irumide B.,Zm	Mutangoshi (or grey) biotite granite	1009	12	1021	997	zircon	shrimp U-Pb	De Waele & Mapani, 2002
4		Mutangoshi granite, N Irumide B.,Zm	Mesocratic, fine-grained granite	1021	3	1024	1018	zircon	shrimp U-Pb	De Waele & Mapani, 2002
5		G4 gtd. W Irumide B.,Zm	Anorogenic porph biot granite gneiss	1027	13	1040	1014	zircon	shrimp U-Pb	De Waele et al, 2003c
6		G4 gtd Irumide B.,Zm	Coarse biotite granite	1036	13	1049	1023	Nd isotop	shrimp U-Pb	De Waele et al, 2003b
7		G4 gtd Irumide B.,Zm	Coarse biotite granite	1037	16	1053	1021	Nd isotop	shrimp U-Pb	De Waele et al, 2003b
8		G4 gtd Irumide B.,Zm	Coarse biotite granite	1042	47	1042	948	zircon	shrimp U-Pb	De Waele et al, 2003c
9		Mutangoshi granite, N Irumide B.,Zm	Coarse-grained felsic granite	1053	7	1060	1046	zircon	shrimp U-Pb	De Waele & Mapani, 2002
10		G4 gtd. W Irumide B.,Zm	Anorogenic porph biot granite gneiss	1055	13	1068	1042	zircon	shrimp U-Pb	De Waele et al, 2003c
11		G4 gtd Irumide B.,Zm	Coarse biotite granite	1055	13	1068	1042	zircon	shrimp U-Pb	De Waele et al, 2003c
12		Mivula Hill, Central Irumide B., Zm	Syenite	1341	16	1357	1325	w.r.	Rb-Sr	Tembo in De Waele et al, 2000a
13		Magmatic event in Irumide B., Zm	Large syntectonic granite bodies	1407	39	1446	1368	w.r.	Rb-Sr	Daly, 1986; De Waele et al, 2000a
14		G2 gtd. Lubu Gt, W Irumide B.Zm	Granite gneiss	1551	33	1584	1518	zircon	shrimp U-Pb	De Waele et al, 2003c
15		G2 Mutangoshi/Musalango gn, N Irumide B.Zm	Anorogenic porph biot granite gneiss	1610	26	1636	1584	zircon	shrimp U-Pb	De Waele et al, 2003c
16		G2 Lukamfwa Hill gtd.W Irumide B.,Zm	Anorogenic porph biot granite gneiss	1627	12	1639	1615	zircon	shrimp U-Pb	De Waele et al, 2003c
17		G2 Lukamfwa Hill gtd.W Irumide B.,Zm	Anorogenic porph biot granite gneiss	1639	14	1653	1625	zircon	shrimp U-Pb	De Waele et al, 2003c
18		G2 Lukamfwa Hill gtd.W Irumide B.,Zm	Anorogenic porph biot granite gneiss	1650	4	1654	1646	zircon	shrimp U-Pb	De Waele et al, 2003c
19		G2 Lukamfwa Hill gtd.W Irumide B.,Zm	Anorogenic porph biot granite gneiss	1664	4	1668	1660	zircon	shrimp U-Pb	De Waele et al, 2003c
20		Manshya River Group, Irumide B., Zm	Rhyolitic tuff	1856	4	1860	1852	zircon	shrimp U-Pb	De Waele et al, 2003c
21		Mansa, Irumide B., Zm	Undeformed biot. Gt into Luapula volcs.	1860	13	1873	1847	zircon	shrimp U-Pb	De Waele et al, 2003c
22		Mansa, Irumide B., Zm	Undeformed biot. Gt into Luapula volcs.	1862	8	1870	1854	zircon	shrimp U-Pb	De Waele et al, 2003c
23		Mansa, Irumide B., Zm	Luapula acid volcanics	1862	19	1881	1843	zircon	shrimp U-Pb	De Waele et al, 2003c
24		Mansa, Irumide B., Zm	Undeformed biot. Gt into Luapula volcs.	1866	9	1875	1857	zircon	shrimp U-Pb	De Waele et al, 2004a
25		Mansa, Irumide B., Zm	Luapula acid volcanics	1868	7	1875	1861	zircon	shrimp U-Pb	De Waele et al, 2003c
26		Manshya River Group, Irumide B., Zm	Rhyolitic tuff	1879	13	1892	1866	zircon	shrimp U-Pb	De Waele et al, 2003c
27		Muva sequence, SW Chinsali, Zm	Conformable metarhyolite	1880	12	1892	1868	zircon	shrimp U-Pb	De Waele & Mapani, 2002
28		Luwalizi Granite, NE Irumide B., Zm	Weakly deformed granite	1937	10	1947	1927	zircon	shrimp U-Pb	De Waele et al, 2003c
29		Luwalizi Granite, NE Irumide B., Zm	Weakly deformed granite	1942	6	1948	1936	zircon	shrimp U-Pb	De Waele et al, 2003c
30		Mansa, Irumide B., Zm	Luapula acid volcanics (Model age)	2095	9	2104	2086	Nd isotop	Tchur	De Waele et al, 2003b
31		Mansa, Irumide B., Zm	Undeformed biot. Gt (Model age)	2116	11	2127	2105	Nd isotop	Tchur	De Waele et al, 2003b
32		Mansa, Irumide B., Zm	Luapula acid volcanics (Model age)	2135	14	2149	2121	Nd isotop	Tchur	De Waele et al, 2003b
33		Mansa, Irumide B., Zm	Undeformed biot. Gt (Model age)	2159	14	2173	2145	Nd isotop	Tchur	De Waele et al, 2003b
34		G2 Lukamfwa Hill gtd.W Irumide B.,Zm	Anor porph biot granite gn (Model age)	2310	55	2365	2255	Nd isotop	Tchur	De Waele et al, 2003b
35		Luwalizi Granite, NE Irumide B., Zm	Weakly deformed gt (Model age)	2372	23	2395	2349	Nd isotop	Tchur	De Waele et al, 2003b
36		Luwalizi Granite, NE Irumide B., Zm	Weakly deformed gt (Model age)	2400	17	2417	2383	Nd isotop	Tchur	De Waele et al, 2003b
37		Manshya River Group, Irumide B., Zm	Rhyolitic tuff (Model age)	2532	109	2641	2423	Nd isotop	Tchur	De Waele et al, 2003b
38		Irumi Hill, Irumide B.,Zm	Irumi quartzite, oldest detrital age	2720	24	2744	2696	monazite	U-Pb	Snelling et al, 1964; Vail et al, 1968
39		G4 gtd Irumide B.,Zm	Coarse biotite granite (Model age)	2808	35	2843	2773	Nd isotop	Tchur	De Waele et al, 2003b
40		G4 gtd Irumide B.,Zm	Coarse biotite granite (Model age)	2948	18	2966	2930	Nd isotop	Tchur	De Waele et al, 2003b
41		Manshya River Group, Irumide B., Zm	Rhyolitic tuff (Model age)	2961	152	3113	2809	Nd isotop	Tchur	De Waele et al, 2003b
42		G2 Lukamfwa Hill gtd.W Irumide B.,Zm	Anor porph biot granite gn (Model age)	3199	229	3428	2970	Nd isotop	Tchur	De Waele et al, 2003b
43		Manshya River Group, Irumide B., Zm	Rhyolitic tuff (Model age)	3238	55	3293	3183	Nd isotop	Tchur	De Waele et al, 2003b

LUANGWA VALLEY, ZAMBIA

	sample	Site/Event	Rock type	age	error	max	min	material	type	reference
1		Luangwa River, border Mozambique, Zm	Lower intercept, deformed orthogneiss	590	50	640	540	zircon	LAM ICPMS	Cox et al, 2002
2		Luangwa River, border Mozambique, Zm	Metamorphism, deformed orthogneiss	1043	19	1062	1024	zircon	LAM ICPMS	Cox et al, 2002
3		Kamono school, Luangwa Terrane, Zm	Foliated granitoid	2050	10	2060	2040	zircon	LAM ICPMS	Cox et al, 2002
4		Luangwa River, border Mozambique, Zm	Strongly-deformed granodiorite-diorite orthogneiss	2808	14	2822	2794	zircon	LAM ICPMS	Cox et al, 2002

OTHER ZAMBIA

	sample	Site/Event	Rock type	age	error	max	min	material	type	reference
1		Sinda Granite,Zm	Gtd	380	10	390	370	Biotite	Rb-Sr	Snelling et al, 1972
2		Lusandwa Syenite,Zm	Syenite	455	5	460	450	Biotite	Rb-Sr	Snelling et al, 1972
3		Chapalapata, Sasare,Zm	Granite	460		460	460	Biotite	Rb-Sr	Snelling et al, 1972
4		Minga Migmatite, Great East Rd,Zm	Migmatite	470		470	470	Biotite	Rb-Sr	Snelling et al, 1972
5		Bukanda near Luapula River,Zm	Galena	480		480	480	Galena	Pb	Snelling et al, 1972
6		Lundazi,Zm	Mica-beryl pegmatite	485		485	485	Betafite	U-Pb	Snelling et al, 1972
7		Chinyunyu zone,Zm	Sheared granite	500	20	520	480	Biotite	K-Ar	Snelling et al, 1972
8		Chinyunyu zone,Zm	Sheared granite	505	20	525	485	Biotite	K-Ar	Snelling et al, 1972
9		Sachenga mica claims,Zm	Pegmatite	550	20	570	530	Muscovite	K-Ar	Snelling et al, 1972
10		Mivula Syenite,N Province,Zm	Syenite	550	20	570	530	Biotite	K-Ar	Snelling et al, 1972
11		Kamfinsa Quarry,Zm	Pegmatite	560	20	580	540	Biotite	K-Ar	Snelling et al, 1972
12		Migmatitic biotite gneiss,Zm	Migmatitic biotite gneiss,Zm	565	24	589	541	Biotite	K-Ar	Snelling et al, 1972
13		Migmatitic biotite gneiss,Zm	Migmatitic biotite gneiss,Zm	567	24	591	543	Biotite	K-Ar	Snelling et al, 1972
14		Nkombwa Carbonatite,Zm	Fenite	680	25	705	655	Phlogopit	K-Ar	Snelling et al, 1972
15		Mafingi Group Phyllite,Zm	Phyllite	690	20	710	670	w.r.	K-Ar	Snelling et al, 1972
16		Old Millberg Claims,Zm	Galena	695		695	695	Galena	Pb	Snelling et al, 1972
17		Galena veins near Kabwe,Zm	Galena	712		712	712	Galena	Pb	Snelling et al, 1972
18		Chiwanda,Zm	Galena	734		734	734	Galena	Pb	Snelling et al, 1972
19		Mafingi Group Phyllite,Zm	Phyllite	770	25	795	745	w.r.	K-Ar	Snelling et al, 1972
20		Isoka District, Zm	Porphyroblastic biotite gneiss	870	36	906	834	Biotite	K-Ar	Snelling et al, 1972
21		Isoka District, Zm	Porphyroblastic biotite gneiss	890	36	926	854	Biotite	K-Ar	Snelling et al, 1972
22		Northeast of Chinsali,Zm	Biotite gneiss	905	36	941	869	Biotite	K-Ar	Snelling et al, 1972
23		Rufunsa Area, Eastern Zm	Granite	927		927	927	zircon	U-Pb	Barr et al, 1978
24		Rufunsa Area, Eastern Zm	Granite and porphyry	945	30	975	915	zircon	U-Pb	Barr et al, 1978
25		Rufunsa Area, Eastern Zm	Porphyry	955		955	955	zircon	U-Pb	Barr et al, 1978
26		near Kariba Dam, Zm	Amphibolite	960	30	990	930	Bt-w.r.	Rb-Sr	Snelling et al, 1972
27		Phoenix mica claims,Zm	Pegmatite	1045	30	1075	1015	Muscovite	Rb-Sr	Snelling et al, 1972
28		Phoenix mica claims,Zm	Pegmatite	1050	40	1090	1010	Muscovite	Rb-Sr	Snelling et al, 1972
29		Chipata Area, Eastern Zm	Granitic orthogneiss	1071	8	1079	1063	zircon	Pb/Pb	Haslam et al, 1986
30		Mafingi Hills,Zm	Granite gneiss	1120	30	1150	1090	Plagioclas	Rb-Sr	Snelling et al, 1972
31		Mafingi Hills,Zm	Lamprophyre	1145	60	1205	1085	riebeckite	K-Ar	Snelling et al, 1972
32		Lusenga Syenite,Zm	Syenite	1390	200	1590	1190	w.r.	Rb-Sr	Snelling et al, 1972
33		Chewore Ophiolite, Zm	Plagiogranite sheet in ophiolite	1393	22	1415	1371	zircon	shrimp U-Pb	Johnson & Oliver, 2000; Oliver, et al, 1998
34		Ufipa Gneiss near Mbala,Zm	Gneiss	1425	50	1475	1375	Biotite	K-Ar	Snelling et al, 1972
35		Kamfinsa Quarry,Zm	Pegmatite	1550	50	1600	1500	Biotite	K-Ar	Snelling et al, 1972
36		Lumi gneissic granite,Zm	Granite	1590	50	1640	1540	Biotite	K-Ar	Snelling et al, 1972
37		Plateau Series,Zm	Pegmatite cutting Plateau Series	1785	70	1855	1715	K-feldspa	K-Ar	Snelling et al, 1972
38		Orange River Group,Nm		2000		2000	2000			Miller, 1999
39		Changwena River, Irumi Hill,Zm	Monazite	2720	20	2740	2700	Monazite	U-Pb	Snelling et al, 1972
40		Changwena River, Irumi Hill,Zm	Monazite	2720	20	2740	2700	Monazite	U-Pb	Snelling et al, 1972
41		Kapiri Mposhi, Zm	Granite	2738	4	2742	2734	zircon	shrimp U-Pb	De Waele et al, 2003c

TRUE KAMANJAB, NAMIBIA

	sample	Site/Event	Rock type	age	error	max	min	material	type	reference
1	L-795	Ugab River, Nm	Gtd	540	4	544	536	zircon		This report
2		Kamanjab Batholith,Nm	Gtd	558	20	578	538	zircon	U-Pb	Clifford et al, 1969
3		Kamanjab Batholith,Nm	tectonic activity	1580	20	1600	1560	zircon	U-Pb	Burger et al, 1976
4		Franzfontein Granite, Nm	Granite	1662	30	1692	1632	zircon	U-Pb	Burger et al, 1976
5	L-796	Ugab,Nm	inherited zircons in gtd	1700	10	1710	1690	zircon	U-Pb	This report
6		Khoabendus Group,Nm	Felsic metavolcanics	1813		1860	1765	zircon	U-Pb	Burger & Coertze, 1973
7		Franzfontein Granite, Nm	Granite	1838	30	1868	1808	zircon	U-Pb	Burger et al, 1976
8		Gelbingen Farm, Nm	Quartz eye rhyolite	1862	6	1868	1856	zircon	U-Pb	Steven & Armstrong, 2002
9	L-993	Kamanjab Batholith,Nm	Granite	1866	13	1853	1879	zircon	U-Pb	This report
10	L-1013	Kamanjab Batholith,Nm	Quartzmonzonite	1878	15	1863	1893	zircon	U-Pb	This report
11		Kamanjab inlier, Nm	bimodal vulc + intrusion	1880	80	1960	1800	zircon	U-Pb	Burger et al, 1976
12	L-943	Kamanjab Batholith,Nm	Granite	1887	39	1848	1926	zircon	U-Pb	This report
13	L-868	Kamanjab Batholith,Nm	Quartzmonzonite	1937	14	1923	1951	zircon	U-Pb	This report
14	L-855	Kamanjab Batholith,Nm	Granite	1937	19	1918	1956	zircon	U-Pb	This report
15	L-1045	Grootfontein Inlier, Nm	Quartzmonzonite	1939	64	1875	2003	zircon	U-Pb	This report
16	L-969	Kamanjab Batholith,Nm	Foid syenite	1976	42	1934	2018	zircon	U-Pb	This report
17		Khoabendus Formation,Nm	Flow-banded rhyolite	1987	4	1991	1983	zircon	Pb/Pb ev	Hoffman & Kroner, unpub in Seth, 1998
18	L-855	Kamanjab Batholith,Nm	inherited zircons in gtd	2500	19	2481	2519	zircon	U-Pb	This report
19	L-1045	Grootfontein Inlier, Nm	inherited zircons in gtd	2549	78	2471	2627	zircon	U-Pb	This report

KHORIXAS INLIER, NAMIBIA

	sample	Site/Event	Rock type	age	error	max	min	material	type	reference
1		Huab Complex,Nm	Gtd (Tectonic event age)	488		537	437	zircon	U-Pb	Tegtmeyer & Kroner, 1985
2		Oas Farm,Nm	Syenite	736		869	595	zircon	U-Pb	Tegtmeyer & Kroner, 1985
3	L-716	Oas Farm, Nm (basement)	Host gtd	745	5	750	740	zircon	U-Pb	This report
4	PH.11.9	Summas Mountains,Nm	Rhyolitic lava flow	746	2	748	744	zircon	U-Pb	Hoffman et al, 1996
5	PH.12.9	Summas Mountains	Ash-flow tuff	746	2	744	748	zircon	U-Pb	Hoffman et al, 1996
6	PH.11.9	Lower Ugab rhyolite lava	Rhyolite lava	747	2	745	749	zircon	U-Pb	Hoffman et al, 1996
7	L-758	Mesopotamie Farm,Nm	Graphic granite	750	5	755	745	zircon	U-Pb	This report
8	PH.10.9	Oas Farm,Nm	Quartz syenite	756	2	758	754	zircon	U-Pb	Hoffman et al, 1996
9	L-688	Oas Farm,Nm (older intrusive)	Syenite intrusion	762	12	774	750	zircon	U-Pb	This report
10	L-693	Oas Farm, Nm (young intrusive)	Dark subvolcanic intrusive (alkali gtd)	765	4.5	770	761	zircon	U-Pb	This report
11		Oas Farm, Nm	Gtd	783	18	801	765	zircon	U-Pb	Burger & Kroner in Tegtmeyer,1985
12	PRU142	Oas Farm, Nm	Gtd	840	13	853	827	zircon	U-Pb	Kroner in Tegtmeyer,1985
13	L-758	Mesopotamie Farm,Nm	inherited zircons in gtd	1692	10	1702	1682	zircon	U-Pb	This report
14	PRU141	Huab Complex,Nm	Granitic gneiss	1749		1827	1679	zircon	U-Pb	Tegtmeyer & Kroner, 1985
15	L-728	Lofdal Farm,Nm	Foliated Gtd	1750	5	1755	1745	zircon	U-Pb	This report
16	PRU144	Huab Complex,Nm	Gtd	1811		1850	1776	zircon	U-Pb	Tegtmeyer & Kroner, 1985
17	PRU142	Oas Farm,Nm	Syenite, inherited zircons	2124		2192	2070	zircon	U-Pb	Tegtmeyer & Kroner, 1985

ALL KAMANJAB AREA, NAMIBIA (gray is Khorixas)

	sample	Site/Event	Rock type	age	error	max	min	material	type	reference
1		Huab Complex,Nm	Gtd (Tectonic event age)	488		537	437	zircon	U-Pb	Tegtmeyer & Kroner, 1985
2	L-795	Ugab River, Nm	Gtd	540	4	544	536	zircon		This report
3		Kamanjab Batholith,Nm	Gtd	558	20	578	538	zircon	U-Pb	Clifford et al, 1969
4		Oas Farm,Nm	Syenite	736		869	595	zircon	U-Pb	Tegtmeyer & Kroner, 1985
5	L-716	Oas Farm, Nm (basement)	Host gtd	745	5	750	740	zircon	U-Pb	This report
6	PH.11.9	Summas Mountains,Nm	Rhyolitic lava flow	746	2	748	744	zircon	U-Pb	Hoffman et al, 1996
7	PH.12.9	Summas Mountains	Ash-flow tuff	746	2	744	748	zircon	U-Pb	Hoffman et al, 1996
8	PH.11.9	Lower Ugab rhyolite lava	Rhyolite lava	747	2	745	749	zircon	U-Pb	Hoffman et al, 1996
9	L-758	Mesopotamie Farm,Nm	Graphic granite	750	5	755	745	zircon	U-Pb	This report
10	PH.10.9	Oas Farm,Nm	Quartz syenite	756	2	758	754	zircon	U-Pb	Hoffman et al, 1996
11	L-688	Oas Farm,Nm (older intrusive)	Syenite intrusion	762	12	774	750	zircon	U-Pb	This report
12	L-693	Oas Farm, Nm (young intrusive)	Dark subvolcanic intrusive (alkali gtd)	765	4.5	770	761	zircon	U-Pb	This report
13		Oas Farm, Nm	Gtd	783	18	801	765	zircon	U-Pb	Burger & Kroner in Tegtmeyer,1985
14	PRU142	Oas Farm, Nm	Gtd	840	13	853	827	zircon	U-Pb	Kroner in Tegtmeyer,1985
15		Kamanjab Batholith,Nm	tectonic activity	1580	20	1600	1560	zircon	U-Pb	Burger et al, 1976
16		Franzfontein Granite, Nm	Granite	1662	30	1692	1632	zircon	U-Pb	Burger et al, 1976
17	L-758	Mesopotamie Farm,Nm	inherited zircons in gtd	1692	10	1702	1682	zircon	U-Pb	This report
18	L-796	Ugab,Nm	inherited zircons in gtd	1700	10	1710	1690	zircon	U-Pb	This report
19	PRU141	Huab Complex,Nm	Granitic gneiss	1749		1827	1679	zircon	U-Pb	Tegtmeyer & Kroner, 1985
20	L-728	Lofdal Farm,Nm	Foliated Gtd	1750	5	1755	1745	zircon	U-Pb	This report
21	PRU144	Huab Complex,Nm	Gtd	1811		1850	1776	zircon	U-Pb	Tegtmeyer & Kroner, 1985
22		Khoabendus Group,Nm	Felsic metavolcanics	1813		1860	1765	zircon	U-Pb	Burger & Coertze, 1973
23		Franzfontein Granite, Nm	Granite	1838	30	1868	1808	zircon	U-Pb	Burger et al, 1976
24		Gelbingen Farm, Nm	Quartz eye rhyolite	1862	6	1868	1856	zircon	U-Pb	Steven & Armstrong, 2002
25	L-993	Kamanjab Batholith,Nm	Granite	1866	13	1853	1879	zircon	U-Pb	This report
26	L-1013	Kamanjab Batholith,Nm	Quartzmonzonite	1878	15	1863	1893	zircon	U-Pb	This report
27		Kamanjab inlier, Nm	bimodal vulc + intrusion	1880	80	1960	1800	zircon	U-Pb	Burger et al, 1976
28	L-943	Kamanjab Batholith,Nm	Granite	1887	39	1848	1926	zircon	U-Pb	This report
29	L-868	Kamanjab Batholith,Nm	Quartzmonzonite	1937	14	1923	1951	zircon	U-Pb	This report
30	L-855	Kamanjab Batholith,Nm	Granite	1937	19	1918	1956	zircon	U-Pb	This report
31	L-1045	Grootfontein Inlier, Nm	Quartzmonzonite	1939	64	1875	2003	zircon	U-Pb	This report
32	L-969	Kamanjab Batholith,Nm	Foid syenite	1976	42	1934	2018	zircon	U-Pb	This report
33		Khoabendus Formation,Nm	Flow-banded rhyolite	1987	4	1991	1983	zircon	Pb/Pb ev	Hoffman & Kroner, unpub in Seth, 1998
34	PRU142	Oas Farm,Nm	Syenite, inherited zircons	2124		2192	2070	zircon	U-Pb	Tegtmeyer & Kroner, 1985
35	L-855	Kamanjab Batholith,Nm	inherited zircons in gtd	2500	19	2481	2519	zircon	U-Pb	This report
36	L-1045	Grootfontein Inlier, Nm	inherited zircons in gtd	2549	78	2471	2627	zircon	U-Pb	This report

WITVLEI AREA AND POSSIBLE CORRELATIVES IN THE REGION

	sample	Site/Event	Rock type	age	error	max	min	material	type	reference
1		Northeast of Chinsali,Zm	Biotite gneiss	905	36	941	869	Biotite	K-Ar	Snelling et al, 1972
2		Rufunsa Area, Eastern Zm	Granite	927		927	927	zircon	U-Pb	Barr et al, 1978
3	RehBl	Gamsberg, Uitdraai granite, Nm	Ghoab Oos 381	930	70	1000	860	zircon	U-Pb	Hugo & Schalk, 1974
4	RehBl	Gamsberg, Uitdraai granite, Nm	Ghoab Oos 381	932	50	982	882	zircon	U-Pb	Burger & Coertze, 1975
5	RehBl	Gamsberg, Uitdraai granite, Nm	Uitdraai Oos 296	932	50	982	882	zircon	U-Pb	Hugo & Schalk, 1974
6		G4 gtd Irumide B.,Zm	Coarse biotite granite	943	5	948	938	zircon	shrimp U-Pb	De Waele et al, 2003c
7		Rufunsa Area, Eastern Zm	Granite and porphyry	945	30	975	915	zircon	U-Pb	Barr et al, 1978
8	RehBl	Gamsberg S, Nm	Oorwinning 134	948	20	968	928	zircon	U-Pb	Burger & Coertze, 1975
9	KES5	Namibrand-Sesriem area, Nm	Oorwinning 134 granite	948	20	968	928	zircon	U-Pb	Burger & Coertze, 1975
10		Rufunsa Area, Eastern Zm	Porphyry	955		955	955	zircon	U-Pb	Barr et al, 1978
11		Awasib Granite, Sinclair,Nm	A-type slightly peralkaline granite	957	50	1007	907			Hoal, 1990
12		near Kariba Dam, Zm	Amphibolite	960	30	990	930	Bt-w.r.	Rb-Sr	Snelling et al, 1972
13		Chinsali, Irumide B., Zm	Kaunga Granite	970	5	975	965	zircon	U-Pb	Daly, 1986 in De Waele & M, 2002
14	RehBl	Gamsberg S, Nm	Oorwinning 134	976	20	996	956	zircon	U-Pb	Burger & Coertze, 1978
15	KES13	Namibrand-Sesriem area, Nm	Oorwinning 134 porphyry	976	20	996	956	zircon	U-Pb	Burger & Coertze, 1975
16		Chinsali, N Irumide B.,Zm	Mutangoshi (or grey) biotite granite	1009	12	1021	997	zircon	shrimp U-Pb	De Waele & Mapani, 2002
17	RehBl	Gamsberg, Kobos granite, Nm	Nauzerus 1	1010	70	1080	940	zircon	U-Pb	Hugo & Schalk, 1974
18		Namaqua, Nm, Nm	Luderitz Tschaukaib granite	1012	10	1022	1002	zircon	U-Pb	Burger, 1976
19		Serenje area, Zm	Sasa, leucocratic biotite porphyritic granite	1018	6	1024	1012	zircon	shrimp U-Pb	De Waele et al,2001; De Waele & M, 2002
20		Namaqua, Nm, Nm	Luderitz Tschaukaib granite	1018	10	1028	1008	zircon	U-Pb	Burger, 1976
21		Mutangoshi granite, N Irumide B.,Zm	Mesocratic, fine-grained granite	1021	3	1024	1018	zircon	shrimp U-Pb	De Waele & Mapani, 2002
22		Serenje area, Zm	Porphyritic granite	1022	12	1034	1010	zircon	shrimp U-Pb	De Waele et al,2001; De Waele & M, 2002
23		Namaqua, Nm, Nm	Luderitz Glockenberg granite	1022	10	1032	1012	zircon	U-Pb	Burger, 1976
24		Serenje area, Zm	Porphyritic granite	1024	13	1037	1011	zircon	shrimp U-Pb	De Waele et al,2001; De Waele & M, 2002
25		Serenje area, Zm	Porphyritic granite	1025	10	1035	1015	zircon	shrimp U-Pb	De Waele et al,2001; De Waele & M, 2002
26		G4 gtd. W Irumide B.,Zm	Anorogenic porph biot granite gneiss	1027	13	1040	1014	zircon	shrimp U-Pb	De Waele et al, 2003c
27	BK-27	Kaoko belt, Hoanib River, NW Nm	Xenocrystic zircon in augen gneiss	1032	130	1162	902	zircon	U-Pb	Seth et al, 1998
28		Serenje area, Zm	Porphyritic granite	1033	15	1048	1018	zircon	shrimp U-Pb	De Waele et al, 2002b
29		G4 gtd Irumide B.,Zm	Coarse biotite granite	1036	13	1049	1023	Nd isotop	shrimp U-Pb	De Waele et al, 2003b
30		G4 gtd Irumide B.,Zm	Coarse biotite granite	1037	16	1053	1021	Nd isotop	shrimp U-Pb	De Waele et al, 2003b
31		Serenje area, Zm	Porphyritic granite	1038	10	1048	1028	zircon	shrimp U-Pb	De Waele et al,2001; De Waele & M,2002
32		G4 gtd Irumide B.,Zm	Coarse biotite granite	1042	47	1042	948	zircon	shrimp U-Pb	De Waele et al, 2003c
33		Luangwa River, border Mozambique, Zm	Metamorphism, deformed orthogneiss	1043	19	1062	1024	zircon	LAM ICPMS	Cox et al, 2002
34		Phoenix mica claims,Zm	Pegmatite	1045	30	1075	1015	Muscovite	Rb-Sr	Snelling et al, 1972
35		Namaqualand Metamorphic Complex,Nm	Granites and basic to ultrabasic rocks	1050		1200	900			Jackson, 1976; Schreuder & Genis, 1978
36		Phoenix mica claims,Zm	Pegmatite	1050	40	1090	1010	Muscovite	Rb-Sr	Snelling et al, 1972

WITVLEI AREA AND POSSIBLE CORRELATIVES IN THE REGION (cont.)

	sample	Site/Event	Rock type	age	error	max	min	material	type	reference
37	BK-426	Kaoko belt, Hoanib River, NW Nm	Xenocrystic zircon in augen gneiss	1052	4	1056	1048	zircon	U-Pb	Seth et al, 1998
38		Namaqua, Nm, Nm	Townlands tonalitic augengneiss	1052	10	1062	1042	zircon	U-Pb	Burger, 1976
39		Mutangoshi granite, N Irumide B.,Zm	Coarse-grained felsic granite	1053	7	1060	1046	zircon	U-Pb	De Waele & Mapani, 2002
40		G4 gtd. W Irumide B.,Zm	Anorogenic porph biot granite gneiss	1055	13	1068	1042	zircon	shrimp U-Pb	De Waele et al, 2003c
41		G4 gtd Irumide B.,Zm	Coarse biotite granite	1055	13	1068	1042	zircon	shrimp U-Pb	De Waele et al, 2003c
42		Mtuga aplites, Mkushi,Zm	emplacement of aplite	1059	26	1085	1033	zircon	U-Pb	Rainaud, et al, 2004
43		Nuckopf Formation,Nm	Coarse, quartz feldspar porphyries	1061		1090	1032			Burger & Coetze, 1975
44		Omitiomire, Nm	Foliated tonalite	1063	9	1072	1054	zircon	U-Pb	Steven et al, 2000
45	RehBl	Gamsberg, Kobos granite, Nm	Kanaus S 336	1064	20	1084	1044	zircon	U-Pb	Burger & Coertze, 1975
46		Chipata Area, Eastern Zm	Granitic orthogneiss	1071	8	1079	1063	zircon	Pb/Pb	Haslam et al, 1986
47	RehBl	Gamsberg, Gamsberg granite, Nm	Gamsberg 23	1077	26	1202	1010	zircon	U-Pb	Nagel, 2000
48	RehBl	Gamsberg, Gamsberg granite, Nm	Hohenheim 24	1078	30	1108	1048	zircon	U-Pb	Burger & Coertze, 1975
49	RehBl	Gamsberg, Gamsberg granite, Nm	Gamsberg 23	1079	30	1142	1038	zircon	U-Pb	Nagel, 2000
50	RehBl	Gamsberg, Gamsberg granite, Nm	Hohenheim 24	1080	70	1150	1010	zircon	U-Pb	Hugo & Schalk, 1974
51		Namaqua, Nm, Nm	Hottentots Bay Namaqua augengneiss	1080	10	1090	1070	zircon	U-Pb	Burger, 1976
52		Omitiomire, Nm	Chalcocite-bearing amphibole schist	1081	10	1091	1071	zircon	U-Pb	Steven et al, 2000
53		Namaqua, Nm, Nm	Grasplatz quartz monzonitic gneiss	1082	10	1092	1072	zircon	U-Pb	Burger, 1976
54	RehBl	Nauzerus G, Kartatsaus F, Nm	Uitdraai Oos 296	1083	30	1113	1053	zircon	U-Pb	Burger & Coertze, 1975
55	RehBl	Gamsberg, Rostock granite, Nm	Greilingshof 107	1084	8	1092	1076	zircon	U-Pb	Pfurr et al, 1990
56		Namaqua, Nm, Nm	Luderitz Glockenberg granite	1086	10	1096	1076	zircon	U-Pb	Burger, 1976
57		Mkushi Gneiss, Zm	Granitic gneiss (zircon rims)	1088	159	1247	929	zircon	shrimp U-Pb	Robb in De Waele et al,2001a
58	RehBl	Gamsberg, Gamsberg granite, Nm	Abendruhe 411	1089	30	1119	1059	zircon	U-Pb	Burger & Coertze, 1975
59	RehBl	Nauzerus G, Kartatsaus F, Nm	Kaartatsaus 293	1090	30	1120	1060	zircon	U-Pb	Burger & Coertze, 1975
60	RehBl	Nauzerus G, Kartatsaus F, Nm	Kaartatsaus 293	1090	70	1160	1020	zircon	U-Pb	Hugo & Schalk, 1974
61	RehBl	Nauzerus G, Kartatsaus F, Nm	Kaartatsaus 293	1090	70	1160	1020	zircon	U-Pb	Hugo & Schalk, 1974
62	RehBl	Oorlogsende F, Nm	Epukiro area	1094	30	1112	1074	zircon	U-Pb	Hegenberger & Burger, 1985
63		Mpande Dome (south), Southern Zm	Fine-grained granite	1095	12	1107	1083	zircon	U-Pb	De Waele et al, 2000a
64	RehBl	Gamsberg, Gamsberg granite, Nm	Gamsberg 23	1095	30	1216	1074	zircon	U-Pb	Nagel, 2000
65	RehBl	Gamsberg, Rostock granite, Nm	Greilingshof 107	1097	24	1121	1073	zircon	U-Pb	Pfurr et al, 1990
66	L-638	Witvlei Gtd,Nm	Gtd	1098	5.9	1104	1092	zircon	U-Pb	This report
67	RehBl	Gamsberg, Rostock granite, Nm	Greilingshof 107	1099	16	1115	1083	zircon	U-Pb	Pfurr et al, 1990
68		Lusaka Granite,Zm	Granite	1100	70	1170	1030	Plagioclas	Rb-Sr	Snelling et al, 1972
69	RehBl	Gamsberg, Rostock granite, Nm	Rostock S 414	1102	7	1109	1095	zircon	U-Pb	Pfurr et al, 1990
70	RehBl	Gamsberg, Koichas granite, Nm	Kangas 371	1104	20	1124	1084	zircon	U-Pb	Burger & Coertze, 1975
71		Mpande Gneiss, Southern Zm	Granitic orthogneiss	1106	19	1125	1087	zircon	U-Pb	Hanson et al, 1988, 1994
72		Kwebe Mills,Botswana	Ghanzi Rhyolite	1106	2	1108	1104	zircon	U-Pb	Schwartz et al, 1996
73	RehBl	Gamsberg, Biesespoort granite, Nm	Biesiepoort 275	1110	30	1140	1080	zircon	U-Pb	Burger & Coertze, 1978
74	RehBl	Gamsberg, Gamsberg granite, Nm	Nauzerus 1	1110	30	1140	1080	zircon	U-Pb	Burger & Coertze, 1975
75		Namaqua, Nm	Hottentots Bay Namaqua augengneiss	1114	10	1124	1104	zircon	U-Pb	Burger, 1976
76		Namaqua, Nm	Jannelspan F. Garub station, Aus biot schist	1116	10	1126	1106	zircon	U-Pb	Burger, 1976
77		Mafingi Hills,Zm	Granite gneiss	1120	30	1150	1090	Plagioclas	Rb-Sr	Snelling et al, 1972
78	RehBl	Oorlogsende F, Nm	Epukiro area	1127	30	1157	1097	zircon	U-Pb	Burger & Walraven, 1980
79	RehBl	Nauzerus G, Nuckopf F, Nm	Lekkerwater 144	1130	75	1205	1055	zircon	U-Pb	Ziegler & Stoessel, 1993
80		Namaqua, Nm	Luderitz felsic volcanics	1131	10	1141	1121	zircon	U-Pb	Burger, 1976
81	RehBl	Gamsberg, Gamsberg granite, Nm	Gamsberg 23	1132	26	1158	1106	zircon	U-Pb	Ziegler & Stoessel, 1993
82	RehBl	Nauzerus G, Nuckopf F, Nm	Kunineib 378	1132	75	1207	1057	zircon	U-Pb	Hilken, 1977
83		Namaqua, Nm	Luderitz felsic volcanics	1132	10	1142	1122	zircon	U-Pb	Burger, 1976
84	RehBl	Oorlogsende F, Nm	Epukiro area	1144	30	1174	1114	zircon	U-Pb	Burger & Walraven, 1979
85		Mafingi Hills,Zm	Lamprophyre	1145	60	1205	1085	riebeckite	K-Ar	Snelling et al, 1972
86	RehBl	Gamsberg, Ganeib granite, Nm	Danigas 289	1150	30	1180	1120	zircon	U-Pb	Burger & Coertze, 1975
87		Piksteel Granodiorite, Rehoboth,Nm	Med-coarse-grained porphyritic biotite granodiorite	1170	20	1190	1150			Reid et al, 1988
88	KES7	Namibrand-Sesriem area, Nm	Sesriem 134 Eesaam F	1170	30	1200	1140	zircon	U-Pb	Burger & Coertze, 1975
89	CK4	Choma-Kalomo Batholith, Zm	Medium-grained two mica granite	1174	27	1201	1147	zircon	shrimp U-Pb	Bulambo et al, 2004
90	CK12	Choma-Kalomo Batholith, Zm	Gneiss containing mica-rich restites	1177	70	1247	1107	zircon	shrimp U-Pb	Bulambo et al, 2004
91	RehBl	Gamsberg, Kobos granite, Nm	Nauchas 14	1178	20	1198	1158	zircon	U-Pb	Burger & Coertze, 1975
92		Namaqua, Nm	Luderitz Glockenberg granite	1178	10	1188	1168	zircon	U-Pb	Burger, 1976
93	CK25	Choma-Kalomo Batholith, Zm	Foliated, med-coarse-g biotite granite	1181	9	1190	1172	zircon	shrimp U-Pb	Bulambo et al, 2004
94		Namaqua, Nm	Luderitz felsic volcanics	1184	10	1194	1174	zircon	U-Pb	Burger, 1976
95	RehBl	Gamsberg, Gamsberg granite, Nm	Corona 223	1186	30	1240	1147	zircon	U-Pb	Nagel, 2000
96	CK10	Choma-Kalomo Batholith, Zm	Foliated med-coarse-g biotite granite	1188	11	1199	1177	zircon	shrimp U-Pb	Bulambo et al, 2004
97	L-638	Okatjepuiko,Nm xenocrystic	Granitoid	1194	11	1205	1183	zircon	Pb/U shrimp	This report
98	RehBl	Gamsberg, Rostock granite, Nm	Rostock S 414	1194	26	1220	1168	zircon	U-Pb	Pfurr et al, 1990
99		Namaqua, Nm	Luderitz Glockenberg granite	1194	10	1204	1184	zircon	U-Pb	Burger, 1976
100		Basement, Kabompo Dome,Zm	Gtd	1200	50	1250	1150	zircon	U-Pb	AGIP, 1985
101		Lusaka Granite,Zm	Granite	1200	96	1296	1104	Plagioclas	Rb-Sr	Snelling et al, 1972
102	RehBl	Gamsberg, Rostock granite, Nm	Rostock N 393	1207	15	1222	1192	zircon	U-Pb	Pfurr et al, 1990
103	RehBl	porphyry dike, Nm	Marienhof 577	1210	7	1217	1203	zircon	U-Pb	Ziegler & Stoessel, 1993
104	RehBl	Gamsberg S, Nn	Morgenroth 17	1210	8	1218	1202	zircon	U-Pb	Ziegler & Stoessel, 1993
105	RehBl	Nauzerus G, Nuckopf F, Nm	Areb North 202	1221	35	1257	1192	zircon	U-Pb	Schalk, 1970
106		Biesiespoort Granite,Nm	Foliated granite	1222	45	1267	1177			Miller, 1999
107	RehBl	Nauzerus G, Kartatsaus F, Nm	Spitskop F	1232	30	1262	1202	zircon	U-Pb	Burger & Coertze, 1978
108		Namaqua, Nm	Luderitz granite	1233	10	1243	1223	zircon	U-Pb	Burger, 1976
109		Namaqua, Nm	Luderitz granite	1264	10	1274	1254	zircon	U-Pb	Burger, 1976
110	KES231	Namibrand-Sesriem area, Nm	Hebron 136 Neuhof felsic volcanics	1294	25	1319	1269	zircon	U-Pb	Burger & Walraven, 1978
111	KES9	Namibrand-Sesriem area, Nm	Draaihook 119 Nubib granite	1302	20	1322	1282	zircon	U-Pb	Burger & Coertze, 1975
112	RehBl	Oorlogsende F, Nm	Epukiro area	1313	30	1343	1283	zircon	U-Pb	Burger & Walraven, 1980
113	KES6	Namibrand-Sesriem area, Nm	Sesriem 134 Nubib granite	1350	40	1390	1310	zircon	U-Pb	Burger & Coertze, 1975
114	L-638	Okatjepuiko,Nm xenocrystic	Granitoid	1871	6.8	1878	1864	zircon	Pb/Pb shrimp	This report

CENTRAL NAMIBIA

	sample	Site/Event	Rock type	age	error	max	min	material	type	reference
1		Khan-Swakop River, Nm	Schist, cooling age of biotite (350degC)	448		448	448	Biotite	Rb-Sr	Hawkesworth et al, 1983
2		Rossing Mine, Nm	Uraniferous alaskite, late alaskite	458	8	466	450	w.r.	Rb-Sr	Steven et al, 1993
3		Khan-Swakop River, Nm	Schist, cooling age of biotite (350degC)	465	5	470	460	Biotite	Rb-Sr	Hawkesworth et al, 1983
4		Sandamap Mine, Central Zone,Nm	Stanniferous pegmatite	468	14	482	454	w.r.	Rb-Sr	Steven et al, 1993
5		Sandamap Noord, Central Zone,Nm	Pegmatite	473	23	496	450	w.r.	Sr/Sr	Steven et al, 1993
6		Otjozondjou, Nm	Diorite	478	4	482	474	Hornblend	Ar/Ar	Hawkesworth et al, 1983
7		Stinkbank, Central Zone, Nm	Uraniferous leucogranite, scheelite skarn	484	25	509	459	w.r.	Rb-Sr	Steven et al, 1993
8		Navachab Mine, Cental Zone, Nm	Biotite in skarn	490		490	490	Bt	Rb-Sr	Steven et al, 1993
9		Kohero Tin mine, Central Zone, Nm	Stanniferous pegmatite	492	11	503	481	w.r.	Rb-Sr	Steven et al, 1993
10		Uis Mine, Central Zone, Nm	Stanniferous pegmatite	496	30	526	466	w.r.	Rb-Sr	Steven et al, 1993
11		Ohere, Central Zone, Nm	Leucogranite	506	135	641	371	w.r.	Sr/Sr	Steven et al, 1993
12		Goniakontes alaskite, Nm	Alaskite, post-tectonic doming intrusion	508	2	510	506	uraninite,	U-Pb	Briqueau et al, 1980
13		Gamigab Prospect, Central Zone, Nm	Cassiterite veins	510		510	510	Muscovite	Rb-Sr	Steven et al, 1993
14		Rossing Mine, Nm	Uraniferous alaskite, early alaskite	510		510	510	w.r.	Rb-Sr	Steven et al, 1993
15		Khan formation, Goniakonites, Nm	Syn-metamorphic growth	510	3	513	507	monazite	U-Pb	Briqueau et al, 1980
16		Sandamap Noord, Central Zone,Nm	Leucogranite phacolith	512	19	531	493	w.r.	Sr/Sr	Steven et al, 1993
17		Salem Granite, Goas, Nm	Granite, syn-metamorphic intrusion	512	40	552	472	zircon	U-Pb	Allsopp at al, 1983
18		Rubicon mine, Cental Zone, Nm	Petalite in pegmatite	515	36	551	479	Amb, Kfel	Rb-Sr	Steven et al, 1993
19		Goniakontes, red granite, Nm	Granite, syn-metamorphic anatexis	534	7	541	527	zircon, m	U-Pb	Briueu et al, 1980
20		Salem Granite, Ohere Oos, Nm	Granite	542	11	553	531	w.r.	Sr/Sr	Steven et al, 1993
21		Gariep Complex Intrusives,Nm		550		600	500			Miller, 1999
22		Damara syn to post-tectonic intrusives,Nm	Granites	555		650	460			Miller, 1999
23		Damara volcanics,Nm	Alkaline ignimbrites	780		840	720			Miller, 1999
24		Damaran metased, Navachab mine, Nm	Detrital zircons in Damaran metaseds	1962	10	1972	1952	zircon	U-Pb	Jacob et al, 2003
25		Damaran metased, Navachab mine, Nm	Detrital zircons in Damaran metaseds	2360	5	2365	2355	zircon	U-Pb	Jacob et al, 2003
26		Damaran metased, Navachab mine, Nm	Detrital zircons in Damaran metaseds	2428	9	2437	2419	zircon	U-Pb	Jacob et al, 2003
27		Damaran metased, Navachab mine, Nm	Detrital zircons in Damaran metaseds	2870	6	2876	2864	zircon	U-Pb	Jacob et al, 2003
28		Damaran metased, Navachab mine, Nm	Detrital zircons in Damaran metaseds	2872	4	2876	2868	zircon	U-Pb	Jacob et al, 2003

NORTHERNMOST NAMIBIA

	sample	Site/Event	Rock type	age	error	max	min	material	type	reference
1		Epupa Complex,Nm	Augen gneiss	1795		1828	1766	zircon	U-Pb	Tegtmeyer & Kroner, 1985
2		Kunene Complex,Nm	Anorthosites	2100		2100	2100			Miller, 1999
3	sample	Site/Event	Rock type	age	error	maxin	minim	material	type	reference

SOUTHERNMOST NAMIBIA

	sample	Site/Event	Rock type	age	error	max	min	material	type	reference
1	Mo Porp	Marinkas Kwela, Nm	Syenite,gt,cb	520		550	490	zircon	U-Pb	Bernasconi, 1986
2		Rosh Pinah Formation,Nm		700		700	700			Hoffman, 1989
3		Richtersveld Intrusive Complex,Nm		920		920	920			Miller, 1999
4		Haib porphyry Cu deposit,Nm	Metamorphism	1750	20	1770	1730		Rb-Sr	Minnit, 1986; Barr & Reid, 1993
5		Lorelei porphyry Cu-Mo,Nm	Granodiorite	1900	50	1950	1850		inferred	Viljoen, Minnit,Viljoen, 1986
6		Haib porphyry Cu deposit,Nm	Gtd	1900	5	1905	1895	zircon	U-Pb	Reid, personal communication, 2003

KAOKOVELD, NAMIBIA

	sample	Site/Event	Rock type	age	error	max	min	material	type	reference
1	BK-19	Kaoko belt, Hoanib River, NW Nm	Coarse-g monzogranite	551.9	1.5	553	550	zircon	U-Pb	Seth et al, 1998
2	BK-43	Kaoko belt, Hoanib River, NW Nm	Cg late tectonic granite (migmatite)	563.8	1.5	565	562	zircon	Pb/Pb	Seth et al, 1998
3	BK-43	Kaoko belt, Hoanib River, NW Nm	Cg late tectonic granite (migmatite)	565	13	578	552	zircon	Pb/Pb	Seth et al, 1998
4	BK-24	Kaoko belt, Hoanib River, NW Nm	Foliated cg granodioritic gneiss	567.2	1.5	569	566	zircon	U-Pb	Seth et al, 1998
5	BK-17	Kaoko belt, Hoanib River, NW Nm	Metamorphic age in granitic gneiss	578	57	635	521	zircon	U-Pb	Seth et al, 1998
6	BK-426	Kaoko belt, Hoanib River, NW Nm	Granodioritic augen gneiss	580	3	583	577	zircon	U-Pb	Seth et al, 1998
7	BK-43	Kaoko belt, Hoanib River, NW Nm	Xenocrystic zircon in migmatite	584.3	1.6	586	583	zircon	Pb/Pb	Seth et al, 1998
8	BK-19	Kaoko belt, Hoanib River, NW Nm	Xenocrystic zircon in cg monzogranite	588.1	1.4	590	587	zircon	U-Pb	Seth et al, 1998
9	BK-426	Kaoko belt, Hoanib River, NW Nm	Xenocrystic zircon in augen gneiss	620	42	662	578	zircon	U-Pb	Seth et al, 1998
10	BK-43	Kaoko belt, Hoanib River, NW Nm	Xenocrystic zircon in migmatite	625	9	634	616	zircon	U-Pb	Seth et al, 1998
11	BK-426	Kaoko belt, Hoanib River, NW Nm	Xenocrystic zircon in augen gneiss	630	8	638	622	zircon	U-Pb	Seth et al, 1998
12	BK-27	Kaoko belt, Hoanib River, NW Nm	Coarse-grain augen gneiss	656	8	664	648	zircon	U-Pb	Seth et al, 1998
13	BK-426	Kaoko belt, Hoanib River, NW Nm	Xenocrystic zircon in augen gneiss	710	80	790	630	zircon	U-Pb	Seth et al, 1998
14	BK-27	Kaoko belt, Hoanib River, NW Nm	Xenocrystic zircon in augen gneiss	1032	130	1162	902	zircon	U-Pb	Seth et al, 1998
15	BK-426	Kaoko belt, Hoanib River, NW Nm	Xenocrystic zircon in augen gneiss	1052	4	1056	1048	zircon	U-Pb	Seth et al, 1998
16	BK-17	Kaoko belt, Hoanib River, NW Nm	Foliated red granitic gneiss	1507	16	1523	1491	zircon	U-Pb	Seth et al, 1998
17		Kaoko Belt, 45 km NW Sesfontein,Nm	partly sheared monzogranite	1961	0.6	1962	1960	zircon	U-Pb	Hoffman & Kroner, unpub in Seth, 1998
18	BK-439	Kaoko belt, NW Nm	Cg monzogranitic augen gneiss	1961	4	1965	1957	zircon	U-Pb	Seth et al, 1998
19	BK-10	Kaoko belt, Hoanib River, NW Nm	Foliated syenogranitic orthogneiss	1971	7	1978	1964	zircon	U-Pb	Seth et al, 1998
20		Kaoko Belt, 30 km NW Sesfontein,Nm	partly sheared monzogranite	1978	0.6	1978	1977	zircon	U-Pb	Hoffman & Kroner, unpub in Seth, 1998
21	BK-5	Kaoko belt, NW Nm	Dioritic orthogneiss	1985	23	2008	1962	zircon	U-Pb	Seth et al, 1998
22	BK-10	Kaoko belt, Hoanib River, NW Nm	Xenocrystic zircon in syenogranitic orthogneiss	2033		2033	2033	zircon	U-Pb	Seth et al, 1998
23	BK-5	Kaoko belt, NW Nm	Xenocrystic zircon in dioritic orthogneiss	2281	0.9	2282	2280	zircon	U-Pb	Seth et al, 1998
24	BK-5	Kaoko belt, NW Nm	Xenocrystic zircon in dioritic orthogneiss	2287	10	2297	2277	zircon	U-Pb	Seth et al, 1998
25	BK-29	Kaoko belt, NW Nm	Coarse-grained quartz-monzonitic augen gneiss	2584	0.6	2585	2584	zircon	U-Pb	Seth et al, 1998
26	BK-1	Kaoko belt, NW Nm	Grey, coarse-grained monzonitic augen gneiss	2585	1.2	2587	2584	zircon	U-Pb	Seth et al, 1998
27	BK-5	Kaoko belt, NW Nm	Xenocrystic zircon in dioritic orthogneiss	2600		2600	2600	zircon	U-Pb	Seth et al, 1998
28	BK-5	Kaoko belt, NW Nm	Xenocrystic zircon in dioritic orthogneiss	2605	11	2616	2594	zircon	U-Pb	Seth et al, 1998
29	BK-446	Kaoko belt, NW Nm	Quartz-monzodioritic gneiss	2616	5	2621	2611	zircon	U-Pb	Seth et al, 1998
30	BK-3	Kaoko belt, NW Nm	Fol Quartz-monzodioritic orthogneiss	2645	6	2651	2639	zircon	U-Pb	Seth et al, 1998

REHOBOTH INLIER, NAMIBIA

	sample	Site/Event	Rock type	age	error	max	min	material	type	reference
1	RehBI	Gamsberg, Uitdraai granite	Ghoab Oos 381	930	70	1000	860	zircon	U-Pb	Hugo & Schalk, 1974
2	RehBI	Gamsberg, Uitdraai granite	Ghoab Oos 381	932	50	982	882	zircon	U-Pb	Burger & Coertze, 1975
3	RehBI	Gamsberg, Uitdraai granite	Uitdraai Oos 296	932	50	982	882	zircon	U-Pb	Hugo & Schalk, 1974
4	RehBI	Gamsberg S	Oorwinning 134	948	20	968	928	zircon	U-Pb	Burger & Coertze, 1975
5	RehBI	Gamsberg S	Oorwinning 134	976	20	996	956	zircon	U-Pb	Burger & Coertze, 1978
6	RehBI	Gamsberg, Kobos granite	Nauzerus 1	1010	70	1080	940	zircon	U-Pb	Hugo & Schalk, 1974
7	RehBI	Gamsberg, Kobos granite	Kanaus S 336	1064	20	1084	1044	zircon	U-Pb	Burger & Coertze, 1975
8	RehBI	Gamsberg, Gamsberg granite	Gamsberg 23	1077	26	1202	1010	zircon	U-Pb	Nagel, 2000
9	RehBI	Gamsberg, Gamsberg granite	Hohenheim 24	1078	30	1108	1048	zircon	U-Pb	Burger & Coertze, 1975
10	RehBI	Gamsberg, Gamsberg granite	Gamsberg 23	1079	30	1142	1038	zircon	U-Pb	Nagel, 2000
11	RehBI	Gamsberg, Gamsberg granite	Hohenheim 24	1080	70	1150	1010	zircon	U-Pb	Hugo & Schalk, 1974
12	RehBI	Nauzerus G, Kartatsaus F	Uitdraai Oos 296	1083	30	1113	1053	zircon	U-Pb	Burger & Coertze, 1975
13	RehBI	Gamsberg, Rostock granite	Greilingshof 107	1084	8	1092	1076	zircon	U-Pb	Pfurr et al, 1990
14	RehBI	Gamsberg, Gamsberg granite	Abendruhe 411	1089	30	1119	1059	zircon	U-Pb	Burger & Coertze, 1975
15	RehBI	Nauzerus G, Kartatsaus F	Kaartatsaus 293	1090	30	1120	1060	zircon	U-Pb	Burger & Coertze, 1975
16	RehBI	Nauzerus G, Kartatsaus F	Kaartatsaus 293	1090	70	1160	1020	zircon	U-Pb	Hugo & Schalk, 1974
17	RehBI	Nauzerus G, Kartatsaus F	Kaartatsaus 293	1090	70	1160	1020	zircon	U-Pb	Hugo & Schalk, 1974
18	RehBI	Oorlogsende F	Epukiro area	1094	30	1112	1074	zircon	U-Pb	Hegenberger & Burger, 1985
19	RehBI	Gamsberg, Gamsberg granite	Gamsberg 23	1095	30	1216	1074	zircon	U-Pb	Nagel, 2000
20	RehBI	Gamsberg, Rostock granite	Greilingshof 107	1097	24	1121	1073	zircon	U-Pb	Pfurr et al, 1990
21	RehBI	Gamsberg, Rostock granite	Greilingshof 107	1099	16	1115	1083	zircon	U-Pb	Pfurr et al, 1990
22	RehBI	Gamsberg, Rostock granite	Rostock S 414	1102	7	1109	1095	zircon	U-Pb	Pfurr et al, 1990
23	RehBI	Gamsberg, Koichas granite	Kangas 371	1104	20	1124	1084	zircon	U-Pb	Burger & Coertze, 1975
24	RehBI	Gamsberg, Biesespoort granite	Biesiepoort 275	1110	30	1140	1080	zircon	U-Pb	Burger & Coertze, 1978
25	RehBI	Gamsberg, Gamsberg granite	Nauzerus 1	1110	30	1140	1080	zircon	U-Pb	Burger & Coertze, 1975
26	RehBI	Oorlogsende F	Epukiro area	1127	30	1157	1097	zircon	U-Pb	Burger & Walraven, 1980
27	RehBI	Nauzerus G, Nuckopf F	Lekkerwater 144	1130	75	1205	1055	zircon	U-Pb	Ziegler & Stoessel, 1993
28	RehBI	Gamsberg, Gamsberg granite	Gamsberg 23	1132	26	1158	1106	zircon	U-Pb	Ziegler & Stoessel, 1993
29	RehBI	Nauzerus G, Nuckopf F	Kunineib 378	1132	75	1207	1057	zircon	U-Pb	Hilken, 1977
30	RehBI	Oorlogsende F	Epukiro area	1144	30	1174	1114	zircon	U-Pb	Burger & Walraven, 1979
31	RehBI	Gamsberg, Ganeib granite	Danigas 289	1150	30	1180	1120	zircon	U-Pb	Burger & Coertze, 1975
32	RehBI	Gamsberg, Kobos granite	Nauchas 14	1178	20	1198	1158	zircon	U-Pb	Burger & Coertze, 1975
33	RehBI	Gamsberg, Gamsberg granite	Corona 223	1186	30	1240	1147	zircon	U-Pb	Nagel, 2000
34	RehBI	Gamsberg, Rostock granite	Rostock S 414	1194	26	1220	1168	zircon	U-Pb	Pfurr et al, 1990
35	RehBI	Gamsberg, Rostock granite	Rostock N 393	1207	15	1222	1192	zircon	U-Pb	Pfurr et al, 1990
36	RehBI	porphyry dike	Marienhof 577	1210	7	1217	1203	zircon	U-Pb	Ziegler & Stoessel, 1993
37	RehBI	Gamsberg S	Morgenroth 17	1210	8	1218	1202	zircon	U-Pb	Ziegler & Stoessel, 1993
38	RehBI	Nauzerus G, Nuckopf F	Areb North 202	1221	35	1257	1192	zircon	U-Pb	Schalk, 1970
39	RehBI	Nauzerus G, Kartatsaus F	Spitskop F	1232	30	1262	1202	zircon	U-Pb	Burger & Coertze, 1978
40	RehBI	Oorlogsende F	Epukiro area	1313	30	1343	1283	zircon	U-Pb	Burger & Walraven, 1980
41		Alberta Basic Complex,Rehoboth,Nm	Layered gabbroic rocks	1442	32	1474	1410			Reid et al, 1988
42		Rehoboth Area, Nm	Granitic and basic rocks	1545		1670	1420			Miller, and Shalk, 1988
43		Swartmodder Granite,Rehoboth,Nm	Leucocratic granite	1639	25	1664	1614			Reid et al, 1988 and Shalk, 1988
44		Naub Diorite, Rehoboth Area,Nm	hornblende-biotite gneiss	1725	52	1777	1673			Reid et al, 1988
45	RehBI	Nauzerus G, Nuckopf F	Auchas 347	1770	35	1805	1735	zircon	U-Pb	Burger & Coertze, 1978
46	RehBI	Gamsberg, Kobos granite	Kwakwas 251	1775	10	1785	1765	zircon	U-Pb	Nagel, 2000
47		Elim Formation, Rehoboth Area,Nm	Quartzites, siliciclastics and volcanics	1795		1860	1730			Miller, 1999
48		Weener Quartz Diorite,Rehoboth,Nm	Medium-grained quartzdiorite	1871	143	2014	1728			Seifert, 1986

NAMIBRAND-SASRIEM AREA, NAMIBIA

	sample	Site/Event	Rock type	age	error	max	min	material	type	reference
1	KES232	Namibrand-Sesriem area	Hebron 136 Neuhof felsic volcanics	594	10	604	584	zircon	U-Pb	Burger & Walraven, 1978
2	KES5	Namibrand-Sesriem area	Oorwinning 134 granite	948	20	968	928	zircon	U-Pb	Burger & Coertze, 1975
3	KES13	Namibrand-Sesriem area	Oorwinning 134 porphyry	976	20	996	956	zircon	U-Pb	Burger & Coertze, 1975
4	KES7	Namibrand-Sesriem area	Sesriem 134 Eesaam F	1170	30	1200	1140	zircon	U-Pb	Burger & Coertze, 1975
5	KES231	Namibrand-Sesriem area	Hebron 136 Neuhof felsic volcanics	1294	25	1319	1269	zircon	U-Pb	Burger & Walraven, 1978
6	KES9	Namibrand-Sesriem area	Draaihook 119 Nubib granite	1302	20	1322	1282	zircon	U-Pb	Burger & Coertze, 1975
7	KES6	Namibrand-Sesriem area	Sesriem 134 Nubib granite	1350	40	1390	1310	zircon	U-Pb	Burger & Coertze, 1975
8	KES230	Namibrand-Sesriem area	Sesriem 137 Eensam qtz porphyry	1656	40	1696	1616	zircon	U-Pb	Burger & Walraven, 1978

NAMAQUA METAMORPHIC COMPLEX, NAMIBIA (All with 10Ma error for plotting)

	sample	Site/Event	Rock type	age	error	max	min	material	type	reference
1		Namaqua, Nm	Luderitz Tschaukaib granite	1012	10	1022	1002	zircon	U-Pb	Burger, 1976
2		Namaqua, Nm	Luderitz Tschaukaib granite	1018	10	1028	1008	zircon	U-Pb	Burger, 1976
3		Namaqua, Nm	Luderitz Glockenberg granite	1022	10	1032	1012	zircon	U-Pb	Burger, 1976
4		Namaqua, Nm	Townlands tonalitic augengneiss	1052	10	1062	1042	zircon	U-Pb	Burger, 1976
5		Namaqua, Nm	Hottentots Bay Namaqua augengneiss	1080	10	1090	1070	zircon	U-Pb	Burger, 1976
6		Namaqua, Nm	Grasplatz quartz monzonitic gneiss	1082	10	1092	1072	zircon	U-Pb	Burger, 1976
7		Namaqua, Nm	Luderitz Glockenberg granite	1086	10	1096	1076	zircon	U-Pb	Burger, 1976
8		Namaqua, Nm	Hottentots Bay Namaqua augengneiss	1114	10	1124	1104	zircon	U-Pb	Burger, 1976
9		Namaqua, Nm	Jannelspan F. Garub station, Aus biot schist	1116	10	1126	1106	zircon	U-Pb	Burger, 1976
10		Namaqua, Nm	Luderitz felsic volcanics	1131	10	1141	1121	zircon	U-Pb	Burger, 1976
11		Namaqua, Nm	Luderitz felsic volcanics	1132	10	1142	1122	zircon	U-Pb	Burger, 1976
12		Namaqua, Nm	Luderitz Glockenberg granite	1178	10	1188	1168	zircon	U-Pb	Burger, 1976
13		Namaqua, Nm	Luderitz felsic volcanics	1184	10	1194	1174	zircon	U-Pb	Burger, 1976
14		Namaqua, Nm	Luderitz Glockenberg granite	1194	10	1204	1184	zircon	U-Pb	Burger, 1976
15		Namaqua, Nm	Luderitz granite	1233	10	1243	1223	zircon	U-Pb	Burger, 1976
16		Namaqua, Nm	Luderitz granite	1264	10	1274	1254	zircon	U-Pb	Burger, 1976
17		Namaqua, Nm	Luderitz augen gneiss	1742	10	1752	1732	zircon	U-Pb	Burger, 1976
18		Namaqua, Nm	Luderitz augen gneiss	1752	10	1762	1742	zircon	U-Pb	Burger, 1976
19		Namaqua, Nm	Luderitz hbl-gneiss	1755	10	1765	1745	zircon	U-Pb	Burger, 1976
20		Namaqua, Nm	Luderitz Kunguib granodiorite	1952	10	1962	1942	zircon	U-Pb	Burger, 1976
21		Namaqua, Nm	Luderitz Kunguib granodiorite	1978	10	1988	1968	zircon	U-Pb	Burger, 1976

"KIBARAN" ROCKS OF NAMIBIA

	sample	Site/Event	Rock type	age	error	max	min	material	type	reference
1	KES232	Namibrand-Sesriem area	Hebron 136 Neuhof felsic volcanics	594	10	604	584	zircon	U-Pb	Burger & Walraven, 1978
2	RehBl	Gamsberg, Uitdraai granite	Ghoab Oos 381	930	70	1000	860	zircon	U-Pb	Hugo & Schalk, 1974
3	RehBl	Gamsberg, Uitdraai granite	Ghoab Oos 381	932	50	982	882	zircon	U-Pb	Burger & Coertze, 1975
4	RehBl	Gamsberg, Uitdraai granite	Uitdraai Oos 296	932	50	982	882	zircon	U-Pb	Hugo & Schalk, 1974
5	RehBl	Gamsberg S	Oorwinning 134	948	20	968	928	zircon	U-Pb	Burger & Coertze, 1975
6	KES5	Namibrand-Sesriem area	Oorwinning 134 granite	948	20	968	928	zircon	U-Pb	Burger & Coertze, 1975
7	RehBl	Gamsberg S	Oorwinning 134	976	20	996	956	zircon	U-Pb	Burger & Coertze, 1978
8	KES13	Namibrand-Sesriem area	Oorwinning 134 porphyry	976	20	996	956	zircon	U-Pb	Burger & Coertze, 1975
9	RehBl	Gamsberg, Kobos granite	Nauzerus 1	1010	70	1080	940	zircon	U-Pb	Hugo & Schalk, 1974
10		Namaqua, Nm	Luderitz Tschaukaib granite	1012	10	1022	1002	zircon	U-Pb	Burger, 1976
11		Namaqua, Nm	Luderitz Tschaukaib granite	1018	10	1028	1008	zircon	U-Pb	Burger, 1976
12		Namaqua, Nm	Luderitz Glockenberg granite	1022	10	1032	1012	zircon	U-Pb	Burger, 1976
13		Namaqua, Nm	Townlands tonalitic augengneiss	1052	10	1062	1042	zircon	U-Pb	Burger, 1976
14	RehBl	Gamsberg, Kobos granite	Kanaus S 336	1064	20	1084	1044	zircon	U-Pb	Burger & Coertze, 1975
15	RehBl	Gamsberg, Gamsberg granite	Gamsberg 23	1077	26	1202	1010	zircon	U-Pb	Nagel, 2000
16	RehBl	Gamsberg, Gamsberg granite	Hohenheim 24	1078	30	1108	1048	zircon	U-Pb	Burger & Coertze, 1975
17	RehBl	Gamsberg, Gamsberg granite	Gamsberg 23	1079	30	1142	1038	zircon	U-Pb	Nagel, 2000
18		Namaqua, Nm	Hottentots Bay Namaqua augengneiss	1080	10	1090	1070	zircon	U-Pb	Burger, 1976
19	RehBl	Gamsberg, Gamsberg granite	Hohenheim 24	1080	70	1150	1010	zircon	U-Pb	Hugo & Schalk, 1974
20		Namaqua, Nm	Grasplatz quartz monzonitic gneiss	1082	10	1092	1072	zircon	U-Pb	Burger, 1976
21	RehBl	Nauzerus G, Kartatsaus F	Uitdraai Oos 296	1083	30	1113	1053	zircon	U-Pb	Burger & Coertze, 1975
22	RehBl	Gamsberg, Rostock granite	Greilingshof 107	1084	8	1092	1076	zircon	U-Pb	Pfurr et al, 1990
23		Namaqua, Nm	Luderitz Glockenberg granite	1086	10	1096	1076	zircon	U-Pb	Burger, 1976
24	RehBl	Gamsberg, Gamsberg granite	Abendruhe 411	1089	30	1119	1059	zircon	U-Pb	Burger & Coertze, 1975
25	RehBl	Nauzerus G, Kartatsaus F	Kaartatsaus 293	1090	30	1120	1060	zircon	U-Pb	Burger & Coertze, 1975
26	RehBl	Nauzerus G, Kartatsaus F	Kaartatsaus 293	1090	70	1160	1020	zircon	U-Pb	Hugo & Schalk, 1974
27	RehBl	Nauzerus G, Kartatsaus F	Kaartatsaus 293	1090	70	1160	1020	zircon	U-Pb	Hugo & Schalk, 1974
28	RehBl	Oorlogsende F	Epukiro area	1094	30	1112	1074	zircon	U-Pb	Hegenberger & Burger, 1985
29	RehBl	Gamsberg, Gamsberg granite	Gamsberg 23	1095	30	1216	1074	zircon	U-Pb	Nagel, 2000
30	RehBl	Gamsberg, Rostock granite	Greilingshof 107	1097	24	1121	1073	zircon	U-Pb	Pfurr et al, 1990
31	RehBl	Gamsberg, Rostock granite	Greilingshof 107	1099	16	1115	1083	zircon	U-Pb	Pfurr et al, 1990
32	RehBl	Gamsberg, Rostock granite	Rostock S 414	1102	7	1109	1095	zircon	U-Pb	Pfurr et al, 1990
33	RehBl	Gamsberg, Koichas granite	Kangas 371	1104	20	1124	1084	zircon	U-Pb	Burger & Coertze, 1975
34	RehBl	Gamsberg, Biesespoort granite	Biesiepoort 275	1110	30	1140	1080	zircon	U-Pb	Burger & Coertze, 1978
35	RehBl	Gamsberg, Gamsberg granite	Nauzerus 1	1110	30	1140	1080	zircon	U-Pb	Burger & Coertze, 1975
36		Namaqua, Nm	Hottentots Bay Namaqua augengneiss	1114	10	1124	1104	zircon	U-Pb	Burger, 1976
37		Namaqua, Nm	schist	1116	10	1126	1106	zircon	U-Pb	Burger, 1976
38	RehBl	Oorlogsende F	Epukiro area	1127	30	1157	1097	zircon	U-Pb	Burger & Walraven, 1980
39	RehBl	Nauzerus G, Nuckopf F	Lekkerwater 144	1130	75	1205	1055	zircon	U-Pb	Ziegler & Stoessel, 1993
40		Namaqua, Nm	Luderitz felsic volcanics	1131	10	1141	1121	zircon	U-Pb	Burger, 1976
41		Namaqua, Nm	Luderitz felsic volcanics	1132	10	1142	1122	zircon	U-Pb	Burger, 1976
42	RehBl	Gamsberg, Gamsberg granite	Gamsberg 23	1132	26	1158	1106	zircon	U-Pb	Ziegler & Stoessel, 1993
43	RehBl	Nauzerus G, Nuckopf F	Kunineib 378	1132	75	1207	1057	zircon	U-Pb	Hilken, 1977
44	RehBl	Oorlogsende F	Epukiro area	1144	30	1174	1114	zircon	U-Pb	Burger & Walraven, 1979
45	RehBl	Gamsberg, Ganeib granite	Danigas 289	1150	30	1180	1120	zircon	U-Pb	Burger & Coertze, 1975
46	KES7	Namibrand-Sesriem area	Sesriem 134 Eesaam F	1170	30	1200	1140	zircon	U-Pb	Burger & Coertze, 1975
47		Namaqua, Nm	Luderitz Glockenberg granite	1178	10	1188	1168	zircon	U-Pb	Burger, 1976
48	RehBl	Gamsberg, Kobos granite	Nauchas 14	1178	20	1198	1158	zircon	U-Pb	Burger & Coertze, 1975
49		Namaqua, Nm	Luderitz felsic volcanics	1184	10	1194	1174	zircon	U-Pb	Burger, 1976
50	RehBl	Gamsberg, Gamsberg granite	Corona 223	1186	30	1240	1147	zircon	U-Pb	Nagel, 2000
51		Namaqua, Nm	Luderitz Glockenberg granite	1194	10	1204	1184	zircon	U-Pb	Burger, 1976
52	RehBl	Gamsberg, Rostock granite	Rostock S 414	1194	26	1220	1168	zircon	U-Pb	Pfurr et al, 1990
53	RehBl	Gamsberg, Rostock granite	Rostock N 393	1207	15	1222	1192	zircon	U-Pb	Pfurr et al, 1990
54	RehBl	porphyry dike	Marienhof 577	1210	7	1217	1203	zircon	U-Pb	Ziegler & Stoessel, 1993
55	RehBl	Gamsberg S	Morgenroth 17	1210	8	1218	1202	zircon	U-Pb	Ziegler & Stoessel, 1993
56	RehBl	Nauzerus G, Nuckopf F	Areb North 202	1221	35	1257	1192	zircon	U-Pb	Schalk, 1970
57	RehBl	Nauzerus G, Kartatsaus F	Spitskop F	1232	30	1262	1202	zircon	U-Pb	Burger & Coertze, 1978
58		Namaqua, Nm	Luderitz granite	1233	10	1243	1223	zircon	U-Pb	Burger, 1976
59		Namaqua, Nm	Luderitz granite	1264	10	1274	1254	zircon	U-Pb	Burger, 1976
60	KES231	Namibrand-Sesriem area	Hebron 136 Neuhof felsic volcanics	1294	25	1319	1269	zircon	U-Pb	Burger & Walraven, 1978
61	KES9	Namibrand-Sesriem area	Draaihook 119 Nubib granite	1302	20	1322	1282	zircon	U-Pb	Burger & Coertze, 1975
62	RehBl	Oorlogsende F	Epukiro area	1313	30	1343	1283	zircon	U-Pb	Burger & Walraven, 1980
63	KES6	Namibrand-Sesriem area	Sesriem 134 Nubib granite	1350	40	1390	1310	zircon	U-Pb	Burger & Coertze, 1975
64	KES230	Namibrand-Sesriem area	Sesriem 137 Eensam qtz porphyry	1656	40	1696	1616	zircon	U-Pb	Burger & Walraven, 1978
65		Namaqua, Nm	Luderitz augen gneiss	1742	10	1752	1732	zircon	U-Pb	Burger, 1976
66		Namaqua, Nm	Luderitz augen gneiss	1752	10	1762	1742	zircon	U-Pb	Burger, 1976
67		Namaqua, Nm	Luderitz hbl-gneiss	1755	10	1765	1745	zircon	U-Pb	Burger, 1976
68	RehBl	Nauzerus G, Nuckopf F	Auchas 347	1770	35	1805	1735	zircon	U-Pb	Burger & Coertze, 1978
69	RehBl	Gamsberg, Kobos granite	Kwakwas 251	1775	10	1785	1765	zircon	U-Pb	Nagel, 2000
70		Namaqua, Nm	Luderitz Kunguib granodiorite	1952	10	1962	1942	zircon	U-Pb	Burger, 1976
71		Namaqua, Nm	Luderitz Kunguib granodiorite	1978	10	1988	1968	zircon	U-Pb	Burger, 1976

OTHER NAMIBIA

###		Aunis Gneiss, Awasib Mtns,Nm	Tonalite gneiss	1271	62	1333	1209			Hoal, 1990
###		Ababis Inlier, Nm	Basement gneisses	1925		2255	1645	zircon	U-Pb	Jacob et al, 1978
###		Tumas Dome, Nm	Basement gneisses	1945	18	1963	1927	zircon	U-Pb	Jacob et al, 1978, Burger & Jacob, unpub. data in Kroner et al, 1991

OTHER COUNTRIES, RELEVANT TO LUFILIAN PROJECT

	sample	Site/Event	Rock type	age	error	max	min	material	type	reference
1		Kipushi Mine, D.R.Congo	Syn- to post-tectonic metamorphic veins	504.5		496	513	Rutile	U-Pb	Richards, 1988
2		Kipushi Mine, D.R.Congo	Breccia Pipe	546	18	564	528	Zircon	U-Pb	Walraven & Chabu, 1994
3		Kibaran orogeny, D.R.Congo	pegmatites that cut Roan	870	42	912	828	K-feldspa	Rb-Sr	Caen et al, 1984
4		Orue gneisses, S Angola	Gneiss	1334	21	1355	1313	zircon	U-Pb	Bassot et al, 1981
5		Khairab Basalt, Awasib Mtns,Nm	Mafic high-alumina metavolcanic rocks	1460		1460	1460			Hoal, 1990
6		Kate granite, Tanzania	Granite	1725	70	1795	1655	K-feldspa	Rb-Sr	Snelling et al, 1972
7		Etoile mine, D.R.Congo	Roan Group tuff (xenocrystic zircons)	1858	24	1882	1834	zircon	U-Pb	Rainaud, et al, 2004
8		Kinsenda Lufubu Schist, Luina Dome, D.R.Congo	metatrachyandesite	1874	8.3	1882	1865	zircon	U-Pb	Rainaud et al, 2004
9		Etoile mine, D.R.Congo	Roan Group tuff (xenocrystic zircons)	2802	36	2838	2766	zircon	U-Pb	Rainaud, et al, 2004
10		Etoile mine, D.R.Congo	Roan Group tuff (xenocrystic zircons)	2831	16	2847	2815	zircon	U-Pb	Rainaud, et al, 2004

ALL ZAMBIA (COMPILATION OF ALL ZAMBIAN AGES)

	sample	Site/Event	Rock type	age	error	max	min	material	type	reference
1		Nkana mine,Zm	Botryoidal pitchblende vein	235	35	270	200	Pitchblend	U-Pb	Snelling et al, 1972
2		Luanshya mine,Zm	Pitchblende in vein	365	40	405	325	Pitchblend	U-Pb	Snelling et al, 1972
3		Sinda Granite,Zm	Gtd	380	10	390	370	Biotite	Rb-Sr	Snelling et al, 1972
4	L-030	Kabompo Dome, Zm	diorite-granodiorite gneiss	419	250	669	169	zircon	Pb/U shrimp	This report
5		Leopard's Hill area,Zm	Biotite-garnet schist	435	15	450	420	Muscovite	K-Ar	Snelling et al, 1972
6		Hook Granite,Zm	Pegmatite	440	15	455	425	Muscovite	K-Ar	Snelling et al, 1972
7		Hook Granite,Zm	Biotite granite gneiss	450	14	464	436	biotite	K-Ar	Snelling et al, 1972
8		Nkana mine,Zm	Metasediment with uraninite	452	24	476	428	Uraninite	U-Pb	Snelling et al, 1972
9		Lusandwa Syenite,Zm	Syenite	455	5	460	450	Biotite	Rb-Sr	Snelling et al, 1972
10		Nkana mine,Zm	Schistose granulite	455	20	475	435	Biotite	Rb-Sr	Snelling et al, 1972
11		Hook Granite,Zm	Porphyroblastic gneiss	458	122	580	336	Biotite	K-Ar	Snelling et al, 1972
12		Lylands Quarry, Ndola,Zm	Galena	460		460	460	Galena	Pb	Snelling et al, 1972
13		Chapalapata, Sasare,Zm	Granite	460		460	460	Biotite	Rb-Sr	Snelling et al, 1972
14		Hook Granite,Zm	Granite	465	15	480	450	Biotite	K-Ar	Snelling et al, 1972
15		Hook Granite,Zm	Biotite-hornblende granite	465	16	481	449	Biotite	K-Ar	Snelling et al, 1972
16		Minga Migmatite, Great East Rd,Zm	Migmatite	470		470	470	Biotite	Rb-Sr	Snelling et al, 1972
17		Mpande Dome,Zm	Microgranite	476	19	495	457	Muscovite	K-Ar	Snelling et al, 1972
18		Bukanda near Luapula River,Zm	Galena	480		480	480	Galena	Pb	Snelling et al, 1972
19		Nkana mine,Zm	Uraninite in sediment	485	16	501	469	Uraninite	U-Pb	Snelling et al, 1972
20		Leopard's Hill area,Zm	Schist	485	20	505	465	Biotite	K-Ar	Snelling et al, 1972
21		Lundazi,Zm	Mica-beryl pegmatite	485		485	485	Betafite	U-Pb	Snelling et al, 1972
22		Gray's Quarry, Nchanga, Zm	Red granite	490	15	505	475	Biotite	Rb-Sr	Snelling et al, 1972
23		Gray's Quarry, Nchanga, Zm	Red granite	490	20	510	470	Biotite	K-Ar	Snelling et al, 1972
24		Serenje area,Zm	Biotite gneiss	495	20	515	475	Biotite	K-Ar	Snelling et al, 1972
25		Nkana mine, Mindola,Zm	Schistose granulite	495	20	515	475	Biotite	K-Ar	Snelling et al, 1972
26		Kafue Rhyolites,Zm	Sheared tuff	495	35	530	460	w.r.	Rb-Sr	Snelling et al, 1972
27		Hook Granite,Zm	Granite	500	17	517	483	Granite	Rb-Sr	Snelling et al, 1972
28		Chinyunyu zone,Zm	Sheared granite	500	20	520	480	Biotite	K-Ar	Snelling et al, 1972
29		Kansanshi Mine, Zm	Carbonate-molybdenite-monazite veins	502.4	1.7	504	501	Molybden	Re-Os	Torrealday et al, 2003
30		Kansanshi Mine, Zm	Carbonate-molybdenite-monazite veins	503	15	518	488	Brannerite	U-Pb	Darnley, 1961
31		Mufulira West mine, Zm	Basement granite	505	20	525	485	Biotite	K-Ar	Snelling et al, 1972
32		Chinyunyu zone,Zm	Sheared granite	505	20	525	485	Biotite	K-Ar	Snelling et al, 1972
33		Lusaka Granite,Zm	Granite	507	15	522	492	Biotite	Rb-Sr	Snelling et al, 1972
34		Kansanshi mine, Zm	Minzd qz vein	511	11	522	500	zircon	U-Pb	Torrealday et al, 2000
35		Kansanshi Mine, Zm	Cpy-rich veins	512.4	1.2	514	511	Molybden	Re-Os	Torrealday et al, 2003
36		Leopard's Hill area,Zm	Katangan mica quartzite	515	20	535	495	Biotite	K-Ar	Snelling et al, 1972
37		Mufulira West mine, Zm	Basement granite	515	25	540	490	Biotite	Rb-Sr	Snelling et al, 1972
38		Luanshya mine, Zm	Lufubu Schist	515	100	615	415	Actinolite	K-Ar	Snelling et al, 1972
39		Leopard's Hill area,Zm	Sheared gneiss	520	20	540	500	Biotite	K-Ar	Snelling et al, 1972
40		Nkana mine,Zm	Uraninite	520	20	540	500	Uraninite	U-Pb	Snelling et al, 1972
41		Kansanshi mine,Zm	Vein	520	20	540	500	Brannerite	U-Pb	Snelling et al, 1972
42		Luanshya mine, Zm	Lufubu Schist	530	30	560	500	Biotite	K-Ar	Snelling et al, 1972
43		Lusaka Granite,Zm	Granite	531	21	552	510	Biotite	K-Ar	Snelling et al, 1972
44	H-4	Hook Granite, Zm	Post-Tectonic megacrystic granite	533	3	536	530	zircon	U-Pb	Hanson et al, 1993
45		Nkana mine,Zm	Uraninite in Lower Roan	535	21	556	514	Uraninite	U-Pb	Snelling et al, 1972
46		Hook Granite, Zm	tectonic activity	535		540	530	zircon	U-Pb	Hanson et al, 1993
47	H-3	Hook Granite, Zm	Rhyolite dike within Katangan	538	1.5	540	537	zircon	U-Pb	Hanson et al, 1993
48	L-207	Nampundwe,Zm	Gtd	538.2	3.3	542	535	zircon	U-Pb	This report
49		Lusaka Area, Zm	metasediments?	539	20	559	519	w.r.	Rb-Sr	Barr et al, 1978
50		Lusaka Granite,Zm	Granite	540	20	560	520	Biotite	K-Ar	Snelling et al, 1972
51		Kafue Rhyolites,Zm	Rhyolitic tuff	548	32	580	516	w.r.	Rb-Sr	Snelling et al, 1972
52		Sachenga mica claims,Zm	Pegmatite	550	20	570	530	Muscovite	K-Ar	Snelling et al, 1972
53		Mivula Syenite,N Province,Zm	Syenite	550	20	570	530	Biotite	K-Ar	Snelling et al, 1972
54	L-213	Kafue Flats,Zm	Syenite	550	25	575	525	zircon	U-Pb	This report
55	H-5	Hook Granite, Zm	Rhyolite intrusion in Mwembezhi dislocation	551	19	570	532	zircon	U-Pb	Hanson et al, 1993
56		Lusaka Granite,Zm	Granite	551	22	573	529	Biotite	K-Ar	Snelling et al, 1972
57		Lusaka Area, Zm	metasediments?	557	4	561	553	w.r.	K-Ar	Barr et al, 1978
58	H-1	Hook Granite, Zm	Deformed f-mg granite	559	18	577	541	zircon	U-Pb	Hanson et al, 1993
59		Kamfinsa Quarry,Zm	Pegmatite	560	20	580	540	Biotite	K-Ar	Snelling et al, 1972
60	L-158	Konkola Deep Borehole,Zm, resetting age	Foliated pink gtd	562	18	580	544	zircon em	Pb/U shrimp	This report
61		Kafue Rhyolites,Zm	Porphyritic Rhyolite	562	40	602	522	w.r.	Rb-Sr	Snelling et al, 1972
62		Migmatitic biotite gneiss,Zm	Migmatitic biotite gneiss,Zm	565	24	589	541	Biotite	K-Ar	Snelling et al, 1972
63		Hook Granite, Zm	Syntectonic granitic plutonism	565		570	560	zircon	U-Pb	Hanson et al 1993
64	H-2	Hook Granite, Zm	Deformed megacrystic granite	566	5	571	561	zircon	U-Pb	Hanson et al, 1993
65		Lusaka Granite,Zm	Granite	567	23	590	544	Biotite	K-Ar	Snelling et al, 1972
66		Migmatitic biotite gneiss,Zm	Migmatitic biotite gneiss,Zm	567	24	591	543	Biotite	K-Ar	Snelling et al, 1972
67		Nchanga,Zm	Nchanga red granite	583	90	673	493	w.r.	Rb-Sr	Snelling et al, 1972
68		Luangwa River, border Mozambique, Zm	Lower intercept, deformed orthogneiss	590	50	640	540	zircon	LAM ICPMS	Cox et al, 2002
69		Lusaka Series,Zm	Vein in Lusaka series	630		630	630	Galena	Pb	Snelling et al, 1972
70		Serenje area,Zm	Kalonga metasiltite	645	25	670	620	Muscovite	K-Ar	Snelling et al, 1972
71		Mpande Dome,Zm	Microgranite	677	45	722	632	K-feldspa	Rb-Sr	Snelling et al, 1972
72		Nkombwa Carbonatite,Zm	Fenite	680	25	705	655	Phlogopit	K-Ar	Snelling et al, 1972
73		Lusaka Granite,Zm	Granite	681	28	709	653	K-feldspa	Rb-Sr	Snelling et al, 1972
74		Mafingi Group Phyllite,Zm	Phyllite	690	20	710	670	w.r.	K-Ar	Snelling et al, 1972
75		Old Millberg Claims,Zm	Galena	695		695	695	Galena	Pb	Snelling et al, 1972
76		Lusaka Granite,Zm	Granite	700	28	728	672	K-feldspa	Rb-Sr	Snelling et al, 1972
77		Lusaka Granite,Zm	Granite	703	28	731	675	w.r.	Rb-Sr	Snelling et al, 1972
78		Kabompo Dome, Zm	Met event (amphibolite facies)	708	7	715	701		K/Ar	Cosi et al, 1992
79		Galena veins near Kabwe,Zm	Galena	712		712	712	Galena	Pb	Snelling et al, 1972
80	3DA-101	Kasai Shield, Zm	Met event	714	66	780	648	zircon	U-Pb	Key et al, 2001
81		Mpande Dome,Zm	Microgranite	730	50	780	680	w.r.	Rb-Sr	Snelling et al, 1972
82	3DA-51	Kasai Shield, Zm	Met event	734	63	797	671	zircon	U-Pb	Key et al, 2001
83		Chiwanda,Zm	Galena	734		734	734	Galena	Pb	Snelling et al, 1972
84		Luamata, NWZm	Felsic volcanic	735	5	740	730	zircon	U-Pb	Key et al, 2001
85		Kabompo Dome, Zm	Met event (high pressure)	744	8	752	736		Rb/Sr	AGIP, 1985
86		Lusaka Granite,Zm	Granite	745	30	775	715	w.r.	Rb-Sr	Snelling et al, 1972
87		Lusaka Granite,Zm	Granite	745	70	815	675	w.r.	Rb-Sr	Snelling et al, 1972
88	L-047	Mombwezhi Dome, Zm	Quartzmonzonite	745.9	3.4	749	743	zircon	U-Pb	This report

ALL ZAMBIA (COMPILATION OF ALL ZAMBIAN AGES) (cont.)

	sample	Site/Event	Rock type	age	error	max	min	material	type	reference
89		Lusaka Granite,Zm	Granite	746	30	776	716	K-feldspa	Rb-Sr	Snelling et al, 1972
90	L-060	Kansanshi mine, Zm	Diorite	750	5	755	745	zircon	U-Pb	This report
91	L-142	MB-34 intrusives, Kasempa,Zm	Subvolcanic porphyritic intrusive	750	5	755	745	zircon	U-Pb	This report
92		Serenje area,Zm	Pegmatite	755	30	785	725	Muscovite	K-Ar	Snelling et al, 1972
93	L-172c	Nchanga open pit intrusives, Zm	Lamprophyre in borehole	765	3	768	762	zircon	U-Pb	This report
94	L-169	Nchanga open pit intrusives, Zm	Lamprophyre in borehole	765	3	768	762	zircon	U-Pb	This report
95		Lwanu basalt, Mwinilunga, NW Zm	Basalt	765	5	770	760	zircon	U-Pb	Key et al, 2001
96		Lusaka Granite,Zm	Granite	770	25	795	745	w.r.	K-Ar	Snelling et al, 1972
97		Mafingi Group Phyllite,Zm	Phyllite	770	25	795	745	w.r.	K-Ar	Snelling et al, 1972
98		Lusaka Granite,Zm	Granite	790	32	822	758	w.r.	Rb-Sr	Barr et al, 1978
99		Ngoma Gneiss, W Lusaka, Zm	Gneiss	820	7	827	813	zircon	U-Pb	Wilson, 1993 in De Waele et al,2001a
100		Luanshya mine, Zm	Pegmatite in lower Roan	840	40	880	800	Microcline	Rb-Sr	Snelling et al, 1972
101		Lusaka Granite, W Lusaka, Zm	Granite	843	10	853	833			Cahen, 1984 in De Waele & T,1999
102		Lusaka Granite,Zm	Granite	846	68	914	778	zircon	U-Pb	Barr et al, 1978
103		Isoka District, Zm	Porphyroblastic biotite gneiss	870	36	906	834	Biotite	K-Ar	Snelling et al, 1972
104		Nchanga Red Granite,Zm	Gtd	877	5	882	872	zircon	U-Pb	Armstrong et al, in preparation
105		Kafue Rhyolites, W Lusaka, Zm	Rhyolite	879	19	898	860	zircon	U-Pb	Wardlaw in De Waele et al,2001a
106		Nchanga open pit intrusives, Zm	inherited zircons	880	5	885	875	zircon	U-Pb	This report
107		Serenje area,Zm	Kalonga metasiltstone	885	36	921	849	Muscovite	K-Ar	Snelling et al, 1972
108		Isoka District, Zm	Porphyroblastic biotite gneiss	890	36	926	854	Biotite	K-Ar	Snelling et al, 1972
109		Northeast of Chinsali,Zm	Biotite gneiss	905	36	941	869	Biotite	K-Ar	Snelling et al, 1972
110		Rufunsa Area, Eastern Zm	Granite	927		927	927	zircon	U-Pb	Barr et al, 1978
111		G4 gtd Irumide B.,Zm	Coarse biotite granite	943	5	948	938	zircon	shrimp U-Pb	De Waele et al, 2003c
112		Rufunsa Area, Eastern Zm	Granite and porphyry	945	30	975	915	zircon	U-Pb	Barr et al, 1978
113		Rufunsa Area, Eastern Zm	Porphyry	955		955	955	zircon	U-Pb	Barr et al, 1978
114		near Kariba Dam, Zm	Amphibolite	960	30	990	930	Bt-w.r.	Rb-Sr	Snelling et al, 1972
115		Chinsali, Irumide B., Zm	Kaunga Granite	970	5	975	965	zircon	U-Pb	Daly, 1986 in De Waele & Mapani, 2002
116		Chinsali, N Irumide B.,Zm	Mutangoshi (or grey) biotite granite	1009	12	1021	997	zircon	shrimp U-Pb	De Waele & Mapani, 2002
117		Serenje area, Zm	Sasa, leucocratic biotite porphyritic granite	1018	6	1024	1012	zircon	shrimp U-Pb	De Waele et al,2001; De Waele & M, 2002
118		Mutangoshi granite, N Irumide B.,Zm	Mesocratic, fine-grained granite	1021	3	1024	1018	zircon	shrimp U-Pb	De Waele & Mapani, 2002
119		Serenje area, Zm	Porphyritic granite	1022	12	1034	1010	zircon	shrimp U-Pb	De Waele et al,2001; De Waele & M, 2002
120		Serenje area, Zm	Porphyritic granite	1024	13	1037	1011	zircon	shrimp U-Pb	De Waele et al,2001; De Waele & M, 2002
121		Serenje area, Zm	Porphyritic granite	1025	10	1035	1015	zircon	shrimp U-Pb	De Waele et al,2001; De Waele & M, 2002
122		G4 gtd. W Irumide B.,Zm	Anorogenic porph biot granite gneiss	1027	13	1040	1014	zircon	shrimp U-Pb	De Waele et al, 2003c
123		Serenje area, Zm	Porphyritic granite	1033	15	1048	1018	zircon	shrimp U-Pb	De Waele et al, 2002b
124		G4 gtd Irumide B.,Zm	Coarse biotite granite	1036	13	1049	1023	Nd isotop	shrimp U-Pb	De Waele et al, 2003b
125		G4 gtd Irumide B.,Zm	Coarse biotite granite	1037	16	1053	1021	Nd isotop	shrimp U-Pb	De Waele et al, 2003b
126		Serenje area, Zm	Porphyritic granite	1038	10	1048	1028	zircon	shrimp U-Pb	De Waele et al,2001; De Waele & M, 2002
127		G4 gtd Irumide B.,Zm	Coarse biotite granite	1042	47	1042	948	zircon	shrimp U-Pb	De Waele et al, 2003c
128		Luangwa River, border Mozambique, Zm	Metamorphism, deformed orthogneiss	1043	19	1062	1024	zircon	LAM ICPMS	Cox et al, 2002
129		Phoenix mica claims,Zm	Pegmatite	1045	30	1075	1015	Muscovite	Rb-Sr	Snelling et al, 1972
130		Phoenix mica claims,Zm	Pegmatite	1050	40	1090	1010	Muscovite	Rb-Sr	Snelling et al, 1972
131		Mutangoshi granite, N Irumide B.,Zm	Coarse-grained felsic granite	1053	7	1060	1046	zircon	shrimp U-Pb	De Waele & Mapani, 2002
132		G4 gtd. W Irumide B.,Zm	Anorogenic porph biot granite gneiss	1055	13	1068	1042	zircon	shrimp U-Pb	De Waele et al, 2003c
133		G4 gtd Irumide B.,Zm	Coarse biotite granite	1055	13	1068	1042	zircon	shrimp U-Pb	De Waele et al, 2003c
134		Mtuga aplites, Mkushi,Zm	emplacement of aplite	1059	26	1085	1033	zircon	U-Pb	Rainaud, et al, 2004
135		Chipata Area, Eastern Zm	Granitic orthogneiss	1071	8	1079	1063	zircon	Pb/Pb	Haslam et al, 1986
136		Mkushi Gneiss, Zm	Granitic gneiss (zircon rims)	1088	159	1247	929	zircon	shrimp U-Pb	Robb in De Waele et al,2001a
137		Mpande Dome (south), Southern Zm	Fine-grained granite	1095	12	1107	1083	zircon	U-Pb	De Waele et al, 2000a
138		Lusaka Granite,Zm	Granite	1100	70	1170	1030	Plagioclas	Rb-Sr	Snelling et al, 1972
139		Mpande Gneiss, Southern Zm	Granitic orthogneiss	1106	19	1125	1087	zircon	U-Pb	Hanson et al, 1988, 1994
140		Mafingi Hills,Zm	Granite gneiss	1120	30	1150	1090	Plagioclas	Rb-Sr	Snelling et al, 1972
141		Mafingi Hills,Zm	Lamprophyre	1145	60	1205	1085	riebeckite	K-Ar	Snelling et al, 1972
142	CK4	Choma-Kalomo Batholith, Zm	Medium-grained two mica granite	1174	27	1201	1147	zircon	shrimp U-Pb	Bulambo et al, 2004
143	CK12	Choma-Kalomo Batholith, Zm	Gneiss containing mica-rich restites	1177	70	1247	1107	zircon	shrimp U-Pb	Bulambo et al, 2004
144	CK25	Choma-Kalomo Batholith, Zm	Foliated, med-coarse-g biotite granite	1181	9	1190	1172	zircon	shrimp U-Pb	Bulambo et al, 2004
145	CK10	Choma-Kalomo Batholith, Zm	Foliated med-coarse-g biotite granite	1188	11	1199	1177	zircon	shrimp U-Pb	Bulambo et al, 2004
146		Basement, Kabompo Dome,Zm	Gtd	1200	50	1250	1150	zircon	U-Pb	AGIP, 1985
147		Lusaka Granite,Zm	Granite	1200	96	1296	1104	Plagioclas	Rb-Sr	Snelling et al, 1972
148		Lusaka Granite,Zm	Granite	1305	65	1370	1240	Plagioclas	Rb-Sr	Snelling et al, 1972
149		Mivula Hill, Central Irumide B., Zm	Syenite	1341	16	1357	1325	w.r.	Rb-Sr	Tembo in De Waele et al, 2000a
150		Siasikobole granite, Choma-Kalomo,Zm	Granite	1352	14	1366	1338	zircon	U-Pb	Hanson et al, 1998b
151	CK13	Choma-Kalomo Batholith, Zm	Augen (ortho) gneiss	1368	10	1378	1358	zircon	shrimp U-Pb	Bulambo et al, 2004
152		Lusenga Syenite,Zm	Syenite	1390	200	1590	1190	w.r.	Rb-Sr	Snelling et al, 1972
153		Chewore Ophiolite, Zm	Plagiogranite sheet in ophiolite	1393	22	1415	1371	zircon	shrimp U-Pb	Johnson & Oliver,2000; Oliver et al,1998

ALL ZAMBIA (COMPILATION OF ALL ZAMBIAN AGES) (cont.)

	sample	Site/Event	Rock type	age	error	max	min	material	type	reference
154		Magmatic event in Irumide B., Zm	Large syntectonic granite bodies	1407	39	1446	1368	w.r.	Rb-Sr	Daly, 1986; De Waele et al, 2000a
155		Ufipa Gneiss near Mbala,Zm	Gneiss	1425	50	1475	1375	Biotite	K-Ar	Snelling et al, 1972
156		Kamfinsa Quarry,Zm	Pegmatite	1550	50	1600	1500	Biotite	K-Ar	Snelling et al, 1972
157		G2 gtd. Lubu Gt, W Irumide B.Zm	Granite gneiss	1551	33	1584	1518	zircon	shrimp U-Pb	De Waele et al, 2003c
158	3DA-57	Kasai Shield, NW Zm	Aphyric med-g gtd	1561	10	1571	1551	zircon	U-Pb	Key et al, 2001
159		Lumi gneissic granite,Zm	Granite	1590	50	1640	1540	Biotite	K-Ar	Snelling et al, 1972
160		G2 Mutangoshi/Musalango gn, N Irumide B.Zm	Anorogenic porph biot granite gneiss	1610	26	1636	1584	zircon	shrimp U-Pb	De Waele et al, 2003c
161		Mkushi mine, Zm	Aplite	1625	50	1675	1575	zircon	U-Pb	Snelling
162		Mkushi area,Zm	Aplite cutting Mkushi Gneiss	1625	50	1675	1575	w.r.	Rb-Sr	Snelling et al, 1972
163		G2 Lukamfwa Hill gtd.W Irumide B.,Zm	Anorogenic porph biot granite gneiss	1627	12	1639	1615	zircon	shrimp U-Pb	De Waele et al, 2003c
164		Luanshya mine, Zm	Pegmatite in Lufubu	1635	180	1815	1455	K-feldspa	Rb-Sr	Snelling et al, 1972
165		G2 Lukamfwa Hill gtd.W Irumide B.,Zm	Anorogenic porph biot granite gneiss	1639	14	1653	1625	zircon	shrimp U-Pb	De Waele et al, 2003c
166		Serenje area, Irumide B.,Zm	Granite gneiss	1647	10	1657	1637	zircon	shrimp U-Pb	De Waele & Mapani, 2002
167		G2 Lukamfwa Hill gtd.W Irumide B.,Zm	Anorogenic porph biot granite gneiss	1650	4	1654	1646	zircon	shrimp U-Pb	De Waele et al, 2003c
168		Serenje area, Irumide B.,Zm	Granite gneiss	1661	8	1669	1653	zircon	shrimp U-Pb	De Waele & Mapani, 2002
169		G2 Lukamfwa Hill gtd.W Irumide B.,Zm	Anorogenic porph biot granite gneiss	1664	4	1668	1660	zircon	shrimp U-Pb	De Waele et al, 2003c
170		Roan Antelope mine,Zm	Granite	1750	50	1800	1700	K-feldspa	K-Ar	Snelling et al, 1972
171		Plateau Series,Zm	Pegmatite cutting Plateau Series	1785	70	1855	1715	K-feldspa	K-Ar	Snelling et al, 1972
172		Kalumbila, NW Zm	sediments	1845		1860	1830	zircon	U-Pb	Steven & Armstrong, 2000
173		Manshya River Group, Irumide B., Zm	Rhyolitic tuff	1856	4	1860	1852	zircon	shrimp U-Pb	De Waele et al, 2003c
174	L-169	Nchanga Intrusives, Zm	Lamprophyre in borehole (inherited zircons)	1860	10	1870	1850	zircon	U-Pb	This report
175		Mansa, Irumide B., Zm	Undeformed biot. Gt into Luapula volcs.	1860	13	1873	1847	zircon	shrimp U-Pb	De Waele et al, 2003c
176		Mansa, Irumide B., Zm	Undeformed biot. Gt into Luapula volcs.	1862	8	1870	1854	zircon	shrimp U-Pb	De Waele et al, 2003c
177		Mansa, Irumide B., Zm	Luapula acid volcanics	1862	19	1881	1843	zircon	shrimp U-Pb	De Waele et al, 2003c
178	L-075	Muliashi Porphyry,Zm	Rapakivi granite	1865	5.4	1870	1860	zircon	U-Pb	This report
179		Mansa, Irumide B., Zm	Undeformed biot. Gt into Luapula volcs.	1866	9	1875	1857	zircon	shrimp U-Pb	De Waele et al, 2004a
180	L-160	Konkola Deep Borehole,Zm	Undeformed white gtd	1866	5.4	1872	1861	zircon	U-Pb	This report
181	L-160	Konkola Deep Borehole,Zm	Gray gtd	1868	4.8	1873	1863	zircon	shrimp concordia age	This report
182		Mansa, Irumide B., Zm	Luapula acid volcanics	1868	7	1875	1861	zircon	shrimp U-Pb	De Waele et al, 2003c
183	L-213	Old Kafue Basement,Zm	Inherited zircons in syenite	1872	14	1886	1858	zircon	U-Pb	This report
184	L-158	Konkola Deep Borehole,Zm	Foliated pink gtd	1874	14	1888	1860	zircon	U-Pb	This report
185		Manshya River Group, Irumide B., Zm	Rhyolitic tuff	1879	13	1892	1866	zircon	shrimp U-Pb	De Waele et al, 2003c
186		Muva sequence, SW Chinsali, Zm	Conformable metarhyolite	1880	12	1892	1868	zircon	shrimp U-Pb	De Waele & Mapani, 2002
187		Kalumbila, NW Zm	sediments	1887		1896	1878	zircon	U-Pb	Steven & Armstrong, 2000
188		Kalumbila, NW Zm	sediments	1919		1924	1913	zircon	U-Pb	Steven & Armstrong, 2000
189	L-030	Mwinilunga, NW Zm	Foliated Gtd	1928	7.1	1935	1921	zircon	U-Pb	This report
190		Kabompo Dome, Zm	Feldspar-phyric gtd	1934	6	1940	1928	zircon	U-Pb	Key et al, 2001
191		Luwalizi Granite, NE Irumide B., Zm	Weakly deformed granite	1937	10	1947	1927	zircon	shrimp U-Pb	De Waele et al, 2003c
192		Kabompo Dome, Zm	Feldspar-phyric gtd	1940	2.8	1943	1937	zircon	U-Pb	Key et al, 2001
193		Luwalizi Granite, NE Irumide B., Zm	Weakly deformed granite	1942	6	1948	1936	zircon	shrimp U-Pb	De Waele et al, 2003c
194		Kalumbila, NW Zm	sediments	1946		1952	1939	zircon	U-Pb	Steven & Armstrong, 2000
195		Samba Cu prospect,Zm	felsic metavolcanic schist	1964	12	1976	1952	zircon	U-Pb	Rainaud et al, 2004
196		Mufulira Lufubu schist,Zm	blastoporphyritic metavolcanic	1968	9	1977	1959	zircon	U-Pb	Rainaud et al, 2004
197		Mufulira mine,Zm	Mufulira granite	1975	20	1995	1955	Zircon	U-Pb	Snelling et al, 1972
198		Mulungushi bridge, Kabwe,Zm	Augen gneiss	1976	5	1981	1971	zircon	U-Pb	Rainaud, et al, 2004
199		Chambishi basin Lufubu Schist,Zm	Meta-andesite	1980	7	1987	1973	zircon	U-Pb	Rainaud et al, 2004
200		Chambishi granite,Zm	Coarse-grained undeformed monzogranite	1983	5	1988	1978	zircon	U-Pb	Rainaud et al, 2004
201		Mufulira Pink Granite,Zm	Granite	1994	7.1	2001	1987	zircon	U-Pb	Rainaud et al, 2004
202		Kalumbila, NW Zm	sediments	1994		2001	1987	zircon	U-Pb	Steven & Armstrong, 2000
203		Mtuga aplites, Mkushi,Zm	Inherited zircons	1998	18	2016	1980	zircon	U-Pb	Rainaud, et al, 2004
204		Orange River Group,Nm		2000		2000	2000			Miller, 1999
205		Mtuga aplites, Mkushi,Zm	Inherited zircons	2009	4	2013	2005	zircon	U-Pb	Rainaud, et al, 2004
206		Mkushi Gneiss, SE Irumide B.,Zm	Variably deformed biotite granite and highly deformed mylonitic granitoids	2036	7	2043	2029	zircon	shrimp U-Pb	De Waele et al, 2003c
207		Mkushi Gneiss, Zm	Granitic gneiss	2036	22	2058	2014	zircon	shrimp U-Pb	Robb in De Waele et al,2001a
208		Mkushi Gneiss, Zm	Variably deformed biotite granite and highly deformed mylonitic granitoids	2037	12	2049	2025	zircon	shrimp U-Pb	De Waele et al, 2003c
209		Mkushi Gneiss, Zm	Gtd	2049	6	2055	2043	zircon	U-Pb	Rainaud et al, 2004
210		Kamono school, Luangwa Terrane, Zm	Foliated granitoid	2050	10	2060	2040	zircon	LAM ICPMS	Cox et al, 2002
211		Mkushi Gneiss, Zm	Variably deformed biotite granite and highly deformed mylonitic granitoids	2052	13	2065	2039	zircon	shrimp U-Pb	De Waele et al, 2003c
212		Mufulira Lufubu schist,Zm	blastoporphyritic metavolcanic (inherited zircons)	2057	9	2066	2048	zircon	U-Pb	Rainaud et al, 2004
213	3DA-150	Kasai Shield, Zm	Porphyritic gtd	2058	7	2065	2051	zircon	U-Pb	Key et al, 2001
214		Mtuga aplites, Mkushi,Zm	Inherited zircons	2064	15	2079	2049	zircon	U-Pb	Rainaud, et al, 2004
215		Mtuga aplites, Mkushi,Zm	Inherited zircons	2072	9	2081	2063	zircon	U-Pb	Rainaud, et al, 2004
216		Mansa, Irumide B., Zm	Luapula acid volcanics (Model age)	2095	9	2104	2086	Nd isotop	Tchur	De Waele et al, 2003b

ALL ZAMBIA (COMPILATION OF ALL ZAMBIAN AGES) (cont.)

	sample	Site/Event	Rock type	age	error	max	min	material	type	reference
217		Mansa, Irumide B., Zm	Undeformed biot. Gt (Model age)	2116	11	2127	2105	Nd isotop	Tchur	De Waele et al, 2003b
218		Mansa, Irumide B., Zm	Luapula acid volcanics (Model age)	2135	14	2149	2121	Nd isotop	Tchur	De Waele et al, 2003b
219		Mansa, Irumide B., Zm	Undeformed biot. Gt (Model age)	2159	14	2173	2145	Nd isotop	Tchur	De Waele et al, 2003b
220		Samba Cu prospect,Zm	Inherited zircon	2160	25	2185	2135	zircon	U-Pb	Rainaud et al, 2004
221		Kasai Shield, Zm	Porphyritic gtd	2169	5	2174	2164	zircon	U-Pb	This report
222		Kalumbila, NW Zm	sediments	2170		2189	2151	zircon	U-Pb	Steven & Armstrong, 2000
223		Mufulira Lufubu schist,Zm	blastoporphyritic metavolcanic (inherited zircons)	2174	13	2187	2161	zircon	U-Pb	Rainaud et al, 2004
224		G2 Lukamfwa Hill gtd.W Irumide B.,Zm	Anor porph biot granite gn (Model age)	2310	55	2365	2255	Nd isotop	Tchur	De Waele et al, 2003b
225		Samba Cu prospect,Zm	Inherited zircon	2336	9	2345	2327	zircon	U-Pb	Rainaud et al, 2004
226		Mpika, Irumide B.,Zm	Intermediate+mafic volcs (Model age)	2338	109	2447	2229	Nd isotop	Tchur	De Waele et al, 2003b
227		Luwalizi Granite, NE Irumide B., Zm	Weakly deformed gt (Model age)	2372	23	2395	2349	Nd isotop	Tchur	De Waele et al, 2003b
228		Mkushi Gneiss, SE Irumide B.,Zm	Biotite granite (Model age)	2400	17	2417	2383	Nd isotop	Tchur	De Waele et al, 2003b
229		Luwalizi Granite, NE Irumide B., Zm	Weakly deformed gt (Model age)	2400	17	2417	2383	Nd isotop	Tchur	De Waele et al, 2003b
230		Samba Cu prospect,Zm	Inherited zircon	2423	13	2436	2410	zircon	U-Pb	Rainaud et al, 2004
231		Manshya River Group, Irumide B., Zm	Rhyolitic tuff (Model age)	2532	109	2641	2423	Nd isotop	Tchur	De Waele et al, 2003b
232	3DA-100	Kasai Shield, Jimbe Bridge,Zm	Granulite	2535	11	2546	2524	zircon	U-Pb	Key et al, 2001
233	3DA-101	Kasai Shield, NW Zm	Foliated gtd	2538	10	2548	2528	zircon	U-Pb	Key et al, 2001
234	3DA-100	Kasai Shield, Jimbe Bridge,Zm	Granulite	2543	5	2548	2538	zircon	U-Pb	Key et al, 2001
235		Mtuga aplites, Mkushi,Zm	Inherited zircons	2688	8	2696	2680	zircon	U-Pb	Rainaud, et al, 2004
236		Changwena River, Irumi Hill,Zm	Monazite	2720	20	2740	2700	Monazite	U-Pb	Snelling et al, 1972
237		Changwena Hill, Ndabala, SW Serenje,Zm	Quartzite, oldest detrital age	2720	20	2740	2700	monazite,	U-Pb	Snelling et al, 1964
238		Irumi Hill, Irumide B.,Zm	Irumi quartzite, oldest detrital age	2720	24	2744	2696	monazite,	U-Pb	Snelling et al, 1964; Vail et al, 1968
239		Mtuga aplites, Mkushi,Zm	Inherited zircons	2730	7	2737	2723	zircon	U-Pb	Rainaud, et al, 2004
240		Kapiri Mposhi, Zm	Granite	2738	4	2742	2734	zircon	shrimp U-Pb	De Waele et al, 2003c
241		Luangwa River, border Mozambique, Zm	Strongly-deformed granodiorite-diorite orthogneiss	2808	14	2822	2794	zircon	LAM ICPMS	Cox et al, 2002
242		G4 gtd Irumide B.,Zm	Coarse biotite granite (Model age)	2808	35	2843	2773	Nd isotop	Tchur	De Waele et al, 2003b
243		Mpika, Irumide B.,Zm	Intermediate+mafic volcs (Model age)	2909	31	2940	2878	Nd isotop	Tchur	De Waele et al, 2003b
244		G4 gtd Irumide B.,Zm	Coarse biotite granite (Model age)	2948	18	2966	2930	Nd isotop	Tchur	De Waele et al, 2003b
245		Manshya River Group, Irumide B., Zm	Rhyolitic tuff (Model age)	2961	152	3113	2809	Nd isotop	Tchur	De Waele et al, 2003b
246		G2 Lukamfwa Hill gtd.W Irumide B.,Zm	Anor porph biot granite gn (Model age)	3199	229	3428	2970	Nd isotop	Tchur	De Waele et al, 2003b
247		Manshya River Group, Irumide B., Zm	Rhyolitic tuff (Model age)	3238	55	3293	3183	Nd isotop	Tchur	De Waele et al, 2003b

ALL NAMIBIA (COMPILATION OF ALL AGES FROM THE COUNTRY)

	sample	Site/Event	Rock type	age	error	max	min	material	type	reference
1		Khan-Swakop River, Nm	Schist, cooling age of biotite (350degC)	448		448	448	Biotite	Rb-Sr	Hawkesworth et al, 1983
2		Rossing Mine, Nm	Uraniferous alaskite, late alaskite	458	8	466	450	w.r.	Rb-Sr	Steven et al, 1993
3		Khan-Swakop River, Nm	Schist, cooling age of biotite (350degC)	465	5	470	460	Biotite	Rb-Sr	Hawkesworth et al, 1983
4		Sandamap Mine, Central Zone,Nm	Stanniferous pegmatite	468	14	482	454	w.r.	Rb-Sr	Steven et al, 1993
5		Sandamap Noord, Central Zone,Nm	Pegmatite	473	23	496	450	w.r.	Sr/Sr	Steven et al, 1993
6		Otjozondjou, Nm	Diorite	478	4	482	474	Hornblend	Ar/Ar	Hawkesworth et al, 1983
7		Stinkbank, Central Zone, Nm	Uraniferous leucogranite, scheelite skarn	484	25	509	459	w.r.	Rb-Sr	Steven et al, 1993
8		Huab Complex,Nm	Gtd (Tectonic event age)	488		537	437	zircon	U-Pb	Tegtmeyer & Kroner, 1985
9		Navachab Mine, Cental Zone, Nm	Biotite in skarn	490		490	490	Bt	Rb-Sr	Steven et al, 1993
10		Kohero Tin mine, Central Zone, Nm	Stanniferous pegmatite	492	11	503	481	w.r.	Rb-Sr	Steven et al, 1993
11		Uis Mine, Central Zone, Nm	Stanniferous pegmatite	496	30	526	466	w.r.	Rb-Sr	Steven et al, 1993
12		Ohere, Central Zone, Nm	Leucogranite	506	135	641	371	w.r.	Sr/Sr	Steven et al, 1993
13		Goniakontes alaskite, Nm	Alaskite, post-tectonic doming intrusion	508	2	510	506	uraninite,	U-Pb	Briqueau et al, 1980
14		Khan formation, Goniakonites, Nm	Syn-metamorphic growth	510	3	513	507	monazite	U-Pb	Briqueau et al, 1980
15		Gamigab Prospect, Central Zone, Nm	Cassiterite veins	510		510	510	Muscovite	Rb-Sr	Steven et al, 1993
16		Rossing Mine, Nm	Uraniferous alaskite, early alaskite	510		510	510	w.r.	Rb-Sr	Steven et al, 1993
17		Sandamap Noord, Central Zone,Nm	Leucogranite phacolith	512	19	531	493	w.r.	Sr/Sr	Steven et al, 1993
18		Salem Granite, Goas, Nm	Granite, syn-metamorphic intrusion	512	40	552	472	zircon	U-Pb	Allsopp at al, 1983
19		Rubicon mine, Cental Zone, Nm	Petalite in pegmatite	515	36	551	479	Amb, Kfel	Rb-Sr	Steven et al, 1993
20	Mo Porp	Marinkas Kwela, Nm	Syenite,gt,cb	520		550	490	zircon	U-Pb	Bernasconi, 1986
21		Goniakontes, red granite, Nm	Granite, syn-metamorphic anatexis	534	7	541	527	zircon, mo	U-Pb	Briueu et al, 1980
22	L-795	Ugab River, Nm	Gtd	540	4	544	536	zircon		This report
23		Salem Granite, Ohere Oos, Nm	Granite	542	11	553	531	w.r.	Sr/Sr	Steven et al, 1993
24		Gariep Complex Intrusives,Nm		550		600	500			Miller, 1999
25	BK-19	Kaoko belt, Hoanib River, NW Nm	Coarse-g monzogranite	551.9	1.5	553	550	zircon	U-Pb	Seth et al, 1998
26		Damara syn to post-tectonic intrusives,Nm	Granites	555		650	460			Miller, 1999
27		Kamanjab Batholith,Nm	Gtd	558	20	578	538	zircon	U-Pb	Clifford et al, 1969
28	BK-43	Kaoko belt, Hoanib River, NW Nm	Cg late tectonic granite (migmatite)	563.8	1.5	565	562	zircon	Pb/Pb	Seth et al, 1998
29	BK-43	Kaoko belt, Hoanib River, NW Nm	Cg late tectonic granite (migmatite)	565	13	578	552	zircon	Pb/Pb	Seth et al, 1998
30	BK-24	Kaoko belt, Hoanib River, NW Nm	Foliated cg granodioritic gneiss	567.2	1.5	569	566	zircon	U-Pb	Seth et al, 1998
31	BK-17	Kaoko belt, Hoanib River, NW Nm	Metamorphic age in granitic gneiss	578	57	635	521	zircon	U-Pb	Seth et al, 1998
32	BK-426	Kaoko belt, Hoanib River, NW Nm	Granodioritic augen gneiss	580	3	583	577	zircon	U-Pb	Seth et al, 1998
33	BK-43	Kaoko belt, Hoanib River, NW Nm	Xenocrystic zircon in migmatite	584.3	1.6	586	583	zircon	Pb/Pb	Seth et al, 1998
34	BK-19	Kaoko belt, Hoanib River, NW Nm	Xenocrystic zircon in cg monzogranite	588.1	1.4	590	587	zircon	U-Pb	Seth et al, 1998
35	KES232	Namibrand-Sesriem area	Hebron 136 Neuhof felsic volcanics	594	10	604	584	zircon	U-Pb	Burger & Walraven, 1978
36	BK-426	Kaoko belt, Hoanib River, NW Nm	Xenocrystic zircon in augen gneiss	620	42	662	578	zircon	U-Pb	Seth et al, 1998
37	BK-43	Kaoko belt, Hoanib River, NW Nm	Xenocrystic zircon in migmatite	625	9	634	616	zircon	U-Pb	Seth et al, 1998
38	BK-426	Kaoko belt, Hoanib River, NW Nm	Xenocrystic zircon in augen gneiss	630	8	638	622	zircon	U-Pb	Seth et al, 1998
39	BK-27	Kaoko belt, Hoanib River, NW Nm	Coarse-grain augen gneiss	656	8	664	648	zircon	U-Pb	Seth et al, 1998
40		Rosh Pinah Formation,Nm		700		700	700			Hoffman, 1989
41	BK-426	Kaoko belt, Hoanib River, NW Nm	Xenocrystic zircon in augen gneiss	710	80	790	630	zircon	U-Pb	Seth et al, 1998
42		Oas Farm,Nm	Syenite	736		869	595	zircon	U-Pb	Tegtmeyer & Kroner, 1985
43	L-716	Oas Farm, Nm (basement)	Host gtd	745	5	750	740	zircon	U-Pb	This report
44	PH.12.9	Summas Mountains	Ash-flow tuff	746	2	744	748	zircon	U-Pb	Hoffman et al, 1996
45	PH.11.9	Summas Mountains,Nm	Rhyolitic lava flow	746	2	748	744	zircon	U-Pb	Hoffman et al, 1996
46	PH.11.9	Lower Ugab rhyolite lava	Rhyolite lava	747	2	745	749	zircon	U-Pb	Hoffman et al, 1996
47	L-758	Mesopotamie Farm,Nm	Graphic granite	750	5	755	745	zircon	U-Pb	This report
48	PH.10.9	Oas Farm,Nm	Quartz syenite	756	2	758	754	zircon	U-Pb	Hoffman et al, 1996
49	L-688	Oas Farm,Nm (older intrusive)	Syenite intrusion	762	12	774	750	zircon	U-Pb	This report
50	L-693	Oas Farm, Nm (young intrusive)	Dark subvolcanic intrusive (alkali gtd)	765	4.5	770	761	zircon	U-Pb	This report
51		Damara volcanics,Nm	Alkaline ignimbrites	780		840	720			Miller, 1999
52		Oas Farm, Nm	Gtd	783	18	801	765	zircon	U-Pb	Burger & Kroner in Tegtmeyer,1985
53	PRU142	Oas Farm, Nm	Gtd	840	13	853	827	zircon	U-Pb	Kroner in Tegtmeyer,1985
54		Richtersveld Intrusive Complex,Nm		920		920	920			Miller, 1999
55	RehBI	Gamsberg, Uitdraai granite	Ghoab Oos 381	930	70	1000	860	zircon	U-Pb	Hugo & Schalk, 1974
56	RehBI	Gamsberg, Uitdraai granite	Ghoab Oos 381	932	50	982	882	zircon	U-Pb	Burger & Coertze, 1975
57	RehBI	Gamsberg, Uitdraai granite	Uitdraai Oos 296	932	50	982	882	zircon	U-Pb	Hugo & Schalk, 1974
58	RehBI	Gamsberg S	Oorwinning 134	948	20	968	928	zircon	U-Pb	Burger & Coertze, 1975
59	KES5	Namibrand-Sesriem area	Oorwinning 134 granite	948	20	968	928	zircon	U-Pb	Burger & Coertze, 1975
60		Awasib Granite, Sinclair,Nm	A-type slightly peralkaline granite	957	50	1007	907			Hoal, 1990
61	RehBI	Gamsberg S	Oorwinning 134	976	20	996	956	zircon	U-Pb	Burger & Coertze, 1978
62	KES13	Namibrand-Sesriem area	Oorwinning 134 porphyry	976	20	996	956	zircon	U-Pb	Burger & Coertze, 1975
63	RehBI	Gamsberg, Kobos granite	Nauzerus 1	1010	70	1080	940	zircon	U-Pb	Hugo & Schalk, 1974
64		Namaqua, Nm	Luderitz Tschaukaib granite	1018	10	1028	1008	zircon	U-Pb	Burger, 1976
65		Namaqua, Nm	Luderitz Glockenberg granite	1022	10	1032	1012	zircon	U-Pb	Burger, 1976
66	BK-27	Kaoko belt, Hoanib River, NW Nm	Xenocrystic zircon in augen gneiss	1032	130	1162	902	zircon	U-Pb	Seth et al, 1998
67		Namaqualand Metamorphic Complex,Nm	Granites and basic to ultrabasic rocks	1050		1200	900			Jackson, 1976; Schreuder & Genis, 1978
68	BK-426	Kaoko belt, Hoanib River, NW Nm	Xenocrystic zircon in augen gneiss	1052	4	1056	1048	zircon	U-Pb	Seth et al, 1998
69		Namaqua, Nm	Townlands tonalitic augengneiss	1052	10	1062	1042	zircon	U-Pb	Burger, 1976
70		Nuckopf Formation,Nm	Coarse, quartz feldspar porphyries	1061		1090	1032			Burger & Coetze, 1975
71		Omitiomire, Nm	Foliated tonalite	1063	9	1072	1054	zircon	U-Pb	Steven et al, 2000
72	RehBI	Gamsberg, Kobos granite	Kanaus S 336	1064	20	1084	1044	zircon	U-Pb	Burger & Coertze, 1975
73	RehBI	Gamsberg, Kobos granite	Kanaus S 336	1064	20	1084	1044	zircon	U-Pb	Burger & Coertze, 1975
74	RehBI	Gamsberg, Gamsberg granite	Gamsberg 23	1077	26	1202	1010	zircon	U-Pb	Nagel, 2000
75	RehBI	Gamsberg, Gamsberg granite	Hohenheim 24	1078	30	1108	1048	zircon	U-Pb	Burger & Coertze, 1975
76	RehBI	Gamsberg, Gamsberg granite	Gamsberg 23	1079	30	1142	1038	zircon	U-Pb	Nagel, 2000
77		Namaqua, Nm	Hottentots Bay Namaqua augengneiss	1080	10	1090	1070	zircon	U-Pb	Burger, 1976
78		Namaqua, Nm	Hottentots Bay Namaqua augengneiss	1080	10	1090	1070	zircon	U-Pb	Burger, 1976
79	RehBI	Gamsberg, Gamsberg granite	Hohenheim 24	1080	70	1150	1010	zircon	U-Pb	Hugo & Schalk, 1974
80		Omitiomire, Nm	Chalcocite-bearing amphibole schist	1081	10	1091	1071	zircon	U-Pb	Steven et al, 2000
81		Namaqua, Nm	Grasplatz quartz monzonitic gneiss	1082	10	1092	1072	zircon	U-Pb	Burger, 1976
82	RehBI	Nauzerus G, Kartatsaus F	Uitdraai Oos 296	1083	30	1113	1053	zircon	U-Pb	Burger & Coertze, 1975
83	RehBI	Gamsberg, Rostock granite	Greilingshof 107	1084	8	1092	1076	zircon	U-Pb	Pfurr et al, 1990
84		Namaqua, Nm	Luderitz Glockenberg granite	1086	10	1096	1076	zircon	U-Pb	Burger, 1976
85	RehBI	Gamsberg, Gamsberg granite	Abendruhe 411	1089	30	1119	1059	zircon	U-Pb	Burger & Coertze, 1975
86	RehBI	Nauzerus G, Kartatsaus F	Kaartatsaus 293	1090	30	1120	1060	zircon	U-Pb	Burger & Coertze, 1975
87	RehBI	Nauzerus G, Kartatsaus F	Kaartatsaus 293	1090	70	1160	1020	zircon	U-Pb	Hugo & Schalk, 1974
88	RehBI	Oorlogsende F	Epukiro area	1094	30	1112	1074	zircon	U-Pb	Hegenberger & Burger, 1985

ALL NAMIBIA (COMPILATION OF ALL AGES FROM THE COUNTRY)

	sample	Site/Event	Rock type	age	error	max	min	material	type	reference
88	RehBl	Oorlogsende F	Epukiro area	1094	30	1112	1074	zircon	U-Pb	Hegenberger & Burger, 1985
89	RehBl	Gamsberg, Gamsberg granite	Gamsberg 23	1095	30	1216	1074	zircon	U-Pb	Nagel, 2000
90	RehBl	Gamsberg, Rostock granite	Greilingshof 107	1097	24	1121	1073	zircon	U-Pb	Pfurr et al, 1990
91	L-638	Witvlei Gtd,Nm	Gtd	1098	5.9	1104	1092	zircon	U-Pb	This report
92	RehBl	Gamsberg, Rostock granite	Greilingshof 107	1099	16	1115	1083	zircon	U-Pb	Pfurr et al, 1990
93	RehBl	Gamsberg, Rostock granite	Rostock S 414	1102	7	1109	1095	zircon	U-Pb	Pfurr et al, 1990
94	RehBl	Gamsberg, Koichas granite	Kangas 371	1104	20	1124	1084	zircon	U-Pb	Burger & Coertze, 1975
95		Kwebe Mills,Botswana	Ghanzi Rhyolite	1106	2	1108	1104	zircon	U-Pb	Schwartz et al, 1996
96	RehBl	Gamsberg, Biesespoort granite	Biesiepoort 275	1110	30	1140	1080	zircon	U-Pb	Burger & Coertze, 1978
97	RehBl	Gamsberg, Gamsberg granite	Nauzerus 1	1110	30	1140	1080	zircon	U-Pb	Burger & Coertze, 1975
98		Namaqua, Nm	Hottentots Bay Namaqua augengneiss	1114	10	1124	1104	zircon	U-Pb	Burger, 1976
99		Namaqua, Nm	Jannelspan F. Garub station, Aus biot schist	1116	10	1126	1106	zircon	U-Pb	Burger, 1976
100	RehBl	Oorlogsende F	Epukiro area	1127	30	1157	1097	zircon	U-Pb	Burger & Walraven, 1980
101	RehBl	Nauzerus G, Nuckopf F	Lekkerwater 144	1130	75	1205	1055	zircon	U-Pb	Ziegler & Stoessel, 1993
102		Namaqua, Nm	Luderitz felsic volcanics	1131	10	1141	1121	zircon	U-Pb	Burger, 1976
103	RehBl	Gamsberg, Gamsberg granite	Gamsberg 23	1132	26	1158	1106	zircon	U-Pb	Ziegler & Stoessel, 1993
104	RehBl	Nauzerus G, Nuckopf F	Kunineib 378	1132	75	1207	1057	zircon	U-Pb	Hilken, 1977
105	RehBl	Oorlogsende F	Epukiro area	1144	30	1174	1114	zircon	U-Pb	Burger & Walraven, 1979
106	RehBl	Gamsberg, Ganeib granite	Danigas 289	1150	30	1180	1120	zircon	U-Pb	Burger & Coertze, 1975
107		Piksteel Granodiorite, Rehoboth,Nm	Med-coarse-grained porphyritic biotite granodiorite	1170	20	1190	1150			Reid et al, 1988
108	KES7	Namibrand-Sesriem area	Sesriem 134 Eesaam F	1170	30	1200	1140	zircon	U-Pb	Burger & Coertze, 1975
109		Namaqua, Nm	Luderitz Glockenberg granite	1178	10	1188	1168	zircon	U-Pb	Burger, 1976
110	RehBl	Gamsberg, Kobos granite	Nauchas 14	1178	20	1198	1158	zircon	U-Pb	Burger & Coertze, 1975
111		Namaqua, Nm	Luderitz felsic volcanics	1184	10	1194	1174	zircon	U-Pb	Burger, 1976
112	RehBl	Gamsberg, Gamsberg granite	Corona 223	1186	30	1240	1147	zircon	U-Pb	Nagel, 2000
113	RehBl	Gamsberg, Gamsberg granite	Corona 223	1186	30	1240	1147	zircon	U-Pb	Nagel, 2000
114	L-638	Okatjepuiko,Nm xenocrystic	Granitoid	1194	11	1205	1183	zircon	Pb/U shrimp	This report
115		Namaqua, Nm	Luderitz Glockenberg granite	1194	10	1204	1184	zircon	U-Pb	Burger, 1976
116	RehBl	Gamsberg, Rostock granite	Rostock S 414	1194	26	1220	1168	zircon	U-Pb	Pfurr et al, 1990
117	RehBl	Gamsberg, Rostock granite	Rostock N 393	1207	15	1222	1192	zircon	U-Pb	Pfurr et al, 1990
118	RehBl	Gamsberg, Rostock granite	Rostock N 393	1207	15	1222	1192	zircon	U-Pb	Pfurr et al, 1990
119		Weener Quartz Diorite,Rehoboth,Nm	Medium-grained quartzdiorite	1207	170	1377	1037			Reid et al, 1988
120	RehBl	porphyry dike	Marienhof 577	1210	7	1217	1203	zircon	U-Pb	Ziegler & Stoessel, 1993
121	RehBl	Gamsberg S	Morgenroth 17	1210	8	1218	1202	zircon	U-Pb	Ziegler & Stoessel, 1993
122	RehBl	Nauzerus G, Nuckopf F	Areb North 202	1221	35	1257	1192	zircon	U-Pb	Schalk, 1970
123		Biesiespoort Granite,Nm	Foliated granite	1222	45	1267	1177			Miller, 1999
124	RehBl	Nauzerus G, Kartatsaus F	Spitskop F	1232	30	1262	1202	zircon	U-Pb	Burger & Coertze, 1978
125		Namaqua, Nm	Luderitz granite	1233	10	1243	1223	zircon	U-Pb	Burger, 1976
126		Namaqua, Nm	Luderitz granite	1264	10	1274	1254	zircon	U-Pb	Burger, 1976
127		Aunis Gneiss, Awasib Mtns,Nm	Tonalite gneiss	1271	62	1333	1209			Hoal, 1990
128	KES231	Namibrand-Sesriem area	Hebron 136 Neuhof felsic volcanics	1294	25	1319	1269	zircon	U-Pb	Burger & Walraven, 1978
129	KES9	Namibrand-Sesriem area	Draaihook 119 Nubib granite	1302	20	1322	1282	zircon	U-Pb	Burger & Coertze, 1975
130	RehBl	Oorlogsende F	Epukiro area	1313	30	1343	1283	zircon	U-Pb	Burger & Walraven, 1980
131	KES6	Namibrand-Sesriem area	Sesriem 134 Nubib granite	1350	40	1390	1310	zircon	U-Pb	Burger & Coertze, 1975
132		Alberta Basic Complex,Rehoboth,Nm	Layered gabbroic rocks	1442	32	1474	1410			Reid et al, 1988
133	BK-17	Kaoko belt, Hoanib River, NW Nm	Foliated red granitic gneiss	1507	16	1523	1491	zircon	U-Pb	Seth et al, 1998
134		Rehoboth Area, Nm	Granitic and basic rocks	1545		1670	1420			Miller, and Shalk, 1988
135		Kamanjab Batholith,Nm	tectonic activity	1580	20	1600	1560	zircon	U-Pb	Burger et al, 1976
136		Swartmodder Granite,Rehoboth,Nm	Leucocratic granite	1639	25	1664	1614			Reid et al, 1988 and Shalk, 1988
137	KES230	Namibrand-Sesriem area	Sesriem 137 Eensam qtz porphyry	1656	40	1696	1616	zircon	U-Pb	Burger & Walraven, 1978
138		Franzfontein Granite, Nm	Granite	1662	30	1692	1632	zircon	U-Pb	Burger et al, 1976
139	L-758	Mesopotamie Farm,Nm	inherited zircons in gtd	1692	10	1702	1682	zircon	U-Pb	This report
140	L-796	Ugab,Nm	inherited zircons in gtd	1700	10	1710	1690	zircon	U-Pb	This report
141		Naub Diorite, Rehoboth Area,Nm	hornblende-biotite gneiss	1725	52	1777	1673			Reid et al, 1988
142		Namaqua, Nm	Luderitz augen gneiss	1742	10	1752	1732	zircon	U-Pb	Burger, 1976
143	PRU141	Huab Complex,Nm	Granitic gneiss	1749		1827	1679	zircon	U-Pb	Tegtmeyer & Kroner, 1985
144	L-728	Lofdal Farm,Nm	Foliated Gtd	1750	5	1755	1745	zircon	U-Pb	This report
145		Haib porphyry Cu deposit,Nm	Metamorphism	1750	20	1770	1730		Rb-Sr	Minnit, 1986; Barr & Reid, 1993
146		Namaqua, Nm	Luderitz augen gneiss	1752	10	1762	1742	zircon	U-Pb	Burger, 1976
147		Namaqua, Nm	Luderitz hbl-gneiss	1755	10	1765	1745	zircon	U-Pb	Burger, 1976
148	RehBl	Nauzerus G, Nuckopf F	Auchas 347	1770	35	1805	1735	zircon	U-Pb	Burger & Coertze, 1978
149	RehBl	Gamsberg, Kobos granite	Kwakwas 251	1775	10	1785	1765	zircon	U-Pb	Nagel, 2000
150		Epupa Complex,Nm	Augen gneiss	1795		1828	1766	zircon	U-Pb	Tegtmeyer & Kroner, 1985
151		Elim Formation, Rehoboth Area,Nm	Quartzites, siliciclastics and volcanics	1795		1860	1730			Miller, 1999
152	PRU144	Huab Complex,Nm	Gtd	1811		1850	1776	zircon	U-Pb	Tegtmeyer & Kroner, 1985
153		Khoabendus Group,Nm	Felsic metavolcanics	1813		1860	1765	zircon	U-Pb	Burger & Coertze, 1973
154		Franzfontein Granite, Nm	Granite	1838	30	1868	1808	zircon	U-Pb	Burger et al, 1976
155		Gelbingen Farm, Nm	Quartz eye rhyolite	1862	6	1868	1856	zircon	U-Pb	Steven & Armstrong, 2002
156	L-993	Kamanjab Batholith,Nm	Granite	1866	13	1853	1879	zircon	U-Pb	This report
157	L-638	Okatjepuiko,Nm xenocrystic	Granitoid	1871	6.8	1878	1864	zircon	Pb/Pb shrimp	This report
158		Weener Quartz Diorite,Rehoboth,Nm	Medium-grained quartzdiorite	1871	143	2014	1728			Seifert, 1986
159	L-1013	Kamanjab Batholith,Nm	Quartzmonzonite	1878	15	1863	1893	zircon	U-Pb	This report
160		Kamanjab inlier, Nm	bimodal vulc + intrusion	1880	80	1960	1800	zircon	U-Pb	Burger et al, 1976
161	L-943	Kamanjab Batholith,Nm	Granite	1887	39	1848	1926	zircon	U-Pb	This report
162		Haib porphyry Cu deposit,Nm	Gtd	1900	5	1905	1895	zircon	U-Pb	Reid, personal communication, 2003
163		Lorelei porphyry Cu-Mo,Nm	Granodiorite	1900	50	1950	1850		inferred	Viljoen, Minnit,Viljoen, 1986
164		Ababis Inlier, Nm	Basement gneisses	1925		2255	1645	zircon	U-Pb	Jacob et al, 1978
165	L-868	Kamanjab Batholith,Nm	Quartzmonzonite	1937	14	1923	1951	zircon	U-Pb	This report
166	L-855	Kamanjab Batholith,Nm	Granite	1937	19	1918	1956	zircon	U-Pb	This report
167	L-1045	Grootfontein Inlier, Nm	Quartzmonzonite	1939	64	1875	2003	zircon	U-Pb	This report
168		Tumas Dome, Nm	Basement gneisses	1945	18	1963	1927	zircon	U-Pb	Jacob et al, 1978, Burger & Jacob, unpub. data in Kroner et al, 1991
169		Namaqua, Nm	Luderitz Kunguib granodiorite	1952	10	1962	1942	zircon	U-Pb	Burger, 1976

ALL NAMIBIA (COMPILATION OF ALL AGES FROM THE COUNTRY)

	sample	Site/Event	Rock type	age	error	max	min	material	type	reference
170		Kaoko Belt, 45 km NW Sesfontein,Nm	partly sheared monzogranite	1961	0.6	1962	1960	zircon	U-Pb	Hoffman & Kroner, unpub in Seth, 1998
171	BK-439	Kaoko belt, NW Nm	Cg monzogranitic augen gneiss	1961	4	1965	1957	zircon	U-Pb	Seth et al, 1998
172		Damaran metased, Navachab mine, Nm	Detrital zircons in Damaran metaseds	1962	10	1972	1952	zircon	U-Pb	Jacob et al, 2003
172	BK-10	Kaoko belt, Hoanib River, NW Nm	Foliated syenogranitic orthogneiss	1971	7	1978	1964	zircon	U-Pb	Seth et al, 1998
173	L-969	Kamanjab Batholith,Nm	Foid syenite	1976	42	1934	2018	zircon	U-Pb	This report
174		Kaoko Belt, 30 km NW Sesfontein,Nm	partly sheared monzogranite	1978	0.6	1978	1977	zircon	U-Pb	Hoffman & Kroner, unpub in Seth, 1998
175		Namaqua, Nm	Luderitz Kunguib granodiorite	1978	10	1988	1968	zircon	U-Pb	Burger, 1976
176	BK-5	Kaoko belt, NW Nm	Dioritic orthogneiss	1985	23	2008	1962	zircon	U-Pb	Seth et al, 1998
177		Khoabendus Formation,Nm	Flow-banded rhyolite	1987	4	1991	1983	zircon	Pb/Pb ev	Hoffman & Kroner, unpub in Seth, 1998
178	BK-10	Kaoko belt, Hoanib River, NW Nm	Xenocrystic zircon in syenogranitic orthogneiss	2033		2033	2033	zircon	U-Pb	Seth et al, 1998
179		Kunene Complex,Nm	Anorthosites	2100		2100	2100			Miller, 1999
180		Oas Farm,Nm	Syenite, inherited zircons	2124		2192	2070	zircon	U-Pb	Tegtmeyer & Kroner, 1985
181	PRU142	Oas Farm,Nm	Syenite, inherited zircons	2124		2192	2070	zircon	U-Pb	Tegtmeyer & Kroner, 1985
182	BK-5	Kaoko belt, NW Nm	Xenocrystic zircon in dioritic orthogneiss	2281	0.9	2282	2280	zircon	U-Pb	Seth et al, 1998
183	BK-5	Kaoko belt, NW Nm	Xenocrystic zircon in dioritic orthogneiss	2287	10	2297	2277	zircon	U-Pb	Seth et al, 1998
184		Damaran metased, Navachab mine, Nm	Detrital zircons in Damaran metaseds	2360	5	2365	2355	zircon	U-Pb	Jacob et al, 2003
185		Damaran metased, Navachab mine, Nm	Detrital zircons in Damaran metaseds	2428	9	2437	2419	zircon	U-Pb	Jacob et al, 2003
186	L-855	Kamanjab Batholith,Nm	inherited zircons in gtd	2500	19	2481	2519	zircon	U-Pb	This report
187	L-1045	Grootfontein Inlier, Nm	inherited zircons in gtd	2549	78	2471	2627	zircon	U-Pb	This report
188	BK-29	Kaoko belt, NW Nm	Coarse-grained quartz-monzonitic augen gneiss	2584	0.6	2585	2584	zircon	U-Pb	Seth et al, 1998
189	BK-1	Kaoko belt, NW Nm	Grey, coarse-grained monzonitic augen gneiss	2585	1.2	2587	2584	zircon	U-Pb	Seth et al, 1998
190	BK-5	Kaoko belt, NW Nm	Xenocrystic zircon in dioritic orthogneiss	2600		2600	2600	zircon	U-Pb	Seth et al, 1998
191	BK-5	Kaoko belt, NW Nm	Xenocrystic zircon in dioritic orthogneiss	2605	11	2616	2594	zircon	U-Pb	Seth et al, 1998
192	BK-446	Kaoko belt, NW Nm	Quartz-monzodioritic gneiss	2616	5	2621	2611	zircon	U-Pb	Seth et al, 1998
193	BK-3	Kaoko belt, NW Nm	Fol Quartz-monzodioritic orthogneiss	2645	6	2651	2639	zircon	U-Pb	Seth et al, 1998
194		Damaran metased, Navachab mine, Nm	Detrital zircons in Damaran metaseds	2870	6	2876	2864	zircon	U-Pb	Jacob et al, 2003
195		Damaran metased, Navachab mine, Nm	Detrital zircons in Damaran metaseds	2872	4	2876	2868	zircon	U-Pb	Jacob et al, 2003
	sample	Site/Event	Rock type	age	error	max	min	material	type	reference
	sample	Site/Event	Rock type	age	error	max	min	material	type	reference

APPENDIX F
EVENT DIAGRAMS

ZAMBIA	
A23	Hook Granite Batholith, Zambia, 68
A24	NW Zambia, 69
A25	West Lusaka-Kafue Flats Area, Zambia, 70
A26	Environs of the Nchanga Mine, Zambia, 71
A27	Basement to the main Copperbelt, Zambia, 72
A28	Environs of the Mufulira Area, Zambia, 73
A29	All basement to the Copperbelt, Zambia, 74
A30	Luangwa Valley, Zambia, 75
A31	Mkushi-Serenje Area, Zambia, 76
A32	Choma-Kalomo Batholith, Zambia, 77
A33	Irumide Belt, Zambia, 78
A34	Other Zambian reported ages, 79
A35	All Zambian radiometric ages, 80
NAMIBIA	
A36	Kaokoland Area, Namibia, 81
A37	Entire Kamanjab region, Namibia, 82
A38	Khorixas Inlier, Namibia, 83
A39	True Kamanjab Batholith, Namibia, 84
A40	Comparative event diagram for Khorixas Inlier and Kamanjab Batholith, Namibia, 85
A41	Central Namibian Area, 86
A42	Namaqua Metamorphic Complex, Namibia, 87
A43	Witvlei Area and correlatives in the Greater Lufilian Arc, 88
A44	So-called “Kibaran-Age” rocks, Namibia, 89
A45	Southernmost portion of Namibia, 90
A46	Namibrand-Sasriem Area, Namibia, 91
A47	Rehoboth Inlier, Namibia, 92
A48	All Namibian radiometric ages, 93
A49	Radiometric ages of other countries that are related to the Greater Lufilian Arc, 94

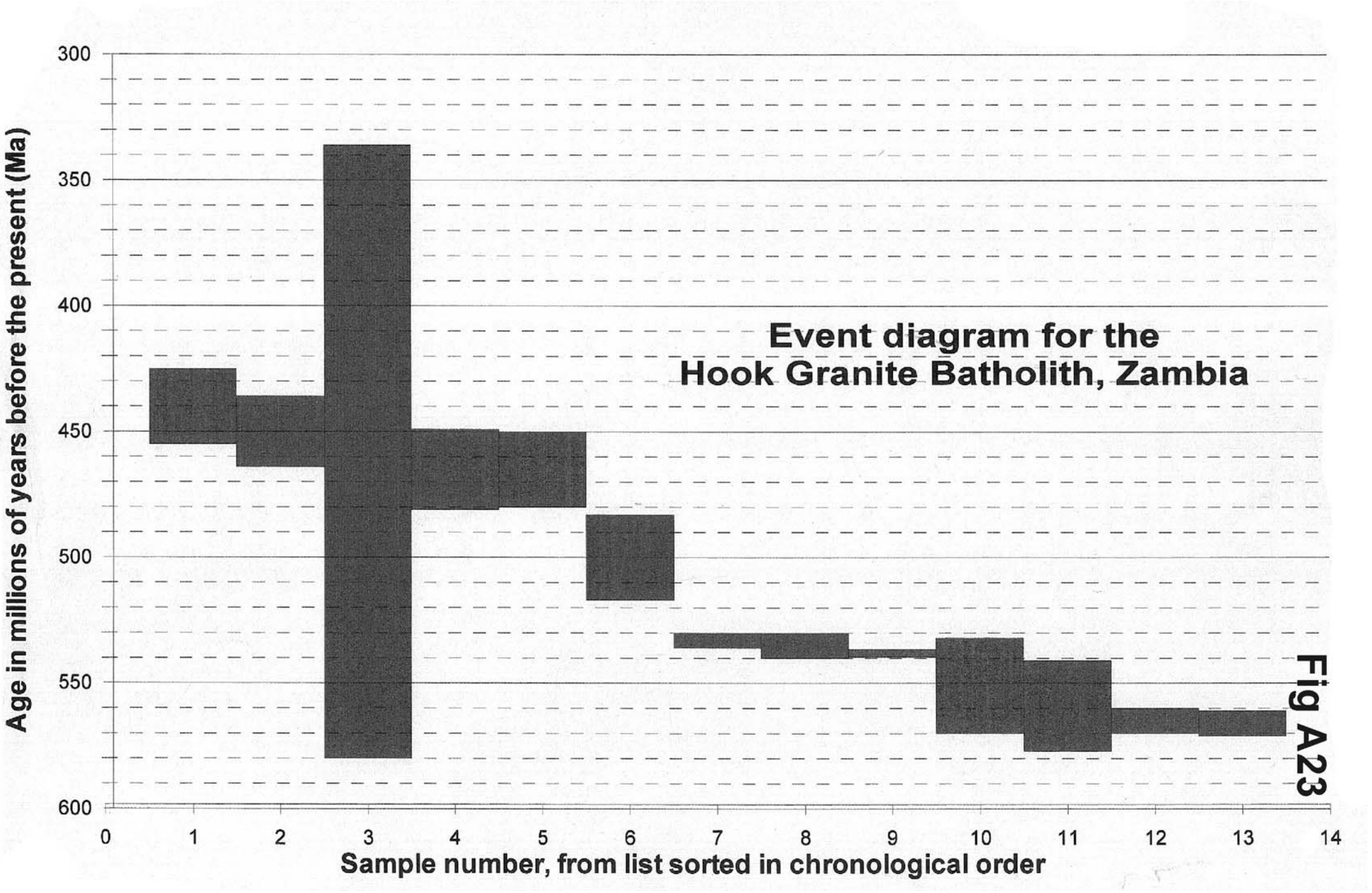
Event diagram for the
Hook Granite Batholith, Zambia
Age in millions of years before the present (Ma)
300
350
400
450
500
550
600
0
1
2
3
4
5
6
7
8
9
10
11
12
13
14
Sample number, from list sorted in chronological order

Fig A23

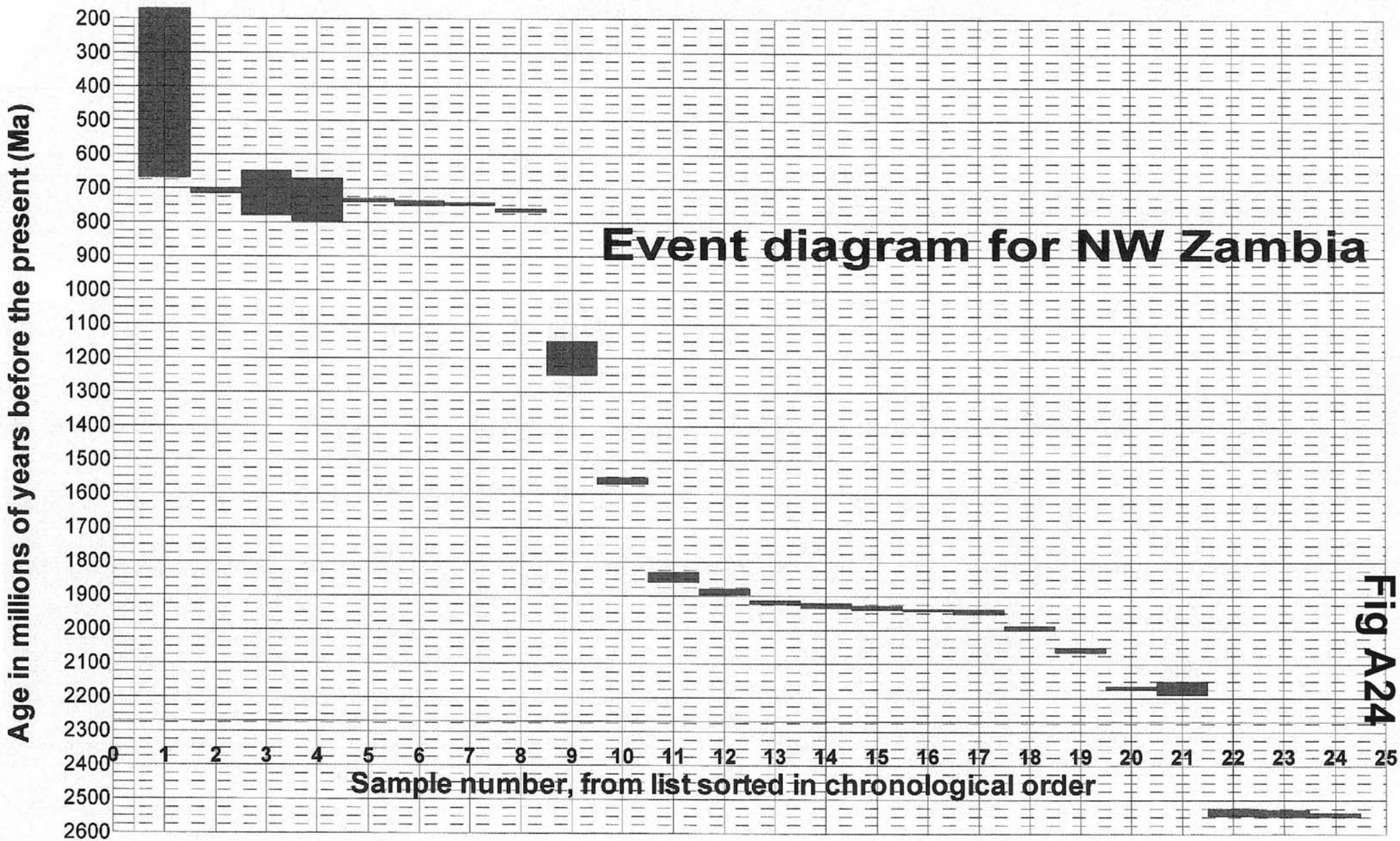
Event diagram for NW Zambia
Age in millions of years before the present (Ma)
200
300
400
500
600
700
800
900
1000
1100
1200
1300
1400
1500
1600
1700
1800
1900
2000
2100
2200
2300
2400
2500
2600
0 1 2 3 4 5 6 7 8 9 10 11 12 13 14 15 16 17 18 19 20 21 22 23 24 25
Sample number, from list sorted in chronological order

Fig A24

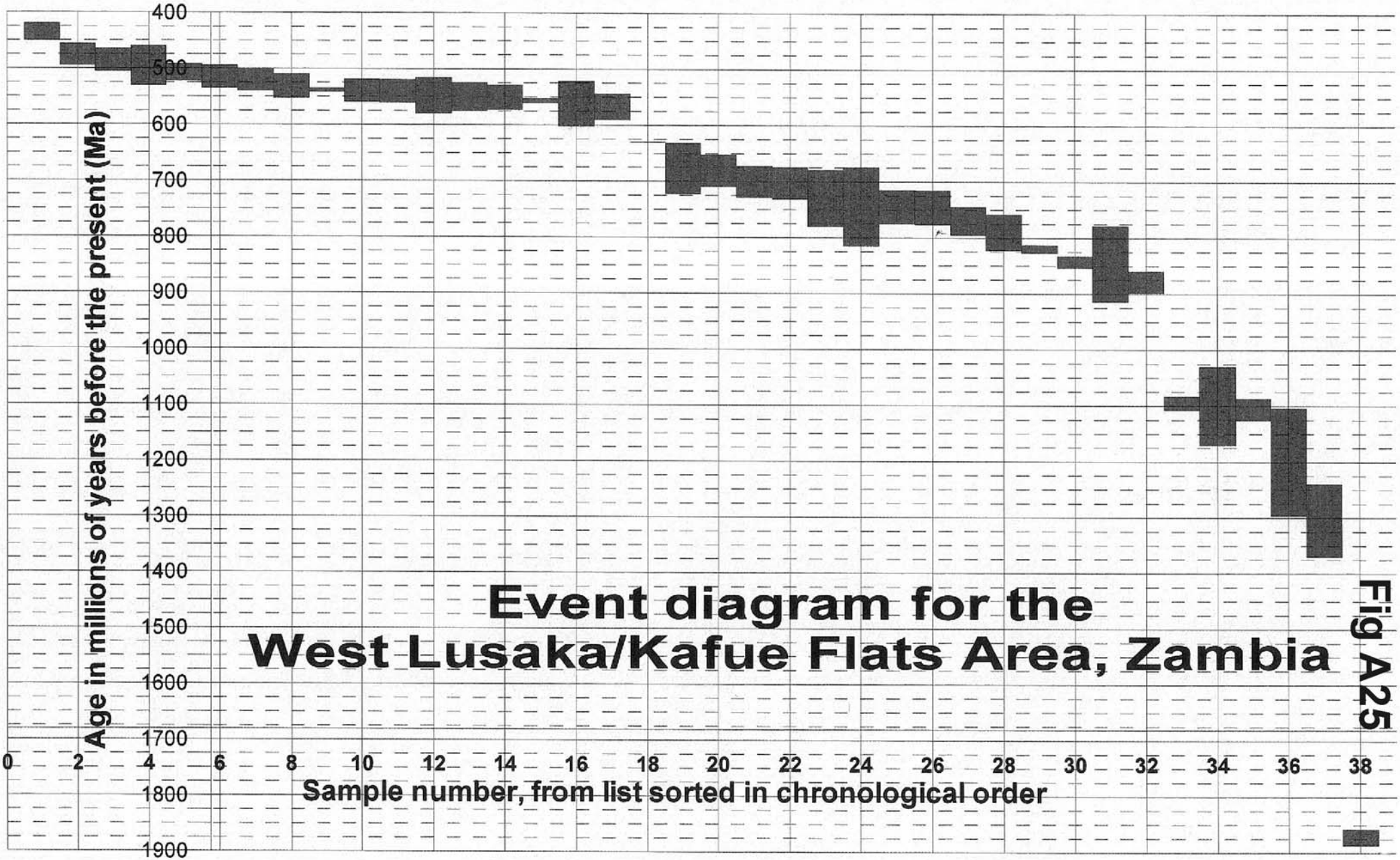

Event diagram for the West Lusaka/Kafue Flats Area, Zambia

Fig A25

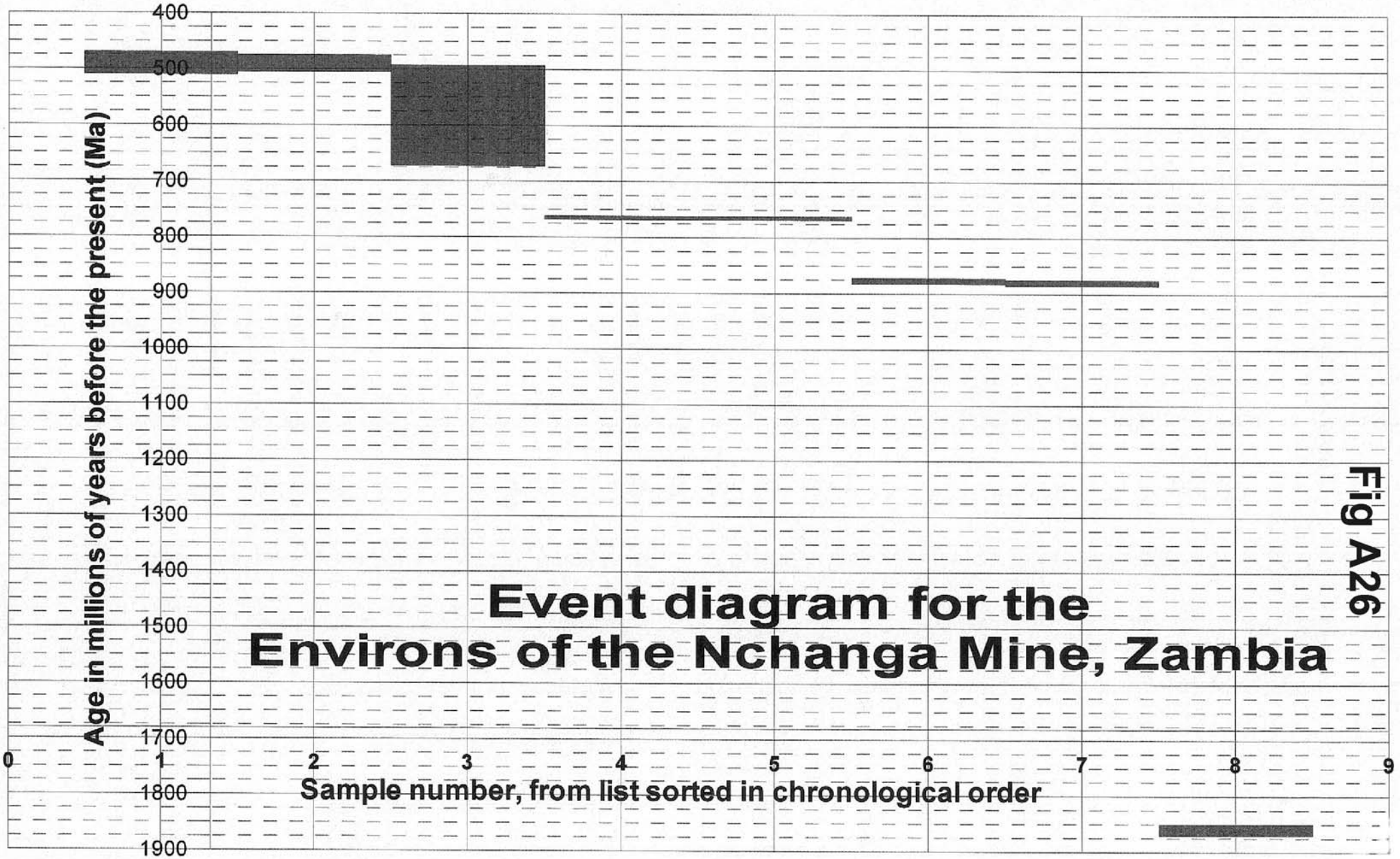

Event diagram for the Environs of the Nchanga Mine, Zambia

Fig A26

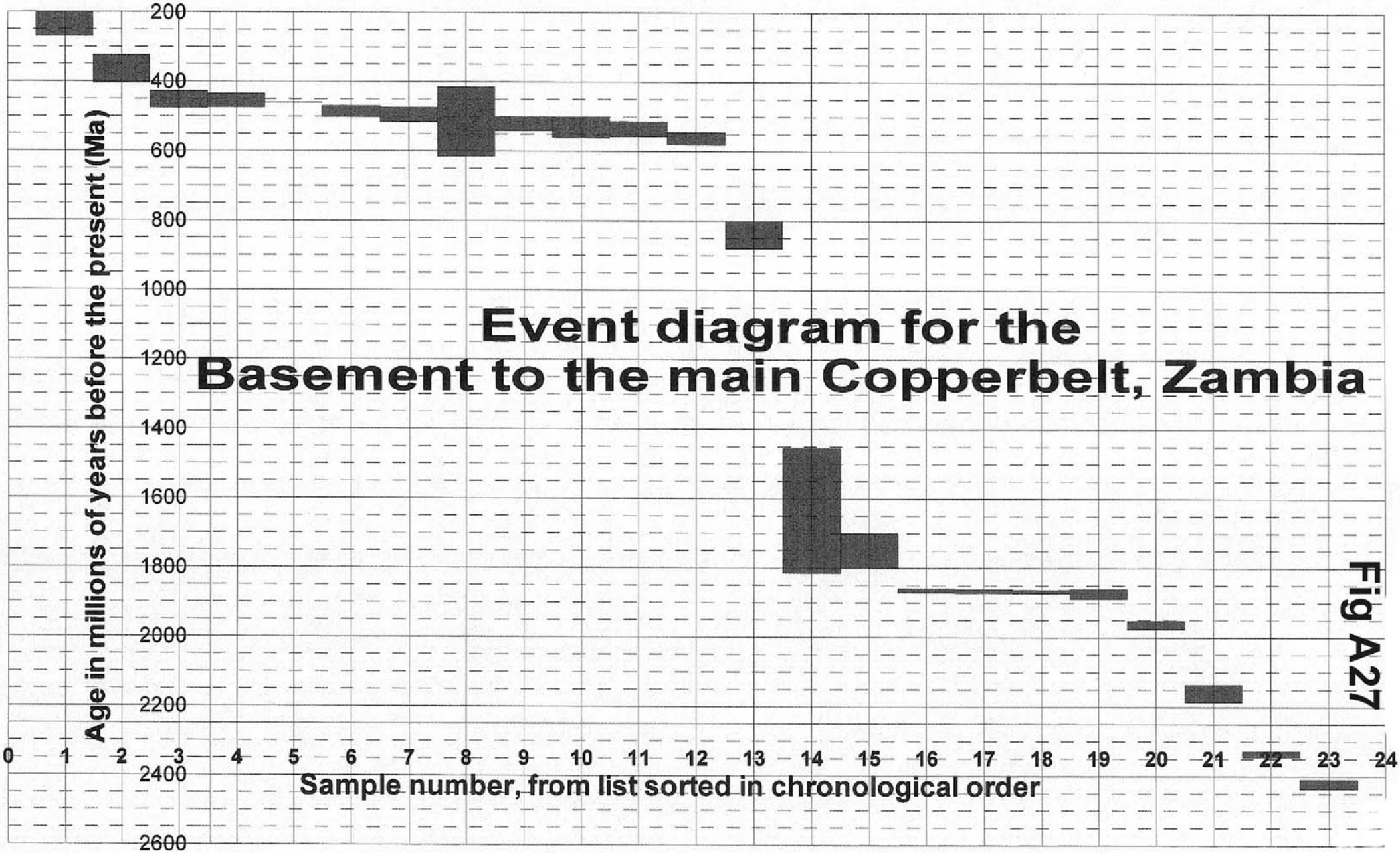
Event diagram for the
Basement to the main Copperbelt, Zambia
Age in millions of years before the present (Ma)
200
400
600
800
1000
1200
1400
1600
1800
2000
2200
2400
2600
0
1
2
3
4
5
6
7
8
9
10
11
12
13
14
15
16
17
18
19
20
21
22
23
24
Sample number, from list sorted in chronological order

Fig A27

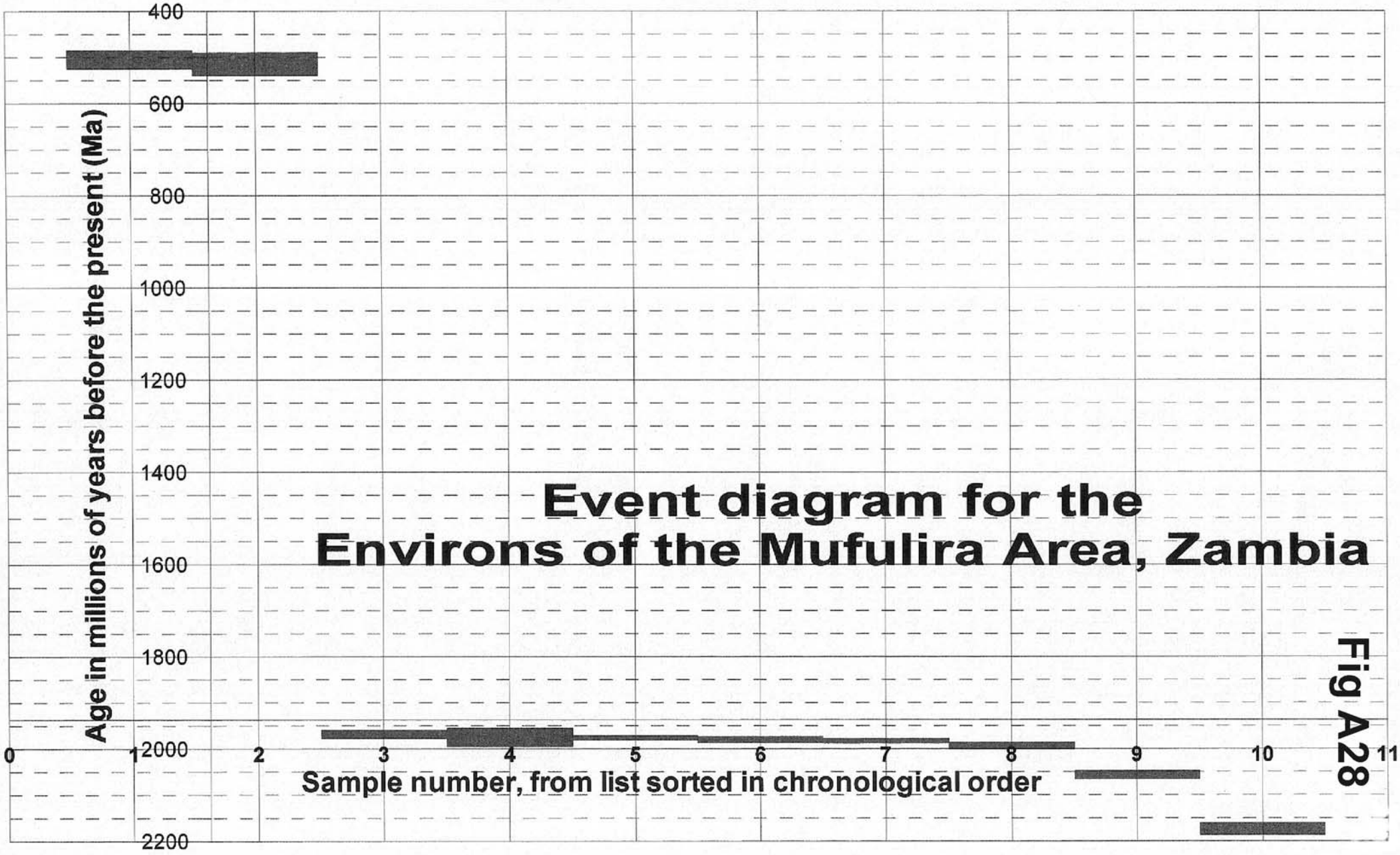
Event diagram for the
Environs of the Mufulira Area, Zambia
Age in millions of years before the present (Ma)
400
600
800
1000
1200
1400
1600
1800
2000
2200
0
1
2
3
4
5
6
7
8
9
10
11
Sample number, from list sorted in chronological order

Fig A28

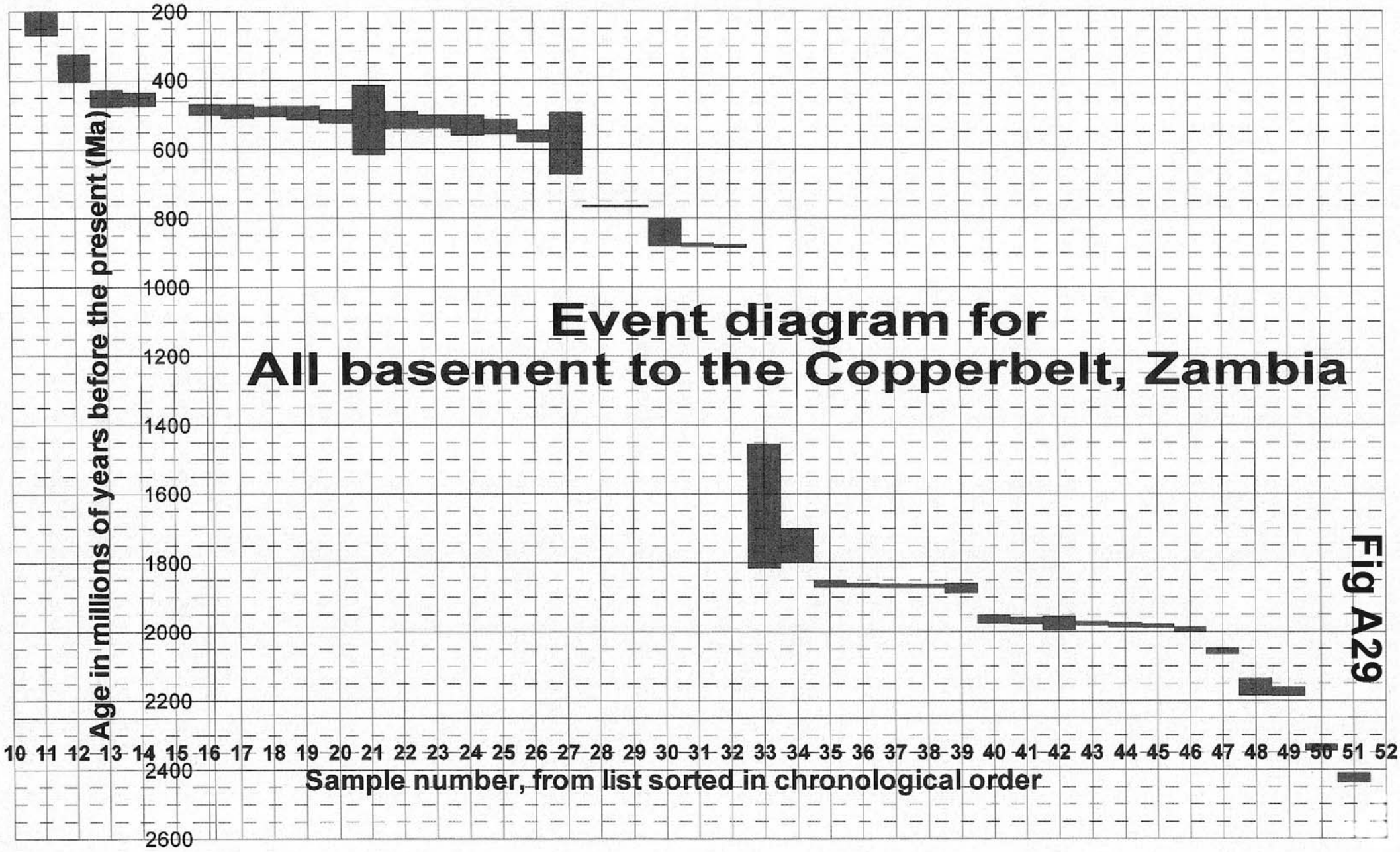
Event diagram for
All basement to the Copperbelt, Zambia
Age in millions of years before the present (Ma)
200
400
600
800
1000
1200
1400
1600
1800
2000
2200
2400
2600
10 11 12 13 14 15 16 17 18 19 20 21 22 23 24 25 26 27 28 29 30 31 32 33 34 35 36 37 38 39 40 41 42 43 44 45 46 47 48 49 50 51 52
Sample number, from list sorted in chronological order

Fig A29

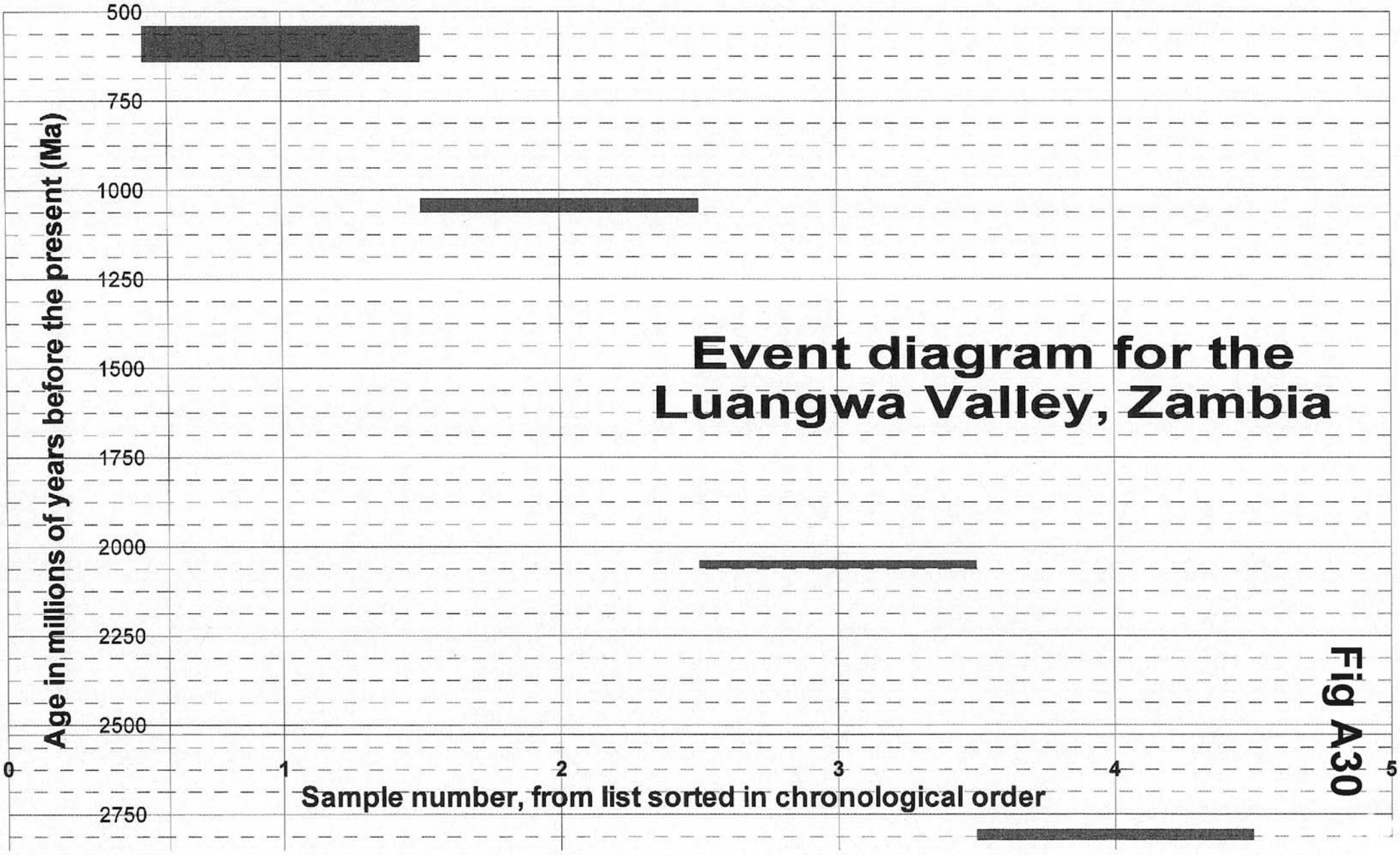
Event diagram for the
Luangwa Valley, Zambia
Age in millions of years before the present (Ma)
500
750
1000
1250
1500
1750
2000
2250
2500
2750
0
1
2
3
4
5
Sample number, from list sorted in chronological order

Fig A30

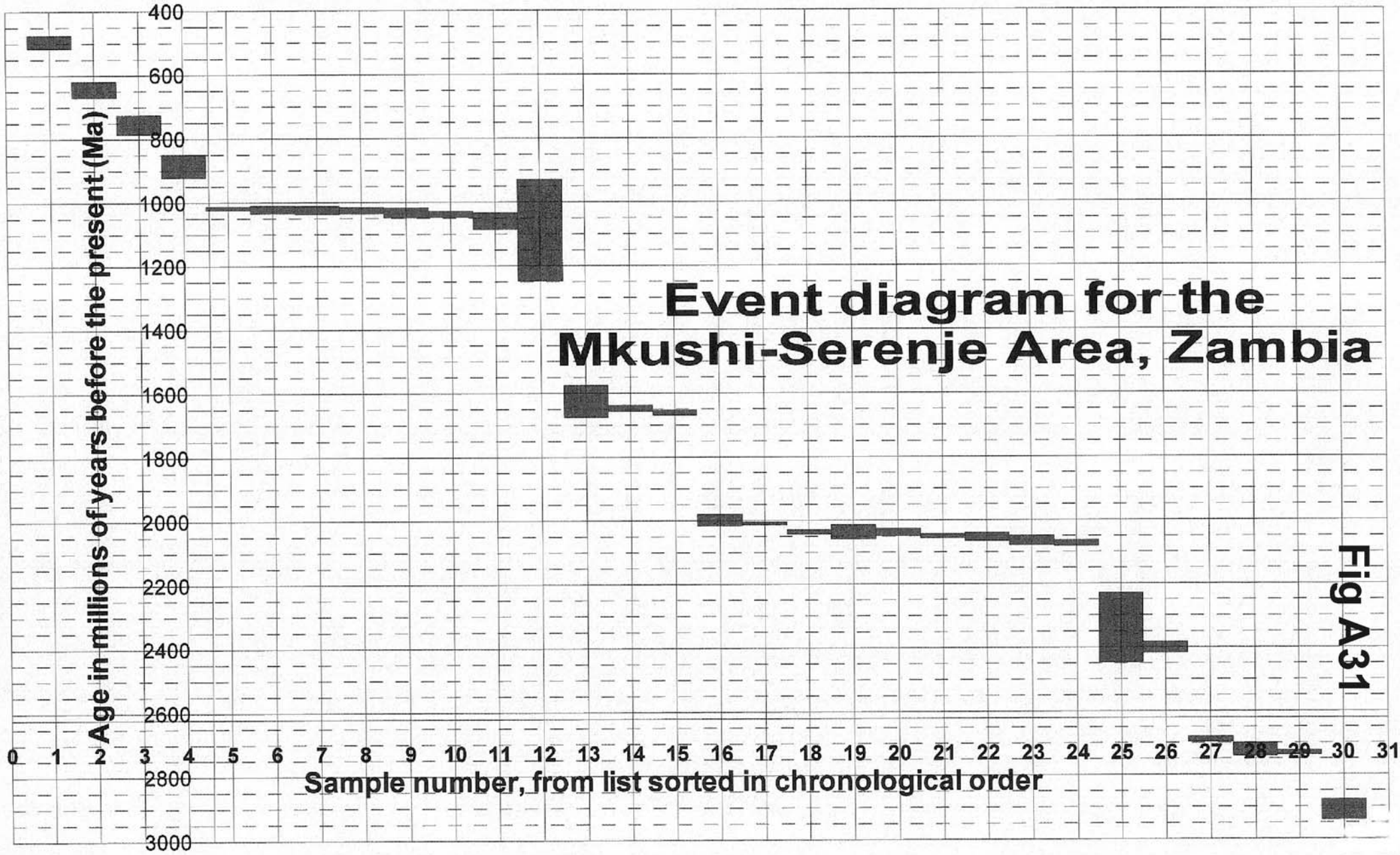
Event diagram for the
Mkushi-Serenje Area, Zambia
Age in millions of years before the present (Ma)
400
600
800
1000
1200
1400
1600
1800
2000
2200
2400
2600
2800
3000
0 1 2 3 4 5 6 7 8 9 10 11 12 13 14 15 16 17 18 19 20 21 22 23 24 25 26 27 28 29 30 31
Sample number, from list sorted in chronological order

Fig A31

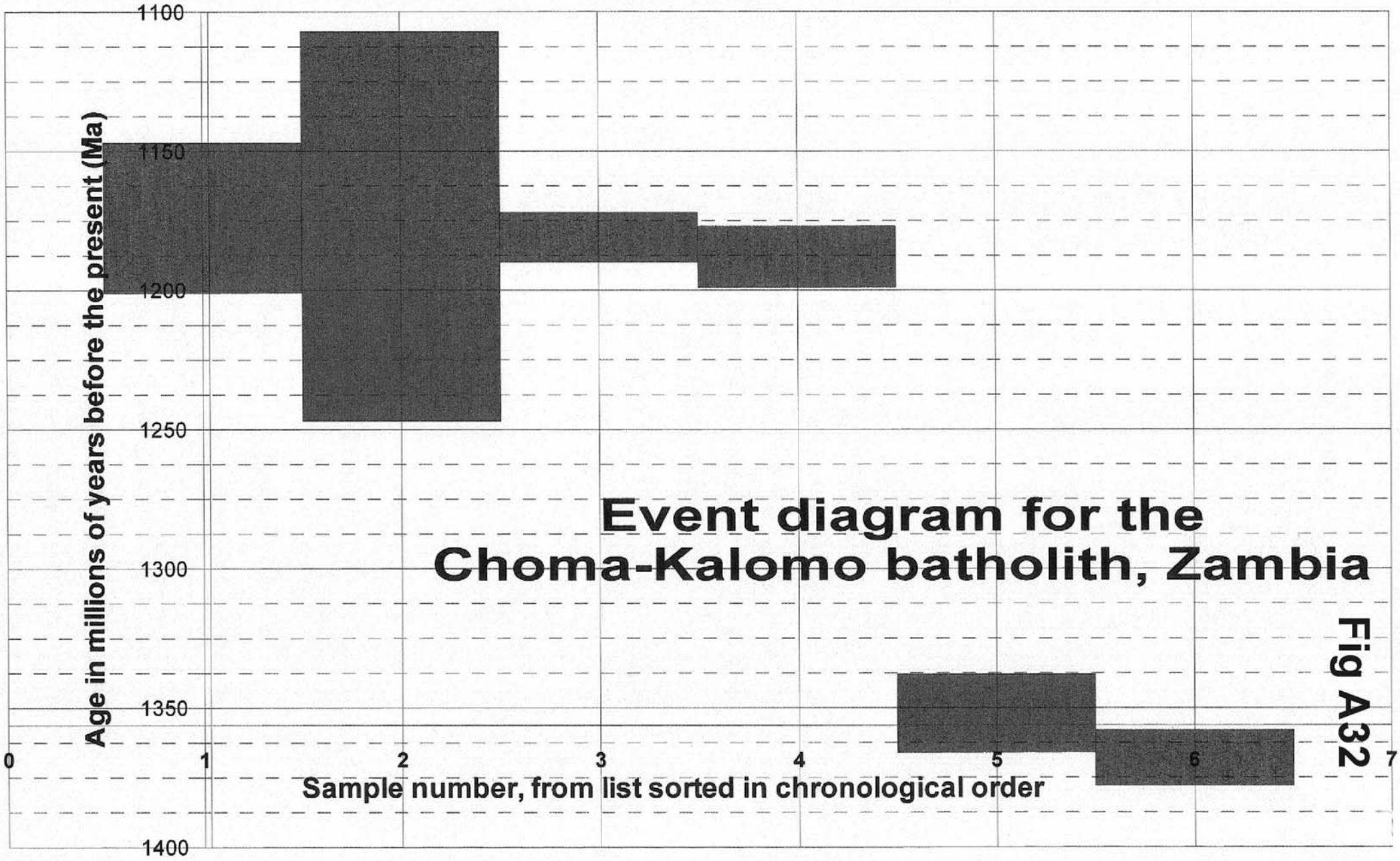

Event diagram for the Choma-Kalomo batholith, Zambia

Fig A32

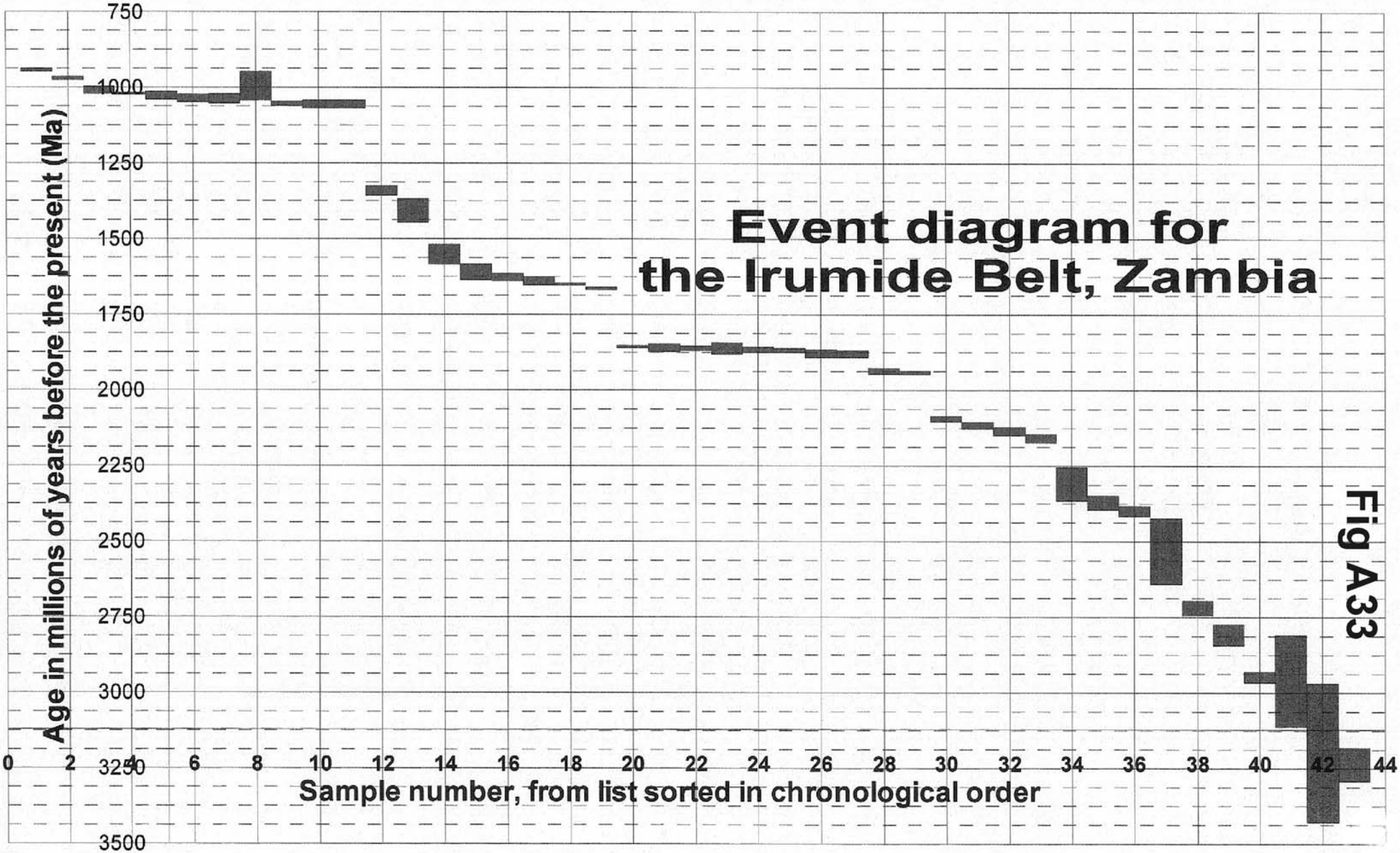
Event diagram for
the Irumide Belt, Zambia
Age in millions of years before the present (Ma)
750
1000
1250
1500
1750
2000
2250
2500
2750
3000
3250
3500
0
2
4
6
8
10
12
14
16
18
20
22
24
26
28
30
32
34
36
38
40
42
44
Sample number, from list sorted in chronological order

Fig A33

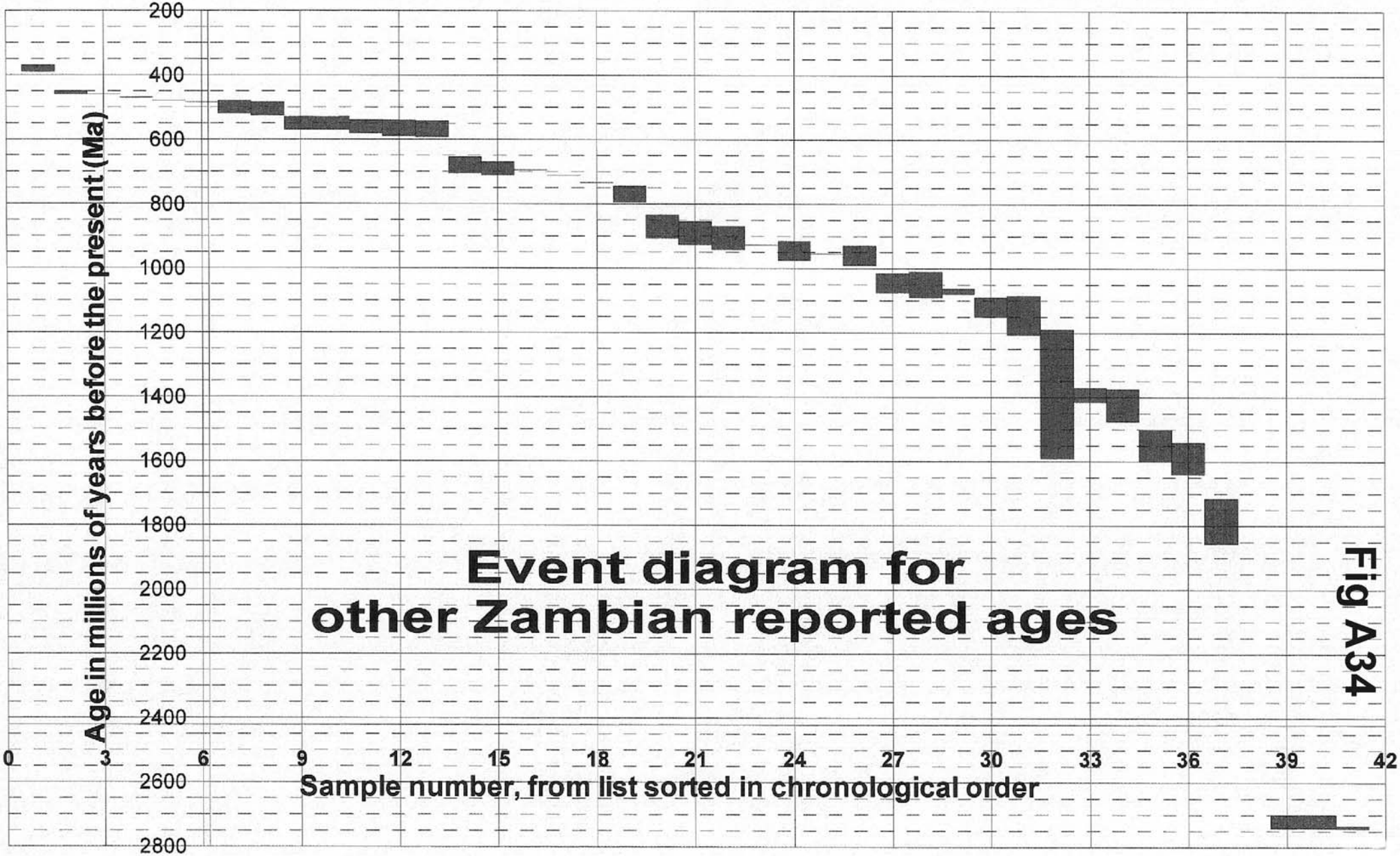
Age in millions of years before the present (Ma)
200
400
600
800
1000
1200
1400
1600
1800
2000
2200
2400
2600
2800
0
3
6
9
12
15
18
21
24
27
30
33
36
39
42
Sample number, from list sorted in chronological order
Event diagram for other Zambian reported ages

Fig A34

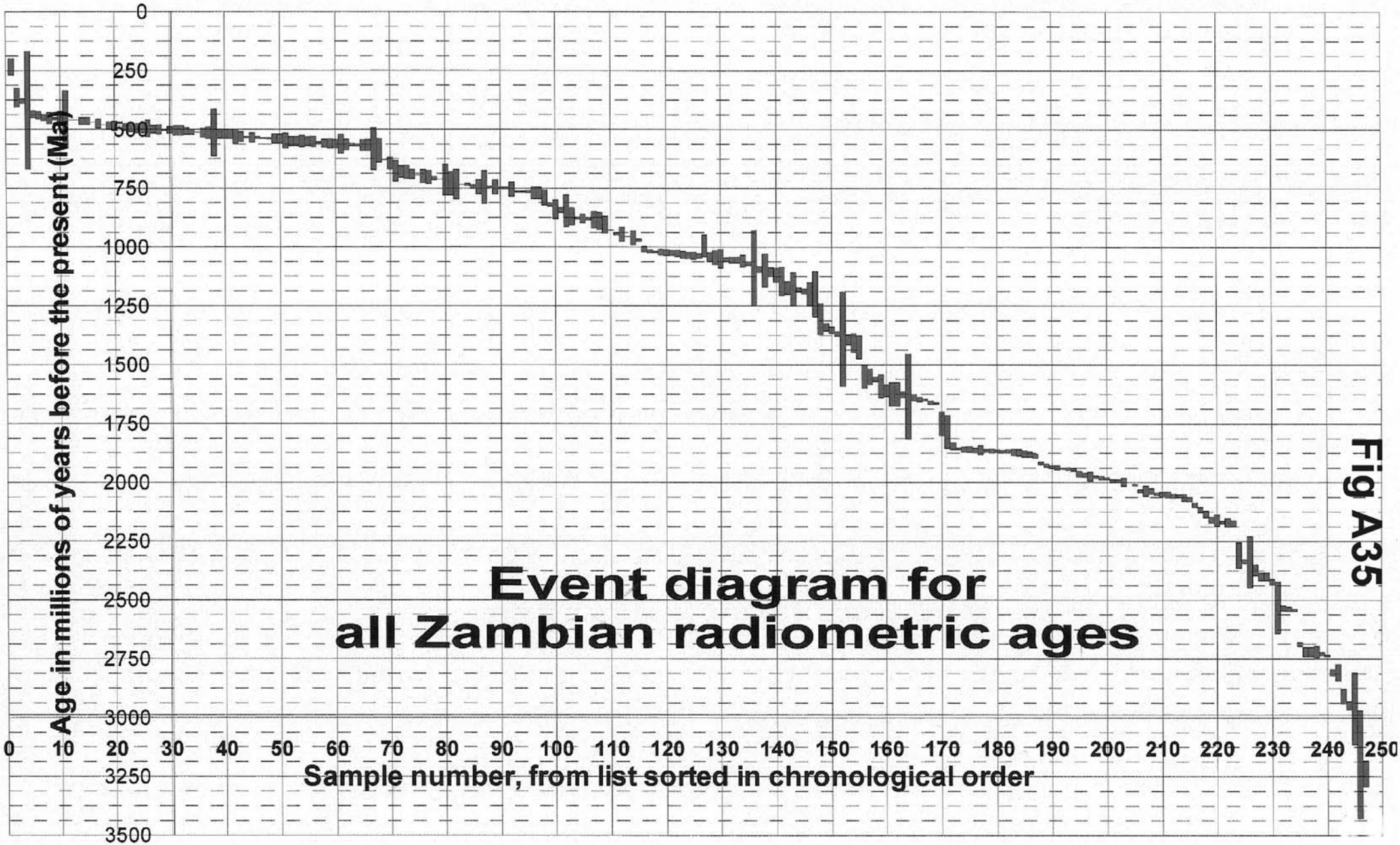
Event diagram for
all Zambian radiometric ages
Age in millions of years before the present (Ma)
0
250
500
750
1000
1250
1500
1750
2000
2250
2500
2750
3000
3250
3500
0 10 20 30 40 50 60 70 80 90 100 110 120 130 140 150 160 170 180 190 200 210 220 230 240 250
Sample number, from list sorted in chronological order

Fig A35

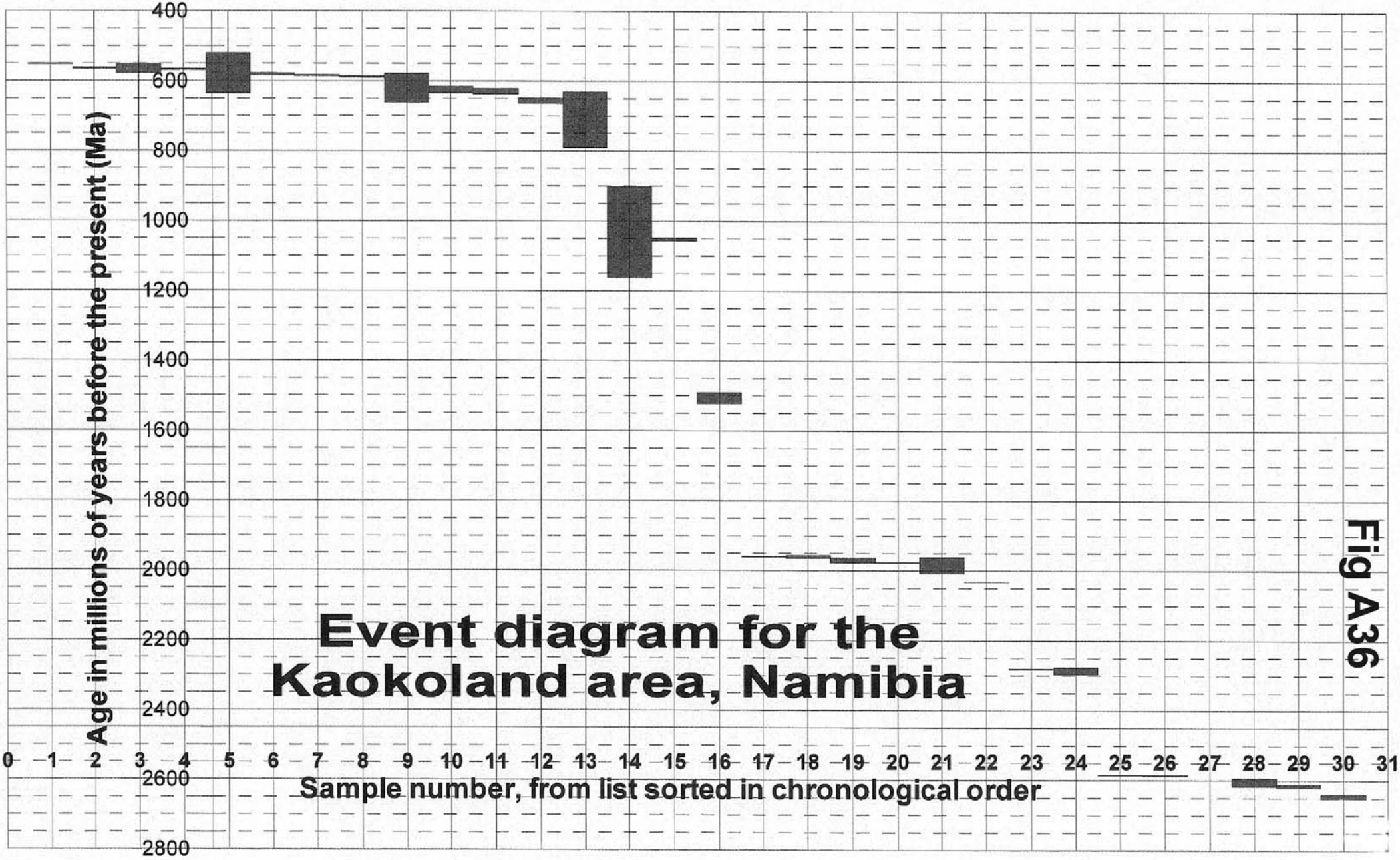
Event diagram for the
Kaokoland area, Namibia
Age in millions of years before the present (Ma)
400
600
800
1000
1200
1400
1600
1800
2000
2200
2400
2600
2800
0 1 2 3 4 5 6 7 8 9 10 11 12 13 14 15 16 17 18 19 20 21 22 23 24 25 26 27 28 29 30 31
Sample number, from list sorted in chronological order

Fig A36

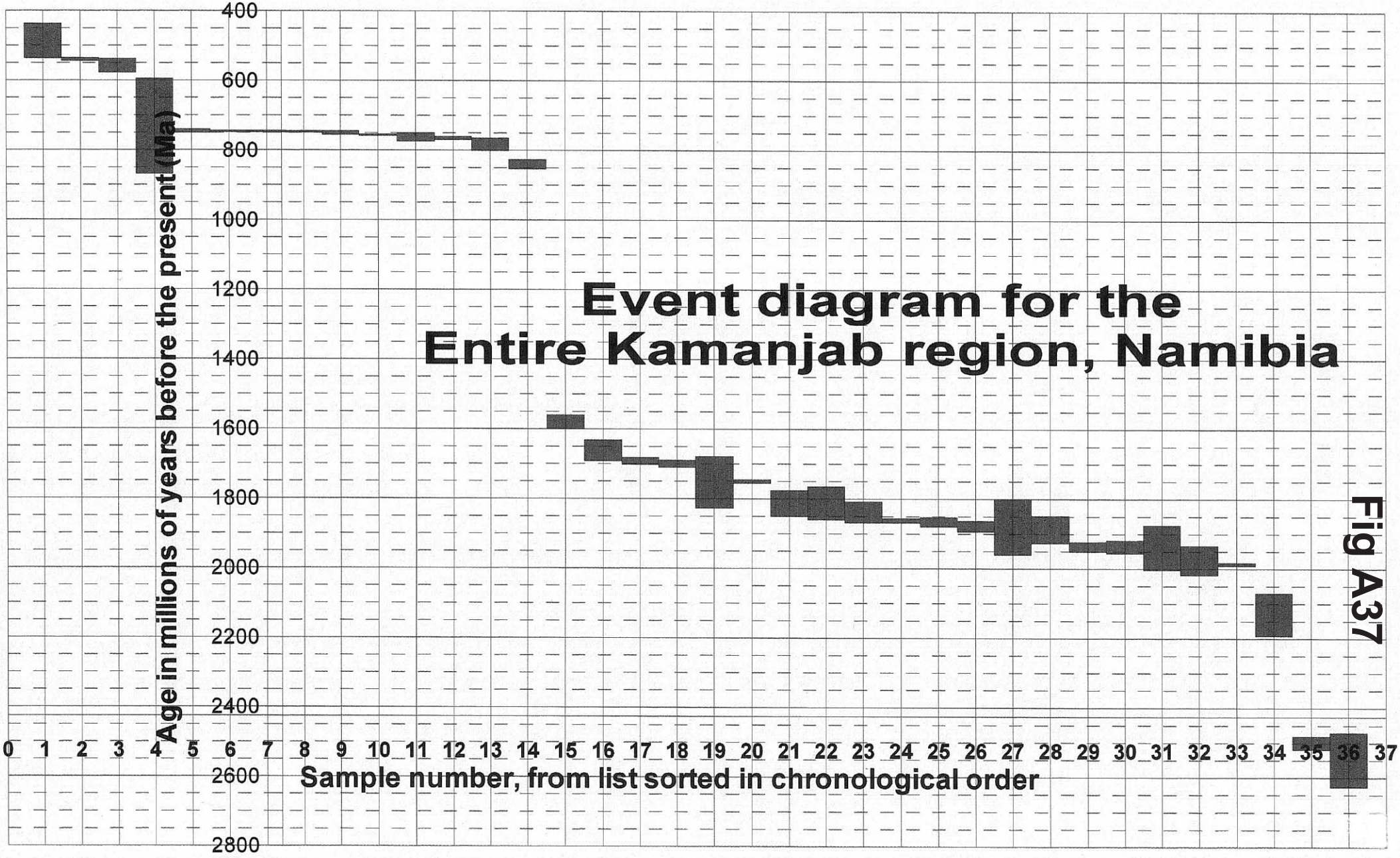
Event diagram for the
Entire Kamanjab region, Namibia
Age in millions of years before the present (Ma)
400
600
800
1000
1200
1400
1600
1800
2000
2200
2400
2600
2800
0 1 2 3 4 5 6 7 8 9 10 11 12 13 14 15 16 17 18 19 20 21 22 23 24 25 26 27 28 29 30 31 32 33 34 35 36 37
Sample number, from list sorted in chronological order

Fig A37

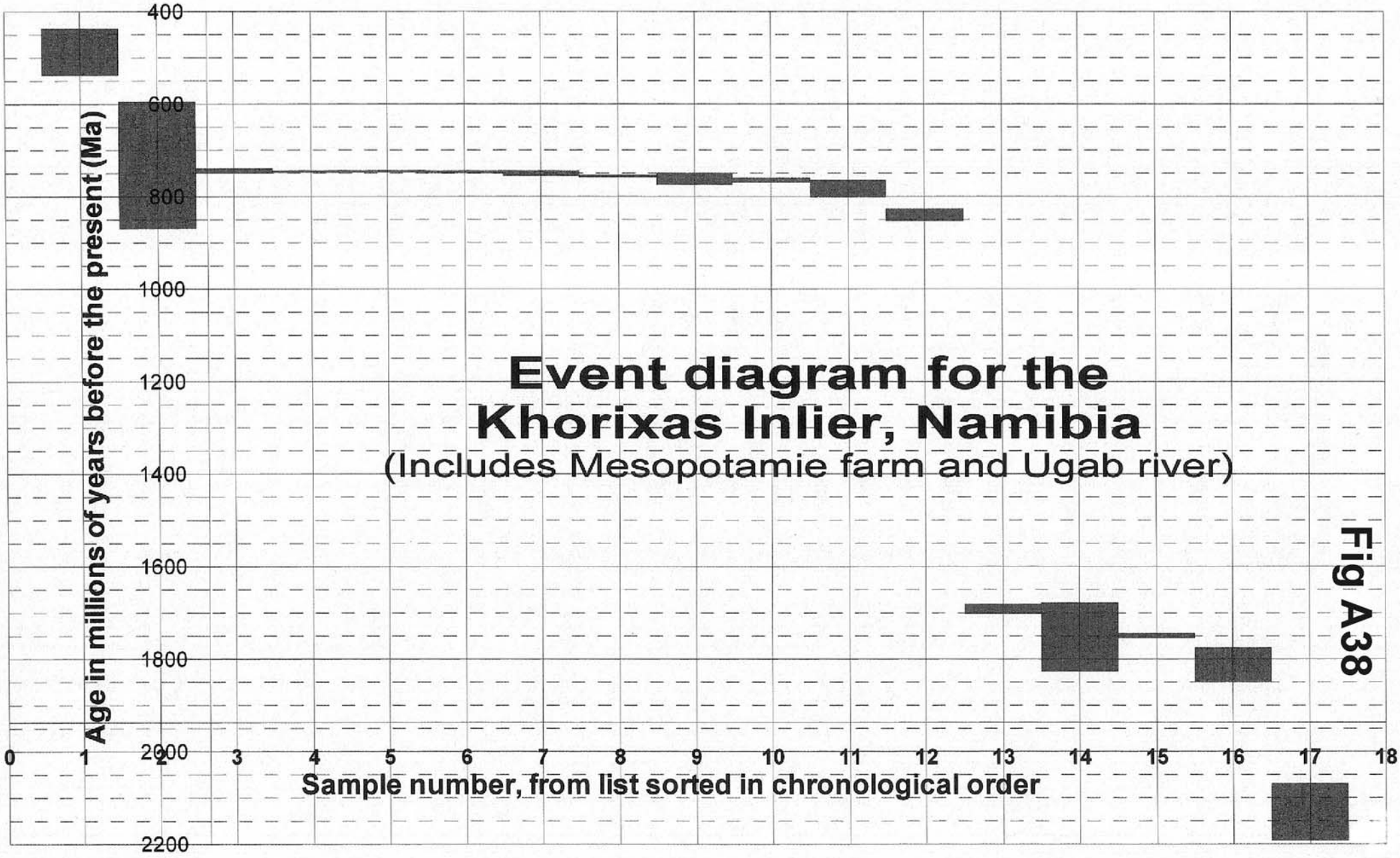
Event diagram for the
Khorixas Inlier, Namibia
(Includes Mesopotamie farm and Ugab river)
Age in millions of years before the present (Ma)
400
600
800
1000
1200
1400
1600
1800
2000
2200
0
1
2
3
4
5
6
7
8
9
10
11
12
13
14
15
16
17
18
Sample number, from list sorted in chronological order

Fig A38

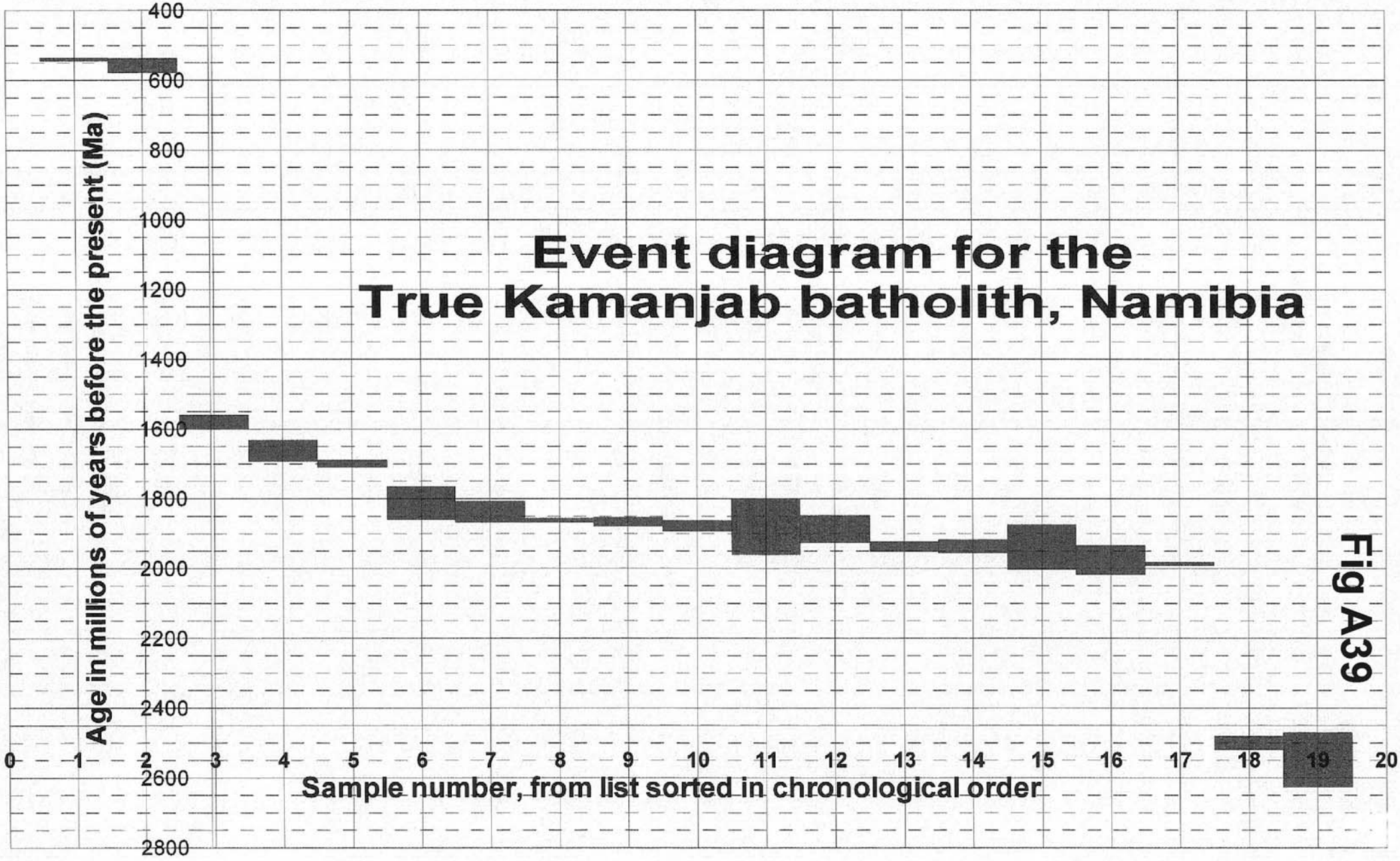
Event diagram for the
True Kamanjab batholith, Namibia
Age in millions of years before the present (Ma)
400
600
800
1000
1200
1400
1600
1800
2000
2200
2400
2600
2800
0
1
2
3
4
5
6
7
8
9
10
11
12
13
14
15
16
17
18
19
20
Sample number, from list sorted in chronological order

Fig A39

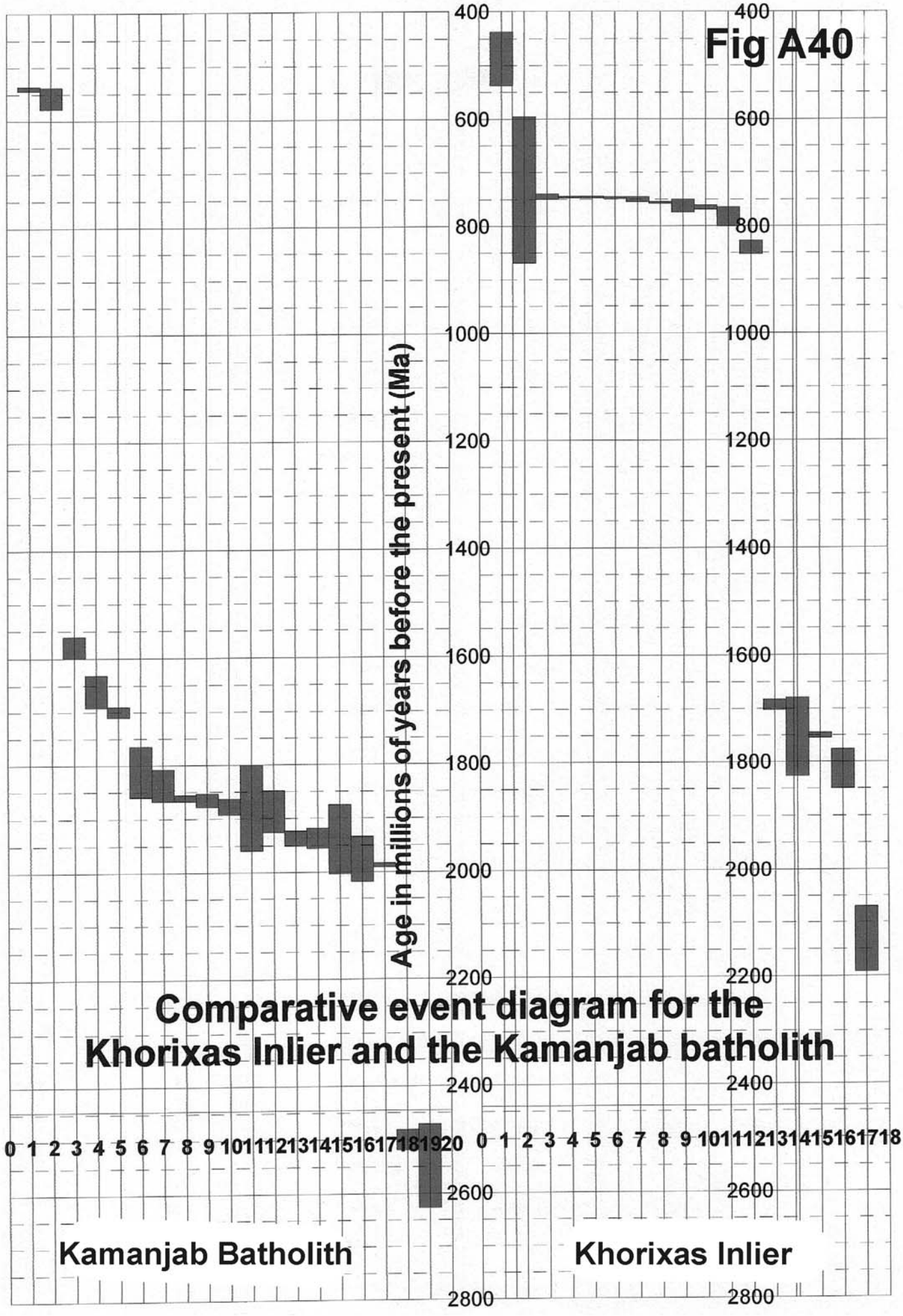

Comparative event diagram for the Khorixas Inlier and the Kamanjab batholith

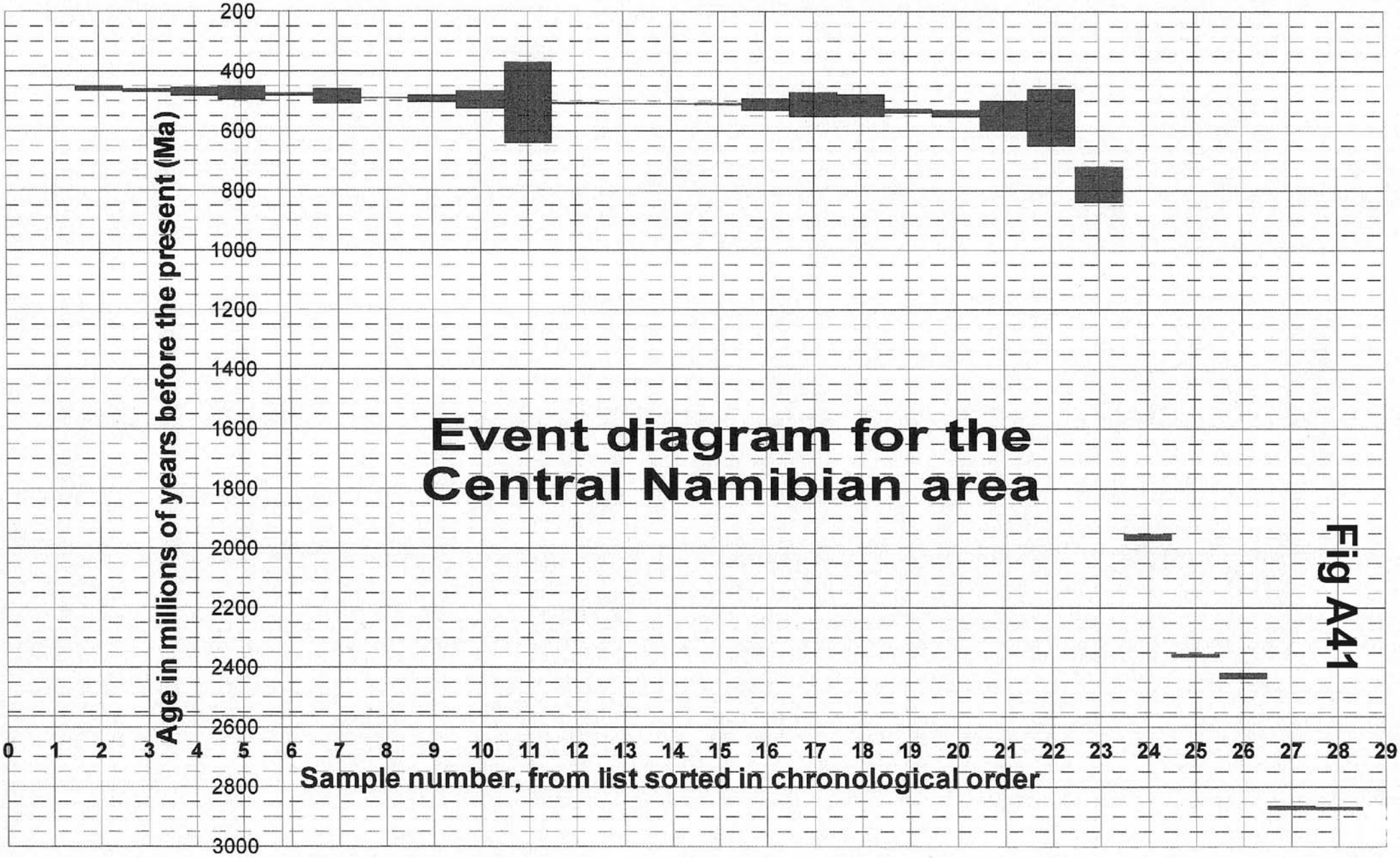
Event diagram for the
Central Namibian area
Age in millions of years before the present (Ma)
200
400
600
800
1000
1200
1400
1600
1800
2000
2200
2400
2600
2800
3000
0 1 2 3 4 5 6 7 8 9 10 11 12 13 14 15 16 17 18 19 20 21 22 23 24 25 26 27 28 29
Sample number, from list sorted in chronological order

Fig A41

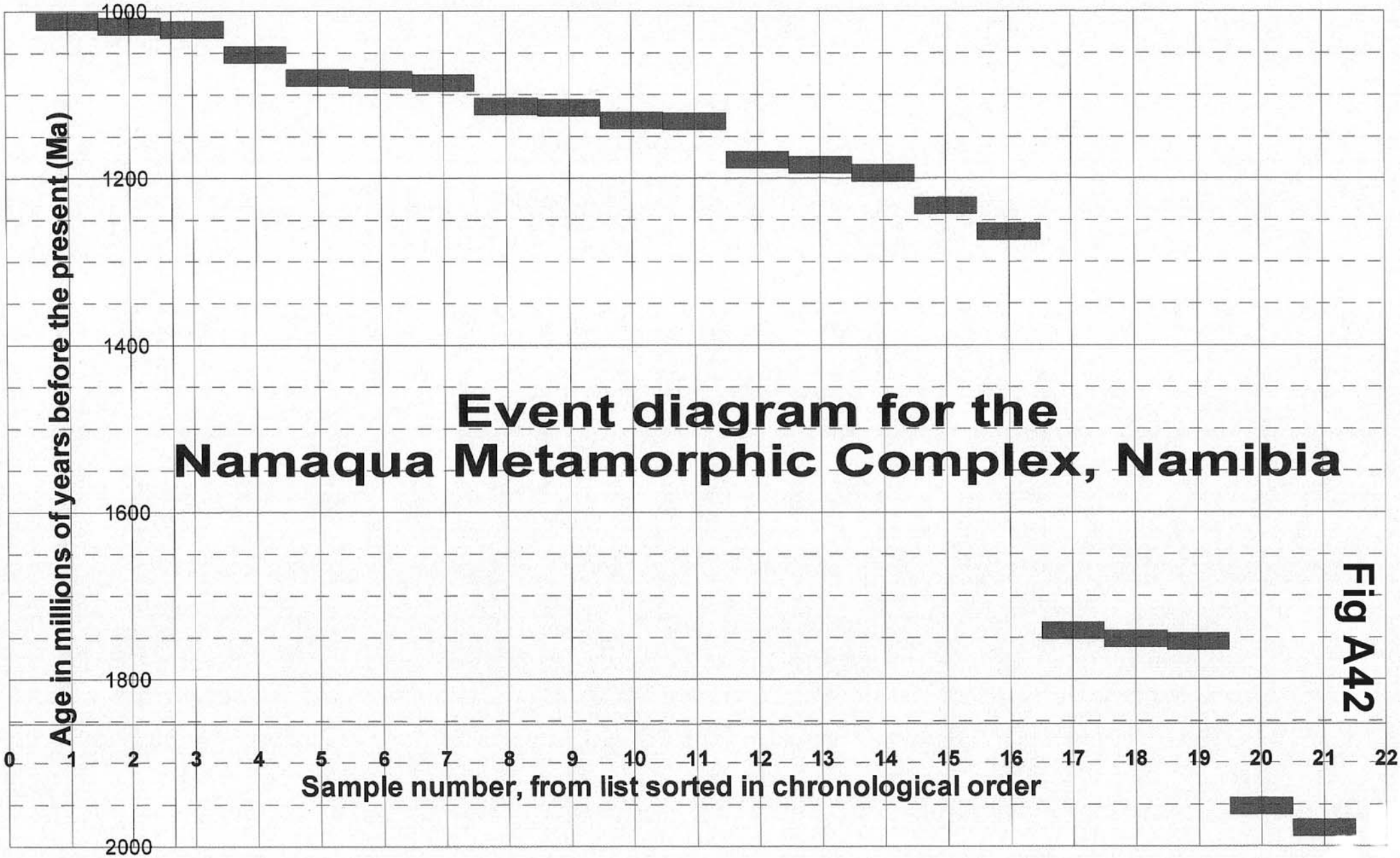
Event diagram for the
Namaqua Metamorphic Complex, Namibia
Age in millions of years before the present (Ma)
1000
1200
1400
1600
1800
2000
0
1
2
3
4
5
6
7
8
9
10
11
12
13
14
15
16
17
18
19
20
21
22
Sample number, from list sorted in chronological order

Fig A42

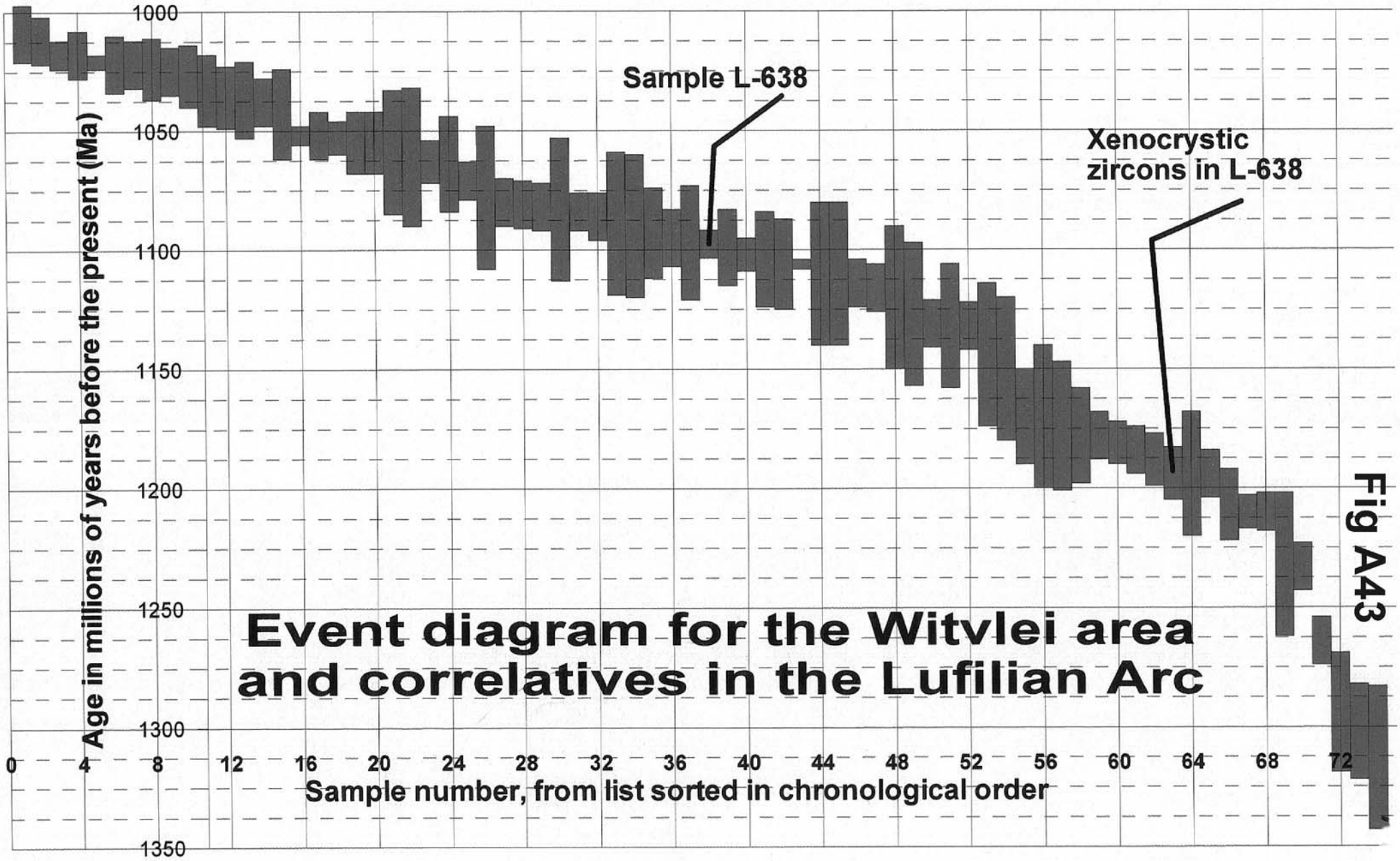

Event diagram for the Witvlei area and correlatives in the Lufilian Arc

Fig A43

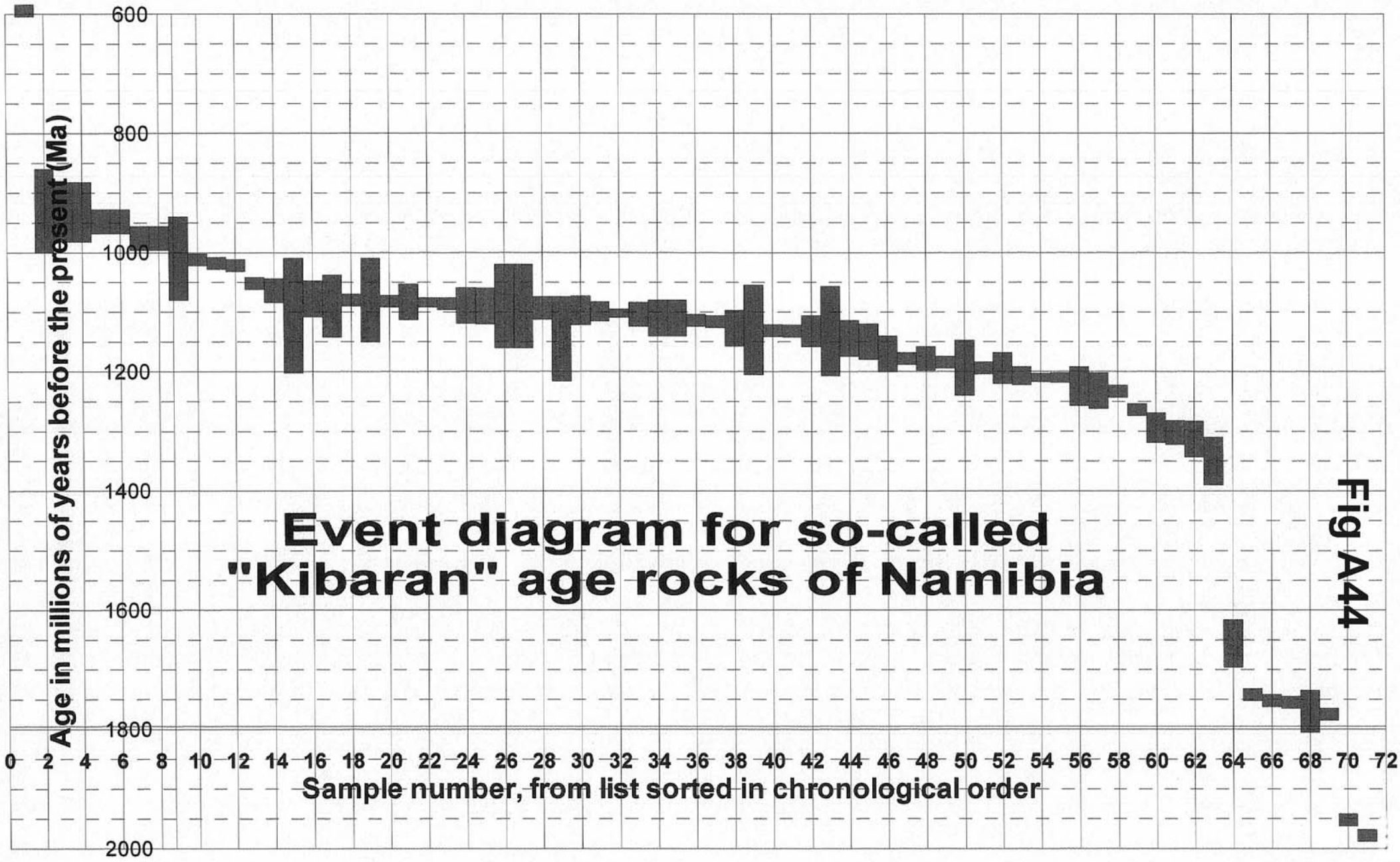
Age in millions of years before the present (Ma)
600
800
1000
1200
1400
1600
1800
2000
0 2 4 6 8 10 12 14 16 18 20 22 24 26 28 30 32 34 36 38 40 42 44 46 48 50 52 54 56 58 60 62 64 66 68 70 72
Sample number, from list sorted in chronological order
Event diagram for so-called
"Kibaran" age rocks of Namibia
Fig A44

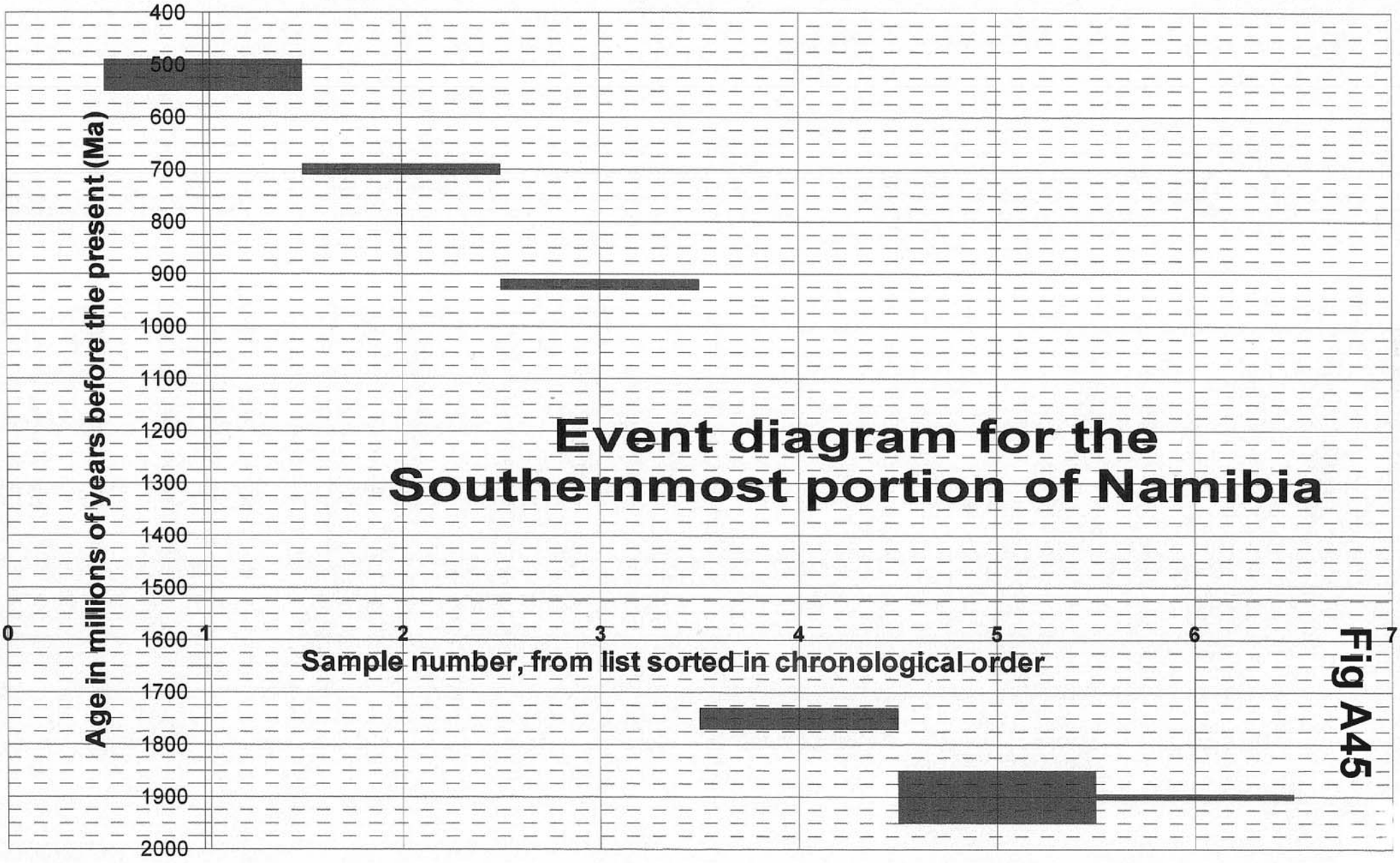
Event diagram for the
Southernmost portion of Namibia
Age in millions of years before the present (Ma)
400
500
600
700
800
900
1000
1100
1200
1300
1400
1500
1600
1700
1800
1900
2000
0
1
2
3
4
5
6
7
Sample number, from list sorted in chronological order

Fig A45

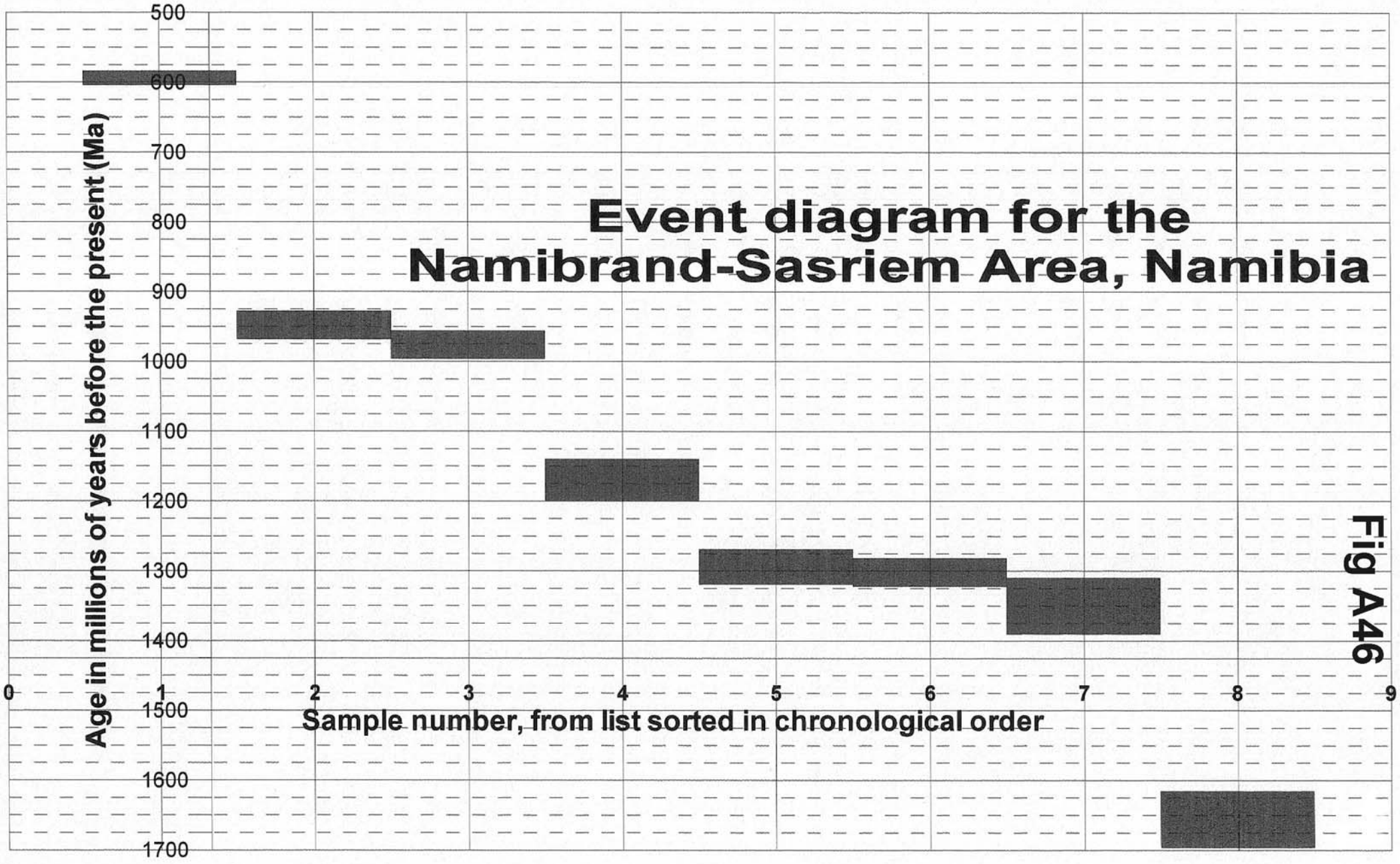
Event diagram for the
Namibrand-Sasriem Area, Namibia
Age in millions of years before the present (Ma)
500
600
700
800
900
1000
1100
1200
1300
1400
1500
1600
1700
0
1
2
3
4
5
6
7
8
9
Sample number, from list sorted in chronological order

Fig A46

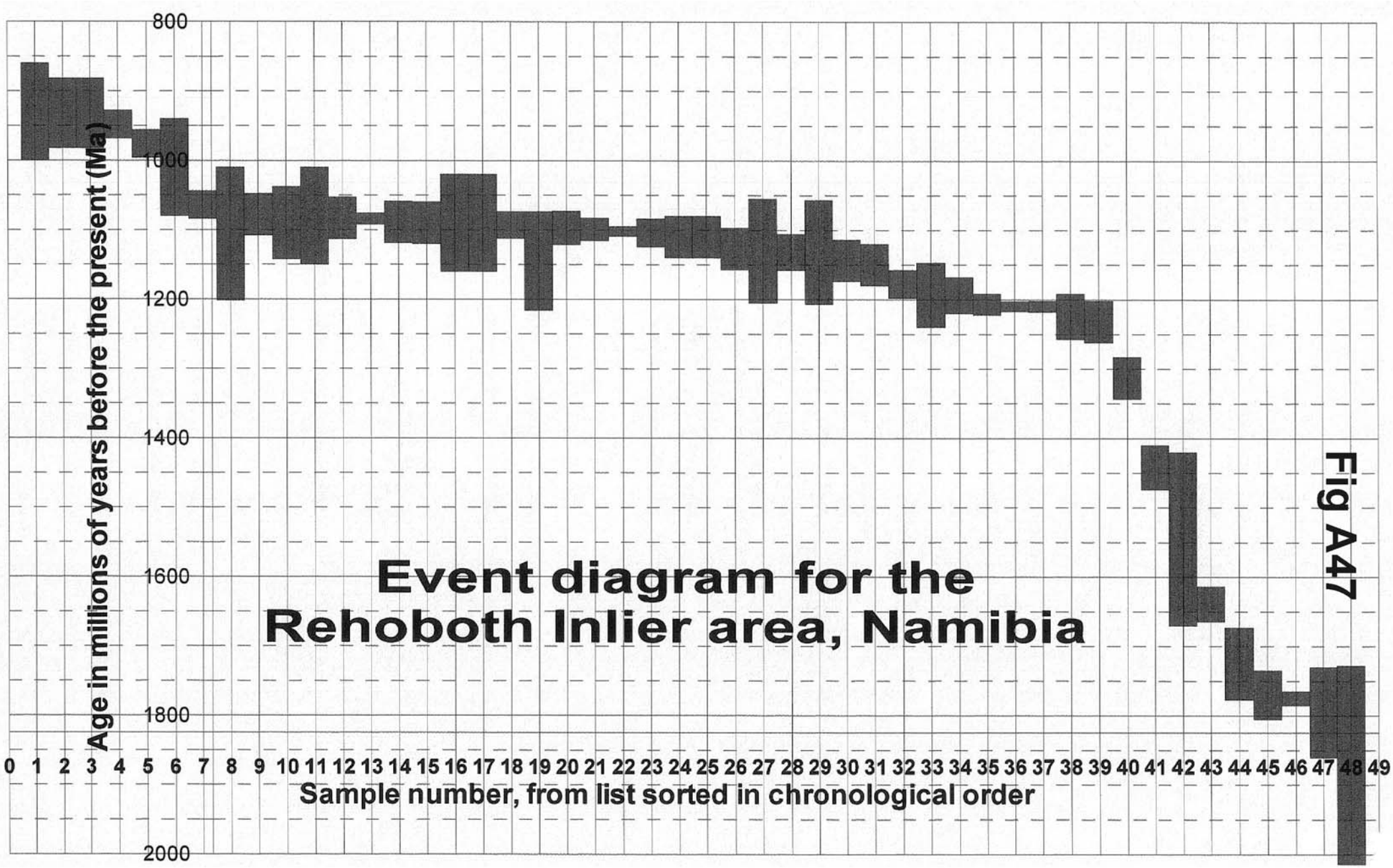
Event diagram for the
Rehoboth Inlier area, Namibia
Age in millions of years before the present (Ma)
800
1000
1200
1400
1600
1800
2000
0 1 2 3 4 5 6 7 8 9 10 11 12 13 14 15 16 17 18 19 20 21 22 23 24 25 26 27 28 29 30 31 32 33 34 35 36 37 38 39 40 41 42 43 44 45 46 47 48 49
Sample number, from list sorted in chronological order

Fig A47

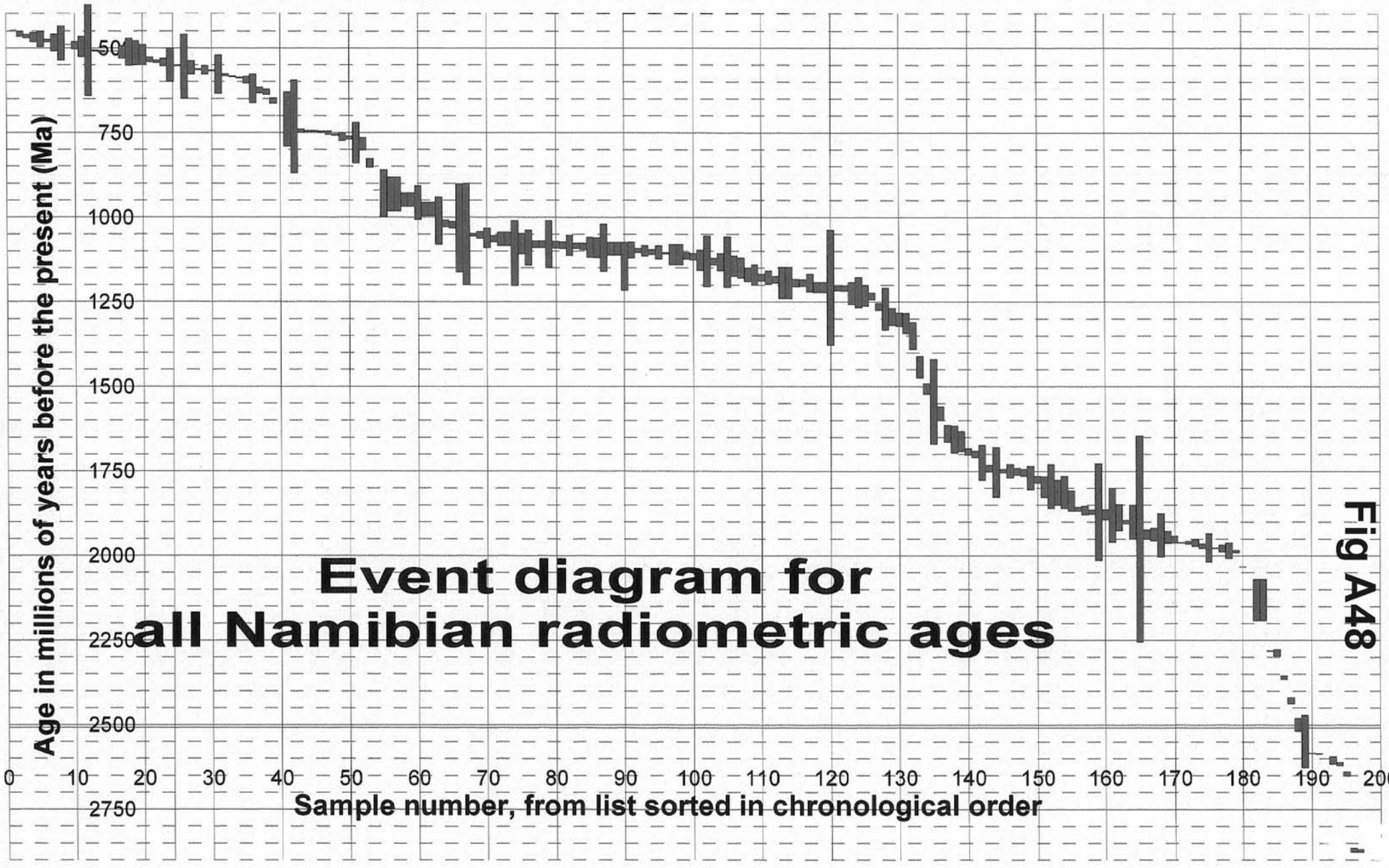
Event diagram for
all Namibian radiometric ages
Age in millions of years before the present (Ma)
500
750
1000
1250
1500
1750
2000
2250
2500
2750
0
10
20
30
40
50
60
70
80
90
100
110
120
130
140
150
160
170
180
190
200
Sample number, from list sorted in chronological order

Fig A48

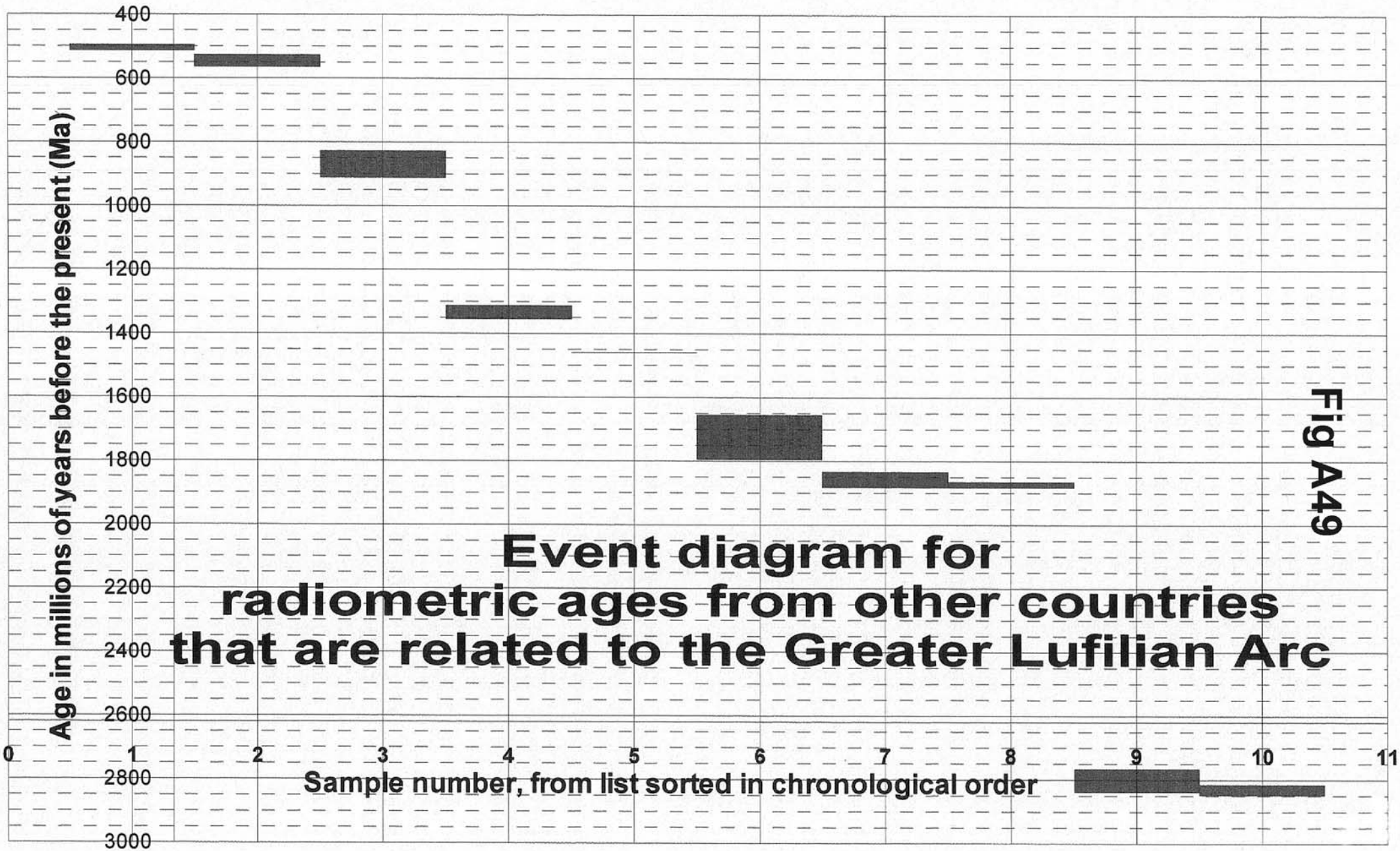

Event diagram for radiometric ages from other countries that are related to the Greater Lufilian Arc

Fig A49

APPENDIX G
TECTONIC ENVIRONMENT OF EMPLACEMENT

A50	Tectonic environment of emplacement for samples from the Greater Lufilian Arc, 96
A51	Results of determination for environment of emplacement of granitoids based on methodology of Maniar & Piccoli, 1989, 102
A52	Results of determination for anorogenic character of granitoids based on the Whalen et al, 1987 plots, 108
A53	Results of determination for environment of emplacement of granitoids based on methodology of Pearce et al, 1984, 113
A54	Discrimination of granitoids following procedure of Harris et al, 1986, 118
A55	Results of determination for environment of emplacement of granitoids based on methodology of Batchelor & Bowden, 1985, 122
A56	Tectonic environment of mafic rocks, Greater Lufilian Arc project, 123

TABLE A50

Discrimination of Rock Samples by their Tectonic Environment of Emplacement

Sample	Maniar	Whalen	Pierce		Maniar	Whalen	Pierce	Mafic	Harris			Batchelor/Bowden
									Rb/10HfTa	Rb/30HfTa	Nb-Ta	
L-012	IAG+CAG	A			IAG+CAG	A			VA-	III	INW-INV	Late Orogenic
L-012A	IAG+CAG	A	O-W1-1		IAG+CAG	A	O-W1-1					Late Orogenic
L-020	POG	A	O3/4		POG	A	O3/4				OUTU	Anorogenic
L-023		N	O3/4			N	O3/4				OUTU	3 limit 2
L-024	RRG	A	V2/4		RRG	A	V2/4	emor			OUTU	Pre-Plate Collision
L-025		N	O3/4			N	O3/4				OUTU	Syn-Collision
L-026	POG	A			POG	A						Syn-Collision
L-027	IAG+CAG	N	V		IAG+CAG	N	V					Pre-Plate Collision
L-028		N	O3/4			N	O3/4				OUTU	Post-Collision Uplift
L-029		N				N						Pre-Plate Collision
L-030	POG	A	S2/4 O2/4		POG	A	S2/4 O2/4		VA-	II	INV	4, corner
L-032		A	O3/4			A	O3/4	wpab			OUTU	Pre-Plate Collision
L-034		A	V1/2			A	V1/2					5 on limit
L-036		A	W			A	W					Mantle Fractionates
L-037		A	O-W 2-2			A	O-W 2-2				OUTU	off left
L-038		A	W			A	W					off left
L-039		A	W			A	W					off left
L-040		A	W			A	W					off left
L-041		A	W			A	W					off left
L-044		A	O-W 2-2			A	O-W 2-2				OUTU	off left
L-045		A	W3/4			A	W3/4		WP	WP	INW	off left
L-046		A	O2/3			A	O2/3				OUTU	off left
L-047	CEUG	A	W3/4		CEUG	A	W3/4				OUTU	Late Orogenic
L-049	IAG+CAG	N	V		IAG+CAG	N	V	wpab				off left
L-050	IAG+CAG	N	V		IAG+CAG	N	V	emor				off left
L-060	POG	A			POG	A		wpab				off left
L-060	POG	A			POG	A		wpt	VA-	III-VA	II-INV	off left
L-060		A	O			A	O					Anorogenic
L-063	IAG+CAG	A	V		IAG+CAG	A	V	?				off left
L-064	IAG+CAG	A	V		IAG+CAG	A	V	wpab				off left
L-065	IAG+CAG	N	V3/4		IAG+CAG	N	V3/4	arc			OUTU	off left
L-075		N	S2/4 O2/4			N	S2/4 O2/4		VA	II	INV	
L-076		A	O-W1-1			A	O-W1-1					Late Orogenic
L-077		A	O3/4			A	O3/4				OUTU	Late Orogenic
L-078		A	O-W1-1			A	O-W1-1					Post-Collision Uplift
L-079			O-W1-1				O-W1-1					Late Orogenic
L-1000		A	O3/4			A	O3/4				OUTU	Late Orogenic
L-1002	RRG	A			RRG	A			VA-	III	OUTU	Anorogenic
L-1003	POG	A	O3/4		POG	A	O3/4		WP	WP	OUTU	Late Orogenic
L-1005	RRG	A	O-W1-1		RRG	A	O-W1-1					Syn-Collision
L-1007		A				A						Post-Collision Uplift
L-1009		A				A						Late Orogenic
L-1010		A				A						Late Orogenic
L-1011		A	O-W1-1			A	O-W1-1					Late Orogenic
L-1012		A	O-W1-1			A	O-W1-1					Late Orogenic
L-1013		A	O3/4			A	O3/4				OUTU	Late Orogenic
L-1014	IAG_CAG	?N			IAG_CAG	?N						Pre-Plate Collision
L-1016	OP	?	V?		OP	?	V?					1 off right
L-1016a	OP	?	V		OP	?	V					1 off right
L-1019	RRG	A	V2/4		RRG	A	V2/4		WP-	WP	INW	Anorogenic
L-1020		A	W			A	W					Late Orogenic
L-1021	RRG	A	W		RRG	A	W					Late Orogenic
L-1022		A	O2/3			A	O2/3	?			OUTU	off left
L-1023	IAG+CAG	?NZn	V		IAG+CAG	?NZn	V	emor				off left
L-1024a		A				A						off upper left
L-1024c		A				A						off upper left
L-1025		A				A		arc	WP	WP	OUTD-INW	off left
L-1027		A	W-O 2-2			A	W-O 2-2	?			OUTU	off left
L-1032		N	V2/4			N	V2/4	emor	WP	WP	OUTU	off left
L-1037		A				A						Late Orogenic
L-1038		A				A						Late Orogenic
L-1039	CEUG	A			CEUG	A						Anorogenic
L-1039a		A	S2/4 O2/4			A	S2/4 O2/4		VA-	VA	INV	
L-1039c	CEUG	A			CEUG	A						
L-1042	POG	A			POG	A			WP-	WP	OUTU	
L-1043	POG	A	O-W 2-2		POG	A	O-W 2-2		WP	WP	OUTU	
L-1044	POG	A	O-W1-1		POG	A	O-W1-1					
L-1045		A	W3/4			A	W3/4				OUTU	
L-1046	POG	A	O-W1-1		POG	A	O-W1-1					
L-139		A				A						Mantle Fractionates
L-150		A	O3/4			A	O3/4	emor			OUTU	Late Orogenic
L-151	RRG	A	W3/4		RRG	A	W3/4		WP-	III	OUTU	Mantle Fractionates
L-153	RRG	A	W		RRG	A	W					Mantle Fractionates
L-154		A	O-W 2-2			A	O-W 2-2		WP-	WP-III	OUTU	Mantle Fractionates
L-155		N	O3/4			N	O3/4				OUTU	Mantle Fractionates
L-157		A				A						Mantle Fractionates
L-158		N	O2/3			N	O2/3		WP-	II	OUTU	Mantle Fractionates
L-159		A	O-W1-1			A	O-W1-1					Syn-Collision
L-160		A	O3/4			A	O3/4				OUTU	Syn-Collision

Sample	Maniar	Whalen	Pierce	Maniar	Whalen	Pierce	Mafic	Harris			Batchelor/Bowden
								Rb/10HfTa	Rb/30HfTa	Nb-Ta	
L-161		A	O-W1-1		A	O-W1-1	wpab-wpt				Late Orogenic
L-162	POG	A		POG	A						Late Orogenic
L-163		N			N		emor				off left
L-166	POG	N	V2/4 O2/4	POG	N	V2/4 O2/4		VA-	III	OUTU	Late Orogenic
L-167		A	W		A	W	wpab				off left
L-168		A?	O2/3		A?	O2/3					Mantle Fractionates
L-170		A	O-W 2-2		A	O-W 2-2				OUTU	Mantle Fractionates
L-172		A	O-W 2-2		A	O-W 2-2		VA-	III-II	INW	Anorogenic
L-173		A	W		A	W					Anorogenic
L-175	POG	A	O3/4	POG	A	O3/4				OUTU	2 joint
L-181	IAG+CAG	N	V	IAG+CAG	N	V	emor				Pre-Plate Collision
L-195	CEUG	A	O-W 2-2	CEUG	A	O-W 2-2				OUTU	Late Orogenic
L-199			O 2/4			O 2/4		WP	WP	INW	
L-207		?			?						Anorogenic
L-208		A			A						Anorogenic
L-209		N			N		emor				off left
L-210	OP	A	V1/2	OP	A	V1/2					Anorogenic
L-212	CEUG	A	O-W1-1	CEUG	A	O-W1-1					Anorogenic
L-213	CEUG	A	O3/4	CEUG	A	O3/4		WP	WP	OUTU	Anorogenic
L-214		A	W		A	W					Anorogenic
L-215		A	V		A	V					Anorogenic
L-217		N?	O2/3		N?	O2/3				OUTU	Mantle Fractionates
L-218	CEUG	A	O3/4	CEUG	A	O3/4		WP	WP	OUTU	Late Orogenic
L-222	CEUG	A	O-W1-1	CEUG	A	O-W1-1					Post-Orogenic
L-223	CEUG	A	O2/3	CEUG	A	O2/3				OUTU	4 limit w/2
L-224	CEUG	A	O-W1-1	CEUG	A	O-W1-1	wpab				Anorogenic
L-237	CEUG	A	O-W1-1	CEUG	A	O-W1-1					Syn-Collision
L-238	CEUG-RRG	A	O3/4	CEUG-RRG	A	O3/4				OUTU	Syn-Collision
L-239		A	O-W1-1		A	O-W1-1					Late Orogenic
L-241		A	O-W 2-2		A	O-W 2-2		VA-	III	INW-INV	
L-242		A	V		A	V					Mantle Fractionates
L-248		A	W		A	W					Pre-Plate Collision
L-248-L0	POG	A	O-W1-1	POG	A	O-W1-1					Late Orogenic
L-249		A	O3/4		A	O3/4				OUTU	Syn-Collision
L-257	POG	A	O-W 2-2	POG	A	O-W 2-2		WP	WP	OUTU	Late Orogenic
L-259		A	W		A	W					Late Orogenic
L-259-B	RRG	A	W	RRG	A	W					Late Orogenic
L-263	IAG+CAG	A	O-W 2-2	IAG+CAG	A	O-W 2-2				OUTU	Post-Collision Uplift
L-311							arc				Post-Collision Uplift
L-313											
L-314											
L-318											
L-321	OP	A	V1/2	OP	A	V1/2					Mantle Fractionates
L-322	RRG	A	O-W1-1	RRG	A	O-W1-1					Anorogenic
L-323	RRG	A	O-W1-1	RRG	A	O-W1-1					Anorogenic
L-324	RRG-CEUG	A	W	RRG-CEUG	A	W					Late Orogenic
L-325	RRG	A	W	RRG	A	W					Late Orogenic
L-341	OP	A	V1/2	OP	A	V1/2					Post-Collision Uplift
L-343		A	S1/2		A	S1/2					Pre-Plate Collision
L-344		A	V1/2		A	V1/2					Post-Collision Uplift
L-345	CEUG-RRG	A	O-W1-1	CEUG-RRG	A	O-W1-1					Late Orogenic
L-346	RRG-CEUG	A	O-W1-1	RRG-CEUG	A	O-W1-1					Late Orogenic
L-347		A	V		A	V	vab				off upper left
L-348		A	V1/2		A	V1/2					Late Orogenic
L-349		A	W		A	W					Late Orogenic
L-352	CEUG	A	O-W1-1	CEUG	A	O-W1-1					Syn-Collision
L-353		A	W		A	W					Late Orogenic
L-354		A	W		A	W					Late Orogenic
L-355	CEUG	A	O-W1-1	CEUG	A	O-W1-1					Late Orogenic
L-357	CEUG	A	W	CEUG	A	W					Late Orogenic
L-358		A	O3/4		A	O3/4				OUTU	Post-Collision Uplift
L-359	CEUG	A		CEUG	A						Late Orogenic
L-360	CEUG	A	O-W1-1	CEUG	A	O-W1-1					Late Orogenic
L-361		A			A						Post-Collision Uplift
L-362		A			A						Pre-Plate Collision
L-363		N			N						Post-Collision Uplift
L-364		A			A						Anorogenic
L-365		A	O-W1-1		A	O-W1-1					Late Orogenic
L-366	CEUG-RRG	A	O-W 2-2	CEUG-RRG	A	O-W 2-2				OUTU	Late Orogenic
L-367		A	W		A	W					Mantle Fractionates
L-368	RRG-CEUG	A		RRG-CEUG	A						Late Orogenic
L-369		A	?		A	?				OUTU	Syn-Collision
L-370	CEUG	A		CEUG	A						Anorogenic
L-371	POG	A	O-W1-1	POG	A	O-W1-1					Late Orogenic
L-372	IAG+CAG	A		IAG+CAG	A		?				Post-Collision Uplift
L-373	POG	N		POG	N			WP	WP	OUTU	Syn-Collision
L-374		N			N						Late Orogenic
L-375	CEUG	A	O-W1-1	CEUG	A	O-W1-1					Anorogenic
L-376	CEUG	A	O-W1-1	CEUG	A	O-W1-1					off left
L-377	CEUG	A	O2/3	CEUG	A	O2/3					Anorogenic
L-378	CEUG-RRG	A	O-W1-1	CEUG-RRG	A	O-W1-1					Anorogenic
L-379		A	O-W1-1		A	O-W1-1					Anorogenic
L-380	CEUG-RRG	A	O3/4	CEUG-RRG	A	O3/4		WP	WP	OUTU	Anorogenic
L-402	CEUG-RRG	A	W	CEUG-RRG	A	W					Pre-Plate Collision

Sample	Maniar	Whalen	Pierce	Maniar	Whalen	Pierce	Mafic	Harris			Batchelor/Bowden
								Rb/10HfTa	Rb/30HfTa	Nb-Ta	
L-403	CEUG	A	W	CEUG	A	W					Late Orogenic
L-405	IAG+CAG	N	V	IAG+CAG	N	V	emor				Pre-Plate Collision
L-406		A	V		A	V	emor				off left
L-407		A	W		A	W	wpt+vab				Post-Collision Uplift
L-408	CEUG	A	W	CEUG	A	W					Syn-Collision
L-409	CEUG-RRG	A	O-W1-1	CEUG-RRG	A	O-W1-1					Late Orogenic
L-410	CEUG	A		CEUG	A						Mantle Fractionates
L-411			V			V	wpab+wpt-cab				off upper left
L-416											Mantle Fractionates
L-416	IAG+CAG	N	V	IAG+CAG	N	V	emor				Mantle Fractionates
L-420	POG	A		POG	A						Late Orogenic
L-421	POG	A		POG	A						Late Orogenic
L-433		A	O-W1-1		A	O-W1-1	wpt				off left
L-434	RRG-CEUG	A		RRG-CEUG	A						Syn-Collision
L-435	CEUG	A	O-W1-1	CEUG	A	O-W1-1					Late Orogenic
L-436	RRG	A	O-W1-1	RRG	A	O-W1-1					Late Orogenic
L-437	CEUG	A	O-W1-1	CEUG	A	O-W1-1	wpab+wpt				Late Orogenic
L-438	IAG+CAG	A	O-W1-1	IAG+CAG	A	O-W1-1	wpab				off left
L-439	RRG	A	W	RRG	A	W					Anorogenic
L-440		A	O-W1-1		A	O-W1-1	wpab				Post-Collision Uplift
L-441	RRG	A	W	RRG	A	W					Late Orogenic
L-442	RRG	A	O-W1-1	RRG	A	O-W1-1					Mantle Fractionates
L-443	CEUG	A	O-W1-1	CEUG	A	O-W1-1					Mantle Fractionates
L-444	RRG	N?	V1/2	RRG	N?	V1/2	emor				Pre-Plate Collision
L-458		A	O-W1-1		A	O-W1-1					Anorogenic
L-459		A			A						Pre-Plate Collision
L-460		A			A						Mantle Fractionates
L-461	POG	?N		POG	?N						Late Orogenic
L-462	POG	N		POG	N						Syn-Collision
L-463		A	V		A	V	wpt				Pre-Plate Collision
L-464	CEUG		V	CEUG		V					off left
L-465	CEUG	A	V	CEUG	A	V					off left
L-466		A			A						Late Orogenic
L-467	RRG-CEUG	A		RRG-CEUG	A						Anorogenic
L-600A	RRG-CEUG	A		RRG-CEUG	A						Anorogenic
L-602		A	O3/4		A	O3/4				OUTU	Syn-Collision
L-605		A			A						Anorogenic
L-606	RRG-CEUG	A		RRG-CEUG	A						Syn-Collision
L-625	POG	A	V1/2	POG	A	V1/2					Late Orogenic
L-626	POG	A		POG	A					OUTU	Late Orogenic
L-633		N?Zn			N?Zn		arc			OUTU	Pre-Plate Collision
L-635	OP	A	V2/4	OP	A	V2/4	wpab			OUTU	Late Orogenic
L-637	OP	A		OP	A			WP	WP	OUTU	Syn-Collision
L-638	RRG	A	S2/4 O2/4	RRG	A	S2/4 O2/4		VA-	VA	INV	Anorogenic
L-641		N?Zn	V		N?Zn	V	wpab				Post-Collision Uplift
L-645	RRG-CEUG	A	V	RRG-CEUG	A	V	wpt				off left
L-648		A	V		A	V					Anorogenic
L-649	RRG	N?	V	RRG	N?	V					Anorogenic
L-668	RRG	A	O-W 2-2	RRG	A	O-W 2-2	wpab	WP-	WP	INW	Late Orogenic
L-669	CEUG	A	W	CEUG	A	W		WP-	WP	INW	Late Orogenic
L-670	RRG	A	O-W 2-2	RRG	A	O-W 2-2	?			OUTU-NEA	off left
L-675	CEUG	A	W3/4	CEUG	A	W3/4	wpab			OUTU	Late Orogenic
L-676	RRG-CEUG	A	W	RRG-CEUG	A	W	wpab				Late Orogenic
L-691	RRG-CEUG	A	W	RRG-CEUG	A	W	wpt				Post-Collision Uplift
L-693	RRG	A	W3/4	RRG	A	W3/4		WP-	WP	INW	Anorogenic
L-694	RRG	A	W	RRG	A	W	wpab				off left
L-695	RRG-CEUG	A	O-W1-1	RRG-CEUG	A	O-W1-1	wpab				off left
L-697	RRG-CEUG	A	w3/4	RRG-CEUG	A	w3/4	wpab	WP-	WP	OUTU-NEA	off left
L-698	RRG-CEUG	A	O-W 2-2	RRG-CEUG	A	O-W 2-2				OUTU	Anorogenic
L-699	CEUG	A	W	CEUG	A	W					off left
L-708	IAG-CAG	A	W?	IAG-CAG	A	W?	wpab				off left
L-712	POG	A	V	POG	A	V					Post-Orogenic
L-713		A	O-W 2-2		A	O-W 2-2		WP	WP	OUTU	Anorogenic
L-714	OP	A	V	OP	A	V					Late Orogenic
L-714		A	V		A	V					Anorogenic
L-715	RRG-CEUG	A	O3/4	RRG-CEUG	A	O3/4				OUTU	Syn-Collision
L-716	CEUG-RRG	A	S2/4 O2/4	CEUG-RRG	A	S2/4 O2/4		VA-	VA	INV	Late Orogenic
L-722		A			A					OUTU	off upper left
L-728	OP	A	?	OP	A	?		WP-	WP	INW	Syn-Collision
L-729	POG	A	O-W1-1	POG	A	O-W1-1					Late Orogenic
L-740	CEUG	A	O3/4	CEUG	A	O3/4	?			OUTU	off left
L-741	CEUG	A	O-W 2-2	CEUG	A	O-W 2-2	wpab			OUTU	off left
L-742		A	O2/3		A	O2/3				OUTU	Late Orogenic
L-754	RRG	N		RRG	N		arc				Mantle Fractionates
L-759		A			A						Late Orogenic
L-772		A			A						Anorogenic
L-773		A	W		A	W					Late Orogenic
L-783		A	O-W1-1		A	O-W1-1					Late Orogenic
L-784	RRG-CEUG	A	O3/4		A	O3/4		WP	WP	OUTU	Syn-Collision
L-789	RRG-CEUG	A	O-W 2-2	RRG-CEUG	A	O-W 2-2				OUTU	Late Orogenic
L-791	RRG-CEUG	A	W3/4	RRG-CEUG	A	W3/4		WP-	WP	INW	Anorogenic
L-791			W			W					Anorogenic
L-793	POG	A	W3/4	POG	A	W3/4		WP-	WP	OUTU	Late Orogenic
L-797	RRG-CEUG	A		RRG-CEUG	A						Anorogenic

Sample	Maniar	Whalen	Pierce	Maniar	Whalen	Pierce	Mafic	Harris			Batchelor/Bowden
								Rb/10HfTa	Rb/30HfTa	Nb-Ta	
L-798	POG	A		POG	A						Syn-Collision
L-799		A			A						Late Orogenic
L-802		N			N						Syn-Collision
L-808	IAG-CAG	N	S2/4 O2/4	IAG-CAG	N	S2/4 O2/4		VA-	II	INV	Late Orogenic
L-809	IAG-CAG	A		IAG-CAG	A						Late Orogenic
L-810		A			A						Late Orogenic
L-812		A			A						4-2
L-813		A			A						Late Orogenic
L-814											1 off right
L-815		A	O-W1-1		A	O-W1-1					Late Orogenic
L-816	POG	A		POG	A			WP	WP	OUTU	Syn-Collision
L-832	POG	A		POG	A						Anorogenic
L-834	CEUG	A	O3/4	CEUG	A	O3/4		WP	WP	OUTU	Late Orogenic
L-835		A			A						Late Orogenic
L-836		A?			A?						Late Orogenic
L-838		N			N						Late Orogenic
L-839		A			A						Post-Orogenic
L-840	POG	A		POG	A						Late Orogenic
L-842		A	O3/4		A	O3/4		WP	WP	OUTU	Late Orogenic
L-843		A	O-W 2-2		A	O-W 2-2		WP-	WP	OUTU	Post-Orogenic
L-844		A			A						Late Orogenic
L-846		A	O2/3		A	O2/3				OUTU	Late Orogenic
L-849	RRG-CEUG	A	O3/4	RRG-CEUG	A	O3/4		WP	WP	OUTU	Anorogenic
L-850	POG	A	O3/4	POG	A	O3/4		WP	WP	OUTU	Syn-Collision
L-855	RRG-CEUG	A		RRG-CEUG	A						Anorogenic
L-857	POG	N		POG	N						Syn-Collision
L-863		A			A						Post-Collision Uplift
L-864		N	S2/4 O2/4		N	S2/4 O2/4		VA-	II	INV	Pre-Plate Collision
L-864											
L-865		A			A						Post-Collision Uplift
L-868		N	S2/4 O2/4		N	S2/4 O2/4		VA-	II	INV	Late Orogenic
L-874	RRG	A	V	RRG	A	V					Late Orogenic
L-874-			O-W1-1			O-W1-1					1 off right
L-875		A?	O3/4		A?	O3/4				OUTU	Late Orogenic
L-877	RRG	A	O-W1-1	RRG	A	O-W1-1					Late Orogenic
L-878		A	O3/4		A	O3/4				OUTU	Late Orogenic
L-895		N?	O3/4		N?	O3/4	wpt+vab-cab			OUTU	off left
L-898	RRG-CEUG	A		RRG-CEUG	A						Late Orogenic
L-899		A			A						Syn-Collision
L-900		A			A						Late Orogenic
L-902	RRG-CEUG	A		RRG-CEUG	A						Anorogenic
L-903		A			A						Anorogenic
L-904	RRG-CEUG	A		RRG-CEUG	A					OUTU	Anorogenic
L-905	POG	N?	O-W1-1	POG	N?	O-W1-1					Anorogenic
L-906	POG	A	O-W1-1	POG	A	O-W1-1					Anorogenic
L-907	POG	A		POG	A						Syn-Collision
L-908	CEUG	A	S2/4 O2/4	CEUG	A	S2/4 O2/4		VA-	III	INV	Anorogenic
L-909	POG	A	O-W1-1	POG	A	O-W1-1				OUTU	Anorogenic
L-910	RRG-CEUG	A	O-W1-1	RRG-CEUG	A	O-W1-1					Anorogenic
L-911		A	O-W1-1		A	O-W1-1					Mantle Fractionates
L-912		A	O-W1-1		A	O-W1-1					Pre-Plate Collision
L-917		A	S2/4 O2/4		A	S2/4 O2/4		VA-	II	INV	Late Orogenic
L-919	RRG			RRG							1 off right
L-920	CEUG	A	O3/4	CEUG	A	O3/4	wpab			OUTU	Anorogenic
L-922		A	O3/4		A	O3/4				OUTU	Late Orogenic
L-923	RRG-CEUG	A	O-W1-1	RRG-CEUG	A	O-W1-1					Late Orogenic
L-924		A	O-W1-1		A	O-W1-1					Syn-Collision
L-938		A	O3/4		A	O3/4		WP	WP	OUTU	Syn-Collision
L-939	CEUG-RRG	N?	O3/4	CEUG-RRG	N?	O3/4				OUTU	Late Orogenic
L-940		N	O3/4		N	O3/4				OUTU	Pre-Plate Collision
L-943	CEUG-RRG	A	S2/4 O2/4	CEUG-RRG	A	S2/4 O2/4		VA-	VA	INV	Anorogenic
L-945	CEUG	A	O3/4	CEUG	A	O3/4				OUTU	Late Orogenic
L-946		A	O-W1-1		A	O-W1-1					Late Orogenic
L-948		A	O-W1-1		A	O-W1-1					Late Orogenic
L-951	OP	A	V2/4	OP	A	V2/4				OUTU	off left
L-952	OP	A	V1/2	OP	A	V1/2					Anorogenic
L-955	OP	A	V3/4	OP	A	V3/4				OUTU	Anorogenic
L-956	OP	A		OP	A					OUTU	Late Orogenic
L-957	POG	A	O3/4	POG	A	O3/4		WP-	WP	OUTU	Pre-Plate Collision
L-958		NZn?	V		NZn?	V	arc				Pre-Plate Collision
L-963	RRG			RRG							1 off right
L-965	CEUG	A	W	CEUG	A	W					Anorogenic
L-966	CEUG-RRG	A		CEUG-RRG	A			VA-	III	INV	Anorogenic
L-967	RRG-CEUG	A	O-W1-1	RRG-CEUG	A	O-W1-1					Late Orogenic
L-967a											
L-968	CEUG-RRG	A	O3/4	CEUG-RRG	A	O3/4		WP	WP	OUTU	Late Orogenic
L-969	CEUG	A	O3/4	CEUG	A	O3/4		WP	WP	OUTU	off left
L-971	CEUG	A	O-W1-1	CEUG	A	O-W1-1					Anorogenic
L-973		A	O3/4		A	O3/4		WP	WP	OUTU	Syn-Collision
L-975	POG	A		POG	A						Anorogenic
L-976	POG	A	O-W 2-2	POG	A	O-W 2-2		WP-	WP	OUTU	Anorogenic
L-977	POG	A		POG	A						Anorogenic
L-978	RRG	A	S2/4 O2/4	RRG	A	S2/4 O2/4		VA-	VA	INV	Anorogenic
L-979	IAG-CAG	N		IAG-CAG	N						Late Orogenic

Sample	Maniar	Whalen	Pierce
L-980	IAG-CAG	N	
L-982	IAG-CAG	N	
L-983	CEUG-RRG	A	
L-985	POG	N	S2/3
L-987a		NZn?	
L-987b		N	V2/3
L-990		N	
L-991		N	V
L-992	IAG-CAG	N	S2/4 O2/4
L-993	POG	N?	S2/4 O2/4
L-994	POG	A	O-W1-1
L-995	RRG	A	V
L-996		N?	S2/4 O2/4
L-997	CEUG	A	O-W 2-2
L-998		A	O3/4
L-999		A	O3/4
LJ1		A	
LL1	IAC+CAG	A	
LL10		A	W
LL11		A	
LL13	OP	A	V
LL14	RRG	A	W
LL15		A	
LL16		A	
LL17a		A	
LL17b	RRG	A	
LL18		A	
LL2a		A	
LL2b		A	
LL3a		A	
LL3b	CCG	A	
LL4	POG	A	O-W1-1
LL5		A	
LL9		A	
P-13			
P-17			
P-25	IAG+CAG		
P-26			
P-28			
P-29			
P-32			
P-33			
P-35	IAG+CAG		
P-39			
P-40i			
P-40ii			
P-46			
P-50			
P-53			
P-57			
P-58			
X-43	CCG-IAG-CAG		
X-44			
X-45			
X-46	IAG+CAG		
X-47			
X-48	IAG+CAG		
X-49			O-W1-1
X-50			
X-51			O3/4
X-52			
X-53			
X-54			
X-55			
X-56	IAG+CAG		
X-57			
X-58			
X-59			
X-60			
X-61	CCG-IAG-CAG		
X-62			
X-63			
X-64			
X-65	IAG+CAG		
X-66	IAG+CAG		
X-67			
X-68			
X-69			
X-70	CCG		
X-71			
X-72			
X-73			
X-74			
X-75			

Maniar	Whalen	Pierce	Mafic	Harris			Batchelor/Bowden
				Rb/10HfTa	Rb/30HfTa	Nb-Ta	
IAG-CAG	N						Late Orogenic
IAG-CAG	N					OUTU	Late Orogenic
CEUG-RRG	A						Late Orogenic
POG	N	S2/3		VA-	VA	OUTD-INV	Syn-Collision
	NZn?		emor	VA-	VA	OUTD	off left
	N	V2/3	morb-iat-cab			OUTU	off left
	N		wpab				off left
	N	V	arc				off left
IAG-CAG	N	S2/4 O2/4	emor	VA-	VA	INV	off left
POG	N?	S2/4 O2/4		VA-	VA	INV	Late Orogenic
POG	A	O-W1-1					Late Orogenic
RRG	A	V	morb-wpt				off left
	N?	S2/4 O2/4		VA-	III	INV	Late Orogenic
CEUG	A	O-W 2-2		WP-	WP	OUTU	Anorogenic
	A	O3/4				OUTU	Late Orogenic
	A	O3/4		WP-	WP	OUTU	Late Orogenic
	A						Late Orogenic
IAC+CAG	A						Syn-Collision
	A	W	wpab				off left
	A						Late Orogenic
OP	A	V	arc				off upper right
RRG	A	W	wpab				off left
	A						off left
	A						Syn-Collision
	A						Late Orogenic
RRG	A						Post-Collision Uplift
	A						Late Orogenic
	A						Anorogenic
	A						Anorogenic
	A						Anorogenic
CCG	A						Anorogenic
POG	A	O-W1-1					Late Orogenic
	A						Pre-Plate Collision
	A						1 off right
				VA-	WP	INW	Late Orogenic
				VA-	WP	INW	Late Orogenic
IAG+CAG			wpab	VA-	III-WP	INV	out left
				OF	WP	OUTD	Anorogenic
				VA-	VA-III	INW-INV	out left
				VA-	III	INW-INV	Late Orogenic
				VA-	VA	INV	Anorogenic
				VA-	III	OUTU-INW	Late Orogenic
IAG+CAG				VA-	VA	INV	Late Orogenic
				VA-	VA-	INW-INV	Anorogenic
				VA-	VA	INV	Late Orogenic
				VA-	III	INW-INV	Late Orogenic
				VA-	VA-	INW-INV	Anorogenic
				VA-	III	OUTD-INW	Late Orogenic
				VA-	II	INV-INW	5 limit 4
				VA-	VA-	INW-INV	far out left
				VA-	III	INV-INW	Late Orogenic
CCG-IAG-CAG							
IAG+CAG							
IAG+CAG							
		O-W1-1					
		O3/4					
IAG+CAG							
CCG-IAG-CAG							
IAG+CAG							
IAG+CAG							
CCG							

Sample	Maniar	Whalen	Pierce
X-76	RRG		O-W1-1
X-77	RRG		O-W1-1
X-78		A	
X-79		A	V1/2
X-80	RRG	A	W
X-81	RRG	A	W
X-82	RRG	A	V1/2
X-83	RRG	N	
X-84		A	V1/2
X-85		N	V1/2
X-86	RRG	N	V1/2
X-87		N	V1/2
X-88		N	
X-89		N	W

Maniar	Whalen	Pierce	Mafic	Harris			Batchelor/Bowden
				Rb/10HfTa	Rb/30HfTa	Nb-Ta	
RRG		O-W1-1	wpab				Late Orogenic
RRG		O-W1-1	wpab				Late Orogenic
	A		wpab				Late Orogenic
	A	V1/2	wpab				Pre-Plate Collision
RRG	A	W	wpab				off left
RRG	A	W	wpab				off left
RRG	A	V1/2	wpab				off left
RRG	N		wpab				off left
	A	V1/2	wpab				off left
	N	V1/2	wpab				off left
RRG	N	V1/2	wpab				off left
	N	V1/2	wpab				off left
	N		wpab				off left
	N	W	wpab				off left

COLOR CODING FOR INTERPRETATION

L-567	XXYX	A	
L-123	XYZ-ABC	N	
LL14	RRG	A	W

incompatible information

information validated in two systems

informationvalidated in three systems

sample that was interpreted as a mafic r

GRANITOIDS

POG	Post-Orogenic Granitoid
IAG+CAG	Island Arc Granitoid + Continental Arc Granitoid
CEUG	Continental Epeirogenic Uplift Granitoid
RRG	Rift-Related Granitoid
OP	Oceanic Plagiogranite
CCG	Continental Collision Granitoid
CCG-IAG-CA	Imposible to define between these three types
CEUG-RRG	CEUG near the margin with RRG
RRG-CEUG	RRG near the margin with CEUG

MAFIC ROCKS

mor	Mid-Ocean Ridge Basalt
emor	E-Type Mid-Ocean Ridge Basalt
wpab	Within-Plate Alkaline Basalt
vab	Volcanic Arc Basalt
wpt	Within-Plate Tholeiite
?	Unknown Environment
-	or
+	and

KEY FOR THE DATA OF HARRIS ET AL

WP	Within-Plate Granitoids
VA	Volkanic Arc Granitoids
II	Type II Collisional Granitoids
VA-	Plots in Volcanic Arc Field but might be Collisional Granitoid
WP-	Plots in Within-Plate Field but might be Collisional Granitoid
OF	Oceanic Floor Granitoid

KEY FOR THE DATA OF BATCHELOR & BOWDEN

1 off right
2 joint
2-4
3 limit 2
3 triple limit
4 limit w/2
4, corner
5 limit 4
5 on limit
Anorogenic
Late Orogenic
Mantle Fractionates
Post-Collision Uplift
Post-Orogenic
Pre-Plate Collision
Syn-Collision

Table A51

Results of Determination for Environment of Emplacement of Granitoids Based on Methodology of Maniar & Piccoli, 1989

	Al vs Si (Fig5)			Fe vs Si (Fig6)			Fe vs Mg			Fe vs Ca			iag+cag+ccg
Sample	R+Ceug	POG	I+Cac+Ccg	R+Ceug	POG	I+Cac+Ccg	R+Ceug	POG	I+Cac+Ccg	R+Ceug	POG	I+Cac+Ccg	op
L-012			v			I			I		P	I	pog
L-012A			v			I			I		P	I	rrg
L-020	R	P		R	P		R	P		R	P		
L-023	v					I				R			
L-024	v			v			R			R			
L-025	R	P			P	I	R	P		R			
L-026	R	P			P	I	R	P		R	P		
L-027			v			I		P	I			I	
L-028	v					I			I	R			
L-029			v			I			I	R	P		
L-030		P	I	R	P			P	I	R	P		
L-032	v					I			I (v)	R			
L-034			v	R			R			R			
L-036				R	P				I			I	
L-037			v	R			R			R	O		
L-038			v	R			R			R			
L-039			v	R			R			R	O		
L-040			v	R			R			R			
L-041			I (v)	R					I			I	
L-044			v	R			R			R	O		
L-045			v	R			R			R			
L-046			v	R			R			R	O		
L-047	v			R			R			R			
L-049	v					v			I			I(v)	
L-050	v					v			I			I(v)	
L-060	R	P		R	P		R	P		R	P		
L-063	v					v			I			I	
L-064	v					v			I			I	
L-065	R (v)					v			I			I	
L-075													
L-076	R					I	R			R			
L-077	R					I	R			R			
L-078	R					I	R			R			
L-079	v					I	R			R			
L-1000			v			I		P	I	R	P		
L-1002	R	P		R			R	P		R	P		
L-1003			v		P	I	R	P		R	P		
L-1005	R			R	P		R	P		R			
L-1007	v					I			I	R			
L-1009	v				P	I	R					I	
L-1010	v					I	R					I	
L-1011	v				P	I	R					I	
L-1012	v					I	R					I	
L-1013	v				P	I	R			R			
L-1014	v					I			I		P	I	
L-1016						I			I			I	
L-1016a						I			I			I	
L-1019	R	P		R			R			R			
L-102	R	P											
L-1020	R				P	I	R			R			
L-1021	R	P		R			R	P		R			
L-1022			v	v			R	P		R	P		
L-1023	v					v			I			I	
L-1024	v			v					I			I	
L-1024c	v			v					I			I	
L-1025	v			v			R					I	
L-1027	v					v			I	R			
L-1029							R						
L-1032	v					v			I	R			
L-1037			v			I			I	R	P		
L-1038			v			I		P	I	R	P		
L-1039	R	P		R			R			R	P		
L-1039a		P	I	R				P	I		P	I	
L-1039c	R	P		R			R			R	P		
L-1042Y	R	P			P	I	R	P		R	P		
L-1043Z	R	P			P	I		P	I	R	P		
L-1044XX	R	P			P	I	R	P		R	P		
L-1045Yb			v	R				P	I			I	
L-1046XX	R	P			P	I	R	P		R	P		
L-105													
L-139	R	P				I			I	R			
L-150	R					I			I	R			
L-151	R	P		R	P		R	P		R			
L-153	R	P		R	P		R	P		R			
L-154	R	P		R					I	R	P		
L-155	R	P				I			I	R	P		
L-157	R	P				I			I	R			
L-158	R	P				I			I	R	P		
L-159	R					I			I	R	P		
L-160	R					I			I	R	P		
L-161			v			I			I	R			
L-162	R	P			P	I		P	I	R	P		
L-163	R					I			I	R			
L-166	R	P			P	I	R	P			P	I	
L-167	v					I			I	R			

	Al vs Si (Fig5)			Fe vs Si (Fig6)			Fe vs Mg			Fe vs Ca		
Sample	R+Ceug	POG	I+Cac+Ccg	R+Ceug	POG	I+Cac+Ccg	R+Ceug	POG	I+Cac+Ccg	R+Ceug	POG	I+Cac+Ccg
L-168	R					I		P	I	R		
L-170			I			I			I	R		
L-172	R	P			P	I		P	I	R		
L-173	R	P			P	I		P	I	R		
L-175	R	P		R	P		R	P		R	P	
L-175	R	P		R	P		R	P		R	P	
L181	v					v			I		P	I
L181	v					v			I		P	I
L-195	v			R			R			R		
L-195	v			R			R			R		
L-199												
L-199												
L-207		P	I	R					I	R		
L-207		P	I	R					I	R		
L-208		P	I	R					I	R		
L-208		P	I	R					I	R		
L-209	v					v					P	I
L-209	v					v					P	I
L-210			v	R			R	P		R	P	
L-210			v	R			R	P		R	P	
L-212			v	R			R	P		R	P	
L-212			v	R			R	P		R	P	
L-213			v	R			R			R		
L-213			v	R			R			R		
L-214			v	R					I	R		
L-214			v	R					I	R		
L-215			I	R					I			I
L-215			I	R					I			I
L-217	R					I			I	R		
L-217	R					I			I	R		
L-218			v	R			R			R		
L-218			v	R			R			R		
L-222	v			R			R			R		
L-222	v			R			R			R		
L-223	v			R			R			R		
L-223	v			R			R			R		
L-224	v			R			R			R		
L-224	v			R			R			R		
L-225							R					
L-237	R	P		R		I	R			R		
L-237	R	P		R		I	R			R		
L-238	R			R		I	R	P		R		
L-238	R			R		I	R	P		R		
L-239	R					I	R			R		
L-239	R					I	R			R		
L-241	v											
L-241	v											
L-242	R					I			I	R		
L-242	R					I			I	R		
L-248	R (v)					I			I	R		
L-248	R (v)					I			I	R		
L-248-LG		P	I	R	P				I near P+I		P	I
L-248-LG		P	I	R	P				I near P+I		P	I
L-249	R				P	I	R	P		R	P	
L-249	R				P	I	R	P		R	P	
L-257	R	P		R	P	I	R	P			P	I
L-257	R	P		R	P	I	R	P			P	I
L-259			v	R		I	R	P			P	I
L-259			v	R		I	R	P			P	I
L-259B	R	P		R		I	R	P		R	P	
L-259-B	R	P		R		I	R	P		R	P	
L-263	v					I		P	I			I
L-263	v					I		P	I			I
L-267												
L-311												I
L312												
L-313												I
L-314												I
L-318							R					I
L-321					P	I	R			R		
L-321	R				P	I		P	I			I
L-322	R	P		R			R			R		
L-322	R	P		R			R					I
L-323	v			R			R			R		
L-323	R			R			R					I
L-324	v			R			R			R		
L-324	R			R			R					I
L-325			v	R			R			R		
L-325			I	R			R					I
L-330	R											
L-340												
L-341	v			R			R					I(v)
L-342										R		I
L-343	v			R			R	P				I
L-344	v					I			I			I
L-345	v			R			R			R		
L-346	R			R			R			R		
L-347	v					v			I(v)		P	I
L-348	v			R			R	P				I
L-349	v			R			R	P				I

iag+cag+ccg
op
pog
rrg

	Al vs Si (Fig5)			Fe vs Si (Fig6)			Fe vs Mg			Fe vs Ca		
Sample	R+Ceug	POG	I+Cac+Ccg	R+Ceug	POG	I+Cac+Ccg	R+Ceug	POG	I+Cac+Ccg	R+Ceug	POG	I+Cac+Ccg
L-352	R			R			R			R		
L-353	v					i	R				P	I
L-354	v					I	R			R		
L-355	R	P		R			R			R	P	
L-357			v	R			R	P		R	P	
L-358	v			R			R	P				I
L-359	v			R			R			R		
L-360	v			R		I	R	P		R		
L-361	v					I	R			R		
L-362	v					I	R					I
L-363	v					I	R			R		
L-364	R				P	I	R	P		R		
L-365	R	P			P	I	R			R		
L-366	v			R			R			R		
L-367	R				P	I		P	I			I
L-368	v						R			R		
L-369	R	P			P	I		P	I			I
L-370	R			R	P		R	P		R		
L-371		P	I		P	I		P	I		P	I
L-372			v			i			I (limit with R)			I
L-373		P	I		P	I		P	I		P	I
L-374		P	I	R			R	P			P	I
L-375	v			R			R			R		
L-376			v	r			R			R		
L-377	v			R			R			R		
L-378	R			R			R	P		R		
L-379	R	P			P	I	R	P		R		
L-380				R			R			R		
L-402	v			R			R	P		R		
L-403	v			R			R			R		
L-405	v					v			I		P	I
L-406	v					v			I	R		
L-407	v			R			R					I
L-408	R			R			R	P		R		
L-409			v	R			R	P		R	P	
L-410	v			R			R			R		
L-411	v					I(v)			I			I
L-416	v					v			I			I
L-416	v					v			I			
L-420	R	P			P	I	R	P		R	P	
L-421					P	I	R	P		R	P	
L-433	v					v			I	R		
L-434	v			R			R	P		R	P	
L-435			v	R			R	P		R		
L-436	R			R			R			R		
L-437	v			v			R			R		
L-438	v					v			I		P	I
L-439	R			R			R			R		
L-440	v					v			I	R		
L-441	v			R			R			R		
L-442	R			R			R			R		
L-443	R			R	P		R			R		
L-444	v					I(v)	R			R		
L-458	R	P		R					I			I
L-459	v					I			I(v)	R		
L-460	R				P	I	R			R		
L-461		P	I	R	P			P	I	R	P	
L-462	R	P		R	P		R	P		R	P	
L-463	v					v			I	R		
L-464	v			v			R			R		
L-465	v			v			R			R		
L-466	R	P		R			R	P			P	I
L-467	R	P		R			R	P		R	P	
L-600A	R	P		R	P		R			R		
L-602	R				P	I	R			R		
L-605	R	P		R			R				P	I
L-606	R	P		R	P		R			R		
L-616	R	P		R	P							
L-625	R	P			P	I	R	P		R	P	
L-626	R	P			P	I	R	P		R	P	
L-633	v						R	P		R		
L-635	v					I	R	P		R		
L-637	v			R			R			R		
L-638	R	P		R	P		R	P		R	P	
L-641	v					v	R	P		R		
L-645	v			v			R			R		I
L-648	R	P			P	I	R			R		
L-649	R			R	P		R			R		
L-668			v	R			R			R		
L-669			v	R			R			R		
L-670	v			v			R			R		
L-675			I	R			R			R	P	
L-676			v	v			R			R		
L-691	v			v			R			R		
L-693	R			R			R			R		
L-694			v	v			R			R		
L-695	v			v			R			R		
L-697			v	v			R			R		
L-698	R			R			R			R		
L-699			v	R			R			R		

iag+cag+ccg
op
pog
rrg

	Al vs Si (Fig5)			Fe vs Si (Fig6)			Fe vs Mg			Fe vs Ca		
Sample	R+Ceug	POG	I+Cac+Ccg	R+Ceug	POG	I+Cac+Ccg	R+Ceug	POG	I+Cac+Ccg	R+Ceug	POG	I+Cac+Ccg
L-708	v					v			I			I
L-712	R	P			P	I		P	I		P	I
L-713		P	I	R				P	I	R		
L-714		P	I	R	P			P	I		P	I
L-715	R	P		R	P		R			R		
L-716	R	P		R	P		R	P		R		
L-722	v			v			R					I
L-728	R			R	P		R					I
L-729	R	P		R	P		R	P		R	P	
L-740			v	v			R			R	P	
L-741			v	v			R			R		
L-742	v					I			I	R		
L-754	v					v	R		I	R		
L-759			I	R					I		P	
L-772		P	I	R				P	I	R		
L-773			I	R	P			P	I		P	
L-783		P	I	R	P		R	P		R	P	
L-784	R	P		R	P		R			R		
L-789	v			R			R			R		
L-791	R	P		R			R			R	P	
L-793	R	P		R	P		R	P		R	P	
L-797	R	P		R	P		R			R	P	
L-798		P	I	R	P		R	P		R	P	
L-799		P	I	R			R			R	P	
L-802			I		P	I		P	I	R	P	
L-808			I		P	I		P	I			I
L-809			I		P	I		P	I		P	I
L-810		P	I	R	P			P	I			I
L-812	R	P			P	I		P	I			I
L-813			I	R	P			P	I			I
L-814	v			R			R					I
L-815			v		P	I	R			R		
L-816	R	P		R	P		R	P		R	P	
L-832	R	P		R	P		R	P		R	P	
L-834	R(v)			v			R			R		
L-835	v					I	R	P		R		
L-836	v					I	R			R		
L-838	v					I	R	P		R		
L-839	R				P	I	R	P		R	P	
L-840	R	P			P	I	R	P		R	P	
L-842	v					I	R			R		
L-843	R	P			P	I		P	I	R		
L-844	v					I	R	P		R	P	
L-846	v					I	R			R		
L-849	R	P		R	P		R	P		R		
L-850	R	P		R	P		R	P		R	P	
L-855	R	P		R	P		R			R	P	
L-857	R	P			P	I		P	I		P	I
L-863	v					I	R			R		
L-864	R(v)					I			I	R		
L-865	v					I			I	R		
L-866												
L-868	v					I	R			R		
L-874	v			v		I	R			R		
L-875	v					I	R			R		
L-877	v			R	P	I	R			R		
L-878	v					I	R			R		
L-882												I
L-895			I(v)			v			I	R		
L-898	v			R			R			R		
L-899	R				P	I		P	I		P	I
L-900	v					I	R			R		
L-902	R	P		R	P		R	P		R		
L-903	R					I	R	P		R		
L-904	R	P		R	P		R	P		R		
L-905	R	P			P	I		P	I	R	P	
L-906	R	P		R	P		R	P		R	P	
L-907	R	P			P	I	R	P		R	P	
L-908			v	R			R	P	I	R		
L-909	R	P			P	I	R	P		R	P	
L-910	R	P		R			R	P		R		
L-911		P	I			I			I	R		
L-912	R	P				I			I	R		
L-917	R	P				I	R			R		
L-919	R(v)			v			R			R		
L-920	R(v)			v			R			R		
L-922	v					I	R			R		
L-923	R			R			R			R		
L-924	R				P	I	R	P		R	P	
L-938	R				P	I	R	P		R	P	
L-939			v	R			R	P		R	P	
L-940	v					I			I			I
L-943	R	P		R	P	I	R			R	P	
L-945			v	R			R	P		R	P	
L-946	v					I	R	P		R	P	
L-948	R				P	I	R	P		R		
L-951			v	R			R			R		
L-952			v	R			R			R		
L-955			v	R			R			R		
L-956				R			R			R		

iag+cag+ccg
op
pog
rrg

	Al vs Si (Fig5)			Fe vs Si (Fig6)			Fe vs Mg			Fe vs Ca		
Sample	R+Ceug	POG	I+Cac+Ccg	R+Ceug	POG	I+Cac+Ccg	R+Ceug	POG	I+Cac+Ccg	R+Ceug	POG	I+Cac+Ccg
L-957	R	P		R	P		R	P			P	I
L-958	v					v			I	R		
L-963	v					v	R			R		
L-965	v			R			R			R		
L-966	v			R			R			R		
L-967	R			R			R	P		R		
L-967a												
L-968	R	P		R			R	P		R	P	
L-969			I(v)	v			R			R		
L-971			v	R			R	P		R	P	
L-973	R			R			R					I
L-975	R	P		R	P		R	P		R	P	
L-976	R	P		R	P		R	P		R	P	
L-977	R	P		R	P		R	P		R	P	
L-978	R			R			R			R		
L-979	v					I			I			I
L-980	v					I			I			I
L-982	R(v)					I			I			I
L-983	R	P		R			R			R	P	
L-985	R	P		R	P		R	P		R	P	
L-987a	v			v			R					I
L-987b	R(v)			v			R					I
L-990	v					I(v)			I	R		
L-991	v					v			I	R		
L-992			I(v)			v			I			I
L-993	R	P			P	I	R	P			P	I
L-994	R	P			P	I		P	I		P	I
L-995	v			v			R			R		
L-996			I	R			R	P			P	I
L-997			v	R			R	P	I	R	P	
L-998	v					I			I	R		
L-999	v					I		P	I	R	P	
LJ1			v			I			I	R	P	
LL1			I		P	I			I			I
LL10			v			I	R			R		
LL11		P	I	R			R			R	P	
LL13	v					I			I			I
LL14	v			R			R	P		R	P	
LL15	v			R			R					I
LL16	R					I			I	R	P	
LL17a		P	I	R			R	P	I			I
LL17b			v	R			R	P		R		
LL18		P	I	R			R					I
LL2a			I	R	P				I			I
LL2b			v	R					I			I
LL3a			I	R	P				I		P	I
LL3b			I			I			I		P	I
LL4		P	I	R	P		R	P		R	P	
LL5			I	R					I			I
LL9			I	R					I			I
P-13	R			R			R		I			I
P-17	R			R			R		I			I
P-25			I			I	R		I		P	I
P-26	R	P		R	P		R					I
P-28	R			R					I			I
P-29				R					I			I
P-32				R					I			I
P-33	R					I			I			I
P-35		P	I		P	I			I			I
P-39									I			I
P-40i	R	P							I			I
P-40ii	R								I			I
P-46	R								I			I
P-50	R								I			I
P-53	R	P							I			I
P-57	R								I			I
P-58	R								I			I
X-43		P	I			I			I			I
X-44	R	P							I			I
X-45	R					I			I			I
X-46		P	I			I			I			I
X-47	R	P				I			I			I
X-48		P	I		P	I			I			I
X-49			I	R					I			I
X-50			I	R					I			I
X-51			I	R					I			I
X-52	R					I			I			I
X-53		P	I	R	P				I			I
X-54						I			I			I
X-55	R	P			P	I limit			I			I
X-56	R	P	I			I			I			I
X-57	R					I			I			I
X-58				R					I			I
X-59	R	P							I			I
X-60	R	P	I	R					I			I
X-61		P	I		P	I			I			I
X-62			I	R					I			I
X-63	R					I			I			I
X-64	R					I			I			I
X-65		P	I			I			I			I

iag+cag+ccg
op
pog
rrg

Sample	Al vs Si (Fig5)			Fe vs Si (Fig6)			Fe vs Mg			Fe vs Ca		
	R+Ceug	POG	I+Cac+Ccg	R+Ceug	POG	I+Cac+Ccg	R+Ceug	POG	I+Cac+Ccg	R+Ceug	POG	I+Cac+Ccg
X-66		P	I		P	I			I			I
X-67	R			R					I			I
X-68	R	P		R					I			I
X-69	R			R					I			I
X-70		P	I		P	I			I			I
X-71	R				P	I			I			I
X-72	R			R					I			I
X-73				R					I			I
X-74	R					I			I			I
X-75			I	R					I			I
X-76	v			R			R			R		
X-77	v					v	R		I	R		
X-78	v					v			I	R		
X-79	v					v			I			
X-80	v			v			R			R		
X-81	v					v	R			R		
X-82	v			v			R			R		
X-83	v			v			R			R		
X-84	v			v			R				P	I
X-85	v					v			I	R		
X-86	v			v			R			R		
X-87	v					v			I	R		
X-88	v					v			I(v)	R		
X-89	R (v)					v			I	R		

iag+cag+ccg
op
pog
rrg

Table A52

RESULTS OF DETERMINATIONS FOR ANOROGENIC CHARACTER OF GRANITOIDS BASED ON THE WHALEN ET AL, 1987 PLOTS

Sample	GavKN/Ca	GavK/Mg	GavNa+K	ZrvFe	ZrvK	GavFe/Mg	GavZn	GavNb	GavY	RESULT
BK10a										
BK12a										
BK14a										
BK16b										
BK19a										
BK1a										
BK1b			n							
BK1c			n							
BK24a										
BK25a			n							
BK27a			a							
BK29a										
BK32a										
BK32b			n							
BK39a										
BK39b										
BK3a										
BK423a			n							
BK425a										
BK425c										
BK428a			n							
BK435b										
BK439a			n							
BK43a										
BK445a			n							
BK445b			n							
BK446a										
BK452a			n							
BK45a										
BK4c										
BK5a										
X-76				a	a					
X-77				a	a					
L-012	n		a	n,a	a	n	n		n	A
L-012A	n		a	n,a	a	n	n		n	A
L-020	a		a	a	a	a	a	a	a	A
L-023	n		n	nog	nog	n	n	n	n	N
L-024	a		a	nog	nog	a	a	a	a	A
L-025	n		n	nfg	nog	n	n		n	N
L-026	n		n	a	a	n	n	n	n	A
L-027	n		n	nog	nog	n	n	n	n	N
L-028	n		n	nog	nog	n	n	n	n	N
L-029	n		n	nog	nog	n	n	n	n	N
L-030	a		n	a limit n	nfg		n	n	n	A
L-032	n	n	n	a	a	n	n		n	A
L-034	a	a	a	a	a		n		a	A
L-036	a	a	a	a	a		a		a	A
L-037	a	a	a	a	a		a		n	A
L-038	a	a	a		a		a,n		n	A
L-039	a	a	a	a	a		a		n	A
L-040	a	a	a	a	a		a		n	A
L-041	a	a	a							A
L-044	a	a	a		a		a		a	A
L-045	a	a	a		a		n		n	A
L-046	a	a	a	a	a		a		n	A
L-047	a		a	a	a	a	a	a	a	A
L-049	n		n	nog	nog	n	a	n	n	N
L-050	a		n	nog	nog	n	n	n	n	N
L-057							n			?
L-060	n		a	nfg	nfg	a	a	a	a	A
L-060	a									A
L-060	a									A
L-063	a		a	nog	nog	a	a	a	a	A
L-064	a		a	nog	nog	a	a	a	a	A
L-065	n		n	nog	nog	n	n	n	n	N
L-075	n			nog limit	nog	n		n		N
L-076	n	n		a	a	n	n	a	n	A
L-077	n	n		a	a	n	n	a	n	A
L-078	n	n	n	a	a	n	n	a	n	A
L-079										
L-1000	n	n	n	a	a	n	n		n	A
L-1002	a	a	a limit	a	nfg	a	n,a		n	A
L-1003	n	n	a	a	a	n	n		n	A
L-1005	n	n	n	a	a	a			n	A
L-1007	n	n	n	a	a	n	n		n	A
L-1009	n	n	a limit	a	a	n	n		n	A
L-1010	n	n	n	a	a	n	n		n	A
L-1011	n	n	a	a	a	n	n		n	A
L-1012	n	n	a	a	a	n	a		n	A
L-1013	n	n	a	a	a	n	n		n	A
L-1014	n	a	n	nfg	nog	n	n		n	?

Sample	GavKN/Ca	GavK/Mg	GavNa+K	ZrvFe	ZrvK	GavFe/Mg	GavZn	GavNb	GavY	RESULT
L-1015							n			?
L-1016	a									?
L-1016a	a									?
L-1019	a		a	a		a	n		n	A
L-1020	a	n	n	a	a	n	n limit a		n	A
L-1021	n		n	a	a		n		a	A
L-1022	a		a	a	a		a		a	A
L-1023	n	n	n	nog	nog	n	a		n	?
L-1024a	a									
L-1024c	a									
L-1025	a		a	a	a		a		a	A
L-1027	a		a	a	a		a		a	A
L-1032	n	n	n			n	a		n	
L-1037	n	n	a	a	a	n	n		n	A
L-1038	n	n	a	a	a	n	n		n	A
L-1039	a		a	a	nfg	a	n		n	A
L-1039a	a		a	a limit fg	nfg	a	n		n	A
L-1039c	a		a		nfg	a	n		n	A
L-1042Y	a	a	a	nfg limits	nfg	n	n		n	A
L-1043Z	a	a	a limit	a	a	n	n		n	A
L-1044XX	a	a	a	nfg limits	nfg	n	n		n	A
L-1045Yb	n	a	n	a	a	n	n		a	A
L-1046XX	a	a	n	a	a	n	n		n	A
L-139	a		a	nfg	a	a	a		a	A
L-143							a			?
L-150	a	a		nog	nfg	a	a	a	a	A
L-151	a	a		a	a	a	a	a	a	A
L-153	a	a		a	a		a	a	a	A
L-154	a				a		a	a	a	A
L-155	n	n	n	nog	nfg	a	n	n	n	N
L-157	a	n	n	nog	a	n	n	n	n	A
L-158	n	n	n	nog	nfg	n	n	n	n	N
L-159	n	n	n	a	a	n	n	a	n	A
L-160	n	n	n	a	a	n	n	a	n	A
L-161	n	n		a	a	n	a	a	n	A
L-162	a	a		nfg	nfg	n	n	n	n	A
L-163	n	n	n	nog	nog	n	a	n	n	N
L-166	n	n		nfg	nog	n	n	n	n	N
L-167	a	a		a		a	a	a	a	A
L-168	a									
L-170	a	a		a	a	a	a	a	a	A
L-172	a			nfg	a	a	a	a	a	A
L-173	a	a		a	a	a	a	a	a	A
L-175	n	n	n	n,a	a	n	n			A
L-181	n	n	n	n		n	n	n	n	N
L-195	a	a	a	a	a	a	a		a	A
L-199										
L-207				nfg						?
L-208	a		a		a		a		a	A
L-209	n	n	n	nfg,a	nog	n	n	n	n	N
L-210	a	n	a	a	a	a	n		n	A
L-212	a	a	a	a	a	a	a		a	A
L-213	a	a	a	a	a	a	a		a	A
L-214	a		a		a		a		a	A
L-215	a		a		a		a		a	A
L-217	n	a	n	n,a	nog	n	n	n	n	?
L-218	a	a	a	a	a	a	a		a	A
L-222	a	a	a	a	a	a	a		a	A
L-223	a	a	a	a	a	a	a		a	A
L-224	a	a	a	a	a	a	a		a	A
L-225					a					A
L-226							a			?
L-237	n	a	n limit	a	a		n		n	A
L-238	n	a	n limit	a	a		n		n	A
L-239	n	a	a	a	a		n		n	A
L-241	a	a								A
L-242	a	a	a	a	a	a	a		a	A
L-248	a	a	a	a	a	a	a		a	A
L-248-LG	a	a	a	a	a	a	a		a	A
L-249	n	a	n limit	a	a	n limit	n		n	A
L-257	a	a	a	a	a	a	a		a	A
L-259	n	a	a	a	a	a limit	n		n	A
L-259-B	a	a	a	a	a	a	a		a	A
L-263	a	a	a	a	a	a	a		a	A
L-321	a		a	a	a	a	a		a	A
L-322	a		a	a	a	a	a		a	A
L-323	a		a	a	a	a	a		a	A
L-324	a		a	a	a	a	a		a	A
L-325			a	a		a	a		a	A
L-341	a		a	a	a	a	a		a	A
L-343	a			a	a	a	a		a	A
L-344	a		a	a	a	a	a		a	A
L-345	a		a limit	a	a	a	a		a	A
L-346	a		a	a	a	a	a		a	A

Sample	GavKN/Ca	GavK/Mg	GavNa+K	ZrvFe	ZrvK	GavFe/Mg	GavZn	GavNb	GavY	RESULT
L-347	a		a	nfg	nog	a	a		a	A
L-348	a		a	a	a	a	a		a	A
L-349	a		a	a	a	a	a		a	A
L-352	a		a	a	a	a	a		a	A
L-353			a	a	a	a	a		a	A
L-354	n		n limit	n,a	a	n limit	n		n	A
L-355	a		a	a	nfg	a	n		n	A
L-357	n		a limit	a	a	n	n	a	n	A
L-358	a		a	a	a	a	a	a	a	A
L-359	a		a	a	a	a	a	a	a	A
L-360	n		a	a	nfg		n	a,n	n	A
L-361	a		n limit	a	a	n	n	n	n	A
L-362	a		n limit	a	a	n	n		n	A
L-363	n		n	nfg	nog		n		n	N
L-364	a		a	a	a	a	a	a	a	A
L-365	a		a	a	a	a	a	a		A
L-366	a		a	a	a	a	a	a	a	A
L-367	n		n	a	a	n	n	a	a	A
L-368	n		n	a	a	n	n	n	n	A
L-369	n		n	nog		n	a		n	A
L-370	a		a	a limit n	a limit a	a	a		a	A
L-371	n		a	nfg	nog	n	n	a	n	A
L-372	n		n	nog limit	a limit n	n	a	n	n	A
L-373	n		n	nfg	nog	n	n	n	n	N
L-374	n		a	nfg	nog	n	n	n	n	N
L-375	a		a	a	a	a	a		a	A
L-376	n		a	a	a	n	n	a	n	A
L-377	a		a	a	a	a	a	a	a	A
L-378	a		a	a	a	a	a	a	a	A
L-379	a		a	nfg	nfg	a	a	a	a	A
L-380	a		a	a	a	a	n	a	n	A
L-402	a		a	a	a	a	a		a	A
L-403	a		a	a	a	a	a		a	A
L-405	n		n	nfg		n	n	n	n	N
L-406	n		n	nfg	nog	a	a	n	n	A
L-407	a		a	a	a	a	a		a	A
L-408	a		a	a	a	a	a		a	A
L-409	n		a	n,a	a	n	n		n	A
L-410	a		n	a	a	a limit	a		n	A
L-411										
L-416		n	n	n		n	n	n	n	N
L-420	a		n	a	a	n	n	a	n	A
L-421	n		a	a		n	n		n	A
L-433	n		n limit	n,a	a	n limit	n limit		n	A
L-434	n		n	n,a	a	n	n	n	n	A
L-435	n		a	a	a	a	n	n	n	A
L-436	a		a	a	a	a			a	A
L-437	a		a	a	a	a	a		a	A
L-438	n		n limit	n,a	a	n	n limit		n	A
L-439	a		a	a	a	a	a		a	A
L-440	a		a	a	a	a	a		a	A
L-441	a		a	a	a	a	a		a	A
L-442	a		n limit		a		n	n	a	A
L-443	a		a	a	a	a	a		a	A
L-444	n		n	nfg	nog	n limit	a		n	?
L-458	a		a		a		n	n	n	A
L-459	a		a	nfg	nog	a	a		a	A
L-460	a		a	a	a	a	a		a	A
L-461	n		a	nfg	nfg	n	n	n	n	?
L-462	n		n	nfg	nog	n	n	n	n	N
L-463	a		a	nfg	nog	a	a		a	A
L-464										
L-465	a		a			a	a		a	A
L-466	a		a	a	nfg	a	a		a	A
L-467	a		a	a	a	a	a		a	A
L-600A	a	a	a	a	nfg		n		n	A
L-602	a	a	n	a	a		n		n	A
L-605	a	a	a	a	nfg		n		a	A
L-606	a	a	a limit	a	a		a		a	A
L-625	n	n	n	a	a	n	n		n	A
L-626	a	n	n	a	a	n	n		n	A
L-633	n	n	n	nfg	nog	n	a		n	?
L-635	n	n	n	a	a	n	n		n	A
L-637	a	a	a	a	a	a	a		a	A
L-637a			n							?
L-638	a	a	n	a	nfg	a			n	A
L-641	n	n	n	nfg	nog	n	a		n	?
L-645	n	n	a limit	a	nog	a	n		n	A
L-648	a	n	a	a	a	n	n		n	A
L-649	a	n	n	nfg	nfg	n	n		n	?
L-668	a		a	a	a	a	a		a	A
L-669	a		a	a	a	a	a		a	A
L-670	a		a	a	a	a	a		a	A
L-675	a		a	a		a	a		a	A

Sample	GavKN/Ca	GavK/Mg	GavNa+K	ZrvFe	ZrvK	GavFe/Mg	GavZn	GavNb	GavY	RESULT
L-676	a		a	a	a	a	a		a	A
L-691	a		a	a	a	a	a		a	A
L-693	a		a	a		a	a		a	A
L-694	a	n	a	a	a	n	a			A
L-695	n		a		a	a	a		a	A
L-697	a		a	a	a	a	a		a	A
L-698	a		a	a		a	a		a	A
L-699	a		a	a		a	a		a	A
L-708	a		a	a	a	a			a	A
L-710		n								?
L-712	a		a	nog		a	a		a	A
L-713	a		a	a		a	a		a	A
L-714	a		a		a	a	a		a	A
L-715	a		a	a	a	a	a limit n		a	A
L-716	a		n	a	a	n	n		n	A
L-722	a									A
L-728	a		a	a	a	a	a		a	A
L-729	a									A
L-740	a		a	a			a		a	A
L-741	a		a	a	a		a		a	A
L-742	a		a	a			a		a	A
L-754	n	n	n	nog	nog	n	a		n	?
L-759	a	a	a	a		a	n		n	A
L-772	a	a	a			a	n		n	A
L-773	a	a	n	nfg		n	n			A
L-783	a	n	a	a		n	n		n	A
L-784	n	n	a	a	a	n	n		n	A
L-789	a	a	a	a		a	a		a	A
L-791	a	a	a	a		a	a		a	A
L-793	n	a	a	a	a	a	a		a	A
L-797	n	a	a	a	a	a	a		a	A
L-798	n	a	a	a	a	a	a		a	A
L-799	n	a	a	a	a	a	n		n	A
L-802	n	n	n	nog	nfg	n	n		n	N
L-808	n	n	n limit	nfg	nog	n	n		n	N
L-809	a	a	a			n	n		n	A
L-810	n	a	a			n	n		n	A
L-812	n	a	n	a	a	n	n		a	A
L-813	n	a	a	nfg	nfg limi	n	n		n	A
L-814										
L-815	n	n	a	a		n	n		n	A
L-816	n	n	n	a	a	n	n		n	A
L-832	a	a	a	a	a	a	a		a	A
L-834	a	a	a	a	a	a	a,n,n		n	A
L-835	n	n	a	a	a	n	n		n	A
L-836	a									?
L-838	n	n	n	nfg	nog	n	n		n	N
L-839	a	a	n	nfg	nfg	n	n		n	A
L-840	n	n	a	a	a	n	n		n	A
L-842	n	n	n	a	a	n	n		n	A
L-843	a	a	n	a	a	n	n		n	A
L-844	n	n	n	a	a	n	n		n	A
L-846	n	n	a	a	a	n	n		n	A
L-849	a	a	a	a	a	a on limit	a limit n	a	alimit n	A
L-850	n	n	n	a	a	n	n		n	A
L-855		a	a	a	a	a	n		n	A
L-857	n	n	n,a	nfg	nog	n	n			N
L-859									n	?
L-863	n	n	n,a	a	a		n		n	A
L-864	n	n	n	nog	nog	n	n		n	N
L-865	n,a	n	n,a	a	a	n	n		n	A
L-866				a						?
L-868	n	n	n,a	nfg	nog	n			n	?
L-874	a	n	a,n		nfg		a		a	A
L-874-		n								?
L-875	n	n	n,a	a	a	n,a	n		n	A
L-877	n	n	n limit	a	a	a limit	n		n	A
L-878	n	n	a limit		a	a limit			alimit n	A
L-895	n	n	a	nog	nog	n	n		n	?
L-898		n		a						A
L-899	n	n	n	a	a	n	n		n	A
L-900	n	n	a	a	a	n	n		n	A
L-902	a	a	a	nfg	a	a	n		n	A
L-903	a	a	n	nfg	a	n limit	n		n	A
L-904	a	a	n	nfg	a	a	n		n	A
L-905	a	n	n	nfg	nfg	n	n		n	?
L-906	a	a	a	a	a	a	n		n	A
L-907	n	n	a	a	a	n	n		n	A
L-908	a	a	a	nfg		a	a		a	A
L-909	a	n	a	a	a	n	n		n	A
L-910	a	n	n	a	a	n	n		n	A
L-911	a	n	n	a	a	n	n		n	A
L-912	a	n	n	a	a	n	n		n	A
L-917	a	n	a,n border	nog	nfg	n	n		n	?

Sample	GavKN/Ca	GavK/Mg	GavNa+K	ZrvFe	ZrvK	GavFe/Mg	GavZn	GavNb	GavY	RESULT
L-919										
L-920	a	a	a	nog	nfg	a	a		a	A
L-922	n	n	a	a	a	n	n		n	A
L-923	n	n	a	a	a	n	n		n	A
L-924	n	n	n	a	a	n	n		n	A
L-938	n	n	n	a	a		n		n	A
L-939	n	n	a	nog	nog	n	n		n	?
L-940	n	n	n	nog	nog	n	n		n	N
L-943	a	a	a	a	nfg	a	n		n	A
L-945	n	n	a	a	a	n	n		n	A
L-946	n	n	a	a	a		n		n	A
L-948	n	n	a	a	a	n	n		n	A
L-951	a	n	a	a	a	a	n		n	A
L-952	a	n	a	a	a	a	n		n	A
L-955	a	n	a	a	a		a		n	A
L-956	a	a	a	a	a	a	a		a	A
L-957	n	a	n	a	a	n	n		n	A
L-958	n	n	n,a	nfg	nog	n	a,n		n	?
L-963										
L-965	a	a	a	a	a	a	n,a		a	A
L-966	a	a	a	a	nfg	a	n,a		n	A
L-967	n	n	a	a	a	n	n,a		a	A
L-967a										
L-968	a	a	a	a	a	a	n		n	A
L-969	a	a	a	a	a	n	n		n	A
L-971	a	a	a	a	a	a	n,a		n	A
L-973	a	a	a	a	a	a	a,n,a		n	A
L-975	a	a	a	a	a	n	n		n	A
L-976	a	a								?
L-977	a	a	a	nfg limit	a	n	n		n	A
L-978	a	a	a	a	a	a	a		a	A
L-979	n	n	n	nog	nog	n	n		n	N
L-980	n	n	n	nog	nog	n	n		n	N
L-982	n	n	n	nog	nog	n	n		n	N
L-983	n	a	a	a	nfg	a	n		n	A
L-985	n	n	n	nfg	nog	n	n		n	N
L-987			n							?
L-987a	n		n			n	a,n		n	?
L-987b			n	nog	nog	n	n		n	N
L-990	n	n	n	nog	nog	n	n		n	N
L-991	n	n	n	nog	nog	n	n		n	N
L-992	n	n	n	nog	nog	n	n		n	N
L-993	n	n	a	nfg	nog	n	n		n	?
L-994	n	n	a	a	a	n	n		n	A
L-995	a	a	a			a	a		a	A
L-996	n	n	a	nfg	nog	n	n		n	?
L-997	a	a	a	a	a	n	n		n	A
L-998	n	n	a limit	a	a	n	n		n	A
L-999	n	n	a	a	a	n	n		n	A
LJ1	a			nog	nog					?
LL1	a			a	nfg					A
LL10	a				a					A
LL11	a				nfg					A
LL13	a			nog	nog					A
LL14	a			a	a					A
LL15	a			a	a					A
LL16	a			a	a					A
LL17a	a				nfg					A
LL17b	a			a limit w	a limit nog					A
LL18	a				nfg					A
LL2a	a			a	a					A
LL2b	a				a					A
LL3a	a			a	a					A
LL3b	a			a	a					A
LL4	a			nfg limit	nfg					A
LL5	a				nog					A
LL9	a			a	a					A
X-78				a	a					A
X-79				a	a					A
X-80				a	a					A
X-81				a	a					A
X-82				a	a					A
X-83				ngt	nog					N
X-84				a	a					A
X-85				ngt	nog					N
X-86				ngt	nog					N
X-87				ngt	nog					N
X-88				ngt	nog					N
X-89				ngt	nog					N
N11b			n							N
N12d										
N50b										
N52a										
N8a										

Table A53 Results of Determination for Environment of Emplacement of Granitoids Based on Methodology of Pearce et al, 1982

Sample	Nb vs Y					Ta vsYb					Rb vs Y+Nb				Rb vs Yb+Ta					#	
	WPG	VAG	synCOLG	ORG	Wb	WPG	syn-COLG	VAG	ORG	Wb	WPG	syn-COLG	VAG	ORG	WPG	syn-COLG	VAG	ORG		TYPE	
P-13											W										
P-17											W										
P-25											W										
P-26												S									
P-28											W										
P-29											W										
P-32														O							
P-33											W										
P-35														O							
P-39											W										
P-46											W										
P-50											W										
P-53											W										
P-57											W										
P-58											W										
P-40i											W										
P-40ii											W										
BK10a	x													x					O-W1-1	30	
BK12a		x	x											x						47	
BK14a		x	x											x						47	
BK16b		x	x											x						47	
BK19a		x	x											x						47	
BK1a		x	x										x						V	45	
BK1b		x	x											x						47	
BK1c		x	x											x						47	
BK24a	x													x					O-W1-1	30	
BK25a		x	x											x						47	
BK27a	x													x					O-W1-1	30	
BK29a		x	x											x						47	
BK32a	x													x					O-W1-1	30	
BK32b		x	x											x						47	
BK39a		x	x											x						47	
BK39b		x	x											x						47	
BK3a		x	x											x						47	
BK423a		x	x											x						47	
BK425a		x	x											x						47	
BK425c		x	x											x						47	
BK428a		x	x											x						47	
BK435b		x	x											x						47	
BK439a		x	x											x						47	
BK43a		x	x											x						47	
BK445a		x	x											x						47	
BK445b		x	x										x						V	45	
BK446a		x	x											x						47	
BK452a		x	x											x						47	
BK45a		x	x											x						47	
BK4c		x	x										x						V	45	
BK5a		x	x											x						47	
X-76	x													x					O-W1-1	30	X
X-77	x													x					O-W1-1	30	X
L-012	x						x							x				x		9	
L-012A	x													x					O-W1-1	30	
L-020	x								x					x				x	O3/4	18	X
L-023		x	x						x					x				x	O3/4	40	X
L-024		x	x						x				x		x				V2/4	37	X
L-025		x	x						x					x				x	O3/4	40	X
L-026		x	x											x						47	
L-027		x	x										x						V	45	X
L-028		x	x						x					x				x	O3/4	40	X
L-029		x	x											x						47	
L-030		x	x				x							x				x	S2/4 O2/4	34	X
L-032		x	x						x					x				x	O3/4	40	X
L-034					x								x						V1/2	60	X
L-036					x						x								W	59	
L-037					x				x		x							x	O-W 2-2	56	X
L-038					x						x								W	59	
L-039					x						x								W	59	
L-040					x						x								W	59	
L-041					x						x								W	59	
L-044					x				x		x							x	O-W 2-2	56	X
L-045					x					x	x							x	w3/4	58	
L-046									x		x							x	O2/3	63	
L-047	x					x					x							x	W3/4	3	
L-049		x	x										x						V	45	
L-050		x	x										x						V	45	
L-060	x						x						x					x		8	
L-060		x	x											x						47	
L-060														x					O	65	?
L-063		x	x										x						V	45	
L-064		x	x										x						V	45	
L-065		x	x						x				x				x		V3/4	38	X
L-075		x	x				x							x				x	S2/4 O2/4	34	X
L-076	x													x					O-W1-1	30	
L-077	x								x					x				x	O3/4	18	X
L-078	x													x					O-W1-1	30	
L-079	x													x					O-W1-1	30	
L-1000		x	x						x					x				x	O3/4	40	

	WPG	VAG	synCOLG	ORG	Wb	WPG	syn-COLG	VAG	ORG	Wb	WPG	syn-COLG	VAG	ORG	WPG	syn-COLG	VAG	ORG		TYPE	
L-1002		x	x							x				x				x		42	
L-1003		x	x						x					x				x	O3/4	40	
L-1005	x													x					O-W1-1	30	
L-1007		x	x											x						47	
L-1009		x	x											x						47	
L-1010		x	x											x						47	
L-1011	x													x					O-W1-1	30	
L-1012	x													x					O-W1-1	30	
L-1013		x	x						x					x				x	O3/4	40	
L-1014		x	x											x						47	
L-1016													x						V	64	X?
L-1016a		x	x										x						V	45	
L-1019		x	x		x	x							x					x	V2/4	32	X
L-1020	x										x								W	25	
L-1021	x										x								W	25	
L-1022				x							x							x	O2/3	52	X
L-1023		x	x										x						V	45	
L-1024a	x												x							28	
L-1024c	x												x							28	
L-1025				x						x		x						x		51	
L-1027					x				x		x							x	W-O 2-2	56	X
L-1032		x	x							x			x		x				V2/4	41	X
L-1037		x	x											x						47	
L-1038		x	x											x						47	
L-1039		x	x											x						47	
L-1039a		x	x				x							x				x	S2/4 O2/4	34	X
L-1039c		x	x											x						47	
L-1042Y	x									x				x				x		23	
L-1043Z	x									x				x				x	O-W 2-2	23	X
L-1044XX	x													x					O-W1-1	30	
L-1045Yb	x								x		x				x				W3/4	12	
L-1046XX	x													x					O-W1-1	30	
L-139	x													x					O-W1-1	30	
L-150	x								x					x				x	O3/4	18	
L-151	x					x					x							x	W3/4	3	
L-153	x										x								W	25	
L-154	x									x				x				x	O-W 2-2	23	X
L-155		x	x						x					x				x	O3/4	40	
L-157		x	x											x						47	
L-158		x	x											x				x	O2/3	46	X
L-159	x													x					O-W1-1	30	
L-160	x								x					x				x	O3/4	18	
L-161	x													x					O-W1-1	30	
L-162		x	x											x						47	
L-163		x	x											x						47	
L-166		x	x					x						x				x	V2/4 O2/4	36	X
L-167	x										x								W	25	
L-168		x	x											x				x	O2/3	46	X
L-170					x				x		x							x	O-W 2-2	56	X
L-172					x	x								x				x	O-W 2-2	55	X
L-173					x						x								W	59	
L-175	x								x					x				x	O3/4	18	
L-181		x	x										x						V	45	
L-195	x								x		x							x	O-W 2-2	10	X
L-199	x					x							x					x	O 2/4	4	X
L-207		x	x											x						47	
L-208		x	x											x						47	
L-209		x	x											x						47	
L-210					x								x						V1/2	60	X
L-212	x													x					O-W1-1	30	
L-213					x				x					x				x	O3/4	57	X
L-214					x						x								W	59	
L-215		x	x										x						V	45	
L-215		x	x										x						V	45	
L-217		x	x											x				x	O2/3	46	X
L-218	x								x					x				x	O3/4	18	
L-222	x													x					O-W1-1	30	
L-223	x													x				x	O2/3	29	X
L-224	x													x					O-W1-1	30	
L-237	x													x					O-W1-1	30	
L-238	x								x					x				x	O3/4	18	
L-239	x													x					O-W1-1	30	
L-241	x					x								x				x	O-W 2-2	5	X
L-242		x	x										x						V	45	
L-248	x										x								W	25	
L-248-LG	x													x					O-W1-1	30	
L-249	x								x					x				x	O3/4	18	
L-257	x									x				x				x	O-W 2-2	23	X
L-259	x										x								W	25	
L-259-B	x										x								W	25	
L-263	x								x		x							x	O-W 2-2	10	X
L-321	x												x						V1/2	28	X
L-322	x													x					O-W1-1	30	
L-323	x													x					O-W1-1	30	
L-324	x										x								W	25	
L-325	x										x								W	25	
L-341	x												x						V1/2	28	X
L-343	x											x							S1/2	27	X
L-344	x												x						V1/2	28	X
L-345	x													x					O-W1-1	30	
L-346	x													x					O-W1-1	30	

	WPG	VAG	synCOLG	ORG	Wb	WPG	syn-COLG	VAG	ORG	Wb	WPG	syn-COLG	VAG	ORG	WPG	syn-COLG	VAG	ORG		TYPE	
L-347		x	x										x						V	45	
L-348	x												x						V1/2	28	X
L-349	x										x								W	25	
L-352	x													x					O-W1-1	30	
L-353	x										x								W	25	
L-354	x										x								W	25	
L-355	x													x					O-W1-1	30	
L-357	x										x								W	25	
L-358		x	x						x					x				x	O3/4	40	
L-359	x	x	x											x						1	
L-360	x													x					O-W1-1	30	
L-361		x	x											x						47	
L-362		x	x											x						47	
L-363		x	x											x						47	
L-364		x	x											x						47	
L-365	x													x					O-W1-1	30	
L-366	x									x				x				x	O-W 2-2	23	X
L-367	x										x								W	25	
L-368		x	x											x						47	
L-369	x										x							x	?	24	
L-370		x	x											x						47	
L-371	x													x					O-W1-1	30	
L-372		x	x											x						47	
L-373		x	x											x						47	
L-374		x	x											x						47	
L-375	x													x					O-W1-1	30	
L-376	x													x					O-W1-1	30	
L-377	x													x				x	O2/3	29	X
L-377	x													x					O-W1-1	30	
L-379	x													x					O-W1-1	30	
L-380	x								x					x				x	O3/4	18	
L-402	x										x								W	25	
L-403	x										x								W	25	
L-405		x	x										x						V	45	
L-406		x	x										x						V	45	
L-407	x										x								W	25	
L-408	x										x								W	25	
L-409	x													x					O-W1-1	30	
L-410					x									x						61	
L-411		x	x										x						V	45	
L-416		x	x										x						V	45	
L-420	x													x					O-W1-1	30	
L-421		x	x											x						47	
L-433	x													x					O-W1-1	30	
L-434		x	x											x						47	
L-435		x	x											x						47	
L-436	x													x					O-W1-1	30	
L-437	x													x					O-W1-1	30	
L-438	x													x					O-W1-1	30	
L-439	x										x								W	25	
L-440	x													x					O-W1-1	30	
L-441	x										x								W	25	
L-442	x													x					O-W1-1	30	
L-443	x													x					O-W1-1	30	
L-444	x												x						V1/2	28	X
L-458	x													x					O-W1-1	30	
L-459		x	x											x						47	
L-460		x	x											x						47	
L-461		x	x											x						47	
L-462		x	x											x						47	
L-463		x	x										x						V	45	
L-464		x	x										x						V	45	
L-465		x	x										x						V	45	
L-466					x									x						61	
L-467		x	x											x						47	
L-600A		x	x											x						47	
L-602	x								x					x				x	O3/4	18	
L-605		x	x											x						47	
L-606		x	x											x						47	
L-625	x												x						V1/2	28	X
L-626	x								x				x		x					14	
L-633		x	x						x					x	x					39	
L-635		x	x						x				x		x				V2/4	37	X
L-637	x									x			x		x					22	
L-638		x	x				x							x				x	S2/4 O2/4	34	X
L-641		x	x										x						V	45	
L-645		x	x										x						V	45	
L-648		x	x										x						V	45	
L-649		x	x										x						V	45	
L-668					x				x		x							x	O-W 2-2	56	X
L-669					x	x					x								W	53	
L-670					x				x		x							x	O-W 2-2	56	X
L-675									x		x				x			x	W3/4	62	
L-676					x						x								W	59	
L-691	x										x								W	25	
L-693					x	x					x							x	W3/4	54	
L-694					x						x								W	59	X
L-695	x													x					O-W1-1	30	
L-697					x					x	x							x	w3/4	58	
L-698					x				x		x							x	O-W 2-2	56	X
L-699					x						x								W	59	

	WPG	VAG	synCOLG	ORG	Wb	WPG	syn-COLG	VAG	ORG	Wb	WPG	syn-COLG	VAG	ORG	WPG	syn-COLG	VAG	ORG		TYPE	
L-708	x																		W?	31	
L-712		x	x										x						V	45	
L-713					x				x		x							x	O-W 2-2	56	X
L-714		x	x										x						V	45	
L-714													x						V	64	X?
L-715	x								x					x				x	O3/4	18	
L-716		x	x				x							x				x	S2/4 O2/4	34	X
L-722	x								x			x			x					13	
L-728	x					x												x	?	7	
L-729	x													x					O-W1-1	30	
L-740				x					x		x							x	O3/4	50	
L-741					x				x		x							x	O-W 2-2	56	X
L-742	x								x									x	O2/3	20	X
L-754		x	x											x						47	
L-759		x	x											x						47	
L-772		x	x											x						47	
L-773	x										x								W	25	
L-783	x													x					O-W1-1	30	
L-784	x								x					x				x	O3/4	18	X
L-789					x				x		x							x	O-W 2-2	56	X
L-791	x					x					x							x	W3/4	3	
L-791	x										x								W	25	
L-793	x									x	x							x	W3/4	21	
L-797					x									x						61	
L-798					x									x						61	
L-799		x	x											x						47	
L-802					x									x						61	
L-808		x	x				x							x				x	S2/4 O2/4	34	X
L-809		x	x											x						47	
L-810		x	x											x						47	
L-812	x	x	x											x						1	
L-813		x	x											x						47	
L-814		x	x																	49	CHECK OTHERS
L-815	x													x					O-W1-1	30	
L-816	x								x				x					x		17	
L-832		x	x											x						47	
L-834	x								x					x				x	O3/4	18	X
L-835		x	x											x						47	
L-836		x	x											x						47	
L-838		x	x											x						47	
L-839		x	x											x						47	
L-840		x	x											x						47	
L-842		x	x						x					x				x	O3/4	40	
L-843	x									x				x				x	O-W 2-2	23	X
L-844		x	x											x						47	
L-846		x	x											x				x	O2/3	46	X
L-849					x				x					x				x	O3/4	57	
L-850		x	x						x					x				x	O3/4	40	
L-855		x	x											x						47	
L-857		x	x											x						47	
L-863		x	x											x						47	
L-864		x	x				x							x				x	S2/4 O2/4	34	X
L-864		x	x											x						47	
L-865		x	x											x						47	
L-868		x	x				x							x				x	S2/4 O2/4	34	X
L-874		x	x										x						V	45	
L-874-	x													x					O-W1-1	30	
L-875	x								x					x				x	O3/4	18	
L-877	x													x					O-W1-1	30	
L-878	x								x					x				x	O3/4	18	
L-895		x	x						x					x				x	O3/4	40	
L-898		x	x											x						47	
L-899		x	x											x						47	
L-900		x	x											x						47	
L-902		x	x											x						47	
L-903		x	x											x						47	
L-904		x	x							x				x				x		42	
L-905	x													x					O-W1-1	30	
L-906	x													x					O-W1-1	30	
L-907		x	x											x						47	
L-908		x	x				x							x				x	S2/4 O2/4	34	X
L-909	x													x					O-W1-1	30	
L-910	x													x					O-W1-1	30	
L-911	x													x					O-W1-1	30	
L-912	x													x					O-W1-1	30	
L-917		x	x				x							x				x	S2/4 O2/4	34	X
L-919		x	x											x						47	
L-920		x	x						x					x				x	O3/4	40	
L-922	x								x					x				x	O3/4	18	
L-923	x													x					O-W1-1	30	
L-924	x													x					O-W1-1	30	
L-938	x								x					x				x	O3/4	18	
L-939		x	x						x					x				x	O3/4	40	
L-940		x	x						x					x				x	O3/4	40	
L-943		x	x				x							x				x	S2/4 O2/4	34	X
L-945	x								x					x				x	O3/4	18	
L-946	x													x					O-W1-1	30	
L-948	x													x					O-W1-1	30	
L-951	x								x				x				x		V2/4	16	X
L-952	x												x						V1/2	28	X
L-955		x	x						x				x				x		V3/4	38	

	WPG	VAG	synCOLG	ORG	Wb	WPG	syn-COLG	VAG	ORG	Wb	WPG	syn-COLG	VAG	ORG	WPG	syn-COLG	VAG	ORG		TYPE	
L-956	x								x				x			x				15	
L-957		x	x						x					x				x	O3/4	40	
L-958		x	x										x						V	45	
L-963		x	x											x						47	
L-965	x										x								W	25	
L-966	x					x								x						6	
L-967	x													x					O-W1-1	30	
L-967a														x						65	CHECK OTHERS
L-968		x	x						x					x				x	O3/4	40	
L-969	x								x					x				x	O3/4	18	
L-971	x													x					O-W1-1	30	
L-973	x								x					x				x	O3/4	18	
L-975		x	x											x						47	
L-976	x									x				x				x	O-W 2-2	23	X
L-977		x	x											x						47	
L-978		x	x				x							x				x	S2/4 O2/4	34	X
L-979		x	x																	49	CHECK OTHERS
L-980		x	x																	49	CHECK OTHERS
L-982		x	x															x		48	
L-983		x	x																	49	CHECK OTHERS
L-985		x	x				x											x	S2/3	35	X
L-987a		x	x				x						x					x		33	?
L-987b		x	x										x		x				V2/3	43	X
L-990		x	x										x					x		44	
L-991		x	x										x						V	45	
L-992		x	x				x							x				x	S2/4 O2/4	34	X
L-993		x	x				x							x				x	S2/4 O2/4	34	X
L-994	x													x					O-W1-1	30	
L-995		x	x										x						V	45	
L-996		x	x				x							x				x	S2/4 O2/4	34	X
L-997	x									x				x				x	O-W 2-2	23	X
L-998		x	x						x					x				x	O3/4	40	
L-999	x								x					x				x	O3/4	18	
LJ1														x						65	CHECK OTHERS
LL1		x	x											x						47	
LL10					x						x								W	59	
LL11		x	x											x						47	
LL13		x	x										x						V	45	
LL14					x						x								W	59	
LL15					x									x						61	
LL16					x									x						61	
LL17a		x	x											x						47	
LL17b		x	x											x						47	
LL18		x	x											x						47	
LL2a		x	x											x						47	
LL2b		x	x											x						47	
LL3a		x	x											x						47	
LL3b		x	x											x						47	
LL4	x													x					O-W1-1	30	
LL5		x	x											x						47	
LL9		x	x											x						47	
X-78					x									x						61	
X-79					x								x						V1/2	60	X
X-80	x				x						x								W	2	
X-81	x				x						x								W	2	
X-82					x								x						V1/2	60	X
X-83					x									x						61	
X-84					x								x						V1/2	60	X
X-85					x								x						V1/2	60	X
X-86					x								x						V1/2	60	X
X-87					x								x						V1/2	60	X
X-88		x	x											x						47	
X-89					x						x								W	59	
N11b		x	x											x						47	
N12d		x	x											x						47	
N50b		x	x											x						47	
N52a		x	x											x						47	
N8a		x	x											x						47	

Appendix A54

DISCRIMINATION OF GRANITOIDS FOLLOWING PROCEDURE OF HARRIS ET AL, 1986

Sample	Rb/10HfTa	Rb/30HfTa	Nb-Ta	norm Hf	norm Tax3	norm Rb/10	norm Hf	norm Tax3	norm Rb/30	Nb	Ta
Kafue Park, Zambia											
L-238			OUTU	0.00	84.72	15.28	0.00	98.23	1.77	2.60	96.79
L-241	VA-	III	INW-INV	8.22	8.88	82.90	32.38	34.97	32.65	2.41	2.66
L-249			OUTU	0.00	77.19	22.81	0.00	97.13	2.87	2.30	66.05
L-257	WP	WP	OUTU	3.44	50.74	45.81	5.86	86.34	7.80	2.50	37.63
L-263			OUTU	0.00	75.94	24.06	0.00	96.93	3.07	2.6	41.571
West Lusaka, Zambia											
L-175			OUTU	0.00	62.87	37.13	0.00	94.42	5.58	2.9	59.393
L-195			OUTU	0.00	93.62	6.38	0.00	99.32	0.68	8	207.32
L-199	WP	WP	INW	48.62	35.84	15.54	56.53	41.66	1.81	4.6596	3.7872
L-213	WP	WP	OUTU	10.41	74.21	15.38	12.09	86.13	1.79	3.9	55.911
L-217			OUTU	0.00	80.96	19.04	0.00	97.70	2.30	1	83.714
L-218	WP	WP	OUTU	2.77	72.38	24.85	3.57	93.23	3.20	5.3	93.393
L-223			OUTU	0.00	82.72	17.28	0.00	97.95	2.05	2.8	237.14
Hook Granite, Zambia											
HOOK-1	VA-	III	INW-INV	8.89	8.86	82.25	34.24	34.10	31.66	2.9177	2.242
L-175			OUTU							2.9	59.393
L-195				0.00	93.62	6.38	0.00	99.32	0.68	8	207.32
L-199	WP	WP	INW	48.62	35.84	15.54	56.53	41.66	1.81	4.6596	3.7872
L-213	WP	WP	OUTU	10.41	74.21	15.38	12.09	86.13	1.79	3.9	55.911
L-217			OUTU							1	83.714
L-218	WP	WP	OUTU	2.77	72.38	24.85	3.57	93.23	3.20	5.3	93.393
L-223			OUTU							2.8	237.14
L-238			OUTU							2.6	96.786
L-241	VA-	III	INW-INV	8.22	8.88	82.90	32.38	34.97	32.65	2.4061	2.6586
L-249			OUTU	0.00	77.19	22.81	0.00	97.13	2.87	2.3	66.054
L-257	WP	WP	OUTU	3.44	50.74	45.81	5.86	86.34	7.80	2.5	37.625
L-263			OUTU							2.6	41.571
39	VA-	VA-	INW-INV	6.57	4.93	88.50	32.29	24.22	43.49	5.9	3.5714
40i	VA-	VA	INV	16.95	6.01	77.04	55.28	19.60	25.13	2.7	1.8571
40ii	VA-	III	INW-INV	12.81	11.53	75.67	40.15	36.13	23.72	5.2	4.7143
46	VA-	VA-	INW-INV	7.23	5.52	87.24	33.67	25.71	40.61	5.3	4
50	VA-	III	OUTD-INV	6.25	6.67	87.08	28.91	30.84	40.26	10.7	4.5714
53	VA-	II	INV-INW	3.90	4.88	91.22	21.79	27.24	50.97	4.8	3.5714
57	VA-	VA-	INW-INV	11.73	8.32	79.96	41.83	29.66	28.52	4.8	3.7143
58	VA-	III	INV-INW	7.29	7.65	85.05	31.09	32.64	36.27	3	3
Kalengwa Area, Zambia											
13	VA-	WP	INW	19.11	17.20	63.69	44.78	40.30	14.93	3	3.8571
17	VA-	WP	INW	15.73	14.15	70.12	42.63	38.37	19.01	3.2	3.4286
25	VA-	III-WP	INV	8.25	16.09	75.65	25.86	50.43	23.71	1.4	1.8571
26	OF	WP	OUTD	64.94	30.17	4.89	67.93	31.56	0.51	24.3	6.8571
Mwinilunga-Kalene Area, Zambia											
L-020			OUTU							1.9	104.5
L-023			OUTU							1.3	87.464
L-024			OUTU							1.1	559.11
L-025			OUTU							1	35.071
L-028			OUTU							1.6	136.07
L-030	VA-	II	INV	4.21	3.91	91.87	24.33	22.61	53.06	1.6168	1.7706
L-047			OUTU							10.5	97.857
L-060	VA-	III-VA	II-INV	7.10	6.08	86.82	32.50	27.80	39.71	0.9536	1.661
L-065			OUTU							0.8	101.43
L-358			OUTU							1.3	140.18
L-366			OUTU							1.9	125.89
L-369			OUTU							2.5	33
L-373	WP	WP	OUTU	2.91	60.90	36.19	4.31	90.32	5.37	0.8	30.446
L-380	WP	WP	OUTU	0.36	69.06	30.58	0.49	95.29	4.22	2.8	63.446
Nepheline Sodalite Quarry, Zambia											
L-032			OUTU							2.3	137.32
L-037			OUTU							10.1	72.429
L-044			OUTU							17.8	53
L-045	WP	WP	INW	4.68	57.19	38.12	7.13	87.07	5.80	9.7615	13.861
L-046			OUTU							8.2	63.393

Sample	Rb/10HfTa	Rb/30HfTa	Nb-Ta	norm Hf	norm Tax3	norm Rb/10	norm Hf	norm Tax3	norm Rb/30	Nb	Ta
Nchanga Granite, Zambia											
L-075	VA	II	INV	2.39	4.20	93.41	15.00	26.37	58.63	1.6788	1.1558
L-077			OUTU							2.2	107.32
L-150			OUTU							2.8	315.36
L-151	WP-	III	OUTU	4.21	24.72	71.07	11.69	68.58	19.72	9.1	19.375
L-154	WP-	WP-III	OUTU	1.86	15.52	82.62	7.26	60.52	32.22	5.8	14.25
L-155			OUTU							1.3	52.018
L-158	WP-	II	OUTU	2.01	23.63	74.36	6.08	71.44	22.48	1.6	11.75
L-160			OUTU	0.00	48.76	51.24	0.00	90.49	9.51	3.2	39.875
L-166	VA-	III	OUTU	3.70	12.02	84.27	15.34	49.77	34.89	1.8	4.7321
L-170			OUTU							7.9	66.411
L-172	VA-	III-II	INW	4.14	7.99	87.87	19.79	38.21	42.00	8.5	4.5669
28	VA-	VA-III	INW-INV	8.17	6.46	85.37	35.26	27.88	36.86	6.4	4.1429
29	VA-	III	INW-INV	5.70	6.27	88.03	27.44	30.18	42.38	4.6	3.1429
Serenje, Zambia											
32	VA-	VA	INV	3.39	2.29	94.32	22.43	15.14	62.43	1.2	1.2857
33	VA-	III	OUTU-INV	4.55	8.19	87.25	21.20	38.16	40.64	1.9	3.4286
35	VA-	VA	INV	9.41	3.77	86.82	43.06	17.22	39.71	0.6	0.5714
Kamanjab Inlier, Namibia											
L-834	WP	WP	OUTU	0.87	70.45	28.68	1.18	94.96	3.87	2	110.36
L-842	WP	WP	OUTU	0.62	79.56	19.82	0.76	96.83	2.41	1.6	89.821
L-843	WP-	WP	OUTU	4.48	33.87	61.65	10.07	76.08	13.85	2	14.214
L-846			OUTU							1.6	71.964
L-849	WP	WP	OUTU	0.61	61.20	38.18	0.93	93.25	5.82	2.7	48.089
L-850	WP	WP	OUTU	2.44	52.46	45.10	4.11	88.30	7.59	1.5	48.75
L-864	VA-	II	INV	3.80	6.85	89.34	19.42	34.98	45.60	1.1938	1.1846
L-868	VA-	II	INV	2.10	4.15	93.76	13.44	26.54	60.02	1.5329	0.7892
L-875			OUTU							2.3	109.46
L-878			OUTU							1.9	80.143
L-895			OUTU							0.7	140.89
L-904			OUTU							1.8	10.268
L-908	VA-	III	INV	5.45	8.52	86.02	24.15	37.75	38.10	1.5507	1.5128
L-917	VA-	II	INV	3.26	6.65	90.09	17.25	35.14	47.61	1.5172	1.3185
L-920			OUTU							1.5	26.982
L-922			OUTU							2.7	88.036
L-938	WP	WP	OUTU	2.24	80.16	17.60	2.66	95.25	2.09	1.9	54.946
L-939			OUTU							1.1	110.71
L-940			OUTU							1.2	113.93
L-943	VA-	VA	INV	6.51	3.05	90.44	35.00	16.39	48.60	0.7212	0.7333
L-945			OUTU							1.8	87.375
L-951			OUTU							2.4	69.339
L-955			OUTU							1.7	61.125
L-956			OUTU							1.4	424.46
L-957	WP-	WP	OUTU	4.79	32.30	62.91	11.05	74.45	14.50	2	10.268
L-966	VA-	III	INV	5.70	6.60	87.70	27.05	31.32	41.63	1.7104	1.7212
L-968	WP	WP	OUTU	2.26	61.96	35.78	3.33	91.39	5.28	1.5	37.375
L-969	WP	WP	OUTU	2.26	56.67	41.08	3.58	89.90	6.52	2.4	86.054
L-973	WP	WP	OUTU	2.87	53.67	43.46	4.71	88.15	7.14	1.9	52.143
L-976	WP-	WP	OUTU	2.98	37.03	59.99	6.47	80.49	13.04	2.1	19.107
L-978	VA-	VA	INV	9.38	5.63	84.99	39.88	23.97	36.15	1.6898	1.462
L-982			OUTU							1.2	76.804
L-985	VA-	VA	OUTD-INV	3.43	1.31	95.26	24.03	9.18	66.80	0.6062	0.2684
L-987a	VA-	VA	OUTD	6.54	1.08	92.38	38.79	6.42	54.79	0.1893	0.0403
L-987b			OUTU							0.4	406.07
L-992	VA-	VA	INV	3.19	1.65	95.16	22.21	11.49	66.30	0.3362	0.1843
L-993	VA-	VA	INV	5.60	4.15	90.25	29.82	22.12	48.07	1.1471	0.8393
L-996	VA-	III	INV	5.10	5.51	89.39	26.08	28.20	45.72	1.3872	1.1853
L-997	WP-	WP	OUTU	5.08	40.29	54.63	10.00	79.25	10.75	2.2	15.804
L-998			OUTU							1.5	90
L-999	WP-	WP	OUTU	0.92	70.91	28.17	1.23	94.99	3.77	2	55.946
L-1000			OUTU							1.8	117.07
L-1002	VA-	III	OUTU	4.21	20.33	75.46	13.13	63.35	23.52	2.2	7.6964
L-1003	WP	WP	OUTU	1.76	65.14	33.09	2.51	92.78	4.71	1.6	45.304
L-1013			OUTU							1.6	68.893

Sample	Rb/10HfTa	Rb/30HfTa	Nb-Ta	norm Hf	norm Tax3	norm Rb/10	norm Hf	norm Tax3	norm Rb/30	Nb	Ta
Ugab River 2, Namibia											
L-793	WP-	WP	OUTU	1.05	49.97	48.98	1.88	89.36	8.76	7.8	40.643
Khorixas Inlier, Namibia											
Oas Farm, Namibia											
L-668	WP-	WP	INW	3.88	60.98	35.15	5.67	89.19	5.14	19.3	33.321
L-669	WP-	WP	INW	9.89	44.24	45.87	16.84	75.35	7.81	20.436	17.562
L-670			OUTU-NEAR INW							45.8	105.71
L-675			OUTU							34.5	340
L-693	WP-	WP	INW	6.06	31.96	61.97	13.71	72.27	14.01	10.526	7.0606
L-697	WP-	WP	OUTU-NE	0.45	84.79	14.76	0.52	97.78	1.70	43.2	154.11
L-698			OUTU							12.4	131.61
L-713	WP	WP	OUTU	0.85	64.81	34.34	1.23	93.80	4.97	7.1	35.054
L-715			OUTU	0.00	74.79	25.21	0.00	96.74	3.26	2.5	55.571
L-716	VA-	VA	INV	20.66	6.90	72.44	59.37	19.82	20.81	1.5874	1.0463
L-1019	WP-	WP	INW	24.20	21.03	54.77	47.73	41.47	10.80	4.6873	3.0241
Lofdal Farm, Namibia											
L-722			OUTU							1.3	327.5
L-728	WP-	WP	INW	29.23	34.82	35.95	43.21	51.47	5.31	3.3008	3.6028
L-740			OUTU							56.3	163.93
L-741			OUTU							33.7	181.43
L-742			OUTU							2.6	102.68
L-1022			OUTU							24.9	134.82
L-1025	WP	WP	OUTD-INV	8.35	83.33	8.31	9.03	90.07	0.90	142.54	48.008
L-1027			OUTU							22	134.64
L-1032	WP	WP	OUTU	4.74	90.79	4.48	4.93	94.60	0.47	0.9	32.179
Mesopotamie Farm, Copper Vallei Mine, Namibia											
L-784	WP	WP	OUTU	0.79	65.50	33.71	1.14	94.02	4.84	2.3	59.518
Summas Mountains, Namibia, (Volcanic Rocks)											
L-789			OUTU							14.9	182.32
L-791	WP-	WP	INW	2.87	30.84	66.29	7.12	76.44	16.43	13	10.411
Otjiwarongo Environs, Namibia											
L-1039a	VA-	VA	INV	2.25	0.42	97.33	18.13	3.38	78.49	0.2095	0.1147
AVMIN Pegmatitic Granitoids, Namibia											
L-808	VA-	II	INV	2.29	7.11	90.61	12.38	38.51	49.11	1.3919	1.7372
Grootfontein Inlier, Otavi Mountains, Namibia											
L-1014										0.2549	
L-1042Y	WP-	WP	OUTU	1.91	42.55	55.54	3.81	85.09	11.10	1.7	38.554
L-1043Z	WP	WP	OUTU	0.84	54.20	44.97	1.41	91.04	7.55	1.7	52.804
L-1045Yb			OUTU							2.4	425.36
Okatjepuiko, Witvlei, Namibia											
L-626			OUTU							3	55.107
L-633			OUTU							1.3	320
L-635			OUTU							1.9	128.93
L-637	WP	WP	OUTU	2.96	91.98	5.06	3.10	96.37	0.53	2.9	49.054
L-638	VA-	VA	INV	17.16	5.98	76.86	55.67	19.39	24.93	1.7538	0.7226
L-816	WP	WP	OUTU	1.05	86.39	12.56	1.19	97.40	1.42	3.2	46.946
Owka River, Botswana											
L-602			OUTU							2.6	75.982
STANDARDS											
Tsucany	OF	WP	INW-INV	71.87	26.71	1.41	72.80	27.06	0.14	20	2.1
Smartville	OF	WP	INV	72.24	25.71	2.04	73.60	26.20	0.21	14	1.4
Mar-45			INW	43.35	54.75	1.90	44.10	55.71	0.19	42	3.2
Troodos	OF	WP	INV	66.12	25.71	8.16	71.37	27.75	0.88	5	0.35
Oman	OF	VA	INV	80.73	10.39	8.88	87.74	11.29	0.97	2	0.13
Little Port										6	
Jamaica	VA-	III-VA?	INV	11.01	9.03	79.97	39.27	32.20	28.53	9	0.79
Chile	VA-	III-VA?	INV	8.51	7.80	83.69	34.49	31.60	33.91	17	1.75
Oslo	WP-	WP	INW	14.03	30.07	55.90	28.24	60.51	11.25	226	15
sabaloka	VA-	WP	INW	23.19	13.47	63.34	53.94	31.32	14.73	56	3
skaergaard	VA-	WP	INW	16.68	10.42	72.90	48.51	30.29	21.20	24	1.54
mull	VA-	VA	INW	17.79	7.58	74.63	54.19	23.08	22.73	21	2.11
ascension	WP	WP	INW	34.62	39.56	25.82	45.10	51.54	3.36	168	16

Sample	Rb/10HfTa	Rb/30HfTa	Nb-Ta	norm Hf	norm Tax3	norm Rb/10	norm Hf	norm Tax3	norm Rb/30	Nb	Ta
Yunnan	VA-	VA	INV	6.34	2.35	91.31	35.58	13.18	51.24	6	0.6
Gabug	VA-	III	OUTU	4.26	8.41	87.33	19.90	39.29	40.81	16	2.6
SWEngland	VA-	III	II	1.83	2.73	95.44	12.98	19.35	67.67	13	1.55
Novate	VA-	II	II	3.47	13.57	82.96	13.70	53.56	32.75	4	1.89
Barousse	VA-	III	II	1.80	12.81	85.39	7.79	55.33	36.89	10	1.8
Vedrette	VA-	III	II	4.71	11.47	83.82	19.16	46.71	34.13	16	2.6
Querigut	VA-	III	II	4.62	8.09	87.29	21.56	37.72	40.72	14	2.45
Oman	VA-	III	INV	8.79	8.79	82.43	34.03	34.03	31.93	8	0.9
Bolivia	VA-	II	INV	2.46	2.87	94.67	16.62	19.38	64.00	12	1.4

Maybe a lot of the samples that plot as a group on the Nb-Ta diagram might be of a similar origin. These may be a particular type of rocks from anorogenic environment. They are the ones with OUTU classification.

WP	Within-Plate Granitoids
VA	Volkanic Arc Granitoids
II	Type II Collisional Granitoids
VA-	Plots in Volcanic Arc Field but might be Collisional Granitoid
WP-	Plots in Within-Plate Field but might be Collisional Granitoid
OF	Oceanic Floor Granitoid

Table A55 Results of Determination for Environment of Emplacement of Granitoids Based on Methodology of Batchelor & Bowden, 1985

Sample	RESULT	Sample	RESULT	Sample	RESULT	Sample	RESULT	Sample	RESULT
13	Late Orogenic	L-1010	Late Orogenic	L-359	Late Orogenic	L-715	Syn-Collision	L-967	Late Orogenic
17	Late Orogenic	L-1011	Late Orogenic	L-360	Late Orogenic	L-716	Late Orogenic	L-968	Late Orogenic
25	out left	L-1012	Late Orogenic	L-361	Post-Collision Uplift	L-722	off upper left	L-969	off left
26	Anorogenic	L-1013	Late Orogenic	L-362	Pre-Plate Collision	L-728	Syn-Collision	L-971	Anorogenic
28	out left	L-1014	Pre-Plate Collision	L-363	Post-Collision Uplift	L-729	Late Orogenic	L-973	Syn-Collision
29	Late Orogenic	L-1016	1 off right	L-364	Anorogenic	L-740	off left	L-975	Anorogenic
32	Anorogenic	L-1016a	1 off right	L-365	Late Orogenic	L-741	off left	L-976	Anorogenic
33	Late Orogenic	L-1019	Anorogenic	L-366	Late Orogenic	L-742	Late Orogenic	L-977	Anorogenic
35	Late Orogenic	L-1020	Late Orogenic	L-367	Mantle Fractionates	L-754	Mantle Fractionates	L-978	Anorogenic
39	Anorogenic	L-1021	Late Orogenic	L-368	Late Orogenic	L-759	Late Orogenic	L-979	Late Orogenic
46	Anorogenic	L-1022	off left	L-369	Syn-Collision	L-772	Anorogenic	L-980	Late Orogenic
50	Late Orogenic	L-1023	off left	L-370	Anorogenic	L-773	Late Orogenic	L-982	Late Orogenic
53	5 limit 4	L-1024a	off upper left	L-371	Late Orogenic	L-783	Late Orogenic	L-983	Late Orogenic
57	far out left	L-1024c	off upper left	L-372	Post-Collision Uplift	L-784	Syn-Collision	L-985	Syn-Collision
58	Late Orogenic	L-1025	off left	L-373	Syn-Collision	L-789	Late Orogenic	L-987a	off left
40i	Late Orogenic	L-1027	off left	L-374	Late Orogenic	L-791	Anorogenic	L-987b	off left
40ii	Late Orogenic	L-1032	off left	L-375	Anorogenic	L-791	Anorogenic	L-990	off left
BK10a	Late Orogenic	L-1037	Late Orogenic	L-376	off left	L-793	Late Orogenic	L-991	off left
BK12a	Syn-Collision	L-1038	Late Orogenic	L-377	Anorogenic	L-797	Anorogenic	L-992	off left
BK14a	Mantle Fractionates	L-1039	Anorogenic	L-378	Anorogenic	L-798	Syn-Collision	L-993	Late Orogenic
BK16b	Mantle Fractionates	L-139	Mantle Fractionates	L-379	Anorogenic	L-799	Late Orogenic	L-994	Late Orogenic
BK19a	3 triple limit	L-150	Late Orogenic	L-380	Anorogenic	L-802	Syn-Collision	L-995	off left
BK1a	Pre-Plate Collision	L-151	Mantle Fractionates	L-400B	Late Orogenic	L-804	1 off right	L-996	Late Orogenic
BK1b	Pre-Plate Collision	L-153	Mantle Fractionates	L-402	Pre-Plate Collision	L-808	Late Orogenic	L-997	Anorogenic
BK1c	Syn-Collision	L-154	Mantle Fractionates	L-403	Late Orogenic	L-809	Late Orogenic	L-998	Late Orogenic
BK24a	Pre-Plate Collision	L-155	Mantle Fractionates	L-405	Pre-Plate Collision	L-810	Late Orogenic	L-999	Late Orogenic
BK25a	Anorogenic	L-157	Mantle Fractionates	L-406	off left	L-812	4-2	LJ1	Late Orogenic
BK27a	Late Orogenic	L-158	Mantle Fractionates	L-407	Post-Collision Uplift	L-813	Late Orogenic	LL1	Syn-Collision
BK29a	Post-Collision Uplift	L-159	Syn-Collision	L-408	Syn-Collision	L-814	1 off right	LL10	off left
BK32a	Late Orogenic	L-160	Syn-Collision	L-409	Late Orogenic	L-815	Late Orogenic	LL11	Late Orogenic
BK32b	Pre-Plate Collision	L-161	Late Orogenic	L-410	Mantle Fractionates	L-816	Syn-Collision	LL13	off upper right
BK39a	Anorogenic	L-162	Late Orogenic	L-411	off upper left	L-832	Anorogenic	LL14	off left
BK39b	Mantle Fractionates	L-163	off left	L-416	Mantle Fractionates	L-834	Late Orogenic	LL15	off left
BK3a	Pre-Plate Collision	L-166	Late Orogenic	L-420	Late Orogenic	L-835	Late Orogenic	LL16	Syn-Collision
BK423a	2-4	L-167	off left	L-421	Late Orogenic	L-836	Late Orogenic	LL17a	Late Orogenic
BK425a	Mantle Fractionates	L-168	Mantle Fractionates	L-433	off left	L-838	Late Orogenic	LL17b	Post-Collision Uplift
BK425c	Mantle Fractionates	L-170	Mantle Fractionates	L-434	Syn-Collision	L-839	Post-Orogenic	LL18	Late Orogenic
BK428a	Syn-Collision	L-172	Anorogenic	L-435	Late Orogenic	L-840	Late Orogenic	LL2a	Anorogenic
BK435b	Pre-Plate Collision	L-173	Anorogenic	L-436	Late Orogenic	L-842	Late Orogenic	LL2b	Anorogenic
BK439a	Late Orogenic	L-175	2 joint	L-437	Late Orogenic	L-843	Post-Orogenic	LL3a	Anorogenic
BK43a	Syn-Collision	L-181	Pre-Plate Collision	L-438	off left	L-844	Late Orogenic	LL3b	Anorogenic
BK445a	Pre-Plate Collision	L-195	Late Orogenic	L-439	Anorogenic	L-846	Late Orogenic	LL4	Late Orogenic
BK445b	Mantle Fractionates	L-200B	Late Orogenic	L-440	Post-Collision Uplift	L-849	Anorogenic	LL5	Pre-Plate Collision
BK446a	Pre-Plate Collision	L-207	Anorogenic	L-441	Late Orogenic	L-850	Syn-Collision	LL9	1 off right
BK452a	Pre-Plate Collision	L-208	Anorogenic	L-442	Mantle Fractionates	L-855	Anorogenic	MUF1/15	Late Orogenic
BK45a	Mantle Fractionates	L-209	off left	L-443	Mantle Fractionates	L-857	Syn-Collision	MUF2/04	Pre-Plate Collision
BK4c	Mantle Fractionates	L-210	Anorogenic	L-444	Pre-Plate Collision	L-863	Post-Collision Uplift	MUF3/02	off left
BK5a	Pre-Plate Collision	L-212	Anorogenic	L-458	Anorogenic	L-864	Pre-Plate Collision	MUF3/03	off left
CH5/01	Late Orogenic	L-213	Anorogenic	L-459	Pre-Plate Collision	L-865	Post-Collision Uplift	MUF3/09	off left
CH5/05	Late Orogenic	L-214	Anorogenic	L-460	Mantle Fractionates	L-868	Late Orogenic	MUF3/11	off left
HOOK-1	Late Orogenic	L-215	Anorogenic	L-461	Late Orogenic	L-874	Late Orogenic	MUF3/13	off left
HOOK-2	Late Orogenic	L-217	Mantle Fractionates	L-462	Syn-Collision	L-874	1 off right	MUF4/01	off left
L-005A	Syn-Collision	L-218	Late Orogenic	L-463	Pre-Plate Collision	L-875	Late Orogenic	MUF4/02	off left
L-020	Anorogenic	L-222	Post-Orogenic	L-464	off left	L-877	Late Orogenic	MUF4/03	off left
L-023	3 limit 2	L-223	4 limit w/2	L-465	off left	L-878	Late Orogenic	MUF4/09	off left
L-024	Pre-Plate Collision	L-224	Anorogenic	L-466	Late Orogenic	L-895	off left	MUF4/17	off left
L-025	Syn-Collision	L-228	off upper left	L-467	Anorogenic	L-898	Late Orogenic	N11b	Mantle Fractionates
L-026	Syn-Collision	L-237	Syn-Collision	L-597A	Late Orogenic	L-899	Syn-Collision	N12d	Mantle Fractionates
L-027	Pre-Plate Collision	L-238	Syn-Collision	L-600A	Anorogenic	L-900	Late Orogenic	N50b	Pre-Plate Collision
L-028	Post-Collision Uplift	L-239	Late Orogenic	L-602	Syn-Collision	L-902	Anorogenic	N52a	Syn-Collision
L-029	Pre-Plate Collision	L-242	Mantle Fractionates	L-605	Anorogenic	L-903	Anorogenic	N8a	Pre-Plate Collision
L-030	4, corner	L-248	Pre-Plate Collision	L-606	Syn-Collision	L-904	Anorogenic		
L-032	Pre-Plate Collision	L-248A	Late Orogenic	L-608	Mantle Fractionates	L-905	Anorogenic		
L-036	5 on limit	L-249	Syn-Collision	L-609	1 limit 4	L-906	Anorogenic		
L-037	Mantle Fractionates	L-257	Late Orogenic	L-625	Late Orogenic	L-907	Syn-Collision		
L-037	off left	L-259Brow	Late Orogenic	L-626	Late Orogenic	L-908	Anorogenic		
L-038	off left	L-259Grey	Late Orogenic	L-633	Pre-Plate Collision	L-909	Anorogenic		
L-039	off left	L-263	Post-Collision Uplift	L-635	Late Orogenic	L-910	Anorogenic		
L-040	off left	L-268	Mantle Fractionates	L-637	Syn-Collision	L-911	Mantle Fractionates		
L-041	off left	L-269	Mantle Fractionates	L-638	Anorogenic	L-912	Pre-Plate Collision		
L-044	off left	L-273	Pre-Plate Collision	L-641	Post-Collision Uplift	L-917	Late Orogenic		
L-045	off left	L-279	Pre-Plate Collision	L-645	off left	L-919	1 off right		
L-046	off left	L-311	Post-Collision Uplift	L-648	Anorogenic	L-920	Anorogenic		
L-047	Late Orogenic	L-321	Mantle Fractionates	L-649	Anorogenic	L-922	Late Orogenic		
L-049	off left	L-322	Anorogenic	L-668	Late Orogenic	L-923	Late Orogenic		
L-050	off left	L-323	Anorogenic	L-669	Late Orogenic	L-924	Syn-Collision		
L-060	off left	L-324	Late Orogenic	L-670	off left	L-938	Syn-Collision		
L-060	off left	L-325	Late Orogenic	L-675	Late Orogenic	L-939	Late Orogenic		
L-060	Anorogenic	L-341	Post-Collision Uplift	L-676	Late Orogenic	L-940	Pre-Plate Collision		
L-063	off left	L-343	Pre-Plate Collision	L-691	Post-Collision Uplift	L-943	Anorogenic		
L-064	off left	L-344	Post-Collision Uplift	L-693	Anorogenic	L-945	Late Orogenic		
L-065	off left	L-345	Late Orogenic	L-694	off left	L-946	Late Orogenic		
L-076	Late Orogenic	L-346	Late Orogenic	L-695	off left	L-948	Late Orogenic		
L-077	Late Orogenic	L-347	off upper left	L-697	off left	L-951	off left		
L-078	Post-Collision Uplift	L-348	Late Orogenic	L-698	Anorogenic	L-952	Anorogenic		
L-079	Late Orogenic	L-349	Late Orogenic	L-699	off left	L-955	Anorogenic		
L-1000	Late Orogenic	L-352	Syn-Collision	L-700B	Late Orogenic	L-956	Late Orogenic		
L-1002	Anorogenic	L-353	Late Orogenic	L-708	off left	L-957	Pre-Plate Collision		
L-1003	Late Orogenic	L-354	Late Orogenic	L-712	Post-Orogenic	L-958	Pre-Plate Collision		
L-1005	Syn-Collision	L-355	Late Orogenic	L-713	Anorogenic	L-963	1 off right		
L-1007	Post-Collision Uplift	L-357	Late Orogenic	L-714	Late Orogenic	L-965	Anorogenic		
L-1009	Late Orogenic	L-358	Post-Collision Uplift	L-714	Anorogenic	L-966	Anorogenic		

Appendix A56 TECTONIC ENVIRONMENT OF MAFIC ROCKS, LUFILIAN ARC PROJECT

Sample	Ca+Mg	Pierce TiZrY	Pierce ZrTi	Meschede NbZrY	Shervais	Shervais2	Wood HfThTa	Pierce TiZrSr	interp name
Kasempa, Zambia, Dale Janneker's									
CH5/01	4.39	CAB	off	W-P Alk Bas and W-P Tho	W-P Alk Bas			off	wpab
CH5/05	6.86	off	off	W-P Alk Bas	W-P Alk Bas			off	wpab
MUF1/15	8.53	W-P Bas	off	W-P Alk Bas	W-P Alk Bas			MORB	wpab
MUF2/04	15.82	W-P Bas	off	W-P Alk Bas	Aoff			MORB	wpab
MUF3/02	11.09	W-P Bas	off	W-P Alk Bas and W-P Tho	Aoff			off	wpab
MUF3/03	11.08	W-P Bas	off	W-P Alk Bas and W-P Tho	Aoff			off	wpab
MUF3/09	7.09	off	off	W-P Alk Bas and W-P Tho	A			off	wpab
MUF3/11	11.81	W-P Bas	off	W-P Alk Bas and W-P Tho	W-P Alk Bas			off	wpab
MUF3/13	12	W-P Bas	off	W-P Alk Bas	Aoff			MORB	wpab
MUF4/01	15.51	W-P Bas	off	W-P Alk Bas	Aoff			off	wpab
MUF4/02	12.8	W-P Bas	off	W-P Alk Bas and W-P Tho	Aoff			MORB	wpab
MUF4/03	14.05	W-P Bas	off	W-P Alk Bas	Aoff			MORB	wpab
MUF4/09	15.08	W-P Bas	OFBas	W-P Alk Bas and W-P Tho	A			off	wpab
MUF4/17	17.49	W-P Bas	off	W-P Alk Bas	W-P Alk Bas			off	wpab
West Lusaka, Zambia									
L-181	17.58	MORB, I-A Thol and CAB	B	E-Type MORB	E			MORB	emor
L-209	18.97	MORB, I-A Thol and CAB	off	E-Type MORB	MORB and W-P Tho	OI+AB		off	emor
L-224	0.69	off	off	W-P Alk Bas	W-P Alk Bas			off	wpab
Hook Granite, Zambia									
L-347	25.11	CAB	off	W-P Thol and VAB	E			I-A Thol	vab
L-405	14.28	CAB	CAB	E-Type MORB	W-P Alk Bas			CAB	emor
L-406	16.72	MORB, I-A Thol and CAB	B	E-Type MORB	MORB and W-P Thol			I-A Thol	emor
L-407	9.76	off	off	W-P Thol and VAB	A			off	WPT+VAB
L-411	48.52	CAB	off	W-P Alk Bas and W-P Tho	A			CAB	WPAB+WPT-CAB
L-416	19.7	MORB, I-A Thol and CAB	B	E-Type MORB	E			I-A Thol	emor
L-433	12.9	CAB	off	W-P Thol and VAB	MORB and W-P Tho	MORB+BAB		MORB	wpt
L-437	7.88	CAB	off	W-P Alk Bas and W-P Tho	A			off	WPAB+WPT
L-438	13.75	off	off	W-P Alk Bas	A			off	wpab
L-440	11.96	off	off	W-P Alk Bas	W-P Alk Bas	OI+AB		CAB	wpab
L-444	11.04	MORB, I-A Thol and CAB	off	E-Type MORB	A			MORB	emor
L-463	14.94	W-P Bas	off	W-P Thol and VAB	A			MORB	wpt
Kalengwa Area, Zambia									
L-311	10.01	CAB	off	W-P Thol and VAB	E			off	arc
25	9.19	W-P Bas	off	E-Type MORB	Aoff		Alk-Within Plate	I-A Thol	wpab

Sample	Ca+Mg	Pierce TiZrY	Pierce ZrTi	Meschede NbZrY	Shervais	Shervais2	Wood HfThTa	Pierce TiZrSr	interp name
Mwinilunga-Kalene Area, Zambia									
L-024	13.67	MORB, I-A Thol and CAB	OFBas	E-Type MORB	E			off	emor
L-049	15.92	MORB, I-A Thol and CAB	off	W-P Alk Bas	W-P Alk Bas			I-A Thol	wpab
L-050	15.66	MORB, I-A Thol and CAB	off	E-Type MORB	W-P Alk Bas			MORB	emor
L-060	15.6	off	off	W-P Alk Bas and W-P Tho	Aoff			off	wpab
L-060	15.73	W-P Bas	off	W-P Alk Bas and W-P Tho	A			off	wpt
L-063	15.66	off	CAB	off	A			off	?
L-064	15.14	off	CAB	W-P Alk Bas	MORB and W-P Thol			off	wpab
L-065	21.02	CAB	CAB	W-P Thol and VAB	MORB and W-P Tho	AT		CAB	arc
L-372	10.24	off	off	off	A			CAB	?
Nepheline Sodalite Quarry, Zambia									
L-032	8.08	off	off	W-P Alk Bas	E			CAB	wpab
Nchanga Granite, Zambia									
L-150	10.77	MORB, I-A Thol and CAB	OFBas	E-Type MORB	E			off	emor
L-161	8.69	off	off	W-P Alk Bas and W-P Tho	A			off	WPAB-WPT
L-163	15.95	MORB, I-A Thol and CAB	OFBas	E-Type MORB	MORB and W-P Tho	MORB+BAB		MORB	emor
L-167	12.98	off	off	W-P Alk Bas	W-P Alk Bas			off	wpab
Kamanjab Inlier, Namibia									
L-895	7.66	CAB	CAB	W-P Thol and VAB	E			MORB	WPT+VAB-CAB
L-920	0.51	off	off	W-P Alk Bas	W-P Alk Bas			off	wpab
L-958	15.26	MORB, I-A Thol and CAB	CAB	N-Type MORB and VAB	E	AT		MORB	arc
L-967a	0				E				?
Cu-Mineralized System 3, Namibia									
L-987a	14.63	MORB, I-A Thol and CAB	OFBas	E-Type MORB	E			MORB	emor
L-987b	16.94	MORB, I-A Thol and CAB	off	off	A			off	MORB-IAT-CAB
L-990	15.81	CAB	off	W-P Alk Bas and W-P Tho	W-P Alk Bas			CAB	wpab
L-991	20.77	MORB, I-A Thol and CAB	B	E-Type MORB	E	AT		I-A Thol	arc
L-992	14.95	MORB, I-A Thol and CAB	Low K Thol	E-Type MORB	MORB and W-P Tho	AT	VAB	off	emor
L-995	18.03	MORB, I-A Thol and CAB	off	off	MORB and W-P Tho	CFB		off	MORB-WPT

Sample	Ca+Mg	Pierce TiZrY	Pierce ZrTi	Meschede NbZrY	Shervais	Shervais2	Wood HfThTa	Pierce TiZrSr	interp name 3/4
Khorixas Inlier, Namibia; Oas Farm									
L-668	2.52	off	off	W-P Alk Bas	E		off	off	wpab
L-670	3.75	off	off	off	A		off	off	?
L-675	1.07	off	off	W-P Alk Bas	MORB and W-P Thol		off	off	wpab
L-676	3.29	off	off	W-P Alk Bas	MORB and W-P Thol			CAB	wpab
L-691	10.66	W-P Bas	off	W-P Alk Bas and W-P Tho	MORB and W-P Tho	OI+AB		CAB	wpt
L-694	3.49	off	off	W-P Alk Bas	A			off	wpab
L-695	8.11	W-P Bas	off	W-P Alk Bas and W-P Tho	W-P Alk Bas	OI+AB		MORB	wpab
Sample	Ca+Mg	Pierce TiZrY	Pierce ZrTi	Meschede NbZrY	Shervais	Shervais2	Wood HfThTa	Pierce TiZrSr	interp name
L-697	3.05	off	off	W-P Alk Bas	A		off	off	wpab
L-708	27.27	off	off	W-P Alk Bas and W-P Tho	MORB and W-P Tho	AT		off	wpab
Lofdal Farm, Namibia									
L-740	1.24	off	off	off	E		off	off	?
L-741	3.89	off	off	off	W-P Alk Bas			off	wpab
L-754	14.03	MORB, I-A Thol and CAB	OFBas	E-Type MORB	Arc Bas	AT		MORB	arc
L-1022	2.28	off	off	off	A		off	off	?
L-1023	18.6	MORB, I-A Thol and CAB	B	E-Type MORB	E	AT		I-A Thol	emor
L-1025	20.2	off	off	off	Arc Bas	AT-CAB	off	off	arc
L-1027	5.92	off	off	off	A		off	off	?
L-1032	16.06	MORB, I-A Thol and CAB	OFBas	E-Type MORB	MORB and W-P Tho	CFB-MORB+BAB		MORB	emor
Otjiwarongo Environs, Namibia									
LL10	5.74	off	off	W-P Alk Bas	E		off	off	wpab
LL13	21	CAB	CAB	N-Type MORB and VAB	W-P Alk Bas			CAB	arc
LL14	4	off	off	W-P Alk Bas	A			off	wpab
Okatjepuiko, Witvlei, Namibia									
L-633	13.86	MORB, I-A Thol and CAB	OFBas	W-P Thol and VAB	E			MORB	arc
L-635	6.57	CAB	off	W-P Alk Bas and W-P Tho	W-P Alk Bas			off	wpab
L-641	13.81	off	off	off	W-P Alk Bas	OI+AB		off	wpab
L-645	6.29	W-P Bas	off	W-P Thol and VAB	A			off	wpt
Barbara Seth's Samples, NW Namibia									
BK446a	8.81	CAB	CAB	W-P Alk Bas and W-P Thol	E			CAB	wpt
BK425a	8.43	CAB	off	W-P Alk Bas and W-P Thol	MORB and W-P Thol			CAB	wpt
N50b	11.68	CAB	off	W-P Alk Bas and W-P Thol	MORB and W-P Thol		VAB	CAB	wpt
BK5a	11.05	CAB	CAB	W-P Thol and VAB	MORB and W-P Thol			CAB	wpt
BK32a	5.55	off	off	E-Type MORB	W-P Alk Bas			off	EMORB-WPAB
BK435b	7.16	CAB	CAB	W-P Thol and VAB	W-P Alk Bas			CAB	WPT+VAB-WPAB
BK439a	4.38	off	off	off	W-P Alk Bas	AT		off	WPAB?
BK445a	6.2	off	off	off	MORB and W-P Thol	AT		off	MORB-WPT
BK452a	8.51	off	CAB	W-P Alk Bas	Arc Bas	AT		CAB	arc
N8a	8.92	CAB	CAB	W-P Thol and VAB	Arc Bas	AT		CAB	arc

TECTONIC ENVIRONMENT OF MAFIC ROCKS, LUFILIAN ARC PROJECT

CAB	Calc-Alkaline Basalt
MORB	Mid-Ocean Ridge Basalt
W-P Thol	Within-Plate Tholeiite
VAB	Volcanic Arc Basalt
W-P Alk Bas	Within-Plate Alkaline Basalt
I-A Thol	Island-Arc Tholeiite
VAB	Volcanic Arc Basalt
OFBas	Ocean-Floor Basalt
Arc Bas	Arc Basalt
off	Sample plots out of discrimination polygons
A	Parameter of lower Shervais scheme
E	Parameter of left Shervais scheme
OI	Ocean-Island
AB	Alkali Basalt
BAB	Back-Arc Basin Basalt
CFB	CFB
AT	AT
	Environment that coincides

emor
wpab
vab
wpt

POG	Post-Orogenic Granitoid
IAG+CAG	Island Arc Granitoid + Continental Arc Granitoid
CEUG	Continental Epeirogenic Uplift Granitoid
RRG	Rift-Related Granitoid
OP	Oceanic Plagiogranite
CCG	Continental Collision Granitoid
CCG-IAG-CAG	Imposible to define between these three types
CEUG-RRG	CEUG near the margin with RRG
RRG-CEUG	RRG near the margin with CEUG

APPENDIX A SAMPLE MAPS

M1	Key for Zambian Sample Maps, 128
M2	Sample map, Hook Granite Batholith, Zambia over 1:1'000,000 geological map, 129
M3	Sample map, Hook Granite Batholith, Zambia over 1:100,000 geological sheets, 130
M4	Enlarged sample map, Hook Granite Batholith, Zambia over 1:100,000 geological sheets, (See Fig 4.15)
M5	Enlargement of sample, Hook Granite Batholith, northern portion, 131
M6	Enlargement of sample, Hook Granite Batholith, southern portion, 132
M7	Sample map of the Kafue Flats area, Zambia, 133
M8	Sample map, Kalengwa mine environs, Zambia, 134
M9	Sample map, Kasempa environs, Zambia, 135
M10	Sample map, Kalene Hill and Kabompo Dome, NW Zambia, 136
M11	Sample map of Kalene Hill and environs, NW Zambia, 137
M12	Sample map, Domes Area, Zambia, 138
M13	Sample map, Kabompo and Mwombezhi Domes, Zambia, 139
M14	Sample map SE of Mwinilunga, 140
M15	Sample map, Solwesi Dome environs, Zambia, 141
M16	Sample map of the Nchanga Granite, Zambia, 142
M17	Sample map of the Chambishi-Mufulira Area, Zambia, 143
M18	Sample map of the Serenje area, Zambia, 144
M19	Key for Namibian Sample Maps, 145
M20	Sample map of the Khorixas inlier and the Mesopotamie farm, Namibia, 146
M21	Sample map of the Oas and Lofdal farms, Khorixas Inlier, Namibia, 147
M22	Sample map of the Summas Mountains and Ugab River, Namibia, 148
M23	Sample map, Otjiwarongo environs, Namibia, 149
M24	Close-up of sample map, Otjiwarongo environs, Namibia, 150
M25	Sample map, Otavi Mountains, Namibia, 151
M26	Sample map, Witvlei environs, Namibia, 152
M27	Key for Kamanjab Batholith sample maps, Namibia, 153
M28	K-14 portion of sample map, Kamanjab Batholith, Namibia, 154
M29	K-15 portion of sample map, Kamanjab Batholith, Namibia, 155
M30	K-16 portion of sample map, Kamanjab Batholith, Namibia, 156
M31	K-17 portion of sample map, Kamanjab Batholith, Namibia, 157
M32	K-18 portion of sample map, Kamanjab Batholith, Namibia, 158
M33	K-19 portion of sample map, Kamanjab Batholith, Namibia, 159
M34	K-20 portion of sample map, Kamanjab Batholith, Namibia, 160
M35	K-21 portion of sample map, Kamanjab Batholith, Namibia, 161
M36	K-22 portion of sample map, Kamanjab Batholith, Namibia, 162
M37	K-23 portion of sample map, Kamanjab Batholith, Namibia, 163
M38	K-24 portion of sample map, Kamanjab Batholith, Namibia, 164
M39	K-25 portion of sample map, Kamanjab Batholith, Namibia, 165

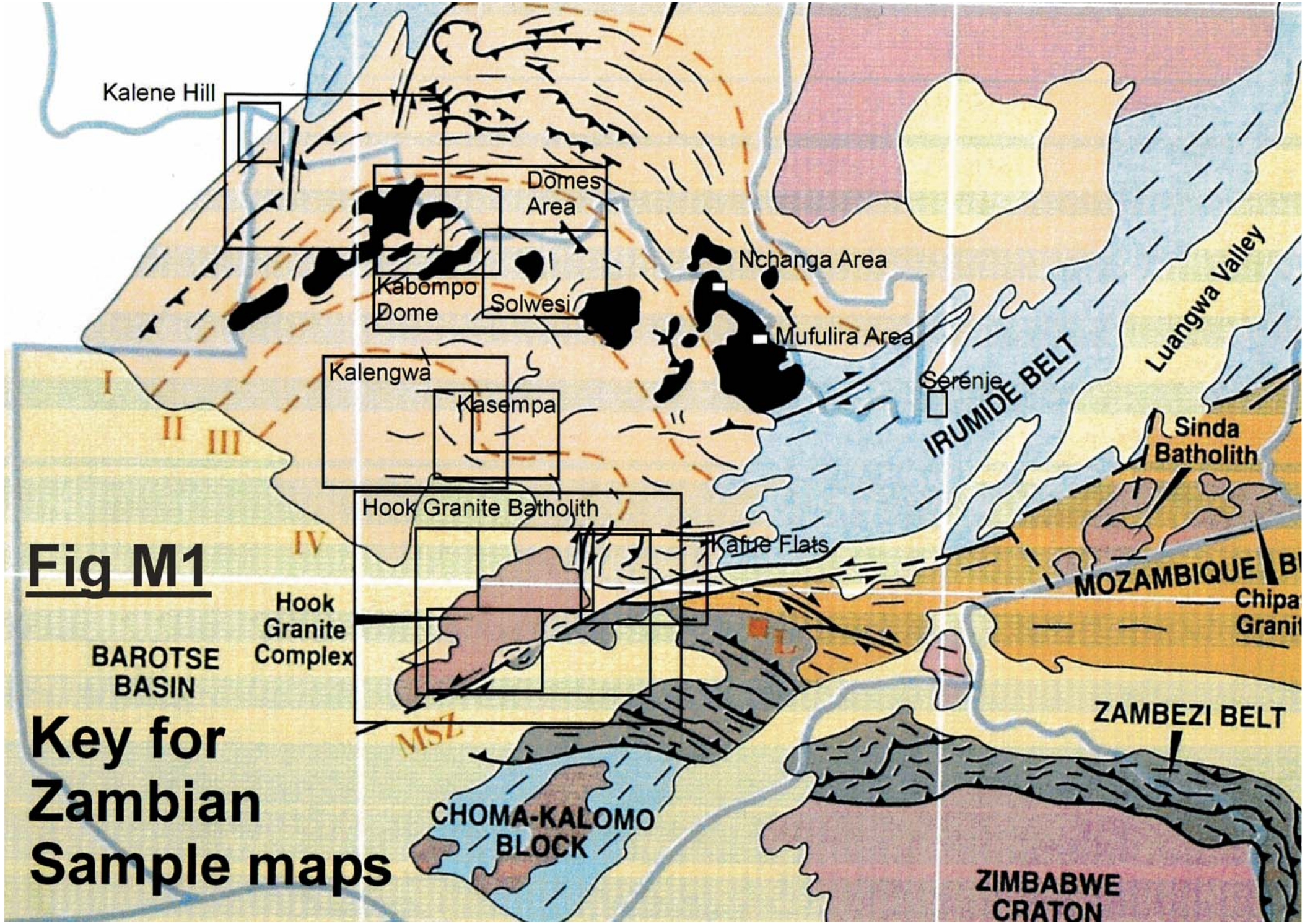
Kalene Hill
Domes Area
Kabompo Dome
Solwesi
Nchanga Area
Mufulira Area
Kalengwa
Kasempa
Serenje
IRUMIDE BELT
Luangwa Valley
Sinda Batholith
Hook Granite Batholith
Kafue Flats
MOZAMBIQUE
Chipa
Granit
I
II
III
IV
Fig M1
Hook Granite Complex
BAROTSE BASIN
MSZ
ZAMBEZI BELT
CHOMA-KALOMO BLOCK
ZIMBABWE CRATON
Key for Zambian Sample maps

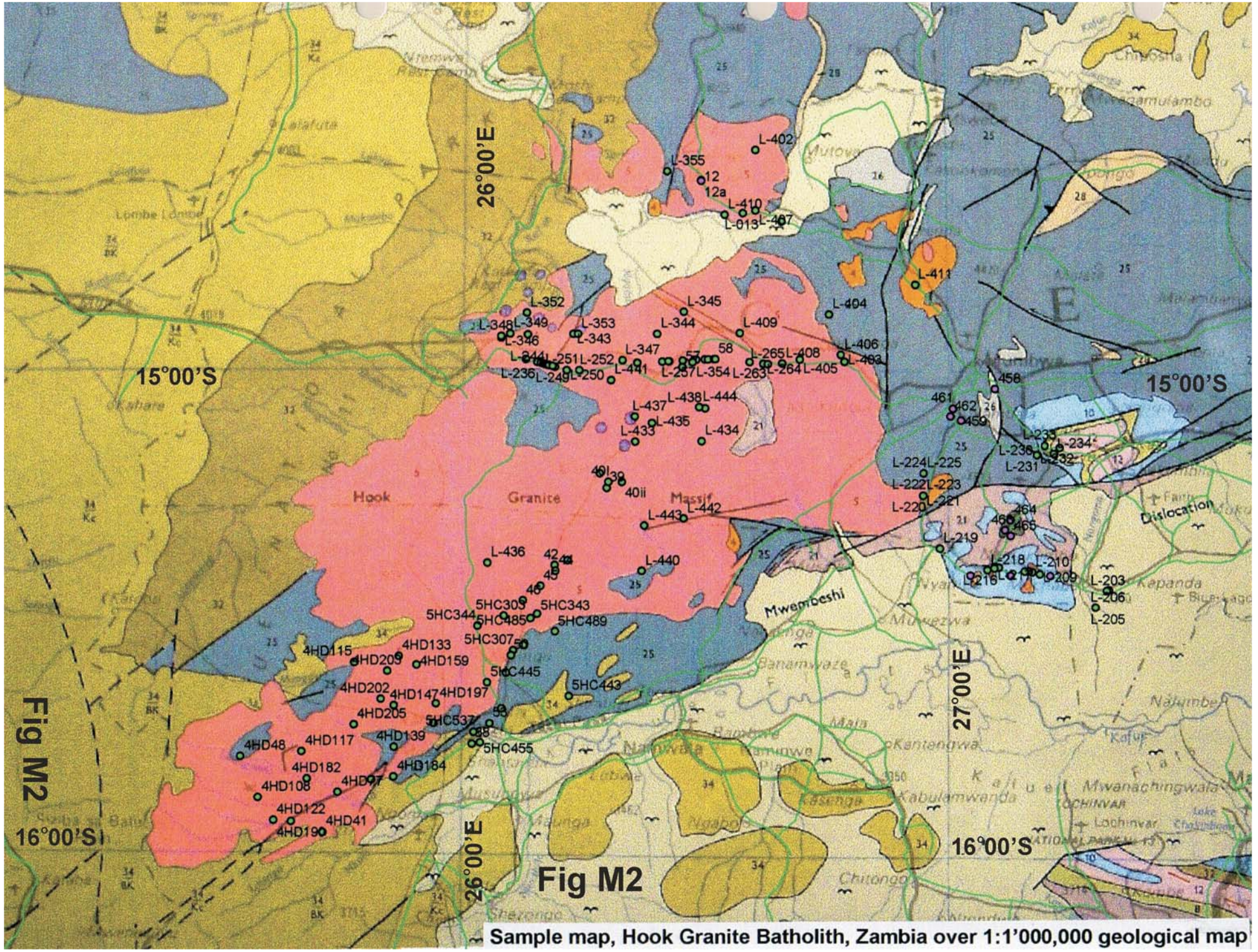

Sample map, Hook Granite Batholith, Zambia over 1:1'000,000 geological map

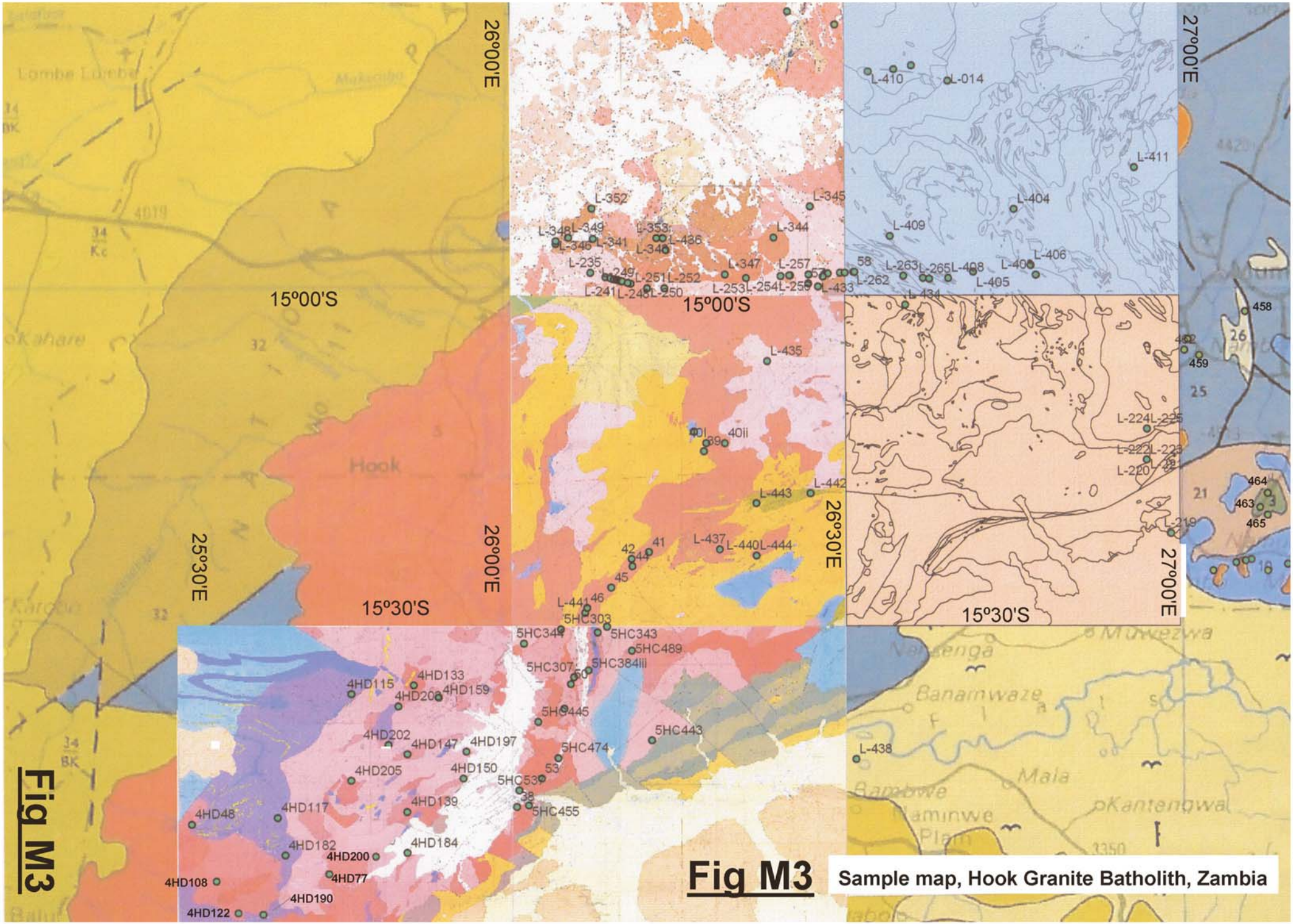
26°00'E
27°00'E
15°00'S
15°30'S
25°30'E
26°30'E
L-410
L-014
L-411
L-404
L-409
L-406
L-405
L-352
L-345
L-348
L-349
L-353
L-344
L-346
L-341
L-436
L-340
L-235
L-347
L-257
L-262
L-263
L-265
L-408
L-400
L-241
L-248
L-250
L-251
L-252
L-253
L-254
L-259
L-433
L-434
L-435
L-224
L-225
L-222
L-223
L-220
L-219
L-442
L-443
L-437
L-440
L-444
L-441
458
459
464
463
465
Hook
Banamwaze
Mala
Kantenowa
5HC303
5HC344
5HC343
5HC489
5HC307
5HC384iii
5HC445
5HC443
5HC474
5HC539
5HC455
4HD115
4HD133
4HD159
4HD208
4HD202
4HD147
4HD197
4HD205
4HD150
4HD139
4HD48
4HD117
4HD182
4HD200
4HD184
4HD77
4HD108
4HD190
4HD122
L-438
Fig M3
Fig M3
Sample map, Hook Granite Batholith, Zambia

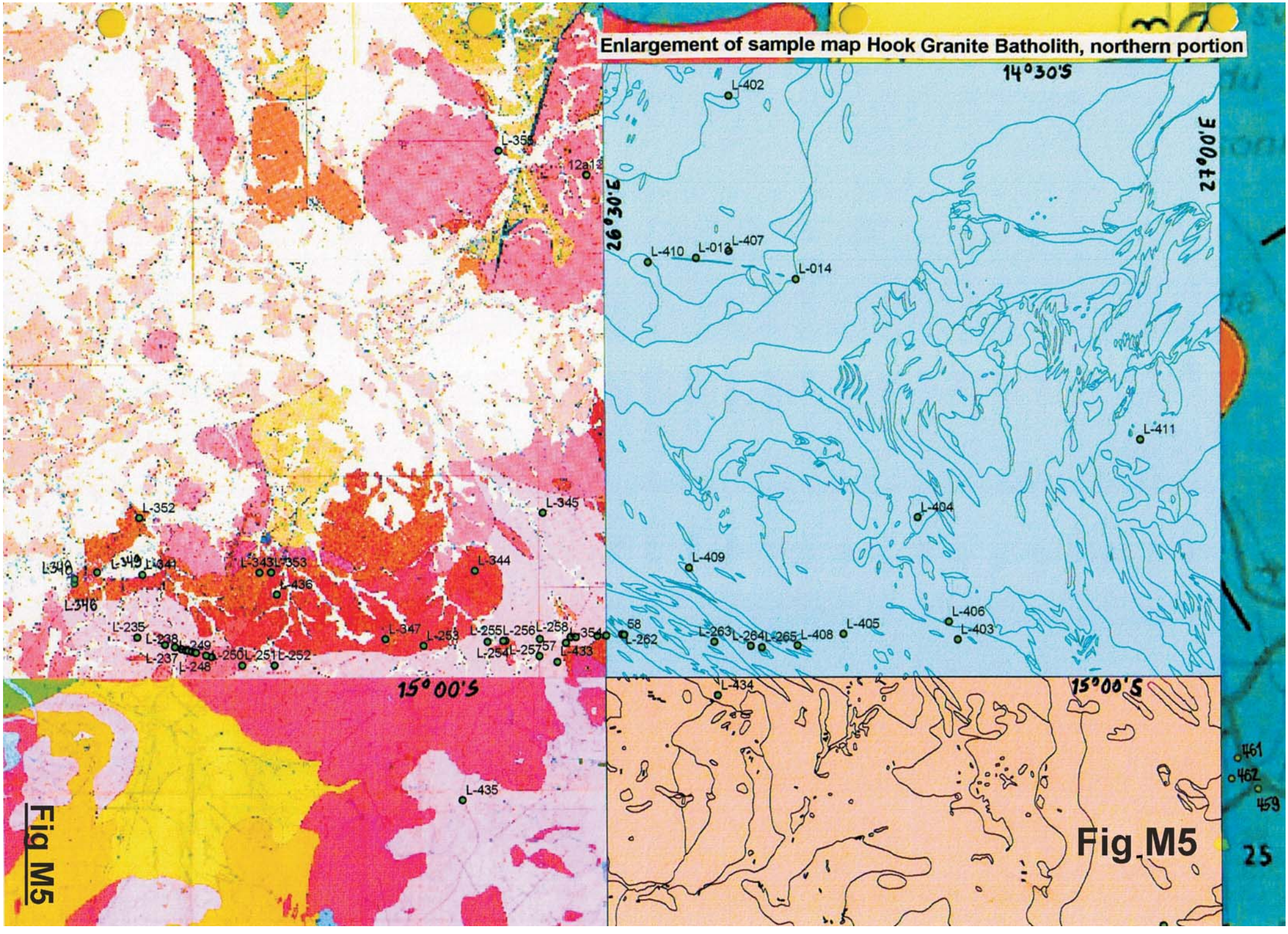
Enlargement of sample map Hook Granite Batholith, northern portion
14°30'S
27°00'E
26°30'E
15°00'S
L-402
L-355
12a12
L-410
L-013
L-407
L-014
L-411
L-404
L-409
L-406
L-403
L-405
L-408
L-263
L-264
L-265
L-262
58
L-354
L-433
L-257
L-254
L-255
L-256
L-258
L-253
L-347
L-235
L-238
L-249
L-237
L-248
L-250
L-251
L-252
L-436
L-343
L-353
L-341
L-340
L-339
L-346
L-352
L-345
L-344
L-435
L-434
461
462
459
Fig M5
Fig M5
25

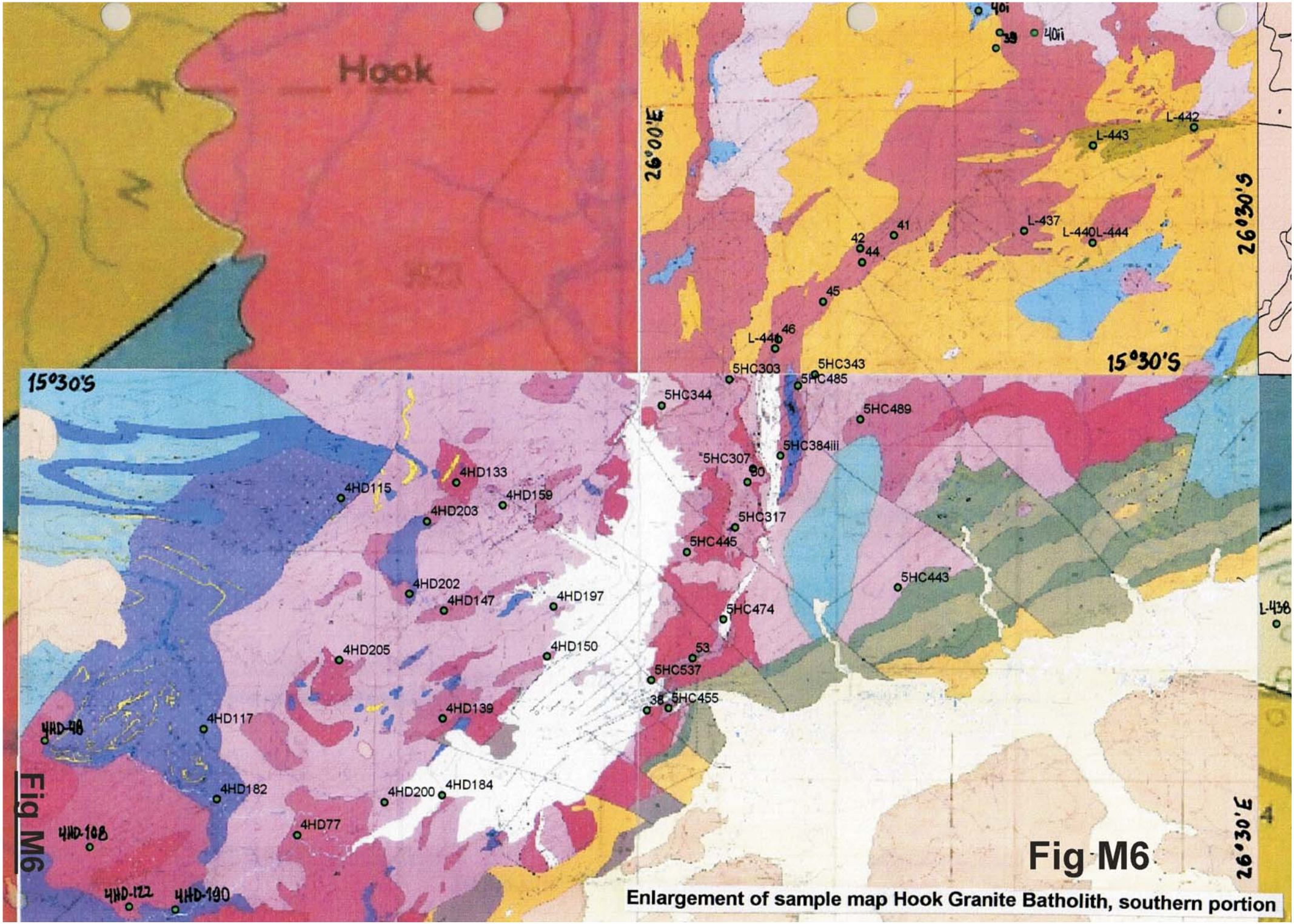
Hook
26°00'E
26°30'S
15°30'S
40i
40ii
39
L-442
L-443
L-437
L-440
L-444
41
42
44
45
46
L-445
5HC303
5HC343
5HC485
5HC344
5HC489
5HC384iii
5HC307
50
5HC317
5HC445
5HC443
5HC474
L-438
53
5HC537
38
5HC455
4HD133
4HD115
4HD159
4HD203
4HD202
4HD147
4HD197
4HD205
4HD150
4HD139
4HD117
4HD-98
4HD182
4HD200
4HD184
4HD77
4HD-108
4HD-122
4HD-190
Fig M6
Fig M6
Enlargement of sample map Hook Granite Batholith, southern portion

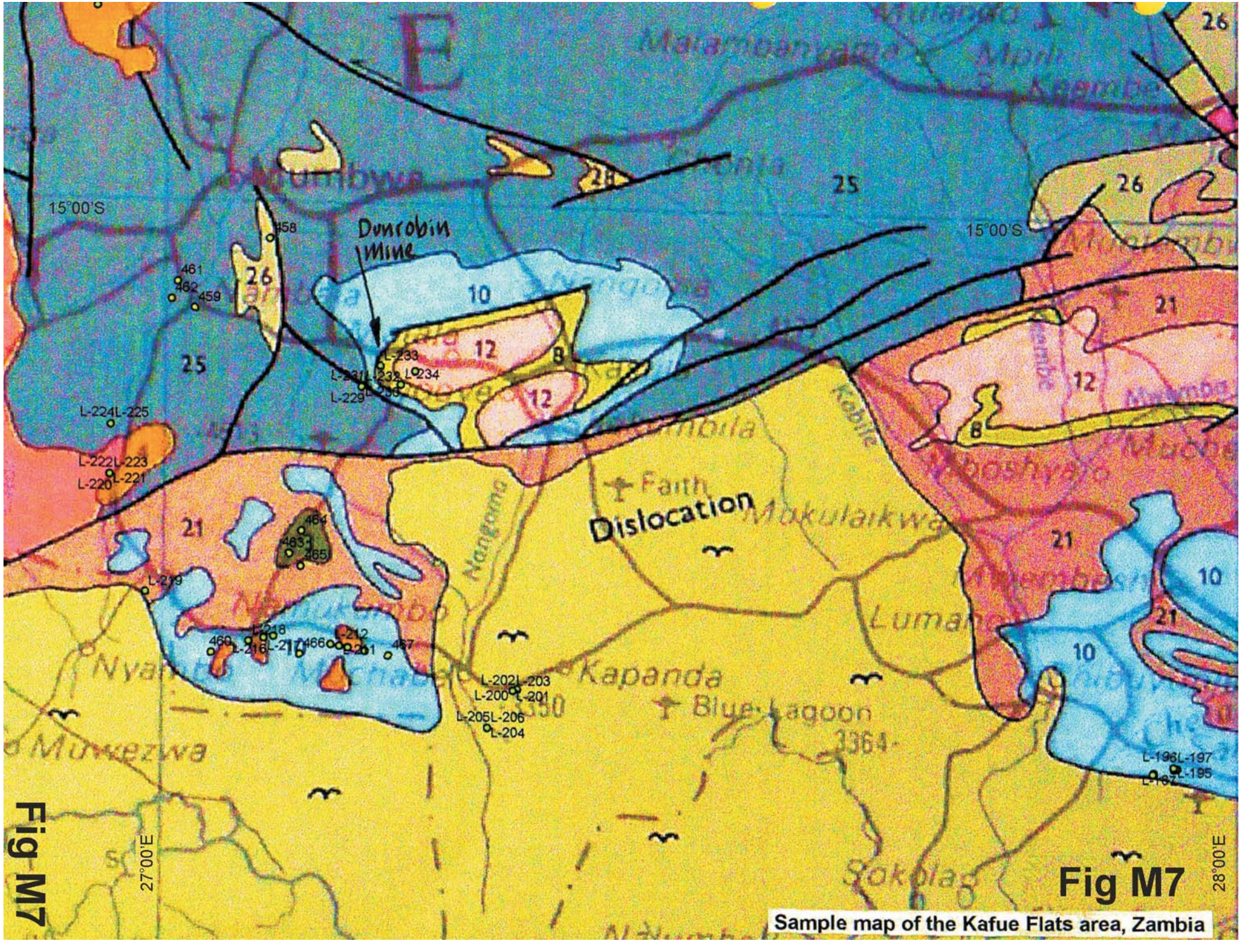
Dunrobin Mine
Dislocation
15°00'S
27°00'E
28°00'E
Fig M7
Fig M7
Sample map of the Kafue Flats area, Zambia

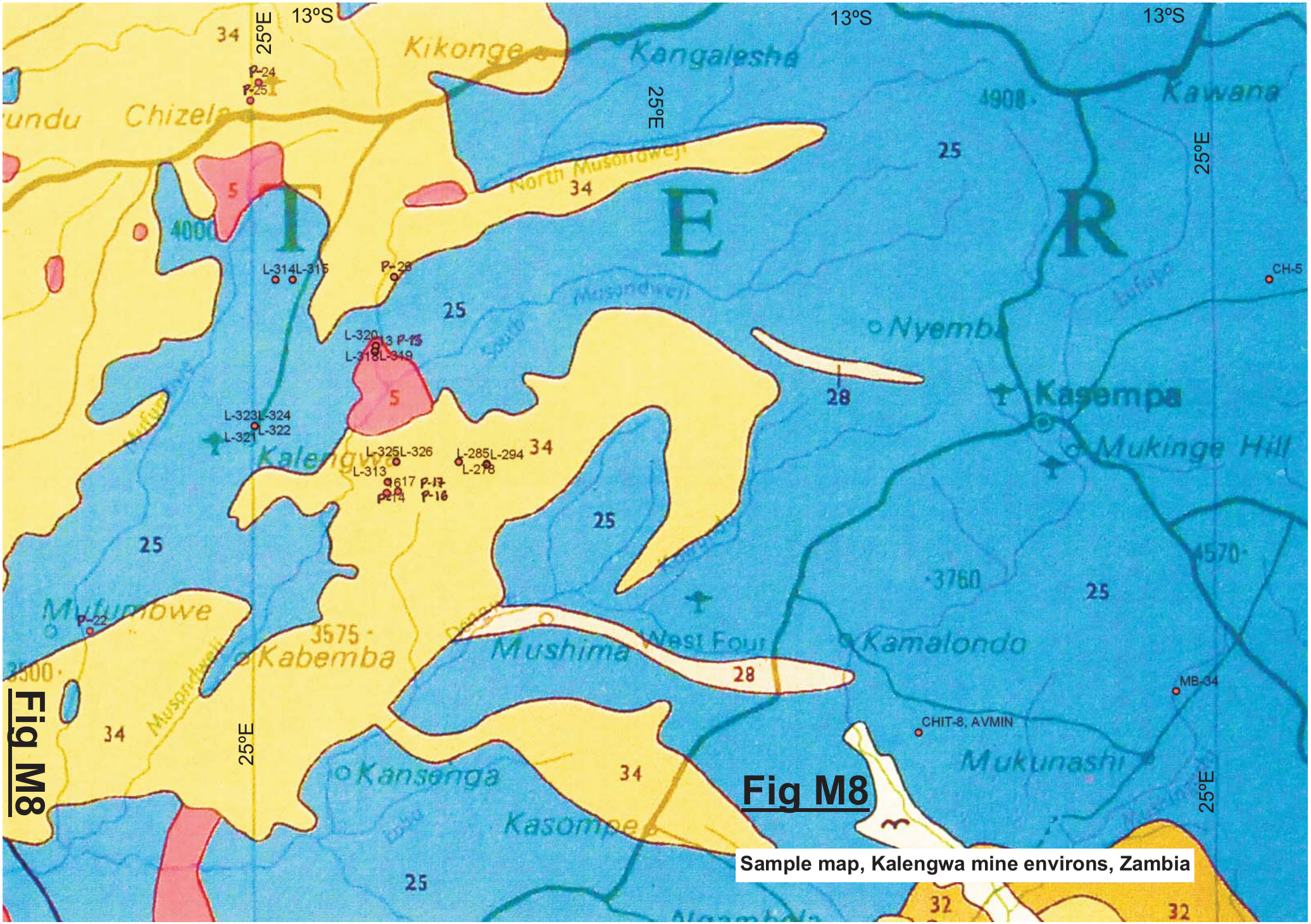
13°S
25°E
Kikonge
Kangalesha
Kawana
Chizela
North Musondweji
Musandweji
Nyemba
Kasempa
Mukinge Hill
Kalengwa
Mushima
Nest Four
Kamalonda
Kabemba
Mukunashi
Kansenga
Kasompe
Mufumbwe
Musondweji
L-314
L-315
P-24
P-25
P-26
L-320
L-318
L-319
L-323
L-324
L-322
L-321
L-325
L-326
L-313
L-285
L-294
L-278
P-17
P-16
P-22
CH-5
MB-34
CHIT-8, AVMIN
4000
3575
3760
4570
4908
Fig M8
Fig M8
Sample map, Kalengwa mine environs, Zambia

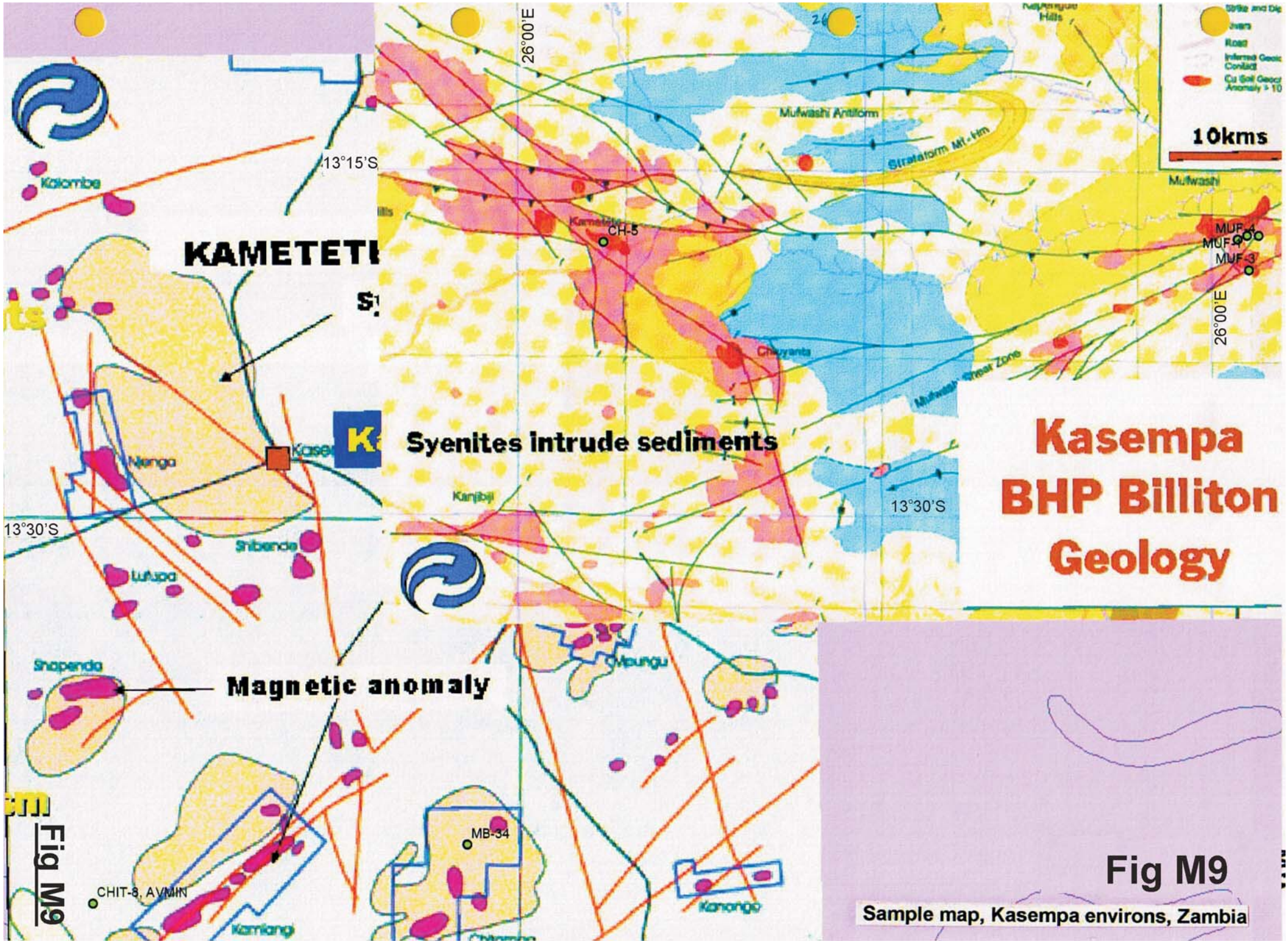
26°00'E
13°15'S
Kalombo
KAMETETI
Syenites intrude sediments
Kasempa
Nenga
13°30'S
Shibende
Lufupa
Shapenda
Magnetic anomaly
Mpungu
MB-34
CHIT-8, AVMIN
Kamiangi
Kanongo
Fig M9
Mufwashi Antiform
Stratiform Mf-Hm
CH-5
Mufwashi
MUF-4
MUF-2
MUF-3
Chisyanta
Mufwashi Shear Zone
Kanjibji
10kms
Kasempa
BHP Billiton
Geology
Fig M9
Sample map, Kasempa environs, Zambia

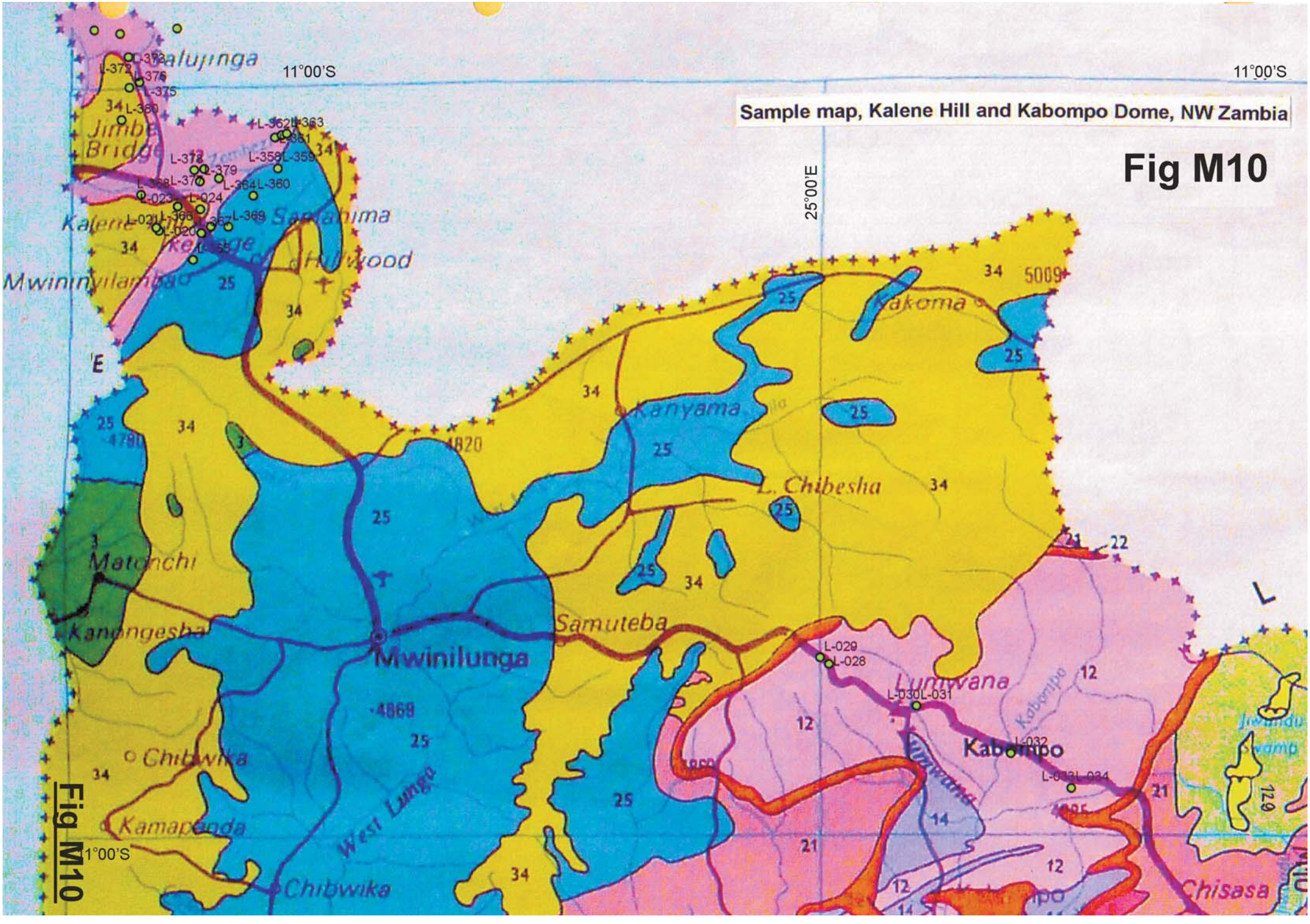
Sample map, Kalene Hill and Kabompo Dome, NW Zambia
Fig M10
11°00'S
25°00'E
Mwinilunga
Kabompo
Matonchi
Kanongesha
Chibwika
Kamapanda
West Lunga
Kanyama
L. Chibesha
Samuteba
Kakoma
Lunwana
Chisasa
Jimbe
Bridge
Kalene Hill
Sakahima
Hollywood
Fig M10

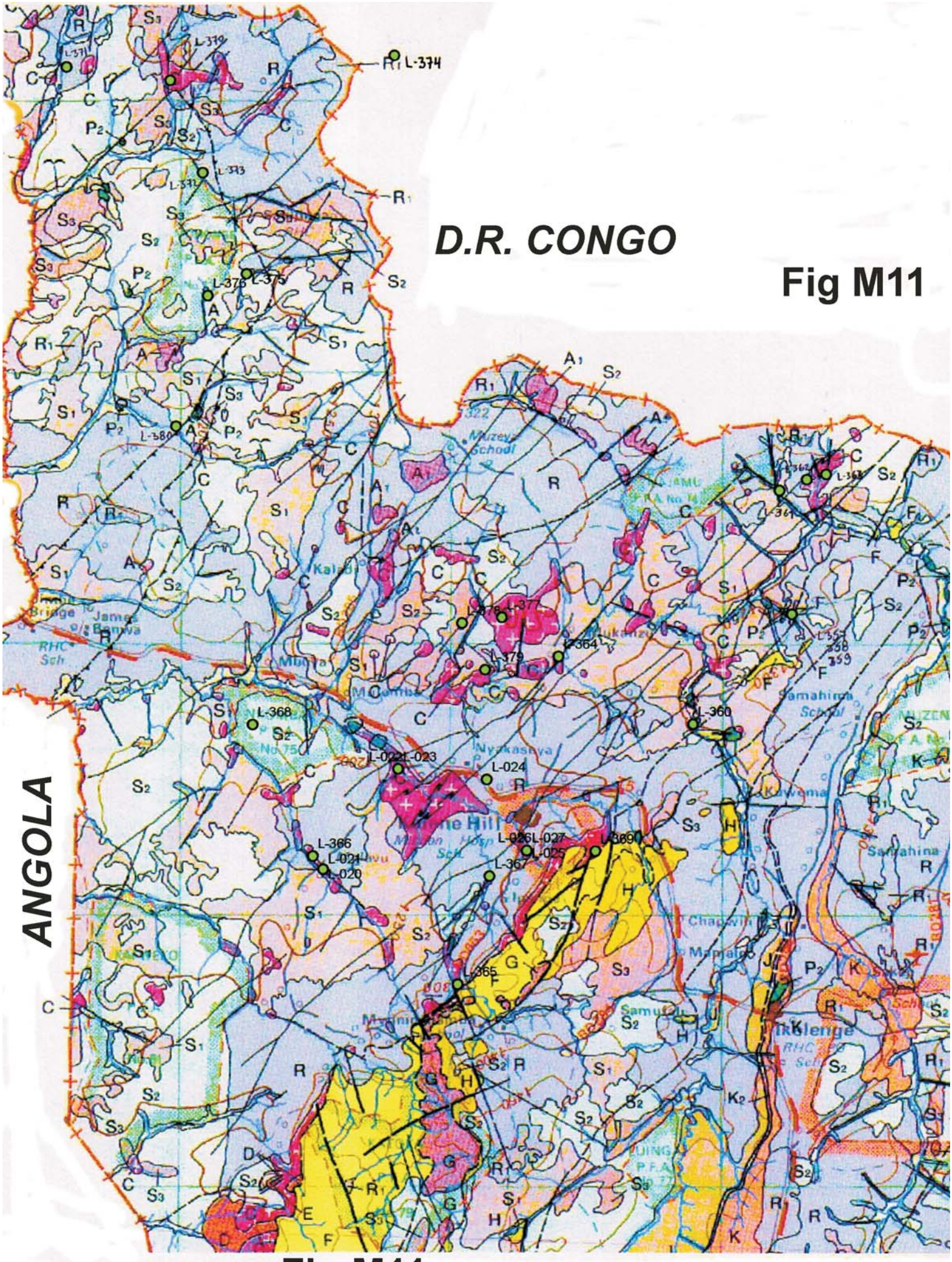

Fig M11

Fig M11 Sample map of Kalene Hill and environs, NW Zambia

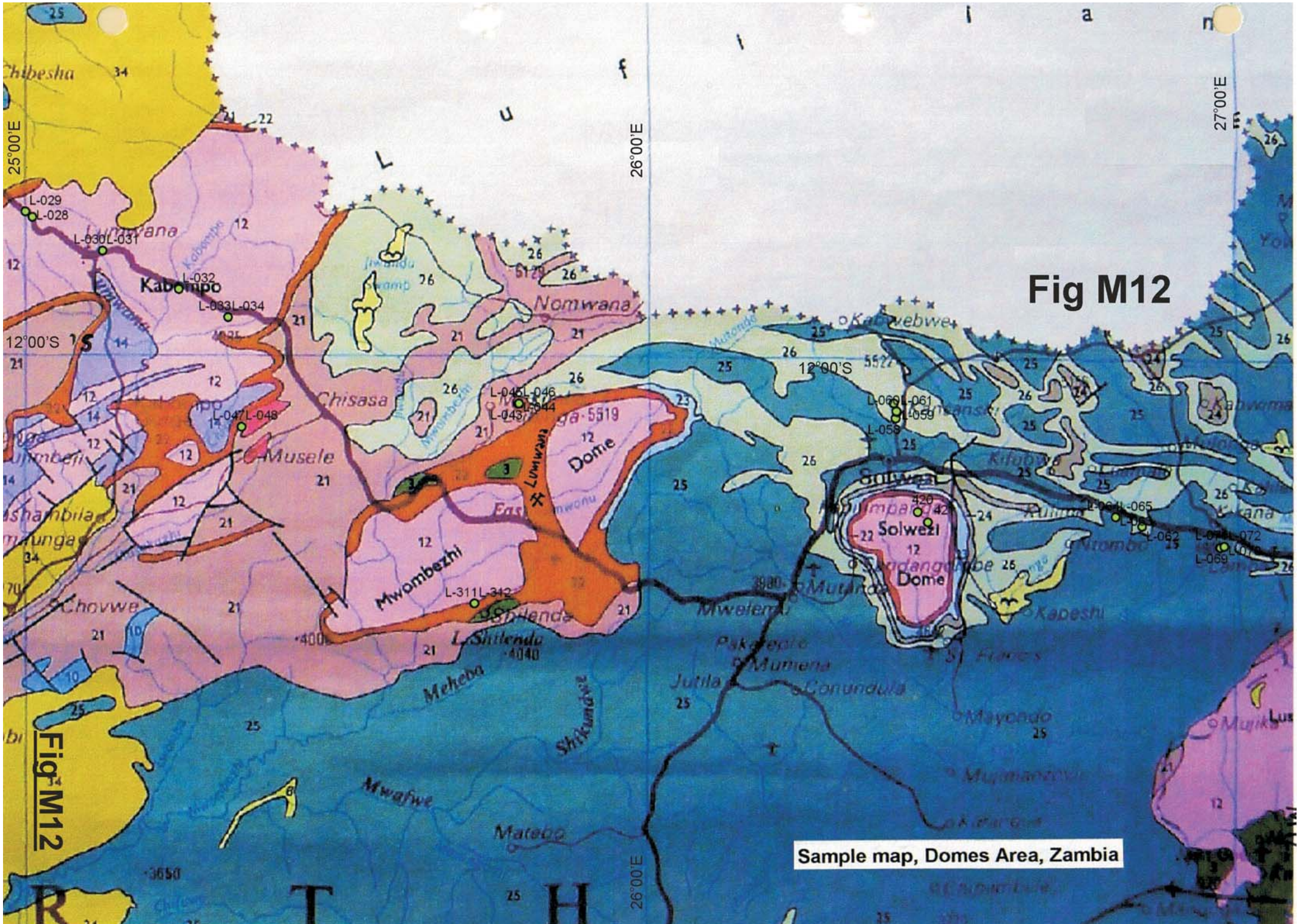
Fig M12
Sample map, Domes Area, Zambia
Fig M12
25°00'E
26°00'E
27°00'E
12°00'S
Kabompo
Nomwana
Chisasa
Musele
Mwombezhi
Dome
Solwezi
Dome
L. Shitlendo
Mwafwe
Mateo
Meheba
Chovwe
Mwelena
Mayondo
L-029
L-028
L-030
L-031
L-032
L-033
L-034
L-045
L-046
L-044
L-043
L-047
L-048
L-311
L-312
L-058
L-061
L-059
L-064
L-065
L-062
L-072
L-069

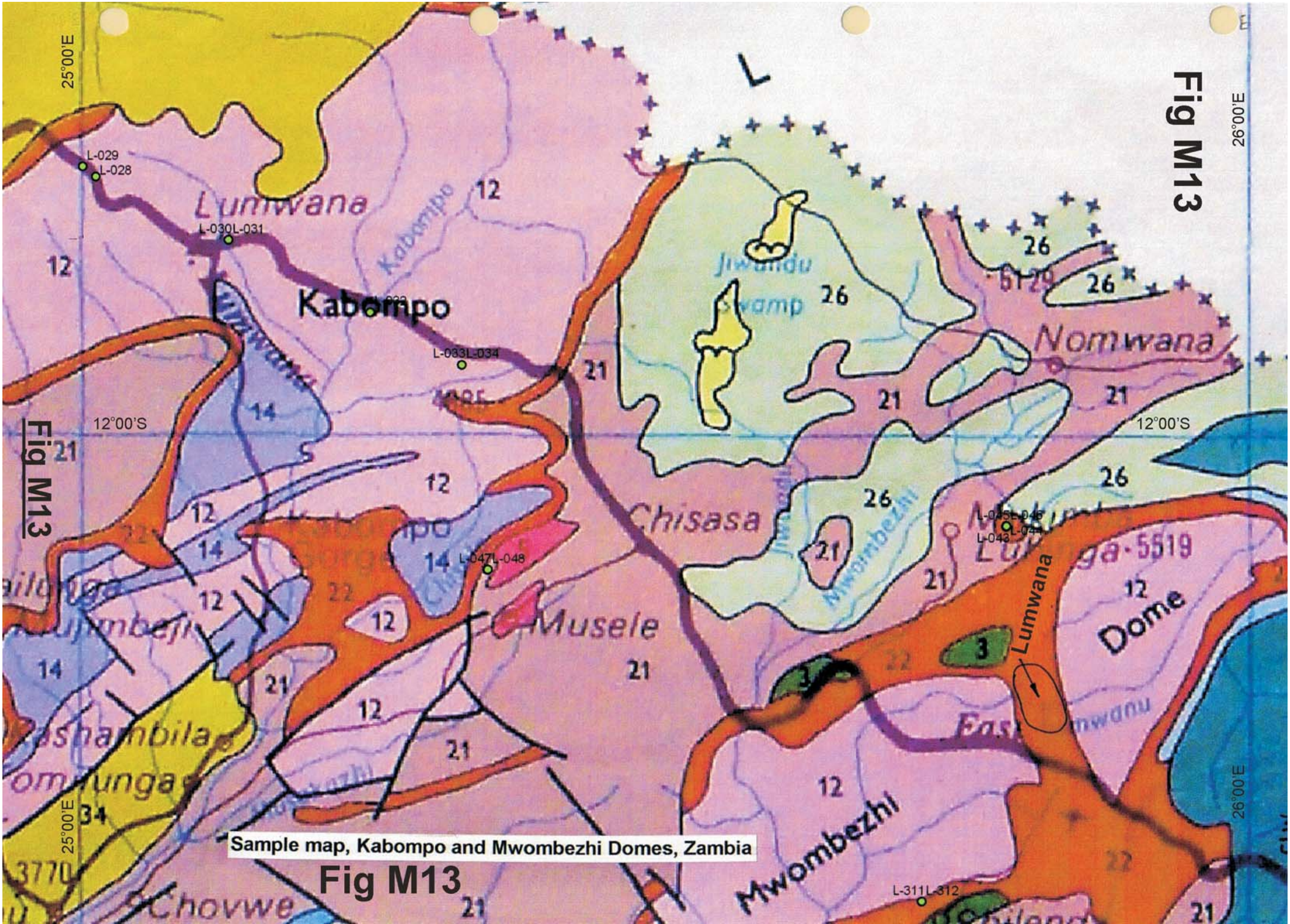

Sample map, Kabompo and Mwombezhi Domes, Zambia

Fig M13

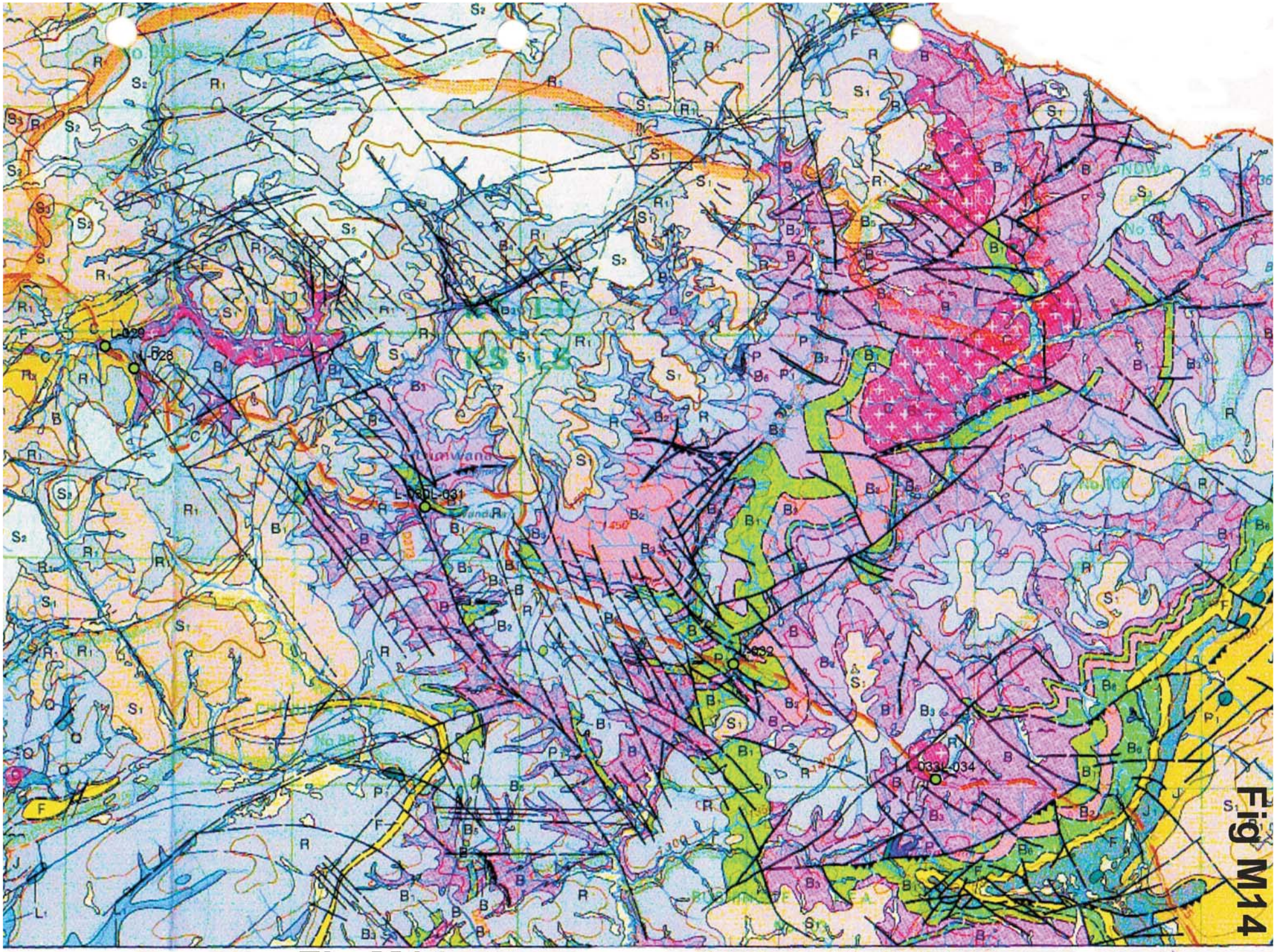

Fig M14

Sample map SE of Mwinilunga, Zambia

Fig M14

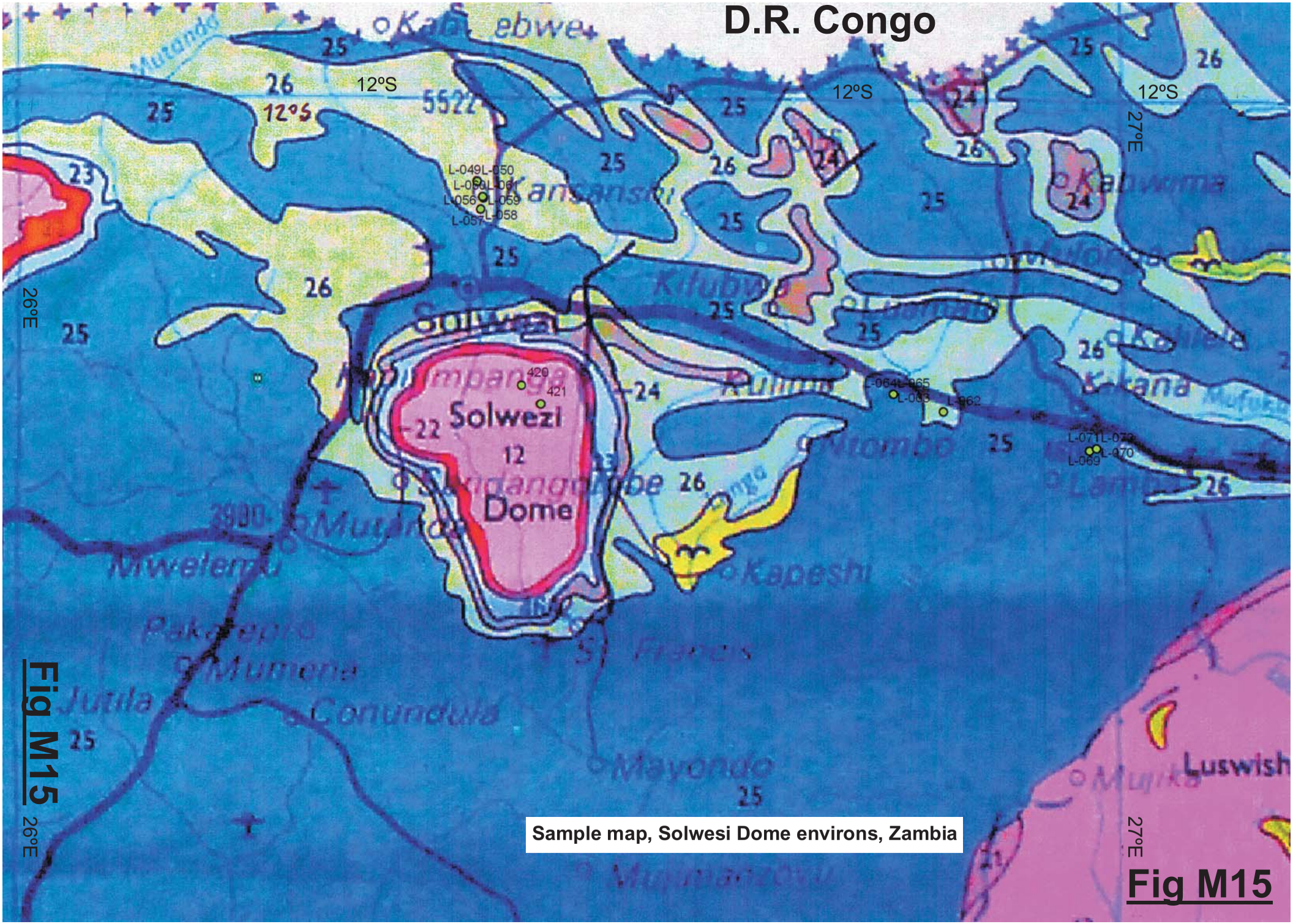
D.R. Congo
12ºS
26ºE
27ºE
Solwezi
Dome
Sample map, Solwesi Dome environs, Zambia
Fig M15

Fig M15

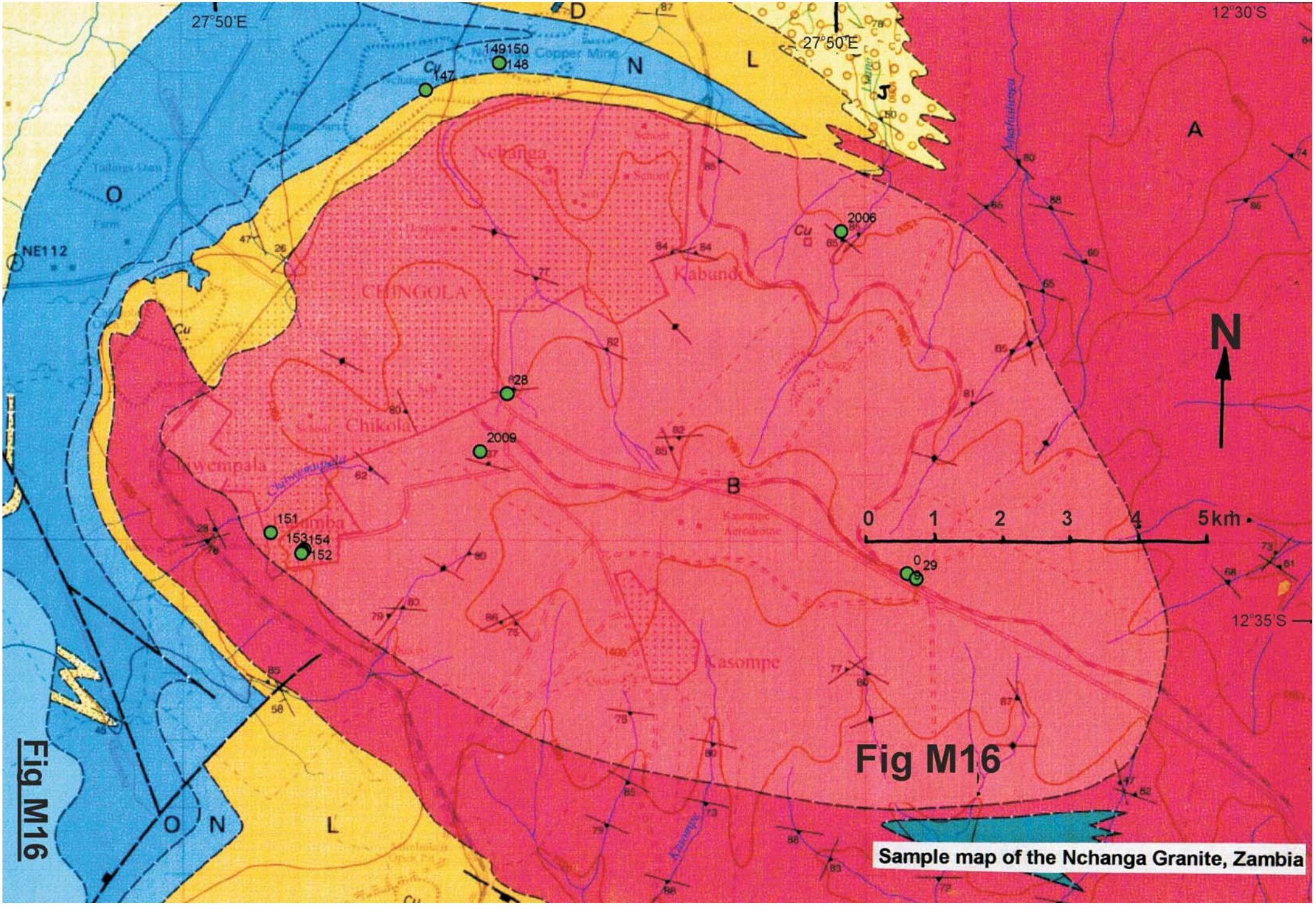
27°50'E
12°30'S
27°50'E
12°35'S
149150
148
147
2006
2009
28
29
151
153154
152
NE112
CHINGOLA
Nchanga
Kabundi
Chikola
Kasompe
Kawempala
Nchanga Copper Mine
D
N
L
J
A
O
B
Cu
N
0 1 2 3 4 5km
Fig M16
Fig M16
Sample map of the Nchanga Granite, Zambia

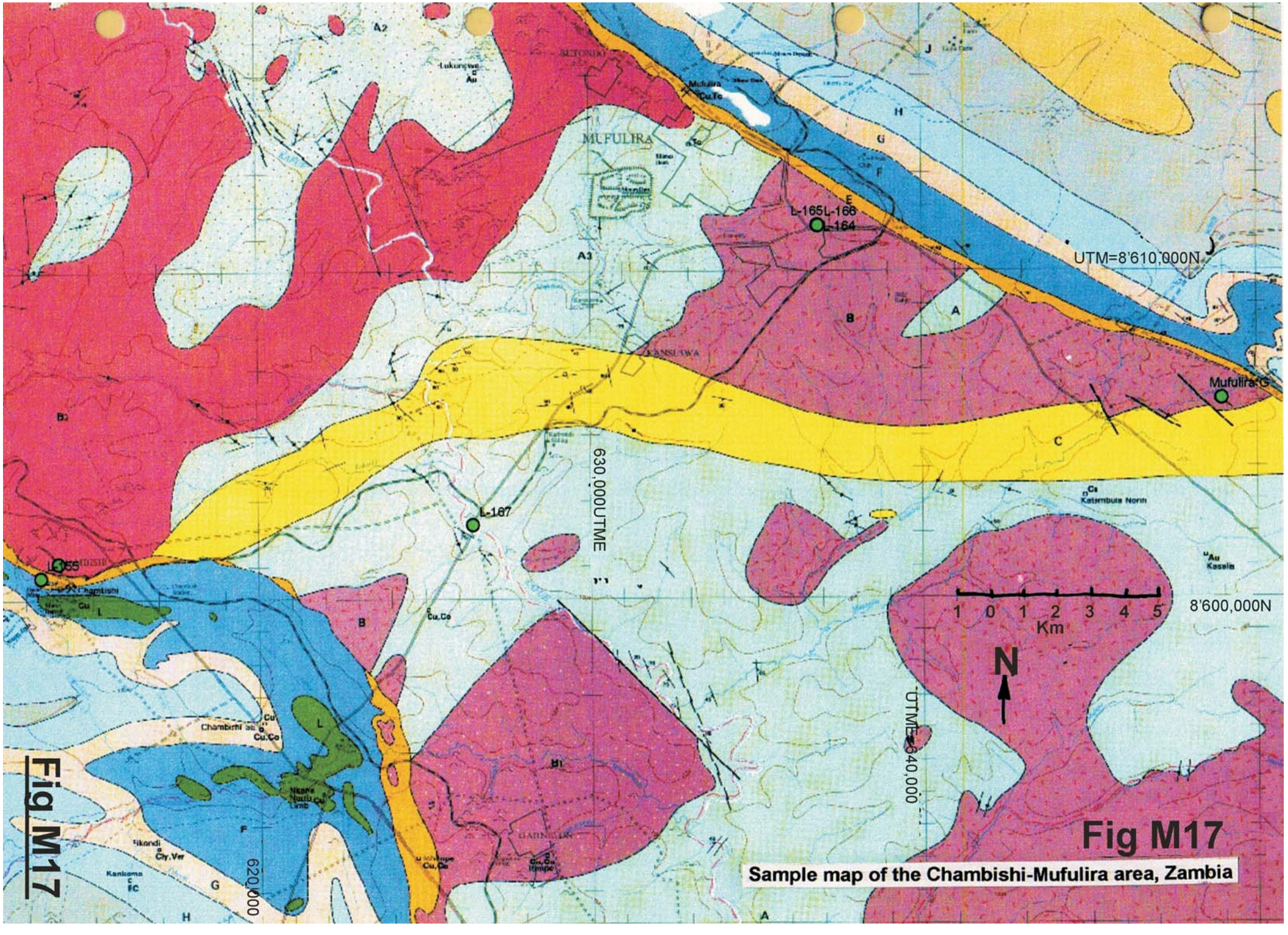
MUFULIRA
L-165
L-166
L-164
L-167
L-155
UTM=8'610,000N
8'600,000N
630,000UTME
640,000
620,000
1 0 1 2 3 4 5
Km
N
Mufulira 'G'
Chambishi
Nkana
Nkana North Limb
Ikandi
Kankoma
Katembula North
Kasale
Fig M17
Sample map of the Chambishi-Mufulira area, Zambia

Fig M17

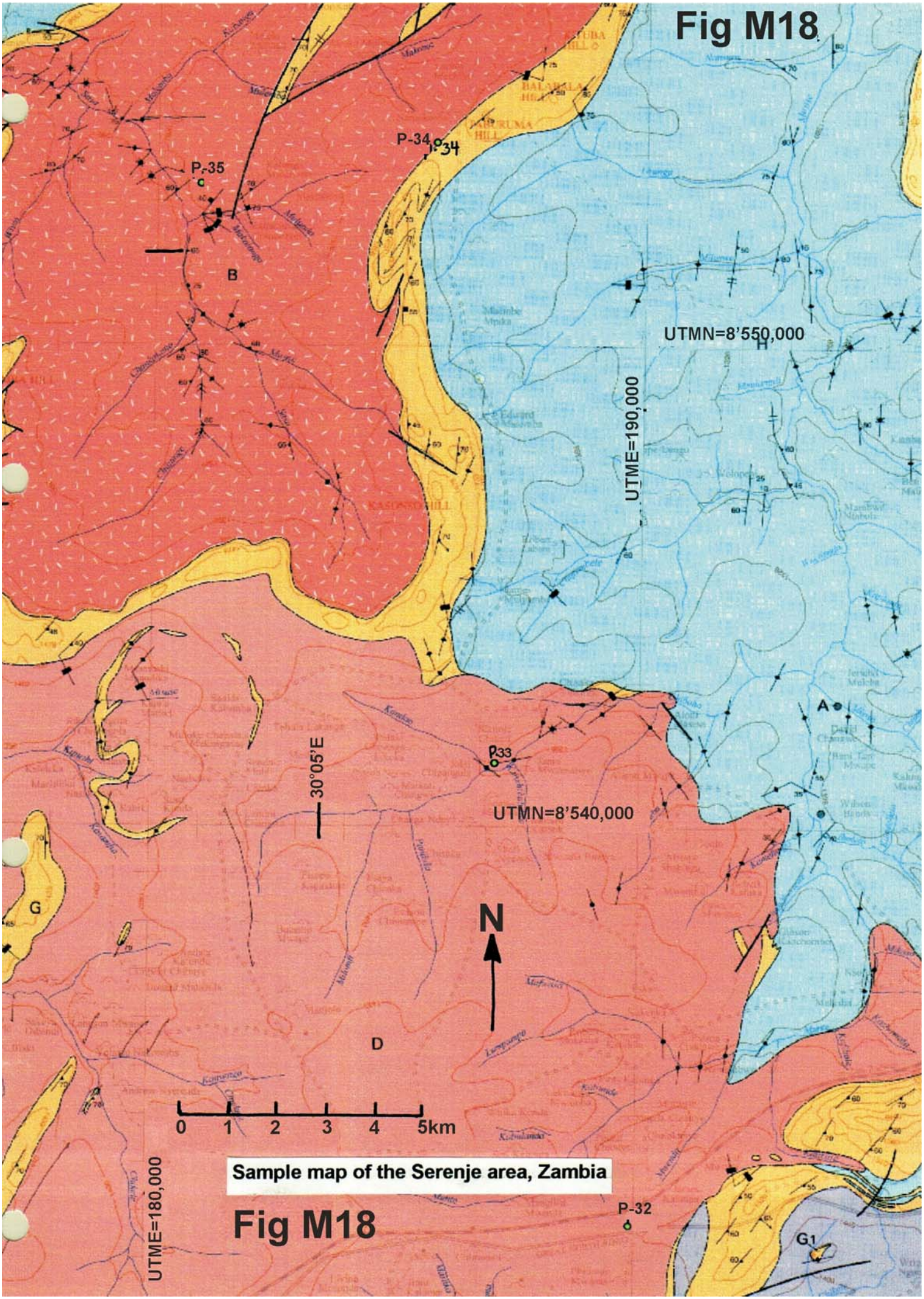

Sample map of the Serenje area, Zambia

Fig M18

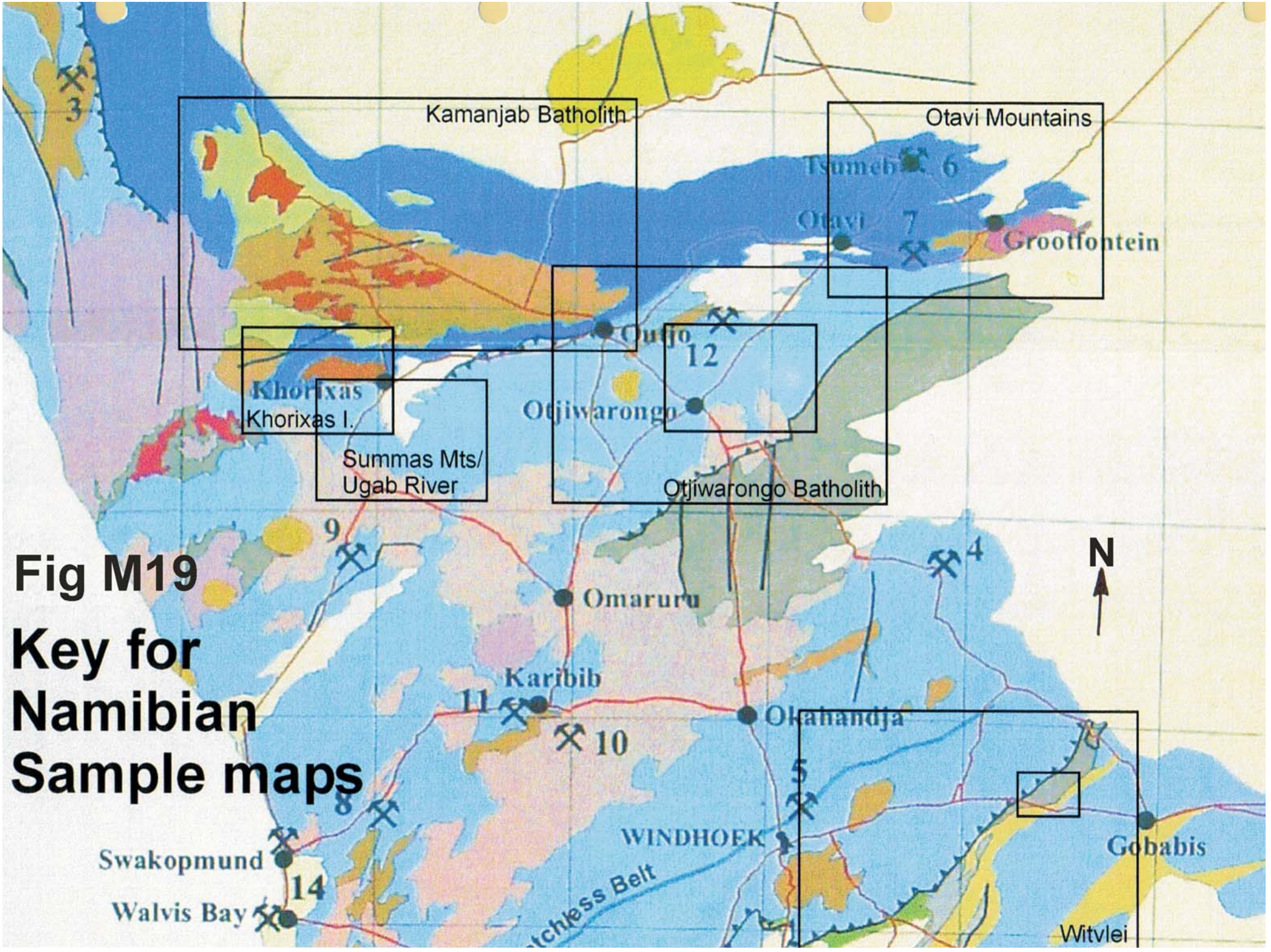

Fig M19

Key for Namibian Sample maps

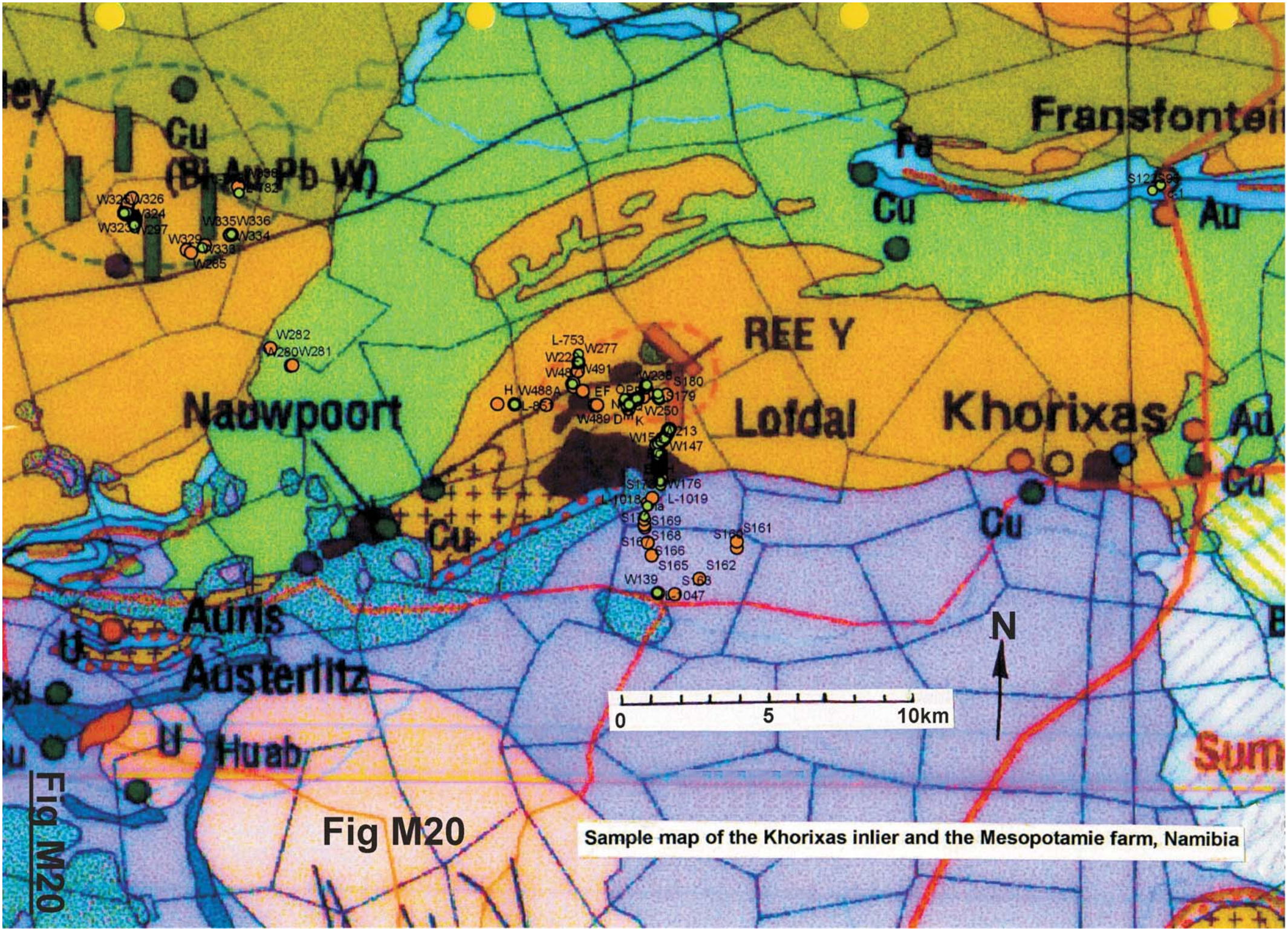

Fig M20

Sample map of the Khorixas inlier and the Mesopotamie farm, Namibia

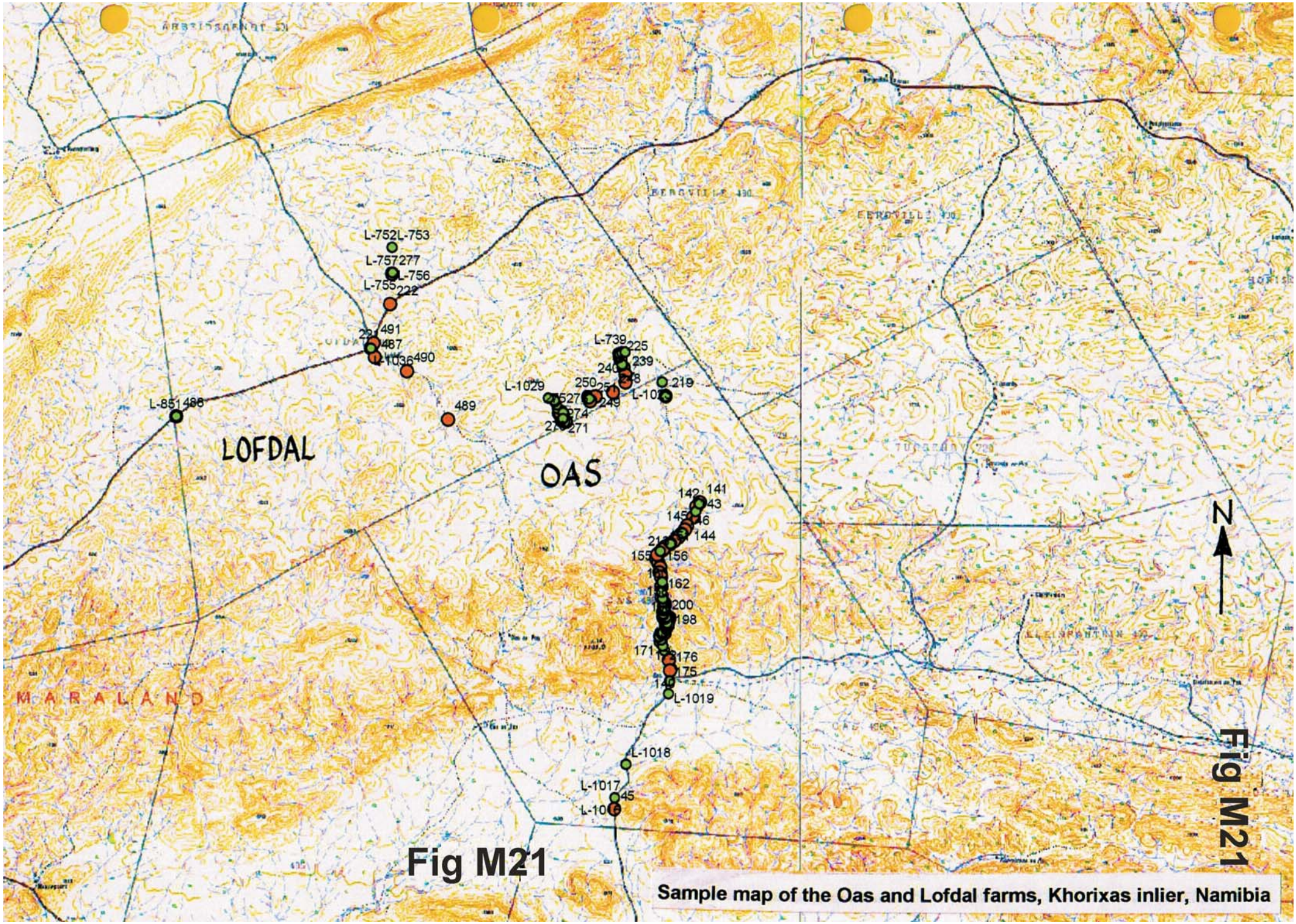

Fig M21

Sample map of the Oas and Lofdal farms, Khorixas inlier, Namibia

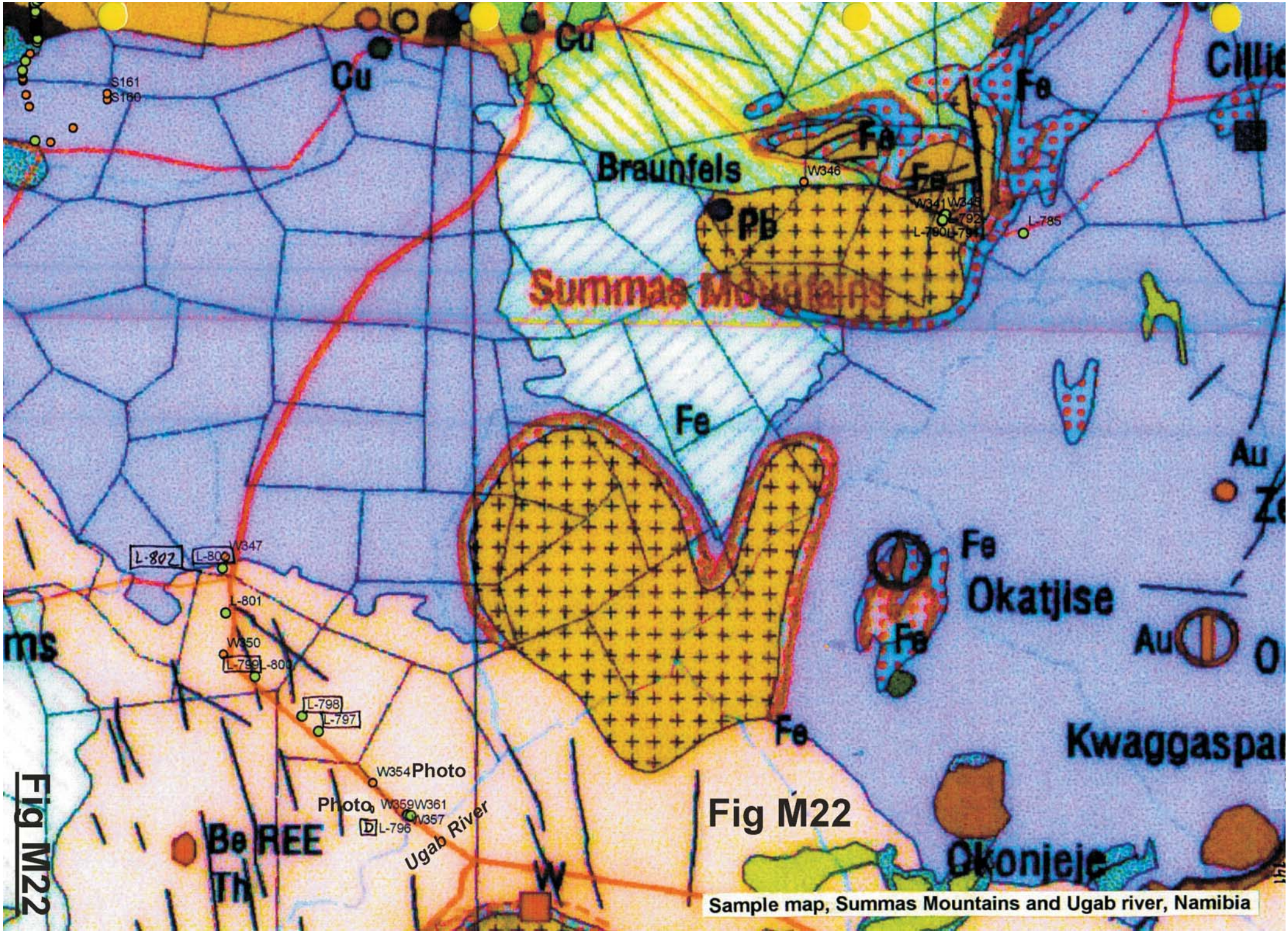
Cu
Cu
S161
S160
Fe
Fe
Fe
Braunfels
W346
PB
W341
W345
L-792
L-790
L-791
L-785
Summas Mountains
Fe
Au
Fe
Okatjise
Fe
Au
L-802
L-800
W347
L-801
W350
L-799
L-800
L-798
L-797
Fe
Kwaggaspa
W354
Photo
Photo
W359
W361
W357
L-796
Ugab River
Be
REE
Th
W
Okonjeje
Fig M22
Fig M22
Sample map, Summas Mountains and Ugab river, Namibia

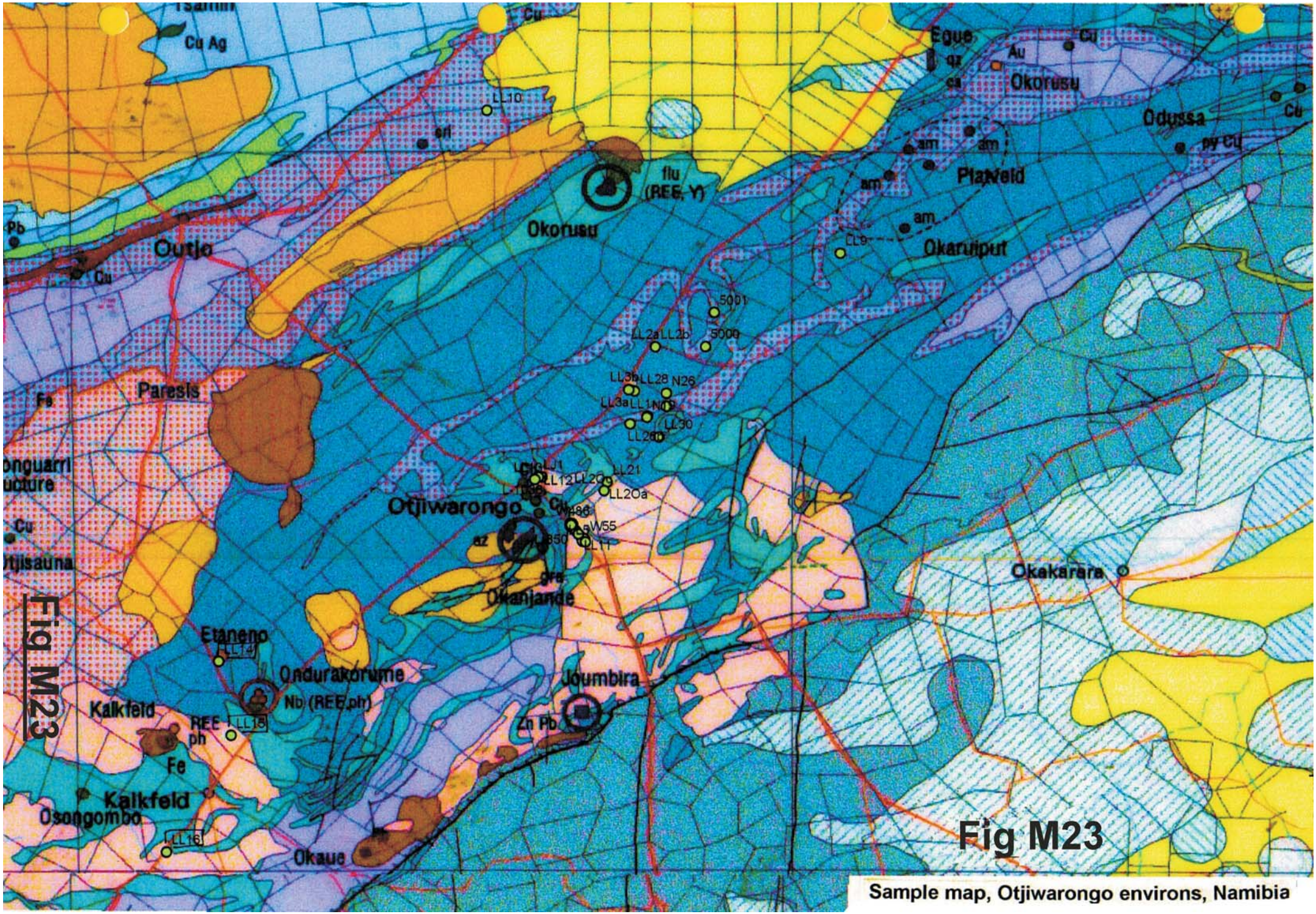

Fig M23

Sample map, Otjiwarongo environs, Namibia

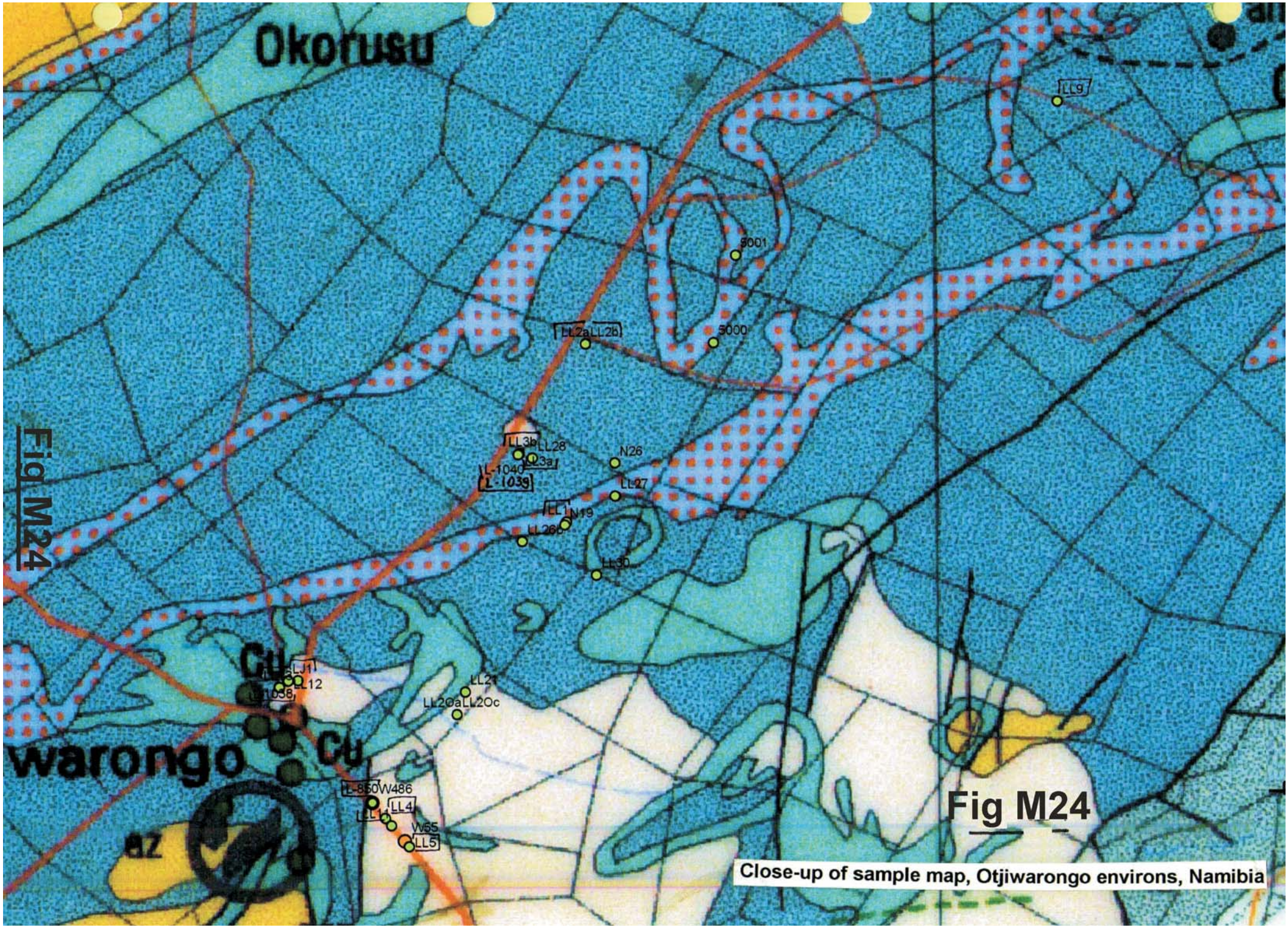

Close-up of sample map, Otjiwarongo environs, Namibia

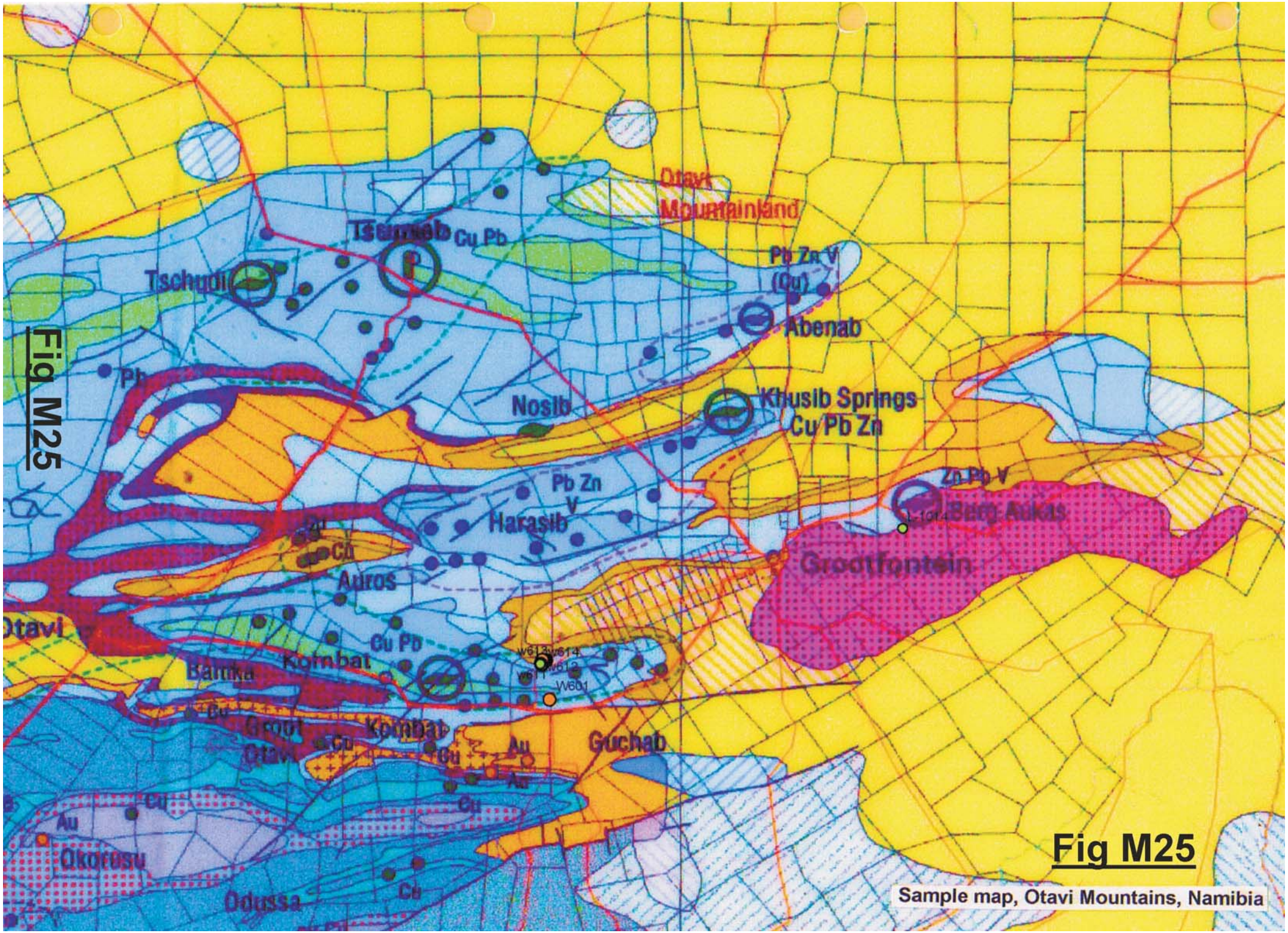
Fig M25
Otavi Mountainland
Tsumeb Cu Pb
Tschudi
Pb Zn V (Cu)
Abenab
Pb
Nosib
Khusib Springs Cu Pb Zn
Pb Zn V
Harasib
Zn Pb V
Berg Aukas
Grootfontein
Cu
Auros
Otavi
Cu Pb
Kombat
Bamika
Cu
Groot Otavi
Cu
Kombat
Au
Guchab
Cu
Au
Au
Okotusu
Odussa
Cu
Fig M25
Sample map, Otavi Mountains, Namibia

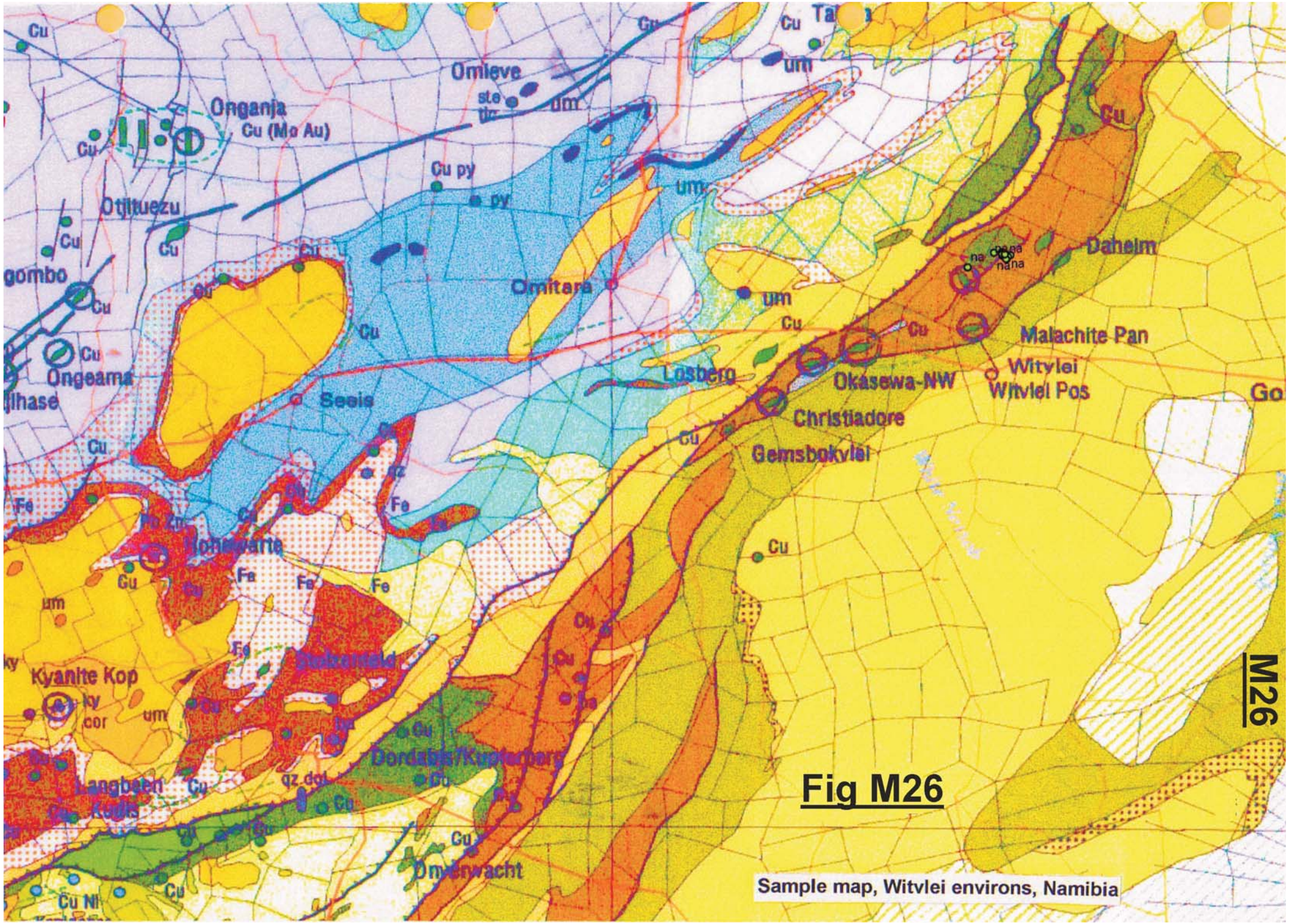
Omieve
Onganja
Cu (Mo Au)
Cu py
Otjituezu
Omitara
Daheim
Malachite Pan
Witvlei
Witvlei Pos
Losberg
Okasewa-NW
Christiadore
Gemsbokvlei
Seeis
Ongeama
Kyanite Kop
Dordabis/Kupferberg
Omeiwacht
Fig M26
Sample map, Witvlei environs, Namibia
M26

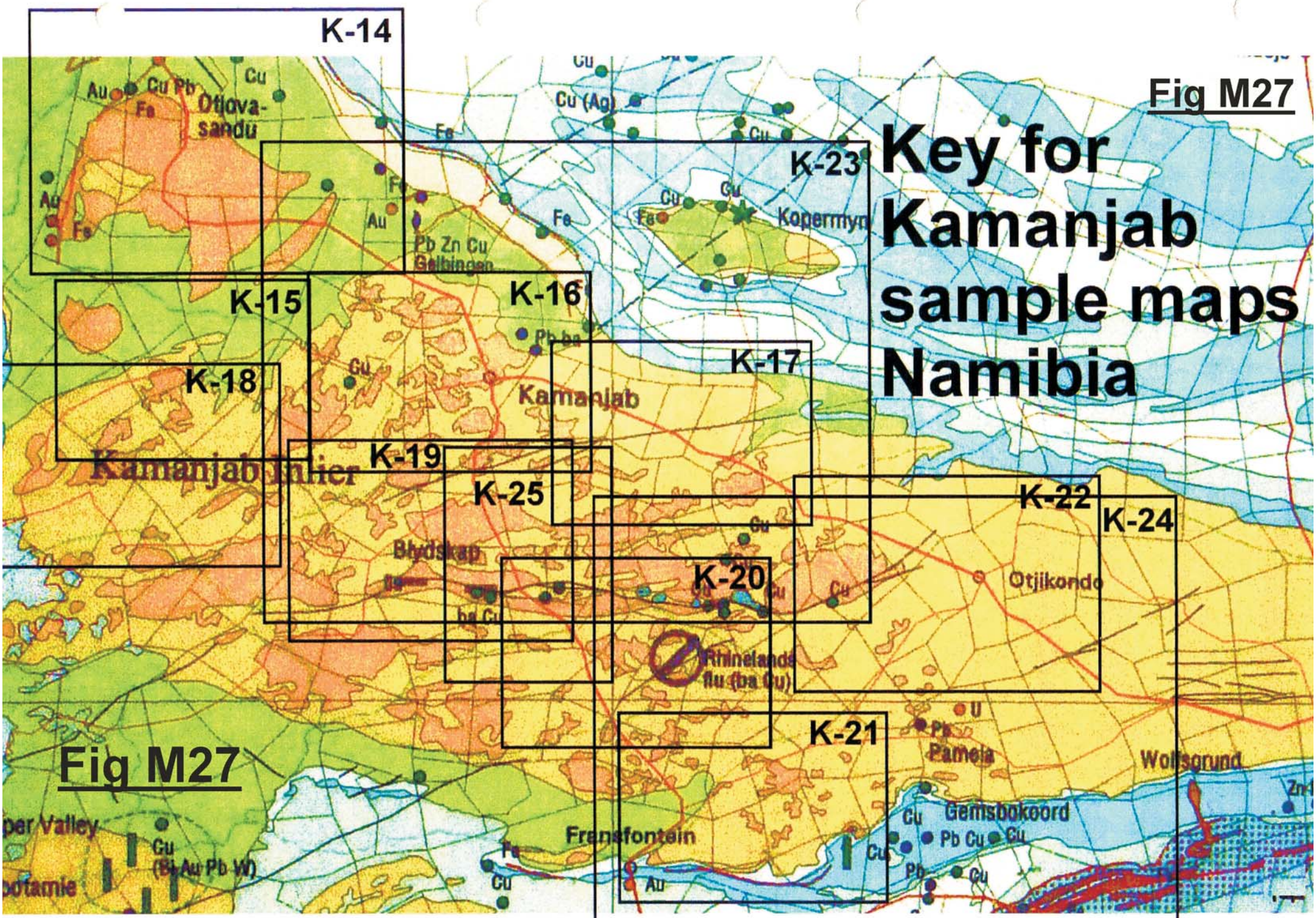
Fig M27
Key for Kamanjab sample maps Namibia
K-14
K-15
K-16
K-17
K-18
K-19
K-20
K-21
K-22
K-23
K-24
K-25
Fig M27
Otjova-sandu
Kamanjab
Kamanjab Inlier
Blydskap
Rhinelands flu (ba Cu)
Otjikondo
Pamela
Wolfsgrund
Gemsbokoord
Fransfontein
Kopermyn
Pb Zn Cu Gelbingen

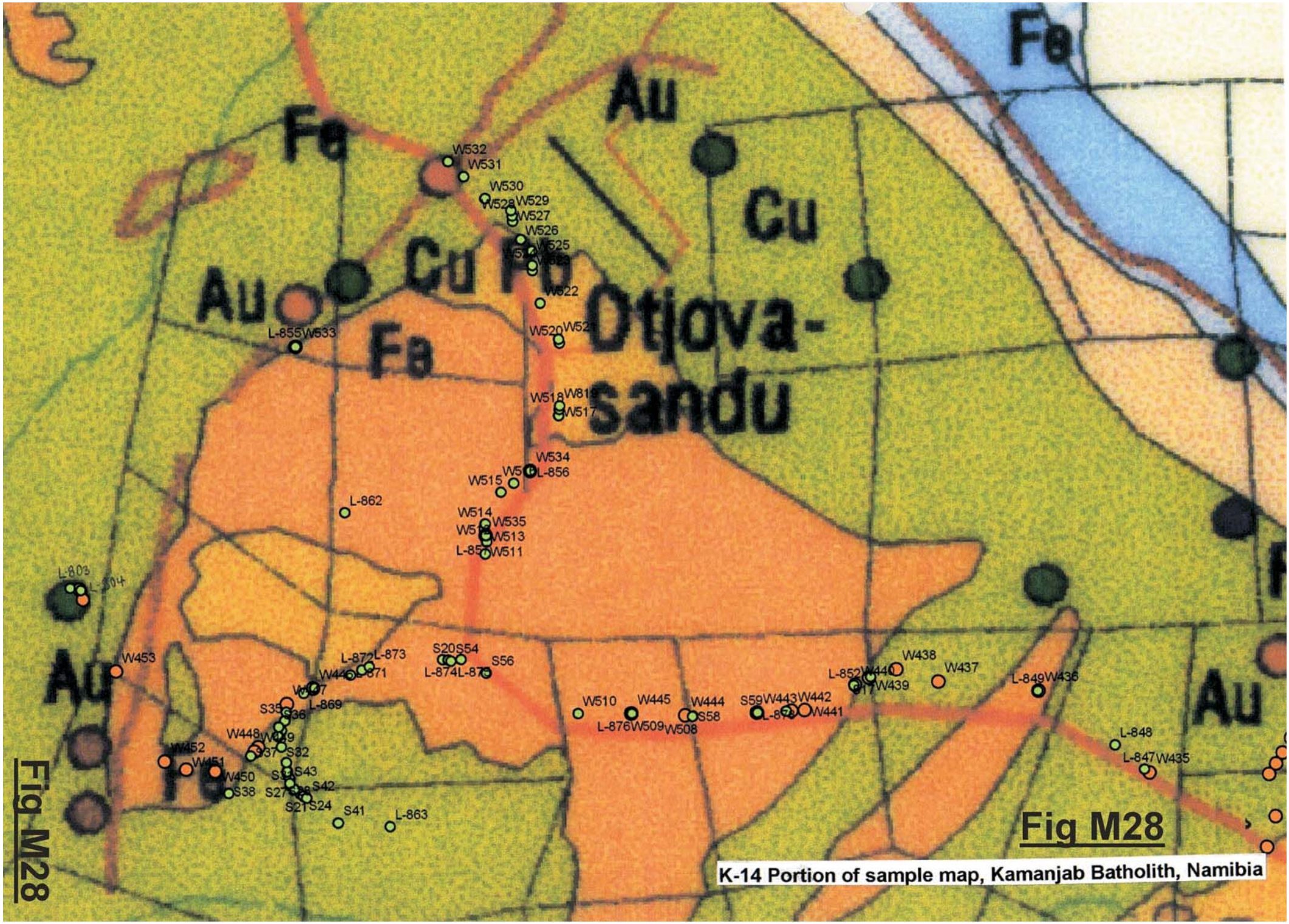
Fig M28
Fig M28
K-14 Portion of sample map, Kamanjab Batholith, Namibia

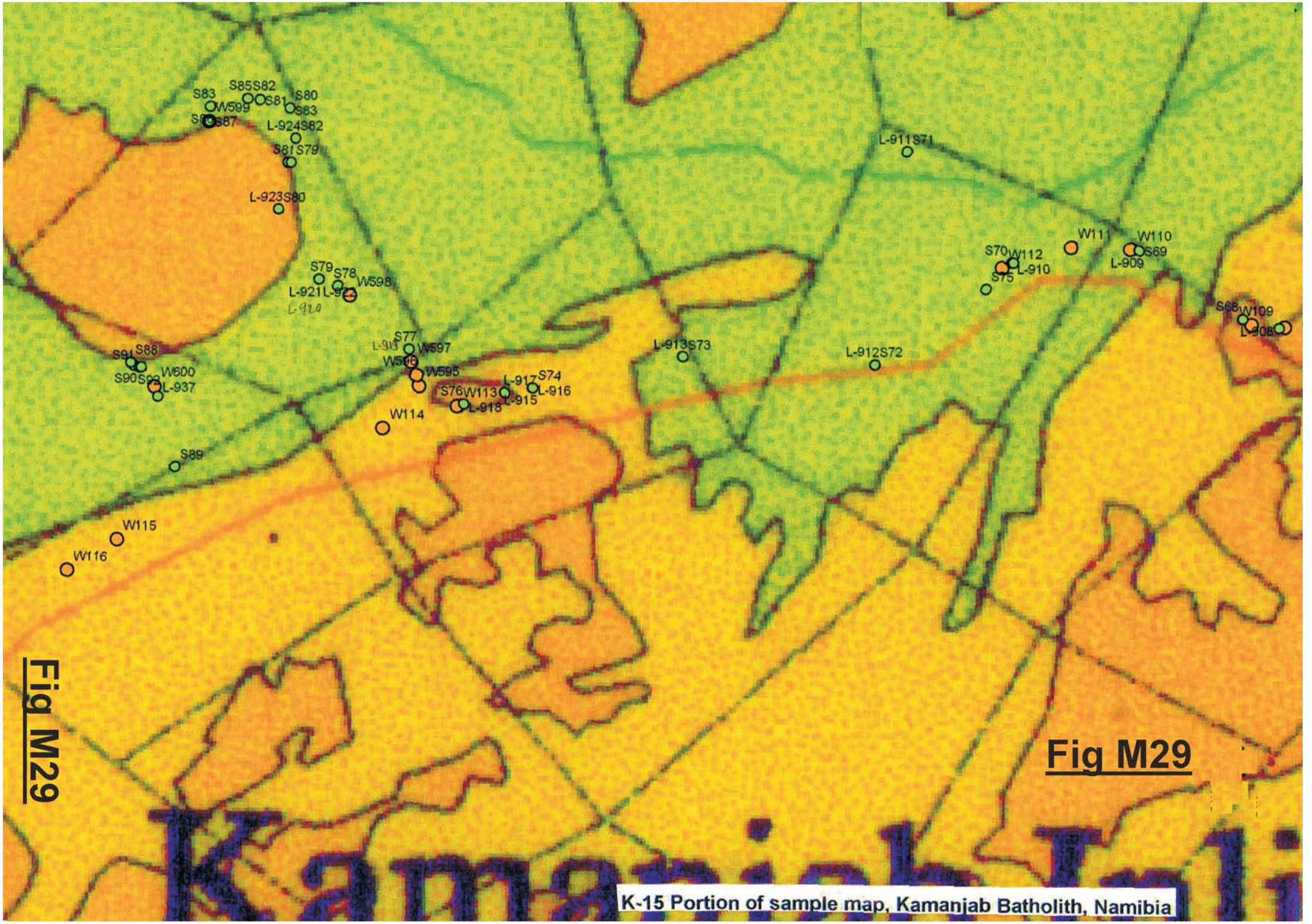
S83
S85S82
S81
S80
W599
S83
L-924S82
S81S79
L-923S80
S79
S78
W598
L-921
L-920
S77
L-919
W597
W596
W595
S76
W113
L-918
L-917
S74
L-916
L-915
W114
S91
S88
S90
W600
L-937
S89
W115
W116
L-911S71
W111
W110
S70
W112
S69
L-910
L-909
S75
L-913S73
L-912S72
S68
W109
L-908
Fig M29
Fig M29
K-15 Portion of sample map, Kamanjab Batholith, Namibia

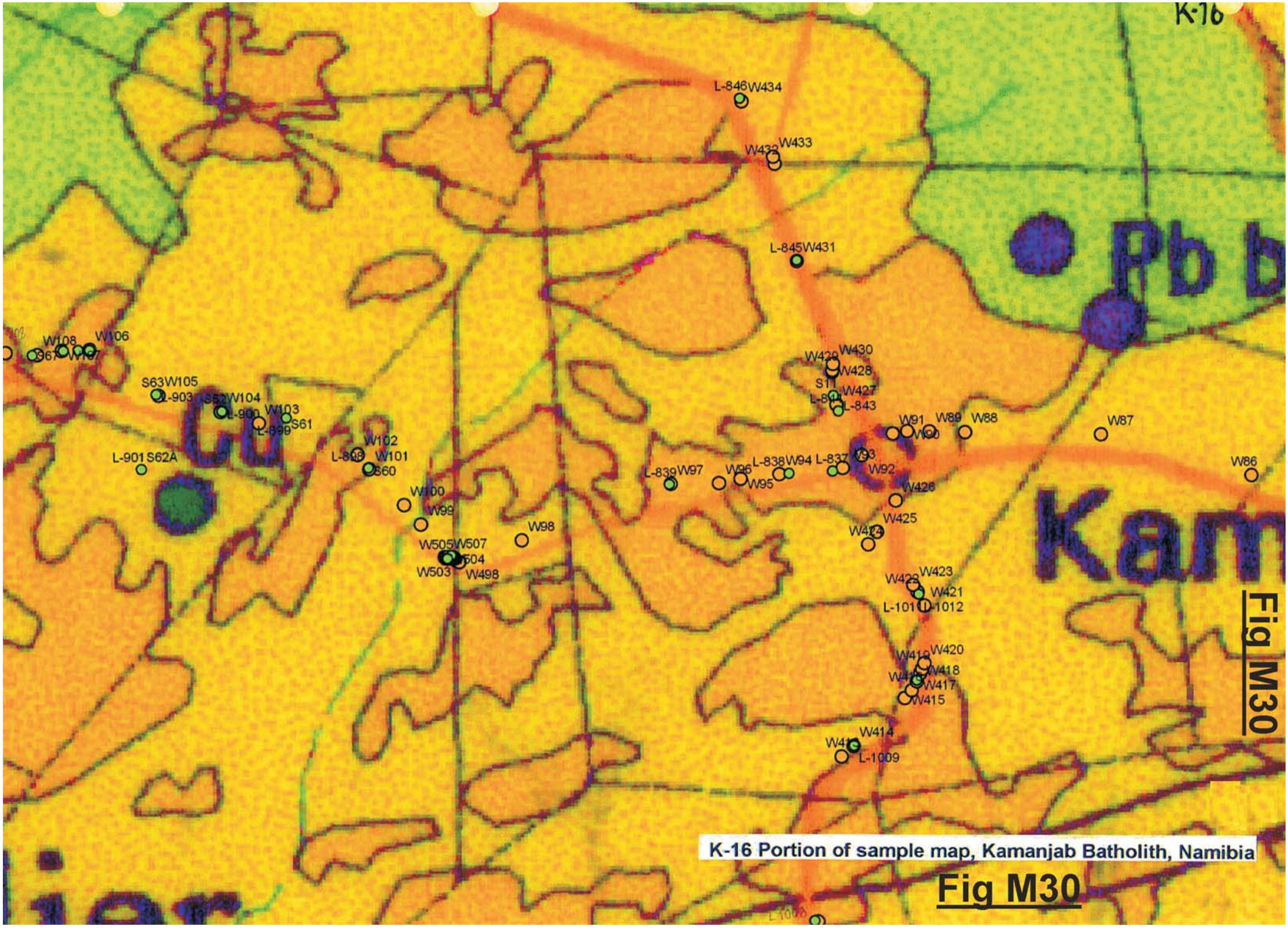

K-16 Portion of sample map, Kamanjab Batholith, Namibia

Fig M30

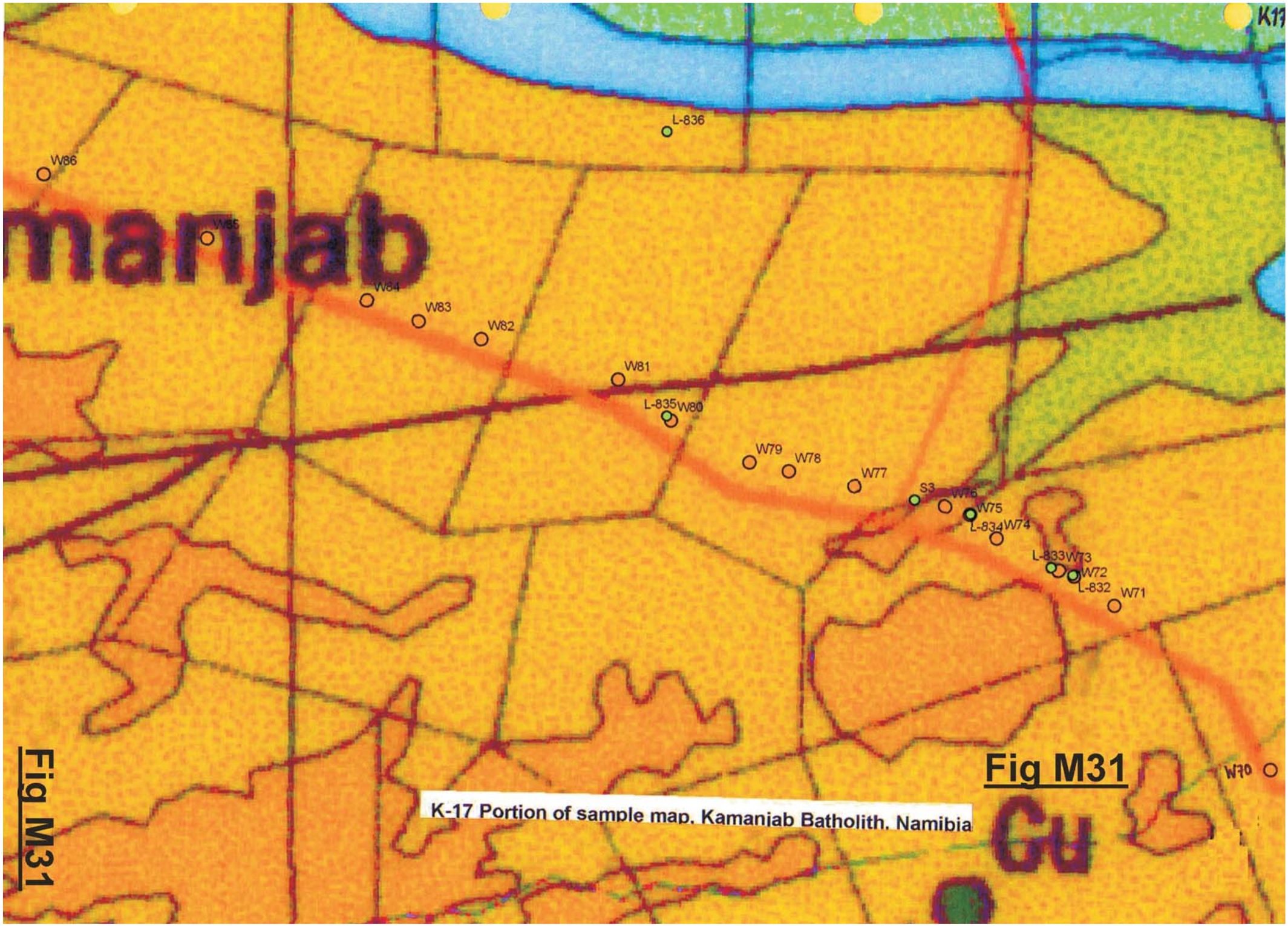

Fig M31

K-17 Portion of sample map, Kamanjab Batholith, Namibia

Fig M31

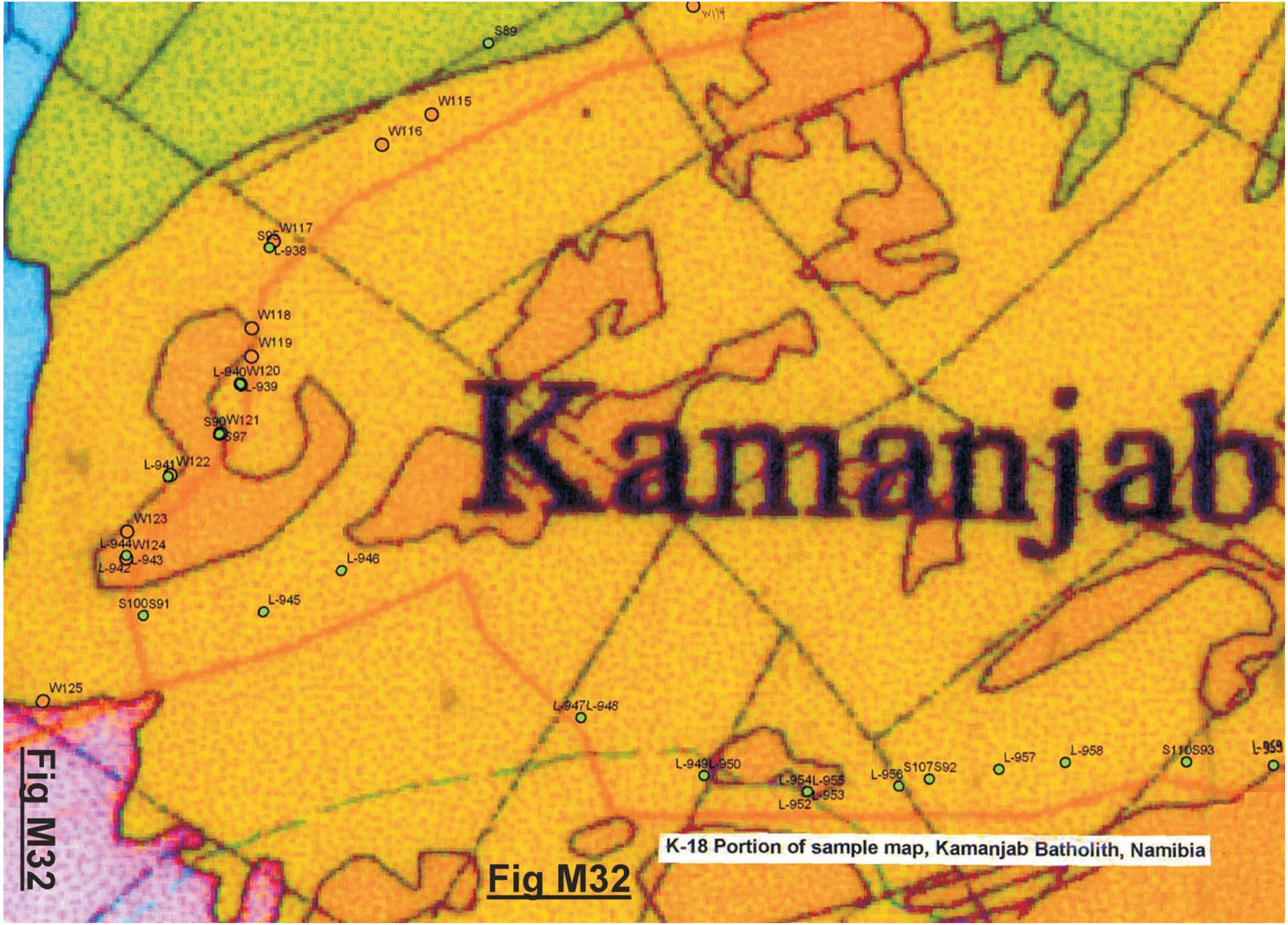

Fig M32

K-18 Portion of sample map, Kamanjab Batholith, Namibia

Fig M32

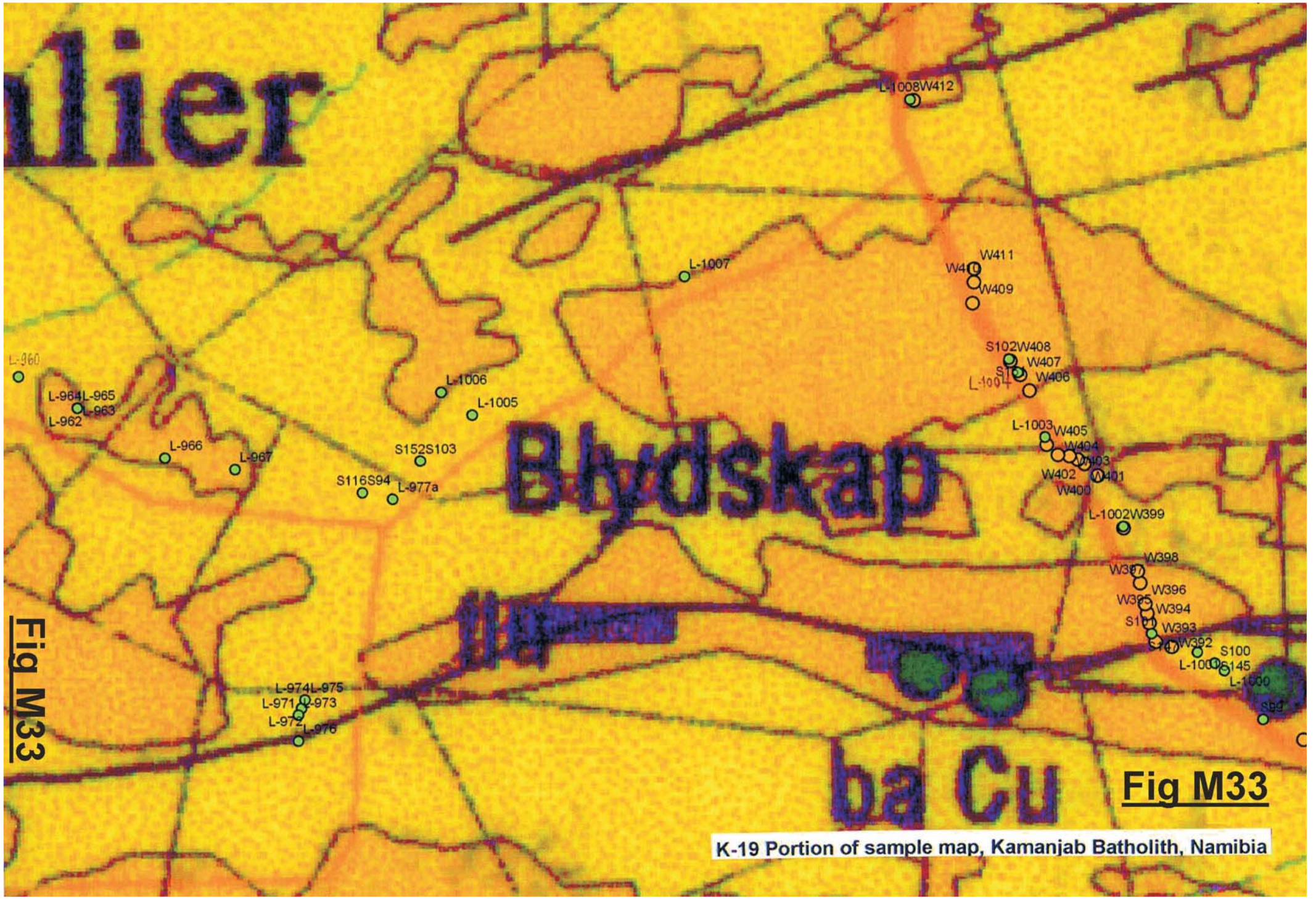

Fig M33

K-19 Portion of sample map, Kamanjab Batholith, Namibia

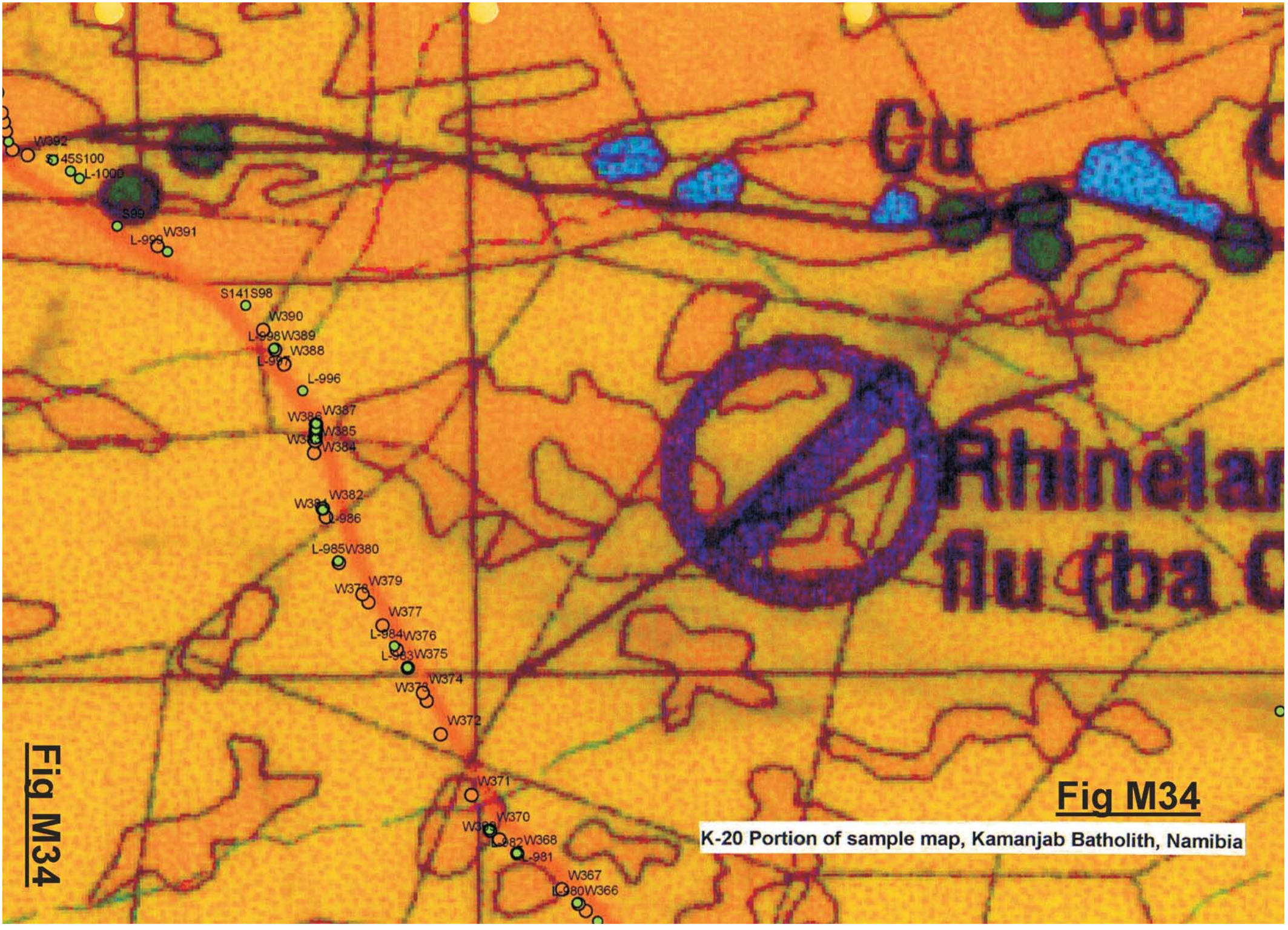

Fig M34

Fig M34

K-20 Portion of sample map, Kamanjab Batholith, Namibia

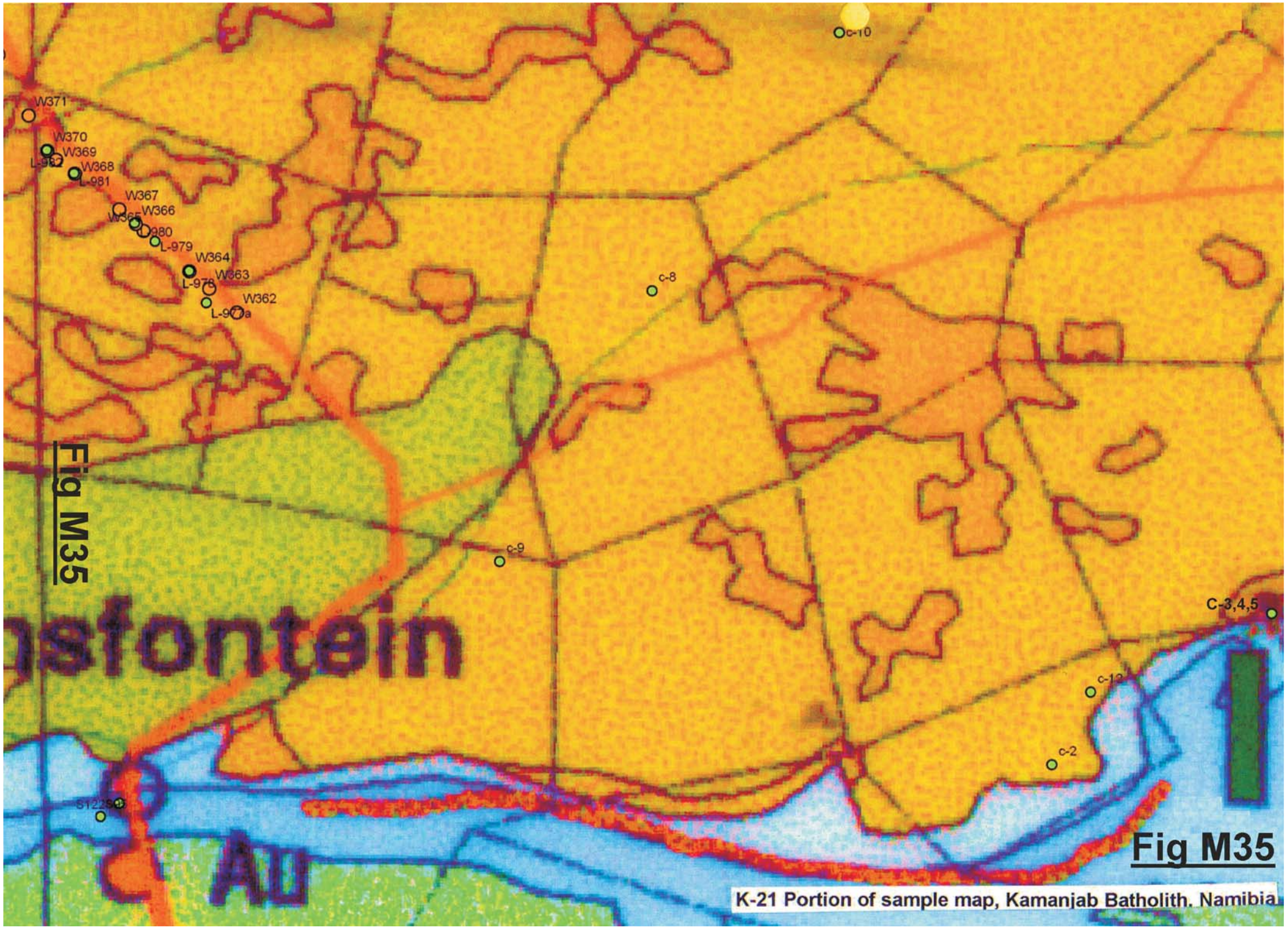

Fig M35

K-21 Portion of sample map, Kamanjab Batholith, Namibia

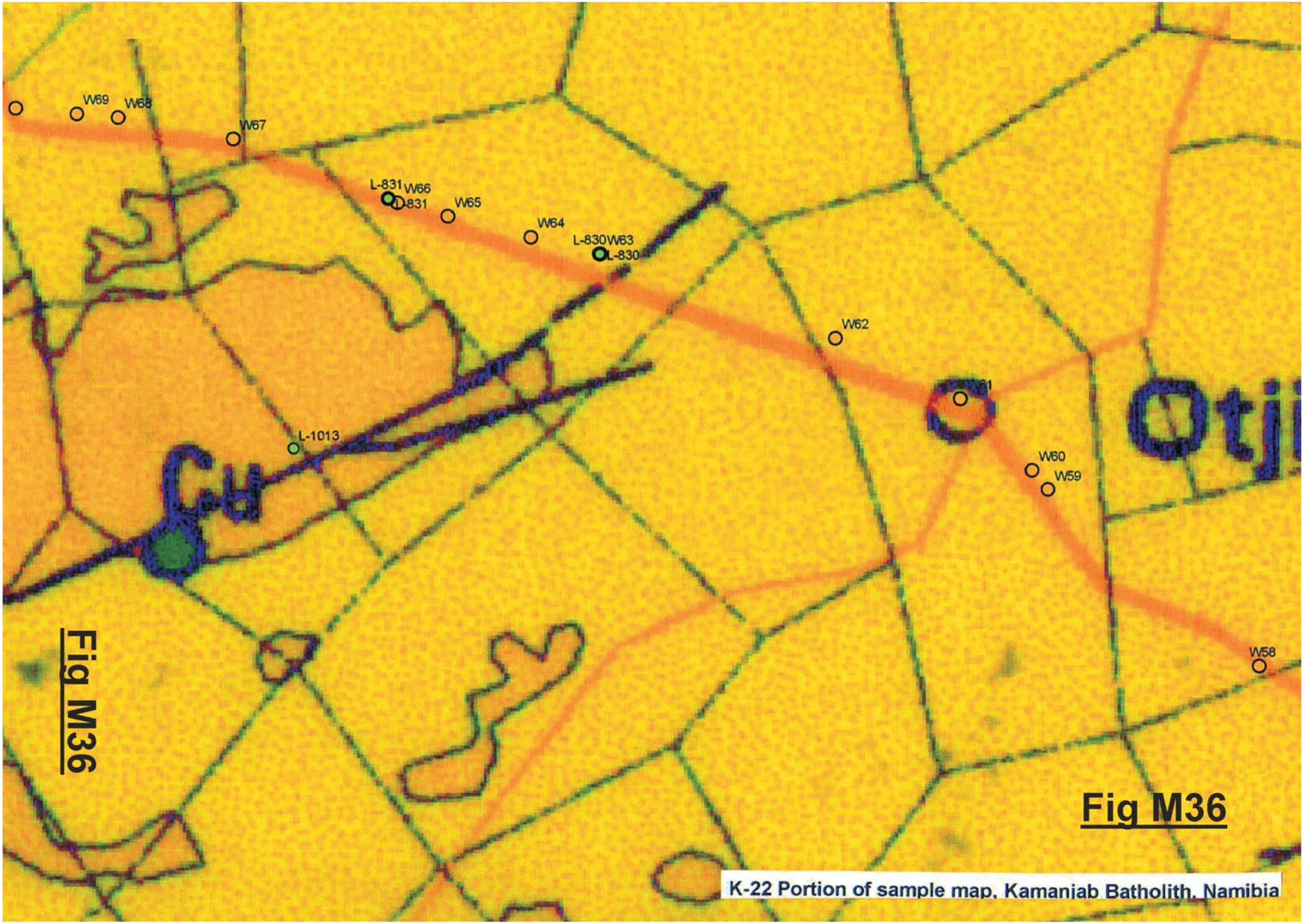

K-22 Portion of sample map, Kamaniab Batholith, Namibia

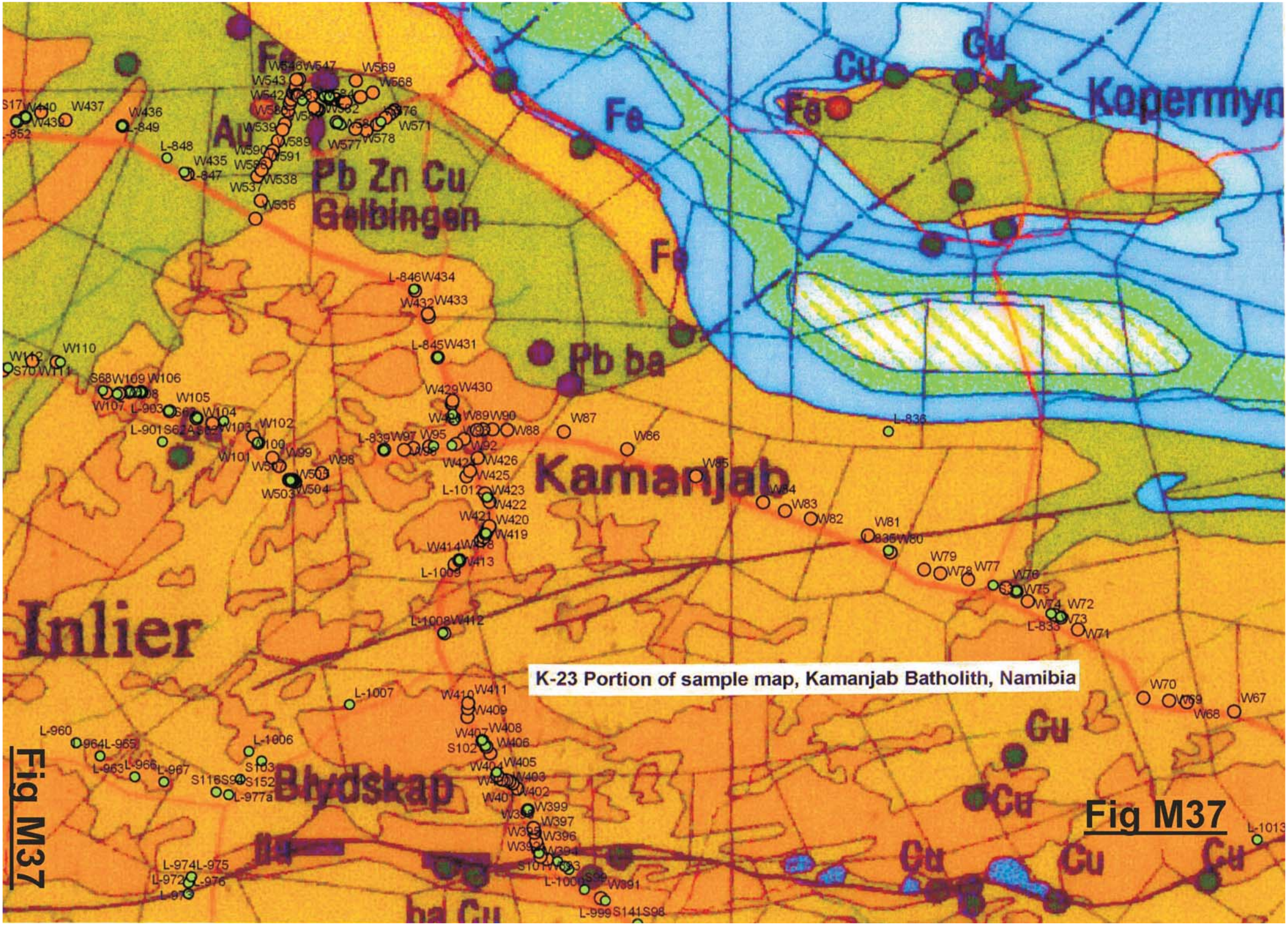
Fe
Cu
Cu
Fe
Kopermyn
Fe
Au
Pb Zn Cu
Gelbingen
Fe
Pb ba
Kamanjab
Inlier
Blydskap
Gu
Cu
Cu
Cu
Cu
K-23 Portion of sample map, Kamanjab Batholith, Namibia
Fig M37
Fig M37

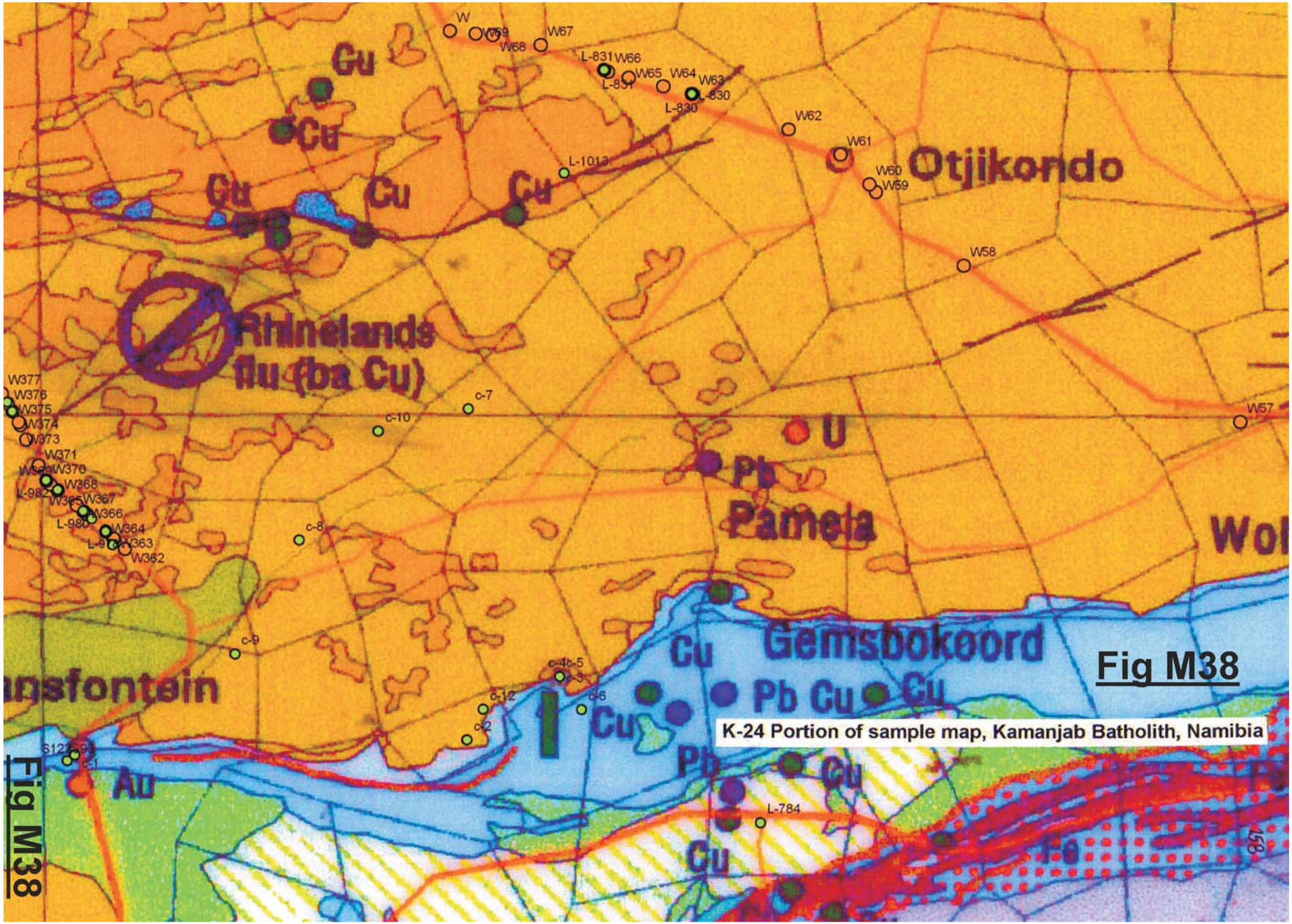
Fig M38
K-24 Portion of sample map, Kamanjab Batholith, Namibia
Otjikondo
Rhinelands
flu (ba Cu)
Pamela
Gemsbokoord
Cu
Pb
U
Au
W
W67
W68
W66
W65
W64
W63
W62
W61
W60
W59
W58
W57
L-831
L-830
L-1013
L-784
c-7
c-10
c-8
c-9
c-12
c-2
c-6
c-4
c-5
c-3
W377
W376
W375
W374
W373
W371
W370
W368
W367
W366
W364
W363
W362
L-982
L-980
158

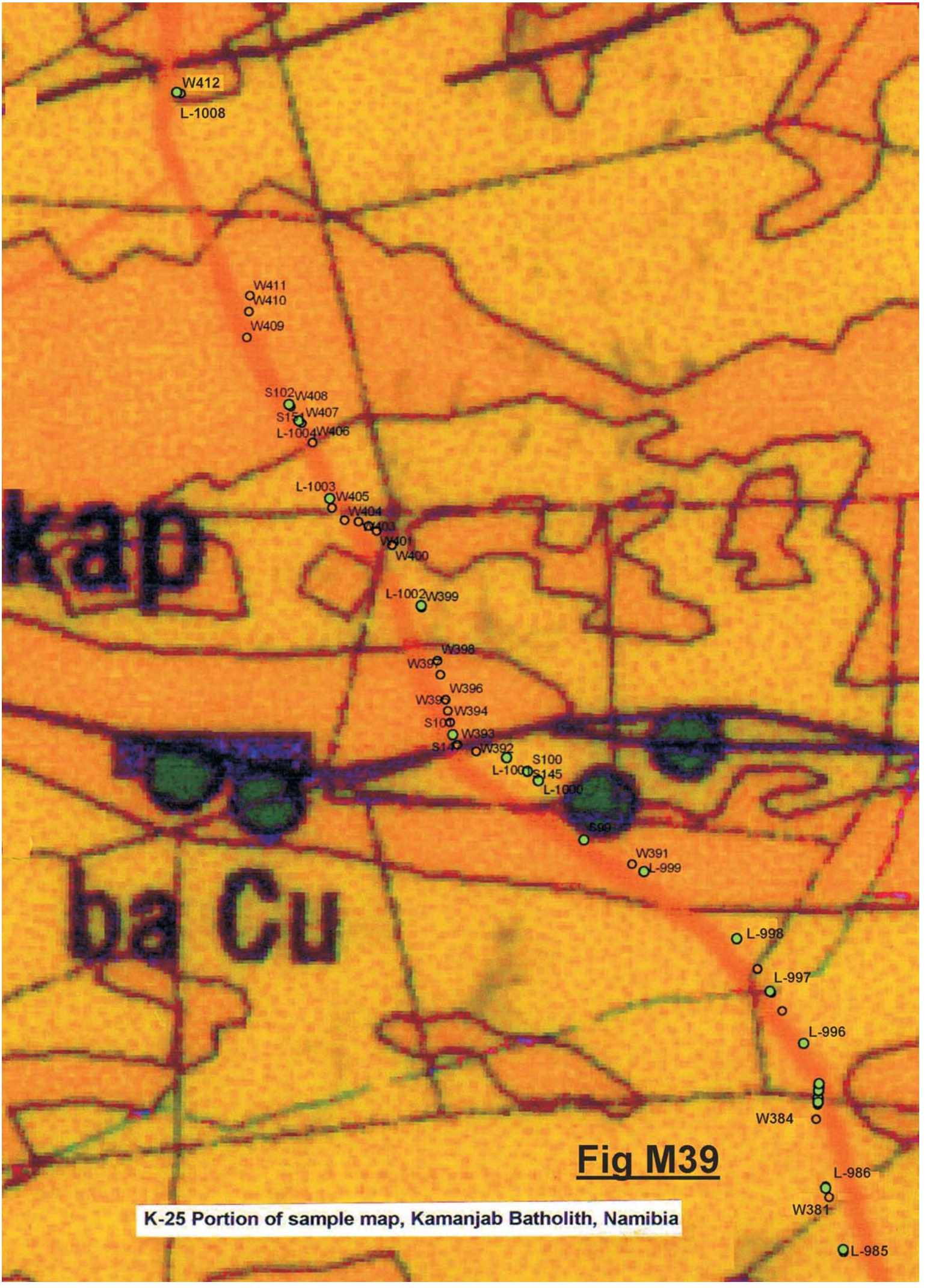

Fig M39

K-25 Portion of sample map, Kamanjab Batholith, Namibia

APPENDIX B
TAS DIAGRAM FOR SUITES OF THE KAMANJAB BATHOLITH, NAMIBIA

F1	Suite A, 166
F2	Suite B, 167
F3	Suite C, 168
F4	Suite D, 169
F5	Suite E, 170
F6	Suite F, 171
F7	Suite G, 172
F8	Suite H, 173
F9	Suite I, 174
F10	Suite J, 175
F11	Suite K, 176
F12	Suite L, 177
F13	Suite M, 178
F14	Suite N, 179
F15	Suite P, 180
F16	Suite Q, 181

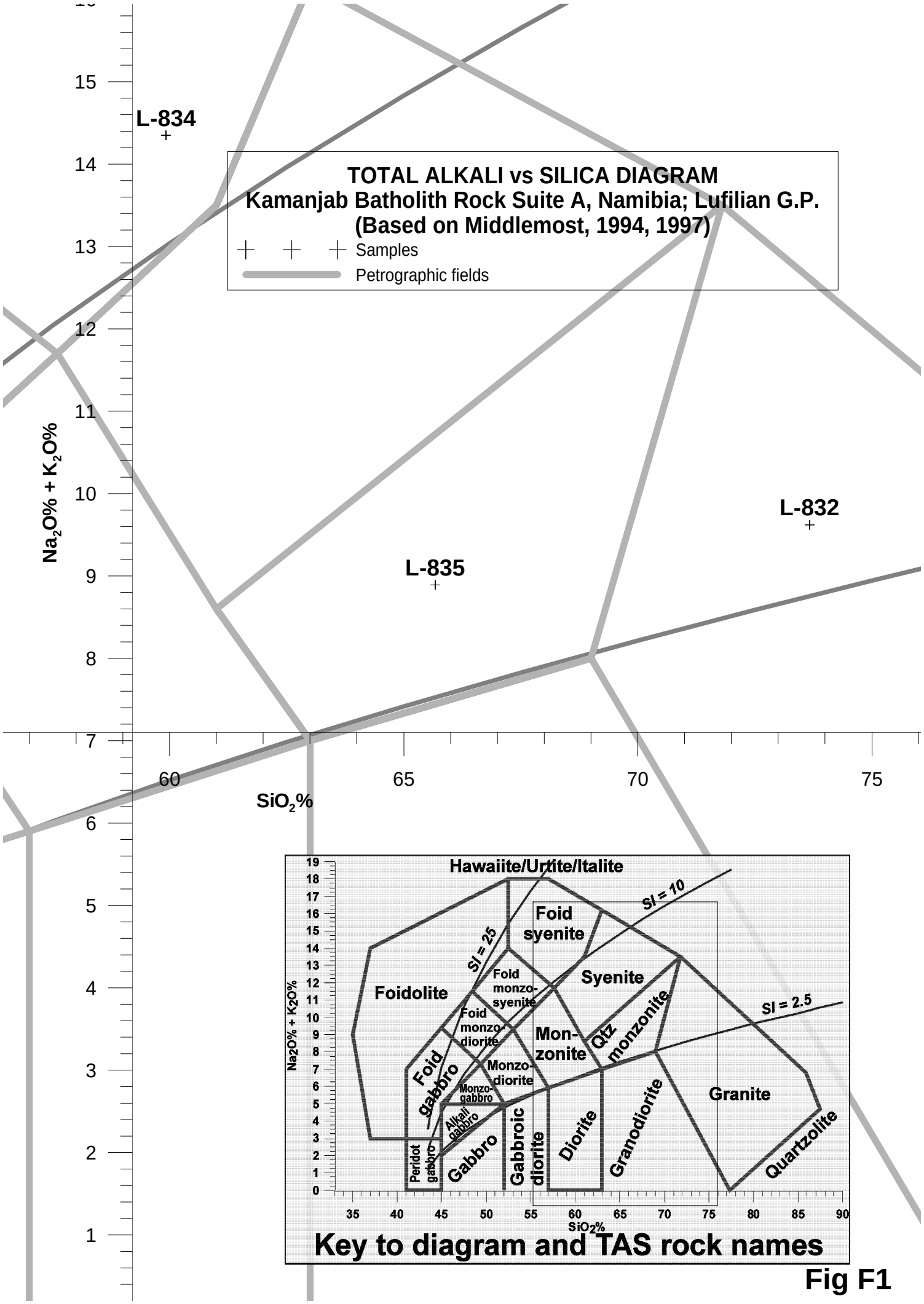
TOTAL ALKALI vs SILICA DIAGRAM
Kamanjab Batholith Rock Suite A, Namibia; Lufilian G.P.
(Based on Middlemost, 1994, 1997)
Samples
Petrographic fields
L-834
L-832
L-835
Na2O% + K2O%
SiO2%
Hawaiite/Urtite/Italite
Foid syenite
Syenite
Foidolite
Foid monzo-syenite
Foid monzo-diorite
Mon-zonite
Qtz monzonite
Granite
Foid gabbro
Monzo-diorite
Monzo-gabbro
Alkali gabbro
Peridot gabbro
Gabbro
Gabbroic diorite
Diorite
Granodiorite
Quartzolite
SI = 10
SI = 25
SI = 2.5
Key to diagram and TAS rock names

Fig F1

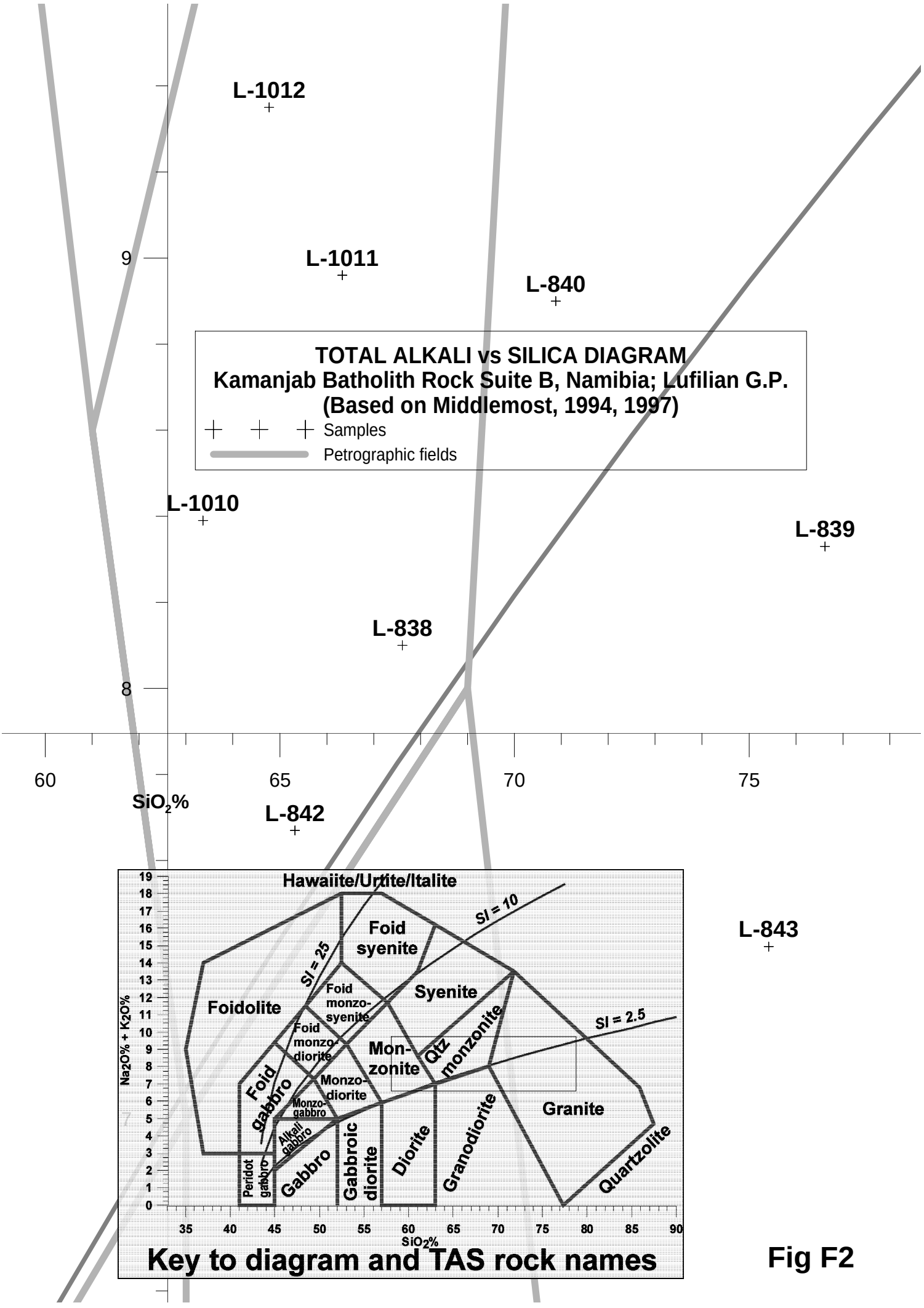
L-1012
L-1011
L-840
TOTAL ALKALI vs SILICA DIAGRAM
Kamanjab Batholith Rock Suite B, Namibia; Lufilian G.P.
(Based on Middlemost, 1994, 1997)
Samples
Petrographic fields
L-1010
L-839
L-838
L-842
L-843
9
8
60
65
70
75
SiO2%
Hawaiite/Urtite/Italite
Foid syenite
Sl = 10
Sl = 25
Sl = 2.5
Foidolite
Foid monzo-syenite
Syenite
Foid monzo-diorite
Mon-zonite
Qtz monzonite
Foid gabbro
Monzo-diorite
Monzo-gabbro
Granite
Alkali gabbro
Peridot gabbro
Gabbro
Gabbroic diorite
Diorite
Granodiorite
Quartzolite
Na2O% + K2O%
SiO2%
Key to diagram and TAS rock names

Fig F2

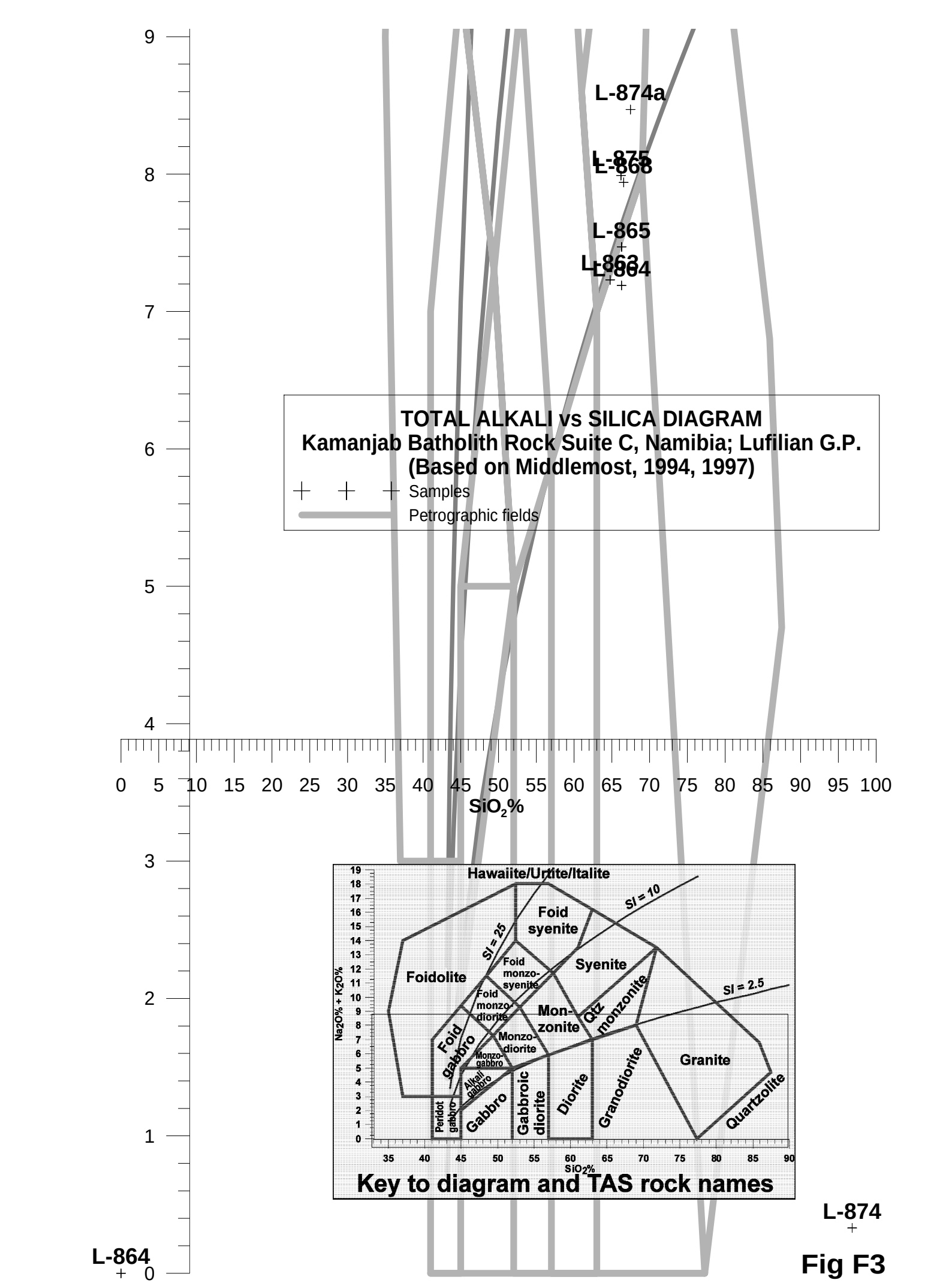
L-874a
L-875
L-868
L-865
L-863
L-864
TOTAL ALKALI vs SILICA DIAGRAM
Kamanjab Batholith Rock Suite C, Namibia; Lufilian G.P.
(Based on Middlemost, 1994, 1997)
Samples
Petrographic fields
SiO2%
Hawaiite/Urtite/Italite
Sl = 10
Sl = 25
Sl = 2.5
Foid syenite
Foid monzo-syenite
Syenite
Foidolite
Foid monzo-diorite
Mon-zonite
Qtz monzonite
Foid gabbro
Monzo-diorite
Monzo-gabbro
Granite
Alkali gabbro
Peridot gabbro
Gabbro
Gabbroic diorite
Diorite
Granodiorite
Quartzolite
Na2O% + K2O%
SiO2%
Key to diagram and TAS rock names
L-874
L-864

Fig F3

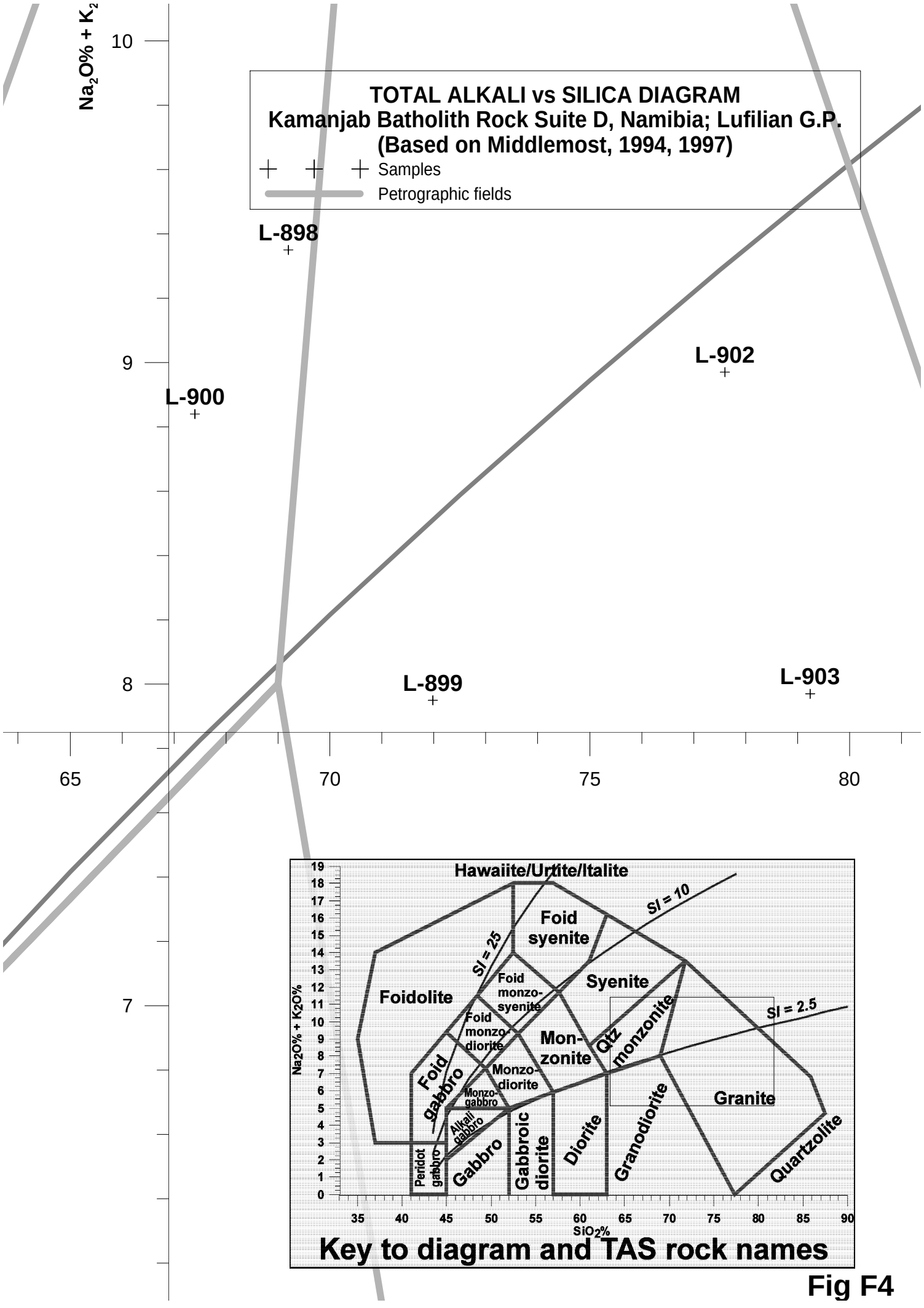
TOTAL ALKALI vs SILICA DIAGRAM
Kamanjab Batholith Rock Suite D, Namibia; Lufilian G.P.
(Based on Middlemost, 1994, 1997)
Samples
Petrographic fields
Na2O% + K2
10
9
8
7
65
70
75
80
L-898
L-902
L-900
L-899
L-903
Hawaiite/Urtite/Italite
Sl = 10
Sl = 25
Sl = 2.5
Foid syenite
Foidolite
Foid monzo-syenite
Syenite
Foid monzo-diorite
Mon-zonite
Qtz monzonite
Foid gabbro
Monzo-diorite
Monzo-gabbro
Granite
Alkali gabbro
Peridot gabbro
Gabbro
Gabbroic diorite
Diorite
Granodiorite
Quartzolite
Na2O% + K2O%
SiO2%
Key to diagram and TAS rock names

Fig F4

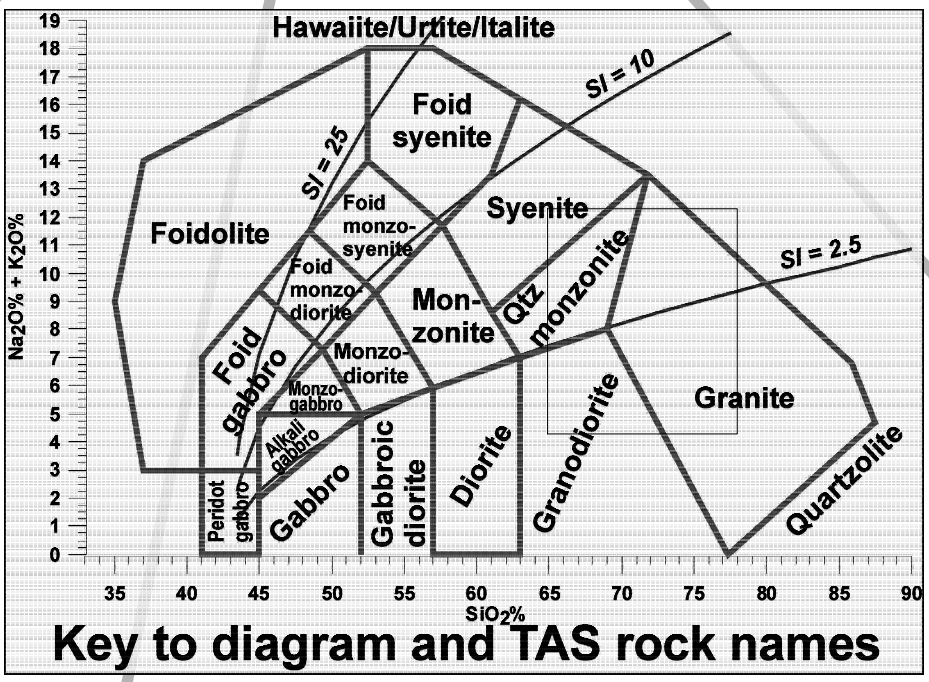

TOTAL ALKALI vs SILICA DIAGRAM
Kamanjab Batholith Rock Suite E, Namibia; Lufilian G.P.
(Based on Middlemost, 1994, 1997)

Samples

Petrographic fields

Fig F5

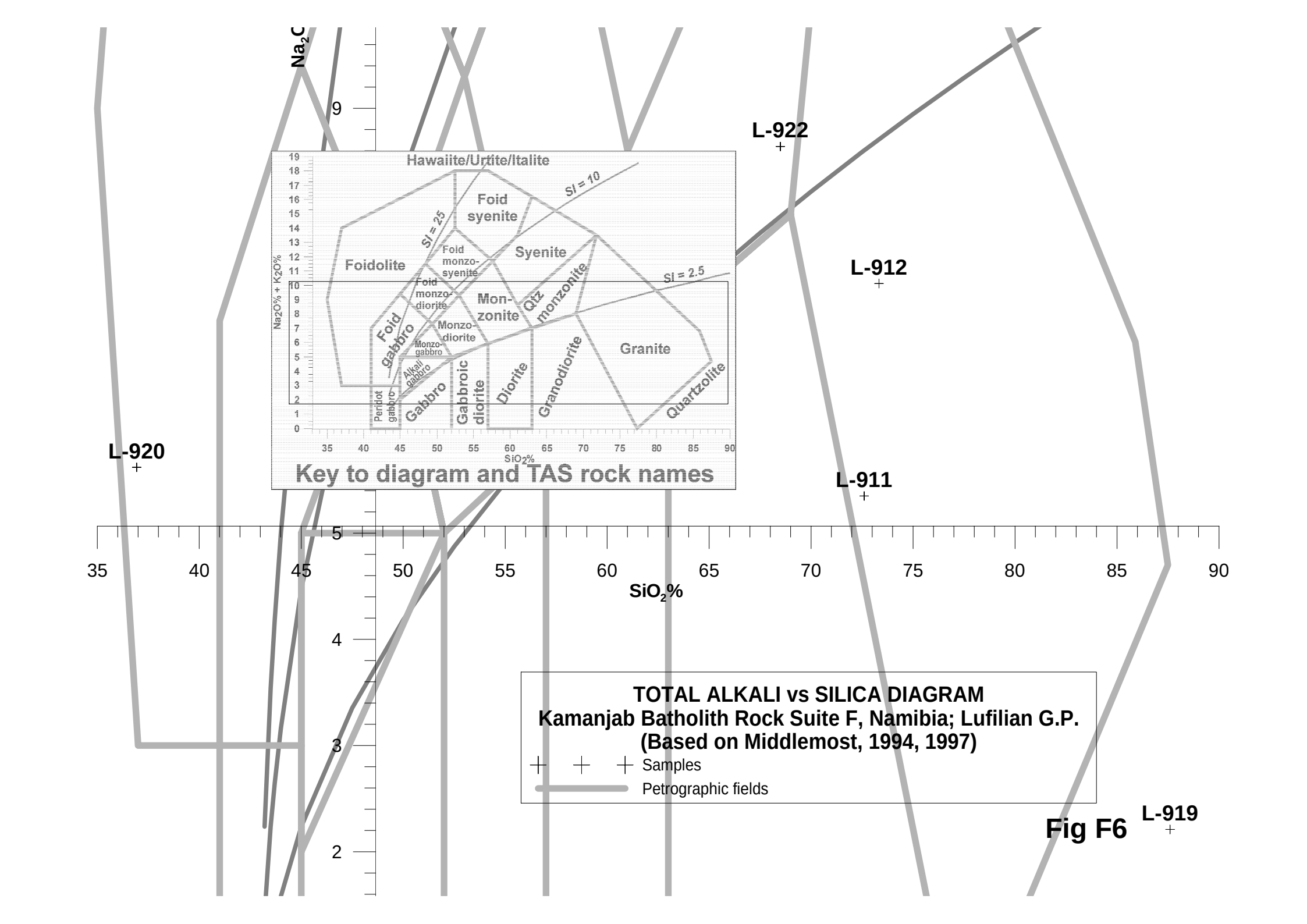
Hawaiite/Ultite/Italite
SI = 10
SI = 25
SI = 2.5
Foid syenite
Foid monzo-syenite
Syenite
Foidolite
Foid monzo-diorite
Mon-zonite
Qtz monzonite
Monzo-diorite
Foid gabbro
Monzo-gabbro
Alkali gabbro
Peridot gabbro
Gabbro
Gabbroic diorite
Diorite
Granodiorite
Granite
Quartzolite
Na2O% + K2O%
SiO2%
Key to diagram and TAS rock names
L-922
L-912
L-920
L-911
L-919
SiO2%
TOTAL ALKALI vs SILICA DIAGRAM
Kamanjab Batholith Rock Suite F, Namibia; Lufilian G.P.
(Based on Middlemost, 1994, 1997)
Samples
Petrographic fields

Fig F6

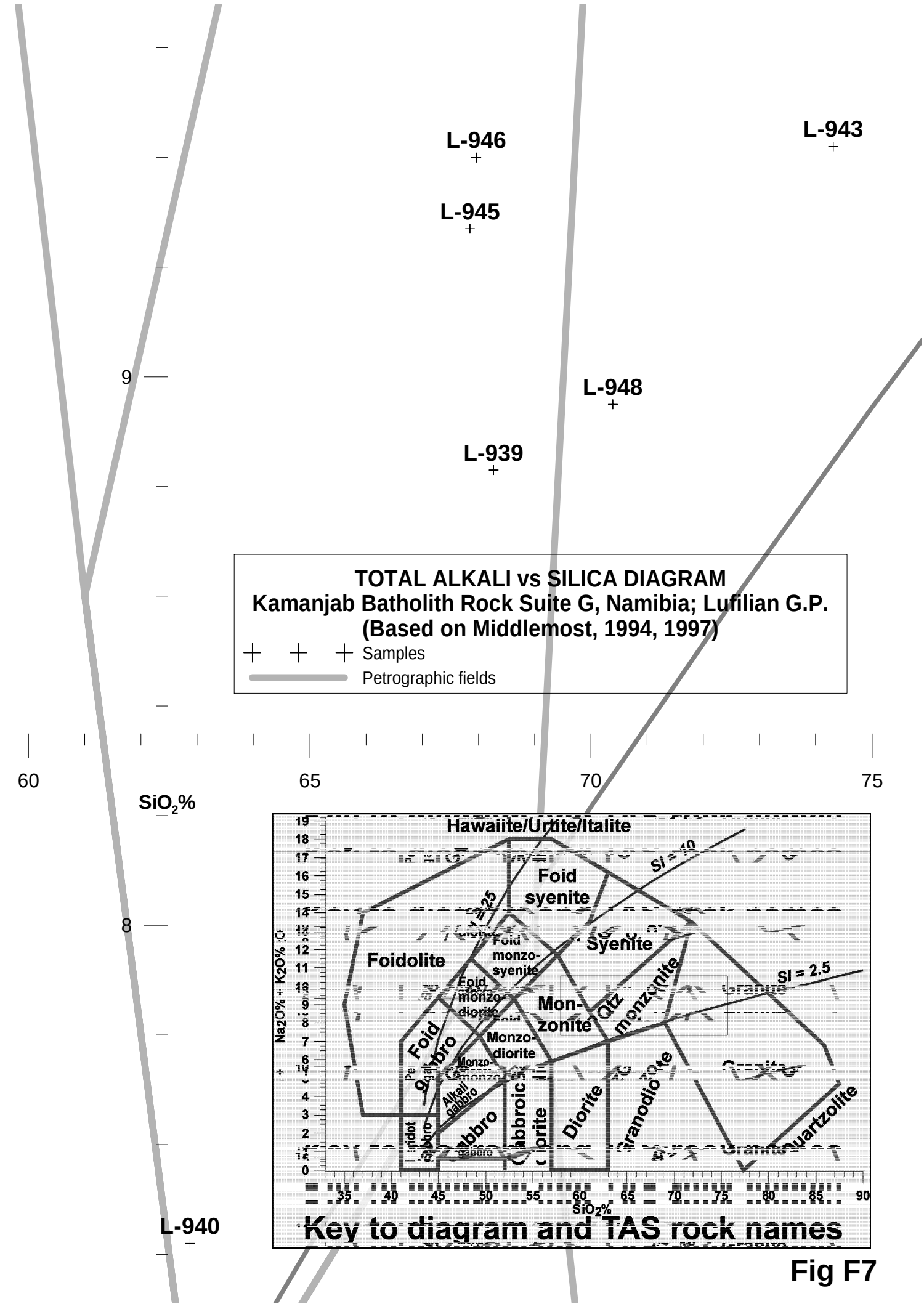
L-946
L-943
L-945
9
L-948
L-939
TOTAL ALKALI vs SILICA DIAGRAM
Kamanjab Batholith Rock Suite G, Namibia; Lufilian G.P.
(Based on Middlemost, 1994, 1997)
Samples
Petrographic fields
60
65
70
75
SiO2%
8
L-940
Hawaiite/Urtite/Italite
Foid syenite
Sl = 10
Sl = 2.5
Foidolite
Foid monzo-syenite
Syenite
Foid monzo-diorite
Mon-zonite
Qtz monzonite
Granite
Monzo-diorite
Foid gabbro
Monzo-gabbro
Alkali gabbro
Gabbro
Gabbroic diorite
Diorite
Granodiorite
Granite
Quartzolite
Na2O% + K2O%
SiO2%
Key to diagram and TAS rock names

Fig F7

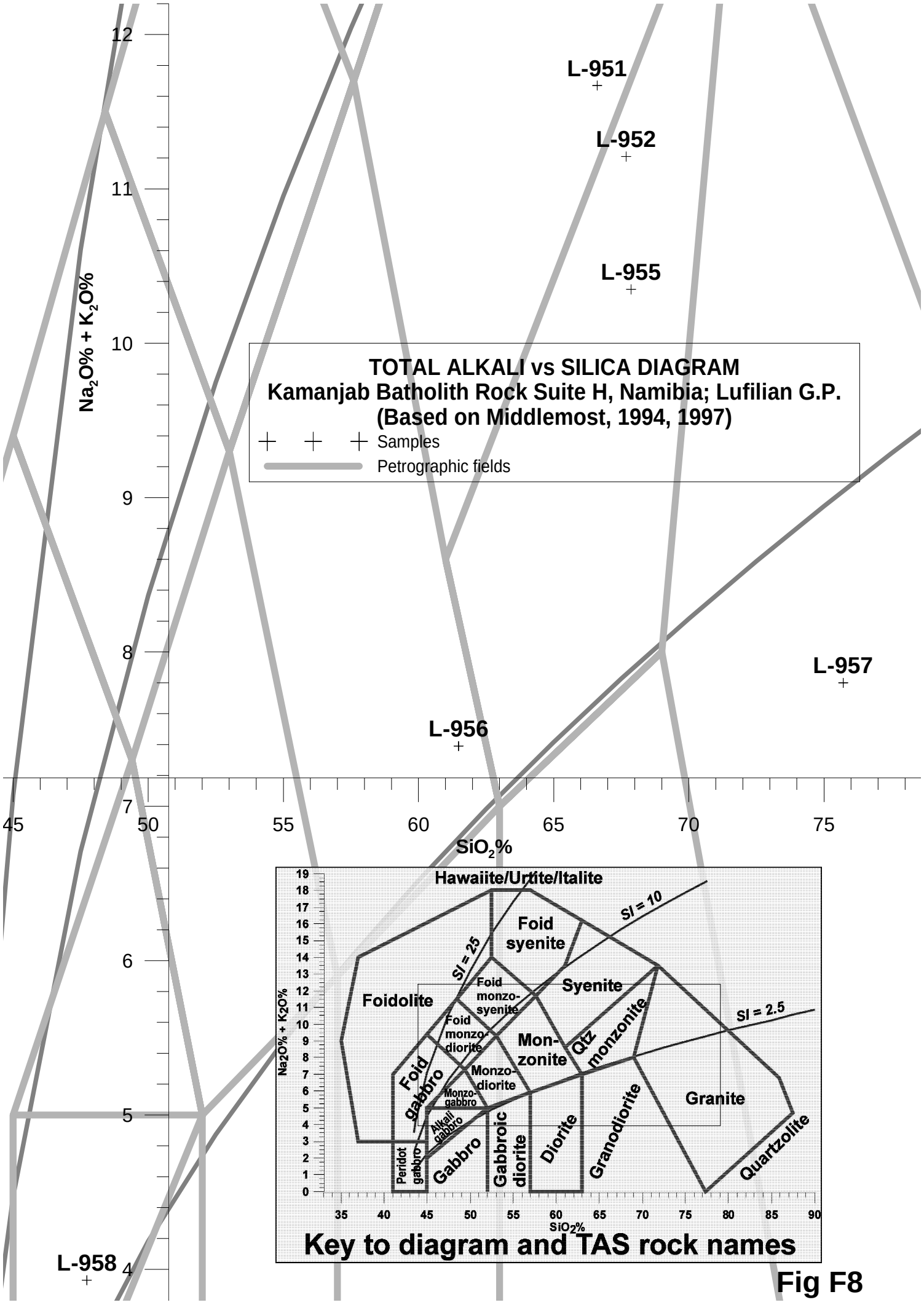
TOTAL ALKALI vs SILICA DIAGRAM
Kamanjab Batholith Rock Suite H, Namibia; Lufilian G.P.
(Based on Middlemost, 1994, 1997)
Samples
Petrographic fields
L-951
L-952
L-955
L-957
L-956
L-958
Na2O% + K2O%
SiO2%
12
11
10
9
8
7
6
5
4
45
50
55
60
65
70
75
Hawaiite/Urtite/Italite
Sl = 10
Sl = 25
Sl = 2.5
Foid syenite
Syenite
Foidolite
Foid monzo-syenite
Foid monzo-diorite
Mon-zonite
Qtz monzonite
Foid gabbro
Monzo-diorite
Monzo-gabbro
Granite
Alkali gabbro
Gabbroic diorite
Diorite
Granodiorite
Peridot gabbro
Gabbro
Quartzolite
Key to diagram and TAS rock names

Fig F8

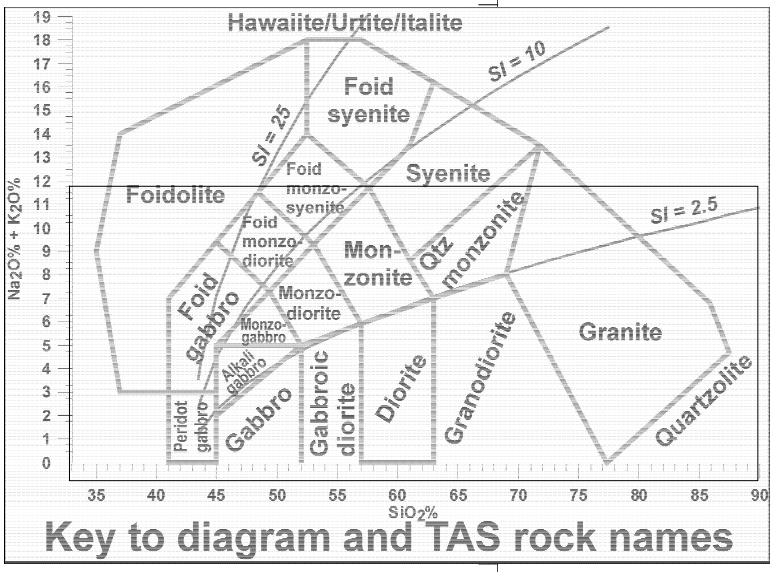
Hawaiite/Urtite/Italite
Foid syenite
Syenite
Foidolite
Foid monzo-syenite
Foid monzo-diorite
Mon-zonite
Qtz monzonite
Monzo-diorite
Monzo-gabbro
Foid gabbro
Alkali gabbro
Peridot gabbro
Gabbro
Gabbroic diorite
Diorite
Granodiorite
Granite
Quartzolite
Sl = 10
Sl = 25
Sl = 2.5
Na2O% + K2O%
SiO2%
Key to diagram and TAS rock names

Na2O% + K2O%
SiO2%
L-966
L-965
L-967
L-963
L-967a
TOTAL ALKALI vs SILICA DIAGRAM
Kamanjab Batholith Rock Suite I, Namibia; Lufilian G.P.
(Based on Middlemost, 1994, 1997)
Samples
Petrographic fields

Fig F9

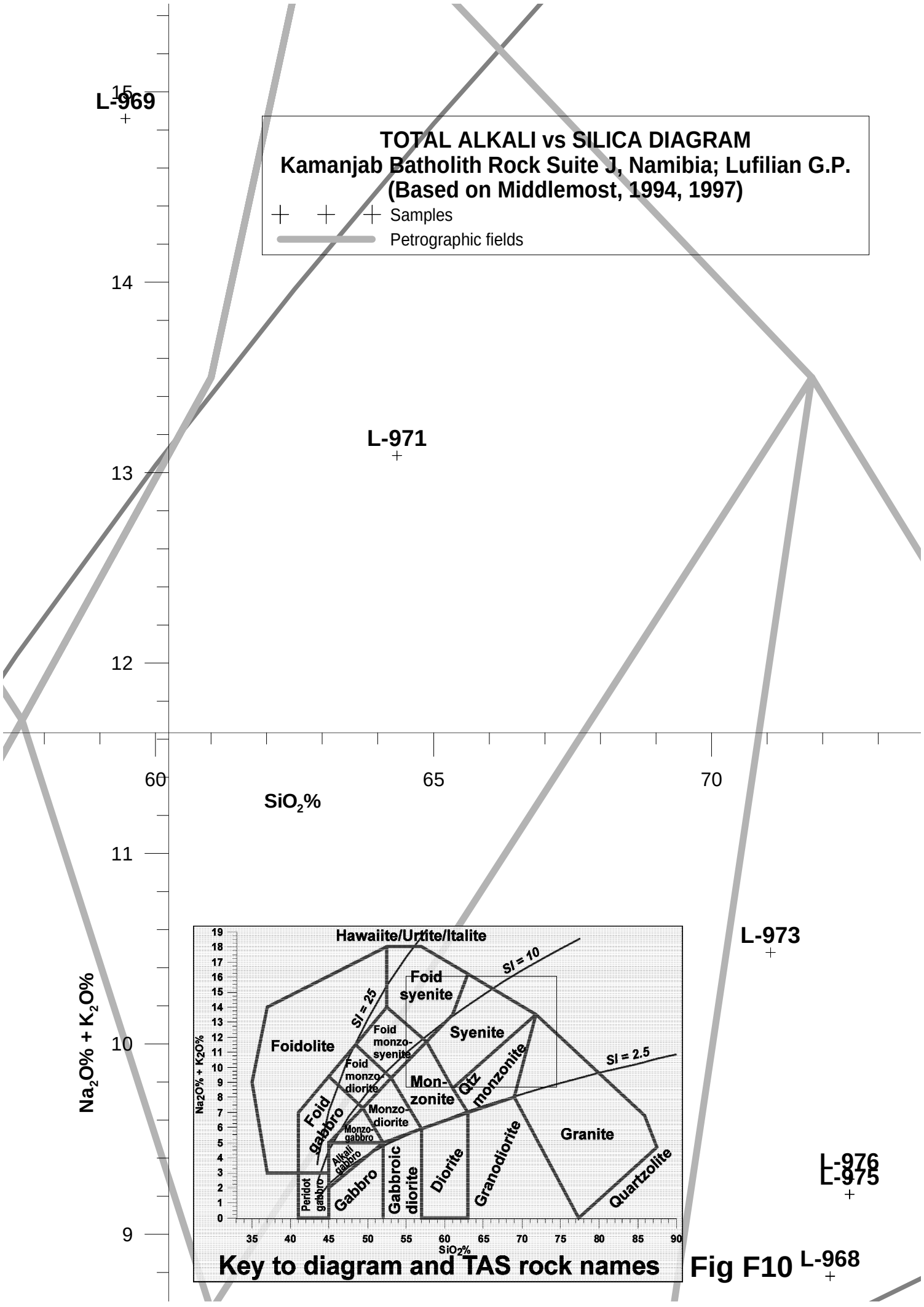
TOTAL ALKALI vs SILICA DIAGRAM
Kamanjab Batholith Rock Suite J, Namibia; Lufilian G.P.
(Based on Middlemost, 1994, 1997)
Samples
Petrographic fields
L-969
L-971
L-973
L-976
L-975
L-968
15
14
13
12
11
10
9
60
65
70
SiO2%
Na2O% + K2O%
Hawaiite/Urtite/Italite
Foid syenite
Syenite
Foidolite
Foid monzo-syenite
Foid monzo-diorite
Mon-zonite
Qtz monzonite
Monzo-diorite
Monzo-gabbro
Foid gabbro
Alkali gabbro
Peridot gabbro
Gabbro
Gabbroic diorite
Diorite
Granodiorite
Granite
Quartzolite
SI = 10
SI = 25
SI = 2.5
Key to diagram and TAS rock names

Fig F10

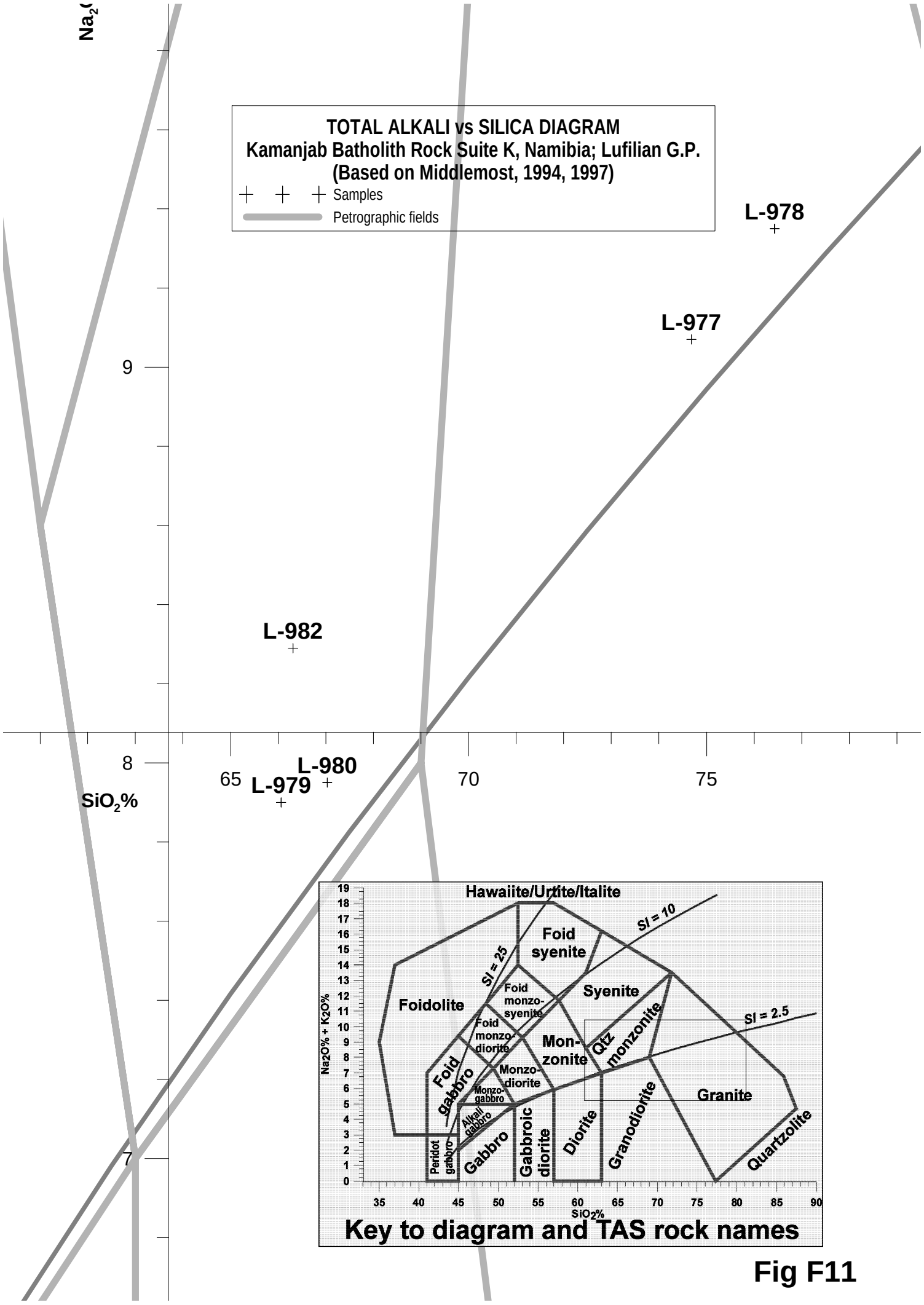
TOTAL ALKALI vs SILICA DIAGRAM
Kamanjab Batholith Rock Suite K, Namibia; Lufilian G.P.
(Based on Middlemost, 1994, 1997)
Samples
Petrographic fields
L-978
L-977
L-982
L-980
L-979
9
8
7
65
70
75
SiO2%
Hawaiite/Urtite/Italite
Sl = 10
Sl = 25
Sl = 2.5
Foid syenite
Syenite
Foidolite
Foid monzo-syenite
Foid monzo-diorite
Mon-zonite
Qtz monzonite
Monzo-diorite
Monzo-gabbro
Foid gabbro
Alkali gabbro
Granite
Peridot gabbro
Gabbro
Gabbroic diorite
Diorite
Granodiorite
Quartzolite
Na2O% + K2O%
SiO2%
Key to diagram and TAS rock names

Fig F11

TOTAL ALKALI vs SILICA DIAGRAM
Kamanjab Batholith Rock Suite L, Namibia; Lufilian G.P.
(Based on Middlemost, 1994, 1997)

Samples

Petrographic fields

$Na_2O\% + K_2O\%$

11

10

9

8

7

6

5

70

L-983

L-985

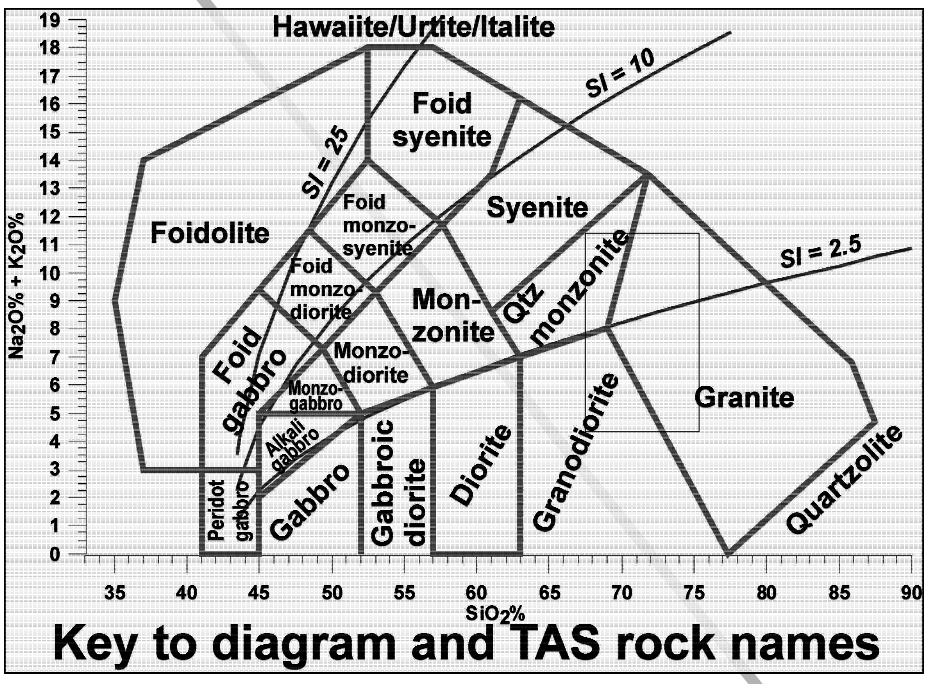

Fig F12

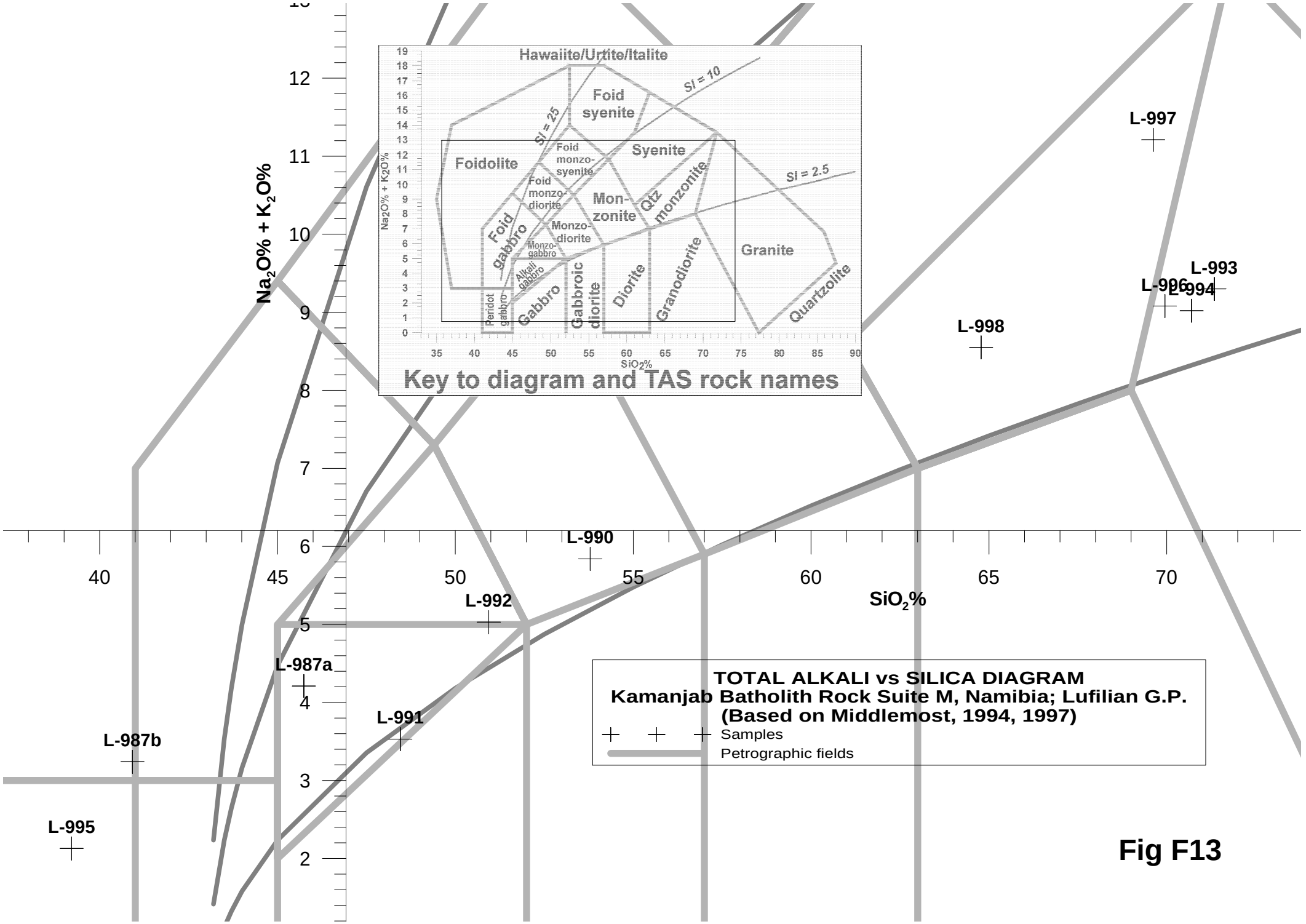
Hawaiite/Urtite/Italite
Foid syenite
SI = 10
SI = 25
SI = 2.5
Foidolite
Foid monzo-syenite
Syenite
Foid monzo-diorite
Mon-zonite
Qtz monzonite
Foid gabbro
Monzo-diorite
Monzo-gabbro
Granite
Alkali gabbro
Peridot gabbro
Gabbro
Gabbroic diorite
Diorite
Granodiorite
Quartzolite
Na2O% + K2O%
SiO2%
Key to diagram and TAS rock names
Na2O% + K2O%
SiO2%
L-997
L-993
L-994
L-996
L-998
L-990
L-992
L-987a
L-991
L-987b
L-995
TOTAL ALKALI vs SILICA DIAGRAM
Kamanjab Batholith Rock Suite M, Namibia; Lufilian G.P.
(Based on Middlemost, 1994, 1997)
Samples
Petrographic fields

Fig F13

TOTAL ALKALI vs SILICA DIAGRAM
Kamanjab Batholith Rock Suite P, Namibia; Lufilian G.P.
(Based on Middlemost, 1994, 1997)

Samples

Petrographic fields

$Na_2O\% + K_2O\%$

10

8

L-1003

L-1000

L-999

70

75

L-1002

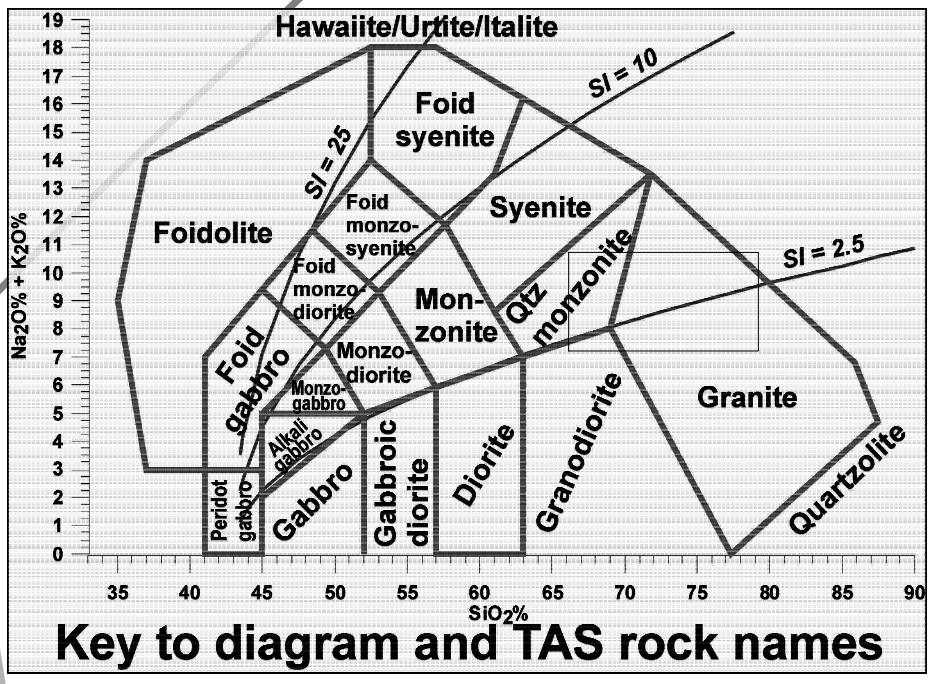

Fig F14

TOTAL ALKALI vs SILICA DIAGRAM
Kamanjab Batholith Rock Suite P, Namibia; Lufilian G.P.
(Based on Middlemost, 1994, 1997)

Samples

Petrographic fields

$Na_2O\% + K_2O\%$

10

9

7

65 8

70

75

C-2

C-4

C-3

C-5

C-6

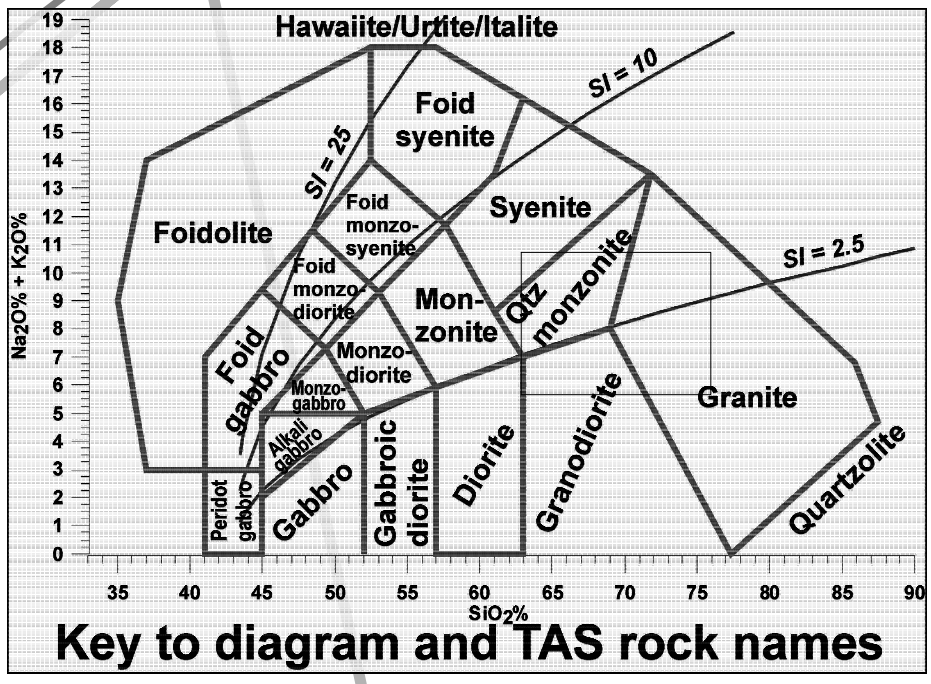

Key to diagram and TAS rock names

Fig F15

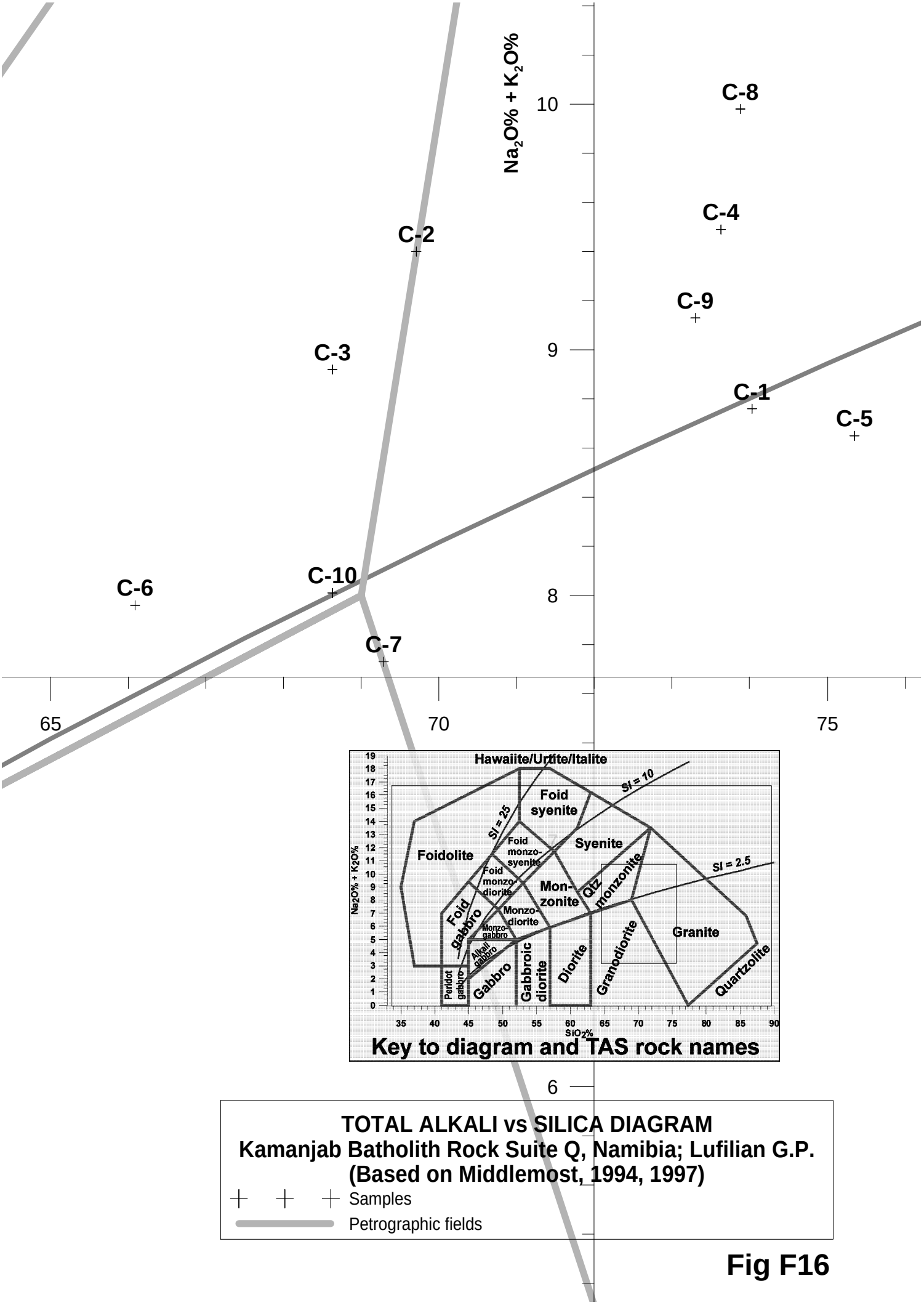

TOTAL ALKALI vs SILICA DIAGRAM
Kamanjab Batholith Rock Suite Q, Namibia; Lufilian G.P.
(Based on Middlemost, 1994, 1997)

Samples

Petrographic fields

Fig F16

APPENDIX H
PARTIAL TRANSCRIPTION OF FIELD NOTES

ZAMBIA

A57	Field notes taken along E-W transect of the Hook Granite Batholith, 184
A58	Abbreviated description of samples collected in the Hook Granite Batholith by Pepper, 2001, 186
A59	Comments from published Zambian geological survey reports and maps on iron oxide bodies, quartz pods, associated granitoids and round-pebble hydrothermal breccias, 188
A60	Sample description and field relationships in the West Lusaka-Kafue Flats Area, Zambia, 189
A60.1	Quartz pods, 189
A60.2	Granitoids, 189
A60.3	Gabbroids, 190
A60.4	Iron oxide bodies, 191
A60.5	Contact metamorphic rocks, 191
A61	Descriptions of samples from the Kalengwa Area, Zambia by Pepper, 2001, 192
A62	Descriptions of samples collected in the field, Kalene Hill Area, NW Zambia, 193
A63	Field descriptions of samples L-032 to L-034, Kabompo dome, NW Zambia, 194
A64	Petrography of the Chitungulu sodalite syenites, Mwombezhi Dome, NW Zambia, 195

NAMIBIA

A65	Field notes for a few suites of Cu-mineralized rocks in the Kamanjab Batholith, Namibia, 196
A65.1	Suite G, 196
A65.2	Suite H, 196
A65.3	Suite M, 197
A65.4	Suite N, 198
A66	Field notes on the N-S transect through the Oas Farm, Namibia, 199
A67	Field notes from the Lofdal farm, Namibia, 207
A67.1	Cross section through series of ultramafic dikes, Lofdal farm, Namibia, 210
A67.2	Magnetite-cemented, polymictic hydrothermal breccia that makes a diatreme, 211
A68	Partial field notes collected at the Mesopotamie farm, Namibia, 213
A69	Field notes, Ugab River, Namibia, 214
A70	Field notes, Okwa River, Botswana, 217
A71	Field notes Grootfontein Inlier, Namibia, 218
A72	Field notes from Okatjepuiko, Witvlei, Namibia, 219

APPENDIX A57

TRANSCRIPTION OF FIELD NOTES TAKEN ALONG THE E-W TRANSECT OF THE HOOK GRANITE BATHOLITH, ZAMBIA

(Underlined sample numbers have chemical analysis)

WPT 194. **L-235**.
WPT 192. **L-236**: Hornfels.
WPT 191. **L-237**: Large outcrop of peraluminous mesocratic potassic ferriferous granite.
WPT 190. **L-238**: Coarse metaluminous mesocratic potassic ferriferous granodiorite with sulfides.
WPT 189. **L-239**: Coarse-grained metaluminous mesocratic potassic ferriferous granite. **L-240** 2 samples of granitoid.
WPT 188. **L-241**: Granitoid with disseminated sulfides.
WPT 187. **L-242**: Two samples of angular breccia made of red peraluminous mesocratic potassic ferriferous granodiorite clasts with a black matrix. The rock has may have been subject to extreme potassic alteration. **L-243**. Gray granitoid.
L-244 and **L-245**: Two samples of pink granitoid. **L-246**. Gray coarse-grained granite.
WPT 185. **L-247**: 2 samples of oriented medium-grained, foliated granitoid. 150/78° E.
Xenoliths in pink, coarse-grained granitoid. Photo of emplacement; scale is an aluminium writing pad. Close-up photo of xenolith from previous photo. The foliation in the granitoid varies with location, as if several portions 'flowed' within each other in a series of aleatory whirlpools.

L-248: Two fragments of xenoliths. Darker material. **L-248** is a dark, peraluminous mesocratic sodic ferriferous granodiorite, while **L-248LG** is a peraluminous mesocratic socid potassic granite. **L-249**: "Normal" pink peraluminous mesocratic sodic-potassic ferriferous granite.
WPT 181. Very large outcrop by the road. Approximately 500 m in diameter. **L-250**: Medium-grained granitoid with epidote and abundant disseminated sulfides. **L-251**: other granitoids.
WPT 177. **L-252**. Large granitoid outcrop.
WPT 176, WPT 175.
WPT 174. **L-253**. Pink-purple quartz pods; many quartz in boulders. The quartz extends to WPT 201 and WPT 172 and 173.
WPT 170. **L-254**. Under bridge with large mammal grazers. Fine to medium-grained gray granite.
WPT 168. **L-255**: Medium-grained, brown granitoid with disseminated sulfides.
L-256. Excellent exposure, large outcrop with intrusives, dikes and xenoliths and foliation. Larger than 500 meters in diameter. Deserves to return, measure and take photos. With coarse biotite phenocrystals.
WPT 203. **L-257**. Very good outcrop of pink, fine-grained granitoid. Look for purple mineral. Good, large outcrop on both sides of the road.
WPT 164. L-258: Light gray, medium-to fine-grained granitoid. Large outcrop on both sides of the road. Contains sulfides.
WPT 163. **L-259**: Brown, medium-grained peraluminous subleucocratic potassic ferriferous granite**. L-260**: Light brown granitoid with sulfides.
WPT 160. **L-261**: Gray to pink medium-grained granitoid with disseminated chalcopyrite crystals.
WPT 157. **L-262**: Large, good outcrop. Worth returning and observing the textures in detail. Very good exposure. Foliated granitoid with disseminated sulfides (?)
WPT 148. **L-263**: Foliated gray metaluminous subleucocratic potassic magnesic quartzmonzonite with quartz porphyroblasts. The same type of outcrop on both sides of bridge.
WPT 147. **L-264**: Extremely foliated granitoid. There is no time to take a better sample. Due to excess hammering, my hand feels like it is breaking apart.
WPT 146. **L-265**: Boulders of brown, fine-grained granitoid.

L-411, collected from a syenite ring complex that is isolated from the main Hook Granite. It is a carbonatite that is not enriched in any rare earth. See Fig 4.8 for location. That syenitic body has a very high and large magnetic anomaly on the airborne geophysical image of the Hook Granite Batholith published by Nesbit et al, 2004. The sample available lacks any metal enrichment. Only Sc values are high. See further evaluation along with other carbonatite rocks from the Lofdal farm.

Cikin, 1972 describes syenite satellite intrusions in the Hook Granite batholith, including some petrography (p. 13-14). One of the samples, which he called a "bostonite" turned out to be a carbonatite (**L-411**).

> "Of the satellite intrusives, the syenites (…) show a wide range of mineral composition and vary in color from red and white to pink and gray. The more dioritic types are green to dark green. The

syenites are usually medium- to fine-grained, and very rarely coarse. They are hypautomorphic-granular and, in the margins of the bodies, porphyritic to some extent". P. 13.

"Fine-grained bostonites (5GD229[1]) are associated with syenite and related rocks. Where orthoclase is the main constituent the bostonites are usually red to pink, but are green in colour when mafic minerals are more common. The bostonites are, in many cases, highly altered and iron stained. Abundant phenocrystals of orthoclase up to 2.5 mm long set in a trachytic groundmass are seen in thin section (5GD 223, 276). The mafic minerals are usually confined to the groundmass, but in some bostonite dikes which cut the syenites along the Mumbwa-Mankoya road in the eastern part of the area, phenocrysts of chloritized amphybole, and less commonly, biotite, are plentiful (5GD276)." P. 14.

[1] Sample number from the Zambian Geological Survey sample repository. Sample 5GD229 a "fine-grained bostonite" as described by Cikin, 1972 was collected from the Zambian Geological Survey and analysed for this project with sample number L-411. It turned out to be a carbonatite.

APPENDIX A58

ABBREVIATED DESCRIPTION OF SAMPLES COLLECTED BY LEE PEPPER IN THE HOOK GRANITE, ZAMBIA (PEPPER, 2001)

(Underlined samples were analysed. Chemical analyses appear on Table A3).

P-38 Very coarse-grained holocrystalline, porphyritic granitoid with slightly-rounded, large (up to 3 cm wide) pink K-feldspar phenocrystals in a dark grey to black feldspar + quartz matrix. Feldspars are slightly weathered. Field allignment of phenocrystals is 240°; that might be an igneous allignment.
Macroscopic mineral composition: 45% feldspar phenocrysts, 15-20% quartz, 10% feldspar in matrix, 10% biotite, <5% alteration products.

P-39 White (with black crystals) holocrystalline, equigranular, medium to coarse-grained, metaluminous subleucocratic sodic ferriferous alkali granite. It shows little alteration, minor chlorite in places, and no pronounced fabric or crystal allignment.
Macroscopic mineral composition: 40% feldspar (plagioclase), 35% quartz, 15% biotite, <2% chlorite.
Microscopic description: Microgranite. Minor alteration of the feldspars to sericite. Low strain, quite fresh, minor weathering.
Microscopic mineral composition: 45% quartz, 20% perthite, 10% plagioclase, 10% biotite, <5% chlorite, <5% opaques, <5% sericite (alteration of feldspars).

P-40i Light grey, holocrystalline, medium-grained, granular to equigranular, leucocratic micro-metaluminous leucocratic sodic ferriferous granite with no visible alteration or obvious fabric. Found in the same outcrop as P-40ii (same rock or P-40ii is a xenolith?).
Macroscopic mineral composition: 50% feldspar (plag), 40% quartz, 5-10% biotite, <2% unknown minerals.
Microscopic description: Granite. Little alteration. Low mafic content. Fractures in quartz. Secondary chlorite wraps around quartz and feldspars. Granular texture.
Microscopic mineral composition:50% quartz, 30-35% plagioclase, 10% perthite (micro-), <5% microcline, <2% chlorite, <1% opaques, <1% amphibole.

P-40ii Dark grey to black, holocrystalline metaluminous sodic to potassic ferriferous quartz syenite. Average crystals are 3 mm but they reach 6mm. It has minor alteration (chlorite from biotite?). No obvious fabric or foliation. One fine quartz vein cuts the specimen. It is slightly coarser and much darker than microgranite P-40i; looks very different from it, but was found in same outcrop. P-40ii is hard, but softer than P-40i. There is no sharp field contact with P-40i, diffuse over approximately 7 cm. Confusing rock.
Macroscopic mineral composition: 55% felspar (plag), 25% biotite, 15% quartz, 5% chlorite, <5% unknown minerals.
Microscopic description: Granitoid. Some minor phenocrysts. Brown iron oxide alteration in parts of the matrix. Pyroxene with alteration to fron oxide. Small sphene crystal.
Microscopic mineral composition: 35% quartz, 30% perthite, 15% plagioclase, ~10% biotite, ~10% pyroxene, <5% opaques, <5% chlorite, <2% allanite, <2% zircon.

P-41 Light pink, weathered and highly altered, coarse-grained, porphyritic granite, with quartz phenocrysts up to 13 mm wide. Abundant quartz veins were seen in the field, and they are oriented from 016-96°.
Macroscopic mineral composition: 60% feldspar (plag), 35% quartz, 5% biotite, <2% unknown minerals.

P-42 Cream-pinkish, coarse porphyroblastic, augen gneiss with feldspar porphyroblasts up to 2 cm in size. A granitic rock was highly strained to produce this gneiss. Foliation is oriented 60-240º. The sample was collected from a shear zone that runs through the Hook Granite Batholith.
Macroscopic mineral composition: 60%, Feldspar (plag), 25% quartz, 15% biotite, <1% unknown minerals.

P-44 Pink, partially weathered, tectonized granitoid, with a pronounced fabric. Deformed K-feldspar phenocrystals up to 4 cm long occur in a darker gray matrix of clear quartz and biotite. The sample was probably affected by a branch of the Mwembeshi shear zone.
Macroscopic mineral composition: 50% Feldspar, 35% quartz, <10% Biotite, <10% alteration products.

P-45 Pink, coarse-grained, holocrystalline granite with pink feldspar phenocrystals and clear to grey subhedral quartz. Very slight foliation, weathering and alteration.
Macroscopic mineral composition: 50% feldspars, 40% quartz, <5% alteration products, <5% unknown minerals.

P-46 Slightly pink/cream speckled, coarse-grained, holocrystalline, porphyritic metaluminous mesocratic potassic ferriferous alkali granite with a weak fabric. Feldspars up to 12 mm wide show minor alteration and

weathering. A moderate fabric can be detected by biotite alignment. Field orientation is 350-170°. There are some similarities with **P-50**.
Macroscopic mineral composition: 60% feldspars (plag), 35% quartz, 10-15% biotite, <2% chlorite + epidote, <2% unknown minerals.

P-50 Pink, speckled, medium- to coarse-grained, holocrystalline, metaluminous subleucocratic sodic ferriferous granite with a weak fabric and minor epidote alteration. Granular quartz and felspars with moderate fabric are bordered by darker bands of biotite and minor amphibole. This type of rock produces large, rounded outcrops.
Macroscopic mineral composition: 55-60% feldspars (plag), 30% quartz, 10% biotite, <5% amphibole, <2% epidote, <1% unknown minerals.

P-53 Yellow to pink, medium- coarse-grained (up to 6mm) holocrystalline, altered, metaluminous subleucocratic sodic ferriferous granite with minor feldspar alteration that weathers to clay near the surface. Moderate fabric detected from biotite. Granular quartz with larger elongated feldspars.
Macroscopic mineral composition: 60% feldspars (plag), 25% quartz, 10% biotite, <5% alteration product, <1% unknown minerals.
Microscopic description: Altered granite. Some myrmekitic intergrowth of feldspars. Some sericite alteration and iron oxide staining. Minor foliation. Most biotites in the slide have the same allignment.
Microscopic mineral composition: 40% quartz, 30% perthite (micro-), 10% plagioclase, <10% biotite, <5% amphibole, <5% muscovite, <5% microcline, <5% sericite alteration, <2% opaques.

P-57 Dark pink to brown, speckled, coarse-grained (crystals up to 10 mm wide), holocrystalline, equigranular, massive, non-foliated, metaluminous subleucocratic sodic ferriferous nepheline syenite. With some alteration of feldspars.
Macroscopic mineral composition: 65% feldspars (plag), 25% quartz, 10% biotite, <1% unknown minerals.
Microscopic description: Feldspar-rich granite. Quartz and feldspar-rich holocrystalline igneous rock. Large (up to 3-4 mm) feldspars (perthite & microcline) with smaller quartz and plagioclase. Abundant quartz and feldspar intergrowths.
Microscopic mineral composition: 40% quartz, 25% microperthite, 15% microcline, 10% plagioclase, ~5% biotite, <5% opaques, <5% chlorite, <2% allanite, <2% unknown minerals, <1% zircon, <1% rutile, <1% sphene.

P-58 Fresh, pink, speckled, weakly foliated, holocrystalline, coarse-grained (up to 10 mm feldspars), slightly foliated, metaluminous mesocratic sodic, ferriferous granite with pink feldspar phenocrysts in a darker matrix and slight segregation into more mafic bands. Feldspars are aligned 002° in the field.
Macroscopic mineral composition: 60% feldsapars (plag), 20% quartz, 15-20% biotite, <1% unknown minerals.
Microscopic description: Porphyritic granite. Some alteration of the plagioclases giving them a special look. Minor fractures in some crystals.
Microscopic mineral composition: 35% quartz, 30% plagioclase, 20% microcline, <5% microperthite, 10% biotite, <5% muscovite, <5% chlorite, <2% opaques, <2% allanite, <2% amphibole.

APPENDIX A59

COMMENTS FROM PUBLISHED ZAMBIAN GEOLOGICAL SURVEY REPORTS AND MAPS ON IRON OXIDE BODIES, QUARTZ PODS, ASSOCIATED GRANITOIDS AND ROUND-PEBBLE HYDROTHERMAL BRECCIAS

Iron oxide bodies were clearly identified and described in some geological reports that accompany geological sheets covering the Hook Granite batholith. Although quartz pods were not identified as such in reports; they are well described. The following are some examples. On sheet 1526NW, iron oxide bodies are associated to fractures and to unit H, which is made by "sheared leucogranites, myarolitic in places with banded cryptocrystalline silica filling cavities and fractures." The cryptocrystalline silica is akin to quartz pods. A similar type of rock was observed near the Hippo Mine.

Unit "H" from sheet 1526NW corresponds with unit 3, and samples **L-341**, **L-343**, **L-346**, **L-347**, **L-348**, **L-352** and **L-355** are supposed to represent it, as shown on Table 4.11.

Several bodies of iron oxide are also present on unit "A".
The fractures on unit H are oriented E-W.
Unit "A" also has some 'quartz veins' that may well be the quartz pods of this research paper. These are also oriented E-W.
Iron oxide bodies and quartz seem to be superimposed on type "A" intrusive rocks.
Quartz pods occur in the same environment (and along the same structures) as the iron oxide bodies in map sheet 1526NW. This makes sense with the hypothetic genesis for both iron oxide bodies and quartz pods.

Another fracture system with leucogranite is on the southeastern corner of sheet 1526NW that extends eastward into 1526NE and westward into 1526SW.

Mapped quartz pods are different from quartz veins; they are too round and isolated to be typical quartz veins.
Quartz pods occur on coordinates: 445000/8309500, 423000/8304500 and 420000/8300500.
Iron oxide bodies occur on coordinates: 440000/8309000 (500m diameter), 429200/83339500 (150 m diameter), 428000/8335000, 429500/8334200, 441000/8338000.

The next map sheet to the east, 1526NE, has a continuation of the E-W fault systems; and siliceous breccias as well as quartz pods occur along them. Quartz pods (mapped as "d" bodies) occur on UTM coordinates 454000/8298500, 448200/8310000, 449800/8310400, 851400/8311000. Small bodies of quartz feldspar porphyry also occur along the same E-W fracture on UTM coordinates 451200/8310700.

The intersection of fractures in sheet 1526NE are very interesting. A triangular zone exists that lifts up the Bulala Hills, Kwako Hills and Chalobeti Hills. Elongated quartz feldspar porphyries occur along the fractures in that region, on UTM coordinates 462000/8300000, 470000/8304000, 467600/8302400 and 474000/8304200.

Many iron oxide bodies occur in and around the Hook Granite batholith. These bodies are commmonly related to quartz, sulfides and various types of hydrothermal brecciation. Some of the iron oxide bodies measure around 500 m in diameter. The following are UTM coordinates of the center of such bodies: 499000/831350 and 499000/831500, 468100/8303000, 468100/8303600, 466000/8302000, 465600/8301250, 463300/8300500, and 859600/8296600. Many more un-mapped bodies probably occur. Part of them are magnetic.

Round-pebble hydrothermal breccias were mapped as conglomerates and a long stretch of such rocks outcrops on 465000/8303000.

Large bodies of massive iron oxide occur along major fault systems within the Hook Granite Batholith. For example, the SW extension of a fault system contains large iron oxide bodies on 449000/8292000, 497000/8330200, and 495000/8333500, large syenite bodies on 453000/8303000, and smaller ones on 453000/8290500 3 (km x 500 m.) A NW-SE fracture comes from map 1426SE towards the SW and is associated to iron oxide bodies in 453500/8340000, Pempela Hill 457300/8338400, 463150/8334600, 449700/8344500, and 449200/8345300. Another NW-SE fracture is on 467000/8342000 and is associated to iron oxide bodies on 470200/8342000, 470550/8340000. 472400/8342000.

The abandoned Rhino mine is associated to the fracture MO-203, MT 123. It extends to the NW into map sheet 1426SE and contains many small syenitic bodies (476200/8346600) and iron oxide bodies (483500/8343000).

APPENDIX A60

SAMPLE DESCRIPTION AND FIELD RELATIONSHIPS IN THE WEST LUSAKA/KAFUE FLATS AREA, ZAMBIA

This presentation has been grouped into quartz pods, granitoids, gabbroids, iron oxide bodies and contact metamorphic rocks. The descriptions also refer to geochemistry and other geological data from the various rock suites. Detailed coordinates of all the sampling sites are listed on Table A16 in the Appendix.

4.1.2.3.2 Quartz Pods

Many extensive blocks of massive white, coarse quartz with sugary texture that make quartz pods were observed (For example, samples **L-174**). Abundant fragments of quartz were found around 0520255/8256073;1012m (between **L-209** and **L-210**). On UTM coordinates 0622333/8310267;1164m, an isolated outcrop of foliated granitoid is surrounded by massive quartz pods. Most of the hill is made of only milky, sugary quartz.

Samples **L-176** to **L-178** are quartz pods. **L-177** is a massive pink quartz pod, and **L-178** is made of massive white quartz with some iron oxide staining and a spherical fragment of hematite. **L-179** is a mafic dike of unknown composition (tremolite-actinolite+quartz but no feldspars?). **L-180** is a foliated granitoid collected from the top of the hill and completely surrounded by quartz pods.

4.1.2.3.3 Granitoids

L-195 is a red, metaluminous mesocratic sodic ferriferous syenite collected from one of the low-lying hills shown on the foreground of Fig 8.12. The size of the outcrops is approximately 1 km in diameter. **L-195** contains very high Zr and high Y, Na_2O, Ba and Nb. It seems to have formed in a continental epeirogenic uplift environment. Syenites outcrop all along the road from GPS WPT 133 to GPS WPT 135.

L-199 is another intensely weathered syenite from one of many small outcrops of similar lithology that are associated with very small bodies of gabbro (**L-198**), and are shown on the foreground of Fig 8.12. Very weathered small bodies of syenite and gabbro occur together. Part of the siliciclastic rocks (including sandstone) display coarse, specular hematite specks and thin veinlets. **L-199** has high content of the light rare earths (Nd, Pr, Ce, La, Hf, Eu) as well as high Sr, Zr and Nb. It is a high heat producer. Small bodies of gabbro with epidote and pink feldspar are ubiquitous. They seem to be related to the widespread hydrothermal iron oxide alteration. Their genesis is probably related. The environment of formation for the gabbroids is not clear.

L-200 and **L-201** are many chips of fresh, hard, granitoid rocks. Maybe the “freshness” is due to induration by albitization, such as in other cases. This has not been verified by chemical analyisis.

Samples **L-207***, **L-208** and **L-209** were collected under a small bridge, in a region with extremely rare outcrops. **L-207*** is a very red, fine-grained, metaluminous leucocratic sodic to potassic ferriferous alkali granite with intense red color and abundant myarolitic cavities that is closely associated with small bodies of alkali gabbro (**L-209**). **L-208** is a coarser-grained, red, alkali granite, very similar to that of **L-207***. Both seem to have formed in an anorogenic environment, but greater precision of their environment of formation is not possible now. **L-209** is a medium-grained, metaluminous sodic ferriferous alkali gabbro that formed in a mid ocean ridge environment, according to geochemical comparisons carried out during this study. There is a close association between all three samples; they are all fresh and contain epidote. Very little or nothing was visible along the way to this site, not even float.

L-210 is a fresh, fine-grained, pink peraluminous mesocratic sodic ferriferous syenite, that outcrops very badly. Nevertheless, the sample was collected from the only rock outcrop for a few kilometers along the road. From then onward, pink syenite is found, and it extends up to 051530/8296501. The sample contains anomalous enrichment in Na, Cu, Th, Ce, La, Zr, and very low Mn. Shimyoka North and South boreholes were drilled by Billiton and are located around here.

A potential environment of formation for this syenite is not yet clear. It has anorogenic features, and may have formed in an oceanic plateau.

L-211 a boulder of somewhat-weathered, foliated, porphyritic syenite with epidote found along the road. It is the only sample available for a long distance.

L-212 is a large red, metaluminous subleucocratic potassic ferriferous quartz syenite boulder that intrudes Katangan limestones. It seems to have formed in a continental epeirogenic uplift environment.

L-213, **L-214** and **L-215** are all red syenites from abundant in situ large boulders that outcrop for more than 500m in diameter. Parts of these rocks carry disseminated hematite (especially **L-214**). They have widely varying compositions, as shown on Table 4.1.2.3 for tectonic environment and Debon & LeFort names. They formed during a continental epeirogenic uplift; in any case, samples **L-212** to **L-215** formed in an anorogenic environment. All three samples have anomalous Na, Zr, extremely high Th values, some Nb and Cu.

Large syenite outcrops all along (WPT 140, 139) Samples **L-216**, brown, non-oriented, fine-grained syenite and **L-217*** were collected from there. **L-217*** is an outcrop of red, fine-grained, peraluminous subleucocratic potassic magnesic granodiorite that seems to be altered. It was considered to be a red syenite in the field. The environment of emplacement of **L-217*** cannot be be discerned from the chemistry. It contains high Mg, Cr and Pr; anomalous Co and Ni; Low Th and Al; no Cu; and produced a high LOI.

L-218 is a fine-grained, pink, metaluminous mesocratic sodic ferriferous quartz syenite with black needles of possible tourmaline. It is one of many large boulders and outcrops just by a village. The outcrops are limited by carbonates in all directions. **L-218** formed in a continental epeirogenic uplift environment.

L-220, **L-221**, **L-222**, **L-223** were collected from pink granitoid boulders with slight alteration, chloritization and specular hematite veinlets in many directions; they also contain tourmaline veinlets and networks. Plagioclases weather to a pink clay. Quartz is also common in the rock samples, and is evident in the field. **L-222** is a peraluminous subleucocratic potassic ferriferous alkali granite, and **L-223** is a peraluminous mesocratic potassic ferriferous granite. These samples were not oriented, because there is no formal outcrop present. Both seem to have formed in a continental epeirogenic uplift environment.

L-224 and **L-225** were collected from true outcrop of coarse, very intensely-veined, red-altered, peraluminous mesocratic potassic ferriferous alkali granite with black tourmaline stockwork. Large fragments were selected to evaluate textures and vein relationships. These three anomalous samples (**L-222**, **L-223** and **L-224**) are located around (or within?) a small syenite body that is a satellite of the main Hook Granite batholith (Fig 4.8). They have a high LOI and contain anomalous Rb enrichment, and seem to have formed in a continental epeirogenic uplift environment.

Samples **L-458**, **L-460**, **L-461**, **L-466** and **L-462** are granites and alkali granites of varying compositions, collected from the Zambian Geological Survey. Their chemical characteristics are listed on Tables 4.1.2.2 and 4.1.2.3.

4.1.2.3.4 Gabbroids

Many gabbros outcrop in the West Lusaka/Kafue Flats region. Only a few of these abundant gabbroid rock outcrops were analysed. They contain significant metal mineralization and may be source for copper, zinc and other economic metallic enrichment in the region. Some occur as small isolated bodies that intersect any type of rock, others appear as dikes or sills with various granitoids, and yet others are gabbro only ring complexes. In addition to gabbroids already discussed, the following were observed and studied.

L-181 is a metaluminous sodic ferriferous, saturated olivine gabbro taken from a site shown on Fig 8.12. Iike most gabbroids in the region, it contains Co, Ni, Cu, Zn, V and Sc. The not very foliated metagabbros with metamorphosed pyroxene seem to intrude only below the dolomitic Lusaka Formation. They are said to be “Pre-Lusaka”. Samples **L-181** and **L-182** are examples of such rocks, and both contain red garnets.

According to the studies done, chemistry of **L-181** and **L-209** is compatible with mid ocean ridge basalts.

L-203 is another gabbroid sample.

L-416 is a metaluminous sodic magnesic gabbro-norite from one of the abundant small gabbroic bodies found in the region. It contains high Cu, Co, Ni, V and Cr; and is interpreted to have formed as a within-plate alkaline basalt.

L-463 is another metaluminous sodic ferriferous gabbro from a large mapped body of gabbroids. It probably constitutes an only-gabbro ring complex.

4.1.2.3.5 Iron Oxide Bodies

Gabbroids and what seem to be massive hematite plugs are hosted by Katangan limestones and dolostones. Sometimes the entire soil is made of only magnetite sand and gravel (WPT 131 to 132). Samples **L-183** to **L-187** were collected from massive iron oxide bodies that sometimes contain blue and green iridiscent minerals. They may contain metals besides Fe, including Cu, Mn and others (See analysis of **L-464** and **L-465)**. Several samples from this site were sent to the University of Quebec in Montreal for detailed chemical studies. The aim of that research is to find particular chemical signatures in iron oxide bodies from mineralized areas, to aid in mineral exploraiton. Results are not complete yet.

Many of the iron oxide bodies are made of breccioid material. In some samples, hydrothermal breccias are flooded by coarse, metallic hematite or magnetite. There is a relict igneous texture in some of the iron oxide bodies. This may be due to progressive overprinting and replacement of the silicates by iron oxides.

Samples **L-183** to **L-194** were collected from massive magnetite-hematite bodies and bordering angular hydrothermal breccias/magnetite-specularite stockworks that occur on the contact between the iron oxide bodies and Katangan carbonates.

L-204 is a sample of magnetite-hematite from the hill of magnetite in Fig 8.12, that is used by Mamba Collieries to wash coal. Only the hill is made of massive magnetite. Note flat topography in the surrounding area.

4.1.2.3.6 Contact Metamorphic Rocks

L-196 and **L197** are contact metamorphic rocks. Probably carbonates that were transformed by the heat of intrusions. **L197** is a dolomite.

L-202 is a sandstone with coarse specular hematite disseminated crystals and veinlets.

L-205 is a skarn with tremolite-actinolite and sulfides. **L-206** is made of several other skarn samples. There are also some minor amethyst veins at the quarry.

There are no outcrops along the way from **L-206** to **L-207**. Only occasional quartz float from vein fragments and nothing else but flood plain sands from the Kafue River.

APPENDIX A61

DESCRIPTIONS OF SAMPLES FROM THE KALENGWA AREA, ZAMBIA, BY (PEPPER, 2001)
(Underlined samples were analysed) Formal rock names were modified, after studies of this project.

P-13 Medium-to coarse-grained, slightly pinkish to cream, metaluminous mesocratic sodic ferriferous quartz syenite with no apparent fabric and some iron oxide stains. No evidence of deformation. Thin quartz vein (max 2mm wide). Isolated pyrite crystals (2 x 1mm visible in 6cm x 7cm x 3cm sample). Dark brown to orange surface weathering color.
Macroscopic mineral composition: 40% quartz, 40% plagioclase, 10% biotite, <3% chlorite, <2% amphibole, <3% other (including pyrite).
Microscopic description: Granite. Garnets with brown alteration halo. Chlorite alteration after biotite.
Microscopic mineral composition: 40% quartz, 30% plagioclase, 10% biotite, 5% isotropic mineral (garnet); <5% chlorite, ~5% amphibole, 5-10 in fractures calcite, <5% garnet, <2% rutile.

P-14 Dense, medium-grained, magnetic, massive, dark gray/black ironstone with metallic lustre and no apparent fabric. Some iron oxide on surface faces. Heavily weathered surfaces. One minor quartz vein max 2 mm thick. Exposures of this rock were found in close proximity to large igneous plutons.
Estimated composition of hand specimen: 55% hematite, 15% magnetite, 25% silica, 5% goethite; unknown minerals: <5%.

P-16 Light pink, holocrystaline, heavily altered, medium- to coarse grained granitoid with iron oxide on surface faces and no detectable foliation. There are small cavities on the surface and between some crystals. (miarolites? or weathered sulfides?)
Macroscopic mineral composition: 60% altered plagioclase, 10% quartz, 10-15% biotite, 10% chlorite, <5% amphibole, <5% other.

P-17 Very red-pink, holocrystaline, heavily altered, medium- to coarse-grained, metaluminous mesocratic sodic-potassic ferriferous quartz syenite with iron oxide on surface faces and no detectable foliation. Small cavities on the surface and between some crystals (miarolites? or weathered sulfides?). Six small pyrite grains up to 1mm in size on one face of the sample. Chloritized biotite.
Macroscopic mineral composition: 65% plagioclase, 15% quartz, 15% biotite, <5% amphibole, <5% chlorite, <0.5% pyrite grains.
Microscopic description: Microgranite with iron oxides. Slightly altered plagioclase and microperthite feldspars. Some granophyric intergrowths. No fabric. Iron oxide stain around crystal boundaries.
Microscopic mineral composition: 30% microperthite, 25-30% plagioclase, 20% quartz, 10% biotite, 5% muscovite, ~3% garnet, < 2% amphibole, <2% chlorite.

P-22 Light tan (yellow/brown), fine to medium-grained siltstone with weak lamination that conforms country rock. Sample is speckled with (hydrothermal?) specular hematite that covers surfaces, cuts weak lamination and also permeates into the rock. Some radiating specular hematite crystals on fracture surfaces. Some bladed crystals are up to 1 cm in length.

P-24 Dense, dark grey/green medium- to coarse grained crystalline igneous rock, with distinct mineral bands. Dark minerals concentrate in bands; there is a biotite-rich augen with laterally extending mafic-rich bands. Some silica and minor pyrite in larger of two samples. Abundant orange iron oxide on exposed surfaces. Chorite, epidote and sericite alteration. Mixing of igneous and sedimentary rock? Very uncertain about origin and exact mineralogy.

P-25 Dark grey/green, highly altered and weathered, medium- to coarse-grained metaluminous mesocratic sodic ferriferous essexite. It displays conchoidal fracture. Contains some pyrite grains that are up to 2.5 mm across. The sample has a darker, mafic-rich portion.
Macroscopic mineral composition: 40% plagioclase, 20% chlorite, 10% epidote, 10% sericite, 10% amphibole, ~5% quartz, <2% pyrite.

P-26 Light colored to pink, holocrystaline, medium-grained, felsic-rich, metaluminous leucocratic sodic ferriferous quartz syenite with little alteration and minor iron oxide on the surfaces. It contains many small cavities between grains that account for <2% of the volume.
Macroscopic mineral composition: 45% plagioclase, 40% quartz, <5% mafics (biotite + amphibole).
Microscopic description: Felsic-rich leucogranite. Subhedral feldspars. Anhedral quartz. Fresh sample. Very little mafic minerals. Some quartz-feldspar intergrowths.
Microscopic mineral composition: 45% quartz, 40% perthite, <10% plagioclase, <5% microcline, <5% biotite, <2% allanite.

APPENDIX A62

DESCRIPTION OF SAMPLES COLLECTED IN THE FIELD, KALENE HILL AREA, NW ZAMBIA

Below is a description of the samples collected in the field by the author. Underlined sample numbers were analysed.

L-020 is a thorium-rich, medium-grained, peraluminous subleucocratic potassic ferriferous alkali granite taken from a rounded boulder along a creek where both banks of the river and the riverbed are clayey. The sample was taken 10 meters south from a concrete bridge located on UTM coordinates 35L 0185354/8761659, along a main road, just after Malovu village, as shown on the map of Figs M13 and M14. It seems to have formed in a post-orogenic environment, as shown on Table 4.1.4.5. **L-021** is another portion of the same rock.

Soil near the river is a non-indurated, light gray clay with quartz fragments. Broad-based termite mounds 8 m high are very abundant. Also some minor light gray thin termite columns.

An extensive outcrop of fresh granodiorite (at least 20 x 15 m) was found along both sides of a river bed used by local people for bathing. The rock displays onion ring exfoliation. It is located on UTM coordinates 35L 0188112/8765321. Note the large granite outcrop on the 1:250,000 Mwinilunga geological map sheet. The rock is cut by several subparallel white aplite dikes, 5 to 15 cm wide, oriented N18E/90°. One generation of black dike, 27 cm wide is cut by a 15 cm pink aplite vein. It is also dextrally displaced 1.8 m along strike. See Fig below of the main orientation of elongated plagioclase porphyroblasts, with hammer and chisel for scale. The main orientation of foliation along the plane of the outcrop is 045° and probably was produced by flow.

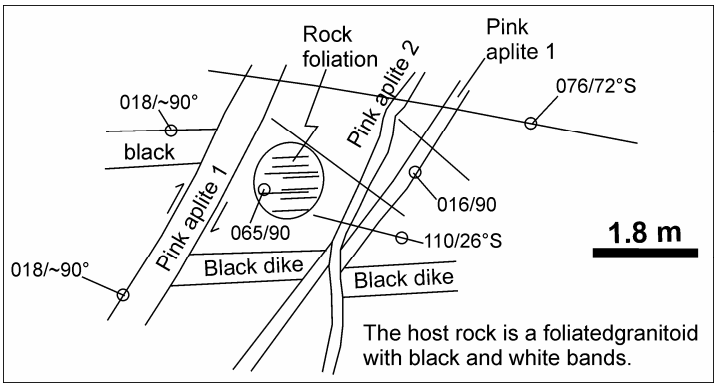

Fig to show main features of the outcrop where L-022 and L-023 were collected.
More descriptions on the text.

Oriented sample **L-022** was collected with a north arrow along a true horizontal line. It is a fresh rock with abundant pink, granular quartz, light green-opaque feldspars, muscovite and large euhedral plagioclase crystals of two types: perlatic white and light gray-green.

L-023 was taken from a metaluminous sodic ferriferous granodiorite to show surface differential weathering of plagioclase. The surface of the photograph was a horizontal joint. There seems to be deformation prior to the emplacement of the large plagioclase phenocrystals. The rock weathers to a dull, light gray color. Cr and Pr are enriched in the sample.

L-024 was collected from one of a series of fresh, massive, black, metaluminous sodic ferriferous gabbro outcrops along the road and under a bridge. The sampling site was located on UTM 35L 0191378/8764946, as shown on Fig M11. Geometry and relationship of the gabbros to other rocks does not outcrop, but they are inferred to be pod-like bodies or short dikes. This sample contains a high amount of copper. It also is anomalously enriched in Co, Ni, Zn, V and Ta. The rock seems to have formed in a rift-related environment.

L-025, **L-026** and **L-027** were collected from large, extremely fresh granitoid boulders located under a bridge. No *in situ* outcrops were found. These granites and granodiorites represent the variety of lithologies that occur. The collection site is shown on Fig M11. Note polished slabs of this rock on main chapter. **L-027**, a metaluminous sodic ferriferous granodiorite is enriched in chrome and strontium, and formed in a magmatic arc. **L-025** and **L-026** are mesocratic sodic-potassic ferriferous granites that probably formed in a magmatic arc and contain abundant barium. **L-026** is enriched in zirconium.

APPENDIX A63

FIELD DESCRIPTION OF SAMPLES L-032 TO L-034, KABOMPO DOME, NW ZAMBIA

L-032 was collected under a concrete bridge. A good outcrop of rocks can be seen along the riverbed, on UTM location 35L 0309413/8685473, at 1332 mosl. In hand specimen, rocks are amphibolite-facies gneisses. They are extremely fresh and very hard. Joints are extremely separated to very separated from each other. Main minerals of the rock are quartz, amphibole and white plagioclase. Very large boulders, with diameters over 5 m can be seen along the river bed. The *in situ* general plane of foliation is 056/07°NW. Weathering on the surface and enhancement of the plagioclases over amphibole on the surface is one of the features of this rock. The orientation and zonation of plagioclases is very clear. At the time of writing this report, very little petrographic work has been carried out on this sample. No chemical analysis has been done.

Good granitoid outcrops were expected to occur around UTM 35L 0318288/9690411; 1459 mosl. That is the center of a large circular outcrop of intrusive rocks, according to the 1:250,000 geological sheet. There is nothing to be seen on the ground, except for a light gray, sandy soil. Many holes to obtain drinking/cooking water were visited. The material is quite clayey, and natives were using it to manufacture adobe bricks to build a church. Red soil lies outside of the area of gray soil. Maybe the map was based on the color of the soil more than on true rock outcrop. Native peoples mention that very little vegetation grows on the soil that lies in the mapped circle of granitoid rocks. Plants grow much shorter there; physiography is mainly flat grassland and small swamps.

To make up for the lack of granitoid rock sample, **L-033** was collected from soil on the north side of the road, just beside the GPS site, in the gray soil just described. **L-034** was taken from a termite mound near the GPS site, towards the center of the outcrop to check for zircons and minerals that can help detect rock type and/or date it.

APPENDIX A64

PETROGRAPHY OF THE CHITUNGULU SODALITE SYENITES, MWOMBEZHI DOME, NW ZAMBIA [MULELA, 1980 - 1998 #949]

Below are some extracts from a recently re-edited report on the petrography of typical rocks from the Chitungulu sodalite syenite quarry. These have been taken directly from Mulela (1980 – 1998) pp. 12-13. According to the authors, the proper petrographical name for the sodalite syenite is aegirine ditroite.

Major constituents of the typical syenite are microcline, albite, pyroxene, nepheline and sodalite. Minor and accessory minerals include zircon, calcite, quartz, biotite, cancrinite, perovskite, magnetite and hematite. Microcline is the most abundant mineral; it tends to be tabular, but also forms crudely radiating groups. Cores of some anhedral microcline crystals are clouded but the margins are clear. Much of it has been replaced by albite. In some grains the replacement is along irregular zones, but in others only the margins have been replaced. There are also cases of oriented intergrowths in which inclusions of plagioclase are enclosed in potassium feldspar and could be termed perthite. Mulela (1980 – 1998), identified string, ribbon, interpenetrant and braid perthite that developed during exsolution, according to Allings (1938) shape classification of igneous perthites in Mulela (1980 – 1998).
"Plagioclase, in the range albite to acid oligoclase, is generally anhedral and shows no multiple twinning, except in the larger grains, which are well twinned. Where the microcline has been almost entirely replaced, albite is lamellar and in laths up to 4mm. Only a little albite formed outside the microcline crystals. Pale green-brown pleochroic aegirine-augite is present, commonly in isolated rods, irregular bundles or fibrous aggregates, although subhedral crystals with prisms are also developed. Most thin sections have small extinction angles (up to 7°), but some have almost straight extinction. The lower index of refraction, determined by immersion by Adams & Osborne (1932) is 1.72 and the birrefringence, estimated in thin section from a grain showing central emergence of the optic normal, is about 0.03. It is optically negative with an optic-axial angle of 65° and a strong dispersion. Several small grains with distinct hornblende cleavage (probably afverdsonite), occur in the margins of pyroxene grains. Nepheline occurs as clear or slightly clouded grains interstitial to the feldspar. It is replaced around its margins by large individual crystals or granular aggregates of sodalite". [Mulela (1980 – 1998) pp. 12-13]

"Sodalite is particularly abundant in some places, amounting to 35% of the rock. Much of it is interstitial to lath-shaped sections of microcline-perthite, but some of it occurs as euhedral rhombododecahedrons embedded in the feldspar. It is probably primary in origin. The sodalite contains small myrmekite-like anhedral inclusions of nepheline, microcline and albite, which are parallel to adjacent grains of the corresponding minerals. Similar inclusions are not found in the nepheline, which suggests that the sodalite formed at the expense of nepheline, microcline and albite along grain boundaries, particularly those of the nepheline. In such cases it is probable that the sodalite formed from nepheline by a later (pneumatolytic) process." [Mulela (1980 – 1998) p. 13].

"Zircon occurs in rounded and equidimensional grains. Perovskite is present in rounded isotropic grains of very high refractive index. The cores of the larger grains are colourless, grading to pale red at the margins. Very rarely, syenite contains aggregates of cancrinite and its relationship to the nepheline indicate that it is an alteration product of the latter. Biotite forms small flakes with intense pleochroism in brown colours. Calcite occurs as an accessory mineral and is usually associated with the pyroxene or replaces feldspar. Rarely, quartz in small anhedral grains and sphene in subhedral crystals are present. Magnetite occurs as minute octahedra near the pyroxene. Larger aggregates of magnetite and magnetite oxidized to hematite are interstitial to the silicate minerals." [Mulela (1980 – 1998) p. 13].

Mulela & Siefert present the chemical analysis of a phonolite from Malawi that has very similar major oxide composition to rocks from the sodalite nepheline quarry (Table below). According to them, the proper petrographical name for the nepheline syenite from the Mwembezhi Dome is aegirine ditroite [Mulela, (1980 – 1998), p. 13].

Chemical analysis of the sodalite nepheline syenite quarry, Zambia From Mulela (1980 – 1998) p. 13.

Sample	SiO2	TiO2	Al2O3	Fe2O3	FeO	MnO	MgO	CaO	Na2O	K2O	P2O5	H2O+	H2O-	CO2	ZrO2	SO3	Cl
I	58.04	Tr	20.76	4.45		0.2	0.09	0.95	9.22	4.81	Tr		1.99				
II	56.31	Tr	19.89	4.28	0.3	0.16	0.26	0.74	8.33	5.75	n.d.	0.68	0.13	1.27	0.16	0.19	1.13
III	57.87	0.5	18.46	4.63	0.4	0	0.61	1.03	8.83	5.74	0.14	0.9	0.7				0.62

NOTES: I is a nepheline sodalite syenite collected by D. Mulela and analysed by S.K. Mukhopadhyay.
II is a nepheline sodalite syenite collected at the Mwombezhi Dome syenites by Adams & Osborne (1932), in Mulela (1980 – 1998)
III is a phonolite from the Patabwa River, near Utanjiva, Malawi, analysed by E. Lehmann.

APPENDIX A65

TRANSCRIPTION OF FIELD NOTES FOR A FEW SUITES OF COPPER-MINERALIZED ROCKS IN THE KAMANJAB BATHOLITH

The nature of field work carried out in the Kamanjab batholith was merely of reconnaissance quality. No detailed work or mapping whatsoever was done. The field observations described below have to be understood as such. Some additional work has been done on the samples after laboratory work for the Greater Lufilian Arc granitoid project, but that will not be included here.

Suite of rocks G, Kamanjab batholith (Fig F7).

S-96. Well exposed outcrop is made by a series of inselbergs. Several key textures and intrusive relationships are evident. **L-939**: Coarse-grained gray, slightly foliated peraluminous mesocratic sodic to potassic ferriferous biotite granite with abundant xenoliths of black amphibolitic material that show preferential flow orientation. The rock does not show very evident foliation on the outcrop scale, except for the presence of its elongated mafic enclaves. At short distance, a slight foliation is detectable; it is especially enhanced by the orientation of biotite and amphibole phenocrystals and micro enclaves.

L-940: Enclaves of black amphybolitic metaluminous mesocratic sodic ferriferous gabbro-diorite that are hosted in **L-939**. All enclaves are elongated and they follow a general trend of flow inside the rock.

S-97. Same rock and features that outcrop on a big outcrop. Abundant enclaves. Very similar texture and macroscopic characteristics to the Jurassic Ibagué Batholith in Tolima, Colombia.

S-98. Same rock. **L-941**. Slightly stronger foliation and the same enclaves.

S-99. **L-942**: Foliated, coarse-grained granitoid (same as L-945 and 939) that is intersected by felsic dikes of a fine-grained metaluminous leucocratic potassic ferriferous biotite-amphibole granite (**L-943**) collected for chemical analysis. It also has white pegmatitic veins made of quartz and light blue-gray feldspars (**L-944**).

S-100. Very weathered, coarse-grained porphyritic, foliated granitoid. Same as **L-945**.

S-101. Outcrop of **L-945**: Foliated, coarse-grained, porphyritic, peraluminous mesocratic sodic ferriferous biotite granite (same as **L-945** and **L-939**). Large enclaves are overprinted by large potassium feldspar porphyroblasts that overprint previous texture, foliation, veins and enclaves. Regrowth might mean some sort of autometasomatism or regional hydrothermal alteration. Potassic alteration was confirmed by the chemical analysis.

S-102. **L-946**: Small isolated outcrop of what seemed to be the same rock as **L-945** (extremely fresh metaluminous mesocratic sodic ferriferous biotite-amphibole granite). It is almost identical to **L-945**.

S-103. Small isolated outcrop of two granitoids. The coarse-grained, non-foliated (un-deformed?) one (**L-947**), seems to intrude the foliated, coarse-grained metaluminous mesocratic sodic ferriferous biotite granite (**L-948**).

Suite of Rocks H (See Fig F8).

S-104. Small outcrop of non-porphyritic, fine-grained silicate black rock with some large angular vugs. Probably a volcanic rock. It does not have any identifiable crystals. **L-949** and **L-950** were collected here. The standard black rock is **L-950**. It may be a basalt, but none of the samples were analysed.

S-104. **L-951**: Small outcrop of an extremely fresh, slightly foliated, metaluminous subleucocratic sodic ferriferous nepheline syenite. Maybe “freshness” is due to albitization.

There are two facies of banding in the coarse-grained porphyritic granitoid. **L-952** is a white, metaluminous sodic ferriferous nepheline syenite, and **L-953** is a pink portion of the same rock. Both are intruded by a dark green, slightly foliated, fine-grained rock (**L-954**), and by **L-955**, a fine-grained (volcanic-looking) slightly-foliated, very felsic, metaluminous subleucocratic sodic ferriferous nepheline syenite with high Cu, Na, Zn, and Al. It was not posible to figure out the intrusive relationship between the two young rocks.

S-106. Small outcrop of similar situation as the previous outcrop. Relationships between rock types are not clear; no cross-cutting evidence has been spotted. Again, the mafic rock is extremely fresh and lacks foliation.

Maybe the black, fine-grained rock is part of large xenoliths (?) in the **L-956**, coarse-grained, foliated, metaluminous mesocratic sodic ferriferous syenite with high Fe, Ti, Na, Al and P2O5.

Mafic enclaves with overgrowth of potassic feldspar were seen on an outcrop of the coarse-grained porphyritic rock. No mafic or felsic dikes were seen.

S-107. Large outcrop of coarse-grained, porphyritic, foliated rock intruded by mafic dikes in different style of foliation. The rocks may have been sheared repeatedly. Some quartz veins with the same orientation, along the same foliation were also seen. The average foliation of the mafic rocks is 090° dipping vertically; the rocks in this case are schists, more strongly foliated than before and coarser-grained. The quartz veins strike 090° and dip 64°S.

S-108. Complex relationship between various schists (after volcanic rocks?) and phases of the coarse-grained porphyritic, foliated granitoid.

The felsic material previously called a dike is also present. Now **L-957**, another sub-volcanic (?) silicic, very fine-grained, glassy, pink, metaluminous, leucocratic potassic ferriferous granite with some rare coarse crystals. It may also be a metamorphosed volcanic rock. The sample is extremely fresh for chemical analysis.

Suite of rocks M (See Fig F13).

S-134. **L-987a**: Fresh, non-foliated, metaluminous mesocratic sodic ferriferous alkali gabbro with disseminated pyrite. It looks like the porphyry copper rock type. Strangely, the rock is unweathered and its sulfides are fresh. It probably is a subvolcanic rock, more mafic than other seen today. The outcrop is not very good or clear; better relationships may well be exposed in other nearby outcrops. **L-987b**: Another pink, porphyritic, fine-grained, porphyritic, metaluminous mesocratic sodic ferriferous theralite with abundant sulfides. All samples from this outcrop contain disseminated sulfides.

S-135. **L-988**: Coarse-grained gabbroid with disseminated copper sulfides (mainly pyrite)
L-989: Finer-grained gabbroid with disseminated copper sulfides.
L-990: Coarse-grained, metaluminous mesocratic sodic magnesic monzogabbro with a white band of plagioclase and high Cu content.
L-991: Coarse-grained, metaluminous mesocratic sodic ferriferous undersaturated olivine gabbro with a white plagioclase band and high Cu content.

S-136. **L-992**: Intermediate to mafic, medium- to coarse-grained, metaluminous sodic magnesic under-saturated olivine gabbro without sulfides.

None of the rocks from the past three outcrops had any type of foliation. They might be very young, or at least younger than the main events of deformation and metamorphism in the Kamanjab batholith. If these magmas intruded favorable, reactive host rocks, an economic deposits could have formed. Favorable rocks could be: carbonates, porous volcanics, mafic fractured rocks, porous felsic intrusives, brecciated granitoids, and/or major fracture zones, among others.

S-137. Photo with hammer of the type of low-lying outcrops. Photo of the general oxidation and alteration features. Photo with hammer of xenoliths in dioritic rock; the same type, but with less sulfides. The xenoliths are still more mafic (gabbroic).
3 panoramic photos of small outcrops on the flat part of the valley that contains the disseminated sulfidation. Taken towards the south. The road to Fransfontein is in the middle of photo.

L-993*: Fresh, pink, fine-grained, porphyritic metaluminous subleucocratic sodic to potassic ferriferous granite with blue quartz porphyroblasts and disseminated sulfides including chalcopyrite. Several angular mafic xenoliths are evident.
L-994: Fresh, same as above, with visible chalcopyrite.
L-995: Black to dark gray, metaluminous mesocratic sodic ferriferous alkali gabbro with disseminated pyrite and chalcopyrite; it contains high Ti, Fe, Ca and Cu.

S-139. Not very good outcrop. **L-996**: Medium-grained, metaluminous subleucocratic sodic ferriferous biotite granite with high copper content.

S-140. Bridge over dry river with good outcrop of granitoids on the Guab River. Very clear, visible contact between a medium- to coarse-grained, very slightly foliated, pink, metaluminous leucocratic sodic ferriferous

quartz syenite (**L-997**) and a very coarse, foliated, porphyritic, brown, metaluminous mesocratic sodic ferriferous quartzmonzonite with large, spherical, golf-ball-sized pink plagioclase porphyroblasts (**L-998**). The pink rock intrudes the brown rock.

Suite of rocks N (See Fig F14)

S-141. Up to here, foliated, coarse-grained porphyritic granitoid.

S-142. **L-999**: strongly foliated metamorphic rocks including a foliated, metaluminous mesocratic sodic ferriferous biotite granite with hexagonal megacrysts. Neither apatite nor zircon seem reasonable from the chemical data. Quartz is not a possibility either.

S-143. Small outcrop on both sides of the road.

S-144. **L-1000**: Fresh, medium-grained, peraluminous subleucocratic sodic ferriferous biotite granite that outcrops on both sides of the road. It contains abundant Cu. Schists are hosting the granite, and they outcrop on both sides of the road.

S-145. Flat area covered by abundant coarse quartz (>50 cm diameter in some cases) and inclusions of green and black schistose rocks. It may be a breccia zone filled with quartz. No sulfides or iron oxides of any type were found. The last zone, located between 19°52.5'S and 19°51.8'S was thought to be the continuation of a main regional mineralized fracture zone, as seen on Fig 4.2.1.6. That fracture is the same that has the copper sulfide disseminations and abundant vugs after sulfidation.

S-146 **L-1001**: Quartz with schistose black/green rock with abundant vugs.

S-147. Foliated, coarse-grained granitoids from the local basement.

S-148. Outcrop on a box cut for road. **L-1002**: Intensely-fractured and quartz-veined massif of medium-grained, pink, metaluminous leucocratic sodic to potassic ferriferous alkali granite with biotite and amphibole. Very altered and possibly hydrothermally altered. The sample is the freshest rock available.

S-149. **L-1003**: Slightly foliated, coarse-grained, metaluminous subleucocratic sodic ferriferous quartz latite from the basement. This rock correlates very well with the group of quartzmonzonites.

S-150. Large hill with outcrop on the road. Myarolitic cavities are visible in a large extension of the outcrop. Fine-grained subvolcanic granitoid (**L-1004**).

S-151. The rock of **L-1004** is cutting through the brown, foliated, coarse-grained porphyritic granitoid that was seen on the Guab River. Maybe it is the same granitoid that was seen there too. It still has the angular myarolitic cavities and ocassionally grades into a breccia.

APPENDIX A66

FIELD NOTES ON THE N-S TRANSECT THROUGH THE OAS FARM, NAMIBIA

From WPT 176 to WPT 175 there is abundant magnetite in the sand that covers the ground.

On WPT 174, **L-666** pan concentrate of magnetite from the sand, to look for metals. **L-667** is another sample of magnetic substances collected with a strong hand magnet.

L-668. Reasonably fresh, brown, medium-grained, metaluminous mesocratic sodic ferriferous syenite, with 2 feldpars and low quartz content. The rock has small clusters of biotite, amphibole and magnetite. The dominant minerals are pink potassic feldspar and light gray, transparent plagioclase. The rock is cut by a 1.5cm wide quartz+magnetite veinlet that is more magnetic than rest of the rock; it is accompanied by a stockwork of 1-3mm similar magnetite-rich veinlets. There were no apparent sulfides.

This sample was collected from a series of dense veins of a darker intrusive material around a pink, coarse-grained granitoid (See Fig photos).

L-669. Angular (hydrothermal?) breccia of pink, medium-grained, metaluminous mesocratic sodic ferriferous syenite, cemented by a black quartz+magnetite (mafic-rich) intrusive material. The rock is not very fresh. It was intersected by later 1mm veinlet network that does not carry sulfides. Another portion of the sample shows round clast breccia and angular breccia cemented by quartz+magnetite (dark-black) material. The rock was later overprinted by a network of fine black veinlets filled by quartz+magnetite. A portion has a boxwork of magnetite blades with dark-colored quartz in the middle.

This intensely-fractured and re-cemented pink coarse- to medium-grained granitoid seems to make most of the rock in the massif. The massif has approximately 150 meters in diameter, it is located to the east of WPT 172, and makes a rock outcrop along the road (Fig 4.2.2.1).

WPT 177, **L-670**. Fresh, medium-grained, light gray to pink, metaluminous mesocratic sodic ferriferous nepheline syenite with clusters of light green (epidote and/or chloritized biotite)+magnetite+biotite. Some very long pink plagioclase blades (Potassium feldspar?) 2-3cm. Might have contained small sulfides, now oxidized. It comes from the massif of body E. The rock is a high-heat producing syenite.

WPT 178, **L-671**. Fine-grained, red-brown intrusive rock with sulfides (may have “brown-rock” alteration). It is cut by a 1-1.5cm quartz veinlet with sulfides (now angular vugs+gossans) and magnetite. It also contains very brittle minerals with silvery, metallic luster (sulfide or sulfosalt) that couldn’t be identified. The sulfide is hard to scratch; the scratch is not red, yellow, black or white in color. Thin, 1mm thick quartz veinlets radiate out of the 1.5cm quartz vein.

L-672. Quartz from a vein with very thin, non-oriented, red iron oxide-filled joints and angular vugs after sulfides; some vugs are gossanous. The vein cuts through a fine-grained red, sulfide-bearing intrusive rock. The sample was collected for fluid inclusion studies.

By WPT 171 the abundance of ferromagnesians in the rock increases. Amphiboles and magnetite make 0.5 cm to 0.7 cm diameter clusters. The rock is spotted and looks like the skin of a dalmatian.

WPT 179. Massive magnetite fragments, such as that of **L-673** begin to appear. Massive magnetite from a quartz+magnetite vein. The magnetite contains some gossanous vugs where sulfides might have previously resided. Part of the quartz has a dark gray to almost black color.

WPT 179, **L-674**. Medium- to fine-grained pink granitoid intersected by stockwork of quartz+magnetite veinlets; some 1cm, most a few mm wide. It contained disseminated very small (<1mm) sulfides that now are leached. It also has disseminated clusters of mafic minerals including magnetite.

L-675. Medium-grained, peraluminous, subleucocratic sodic ferriferous syenite with a “black-white” dot texture. Abundant magnetite clusters conform “black” and plagioclases+quartz+muscovite make the rest = “white”. This rock is similar to others seen at WPT 171. There may be some type of iron oxide flooding that altered a previous rock, replacing all the mafics: biotite, amphibole, etc. The rock has a small, more felsic dike with flow textures that is also partially replaced by magnetite. A magnetite vein cuts across the sample and carried sulfides, now represented by gossanous vugs. Thin magnetite veinlets branch from the magnetite veinlet. This rock is a very high heat producer due to high Th.

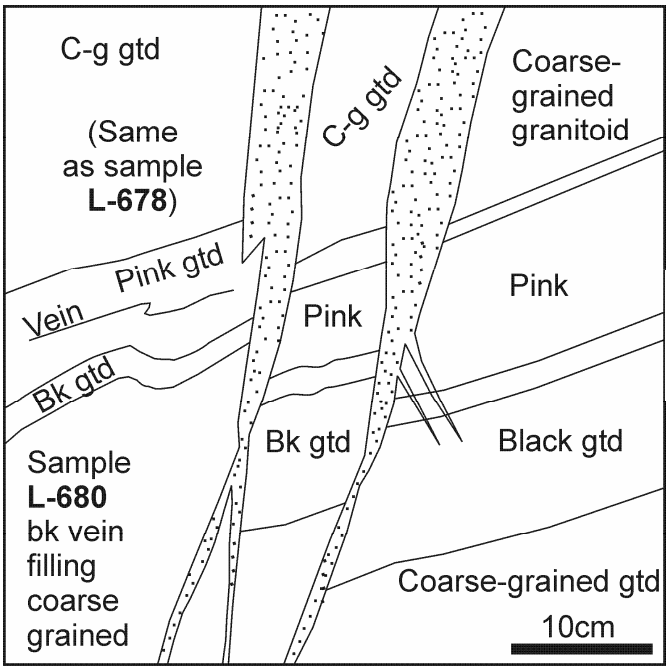

WPT 183. **L-676**. Metaluminous mesocratic sodic ferriferous syenite. It contains a large mass of partly martitized magnetite from ~10cm wide veinlet with some vugs that might have been sulfides or other minerals immersed into the magnetite. The vein seems displays flow texture or banding. Note the abundant angular vugs and boxwork textures in the photo.

From WPT 171 to WPT 170 to the west, small hill of granitoid rocks.

WPT 180, 947m (highest point). **L-677**. Fragment of quartz vein with hematite in 2mm thick blades and very abundant vugs after sulfides. The sample is hosted by deeply hematitized, red intrusive rock. It was collected to slab and look at the iron oxide mineralization; it could also be used to carry out fluid inclusion studies. Two of the veins intersect. There is iron oxide + mineralization at the intersection. The massive iron oxide vein system was oriented 110/72° N. This was measured using the magnetic needle of a Brunton compass set to 0°; it should be corrected for magnetic declination and for error due to nearby magnetic ironstones. Veins have an irregular texture, they normally are 4-12 cm wide but may open up to 40 cm, and were also oriented in many other directions. No clear quartz veins are visible.

WPT 181, 948m. ***L-678***. Fresh, medium-grained, pink-black granitoid with twinned plagioclase (or nepheline?) elongated phenocrystals in tabular shapes. Some of the blades are 3-4cm long and 4-5mm thick. The rock has clusters of mafic minerals with magnetite, and is intersected by diffuse 0.5cm thick magnetite-rich veinlets. It represents the whole hill. The sample has a xenolith of a finer-grained, pink rock without the plagioclase blades.

WPT 180, **L-679**. Pink granitoid with black accumulations of mafic minerals including magnetite. It is cut by two dark quartz+magnetite parallel veins, oriented as measured on WPT 180. Indicated with blue marker. The veins seem to have carried sulfides.

Photo of the fracturing style with N and scale, taken 1 m away from WPT 181. There is a diagram (page 23 of field notebook) of the main rock relationships. See photo on WPT 182, 943m. Relationships of **L-678**, **L-681**, and **L-680** are indicated on the diagram. Black, lensoid veinlets cut the other granitoids almost perpendicularly.

L-680. Fragment of a quartz+feldpar rock with abundant very fine-grained, black magnetite. It comes from a vein.

L-681. Massive black magnetite vein with angular fragments of host pink rock (**L-678**) in a breccia fashion. The rock has flow foliation. Its fragments are elongated and show slight imbrication. A dense network of magnetite veinlets was seen nearby. The host rock is a pink medium to fine-grained granitoid with very little observable texture that seems to grade from L-678. The vein's width varies from 1 to 5cm in the hand sample. Some very vuggy textures with black-dark brown gossanous surfaces after sulfides. The gossanous vugs occur both on the pink host rock and black vein.

L-682. Grab samples of a fine- to medium-grained, light gray to pink granitoid (**L-678**) intersected by a 0.7-1.5cm magnetite-rich black veinlet with minor quartz. Fine black veinlets <1mm radiate from the main black vein. The host rock has some clusters of mafic minerals, most with iron oxide (earthy goethite) on outer surface.

L-683. Medium-grained, pink-brown granitoid (like **L-678**) with bladed twinned plagioclases. It is intersected by series of sub-parallel very fine (<1mm) black magnetite-rich veinlets+sulfides that account for a thickness of 4cm. The outcrop showed a 3 cm black vein with internal subparallel banding and many gossanous vugs. The sample might carry free gold and needs to be assayed. Gossanous vugs are also present in the pink host rock. Disseminated magnetite is also present in the pink rock.

L-684. Massive magnetite with angular breccioid fragments. Probably derived from vein. Continuous, very large vugs and abundant small vugs with gossanous textures after leached sulfides.

All of the previous samples come from the “hill”. Its perimeter was walked and recorded with the GPS to note its map outcrop and surface. WPTS A to I (Fig 4.2.2.1).

WPT 170. Coarse “dalmatian” rock and fine-grained pink intrusive with stockwork of magnetite fractures.

WPT 184, 950m. Quartz veins with hematite and vugs after sulfides begin to appear. **L-685** has the intersection of several such veins. It is a large sample of braided network of approximately 1cm wide quartz+hematite+sulfide veins. The host rock seems to be a fine-grained volcanic rock (or dike?). It has abundant little dips like pin pricks on a weathered surface, after weathered disseminated sulfides. **L-686** was collected from same site; **L-687** from approximately 10 m to the east. The host rock is a fine-grained granitoid.

L-686. Braided, 6-7 cm wide quartz veins with hematite and very abundant, open gossanous vugs hosted in what seems to be a very fine-grained volcanic rock. The sample might contain free gold if the rock ever did. Nothing in the sample is magnetic.

L-687. Quartz vein with large clusters of hematite and associated angular vugs after sulfides. Hosted by a fine-grained, and intensely brown-altered, gossanous rock.

WPT 185, 971m. **L-688**. Fresh, brown-colored fine- to medium-grained granitoid with little visible quartz. It is a slightly magnetic rock cut by a 0.5mm quartz-magnetite veinlet. Fresh samples were hard to find due to intense fracturing and weathering. This rock was dated by SHRIMP at 762±12 Ma. Structural relationships indicate that the rock is older than **L-689**.

L-689. Quartz vein with a black, 2-3cm tabular interlayer of massive hematite. The vein contains mineral inclusions of minerals, angular rock fragments and maybe fluid inclusions. It has coarse angular vugs and gossans. Part of the sample is a quartz vein with less hematite, very thin red and black joints, and vuggy texture on one surface.

WPT 186, 967m. 2 photos (ED 10120005.jpg) of very thin 1.2 mm hematite with the veinlets (**L-690**) on a wet surface. Less dense fracture pattern and thinner veinlets. The main vein orientation is 070/69° N. There are other minor sets.

L-690 Relatively fresh, medium-grained intrusive rock with clusters of mafic minerals+magnetite, that is cut by a 0.5mm magnetite veinlet.

WPT 187, 965m. **L-691**. Small (~1m wide) non-porphyritic, very dense, black to dark green, very fine-grained, metaluminous sodic ferriferous monzonitic dike that runs E-W. It contains high copper values and was identified in the field as a fine-grained gabbroid with none to very low magnetism.

By WPT 168 to the W there is another intrusive body that makes a small hill. Abundant massive hematite and magnetite fragments and black veinlets cutting the coarse intrusive rocks.

L-692. Very fine-grained black rock with abundant angular (mostly cubic) vugs 0.5-0.8mm∅ uniformily spread out. It is a 3-D silica rock, with white scratch mark and conchoidal fracture. It is intersected by some 0.5mm hematite veinlets and one 3mm quartz+hematite veinlet. The origin of the rock is unknown. It could be a subvolcanic sulfide-rich dike, a fine-grained nepheline syenite, or a leached carbonatite. In the field, it was thought to be a “porous” hematite (after sulfides?) but that turned out to be wrong. The rock displays textures similar to angular breccias and contains very high silica.

WPT 188, 998m. Photograph of a subvolcanic rock (or something that looks like it) that intersects the main granitoid body and has a contact breccia. Several sub-parallel dikes, **L-693***. Fresh, fine-grained, medium gray, metaluminus mesocratic sodic ferriferous, biotite-rich, non-calcareous alkali granite, with strong magnetic content (very fine magnetite, not seen with bare eye) and high silica. It has no other particular macroscopic features. This rock was dated by SHRIMP at 765±4.5 Ma. Structural relationships indicate that the rock is younger than **L-688***.

WPT 189, 996m. Site of same dark subvolcanic intrusive as **L-693***, with xenoliths and flow textures, located on the hilltop. The strike of the subvertical rock is N70°E. It is 25-30 cm wide. The dike is finer-grained on the margins.

WPT 190, 982m. **L-694**. Fresh, medium-grained, medium-gray, slightly magnetic, metaluminous sodic ferriferous nepheline syenite with low quartz content, clusters of mafic minerals and minor magnetite. The entire hill is made of this material.

WPT 191, 991m. Highest elevation of small hill 2. 15 to 10 cm wide black dike oriented 077/69°N that cuts across the coarse granitoid (same as **L-694**). **L-695**: very fine-grained, black, metaluminous sodic ferriferous nepheline syenite with no magnetic signature, intersected by at least 2 families of very thin <<1mm quartz+hematite veinlets. It has some minor open vugs that on fresh surface seem to correspond with red hematite small clusters in 3-D. The rock matrix scratches white. See diagram of the hills on pg 25 of field notebook.

WPT 192, 979m. Located on top of the third, smaller hill and granitoid outcrop. Same rock type and orientation of dikes as on hill 2 = 69/80°N.

After WPT 167, going up, we begin to see yet another hill composed of intrusive rocks. Maybe it is another intrusive pipe of a system. At WPT 193, 975m is the base of this new hill. The road turns around it.

WPT 194, 982m. **L-697**: Fresh, representative medium-grained, light brown to pink, metaluminous sodic ferriferous syenite with clusters of mafic minerals+hematite, cut by network of magnetite-rich dark gray to black granitoid veins 0.6-0.8cm wide. The rock is a high-heat producer due to its high Th content.

WPT 195, 977m. The hill of body B is surrounded by quartz veins. **L-696**. 5mm quartz veinlet that intersects medium- to fine-grained syenitoid rock, as in the other hills. Also cut by 1mm hematite+quartz veinlets. The sample was slabbed to see textures better. Also photo of breccia vein/dike with hematite and angular fragments.

WPTS 196, 988m, 197, 980m, 198, 978m, 199, 978m, 200, 987m, and 201, 994m close the perimeter around the base of the hill. There is a similar hill further east that was not studied in great detail.

Photo taken towards the S from WPT 201 of the three hills and intrusives of p. 25, taken towards the N. Note general geomorphology of the small intrusive bodies.

WPT 201. Black to dark gray dike, 15 cm wide and oriented 150/90° that intersects other dikes 40 cm wide. **L-698**. Fresh, fine-grained light brown-gray metaluminous sodic ferriferous alkali granite with disseminated py clusters in very fine nuclei. Slightly foliated in the same orientation as the host rock. Need to slab to describe better.

WPT 202, 985m. **L-699**. Medium-grained, brown, metaluminous sodic ferriferous syenite with clusters of dark gray quartz+magnetite (and also transparent quartz). Slightly magnetic, medium color index. It was difficult to find a fresh sample of this rock. It is a high heat producing syenite due to high Th content. The sample comes from a very large ring complex (body H) with the same composition. The same rock is host to bodies bodies A, B and C.

WPT 203, 990m. **L-700**. Very vuggy, gossanous quartz vein that contained sulfides.

WPT 204, 977m. **L-701**. Massive, very fresh, black, non-magnetic intrusive with extremely fine needles of acicular crystals in all directions (like rutile) that make 10-12 cm veins. Some of the vugs contain quartz druzes. The origin of the vugs is uncertain; could be miarolitic cavities or amygdules. Some of the vugs have gossanous textures. There are many similar bodies of rock lying around.

WPT 205, 981m. **L-702**. Large sample to slab. Quartz druzes and quartz veins 10-15 cm wide with gossanous vugs. This sample might have carried sulfides and gold. Collected to be slabbed and assayed.

WPT 206, 988m. **L-703**. Large sample to slab, same as previous sample.

Red rock alteration was observed on both sides of the road, up to WPT 165.

After WPT 165 to the west, outcrops of calcareous schists with many red veinlets and red rock iron oxide alteration. Any carbonate rock like this makes a good host for mineralization.

WPT 207, 992m. Sheeted, subparallel, 1mm quartz + hematite veinlets in fine-grained igneous rock that is hard to identify (**L-704**). There is at least one other perpendicular family of joints with black iron oxide minerals.

WPT 208, 993m. Very fine-grained intrusive rock (originally mis-identified as a quartzite) with abundant iron oxide veining stockwork and main system of sheeted veins. **L-705** and **L-706** were collected there. **L-705** is a brown very fine-grained intrusive rock with thin, braided quartz black hematite (?) veinlets. **L-706** is a 6cm vein (dike?) filled by very fine-grained green intrusive material. It contains massive hematite, rounded vugs and gossanous textures. Both of these samples might carry economic metal mineralization and they should be assayed. The same kind of veining occurs in several types of rocks on the way up the road. Red rock alteration also continues along the route.

WPT 208, 986m. Very “dirty” dark gray quartz vein collected for fluid inclusion studies. **L-707** Pink, medium-grained, granitoid intersected by dense reticle of quartz veins in all directions.

WPT 164. Red rock alteration in foliated quartzites.

WPT 209, 994m. **L-708**. Dark green-black, fine- to medium-grained, non-magnetic, metaluminous sodic ferriferous pyroxenite. It contains some disseminated sulfides. The surface is strongly covered by gossans and weathers orange. It also contains some carbonates. It is chloritized.

WPT 210, 1010m. Fine-grained intrusive rock. (same as **L-705**) **L-709**. Fine-grained pink intrusive rock cut by a series of sub-parallel and braided, 1mm quartz + chlorite veinlets. At least seven veinlets identified on sample; one is 3-5mm wide. The sample has red-rock alteration. It was marked in blue to slab and carry out petrographic studies.

WPT 163. Some massive iron oxide rocks and vuggy quartz veins, as well as extensive iron oxide alteration. Lots of gossan on some surfaces; see **L-710**. Collected to slab and observe the source of gossan. Dark green-gray, fine-grained, non-magnetic intrusive intersected by multiple sub-parallel 1-2mm veinlets of quartz + hematite + vugs that probably carried sulfides. Weathered surfaces show abundant irregular vugs and gossanous textures. The rock reacts with HCl; it might be a carbonatite dike.

Abundant gossanous surfaces on the way up. Iron oxide alteration in all rocks.

L-711. Fine-grained, foliated, dark granitoid (gabbroid?) with network of braided quartz+earthy goethite (red-orange) <<1mm veinlets. Stockwork texture. Most veinlets open to show crusty hematite-dusty red hematite and gossanous textures. The sample might carry free gold.

WPT 211, 1021m. Vuggy, white rock with gossan and dusty limonite. This rock should be assayed for gold and base metals. It is macroscopically very similar to **L-709**.

WPT 212, 1005m. Some gneissose textures (granulites?) with quartz in veinlets. **L-712**. Non-magnetic, fine- to medium-grained, foliated, peraluminous leucocratic sodic ferriferous alkali granite cut by 1cm thick, white quartz veinlets. Maybe the “foliation” is due to very close quartz braided veining in a non-foliated granitoid.

WPT 162. Many very thin quartz veinlets (2-5 cm wide) and persistent red iron oxide surfaces. The veins might have contained sulfides. There are no evident fresh sulfides.

WPT 161. **L-713**. Fine- to medium-grained, brown to dark gray, non-magnetic, metaluminous sodic ferriferous quartz syenite, with abundant gray smoky quartz. the rock might have carried some sulfides, now oxidized. It contains 1 cm-diameter plagioclase phenocrystals with ghost borders and general fuzzy texture. This rock probably is intensely hydrothermally altered.

From here onward, less iron oxide on the rock surfaces. Less gossanous textures. Migmatitic rocks ~ foliated.

WPT 160. Brown, coarse-grained intrusive rock.

WPT 159. Fine grained, brown, peraluminous sodic ferriferous, biotite alkali granite. Ten meters after that, **L-714**: foliated, medium- to coarse-grained, pink, metaluminous leucocratic sodic magnesian granite with series of sub-parallel, black, braided very thin <<1mm veinlets of quartz+sulfides that are now gossanous vugs and coarse quartz elongated crystals. Several orientations of intersecting fractures. Some with minor black hematite. After WPT 159, red rock alteration increases once more.

Up to WPT 158, foliated intrusive rocks (?). Similar brown, fine-grained intrusives with very thin, <1mm quartz veinlets.

WPT 157. Red-rock and brown-rock alteration persists. Pink granitoids with some minor foliation planes and minor dark facies.

WPT 156. Abundant subparallel 1 cm quartz veining.

WPT 155. Red rock alteration persists. Some strongly-banded cemented rocks. ~ submillimetric black and white banding.

Brown rock. Red color does not continue further. No coarse quartz veins. No gossans. Ocassional dark-green to black gabbros.

WPT 154. Foliated, banded, black-pink granitoids. After sedimentary rocks?

WPT 213, 1044m. Gossanous rocks with quartz veinlets; red rocks.

WPT 153. Banded intrusive rocks (gneissose). With black iron oxide banding.

WPT 153. Outcrops of hematite pods. There are some quartz vuggy veins with massive black hematite and gossans; probably after sulfides. Red rock alteration is abundant. Some of the red granitoids have subparallel black hematite veinlets.

Banded black and white igneous (?) rocks along the way. No hills or evidence of granite plugs.

WPT 214, 1046m. **L-715**: Very magnetic sample of black and white, foliated, metaluminous mesocratic sodic-potassic ferriferous biotite granite. Gneiss-like texture with black bands of biotite + magnetite + quartz. Seems to have a metamorphic segregation origin. The main rock is a pink coarse-grained granitoid.

WPT 152. Some quartz float.

Black and white dike 25-30 cm wide, 18m after fence.

Banded intrusive rocks.

WPT 150. Same as before. Quartz float and red-rock alteration. Some gossanous rocks.

WPT 149. Some black, foliated dikes.

WPT 215, 1043m. **L-716***. Fresh, gneissic brown to pink/black, fine-grained, metaluminous subleucocratic sodic ferriferous biotite granite with evident rock foliation. Pink potassium feldspar + quartz + biotite + no appreciable magnetite. Very strongly oxidized, with gossanous surfaces and no visible sulfides. The rock is similar to others seen before. There is some quartz float lying around. **L-716*** was dated by SHRIMP at 745±5 Ma.

WPT 148. Quartz float is abundant and rocks have brown-rock alteration.

Foliated granitoids.

Dark green “porous” gabbros with red oxidation.

WPT 147. Very abundant quartz float. No good outcrops available.

WPT 146. Coarse quartz float and gabbros. Red iron oxide on most rock surfaces.

WPT 216, 1028m. **L-717**. Abundant quartz float is present in the environs. Quartz milky fragments, some with joints filled by black material. They were collected for fluid inclusion work. Maybe the fluid inclusions in the quartz can be used as an exploration tool for iron oxide-copper-gold (or other types?) of mineralization.

WPT 145. Some gabbro (green) fragments are present in the environs. No in situ outcrop. Only angular gravel terraces. Minor iron oxide in coarse, angular gravel. Relatively flat topography.

WPT 143. Not much outcrop. Some dark green dikes.

WPT 217, 1029m. Abundant coarse quartz float. **L-718**. Milky white quartz in part with coarse "sugary" texture is found on the ground. Collected for fluid inclusion work. No true outcrops along the way.

WPT 142. Abundant quartz float.

WPT 218, 1036m. Fine-grained pink intrusives. **L-719**.

S160 (See on Fig M21). All the way up to here from the main road from Khorixas there is a lot of coarse quartz with gossanous vugs.

S161. Outcrop of fine-grained schists after volcanic rocks, with some plagioclase porphyroclasts. Abundant quartz with gossanous vugs lies on the ground. There might be some sort of epithermal mineralization, there is no more time available for evaluation.

The road is rough for a 4WD vehicle.

Good outcrops on the hills. They are easy to traverse and have very little vegetation.

Flat plateaus full of quartz. Photos with abundant quartz.

S162. Photo with hammer and Welwitschia for scale. Another photo with car for scale in a flat flateau that is 100% made of quartz from quartz pod.

S163. Extremely iron oxide-rich fracture (?) in shales or volcanic rocks. Outcrop along a dry creek bed.

S164, 807m. Entrance to road to Oas farm from the main road. Hand sample for example of stockwork in brittle quartzites **L-1047.**

S165. Very abundant quartz with gossanous vugs. Also abundant rocks such as **L-1047** with many intersecting quartz veins.

S166. Brown rock alteration and abundant quartz veins with gossanous vugs.

S167. Abundant calcrete covers rocks. Some quartz is still visible.

S168, 876m. Entrance to Oas farm. Calcrete and brown rock alteration.

S169. Quartz and brown-rock altered, fine-grained rock make all the ground. Maybe the quartz is evidence of silicification ~ veining.

S170, 889m. Outcrop of strange rock (**L-1016**) that after microscopic analysis turned out to be a quartzite. Glassy, very fine-grained with subparallel vugs, such as vesicular lava would have, intersected by abundant network of quartz veins. The surface color is brown; inside its color is white or light gray. Very fresh; it gives a bell tinge when struck by the hammer. **L-1047** is from that same type of rock.

Photo (photo 03080007) with pencil of sub-parallel vugs and stockwork of of quartz veins. **L-1015** for chemical analysis.

Much of the quartz in veins of the brown-surface rock has vuggy textures, after sulfides.

Photo (photo 03080008) with hammer that shows aspects of the quartz stockwork in brown-white rock. Veins with abundant iron oxide and vugs after sulfides. **L-1017**.

S171. **L-1018**. Magnetite from sand found in the active bed of a dry creek. Several samples of subvolcanic intrusions were observed along the creek.

S172. Another dry creek with subvolcanic intrusives along it.

S173, 199m. Sand-covered flat savannah with abundant magnetite clasts concentrated along drainage.

S174. **L-1019**. Foliated, fine-grained, metaluminous, subleucocratic sodic alkali granite with pyroxene and amphibole. Its chemical composition is similar to **L-1021**. Goats without earings were observed on the site. The “earings” are special appendices that hang from the goat’s neck when they feed on soils with high arsenic content.

S175. Farm house. **L-1020**. Foliated, metaluminous mesocratic sodic amphibole-rich granite with high sodium and copper contents.

S176. Many quartz veins that cut gneissic, metaluminous subleucocratic sodic biotite granite **L-1021**.

S177, 993m. Sulbvolcanic porphyritic, peraluminous mesocratic sodic-potassic ferriferous nepheline syenite dike that runs @ 070° strike 2 m wide, cuts road. **L-1022**. It is very similar in composition to **L-161**.

L-716* was considered to be a representative sample of the “basement” to the syenite intrusions of the Oas farm, but it turned out to be much younger. A definitive age for this sample is not yet completely interpreted. Nevertheless, several xenocrystic zircons with an age of 1692 Ma were found.

APPENDIX A67

FIELD NOTES FROM THE LOFDAL FARM, NAMIBIA

WPT 220, 1022m. Large outcrop of gossanous, strongly magnetic, silicified, angular clast, polymictic hydrothermal breccia. Some of the clasts have diameter greater than 20 cm.

L-719. Fresh, very fine-grained pink granitoid, with no magnetite.

WPT 223, 973m. Large fragments of magnetite that is turning into hematite (martite). **L-720**. The outcrop is located in front of a house. Massive magnetite with internal layering is intersected by a white carbonate veinlet. All surfaces are strongly altered and full of vugs.

L-721. Small quartz fragments with coarse magnetite/hematite clusters inside. Pebble of vuggy white quartz, with round nugget of enclosed hematite. This is the surface expression of a quartz pod.

WPT 224, 972m. **L-722**. Brown, fine- to medium-grained, massive intrusive carbonate rock. It has white calcite veinlets, inclusions of black magnetite and xenoliths of some siliceous, igneous-looking rocks. All constituent minerals seen are brown-colored carbonates and abundant red, dusty hematite. Nothing else is visible, except for magnetite. See photo on Fig 4.4.2.18. The rock is a carbonatite.

The environs contain abundant black magnetite-hematite ~1mm wide veinlets in a brown carbonatite, just as sampled above. There is abundant float of ankerite and iron oxide gossans.

WPT 225, 1980m. Many piled fragments of unidentified coarse white micas, pink plagioclase, quartz and light green minerals that cannot be recognized in what seem to be pegmatites. These minerals were mined for their rare earth content.

WPT 226, 985m. Up to here, abundant quartz float. **L-723**. Milky white quartz with abundant very thin <<1mm black iron oxide veinlets. The sample was taken for fluid inclusions studies. It may be part of a mineralized system.

L-724. Milky, white quartz intersected by a dense set of braided, 0.1 – 3mm, somewhat hematitized magnetite veinlets, with very porous vuggy textures and gossanous vugs. These probably were sites of old sulfides. Collected to slab and make thin/opaque section.

WPT 227, 986m. Coarse white body of quartz with sheeted hematite veins that may carry gold.

WPT 228, 987m. Coarse crystals of tan-pink plagioclase. **L-725**. Very coarse (10cm∅), single plagioclase crystal with coarse quartz inclusions. Part of a pegmatite.

Some float of quartz veins with disseminated “dalmatian” hematite spots 3-6mm diameter. Veins are 5 cm wide.

WPT 229, 1000m. **L-726**. Coarse- to fine-grained granitoid with abundant myarolitic cavities filled by brown, druzy hematite. The rock is spongy and has light density as if leached. It might carry gold. Quartz and feldspar in coarse pegmatite with hematite/limonite vugs that may be sulfide remnants. Located just by a ridge of intrusive rocks. The rocks seems to have been etched by an acid selectively disolving a portion of the rock out.

WPT 230, 1002m. **L-727**. Gossanous fractures with goethite in light, foliated, fine-grained, pink granitoid; densely intersected by quartz-hematite veinlets with abundant gossanous vugs after sulfides. Part of the quartz in the veins is dark and smokey. This rock might contain gold. Quartz and pink potassium feldspar react slowly to HCl along the pores.

WPT 231, 1002m. **L-728***. Fresh sample of fine-grained, banded, dark pink to red-brown, fine-grained, metaluminous, subleucocratic sodic ferriferous granite. Same as described above for **L-727**. Intersected by two (at least) very fine quartz veins and brown-ochre hematite-rich veinlets. Zircons from this sample were dated by SHRIMP U-Pb at 1750±5 Ma.

WPT 232. 1002m. **L-730**. Large sample of intensely-fractured, fine- to medium-grained intrusive rock cut by a dense 3-D network of gossanous, vuggy quartz + hematite + sulfides (?) veinlets ~1mm wide. The sample seems to have carried sulfides. It was collected for slabbing and detailed observation. Breccioid texture.

L-729. Breccia of similar characteristics to the previous sample (**L-730**). Fine- to medium-grained, pink, metaluminous subleucocratic sodic to potassic ferriferous biotite granite. The sample is cut by several subparallel sets of 1mm or thinner quartz veinlets with abundant vugs and gossanous texture. Collected for slabbing and observing textures.

WPT 233, 993m. Photo that was taken towards 064° of a fracture-fill breccia with leached sulfide vugs and gossanous surfaces. The fracture zone is approximately 1m wide.

Fig (Photo) shows a subvertical, 25-30 cm breccioid vein with abundant dusty goethite-filled vugs after sulfides. It contains quartz, black, massive hematite and sulfides. There is calcite in the veins. Note coarse texture of the breccia vein, angular fragments, etc. Taken from S to N and downward from WPT 233. Orientation of veins is 150°.

Close-up photo of the same breccia vein, with card for scale and no north arrow.

L-731. Abundant 2-3 cm-wide, non-magnetic, coarse-grained, brown to deep red carbonatitic dikes that run subparallel to each other in 165/80°W. Dikes are spaced every 40-45 to 80 cm and occur in large numbers. The carbonatite dikes contain plagioclase, clear calcite and quartz needles as intra-fragments. Dikes intersect a medium- to coarse-grained, porphyritic, white to light gray granitoid rock. Both contacts are present in sample. Some vugs in the host rock now are filled by red material. See also photo in section 4.2.2 with camera bag for scale, for a general image of the dikes. Located 80 m N of WPT 233.

Dark green (brown) dikes 065/79°S subparallel.

65 m N, from WPT 233. Foliated, dark gray carbonatite dikes 2.5 cm wide, 15-20 cm wide, sub-parallel to each other. Some run parallel and attached to white quartz veinlets. See **L-732**. 2-3mm lens of quartz enclosed by carbonatite (Fig 4.2.2.19 photo L-732; a close-up view of slabbed sample can be seen on Fig 4.2.2.16). These are not simple ankerite veins, because at times the dikes thicken and display clear igneous textures.

L-733. Tabular magnetite crystals, 5 mm thick and 10 cm long, with aleatory orientation. They occur in a brown carbonatite dike with white calcite porphyroclasts or xenocrysts (Fig, photo **L-733d**). Located 50 m NE of WPT 233. Elephant skin weathering texture on surface. Note white color of the fresh surface and dense network of magnetite-filled fractures.

L-734. White quartz veinlet with angular crystals of magnetite, brown dolomite, corroded fragments of slightly magnetic hematite, and transparent calcite xenocrysts. It looks like the “slurry veins” that are common in Carlin mineralized environments, Nevada, U.S.A.

L-735. Non-magnetic, angular breccia vein from WPT 233 with gossanous vugs and some 1-2 mm hematite veinlets and quartz. Medium-grained pink igneous rock (syenite?) that seems to have been “chewed up” by something. Some 1cm∅, clusters of brown calcite are found within the intrusive texture. Very irregular outer surface, with black iron oxide-rich layer. Collected to slab and observe textures.

WPT 234, 998m. **L-736**. Foliated medium- to fine-grained biotite-rich granitoid cut by at least two different families of 1-2 mm wide very vuggy, gossanous quartz–magnetite-sulfides veinlets that make a dense mineralized stockwork. The veinlets display red iron oxide alteration haloes. This sample may be mineralized with disseminated precious metals.

WPT 235, 998m. **L-737**. White quartz veinlet intersected by three families of magnetite banded veinlets. There is paired zonation from the center outward. The thicker vein is 8-9mm wide; thinner ones are millimetric. The quartz is full of voids, like big bubbles. Try fluid inclusion studies.

WPT 236, 1002m. Photos (several, 1 close-up, one long distance, another short distance. All with hammer for scale.)

L-738. For slabbing. Fine-grained, foliated, pink granitoid intersected by braided (or sheeted) magnetite+hematite+quartz veinlets 1-0.3 cm wide, that intersect each other and anastomose. Note iron oxide alteration of host rock near some veinlets and progressive overprinting from one side of the sample to the

other. Almost every single vein has vugs with gossanous infill that probably contained sulfides. Magnetite is partially martitized. Foliation is 130/76°N. The same orientation and similar features are often seen around this site. The rock is very similar to rocks from around the Hook Granite batholith, Zambia and to mineralized stockworks from the Tevrede iron oxide-copper-gold deposit in Namibia.

WPT 237, 997m. **L-739**. Extremely vuggy coarse-grained igneous rock in a gossanous breccia vein. Very similar to that of WPT 233, collected to compare. Probable orientation = 070°. No reaction to HCl. The sample is intersected in multiple directions by thin (<<1mm) magnetite-quartz veinlets that probably contained sulfides. An important portion of the rock seems to have been dissolved out. It should be assayed for gold.

APPENDIX A67.1

Cross Section Through Series of Ultramafic Dikes, Lofdal farm, Namibia

WPT 238, 997m.
WPT 239, 980m. Near farm worker's house.
WPT 240, 963m.

WPT 241, 1007m. **L-740**. Fresh, very fine-grained, glassy, gray-reddish to dark pink-brown, ~1m wide, peraluminous sodic ferriferous trachy phonolite dike with disseminated fine magnetite and no reaction to HCl, that runs 056° azimuth. It has conchoidal fracture and sharp edges. Well indurated.

WPT 242., 1005m. **L-741**. Subvertical, magnetic, dark gray to black subvolcanic, metaluminous potassic ferriferous trachy phonolite dike. It has an extremely fine-grained matrix, plagioclase porphyries, open vacuoles, and does not react to HCl. The dike is oriented 078°. Typical nepheline blades are 2-3mm wide, but range up to 2cm. The rock has a strong chloritic alteration.

WPT 243, 1052m. Black to dark brown carbonatite dike with hematitic banding along the foliation, coarse hematite clusters and gossanous texture. Oriented 60°/78°S. Very abundant iron oxides.

WPT 244, 1002m. **L-742**. Fresh, very fine-grained, medium gray, foliated, metaluminous sodic magnesian biotite granite, with slightly magnetic character. It lies exactly halfway between consecutive subparallel carbonatite dikes. Maybe the magnetism is due to hydrothermal alteration.

WPT 245, 1002m. **L-743**. Very magnetic, approximately 1m wide, brown carbonatite dike with abundant earthy goethite (after sulfides?), that seems to have internal flow banding. Oriented 085/52° S. It reacts to HCl. No more macroscopic features visible.

L-744. Non-magnetic, somewhat foliated, medium- to coarse-grained pink granitoid cut by by quartz veinlets. The rock is reasonably fresh for petrography and dating. It should be the same rock as L-742, and was collected to check for hydrothermal alteration and chemical variation in the host rock due to carbonatitic dikes.

WPT 246, 1012m. **L-745**. Fresh 4-5 cm wide, strongly magnetic, very fine-grained, medium gray carbonatite dike with internal flow banding and no visible iron oxides that intersects rock **L-742**. Orientation is 095/49°S. This rock could be dated. There is an alteration halo around the dike, and the sample has two "quenched" margins. It was slabbed across for detailed petrographic study. The sample has dip and strike indications written on it to correct for erroneous compass measurement. The average strike was defined using several GPS readings, to bypass rock magnetism.

WPT 247, 1002m. Carbonatite dike with abundant foliated (or braided?), black magnetite bodies that might contain sulfide mineralization. It runs parallel to the road and produces an elongated ridge. Oriented 064/83°S. As seen on photo, the iron oxides seem to be foliated along the dike. WPTs 248, 249 and 250 were taken are along the same dike. Minimun outcrop length is 400 m. Compare the orientation with that measured by the compass. **L-746** was collected across the northern half of the carbonatite dike. Note the orientation of the sample. It contains an iron oxide gossan on one side. The weathering surfaces show clusters of iron oxide-rich substance that do not weather as much; that is due to magnetite-alteration. The surface is brown/yellow and has a very irregular texture like lapiez corrosion in karstic environments. Dozens of satellite dikes run subparallel to the main ones that were sampled.

A typical cross section of the various dikes is shown and discussed on section 4.2.2, Fig 4.2.2.15. In other locations, dikes are closer together and very abundant.

WPT 251, 1001m. Site of another subvertical carbonatite dike. 25-30 cm wide with abundant iron oxide and red-rock alteration in the host rocks.

WPT 252, 1002m. Subvertical, 10-15 cm wide, quartz vein with iron oxide and black fractures that is oriented 050°. It seems to be younger than other nearby, quartz-less, carbonatite dikes sampled; but that is not proven, due to insufficient outcrop. It could also be contemporary with the ultramafic dikes. Sample **L-747** of quartz with red stain and thin red-filled joints and some black-filled joints, taken to study fluid inclusions.

APPENDIX A67.2

Magnetite-Cemented, Polymictic Hydrothermal Breccia that Makes a Diatreme

WPT 220. **L-748**. Highly magnetic, coarse-grained, polymictic, angular hydrothermal breccia with gossanous surface. It is extremely difficult to find a fresh representative sample. Many of the clasts display corrosion edges and hydrothermal alteration. Most of the sample surfaces are magnetic. The dimensions of the sample collected were 25 x 15 x 20 cm. It was slabbed every 2cm to study clast composition and angular variation. The gossanous surface was all left of the abundant contained sulfides. It may carry economic metallic mineralization and it should be evaluated. See Photos on Chapter 8.

WPT 635. Photo with hammer and view of the flat land. Note textures.

WPT 636. 2 photos of bare outcrop.

WPT 637. **L-1024**. Outcrop of carbonatite inside the breccia body. This rock does not seem to be a dike, but a massive volume of carbonatite. The sample contains high values of rare earths, Y, Cu, Sc, Ce and La; low Al_2O_3, Na_2O and Rb.

WPT 636, 639, 640 (from south to north end) waypoints along a subvertical, black, magnetic, metaluminous, sodic ferriferous undersaturated olivine gabbro dike with extremely large radial pyroxene crystals. **L-1025** was collected from the dike, on WPT 639. The rock has a decimetric, radial, conic crystal structure. It might indicate paleo-orientation of verticality at the time of emplacement. The sample has anomalous enrichement in Ti, P, Zn and V; very high Sr, Sr and Nb; low Al_2O_3, K, Na and Rb. Its copper content is also significant. The dike is two meters wide at times, but thins. The field map of Fig 4.2.2.20 shows it location.

WPT 641. **L-1026**. Massive magnetite.

WPT 642. **L-1028**. Abundant massive black magnetite with gossanous vugs after sulfides and occasional quartz veins.

WPT 643. **L-1027**. First outcrop of possible host rock to the diatreme. It is a coarse-grained, metaluminous mesocratic potassic ferriferous nepheline syenite with lots of circular vugs, and contains high K, LOI, Zr, Zn and Nb.

WPT 644. Abundant fragments of magnetite lying on the ground. Most with gossanous textures and quartz or white clay.

WPT 645. All the way from WPT 644 with abundant gossanous magnetite. **L-1029**, massive magnetite with small hole.

WPT 646. 2 samples of magnetite-matrix, very coarse-grained, round-clast, polymictic hydrothermal breccia for chemical analysis and assaying. **L-1030** is large, **L-1031** is small. Both for slabbing and assaying.

WPTs 647, 648, 649. These waypoints were made along the strike of the foliation of **L-1032**, a massive, very dark, green to black, foliated, metaluminous mesocratic sodic ferriferous undersaturated olivine gabbro that seems to conform the host rock of the magnetite breccia body (diatreme). The average dip of the foliation is 65° to the SE; measured indirectly, due to the rock's strong magnetism. The rock has similar chemistry to **L-1023** and **L-754**.

WPT 650. **L-1033**. Magnetite-matrix in coarse-grained, polymictic hydrothermal breccia to slab, assay, and evaluate composition of fragments and matrix.

WPT 652. **L-1034**. Magnetite-matrix, coarse-grained polymictic hydrothermal breccia with igneous clasts and abundant chlorite. Sampled to evaluate corrosion of clast margin and assay.

WPT 653. **L-1035**. Center of a large magnetite-matrix, coarse-grained polymictic hydrothermal breccia outcrop with well-packed angular fragments.

L-1036, Very large sample of the magnetite-cemented breccia. Collected to make large-area slabs and study the corrosion of round clasts. Also for assaying.

WPT 277. Pitch black dike or vein with quartz to be described later.

WPT 278, 970m. **L-754**. A one-meter wide, fine-grained, dark gray to black, metaluminous potassic, ferriferous diorite dike that produces a slight reaction with HCl and does not contain quartz (Fig photo **L-754**). Strongly-foliated: 070/55°S. The surface weathers with subparallel ridges and valleys. Other nearby dikes seem to have lamprophyric composition.

L-749. Quartz with minor light green micas in small batches. This comes from a rare-earth-bearing pegmatite.

WPT 279, 970m. **L-755**. Pitch black, non-magnetic, ~40 cm wide, extremely fine-grained dike, oriented 076/74°S. It is made of an unidentified black silicate substance that scratches white. The black material is full of very small vugs, and many submillimetric veinlets of braided quartz. Some 5mm, white quartz lenses; coarser portions show prismatic amphiboles+quartz+plagioclases. Another portion of the sample has more quartz and less black material. The sample was slabbed to observe its texture in detail. No massive hematite was present in the rock and it did not produce any reaction to 10% HCl. The rock extends for at least 50 m along strike. There are a few astomosing black veinlets in white quartz. One part of the sample is a quartz pod, the other part is a breccia.

WPT 281, 883m. Site along a dry creek with dense 3-D network of quartz veinlets. Some of them are vuggy. The host rock is a silicified, fine-grained granitoid.

WPT 282. Abundant quartz is lying on the ground, located by a farm gate. It may be from a quartz pod or a pegmatite.

WPT 283. Granitic rock outcrop. 0443882/7762969

WPT 284. End of igneous rock outcrop. 0443718/7762833.

L-756. Quartz with hematite 1-2cm∅ particles intersected by network of at least 2 families of braided, submillimetric black hematite veinlets. All (particles and veinlets) contain gossanous vugs after sulfides, and should be assayed for their gold/metal/rare earth content.

S175. Farm house. **L-1020**. Mafic, foliated rock with high Na and Cu.

WPT 151 is a gate in the fence.

S176. Many quartz veins cut gneissic, metaluminous, subleucocratic sodic ferriferous biotite granite (**L-1021**). Similar to **L-1019**.

S177, 993m. **L-1022**. Outcrops of a subvolcanic, porphyritic, peraluminous mesocratic sodic-potassic ferriferous trachytic dike. It is 2m wide, strikes 070°, and cuts the road. Its chemistry is similar to **L-161**.

S178 WPT 623, 995m. Just by windmill, gate of fence.

S179. Entrance to site of abandoned water borehole that is marked #W96911. Cased in 6-inch diameter iron pipe. A stratigraphic column of the borehole might be available with the farm owner or a Namibian government institution. Many magnetic dikes were seen around here.

WPT 624. House on road. WPT 625. Located on the road.

WPT 626. On dry river. **L-1023**. Reasonably fresh, flat-lying, black, non-magnetic, foliated rock. It might be a pyroxenite? If it is a dike, it is more than 5 meters wide. The chemistry of this sample is very similar to that of **L-1032** and **L-754**. It contains high Ca, Fe2O3, Co, Ni, Zn, and V.

WPT 627. Along road, several mafic or ultramafic black dikes were crossed.

S180 Gate on fence to enter the Lofdal farm. Black ultramafic rock makes the ground.

Zinc enrichment seems to be a particular feature of some syenites. Nepheline syenites from the sodalite syenite quarry in Zambia also contain high zinc. Gabbroic rocks in general are zinc-enriched; high-Zn rocks from other suites in the Greater Lufilian Arc tend to be gabbroids. Such is the case for the Kamanjab batholith and Okatjepuiko.

APPENDIX A68

PARTIAL FIELD NOTES COLLECTED AT THE MESOPOTAMIE FARM, NAMIBIA

WPT 312, 726m. **L-758**. Gossanous, quartz-rich, white, coarse-grained granite with graphic texture. There are several pegmatitic phases of the same rock made of coarse biotite, plagioclase and quartz that display partial graphic texture; its crystals vary from 5-10 cm in diameter. A zircon concentrate of this sample was dated using SHRIMP U-Pb methods and gave an age of emplacement of 750±5 Ma. Xenocrystic zircons produced an age of 1692±10 Ma. They record the igneous protolith from which the graphic granite was made. The sample was collected near the NW corner of the farm, as seen on Fig 4.2.3.3.

WPT 327, 682m. **L-759**. Peraluminous leucocratic potassic ferriferous, muscovite-rich granite that intersects schists. It is very similar to the previous outcrops along road (**L-758**).

On 0439579/7764129, 703m on a hill located just above the old mine plant site, **L-772** is one of several light gray to white, 70 cm wide, metaluminous potassic ferriferous graphic alkali granite veins that intrude a coarse, pegmatitic peraluminous leucocratic sodic ferriferous pegmatitic granite (**L-773**). The main orientation of the veins is 032/82° NW. They have many 2-3 cm long tabular white to light pink plagioclase phenocrystals.

WPTs 283 to 284 **L-779**. Outcrop of an intensely-fractured and hard to sample gneissose granitoid rock that probably is the regional basement.

On the NE corner of the Mesopotamie farm, several quartz pods were observed. **L-780** to **L-782** come from quartz pods.

WPT 337, **L-783**. Peraluminous mesocratic sodic to potassic ferriferous, muscovite-biotite gneissic granite outcrop on the northeastern portion of the Mesopotamie farm.

WPT 338, 790m. **L-784** comes from a coarse-grained, metaluminous mesocratic sodic to potassic ferriferous augen granite gneiss that probably makes the regional basement. It has pink potassium feldspar phenocrystals (with white nucleus) in a biotite+amphybole+plagioclase, dark gray, fine-grained matrix. The granitoid's main foliation is 154/51° E. It is macroscopically very similar to **L-779**.

APPENDIX A69

FIELD NOTES, UGAB RIVER, NAMIBIA

WPT 346. Gate
WPT 347. Flat outcrop of granitoids.
WPT 348.
WPT 349. E flat outcrop of granitoids
WPT 350. NE flat
WPT 351.
WPT 352. S outcrop
WPT 353. S Good, large outcrop

WPT 354. Long, panoramic photograph radiating from 070° to 045°. To the left, in the Ugab River valley, there are small, red intrusive bodies that seem to be young (L-793, L-796 and L-797). Next comes a soft, round hill, the road, and other small hills that are probably made of the same red intrusive rock. The large rolling hills to the right are made by gray, old intrusive rocks (L-795, L-798, L-799 and L-802).

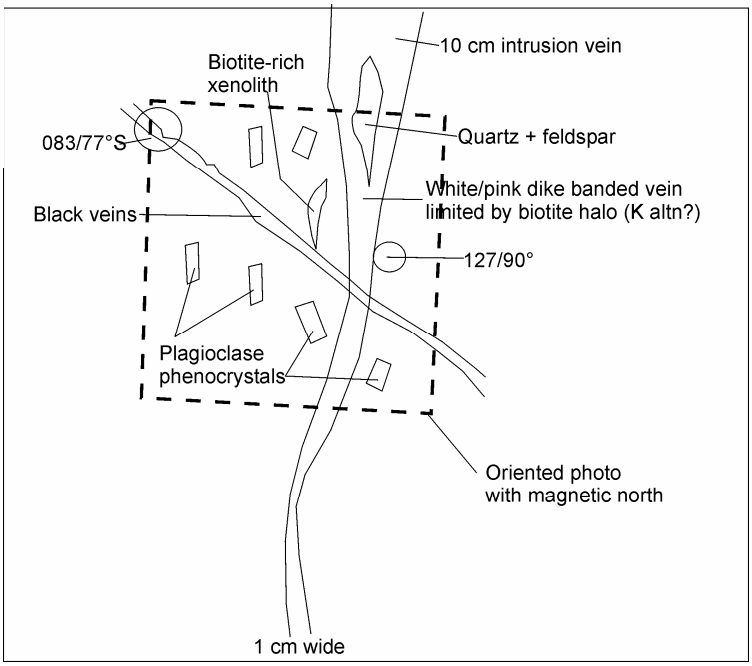

Fig Field drawing of some structural relationships at the Ugab River site, Namibia*. Located on geological station WPT 359, as described in the text. See photograph of the same outcrop on the next page.*

WPT 359, 648 m. Oriented photograph of porphyritic "gray" granitoid. The arrow points toward magnetic north. It has a 10 cm thick vein that contains a quartz + feldspar inclusion. A white/pink, banded dike is limited by a biotite halo (K alteration?). There is also a black, biotite-rich xenolith. The orientation of the dike is 127/90°. Some thin, black veins are oriented 083/77° S. All is shown on the Fig above. The photograph is perpendicular to the main rock foliation in this place, but few locations show similar foliation. The "foliation" might be due to local flow textures.

Roy Miller, consultant to the Namibian Geological Survey, suggested that I should visit the well-exposed outcrop of intrusive rocks near the Ugab River bridge. It is a good site to observe the contact between two intrusive bodies. The river was completely dry at the time of the visit.

WPT 361, 614 m. Parking spot.

WPT 355, 633 m. **L-793**. Coarse pink, metaluminous sodic ferriferous biotite granite with magnetite in abundant clusters. It may be a coarse facies of the pink intrusive body.

WPT 356, 630 m. **L-794**. Typical texture of the pink granitoid with very little magnetite. The rock has a slight foliation due to deformation; deformation is especially seen on the quartz. The rock is not extremely fresh, but is the best available for sampling.

WPT 357, 632 m. Fig is a photograph of contact the between both intrusive rocks. The red intrusive is fine grained near the contact (~chill margins). The gray granitoid is older, as observed on the outcrop.

WPT 358, 646 m. **L-795***. Two fragments of the gray, coarse, porphyritic intrusive body with abundant biotite and magnetite clusters. Most of the rock has intense chemical and mechanical weathering. A zircon concentrate from the sample was dated by U-Pb SHRIMP II at approximately 540 Ma; it also contained xenocrystic zircons with ages around 1200 Ma. Geochronology has not been completed at the time of writing this document.

WPT 360, 647 m. **L-796***. Fresh pink granitoid from opposite side of the road, behind a small, informal crafts shop. The sample contains red quartz clusters, no magnetite and zoned red plagioclase. A zircon concentrate from the sample was dated by U-Pb SHRIMP II at approximately 750 Ma. That age came as a surprise, for the foliated, porphyritic rock seemed to be older. There might be two generations of pink granitoids at the Ugab River outcrops.

WPT 353. **L-797**. Fresh, pink, medium-grained, peraluminous sodic-potassic ferriferous biotitic granite with pink feldspars, rare magnetite and red quartz.

WPT 352. **L-798**. Very fresh, fine to medium-grained, gray, peraluminous leucocratic sodic-potassic ferriferous granite with no pink feldspar present. It may be facies of the “pink” granitoid (**L-796**, **L-797**).

WPT 351. Two types of granitoids. A non-magnetic, medium-grained, gray granitoid with coarser-grained gray/pink feldspar (**L-800**, the same as on WPT 350) that intrudes medium- to coarse-grained, brown, porphyritic, peraluminous sodic-potassic ferriferous biotite granite (**L-799**) with yellow quartz, some magnetite and transparent to yellow plagioclase.

WPT 349. **L-801** Granitoid with dark red, tabular, soft macrocrystals and medium gray quartz. The gray granitoid progressively changes into a more pink rock.

WPT 348. **L-802**. Fine to medium-grained, pink, non-magnetic, peraluminous sodic-potassic ferriferous granite that grades from the previous gray granitoid (L-801). It contains small spindle-shaped, biotite- rich xenoliths and coarse biotite “eyes”.

APPENDIX A70

FIELD NOTES, OKWA RIVER, BOTSWANA

WPT 001 Car stop near a “bridge” over a dry river bed.

Very low profile outcrops as rock pavement surrounded by calcrete.

WPT 002. Granite outcrop
WPT 003. Granite outcrop
WPT 004. Calcrete cover
WPT 005. Granite outcrop
WPT 006. Boulder of calcrete with granite clasts in it. ***(See map on page 8.)***
WPT 007. Granite outcrop along the river bed
WPT 008-012. Delimit the perimeter of foliated granite outcrop. Main rock foliation is 131/87°N.

WPT 013. Small 10m diameter outcrop (**L-600A**) Fresh, light pink, slightly foliated, porphyritic, peraluminous sodic-potassic ferriferous alkali granite that is cut by a pink dike. Note zoned plagioclases and intense brown alteration in the fine-grained matrix.

WPT 014. L-601, Foliated granitoid sampled *in situ* from the freshest rock possible. Main rock foliation is 121/88°N.

WPT 015. **L-602**: Dark gray-greenish, fine- to medium-grained, metaluminous mesocratic sodic-potassic ferriferous granite. This rock was so dark that in the field, it was considered to be a gabbroid instead of a granite.

WPT 016. **L-603**. Fresh, non-foliated, fine-grained intrusive surrounded by foliated, coarse-grained (dike?).

WPT 017. **L-604**. Fresh, foliated granitoid.

WPT 018. **L-605**. Coarse-grained, foliated, metaluminous leucocratic sodic ferriferous clinopyroxene granite.

WPT 019. **L-606**. Composite, medium-grained, metaluminous mesocratic sodic ferriferous biotite granite that is not as strongly foliated.

Most of the foliated rocks contain dark gray to black xenoliths.

Abundant fragments of green, glassy volcanic rock are lying in the ground. These probably are Karoo age volcanic rocks.

This type of rock turned out to be quite common and widespread, as indicated on the main text of the chapter comparing Okwa River rocks to those from the Grootfontein Inlier, the Ugab River and others.

APPENDIX A71

FIELD NOTES, GROOTFONTEIN INLIER, NAMIBIA

WPT 602. Site where vehicle was parked.
WPT 603 to 610, 620 and 621: route along a railroad.
WPT 611 and WPT 612 traversed over coarse granitoids.
WPT 613. Over fine-grained porphyritic granitoid.
WPT 614. Over coarse-grained granitoid in forest.
WPT 615 and 616. From the highest point reached. *In situ* outcrop of carbonates with no evidence of intrusions or metamorphism. Bedding planes have normal polarity.

WPT 617. **L-1041**: Carbonate breccia from the base of the Otavi sequence with fragments of rounded granitoids. This is evidence that the Katangan rocks were unconformably laid over the granitoids.

WPT 618. **L-1042**: Coarse-grained, porphyritic, slightly foliated, peraluminous subleucocratic potassic ferriferous biotite granite with fuzzy mineral borders and 1cm long euhedral white to light yellow plagioclase phenocrystals. The sample was the least altered rock that could be found.

L-1043*: Fine, felsic, porphyritic, almost un-foliated, peraluminous, subleucocratic potassic ferriferous biotite granite. Zircons concentrated from this rock were dated by laser ablation ICPMS at the Memorial University in Newfoundland, Canada. They gave a U-Pb age of 1939±64 Ma, with xenocrystic zircons that dated 2544±78 Ma. Geochronological data for this sample was extremely complex to interpret, and further work may end up refining the ages.

WPT 619. The rock represented by **L-1043*** intrudes into **L-1044** in several locations. **L-1044** is a coarse-grained, porphyritic, peraluminous leucocratic sodic ferriferous biotite granite with alligned 2-3 cm long, pink feldspar euhedral phenocrystals.

L-1045: Fresh, very light gray to light yellow-pink, very fine-grained, metaluminous sodic ferriferous clinopyroxene quartzmonzonite with small vugs that may be sulfides (?).

L-1046: Fresh, porphyritic, gneissose, peraluminous subleucocratic potassic ferriferous biotite granite with white to yellow-pink potassic feldapar augen phenocrystals.

APPENDIX A72

TRANSCRIPTION OF FIELD NOTES FROM OKATJEPUIKO, NAMIBIA

Route with several fences and brooches. Sparse outcrop.
WPT 26 + 27 Outcrop.

WPT 28, brooch.

WPT 29 Borehole OP-2-17-100 100-17m 0243000/7537055 1544 m

WPT 30 Borehole OP-1, (to south). There is a pole with rock outcrop. The salt pan (called "malachite pan") is located to the east of WPT 30. The coordinates that I get for borehole OP-1 are 0243351/7537256±1544 meters of elevation.

WPT 31 **L-624**: Medium- to fine-grained fresh intrusive rocks
L-625: Metaluminous subleucocratic potassic ferriferous granite.

WPT 32 **L-626**: Fresh, medium- to fine-grained, peraluminous mesocratic potassic ferriferous granite with iron oxide veins. Large sample, packed in two bags.

WPT 33 Pole on OP-2 steel material over a concrete BM. This is the location of borehole OP-2.

WPT 034 Small outcrops of similar intrusive rock. Maybe outcrop is 20 m in diameter around all above stations.

WPT 035 [34K 0243343/7537284] **L-627**, **L-628**, **L-629** and **L-630** were collected here. They are different hand samples with iron oxide, black hematite and fine- to medium-grained, chloritized igneous rock.

On WPT 036: A dark green-black, fine grained gabbro cuts a much lighter gabbro with foliation.

WPT 037 **L-631**: Red jasper breccia

WPT 038 Site to sample later.

WPT 039 **L-632**: Gabbro or basalt (?) with white porphyries of plagioclase (or amygdules) in a very fine-grained, dark green matrix.

WPT 041 **L-633**: Fine of medium-grained metaluminous mesocratic potassic ferriferous monzo-gabbro with chlorite veinlets.

WPT 042 Outcrop of medium-grained gabbro or amphibole-rich rock. **L-639**: Black to dark green gabbro to NE of power line.

WPT 043 and 040 Poles for power line. Cables. L-634: Gabbro cut by thin, lighter 2mm intrusive veinlet.

WPT 044 Power line tower. **L-635**: Medium gray, porphyritic metaluminous potassic ferriferous quartz latite. It outcrops in a 10 m diameter around wpt.

L-636: Dark gabbro with pink veinlets.

L-637: Lighter (than **L-636**) fine-grained, metaluminous mesocratic potassic ferriferous biotite granite with higher plagioclase content and very slight foliation (or flow-banding?). In the field it seemed to be a different facies of the same gabbroic body of **L-636**. Fig (photo **L-637A**) shows the main features of the rock and illustrate the surface weathering and strong red surface coloration.

WPT 045 **L-638**: Pink, fresh, medium- to fine-grained, metaluminous leucocratic potassic ferriferous alkali granite. Contains fine green (chlorite?) and black (magnetite+biotite?) veinlets. It outcrops along the road, beneath a power line.

WPT 046 **L-640**: Pink and fine grained granitoid with black gabbro xenoliths ~rounded edges. Also some black hematite (?) veinlets.

In the same site, **L-641**: Fine-grained, dark green to dark gray, metaluminous mesocratic potassic ferriferous monzo-gabbro. Seems to be a xenolith into the pink granitoid of **L-640**.

WPT 048 **L-642**: Small fragments of fine-grained, black gabbro. Foliated rock with massive iron oxide alteration (hematitization) of sedimentary rock or foliated metamorphic rock. Also contains fragment of quartz + iron oxide pod. None of the samples are *in situ*, but collected from 5 m diameter around the WPT.

WPT 049 **L-643**: Small sample of granitoid with iron oxide veinlets. No more outcrop available at site of sample #130 of Eckhart Freyer.

On WPT 050 and 10 m around it, many samples of intensely-hematitized rock with quartz veins, vuggy quartz veins, calcite veinlets in networks, near a "T" junction and fence intersection. Deep red color extends along the road.

Some of the rocks display round-clast brecciation overprinted by extreme red hematite alteration. (See **L-644** and **L-645**: Brown-red, metaluminous mesocratic potassic ferriferous nepheline syenite) with strong hydrothermal alteration. The rock name is probably wrong. Intense sodic alteration, added to the large iron oxide hydrothermal input have largely modified the original rock chemistry. The trace element chemistry is not from a nepheline syenite. The original type of rock was hard to identify in the field. It seemed to have been fine-grained gabbro, or a dark sedimentary rock. It could also be a hydrothermal breccia cemented by nepheline syenite. As seen on Fig the photograph, the original clastic texture of the rock has almost vanished, to be replaced by a pervasive brown-red hematite alteration that progressively replaces matrix and clasts of the breccia. The photograph of **L-645** also helps to illustrate the red-rock alteration. In this case, original texture is easier to identify. Both **L-644** and **L-645** are massive, extremely well cemented rocks.

L-646 (Big sample): has deep purple-brown iron oxide color that masks previous rock texture out completely. A vuggy, white quartz vein intersects it and the oxidized vugs seem to have contained some sort of sulfides.

L-647: Red-rock altered rock with calcite thin veinlets in a stockwork fashion.

L-648: Brown iron oxide massive alteration in metaluminous mesocratic potassic ferriferous alkali granite with some Cu stains & gossans.

L-649: Fine-grained, metaluminous subleucocratic potassic ferriferous granite with silicification and massive iron oxide alteration; with chlorite and possible $CuCO_3$ stains. Very difficult to identify in the field. As shown on the photograph of **L-649**, a very dense three dimensional network of iron oxide-rich sub-millimetric veinlets, along with chlorite and sulfides of copper and iron were overprinted on a granitoid rock.

L-650: Breccia of brown-altered rock with quartz and calcite veins.

On WPT 051 entering the pan along a road, there is a ~20 m diameter outcrop of black to dark green and dark brown/red possible porphyritic (mafic?) volcanic rocks with massive iron oxide alteration. Some rocks even display massive metallic hematite.

L-651: Several grab samples with metallic iron oxide (hematite).

L-652: Several grab samples of the different varieties of rock in the outcrop. Note possible vacuoles and porphyroblasts as well as flow textures and/or bedding. Some rocks may be breccioid, but their texture is masked by pervasive iron oxide alteration. The rocks are immersed in white $CaCO_3$ calcrete.

Light gray color in roads that cover the pan. Some with Cu stains!

WPT 052 On the change of road, ballast color varies from from red/brown to light gray. This might indicate the areal extension of iron oxide alteration.

WPT 053 Change of soil color from brown to ochre. The brown soil has large rock boulders that were not sampled, but are thought to be similar to the brown rock iron oxide pervasive alteration that was previously described.

WPT 054 Entrance to farm house. Very friendly manager.

WPT 055 Possible intrusive rocks.

APPENDIX I
OTHER INFORMATION

A73	Persons interviewed for preparation of fieldwork, during fieldwork, and when processing information, 223
A74	Rock names of samples from the Greater Lufilian Arc Granitoid project, 224
A75	Experiment to test quality of chemical laboratory, 229
A76	Heat production capacity of intrusive rocks from the Greater Lufilian Arc at the time of their emplacement, 231

APPENDIX A73

PERSONS INTERVIEWED FOR PREPARATION OF FIELD WORK, DURING FIELD WORK AND WHEN PROCESSING INFORMATION

Armstrong, David; Kitwe, Mopani Copper Mines Ltd.
Ashwall, Lew; Johannesburg, University of the Witwatersrand
Badenhorst, Frik; Navachab mine, Anglogold Corporation, Namibia
Bantu-Bonse, Frederick; Kalulushi, Zambian Chamber of Mines
Borg, Gregor; Windhoek, Johannesburg, Martin Luther University, Halle, Germany
Bouda, Steven; Lumwana, Equinox Corporation, Zambia
Buxton, Mike; Johannesburg, Windhoek, Lubumbashi, Anglo American Corporation South African exploration office
Carruthers, Hugh; Kitwe, First Quantum Corporation
Clark, Alan, H., Queen's University, Kingston, Ontario, Canada; met in Toronto
Corner, Branko; Swakopmund, Private consultant in applied geophysics
Corrans, Roy; Johannesburg, geological consultant
Freyer, Eckart; Windhoek, Manager of AngloAmerican Corporation exploration office in Namibia
Greyling, Lynette; University of the Witwatersrand
Günzel, Arno; Windhoek, Otavi, Lubumbashi, Ongopolo Corporation
Hoffmann, Karl; Windhoek, Namibian Geological Survey
Hunt, John Paul; University of the Witwatersrand
Injoque, Jorge; Lima, via e-mail, geological consultant, Lima, Peru
Jebrak, Michel, University of Quebec in Montreal, Canada
Kabengele, Matthias, Lubumbashi, D.R. Congo
Kamona, Fred; Windhoek and Lubumbashi, University of Namibia
Khunuchab, Julius
Kinnaird, Judith; Johannesburg, Zambia, University of the Witwatersrand
Klinge, Thoren; Kumba Resources, South Africa
Lauderdale, John, Kitwe, Lubumbashi, AVMIN exploration office in Zambia
Liyungu, Kennedy; Lusaka, Director, Zambian Geological Survey
Lombaard, Andrus; Otavi, geological consultant to Ongopolo Corporation
Lombard, Anton; Windhoek, manager of AVMIN exploration office in Namibia
MacKenzie, Chris; Windhoek, Manager of BAFEX corporation
Mann, Peter; Kitwe, Anglo American Corporation exploration office in Zambia
Mariano, Anthony; Windhoek, geological consultant
Martin, Robert, McGill University, Montrea, Canada
Master, Sharad; Johannesburg, various portions of Zambia and Botswana, Lubumbahi, University of the Witwatersrand
Matthews, Alexander, Kitwe, Lusaka, Lubumbashi, AVMIN exploration office in Zambia
Mendelsohn, Felix; Johannesburg, geological consultant
Miller, Roy; Windhoek, Geological consultant to the Namibian Geological Survey
Murphy, John; Johannesburg, AVMIN
Mweti, Albert
Nex, Paul; Johannesburg, University of the Witwatersrand
Niku-Paavola, Vicky; Windhoek, Namibian Geological Survey
Nyambe, Imasiku; Lusaka, Lubumbashi, Johannesburg, University of Zambia
Pelly, Peter; Johannesburg, Kitwe, Windhoek, Lubumbashi, BHPBilliton exploration office in South Africa
Philpot, Hilton; Johannesburg, Exploration Manager, AVMIN
Porada, Hubertus; via e-mail, University of Würsburg, Germany
Prinsloo, Tinus; Kombat Mine, Ongopolo Corporation
Rainaud, Christine; Johannesburg, University of the Witwatersrand
Richards, Michael; Lumwana, Equinox Corporation
Schneider, Gaby; Windhoek, Director, Namibian Geological Survey
Sillitoe, Richard; Kitwe, geological consultant
Steven, Nick; Johannesburg, private geological consultant, Capetown
Tembo, Francis; Lusaka, Head of Geology, University of Zambia
Tsengua, Simon
Whitfield, Gavin; Johannesburg, geological consultant
Williams, Tim; Chingola, Nchanga Mine, Nchanga Copper Corporation
Wilton, John; Otjiwarongo, AVMIN exploration office in Namibia
Woodhead, John; Kitwe, Lubumbashi, Anglo American Corporation exploration office in Zambia

TABLE A74 ROCK NAMES, GRANITOID SAMPLES COLLECTED, LUFILIAN PROJECT, ZAMBIA AND NAMIBIA

By Alberto Lobo-Guerrero S, Geologist, M.Sc., Min.Ex., Feb. 2004, Johannesburg

Sample	Middlemost	de la Roche	IUGS		Sample	Middlemost	de la Roche	IUGS
L-005a		granite			L-163	foid gabbro	syeno-gabbro	foid diorite
L-012	syenite	quartz syenite	syenite		L-166	granite	granite	granite [high-K]
L-012A	syenite	quartzmonzonite	syenite		L-167	foid monzodiorite	syeno-diorite	foid monzodiorite
L-020	granite	alkali granite	granite [high-K]		L-168	granite	alkali granite	granite [high-K]
L-023	granodiorite	granodiorite	tonalite		L-170	granodiorite	granite	granite [high-K]
L-024	gabbro	gabbro-diorite	gabbro [subalkali]		L-172	granite	alkali granite	granite [high-K]
L-025	granite	granite	granite [high-K]		L-173	granite	alkali granite	granite [high-K]
L-026	granite	granite	granite [high-K]		L-175	granite	granite	granite [high-K]
L-027	granodiorite	granodiorite	granodiorite [medium-K]		L-181	gabbro	s. olivine gabbro	gabbro [subalkali]
L-028	monzonite	quartz monzonite	monzonite [Na2O-2<K2O]		L-195	syenite	syenite	syenite
L-029	granodiorite	tonalite	granodiorite [medium-K]		L-199			
L-030	granite	granite	granite [high-K]		L-207	granite	alkali granite	granite [Peralkaline, Al2O3>1.33Fe+4.4]
L-032	diorite	gabbro-diorite	diorite [high-K]		L-208	granite	alkali granite	granite [high-K]
L-034	syenite	?	syenite		L-209	gabbro	alkali gabbro	gabbro [alkali]
L-036	granodiorite	syenite	granodiorite [low-K]		L-210	quartzmonzonite	syenite	syenite
L-037	foid syenite	out of plot (far from gtd field)	nepheline sodalite syenite [peralkaline]		L-212	syenite-quartzmonzonite	quartz syenite	syenite
L-038	foid syenite	nepheline syenite	nepheline sodalite syenite [peralkaline]		L-213	syenite	syenite	syenite
L-039	foid syenite	nepheline syenite	nepheline sodalite syenite		L-214	syenite	syenite	syenite
L-040	foid syenite	nepheline syenite	nepheline sodalite syenite [peralkaline]		L-215	granite	syenite	granite [Peralkaline, Al2O3>1.33Fe+4.4]
L-041	foid syenite	nepheline syenite	nepheline sodalite syenite		L-217	granite-granodiorite	granodiorite	granite [medium-K]
L-044	foid syenite	nepheline syenite	nepheline sodalite syenite [peralkaline]		L-218	quartzmonzonite	quartz syenite	syenite
L-045	foid syenite	nepheline syenite	nepheline sodalite syenite		L-222	granodiorite	alkali granite	tonalite
L-046	foid syenite	nepheline syenite	nepheline sodalite syenite		L-223	granodiorite	granite	tonalite
L-047	quartzmonzonite	quartz syenite	syenite		L-224	diorite	alkali granite	tonalite
L-049	gabbro	saturated olivine gabbro	gabbro [alkali]		L-237	granite	granite	granite [high-K]
L-050	gabbro	undersaturated olivine gabbro	gabbro [alkali]		L-238	granite	granodiorite	granite [high-K]
L-060	gabbro	saturated olivine gabbro	gabbro [subalkali]		L-239	granite	granite	granite [high-K]
L-060	gabbro	saturated olivine gabbro	gabbro [subalkali]		L-241	foid out of plot		
L-060	granite	granite	granite [Peralkaline, Al2O3>1.33Fe+4.4]		L-242	granite	out of plot granodiorite	granite [medium-K]
L-063		essexite	foid gabbro (ol<10%)		L-248	granodiorite	granodiorite	granodiorite [medium-K]
L-064		essexite	foid gabbro (ol<10%)		L-248-LG	granite	granite	granite [high-K]
L-065		theralite	nepheline syenite		L-249	granite	granite-granodiorite	granite [high-K]
L-075			quartzmonzonite		L-257	granite	granite	granite [high-K]
L-076	quartzmonzonite	quartz monzonite	quartzmonzonite		L-259	quartzmonzonite	granite	granite [high-K]
L-077	quartzmonzonite	quartz monzonite	quartzmonzonite		L-259-B	quartzmonzonite	granite	granite [high-K]
L-078	granodiorite		tonalite		L-263	quartzmonzonite	quartzmonzonite	quartzmonzonite
L-079	quartzmonzonite	granite - limit with granodiorite	quartzmonzonite		L-268	granodiorite	granite?	
L-079		granite			L-269	granite	granite?	
L-139	granite	alkali granite	granite [high-K]		L-273	granodiorite	granodiorite	
L-150	monzodiorite	syeno-diorite	monzodiorite [Na2O-2<K2O]		L-279	granodiorite	granodiorite	
L-151	granite	alkali granite	granite [high-K]		L-311	gabbro	monzonite	gabbro [subalkali]
L-153	granite	alkali granite	granite [high-K]		L-313			
L-154	granite	alkali granite	granite [high-K]		L-314			
L-155	granite	granite	granite [high-K]		L-318	off graph foid?		
L-157	granite	granite	granite [high-K]		L-321	granodiorite	granodiorite	
L-158	granite	granite	granite [high-K]		L-321	granodiorite	off diagram (granodiorite?)	granodiorite [low-K]
L-159	granodiorite	granodiorite-granite	granite [high-K]		L-322	granite	alkali granite	
L-160	quartzmonzonite	granite	granite [high-K]		L-322	granite	alkali granite	granite [high-K]
L-161	monzodiorite	syeno-diorite	monzodiorite [Na2O-2<K2O]		L-323	quartzmonzonite	alkali granite	
L-162	granite	granite	granite [high-K]		L-323	quartzmonzonite	alkali granite	quartzmonozonite

Sample	Middlemost	de la Roche	IUGS
L-324	syenite	quartz syenite	
L-324	syenite	quartz syenite	syenite
L-325	monzonite	granite	
L-325	monzonite	granite	monzonite [Na2O-2<K2O]
L-341	quartzmonzonite	monzonite	syenite
L-343	granodiorite	gabbro-diorite	granodiorite [low-K]
L-344	monzonite	monzonite	syenite
L-345	syenite	quartz syenite	syenite
L-346	granite	granite	granite [high-K]
L-347	gabbro	out of plot (gabbro)	gabbro [alkali]
L-348	quartzmonzonite	granodiorite-quartzmonzonite	granite [high-K]
L-349	quartzmonzonite	quartzmonzonite	granite [high-K]
L-352	granite	granite	granite [high-K]
L-353	quartzmonzonite	quartzmonzonite	syenite
L-354	granodiorite	granodiorite	tonalite
L-355	granite	granite	granite [high-K]
L-357	quartzmonzonite	quartz monzonite	syenite
L-358	granodiorite	quartz monzonite	granodiorite [medium-K]
L-359	quartzmonzonite	granite	quartzmonzonite
L-360	quartzmonzonite	granite	granite [high-K]
L-361	granodiorite	quartz monzonite	granodiorite [medium-K]
L-362	granodiorite	granodiorite	granodiorite [medium-K]
L-363	granodiorite	granodiorite	tonalite
L-364	granite	alkali granite	granite [high-K]
L-365	granite	granite	granite [high-K]
L-366	quartzmonzonite	granite	quartzmonzonite
L-367	granodiorite	granodiorite	granite [medium-K]
L-368	quartzmonzonite	granite	quartzmonzonite
L-369	granite	granite	granite [high-K]
L-370	granite	granite	granite [high-K]
L-371	granite	granite	granite [high-K]
L-372	monzo-diorite	monzo-gabbro	monzodiorite [Na2O-2>=K2O]
L-373	granite	granite	granite [high-K]
L-374	granite	granite	granite [high-K]
L-375	granite	granite	granite [high-K]
L-376	syenite	syenite	syenite
L-377	quartzmonzonite	quartz syenite	granite [peralkaline, Al2O3>1.33Fe+4.4]
L-378	granite	granite	granite [high-K]
L-379	granite	alkali granite	granite [peralkaline, Al2O3>1.33Fe+4.4]
L-380	granite	alkali granite	granite [high-K]
L-402	granodiorite	granodiorite	granodiorite [low-K]
L-403	quartzmonzonite	quartzmonzonite	syenite
L-405	gabbroic diorite	s. olivine gabbro	gabbroic diorite [medium-K]
L-406	gabbro	alkali gabbro	gabbro [alkali]
L-407	monzonite	gabbro-diorite	monzonite [Na2O-2<K2O]
L-408	granite	granite	granite [high-K]
L-409	quartzmonzonite	granite-alkali granite	granite [high-K]
L-410	granodiorite	granite	tonalite
L-411	out of plot, foid	off plot, ultramafic	foidolite
L-416	gabbro-diorite	gabbro norite	gabbroic diorite [medium-K]
L-420	granite	granite	granite [medium-K]
L-421	quartzmonzonite	granite	granite [high-K]
L-433	monzodiorite	syeno gabbro	monzodiorite [Na2O-2<K2O]
L-434	granodiorite	granodiorite	granite [high-K]

Sample	Middlemost	de la Roche	IUGS
L-435	quartzmonzonite	quartz syenite	syenite
L-436	granite	granite	granite [Peralkaline, Al2O3>1.33Fe+4.4]
L-437	monzonite	syeno diorite	monzonite [Na2O-2<K2O]
L-438	monzodiorite	monzogabbro	monzodiorite [Na2O-2<K2O]
L-439	granite	alkali granite	granite [high-K]
L-440	monzogabbro	gabbro-diorite	monzodiorite [Na2O-2<K2O]
L-441	quartzmonzonite	quartzmonzonite	syenite
L-442	granite	alkali granite	granite [high-K]
L-443	granite		granite [high-K]
L-444	monzodiorite	gabbro-diorite	monzodiorite [Na2O-2<K2O]
L-458	granite	alkali granite	granite [high-K]
L-459	diorite	tonalite	diorite [medium-K]
L-460	granite	granite	granite [medium-K]
L-461	granite	granite	granite [high-K]
L-462	granite	granite	granite [high-K]
L-463	gabbro	gabbro-diorite	gabbro [subalkali]
L-464	out of plot, foid		melilite nephelinite or melilite leucitite
L-465	out of plot, foid	out of plot (foid)	foidolite
L-466		granite	granite [high-K]
L-467	granite	alkali granite	granite [high-K]
L-600A	granite	alkali granite	granite [peralkaline, Al2O3>1.33Fe+4.4]
L-602	granite	granite	granite [high-K]
L-605	granite	granite	granite [high-K]
L-606	granite	granite	granite [high-K]
L-625	granite	granite	granite [medium-K]
L-626	granite	granite	granite [low-K]
L-633	monzo-gabbro	monzo-gabbro	monzogabbro [Na2O-2>=K2O]
L-635	monzonite	quartzmonzonite	syenite
L-637	granodiorite	granite	granite [low-K]
L-638	granite	alkali granite	granite [high-K]
L-641	gabbro	monzo-gabbro	gabbro [subalkali]
L-645	monzonite	nepheline syenite	monzonite [Na2O-2>=K2O]
L-648	granite	alkali granite	granite [peralkaline, Al2O3>1.33Fe+4.4]
L-649	granite	alkali granite	granite [medium-K]
L-668	diorite	syenite	syenite
L-669	granodiorite	syenite	syenite
L-670	diorite-gabbroic diorite	nepheline syenite	monzonite [Na2O-2>=K2O]
L-675	diorite	syenite	syenite
L-676	diorite	syenite	syenite
L-691	gabbro	monzonite	monzodiorite [Na2O-2<K2O]
L-693	granodiorite	alkali granite	granite [peralkaline, Al2O3>1.33Fe+4.4]
L-694	diorite	nepheline syenite	syenite
L-695	gabbro	nepheline syenite	foid diorite
L-697	diorite	syenite	syenite
L-698	granodiorite	alkali granite	granite [peralkaline, Al2O3>1.33Fe+4.4]
L-699	granodiorite	syenite	syenite [comenditic]
L-700B	granodiorite	quartz monzonite	
L-708	gabbro	out of plot, gabbro	gabbro [alkali]
L-712	granite	alkali granite	granite [medium-K]
L-713	granodiorite	quartz syenite	granite [peralkaline, Al2O3>1.33Fe+4.4]
L-714	granite	granite-alkali granite	granite [high-K]
L-714	granodiorite	granite	granite [high-K]
L-715	granite-granodiorite	granite	granite [high-K]
L-716	granite	granite	granite [high-K]

Sample	Middlemost	de la Roche	IUGS
L-722	out of plot, high Ca	out of plot, high Ca	foidolite
L-728	granite	granite	granite [peralkaline, Al2O3>1.33Fe+4.4]
L-729	granite	granite	granite [high-K]
L-740	monzodiorite	nepheline syenite	monzonite [Na2O-2<K2O]
L-741	foid monzosyenite	nepheline syenite	foid monzosyenite
L-742	granodiorite	granite	granodiorite [low-K]
L-754	gabbroic diorite	gabbro diorite	gabbroic diorite [medium-K]
L-759	granite	granite	granite [high-K]
L-772	granite	alkali granite	granite [peralkaline, Al2O3>1.33Fe+4.4]
L-773	granite	granite	granite [medium-K]
L-783	granite	granite	granite [high-K]
L-784	granite	granite	granite [high-K]
L-789	syenite	quartz syenite	syenite
L-791	granite	alkali granite	granite [high-K]
L-791	granite	alkali granite	granite [high-K]
L-793	granite	granite	granite [high-K]
L-797	granite	granite	granite [high-K]
L-798	granite	granite	granite [high-K]
L-799	granite	granite	granite [high-K]
L-802	granite	granite	granite [high-K]
L-808	granite	granite	granite [high-K]
L-809	granite	alkali granite	granite [high-K]
L-810	granite	granite	granite [high-K]
L-812	granite	granite	granite [high-K]
L-813	granite	granite	granite [high-K]
L-814	out of plot, high Si	out of plot,high Si	granite [low-K]
L-815	granite-quartz monzonite	granite	granite [high-K]
L-816	granite	granite	granite [medium-K]
L-816	granite		
L-832	granite	alkali granite	granite [peralkaline, Al2O3>1.33Fe+4.4]
L-834	foid syenite	syenite	foid syenite
L-835	quartzmonzonite	quartzmonzonite	syenite
L-836	quartzmonzonite	granite	quartzmonzonite
L-838	quartzmonzonite	granite	quartzmonzonite
L-839	granite	alkali granite	granite [high-K]
L-840	granite	granite	granite [high-K]
L-842	quartzmonzonite	granite	
L-843	granite	alkali granite	granite [high-K]
L-844	quartzmonzonite	granite	granite [high-K]
L-846	quartzmonzonite	granite	quartzmonzonite
L-849	granite	alkali granite	granite [high-K]
L-850	granite	granite	granite [high-K]
L-855	granite	alkali granite	granite [peralkaline, Al2O3>1.33Fe+4.4]
L-857	granite	granite	granite [high-K]
L-863	granodiorite	granodiorite	tonalite
L-864	n.d.		
L-864	granodiorite	granodiorite	tonalite
L-865	granodiorite	granodiorite	tonalite
L-868	quartzmonzonite	granite	quartzmonzonite
L-874	off plot	out of plot, high Si	granite [low-K]
L-874-	quartzmonzonite	granite	quartzmonzonite
L-875	quartzmonzonite	granodiorite	quartzmonzonite
L-877	quartzmonzonite	granite	quartzmonzonite
L-878	quartzmonzonite	granite	granite [high-K]

Sample	Middlemost	de la Roche	IUGS
L-895	monzonite	syeno-diorite	monzonite [Na2O-2<K2O]
L-898	quartzmonzonite	granite	granite [high-K]
L-899	granite	granite	granite [high-K]
L-900	quartzmonzonite	quartzmonzonite	syenite
L-902	granite	alkali granite	granite [peralkaline, Al2O3>1.33Fe+4.4]
L-903	granite	alkali granite	granite [high-K]
L-904	granite	alkali granite	granite [high-K]
L-905	granite	alkali granite	granite [high-K]
L-906	granite	alkali granite	granite [high-K]
L-907	granite	granite	granite [high-K]
L-908	syenite	syenite	
L-909	granite	alkali granite	granite [high-K]
L-910	granite	alkali granite	granite [high-K]
L-911	granite	out of plot, high Si	granite [high-K]
L-912	granite	granite	granite [high-K]
L-917	granite	granite	granite [high-K]
L-919	out of plot, high Si	out of plot, high Si	granite [high-K]
L-920	foidolite	syenite	foidolite
L-922	quartzmonzonite	granite	quartzmonzonite
L-923	granite	granite	granite [high-K]
L-924	granite	granite	granite [high-K]
L-938	granite	granite	granite [high-K]
L-939	quartzmonzonite	granite	quartzmonzonite
L-940	quartzmonzonite	gabbro-diorite	syenite
L-943	granite	granite	granite [high-K]
L-945	quartzmonozonite	granite	granite [high-K]
L-946	quartzmonozonite	granite	granite [high-K]
L-948	granite	granite	granite [high-K]
L-951	syenite	nepheline syenite	syenite [comenditic]
L-952	quartz monzonite	nepheline syenite	syenite [comenditic]
L-955	quartz monzonite	nepheline syenite	syenite [comenditic]
L-956	monzonite	syenite	monzonite [Na2O-2>=K2O]
L-957	granite	granite	granite [high-K]
L-958	gabbro	under-saturated olivine gabbro	gabbro [subalkali]
L-963	out of plot, high Si	out of plot, high Si	granite [low-K]
L-965	quartz monzonite	quartz syenite	quartzmonzonite
L-966	quartz monzonite	quartz syenite	quartzmonzonite
L-967	granite	granite	granite [high-K]
L-967a	gabbro		
L-968	granite	granite	granite [high-K]
L-969	foid syenite	nepheline syenite	foid syenite
L-971	syenite	nepheline syenite	syenite
L-973	granite	granite	granite [high-K]
L-975	granite	granite	granite [high-K]
L-976	granite	alkali granite	granite [high-K]
L-977	granite	alkali granite	granite [peralkaline, Al2O3>1.33Fe+4.4]
L-978	granite	alkali granite	granite [peralkaline, Al2O3>1.33Fe+4.4]
L-979	quartzmonzonite	quartzmonzonite	quartzomonzonite
L-980	quartzmonzonite	quartzmonzonite	quartzomonzonite
L-982	quartzmonzonite	quartzmonzonite	syenite
L-983	granite	granite	granite [high-K]
L-985	granite	granite	granite [high-K]
L-987a	gabbro	alkali gabbro	gabbro [alkali]
L-987b	foidolite	theralite	foid diorite

Sample	Middlemost	de la Roche	IUGS
L-990	monzodiorite	monzo-gabbro	diorite [high-Mg, low-alkali, Boninite]
L-991	gabbro	under-saturated olivinie gabbro	gabbro [subalkali]
L-992	monzogabbro	under-saturated olivinie gabbro	monzogabbro [k mzgb., Na2O-2<K2O]
L-993	granite	granite	granite [high-K]
L-994	granite	granite	granite [high-K]
L-995	out of plot	alkali gabbro	foidolite
L-996	granite	granite	granite [high-K]
L-997	quartzmonzonite	quartz syenite	granite [peralkaline, Al2O3>1.33Fe+4.4]
L-998	quartzmonzonite	quartzmonzonite	syenite
L-999	quartzmonzonite	granite	granite [high-K]
L-1000	quartzmonzonite	granite	granite [high-K]
L-1002	granite	alkali granite	granite [high-K]
L-1003	quartzmonzonite	quartzmonzonite	syenite
L-1005	granite	granite	granite [high-K]
L-1007	quartzmonzonite	quartzmonzonite	syenite
L-1009	quartzmonzonite	quartzmonzonite	quartzmonzonite
L-1010	quartzmonzonite	quartzmonzonite	syenite
L-1011	quartzmonzonite	quartzmonzonite	syenite
L-1012	quartzmonzonite	quartzmonzonite	syenite
L-1013	quartzmonzonite		quartzmonzonite
L-1014	granodiorite	granodiorite	granite [high-K]
L-1016	granite	out of plot, high Si	granite [lok-K]
L-1016a	granite	out of plot, high Si	granite [peralkaline, Al2O3>1.33Fe+4.4]
L-1019	granite	alkali granite	granite [peralkaline, Al2O3>1.33Fe+4.4]
L-1020	granite	granite	granite [high-K]
L-1021	granite	granite	granite [high-K]
L-1022	foid monzosyenite	nepheline syenite	foid syenite
L-1023	gabbro	under-saturated olivine gabbro	gabbro [alkali]
L-1024a	out of plot, high Ca	out of plot, high Ca	foidolite
L-1024c	out of plot, high Ca	out of plot, high Ca	foidolite
L-1025	peridot gabbro	alkali gabbro	peridot gabbro
L-1027	foid monzosyenite	nepheline syenite	foid monzosyenite
L-1032	gabbro	alkali gabbro-under saturated oliv	gabbro [alkali]
L-1037	quartzmonzonite	quartzmonzonite	syenite
L-1038	quartzmonzonite	granite	quartzmonzonite
L-1039	granite	alkali granite	granite [high-K]
L-1039a	granite		granite [high-K]
L-1039c	granite		granite [high-K]
L-1042Y	granite	granite	granite [high-K]
L-1043Z	granite	granite	granite [high-K]
L-1044XX	granite	granite	granite [high-K]
L-1045Yb	quartzmonzonite	quartzmonzonite	syenite
L-1046XXb	granite	granite	granite [high-K]
LJ1	quartzmonzonite	granite	quartzmonzonite
LL1	granite	granite	granite [high-K]
LL10	monzonite	nepheline syenite	monzonite [Na2O-2>=K2O]
LL11	granite	granite	granite [high-K]
LL13	diorite	out of plot, high Ca, high Si	diorite [low-K]
LL14	monzonite	nepheline syenite	monzonite [Na2O-2>=K2O]
LL15	syenite	syenite	syenite
LL16	granite	granite-granodiorite	granite [high-K]
LL17a	granite	granite	granite [high-K]
LL17b	quartzmonzonite	granodiorite	quartzmonzonite
LL18	granite	granite	granite [high-K]

Sample	Middlemost	de la Roche	IUGS
LL2a	granite	alkali granite	granite [high-K]
LL2b	syenite	quartz syenite	granite [high-K]
LL3a	granite	alkali granite	granite [high-K]
LL3b	quartzmonzonite	alkali granite	granite [high-K]
LL4	granite	granite	granite [high-K]
LL5	granite	granite	granite [medium-K]
LL9	granite	out of plot, granite	quartzmonzonite
P-13	quartzmonzonite	quartz syenite	syenite
P-17	quartzmonzonite	quartz syenite	syenite
P-25	monzodiorite	essexite	monzodiorite [Na2O-2>=K2)]
P-26	granite	quartz syenite	granite [Peralkaline, Al2O3>1.33Fe+4.4]
P-28	syenite	nepheline syenite	syenite [comenditic]
P-29	granite	granite	granite [high-K]
P-32	granite	alkali granite	granite [peralkaline, Al2O3>1.33Fe+4.4]
P-33	quartzmonzonite	quartz syenite	syenite [comenditic]
P-35	granite	granite	granite [high-K]
P-39	granite	alkali granite	Granite [Peralkaline, Al2O3>1.33Fe+4.4]
P-40i	granite	granite	granite [high-K]
P-40ii	quartzmonzonite	quartz syenite	syenite [comenditic]
P-46	granite	alkali granite	granite [Peralkaline, Al2O3>1.33Fe+4.4]
P-50	granite	granite	granite [Peralkaline, Al2O3>1.33Fe+4.4]
P-53	granite	granite	granite [high-K]
P-57	out of plot, foid	nepheline syenite	foid syenite [peralkaline]
P-58	quartzmonzonite	granite	quartzmonzonite
X-43			granite [high-K]
X-44			granite [high-K]
X-45			quartzmonzonite
X-46			granite [high-K]
X-47			granite [high-K]
X-48			granite [high-K]
X-49			syenite
X-50			syenite
X-51			syenite
X-52			quartzmonzonite
X-53			granite [high-K]
X-54			granite [high-K]
X-55			granite [high-K]
X-56			tonalite
X-57			quartzmonzonite
X-58			granite [high-K]
X-59			granite [high-K]
X-60			granite [high-K]
X-61			granite [high-K]
X-62			syenite
X-63			syenite
X-65			granite [high-K]
X-66			granite [high-K]
X-67			granite [high-K]
X-68			granite [high-K]
X-69			monzonite [Na2O-2<K2O]
X-69			granite [high-K]
X-70			granite [high-K]
X-71			granite [high-K]
X-72			granite [high-K]

Sample	Middlemost	de la Roche	IUGS					
X-73			quartzmonzonite					
X-74			syenite					
X-75			quartzmonzonite					
X-76	syenite	quartz syenite	syenite					
X-77	monzonite	quartzmonzonite	monzonite [Na2O-2<K2O]					
X-78	monzodiorite	syenite	monzodiorite [Na2O-2<K2O]					
X-79	gabbro	gabbro-diorite	gabbro [subalkali]					
X-80	foid-gabbro	nepheline syeniete	foid diorite					
X-81	foid-gabbro	essexite	foid diorite					
X-82	foid-monzodiorite	nepheline syenite	foid monzonite					
X-83	foid-gabbro	syeno diorite	foid diorite					
X-84	foid-gabbro	essexite	foid Gabbro (ol<10%)					
X-85	gabbro	syeno gabbro	gabbro [alkali]					
X-86	monzogabbro	syeno diorite	monzogabbro [Na2O-2>=K2O]					
X-87	monzogabbro	syeno gabbro	monzogabbro [Na2O-2>=K2O]					
X-88	foid-gabbro	essexite	melanephelinite					
X-89	foid-gabbro	essexite	foid diorite					

APPENDIX A75

EXPERIMENT TO TEST THE QUALITY OF THE CHEMICAL LABORATORY:

An experiment was carried out to test the chemical laboratory of the School of Geosciences of the University of the Witwatersrand. Samples **L-012** and **L-012A** were used as double control samples. The test was also designed to evaluate the representativity of single rock analysis on the various diagrams used for geochemical interpretation in the Greater Lufilian Arc granitoid research project.

Five kilograms of rock sample were collected from two outcrops of a large, well exposed pluton in the Hook Granite Batholith, Zambia. Macroscopically, the outcrop seemed to be very uniform in composition and grain size.

Two types of experiments were carried out during the Lufilian Arc Granitoid project. Some were intended to evaluate the representativity of single samples in a large outcrop. Another one was designed to evaluate the accuracy of the laboratory. Only the second experiment will be described here. Samples **L-012** and **L-012A** were carefully crushed, ground and quartered. Three samples were obtained from the fine powder of **L-012** and sent along with the first three batches of samples for analysis at the laboratory. These were labeled **L-200B**, **L-400B** and **L-700B**. **L-012** and **L-012A** were analysed in the same batch of samples.

Laboratory results are listed on Table 1. They plot as shown on Figs 1 and 2 on a logarithmic scale. Arithmetic scales display similar results. Fig 3 shows arithmetic-scale diagrams of major oxides and trace elements for the five samples.

Main conclusions of the experiment were: 1) The quality of the laboratory is acceptable for the type of research intended, 2) Sample repeatability and general quality control of the laboratory were adequate for the type of research, 3) The samples collected may be taken as representative of large granitoid bodies, and 4) Dispersion in results from analysis of the major oxides was very small.

Assuming that instrumental error is negligible, some oxides tend to have greater dispersion than others. For example, TiO_2, MnO, Na_2O and P_2O_5 are more variable than SiO_2, Al_2O_3, MgO or K_2O (Figs 1 and 3). Minor elements show somewhat similar results: Co, Ni, Cu, Zn and V display large dispersion, while Rb, Sr, Y,Zr, Cr and Ba are almost the same in all cases (Figs 1 and 3). The variation may be due to the minerals that contain the given elements, and the size of those minerals in the rock. A few coarse-grained minerals contain a large proportion of the total iron, Mn, P, Co, Cu, Zn, V and Cr.

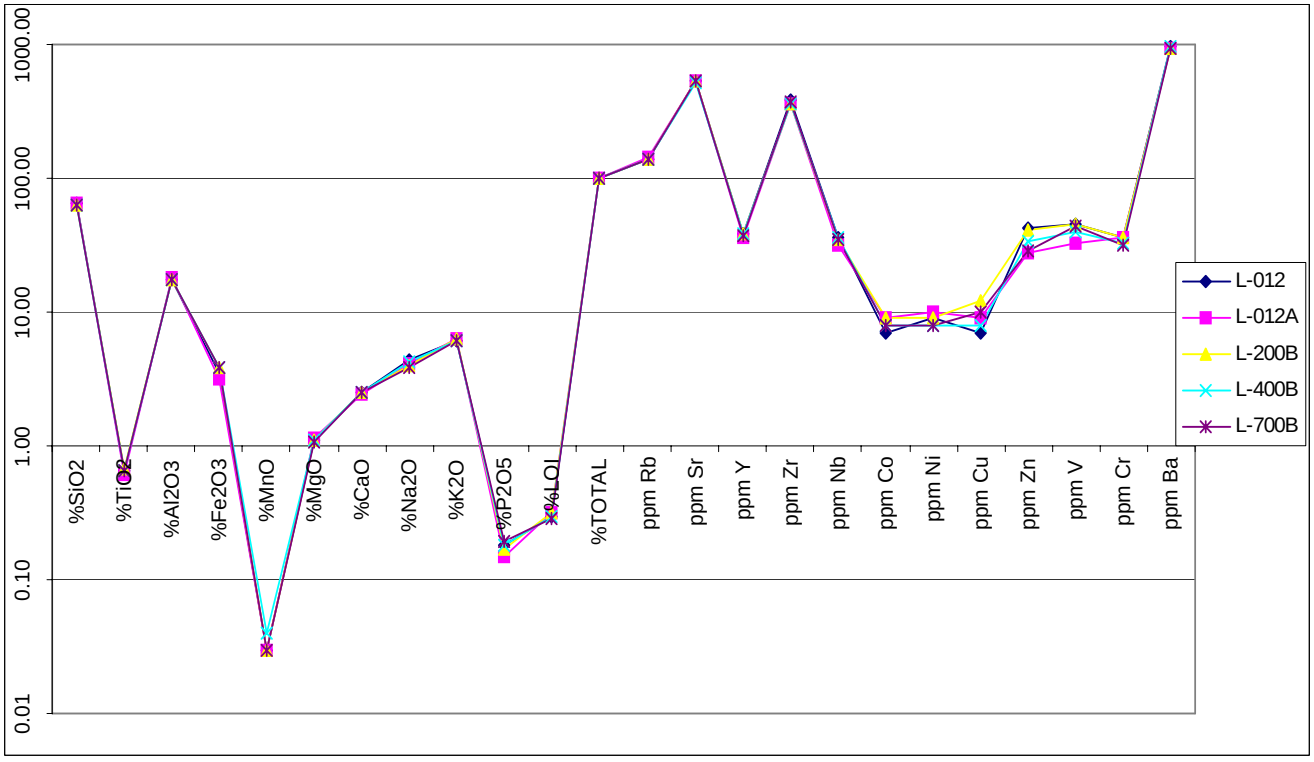

Fig 1 Logarithmic chemical data diagram for five portions of the same sample.

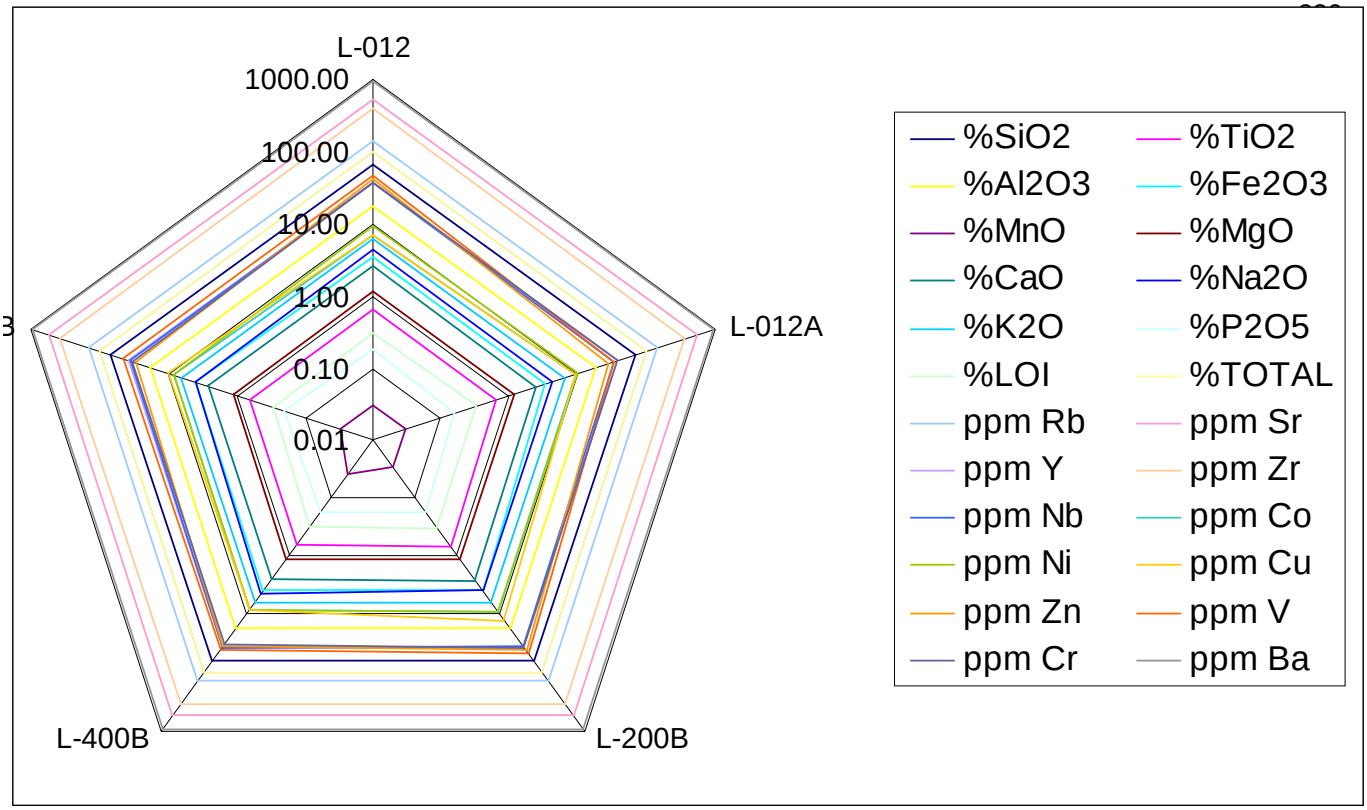

Fig 2 Logarithmic web representation of chemical data for five portions of the same sample

Table 1. Duplicate analysis to evaluate precision of analytical results

Sample	SiO2	TiO2	Al2O3	Fe2O3	MnO	MgO	CaO	Na2O	K2O	P2O5	LOI	TOTAL	Rb	Sr	Y	Zr	Nb	Co	Ni	Cu	Zn	V	Cr	Ba
L-012	64.19	0.66	17.47	3.45	0.030	1.12	2.55	4.34	6.14	0.18	0.30	100.43	141	529	38	387	36	7	9	7	42	46	36	968
L-012A	64.38	0.61	17.86	3.18	0.030	1.13	2.40	4.10	6.24	0.15	0.32	100.40	143	536	36	360	32	9	10	9	28	33	36	940
L-200B	63.93	0.67	17.66	3.89	0.030	1.10	2.55	3.98	6.22	0.17	0.32	100.52	140	527	38	362	35	9	9	12	41	46	36	940
L-400B	63.85	0.65	17.33	3.84	0.040	1.11	2.49	4.27	6.06	0.18	0.30	100.12	139	526	38	357	36	8	8	8	34	40	33	956
L-700B	64.12	0.66	17.78	3.83	0.030	1.06	2.53	3.91	6.08	0.19	0.29	100.48	140	529	37	374	35	8	8	10	29	44	32	944
Average	64.09	0.65	17.62	3.64	0.032	1.10	2.50	4.12	6.15	0.17	0.31	100.39	140.6	529.4	37.4	368	34.8	8.2	8.8	9.2	34.8	41.8	34.6	949.6

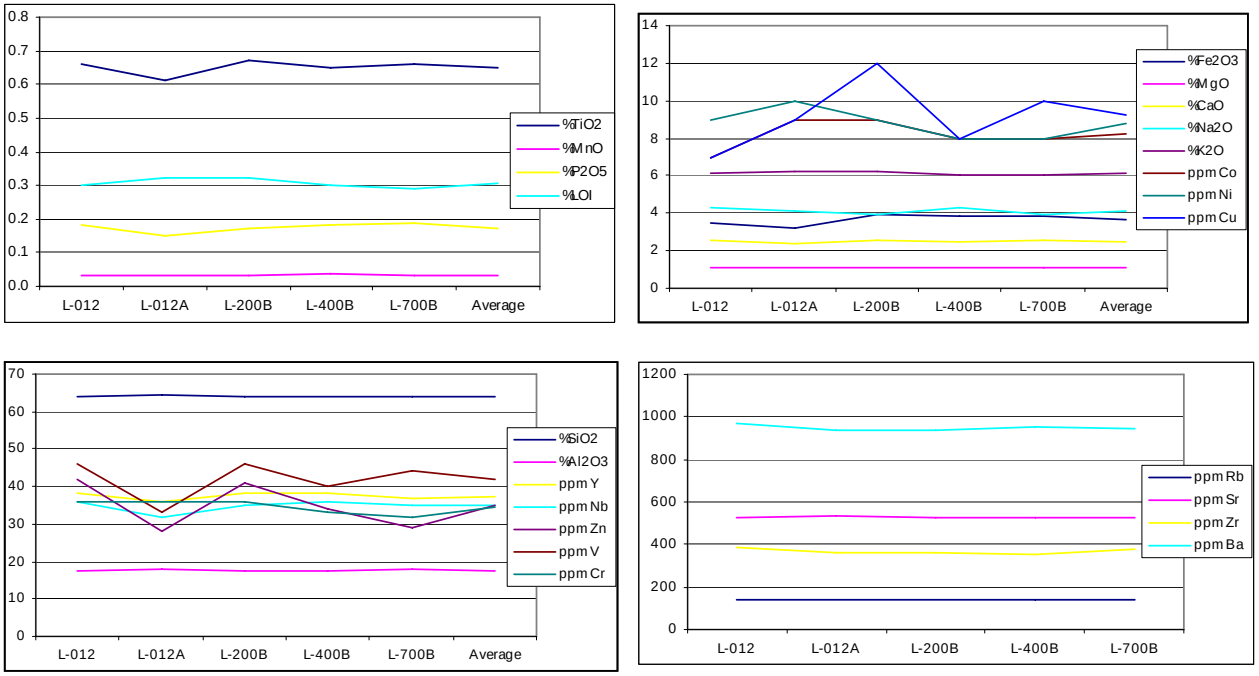

Fig 3 Distribution of major oxides and minor elements for five portions of the same sample.

Table A76 Heat production capacity of intrusive rocks from the Greater Lufilian Arc at the time of their emplacement (Based on equation No. 4 by Gibson, 2002***)***

Sample number	U (ppm)	Th (ppm)	K (%)	Time (BA)	Heat producing value (H(t) muW-m3)	U/Th
	ppm	ppm	(%)	t (BA)	H(t) muW-m	U/Th
West Lusaka, Zambia						
L-175	3	25	4.6	0.55	2.400	0.12
L-181	3	7.5	0.24	0.55	0.635	0.40
L-195	8	7.5	5.03	0.55	1.389	1.07
L-199	8.85	38.67	0	0.55	2.927	0.23
L-207	0	0	6.27	0.55	0.799	
L-207 pr	9	132	6.27	0.55	10.181	0.07
L-208	9	132	6.13	0.55	10.163	0.07
L-209	3	7.5	1.91	0.55	0.848	0.40
L-210	7	74	0.09	0.55	5.327	0.09
L-212	8	79	7.04	0.55	6.587	0.10
L-213	12	163	4.87	0.55	12.232	0.07
L-214	7	104	3.92	0.55	7.889	0.07
L-215	3	193	0.19	0.55	13.450	0.02
L-217	3	7.5	2.97	0.55	0.983	0.40
L-218	8	99	5.43	0.55	7.764	0.08
L-222	7	20	4.74	0.55	2.187	0.35
L-223	8	21	5.2	0.55	2.344	0.38
L-224	8	19	5.69	0.55	2.268	0.42
L-416	6	7.5	0.73	0.55	0.784	0.80
X-90			5.9	0.55	0.752	
X-90 pro	8	19	5.9	0.55	2.295	0.42
Hook Granite, Zambia						
L-012	4.27	50.39	6.14	0.55	4.388	0.08
L-012A	3	49	6.24	0.55	4.268	0.06
L-079	0	0	4.98	0.55	0.635	
L-237	3	26	5.44	0.55	2.576	0.12
L-238	6	24	6.16	0.55	2.616	0.25
L-239	6	24	6.16	0.55	2.616	0.25
L-242	7	7.5	1.96	0.55	0.969	0.93
L-248	6	7.5	2.1	0.55	0.958	0.80
L-248-LC	3	27	4.49	0.55	2.525	0.11
L-249	3	20	4.5	0.55	2.042	0.15
L-257	16	74	5.29	0.55	6.248	0.22
L-259	7	21	6.11	0.55	2.431	0.33
L-259-B	10	29	5.35	0.55	2.973	0.34
L-263	3	19	5.55	0.55	2.107	0.16
L-341	3	20	0.95	0.55	1.590	0.15
L-343	3	35	1.11	0.55	2.647	0.09
L-344	6	24	1.83	0.55	2.064	0.25
L-345	6	7.5	7.65	0.55	1.665	0.80
L-346	11	24	5.99	0.55	2.738	0.46
L-347	9	29	0.45	0.55	2.320	0.31
L-348	3	40	3.37	0.55	3.280	0.08
L-349	3	23	4.97	0.55	2.309	0.13
L-352	3	19	4.96	0.55	2.031	0.16
L-353	6	20	5.05	0.55	2.198	0.30
L-354	3	22	4.06	0.55	2.124	0.14
L-355	8	21	5.57	0.55	2.391	0.38
L-402	6	21	1.14	0.55	1.769	0.29
L-403	8	17	4.38	0.55	1.963	0.47
L-405	3	7.5	1.08	0.55	0.742	0.40
L-406	3	7.5	0.8	0.55	0.706	0.40
L-407	7	26	3.86	0.55	2.490	0.27
L-408	12	32	5.24	0.55	3.224	0.38
L-409	13	53	5.43	0.55	4.728	0.25
L-410	7	32	4.34	0.55	2.966	0.22
L-411	3	7.5	0.35	0.55	0.649	0.40
L-433	7	7.5	2.33	0.55	1.016	0.93
L-434	3	7.5	4.77	0.55	1.212	0.40
L-435	3	7.5	6.45	0.55	1.426	0.40
L-436	26	99	4.81	0.55	8.202	0.26
L-437	3	7.5	4.4	0.55	1.165	0.40
L-438	7	22	3.75	0.55	2.199	0.32
L-439	19	90	5.46	0.55	7.462	0.21
L-440	3	7.5	2.19	0.55	0.884	0.40
L-441	6	19	5.3	0.55	2.161	0.32
L-442	3	44	7.61	0.55	4.097	0.07
L-443	3	100	6.79	0.55	7.863	0.03
L-444	6	7.5	1.98	0.55	0.943	0.80
L-458	8	7.5	6.94	0.55	1.632	1.07
L-459	3	7.5	1.16	0.55	0.752	0.40
L-460	3	20	2.33	0.55	1.765	0.15
L-461	3	15	5.34	0.55	1.803	0.20
L-462	3	16	5.19	0.55	1.853	0.19
L-463	3	7.5	1.01	0.55	0.733	0.40
L-464	29	7.5	0.52	0.55	1.417	3.87
L-465	24	7.5	0.43	0.55	1.262	3.20
L-466	3	23	4.5	0.55	2.249	0.13
L-467	3	67	5.45	0.55	5.412	0.04
X-43			5.46	0.55	0.696	
X-44			5.77	0.55	0.735	
X-45			4.63	0.55	0.590	
X-46			4.57	0.55	0.582	
X-47			6.08	0.55	0.775	
X-48			4.44	0.55	0.566	
X-49			4.57	0.55	0.582	
X-50			6.04	0.55	0.770	
X-51			7	0.55	0.892	
X-52			5.3	0.55	0.675	
X-53			5.64	0.55	0.719	
X-54			5.49	0.55	0.700	
X-55			5.6	0.55	0.714	
X-56			4.6	0.55	0.586	
X-57			5.1	0.55	0.650	
X-58			6.3	0.55	0.803	
X-59			5.5	0.55	0.701	
X-60			5.5	0.55	0.701	
X-61			4.65	0.55	0.593	
X-62			6.03	0.55	0.768	
X-63			4.3	0.55	0.548	
X-64			3.3	0.55	0.421	
X-65			5.35	0.55	0.682	
X-66			5.25	0.55	0.669	
X-67			5.9	0.55	0.752	
X-68			7.44	0.55	0.948	
X-69			7.36	0.55	0.938	
X-70			5.91	0.55	0.753	
X-71			7.33	0.55	0.934	
X-72			6.03	0.55	0.768	
X-73			3.53	0.55	0.450	
X-74			3.07	0.55	0.391	

Sample number	U	Th	K	Time	Heat Cap	U/Th
X-75			4.92	0.55	0.627	
P-39	19	71	5.57	0.55	6.163	0.27
P-46	10	46	6.89	0.55	4.345	0.22
P-50	62	256	4.88	0.55	20.096	0.24
P-53	21	43	5.92	0.55	4.329	0.49
P-57	10	51	5.52	0.55	4.516	0.20
P-58	4	24	4.27	0.55	2.318	0.17
P-40i	6	20	4.05	0.55	2.071	0.30
P-40ii	1	15	5.77	0.55	1.801	0.07
Kalengwa-Kasempa Area, Zambia						
L-139	3	26	7.87	0.55	2.886	0.12
L-311	8	7.5	0.84	0.55	0.855	1.07
L-313	7	7.5	0.8	0.55	0.821	0.93
L-314	3	7.5	0.36	0.55	0.650	0.40
L-318	3	7.5	0.56	0.55	0.676	0.40
L-321	3	7.5	0.05	0.55	0.611	0.40
L-322	3	27	7.57	0.55	2.917	0.11
L-323	3	30	8.21	0.55	3.206	0.10
L-324	13	48	6.29	0.55	4.492	0.27
L-325	6	27	6.75	0.55	2.899	0.22
P-13	10	56	3.89	0.55	4.653	0.18
P-17	11	48	5.62	0.55	4.350	0.23
P-25	1	2	1.71	0.55	0.385	0.50
P-26	6	76	0.03	0.55	5.429	0.08
X-76			7.34	0.55	0.935	
X-77			5.07	0.55	0.646	
X-78			4.48	0.55	0.571	
X-79			1.14	0.55	0.145	
X-80			3.32	0.55	0.423	
X-81			2.96	0.55	0.377	
X-82			1.05	0.55	0.134	
X-83			3.2	0.55	0.408	
X-84			0.87	0.55	0.111	
X-85			0.61	0.55	0.078	
X-86			1.46	0.55	0.186	
X-87			0.32	0.55	0.041	
X-88			5.24	0.55	0.668	
X-89			2.7	0.55	0.344	
Northwestern Zambia Region, Zambia						
Archean rocks						
L-372	3	7.5	2.25	2.3	1.412	0.40
L-373	3	17	4.2	2.3	2.724	0.18
L-375	3	21	5.81	2.3	3.541	0.14
L-376	3	7.5	4.94	2.3	2.316	0.40
Paleoproterozoic rocks						
L-027	3	7.5	1.72	1.89	1.099	0.40
L-023	3	7.5	3.6	1.89	1.602	0.40
L-025	3	7.5	4.8	1.89	1.924	0.40
L-026	3	7.5	4.51	1.89	1.846	0.40
L-362	3	7.5	2.15	1.89	1.214	0.40
L-363	3	7.5	3.37	1.89	1.541	0.40
L-369	3	7.5	3.83	1.89	1.664	0.40
L-370	9	52	4.07	1.89	5.045	0.17
L-377	8	45	5.45	1.89	4.890	0.18
L-364	8	44	5.07	1.89	4.719	0.18
L-365	3	26	4.87	1.89	3.221	0.12
L-378	6	33	4.18	1.89	3.641	0.18
L-020	10	62	5.85	1.89	6.253	0.16
L-379	10	7.5	2.92	1.89	1.701	1.33
Other						
L-367	3	7.5	2.41	1.89	1.284	0.40
L-023	3	7.5	3.6	1.89	1.602	0.40
L-024	6	7.5	0.43	1.89	0.874	0.80
L-028	3	17	3.07	1.89	2.117	0.18

Sample number	U	Th	K	Time	Heat Cap	U/Th
L-029	3	7.5	2.5	1.89	1.308	0.40
L-030	16	40	5.91	1.89	4.989	0.40
L-047	6	7.5	4.75	1.89	2.031	0.80
L-049	3	7.5	0.93	1.89	0.888	0.40
L-050	3	7.5	0.89	1.89	0.877	0.40
L-060	4.91	46.54	1.12	1.89	3.714	0.11
L-060	3	7.5	5.74	1.89	2.175	0.40
L-060			1.09	1.89	0.292	
L-063	3	7.5	0.15	1.89	0.679	0.40
L-064	3	7.5	0.05	1.89	0.652	0.40
L-065	3	7.5	0.12	1.89	0.671	0.40
L-357	3	7.5	3.59	1.89	1.600	0.40
L-358	3	7.5	2.31	1.89	1.257	0.40
L-359	3	7.5	4.84	1.89	1.934	0.40
L-360	3	7.5	6.02	1.89	2.250	0.40
L-361	3	7.5	2.06	1.89	1.190	0.40
L-366	3	7.5	4.28	1.89	1.785	0.40
L-368	3	7.5	4.64	1.89	1.881	0.40
L-371	3	7.5	4.06	1.89	1.726	0.40
L-374	3	7.5	3.92	1.89	1.688	0.40
L-380	3	18	5.94	1.89	2.955	0.17
L-420	13	37	2.98	1.89	3.876	0.35
L-421	3	57	6.69	1.89	5.851	0.05
Nepheline Sodalite Quarry, Zambia						
L-032	3	7.5	3.13	0.5	0.992	0.40
L-034	3	20	4.47	0.5	2.022	0.15
L-036	3	36	0.25	0.5	2.605	0.08
L-037	9	17	5.51	0.5	2.114	0.53
L-038	8	32	4.32	0.5	2.975	0.25
L-039	9	30	4.63	0.5	2.903	0.30
L-040	8	30	6.14	0.5	3.062	0.27
L-041	11	22	5.41	0.5	2.504	0.50
L-044	10	31	4.28	0.5	2.957	0.32
L-045	7.24	17.82	4.16	0.5	1.953	0.41
L-046	3	29	5.27	0.5	2.743	0.10
Basement to the Copperbelt, Zambia						
Muliashi Porphyry						
L-075	3	16	5.1	1.9	2.600	0.19
L-076	3	17	5.1	1.9	2.669	0.18
L-077	3	14	5.06	1.9	2.451	0.21
L-078	3	18	3.78	1.9	2.382	0.17
L-157	3	18	6.95	1.9	3.236	0.17
L-158	6	26	7.11	1.9	3.952	0.23
L-159	11	24	6.8	1.9	3.932	0.46
L-160	3	15	5.69	1.9	2.689	0.20
X-01			4.83	1.9	1.300	
X-02			6.12	1.9	1.648	
X-03			3.03	1.9	0.816	
X-04			2.13	1.9	0.573	
X-05			4.7	1.9	1.265	
Chambishi Mine Area						
L-155	3	7.5	6.03	0.5	1.351	0.40
X-42			4.04	0.5	0.501	
X-06			2.5	0.5	0.310	
X-07			0.66	0.5	0.082	
X-08			0.2	0.5	0.025	
X-09			0.2	0.5	0.025	
X-10			1.55	0.5	0.192	
X-11			1.4	0.5	0.174	
Samba "Porphyry"				0.5	0.000	
L-268	3	19	4.53	1.9	2.653	0.16
L-269	3	7.5	3.67	1.9	1.627	0.40
L-273	3	7.5	3.12	1.9	1.479	0.40

Sample number	U	Th	K	Time	Heat Cap	U/Th
L-279	6	20	3.08	1.9	2.453	0.30
Nchanga Granite						
X-34			5.01	0.88	0.766	
X-35			4.9	0.88	0.750	
X-36			4.4	0.88	0.673	
X-37			4.9	0.88	0.750	
X-38			2.9	0.88	0.444	
X-39			11.9	0.88	1.821	
X-40			15.5	0.88	2.371	
P-28	13	98	5.32	0.88	7.989	0.13
P-29	9	65	5.56	0.88	5.621	0.14
L-151	11	65	5.54	0.88	5.680	0.17
L-153	11	44	4.89	0.88	4.129	0.25
L-154	3	44	5.78	0.88	4.018	0.07
L-162	3	7.5	4.92	0.88	1.364	0.40
Nchanga Mine						
L-150	6	7.5	6.12	0.5	1.447	0.80
L-167	12	37	8.7	0.5	3.977	0.32
L-168	3	7.5	7.61	0.5	1.547	0.40
L-170	10	7.5	5.02	0.5	1.425	1.33
L-172	5.31	48.48	7.48	0.5	4.429	0.11
L-173	7	58	7.51	0.5	5.139	0.12
Mufulira Granite						
X-41			4.65	0.5	0.576	
L-166	3	15	4.54	0.5	1.685	0.20
Other						
L-163	3	7.5	3.69	0.5	1.061	0.40
L-161	3	30	6.26	0.5	2.935	0.10
X-12				0.5	0.000	
X-13			0.8	0.5	0.099	
X-14			0.86	0.5	0.107	
Serenje, Zambia						
P-32	1	7	6.61	1.8	2.206	0.14
P-33	1	16	6.09	1.8	2.696	0.06
P-35	2	8	2.54	1.8	1.278	0.25
X-15			5.21	1.8	1.327	
Kamanjab Inlier, Namibia						
L-832	3	19	5.23	1.8	2.762	0.16
L-834	7	25	14.1	1.8	5.582	0.28
L-835	3	15	4.48	1.8	2.295	0.20
L-836	0	0	4.77	1.8	1.215	
L-838	3.98	21.25	4.48	1.8	2.765	0.19
L-839	3	16	5.28	1.8	2.568	0.19
L-840	3	18	4.93	1.8	2.617	0.17
L-842	3	16	3.5	1.8	2.114	0.19
L-843	3	21	4.39	1.8	2.687	0.14
L-844	6	16	4.35	1.8	2.448	0.38
L-846	3	19	4.59	1.8	2.599	0.16
L-849	3	16	5.57	1.8	2.642	0.19
L-850	3	46	4.96	1.8	4.560	0.07
L-855	3	7.5	4.06	1.8	1.670	0.40
L-857	3	7.5	4.21	1.8	1.708	0.40
L-863	3	17	3.86	1.8	2.275	0.18
L-864	3.14	13.43	4.14	1.8	2.105	0.23
L-864	3	7.5	0	1.8	0.636	0.40
L-865	3	16	4.38	1.8	2.339	0.19
L-868	3	7.5	4.38	1.8	1.751	0.40
L-874	6	17	0.31	1.8	1.488	0.35
L-874a			4.99	1.8	1.271	
L-875	3	7.5	4.25	1.8	1.718	0.40
L-877	3	17	4.74	1.8	2.499	0.18
L-878	3	17	4.58	1.8	2.459	0.18
L-895	3	7.5	4.61	1.8	1.810	0.40

Sample number	U	Th	K	Time	Heat Cap	U/Th
L-898			5.14	1.8	1.309	
L-899	3	16	3.72	1.8	2.170	0.19
L-900	3	16	4.01	1.8	2.244	0.19
L-902	3	25	4.81	1.8	3.070	0.12
L-903	3	25	4.99	1.8	3.116	0.12
L-904	3	21	4.81	1.8	2.794	0.14
L-905	3	22	1.54	1.8	2.030	0.14
L-906	3	19	5.97	1.8	2.951	0.16
L-907	3	16	5.07	1.8	2.514	0.19
L-908	3	15	2.63	1.8	1.824	0.20
L-909	3	18	4.96	1.8	2.625	0.17
L-910	3	7.5	4.24	1.8	1.715	0.40
L-911	3	19	5.19	1.8	2.752	0.16
L-912	3	16	5.3	1.8	2.573	0.19
L-917	3	7.5	4.48	1.8	1.777	0.40
L-919	3	7.5	2.09	1.8	1.168	0.40
L-920	3	7.5	2.72	1.8	1.328	0.40
L-922	3	16	4.88	1.8	2.466	0.19
L-923	3	21	4.67	1.8	2.758	0.14
L-924	3	19	3.97	1.8	2.442	0.16
L-938	3	7.5	4.11	1.8	1.682	0.40
L-939	3	7.5	5.28	1.8	1.980	0.40
L-940	3	7.5	3.4	1.8	1.501	0.40
L-943	3	28	5.72	1.8	3.509	0.11
L-945	3	19	5.08	1.8	2.724	0.16
L-946	3	7.5	5.01	1.8	1.912	0.40
L-948	3	15	4.47	1.8	2.292	0.20
L-951	3	22	0.33	1.8	1.722	0.14
L-952	3	7.5	0.35	1.8	0.725	0.40
L-955	3	7.5	0.19	1.8	0.684	0.40
L-956	3	7.5	0.01	1.8	0.638	0.40
L-957	3	26	4.9	1.8	3.162	0.12
L-958	3	7.5	0.36	1.8	0.727	0.40
L-963	3	7.5	1.77	1.8	1.086	0.40
L-965	7	30	5.73	1.8	3.806	0.23
L-966	5.82	27.15	5.68	1.8	3.551	0.21
L-967	8	36	5.05	1.8	4.087	0.22
L-967a	3	20	0	1.8	1.500	0.15
L-968	3	23	4.79	1.8	2.927	0.13
L-969	6	29	14.3	1.8	5.883	0.21
L-971	3	7.5	8.51	1.8	2.803	0.40
L-973	3	18	9.97	1.8	3.901	0.17
L-975	3	21	5.4	1.8	2.944	0.14
L-976			5.29	1.8	1.347	
L-977	3	16	5.21	1.8	2.550	0.19
L-978	3.59	19.11	5.19	1.8	2.783	0.19
L-979	3	7.5	3.67	1.8	1.570	0.40
L-980	3	7.5	3.48	1.8	1.522	0.40
L-982	3	7.5	3.57	1.8	1.545	0.40
L-983	3	19	4.95	1.8	2.691	0.16
L-985	1.49	17.09	4.25	1.8	2.322	0.09
L-987a	3	7.5	1.59	1.8	1.040	0.40
L-987b	3	7.5	0.79	1.8	0.837	0.40
L-990	3	7.5	0.32	1.8	0.717	0.40
L-991	3	7.5	0.46	1.8	0.753	0.40
L-992	0.24	0.89	1.87	1.8	0.547	0.27
L-993	3	17	5.33	1.8	2.650	0.18
L-994	3	7.5	5.07	1.8	1.927	0.40
L-995	3	7.5	0.53	1.8	0.770	0.40
L-996	2.82	14.88	4.78	1.8	2.356	0.19
L-997	3	33	5.33	1.8	3.756	0.09
L-998	3	7.5	4.03	1.8	1.662	0.40
L-999	3	16	4.65	1.8	2.407	0.19
L-1000	3	20	5.11	1.8	2.801	0.15

Sample number	U	Th	K	Time	Heat Cap	U/Th
L-1002	3	28	4.97	1.8	3.318	0.11
L-1003	3	15	5.26	1.8	2.494	0.20
L-1005	3	18	4.47	1.8	2.500	0.17
L-1007	3	22	3.92	1.8	2.636	0.14
L-1009	3	16	4.42	1.8	2.349	0.19
L-1010	3	7.5	4.24	1.8	1.715	0.40
L-1011	3	17	4.43	1.8	2.420	0.18
L-1012	3	17	3.94	1.8	2.296	0.18
L-1013	3	19	4.72	1.8	2.633	0.16
C-1			5.09	1.8	1.296	
C-2			5.3	1.8	1.350	
C-3			4.42	1.8	1.126	
C-4			6.35	1.8	1.617	
C-5			5.5	1.8	1.401	
C-6			4.71	1.8	1.200	
C-7			4.4	1.8	1.121	
C-8			5.93	1.8	1.510	
C-9			5.67	1.8	1.444	
C-10			3.6	1.8	0.917	
C-11			5.2	1.8	1.324	
C-13 (weath 1)			5.71	1.8	1.454	
C-14			1.05	1.8	0.267	
Felsic volcanics, Namibia						
X-16			0.13	1.8	0.033	
X-17			0.3	1.8	0.076	
X-18			5.36	1.8	1.365	
X-19			5.18	1.8	1.319	
X-20			5.02	1.8	1.279	
Ugab River 2, Namibia						
L-793	12	61	5.24	0.75	5.322	0.20
L-797	6	37	4.63	0.75	3.396	0.16
L-798	7	27	5.17	0.75	2.812	0.26
L-799	7	7.5	4.84	0.75	1.417	0.93
L-802	3	15	4.55	0.75	1.774	0.20
Owka River, Botswana						
L-600A	3	43	5.55	0.75	3.852	0.07
L-602	3	36	4.54	0.75	3.225	0.08
L-605	3	42	5.47	0.75	3.772	0.07
L-606	3	38	5.19	0.75	3.455	0.08
Summas Mountains, Namibia, (Volcanic Rocks)						
L-789	8	15	5.21	0.75	2.018	0.53
L-791a	6	32	5.16	0.75	3.126	0.19
L-791b	8	17	5.85	0.75	2.248	0.47
Oas Farm, Namibia						
L-668	7	22	4.79	0.75	2.412	0.32
L-669	9	31	4.8	0.75	3.096	0.29
L-670	17	46	3.35	0.75	4.166	0.37
L-675	10	78	6.41	0.75	6.603	0.13
L-676	3	19	5.55	0.75	2.193	0.16
L-691	3	7.5	2.82	0.75	1.010	0.40
L-693	2.29	8.612	4.46	0.75	1.299	0.27
L-694	3	7.5	4.89	0.75	1.304	0.40
L-695	3	7.5	3.51	0.75	1.108	0.40
L-697	15	51	4.59	0.75	4.628	0.29
L-698	3	7.5	4.1	0.75	1.192	0.40
L-699	15	50	4.73	0.75	4.579	0.30
L-708	3	7.5	1.77	0.75	0.860	0.40
L-712	3	7.5	1.95	0.75	0.886	0.40
L-713	3	7.5	5.66	0.75	1.414	0.40
L-714	3	16	0.76	0.75	1.304	0.19
L-714a	0	0	0.94	0.75	0.134	
L-715	3	19	4.88	0.75	2.098	0.16
L-716	7	24	3.98	0.75	2.435	0.29
L-1016	3	7.5	0.09	0.75	0.621	0.40

Sample number	U	Th	K	Time	Heat Cap	U/Th
L-1016a	3	7.5	0.13	0.75	0.627	0.40
L-1019	1.82	17	3.79	0.75	1.769	0.11
L-1020	3	19	3.14	0.75	1.850	0.16
X-21			5.27	0.75	0.750	
X-22			5.64	0.75	0.803	
X-23			6	0.75	0.854	
X-24			5.19	0.75	0.739	
X-25			0.77	0.75	0.110	
X-26			1.1	0.75	0.157	
Lofdal Farm, Namibia						
L-722	6	27	0	0.75	2.046	0.22
L-728	4.64	20.88	0.86	0.75	1.704	0.22
L-729			4.96	0.75	0.706	
L-740	27	18	4.68	0.75	2.719	1.50
L-741	19	7.5	7.21	0.75	2.114	2.53
L-742	3	21	1.17	0.75	1.708	0.14
L-754	3	7.5	1.02	0.75	0.753	0.40
L-1021	3	18	4.02	0.75	1.906	0.17
L-1022	8	7.5	7.25	0.75	1.790	1.07
L-1023	3	7.5	0.87	0.75	0.732	0.40
L-1024a	19	20	0.15	0.75	1.973	0.95
L-1024c	20	18	0.04	0.75	1.849	1.11
L-1025	86.4	19.53	0.56	0.75	4.017	4.42
L-1027	3	7.5	6.88	0.75	1.588	0.40
L-1032	3	7.5	0.75	0.75	0.715	0.40
LR25	24	7730	0.01	0.75	535.017	0.00
LR23	15	130	0.1	0.75	9.450	0.12
LR20	0	36	0.04	0.75	2.494	0.00
LR5	26	2347	0.53	0.75	163.080	0.01
LR4	28	1593	0.04	0.75	110.953	0.02
AM-1	11	1019		0.75	70.777	0.01
Mesopotamie Farm, Copper Vallei Mine, Namibia						
L-759	3	7.5	5.54	0.75	1.397	0.40
L-772	3	7.5	10.1	0.75	2.042	0.40
L-773	3	7.5	3.07	0.75	1.045	0.40
L-783	3	27	5.15	0.75	2.689	0.11
L-784	7	26	5.07	0.75	2.729	0.27
Other alkaline and gabbroic rocks to compare with (used by Frets)						
X-27			0.75	0.75	0.107	
X-28			3.81	0.75	0.542	
X-29			5.57	0.75	0.793	
X-30			5.86	0.75	0.834	
X-31			4.4	0.75	0.626	
X-32			5.1	0.75	0.726	
X-33			5.36	0.5	0.664	
Otjiwarongo Environs, Namibia						
L-1037	3	105	7.49	0.55	8.298	0.03
L-1038	3	112	6.45	0.55	8.649	0.03
L-1039	3	26	5.51	0.55	2.585	0.12
L-1039a	3	7.5	6.14	0.55	1.387	0.40
L-1039c	3	32	5.94	0.55	3.055	0.09
LJ1	1	95	7.17	0.55	7.509	0.01
LL1	0	5	6.24	0.55	1.141	0.00
LL10	9	25	4.86	0.55	2.606	0.36
LL11	3	55	6	0.55	4.652	0.05
LL13	4	5	0	0.55	0.460	0.80
LL14	22	83	5	0.55	7.005	0.27
LL15	3	26	5	0.55	2.520	0.12
LL16	3	33	5	0.55	3.004	0.09
LL17a	5	3	7	0.55	1.243	1.67
LL17b	4	18	5	0.55	1.996	0.22
LL18	5	4	7	0.55	1.312	1.25
LL2a	2	4	4.86	0.55	0.953	0.50
LL2b	0	2	10.4	0.55	1.464	0.00

Sample number	U	Th	K	Time	Heat Cap	U/Th
LL3a	0	7	5.93	0.55	1.240	0.00
LL3b	1	0	9.09	0.55	1.187	
LL4	4	52	5.74	0.55	4.440	0.08
LL5	5	11	3.46	0.55	1.345	0.45
LL9	2	3	5.63	0.55	0.982	0.67
AVMIN Pegmatitic Granitoids, Namibia						
L-808	3	7.5	3.67	0.55	1.072	0.40
L-809	3	7.5	7.52	0.55	1.563	0.40
L-810	3	7.5	5.44	0.55	1.298	0.40
L-812	17	30	4.17	0.55	3.093	0.57
L-813	13	21	5.59	0.55	2.537	0.62
L-814	3	7.5	0.31	0.55	0.644	0.40
L-815	42	16	5.59	0.55	3.024	2.63
Grootfointein Inlier, Otavi Mountains, Namibia						
L-1014						
L-1042	3	35	6.14	0.55	3.288	0.09
L-1043	3	44	5.77	0.55	3.863	0.07
L-1044	3	36	5.94	0.55	3.331	0.08
L-1045	3	57	1.7	0.55	4.243	0.05
L-1046	3	42	5.45	0.55	3.684	0.07
Okatjepuiko, Witvlei, Namibia						
L-625	3	7.5	2	1.1	0.961	0.40
L-626	3	7.5	1.04	1.1	0.795	0.40
L-633	3	7.5	1.69	1.1	0.908	0.40
L-635	3	7.5	0.22	1.1	0.654	0.40
L-637	3	7.5	0.76	1.1	0.747	0.40
L-638	3	7.5	3.73	1.1	1.260	0.40
L-641	3	7.5	0.62	1.1	0.723	0.40
L-645	3	7.5	0.16	1.1	0.643	0.40
L-648	3	7.5	1.32	1.1	0.844	0.40
L-649	3	7.5	1.86	1.1	0.937	0.40
L-816	3	7.5	1.96	1.1	0.954	0.40
Spitzkoppe Complexes, Namibia						
X-92			5.23	0.2	0.549	
X-93			4.93	0.2	0.517	
X-94			4.84	0.2	0.508	
X-95			6.29	0.2	0.660	
Erongo Complex, Namibia				0.2	0.000	
X-96			5.07	0.2	0.532	
Brandberg Complex, Namibia				0.2	0.000	
X-97			4.69	0.2	0.492	
X-98			5.53	0.2	0.580	
X-99			5.6	0.2	0.588	
X-100			5.66	0.2	0.594	
X-101			5.15	0.2	0.541	
Nigerian Ring Complexes				0.2	0.000	
AMN24		27	5.74	0.15	2.452	0.00
RN75		111	4.31	0.15	8.112	0.00
PAN112		25	5.17	0.15	2.256	0.00
JON147		41	5.32	0.15	3.377	0.00
B34		40	5.77	0.15	3.354	0.00
MD333		66	4.53	0.15	5.024	0.00
NG208		63	5.1	0.15	4.875	0.00
T15A		69	4.59	0.15	5.238	0.00
DR11		61	3.58	0.15	4.582	0.00
DW1		42	3.56	0.15	3.267	0.00
FG5		39	4.45	0.15	3.150	0.00
KD12		36	4.39	0.15	2.937	0.00

APPENDIX J
RAW DATA FOR NEW GEOCHRONOLOGY

A77.1	Raw data obtained for SHRIMP II U-Pb dating at the Australian National University, Canberra, 238
	L-030, 238
	L-075, 238
	L-158, 238
	L-160, 239
	L-207, 239
	L-213, 240
	L-638, 240
	L-688, 241
A77.2	Raw data and processing for zircon dating using U-Pb laser-ablation ICP-MS technique, 242
	L-855, 242
	L-868, 242
	L-943, 242
	L-969, 242
	L-993, 243
	L-1013, 243
	L-1043, 243
A78	**CONCORDIA DIAGRAMS, 244**
A78.1	Sample L-030, 244
A78.2	Sample L-047, 244
A78.3	Sample L-075, 245
A78.4	Sample L-158, 245
A78.5	Sample L-160, 246
A78.6	Sample L-207, 246
A78.7	Sample L-213 Concordia diagram for high U zircons + rims, 247
A78.8	Sample L-213 Concordia diagram for cores and rims, 247
A78.9	Sample L-638 Concordia diagram for all zircons including xenocrysts, 248
A78.10	Sample L-638 Concordia diagram for main cluster of zircons, 248
A78.11	Sample L-688 Concordia diagram for all zircons, 249
A78.12	Sample L-688 Histogram of all 12 ages in main cluster, 249
A78.13	Sample L-693, 250
A78.14	Sample L-868, 250
A78.15	Sample L-855 Concordia diagram for all zircons, 251
A78.16	Sample L-855 Concordia diagram for main cluster of ages, 251
A78.17	Sample L-943 Concordia diagram for all zircons, 252
A78.18	Sample L-943 Concordia diagram for main cluster of zircons, 252
A78.19	Sample L-969, 253
A78.20	Sample L-993, 253
A78.21	Sample L-1013 first, 254
A78.22	Sample L-1013 second, 254
A78.23	Sample L-1043 concordia diagram for older group of zircons, 255
A78.24	Sample L-1043 concordia diagram for younger group of zircons, 255
A78.25	Sample L-1043 concordia diagram for all zircons 2, 256
A78.26	Sample L-1043 concordia diagram for all zircons 1, 256

Table A77.1 ***Raw data obtained for SHRIMP II U-Pb dating at the Australian National University, Canberra***
Data provided by Richard Armstrong, PRISE Institute.

(Errors are 1-sigma; Pbc and Pb* indicate the common and radiogenic portions, respectively. (1) Common Pb corrected using measured 204Pb.)

	Grain spot	% 206Pbc	ppm U	ppm 232Th/ 238U	232Th/ 238U	ppm20 6Pb*	(1) 206Pb/ 238U	error	(1) 207Pb/2 06Pb	error	% discordant	(1) 207Pb/206 Pb	±%	(1) 207Pb/2 35U	±%	(1) 206Pb/2 38U	±%	err corr
L-030	1.1	0.04	827	452	0.56	235	1841	15	1925	4.4	5	0.11793	0.25	5.375	0.94	0.3306	0.91	0.964
	2.1	8.18	319	82	0.27	61.6	1209	19	1868	180	54	0.114	10.00	3.25	10.00	0.2064	1.80	0.172
	3.1	1.53	3305	732	0.23	495	1021.8	9.4	1609	64	57	0.0992	3.40	2.349	3.60	0.1718	10.00	0.28
	4.1	2.40	2406	315	0.14	441	1220	14	1655	140	36	0.1017	7.40	2.92	7.60	0.2083	1.30	0.17
	5.1	0.03	520	272	0.54	149	1859	14	1932.6	6.1	4	0.11842	0.34	5.459	0.92	0.3343	0.85	0.928
	6.1	0.51	523	465	0.92	122	1543	12	1935	12	25	0.11861	0.66	4.421	1.10	0.2703	0.88	0.798
	7.1	2.18	2193	255	0.12	286	893	7	1706	48	91	0.1045	2.60	2.141	2.80	0.1486	0.84	0.306

	Grain spot	% 206Pbc	ppm U	ppm 232Th/ 238U	232Th/ 238U	ppm20 6Pb*	(1) 206Pb/ 238U	error	(1) 207Pb/2 06Pb	error	% discordant	(1) 207Pb/206 Pb	±%	(1) 207Pb/2 35U	±%	(1) 206Pb/2 38U	±%	err corr
L-075	1.1	0.08	194	176	0.94	55.8	1858	11	1864.9	8.9	0	0.11405	0.49	5.253	0.84	0.334	0.68	0.812
	2.1	0.06	171	135	0.81	49.7	1872	11	1856.1	8.2	-1	0.11349	0.45	5.273	0.82	0.3369	0.68	0.833
	3.1	0.09	116	81	0.72	33.5	1869	17	1863	11	0	0.11392	0.63	5.284	1.20	0.3364	1.10	0.862
	3.2	0.06	174	99	0.59	52	1924	13	1869.1	9.5	-3	0.11431	0.53	5.482	0.92	0.3478	0.75	0.819
	4.1	0.06	175	130	0.77	51	1884	12	1857.1	9.3	-1	0.11356	0.52	5.315	0.88	0.3395	0.72	0.811
	5.1	0.01	226	206	0.94	63.6	1828	11	1869.7	7.4	2	0.11435	0.41	5.168	0.80	0.3278	0.69	0.859
	6.1	0.04	281	231	0.85	82.2	1889	12	1870.8	7	-1	0.11442	0.39	5.373	0.84	0.3406	0.74	0.886
	7.1	0.06	142	143	1.04	41.2	1878	12	1860	11	-1	0.11373	0.61	5.304	0.97	0.3382	0.75	0.774
	8.1	0.08	143	136	0.98	40.6	1837	12	1862.6	9.4	1	0.1139	0.52	5.178	0.91	0.3297	0.75	0.822
	9.1	0.41	361	401	1.15	93.8	1696.8	9.6	1859	23	10	0.1137	1.20	4.719	1.40	0.3011	0.64	0.457
	9.2	0.24	163	148	0.94	43.2	1729	14	1882	14	9	0.11514	0.75	4.885	1.20	0.3077	0.95	0.782
Error in Standard calibration was 0.23% (not incuded in above errors, but required when comparing data from different mounts																		

	Grain spot	% 206Pbc	ppm U	ppm 232Th/ 238U	232Th/ 238U	ppm20 6Pb*	(1) 206Pb/ 238U	error	(1) 207Pb/2 06Pb	error	% discordant	(1) 207Pb/206 Pb	±%	(1) 207Pb/2 35U	±%	(1) 206Pb/2 38U	±%	err corr
L-158	2.1	2.84	159	153	1.00	32.7	1347	12	1893	59	29	0.1158	3.30	3.71	3.40	0.2324	0.98	0.286
	2.2	0.06	340	320	0.97	99.7	1891	16	1865.7	7	-1	0.1141	0.39	5.362	1.00	0.3408	0.95	0.925
	3.1	0.01	118	153	1.34	34.7	1897	19	1891	11	0	0.11574	0.62	5.461	1.30	0.3422	1.10	0.878
	3.2	0.05	121	216	1.84	34.6	1847	27	1872.3	9.1	1	0.11452	0.50	5.239	1.80	0.3318	1.70	0.959
	4.1	0.72	173	286	1.71	47.6	1785	15	1914	22	7	0.1172	1.20	5.155	1.60	0.3189	0.94	0.603
	5.1*	32.83	3365	244	0.07	392	562	18	1360	1200	142	0.087	62.00	1.09	64.00	0.0911	3.30	0.052
	6.1	0.17	320	364	1.17	92.7	1872	26	1883.4	7.7	1	0.11522	0.43	5.352	1.70	0.3369	1.60	0.967
	7.1	0.10	108	150	1.44	31.3	1873	27	1879.5	9.3	0	0.11498	0.51	5.345	1.70	0.3372	1.60	0.955
	8.1	4.32	607	154	0.26	127	1349	22	1745	92	23	0.1067	5.00	3.43	5.30	0.2328	1.80	0.334
	9.1	0.71	196	224	1.18	50	1666	24	1862	17	11	0.1139	0.96	4.629	1.90	0.2949	1.60	0.859
	10.1	0.08	224	274	1.26	63.8	1843	27	1868.3	7.2	1	0.11427	0.40	5.214	1.70	0.3309	1.70	0.973
	11.1	0.05	258	306	1.23	70.4	1775	25	1873.9	6.1	5	0.11462	0.34	5.01	1.60	0.317	1.60	0.978
	12.1	0.24	158	236	1.54	42.5	1749	25	1852	13	6	0.11324	0.70	4.867	1.80	0.3117	1.60	0.92
	13.1	5.88	144	153	1.10	33.7	1473	23	1808	120	19	0.1105	6.80	3.91	7.00	0.2568	1.70	0.249
	14.1	3.09	223	210	0.97	50	1454	21	1825	63	20	0.1116	3.50	3.89	3.80	0.253	1.60	0.423
* = embayment.																		

Raw data obtained for SHRIMP II U-Pb dating at the Australian National University, Canberra

Data provided by Richard Armstrong, PRISE Institute.

(Errors are 1-sigma; Pbc and Pb* indicate the common and radiogenic portions, respectively. (1) Common Pb corrected using measured 204Pb.)

	Grain spot	% 206Pbc	ppm U	ppm 232Th/ 238U	232Th/ 238U	ppm206 Pb	206Pb/ 238U	error	207Pb/2 06Pb	error	% discordant	207Pb/206 Pb	±%	207Pb/2 35U	±%	206Pb/2 38U	±%	err corr
L-160	1.1	0.03	201	172	0.89	59.3	1906	15	1860.1	7.6	-2	0.11374	0.42	5.394	1.00	0.3439	0.93	0.91
	2.1	0.04	201	154	0.79	59.1	1896	13	1863.6	8.4	-2	0.11397	0.47	5.375	0.92	0.342	0.79	0.862
	3.1	0.18	39	62	1.61	11.4	1862	18	1874	21	1	0.1146	1.20	5.293	1.60	0.3349	1.10	0.691
	4.1	0.04	181	171	0.98	52.1	1866	12	1871.9	8.4	0	0.11449	0.46	5.299	0.85	0.3357	0.71	0.841
	5.1	0.04	220	181	0.85	63.5	1865	11	1866.9	7.6	0	0.11418	0.42	5.281	0.81	0.3354	0.69	0.853
	6.1	0.04	435	344	0.82	124	1851	10	1871.4	5.5	1	0.11446	0.31	5.25	0.70	0.3326	0.63	0.898
	7.1	0.06	149	151	1.05	43.6	1892	14	1868	10	-1	0.11427	0.57	5.373	1.00	0.341	0.85	0.831
	7.2	0.03	111	108	1.01	31.9	1863	16	1857	10	0	0.11357	0.58	5.246	1.10	0.335	0.98	0.86
	7.3	0.01	259	237	0.95	73.9	1851	15	1869.4	7	1	0.11433	0.39	5.244	0.99	0.3327	0.91	0.921
	8.1	0.04	287	184	0.66	77.8	1767	10	1856.7	6.8	5	0.11353	0.38	4.938	0.75	0.3154	0.65	0.864
Error in Standard calibration was 0.23% (not incuded in above errors, but required when comparing data from different mounts																		

	Grain spot	% 206Pbc	ppm U	ppm 232Th/ 238U	232Th/ 238U	ppm20 6Pb*	(1) 206Pb/ 238U	error	(1) 207Pb/2 06Pb	error	% discordant	(1) 207Pb/206 Pb	±%	(1) 207Pb/2 35U	±%	(1) 206Pb/2 38U	±%	err corr
	1.1	0.03	3670	619	0.17	266	521.5	2.8	544.4	6.4	4	0.05839	0.29	0.6784	0.64	0.0843	0.57	0.888
	2.1	-	4107	924	0.23	302	529.8	2.9	541.3	6.5	2	0.05831	0.30	0.6887	0.64	0.0857	0.57	0.887
	3.1	-	4469	997	0.23	326	525.2	2.9	540.9	5.1	3	0.05829	0.24	0.6882	0.61	0.0849	0.57	0.923
	4.1	0.02	3236	415	0.13	239	531.1	2.9	536	6.3	1	0.05817	0.29	0.6887	0.64	0.0859	0.57	0.893
	5.1	0.02	1592	217	0.14	117	528.4	3.1	534	12	1	0.05811	0.55	0.6884	0.82	0.0854	0.61	0.741
	6.1	0.01	1392	760	0.23	242	513.5	3	550.2	6.3	7	0.05854	0.29	0.6693	0.67	0.0829	0.60	0.901
	7.1	-	5836	1568	0.28	435	536	2.9	542	4.5	1	0.05833	0.21	0.6973	0.60	0.0867	0.56	0.939
L-207	8.1	-	3562	1465	0.42	257	520	2.8	537.8	5.7	3	0.05821	0.26	0.6742	0.63	0.0884	0.57	0.908
	9.1	0.00	17119	29182	1.76	1530	637	16	531.8	4.2	-17	0.05805	0.19	0.831	2.70	0.1038	2.70	0.997
	10.1	0.00	3280	362	0.11	237	520.4	3.3	531.7	6.3	2	0.05805	0.27	0.6729	0.72	0.0841	0.66	0.916
	11.1	0.01	2305	482	0.22	165	515.6	3	547.1	8.6	6	0.05846	0.40	0.6712	0.72	0.0833	0.60	0.834
	12.1	0.00	1076	235	0.23	79.5	531.8	3.2	536	11	1	0.05816	0.50	0.6896	0.80	0.086	0.62	0.776
	13.1	0.00	659	96	0.15	48.9	533.3	3.2	540	13	1	0.05827	0.61	0.6928	0.87	0.0862	0.63	0.72
	14.1	0.08	749	60	0.08	54.5	524.4	3.1	530	16	1	0.05802	0.72	0.6779	0.95	0.0847	0.63	0.655
	15.1	0.03	2825	625	0.23	204	519.9	2.9	524	7.2	1	0.05785	0.33	0.6699	0.67	0.084	0.58	0.869
Error in Standard calibration was 0.23% (not incuded in above errors, but required when comparing data from different mounts																		

Data provided by Richard Armstrong, PRISE Institute.

(Errors are 1-sigma; Pbc and Pb* indicate the common and radiogenic portions, respectively. (1) Common Pb corrected using measured 204Pb.)

	Grain spot	% 206Pbc	ppm U	ppm 232Th/ 238U	232Th/ 238U	ppm206Pb*	(1) 206Pb/ 238U	error	(1) 207Pb/206Pb	error	% discordant	(1) 207Pb/206Pb	±%	(1) 207Pb/235U	±%	(1) 206Pb/238U	±%	err corr
L-213	1.1	2.76	441	945	2.21	23.7	380.3	3.9	517	150	26	0.0577	7.00	0.483	7.10	0.0608	1.10	0.149
	2.1c	0.05	308	263	0.88	90.5	1895	14	1869.6	6.4	-1	0.11435	0.36	5.388	0.95	0.3418	0.88	0.927
	2.2c	0.06	781	486	0.64	235	1933	27	1864.7	3.9	-4	0.11404	0.22	5.498	1.60	0.3497	1.60	0.991
	3.1	0.15	447	503	1.16	32	516	4.4	562	23	8	0.05886	1.00	0.6764	1.40	0.0833	0.89	0.647
	3.2	0.18	492	791	1.66	34.6	506.4	7.8	537	20	6	0.05818	0.90	0.656	1.80	0.0817	1.60	0.873
	4.1	0.14	336	315	0.97	24.1	515.9	5.3	555	29	7	0.05866	1.30	0.674	1.70	0.0833	1.10	0.62
	5.1	1.64	595	1616	2.81	46.6	553.8	5	521	82	-6	0.0578	3.70	0.715	3.90	0.0897	0.95	0.245
	6.1c	0.14	216	256	1.23	60.8	1826	26	1877.9	8.1	3	0.011487	0.45	5.188	1.70	0.3275	1.60	0.963
	7.1	4.18	685	1617	2.44	46.8	473.7	7.4	486	200	3	0.0569	8.90	0.598	9.10	0.0763	1.60	0.179
	8.1	7.00	2457	7179	3.02	69.5	194.4	3.5	522	330	63	0.0578	15.00	0.244	15.00	0.0306	1.90	123
	9.1c	0.03	157	215	1.41	43.8	1812	26	1891.7	7.1	4	0.11576	0.39	5.181	1.70	0.3246	1.60	0.972
	9.2c	0.01	167	205	1.26	43	1687	24	1882.8	7.6	10	0.11519	0.42	4.75	1.70	0.2991	1.60	0.968
	10.1	0.46	601	899	1.54	40.1	479.3	8.1	575	47	17	0.0592	2.20	0.63	2.80	0.0772	1.70	0.625
	11.1c	0.02	457	260	0.59	124	1764	25	1863.5	6.3	5	0.11396	0.35	5.945	1.60	0.3147	1.60	0.977
	12.1	####	2336	6723	2.97	183	500.9	8.5	694	490	28	0.063	23.00	0.7	23.00	0.0808	1.80	0.076
c = core																		

	Grain spot	% 206Pbc	ppm U	ppm 232Th/ 238U	232Th/ 238U	ppm206Pb*	(1) 206Pb/ 238U	error	(1) 207Pb/206Pb	error	% discordant	(1) 207Pb/206Pb	±%	(1) 207Pb/235U	±%	(1) 206Pb/238U	±%	err corr
L-638	1.1	0.60	171	91	0.55	27.5	1105.1	10	1095	16	-1	0.076	0.80	1.96	1.30	0.187	1.00	0.785
	2.1	1.43	258	149	0.60	42	1104.7	9.6	801	68	-28	0.0658	3.20	1.7	3.40	0.1869	0.90	0.281
	3.1	0.02	462	439	0.98	73.9	1098.9	8.8	1102	11	0	0.0763	0.50	1.95	1.00	0.1859	0.90	0.854
	4.1	0.13	188	109	0.60	29.7	1087	11	1090	23	0	0.0758	1.10	1.92	1.50	0.1837	1.10	0.683
	5.1	0.05	133	86	0.67	32.2	1193.9	11	1133	17	-5	0.0775	0.80	2.17	1.30	0.2035	1.00	0.768
	6.1	-	291	252	0.90	46.5	1101.3	9.1	1095	12	-1	0.076	0.60	1.95	1.10	0.1863	0.90	0.843
	7.1	0.01	164	99	0.62	25.8	1083	9.5	1086	15	0	0.0757	0.80	1.91	1.20	0.1829	1.00	0.786
	8.1	-	275	257	0.96	78.5	1849.7	14.2	1871	6.8	1	0.1144	0.40	5.24	1.00	0.3323	0.90	0.92
	9.1	-	205	131	0.66	33	1107.1	9.8	1091	18	-1	0.0759	0.90	1.96	1.30	0.1874	1.00	0.733
	10.1	0.17	167	100	0.62	26.9	1105.3	11	1100	24	0	0.0762	1.20	1.97	1.60	0.187	1.10	0.662
	11.1	0.08	347	309	0.92	54.2	1076	8.8	1090	12	1	0.0758	0.60	1.9	1.10	0.1817	0.90	0.827
	12.1	0.03	311	241	0.80	50.3	1111.6	9.1	1094	11	-2	0.076	0.60	1.97	1.10	0.1882	0.90	0.842
	13.1	-	299	232	0.80	48	1105.9	9.1	1113	11	1	0.0767	0.60	1.98	1.10	0.1871	0.90	0.844
Error in Standard calibration was 0.29% (not incuded in above errors, but required when comparing data from different mounts																		

Raw data obtained for SHRIMP II U-Pb dating at the Australian National University, Canberra

Data provided by Richard Armstrong, PRISE Institute.

(Errors are 1-sigma; Pbc and Pb* indicate the common and radiogenic portions, respectively. (1) Common Pb corrected using measured 204Pb.)

	Grain spot	% 206Pbc	ppm U	ppm 232Th/ 238U	232Th/ 238U	ppm20 6Pb*	(1) 206Pb/ 238U	error	(1) 207Pb/2 06Pb	error	% discordant	(1) 207Pb/206 Pb	±%	(1) 207Pb/2 35U	±%	(1) 206Pb/2 38U	±%	err corr
L-688	1.1	6.61	2382	1633	0.71	90.44	260.6	2.4	647	280	60	0.0612	13.00	0.348	13.00	0.0413	0.95	0.072
	2.1	0.20	216	67	0.32	22.6	738.9	6.6	774	31	5	0.06499	1.50	1.088	1.80	0.1214	0.95	0.537
	3.1	7.34	2563	3230	1.30	123	324.5	3.1	745	300	56	0.0641	14.00	0.456	14.00	0.0516	0.98	0.069
	4.1	0.04	283	265	0.97	29.8	746.1	7.1	745	18	0	0.06411	0.85	1.085	1.30	0.1227	1.00	0.763
	5.1	0.00	189	135	0.74	20.5	765.3	8.2	754	20	-1	0.06436	0.93	1.119	1.50	0.126	1.10	0.772
	6.1	0.07	175	148	0.87	19.2	774.1	7.2	775	22	0	0.06503	1.00	1.144	1.40	0.1276	0.98	0.689
	7.1	0.66	229	78	0.35	21.3	658.2	6	726	51	9	0.0635	2.40	0.941	2.60	0.1075	0.96	0.368
	7.2	0.41	509	381	0.77	48.7	678	5.6	738	27	8	0.0639	1.30	0.977	1.50	0.1109	0.88	0.57
	8.1	7.64	1536	2115	1.42	91.9	401.9	3.9	732	310	45	0.0637	15.00	0.565	15.00	0.0643	0.99	0.068
	9.1	0.31	397	451	1.17	39.7	707	6	764	24	7	0.06468	1.20	1.034	1.50	0.1159	0.89	0.612
	10.1	0.11	171	137	0.83	18.4	758.7	7.4	755	24	0	0.06442	1.20	1.109	1.50	0.1249	1.00	0.666
	11.1	-	275	234	0.88	29.7	763.4	8.2	771	16	1	0.0649	0.78	1.125	1.40	0.1257	1.10	0.825
	12.1	0.16	152	102	0.70	15.2	708.3	6.7	754	30	6	0.06436	1.40	1.031	1.70	0.1161	1.00	0.581
	13.1	0.00	78	37	0.49	8.11	735	14	770	31	5	0.06488	1.50	1.08	2.50	0.1207	2.00	0.8
	14.1	0.01	608	399	0.68	64.8	754.2	6.1	769	12	2	0.06483	0.56	1.109	1.00	0.1241	0.86	0.84
Error in Standard calibration was 0.29% (not incuded in above errors, but required when comparing data from different mounts																		

Table No. 77.2 Raw data and processing for zircon dating using U-Pb laser-ablation ICP-MS techniques.

Work was done by Marc Poujol at the Memorial University of Newfoundland, Canada.

SAMPLE		CONCORDIA COLUMNS								2 σ %	2 σ %	2 σ %	AGES Ma					
spot #	file	207/235	7/5 err	206/238	6/8 err	Rho		207/206	7/6 err	207/235	206/238	207/206	7/5 age	1 sigma	6/8 age	1sigma	7/6 age	1 sigma
		I N T E R C E P T V A L U E S																
L-855																		
17	de07a73 1	3.8861689	0.2723272	0.2181177	0.0154914	0.5719453	0.0474051	0.1490011	0.0151776	14.015202	14.20461	20.372445	1610.8123	56.591665	1271.9214	81.982128	2334.4934	174.38964
18	de07a74 1	5.8943952	1.0937442	0.3293116	0.1008497	0.9584352	0.95	0.12692	0.0115705	37.111329	61.248819	18.232759	1960.409	161.08292	1835.0441	489.06453	2055.7429	160.90729
20	de07a76 1	5.7359715	0.4308339	0.3494882	0.0222455	0.8483357	-0.148335	0.1222516	0.0048565	15.022176	12.730309	7.9451708	1936.8046	64.944072	1932.154	106.26507	1989.3445	70.655851
21	de07a78 1	5.9298652	0.4346084	0.3630994	0.022412	0.8827698	0.7536593	0.1175504	0.0038614	14.658289	12.344814	6.5698489	1965.6195	63.680024	1996.8483	105.99144	1919.3124	58.908056
22	de07a79 1	5.5746854	0.2218629	0.3430592	0.0106765	0.7941551	0.9566402	0.1215528	0.0028948	7.9596572	6.2242983	4.763049	1912.1965	34.264127	1901.37	51.245124	1979.1435	42.407829
25	de07a82 1	5.7703022	0.34888	0.3647025	0.0199801	0.8351765	0.3830381	0.1172916	0.0042315	12.092261	10.956951	7.2153921	1941.9665	52.323639	2004.425	94.379716	1915.3593	64.726662
26	de07a83 1	2.2541158	0.2621079	0.1059486	0.0163581	0.9519029	0.95	0.1559413	0.0077499	23.255937	30.879257	9.9394641	1198.0714	81.785625	649.17625	95.348855	2412.1205	84.400941
27	de07a84 1	5.6765228	0.4230757	0.3652015	0.0203673	0.8606453	0.95	0.1176787	0.003883	14.906155	11.154012	6.5993234	1927.8035	64.342452	2006.7819	96.173431	1921.269	59.158596
28	de07a85 1	6.0652984	0.3150475	0.3533505	0.0213286	0.828722	-0.730174	0.1235805	0.0050376	10.388523	12.072204	8.1527167	1985.2721	45.276764	1950.5777	101.5945	2008.5532	72.340187
L-868																		
27	de07a59 1	5.6814046	0.2714572	0.3477042	0.0193947	0.8395116	-2.092603	0.1261072	0.0045526	9.5559906	11.155887	7.2202198	1928.5457	41.253764	1923.6262	92.770017	#########	#########
4	de07a60 1	5.8364594	0.2499059	0.3562104	0.0136202	0.7730637	-1.409699	0.1176722	0.0036919	8.5636146	7.6472704	6.2748793	1951.8403	37.117204	1964.1861	64.740227	1921.1691	56.250835
5	de07a61 1	5.6451029	0.2597258	0.3525353	0.0138085	0.1532033	-13.67142	0.1777832	0.044917	9.201811	7.8338504	50.530055	1923.0138	39.686553	1946.6933	65.813874	2632.2986	419.82811
7	de07a70 1	5.5665511	0.3622369	0.3634626	0.0151121	0.6938889	0.2887536	0.1145689	0.0049434	13.014769	8.3156224	8.6295234	1910.9395	56.012536	1998.5654	71.449538	1873.1152	77.804437
8	de07a64 1	5.5555309	0.3968726	0.3497276	0.0188052	0.8562946	0.4650214	0.1194884	0.0038753	14.287475	10.754187	6.48656	1909.234	61.4714	1933.2978	89.815153	1948.5864	57.960307
9	de07a65 1	5.7973008	0.4583302	0.3465556	0.0261189	0.4123277	-0.137801	0.15018	0.0250085	15.811847	15.073443	33.304681	1946.0076	68.465513	1918.1299	125.04009	2347.9771	284.68857
10	de07a66 1	5.7187663	0.3694023	0.3596408	0.0198537	0.6735214	0.6411648	0.1153613	0.0069892	12.918951	11.040878	12.117002	1934.2078	55.826444	1980.4708	94.131841	1885.5348	109.08495
11	de07a67 1	5.827115	0.3255682	0.3380223	0.0246191	0.8456335	-1.330556	0.1288558	0.0059238	11.174251	14.566574	9.1944238	1950.4515	48.421108	1877.1482	118.61172	2082.4203	80.896854
12	de07a68 1	5.6436119	0.353291	0.3624487	0.0171024	0.7614459	0.8891728	0.1151226	0.0046244	12.520033	9.4371225	8.0339408	1922.786	53.995586	1993.77	80.91968	1881.804	72.359016
13	de07a69 1	5.8262672	0.3385881	0.3611168	0.0174379	0.71151	0.7020767	0.1181978	0.0056368	11.622816	9.6577658	9.5378563	1950.3254	50.363787	1987.4652	82.588044	1929.1557	85.420724
L-943																		
1	de07a37 1	5.5790795	0.3447373	0.3394403	0.015608	0.3102493	-0.745717	0.1441734	0.0203134	12.358215	9.196332	28.179083	1912.8749	53.205077	1883.9764	75.117806	2277.9373	242.66225
4	de07a32 1	5.2631163	0.2877905	0.3381076	0.0218543	0.8463948	-0.761206	0.1215086	0.0049418	10.936126	12.927443	8.1340149	1862.9008	46.656902	1877.5594	105.28458	1978.4959	72.426712
5	de07a33 1	5.1460642	0.2912204	0.2320183	0.0126158	0.7475899	0.6604485	0.169195	0.0081732	11.31818	10.87487	9.6612601	1843.7446	48.112136	1345.0685	66.011168	2549.6957	80.915097
6	de07a34 1	5.1903189	0.3398781	0.2870648	0.0227464	0.5482055	0.3639471	0.1541875	0.0186391	13.096616	15.847592	24.177127	1851.0297	55.749379	1626.8446	113.92814	2392.8942	205.70575
7	de07a35 1	5.1738748	0.4968662	0.3364605	0.02677	0.2080789	0.4083423	0.1001822	0.0374684	19.206733	15.912698	74.80048	1848.3288	81.716828	1869.6195	129.12491	1627.4691	695.38114
11	de07a40 1	7.9292555	0.9601647	0.3533551	0.0426658	0.9740681	0.9967587	0.1660353	0.0046567	24.218281	24.148969	5.6092835	2223.0117	109.18435	1950.5999	203.22936	2518.069	47.12564
12	de07a41 1	4.8701803	0.3640734	0.2875914	0.0244424	0.9167832	-0.128503	0.1300729	0.0048159	14.951126	16.998001	7.4049702	1797.1116	62.974889	1629.4816	122.37251	2098.9476	65.03097
13	de07a42 1	5.1178	0.3229215	0.3369483	0.018361	0.8206989	-0.721338	0.1173243	0.0044509	12.619545	10.898382	7.5873253	1839.0644	53.595908	1871.9716	88.531713	1915.8598	68.059091
14	de07a43 1	5.0802446	1.1563019	0.3410673	0.0732018	0.9616655	0.95	0.1171194	0.0071679	45.521506	42.925103	12.240373	1832.812	193.09904	1891.8022	351.87556	1912.7224	109.83837
15	de07a44 1	6.1755834	0.5920532	0.3012298	0.034479	0.7555957	0.7820836	0.1770828	0.0175715	19.174	22.892148	19.845575	2000.9992	83.778658	1697.4041	170.81211	2625.7373	164.99018
L-969																		
1	de07a09 1	5.2244037	0.3166229	0.3280679	0.0179158	0.8656311	-1.089433	0.114913	0.0036297	12.120919	10.922004	6.3173037	1856.6052	51.650491	1829.0099	86.962896	1878.5201	56.920284
6	de07a05 1	5.5423445	0.6026643	0.3254451	0.0125216	0.3007831	0.4711928	0.1421572	0.0173422	21.747631	7.6950477	24.398673	1907.1895	93.53453	1816.2665	60.899754	2253.6501	210.65463
8	de07a07 1	5.5265467	0.2904833	0.3334539	0.0188007	0.3436379	-2.983624	0.1381832	0.0212915	10.512291	11.27636	30.816316	1904.7347	45.192637	1855.1006	90.889756	2204.5608	267.4816
9	de07a08 1	5.0661801	0.3795521	0.3070497	0.0223789	0.8658847	0.1220115	0.1192419	0.0050209	14.983757	14.576717	8.4213412	1830.4606	63.531041	1726.172	110.37341	1944.8949	75.281166
10	de07a18 1	5.0433297	0.2765725	0.3246592	0.0154257	0.7143129	-4.791581	0.1135063	0.0052837	10.967854	9.5027038	9.309986	1826.6286	46.468927	1812.4431	75.068716	1856.2954	84.110027
13	de07a12 1	5.481676	0.5443276	0.3209244	0.0197536	0.6355912	0.2026786	0.1269908	0.0094944	19.859897	12.310422	14.952949	1897.7297	85.271314	1794.2419	96.401969	2056.7277	131.94758
15	de07a14 1	5.354477	0.3405239	0.3228988	0.0203466	0.888929	-0.663536	0.1157783	0.0037592	12.719222	12.602441	6.4937525	1877.6053	54.412378	1803.8702	99.147705	1892.0283	58.415426
16	de07a15 1	5.6757555	0.2567558	0.3318133	0.020104	0.8558245	-1.760238	0.1202999	0.0044054	9.0474575	12.117647	7.3239908	1927.6868	39.052579	1847.1645	97.309882	1960.6726	65.350245
17	de07a16 1	5.6701703	0.2306803	0.3128281	0.0181811	0.8590636	-2.86665	0.1268333	0.0043922	8.1366286	11.623671	6.925907	1926.837	35.115882	1754.6086	89.274903	2054.5367	61.130755

SAMPLE		CONCORDIA COLUMNS								2 σ %	2 σ %	2 σ %	AGES Ma					
spot #	file	207/235	7/5 err	206/238	6/8 err	Rho		207/206	7/6 err	207/235	206/238	207/206	7/5 age	1 sigma	6/8 age	1sigma	7/6 age	1 sigma
L-993																		
10	de07a18 1	5.0433297	0.2765725	0.3246592	0.0154257	0.7143129	-4.791581	0.1135063	0.0052837	10.967854	9.5027038	9.309986	1826.6286	46.468927	1812.4431	75.068716	1856.2954	84.110027
18	de07a17 1	5.2155825	0.2930756	0.3158416	0.0173751	0.4079038	-0.71912	0.1355637	0.0166927	11.238462	11.002402	24.627049	1855.1652	47.877094	1769.3888	85.121921	2171.2761	214.54103
22	de07a21 1	5.0282414	0.243085	0.31959	0.0166628	0.8518812	0.284619	0.1125839	0.0036088	9.6687875	10.427599	6.4108689	1824.0903	40.944674	1787.7268	81.400434	1841.5386	58.021946
23	de07a22 1	4.9479696	0.3144167	0.3282694	0.0143464	0.7705624	-0.420794	0.1091408	0.0039453	12.708916	8.7405969	7.2297144	1810.4787	53.674341	1829.9881	69.626338	1785.1235	65.88648
24	de07a23 1	5.2793953	0.2655679	0.3357591	0.0120442	0.6889278	0.3933588	0.1125297	0.004247	10.060544	7.1743009	7.5481758	1865.5366	42.94254	1866.235	58.125594	1840.6674	68.322438
25	de07a24 1	5.3047917	0.2611458	0.3246616	0.0179237	0.8383324	-15.7668	0.1175756	0.0042211	9.8456579	11.041485	7.1801703	1869.6349	42.057383	1812.4545	87.225132	1919.6971	64.377516
26	de07a25 1	5.1905442	0.2834624	0.3196162	0.0178786	0.8516318	0.6341477	0.115049	0.0039608	10.922261	11.187545	6.885422	1851.0667	46.493958	1787.8544	87.338171	1880.6523	62.023267
27	de07a26 1	4.9359082	0.3400392	0.3238592	0.0164922	0.7417392	-0.175981	0.1101967	0.0050741	13.778182	10.184811	9.2092143	1808.4176	58.166337	1808.5487	80.307412	1802.6527	83.745301
28	de07a27 1	5.5585206	0.2408556	0.3244011	0.0178945	0.7820466	0.2933926	0.1163312	0.0051138	8.6661749	11.03234	8.7917715	1909.697	37.288997	1811.1866	87.100089	1900.5956	79.006617
L-1013																		
1	de07a88 1	5.3112417	0.2912953	0.3155266	0.0232072	0.9275001	0.95	0.1191242	0.0035313	10.96901	14.710171	5.9288395	1870.6731	46.864998	1767.8454	113.72142	1943.1291	53.010899
4	de07a91 1	5.1785406	0.2955598	0.3304206	0.0140517	0.9067522	0.95	0.1152943	0.0022801	11.414792	8.5053578	3.9552178	1849.0959	48.572383	1840.4198	68.086175	1884.4879	35.611853
5	de07a92 1	4.8936428	0.4375046	0.3210772	0.020323	0.8464205	0.95	0.1070732	0.0042639	17.880529	12.659236	7.9644026	1801.1619	75.375243	1794.9877	99.169235	1750.1876	72.897143
6	de07a93 1	5.0513482	0.4307734	0.3277303	0.0169057	0.7531384	0.95	0.1106088	0.0049839	17.055781	10.316809	9.0116747	1827.9749	72.281423	1827.3711	82.080564	1809.4393	81.880738
7	de07a94 1	4.8492316	0.4395616	0.3218411	0.018785	0.8392279	0.95	0.1092804	0.0041329	18.129123	11.673447	7.5638402	1793.4815	76.304618	1798.714	91.611408	1787.4518	68.911665
8	de07a95 1	4.8370614	0.5257475	0.307162	0.0226887	0.9289885	0.95	0.1167672	0.0034362	21.7383	14.77314	5.8856102	1791.3667	91.456131	1726.7262	111.89203	1907.3169	52.848229
9	de07a96 1	5.3529454	0.3228036	0.3255053	0.0239632	0.8558893	0.9904111	0.117708	0.005236	12.060783	14.723663	8.896568	1877.3606	51.593275	1816.5593	116.54153	1921.7153	79.74766
10	de07a97 1	4.9559367	0.3235049	0.2999937	0.0234993	0.8794396	0.200595	0.1199461	0.0050856	13.055245	15.6665	8.4797405	1811.8378	55.15192	1691.2775	116.52821	1955.4162	75.709431
14	de07a87 1	5.1252415	0.4973133	0.3362542	0.0247572	0.8885686	0.95	0.1134834	0.0043136	19.406434	14.725259	7.6022493	1840.2987	82.439771	1868.6244	119.43451	1855.9312	68.684696
L-1043																		
1	de07a45 1	5.4648859	0.2598163	0.3256634	0.0216861	0.9041929	-0.528848	0.1243149	0.0039105	9.5085734	13.318089	6.2912223	1895.0961	40.807079	1817.3278	105.45465	2019.0614	55.755188
2	de07a46 1	5.2914589	0.2751321	0.3165815	0.0166182	0.2904635	-2.796617	0.1632353	0.028228	10.399102	10.498507	34.585671	1867.4854	44.403767	1773.0127	81.367973	2489.4508	291.39556
3	de07a49 1	~~12.092751~~	~~0.7941725~~	~~0.5029125~~	~~0.0425009~~	~~0.9605512~~	0.95	0.1830016	0.0044776	13.134686	16.901918	4.8935183	2611.6248	61.590513	2626.3006	182.29843	2680.2618	40.47313
4	de07a50 1	4.0401862	0.4094227	0.2286349	0.0284983	0.8858599	0.9988996	0.1394286	0.009102	20.267518	24.929046	13.056127	1642.3242	82.481257	1327.3408	149.52492	2220.1229	113.13371
5	de07a51 1	4.6064705	0.3039321	0.2443014	0.014603	0.9654131	0.95	0.1452107	0.0023441	13.195879	11.954915	3.2286111	1750.4406	55.044886	1409.0203	75.654564	2290.2762	27.766459
6	de07a52 1	5.1658876	0.5445519	0.2565876	0.0203743	0.9276599	0.95	0.1526757	0.0048802	21.082608	15.881005	6.3928395	1847.0144	89.675457	1472.3597	104.52233	2376.1119	54.486401
7	de07a53 1	3.8084903	0.6267278	0.1967121	0.011892	0.2083014	0.95	0.1361647	0.0386512	32.912138	12.090734	56.771199	1594.5405	132.34274	1157.6334	64.05931	2178.9799	494.14889
8	de07a54 1	~~9.3724075~~	~~0.5987481~~	~~0.4068449~~	~~0.0320976~~	~~0.9708126~~	0.95	0.1718203	0.0033489	12.776826	15.778799	3.8981554	2375.1324	58.613073	2200.4807	147.07702	2575.4537	32.565816
9	de07a55 1	~~3.0315512~~	~~0.2247834~~	~~0.1914939~~	~~0.0141233~~	~~0.7243399~~	0.9441589	0.1259064	0.0088386	14.829594	14.750626	14.039977	1415.5975	56.613747	1129.4624	76.412022	2041.5793	124.10601
10	de07a58 1	~~6.6686291~~	~~0.7825919~~	~~0.2888674~~	~~0.0430327~~	~~0.9921435~~	-0.231836	0.1661435	0.0031209	23.470849	29.794058	3.7568973	2068.4753	103.62094	1635.8667	215.23263	2519.1632	31.559646
11	de09a12 1	~~6.0133045~~	~~1.3234738~~	~~0.3703881~~	~~0.0462822~~	~~0.7741406~~	0.95	0.1262575	0.0129005	44.018187	24.99118	20.435255	1977.7722	191.61194	2031.2265	217.71506	2046.5007	180.53518
12	de09a17 1	4.8438518	0.7226037	0.2615149	0.0351093	0.8375949	0.9771022	0.1416091	0.0123996	29.835913	26.850671	17.512405	1792.5472	125.5541	1497.588	179.41034	2246.9769	151.30817
13	de09a18 1	~~5.7567967~~	~~1.6103982~~	~~0.2498894~~	~~0.064653~~	~~0.9839455~~	0.95	0.1611289	0.0075615	55.947718	51.745251	9.3856202	1939.939	242.00388	1437.9055	333.45328	2467.5409	79.250877
14	~~de09a15 1~~	~~5.9249064~~	~~0.9703973~~	~~0.2470443~~	~~0.1672451~~	~~0.9129523~~	~~0.95~~	~~0.1528901~~	~~0.0462637~~	~~32.756545~~	~~135.3968~~	~~60.518887~~	~~1964.8927~~	~~142.28712~~	~~1423.2149~~	~~864.54897~~	~~2378.5034~~	~~515.67701~~
15	de09a16 1	~~3.8012578~~	~~0.6072876~~	~~0.259721~~	~~0.0343578~~	~~0.7506087~~	0.95	0.1101086	0.0128221	31.951928	26.457439	23.289993	1593.0121	128.43083	1488.4143	175.82017	1801.198	211.82872
16	de09a13 1	~~6.8573273~~	~~0.5616457~~	~~0.3853195~~	~~0.0366172~~	~~0.8925806~~	0.9995402	0.1305711	0.006268	16.380893	19.006139	9.6009701	2093.1579	72.580095	2101.0848	170.39354	2105.66	84.252757
17	de09a14 1	~~5.3946515~~	~~0.3896944~~	~~0.3471454~~	~~0.024745~~	~~0.7886113~~	0.9875615	0.1214013	0.0067474	14.447437	14.256249	11.115812	1884.0046	61.87814	1920.953	118.41056	1976.9224	98.99534
16	de07a45 1	5.4648859	0.2598163	0.3256634	0.0216861	0.9041929	-0.528848	0.1243149	0.0039105	9.5085734	13.318089	6.2912223	1895.0961	40.807079	1817.3278	105.45465	2019.0614	55.755188
17	de07a46 1	5.2914589	0.2751321	0.3165815	0.0166182	0.2904635	-2.796617	0.1632353	0.028228	10.399102	10.498507	34.585671	1867.4854	44.403767	1773.0127	81.367973	2489.4508	291.39556
20	de07a49 1	12.092751	0.7941725	0.5029125	0.0425009	0.9605512	0.95	0.1830016	0.0044776	13.134686	16.901918	4.8935183	2611.6248	61.590513	2626.3006	182.29843	2680.2618	40.47313
21	de07a50 1	4.0401862	0.4094227	0.2286349	0.0284983	0.8858599	0.9988996	0.1394286	0.009102	20.267518	24.929046	13.056127	1642.3242	82.481257	1327.3408	149.52492	2220.1229	113.13371
22	de07a51 1	4.6064705	0.3039321	0.2443014	0.014603	0.9654131	0.95	0.1452107	0.0023441	13.195879	11.954915	3.2286111	1750.4406	55.044886	1409.0203	75.654564	2290.2762	27.766459
23	de07a52 1	5.1658876	0.5445519	0.2565876	0.0203743	0.9276599	0.95	0.1526757	0.0048802	21.082608	15.881005	6.3928395	1847.0144	89.675457	1472.3597	104.52233	2376.1119	54.486401
24	de07a53 1	3.8084903	0.6267278	0.1967121	0.011892	0.2083014	0.95	0.1361647	0.0386512	32.912138	12.090734	56.771199	1594.5405	132.34274	1157.6334	64.05931	2178.9799	494.14889
25	de07a54 1	9.3724075	0.5987481	0.4068449	0.0320976	0.9708126	0.95	0.1718203	0.0033489	12.776826	15.778799	3.8981554	2375.1324	58.613073	2200.4807	147.07702	2575.4537	32.565816
26	de07a55 1	3.0315512	0.2247834	0.1914939	0.0141233	0.7243399	0.9441589	0.1259064	0.0088386	14.829594	14.750626	14.039977	1415.5975	56.613747	1129.4624	76.412022	2041.5793	124.10601
30	de07a58 1	6.6686291	0.7825919	0.2888674	0.0430327	0.9921435	-0.231836	0.1661435	0.0031209	23.470849	29.794058	3.7568973	2068.4753	103.62094	1635.8667	215.23263	2519.1632	31.559646

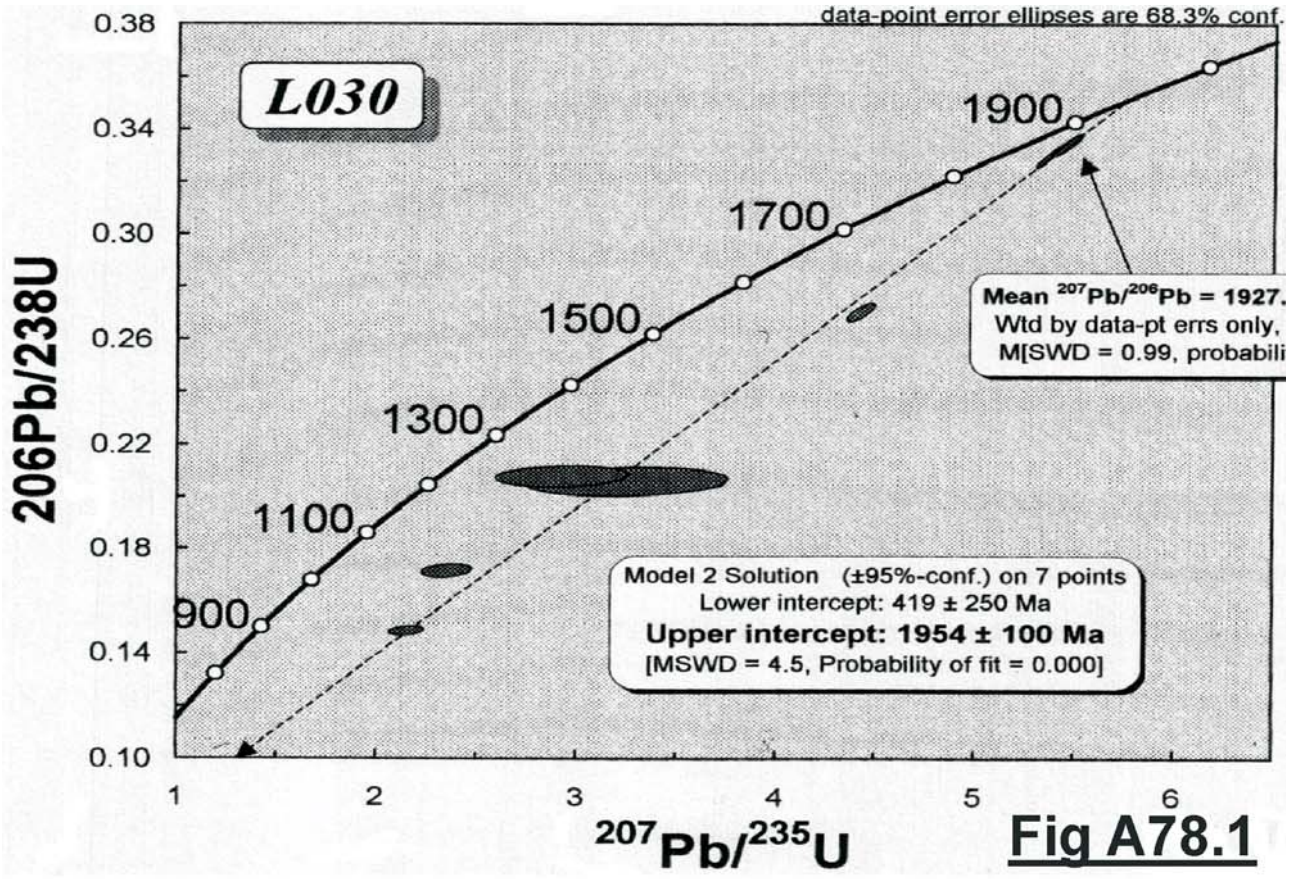

Fig A78.1

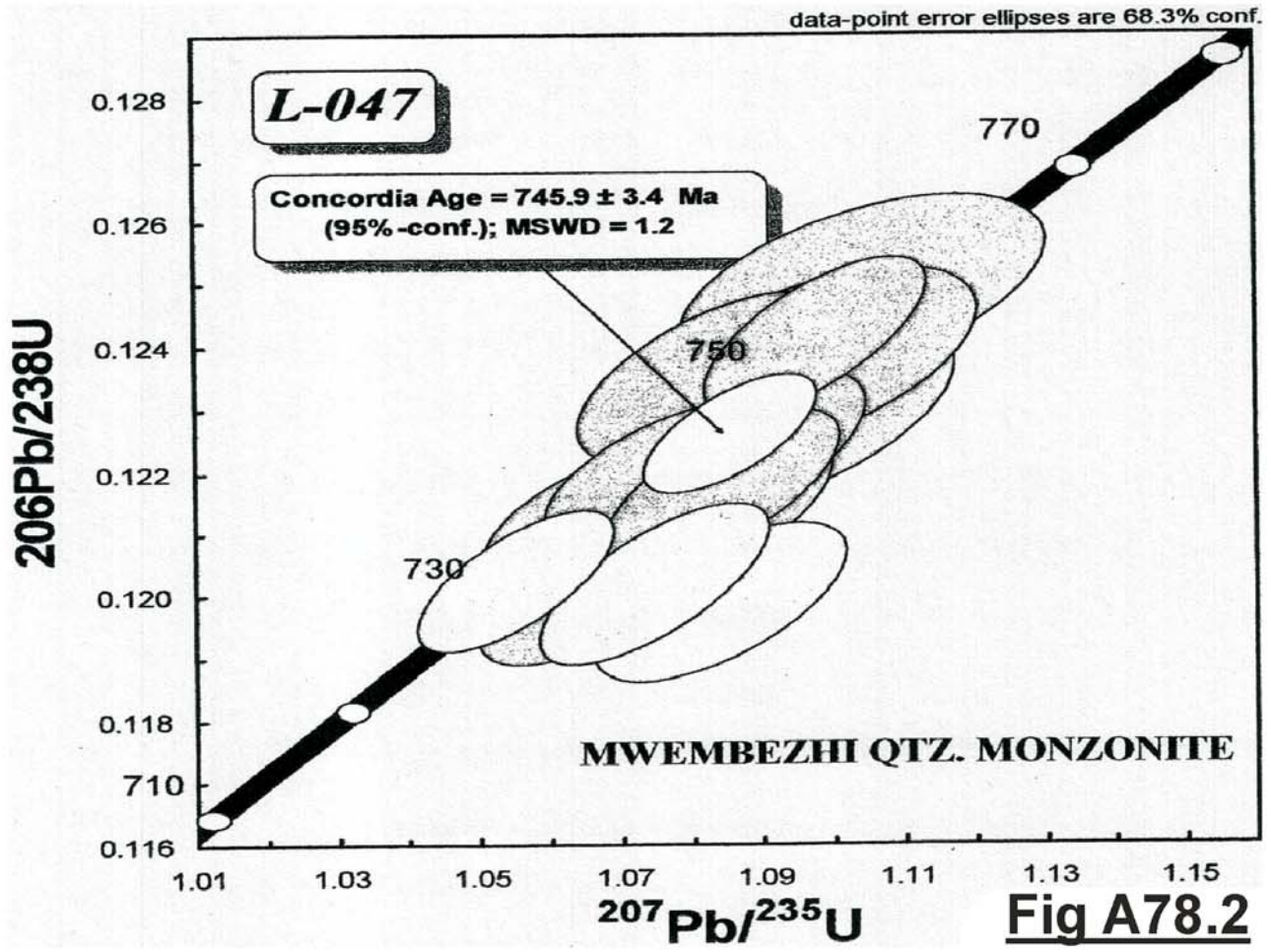

Fig A78.2

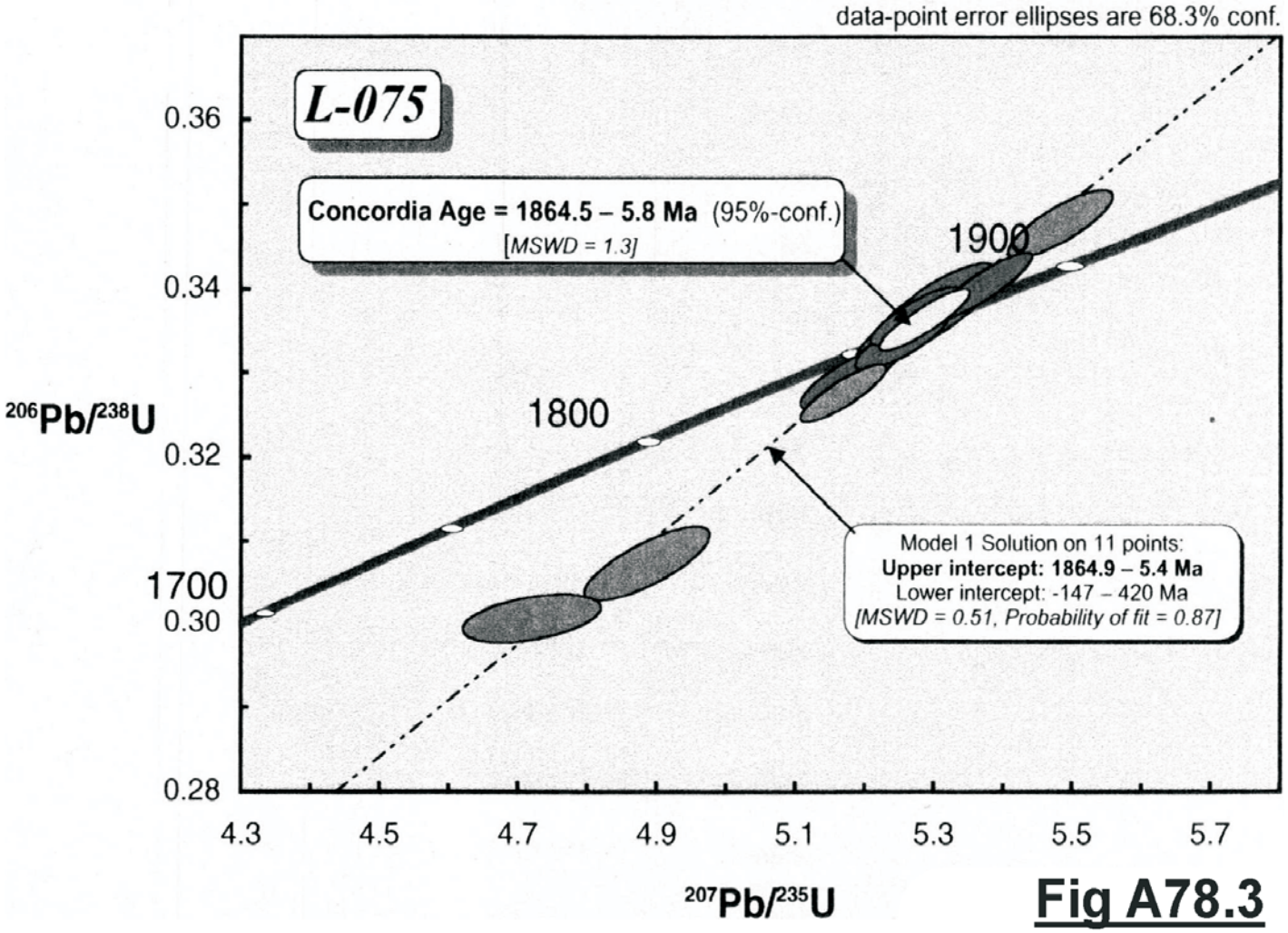

Fig A78.3

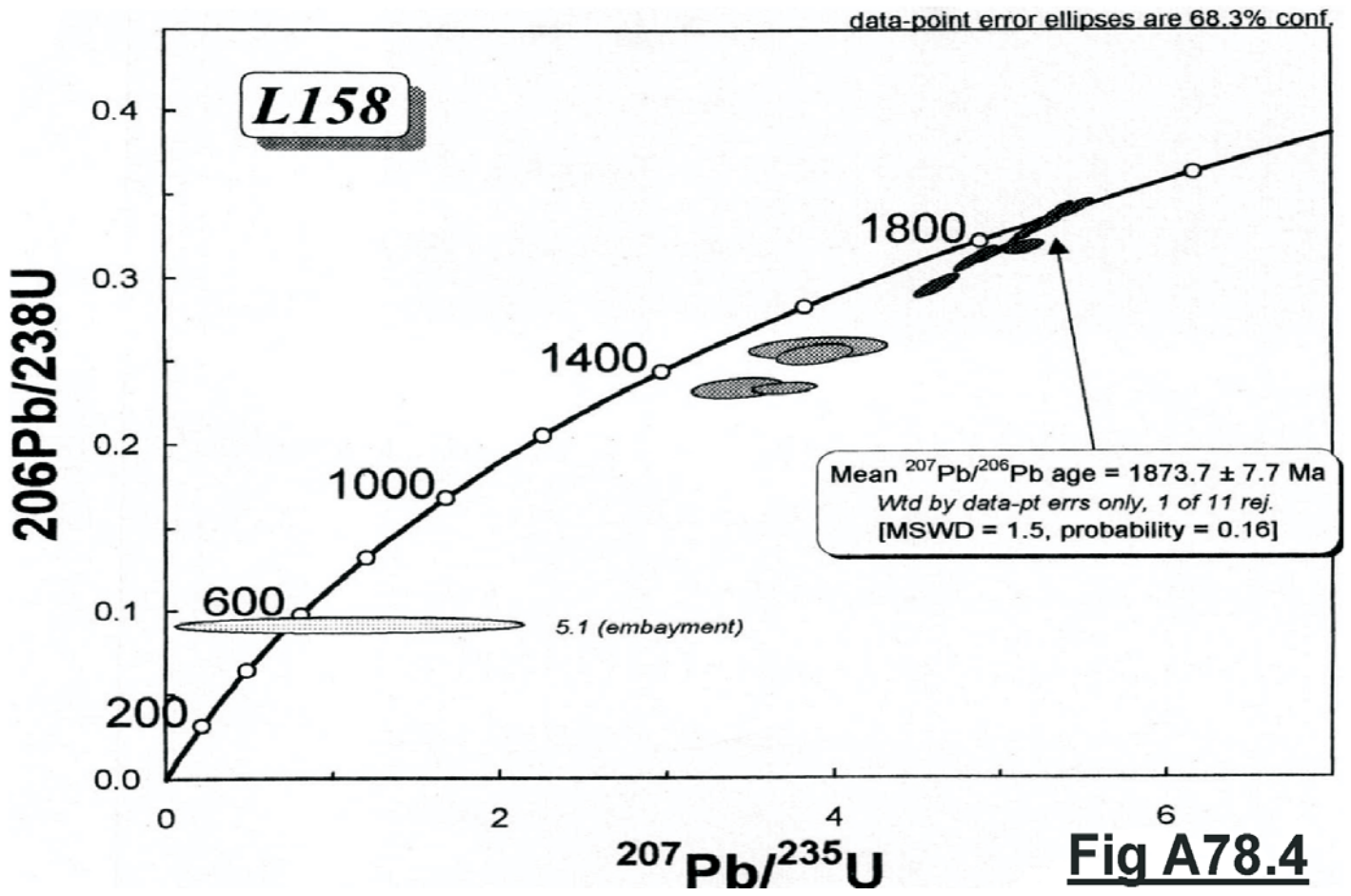

Fig A78.4

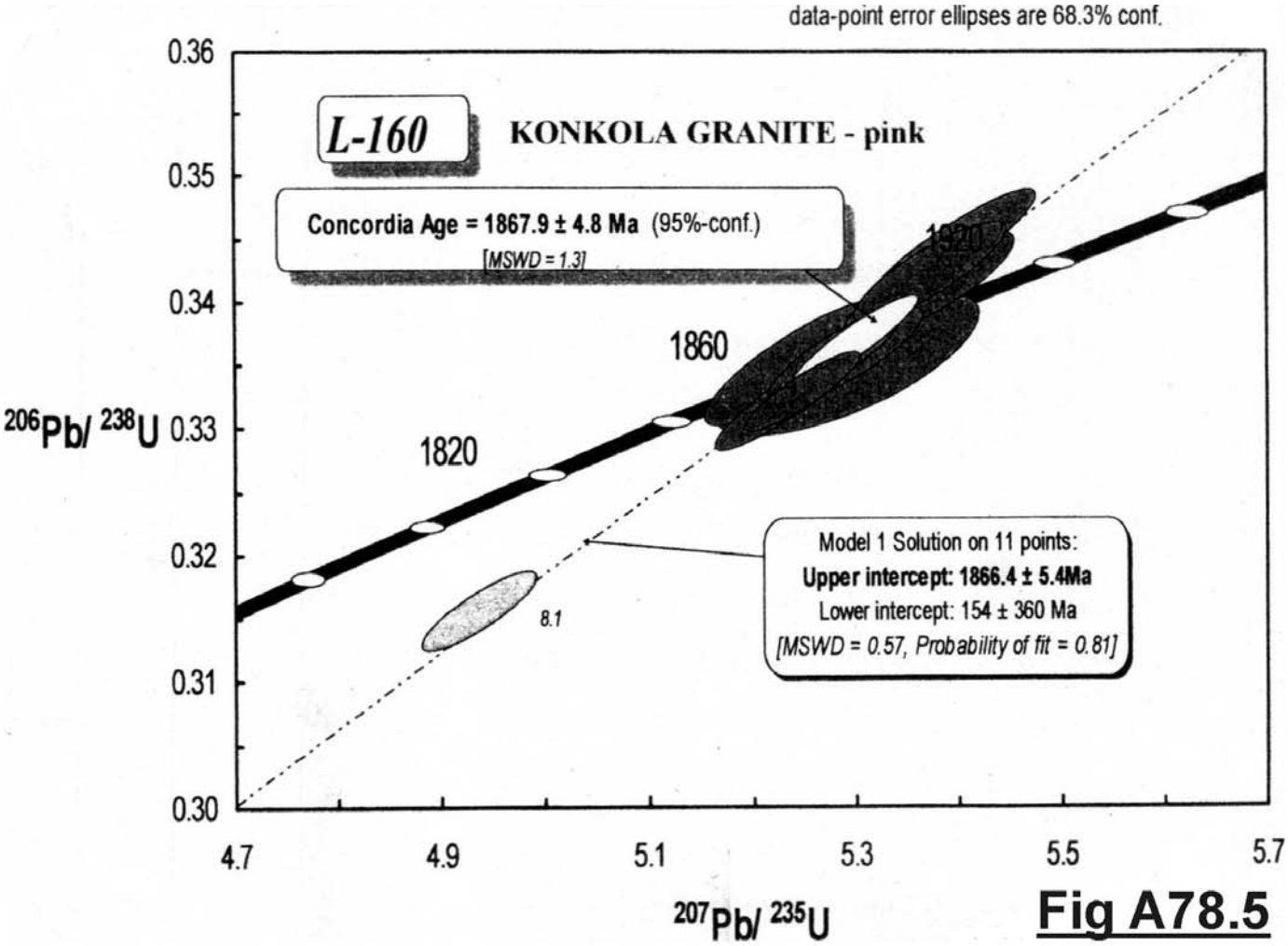

Fig A78.5

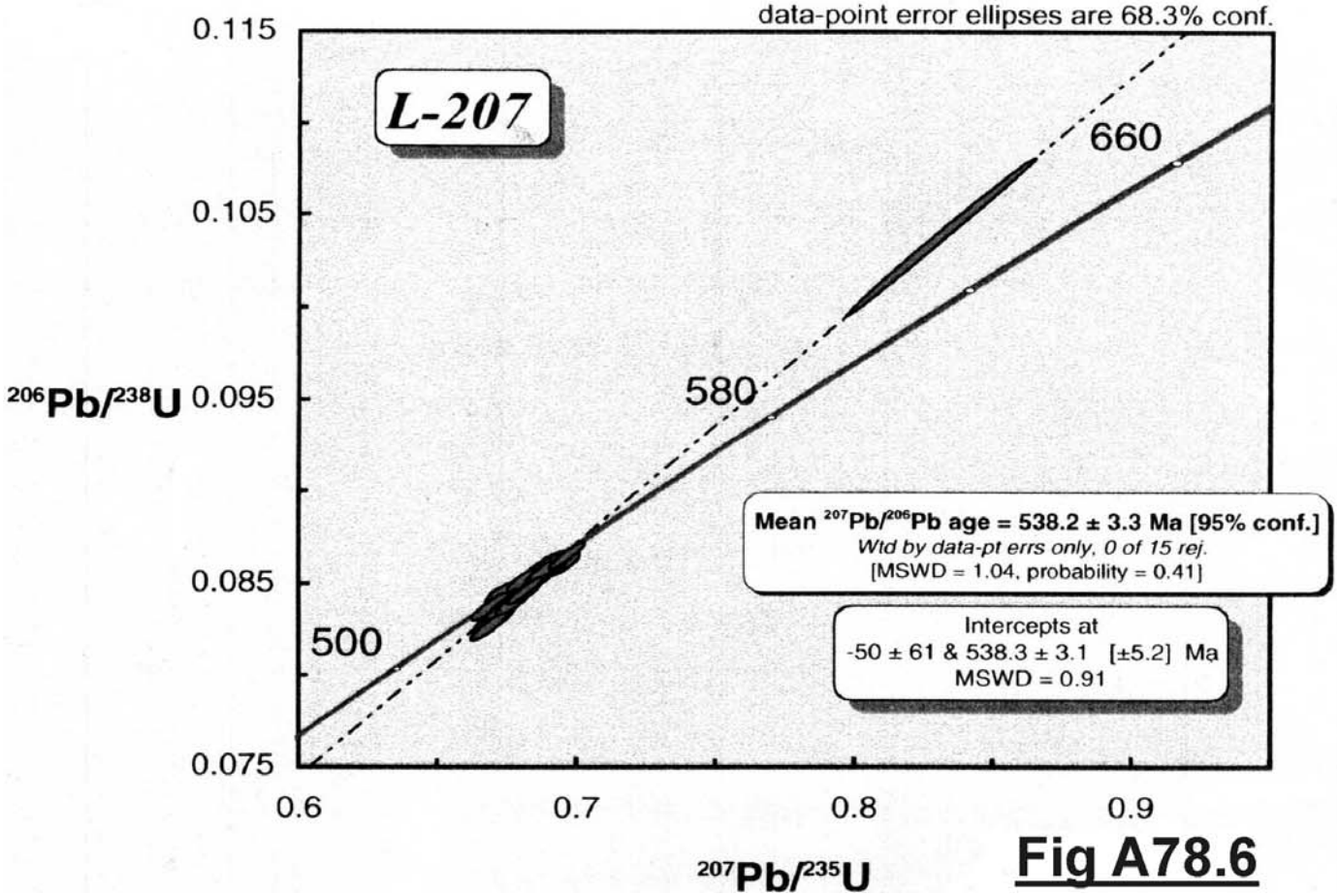

Fig A78.6

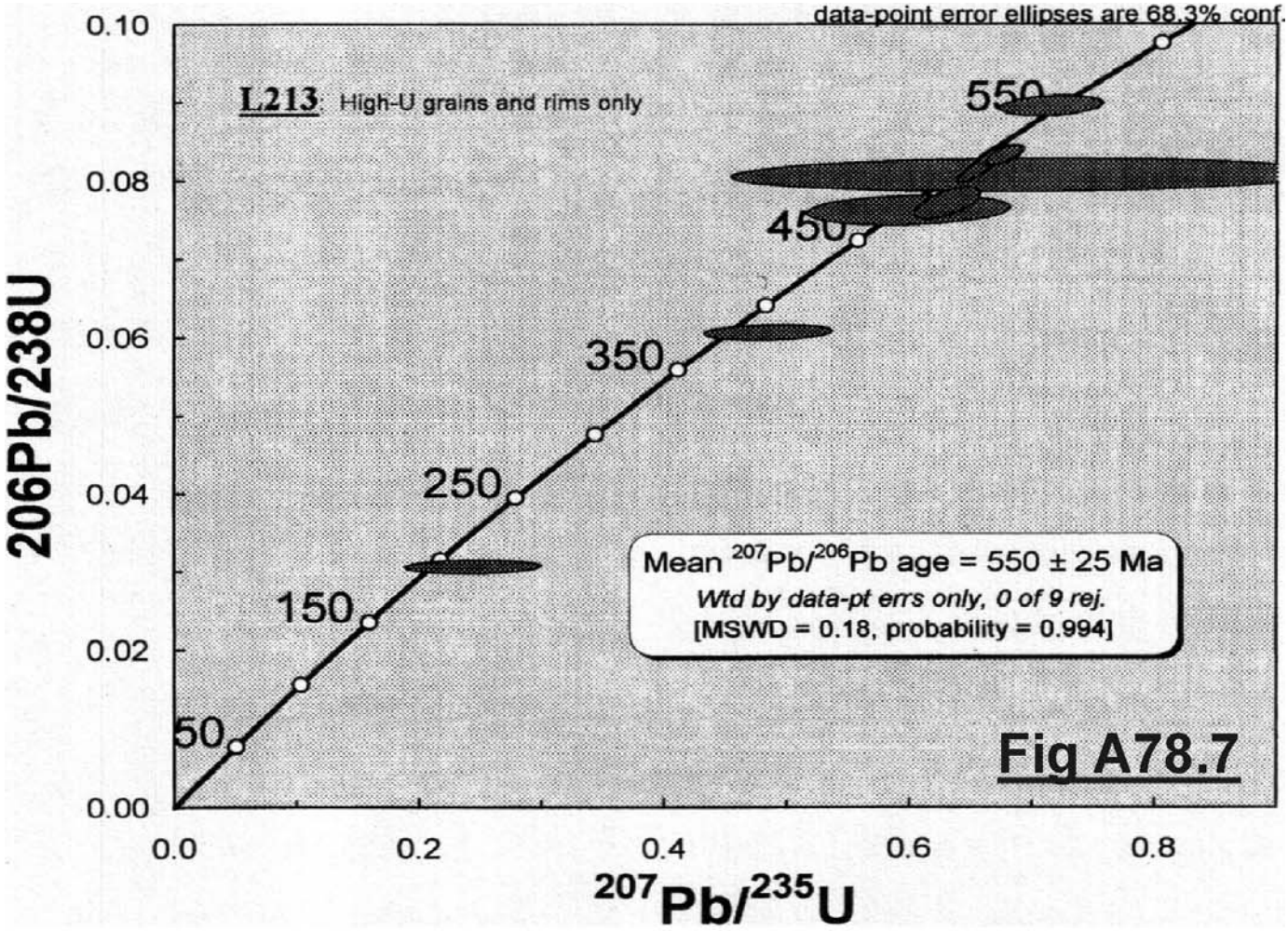
data-point error ellipses are 68.3% conf.
L213: High-U grains and rims only
550
450
350
250
150
50
Mean 207Pb/206Pb age = 550 ± 25 Ma
Wtd by data-pt errs only, 0 of 9 rej.
[MSWD = 0.18, probability = 0.994]
Fig A78.7
206Pb/238U
207Pb/235U
0.10
0.08
0.06
0.04
0.02
0.00
0.0
0.2
0.4
0.6
0.8

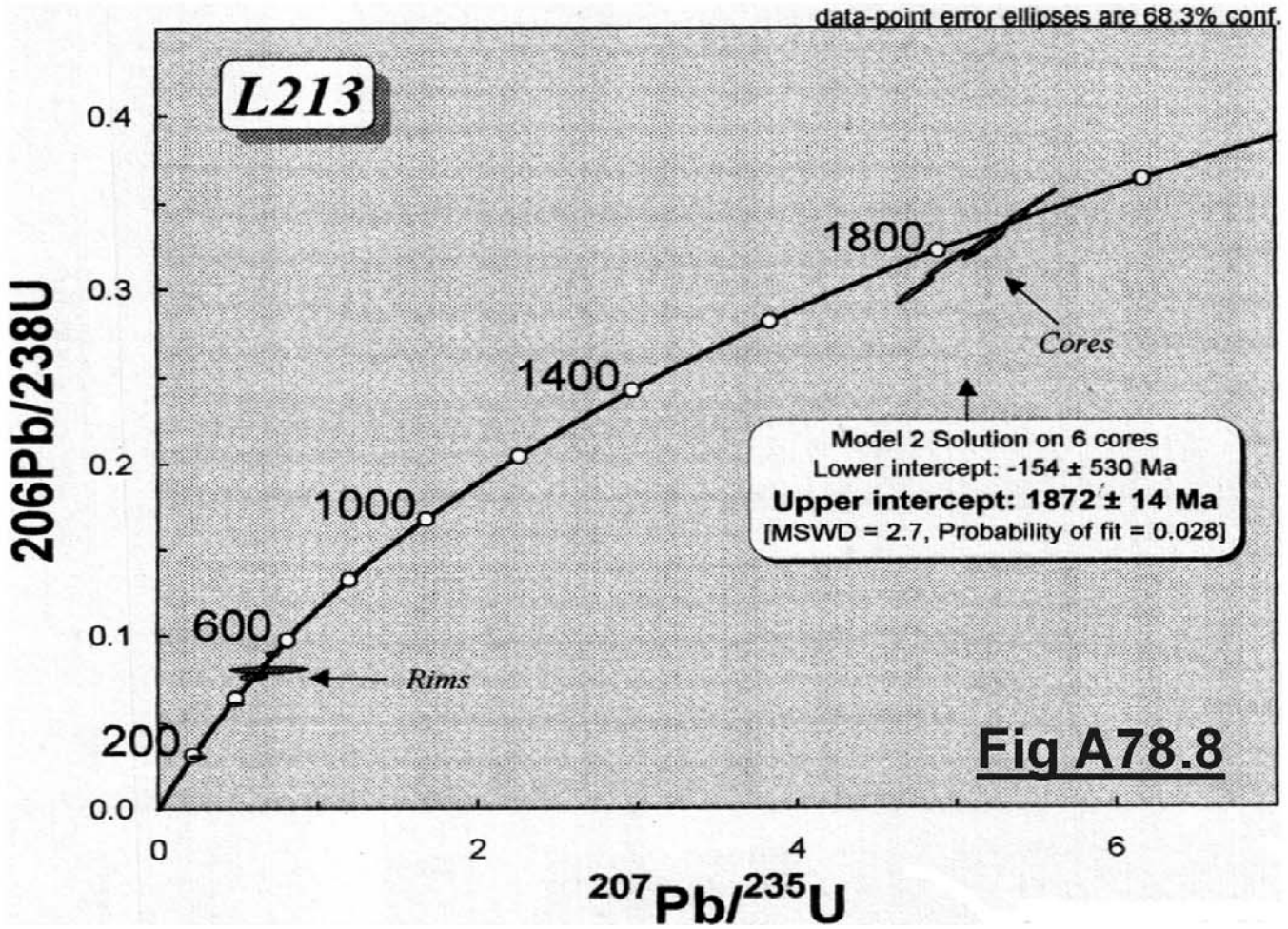
data-point error ellipses are 68.3% conf.
L213
1800
1400
1000
600
200
Cores
Rims
Model 2 Solution on 6 cores
Lower intercept: -154 ± 530 Ma
Upper intercept: 1872 ± 14 Ma
[MSWD = 2.7, Probability of fit = 0.028]
Fig A78.8
206Pb/238U
207Pb/235U
0.4
0.3
0.2
0.1
0.0
0
2
4
6

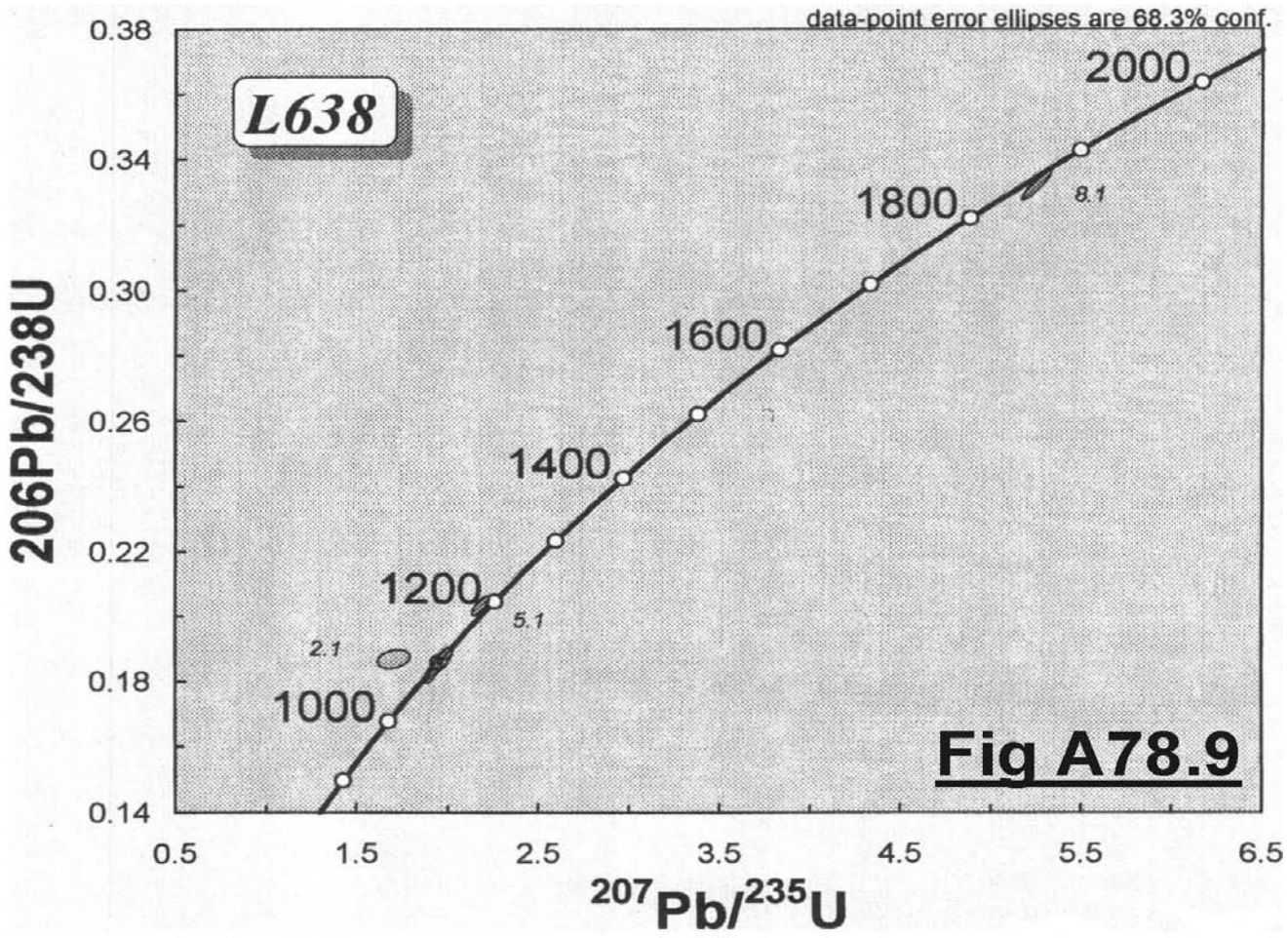

Fig A78.9

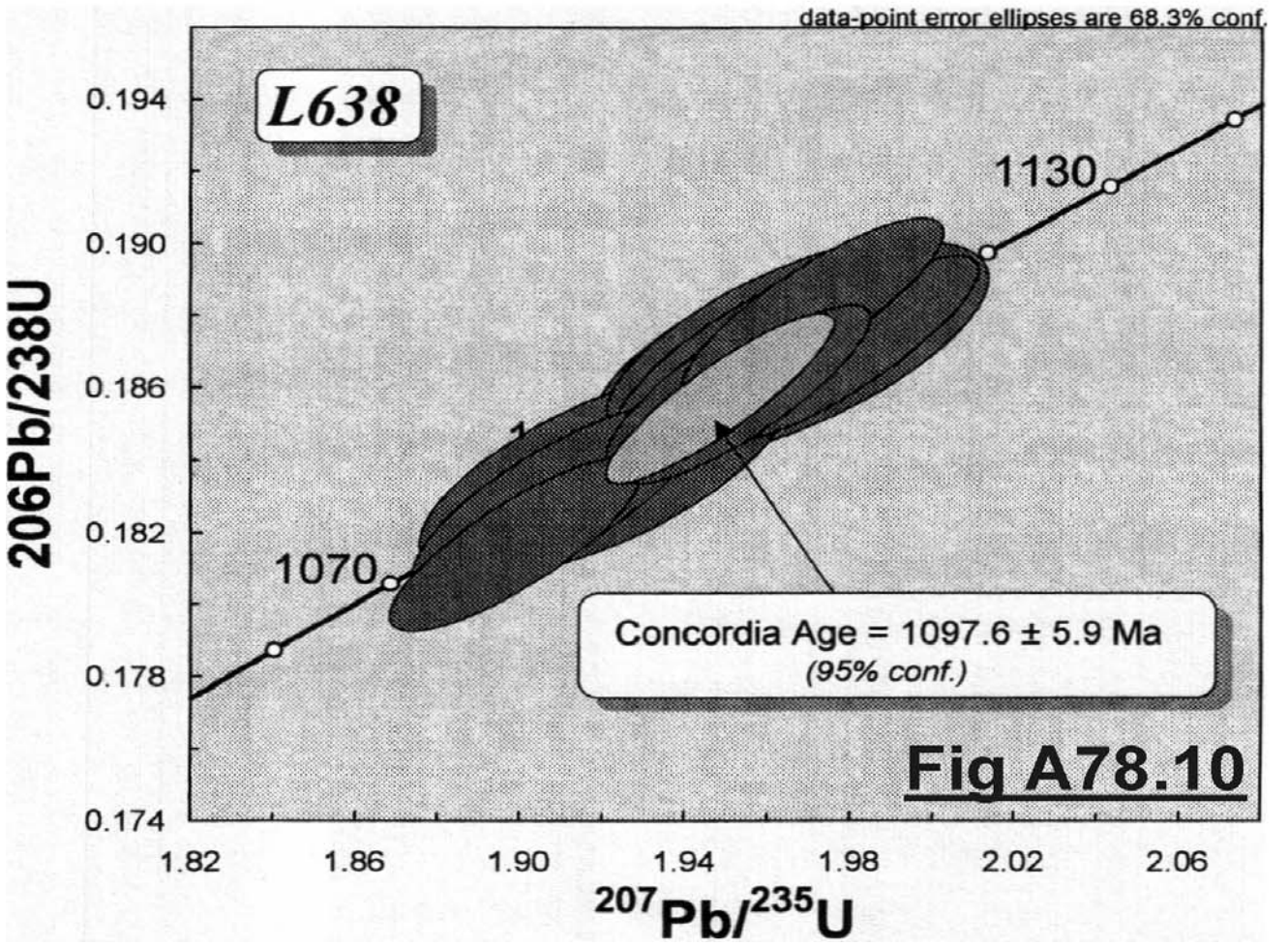

Fig A78.10

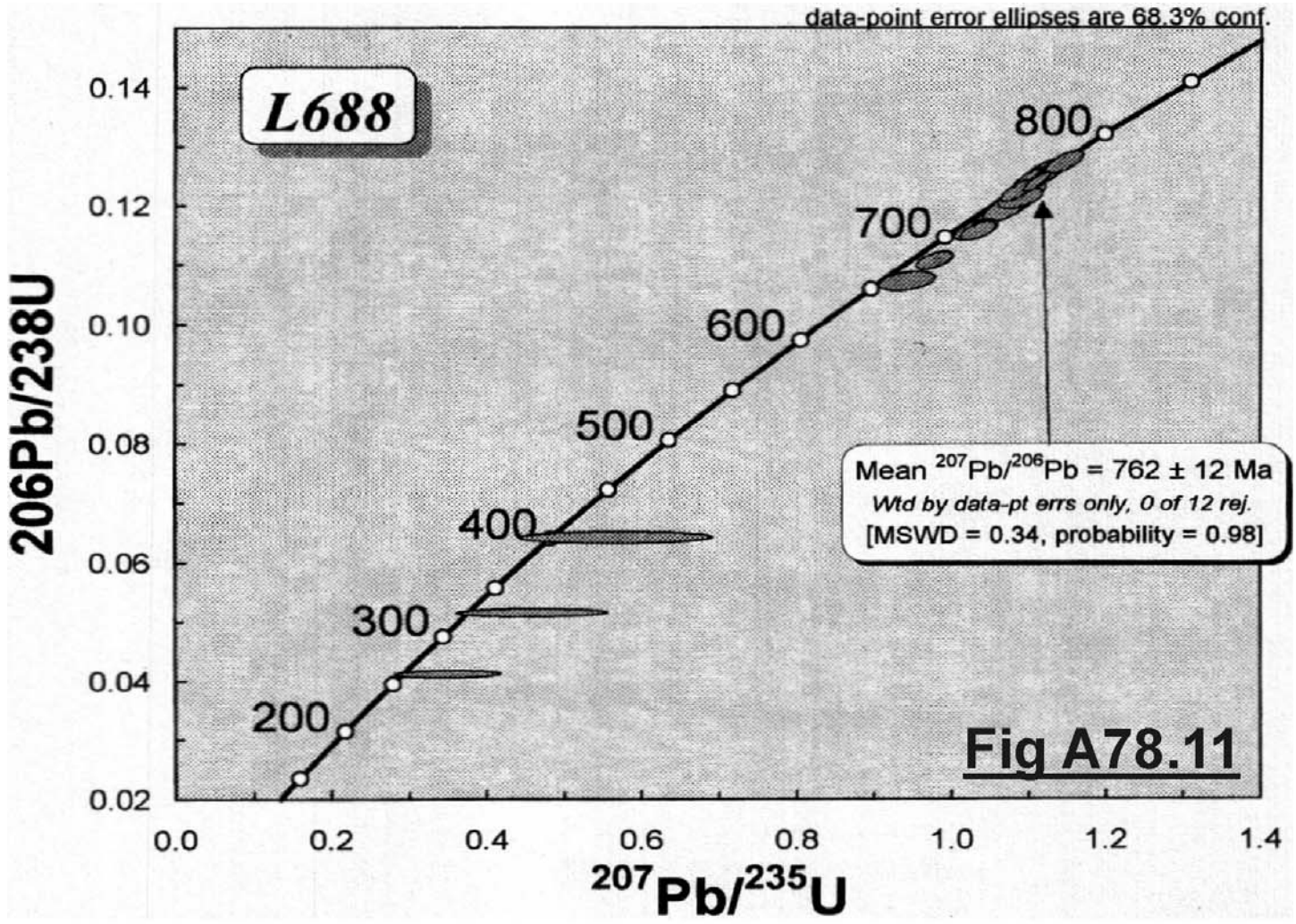

Fig A78.11

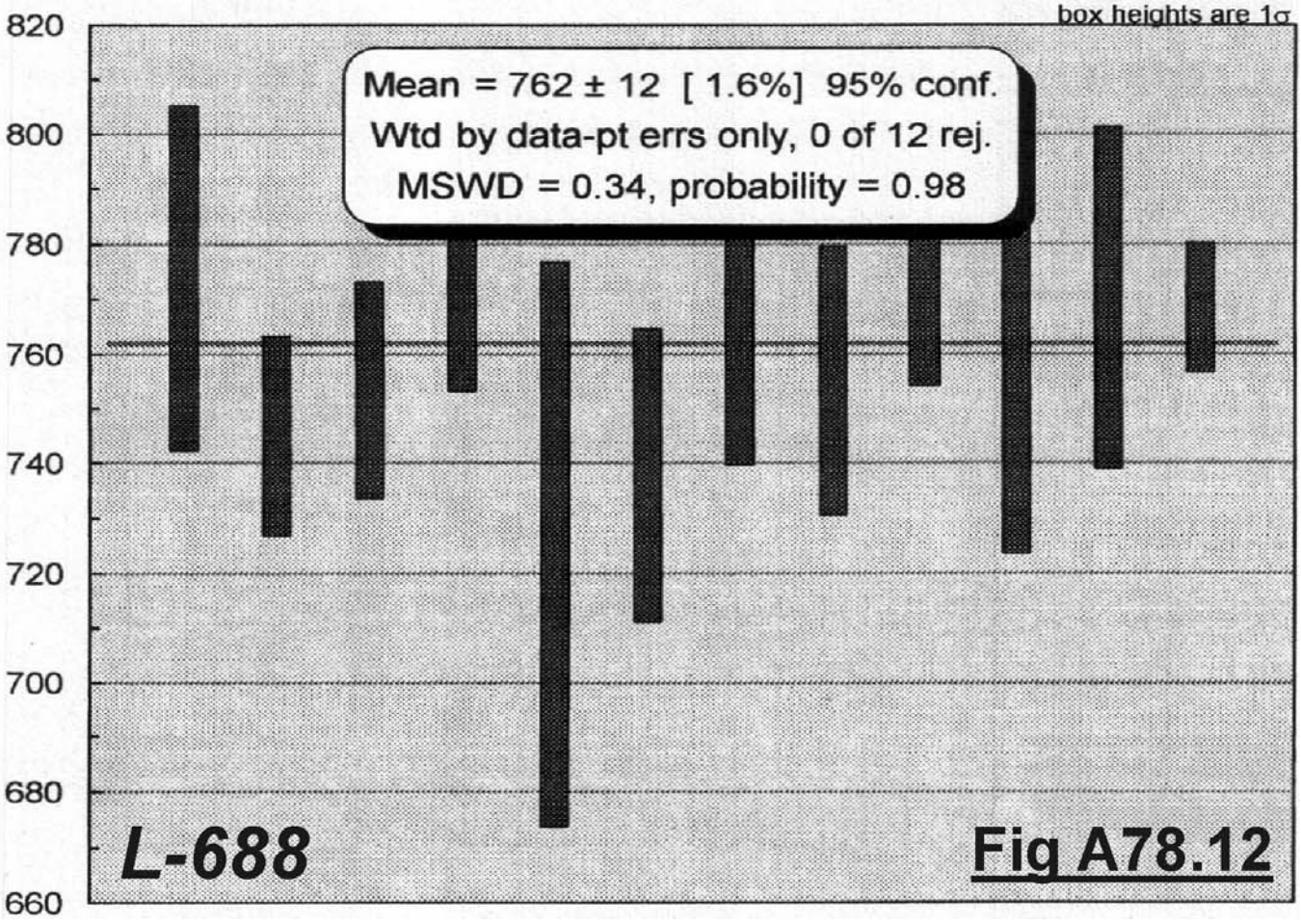

Fig A78.12

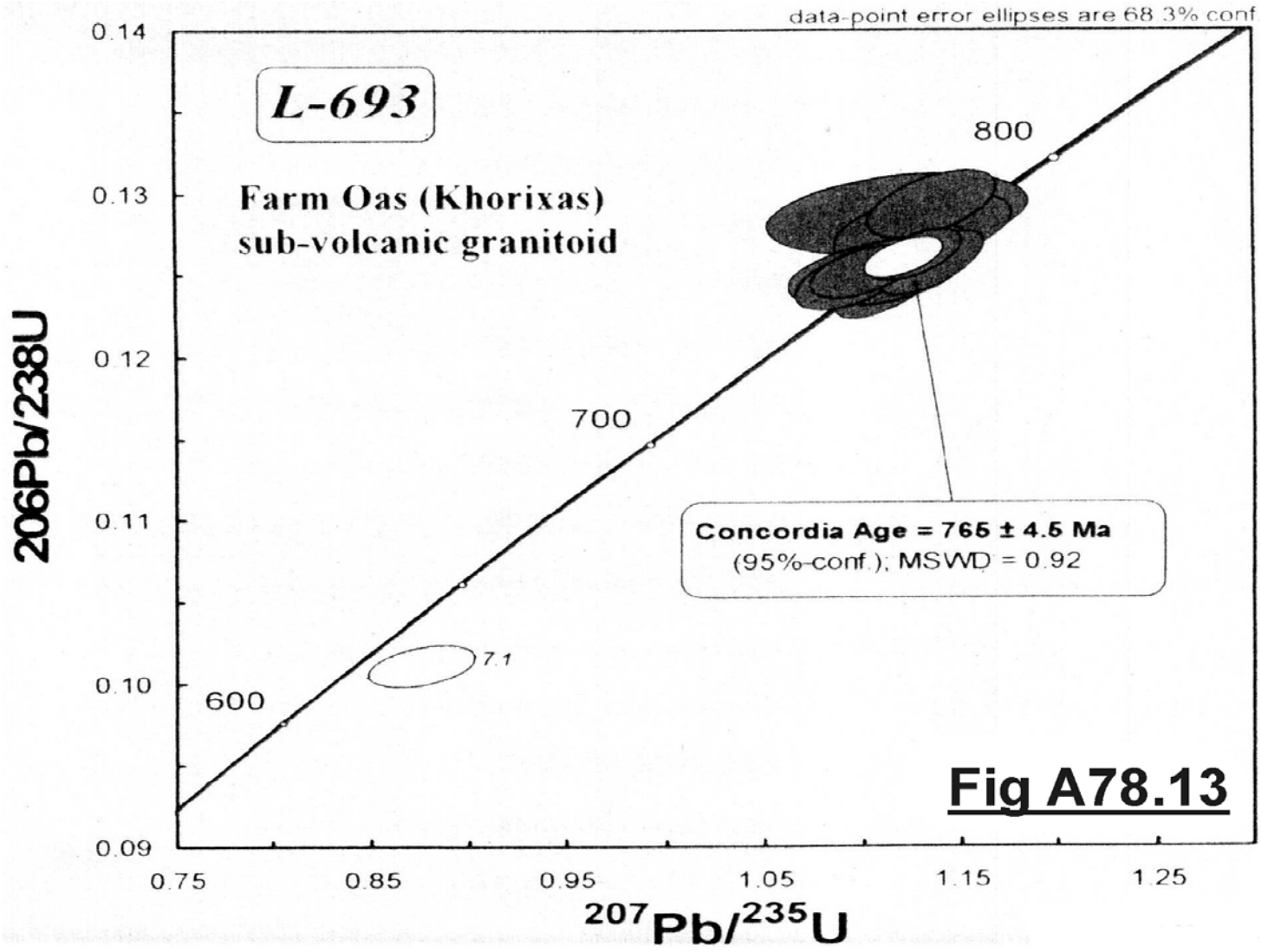

Fig A78.13

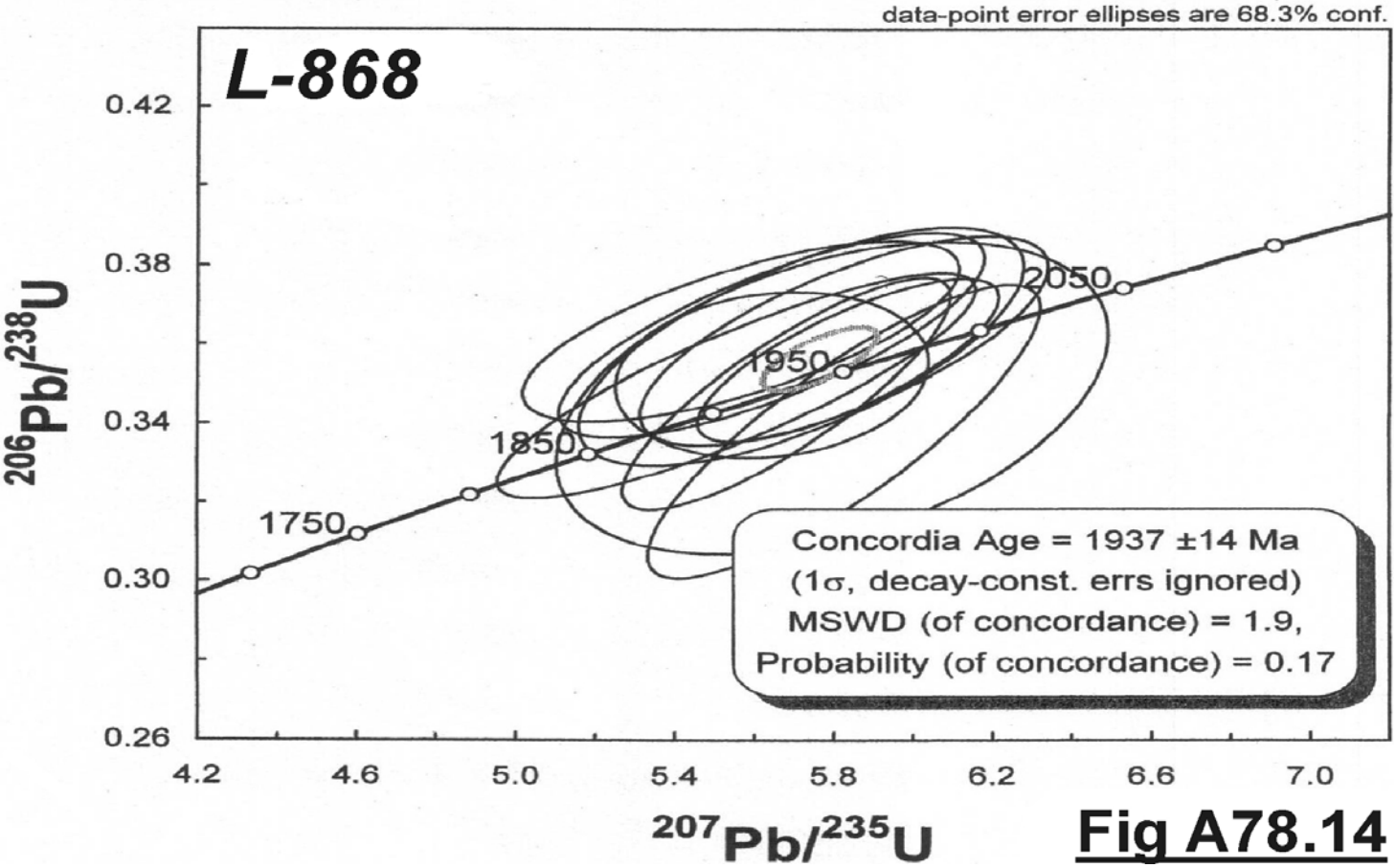

Fig A78.14

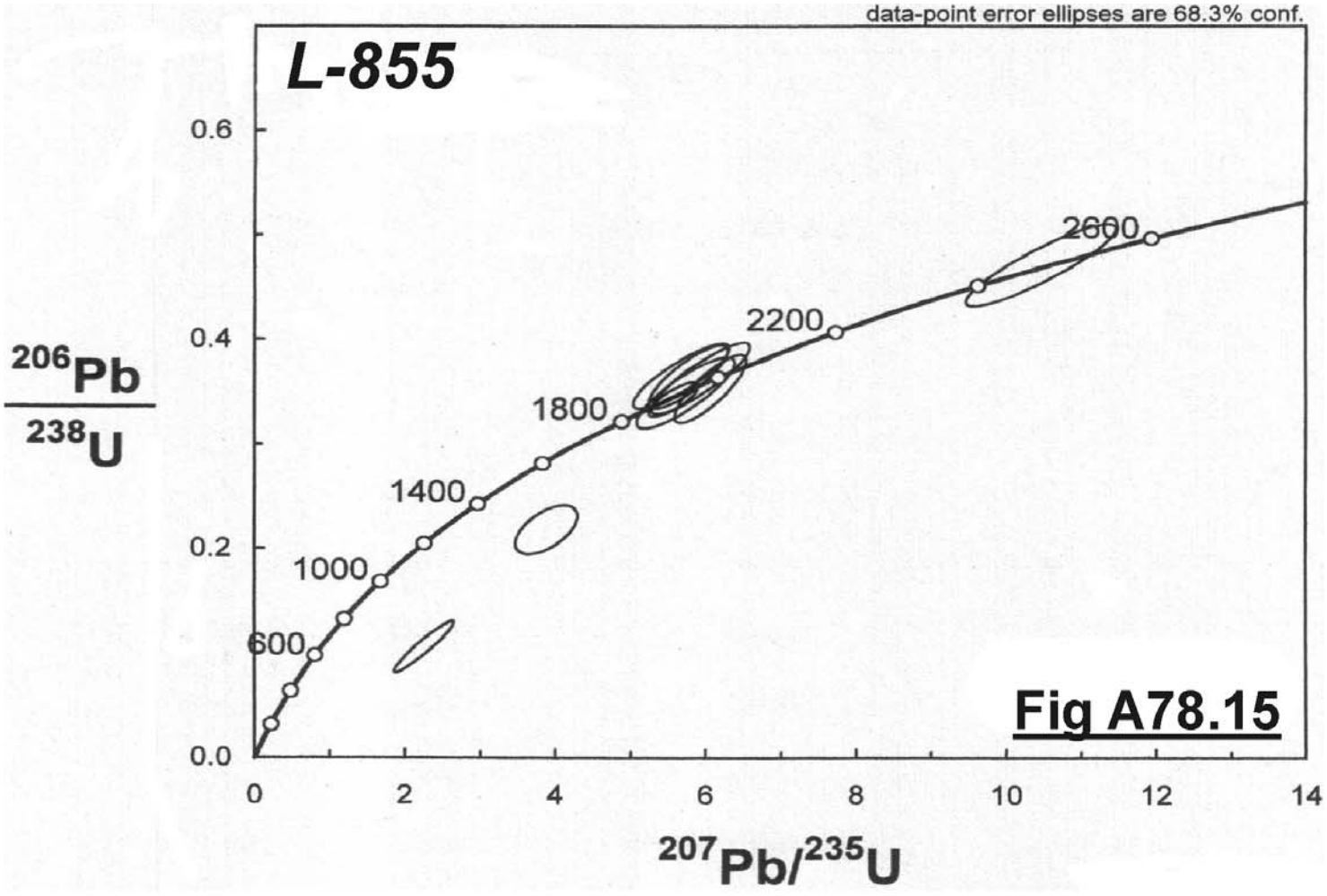

Fig A78.15

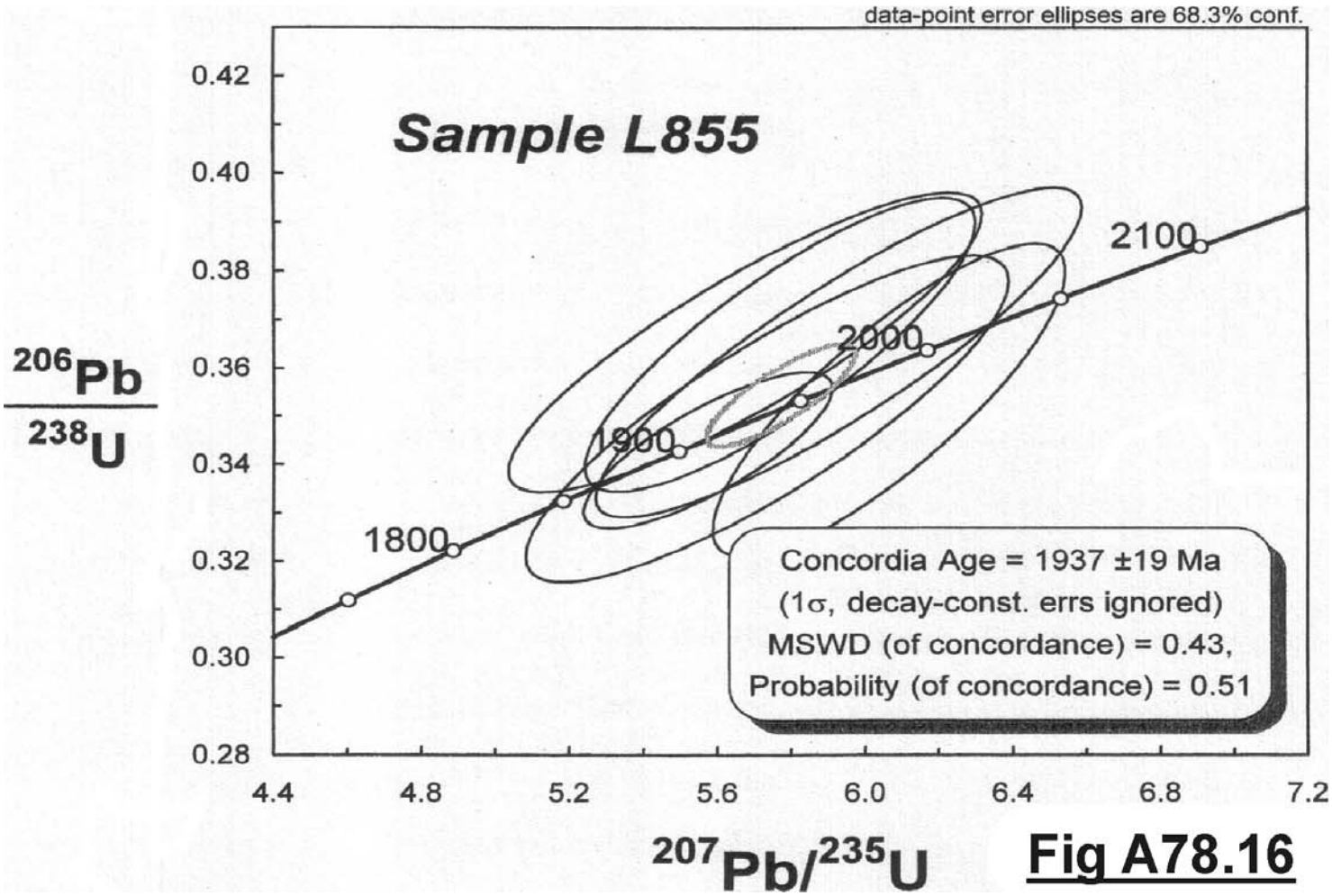

Fig A78.16

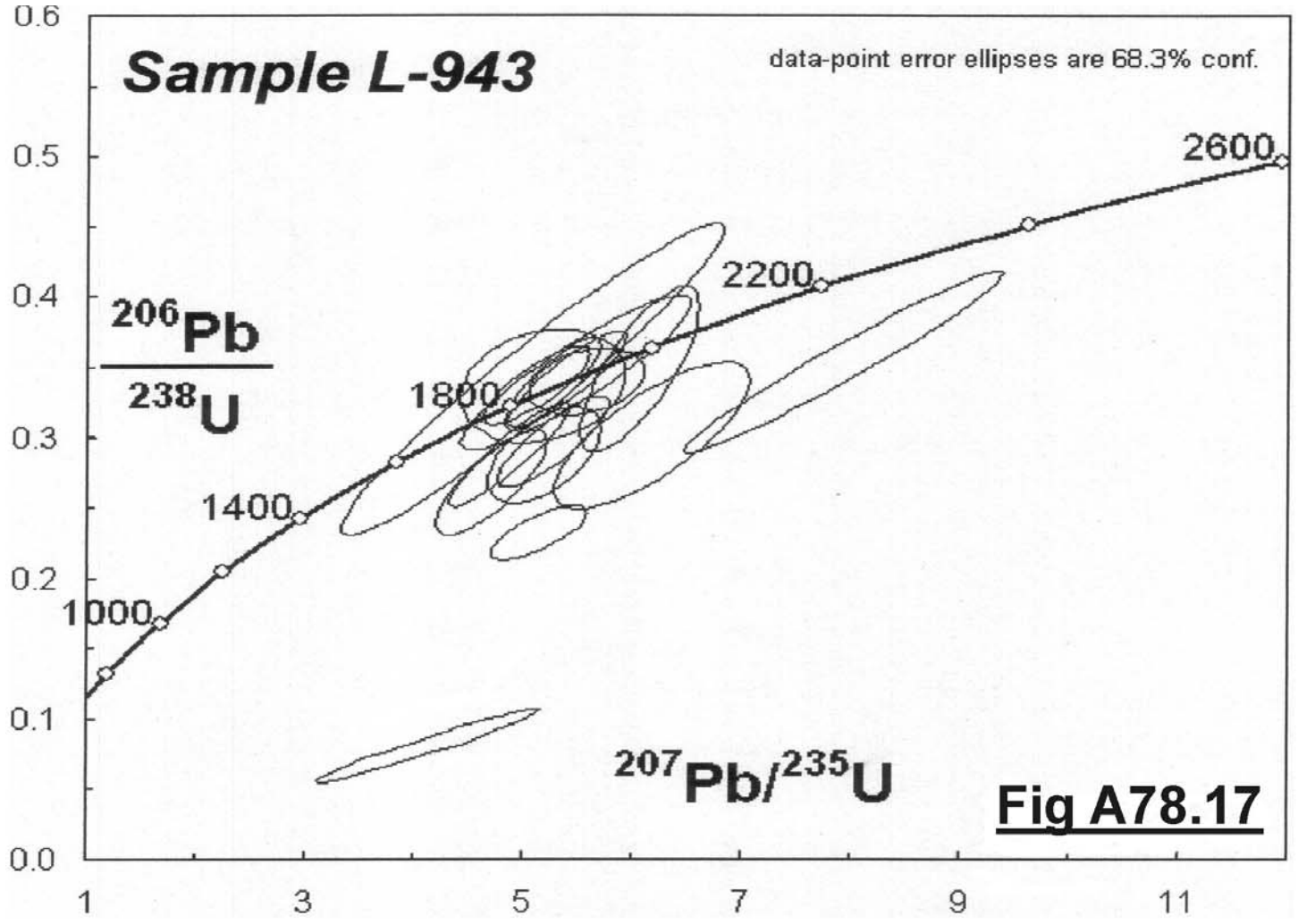

Fig A78.17

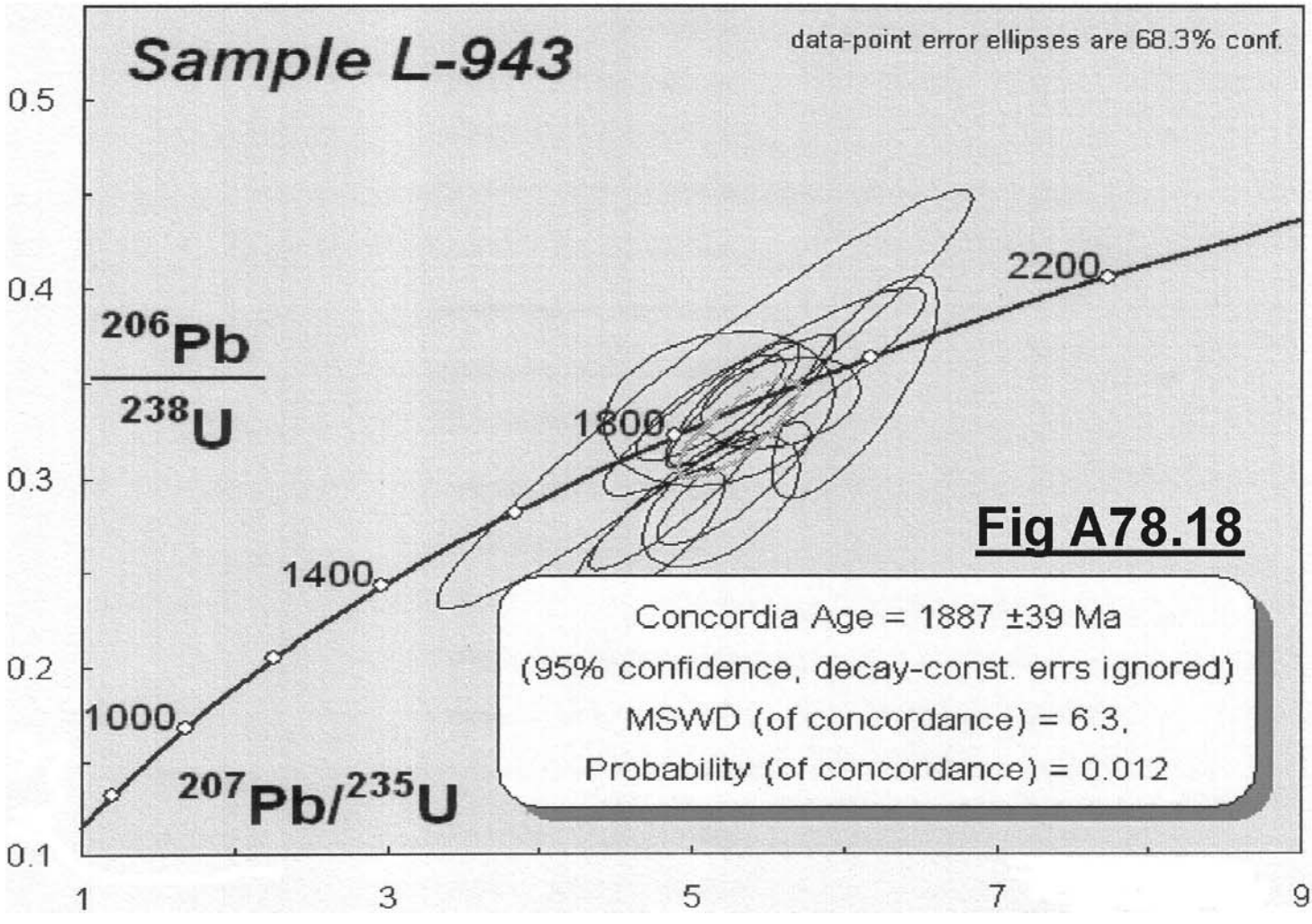

Fig A78.18

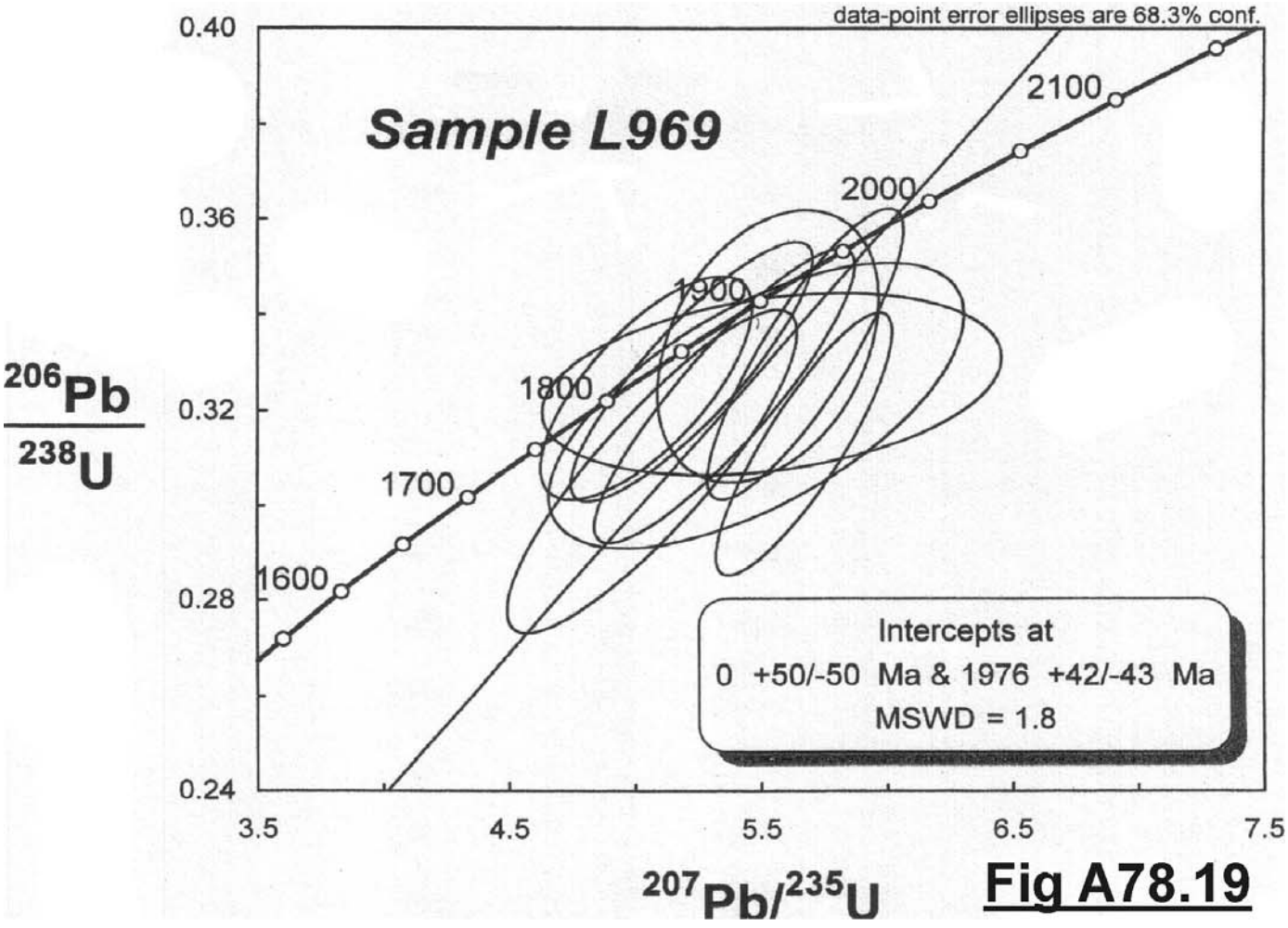

Fig A78.19

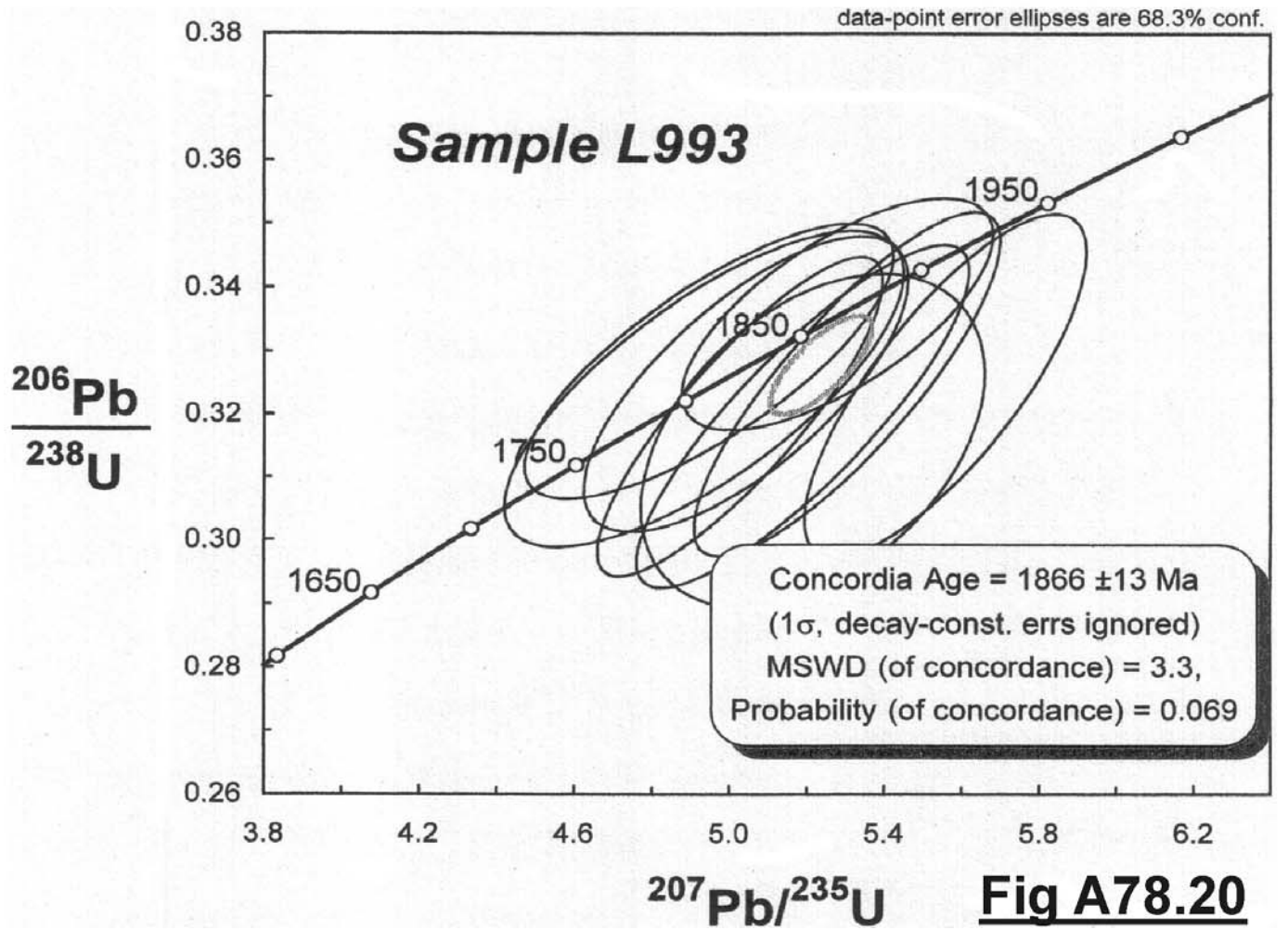

Fig A78.20

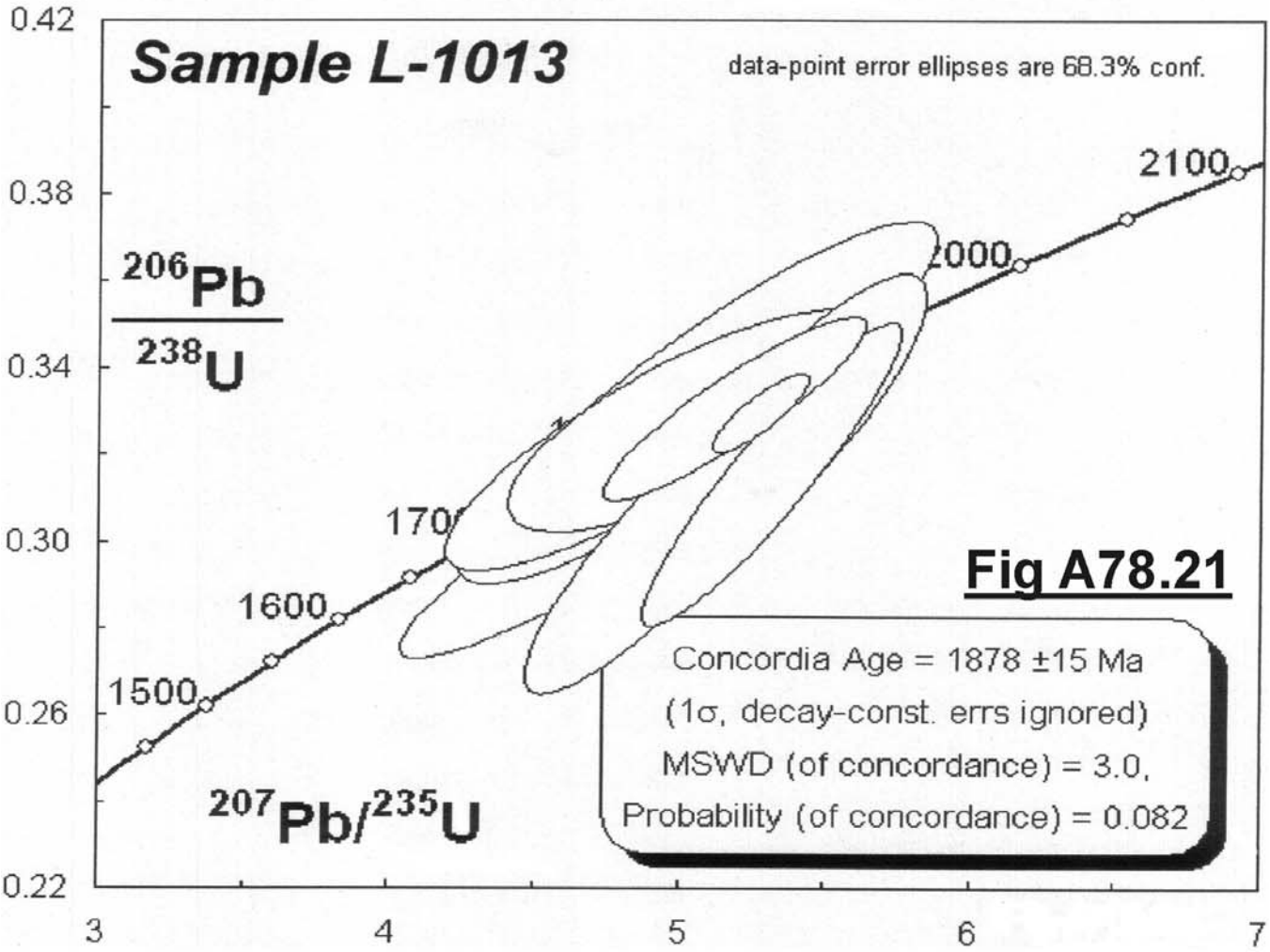

Fig A78.21

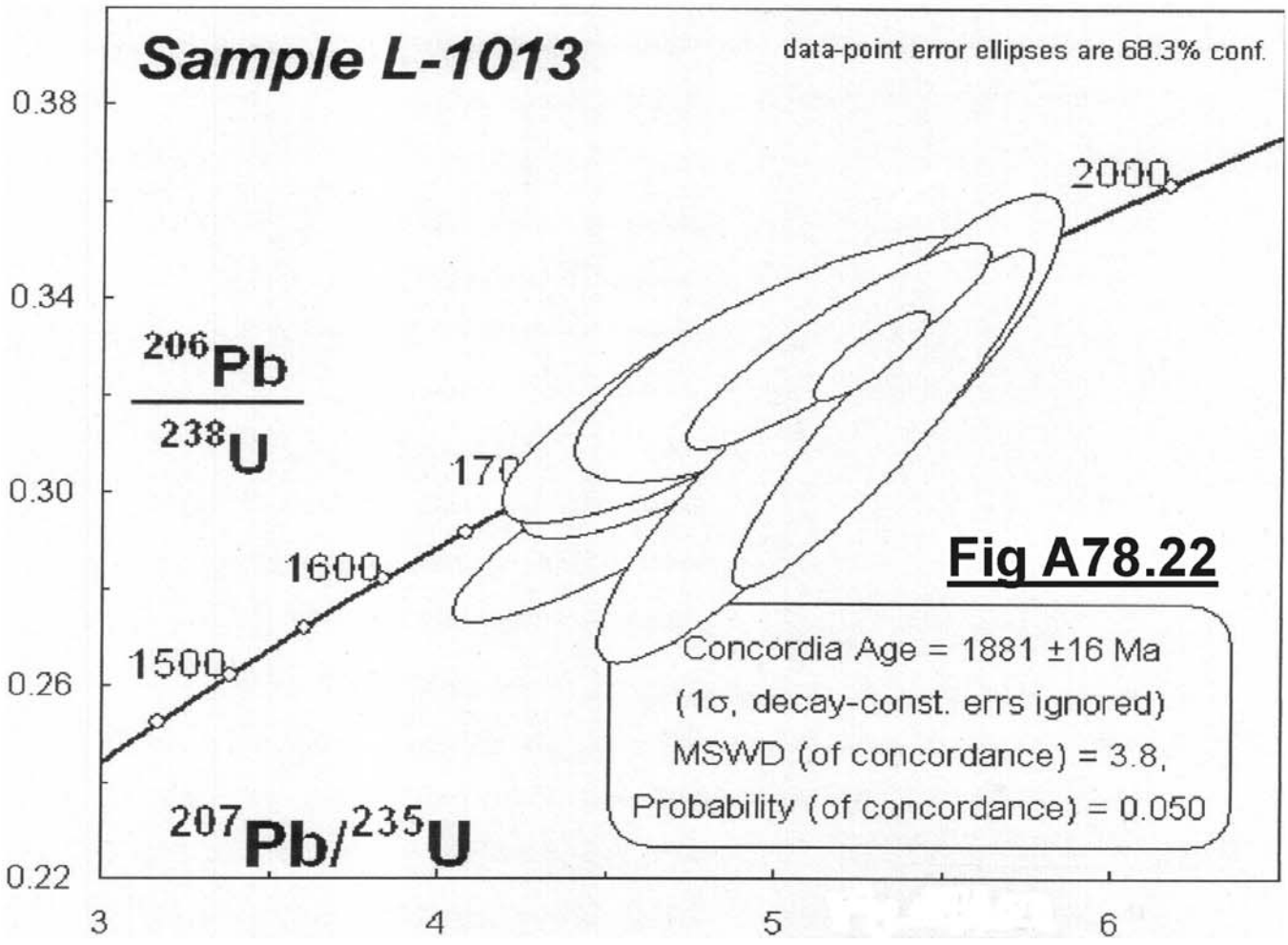

Fig A78.22

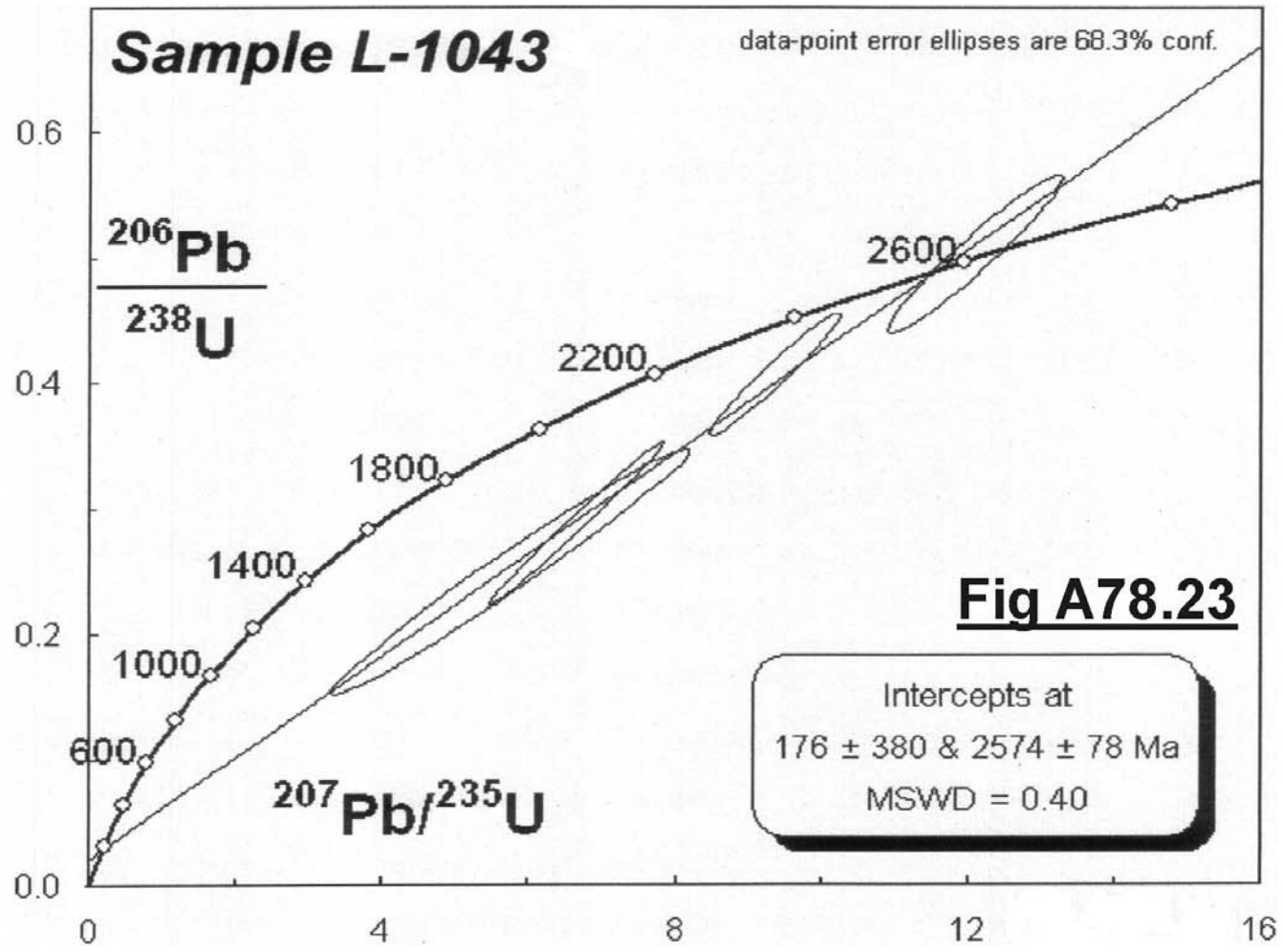

Fig A78.23

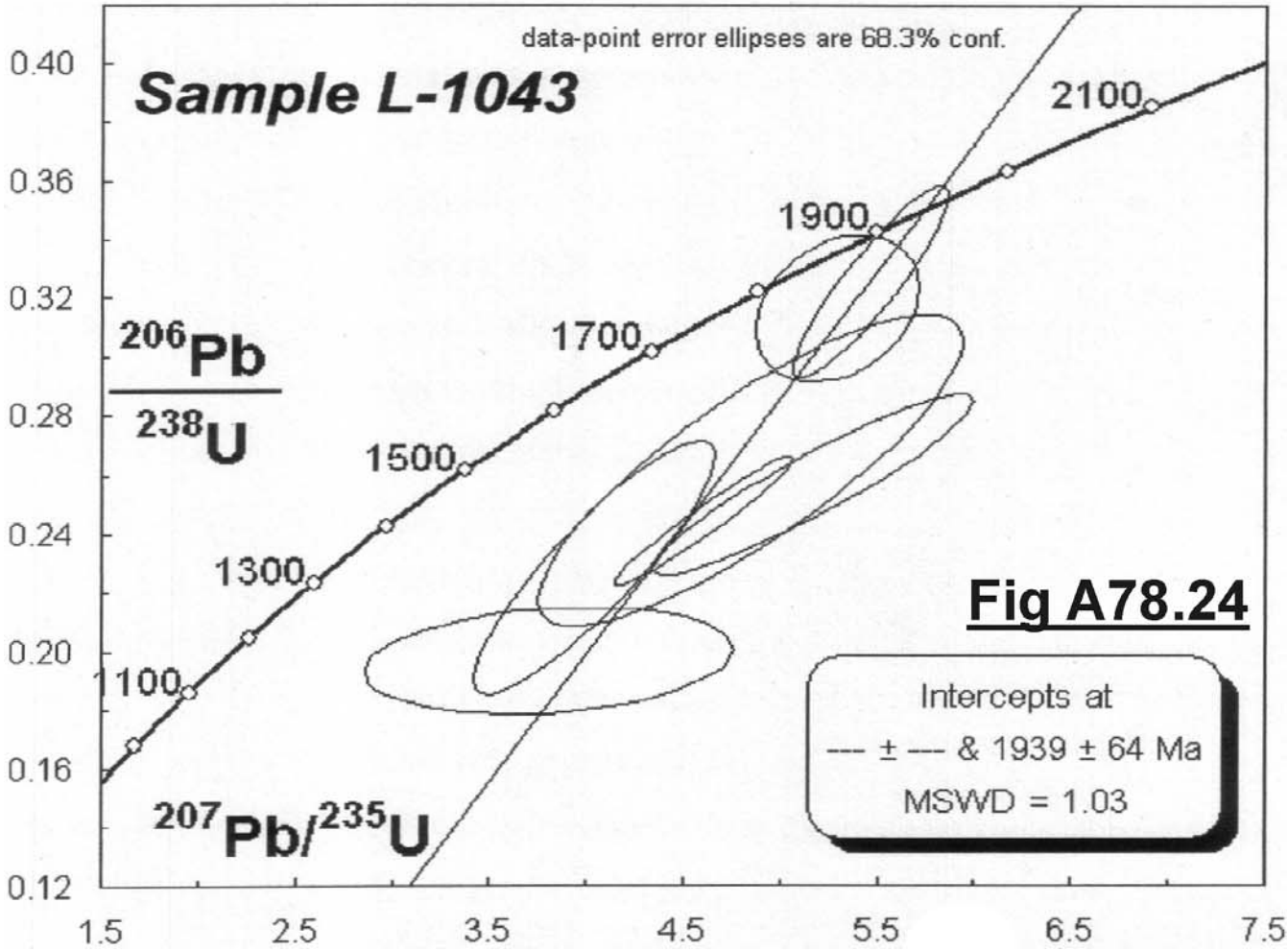

Fig A78.24

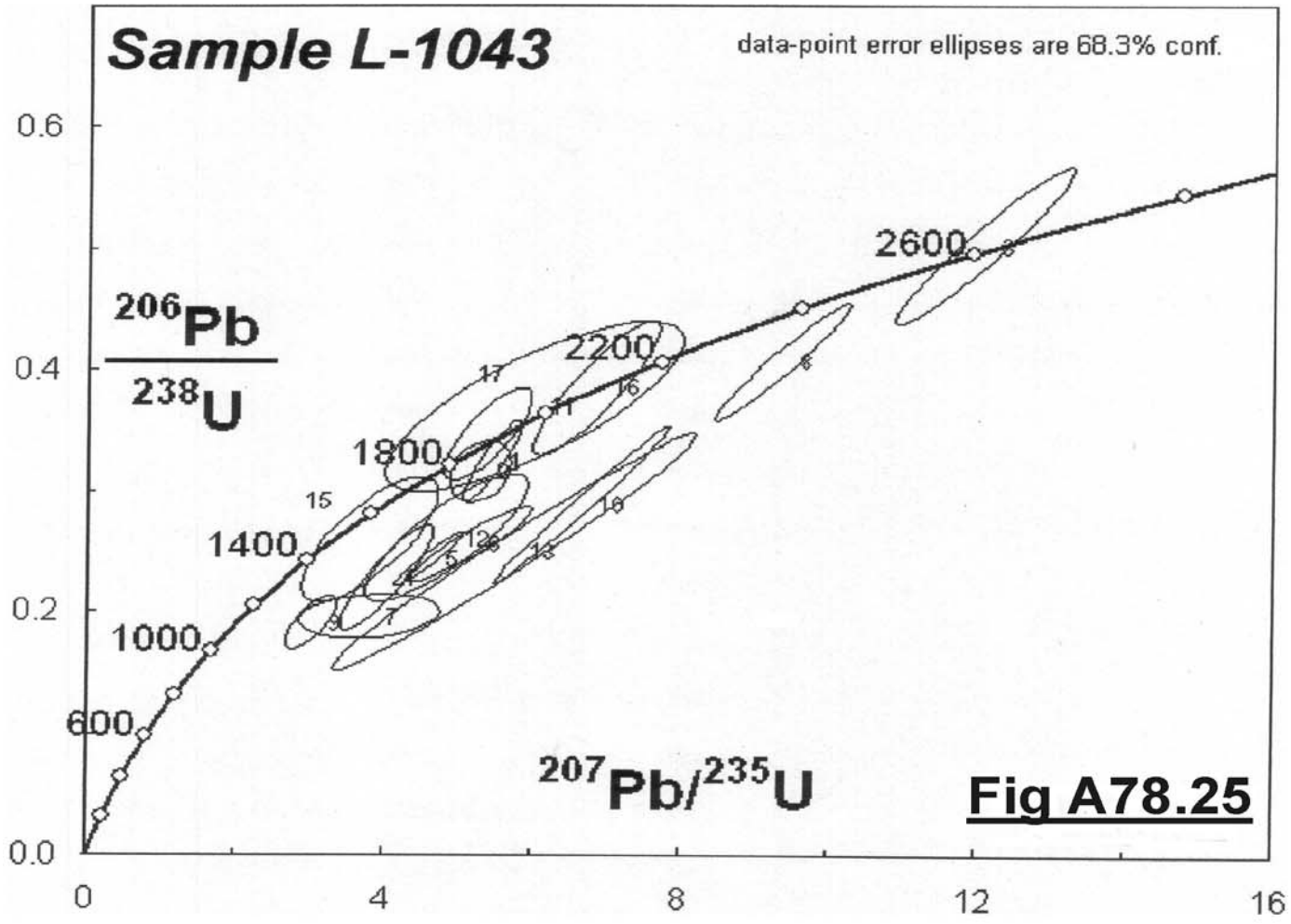

Fig A78.25

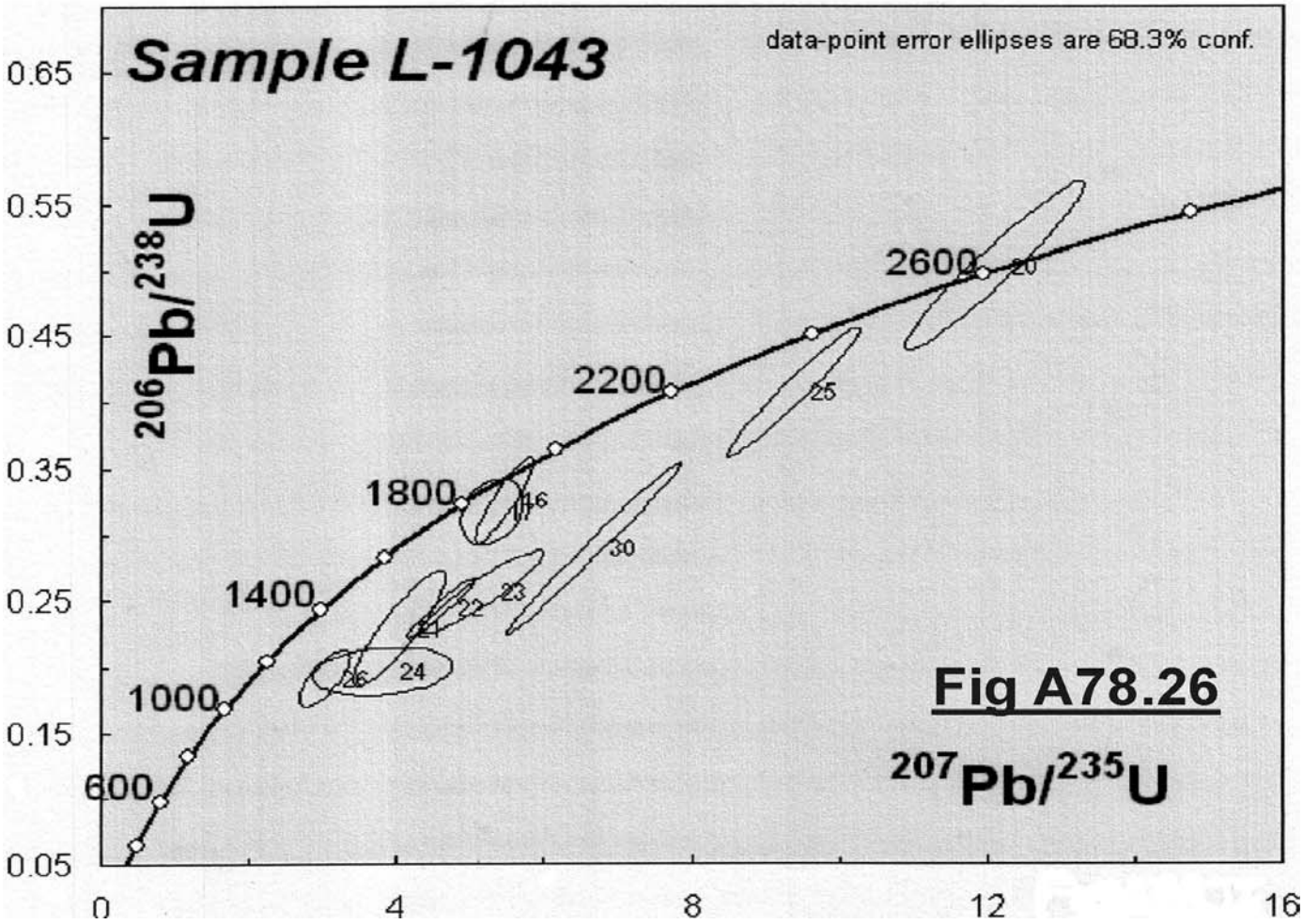

Fig A78.26

APPENDIX K
GEOCHRONOLOGICAL CORRELATION DIAGRAMS

A79	Correlation of dated events, Zambian locations, 258
A80	Correlation of dated events, Namibian locations, 259
A81	Correlation of dated events, Greater Lufilian Arc, 260
A82	Correlation of dated events, Greater Lufilian Arc, first portion (3000 to 1400 Ma), 261
A83	Correlation of dated events, Greater Lufilian Arc, second portion (1400 to 0 Ma), 262

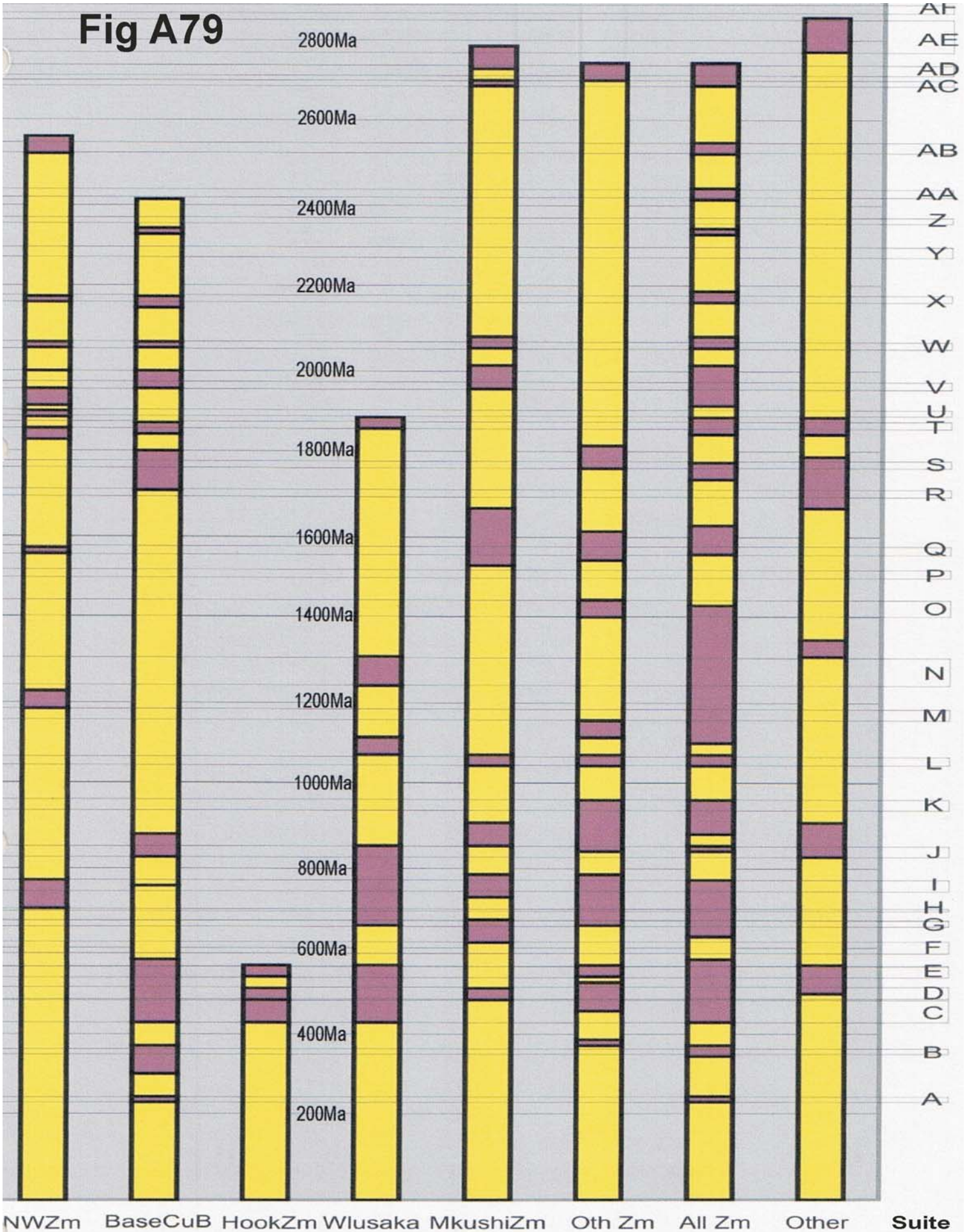

Correlation of dated events, Zambian Locations

Fig A80

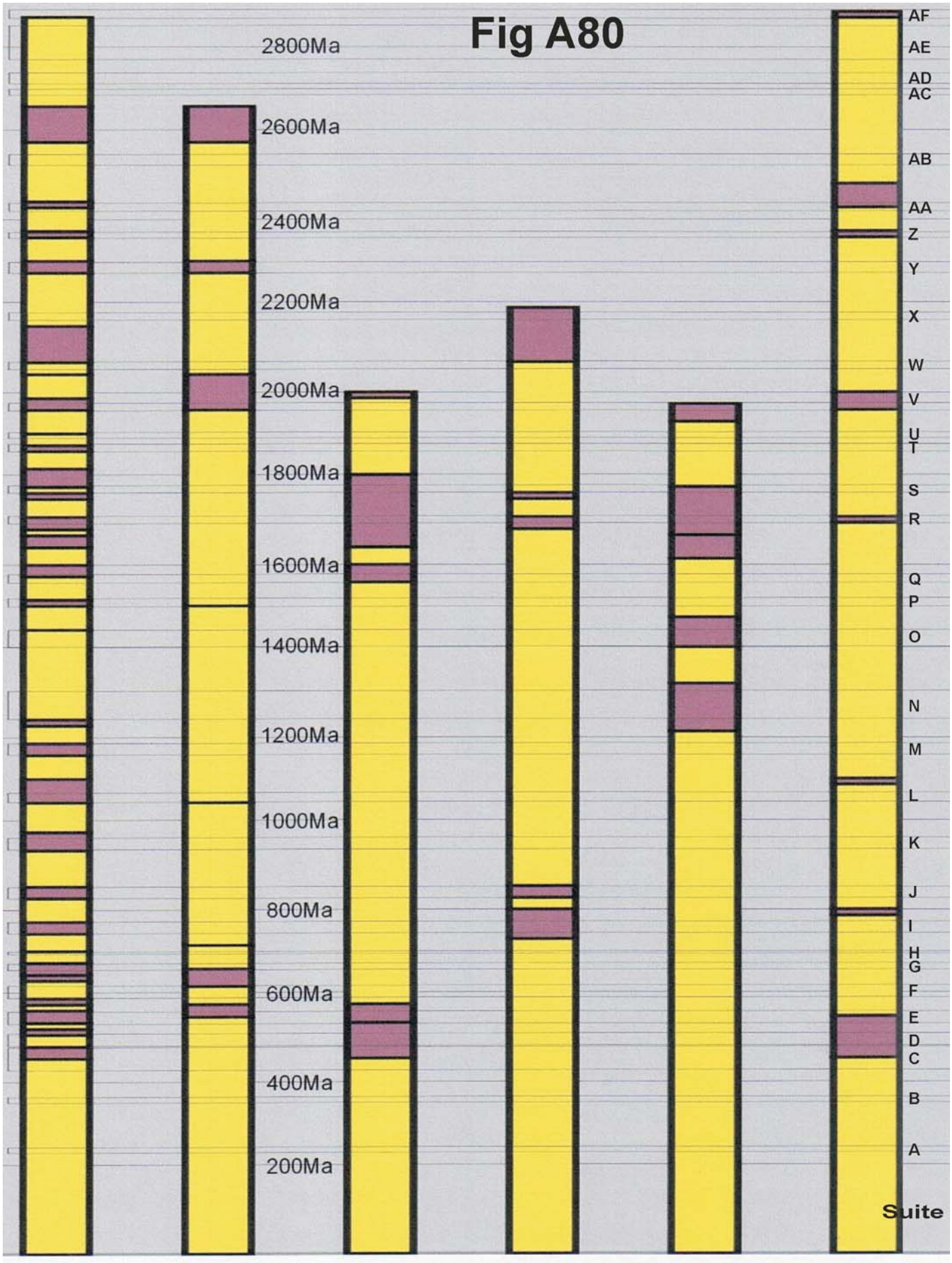

Correlation of dated events, Namibian Locations

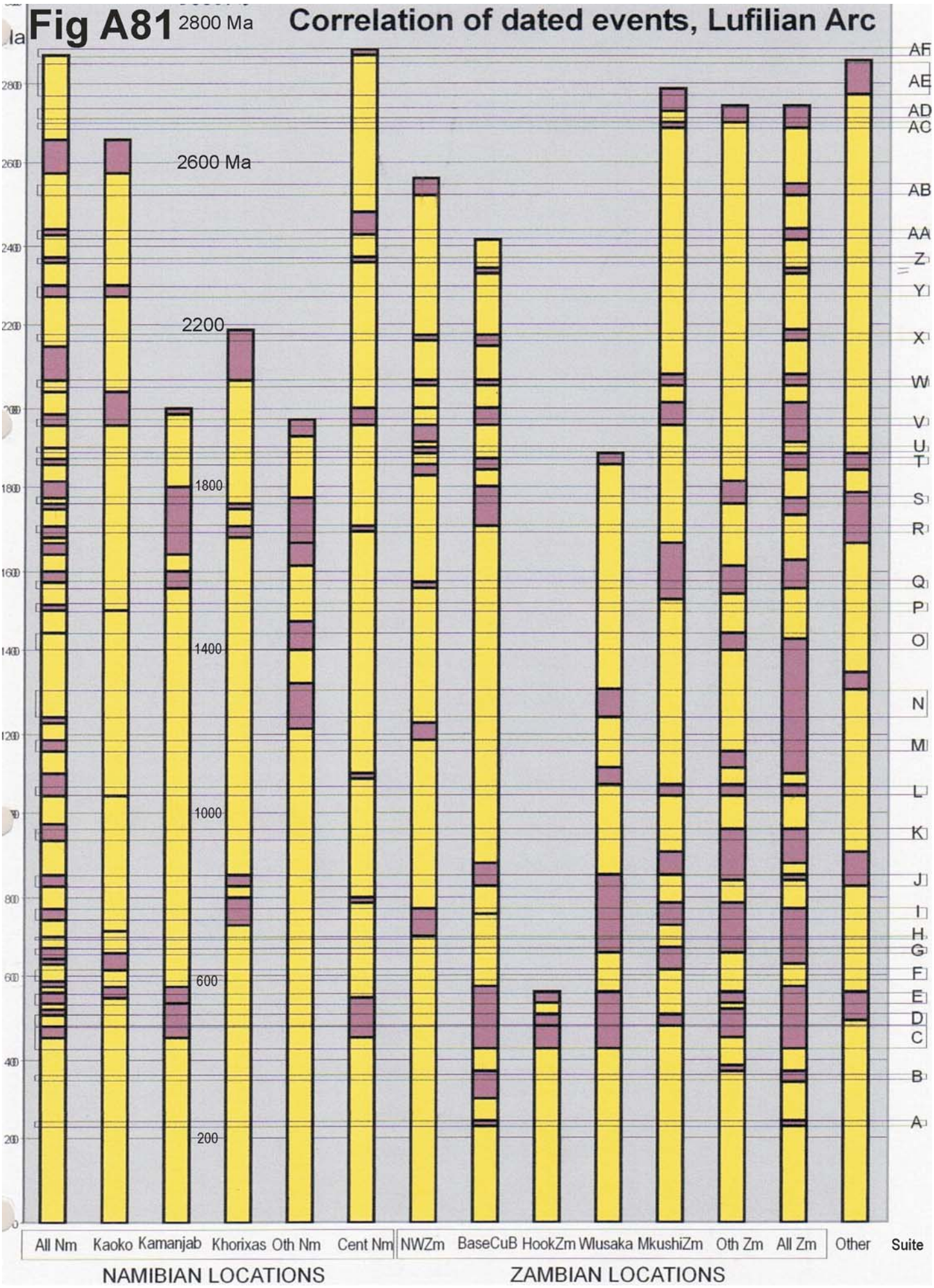
Fig A81
2800 Ma
Correlation of dated events, Lufilian Arc
2600 Ma
2200
1800
1400
1000
600
200
AF
AE
AD
AC
AB
AA
Z
Y
X
W
V
U
T
S
R
Q
P
O
N
M
L
K
J
I
H
G
F
E
D
C
B
A
All Nm
Kaoko
Kamanjab
Khorixas
Oth Nm
Cent Nm
NWZm
BaseCuB
HookZm
Wlusaka
MkushiZm
Oth Zm
All Zm
Other
Suite
NAMIBIAN LOCATIONS
ZAMBIAN LOCATIONS

Fig A82 Correlation of dated events, Lufilian Arc

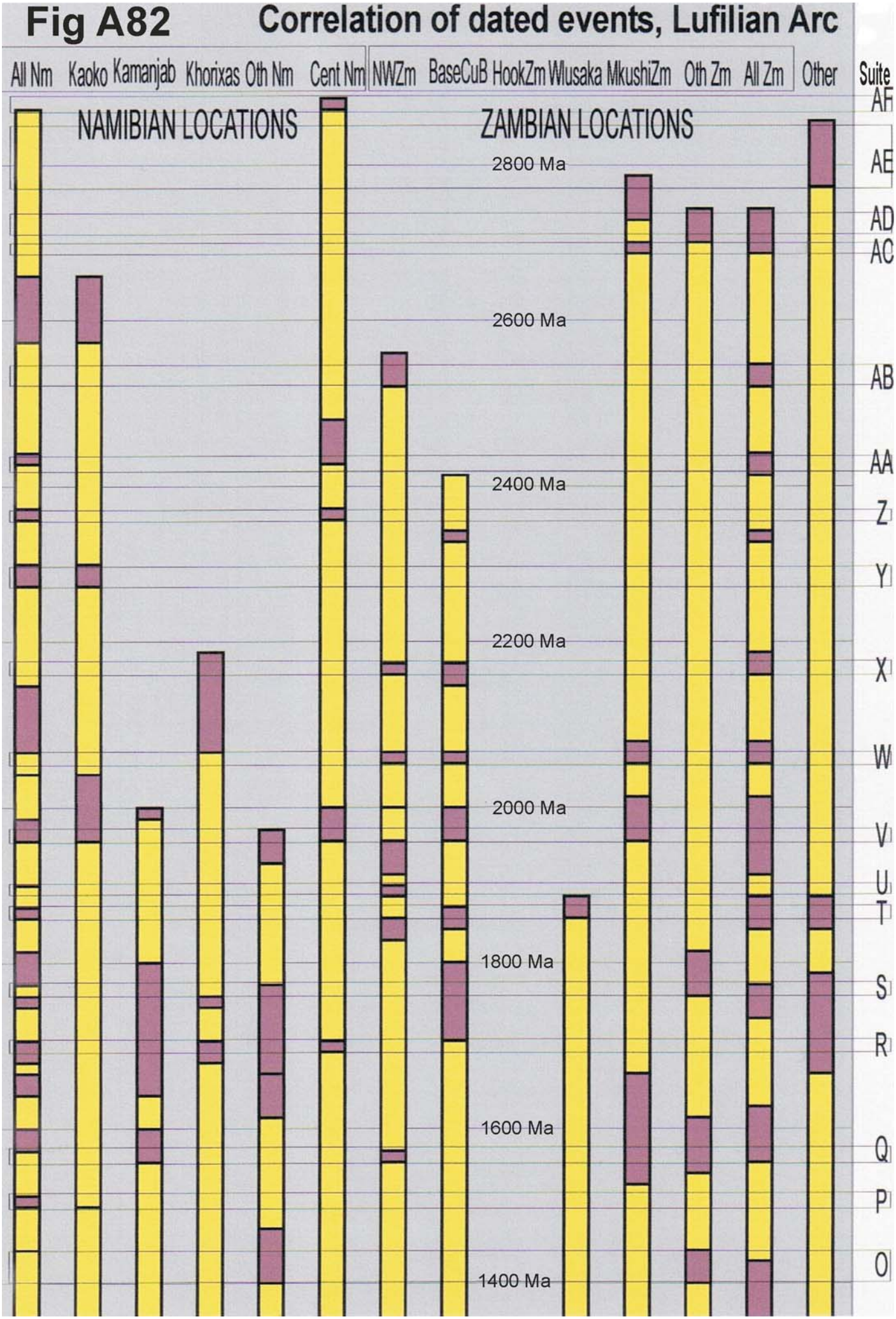

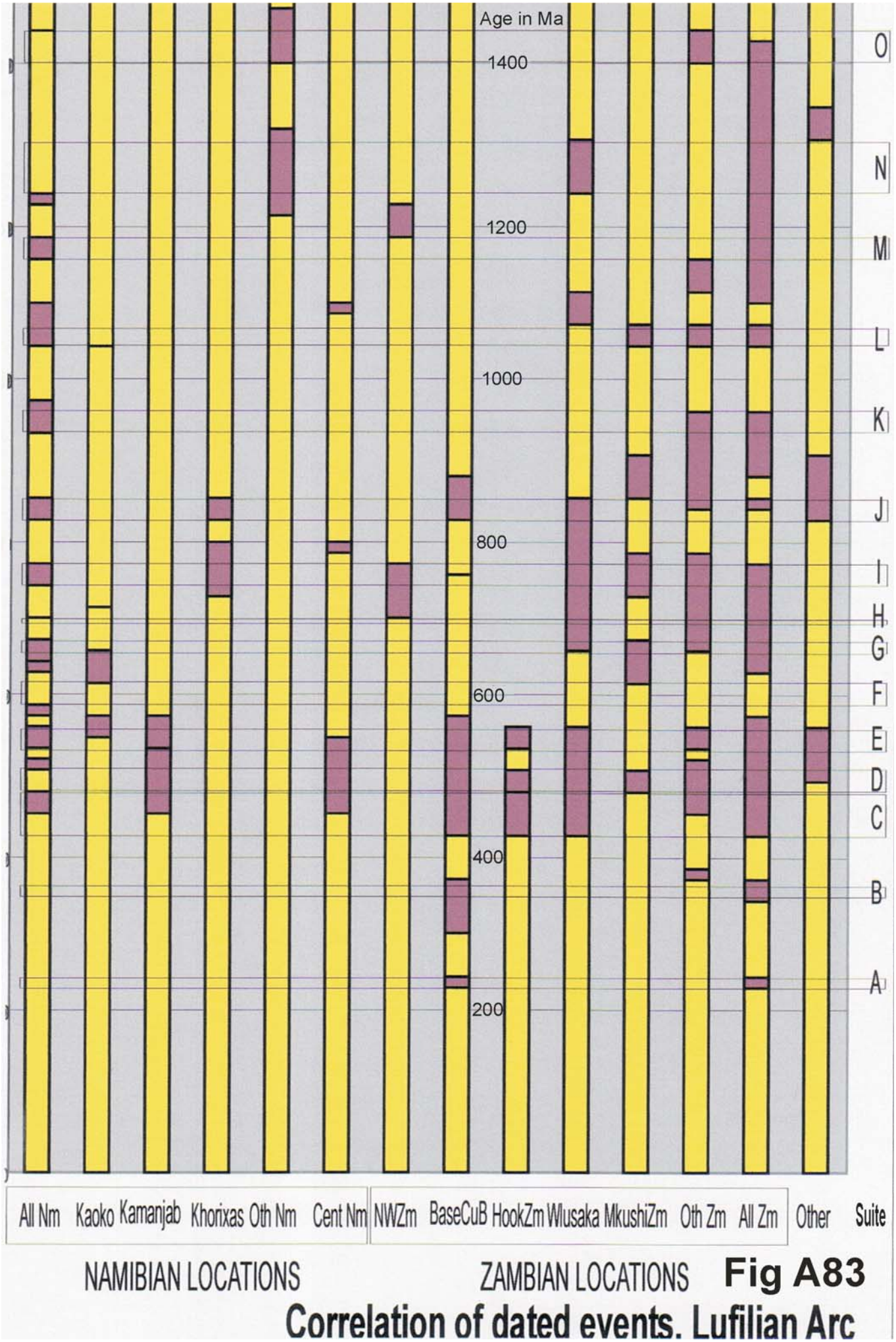

Fig A83

Correlation of dated events. Lufilian Arc

Contact information of the author

Last Name: **Lobo-Guerrero Sanz**

Name: **Alberto**

e-mail addresses: **ageo@iname.com**

ageo@logemin.com

Paper mail address: **Calle 127A No. 53A-28, office 309**
Bogota, Colombia

Home address: **Calle 109 No. 13-98**
Bogota, Colombia

Business telephone: **+57-1-6435364**

Home telephone: **+57-1-6586040**